# NUCLEAR SCIENCE ABSTRACTS

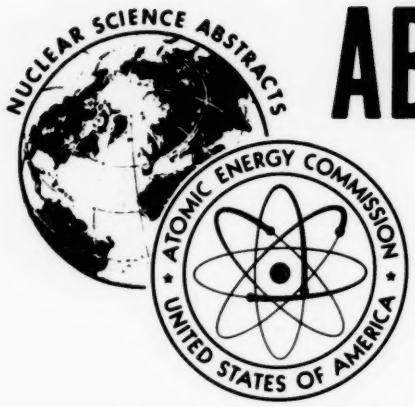


Volume 25 Number 23

Abstracts 54396-57296

December 15, 1971

UNITED STATES ATOMIC ENERGY COMMISSION
Division of Technical Information

XUM

# REPORT COLLECTIONS IN THE UNITED STATES

The libraries listed below purchase and maintain microfiche collections of USAEC and foreign reports that are abstracted in *NSA*. Their collections also include *NSA* and its indexes, AEC's Technical Progress Reviews, AEC-sponsored translations, conference proceedings published by AEC, and various bibliographic tools. Most of these libraries have microfiche reader-printers or other photocopy facilities with which to reproduce enlarged copies from microfiche. Charges for reproduction services vary.

**ALABAMA**
Auburn, Auburn University
Tuskegee Institute, Tuskegee Institute

**ALASKA**
College, University of Alaska

**ARIZONA**
Tucson, University of Arizona

**ARKANSAS**
Fayetteville, University of Arkansas

**CALIFORNIA**
Davis, University of California
Los Angeles, University of California

**COLORADO**
Boulder, University of Colorado

**DISTRICT OF COLUMBIA**
Washington, Library of Congress

**FLORIDA**
Gainesville, University of Florida

**GEORGIA**
Atlanta, Georgia Institute of Technology

**HAWAII**
Honolulu, University of Hawaii

**IDAHO**
Pocatello, Idaho State University

**ILLINOIS**
Evanston, Northwestern University
Urbana, University of Illinois

**INDIANA**
Lafayette, Purdue University

**IOWA**
Ames, Iowa State University

**KANSAS**
Manhattan, Kansas State University

**KENTUCKY**
Lexington, University of Kentucky
Louisville, University of Louisville

**LOUISIANA**
Baton Rouge, Louisiana State University
New Orleans, Tulane University

**MARYLAND**
Baltimore, Johns Hopkins University
College Park, University of Maryland

**MASSACHUSETTS**
Cambridge, Massachusetts Institute of Technology
Worcester, Worcester Polytechnic Institute

**MICHIGAN**
Ann Arbor, University of Michigan

**MISSISSIPPI**
State College, Mississippi State University

**MISSOURI**
Kansas City, Linda Hall Library

**NEVADA**
Las Vegas, University of Nevada

**NEW JERSEY**
Princeton, Princeton University

**NEW MEXICO**
Albuquerque, University of New Mexico

**NEW YORK**
Albany, New York State Library
Albany, State University at Albany
Buffalo, State University of New York at Buffalo
Ithaca, Cornell University
New York, Columbia University
Rochester, University of Rochester
Syracuse, Syracuse University
Troy, Rensselaer Polytechnic Institute

**NORTH CAROLINA**
Raleigh, North Carolina State University

**OHIO**
Cincinnati, University of Cincinnati
Cleveland, Cleveland Public Library
Columbus, Ohio State University
Toledo, University of Toledo

**OKLAHOMA**
Norman, University of Oklahoma

**PENNSYLVANIA**
Philadelphia, University of Pennsylvania
Pittsburgh, Carnegie Library
University Park, Pennsylvania State University

**PUERTO RICO**
San Juan, University of Puerto Rico

**SOUTH CAROLINA**
Columbia, University of South Carolina

**TENNESSEE**
Knoxville, University of Tennessee
Nashville, Joint University Libraries
Oak Ridge, Oak Ridge Associated Universities

**TEXAS**
Austin, University of Texas
College Station, Texas A & M University
Houston, Rice University

**UTAH**
Salt Lake City, University of Utah

**VIRGINIA**
Blacksburg, Virginia Polytechnic Institute
Charlottesville, University of Virginia

**WASHINGTON**
Pullman, Washington State University
Seattle, University of Washington

**WEST VIRGINIA**
Morgantown, West Virginia University

**WISCONSIN**
Madison, University of Wisconsin

**WYOMING**
Laramie, University of Wyoming

The following governmental and international organizations offer for sale USAEC reports abstracted in *Nuclear Science Abstracts:*

National Technical Information Service, U. S. Department of Commerce
Springfield, Virginia 22151
International Atomic Energy Agency, Vienna, Austria
National Lending Library, Boston Spa, England

XUM

Volume 25, Number 23, December 15, 1971

# NUCLEAR SCIENCE ABSTRACTS

*A semimonthly publication of the USAEC Division of Technical Information, Edward J. Brunenkant, Director, Published by the USAEC Division of Technical Information Extension, Robert L. Shannon, Extension Manager.*

*Nuclear Science Abstracts* provides the only comprehensive abstracting and indexing coverage of international nuclear science literature. *Nuclear Science Abstracts* covers scientific and technical reports of the U. S. Atomic Energy Commission and its contractors, other U. S. Government agencies, other governments, universities, and industrial and research organizations. In addition, books, conference proceedings, individual conference papers, patents, and journal literature on a worldwide basis are abstracted and indexed. Each issue of *Nuclear Science Abstracts* includes four indexes: subject, personal author, corporate author, and report number.

The following organizations scan and abstract the nuclear science literature in their respective countries:

Atomic Energy of Canada Limited
Australian Atomic Energy Commission
Danish Atomic Energy Commission
Finnish Atomic Energy Commission
French Atomic Energy Commission
Japan Atomic Energy Bureau–Atomic Energy Research Institute
Institutt for Atomenergi (Norway)
Aktiebolaget Atomenergi (Sweden)
United Kingdom Atomic Energy Authority

Numerous organizations, societies, and publishers throughout the world provide *Nuclear Science Abstracts* with advance page-proof copy of their publications, e.g., in the United States the American Institute of Physics provides page-proof copy of its publications.

A list of the journals scanned regularly and the abbreviations used appears in Issue 1 (January 15) of each volume of *Nuclear Science Abstracts* and is supplemented in Issues 7, 13, and 19. Issue 1 of each volume also describes the scope and arrangement of the subject matter covered in *Nuclear Science Abstracts*. The subject matter covered is also described in TID-4552, *Subject Scope of Nuclear Science Abstracts*, available free from the USAEC Division of Technical Information Extension, P.O. Box 62, Oak Ridge, Tennessee 37830. An outline of the subject categories appears in the Contents of each issue.

## AVAILABILITY OF PUBLICATIONS ABSTRACTED

Public availability of all U. S. Atomic Energy Commission reports is indicated in the report number indexes. The availability of other reports, when known, is also indicated. The availability of some unnumbered reports is given in the abstract.

Dissertations abstracted in *Dissertation Abstracts* and included in *Nuclear Science Abstracts* are available from University Microfilms, Inc., 315 N. First Street, Ann Arbor, Michigan 48103.

Information on the availability of the published literature and unpublished conference papers abstracted in *Nuclear Science Abstracts* can be obtained from the USAEC Division of Technical Information Extension, P.O. Box 62, Oak Ridge, Tennessee 37830.

## HOW TO OBTAIN NUCLEAR SCIENCE ABSTRACTS

*Nuclear Science Abstracts* is available to the public on a subscription basis from the Superintendent of Documents, U. S. Government Printing Office, Washington, D. C. 20402.

For the 24 regular issues, the yearly rate is $42.00 for domestic subscribers and $52.50 for foreign subscribers. A single issue costs $1.75, domestic rates, or $2.19, foreign rates. Domestic rates apply to the United States, Canada, Mexico, and Central and South American countries except Argentina, Brazil, Guyana, French Guiana, Surinam, and British Honduras.

For a yearly subscription to the cumulative indexes, the rates are $34.50 for domestic subscribers and $43.00 for foreign subscribers.

The following cumulative indexes are available:

From Johnson Reprint Corporation, 111 Fifth Avenue, New York, N. Y. 10003:

**Vols. 1–4, Subjects and Authors (1948–1950),** $30.00.

From Superintendent of Documents, U. S. Government Printing Office, Washington, D. C. 20402:

**Vols. 5–10, Subjects and Authors (1951–1956),** $5.25.

**Vols. 11–15, Subjects (1957–1961),** $19.00.
**Vols. 11–15, Personal Authors (1957–1961),** $14.25.
**Vols. 11–15, Corporate Authors (1957–1961),** $2.50.

**Vols. 16–20, Subjects (1962–1966),** $36.00.
**Vols. 16–20, Personal Authors (1962–1966),** $22.50.
**Vols. 16–20, Corporate Authors (1962–1966),** $3.75.

**Vol. 21, Subjects and Authors (1967),** $16.00.
**Vol. 22, Subjects and Authors (1968),** $26.00.
**Vol. 23, Subjects and Authors (1969),** $25.75.
**Vol. 24, Subjects and Authors (1970),** $22.50.
**Vol. 24, Authors (1970), Suppl.,** $2.00.

**Cumulative Report Number Index, Vols. 1–15 Revised,** $4.00.
**Cumulative Report Number Index, Vols. 16–20 Revised,** $5.50.
**Cumulative Report Number Index, Vols. 21–24,** $4.25.

*Nuclear Science Abstracts* is available on an exchange basis to universities, research institutions, industrial firms, and publishers of scientific information. Government agencies may obtain *NSA* free of charge. Inquiries should be directed to the USAEC Division of Technical Information Extension, P. O. Box 62, Oak Ridge, Tennessee 37830.

XUM

*Nuclear Science Abstracts* is also available on 16-mm microfilm in open reels or cartridges from Princeton Microfilm Corporation, Alexander Road, Princeton, New Jersey 08540. The backfile, which includes *Abstracts of Declassified Documents* (1947–1948), *Nuclear Science Abstracts* (1948–1969), *Nuclear Science Abstracts* cumulative indexes (1948–1966), and *Nuclear Science Abstracts* annual indexes (1967–1969), is $975. Yearly backfiles, beginning with 1970, and subscriptions, including cumulative indexes, are $125 per year.

## INDEXES TO NSA

Comprehensive indexes appear in each issue and are cumulated quarterly and annually. Multivolume cumulations have been issued as indicated above.

All documents abstracted are indexed by subjects and personal authors. Report literature is indexed also by corporate author and report number. Each of these indexes in every issue is preceded by an introduction explaining in detail the organization of the index and the principles by which it is compiled. The reader is referred to these explanations for information not found in the brief summary below.

### Personal Authors

Each author's name is indexed in the form appearing on the document abstracted:

**NEWCOMB, William A.,** Stability of a magnetic well, 25:1239
**NEWKIRK, L. R.,** Superconductivity in the pseudobinary alloys $V_3Si$—$Nb_3Al$, 25:1093 (CALT-822-13)
**NEWLAND, E. A.,** Radiation treatment of sewage, 25:140 (AAEC/LIB/Bib-254)

### Subjects

The subject index consisting of specific materials, objects, and processes is arranged alphabetically. Modifying phrases specific to these subjects in turn are arranged alphabetically under the subjects.

**TRANSURANIUM ELEMENTS**
determination in bone ash, radiochemical method for, 25:40 (IDO-12073, pp 28-36)
separation by ion exchange and complex-formation elution, 25:251(P)

**TRIETHYLENETETRAMINE**
complexes with cobalt(III) and rhodium(III) chlorides, radiation effects on labeled, thermal-neutron, 25:137
**TRITIUM**
content in Cattaraugus Creek near West Valley Processing Plant, July through Dec. 1969, 25:258 (DOCKET-50201-48)
content in Cattaraugus Creek near West Valley Processing Plant, Jan. to July 1970, 25:259 (DOCKET-50201-49)
determination in luminescent material by scintillation counting, 25:40 (IDO-12073, pp 28-36)

### Corporate Authors

Technical report literature is indexed from the name of the organization or institution responsible for the issuance of the report.

372 (UCRL-72739) CONSTRUCTION OF A UNIQUE UNDERGROUND WHOLE BODY COUNTER. Griffith, R. V.; Anderson, A. L.; Lindeken, C. L. **(California Univ., Livermore. Lawrence Radiation Lab.).** Oct 1970. 27p. (CONF-701009-1). Dep. NTIS.

is indexed as:

**CALIFORNIA UNIV., LIVERMORE. LAWRENCE RADIATION LAB.**
Construction of a unique underground whole body counter, 25:372 (UCRL-72739)

### Report Numbers

Technical report literature is also indexed by report numbers. This index includes information on where individual reports may be obtained. While not reports, patents and conference papers are indexed here as a matter of convenience.

| | | |
|---|---|---|
| **ORNL-** | | |
| 4270(Vol.2) | 25-614 | Dep. NTIS |
| 4606 | 25-1530 | Dep. NTIS |
| **ORNL-IBP-** | | |
| 70-3 | 25-2025 | Dep. NTIS |
| **ORNL-IIC-** | | |
| 21 | 25-261 | Dep. NTIS |
| 30(Pt.2) | 25-331 | Dep. NTIS |
| **ORNL-NSIC-** | | |
| 78 | 25-1912 | Dep. NTIS |

# TABLE OF CONTENTS

Volume 25, Number 23, December 15, 1971


| Category | Page |
|---|---|
| **CHEMISTRY** | 5345 |
| Analytical Chemistry | 5345 |
| *Chemical and Spectral Procedures* | 5345 |
| *Radiometric and Radiochemical Procedures* | 5349 |
| *Activation Procedures* | 5350 |
| Inorganic, Organic, and Physical Chemistry | 5359 |
| *Chemical Properties* | 5359 |
| *Isotope Effects and Exchange* | 5361 |
| *Physical Chemistry* | 5364 |
| Radiation and Nuclear Chemistry | 5365 |
| *Radiation Effects* | 5366 |
| *Radiation Processes* | 5367 |
| *Radiolysis* | 5369 |
| *Radioisotope Production* | 5374 |
| *Recoil Production and Reactions* | 5374 |
| Radiochemistry | 5376 |
| Separation Processes | 5377 |
| **EARTH SCIENCES** | 5383 |
| Geology and Hydrology | 5383 |
| Meteorology | 5385 |
| Mineralogy and Exploration | 5388 |
| Oceanography | 5389 |
| Seismology | 5389 |
| **ENGINEERING** | 5390 |
| Nuclear Explosions | 5390 |
| Facilities and Equipment | 5391 |
| Heat Transfer and Fluid Flow | 5394 |
| Isotope Technology | 5397 |
| Materials Testing | 5401 |
| Protective Structures | 5402 |
| Radioactive Material Handling | 5402 |
| Vacuum Engineering | 5408 |
| **INSTRUMENTATION** | 5409 |
| Radiation Detection Instruments | 5409 |
| *General Detectors and Monitors* | 5409 |
| *Nuclear Spectroscopic Instrumentation* | 5412 |
| *High Energy Physics Instrumentation* | 5413 |
| Radiation Dosimeters | 5414 |
| Radiometric Instruments | 5415 |
| Miscellaneous Instruments and Components | 5415 |
| Radiation Effects on Instruments and Instrument Components | 5418 |
| **LIFE SCIENCES** | 5420 |
| Biochemistry, Physiology, and Molecular Biology | 5420 |
| *Basic Processes* | 5420 |
| *Metabolism, Physiology, and Toxicology* | 5420 |
| *Radiation Effects* | 5422 |
| *Immunology* | 5424 |
| Ecology | 5425 |
| Genetics and Cytogenetics | 5427 |
| Health Physics and Safety | 5431 |
| *Radioactive Contamination and Decontamination* | 5431 |
| *Dosimetry and Monitoring* | 5432 |
| *Radiation Protection* | 5436 |
| *Safety Procedures* | 5437 |

| Category | Page |
|---|---|
| **LIFE SCIENCES (Cont'd.)** | |
| *Legal Aspects* | 5437 |
| Medicine | 5438 |
| *Protective Substances* | 5438 |
| *Radiation Sickness and Injuries* | 5439 |
| *Radiodiagnosis* | 5440 |
| *Radiotherapy* | 5442 |
| *Blast and Thermal Effects* | 5443 |
| Radiation Effects on Animals | 5443 |
| *Invertebrates* | 5444 |
| *Vertebrates* | 5444 |
| *Man* | 5447 |
| Radiation Effects on Plants | 5448 |
| Radiation Effects on Microorganisms | 5448 |
| Radiosterilization and Radiopreservation | 5450 |
| **METALS, CERAMICS, AND OTHER MATERIALS** | 5451 |
| Metals and Alloys | 5451 |
| *Corrosion and Erosion* | 5451 |
| *Preparation and Fabrication* | 5454 |
| *Properties Evaluations* | 5457 |
| *Structure and Phase Studies* | 5467 |
| *Radiation Effects* | 5471 |
| Ceramics and Cermets | 5473 |
| *Corrosion and Erosion* | 5473 |
| *Preparation and Fabrication* | 5473 |
| *Properties Evaluations* | 5475 |
| *Structure and Phase Studies* | 5479 |
| *Radiation Effects* | 5479 |
| Plastics and Other Materials | 5481 |
| **PHYSICS (GENERAL)** | 5483 |
| Astrophysics and Cosmology | 5483 |
| *Cosmic Ray Exposure Ages* | 5483 |
| *Stars* | 5483 |
| *Quasi-Stellar, Radio, and X-Ray Sources* | 5487 |
| *Solar Phenomena* | 5489 |
| *Galaxies* | 5494 |
| *Cosmology* | 5496 |
| *Planetary Phenomena* | 5497 |
| Atomic and Molecular Physics | 5497 |
| *Atomic, Electron, Ion, and Molecular Beams and Their Reactions* | 5497 |
| *Atomic and Molecular Properties* | 5498 |
| *Positronium, Muonium, and Mesic Atoms and Molecules* | 5499 |
| *Collision Phenomena* | 5499 |
| *Atomic Theory* | 5504 |
| Cosmic Radiation | 5505 |
| Direct Energy Conversion | 5507 |
| Fluid Physics | 5507 |
| Geophysics (Upper Atmosphere) | 5511 |
| Low-Temperature Physics and Cryogenic Equipment | 5522 |
| *Superfluidity* | 5522 |
| *Superconductivity* | 5523 |
| *Equipment and Devices* | 5528 |
| Plasma and Thermonuclear Physics | 5529 |
| *Confinement and Heating* | 5529 |
| *Diagnostics* | 5530 |


XUM

# TABLE OF CONTENTS (continued)


| Category | Page |
|---|---|
| **PHYSICS (GENERAL) (Cont'd.)** | |
| *Kinetics (General)* | 5531 |
| *Kinetics (Experimental)* | 5532 |
| *Kinetics (Theoretical)* | 5533 |
| *Production* | 5537 |
| *Stability* | 5537 |
| *Thermonuclear Processes* | 5538 |
| *Wave Phenomena* | 5540 |
| Shielding | 5543 |
| Solid-State Physics | 5545 |
| *Radiation Effects* | 5545 |
| *Physical Properties* | 5552 |
| *Moessbauer Effects and NMR* | 5554 |
| *Theory* | 5557 |
| Theoretical Physics | 5557 |
| **PHYSICS (HIGH-ENERGY)** | 5559 |
| Particle Interactions and Properties (Experimental) | 5559 |
| *Electromagnetic* | 5559 |
| *Weak* | 5559 |
| *Strong (Baryon-Induced)* | 5559 |
| *Strong (Meson-Induced)* | 5560 |
| Particle Interactions and Properties (Theoretical) | 5561 |
| *General* | 5561 |
| *Electromagnetic* | 5562 |
| *Weak* | 5563 |
| *Strong (General)* | 5564 |
| *Strong (Baryon No. = 0)* | 5565 |
| *Strong (Baryon No. = 1)* | 5566 |
| *Strong (Baryon No. ≥ 2)* | 5568 |
| Particle Invariance Principles and Symmetries | 5569 |
| *General* | 5569 |
| *Applications (Electromagnetic and Weak)* | 5569 |
| *Applications (Strong)* | 5569 |
| Field Theories | 5569 |
| *General* | 5569 |
| *Quantum Field Theory* | 5569 |
| *Gravitation and General Relativity* | 5571 |
| Scattering Theory | 5572 |
| Particle Accelerators | 5572 |
| **PHYSICS (NUCLEAR)** | 5576 |
| Neutron Interactions with Matter | 5576 |
| Nuclear Properties and Reactions, A ≤ 5 | 5579 |

| Category | Page |
|---|---|
| **PHYSICS (NUCLEAR) (Cont'd.)** | |
| Nuclear Properties and Reactions, 6 ≤ A ≤ 19 | 5580 |
| Nuclear Properties and Reactions, 20 ≤ A ≤ 89 | 5584 |
| Nuclear Properties and Reactions, A ≥ 90 | 5589 |
| Nuclear Theory | 5597 |
| **REACTOR TECHNOLOGY** | 5604 |
| Commercial Power Reactors | 5604 |
| *Operation and Economics* | 5605 |
| *Safety and Siting* | 5607 |
| Power Reactor Development | 5610 |
| *Kinetics and Dynamics* | 5614 |
| *Control Systems* | 5614 |
| *Shielding* | 5615 |
| *Cooling Systems* | 5615 |
| *Fuels* | 5616 |
| *Auxiliary and Emergency Systems* | 5618 |
| *Operation and Economics* | 5618 |
| *Safety and Siting* | 5619 |
| *Power Conversion Systems* | 5624 |
| Research and Test Reactors | 5624 |
| Rocket and Space Reactors | 5626 |
| Process Heat and Desalination Reactors | 5626 |
| Marine and Portable Power Reactors | 5626 |
| Production Reactors | 5627 |
| Reactor Theory | 5627 |
| *Kinetics* | 5630 |
| *Dynamics* | 5631 |
| *Experimental Applications* | 5631 |
| Reactor Components, Fuels, and Accessories | 5632 |
| **GENERAL** | 5634 |
| **CORPORATE AUTHOR INDEX** | INDEX-1 |
| **PERSONAL AUTHOR INDEX** | INDEX-13 |
| **SUBJECT INDEX** | INDEX-75 |
| **REPORT NUMBER INDEX** | INDEX-178 |

## STAFF OF NUCLEAR SCIENCE ABSTRACTS

John W. Norris
*Managing Editor*

Donald D. Davis
*Assistant Managing Editor*

David E. Bost
*Production Manager*

Sidney F. Lanier
*Subject Heading Specialist*

J. Paul Meredith
*Descriptive Cataloging Specialist*

Frederick E. Marsh, Jr.
*Computer Index Coordinator*

Clara L. Fox
*Corporate Author Specialist*

Helen W. White
*Report Number Specialist*

### Section Editors

Everett J. Hoffman
*Chemistry*

Robert C. Kelly
*Engineering; Earth Sciences; Metals, Ceramics, and Other Materials*

Lee M. Thompson
*General Physics*

Charles E. Stuber
*High Energy Physics; Instrumentation*

Donald D. Davis
*Life Sciences*

Lawrence T. Whitehead
*Nuclear Physics*

James M. Jacobs
*Reactor Technology*

### Evaluators

Thomas S. Chapman
John H. Mitchell
Mary H. Newman
Polly C. Summers

### Abstractors

F. S. Armstrong*
Ellis R. Bedford
Jane G. Buchanan
D. Lamar Cason
Gloria M. Caton
David C. Cunningham
James R. Dulaney
Helga B. Gerstner
Mary C. Grissom
Phyllis C. Hansen
Carolyn D. Houston
Elaine E. Huber
W. Hugh Kinser, Jr.
Lisbeth C. Lieberman
Betty L. McDowell
Fay M. Martin
William D. Matheny
Dora H. Moneyhun
Jean F. Peckham
Henry D. Raleigh
Mona H. Raridon
Julia S. Redford
Jessie W. Rushing
Robert W. Rutkowski
Francis L. Sachs
Lila B. Smith
Anne G. Ward
Helen L. Ward
Kenneth S. Warren
Milton O. Whitson
Juanita Wilson

*Atomic Energy of Canada, Ltd.

Charles R. Bruce
*Publishing Coordinator*

**Communication concerning the editorial policy and content of *Nuclear Science Abstracts* should be addressed to the Managing Editor, *Nuclear Science Abstracts*, USAEC Division of Technical Information Extension, P. O. Box 62, Oak Ridge, Tennessee 37830.**

*Use of funds for printing this publication approved by the Director of the Bureau of the Budget, June 26, 1969.*

XUM

Volume 25, Number 23 December 15, 1971

# NUCLEAR SCIENCE ABSTRACTS

# CHEMISTRY

## Analytical Chemistry

*Refer also to abstracts 54587, 54711, 54734, 55369, 56752, and 57127.*

**54396** (ORNL-4682, pp 242-9) MISCELLANEOUS PROGRAMS. (Oak Ridge National Lab., Tenn.).

In Chemical Technology Division annual progress report.

Research progress is reported on: the quality assurance program, evaluation of the radiation resistance of selected protective coatings (paints), resource studies, environmental quality program on the productive uses of waste heat, systems analysis of a nuclear engineering center, applications of $^{252}Cf$. (M.C.G.)

**54397** ION EXCHANGE IN ANALYTICAL CHEMISTRY. Riemann III, William; Walton, Harold F. International Series of Monographs in Analytical Chemistry, Volume 38. Oxford; Pergamon Press (1970). 293p. £7.50.

One chapter, that dealing with nonchromatographic applications is in scope for NSA. Among other subjects discussed in this chapter, on removal of interfering constituents, is the determination of Ru, U, In (by activation analysis), Y, and rare earths in steel and the removal of U from alkali and alkaline-earth metals. In the section on concentrating trace constituents the determination of $^{131}I$ in drinking water and $^{90}Sr$ in milk are among subjects considered. (UK)

**54398** THIRD RUSSIAN-ITALIAN SYMPOSIUM ON CHROMATOGRAPHY, TBILISI, USSR, OCTOBER 26th-29th, 1970. J. Chromatogr.; 58: No. 1, 1-135(10 Jun 1971). (CONF-701051).

Sixteen papers presented at the conference are included. A separate abstract was prepared for one paper. (M.C.G.)

*For an abstract of an individual paper see: 54727.*

**54399** DETERMINATION OF SMALL AMOUNTS OF IMPURITIES IN MOLYBDENUM AND ITS COMPOUNDS. Horkay-Borsos, Klara; Hegedus, Andras J. (United Incandescent Lamp and Electricity Co., Budapest). Kem. Kozlem.; 34: 107-21(1970). (In Hungarian).

Various methods used for the determination of impurities in molybdenum, including the starting materials used for fabrication, and the intermediate products, were evaluated on the basis of material published in Chemical Abstracts during the 1948 to 1968 period. Most of the effort was spent on the determination of rhenium. The number of papers on radiochemical and spectrophotometric techniques is of the same order of magnitude as that of emission spectroscopic studies. Radiochemical determinations are most sensitive, exceeding the level of spectroanalytical methods by 1 to 2 orders of magnitude. The radiochemical method is highly selective; it allows the determination of several elements on the basis of a single measurement and has an excellent precision without requiring a preliminary chemical separation. The x-ray fluorescence technique also presents several advantages. The mass spectroscopic method is in a period of rapid growth but requires the use of an expensive instrument. (233 references). (TTT)

### Chemical and Spectral Procedures

*Refer also to abstract 54529.*

**54400** ULTRAVIOLET SPECTROPHOTOMETRIC DETERMINATION OF TELLURIUM. Looyenga, Robert W.; Boltz, D. F. (Wayne State Univ., Detroit). Microchim. Acta; No. 3, 507-12 (1971).

An ultraviolet spectrophotometric method for the determination of tellurium is proposed. It is based on the formation of tetrakis-1-pyrrolidinecarbodithioate tellurium(IV), which is extractable with chloroform. Conformity to Beer's law was observed. The molar absorptivity at 257 nm is $8.12 \cdot 10^4$ l./mole$^{-1}$/cm$^{-1}$. (auth)

**54401** SEPARATION OF RHENIUM FROM MOLYBDENUM AND OTHER HEAVY METALS BY SOLVENT EXTRACTION. Yatirajam, V.; Kakkar, L. R. (Kurukshetra Univ., India). Mikrochim. Acta; No. 3, 479-88(1971).

Two methods are presented for the extractive separation of rhenium from molybdenum and other heavy metals in hydrochloric acid solution. In the first method, Mo(VI) and Re(VII) are reduced by hydrazine in strong hydrochloric acid solution to Mo(V) and Re(IV). The former is then extracted into iso-amyl acetate. The Re(IV) remaining in the aqueous phase is oxidized to Re(VII) and determined by known procedures. In the second method, Re(VII) and other ions in 1 to 1.3 N HCl are boiled with hydrazine sulphate for 5 minutes. After adding EDTA to complex Mo(V) and adjusting the solution to 0.33 N HCl, rhenium is extracted into chloroform containing 1% tribenzylamine, and is recovered by shaking with water having sufficient ammonia to neutralise the acid and a little hydrogen peroxide. (auth)

**54402** ANOMALOUS ION-EXCHANGE BEHAVIOR EXHIBITED BY AGED ACID-FREE URANYL NITRATE SOLUTIONS. Perez-Bustamante, J. A. (Junta de Energia Nuclear, Madrid). Mikrochim. Acta; No. 3, 455-63(1971).

A comparison of the ion-exchange behaviour of stoichiometric acid-free freshly prepared and strongly aged (7 to 8 years) uranyl nitrate solutions was made by means of different cation-exchange and anion-exchange resin systems. While the freshly prepared solutions undergo completely normal stoichiometric anionic and cationic exchange when percolated through strongly acidic or basic ion-exchange resins, the aged solutions show a strikingly anomalous cation-exchange behavior since the uranyl cation exhibits an apparent net electrical charge of about 4+. On the basis of these findings it was concluded that proper attention should be paid to possible restrictions in the applicability of cation-exchange resins for the determination of free acidity in uranyl nitrate solutions, especially when dealing with aged solutions of very low free acidity. (auth)

**54403** CHEMICAL METHODS OF ROCK ANALYSIS. Jeffrey, Paul G. London; Pergamon Press Ltd. (1970). 514p. £7.00.

Several chapters come within NSA scope, including molybdenum and tungsten (occurrence, determination by photometric methods, and determination in silicate rocks), niobium (occurrence, determination, determination in carbonatites with hydrogen peroxide, in silicate rocks with thiocyanate, with 4-(2-pyridylazo)-resorcinol), occurrence and determination of tantalum, scandium (occurrence and determination in silicate rocks), yttrium (occurrence and determination), lanthanide rare earths (occurrence, gravimetric determination in silicate and carbonatite rocks, and photometric determination in silicate rocks), occurrence and determination of tellurium, strontium (occurrence, determination, determination by flame photometry and by atomic absorption spectroscopy), thorium (occurrence, determination by gravimetric and photometric methods, separation methods, and in silicate rocks), uranium (occurrence, determination, photometric methods,



XUM

separation and determination in silicate rocks) and zirconium (occurrence, gravimetric determination in silicate rocks, phosphate method, other gravimetric methods and photometric methods). (UK)

**54404** MASS-SPECTROMETRIC ANALYSIS OF THE ISOTOPIC COMPOSITION OF IRON IN THE GAS PHASE. Ivlev, A. A.; Knyazev, D. A.; Galimov, E. M. (Moscow Inst. of the Petrochemical and Gas Industry. Moscow Inst. of Chemical Engineering). Russ. J. Phys. Chem. (Engl. Transl.); 45: No. 2, 130-2(Feb 1971).

Translated from Zh. Fiz. Khim.; 45: No. 2, 230-3(Feb 1971).

A method was developed for the accurate gas-phase mass-spectrometric analysis of iron isotopes based on the use of iron pentacarbonyl. The optimum conditions for synthesis of iron pentacarbonyl from small amounts of the starting materials were chosen. Accurate mass-spectrometric analysis is ensured by employing a two-channel filling system with a block of magnetically operated valves and a commutating device. The accuracy is estimated as ±0.1%. (auth)

**54405** STANDARD METHOD OF TEST FOR CONSUMPTION OF POTASSIUM PERMANGANATE BY IMPURITIES IN DEUTERIUM OXIDE. ASTM D2033-68. Philadelphia; American Society for Testing and Materials (1968). 2p. Available from American Society for Testing and Materials, Philadelphia.

A titrimetric measurement of impurities in $D_2O$ is described. A measured amount of $D_2O$ is reflexed with $KMnO_4$ in an acid medium. Standard oxalic acid is added and the mixture back-titrated with standard $KMnO_4$. (M.C.G.)

**54406** IODINE-SPECIFIC DETECTOR FOR A GAS CHROMATOGRAPH. Gutsche, Brigitte; Herrmann, Roland (Univ., Giessen, Ger.). Z. Anal. Chem.; 253: No. 4, 257-62(1971). (In German)

The in-flame detector earlier applied to the specific chlorine (359.9 nm) and bromine (372.7 nm) analysis has now been employed for the iodine determination at 409.9 nm. It is shown that the resolution power of a GC column can be improved by such a specific detector. After calibration quantitative measurements of the iodine contents of the GC fractions are possible. The detection limits are 0.01 to 1.4 μg of iodine. (auth)

**54407** PHOTOMETRIC DETERMINATION OF SMALL AMOUNTS OF CHLORIDE IN SELENIUM, TELLURIUM, GALLIUM, AND BISMUTH. Scheubeck, E.; Ernst, O. (Siemens AG, Erlangen, Ger.). Z. Anal. Chem.; 254: No. 3, 185-7(1971). (In German).

The sample is dissolved in nitric acid in the presence of silver nitrate. Silver chloride is separated by centrifuge and decomposed in a glass equipment by chromosulphuric acid. Resulting volatile compounds of chlorine are oxidized by potassium permanganate in sulphuric acid solution to chlorine, which forms with o-tolidine a yellow oxidation product. The absorbance of this coloration is measured by photometry and corresponding amounts of chloride are found out by calibration curves. One to 100 μg of chloride can be determined in the range of 1 to 10 ppm Cl with a standard deviation of ±0.6 ppm Cl and at approximately 200 ppm Cl with ±2.8 ppm Cl. (auth)

**54408** DETERMINATION OF METALS IN RIVER SLUDGE BY MEANS OF X-RAY FLUORESCENCE AND ITS APPLICATION IN ACTUAL PRACTICE. Hellmann, H. (Bundesanstalt fuer Gewaesserkunde, Coblenz). Z. Anal. Chem.; 254: No. 3, 192-5 (1971). (In German).

The occurrence of metals in the sediments of the Rhine basin was investigated with the aid of x-ray fluorescence. In addition to trace metals such as zirconium, strontium, and rubidium, which are encountered in non-varying concentrations, the heavy metals copper, lead and, in particular, zinc were found to occur in concentrations that vary considerably from one region to the other. Concentrations beyond the normal background limits are due to influent waste water. (auth)

**54409** ANALYSIS COMPARISONS OF SOME THERMAL AND SURFACE WATERS BY MASS SPECTROMETRY AND U. V. ABSORPTION SPECTROMETRY. Klose, M. (Forschungsstelle der Saechsische Akademie, Freiberg, Ger.). Z. Anal. Chem.; 254: No. 3, 195-8(1971). (In German).

The results of mass-spectrographic analyses of powdered residues of some thermal and surface waters, as well as their uv absorption spectra are reported. According to these results, a comparatively higher number of elements (up to 10 additional elements in our examples), which is typical of the minerals existing in the reservoir rock bearing thermal waters, is a characteristic of the thermal waters. Parallel to this, the uv transmission of the thermal waters examined was measured, which (with the occurrence of weak fluorescence) proved to be more intensive because of their chemical constituents and suggests their application in connection with uv radiotherapy as useful. (auth)

**54410** TRIPHENYLMETHANE DYES AS REDOX INDICATORS IN DICHROMETRY. Rao, N. Venkateswara; Dutt, V. V. S. Eswara (Andhra Univ., Waltair, India). Z. Anal. Chem.; 254: No. 2, 110-14(1971).

The use of some triphenylmethane dyes, Erioglaucine A, Eriogreen B, Xylenecyanol FF, Setoglaucine O, Setocyanine Supra, Fast Green FCF, and Night Blue as redox indicators in the dichrometric titration of iron(II), ferrocyanide, uranium(IV), molybdenum(V), and hydroquinone in hydrochloric acid, sulfuric acid, and perchloric acid media was studied. Conditions for the satisfactory titrations employing these indicators were established. (auth)

**54411** INDIRECT POTENTIOMETRIC METHOD FOR THE DETERMINATION OF PLUTONIUM. Rao, C. L.; Nair, G. M.; Singh, N. P.; Ramaniah, M. V.; Srinivasan, N. (Bhabha Atomic Research Centre, Trombay, India). Z. Anal. Chem.; 254: No. 2, 126-7(1971).

A procedure was developed for determination of Pu based on the following principle: oxidation of Pu to Pu(VI) by AgO, destruction of excess oxidant by sulfamic acid, reduction of Pu(VI) by known excess of Fe(II) and potentiometric titration of remaining Fe(II) with Ce(IV). The accuracy of the method was <0.2%. Large quantities of U were found to affect the results tending to give higher values. The entire operation takes about 15 min. (M.C.G.)

**54412** RUTHENIUM AND OSMIUM SEPARATE SPECTROPHOTOMETRIC DETERMINATION BY THE USE OF 4-(2-PYRIDYLAZO)-RESORCINOL. Bogdanovich, L. I.; Busev, A. I.; Ivanov, V. M. Vestn. Mosk. Univ., Ser. II. Khim.; 12: No. 2, 197-200(Mar-Apr 1971). (In Russian).

A spectrophotometric method was used for the determination of ruthenium and osmium without their separation. The method was used for the determination of ruthenium (7.9 to 71 mkg) in the presence of 7.4 to 103.9 mkg osmium. (auth)

**54413** DETERMINATION OF STRONTIUM IN BARIUM MINERALS BY ATOMIC ABSORPTION SPECTROSCOPY. Michalewska, Malgorzata; Kazimierczyk, Stefania (Pilot Plant of Copper Mining and Metallurgic Works, Lubin, Poland). Chem. Anal. (Warsaw); 16: No. 3, 573-80(1971). (In Polish).

Atomic absorption spectrophotometry was used for the determination of strontium in barium minerals. Uvispek H-700 spectrophotometer manufactured by Hilger and Watts with acetylene–air flame was used. Absorption of strontium in the presence of interfering cations and anions was measured and the possibility of applying an inhibiting agent was investigated. It was found that the effect of titanium and aluminum on absorption of the strontium line could be eliminated by addition of 300 ppM of calcium or mixed buffer (ammonium salt of EDTA + 2000 ppM $La_2O_3$) respectively. The method is valid for a strontium concentration range of 0.5 to 40.0 ppM. The relative standard deviation did not exceed ±5%. (auth)

**54414** DETERMINATION OF IMPURITIES IN HIGH PURITY TELLURIUM. III. SPECTROPHOTOMETRIC DETERMINATION OF COPPER AS ROSE BENGAL–BIS(PHENANTHROLINE)–COPPER(II) COMPLEX. Kasterka, Barbara; Dobrowolski, Jan (Politechnika, Danzig). Chem. Anal. (Warsaw); 16: No. 3, 619-30(1971). (In Polish).

A spectrophotometric method for the determination of traces of copper in high purity tellurium as a ternary complex: $[Cu(phen)_2]$ Bengal Rose developed. Molar absorptivity amounted to $\epsilon = 58.8 \times 10^3$ at $\lambda_{max} = 570$ nm. The limit of determination for copper was found to be $4.2 \times 10^{-2}$ μg/ml, at the cell thickness 10 mm and the confidence level of 99% for n = 6. The optimum pH was found to be 8 to 10. The precision of the standard addition method expressed in terms of standard deviation amounted $s = 4.9 \times 10^{-2}$. The method was rendered specific for copper. Tellurium at concentrations lower than 50 mg did not interfere. The coefficient of the preconcentration of copper was found to be $1.1 \times 10^2$. From $10^{-5}$ to $10^{-6}$% of copper in tellurium can be determined by this method. (auth)

**54415** ANALYTICAL USES OF LANTHANIDE NITRITE COMPLEXES. II. DETERMINATION OF CESIUM AS CESIUM SILVER HEXANITRITOCERITE(III). Richter, Malgorzata; Cyganski, Andrzej (Politechnika, Lodz, Poland). Chem. Anal. (Warsaw); 16: No. 3, 637-41(1971). (In Polish).

XUM

A method for gravimetric and indirect titrimetric determination of cesium was developed. The method consists of precipitation of cesium in the form of $Cs_2Ag[Ce(NO_2)_6]$ by addition of the precipitating agent (15 g $Ce(NO_3)_3 \cdot 6H_2O$, 20 g $NaNO_2$, and 1.5 g $AgNO_3$ in 100 $cm^3$ of the solution). The precipitate is dried at 100°C or dissolved in $HNO_3$ (1 + 1), followed by the determination of silver by Volhard's method. The method can be used in the presence of potassium, lithium, ammonium ions, magnesium, and calcium. (auth)

**54416** GRAVIMETRIC DETERMINATION OF TELLURIUM IN SILICON–MAGNESIUM MASTER ALLOYS. Nowak, Teresa. Pr. Inst. Odlew., Zesz. Specjalne; No. 1, 38-47(1970). (In Polish).

Te was determined in 2 samples containing Ca 7.20, C 2.31, Mg 12.16, Ce 16.50, Si 10.00, and Te ~14% (Fe balance) and Ca 13.60, C 1.58, Mg 19.45, Ce 18.70, Si 26.50, and Te ~0.30% (Fe balance) and in a number of synthetic samples prepared from a Si–Mg alloy (Si 47.7, Mg 9.95, Ce 1.05, and Fe 30.16%) and specified amounts of standard solution of Te. The sample is fused with NaOH at 300 to 600°C, leached with $H_2O$, and evaporated twice with HCl. The precipitated silicic acid is filtered off and the filtrate evaporated with $HClO_4$. Te is reduced with hydrazine sulfate, filtered on a Gooch filter, dried for 1 hr, and weighed. Precision of the method is satisfactory for larger concentrations of Te, but for Te <0.5% there is considerable scatter of results. (Selenium-Tellurium Abstr.)

**54417** X-RAY SPECTRAL DETERMINATION OF LANTHANUM, CERIUM, PRASEODYMIUM, AND NEODYMIUM IN INTERMEDIATE PRODUCTS OF RARE EARTH PRODUCTION. Rekhkolainen, G. I. Nauch. Tr., Gos. Nauch.-Issled. Proekt. Inst. Redkometal. Prom.; 22: 240-4(1968). (In Russian).

A method is described for determining La, Ce, Pr, and Nd directly in solutions without preliminary processing of the test sample. Total rare earth content of a preparative sample may be from 20 to 300 g/l. A standard x-ray machine was used with slight modification. Solution cuvettes were plastic, 25 mm in diameter, with a 20 micron polyethylene bottom. The x-ray tube was operated with an iron anode at 35 kV and a current of 10 ma. Chromium was chosen as the internal standard; for aqueous solutions $K_2Cr_2O_7$ was used. Standard samples of each rare earth was prepared using the same acidities and organic contaminants as would be expected in the test samples. Sensitivity of the determination varied from 0.3 to 1.0 g/l (~5%), and the time required for one sample was about 15 minutes. (K.S.W.)

**54418** FEASIBILITY STUDY OF THE DETERMINATION OF OXYGEN IN LIQUID ALKALI METALS BY ZIRCONIUM GETTERING. Klueh, R. L. (Oak Ridge National Lab., Tenn.). J. Nucl. Energy; 25: No. 6, 253-61(Jun 1971).

The partitioning of oxygen between zirconium and liquid potassium and sodium was studied in order to assign a lower limit to $\kappa^o$ the ratio of oxygen in zirconium to that in the liquid metal at equilibrium. For both systems $\kappa^o_{815°C} \gg 1$. This property was applied to the determination of oxygen in potassium or sodium by exposing the liquid metal to zirconium and determining the amount of oxygen gettered. The technique, termed gettering-vacuum-fusion (GVF), was tested at 815°C by exposing zirconium to potassium and sodium containing known amounts of oxygen. Recoveries above 90% were obtained for oxygen concentrations (in K or Na) in the range 25 to 1000 ppM. Reasons are given for the decrease in accuracy outside this oxygen range. (auth)

**54419** EMISSION-SPECTROMETRIC DETERMINATION OF TRACE NON-RARE EARTH ELEMENTS IN YTTRIUM OXIDE USING AgF–$Ga_2O_3$ MIXED CARRIER. Osumi, Y.; Kato, A.; Miyake, Y. (Government Industrial Research Inst., Osaka). Z. Anal. Chem.; 255: No. 2, 103-9(1971).

An emission-spectrometric method is described for the quantitative determination of traces of non-rare earth elements in yttrium oxide, employing addition of AgF–$Ga_2O_3$ mixed carrier. This addition effects an increase of the rate of evaporation of the analytical elements and of the number of atoms in the arc plasma. It enhances the sensitivity of the analytical elements to a larger extent than other carriers and permits the determination of microquantities of the elements (Mg, Ca, Mn, Co, Fe, Pb, Cu, Cd, Al, B, Sn, As, Bi) within limits of detection from 0.1 to 13 ppM in high-purity yttrium oxide. The coefficients of variation are less than 20%. (auth)

**54420** STUDIES ON THE EXTRACTION AND DETERMINATION OF METAL SALTS WITH METHYLISOBUTYL KETONE. XV. SPECTROPHOTOMETRIC DETERMINATION OF MICROAMOUNTS OF URANIUM IN THORIUM DIOXIDE WITH ARSENAZO III. Ichinose, Norio (Yamaguchi Univ., Japan). Z. Anal. Chem.; 255: No. 2, 109-13(1971).

A sensitive and selective spectrophotometric method with Arsenazo III was developed for the determination of microamounts of uranium in high-purity thorium dioxide for nuclear fuel. Interferences by thorium and impurities in not more than 1 g of thorium dioxide are effectively eliminated by the preliminary extraction process in methyl isobutyl ketone–hydrochloric acid and the masking actions of disodium hydrogen phosphate and ascorbic acid in colorimetry. This method can be successfully applied to the determination of uranium in a 1 g sample of thorium dioxide in the range of 1 to 50 ppM ($U/ThO_2$). (auth)

**54421** POLAROGRAPHIC DETERMINATION OF CADMIUM, LEAD, NICKEL, THALLIUM, AND URANIUM(VI) IN ISOQUINOLINE FORMATE. Rao, A. L. J.; Puri, B. K. (Punjabi Univ., Patiala, India). Z. Anal. Chem.; 255: No. 1, 20-1(1971).

The polarographic behavior of Cd, Pb, Ni, Tl, and U(VI) is described in 0.1 M isoquinoline formate as base electrolyte. In all cases well defined reversible waves were obtained and determinations are possible in the presence of Mo, Co, Zn, Mn, Te, In, Se, Fe, Cr, V, Th, Zr, As, Sb, Ag, Hg, and Cu. (auth)

**54422** OXIDATIVE DECARBOXYLATION OF POLYAMINOCARBOXYLIC ACIDS. II. A COMPARATIVE KINETIC STUDY OF THE OXIDATION OF NTA, EDTA, CDTA, AND DTPA WITH CERIUM(IV) IN SULFURIC ACID MEDIA. Hanna, Samir B.; Hessley, Rita; Webb, William H.; Carroll, William R. (Univ. of Missouri, Rolla). Z. Anal. Chem.; 255: No. 1, 30-2(1971).

The rates of oxidation of four chelating agents, NTA, EDTA, CDTA, and DTPA with Ce(IV), in sulfuric acid media, were determined spectrophotometrically by a stopped-flow technique. The reductive ability is in the order CDTA > EDTA > DTPA > NTA. The influence of varying the acidity of the medium was studied, and in each case a maximum in the rate constant vs $[H^+]$ plot was observed. A possible interpretation of the reactivities and the influence of acidity is advanced. (auth)

**54423** SPECTROPHOTOMETRIC DETERMINATION OF URANIUM(VI) WITH BENZOYLACETANILIDE. Chaudhuri, N. K.; Das, J. (Univ. of Burdwan, Bengal, India). Z. Anal. Chem.; 255: No. 1, 34-5(1971).

The yellow-colored U(VI) benzoylacetanilide complex was used for spectrophotometric determination of uranium. Isobutyl methyl ketone proved to be the most suitable extracting agent. A straight-line calibration curve was obtained up to 40 μg of U(VI)/ml. (M.C.G.)

**54424** INSTRUMENT FOR MEASURING THE HYDROGEN CONTENT OF METALS. Condon, J. B.; Strehlow, R. A.; Powell, G. L. (Union Carbide Corp., Oak Ridge, Tenn.). Contract W-7405-eng-26. Anal. Chem.; 43: No. 11, 1448-52(Sep 1971).

An instrument was developed to measure the hydrogen content of metals in the range from 0.01 to 100 wppM. The instrument requires a 0.1-gram to 5.0-gram sample size and records, as a function of time, both the rate at which hydrogen is thermally evolved from the sample and the total amount of hydrogen evolved. Examples are given for uranium and uranium alloys. (auth)

**54425** SPECTROPHOTOMETRIC DETERMINATION OF NIOBIUM WITH 4-(2-PYRIDYLAZO)RESORCINOL AND COLORED COMPLEXES SEPARATED FROM OXALIC AND TARTARIC ACID SYSTEMS. Siroki, Marija (Univ., Zagreb); Djordjevic, Cirila. Anal. Chem.; 43: No. 11, 1375-8(Sep 1971).

Niobium complex species involved in the spectrophotometric determination of Nb(V) with 4-(2-pyridylazo)resorcinol, (PAR = $H_2R$), in oxalic and tartaric acid media were separated in solid state. Oxooxalato-4(2-pyridylazo)resorcinol niobate(V) was extracted from aqueous solutions in chloroform by tetraphenyl phosphonium and tetraphenyl arsonium chloride, respectively, and compounds of the formula $(C_6H_5)_4X[NbOC_2O_4)R]$, where X = P, As; and R = $C_{11}H_7N_3O_2^{2-}$, were obtained. From aqueous tartaric acid solutions, at pH 1 to 2, a substance corresponding to the formula $NbO(C_4H_4O_6)(HR) \cdot H_2O$ was prepared. The compounds were characterized by analysis, ir and visible spectra, conductivity measurements, and powder photographs. It was shown that colored species in oxalic and tartaric acid media, absorbing between 560 to 520 nm, involve mixed ligand spheres, containing coordinated PAR along with an oxalato and tartrato ligand, respectively. (auth)

**54426** DETERMINATION OF OXYGEN, HYDROGEN, AND NITROGEN IN HIGH-MELTING METALS. VI. OXYGEN DETERMINATION IN MOLYBDENUM WITH THE EXHALOGRAPH EAO-201. Lassner, E.; Schedle, H. (Metallwerk Plansee AG, Reutte, Austria). J. Less-Common Metals; 25: No. 2, 171-4(Oct 1971). (In German).

XUM

The method, previously proposed, of oxygen determination in metallic molybdenum by melting without an auxiliary metal as $Mo_2C$–C-eutectic has assumed great importance by use of the new apparatus Exhalograph EAO-201. The test method is described in detail and statistical data and analysis time are given. (auth)

**54427** ROTATED MERCURY CELL FOR CONTROLLED POTENTIAL COULOMETRY. ELIMINATION OF BACKGROUND CURRENT BY DIGITAL NORMALIZATION. Clem, Ray G.; Jakob, Fredi; Anderberg, Dane H.; Ornelas, Lawrence D. (Univ. of California, Berkeley). Anal. Chem.; 43: No. 11, 1398-1405 (Sep 1971).

A cell that is rotated at high speeds and contains a thin-layer, mercury, working electrode was developed for controlled-potential coulometric determinations. The cell, which is the first successful departure from stirred mercury pool types, has several advantageous features. Constant mercury geometry assures very low noise operation and background currents that are substantially less than most stirred mercury pool cells. A large solution surface area to solution volume ratio results in sparging times that can be as short as 20 sec. Electrolytic rate constants of 0.020, 0.017, and 0.012 $sec^{-1}$ were obtained for the determination of Pb, Cd, and U, respectively. A unique arrangement of the reference and auxiliary electrodes was developed. This very compact combination contains both reference and auxiliary electrodes in a single probe configuration. With this electrode, it should be possible to produce scaled down versions of the rotated mercury cell, which currently requires 2 ml of mercury and 2 ml of solution. A procedure termed "normalization" that requires the use of digital equipment permits the elimination of the continuous background current from individual titrations. The result is improved precision. (auth)

**54428** ANALYTICAL APPLICATIONS OF X-RAY EXCITED OPTICAL FLUORESCENCE. DIRECT DETERMINATIONS OF RARE EARTH NUCLEAR POISONS IN URANIUM AT THE PART PER GIGA (1 IN $10^9$) LEVEL. D'Silva, Arthur P.; Fassel, Velmer A. (Ames Lab., Iowa). Anal. Chem.; 43: No. 11, 1406-10(Sep 1971).

An x-ray excited optical fluorescence method for the direct quantitative determination of Gd, Sm, Dy, Eu, and Pr at the part per giga level (1 in $10^9$) in nuclear grade uranium is described. The $UO_2$ or $U_3O_8$ samples are incorporated into a quaternary oxide host system, $2\,Li_2O \cdot SrO \cdot UO_2 \cdot 2WO_3$, prepared by heating stoichiometric proportions of $Li_2CO_3$, $Sr(NO_3)_2 \cdot UO_2$ or $U_3O_8$, and $WO_3$ at 825°C for 3 hours. The internal reference element Er corrects for preparative and excitation variables. The analytical curves extend over the following concentration ranges: 0.005 to 0.5 ppM Gd, 0.005 to 0.2 ppM Dy, 0.01 to 0.5 ppM Pr, and 0.02 to 0.5 ppM for Eu and Sm. (auth)

**54429** TENTATIVE METHOD FOR COLORIMETRIC DETERMINATION OF TECHNETIUM IN AQUEOUS SOLUTIONS. ASTM E417-70T. Philadelphia; American Society for Testing and Materials (1970). 5p. Available from American Society for Testing and Materials, Philadelphia.

The method is applicable to known volumes from the processing of irradiated nuclear fuel and from laboratory studies on irradiated nuclear fuel. It can be used for solutions that contain as little as 0.4 $\mu g$. The method is based on measurement of the absorbance of the technetium thiocyanate complex in chloroform. Two comparison standards bracketing the unknown are used. (M.C.G.)

**54430** STANDARD METHOD OF TESTING DEUTERIUM OXIDE. ASTM D2184-68. Philadelphia; American Society for Testing and Materials (1968). 6p. Available from American Society for Testing and Materials, Philadelphia.

Measurement of the isotopic composition of hydrogen in heavy water is described. Measurement of the specific gravity of heavy water is a precise and accurate method for determining the isotopic composition to ±0.03 at. % deuterium. (M.C.G.)

**54431** PRACTICAL ANALYSIS OF HIGH-PURITY CHEMICALS. VI. EMISSION SPECTROGRAPHIC ANALYSIS OF HIGH-PURITY ACIDS. Kershner, N. A.; Joy, E. F.; Barnard, A. J. Jr. (J. T. Baker Chemical Co., Phillipsburg, N. J.). Appl. Spectrosc.; 25: No. 5, 542-9(Sep-Oct 1971).

The spectrographic analysis of volatile acids in a high-purity form is reviewed and a procedure presented that involves evaporation of a 100-g sample under temperature controlled contamination-free conditions and emission spectrography using dc-arc excitation under controlled atmosphere. In the evaporation, graphite (10 mg) is added as a collector, sulfuric acid to convert to less volatile sulfates (with acetic, hydrochloric, and nitric acids), and also mannitol to retain boron (with hydrochloric and hydrofluoric acids). Indium is added as an internal standard. Spectra are examined for 33 elements against a multielement standard in graphite containing indium as an internal standard. Among the elements for which analytical lines and detection limits are given are: Mo, Nb, Sr, V, and Zr. For the concurrent analysis of three samples, the elapsed time is 4 to 10 h and the actual working time 3 to 5 h. Recovery studies are reported as well as the use of the procedure in the assessment of the leaching of borosilicate glass by concentrated mineral acids. (auth)

**54432** MEASUREMENTS OF THE ISOTOPIC RATIO OF BORON. Gensho, Reisuke; Honda, Masatake (Tokyo Univ.). Shitsuryo Bunseki; 19: No. 2, 134-43(Jun 1971). (In Japanese).

A method of boron isotope analysis using the $M_2BO_2^+$ ion (M is the alkaline metal) was investigated. In the case of the $M_2BO_2^+$ where the alkaline metal has two or more isotopes, this method has the following characteristics: (1) Three or more peaks are obtained from the combination of isotopes of boron and the alkaline metal. (2) Using the enriched isotopes of the alkaline metal, the relative peak heights can be adjusted so as to read with minimum errors. (3) The discrimination effect may be corrected from the known isotopic composition of the alkaline metal. (4) The error of measurements can be examined by a pair of the appropriate combination of peak heights. As results of the investigation on a series of alkaline borates, it was concluded that the $Rb_2BO_2^+$ ion has the most appropriate combination of peak heights. In the case of $Rb_2BO_2^+$, four peaks of m/e 212 to 215 are effectively obtained. The error of measurements can be examined from the relation 213/212 = 215/214. The discrimination effect for the measured boron isotopic ratio $^{11}B/^{10}B$ = 213/212 may be corrected using the measured value of 215/213 = $^{87}Rb/^{85}Rb + {}^{18}O/{}^{16}O$ and the standard isotopic ratio of rubidium and oxygen. In this method, the examination of the error of measurements is always feasible, but the correction of the discrimination effect may be significant only when the deviation of the observed value due to the discrimination effect is greater than the statistical fluctuation or the variation of the standard isotopic composition due to the fractionation effect. (auth) (Japan)

**54433** USE OF $OsO_4$ AS A CATALYST IN TITRIMETRY. COMMUNICATION 11. POTENTIOMETRIC DETERMINATION OF PERIODATE, IODATE, AND IODINE MONOCHLORIDE WITH ARSENITE. Norkus, P. K.; Shimkyavichyute, G. S. (Inst. of Chemistry and Chemical Tech., Vilnyus, USSR). Zh. Anal. Khim.; 26: No. 6, 1076-8(Jun 1971). (In Russian).

Conditions were found and a method developed for the potentiometric titration of periodate, iodate, and iodine monochloride by reducing them to free iodine with arsenite in an acid (1 to 5 N $H_2SO_4$, $H_3PO_4$, or $HClO_4$) medium. The potentiometric titration of $IO_4^-$ and $IO_3^-$ is improved in the presence of $OsO_4$ as a catalyst. The possibility of successive potentiometric determination of periodate and iodate in the same sample is shown. (auth)

**54434** QUATERNARY AMMONIUM BASES AS ANALYTICAL REAGENTS. COMMUNICATION 2. GRAVIMETRIC DETERMINATION OF CERIUM BY MEANS OF N-BENZYLQUINOLINIUM NITRATE. Markov, G. S.; Nikol'skii, B. P.; Posvol'skii, M. V. (Inst. of Radium, Leningrad). Zh. Anal. Khim.; 26: No. 6, 1215-17(Jun 1971). (In Russian).

A gravimetric method for determining cerium is suggested. The method is based on cerium precipitation as $(C_{16}H_{14}N)_2[Ce(NO_3)_6]$ from 6 to 8 M $HNO_3$ solutions by means of N-benzylquinolinium nitrate in the presence of potassium bromate. The method ensures most complete separation of cerium from the rare earths. (auth)

**54435** SPECTROGRAPHICAL ANALYSIS OF $^{235}U$ WITH A HOLLOW CATHODE DISCHARGE TUBE. Sonoda, Takenori (Kyoto Univ.); Nakagawa, Isamu; Nishihara, Kiyokado. Bunko Kenkyu; 20: No. 2, 98-104(Apr 1971). (In Japanese).

The content of $^{235}U$ in natural uranium is spectrographically determined using a hollow cathode discharge tube. A new technique is developed in loading the sample into the cathode cavity of the discharge tube. The uranium sample to be analyzed is electrodeposited onto the cavity wall in a chemical form of $2UO_3 \cdot NH_2 \cdot 3H_2O$ using aqueous uranyl nitrate solution as the electrolyte. In the power supply for the hollow cathode discharge tube, a half-wave rectifier is used instead of an ordinary full-wave rectifier, in order to stabilize the discharge. The operating conditions of the discharge tube are: 250 volt 350 mA in argon at 3 mmHg. After a predischarge for 20 minutes, three exposures (3-minutes each) are carried out successively. The spectrograms are obtained with a Jarrell–Ash 3.4-meter Ebert-type spectrograph, equipped with a prism order-sorter. The grating used has 7500 grooves per inch, and is blazed at 18.3°. The reciprocal dispersion at 4244 Å is 1.86 Å/mm, which makes it possible to separate

XU

the uranium lines at 4244.124 Å ($^{235}$U) and 4244.372 Å ($^{238}$U) completely. The analytical calibration curve made in the range 0.712 to 20.26% of $^{235}$U shows that the C. V. value is good as 0.7 to 5.9%. (auth) (Japan)

## Radiometric and Radiochemical Procedures

*Refer also to abstracts 54757, 55003, 55024, 55027, 55035, and 55197.*

**54436** (ORNL-TM-3463) TECHNIQUES USED AT OAK RIDGE NATIONAL LABORATORY FOR UNFOLDING NEUTRON AND GAMMA-RAY PULSE-HEIGHT SPECTRA. Peelle, R. W. (Oak Ridge National Lab., Tenn.). Aug 1971. 27p. (CONF-710606-13). Dep. NTIS.

From the seventeenth annual meeting of the American Nuclear Society: Boston, Mass. (13 Jun 1971).

Some unscrambling methods, which have been used in recent years at the Oak Ridge National Laboratory, are discussed and illustrated. For discrete sources, radioanalysts studying weak samples with NaI(Tl) utilize iterative least-squares spectrum resolution, while for gamma spectra from (n,n'γ) reactions another group performs peak stripping on Ge(Li) spectra with the aid of a computer-driven interactive display. To show that unfolding methods are more broadly applicable, the effect is illustrated of processing the data from two-dimensional radiodiagnostic positional scans. The energy-sensitive detector for neutron capture gamma rays is discussed as an unscrambling analysis using an inverted triangularized response matrix. For continuous spectral sources, the formulation of Burrus in terms of "window functions" is described from a simplified operational point of view. Reference is made to comparisons with flight-time spectra and with spectra unfolded using hand-guided iterative refolding. Distinctions are made among the FERDoR, FERD, and OPTIMO codes of Burrus. Clearer documentation and more incisive procedures for error estimation are considered the greatest current needs for generally improved unfolding of continuous spectra. The method chosen for a particular problem should match its needs and the investigator's style. (auth)

**54437** (RFP-Trans-82) DETERMINATION OF BORON IN BORIC GLASSES BY THE NEUTRON ABSORPTION METHOD. Dillinger, Pavel; Tolgyessy, Juraj. Translated for Dow Chemical Co., Rocky Flats Div., from Silikaty; 13: 339-46(1969). 11p. Dep. NTIS.

A method is given for determining $B_2O_3$ content (or boron content) by the neutron absorption method with the help of a calibration curve obtained by measuring neutron radiation in reference samples of fine glass cullet with various additions of boric acid in the concentrations from 0 to 12.87% by wt. of $B_2O_3$ (i.e., from 0 to 4% by wt. of B). In the analysis a Pu–Be neutron source with a flux of $5.6 \times 10^6$ n · sec$^{-1}$ and detection of thermal neutron flux with the help of activation detectors was used. The mean square error of the measurements did not exceed ±1.5% of the determined value and the maximum deviation observed in determining 8.69% of $B_2O_3$ was 0.58% by wt. This is a smaller deviation than that given in classical analytical determinations of boron in these materials. The reproducibility of the results is also satisfactory. (auth)

**54438** SOME ASPECTS OF THE MEASUREMENT OF $^{32}$P CHERENKOV RADIATION IN WATER BY A LIQUID SCINTILLATION SPECTROMETER. Wiebe, L. I.; Noujaim, A. A.; Ediss, C. (Univ. of Alberta, Edmonton). Int. J. Appl. Radiat. Isotop.; 22: No. 8, 463-7(Aug 1971).

The shift of the pulse height spectrum and the relative counting efficiency of $^{32}$P Čerenkov radiation in water were examined using a liquid scintillation spectrometer. This shift was related to the spectrophotometric absorbancy of samples containing various dyes. The isotope channels ratio method of producing a counting efficiency correction curve was found to be effective for colored samples. Although the addition of some chemicals to the sample caused little change in the counting efficiency, a suspending agent (Cabo-sil®) produced a counting efficiency and spectral shift different from those obtained for the samples containing dyes. The absolute counting efficiency for $^{32}$P in water was found to be 30.5%. (auth) (UK)

**54439** ACID DETERMINATION WITH THE HELP OF RADIOIODINE. Gimesi, O.; Weber, O.; Szabadvary, F. (Technische Univ., Budapest). J. Radioanal. Chem.; 6: No. 2, 457-60(Dec 1970). (In German).

To acids ranging from 0.1 to 0.0001 normality, a mixture of potassium iodate and $^{131}$I-labeled potassium iodide was added. To the end volume of 10 ml were then added 3 to 4 ml of a mixture comprising one part pyridine and ten parts chloroform. After thorough shaking, samples of the organic phase were measured in a well counter. Results showed a strictly linear relationship between radioactivity and acidity. The described method permitted measurements on a micro- as well as an ultramicro scale. (tr-auth)

**54440** RADON EMANATION FROM THE LUNAR SURFACE. Lindstrom, Richard M.; Evans, John C. Jr.; Finkel, Robert C.; Arnold, James R. (Univ. of California, San Diego, La Jolla). Earth Planet. Sci. Lett.; 11: No. 4, 254-6(Jul 1971).

The radon daughter $^{210}$Pb in surface samples of lunar soil and rock is in equilibrium with its parent uranium to within five percent. The lack of a surface excess in these samples, if real, implies an effective diffusion coefficient for radon of less than $10^{-6}$ that observed in terrestrial soils. A low-level coincidence β-scintillation spectrometer was used to detect the 1.16 MeV β- of the $^{210}$Bi daughter. (auth)

**54441** MODEL SIMULATION OF A RADIOACTIVE PROCESS WITH A COMPUTER. Akalaev, G. G. At. Energ. (USSR); 30: No. 5, 459-60(May 1971). (In Russian).

A mixture of radioisotopes, each distinguished by its decay constant λ, may be analyzed by determining the decay time of each component experimentally with a γ spectrometer and pulse-height analyzer. A mixture of n isotopes that release γ quanta, taken together with the basic radioactive decay law, furnishes a mathematical model based on the probability for the process. Algorithms are employed with the model in order to obtain the γ spectrum of a multicomponent mixture. Model simulation of radioactive decay processes with an electronic computer tends to eliminate errors and to decrease the degree of difficulty of the experiment. The sources of possible errors inherent in model simulation are discussed. (K.S.W.)

**54442** NEW METHOD FOR RADIOCHEMICAL ANALYSIS OF IODIDE AND IODATE IN ENVIRONMENTAL WATER. Ikeda, Nagao; Takahashi, Yasuko; Tanaka, Kiriko; Kimura, Kan (Tokyo Kyoiku Univ.). Radioisotopes (Tokyo); 20: No. 7, 336-7(Jul 1971).

A new analytical method using isotope exchange is given for the individual determination of radioactive iodide and iodate in seawater and rain water. (D.P.O.)

**54443** RADIOMETRIC METHOD FOR SULFATE DETERMINATION. Klehr, Edwin H. (Univ. of Oklahoma, Norman). Isotop. Radiat. Technol.; 9: No. 1, 44-7(Fall 1971).

A radiometric method for the determination of sulfate in fresh water is described. The sulfate is precipitated with a barium chloride solution containing $^{133}$Ba, and the resulting barium sulfate is filtered off and counted. The radioactivity of the supernatant liquid is also determined and can be used as a measure of the sulfate content. A comparison of the radiometric method to the standard gravimetric and turbidimetric methods showed that the precision and accuracy of all three methods were similar. (auth)

**54444** TENTATIVE METHODS FOR MEASURING FAST NEUTRON FLUX FOR ANALYSIS FOR $^{140}$Ba PRODUCED BY $^{238}$U FISSION. ASTM E393-69T. Philadelphia; American Society for Testing and Materials (1969). 7p. Available from American Society for Testing and Materials, Philadelphia.

Two procedures are described for measurement of fast neutron fluxes by determining $^{140}$Ba from the $^{238}$U(n,f) fission product reaction. One method is the nondestructive determination of $^{140}$Ba by direct counting of $^{140}$La several days after the irradiation. The second method is chemical separation of $^{140}$Ba and subsequent counting of it or its daughter $^{140}$La. Neutron fluxes can be measured in the range from $10^7$ to $10^{14}$ n/cm$^2$ sec. (M.C.G.)

**54445** DETERMINATION OF THE CONCENTRATION OF URANIUM IN DIFFERENT MATERIALS BY THE MEASUREMENT OF ALPHA, BETA, AND GAMMA RADIATIONS. Niederkorn, I. (Research Center for Radioactive Metals, Bucharest). Rev. Roum. Chim.; 16: No. 4, 631-9(Apr 1971). (In French).

Gamma spectrometric analysis of samples obtained by the treatment of a uranium mineral with sulfuric acid or a solution of sodium carbonate and a solution of impure uranium nitrate by TBP has made it possible to establish the distribution of the disintegration products of uranium in different liquid and solid phases. In the treatment of the uranium mineral with sulfuric acid or sodium carbonate, only uranium, thorium, and protactinium enter the liquid phase. All the other products of disintegration, beginning with radium, remain in the residue. After the treatment of the uranium mineral in the liquid phase, the uranium, thorium, and protactinium were found in a nonequilibrium state. The degree of disequilibrium of the solutions differs as a function of the conditions of the treatment. By purification of a technical concentrate (equilibrium) by

XUM

TBP, only uranium, thorium, and protactinium were found in the final liquid phase in a nonequilibrium disintegration yield. It is shown that the measurement of the alpha or beta radiation of the products that contain uranium and that were subjected to physicochemical treatments cannot be used for the determination of the uranium concentration (at least four months after the treatment), the ratios between the emitters of radiations being practically unknown. (tr-auth)

**54446** NATURALLY UNSTABLE NUCLIDES, THEIR RADIOMETRIC DETERMINATION AND POSSIBILITIES OF THEIR UTILIZATION. Zaduban, Milan (Univ. Sefarika, Kosice, Czech.). Chem. Listy; 65: No. 4, 337-73(Apr 1971). (In Slovak).

The most important characteristics of naturally unstable nuclides having an experimentally confirmed and theoretically possible instability are presented. The following relationships were studied: dependence of half-life period on Z, line of stability, dependence of the type of emitted radiation on Z, of $(N-Z)/Z$ value on Z, of the value of the $\alpha$- and $\beta$-radiation energies on Z, and the dependence of the frequency of the naturally unstable nuclides on the values of total detection efficiency of their amount in the compound. (294 references). (auth)

**54447** STANDARD METHOD OF TEST FOR RADIOACTIVE TRITIUM IN WATER. ASTM D2476-70. Philadelphia; American Society for Testing and Materials (1970). 3p. Available from American Society for Testing and Materials, Philadelphia).

A method is described for the liquid scintillation measurement of tritium radioactivity in water, $T_2O$ or HTO. The minimum detectable activity is 2 pCi/ml for a 50-ml sample counted for 20 min in a counter where the background is 30 cpm and the efficiency is 13.5%. Multiple solutes are used in the scintillator to provide the best combination of wavelength and pulse height for this application. (M.C.G.)

**54448** NEW RADIOMETRIC TITRATION METHOD BASED ON SEPARATION BY MEANS OF ION-EXCHANGE. IV. THE DETERMINATION OF THALLIUM. Heijink, A.; Polak, H. L. (Univ., Amsterdam). J. Radioanal. Chem.; 7: No. 2, 261-9 (Mar 1971).

The determination of thallium with potassium chlorate is chosen as an example for the previously suggested radio-oxidimetric titration procedure in which phase separation is achieved by means of a strongly basic anion exchanger in the solution. Concentrations of thallium down to $2 \times 10^{-6}$ M were determined. Special care has to be taken for concentrations lower than $10^{-5}$ M as uv radiation is a disturbing factor. Other oxidizing agents were also tested. (auth)

**54449** SYSTEMATIC RADIOCHEMICAL ANALYSIS OF FISSION PRODUCTS. Natsume, H.; Umezawa, H.; Suzuki, T.; (and others) (Japan Atomic Energy Research Inst., Ibaraki). J. Radioanal. Chem.; 7: No. 2, 189-202(Mar 1971).

A scheme for the sequential separation of fission products was developed on the basis of ion-exchange techniques. It consists of a main cation-exchange process for group separation and subsidiary processes of cation or anion exchange for further separations or purifications of the individual fission products. By the present method, Zn, Rb, Sr, Y, (Zr), Mo, Pd, Cd, Te, Cs, Ba, La, Ce, Pr, Nd, Pm, Sm, Eu, and Tb can be separated simultaneously from an irradiated uranium sample. Of these, alkali, alkaline earth, and rare earth metal ions are separated quantitatively. A polarographic method was applied to determine the recoveries of Zn, Mo, Pd, Cd and Te, which were not separated quantitatively. (auth)

## *Activation Procedures*

*Refer also to abstracts 54692, 55065, 55066, and 55106.*

**54450** (TID-25773) NONMETALLIC TOOLS FOR SAMPLING FROZEN TISSUES FOR TRACE METAL ANALYSES. Folsom, T. R. (Scripps Institution of Oceanography, La Jolla, Calif. Soledad Lab.). 20 Jul 1971. 6p. Dep. NTIS.

The development of several types of plastic tools for use in sampling frozen tissues for analysis by neutron activation is reported. (D.H.M.)

**54451** ANALYTICAL EVALUATION OF PROMPT GAMMA RADIATION AFTER NEUTRON CAPTURE. Henkelmann, R. (Technische Univ., Garching, Ger.). Radiochim. Acta; 15: No. 4, 169-80(Jun 1971). (In German).

The neutron capture gamma radiation was checked on its analytical use. From the prompt gamma spectra of 24 elements data on the energy and the intensity of the prompt gamma rays are given, also the detection limits of these elements. Boron and rare earths in rocks were analyzed experimentally. Some other applications of the neutron capture gamma activation analysis are discussed. (auth)

**54452** NEW TECHNIQUE FOR DETERMINING THE CONCENTRATION AND DISTRIBUTION OF LEAD IN MATERIALS. Hamilton, E. I. (Radiological Protection Board, Sutton, Eng.). Nature (London); 231: No. 5304, 524-5(25 Jun 1971).

A method is described for determining trace quantities of Pb, such as in bone and biological tissues. Compacted powders of the material to be analysed, in the form of thin sections or briquettes, are irradiated with about 30-MeV $\alpha$ particles, whereby Pb isotopes are converted to Po isotopes by $(\alpha,n)$ reactions. The $\alpha$ particles emitted by the Po are registered as tracks in sheet cellulose nitrate, which is insensitive to the other active nuclides that are also produced. Only $^{210}$Po is important, because of its relatively high capture cross section and short half-life. The advantage of the technique lies mainly in the method of registering the $\alpha$ particles, and the detection can be improved by prolonged contact of the irradiated sample with the cellulose nitrate detector. Fading of the latent track image does not appear significant. Details of the technique are given, together with precautions. For the examples given the exposure period was 6 weeks. The number of tracks produced is proportional to the lead concentration and the sample density. NaOH was used for detector etching purposes. A suitable Pb standard was used for comparison purposes. More precise measurements can be made, however, if another element is used as an internal flux monitor, for example employing the $^{44}Ca(\alpha,p)^{47}Sc$ reaction or $^{59}Co(\gamma,n)^{58}Co$. Comparisons are made with activation analysis for several specimens. (UK)

**54453** DETERMINATION OF TRIIODOTHYRONINE AND THYROXINE IN BLOOD SERUM BY ACTIVATION ANALYSIS. Schmoelzer, G.; Mueller, K. (Technische Hochschule, Graz). Int. J. Appl. Radiat. Isotop.; 22: No. 8, 509-10(Aug 1971).

The two hormones are jointly isolated from serum by ion exchange, and their total iodine determined as previously described (Schmaelzer, G. et al, 1970); triiodothyronine ($T_3$) is then separated by further exchange processes and its iodine determined by the same method. A small amount of $^{131}$I-labelled $T_3$ is added in order to ascertain any necessary correction factors. The $^{128}$I photopeak is measured by two methods, one of them computerised. Means of ten samples show deviations of about ±15% for $T_3$ and ±6% for $T_4$, and good agreement with chemical determinations. (UK)

**54454** DETERMINATION OF CADMIUM, MERCURY, THALLIUM, AND BISMUTH IN TERRESTRIAL ROCKS BY NEUTRON ACTIVATION ANALYSIS. Marowsky, Gerd (Univ., Goettingen, Ger.). Z. Anal. Chem.; 253: No. 4, 267-71(1971). (In German).

In a series of U. S. Geological Survey standard rocks and high purity quartzes the trace elements Cd, Hg, Tl, and Bi were determinated by thermal neutron activation analysis. The bulk activity of the samples was removed by ion exchange. Cd and Hg were purified as far as necessary for Ge(Li) $\gamma$ spectrometry. The $\beta$-emitters $^{204}$Tl and $^{210}$Bi were separated in radiochemical purity. For a 3 day irradiation at a thermal neutron flux of $6 \times 10^{13}$ cm$^{-2}$ $\times$ sec$^{-1}$ the detection limits were 0.1 ppB for Hg and Tl, and 1 ppB for Cd and Bi. (auth)

**54455** NEUTRON ACTIVATION ANALYSIS OF A STANDARDIZED Al-Si ALLOY. II. DETERMINATION OF CHROMIUM, ZINC, IRON, COBALT, SCANDIUM, HAFNIUM, AND NICKEL. Becker, R.; Sorantin, H. (Univ., Vienna. Oesterreichische Studiengesellschaft fuer Atomenergie, Seibersdorf). Z. Anal. Chem.; 254: No. 4, 281-6(1971). (In German).

An Al-Si-alloy (No. 87a), standardized by the National Bureau of Standards, Washington, was activated by thermal neutrons and the radionuclides produced first analyzed with a Ge(Li) detector. Besides the expected radionuclides, $^{46}$Sc, $^{60}$Co, and $^{181}$Hf were also found. Afterwards the sample was dissolved and the radionuclides separated by extraction with trioctyl phosphinoxide or tributyl phosphate, supported on polytrifluoromonochloroethylene columns. The isolated radionuclides were also identified and determined by $\gamma$ spectrometry, with a NaI(Tl) detector. The results of both methods showed good agreement and the deviations of the standard values were between ±0.6 and 3.7%. (auth)

**54456** DIURNAL VARIATION OF AEROSOL TRACE ELEMENT CONCENTRATIONS IN LIVERMORE, CALIFORNIA. Rahn, K.; Wesolowski, J. J.; John, W.; Ralston, H. R. (Univ. of California, Livermore). J. Air Pollut. Contr. Ass.; 21: No. 7, 406-9(Jul 1971).

Concentrations of 15 atmospheric aerosol trace elements in Livermore, California, were measured by neutron activation analysis in 2-hour filter samples for 58 hours during 3 typical

XUM

summer days. All elements showed cyclic patterns with concentration variations of factors of 3 to 10. Three basic patterns were seen: Na and Cl in phase with each other and nearly perfectly out of phase with the others, with a late night maximum for both; all other elements except Br, showing a midafternoon maximum; and Br, which had morning and evening peaks suggestive of automotive sources. Details of the patterns suggest a diurnal circulation model for the Livermore Valley involving alternation between fresh and aged marine air. Comparison of the trace element patterns with those of CO, $NO_2$, and oxidant was not definitive. (auth)

**54457** ACTIVATION ANALYSIS IN GEOCHEMISTRY AND COSMOCHEMISTRY. Proceedings of a Conference Held at Kjeller, Norway, September 7–12, 1970. Brunfelt, Arild O.; Steinnes, Eiliv (eds.). Oslo; Universitetsforlaget (1971). 468p. (CONF-700968).

The application of activation analysis to geological material started about 1950, and has since contributed significantly to the present understanding of trace element distribution in geological materials. This is the first scientific meeting devoted to activation analysis in geochemistry and cosmochemistry. The opening address briefly surveys the history of activation analysis. Norway's background in geochemistry and cosmochemistry is mentioned and the Norwegian geotraverse project briefly described. Forty-three separate abstracts have been submitted. Three papers dealing with the chemical evidence relating to the origin of returned lunar material, rare earths in meteoritic, terrestrial, and lunar material, and the relationships among pyroxene-plagioclase achondrites, were not within the scope of NSA. (Norway)

*For abstracts of individual papers see: 54458–54497, 54765, 54810, and 55781.*

**54458** PLACE OF ACTIVATION ANALYSIS IN GEOCHEMISTRY AND COSMOCHEMISTRY. Smales, A. A. (Atomic Energy Research Establishment, Harwell, Eng.). pp 17–24 of Activation Analysis in Geochemistry and Cosmochemistry. /Brunfelt, Arild O. (ed.). Oslo; Universitetsforlaget (1971).

From Conference on activation analysis in geochemistry and cosmochemistry; Kjeller, Norway (7 Sep 1970). See CONF-700968.

The desirable attributes of the perfect method for analysing rocks and meteorites are discussed and existing available methods are considered in relation to those attributes. Some of the results of the analysis of Apollo 11 lunar fines as published in Science 1970, 167, 449 to 780 are used to put activation analysis and other methods "in their place". (Norway)

**54459** IN-SITU CHEMICAL ANALYSIS OF EXTRA-TERRESTRIAL OBJECTS SUCH AS THE MOON AND MARS BY THE USE OF ALPHA PARTICLES. Turkevich, A. (Univ. of Chicago). pp 25–41 of Activation Analysis in Geochemistry and Cosmochemistry. /Brunfelt, Arild O. (ed.). Oslo; Universitetsforlaget (1971).

From Conference on activation analysis in geochemistry and cosmochemistry; Kjeller, Norway (7 Sep 1970). See CONF-700968.

The state of development of the alpha-scattering technique of chemical analysis is reviewed. The method can determine about 99% of the atoms (other than hydrogen) usually found in rocks. The accuracy and precision of the technique, as determined by analysis of eleven igneous rocks of known composition, is usually less than half an atom percent. The performance of the alpha-scattering instruments on the Surveyor lunar missions, the data obtained, and examples of the important geochemical information that can be deduced from such in-situ chemical analyses are reviewed. The agreement of the Surveyor analytical results on lunar mare material with the composition of the powdered samples brought back by the Apollo 11 and 12 astronauts is good. It indicates gross similarity in chemical composition of many lunar mare. Finally, the present status of work to adapt the Surveyor instrument for a possible in-situ analysis of Mars is given. (auth) (Norway)

**54460** INSTRUMENTAL ACTIVATION ANALYSIS OF COLUMBIA RIVER BASALTS AND OF LUNAR ROCKS. Goles, G. G. (Univ. of Oregon, Eugene). pp 45–50 of Activation Analysis in Geochemistry and Cosmochemistry. /Brunfelt, Arild O. (ed.). Oslo; Universitetsforlaget (1971).

From Conference on activation analysis in geochemistry and cosmochemistry; Kjeller, Norway (7 Sep 1970). See CONF-700968.

Applications of instrumental activation analysis to Columbia River basalts and Apollo 11 lunar specimens are reviewed. Picture Gorge basalt flows may be sub-divided into two compositionally-distinct types. The lower of these flows is very similar in composition to abyssal basalts. A secular progression is observed from basalts with these primitive characteristics to typical continental basalts (the Late Yakima flows). Some of these basalts were erupted from vents which are found in a roughly oval area at least 200 km by 500 km. Salient interpretations and speculations derived from instrumental activation analysis data on Apollo 11 specimens include suggestions that the Moon's surface regions have always been very dry, that residual melts have played an important rôle in generating Eu anomalies, and that a cryptic component, compositionally somewhat like Apollo 12 olivine basalts, is a major contributor to Apollo 11 "soil". Preliminary data on Apollo 12 specimens suggest that a similar cryptic component is present there. (auth) (Norway)

**54461** MULTIELEMENT NEUTRON ACTIVATION ANALYSIS OF GEOLOGICAL AND LUNAR MATERIAL USING CHEMICAL GROUP SEPARATIONS AND HIGH RESOLUTION GAMMA SPECTROMETRY. Morrison, G. H. (Cornell Univ., Ithaca, N. Y.). pp 51–4 of Activation Analysis in Geochemistry and Cosmochemistry. /Brunfelt, Arild O. (ed.). Oslo; Universitetsforlaget (1971).

From Conference on activation analysis in geochemistry and cosmochemistry; Kjeller, Norway (7 Sep 1970). See CONF-700968.

Instrumental neutron activation analysis and neutron activation analysis with a high-resolution lithium-drifted germanium detector, chemical group separations, and a coincidence-anticoincidence system are used to determine 42 elements in terrestrial rocks, meteorites, and lunar samples. The elemental abundances of the lunar materials are compared with terrestrial basalts and basaltic achondrites. (auth) (Norway)

**54462** DETERMINATION OF TRACE ELEMENTS IN IGNEOUS ROCKS BY NUCLEAR TECHNIQUES. Whitley, J. E. (Scottish Research Reactor Centre, East Kilbride); Bowden, P.; Angus, N. S. pp 55–64 of Activation Analysis in Geochemistry and Cosmochemistry. /Brunfelt, Arild O. (ed.). Oslo; Universitetsforlaget (1971).

From Conference on activation analysis in geochemistry and cosmochemistry; Kjeller, Norway (7 Sep 1970). See CONF-700968.

The philosophy of using established techniques, whenever practicable, in a laboratory processing a wide variety of samples is explained, and results of some recent geochemical work at the Scottish Research Reactor Centre presented. Nine elements were determined in AGV-1, GSP-1 and G-2, and comments are offered on their agreement with other results. A similar set of elements were determined in granitic rocks from the Tyrone Igneous Series, and the results appear to support the conclusions of major element analysis. Details are also given of the accuracy attainable in the determination of boron by neutron-capture gamma-ray analysis, and preliminary results of the analysis of peralkaline lavas compared with those obtained by emission spectrographic and chemical methods. (auth) (Norway)

**54463** ROUTINE DETERMINATIONS ON ROCKS AND SEDIMENTS BY ACTIVATION ANALYSIS. Das, H. A.; Zonderhuis, J. (Reactor Centrum Nederland, Petten). pp 65–71 of Activation Analysis in Geochemistry and Cosmochemistry. /Brunfelt, Arild O. (ed.). Oslo; Universitetsforlaget (1971).

From Conference on activation analysis in geochemistry and cosmochemistry; Kjeller, Norway (7 Sep 1970). See CONF-700968.

Some possibilities of activation analysis as a routine method in geochemistry are discussed. The system here is based on activation with thermal and fast neutrons and with photons. The elements are divided into three groups: elements that can be determined by instrumental analysis on great series of samples; elements requiring a simple chemical separation but which can be analyzed rapidly; and special analyses involving more work and which are restricted to small groups of samples. The outline of the system for the instrumental analysis is given. In addition, one case for the other categories is discussed, namely: the determination of vanadium in rocks as an example of a simple chemical separation, and the determination of the lanthanides by high-pressure ion-exchange, as a representative of the more complicated analyses. (auth) (Norway)

**54464** INSTRUMENTAL NEUTRON ACTIVATION ANALYSIS OF SOME NEW STANDARD ROCKS. Cojocaru, V.; Ispas, M. (Inst. for Atomic Physics, Bucharest). pp 73–7 of Activation Analysis in Geochemistry and Cosmochemistry. /Brunfelt, Arild O. (ed.). Oslo; Universitetsforlaget (1971).

From Conference on activation analysis in geochemistry and cosmochemistry; Kjeller, Norway (7 Sep 1970). See CONF-700968.

By means of high resolution Ge(Li) detectors and neutron activa-

XUM

tion analysis, 24 elements were determined in six standard rocks: GM (granite), KH (limestone), TB (argillite), BM (basalt) and an anhydrite, prepared in D.D.R., and a magnesite prepared in Czechoslovakia. (auth) (Norway)

**54465** 14 MeV NEUTRON ACTIVATION ANALYSIS OF ROCKS AND METEORITIES. Morgan, J. W.; Ehmann, W. D. (Univ. of Kentucky, Lexington). pp 81-97 of Activation Analysis in Geochemistry and Cosmochemistry. /Brunfelt, Arild O. (ed.). Oslo; Universitetsforlaget (1971).

From Conference on activation analysis in geochemistry and cosmochemistry; Kjeller, Norway (7 Sep 1970). See CONF-700968.

Activation analysis using 10-MeV neutrons has certain unique advantages for the nondestructive analysis of rocks and meteorites. The principles of the method are outlined, and the techniques for the precise and accurate analyses are summarized. Some current and future applications are described. (auth) (Norway)

**54466** NON-DESTRUCTIVE ACTIVATION ANALYSIS OF SOME ELEMENTS IN STONY METEORITES BY PROTON AND BREMSSTRAHLUNG-IRRADIATION. van Zelst, L. (Instituut voor Kernphysisch Onderzoek, Amsterdam). pp 99-104 of Activation Analysis in Geochemistry and Cosmochemistry. /Brunfelt, Arild O. (ed.). Oslo; Universitetsforlaget (1971).

From Conference on activation analysis in geochemistry and cosmochemistry; Kjeller, Norway (7 Sep 1970). See CONF-700968.

The elements Fe, Ni, Cr, and Ca were determined in stony meteorites by activation with bremsstrahlen, obtained from the IKO linear electron accelerator. The same elements, together with Ti, were determined by activation with protons from the IKO synchrocyclotron. Advantages and disadvantages of both methods are discussed. (auth)

**54467** DETERMINATION OF BERYLLIUM IN ROCKS BY ACTIVATION ANALYSIS, USING THE $^{9}Be(\alpha,\gamma)^{12}C$ REACTION WITH $^{210}Po$. Flakus, F. N.; Kim, J. I.; Born, H.-J. (Technische Univ., Munich). pp 105-112 of Activation Analysis in Geochemistry and Cosmochemistry. /Brunfelt, Arild O. (ed.). Oslo; Universitetsforlaget (1971).

From Conference on activation analysis in geochemistry and cosmochemistry; Kjeller, Norway (7 Sep 1970). See CONF-700968.

The following method has been devised to determine beryllium: extracted beryllium in solvent is passed through an alpha source, $^{210}Po$ deposited spontaneously on copper grains, and the prompt gamma rays resulting from the $^{9}Be(\alpha,n\gamma)^{12}C$-reaction are measured. By application of the method, beryllium contents in geological samples from various places in the East Alps were determined. Extraction of beryllium from the samples is undertaken by HF digestion, anion exchange in HCl, and cation exchange in HCl–ethanol mixture. The sensitivity of the method depends on the intensity of the alpha source, with 100-mC $^{210}Po$, the limit of detection can reach ca. 10 ppM. (auth) (Norway)

**54468** EPITHERMAL NEUTRON ACTIVATION ANALYSIS OF GEOLOGICAL MATERIAL. Steinnes, E. (Institutt for Atomenergi, Kjeller, Norway). pp 113-28 of Activation Analysis in Geochemistry and Cosmochemistry. /Brunfelt, Arild O. (ed.). Oslo; Universitetsforlaget (1971).

From Conference on activation analysis in geochemistry and cosmochemistry; Kjeller, Norway (7 Sep 1970). See CONF-700968.

The determination of minor and trace elements in geological material by activation analysis with epithermal neutrons is reviewed. The theoretical background of epithermal activation is outlined, and the feasibility of the technique for elements of interest in activation analysis is calculated and tabulated. Previous work on geological material using epithermal neutron activation is summarized, and some new applications are briefly described. Sources of error in epithermal activation analysis are discussed, with particular emphasis on neutron absorption effects. (auth)

**54469** NEUTRON ACTIVATION ANALYSIS OF INTACT DRILL CORE. Evans, D. J. R.; Herage, T. I. (Atomic Energy of Canada Ltd., Ottawa). pp 129-34 of Activation Analysis in Geochemistry and Cosmochemistry. /Brunfelt, Arild O. (ed.). Oslo; Universitetsforlaget (1971).

From Conference on activation analysis in geochemistry and cosmochemistry; Kjeller, Norway (7 Sep 1970). See CONF-700968.

The recent development of portable high output isotopic neutron sources (output $>10^{10}$ thermal neutrons/second) permits rapid nondestructive field analysis of exploration drill core. Neutron activation analysis provides more accurate assays of intact drill core than are obtained by x-ray fluorescence techniques. The method was used to obtain a copper assay profile down a length of drill core and has measured copper contents below 0.1%. A comparison of activation analyses with assays by x-ray fluorescence (intact and powdered samples) and chemical analysis is presented. (auth) (Norway)

**54470** PRACTICAL ASPECTS OF ACTIVATION ANALYSIS WITH FAST NEUTRONS AND PHOTONS. Das, H. A.; Zonderhuis, J. (Reactor Centrum Nederland, Petten). pp 135-41 of Activation Analysis in Geochemistry and Cosmochemistry. /Brunfelt, Arild O. (ed.). Oslo; Universitetsforlaget (1971).

From Conference on activation analysis in geochemistry and cosmochemistry; Kjeller, Norway (7 Sep 1970). See CONF-700968.

Activation analysis with fast neutrons and photons is a useful complement to the determinations by thermal neutron-induced reactions. The isotope production cyclotron of Philips–Duphar at Petten and the linear accelerator of the Institute for Nuclear Physics Research in Amsterdam are used for this purpose. In the cyclotron a rabbit system has been constructed that makes irradiation possible with conversion neutrons produced by the internal beam of the cyclotron. The linear accelerator is used for the instrumental determination of four elements. (auth) (Norway)

**54471** COMPUTER DATA REDUCTION IN ACTIVATION ANALYSIS. Yule, H. P. (National Bureau of Standards, Washington, D. C.). pp 145-66 of Activation Analysis in Geochemistry and Cosmochemistry. /Brunfelt, Arild O. (ed.). Oslo; Universitetsforlaget (1971).

From Conference on activation analysis in geochemistry and cosmochemistry; Kjeller, Norway (7 Sep 1970). See CONF-700968.

Methods of result computation with activation analysis gamma spectra are reviewed, emphasizing recent developments. For NaI(Tl) detector spectra, the multiple linear regression technique is reported. For Ge(Li) detector, methods of peak location, net peak area computation, and complex peak resolution are indicated. Each technique is discussed for applicability and difficulties in utilization. General features of result computation and of various numerical analytic techniques are discussed. (auth) (Norway)

**54472** COMBINED PEAKSEARCH AND PEAKFIT IN DATA PROCESSING OF $\gamma$-SPECTRA. Freiburg, C.; Erdtmann, G.; Petri, H. (Kernforschungsanlage, Juelich, Ger.). pp 167-73 of Activation Analysis in Geochemistry and Cosmochemistry. /Brunfelt, Arild O. (ed.). Oslo; Universitetsforlaget (1971).

From Conference on activation analysis in geochemistry and cosmochemistry; Kjeller, Norway (7 Sep 1970). See CONF-700968.

Automatic computer search and fit of distinct peaks in complex multicomponent $\gamma$ spectra are important with respect to comfort of evaluation and are essential for objective judgement of resolution and detection limit. The problem of resolution is constituted in terms of reliability of the parameters of superimposed peaks, while the problem of detection limit is solved by checking the threefold background variance against the peak area. The combination of peaksearch and peakfit procedures is a versatile tool though rather laborious to program because of data reduction problems. (auth) (Norway)

**54473** DIGITAL METHODS OF PHOTO PEAK INTEGRATION IN ACTIVATION ANALYSIS. Baedecker, P. A. (Univ. of California, Los Angeles). pp 175-82 of Activation Analysis in Geochemistry and Cosmochemistry. /Brunfelt, Arild O. (ed.). Oslo; Universitetsforlaget (1971).

From Conference on activation analysis in geochemistry and cosmochemistry; Kjeller, Norway (7 Sep 1970). See CONF-700968.

A study of the precision attainable by several methods of gamma photopeak integration was carried out. The "total peak area" method, the methods proposed by Covell, Sterlinski, and Quittner, and some modifications of these methods were considered. A modification by Wasson of the total peak area method is considered to be the most advantageous due to its simplicity and the relatively high precision obtainable with this technique. A computer routine for the analysis of spectral data from nondestructive activation analysis experiments employing a Ge(Li) detector-spectrometer system is described. The routine processes the spectral data, applies appropriate corrections for decay, and provides a readout in concentration units. (auth) (Norway)

**54474** ON-LINE COMPUTERS FOR GAMMA SPECTROMETRY AND ACTIVATION ANALYSIS. Webster, R. K. (Atomic Energy Research Establishments, Harwell, Eng.). pp 183-97

XUM

of Activation Analysis in Geochemistry and Cosmochemistry. /Brunfelt, Arild O. (ed.). Oslo; Universitetsforlaget (1971).

From Conference on activation analysis in geochemistry and cosmochemistry; Kjeller, Norway (7 Sep 1970). See CONF-700968.

Small computer systems can be developed to operate as $\gamma$ spectrometers, and offer an attractive alternative to the use of multichannel analysers, often at comparable costs. A computer system can combine the main features of a multichannel analyser with the advantages of on-line data processing, high speed peripherals, etc., and the high degree of flexibility in layout and operation minimises any risk of obsolescence. A brief outline is given of the operation and control of a small computer, and single and multi-$\gamma$-spectrometer systems are discussed as examples. (auth)

**54475** IMPROVED TECHNIQUES FOR SEPARATION AND DETERMINATION OF RARE-EARTH ELEMENTS IN EXTRATERRESTRIAL MATERIAL. Absel-Rassoul, A. A.; Herpers, U., Herr, W. (Univ., Cologne). pp 219-26 of Activation Analysis in Geochemistry and Cosmochemistry. /Brunfelt, Arild O. (ed.). Oslo; Universitetsforlaget (1971).

From Conference on activation analysis in geochemistry and cosmochemistry; Kjeller, Norway (7 Sep 1970). See CONF-700968.

Improved techniques for the separation and determination of the rare earth elements in lunar fines (No. 10084) from the Apollo 11 mission are presented. The procedures developed are based independently on ion-exchange chromatography and on high-voltage electrophoresis. In both cases, group preseparation was carried out followed by a short and a long neutron irradiation. The short-lived radionuclides $^{153}$Sm, $^{152m_1}$Eu and $^{165}$Dy could be directly assayed. Using a special resin (Aminex-A5), and $\alpha$-hydroxyisobutyric acid as eluant, excellent separation was achieved. Fast high-voltage electrophoresis, however, was also found useful for optimal separation and quantitative determination. The methods have been compared and the analytical data are found to be reliable. (auth) (Norway)

**54476** RARE EARTH ABUNDANCES IN MESOZOIC DOLERITE DIKES FROM EASTERN UNITED STATES. Ragland, P. C.; Brunfelt, A. O.; Weigand, P. W. (Mineralogisk-Geologisk Museum, Oslo). pp 227-40 of Activation Analysis in Geochemistry and Cosmochemistry. /Brunfelt, Arild O. (ed.). Oslo; Universitetsforlaget (1971).

From Conference on activation analysis in geochemistry and cosmochemistry; Kjeller, Norway (7 Sep 1970). See CONF-700968.

Ten Mesozoic dolerite dikes from eastern United States were analyzed for eight rare earth elements. Three distinct REE distribution patterns, which can be related to petrochemistry, are evident: (1) moderately fractionated REE pattern relative to chondrites and highest absolute REE abundance (high-Ti quartz-tholeiitic dolerites); (2) relatively unfractionated pattern and lowest REE abundance (olivine-tholeiitic dolerites); and (3) intermediate pattern and absolute abundance (low-Ti quartz-tholeiitic dolerites). The olivine tholeiites are depleted in absolute REE with respect to most continental and oceanic-ridge tholeiites. Models involving simple crystal fractionation are not adequate to explain the relative distribution patterns; a process such as selective diffusion from crustal country rocks into the magmas prior to emplacement may have been operative. (auth)

**54477** DETERMINATION OF TRACE ELEMENTS IN METEORITIC PHASES BY NEUTRON ACTIVATION ANALYSIS. Kiesl, W. (Univ., Vienna). pp 243-51 of Activation Analysis in Geochemistry and Cosmochemistry. /Brunfelt, Arild O. (ed.). Oslo; Universitetsforlaget (1971).

From Conference on activation analysis in geochemistry and cosmochemistry; Kjeller, Norway (7 Sep 1970). See CONF-700968.

The activities of the Analytical Institute of the University of Vienna in meteoritics are discussed. Trace elements in meteorites and meteoritic phases were determined either by nondestructive techniques or after a chemical separation. Ge was determined after a reactor-pulse in the automatic pneumatic tube system of 15 msec transfer time, and a nondestructive determination of Cu, As, Au, and Ga in the metal phase was carried out after a 5 to 10 min irradiation. About 25 trace elements as well as the majority of the rare earths were determined using chemical separations after long-time irradiation in the reactor. Trace element distributions between the four main-phases of Cañon Diablo and Odessa are discussed. Activation analysis for some trace elements in these phases was supported by microprobe investigations. Their very inhomogeneous distribution is demonstrated in the case of Odessa and Cañon Diablo troilite. (auth) (Norway)

**54478** ELEMENTAL ABUNDANCE TRENDS IN THE AUSTRALITE STREWN FIELD BY NON-DESTRUCTIVE NEUTRON ACTIVATION. Ehmann, W. D.; Showalter, D. L. (Univ. of Kentucky, Lexington). pp 253-60 of Activation Analysis in Geochemistry and Cosmochemistry. /Brunfelt, Arild O. (ed.). Oslo; Universitetsforlaget (1971).

From Conference on activation analysis in geochemistry and cosmochemistry; Kjeller, Norway (7 Sep 1970). See CONF-700968.

Neutron activation and gamma-ray spectrometry utilizing high resolution lithium-drifted germanium detectors were used to determine the abundances of 10 elements in 86 different Australian tektites from 41 documented sites. Elements determined include Na, Fe, Th, Cr, La, Hf, Cs, Sc, Co, and Eu. Little variation was observed in the site to site abundances of most of these elements. However, wide ranges of abundances from site to site were recorded for Cr (41 to 233 ppM) and Co (9 to 31 ppM) with australites high in Cr being invariably high in Co. In addition, Si was determined by 14 MeV neutron activation and Au and Hg by thermal neutron activation and radiochemical separations. Implications of the data to the existence of australite chemical subgroups and to the identification of a suitable parent material for the australites will be discussed. (auth) (Norway)

**54479** COINCIDENCE COUNTING APPLIED TO THE ACTIVATION ANALYSIS OF METEORITES AND ROCKS. Ehmann, W. D.; McKown, D. M.; Morgan, J. W. (Univ. of Kentucky, Lexington). pp 267-83 of Activation Analysis in Geochemistry and Cosmochemistry. /Brunfelt, Arild O. (ed.). Oslo; Universitetsforlaget (1971).

From Conference on activation analysis in geochemistry and cosmochemistry; Kjeller, Norway (7 Sep 1970). See CONF-700968.

The use of gamma–gamma coincidence spectrometry in the instrumental activation analysis of materials of geochemical interest can offer advantages of improved sensitivity and precision for certain elements over other counting techniques. In other cases coincidence spectrometry may be used to test other counting techniques for the presence of unresolved interferences. An introduction to some of the theory and the practical considerations involved in the establishment of gamma–gamma coincidence counting systems is presented. Previous applications of this technique to the activation analysis of meteorites and rocks are reviewed and some future applications are proposed. (auth) (Norway)

**54480** NEUTRON ACTIVATION ANALYSIS OF TIN IN GEOCHEMICAL AND COSMOCHEMICAL MATERIAL, USING 40 MINUTE $^{123}$Sn. Schmidt, D. (Max Planck-Institut fuer Kernphysik, Heidelberg). pp 293-7 of Activation Analysis in Geochemistry and Cosmochemistry. /Brunfelt, Arild O. (ed.). Oslo; Universitetsforlaget (1971).

From Conference on activation analysis in geochemistry and cosmochemistry; Kjeller, Norway (7 Sep 1970). See CONF-700968.

A method for the neutron-activation determination of tin in geological material, based on the gamma-emitting isotope $^{123}$Sn, was developed. The short half-life of 40 minutes requires an improved, more rapid radiochemical separation procedure. After alkaline fusion of the irradiated samples, tin is separated by liquid-liquid-extractions with thenoyltrifluoroacetone in methyl isobutyl ketone and with tartaric acid, and purified by precipitation of $SnS_2$. Chemical yields of 70% and 2 hours overall processing time are sufficient to determine tin down to the 0.1 ppM range. Analyses are reported for chondrites and achondrites, and for some tektites and related natural glasses. (auth) (Norway)

**54481** REVIEW OF THE APPLICATION OF ACTIVATION ANALYSIS IN OCEANOGRAPHY. Hoegdahl, O. (Central Inst. for Industrial Research, Oslo). pp 301-10 of Activation Analysis in Geochemistry and Cosmochemistry. /Brunfelt, Arild O. (ed.). Oslo; Universitetsforlaget (1971).

From Conference on activation analysis in geochemistry and cosmochemistry; Kjeller, Norway (7 Sep 1970). See CONF-700968.

On the basis of an incomplete although illustrative picture of the present state of knowledge in oceanography, and a bibliographic compilation of papers on the application of activation analysis in oceanography, the advantages, limitations, and possibilities of this analytical technique are discussed. (auth) (Norway)

**54482** ANALYSIS OF OCEANOGRAPHIC SAMPLES FROM THE GLOMAR CHALLENGER VOYAGE. Kuykendall, W. E. Jr.; Hoffman, B. W.; Wainerdi, R. E. (Texas A and M Univ., College Station). pp 321-32 of Activation Analysis in Geochemistry and Cosmochemistry. /Brunfelt, Arild O. (ed.). Oslo; Universitetsforlaget (1971).

XUM

From Conference on activation analysis in geochemistry and cosmochemistry; Kjeller, Norway (7 Sep 1970). See CONF-700968.

Equipment and procedures used for the nondestructive analysis of ocean sediment samples by 14-MeV neutron activation are discussed. A computer routine that analyzes gamma ray spectra on the basis of both energy and half-life is described. Results obtained when the procedures were tested on USGS standard rock samples are given along with results of analyses of selected core samples from the NSF Deep Sea Drilling Project. (auth) (Norway)

**54483** ACTIVATION ANALYSIS OF PHILIPPINE MAGNETITE SANDS. Santos, G. G. Jr.; Walters, L. J. Jr. (Philippine Atomic Energy Commission, Manila. Bowling Green State Univ., Ohio). pp 333-5 of Activation Analysis in Geochemistry and Cosmochemistry. /Brunfelt, Arild O. (ed.). Oslo; Universitetsforlaget (1971).

From Conference on activation analysis in geochemistry and cosmochemistry; Kjeller, Norway (7 Sep 1970). See CONF-700968.

Results obtained using activation analysis techniques show that the vanadium contents of magnetite from beach and river sands are strikingly similar and are in close agreement with the vanadium concentrations of magnetites found in recent volcanic sedimentary rocks. The sulfide-associated magnetites coming from copper–gold and iron–copper areas contain about half the amount of vanadium as compared to the river and beach magnetites. The manganese concentration of the beach and river magnetites is higher than those of the volcanic rocks and sulfide-associated magnetites. The beach magnetic sands from northern and western Luzon may well have been derived from the north-south trending Cordillera Central and the Zambales alpine-type peridotite complexes in western central Luzon. (auth) (Norway)

**54484** NEUTRON ACTIVATON ANALYSIS FOR NOBLE METALS IN GEOCHEMISTRY. Crocket, J. H. (McMaster Univ., Hamilton, Ont.). pp 339-51 of Activation Analysis in Geochemistry and Cosmochemistry. /Brunfelt, Arild O. (ed.). Oslo; Universitetsforlaget (1971).

From Conference on activation analysis in geochemistry and cosmochemistry; Kjeller, Norway (7 Sep 1970). See CONF-700968.

The sensitivity of neutron activation for platinum group metals and gold, and its application to their determination in meteorites, terrestrial rocks, sediments, ores and lunar samples are reviewed. The method accounts for some 80% of the Pd, Os, Ir, and Au and about 30% of the Ru and Pt data on meteorites. For terrestrial samples the sensitivity is sufficiently high for determination of Au, Ir, Pd, and generally Os, in basic and ultrabasic rocks where average concentrations range from approximately 0.5 to 5 ppB. Gold is far more extensively analysed than any other noble metal. Sensitivity is low for Ru and Pt, and Ru is subject to serious interference from fission products, particularly in acidic rocks. In sulfide ores higher concentrations and low uranium contents allow determination of all noble metals. (auth) (Norway)

**54485** NEUTRON ACTIVATION ANALYSIS PROCEDURE FOR THE DETERMINATION OF THE NOBLE METALS IN GEOLOGICAL SAMPLES. Millard, H. T. Jr.; Bartell, A. J. (Geological Survey, Denver). pp 353-8 of Activation Analysis in Geochemistry and Cosmochemistry. /Brunfelt, Arild O. (ed.). Oslo; Universitetsforlaget (1971).

From Conference on activation analysis in geochemistry and cosmochemistry; Kjeller, Norway (7 Sep 1970). See CONF-700968.

A procedure was developed for the determination of Pd, Pt, Au, Ru, Os, and Ir in a single geological sample. The sample is irradiated for eight hours in a neutron flux of $2 \times 10^{12}$ n $cm^{-2}$ $sec^{-1}$, then fused with peroxide, and a modified fire assay procedure is used to extract the noble metals into a metallic lead button. The lead button is fused with peroxide and Os and Ru distilled. Pd, Au, Pt, and Ir are then separated from each other by anion exchange and precipitation. Carrier yields are determined by re-irradiation of the various fractions. Results obtained for the USGS standard rock PCC-1 agree well with values reported in the literature. (auth) (Norway)

**54486** NEUTRON ACTIVATION ANALYSIS FOR OSMIUM, RUTHENIUM, AND IRIDIUM IN SOME SILICATE ROCKS AND ROCK-FORMING MINERALS. Gijbels, R.; Millard, H. T. Jr.; Desborough, G. A.; Bartel, A. J. (State Univ., Ghent). pp 359-70 of Activation Analysis in Geochemistry and Cosmochemistry. /Brunfelt, Arild O. (ed.). Oslo; Universitetsforlaget (1971).

From Conference on activation analysis in geochemistry and cosmochemistry; Kjeller, Norway (7 Sep 1970). See CONF-700968.

A method is described for the simultaneous determination of osmium, iridium, and ruthenium by thermal neutron activation analysis. After dissolution of the sample by peroxide fusion in the presence of carriers, osmium and ruthenium were separated by two distillations and two precipitations each. Iridium was separated by anion-exchange adsorption and batch extraction. Radioactivity measurements were carried out with a Ge(Li) detector, and using ($x\gamma$) and ($\gamma\gamma$) coincidence techniques. Chemical yields were determined by reactivation. The uranium content of the samples was estimated by the fission track technique, in order to correct for fission $^{103}Ru$. The method was applied to chromite, plagioclase, and orthopyroxene cumulates from the central sector of the eastern Bushveld Complex, South Africa. The concentration ranges measured were: osmium 0.06 to 114 ppB; iridium 0.08 to 105 ppB; ruthenium 3.0 to 680 ppB. Results are also given for the USGS standard rocks DTS-1 and PCC-1. (auth) (Norway)

**54487** DIRECT DETERMINATION OF THE NOBLE METALS BY ACTIVATION ANALYSIS UTILIZING HIGH-RESOLUTION GAMMA SPECTROMETRY. De Wet, W. J.; Turkstra, J.; Toerien, F. V. S. (Atomic Energy Board, Pretoria). pp 371-9 of Activation Analysis in Geochemistry and Cosmochemistry. /Brunfelt, Arild O. (ed.). Oslo; Universitetsforlaget (1971).

From Conference on activation analysis in geochemistry and cosmochemistry; Kjeller, Norway (7 Sep 1970). See CONF-700968.

Instrumental reactor activation analysis using a Ge(Li) detector was investigated for the nondestructive determination of the noble metals in lead beads, matte, and platinum-bearing ores. The results obtained have recently been published and are reviewed. The important aspects of the study are discussed, and advantages and limitations of the method are emphasized. To improve the precision of determination of the important noble metals platinum and palladium, it seems necessary to resort to chemical separations. Progress made along these lines is indicated. (auth)

**54488** DETERMINATION OF GOLD IN GEOLOGICAL MATERIALS BY NEUTRON ACTIVATION ANALYSIS. Wood, E. D.; Hood, D. W. (Univ. of Alaska, College). pp 381-90 of Activation Analysis in Geochemistry and Cosmochemistry. /Brunfelt, Arild O. (ed.). Oslo; Universitetsforlaget (1971).

From Conference on activation analysis in geochemistry and cosmochemistry; Kjeller, Norway (7 Sep 1970). See CONF-700968.

Gold concentrations in geological material subsamples of less than one gram often show great variability due to the inhomogeneity caused by gold being present in the metallic form. Sensitive and accurate determinations of gold in 100 gram sediment samples from southeast Alaska were obtained by sieving the samples and separating the gold from the fractions prior to analysis by neutron activation. A multichannel analyzer-Ge(Li) detector system was used to measure the 412-keV photopeak of the (n,$\gamma$) product, $^{198}Au$, and the 99-keV photopeak of $^{195}Au$ added to each sample prior to fusion to monitor the separation efficiency. The particle size of the gold decreased with distance from the source in the Gold Creek-Gastineau Channel system, but the total gold in the sediment remained constant at 0.104 ± 0.004 ppM. The highest gold concentration was in the 4 phi size fraction, 1.8 ppM. (auth) (Norway)

**54489** SENSITIVITY RANGES IN NEUTRON ACTIVATION ANALYSIS OF SOME RARE TRACE ELEMENTS (Cd, Hg, Tl, Bi) IN SILICATE SAMPLES. Marowsky, G. (Univ., Goettingen, Ger.). pp 391-6 of Activation Analysis in Geochemistry and Cosmochemistry. /Brunfelt, Arild O. (ed.). Oslo; Universitetsforlaget (1971).

From Conference on activation analysis in geochemistry and cosmochemistry; Kjeller, Norway (7 Sep 1970). See CONF-700968.

The determination of the geochemically interesting rare trace elements Cd, Hg, Bi, and Tl imposes considerable difficulties when the ppB range is approached. Neutron activation analysis in combination with low level $\beta$ counting and semiconductor $\gamma$ spectrometry was used to determine these elements in a series of rock samples, including some USGS standard rocks. The four elements were determined simultaneously, employing traditional carrier techniques and radiochemical separation. After removal of the bulk activity in an anion exchange step, Cd and Hg were separated as far as necessary for Ge(Li) $\gamma$ spectrometry. The $\beta$-emitters $^{204}Tl$ and $^{210}Bi$ were brought to radiochemical purity before low level counting. For three days' irradiation at a thermal neutron flux of $6 \times 10^{13}$ $cm^{-2}$ $sec^{-1}$, the limit of detection was 0.1 ppB for Hg and Tl, and 1 ppB for Cd and Bi. High purity quartz was used to examine the sensitivity limits with particular reference to coinciding $\gamma$ lines from background activities. (auth) (Norway)

**54490** STUDY ON THE MONOSTANDARD ACTIVATION ANALYSIS AND ITS APPLICATION TO GEOLOGICAL SAMPLES:

XUM

INVESTIGATION OF SCHEELITE DEPOSITS IN THE EAST ALPS. Kim, J. I.; Staerk, H. (Technische Univ., Munich). pp 397-410 of Activation Analysis in Geochemistry and Cosmochemistry. /Brunfelt, Arild O. (ed.). Oslo; Universitetsforlaget (1971).

From Conference on activation analysis in geochemistry and cosmochemistry; Kjeller, Norway (7 Sep 1970). See CONF-700968.

The monostandard method with the use of Ge(Li) gamma spectrometry was studied by critical evaluation of nuclear data involved in activation and activity measurement. The method was applied to investigate the recently discovered scheelite deposits in the East Alps. W contents in 18 samples of different origin were determined, and simultaneously 14 other elements which are usually associated with scheelite deposits were analysed. The results are compared with data obtained by the relative method to prove the accuracy and reproducibility of the monostandard technique. (auth) (Norway)

**54491** NON-DESTRUCTIVE ANALYSIS OF HAFNIUM IN ZIRCONS BY NEUTRON ACTIVATION AND GAMMA SPECTROMETRY OF $^{179m}$Hf. Voldet, Pia (Inst. of Mineralogy, Geneva). pp 411-16 of Activation Analysis in Geochemistry and Cosmochemistry. /Brunfelt, Arild O. (ed.). Oslo; Universitetsforlaget (1971).

From Conference on activation analysis in geochemistry and cosmochemistry; Kjeller, Norway (7 Sep 1970). See CONF-700968.

A nondestructive method for the determination of hafnium in zircons, based on the formation of $^{179m}$Hf (half-life 19 sec), is proposed. For a neutron flux of $10^9$ n cm$^{-2}$ sec$^{-1}$ and an irradiation time of 60 sec, the limit of detection is about $1 \times 10^{-7}$ g. The method is rapid and very selective. Results of some hafnium determinations are reported. (auth) (Norway)

**54492** MEASUREMENT OF ISOTOPE ABUNDANCE SHIFTS BY MEANS OF NEUTRON ACTIVATION ANALYSIS. Goerlich, W.; Moeller, P.; Schneeweiss, F. (Hahn-Meitner Inst., Berlin). pp 423-8 of Activation Analysis in Geochemistry and Cosmochemistry. /Brunfelt, Arild O. (ed.). Oslo; Universitetsforlaget (1971).

From Conference on activation analysis in geochemistry and cosmochemistry; Kjeller, Norway (7 Sep 1970). See CONF-700968.

The nuclear reactions $^{44}$Ca(n,$\alpha$)$^{41}$Ar, $^{40}$Ca(n,$\alpha$)$^{37}$Ar, $^{41}$K(n,p)$^{41}$Ar, and $^{39}$K(n,p)$^{39}$Ar are used for the isotope analysis of Ca and K, respectively. The standard deviation of the ratio $^{41}$Ar/$^{37}$Ar, which is proportional to the ratio $^{44}$Ca/$^{40}$Ca, is $\pm 3\%$ when using 0.5 g $CaCO_3$ and depends on the fast neutron flux of BER I ($10^{12}$ n cm$^{-2}$ sec$^{-1}$). The standard deviation of $\delta$ ($^{41}$K) is $\pm 4\%$. In routine application 2 to 3 samples plus their standards can be analysed by one person per day. From the point of view of time consumption and accuracy the activation method is superior to an analysis by mass-spectrometry. (auth) (Norway)

**54493** MULTI-ELEMENT SEPARATION FOR ACTIVATION ANALYSIS USING COUNTERCURRENT ELECTROLYSIS. Behne, D. (Hahn-Meitner Inst., Berlin). pp 431-5 of Activation Analysis in Geochemistry and Cosmochemistry. /Brunfelt, Arild O. (ed.). Oslo; Universitetsforlaget (1971).

From Conference on activation analysis in geochemistry and cosmochemistry; Kjeller, Norway (7 Sep 1970). See CONF-700968.

A separation method based on differences in the velocities of electromigrating ions is applied to activation analysis. The procedure, which is performed in a single step, is independent of the number of elements to be determined and is therefore generally applicable. The elements in question are either separated completely or split into different groups. A simple, remote-controlled apparatus is used which allows the processing of samples with high radiation levels. The method was tested in the separation of fifteen elements. (auth) (Norway)

**54494** FELDSPAR ANALYSIS BY NEUTRON ACTIVATION. Nissen, H.-U.; Rybach, L. (Eidgenoessiche Technische Hochschule, Zurich). pp 437-43 of Activation Analysis in Geochemistry and Cosmochemistry. /Brunfelt, Arild O. (ed.). Oslo; Universitetsforlaget (1971).

From Conference on activation analysis in geochemistry and cosmochemistry; Kjeller, Norway (7 Sep 1970). See CONF-700968.

A rapid procedure for the simultaneous neutron activation analysis of Na, K, and Ba designed for application to rock-forming minerals (feldspars) is described. Fragments of feldspars,(10 to 50 mg) are irradiated in a thermal flux of $5 \times 10^{12}$ ncm$^{-2}$ sec$^{-1}$ for 10 to 40 minutes. Na, Ba, and K contents, all major components of feldspars, are determined by measuring the gamma ray spectra of $^{24}$Na, $^{42}$K, and $^{139}$Ba with drift-stabilized multichannel equipment. The results are compared with electron microprobe, wet chemical, and optical analyses of the same specimens. The accuracy and precision are similar to those of the other analytical methods. The advantages of activation analysis of feldspars are easy sample preparation, low time consumption, nondestructiveness and opportunities to use computer programs for the automation of data handling. This permits analysis of extensive series of specimens, as needed in modern petrological and mineralogical studies. Examples are given, especially from the Swiss Alps. (auth) (Norway)

**54495** URANIUM AND THORIUM IN SOME BASIC AND ULTRA BASIC ROCKS OF POSSIBLE DEEP-SEATED ORIGIN. Morgan, J. W.; Lovering, J. F. (Univ. of Kentucky, Lexington). pp 445-54 of Activation Analysis in Geochemistry and Cosmochemistry. /Brunfelt, Arild O. (ed.). Oslo; Universitetsforlaget (1971).

From Conference on activation analysis in geochemistry and cosmochemistry; Kjeller, Norway (7 Sep 1970). See CONF-700968.

Neutron activation analyses are reported for 50 rocks, which are possibly representative of the lower continental crust or of the upper mantle. The radionuclides $^{239}$Np and $^{233}$Pa were used as indicators for uranium and thorium respectively. The rock types studied were: a) Kimberlites and xenoliths from several locations, chiefly in Africa. b) Basic and ultrabasic rocks from basaltic intrusions in south eastern Australia. c) A basalt and inclusions from the Hawaiian Islands. d) Crustal and intrusive eclogitic and ultrabasic rocks. (auth)

**54496** DETERMINATION BY NEUTRON ACTIVATION ANALYSIS OF ALKALI AND OTHER TRACE ELEMENTS IN ULTRAMAFIC ROCKS. Oosterom, M. G.; Das, H. A. (Univ., Utrecht). pp 455-9 of Activation Analysis in Geochemistry and Coscochemistry. /Brunfelt, Arild O. (ed.). Oslo- Universitetsforlaget (1971).

From Conference on activation analysis in geochemistry and coscochemistry; Kjeller, Norway (7 Sep 1970). See CONF-700968.

Aluminum and iron and minor amounts of manganese, sodium, potassium, scandium, cobalt, and copper can be determined by a sensitive neutron activation method by means of thermal neutrons and $\gamma$ spectrometry. This method was applied on samples of ultramafic rocks and serpentinites from Northern Greece with extremely low contents (10 to 100 ppM) of sodium and potassium. Accurate and sensitive determination of alkali contents is pertinent to the problem of distinguishing between ultramafic rock types of different genesis. (auth) (Norway)

**54497** DETERMINATION OF THE TRACE ELEMENT DISTRIBUTION IN COEXISTING CALCITE AND DOLOMITE BY NEUTRON ACTIVATION ANALYSIS. Braetter, P.; Moeller, P.; Roesick, U. (Hahn-Meitner Inst., Berlin). pp 461-5 of Activation Analysis in Geochemistry and Cosmochemistry. /Brunfelt, Arild O. (ed.). Oslo; Universitetsforlaget (1971).

From Conference on activation analysis in geochemistry and cosmochemistry; Kjeller, Norway (7 Sep 1970). See CONF-700968.

A nondestructive determination of twenty elements in coexisting calcite and dolomite was carried out by means of a large volume Ge(Li)-detector for high-resolution $\gamma$ spectrometry. Furthermore the phosphorus content was determined by Cherenkov-counting of the chemically separated radionuclide $^{32}$P. The trace element content of the "pure" phases calcite and dolomite was obtained by an extrapolation method. From the data, enrichment factors were calculated which can be correlated to the ionic radii. The distribution pattern and our investigations on ionic diffusion in single crystals of calcite seem to indicate that dolomite is formed via a solution phase and not by solid state diffusion. (auth) (Norway)

**54498** RATIONAL METHODS OF DECIPHERING TRICOMPONENT ACTIVITY INDUCED BY A COMPETING REACTION. Kryzhenkova, N. A.; Zhuk, L. I.; Kist, A. A.; Kirzhner, M. A.; Sattarov, M. G. (Inst. of Nuclear Physics, Tashkent). Izv. Akad. Nauk Uzb. SSR, Ser. Fiz.-Mat. Nauk; No. 1, 67-9(1971). (In Russian).

Competing reactions seriously hamper the methods of activation analysis. With fixed conditions of exposure and component concentrations, however, it is still possible to achieve quantitative separation of the induced activity of the product nucleus. A mathematical treatment is presented by which the analytical difficulties are generally avoided. (K.S.W.)

**54499** SEPARATION OF MERCURY FROM SOLUTIONS BY MEANS OF MERCURATION REACTIONS. Bock, Rudolf; Puff,

XUM

Hans-Juergen (Johannes Gutenberg-Univ., Mainz). Z. Anal. Chem.; 255: No. 1, 14-19(1971). (In German).

Divalent mercury reacts in weakly acidic, acetate containing solution with 2-methylthiophen. The 2-methylthiophen-5-mercury acetate is extracted by organic solvents, and Hg can be determined in the organic phase by photometry or activation analysis. All elements normally associated with mercury are separated by this method. Furthermore, divalent mercury reacts in alcoholic-alkaline solution with trichloro-ethylene to mercury-bis-trichloro-ethylene. This compound is less suited for the separation of mercury than the above mentioned 2-methylthiophen compound. (auth)

54500 DETERMINATION OF CHLOROBIPHENYL IN RAT ADIPOSE TISSUE BY NEUTRON ACTIVATION ANALYSIS. Manri, Teruo; Shinbori, Yoshio; Murakawa, Shoichiro; Mochizuki, Yoshio (Musashi Inst. of Tech., Kawasaki, Japan. National Inst. of Radiological Sciences, Chiba, Japan). Radioisotopes (Tokyo); 20: No. 8, 371-5(Aug 1971). (In Japanese).

A method for the determination of chlorobiphenyl in rat adipose tissue by neutron activation analysis is described. Adipose tissue from the tritiated chlorobiphenyl loaded rat was extracted with n-hexane, and the extract was partially purified by thin layer chromatography. Both crude and partially purified extract were used for analysis. The extracted material was sealed in a quartz ampoule while cooling with dry ice, and activated in a research reactor, Model TRIGA-II, at $4.4 \times 10^{12}$ n/cm$^2$ · sec for 30 minutes. After cooling, the ampoule was cleaned with diluted nitric acid, distilled water and acetone, and heated in an electric furnace at 650°C for 10 minutes for pyrolysis of extract. The ampoule was then broken in 5% NaOH and $H_2O_2$ solution (30 : 1/v : v) containing $NH_4Cl$ as a chlorine carrier to recover $^{38}Cl$ in solution. To eliminate $^{24}Na$ contamination chlorine was precipitated as AgCl and the precipitate was washed with $HNO_3$ and distilled water followed by redissolving in ammonium solution. Precipitating and washing were repeated again to get the final precipitate for assay of radioactivity. The radioactivity measured was the $^{38}Cl$ γ spectrum and its half life of 37.5 minutes. The sensitivity of the method was 0.1 microgram. The value of chlorobiphenyl in adipose tissue was calculated assuming that it exists in fat without any changes in structure. At the same time, a method of measuring tritium-labeled chlorobiphenyl with a liquid scintillation counter was carried out and a comparative study of both measured values made. The validity of values obtained by this assay procedure was confirmed by the demonstration that the value agreed with those determined independently by the analysis based on the amount of tritium activity in the extracted material. (auth)

54501 DEVELOPMENT OF A FAST-NEUTRON ACTIVATION METHOD FOR THE DETERMINATION OF NITROGEN IN NIOBIUM, TANTALUM, AND TITANIUM. Kudinov, B. S.; Pronman, I. M.; Shchulepnikov, M. N. Nauch. Tr., Gos. Nauch.-Issled. Proekt. Inst. Redkometal. Prom.; 22: 52-65(1968). (In Russian).

Two methods for N determination in Nb, Ta, and Ti by means of fast-neutron activation are described, wherein the cross section for 14-MeV neutrons is about 7 mbarns for $^{14}N$. Activation is based on the reaction: $^{14}N(n,2n)^{13}N$. In the first method the activating neutrons were generated by bombarding a Zr-T target with accelerated deuterium ions to produce the reaction: $T(D,^4He)n$ at a rate of about $10^{10}$ n/sec. In the second method, which is nondestructive, the test sample and the melamine standard were placed 12 mm from the target, and the coincidence of quanta annihilation was subsequently recorded. In the first method, the irradiated sample was dissolved and the $^{13}N$ activity was measured by triple coincidence, a positron and two quanta annihilation after radiochemical separation of the nitrogen. (K.S.W.)

54502 RADIOACTIVE DETERMINATION OF OXYGEN IN GERMANIUM AND SILICON. Aleksandrova, G. I.; Pleshakova, G. P.; Sukhov, G. V.; (and others). Nauch. Tr., Gos. Nauch.-Issled. Proekt. Inst. Redkometal. Prom.; 22: 70-9(1968). (In Russian).

The determination of oxygen in Ge and Si described is based on cyclotron-irradiation of samples with $^3He$ ions, wherein $^{16}O$ undergoes nuclear reactions leading to $^{18}F$. The positron activity of the $^{18}F$ with a half-life of 112 min is measured by means of γ-γ coincidence with a NaI crystal. Interaction of $^3He$ with $^{30}Si$ produces beta emitters; other Si isotopes form isotopes with very short half-lives. Interference with the γ-γ coincidence 0 determination is thus negated. Interaction of $^3He$ with Ge formed the following positron emitters: $^{73}Se$, $^{71}As$, and $^{69}Ge$, with $10^8$, $10^7$ and $10^6$ cpm, respectively. A procedure is given for isolation of the $^{18}F$ from the latter contaminating isotopes before proceeding to the measurement of $^{18}F$ activity. (K.S.W.)

54503 SIMULTANEOUS DETERMINATION OF OXYGEN, FLUORINE, AND ALUMINUM IN ALUMINUM ELECTROLYTIC BATH BY FAST-NEUTRON ACTIVATION. Tamura, Mituhisa (National Research Inst. for Pollution and Resources, Kawaguchi, Japan); Taira, Shigenobu; Nakamura, Yutaka; Takatsuna, Toshio; Honma, Takashi. Radioisotopes (Tokyo); 20: No. 7, 310-16 (Jul 1971). (In Japanese).

A rapid and nondestructive determination of oxygen, fluorine, and aluminum in aluminum electrolytic bath was studied by the use of 14-MeV neutron activation, together with the flux monitoring and the calculation of the photopeaks in the presence of non-linear backgrounds. A standard sample ($AlF_3$) for the flux monitoring and an unknown sample were irradiated under neutron fluxes of $3.3 \times 10^6$n/cm$^2$/sec and $1.3 \times 10^7$n/cm$^2$/sec, respectively, both for about 100 seconds. The following reactions and radiations from the products were used: $^{16}O(n,p)^{16}N$, 4-8 MeV β and γ rays; $^{19}F(n,2n)^{18}F$, 0.51 MeV annihilation photon; $^{27}Al(n,p)^{27}Mg$, 0.84 MeV γ rays. The photopeak counts and the concentrations of oxygen, fluorine, and aluminum were calculated with a computer. Fluorine in the monitor ($AlF_3$) was used also as the oxygen standard, because the $^{19}F(n,\alpha)^{16}N$ reaction gives $^{16}N$ as well as does the $^{16}O(p,n)^{16}N$ reaction. The relative standard deviations were about 3% for fluorine and aluminum, and about 6% for oxygen. It took about 17 minutes for the determination including the irradiation and measurement. (auth)

54504 ACTIVATION ANALYSIS OF LANTHANIDE ELEMENTS IN NATURAL WATER. Nagatsuka, Sumiko; Suzuki, Hamaji; Nakajima, Kiyoshi (Tokyo Metropolitan Isotope Research Center). Radioisotopes (Tokyo); 20: No. 7, 305-9(Jul 1971).

In the determination by activation analysis of rare earth elements contained in Tama river and sea water in Tokyo Bay, a simple chemical group separation made it possible to determine La, Ce, Sm, Eu, Tb, Dy, Tm, Yb, and Lu by γ spectrometry using a Ge(Li) detector. The distribution pattern of these rare earth elements expressed by chondrite normalized pattern for the sample waters showed that there is a characteristic difference in the pattern between river and sea water. When these patterns are compared with that of ocean water, the pattern of sea water has intermediate characteristics between those of river and ocean water. (auth)

54505 PARTICLE SIZE DISTRIBUTIONS OF TRACE ELEMENTS IN POLLUTION AEROSOLS. Nifong, Gordon Dale. Ann Arbor, Mich.; Univ. of Michigan (1970). 277p. University Microfilms Order No. 71-15,250.

Thesis.

Trace element content of particle size fractions of pollution aerosols was determined within a polluted source area in order to better understand aerosol source processes, atmospheric transformation, and removal mechanisms, or, the aerosol "life cycle." With the excellent sensitivities available for many elements through nondestructive neutron activation analysis, the analysis of particle size fractions for 29 elements has been accomplished. The technique consisted of giving each size fraction neutron irradiations for 5 minutes at $2 \times 10^{12}$ n/cm$^2$ and for 2 hours at 10-fold higher neutron flux. Amounts of each element were calculated from short-lived and long-lived induced radioactivity measured by Ge(Li) gamma-ray spectrometry in a sequence of counts over a 3-week period. Two of the 29, iron and zinc, were also quantitated by atomic absorption spectroscopy, with excellent agreement found between the methods. Forty-four samples at 11 locations in the industrial atmosphere of Northwest Indiana, and 6 samples at 1 location in urban Ann Arbor, Michigan, were collected using 7-stage cascade impactors equipped with in-line backup filters. Analytical data obtained from these samples were used in an attempt to determine types of source processes involved in production, degree of transformation in the atmosphere, and differential removal of the elemental components, particularly by dry fallout. Twenty-five of the elements were found to fall into one of several observed groupings, based on similarities in appearance of size distributions of aerosols with which the elements were associated. The steel complex of Northwest Indiana accounts for much of the particulate matter present in the atmosphere in the source area, and, comparing these data with the "Junge mass distribution", dM/d(log r) = Constant, the steel-related elements, iron, manganese, chromium, and cobalt, in addition to scandium and thorium, show a distinct large particle preference suggesting a predominantly dispersion source process. In contrast, zinc, antimony, arsenic, and indium appear mostly on small particles, suggesting a process of vapor condensation at high supersaturation, but a process also located within the steel industry. Some elements, Na, K, Br, Cl, rapidly approach a "Junge distribution" while airborne; others, Fe, Cr, Ca, Al, do not. Elements likely to be associated with condensation source processes tend to be more "Junge distributed" than do those arising by dispersion processes. It is suggested that primary particle size distributions determined by source processes may be modified by coagulation and sedimenta-

XUM

tion of aerosol particles within the urban area studied. Rough calculations of fallout indicate that both gravitational settling and turbulent impaction are important mechanisms of aerosol removal by fallout. Knowledge of elemental content of particle size fractions serves to establish natural tracers for certain emission processes; for example, Mn/Fe or Sb/Zn ratios may be used as indicators of steel plant emissions. This work suggests that other elements or combinations of elements added to the urban atmosphere may also be useful tracers of aerosol particle diffusion. (Diss. Abstr. Int., B)

**54506** NEUTRON ACTIVATION AND ON-STREAM ANALYSIS IN THE MINERAL INDUSTRIES USING SHERLOCK III. Godfrey, K. V. (British Columbia Research, Vancouver); Downs, W. E. Isotop. Radiat. Technol.; 9: No. 1, 23-30(Fall 1971).

The SHERLOCK III neutron irradiator is a simple, safe neutron activation unit that generates a neutron flux of $10^8$ n/(cm$^2$)(sec) by the $^{124}$Sb($\gamma$,n) reaction in beryllium. The irradiator, which can be used either for continuous on-stream analysis or for batch irradiations, is described, and some applications of the unit in the continuous analysis of ore slurries in the mineral industries are discussed. (auth)

**54507** USE OF RADIOISOTOPIC NEUTRON SOURCES FOR PROCESS-CONTROL ACTIVATION ANALYSIS. Kuusi, J. (Technical Univ. of Helsinki, Otaniemi, Finland). Isotop. Radiat. Technol.; 9: No. 1, 48-53(Fall 1971).

Neutron activation using a radioisotopic source for the determination of chromium in process and quality control during ore beneficiation is described. Characteristics of radioisotopic neutron sources are reviewed, and other potential applications of these sources are illustrated. (auth)

**54508** DETERMINATION OF MERCURY IN BIOLOGICAL AND ENVIRONMENTAL SAMPLES BY NEUTRON ACTIVATION ANALYSIS. Pillay, K. K. Sivasankara; Thomas, Charles C. Jr.; Sondel, James A.; Hyche, Carolyn M. (State Univ. of New York, Buffalo). Anal. Chem.; 43: No. 11, 1419-25(Sep 1971).

A neutron activation analysis procedure for the determination of trace levels of mercury in a variety of samples was developed. Problems associated with mercury losses throughout sampling and analysis were systematically examined. After neutron activation, the samples are wet ashed with mercury carrier. A preliminary precipitation is followed by further purification, and electrodeposition or precipitation is used to isolate mercury. The radioactivities $^{197}$Hg and $^{197m}$Hg are measured by scintillation spectrometry using a thin sodium iodide detector. The results of the analysis of several fish species and other aquatic environment samples from Lake Erie are reported. Comparison of the results of this analytical procedure with other techniques was made. (auth)

**54509** APPLICATION OF AN IODIDE-SPECIFIC RESIN TO THE DETERMINATION OF IODINE IN BIOLOGICAL FLUIDS BY ACTIVATION ANALYSIS. Heurtebise, Michel; Ross, W. J. (Instituto Venezolano de Investigaciones Cientificas, Caracas). Anal. Chem.; 43: No. 11, 1438-41(Sep 1971).

A reliable method was developed for the determination of iodine in biological fluids that incorporates the high sensitivity of neutron activation analysis with a very simple, economical, and rapid radiochemical separation procedure. Through the use of a novel and specific "iodinated" resin, $^{128}$I is separated from all other radioactive components of an activated sample. The high degree of isolation achieved permits the determination of this isotope with the maximum sensitivity that can be attained by means of gamma spectrometry. The method was applied to the routine analysis of urine, blood serum, PBI, and saliva. (auth)

**54510** TENTATIVE GUIDE FOR SELECTION OF NEUTRON ACTIVATION DETECTOR MATERIALS. ASTM E419-70T. Philadelphia; American Society for Testing and Materials (1970). 5p. Available from American Society for Testing and Materials, Philadelphia.

A guide is presented to bring about more uniformity in materials used for neutron activation detectors. The thickness, self-shielding, self-absorption, outer flux depression, fission fragment loss, diameter, shape and mass, and purity of foils are discussed. Alloys, other forms of detectors, and thermal neutron shields are considered. Commonly used detector materials are listed. (M.C.G.)

**54511** DETERMINATION OF MERCURY IN SMALL TERRESTRIAL AND NONTERRESTRIAL ROCK SAMPLES BY ATOMIC-ABSORPTION SPECTROSCOPY, AND THE STUDY OF MERCURY RELEASE AT ELEVATED TEMPERATURES. Goleb, Joseph A. (Argonne National Lab., Ill.). Appl. Spectrosc.; 25: No. 5, 522-5 (Sep-Oct 1971).

An atomic-absorption method was developed for determining subnanogram amounts of mercury in 100 mg of samples and for studying the release of mercury at elevated temperatures. The rock samples were contained in a sidearm of a quartz cell, and the mercury released by heating was determined by measuring the absorption of 2537-Å light passed through the cell. For a number of terrestrial and nonterrestrial samples analyzed, the results obtained agreed within a factor of 2 with neutron activation methods. This agreement is considered satisfactory since samples are not homogeneous. For a lunar sample that contained 1.79 ppB of mercury, the precision expressed as standard error is ±0.05 ppB. The sensitivity of this method for 1% light absorption is 0.03 ng; the limit of detectability is of the order of 0.01 ng. Mercury-release patterns obtained by atomic absorption methods also were in reasonable agreement with mercury-release patterns obtained by neutron-activation methods. (auth)

**54512** RADIOACTIVATION DETERMINATION OF IMPURITIES IN THE EPITAXIAL FILMS OF GALLIUM ARSENIDE. Shulepnikov, M. N.; Shmanenkova, G. I.; Yakovlev, Yu. V.; Dogadkin, N. N. (State Scientific-Research and Design Inst. of the Rare Metal Industry, Moscow. Inst. of Geochemistry and Analytical Chemistry, Moscow). Zh. Anal. Khim.; 26: No. 6, 1167-70(Jun 1971). (In Russian).

A method was developed for the neutron–activation determination of chromium, manganese, cobalt, nickel, copper, and zinc in epitaxial films of gallium arsenide with a sensitivity of $1.10^{-8}$ to $1.10^{-5}$%. The method is based on the radiochemical separation of macrocomponents and purification of the impurities by extraction chromatography in the systems tributyl phosphate–hydrochloric acid and trioctylamine–hydrochloric acid, followed by the $\gamma$ spectrometric determination. (auth)

**54513** TRACE ELEMENT CORRELATION OF VOLCANIC ASH SOILS. Borchardt, G. A.; Harward, M. E. (Oregon State Univ., Corvallis). Contract AT(45-1)-2062. Soil Sci. Soc. Amer., Proc.; 35: No. 4, 626-31(Jul-Aug 1971).

Neutron activation of volcanic ash followed by gamma-ray detection with a Ge(Li) semiconductor detector and 4096 multichannel analyzer produced rapid analysis for 19 elements. This was demonstrated to be useful for correlating soil parent materials. The trace element compositions of volcanic glass from C horizons of soils along a 450-km transect in Oregon correlate with known ejecta from Mt. Mazama. Concentration of transition metals in upper horizons relative to C horizons occurred in the order Cr > Co > Fe = Sc. Ratios of Na/Fe and Na/Co increased with depth. The abundances of Hf, Th, and the rare earth elements, as well as Sc/Fe ratios, were relatively constant with depth. Stable elemental ratios unique to Mazama ash aided correlation of weathered soil horizons. Some of the soils of northeastern Oregon may have small amounts of St. Helens ash in upper horizons in addition to the predominant Mazama ash. (auth)

**54514** NEUTRON ACTIVATION ANALYSIS FOR ALUMINUM IN ANIMAL TISSUE. Fritze, K.; Robertson, R. (McMaster Univ., Hamilton, Ont.). J. Radioanal. Chem.; 7: No. 2, 213-20 (Mar 1971).

A method for neutron activation determination of aluminum in animal tissue was developed which through pre-irradiation chemistry eliminates otherwise interfering nuclear reactions. The procedure gives a precision of ±0.1 ppM in samples of a few hundred milligrams dry tissue containing about 1 ppM Al. Bowen's standard kale was analyzed instrumentally and a value of 45 ± 4 ppM Al was found. Difficulties specifically related to the aluminum analysis of this material are discussed. (auth)

**54515** SIMULTANEOUS DETERMINATION OF ANTIMONY, ARSENIC, AND COPPER BY NEUTRON ACTIVATION ANALYSIS. Qureshi, I. H.; Nagi, F. I.; Nasra, M.; Cheema, M. N. (Atomic Energy Centre, Lahore). J. Radioanal. Chem.; 7: No. 2, 221-6 (Mar 1971).

A rapid procedure was developed for the mutual separation of antimony and arsenic using tribenzylamine as the extracting agent. The extraction behaviors of Sb(III), Sb(V), As(III), As(V), and Au(III) were studied as a function of the acidity of the aqueous phase. Various factors which affect the extraction of these complexes were studied and optimized. The procedure was then applied to lead base alloy for the simultaneous determination of antimony, arsenic, and copper. Chemical recoveries were quantitative and only about one hour is required for the chemical processing of duplicate samples. (auth)

**54516** SEMI-AUTOMATED DETERMINATION OF IODINE IN BIOLOGICAL FLUIDS BY ACTIVATION ANALYSIS. Heurtebise, M. (Instituto Venezolano de Investigaciones Cientificas, Caracas). J. Radioanal. Chem.; 7: No. 2, 227-33(Mar 1971).

XUM

A simple automated system was built that permits the selective separation of radioiodine by ion-exchange in eight samples simultaneously and the regeneration of the resin columns in fifteen minutes. Iodine is subsequently determined by γ-spectrometry. (auth)

**54517** WET-CHEMICAL ANALYSIS AND DETERMINATION OF TRACE ELEMENTS BY NEUTRON ACTIVATION IN METEORITES. Seitner, H.; Kiesl, W.; Kluger, F.; Hecht, F. (Univ., Vienna). J. Radioanal. Chem.; 7: No. 2, 235-48(Mar 1971).

As a study of the cosmochemical distribution of elements, 35 meteorites of collections in Vienna were analyzed. In the meteorites main and minor constituents were determined by wet-chemical methods, whereas for the determination of about 16 trace elements neutron activation analysis was employed. (auth)

**54518** NEUTRON ACTIVATION ANALYSIS OF IMPURITIES IN THORIUM AND ZIRCONIUM MATRICES. Oerdoegh, M.; Csath, G.; Szabo, E. (Central Research Inst. for Physics, Budapest). J. Radioanal. Chem.; 7: No. 2, 249-59(Mar 1971).

A neutron activation method is described for the determination of small concentrations of Cu, Cd, Mn, Co, Cr, and Zn contaminants in thorium and zirconium compounds used for telecommunication and reactor techniques. The thorium matrix is separated from the contaminants by pre-irradiation paper chromatography and the $^{233}Pa$ is isolated after irradiation by extraction into methyl isobutyl ketone and precipitation with cupferron. For the analysis of the contaminant in zirconium compounds only precipitation with cupferron is used after irradiation. The individual impurities are determined by γ spectrometry following separation. (auth)

**54519** ACTIVATION ANALYSIS OF SILICON IN STEEL WITH FAST NEUTRONS. Santner, E. (Bundesanstalt fuer Materialpruefung, Berlin). J. Radioanal. Chem.; 7: No. 2, 271-80 (Mar 1971). (In German).

Three experimentally different methods for determining silicon in steel by activation with fast neutrons are described. By bombardment of $^{29}Si$ with fast neutrons $^{28}Al$ is obtained after a (n,p) reaction. $^{28}Al$ emits γ radiation at 1.78 MeV. The difficulty lies in discriminating the 1.78-MeV peak out of the emitted radiation. The first method consists in determining the ratio of the 1.8-MeV peak to the 2.1-MeV peak of an activated iron sample. From this ratio the contribution of $^{28}Al$ to the 1.8 MeV peak of a silicon-containing sample can be deducted. The other method of separation makes use of the different half lives of the 1.78-MeV γ rays from $^{28}Al$ and the 1.81-MeV γ rays from $^{56}Mn$. The direct separation of the peaks with a Ge(Li) detector is the third method. The possibilities of activation analysis with fast neutrons are illustrated. For this reason the values measured are compared with the results of chemical analyses. (auth)

**54520** DETERMINATION OF Be, B, C, N, O, AND F BY p, d, $^{3}He$, AND α ACTIVATION. II. RELATIVE IMPORTANCE OF PRINCIPLE NUCLEAR INTERFERENCES. OPTIMAL IRRADIATION CONDITIONS. Engelmann, Ch. (CEN, Saclay, France). J. Radioanal. Chem.; 7: No. 2, 281-98(Mar 1971). (In French).

Curves and numerical values are given, representing the relative importance of the main nuclear interferences involved in the determination of Be, B, C, N, O, and F by p, d, $^{3}He$, and α activation. The possibilities offered by these charged particles and γ photons are compared, taking into account detection sensitivities on the one hand and interferences on the other. It is then possible to define the optimum irradiation conditions for the standard determination of each of these light elements. (auth)

**54521** CUPEL ASSAY OF GOLD BY AN ACTIVATION METHOD. Leipunskaya, D. I.; Savosin, S. I.; Drynkin, V. I.; (and others) (State Research Inst. of Nuclear Geophysics and Geochemistry, Moscow. Central Mining and Prospecting Research Inst. of Non-Ferrous, Rare, and Noble Metals, Moscow). J. Radioanal. Chem.; 7: No. 2, 299-308(Mar 1971).

The difficulties of determining gold in rocks and ores are due to two causes: low gold concentrations in rocks (Clark 1 to $4 \times 10^{-7}$%), and nonuniform distribution of gold in ores. A method is proposed based on neutron activation of the lead alloy obtained by cupel melting in the procedure of determining gold by cupel assay. Samples of 50 to 100 g are used for cupel melting. Such large samples guarantee that they will be representative. Discs of 2 to 3 g are cut from the lead alloy block and activated in a neutron flux of $10^{11}$ to $10^{13}$ $n \cdot cm^{-2} sec^{-1}$. The gold content is determined from the photopeak of $^{198}Au$ using a standard for comparison. The sensitivity of the method is 0.02 g/metric ton, its accuracy at a gold content in the order of 1.0 g/metric ton is 10% relative. The method is distinguished by the fact that it is fast and requires little labor. (auth)

**54522** ALPHA ACTIVATION OF CALCIUM AND ITS POSSIBLE USE FOR ANALYSIS. Pretorius, R.; Schweikert, E. A. (Texas A and M Univ., College Station). J. Radioanal. Chem.; 7: No. 2, 319-27(Mar 1971).

This method is based on measurement of 3.95-hr $^{43}Sc$, which is formed during α activation from $^{40}Ca$, the most abundant (96.8%) isotope of calcium. The excitation function for the $^{40}Ca(\alpha,p)^{43}Sc$ reaction was determined and the maximum yield of $^{43}Sc$ (about $10^7$ cpm per mg of calcium for a 1-hr irradiation at a beam current of 1 μA) was obtained at an irradiation energy of 14 MeV. The interference free sensitivity of the method at this energy was found to be $8.5 \cdot 10^{-12}$ g, for a 1-hr irradiation at a beam current of 10 μA. The elements most likely to interfere with the determination are potassium and scandium. The extent of this interference was investigated as a function of irradiation energy and methods to eliminate or subtract the activity formed from these elements are discussed. An attempt was made to determine nondestructively the calcium content of very pure silicon and aluminum and upper limits for the concentration of calcium in these samples were set at 0.27 and 6.9 ppB, respectively. Magnesium, thulium oxide, and yttrium oxide samples of known calcium content were also analyzed. (auth)

**54523** COMPUTER-ASSISTED QUALITATIVE ANALYSIS OF GAMMA-RAY SPECTRA. Adams, F.; Dams, R. (Ghent Univ.). J. Radioanal. Chem.; 7: No. 2, 329-40(Mar 1971).

A computer program is described to perform the identification of isotopes in neutron-activated samples. The γ energies as obtained from a Ge(Li) γ spectrum are compared with those of a library, containing data for about 250 isotopes. Isotopes whose γ energies match closely with the unknowns are selected as possible constituents. Unlikely attributions are then eliminated by a careful inspection of the γ rays found. Further exploitation of half-life, the way of production, and the sensitivity for the given irradiation and measurement conditions, allow selection of the most likely constituents in the source. The results of the automated identification agree closely to those obtained by an experienced investigator. The program is written in FORTRAN IV for a PDP-9 computer with a 16 K word memory. (auth)

**54524** 14 MeV NEUTRON ACTIVATION ANALYSIS APPLIED TO A NON-AQUEOUS FLOWING SYSTEM. Hayward, C. C.; Oldham, G.; Ware, A. R. (Loughborough Univ. of Tech., Eng.). J. Radioanal. Chem.; 7: No. 2, 341-6(Mar 1971).

The feasibility and advantages of fast neutron activation analysis in a nonaqueous flowing system, using economical irradiation techniques, are outlined. The application of the method to determination in solution of elements producing isotopes with half-lives in the range 588 to 29.4 sec, the selection of the optimum flow rate to minimize interferences for each element, and their limits of detection are given. A method for prediction of the optimum flow rate, on a given system, for the determination of any element producing an isotope of known half-life is also given. (auth)

**54525** CONCENTRATION AND DETERMINATION OF RARE EARTH IMPURITIES IN AN YTTRIUM MATRIX. Kulus, E.; Molnar, F.; Szabo, E. (Central Research Inst. for Physics, Budapest). J. Radioanal. Chem.; 7: No. 2, 347-9(Mar 1971).

The anion exchange separation of rare earth impurities from an yttrium matrix was studied. Activation analysis was used to determine these rare earths after separation from a high-purity matrix. (M.C.G.)

**54526** DEPENDENCE OF ACTIVATION UPON THE PULSE FORM IN A PULSED NEUTRON GENERATOR. Sterlinski, S. (Inst. of Nuclear Research, Warsaw). J. Radioanal. Chem.; 7: No. 2, 351-4(Mar 1971).

If the neutron yield during a pulse is fixed, the activity of the sample at the end of pulse will depend on pulse shape. It is shown that the narrower the neutron pulse the better the utilization of the generator target. (M.C.G.)

**54527** CALCULATIONS OF INDUCED ACTIVITY IN THE CASE OF INTERMITTENT IRRADIATION. Mednis, I. V. (Inst. of Physics, Riga). J. Radioanal. Chem.; 7: No. 2, 355-63(Mar 1971).

A survey is made of methods of calculation of induced activity in the case of intermittent irradiation when the periods of irradiation and cooling of the samples are equal and also for different time intervals. To simplify and speed up the calculations, formulas and graphs are given. Examples are given for every calculation method illustrating its practical use. (auth)

**54528** USE OF ACCELERATED CHARGED PARTICLES (α PARTICLES AND PROTONS) FOR THE DETERMINATION OF THE CONCENTRATION OF CERTAIN LIGHT ELEMENTS. Baskova, K. A.; Vasil'ev, S. S.; Dzhemard'yan, Yu. A.; (and others). At. Energ. (USSR); 30: No. 4, 398-9(Apr 1971). (In Russian).

Reactions that may be excited by low- and medium-energy charged particles may be used to determine the concentration of light elements. Thus, the boron and oxygen content of semiconductor-type silicon was determined by means of cyclotron-generated 6.25-MeV protons and 25-MeV $\alpha$ particles. The silicon specimens were bombarded by the particles and the induced positron activity recorded by means of a $\gamma$-$\gamma$ coincidence spectrometer. The boron was determined by the induced activity of $^{11}C$ from the $^{11}B(p,n)^{11}C$ reaction, with a threshold sensitivity of $10^{-6}$%. The oxygen was determined on the basis of $^{18}F$, formed by the $^{16}O(\alpha,d)^{18}F$ and $^{16}O(\alpha,pn)^{18}F$ reactions with a sensitivity of $5 \times 10^{-6}$%. Optical grade quartz was used as reference. The reproducibility of the determinations was not worse than 20%. The selectivity of the analysis was facilitated by the resonance character of the $(p,\gamma)$ and $(p,\alpha\gamma)$ reactions induced by ~1-MeV protons. (TTT)

# Inorganic, Organic, and Physical Chemistry

*Refer also to abstracts 54587, 54600, 54711, 54719, 54982, 55369, and 56380.*

**54529** STANDARD SPECIFICATIONS FOR DEUTERIUM OXIDE. ASTM D2032-68. Philadelphia; American Society for Testing and Materials (1968). 2p. Available from American Society for Testing and Materials (1968).

Specifications are given for minimum requirements for $D_2O$ to be used as a moderator in heavy water-moderated reactors. These include: isotopic content of deuterium to equal or exceed 99.75 at. %, electric conductivity not to exceed 15 $\mu$ Ohms/cm, consumption of $KMnO_4$ not to exceed $1 \times 10^{-5}$ g/ml, turbidity not to exceed 5 nephelos units, total solids not to exceed 12 mg/l, and chlorides not to exceed 0.1 mg/l. Methods of testing are listed. (M.C.G.)

## Chemical Properties

*Refer also to abstracts 55193, 55592, 55822, and 57103.*

**54530** (LA-DC-12469) ELECTROCHEMICAL REDUCTION OF EUROPIUM AT A POROUS CARBON CATHODE WITH FLOWING ELECTROLYTE. Onstott, E. I.; McClenahan, C. R. (Los Alamos Scientific Lab., N. Mex.). [1968]. 9p. (CONF-711001-2). Dep. NTIS.

From ninth rare earth research conference; Blacksburg, Va. (10 Oct 1971).

$EuBr_3$ electrolytes were electrolyzed between porous carbon electrodes with the electrolyte flowed through the electrodes. Current–voltage curves were obtained under precisely controlled flow conditions with dissolved oxygen removed. $Eu^{3+}$ reduction to $Eu^{2+}$ started at cell potentials greater than about 1.4 volts. At higher cell potentials, limiting current regions were demonstrated, indicating complete formation of $Eu^{2+}$ at the cathode. Relatively high cell potentials were required to obtain quantitative $Eu^{2+}$ formation when the electrolyte flows were high, and/or when the $Eu^{3+}$ concentrations were high. Eighty-three % of the current could be accounted for by bulk flow of electrolyte to the cathode, and the remaining 17% was attributed to migration effects. The cathode reaction appeared to be reversible in the sense that electron transfer was not rate limiting, but irreversible in the sense that overvoltage was necessary to overcome cell resistance. (auth)

**54531** (ORNL–4717) REACTOR CHEMISTRY DIVISION ANNUAL PROGRESS REPORT FOR PERIOD ENDING MAY 31, 1971. (Oak Ridge National Lab., Tenn.). Aug 1971. Contract W-7405-eng-26. 141p. Dep. NTIS.

Progress is reported in eight sections and a separate abstract was prepared for each section. (D.H.M.)

*For abstracts of individual sections see: 54532–54535, 54599, 54758, 55647, and 57090.*

**54532** (ORNL–4717, pp 1-27) MOLTEN SALT CHEMISTRY. (Oak Ridge National Lab., Tenn.).

In Reactor Chemistry Division annual progress for period May 31, 1971.

Progress is reported for research on molten salt chemistry including fluoride systems; structural studies; electrochemical studies; oxide–fluoride systems; noble metal fluorides; and fluoroborates. (D.H.M.)

**54533** (ORNL–4717, pp 29-41) CHEMICAL BEHAVIOR SALT REACTOR EXPERIMENT. (Oak Ridge National Lab., Tenn.).

In Reactor Chemistry Division annual progress for period May 31, 1971.

Fuel, coolant, and moderator chemistry and fission product distribution and behavior are discussed. (D.H.M.)

**54534** (ORNL–4717, pp 43-56) MOLTEN SALT BREEDER STUDIES. (Oak Ridge National Lab., Tenn.).

In Reactor Chemistry Division annual progress for period May 31, 1971.

Research progress is reported on reductive extraction studies, other separations, graphite, tritium behavior, and special studies. (D.H.M.)

**54535** (ORNL–4717, pp 57-82) AQUEOUS STUDIES. (Oak Ridge National Lab., Tenn.).

In Reactor Chemistry Division annual progress for period May 31, 1971.

Research progress is reported on high temperature equilibria, surface, and corrosion studies. (D.H.M.)

**54536** N-SUBSTITUTED UREA COMPLEXES OF THORIUM AND URANIUM TETRAHALIDES. Bagnall, K. W. (Univ. of Manchester, Eng.); du Preez, J. G. H.; Gibson, M. L. J. Chem. Soc., A; No. 13, 2124-31(1971).

Uranium tetrachloride and tetrabromide form 1:2 complexes with NNN'N'-tetramethylurea (tmu), NNN'N'-tetraethylurea (teu), NN'-dimethyl-NN'-diethylurea (ddeu) and NN'-dimethyl-NN'-diphenylurea (ddu), whereas uranium tetrachloride forms 1:4 complexes with NN'-dimethylurea (dmu) and with NNN'-trimethylurea (trmu). In contrast, the thorium tetrahalides form the 1:3 complexes $ThCl_4$,3ddu, $ThCl_4$,3tmu, and $ThBr_4$,3tmu, as well as the 1:6 complex $ThCl_4$,6dmu and the 1:4 complex $ThCl_4$,4trmu, the last being the only compound isolated for the thorium halides that is of the same stoichiometry as the uranium analogue. Ir spectroscopic and magnetic susceptibility results are reported for these complexes. (auth) (UK)

**54537** EQUILIBRIUM BETWEEN SODIUM HYDROGEN ACETYLIDE AND DISODIUM ACETYLIDE. Addison, C. C.; Hobdell, M. R.; Pulham, R. J. (Univ. of Nottingham, Eng.). J. Chem. Soc., A; No. 11, 1700-3(1971).

Attempts to determine the equilibrium pressure of acetylene over the solid phases in the system $2NaHC_2 \rightleftharpoons Na_2C_2 + C_2H_2$ were unsuccessful when appreciable dissociation (>5%) of the hydrogen acetylide occurred; this is due to the polymerization of acetylene, which is catalysed by the hydrogen acetylide. True dissociation pressures (P) are obtainable when dissociation is small (<0.5%). These are given by $\log_{10} P/mm = 9.942 - 3363/T$, and the heat of dissociation is +15.4 kcal/mol. Dissociation rates for the forward reaction were measured for the temperature range 120 – 170°C, and activation energies for the forward and back reactions found to be 30.8 and 15.4 kcal/mol respectively. (auth) (UK)

**54538** REACTION OF RHENIUM AND TECHNETIUM METALS WITH MOLTEN LITHIUM PERCHLORATE AND THE RAMAN SPECTRA OF THE CORRESPONDING MELTS. Cohen, D.; Fried, S.; Selig, H. (Argonne National Lab., Ill.). J. Inorg. Nucl. Chem.; 33: No. 8, 2687-8(Aug 1971).

Melts containing rhenium and technetium in molten $LiClO_4$ were examined by Raman spectroscopy and the spectra showed that perrhenate and pertechnetate ions were formed. The results are tabulated. The spectra were found to be very similar to those of aqueous solutions, except for a strong shift of about $20cm^{-1}$ towards shorter wavelengths for the totally symmetric vibrations. (UK)

**54539** STUDIES ON YTTRIUM, THORIUM, AND URANIUM SALICYLALDEHYDE COMPLEXES. Deshpande, Y. H.; Rao, V. Ramachandra (Marathwada Univ., Aurangabad, India). Curr. Sci. (India); 40: No. 16, 432-3(20 Aug 1971).

Details of the preparation and a study of spectral properties of yttrium, thorium, and uranium salicylaldehyde complexes are reported. The preparation involves the addition of a calculated amount of salicylaldehyde to the metal cation in ethanol medium and a subsequent addition of alcoholic ammonia to act as a hydrogen ion acceptor. The absorption spectra of the ligand and the chelates in the ultraviolet and visible region were recorded. (J.G.B.)

**54540** PREPARATION AND THE ABSORPTION SPECTRA OF URANIUM(III) IN VARIOUS ACID SOLUTIONS. Suzuki, Kazunori; Nakamura, Shigeru; Fukutomi, Hiroshi (Tokyo Inst. of Tech.). Bull. Tokyo Inst. Technol. (Engl. Ed.); No. 102, 63-7 (Mar 1971).

An attempt to prepare uranium(III) from uranium(VI) in various acid solutions was made by means of electrolytic reduction with a mercury cathode and cation exchange membrane. Nearly complete reduction was obtained in hydrochloric, perchloric, and sulfuric acid solutions. The molar extinction coefficient at 495 m$\mu$ in phos-

XUM

phoric acid markedly increased with the acid concentration, which might imply a formation of complex. (auth) (Japan)

**54541** INVESTIGATION OF A $U^{+5}$ SYSTEM: $(C_5H_5N)_2UOCl_5$. Maier, Mary Louise. Ann Arbor, Mich.; Univ. of Michigan (1970). 82p. University Microfilms Order No. 71-15,226. Thesis.

Pyridinium oxochlorouranate (V) was first synthesized by Bradley et al., in 1956, but no investigation of this compound beyond a stoichiometric analysis followed. An investigation verified the stoichiometry and established the monomeric nature of the compound. It includes confirmation of the oxidation state of uranium(V) by means of potentiometric titration as well as magnetic susceptibility measurements, which indicate the presence of one unpaired electron, with $\mu_{eff} = 1.90 + 0.03$, slightly greater than a spin-only value. ESR spectra of U(V) are generally broad lines with low g values. The ESR spectrum has such low intensity that it could not be due to the bulk sample but to a trace paramagnetic component with a g value near 2. Correlation of the absorption spectrum with the magnetic susceptibility suggested that a system with low symmetry and reduced spin-orbit coupling was present. Comparison of the uranium compound with its tungsten analog supports the commonly accepted theory that the unpaired electron of U(V) is a 5f rather than 6d electron. (Diss. Abstr. Int., B)

**54542** TECHNIQUE FOR EFFICIENTLY CONVERTING $^{13}CH_4$ INTO PYROLYTIC $^{13}C$. Goosman, D. R. (Brookhaven National Lab., Upton, N. Y.). Rev. Sci. Instrum.; 42: No. 10, 1468-71(Oct 1971).

A method is described for producing pyrolytic carbon with efficiencies suitable for use with highly enriched isotopes. Dense cylinders 14 cm long × 1.4 cm in diameter were produced with 97% efficiency by the pyrolysis of $^{13}CH_4$. A process for converting $^{13}CO$ into $^{13}CH_4$ is also described briefly. Some applications for nuclear spectroscopy are discussed. (auth)

**54543** CHEMICAL STABILITY OF DIBORIDES OF THE TRANSITION METALS FROM GROUPS IV–V OF THE PERIODIC SYSTEM. Kugai, L. N.; Nazarchuk, T. N. (Inst. of Materials Science, Kiev). Sov. Powder Met. Metal Ceram. (Engl. Transl.); 10: No. 3, 212-15(Mar 1971).

Translated from Porosh. Met., Akad. Nauk Ukr. SSR; 10: No. 3, 51-5(Mar 1971).

The decomposition of $TiB_2$, $ZrB_2$, $HfB_2$, $VB_2$, $NbB_2$, and $TaB_2$ in nonoxidizing and oxidizing acids and their mixtures was investigated. The dissolution and gas evolution were studied in more detail in 1:1 HCl and 1:1 $H_2SO_4$, using a $N_2$ stream, and the stability of the corresponding metals was also studied for comparison. The results show that the diborides of the group V are less stable than those of group IV, with $TaB_2$ being the most resistant to acids, and that the borides are stronger reducing agents than boron and the corresponding metals. (D.L.C.)

**54544** THERMAL DECOMPOSITION OF THORIUM OXALATE. Saito, Yasutoshi (Akita Univ., Japan). Funtai Oyobi Funmatsuyakin; 17: No. 6, 235-42(Mar 1971). (In Japanese).

Thermal decomposition of thorium oxalate hexahydrate, $Th(C_2O_4)_2 \cdot 6H_2O$, was studied by thermogravimetry (TG) and differential thermal analysis (DTA) in air and argon. The thermal decomposition took place in three steps. At temperatures below about 300°C, plateaus in TG and endothermic peaks in DTA indicated the appearance of the dihydrate and monohydrate at the first two steps, respectively. At higher temperatures the monohydrate decomposed to the oxide at the third step. In argon the dehydration processes were essentially the same as those in air, but the decomposition to the oxide was sluggish. This might be due to the deposition of carbon caused by the disproportionation of primarily evolved CO. The decomposition to the oxide gave an endothermic peak in DTA in argon, but in air exothermic peaks due to the oxidation of CO and carbon were observed. Hahn's emanation technique using thoron 54.5-second was applied to the studies of thermal decomposition. Three peaks were observed in the emanation curves and corresponded to the three steps as determined both in TG and DTA. In the electron microscope the oxalate particles were square platelets of a few microns, and the oxide appeared as the skeleton particles of the original oxalate. (auth) (Japan)

**54545** PHYSICAL AND CHEMICAL CHARACTERISTICS OF AEROSOLS PRODUCED FROM SOLUTIONS OF POLYVALENT METALLIC NUCLIDES. Kanapilly, G. M.; Raabe, O. G.; Newton, G. J. (Lovelace Foundation for Medical Education and Research, Albuquerque, N. Mex.). Contract AT(29-2)-1013. pp 171-97 of Health Physics Aspects of Nuclear Facility Siting. Vol. I. /Voilleque, Paul G. (comp.). Idaho Falls, Idaho; Burton R. Baldwin, Publications Chairman (1971).

From fifth annual midyear topical symposium on health physics aspects of nuclear facility siting; Idaho Falls, Idaho (3 Nov 1970).

The physical and chemical nature of radioactive aerosols influences the relative health hazards of inhaled radionuclides. The character of the aerosols produced from solutions of metallic ions is influenced by (a) the composition of the solution, (b) the droplet sizes, (c) the rate of drying of the droplets, and (d) the rates of heating and cooling when degradation or sintering is involved. The relative effects of these factors were investigated with aqueous solutions of metallic ions of Co, La, Ce, Y, Sb, Ru, Zr, and Mo in one or more anionic forms including chloride, lactate, citrate, acetate, EDTA, hydroxide, oxalate, acetylacetonate, and tartrate. Production of aerosols consisted of nebulization, drying, degradation at temperatures up to 1150°C, and cooling. Electron microscopic studies and determination of aerodynamic properties were used in physical characterization. The chemical nature of aerosols was studied by tracer techniques, and other methods as applicable for specific cases. The probable physical and chemical characteristics of aerosols that may be produced in some nuclear industrial accidents involving solutions of polyvalent nuclides are predicted using the general information obtained in this study. (auth)

**54546** AMOUNT AND CHARACTERISTICS OF PLUTONIUM MADE AIRBORNE UNDER THERMAL STRESS. Mishima, J.; Schwendiman, L. C. (Battelle-Northwest, Richland, Wash.). Contract AT(45-1)-1830. pp 198-207 of Health Physics Aspects of Nuclear Facility Siting. Vol. I. /Voilleque, Paul G. (comp.). Idaho Falls, Idaho; Burton R. Baldwin, Publications Chairman (1971).

From fifth annual midyear topical symposium on health physics aspects of nuclear facility siting; Idaho Falls, Idaho (3 Nov 1970).

The quantity and nature of the particles airborne when plutonium metal or compounds are subjected to thermal stresses are under study. A retrospective review of incidents that have occurred in operations involving plutonium helped orient the investigation towards situations which may be most productively studied. An analysis was made of circumstances surrounding 46 incidents occurring in the nuclear industry, 1952 to 1967, and the incidents cataloged as to nature of the material involved, initiating event, and consequences. A series of laboratory studies was conducted to investigate the behavior of plutonium and its compounds when subjected to thermal stresses which might occur in overheating situations. Fractional release rate was measured for plutonium metal, plutonium nitrate, plutonium fluoride, and plutonium oxide when subjected to temperatures up to 1000°C. Release from heated solutions of plutonium nitrate was measured for several heating rates. Rate of release from combustion of small samples of four materials impregnated with powder or with nitrate was measured. The range of release rates is presented. Large scale experiments are planned using uranium compounds as simulants for plutonium. Conditions which reflect the type of thermal stresses typical of those postulated for some serious incidents will be imposed. Emphasis is to be given to those situations currently regarded as potentially serious when plutonium or its compounds in shipment are involved in a petroleum fire. The information gathered has given insight into the potential for release of plutonium and its compounds under various conditions. (auth)

**54547** IODINE CHEMISTRY IN STEAM AIR ATMOSPHERES. Keller, J. H.; Duce, F. A.; Pence, D. T.; Maeck, W. J. (Idaho Nuclear Corp., Idaho Falls). pp 764-83 of Health Physics Aspects of Nuclear Facility Siting. Vol. III. /Voilleque, Paul G. (comp.). Idaho Falls, Idaho; Burton R. Baldwin, Publications Chairman (1971).

From fifth annual midyear topical symposium on health physics aspects of nuclear facility siting; Idaho Falls, Idaho (3 Nov 1970).

In the event of a loss-of-coolant accident in a power reactor and the subsequent release of fission products to the containment vessel, the airborne iodine may be the controlling factor in the downwind dose. Based on experiments in the laboratory and in an 86 $ft^3$ test vessel, hypoiodous acid can be the major airborne iodine species after the initial rapid washout of elemental iodine from a steam–air atmosphere. The equilibria concerned with the hydrolysis of iodine are discussed to show that hypoiodous acid is a major species in solution. Relationships are given for the ratio of hypoiodous acid to total iodine in solution as a function of pH and temperature. Airborne hypoiodous acid can be produced by injection of elemental iodine into a steam–air atmosphere or by purging a dilute aqueous solution of iodine in water with air or other gas. Laboratory experiments confirming the volatility of hypoiodous acid by means of a specific chemical reaction are discussed. In a water-cooled power reactor, the accident released fission products will contact a heated water solution at a pH of 7 to 10 and then be transported into a steam–air atmosphere. These conditions seem ideal for the formation and stable existence of hypoiodous acid in

XUM

the vapor state. Thus, it, rather than methyl iodide, could well be the major long-term hazardous species from the biological standpoint. Hypoiodous acid, like methyl iodide, penetrates various adsorbents including silver surfaces commonly used in atmospheric sampling devices and thus may explain the abnormally high organic fraction reported by other investigators. (auth)

**54548** BROENSTED TYPE EQUATION FOR SOLVOLYSIS OF TERT-BUTYL HALIDES UNDER THE ACTION OF METAL IONS (LEWIS ACIDS). Rudakov, E. S.; Kozhevnikov, I. V. (Inst. of Catalysis, Novosibirsk, USSR). Reakts. Sposobnost Org. Soedin., Tartu. Gos. Univ.; 7: No. 3, 771-8(Oct 1970). (In Russian).

A general Brönsted type correlation, $\log(k_1/k_0) = -0.7 + 0.84 \log K_{YCT}$, was found for solvolysis of tert-butyl halides under the action of metal ions (Lewis acids) ($k_1$, $k_0$, and $K_{YCT}$ are rate constants of the reaction with the metal ion and solvent respectively, and stability constant of the metal halide complexes, which are all measured at the same solvent). This equation embraces variation of ion [H(1), Mg(2), Al(3), Ga(3), In(3), Tl(1), Pb(2), Bi(3), Cu(2), Ag(1), Zn(2), Cd(2), Sc(3), Zr(4), Th(4), Mn(2), Fe(3), Co(2)], alkyl halide RX (R = tert-Bu; X = F, Cl, Br; where different X have different sets of active metal ions), and solvent ($H_2O$, $H_2O$–EtOH, $CH_3NO_2$). Such a generality is conditioned by the use of the value of $k_1/k_0$ as the measure of the activity of the metal ion. The slope of the correlation ($\beta = 0.84$) is discussed in connection with the position of transition state along the reaction coordinate (related to the initial and final states). This correlation allows prediction of widely varying effects of electrophilic catalysis for the $S_N1$-type and similar reactions. (auth)

## *Isotope Effects and Exchange*

*Refer also to abstracts 54442, 54651, 54686, 54727, 54735, 54748, and 55826.*

**54549** INVESTIGATION OF THE KINETICS OF OXYGEN ISOTOPIC EXCHANGE BETWEEN WATER AND CARBON DIOXIDE IN THE PRESENCE OF SOLUBLE ADDITIVES. Andreev, B. M.; Gumenyuk, T. D.; Sel'venskii, Ya. D.; Meretskii, A. M. Isotopenpraxis; 7: No. 5, 180-4(May 1971). (In Russian).

In a circulating plant the influence of additives, such as the inorganic salts $Na_2SO_3$, $Na_2SeO_3$, and $Na_2TeO_3$, the amines MEA, TEA, and EDA, as well as of piperidine and hexamethylenimine on the isotopic exchange velocity was investigated at atmospheric pressure. Information on the correlation between exchange velocity and salt concentrations up to saturated solutions and temperatures ranging from 20 to 50°C was obtained. In the S–Se–Te series exchange velocity increased with the atomic number of elements. In the presence of piperdine and hexamethylenimine an increase of amine concentration was accompanied by increase of exchange velocity. When exchange is going on with MEA, TEA, and EDA present, exchange velocity shows extreme dependence on amine concentration, which is caused by increased viscosity of the solutions. (auth)

**54550** INFLUENCE OF ROTATIONAL ENERGY ON ION–MOLECULE CROSS SECTIONS: ORTHO AND PARA HYDROGEN AND DEUTERIUM. Hyatt, D. (Northern Polytechnic, London); Stanton, L. Chem. Phys. Lett.; 10: No. 1, 10-12(1 Jul 1971).

The influence of the rotational isotope on the cross section of the reaction of $Ar^+$ with ortho or para hydrogen (or deuterium) was calculated using a multipole interaction potential. The ratio $\sigma(J = 0)/\sigma(J = 1)$ is predicted to be close to unity at relative collision energies around 1 eV but to increase with decreasing collision energy. (auth)

**54551** VIBRATION–ROTATION–TRANSLATION ENERGY TRANSFER IN HF–HF AND DF–DF. Shin, H. K. (Univ. of Nevada, Reno). Chem. Phys. Lett.; 10: No. 1, 81-5(1 Jul 1971).

The vibrational relaxation times of HF and DF were calculated on the basis of the vibration-rotation-translation energy transfer theory over the temperature range from 400 to 4000°K. Up to about 2500°K, DF molecules always relax slowly compared to HF, but at still higher temperatures they relax faster. This alternation in the isotope effect is due to the increased efficiency of the translational motion in removing the vibrational energy at elevated temperatures in DF-DF. In HF-HF the maximum value of the relaxation time at 1 atm appears at ≈800°K, and in DF-DF it occurs at ≈700°K. The appearance of the maximum values is due to the dipole-dipole attraction. The calculated values are in reasonable agreement with experiment. (auth)

**54552** CATALYSIS BY METAL VAPORS. IV. HOMOMOLECULAR HYDROGEN ISOTOPE EXCHANGE REACTION. Peretyaka, A. R.; Danchevskaya, M. N.; Kobozev, N. I. (Moscow State Univ.). Russ. J. Phys. Chem. (Engl. Transl.); 45: No. 2, 216-18(Feb 1971).

Translated from Zh. Fiz. Khim.; 45: No. 2, 391-4(Feb 1971).

The catalytic effect of zinc, cadmium, and thallium vapors on homomolecular hydrogen isotope exchange was investigated in the temperature range 300 to 500°C. Only zinc vapor proved to be catalytically active. The isotope exchange in zinc vapor is a first-order reaction with an activation energy of 15 ± 1 kcal $mole^{-1}$. (auth)

**54553** DETERMINATION OF THE ASSOCIATION CONSTANTS OF IONS FROM THE RATE OF OXYGEN EXCHANGE BETWEEN ANIONS AND WATER. Tereshkevich, M. O.; Volkova, S. A.; Kuratova, T. S.; Dlugach, R. E. (Dnepropetrovsk State Univ., USSR). Russ. J. Phys. Chem. (Engl. Transl.); 45: No. 2, 227-9(Feb 1971).

Translated from Zh. Fiz. Khim.; 45: No. 2, 413-16(Feb 1971).

The effect of the concentration of the solution on the rate of oxygen exchange between $Na_2SeO_4$, $Ni(NO_3)_2$, and $LiBrO_3$, on the one hand, and water containing oxygen-18, on the other, was studied at temperatures between 100 and 170°C. The rate of reaction passes through a maximum as the concentration of electrolyte increases and then after a fall begins to increase again. Ionic association constants were calculated at different temperatures. A relation between ion hydration and their capacity for association was postulated. (auth)

**54554** MECHANISM OF ISOTOPE EXCHANGE IN THE SYSTEM $H_2$–$H_2O$ ON SOME OXIDE CATALYSTS. Rachkovskii, E. E.; Boreskov, G. K. (Inst. of Catalysis, Novosibirsk, USSR). Kinet. Katal. (USSR) (Engl. Transl.); 11: No. 6, 1176-82(Nov-Dec 1970).

Translated from Kinet. Katal.; 11: No. 6, 1410-18(Nov-Dec 1970).

On samples of $Fe_3O_4$, $Cr_2O_3$, and $CuCr_2O_4$, the rates of interaction of the catalyst surfaces with $H_2$ and with $H_2O$ in the stationary state and the rates of isotope exchange between deuterium and protium in the system $H_2$–$H_2O$ were measured at 4.6 mm Hg pressure of the components and at temperatures of 400 and 350°C for $Cr_2O_3$, and 200°C for $CuCr_2O_4$. It is shown that a stepwise mechanism is given only on iron (II, III) oxide. (auth)

**54555** KINETIC ISOTOPE EFFECT UPON HYDROGEN EXCHANGE OF m-CARBORANE WITH BASES. Yakushin, F. S.; Vukmirovich, Z.; Yakovleva, E. A.; (and others) (Physical-Chemical Inst., Moscow. Inst. of Heteroorganic Compounds, Moscow). Kinet. Katal. (USSR) (Engl. Transl.); 11: No. 6, 1189-92(Nov-Dec 1970).

Translated from Kinet. Katal.; 11: No. 6, 1426-30(Nov-Dec 1970).

Primary kinetic isotope effects (KIE) were determined for the isotope exchange reaction in the C–D (T) bond of m-carborane with liquid ammonia, and also with ethanol and t-butanol on catalysis with the corresponding basic metal alkoxides. It was found that the ratio $k_D/k_T = 1.0$ (at 25°C) in all cases, and a comparison was carried out of it with the values of $k_D/k_T$ for exchange reactions of fluorene with the same bases, where $k_D/k_T \approx 2$. Possible reasons for the absence of a KIE in the case of m-carborane are discussed. (auth)

**54556** DETERMINATION OF DIFFUSION COEFFICIENTS IN LIQUID METALS BY ISOTOPE EXCHANGE THROUGH THE GAS PHASE. Kryukov, S. N.; Soldatov, E. A.; Irkov, V. I. Vestn. Mosk. Univ., Ser. II. Khim.; 12: No. 2, 224-5(Mar-Apr 1971). (In Russian).

Diffusion coefficients in liquid metals were measured by an experimental technique based on isotope exchange in the gaseous phase. The method assures the best boundary conditions and also permits the study of vaporization in addition to diffusion. One of two metal samples, designated the donor, contained a radioactive isotope; the other was designated the acceptor. Detailed conditions of the experiment are lacking; however, the kinetics of the isotope exchange are defined by three processes: condensation on the exchange surface of the acceptor, evaporation from the surface, and diffusion from the surface into the interior of the sample. The pertinent mathematical relationships were developed. One of the basic equations was tested by determining the distribution of the radioisotope Zn-65 in an acceptor made of the natural mixture of Zn isotopes (self-diffusion). (K.S.W.)

**54557** PALLADIUM(II)-CATALYZED EXCHANGE AND ISOMERIZATION REACTIONS. I. THE EXCHANGE OF ENOL ACETATES WITH ACETIC ACID CATALYZED BY PALLADIUM-(II) CHLORIDE. Henry, Patrick M. (Hercules Inc., Wilmington, Del.). J. Amer. Chem. Soc.; 93: No. 16, 3853-9(11 Aug 1971).

The main Pd(II)-catalyzed exchange of $CH_2{=}CHOOCCD_3$ with $CH_3COOH$ was found to obey the following rate expression:

XUM

$-d[C_2H_3OOCCD_3]/dt = ([Li_2Pd_2Cl_6][C_2H_3OOCCD_3]/[LiCl])$ $(k_1 + k_2[LiOAc])$. There may be a small contribution from a reaction with a higher LiCl inhibition. A study of the rates of isomerization and vinyl ester exchange of cis- and trans-1-acetoxyl-1-propene showed that exchange occurs only with isomerization. The kinetics and stereochemical results are consistent with an oxypalladation–deoxypalladation mechanism for exchange: $C_2H_3OOCCD_3 + PdOOCCH_3 \rightarrow PdCH_2CH(OOCCD_3)(OOCCH_3) \rightarrow PdOOCCD_3 + C_2H_3OOCCH_3$. This mechanism predicts that cyclic enol acetates should not exchange. It was found that 1-acetoxyl-1-cyclopentene in fact did not exchange. Substitution on vinyl carbon strongly inhibits exchange. The relative rates for vinyl acetate, trans-1-acetoxyl-1-propene isopropenyl acetate, and cis-2-acetoxy-2-butene are $1 : 2.5 \times 10^{-2} : 3.3 \times 10^{-3} : 1.6 \times 10^{-6}$. (auth)

**54558** RADIOISOTOPIC EXCHANGE OF LIGANDS IN CHLORO- AND THIO-CYANATOMOLYBDATES(III). Wajda, Stanislaw; Pruchnik, Florian; Zarzeczny, August (Univ. of Wroclaw). Nukleonika; 16: No. 3-4, 125-31(1971).

The kinetic of exchange of radiocarbon or radiochlorine in the $[MoX_6]^{3-}$–$^*X^-$ systems is examined, where X = $NCS^-$ or $Cl^-$. On the basis of experimental data the mechanism of isotopic exchange is proposed. The magnitude of the activation energy in both systems suggests that the Mo–X bonds are covalent. Recapitulating, it should be noted that the stability of octahedral transition metal complexes is most significantly affected by the central ion electron structure, a strong covalent bonding being exhibited by the complexes containing the central ions with the $d^3$-electron structure. (auth)

**54559** SOLVOLYSIS OF SULFONATE ESTERS IN SOLVENTS OF LOW NUCLEOPHILICITY. Dafforn, Geoffrey Alan. Berkeley, Calif.; Univ. of California (1970). 150p. University Microfilms Order No. 71-15,749.

Thesis.

A study of the solvolyses of primary alkyl and aryl trifluoromethanesulfonates and related systems was undertaken, primarily in solvents of low nucleophilicity, in order to determine the degree of limiting character in their solvolyses. In order to demonstrate qualitatively the low nucleophilicity of trifluoroacetic acid, secondary deuterium effects for isopropyl p-toluenesulfonate were determined in it. Isotope effects of $(k_H/k_D)_\alpha = 1.22 \pm .02$ and $(k_H/k_D)_{\beta\text{-}d_6} = 2.12 \pm .10$ indicate that solvolysis of isopropyl p-toluenesulfonate is much nearer limiting in trifluoroacetic acid than in acetic acid or trifluoroethanol. The rate constant for trifluoroethanolysis of ethyl trifluoromethanesulfonate is $k_1 = 8.21 \pm .44 \times 10^{-5}$ $sec^{-1}$ at 34.98° with isotope effects of $(k_H/k_D)_{\alpha\text{-}d_2} = 1.13 \pm .05$ and $(k_H/k_D)_{\beta\text{-}d_3} = 1.09 \pm .05$. For trifluoroacetolysis, the rate is $k_1 = 1.34 \pm .04 \times 10^{-5}$ $sec^{-1}$ at 50°, with isotope effects of $(k_H/k_D)_{\alpha\text{-}d_2} = 1.13 \pm .04$ and $(k_H/k_D)_{\beta\text{-}d_3} = 1.15 \pm .04$. These isotope effects are interpreted as indicating that these solvolyses proceed with only a slight degree of limiting character. n-Propyl trifluoromethanesulfonate rearranges to isopropyl trifluoroacetate in trifluoroacetic acid (>90%), as does n-propyl p-toluenesulfonate. The enhanced rate of trifluoroacetolysis of the propyl ester ($k_1 = 1.39 \pm .14 \times 10^{-4}$ $sec^{-1}$ at 50°) indicates that the rearrangement is probably concerted with ionization. Phenyl trifluoromethanesulfonate does not react in ethanol (285 hr, 161°) or in trifluoroethanol below its critical temperature (157 hr, 150°). Reaction in ethylene glycol (18 hr, 244°) and trifluoroacetic acid (2 days, 161°) gave no identifiable major products. Reaction in trifluoroethanol (217 hr, >244°) gives phenol, as does reaction with 3M $NaOCH_3$ at ~35°. 2-n-Propylphenyl trifluoromethanesulfonate decomposes in Sulfolane at 276° (179 hr), but does not yield indan (the expected product fron. cyclization of an aryl cation). These results indicate that aryl trifluoromethanesulfonates are too subject to side reactions at their high decomposition temperatures to be useful for generation of aryl cations. (Diss. Abstr. Int., B)

**54560** SOLVENT ISOTOPE EFFECTS ON DECOMPOSITION OF N,N-DIALKYLDITHIOCARBAMIC ACIDS. Aspila, K. I.; Joris, S. J.; Chakrabarti, C. L. (Carleton Univ., Ottawa). Anal. Chem.; 43: No. 11, 1529-30(Sep 1971).

The solvent isotope effects on decomposition rates of dialkyldithiocarbamic acids are compared. Results show that the $K_{D_2O}/K_{H_2O}$ for dimethyldithiocarbamic acid is 2.80; diethyldithiocarbamic acid is 2.54; dibutyldithiocarbamic acid is 1.81; and diisopropyldithiocarbamic acid is 0.42. (D.H.M.)

**54561** FLASH PHOTOLYSIS OF A SUBSTITUTED HEXAARYLBIIMIDAZOLE AND REACTIONS OF THE IMIDAZOLYL RADICAL. Riem, R. H.; MacLachlan, A.; Coraor, G. R.; Urban, E. J. (E. I. du Pont de Nemours and Co., Wilmington, Del.). J. Org. Chem.; 36: No. 16, 2272-5(13 Aug 1971).

The rate of reaction of 2-(o-chlorophenyl)-4,5-diphenylimidazolyl radicals (L·) with additives was studied in various solvents. Evidence based on measured rate constants, including kinetic deuterium isotope effects, prove that the rate-determining step in the reaction L· + aromatic amine is an electron exchange reaction at the amino nitrogen, while in the reaction L· + hydroquinone the rate-determining step is hydrogen abstraction. (auth)

**54562** DYNAMIC SAMPLING OF THE DEUTERIUM HYDRIDE SELF-EXCHANGE BEHIND REFLECTED SHOCK WAVES. Kern, R. D.; Nika, G. G. (Louisiana State Univ., New Orleans). J. Phys. Chem.; 75: No. 17, 2541-6(19 Aug 1971).

The self-exchange reaction of deuterium hydride diluted in neon was studied over the temperature range 1800 to 2800°K. Dynamic sampling of the reflected shock zone at 20-$\mu$sec intervals was performed with a time-of-flight mass spectrometer. Sixty-one experiments covering a total density range $1.7\text{-}3 \times 10^{-6}$ mol $cm^{-3}$ were analyzed during typical reaction times of 500 $\mu$sec. During the observation period of runs exceeding 2600°K, an equilibrium condition was observed. The time dependence of product formation was found to be nonlinear. An average mole fraction basis was used for product formation. The reaction profiles were fit to the equation $[1 - 4f_{av}] = \exp(-k'[M]t^2)$; $k' = 10^{16.67\pm0.21} \exp(-40{,}980 \pm 2250/RT)$ $cm^3$ $mol^{-1}$ $sec^{-2}$. The equilibrium constant for the $H_2 + D_2 \rightleftharpoons 2HD$ system was obtained using the previously reported rate constant for the forward reaction along with the self-exchange rate constant reported here. Agreement with the calculated equilibrium constant was obtained within the experimental errors associated with the kinetic results. (auth)

**54563** INFRARED SPECTRA OF $LiAlF_4$ AND $NaAlF_4$. Cyvin, S. J. (Technical Univ. of Norway, Trondheim); Cyvin, B. N.: Snelson, A. J. Phys. Chem.; 75: No. 17, 2609-15(19 Aug 1971).

The infrared spectra of the vapors over heated mixtures of $^7LiF + AlF_3$, $^6LiF + AlF_3$, and $NaF + AlF_3$ were obtained using the matrix isolation technique. In the spectral region 4000 to 190 $cm^{-1}$, eight frequencies were assigned to $LiAlF_4$, and seven frequencies to $NaAlF_4$. A normal coordinate analysis, based on a molecular model with $C_{2v}$ symmetry, was performed. Agreement between the observed and calculated frequencies, though fairly good, was insufficient to prove the assumed molecular geometry. Mean amplitudes of vibration based on the assumed force fields are given for both compounds. A possible structure for the $(MAlF_4)_2$ dimer is suggested. (auth)

**54564** RAMAN SPECTRAL STUDY OF BISULFATE–SULFATE SYSTEMS. II. CONSTITUTION, EQUILIBRIA, AND ULTRAFAST PROTON TRANSFER IN SULFURIC ACID. Chen, H.; Irish, D. E. (Univ. of Waterloo, Ont.). J. Phys. Chem.; 75: No. 17, 2672-81 (19 Aug 1971).

Species concentrations are reported for aqueous solutions of $H_2SO_4$ and $H_2SO_4$ + NaOH (or HCl) mixtures. These were obtained from the relative integrated intensities of the 981-$cm^{-1}$ Raman line of $SO_4^{2-}$. The apparent concentration quotients, $Q_c$, for the equilibrium were computed and attempts to estimate $K_2$ from the data are discussed. Half-widths of the 981-$cm^{-1}$ line and the 1050-$cm^{-1}$ line of $HSO_4^-$ were also measured, and correlated with proton transfer processes occurring in the solutions. An apparent rate law, $rate_R = k_R[H_3O^+](a_w)^x[SO_4^{2-}]$, was inferred, with $k_R^H = 6.4 \times 10^{11}$ $M^{-1}$ $sec^{-1}$. For $KDSO_4$–$D_2O$ solutions $k_R^D = 10.4 \times 10^{11}$ $M^{-1}$ $sec^{-1}$. It is believed that for this system the Raman effect is providing uniquely detailed information about the mechanism of proton transfer along a chain of oriented water molecules. (auth)

**54565** INFRARED STUDY OF SURFACE PROPERTIES OF $\alpha$-CHROMIA. I. PREPARATION AND ADSORPTION OF WATER, HEAVY WATER, AND CARBON MONOXIDE. Zecchina, A.; Coluccia, S.; Guglielminotti, E.; Ghiotti, G. (Univ., Turin). J. Phys. Chem.; 75: No. 18, 2774-83(2 Sep 1971).

Samples of $\alpha$-chromia of high surface area and suitable for spectroscopic work were prepared in a controlled manner. Crystals mainly expose the (001) face on which the adsorption of $H_2O$, $D_2O$, and CO was studied. At low coverages, water adsorption at room temperature is dissociative and hydroxyl groups are formed. At higher coverages a nondissociative chemisorption is observed and discussed. Carbon monoxide is adsorbed onto surface $Cr^{3+}$ ions to form $\sigma$ adducts, and the adsorbed amount solely depends on surface dehydration. (auth)

**54566** EQUILIBRIUM DEUTERIUM ISOTOPE EFFECTS ON THE IONIZATION OF THIOL ACIDS. Jencks, William P.; Salvesen, Karin (Brandeis Univ., Waltham, Mass.). J. Amer. Chem. Soc.; 93: No. 18, 4433-6(8 Sep 1971).

Isotope effects on the ionization of the thiol groups of pentafluorothiophenol, thioacetic acid, 4-nitrothiophenol, thiophenol, methyl mercaptoacetate, mercaptoethanol, and mercaptoacetate

XUM

in water and deuterium oxide range from $K_{RSH}/K_{RSD} = 2.0$ to 2.5 and approximately follow the equation $\Delta pK = 0.26 + 0.012\ pK_a$. Bending as well as stretching frequencies contribute significantly to the isotope effects for reactions of thiols. The increase in the isotope effect with decreasing acidity of the thiol and the magnitude of the difference in the isotope effects for the ionization of RSH and ROH provide evidence that isotope effects on the interaction of $RS^-$ and $RO^-$ with the solvent contribute significantly to the observed effects. (auth)

**54567** SILICON–TRANSITION METAL CHEMISTRY. VI. KINETICS AND MECHANISM OF THE REPLACEMENT OF TRIPHENYLSILANE BY TRIPHENYLPHOSPHINE IN HYDRIDOTRIPHENYLSILYL(π-CYCLOPENTADIENYL)DICARBONYLMANGANESE. Hart-Davis, A. J.; Graham, W. A. G. (Univ. of Alberta, Edmonton). J. Amer. Chem. Soc.; 93: No. 18, 4388-93(8 Sep 1971).

The kinetics and mechanism of the replacement of triphenylsilane by ligands such as triphenylphosphine from hydridotriphenylsilyl(π-cyclopentadienyl)dicarbonylmanganese were studied in n-heptane, toluene, and tetrahydrofuran. The initial process is the rate-determining dissociation of the silane molecule, for which activation parameters (in n-heptane) are $\Delta H^{\ddagger} = 29.2$ kcal/mol, $\Delta S^{\ddagger} = 16.3$ eu. The reaction is retarded by added triphenylsilane, and competition experiments indicate that triphenylphosphine is 3.6 times as reactive as triphenylsilane toward the intermediate π-cyclopentadienyldicarbonylmanganese. The kinetic isotope effects for both forward and back reactions are small but significant and consistent with the proposed mechanism of a concerted single-stage mechanism for silane dissociation. (auth)

**54568** DEUTERIUM ISOTOPE EFFECTS ON THERMAL CYCLOBUTENE ISOMERIZATIONS. AN INVESTIGATION OF COMPETITIVE CONROTATORY RING OPENINGS. Winter, Rudolph Ernest K. (Univ. of Missouri, St. Louis); Honig, Milton L. J. Amer. Chem. Soc.; 93: No. 18, 4616-17(8 Sep 1971).

A study was made of isotope effects in the isomerization of 1,2-bis(trimethylsiloxy)cyclobutene in an effort to describe the mechanism of thermal isomerization of cyclobutenes. (D.H.M.)

**54569** CATALYTIC OXIDATION. IV. ETHYLENE AND PROPYLENE OXIDATION OVER GOLD. Cant, Noel W.; Hall, W. Keith (Carnegie-Mellon Univ., Pittsburgh). J. Phys. Chem.; 75: No. 19, 2914-21(16 Sep 1971).

The heterogeneous oxidation of $C_2H_4$ and $C_3H_6$ was studied over several gold catalysts. The principal products from $C_2H_4$ were $CO_2$ and $H_2O$, but small amounts of acetic acid and acetaldehyde were also found. In addition to these products, up to 3% acetone and 50% acrolein were obtained from $C_3H_6$. Gold sponge and Au/$SiO_2$ were much more selective for acrolein formation than Au/$\alpha$-$Al_2O_3$. For both olefins, the rate of total oxidation was first order in oxygen pressure and zero order in olefin pressure at low pressures. The apparent activation energies (except for $C_2H_4$ over Au sponge) ranged from 17 to 22 kcal $mol^{-1}$. Acrolein formation had a much lower apparent activation energy (9 to 12 kcal $mol^{-1}$), was also first order in $O_2$, but showed a maximum rate for $C_3H_6$ pressures near 30 Torr. Oxidation of propylene-1-$^{13}C$ produced acrolein molecules in which the $^{13}C$ was equally distributed between the end positions. Similarly, $CD_3CHCH_2$ and $CH_3CHCD_2$ both yielded $CH_2CHCDO$ and $CD_2CHCHO$ in about equal amounts, although the rate of the reaction with the former olefin was only about 40% that of the latter or that of $CH_3CHCH_2$. These results indicated that the rate-determining step in acrolein formation was abstraction of a methyl hydrogen (or deuterium) to yield a symmetrical allylic intermediate. The modes of fragmentation of acrolein during mass spectral analysis are discussed on the basis of high-resolution measurements of the labeled acroleins formed. (auth)

**54570** HYDROGEN ISOTOPE EFFECT IN THE REACTION OF TRITYL RADICALS WITH THIOPHENOL. Lewis, E. S.; Butler, M. M. (Rice Univ., Houston). J. Org. Chem.; 36: No. 18, 2582-4(10 Sep 1971).

Excess thiophenol reacts at room temperature with 4-triphenylmethyl-1-diphenylmethylene-2,6-cyclohexadiene (I) to produce triphenylmethane and phenyl triphenylmethyl sulfide. At −20 and −40°, p-benzyhydryltetraphenylmethane (II), an isomer of I, is also formed. When tritium is present in the SH position, both triphenylmethane and II are labeled, and an isotope effect for the hydrogen transfer from sulfur to carbon is found with $k_H/k_T = 14.9$. Between 0 and 40°, the temperature dependence of the isotope effect is normal, but the measured isotope effect is apparently too low both at high temperatures (60°) and low (−20 and −40°). An explanation is offered for the high-temperature deviation in terms of failure of the competitive method. Low-temperature deviations are attributed to reversibility. An extremely rough estimate of the rate of this nearly thermoneutral hydrogen atom transfer, $k = 1\ M^{-1}\ sec^{-1}$, is presented. (auth)

**54571** RING-OPENING REACTIONS OF TRIPHENYLCYCLOPROPYLLITHIUM COMPOUNDS. Mulvaney, J. E.; Savage, Dennis (Univ. of Arizona, Tucson). J. Org. Chem.; 36: No. 18, 2592-6(10 Sep 1971).

The compound, trans-1,2,3-triphenylcyclopropane undergoes ring opening with n-BuLi to give, after treatment with $D_2O$, a mixture of cis- and trans-stilbenes in which the trans isomer prevails. The use of N,N,N′,N′-tetramethylethylenediamine (TMEDA) did not effect polymetalation of the cyclopropyl ring. Although attempts to trap a cyclopropyl anion in the above experiment were unsuccessful, the 1,2,3-triphenylcyclopropyl anion can form without immediately undergoing ring opening. This was demonstrated by hydrogen–deuterium exchange of the cyclopropyl hydrogens in both cis- and trans-1,2,3-triphenylcyclopropane, accompanied by isomerization of the cis isomer to the trans, using potassium tert-butoxide in dimethyl sulfoxide-$d_6$. Treatment of triphenylcyclopropene with n-butyl- or tert-butyllithium–TMEDA resulted in addition to the cyclopropenyl double bond followed by ring opening to give a mixture of stilbenes. Attempts to prepare the anti aromatic triphenylcyclopropenyllithium with triptycyllithium TMEDA and triphenylcyclopropene were unsuccessful. (auth)

**54572** INFRARED SPECTRA AND VAPOR PRESSURE ISOTOPE EFFECT OF CRYSTALLIZED AMMONIA AND ITS DEUTERIUM DERIVATIVES. Wolff, H.; Rollar, H.-G.; Wolff, E. (Univ., Heidelberg). J. Chem. Phys.; 55: No. 3, 1373-8(1 Aug 1971).

The infrared spectra of crystalline $NH_3$, $NH_2D$, $ND_2H$, and $ND_3$, which were thoroughly studied by Reding and Hornig in 1951 and 1955 were reinvestigated. The antisymmetric stretching bands of $NH_3$ and $ND_3$ are found to be split. Their shifts relative to the values for the gas phase found to be approximately equal by the previous measurements are now shown to be distinctly different. The antisymmetric stretching vibrations of $NH_2D$ and $ND_2H$ were observed separately from those of $NH_3$ and $ND_3$. The ND stretching vibration of $NH_2D$ consists of a triplet composed of the unperturbed vibrational center band and of two satellite bands due to correlation field splitting. It was derived from this splitting that intermolecular coupling between the ammonia molecules is weak. The equality of the NH and ND stretching force constants in $NH_2D$ and $ND_2H$ as well as in $NH_3$ and $ND_3$ follows from two facts: (1) The NH stretching vibration of $ND_2H$ lies in the middle of the $NH_2$ stretching vibrations of $NH_2D$, also the ND stretching vibration of $NH_2D$ lies in the middle of the $ND_2$ stretching vibrations of $ND_2H$; (2) only single NH and ND stretching bands are observed. Therefore, the unequal shifts of the symmetric and of the antisymmetric stretching vibrations of $NH_3$ and $ND_3$ relative to the values observed in the gas phase cannot be explained by an asymmetric change of stretching force constants during crystallization. They must be explained by Fermi resonance of the symmetric stretching vibration with the parallel component of the overtone of the deformational vibration. The calculation of the vapor pressure isotope effect of crystalline $NH_3$ and $ND_3$ by using the corrected vibrational frequencies shows further evidence in support of these explanations. (auth)

**54573** REACTIONS OF HYDROGEN AND DEUTERIUM ATOMS FORMED IN THE PHOTOLYSIS OF METHANE AND PERDEUTERATED METHANE AT 123.6 nm. Hellner, Lucette; Masanet, Jeannine; Vermeil, Catherine (CNRS, Paris). J. Chem. Phys.; 55: No. 3, 1022-8(1 Aug 1971).

The photolysis of methane and perdeuterated methane was carried out at 123.6 nm, in the presence of interceptors (deuterium in the case of methane, and hydrogen in the case of deuterated methane). The hydrogen and deuterium atoms formed are statistically in thermal equilibrium with the reaction medium; it follows that the photodissociation into $CH_3$ and H has a probability close to zero at 123.6 nm. In addition, it is confirmed that $CH_4$ and $CD_4$ have different photolytic behaviors insofar as the quantum yields of hydrogen and deuterium are concerned with $\phi_H > \phi_D$. (auth)

**54574** $ReO_4^-$–$H_2O$ EXCHANGE KINETICS IN METHANOL USING $^{18}O$. Murmann, R. Kent (Univ. of Missouri, Columbia). J. Amer. Chem. Soc.; 93: No. 17, 4184-6(25 Aug 1971).

The $^{18}O$ exchange between $ReO_4^-$ and $H_2O$ was studied in methanol solution. The kinetic expressions are basically the same as those with water as a solvent. In methanol the rate is relatively insensitive to $[H_2O]$ in the neutral and acidic regions. This suggests that the mechanism of oxygen exchange is closer to a dissociation facilitated by solvent hydrogen bonding than a displacement. Isotope fractionation factors are also presented. (auth)

**54575** BELL-SHAPED pH-RATE PROFILE FOR AN OXIDATION. THE REACTION OF PERMANGANATE WITH HYDROXYCYCLOHEXANECARBOXYLIC ACIDS. Stewart, Ross; MacPhee, J. Anthony (Univ. of British Columbia, Vancouver). J. Amer. Chem. Soc.; 93: No. 17, 4271-5(25 Aug 1971).

XUM

The effect of a neighboring carboxyl group on the oxidation of a number of cyclohexanols by aqueous permanganate was examined. cis-2-Hydroxycyclohexanecarboxylic acid (1) and its cis-5-tert-butyl derivative (3) exhibit pronounced rate accelerations at intermediate pH values, producing bell-shaped pH–rate profiles. A substantial isotope effect (7 to 8 : 1) is observed when the alcoholic carbon of 1 is substituted by deuterium. A solvent isotope effect is also observed. Compounds (1) and (3) exist predominantly in conformations that allow the carboxylate ion to participate in the removal of the hydrogen from the alcoholic carbon atom. A mechanism is proposed in which a carboxylate–permanganate adduct, $C^-$, is formed between the neutral hydroxy acid and permanganate ion. Dissociation of $C^-$ gives $C^{2-}$ which decomposes to products. Rate equations were derived, based on the steady-state approximation, which give satisfactory agreement with experiment. (auth)

**54576** OXIDATION OF ALCOHOLS BY FENTON'S REAGENT. THE EFFECT OF COPPER ION. Walling, Cheves; Kato, Shin'ichi (Univ. of Utah, Salt Lake City). J. Amer. Chem. Soc.; 93: No. 17, 4275-81(25 Aug 1971).

The oxidation of alcohols in $Fe^{2+} - H_2O_2$ systems was reexamined and a new kinetic analysis developed. Relative reactivities of methyl, ethyl, isopropyl, and tert-butyl alcohols are in good agreement with those from radiolysis experiments. The analysis and product studies indicate attack on both $\alpha$- and $\beta$-hydrogens of ethyl and isopropyl alcohols. The $\beta$-hydroxyalkyl radicals are not oxidized by $Fe^{3+}$, but dimerize, terminating kinetic chains. They are, however, oxidized by $Cu^{2+}$ to yield glycols with chain propagation. Thus the oxidation of tert-butyl alcohol is converted to a long-chain process by $Cu^{2+}$. We suggest that, in these systems, radical oxidation by $Fe^{3+}$ is an electron-transfer process, but, with $Cu^{2+}$, involves either ligand transfer or an organocopper intermediate. The $Fe^{3+}$ oxidation is evidently reversible in some cases, since solvolysis of ethyl trifluoromethanesulfonate in the presence of $Fe^{2+}$ yields significant amounts of $Fe^{3+}$ and butane. A large kinetic isotope effect was observed in the oxidation of isopropyl alcohol when deuterium was substituted in the alcohol. (auth)

**54577** ISOTOPE EFFECTS AFTER THE RATE-DETERMINING STEP. THE ROLE OF ROTATIONAL ISOMERISM IN A HYDROGEN TRANSFER. Cohen, Theodore; Smith, Katherine W.; Swerdloff, Michael D. (Univ. of Pittsburgh). J. Amer. Chem. Soc.; 93: No. 17, 4303-4(25 Aug 1971).

A study was made using competitive isotope effects in steps following the rate-determining step to discern whether or not a bond to hydrogen was broken during the product-determining competition. When this concept was applied in previous studies to the 1,5-hydrogen atom transfer that occurs in the radical produced by the cuprous oxide promoted decomposition of the diazonium ion 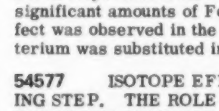 evidence was provided that the rate of internal transfer was greater than that of rotation about the carbonyl CN bond but less than the rate of rotation about the methyl CN bond. Results are now reported that can be interpreted in terms of the behavior of the CC bond during this transfer. (D.H.M.)

## *Physical Chemistry*

*Refer also to abstracts 54673, 54736, 55092, 55489, 55525, and 56384.*

**54578** (ORNL–4682, pp 215-17) SPECTROPHOTOMETRIC STUDIES OF SOLUTIONS OF LANTHANIDES AND ACTINIDES. (Oak Ridge National Lab., Tenn.).

In Chemical Technology Division annual progress report.

Research progress is reported on: high-energy absorption bands of $H_2O$ and $D_2O$, spectral studies of actinides, emission spectra of actinides, densities of aqueous rare earth solutions to 340°C, and protonic wave functions and spectra. (M.C.G.)

**54579** GROWTH AND STRUCTURE OF $RbUO_2(NO_3)_3$ CRYSTALS. Kvapil, Josef; Kvapil, Jiri; Tethal, Tomas (Inst. of Nuclear Research, Rez, Czech.). J. Cryst. Growth; 10: No. 3, 279-80(Aug 1971).

The growth conditions and structure of $RbUO_2(NO_3)_3$ crystals are reported. The crystals were grown from an equimolar solution of the cation components containing 37 to 40% $HHO_3$. The crystals were found to be monoclinic with a = 8.321 ± 0.015 Å, b = 9.374 ± 0.012 Å, c = 6.257 ± 0.018 Å, $\beta$ = 100° 30′ 32″ ± 18″; space group C2/m. (auth)

**54580** PRECIPITATION OF URANIUM FROM A MELT OF FUSED HALIDES WITH A MOLTEN ZINC CATHODE. Volkovich, A. V.; Nichkov, I. F.; Raspopin, S. P.; Kanashin, Yu. P. This paper was summarized in At. Energ. (USSR); 29: No. 4, 284-5 (Oct 1970) as paper No. 432/5415. (In Russian).

Polarization of a molten zinc cathode in an equimolar mixture of KCl–NaCl containing 1.0, 2.9, 3.5, and 6.8 wt. % uranium was studied at 700°C. The uranium content in the electrolyte was 3.0 wt. % in experiments designed to study the effect of the fluoride ion on cathodic polarization, and the fluorine content (converted to NaF content) was 1.66, 2.14, 2.66, 3.17, and 5.5 wt. %. Uranium deposition on the molten zinc cathode was found to take place accompanied by depolarization. A strongly bonded intermetallic compound $U_2Zn_{17}$ exists in the system Zn–U. This is what is responsible for the depolarization observed, which amounts to 0.3 V by comparison with a solid molybdenum cathode. At a uranium concentration of 6.8 wt. %, a new wave appears on the polarization curve at E = –2.5 V, corresponding to precipitation of uranium just as when a solid cathode is used. This provides evidence to the effect that the discharge rate of the $U^{3+}$ ions is greater than the rate at which interaction products shift from the surface into the bulk phase of the cathode. Raising the temperature above 800°C had no effect on the shape of the polarization curves, and only shifted the cathode potential more positive. The presence of fluoride ions in the electrolyte resulted in a decline in the limiting diffusion currents in the discharge of $U^{3+}$ ions, in a slight increase in cathodic polarization, and in a shift of the cathodic potential negative. The shape of the polarization curves was not affected. (auth)

**54581** INVESTIGATION OF U(IV) COMPLEXING WITH ACETATE AND FORMATE IONS. Lobanova, T. S.; Dunaeva, K. M.; Ippolitova, E. A. Vestn. Mosk. Univ., Ser. II. Khim.; 12: No. 2, 229-31(Mar-Apr 1971). (In Russian).

Stability constants of the ions $[U(Lig)]^{3+}$ and $[U(Lig)_2]^{2+}$ in the system benzene–water–carboxylic acid were determined by a distribution method. All the constants were determined at 20°C and ionic strength 2. (auth)

**54582** EXPERIMENTAL STUDY OF THE EQUATION OF STATE OF URANIUM HEXAFLUORIDE. Malyshev, V. V. (Inst. of Atomic Energy, Moscow). Dokl. Akad. Nauk SSSR; 197: No. 1, 73-4(1 Mar 1971). (In Russian).

The constant-volume piezometric technique was used to study the equation of state of $UF_6$ in the 99.1 to 320.3°C temperature range at densities up to 2.1 g/cm³. In order to reduce corrosion losses, the internal surface of the Monel metal used for the fabrication of the piezometer was passivated with fluorine at 300°C for 10 days. The $UF_6$ used was not less than 99.98% pure. The expression obtained for the temperature dependence of the vapor pressure of saturated $UF_6$ ($P_s$) in °K: $\lg P_s = 4.5830 - 1476.24/T$, agrees with previously published data. The heat of evaporation of liquid $UF_6$, calculated by the Clausius–Clapeyron equation and the experimentally obtained vapor density data agreed within 4 to 6% with earlier values. The critical parameters of the system were also determined. (TTT)

**54583** SOLUBILITY OF HELIUM AND ARGON IN LIQUID SODIUM. Veleckis, Ewald; Dhar, Sanat K.; Cafasso, Fred A.; Feder, Harold M. (Argonne National Lab., Ill.). J. Phys. Chem.; 75: No. 18, 2832-8(2 Sep 1971).

The solubilities of helium and argon in liquid sodium were determined as functions of pressure and temperature. The data obeyed Henry's law to at least 9 atm. In the temperature range 330 to 550°C, the solubilities may be represented by the following linear equations: helium, $\log \lambda = 0.516 - 3078T^{-1}$; argon, $\log \lambda = 1.08 - 4462T^{-1}$; where $\lambda$ is the Ostwald coefficient. The 95% confidence limits of the mean value of $\lambda$ predicted by these equations are ±4% for helium and ± 16% for argon. For the standard state defined as 1 mol of ideal gas confined to a volume equal to the molar volume of sodium, the heats of solution are 14.1 ± 0.6 kcal/mol for helium and 20.4 ± 2.1 kcal/mol for argon. The results are compared with experimental data of others and with calculations based on existing theoretical models. (auth)

**54584** HIGH-TEMPERATURE THERMODYNAMIC PROPERTIES OF URANIUM MONOSULPHIDE. MacLeod, A. C. (Univ. of Strathclyde, Glasgow). J. Inorg. Nucl. Chem.; 33: No. 8, 2419-25(Aug 1971).

The enthalpy of uranium monosulphide was measured from 400 to 1400°K in an adiabatic drop calorimeter. The data are represented by the equation $(H_T - H_{298.15}) = 12.633T + 7.7865 \times 10^{-4}T^2 + 9.0413 \times 10^4T^{-1} - 4139$ cal mole$^{-1}$ with a mean deviation of 0.55%. Molar thermodynamic properties from 300 to 2000 K were calculated and a value of –80 kcal mole$^{-1}$ is derived for the heat of formation from the solid elements at 298.15°K. (auth)

**54585** DISPROPORTIONATION AND ECE MECHANISMS. III. ASYMMETRICAL POTENTIAL-SCAN METHOD: DIAGNOSTIC CRITERIA AND RATE-DETERMINATION PROCEDURES AND APPLICATION TO THE REDUCTION MECHANISM OF THE URANYL CATION IN PERCHLORIC ACID. Nadjo, L.; Saveant,

XUM

J. M. (Ecole Normale Superieure, Paris). Electrochim. Acta; 16: No. 7, 887-900(Jul 1971).

The duality of ECE (electrochemical-chemical-electrochemical) and disproportionation mechanisms is studied in conditions of double-scan polarization of the working electrode. Formal kinetics are analysed for trapezoidal and triangular scanning, the anodic stage being much shorter than the cathodic one (for the example of a reduction process and conversely for an oxidation process). Diagnostic criteria are established that allow the distinction between the two possible reaction schemes. Procedures for measurement of the kinetic parameters characterizing each reaction path are described. The method is then applied to the analysis of the reduction process of the uranyl cation in perchloric acid. The results obtained previously in this respect with single sweep voltammetry are confirmed, the accuracy in the determination of rate factors being better with the double-scan technique. (auth) (UK)

**54586** STANDARD POTENTIAL AND ENTHALPY VALUES OF METALS AND THEIR COMPOUNDS BASED ON ELECTRODE POTENTIALS. Krupkowski, A. (Inst. for Metal Research, Krakow). Bull. Acad. Pol. Sci., Ser. Sci. Tech.; 19: No. 4, 327-34(1971).

The formulas representing the dependence of basic molar functions of elements and their compounds on temperature are given. An analysis of these formulas proves that the values of two thermodynamic functions—those of the potential and enthalpy—cannot be calculated because they contain an unknown standard enthalpy $H^0_{298}$. A method is given for calculating the standard potentials and enthalpies of metals during oxidation and chlorination processes. The calculations were based on the assumption that the potentials of oxygen and oxides, as well as those of chlorine and chlorides, assume the zero value for a given group of metals. (auth)

# Radiation and Nuclear Chemistry

**54587** (AECL-3909) CHEMISTRY AND MATERIALS DIVISION PROGRESS REPORT, JANUARY 1–MARCH 31, 1971. (Atomic Energy of Canada Ltd., Chalk River (Ontario). Chalk River Nuclear Labs.). 92p. (PR-CMa-16). Dep. NTIS (U. S. Sales Only). AECL $2.00.


ALUMINUM ALLOYS—Al-base–Mn, binding energy and entropy of vacancies in
CARBON MONOXIDE—CO–O, radiolysis of, electron pulse
COBALT—deposition on surfaces, basic chemistry in
CORROSION—research progress on
DEUTERIUM—determination of, evaluation of methods for
—separation from hydrogen, electrochemical
—exchange between water-d and hydrogen, catalytic effects of platinum on
DIFFUSION—research progress on, in solids
ELECTRON MICROSCOPES—lens of, spatial frequency of
ELECTRONS—effects of pulsed, on heavy water–water systems
—effects of pulsed, on carbon monoxide–oxygen mixtures
HELIUM IONS—scattering by sodium chloride crystals, channeling in
HYDROGEN IONS—scattering by sodium chloride crystals, channeling in
INDIUM—superconducting transition temperature of, effects of compression deformation on
MASS SPECTROGRAPHY—research progress on
METALS—surface relaxations in cubic
NICKEL—sorptive properties for tellurium
NICKEL OXIDES—preparation of uniform particles of, for fission product deposition studies
NUCLEAR CHEMISTRY—research progress in
PLUTONIUM-239—neutron fission of, yields from thermal
REACTORS, RESEARCH—radioactivity in cooling water of Slowpoke
SODIUM CHLORIDES—ion scattering by crystals of, channeling in
SOLIDS—diffusion in, research progress on
SPECTROSCOPY—research progress on
SURFACES—chemistry of, research progress on
TANTALUM OXIDES—ion implantation in anodic
TELLURIUM—sorption on nickel
THORIUM OXIDES $ThO_2$—spectra of, color center identification in
—radiation effects on thermoluminescence of
URANIUM-233—neutron fission of, yields from thermal
WATER—$D_2O$–$H_2O$, radiolysis of, isotopic separation factor for electron pulse
ZIRCALOY-2—oxidation of, effects of coatings on high-temperature
ZIRCONIUM ALLOYS—corrosion studies on (M.C.G.)


**54588** (CONF-700652-(Vol.1)) PROGRESS AND PROBLEMS IN CONTEMPORARY RADIATION CHEMISTRY. Proceedings of the Tenth Czechoslovak Annual Meeting Held as an International Discussion at Marianske Lazne, Czechoslovakia, June 22–25, 1970. Teply, J. (ed.) (Ceskoslovenska Akademie Ved, Rez. Ustav Jaderneho Vyzkumu). Mar 1971. 258p.

An abstract was prepared for each of the 4 papers included in this volume. (M.C.G.)

*For abstracts of individual papers see: 54589–54591, and 54626.*

**54589** (CONF-700652-(Vol.1), pp 19-49) APPROACHES TO TRACK STRUCTURE. Boag, John W. (Institute of Cancer Research, Sutton (England). Surrey Branch).

From tenth meeting on radiation chemistry; Marianske Lazne, Czechoslovakia (22 Jun 1970).

In Progress and problems in contemporary radiation chemistry.

A search was made for a satisfactory formulation of track structure in liquids and solids. Suitable parameters that can be measured independently were sought, and a theoretical model based on these was developed. For high LET tracks a model based on a Gaussian distribution with cylindrical symmetry may be adequate. For low LET radiation, advantages of a statistical model that defines only the distribution of nearest neighbor spacings of the molecular species of interest are considered. Various methods used in studying tracks are discussed. (M.C.G.)

**54590** (CONF-700652-(Vol.1), pp 51-136) CURRENT STATE OF A PRIORI YIELD PREDICTIONS. Santar, Ivan (Ceskoslovenska Akademie Ved, Rez. Ustav Jaderneho Vyzkumu).

From tenth meeting on radiation chemistry; Marianske Lazne, Czechoslovakia (22 Jun 1970).

In Progress and problems in contemporary radiation chemistry.

Yield predictions based on input data independent of radiation-chemical evidence and stemming from studies of the elementary processes involved are discussed. A search was made for the distribution spectrum of yields for primary activations of all types formed during the physical stage of radiolysis. A continuous slowing-down approximation for use in the calculations and a description of the actual course of energy degradation are given. (M.C.G.)

**54591** (CONF-700652-(Vol.1), pp 221-58) SOME PROBLEMS OF ION-ELECTRON RECOMBINATION. Schiller, Robert (Magyar Tudomanyos Akademia Kozponti Fizikai Kutato Intezete, Budapest).

From tenth meeting on radiation chemistry; Marianske Lazne, Czechoslovakia (22 Jun 1970).

In Progress and problems in contemporary radiation chemistry.

The nature of charge carriers in irradiated materials is discussed. Both positive and negative charge carriers can be regarded as massive ions having the same properties as dissolved electrolytes for calculations. The kinetics of ion-recombination processes are discussed. Steady-state charge carriers are shown to be faster than massive negative ions and much slower than quasi-free electrons. Transient charge carriers cannot unequivocally be considered as quasi-free electrons on the basis of their mobilities. The differences in values for steady-state and transient charge carriers may be explained by the possible formation of metastable bubbles and by different rates of localization. (M.C.G.)

**54592** (CONF-700652-(Vol.2)) PROGRESS AND PROBLEMS IN CONTEMPORARY RADIATION CHEMISTRY. Proceedings of the Tenth Czechoslovak Annual Meeting Held as an International Discussion at Marianske Lazne, Czechoslovakia, June 22–25, 1970. Teply, J. (ed.) (Ceskoslovenska Akademie Ved, Rez. Ustav Jaderneho Vyzkumu). Mar 1971. 214p.

An abstract was prepared for each of the five papers included in this volume. (M.C.G.)

*For abstracts of individual papers see: 54593, 54594, 54598, 54627, and 54628.*

**54593** (CONF-700652-(Vol.2), pp 261-93) NATURE AND PROPERTIES OF TRAPPED ELECTRONS IN POLAR SUBSTANCES. Ershov, B. G. (Akademiya Nauk SSSR, Moscow. Institut Fizicheskoi Khimii).

From tenth meeting on radiation chemistry; Marianske Lazne, Czechoslovakia (22 Jun 1970).

In Progress and problems in contemporary radiation chemistry.

The optical absorption of trapped electrons, their EPR spectra, the effects of structure on the formation process of trapped electrons, the effects of linear transition on their yield and spatial distribution, kinetics of photostimulated and thermal decay of trapped electrons, and reactions of thermalized and trapped electrons in aqueous alkaline glasses are discussed. (M.C.G.)

**54594** (CONF-700652-(Vol.2), pp 331-64) ELECTRONS IN NON-POLAR SOLIDS. Albrecht, A. C. (Cornell Univ., Ithaca, N. Y. Dept. of Chemistry).

XUM

From tenth meeting on radiation chemistry; Marianske Lazne, Czechoslovakia (22 Jun 1970).

In Progress and problems in contemporary radiation chemistry.

The behavior of electrons in nonpolar rigid amorphous solids appears to be governed by two basic properties of such solids: long-range Coulomb fields and the ability to trap electrons for very long periods of time. Both theoretical and experimental considerations indicate a second state, in addition to trapped, of the electrons in these solids. This is a mobile or quasi-free condition. Coulomb well matrix trapped electrons exhibited dual behavior: inward flow to give recombination luminescence and outward flow to give photocurrents. The effects of applied electric fields on the trapped electrons are discussed. (M.C.G.)

**54595** (CONF-700652-(Vol.3)) PROGRESS AND PROBLEMS IN CONTEMPORARY RADIATION CHEMISTRY. Proceedings of the Tenth Czechoslovak Annual Meeting Held as an International Discussion at Marianske Lazne, Czechoslovakia, June 22-25, 1970. Teply, J. (ed.) (Ceskoslovenska Akademie Ved, Rez. Ustav Jaderneho Vyzkumu). Mar 1971. 216p.

An abstract was prepared for each of 4 of the 5 papers included in this volume. The remaining paper covered photodissociation of an $e^-_{aq}$ complex in $H_2$-saturated alkaline solutions. (M.C.G.)

*For abstracts of individual papers see: 54629-54632.*

**54596** POTENTIAL ROLE OF THE TUNNEL EFFECT IN POSTRADIATION REACTIONS IN SOLID ORGANIC MATERIALS. Mikhailov, A. I. (Inst. of Chemical Physics, Moscow). Dokl. Akad. Nauk SSSR; 197: No. 1, 136-9(1 Mar 1971). (In Russian).

The relatively long time of mutual contact, $\tau_m$, of the reacting particles in solid-state reactions may result in the increase of the reaction cross section. This may be conveniently shown in recombination reaction of ions stabilized during low-temperature radiolysis. The electron of the negative ion $A^-$ was assumed to be stabilized in the potential well, considered to be rectangular and one-dimensional with a depth of $I_0$, and located in the Coulomb field of the positive ion $B^+$. If the ionization potential $I^+$ is larger than $I_0$, the tunnel transition of the electron may lead to the recombination of the ions. The calculations indicated that the tunnel effect may be an important factor at low ion concentrations stabilized at low-temperature radiolysis. Tunnel transitions in radiation and postradiation reactions may lead to specific chemical and kinetic effects. They also may be involved in other reactions based on electron transport, such as ionic polymerization, therefore the long cortact time of the reacting particles in the condensed state must be taken into account. (TTT)

**54597** PHOTOELECTRON-INDUCED DECOMPOSITION OF ETHANE. Hutchins, Robert R.; Kuntz, Robert R. (Univ. of Missouri, Columbia). J. Phys. Chem.; 75: No. 19, 2903-8 (16 Sep 1971).

The decomposition of ethane by low-energy electrons was investigated using photoelectrons accelerated by electric fields. The mechanism of this decomposition is characterized by formation of neutral excited states and the absence of major ionic processes. Isotope and inhibition experiments establish the similarity between this decomposition and that which accompanies vacuum-uv and applied field radiolysis studies. Evidence is presented suggesting that superexcited states contribute significantly to the decomposition. Apparent differences between the electron energy degradation spectrum caused by ionizing radiation and the energy distribution resulting from acceleration of electrons in an electric field do not substantially alter the neutral processes. (auth)

## Radiation Effects

*Refer also to abstract 54727.*

**54598** (CONF-700652-(Vol.2), pp 423-75) POSTLUMINESCENCE OF ORGANIC SOLID SOLUTIONS. Magat, Michel (Paris Univ., Orsay (France). Laboratoire de Physico-Chimie des Rayonnements).

From tenth meeting on radiation chemistry; Marianske Lazne, Czechoslovakia (22 Jun 1970).

In Progress and problems in contemporary radiation chemistry.

Conclusions that can be drawn from postluminescence studies are discussed. The process of neutralization and its consequences are considered. Radiothermoluminescence of cyclohexane crystals is described as an example. Data for other compounds and systems are reviewed. (M.C.G.)

**54599** (ORNL-4717, pp 117-24) SPECIAL RESEARCHES. (Oak Ridge National Lab., Tenn.).

In Reactor Chemistry Division annual progress for period May 31, 1971.

Research progress is reported on economic aspects of environmental degradation; participation in plowshare activities; radiation-induced reactions of hydrocarbons; development of radiation-resistant insulators; fast-neutron irradiation effects on electrical insulators; and helium release experiments. (D.H.M.)

**54600** (UCLA-34-P-88-32) INTRA- AND INTER-MOLECULAR ENERGY TRANSFER STUDIES. Progress Report, May 1, 1970-May 31, 1971. McMillan, W. G.; Hardwick, E. R.; Nicol, M. F. (California Univ., Los Angeles. Dept. of Chemistry). 15 Jul 1971. Contract AT(04-3)-34. 28p. Dep. NTIS.

Research is being carried out to develop a more complete understanding of nonradiative energy transfer in atomic and especially molecular systems through intensive experimental and theoretical investigations. The research is now focused on several specific problems including: dependence of the efficiency of energy transfer on the separation between donor and acceptor molecules; displacement of absorption and luminescence bands by the molecular environment; vibrational relaxation of excited molecules; intramolecular energy transfer, photochromism, and chemiluminescence; and radiation damage of scintillators. Spectroscopic studies were made of the perturbations of intermolecular energy transfer processes in rigid media resulting from application of high pressures and the resulting compression of intermolecular distances. Studies in progress during this period included comparison of solvent- and pressure-induced spectral shifts of polar and triplet chromophors, development of a time-resolved high-pressure spectrofluorimeter, determination of the kinetics of $\alpha$-particle radiation damage of crystals and polymeric solutions of anthracene, examination of a theoretical model of inelastic scattering from simple molecules, and experimental and theoretical analysis of the effects of compression on the structures and lattice dynamics of simple solids. (auth)

**54601** ELECTRONIC PROPERTIES OF THE ANODIZED ALUMINUM ELECTRODE: RADIATION-INDUCED GALVANIC PHENOMENA. Zagorski, Z. P.; Panta, P. P. (Inst. of Nuclear Research, Warsaw). Electrochim. Acta; 16: No. 8, 1261-7(Aug 1971).

The effect of emf and current generation in the cell $Al/Al_2O_3$-electrolyte-Al in a high energy radiation field is explained in the light of the p-i-n structure of the oxide layer. Several parameters of the layer are estimated, $G^-_c = 7$, internal electric field maximum $10^6$ V/cm, density of electronic states $10^{12}$ cm$^{-2}$, stoichiometry deviation 0.001 of the monolayer of the adsorbed oxygen ions. Proposed applications of the effect are of both applied and basic character. (auth) (UK)

**54602** EFFECT OF NEUTRON IRRADIATION ON THE CHARACTERISTICS OF THE HYDROGEN ELECTRODE IN A LOW-TEMPERATURE FUEL CELL. Zimakov, I. E.; Pletnev, V. P.; Chernyshov, A. M.; (and others) (Inst. of Physical Chemistry, Moscow). Kinet. Katal. (USSR) (Engl. Transl.); 11: No. 6, 1322-3(Nov-Dec 1970).

Translated from Kinet. Katal.; 11: No. 6, 1583-4(Nov-Dec 1970).

It was found that irradiation of hydrogen electrodes with neutrons improves the electrochemical characteristics of the electrodes in the initial period of operation. The variation of the electrocatalytic properties is evidently due to formation of structural defects in the crystal lattice of the catalyst. (auth)

**54603** GAS-CHROMATOGRAPHIC STUDY OF THE EFFECT OF RADIOACTIVE RADIATION AND HEAT TREATMENT ON THE ADSORPTIVE PROPERTIES OF MAGNESIUM SULFATE. Belyakova, L. D.; Kiselev, A. V.; Mikhailenko, I. E.; Soloyan, G. A.; Spitsyn, V. I. (Inst. of Physical Chemistry, Moscow. Moscow State Univ.). Dokl. Akad. Nauk SSSR; 197: No. 1, 88-90(1 Mar 1971). (In Russian).

A fast and sensitive gas-chromatographic method was developed to determine the dispersion and adsorptive properties of solids possessing a low specific activity, using nonradioactive $MgSO_4$ and $Mg^{35}SO_4$ specimens prepared under identical conditions and calcined at 400°C for 2 hours. The specific surface of the 2 types of materials was 8.4 and 9.5 m$^2$/g, respectively. The measurements involved determination of their adsorption of n-octane, n-nonane, and benzene. It was found that the materials containing $^{35}S$ adsorb more strongly hydrocarbons with molecules belonging to both the B group (containing $\pi$ ones) and the A group (containing only $\sigma$ bonds) than the nonradioactive material. Removal of water and increase of the calcination temperature increased the adsorption of both types of hydrocarbons. Extended high-temperature calcination reduced the adsorption of the radioactive material, but the specific adsorptivity toward aromatic hydrocarbons, due to the presence of positive charge at the surface, was preserved. (TTT)

XUM

**54604** INFRARED INVESTIGATION OF THE ACTION OF IONIZING RADIATION ON CARBON-CHAIN POLYMERS. Goryachev, A. N.; Pankratova, L. N. (Moscow State Univ.). High Energy Chem. (USSR) (Engl. Transl.); 4: No. 6, 491-5 (Nov-Dec 1970).

Translated from Khim. Vys. Energ.; 4: No. 6, 542-3(Nov-Dec 1970).

The action of protons and γ radiation on polyethylene films was compared. The investigation of the action of protons and γ radiation on low (LPPE) and high (HPPE) pressure polyethylene films was carried out on a UR-20 IR spectrometer in the region 400 to 4000 $cm^{-1}$. The spectra of each sample were recorded prior to and after irradiation. The thickness of the polyethylene films, 50 to 60 μ, was measured on the IR spectrometer using their interference patterns. (auth)

**54605** OXIDATION AND REDUCTION OF ORGANIC COMPOUNDS BY IONIZING RADIATION: L-PENICILLAMINE HYDROCHLORIDE. Budzinski, Edwin E.; Box, Harold C. (Roswell Park Memorial Inst., Buffalo). Contract AT(30-1)-3558. J. Phys. Chem.; 75: No. 17, 2564-70(19 Aug 1971).

ESR measurements on single crystals of L-penicillamine HCl x-irradiated and observed at 4.2°K reveal one reduced and two oxidized products. The oxidized products are "sulfur" radicals $SC(CH_3)_2CH(NH_3Cl)COOH$ and chlorine atoms. The reduced product is the anion $HSC(CH_3)_2CH(NH_3Cl)C(OH)O^-$. On warming, the yield of "sulfur" radicals is augmented by hole transfer from chlorine atoms to sulfur atoms. Dissociation of the anion also occurs on warming, producing the radical $HSC(CH_3)_2CHCOOH$. At room temperature the latter radical also disappears, and the final absorption is entirely due to "sulfur" radicals. It appears that processes initiated by both oxidation and reduction contribute to the formation of "sulfur" radicals. Altogether nine paramagnetic absorption spectra were observed including several due to different conformations of the aforementioned radicals. (auth)

**54606** ELECTRON SPIN RESONANCE OF ATOMIC SILVER ON POROUS GLASS AND SILICA GEL SURFACES. Starkie, H. C.; Symons, M. C. R. (Univ. of Leicester, Eng.). J. Phys. Chem.; 75: No. 17, 2705-6(19 Aug 1971).

Reasons are presented to support the suggestion that two types of silver atoms are trapped in γ-irradiated alcoholic silver nitrate on porous glass or silica gel surfaces. (D.H.M.)

**54607** REPLY TO ELECTRON SPIN RESONANCE OF ATOMIC SILVER ON POROUS GLASS AND SILICA GEL SURFACES BY H. C. STARKIE AND M. C. R. SYMONS. Gardner, C. L.; Casey, E. J.; Grant, C. W. M. (Defense Research Board, Ottawa). J. Phys. Chem.; 75: No. 17, 2706-7(19 Aug 1971).

A rebuttal is presented to the communication by Starkie and Symons questioning the interpretation of the ESR spectra of silver atoms on porous glass and silica gel surfaces. The present authors retain the opinion that one silver atom species is trapped in γ-irradiated silver nitrate on porous glass or silica gel surfaces. (D.H.M.)

**54608** FORMATION OF OZONIDE IONS IN γ-IRRADIATED AQUEOUS SOLUTIONS OF ALKALI HYDROXIDES. Rao, K. V. S.; Symons, M. C. R. (Univ. of Leicester, Eng.). J. Phys. Chem.; 75: No. 19, 3030-1(16 Sep 1971).

ESR studies of the exposure of 1 M aqueous solutions of alkali metal hydroxides to $^{60}Co$ γ radiation at 77°K showed no feature that could possibly be associated with hyperfine coupling to alkali metal nuclei. There was detected a fairly long-lived radical having three g-value features at 77°K that average to a single feature on warming, together with a weak single line that appears just below the free-spin region. The principal values of the g tensor for the low-field species are close to those for $O_3^-$ in a variety of different environments. It was not possible to identify the second species detected in the spectra, since it has only a single line in the free-spin region, it seems reasonable to assume that it is an impurity radical, such as $CO_3^-$ or $CO_2^-$ formed from carbonate impurity. (D.H.M.)

**54609** REPLY TO FORMATION OF OZONIDE IONS IN γ-IRRADIATED AQUEOUS SOLUTIONS OF ALKALI HYDROXIDES. Nazhat, N. B.; Weiss, J. J. (Univ. of Newcastle Upon Tyne, Eng.). J. Phys. Chem.; 75: No. 19, 3031(16 Sep 1971).

**54610** ESR STUDY OF X-RAY IRRADIATED CRYSTALS OF COPPER ACETATE MONOHYDRATE. Kawamori, Asako; Miyagawa, Ichiro (Univ. of Alabama, University). J. Chem. Phys.; 55: No. 3, 1336-42(1 Aug 1971).

Two single crystals of copper acetate monohydrate were irradiated by x rays at 80 and 290°K, respectively. In the paramagnetic centers produced at both temperatures, a single copper nucleus was found to contribute to the hyperfine structure. Spin Hamiltonian parameters of $^{63}Cu$ of the center produced at 80°K were determined to be $g_z = 2.364$, $g_x = 2.047$, $g_y = 2.086$, $A_z = -126.8$, $A_x = 32.1$, $A_y = -11.3$, and $Q = 7.3$, and those for the center produced at 290°K to be $g_z = 2.387$, $g_x = 2.069$, $g_y = 2.062$, $A = -131.4$, $|A_x| = 7.0$, $|A_y| = 5.0$, and $Q = 9.0$, the A and Q tensors being given in units of $10^{-4}$ $cm^{-1}$. The result was compared with that of zinc-doped copper acetate and was interpreted in terms of molecular orbitals between copper and acetate oxygens. A small mixing of the $d_{z^2}$ orbital to the ground $d_{x^2-y^2}$ orbital was shown to account for the large anisotropies of both the g tensor and A tensor for the sample irradiated at 80°K. The paramagnetic center produced at 80°K was converted irreversibly at about 150°K to another species, which was found to be identical to that produced at 290°K. (auth)

**54611** IRRADIATION PROCESS FOR REDUCING THE MOLECULAR WEIGHT OF POLYOXYMETHYLENE AND THEREBY INCREASING THERMAL STABILITY. Marans, Nelson Samuel (to W. R. Grace and Co.). U. S. Patent 3,594,293. 20 Jul 1971. Filed 24 May 1968.

A process for rendering polyoxymethylene polymers and copolymers thermally stable while simultaneously reducing their molecular weights is described. Polyoxymethylene of a high molecular weight is subjected to ionizing radiation of about 0.000015 to 5 MeV at a dosage of about 0.01 to 2.0 megarads. The irradiated polymer has a much greater thermal stability than the nonirradiated polymer, as well as a substantially reduced molecular weight. (auth)

## *Radiation Processes*

*Refer also to abstract 55658.*

**54612** RADIATION TELOMERIZATION OF ETHYLENE BY PROPIONIC ACID. Freidlina, R. Kh.; Zagorets, P. A.; Bryantsev, I. N.; Terent'ev, A. B. (Inst. of Organometallic Compounds, Moscow). Dokl. Akad. Nauk SSSR; 197: No. 1, 105-8(1 Mar 1971). (In Russian).

Radiation initiation of the reaction was used to study the kinetics of the telomerization of ethylene by propionic acid, because under such conditions the initiation rate may be kept constant and a broad temperature range may be covered. The telomerization was carried out in 100-ml glass ampoule placed in an autoclave. The doses used ranged from 26 to 136 rad/sec; the temperature was kept at 100, 150, and 175°C. The products of the γ-initiated reaction were found to be identical with those of the peroxide-initiated reaction. The data indicated that in case of low-efficiency telogens, the polar effect of the substituent in the growing radicals affects relatively slightly the partial transfer constants. These constants and the isomerization constants obtained in the case of telomerization of ethylene with propionic acid were found to lie close to the corresponding values of the reaction with methyl propionate. (TTT)

**54613** EFFECT OF DOSE RATE ON THE RADIATION GRAFT POLYMERIZATION OF ACRYLONITRILE ONTO POLY(VINYL CHLORIDE) FIBER. Kageyama, Eiichi; Kusama, Yasuo; Udagawa, Akira; Hashimoto, Shoji (Japan Atomic Energy Research Inst., Takasaki). Kogyo Kagaku Zasshi; 74: No. 6, 1237-40(Jan 1971). (In Japanese).

The effect of dose rate on the radioinduced grafting of acrylonitrile on poly(vinyl chloride) was studied. Undrawn polyvinyl-chloride fiber was immersed in acrylonitrile–n-hexane (1 : 1) mixture and irradiated. $^{60}Co$ source was used for lower dose rate ($10^4$ to $10^6$ rad/hr) experiments and an accelerator for higher dose rate ($10^7$ to $10^9$ rad/hr) experiments. The following results were obtained. (1) Either by lower dose rate or higher dose rate, grafting to an extent of 100% is easily obtained. By higher dose rate it is achieved in a period of 2 or 3 minutes. (2) The initial rate of grafting is proportional to the dose rate at lower dose rates, i.e., $R \propto I^1$, but at higher dose rates, it is a function of the dose rate with decreasing power from 0.3 to 0, as the dose rate increases, i.e., $R \propto I^{0.3}-I^0$. (3) The temperature dependency of initial rate is very small. (4) The post irradiation effect is very small. (5) Higher graft efficiencies are obtained at higher dose rates. (6) The effect of atmosphere is observed only in the early stage of grafting. (auth) (Japan)

**54614** STUDIES OF LIGNIN–CELLULOSE–STYRENE GRAFT COPOLYMERIZATION REACTIONS. Phillips, Richard Busbee. Raleigh, N. C.; North Carolina State Univ. (1970). 297p. University Microfilms Order No. 71-15,940.

Thesis

The effect of lignin structure, chemical nature of the free radicals formed on lignin, and degree of swelling and solution of lignin on the γ-radiation- and chemical-induced graft copolymerization of styrene to lignin was studied. In addition, char-

XUM

acterization of kraft lignin-polystyrene graft copolymers was made. Finally, the role of lignin in the radiation-induced graft copolymerization of styrene to lignin-containing pulps was studied. (Diss. Abstr. Int., B)

**54615** MECHANISM OF RADIOLYTIC HYDROCARBONS FORMATION FROM METHANE IN DILUTE SOLUTIONS IN LIQUID ARGON. Sheridan, Michael Eugene. Los Angeles; Univ. of California (1970). 90p. University Microfilms Order No. 71-16,362.

Thesis.

A mechanism for the polymerization of methane in dilute solutions in liquid argon was studied. Cobalt-60 gamma rays gave a polymer with an average formula of about $C_{22}H_{44}$. To aid in the determination of the mechanism, a similar set of reactions was carried out with ethane and ethylene as reactants. The polymer was formed with G(polymer) values of 0.06, 0.20 and 0.70 from methane, ethane, and ethylene respectively. Analysis of the lighter products showed a lack of unsaturated or branched light hydrocarbons from methane and ethane. Increased branching and unsaturation were observed in the light products from ethylene and from mixtures of the reactant hydrocarbons. An attempt was made to replace argon as solvent. Nitrogen was used and gave a polymer with about 40% nitrogen incorporated into the polymer molecules. Several possible mechanisms for the formation of the polymer are discussed. It was concluded that a combination of ionic reactions, free-radical reactions, and hydride ion abstraction reactions best account for the requirements of the mechanism. The Auger processes in argon may give some assistance to the polymer formation by a local heating effect. The role of each type of reaction is discussed. (Diss. Abstr. Int., B)

**54616** AUTOMATIC DILATOMETER FOR RADIATION POLYMERIZATIONS. Niezette, J.; Desreux, V. (Univ., Liege). J. Appl. Polym. Sci.; 15: No. 8, 1981-3(Aug 1971).

An automatic dilatometer particularly suitable for radiation polymerizations is described. The volume contraction may be followed outside the irradiation room by two methods with great accuracy. (auth)

**54617** RADIATION CHEMICAL SYNTHESIS OF ORGANIC COMPOUNDS IN LIQUID NONAQUEOUS SYSTEMS (SURVEY). Vereshchinskii, I. V. High Energy Chem. (USSR) (Engl. Transl.); 4: No. 6, 437-50(Nov-Dec 1970).

Translated from Khim. Vys. Energ.; 4: No. 6, 483-98(Nov-Dec 1970).

This survey of radiation chemical processes is divided into two groups: I) chain processes of synthesis, characterized by substantial values of $6 \gg 10$; II) processes of synthesis of a radical and (or) ionic nature, the value of G which does not exceed 10. The processes of synthesis in group I include chlorination, bromination, sulfoxidation, sulfochlorination, oxidation, addition to olefins and derivatives, synthesis of chlorosilanes, phenylphosphanates, and dialkyltin dibromides. Group II includes the synthesis of perchlorocarbons, fluorination, carbonylation, carboxylation, synthesis of organic sulfur compounds, nitrosylation, synthesis of diamines, amidation, synthesis of alkyl (cycloalkyl) chlorophosphines, and the synthesis of quaternary phosphonium salts. (D.P.O.)

**54618** KINETIC STUDY OF THE PHOTOSENSITIZED ELECTRON EXCHANGE REACTION BETWEEN URANIUM(IV) AND URANIUM(VI) IN HYDROCHLORIC ACID. Kato, Yasuyoshi; Fukutomi, Hiroshi (Tokyo Inst. of Tech.). Bull. Tokyo Inst. Technol. (Engl. Ed.); No. 12, 55-62(Mar 1971).

The photo-acceleration on the U(IV)–U(VI) electron exchange reaction was studied in aqueous hydrochloric acid. The observed quantum yield is given by $1/\phi = k(I_{abs})^{0.38}\{1/k_1[U(VI)] + 1/k_2[U(IV)]\}$. On the assumption that uranium(V) is formed as intermediate, exchange mechanism is proposed to interpret this result. (auth) (Japan)

**54619** TREATMENT OF ELASTOMERS. Laizier, Jacques; Noel, Marie-Therese; Pordes, Maurice; Veber, Andre (to Commissariat a l'Energie Atomique). French Patent 2,040,614. 11 Jan 1971. Filed 4 Apr 1969. (In French).

This method for the treatment of emulsions or dispersions of natural or synthetic elastomers consists of incorporating in a latex suspension halogenated compounds and/or a polymerizable monomer, adding sulfur or thioorganic compounds, and irradiating and drying the mixture. (France)

**54620** MECHANISM OF THE RADIATION-INDUCED DECHLORINATION OF 1,1,1-TRICHLORO-2,2-bis(p-CHLOROPHENYL)ETHANE IN ALCOHOLIC SOLUTION. Evans, Rudolph; Nesyto, Edwin; Radlowski, Cecilia; Sherman, Warren V. (Chicago State Univ., Ill.). J. Phys. Chem.; 75: No. 18, 1762-5(2 Sep 1971).

1,1,1-Trichloro-2,2-bis (p-chlorophenyl)ethane (DDT) undergoes dechlorination to 1,1-dichloro-2,2-bis(p-chlorophenyl)ethane (DDD) in γ-irradiated 2-propanol solution. The large G yields obtained indicate a chain mechanism for the process. Reduction in yield in the presence of small concentrations of free-radical scavengers shows the participation of free radicals as chain carriers, while the dependence of yield on dose rate is consistent with chain termination via bimolecular reaction of these radicals. A detailed mechanism is proposed for the reaction. (auth)

**54621** FUNDAMENTAL STUDIES ON CATIONIC POLYMERIZATIONS: MOLECULAR WEIGHTS AND MOLECULAR WEIGHT DISTRIBUTIONS OF POLYISOBUTYLENES PRODUCED BY γ-IRRADIATION (FREE IONS) AND CHEMICAL CATALYSIS (ION PAIRS). Kennedy, Joseph P. (Univ. of Akron, Ohio); Shinkawa, Akihiro; Williams, Ffrancon. J. Polym. Sci., Part A-1; 9: No. 6, 1551-61(Jun 1971). (ORO-2968-55).

The molecular weights ($\overline{M}_n$, $\overline{M}_v$, and $\overline{M}_w$) and molecular weight distributions of polyisobutylenes synthesized by γ-irradiation in the range 29 to −78°C were determined. The plots of log $\overline{M}_n$, log $\overline{M}_v$, and log $\overline{M}_w$ versus 1/T are linear and parallel ($E_{\overline{M}} = -6.3_6 \pm 0.5$), and $\overline{M}_w/\overline{M}_n \approx 3.0 \pm 0.5$ over this temperature range. The viscosity-average molecular weights of polyisobutylenes obtained by γ-irradiation were compared with those of polymers prepared by $BF_3$, $EtAlCl_2$, and $AlCl_3$. It was found that, at the same polymerization temperature, the $\overline{M}_v$ of radioinduced polyisobutylenes, which propagate by free carbonium ions, is significantly higher than that of those synthesized by the Lewis acids, which probably propagate via ion pairs. The implications of these findings are discussed, and it is concluded that the counterion in the proximity of the growing cation impedes propagation to a greater extent than it does the competing process of chain transfer to monomer. (auth)

**54622** TRIAD TACTICITY OF POLYACRYLONITRILE. Matsuzaki, Kei; Okada, Munehisa; Uryu, Toshiyuki (Tokyo Univ.). J. Polym. Sci., Part A-1; 9: No. 6, 1701-14(Jun 1971).

The high-resolution NMR spectra of polyacrylonitrile-$\beta,\beta$-$d_2$ prepared by radical polymerization were determined, and the stereoregularity of the polymer was studied. The NMR spectra of methine protons of polyacrylonitrile-$\beta,\beta$-$d_2$ in dimethyl sulfoxide-$d_6$ and a mixture of nitromethane-$d_3$ and ethylene carbonate showed three partially resolved multiplets. The deuterium-decoupled spectra of the polymer were measured, and three well-resolved peaks were observed in the two solvents and dimethylformamide-$d_7$. These three peaks were analyzed by comparison with the NMR spectra of model compounds and polyacrylonitrile-α-d, and they were assigned to isotactic, heterotactic, and syndiotactic triads with decreasing magnetic field. This order seems to be unchanged in other solvents. Triad stereoregularity of the polymer was determined according to the assignment. Polymerizations of acrylonitrile-$\beta,\beta$-$d_2$ by radical initiators between −78°C and 60°C were explained by the Bernoulli trial propagation step. The polymers had an atactic structure, independent of polymerization temperature. This shows that in free-radical polymerization of acrylonitrile, the chain end is not represented as having any particular stereochemistry. Other stereochemical control is necessary to produce tactic polymers. The triad tacticity of isotactic polyacrylonitrile was also determined. (auth)

**54623** INFLUENCE OF SAMPLE SIZE ON RADIATION DAMAGE OF POLYETHYLENE. Malliaris, Angelos; Turner, D. T. (Drexel Univ., Philadelphia). J. Polym. Sci., Part A-1; 9: No. 6, 1765-7(Jun 1971).

The powder and cuttings from the crystalline polyethylene films, of area ca 0.1 $cm^2$, were degassed and, together, sealed in vacuum in ampules. The ampules were exposed to $^{60}Co$ γ rays at ambient temperature at a dose rate of 3.2 Mrad/hr. Several days after irradiation the ampules were heated at 80°C for 24 hours to remove trapped radicals and the samples then exposed to air. Samples were examined in an atmosphere of nitrogen at a heating rate of 20°C/min by differential thermal analysis. It is concluded that at low doses of γ rays the damage of polyethylene is not noticeably dependent on sample geometry. By contrast, at higher doses the damage is smaller in samples of low surface to volume ratio. It is suggested that these effects are due to the back reactions of trapped polymer radicals with mobile species such as hydrogen atoms and gaseous molecules. (J.G.B.)

**54624** PHYSICO-CHEMICAL PROPERTIES OF POLY(VINYL FLUORIDE) OBTAINED BY γ-IRRADIATION. Usmanov, Kh. U.; Yulchibaev, A. A.; Sirlibaev, T. (Tashkent State Univ.). J. Polym. Sci., Part A-1; 9: No. 6, 1779-83(Jun 1971).

The infrared spectra, thermomechanical properties, solubility, and thermal stability of poly(vinyl fluoride) produced by radiation and chemical polymerization under various conditions were studied. Results indicate that differences in the solubility, thermomechani-

XUM

cal properties, and thermal stability of radiation-polymerized poly(vinyl fluoride) are caused by the branching of the macromolecules. (auth)

**54625** MANUFACTURE OF ALIPHATIC ALDEHYDES BY RADIOLYSIS. Battaerd, Hendrik Adriaan Jacobus (to Imperial Chemical Industries). U. S. Patent 3,591,476. 6 Jul 1971. Priority date 12 Dec 1966, Australia.

A process is described for converting alcohols into aldehydes that comprises irradiating the alcohol with a source of high-energy radiation in the presence of a solid energy transfer catalyst selected from the group consisting of CdO, ZnO, alpha alumina $Al_2O_3$, PbO, $Pb_3O_4$, $Sb_2O_3$, $Bi_2O_3$, $V_2O_5$, $WO_3$, MoO and copper, surface-oxidized to cuprous oxide. (auth)

## Radiolysis

*Refer also to abstracts 54705, 55053, 55130–55132, 55135, 55139, and 56318.*

**54626** (CONF-700652–(Vol.1), pp 139-219) COMMENTS ON THE ACTIVATED SPECIES IN IRRADIATED ORGANIC MEDIA. Voltz, Rene (Centre National de la Recherche Scientifique, Strasbourg (France). Laboratoire de Physique des Rayonnements et d'Electronique Nucleaire).

From tenth meeting on radiation chemistry; Marianske Lazne, Czechoslovakia (22 Jun 1970).

In Progress and problems in contemporary radiation chemistry.

The early effects of high-energy radiation in condensed organic materials were studied. It is suggested that excited states should predominate as early species in aromatic media, while charge–separated states are likely to be comparatively more important in aliphatic compounds. The very primary excited states in irradiated organic compounds are largely collective but rapidly decay producing highly excited states of individual molecules. The various electronic relaxation processes that reduce the primary excitation of the molecules and finally produce more stable species having lower excitation energies are discussed. Some typical experimental data obtained with aromatic and aliphatic hydrocarbons in the condensed phase are examined. For aromatics the intermediates are mainly neutral excited molecules. For aliphatics the charge-separated states appear to be comparatively more significant. (M.C.G.)

**54627** (CONF-700652–(Vol.2), pp 295-330) RECENT EXPERIMENTS ON STEADY STATE AND PULSE RADIOLYSIS OF ALKALINE AQUEOUS SYSTEMS. Buxton, G. V.; Cattell, F. C.; Dainton, F. S.; Lantz, T. E.; Sargent, F. P. (Leeds Univ. (England)).

From tenth meeting on radiation chemistry; Marianske Lazne, Czechoslovakia (22 Jun 1970).

In Progress and problems in contemporary radiation chemistry.

The effects of light and heat on $\gamma$-irradiated alkaline glasses and the nature of electron traps in these glasses were studied. The kinetics of photobleaching of trapped electrons in 10M hydroxide glasses are discussed. Light-induced spectroscopic changes and heat-induced spectral changes are considered. Pulse radiolysis studies are described. Data indicated that roughly 3.3 electrons and hydrogen atoms escape recombination in the spur within $10^{-7}$ sec at room temperature. Further, the number of electrons and hydrogen atoms that are destroyed in spur reactions is at least 1.7 and the number of electrons that can be trapped in a rigid 10M hydroxide glass in the temperature range 77 to 140°K is 2.6. Examination of the spectrum of the spur electrons during recombination indicated that these electrons were fully solvated. (M.C.G.)

**54628** (CONF-700652–(Vol.2), pp 367-420) HYDROGEN ATOMS AS STUDIED BY ESR. Vacek, Karel (Ceskoslovenska Akademie Ved, Rez, Ustav Jaderneho Vyzkumu).

From tenth meeting on radiation chemistry; Marianske Lazne, Czechoslovakia (22 Jun 1970).

In Progress and problems in contemporary radiation chemistry.

The formation of hydrogen in the radiolysis of compounds containing X–H bonds may occur by four different mechanisms: homolytic dissociation of excited X–H bonds, protonation of electrons, ionization of hydride anion, and abstraction of hydrogen atom from molecule of hydrogen by a reactive radical. Reactions of radiolytic hydrogen atoms are discussed. (M.C.G.)

**54629** (CONF-700652–(Vol.3), pp 479-521) PROGRESS AND PROBLEMS IN THE RADIOLYSIS OF ALCOHOLS. Freeman, Gordon R. (Alberta Univ., Edmonton. Dept. of Chemistry).

From tenth meeting on radiation chemistry; Marianske Lazne, Czechoslovakia (22 Jun 1970).

In Progress and problems in contemporary radiation chemistry.

Radiolysis of alcohols in the gaseous, liquid, and solid phases is discussed. Free ion yields, nonhomogeneous kinetics, and decomposition of solvated electrons in alcohols and water are described. (M.C.G.)

**54630** (CONF-700652–(Vol.3), pp 523-98) ROLE OF IONS IN THE RADIOLYSIS OF HYDROCARBONS. Kroh, Jerzy (Technical Univ., Lodz (Poland). Inst. of Radiation Chemistry).

From tenth meeting on radiation chemistry; Marianske Lazne, Czechoslovakia (22 Jun 1970).

In Progress and problems in contemporary radiation chemistry.

Ionic processes in radiolysis of hydrocarbons are reviewed. Geminate recombination and ion scavenging are discussed and these phenomena illustrated for several hydrocarbons. It was concluded that the Hummel approximation offers the best description of scavenging processes in some cases; in others homogeneous kinetics may turn out to be quite sufficient for description of the scavenging processes. (M.C.G.)

**54631** (CONF-700652–(Vol.3), pp 601-48) REACTIONS OF THE HYDRATED ELECTRON WITH ORGANIC COMPOUNDS. Hart, Edwin J. (Argonne National Lab., Ill.).

From tenth meeting on radiation chemistry; Marianske Lazne, Czechoslovakia (22 Jun 1970).

In Progress and problems in contemporary radiation chemistry.

The structural properties of organic molecules affecting $e^-_{aq}$ reactivity are discussed and the nature of the reduced species considered. General mechanisms of solvated electron reduction reactions, correlations of $e^-_{aq}$ reactions, and reactions producing hydrocarbons are reviewed. The radiolysis of aqueous benzene is described. The techniques needed for studying single and double $e^-_{aq}$ addition to organic molecules are discussed. (M.C.G.)

**54632** (CONF-700652–(Vol.3), pp 649-92) PULSE RADIOLYSIS OF ORGANIC COMPOUNDS IN AQUEOUS SOLUTIONS. Henglein, Arnim (Hahn-Meitner-Institut fuer Kernforschung, Berlin (West Germany)).

From tenth meeting on radiation chemistry; Marianske Lazne, Czechoslovakia (22 Jun 1970).

In Progress and problems in contemporary radiation chemistry.

Reactions of hydrated electrons and OH radicals with organic solutes and the disappearance of second generation products are discussed. Solutions were irradiated to investigate autooxidation of organic compounds in aqueous solutions and the formation of hydrated nitroso compounds. (M.C.G.)

**54633** (ORO–3660-4) PROGRESS REPORT [ON RADIATION INDUCED DECOMPOSITION OF INORGANIC MOLECULAR IONS]. Johnson, Everett R. (Maryland Univ., College Park. Dept. of Chemical Engineering). [1970]. Contract AT(40-1)-3660. 10p. Dep. NTIS.

Research progress is reported on a comparison of the Ceric and Shinn methods for determining the nitrite ion produced from the irradiation of sodium nitrate; production of $^{18}O$-labeled compounds by irradiation of $KClO_3$, $KNO_3$, $KClO_4$, $KBrO_3$, and $KIO_3$ in the presence of $^{18}O$; and the mechanism of formation of nitrate ion on the surface of KBr crystals irradiated in air. (D.H.M.)

**54634** ESR SINGLE-CRYSTAL STUDY OF RADICAL AND RADICAL-PAIR FORMATION IN SOME $\gamma$-IRRADIATED VINYL MONOMERS. Gillbro, T.; Kinell, P.-O.; Lund, A. (Aktiebolaget Atomenergi, Studsvik, Sweden). J. Polym. Sci., Part A-2; 9: No. 8, 1495-1507(Aug 1971).

Single crystals of methyl methacrylate (MMA), methyl acrylate (MA), and acrolein (A) were prepared by a low-temperature technique. After irradiation with $\gamma$ rays at 77°K, the paramagnetic species were identified by ESR spectroscopy. MMA gave a seven-line single spectrum from radicals formed by hydrogen addition. The hyperfine coupling constants are slightly anisotropic with a mean value of 22 G. Radical pairs were observed as $\Delta M_s = 1$ and $\Delta M_s = 2$ transitions; the hyperfine coupling was 11 G. From the strongly anisotropic dipolar interaction, upper limits for the distances between the pair components were calculated to be 5.45 Å and 6.3 Å. MA gave a five-line main spectrum with the same hyperfine coupling values and two radical pairs, one with a distance 5.9 Å between the components. In A there was also a strongly anisotropic interaction. The hyperfine coupling of the $\Delta M_s = 2$ transition was 9.8 G. The number of radical pairs compared to the total number of radicals increases only slightly with the radiation dose. This makes it likely that pair formation occurs in the spurs and blobs formed by the $\gamma$ radiation. At an increased temperature the radical pairs disappeared; the spectrum of MMA changed to that characteristic of propagating polymer radicals. (auth)

**54635** EFFECTS OF IONIZING RADIATIONS ON MATTER IN THE SOLID STATE. PART I. RADIOLYSIS OF ORGANIC MOLE-

XUM

CULES IN THE SOLID STATE. Van de Vorst, Albert (Univ. Liege, Sart-Tilman, Belg.). Acad. Roy. Belg., Cl. Sci., Mem., Collect. 8; 39: 9-89(1970). (In French).

A study of the radiolysis of organic molecules in the solid state showed that factors determining the behavior of an organic molecule under the direct action of ionizing radiation are electron dislocation and the molecular dimension. This behavior can also be modified by the presence of certain additives, among which are the paramagnetic ions. Study of the evolution of radioresistance in a series of chelates showed that for these complexes the paramagnetism of the central ion is shown by an increase of the radioresistance of the organic part. (tr-auth)

**54636** EFFECTS OF IONIZING RADIATIONS ON MATTER IN THE SOLID STATE. PART II. ORIGIN OF RADIORESISTANCE OF NUCLEIC ACIDS IN THE SOLID STATE. Van de Vorst, Albert (Univ. Liege, Sart-Tilman, Belg.). Acad. Roy. Belg., Cl. Sci., Mem., Collect. 8; 39: 91-136(1970). (In French).

The origin of the radioresistance of DNA in the solid phase was analyzed by first considering the constituents of DNA and then the acid itself. Analysis showed that electron dislocation and molecular weight are primary factors in radioresistance. The effect of the electron-$\pi$ dislocation is shown directly at the level of the bases that have a radioresistance 10 to 100 times higher than phosphate pentose. A clear decrease in free radical yield is detected when the mass increases. (J.S.R.)

**54637** EFFECTS OF NITROUS OXIDE AND ETHYLENE ON THE GAS YIELDS AND GEL FORMATION FROM $\gamma$-IRRADIATED POLYPROPYLENE. Pinkerton, D. M. (Australian Defence Scientific Service, Ascot Vale). Aust. J. Chem.; 24: No. 8, 1619-32(Aug 1971).

Isotactic and atactic polypropylene were $\gamma$-irradiated in a vacuum, in nitrous oxide, and in ethylene, and also in the presence of mixtures of these two gases. The $\gamma$-irradiation of the isotactic polypropylene in a vacuum gives a $H_2$ yield that is nonlinear with dose, whereas the $CH_4$ yield is linear with dose. Yields of $H_2$ and $CH_4$ from atactic polypropylene obey a linear relationship with the dose delivered. Both $N_2O$ and ethylene depress the $G(H_2)$ obtained from vacuum irradiations of isotactic polypropylene, the former due to electron scavenging and the latter to hydrogen atom scavenging. The scavenger studies lead to $G(e^-) = 0.7 \pm 0.1$, $G(H)_{thermal} = 1.0 \pm 0.1$, and $G(H_2)_{molecular} = 1.86 \pm 0.05$. Compared to vacuum irradiations, $N_2O$ enhances, and ethylene suppresses completely the crosslinking yield in isotactic polypropylene. In equimolar mixtures of $N_2O$ and ethylene the crosslinking yield is suppressed completely. It is suggested that $N_2O$ enhances the crosslinking mechanism through an energy transfer and dehydrogenation process and that ethylene interferes by radical scavenging. In mixtures, the results are consistent with ethylene participating in the energy transfer reaction in preference to the $N_2O$ and so inhibiting the additional crosslinking that $N_2O$ causes through the dehydrogenation reaction. A tentative reaction sequence is proposed. (auth) (Australia)

**54638** RADIOLYSIS OF CRYSTALLINE ALKALINE AZIDES, BROMATES, AND NITRATES. Boldyrev, V. V. (Inst. of Chemical Kinetics and Combustion, Novosibirsk, USSR). Int. J. Radiat. Phys. Chem.; 3: No. 2, 155-69(Aug 1971). (In Russian).

Radiolytic stability at room temperature of crystalline alkaline azides, bromates and nitrates was compared to their respective thermal stability. The observed variation of radiation yields (of $N_2$ and $Me^0$ in azides, of $Br^-$ and $O_2$ in bromates, and of $NO_2^-$ in nitrates) is accounted for by a correspondence between the size of radiolytic fragments and the "free volume" in the crystal lattice. The dependence of radiation yield on LET (linear energy transfer) was investigated, irradiation sources being $^{60}Co$ (dose rate $29 \times 10^{16}$ eV/gs) and a 4.7 MeV proton beam (average rate 0.5 to $1.5 \times 10^{19}$ eV/gs). The hypothesis concerning the predominant role of thermal spikes in the radiolysis of ionic salts is critically analyzed, and experimental data which are not in agreement with the "hot spike" hypothesis are given. Radiolytic yields from alkali azides radiolysis decrease to one-third when LET increases in spite of the high positive temperature coefficient of azide radiolysis. On the contrary the radiolytic yields in alkali perchlorates increase when LET decreases despite the low corresponding temperature coefficient. In sodium nitrate radiolysis two temperature regions of LET effect are observed: thermal effects in tracks are predominant in the low temperature region (20 to 100°C), whereas above 180°C secondary reactions are of increasing importance. Action of additives incorporated into the lattice of silver oxalate and potassium nitrate on the radiolysis of these salts was examined. The inhibiting action of cadmium ions introduced into silver oxalate is explained by a diminution of the interstitial silver ion concentration. The effect of $Tl^+$, $Sr^{2+}$, $Pb^{2+}$, $Ce^{3+}$, $La^{3+}$, $Pr^{3+}$, $Nd^{3+}$ ions on the radiolysis of potassium nitrate is regarded as resulting from ionic defects produced by the incorporation of these additives into the lattice; the resulting defects increase the radiation yield due to localization of excitation or to local increase of the free volume in the lattice but, in addition, they can improve the annealing of radiation defects. Doping of potassium nitrate with additives which can act as electron donors ($Tl^+$, $Ce^{3+}$, $Pr^{3+}$) increases the radiation yields. Doping of nitrates in the anionic sublattice (e.g. with $SO_4^{2-}$) does not change the radiation yields. (auth)

**54639** ELECTRON SPIN RESONANCE STUDIES OF PRIMARY PROCESSES IN RADIATION-INDUCED REACTIONS. II. SINGLE CRYSTAL 1,3-BUTADIENE. Shiga, Tetsuo; Lund, Anders; Kinell, Per-Olof (Swedish Research Councils' Lab., Studsvik). Int. J. Radiat. Phys. Chem.; 3: No. 2, 145-53(Aug 1971).

This work aims at elucidating the reactions induced in 1,3-butadiene by radiation in the solid state. The radical $-CH_2-\dot{C}H-CH=CH-CH_2-$ was identified in the single crystal and polycrystal samples by ESR spectroscopy following $\gamma$ irradiation at 77°K. The geometric conformation of this radical is the trans-form

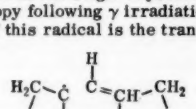

The observations of hyperfine coupling anisotropy and transconformity for the radical suggest that it is located in an oligomer produced by trans-1,4-addition. The possible existence of radical pairs at 77°K was indicated. (auth)

**54640** ELECTRON SPIN RESONANCE STUDIES OF PRIMARY PROCESSES IN RADIATION-INDUCED REACTIONS. I. 1,3-BUTADIENE ADSORBED ON SILICA GEL. Shiga, Tetsuo; Lund, Anders; Kinell, Per-Olof (Swedish Research Councils' Lab., Studsvik). Int. J. Radiat. Phys. Chem.; 3: No. 2, 131-44(Aug 1971).

Following $\gamma$ irradiation of 1,3-butadiene adsorbed on silica gel, three kinds of radicals were observed at 77°K. The first is the cation radical $[CH_2-CH=CH-CH_2]^+$, whose ESR spectrum consists of a quintet of lines separated by about 11G. The cation radical initiates polymerization of butadiene in the adsorbed state at 77°K. Propagation proceeds cationically. The second radical is the allyl-type radical, $CH_2=CH-CH-CH_2-R$, which is located at the end of the polymer chains. The radical shows a change of the line profile with temperature. The third radical is also of the allyl type, $CH_2-CH-CH=CH_2$, and is a hydrogen atom addition-type radical. This radical is observed either with decreasing butadiene concentration or with a lower preheating temperature of the silica gel. (auth)

**54641** INFLUENCE OF THE NUCLEAR ZEEMAN TERM ON ANISOTROPIC HYPERFINE PATTERNS IN ELECTRON SPIN RESONANCE. Poole, Charles P. Jr.; Farach, Horacio A. (Univ. of South Carolina, Columbia). J. Magn. Resonance; 4: No. 3, 312-21(Jun 1971).

The spin Hamiltonian for the two spin system $S = \frac{1}{2}$, $I = \frac{1}{2}$ was solved taking into account the electronic Zeeman, nuclear Zeeman, and hyperfine interactions. The two Zeeman terms were assumed to be isotropic and the hyperfine interaction was completely anisotropic. The spectrum is a symmetric quartet with the splitting of the outer pair $T_0$ related to that of the inner pair $T_i$ through the relations $T_0^2 + T_i^2 = T^2 + (2g_n\beta_n H)^2$, and $T_0T_i = |2g\beta_n HT_{zz}|$, where T is the true hyperfine coupling constant and $T_{zz}$ is its zz component. The two doublets have the respective intensities $I_0 = [T_0^2 - (2g_n\beta_n H)^2]/(T_0^2 - T_i^2)$, and $I_i = [(2g_n\beta_n H)^2 - T_i^2]/[T_0^2 - T_i^2]$. At X-band twice the nuclear Zeeman term $2g_n\beta_n H$ amounts to eleven gauss, so for typical irradiated organic single crystals the outside doublet is strongest. In such samples the weak doublet is ordinarily only observed at particular orientations. An analysis was made of the errors that arise when the nuclear Zeeman term is neglected. For typical irradiated organic single crystals at X-band the errors in many hitherto reported coupling constants amount to several percent. (auth) (UK)

**54642** TOPOGRAPHY OF THE EVOLUTION OF THE RADIOLYSIS PRODUCTS OF LEAD AZIDE ($PbN_6$). Ryabykh, S. M.; Zakharov, Yu. A.; Lysykh, A. P. (Tomsk Polytechnic Inst., USSR). Russ. J. Phys. Chem. (Engl. Transl.); 45: No. 2, 180-1(Feb 1971).

Translated from Zh. Fiz. Khim.; 45: No. 2, 327-9(Feb 1971).

In the radiolysis of $PbN_6$ metallic lead and gaseous nitrogen are formed mainly in the surface layer, the thickness of which increases with temperature and radiation dose. In the interpretation of this finding, it was postulated that azide radicals (holes),

which have an effective positive charge, migrate towards the surface, which is negatively charged. (auth)

**54643** EFFECT OF SOME OXYGEN-CONTAINING COMPOUNDS ON THE RADIOLYSIS OF GASEOUS ETHYLENE. Niedzielski, Jan; Gawlowski, Janusz (Univ. of Warsaw). Nukleonika; 16: No. 3-4, 143-55(1971).

The effect of oxygen containing compounds, having great proton affinities, viz. ethyl alcohol, diethyl ether, and dimethyl ether on the gas-phase radiolysis of ethylene was studied. These additives act as positive ion scavengers (their effect resembling that of ammonia). The increase of methyl radical yield at the expense of the ethyl one in the presence of dimethyl ether is probably due to the neutralization processes; neutralization of $(CH_3)_2OH^+$ ions yields methyl radicals instead of hydrogen atoms. (auth)

**54644** RADIOLYSIS OF DILUENT–TBP–$HNO_3$ SYSTEMS. Nowak, Zofia (Inst. of Nuclear Research, Warsaw). Nukleonika; 16: No. 3-4, 133-42(1971).

The effect of nitric acid on the radiolysis of n-dodecane–TBP, mepasine–TBP, and odorless kerosene–TBP systems was studied. Yields of nitration products increased with growing nitric acid concentration, whereas the yields of oxidation products reached a maximum for 2 to 3 M $HNO_3$. From the results of the investigation for one and two-phase systems as well as for systems free from TBP the conclusion may be drawn that nitration precedes chiefly at the cost of the nitric acid forming a TBP complex. (auth)

**54645** FEASIBILITY OF THE THERMAL DECOMPOSITION OF METHYL ALCOHOL IN FISSION FRAGMENT TRACKS. Borisov, E. A.; Bulanov, L. A.; Starodubtseva, E. V. (Inst. of Physics and Chemistry, Moscow). High Energy Chem. (USSR) (Engl. Transl.); 4: No. 6, 501-2(Nov-Dec 1970).

Translated from Khim. Vys. Energ.; 4: No. 6, 550-1(Nov-Dec 1970).

Computations were performed on the temperature of a fission fragment track in a methanol atmosphere to test the feasibility of thermal decomposition of methanol in the track. It was assumed that the heat generated in the reaction is small compared to the heat resulting from the fission fragment and that temperature equilibration in the track obeys the law of convective thermal diffusion. The calculated results agree with the literature values and suggest that the characteristics of formation of methanol decomposition products observed during radiolysis by fission fragments can be explained by the thermal chemical action of the fragments. (D.P.O.)

**54646** YIELDS OF HYDROGEN PEROXIDE IN AQUEOUS SOLUTIONS OF THALLIUM SULFATE. Nichiporov, F. G. (Inst. of Theoretical and Experimental Physics, Moscow). High Energy Chem. (USSR) (Engl. Transl.); 4: No. 6, 498(Nov-Dec 1970).

Translated from Khim. Vys. Energ.; 4: No. 6, 548(Nov-Dec 1970).

The yields of hydrogen peroxide in $\gamma$ radiolysis of air-saturated solutions of $Tl_2SO_4$ ($1 \times 10^{-4}$ to $1 \times 10^{-2}$M) were determined. The yields are independent of the pH of the medium. (D.P.O.)

**54647** REACTIVITY OF $Ce^{4+}$ IONS IN IRRADIATED AQUEOUS SOLUTIONS OF SULFURIC ACID. Nichiporov, F. G.; Byakov, V. M. (Inst. of Theoretical and Experimental Physics, Moscow). High Energy Chem. (USSR) (Engl. Transl.); 4: No. 6, 596-7(Nov-Dec 1970).

Translated from Khim. Vys. Energ.; 4: No. 6, 546-7(Nov-Dec 1970).

The competitive acceptor method was used to determine the value of the rate constant of the reaction: $H + Ce^{4+} \rightarrow H^+ + Ce^{3+}$ in irradiated solutions. The results were compared with rate constants determined from the linear dependences ($G_M$) of the radiation yields of the molecular radiolysis products of water ($H_2$, $H_2O_2$) on the cubic root of concentration $C_s$ of the dissolved substances, $G_n = G_M^0 - qC_s^{1/3}$, where q is an empirical coefficient, depending on the type of dissolved substance. (D.P.O.)

**54648** REACTIONS AND IDENTIFICATION OF RADICALS PRODUCED BY PHOTOCHEMICAL METHODS AND GAMMA IRRADIATION IN BRANCHED ALKANE GLASSES. Arce Quintero, Rafael Angel. Madison, Wisc.; Univ. of Wisconsin (1971). 194p. University Microfilms Order No. 71-12,674.

Thesis.

Studies were made on: (1) photochemical reactions of chlorine, hydrogen iodide, and peroxy radicals in organic glasses between 77 and 97°K; (2) thermal decay of matrix radicals by reaction with each other and with oxygen and chlorine added to the matrix; (3) the identification of the free radicals formed from a series of branched alkane glasses by hot hydrogen attack during photolysis of HI. Illumination of $Cl_2$ in glassy 3-methylpentane (3MP) at 77°K with 3300 Å light produces trapped $C_6H_{1,3}$ radicals with a quantum yield of 0.013 accompanied by chlorine disappearance with a quantum yield of 0.7. Gas chromatographic analysis after melting shows that alkyl chlorides are produced with a yield of ca. 0.60 and dodecanes with a yield of less than 0.005. These data indicate that much of the chlorine reacts in a concerted reaction to form RCl + HCl. The quantum yields for chlorine disappearance at 80, 83, 87, 97, 199, and 300°K are 1.5, 2.2, 4.2, 270, $5 \times 10^3$ and $1.9 \times 10^4$ respectively, indicating a chain reaction which increases in length with increasing temperature. During decay of the radicals 77°K to 87°K an optical absorption grows at 2600 Å. This is attributed to a radical-chlorine complex (R-$Cl_2$). Trapped $C_6H_{1,3}$ radicals produced by $\gamma$ irradiation of 3MP glass at 77°K containing dissolved oxygen or chlorine decay by reaction with diffusing molecules of the additive at rates which indicate diffusion coefficients of $4.9 \times 10^{-16}$ $cm^2$ $sec^{-1}$ and $1.4 \times 10^{-16}$ $cm^2$ $sec^{-1}$ for oxygen and chlorine, respectively. Peroxy radicals are formed by the reaction of oxygen with the radicals. These can be photochemically decomposed with 2700 Å light, but the reaction is reversed in the dark. Comparison of the ESR spectra of radicals produced by the photolysis of HI in ten branched alkanes at 77°K, indicates that there is a high selectivity for H abstraction from a particular type of secondary C–H bond. The secondary 3-methylpentyl radical is preferentially formed from 3MP. The radicals produced by HI photolysis in at least three of the alkanes decay by composite first order kinetics by reacting with the geminate iodine atom. (Diss. Abstr. Int., B)

**54649** EFFECT OF WATER ON THE RADIATION CHEMICAL STABILITY OF CRYSTALLINE $NaNO_3$. Lykhin, V. M. (Polytechnic Inst., Moscow). High Energy Chem. (USSR) (Engl. Transl.); 4: No. 6, 489-90(Nov-Dec 1970).

Translated from Khim. Vys. Energ.; 4: No. 6, 541-2(Nov-Dec 1970).

Comparison of results from the radiolysis of solid anhydrous salts, their crystal hydrates, and aqueous solutions shows that the yield of products is higher in the presence of water. The effect of adsorbed water on the radiolysis of $NaNO_3$, as one of the most hygroscopic salts in the alkali metal nitrate series, was studied and the results are reported. (auth)

**54650** EFFECT OF IONIZING RADIATION AND UV LIGHT ON N-ACETYGLYCINE IN THE PRESENCE OF AMMONIA. Dose, Klaus; Ponnamperuma, Cyril (Ames Research Center, Moffett Field, Calif.). Biophysik; 7: 311-21(1971).

Aqueous solutions of 1-$^{14}$C-N-acetylglycine and ammonia were irradiated with 7.5-MeV fast electrons, $^{60}$Co $\gamma$ rays, and uv light (low pressure mercury lamp). The products and their hydrolyzates were separated by electrophoresis, paper chromatography, and ion exchange chromatography. Among the main reactions are: decarboxylations, aminations yielding diglycine, dimerizations giving rise to diaminosuccinic acid, succinic acid, aspartic acid, $\beta$-aspartylglycine, $\beta$-alanylglycine, and the N-acetyl derivatives of these compounds. Methylations yield $\alpha$-alanine, and a reductive transacetylation yields threonine. The results are briefly discussed with respect to the effect of different concentrations and the use of different qualities of radiation. The results also point to a possible pathway to the prebiotic origin of a number of biologically important micromolecules, including oligopeptides. The results indicate, however, that a prebiotic formation of polypeptides or protein-like macromolecules by the action of ionizing radiations or uv light upon aqueous solutions of monomers is unlikely under the conditions of this investigation. (auth)

**54651** REACTIVITY TREND SEEN IN THE REDUCTION OF TRANSITION METAL COMPLEXES BY OUTER-SPHERE REACTANTS VERIFIED FOR HYDRATED ELECTRON REACTIONS; PULSE RADIOLYSIS STUDIES OF COBALT(III) COMPLEXES. Venerable II, G. D. (Argonne National Lab., Ill. Univ. of Chicago. Univ. of California, Los Angeles). Contract AT(04-1)-Gen-12. Inorg. Chem.; 10: No. 9, 1999-2002(Sep 1971).

Hydrated electrons ($e^-_{aq}$) generated in the pulse radiolysis of aqueous solutions of cobalt(III) cyanide complexes react with the cobalt solute at rate constants in the $10^9$ to $10^{10}$ $M^{-1}$ $sec^{-1}$ region. Of particular interest is a correlation between the rate constant for $e^-_{aq} + Co(CN)_5X^{3-}$ and the magnitude of the ligand field splitting parameter ($\Delta$) of the heteroligand $X^-$. Within the standard outer-sphere–inner-sphere terminology, an attempt was made to provide a useful way of looking at the transition state consisting of $e^-_{aq}$ and the metal complex. (auth)

**54652** ELECTRON SPIN RESONANCE AND RELAXATION STUDIES OF INTERNAL MOTION IN $CH_2CO_2^-$ RADICALS TRAPPED IN $\gamma$-IRRADIATED SODIUM ACETATE CRYSTALS. Fujimoto, M.; Janecka, J. (Univ. of Guelph, Ont.). J. Chem. Phys.; 55: No. 1, 5-11(1 Jul 1971).

XUM

$CH_2CO_2^-$ radicals are stable in γ-irradiated sodium acetate crystals. The ESR spectra of $CH_2CO_2^-$ and carbon-13-labeled radicals, $CH_2{}^{13}CO_2^-$ and $^{13}CH_2CO_2^-$, were studied in detail in the temperature range of 77°K to room temperature. The $CH_2$ group executes an internal motion, which is characterized by proton exchange in the oriented radicals. The motion is slowed on lowering the temperature, giving rise to an electron spin relaxation time of the order of microseconds at 77°K. The correlation time for the motion was found to be temperature dependent, varying as exp (V/kT) with an activation energy V of the order of 3 kcal $mole^{-1}$. (auth)

**54653** ESR STUDY OF IRRADIATED GLYCINE AT LOW TEMPERATURES. Sinclair, James (Utah State Univ., Logan). J. Chem. Phys.; 55: No. 1, 245-51(1 Jul 1971).

Single crystals of glycine, glycine-$d_3$, and glycine-$d_5$ were x irradiated at liquid-nitrogen temperatures and the paramagnetic fragments produced examined as a function of temperature by electron spin resonance techniques. The radicals observed in the temperature range 77 to 300°K include: $\dot{C}H_2N^+H_3$, $N^+H_3\dot{C}H_2COO^-$(H), $\dot{C}H_2COO$(H), $\dot{N}H_2^+CH_2COO^-$, and $N^+H_3\dot{C}HCOO^-$. The production of these radicals can be rationalized by a sequence of reactions which involve initially formed cation and anion radicals. (auth)

**54654** EFFECTS OF IONIZING RADIATION ON POTASSIUM HYDROGEN MALONATE. Box, Harold C.; Budzinski, Edwin E.; Potter, William (Roswell Park Memorial Inst., Buffalo). J. Chem. Phys.; 55: No. 1, 315-9(1 Jul 1971).

Electron spin resonance spectroscopy was used to observe the primary effects of x rays on a single crystal of KOOC-$CH_2$-COOH irradiated at 4.2°K. Three effects were observed: anions are formed by the addition of an electron to the oxygen of the carbonyl group; a unique paramagnetic center results from the loss of a hydrogen atom shared between two molecules; and, pairs of radicals are created by the removal of a hydrogen atom from the $CH_2$ groups of each of two adjacent molecules. In order to explain the hyperfine pattern associated with the radical pair absorption it is necessary to develop the theory of forbidden transitions for the triplet state. (auth)

**54655** EFFECT OF OLEFINS ON THE REACTIONS OF NITROUS OXIDE IN γ-IRRADIATED LIQUID CYCLOPENTANE. Busi, Fabio; Freeman, Gordon R. (Univ. of Alberta, Edmonton). J. Phys. Chem.; 75: No. 17, 2560-4(19 Aug 1971).

Addition of propylene or cyclopentene to solutions of nitrous oxide in cyclopentane has no effect on the nitrogen yields when the nitrous oxide concentration is <1 mol %, but it appears to increase the nitrogen yields slightly at nitrous oxide concentrations >1 mol %. The kinetics of the olefin effect cannot be explained by the association of an electron with an olefin molecule followed by transfer of the electron to nitrous oxide, as previously suggested. The effect is small, and if it is not an experimental artifact it must be due to unknown secondary reactions. Nitrous oxide does not react appreciably with hydrogen atoms, and monoolefins do not interact to a significant extent with electrons in the radiolysis of liquid saturated hydrocarbons at 25°C. The initial yield of hydrogen from pure cyclopentane appears to be $G(H_2)_i$ = 5.7. Essentially all ion–electron neutralizations in pure cyclopentane lead to hydrogen formation: G(H, olefin scavengable) ≈ 2.9; k(H + olefin)/k(H + c-$C_5H_{10}$) = 140 for both propylene and cyclopentene. (auth)

**54656** ELECTRON SPIN RESONANCE STUDY OF IRRADIATED AQUEOUS SOLUTIONS OF FUMARATE ION. THE USE OF FUMARATE FOR RADICAL TRAPPING. Neta, P. (Carnegie-Mellon Univ., Pittsburgh). J. Phys. Chem.; 75: No. 17, 2570-4(19 Aug 1971).

Radicals produced by the reaction of fumarate ions with hydrated electrons, hydrogen atoms, hydroxyl radicals, carboxyl radicals, and a series of substituted alkyl radicals were studied by electron spin resonance. The technique of in situ electron irradiation of aqueous solutions was used for the formation of the radicals. Radicals produced from fumarate show a relatively slow second-order disappearance due to the double charge and were thus present at high steady-state concentrations. Spectra of three radicals were observed in irradiated dilute solutions of fumarate: $^-OOC\dot{C}HCH(OH)COO^-$ formed by addition of OH, $^-OOC\dot{C}HCH_2COO^-$ formed by addition of H, and

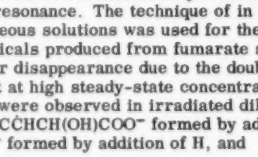

formed by reaction with $e_{aq}^-$. In concentrated solutions an additional spectrum was observed that was formed by addition of $^-OOC\dot{C}HCH_2COO^-$ and $^-OOC\dot{C}HCH(OH)COO^-$ to fumarate. The high radical concentrations found with fumarate suggest the use of this compound for radical trapping. The radicals $\dot{C}H_3$, $\dot{C}H_2Cl$, and $\dot{C}F_3$, which could not be observed in aqueous solutions directly, were successfully trapped by fumarate and the adduct positively identified through the hyperfine splittings of the hydrogen and halogen atoms. The rate constant for the addition of alcohol radicals to fumarate is estimated to be $10^7$ $M^{-1}$ $sec^{-1}$. (auth)

**54657** KINETICS OF THE LOW-DOSE RADIOLYSIS OF CONCENTRATED AQUEOUS ACIDIC SOLUTIONS OF SODIUM NITRATE. Podzorova, E. A.; Orekhov, V. D.; Vereshchinskii, I. V.; Kabakchi, A. M. High Energy Chem. (USSR) (Engl. Transl.); 4: No. 5, 425-6(Sep-Oct 1970).

Translated from Khim. Vys. Energ.; 4: No. 5, 471-2(Sep-Oct 1970).

The radiolysis kinetics of 4 M sodium nitrate with added acetic acid (pH ≥ 2) were studied during exposure to $^{60}Co$ gamma radiation in doses from $3 \times 10^{15}$ to $1 \times 10^{17}$ ev/ml. The radiation yield of nitrite ions was measured both in the presence of, and in the absence of, diazo reagents such as α-nephthylamine ans p-aminobenzoic acid. Measurements of $G_{NO_2^-}$ were also made in one-phase (acetic acid) and in two-phase ($H_2O$ + n-butanol) systems. The experiments with solutions of $NaNO_3$ containing azo-forming compounds showed that they have no effect on the radiochemical conversion of nitrate into nitrite. The presence of organic solvents does not influence the color formation. The initial $G_{NO_2^-}$ value was 2.9 ± 0.1 ion/100 eV, but this value decreased with increased radiation dose. This was explained by the increased role of the reverse of the radiolytic reaction: $NO_2^- + H_2O_2 \rightarrow NO_3^- + H_2O$. (K.S.W.)

**54658** ABSORPTION SPECTRUM OF $e_{aq}^-$ IN THE TEMPERATURE RANGE −4 TO 390°. Michael, B. D.; Hart, Edwin J.; Schmidt, Klaus H. (Argonne National Lab., Ill.). J. Phys. Chem.; 75: No. 18, 2798-2805(2 Sep 1971).

The effect of temperature on the absorption spectrum of $e_{aq}^-$ was determined from −4 to 390°C. Measurements below 100° were made using conventional pulse radiolysis techniques. Above 100° solutions were sealed into thick-walled high purity silica capillaries and irradiation took place within a thermostatically controlled oven. Absorptions were detected to 1.7 μ using a germanium infrared diode and a pulsed xenon arc light source. In the range −4 to 90° the shift of peak absorption energy is −0.003 eV/°C, in good agreement with earlier work. The half-intensity width of the absorption is 0.885 ± 0.03 eV and no significant temperature dependence exists. The product $G\epsilon_{max}$ is 5.23 ± 0.09 × $10^4$ (molecules/100 eV) × ($M^{-1}$ $cm^{-1}$) at 25°, with a linear temperature dependence of 19 ± 11 per °C. Above 100° the $e_{aq}^-$ ($D_2O$) absorption maximum shifts continuously to lower energies with increasing temperature to and above the critical temperature (371°), the rate being −0.0015 eV/°C at 350°. The half-width of the absorption shows little change between 200 and 390° (average value 0.82 eV); however, the absorption becomes markedly less symmetrical with increasing temperature, favoring high-energy transitions. Over this broad temperature range where the structure of water changes drastically, our spectrum indicates that the electron interacts strongly with the surrounding water molecules and produces a stable entity. The trapping of electrons at supercritical temperatures where water is >95% monomeric indicates that preformed traps are not required for this process. (auth)

**54659** RADIOLYSIS OF LIQUID n-BUTANE. Fujisaki, Noboru; Shida, Shoji; Hatano, Yoshihiko; Tanno, Kuniyasu (Tokyo Inst. of Tech.). J. Phys. Chem.; 75: No. 18, 2854-60(2 Sep 1971).

The effects of radical scavenger ($O_2$) and electron scavenger ($SF_6$) on the yields of $C_1$–$C_4$ products formed in the radiolysis of liquid n-butane at 0°C were examined. Furthermore, the isotopic analysis of hydrocarbon products, methane, ethane, ethylene, and propane, formed in the radiolysis of equimolar mixtures of n-$C_4H_{10}$–n-$C_4D_{10}$ was made in the presence and absence of the scavengers. It is shown that some 60% of methane formed from n-butane containing 0.02 M $O_2$ is produced by bimolecular processes, the formation of which is interpreted in terms of the hydrogen abstraction of hot methyl radicals. By assuming that the isotopically mixed ethanes and propanes from n-$C_4H_{10}$–n-$C_4D_{10}$–0.02 M $O_2$ systems represent products formed by ion-molecule reactions, the yields of fragment ions, $C_2H_4^+$, $C_2H_5^+$, n-$C_3H_7^+$, sec-$C_3H_7^+$, and $C_3H_6^+$, were estimated. These yields are generally small (G ≤ 0.2) and suggest that the fragmentation of the parent ions does not occur extensively in the liquid-phase radiolysis of n-butane. The fact that the G value of nitrogen formed from n-$C_4H_{10}$–(0.08 M) $N_2O$ decreased from 3.5 to 2.5 upon the addition of 0.22 M $O_2$ suggests that oxygen of high concentrations scavenges electrons as well as free radicals in irradiated liquid alkanes. (auth)

XUM

**54660** γ RADIOLYSIS OF LIQUID ETHANOL. YIELDS OF HYDROGEN AND FREE IONS. SOLVATED ELECTRON RATE CONSTANTS. Akhtar, S. M. S.; Freeman, G. R. (Univ. of Alberta, Edmonton). J. Phys. Chem.; 75: No. 18, 2756-62 (2 Sep 1971).

The initial hydrogen yield from pure ethanol at 20° is $G(H_2)_0 = 5.9$; the free ion yield is $G(e^-_{solv})_{fi} = 1.7$. Most of the values reported earlier were lower than these and seem to have been affected by impurities in the alcohol. The dose dependence of the hydrogen yields and the yields of hydrogen and nitrogen from nitrous oxide solutions agree with calculations based on $G(H_2)_0 = 5.9$, $G(e^-_{solv})_{fi} = G(H_2)^{max}_{fi} = G(N_2)^{max}_{fi} = 1.7$, using independently measured values of the rate constants. For the free ion reaction, 1.0 nitrogen molecule is formed for each solvated electron scavenged by nitrous oxide in ethanol. Rate constant ratios for reactions of solvated electrons were determined by competition kinetics. Using the previously reported value $k(e^-_{solv} + CH_3(CHO) = 4 \times 10^9\ M^{-1}\ sec^{-1}$, the following values of k for other solutes were obtained at 20°, in units of $10^9\ M^{-1}\ sec^{-1}$: $N_2O$, 7; $C_2H_5OH_2^+$, 29; $C(NO_2)_4$, 19; $CCl_4$, <9; n-$C_3H_7Br$, ≤1.3. Pulse-spectroscopic measurements gave higher values for the last three compounds: $C(NO_2)_4$, 35; $CCl_4$, 11; n-$C_3H_7Br$, 3.0. (auth)

**54661** KINETIC STUDY OF SPECIES FORMED DURING THE PULSED RADIOLYSIS OF AMMONIA. Clerc, M.; Schmidt, M.; Hagege-Temman, J.; Belloni, J. (Centre d'Etudes Nucleaires de Saclay, Gif-sur-Yvette, France). J. Phys. Chem.; 75: No. 19, 2908-14(16 Sep 1971).

Pulsed radiolysis of $NH_3$ by 560-keV electrons at pressures ranging from 0.1 to 760 Torr was used to study the reactions of the excited species $NH(c^1\Pi)$ and $NH(A^3\Pi_i)$ and the ground state $NH(X^3\Sigma^-)$. The radiative lifetimes of the excited species were measured and the values $\tau = 500 \pm 100$ and $500 \pm 60$ nsec found for $NH(c^1\Pi)$ and $NH(A^3\Pi_i)$, respectively. The radical $NH_2$ was also observed in absorption but could not be studied quantitatively. The radiolytic yield of hydrazine formation was measured at different ammonia pressures and the influence of $N_2H_4$ in the $NH(X^3\Sigma^-)$ disappearance kinetics was demonstrated. The reactions of the radical $NH(X^3\Sigma)$ are more complex than would appear from previous studies; the addition of rare gases has shown its disappearance kinetics to be a function of its rotational and vibrational temperature. (auth)

**54662** ELECTRON SPIN RESONANCE STUDIES OF SHORT-LIVED RADICALS GENERATED BY FAST FLOW TECHNIQUES IN AQUEOUS SOLUTIONS. Czapski, Gideon (Carnegie-Mellon Univ., Pittsburgh). J. Phys. Chem.; 75: No. 19, 2957-67(16 Sep 1971).

The application of fast reaction flow systems with ESR detection to studies of free radicals in aqueous solution is analyzed in detail. It is shown that for short-lived radicals it is essential that the chemical reactions which produce the intermediates proceed within the cavity and that few radicals will be observed if the reactions responsible for the radical formation are complete immediately after mixing. The assumption frequently made in these studies, that this reaction is complete before the solution enters the cavity, is shown to be incorrect. It is believed that many of the controversies in the literature can be readily cleared up by analysis of the kinetics as is done here. (auth)

**54663** RADIATION CHEMISTRY OF SUPERCOOLED WATER. Kules, Inna; Schiller, Robert (Central Research Inst. for Physics, Budapest). J. Phys. Chem.; 75: No. 19, 2997-9(16 Sep 1971).

Dilute aqueous solutions were irradiated between room temperature and −8° in the liquid phase to determine the primary radiation chemical yields of the decomposition products of water. The application of normal scavenger methods showed a linear decrease in $G_H$ and $G_{OH}$ and an increase in $G_{\bar{e}_{aq}}$ with decreasing temperature below 0°, although these yields were temperature independent above the equilibrium melting point. This seems to be the first observation of an abrupt discontinuity due to supercooling in any property of water. $G_{H_2O_2}$ was not affected by supercooling, which suggests that the mechanism of $H_2O_2$ formation is probably not the combination of two OH radicals. (auth)

**54664** REACTIVITY OF HYDROGEN ATOMS AND HYDRATED ELECTRONS TOWARD AQUEOUS ERYTHROSIN. X-RADIOLYSIS. Chrysochoos, John; Shihabi, David S. (Univ. of Toledo). J. Phys. Chem.; 75: No. 19, 3020-2(16 Sep 1971).

A study of the x-radiolysis of aqueous erythrosin (2′,4′,5′,7′-tetraiodofluorescein) is reported that includes the absorption spectra of deaerated aqueous erythrosin in the presence of isopropyl alcohol and of air-saturated aqueous erythrosin in the presence of bromide. Dye bleaching, given in terms of G(−S), was used to study the mechanism of the radiolysis. (D.H.M.)

**54665** ESR OF RADICAL PAIR FORMED FROM PRIMARY IONIC SPECIES PRODUCED BY IONIZING RADIATION. Iwasaki, Machio; Minakata, Kayoko; Toriyama, Kazumi (Government Industrial Research Inst., Nagoya, Japan). J. Chem. Phys.; 55: No. 3, 1472-4(1 Aug 1971).

Clear evidence for a dissimilar radical pair was found in a single crystal of potassium hydrogen fumarate irradiated at 77°K. The most probable formula of the radical pair is given. (M.C.G.)

**54666** EPR STUDIES OF MULTIPLE $Ag^0$ TRAPPING SITES PRODUCED IN GAMMA-IRRADIATED FROZEN $AgNO_3$ ICES. Bales, Barney L. (San Fernando Valley State Coll., Northridge, Calif.); Kevan, Larry. J. Chem. Phys.; 55: No. 3, 1327-36 (1 Aug 1971).

EPR studies show that gamma-irradiated $AgNO_3$–KF and $AgNO_3$ ices at 77°K form $Ag^0$ in several magnetically distinct sites. Temperature and optical excitation cause conversions among these sites with little loss of $Ag^0$. From 77 to 150°K the predominant change is from a matrix site characterized by a symmetric electric field to a matrix site characterized by an asymmetric electric field. This is explained in terms of water dipole rotation in response to the removal of the electric field of $Ag^+$ on formation of $Ag^0$. Then the change in electric field due to water dipole rotation semiquantitatively accounts for the change in magnetic parameters of the $Ag^0$ sites. The activation energy for the dipole rotation process is 0.12 eV. At higher temperature $Ag^0$ is converted to $Ag_2^+$ with an activation energy of 0.32 eV, and finally $Ag_2^+$ decays with an activation energy of ~0.5 eV. These activation energies are discussed in terms of L-defect formation and motion of ice matrix. Optical studies show that uv light converts $Ag_2^+$ to $Ag^0$ in a symmetric site and that visible light converts $Ag^0$ from a symmetric to an asymmetric site and partly back to $Ag_2^+$. (auth)

**54667** ELECTRON SPIN RESONANCE SPECTRUM AND STRUCTURE OF THE RADICAL ANION OF PHOSPHORUS OXYCHLORIDE. Kerr, Carolyn M. L.; Williams, Ffrancon (Univ. of Tennessee, Knoxville). Contract AT(40-1)-2968. J. Phys. Chem.; 75: No. 19, 3023-4(16 Sep 1971). (ORO-2968-63).

ESR evidence for the formation of $POCl_3^-$ in γ-irradiated $POCl_3$ is presented. It was concluded that the structure of $POCl_3^-$ is similar to that of other valence electron radicals, i.e., $PCl_4^-$, $PF_4^-$, $PO_4^{3-}$. The structure is most easily visualized as a distorted bipyramid, and in this representation it is probable that the unpaired electron, the oxygen, and the chlorine giving the smaller splitting are in equatorial positions and the two remaining chlorines are axially placed. (D.H.M.)

**54668** KINETICS OF CHARGE SCAVENGING IN γ-IRRADIATED LIQUID CYCLOHEXANE: A COMPARISON BETWEEN DIFFERENT ION–ELECTRON SPACIAL DISTRIBUTION FUNCTIONS USED WITH TWO DIFFUSION APPROXIMATIONS. Dodelet, J.-P.; Freeman, G. R. (Univ. of Alberta, Edmonton). Can. J. Chem.; 49: 2643-50(15 Aug 1971).

The form of the spacial distribution function of ions and electrons in an irradiated liquid is not accurately known and several types of function were assumed by different workers. The various forms are compared and used in the calculation of electron–solute reaction yields in liquid cyclohexane. Our previously used semi-empirical distribution function (YSE) and a power function (YP) give satisfactory results, but a three dimensional, single parameter Gaussian (YGl) and a delta function (YD) do not. The prescribed diffusion approximation was also inserted into the model for comparison with earlier work. No improvement was obtained. Whereas our previous approximations may lead to an underestimate of the germinate neutralization times, the prescribed diffusion approximation may lead to an overestimate of them. (auth) (Canada)

**54669** OXIDATION OF BENZOATOPENTAAMMINECOBALT(III) BY HYDROXYL RADICALS. Cohen, H.; Meyerstein, D. (Nuclear Research Centre, Beersheba, Israel). J. Amer. Chem. Soc.; 93: No. 17, 4179-83(25 Aug 1971).

The reaction of hydroxyl radicals with benzoatopentaamminecobalt(III) yields a radical formed by the addition of the OH to the aromatic ring. The spectrum of the radical formed is very similar to that formed by the reaction of OH radicals with free benzoate ions. The specific rates of formation and disappearance of the radical were measured. The disappearance follows a second-order mechanism. The yield of $Co^{2+}$ depends on the steady-state concentration of the radicals formed and is always considerably less than one, based on the concentration of OH radicals introduced. It is concluded that the overlap between the orbitals on the central Co(III) atom and the conjugated double bond system of the radical is small. Furthermore, if an inner-electron trans-

XUM

fer from the radical to the central Co(III) atom takes place, the specific rate of this reaction is less than $10^2$ $sec^{-1}$. (auth)

**54670** CONCENTRATION DEPENDENCE IN BINARY SYSTEMS IN THE CASE OF INDIRECT ACTION VIA AN ION-PAIR MECHANISM. Berlin, Yu. A.; Talroze, V. L. (Inst. of Chemical Physics, Moscow). Int. J. Radiat. Phys. Chem.; 3: No. 2, 97-115(Aug 1971). (In Russian).

A quantitative theory was devised for description of concentration dependence in the case when indirect action of radiation occurs via an ion pair mechanism. The resulting expression for the yield of donor decomposition ($G_D$) vs. scavenger concentration ($c_S$) cannot be integrated mathematically. The results of numerical integration by electronic computing showed three different regions of concentration dependence. The proposed approximations, which described $G_D = f(c_S)$ rather accurately, led to a square-root dependence for the first region, for the second region the dependence was approximately linear, and for the third exponential. Inequalities were obtained that determine approximate bounds of every region in terms of microscopic constants. The comparison of this theory with experimental data on radiolysis of cyclohexane with $N_2O$ and $CCl_4$ as scavengers showed a good agreement between theory and experiments. Parameters that quantitatively characterize the dependences obtained are $(G_0/G)_{extrap}$ and $\xi' = 1{,}08(k_S r_0^2/\alpha D)$, where $(G_0/G)_{extrap}$ is the value of the intercept, obtained by extrapolation of concentration dependence to $c_S = 0$; D, the diffusion constant of charges in ion pairs, $D = D_+ + D_-$; $\alpha$, the Onsager radius; $r_0$, the average initial separation between components of ion pairs; and $k_S$, the rate constant of the reaction between ion pair component and acceptor molecule. (auth)

## Radioisotope Production

*Refer also to abstract 54739.*

**54671** (ORNL-4682, pp 114-32) TRANSURANIUM-ELEMENT PROCESSING. (Oak Ridge National Lab., Tenn.).

In Chemical Technology Division annual progress report.

Research progress is reported on: TRU operations, isolation and purification of TRU products, special projects, development of chemical processes, and transplutonium elements. (M.C.G.)

**54672** CHEMICAL PROBLEMS IN THE PRODUCTION OF SUPERHEAVY ELEMENTS BY NUCLEAR REACTIONS. Baechmann, K.; Hoffmann, P. (Technische Hochschule, Darmstadt, Ger.). Radiochim. Acta; 15: No. 4, 153-63(Jun 1971). (In German).

A survey is presented of the chemical problems arising in on-line separation of short-lived nuclides. The different methods are discussed in the light of a fast separation of superheavy elements. The properties of methyl ethyl compounds and hydrides were extrapolated. This was done by calculating electronegativities and atomic volumes of the elements 104 to 118. The fast separation of methyl compounds and volatile chlorides is mentioned in more detail. (auth)

**54673** ELECTRODEPOSITION OF THORIUM, URANIUM, AND NEPTUNIUM FROM AMMONIUM SULPHATE SOLUTIONS. Morgan, J. W. (Australian Atomic Energy Commission Research Establishment, Sutherland). Radiochim. Acta; 15: No. 4, 190-3(Jun 1971).

A method for the preparation of high quality sources of thorium, uranium, and neptunium for alpha particle spectrometry is described. Electrodeposition from ammonium sulfate solution to stainless steel gives quantitative recovery of thorium in 6 h, uranium in 3 h, and neptunium in 2 h. For the deposition of "thick" uranium sources, (5-20 $\mu g\ cm^2$), the addition of oxalate to the plating solution is recommended. (auth)

**54674** $^{237}Pu$ PRODUCTION BY THE $^{235}U(\alpha,2n)$ REACTION. Jenkins, J. L.; Wain, A. G. (Atomic Energy Research Establishment, Harwell, Eng.). Int. J. Appl. Radiat. Isotop.; 22: No. 7, 429-30(Jul 1971).

$^{237}Pu$ was obtained by irradiating $^{235}U$ with helium ions. Dimensions and composition of the uranium target are given and the target design described. The experimental technique including dissolving the irradiated target and deposition of plutonium III, subsequently oxidised to plutonium (IV), is explained. The amount of $^{237}Pu$ isolated was found to correspond to an irradiation yield of ~5.4 $\mu$ Ci/100 $\mu$A. A table of $\alpha$ emitters in the $^{237}Pu$ product and their probable origins is included. (UK)

**54675** SYSTEM FOR THE ROUTINE PRODUCTION OF CONCENTRATED $^{99m}Tc$ BY SOLVENT EXTRACTION OF $^{99}Mo$. Baker, R. J. (Inst. of Medical and Veterinary Science, Adelaide). Int. J. Appl. Radiat. Isotop.; 22: No. 8, 483-5(Aug 1971).

Apparatus for use in producing concentrated $^{99m}Tc$, by solvent extraction from $^{99}Mo$ is shown diagramatically and its mechanics and operation explained. Radiation protection methods are noted and the technique of loading weekly supplies of molybdenum into the apparatus is described. Precautions against the possibility of contamination of the $^{99m}Tc$ with $^{99}Mo$ are noted. The efficiency of the first extraction each day is 63% to 79%, depending on specific activity of the molybdate used. The system is suitable for the routine daily production of $^{99m}Tc$ with minimum radiation dose to the operator, since it can be left unattended during the extraction process. The cost/mCi is much reduced compared with the conventional alumina generator. The pertechnetate can be dissolved in any required volume of physiological saline so that small volumes can be used for dynamic studies with the gamma camera. The system could be easily modified for automatic operation. (UK)

**54676** PRODUCTION OF $^{52}Fe$ BY THE $^{55}Mn(p,4n)^{52}Fe$ REACTION FOR MEDICAL USE. Saha, G. B.; Farrer, P. A. (Royal Victoria Hospital, Montreal. McGill Univ., Montreal). Int. J. Appl. Radiat. Isotop.; 22: No. 8, 495-8(Aug 1971).

The radioactive properties of $^{52}Fe$ and its decay scheme are given. The advantages of this isotope for bone marrow imaging are enumerated. A $MnO_2$ target, irradiated with 65-MeV protons, was used to produce $^{52}Fe$ by the $^{55}Mn(p,4n)^{52}Fe$ reaction. $^{52}Fe$ was then separated by ion exchange. The irradiation technique and separation methods are detailed. The total $^{52}Fe$ activity obtained was ~160 $\mu$Ci/$\mu$A-hr. Maximum possible doses are noted and the method of checking the purity of resulting Fe samples, using a 3 in. × 3 in. NaI(Tl) crystal coupled to a 400 channel pulse-height analyzer noted. A sample spectrum figure and decay curve are given. Specific activity was 1.2 to 1.3 $\mu$Ci/$\mu$gm of Fe. The medical advantages of injected doses of 80 $\mu$Ci of $^{52}Fe$ are outlined. (UK)

**54677** YIELDS OF $^{48}V$ IN NUCLEAR REACTIONS ON A CYCLOTRON. Dmitriev, P. P.; Konstantinov, I. O.; Krasnov, N. N. This paper was summarized in At. Energ. (USSR); 29: No. 3, 205(Sep 1970) as paper No. 426/5755. (In Russian).

The yields of $^{48}V$ for various methods were measured on a cyclotron. Stacks of titanium foils and thick samples of titanium, scandium, and chromium were irradiated by the deflected beam in the chamber. The activity of $^{48}V$ was measured by a scintillation $\gamma$ spectrometer. The total error of the values of the yield was 11 to 13%. The results obtained, as well as literature data, are given. (M.C.G.)

## Recoil Production and Reactions

*Refer also to abstracts 54694, 54704, and 56381.*

**54678** HOT TRITIUM REACTIONS IN THE $CH_4 + SiH_4$ SYSTEM. Castiglioni, M.; Volpe, P.; Ramonda, G. (Univ., Turin). Radiochim. Acta; 15: No. 4, 164-6(Jun 1971).

Study on the system $CH_4 + SiH_4 + T$ confirms by direct comparison the data obtained from the Hot Atom Kinetic theory for the single systems $CH_4 + T$ and $SiH_4 + T$. Moreover, the study of the mixed system can give further information on kinetic parameters of the reactants. The logarithmic average energy loss for the monosilane is experimentally determined. The dependence of the excitation functions on energy for substitution reactions in $CH_4$ and $SiH_4$ is compared. (auth)

**54679** INFLUENCE OF IONISING RADIATION ON THERMAL ANNEALING IN THE CROSSOVER REGION OF POTASSIUM CHROMATE. Collins, C. H.; Collins, K. E. (National Tsing Hua Univ., Hsinchu, Taiwan). Nature (London) Pphys. Sci.; 232: No. 31, 109-10(2 Aug 1971).

It has been suggested that the "crossover reaction" in neutron-irradiated $K_2CrO_4$, characterised by a conversion of Cr(III)-dimir+polymer species to Cr(III)-monomer species during annealing in the temperature range 0 to 100°C, may be related to either the presence of irradiation-produced bulk structural and/or electronic species, or to local damage created by the recoil atom, or both. The studies described showed that this reaction is not sensitised by bulk-irradiation-produced defects, but the results suggested that the "crossover reaction" occurs only in the presence of crystal defects formed in the immediate vicinity of the nuclear activation event by the recoil atom. It also appeared that the recoil-related defects that promoted the "crossover reaction" were sensitive to the presence of crystallisation-produced defects. It may also be that thermal annealing processes that occur at temperatures of 0 to 100°C are the only "hot atom" recoil affected annealing processes occurring in neutron-irradiated $K_2CrO_4$. (UK)

**54680** OBSERVATION OF NEUTRON DOSE DEPENDENCE OF THE APPARENT INITIAL RETENTION IN CHLOROINDIUM

CHLOROPHTHALOCYANINE. Kudo, Hiroshi; Yoshihara, Kenji (Japan Atomic Energy Research Inst., Tokai). Radiochim. Acta; 15: No. 4, 167-9(Jun 1971).

Chloroindium chlorophthalocyanine, (InCl)PcCl, was irradiated at dry ice temperature in a nuclear reactor and the Szilard-Chalmers process investigated. Neutron dose dependence of the apparent initial retention was observed in the range of neutron dose between $3 \times 10^{14}$ and $6.4 \times 10^{15}$ n/cm$^2$. The results are discussed in terms of internal radiation effects and thermal annealing during neutron irradiation. (auth)

**54681** EFFICACY OF VARIOUS SCAVENGERS IN THE STUDY OF HOT CHLORINE REACTIONS. Alfassi, Zeev B.; Amiel, Saadia (Soreq Nuclear Research Centre, Yavne, Israel). Radiochim. Acta; 15: No. 4, 201-4(Jun 1971).

Various scavengers used in the study of hot halogen reactions were tested for the system $^{38}Cl + CH_3Cl \rightarrow CH_3{}^{38}Cl + Cl$, where the hot chlorine originated from neutron capture. A 1 to 2% concentration of $Br_2$ or $I_2$ was an effective scavenger and removed radicals, thermal atoms, and ions. Other scavengers tried required a mixture of a radical scavenger and a thermal halogen scavenger to obtain the true "hot" reaction yield. A value of 3.4 ± 0.25% was obtained for the yield of the above hot atom reaction. (auth)

**54632** CORRELATED ANNEALINGS OF $^{60}$Co RECOILED ATOMS IN CATIONIC AND ANIONIC SITES OF NEUTRON-IRRADIATED CRYSTALS OF cis-[Co en$_2$(NO$_2$) CNS][Co EDTA]2H$_2$O. Lazzarini, E.; Fantola-Lazzarini, A. L. (Politecnico, Milan). Lett. Nuovo Cim.; 2: No. 11, 541-4(11 Sep 1971).

Thermal annealing of atoms recoiled as a consequence of an $(n,\gamma)$ reaction was investigated in Co complexes in which the recoiled atom can anneal in two different kinds of lattice sites. The compound cis-[Coen$_2$NO$_2$CNS][CoEDTA]2H$_2$O was irradiated for 100 min at $4.5 \times 10^{\prime\prime}$ n/cm$^2$/sec for thermal neutron flux, $1.5 \times 10^{\prime\prime}$ n/cm$^2$/sec fast neutron flux, and ~1 Mrad/hr gamma dose and then annealed. Data are presented to support the prediction that the thermal annealings of recoils are correlated and are related to the changes in crystal lattice structure subsequent to the removal of the crystallization water. (M.C.G.)

**54683** RECOIL SYNTHESIS OF HIGH SPECIFIC ACTIVITY $^{11}$C-CYANIDE. Lamb, J. F.; James, R. W.; Winchell, H. S. (Univ. of California, Berkeley). Int. J. Appl. Radiat. Isotop.; 22: No. 8, 475-9(Aug 1971).

The low radiation dose associated with the short half-life of $^{11}$C (20.4 min), the good spatial resolution possible in imaging $\beta^+$ emission and the chemical identity of $^{11}$C-containing compounds to their $^{12}$C homologues, make $^{11}$C labeled organic compounds very attractive for use in nuclear medicine. As an initial step in the synthesis of $^{11}$C amines and amino acids, methods for direct recoil synthesis of large quantities of $^{11}CN^-$ were developed. The $^{11}N(p,\alpha)^{11}C$ reaction with bombardment of solid $LiNH_2$ or a gas target containing 99% $N_2$ and 1% $H_2$ was used. Using a continuous flow of $N_2 + H_2$ through a quartz-lined gas target over 500 mCi of $^{11}CN^-$ were routinely recovered in the gas flow from the target following bombardment with 15 to 30 μA of 15 MeV protons for 30 to 45 min. Analysis of all of the $^{11}$C activity in the gas stream from the target during bombardment showed ~61% H$^{11}$CN, ~28% $^{11}$C hydrocarbons, ~9% CO and ~2% $CO_2$. The total H$^{11}$CN recovered amounted to ~20% of the total theoretical yield in the target. (auth) (UK)

**54684** KINETIC ISOTOPE EFFECT OF REACTIONS OF HOT ATOMS IN GASEOUS MIXTURES. Brodskii, A. M.; Temkin, A. Ya. (Inst. of Electrochemistry, Moscow. Inst. of Petrochemical Synthesis, Moscow). High Energy Chem. (USSR) (Engl. Transl.); 4: No. 6, 451-5(Nov-Dec 1970).

Translated from Khim. Vys. Energ.; 4: No. 6, 499-504(Nov-Dec 1970).

The dependence of the HT/DT yield ratio on the concentration of inert inhibitor was calculated for reactions of T recoil atoms in a gaseous mixture of $C_2H_6$, $CD_4$, and Ne on the basis of a model of two shifted resonances. This model provides a natural explanation of the inhibiting effect of $C_2H_6$ on the reaction of tritium with $CD_4$. The dependence is in good agreement with the experimental results and is a serious argument in favor of the hypothesis of a resonance mechanism for the reactions of hot atoms. It is shown that the inhibition effect can play a significant role in the radiolysis of hydrocarbon mixtures by affecting the reaction rates of hot hydrogen atoms. The dependence of the inhibiting effect characteristic for this case on the concentration of the inhibiting component was obtained. The yields and isotope effect of the reactions of hot H atoms were calculated on the basis of the well-known values of these parameters for hot T atoms. (auth)

**54685** MECHANISM OF THE FORMATION OF $C_1$–$C_4$ ALKANES IN THE ACTION OF RECOIL TRITIUM ATOMS ON CYCLOHEXANE. Avdonina, E. N. (Moscow State Univ.). High Energy Chem. (USSR) (Engl. Transl.); 4: No. 6, 479-82 (Nov-Dec 1970).

Translated from Khim. Vys. Energ.; 4: No. 6, 531-4(Nov-Dec 1970).

The yields of labeled alkanes formed in the action of recoil tritium atoms on cyclohexane were measured. These compounds are formed in reactions of the excited labeled alkyl radicals arising by the insertion of a recoil tritium atom into a C–C bond of cyclohexane. Proofs of the occurrence of these reactions in the radiolysis of cyclohexane, as well, are given. (auth)

**54686** RELATIVE RATES OF HYDROGEN ATOM ABSTRACTION BY NEAR-THERMAL $^{18}$F ATOMS. Williams, Ronald L.; Rowland, F. S. (Univ. of California, Irvine). Contract AT(04-3)-34. J. Phys. Chem.; 75: No. 17, 2709-10(19 Aug 1971).

A series of measurements of the relative rates of the hydrogen abstraction reaction by near-thermal $^{18}$F atoms with $H_2$, $D_2$, $CH_4$, $CD_4$, $C_2H_6$, and $CH_3CF_3$ are reported. The $^{18}$F atoms were formed as high kinetic energy atoms by the nuclear reaction $^{19}F(n,an)^{18}F$ and 98% of them were moderated to near thermal energies through multiple collisions with $SF_6$. Earlier measurement of the relative rates of hydrogen abstraction by fluorine atoms showed only small variations for different RH molecules [about a factor of 2 per H atom from the most easily abstracted (tertiary H in isobutane) to the least easily abstracted ($H_2$)]. Relative rates for the sequence $C_2H_6 - CH_4 - H_2$ show a somewhat wider variation than that found earlier, and the total range of about a factor of 25 per bond between HI and $CH_3CF_3$. The isotope effects for the relative rates of abstraction are 1.6 ± 0.2 for methane and 1.8 ± 0.2 for molecular hydrogen. (D.H.M.)

**54687** CHEMICAL EFFECTS OF THE NUCLEAR REACTION $^{14}N(n,p)^{14}C$ IN POTASSIUM AZIDE. Vaughan, John D.; Springborn, Richard L.; Vaughan, Virginia L. (Colorado State Univ., Fort Collins). J. Phys. Chem.; 75: No. 17, 2551-5(19 Aug 1971).

The distribution of labeled products resulting from $^{14}N(n,p)^{14}C$ in potassium azide was investigated. The chief products found with water dissolution of the target were $^{14}CN^-$, $^{14}CN_2^{2-}$, and $^{14}CH_3NH_2$. Thermal anneal at 300°C for periods of 1 to 8 hr resulted in a large increase in $^{14}CN_2^{2-}$ and in decreases in other products. Thermal decomposition of target at 400°C gave principally $^{14}CN_2^{2-}$. (auth)

**54688** REPLACEMENT REACTIONS OF HOT CHLORINE ATOMS IN CHLOROFLUOROMETHANES. Lee, S. C.; Hower, C. O. (Univ. of Idaho, Moscow). J. Phys. Chem.; 75: No. 17, 2685-7(19 Aug 1971).

Results are reported of measurements made on the absolute yields of hot replacement products in chlorine atom reactions with chlorofluoromethanes. The hot $^{38}$Cl was produced by means of the $^{37}Cl(n,\gamma)^{38}Cl$ reaction. The reactants included $CF_3Cl$, $CF_2Cl_2$, $CFCl_3$, and $CCl_4$ for Cl replacement and $CF_4$, $CF_3Cl$, $CF_2Cl_2$, and $CFCl_3$ for the Cl for F replacement. Cl for Cl replacement increased as the number of Cl atoms increased until there was an abrupt decrease with $CCl_4$. The yields of Cl for F replacement products followed the trend expected from steric and inertial considerations. (D.H.M.)

**54689** THERMAL ANNEALING BEHAVIOR OF THE RECOIL $^{57}$Co FORMED BY THE DECAY OF $^{57}$Ni-LABELED HEXAMMINENICKEL(II) COMPLEXES. Omori, Takashi; Wu, Shaw-chii; Shiokawa, Takanobu (Tohoku Univ., Sendai). Bull. Chem. Soc. Jap.; 44: No. 4, 1014-17(Apr 1971).

Thermal annealing reactions of $^{57}$Co formed by the EC and $\beta^+$-decay of the $^{57}$Ni-labeled hexaamminenickel(II) halide complexes were investigated in detail by means of ion-exchange techniques. When the annealing is carried out at high temperatures, the chemical behavior of $^{57}$Co is remarkably affected by the thermal decomposition of the parent and daughter complexes. In the intrinsic annealing, however, the annealing curves have characteristic shapes and the plateau yields of $^{57}Co(NH_3)_6^{3+}$ ion are independent of the temperature, depending on the nature of the outer-sphere anion. The unusual oxidation reaction of the recoil $^{57}$Co(II) species is explained by the action of the crystal defects in the near-neighborhood of the recoil site. (auth)

**54690** RECOIL BROMINE REACTION. THE ISOMERIZATION OF EXCITED CYCLOPROPYL BROMIDE. Wai, C. M.; Jennings, R. L. (Univ. of Idaho, Moscow). J. Phys. Chem.; 75: No. 17, 2698-2700(19 Aug 1971).

The isomerization of excited cyclopropyl bromide to allyl bromide induced by recoil $^{80m}$Br substitution is reported. The gas-phase results suggest that nearly every excited c–$C_3H_5{}^{80m}$Br

XUM

molecule formed by recoil $^{80m}Br$ substitution for H or for Br in the cyclopropyl ring undergoes secondary isomerization to allyl bromide; however, an appreciable amount of $c-C_3H_5{}^{80m}Br$ is present in the liquid phase experiments. Yields are also given for radioactive products from recoil $^{80m}Br$ reactions with cyclopropane–$Br_2$. Possible mechanisms of the reactions are considered. (D.H.M.)

**54691** METHODS OF OBTAINING $^{51}Cr$ ON A CYCLOTRON. Dmitriev, P. P.; Konstantinov, I. O.; Krasnov, N. N. This paper was summarized in At. Energ. (USSR); 29: No. 3, 206(Sep 1970) as paper No. 427/5756. (In Russian).

Carrier-free $^{51}Cr$ can be obtained on a cyclotron in nuclear reactions with charged particles. A comparative analysis of the various methods of obtaining it was carried out. The measured values of the yield are given and curves are shown. The results obtained are compared with the data cited by other authors. The most effective methods are (V + p) and (V + d). (M.C.G.)

## Radiochemistry

*Refer also to abstracts 54440, 54676, 54914, and 56742.*

**54692** (NYO–3417-15) PROGRESS REPORT [ON RADIOCHEMISTRY], JUNE 1, 1970–MAY 31, 1971. Finston, Harmon L. (Brooklyn Coll., N. Y. Dept. of Chemistry). Contract AT(30-1)-3417. 11p. Dep. NTIS.

ANTIMONY—determination by x-ray counting after neutron activation
ARSENIC—determination by x-ray counting after neutron activation
1,3-BUTANEDIONE, 4,4,4-TRIFLUORO-1-(2-THIENYL)—complexes with iron, spectrophotometric study of
IRON—separation of ferric, by solvent extraction using TTA, effects of TOPO on
—complexes with TTA, spectrophotometric study of
LEAD—determination by x-ray counting after neutron activation
RADIOISOTOPES—neutron cross sections for, thermal

**54693** METHOD FOR PREPARING MOLECULES LABELED WITH TRITIUM. Hung Lam Thanh; Morgat, Jean-Louis (to Commissariat a l'Energie Atomique). French Patent 2,039,530. 4 Jan 1971. Filed 2 Apr 1969. (In French).

A method of tritiating polypeptides is described; it consists of the iodidation of the polypeptide by iodine monochloride and the catalytic removal of halogens from the iodinated polypeptide by gaseous tritium in the presence of a catalyst on an alkaline support. (auth)

**54694** MECHANISM OF $\beta$ RECOIL. Mundschenk, H. (Univ., Mainz). Radiochim. Acta; 15: No. 4, 193-200(Jun 1971). (In German).

Beta recoil studies on solid substrates were performed using $^{212}Pb$ or $^{214}Pb$ as parent nuclide. Several parameters that severely influence the recoil yield were investigated thoroughly. The diffusion coefficients D, activation energies Q, and desorption energies A of the processes were calculated. From the findings obtained, a tentative explanation of the state of binding of the parent nuclide within the emitter surface before and after decay was given. Beta recoil may be used to separate short-lived fission products. (auth)

**54695** SOLUBILITY PRODUCTS AND COLLOID FORMATION OF RADIOELEMENTS. Davydov, Yu. P. (Inst. of Atomic Energy, Minsk). Dokl. Akad. Nauk BSSR; 15: No. 2, 147-50(Feb 1971). (In Russian).

Analysis of published experimental data showed that low-molecular-weight polymers such as dimers, trimers, etc., exhibit properties characteristic of colloids. It was concluded from this that the solubility product cannot be formally prevalent in all manifestations of colloidal properties—from dimers to hydroxide precipitates. No connection was observed between the solubility product values of hydroxides and the incipient formation of negatively charged colloidal radioelements. (K.S.W.)

**54696** COULOMB FRAGMENTATION IN InI AND $InI_3$. Schumacher, M.; Borchert, I.; Langhoff, H. (Univ., Goettingen, Ger.). Z. Phys.; 246: No. 5, 396-406(1971).

The fragmentation of InI and $InI_3$ initiated by electron capture in $^{114m}In$ was studied by investigating the profile of the 558-keV $\gamma$ line emitted by the $^{114}Cd$ nuclei. The profile was deduced from measured cross sections for the resonant scattering of the 558-keV quanta in coincidence with the preceding 724-keV quanta. Predictions using a simple model for the fragmentation are in agreement with the experimental results for InI. The average energy of the fragments amounts to about 120 eV. (auth)

**54697** ABSOLUTE MEASUREMENT OF THE RADIOACTIVITY OF PURE $\beta$ EMITTERS WITH LIQUID SCINTILLATORS. Spahr, Juerg; Binkert, Thomas (Univ., Bern). Z. Angew. Math. Phys.; 22: No. 3, 472-84(25 May 1971). (In German)

The use of liquid scintillation counting for the absolute standardization of pure $\beta$-emitting radionuclides by means of the efficiency-tracing method is investigated. Special effects occurring by the use of liquid scintillators do not lead to important errors. Results of measurements of the nuclides $^{35}S$ and $^{45}Ca$ are given. (auth)

**54698** RADIOCHEMICAL STUDY OF THE STABILITY OF SELENOMETHIONINE $^{75}Se$. Besnard, Madeleine; Frapart, P.; Cohen, Y. (CEN de Saclay, Gif-sur-Yvette, France). Int. J. Appl. Radiat. Isotop.; 22: No. 8, 469-74(Aug 1971). (In French).

The radiochemical purity of selenomethionine $^{75}Se$ by ascending chromatographs was determined. The system paper Whatman No. I, solvent: n butanol/acetic acid/ethanol/water (10/1/0, 3/3) gave the best results. This system allows the separation of selenomethionine $^{75}Se$/selenious acid/selenomethionine oxides. The percentage of damage attributable to the chromatographic manipulation comes to 3% of the analyzed selenomethionine. With this sytem, the autoradiolysis and the action of oxygen at different temperatures were studied. Selenious acid, methionine selenone, and methionine selenoxide were formed. (auth) (UK)

**54699** DETERMINATION OF THE ACTIVITY OF FISSION PRODUCTS. Amadesi, P.; Cazzoli, S.; Cucchi, G. (CNEN, Bologna). Minerva Fisiconucl.; 13: 271-5(Oct-Dec 1969). (In Italian).

A simplified formalism for calculation of the activity of fission products is described. The activity of fission products can thus be evaluated in some common cases found in research laboratories. (J.S.R.)

**54700** DISINTEGRATION RATE DETERMINATION OF $^{241}Am$ BY LIQUID SCINTILLATION COUNTING. Yura, Osamu (Electrotechnical Lab., Tokyo). Radioisotopes (Tokyo); 20: No. 8, 383-4(Aug 1971).

Experimental results are presented with an emphasis on sample preparation technique in the absolute measurement of Am-241 disintegration rate by liquid scintillation counting. Three systems (A, B, C) of counting solution were prepared using two types of scintillator solutions. Results of counting efficiencies showed that no deviation of any type of method exceeded 1% of expected values. (J.G.B.)

**54701** METHOD FOR CALCULATING CROSS-CONTAMINATION IN COLUMN CHROMATOGRAPHIC SEPARATION OF RADIOACTIVE PARENT–DAUGHTER PAIRS. Karol, P. J. (Carnegie-Mellon Univ., Pittsburgh). Anal. Chem.; 43: No. 11, 1383-90(Sep 1971).

In the chromatographic separation of two species where one is the radioactive precursor of the other, radioactive transformation while on the column modifies the parent–daughter elution curve from that expected of stable isotopes of the same elements. Precise determination of the amount of daughter species produced by other mechanisms such as nuclear reactions or decay of an alternate (independent) precursor necessitates an accurate calculation of hereditary contamination in the daughter fraction. The extent of this contamination, which can be quite considerable, is a function of the column elution rate and the half-lives of the parent and daughter isotopes. The theoretical plate concept of column chromatography is applied to radioactive systems and used to derive a general expression for the modified elution curve from which the amount of contamination may be determined. (auth)

**54702** PARTIAL DEGRADATION OF 1,3,5-CYCLOHEPTATRIENE-$^{14}C$ OBTAINED FROM HOT-ATOM, PHOTOLYTIC, AND THERMAL REACTIONS. Pohlit, Helmut M.; Lemmon, Richard M. (Univ. of California, Berkeley). J. Phys. Chem.; 75: No. 17, 2558-60(19 Aug 1971).

1,3,5-Cycloheptatriene-$^{14}C$ (CHT), one of the prominent products of fast $^{14}C$ atoms in benzene, was produced with $^{14}C^+$ ions (kinetic energies of 5, 31, and 100 eV) and was partially degraded. In the 5- to 100-eV energy range, over which the yield varies by a factor of about 6 to 8, the distribution of $^{14}C$ activity in the CHT product seems constant, i.e., 31% in carbons 2–5. This value is compared with 45% obtained from 5000-eV $^{14}C^+$ ions, indicating secondary isomerization of CHT-$^{14}C$, at the higher energy, after its formation. In contrast, these same four carbons contain only 3.5% of the activity in CHT prepared by the photolysis of $^{14}CH_2N_2$ in benzene, and only 2.5% of the activity when the CHT is prepared

by the catalytic decomposition of $^{14}CH_2N_2$ in benzene. It is concluded that (1) over the energy range from 5 to 100 eV only one mechanism is operative, (2) the last step, presumably the insertion reaction of $CH_2$ into benzene, does not proceed at energies above 5 eV, and (3) the effective energy available to the photolytically produced $CH_2$ must be well below 5 eV. (auth)

**54703** HOT-ATOM CHEMISTRY OF $^{14}C$ IN SOLID BENZENE AT KINETIC ENERGIES BETWEEN 5 AND 100 ELECTRON VOLTS. Pohlit, Helmut M.; Erwin, Wallace; Lin, Tz-hong; Lemmon, Richard M. (Univ. of California, Berkeley). J. Phys. Chem.; 75: No. 17, 2555-7(19 Aug 1971).

The yields of seven major hydrocarbon products from the interaction of energetic $^{14}C$ ions with solid benzene (−196°C) were determined for carbon ion energies between 5 and 100 eV. Toward the lower kinetic energy, the yields of benzene, biphenyl, and diphenylmethane appear to remain essentially constant, that of phenylcycloheptatriene appears to increase, and those of toluene, cycloheptatriene, and phenylacetylene definitely decrease by a factor of 5 to 10. These results are additional support for previously postulated mechanisms and lead to the conclusions that (1) hydrogen and carbon pickup reactions proceed up to rather high kinetic energies (50 to 100 eV), and (2) insertion into carbon–hydrogen or carbon–carbon bonds with preservation of the adduct is limited to energies below 5 eV. (auth)

**54704** $^{129}I$ MOESSBAUER STUDIES OF THE CHEMICAL EFFECTS OF NUCLEAR TRANSFORMATIONS IN COMPOUNDS OF TELLURIUM. Warren, J. L.; Jones, C. H. W.; Vasudev, P. (Simon Fraser Univ., British Columbia, Can.). J. Phys. Chem.; 75: No. 18, 2867-79(2 Sep 1971).

The chemical effects of the $^{129m}Te \rightarrow {}^{129}Te$ isomeric transition and the $^{128}Te(n,\gamma)^{129}Te$ nuclear reaction were studied in telluric acid and several related tellurium–oxygen compounds, using the $^{129}I$ 27.8-keV 15-nsec Moessbauer transition as a probe. The $^{129}I$ Moessbauer emission spectra of the following compounds, labeled in separate experiments with $^{129}Te$ and $^{129m}Te$, were recorded against $Na^{129}I$ absorber: $H_6TeO_6$, $(H_2TeO_4)_n$, $\alpha$-$TeO_3$, tetragonal $TeO_2$, $H_2TeO_3$, and Te metal. The neutron irradiation of $H_6TeO_6$, $TeO_2$, and Te metal with the production of $^{129}Te$-labeled sources was also studied. Chemical effects of the isomeric transition and $(n,\gamma)$ reaction were clearly observed in $H_6TeO_6$ and $(H_2TeO_4)_n$ but not in $TeO_2$, $H_2TeO_3$, or Te metal. Where molecular decomposition was observed, a single decomposition product, apparently the $TeO_3^{2-}$ ion, was identified. On heating telluric acid containing the $^{129}TeO_3^{2-}$ recoil product, a single-step annealing reaction was observed in which $^{129}TeO_3^{2-} \rightarrow {}^{129}Te(VI)$. The results of these Mössbauer studies are compared with those of previous radiochemical studies of similar transformation schemes. An analysis of the data for the $^{129}Te$-labeled sources provides further estimates of the parameter $[(q_{at}(Te(Q^{125})/(q_{at}(I)Q^{129})](1+\eta^2/3)$ and $\rho^{125}Te/\rho^{129}I$, the radius ratio for $^{125}Te$ and $^{129}I$, and also allows a comparison of the bonding in tetragonal and orthorhombic $TeO_2$. The study of tellurium compounds using double labeling with $^{125}Te$ and $^{129}Te$ is illustrated. (auth)

**54705** REACTIONS OF IODINE WITH OLEFINS. II. RADIATIVE NEUTRON CAPTURE INDUCED REACTIONS OF $^{128}I$ WITH VARIOUS $C_5$ ISOMERS: EVIDENCE FOR A MECHANISM OTHER THAN AUTORADIOLYSIS IN THE CONDENSED STATE. Ayres, R. L.; Gadeken, O. C.; Rack, E. P. (Univ. of Nebraska, Lincoln). J. Phys. Chem.; 75: No. 18, 2880-2(2 Sep 1971).

The respective organic yields and product distribution resulting from the $(n,\gamma)$ activation of $^{127}I$ in n-pentane, 1-pentene, cis-2-pentene, and trans-2-pentene are compared with the corresponding $^{131}I$ product distribution obtained by radiolytic processes in similar binary $I_2$–olefin systems. Two major differences between the relative quantities of the various products produced by these dissimilar processes are a significant increase in the relative yields of the individual fragmentation products, in most instances ≥50% produced by the $(n,\gamma)$ activation process in comparison to the radiolytically produced fragmentation products, and a lower sensitivity of the $C_5$ iodides produced by the radiolysis process to the isomeric composition of the $C_5$ hydrocarbon, whereas the yields of the $C_5$ iodides obtained from the $(n,\gamma)$ activation show a definite preference for addition of the activated iodine at the position of the double bond. (D.H.M.)

## Separation Processes

*Refer also to abstracts 54534, 54546, 54587, 54671, 54692, 54847, 54937, 55376, 55389, 55390, 57001, and 57127.*

**54706** (BNWL-SA-3345) INTEGRATED LANTHANIDE–ACTINIDE SOLVENT EXTRACTION PROCESS. Schulz, Wallace W.; Richardson, Gerald L. (Battelle-Northwest, Richland, Wash. Pacific Northwest Lab.). 1 Jun 1970. Contract AT(45-1)-1830. 25p. Dep. NTIS.

A conceptual solvent extraction scheme for integrated recovery of product (U,Pu) and selected byproduct (Np, Am, Cm, and fission product rare earths) from irradiated LMFBR fuel is described. This scheme, termed the Lacex Process, uses dibutyl butylphosphonate as the extractant. Results of limited batch tests that demonstrate technical feasibility of the process are presented and discussed. Envisioned and discussed also is application of the Lacex Process in a short-cooled, head-end treatment plant to fractionate the various product and byproduct candidates into crude cuts that could be "sold" to other purification plants or that could be purified by rework in the head end facility itself. (auth)

**54707** (CONF-710401–, pp 300-6) PROBLEMS ASSOCIATED WITH $^{238}Pu$ PROCESSING. Case, A. H. (Atlantic Richfield Hanford Co., Richland, Wash.). 14 Apr 1971.

From Rocky Flats symposium on safety in plutonium handling facilities; Golden, Colo. (13 Apr 1971).

The characteristics of $^{238}Pu$, which differ from those of $^{239}Pu$ and require different operating techniques and safety precautions that were observed during the conversion of plutonium nitrate solution to oxide via oxalate precipitation and calcination, are described. The high specific alpha activity of $^{238}Pu$ caused several unusual problems in handling and processing of this isotope. The problems resulted from the self-heating effect, the generation of gases by radiolysis of nitric acid solutions, and the neutron field produced through $(\alpha,n)$ reactions. However, it was concluded that $^{238}Pu$ can be handled safely provided the proper techniques are used and the necessary precautions are taken. (P.C.H.)

**54708** (CONF-710401–, pp 369-85) PROCESSING OF PLUTONIUM-CONTAMINATED LIQUID WASTES AT LOS ALAMOS. Emelity, L. A.; Christenson, C. W. (Los Alamos Scientific Lab., N. Mex.). 15 Apr 1971.

From Rocky Flats symposium on safety in plutonium handling facilities; Golden, Colo. (13 Apr 1971).

Various aspects of control in the processing of liquid industrial wastes that are contaminated by plutonium are discussed. Descriptions and operations of the two facilities used for waste processing are given. Safety considerations are also discussed. (P.C.H.)

**54709** (CONF-710401–, pp 386-91) WASTE REDUCTION STUDIES. Ziegler, D. L. (Dow Chemical Co., Golden, Colo. Rocky Flats Div.). 15 Apr 1971.

From Rocky Flats symposium on safety in plutonium handling facilities; Golden, Colo. (13 Apr 1971).

The waste process development efforts at Rocky Flats are described. The main objectives are: to decrease the amount or bulk volume of radioactive waste generated in the operation of the plant; to decrease the amount of Pu and Am contained in the wastes; and to convert the radioactive waste into forms that will provide for maximum isolation of radionuclides from man's biological environment. (P.C.H.)

**54710** (DOCKET-50201-86) WEST VALLEY REPROCESSING PLANT. Addendum, Site Environmental Studies. (Nuclear Fuel Services, Inc., West Valley, N. Y.). 15 Sep 1971. 9p. Dep. NTIS.

Results of additional geologic studies performed for the proposed expansion of an existing nuclear spent fuel reprocessing facility at West Valley, New York, are given. A structure contour map, based on more detailed data than was originally available, is presented, which will permit an accurate definition of the orientation and extent of the bifurcation. Revised response spectra at 12% and 6% of gravity (horizontal) are presented, which incorporate an amplification factor of 3.5 at 2% damping in the period range of 0.1 to 0.5 sec. (M.C.G.)

**54711** (ORNL-4682) CHEMICAL TECHNOLOGY DIVISION ANNUAL PROGRESS REPORT FOR THE PERIOD ENDING MARCH 31, 1971. (Oak Ridge National Lab., Tenn.). Jul 1971. Contract W-7405-eng-26. 294p. Dep. NTIS.

Research progress is reported on: molten-salt reactor processing, development of aqueous processes for LMFBR fuels, development of methods for reprocessing HTGR fuels, waste treatment and disposal, transuranium element processing, development of the thorium fuel cycle, sol-gel processes for the uranium fuel cycle, conversion studies in the LMFBR fuel cycle, preparation of $^{233}UO_2$ for light-water breeder reactors, separations chemistry, chemical applications of nuclear explosives, biochemical technology, spectrophotometric studies of lanthanides and actinides, preparation and properties of actinide oxides, chemical engineering research, reactor evaluation studies, and miscellaneous pro-

XUM

grams. Separate abstracts were prepared for 16 of the 17 sections. Bicochemical technology, not covered separately, includes macromolecular separations, body fluids analyses programs, and water pollution studies. (M.C.G.)

*For abstracts of individual sections see: 54396, 54578, 54671, 54712–54719, 54816, 55592–55594, and 57062.*

**54712** (ORNL–4682, pp 1-38) MOLTEN-SALT REACTOR PROCESSING. (Oak Ridge National Lab., Tenn.).

In Chemical Technology Division annual progress report.

Progress is reported on molten-salt breeder reactor flowsheet analysis, measurement of distribution coefficients in molten salt-metal systems, estimation of free energies of formation of some lanthanide and actinide halides using distribution coefficient data, solubilities of thorium and neodymium in Li–Bi systems, protactinium oxide precipitation studies, reductive extraction engineering studies, development of the metal transfer process for removing rare earths, contactor studies of a simulated molten salt–liquid Bi system, axial dispersion in simulated continuous fluorinators, development of a frozen-wall continuous fluorinator, design of a processing materials test stand and the first molybdenum reductive extraction equipment, removal of U from molten salt by oxide precipitation, reduction of iron fluoride in molten salt by countercurrent contact with hydrogen in a packed column. (M.C.G.)

**54713** (ORNL–4682, pp 39-79) DEVELOPMENT OF AQUEOUS PROCESSES FOR LMFBR FUELS. (Oak Ridge National Lab., Tenn.).

In Chemical Technology Division annual progress report.

Research progress is reported on: shipping, head-end processing, removal of volatile fission products, dissolution and feed preparation, solvent extraction with TBP, off-gas treatment, radiation, shielding, and criticality studies, and engineering studies. (M.C.G)

**54714** (ORNL–4682, pp 80-94) DEVELOPMENT OF METHODS FOR REPROCESSING HTGR FUELS. (Oak Ridge National Lab., Tenn.).

In Chemical Technology Division annual progress report.

Research progress is reported on: head-end reprocessing studies with irradiated and unirradiated fuels, procurement of fuel for head-end studies, and design support for head-end studies. (M.C.G.)

**54715** (ORNL–4682, pp 95-113) WASTE TREATMENT AND DISPOSAL. (Oak Ridge National Lab., Tenn.).

In Chemical Technology Division annual progress report.

Research progress is reported on: radioactive waste repository; engineering, economic and safety evaluations; high-level radioactive waste; combustion of plutonium-bearing solid wastes; and incorporation of intermediate-level wastes in polyethylene. (M.C.G.)

**54716** (ORNL–4682, pp 133-43) DEVELOPMENT OF THE THORIUM FUEL CYCLE. (Oak Ridge National Lab., Tenn.).

In Chemical Technology Division annual progress report.

Research progress is reported on: recycle of the alcohol used in the microsphere-forming column, development of prototype equipment for TURF, preparation of microspheres in nonfluidized-bed columns, preparation of test materials, and $^{233}U$ storage, purification, and distribution. (M.C.G.)

**54717** (ORNL–4682, pp 160-2) CONVERSION STUDIES IN THE LMFBR FUEL CYCLE. (Oak Ridge National Lab., Tenn.).

In Chemical Technology Division annual progress report.

Technical and economic evaluations were made of conversions in the LMFBR fuel cycle. Conversion by homogeneous reduction is discussed. (M.C.G.)

**54718** (ORNL–4682, pp 168-81) SEPARATIONS CHEMISTRY RESEARCH. (Oak Ridge National Lab., Tenn.).

In Chemical Technology Division annual progress report.

Research progress is reported on: new separations agents, recovery of uranium from commercial phosphoric acid, high-resolution rare earth separations, displacement elution with amino-polyacetic acids, isotope enrichment by (n,γ) reactions in molecular sieves, distribution equilibria and mechanisms, relative potentials of the Bk(IV)–Bk(III) and Ce(IV)–Ce(III) couples, lanthanide and actinide hydroxides, and kinetics of metal ion extractions by organophosphorus acids. (M.C.G.)

**54719** (ORNL–4682, pp 229-39) CHEMICAL ENGINEERING RESEARCH. (Oak Ridge National Lab., Tenn.).

In Chemical Technology Division annual progress report.

Research progress is reported on: mass transfer of water from sol droplets, dehydration of individual sol droplets in a minicolumn, production of sol-gel microspheres of small uniform size, pulsed clone contactor, axial dispersion in packed columns for contacting liquids with a high density difference, multicomponent mass transfer in electrolyte systems, chemical engineering research studies related to MSR processing. (M.C.G.)

**54720** (UJV–2550-Ch) CALCULATION OF THE SORPTION KINETICS OF RADIOACTIVE MICROCOMPONENT ON A CATION EXCHANGER IN THE PRESENCE OF COMPETING IONS IN A BATCH ARRANGEMENT. Uher, E. (Ceskoslovenska Akademie Ved, Rez. Ustav Jaderneho Vyzkumu). Feb 1971. 58p. (In Czech). Dep. NTIS (U. S. Sales Only).

For a solution whose composition by definition is $C_{Sr} = 10^{-6}$, $C_{Fe} = 10^{-3}$, and $C_H = 0.1$ meq/cm$^3$, principles were derived governing the sorption kinetics of radioactive microcomponent ($Sr^{2+}$) in the medium of strong acid and in the presence of competing ion ($Fe^{3+}$) on a strong acid cation exchanger in the H-form from an infinite solution volume. It was found that if the internal (particle) diffusion was rate limiting, the kinetic law was the same as in the well known case of an univalent ion in the absence of other ions. For the external (film) diffusion or the rate of the exchange reaction proper as rate-governing mechanisms, a system of complicated differential equations was derived, whose numerical integration (by computer) indicated that the time dependence of Sr concentration in the solid phase ran through a maximum. The numerical solution was demonstrated by numerous graphs. Modification of the calculation for elements of other valencies was described. (auth)

**54721** DEPENDENCE OF THE ISOTOPE SEPARATION FACTOR OF THE HYDROGEN-EVOLUTION REACTION UPON POTENTIAL: MECHANISM EVIDENCE FOR TRANSITION-METAL SUBSTRATES. Haynes, R. (Univ. of Pennsylvania, Philadelphia). Electrochim. Acta; 16: No. 8, 1129-42(Aug 1971).

A linear variation of the separation factor of hydrogen isotopes with overpotential was observed only on the high overpotential metals, where the discharge step is rate-determining, and seems to depend on a change in shape of the potential-energy barrier of the rate-determining discharge step with potential, resulting in change of the degree of tunnelling for protium and tritium. The variation of the separation factor with overpotential on medium and low overpotential metals is associated with the change of the rate-determining step and/or mechanism. (auth) (UK)

**54722** DOUBLE-BED PROCESS FOR THE REMOVAL OF CATIONIC FISSION PRODUCTS FROM MILK. Glascock, R. F.; Bryant, D. T. W. (National Inst. for Research in Dairying, Shinfield, Eng.). J. Dairy Res.; 38: No. 2, 217-(1971).

A process for the removal of cationic fission products from milk is described in which no prior acidification is necessary. The milk is treated at 40°C by 2 beds of suitably charged cation exchange resins, one of which is of the carboxylic acid type and the other of the sulphonic acid type. On the first bed all the metallic cations of the milk are replaced by $K^+$ and $H^+$, and on the second the ionic composition is restored. During processing the pH is reduced from 6.8 to approximately 6.2 and is restored to 6.8 by the addition of alkali metal carbonates to the milk after treatment. On a pilot plant of capacity 1600 l (30 resin bed volumes) per 5-h day it was found that the radiochemical efficiency was approximately 80% for $^{85}Sr$ and 97% for $^{137}Cs$. The process caused some losses of vitamins, especially of thiamine, and an increase in the lead, copper, and iron contents all of which, however, were at an acceptable level. Other changes in chemical composition were negligible and enzymic clotting time remained unchanged. Flavour and appearance of the product were satisfactory and it was satisfactorily both roller- and spray-dried. The process is discussed with reference to an earlier method in which prior acidification is necessary. It is concluded that the double-bed process is somewhat more efficient for the removal of fission products and that a full-scale plant would be little or no more expensive to erect and only slightly more expensive to operate. (auth) (UK)

**54723** ISOLATION OF PROMETHIUM BY DISPLACEMENT CHROMATOGRAPHY DUE TO COMPLEX FORMATION. Chmutov, K. V.; Nazarov, P. P.; Masslova, G. B.; Sheptunov, V. N. (Inst. of Physical Chemistry, Moscow). J. Chromatogr.; 59: No. 2, 415-22(22 Jul 1971).

The separation of a mixture of rare earth elements by means of solutions of ethylenediaminetetraacetic, diethylenetriaminepentaacetic, and nitrilotriacetic acids was carried out. It was found that nitrilotriacetic acid has the minimum value for the height equivalent to a theoretical plate. The high separation power of nitrilotriacetic acid was accounted for by the greater velocity of the diffusion processes as compared to the other complexones. The influence of kinetic factors on the height equivalent to a theoretical plate value in the elution of cerium and neodymium by diethylenetriaminepentaacetic acid solution was investigated as an example. The limiting stage for elution from a resin containing no more than

12% divinylbenzene was found to be the outer diffusion inhibition. The method was used for the isolation of promethium-147 from fission products. (auth)

**54724** SEPARATION OF SELENIUM AND TELLURIUM BY MEANS OF BISMUTHIOL II. Bock, Rudolf; Spalek, Ursula (Johannes Gutenberg-Univ., Mainz). Z. Anal. Chem.; 254: No. 3, 183-5(1971). (In German).

Tellurium(IV) can be separated from selenium(IV) by extracting the Bismuthiol II complex with chloroform at pH 4.5 to 4.7 of the aqueous solution. The addition of the organic reagent must be made after adjusting the pH. (auth)

**54725** SEPARATION OF THE ALKALINE EARTH METAL IONS BY IONOPHORESIS ON FILTER PAPER AND POLY-(VINYL ALCOHOL). Maslowska, Joanna; Hermanowicz, Ryszard (Politechnika, Lodz, Poland). Chem. Anal. (Warsaw); 16: No. 3, 603-9(1971). (In Polish).

The separation of alkaline earth metal ions by ionophoresis on No. 1 Whatman paper and on layers of poly(vinyl alcohol) (PVA) as supports was investigated. A large number of supporting electrolyte solutions such as KCl, $NaNO_3$, $NaNO_2$, KNCS, $(NH_4)_2C_2O_4$, $HClO_4$, and KCl in aqueous alcohol was employed. A good separation was obtained on layers of (PVA) in 0.25M $NaNO_3$ after 60 min. at 5.56 V/cm. The shift of the separate ions amounted to: $Mg^{2+}$ – 2.03, $Ca^{2+}$ –2.81, $Sr^{2+}$ –2.46, and $Ba^{2+}$ –1.31 cm respectively. (auth)

**54726** PRELIMINARY CONSIDERATIONS ON THE CONDITIONING OF HIGH ACTIVITY LIQUID WASTES PRODUCED IN THE REPROCESSING OF IRRADIATED FUELS. Bocola, W.; Boenzi, D.; Cagnetti, P. (CNEN, Rome). Minerva Fisiconucl.; 13: 282-91(Oct-Dec 1969). (In Italian).

The possibility of encasing fission products from the reprocessing of irradiated fuel in glass cylinders was considered. The final product in the form of compact solids is made safe for storage with a high degree of security. Calculations were made to evaluate the maximum temperature reached in the interior of such cylinders as a function of the thermal power density associated with the decay of the fission products, assuming an external cooling of the cylinder by free convection in air. On the basis of the results of these calculations, the maximum concentration factor attainable in the reprocessing was evaluated for a mixture of fission products from power reactors presently in operation in Italy, compatible with a prefixed cooling period for the mixture itself. (tr-auth)

**54727** AUTOMATION OF CHROMATOGRAPHY OF RADIOACTIVE SUBSTANCES. Barnov, V. A.; Tsetskhladze, T. V.; Shrabshtein, S. A. (Inst. of Physics, Tbilisi, USSR). J. Chromatogr.; 58: No. 1, 5-10(10 Jun 1971).

From third Russian–Italian symposium on chromatography; Tbilisi, USSR (26 Oct 1970). See CONF-701051.

A technique for automation of the registration of data of a chromatographic separation of radioactive substances is described in which a device is used for delivery of information to a punched tape. The results of computer processing of the data are shown for an actual example, the study of the influence of nuclear radiation on isotopic exchange in the gaseous phase. (auth)

**54728** CATION-EXCHANGE SEPARATION OF URANIUM IN DIMETHYLSULPHOXIDE MEDIUM. Janauer, Gilbert E.; Korkisch, J.; Hubbard, S. A. (State Univ. of New York, Binghamton). Talanta; 18: No. 8, 767-72(Aug 1971).

Cation-exchange chromatography in a dimethyl sulphoxide (DMSO) medium is a suitable means for separating uranium from metal ions, including copper, iron, nickel and molybdenum. Quantitative separations of uranium from 26 elements can best be effected on a column of Dowex 50W-X8 (200–400 mesh), using as the eluent a 20% v/v DMSO solution which is 0.6M in hydrochloric acid and 0.25M in sodium acetate. Only calcium is eluted with the uranium and all other elements studied are eluted either before or after uranium. The elution characteristics of uranium and of other metal ions were investigated with respect to changes in eluent and resin compositions. Separations were much less effective at higher concentrations of sodium ion or DMSO. None of the organic solvents methanol, ethanol, methyl glycol, acetone, dioxan or acetic acid was found to produce favorable separation conditions. Results with Dowex 50 resins of lower or higher cross-linkage were inferior to those obtained with the X8 resin. (auth)

**54729** ESTIMATION OF THE SINGLE-STAGE ISOTOPE SEPARATION FACTOR IN THE ELECTROMIGRATION OF ISOTOPIC IONS THROUGH AN ION-EXCHANGE MEMBRANE. Tikhomirov, I. A.; Doronin, V. T.; Vergun, A. P.; Larionov, V. V. (Tomsk Polytechnic Inst., USSR). Russ. J. Phys. Chem. (Engl. Transl.); 45: No. 2, 248-9(Feb 1971).

Translated from Zh. Fiz. Khim.; 45: No. 2, 448-9(Feb 1971).

An equation was derived for the determination of the isotope separation factor in the electromigration of an isotopic ion through an ion-exchange membrane-solution system. (auth)

**54730** DETERMINATION OF THE RELATIVE DIFFERENCE BETWEEN THE MOBILITIES OF ISOTOPIC LITHIUM IONS IN AN ION-EXCHANGE RESIN–SOLUTION SYSTEM. Kurin, M. N.; Tikhomirov, I. A.; Prikhod'ko, V. A.; Vergun, A. P. (Tomsk Polytechnic Inst., USSR). Russ. J. Phys. Chem. (Engl. Transl.); 45: No. 2, 221-2(Feb 1971).

Translated from Zh. Fiz. Khim.; 45: No. 2, 400-1(Feb 1971).

Experimental data were obtained for the relative difference between the mobilities of isotopic lithium ions in an ion-exchange resin-solution system. The separation factor for lithium isotopes in the systems lithium sulfate–KU-2 resin and lithium acetate–KU-2 resin is higher than in the system lithium chloride–KU-2 resin. (auth)

**54731** SYNERGISTIC SOLVENT EXTRACTION OF RARE EARTHS BY MIXTURES OF THENOYLTRIFLUOROACETONE AND ACETYLACETONE. Woo, Ching; Wagner, William F.; Sands, Donald E. (Univ. of Kentucky, Lexington). J. Inorg. Nucl. Chem.; 33: No. 8, 2661-6(Aug 1971).

Synergistic extraction of the thenoyltrifluoroacetonates of neodymium, samarium, gadolinium, dysprosium, and erbium by acetylacetone was studied using mixtures of the two $\beta$-diketones. The synergistic shift of the extraction curves decreases the separability of the rare earth chelates. (auth)

**54732** SOLVENT EXTRACTION STUDY OF LANTHANUM AND EUROPIUM BY ACIDIC ESTERS OF AMINOPHOSPHONIC ACIDS. Jagodic, V.; Herak, M. J.; Sipalo, B.; Radosevic, J. (Rudjer Boskovic Inst., Zagreb). J. Inorg. Nucl. Chem.; 33: No. 8, 2651-9(Aug 1971).

The extraction of lanthanum and europium by monooctyl esters of $\alpha$-anilinobenzylphosphonic acid (MOABP) and of $\alpha$-(2-carboxyanilino)benzylphosphonic acid (MOCABP) was studied. Petroleum ether, carbon tetrachloride, or chloroform were used as solvents and their influence on the metal extraction is discussed. The metal–ligand ratios were determined and it was found that the extractions are unaffected by addition of sodium chloride. An inverse third-power relation is observed between D and the hydrogen ion concentration for varying HCl concentrations. However, for 1.0 M (HCl + NaCl) aqueous solutions this is sometimes less. This phenomenon is discussed in terms of the complexing of metals with chloride ions in the aqueous phase and the competition between sodium and hydrogen ions in the extractable complexes. (auth)

**54733** BEHAVIORS OF NEPTUNIUM IN AQUEOUS SOLUTIONS. I. STABILITY OF TETRAVALENT NEPTUNIUM ION. Chang, Chau-ting; Liaw, Chiu-fong (National Tsing Hua Univ., Hsinchu, Taiwan). J. Inorg. Nucl. Chem.; 33: No. 8, 2623-30 (Aug 1971).

The solvent extraction behavior of the system $N_p(IV)-HNO_3-$ EDTA–TTA–benzene was investigated. The distribution ratio of the predominant reaction may be written as: $D = \{[NpT_4]_o/[Np(IV)]_{aq}^{4+}[NpY]_{aq}\}$. The hydrogen ion activity of the aqueous phase was kept above 0.45 M and the TTA activity in the benzene phase was maintained below 0.09 M. Taking the present and earlier experiments into consideration thermodynamic data of the possible reactions were estimated. (auth)

**54734** SEPARATION OF THE TRACE ELEMENTS BY PRECIPITATION AND EXTRACTION. Upor, Endre (Mecsek Ore Mining Enterprise, Pecs, Hungary). Kem. Kozlem.; 34: 45-71 (1970). (In Hungarian).

The sorption phenomena of separation of trace elements by precipitation are reviewed, examining specifically the sorption of $UO_2^{2+}$ on metal hydroxides in carbonate media. It was found that in the presence of $Fe(OH)_3$, the sorption of uranium decreases to a certain level as the $CO_3^{2-}$ concentration is increased. Experiments with alkali metal and alkaline earths hydroxides revealed that above a certain pH value the corresponding hydroxide is precipitated with the diuranate. The desorbing effect of thorium in case of sorption of U(VI) and the sorption of $Th^{4+}$, $Zr^{4+}$, $Sc^{3+}$, and $RF^{3+}$ ions in carbonate medium were examined, determining the effect of pH and the $CO_3^{2-}$ concentration on the dissolution in the presence of $Fe(OH)_3$. Extraction by alkyl phosphate esters was reviewed on the basis of synergistic and antagonistic phenomena, considering the partition equilibria, chelation, and similar processes involving, Th, Zr, and rare earths. Arsenaso III and extraction-photometric methods, neutron activation, and derivatography were used to determine trace elements. (92 references) (TTT)

**54735** TRITIUM FRACTIONATION IN WATER-CARBIDE TO BENZENE REACTION. Hoehndorf, A.; Oro, F. (Bundesanstalt

XUM

fuer Bodenforschung, Hanover). Earth Planet. Sci. Lett.; 11: No. 4, 265-8(Jul 1971).

The fractionation of tritium in the synthesis of benzene from the water–calcium carbide reaction was measured using liquid scintillation counting techniques. An isotope effect of $-31.4 \pm 1.2\%$ was found in the synthesized benzene and this fractionation was reproducible in four different experiments within the counting statistics of $\pm 0.15\%$. It was also indicated in these experiments that the isotope fractionation of the fast reacting first fraction of the generated acetylene is equal to that of the slowly reacting fraction, i.e., the isotope fractionation of the $H_2O \rightarrow C_2H_2$ reaction is almost independent of the yield of this reaction. (auth)

**54736** KINETICS OF THE REACTION OF $UO_2$, $NpO_2$, AND $(U,Pu)O_2$ WITH FLUORINE AND ITS CHLORINE DERIVATIVES. Henrion, P. N.; Leurs, A. (SCK-CEN, Mol, Belg.). J. Nucl. Mater.; 41: No. 1, 1-22(Oct 1971).

Fluorination of oxide fuels has repeatedly been considered as a basis for the reprocessing of spent fuels. In order to test the feasibility of this suggestion, the kinetics of the reactions between $F_2$, $ClF_3$, or ClF with various simulated oxide fuel compositions was investigated by thermogravimetry. The influence on the kinetics of temperature, particle size, porosity, rate of heat removal, etc., was examined, and the work was complemented by chemical analysis, micrography, and x-ray diffraction. By means of the fluorine reaction, uranium and plutonium can be separated from nonvolatile fission products, though the separation of uranium and plutonium from each other is incomplete. (auth)

**54737** CALCULATION AND OPTIMIZATION OF THE DEMINERALIZATION OF WATER FOR REACTORS BY ION EXCHANGE. Komarova, I. V.; Nikashina, V. A.; Rubinshtein, R. N.; Senyavin, M. M. At. Energ. (USSR); 30: No. 4, 343-7 (Apr 1971). (In Russian).

Simple experimental data are not sufficient to determine the optimum conditions for demineralizing feed waters for reactor use because this multicomponent, nonequilibrium system requires complex calculations. Selections of the best resin depends on the desired purity of the water and the needed rate of production of pure water. The removal of cations and anions from waters containing chlorides and sulfates by ion exchange resins was studied by means of a mathematical model, using a computer program for optimizing the operations. Similar calculations were carried out for the purifications for other salt-containing starting solutions. It was found that by keeping the demineralization rate constant, if the salt constant of the initial solution is decreased, the flow rate and the thickness of the bed may be reduced. If the purity of the produced water is kept constant, the optimum rate is increased and the depth of the resin bed is decreased if the salt content of the starting solution is lowered. Optimum conditions for ion exchange resins are shifted toward the higher flow rates and reduced lengths of the column. (TTT)

**54738** SEPARATION OF URANIUM FROM SEAWATER BY ADSORBING COLLOID FLOTATION. Kim, Young S.; Zeitlin, Harry (Univ. of Hawaii, Honolulu). Anal. Chem.; 43: No. 11, 1390-3(Sep 1971).

A procedure is described for the separation from seawater of uranium present as the stable tricarbonatouranyl anion by an adsorbing colloid flotation technique which utilizes a collector-surfactant-air system. At pH $6.7 \pm 0.1$ the uranium is adsorbed effectively on the positively charged ferric hydroxide collector. On addition of the anionic surfactant, sodium dodecyl sulfate, and the bubbling of air through the seawater, the colloidal particulates of ferric hydroxide enriched with uranium by absorption are floated within 2 to 3 minutes to the surface as a stable froth which is easily removed. Uranium was analyzed spectrophotometrically using Rhodamine B. Average recovery of uranium from seawater by this method is 82%. (auth)

**54739** RECOVERY OF $^{147}Pm$ FROM SAVANNAH RIVER PLANT WASTE. Isotop. Radiat. Technol.; 9: No. 1, 1-8(Fall 1971).

Batch solvent extraction procedures were developed for recovering $^{147}Pm$, as a mixture of fission-product lanthanides, from the aqueous wastes obtained in processing irradiated nuclear fuels. Extraction of the lanthanides and plutonium with 50% tributyl phosphate (TBP) from concentrated $Al(NO_3)_3$ and/or $NaNO_3$ solution is followed by back extraction into dilute nitric acid. By-product plutonium isotopes are separated from the trivalent lanthanides by extraction, as Pu(IV), into TBP from strong nitric acid. Cerium-144 is separated from the mixture by equilibration of $^{144}Ce$(III) with stable Ce(IV) and extracting $^{144}Ce$(IV) formed with 50% TBP. Approximately 3 kg of $^{147}Pm$ was recovered in two plant tests. (auth)

**54740** RADIOCHEMICAL STUDIES ON THE SOLVENT EXTRACTION OF SEVERAL ELEMENTS IN $Mn(NO_3)_2.6\,H_2O$– AND $CaCl_2.6\,H_2O$–TRI-n-BUTYL PHOSPHATE SYSTEMS. Akatsu, Eiko; Asano, Masaharu (Japan Atomic Energy Research Inst., Tokai). Anal. Chim. Acta; 55: No. 2, 333-40(Jul 1971).

A solvent extraction study was carried out at 30°C with organic phases of tri-n-butylphosphate (TBP) in dodecane and inorganic phases of molten manganese nitrate hexahydrate (m.p. 25.8°). Distribution ratios of several rare earth and actinide elements and fission products were determined with TBP solutions of various concentration. The values obtained were higher than those in the TBP–nitric acid system. Calcium chloride hexahydrate (m.p. 299°) was also used in a similar way. (auth)

**54741** FINISHING OF CRUDE PYROCHLORE CONCENTRATES. Tarasova, T. B. Tsvetn. Metal.; No. 7, 81-3(Jul 1971). (In Russian).

A schedule of physical and chemical operations is proposed for the beneficiation of a niobium concentrate. These include electric, magnetic separation, classification, magnetizing-calcining, and lixiviation processes, which assure a conditioned concentrate for the recovery of $Nb_2O_3$, 89.5%. (tr-auth)

**54742** COUNTERCURRENT ELECTROPHORESIS. Wagener, K.; Freyer, H. D.; Bilal, B. A. (Nuclear Research Center, Juelich, Ger.). Separ. Sci.; 6: No. 4, 483-503(Aug 1971).

Historical development, principal operation, different ways of experimental realization, and typical examples of application of countercurrent electrophoresis are reviewed. The separation process is principally capable of being applied to all types of ions, as far as any difference is shown in their ionic behavior. Different types of columns can be adapted to varying amounts of substance from approximately $10^{-6}$ mole up to several moles (in the laboratory scale). The production of high-purity components and the use of the column as an absolute ion filter are further possible applications. Some examples included are: isotope separation ($^{39}K$–$^{41}K$), ($^{6}Li$–$^{7}Li$), ($^{85}Rb$–$^{87}Rb$), and ($^{12}C$–$^{14}C$); extraction of $^{7}Be$ from rainwater; preparation of strontium and rare earths; and radiochemical nuclide generators. (auth)

**54743** RAPID ADSORBING COLLOID FLOTATION METHOD FOR THE SEPARATION OF MOLYBDENUM FROM SEAWATER. Kim, Young S.; Zeitlin, Harry (Univ. of Hawaii, Honolulu). Separ. Sci.; 6: No. 4, 505-13(Aug 1971).

A procedure is described whereby the molybdenum in a 500-ml seawater sample is brought to the surface in 5 min by an adsorbing colloid flotation process which utilizes iron(III) hydroxide, sodium dodecyl sulfate, and air. Statistical studies on a test series for recovery of molybdenum by means of spectrophotometric analysis show a mean recovery of 95.3% and a relative standard deviation of 2.6%. (auth)

**54744** QUANTITATIVE SEPARATION OF MAGNESIUM AND PALLADIUM FROM NUMEROUS METAL IONS ON TITANIUM TUNGSTATE PAPERS BY ELECTROCHROMATOGRAPHY. Qureshi, Mohsin; Varshney, K. G.; Khan, Fahmida (Aligarh Muslim Univ., India). Separ. Sci.; 6: No. 4, 559-72(Aug 1971).

Electrochromatography of 46 metal ions was performed in fifteen electrolytes on papers impregnated with titanium tungstate by applying different electric potentials and allowing different time intervals for migration. On the basis of the differential mobility of the cations, which depend on the nature of the complexes formed with the background electrolytes and the ion exchange properties of titanium tungstate, a large number of binary and ternary separations were achieved. The separations of one metal ion from numerous metal ions were also accomplished. For example, the following difficult and important separations were made: $Cu^{2+}$–$Cd^{2+}$–$Bi^{3+}$, $Ag^{+}$–$Cu^{2+}$–$Au^{3+}$, $Pd^{2+}$–$Pt^{4+}$–$Ir^{4+}$, $Hg^{2+}$–$Cd^{2+}$–$Zn^{2+}$, $Ag^{+}$–$Pt^{4+}$, $Au^{3+}$–$Pt^{4+}$, $Cd^{2+}$–$Bi^{3+}$, $Bi^{3+}$–$Pb^{2+}$, $Bi^{3+}$–$Hg^{2+}$, $Pd^{2+}$–$Ru^{3+}$, $Ga^{3+}$–$In^{3+}$, $La^{3+}$–$Ce^{4+}$, $Hg_2^{2+}$–$Hg^{2+}$, $Mg^{2+}$–$Al^{3+}$, $Mg^{2+}$–$Sr^{2+}$, $Ga^{3+}$–$Fl^{+}$, $Ir^{4+}$–$Ru^{3+}$, $Bi^{3+}$–$UO_2^{2+}$, $Ru^{3+}$–$Pt^{4+}$, $Hg^{2+}$ from 45 cations, $Au^{3+}$ from 41 cations, $Pd^{2+}$ from 43 cations and $Mo^{6+}$ from 27 cations. Magnesium and palladium were quantitatively separated in 100 to 200 $\mu$g quantities from binary mixtures as well as from synthetic mixtures containing commonly interfering metals. (auth)

**54745** LIQUID–LIQUID CHROMATOGRAPHIC SEPARATION OF NEODYMIUM, SAMARIUM, AND GADOLINIUM. Winget, J. O.; Lindstrom, R. E. (Bureau of Mines, Reno, Nev.). Separ. Sci.; 6: No. 4, 573-81(Aug 1971).

Neodymium, samarium, and gadolinium were separated by a liquid–liquid chromatographic technique. Sulfuric acid was more effective than hydrochloric or nitric acid as an eluent with di(2-ethylhexyl) phosphoric acid (EHPA) as the stationary phase. Recovery of 45% of the neodymium as >90% $Nd_2O_3$, 84% of the samar-

ium as >99% $Sm_2O_3$, and 50% of the gadolinium as >99% $Gd_2O_3$ was achieved. The degree of separation and the time required for the separation can be varied by changing the concentration of the eluent and the number of stages in the system. A system comprising a primary amine organic extractant and an aqueous eluent containing diethylenetriaminepentaacetic acid (DTPA) was less effective for separating the rare earths. (auth)

**54746** REVERSE PHASE PARTITION CHROMATOGRAPHY ON PAPER IMPREGNATED WITH 2-THENOYLTRIFLUOROACETONE. De, Anil K.; Bhattacharyya, Chitta R. (Dept. of Chemistry, Santiniketan, India). Separ. Sci.; 6: No. 4, 621-5 (Aug 1971).

Interesting separations of metal ions were observed by using the technique of reverse phase partition chromatography on 2-thenoyltrifluoroacetone-impregnated paper. Ketone–hydrochloric acid mixtures in different proportions were used as the developing solvent for the separations of different metal ion mixtures. The $R_F$ values of metal ions separated are given and the superiority of separation over that of ordinary filter paper is discussed. (auth)

**54747** CHEMICAL DECANNING OF FUEL ELEMENTS BY MEANS OF $HF/O_2$ MIXTURES. Dumont, G.; Goossens, W. (SCK/CEN, Mol, Belg.). Chem.-Ing.-Tech.; 43: No. 14, 800-3(Jul 1971). (In German).

The stainless steel casing of spent fuel elements must be removed prior to reprocessing. For this purpose a mixture of hydrogen fluoride and oxygen was used, a fluid bed of aluminum being employed in some experiments in order to achieve a better temperature control. At HF contents above 80 vol % only the casing is removed; at lower HF concentrations the $UO_2$ pellets are also pulverized. Since the rate of permeation decreases with increasing temperature, after a certain time the temperature assumes a constant value which depends on the experimental conditions, the geometrical dimensions of the bundle exerting a particularly large influence. (auth)

**54748** OPTIMIZATION OF A HEAVY-WATER ENRICHMENT PLANT BASED ON $H_2/NH_3$ EXCHANGE AND OPERATING BY THE HOT/COLD PRINCIPLE. Lang, Gerhard (Friedrich Uhde GmbH, Dortmund, Ger.); Schindewolf, Ulrich. Chem.-Ing.-Tech.; 43: No. 14, 804-10(Jul 1971). (In German).

The operating conditions for a hot-cold plant for enrichment of heavy water employing ammonia–hydrogen as the exchange pair were optimized with regard to minimum production costs; attention was paid not only to the known separation factors and the experimentally determined exchange performance and gas loading of the plates but also to cost factors for plant components and energy based on estimates provided by the relevant industries. The optimization embraces one- to three-stage enrichment systems, a three-stage enrichment series with a stripping unit, and a three-stage enrichment-stripping system with a transfer column using hydrogen as deuterium source, as well as a three-stage enrichment-stripping series with a regenerating column that uses water as starting material. It is shown that the production prices achievable in relatively small, carefully optimized plants are considerably lower than the current price of heavy water. (auth)

**54749** PROCESS FOR REMOVING CERIUM AND THORIUM FROM THE OTHER RARE EARTH METALS. Chiola, Vincent; Kamin, George J. (to Sylvania Electric Products Inc.). U. S. Patent 3,594,117. 20 Jul 1971. Filed 30 Oct 1968.

A process for separating impurities selected from the group consisting of cerium, thorium, and mixtures thereof from an impure material useful for cathodoluminescent phosphor production is disclosed, the process comprising a dissolution of the impure material in a mineral acid, oxidizing the impurities, forming the insoluble iodates of the impurities and removing the impurities as solid iodates from the solution containing the purified luminescent materials. (auth)

**54750** SEPARATION OF YTTRIUM AND CERIUM. Dodds, Phyllis R. (to Sylvania Electric Products Inc.). U. S. Patent 3,594,118. 20 Jul 1971. Filed 20 Oct 1968.

A process for recovering a purified material containing yttrium values from an impure material containing yttrium and cerium is disclosed. The process comprises dissolving the impure material in an aqueous solution of a mineral acid having a critical concentration of acid, contacting the resulting solution with an organic solution containing a critical concentration of di-2-ethylhexylphosphoric acid for sufficient time to extract yttrium into the organic solution, separating the organic and the aqueous solutions, contacting the organic solution with an aqueous nitric acid solution having a concentration of nitric acid of at least 3.5 moles/liter for a time sufficient to remove the yttrium into the aqueous solution, and recovering the purified yttrium values that contain less than 50 ppM of cerium. (auth)

**54751** REGULARITIES OF EXTRACTION OF URANYL THENOYLTRIFLUOROACETONATE INTO A NUMBER OF SOLVENTS. Akiba, K.; Suzuki, N.; Asano, H.; Kanno, T. (Tohoku Univ., Sendai). J. Radioanal. Chem.; 7: No. 2, 203-11(Mar 1971).

Extraction equilibria were investigated of the thenoyltrifluoroacetone (TTA) chelate of uranyl ion between aqueous perchlorate medium and thirteen organic solvents. The extracted species was shown to be $UO_2A_2$. The solubility parameter of the chelate was estimated from the partition data and it was confirmed that the relationship $\lg P_M = n \lg P_{HA} +$ const. holds for the present system. When the extraction constant ($K_{ex}$) is considered in relation to the distribution coefficients, the $K_{ex}$ values are expected to be constant under certain conditions for all of the solvents; the $\lg K_{ex}$ values were found to be constant ($\lg K_{ex} = -2.85 \pm 0.17$). (auth)

**54752** STUDIES ON THE UTILIZATION OF PEGMATITIC ORES. Baba, Riichi; Imagawa, Koji (Resources Research Inst., Kawaguchi, Japan). Shigen Gijutsu Shikenjo Hokoku; No. 75, 133(Sep 1969). (In Japanese).

Experiments on the leaching and recovery of valuable elements from domestic low-grade pegmatitic ore, some properties of the recovered niobium and tantalum oxides, and the production of Nb metal are discussed. Recovery of $(Nb, Ta)_2O_5$ was about 95% with hydrofluoric acid above 20N, while rare earth elements were precipitated as fluoride. The recoveries of rare earth elements and U with sulfuric acid solution (50%) were about 87% and 80%, respectively. Generally, hydrofluoric acid dissolution of the pegmatitic ore, liquid–liquid extraction for high-grade pregnant liquor, and ion exchange for low-grade liquor or slurry are suitable for the leaching of Nb and Ta. (Japan)

**54753** LIQUID WASTE EFFLUENTS FROM A NUCLEAR FUEL REPROCESSING PLANT. Magno, P.; Reavey, T.; Apidianakis, J. (Dept. of Health, Education, and Welfare, Winchester, Mass.). pp 208-20 of Health Physics Aspects of Nuclear Facility Siting. Vol. I. /Voilleque, Paul G. (comp.). Idaho Falls, Idaho; Burton R. Baldwin, Publications Chairman (1971).

From fifth annual midyear topical symposium on health physics aspects of nuclear facility siting; Idaho Falls, Idaho (3 Nov 1970).

The liquid waste effluents from Nuclear Fuel Services were studied in detail during a six-month period May through October 1969. The concentrations and amounts of individual radionuclides discharged from the plant were measured and the amounts of sedimentation of individual radionuclides in the lagoon system estimated. Tritium, $^{106}Ru$, $^{90}Sr$, $^{137}Cs$, and $^{134}Cs$ were the principal radionuclides discharged to the environment during this period. No relationship could be established between the amount and burnup of fuel processed and the amount of activity discharged from the plant to the lagoon system during this study. For the Yankee fuel campaign of May to August 1969, the waste management practice and not the amount of fuel processed was the controlling factor in the amount of activity discharged from the plant to the lagoon system. During June and November 1969 simultaneous sampling was carried out at the point of discharge of the waste and several locations on the Buttermilk and Cattaraugus Creeks. Tritium, $^{106}Ru$, and $^{90}Sr$ were the radionuclides present in the highest concentrations in these streams during these periods. Stream dilution and absorption factors were calculated for individual radionuclides at various locations along the stream system. A comparison of the concentrations of the radionuclides in Cattaraugus Creek with 10CFR20 discharge concentration limits showed that $^{90}Sr$ was about 20% of the concentration limit during both sampling periods. All other radionuclides were less than 10% of the concentration limits during these periods. (auth)

**54754** RADIOACTIVITY RELEASED FROM A LIQUID METAL FAST BREEDER REACTOR FUEL RECYCLE COMPLEX. Cook, E. M.; Stoddart, P. G. (Argonne National Lab., Idaho Falls, Idaho). pp 221-5 of Health Physics Aspects of Nuclear Facility Siting. Vol. I. /Voilleque, Paul G. (comp.). Idaho Falls, Idaho; Burton R. Baldwin, Publications Chairman (1971).

From fifth annual midyear topical symposium on health physics aspects of nuclear facility siting; Idaho Falls, Idaho (3 Nov 1970).

Argonne National Laboratory's Fuel Cycle Facility and associated analytical chemistry facilities for Experimental Breeder Reactor II produced mainly solid radioactive wastes during the operation of a closed fuel cycle in 1966 to 1969, owing to the nature of the pyrochemical fuel-refining process used. The quantities and isotopic identification of the routinely released radioactive wastes

XUM

are reported. The solid wastes consisted primarily of fission products deposited in the melt-refining fume traps and activated stainless-steel scrap from the fuel subassemblies. This high-level waste, amounting to several million curies per year, is stored in the EBR-II High Level Waste Storage Facility with retrieval capability. Liquid wastes, predominantly from the analytical chemistry facilities, amounted to less than 1.5 Ci/yr. Gaseous wastes released to the atmosphere consisted mainly of Kr. (auth)

XUM

# EARTH SCIENCES

## Geology and Hydrology

*Refer also to abstracts 54495, 54513, 54531, 54753, 54754, 54784, 54937, 55066, and 55150.*

**54755** (CONF-710401–, pp 320-7) MEASUREMENT OF PLUTONIUM IN SOIL AROUND THE NEVADA TEST SITE. Bliss, Wayne; Dunn, Leslie (Southwestern Radiological Health Lab., Las Vegas, Nev.). 15 Apr 1971.

From Rocky Flats symposium on safety in plutonium handling facilities; Golden, Colo. (13 Apr 1971).

Experiments conducted at the Atomic Energy Commission's Nevada Test Site between 1951 and 1963, using plutonium in both critical and sub-critical configurations, have resulted in distribution of plutonium beyond the boundaries of the Test Site. The Southwestern Radiological Health Laboratory of the Environmental Protection Agency is conducting a survey to assess the distribution and concentration of plutonium in the off-site environment. Special sampling methods were devised since desert soil is too coarse and dry for auger and cookie cutter sampling techniques. Soil sample analyses are performed by a dissolution, ion exchange, electrodeposition procedure followed by alpha spectroscopy. Plutonium has been detected in four locations around the Nevada Test Site. These locations correspond to fallout areas previously identified for the various test series. Plutonium concentrations in the top 3 cm of soil were 10 to 100 times greater than the concentration in soils from areas not subject to contamination by these series. (auth)

**54756** (CONF-710401–, pp 411-29) SOLUBILITY OF PLUTONIUM IN SOIL/WATER ENVIRONMENTS. A Theoretical Study. Polzer, W. L. (Idaho Operations Office (AEC), Idaho Falls. Health Services Lab.). 16 Apr 1971.

From Rocky Flats symposium on safety in plutonium handling facilities; Golden, Colo. (13 Apr 1971).

The phase relations of the various plutonium species, both solid and aqueous, are evaluated as a function of hydrogen ion concentration (pH) and oxidation-reduction potential (Eh) for conditions normally found in soil/water environments. The evaluation is based on theoretical considerations and laboratory data obtained from the literature. Concentrations of dissolved plutonium are calculated from the evaluated phase relations. The significance of plutonium complexes on the concentration of dissolved plutonium is discussed and the effect of plutonium carbonate on dissolved plutonium evaluated. (auth)

**54757** (MIT–1381-18) VARIATIONS IN ISOTOPIC ABUNDANCES OF STRONTIUM, CALCIUM, AND ARGON AND RELATED TOPICS. Eighteenth Annual Progress Report for 1970. (Massachusetts Inst. of Tech., Cambridge. Dept. of Earth and Planetary Sciences). 1 Dec 1970. Contract AT(30-1)-1381. 159p. Dep. NTIS.

Geochronological studies based on measurements of the isotopic abundances in rocks from worldwide locations such as Korea, Venezuela, Vermont, Guyana, Liberia, Sierra Leone, Maine, eastern USA, and east Africa, are presented. Three doctoral theses investigations on the roles of lherzolite and garnet pyroxenite in the constitution of the upper mantle, the ages and trace element compositions of the Canadian Precambrian iron formations, and age and paleomagnetic investigation on precambrian diabase dikes are included. Techniques and standards for measuring isotopic abundances, particularly x-ray fluorescence and mass spectrometric analyses of Rb and Sr in silicate standards, are described. Abstracts of papers presented at meetings and additions to the project bibliography are included. (L.C.L.)

**54758** (ORNL–4717, pp 109-15) SALT MINE REPOSITORY. (Oak Ridge National Lab., Tenn.).

In Reactor Chemistry Division annual progress for period May 31, 1971.

Research progress is reported on gas flow characterization of unconsolidated beds; volatility enhancement of fission product oxides in the presence of water vapor; surface diffusion of oxides on sodium chloride; solid state diffusion of plutonium in sodium chloride; radiolysis and hydrolysis of salt mine brines. (D.H.M.)

**54759** POSSIBILITY OF GAMMA SPECTROSCOPY IN WELL LOGGING IN THE PRESENCE OF RADON. Serdyukova, A. S.; Doshchechkin, V. P. (Moscow Geological Prospecting Inst.). Izv. Vyssh. Ucheb. Zaved., Geol. Razved.; 12: No. 12, 134-7 (1969). (In Russian).

Experiments were performed to investigate the feasibility of using gamma spectrometry for the bore-hole surveying of wells when Rn is present. It was concluded that gamma spectrometry can be used for bore-hole surveying to determine the U content in ores, even in the presence of Rn, if the range of energies is from 180 to 230 keV or from 580 to 630 keV. (L.C.L.)

**54760** STUDY OF AGE DETERMINATION METHOD ON SOME MINERALS AND GLASSES BY FISSION-TRACK REGISTRATION. Nishimura, Susumu (Kyoto Univ.). Ganseki Kobutsu Kosho Gakkaishi; 64: No. 6, 173-81(Dec 1970). (In Japanese).

Recent developments in the fission track method have provided geologists and archaeologists with a promising new tool with which various igneous rocks or many baked relics can be dated. However, in actual analysis of fission tracks, several questions still remain. Therefore, the effects of various geophysical variables on track formation and stability were studied. It was found that the replica method can be used for identification of the fission tracks. Impurities in etching solution sometimes speed up the etching process, so that it is necessary to use fresh etching solutions. Fading of range distribution due to surrounding temperature to which samples have been exposed for ages, can be corrected if it is small. It was found that mica is unstable in the determination of fission track age if it has been under partial pressure. Correction to effect of natural radiation is also mentioned. (auth) (Japan)

**54761** FISSION TRACK DATING OF ANCIENT GLASSES. Shima, Makoto (Inst. of Physical and Chemical Research, Yamato, Japan). Seramikkusu; 5: No. 12, 1041-6(Dec 1970). (In Japanese).

Fission tracks are left as radiation damage in the interior of solids when heavy charged particles with high energy collide with or pass through them. The mechanism of their formation has not yet been established. However, various applications of this phenomenon have been suggested because it is believed that age determination is possible throughout the geologic ages with simple experimental operations and apparatus and also with low-cost research. Significant interpretation can be given to ancient glasses if measuring errors from 20 to 30% of the method and thermal history of samples are taken into account. Several attempts in this direction are reviewed. Examples of actual measurement and necessary caution to be given in this method are given. (auth) (Japan)

**54762** SENSITIVE METHOD FOR THE SELECTIVE MEASURING OF ARTIFICIAL $\alpha$-EMITTERS IN THE PRESENCE OF NATURAL $\alpha$ ACTIVITY. Lembo, G. (CNEN, Rome). Minerva Fisiconucl.; 13: 225-35(Jul-Sep 1969). (In Italian). CONF-680535-25).

From fourteenth national conference of the Italian Association for Health Physics and Protection from Radiation; Formia, Italy (29 May 1968).

A method, based on the discrimination of artificial $\alpha$ emitters from natural emitters because of the difference in energy of the emission, is proposed for the measurement of artificial emitters in the presence of natural $\alpha$ emitters. The results obtained with this method show that 1 hr sampling is sufficient to detect 1 MPC of $^{239}Pu$ and 0.5 MPC of natural U and $^{235}U$. (J.S.R.)

**54763** OCHERKI PO GEOLOGII I GEOKHIMII RUDNYKH MESTOROZHDENII. (Essays on the Geology and Geochemistry of Ore Deposits). Shcherbakov, D. I. (ed.). Moscow; Izdatel'stvo Nauka (1970). 316p.

The formation and mechanisms of distribution of endogenic deposits of a number of non-ferrous and rare metals are considered in this collection of twenty-three articles by different authors. Problems of mineralization with magmas, and the depth of formation of hydrothermal mineralization are discussed, with particular reference to different epochs of ore formation. The geology of uranium deposits constitutes an important portion of the book, accompanied by an account of the radioactive ores of the Tyuya Muyun Ridge and Aravan River Valley, their mineralogy and genesis. The structural and thermal conditions of localization of hydrothermal uranium deposits in carbonate rocks are discussed. A number of essays treat ore deposits of Sb, Hg, Sn, Mo, Se, F, and Th, with some new data on the geochronology of intrusion formations in middle Asia. (K.S.W.)

**54764** THERMOLUMINESCENT DATING PRINCIPLES AND APPLICATION. Fleming, S. J. (Research Lab. for Archaeology and History of Art, Oxford). Naturwissenschaften; 58: No. 7, 333-8(Jul 1971).

XUM

The physical process of thermoluminescence is outlined with particular reference to the behavior of the common crystalline minerals found in pottery, like quartz and feldspars. Though the internal radiation dosimetry of pottery is complex two experimental techniques have been developed which allow accurate pottery dating and are believed to surmount the worst of the problems discussed. Application of thermoluminescent dating covers results for Central European Neolithic pottery and for authenticity studies of art ceramics. (auth)

**54765** DETERMINATION OF GEOLOGICAL TIME WITH A NUCLEAR REACTOR AND A MASS SPECTROMETER. York, D.; Yanase, Y.; Berger, G. W. (Univ. of Toronto). pp 419-22 of Activation Analysis in Geochemistry and Cosmochemistry. /Brunfelt, Arild O. (ed.). Oslo; Universitetsforlaget (1971).

From Conference on activation analysis in geochemistry and cosmochemistry; Kjeller, Norway (7 Sep 1970). See CONF-700968.

In 1965 Merrihue proposed that a number of improvements could be wrought in conventional K–Ar dating with the aid of neutron irradiation. The $^{39}K(n,p)^{39}Ar$ reaction converts the potassium analysis into an argon determination to be done mass spectrometrically. Using total fusions of irradiated minerals, the manufacture of $^{38}Ar$ spikes and the need of conventional potassium analysis are eliminated. More importantly, when used in incremental heating experiments, the approach has considerable potential for elucidating the thermal history of rocks. The applicability of the method is tested with muscovite, nepheline and basalt. (auth) (Norway)

**54766** NEW MEASUREMENT OF THE RADON CONTENT OF THE WATERS AT BAD BRAMBACH. Herrmann, D. B. Arch. Phys. Ther. (Leipzig); 20: No. 1, 29-32(Jan-Feb 1968). (In German).

The radon content of the springs at Bad Brambach was determined with a double ionization chamber. The measuring equipment and method are described. One of the springs was measured first in 1911 and showed a surprisingly high radon content of $8.26 \times 10^{-7}$ Ci/l. In the interim, the springs were measured several times. The present measurements on each of four springs yielded values from $1.69 \times 10^{-7}$ to $7.04 \times 10^{-7}$ Ci/l. It was concluded that the radon content of the spring water did not change significantly throughout several decades. (H.B.G.)

**54767** PROCEEDINGS OF THE SIXTH INTERNATIONAL SYMPOSIUM ON REMOTE SENSING OF ENVIRONMENT. VOLUME I. Conference Held at Ann Arbor, Michigan, October 13–16, 1969. Ann Arbor, Mich.; University of Michigan (1969). 697p. (CONF-691065-(Vol.1)).

Thirty-seven of the papers presented at the conference are included in Volume 1. A separate abstract was prepared for one paper on airborne spectral gamma radiation measurements. The remaining papers were not in scope for NSA. (R.C.K.)

*For an abstract of an individual paper see: 54768.*

**54768** COMPARISON OF AIRBORNE SPECTRAL GAMMA RADIATION DATA WITH FIELD VERIFICATION MEASUREMENTS. Purvis, A. E.; Buckmeier, F. J. (Texas Instruments Inc., Dallas). pp 553-64 of Proceedings of the Sixth International Symposium on Remote Sensing of Environment. Vol. 1. Ann Arbor, Mich.; Univ. of Michigan (1969).

From sixth international symposium on remote sensing of environment; Ann Arbor, Mich. (13 Oct 1969). See CONF-691065-(Vol.1).

In recent experiments, potassium-40 counting rate data from airborne measurements showed good correlation with the available field gamma radiation data and soil type information. From field measurements, sandy surface material exhibited a potassium-40 counting rate of 21,700 ± 3,600 counts/10 minutes while clay surface materials exhibited counting rates of 33,800 ± 3,500 counts/10 minutes. The investigation included measurements to determine the effect of aircraft altitude on the observed gamma radiation flux. Also studied was the interrelationships between the flux observed by a detector suspended from a tripod 8 feet above the surface and the concentrations of thorium, uranium and potassium obtained from laboratory analyses of soil samples. (auth)

**54769** METHOD AND APPARATUS FOR MEASURING NEUTRON CHARACTERISTICS OF A MATERIAL SURROUNDING A WELL BORE. Nelligan, William B. (to Schlumberger Technology Corp.). U. S. Patent 3,566,116. 23 Feb 1971. Filed 8 Nov 1966.

In the invention described, the formation surrounding a well bore is irradiated with a burst of neutrons and the neutron concentration is observed during selected time intervals after irradiation to determine the thermal neutron decay time characterizing the formation. In one method, the neutron concentration is observed during a first interval one decay time long and during a second and subsequent interval two decay times long which starts immediately after the first interval. In another method the two intervals are spaced by one decay time. (Official Gazette)

**54770** IZOTOPY SVINTSA V GEOKHIMII I KOSMOKHIMII. (Lead Isotopes in Geochemistry and Cosmochemistry). Sobotovich, E. V. Moscow; Atomizdat (1970). 352p.

Studies of the distribution of lead isotopes in the earth's surface and in cosmic substances with consideration being given to certain geochemical and cosmochemical laws that are derived from the isotope data are described. The latest methods for the analysis of materials with minimum concentrations of lead are discussed. Attention is given to the lead-isochronic method for dating rocks, ores, and meteorites. The existing hypotheses for the origin of meteorites and tektites are considered; in particular the solar origin of iron meteorites is substantiated. Prospects for studies of unsolved problems in cosmic chemistry and planetary geochemistry are discussed. (tr-auth)

**54771** FISSION TRACK AND ALPHA-PARTICLE RECOIL TRACK DATING. Shima, Makoto. Dai-4-Ki Kenkyu; 6: 134-40(1967). (In Japanese).

The application and principles of fission track and alpha-particle recoil techniques to dating of Quaternary materials are reviewed. Results are cited from fission track dating of volcanic glass and man-made glasses. Ages of volcanic glass from a deep-sea core are compared with paleomagnetic results. (Geophys. Abstr.)

**54772** GAMMA-LOGGING METHOD IN COAL FIELD. Katayose, K. (Ube Industries, Ltd., Yamaguchi, Japan). Butsuri Tanko; 22: 237-41(Sep 1969). (In Japanese).

The results of gamma-ray logging in coal fields in Japan are summarized. The instrumentation, accuracy of measurement, effects of temperature, method for utilization in coal prospecting, and some defects of the method are discussed. The main parts of the measuring device are a GM tube and a scintillation counter which can be used alternately as needed, and which are connected to several accessory instruments. The scintillation counter is preferable for securing the higher counting rate that is required for higher accuracy measurement. For avoiding high temperature effects in some deep bore holes, the scintillation counter is provided with a protective tube. The GM tube is of a heat-resisting type. An example of the gamma logging chart of representative coal-bearing beds is presented. The minimum thickness of a coal seam that is detectable by this method is estimated as 20 cm. (Japan)

**54773** FISSION TRACK DATING AND URANIUM CONTENTS OF OBSIDIAN. 2. Suzuki, Masao (Tokyo Univ.). Dai-4-Ki Kenkyu; 9: No. 1, 1-6(May 1970). (In Japanese).

Obsidian specimens from seven geologic localities in the Central Honshu and Izu Islands of Japan were submitted for dating. While the non-flake quality obsidian contains many bubbles, second phase particles, and string-like microlites that make the counting of spontaneous fission tracks difficult, it is easy to determine the time of eruption of the compact flake quality obsidian. Wada-pass, Kirigamine, Hakone (Hatajuku, Ashinoyu), and Horaiji yield the flake quality obsidian. The time of eruption and the uranium content of obsidian specimens from these localities were measured. The results show that the fission track dates and uranium contents differ from each other. Accordingly, when obsidian materials from archaeological sites are measured for the time of eruption and the uranium content, it is likely that the geologic sources of these materials may be identified by comparing the results with those for previously measured geologic sources. (auth)(Japan)

**54774** CONTRIBUTION TO THE STUDY OF NATURAL RADIONUCLIDES IN WASTE AND SURFACE WATERS. Mansfeld, A.; Ruzicka, J.; Hanslik, E. (Vyzkumny Ustav Vodohospodarsky, Prague. Ustredi Statni Vodohospodarske Inspekce, Prague). Radioisotopy; 11: No. 5, 715-23(1970). (In Czech).

The $^{210}Pb$, $^{210}Po$, $^{226}Ra$, $^{222}Rn$, Th, and U content in river waters in Czechoslovakia was measured as part of a water management research program. The results are presented. (tr-auth)

**54775** ROLE OF RADIOHYDROCHEMICAL INDEXES IN THE STUDY OF REGIONAL TECTONIC ACTIVITY. Tyminskii, V. G. (All-Union Scientific Research Inst. of Nuclear Geophysics and Geochemistry, Moscow). Geokhimiya; No. 1, 107-10(Jan 1971). (In Russian).

XUM

It was recently discovered that an earthquake may change the U isotope ratios and the concentration of radiogenic gases, He and Rn, in ground water. For example, data from a Tashkent earthquake showed that an increase in Rn content in mineral water preceded the earthquake and that the He content and U isotope ratios in ground water were changed after the earthquake. (tr-auth)

**54776** EVALUATION OF APPARENT IONIUM AGES OF SOME HERMATYPIC CORALS. Omura, Akio; Konishi, Kenji (Kanazawa Univ., Japan). Chishitsugaku Zasshi; 76: 389-97 (Aug 1970). (In Japanese).

In order to evaluate criteria for reliable dating by the ionium ($^{230}$Th) growth method, changes of uranium and thorium isotopic contents due to diagenetic processes in partially calcified but otherwise aragonitic exoskeletons of some fossil hermatypic corals were examined using $\alpha$-spectrometry. All the samples examined contained measurable amounts of thorium isotopes. Although the uranium ($^{238}$U) content varied in entirely aragonitic coral colonies, variation in $^{230}$Th/$^{234}$U was too small to cause any appreciable discordance in ionium dates. Calcification of aragonitic skeletons usually tends to deplete both uranium and thorium isotopes. The depletion of uranium may be attributed to crystallographic control of uranium in carbonate polymorphs. The reason of the apparently young dates of $^{230}$Th/$^{234}$U in the calcified part is explained by the almost Th-free nature of the calcite, when compared with the aragonitic part. Thus, the criteria to be fulfilled for reliable dating of fossil corals by the ionium growth method are the following: neither terrigenous nor any other source of contamination such as epilithic organic material should be noticeable in the pores and/or on the surface of sample; the sample should be entirely composed of aragonite; uranium ($^{238}$U) concentration in the sample should be from 2 to 3.5 ppM, the same as that in recent corals; the $^{234}$U/$^{238}$U activity ratio in the sample ranges from 1.15 to 1.00, and thorium ($^{232}$Th) concentration in the sample should be less than that in recent corals from the same area where the fossil corals were collected. (auth) (Japan)

**54777** GEOLOGIC AND SEISMIC CONSIDERATIONS AFFECTING NUCLEAR POWER PLANT SITE SELECTION. Waldron, H. H. (Geological Survey, Denver); Coulter, H. W. pp 83-92 of Health Physics Aspects of Nuclear Facility Siting. Vol. I. /Voilleque, Paul G. (comp.). Idaho Falls, Idaho; Burton R. Baldwin, Publications Chairman (1971).

From fifth annual midyear topical symposium on health physics aspects of nuclear facility siting; Idaho Falls, Idaho (3 Nov 1970).

Geologic and seismic aspects of siting are important factors in selecting and evaluating sites for any large power plant, and especially those for nuclear plants. Before engineering design criteria can be established for a proposed facility, the engineering geologist must provide reasonable assurance that the site is feasible. Ideally a site should be in a geologically stable area—one low in seismicity, free of active faults, underlain by competent foundation materials, and free from the adverse effects of other geologic hazards. Deficiencies in any of these aspects must be compensated for by engineering design. Brief descriptions are presented of some of the current procedures and some of the seismic and geologic criteria that are being used in evaluating nuclear power plant sites, with emphasis placed on earthquake criteria and on procedures required for determining the likelihood of surface displacement occurring on a fault. (P.C.H.)

**54778** DIFFERENTIAL Sr–Ca BONDING ON SOIL AS INFLUENCED BY BONDING SITE. Elgawhary, S. M.; Barber, S. A. (Purdue Univ., Lafayette, Ind.). Contract AT(11-1)-1495. Soil Sci. Soc. Amer., Proc.; 35: No. 4, 566-71(Jul-Aug 1971).

The Sr−Ca selectivity coefficient, $k_{Sr/Ca}$, was used to interpret the differential Sr−Ca bonding of cation exchange sites in two soils. A dominant complementary cation, K, was used to place the Sr and Ca on sites which favored Sr and Ca over K. As the equivalent fraction of Sr plus Ca in the equilibrium solution was reduced, $k_{Sr/Ca}$ decreased, indicating that organic exchange sites were the first to be filled. When the complementary ion was Mg or Ba, $k_{Sr/Ca}$ was much larger, indicating that these complementary ions competed more nearly equally with Sr and Ca for all exchange sites. There was a relationship between the log of the equivalent fraction of Sr plus Ca and $k_{Sr/Ca}$ that was linear over segments of the range of equivalent fraction used. Chromatographic separation of Sr and Ca on a Sidell soil reflected the $k_{Sr/Ca}$ of this soil at low Sr plus Ca saturations. Little Sr and Ca separation occurred with the Edwards muck apparently because of the over-shadowing of the readily exchangeable cations by Sr and Ca adsorbed in very slowly exchangeable positions resulting in little movement of these ions. (auth)

## Meteorology

*Refer also to abstracts 54815, 54908, 54964, 55157, and 55193.*

**54779** (CONF-710401–, pp 347-51) ENVIRONMENTAL SAMPLING. A Critical Look at Common Procedures. Hazle, A. J.; Siek, R. D. (Colorado State Dept. of Public Health, Denver). 15 Apr 1971.

From Rocky Flats symposium on safety in plutonium handling facilities; Golden, Colo. (13 Apr 1971).

A discussion on environmental sampling is presented in which the subjectivity of commonly used procedures is reviewed. Although this review is not as thorough as may be deemed desirable, it does raise questions as to procedures that are subjective versus results that are used objectively. The poorest trained personnel are usually delegated the responsibility for sample collection and the comparison is, unfortunately, always with existing standards. Investigators should know the limitations of their surveillance systems and the resultant data. Comprehensive knowledge with positive thinking regarding the use of pertinent data brings subjective environmental sampling into the realm of objectivity. (auth)

**54780** (CONF-710505-6) PLUME RISE CALCULATIONS USING SELECTED FUNCTIONAL FORMS AND THE TABULATION PREDICTION TECHNIQUE. Moses, Harry; Kraimer, Martin R. (Argonne National Lab., Ill.). [1971]. 42p. Dep. NTIS.

From American industrial hygiene conference; Toronto, Ontario, Canada (27 May 1971).

This study is based on single stack plume rise data taken from a wide range of stack sizes with complete information on meteorological and engineering stack parameters. The functional forms of conventional plume rise equations were examined and improved coefficients were obtained based on least squares techniques. The tabulation prediction technique, a new method for determining plume rise, is also given. The plume rise is determined from a multivariate contingency table in which values of the independent variables are arranged in an ordered sequence and relevant statistical features of the dependent variables are given. This method has definite advantages over conventional plume rise formulas. (auth)

**54781** (JPRS-53174) GLOBAL CONTAMINATION OF THE ATMOSPHERE BY $^{85}$Kr FROM WORLDWIDE NUCLEAR POWER PLANTS AND THE RADIATION DANGER. Karol, I. L.; Ivanov, V. M.; Kolobashkin, V. M.; Leypunskii, O. I.; Nekrasov, V. I.; Gudkov, A. N.; Ushakova, N. P. (Institute of Experimental Meteorology, Obninsk (USSR)). Translation of Global'noe Zagryaznenie Atmosfery $^{85}$Kr ot Mirovoy Yadernov Energetiki i Ego Radiatsionnaya Opasnost. 17p. NTIS.

The sources of $^{85}$Kr contamination in the earth's atmosphere, including cosmic radiation, nuclear explosions, and the release of $^{85}$Kr from worldwide nuclear power plants, are described. A numerical model for the global distribution of atmospheric $^{85}$Kr is presented. The results of calculations for the zonal distribution of $^{85}$Kr released into the atmosphere by nuclear power plants and the expected annual radiation dose to the year 2000 from the maximum allowable $^{85}$Kr concentrations are discussed. (L.C.L.)

**54782** (UCRL-51054) COMPARISON OF U.S. AND U.S.S.R. METHODS OF CALCULATING THE TRANSPORT, DIFFUSION, AND DEPOSITION OF RADIOACTIVITY. Knox, J. B.; Crawford, T. V.; Peterson, K. R.; Crandall, W. K. (California Univ., Livermore. Lawrence Radiation Lab.). 24 May 1971. Contract W-7405-eng-48. 52p. Dep. NTIS.

Because of possible future applications of peaceful nuclear explosives (PNE) in constructing harbors and canals and developing water resources, calculational techniques have been devised for predicting the distribution of PNE debris downwind from the point of application. It is essential that radiation levels from such applications remain within existing international standards. With this in mind, both the United States and the Soviet Union have independently developed prediction methods that differ in approach and parameter selection. It is desirable that the calculational techniques of countries performing PNE applications yield results that are in reasonable agreement, or whose differences, where they exist, are defined and physically understood. The U. S. and Russian prediction methods are compared. Five previous case studies of diffusion and deposition of debris clouds have shown that the U. S. method consistently calculates cloud center concentrations, surface concentrations under the cloud center, and the corresponding deposition on the ground to within factors of 2 to 3 for times up to 50 to 100 hr downwind. Studies on the Schooner experiment indicate that, taking into account the weather conditions along the cloud path, the U. S. method gives predictions to about the same accuracy for times of 200 to 300 hr. It is believed that this good calculational accuracy at very long ranges is in part due to the ever-increasing width of the debris cloud; thus, average values of diffusion coefficients on this spatial scale are not sensitive to distance along the cloud path, provided large-scale wet deposition has not previously deposited the cloud

XUM

at shorter ranges. The U. S. and the U.S.S.R. methods were examined and their predictions with medium and long range measurements of radioactivity from the Schooner cratering experiment were compared. The major result of this comparison was that if the vertical integral of radioactivity through the Schooner debris cloud center was considered, it was found that the two prediction methods within about a factor of 2 at long ranges (more than 1000 km downwind), provided that extensive precipitation scavenging has not occurred previously. At distances of 400 to 1000 km, the vertical integral obtained by the U. S. method was as much as several times higher than the U.S.S.R. estimates. The two calculational techniques as applied to Schooner showed differences of as much as two orders of magnitude for dry deposition, particularly at distances less than 1000 km downwind. These large differences are primarily attributable to the U.S.S.R.'s treatment of the debris cloud as an instantaneous point source and the inability of their method to account for changes in diffusion environment of the cloud caused by topography, diurnal variations in vertical diffusivity, inversions beneath the cloud, and scavenging processes. In order to illustrate and evaluate the differences in the U. S. and the U.S.S.R. solutions for different along-the-cloud-path diffusion conditions and initial conditions, the hypothetical case of a nuclear excavation of a canal at the Isthmus of Kra is also presented. (P.C.H.)

**54783** EVALUATION OF THE ATMOSPHERIC DIFFUSION PARAMETERS AT THE CASACCIA SITE BY SMOKE PLUME PHOTOGRAPHY. Cagnetti, P. (CNEN, Rome). Minerva Fisiconucl.; 13: 192-203(Jul-Sep 1969). (In Italian). (CONF-680535-21).

From fourteenth national conference of the Italian Association for Health Physics and Protection from Radiation; Formia, Italy (29 May 1968).

The evaluation of the atmospheric diffusion parameters by use of smoke plume photography is based on the Roberts opacity theory. After a discussion of this theory, its practical application in calculating, under given stability conditions, the diffusion parameters on the Casaccia site is outlined. Photography with exposures of several minutes and crossed polarized filters with variable angles calibrated with a microphotometer was used. The results obtained, taken in relation with the stability conditions shown by the instruments placed on the 40-m high meteorological tower at Cassacia, were analyzed and compared with results obtained under various conditions by other investigators. (tr-auth)

**54784** LA SURVEILLANCE COURANTE DES RADIONUCLEIDES DANS L'AIR ET DANS L'EAU. (Surveillance of Radionuclides in the Air and Water at the Present Time). Geneve: Organisation Mondiale de la Sante (1969). 72p.

The World Health Organization reviews current practices in the surveillance of radionuclides in the air and water. The contribution of natural and artificial radioactivity is estimated. The behavior of wastes released in the environment is described. The characteristics of the most important radionuclides are summarized. Directives and standards applicable to radioactive contaminants are discussed. The organization of a surveillance program is outlined. (J.S.R.)

**54785** $^{181}$W AND OTHER SHORT LIVED FISSION PRODUCTS IN GROUND-LEVEL AIR IN NORTH GERMANY AND NORTH NORWAY. Kolb, W. (Physikalisch-Technische Bundesanstalt, Brunswick). Nature (London); 232: No. 5312, 552-3(20 Aug 1971).

Analytical data are given for samples of atmospheric dust collected in 1970 and 1971 at 1.5m above ground in Brunswick and in Tromso. The concentrations of various fission products and some cosmogenic radionuclides were evaluated from the $\gamma$-spectra. Fresh fission products were recently detected on three occasions. Ten days after the eleventh Chinese nuclear test, $^{131}$I was found in a rain sample at a concentration of 2pCi/l, and during the following days dust samples both from Brunswick and Tromso contained $^{140}$Ba + $^{140}$La, $^{147}$Nd and $^{237}$U. Data are also given for $^{95}$Zr, $^{95}$Nb, $^{103}$Ru, $^{106}$Ru, $^{137}$Cs, $^{141}$Ce, and $^{144}$Ce. An increasing ratio $^{103}$Ru/$^{106}$Ru indicated that most of these Chinese fission products reached the surface through the stratosphere during the spring peak. Samples from both localities later contained small concentrations of $^{131}$I, together with some $^{132}$Te and $^{140}$Ba + $^{140}$La, probably produced by the US underground nuclear test in Dec. 1970. Still later, $^{140}$Ba + $^{140}$La and $^{181}$W were detected, the last named at a concentration of 0.27 to 0.38 pCi/m$^3$ ± 20%. Tungsten-181 was also found in ground level air in other parts of the world after an underground nuclear test carried out in Nevada in 1968. It cannot, however, be concluded with certainty that the fission products, and the $^{181}$W, arose from a USSR underground test. (UK)

**54786** ESTIMATE OF THE INFLUENCE OF THE NATURAL RADIOACTIVITY ON THE ION BALANCE IN THE ATMOSPHERE. Krasnopevtsev, Yu. V. Izv. Akad. Nauk SSSR, Fiz. Atmos. Okeana; 6: No. 10, 1069-72(Oct 1970). (In Russian).

Following up earlier studies on the role of radioactive materials in the ionization of the surface layer of the atmosphere, attempts were made to calculate the ionization due to the action of natural radioactive materials. Distribution of these materials in the atmosphere and the simultaneously determined variations in the vertical direction of the conductivity of the air as a function of the altitude were used for the calculation. The sampling technique used to determine the radioactivity of the particles captured on the filter indicated only the activity to $\alpha$ and $\beta$ decay of the aerosol components of the radon series. Actually, only the $\alpha$-emitting components such as RaA and RaC′ and the radon itself had to be taken into account because their total emitted energy is much higher than that of the $\beta$-emitting RaB and RaC. The ionization corresponding to the total $\alpha$ activity of the aerosols was taken as ~$1 \times 10^{-12}$ Ci/l, corresponding to $3.7 \times 10^{-6}$ disintegration/sec. cm$^3$. Under equilibrium conditions, RaA and RaC′ each account for one-half of the activity; the total energy was calculated as $U_\Sigma$ = 35 eV/sec. cm$^3$. It was concluded from the conductivity and aerosol concentration data that regions of high concentrations of radioactive aerosols in the presence of delaying layers occur frequently; they are responsible for the ionization to relative high altitudes. This must be taken into account when calculating the ionization balance of the free atmosphere. (TTT)

**54787** STATIONARY VERTICAL PROFILES OF RADON AND THORON DECAY PRODUCT CONCENTRATIONS IN THE SURFACE LAYER OF THE ATMOSPHERE. Belekhova, N. G. (Moscow Engineering-Physics Inst.). Izv. Akad. Nauk SSSR, Fiz. Atmos. Okeana; 6: No. 10, 1073-6(Oct 1970). (In Russian).

Previous studies on the propagation of radioactive emanation in the atmosphere near the ground were continued. A mathematical model of the turbulent diffusion of the decay products of emanation was derived and solved on the basis of conditions used in the vertical propagation model, taking the dry fallout rate into account. A boundary condition, $K_z$ was established to consider the interaction of the aerosols with the subjacent surface. The effects of the linear growth of $K_z$ near the surface on the emanation and its decay product, the concentration ratio of radon thoron and their decay products at a height of 1 m were calculated. Systematic measurements revealed that $K_z$ increased with the altitude up to H = 200 to 500 m; a value of H = 100 m was used in the calculations. The data allowed to determine disturbances in the radioactive equilibrium between emanation and its short-lived decay products. The reported daily oscillations of the RaB/RaA and RaC/RaA ratio from 0.5 to 0.9 were attributed to daily changes of the concentration of radon and its decay products which have not been taken into account in the present stationary scheme. (TTT)

**54788** BALANCE OF $^{90}$Sr OVER ANTARCTICA: EXISTENCE OF PROTECTED AREA. Lambert, G. (CNRS, Gif-sur-Yvette, France); Ardouin, B.; Brichet, E.; Lorius, C. Earth Planet. Sci. Lett.; 11: No. 4, 317-23(Jul 1971).

The study of firn cores from Terre Adélie and from stations located along the Mirny–Vostok axis made possible new calculations of $^{90}$Sr accumulation in Antarctica, i.e., 25.10$^3$ Ci as of Jan. 1964. Despite the scarcity of sampling stations, an inhomogeneous geographical distribution may be observed which shows the existence of a low contamination area. Moreover, a linear relationship seems to exist in many cores between $^{90}$Sr and water accumulations. Thus it could be possible to extrapolate some geochemical measurements made in Antarctica to the rest of the Southern Hemisphere. (auth)

**54789** RESEARCHES ON RADIOCONTAMINATION IN HOKKAIDO. 9. THE EFFECT OF THE TENTH NUCLEAR TEST BY THE PEOPLE'S REPUBLIC OF CHINA. Ando, Yoshiaki (Hokkaido Inst. of Public Health, Sapporo); Kawahara, Hosaku. Hokkaidoritsu Eisei Kenkyushoho: No. 20, 232-3(Jun 1970). (In Japanese).

The tenth nuclear test of the People's Republic of China was carried out on September 29, 1969, according to the news reports. The first arrival of the fallout was not detected at ground level in the Honshu District, but abnormally high radioactivity was detected in the rainwater which was collected on October 1, 1969 in Hakadate, Hokkaido. The intensity of the radioactivity was found to be as high as 17 pCi/ml. The initial half-life was estimated from the decay curve to be about 2 days. The gamma-ray spectrum, measured 7 days after collection, showed the existence of the following nuclides: $^{141}$Ce + $^{144}$Ce, $^{103}$Ru + $^{106}$Ru, $^{140}$Ba, and $^{95}$Zr + $^{95}$Nb. (auth) (Japan)

**54790** VERTICAL DISTRIBUTION OF THE INTENSITY OF IONIZATION DUE TO TERRESTRIAL GAMMA-RADIATION.

Minato, Susumu; Kawano, Minoru (Nagoya Univ., Japan). J. Radiat. Res.; 11: 138-44(Sep-Dec 1970).

Formulas concerning the intensity of ionization due to the terrestrial gamma radiation which include both the primary gamma radiation from radioisotopes in the ground and radiation scattered in soil and air were obtained by using buildup data with respect to aluminum and water for a point source. The intensities of ionization due to terrestrial gamma radiation above and below the ground surface were calculated by the formulas with the aid of the "true" photon spectrum of the radiation in the air on the campus of Nagoya University, and the relation between the ionization intensity and altitude or depth was obtained. (auth)

**54791** 13th REPORT OF THE FEDERAL COMMISSION ON THE MONITORING OF RADIOACTIVITY FOR THE YEAR 1969 DELIVERED TO THE FEDERAL COUNCIL. Huber, P.; Halter, J. Bull. Eidgenoess. Gesundh., Beil B; No. 4, 1-82(5 Sep 1970). (In German and French).

Early fission products from the Chinese H-bomb explosion of December 1968 could be detected in the stratosphere at the end of January 1969. Increase of surface air activity became noticeable only after the spring stratosphere/troposphere exchange. In September 1969, a 3 megaton H-bomb was exploded at Lop Nor, China. Fission products could be detected in the upper troposphere during October. Surface-near activity increased only to a minor degree. The incidents at the Lucens nuclear center on January 21, 1969, triggered general radioactive monitoring. A few hours following the incident, it was established that the general population was not endangered. To clarify the situation, numerous measurements were conducted subsequently in the laboratories at Fribourg and Basel, Switzerland. Data are presented in graphs and tables. (H.B.G.)

**54792** YEARLY COURSE OF RADON AND THORON INDUCTIONS AND THE LONG LASTING RADIOACTIVITY OF AEROSOLS IN PLOVDIV. Genkov, D.; Stefanova, M. (Higher Medical Inst., Plovdiv, Bulgaria). Folia Med. (Plovdiv); 11: 214-21(1969).

The average monthly values of Ra and thoron content and the beta activity of atmospheric aerosols measured at Plovdiv, Bulgaria throughout 1966, 1967, and 1968 are presented and discussed. (L.C.L.)

**54793** METEOROLOGICAL QUESTIONS CONCERNING PLANT SITING. Slade, David H. (Atomic Energy Commission, Washington, D. C.). pp 56-82 of Health Physics Aspects of Nuclear Facility Siting. Vol. I. /Voilleque, Paul G. (comp.). Idaho Falls, Idaho; Burton R. Baldwin, Publications Chairman (1971).

From fifth annual midyear topical symposium on health physics aspects of nuclear facility siting; Idaho Falls, Idaho (3 Nov 1970).

Methods for obtaining the engineering estimates of diffusion frequently used in nuclear plant site safety analyses are discussed. It is suggested that some of the meteorological knowledge is not reflected in these techniques. (auth)

**54794** STEADINESS OF THE WIND DURING STABLE CONDITIONS. Singer, Irving A.; Nagle, Constance (Brookhaven National Lab., Upton, N. Y.). pp 447-62 of Health Physics Aspects of Nuclear Facility Siting. Vol. II. /Voilleque, Paul G. (comp.). Idaho Falls, Idaho; Burton R. Baldwin, Publications Chairman (1971).

From fifth annual midyear topical symposium on health physics aspects of nuclear facility siting; Idaho Falls, Idaho (3 Nov 1970).

An important aspect of nuclear facility siting is the steadiness of the wind direction in evaluating potential doses. In an earlier investigation steadiness, S, was studied as a function of time regardless of meteorological conditions where, S, is defined as the mean vector wind divided by the mean scalar wind $\bar{V}/\bar{V}$. A series of recurrence interval maps of (S) for the U. S. showing wind-direction persistence patterns for periods of 2, 4, and 8 days were presented in the Jan.–Feb. issue of Nuclear Safety. Recent studies using meteorological tower data from 4 stations with differing terrain have concentrated on wind direction persistence only during stable hours. The results showed that during stable conditions the wind direction will not change significantly for periods less than 12 hours. For periods of 12 hours or greater, persistence is a function of terrain configuration. Persistence values for smooth terrain, river valleys, and shore sites as a function of height will be presented. (auth)

**54795** COMPARATIVE DIFFUSION AND DEPOSITION OF URANIN DYE, MOLECULAR IODINE GAS, AND METHYL IODIDE GAS. Start, G. E. (National Oceanic and Atmospheric Administration, Idaho Falls, Idaho). pp 463-74 of Health Physics Aspects of Nuclear Facility Siting. Vol. II. /Voilleque, Paul G. (comp.). Idaho Falls, Idaho; Burton R. Baldwin, Publications Chairman (1971).

From fifth annual midyear topical symposium on health physics aspects of nuclear facility siting; Idaho Falls, Idaho (3 Nov 1970).

A set of paired diffusion tests for continuous 30 minute point source releases was conducted to gain an initial indication of whether or not significant differences might exist between the diffusion and deposition of uranin dye and molecular iodine gas. To avoid interaction and a loss of independent diffusion of uranin dye and molecular iodine gas, each tracer was released during separate tests. To normalize the diffusion results for expected differences in atmospheric diffusing conditions, a third tracer, methyl iodide gas, was released during each test. The tests were conducted during afternoons under temperature lapse conditions and southwesterly windspeeds of 3 to 8 mps. The first paired tracer release was a simultaneous release of uranin dye and methyl iodide gas. The second paired release involved molecular iodine and methyl iodide gases. The lateral plume spreadings and crosswind integrated concentrations were compared for measurements from five sampling arcs between 100 and 1600 meters downwind of the tracer release points. A total of 24 samples, from four 100 foot towers near 400 meters downwind, were also compared. The lateral spreads of the effluent materials were nearly the same, with molecular iodine gas having the greatest spread and uranine dye the least. Plume centerline concentrations of molecular iodine gas were greater than uranin dye plume centerline concentrations. Before these numerical comparisons can gain a stable statistical basis, many additional sets of measurements are needed. The assumption that deposition produces air concentrations of molecular iodine gas which are less than the corresponding measured air concentrations of uranin dye appears to be invalid, at least some of the time. (auth)

**54796** PHOTON ENERGY AND AIR SHIELDING IN CLOUD GAMMA DOSE CALCULATIONS. Willis, C. A. (McDonnell Douglas Astronautics Co.-West, Huntington Beach, Calif.). pp 540-54 of Health Physics Aspects of Nuclear Facility Siting. Vol. III. /Voilleque, Paul G. (comp.). Idaho Falls, Idaho; Burton R. Baldwin, Publications Chairman (1971).

From fifth annual midyear topical symposium on health physics aspects of nuclear facility siting; Idaho Falls, Idaho (3 Nov 1970).

In calculating the radiation dose from a passing cloud of radioactive material it is usually necessary to approximate the gamma energy spectrum by a number of energy groups for air attenuation considerations. A study was undertaken to determine the importance of these approximations. It was found that cloud centerline doses do not vary by more than a factor of 2 for gamma energy variations from 0.1 to 10 MeV. Since far-off-centerline doses (which could be greatly affected by gamma energy) are rarely critical, it was concluded that a single-kernel representation for air attenuation is adequate for most applications. (auth)

**54797** CLOUD GAMMA CALCULATIONS. Wenzel, D. R. (Idaho Nuclear Corp., Idaho Falls). pp 555-63 of Health Physics Aspects of Nuclear Facility Siting. Vol. III. /Voilleque, Paul G. (comp.). Idaho Falls, Idaho; Burton R. Baldwin, Publications Chairman (1971).

From fifth annual midyear topical symposium on health physics aspects of nuclear facility siting; Idaho Falls, Idaho (3 Nov 1970).

An integral part of a reactor siting evaluation is the calculation of whole-body doses that could be received from an airborne plume of radioactive material as a result of an accident. The interest generated during the past few years over the methods used for cloud gamma calculations has prompted improvements in the Radiological Safety Analysis Computer (RSAC) Program. An exact solution to the equation developed for a finite cloud has not been found. Either simplifying assumptions must be made or a generalized numerical solution is necessary. The use of a numerical integration approach to obtain a precise solution has been criticized as being impractical because it would take unreasonably long running time on the computer. An improved version of the RSAC Program is discussed which not only requires short computer running time but also improves the accuracy of the calculations. (auth)

**54798** SAMPLING OF $^{3}H$-WATER VAPOR BY MOLECULAR SEIVES AND MEASUREMENT WITH A MULTIPLE COINCIDENCE LIQUID SCINTILLATOR. D'Adamo, D.; de Bortoli, M.; Dominici, G. (CCR-EURATOM, Ispra, Italy). Minerva Fisiconucl.; 14: 31-7(Jan-Mar 1970). (In Italian). (CONF-690929-7).

From fifteenth national congress of the Italian Association for Health Physics and Protection Against Radiation; Cagliari, Italy (Sep–Oct 1969).

A selective sampling procedure for water vapor in air is described in which moisture is trapped in a column of 3 A molecular sieve. The collection efficiency does not depend on the vapor concentration within the investigated limits, but it is influenced by the velocity of air through the column. The recovery is 100% up to a velocity of about 1 m/sec. The $^{3}H$ concentration

XUM

in the water sampled is measured in a liquid scintillator by means of an instrument developed in the laboratory. The instrument is based on the counting of the coincidences produced among three photomultiplier tubes, disposed at 120° around the scintillation cell. The ratio between simple and composed coincidences allows for an energy discrimination of the beta particles. The overall sensitivity of the method is about $3 \times 10^{-9}$ $\mu Ci/cm^3$ and hence adequate also for the surveillance of $^3H$ vapor air contamination in the vicinity of nuclear installations. (auth)

**54799** COLLOQUIUM ON THE PHYSICS AND CHEMISTRY OF AEROSOLS, FONTENAY-AUX-ROSES, FRANCE, SEPTEMBER 24–25, 1970. J. Aerosol. Sci.; 2: No. 2, 131-280(Jun 1971). (In French and English). (CONF-700967).

Eighteen papers were presented at the colloquium of which four were in scope for NSA and for which separate abstracts were prepared. (UK)

*For abstracts of individual papers see: 54800–54802, and 55032.*

**54800** MEASUREMENT OF MOBILITY AND MASS OF ATMOSPHERIC IONS. Huertas, M. L.; Marty, A. M.; Fontan, J.; Alet, I.; Duffa, G. (Laboratoires Associes de Physique des Aerosols, Toulouse). J. Aerosol. Sci.; 2: No. 2, 145-50(Jun 1971).

From Conference on the physics and chemistry of aerosols; Fontenay-aux-Roses, France (24 Sep 1970). See CONF-700967.

The evolution in atmospheric air of small radioactive or gaseous ions was studied, for ionic ages ranging from $10^{-4}$ sec to a few seconds. Different mobility values were found. The influence of various phenomena on the evolution of the ions was investigated: water vapor, gaseous impurities. To specify the nature and the structure of ionic agglomerates, a mass spectrometer was used to measure ionic masses. Preliminary experimental results are given. (auth)

**54801** STUDY OF THE MOBILITY OF IONS IN AIR. Bricard, J.; Cabane, M.; Madelaine, G.; Vigla, D. (Faculte des Sciences, Paris). J. Aerosol. Sci.; 2: No. 2, 193-9(Jun 1971). (In French).

From Conference on the physics and chemistry of aerosols; Fontenay-aux-Roses, France (24 Sep 1970). See CONF-700967.

A method is described for establishing the mobility spectrum at atmospheric pressure of small ions produced by $\alpha$-particles. The effects of time of exposure to air and of the humidity of the air are investigated. (auth)

**54802** EXPERIMENTAL CHECK ON THE REMOVAL OF RADON. Dalu, G.; Dalu, G. A. (Istituto di Fisica dell'Atmosfera, Rome). J. Aerosol. Sci.; 2: No. 2, 241-6(Jun 1971).

From Conference on the physics and chemistry of aerosols; Fontenay-aux-Roses, France (24 Sep 1970). See CONF-700967.

Experiments in the past suggested that a partial removal of radon from the atmosphere occurs by wash-out. To test this, direct measurements were made of radon concentration in an isolated environment which was enriched with this gas and in which fog was produced artificially. Similar measurements were also made in the presence of a high potential gradient. From these experiments, it was established that the only process which eliminates radon from the atmosphere is the radioactive decay of the radon itself. (auth)

**54803** RECOGNITION OF THE FRAGMENT NUCLIDES $^{90}Sr$ AND $^{89}Sr$ ON THE BASIS OF RADIOACTIVITY. PART II. Santholzer, Vilem; Stransky, Pravoslav; Knaifl, Josef; Kuncova, Vlasta (Charles Univ., Hradci Kralove, Czech.). Jad. Energ.; 17: No. 4, 113-17(Apr 1971). (In Czech).

A method for recognizing $^{89}Sr$ and $^{90}Sr$ fallout is described based upon the increase of $^{90}Y$ activity in conjunction with the decay of $^{89}Sr$, and upon the characteristic decay of both radioisotopes of Sr. This method was employed for detecting atmospheric fallout in 1969 to 70. The quantity of $^{95}Zr + {}^{95}Nb$ was determined by spectrometry, and from this the fractionation factor for $^{90}Sr/^{89}Sr$ was obtained. (tr-auth)

## Mineralogy and Exploration

*Refer also to abstract 54913.*

**54804** URANIUM IN TEXAS. Eargle, D. Hoye. Houston Geol. Soc. Bull.; 13: No. 2, 18-27(1970).

Five geographic areas of Texas where at least some uranium has been found are listed, the nature of the mineralization summarized, and their potential considered briefly. The areas are: Trans-Pecos; Panhandle, in Triassic sandstones and conglomerates filling channels; Red River region, in channels and carbonaceous sandstones in outcrops of Permian redbeds, potential low; Llano Uplift, little prospecting done, potential seems low; and Coastal Plain, the only area in which economic deposits have been exploited. These deposits are in Tertiary beds extending from Fayette County in east-central Texas to Starr County on the Rio Grande, but principal deposits are in Karnes County. Several prospects and mines are described. Current exploration is by boring, logging, and core sampling. Many anomalies are found along faults, discovered by photointerpretation. (Abstr. N. Amer. Geol.)

**54805** POISKI URANOVYKH MESTOROZHDENII V USLOVIYAKH GORNOI TAIGI. (Prospecting for Uranium Deposits in Mountainous Taiga). Sharkov, Yu. V. Moscow; Atomizdat (1971). 216p.

Prospecting for uranium deposits under complex mountainous conditions is discussed, with some attention given to methods such as radiometric prospecting. The remainder of the book deals with the geology of uranium ore bodies, first and second oreoles in the distribution of deposits, and factors controlling the distribution of uranium by aqueous precipitation and dispersion currents. Methods of mapping and districting territory in mountainous regions based on prospecting information is the subject of one of the major sections of the book. (K.S.W.)

**54806** URANIFEROUS BED IN MIZUSAWA AREA. Komura, Kohjiro; Natori, Hiroo (Geological Survey of Japan, Kawasaki). Chishitsu Chosajo Geppo; 20: 729-37(Nov 1969). (In Japanese).

A geological reconnaissance was made of the uraniferous bed in Mizusawa area, Iwate prefecture, in August, 1967. This area is composed of the pre-Tertiary formation which is presumably of Paleozoic in age, granodiorite, Tertiary formation, and some kinds of dike. The granodiorite intrudes into the pre-Tertiary formation, and is overlain unconformably by the Tertiary formation which can be divided by the "Sennin fault" into two groups, i.e., Oarasawa and Oishi formations, both of which are of Miocene in age. The uraniferous beds seem to be intermittently scattered in the basal part of Oarasawa formation, and contain some pieces of silicified wood, sulfide and clay mineral such as kaoline, sericite, and chlorite. The maximum thickness of the beds is estimated at about 2 m, but its extension is unknown because of the deficiency of data. The results of chemical analysis suggest that the ore grade changes with the maximum value being 0.02% $U_3O_8$. (Japan)

**54807** SIGNIFICANCE OF ZIRCON AND THORITE IN URANIUM AND THORIUM GEOCHEMISTRY OF VOLCANIC ROCKS ASSOCIATED WITH THE CULM OF THE SOURTHERN VOSGES. Stussi, Jean-Marc (Nancy Univ.). Compt. Rend., Ser. D; 271: 2255-8(21 Dec 1970). (In French).

The important part played by zircons and thorites, of early or late formation, in the geochemistry of uranium and thorium is shown. These two minerals, together with the total U and Th concentrations recorded in the rocks considered, entitle the hercynian magnetic region of the southern Vosges to be considered as thoriferous. (auth) (France)

**54808** INTERPRETING $\gamma$-MEASUREMENTS OF AN EXOGENOUS EPIGENETIC URANIUM DEPOSIT. Pritchin, B. P. This paper was summarized in At. Energ. (USSR); 26: 456-7 (May 1969) as paper No. 299/4686. (In Russian).

Changes in the radioactive element content were found in a study of deposits connected with stratified oxidation zones. Methods for interpreting the data from $\gamma$-cores and $\gamma$-assays were developed on the basis of these changes. The distribution of uranium and radium contents over a transverse cross-section of the deposit regions separated by an oxidation zone was constructed by statistical generalization. The generalized radium distributions for various wing thicknesses were used as initial data from which methods for finding the ore boundaries are determined, after calculation of the theoretical $\gamma$-intensity. The boundary on the oxidation-zone side corresponds to the point where the $\gamma$-intensity is 0.75 the maximum; at the opposite boundary, the ratio $I_{bdry}/I_{max}$ varies from 0.3 to 0.7, inversely proportional to the wing thickness. The ore boundary on the unoxidized-rock side can be found in terms of this intensity. This method is applicable for all deposits, not only for wings. It is convenient because the ore is practically uniform in all the layers in the zone bounding the unoxidized rock, i.e., the value of this intensity is the same in all layers. An area-ratio method is proposed for determining the uranium content. The areas are computed from the theoretical $\gamma$-intensity curves, and the area ratio is given as a function of the ore strength. (L.C.L.)

**54809** DISTRIBUTION OF URANIUM IN SOME BASIC IGNEOUS CUMULATES AND ITS PETROLOGICAL SIGNIFICANCE. Henderson, P. (Chelsea Coll. of Science and Tech., Eng.); Mackinnon, A.; Gale, N. H. Geochim. Cosmochim. Acta; 35: No. 9, 917-25(Sep 1971).

The distribution of uranium in the minerals and rocks of the Skaergaard, Rhum, and Bushveld layered igneous intrusions was investigated by the delayed-neutron analytical technique. The uranium concentration in the minerals depends, in part, upon the nature of the cumulate from which they were separated. In those minerals from adcumulates, pyroxene contains the most uranium and olivine the least. The uranium content of a basic igneous cumulate is shown to be useful as an indicator of the relative amount of mesostasis in the rock, provided uranium-bearing cumulus minerals such as apatite are absent. The amount of mesostasis sometimes changes rapidly from one layer to another. (auth)

## Oceanography

*Refer also to abstracts 54481 and 55252.*

**54810** MARINE GEOCHEMISTRY OF THE URANIUM ISOTOPES, $^{230}Th$ AND $^{231}Pa$. Turekian, K. K.; Chan, L. H. (Yale Univ., New Haven). pp 311-20 of Activation Analysis in Geochemistry and Cosmochemistry. /Brunfelt, Arild O. (ed.). Oslo; Universitetsforlaget (1971).

From Conference on activation analysis in geochemistry and cosmochemistry; Kjeller, Norway (7 Sep 1970). See CONF-700968.

The supply rate of $^{234}U$ and $^{238}U$ by streams and the diffusion rate of $^{234}U$ from deep-sea sediments are shown to form a self-consistent pattern when the following values of the critical quantities are used: average stream concentration of U = 0.3 $\mu g/l$; average $^{234}U/^{238}U$ activity ratio of streams = 1.19; average $^{234}U$ diffusion rate from deep-sea sediments = 0.3 $dpm/cm^2/1000$ yr. Other values of these parameters are also self-consistent, but some suggested regional values are found not to be. The uranium-to-salinity ratio of the oceans is constant within 4% at a $9.21 \times 10^{-8}$ g U/salinity corresponding to 3.2 $\mu g$ U/l for sea water of 35‰ salinity. $^{230}Th$ and $^{231}Pa$ are proportionated between deep-sea sediments and manganese nodules, particularly in the Pacific Ocean. Approximately 25% of the ocean surface (excluding the Atlantic) should show manganese nodules if their growth takes place primarily at the sediment-water interface and recent sediment masking has not occurred. (auth) (Norway)

**54811** STUDY OF THE ABSORBING SURFACE OF THE SUSPENSIONS IN SEA WATER BY MEANS OF RADIOISOTOPES. Ivanov, V. N. (Biological Inst. of the Southern Seas, Sevastopol, USSR). Dokl. Akad. Nauk SSSR; 195: 1441-2(21 Dec 1970). (In Russian).

Adsorption processes play an important role in the accumulation of radioisotopes in seawater. This distribution of radionuclides in the water-hydrobiont system depends on the buildup factor and the biomass of the organisms. The problem was studied by determining the adsorption of $^{144}Ce$ during the first trip of the research ship Akademician Vernadskii to tropical areas of the Atlantic Ocean during the fall of 1969. The seawater samples were taken at noon and at midnight, introducing into the 0.5 l sample 1 ml of a pH = 1 areal $^{144}CeCl_3$ solution. After the addition, the pH of the seawater was 8 and its activity $10^{-6}$ Ci/l. The adsorption on glass and plastic was determined with the sample solution and also after filtration through a membrane. The adsorption coefficients of $^{144}Ce$ were found to be higher on the weak cation exchanger glass than on the neutral hydrophobic surface of the plastic. Filtering of the samples collected during the night revealed that 1.84 times more activity was retained on the filter than with samples collected during the day. This indicated that the biomass in the surface layer of the ocean increased by the same factor during the night. The method may be used to compare changes of the adsorbing surface in waters collected at various depths and to follow the seasonal, daily, and geographic changes. (TTT)

## Seismology

*Refer also to abstracts 54775 and 54820.*

**54812** (NVO-1163-TM-30) PREDICTED SAN FERNANDO EARTHQUAKE SPECTRA: GLENDALE AREA. Murphy, J. R.; Lynch, R. D.; O'Brien, L. J. (Environmental Research Corp., Las Vegas, Nev.). Aug 1971. 34p. Dep. NTIS.

An analysis of selected aftershocks of the San Fernando earthquake recorded at damage sites in the city of Glendale, California indicates that significant variability in the ground motion spectra occurs within this rather small geographical area. This variability is quantified and used to estimate the main shock ground motion spectra at a number of sites of interest which did not record the main shock. (auth)

**54813** (PNE-R-51) RULISON GROUND MOTIONS RECORDED AT THE TOSCO MINE AND TOWER STATIONS. Hays, Walter W. (Environmental Research Corp., Las Vegas, Nev.). 30 Jul 1971. 6p. Dep. NTIS.

Two graphs of the 5% PSRV spectra of ground motions measured at the Tosco mine and tower stations following the Rulison Event are presented. (L.C.L.)

**54814** RADIATION PATTERNS OF S WAVES FROM UNDERGROUND NUCLEAR EXPLOSIONS. Hirasawa, Tomowo (Massachusetts Inst. of Tech., Cambridge). J. Geophys. Res.; 76: No. 26, 6440-54(10 Sep 1971).

Use is made of polarization angles of S waves from the Greeley, Boxcar, and Benham events to determine focal mechanisms of earthquakes presumably triggered almost instantaneously by the events. Although other possibilities are not completely excluded, the observed S waves are interpreted as mixed waves of direct S phase and reflected phases (sS, pS) from a composite source of explosion and double-couple force. Assuming a vertical strike slip, the strike of the P-wave nodal plane and the relative strength of the double-couple source compared with that of the explosion are determined. The seismic moments of triggered earthquakes are calculated as $3.9 \sim 6.3 \times 10^{23}$ dyne cm for Boxcar and $1.4 \sim 2.3 \times 10^{24}$ dyne cm for Benham. Particularly in the case of Benham, the rise time of about 2 sec together with the seismic moment of $2.3 \times 10^{24}$ dyne cm is compatible with the observations of seismic waves. The possibility of estimating the pre-existing tectonic shear stress is suggested in the case of Boxcar. The tectonic stress is estimated at 130 bars from the assumption of stress relaxation due to a cavity created by the nuclear detonation. (auth)

XUM

# ENGINEERING

## Nuclear Explosions

*Refer also to abstracts 54599, 54782, 54789, 54813, 54814, 54993, 55124, and 55249.*

**54815** (AD-722031) POSSIBLE EFFECTS OF ATMOSPHERIC PARTICLES ON FIREBALL EMISSIONS. Ory, Hal A.; Gilmore, Forrest R. (RAND Corp., Santa Monica, Calif.). Feb 1971. Contract DASA01-71-C-0012. 19p. (DASA-2612). NTIS.

In order to investigate the possible effects of natural atmospheric particles on fireball emission, the available data on particle distribution in the atmosphere are used to calculate the mass fraction as a function of altitude for sulfate particles and particles of meteoritic origin. For altitudes below 20 km the mass fraction of sulfate particles is 10 to the (−10) power to 10 to the (−9) power; above 20 km, the mass fraction decreases rapidly with altitude. The mass fraction of $SO_2$ vapor is probably more than an order of magnitude greater, based on observations at low altitudes. The meteoritic mass fraction shows practically no altitude dependence, and is approximately $1.3 \times 10$ to the (−10) power over the entire range of interest. Based on a simple thermodynamic model, the mass of meteoritic material vaporized in a fireball is less than half a pound per megaton of bomb yield. Within the limitations of the data used in the calculations, the following conclusions were reached concerning possible effects of atmospheric particles on fireball emission: the contribution of sulfate particles is probably negligible compared with that of atmospheric $SO_2$ vapor, which itself has negligible effect; and the contribution of meteoritic particles is negligible compared with that of bomb debris material. (auth) (USGRDR)

**54816** (ORNL-4682, pp 182-6) CHEMICAL APPLICATIONS OF NUCLEAR EXPLOSIVES. (Oak Ridge National Lab., Tenn.). in Chemical Technology Division annual progress report.

Fracturing of copper ores by nuclear explosions, recovery of oil from shale, and natural-gas storage reservoirs produced by nuclear explosions are discussed. (M.C.G.)

**54817** (PNE-R-52) PROJECT RULISON. POST-SHOT WELL TEST DATA. (Austral Oil Co., Inc., Houston, Tex.). [nd]. 52p. Dep. NTIS.

All flow and pressure build-up data collected between Sept. 69 and June 71 on the two wells associated with Project Rulison are presented. All surface pressures shown were measured either with a dead weight tester or with conventional pressure gages. Bottom hole pressures were measured using an Amerada Type RPG-3 bottom hole pressure gage. Flow rates were measured by using either a conventional orifice flow meter or a critical flow prover. The results of Rulison Project gas analyses, both chemical and radiochemical, are also tabulated. (auth)

**54818** (UCRL-Trans-10543) FRENCH AND SOVIET PAPERS PRESENTED AT THE SECOND PANEL ON THE PEACEFUL USES OF NUCLEAR EXPLOSIONS, VIENNA, AUSTRIA, JANUARY 18-22, 1971. Translation of French and Russian papers. 116p. (CONF-710108). Dep. NTIS.

Eight French and Soviet papers on peaceful uses of nuclear explosions were presented at the conference. A separate abstract was prepared for each paper. (L.C.L.)

*For abstracts of individual papers see: 54819–54826.*

**54819** (UCRL-Trans-10543, pp 1-3) NUCLEAR EXPLOSIONS FOR PEACEFUL PURPOSES. Therene, P. (Commissariat a l'Energie Atomique, Paris (France)). Translation of French paper.

The current status and future plans of the French program for peaceful uses of underground nuclear explosions are described briefly. Primary efforts are being directed toward using deep contained underground nuclear explosions for creating underground storage facilities, stimulating oil field production, and extracting minerals. Educational programs concerned with industrial uses of nuclear explosions are mentioned. (L.C.L.)

**54820** (UCRL-Trans-10543, pp 4-35) MECHANICAL EFFECTS OF A CONTAINED NUCLEAR EXPLOSION. Ferrieux, H.; Guerrini, C. Translation of French paper.

The 120-kt nuclear blast Monique was detonated in the Tan Afella (Sahara) granite massif. The ground movements caused by the explosion were recorded at distances of from several meters to 50 km. The evolution of the shock wave was followed all along this path. Different types of recordings were made during the experiment (measurements of shock-wave arrival times, acceleration, material velocity and displacement, the pressure being determined by an indirect method). These different parameters are compared to the general experimental laws arrived at for all of the contained Sahara blasts. Several types of measurements taken after the nuclear blast made it possible to study the changes in and damage to the environment that Monique produced. (auth)

**54821** (UCRL-Trans-10543, pp 36-41) STATUS REPORT ON THE PROGRAM OF CONTAINED NUCLEAR EXPLOSIONS FOR USE IN INDUSTRY. Kedrovskii, O. L. Translation of Russian paper.

The USSR program for developing industrial uses of contained underground nuclear explosions is reviewed. These uses are primarily creation of underground storage cavities, ore crushing, gas and petroleum production stimulation, and the extinguishing runaway gas and oil wells. After 10 years of study and testing it is concluded that it will soon be possible to use underground nuclear explosions on a broad industrial scale. (L.C.L.)

**54822** (UCRL-Trans-10543, pp 42-55) USE OF CONTAINED NUCLEAR EXPLOSIONS TO STIMULATE PETROLEUM OUTPUT. Kedrovskii, O. L. Translation of Russian paper.

A description is given of nuclear explosions detonated in a nonuniform carbonate reservoir confined to one of the oil fields of the USSR. The three explosions, one with a yield of 8 kt, the other two of 2.3 kt each, were intended to provide information on, and confirm the possibility of, the use of nuclear explosions to increase a field's yield. Included are data on the geologic structure of the test region, the increased petroleum output after the explosions, and on the absence of any complications in the form of radioactive contamination of the petroleum. The studies made indicate a possibility of substantially increasing the day-to-day output, and shortening the depletion time. Several very promising methods for working oil and gas-condensate deposits with the aid of underground nuclear explosions are discussed. (auth)

**54823** (UCRL-Trans-10543, pp 56-69) MAKING CONTAINED NUCLEAR EXPLOSIONS RADIATION-SAFE. Kedrovskii, O. L. Translation of Russian paper.

Conditions that could lead to radiation hazards after contained nuclear explosions are discussed. A method for determining the minimum charge-emplacement depth ensuring radiation safety is described. Some radiation-safety measures are enumerated. A method is described for continuous telerecording of the gamma-radiation dose rate of radioactive gases in the shothole and producing wells following nuclear explosions in gas and oil fields. Results are given of the petroleum-contamination studies made after one underground nuclear explosion. The experimental research conducted in the laboratory and under natural conditions indicates that underground nuclear explosions can be safely used in oil fields. (auth)

**54824** (UCRL-Trans-10543, pp 70-80) CREATING UNDERGROUND STORAGE CAVITIES WITH CONTAINED NUCLEAR EXPLOSIONS DETONATED IN ROCK SALT. Myasnikov, K. V. Translation of Russian paper.

The feasibility of using nuclear explosions to create underground storage cavities in rock salt is reported. The problems involved in developing the appropriate industrial techniques are discussed. Results are given of studies made of two nuclear explosions in rock salt (their respective yields 1.1 and 25 kt), on the basis of which some of the engineering problems have been solved. The conclusion is drawn that further research will be necessary before the new method can start to be used by industry. (auth)

**54825** (UCRL-Trans-10543, pp 81-98) USE OF CONTAINED NUCLEAR EXPLOSIONS TO STOP RUNAWAY OIL AND GAS WELLS. Kedrovskii, O. L. Translation of Russian paper.

The problems of the industrial application of contained nuclear explosions for the stopping of two complex runaway gushers at gas fields are outlined. The main conditions for an effective application of explosions to stop runaway gushers are described. The main principles of calculations on stopping gushers and gas crossflows are given and the mechanism of well closure under the action of an explosion is indicated. Finally, specific geologic and engineering details are given concerning two contained nuclear explosions as a result of which runaway wells were closed and gas gushers stopped. (auth)

**54826** (UCRL-Trans-10543, pp 99-116) DISTRIBUTION OF RADIOACTIVE PRODUCTS IN ROCK CRUSHED BY CONTAINED

NUCLEAR EXPLOSIONS AND CALCULATION OF POSSIBLE CONTAMINATION OF PETROLEUM WHOSE OUTPUT IS STIMULATED BY SUCH EXPLOSIONS. Izrael, Yu. A.; Pressman, A. Ya.; Bataev, K. G.; Stukin, E. D. Translation of Russian paper.

The distribution of volatile radioactive products or of ones having gaseous precursors in rock crushed by a contained underground nuclear explosion is described. The amount of such isotopes in the zone of fracturing and in the rubble-filled chimney depends largely on the time of collapse of the cavity. A scheme is given for the possible contamination of the petroleum by the radioactive isotopes, and the rate of penetration of these products together with the petroleum into producing wells in the region of the explosion. The calculated strontium-89 and cesium-137 concentrations in the petroleum are in good agreement with experimental data. (auth)

**54827** FRACTIONAL BURNUP IN A THERMONUCLEAR EXPLOSION. Mitra, Ved (MNR Engineering Coll., Allahabad, India). Energ. Nucl. (Milan); 18: No. 9, 473-7(Sep 1971).

The fractional burnup of fusion fuel in a thermonuclear explosion is obtained, assuming it to be an expanding ball of D–T plasma with Maxwellian velocity distribution, in which the temperature is maintained at the optimum value for the D–T fusion reaction. It is found that such temperature control in the fireball is possible, if during fusion the tritium quantity is maintained constant by regeneration, so that generated power is equal to lost power. (auth)

**54828** PEACEFUL NUCLEAR EXPLOSIONS. Johnson, G. W. (Gulf General Atomic, Inc., San Diego, Calif.). Progr. High Temp. Phys. Chem.; 4: 85-97(1971).

For the past decade the United States has been conducting a program of research and development devoted to the study of potential engineering and scientific uses of nuclear explosives. A large number of possibilities have been examined, extending from basic scientific experiments in seismology, transuranic element production, and neutron physics, to such engineering fields as large-scale excavation, natural gas stimulation and storage, and recovery of minerals. Yields, diameter and likely costs for thermonuclear explosions are tabulated. Work carried out under the Plowshare Program to decrease fallout in cratering events and to develop a basic understanding of cratering through theoretical and experimental approaches is outlined. It is suggested that, because of the problems which would be posed by the release of even small quantities of radioactivity, it seems likely that deeply buried nuclear explosions will probably be the first type to become useful. The advantages and uses of the three general classes, shallow burial (up to 600 m), intermediate depth burial (900 to 1800 m) and deep burial (2500 to 3000 m) into which such applications roughly fall are discussed. (UK)

**54829** ARMS CONTROL AND DISARMAMENT. Curr. Notes Int. Aff.; 41: 253-66(May 1970).

A history of arms control negotiations following the formation of the Ten Nation Disarmament Committee in Geneva in 1959 is summarized, beginning with a description of the goals of a joint statement of agreed principles for guidance on disarmament negotiations, submitted to the U. N. General Assembly by the U.S.S.R. and the U.S.A. The formation of the Eighteen Nation Committee on Disarmament and its evolution to the Conference of the Committee on Disarmament is reviewed. The relation of the official Australian viewpoint to ENDC's objectives with regard to nuclear weapons testing and the nonproliferation of nuclear weapons is partially delineated (principally by statements relating to the NPT). Descriptions are given of the principles of treaties which lead up to the NPT (Antarctic treaty; Outer Space treaty; the treaty for the prohibition of nuclear weapons in Latin America) and those which have followed it (strategic arms limitation talks; draft treaty for arms control of the sea-bed). A short history of efforts made to limit chemical and biological warfare, following the 1925 Geneva Protocol, is also presented. (Australia)

**54830** DIE FRIEDLICHE ANWENDUNG VON NUCKEAREN EXPLOSIONEN. EIN BERICHT UEBER DAS FORSCHUNGS-PROGRAMM PLOWSHARE. (Peaceful Application of Nuclear Explosions. A Report on the Plowshare Research Program). Ginsburg, Theo. Thiemig-Taschenbuecher, Band 21. Muenchen; Verlag Karl Thiemig KG (1965). 255p. DM 14,80.

The following aspects of the Plowshare research program are discussed: characteristics of nuclear explosions; production of electric energy by nuclear explosions; nuclear explosions as peaceful detonators; production of raw materials; scientific applications of nuclear explosions; and present status and future outlook. Special emphasis is given to release of geothermical energy sources, excavation of large harbors and channels, construction of dams, subterranean storage of liquids, desalination of seawater, economic exploitation of thus far inaccessible oil deposits, and the uncovering of deeply deposited coal and ore bodies for pit mining. With respect to scientific applications, studies of the inner structure of the earth, atmosphere and weather, production of high neutron densities, new elements, and isotopes of high activity are discussed. (H.B.G.)

## Facilities and Equipment

*Refer also to abstracts 55086, 55087, 55234, 55440, 55454, 55596, 56120, and 57054.*

**54831** (RDT-E-3-3-T) VERTICAL, SHAFT-SEALED, MOTOR DRIVE, SINGLE-STAGE CENTRIFUGAL PUMP. (Division of Reactor Development and Technology (AEC), Washington, D. C.). Oct 1970. 27p. RSO.

A standard prescribing requirements for a vertically mounted, single-stage, shaft-sealed, electric motor-driven, centrifugal pump classified as a Class I pump as required by paragraph 130 of the draft ASME Code for Pumps and Valves for Nuclear Power for service in water-cooled reactor systems is presented. (auth)

**54832** (RDT-E-4-17-T) HEAT EXCHANGER, CLASS 2, WATER-TO-WATER, STRAIGHT, OR U-TUBE. (Division of Reactor Development and Technology (AEC), Washington, D. C.). Jul 1971. 28p. RSO.

A standard prescribing requirements for construction and acceptance of water-to-water, shell and tube heat exchangers meeting the Class 2 requirements of the ASME Boiler and Pressure Vessel Code, Section III, Nuclear Power Plant Components is presented. It includes U-tube, straight tube, and special configuration types of heat exchangers. (auth)

**54833** (RDT-E-4-18-T) AIR-COOLED HEAT EXCHANGER FOR NUCLEAR STEAM-SUPPLIED SYSTEMS. (Division of Reactor Development and Technology (AEC), Washington, D. C.). Mar 1971. 30p. RSO.

A standard prescribing requirements for the mechanical design, thermal and hydraulic analyses, materials, fabrication, inspection, and testing of air-cooled heat exchanger assemblies for nuclear power plant applications is presented. (auth)

**54834** (WAPD-331) BIBLIOGRAPHY ON ELECTRICAL DISCHARGE MACHINING AND ELECTROCHEMICAL MACHINING. Wahl, W. C.; Tafel, Linda L. (Bettis Atomic Power Lab., Pittsburgh, Pa.). Sep 1971. Contract AT(11-1)-Gen-14. 215p. Dep. NTIS.

A bibliography containing over 1000 references to publications published from 1950 to 1970 on electrical discharge machining and electrochemical machining is presented. The indexes and journals reviewed as bibliographic source material are listed. Author and subject indexes are included. (L.C.L.)

**54835** APPARATUS FOR IRRADIATING MATERIALS WITH ELECTRONS. Noltingk, Bernard Edward; Davidson, William Henry Thomas (to TI (Group Services) Ltd.)). British Patent 1,243, 625. 25 Aug 1971. Filed 26 Jul 1967.

An apparatus for use in the electron irradiation of materials on the industrial scale, and in particular to the provision of improved beam exit windows is described. The electron permeable window structure described comprises a rectangular frame, provided with an array of tubes extending across it, with connections for the passage of coolant. The frame is covered by a thin membrane of electron permeable material pressed into close thermal contact with the cooling tubes when a pressure differential exists across the window. The tubes are preferably of oval or elongated cross-section, with the shorter axis across the electron beam, so as to present a minimum target area for a given cross-section. An electrode, taking the form of a grid of wires, may be located inside the window and clear of the tubes, arrayed to shadow the array of tubes, the applied potential being such as to divert the electrons away from the tubes and towards the clear areas of foil. In order to ensure good thermal contact between the tubes and window a suitable low melting metal of good thermal conductivity may be used. Thermal contact may be further assisted by placing a further grid on the outside of the foil window to press the window tightly against the tubes. (UK)

**54836** FORCED-FLOW STEAM GENERATOR TO BE HEATED BY PRESSURIZED COOLANT OF A NUCLEAR REACTOR. Michel, Rupprecht (to Siemens Aktiengesellschaft). U. S. Patent 3,596,638. 3 Aug 1971. Filed 15 Oct 1968.

XUM

A forced-flow steam generator which is to be heated by pressurized water or other nuclear-reactor pressurized coolant is comprised of a vertically elongated heat exchanger whose pressure-resistant vessel structure encloses a system of vertically parallel tubes which extend from a plenum chamber at the vessel bottom upwardly to a plenum chamber at the vessel top. The tubes are all straight and have no mixing points between the two plenum chambers. At least one of the two structures that form the respective plenum chambers is movably connected with the wall structure of the heat exchanger vessel to permit a heat-responsive movement. Preferably one of the conduits entering into the vessel to communicate with one of the plenum chambers is joined with an outlet of the chamber by a movable or overlapping joint which is sealed by means of an expansible diaphragm such as a corrugated sealing tube. (Official Gazette)

**54837** GAMMA-RAY IRRADIATION EQUIPMENT. Srapenyants, R. A.; Voropaev, Yu. V.; Lur'e, L. S.; Khrushchev, V. G.; Kaushanskii, D. A. Russian Patent 270,114. 8 May 1970. Filed 4 Apr 1966. (In Russian).

An installation for irradiating tubers without first having to put them into sacks is described; to increase output and reduce the size and complexity of the device, the irradiation chamber is built sloping toward the unloading mechanism. (R.W.R.)

**54838** IMPROVEMENTS TO SHEARS USED WITH IRRADIATED FUEL ELEMENTS. Cherel, Guy (to Saint-Gobain Techniques Nouvelles, SA). French Patent 2,034,223. 11 Dec 1970. Filed 26 Feb 1969. (In French).

Shears for a fuel reprocessing plant are described. The device is of the type consisting of equipment for advancing the element into the shears. A characteristic of the shears is the position of their face with respect to the clamp. The face consists of at least one protruding part and a hollow part separated by a distance greater than the pitch of the element advancing device. A reprocessing plant consisting of a sawing machine, shears and a dissolver is presented. (France)

**54839** LUXEMBOURG SODIUM TEST FACILITY. Sims, J. (Gradel SA, Luxembourg). Nucl. Eng. Int.: 16: 415-16(May 1971).

The general arrangement of the Luxatom mechanical components Na test facility is shown. The temperature is normally 200°C, but may reach 350°C. Rigs are subjected only to convection flow and Na transfer is by pressure differential. The blanket gas is argon. The total volume of Na is 100 liters and those parts of the circuit in contact with Na are of 316 stainless steel. All welds are produced by argon-arc. Brief reference is made to purification, level control, leak detection and rig cleaning. (UK)

**54840** PEGASE AND OSIRIS HIGH TEMPERATURE IRRADIATION LOOPS. Bull. Inform. Sci. Tech. (Paris); No. 153-154, 140-50(Nov-Dec 1970). (In French).

Improvements made to the Pegase loops and the results obtained from the following tests are described: helium tightness tests, blowing tests, and thermal insulation tests. The BABAR device is based on the principle of the injection pump (also used in the Osiris Spitfire loop). The Osiris Aida loop is mobile and situated in the Osiris pool, while the Othello loop is fixed in the core. The loops consist of an immersed gas circuit connected to a nonimmersed circuit. (France)

**54841** IMPROVEMENTS IN OR RELATING TO HOPPER FEEDERS. Tindale, John Basil; Ridout, Edmund Umfreville (to United Kingdom Atomic Energy Authority). British Patent 1,227,540. 7 Apr 1971. Filed 22 Dec 1967.

In applications of hopper feeders to nuclear fuel, particularly in the form of cylindrical ceramic pellets, damage may occur due to the pellets jamming against one another or against the sides of the hopper outlet; the hopper feeder described was designed to alleviate this problem. It has a discharge means having a resilient surface and opposing walls extending upwardly away from this surface. The lower edges of the walls define gaps between the walls and the resilient surface for the passage of material, and means are provided for producing an oscillating motion of the discharge means in a direction across these edges. The resilient surface may be curved and may comprise a thin outer layer of solid flexible material and a thicker inner layer of spongy resilient material. The outer layer may comprise solid rubber and the inner layer sponge rubber. (UK)

**54842** DESIGN OF THE VALVES FOR NUCLEAR POWER GENERATION. Wada, Susumu (Okano Valve Mfg. Co. Ltd., Kitakyushu, Japan). Haikan To Sochi; 10: No. 4, 32-47(Apr 1970). (In Japanese).

The nuclear power plants in Japan employ mainly BWR's and PWR's. Compared with conventional power plants, the following are important for the valves of nuclear use. An extended endurance or life is necessary because of larger capital cost, and higher performance required against radiation effects. According to the ASME's code for pumps and valves, the valves for nuclear use are classified into A-class, including the inlet and outlet valves of recirculation pumps and main steam control valves, B-class including the other than above, and C-class such as those for the cooling lines for reactor buildings. The design features of these valves used for a BWR are described. A-class valves (materials, valve body, stresses, fatigue, and cycle rating); B- and C-class, and other valves (stuffing box, gland packing, and electric valves); and the general requirement for valves are discussed. (Japan)

**54843** NEW WRINKLE IN SOLID-WASTE DISPOSAL. Power 115: No. 7, 86-7(Jul 1971).

A pilot plant recovery system is described in which solid wastes are transported by sewer mains. The goal of the investigation is to develop a plant in which useful materials now being discarded can be recovered. No waste fraction is to be returned to air or water as a pollutant. A flow diagram is included. (J.R.D.)

**54844** LARGE GAMMA FACILITY UGU-200. Krasin, A. K.; Salamatov, I. I.; Borisevich, V. A.; (and others). At. Energ. (USSR); 31: No. 3, 205-7(Sep 1971). (In Russian).

The multicell gamma irradiation plant was put into operation. Two dry cells can be supplied by one source separately or by two sources simultaneously. The volume of each cell is 35 $m^3$. The cell shielding is designed for work with the sources on 210,000 gram-equivalents of radium. Two sources are used in this plant. Their total activity is about 400,000 gram-equivalents of radium. There is a water pool for keeping and assembling of sources. This pool serves as the third irradiation cell. It is possible to modify the shape of the source in a short time. (auth)

**54845** FLUID SEALING DEVICES. Pettinger, Donald Stanley (to United Kingdom Atomic Energy Authority). British Patent 1,233,548. 26 May 1971. Filed 3 Nov 1967.

Reference is made to fluid sealing devices for sealing elongated bodies within pressure tubes. The device described is stated to be particularly suitable for nuclear reactor applications under high temperature and pressure conditions, and an example is its use for sealing a closure plug within a pressure tube of a stream generating nuclear reactor. The device comprises a stack of at least three nested identical metallic cups each having a central opening for sealed engagement by the elongated body, and a flexible wall with an unbroken rim to make peripheral and sliding contact with the pressure tube. At least two cups are in contact with the surfaces of adjacent cups. In use the interiors of the cups are directed towards fluid pressure so that they are expanded into sealing contact with the pressure tube. (UK)

**54846** EXPERIMENTAL STRESS ANALYSIS AND ITS INFLUENCE ON DESIGN. Proceedings of the Fourth International Conference, Cambridge, England, 6th-10th April 1970. Meyer, M. L. (ed.). London; Institution of Mechanical Engineers (1971). 584p. (In several languages). (CONF-700427).

Forty-two papers were presented at the conference. Sessions were devoted to discussions of civil engineering structures; inclusions and photoelastic coatings on concrete; hydrotechnical structures, bridges, and plates; girders; photoelastic techniques; Moire techniques; welds and internal stresses; strain gages and pressure vessels; stress distributions in thin-walled pressure vessels; tubes and flanges; thermal loading; rotating machines and the use of polythene; and notches and pins. (R.C.K.)

**54847** NOMOGRAM FOR DETERMINING THE NUMBER OF SEPARATORS IN THE COMBINATION OF RADIOMETRIC LUMP AND BATCH SEPARATION OF RADIOACTIVE ORES. Lubyanskii, Ya. M.; Malakhov, S. S. (Moscow Geological-Prospecting Inst.). Izv. Vyssh. Ucheb. Zaved., Geol. Razved.; 13: No. 7, 125-8(1970). (In Russian).

Nomograms are given for determining the number of separators to be used in combined radiometric lump and batch separation for industrial processing of radioactive ores. The theoretical basis of the efficiency of the combined lump and batch separation method and of the optimum conditions for such combined operations is discussed. (R.V.J.)

**54848** RELUCTANCE MOTOR FOR DRIVING CONTROL RODS OF NUCLEAR REACTOPS. Saban, J. (Rade Koncar, Zagreb). Elektrotehnika (Zagreb); 12: No. 2, 124-32(1969).

Problems concerning the use of reluctance motors and their

construction materials for use in nuclear reactors are described. The questions of the use and construction of these motors that are rarely found in literature, or are treated in a somewhat different way are discussed. The two-axis theory is not discussed because it is already known. (Bull. Sci., Sect. A)

**54849** METHODS OF AND APPARATUS FOR IRRADIATION OF ARTICLES BY RADIOACTIVE PANELS. **Balanca, Pierre; Frignet, Georges; Pierlas, Rene (to Saint-Gobain Techniques Nouvelles). U. S. Patent 3,566,113. 23 Feb 1971. Priority date 2.Dec 1964, France.**

A method and apparatus are described for the irradiation of containers and articles therein, by radioactive panels. A chamber defined by a shielded top, bottom and sidewalls, and one end wall, supports a radioactive panel in vertically-erect position midway between and parallel with the sidewalls, to define two corridors side by side. The otherwise open end of the chamber is closed by a cylindrical housing rotatable about its vertical central axis. The housing has four compartments separated and defined by shielded walls. In one of two 180° positions of the housing, two of these compartments register with the respective corridors while the other two face outwardly for loading and unloading. In a second 180° position the locations of the compartments are reversed. Conveyors support the containers and move them in and along one corridor, past the radioactive panel, translate them without rotation at and along the end wall, then in a return translation pass in and along the corridor at the other side of the panel, to thus complete a cycle. Opposite sides of each container are thus directly and equally exposed to radiation during a cycle. The bottom wall of the chamber has an opening into which fits a shielded housing for enclosing the panel during transport. Means are provided for elevating the panel from the housing into the chamber, through the opening, when the chamber and housing are in interfitting relation. The panel may be in upper and lower sections and connected for relative vertical translation. When collapsed, the panel sections fit snugly into the housing. When moved from the housing into the chamber, the sections automatically move vertically and relatively and when fully emplaced in the chamber, form what is in effect a single panel of double the area of the sections. Suitable safety interlocks provide complete protection for operating personnel and indicate and assure proper functioning of the apparatus. The invention is of particular value because it may be transported in sections from one place of use to another. (Official Gazette)

**54850** STRESS CALCULATION FOR THE PIPING SYSTEMS IN A NUCLEAR REACTOR PLANT. **Uchiyama, Yuichi (Hitachi Ltd., Ibaraki, Japan). Haikan Gijutsu; 12: No. 9, 69-76(Sep 1970). (In Japanese).**

The thermal stress analysis and earthquake stress analysis of the piping systems in a nuclear reactor plant are described. The importance of the stress analysis for the piping systems with regard to the characteristics of a nuclear reactor plant is described. The theory of thermal stress analysis is briefly presented. Earthquake stress analysis is described as follows: the piping systems are classified according to their degree of importance; the theory of the vibration analysis for the piping systems by the dynamic transfer matrix method is presented; the program for the analysis of earthquake response is outlined; and finally, the calculated and the experimental results for a model piping system are compared. Important piping systems should be supported as rigidly as thermal stresses permit, and should be divided in small sections by providing anchor points. (Japan)

**54851** IRRADIATION AND CALIBRATION DEVICES. **Candes, P. (CEA, Saclay, France). Radioprotection; 5: 323-8(1970). (In French). (CONF-700505-25).**

From second Congress of the International Radiation Protection Association, Brighton, England.

The irradiation station at Cadarache (STIRCA) is described; this station is concerned with developing radiation dosimetry techniques for nuclear installations. The calibrated sources available are thermal neutrons, 14-MeV neutrons, and $\gamma$ radiation sources. In addition, the station contains an experimental hall constructed of light material and an underground building. The thermal neutron source SIGMA contains a graphite stack. (auth) (France)

**54852** OPTIMUM PLANNING FOR RADIATION FACILITIES. MEDICAL FACILITIES. **Iwaki, I. (Ministry of Health and Welfare, Tokyo). Genshiryoku Kogyo; 16: No. 5, 11-16(Mar 1970). (In Japanese).**

Radiation facilities for medical use require various measures for shielding and contamination protection according to the nature of radiation employed. A review of the special conditions required for designing such facilities is presented. In accordance with the Medical Facilities Regulations, these facilities are classified into x-ray apparatus, radiation apparatus, radiation equipment, and radioisotope apparatus. The equipment using high-energy radiation, radiocobalt, and radium are regulated by law for prevention of radiation damage and requires a legal permit for operation. The planning and designing of radiotherapy facilities for x-ray, radiation, and radioisotope therapy are explained. Brief explanations are given for flow plans itemized as fundamental policy of designing, central control system, establishment of management area, separation of radiation area and contamination area, ground floor or basement plans, and area conditions and future plans. Enforcement regulations set the permissible dose of 100 mrem/week for radiology technicians, 30 mrem/week for hospital workers, and 10 mrem/week for people in general. (Japan)

**54853** COMBINATION LINEAR LIFTING AND TRANSLATION MECHANISM. **Rutkauskas, Vincent J. (to United States Atomic Energy Commission). U. S. Patent 3,556,486. 19 Jan 1971. Filed 7 Feb 1969.**

A laboratory manipulator for the remote handling of objects in a controlled environment is described. A plurality of blocks are attached to one side of a flexible band. One end of the band is attached to a rotatable drum and a gripping means is attached to the other end of the band. (Official Gazette)

**54854** METHOD FOR CONSTRUCTING A LINED UNDERGROUND CAVITY BY UNDERREAMING, GROUTING, AND BORING THROUGH THE GROUTING. **Johnson, Walter H. (to United States Atomic Energy Commission). U. S. Patent 3,559,409. 2 Feb 1971. Filed 24 Jun 1969.**

A method is described for constructing a lined underground cavity by drilling a borehole, locating a casing in the borehole, filling the space between the casing and the borehole with grout, underreaming a large borehole beneath the grout, underreaming the large borehole, filling the large underreamed borehole with additional grout that binds with the previously underreamed grout, drilling a small borehole from the casing into the added grout, and underreaming the small borehole but leaving a wall of grout to form a lined cavity. (Official Gazette)

**54855** IRRADIATION APPARATUS. **(to Sulzer Brothers Ltd.). British Patent 1,229,375. 21 Apr 1971. Priority date 20 Sep 1968, Switzerland.**

An irradiation apparatus is described which includes a chamber surrounded by shielding, equipment for placement of radiation exposure specimens, and a rotary lock in the shield wall having recess for receiving charges to be irradiated. (J.R.D.)

**54856** GAS TURBINE PLANT. **Suter, Peter (to Sulzer Brothers Ltd.). British Patent 1,230,005. 28 Apr 1971. Priority date 27 Jul 1967, Switzerland.**

A gas turbine plant is described having at least two shafts, at least two stages of compression with interstage cooling, at least two stages of expansion with interchange reheating, a controllable throttle upstream of the low-pressure compressor, and a further expansion turbine connected to the high-pressure shaft and connected in parallel with the throttle. (J.R.D.)

**54857** CIRCULATION PUMPS FOR NUCLEAR USE. **Ezaki, Y. (Fuji Electric Co. Ltd., Suzuka, Japan). FAPIG (Tokyo); No. 54, 131-5(Sep 1969). (In Japanese).**

Glandless motor pump units (GMPU) are described. In the circulation pumps for PWR's, leaks from glands are not permitted and perfect nonleakage from the pumps is required. In the GMPU, the pump and motor are completely encased, and the impeller is fixed to the end of a motor axis by overhanging. The GMPU's are of two types; in the dry stator unit (DSU) the stator winding of a motor is separated from the liquid by thin canning, and in the wet stator unit (WSU) the winding is in direct contact with it. The advantages and disadvantages of DSU and WSU are described, including also the structural materials. The stator winding, canning for the DSU, bearings, and motor cooling are also discussed. The procedure of testing the GMPU's is outlined. (Japan)

**54858** INTRODUCTION OF HYDROGEN ISOTOPES IN METALS BY MEANS OF A MINIATURIZED CATHODE LOADING CELL. **Bretin, Lucien (CEA, Bruyeres-Le-Chatel, France); Broudeur, Robert; Fidelle, Jean-Pierre. Compt. Rend., Ser. C; 272: 516-9(8 Feb 1971). (In French).**

A miniaturized cell was built for hydrogen, deuterium, and tritium cathode loading. The first tests carried out with hydrogen and deuterium gave satisfactory results in spite of the strict conditions imposed by the prospective use of tritium. (auth) (France)

**54859** ELECTROCHEMICAL PROCESS FOR DETECTING MICROPOROUS ZONES IN FILM MATERIAL SUCH AS INSUL-

XUM

ATING FILMS. Chapron, Yves; Chapuis, Anne-Marie; Francois, Henri (to Commissariat a l'Energie Atomique). British Patent 1,230,301. 28 Apr 1971. Priority date 29, Mar 1968, France.

The film surface to be evaluated for microporosity is brought into contact with ions designated as X while the opposite surface is brought into contact with a reagent containing ions designated Y. If X ions diffuse through the film, a colored XY compound results which shows the porous area. The process is applicable to gloves and can be used with Ni salts and dimethylglyoxime. (J.R.D.)

**54860** SUBSTANTIALLY FLUID TIGHT CLOSURE DEVICE BETWEEN TWO COAXIAL WALLS. Derussit, Richard; Thomas, Bernard (to Commissariat a l'Energie Atomique). British Patent 1,229,773. 28 Apr 1971. Priority date 12 Aug 1968, France.

It is noted that when two coaxial walls are subjected to different temperature conditions or have different coefficients of expansion, their connection or the closure of the space separating them must be ensured by a resilient member. A device is described in which stresses in such systems are eliminated by circumferentially fractioning of the various members in such a way that the relative movements of the two walls are absorbed while seal-tightness is maintained. (J.R.D.)

## Heat Transfer and Fluid Flow

*Refer also to abstracts 54888, 54916, 57031, 57032, 57034–57036, and 57094.*

**54861** (AEEW-R-705) INVESTIGATION INTO THE EFFECT OF "CRUD" DEPOSITS ON SURFACE TEMPERATURE, DRY-OUT AND PRESSURE DROP, WITH FORCED CONVECTION BOILING OF WATER AT 69 BAR IN AN ANNULAR TEST SECTION. Macbeth, R. V.; Trenberth, R.; Wood, R. W. (Atomic Energy Establishment, Winfrith (England)). May 1971. 19p. Dep. NTIS (U. S. Sales Only).

Water boiling surfaces usually acquire deposits of one kind or another, often referred to as "crud". With the greatly increased heat transfer rates that have become common practice in recent years, both in fossil and in nuclear fired boilers, these crud deposits have, on occasions, led to severe overheating and failure of boiler tubes and boiling water reactor fuel elements. The remedy being adopted is to introduce better water quality control. While this is proving reasonably effective it is nevertheless an expensive procedure and it is not clear to what extent the blanket operation of water purification is justified. A research programme has been started at AEE Winfrith to investigate the subject, and some initial results of the heat transfer performance of crudded rods are presented. The crud deposits were prepared to a close specification so that their chemical and physical structure was known. The crudded rods were tested at 69 bar in an annular test section with forced convection boiling at mass velocities in the range 1360 to 3400 kg/m$^2$s and with inlet subcooled temperatures from 3°C to 60°C. The effect of the deposits on dry-out, metal surface temperature and frictional pressure drop are reported. (auth) (UK)

**54862** (AEEW-R-711) BOILING ON SURFACES OVERLAID WITH A POROUS DEPOSIT: HEAT TRANSFER RATES OBTAINABLE BY CAPILLARY ACTION. Macbeth, R. V. (Atomic Energy Establishment, Winfrith (England)). Jun 1971. 10p. Dep. NTIS (U. S. Sales Only).

It is becoming apparent that wick-boiling is probably the principal mode of boiling in many common situations, including power station boilers and boiling water nuclear reactors, although this has not been generally realized until recently. Deposits of porous magnetite, which tend to be found in most water boiling circulation systems, are the cause of wick-boiling being present. The evidence against the presently held view of what constitutes convective boiling is examined, and a detailed description and analytical model are presented of the process that is considered more likely to be taking place where porous magnetite deposits are found. (auth) (UK)

**54863** (AI-AEC-13010) FORCED-FLOW SODIUM BOILING IN MULTIPLE CHANNELS. Logan, D.; Baroczy, C. J.; Morewitz, H. A. (Atomics International, Canoga Park, Calif.). 15 Sep 1971. Contract AT(04-3)-701. 43p. Dep. NTIS.

Experimental data are presented for the boiling sodium pressure drop-flow characteristic, at fixed power, for a group of interconnected channels formed by three heated 0.25-in. diameter pins located in a cloverleaf-shaped channel. Comparison of the data with a multichannel boiling sodium code shows reasonable agreement; however, the curve shape is shown to be very sensitive to small changes in flow-channel dimensions or geometry. Numerical results demonstrate that the pressure drop-flow behavior of a group of geometrically identical channels can, under nonuniform heat input conditions, be substantially different from that normally observed for a single channel. Boiling behavior and burnout heat flux data at 5 psia are also presented for a test section consisting of constant-geometry, equal-length, heated and unheated sections, with and without wire-wrap spacers. When the burnout heat flux data were corrected to constant pressure, velocity effects were negligible, while the effects of local subcooling were large. (auth)

**54864** (ANL–7754) ENGINEERING RELATIONSHIPS FOR TURBULENT FORCED-CONVECTION HEAT TRANSFER IN DUCTS WITH FLUX TRANSIENTS. Stein, Ralph P. (Argonne National Lab., Ill.). Jun 1971. Contract W-31-109-eng-38. 31p. Dep. NTIS.

Engineering relationships to account for turbulent forced-convection heat transfer in ducts during heat-flux transients and steady flow are derived. These relationships are suggested as more accurate replacements for the simple heat-transfer-coefficient expression $t_s - \bar{t} = q/h$ currently used in most engineering computations involving transients. The new relationships have the form $t_s - \bar{t} = (q/h) + (D^2R_1/2k\beta)\,[(\partial q/\partial\bar{t}) + (1/\bar{u})(\partial q/\partial\tau)] + \ldots$, where $R_1$ and $\beta$ are dimensionless coefficients depending on Reynolds and Prandtl numbers and on duct shape. Tabulated values of these coefficients for the circular tube, parallel-plane duct, and pin bundle are given for wide ranges of Reynolds and Prandtl numbers, with emphasis on liquid metals. (auth)

**54865** (CEA-CONF–1758) NUCLEAR THERMAL STUDIES IN FRANCE AND THEIR APPLICATIONS TO OTHER FIELDS. Mondin, Henri (Commissariat a l'Energie Atomique, Grenoble (France). Centre d'Etudes Nucleaires). 1971. 16p. (In French). (CONF-710317–2). Dep. NTIS (U. S. Sales Only).

From sixteenth nuclear congress; Rome Italy (25 Mar 1971).

The principal heat transfer studies made in relation with the French nuclear program are outlined and the results obtained are given. The information acquired is enumerated. Nonnuclear applications are classified by the nature of the applied information and the needs of the users. An important role is played by the fundamental aspects and the scientific potential and technology acquired by the teams studying thermal techniques in making use of new concepts. The liaison with the CEA and the nonnuclear industry with regards to reciprocal information, financing of contracts, and the interchange of knowledge, is discussed. (auth) (France)

**54866** (EIR–198) CONVECTIVE HEAT TRANSFER IN LONGITUDINAL FLOW THROUGH TUBES AND ROD BUNDLES. Markoczy, G. (Eidgenoessisches Institut fuer Reaktorforschung, Wuerenlingen (Switzerland)). Apr 1971. 154p. (In German). Dep. NTIS (U. S. Sales Only).

Convective heat transfer in tubes and rod bundles was theoretically and experimentally studied under forced axial turbulent flow. It was shown that heat transfer coefficients under these complex conditions could not be determined by means of geometry-dependent correction functions. Therefore, new relationships were developed which described with sufficient accuracy local heat transfer in bundles of various arrangements. Two mathematical procedures were developed and tested on 2000 experimental measurements. The first one is an involved analytical procedure, while the second is simple and semi-empirical. (68 references) (tr-auth)

**54867** (EUR–4683) PRESSURIZED AND BOILING WATER LOOP OF THE TECHNOLOGY DIVISION AT ISPRA. Herkenrath, H.; Moerk-Moerkenstein, P. (European Atomic Energy Community, Ispra (Italy). Joint Nuclear Research Center). 2 Apr 1971. 36p. Dep. NTIS (U. S. Sales Only). EUR FF 7.75.

The pressurized and boiling water loop of the Technology Division at Ispra is described. This loop is specially designed for the investigation of heat transfer to water at pressures up to 250 bar, and allows investigations of test sections of realistic dimensions with a maximum power input of 3.0 MW. The detailed description of all elements of the loop demonstrates its great versatility. (auth)

**54868** (EURFNR–897) EXPERIMENTAL STUDY OF INCIPIENT BOILING SUPERHEAT OF SODIUM ON ARTIFICIAL SURFACE ROUGHNESSES. Schultheiss, G. F. (Kernforschungszentrum, Karlsruhe (West Germany). Institut fuer Reaktorentwicklung). Translation of report KFK–1332. 113p. Dep. NTIS.

Work Performed under United States–Euratom Fast Reactor Exchange Program.

The equipment, procedures, and results of experiments performed to investigate the effects of test surface material, surface roughness, and sodium oxide concentration on the amount of superheating required for the incipient boiling of sodium are described in detail. The surface materials used included stainless steel, pure nickel, iron, and chromium. Changes in surface roughness were achieved by cutting cylindrical cavities of varying depths and diameters into the surface materials. The results showed: little change in the surface cavities after long-time boiling; that decreasing the depth-to-dia. ratio of the cavities slightly increases the incipient boiling superheat; the hot-trap purified sodium experimental results are in good agreement with theoretical values of incipient boiling superheat calculated from the vapor pressure to surface-tension equilibrium (critical radius of the nucleus equal to cavity radius); incipient boiling superheat depends on oxide concentration as well as on the test-surface material; and for stainless steel, superheat has a typical maximum at about 127°C cold-trap temperature corresponding to 2 ppM $Na_2O$ obviously caused by the chromium content. Pure iron and nickel did not show such a maximum. Pure chromium behaves like stainless steel. Pure iron shows generally very small superheat not influenced by oxide concentration. For nickel, superheat decreases with increasing oxide concentration and approaches the same constant value as stainless steel. (L.C.L.)

**54869** (FEI–217) CRISIS OF HEAT TRANSFER IN PIPES. Zenkevich, B. A.; Peskov, O. L.; Sapankevich, A. P. (Gosudarstvennyi Komitet po Ispol'zovaniyu Atomnoi Energii SSSR, Obninsk. Fiziko-Energeticheskii Institut). 1970. 35p. (In Russian). Dep. NTIS (U. S. Sales Only).

Experiments were performed to study the effects on the heat transfer crisis of film and diffusion components in two-phase flow in the dispersion-annular flow regime. Experimental data obtained in uniformly heated tubes and in tubes with axial cosinusoidal distribution of the heat flow are presented. Analysis of experimental data under other axial distributions of the heat flow showed the presence of feedback between the local critical heat flow and the local rate of flow of the liquid to the cross section of the crisis. The coefficients of mass transfer by influx were analyzed and used to calculate recommended local critical thermal flows in pipes. (JPRS)

**54870** (GEAP–10347) TWO-PHASE FLOW AND HEAT TRANSFER IN MULTIROD GEOMETRIES. Final Report. Janssen, E. (General Electric Co., San Jose, Calif. Atomic Power Equipment Dept.). Mar 1971. Contract AT(04-3)-189. 76p. Dep. NTIS.

An investigation of two-phase flow in multirod coolant channels characteristic of a large class of modern water-cooled nuclear reactors is described. Its purpose is the more accurate determination of the mechanisms associated with boiling heat transfer which ultimately limit the rate of heat transfer from the rods to the coolant. Detailed measurements were made of pressure drop/wall shear stress, liquid film thickness, liquid film flow rate, local mass velocity, and local quality for fully developed adiabatic flow in both simple and multirod channels. A model of fully developed annular-dispersed flow was developed based on these and other results which shows, for example, the relationship between entrainment fraction and pressure gradient, correlates much of the world data pertaining to entrainment fraction in simple channels, and shows the presence of anomalies in some of the remainder of the world data. Measurements were made of critical heat flux in a clean nine-rod channel, trends in the data with certain parameters were pointed out, and various schemes for correlating multirod critical heat flux (CHF) data were assessed. It was concluded that the schemes using average channel conditions had serious limitations, but that a scheme considering individual subchannel conditions would provide the means for a more general correlation of multirod CHF data. Measurements were made of pressure drop, liquid film thickness, and liquid film flow rate for developing diabatic flow in simple channels, and subchannel and pressure drop measurements were made for both adiabatic and diabatic developing flow in a nine-rod channel. These latter measurements provide essential, and previously lacking, inputs to subchannel schemes for predicting multirod CHF. Finally, measurements were made of CHF in a nine-rod channel fitted with grid-type spacers characteristic of modern water-cooled reactors. The tests were run with various axial arrangements of the spacers with respect to the heated length, to better understand their effect on CHF. The results showed, for example, that CHF prefers to occur directly ahead of a spacer. An analysis and some simple experiments in a shallow water channel identified mechanisms which would cause dryout directly ahead of an obstruction, and so help to explain some of the findings. (auth)

**54871** (IFA-TR-58) BURN-OUT HEAT FLUXES AT SUBCOOLED BOILING. Mihaila, A.; Dobrescu, C.; Luca, L.; Pana, M. (Institutul de Fizica Atomica, Bucharest (Romania)). 1970. 12p. Dep. NTIS (U. S. Sales Only).

The equipment and methods used and heat fluxes measured in experiments performed to study burnout heat fluxes during subcooled boiling are described. (L.C.L.)

**54872** (JUL–740-RB) MEASUREMENT OF HEAT TRANSFER IN THE BUBBLE BOILING OF WATER IN METALLIC TUBES. Fedders, Heinrich (Kernforschungsanlage, Juelich (West Germany). Institut fuer Reaktorbauelemente). Feb 1971. 111p. (In German). Dep. NTIS (U. S. Sales Only).

Heat transfer measurements with bubble boiling were made in order to clarify some input parameters and to prove heat transfer relations developed in previous studies. The experimental method, one using direct heating, was selected in order to investigate the heat transfer at high heat current densities in a range of atmospheric pressure up to 150 bar. The effect of heat surface roughness on the heat transfer was also investigated. The dependence found by Stephan, in which the heat transfer coefficient is $\alpha \sim R_p^{0.13}$, was verified. If the heat current density is increased the effect of the roughness is decreased. (J.S.R.)

**54873** (RD/B/N–1967) ESTIMATION OF FRICTION FACTOR OF ROUGH SURFACES FROM THE PRESSURE DISTRIBUTION AROUND A ROUGHNESS ELEMENT. Kacker, S. C. (Central Electricity Generating Board, Berkeley (England). Berkeley Nuclear Labs.). Apr 1971. 25p. Dep. NTIS (U. S. Sales Only).

A method for estimating the friction factor of rough surfaces from pressure measurements around a roughness element is described. The present method is suitable for developing boundary layers over rough surfaces, and it can be applied to study the effect of roughness element geometry and shapes on drag coefficients. (auth) (UK)

**54874** (RD/B/N–1980) THE USE OF AN EDDY VISCOSITY MODEL TO PREDICT THE HEAT TRANSFER AND PRESSURE DROP PERFORMANCE OF ROUGHENED SURFACES. Lawn, C. J. (Central Electricity Generating Board, Berkeley (England). Berkeley Nuclear Labs.). May 1971. 20p. Dep. NTIS (U. S. Sales Only).

Calculations were made of the velocity and temperature profiles for fully-developed turbulent flow in annular channels with roughened core rods. A unique set of boundary values for dimensionless velocity and temperature, together with a universal eddy viscosity model, serve to predict the friction factors and Stanton numbers of one particular surface in a wide variety of flow channels. The necessity for transformation of data in making comparisons of single pin performance is thus avoided. (UK)

**54875** (RT/ING–71-8) PHOTOGRAPHIC STUDY OF TWO-PHASE HIGHLY DISPERSED FLOWS. Cumo, M.; Ferrari, G.; Farello, G. E. (Comitato Nazionale per l'Energia Nucleare, Rome (Italy)). 24 Mar 1971. 22p. Dep. NTIS.

A post-burnout two-phase flow of a highly dispersed mixture of Freon-12 (reduced pressure 0.3) was analyzed by means of high speed cinematography. The Freon was electrically heated in a loop where, downstream from the heating section, a visualized test section was placed through which high-speed films were taken. The photographs were analyzed, taking into account the characteristics of the droplet population such as droplet dimensional distribution, velocity, trajectories etc. The main conclusions were: there is photographic evidence of a thermodynamic disequilibrium up to calculated qualities of 200% in post burn-out two-phase flows; the droplet mean diameter decreases with the heat flux (of the test section uniformly heated by Joule effect) and the vapor specific mass flowrate; the droplet velocity is independent of droplet diameter and is almost equal for all droplets (theoretical equations of droplet entrainment have been confirmed); the droplet transversal velocity profiles are very close to the vapor velocity profiles theoretically deduced (the local slip ratios are very close to 1); and droplet trajectories (graphically deduced from the photographs and plotted) are straight and parallel to the flow. Many diagrams of droplet dimensional distribution dependent on specific mass flowrate, quality and heat flux were plotted, analyzing more than 10,000 droplets. With increasing flowrate and heat flux the dimensional distribution curves decrease towards minor diameters. (auth)

**54876** (RT/ING–(71)11) SPACE TIME TEMPERATURE DISTRIBUTION IN A SEMI INFINITE MEDIUM UNDER PARTICULAR CONDITIONS OF THERMAL TRANSIENT. Musso, B.; Zona, R. (Comitato Nazionale per l'Energia Nucleare, Rome (Italy)). 23 Apr 1971. 27p. (In Italian). Dep. NTIS (U. S. Sales Only).

Numerical and analytical methods for calculating the space-time temperature distribution in a semi-infinite medium under

XUM

conditions of thermal transients (sudden contract with a hot fluid) are outlined. (tr-auth)

**54877** (SGAE-RT-38/1971) INVESTIGATIONS OF THE DYNAMICS OF HEAT TRANSFER. PART 2. MODEL OF AXIAL HEAT TRANSFER IN TURBULENT TUBE FLOW. 5th Work Report, 1971. Schmidl, H. (Oesterreichische Studiengesellschaft fuer Atomenergie G.m.b.H., Seibersdorf. Institut fuer Reaktortechnik). Mar 1971. 109p. (In German). Dep. NTIS (U. S. Sales Only).

The dynamic behavior of a heat transfer medium is difficult to determine. Therefore, in order to facilitate a solution to the problem a selected tube flow was treated with only two dimensions. The principles of heat transfer in turbulent flow of an incompressible medium were determined. A model for axial heat transfer with turbulent tube flow was derived. (J.S.R.)

**54878** ACCURATE CHARACTERIZATION OF THE HIGH-PRESSURE ENVIRONMENT. Proceedings of a Symposium Held at Gaithersburg, Md., October 14–18, 1968. Lloyd, Edward C. (ed.). National Bureau of Standards Special Publication 326. Washington, D. C.; National Bureau of Standards (1971). 344p. (NBS-SPEC.PUBL.-326; CONF-681005). GPO $4.50.

The conference was intended to provide an authoritative survey of precise measurement problems and techniques now in use or proposed. It was hoped that the conference would permit critical evaluation of the need for efforts toward the development of improved measurement standards, and identification of probable fruitful lines of investigation toward establishment of such standards. The survey should provide the information needed to evaluate the feasibility of obtaining early agreement on a provisional pressure scale. Thirty-eight papers were presented, and four panel sessions held, covering research at high pressures in static systems and in shock wave experiments. The importance of improved accuracy in measurements at high pressures and in calibrations relevant to such measurements was emphasized. The point was made that in current work, involving a wide range of phenomena and many types of apparatus, a series of "interlocking" standards is needed. About one-fourth of the papers dealt with matters relevant to selection of reproducible and reversible reference points on the pressure scale — so-called "fixed points" — indicated by phase changes in selected substances. The importance attached to establishing such agreed-on fixed points was indicated. (R.C.K.)

**54879** CRITICAL HEAT FLUXES ENCOUNTERED IN THE CASE OF BOILING OF ORGANIC HEAT TRANSFER AGENTS WITH A HIGH BOILING POINT. Sterman, L. S. (Moscow Energetic Inst.); Korychanek, Ya. At. Energ. (USSR); 29: 374-6(Nov 1970). (In Russian).

The critical heat fluxes were studied on surfaces immersed into mixtures of terphenyls which exhibit vapor pressures of only 3 to 4 bars at temperatures up to 420°C and are stable against pyrolytic and radiolytic decomposition. Mixtures of compounds manufactured in Czechoslovakia (Delowax S, Delowax OM), hydroterphenyl and their components, ortho-, meta-, and para-terphenyl, and diphenyl were used for the bulk boiling experiments, during which the pressure was varied from 0.1 to 4.0 bar. It was found that the value of $q_{crit}$ of pure terphenyls had the same relation to pressure as the other heat transfer agents; however, the pressure affected only slightly the $q_{crit}$ of these high-boiling liquids while it exerted a strong effect on the critical heat flux of low-boiling-point organic compounds and water. Comparison of experimental and calculated data showed good agreement in the neighborhood of atmospheric pressure, indicating that in case of the boiling of high-boiling point organic compounds at elevated temperatures, processes which lead to an early establishment of critical boiling conditions occur. This early transition to film boiling may be due to the pyrolytic decomposition of the microlayer near the walls. This behavior was confirmed also at pressures of $p < 1$ bar. (TTT)

**54880** EFFECT OF THE DIMENSIONS OF THE FUEL ELEMENT OF THE HEAT TRANSFER AT SUPERCRITICAL PRESSURES. Kafengauz, N. L.; Fedorov, M. I. At. Energ. (USSR); 29: 293-4(Oct 1970). (In Russian).

It was found during previous studies on heat transfer of liquids flowing through ducts at supercritical pressures that heat transfer is improved only if the liquid is subject to thermal decomposition, forming lighter components. Results of the current work revealed that an improvement may be obtained in the heat transfer rate, regardless of the decomposition of the liquid; the heat transfer is affected primarily by the flow parameters, such as pressure and flow rate, and the dimensions of the fuel element together with other design features. The heat transfer experiments were carried out under forced circulation of the liquid, using an electrically heated stainless steel pipe in the horizontal position to mockup the fuel element; diisopropyl cyclohexane served as the heat transfer liquid. It was found during the test, carried out at temperatures between 300 and 350°C, that the wall temperature at which the heat transfer is improved depends on the diameter and the length of the heated portion of the fuel element. The experimental conditions used included a pressure of 3.9 MN/m², a flow rate of 5 to 20 m/sec and a fuel element of 30 mm. An increase of the temperature resulted in a similar increase of the heat transfer; this was especially noticeable at low flow rates. Decrease of the length had a similar effect. The shape of the channel was found to be the most important factor. The improvement of the heat transfer was accompanied by a high-frequency pressure oscillation with a frequency of 5 to 20 kHz and an amplitude between 0.2 and 4 MN/m²; these oscillations may be responsible for the observed effect. Parameters of the oscillations are probably due to acoustical properties of the 2-phase stream and the geometric dimensions of the system. (TTT)

**54881** ONSET OF FREE CONVECTION IN ANNULI. Nagendra, H. R.; Tirunarayanan, M. A.; Ramachandran, A. (Indian Inst. of Science, Bangalore). Nucl. Eng. Des.; 15: 1-16(Mar 1971).

The onset of free convection in a fluid contained in a vertical annular space with its top and bottom ends open was investigated. Under the limiting conditions of onset, heat transfer across the annular gap is governed by Laplace's heat conduction equation. Closed form analytical solutions for this steady axisymmetric heat conduction equation, under four different boundary conditions were obtained. An analysis of the results indicates that the effect of the height to radial clearance ratio on Nusselt number is negligibly small. Criteria for the lower limit of onset were developed. Experiments were conducted using platinum wires in a brass tube and stainless steel cylinder in glass tubes to check the analytical results. The experimental results presented herein are in good agreement with the analytical results. (auth)

**54882** USE OF AN ELEMENT METHOD PROGRAM FOR SOLUTION OF TEMPERATURE DISTRIBUTION PROBLEMS. Crastan, Valentin (Schweizerische Elektrizitaets- und Verkehrsgesellschaft, Basel). Nucl. Eng. Des.; 15: 54-64(Mar 1971). (In German).

A computer program was developed which can solve 2- or 3-dimensional structural problems and general boundary value problems for scalar and vector fields, based on the finite element techniques. As an example of its application to scalar fields, heat conduction problems for isotropic and anisotropic bodies are treated. It is also shown that the finite element method does not require the existence of a variational principle and can be applied to non-symmetric problems like temperature distributions in slowly moving fluids or to nonlinear problems like temperature distributions in a solid with temperature dependent thermal conductivity. (auth)

**54883** CALCULATION OF STABLE HEAT TRANSFER FROM ROD BUNDLES IN LONGITUDINAL FLOW. Kokorev, L. S.; Korsun, A. S.; Petrovichev, V. I. Heat Transfer-Sov. Res.; 3: 44-55(Jan-Feb 1971).

The method for calculating heat transfer in a uniform rod bundle placed in a longitudinal turbulent coolant flow is presented. The method involves integrating the heat transfer equation in the coolant along the coordinate normal to the heated surface within the limits from the wall to the minimum-temperature curve, to obtain an expression for the coolant mean-temperature distribution $t^h$ along the channel perimeter; and then using the second integral transformation of the heat transfer equation (a Lyon-type transformation) for calculating the local heat transfer coefficient, i.e., for relating the local heat flux at the wall to the difference of local wall temperatures and $t - t^h$. The equations obtained in the above manner are formally equivalent to the starting heat transfer equation in the coolant and can be used for simultaneous solution with the heat conduction equation in the fuel element, as well as calculating the average heat-transfer variables in the channels, when boundary conditions at the heated surface are given. (auth)

**54884** HYDRAULIC DRAG AND HEAT TRANSFER IN TURBULENT FLOW OF LIQUIDS IN TRIANGULAR CHANNELS. Kokorev, L. S.; Korsun, A. S.; Kostyunin, B. N.; Petrovichev, V. I. Heat Transfer-Sov. Res.; 3: 56-65(Jan-Feb 1971).

Calculations of the velocity and heat transfer distributions in turbulent flow of a liquid in a channel with triangular cross section in the form of an isosceles triangle with an acute vertex angle (11.5°) are presented. Such a channel has almost all the characteristic properties of hydraulics and heat transfer in noncircular channels. The momentum and heat transfer in the cross section of a triangular channel is basically two-dimensional. A

XUM

pronounced nonuniformity is observed in the tangential-stress and temperature distributions over the channel perimeter. Heat fluxes along the channel walls are responsible for the effect on heat transfer to the coolant flow of the geometry and physical properties of the wall material. In addition, it is possible to have laminar coolant flow in the domain enclosed by the acute angle of the channel even when the flow is turbulent in the rest of the channel. Triangular channels were studied extensively. A number of experimental studies of the hydraulics and heat transfer in turbulent flows in triangular channels were published. Hence calculations are of interest from the point of view of comparing the calculated with the published experimental data. (auth)

**54885** CALCULATION OF HEAT TRANSFER IN SLENDER BODIES. Voskresenskii, K. D.; Turilina, E. S. Heat Transfer-Sov. Res.; 3: 87-94(Jan-Feb 1971).

The calculation of heat transfer in bodies of different shapes, having small Biot numbers along some directions are encountered in nuclear and instrument engineering, and are usually solved by setting up differential equations for each specific case. In order to simplify these calculations, bodies with Bi $\ll 1$ were classified into 3 groups termed as slender spheres, slender rods, and slender shells. Curved rods and twisted shells were excluded. It was assumed that the bodies were of homogeneous and isotopic materials whose physical properties do not change with temperature and whose geometry and shape do not change with time. The heat transfer equations for each of the three classifications with the assumed conditions are presented. (L.C.L.)

**54886** COMPUTER PROGRAM FOR THE DYNAMIC CALCULATION OF PRESSURE OVER TIME DURATION IN COUPLED VOLUMES. Kueper, K. D.; Langhans, J. (Gutehoffnungshuette Sterkrade AG, Oberhausen, Ger.). Atomkernenergie; 17: 163-6 (May 1971). (In German).

A digital computer program is described, which is used to determine pressure and temperature over time duration within any coupling of volumes. The volumes can have different pressures and temperatures at the starting-point and can be connected in the latest standard by two physically differing openings. Various gases can be mixed during the transient time. The results of an example are demonstrated and discussed. (auth)

## Isotope Technology

*Refer also to abstracts 54506, 54507, 54849, 54851, 54924, 54927, 54930, 54983, 55041, 55070, 56584, and 57127.*

**54887** (BNWL-1308-6) PACIFIC NORTHWEST LABORATORY, DIVISION OF ISOTOPES DEVELOPMENT PROGRAMS QUARTERLY REPORT: FEBRUARY-APRIL 1971. Hansen, J. E. (comp.) (Battelle-Northwest, Richland, Wash. Pacific Northwest Lab.). Jun 1971. Contract AT(45-1)-1830. 51p. Dep. NTIS.

The results of the isotopic fuels program and related research conducted at the Pacific Northwest Laboratory from Feb. through April 1971 are reported. The subjects studied included: encapsulation of fission-product Cs and Sr for process radiation sources; determination of the half-life of $^{107m}$Rh; evaluation of potential radiological hazards from $^{107}$Pd; evaluation of large scale uses for purified fission product Xe; methods for stimulating a market for $^{137}$Cs and $^{90}$Sr sources; $^{146}$Pm burnout; neutron radiography using $^{252}$Cf; preparation of alpha-photon sources; development of radioisotope-powered circulatory support systems; and evaluation of nuclear techniques for seabed mineral exploration. (L.C.L.)

**54888** (CONF-700557-5) KINETIC THEORY OF FLOW BETWEEN ROTATING CYLINDERS: THE GAS CENTRIFUGE. Morse, T. F. (Deutsche Forschungs- und Versuchsanstalt fuer Luft- und Raumfahrt e. V., Porz-Wahn (West Germany)). [1970]. 23p. Dep. NTIS (U. S. Sales Only).

From Meeting on mechanical flow processes in gas centrifuges; Porz-Wahn, Germany (14 May 1970).

A moment method was used to obtain approximate solutions to the velocity distribution function for the problem of quasi-linear cylindrical Couette flow. This problem contains many of the essential flow features of the gaseous centrifuge, and although in this particular study, the effects of countercurrent flow were neglected, the strong assumption of the continuum equations was relaxed. The solution is uniformly valid for all ranges of the mean free path, as it must be in order to describe the flow both in the inner rarefied region and the outer continuum region. All of the macroscopic variables were reduced to a quadrature, and work is presently in progress to obtain these numerical results. The simple process factor for the separation of two isotopes has also been reduced to a quadrature for the case of no collisions, and it will be possible to compare this limiting case with experimental data on Couette flow. (auth)

**54889** (INR-P-1325) PREPARATION OF HIGH PURITY CARRIER-FREE $^{131}$Cs SOURCE FOR SPECTROSCOPIC MEASUREMENTS. Kotlinska-Filipek, Barbara; Myslek, Bogumila; Stryczniewicz, Kamila (Institute of Nuclear Research, Warsaw (Poland)). 1971. 10p. Dep. NTIS (U. S. Sales Only).

A $^{131}$Cs carrier-free source of very high purity was obtained as a daughter product of $^{131}$Ba. The latter was produced through the reaction $^{130}$Ba(n,$\gamma$)$^{131}$Ba. The natural barium was irradiated in the reactor and then purified to remove the $^{132}$Cs and possibly $^{137}$Cs isotopes present in the sample. About 15 days later the $^{131}$Cs was isolated and purified by ion exchange chromatography. Sources for electron spectroscopy were prepared by a microcolumn technique. The admixture of other active Cs isotopes and $^{131}$Ba in the $^{131}$Cs source measured immediately after the chemistry was found to be less than $10^{-7}$ per $^{131}$Cs decay. (tr-auth)

**54890** (K-Trans-61-3) RADIAL FLOW THROUGH A ONE-DIMENSIONAL GAS CENTRIFUGE. Hirschel, E. H. Translated for Oak Ridge Gaseous Diffusion Plant, Tenn., from pp 121-45 of Stroemungsmechanische Vorgaenge in Graszentrifugen, DFVLR-Kolloquium, om 14 Mai 1970, Porz, Wahn, Germany. 21p. (CONF-700557-7). Dep. NTIS.

The radial flow of a compressible, two-component gas through a centrifuge was investigated with the use of a numerical solution of the Navier-Stokes equation for the nonstationary case and an analytical solution for the case of small throughput with stationary flow. It was assumed that the gas had thermally ideal characteristics and that dilution effects were small in the internal part of the centrifuge, so that adhesion conditions could be expected on the internal cylinder. The internal degrees of freedom of the gas molecule were considered to be in equilibrium and once as frozen. The flow fields and diffusion processes formed in the centrifuge are discussed. (auth)

**54891** (K-Trans-61-5) DETERMINATION OF THE TEMPERATURE AND FLOW RELATIONSHIPS IN THE INTERIOR OF A GAS CENTRIFUGE ROTOR. Jung, E. Translated for Oak Ridge Gaseous Diffusion Plant, Tenn., from pp 147-161 of Stroemungsmechanische Vorgaenge in Graszentrifugen, DFVLR-Kolloquium, om 14 Mai 1970, Porz, Wahn, Germany. 16p. (CONF-700557-8). Dep. NTIS.

The flow and temperature relationships in a very dilute gas in the interior of a rotating hollow cylinder (a gas centrifuge) were investigated in the absence of feed and withdrawal. The flow is driven solely by a prescribed radially symmetric temperature distribution on the wall of the cylinder. The system of equations under consideration — Navier-Stokes and the heat conduction equation — is solved numerically after transformation into a two-dimensional problem, omitting, of course, the equation of continuity (direct thermal drive). The numerical process itself is an iteration process combined with Fourier expansions. It is demonstrated here by two temperature cases. In addition, methods for automatic calculation (Fortran) are sketched. (auth)

**54892** (LA-4745) STUDY OF A THERMAL NEUTRON CALIBRATOR. Hankins, Dale E. (Los Alamos Scientific Lab., N. Mex.). Aug 1971. Contract W-7405-eng-36. 6p. Dep. NTIS.

A study was made of the neutron fluences obtained with a thermal neutron calibrator made of paraffin. Variations of 40% in the thermal neutron fluences were found when six different types of $\alpha$-n neutron sources were used. Significant variations in the thermal neutron fluences were observed from four $^{239}$PuBe sources. A similar calibrator should have a thermal fluence within 10% of the values given for sources of the types studied. If the calibrator is used with the probe inside and the source outside the calibrator (the reverse of the locations normally used), an increase in the neutron fluence of from 4.5 to 7 times results. The count rate of the cadmium-covered probe is small and only a small error would be made if it were not considered. Placing the calibrator on a 1-in.-thick wood table top increases the thermal fluences outside the moderator from 10 to 40% depending upon the distance of the probe from the calibrator. (auth)

**54893** (MLM-1736) SUPPLEMENT TO SUMMARY REPORT ON SNAP-19B (IRHS) PROGRAM. Loyer, D. E.; Davenport, C. H. (Mound Lab., Miamisburg, Ohio). 25 May 1970. Contract AT-33-1-GEN-53. 57p. Dep. NTIS.

Two fueled SNAP-19B (IRHS) heat sources were fabricated for application to the NIMBUS B mission. Each source had a thermal power of 623 ± 9 W and was designed to remain intact under reentry conditions. The same design characteristics and fabrication procedures were used for these heat sources as were used pre-

XUM

viously for four SNAP-19B (IRHS) heat sources. A zirconia frit filter was incorporated into one end of each capsule to provide continuous venting and to preclude failure due to pressure buildup during reentry or while in operation. The only difference in the new heat sources was in thermal power, 623 ± 9 W as compared with the earlier 570 ± 17 W. (auth)

**54894** (ORNL-IIC-37(Pt.2)) SELECTED ABSTRACTS OF WORLD LITERATURE ON PRODUCTION AND INDUSTRIAL USES OF RADIOISOTOPES (FROM NSA, APRIL-JUNE 1971). Gerrard, Martha; Baker, P. S. (Oak Ridge National Lab., Tenn.). Sep 1971. 45p. Dep. NTIS.

Approximately 400 abstracts of domestic and foreign publications on production and use of radioisotopes and radiation, selected from the April-June 1971 issues of Nuclear Science Abstracts, are presented. (auth)

**54895** (SC-RR-710353) THERMAL ANALYSIS OF THE INTACT SNAP-19/NIMBUS B/AGENA SYSTEM. Klett, R. D. (Sandia Labs., Albuquerque, N. Mex.). Jul 1971. 103p. Dep. NTIS.

The parametric safety studies conducted to aid in the design of the intact SNAP-19 radioisotopic thermoelectric generator and the final aerothermal safety assessment of the generator on the Nimbus B/SNAP-19 mission are presented. The safety analysis includes ablation and temperature predictions for a launch pad abort fire and for abort and orbital reentries. (auth)

**54896** PROMETHIUM SOURCES. (to Atomic Energy of Canada Ltd.). British Patent 1,243,471. 18 Aug 1971. Priority date 2 Aug 1968, Canada.

A method for Pm deposition is described. The method may be used in the preparation of Pm beta sources for use in nuclear batteries, thickness gages, and luminous sources. An outline of the preparation process is given as a series of steps. (J.R.D.)

**54897** CHARGE REMOVAL FROM POWDER USING $\beta$-RADIATION. 1. Sakanushi, Katsuhiro (Research Inst. of Industrial Safety, Tokyo). Funtai Kogaku; 7: No. 12, 37-43 (Dec 1970). (In Japanese).

Charge removal from stationary powders by $\beta$-rays was studied. Flour was charged positively by friction while falling through a long spout into a polyethylene container; the charge distribution in it was uniform. The radioisotopes used were $^{90}Sr$ and $^{147}Pm$, and the distance from the source to powder bottom was 35 cm. It was found that when the charge on the powder is not large, residual charge is negative. This is due mainly to attaching negative beta particles to the powder. The residual charge increases with the increasing charge on the powder, because of insufficient ionization of ambient air. When the powder is irradiated for long period of time, it is charged negatively. $^{90}Sr$, emitting large-energy particles, is superior to $^{147}Pm$ for the charge removal. The effect of charge removal is not influenced by the charge density, nor by the powder thickness. (Japan)

**54898** DETERMINATION OF THE RATE OF MOVEMENT OF THE CHARGE IN ROTARY KILNS BY MEANS OF RADIOACTIVE ISOTOPES. Shevtsov, B. I.; Kubyshev, N. N.; Cherepivskii, A. A.; Bogdanov, Yu. Yu. Int. Chem. Eng.; 11: 252-4(Apr 1971). Translated from Tsvetn. Metal.; 43: No. 9, 21-3(1970).

Cobalt-60 was used as a radiation source to determine the residence time of a charge in the various zones of a rotary kiln. It was established experimentally that with an increase in the rotational speed of the kiln the residence time of the material in the kiln decreases as a result of the increase of the rate of movement of the material. (auth)

**54899** PREPARATION OF STABLE IOSOTPES FOR SCIENTIFIC RESEARCH PURPOSES. Bochin, V. P.; Romanov, V. S.; Zolotarev, V. S. Isotopenpraxis; 7: No. 5, 185-8(May 1971). (In Russian).

Separated stable isotopes are being more widely used in science and engineering. To provide the basic research necessary, work in nuclear physics, solid state physics, and reactor technology, the production of thin foils, pure metals, monocrystals, rolled material, ceramics, and separated isotopes has been initiated. Centralized preparation of stable isotopes helps physical researchers to save time and permits working with minimum losses of costly isotopic material. (tr-auth)

**54900** NON-CONTACT THREAD VELOCITY MEASUREMENT THROUGH POINT LABELLING. Zeidler, H.; Felber, G. (Forschungsinstitut fuer Textiltechnologie, Karl-Marx-Stadt, Ger.). Isotopenpraxis; 7: No. 5, 171-4(May 1971). (In German).

A method is described which is suitable for measuring the velocity of a running thread. The measurement is carried out without touching the thread. Before measuring, individual spots on the thread are marked using radioactive phosphoric acid ($^{32}P$). The measurement of speed is made by measuring the time interval. Commercial devices are used which are connected to a definite functional scheme through their inputs and outlets. As a practical example, measurements on a false-twist texturing machine are given. (tr-auth)

**54901** USE OF $^{40}K$ AND $^{87}Rb$ IN RADIONUCLIDE METROLOGY. Zaduban, M. (Safarik, Univ., Kosice, Czech.). Isotopenpraxis; 7: No. 5, 160-6(May 1971). (In German).

The possibility of using some naturally unstable nuclides in metrology is discussed on the basis of nuclear characteristics. $^{40}K$ and $^{87}Rb$ are very suitable as standards. The most suitable potassium and rubidium salts were chosen with regard to the criteria for standards. Several examples of their practical use are presented. (tr-auth)

**54902** PROJECTOR FOR RADIOACTIVE SOURCES USED IN PLESIOTHERAPY FOR NONRADIOACTIVE PREPARATION TECHNIQUE. Chassagne, Daniel; Delouche, Gilles; Fradin, Jean; Rocoplan, Jean Antoine (to Commissariat a l'Energie Atomique). French Patent 2,033,653. 23 Nov 1970. Filed 28 Feb 1969. (In French).

A projector for radioactive sources used in plesiotherapy for the nonradioactive preparation technique, which is completely safe for the operating personnel, is described. This apparatus is a multipurpose projector for the treatment of lesions in gynecology. It consists of a body resting on a trolley, surrounded by heavy metal shielding for protection against the radioactive sources, and an electromechanical device for moving the sources. An external control panel is provided and is fixed to the body. The accessories moving the sources consist of four source holders intended to be placed in the region of the cancerous tissue. They are linked by a rapid connecting device to a cable motor, operated by an electromechanical transfer device. Four sterilizable flexible external tubes which can be thrown away after use, and a remote control device for the source holder, are included. (France)

**54903** MECHANICAL SURFACE AERATOR EVALUATION USING RADIO-KRYPTON AS A STANDARD INDICATOR OF MASS TRANSFER. Gordon, John Albert. Lafayette, Ind.; Purdue Univ. (1970). 173p. University Microfilms Order No. 71-2605.

Thesis.

A review of the literature on methods for rating mechanical surface aerators had shown that a satisfactory testing method was not available for use under all conditions. The research studies were concerned with developing apparatus and methodology which would allow radiokrypton to be used as a standard indicator of oxygen mass transfer. Laboratory studies were the first step in the research. Preliminary laboratory studies of a $^1/_{30}$ hp model surface aerator operating in a 14 liter basin of tap water revealed that the simultaneous transfer of krypton oxygen were related by a ratio between the krypton mass transfer constant, K, and the oxygen mass transfer constant, $K_La$, of 0.80 with the transfer of krypton being the slower process. The accepted ratio of 0.81 was within one standard deviation of the determined value. Activated sludge and an artificial waste were then added to the model basin and simultaneous testing of two methods for determining $K_La$ were compared with the krypton method. Testing revealed that the $K_La$ results obtained by reaeration of oxygen depleted aerobic biological sludge and by steady-state measurement of oxygen uptake rate were not compatable. The necessary factors $\alpha$, $\beta$, and initial D.O. proved troublesome to assess. The techniques and partial results of the preliminary laboratory studies provided sufficient information for the design of the pilot-scale studies. Pilot-scale studies of a two horsepower Welles floating surface aerator in a 2000 gallon basin of tap water produced a ratio of 0.817 between the value of the krypton mass transfer constant, K, and the oxygen mass transfer constant, $K_La$, for simultaneous testing. The standard deviation of the $K_La$ values obtained by the reaeration method was of the same order of magnitude as that from the krypton stripping method. Both methods were about equally precise when used to evaluate surface aerator performance in tap water. The tap water pilot studies were followed by biologically active wastewater studies. The addition of 100 mg/l B.O.D. and 1,100 mg/l activated sludge to the basin depressed the measured values of mass transfer. Oxygen transfer was depressed 20 percent while krypton transfer was depressed 10 percent. The standard deviation of the $K_La$ values obtained by the reaeration of the biologically active wastewater was much greater than the standard deviation of the K values determined by the krypton stripping method. The precise nature of the K values obtained by the krypton tracer method did not decrease when the tests were per-

XUM

formed on the aerator after B.O.D. and MLSS were added. Complete mixing at one hp per 1000 gallons was indicated by identical results obtained from two sampling points within the basin. A comparison of $K_La$ values obtained by the reaeration method at 19.5 and 0.8°C showed that the values at 0.8° could be converted to those at 19.5° with a $\theta$ value of 1.030. Radiological safety during the krypton stripping tests was studied by personnel and area monitoring using portable G–M monitors, dosimeters, and $\beta$, $\gamma$, film badges. Potential exposures indicated were not considered to be hazardous to persons in the area. A standard method for rating surface aerators which are fully operational was postulated. The method specified the use of the krypton stripping method for assessing $K_La$ when the aerator was isolated in a mixing volume of 1 hp/1000 gallons and the flow pick-up point for the G–M tube located at middepth and ½ of the distance from the aerator to edge of the isolation area. (Diss. Abstr. Int., B)

**54904** STUDY OF THE DEVELOPMENT OF LEAKS IN FUEL ELEMENT CLADDING BY MEANS OF $^{88}Kr$. Kotel'nikov, G. A.; Leonov, V. F. At. Energ. (USSR); 29: 291-3(Oct 1970). (In Russian).

The krypton isotope $^{88}Kr$, with the short half-life of 2.8 years, was chosen for the continuous and remote detection of leaks in fuel element cladding; the water loop of the MR reactor of the Kurchatov Institute was used for the tests. The course of the increasing leak rate of the stainless steel-clad, uranium-aluminum fuel elements was followed up by means of a Ge(Li) spectrometer for a 2-month period on the basis of the $\gamma$ radiation of fission fragments. The radiation spectrum was measured in the $E_\gamma > 1$ MeV range with a resolution of 15 keV, identifying the total $\gamma$ absorption peaks of $^{88}Kr$ and $^{138}Cs$, together with the corrosion product $^{60}Co$. The effect of the latter material was eliminated by using a low-energy discrimination threshold of 1.6 MeV for recording the fission products; in this range, $^{88}Kr$ was the main product. It was found that escape of the gas is strongly increased by a rapid rise of the reactor power level. During extended shutdown of the reactor, the pressurized water entered the cracks and was removed during the subsequent rise to power. The escaping steam widened the flaws and helped to expel the radioactive gas. (TTT)

**54905** NUCLEAR-THERMIONIC LUNAR BASE POWER SUPPLY. Levedahl, William J.; Schumann, Frederick A.; Scicchitano, Edward A. (to Teledyne, Inc.). U. S. Patent 3,564,302. 16 Feb 1971. Filed 5 Nov 1964.

A nuclear powered direct energy converter system is described employing a cylindrical radiator removed from the converter which is particularly well suited for lunar applications. One embodiment is adapted to be positioned in a lunar crater which incorporates radiation shielding, while another is adapted to receive radiation shielding in the form of lunar material. Reflectors positioned at an angle with respect to the cylindrical radiator reflect thermal radiation received from the radiator in an axial direction. (Official Gazette)

**54906** RADIOISOTOPES IN BLAST-FURNACE IRONMAKING OPERATIONS. Pavlik, W. R. (Republic Steel Crop., Cleveland). Isotop. Radiat. Technol.; 9: No. 1, 8-21(Fall 1971).

Background material on the blast-furnace process is provided and current uses of radioisotopes for on-line analysis of raw materials, raw-materials handling, in-furnace process gaging, process tracing, and quick product analysis are reviewed. Some possible future uses of radioisotopes are suggested. (auth)

**54907** HIGHWAY APPLICATIONS OF NUCLEAR TECHNIQUES. Isotop. Radiat. Technol.; 9: No. 1, 21-3(Fall 1971).

During 1970, the Highway Research Board Committee A2-HO1 (concerned with nuclear principles and applications) contacted the 50 state-highway departments of the United States concerning the possession and usage of nuclear equipment for surface testing with the intent of determining the current status of nuclear testing. These findings are summarized. It is of interest to note that all of the state-highway departments at one time or another have used nuclear testing either in research or for field control, or both. California, Pennsylvania, and Virginia are the three leading states in numbers of gages used for moisture–density testing on soils and aggregates, with 137, 125, and 102 devices, respectively. The growth of nuclear gaging as far as highway applications are concerned is shown. (L.C.L.)

**54908** ATMOSPHERIC TRACER TECHNIQUE EMPLOYING $^{85}Kr$ AND USE OF THIS TECHNIQUE IN DEFINING PUFF DIMENSIONS AND TRANSPORT SPEED. Nickola, P. W.; Ludwick, J. D.; Ramsdell, J. V. Jr. (Battelle-Northwest, Richland, Wash.). Isotop. Radiat. Technol.; 9: No. 1, 65-71(Fall 1971).

An atmospheric tracer technique has been developed in which $^{85}Kr$ is released and subsequently monitored on a real-time basis at 64 field stations, located at distances of up to 800 m from the release point and at elevations of up to 21 m. The technique includes both instantaneous- (puff) and continuous- (plume) release techniques. Data from six puff releases are summarized and analyzed. The effective transport height of puffs released at ground level increases with distance but increases least in a stable atmosphere. In stable atmospheres, the growth rate of a puff in the downwind direction continues to be greater than the growth rate in the crosswind direction as the puff travels from 200 m to 800 m from the release point. However, in less-stable atmospheres, even though the downwind dimension remains greater than the crosswind dimension, puffs become more symmetrical in shape as they move from 200 m to 800 m. (auth)

**54909** RADIOISOTOPE GENERATOR OF THE MOTHER-DAUGHTER TYPE HAVING QUICK-DETACHABLE MEMBERS. Arlman, Jan Jacob; Nonhebel, Dirk (to U.S. Philips Corp.). U. S. Patent 3,564,256. 16 Feb 1971. Priority date 6 Mar 1966, Netherlands.

A device is described for obtaining fluids containing radioactive constituents particularly suitable for medical purposes. The device includes a holder for a substance having radioactive constituents and which is provided at the upper and lower ends with a portion of a quick-coupling member. In operation, a vessel for a flushing liquid is connected with the upper coupling portion and the vessel for the fluid to be collected is connected with the lower coupling member portion to facilitate washing of the holder and collection of the fluid from the holder while avoiding contamination of the fluid in the holder. (Official Gazette)

**54910** IMPLANTABLE RADIOISOTOPE-FUELED STIRLING ENGINE. Goranson, Richard B.; Johnston, Richard P.; Martini, William R.; McDill, William H.; Noble, Jack E.; White, Maurice A. (to McDonnell Douglas Corp.). U. S. Patent 3,563,028. 16 Feb 1971. Filed 22 Jul 1968.

A long-life, radioisotope-fueled, thermal regenerative engine for driving a blood pump is used in a circulatory support unit which is implantable in an animal. The engine includes an encapsulated radioisotopic heat source with a thermal reservoir, a thermodynamic converter, a heat exchanger using blood as the cooling medium, and a control device to regulate engine power output. The converter includes a cylinder containing a regenerator and drive plug assembly suspended from a counterbalanced linkage. The control device includes an adjustable bypass valve which regulates the pressure difference appearing across the plug to control engine speed and, therefore, its power output. (Official Gazette)

**54911** RADIOACTIVE ISOTOPE DISTILLATION SYSTEM FOR RECOVERING WATER FROM WASTE IN A SPACECRAFT. Metzger, Courtney A.; Hearld, Albert B. (to Secretary of the Air Force). U. S. Patent 3,558,437. 26 Jan 1971. Filed 11 Jun 1969.

An improved system is described for obtaining potable water from human waste and involving two evaporators having a waste inlet in common and a vapor outlet in common but segregated functionally by suitably positioned control valves. Each evaporator is of cylindrical shape, formed of several compartments of different diameters, two of which are secured together by a conical housing. The lowermost compartment is hemispherical in shape and is detachably secured to the adjacent compartment. There are four isotopes in the lowermost compartment, also a single isotope in the uppermost compartment. The waste material is pumped into the lowermost compartment where it is heated and the vapor is forced to pass through, in succession, a heavy layer of "wicking" material, also a pair of horizontally disposed filters, in addition to a circumferential filter. Upon reaching the uppermost compartment, the vapor is heated by the single isotope enclosed in a casing from which a number of vanes radiate to distribute the heat. The space between the vanes is filled with an oxidizing catalyst. The vapor is fed into a coiled pipe located in the lowermost compartment where it gives up its heat to the surrounding waste material. The vapor is then conducted through a water-cooled condenser, and finally to a storage tank for consumption. The hemispherical compartment receives the semi-solid precipitate and is adapted to be cleaned by the astronaut by removing the same at the detachable connection, after a "switch over" to the other evaporator has been effected by the various valves. (Official Gazette)

**54912** PARTIALLY IONIZED PLASMA CENTRIFUGE. Lehnerg, B. (Kungliga Tekniska Hoegskolan, Stockholm). Phys. Scr.; 2: 106-7(1970).

A possibility to improve the efficiency of the gas centrifuge by

XUM

an electric discharge across the magnetic field in a partially ionized plasma which consists mainly of neutral gas is presented. Conditions under which it is possible to control the neutral gas rotation are estimated and a system is outlined in which it is possible to keep a neutral gas mixture at a high rotational speed and to control its spatial velocity distribution by electric means. (auth) (Sweden)

**54913** NEUTRON CAPTURE GAMMA RAY STUDIES OF METALS, MIXTURES, ORES, AND MARINE SAMPLES USING $^{252}Cf$. Wiggins, Peter Frederick. College Park, Md.; Univ. of Maryland (1970). 171p. University Microfilms Order No. 71-4099.

Thesis.

A technique to show the feasibility of using californium-252, as an isotopic neutron source for mineral exploration by neutron capture gamma rays was investigated. Initial studies of pure manganese dioxide and a marine manganese nodule used the thermal column of the University of Maryland Nuclear Reactor (UMR) to provide the thermal neutrons for irradiating the relatively small samples to produce the capture gamma ($\gamma$) rays which identified elements present. A lithium-drifted germanium detector, Ge(Li), approximately 40 $cm^3$, was connected to a 1024 channel pulse height analyzer to measure the high energy photon emissions from the sample. The aim of this study was to obtain the capture gamma spectral signatures for a series of known elements which were to be used as standards for analytical studies of known mixtures, ores, and ocean samples of unknown elemental content. The detection system for this study consisted of a 30 $cm^3$ Ge(Li) detector connected to a 400 channel pulse height analyzer. The results of the pure manganese dioxide and marine manganese nodule using $^{252}Cf$ as the neutron source were compared to the (UMR) reactor studies. A marine sample from the Indian Ocean was also studied. This spectrum contained many identifiable energy peaks. The most prominent energy lines were used to identify Cl, Fe, Al, Ca, K, Mn, Cr, and Si. However, these samples are complex and the interpretation of the spectrum is difficult. To simulate an in situ marine investigation unit, a Lucite tank, 26 inches by 19 inches by 22 inches, was filled with seawater. The bottom of the tank contained a three inch layer of silica sand. Marine manganese nodules were studied in this ocean environment. The strong energy lines of the chlorine from the seawater made it difficult to identify many of the other elements present. However, by examining the sections of the spectrum where (I-In) $\sigma/A$ was high for manganese, it could be identified. Two marine exploration units are proposed for future in situ exploration of the vast unexplored areas under the sea. (TSS) (Diss. Abstr. Int., B)

**54914** GAMMA RADIATION DOSE RATE IN THE EMITTER OF A RADIATION-CHEMISTRY DEVICE PROVIDED WITH A URANIUM-BASED RADIATION CIRCUIT. Breger, A. Kh.; Starizznyi, E. S. (Physical-Chemical Inst., Moscow). Dokl. Akad. Nauk SSSR; 195: 1385-7(21 Dec 1970). (In Russian).

In order to develop a high-intensity and economical radiation source for industrial irradiation processes, a circulating irradiation device based on fission fragments, has been proposed. The $\gamma$ radiation intensity $W_\gamma$ is related to the heat intensity in the reactor by the Way-Wigner equation. The calculations showed that the most efficient radiation chemical devices are those in which the nuclear fuel is circulated continuously; the AVR type fuels were especially effective in this respect. A new method was developed for determining $W_\gamma$, with a residence time $t_r$ of the fuel in the reactor of $t_r \leq 1$ hr at various ratios of residence times in the emitter and in the circuit. The authors' earlier data on the measurements of the $\gamma$ activity or the fission fragments as a function of time were used for the calculation. The proposed method was found to yield higher $\gamma$ intensity values than earlier methods, resulting in a corresponding decrease of the cost of the $\gamma$ emitter without increasing the required capital investment. (TTT)

**54915** METHOD OF PRODUCING ENCAPSULATED RADIOACTIVATED LIGHT SOURCES. (to Merz and Benteli AG). British Patent 1,230,258. 28 Apr 1971. Priority date 22 Aug 1968, Switzerland.

A method of producing encapsulated radioactivated light sources is described. A glass tube containing a luminophore and a radioactivated gas is divided into a number of sealed, separate lengths by a laser beam. These sections serve as light sources. (J.R.D.)

**54916** HEAT-REJECTION RADIATOR MASS AND ITS INFLUENCE IN SPACE POWER SYSTEMS. Bonneville, Jacques M. (Electronics Research Center, Cambridge, Mass.). Int. J. Heat Mass Transfer; 14: 387-93(Mar 1971).

The influence of radiators on space nuclear power system mass was studied by determining this mass as a function of the parameter $K_R$ = radiator mass/area. Four power-conversion schemes are considered: Brayton, Rankine, thermoelectric, and thermionic, over the power range 200 to 1000 kW. The total system includes power processing equipment and the secondary radiator. The Brayton cycle becomes competitively light (improvements by factors up to 5), and the power range of interest for thermoelectric systems increases significantly with achievable values of $K_R$. The power processor, secondary radiator, and shield render present thermionic systems massive, so that other concepts promise lower mass if $K_R$ can be reduced to less than 0.5 $kg/m^2$. (auth)

**54917** THEORY OF ASYMMETRIC SEPARATION CASCADES WITH AN ARBITRARY ENRICHMENT IN THE SEPARATION ELEMENT. Kolokol'tsov, N. A.; Laguntsov, N. I. At. Energ. (USSR); 29: 300-1(Oct 1970). (In Russian).

The authors' previous paper on the structure of symmetric cascades with a large, arbitrary enrichment per stage was further generalized to cover asymmetric cascades. These cascades present advantages at low enrichment; it was expected that under certain conditions they might be more advantageous to use also in case of high enrichment. The calculation revealed that it is possible to design an ideal, asymmetric cascade, with any desired enrichment per stage. Care must be taken for the specific case of symmetric cascades when the enrichment per stage is low. Formulas were obtained to indicate the lowest total flow for cascades without mixing the concentrations at the output, although it was not found possible to calculate the most favorable parameters. (TTT)

**54918** LOW PRESSURE STRIPPING. Nazzer, D. B.; Thayer, V. R. (to Canadian General Electric Co., Ltd.). Canadian Patent 865,022. 2 Mar 1971.

$H_2S$ is stripped from hot effluent, in a heavy water separation plant using the dual temperature process, by taking liquid effluent from the hot tower before passage through the humidifier. The liquid is then passed through one or more throttle devices to flash off the $H_2S$ gas content, after which the gas is fed into an absorption tower containing incoming feed water, for recycling of the gas through the process. (F.S.A.)

**54919** NEW VISTAS FOR ISOTOPE SEPARATION. Wick, Gerald. New Sci. Sci. J.; 51: No. 770, 692-4(23 Sep 1971).

Commercial interest at the moment is focussed on gas diffusion and gas contrifugation as a means of separating uranium isotopes. However, isotopes of the same element have been separated using rotating hot plasmas, laser techniques, and gas chromatography. These techniques are discussed and their possible extension to uranium separation which could be used for military purposes considered. The personal responsibilities of a scientist, who can forsee the use his discoveries might be put to, is considered in the light of this latest work on isotope separation. (UK)

**54920** ION OPTICS OF A THREE-STAGE INHOMOGENEOUS MAGNETIC FIELD ISOTOPE SEPARATOR. Whitehead, Thomas Wilson Jr. Troy, N. Y.; Rensselaer Polytechnic Inst. (1970). 255p. University Microfilms Order No. 71-3936.

Thesis.

The electromagnetic isotope separator has become an increasingly important instrument complementing research activities in the natural and physical sciences. The beginnings of isotope separations in the 1930's are traced to today's machines. The evolution of the "calutron," which was important in World War II construction of a nuclear weapon, is related to Manhattan District activities. The current ORNL isotopic separations program is considered. Early work at Copenhagen, Denmark in the 1940's led to the development of the Scandinavian type of isotope separator which has seen widespread acceptance for laboratory applications. This activity is traced, and a tabulation of many of the installations currently using isotope separators is given. Enriched stable isotopes and the separators which provide them have found many applications in diverse scientific fields. A study of some of the more common uses in nuclear science, biology and medicine, environmental science, geology, and chemistry reveals the importance of separated isotopes. In much research the quantity of material required is small, and evidence is presented to support the contention that there is merit in seeking high enrichments. The design criteria for the RPI isotope separator were determined on the basis of developing a separator capable of separating microgram to milligram quantities of pure stable nuclides. The selection of parameters is explained and the rationale for constructing this instrument is presented. The RPI isotope separator uses a unique ion-optical system of three magnetic lenses to accomplish the goal of maximum isotopic purity. Magnetic focusing is important in isotope separator design because of the beam transmission requirements. The problem of evaluating beam focusing by a generalized sector magnetic field is studied.

XUM

This problem is solved by resorting to direct application of the principle of least action to determine a general relationship between focal lengths, field inhomogeneity, and deflection angle. The results of this calculation, excluding fringing field effects, are graphed for three magnet angles; and a relationship between mass dispersion, using the general case of unsymmetric object-image position, is derived. A $\frac{1}{6}$-scale model magnet was used to find field shaping constants for improved focusing and transmission. A detailed analysis of magnetic field measurements permitted the use of computer calculations to find the exact ion trajectories. The Runge–Nystrom method was used to solve the differential equations. Two methods for data utilization were developed which were used to compute three-dimensional ion trajectories based on measurements taken in a plane of symmetry. Expansions for off-midplane field coefficients in both Cartesian and polar coordinates were found through the fourth-order of approximation. Magnetic measurements were made using Hall transducers, and the problems associated with one-part-in-$10^4$ field mappings were considered. The need for temperature compensation schemes and a temperature-regulated environment for Hall probe is important. Probe calibration was by nuclear magnetic resonance. A method using magnetic potential functions was employed to determine the contour of an iron pole piece required to produce the predetermined magnetic field configuration. The method of magnetic equipotentials and potential gride calculations was used to design the magnet pole pieces. An appendix contains several computer programs written in FORTRAN which were used specifically for the RPI magnet studies, but which have general applicability in magnet design and particle trajectory analysis. (Diss. Abstr. Int., B)

**54921** SWEDISH STUDIES ON THE ECONOMICS OF URANIUM ENRICHMENT. Martensson, M. (Aktiebolaget Atomenergi, Nykoeping, Sweden). J. Brit. Nucl. Energy Soc.; 10: No. 3, 191-206(Jul 1971).

An account is given of two Swedish investigations, based on computer programs, for optimizing separation cascades for the large-scale production of enriched U. One program is designed for a cascade using the gaseous diffusion process and the other for a cascade made up of gas centrifuges. A broad survey of both programs is presented. Some results of computation are given. (UK)

**54922** NUCLEAR POWER SOURCE. (to Atomic Energy of Canada Ltd.). British Patent 1,224,599. 10 Mar 1971. Priority date 18 Jun 1969, Canada.

A nuclear electric power source is described which utilizes in particular, but not exclusively, beta-emitting radioisotopes. The power source may be fabricated with a minimum requirement for close-tolerance dimensions and may be assembled quickly and simply. Promethium-147 in the form of plates is the power source. (J.R.D.)

**54923** STUDY OF DOSE DISTRIBUTION SURROUNDING A SEALED LINEAR RADIUM SOURCE BY MEANS OF ELECTRONIC CALCULATIONS. Maurenzig, P. R.; Renzi, R. (Univ., Florence). Minerva Fisiconucl.; 13: 236-48(Jul-Sep 1969). (In Italian). (CONF-680535-26).

From fourteenth national conference of the Italian Association for Health Physics and Protection from Radiation; Formia, Italy (29 May 1968).

The dose distribution was calculated by using in the calculation of the Sievert integral the variation of the absorption coefficient in platinum with the thickness of platinum effectively crossed, by considering the real geometry of the source at its extremities, and by expressing the distribution of the dose intensity not only in R/hr but in rad/hr. Examples of the results obtained for the dose intensity distribution in water are given. (J.S.R.)

## Materials Testing

*Refer also to abstracts 54839, 54840, 54850, 54937, 54964, 54970, 54976, 55575, 55659–55665, and 56882.*

**54924** (SC-DR-710178) NEUTRON RADIOGRAPHY AT SANDIA LABORATORIES: ITS TECHNIQUES AND INSTRUMENTATION. Yoshimura, R. H.; Moody, H. D. (Sandia Labs., Albuquerque, N. Mex.). Aug 1971. 46p. (CONF-701217-1). Dep. NTIS.

From Measurements and instrumentation symposium; Albuquerque, N. Mex. (9 Dec 1970).

Neutron radiography, a relatively new and versatile tool for nondestructive testing, has some unusual measurements and instrumentation requirements. Several of the most meaningful parameters are derived using somewhat unconventional techniques. The ACPR (Annular Core Pulse Reactor) facility and the californium-252 neutron camera/source container facility at Sandia Laboratories are reviewed. Facility evaluation parameters, neutron radiography techniques, typical instrumentation and measurement procedures are emphasized, along with their current limitations and calibration problems. (auth)

**54925** STUDIES ON THE ULTRASONIC FLAW TESTING METHOD FOR A REACTOR PRESSURE VESSEL USING A MOCK-UP. Futamura, Yoshiaki (Japan Atomic Energy Research Inst., Tokai); Umeda, Minoru; Ootsuka, Ryoichi; Takeuchi, Kunito. Karyoku Hatsuden; 20: 1239-47(Dec 1969). (In Japanese).

Studies have been made using the ultrasonic flaw testing method, on the internal surface of a nozzle for a reactor pressure vessel mockup. The studies were conducted to establish a testing technique with a choice of probes and to establish the relations of echoes with flaws. The results of preliminary experiments and feasibility tests are described. The mockup of the nozzle was the same size and shape as the actual one. The kinds of flaws prepared, including shape and size, were those which might occur in the internal clad, both radially perpendicular to the nozzle. The ultrasonic testing equipment employed was of the UM-721 type, with frequencies 1, 2.25, and 5 MHz with dc pulse indication and A scope. The probing may be done with one or two probes. (Japan)

**54926** ULTRASONIC TESTING OF NUCLEAR FUEL CLADDING TUBES. Shiraiwa, Toshio; Yamaguchi, Hisao (Sumitomo Metal Industries, Ltd., Amagasaki, Japan). Sumitomo Kinzoku; 22: No. 4, 476-84(Oct 1970). (In Japanese).

In nuclear power stations under construction in Japan Zircaloy tubes are to be used for nuclear fuel cladding, and in fast breeder reactors, stainless steel tubes are going to be utilized. Ultrasonic inspection of high accuracy is required for these cladding tubes. Results of high-speed shear wave testing applied on the cladding tube are described. Apparatus, testing conditions, sensitivity, examples of detected natural flaws, and ultrasonic continuous measurement of thickness are discussed. In both the Zircaloy tubes and stainless steel tubes, longitudinal and transversal flaws of 20 $\mu$ depths on the inner and outer surface can be detected at 3000 rpm. In stainless steel tubes, fine grain is desirable for ultrasonic inspection because ultrasonic noise (echo) appears in coarse grain size which is smaller than ASTM #7. (auth) (Japan)

**54927** NONDESTRUCTIVE INSPECTION OF JET ENGINES WITH RADIOISOTOPES. Watanabe, Kiyokazu (Japan Air Lines Co. Ltd., Tokyo). Nainen Kikan; 9: No. 104, 55-62(Nov 1970). (In Japanese).

The nondestructive inspection of jet engines is being carried out by Japan Airlines, and improvement of safety and cost reduction are being achieved. Inspection of the bending of a guide vane in a first-stage turbine nozzle is conducted aboard by remote operation. The $\gamma$-ray from $^{192}Ir$ is used for penetration radiography. Principles of nondestructive testing are reviewed including, the difference in the absorption of gamma-ray energy which produces the contrast in radiography, the energy loss due to photoelectric effect, Compton effect, and the production of electron pairs. Two modes of engine radiography, such as a source in an engine shaft, and outside a jet engine, are used and the source is handled by remote operation to avoid radiation exposure. Considerations are given to exposure time, radiation sources, film, and sensitizing screen. (Japan)

**54928** ULTRASONIC EXAMINATION OF THIN WALL TUBE TO TUBE BUTT WELDS USING ASSISTED HAND SCANNING METHODS. Abrahams, C. J. Brit. J. Non-Destruct. Test.; 13: No. 6, 141-7(Sep 1971).

Recent advances in the manufacture and erection of both nuclear and conventional boiler plants indicate a need for an acceptable system of ultrasonic inspection of thin-wall butt-welds suitable for use in works or on site. One particular system is outlined which is being used in the examination of butt-welds in carbon and ferritic tubes in thickness down to and including 10 S.W.G. (0.128 in.), and in austenitic G.316 in the thickness range 0 to 10 S.W.G. (0.342 in. to 0.128 in.). The ultrasonic examination of such welds cannot be precise in a strictly tool room sense by virtue of the approximations which have to be made, but by the use of specific aids it can be made sufficiently accurate to make the process well worth while. Provided care is taken to ensure the maximum degree of accuracy at all stages where this is possible, the effect of the approximations can be reduced to a minimum, thereby making the method attractive where the intention is to prove the welding technique, as a quality control

XUM

tool, or when large numbers of welds and a time factor are involved. A major consideration is the type and position of any defects likely to be present, differing welding processes produce different defects. The weld preparation also may have a distinct bearing upon the type of defect. The system developed has the necessary flexibility to accommodate the physical variables, which by the very nature of the fabricating process are bound to occur from time to time. (auth)

**54929** EXPERIMENTAL APPROACH TO THE DETERMINATION OF RADIOGRAPHIC TECHNIQUE FOR LIGHT ALLOY SPECIMENS OF 3-30 mm THICKNESS. Dowd, M. (Royal Armament Research and Development Establishment, Fort Halstead, Eng.). Brit. J. Non-Destruct. Test.; 13: No. 5, 153-5(Sep 1971).

A practical approach to the problem of devising a technique which will produce the best attainable flaw-sensitivity within a reasonable economic exposure-time is described. A method for determining the optimum combination of source-film distance (s.f.d.) and kilovoltage to be used within a standardised framework of exposure-time, extra fine-grain radiographic film and a particular focal-spot size, in order to produce the best radiographs on specimens in the thickness range 3 to 30 mm of aluminum where very fine cracks might be present is considered. (auth)

**54930** NEUTRON RADIOGRAPHY FOR NONDESTRUCTIVE TESTING. Berger, Harold (Argonne National Lab., Ill.). Electron. World; 86: No. 2, 40-1(Aug 1971).

Development and uses of neutron radiography are discussed with emphasis on applications in the electronic field. Examples of applications are given and information is included on neutron sources and radiation detectors. A number of organizations offering neutron radiography service are listed. (J.R.D.)

**54931** IMPROVEMENTS IN OR RELATING TO NEUTRONGRAPHY EQUIPMENT. (to Thomson - C S F). British Patent 1,226,928. 31 Mar 1971. Priority date 4 Mar 1969, France.

A neutron radiography bench is described. The equipment includes a neutron source, a neutron moderator, an image converter, a shutter located past the moderator, and a means of neutron pulse control. A time delay is incorporated between the beginning of the pulse and initiation of shutter opening. (J.R.D.)

## Protective Structures

*For an abstract of an individual paper see: 54933.*

**54932** PROCEEDINGS OF THE INSTITUTE OF ENVIRONMENTAL SCIENCES 1970 ANNUAL TECHNICAL MEETING, BOSTON, MASSACHUSETTS, APRIL 12–16, 1970. Mt. Prospect, Ill.; Institute of Environmental Sciences (1970). 540p. $20.00. (CONF-700402).

Eighty-nine papers were presented at the conference. A separate abstract was prepared for one paper dealing with environmental problems of fallout shelters. The remaining papers were not in scope for NSA. (R.C.K.)

**54933** ENVIRONMENTAL PROBLEMS OF FALLOUT SHELTERS. Jerger, E. W. (Univ. of Notre Dame, Ind.). pp 189-91 of Proceedings of the Institute of Environmental Sciences 1970 Annual Technical Meeting, Boston, Massachusetts, April 12–16, 1970. Mt. Prospect, Ill.; Inst. of Environmental Sciences (1970).

From sixteenth annual meeting and equipment exposition; Boston, Mass. (12 Apr 1970). See CONF-700402.

Fallout shelters are shielded areas designated to provide protection to inhabitants from nuclear radiation. Since shelters are inhabited for appreciable periods of time only in emergency situations, and because this habitation must be under crowded and closed conditions, the environmental problems are formidable. Design of fallout shelters is discussed from shielding, physiological, heat transfer, and water and sanitation standpoints. (R.C.K.)

## Radioactive Material Handling

*Refer also to abstracts 54707–54709, 54755, 54756, 54758, 54779, 55004, 55193, 55204, 55252, 55253, 55657, and 57001.*

**54934** (BNWL–1598) NUCLEAR POWER PLANT IN THE NUCLEAR MATERIAL SAFEGUARDS ACCOUNTING SYSTEM. Clark, R. G.; Svoboda, H. J.; Uotinen, V. O.; Wolkenhauer, W. C. (Battelle Pacific Northwest Labs., Richland, Wash.). 30 Jun 1971. Contract AT(45-1)-1830. 48p. Dep. NTIS.

The function of the reactor, as opposed to the reprocessing plant, in the nuclear materials safeguards system was studied. A brief review is given of the whole fuel cycle and the place of the nuclear reactor in that cycle, of systems analysis as applied to safeguards analysis, of types of nuclear power plants, and of data available from power reactors. The effect of the mission of the reactor on the nuclear materials accounting system and the opportunities and relative probabilities of diversion from a nuclear power plant are discussed. It is concluded that, although diversion from the nuclear reactor portion of the fuel cycle is unlikely, the nuclear reactor plays an important role in the safeguards system. (L.C.L.)

**54935** (BNWL–1599) STATUS OF BURNUP CALCULATIONAL TECHNOLOGY AS APPLIED TO THE NUCLEAR MATERIALS SAFEGUARDS ACCOUNTING SYSTEM. Clark, R. G.; Svoboda, H. J.; Uotinen, V. O.; Wolkenhauer, W. C. (Battelle Pacific Northwest Labs., Richland, Wash.). 30 Jun 1971. Contract AT(45-1)-1830. 27p. Dep. NTIS.

A study was made of the state of the technology in burnup calculations and how this technology can be applied to the nuclear materials safeguards program. Several factors were considered in assessing how accurately power reactor core isotopic inventory can be predicted and included: power plant operational codes and standards; reactor instrumentation; calculation limitations; and theory–experiment correlations. These factors were used to develop tabulated data on the future capability and current performance standards for the burnup problem. It is concluded that significant contributions to the nuclear materials safeguards program can be expected from application of burnup technology. (L.C.L.)

**54936** (BRH/DMRE–71-3) STORAGE AND HANDLING DEVICES FOR RADIUM. (Bureau of Radiological Health, Montgomery, Ala. Div. of Medical Radiation Exposure). Jun 1971. 9p. GPO $0.30.

Difficulties met during radium storage and research operations at the Southeastern Radiological Health Lab. in Montgomery, Ala., have resulted in the development of many new and improved handling techniques for radium-226 sources. Some of these innovations are described and include devices and methods that reduce personnel exposure during the handling and storage of radioactive materials. (auth)

**54937** (CONF-710401) PROCEEDINGS OF THE ROCKY FLATS SYMPOSIUM ON SAFETY IN PLUTONIUM HANDLING FACILITIES, APRIL 13–16, 1971. (Dow Chemical Co., Golden, Colo. Rocky Flats Div.). 463p. Dep. NTIS.

Forty-two articles are included; separate abstracts were prepared for 40. The remaining two articles on use of aerial surveys for determining Pu contamination and estimating natural terrestrial background in the 17- and 60-keV energy regions from the Compton continuum peak were previously included in NSA as 25: 34862 and 34727, respectively. (P.C.H.)

*For abstracts of individual papers see: 54707–54709,54755, 54756, 54779, 54938–54967, 55150, 55195, 55204, and 55243.*

**54938** (CONF-710401–, pp 4-16) HUMAN ELEMENT DESIGN CONSIDERATIONS WITH GLOVEBOXES AT THE ATLANTIC RICHFIELD HANFORD COMPANY. Anderson, R. D.; Olson, R. E. (Atlantic Richfield Hanford Co., Richland, Wash.). 13 Apr 1971.

From Rocky Flats symposium on safety in plutonium handling facilities; Golden, Colo. (13 Apr 1971).

Considerations given to the human element in design of glove boxes at HAPO are outlined. The discussions span the era of several contractors and include consideration of radiation control and plant production needs. (J.R.D.)

**54939** (CONF-710401–, pp 17-25) GLOVEBOX FIRE-RESISTANT MATERIALS AND FIRE SUPPRESSION TESTS. Fisher, F. D. (Nuclear Materials and Equipment Corp., Apollo, Pa.). 13 Apr 1971.

From Rocky Flats symposium on safety in plutonium handling facilities; Golden, Colo. (13 Apr 1971).

The activities of a committee that was formed to test and report on glove box window materials and fire suppression systems are described. The committee's study will include input from glove box users, glove box fabricators, glazing materials experts, fire suppression systems suppliers, a professional fire protection engineer, and representatives from the AEC. The testing program is intended to complement those studies done at Rocky Flats and elsewhere. Since the NUMEC testing program is primarily oriented around the manufacture of $PuO_2$–$UO_2$ fuels for power reactors, rather than the manufacture of metallic plutonium assemblies, the emphasis of the testing program is expected to differ somewhat from similar programs done at Rocky Flats. (J.R.D.)

**54940** (CONF-710401–, pp 26-43) GLOVEBOX DESIGN AND OPERATION. GLOVEBOX MATERIALS STUDIES. Lindsay, John W. (Dow Chemical Co., Golden, Colo. Rocky Flats Div.). 13 Apr 1971.

From Rocky Flats symposium on safety in plutonium handling facilities; Golden, Colo. (13 Apr 1971).

Because of the many environmental implications associated with plutonium, provision of maximum protection to plutonium handling facilities is of utmost importance. Such protection begins with the design of as failproof a glovebox system as possible. Proper design of a glovebox requires that potential hazards associated with the processes and materials it is intended to contain be well known. Once these hazards have been elucidated, the best available materials of construction for the system can be chosen, and the safest possible glovebox configuration designed. (auth)

**54941** (CONF-710401–, pp 44-55) GLOVEBOX GLOVES. Giebel, R. E. (Dow Chemical Co., Golden, Colo. Rocky Flats Div.). 13 Apr 1971.

From Rocky Flats symposium on safety in plutonium handling facilities; Golden, Colo. (13 Apr 1971).

Important or desirable properties of glovebox gloves are presented. A need to determine these properties has resulted in a program for glove evaluation and procurement. Gloves are most vulnerable to a glovebox fire. Burning properties and means of decreasing vulnerability are discussed. (auth)

**54942** (CONF-710401–, pp 56-67) DESCRIPTION OF ARHCO'S NEW COMPACT PLUTONIUM STORAGE FACILITY. Moulthrop, H. A.; Kemp, J. L. (Atlantic Richfield Hanford Co., Richland, Wash.). 13 Apr 1971.

From Rocky Flats symposium on safety in plutonium handling facilities; Golden, Colo. (13 Apr 1971).

A new plutonium storage facility has been constructed at Richland which has a shielded cubicle arrangement for reducing radiation dose rates. Reduction in radiation exposure by a factor of ten is expected in the vaults from that experienced in plutonium storage vaults previously used. A products-of-combustion fire detection system throughout the facility and a sprinkler system in the scrap storage area provides continuous fire protection. A preliminary emphasis is placed on fuel reduction with all concrete construction. Compartmentation within cubicles reduces the amount of plutonium exposed to combustion if a fire should occur. A storage density of 2.1 spots per square foot is realized for the overall facility. The engineered construction of interconnecting precast concrete panels to form the basic structure and the shielded storage cubicles provides increased safety at decreased unit cost. (auth)

**54943** (CONF-710401–, pp 69-82) APPLICATION OF AN INERT ATMOSPHERE TO A PLUTONIUM PROCESSING SYSTEM. Calkins, K. W.; Bogard, C. F. (Dow Chemical Co., Golden, Colo. Rocky Flats Div.). 13 Apr 1971.

From Rocky Flats symposium on safety in plutonium handling facilities; Golden, Colo. (13 Apr 1971).

Design of an inerting gas system for the Rocky Flats plutonium processing plant is described. The design calls for the use of pure nitrogen as the inerting gas. Slides are used to illustrate the design. (J.R.D.)

**54944** (CONF-710401–, pp 83-97) AIR LEAKAGE INTO PLUTONIUM GLOVEBOXES AND ITS EFFECT ON INERT OPERATIONS. Matheson, L. A.; Johnson, T. C.; Oliver, A. J. (Dow Chemical Co., Golden, Colo. Rocky Flats Div.). 13 Apr 1971.

From Rocky Flats symposium on safety in plutonium handling facilities; Golden, Colo. (13 Apr 1971).

To develop quantitative information on air leakage, a material balance method has been developed to relate air leakage through openings into gloveboxes to resultant increases in water vapor or oxygen concentration. The analysis of the nitrogen requirements using the water vapor material balance method to determine leakage, and other considerations that arise during conversion of a glovebox system to an inert atmosphere are described. Results of investigations show that the material balance method developed for glovebox leakage analysis provides an empirical method for determining leakage into existing glovebox systems. Water vapor leakage into gloveboxes instead of oxygen will determine nitrogen usage for machining operations which are maintained at low humidities. Optimum economic operation will be a balance between extra maintenance and operating labor and the cost of the nitrogen supplied to the system. Improved equipment, operation, and leak detection will lower leakage factors and minimize nitrogen cost. A larger nitrogen supply increases the safety of the inerting by assuring an adequate supply under a greater range of circumstances. (auth)

**54945** (CONF-710401–, pp 98-105) INERT ATMOSPHERE MANAGEMENT AND SURVEILLANCE AT THE ARGONNE NATIONAL LABORATORY FUELS TECHNOLOGY CENTER. Livernash, William H. (Argonne National Lab., Ill.). 13 Apr 1971.

From Rocky Flats symposium on safety in plutonium handling facilities; Golden, Colo. (13 Apr 1971).

Argon and nitrogen atmosphere gloveboxes and nitrogen atmosphere hot cells are in operation at the Fuels Technology Center at Argonne National Laboratory to evaluate plutonium alloys, compounds, or mixtures, and the techniques necessary to produce or investigate these materials. A two-cell cave facility and approximately 80 gloveboxes with inert atmosphere are currently in use. This equipment is installed in three separate areas of the building and operated independently. All enclosures in which plutonium is handled are maintained at a pressure that is negative with respect to the room and are ventilated with inert gas on a low-flow, once-through basis. This technique is possible because of the extremely low leak rate of the enclosures. A discussion is presented of the design features, administrative controls, and techniques employed that provide and maintain inert atmospheres for the main purpose of fire prevention. As a secondary benefit, a high-purity atmosphere is useful in working with reactive materials such as sodium, NaK, or plutonium-bearing materials. (auth)

**54946** (CONF-710401–, pp 106-17) PLUTONIUM IGNITION IN INERT ATMOSPHERES. Musgrave, L. E. (Dow Chemical Co., Golden, Colo. Rocky Flats Div.). 13 Apr 1971.

From Rocky Flats symposium on safety in plutonium handling facilities; Golden, Colo. (13 Apr 1971).

The prevention of ignition is an important consideration in handling plutonium. In order to determine fire safe, inert atmospheres in which plutonium can be handled, the ignition of plutonium has been studied in nitrogen-air and carbon dioxide-air mixtures. The results show that such mixtures are effective in preventing plutonium ignition when the oxygen concentration is below about 5 percent. The maximum allowable oxygen concentration in which plutonium ignition is prevented is higher as the specific surface area decreases. It is also higher in nitrogen-air than in carbon dioxide-air mixtures. (auth)

**54947** (CONF-710401–, pp 118-32) FILTRATION FOR THE EXHAUST VENTILATION OF PLUTONIUM RECOVERY FACILITIES. Taylor, Charles L. (Vitro/Hanford Engineering Services, Richland, Wash.). 13 Apr 1971.

From Rocky Flats symposium on safety in plutonium handling facilities; Golden, Colo. (13 Apr 1971).

A discussion is presented on peripheral high efficiency particulate air (HEPA) filter components and their application to plutonium recovery facility exhaust ventilation systems. It is apparent that the same components are also applicable to many types of nuclear plant exhaust systems to maintain continuous operation under adverse conditions, hold radioactive effluents to a minimum, and provide for relatively simple servicing without interruption of operation. It is pointed out that it is possible to design and construct, using present technology and equipment, a filtration system for exhaust ventilation of plutonium recovery facilities or for any nuclear plant exhaust system. (J.R.D.)

**54948** (CONF-710401-, pp 133-48) VENTILATION SYSTEMS AT MOUND LABORATORY "PP" BUILDING. Kleine, P. J. (Mound Lab., Miamisburg, Ohio). 13 Apr 1971.

From Rocky Flats symposium on safety in plutonium handling facilities; Golden, Colo. (13 Apr 1971).

Information is presented on the plutonium processing building ventilation systems at Mound Laboratory and the safety measures taken to ensure the integrity of the ventilation systems, thereby preventing the release of radioactive material to the environment. Discussions are included on the differential pressures between the ventilation systems used to restrict the radioactive contaminants from spreading through the building; the high-efficiency air filtration system used throughout the building; and the fire protection for glove boxes including the design and installation of a Halon 1301 automatic fire detection and protection system. (J.R.D.)

**54949** (CONF-710401–, pp 149-61) DIFFERENT TYPE GLOVEBOX FILTERS USED FOR $^{238}Pu$ WORK AT MOUND LABORATORY. Anderson, H. F. (Mound Lab., Miamisburg, Ohio). 13 Apr 1971.

From Rocky Flats symposium on safety in plutonium handling facilities; Golden, Colo. (13 Apr 1971).

A review is presented of the different type glove box filters that have been used with plutonium-238 glove boxes at Mound Laboratory. Filter installation types discussed include box-type filter mounted inside a small housing on top of glove box, cylindrical filter with 2-in. diameter threaded pipe at one end

XUM

designed to screw into exhaust line inside glove box, and dual cylindrical filters with molded rubber gaskets designed to fit inside a stainless steel or fiber glass tube below glove box. Each type filter installation is discussed in terms of filtration adequacy, sources of leaks, ease of filter change, contamination control problems during filter change, and interference with glove box operations. (auth)

**54950** (CONF-710401–, pp 162-80) DESIGN OF FILTER PLENUM HEAT EXCHANGERS. Domning, W. E. (Dow Chemical Co., Golden, Colo. Rocky Flats Div.). 13 Apr 1971.

From Rocky Flats symposium on safety in plutonium handling facilities; Golden, Colo. (13 Apr 1971).

Results of investigations conducted in the plenum of the Rocky Flats fire test facility are presented which show that heated air generated by a fire within a radioactive processing building is likely to damage the exhaust filters. The application of water sprays to the face of high efficiency particulate air (HEPA) filter banks is likely to result in breakthrough of contamination. Therefore, it is preferable to cool the heated air with a heat exchanger prior to filtration. It is necessary that the distribution of the air flow be uniform so that the contact time within the spray field is maximized for all portions of the air stream. In order to optimize the heat exchanger design for each filter plenum, it is necessary to determine the exchanger inlet temperatures. This can be done by a survey of the combustible material in the area served by the filter plenum, and knowledge of the relative heats of combustion and burning rates. The design can be further optimized for the specific case by considering the effect of dilution air and knowing more accurately the heat loss through the ducting. Based on the assumptions used for the example which approximates a general case, a heat exchanger length of 5 to 6 feet appears necessary for protection of the filters for a 1-hour fire. (J.R.D.)

**54951** (CONF-710401–, pp 181-202) PERFORMANCE OF HIGH EFFICIENCY PARTICULATE AIR FILTER FOR FUME FROM BURNING PLUTONIUM METAL. Woodard, R. W.; Robinson, H. N.; Baker, H. M. (Dow Chemical Co., Golden, Colo. Rocky Flats Div.). 13 Apr 1971.

From Rocky Flats symposium on safety in plutonium handling facilities; Golden, Colo. (13 Apr 1971).

A study was conducted to determine the efficiency of a commercial high-efficiency particulate air (HEPA) filter in retaining plutonium aerosols from burning plutonium metal. Penetration of the test filter ranged from 0 to 0.0003 percent. Particle samples collected on electron microscope grids by means of a point-to-plane electrostatic precipitator revealed a size range of 0.01 to 0.1 $\mu$ for individual particles. The particulate matter was typically found in aggregates containing hundreds to thousands of particles. The cross section of aggregates measured 3 to 15 $\mu$. Samples of particulate matter collected on membrane filters and transferred to electron microscope grids also revealed the preponderance of particles in the form of aggregates. (auth)

**54952** (CONF-710401–, pp 204-7) ORGANIZATION AND PLANNING FOR FIRE CONTROL. Spencer, R. I. (Factory Insurance Association, Chicago, Ill.). 14 Apr 1971.

From Rocky Flats symposium on safety in plutonium handling facilities; Golden, Colo. (13 Apr 1971).

A hypothetical fire episode is presented to stimulate thought on plant fire prevention methods. Aspects of the conditions associated with the fire are further discussed as related to management attitude, emergency preplanning, inspection programs, plant emergency squads, and cooperation with public fire departments. (J.R.D.)

**54953** (CONF-710401–, pp 208-11) THE CATEGORIZATION AND POSTING OF NUCLEAR FACILITIES FOR FIRE PROTECTION PURPOSES AT WADCO. Gough, R. M. (Hanford Engineering Development Lab., Richland, Wash.). 14 Apr 1971.

From Rocky Flats symposium on safety in plutonium handling facilities; Golden, Colo. (13 Apr 1971).

The responsibilities for this program are divided among three groups in WADCO. The Nuclear Safety Organization classifications for facilities comprise four categories. This categorization is done with the idea of obtaining the least possible restrictions on the use of water consistent with criticality safety. Each building is reviewed and audited periodically to see that their criteria are observed and up to date. Adjustments have been made in inventories and processes in order to reduce restrictions. Other details of organization and categorization are included along with an evaluation of the program results. (J.R.D.)

**54954** (CONF-710401–, pp 212-20) FIRE DETECTION AND SUPPRESSION IN GLOVE BOX SYSTEMS. Hill, A. J. (Du Pont de Nemours (E. I.) and Co., Aiken, S. C. Savannah River Lab.). 14 Apr 1971.

From Rocky Flats symposium on safety in plutonium handling facilities; Golden, Colo. (13 Apr 1971).

An automatic fire-extinguishing system has been designed and tested for protection against non-metallic fires in glove boxes at the Savannah River Laboratory. The extinguishing agent is Halon 1301 (bromotrifluoromethane). A number of glove boxes are presently protected by manually actuated systems pending conversion to automatic systems as operations permit. (auth)

**54955** (CONF-710401–, pp 221-36) FIRE DETECTION SYSTEMS IN GLOVEBOXES. Orihood, Glenn M. (Vitro/Hanford Engineering Services, Richland, Wash.). 14 Apr 1971.

From Rocky Flats symposium on safety in plutonium handling facilities; Golden, Colo. (13 Apr 1971).

An investigation is described which served to develop two new devices for inclusion in an already extensive line of fire detection units. Both have the inherent resistivity necessary for installation in high acid environments. It is also felt that they have the necessary capability for reliable fire detection under these circumstances, since they have demonstrated in the tests that they reliably detect both Class A and Class B fires before glove box integrity becomes a factor. (auth)

**54956** (CONF-710401–, pp 237-47) FIRE PROTECTION TEST FACILITY FOR CELLS AND CAVES. Lee, H. A. (Atlantic Richfield Hanford Co., Richland, Wash.). 14 Apr 1971.

From Rocky Flats symposium on safety in plutonium handling facilities; Golden, Colo. (13 Apr 1971).

A fire protection test facility has been constructed by ARHCO at Richland consisting of a simulated hot cell and a filtered exhaust system. The purpose is to study fires and fire protection components and systems under conditions similar to those of typical heavily shielded remote or manipulator operated hot cells and in their filtered ventilation exhaust systems. Tests are planned to establish criteria for effective fire protection systems, components, and methods of operation for both the hot cells and their exhaust systems. (auth)

**54957** (CONF-710401–, pp 248-56) ENGINEERING FIRE-SUPPRESSION SYSTEMS FOR LARGE VOLUMES USING HALON 1301. Gaskill, J. R.; Harder, C. A.; Nelson, G. O. (California Univ., Livermore. Lawrence Radiation Lab.). 14 Apr 1971.

From Rocky Flats symposium on safety in plutonium handling facilities; Golden, Colo. (13 Apr 1971).

Engineering studies of Halon 1301 fire-suppression systems for large volumes (up to 10,000 cu ft) are summarized and the results are presented. Guidelines are given for designing such a system, with particular attention paid to fire detectors, alarms and controls, and the Halon distribution arrangement. (auth)

**54958** (CONF-710401–, pp 258-66) SAFETY CONSIDERATIONS AT THE BABCOCK AND WILCOX PLUTONIUM DEVELOPMENT LABORATORY. Carlson, R. V.; Goodman, W. K. (Babcock and Wilcox Co., Lynchburg, Va. Research and Development Div.). 14 Apr 1971.

From Rocky Flats symposium on safety in plutonium handling facilities; Golden, Colo. (13 Apr 1971).

Since 1966, Babcock & Wilcox has conducted research and development programs in its Plutonium Development Laboratory (PDL). The PDL was designed to handle plutonium-bearing oxides and solutions in a wide variety of processes, on both bench and pilot-plant scales. A description is presented of the PDL safety organization, the administrative procedures and controls, and several systems that allow maximum flexibility in operations without compromising safety. Two glovebox accessories designed by B&W are also described. The first, a specially designed manometer, protects the gloveboxes from inadvertent overpressurization resulting from a malfunction of the compressed inlet air supply or the outlet filter system. The other, a sphincter-type valve, which is used in rapid filter changes to minimize risk of spreading contamination. (auth)

**54959** (CONF-710401–, pp 280-92) BATTELLE'S RESEARCH PLUTONIUM FACILITY ENVIRONMENTAL CONTROL AND SAFETY. Freas, D. G.; Dunlap, J. H.; Ottman, R. J.; Kruger, O. L. (Battelle Memorial Inst., Columbus, Ohio). 14 Apr 1971.

From Rocky Flats symposium on safety in plutonium handling facilities; Golden, Colo. (13 Apr 1971).

Research and development studies of plutonium-bearing materials are conducted in the Battelle-Columbus Plutonium Facility located at West Jefferson, Ohio. The facility provides nearly 7500 $ft^2$ of laboratory space and is operated with a philosophy for total material containment which provides safe conditions for both laboratory personnel and the surrounding environment. Through the use of numerous safety systems and close supervision of personnel activities, research is conducted in an efficient manner. Education and training are provided by frequent

seminars and lectures as well as by on-the-job supervision by qualified personnel. Alarm systems and established procedures are the main safeguards in preventing serious personnel injuries and in attending to emergency situations when they exist within the facility. (auth)

**54960** (CONF-710401–, pp 293-6) ADMINISTRATIVE PROCEDURES AND CONTROLS IN PLUTONIUM PRODUCTION AREAS. Hauschildt, W. H. (Dow Chemical Co., Golden, Colo. Rocky Flats Div.). 14 Apr 1971.

From Rocky Flats symposium on safety in plutonium handling facilities; Golden, Colo. (13 Apr 1971).

The development of administrative procedures for operation of the Rocky Flats Plant subsequent to the May 11, 1969, fire is described. (J.R.D.)

**54961** (CONF-710401–, pp 297-9) SAFETY CONSIDERATIONS IN THE NEW ROCKY FLATS PLUTONIUM RECOVERY PLANT. Carpenter, J. D. (Dow Chemical Co., Golden, Colo. Rocky Flats Div.). 14 Apr 1971.

From Rocky Flats symposium on safety in plutonium handling facilities; Golden, Colo. (13 Apr 1971).

A new chemical recovery facility will incorporate improved health, fire, and safety requirements as determined by the Atomic Energy Commission and The Dow Chemical Company. An architect-engineer will study four construction alternatives. Of the proposed alternatives, Dow feels that only a new building complex can meet these improved standards. These standards require lower exposure, reduced fire potential, and reduced contamination. (auth)

**54962** (CONF-710401–, pp 307-10) MATERIALS FOR SHIELDING NUCLEAR RADIATIONS FROM PLUTONIUM PROCESSING. Hall, Wm. Cornelius; Peterson, J. Merriam (Chemtree Corp., Central Valley, N. Y.). 14 Apr 1971.

From Rocky Flats symposium on safety in plutonium handling facilities; Golden, Colo. (13 Apr 1971).

The most efficient attenuation materials for neutrons from plutonium processing have both hazards and high cost. The less costly materials initially have not proved fire safe, and therefore they are ultimately more costly. Material of comparable efficiency and cost, with good fire retardant properties would seem the most sensible choice. Accordingly, the most nearly ideal materials appear to be the new Chemtree materials having high attenuation efficiency, competitive cost, and noncombustible characteristics. It appears that no other single step can add as much to the safety of plutonium handling as can the substitution of the new improved CHEMTREE 1-5-20 for the previously used combustible materials. (auth)

**54963** (CONF-710401–, pp 311-15) DESIGN FEATURES OF MOUND LABORATORY'S MEDICAL DECONTAMINATION FACILITY. McMannon, R. U.; Musen, L. G. (Mound Lab., Miamisburg, Ohio). 14 Apr 1971.

From Rocky Flats symposium on safety in plutonium handling facilities; Golden, Colo. (13 Apr 1971).

The new medical decontamination facility at Mound Laboratory is described. The facility was constructed to provide maximum medical and health physics care for injured radiation workers. Many of the design features were based on experience in working with radioactive materials and monitoring of injuries involving contamination. These features are intended to control radioactive contamination and to prevent its release to uncontrolled areas. The new facility is located next to the medical facility which provides quick response by medical personnel, and is also adjacent to the whole body counting facility. The services of both of these facilities are available if required. Ventilation in the facility is provided by an air conditioning unit located on the roof of the building. Exhaust air from each room passes through a roughing filter and an absolute filter to remove airborne contamination. An air sampling probe is installed in the exhaust duct on the roof to monitor the effluent air if required. A water collection system consisting of two 400-gallon tanks collects all waste water. The full tank alarm and control panel for the pumps are located in the south entry room. A decontamination table equipped with running water and a drain is available for highly contaminated persons with serious injuries. It is perforated to provide positive drainage. All water is collected in the holding tanks. (R.C.K.)

**54964** (CONF-710401–, pp 316-19) ROCKY FLATS ENVIRONMENTAL RESEARCH. Bright, W. C. (Dow Chemical Co., Golden, Colo. Rocky Flats Div.). 14 Apr 1971.

From Rocky Flats symposium on safety in plutonium handling facilities; Golden, Colo. (13 Apr 1971).

A major concern of the environmental research group is to ensure that Rocky Flats operations have the least possible adverse effect upon the environment. The term environment is here used broadly to include not only the environment external to the plant buildings, but also to that within the buildings as it relates to employee safety and to the proper containment and management of toxic materials. Plutonium is the material of primary concern but various chemical hazards are also under study. (auth)

**54965** (CONF-710401–, pp 365-8) OPERATION OF A TRANSURANIC STORAGE AREA AT NRTS. Nichols, C. E. (Idaho Nuclear Corp., Idaho Falls). 15 Apr 1971.

From Rocky Flats symposium on safety in plutonium handling facilities; Golden, Colo. (13 Apr 1971).

The Improved Temporary Storage Area No. 1 was constructed adjacent to the NRTS burial grounds for the temporary storage of transuranics. In utilizing this above-grade storage area outside the boundaries of the present burial grounds for transuranics, the life expectancy of the NRTS burial grounds has been increased by several years. The methods used in the operation of the Improved Temporary Storage Area No. 1 (ITSA No. 1) for transuranic waste are described. (auth)

**54966** (CONF-710401–, pp 430-7) ADMINISTRATIVE PROCEDURES FOR CRITICALITY PREVENTION IN PLUTONIUM OPERATIONS. Crawley, D. T.; Ridgway, K. R. (Atlantic Richfield Hanford Co., Richland, Wash.). 16 Apr 1971.

From Rocky Flats symposium on safety in plutonium handling facilities; Golden, Colo. (13 Apr 1971).

Increasing amounts of plutonium are being handled by an increasing number of facilities throughout the country. Increased amounts and varieties of plutonium materials at ARHCO have served to indicate new problem areas that can be encountered by others. Scrap materials are of particular concern for all aspects of plutonium handling, as well as for criticality prevention. To effectively administer a plutonium processing facility, criticality prevention must be integrated into the facilities, procedures, and training. (auth)

**54967** (CONF-710401–, pp 438-53) SAFETY CRITERIA FOR THE DESIGN OF FACILITIES PROCESSING PLUTONIUM. Biles, M. B.; Patterson, D. E.; Brown, B. P. (Division of Operational Safety (AEC), Washington, D. C.). 16 Apr 1971.

From Rocky Flats symposium on safety in plutonium handling facilities; Golden, Colo. (13 Apr 1971).

Development of criteria for Pu processing safety has objectives such as public safety, employee safety, program continuity, and minimization of property loss. These objectives are discussed and illustrated by drafts of safety criteria prepared by the AEC's Division of Operational Safety. (J.R.D.)

**54968** (IAEA-R-878-F) ANALYSIS OF THE SAFEGUARDS CAPABILITIES OF MATERIAL BALANCE ACCOUNTING SYSTEMS IN SELECTED URANIUM AND PLUTONIUM SCRAP PROCESSING. Final Report, December 30, 1969–December 29, 1970. Johnson, E. R. (Nuclear Audit and Testing Co., Washington, D. C.). Sep 1970. 93p.

A series of material balance models was constructed for commercial uranium and plutonium scrap processing facilities. These included models for single-purpose facilities for the processing of LWR fuel fabrication scrap, HTGR fuel fabrication scrap, U–Al alloy fuel fabrication scrap, plutonium recycle (LWR) fuel fabrication scrap, FBR fuel fabrication scrap and Pu–Al alloy fuel fabrication scrap—as well as models for an integrated uranium scrap processing facility and an integrated plutonium scrap processing facility. The effectiveness of material balance accounting in detecting a loss of uranium or plutonium during a scrap processing campaign for each of the scrap processing systems studied is tabulated. The variance of materials unaccounted for (MUF) is shown in terms of the relative standard deviation as a percent of plant input during the campaign period. The performance indices ($\sigma_{MUF}$ as a percent of plant input) for uranium scrap processing facilities range from 0.17 to 0.38%, while those for plutonium scrap processing facilities range from 0.19 to 0.34%. The capability indices for uranium scrap processing facilities range from 0.10 to 0.17%, while those for plutonium scrap processing facilities range from 0.12 to 0.17%. The limiting factor in reducing the variance of MUF is the systematic error associated with the analysis, sampling and volume (or weight) measurement of dissolver filtrates, and recovered products. The contributions of inventory, recycle washings and waste measurements are small because of the relatively small quantities involved. However, when those streams increase in size (particularly the inventory) such measurement errors become an important contribution to the variance of MUF. The major contribution to the MUF variance in the cases studied was found to be due to systematic error. Although the results of this study showed that a material balance accounting system would be an ef-

XUM

fective tool for the detection of a diversion of special nuclear materials in both uranium and plutonium scrap processing facilities, it should be pointed out that at the present time the measurement of input to the scrap processing systems is made after considerable head-end treatment of scrap material which precedes such measurement and that such operations are not subject to monitoring by material balance accounting techniques. At the present time there is no reliable method for obtaining an independent check on a scrap processing facility accounting system for uranium or plutonium input, because the facility generating the scrap does not have accurate or reliable methods for determining the uranium or plutonium content of the generally heterogeneous scrap materials. However, a good independent check is available for uranium and plutonium product materials through the use of receiver analyses which, when combined with the results of the scrap processor's analyses, provide a relative standard deviation of 0.06% of the quantity of either uranium or plutonium which is transferred from the scrap processing facility in the capability model. The performance model shows a slight difference between the uranium and plutonium processes, providing a relative standard deviation of 0.08% of the quantity transferred from the scrap processing facility for uranium and 0.11 to 0.13% for plutonium. This range between uranium and plutonium reflects the greater difficulties of handling and measuring plutonium in a typical production facility. (auth)

**54969** (JUL-766-CT) ENERGY ACCUMULATION IN SOLID BODIES THROUGH NUCLEAR RADIATION BY STORAGE OF HIGHLY RADIOACTIVE SCRAP. Laser, M.; Merz, E. (Kernforschungsanlage, Juelich (West Germany). Institut fuer Chemische Technologie). May 1971. 25p. (In German). Dep. NTIS (U. S. Sales Only).

The hazards of a sudden energy release from solidified radioactive wastes as well as from salt in which the material is stored are analyzed. The discussion includes energy storage in solids, interaction between nuclear radiation and solid material, and defect formation in solids. Subsequently, energy storage in salt and glasses used for final disposition of highly radioactive waste is assessed. Glasses are treated with respect to absorption, release, and longtime storage of energy. Salt is considered as a vehicle for energy storage. (H.B.G.)

**54970** (KY-631) ADDITIONAL TESTING OF TEN-TON URANIUM HEXAFLUORIDE CYLINDERS. Richardson, E. W.; Bernstein, S. (Paducah Gaseous Diffusion Plant, Ky.). 15 Sep 1971. Contract W-7405-eng-26. 17p. Dep. NTIS.

Work on the destructive testing of model 48A 10-ton Type P uranium hexafluoride shipping containers at the Paducah cylinder test facility is reported. The two tests were conducted to provide additional data for use in the design of a Type B package for the 10-ton cylinder. The results of 12 previous tests were reported in KY-500. (auth)

**54971** (ORNL-4665) SAFETY ANALYSIS OF WASTE DISPOSAL BY HYDRAULIC FRACTURING AT OAK RIDGE. de Laguna, W.; Binford, F. T.; Weeren, H. O.; Witkowski, E. J.; Struxness, E. G. (Oak Ridge National Lab., Tenn.). Sep 1971. Contract W-7405-eng-26. 41p. Dep. NTIS.

The concept of hydraulic fracturing as a method for the permanent disposal of radioactive waste solutions is founded upon methods developed by the petroleum industry. The basic procedure is to generate a horizontal fracture in the impermeable shale which is located several hundred feet underground. This is done by pumping water at high pressure down into a cased well and out into the shale through slots cut in the well casing. A mixture of waste solution, portland cement, and clay is then pumped into the fracture, the well closed in, and the cement mixture allowed to set up, forming a solid sheet of hardened grout which becomes essentially part of the host rock. The facilities which have been designed and constructed at ORNL for this purpose, together with information concerning ORNL experience with 14 injections performed between February 1964 and September 1970 are described. The safety analysis leads to the conclusion that, within the operating limits specified, hydrofracture disposal of radioactive waste can be carried out in a safe and orderly manner with no significant present or future hazard to the public or to the environment. (auth)

**54972** (ORNL-TM-2723) ENGINEERING EVALUATION OF LMFBR FUEL SHIPMENT. Irvine, A. R. (Oak Ridge National Lab., Tenn.). Sep 1971. Contract W-7405-eng-26. 64p. Dep. NTIS.

The shipment of short-decayed LMFBR spent fuel will require exceptional containment that is resistant to all credible hazards. Results of tests and calculations indicate that it would be possible to construct overland shipping systems which can remain sealed under extreme impact conditions and exposure to relatively long-duration fires. Shipment by barge can avoid exposure to fire and significant impact. Adequate cooling of large loads of short-decayed fuel can be obtained through the use of a low-vapor-pressure liquid metal as the primary coolant. (auth)

**54973** (RT/PROT-71-11) HEALTH PROTECTION ANALYSIS OF TRANSPORTATION OF RADIOACTIVE SUBSTANCES THROUGH TUNNELS: THE MONT BLANC TUNNEL. Faloci, C.; Lucci, F.; Susanna, A. (Comitato Nazionale per l'Energia Nucleare, Rome (Italy)). 14 Apr 1971. 34p. Dep. NTIS (U. S. Sales Only).

A study was carried out to evaluate the possibility of admitting vehicles transporting radioactive substances to travel through the Mont Blanc tunnel. The assumptions on which the reference accident in the IAEA recommendations on transportation of radioactive substances are based were examined. Furthermore, by considering the characteristics of the tunnel as well as the accidents which have happened there, the maximum credible accident that might take place in the tunnel was determined and compared with the IAEA reference accident. The conclusion was that, except for substances defined as exempted in the IAEA recommendations, radioactive substances transported in Type B packages, radioactive substances in special form and not in special form up to certain radioactivity levels transported in Type A packages, those having low specific activity, and those of groups V, VI, VII, and VIII as classed in the ADR, may be admitted for transit through the tunnel subject to certain restrictions. Other substances not in special form having a higher activity than those above mentioned and being transported in Type B packages must not be allowed to enter the tunnel. (auth)

**54974** (SC-M-71-241) ENVIRONMENT EXPERIENCED BY CARGO DURING NORMAL RAIL AND TRUCK TRANSPORT: COMPLETE DATA. Foley, J. T.; Gens, M. B. (Sandia Labs., Albuquerque, N. Mex.). Aug 1971. 318p. Dep. NTIS.

This document presents data reduced from that obtained by the Sandia Laboratories' Environmental Criteria Group during the transportation of a Radioactive Material (RAM) cask by rail and by truck in Kentucky and Tennessee in 1968. It provides background for the reports and analyses which were published elsewhere. (auth)

**54975** (WASH-1167) COMPACTION OF RADIOACTIVE SOLID WASTE. (Atomic Energy Commission, Washington, D. C.). Jun 1970. 41p. Dep. NTIS.

A study was made of methods of compacting Pu- or transuranium nuclide-containing solid radioactive waste in order to comply with new AEC requirements that such waste be stored separately and be retrievable for subsequent relocation or reprocessing. From this study it was concluded that: at least half of AEC site-generated solid radioactive waste can be compacted and reduced to from 0.2 to 0.1 of the original volume; cost savings can be realized by compaction prior to shipment, i.e., compaction should be done at the waste production site; compaction equipment is commercially available, needs little modification for handling radioactive wastes, is relatively cheap, and should be used under conditions which protect the operators from airborne contamination; and the overall cost advantages of compaction must consider methods used for handling the waste after compaction and storage costs. The performance testing of compacting equipment is recommended. (L.C.L.)

**54976** FRENCH REGULATION ON THE TRANSPORT OF GAMMA SOURCES IN SEALED CAPSULES OF SPECIAL FORM (USED PARTICULARLY IN RADIOGRAPHY). Bull. Inform. A.T.E.N. (Ass. Tech. Energ. Nucl.), Suppl.; Nos. 79 and 80, 13-35 (Sep-Dec 1969). (In French).

An analysis of regulations for the transport of radioactive material on French territory by land carriers is presented. The various regulations in force concerned with the transport of sources commonly used in gammagraphy are compiled. (tr-auth)

**54977** IMPROVED CONTAINER FOR RADIOACTIVE SUBSTANCES. Bochard, Camille (to Robatel SLPI). British Patent 1,243,486. 18 Aug 1971. Priority date 12 Aug 1969, France.

A double-walled container for radioactive substances is described which has an outer metal casing, an inner wall of lead for shielding, and an interlayer composed of hydrated $Al_2O_3$–$Fe_2O_3$ forming a solid mass. The hydrated mixture serves as a protective layer to prevent melting of the lead in accidents involving fire. (J.R.D.)

**54978** PROTECTING BOX. (to Societe Belge Pour l'Industrie Nucleaire SA). British Patent 1,235,745. 16 Jun 1971. Priority date 21 Dec 1967, Belgium.

The design of box-type sealed enclosures for handling radioactive or poisonous materials is described. It is noted that in

dealing with rather large objects it may be advantageous to insert them only partially in the box. Provision is made for insertion of only one end of rod-shaped articles through the box wall which incorporates a seal. The specimen can be rotated. (J.R.D.)

**54979** SOLIDIFICATION OF RADIOACTIVE WASTES WITH CEMENT. Kikukawa, Hiroji (Meijo Univ., Nagoya, Japan); Murata, Jiro; Ohtsuka, Shigeo. Semento Konkurito; No. 284, 26-31(Oct 1970). (In Japanese).

For disposal of radioactive wastes in the ocean, the wastes are put into reinforced concrete containers or are solidified with cement. To investigate the optimum proportion of cement–waste mixture, a series of mixing tests was made with some admixture and concentrated liquid waste and filtrated sludge from BWR power stations. The mechanical properties of cemented wastes were also studied with a triaxial compression test apparatus. This equipment was used to study the stability of the solidified wastes under high pressure of the deep sea. The optimum proportion of mixture was determined for both wastes. For the solidification of the concentrated liquid waste, blast-furnace cement was the most suitable from the point of chemical stability. In this case the fine shale dust, which is a by-product of an expanded shale aggregate factory, was more effective than bentonite as a preventive admixture against segregation of the mixture. The properties of the solidified waste were influenced by temperature of the concentrated liquid waste. To solidify the filtrated sludge, Portland cement was suitable from the points of time required for hardening and strength. The radial modulus of elasticity of the solidified wastes under triaxial compression was found to be almost the same as the axial one. (Japan)

**54980** RADIOACTIVE WASTE DISPOSAL AT A PWR POWER PLANT. Kohri, Masaharu (Mitsubishi Heavy Industries, Ltd., Tokyo). Karyoku Hatsuden; 21: No. 12, 1316-21(Dec 1970). (In Japanese).

Problems of radioactivity and control of primary coolant water in a PWR plant are reviewed, and waste disposal practices are explained. Liquid waste sources are: sewage from washing and shower; drainage from laboratories; leakage from the primary coolant loop; and liquid from decontamination. Gaseous wastes are nitrogen cover gas ejected from the primary coolant storage tank, and gases evolved from the primary coolant in boric-acid control. Solid wastes emerge as paper, wood, glass, filter and cartridge wastes, used ion-exchange resin, concentrated solutions mixed in concrete, etc. Finally, measures taken to protect plant operators and the nearby populace are briefly explained. (Japan)

**54981** PLANT PROJECT FOR FIXATION OF RADIOACTIVE WASTES INTO BITUMEN. Napravnik, J.; Ralkova, J. (Nuclear Research Inst., Rez, Czech.). Jad. Energ.; 17: No. 6, 188-91(Jun 1971). (In Czech).

Based on theoretical calculations and laboratory results which proved the usefulness of asphalt emulsions for the fixation of high level radioactive wastes, a pilot plant was designed, the principal unit of which is the mixer-evaporator. (auth)

**54982** PRODUCTION OF RELATIVELY MONODISPERSE AEROSOLS FOR INHALATION EXPERIMENTS BY AEROSOL CENTRIFUGATION. Kotrappa, P. (Lovelace Foundation for Medical Education and Research, Albuquerque, N. Mex.); Moss, Owen R. Health Phys.; 21: No. 4, 531-5(Oct 1971).

Stöber's aerosol spectrometer, based on a spinning spiral duct, was used as an aerosol centrifuge to separate narrow size groups of insoluble aerosols starting from polydisperse distributions. The samples collected were resuspended in water and aerosolized with a Lovelace nebulizer to produce relatively monodisperse aerosols. Working with near-spherical fused clay particles, aerosols were obtained with geometric standard deviations of less than 1.1 and with number concentrations that would be practical for use in inhalation experiments. A formula for dilution of monodisperse suspensions for aerosolization was used to calculate the maximum number concentration that could be aerosolized from a suspension for a particular nebulizer, to obtain 95% singlets. This method appears to be particularly adaptable for the aerosols of oxides of transuranic elements. Estimated respiratory deposition of the oxides of $^{239}Pu$, $^{238}Pu$, $^{244}Cm$, and $^{241}Am$ for beagle dogs breathing the monodisperse aerosols for 1 hr are given for aerodynamic sizes ranging from 0.5 to 3.0 $\mu$m. (auth)

**54983** METHOD AND MEANS FOR CHANGING RADIOACTIVE SOURCES. Santoro, Michael P.; Boyko, Stephen (to Automation Industries, Inc.). U. S. Patent 3,562,532. 9 Feb 1971. Filed 26 Oct 1967.

A method and means to permit the use of a radioactive source capsule with storage units of different sizes are described. An extension cable is detachably connected to a main cable holding the source capsule. The extension cable is detached from the main cable when the source capsule is disposed within the smaller unit and is attached to the main cable when the source capsule is disposed within the larger unit. (Official Gazette)

**54984** RECORD-KEEPING IN A RADIATION SAFETY OFFICE BY TIMESHARING DIGITAL COMPUTER. Ibbott, Geoffrey S.; Hendee, William R.; Crusha, Kenneth L.; Hall, G. Richard (Univ. of Colorado, Denver). Health Phys.; 21: No. 4, 581-4(Oct 1971).

Computer programs in BASIC language were written for the maintenance of an accurate and current inventory of radioactive materials on the campus of the University of Colorado Medical Center. Data files stored in the computer are updated daily for decay of radioactive sources and for influx and outflux of radioactive materials in the Center, and a listing of these files provides a record of the current possession of radionuclides by each authorized user in the institution. Use of these programs not only has enhanced the service and regulatory functions of the Radiation Safety Office, but also has increased the accuracy of record-keeping and reduced the accumulation of radioactive waste in clinical and research laboratories in the Medical Center. (auth)

**54985** RADIOACTIVE WASTE. Kuehn, K. (Gesellschaft fuer Strahlenforschung mbH, Munich). Neue Tech.; 13: 61-8(Feb 1971). (In German).

Radioactive waste disposal procedures are surveyed. Producers, treatment, and final disposal of radioactive waste are discussed. Disposal in salt mines is emphasized. The Asse salt mine near Braunschweig, Germany has been used for this type of disposal since 1967. Starting with the summer of 1971, low-level radioactive waste will be disposed routinely in the mine, and medium-level waste will be stored experimentally. Other forms of disposal such as hydraulic fracturing, placement at ocean bottom, and burying in soil are discussed briefly. (H.B.G.)

**54986** PRODUCTION OF GASES OF KNOWN SPECIFIC ACTIVITY IN A REACTOR FOR CALIBRATING GASEOUS EFFLUENT MONITORS. Bowman, Worth B.; Caruthers, L. T.; Maxwell, Ronald B. (North Carolina States Univ., Raleigh). Health Phys.; 20: 337-9(Mar 1971).

An investigation is reported of activation of a continuously flowing gas in the neutron flux of a reactor for the purpose of generating a gas whose specific activity at the stack monitor detector is known. Calibration is thereby done with the detector in its normal operating configuration and storage of radioactive gas is not required. The importance of flow rate regulation is shown to be small for most gases. (auth) (UK)

**54987** RADIOACTIVITY INDUCED IN COMMONLY USED MATERIALS BY VARIOUS PARTICLE FLUX. Barbier, Marcel (European Organization for Nuclear Research, Geneva). Ind. At.; 14: No. 9/10, 34-40(Sep-Oct 1970). (In French).

An account is given of recent research enabling the induced radioactivity, and the probable doses received by personnel in the vicinity of activated objects, to be calculated. (auth) (France)

**54988** DEVICE FOR THE LEAK-TIGHT TRANSFER OF OBJECTS TO A CONTAINER THROUGH AN ENCLOSURE WALL. Godart, Michel (to Commissariat a l'Energie Atomique). British Patent 1,230,550. 5 May 1971. Priority date 10 Mar 1969, France.

A device for use in leak-tight transfer of objects into containers through enclosing walls is described. The device comprises tubes which penetrate the container walls in such a way that they are leaktight. Tapes corresponding to the diameters of the tubes are used in which holes are punched to act as conveyer carriers. (J.R.D.)

**54989** SEALED CONTAINER WITH PRESSURE RELIEF FOR HAZARDOUS MATERIAL. Wilkins, Charles A.; King, Franklin D. R. (to United States Atomic Energy Commission). U. S. Patent 3,573,462. 6 Apr 1971. Filed 4 Feb 1969.

A sealed vessel for containing a hazardous liquid or a liquid shield for radioactive material is provided with fusible plug assemblies within the vessel walls for melting and relieving internal pressure on high-temperature exposure without loss of unvaporized liquid. The fusible plug assemblies are designed such that only those fusible plugs contacting the vapor space above the liquid will melt and are arranged such that at least one fusible plug will contact the vapor space regardless of container orientation. (Official Gazette)

XUM

54990 SEALED MANIPULATOR THROUGH TUBE. (to Central Research Labs., Inc.). British Patent 1,226,690. 31 Mar 1971. Priority date 8 Nov 1968, United States.

A description is presented of a sealed manipulator which operates through the tube of a remote master-slave device whose motions are transmitted from a master arm on one side of a barrier wall to a slave arm on the opposite side of the wall. Linear motion of the handle on the master arm is converted to rotary motion, transmitted through the support, then reconverted to linear motion of the tong on the slave arm. (J.R.D.)

54991 METHOD FOR THE CALCULATION OF FIELD DOSE OF A URANIUM RADIATION LOOP LINEAR SOURCE OF $\gamma$-RADIATION. Stariznyi, E. S.; Breger, A. Kh. This paper was summarized in At. Energ. (USSR); 26: 451-2(May 1969) as paper No. 239/4874. (In Russian).

Mathematical relations for calculation of doses in uniformly irradiating reaction volumes of U radiation loops are presented. (J.R.D.)

## Vacuum Engineering

*Refer also to abstract 56141.*

54992 ULTRA HIGH VACUUM METROLOGY, DESCRIPTION OF A CALIBRATION BENCH AND THE ASSOCIATED MEASURING EQUIPMENT. Lefevre (Laboratoire Central de l'Armement, Paris). Bull. Inform. Bur. Nat. Metrol.; 2: No. 4, 7-8(Apr 1971). (In French).

Two molecular manometers coupled to the calibration unit enabled the operation of the molecular manometer and the accuracy of the bench to be checked. The precision of the calibration bench was demonstrated to be the same as that of the molecular manometer. This manometer was classified as a primary standard, within the pressure range $10^{-1}$ to $10^{-4}$ Pa. The coupling of this manometer to the calibration bench enabled double control calibrations down to $10^{-5}$ Pa; a thermomolecular manometer enabled calibrations by comparison down to $10^{-7}$ Pa. (France)

# INSTRUMENTATION

## Radiation Detection Instruments

*Refer also to abstracts 54798, 54799, and 54986.*

### General Detectors and Monitors

*Refer also to abstracts 54892, 55071, 55157, 55205, 55217, 55225, 55239, 55273, 55278, 56609, 57025, 57124, and 57201.*

**54993** (AD-720974) NUCLEAR YIELD MEASURING DEVICES. Materiel Test Procedure. (Army Test and Evaluation Command, Aberdeen Proving Ground, Md.). 25 Sep 1969. 14p. (MTP-6-2-332). NTIS.

The objective of this material test procedure is to describe the engineering tests required to determine the technical performance and safety characteristics of nuclear yield measuring equipment and their associated maintenance package relative to criteria contained in applicable Qualitative Materiel Requirements, Small Development Requirements, Technical Characteristics, and other appropriate technical specifications, and to determine their suitability for military use. (auth) (USGRDR)

**54994** (EGG-1183-2283) MONTE CARLO CALCULATION OF SODIUM IODIDE SCINTILLATION DETECTOR RESPONSE FUNCTION. O'Dell, A. A. ([EG and G, Inc., Goleta, Calif.]). [nd]. 15p. (CONF-711009-6). Dep. NTIS.

From Joint meeting of the American Nuclear Society; Miami, Fla. (17 Oct 1971).

An outline for oral presentation is given. The SORS-G Monte Carlo code is described. (W.H.K.)

**54995** (EUR-4611) NEUTRON COINCIDENCES COUNTING SYSTEM. Pedroli, G. (European Atomic Energy Community, Ispra (Italy). Joint Nuclear Research Center). 29 Mar 1971. 32p. (In Italian). Dep. NTIS (U. S. Sales Only). EUR Lit. 620.-.

A counting system for neutron coincidences is described. It allows distinguishing between fission neutrons and those produced by ($\alpha$,n) reactions. As a first approach a counter developed in the Brookhaven Laboratory is studied and a more elaborated version is described. Also a new counter based on a logic that allows measuring all the useful parameters using only two scalers instead of three and also minimizing the statistical error is described. (auth)

**54996** (IKF-28) GROWING AND INVESTIGATION OF SILVER CHLORIDE CRYSTALS: A CONTRIBUTION TO THE DEVELOPMENT OF A PRECIPITATION DETECTOR FOR TRACKS OF IONIZING PARTICLES. Zoergiebel, Friedrich (Frankfurt Univ. (West Germany). Institut fuer Kernphysik). Feb 1971. 93p. (In German). Dep. NTIS (U. S. Sales Only).

Thesis.

A method for growing large series of doped AgCl crystal sheets is described. The microhardness of Cd-doped AgCl crystals, their optical absorption, and their behavior within the beam of an electron microscope are studied. The AgCl crystals have been doped with 32 elements in order to examine their suitability as track detectors. Computations for the $\delta$-ray theory are presented for AgCl. Tracks obtained experimentally are compared with the theory. In conclusion, a hypothesis for the atomistic mechanism of track formation in the AgCl : Cd detector is given. (auth)

**54997** (INS-J-128) METHOD OF CORRECTION ON A SPECTRUM DISTORTED BY ACCIDENTAL COINCIDENCE IN AN ADDRESS-MATRIX OF A COUNTER ARRAY. Kokame, Jun (Tokyo Univ. (Japan). Inst. for Nuclear Study). 2 Jul 1971. 21p. Dep. NTIS (U. S. Sales Only).

The effects of an accidental coincidence in a matrix circuit for conversion of position-counter addresses in decimal to binary are discussed. A method of analysis and correction of the effects on spectra is given with some examples. (auth)

**54998** (JINR-P13-5970) INVESTIGATION OF THE SILICON SURFACE-BARRIER $\Delta$E-DETECTOR CHARACTERISTICS FOR THE NUCLEAR REACTION STUDYING. Zorin, G. N.; Kushniruk, V. F. (Joint Inst. for Nuclear Research, Dubna (USSR). Lab. of Nuclear Reactions). 1971. 17p. (In Russian). Dep. NTIS (U. S. Sales Only).

The technique of designing semiconductor surface-barrier $\Delta$E-detectors, 15 to 140 $\mu$m thick, having plane-parallelism not worse than 0.5 $\mu$m at diameter of 20 to 28 mm and a working area of 0.2 to 1.5 cm$^2$, is described. The results of measurements of these detector characteristics are given and analyzed. (auth)

**54999** (N-71-26447) COMMENTS OF A PAPER ON ELASTICALLY SCATTERED RECOIL NUCLEI IN SOLID STATE DETECTORS. Maurette, M.; Walker, R. M. (Washington Univ., St. Louis, Mo. Lab. for Space Physics). May 1969. Contracts NAS9-8165; Z80058T. 16p. (NASA-CR-118657; SPP-20). NTIS.

The use of elastically scattered recoil nuclei to measure the registration characteristics of solid state track detectors is discussed. To support this, pictures of tracks in mica were attributed to elastically scattered K and Fe nuclei produced by an irradiation with 32 MeV $^{16}$O ions. It is shown that the measured characteristics of the tracks do not match the theoretically predicted features for elastic processes and that the experimental features are consistent with those predicted for inelastic (mostly compound nucleus) reactions. The possibility that they are produced by contaminant ions present in the incident beam is not ruled out. (auth) (STAR)

**55000** (NP-19008) INVESTIGATION INTO SOME PROPERTIES AND APPLICATIONS OF SEMICONDUCTOR NUCLEAR RADIATION DETECTORS. Lauber, Alexander (Kungliga Tekniska Hogskolan, Stockholm (Sweden)). 1970. 26p. Dep. NTIS (U. S. Sales Only).

A summary of different types of semiconductor nuclear radiation detectors is given, as well as a review of the fields of application. Summaries are given of papers published earlier on the mechanism of compensation in lithium drifted detectors, the measurement of (n,p) and (n,$\alpha$) reaction cross sections by means of silicon surface barrier detectors, and the development of lithium drifted silicon detectors for the measurement of tracer activity in living tissue. (Sweden)

**55001** (NP-19011) FORTRAN PROGRAMS FOR Ge(Li) DETECTOR TIME CHARACTERISTICS. Poenaru, D. N. (Institutul de Fizica Atomica, Bucharest (Romania)). [1970]. 39p. (CRD-44-1970). Dep. NTIS (U. S. Sales Only).

FORTRAN programs for calculating the charge collection properties of coaxial and planar Ge(Li) detectors are given. Some programs are written for the IBM 1800 and others for the IBM 360/65. (W.H.K.)

**55002** (NYO-2740-8, pp 7-146) RADIOLOGICAL PHYSICS. (Columbia Univ., New York. Radiological Research Lab.).

In Annual report on research project.

CHARGED-PARTICLES—dosimetry using tissue-equivalent wall-less proportional detectors
GAMMA RADIATION—dosimetry using tissue-equivalent wall-less proportional detectors
IRRADIATION FACILITIES—description of alpha, for irradiating mammalian cells
LINEAR ENERGY TRANSFER—analysis of, algorithm for
NEUTRON SOURCES—isodose curves for californium-252
NEUTRON SPECTROMETERS—development of NE-213 scintillation
NEUTRONS—dosimetry for irradiation of biological materials—dosimetry using tissue-equivalent wall-less proportional detectors
RADIATION DETECTORS, PROPORTIONAL—wall effects in, theory of
RADIATION DOSIMETERS—development at Columbia Univ.
VAN DE GRAAFF ACCELERATORS—development and operation of RARAF, for radiological research
X-RADIATION—dosimetry using tissue-equivalent wall-less proportional detectors (W.H.K.)

**55003** (UCRL-73128) FACILITY FOR THE DETERMINATION OF LOW-LEVEL TRITIUM IN BIOLOGICAL AND ENVIRONMENTAL SAMPLES. Hutchin, W. H.; Bradley, A. E.; Morimoto, E. M.; Wadleigh, W.; Willes, E. (California Univ., Livermore. Lawrence Radiation Lab.). 22 Jul 1971. 10p. (CONF-710809-2). Dep. NTIS.

From Tritium symposium; Las Vegas, Nev. (30 Aug 1971).

A facility for the routine determination of low levels of tritium in biological and environmental samples has been established at LLL. Variations in the types of samples (e.g., animal and vegetable tissues, soil, water, and air) submitted and their tritium content necessitate a wide range of sample-preparation techniques. Among these are electrolytic enrichment, conversion of water to hydrogen gas, freeze-drying, and combustion of organic matter to water. Liquid scintillation and internal gas

proportional counting are the tritium measurement methods used. Detection limits may be enhanced by a factor of 75 when electrolytic enrichment is used. Routine analysis of samples having tritium levels as low as 1 TU are performed. Appropriate measures are taken to avoid contamination from ambient tritium. (auth)

**55004** (WCAP-7562-4) PLANT INSTRUMENTATION PROGRAM. Final Quarterly Progress Report for the Period Ending March 31, 1971. Limpert, J. C. (Westinghouse Electric Corp., Pittsburgh, Pa.). May 1971. Contract AT(30-1)-64. 45p. Dep. NTIS.

Both active and passive assay techniques were investigated for the analysis of fuel rods and fabrication waste. The data indicate that fuel rod analyses can be performed with a precision of ±1 percent, relative, or better by both passive gamma scanning and active neutron scanning. Passive neutron scanning of rods, unsuccessful with current equipment, would be feasible with changes in the number of detectors and improved electronics. Data from related waste studies, projected to fuel rods, indicates a precision might be realized of the order of ±2 percent, relative. Active neutron, passive neutron, and passive gamma interrogation methods were investigated for the assay of low-level waste in drums, low-level waste in packages, and hard scrap in packages. With reasonable segregation of waste, a limit of error for the passive gamma assay of low-level waste in 55-gallon drums was determined to be of the order of ±10 percent, relative, over the concentration range of 0.5 to 10.0 grams of plutonium. Without segregation, this error increases by a factor of 2.5. Low-level waste packages can be assayed with a limit of error of the order of ±5 percent, relative, over the concentration range of 0.2 to 5.0 grams Pu. The package scanning technique was successfully improved by scanning groups of packages in a standardized geometry. The use of such techniques for waste is questionable. Passive neutron scanning utilizing a neutron coincidence well counter was determined to be effective for both low-level waste and hard scrap. The limit of error was found to be less than ±5 percent, relative. (R.W.R.)

**55005** PERFORMANCE IN RECORDING OF X- AND GAMMA-RAYS BY COMBINED DETECTORS. Podgornyi, V. N.; Mandel'tsvaig, Yu. B. (Moscow X-Radiological Research Inst. All-Union Medical Instrumentation Research Inst., Moscow). Sov. J. Nondestruc. Test. (Engl. Transl.); No. 4, 367-70(Jul-Aug 1969). Translated from Defektoskopiya; No. 4, 1-7(Jul-Aug 1969).

Factors governing the response of a combined detector are discussed, with allowance for stability requirements. Examples of detector designs based on the combination of solar batteries with scintillators are given. (auth)

**55006** REAL TIME TREATMENT OF INFORMATION PROVIDED BY ATMOSPHERIC CONTAMINATION DETECTORS. Lebouleux, Ph. (CEN de Saclay, Gif-sur-Yvette, France). Radioprotection; 4: 267-77(1969). (In French).

Systems for the processing of data from atmospheric contamination detectors are reviewed. The number of pulses delivered by the detector for which a signal is sent toward the computer is then calculated. This pre-regulated counting corresponds to an elementary exposure to the atmospheric contamination of about one thousandth of the mean weekly maximum permissible limit. The analysis of the organization of the system is illustrated by the organization chart of the data processing for filter paper band detectors in continuous operation and for fixed filter detectors. It is shown that it is often possible to process data in real time and thus make possible the direct expression of the measurement of the atmospheric air contamination in $Ci/m^3$ and the exposure to atmospheric contamination. (tr-auth)

**55007** SCHOTTKY BARRIER ATOMIC PARTICLE AND X-RAY DETECTOR. Baertsch, Richard D. (to General Electric Co.). U. S. Patent 3,598,997. 10 Aug 1971. Filed 5 Jul 1968.

A solid-state atomic particle and x-ray detector comprising an N-type semiconductor crystal of high atomic number, coated with a metallic film of low atomic number, is described. By making the metal-to-semiconductor interface abrupt, a Schottky barrier-type junction is produced. Atomic particles or x-rays can easily penetrate the metallic film but are absorbed in the semiconductor near the interface, producing electron-hole pairs in the depletion region. Holes which diffuse beyond the depletion region give rise to a current indicative of detection of x-rays or atomic particles. (auth)

**55008** APPARATUS FOR MEASURING AND EVALUATING THE ACTIVITY OF MEASURING PROBES IRRADIATED IN A NUCLEAR REACTOR. Haebler, Dietrich V.; Jahn, Gunther (to Siemens Aktiengesellschaft). U. S. Patent 3,598,996. 10 Aug 1971. Priority date 11 Mar 1967, Germany.

A plurality of measuring probes are sequentially positioned in a conveyer tube in the vicinity of a measuring and evaluating device for determining the activity in each probe. The probes are moved in sequence by a control unit into operative proximity with the measuring and evaluating device. The control unit comprises an elastic wire in the tube blocking the probes and a moving device for controllably withdrawing the wire from the tube. (auth)

**55009** NEUTRON DETECTOR. Kozlov, Stanislav Fedorovich (to Fizichesky Institut Imeni PN Lebedeva Akademii Nauk Sssr). British Patent 1,246,372. 15 Sep 1971. Priority date 3 Oct 1968, Russia.

A neutron detector is described which employs a radiator foil and a diamond crystal detector. The radiator may consist of boron-10, lithium-6, or fission foils. (W.H.K.)

**55010** TRACK REGISTRATION PROCESS. Crawford, Wayne Thomas; Humphrey, Joseph Stevenson Jr. (to General Electric Co.). British Patent 1,240,767. 28 Jul 1971. Priority date 28 Jun 1968, United States.

In the processing of dielectric track radiation detectors, the step is proposed of exposing the dielectric to ultraviolet light in the presence of oxygen after irradiation and before the tracks have been treated with etchant. This procedure results in greatly increased etching of the altered material along the tracks. (R.W.R.)

**55011** GAMMA FLUX DETECTOR AND METHOD OF MANUFACTURE THEREOF. (to Atomic Energy of Canada Ltd.). British Patent 1,241,614. 4 Aug 1971. Priority date 29 Nov 1968, United States.

The manufacture of a self-powered gamma detector is described; increased sensitivity, durability, and uniformity of response are achieved by using an oxidized coherent surface layer of emitter material as the electrically insulating material. (R.W.R.)

**55012** NEUTRON SCINTILLATION DETECTOR. Kozodaeva, N. M.; Korotin, B. A.; Nemirovskii, B. V. Russian Patent 269,344. 17 Apr 1970. Filed 4 Sep 1967. (In Russian).

This neutron detector has a converter material, which emits heavy particles upon neutron irradiation, and a scintillator sensitive to the latter. For calibration purposes a layer of scintillator sensitive to a weakly penetrating ionizing radiation is utilized. (R.W.R.)

**55013** PREPARATION AND OPERATION OF SILICON AND GERMANIUM SEMICONDUCTOR COUNTERS. Anishchenko, Yu. V.; Belkin, I. L.; Volkov, A. N.; (and others). Tr. Fiz. Inst., Akad. Nauk SSSR; 53: 239-52(1971). (In Russian).

The preparation of silicon surface-barrier and Ge(Li) semiconductor counters is described, along with their application in polarization-measuring equipment in accelerators. Maintenance of spectrometric characteristics during radiation doses of $10^{11}$ to $10^{12}$ particles/$cm^2$ is described. Cryostat design for use with Ge counters is outlined, and recording circuitry for providing coupling between accelerator and analyzer is discussed. A mathematical analysis of the pertinent circuitry is given. (tr-auth)

**55014** NEUTRON COUNTERS. Goodings, Anthony; Leake, John Walgate (to United Kingdom Atomic Energy Authority). British Patent 1,240,379. 21 Jul 1971. Filed 1 Jul 1969.

Disadvantages of conventional neutron counters, employing the $^{10}B(n,\alpha)^7Li$ reaction, are stated; these instruments as constructed hitherto have a somewhat limited operational life, and the object of the arrangement described is to provide an improved design. It comprises a metal body containing an anode, with a ceramic/metal seal through which electrical signals from the anode are led via an insulated conductor; the ceramic/metal seal has a ceramic portion protruding into the body of the instrument. This ceramic portion is preferably shielded from the body portion by a shroud. One effect of this arrangement is to postpone bridging by migrating braze material; it also provides a greater surface area for possible metal plate out, so that deposition is not onto a concentrated sensitive area. A $BF_3$ gas-filled counter incorporating this arrangement is described in detail together with several alternative design modifications. (UK)

**55015** IONIZATION CHAMBER RESPONSE FOR PULSED RADIATION AND DRIFT VELOCITY DISTRIBUTION OF FILLING GAS. Mikado, Tomohisa; Tomimasu, Takio; Tsuchiya, Yoshio (Electrotechnical Lab., Tanashi, Japan). Denshi Gijutsu Sogo Kenkyusho Iho; 35: No. 1, 81-91(Jan 1971). (In Japanese).

The saturation current of an ionization chamber exposed to a pulsed radiation beam degrades slightly with increasing repetition rate of radiation pulse even though the radiation intensity per pulse and the applied voltage to the chamber are kept constant. The repetition rate dependence of the saturation characteristic varies

with each filling gas. This phenomenon is commonly seen in ten kinds of gases including air, Ar, $N_2$, $CO_2$, He, 95% Ar + 5% $CO_2$, 90% Ar + 10% $CO_2$, 80% Ne + 20% He, $CCl_2F_2$, and $SF_6$. In order to explain the experimental results mentioned above, it has been assumed that the drift velocity of ions produced by the radiation has a certain distribution and that the deviation from the mean velocity depends upon the kind of gases. To confirm the above-mentioned hypotheses, the ionization chamber was operated as an ion pulse chamber and its output pulses were directly observed with an oscilloscope and photographed for each filling gas with varying applied voltages. For a given gas and applied voltage, an FWHM of a real output pulse (represented by $\Gamma_r$) was obtained from a photograph. On the other hand, an FWHM of an idealized pulse (represented by $\Gamma_i$) was calculated for the corresponding gas and applied voltage. From these values and the following equation, $\Gamma_w$ was calculated to describe the broadness of the real output pulse compared with the idealized one, in a simplest approximation, for eight kinds of gases except for He and 90% Ar + 10% $CO_2$: $\Gamma_w^2 = \Gamma_r^2 - \Gamma_i^2$. A relationship between $\Gamma_{w/2t_0}$ ($2t_0$ representing the time interval during which all the ions produced in the chamber are assumed to be collected) and the repetition rate dependence of the saturation characteristic was found. (auth) (Japan)

**55016** TRACK-EFFECT THEORY OF SCINTILLATION EFFICIENCY. Luntz, Myron (State Univ. of New York, Fredonia). Phys. Rev., B; 4: No. 9, 2857-68(1 Nov 1971).

A theoretical account is presented of the pulse-height characteristics of NaI(Tl) scintillation counters subjected to energetic heavy-ion bombardment ($Z \geq 5$, $E/A = 1-10$ MeV/nucleon) at room temperature. The falling off of scintillation efficiency dL/dE with decreasing energy and the charge dependence at fixed energy are simultaneously accounted for by introducing the concept of a cylinder of high energy-deposit density surrounding the particle track. Inside the cylinder competitive events, favored by high ionization density, are assumed to dominate those which produce the characteristic luminescence emission. Agreement with experiment is best for high-Z particles. Cylinder radii vary over the range $110 \lesssim R_c(Z,v) \lesssim 390$ Å. Estimates of the fraction of the total energy loss available for efficient light production yield the values $0.20 \lesssim F_0(Z,v) \lesssim 0.50$, while the critical value of energy-deposit density defining the high-density cylinder is approximated to be $5.32 \times 10^7$ erg/cm$^3$. Also, a brief discussion is presented regarding interpretation of the heavy-ion pulse-height characteristics of pure alkali halides at low temperature, and those of anthracene and NE 102 plastic scintillators, in terms of the track-effect theory. (auth)

**55017** ASYMPTOTIC BEHAVIOR OF NEUTRON PULSES IN A HARD MULTIPLYING SYSTEM. Platovskikh, Yu. A.; Sergeev, I. V. At. Energ. (USSR); 30: No. 5, 454-5(May 1971). (In Russian).

An attempt was made to find an asymptotic behavior of fission chamber readings m(t) under specified conditions. The system considered is "hard," i.e., free of thermal neutrons. By applying the Laplace transform to an equation involving neutron density, the fission spectrum, and an operator which describes neutron moderation and allows for leakage ($DB^2$), a relationship is developed which suggests that three types of detector readings are possible: the absence of an exponent, when both components play approximately equal roles at the time of observation; nearly exponential behavior of m(t) with constant time $\alpha + \Lambda_0$, dependent upon the subcriticality; and nearly exponential behavior of m(t) with constant time $\alpha$, independent of criticality. (K.S.W.)

**55018** MINIATURIZED PROBE FOR DETECTING RADIOACTIVITY AT THYROID SURGERY. Morris, A. C. Jr.; (Oak Ridge Associated Universities, Inc., Tenn.); Barclay, T. R.; Tanida, R.; Nemcek, J. V. Phys. Med. Biol.; 16: No. 3, 397-404(Jul 1971).

A miniaturized scintillation probe was developed to assist the surgeon in finding remnants of normal or cancerous thyroid tissue. At an appropriate time before surgery, the patient is given a dose of $^{131}I$ or $^{125}I$. During the operation, the surgeon removes as much tissue as he can see or feel and then uses the probe to help him find the remainder. Beta and gamma rays are detected by a small CsI(Tl) crystal, collimated for directivity by the use of an annular, removable, platinum shield. Circuits receiving pulses from the probe convert the counting rate to a loud-speaker sound of varying pitch. With increased counting rate as the probe tip nears an active area, the audio pitch rises; the surgeon can thus hear the response while he watches the position of the probe. (auth) (UK)

**55019** NEUTRON FLUX MONITOR. (to United States Atomic Energy Commission). British Patent 1,245,917. 15 Sep 1971. Priority date 15 Apr 1969, United States.

An activation neutron flux monitor available for use at high temperatures which consists of a pressed and sintered pellet containing about 99% finely ground, high-purity magnesium oxide as matrix material and about 1% finely ground, high-purity nickel monooxide or cobaltous oxide uniformly distributed in the matrix material as activation compound is described. (auth)

**55020** MESURES EN RADIOACTIVITE. MANUEL PRATIQUE D'UTILISATION DES RAYONS NUCLEAIRES. (Radioactivity Measurements. Practical Manual on the Uses of Nuclear Radiation). Briere, Michel; Jouve, Bernard; Paulin, Robert. Paris; Hermann (1970). 261p.

A manual on the detection and measurement of radioactivity is presented. The various procedures for the detection of radioactivity and the associated electronic technology are first considered. Techniques for the preparation and utilization of radioisotopes are summarized. The basic mathematical concepts are reviewed. (J.S.R.)

**55021** TELEVISION MONITOR FOR DOSIMETRIC AND SPECTROMETRIC MEASUREMENT BY METHOD OF NUCLEAR-TRACK EMULSIONS. Havelkova, V.; Bradna, F. (Radiologicka Dozimetrie Ustavu Jaderneho Vyzkumu CSAV, Prague). Radioisotopy; 11: No. 5, 767-75(1970). (In Czech).

A television system for nuclear emulsion scanning is described. The results of the measurement of track parameters of recoil protons are presented, and the accuracy of the dosimetric evaluation of emulsions by the television monitor in comparison with the optical microscopy is discussed. The measuring time is decreased by 27%. (auth)

**55022** INFLUENCE OF STOPPING POWER ON THRESHOLD SENSITIVITY OF NUCLEAR EMULSIONS FOR MEASUREMENT OF SPECTRA AND DOSIMETRY OF FAST NEUTRONS. Bradna, F.; Havelkova, V. (Radiologicka Dozimetrie UJV CSAV, Prague). Radioisotopy; 11: No. 5, 725-38(1970). (In Czech).

The study solves the problems of estimation and influence of the stopping power on threshold sensitivity of gelatin and polymer-gelatin hydrogen-enriched nuclear emulsions, for measuring spectra of fast neutrons. The physical and chemical calibration of both emulsions is described, their elementary composition is quoted, and the stopping power from analytical data is counted. The experimental verification has proved the decrease of stopping power of the polymer-gelatin emulsion and the extension of its threshold sensitivity up to the energy 0.12 MeV. (auth)

**55023** WHOLE BODY RADIOACTIVITY COUNTER FOR MULTIPURPOSE USE IN CLINICAL DIAGNOSIS AND RESEARCH. Schnippering, H. G. (Kernforschungsanlage, Juelich, Ger.). Kerntech. Atomprax.; 13: No. 7-8, 297-306(Jul-Aug 1971). (In German and English).

The design and performance features of the whole-body radioactivity counter at the Medical Institute of the Kernforschungsanlage, Jülich are described. The possibilities of using this system as a whole-body counter, as a multi-detector function test stand, and as a whole-body scanner are described with reference to measurements carried out so far. Also, the methods used for the mathematical processing and for the automatic plotting of measured values with the aid of the available data processing facility IBM 360/75 are described. (auth)

**55024** CHOICE OF AN OPTIMUM DETECTOR AND AN OPTIMUM ADJUSTMENT OF THE APPARATUS FOR THE DETECTION OF VERY LOW GAMMA ACTIVITIES. Husak, V. (Radioizotopove Oddeleni Lekarske Fakulty a Fakultni Nemocnice, Olomouc, Czech.). Radioisotopy; 11: No. 5, 911-32(1970). (In Czech).

The performance of various crystal scintillation detectors and various geometries for determining low specific gamma activities in relatively large volumes is studied. Sensitivity, efficiency, background, and maximum measurable volume are compared for system design optimization. (W.H.K.)

**55025** THERMAL RESISTANCE AND DEPENDENCE OF SCINTILLATION DETECTORS AT ELEVATED TEMPERATURES. Silar, Josef; Lomberska, Ljuba (Vyzkumny Ustav Pristroju Jadernae Techniky, Prague). Radioisotopy; 11: No. 5, 873-907 (1970). (In Czech).

The temperature effects in the range of 20°C to 70°C on scintillation counters with NaI(Tl) crystals 40 × 40 mm and photomultipliers of the new type 61 PK 413-415 or photomultipliers of the type 66 PK 512 being in the developing state are studied. (auth)

**55026** ALPHA DOSIMETRY AND SPECTROMETRY BY SOLID-STATE NUCLEAR TRACK DETECTOR. Novotny, J.

XUM

(Katedra Dozimetrie a Aplikace Ionizujiciho Zareni FJFI, Prague). Radioisotopy; 11: No. 5, 777-86(1970). (In Czech).

A new method of alpha particle dosimetry and spectrometry by triacetate cellulose plastic is described on the basis of general tracks studies in the detector. The factors having influence on the registration efficiency and various dosimetric application of alpha particle detectors are discussed. (auth)

**55027** PROCESS AND DEVICE TO IMPROVE COUNTING STATISTICS IN A RADIOACTIVE SAMPLING APPARATUS. (to Packard Instrument Co. Inc.). French Patent 1,566,661. 31 Mar 1969. Filed 26 Mar 1968. (In French).

A device for the precise centering of a flask containing the sample to be analyzed in a liquid scintillation detection system is described. The device assures a slow continuous rotation of the flask on an axis. The device and procedure assure that the errors due to lack of symmetry and homogeneity are eliminated. (J.S.R.)

**55028** USE OF LIQUEFIED NOBLE GASES: A NEW PROSPECT FOR X RAY AND $\gamma$ RAY LOCALIZATION DETECTORS. Allemand, R.; Laval, M.; Prunier, J. F. (CEN, Grenoble, France). Int. J. Appl. Radiat. Isotop.; 22: No. 10, 633(Oct 1971).

Gas filled neutron localization detectors can be used for the direct viewing of x-ray and $\gamma$-ray emitters for organ dynamic study or mapping. Although simpler than scintillation cameras the poor efficiency of such devices restricts their use to radioisotopes with energies below 100 keV. With a direct charge collection argon-filled chamber to study conduction processes in liquefied gases, the existence of high mobility carriers required for electron avalanche and the strong dependence of the amount of collected charges with applied electric field and liquid purity were demonstrated. (UK)

**55029** USING A PHOTOELECTRIC COLORIMETER FOR COUNTING CHARGED PARTICLE TRACKS ON THE SURFACE OF GLASS DETECTORS. Khovanovich, A. I.; Pikalov, G. L.; Kryvokrysenko, I. F. This paper was summarized in At. Energ. (USSR); 29: No. 5, 367(Nov 1970) as paper No. 443/5530. (In Russian).

A method for counting tracks using the type FÉK-M photoelectric colorimeter is examined. This method is based on the dependence of the change in the optical density of the detector on the number of tracks and the regimes of its chemical processing. The method is simple, dependable in practice, and does not require large time expenditures for scanning the detectors. The range of measured track densities depends on the etching regime and equals $5 \cdot 10^3$ to $10^7$ $cm^{-2}$. The root-mean-square error of a single measurement of track densities with a confidence coefficient of 0.7 is not greater than ±8%. (auth)

**55030** STUDY OF $^{37}Ar$ DISINTEGRATION WITH VARIOUS TYPES OF ORGANIC SCINTILLATORS. Iorgulescu, Adriana (Inst. of Atomic Physics, Bucharest). Stud. Cercet. Fiz.; 23: No. 3, 359-66(1971). (In Rumanian).

$^{37}Ar$ was detected by scintillation spectrometry. The $^{37}Ar$ disintegration process is realized by electron capture with 100% probability, and the de-excitation energy for the K shell is 0.0028 MeV. Experiments were done with a Tri-Carb 3375 Packard Instruments spectrometer using organic scintillator detectors furnished by Nuclear Enterprises. In view of optimizing the work geometry, first measurements were made with plastic scintillators. Comparative subsequent measurements with liquid scintillator detectors indicated an increase of counting efficiency. This increase was assigned to the argon solubility in aromatic compounds. The usefulness of the conventional method is increased at low energies. (auth)

**55031** CHERENKOV DETECTORS FOR BETA RADIATION DETECTION IN WATER AND THEIR PRESENT APPLICATIONS. Silar, Josef. Radioisotopy; 11: No. 3, 353-426(1970). (In Czech).

Based on the study of available literature, the problems of detection of Cherenkov radiation and the present state of applications of Cherenkov detectors for the detection of beta particles in water are dealt with. (40 references) (auth)

**55032** AUTOMATIC COUNTER FOR DIRECT MEASUREMENTS OF RADON CONCENTRATION. Dalu, G.; Dalu, G. A. (Istituto di Fisica dell'Atmosfera, Rome). J. Aerosol. Sci.; 2: No. 2, 247-55(Jun 1971).

From Conference on the physics and chemistry of aerosols; Fontenay-aux-Roses, France (24 Sep 1970). See CONF-700967.

Essentially the counter consists of a brass chamber, into which the air to be examined flows continuously at 4 l/min. Within the chamber there is a ZnS(Ag) scintillator, optically coupled with a photomultiplier. The scintillator is coated with a thin film of gold to render it conductive and, between the chamber and the scintillator, a potential of 1000 V is applied. The positive RaA ions are thus electrostatically collected on the scintillator, where their subsequent alpha decays and those of RaC' produce scintillations. The construction and the calibration of the counter are described. The calibration is achieved by admitting into the chamber known amounts of radon grown from a radium chloride solution. Finally, the methods of sampling and measurement for the evaluation of radon atmospheric concentrations are described. (auth) (UK)

## *Nuclear Spectroscopic Instrumentation*

*Refer also to abstracts 54436, 54472, 54474, 56365, 56367, 56370, and 56629.*

**55033** (COO-2049-6) DEVELOPMENT OF AN NE-213 FAST-NEUTRON TAC SPECTROMETER SYSTEM UTILIZING OFF-LINE GAMMA-RAY DISCRIMINATION. Seck, Richard E.; Meyer, Walter; Krick, Merlyn S. (Kansas State Univ., Manhattan, Dept. of Nuclear Engineering). 30 Jul 1971. Contract AT(11-1)-2049. 90p. Dep. NTIS.

An attempt is made to optimize the gamma discrimination process in fast neutron spectroscopy by off-line computer analysis of the data from a TAC spectrometer system. In the system developed, the linear signal from an NE-213 detector is integrated and double differentiated to produce a bipolar pulse whose cross over point is a function of the original pulse shape. A time to amplitude converter (TAC) converts the zero cross-over time of the bipolar pulse to a pulse height. The TAC signal and the NE-213 linear signal are fed to a 4096 channel multiparameter analyzer operated in a two parameter mode. The analyzer produces a 64 × 64 array of data in which neutrons and gammas lie in two "ridges". The 64 × 64 array of data is analyzed by a specifically constructed computer code and the neutron and gamma information are separated. In the low energy region, an attempt is made to optimize the gamma discrimination by an iterative weighted least squares gaussian fitting routine. (W.H.K.)

**55034** (COO-2049-7) FAST NEUTRON SPECTROSCOPY IN AQUEOUS MEDIA USING AN NE-213 PROTON-RECOIL NEUTRON SPECTROMETER SYSTEM. Coolbaugh, M. J.; Faw, R. E.; Meyer, Walter (Kansas State Univ., Mahnattan, Dept. of Nuclear Engineering). 30 Jul 1971. Contract AT(11-1)-2049. 144p. Dep. NTIS.

The design, calibration, and operation of an NE-213 organic scintillation proton-recoil neutron spectrometer for operation in an aqueous medium up to 20 feet deep are described. A data unfolding technique based on a derivative method and considering the effects of varying scintillator size is also described. The system was tested in a mockup of the KSU Triga reactor core, and the results are discussed. (W.H.K.)

**55035** (DP-1275) GELI2 AND SPAN 2: FORTRAN PROGRAMS TO CALCULATE NUCLIDE ABUNDANCES FROM MULTICHANNEL GAMMA RAY SPECTRA. Slates, R. V. (Du Pont de Nemours (E. I.) and Co., Aiken, S. C. Savannah River Lab.). Oct 1971. Contract AT(07-2)-1. 40p. Dep. NTIS.

A FORTRAN computer program incorporating a second difference peak search was developed to calculate nuclide abundances from gamma ray spectra on magnetic tape without applying iterative fitting techniques. Peak areas are obtained by summing counts above a statistically justified cubic or linear equation background, and confidence limits are determined for all analytical results. (auth)

**55036** (HASL-244) USER'S GUIDE TO SWIFT, A MONTE CARLO TECHNIQUE FOR UNFOLDING NEUTRON SPECTRA. Sanna, Robert S. (New York Operations Office (AEC), N. Y. Health and Safety Lab.). Jul 1971. 12p. Dep. NTIS.

SWIFT is a Fortran IV program written for the CDC-6600, which uses a random number generator to generate neutron spectra whose measurement distributions for a given spectrometer are calculated using appropriate response data. These calculated distributions are then compared with actual measurements. This process is repeated a large number of times and the spectrum whose calculated distribution best agrees with the measurements is said to be the unfolded neutron spectrum. This user's manual describes the input data format required to obtain unfolded spectra from measurement distributions obtained with the multisphere spectrometer. The multisphere spectrometer consists of six $^6LiF$ crystals which are bare or cadmium-covered and with polyethylene moderators. As an aid to understanding the data the input and output of a sample problem are presented with comments. (auth)

**55037** (JUL-737-FF) OPTIMIZATION OF THE RESOLVING POWER AND THE INTENSITY OF PARTICLE SPECTROMETERS USING AS THE EXAMPLE THE PARABOLIC SPECTROGRAPHS. Fiebig, Guenter (Kernforschungsanlage, Juelich (West Germany). Institut fuer Festkoerperforschung). Feb 1971. 120p. (In German). Dep. NTIS (U. S. Sales Only).

The purpose of ion-optical calculations for the design of particle spectrometers, consisting of magnetic and electrical defection fields, is the optimum determination of the system parameters so that for a given mass or energy resolving power maximum intensity is attained in the detection plane. The focusing properties of the system result from the orbit equation of the nth approximation (n = 1,2,...) for the three-dimensional motion of an ion which was emitted from an expanded source in a given spatial direction in the system. Under the assumption that the orbit equations for the particle spectrometer considered are known on the basis of the ion-optical theory, the resolving power is defined with respect to the base width and the variance of the determinant line formed at the site of the focus. The two definitions of the resolving power serve as design functions for determination of the system parameters. It is shown that both design functions represent an alternative to the optimum parameter values. In contrast to the usual methods in the optimization of the resolving power by consideration of the several individual image aberration terms, the effect of all image errors on the resolution power is determined and corrected simultaneously. The dependence of the focusing length on the dispersion properties of the system is considered in the optimization of the resolving power. After establishment of all apparatus sizes, the beam intensity is maximized for a required resolution capacity in which the source slot and the outlet plane are suitably dimensioned. For numerical calculation of the optimization, which represents a non-linear multi-dimensional problem with non-linear secondary condition, a direct searching method and a stochastic approximation method are used. (tr-auth)

**55038** (LA-DC-12314) INSTITUTING A NEUTRON SPECTRUM UNFOLDING CAPABILITY. Robba, A. A.; Fullwood, R. R.; Veeser, L. R. (Los Alamos Scientific Lab., N. Mex.). [1971]. 17p. (CONF-710606-12). Dep. NTIS.

From seventeenth annual meeting of the American Nuclear Society; Boston, Mass. (13 Jun 1971).

The considerations leading to the application of an unfolding technique to the problem of determining the neutron spectrum from a thick $^{238}U$ target, bombarded by 750-MeV protons, are presented. The relative merits of various neutron spectrometers are also presented. The use of spectrum unfolding leads to problems associated with gamma rejection, response matrices, and unfolding techniques. (auth)

**55039** (LB/G-3040) THE TECHNIQUE OF AVERAGE $\bar{\nu}$ MEASUREMENT WITH THE NEUTRON TIME-OF-FLIGHT SPECTROMETER. Ryabov, Yu. V.; Chikov, N. (Joint Inst. for Nuclear Research, Dubna (USSR). Lab. of Neutron Physics). Translated by W. G. Stripp (Atomic Energy Research Establishment, Harwell, Eng.), from report JINR-P3-5119. 16p. Dep. NTIS (U. S. Sales Only).

A large cadmium-loaded liquid scintillation detector with a fission neutron detection efficiency of about 90% is used for measuring the average number of neutrons per fission. The time-of-flight system is described. (W.H.K.)

**55040** (NP-18994) PROPOSAL FOR INSTALLATION OF A VERSATILE $e^- - e^+ - \gamma$ SPECTROMETER FOR NEUTRON CAPTURE SPECTROSCOPY. Pepelnik, R.; Michaelis, W.; Fanger, U. (Kernforschungszentrum, Karlsruhe (West Germany). Institut fuer Angewandte Kernphysik). Oct 1970 15p. Dep. NTIS (U. S. Sales Only).

To obtain the multipolarity of high-energy transitions for unique level spin and parity assignments, the utilization of the internal-pair formation process may be preferable. This process exceeds that of internal conversion in a wide range of the Z-E plane. Also the discrimination of E2 and M1 radiation and of E1 and M1 transitions by internal pair formation is higher than that of the internal conversion. An electron-pair-spectrometer with two Si(Li)-detectors and a superconducting magnet has been designed. Measurements of coincidences between conversion electrons, between conversion electrons and gamma rays, of conversion electrons into solid angles of $2 \times 2\pi$ and of internal pairs are feasible. (auth)

**55041** (ORNL-TM-3509) ENERGIES AND INTENSITIES OF GAMMA RAYS EMITTED BY A $^{226}Ra$ SOURCE. Dickens, J. K. (Oak Ridge National Lab., Tenn.). 13 Aug 1971. 17p. Dep. NTIS.

Energies and intensities of 64 gamma rays emitted by $^{226}Ra$ and its decay products were measured for gamma-ray energies between 186 and 2979 keV. The tabulated results are of primary use for efficiency calibration of Ge(Li) detectors. (auth)

**55042** (RD/B/N-1963) MIMUSA: A FORTRAN IV SUBROUTINE FOR UNFOLDING SPECTRA. PART 2. PROGRAM DETAILS AND USER INSTRUCTIONS. Longworth, J. P. (Central Electricity Generating Board, Berkeley (England). Berkeley Nuclear Labs.). May 1971. 39p. Dep. NTIS (U. S. Sales Only).

SUMI (Spectrum Unfolding by Matrix Iteration) is a FORTRAN IV computer code for analyzing data from spectrometers with non-singular responses. The code consists of three subroutines: NFLO preprocesses TLD data; TESTY preprocesses test spectra for input into MIMUSA; and MIMUSA unfolds spectra. Full details of the program and required data for the subroutines MIMUSA and TESTY are given together with details of how to use NFLO, TESTY, and MIMUSA, either together or independently, as part of SUMI. (auth)

**55043** (RD/B/N-2034) DELTA SPECTROMETER RESULTS ON WATER REACTOR SHIELDS. Longworth, J. P. (Central Electricity Generating Board, Berkeley (England). Berkeley Nuclear Labs.). Jun 1971. 20p. Dep. NTIS (U. S. Sales Only).

The DELTA spectrometer is a neutron flux spectrometer with nearly constant sensitivity within the range from thermal to fission energies. The results are analyzed using the computer codes NFLO and MIMUSA. This note presents the results obtained with the DELTA spectrometer outside six shield configurations on water reactors. (auth)

## *High Energy Physics Instrumentation*

*Refer also to abstract 56566.*

**55044** (JINR-E1-5818) READOUT ELECTRONICS FOR THE $\pi$-e EXPERIMENT AT 50 GeV. Guzik, Z.; Popielska, E.; Popielski, W.; Starchenko, B. M.; Tsyganov, E. N.; Turala, M. (Joint Inst. for Nuclear Research, Dubna (USSR). Lab. of High Energy). 1971. 18p. Dep. NTIS (U. S. Sales Only).

The readout electronics for the $\pi$-e experiment controls the operation of the experimental set up, digitizes data from the detectors, and transfers them to the computer. The following parameters have been obtained: (a) accuracy of the track localization in the spark chamber $\pm(0.2 + 0.4)$ mm; (b) space resolution for one pick-up coil—about 5 mm; (c) counting speed of the accumulators—20 MHz; (d) time resolution of the proportional chambers $2\tau \geq 80$ nsec for efficiency close to 100%; (e) time resolution of the latches—20 nsec; and (f) accuracy of the high voltage measurements $10^{-4}$ (or accuracy of dividers). (auth)

**55045** (LUIP-CR-71-2) DESCRIPTION OF THE LOGIC UNIT OF THE PHOTOMETER SYSTEM SFIL 70. Behrnetz, S.; Lindstam, S.; Mathiesen, O.; Soederstroem, K. (Lund Univ. (Sweden). Inst. of Physics). Feb 1971. 85p. (In Swedish). Dep. NTIS (U. S. Sales Only).

A new electronic gate system to an earlier developed nuclear track photometer is described. Output current from a photomultiplier passes via a dc-amplifier to the electronic gate system and from there via a digital voltmeter to a paper tape punch. The logic unit is desired (1) to activate those rotary magnets, which control the position of the mirrors and the slits, (2) to connect the desired analog and digital signal source to the data acquisition system, and (3) to supply input pulses to this system. To make it possible to connect one more measuring unit, a queue circuit is designed. The logic is built of integrated circuits. (auth)

**55046** (N-71-16750) CALIBRATION OF THE NASA-GSFC HIGH ENERGY COSMIC RAY EXPERIMENT. Whiteside, H.; Crannell, C. J.; Ormes, J. F.; Ryan, M. J. (National Aeronautics and Space Administration, Greenbelt, Md. Goddard Space Flight Center). Jan 1971. 38p. (NASA-TM-X-65440; X-661-71-36). NTIS.

The experimental conditions under which the NASA-GSFC High Energy Cosmic Ray Experiment was calibrated with the G-10 + 4.7 deg test beam at the Brookhaven AGS are described. A detailed discussion is given of the momentum of the test beam used. In addition, summaries of the data runs taken are included. (STAR)

**55047** AUTOMATIC MEASUREMENT OF FILM FROM HIGH-ENERGY PHYSICS EXPERIMENTS. Burren, J. W. (Rutherford High Energy Lab., Chilton, Eng.). pp 2.1-4 of Computational Physics. Vols. I and II. London; Her Majesty's Stationery Office (1969).

From Conference on computational physics; Culham, England (28 Jul 1969). See CONF-690706-(Vols.1 and 2).

In many high energy physics experiments the data are recorded

on film as the images of trails of sparks or bubbles made by charged particles in a detector. Automatic measuring machines transmit a digital representation of the information on the film into a computer. The problems of programming the computer to recognize the information of interest on the film and to filter out the background are dealt with and the problems of running a large production system which contains as one of its basic parts, a procedure that can give unreliable answers are discussed. (auth) (UK)

**55048** TRACK FINDING IN WIRE SPARK CHAMBER DATA. Ellis, R. J. (Rutherford High Energy Lab., Chilton, Eng.); Sherman, H. pp 3.1-4 of Computational Physics. Vols. I and II. London; Her Majesty's Stationery Office (1969).

From Conference on computational physics; Culham, England (28 Jul 1969). See CONF-690706-(Vols.1 and 2).

A method of stringing is described which finds particle tracks in an array of coordinates obtained from digitized wire spark chamber data. It was developed to resolve two, three or more beam tracks per event within a beam spot of 5 × 2 cms. The $\pi^- p \rightarrow K^+ \Sigma^-$, $\Sigma^- \rightarrow n\pi^-$, $\Sigma^- \rightarrow ne^-\nu$ interaction was studied, in which the incident $\pi^-$, $K^+$ and charged $\Sigma^-$ decay product were observed. (auth) (UK)

**55049** LEAST-SQUARES FITTING OF WIRE SPARK CHAMBER EVENTS. Sherman, H. (Queen Mary Coll., London); Ellis, R. pp 24.1-3 of Computational Physics. Vols. I and II. London; Her Majesty's Stationery Office (1969).

From Conference on computational physics; Culham, England (28 Jul 1969). See CONF-690706-(Vols.1 and 2).

A method of reconstructing wire spark chamber events, consisting of calculating the interaction or decay point and track parameters by means of the non-linear least squares method is discussed. It was applied to events of the type $\pi^- + p \rightarrow K^+ + \Sigma^-$, $\Sigma^- \rightarrow N + \pi^-$ where the incident $\pi^-$, $K^+$ and decay $\pi^-$ tracks were recorded. The method is applied to obtain the interaction point, the sigma decay point and the track parameters of the incident $\pi^-$, $K^+$ and decay $\pi^-$ tracks. The criteria used for distinguishing between events of the above topology and two prong events are discussed. (auth) (UK)

**55050** COMPUTERS AND COMPUTATION IN EXPERIMENTAL HIGH-ENERGY PHYSICS. Macleod, G. R. (CERN, Geneva). pp B.0-35 of Computational Physics. Vols. I and II. London; Her Majesty's Stationery Office (1969).

From Conference on computational physics; Culham, England (28 Jul 1969). See CONF-690706-(Vols.1 and 2).

A brief survey is given of the various uses of computers and the kind of computations made in high energy physics experiments. The successive stages of experiments, from the initial design to the final analysis of data, are described with examples chosen from recently completed experiments to illustrate the varied computing techniques used. Finally some future trends to be expected are indicated, with particular reference to their dependence on developments in computer technology. (auth) (UK)

## Radiation Dosimeters

*Refer also to abstracts 55002, 55026, 55205, 55208, 55234, and 55235.*

**55051** INDIVIDUAL DOSIMETER. Mukhin, G. I.; Klyukin, L. P. (to All-Union Scientific Research Inst.). Russian Patent 265,300. 9 Mar 1970. Filed 9 Dec 1965. (In Russian).

A personal dosimeter, designed for many uses, is described. In order to reduce light loss, the optical system is placed inside the condenser; the ionization chamber is put at the end of the dosimeter and is detachable. (R.W.R.)

**55052** BATTERY-OPERATED UNIVERSAL DOSIMETER. Allewaert, J. (Univ., Ghent). Strahlentherapie; 141: No. 6, 715-17(Jun 1971).

A battery-operated dosimeter is described that can be used with different commercially available ionization chambers. The electrometer circuit and calibration procedures are described. (W.H.K.)

**55053** DOSIMETRY BY MEANS OF FORMATION OF RADIOLYTIC GASES FROM FLUOROCARBONS. Proksch, E. (Institut fuer Chemie, Seibersdorf, Austria). Int. J. Appl. Radiat. Isotop.: 22: No. 7. 441-4(Jul 1971).

Fluorocarbons are insensitive to neutrons and are thus suitable for $\gamma$ dosimetry in the range $10^6$ to $10^9$ rad by radiolytic gas production. Three liquid fluorocarbons available commercially were studied in order to find an inexpensive yet accurate and sensitive one. Irradiation with $^{60}$Co $\gamma$ at 3 to 40 Mrad, followed by gas chromatography, showed $CF_4$ as the main product. Sensitivity was the same as for perfluoro-n-hexane used earlier, but the reproducibility was not good, except for perfluoromethylcyclohexane. The latter compound was further studied and found equal to perfluoro-n-hexane in performance while being cheaper and having no large behavior variation with dose or dose rate. (UK)

**55054** SIMPLE SOLID-ELECTROLYTE GAMMA-RAY AND RELATIVISTIC-CHARGED PARTICLE DOSIMETER. Roberts, Thomas G.; Rust, Charles M. (to Secretary of the Army). U. S. Patent 3,585,389. 15 Jun 1971. Filed 1 Dec 1969

A gamma-ray and relativistic-charged-particle detector and a method for measuring the amount of radiation passed through the detector are described. The detector is a dosimeter comprising a plurality of equally spaced batteries disposed to form a series of columns and rows within a plane having vertical and horizontal rectangular coordinate axes. The batteries, radiation sensors, can be repeatedly charged and discharged with very little characteristic change in the discharge curve. The batteries have a solid electrolyte and a low-voltage output. Radiation passing through the electrolyte causes partial ionization of the electrolyte, which reduces the battery terminal voltage in proportion to the amount and type of radiation that passed through it. Before and after being exposed to radiation, the batteries are placed in a test stand, and the individual battery voltages are simultaneously measured and recorded. A change in voltage across the battery terminals, after exposure to a known type of radiation, is proportional to the radiation passed. Thus, differential voltage, displayed as a contour map or picture of the radiation pulse, is representative of the radiation intensity passing through the detector. (auth)

**55055** THERMAL LUMINESCENT MATERIAL FOR IONIZING RADIATION DOSIMETRY. Carpentier, Serge; Dajlevic, Radovan; Delarue, Roger; (and others) (to Commissariat a l'-Energie Atomique). U. S. Patent 3,600,579. 17 Aug 1971. Priority date 12 Mar 1968, France.

The material essentially consists of alumina $Al_2O_3$ in the form of particles smaller in size than 400 $\mu$. A proportion higher than 80% by weight should be in the form of alpha crystals. A proportion of particles at least equal to 60% has a size higher than 10 $\mu$. The alumina may be used in powdered form or included in a construction material. (auth)

**55056** APPLICABILITY OF A SOLID-STATE BRAGG-GRAY CAVITY CHAMBER FOR LUMINESCENCE DEGRADATION DOSIMETRY. Ilic-Popovic, J. (Danish Atomic Energy Commission Research Establishment, Risoe). Int. J. Appl. Radiat. Isotop.: 22: No. 8, 457-61(Aug 1971).

Anthracene-gelatine film was used as a solid-state analogue of a Bragg–Gray cavity ionization chamber. A thin anthracene-gelatine film supported on Ozatex was sandwiched between plates of carbon, aluminium, copper, silver, tin, wolfram, and lead. Irradiations in the absorbed dose range 0.5 to 10 Mrad were performed with $\gamma$ rays from a $^{60}$Co-source. The influence of the thickness of the anthracene-gelatine film on the dose response was investigated for lead relative to carbon. The results are in agreement with values predicted by Burlin's theory of cavity ionization. (auth) (UK)

**55057** UTILIZATION OF POLYMER-GELATIN NUCLEAR EMULSIONS FOR FAST NEUTRON DOSIMETRY. Nikodemova, D. (Vyzkumny Ustav Hygieny Prace a Chorob z Povolani, Bratislava); Bradna, F. Radioisotopy; 11: No. 5, 739-53(1970). (In Czech).

Nuclear emulsions are still the most widely used technique for personnel dosimetry. The results and characteristics of fast neutron dosimetric measurements, using the new type of sensitive polymer-gelatine nuclear emulsion, are discussed. Furthermore, the calibration with four neutron sources, processing, and the limitations of this nuclear emulsion are described. Measurements on the phantom and on the direction dependence were performed. The number of proton tracks as a function of dose equivalent for the generally used neutron sources was investigated and compared with theoretical calculations of the doses. (auth)

**55058** ASSESSMENT OF WALL EFFECTS IN MICRODOSIMETRIC MEASUREMENTS. Kellerer, Albrecht M. (Columbia Univ., New York). Contract AT(30-1)-2740. Radiat. Res.; 47: No. 2, 377-86(Aug 1971).

Proportional counters with solid walls exhibit distortions of pulse height distributions due to the so-called wall effects. With heavy charged particles these wall effects mainly affect the indirect events of energy deposition, i.e., those events where the heavy charged particle does not actually enter the cavity but merely injects some delta rays into it. The percentage of absorbed dose due to these distorted pulses is calculated for charged particles of different energy and for neutron fields. For neutrons below 10 MeV the wall effects are generally small, and conventional proportional counters are applicable. (auth)

XUM

## Radiometric Instruments

*Refer also to abstracts 55070, 55111, and 55213.*

**55059** LINEARIZATION OF RADIATION GAUGES FOR MEASURING THE QUANTITY OF FLUIDIC MATERIALS IN CONTAINERS. Shoemaker, David J. (to Industrial Nucleonics Corp.). U. S. Patent 3,594,575. 20 Jul 1971. Filed 30 Aug 1968.

Specifically disclosed are a method and apparatus for linearizing the output of a nuclear-radiation tank level gage. A plurality of radiation detectors are vertically spaced along one side of the tank to produce separate signals, which are fed to a summing amplifier, and a point source is located on the opposite side of the tank. The summing amplifier has individually adjustable input resistors whereby each signal is individually weighted to produce an amplifier output signal that is linearized with respect to the liquid level in the tank. For standardization, when the liquid level is below the top detector, the signal from the top detector is separately fed to the amplifier input in substitution for the multiple input signals; and the gain of the measuring system is adjusted to compensate for changed parameters of the system. (auth)

**55060** RADIATION GAUGE CALIBRATION. Doering, George I. (to Industrial Nucleonics Corp.). British Patent 1,242,419. 11 Aug 1971. Priority date 11 Oct 1967, United States.

It has been found that different radiation gages have different frequency responses and that the frequency response is an important parameter in determining the characteristics of a product being manufactured. Frequency response is important because spectral information can provide additional data regarding the operation of the process. A method and system are described for frequency-response standardization of a radiation gage. In this way the characteristics of a radiation gage are maintained uniformly consistent to a given property over an extended period of operation. With the gage zero and source standardized, the gage response is modulated at a predetermined frequency or group of frequencies, and an indication of the attenuation introduced by the gage on the modulation components is obtained. If the gage output indication differs from a desired, predetermined level at the modulation frequencies, frequency determining elements of the gage are varied, either manually or automatically, to correct the gage output indication to the desired response level for that frequency. The invention can be used with several gages making measurements simultaneously. (R.W.R.)

**55061** PASSIVE MOISTURE METER. Kastner, Jacob; Oltman, Billie G.; Feige, Yehuda (to United States Atomic Energy Commission). U. S. Patent 3,602,713. 31 Aug 1971. Filed 8 Jul 1970.

A passive moisture meter measures the number of thermal neutrons present in a material as a result of natural radiation, such as cosmic rays, to determine the moisture content of the material The thermal neutron flux in a control region of known moisture content is also measured to determine the magnitude of the high-energy neutron flux developed by the natural radiation. (auth)

**55062** APPARATUS FOR CONTINUOUSLY MEASURING THE CROSS-SECTION OF WIRE. Knufelmann, Manfred; Seidel, Ingo (to Gesellschaft fuer Nucklearmesstechnik. Industrie-Electronik M. Knufelmann and Co. mbH). British Patent 1,247,138. 22 Sep 1971. Priority date 23 Apr 1969, Germany.

A radioisotope source, shielding, collimator, and radiation detector system for measuring the thickness and uniformity of wires is described. (W.H.K.)

**55063** METHOD AND APPARATUS FOR DETECTING GAS LEAKS USING RADIOACTIVE TECHNIQUES. Harman, Randall W.; Rusch, Roger J.; Wakeman, James F. (to TRW Inc.). U. S. Patent 3,597,611. 3 Aug 1971. Filed 20 Jun 1967.

A gas leak detector is described where a trace of radioactive gas is mixed with a functional gas, the leak rate of which is to be determined, and includes means to cause the flow of a portion of an entrapped volume of leaked gas into the vicinity of a radiation detector in which radiation energy is converted into voltage pulses, and means to determine the count rate of change of the pulses in consecutive time periods and from which the leakage rate of the functional gas is determined. (auth)

**55064** RADIOMETRIC METHOD AND APPARATUS FOR MEASURING AND CONTROLLING FOUNDRY SAND MOISTURE. Glaza, Donald D.; Block, Arthur D. (to General Motors Corp.). U. S. Patent 3,600,574. 17 Aug 1971. Filed 12 May 1969.

To measure the amount of water present in foundry sand continuously flowing through a chute, a probe within the chute carries a fast neutron source and a slow neutron detector to detect the amount of water in the sand. A gamma source in the probe and a gamma detector outside the chute measure the sand density. The detector output signals are arithmetically combined to give a signal proportional to percent moisture by weight. The signal may be used to control water addition to the sand. (auth)

**55065** RECENT DID RADIOMETRIC-TECHNIQUE DEVELOPMENTS. Gerrard, Martha. Isotop. Radiat. Technol.; 9: No. 1, 31-40(Fall 1971).

The status of several DID radiometric-technique projects is reviewed including a nuclear helicoptor lift indicator, an isotopic shock-wave-position sensor, tracer measurements of turbine and pump discharge, an airborne system for measuring the snow cover, and application of activation analysis to identification of paper and bullets and detection of gunpowder. (auth)

**55066** GAMMA–GAMMA-METOD V RUDNICHNOI-GEOLOGII. (Gamma–Gamma Method in Mining Geology). Evdokimov, Yu. D. (ed.). Moscow; Atomizdat (1971). 104p.

The gamma-gamma method is useful for investigating the composition and density of ores, and is based upon the measurement of gamma-radiation supplied from an external source which has been scattered by the material being studied. The source consists of a radioisotope with a gamma energy of tens or hundreds of keV, and either Compton scattering or photoelectric absorption may result. After a thorough treatment of the fundamentals of the technique and how it is used to determine the atomic number or the percentage of a given element in an ore body, the practical aspects of working equipment are considered. Scintillation radiometers, probes, radiation sources, and standardization and interpretation of field results are described. 43 references. (K.S.W.)

**55067** GAMMA RAY DENSITY GAUGING. Hoel, John E.; Novitsky, Thomas W. (IBM Systems Manufacturing Div., Endicott, N. Y.). pp 387-94 of Modern Developments in Powder Metallurgy. Vol. 5. /Hausner, Henry H. (ed.). New York; Plenum Publishing Corp. (1971).

From International powder metallurgy conference; New York, N. Y. (12 Jul 1970).

The density of pressed powder metal parts can be rapidly and nondestructively measured by means of gamma transmission techniques. General considerations of gamma density gaging are discussed from an applications viewpoint. Specific applications and results discussed include the density of green, sintered, and repressed iron parts and of bronze and other alloys. (auth)

## Miscellaneous Instruments and Components

*Refer also to abstracts 54767, 54768, 54992, 54993, 55004, 56214, 56347, and 57191.*

**55068** (AEC-tr-7240) PROCESS FOR THE MEASUREMENT OF A DISPLACEMENT AND DEVICE FOR ITS USE. Laffon, Jean-Louis; Masson, Maurice. Translated from French Patent 1,467,228. 13p. Dep. NTIS.

A displacement gage for use in a reactor is described. The displacement measurement is based on the variation of the tuning frequency of a hf resonance cavity. (W.H.K.)

**55069** (ANL-7804) BEHAVIOR AND CALIBRATION OF DEVICES FOR MONITORING IMPURITIES IN SODIUM. Humphreys, J. Ross Jr.; Filewicz, E. C.; Greenberg, S.; Skladzien, S. B.; Vilinskas, P. (Argonne National Lab., Ill.). Jul 1971. Contract W-31-109-eng-38. 36p. Dep. NTIS.

The sodium analytical loop (SAL) was used to study the behavior of two United Nuclear Corporation (UNC) oxygen meters and a dc resistivity meter. Oxygen was added to the loop in the form of sodium hydroxide and was removed by uranium getter tabs. Oxygen concentration in the sodium was periodically determined using in situ vacuum distillation. The resistivity meter was not calibrated, but was confirmed to be sensitive to hydrogen concentration and relatively insensitive to oxygen concentration. The average value for the uranium oxidation coefficient was found to be 16.9 $\mu g\ cm^{-3}hr^{-1}ppM^{-1}$ (range: 14.1–20.9). During the experiment, zirconium wire (in excess of the amount required to form $ZrH_2$ based upon total hydrogen addition in the form of hydroxide) was used as a hydrogen getter. Thirty-eight percent of the hydrogen produced was absorbed. (auth)

**55070** (BHO-67-2) FABRICATION AND EVALUATION OF ISOTOPIC SOURCE NEUTRON INTERROGATION ASSAY SYSTEM (ISAS). Quarterly Technical Report, July 1, 1970–October 9,

XUM

1970. Gallagher, W. J. (United Nuclear Corp., New Haven, Conn. Commercial Products Div.). 12 Oct 1970. Contract AT(30-1)-67. 10p. Dep. NTIS.

The design, fabrication, and preliminary testing were completed for two Isotopic Source Assay Systems (ISAS), each capable of separately measuring the $^{235}U$ and $^{238}U$ content of highly enriched uranium material. The ISAS units were released for shipment to the United Nuclear Corp. which is preparing enriched uranium calibration standards to be used with the ISAS units. (L.C.L.)

**55071** (CEA-N-1433) ELECTRICAL EQUIPMENT FOR MEASURING SMALL CURRENTS. APPLICATIONS TO DOSIMETRY USING CLASSICAL IONIZATION CHAMBERS, LIQUID DIELECTRIC IONIZATION CHAMBERS, AND ELECTRIC CHARGE MEASUREMENTS IN CONNECTION WITH AEROSOL STUDIES. Prigent, Raymond; Bouet, Joseph (Commissariat a l'Energie Atomique, Fontenay-aux-Roses (France). Centre d'Etudes Nucleaires). Apr 1971. 15p. (In French). Dep. NTIS (U. S. Sales Only).

Studies undertaken at STEP led to the development of a d-c amplifier, which can be used with various detectors and is capable of measuring currents between $10^{-15}$ and $10^{-13}$A. Essentially, the equipment consists of a basic amplifying unit and a h-v supply for operating the liquid-dielectric ionization chamber. A stabilized 5000-volt h-v source is incorporated which can be replaced by a variable (h-v) source when this is desirable. Matching to the different types of detector is effected by an interchangeable preamplifier. The appropriate preamplifier can be connected to the unit with 50 meters of cable. Two distinct types of measurement can be made, absorbed dose and integrated absorbed dose. The type of operation desired is selected by a two-position commutator mounted in the assembly. The assembly weighs 5 kg, and its dimensions are 330 × 170 × 100 mm. The preamplifier is 100 × 65 × 65 mm, easy to use and conveniently transported. (auth) (France)

**55072** (FRNC-TH-54) IMPROVEMENTS TO THE PLANAR ELECTROSTATIC ANALYZER FOR SLOW ELECTRONS. Regnaut, Christian (Paris Univ. (France). Faculte des Sciences). 1970. 97p. (In French). Dep. NTIS (U. S. Sales Only).

Thesis.

Grid techniques were used to improve the selective properties of an electrostatic analyzer intended for surface studies. Theoretical and experimental results indicate that a selector which possesses a grid about which the electrons are reflected tangentially, presents optimum operating conditions which depend upon the mean energy of the equipotentials near the grid. The electric field is uniform in the selector except in the region very near the grid and the principal motion remains unchanged; this explains the linear characteristics of the operation of the apparatus. The decreasing slopes occurring with increasing penetration of the opposing field represent the overall action of the grid. Near the peaks of the trajectories the profile of the equipotentials determines the angles of reflection and diffraction of the electrons; it is thus possible to treat the problems as a diffraction grating. A spreading out is possible for the slow electrons but for these the perturbation is on the average less significant since their height in the selector is small. The improvement obtained was about 30 percent without the necessity of reducing the apertures or slits of the selector. (France)

**55073** (INR-1315) INTEGRAL DISCRIMINATOR FOR AMPLITUDE ANALYZERS. Kulka, Zbigniew (Institute of Nuclear Research, Warsaw (Poland)). 1971. 9p. (In Polish). Dep. NTIS (U. S. Sales Only).

The construction of an integral discriminator with pulse shaper and its principles of operation are described. The circuits produce a normalized digital output pulse for every input pulse with an amplitude exceeding a preselected threshold. The discriminator threshold, 0.25 to 10 V, is selected by a 10-turn precision potentiometer. Integral linearity better than ±0.1%; temperature stability, 1.5 mV/°C; and dead time, 80 nsec are obtained. Some results of measurements are given. This discriminator is designed for pulse-height analysis. (auth)

**55074** (JUL-Conf-5) SIEMENS PROCESS CALCULATOR UTILIZATION CONFERENCE, JUNE 29-JULY 1, 1970, JUELICH, GERMANY. Mueller, Klaus-Dieter; Tenten, Walter (Kernforschungsanlage, Juelich (West Germany)). Mar 1971. 231p. (In German). (CONF-700658).

Twenty-one papers concerning the development and uses of Siemens process calculators are presented. Both hardware and software are discussed including peripheral systems. (W.H.K.)

**55075** (K-1817) SOLID-STATE AUTOMATIC BEAM POSITIONER FOR MASS SPECTROMETERS. Jones, H. C. (Oak Ridge Gaseous Diffusion Plant, Tenn.). 16 Aug 1971. Contract W-7405-eng-26. 7p. Dep. NTIS.

An all-solid-state electronic beam positioner for isotopic ratio mass spectrometers has been developed and operated for several months without requiring service or adjustment. Low-frequency modulation of the spectrometer ion accelerating potential with phase sensitive detection of beam position is used to apply an automatic correction signal to the accelerating potential and maintain precise beam position in the collector slit. The operational amplifiers, power supply, and unijunction transistor oscillator utilized in the instrument are of all-solid-state design. Total power dissipation is approximately 12 watts which contributes to the temperature stability of the electronic control and measuring circuitry of the mass spectrometer. (auth)

**55076** (LA-DC-12576) FULLY INTERACTIVE GRAPHICS DATA RETRIEVAL SYSTEM. Stephenson, Dwight L. (Los Alamos Scientific Lab., N. Mex.). [1971]. 10p. (CONF-710912-1). Dep. NTIS.

From Instrumentation fair conference; Washington, D. C. (9 Sep 1971).

The application of interactive graphics technology is a highly effective means of rapid data retrieval, meaningful visual display, and simultaneous viewing of large numbers of related measurements. The interactive capability inherent to such a system allows the viewer to add pertinent commentary and annotation in the data presentation at appropriate points. Scale expansions of the entire data plot or selected portions thereof are easily accomplished under interactive control. Such data manipulations as integration, curve fitting, calibration corrections, smoothing, editing, and many other techniques for data massaging are readily accomplished under function key callable programs. The speed of the processor is such that data manipulation appears to occur in real time. The operator therefore has a powerful real time data processing capability at his fingertips, and data analysis is significantly expedited. The use of the interactive and computational capabilities of the system allows the user to prepare his data in final format including coordinate calibration in scientific or engineering terminology, superposition of several related measurements, legend, grid, etc., and to view the data in its final form prior to hard copy production. A high speed printer/plotter is included within the system for hard copy production. Archive record files are outputted as high density magnetic tape, and archive record control and retrieval is also under program control. The system is described. (auth)

**55077** (LA-tr-71-71) TEMPERATURE MEASUREMENT BASED ON THERMAL NOISE. Brixy, Heinz G. (Kernforschungsanlage, Juelich (West Germany). Institut fuer Reaktorentwicklung). Translated for Los Alamos Scientific Lab., N. Mex., from report JUL-635-RG. 61p. Dep. NTIS.

The Nyquist formula is used for determining the temperature. The noise voltages of two resistors are compared, the one at the unknown temperature, the other at room temperature. The ratio of the resistances, when the noise voltages from the two resistors are equal, determines the ratio of their absolute temperatures. Several temperatures are measured in the range from 300°K to 1100°K with an accuracy better than 0.2 percent. The noise thermometer is independent of the material from which it is made or its previous thermal and mechanical treatment. It is also independent of the environment like nuclear radiation and therefore especially suitable for temperature measurement in nuclear reactors. (auth)

**55078** (NYO-3906-5) ULTRASONIC THERMOMETRY IN LMFBR SYSTEMS. Fifth Quarterly Progress Report Covering the Period Ending December 1968. Fam, S.; Lynnworth, L. C.; Carnevale, E. H. (Panametrics, Inc., Waltham, Mass.). Contract AT(30-1)-3906. 11p. Dep. NTIS.

Agreement was reached on the location and type of test that would provide the closest available simulation of the operating conditions obtained in LMFBR's, with particular emphasis on fuel temperature determination. Pre- and post-irradiation test procedures as well as methods of sensor retrieval were discussed, and a tentative test schedule was drawn up. Continuing efforts to produce nuclear hardened transducers by anodization have succeeded in obtaining fine reproducible layers of oxide insulation on Al. The basic design parameters of the composite ultrasonic/thermocouple temperature probe were worked out. Room-temperature sound-velocity measurements were made on three Re-Os alloy samples, viz. Re-5% Os, Re-10% Os, and Re-15% Os. (R.W.R.)

XUM

**55079** (SC-DC-713696) METHOD FOR THE ROUTINE MEASUREMENT OF DIELECTRIC PHOTOCONDUCTIVITY. Sullivan, W. H.; Ewing, R. L. (Sandia Labs., Albuquerque, N. Mex.). [1971]. 32p. (CONF-710709-3). Dep. NTIS.

From Annual conference on nuclear and space radiation effects; Durham, N. H. (20 Jul 1971).

An instrumentation and data-reduction technique for the routine analysis of dielectric photoconductivity data was developed. This technique provides detailed results for conductivity versus time during and shortly after an ionizing radiation pulse. This technique was used to measure the peak conductivity of H-film and Teflon at dose rates greater than $10^{11}$ rads per second. The results of these experiments and details of the analysis technique used are described. (R.W.R.)

**55080** (TRG-Report-2086) REMOTE-READOUT BALANCE FOR USE IN A HIGHLY RADIOACTIVE ENVIRONMENT. Robertson, A.; Butler, J. K. (United Kingdom Atomic Energy Authority, Dounreay (Scotland). Reactor Group). 18 Aug 1970. 6p. Dep. NTIS (U. S. Sales Only). UK 9p.

A balance is described which is used to weigh irradiated DFR experimental fuel pins. The optical readout system of a commercially available balance has been replaced by a transducer giving an output in the form of a digital display. (auth)

**55081** MASS-SPECTROMETRIC ION SOURCE FOR HIGH-TEMPERATURE INVESTIGATIONS. Fesenko, V. V.; Gordienko, S. P.; Lysenko, A. A. (Inst. of Materials Science, Kiev). Sov. Powder Met. Metal Ceram. (Engl. Transl.); 10: No. 1, 82-3(Jan 1971).

Translated from Porosh. Met., Akad. Nauk Ukr. SSR; 10: No. 1, 103-5(Jan 1971).

A new high-temperature molecular-stream ion source for the MI-1305 mass spectrometer for investigations of refractory materials up to 2500°K is described. (W.H.K.)

**55082** ELECTROSTATIC SPECTROMETER. PART I. Delage, Y.; Carette, J.-D. (Laval Univ., Quebec). Can. J. Phys.; 49: 2118-31(15 Aug 1971). (In French).

A second-order approximation equation for the trajectory of a charged particle in a 1/r electrostatic field is presented. Then a method to evaluate the curve of the energy distribution of the electrons transmitted by an electrostatic spectrometer is proposed. This method is used to evaluate the energy spectrum of two particular cylindrical spectrometers, whose utilization is widely spread in many laboratories. The properties of the electron beam, such as the electron distribution as a function of the exit angle, are studied with the aid of the proposed method of calculation. Also the method of analyzing or measuring the electron energy spectrum, as done by experimenters, is studied in order to evaluate the precision of these measurements. (auth) (Canada)

**55083** ELECTROSTATIC SPECTROMETER. PART II. Allard, P.; Carette, J.-D. (Laval Univ., Quebec). Can. J. Phys.; 49: 2132-7(15 Aug 1971). (In French).

In this paper results of measurements done in order to verify the conclusions of a study concerning the cylindrical condenser used as an electrostatic electron spectrometer are presented. The measurements are related to the angular electron distribution at the exit of the spectrometer, to the average value of the electron energy as a function of the exit angle, to the method of measuring the whole energy distribution of transmitted electrons, and, finally, to the linearity of the transmission characteristics of this spectrometer. (auth) (Canada)

**55084** ELECTROSTATIC SPECTROMETER. PART III. Roy, D.; Carette, J.-D. (Laval Univ., Quebec). Can. J. Phys.; 49: 2138-59(15 Aug 1971). (In French).

The method of calculating the energy distribution of electrons selected electrostatically, presented in Part I, was used to calculate the distribution profiles for the principal types of electrostatic spectrometers: toroidal, cylindrical 127°, and spherical 180° spectrometers and parallel-plate and cylindrical mirrors. The calculations were performed as a function of the most important geometrical parameters of the spectrometers: the slit width and the angular aperture. They were made in a generalized form by expressing these geometrical parameters as a function of the main dimension of each apparatus: main radius in the case of toroidal-type spectrometers, distance between the slits in the case of mirrors. In this way results presented may be extended to spectrometers of any size. Similarly, as calculations were performed for a nominal energy of the electron beam of 1 eV, the energy scale may be considered as arbitrary, and it suffices to multiply it by the nominal energy of interest. For each type of spectrometer, equations used in calculations are given. For various slit widths and angular apertures of spectrometers, numerous energy distribution profiles are presented with the usual characteristics of energy distribution, that is, half-intensity width (FWHM or $\Delta E_{\frac{1}{2}}$), base width (FWB or $\Delta E_B$), and arbitrary transmitted current ($I_t$). (auth) (Canada)

**55085** HOROLOGICAL MOVEMENT UTILIZING A RADIOACTIVITY DETECTOR AND SOURCE. Wuthrich, Paul (to Timex Corp.). U. S. Patent 3,601,975. 31 Aug 1971. Filed 23 Apr 1969.

A horological instrument with an oscillating member as its time base is described. The oscillator, for example, a balance wheel, carries a radioactive source. The path of movement of the radioactive source is within the range of a radiation detector fixed to the base of the instrument. The radiation detector controls an electronic switch which is connected to a power source and provides an impulse to a coil. The coil provides a driving impulse to the oscillator. (auth)

**55086** QUALITY FACTOR OF SUPERCONDUCTING LUMPED-PARAMETER CIRCUITS. Anan'ev, L. L.; Gerasimov, N. P.; Reinov, N. M. (Ioffe Inst. of Physics and Tech., Leningrad). Sov. Phys.-Tech. Phys. (Engl. Transl.); 16: No. 2, 303-4(Aug 1971).

Translated from Zh. Tekh. Fiz.; 41: No. 2, 401-3(Feb 1971).

Experimental studies of superconducting oscillator circuits in the magnetic field of the Earth are described. A Q factor of $10^6$ can be obtained. (auth)

**55087** 4th CONGRESS OF IFAC, WARSAW, 16–21 JUNE 1969. Abstracts of Papers Delivered at Congress Sessions. Duesseldorf; International Federation of Automatic Control (1971). 348p. (CONF-690603-(Absts.)).

**55088** DEVICE FOR MEASURING THE THERMAL CONDUCTIVITY OF URANIUM DIOXIDE SINTERED PELLETS UNDER IRRADIATION IN REACTOR. Avram, Magdalena (Institutul de Fizica Atomica, Bucharest). Stud. Cercet. Fiz.; 23: No. 2, 227-34(1971). (In Rumanian).

Two experiments to measure the thermal conductivity of sintered uranium dioxide under irradiation at a temperature in the central region of the specimens of 300 and 560°C are described. Two devices that permit continuous measurements of the heat output from the specimen were used. The two devices are based on the method of radial heat flow in permanent conditions. The specimens had the shape of cylindrical pellets. To produce the temperature gradient in the pellets, the heat released in the reaction of nuclear fission of $^{235}U$ was used. The results obtained with each of the two devices are given. (auth)

**55089** ULTRALOW TEMPERATURE ROTATING POLARIZATION SYSTEM. Krane, K. S.; Sites, James R.; Steyert, W. A. (Los Alamos Scientific Lab., N. Mex.). Rev. Sci. Instrum.; 42: No. 10, 1475-9(Oct 1971).

A system has been constructed to study very small asymmetries in the directional distribution of $\gamma$ radiation from polarized nuclei. The system combines the ultralow temperatures of a $^3He-^4He$ dilution refrigerator (down to 14 mK) and the large hyperfine field of a ferromagnetic host lattice. The hyperfine field direction is smoothly and continuously rotated by means of an external field to compare the $\gamma$-ray intensity in different directions. Many experimental tests have been performed, and upper limits are placed on various sources of spurious asymmetry. (auth)

**55090** ELECTRONIC PARTICLE COUNTING AND DISPENSING DEVICE FOR USE IN ANIMAL INJECTION EXPERIMENTS. Mullaney, P. F.; Coulter, J. R. (Los Alamos Scientific Lab., N. Mex.). Rev. Sci. Instrum.; 42: No. 10, 1434-6 (Oct 1971).

An electrical resistance counter of the Coulter type has been designed to count particles intended for animal injections and to dispense them into a package (a length of polyethylene medical tubing). The packaged particles are used for injections at a later date. In a typical application, two thousand 10 $\mu$ spheres can be counted and loaded into a 61 cm length of PE-50 tubing (total volume 0.25 ml) in about 5 sec. The accuracy of the count has been determined by an independent method. (auth)

**55091** MICROWAVE RECEIVERS FOR MOLECULAR LINE RADIO ASTRONOMY. Buhl, David (National Radio Astronomy Observatory, Green Bank, W. Va.); Snyder, Lewis E. Nature (London) Phys. Sci.; 232: No. 34, 161-3(23 Aug 1971).

The development of electronic receivers, resulting in the discovery of interstellar molecular lines, has encouraged further instrumental improvements. Some aspects of the NRAO spectral line receivers are discussed. (auth)

XUM

**55092** CALORIMETER TO INVESTIGATE THE SATURATION BEHAVIOR OF HEAVY WATER AND OTHER FLUIDS TO THEIR RESPECTIVE CRITICAL POINTS. Nowak, E. S. (Univ. of Western Ontario, London). pp 89-95 of Proceedings of the Fifth Symposium on Thermophysical Properties. /Bonilla, C. F. (ed.). New York; American Society of Mechanical Engineers (1970).

From fifth symposium on thermophysical properties; Boston, Mass. (Sep-Oct 1970). See CONF-700901.

The design, construction and performance of an Osborne adiabatic calorimeter to investigate the thermal behavior of saturated heavy water and other engineering coolants from their respective triple to critical points are herein described. By conducting three thermodynamic processes on this single apparatus and by making measurements of the heat addition per unit mass and the temperature rise, information may be gained on the following three parameters $\Delta(h_f - v_f TdP/dT)$, $v_f TdP/dT$ and $v_g TdP/dT$. Preliminary measurements of the parameter $\Delta(h_f - v_f TdP/dT)$ have been obtained for both saturated light and heavy water liquid from 50 to 300°C. The obtained data on $\Delta(h_f - v_f TdP/dT)$ for ordinary water are in excellent accord and in all cases are entirely within the scatter of the individual Osborne et al experimental data. (auth)

**55093** USE OF INTERACTIVE COMPUTER GRAPHICS IN HIGH-ENERGY PHYSICS. Chau, A. Y.; Davies, B. W.; Richmond, P. M.; Zacharov, B. (Daresbury Nuclear Physics Lab., Eng.). pp 1.1-4 of Computational Physics. Vols. I and II. London; Her Majesty's Stationery Office (1969).

From Conference on computational physics; Culham, England (28 Jul 1969). See CONF-690706-(Vols.1 and 2).

Many computing problems encountered in a high energy physics environment can profitably be solved by some form of iterative procedure. In such problems it is normally an advantage if the user can be placed on line to the computer with facilities for observing and if necessary modifying the course of execution of a program. Illustrations of the use of computer graphics in this field are given by reference to work currently in progress at Daresbury Nuclear Physics Laboratory. Several areas of application covering both experimental and theoretical physics are mentioned. The design of magnet systems for beam optics configurations, particularly magnet spectrometers, is described. It was found useful to display ambiguous events detected in spark chamber experiments and allow the user to clarify them before submitting them to an analysis program. Brief descriptions are given of a program which enables a user to create, examine and manipulate statistical aggregates arising from experimental data, and of an aid to theorists in which a user can vary the parameters of a mathematical function which is superimposed on a display of experimental data. Comments are made on user experience and an indication is given of the reduction in overall turn round time which was achieved by the introduction of interactive graphics. (auth) (UK)

**55094** COMPUTER CONTROL OF EXPERIMENTS IN ATOMIC PHYSICS. Clout, P. N.; Heddle, D. W. O.; Watkins, R. D. (Univ. of York, Eng.). pp 23.1-3 of Computational Physics. Vols. I and II. London; Her Majesty's Stationery Office (1969).

From Conference on computational physics; Culham, England (28 Jul 1969). See CONF-690706-(Vols.1 and 2).

A system using a Digico Micro 16 computer to control three atomic collision experiments is described. The computer, through six peripherals, controls certain experimental parameters (e.g., the electron energy acceptance and angular setting of the scattering detector) and also records and analyzes the data. (auth) (UK)

## Radiation Effects on Instruments and Instrument Components

*Refer also to abstract 56338.*

**55095** (COO-1624-41) NUCLEAR RADIATION EFFECTS ON SILICON P-N JUNCTIONS. Goben, Charles A. (Missouri Univ., Rolla. Space Sciences Research Center). Jul 1971. Contract AT(11-1)-1624. 53p. Dep. NTIS.

Experimental discoveries and theoretical developments clearly defined the role of the space-charge region of a p-n junction in semiconductor device degradation. A rate of space-charge volume damage introduction was defined, and its dependence on the neutron fluence and electric field of the junction (i.e., bias during irradiation) was determined. Equations that accurately predict the behavior of the p-n junction were developed. (R.W.R.)

**55096** (N-71-24635) REACTOR IRRADIATION OF THERMIONIC SHEATH INSULATORS. Mayer, John T. (National Aeronautics and Space Administration, Cleveland, Ohio. Lewis Research Center). May 1970. 23p. (NASA-TM-X-2271). NTIS.

Two beryllia- and two alumina-bonded trilayers (with niobium as the inner and outer layers) were irradiated at an average temperature of about 1200°K. The total fast fluence was between $2.3 \times 10^{21}$ and $2.6 \times 10^{21}$ neutrons/cm$^2$ (energy > 160 fJ (1 MeV)). None of the trilayers showed any gross changes in either the ceramic or in the metal/ceramic bond, although the alumina did show signs of grain boundary weakening. The sample diameters grew by 0.4 to 0.9%. Postirradiation ac resistance at 1275°K was higher than pretest values by as much as a factor of five. (auth) (STAR)

**55097** (N-71-25389) EFFECTS OF NUCLEAR RADIATION ON A HIGH-RELIABILITY SILICON POWER DIODE. 3. JUNCTION CAPACITANCE. Been, Julian F.; Myers, Ira T.; Godlewski, Michael P. (National Aeronautics and Space Administration, Cleveland, Ohio. Lewis Research Center). May 1971. 19p. (NASA-TN-D-6330). NTIS.

The effects of nuclear radiation on the junction capacitance of a 35-A, 600-PIV $n^+$-p-$p^+$ power diode were determined for fast-neutron fluences up to $4.6 \times 10^{13}$ n/cm$^2$. Capacitance changes ranging from a small decrease to as much as 50% increase were found for small reverse biases. These changes are probably due to channel formation. At large reverse biases, the junction capacitance remained essentially unchanged with radiation. (auth) (STAR)

**55098** (N-71-26389) SOLAR CELL RADIATION DAMAGE EXPERIMENT. Quarterly Report, December 28, 1970-March 27, 1971. (Hughes Aircraft Co., El Segundo, Calif. Space Systems Div.). 19 Apr 1971. Contract NAS5-11677. 33p. (NASA-CR-118660). NTIS.

The design and testing are described for the solar cell radiation damage experiment, scheduled for launch on the ATS-F spacecraft, which is to provide high accuracy data for technical evaluation of the effects of the space radiation environments on solar cells. The flight experiment consists of a small solar panel mounted externally on the environmental measurements experiment package, which is to interface with the spacecraft. The solar panel has a total of 80 solar cells, representing 16 solar cell configurations. Thirteen solar cell configurations are to be mounted to the rigid panel portion of the solar panel (infinite back-shielding), and three configurations are to be mounted to the flexible panel (2 mils of a Kapton-fiberglass substrate). In addition, the experiment has two signal processor units required for data sampling and telemetry. The solar cell experiment is to be activated at programmed intervals to obtain voltage-current data for each individual solar cell and to obtain temperature and calibration data. The ground test program includes evaluation of the effects on solar cells and solar cell assemblies under an environment which simulates both electrons and low energy protons. (auth) (STAR)

**55099** HEAVY-PARTICLE RAY DAMAGE TO A Si SOLAR BATTERY. Nashiyama, Isamu; Teranishi, Eizo; Kageyama, Misao; Sekiguchi, Hiroyoshi (Electrotechnical Lab., Tokyo). Uchu Kagaku Gijutsu Koenkai Koenshu; No. 13, 53-6(Jan 1970). (In Japanese).

The damage done by high-energy protons to a Si solar battery was studied. To approach the actual situation as far as possible, the recombination centers due to Rutherford scattering at high energy and to potential scattering at low energy, and also the relation between flight path length and energy were utilized. The short-circuit current in a solar battery was measured with a monochromatic light-ray through a filter; the dependence of the damage effect on the wavelength as well as on radiation energy and dose were obtained, and the result is compared with the theory. The model employed was able to explain adequately the dependence of the heavy-particle damage in a solar battery upon energy, dose, and wavelength. It was further shown both experimentally and theoretically that the shorter the wavelength of light used for the solar battery the less the short-circuit deterioration. (Japan)

**55100** SOME REGULARITIES IN MEASUREMENT OF CHARACTERISTICS OF SILICON DIODES UNDER THE ACTION OF RADIATION. Korshunov, F. P. (Inst. of Physics of Solids and Semiconductors, Minsk). Vestsi Akad. Navuk BSSR, Ser. Fiz.-Mat. Navuk; No. 6, 115-21(1970). (In Belorussian).

Expressions describing stable changes of forward volt-ampere characteristics of silicon diodes under irradiation were obtained on the basis of the theory of diodes with thin and thick base, with the conditions of irradiation taken into account. In terms of the criterion of conservation of modulation of base conductivity, relations were obtained which established the interdependence of the base thickness with the diffusion length of minority carriers and

the limiting integral radiation flux, up to which the volt–ampere characteristic remains essentially the same. Comparison of the calculated and experimental relations shows good agreement. (tr-auth)

**55101** EXPERIMENTAL STUDY OF GAMMA-IRRADIATION EFFECT ON ELECTRICAL PROPERTIES OF B-TYPE INSULATOR. Chun, Hee Young; Sung, Young Kwon; Lee, Duck Chool. J. Korean Inst. Elec. Eng.; 18: No. 2, 15-20(1969).

Mica was selected as typical of the B-type insulators. Dc, ac, and impulse voltage was applied to the γ-ray-irradiated samples after constant-time doses and time-variable doses. The dielectric breakdown voltage and dielectric constant were measured; it was found that the dielectric breakdown voltage variations are relatively large, but the dielectric constants are almost constant. The above result is useful for the selection and application of the inorganic insulators under irradiation, and it is expected that the result can apply to not only B-type insulators but also inorganic insulators. (TSS) (Korean Sci. Abstr.)

**55102** GAS DESORPTION FROM VARISTORS OF BLACK SILICON CARBIDE STIMULATED BY GAMMA RADIATION. Kashukeev, N.; Ribarov, S.; Krezhov, K. (Physical Inst., Sofia). Compt. Rend. Acad. Bulg. Sci.: 24: No. 3, 295-8(1971). (In Russian).

In an investigation of the gas desorption behavior of silicon carbide varistors, samples of the latter were maintained in a vacuum of $10^{-3}$ mm Hg for several days, and then exposed to $^{60}$Co gamma radiation (10 R/sec). From pressure measurements, it was noted that gas was continuously evolved from the varistors during the exposure period of 850 minutes. A correlation was established between conductivity changes and sorption processes. (K.S.W.)

**55103** CHANGES IN THE NONLINEAR PROPERTIES OF SEMICONDUCTOR RESISTORS (VARISTORS) OF BLACK SILICON CARBIDE AFTER REACTOR-NEUTRON IRRADIATION. Ribarov, S. (Physical Inst., Sofia). Compt. Rend. Acad. Bulg. Sci.; 24: No. 3, 299-302(1971). (In Russian).

Changes in the volt–ampere characteristic of black silicon-carbide semiconductor resistors were determined as a result of exposure to reactor neutrons, while being maintained at 40 to 50°C. For a given constant applied voltage, the relationship between the current through a varistor and the neutron flux was an exponential function. An effort was made to anneal the radiation defects by heating at different temperatures from 100 to 700°C, but the only result observed was a progressive increase in the resistance; at 700°C the resistance became practically infinite. (K.S.W.)

**55104** IZMERENIE TEMPERATURY S POMOSHCH'YU OBLUCHENNOGO ALMAZA. (Use of Irradiated Diamonds for Temperature Measurement). Karpukhin, V. I.; Nikolaenko, V. A. Moscow; Atomizdat (1971). 72p.

A novel method of temperature measurement employing irradiated diamond as an indicator is presented. Radiation damage in diamond, change of properties, and principles of application are considered. Point defects in the majority of materials are preserved at low temperatures of radiation. At room temperatures and higher these defects are transformed into more complex combinations or are annealed out. X-ray diffraction patterns are taken from irradiated diamonds in various stages of annealing and compared with standards. Concrete examples of indicator use are analyzed, such as temperature measurement in gas turbine rotors, drilling and milling tools, piston rings, and fuel elements. The concluding chapter focuses attention on temperature determination in nuclear reactors, their active zones, and diamonds as reference standards under radiation conditions. 200° to 800°C is a working range for this technique. (65 references.) (K.S.W.)

XUM

# LIFE SCIENCES

## Biochemistry, Physiology, and Molecular Biology

55105 APPLICATION OF THE MOESSBAUER EFFECT IN BIOLOGY. Lang, G. (United Kingdom Atomic Energy Research Establishment, Harwell, Eng.). pp 637-54 of Proceedings of the Conference on the Application of the Moessbauer Effect. /Dezsi, I. (ed.). Budapest; Akademiai Kiado (1971).

From Conference on the application of the Moessbauer effect; Tihany, Hungary (17 Jun 1969).

Application of Moessbauer spectroscopy in biology has spanned a wide range, extending from observation of the movements of insects, through the study of the motion of ear structures, the chemical properties of whole bacteria, to the examination of isolated biological compounds and elucidation of their low lying electronic states. The present paper is concerned with the latter part of this range, where most research effort has been concentrated. Much of the early work was on iron prophyrins and haem proteins, only quadrupole spectra being observed initially. While reasonable trends were observed, the theoretical treatment suffers from the usual difficulties common to quadrupole and isomer shift calculations, often compounded by the large covalent effects. In some cases even identification of the charge and spin state has been ambiguous. With the observation of paramagnetic spectra, some of the difficulties have been overcome. Detailed agreement with ESR measurements on pure low-spin and high-spin compounds has been achieved, while the postulated pH and temperature-dependent mixtures of high- and low-spin species have been observed in others. Most haem protein work has concentrated on haemoglobin, but myoglobin, cytochrome c, cytochrome c peroxidase, and other peroxidases have received significant attention. The high oxidation states of the peroxidases are beginning to be understood, again with some help from magnetic spectra. Work on iron sulfur proteins (ferredoxins, xanthine oxidase) has been hampered somewhat by difficulties in preparation, but it appears that the key to their understanding will be by way of Moessbauer and other spectroscopic studies of the paramagnetic forms. An interesting feature here is that pairs of iron atoms appear to share a single unpaired electron. Moessbauer spectroscopy also has been successfully applied to transferrin, ferritin, ferrochrome A, and many other biological molecules. It appears that thus far only a fraction of its potentialities have been realized. (20 references) (auth)

### Basic Processes

*Refer also to abstract 55090.*

55106 NEUTRON-ACTIVATION ANALYSIS OF THE CONTENT OF CALCIUM, PHOSPHORUS, AND SODIUM IN THE BONES IN TUMORS OF THE SKELETON AND OSTEOMYELITIS. Proshin, V. V.; Mel'nik, A. D.; Ryabukhin, Yu. S.; Bizer, V. A. Med. Radiol.; 16: No. 8, 45-9(Aug 1971). (In Russian).

By means of the neutron activation method, the mean concentrations of calcium, phosphorus, and sodium in normal human tissues, tumors of the skeleton, and in the focus of inflammation in chronic osteomyelitis were determined. The authors established the differences by the mean concentrations or by the mean ratios of concentrations of trace elements between the normal and pathological tissues, as well as between different pathological tissues. (auth)

55107 TWENTY-FIVE YEARS OF ISOTOPES IN LIFE SCIENCES. Kuranz, John L. (Amersham/Searle Corp., Arlington Heights, Ill.). Isotop. Radiat. Technol.; 9: No. 1, 113-15(Fall 1971).

The applications of radioisotope technology in the life sciences over the past 25 yrs are briefly discussed. The rapid expansion of radioisotope applications during this time was the result of many factors including their fundamental usefulness in living systems, early interest on the part of investigators, the introduction of isotope technology by educators into the life science curriculum, and the fashionability of the new technique. Advances in radioisotope technology should insure at least the same rate of growth of isotope applications in the life sciences in the future. (E.R.B.)

### Metabolism, Physiology, and Toxicology

*Refer also to abstracts 54982, 55043, 55153, 55157, and 55319.*

55108 (BNWL-SA-3747) COMPARATIVE METABOLISM OF INTRAVENOUSLY INJECTED PROMETHIUM IN SWINE AND HUMANS. McConnon, D.; Cole, C. R.; Smith, V. H. (Battelle-Northwest, Richland, Wash. Pacific Northwest Lab.). [nd]. Contract AT(45-1)-1830. 14p. (CONF-710710-10). Dep. NTIS.

From sixteenth annual Health Physics Society meeting, New York, N. Y. (12 Jul 1971).

Assessment of the extent of internal deposition of $^{147}Pm$ was by analysis of excreta samples and the use of excretion models based on results of metabolism studies. A kinetic model of the metabolism of $PmCl_3$ in man was developed with the aid of an analog computer. The model was constructed from the results of swine experiments for tissue distribution at sacrifice, urinary and fecal excretion, whole blood activity measurements and whole body counting data. Data are presented on computer-derived predictions of the activity in the following compartments: blood, urine, feces, bone, liver, and whole body. Results indicate that: the metabolic data in swine are quite similar to those found in humans; the ICRP value for the biological half life of promethium in bone may be low by as much as a factor of 8; and liver deposition of promethium following intravenous injection of $PmCl_3$ may be higher than the ICRP recommended value by a factor of 5. (H.L.W.)

55109 (COO-1231-67) METABOLISM AND REMOVAL OF RADIOSTRONTIUM IN MAN. Spencer, Herta; Kramer, Lois; Samachson, Joseph (Veterans Administration Hospital, Hines, Ill.). [1971]. Contract AT(11-1)-1231-67. 22p. Dep. NTIS.

The pathways of excretion of intravenously and orally administered radiostrontium ($^{85}Sr$), the factors which influence its absorption and retention in the body, and the compounds which affect its removal in man are described. The main pathway of excretion of intravenously administered $^{85}Sr$ and of the orally absorbed dose is via the kidney. During low calcium intake, the major portion of the ingested $^{85}Sr$ is unabsorbed and an average of 20% of the orally administered dose is absorbed. Increasing the calcium intake about 10-fold did not consistently or significantly decrease this absorption while phosphate added to either a low or high calcium diet moderately decreased radiostrontium absorption. Stable strontium, vitamin D, lactose, and lysine did not affect the absorption of $^{85}Sr$. Parathyroid extract (PTE) had no effect on the absorption of $^{85}Sr$ while the functional state of the thyroid influenced strikingly its absorption, i.e., the absorption was markedly increased following the correction of hyperthyroidism and of induced hypermetabolism. Aluminum phosphate gel markedly inhibited the intestinal absorption of $^{85}Sr$, the effect being greatest when this compound was given immediately prior to the oral dose of $^{85}Sr$. The absence or presence of food markedly affects the absorption of radioactive strontium in man. In the absence of food this absorption is increased by a factor of 2 to 3 as compared to the absorption of the tracer ingested with food. $^{90}Sr$ balance studies have shown that the net absorption of $^{90}Sr$ averaged 15% and that stable calcium did not significantly decrease this absorption. (auth)

55110 (TID-25801) EFFECTS OF $^{3}H$-THYMIDINE AS A DNA LABEL IN THE RAT LIVER. Progress Report. Post, Joseph (New York Univ., N. Y. School of Medicine. Goldwater Memorial Hospital, New York). 1 Sep 1971. Contract AT(30-1)-2778. 48p. Dep. NTIS.

In vivo experiments were conducted on the effects of $^{3}HTdR$ on cell renewal patterns using rat liver cells and spleen lymphocytes. The rads per day per DNA of labeled nucleus could be estimated at different dose levels, 1, 2, and 10 $\mu Ci/g$ in 3 week old male rats. The results showed a good correlation between labeling dose and absorbed radiation. In vitro experiments using HeLa cells were conducted, and a better correlation was seen between the labeling levels and the incorporated radioactivity levels than in the in vivo experiments. Effects of perturbation of cell replication by $^{3}HTdR$ on cell function were studied using altered spleen lymphocyte response to sheep erythrocytes. When tumor explants were grown in culture, profound alterations occurred in cell cycle kinetics. Kinetic data from cell cultures from MCA-sarcomas suggested cycle times of 16 to 20 hrs and S times of 8 to 10 hrs. Studies are in progress on techniques for in vivo labeling of human tumors with $^{3}HTdR$. Studies on alterations in cell renewal patterns included effects of nitrogen mustard, iododeoxyuridine, methotrexate, and hydrocortisone on replication of normal and tumor cells. (H.L.W.)

55111 DISTRIBUTION OF $^{59}Fe$ IN THE HUMAN ORGANISM ACCORDING TO WHOLE-BODY RADIOMETRY. Gorobets, V. F.; Gabuniya, R. I.; Sereda, M. G. (Scientific Research Inst. of Medical Radiology, Obninsk, USSR). Med. Radiol.; 16: No. 8, 36-42(Aug 1971). (In Russian).

An original technique of studying the distribution of absorbed radioactive iron in the human organism based on radiometry of the whole body and separate organs is presented. The method enables determination of the content of $^{59}Fe$ in the blood, in tissues of the liver and spleen, and in the coccygeal bone marrow with the aid of external measurement of the radioactivity. The referred to method makes it possible to evaluate the functional activity of the erythropoietic system. (auth)

**55112** $^{103}Pd$ DISTRIBUTION IN THE ANIMAL ORGANISM FROM AN INTRODUCED RESORBING FILM. Kir'yakov, M. A.; Dedenkov, A. N.; Levin, V. I.; Marygina, A. B. (Inst. of Biophysics of the Ministry of Public Health, Moscow). Med. Radiol.; 16: No. 9, 61-4(Sep 1971). (In Russian).

Films of colloidal $^{103}Pd$ with a carrier and without a carrier were introduced in the thigh muscle of rats for the purpose of studying the migration of the radioisotope. Samples of the bone, blood, liver, muscle, spleen, urine, and feces were subjected to radiometry with a scintillation counter and NaI crystal. Colloidal $^{103}Pd$ with a carrier remained at the site of introduction, whereas $^{103}Pd$ chloride without a carrier was chiefly resorbed by the tissues. The degree of resorption of $^{103}Pd$ depends on the solubility of the Pd compound used in the preparation. (KSW)

**55113** EFFECTIVENESS OF A NUMBER OF CHEMICAL SUBSTANCES IN POISONING WITH A MIXTURE OF RADIOISOTOPES OF CESIUM AND STRONTIUM. Ramzaev, P. V.; Korzun, V. N.; Danetskaya, E. V.; (and others) (Leningrad Scientific Research Inst.). Med. Radiol.; 16: No. 9, 49-53 (Sep 1971). (In Russian).

In experimental and clinical conditions, a number of substances (sodium alginate, Prussian blue, calcium phosphate, methionine, and their complexes) were tested for the purpose of elucidating the assimilation of radioisotopes of cesium and strontium in their combined single intake with food. The most effective proved to be a complex of substances consisting of Prussian blue, sodium alginate, and calcium phosphate that was called antistroncesit. The intake of this substance with food containing radionuclides decreased the absorbed doses in the skeleton and whole body by 7 to 10 times with a simultaneous increase of the dose rate in the intestine from $^{134}Cs$ during the first three days by 40 times. (auth)

**55114** DISTRIBUTION OF $^{134}Cs$ IN THE CONCEPTUS OF THE PREGNANT RAT. Wykoff, M. H. (Univ. of Tennessee, Oak Ridge). Radiat. Res.; 47: No. 3, 628-34(Sep 1971).

Three groups of 25 pregnant rats each were injected with 25 $\mu$Ci $^{134}Cs$ as follows: one group was injected on day 12, another on day 14, and the third group on day 16 of gestation. A fourth group of 15 pregnant rats was injected on day 18 of pregnancy (day 0 = day plug observed). The effect of time after injection on the conceptual burden $^{134}Cs$ and its distribution in the placenta, embryo or fetus, and fetal fluids was estimated by euthanizing five females daily and examining six conceptuses from each. This was done beginning with the first day and then day by day through the fifth day after the mother was injected. An exception was made with the females dosed on day 18 of pregnancy because of ensuing parturition which allowed only 3 days for such observations. The conceptus $^{134}Cs$ burden was observed to be related to the size of the conceptus on the day when the mother was injected. This $^{134}Cs$ burden was further observed to remain constant throughout each observation period. However, the distribution of placenta, embryo or fetus, and fetal fluids was found to be related to the day of gestation. (auth)

**55115** STUDIES ON SHORT-LIVED INTERNAL $\alpha$-EMITTERS IN MICE AND RATS. PART I. $^{224}Ra$. Mueller, Walter A. (Gesellschaft fuer Strahlen-und Umweltforschung mbH, Munich). Int. J. Radiat. Biol.; 20: No. 1, 27-38(1971).

The distribution of intraperitoneally injected $^{224}Ra$ was studied in NMRI mice and Wistar rats. The highest activity concentrations were found in the skeleton. High radium concentrations were also obtained in the spleen (in mice higher than in rats, increasing with age). The calculated values were 12 rads/day for initial skeletal dose-rate and 30 rads for total averaged skeletal dose by supporting 1 $\mu$Ci/kg $^{224}Ra$. The dose relationships of the short-lived $^{224}Ra$ were contrasted to those of the long-lived $^{226}Ra$. Osteosarcoma-induction related to skeletal dose is discussed and compared with results of $^{226}Ra$ known from the literature. (auth)

**55116** INCORPORATION OF $^{239}Pu$ INTO THE HAIR. Jaworowski, Z.; Bilkiewicz, J.; Zylicz, E. (Central Lab. for Radiological Protection, Warsaw). Int. J. Radiat. Biol.; 20: No. 1, 79-83(1971).

Plutonium-239 was given to three groups of red haired New Zealand rabbits (16 in all). Doses of 0.1, 1.0 and 10.0 $\mu$Ci were administered by subcutaneous injection of $^{239}Pu$ chloride dissolved in 0.9% sodium chloride-water solution containing 0.5% of phenol and of pH 5.5. The mean incorporation rate of $^{239}Pu$ in the anagen hair of the first fleece, (grown during 22 days after dose), ranged from 1.22 to $2.73 \times 10^{-3}$% of the dose per gram of hair. This was twice as high at the level of 0.1 $\mu$Ci per animal, as at 1.0 and 100 $\mu$Ci per animal. In the growth of the second fleece, the rate of incorporation was 10 times lower at 10.0 $\mu$Ci than at the lower doses. At dose-levels studied, the concentrations of $^{239}Pu$ found in hair were similar to those in muscle, but several tens to several hundred times lower than in bone and liver. Assuming the results could be valid for humans, it was calculated that the lowest amount of $^{239}Pu$ entering the blood and detectable by hair analysis is 0.0007 $\mu$Ci. (UK)

**55117** BODY BURDEN, DISTRIBUTION, AND INTERNAL DOSE OF $^{210}Pb$ AND $^{210}Po$ IN A URANIUM MINER POPULATION. Blanchard, R. L.; Moore, J. B. (Radiological Engineering Lab., Cincinnati). Health Phys.; 21: No. 4, 499-518(Oct 1971).

Concentrations of $^{210}Pb$ and $^{210}Po$ in tissues from 41 uranium miners and 11 unexposed individuals are reported. The tissues studied were bone, liver, lung, kidney, spleen, testes, heart, muscle, pancreas, lymph nodes, small intestine, stomach, aorta, brain, spinal cord, adrenal gland, prostate, thyroid, and blood. Observations relative to individual tissue types are discussed, and comparisons are made between the levels observed in the exposed and unexposed populations. Relative tissue concentrations and the fractional body burdens of each tissue were determined. The largest amount of $^{210}Po$ and $^{210}Pb$ in the body was observed to be in skeleton, about 78%, while the important soft tissue reservoirs were the lung, liver, muscle, lymph nodes, kidney, and blood. Body burdens of the miners were 4 to 50 times those of the non-miners, approaching 33 nCi $^{210}Pb$ and 23 nCi $^{210}Po$; the latter was 46% of the maximum permissible body burden. The dose calculated for $^{210}Po$ to bone assuming an RBE of 10 and a relative damage factor of 5 may exceed in some cases the maximum permissible dose-rate of 30 Rem/yr. The doses to soft tissues were in all cases below the maximum permissible limits set by ICRP. Relationships observed between the concentration of $^{210}Pb$ and $^{210}Po$ in the blood and various body organs are discussed, and the results indicate that blood may be a reasonable index of these nuclides in the body. (auth)

**55118** URINARY EXCRETION OF $^{241}Am$ UNDER DTPA THERAPY. Fasiska, Barbara C. (Univ. of Pittsburgh); Bohning, D. E.; Brodsky, A.; Horm, J. Health Phys.; 21: No. 4, 523-9(Oct 1971).

Over 2.5 yr of complete urinary excretion data now indicate the continued effectiveness of DTPA in removing americium originally inhaled in oxide form. This interim report presents a summary of the urinary excretion data, together with a description of a method using the principle of maximum likelihood to attempt a fit of the Healy two-compartment model to the first year of urinary data. The result indicates that a two-compartment model would be insufficient for even an empirical description of the urinary excretion curve in the present case. (auth)

**55119** SUBCELLULAR DISTRIBUTION OF RADIOACTIVITY IN NEURONAL AND GLIAL-ENRICHED FRACTIONS AFTER INCORPORATION OF [$^3$H]LEUCINE IN VIVO AND IN VITRO. Hamberger, A.; Blomstrand, C.; Yanagihara, T. (Univ. of Goteborg). J. Neurochem.; 18: No. 8, 1469-78(Aug 1971).

The distribution of protein-bound radioactivity among subcellular organelles of cerebral cortex was followed after intravenous administration of [$^3$H]leucine and after incubation of brain slices in the presence of [$^3$H]leucine. Neuronal and glial cell-enriched fractions were prepared by discontinuous sucrose–Ficoll gradient centrifugation of cerebral cortex cell suspensions. Subcellular fractions were obtained from each of the cell preparations and the protein-bound radioactivity determined after in vivo and in vitro incorporation of [$^3$H]leucine. The unfractionated neuronal material had a considerably higher level of protein-bound radioactivity than the glial material. The most marked neuronal–glial differences were observed in microsomes and soluble proteins, while the radioactive labelling of the nuclear and mitochondrial fractions was similar for the two cell types. (auth)

**55120** UPTAKE AND RELEASE OF $^{45}Ca$ BY BRAIN MICROSOMES, SYNAPTOSOMES, AND SYNAPTIC VESICLES. Diamond, I. (Univ. of California, San Francisco); Goldberg, A. L. J. Neurochem.; 18: No. 8, 1419-31(Aug 1971).

Microsomes and synaptosomes from rat brain accumulated $^{45}Ca$ against a concentration gradient by an ATP-dependent process. Calcium accumulation occurred to the same extent in microsomes prepared from white matter and from grey matter, an observation suggesting that calcium uptake may be in part an activity of the axonal membrane. Microsomes and synaptosomes accumulated

XUM

calcium to a similar extent but less actively than mitochondria. By contrast, synaptic vesicles showed relatively little calcium accumulation. Isotopic concentrations of sucrose, NaCl, KCl and choline chloride inhibited calcium accumulation, with NaCl and KCl the least effective of these inhibitory agents. No consistent effects on calcium uptake were obtained with adenosine 3′,5′-monophosphate, dibutyryl cyclic AMP or the methyl xanthines. Incubation of prelabelled microsomes resulted in a release of $^{45}Ca$, and ATP inhibited this release process. In the absence of added ATP, isotonic NaCl promoted calcium release to a significantly greater extent than KCl choline chloride or sucrose. In the presence of ATP, these agents all promoted a similar degree of release. Adenosine 3′,5′-monophosphate or agents that affect its metabolism did not significantly affect calcium release. Magnesium ions reduced calcium release under all conditions tested. (auth)

**55121** RESPIRATION OF BRAIN SLICES IN HEAVY WATER. Ebstein, B. S.; Samuel, D. (Weizmann Inst. of Science, Rehovot, Israel). J. Neurochem.; 18: No. 8, 1597-8(Aug 1971).

There was a decrease in the respiratory rate of slices of rat brain with increase in $D_2O$ concentration. This decrease was significant when the $D_2O$ concentration was greater than 15%. The same decrease in respiratory rate was obtained by measuring $^{14}Co_2$ production instead of $O_2$ consumption, and similar ones were also obtained when the brain slice thickness was varied. Preliminary observations in experiments with $^{14}C$ in which the amount of tissue per flash was varied, suggested that the effect of $D_2O$ on respiration was dependent of the ratio of tissue mass to the amount of Krebs–Ringer-phosphate medium. (UK)

**55122** GLOMERULAR FILTRATION RATE DETERMINED BY $^{51}Cr$-EDTA. Ditzel, Joern; Vestergaard, Per; Brinkloev, Morten. Nord. Med.; 85: No. 21, 650-3(1971). (In Swedish).

Measurements of the glomerular filtration rate (GFR) in 20 patients with normal and impaired renal function using single injection of the indicator substance $^{51}Cr$-EDTA revealed an accurate correlation to the classical method of continuous inulin infusion are described. The calculations showed that the plasma disappearance curve of the indicator substance, on which the mathematical calculation of the clearance is based, may be drawn from only four plasma activity measurements when the study period extends over at least four hours. This affords a practical, simple, and reproducible clinical method for determining the GFR. (auth)

**55123** HEPATIC BLOOD FLOW IN DOGS MEASURED BY $^{133}Xe$ CLEARANCE TECHNIQUE. Danielson, B. G.; Karlmark, B. (Uppsala Univ.). Acta Soc. Med. Upsal.; 75: No. 3-4, 171-80(1970).

The $^{133}X$ clearance technique after intraportal injection was used to study liver blood flow in dogs. The wash-out curves were analysed and found to have a biexponential or sometimes a monoexponential appearance. The half-times of the two components were determined as well as the half-times of the initial slope. The half-times of the initial slopes were significantly greater than the corresponding values of the fast component. As there are reasons to believe that the slow component represents extrahepatic activity it seemed more correct to calculate the blood flow from the fast component of the wash-out curve. Liver blood flow rates were about 80 ml/min · 100 g liver in anaesthetized dogs after intraportal injections of $^{133}Xe$, as calculated from the fast components. (auth)

**55124** RETENTION AND EXCRETION BY PIGS OF RADIONUCLIDES PRODUCED BY THE PLOWSHARE EVENT SCHOONER. Chertok, Robert J.; Lake, Suzanne (Univ. of California, Livermore). pp 475-6 of Health Physics Aspects of Nuclear Facility Siting. Vol. II. /Voilleque, Paul G. (comp.). Idaho Falls, Idaho; Burton R. Baldwin, Publications Chairman (1971).

From fifth annual midyear topical symposium on health physics aspects of nuclear facility siting; Idaho Falls, Idaho (3 Nov 1970).

In order to determine the whole-body retention and excretion of radioisotopes produced by the Schooner Event, peccaries were given daily doses of debris from the event by ingestion. Data on the whole-body retention and excretion (as % of initial dose) are presented in tabular form. (E.R.B.)

**55125** RELATIVE HAZARDS FROM $^{95}Zr$ AND $^{95}Nb$ BASED UPON INHALATION OF PARTICLES FORMED UNDER VARIOUS THERMAL CONDITIONS. Thomas, R. G.; Walker, S. A.; McClellan, R. O. (Lovelace Foundation for Medical Education and Research, Albuquerque, N. Mex.). Contract AT(29-1)-1013. pp 578-89 of Health Physics Aspects of Nuclear Facility Siting. Vol. III. /Voilleque, Paul G. (comp.). Idaho Falls, Idaho; Burton R. Baldwin, Publications Chairman (1971).

From fifth annual midyear topical symposium on health physics aspects of nuclear facility siting; Idaho Falls, Idaho (3 Nov 1970).

Inhalation exposure is a common route of potential entry into the body for radionuclides released in nuclear industry accidents. This paper reports a study with mice exposed via inhalation that emphasizes the importance of physical-chemical forms (as influenced by heat treatment) of aerosols on their behavior within the body and the subsequent radiation dose. Aerosol droplets containing a near-equilibrium mixture of $^{95}Zr$ and $^{95}Nb$ in oxalic acid were passed through a heating column at 100, 250, 600, or 1100°C, respectively, producing particles of various chemical forms to which mice were then exposed (particle size about 1.6 μm activity median aerodynamic diameter). The mice were routinely whole-body counted and measurements were made to determine the ratio of $^{95}Nb$ to $^{95}Zr$ in the live animals and in certain organs following sacrifice. At the two highest temperatures, the inhaled and deposited particles were retained tenaciously in the lung and maintained the initial solution $^{95}Nb/^{95}Zr$ ratio of approximately 1.9. At 100°C, the radionuclide was translocated from lung to skeleton, with a ratio of 1.3, indicative of an excess burden of $^{95}Zr$. At 250°C, the pattern was similar but less pronounced. The differential patterns of retention resulted in significant differences in radiation dose pattern; at the lowest temperature the highest radiation doses were received by skeleton, lung, and liver, while the higher temperature aerosol exposures resulted in the radiation dose being delivered almost exclusively to lung. (auth)

## *Radiation Effects*

*Refer also to abstracts 54636, 55351, and 55353.*

**55126** IN VITRO UPTAKE OF MODEL AMINO ACIDS BY RAT LIVER FOLLOWING WHOLE-BODY γ-IRRADIATION. Yang, Kuopao; Neuhaus, Otto W. (Univ. of South Dakota, Vermillion). Contract AT(11-1)-1754. Radiat. Res.; 47: No. 2, 500-10(Aug 1971).

Previous in vivo studies demonstrated a stimulated hepatic capture of α-aminoisobutyric acid (AIB) following exposure of rats to whole-body γ irradiation. This observation has been confirmed by the present in vitro studies using liver slices for the study of amino acid uptake. AIB accumulated inside the cell against a concentration gradient which required an endogenous source of energy. This transport mechanism was observed to be $Na^+$ and $K^+$-dependent and sensitive to ouabain. Protein synthesis was needed for the stimulated AIB transport. The radiation-induced stimulation of hepatic amino acid capture was also observed with a second model amino acid, cycloleucine. However, it still remains to be established if these observations are generally applicable to the hepatic uptake of natural amino acids. (auth)

**55127** INITIAL EFFECT OF X RADIATION ON THYMIDINE INCORPORATION INTO DNA IN THYMUS CELLS. Myers, D. K. (Chalk River Nuclear Labs., Ont.). Radiat. Res.; 47: No. 3, 731-40(Sep 1971).

The initial effects of x radiation on thymidine incorporation into DNA in rat thymocytes in vitro were highly dependent upon the incubation medium used. In general, media that promote chromatin condensation tended to increase the apparent radiosensitivity of thymidine incorporation. The effect of low radiation doses could be altered from inhibition to stimulation of thymidine incorporation simply by altering $Na^+$ concentration or pH. The radiosensitivity of protein and RNA synthesis was not appreciably affected under these conditions. The addition of nicotinamide, caffeine, and related compounds after x irradiation protected the thymus cells against the initial effects of high doses of x radiation on nucleic acid synthesis and also retarded the degeneration that occurs during more prolonged incubation of the irradiated cells. It seems probable that three processes affecting thymidine incorporation into DNA are evoked by x irradiation of thymus cells: two distinct and counteracting processes are probably involved in the initial effects of low doses, while the third deleterious process is initially evident only at much higher doses and can be delayed by nicotinamide or caffeine. (auth)

**55128** EFFECT OF IONIZING RADIATION ON THE SUCCINATE DEHYDROGENASE ACTIVITY OF RAT LIVER. Jordana, R.; Lamsfus, Carmen (Univ. of Navarra, Pamplona, Spain). Rev. Espan. Fisiol.; 27: No. 2, 163-4(Jun 1971).

Rat liver slices were x-irradiated and divided into two groups. In the first group, the tissue was homogenized and the succinate dehydrogenase activity was measured immediately following irradiation. In the second group, the irradiated tissue slices were incubated for three hours, then homogenized and the succinate dehydrogenase activity measured. In the first experiment the enzyme activity was not affected, but the activity was inhibited in the second experiment. The relationship of the results to changes in the struc-

XUM

ture and permeability of mitochondrial membranes is discussed. (H.L.W.)

**55129** RADIATION EFFECTS ON MACROMOLECULAR SYNTHESIS IN CONTACT INHIBITION-SENSITIVE CELLS SYNCHRONIZED BY MEDIUM CHANGE. Yoshikura, H. (Faculte des Sciences, Orsay, France). Radiat. Res.; 47: No. 2, 548-61(Aug 1971).

A cell line originating from the kidney tissue of a newborn C3H/He mouse (C3H2K cell line) was sensitive to contact inhibition of cell growth. After renewal of culture medium, the cells in the stationary phase divided in a synchronized fashion. Immediately after medium change, there was a stimulation of RNA synthesis followed by a stimulation of protein synthesis. The conclusions obtained by studying radiation effects on the macromolecular synthesis in this synchronized culture were as follows: Both ultraviolet light (uv) and $\gamma$ rays inhibited DNA synthesis more strongly when applied before the onset of DNA synthesis than when applied during the DNA synthesis. Irradiation by uv immediately inhibited RNA synthesis stimulated by medium change. Protein synthesis which followed RNA synthesis was more strongly inhibited when the cells were irradiated before induction of RNA synthesis than after induction of RNA synthesis. On the contrary, to $\gamma$ rays, dose response of $^3$H-uridine incorporation was bimodal, and protein synthesis remained unaffected up to an exposure as high as 25 kR. (auth)

**55130** CRYSTAL STRUCTURE DEPENENCE OF RADIATION-INDUCED RADICALS IN THYMINE: AN ESR STUDY. Dulcic, Antonije; Herak, Janko N. (Institute Rudjer Boskovic, Zagreb). Radiat. Res.; 47: No. 3, 573-80(Sep 1971).

Electron spin resonance spectroscopy was used to investigate radiation damage in single crystals of thymine. The 5-thymyl radicals were observed in thymine monohydrate as well as in thymine anhydrate, demonstrating that thymine molecules are donors as well as acceptors of hydrogen atoms. A detailed analysis of the 5-thymyl radicals in both of these crystal systems was done. No difference in either electronic structure or conformation of the radical in the two crystals was observed. Another radical species present was not analyzed. (auth)

**55131** FACTORS AFFECTING THE RATE OF HYDRATED ELECTRON ATTACK ON POLYNUCLEOTIDES. Shragge, P. C.; Michaels, H. B.; Hunt, J. W. (Univ. of Toronto). Radiat. Res.; 47: No. 3, 598-611(Sep 1971).

The rate constants for the attack of $e^-_{aq}$ on adenine, cytosine, and several derivatives were measured in the pH range 6 to 14. The rate constants at neutral pH are $0.9 \times 10^{10}$ $M^{-1}s^{-1}$ and $1.3 \times 10^{10}$ $M^{-1}s^{-1}$ for adenine and cytosine, respectively. The rate constants, per base, for the attack of $e^-_{aq}$ on polynucleotides are much lower. At pH 7 they are $7.5 \times 10^8$ $M^{-1}s^{-1}$, $2.5 \times 10^8$ $M^{-1}s^{-1}$, and $1.3 \times 10^8$ $M^{-1}s^{-1}$ for poly U, poly A, and poly (A + U), respectively. It is shown that the low overall reactivity of polynucleotides results from a lowered collision frequency with $e^-_{aq}$. Secondary structure is an important factor, responsible for the observed differences in the values of the rate constants for the polynucleotides studied. Poly (A + U), which has a double helical structure, is least reactive, and poly U, an unstacked random coil, is most reactive. The inherent reactivity of bases in a polynucleotide also determines the rate constant to some extent. (auth)

**55132** RATE CONSTANTS FOR REACTION OF HYDROGEN ATOMS WITH COMPOUNDS OF BIOCHEMICAL INTEREST. Neta, P.; Schuler, Robert H. (Carnegie-Mellon Univ., Pittsburgh). Radiat. Res.; 47: No. 3, 612-27(Sep 1971).

The rate constants for the reaction of hydrogen atoms with a large number of amino acids, hydroxy acids, sugars, purines, pyrimidines, sulfur-containing compounds, and related substances were determined in aqueous solution at pH 1 by an in situ radiolysis steady-state ESR method. These rate constants vary from $<10^5$ $M^{-1}$ $sec^{-1}$ for urea, glycine, and acetic acid to about $5 \times 10^9$ $M^{-1}$ $sec^{-1}$ for the sulfur-containing compounds. The patterns of reactivity are discussed in some detail and in particular the strong deactivating effect of the $NH_3^+$ group on hydrogen atoms in the $\alpha$, $\beta$, and even $\gamma$ positions of the aliphatic compounds is noted. The OH group is shown to activate the hydrogen atoms on the same carbon atom but deactivate those in the $\beta$ position. The carboxyl group produces a small deactivating influence on adjacent hydrogen atoms. In general the amino acids react with hydrogen atoms one to two orders of magnitude more slowly than do the hydrocarbons of the same skeletal structure. The pyrimidine bases and other nitrogen heterocycles similarly exhibit rate constants (about $10^8$ $M^{-1}$ $sec^{-1}$) that are an order of magnitude less than those for the related aromatic substances. The high reactivity of the sulfur-containing compounds relative to their oxygenated analogs demonstrates that the H atom attack occurs directly at the site of the sulfur atom. Sufficient rate information is now available that generalizations can be given from which it is possible to make reasonable predictions of the rate constants for reaction of H atoms with most organic substances. (auth)

**55133** RADIATION-INDUCED SINGLE-STRAND BREAKS IN DOUBLE-STRANDED CIRCULAR DNA. Kessler, B.; Bopp, A.; Hagen, U. (Inst. fuer Strahlenbiologie, Karlsruhe, Ger.). Int. J. Radiat. Biol.; 20: No. 1, 75-8(1971).

Supertwisted SV40 DNA was $\gamma$ irradiated in dilute aqueous solution (21 $\mu$g/ml) in the dry state, and single strand breaks subsequently measured in neutral and alkaline solutions by band sedimentation. Dose-effect curves are presented from 0 to 650 rads. The occurrence of alkali induced single strand breaks in DNA was confirmed in dilute solution, but no enhancement of chain breakage could be seen in the dry state after alkali treatment. (UK)

**55134** VOPROSY RADIOBIOLOGII. (Problems in Radiobiology). Rokitskii, P. F. (ed.). Minsk; Izdatel'stvo Bgu im. V. I. Lenina (1969). 240p.

A collection of papers is presented that was under discussion at a meeting of radiobiologists at Minsk in June 1967. About two-thirds of the papers are grouped under the topic heading "radiation biochemistry and physiology," and include such subjects as x- and neutron radiation effects on protein metabolism in the brain and liver, and the effects of ionizing radiation on corticosteroid levels, serotonin content in tissues, and glutamic acid metabolism. In connection with radiation sickness, the protective action of DNA, experimental therapy, and the combined effects of thermal burns and radiation are considered. The remainder of the papers are collectively described as "radiation genetics," and is concerned with the genetic effects of slow protons, intermediate neutrons, high energy radiation, induced mutation in Drosophila by gamma radiation, and the biological effects of nuclear collisions. Each of the 38 papers has its own bibliography. (K.S.W.)

**55135** $\gamma$ IRRADIATION OF DDT: RADIATION PRODUCTS AND THEIR TOXICITY. Kimbrough, Raymond D. Jr. (Georgia Inst. of Tech., Atlanta); Gaines, Thomas B. J. Agr. Food Chem.; 19: No. 5, 1037-8(Sep-Oct 1971).

The irradiation products found were what would be expected. The DDT is fairly resistant to ionizing irradiation. The only product formed in appreciable quantity was hydrogen, which presumably arose primarily from the action of the radiation on the alkyl tails of the tristearin. The G value obtained for hydrogen, 5.7, is in the same region as that for the $\gamma$ irradiation of alkanes, 5.55 and 5.85. This figure cannot be compared to the G-value of 1.01 for hydrogen production in the irradiation of methyl oleate because the olefinic linkage in methyl oleate which is particularly susceptible to reaction on irradiation is not present in the tristearin used here. The $LD_{50}$ values of the irradiated DDT, 271 to 378 mg/kg, and of the nonirradiated DDT, 263 to 354 mg/kg, are the same within experimental error. Hence it may be concluded that the irradiation of technical DDT had no effect upon its acute oral toxicity in adult female rats. (auth)

**55136** PHYSICAL, CHEMICAL, AND MOLECULAR BIOLOGICAL PROCESSES IN ULTRAVIOLET IRRADIATION OF BIOLOGICAL OBJECTS. Fahr, Egon (Univ., Wuerzburg, Ger.). Strahlentherapie; 141: No. 6, 718-27(Jun 1971). (In German).

Ultraviolet irradiation of nucleic acids leads to the following primary processes: stimulation of singlet- and triplet-conditions and formation of excimers. The latter imply the photochemical formation of cyclobutane-dimers and the addition of water into the 5,6-double bond of the cytosine or uracil to 6-hydroxy-dihydropyrimidine derivatives. Furthermore, irradiation products with a characteristic absorption maximum around 320 nm, changes of the secondary structure of the nucleic acids as well as inner- and intermolecular main valency bindings between nucleic acid chains were observed. Bindings of main valencies between nucleic acids and protein during ultraviolet irradiation of biological objects likewise have to be considered. The photochemical formation of cyclobutane-dimers causes the inhibition of DNA reduplication. It permits the molecular biological explanation of the reactivation of ultraviolet-injured microorganisms through short-wave radiation, in the way of enzymatic or dark-reactivation or as photoreactivation. The water addition into the cytosine portion of the DNA presumably triggers mutations caused by ultraviolet radiation. The formation of cyclobutane-dimers also takes place during ultraviolet irradiation of the human skin. (auth)

**55137** ULTRAVIOLET LIGHT-INDUCED CHANGES IN RIBONUCLEASE CONFORMATION. Aktipis, Stelios; Iammartino,

XUM

Albert J. (Loyola Univ., Maywood, Ill.). Biochem. Biophys. Res. Commun.; 44: No. 4, 918-24(20 Aug 1971).

Ultraviolet light-induced inactivation of RNase A is accompanied by a decrease in the circular dichroism (CD) at the extrema observed at 239 nm and 275 nm. As inactivation progresses a new CD band centered near 325 nm also develops. For RNase maintaining up to one half of its original activity, an isoelliptic point may be noted near 257 nm. These findings are consistent with initial normalization of a buried tyrosyl residue followed by chemical modification of the protein. Further chemical change and extensive conformational reorganization of the protein appear to accompany advanced inactivation. (auth)

55138 SIZE AND LOCATION OF RIBOSOMAL RNA SEGMENTS IN RIBOSOMAL PRECURSOR RNA OF YEAST. Van den Bos, R. C.; Retel, J.; Planta, R. J. (Vrije Univ., Amsterdam). Biochim. Biophys. Acta; 232: 494-508(Mar 1971).

The order of the different segments of the 42-S ribosomal precursor RNA of yeast was investigated. For that purpose first the lengths of the rRNA stretches were measured. These were inferred from the relative amounts of oligonucleotides present in complete pancreatic ribonuclease digests of the two large rRNA components, and in this way were found to be 1600 and 3200 nucleotides, respectively. Next the influence of ultraviolet irradiation on the synthesis of both rRNA components in yeast cells was determined. It was found that the synthesis of 26-S rRNA is about 1.65 times more sensitive to ultraviolet damage of the DNA than the synthesis of 17-S rRNA. On the basis of these data the construction of the 42-S ribosomal precursor RNA was derived. (auth)

55139 X-RADIOLYSIS OF AQUEOUS ERYTHROSIN. Chrysochoos, John; Shihabi, David S. (Univ. of Toledo). Radiat. Res.; 47: No. 2, 392-401(Aug 1971).

X-radiolysis of aqueous erythrosin (2',4',5',7'-tetraiodofluorescein) under reducing conditions (complete removal of OH radicals) has given rise to dye-bleaching and formation of leucoerythrosin, due to reactions of erythrosin with $e^-_{(aq)}$ and H atoms. The reaction rate constant between erythrosin and H atoms was found to be $4.4 \times 10^9$ $M^{-1}$ $sec^{-1}$. Scavenging of OH radicals with formate, and subsequent reactions of erythrosin with the formate radical ion, $CO_2^-$, give rise to both semireduced dye and dehalogenation of the dye in an approximate ratio of 1 : 2. Radiolysis of erythrosin under oxidizing conditions gives rise to products whose absorption spectra overlap strongly with the absorption spectra of erythrosin. Under these conditions, the true dye-bleaching cannot be determined. The apparent dye-bleaching is very low. Apparent and true values of dye-bleaching under various conditions are being discussed. (auth)

55140 ACTIVITY OF HEXOKINASE IN THE ERYTHROCYTES, LIVER, AND BRAIN OF NORMAL, X-IRRADIATED, GUERIN-TUMOR-BEARING RATS, AND RATS WITH CYANIDE-INDUCED CHRONIC HYPOXIA. Cernatescu, C.; Trandafirescu, M.; Haulica, A. Fiziol. Norm. Patol. (Bucharest); 17: No. 1, 85-90 (1971).

Chronic administration of KCN produced a state of metabolic hypoxia in rats. In the treated animals an increase was noted in the glycolytic capacity of the red blood cells. A similar increase was observed in Guérin tumor-bearing animals. The activity of hexokinase, an enzyme regulating cellular glycolysis, increases in the red blood cells and liver of both tumor-bearing animals and those with KCN-induced hypoxia. A parallel is drawn between the hypothesis of O. Warburg on hypoxia as a primary cause of malignant transformation and the results obtained by the authors, which opens up a new route of investigation. (Rom. Sci. Abstr.)

## Immunology

*Refer also to abstracts 55267 and 55292.*

55141 RADIOIMMUNOASSAY OF PLASMA ANGIOTENSIN II IN PATIENTS WITH HYPERTENSION, IN RENAL TRANSPLANT RECIPIENTS, AND IN ANEPHRIC PATIENTS. Fyhrquist, F. (Minerva Foundation Inst. for Medical Research, Finland). Ann. Acad. Sci. Fenn., Ser. A IV; No. 39, 1-52(1971).

A modified radioimmunoassay for human plasma angiotensin II is reported. This method was applied to clinical studies on 75 hospitalized patients. Significantly higher peripheral venous plasma angiotensin II levels, both at recumbency and after 2 hours of upright posture and 20 mg of furosemide i.m., were obtained in malignant hypertension and hypertension associated with renal parenchymal or renal artery diseases, when compared with controls and patients with essential hypertension. The patients with primary aldosteronism had suppressed venous plasma angiotensin II values both at recumbency and after upright posture and furosemide. In renal transplant recipients venous plasma angiotensin II increased significantly in response to upright posture and furosemide. During renal transplantation a peak of peripheral venous plasma angiotensin II was observed within 1 minute after revascularization of the transplant. Peripheral venous plasma angiotensin II was undetectable in anephric patients. Considerably raised plasma angiotensin II values were observed in the renal vein of the affected kidney in hypertensive patients with unilateral renal parenchymal diseases or renal artery lesions. In essential hypertension almost equal plasma angiotensin II values were obtained from both renal veins. (auth)

55142 RADIOIMMUNOASSAY OF ARGININE VASOPRESSIN IN HUMAN PLASMA. Beardwell, C. G. (Univ. of Manchester, Eng.). J. Clin. Endocrinol. Metab.; 33: No. 2, 254-60(Aug 1971).

A sensitive double-antibody radioimmunoassay for the measurement of arginine vasopressin (AVP) in plasma is described. Vasopressin has been extracted from plasma by adsorption to Florisil followed by elution with acid-acetone. Assay of serial dilutions of such extracts shows that they behave in the assay system in the same way as synthetic AVP standards. Recovery of added vasopressin from plasma averaged 45.7 ± 8.1% (SD). Plasma AVP concentration (uncorrected for recovery) in mildly dehydrated subjects ranged from less than 1 to 4.3 pg/ml, and showed a good correlation with plasma osmolality. After nicotine, concentrations up to 21.8 pg/ml were found, and in 4 subjects with the syndrome of inappropriate ADH secretion levels ranged from 24.0 to 102.1 pg/ml. (auth)

55143 CLASSIC BIOASSAY STATISTICAL PROCEDURES APPLIED TO RADIOIMMUNOASSAY OF BOVINE THYROTROPIN, GROWTH HORMONE AND PROLACTIN. Vivian, Stanley R.; LaBella, Frank S. (Univ. of Manitoba, Winnipeg). J. Clin. Endocrinol. Metab.; 33: No. 2, 225-33(Aug 1971).

A double antibody radioimmunoassay (RIA) was used to determine bovine thyrotropin, growth hormone and prolactin in anterior pituitary incubation medium. Each particular assay was found to be specific for the respective hormone only, except for a controllable LH cross reactivity in the assay for TSH. As an integral part of the RIA, classic bioassay statistical procedures for estimates of potency with their confidence limits were applied. The validity of applying the statistical procedures to RIA was verified by considering a number of samples of known potency as unknowns, assaying them, and observing that about the right proportion of the confidence limits from these "known unknowns" contained their true potencies. A test of parallelism between the slopes of unknown and standard dose response curves was used as an operational specificity criterion. (auth)

55144 RADIOIMMUNOASSAY OF THE F PROSTAGLANDINS. Caldwell, Burton V.; Burstein, Sumner; Brock, William A.; Speroff, Leon (Yale Univ., New Haven). J. Clin. Endocrinol. Metab.; 33: No. 2, 171-5(Aug 1971).

Antibodies to prostaglandin $F_{2\alpha}$ ($PGF_{2\alpha}$) were produced in rabbits immunized with a conjugate of $PGF_{2\alpha}$ covalently linked to bovine serum albumin (BSA) by reaction with carbodiimide reagent. A radioimmunoassay was developed using dextran-coated charcoal to separate the free from antibody-bound $PGF_{2\alpha}$-$^3H$. The sensitivity of the method was about 100 pg. Butanol was used for extraction of plasma and the various classes of prostaglandins were separated on a small silicic acid column. Recovery of $PGF_{2\alpha}$-$^3H$ through the extraction and separation procedures was 75 to 85%. Equilibration of $PGF_{1\alpha}$, $PGE_2$, $PGE_1$, $PGA_2$ and $PGB_1$ with antiserum and $PGF_{2\alpha}$-$^3H$ showed a progressive loss of ability to displace the labeled prostaglandin from the antibodies related to the degree of differences in molecular configuration from the hapten used in the immunization. The method should be sufficiently sensitive, precise, and simple to allow its use in the routine estimation of the F prostaglandins from biological samples. (auth)

55145 MATHEMATICAL ANALYSIS OF KINETICS OF RADIOLIGAND ASSAYS: IMPROVED SENSITIVITY OBTAINED BY DELAYED ADDITION OF LABELED LIGAND. Rodbard, David (National Institutes of Health, Bethesda, Md.); Ruder, H. J.; Vaitukaitis, J.; Jacobs, H. S. J. Clin. Endocrinol. Metab.; 33: No. 2, 343-55(Aug 1971).

A theoretical analysis of the transient state (kinetics) of radioligand assay systems leads to a system of 5 first order, nonlinear differential equations and 3 equations for conservation of mass. Numerical solution to these equations makes it possible to predict the position of the standard curve for radioimmunoassays (RIA) and radioligand assays (RLA) as a function of time under a variety of boundary conditions. Three special cases have been considered: (a) Labeled antigen, unlabeled antigen, and antibody or binding protein are added simultaneously; (b) unlabeled antigen and anti-

XUM

body react to equilibrium in a preincubation, and then labeled antigen is added; and (c) labeled antigen and antibody react until equilibrium is reached and then unlabeled antigen is added. This kinetic analysis, aided by computer simulation studies, demonstrates that improved sensitivity can be achieved by delayed addition of labeled antigen (case b, above), providing a theoretical basis for the improved sensitivity of nonequilibrium assays. This analysis also indicates that the order of addition of reagents and/or failure to reach equilibrium may be an important source of variability (scatter around the standard curve) and loss of precision. The present theory also makes it possible to study the effect of nonequilibrium on the apparent Scatchard plot, affinity constant and binding capacity. The major predictions of this model have been validated using the uterine cytosol binding assay for estradiol, and RIAs for human growth hormone and human luteinizing hormone. A computer program has been developed for numerical evaluation of the per cent bound (or any other response variable) as a function of time for any specified equilibrium constant, and concentrations of labeled hormone, unlabeled hormone, and antibody. (auth)

**55146** RADIOMMUNOASSAY OF TRIIODOTHYRONINE IN UNEXTRACTED HUMAN SERUM. Mitsuma, Terunori; Gershengorn, Marvin; Colucci, John; Hollander, Charles S. (New York Univ., N. Y.). J. Clin. Endocrinol. Metab.; 33: No. 2, 364-7(Aug 1971).

L-3,5,3′-triiodothyronine ($T_3$) was measured by a radioimmunoassay the special features of which permit determinations in unextracted serum. These include the use of tetrachlorthyronine which appears to inhibit the binding of $T_3$ to thyroxine binding globulin but does not affect the binding of $T_3$ to antibody and utilization of a $T_3$-free serum prepared in vitro for the construction of a serum standard curve. Mean $T_3$ levels were 60 ng% in hypothyroidism, 139 ng% in normal subjects, and 587 ng% in hyperthyroidism. (auth)

**55147** RECOVERY OF THE ANTIGEN RETENTION MECHANISM AFTER SUBLETHAL X-IRRADIATION IN MICE RECEIVING CELLS FROM VARIOUS SOURCES. Nettesheim, P.; Hammons, Anna S. (Oak Ridge National Lab., Tenn.). J. Immunol.; 107: No. 2, 518-25(Aug 1971).

The intravenous injection of spleen or peritoneal exudate cells into mice x-irradiated with 600 R leads to rapid partial restoration of the x-ray damaged antigen retention system. This effect was already clearly discernible when $^{125}$I-AHGG was injected 1 day after cell infusion, and became very pronounced when the labeled antigen was given 8 days after cell infusion. In contrast, no significant recovery was observed in mice receiving either thymus cells, bone marrow cells or no cells after x-irradiation. The cell doses were approximately equivalent to one-third spleen, one thymus, one femur and the peritoneal cavity cells recoverable from one mouse. The weight, histologic and autoradiographic studies suggest that spleen and peritoneal exudate cell suspensions contain cells (or their precursors) instrumental in recovery of (and probably also in unimpaired) follicular antigen localization. Further studies are needed to determine the nature of the cells involved and precisely what role they play in the enhancement of recovery of antigen localization after x-irradiation. (auth)

**55148** APPLICATION OF γ IRRADIATED HETEROGENIC BOVINE FASCIA IN THE FILLING OF BRAIN DURA DEFECTS IN DOGS. Czochra, M.; Misiuna, P.; Chibowski, D.; Kaminski, S. Neurol., Neurochir, Psychiat. Pol.; 4: No. 6, 693-8(Nov–Dec 1970). (In Polish).

Heterogenic transplants of bovine fascia that were irradiated with gamma rays were performed in 10 dogs for the purpose of filling a defect of the brain dura mater. The histopathological results in the period from 3 weeks to 12 months are discussed. It was concluded that heterogenic fascia can be successfully employed in the covering of dura mater defects in humans. (auth)

# Ecology

*Refer also to abstracts 54753, 54754, 5[illegible]7, and 57098.*

**55149** (BNWL-SA-4048) INFLUENCE OF THE PHYSICO-CHEMICAL FORMS OF RADIONUCLIDES AND STABLE TRACE ELEMENTS IN SEAWATER IN RELATION TO UPTAKE BY THE MARINE BIOSPHERE. Robertson, D. E. (Battelle Pacific Northwest Labs., Richland, Wash.). 8 Sep 1971. Contract AT(45-1)-1830. 60p. Dep. NTIS.

The following sources of radioactivity in the oceans are discussed: atmospheric fallout from nuclear weapons testing; discharges from nuclear processing plants; discharges from power reactors; and releases from nuclear powered ships. Physico-chemical species of radionuclides and trace elements in the oceans are classified into three categories: species in true solution, colloidal species, and particulate forms. Important artificial radionuclides in the marine environment are discussed with emphasis on those with long half-lives such as $^{137}$Cs and $^{90}$Sr. It is pointed out that neutron activation products of biologically essential transition elements are important radionuclides in the marine environment because they are accumulated to a very high degree by the biosphere. The most predominant activation products observed in effluents from nuclear power reactors include $^{55}$Fe, $^{65}$Zn, $^{60}$Co, and $^{54}$Mn. A discussion is presented of factors necessary for predicting the dispersion of long-lived radionuclides through the marine food chain. These factors are the stable element chemistry of organisms constituting the links in the marine food chain and the specific activity ratio of the element at the source of its entry into the food chain. Case studies of the influence of physico-chemical forms of radionuclides and trace elements in relation to biological uptake are described and the role of physico-chemical speciation of $^{55}$Fe and stable iron in relation to biological assimilation by marine organisms is discussed. The behavior of $^{65}$Zn, $^{106}$Ru, $^{238}$Pu, $^{239}$Pu, and $^{240}$Pu is also discussed. (H.L.W.)

**55150** (CONF-710401–, pp 407-10) PLUTONIUM MOVEMENT IN AQUATIC SYSTEMS: A REVIEW. Paine, D.; Johnson, J. E.; Watters, R. L. (Colorado State Univ., Fort Collins. Dept. of Radiology and Radiation Biology). 16 Apr 1971.

From Rocky Flats symposium on safety in plutonium handling facilities; Golden, Colo. (13 Apr 1971).

Two marine studies, specific to Pu movement and distribution, are reviewed, as well as the current study now being conducted at Colorado State University on the Rocky Flats environs. The two studies are Pillai, Smith, and Folsoms' "Pu in the Marine Environment" published in Nature, Aug. 1964 and Aarkrog's "Radioecological Investigations of Pu in an Arctic Marine Environment" published in Health Physics, Jan. 1971. Measurements proposed for the Rocky Flats study are mentioned. (P.C.H.)

**55151** (CONF-710817–1) CONCENTRATIONS OF PLUTONIUM, COBALT, AND SILVER RADIONUCLIDES IN SELECTED PACIFIC SEAWEEDS. Wong, K. M.; Hodge, V. F.; Folsom, T. R. (Scripps Institution of Oceanography, La Jolla, Calif.). [1971]. 11p. Dep. NTIS.

From Plutonium symposium; Los Alamos, N. Mex. (5 Aug 1971).

It was found that all species of seaweeds concentrate plutonium and that seaweeds may be a sensitive indicator for the detection of variations of plutonium concentration in the marine environment; also, further work should be done to correlate Pu concentration between seawater and algae, and that a more comprehensive survey of the marine environment is needed. By comparing samples collected near the nuclear plant with samples of the same species on other coastal collection sites no evidence of anomalous $^{239}$Pu was found near the plant, and definite evidence was found that $^{58}$Co, $^{60}$Co, and $^{110m}$Ag had been coming from the plant. By comparing different species collected near the nuclear plant, the red algae, Gelidium and Corallina, and a surf grass, Phyllospadix, accumulated higher concentrations of cobalt and silver radionuclides than did the brown algae. It is interesting to note that one species of sea hare, Aplysia californica, that is believed to prefer red algae as food also shows higher concentrations of $^{58}$Co, $^{60}$Co, and $^{110m}$Ag. Typical concentrations were: 2200, 180, 260 dpm/Kg wet sample respectively. (auth)

**55152** (IS–2658) SURVEY OF ENVIRONMENTAL RADIOACTIVITY, JANUARY 1–JUNE 30, 1971. Voss, Milo D. (Ames Lab., Iowa). Aug 1971. Contract W-7405-eng-82. 20p. Dep. NTIS.

The environmental monitoring program of the Ames Laboratory of the USAEC for the Ames Laboratory Research Reactor (ALRR) is outlined. The environmental program consists of air samples, soil, vegetation, river water, bottom sediment, precipitation, pond water, ALRR outfall, and well water samples. This report covers the period from January 1, 1971 to June 30, 1971. As soil and vegetation samples are collected later in the year (usually August) that data will be reported in the annual report. The ALRR reached full power as of 7/12/65. As of 12/31/70 the ALRR had generated 139,460 megawatt hours of heat. A total of 156,241 megawatt hours of heat has been generated as of 6/30/71. The data indicate that the ALRR has not contributed a significant amount of radioactivity to the environment in the Ames area. The conclusion is reached that radioactivity levels recorded for environmental samples represent background conditions from atmospheric fallout and naturally occurring radioactivity. (auth)

**55153** UPTAKE AND DISTRIBUTION OF $^{65}$Zn IN OYSTERS. Romeril, M. G. (Fisheries Radiobiological Lab., Lowestoft, Eng.). Mar. Biol.; 9: No. 4, 347-54(Jun 1971).

XUM

Over a period of 6 weeks in aquaria, Portuguese oysters, Crassostrea angulata, accumulate $^{65}Zn$ to a greater extent than do native Ostrea edulis, although intake rates for any particular organ in either species are quite similar. The general distribution pattern of radioactivity in the tissues is similar to that observed for stable zinc and $^{65}Zn$ in other oyster species, concentration occurring to the greatest extent in gills and mantle and least in muscle. The observed equilibrium concentrations and biological half-lives are considerably less than those measured in the natural environment, and the significance of this and its bearing on the mechanism of uptake is discussed. Cobalt and iron depress the rate of $^{65}Zn$ uptake by both oyster soft tissues and the shell. The limiting effect in soft tissues is probably due to competition for sites at the actual point of uptake. The distribution of $^{65}Zn$ in tissue subcellular fractions separated by centrifugation shows the greatest concentration of the radioisotope in the insoluble tissue components of gills, mantle and heart. Appreciable amounts of $^{65}Zn$ are associated with tissue proteins. (auth)

**55154** BIOACCUMULATION OF RADIOISOTOPES BY MICROORGANISMS IN THE SEA. Seki, Humitake (Tokyo Univ.). Nippon Kaiyo Gakkaishi; 26: No. 6, 367-72(Dec 1970). (In Japanese).

Contamination of organisms in the sea by radioactive nuclides includes adsorption, absorption, and ingestion through the digestive organs. Retention of nuclides by organisms must take into consideration the biochemical nature of nuclides, location of accumulation, turnover rate, and half-life. Phytoplankton organisms are the greatest pool for retaining radioactive isotopes in the superficial water mass. Zooplankton organisms are large individuals and, once contaminated with radioisotopes, the contamination is retained over a long period of time. The mechanism of the accumulation of various elements by microörganisms differs with the mode of the presence of such elements in the living organism. Analysis was made of the form of contamination by $^{3}H$, $^{14}C$, and $^{32}P$, which are important elements in an organism. Carbon-14 is absorbed and incorporated into phytoplankton and marine microörganisms by photosynthesis, photoreduction, and dark fixation of carbon dioxide, while $^{32}P$ is absorbed by bacteria as a phosphate. Tritium is also thought to be absorbed and incorporated. All of $^{3}H$, $^{14}C$, and $^{32}P$ are taken into the microörganisms through absorption, and less by adsorption on their surface. In the case of radioisotopes other than these biological elements, contamination through adsorption seems to be the most important. Accumulation of radioactive nuclides by Vibrio sp. in pure culture, when not forming a bacterial mass, is made through incorporation into the cells and adsorption on the cellular surface. The amount of radioactive materials enclosed in the bacterial mass is larger than that by accumulation and probably affects concentration of the isotopes. Marine microörganisms have a great tendency to form bacterial mass. Most of the isotopes incorporated into an organism undergo transition inside the suspension which forms a kind of independent ecosystem and are considered to be transported to the deep layer through food chain. (Japan)

**55155** $^{228}Ra$ IN MARINE PHYTOPLANKTON. Shannon, L. V. (Division of Sea Fisheries, Sea Point, South Africa); Cherry, R. D. Earth Planet. Sci. Lett.; 11: No. 4, 339-43(Jul 1971).

Data are given for $^{228}Ra$ in marine phytoplankton collected in the surface waters around South Africa. Phytoplankton associated with the Agulhas Current System contain $^{228}Ra$ at an average level of $7.7 \times 10^{-12}$ g/g dry material, while the average concentration in phytoplankton from other regions is lower at about $1 \times 10^{-12}$ g/g dry material. On the basis of a simple model requiring certain stated assumptions, a biological removal time of radium from the surface waters of the Agulhas Current of about one year is indicated. For the west coast and oceanic regions longer removal times (about eight years) result. These values may be atypically short, but it is nontheless clear that biological uptake of $^{228}Ra$ is a significant process and that Szabo's previously published estimate of the radium residence time in surface sea water is in need of drastic downward revision. (auth)

**55156** STRONTIUM LEVELS IN SWEDISH FISH. Bergstroem, Sug. O. W. (Aktiebolaget Atomenergi, Studsvik, Sweden). Health Phys.; 21: No. 4, 611-12(Oct 1971).

Due to a mistake in the interpretation of the primary information, a figure in a paper by the author published in the proceedings of the Health Physics Society Midyear Topical Symposium, Jan 1968 (1970) actually represents $^{90}Sr$ content in fish bone. On the other hand the illustrated reference level applies to edible parts of the fish. As a consequence, the discussion in the paper that is based on these facts loses its validity. The revised reasoning and results are presented. It is concluded that surveillance of environmental radio-strontium from nuclear plants in a fallout situation by measuring of sample organisms is inadequate and source control combined with calculations based on research data on food chains should be preferred as safer and more generally applicable. (UK)

**55157** HEALTH PHYSICS ASPECTS OF NUCLEAR FACILITY SITING. VOLUME II. Proceedings of the Fifth Annual Health Physics Society Midyear Topical Symposium, Idaho Falls, Idaho, November 3–6, 1970. Voilleque, Paul G.; Baldwin, Burton R. (comps.). Idaho Falls, Idaho; Burton R. Baldwin, Publications Chairman (1971). 288p. (CONF-701106-(Vol.2)).

Seventeen articles are included; separate abstracts were prepared for 14. Two of the articles on quantitative evaluation of environmental factors affecting population exposure near Hanford and distribution and redistribution of airborne particulates from the Schooner cratering event were previously included in NSA as 25: 6661 and 10716, respectively. The other article was on observations of diffusion rates in stable atmospheres from short duration hot puff sources. (P.C.H.)

*For abstracts of individual papers see: 54794, 54795, 55124, 55158–55161, 55200, 55238–55240, and 56978–56980*

**55158** STABLE ELEMENT AND RADIONUCLIDE RECONCENTRATION IN AQUATIC ECOSYSTEMS. I. STABLE ELEMENT EFFECTS IN THE EQUILIBRIUM SITUATION. Peterson, Harold T. Jr. (Dept. of Health, Education, and Welfare, Rockville, Md.). pp 289-328 of Health Physics Aspects of Nuclear Facility Siting. Vol. II. /Voilleque, Paul G. (comp.). Idaho Falls, Idaho; Burton R. Baldwin, Publications Chairman (1971).

From fifth annual midyear topical symposium on health physics aspects of nuclear facility siting; Idaho Falls, Idaho (3 Nov 1970).

Reconcentration by aquatic organisms of radionuclides discharged from nuclear facilities can result in an increased potential hazard to persons consuming these organisms. Knowledge of the factors that can modify the degree of reconcentration is essential to the evaluation of radionuclide discharge criteria and the design of environmental surveillance programs. The concentration of stable elements present in the environment has been shown to greatly affect radionuclide uptake by aquatic organisms. Models of radionuclide and stable element uptake and discrimination processes were developed to explain these findings. These models indicate that concentration factors applied without regard to existing stable element concentrations may be unsuitable for the assessment of uptake by aquatic ecosystems. These models also show that differences may exist between the radionuclide and the isotopic stable element as a result of the increased rate of elimination of the radioisotope from the organism due to radioactive decay. This effect may lead to a lower specific activity of the element in biota than present in the environment. Therefore, the specific activity of the element in the aquatic environment may provide an upper limit to the level that may be attained in the aquatic food chain. This condition will not be true if the stable and radioactive isotopes are not in equilibrium or if they are present in different chemical forms. If these factors are considered, the measurement of stable element concentrations in aquatic organisms and in their environment may provide a means of estimating potential reconcentration effects for isotopic radionuclides. This application indicates the importance of stable element analyses in preoperational surveillance programs for nuclear facilities. (auth)

**55159** ACCUMULATION OF RADIOCESIUM IN RAINBOW TROUT VIA A NON-FOODCHAIN PATHWAY. Gallegos, A. F.; Whicker, F. W.; Hakonson, T. E. (Colorado State Univ., Fort Collins). Contract AT(11-1)-1156. pp 477-98 of Health Physics Aspects of Nuclear Facility Siting. Vol. II. /Voilleque, Paul G. (comp.). Idaho Falls, Idaho; Burton R. Baldwin, Publications Chairman (1971).

From fifth annual midyear topical symposium on health physics aspects of nuclear facility siting; Idaho Falls, Idaho (3 Nov 1970).

Fallout $^{137}Cs$ levels in trout sampled from Colorado mountain lakes during 1966 to 1969 decreased steadily with the exception of East Twin Lake where $^{137}Cs$ levels have remained fairly constant. A series of follow-up studies on East Twin Lake led to a postulate that the rainbow trout population acquires a large fraction of its $^{137}Cs$ burden directly from bottom sediment. Calculations based on fallout $^{137}Cs$ concentrations suggest that the accumulation of this radionuclide that was observed in the trout could be achieved only if amphipods (Gammarus lacustris) and daphnia (Daphnia pulex), their major food items, were consumed daily in quantities that would amount to about 300% of the fish's body weight. The $^{137}Cs$ level, however, was such that only 0.1 g D. W. of East Twin Lake sediment would have to be consumed daily to result in the observed $^{137}Cs$ burdens in trout. Radiocesium labeled sediment from East Twin Lake injected orally into trout resulted in about 60% incorporation of the radionuclide into the soft tissue of the

XUM

fish exclusive of the GI tract over a 96-hr test period. Microscopic examination of East Twin Lake trout stomachs indicated the presence of sediment minerals, whereas ashed Gammarus samples contained no evidence of mineral residues. The cycling of radionuclides in an aquatic ecosystem, therefore, must include a complete analysis of transfer routes since a short circuit in the food chain transfer of radionuclides may alter decisions on permissible levels of radionuclide discharge. (auth)

**55160** MANMADE RADIONUCLIDES IN THE HUDSON RIVER ESTUARY. Lentsch, Jack W.; Wrenn, McDonald E.; Kneip, Theodore J.; Eisenbud, Merril (New York Univ., N. Y.). pp 499-528 of Health Physics Aspects of Nuclear Facility Siting. Vol. II. /Voilleque, Paul G. (comp.). Idaho Falls, Idaho; Burton R. Baldwin, Publications Chairman (1971).

From fifth annual midyear topical symposium on health physics aspects of nuclear facility siting; Idaho Falls, Idaho (3 Nov 1970).

As part of a large scale ecological research program, in progress since 1964, the identity, abundance, and distributions of natural, fallout, and reactor produced radionuclides in the Hudson River estuarine environment were examined. The annual rates of introduction of the most commonly detected radionuclides were estimated for the purpose of placing the importance of the various artificial and natural sources in perspective, and explaining the measured distributions in space and time. Radionuclides investigated include isotopes of cesium, cobalt, and manganese. The $^{137}Cs$ content of fish is in part related to the cumulative deposition in sediments. However, cesium of recent origin appears to be more biologically available. Cobalt-60 accumulates in estuarine sediments with limited, if any, transfer back into aquatic food chains. Manganese-54 deposits by sedimentation in the freshwater regions of the estuary, but leaches from sediments during seasonal salt water intrusions. Sedimentary buildup of $^{54}Mn$ is limited by its 303 day half-life. The maintenance of constant stable manganese concentrations by fish during periods of highly variable aqueous manganese concentrations is indicative of regulated uptake and loss of this element. Accordingly, the use of concentration factors to predict radionuclide concentrations in fish is not strictly appropriate for manganese. The finding that most radionuclides are at least partially associated with sediments further limits the applicability of the concentration factor approach, particularly for cesium. Rooted aquatic plants concentrate all of the radionuclides measured except tritium and are useful stationary integrators of aqueous radioactivity levels. The most important radionuclides with respect to exposure of man from reactor releases appear to be $^{137}Cs$ and $^{134}Cs$, and the critical pathway ingestion of fish. The fraction of maximum permissible intake during 1969 was less than $10^{-4}$. It appears that present regulations restricting the concentrations of radionuclides in cooling water effluents are more than adequate for this aquatic environment. (auth)

**55161** PLUTONIUM CONCENTRATION IN ORGANISMS OF THE ATLANTIC OCEAN. Wong, K. M.; Burke, J. C.; Bowen, V. T. (Woods Hole Oceanographic Institution, Mass.). pp 529-39 of Health Physics Aspects of Nuclear Facility Siting. Vol. II. /Voilleque, Paul G. (comp.). Idaho Falls, Idaho; Burton R. Baldwin, Publications Chairman (1971).

From fifth annual midyear topical symposium on health physics aspects of nuclear facility siting; Idaho Falls, Idaho (3 Nov 1970).

A series of marine organisms, collected about Cape Cod or in the open N. Atlantic Ocean, were analyzed for $^{239}Pu$ and for some other fallout radionuclides. These data are compared with those from analyses of marine aerosols, sediments, and seawater. The results show that $^{239}Pu$ was concentrated in some tissues of each organism so far examined. In fish, $^{239}Pu$ concentrations range from 0.2 to 140 dpm per 100 kg fresh weight; in benthic invertebrates, from 23 to 140 dpm per 100 kg; in plankton, from 130 to 340, and in Sargasso weed, to 1280 dpm per 100 kg. Plutonium-239 ratios to $^{90}Sr$ or $^{137}Cs$ are higher in organisms than in their environment. (auth)

**55162** EFFECT OF TEMPERATURE UPON THE UPTAKE OF $^{144}Ce$ BY CHLAMYDOMONAS. Jacobson, Arnold F. (Bureau of Radiological Health, Rockville, Md.); Cember, Herman. pp 784-95 of Health Physics Aspects of Nuclear Facility Siting. Vol. III. /Voilleque, Paul G. (comp.). Idaho Falls, Idaho; Burton R. Baldwin, Publications Chairman (1971).

From fifth annual midyear topical symposium on health physics aspects of nuclear facility siting; Idaho Falls, Idaho (3 Nov 1970).

A study was performed to determine the effect of temperature on the uptake of $^{144}Ce$ by Chlamydomonas, a species of freshwater unicellular green algae common in polluted water. A simple experimental procedure was devised, and the investigation was performed under controlled conditions. The data obtained were statistically examined using the techniques of analysis of variance and correlation analysis, and significant effects were detected. Of greatest importance, uptake of $^{144}Ce$ by Chlamydomonas exhibited a strong positive temperature effect, increasing by as much as a factor of 15 between 4°C and 22°C. In addition, other factors investigated were found to have significant effects. Uptake increased steadily with time, and did not attain maximum values during the time period of the study, three to four days. The initial $^{144}Ce$ concentration had a significant positive effect, while the cerium specific activity had little if any influence upon uptake. Also, the biological concentration of the aquatic medium had a strong inverse effect upon the cerium uptake, which increased sharply with decreasing biological population. Of these four significant factors, those of greatest individual influence were found to be temperature and biological concentration. In addition, interactions among variables were also found to affect uptake. Temperature exhibited significant interactions with time, biological concentration, and $^{144}Ce$ concentration. However, no three factor interactions were discovered. (auth)

## Genetics and Cytogenetics

*Refer also to abstracts 55134, 55206, 55256, 55260, 55261, and 55360.*

**55163** CYTOGENETIC INVESTIGATION OF INDUSTRIAL WORKERS OCCUPATIONALLY EXPOSED TO GAMMA RAYS. Popescu, H. I.; Stefanescu, D. T. (Inst. of Hygiene and Public Health, Bucharest. Inst. for Pathology and Medical Genetics, Bucharest). Radiat. Res.; 47: No. 2, 562-70(Aug 1971).

The incidence of chromosome aberrations has been studied in blood cells of 16 technicians occupationally exposed to gamma irradiation, 8 of whom had been irradiated with doses higher than allowed and the other 8 with smaller than allowed ones. The blood cell count of all subjects did not present abnormalities at any of the periodical medical check-ups. Although the peripheral blood picture was normal, chromosome aberrations in 48–50-hr cultures of blood were detected. The incidence of chromosome aberrations, mainly fragments, distinctly differed ($p < 0.001$) from that of an equal number of controls. This incidence was also different ($p < 0.001$) between those who had received doses higher than permissible and the other ones. It should be emphasized that although the incidence of chromosome aberrations did not increase in step with the total accumulated dose, the aberrations can be found even as a result of small doses even though the usual hematological parameters were not modified. (auth)

**55164** PERSISTENCE OF HERITABLE CHANGES IN AN IRRADIATED RAT POPULATION AFTER CESSATION OF THE EXPOSURES. Newcombe, Howard B.; McGregor, John F. (Chalk River Nuclear Labs., Ont.). Radiat. Res.; 47: No. 2, 450-60(Aug 1971).

Studies to assess the importance of radiation-induced genetic damage, of kinds that persist following the cessation of repeated ancestral irradiations, imply that the obviously harmful expressions occur only prior to weaning and are not detected in young adults. Reductions in fertile matings and litter size, and an increase in postnatal mortality up to the time of weaning, were observed in a population of rats after 13 generations of parental irradiation and a 14th generation without irradiation. These findings indicate the persistence of induced genetic changes despite a substantial rate of elimination in each generation. Among young adult rats, however, the only observed effect was a small but significant decrease in the body weights of the males. This change is not believed to be indicative of any detriment to the adult animals because the opposite effect was found in adults of the preceding generation. It seems unlikely that both kinds of change, at least to this degree, would be harmful. It is concluded that eliminations of induced genetic changes in mammals take place through deaths that occur mainly during the early part of the life of the organism. (auth)

**55165** INDUCTION OF HETEROALLELIC REVERSIONS AND LETHALITY IN SACCHAROMYCES CEREVISIAE EXPOSED TO RADIATIONS OF VARIOUS LET ($^{60}Co$ $\gamma$ RAYS, HEAVY IONS, AND $\pi^-$ MESONS) IN AIR AND NITROGEN ATMOSPHERES. Raju, M. R.; (Univ. of California, Berkeley, Univ. of Texas, Dallas); Gnanapurani, M.; Stackler, B.; (and others). Radiat. Res.; 47: No. 3, 635-43(Sep 1971).

Induction of heteroallelic reversion in diploid yeast is one of the most radiosensitive processes known. Reversion to arginine independence in a diploid strain BZ34 of Saccharomyces cerevisiae was used to measure the relative biological effectiveness (RBE) of $\pi^-$ mesons and heavy ions. Exposures were also conducted under anoxic conditions to obtain the oxygen enhancement ratio (OER) for these radiations and for $^{60}Co$ $\gamma$ rays. The linear energy transfer (LET) values used covered a range from 3 to 5500 MeV

XUM

$g^{-1}$ $cm^2$. The OER values obtained for $^{60}Co$ $\gamma$ rays and $\pi^-$ mesons were 2.5 and 1.9, respectively. The response of this yeast system was found to be nearly the same at dose rates of 40 rads/hr and 40 rads/min of $^{60}Co$ $\gamma$ rays. With increasing LET, the RBE rose to a maximum value in the region 2000 MeV $g^{-1}$ $cm^2$, corresponding to that of carbon ions. The OER decreased with increasing LET, approaching unity for neon ions. The study was extended to induction of lethality with the heavy ions. The maximum effectiveness still occurred at an LET of 2000 MeV $g^{-1}$ $cm^2$, and no oxygen effect was found at 5500 MeV $g^{-1}$ $cm^2$. The survival curves, unlike those for other diploid yeast strains reported, shifted from a sigmoidal to an exponential type as the LET increased. This is similar to the response of mammalian cell systems. (auth)

**55166** ABSTRACTS OF PAPERS PRESENTED AT THE 1971 MEETINGS OF THE GENETICS SOCIETY OF AMERICA, ROCHESTER, NEW YORK, AUGUST 23–25, 1971. Genetics; 68: No. 1, Suppl., s1-77(1971). (CONF-710813-(Absts.)).

Two hundred and fourteen abstracts of papers presented at the 1971 meeting of the Genetics Society of America are presented. (E.R.B.)

**55167** PROTRACTED MUTAGENESIS INDUCED BY IONIZING IRRADIATION AND ITS DEPENDENCE ON THE WATER CONTENT OF A BIOSYSTEM. Nemtseva, L. S. (Inst. of General Genetics, Moscow). Genetika; 7: No. 8, 19-30(Aug 1971). (In Russian).

Prolonged mutagenesis develops in dry biosystems after sparsely and densely ionizing radiation, the highest mutation rate being observed at 2 to 4% water content. The radiation-induced prolonged mutagenesis persists through one cell generation. The mutation rates depend on those induced at the initial exposure to radiation. The ratio of the mutation rate observed as a result of prolonged mutagenesis to that observed in the case of the initial irradiation is the same irrespective of the water content in seeds. Densely ionizing radiation induces the prolonged mutagenesis both in air-dry and in dry seeds, the mutation rates in case of prolonged mutagenesis increasing at the beginning of the storage and subsequently decreasing. (auth)

**55168** PREMUTATIONAL OXYGEN-SENSITIVE CHANGES OF CHROMOSOMES INDUCED BY IRRADIATION OF SEEDS. Protopopova, E. M.; Shapiro, N. I. (Inst. of Developmental Biology, Moscow. Moscow State Univ.). Genetika; 7: No. 8, 37-45 (Aug 1971). (In Russian).

Oxygen aftereffect under gamma irradiation of Crepis capillaris seeds was studied and characterized by chromosome aberration frequency. The author's previous data suggest that oxygen aftereffect is connected with formation of potential premutational chromosome changes induced by gamma irradiation. The problem was to study the period of existence of potential chromosome damages and to establish whether they replicate in the process of cell reproduction and whether the regeneration of such damages takes place. It was established that potential damages persisted in chromosome structures for a long time and could be detected during at least three successive cell divisions. Analysis of chromosome aberrations due to the oxygen action in cells of 2nd and 3rd postradiated mitosis revealed that potential damages, as well as true chromosome breaks, replicated in the process of cell reproduction. The detection by the oxygen treatment of single and double chromosome aberrations in tetra- and octoploid cells is indicative of the reparation of potential damages in single chromosomes. This reparation was proportional to the time from the moment of damage formation. It was also shown that the growing of irradiated seeds before the oxygen treatment in a solution of $\beta$-alanine (instead of water) increased the possibility of reparation of potential damages. (auth)

**55169** CYTOGENETIC EFFECT OF REPEATED X-IRRADIATION AND STORAGE OF WHEAT SEEDS. Prikhozenko, E. Ya. (Rostov-on-Don State Univ., USSR). Genetika; 7: No. 8, 79-84 (Aug 1971). (In Russian).

A study of the effect of repeated x irradiation combined with the subsequent selection and three yr storage of irradiated seeds of Triticum durum var. aegyptiacum on the frequency of chromosomal aberrations in the subsequent generations was carried out. The selection proceeded on the background of a 2 kR dose of x rays. Soaked seeds were x-irradiated at the beginning of germination. Before the three yr storage, dry seeds were irradiated at test doses of 0.5, 1.0, 1.5, 2.0, and 3.0 kR. It was established that the repeated irradiation of winter durum wheat seeds combined with the selection under field conditions increased the sensitivity to x rays in the subsequent generations. The three yr storage of irradiated seeds enhanced the radiobiological effect of x rays. (auth)

**55170** CYTOLOGICAL INVESTIGATION OF RADIATION-INDUCED CROSSOVERS IN MALES OF DROSOPHILA MELANOGASTER. Mglinets, V. A. (Inst. of Medical Radiology, Obninsk, USSR). Genetika; 7: No. 8, 108-14(Aug 1971). (In Russian).

Cytological analysis of 60 induced crossovers in Drosophila melanogaster males detected in 5th to 15th day broods has revealed that 16 of them are connected with chromosome rearrangements (3 complex interchromosomal aberrations, and 3 inversions, the rest being intrachromosomal duplications). Eleven of the aberrations were induced at the stage of meiosis. The breakage-points of 12 of the chromosome rearrangements are located within the region of the supposed exchange. (auth)

**55171** VARIABILITY OF MYCOBACTERIUM PHLEI IN THE PIGMENT FORMATION INDUCED BY DIFFERENT MUTAGENS. Daraseliya, G. Ya. (All-Union Research Inst. of Agricultural Microbiology, Leningrad). Genetika; 7: No. 8, 137-42(Aug 1971). (In Russian).

Pigment mutations were induced by uv irradiation in Mycobacterium phlei. The highest frequency of such mutations was observed after 60-seconds exposure of cell suspensions to uv at a dose rate of 1710 erg/$mm^2$. The mutagenic effect of N-nitrosomethyl urea was observed after a 6 hr treatment of cell suspensions in distilled water when the rate of survival was 0.0014%. The range of the variation in the pigment formation was wider when the cell suspension was treated with N-nitrosomethyl urea than when it was uv-irradiated. The color of colonies was observed to change under the influence of mutagenic factors, these changes being correlated with the content of carotinoid pigments in cells. An induced mutant of Mycobact. phlei was obtained (as a result of the action of N-nitrosomethyl urea and subsequent selection) capable of synthesizing a 4-fold total amount of carotinoids, including a 5-fold quantity of $\beta$-carotine as compared to the initial culture. The persistence of active mutants in time was tested, and it was established that induced mutants retained their capacity of producing very large quantities of carotinoid pigments for 1, 3, 6, 9, and 12 months. (auth)

**55172** UV-SENSITIVE MUTANTS OF CHLORELLA VULGARIS AND THEIR CAPACITY TO PHOTOREACTIVATION. Ozol, A. A.; Zheleznyakova, N. Yu. (Far East Scientific Research Centre, Vladivostok, USSR. Ioffe Inst. of Physics and Tech., Leningrad). Genetika; 7: No. 8, 143-9(Aug 1971). (In Russian).

Three uv-sensitive mutants were induced by uv-light in wild-type strain B of Chlorella vulgaris. Two of them were also sensitive to x rays. The capacity to photoreactivation of two uv-sensitive mutants was higher as compared to cells of the wild type, while the third mutant was characterized by a lower photoreactivation capacity. For x irradiation of the wild-type strain, all the parameters determining the character of the dose-survival curve were computed according to Haynes' model. The coefficient of repair was: 0.97. The data obtained suggest that the sigmoid character of dose-survival curves for wild strains is indicative of their systems' activity to repair of radiation lesions. (auth)

**55173** TARGET OF RECOMBINATION IN CROSSES OF DIFFERENT MUTANTS OF PHAGE T4. Matvienko, N. I. (Inst. of Molecular Biology, Moscow). Genetika; 7: No. 8, 150-5(Aug 1971). (In Russian).

The frequency of recombination was shown to decrease approximately by an exponential curve in the case where one of the parent mutants was uv-irradiated before the cross. In crosses of point mutants, the slope of the curve of frequency of recombination (determining the target of recombination) did not depend on the parent mutant that was irradiated. In crosses of deletions mutants, the target of recombination correlated with the dimensions of the deletion of the intact parent. (auth)

**55174** PRE-SELECTION OF COMPACT MUTANTS INDUCED BY X-RAY TREATMENT IN APPLE AND PEAR. Visser, T.; Verhaegh, J. J.; De Vries, D. P. (Inst. for Horticultural Plant Breeding, Wageningen, Netherlands). Euphytica; 20: No. 2, 195-207(May 1971).

Mutation breeding of apple and pear started in 1965 using dormant scions which, after irradiation (x-rays), were grafted on rootstocks. The most efficient dose for apple was around 3 krad, for pear between 4.5 and 7 krad. Primarily shoots exhibiting compact traits were selected, defining such shoots as being thicker than normal for their length or shorter than normal for their diameter while having shorter internodes than normal shoots. The selection was carried out on one-season-old shoots of the same trees during three successive seasons, this involved a cut back at the end of the first and second season. The selected compact shoots yielded with apple on average four times more clones with a distinct compact habit than normal appearing shoots; four out of every

XUM

five clones were found to be stable in both apple and pear. Averaging the results for apple, 7% of the surviving trees produced shoots the clones of which showed compact growth, this was only 0.5% for pear. In all several dozens of such clones were obtained of the apple varieties Golden Delicious, Cox's Orange Pippin, Belle de Boskoop and Tydeman's Early and a few distinct compact and some dwarf clones of Beurré Hardy and Doyenné du Comice. (auth)

**55175** METAPHASE ANALYSIS OF CHROMOSOME REARRANGEMENTS IN BARLEY. Sokolov, V. A.; Khvostova, V. V. (Inst. of Cytology and Genetics, Novosibirsk, USSR). Genetika; 7: No. 8, 177-80(Aug 1971). (In Russian).

A method of obtaining preparations of metaphase chromosomes in barley is described. Good preparations are obtained from the first embryonic leaf. After x irradiation of seeds, aberrations of the chromosome type only were observed in cells of embryonal leaves, suggesting that at the moment of irradiation chromosomes were at the $G_1$ stage. (auth)

**55176** EFFECT OF X IRRADIATION ON CHIASMA FREQUENCY IN CHORTHIPPUS BRUNNEUS. Westerman, M. (Univ. of Birmingham, Eng.). Heredity; 27: 83-91(Aug 1971).

The pattern of response of chiasma frequency to x-irradiation was studied in the grasshopper Chorthippus brunneus. In order to relate any observed change to the time of induction, cells undergoing DNA synthesis at the time of irradiation were labeled with $^3$H-thymidine. Tritiated thymidine alone had no effect on mean cell chiasma frequency. Two distinct radiosensitive periods were found. X-irradiation at the first of these, corresponding with premeiotic DNA synthesis, led to a significant reduction in mean cell chiasma frequency when scored at diplotene-diakinesis. The same treatment when given at the time of zygotene-early pachytene gave a significant increase. A slight increase was also noted following x-irradiation given during lepotene-early zygotene. All alterations in mean cell chiasma frequency were the result of changes in the number of chiasmata formed by the longer chromosomes—both metacentrics and telocentrics. No univalents were observed and three smallest bivalents continued to form a single chiasma at all times. It is suggested that different experimental agencies may affect the control mechanisms of chiasma formation differentially. In some organisms a particular treatment may affect only the fine controls of chiasma formation, in others the same treatment may also affect the coarse controls. (auth)

**55177** INHERITANCE OF GAMMA RAY INDUCED CHLOROPHYLL MUTATION IN LINSEED. Seetharam, A. (Univ. of Agricultural Sciences, Bangalore, India). Sci. Cult. (Calcutta); 37: No. 2, 104(Feb 1971).

Various doses of gamma radiation were administered to progeny of linseed variety N. P. (RR)9. Several lines were observed in the $F_2$ generation segregating for the chlorophyll mutations, xantha and viridis. Reciprocal crosses were made between true breeding viridis types and the parent variety. Since normal chlorophyll development was observed in the back-cross progeny, it was suggested that normal green was dominant over viridis. The tabulated data indicate that allelic difference at a single locus determines the two chlorophyll types, normal green being dominant over viridis. (H.L.W.)

**55178** EFFECTS IN VIVO OF IONIZING RADIATIONS ON HUMAN CHROMOSOMES. Mouriquand, C.; Darnault, J.; Patet, J.; Wolff, Ch.; Gilly, C. (Centre d'Etudes Nucleaires, Grenoble, France. Faculte de Medecine, La Tronche, France). Nouv. Rev. Franc. Hematol.; 10: 117-28(Jan-Feb 1970). (In French).

A bibliographic review is presented of the effects of ionizing radiations on human chromosomes. (115 references) (J.S.R.)

**55179** GENETICS LECTURES. VOLUME 2. Bogart, Ralph (ed.). Corvallis, Oreg.; Oregon State University Press (1971). 126p. $4.00.

Separate abstracts were prepared for two lectures; an additional seven lectures are included on various aspects of genetics. (H.L.W.)

*For abstracts of individual chapters see: 55180 and 55181.*

**55180** INDUCED RECOMBINATION IN MITOTIC DIPLOID CELLS OF SACCHAROMYCES. Roman, Herschel (Univ. of Washington, Seattle). pp 43-59 of Genetics Lectures. Vol. 2. /Bogart, Ralph (ed.). Corvallis, Oreg.; Oregon State Univ. Press (1971).

Types of recombination in fungi are described with emphasis on crossing over and gene conversion. Diagrams are presented to show various genotypes of chromosomes in recombination and consequences of gene conversion. Ultraviolet radiation and nitrosoguanidine were used in experiments to stimulate spontaneous recombination frequency in vegetative cells. Following treatment with these agents, data are tabulated for the following: range of sector sizes in red–white colonies; types of sectored colonies induced by ultraviolet radiation during growth of synchronized cells; and genotypes of sectored colonies induced by ultraviolet light and nitrosoguanidine with reference to the distribution of the adenine and fermentation markers. A discussion is presented of the mechanism of gene conversion. (H.L.W.)

**55181** MUTATIONS AND BIOLOGICAL IMPROVEMENT. Gregory, Walton C. (North Carolina State Univ., Raleigh). pp 71-90 of Genetics Lectures. Vol. 2. /Bogart, Ralph (ed.). Corvallis, Oreg.; Oregon State Univ. Press (1971).

An experiment designed to test the hypothesis that induced mutations effected polygenically controlled variation was conducted using a strain of the cultivated peanut, Arachis hypogaea, following x-ray treatment of the dried seeds. The progeny variances in yield of fruits were calculated from designed experiments where control-type plants were randomly selected for progeny testing and where the progenies containing visible mutants were retained and expunged. It was found that mutant plant frequency increased with decreasing magnitude of change. Following intercrossing experiments, it was found that the distribution of the progenies containing visible mutants was symmetrical but the population mean was below that of the control population. The importance of magnitude of change is emphasized with regard to mutation and biological improvement. A discussion is presented of the adaptation sphere and the limitations of plant breeding. Results of mutation breeding of citrus fruits are discussed and experiments are described that test the hypothesis that numerous mutations of extremely small magnitude of effect induced by x rays include effects on resistance to low temperature. Tables are presented to show effects of temperature along the North Carolina coast on several varieties of citrus fruits. It was concluded from these experiments and those of other investigators that only in those instances in which extensive breeding, selection, and testing have been carried out with induced mutants as parental lines have long-lasting and useful varieties been produced. (H.L.W.)

**55182** STUDIES ON THE INDUCTION OF TRANSLOCATIONS IN MOUSE SPERMATOGONIA. IV. EFFECTS OF ACUTE GAMMA-IRRADIATION. Searle, A. G.; Beechey, C. V.; Evans, E. P.; Ford, C. E.; Papworth, D. G. (Medical Research Council, Harwell, Eng.). Mutat. Res.; 12: No. 4, 411-16(Aug 1971).

The rate of induction of reciprocal translocations by 56 to 816 R exposures of mouse spermatogonia to acute $\gamma$-irradiation (95 R/min) was determined by cytological examination of descendant spermatocytes. The dose–response relationship did not differ significantly from linearity and had a regression coefficient of $1.8 \cdot 10^{-4}$ per R with respect to translocations per spermatocyte. Further analysis at exposures below 816 R (considered less likely to produce distortion) showed that the quadratic regression of best fit had too small a square-law component to account for the very low frequency of translocations obtained after chronic $\gamma$-exposures in a previous experiment. The possibility is discussed that there is some extra factor, besides the diminution of the square-law component, which operates to reduce the yield after protracted exposures. The relative biological effectiveness of the $\gamma$- vs x-irradiation for the induction of translocations in spermatogonia was estimated to be $0.62 \pm 0.10$. (auth)

**55183** EFFECTS OF DEHYDRATION ON THE SENSITIVITY OF YEAST TO ULTRAVIOLET LIGHT. Hieda, Kotaro (Rikkyo Univ., Tokyo). Mutat. Res.; 12: No. 4, 365-80(Aug 1971).

The effects of dehydration on the main actions of uv, killing and genetic, were studied, in connection with the expected conformational change of the DNA molecule, with wild-type and mutant strains for uv sensitivity of diploid yeast (Saccharomyces cerevisiae). The dehydration of the cells to various degrees was performed by exposing the completely dried cells to various vapor pressures, ranging from 0 to 22 Torr at 25°. In addition to survival and genetic tests for a series of vapor pressures, the photorepairability was determined for induced damage, under each condition of the vapor pressure, to serve as a criterion by which the properties of the photoproducts were to be characterized. The results may be summarized as follows. The sensitivities to uv action generally increased at low vapor pressures: the ratios of the sensitivity at 0 to 22 Torr were 5.3 (killing) and 17 (genetic) for the wild-type strain; and 2.0 (killing) and 4.7 (genetic) for the uv-sensitive strain. A drastic change in the uv sensitivity occurred around 14 Torr, which roughly coincided with the pressure at which regular steric arrangement of DNA bases undergoes a reversible and drastic change in vitro. Appreciable hysteresis of uv sensitivity was noted in the dehydration–rehydration cycle for the killing effect at 14 Torr, where in vitro DNA showed a similar

XUM

hysteresis with respect to the steric rearrangement of bases. Killing and genetic damage induced at low vapor pressures was scarcely photorepairable indicating that non-photorepairable products would predominantly be formed in a cell under such conditions. Comparison of the dose–effect relation in the uv-sensitive and wild-type strains leads to the inference that dark-repair efficiency for the photoproduct produced at low vapor pressures seems to be less than that for pyrimidine dimers. These results together strongly suggest that the physicochemical behavior of chromosomal DNA has the same vapor-pressure dependence as that of DNA in vitro with respect to the steric arrangement of the bases, and this behavior determines the types of principal photoproducts that cause the killing and the genetic change. (auth)

**55184** SEARCH FOR RADIATION-INDUCED RECESSIVE SEX-LINKED LETHAL AND DETRIMENTAL MUTATIONS IN IMMATURE GERM CELLS OF THE HOUSE MOUSE (MUS MUSCULUS). Schroeder, Johannes Horst (Inst. of Biology, Neuherberg, Ger.). Genetics; 68: No. 1, 35-57(May 1971).

A 3-generation test was carried out to determine the frequency of recessive sex-linked lethal mutations in mice. The sex-linked Tabby gene was used as a marker. The incidence of Tabby-linked recessive lethals was expected to be detected by pre- and/or postnatal loss of grandsons possessing a recessive sex-linked lethal. However, no true recessive sex-linked lethal could be found after screening a total of 1811 irradiated and 1693 control X chromosomes. The expected frequency of Tabby-linked recessive lethals was estimated to be between 0.3% and 3.3% after 600 roentgens (R) to spermatogonia, but the present findings contradict these values. It is suggested that recessive sex-linked lethal mutations are substituted by recessive sex-linked detrimentals in mammals, because a large proportion of sex-linked lethals in mammals may be expected to be partially dominant rather than true recessives. Radiation genetic damage other than recessive sex-linked mutations was determined by comparison of sex-chromosome losses, mean litter-sizes, preweaning mortality, and semisterility of $F_1$ dams. The mean litter-size decreased and the postnatal mortality increased in the 1st and 2nd postirradiation generation after 600 R to spermatogonia and 300 R to oocytes, but no radiation genetic damage could be found in the progeny of $F_1$ females after 1200 R to spermatogonia. (auth)

**55185** X-RAY INDUCED LIFE-SHORTENING MUTATIONS IN HABROBRACON: A GENETIC APPROACH TO SENESCENCE AND DURATION OF LIFE. Baird, M. B.; Clark, A. M. (Masonic Medical Research Lab., Utica, N. Y. Univ. of Delaware, Newark). Exp. Gerontol.; 6: 1-8(1 Feb 1971).

Habrobracon males were exposed to x-radiation. Two mutations which decreased the adult life span of mutant wasps were isolated after screening the first-generation daughters of the irradiated mates. Both lethals produced a substantial decrease in longevity of mutant males. However, the mutations differed from each other as regards the time of onset of mortality, the range in days over which death occurred, and the appearance, or gross pathology, of the dead wasps. The existence of adult lethal mutations is interpreted to offer support for a developmental model for the control of duration of life. Termination of adult life as a consequence of a single gene mutation appears to mimic termination of preadult development through an analogous process. It is concluded that introduction of a genetic variable in the form of life-shortening mutations would prove useful in elucidating the role of genes in the control of adult life span. (auth)

**55186** DOME MORPHOLOGICAL MUTANT LINKED TO THE B INCOMPATIBILITY FACTOR OF SCHIZOPHYLLUM COMMUNE. Chang, Shu-ting; Wai, Chun-chung (Chinese Univ. of Hong Kong). Genetics; 68: No. 1, 13-19(May 1971).

The two dome mutants induced by ultraviolet appeared not to be exactly the same in gross morphology and could be distinguished by the appearance of the margins of the colonies. dm-2 was demonstrated to be linked to the B incompatibility factor, 9.4 map units from B$\alpha$ and 2.6 from B$\beta$. dm-4 was proved not to be linked to either the A or the B factor. The most likely gene order in the B-factor chromosome is ad-6–fir–B$\alpha$–B$\beta$–dm-2–arg-7. (auth)

**55187** MUTANTS OF YEAST DEFECTIVE IN MUTATION INDUCED BY ULTRAVIOLET LIGHT. Lemontt, Jeffrey F. (Univ. of California, Berkeley). Genetics; 68: No. 1, 21-33(May 1971).

Twenty mutants of Saccharomyces cerevisiae, selected for reduced uv-induced site reversion of the highly uv-revertible ochre-suppressible arg4-17 allele, were found to represent only three unlinked recessive genes denoted by rev1, rev2, and rev3. The rev2 locus is about 4.0 cM distal to asp5 on linkage group XII, but neither rev1 nor rev3 is centromere linked. The rev genes confer moderate uv sensitivity and slight x-ray sensitivity. The data suggest that uv-induced mutation in yeast is controlled by a small number of genes, sharing common enzymatic steps with the repair of lethal uv and x-ray damage to DNA. Both rev1-1 and rev3-1 exert a strong effect on uv-induced locus reversion of not only arg4-17 (1/30 the wild-type frequency at 265 erg/mm$^2$), but also of the ochre-suppressible lys1-1 allele (1/10 wild type). The effect of rev2-1 is only 1/4 and 1/2 wild type, respectively. UV reversion of the missense allele arg4-6 is also reduced by rev1-1 and rev3-1 to 1/4 the wild-type frequency at 265 erg/mm$^2$, but is unaffected by rev2-1 at lower uv doses. At 265 erg/mm$^2$ the frequency of arg4-6 reversion in the rev2-1 strain is twice that in wild type. Based on these few data, rev1-1 and rev3-1 may have a general nonspecific action in reducing uv reversion, but rev2-1 might specifically block uv-locus reversion of only ochre-suppressible alleles. (auth)

**55188** COMPARISON OF THE RELATIVE BIOLOGICAL EFFECTIVENESS OF $^{241}$Am AND $^{144}$Ce ON THE PRODUCTION OF CHROMOSOME ABERRATIONS IN THE CHINESE HAMSTER LIVER. Brooks, A. L.; McClellan, R. O.; McKay, L. R. (Lovelace Foundation for Medical Education and Research, Albuquerque, N. Mex.). pp 600-18 of Health Physics Aspects of Nuclear Facility Siting. Vol. III. /Voilleque, Paul G. (comp.). Idaho Falls, Idaho; Burton R. Baldwin, Publications Chairman (1971).

From fifth annual midyear topical symposium on health physics aspects of nuclear facility siting; Idaho Falls, Idaho (3 Nov 1970).

Cerium-144, a beta emitter and $^{241}$Am, an alpha emitter are present in significant quantities in the inventory of an operating reactor or in discharged fuel elements. Their toxicity following intraperitoneal injection was investigated with a view to obtaining a better understanding of the toxicity of each radionuclide and, moreover, to comparing the toxicity of a beta emitter and an alpha emitter that have similar metabolic characteristics. Following intraperitoneal injection of the two radionuclides as a citrate, the whole-body retention of both was characterized by rapid early clearance of less than 25% of the initial activity with the remainder being retained with a long effective half-life. The majority of retained radionuclide was found in liver, with lesser quantities in skeleton. Administration of high levels of activity resulted in early deaths related to bone marrow damage. Based on the average radiation dose to bone, $^{241}$Am was 2.5 times more effective than $^{144}$Ce in producing early mortality. The frequency of chromosome aberrations in liver was investigated using partial hepatectomy to stimulate liver cell division. The efficiency of $^{144}$Ce or $^{241}$Am for producing chromosome aberrations in liver when expressed as aberrations per rad remained relatively constant over the wide range of dose rates studied. Total aberration increased as a linear function of dose for both radionuclides with a coefficient of $3.3 \times 10^{-4}$ and $4.7 \times 10^{-3}$ aberrations per cell per rad for $^{144}$Ce and $^{241}$Am respectively. Thus, on a per rad basis $^{241}$Am was about 14 times more effective than $^{144}$Ce in producing chromosome aberrations in liver. The dose required to produce a significant increase in the frequency of chromosome aberrations above the level measured in controls was 13 rads for $^{241}$Am and 130 rads for $^{144}$Ce. (auth)

**55189** STUDIES ON THE ISOLATION OF AUXOTROPHIC MUTANTS OF BACILLUS SUBTILIS AND ESCHERICHIA COLI. Kim, H. S.; Lee, C. Y.; Lee, K. H. J. Korean Agr. Chem. Soc.; 11: 137-41(1969).

In order to obtain amino acids and nucleic acid derivatives from adenine auxotrophic mutants of Bacillus subtilis and Escherichia coli, vitamins, nucleic acid analogue, streptomycin as well as ultraviolet light were used for the production of adenine auxotrophic mutants and the results showed efficient production of desired mutants. Ultraviolet (2530 Å 2080 erg/mm$^2$) irradiation given to Bacillus subtilis and E. coli at a distance of 30 cm for 80–90 sec. and for 15–20 sec. respectively induced four and eight strains of auxotrophic mutants. Treatment with aminopterine (200 $\mu$g/ml) inhibited the growth of Bacillus subtilis significantly but a subsequent irradiation of ultraviolet light at the above mentioned conditions induced six times as many mutants as compared to the irradiation alone. In case of E. coli a similar tendency was observed with treatment of streptomycin (200 $\mu$g/ml) with doubled induction rate of adenine auxotrophic mutants as compared to the irradiation alone. (Korean Sci. Abstr.)

**55190** VARIATION IN RADIOSENSITIVITY AND THE DOSE-EFFECT RELATIONSHIP IN THE LOW DOSE REGION. Eriksson, Goesta (Royal Coll. of Forestry, Stockholm). Hereditas; 68: No. 1, 101-14(1971).

A study of the variation in radiosensitivity of different stages of development was undertaken by the aid of waxy mutants. The main purpose of the investigation was to study the dose-effect

XUM

relationship in the low dose region. In barley it was shown that irradiation during meiosis caused a considerably higher induction of waxy mutants than during subsequent developmental stages. Furthermore, the amount of mutants was shown to be dependent on the height of tiller at irradiation and on the spikelet position within the spike. In maize a pronounced difference in mutation rate of the pollen grains from individual plants fixed on five consecutive days was observed. This constitutes a complication for the determination of the dose-effect relationship. This complication was circumvented by constructing one dose-effect relationship for the maximum mutation rate of each plant, as well as one dose-effect relationship for the average mutation of five fixing days. Regardless of the way in which the dose-effect relationship was computed it was shown to be linear. The entire investigation comprised the analysis of more than 40 million pollen grains composing more than 30,000 pollen samples. (auth)

**55191** INDUCED TRANSLOCATIONS IN VICIA FABA L. Sjoedin, Jan (Swedish Seed Association, Svaloef, Sweden). Hereditas; 68: No. 1, 1-34(1971).

A total of 198 translocations have been induced in Vicia faba L. with ionizing radiations and chemical mutagens. The ionizing radiations were about five times more effective in inducing translocations as compared with the chemical mutagens. In all, 109 translocations were analysed. These studies revealed that the translocation break points are not randomly distributed over the chromosomes nor within individual chromosomes. Chromosomes 1, 2, and 5 displayed a significantly lower aberration frequency than the other three chromosomes. Quadrivalents in translocation heterozygotes were mostly characterized by a mixture of rings and chains. The average pollen fertility was 56 percent. Gametes and zygotes of translocation homozygotes were fully viable except in six translocation lines, in which they were semi-lethal. Vegetative growth was slightly depressed compared with the parental variety Primus; but the seed yield was reduced by 25 percent. No differences between extreme translocations and others were detected as regards plant vigour. In the $F_1$ offspring of crosses between translocations involving the same two chromosomes, the translocations behaved differently when compared with barley and Zea mays translocations– i.e., quadrivalents occurred in a much higher frequency in Vicia faba. Only when the breaks were in the same arm in both chromosomes, and then in rather close proximity, were six bivalents formed. (auth)

**55192** DYNAMICS OF MITOTIC ABERRATIONS INDUCED IN THE WHITE RAT BY A SINGLE DOSE OF 800 R. Anastasiu, Gh.; Cilievici, O. Arch. Roum. Pathol. Exp. Microbiol.; 29: No. 1-2, 81-9(1970).

With a view to studying cell division in the femur bone marrow, white Wistar rats were exposed to a single dose of 800 R. The study involved determination of the mitotic index, mitotic and chromosomal aberrations and a 60-day observation period of the caryotype, at various time intervals. A single 800 R dose inhibited cell division, led to aberrant mitoses and multiple chromosomal aberrations such as: ruptures, translocations, agglutinations, and polyploidy. Starting with the 15th day, however, the natural restoring mechanisms interferred, tending to bring the mitotic index in the normal range, to eliminate aberrant mitoses and chromosomal aberrations. (Rom. Sci. Abstr.)

# Health Physics and Safety

*Refer also to abstracts 54937–54962, 54964, 54966, 54967, 55157, and 57103.*

**55193** HEALTH PHYSICS ASPECTS OF NUCLEAR FACILITY SITING. VOLUME III. Proceedings of the Fifth Annual Health Physics Society Midyear Topical Symposium, Idaho Falls, Idaho, November 3–6, 1970. Voilleque, Paul G.; Baldwin, Burton R. (comps.). Idaho Falls, Idaho; Burton R. Baldwin, Publications Chairman (1971). 256p. (CONF-701106-(Vol.3)).

Seventeen articles are included; separate abstracts were prepared for 15. One article on reasons for differences in calculated estimates of the cloud dose was previously included in NSA as 25: 8668. The remaining article on basic data on heat dissipation downstream for large heat sources was not in scope for NSA. (P.C.H.)

*For abstracts of individual papers see: 54547, 54796, 54797, 55125, 55162, 55188, 55201, 55202, 55241, 55242, 55253, 55254, 55347, 56981, and 57131.*

## Radioactive Contamination and Decontamination

*Refer also to abstracts 54545, 54753, 54754, 54781, 54823, 54826, 54963, 55117, 55118, 55149, 55151, 55154, and 56582.*

**55194** (70-CNA-641) BIOLOGICAL SIGNIFICANCE OF RADIOACTIVE RELEASES TO THE ENVIRONMENT. Marko, A. M. (Atomic Energy of Canada Ltd., Chalk River (Ontario)). 1970. 12p. (CONF-700564–12). Dep. NTIS (U. S. Sales Only).

From tenth annual international conference of the Canadian Nuclear Association; Toronto, Canada (24 May 1970).

The biological significance of radioactive releases to the environment by the nuclear industry is discussed. The past record of the industry is mentioned and the significance of natural radioactivity and biological concentration processes in the human food chain is estimated. Radioactive releases from Canadian reactors are summarized. (E.R.B.)

**55195** (CONF-710401–, pp 352-64) APPROACH TO PLUTONIUM SURFACE CONTAMINATION LEVELS. Healy, John W. (Los Alamos Scientific Lab., N. Mex.). 15 Apr 1971.

From Rocky Flats symposium on safety in plutonium handling facilities; Golden, Colo. (13 Apr 1971).

A very brief summary of one attempt to obtain surface contamination levels as based on possible radiation doses to people is presented. The models used are crude and require refinement both in detail and in study of the individual factors involved. They do however indicate the possibility of more refined study of the possible impact of contamination and they open the door to consideration of very valuable studies of an applied health physics nature which will greatly expand understanding of the possible problems of control. In particular, it is emphasized that the numerical values obtained should be used only as guides to the professional in investigating particular cases and in establishing limits of sensitivity for routine monitoring. The prospect for deriving general contamination limits for use in release of materials and equipment seems discouraging at the moment because of the lack of definition of the many places these materials can go, the uses to which they are put, and the quantities so moved. It is possible, however, that detailed study of these factors, along with the transfer coefficients, could lead to acceptable models for many situations which could lead to the development of acceptable standards. (auth)

**55196** (LA–4558) SURFACE CONTAMINATION: DECISION LEVELS. Healy, J. W. (Los Alamos Scientific Lab., N. Mex.). Sep 1971. Contract W-7405-eng-36. 115p. Dep. NTIS.

Levels of contamination are derived for over 180 isotopes for the skin and clothing of workers and individuals in the general public as based on the National Council on Radiation Protection and Measurements (NCRP) recommendations on dose limitation. These levels consider the dose to the skin, the possible inhalation or ingestion of the deposited material, and possible absorption through the skin. Estimates of the levels for transfer to the home are based on these mechanisms plus direct external radiation and resuspension using plausible transfer coefficients. The relation of these transfer levels to transfers to other areas is discussed. Readings on several of the more common types of instruments used to measure surface contamination are then derived. Appendices to provide background data on specific subjects include Appendix A, The Skin; Appendix B, Beta Dose to The Skin; and Appendix C, Resuspension. All derived values for the decision levels for individual isotopes are given in Appendix D. (auth)

**55197** DETERMINATION OF $^{239}$Pu AND ENRICHED URANIUM IN THE URINE IN THEIR COMBINED PRESENCE. Golutvina, M. M.; Stepanov, A. P.; Sadikova, N. M.; Blinov, A. P. Med. Radiol.; 16: No. 9, 46-9(Sep 1971). (In Russian).

A method based on the destruction of tests by boiling with nitric acid and hydrogen peroxide, and concentration of isotopes by precipitation and subsequent extraction with precipitates of bismuth phosphate ($^{239}$Pu) and lantan fluoride (enriched uranium) is proposed. In conclusion, mixing of precipitates with a fluorescent compound and measurement of their radioactivity in a layer of hard scintillator are done. The efficacy of registration of alpha-particles comprises 90 to 95%. (auth)

**55198** MISUSE OF THRESHOLD LIMIT VALUES. Major, G. (Univ. of Sydney). Health Phys.; 21: No. 4, 611(Oct 1971).

It is pointed out that Cohen misused the concept of Threshold Limit Values in his recent publication (Health Phys. 19: 637(1970)). It is hoped that intended users of this concept would read the preface of the American Conference of Governmental Industrial Hygienists in which it is stated "that these limits are intended for use in the practice of industrial hygiene" and may not be used for "the establishment of standards for radionuclides in a natural gas supply". (UK)

**55199** PUBLIC HEALTH ASPECTS OF $^{129}$I FROM THE NUCLEAR POWER INDUSTRY. Russell, John L. (Public Health Service, Rockville, Md.); Hahn, Paul B. pp 241-51 of Health Physics Aspects of Nuclear Facility Siting. Vol. I. /Voilleque,

Paul G. (comp.). Idaho Falls, Idaho; Burton R. Baldwin, Publications Chairman (1971).

From fifth annual midyear topical symposium on health physics aspects of nuclear facility siting; Idaho Falls, Idaho (3 Nov 1970).

The production of $^{129}I$ in nuclear power reactors and its subsequent environmental releases during fuel reprocessing represent a potential long-term public health problem. Because of its extremely long half-life, any discharged $^{129}I$ is essentially a permanent contaminant in the biosphere, where it will eventually be found as a fraction of total iodine within a locality and possibly worldwide. This potential problem, its possible geographical scope, and the projected impact on population exposure are discussed along with data from measurements at nuclear power reactors and a fuel reprocessing plant. A concentration of 0.86% $^{129}I$ in total iodine produces the dose limit recommended by the FRC for a suitable sample of an exposed population. The quantity of $^{129}I$ discharged from operating power reactors was estimated from measurements of $^{131}I$ discharges by calculating a $^{129}I/^{131}I$ buildup ratio. This analysis showed the $^{129}I$ discharge from operating power reactors was negligible. Measurements at a fuel reprocessing plant indicated that approximately 10% of the total $^{129}I$ inventory in spent fuel was discharged from the stack during the batch dissolution process. The liquid discharge concentrations were about 2% of the total $^{129}I$ inventory. Iodine-129 levels in deer thyroids taken in the reprocessing plant locality were about 40% of levels of FRC guidance for human thyroids. (auth)

**55200** RECAPITULATION OF EFFLUENT RELEASES AND RELATED CHANGES IN BACKGROUND RADIATION LEVELS AT BROOKHAVEN NATIONAL LABORATORY, AND SOME COMPARISONS WITH THOSE ASSOCIATED WITH NUCLEAR POWER REACTOR PLANTS. Hull, Andrew P. (Brookhaven National Lab., Upton, N. Y.). pp 342-60 of Health Physics Aspects of Nuclear Facility Siting. Vol. II. /Voilleque, Paul G. (comp.). Idaho Falls, Idaho; Burton R. Baldwin, Publications Chairman (1971).

From fifth annual midyear topical symposium on health physics aspects of nuclear facility siting; Idaho Falls, Idaho (3 Nov 1970).

Laboratory operations at Brookhaven since its establishment in 1949 have included the routine release to the environment of gaseous, halogen, air particulate, and $^{3}H$ radioactivity in reactor air effluents and of beta-gamma emitters and $^{3}H$ in low-level liquid wastes in amounts comparable to current releases from power reactors. Past and current surveillance data at BNL were evaluated for short and long-term changes in radiation levels attributable to these operations. The relation between the large amounts ($4.5 \times 10^{6}$ Ci/yr) of $^{41}Ar$ emitted from the 100m BGRR stack and observed downwind radiation levels is indicated and is used to estimate the ground level doses from the smaller amounts of fission gases emitted from power reactors. The data examined for cumulative deposition of long-lived air effluent nuclides include continuous measurements of external background radiation levels, both on and off site, and measurements of gamma-emitters in soil and vegetation and of $^{90}Sr$ and $^{137}Cs$ in milk from close-in and more distant farms. The data examined for the accumulation or uptake of radionuclides contained in liquid effluents include the concentrations and amounts of activity discharged into and released from a sanitary waste treatment facility, average concentrations in water samples from downstream and remote locations, current concentrations of radionuclides in the stream sediments and vegetation, and the current concentrations in samples of water from eleven widely separated on-site supply wells. On the basis of these data, it is concluded that few changes in background should be apparent, even after long-term operation of nuclear power reactors. (auth)

**55201** DETERMINATION OF THE MAXIMUM PERMISSIBLE BODY BURDENS USING THE METHODS OF THE MEDICAL INTERNAL RADIATION DOSE (MIRD) COMMITTEE OF THE SOCIETY OF NUCLEAR MEDICINE. Schadt, Warren W. (Radiological Health Div., Washington, D. C.); Battist, Lewis. pp 590-9 of Health Physics Aspects of Nuclear Facility Siting. Vol. III. /Voilleque, Paul G. (comp.). Idaho Falls, Idaho; Burton R. Baldwin, Publications Chairman (1971).

From fifth annual midyear topical symposium on health physics aspects of nuclear facility siting; Idaho Falls, Idaho (3 Nov 1970).

Maximum permissible body burdens, "q," for 31 radionuclides were calculated using the methods of the Medical Internal Radiation Dose (MIRD) Committee of the Society of Nuclear Medicine in combination with the methods and biological data of ICRP Publication 2. For 24 of these radionuclides, the ICRP method is conservative by a factor ranging from 1.0 for $^{32}P$ in bone to 2.7 for $^{52}Mn$ in the pancreas. Seven of the isotopes considered showed a decrease in the MIRD value of "q." These radionuclides and their ratios of the MIRD "q" to the ICRP "q" are listed. These ratios are dependent upon the decay scheme data and the methods used to determine the energy absorbed in the critical organ per unit energy emitted by the source (absorbed fraction). The dependence of the ratio on decay scheme data is eliminated by using the MIRD decay scheme data in the ICRP formulation. The revised ratio, "Q," is then a function only of the absorbed fraction. The values of "Q" are also shown. Except for $^{113}Sn$ in bone, the ratios for all radionuclides indicate that the ICRP results are conservative by a factor ranging from approximately 1 to 2. (auth)

**55202** ESTIMATION OF THE RELATIVE INHALATION HAZARD OF REACTOR INVENTORY RADIONUCLIDES. Raabe, Otto G. (Lovelace Foundation for Medical Education and Research, Albuquerque, N. Mex.). Contract AT(29-1)-1013. pp 619-33 of Health Physics Aspects of Nuclear Facility Siting. Vol. III. /Voilleque, Paul G. (comp.). Idaho Falls, Idaho; Burton R. Baldwin, Publications Chairman (1971).

From fifth annual midyear topical symposium on health physics aspects of nuclear facility siting; Idaho Falls, Idaho (3 Nov 1970).

The relative hazard in a nuclear reactor accident from inhalation of radioactive aerosols and vapors was considered on the basis of a model of the inventory of radionuclides in a uranium fueled reactor for 1 yr and 5 yrs of sustained operation. The use of plutonium fuel is also discussed. This approach involves estimation of the relative probabilities of accidental release and the relative probabilities of the production of airborne material of soluble or insoluble forms with respect to lung clearance. With the latest information on the distribution and excretion of both soluble and insoluble forms of the radionuclides, the biological solubility probabilities are used to calculate the relative doses of radiation to various organs after inhalation exposure. The inventory model, release probabilities, solubility probabilities, and organ dose calculations are then combined to provide the relative organ dose estimates and relative hazard estimates of the reactor inventory nuclides. (auth)

## *Dosimetry and Monitoring*

*Refer also to abstracts 54784, 54789, 54987, 55002, 55006, 55032, and 55152.*

**55203** (CEA-N-1449) HEALTH PHYSICS DEPARTMENT PROGRESS REPORT FROM THE NEUTRON WORKING GROUP, MARCH 1969–DECEMBER 1970. (Commissariat a l'Energie Atomique, Fontenay-aux-Roses (France). Centre d'Etudes Nucleaires). Jun 1971. 96p. (In French). Dep. NTIS (U. S. Sales Only).

The current program of the Health Physics department DPS (Department de la Protection Sanitaire) on the problems raised by the exposure of the human body to mixed radiations (neutrons, gamma radiation) is discussed. The dosimetric studies, which were largely carried out in collaboration with other services within the working group (CRAC) of the DPSR, concern the evaluation of internal doses, sodium activation within the body, and sulfur activation of the hair, nails, and clothes. Radiological studies were made on the formation of dicentric chromosomes in lymphocytes following in vitro exposure of human blood, the hematological evolution, LD 50 (30 days), weight loss and the pathology of delayed mortality in rats, and the excretion of urinary amino acids and electrolytes in rats. (France)

**55204** (CONF-710401–, pp 267-79) IN-RESIDENCE HEALTH AND SAFETY SUPPORT IN A PLUTONIUM FACILITY. Morse, J. L.; Marshall, A. L.; Celoni, A. M. (California Univ., Livermore. Lawrence Radiation Lab.). 14 Apr 1971.

From Rocky Flats symposium on safety in plutonium handling facilities; Golden, Colo. (13 Apr 1971).

Health and Safety Technicians (monitors) provide in-residence safety services to the metallurgical research and engineering effort of the plutonium facility at the Lawrence Radiation Laboratory, Livermore. The qualifications of these technicians and typical services rendered by them to the facility scientific personnel, such as, contamination control, waste recovery, monitoring of air sampling equipment, frequent smear and swipe samples, radiation surveys, equipment calibration, out-processing of liquid and solid wastes to control fire and criticality hazard, etc., are described. (auth)

**55205** (NYO-2740-8) ANNUAL REPORT ON RESEARCH PROJECT. (Columbia Univ., New York. Radiological Research Lab.). 1 Jul 1971. Contract AT(30-1)-2740. 259p. Dep. NTIS.

Separate abstracts were prepared for the three sections presented. (W.H.K.)

*For abstracts of individual sections see: 55002, 55206, and 55207.*

**55206** (NYO-2740-8, pp 147-219) BIOPHYSICS. (Columbia Univ., New York. Radiological Research Lab.).

In Annual report on research project.

Studies on the theory of dual radiation action were continued. The analysis of the action of ionizing radiation based on the dependence of RBE on absorbed dose is discussed. It is pointed out that the effect probability is over a wide range of doses dependent on the square of the x-ray dose but that the dependence on neutron dose includes linear and quadratic dose terms. Equations are presented to show these relationships. The role of somatic mutations of germinal cells in the lens epithelium in the process of opacification was investigated. Experiments on the effects of split doses of 250 kVp x rays on the production of flecks (subcapsular opacities) in mice were conducted. A comparison of results with the effects of 380 keV neutrons is in progress. Studies on radioinduced translocations in chromosomes of Drosophila melanogaster using x rays, 0.68 MeV neutrons, and 14.3 MeV neutrons were continued. Dominant lethal mutations induced by neutrons and x rays in Drosophila were also studied. Studies were conducted using Tradescantia stamen hairs and pollen to obtain RBE values for neutrons of various energies compared with x rays. These studies included power relations as an expression of RBE in Tradescantia stamen hairs; relations between phenotypic aberrations and loss of reproductive integrity in Tradescantia stamen hairs; dose response curves for somatic aberrations in Tradescantia stamen hairs at very low doses of 0.43 MeV neutrons and x rays; dose response curve and RBE values for pink aberrant events after irradiation with 13.4 MeV neutrons; and pollen abortion in members of the Tradescantia family. Theorems on dose effect relations are described and equations are developed to show the minimum number of events involved in the effect on the cell and the meaning of the slope of the dose effect curve in double logarithmic scale. (H.L.W.)

**55207** (NYO–2740-8, pp 220-59) RADIOBIOLOGY. (Columbia Univ., New York. Radiological Research Lab.).

In Annual report on research project.

Chinese hamster cells were exposed to a range of low dose rates from radium gamma rays or the mixed neutron and gamma-ray emission from $^{252}Cf$. Cell division was inhibited during the prolonged radiation exposures by temporarily reducing the temperature. After irradiation the cells were returned to 37° and survivors identified by their ability to form colonies in a period of 8 days. Graphs are presented to show cell survival estimates. A discussion is presented of the relative biological effectiveness of $^{252}Cf$ neutrons compared with radium and the dependence of tolerance dose on dose rate. Applications of the results in radiotherapy are considered. Experiments on comparison of 210 kV x rays and alpha particles were conducted using cultured hamster cells; survival data are shown by means of graphs and results indicate that the RBE varies as a function of dose. Cultured hamster cells were used to study the radiosensitizing effects of nydrazid, a drug commonly used for the control of tuberculosis. It was found that the drug did not appear to potentiate the effect of x rays at the cellular level. Studies on radioembryology included chromosome studies on irradiated mouse fetuses; the effect of x rays on the monkey fetal heart; immediate and long-term effects of irradiating mouse sperm; and radiation and its consequences to the mammalian embryo and fetus. (H.L.W.)

**55208** (NYO–3510-18) BIOLOGICAL AND CLINICAL DOSIMETRY. Annual Progress Report, July 1, 1970–June 30, 1971. Laughlin, John S. (Sloan-Kettering Inst. for Cancer Research, New York). Contract AT(30-1)-3510. 26p. Dep. NTIS.

The fabrication of the tissue-equivalent absorbed dose calorimeter for neutrons was completed and assembly and testing are in progress. A preliminary comparison was made of the sensitivity of the hexahydroxyethyl pararosaniline cyanide radiochromic dosimeter to γ rays and neutrons. Results indicate that these are approximately equal and that further investigation of this system is desirable. Measurements are continuing of the LET distributions produced by various neutron sources and a search for an optimum method of data smoothing for computer processing of this data is being pursued. Dosimetric studies substantive to a variety of biological experiments utilizing cyclotron produced neutrons and $^{252}Cf$ spontaneous fission sources are in progress. Pulsed electron sources such as 600 kV field emission generators can deliver doses in excess of $10^6$ rads in single pulses having duration times of a few nanoseconds. When these sources are used to irradiate thin layers of cells, the measurement of absorbed dose is complicated by the associated high dose rates, the relatively low electron energy, and the thickness of the sample that may be only a few microns. In this laboratory, the problem of measuring absorbed dose was investigated by the use of thin disks of Pilot-B, a commercially available fast response plastic scintillator. The measurement of light pulses from the scintillator was accomplished with a nanosecond pulse integrator constructed at this laboratory. The determination of the dose delivered to a cell layer made use of an extrapolation technique in which varying thicknesses of a scintillator disk are placed at the irradiation position in the same geometry as the cellular layer. A thin foil absorbed dose calorimeter was constructed to provide a calibration for the scintillator light output. Since the dynamic range of the scintillator system is quite large, it was possible to perform absorbed dose measurements over the large range of doses used for various radiobiological experiments. A small prototype gamma camera based upon a single (2 × 2) cm diode of p-type ultra-pure germanium has reached an operational stage. Two dimensional information from the camera is achieved through the use of the orthogonal strip geometry developed at Sloan–Kettering in a lithium drifted silicon diode. Preliminary data indicate a spatial resolution of within (3.5 × 3.5) mm for $^{57}Co$ (122 keV). Evaluation of image quality is in progress. (auth)

**55209** PARAMETERS OF BETATRON B-30 BREMSSTRAHLUNG. Mil'shtein, R. S.; Kornev, I. I. (Moscow Scientific Research Inst. of Roentgen-Radiological). Med. Radiol.; 16: No. 9, 67-70(Sep 1971). (In Russian).

The use of high-energy bremsstrahlung in the radiation treatment of malignant tumors is associated with features specific to its dose fields in tissue-equivalent media, particularly in a low relative entry dose and depth-distribution of the maximum of radiation. However, these advantages are not completely realized in the instance when the beam contains the electron component. In the beam of bremsstrahlung may be either chamber-accelerated electrons (an accelerating chamber with an external target), or electrons emitted from an aligning filter. Purification of the beam from accelerated electrons may be effected by different methods: an internal target, the use of a magnetic or electrostatic filter. (auth)

**55210** ISODOSE DISTRIBUTION OF A BEAM OF POSITRONS WITH AN ENERGY OF 5 TO 15 MeV. Gumanskii, G. A.; Tarutin, I. G.; Pilyavets, V. I. (Scientific Research Inst. of Oncology, Minsk. Inst. of Medical Radiology, Minsk). Med. Radiol.; 16: No. 9, 64-7(Sep 1971). (In Russian).

The results of investigations of the isodose distribution created by positrons with an energy of 5, 10, and 15 MeV in a water phantom, and the technique are described. The authors compare the derived distributions with analogous distributions for electrons. It is shown that positrons have lesser fields of scattering. (auth)

**55211** PROGRAMMING OF IRRADIATION AND DESCRIPTION OF THE DOSE FIELD. Vainberg, M. Sh. (Inst. of Experimental and Clinical Oncology, Moscow). Med. Radiol.; 16: No. 8, 69-74(Aug 1971). (In Russian).

Diverse techniques in the programming of irradiation and a variety of methods of describing the dose field in the irradiated body hampers the use of information and the exchange of experiences with radiation therapy not only between countries but also within a single country. A survey is presented of measurements that were directed toward systematization and classification of isodose charts. Practical expedients and systems of administering radiation are examined with a view toward standardizing the graphical description of the dose field in an irradiated body. (tr-auth)

**55212** LOCAL IRREGULARITY OF DOSES IN NEUTRON-CAPTURE THERAPY. Zaichik, V. E.; Ivanov, V. N.; Ryabukhin, Yu. S. (Scientific Research Inst. of Medical Radiology, Moscow). Med. Radiol.; 16: No. 8, 63-8(Aug 1971). (In Russian).

The problem of the local irregularity of doses during neutron-capture therapy of malignant neoplasms with the employment of neutron-capturing nuclides yielding heavy loaded particles is discussed. (auth)

**55213** TISSUE EQUIVALENT SCINTILLATORS IN RADIOMETRY OF LONG WAVE X RADIATION. Frolova, A. V.; Kolotilova, V. G.; Krongauz, A. N.; Shagimardanov, N. Sh. (Moscow Scientific Research Radiological Inst.). Med. Radiol.; 16: No. 8, 59-62(Aug 1971). (In Russian).

The results of experimental determination and the calculation of absorbed doses of long-wave x radiation are presented for muscle and bone tissue-equivalents in the form of polystyrene masses that contained certain organic additives capable of scintillation. Three sets of operating conditions were employed with respect to machine voltages and thickness of aluminum filters, and three different thicknesses of the scintillator materials (5, 10, and 15 mm) were used. Curves are presented that portray the distribution of the absorbed dose as a function of various parameters. (KSW)

**55214** CALCULATION OF THE DOSE DISTRIBUTION OF HIGH-ENERGY ELECTRONS IN TISSUE-EQUIVALENT MEDIA. Khvan, G. V.; Azhigaliev, N. A. (Scientific Research Inst. of Oncology and Radiology, Alma-Ata, USSR). Med. Radiol.; 16: No. 8, 54-8(Aug 1971). (In Russian).

XUM

Methods of evaluating the distribution of doses in homogenous and heterogenous body in normal and inclined beam of fast electrons are discussed. Analytical expressions are given for the dose distribution of electrons in the irradiated medium during the use of $\beta$-15 MeV betatron. Since in the referred to values, the relative dose distribution for different fields and energies of irradiation practically proved to be identical, these formulas also could be employed to electron beams up to 35 MeV. (auth)

**55215** RELATION BETWEEN RBE AND LET TO INHIBIT NEURAL IMPULSE CONDUCTION. Gaffey, C. T. (Univ. of California, Berkeley). Radiat. Res.; 47: No. 2, 511-25(Aug 1971).

A dose of 285 krad (average) of 200-kV x rays absorbed by isolated, frog sciatic nerves promptly inactivated impulse transmission. Blockage of neural activity in this type of nerve required 600 krad (average) of 47.5-MeV protons. Protons of this energy have a relative biological effectiveness (RBE) of 0.48 with respect to 200-kV x rays, which have an assigned value of one. Other investigators exposed frog nerves to different types of radiation and reported inactivation doses. RBE values determined from such doses were 0.66 for 910-MeV $\alpha$ particles, 0.87 for 260-kV x rays, and 30.60 for 5.3-MeV $\alpha$ particles. The RBE values to suppress neural activity depended on the linear energy transfer (LET) of the radiation particles. Radiations with high LET values had high RBE values. A plot of the logarithm of RBE vs the logarithm of LET yielded a linear relation for radiations with LET values between 1.3 and 110.0 keV/$\mu$ of tissue. Frog sciatic nerves exposed to either 200-kV x rays or 47.5-MeV protons exhibited bioelectric changes prior to loss of excitability. Conduction velocity decreased and the detection period (stimulus-response interval) increased after nerves absorbed only one-fourth the inactivation dose. The present investigation failed to confirm the observation of others that the action potential amplitude increased with the onset of radiation. The action potential remained unaltered even after nerves absorbed one-fourth the inactivation dose of x rays and one-half the inactivation dose of protons. (auth)

**55216** CALCULATION OF THE ABSORBED DOSE AND DOSE EQUIVALENT INDUCED BY MEDIUM-ENERGY NEUTRONS AND PROTONS AND COMPARISON WITH EXPERIMENT. Armstrong, T. W.; Bishop, B. L. (Oak Ridge National Lab., Tenn.). Radiat. Res.; 47: No. 3, 581-8(Sep 1971).

Monte Carlo calculations were carried out to determine the absorbed dose and dose equivalent for 592 MeV protons incident on a cylindrical phantom and for neutrons from 580 MeV proton–Be collisions incident on a semi-infinite phantom. For both configurations, the calculated depth dependence of the absorbed dose is in good agreement with experimental data. (auth)

**55217** TECHNIQUES OF LIQUID SCINTILLATION AND APPLICATIONS IN RADIOPROTECTION. Gillet, R.; Regibeau, A. (Univ. Catholique, Louvain, Belg.). J. Belge Radiol.; 54: No. 3, 441-5(May-Jun 1971). (In French).

The methods used for the counting of low energy beta emitters and the individual and automatic determination of efficiencies are described. Their current applications in an ionizing radiation control laboratory are reviewed. (auth)

**55218** USES OF THE COMPUTER IN RADIOTHERAPY. III. CALCULATION OF OPPOSED FIXED-FIELD IRRADIATION PLANS IN TELECOBALT-THERAPY. Milanesi, R. (Istituti Ospitalieri, Verona, Italy); Pasoli, A.; Puppini, G.; Cabassa, N. Radiol. Med.; 56: No. 12, 1155-68(Dec 1970). (In Italian).

Employment of an IBM 1130 computer in the calculation of opposed fixed-field irradiation plans in telecobalt-therapy is described. Two of the more common modalities are considered: emission of a 1/1, and a 1/0.5 skin dose from the two points of entry. Two plan versions are presented: the first is linked only to the percent distribution of the second, while the second also takes evaluation uniformity in the dose delivered to various patients into account. The fact that the computer is capable of preparing a treatment plan on the basis of effective per cent values in as little as 5 ÷ 10 s means that the uniformity of evaluation with respect to the dose delivered to series of patients according to the methods described can be obtained. (auth)

**55219** RATIO TISSUE AND MAXIMUM FOR 42 AND 25 MV X-RAYS OF A 42 MeV BETATRON. Fehrentz, Dieter; Herbig, Wolfgang (Univ., Heidelberg). Strahlentherapie; 141: No. 6, 662-5(Jun 1971). (In German).

By means of a Siemens 42-MeV betatron, the tissue/maximum ratio for x rays of 42 and 25 MV was determined. Its dependence on field size, focal distance, and field compensating body was examined. (auth)

**55220** PROGRAM FOR COMPUTATION OF DOSE DISTRIBUTIONS IN TELETHERAPY WITH $^{60}$Co GAMMA RADIATION. II. STRUCTURE AND PROCEDURES OF THE PROGRAM. Leetz, Hans-Karl (Univ. des Saarlandes, Homburg, Ger.). Strahlentherapie; 141: No. 6, 682-90(Jun 1971). (In German).

A computer program for calculating $^{60}$Co $\gamma$ dose distribution in a radiotherapy department with high patient load is described. The program is simple, error-safe, and can be handled by a medical technician. Basic steps are presented in five block diagrams. Input data are presented by punch tape and the drawing of a cross section of the radiation plane. The program covers up to 16 stationary radiation fields, as long as the central beams lie in the same plane. For Pendulum radiation it yields the rotational axis and angular velocity. Printout usually occurs as a drawing of the patient cross section with isodose curves. If desired, printout may also be obtained in table form by typewriter as punch tape. The entire procedure from input to printout requires 10 to 15 minutes for one patient. (H.B.G.)

**55221** PROGRAM USED FOR CALCULATION OF DOSE DISTRIBUTIONS FOR TELETHERAPY WITH $^{60}$Co-GAMMA RAYS. III. EXPERIMENTAL RESEARCH. Leetz, Hans-Karl (Univ. des Saarlandes, Homburg, Ger.). Strahlentherapie; 141: No. 6, 691-5(Jun 1971). (In German).

The construction and mode of action of a calculation program for a digital process calculator in routine calculation of dose distributions for teletherapy with $^{60}$Co-gamma radiation are described. (auth)

**55222** EXPERIMENTS CONCERNING THE STANDARDIZATION OF THE 2- AND 4-AXIAL $^{60}$Co PENDULUM IRRADIATION OF THE SMALL PELVIS. (POSSIBILITIES FOR A SIMPLIFIED CALCULATION OF THE DOSAGE PARAMETER). Welker, Klaus; Eichhorn, Hans-Juergen (Institut fuer Krebsforschung, Berlin). Strahlentherapie; 141: No. 6, 655-61(Jun 1971). (In German).

The routine application of 2- and 4-axial $^{60}$Co pendulum irradiation of the small pelvis is made possible by standardization of irradiation conditions. Standard dosages that are applied under consideration of the tissue's inhomogeneity are suitable to any case with a maximal deviation of 10%. The focal dose capacity, or time of irradiation, dose volume, and relative focal dose volume are determined by measuring the patient's sagittal and frontal diameter in the irradiation plain. Tables are given from which the three mentioned parameters in relation to the 2 diameters can be learned so that the standard dosages can be easily applied to any individual case with a satisfying deviation. (auth)

**55223** CONTENT OF $^{90}$Sr, Ca, AND STRONTIUM UNITS IN SEEDS OF WHEAT HYBRIDS OBTAINED FROM THE CROSS TRITICUM AESTIVUM x TRITICUM DICOCCUM. Kal'chenko, V. A.; Budashkina, E. B.; Khvostova, V. V. (Inst. of General Genetics, Moscow. Inst. of Cytology and Genetics, Novosibirsk, USSR). Genetika; 7: No. 8, 85-9(Aug 1971). (In Russian).

The content of $^{90}$Sr, Ca, and strontium units was studied in plants of interspecific wheat hybrids ($F_3$) obtained from the cross Triticum aestivum × Tr. dicoccum. It is shown that these hybrids, differ in $^{90}$Sr content in seeds. A low content of $^{90}$Sr is characteristic both of the hybrids having the phenotype of Tr. dicoccum and of Tr. aestivum. Hybrids with a low content of $^{90}$Sr in seeds have different numbers of chromosomes (28 to 42). It is shown that the method of hybridization makes it possible to obtain 42-chromosome forms in which the morphological characters and the chromosome number inherent in Tr. aestivum are combined with a low content of $^{90}$Sr in seeds characteristic of Tr. dicoccum. (auth)

**55224** DOSIMETRY OF FAST ELECTRON BEAMS. Renzi, R. (Univ., Florence). Minerva Fisiconucl.; 13: 249-61(Jul-Sep 1969). (In Italian). (CONF-680535-27).

From fourteenth national conference of the Italian Association for Health Physics and Protection from Radiation; Formia, Italy (29 May 1968).

The base dosimetry of fast electron beams is considered from four viewpoints: energy calibration of the beam, evaluation of the dose in irradiated materials and definition of the yield, dose distribution in irradiated materials, and controls. (J.S.R.)

**55225** RESULTS OF THE INTERNATIONAL COMPARATIVE STUDY BY THE MEMBERS OF THE EUROPEAN COMMUNITY ON THE EFFECTIVENESS OF MEASUREMENTS MADE WITH THE HUMAN WHOLE-BODY $\gamma$ COUNTER. Smeets, J. (EURATOM, Luxembourg); Schmier, H. Minerva Fisiconucl.; 13: 292-300(Oct-Dec 1969). (In French). (CONF-680535-28).

From fourteenth national conference of the Italian Association

for Health Physics and Protection from Radiation; Formia, Italy (29 May 1968).

A comparative study was made of the measurements of the total K and $^{137}Cs$ content in the human body. The measurements were made in vivo with whole-body counters on persons of different height and weight who, within a short period, toured all the measurement installations of the European Community. Each laboratory made the measurements by its usual method. In spite of certain divergences, the results are in very good agreement. Some of the installations had difficulty during the measurements because of the very low concentrations of $^{137}Cs$ present in the human body. (tr-auth)

**55226** RADIATION EXPOSURE TO PERSONNEL DURING CARDIAC CATHETERIZATION. A PRELIMINARY STUDY. **Malsky, Stanley J.; Roswit, Bernard; Reid, Cyprian B.; Haft, Jacob (Veterans Administration Hospital, Bronx, N. Y.). Radiology; 100: No. 3, 671-74(Sep 1971).**

The radiation exposure to personnel in the examining room during a complete cardiac catheterization procedure was studied. Commercial film badges and thermoluminescent LiF wafers were worn at several anatomical sites. Data on the examining physician alone indicate an exposure of 50 mrems to the trunk area during a complete cardiac procedure. Exposure levels for two attending physicians, a nurse, and a technician are also given. (auth)

**55227** DOSE DISTRIBUTION FOR SINGLE- AND THREE-PHASE X-RAY EQUIPMENT. **Barone, Gregory J.; Trout, E. Dale (Oregon State Univ., Corvallis). Radiology; 100: No. 3, 663-9(Sep 1971).**

When single- and three-phase systems are operated at equal peak kilovoltages to perform a given radiographic examination, there must be a higher exposure for the single-phase system, and the depth doses within the subject are higher. However, the kilovoltage can be adjusted to provide equivalent x-ray beam quality. There is no appreciable difference in the dose distribution when this is done. (auth)

**55228** BIOLOGICAL DOSIMETRY IN AN INDUSTRIAL RADIOGRAPHY ACCIDENT. **Brown, J. K.; McNeill, J. R. (Australian Atomic Energy Commission Research Establishment, Sutherland). Health Phys.; 21: No. 4, 519-22(Oct 1971).**

A biological assessment was made of the radiation exposures received by two healthy adults who were accidentally exposed to a 22 Ci/$^{192}Ir$ source. Each subject had the same number of dicentric chromosome aberrations in short term peripheral blood cultures at both day 8 and day 21 after exposure. The frequency of dicentrics for each subject was equivalent to an in vitro dose of 29 Rem. The corresponding film badge reading for one subject was 22 Rem. Analysis of the results suggests that this method can be used to give a reasonable estimate of low levels of radiation exposure provided that the size of the chromosome sample is adequate. (auth)

**55229** DOSE AND LET IN A RABBIT AND A RAT. **Jones, T. D. (Oak Ridge National Lab., Tenn.). Health Phys.; 21: No. 4, 553-62(Oct 1971).**

Monte Carlo radiation transport codes were used to study dose and LET distributions in phantoms corresponding to a rabbit and a rat in size. Monoenergetic neutrons of 0.025 eV, 1 eV, 10 eV, 100 eV, 1 keV, 10 keV, 100 keV, 500 keV, 1 MeV, 2.5 MeV, 5 MeV, 7 MeV, 10 MeV, and 14 MeV were assumed to be unilaterally and bilaterally incident in broad, parallel beams. Distributions of dose vs depth are given for contributions from recoil ions and neutron-produced $\gamma$ rays and are complemented by corresponding LET distributions. Doses distributed according to the energy of the incident neutrons are also given for the reactions that are major contributors to dose. (auth)

**55230** ESTIMATION OF GENETICALLY SIGNIFICANT DOSE EQUIVALENT FROM OCCUPATIONAL EXPOSURE TO EXTERNAL SOURCES OF RADIATION IN JAPAN. **Maruyama, Takashi (National Inst. of Radiological Sciences, Chiba, Japan); Kumamoto, Yoshikazu; Nishimura, Akihisa; Hashizume, Tadashi; Yasubuchi, Shiro. Health Phys.; 21: No. 4, 563-9(Oct 1971).**

The genetically significant dose equivalent from occupational exposure in Japan was estimated. The annual individual dose from external x-ray, $\gamma$-ray, and neutron sources in various types of radiation work was evaluated from the personnel monitoring records. Information is presented on the numbers of installations and radiation workers in Japan. The mean annual dose equivalent in medical, industrial, research and educational, and atomic work was 377, 291, 88.6, and 125 mrem per yr, respectively. The genetically significant dose equivalent in medical, industrial, research and educational, and atomic energy work was 0.082, 0.032, 0.0053, and 0.0056 mrem per yr, respectively. (auth)

**55231** EXPOSURE RATES FROM THE PRODUCTS OF THERMAL-NEUTRON FISSION OF $^{235}U$ AT SELECTED TIMES AFTER FISSION. **Sam, Daniel; Bunney, Leland R. (Naval Ordnance Lab., Silver Spring, Md.). Health Phys.; 21: No. 4, 585-9(Oct 1971).**

The exposure rates, in units of (R/hr)/(fission/cm$^2$), at 3 ft above a uniformly contaminated smooth plane were calculated from the recent experimentally determined $\gamma$-ray spectra of the unfractionated products of thermal-neutron fission of $^{235}U$ at nine selected times (1/4, 1/2, 1, 2, 5, 10, 24, 48, and 72 hr) after fission. The photon energy release rate and the average photon energy for the unfractionated products of thermal-neutron fission of $^{235}U$ and fast-neutron fission of $^{235}U$ and $^{238}U$ were calculated and are also given. (auth)

**55232** IN-PHANTOM MICRODOSIMETRY WITH 14.6 MeV NEUTRONS. **Heintz, Philip H.; Robkin, M. A.; Wootton, Peter; Bichsel, Hans (Univ. of Washington, Seattle). Health Phys.; 21: No. 4, 598-602(Oct 1971).**

The spectra of energy deposition of charged particles produced by 14.6 MeV neutrons in a gas filled proportional counter were measured as a function of location in a tissue equivalent medium, and also in free space. A marked dependence of the form of the spectra was found. (auth)

**55233** DOSE FUNCTION OF A PLANE INFINITELY THIN SOURCE SITUATED ON THE DIVIDING BOUNDARY BETWEEN TWO MEDIA. **Osanov, D. P.; Podsevalov, Yu. N. At. Energ. (USSR); 31: No. 3, 287-9(Sep 1971). (In Russian).**

A study was made of the dose function of a plane, infinitely-thin source situated at the interface of two media, one of which being of tissue-equivalent material. Above and below the source the media are considered to be a "scatterer" and an "absorber." The dose coefficient of backscattering was shown to be independent of the limiting energy of the $\beta$-spectrum, but was determined as a function of the absorber thickness and scatterer material. The relation between the dose and numerical coefficients to the atomic number of the scatterer was also determined. Another graph showed the relation of the backscattering coefficient for a tissue-equivalent scatterer to the thickness of the scatterer and absorber. (K.S.W.)

**55234** METHOD OF DOSIMETRY FOR A BULK-GRAIN IRRADIATOR. **Tilton, E. W.; Brower, J. H.; Cogburn, R. R. (Agricultural Research Service, Savannah). Contract AT(49-11)-2676. Int. J. Appl. Radiat. Isotop.; 22: No. 10, 577-80 (Oct 1971).**

The advantages of a lithium fluoride thermoluminescent dosimetry system for use in a bulk-grain irradiator are discussed. Unique problems of dosimetry exist because dosimeters must be mixed with the grain, must have the same flow characteristics as the grain, and must have adequate resistance to breakage. Tests proved that encapsulated LiF dosimeters provide an accurate record of absorbed dose in a mass of wheat treated by a bulk-grain irradiator. Variations in dosage revealed by the dosimeters showed satisfactory treatment of the majority of the wheat, with overexposure of a small percentage. (auth)

**55235** ACCIDENTAL DOSAGE ESTIMATION AT LARGE GAMMA-IRRADIATION FACILITIES. **Chistov, E. D.; Sprygaev, I. F.; Korenkov, I. P.; Terman, A. V.; Sedov, A. V. At. Energ. (USSR); 30: No. 5, 460-2(May 1971). (In Russian).**

The total dosage at any given point in a gamma-irradiation labyrinth is composed of straight-line and reflected radiation, and is defined in a mathematical relationship which involves the following parameters: the gamma-equivalent irradiator, physical distances from the source, concrete shielding thickness, the area of the scattering surface, exposure time, the angle between the normal to the scattering surface, the direction of the incident radiation, and various coefficients. Data calculated from this equation was evaluated using a phantom man and a $^{60}Co$ source with an activity of 4000 $\gamma$-equivalent Ra. The phantom was provided with 22 aluminum phosphate dosimeters. Significant differences between calculated and experimental dosages may be explained by the screening of some portions of the phantom by constructional details of the irradiation facility. (K.S.W.)

**55236** DETECTION OF ALPHA-RADIONUCLIDES IN THE BONE–MARROW AND BLOOD OF MINERS BY THE METHOD OF NUCLEAR EMULSIONS. **Bradna, F. (Radiologicka Dozimetrie Ustavu Jaderneho Vyzkumu CSAV, Prague); Havelkova, V.; Zackova, H.; Prokopec, J. Radioisotopy; 11: No. 5, 755-65 (1970). (In Czech).**

The nuclear emulsion method for the detection of extra low activities in biological materials is discussed. The composition of used nuclear emulsion is described as well as the method of

XUM

optimum time for exposure by biological material (bone-marrow, blood) and the method of microscopic evaluation. Quantitative results for number of tracks of alpha-particles in 24 samples (from three miners and three non-exposed persons) are given. (auth)

**55237** ESTIMATE OF RADIATION DOSES RECEIVED BY INDIVIDUALS LIVING IN THE VICINITY OF A NUCLEAR FUEL REPROCESSING PLANT IN 1968. Shleien, B. (Dept. of Health, Education, and Welfare, Winchester, Mass.). pp 226-40 of Health Physics Aspects of Nuclear Facility Siting. Vol. I. /Voilleque, Paul G. (comp.). Idaho Falls, Idaho; Burton R. Baldwin, Publications Chairman (1971).

From fifth annual midyear topical symposium on health physics aspects of nuclear facility siting; Idaho Falls, Idaho (3 Nov 1970).

The public health implications associated with a nuclear facility can be best evaluated in terms of the radiation dose delivered to persons in the vicinity of the facility. This report attempts, by use of the dose commitment concept and surveillance data previously collected, to estimate radiation doses in 1968 to persons in the vicinity of a fuel reprocessing plant from ingestion and inhalation. The dose commitment accrued in 1968 to a hypothetical typical individual is not thought to differ significantly from that for the typical individual in the rest of New York State and is attributable to fallout. This commitment was 77 millirem from strontium-90 to the bone and 1.7 millirem whole body from cesium-137 delivered over a 50-year period. For the hypothetical maximum individual, the dose commitment to the bone from strontium-90 is 532 millirem and the first-year dose following ingestion is 38 millirem. The whole-body dose from ingestion of cesium-137 and cesium-134 (mostly from deer meat) is 257 millirem. Preliminary data indicate that the external gamma dose above natural background is approximately 1.2 millirem per year to the maximum individual. Estimated doses from tritium and krypton-85 were negligible (about 2 millirem/year). (auth)

**55238** ECOLOGICAL APPROACH TO ENVIRONMENTAL SURVEILLANCE. Bolch, W. E.; Gamble, J. F.; Roessler, C. E.; (and others) (Univ. of Florida, Gainesville). pp 252-65 of Health Physics Aspects of Nuclear Facility Siting. Vol. II. /Voilleque, Paul G. (comp.). Idaho Falls, Idaho; Burton R. Baldwin, Publications Chairman (1971).

From fifth annual midyear topical symposium on health physics aspects of nuclear facility siting; Idaho Falls, Idaho (3 Nov 1970).

An ecologically based environmental surveillance program for radioactivity goes well beyond that necessary to comply with 10 CFR 20. Modeling predictions should be included so that exposure to man can be estimated. At present, it is probably necessary for radiological health trained personnel to enlist the aid of biologists, zoologists, and ecologists to help in the design of a surveillance program. For the future there is an implication that radiological health training should include more ecological considerations. The ICRP Publication 7, International Committee on Radiation Protection is a landmark work. This report should be continually reviewed and incorporated into surveillance programs. The concept of critical nuclides in critical pathways is an extremely important aspect of an ecologically based surveillance program. There should be a continuing investigation into determining which radionuclides are critical and which pathways are critical. The factors may be different for different facilities and different locations, but the concept is basic. (auth)

**55239** IN SITU MEASUREMENTS OF ENVIRONMENTAL RADIOACTIVITY. Gelskey, Dale E.; Plato, Phillip; Jacobson, A. P. (Univ. of Michigan, Ann Arbor). pp 278-88 of Health Physics Aspects of Nuclear Facility Siting. Vol. II. /Voilleque, Paul G. (comp.). Idaho Falls, Idaho; Burton R. Baldwin, Publications Chairman (1971).

From fifth annual midyear topical symposium on health physics aspects of nuclear facility siting; Idaho Falls, Idaho (3 Nov 1970).

An amphibious gamma radiation detection system was designed and constructed to measure radioactivity on land and in sediments of lakes and streams surrounding nuclear power plants. This design meets the need for rapid and accurate radiation surveys of the environment around nuclear facilities. The radiation detector is a NaI crystal coupled to a phototube and placed inside a watertight aluminum vessel that can withstand water depths to 1000 feet. The vessel is mounted inside a large rubber tire that, when towed, moves the radiation detector over an area at a constant distance above the surface. The detection system was operated successfully aboard boats and trucks. The advantages of this system over more conventional environmental monitoring procedures include: large sediment surface areas can be surveyed for radioactivity in short periods of time; larger environmental samples are observed for radioactivity than could be handled conveniently in laboratories; and immediate readout of the levels and types of radioactivity allows emphasis to be placed on areas showing significant radioactivity. (auth)

**55240** USE OF STABLE ELEMENT CONCENTRATIONS IN PRE-OPERATIONAL ENVIRONMENTAL MONITORING. Golden, John C. Jr.; Whipple, G. Hoyt (Univ. of Michigan, Ann Arbor). pp 329-36 of Health Physics Aspects of Nuclear Facility Siting. Vol. II. /Voilleque, Paul G. (comp.). Idaho Falls, Idaho; Burton R. Baldwin, Publications Chairman (1971).

From fifth annual midyear topical symposium on health physics aspects of nuclear facility siting; Idaho Falls, Idaho (3 Nov 1970).

An important aspect of preoperational monitoring for a nuclear facility is selecting the main pathways by which radioactive materials discharged from the facility may reach human food. The principal factor that determines the degree to which a particular radioactive isotope can be concentrated in foods derived from an aquatic environment is the ratio of the concentration of the stable isotope in the edible portion of the food to that in the water. The premise is that the radioactive isotopes can be biologically reconcentrated only to the same degree as are their stable forms. The objectives of the stable element study are to establish the maximum degree to which the radioactive materials discharged to water will be reconcentrated in human food derived from that water, to identify the limiting food pathways to man, and to select suitable monitor organisms for the radiological monitoring program. A monitor organism is a readily obtainable organism with limited mobility, high concentration factors, and low variability of stable element content from sample to sample. Such an organism, if found, provides an estimate of radioactivity in human food more conveniently and reliably than measurements of human food itself. A study of the distribution of stable elements in the environment at a prospective nuclear facility is the best available method for estimating well in advance of operation the potential exposure to man resulting from a release of radioactivity to the hydrosphere. The purpose of this paper is to describe such a stable element program for preoperational environmental monitoring. (auth)

**55241** DERIVATION AND APPLICATION OF LIMITS AND REFERENCE LEVELS FOR ENVIRONMENTAL RADIOACTIVITY IN THE UNITED KINGDOM. Bryant, Pamela M. (United Kingdom Atomic Energy Authority, Harwell, Eng.). pp 634-43 of Health Physics Aspects of Nuclear Facility Siting. Vol. III. /Voilleque, Paul G. (comp.). Idaho Falls, Idaho; Burton R. Baldwin, Publications Chairman (1971).

From fifth annual midyear topical symposium on health physics aspects of nuclear facility siting; Idaho Falls, Idaho (3 Nov 1970).

The basic ICRP Dose Limits for members of the public can seldom be used directly when evaluating the significance of routine discharges of radioactivity into the environment. Secondary standards, expressed in terms of the rate of release of radionuclides or activity concentration in environmental materials, are now in general use in the United Kingdom. These standards are termed "Derived Working Limits (DWLs)"; their calculation is described and examples are given to illustrate how their use facilitates the control of releases and the interpretation of environmental monitoring programs. When uncontrolled releases of radioactivity occur as a result of accidents the radiation exposure of members of the public can be regulated only by countermeasures. "Emergency Reference Levels (ERLs)" of dose and environmental radioactivity were adopted in the United Kingdom as guides to assist in both emergency preplanning and executive decisions on the practical implementation of countermeasures. Their status and applications are described and their derivation given with particular reference to the choice of standard values for dosimetric, metabolic, and agricultural parameters. (auth)

**55242** EXAMINATION OF THE EMERGENCY RADIATION DOSES USED FOR NUCLEAR POWER PLANT SITING EVALUATIONS. Mann, Bruce J. (Univ. of California, Berkeley). pp 644-55 of Health Physics Aspects of Nuclear Facility Siting. Vol. III. /Voilleque, Paul G. (comp.). Idaho Falls, Idaho; Burton R. Baldwin, Publications Chairman (1971).

From fifth annual midyear topical symposium on health physics aspects of nuclear facility siting; Idaho Falls, Idaho (3 Nov 1970).

Attention is given to the basis for and the meaning of the radiation doses used as guidelines for low-probability accident situations postulated for nuclear power reactors. A review of the literature indicates some differences and uncertainties among various countries and agencies concerning the basis for these doses. The practices with regard to both whole-body and thyroid doses are reviewed. Thyroid doses are compared with whole-body doses on the basis of risk estimates. (auth)

## *Radiation Protection*

*Refer also to abstracts 54852 and 55108.*

**55243** (CONF-710401–, pp 392-406) EVALUATION OF RESPIRATOR PERFORMANCE BY DOP MAN TEST. Hyatt, E. C.; Pritchard, J. A.; Richards, C. P. (Los Alamos Scientific Lab., N. Mex.). 16 Apr 1971.

From Rocky Flats symposium on safety in plutonium handling facilities; Golden, Colo. (13 Apr 1971).

Evaluation of respirator performance by quantitative respirator-man tests during simulated working conditions is a new project at LASL, and is supported by the Director of Regulations of the U. S. Atomic Energy Commission. Respirator performance data on twelve types of particulate respirators, approved by the U. S. Bureau of Mines for protection against up to 10 or 100 times the maximum permissible concentration of radioactive and highly toxic contaminants, are presented. Overall respirator performance is evaluated by continuously sampling air from inside the facepiece and recording the dioctyl phthalate (DOP) aerosol penetration, while the subject performs specified exercises in a DOP aerosol chamber. The results indicate that quantitative tests of the fit of the respirator facepiece on the ultimate wearer provide an accurate and meaningful protection factor for that particular person-respirator combination. Comparison of tested respirator facepieces shows a large difference in sizes from different manufacturers, although only one size of each approved device is available. Comfort ratings, which were found to correlate with performance, were recorded. (auth)

**55244** USE OF A STYROFOAM BLOCK CUTTER TO MAKE TISSUE-EQUIVALENT COMPENSATORS. Beck, Gerald; McGonnagle, Warren J.; Sullivan, Carole A. (Chicago Wesley Memorial Hospital, Northwestern Univ., Chicago). Radiology; 100: No. 3, 694-6(Sep 1971).

A Styrofoam cutter and its use in preparing shields to shape an x-ray beam are described. The cutter can be used to make minified compensators that will correct for surface irregularities without sacrificing the skin-sparing characteristics of megavoltage beams. (auth)

**55245** CONDITIONS IN CONNECTION WITH THE POSSESSION, ACQUISITION, AND DISPOSAL OF, USE AND CONVEYANCE OF RADIOACTIVE NUCLIDES. Regulation Gazette No. 1031 1968. Pretoria; Government Gazette (1968). 16p. (In English and Afrikaans). Available from Atomic Energy Board, Pretoria.

Radiation protection regulations of the Union of South Africa are presented. The regulations cover the acquisition, possession, uses, transportation, and disposal of radioactive materials. (C.H.)

## Safety Procedures

*Refer also to abstract 54707.*

**55246** (CEA-Bib-200) ANALYSIS OF THE SAFETY PROBLEMS DUE TO FLUORINE AND FLUORINE COMPOUNDS. Bittel, Robert; Vaubert, Bernadette (Commissariat a l'Energie Atomique, Fontenay-aux-Roses (France). Centre d'Etudes Nucleaires). Jun 1971. 56p. (In French). (EUR-4669). Dep. NTIS (U. S. Sales Only).

Because of their widespread uses in all fields of activities and the practical problems raised by their toxicity, a survey has been made of our present knowledge on the problems raised by the protection of man and his environment against the hazards due to the release of fluorine and fluorine compounds. The main points requiring further study have been brought out: the biochemical origin of the toxicity, long term effects of chronic pollution dose-effect relationships, the setting of limiting levels. (auth)

**55247** (JAERI-Memo-4353) HEALTH AND SAFETY AT OARAI RESEARCH ESTABLISHMENT. Quarterly Report, October 1–December 31, 1970. (Japan Atomic Energy Research Inst., Tokyo). Feb 1971. 26p. (In Japanese). Dep. NTIS (U. S. Sales Only).

This is the quarterly report of Health and Safety at Oarai Research Establishment for the period from Oct. 1 to Dec. 31, 1970. (auth)

**55248** HEALTH PHYSICS ASPECTS OF $^{133}$Xe LUNG STUDIES. Rummerfield, P. S.; Jones, G. R.; Ashburn, W. L. (Univ. of California, San Diego). Health Phys.; 21: No. 4, 547-52(Oct 1971).

Xenon-133 gas is currently being used for a variety of lung scanning studies in the evaluation of patients with pulmonary disease. This radionuclide was selected for a number of reasons: it does not react chemically with body tissues; its physical half-life is such that useful quantities can be supplied from distant sources; its biological half-life is in the order of minutes and the absorbed dose to the patient, even from millicurie amounts, is minimal; only nominal shielding is required for the x and $\gamma$ emissions; and commercial dose calibrators are available that express activity directly in mCi or $\mu$Ci. In the chain of transfers necessary from receipt of the radioactive gas to final disposal of waste, leakage must be continually guarded against. Over several years, leakage, when it occurred, was most often caused by excessive strain on connecting lines. However, film badge exposures for personnel involved were consistently minimal and no overexposures occurred, although as much as 2 Ci per month were handled. Accident preplanning, including careful consideration of containment and dispensing apparatus, ventilation and exhaust requirements, and dry runs, contributed to this record. (auth)

**55249** OFF-SITE MEDICAL PLANNING AND MANAGEMENT FOR AN EXPERIMENTAL UNDERGROUND NUCLEAR DETONATION. Wheeler, Jamie K. (Univ. of New Mexico, Albuquerque); Moore, Raymond T.; Carter, Melvin W. Health Phys.; 21: No. 4, 571-9(Oct 1971).

The Bureau of Radiological Health, U. S. Public Health Service, provides comprehensive off-site radiological safety and medical programs for underground nuclear tests at the Nevada Test Site and for nuclear tests and experiments conducted at other geographical sites for non-weapons research and peaceful purposes. The specific physical requirements for these latter categories of use may preclude their being conducted at the Nevada Test Site. Future underground nuclear detonations for research and peaceful purposes may be held in locations that are not necessarily remote from relatively sizeable civilian populations. It is thus desirable to delineate the particular problems and their management involved in the public health medical planning for population safety, including such aspects as evacuation. These medical planning and management activities and their implementation for Project Sterling, a 350-ton yield underground nuclear detonation, which was conducted for seismic research purposes on 3 December 1966, in the Tatum Salt Dome near Hattiesburg, Mississippi, are described. (auth)

**55250** RADIATION INCIDENTS REGISTRY: PENNSYLVANIA EXPERIENCE. Lubenau, Joel O.; Gerusky, Thomas M. Health Phys.; 21: No. 4, 605-7(Oct 1971).

It is stated that statistical evaluation of ionizing radiation incidents on a national scale in the U. S. is difficult as it involves records from three sources in two different agencies. It is urged that a national registry should be kept to cover all types of ionizing radiation incidents similar to that maintained in Pennsylvania since 1962. The purposes for which this registry has been used are given, including influencing the development of the State Radiation Emergency Assistance Plan and the highlighting of the facts that an excess of accidental exposures was due to x ray equipment, that nearly half of the radioactive materials incidents involved transportation, and that the record keeping of radium source usage in hospitals is poor. (UK)

**55251** RADIATION QUANTITIES IN HEALTH PHYSICS. Wheatley, B. M. (Central Electricity Generating Board, Berkeley, Eng.); Burlin, T. E. Health Phys.; 21: No. 4, 609-10(Oct 1971).

An appraisal of the position concerning the definition of radiation quantities in health physics is given with especial reference to the recent publication of Neufeld (NSA 24: 48563). It is considered that it may be possible to devise a system of radiological protection that retains the concept of permissible organ dose and also sufficient clarity to allow derivation of safe environmental limits. It appears desirable to set out permissible doses for different organs in a way that recognizes their variation with parameters such as radiation quality while expressing them in terms of rads. Current permissible doses in terms of rads are tabulated and it is seen that modifying factors are not always consistently defined but the use of the table overcomes the difficulties that Neufeld showed to be associated with quality factors since LET is a uniquely defined physical quality. It is agreed with Neufeld that QF is not uniquely defined, but his proposal to modify it or replace it with a Quantity Index is not agreed. It is considered that permissible doses should be set out in terms of rads and LET (both simple unambiguous physical quantities) as a necessary and sufficient basis for radiological protection. The Quality Factor is an unsatisfactory concept for radiological protection, and it is considered to be redundant. (UK)

## Legal Aspects

*Refer also to abstract 55299.*

XUM

55252 (NP-18752) NOTEBOOK OF ATOMIC ENERGY LAW. 2. (Institut de Droit Compare de Paris (France)). Oct 1969. 263p. (In French). Dep. NTIS (U. S. Sales Only).

Six articles on atomic energy law—nuclear law in Latin America, excessive doses of radiation as a cause of radiological accidents in French jurisprudence, the complementary research programs of Euratom, the civil responsibility and insurance in the maritime transport of nuclear materials, the reform of C.N.E. in Italy, and the permissive character with respect to international law on the sinking of radioactive wastes in the sea—are presented in full. Abstracts are presented of the most important books and articles appearing in 1968. The titles of additional books and articles are given. (J.S.R.)

55253 RADIATION STANDARDS AND RADIOACTIVE WASTE. Soule, Harvey F. (Atomic Energy Commission, Washington, D. C.). pp 656-66 of Health Physics Aspects of Nuclear Facility Siting. Vol. III. /Voilleque, Paul G. (comp.). Idaho Falls, Idaho; Burton R. Baldwin, Publications Chairman (1971).

From fifth annual midyear topical symposium on health physics aspects of nuclear facility siting; Idaho Falls, Idaho (3 Nov 1970).

National and international radiation standards are essentially performance codes (stating exposures that are not to be exceeded) rather than specification codes (stating how radiation work is to be accomplished). Rational planning thus requires analysis of the established standards against the work to be done. The standards relative to interim and long-term storage of radioactive wastes, particularly nuclear fuel reprocessing wastes and plutonium-contaminated solid wastes are considered. (auth)

55254 CRITICAL REVIEW OF THE ASSUMPTIONS INVOLVED IN ESTABLISHING THE MPD AND MPC'S IN AIR AND WATER. Miller, Carl R.; Inclan-Suarez, Manuel (Georgia Inst. of Tech., Atlanta). pp 667-75 of Health Physics Aspects of Nuclear Facility Siting. Vol. III. /Voilleque, Paul G. (comp.). Idaho Falls, Idaho; Burton R. Baldwin, Publications Chairman (1971).

From fifth annual midyear topical symposium on health physics aspects of nuclear facility siting; Idaho Falls, Idaho (3 Nov 1970).

A critical review is made of the assumptions and methods used by the International Commission on Radiological Protection, the National Council on Radiation Protection, the Federal Radiation Council, the Atomic Energy Commission, and the Public Health Service in establishing values of maximum permissible doses (MPD) due to ionizing radiation and maximum permissible concentrations (MPC) of radionuclides in air and water to which the human body can be exposed. Critiques of the MPD and MPC values are made in regard to the following: the term maximum; safety factors included in the calculations; their past downward trend in magnitude; evidence regarding safeness of the values; the accuracy of the data used in their determination; the factor 1/30 versus 1/100; the different methods used in their determination; and the legal control on environmental limits. It is concluded that: there is a high probability that in the future the present MPD and MPC levels will be found to be too high; these levels are not to be considered dumping limits; and if the actual dumping limits are allowed to approach those levels, a good understanding of the MPC limits and their methods of determination as well as extreme caution must be utilized. (auth)

# Medicine

*Refer also to abstract 56983.*

55255 RADIOISOTOPE IN PHARMAKOKINETIK UND KLINISCHER BIOCHEMIE. (Radioisotopes in Pharmacological and Clinical Biochemistry). Conference Held in Wiesbaden, Germany, September 26–28, 1968. Hoffmann, G.; Ladner, H.-A. (eds.). Nuclear Medicine, Supplement 8. Stuttgart; F. K. Schattauer Verlag GmbH (1970). 757p. (In German and English). (CONF-680933).

At the 6th annual meeting of the German society for nuclear medicine, held at Wiesbaden from September 26 to 28, 1968, 129 papers were presented. Pharmacokinetic and pharmacodynamic aspects of various radioisotopes were covered. Among the topics discussed were studies of norepinephrine turnover, atropine, bile formation, antibody labeling, and digitalis glucosides. Also discussed were isotope methods for function studies of the lungs, central nervous system, and kidneys. In addition, problems were covered which concerned the development of new radiopharmaceuticals, dosimetry and health physics of radioisotopes, and semiconductor detectors for in vivo measurement and whole-body counters. (H.B.G.)

## Protective Substances

*Refer also to abstracts 55189, 55357, and 55361.*

55256 SOME PRINCIPLES OF EVALUATING THE EFFECTIVENESS OF RADIOPROTECTIVE AGENTS IN MAN. Vladimirov, V. G.; Dzharak'yan, T. K.; Berlin, L. B.; Golubentsev, D. A.; Smirnov, A. D. (Leningrad Medical Academy). Med. Radiol.; 16: No. 9, 54-60(Sep 1971). (In Russian).

The radioprotective dose of cystamine chlorhydrate was determined for man by means of extrapolation of the optimal protective dose for mice with due consideration of the quantity of the protector per unit of body surface. It amounts to about 3 gm. It is shown that the intake of tolerable doses of cystamine (0.8 to 1.2 gm) prior to single local irradiation leads to a decrease in the number of chromosomal aberrations in myeloid cells and lymphocytes of the peripheral blood. A number of investigations enabled the authors to assume that prophylactic intake by man of tolerable doses of cystamine chlorhydrate may ensure a noticeable radioprotective effect. (auth)

55257 CHEMICAL PROTECTION OF THE MOUSE AGAINST RADIATION-INDUCED LIFE SHORTENING. Storer, John B. (Oak Ridge National Lab., Tenn. Jackson Lab., Bar Harbor, Me.). Radiat. Res.; 47: No. 2, 537-47(Aug 1971).

The effectiveness of four radioprotective compounds in reducing life shortening from radiation exposure was evaluated for each sex in two inbred strains of mice. Major differences in effectiveness were found which were highly dependent on sex, strain, and radiation dose level. It was concluded that the effectiveness of these agents is determined by whether they protect against the particular radiation-induced lesions that lead to early death. The nature of these lesions apparently varies by sex and strain and possibly radiation dosage. (auth)

55258 RADIOSENSITIZATION WITH 5-BROMODEOXYURIDINE OF CHINESE HAMSTER CELLS X-IRRADIATED DURING DIFFERENT PHASES OF THE CELL CYCLE. Dewey, W. C.; Stone, L. E.; Miller, H. H.; Giblak, R. E. (Colorado State Univ., Fort Collins). Radiat. Res.; 47: No. 3, 672-88(Sep 1971).

Cells synchronized by selecting mitotic cells from an asynchronous population growing in vitro were x-irradiated and then analyzed both for lethality and for chromosomal aberrations. When BUdR incorporation occurred following irradiation, no radiosensitization or synergistic interaction was observed, although the BUdR treatment produced a small additive effect. However, when the cells incorporated BUdR for at least one cycle prior to being synchronized in mitosis, the radiation dose required to obtain a certain amount of damage was reduced by a factor of 1.9 (BUdR enhancement ratio). This BUdR enhancement ratio was observed in terms of both chromosomal aberrations and cell lethality when cells were irradiated either in mitosis, $G_1$, or S. For both end points of damage, the mitotic phase was most sensitive with a linear dose-effect response, the $G_1$ phase was intermediate in sensitivity (dose modifying factors of 1.5 to 2.0 compared with mitotic cells) with a small shoulder on the dose-effect curve, and the S phase was most resistant (dose modifying factors of 2.1 to 3.2 compared with mitotic cells) with a large shoulder on the dose-effect curve. Furthermore, for both untreated and BUdR-treated cells, irradiated either in mitosis, $G_1$, or S, the logarithm of survival was linearly related to the aberration frequency (37% survival occurring when the cells sustained 0.75 aberrations per cell). These relationships add considerable support to the hypothesis that x-ray-induced cell death results from a chromosomal aberration. (auth)

55259 BIOLOGICAL FACTORS AFFECTING THE RADIOPROTECTIVE EFFICIENCY OF S-2-[3-AMINOPROPYLAMINO]-ETHYLPHOSPHOROTHIOIC ACID (WR-2721): $LD_{50(7)}$ DOSES. Yuhas, John M. (Oak Ridge National Lab., Tenn.). Radiat. Res.; 47: No. 2, 526-9(Aug 1971).

The ability of WR-2721 to increase the resistance of four inbred mouse strains to radiation-induced gastrointestinal death was studied in order to compare the effectiveness of this drug in the gastrointestinal system to its effectiveness in the previously studied hematopoietic system. The factor increase in resistance to gastrointestinal death following injection of this drug is largely independent of the resistance of the strain to the drug's toxic side effects, but is dependent on the inherent resistance of the strain to radiation-induced gastrointestinal death. This finding is in direct contrast to the results obtained in the hematopoietic system. The factor increase method for expressing protection in the gastrointestinal tissues appears therefore unjustified. The mechanism controlling this atypical pattern in the gastrointestinal tissues remains to be resolved. (auth)

**55260** POTENTIAL CHANGES OF CHROMOSOMES AS A RESULT OF INTERACTION OF RADIATION AND ALKYLATING COMPOUNDS. Korytova, A. I.; Mikhailov, O. F.; Dubinin, N. P. (Inst. of General Genetics, Moscow. Dnepropetrovsk State Univ., USSR). Genetika; 7: No. 8, 10-18(Aug 1971). (In Russian).

Crepis capillaris seeds were stored for 126 days after x irradiation at doses of 1500 R and 4500 R and subsequent ethylenimine treatment at a concentration of $9.3 \cdot 10^{-3}$ M. After the elapse of a certain time, seeds were germinated and thus the resulting chromosome changes were made liable for studying. The dose-dependence of these changes was observed. In all the cases of seed storage the kinetics of potential changes leading to direct mutations was undulate. It was established that ethylenimine, being applied to seeds previously x-irradiated, behaved as a protective substance reducing to one half the frequency of chromosome-type changes induced with irradiation. A superadditive effect was observed during the few days of storage of seeds treated both with x rays and ethylenimine, whereas in seeds not subjected to storage the frequency of chromosomal changes was below that expected in the case of an additive effect of these two agents. (auth)

**55261** COMBINED TREATMENT OF BARLEY AND WHEAT SEEDS WITH IONIZING RADIATION AND ETHYLENE-IMINE FOR THE INDUCTION OF MUTATIONS. Olimpienko, G. S.; Vorob'eva, E. A.; Mitrofanov, Yu. A. (Inst. of Biology, Petrozavodsk, USSR. Inst. of General Genetics, Moscow). Genetika; 7: No. 8, 68-78(Aug 1971). (In Russian).

The effect of combined treatment of barley and wheat seeds with ionizing irradiation and ethylenimine was studied. The prevalence of the method was a high survival of $M_1$ plants and the increase of mutation frequency of the forms being valuable for breeding. (auth)

**55262** SENSITIVITY OF ARTEMIA EGGS TO $\gamma$ IRRADIATION. IX. A CORRELATION BETWEEN RADIATION-INDUCED FREE RADICALS AND HATCHABILITY IN EGGS EXPOSED TO $\beta$ MERCAPTOETHYLAMINE. Iwasaki, Tamiko (National Inst. of Radiological Sciences, Chiba, Japan). Int. J. Radiat. Biol.; 20: No. 1, 39-47(1971).

Both free-radical and hatchability measurements were made on the same samples of Artemia eggs treated with MEA. MEA present at the time of irradiation protected eggs under both dry and wet conditions, but was not effective when administered after irradiation. Radiation protection was accompanied by a reduction in the number of free radicals. The effect of MEA was to increase the rate of decay of radiation-induced radicals. However, transfer of unpaired electrons to the sulphur nucleus in MEA was not found. The protective mechanism of MEA is discussed in the light of current hypotheses. (auth)

**55263** ORGANOSILICON ENTITIES AS PROPHYLACTIC AND THERAPEUTIC AGENTS. Garson, Lorrin R.; Kirchner, Lucille K. J. Pharm. Sci.; 60: No. 8, 1113-27(Aug 1971).

The chemistry, general biological properties, toxicology, and biological activity of naturally occurring and synthetic organosilicon compounds are discussed. Included in the discussion of biologically active agents are references to the uv-radioprotective properties of skin creams containing polysiloxanes and the possible radioprotective properties of silicon-substituted thiophene derivatives of mercaptoethylamine. (E.R.B.)

**55264** STUDY OF REACTIVITY OF THE ORGANISM EXPOSED TO TRANSVERSE ACCELERATIONS AND RADIOPROTECTANTS. Antipov, V. V.; Vasin, M. V.; Davydov, B. I.; Panchenkova, E. F.; Saxonov, P. P. Aerosp. Med.; 42: No. 8, 837-9(Aug 1971).

It is of interest to study the response of man to certain drugs when exposed to conditions of space flight. This is of considerable importance in connection with the development of indications for drugs, their dosages, and procedures under space flight circumstances. Space flight factors such as weightlessness, accelerations, ionizing radiation, and artificial atmospheres may markedly influence the response of human beings to certain types of drugs. This paper presents the results of a study of the effect of drugs that protect against ionizing radiation on the animal and the tolerance to back-to-chest accelerations. The experiments indicate that drugs that protect against radiation may reduce the tolerance of the animal to acceleration. The implications with regards to the response of human beings are discussed. (auth)

**55265** COMMENT: RADIOSENSITIZATION AND THE SELECTIVE EFFECT. Rubin, Philip. J. Amer. Med. Ass.; 217: No. 7, 952-3(16 Aug 1971).

The search for radiosensitizers and radioprotective agents is a major sphere of activity and concern to those involved in the direction of cancer research. The advantages of combined treatment (combining one chemical compound with another, or with radiation) are based on the principle of increasing the carcinostatic effect selectively, or decreasing histologic toxicity. Until the difference between the neoplastic and host tissue metabolism is understood, improvements in treatment will depend on serendipity directing the investigator. (auth)

**55266** RADIOBIOLOGICAL INVESTIGATIONS WITH FAST NEUTRONS. II. THE RADIOPROTECTIVE ACTION OF DIFFERENT SUBSTANCES ON MALE MICE. Langendorff, H.; Langendorff, M.; Metzner, R.; (and others) (Univ., Freiburg i. B.). Atomkernenergie; 18: No. 1, 83-8(Aug 1971).

The radioprotective action of the following substances was examined on male NMRI-mice irradiated with fast neutrons of 14.7 MeV: cystamine, serotonin, p-aminopropiophenone, lipopolysaccharide of E. coli, chlorotrianisene as well as a combination of chlorotrianisene with cystamine, serotonine or lipopolysaccharide. The effectiveness of these agents was smaller after neutron irradiation than after x irradiation. In the case of chlorotrianisene with or without cystamine, serotonine, or lipopolysaccharide, no protective effect was observed. The highest absolute effectiveness of the substances tested was revealed by cystamine. The value of $1.15 \pm 0.02$ for the dose reduction factor, however, was smaller by the factor of 1.6 than that obtained in experiments with x rays. On the basis of this approach it was found that p-aminopropiophenone and lipopolysaccharide proved to be the most favorable compounds; the effectiveness of both substances in neutron irradiation was only reduced by a factor of 1.2. No essential changes were observed after neutron irradiation in the treated animals regarding the mean survival time as compared with untreated animals. The reduced effectiveness of the tested agents was caused by different factors. One reason is probably due to the higher LET of fast neutrons, which is responsible for special phenomena in aqueous media. (auth)

**55267** UTILIZATION OF A TRYPANOSOMA EQUIPERDUM TEST IN STUDIES ON THE RADIOPROTECTIVE ACTION OF ENDOTOXIN. Foris, Gabriella; Ujhelyi, K.; Fay, K.; Kertai, P. Acta Vet. Acad. Sci. Hung.; 21: No. 1, 31-9(1971).

Rats that had been immunized with $4 \times 10^7$ Trypanosoma equiperdum and treated with formalin, were intravenously challenged with living trypanosomes. The capacity of the whole immune system was assessed on the basis of the time needed to eliminate the parasites from the circulation. This test was used for a study on the immunosuppressive effect of ionizing radiation. As a result of administration of Serratia marcescens endotoxin, radioprotective action, affecting also the immune system, was observed in animals that had been either serially injected prior to x-ray exposure or 250 $\mu$g/100 g b.wt. of endotoxin was injected within 24 hours before or 6 hours after the irradiation of the rats. It was only the serial treatment or the single dose of 250 $\mu$g/100 g of endotoxin, administered 24 hours prior to the irradiation, that exerted radioprotective effect if survival of x-irradiated rats was taken for basis of evaluation. In some other experiments, it was rather the adjuvant action of endotoxin, effective also in the irradiated organism, that was responsible for restoration of adequate immunological responsiveness. (auth)

**55268** THERAPEUTIC EFFECT OF TETRAHYDROFOLIC ACID IN MIDLETHALLY X-IRRADIATED MICE. Okazaki, Masahiko; Sato, Fumiko; Shikita, Mikio; Akaboshi, Sanya (National Inst. of Radiological Sciences, Chiba, Japan). Chem. Pharm. Bull. (Tokyo); 19: No. 6, 1173-7(1971).

Tetrahydrofolic acid exhibited a life-prolonging effect in the midlethally x-irradiated mice, when it was intraperitoneally injected in the animals after the irradiation. In the tetrahydrofolic acid-treated animals, retardation of the growth rate in the body weight was normalized in 5 days after the irradiation. Recovery in spleen and intestine weights as well as in the number of circulating blood leucocytes was more pronounced in the tetrahydrofolic acid-treated animals than in the control animals. However, it failed to increase the survival rate of the x-irradiated HeLa $S_3$ cells, when it was added in the culture medium after the irradiation. In a subsequent experiment, it was clarified that folic acid was devoid of this therapeutic effect. (auth)

## *Radiation Sickness and Injuries*

**55269** RADIATION REACTIONS OF THE NERVOUS SYSTEM IN IRRADIATION OF TUMORS OF THE HEAD: THEIR PROPHYLAXIS AND TREATMENT. Merkova, M. A. (Moscow Scientific Research Radiological Inst.). Med. Radiol.; 16: No. 8, 19-25(Aug 1971). (In Russian).

XUM

The reactions of the nervous system in radiation therapy of tumors of the head in 220 patients were studied. The radiation reaction was manifested by the asthenic syndrome and circulatory disorders with manifestations of intracranial hypertension and vascular hypotension. For the prophylaxis and treatment of asthenic manifestations, tonic treatment with vitamins and psychotropic preparations were used. In dynamic disorders of the cerebrospinal fluid, dehydration and diuretic therapy was employed. In vestibular disturbances, preparations of atropine were used. (auth)

55270 MANAGEMENT OF RADIONECROSIS. Robinson, David W.; Masters, Frank W.; Ketchum, Lynn D. J. Amer. Med. Ass.; 217: No. 7, 950-1(16 Aug 1971).

Damage to bone following radiotherapy for carcinoma is a severe complication. Necrosis is the primary pathological process, but infection and residual cancer often complicate the picture. The pathogenesis, clinical picture, radiographic findings, prophylaxis, and treatment of radionecrosis are discussed. The essentials of treatment are wide removal of the affected bone plus coverage by adequate soft tissue with good blood supply. (E.R.B.)

## Radiodiagnosis

*Refer also to abstracts 55018, 55023, 55028, 55226, 55227, 55236, and 55248.*

55271 (LB/G-3059) RADIOISOTOPE SCANNING WITH $^{75}$Se-SELENOMETHIONINE IN THE MORPHOLOGICAL AND FUNCTIONAL STUDY OF THE PANCREAS. Romanini, A.; Troncone, L. Translated by L. Wittels (Atomic Energy Research Establishment, Harwell, Eng.), from Med. Nucl.-Radiobiol. Lat.; 11: 119-52(1968). 41p. Dep. NTIS (U. S. Sales Only).

Pancreas scintigraphy brought a notable diagnostic help in the field of the morphological and functional study of this organ, not easily explorable in spite of radiological investigation and laboratory test. Data obtained by means of scintigraphy, sometimes unsatisfactory, together with those obtained by means of radiology, give the opportunity of diagnostic improvement. Scintigraphic technique and methodology are described and normal and pathological patterns are examined. (auth)

55272 USE OF EDTA PREPARATIONS LABELLED WITH $^{51}$Cr AND $^{169}$Yb IN RADIOISOTOPE DIAGNOSIS. Zubovskii, G. A.; Mittel'man, V. A.; Naumenko, Yu. I.; (and others) (Moscow Scientific Research Radiological Inst.). Med. Radiol.; 16: No. 9, 8-14(Sep 1971). (In Russian).

Data are presented on the use of a new radioactive preparation—EDTA-$^{169}$Yb—for investigation of glomerular filtration, and scanning of the kidneys and brain. The authors discuss its diagnostic possibilities in comparison with EDTA-$^{51}$Cr, as well as with other compounds. The radiation dose upon introduction of the referred to preparations into the organism is given. (auth)

55273 Si(Li)-DETECTORS OF BETA-RADIATION FOR RADIOISOTOPE DIAGNOSIS OF SURFACE NEOPLASM OF THE SKIN. Petushkov, A. A.; Pryakhin, Yu. F.; Sivoshinskii, D. S.; Zelentsova, M. V.; Vorob'ev, N. I. Med. Radiol.; 16: No. 8, 74-7(Aug 1971). (In Russian).

The practical application of a newly developed Si(Li)-detector in place of the customary scintillation type for measuring surface content of $^{32}$P in neoplasms of the skin is described. This innovation consists of two channels, each of which is a detector-amplifier system with a device for comparing the count rate in both channels. The results of a number of studies made on patients with variously pigmented skin neoplasms are tabulated and discussed. (KSW)

55274 FINNISH RADIOLOGICAL BIBLIOGRAPHY. Unnerus, C. E.; Sainio, M. Ann. Clin. Res.; 3: Suppl. 6, 1-94(1971).

The Finnish Radiological Bibliography contains references about medical radiology published by Finnish authors during 1964 to 1969. The material is listed both by author's name and subject. The subject section is divided into following main groups: Physics, techniques and dosimetry, hazards and protection, radiobiology, radiodiagnosis, radiotherapy, and miscellaneous subjects. (Finland)

55275 ISOTOPIC RENOGRAM BY PATIENTS SUFFERING FROM CERVICAL CARCINOMA. Van Vaerenbergh, P. M.; De Winter, H. (Univ., Ghent). Strahlentherapie; 141: No. 6, 669-76(Jun 1971).

By means of case reports of 110 patients suffering from cervical carcinoma, the significance of isotopic renograms with regard to course control and prognosis is demonstrated. Nine case histories are analyzed. (auth)

55276 RELIABILITY OF LIVER SCANNING WITH $^{198}$Au. Nordman, Eeva (University Central Hospital, Helsinki). Strahlentherapie; 141: No. 6, 677-81(Jun 1971).

A total of 336 liver scans, in which alkaline phosphatase was also studied, are presented. Eighty-two percent of positive scans were correctly positive by the histological investigation. Of the cases for which no histologic diagnosis was available, 60 to 74 percent were evaluated correctly positive on the basis of alkaline phosphatase and survival time. Only 50 percent of the negative scans were correctly negative by the histological investigation. In the group for which no histologic diagnosis was available, 38 to 58 percent were evaluated to be correctly negative on the basis of survival and alkaline phosphatase. Alkaline phosphatase is probably 90 percent more positive than scanning (79 percent) in cases of liver metastases. If both liver scanning and alkaline phosphatase are positive and the cancer patient has no symptoms of cirrhosis of the liver, metastasizing may be regarded as fairly certain. (auth)

55277 NEUTRON RADIOGRAPHY OF THE DENTAL PULP. Weisman, Manuel I. (Veterans Administration Hospitals, Augusta, Ga.); Brown, Mark. Contract AT(07-2)-1. Oral Surg., Oral Med., Oral Pathol.; 32: No. 3, 487-92(Sep 1971).

Neutron radiography permits direct visualization of the hydrogen-rich coronal pulp through relatively radiolucent enamel and dentin. The technique is not believed to have clinical applicability because overlying hydrogenous tissues are likely to obscure important structures, readily accessible neutron sources appropriate for use by practicing dentists are not available at a reasonable cost, and fast neutron image-recording systems are impractical for use in a clinical setting. However, this does not preclude the use of neutron radiography as a research tool for the investigation of endodontic disease processes. (auth)

55278 IMPROVED DETECTOR FOR VIDEO SYSTEMS USED IN RADIONUCLIDE STUDIES. Griffith, James M.; Schall, Gerald L.; Larson, Steven M. (National Institutes of Health, Bethesda, Md.). Radiology; 100: No. 3, 699-700(Sep 1971).

Video systems that use a comparator-type detector for quantitating radionuclide studies are characteristically insensitive at high count rates. A gated oscillator in the detector significantly reduces this nonlinearity and increases the usable dynamic range of the system. (auth)

55279 $^{167}$Tm: A NEW BONE SCANNING AGENT. Chandra, R.; Hernberg, J.; Braunstein, P.; Rosenfeld, W. (New York Univ., N. Y.). Radiology; 100: No. 3, 687-9(Sep 1971).

Thulium-167 has several distinct advantages as a bone scanning agent, including a half-life of 9.8 days, a gamma-ray emission of 208 KeV, which is suitable for imaging with both the Anger camera and the rectilinear scanner, a relatively low radiation dose to the patient, and good localization in bone. (auth)

55280 PANCREAS IMAGING—IS IT WORTH IT? Landman, Silviu; Polcyn, Robert E.; Gottschalk, Alexander (Univ. of Chicago, Ill.). Radiology; 100: No. 3, 631-6(Sep 1971).

In an analysis of 106 pancreatic radionuclide images it was found that a normal study has a high degree of reliability. With abnormal pictures it is difficult or impossible to distinguish between pathologic entities, especially between pancreatitis and carcinoma. Severe diabetes, starvation, or postoperative states will also cause nonvisualization of the pancreas. Since the patency of the excretory ducts seems to be a crucial factor in determining visualization, small tumors not obstructing the duct system will be missed when the lesion size is below the resolution limits of current imaging devices. (auth)

55281 STATISTICAL RELATIONSHIP OF BRAIN SCANS, CERVICOCRANIAL DYNAMIC STUDIES, AND CEREBRAL ARTIOGRAMS. Meschan, I.; Lytle, William O.; Maynard, C. Douglas; (and others) (Wake Forest Univ., Winston-Salem, N. C.). Radiology; 100: No. 3, 623-9(Sep 1971).

Rapid sequence cervicocranial camera images, scans, angiograms, and pneumograms were compared in 146 cases of neurological disorder. It was found that use of imaging is justified as a screening procedure prior to performance of routine radionuclide brain scanning. Further information is offered in a significant number of cases, particularly when this single study is compared with information obtained by cerebral angiography and pneumography. Additionally, the rapid sequence images, when studied with the brain scans, may help establish such diagnoses as arteriovenous malformation, tumor, or infarction. (auth)

**55282** QUANTITATIVE EVALUATION OF THYROID SCINTIGRAMS BY COMPUTER. Habermehl, A.; Eisenhauer, P.; Joseph, K. (Philipps-Univ., Marburg, Ger.). Fortschr. Geb. Roentgenstr. Nuklearmed.; 115: No. 1, 1-13(Jul 1971). (In German).

Computer storage of scintigrams permits not only various modes of data evaluation for better interpretation but also utilization of programs for special organs. Such a method and program is described for thyroid scintigrams and yields, aside from size and storage condition of the organ. These comprise an outline of the organ by fast printing, presentation of the thyroid area with a computed midline, outline of regions in which the radioactivity exceeds a selected threshold, and absolute activities in ten steps, which are illustrated. (tr-auth)

**55283** INVESTIGATIONS ON TUMOR LOCALIZATION USING $^{67}$Ga. Heidenreich, P.; Remplik, V.; Kempken, K.; (and others) (Univ., Munich). Fortschr. Geb. Roentgenstr. Nuklearmed.; 115: No. 1, 14-26(Jul 1971). (In German).

Tumor scanning with $^{67}$Ga was performed in 40 patients. Examined were twelve reticulum cell sarcomas, six carcinomas of the thyroid, and four bronchial carcinomas; some of these had received previous treatment. The best results were achieved with carcinomas of the thyroid and of the bronchus. Intra-abdominal tumors were difficult to evaluate because of the physiological storage of radiogallium in the liver and in the gut. (auth)

**55284** PERFUSION LUNG SCINTIGRAPHY IN PRIMARY VASCULAR PULMONARY HYPERTENSION. Koppenhagen, K.; Ernst, H.; Paeprer, H.; Liebenschuetz, H. W.; Meinhold, H. (Freie Univ., Berlin). Fortschr. Geb. Roentgenstr. Nuklearmed.; 115: No. 1, 27-33(Jul 1971). (In German).

Local pulmonary hypertension has become more common during recent years; this is probably due to the widespread use of appetite depressants, for instance aminorexfumarat. The correct diagnosis of this disorder is possible only by measuring pulmonary arterial pressure, but scintigraphy of the lungs can contribute to it, as was found in 34 patients who took aminorexfumarat. It is necessary to separate functional pulmonary hypertension caused by reversible contraction of the vessels from a later irreversible stage that is characterized by organic vascular changes. If different marked radioactive albumin particles are injected intravenously (iv) before and after iv aminophylline, a 2-phase-scintigraphy with $^{99m}$Tc-labeled albumen and $^{131}$I-labeled albumen can be used to differentiate between the stage of reversible vascular spasm and the irreversible obstruction damage to the blood-vessels. This investigation can be carried out in one session only and can give valuable guidance for the treatment of the condition. (auth)

**55285** QUANTITATIVE ANALYSIS OF LUNG PERFUSION FOLLOWING BRONCHOGRAPHY. Huenermann, B.; Sobbe, A.; Hermanutz, K. D.; Schwabe, H. (Univ., Bonn). Fortschr. Geb. Roentgenstr. Nuklearmed.; 115: No. 1, 34-7(Jul 1971). (In German).

Lung scans using $^{131}$I-labeled albumin macroaggregates (MAA) were obtained in seven patients before, and 24 and 48 hours after bronchography; activity of the right and left lungs was estimated with the help of a digital computer. After 24 hours, perfusion on the side on which the bronchogram had been carried out was reduced by 2 to 19%. After 48 hours, only one patient showed a 3% reduction in perfusion. A relationship between the reduction in perfusion on the one hand and the clinical diagnosis or age of a patient on the other could not be demonstrated. The results indicate the importance of bearing in mind the perfusion changes induced by bronchography. (auth)

**55286** SCINTIGRAPHY OF INFLAMMATIONS USING SILVER ISOTOPES. Jahns, E.; Brase, A. (Medizinische Hochschule, Hanover). Fortschr. Geb. Roentgenstr. Nuklearmed.; 115: No. 1, 38-41(Jul 1971). (In German).

The first investigations in the clinical differential diagnosis of inflammatory lesions using the silver isotope $^{105}$Ag for scanning are reported. Animal experiments are described. Following this, individual clinical cases are described, which confirmed the usefulness of this method, particularly during the acute stage of inflammation. (auth)

**55287** PROFILOGRAPHY OF SACROILIAC JOINTS IN ANKYLOSING SPONDYLITIS. Dihlmann, W.; Klemm, C.; Stockberg, H.; Bueltmann, F.-J. (Technische Hochschule, Aachen). Fortschr. Geb. Roentgenstr. Nuklearmed.; 115: No. 1, 42-53 (Jul 1971). (In German).

Strontium-85 scanning of the sacroiliac joints in ankylosing spondylitis has the following practical advantage: approximately 10% of patients show a normal sacroiliac joint on the radiograph initially. In such patients the $^{85}$Sr quotient of the radiologically normal joint was at an abnormal level, indicating an abnormality not yet demonstrable radiologically. In about 1% of patients, the first radiological signs of ankylosing spondylitis involve the spine and not the sacroiliac joints. One such patient was examined with $^{85}$Sr and showed increased activity over the sacroiliac joints. The use of $^{85}$Sr scanning for evaluating the osteoplastic activity of ankylosing spondylitis is discussed in relation to another patient. The maximum information was obtained by carrying out the scan seven days after the injection of $^{85}$Sr. (auth)

**55288** RESULTS OF SCINTIGRAPHIC INVESTIGATIONS OF PARASTERNAL LYMPH NODES WITH $^{198}$Au IN NORMAL PERSONS. Meyer-Burg, J.; Wilhelmi, U. (Staedt. Krankenhauses, Berlin). Fortschr. Geb. Roentgenstr. Nuklearmed.; 115: No. 1, 54-8(Jul 1971). (In German).

Parasternal lymph nodes can be demonstrated following the para-xyphoidal application of radioactive gold. In this way a lymph node territory can be demonstrated which was previously inaccessible, but which is of importance because of metastatic spread from carcinomas of the breast. The procedure is simple and painless and is of little trouble to the patient. The radiation dose is small and scans can be repeated as often as seems desirable. The value of the method is limited somewhat by the considerable anatomical variation in the number and size of lymph nodes. In addition the present limitation in resolution of the lymph node scan detracts somewhat from the value of the method. When using the method described for searching for metastases, it must also be remembered that there are no features that are specific for deposits and that metastases do not store radioactive material. The unilateral or bilateral silent areas in the parasternal lymph nodes in patients with carcinomas of the breast were found in a high percentage of older, but normal people. It is believed that this finding represents an expression of anatomic variation or is a sign of degenerative change in these lymph nodes. (auth)

**55289** ANGIOGRAPHIC AND ANGIOSCINTIGRAPHIC COMPARISONS IN CEREBRAL VASCULAR PROCESSES. Deisenhammer, E.; Hammer, B. (Wagner-Jauregg-Krankenhaus des Landes Oberoesterreich, Linz, Austria). Fortschr. Geb. Roentgenstr. Nuklearmed.; 115: No. 1, 59-67(Jul 1971). (In German).

A hundred patients suspected on clinical grounds of a cerebral abnormality were examined by carotid angiography and carotid angioscintigraphy with $^{131}$I. Space-occupying lesions and other localized processes, apart from cerebral infarcts, were excluded. In addition to normal angioscintigraphic findings, there were normal hemodynamic varients; occlusion of large cerebral vessels resulted in extensive regions of reduced particle fixation or irregular smaller areas of reduced particle fixation or showing no uptake whatsoever. In 79% of patients, there was agreement between the angioscintigraphic and angiographic findings regarding the cerebral vascular abnormalities. It was concluded that angiographically visible changes in cerebral vessels exert their effect at the capillary level. (auth)

**55290** VALUE OF VENTRICULAR SCINTIGRAPHY FOR DIAGNOSIS OF CEREBRAL TUMORS IN EARLY CHILDHOOD. Sunder-Plassmann, M.; Grunert, V.; Boeck, F.; Lachmann, D. (Univ., Vienna). Fortschr. Geb. Roentgenstr. Nuklearmed.; 115: No. 1, 67-73(Jul 1971). (In German).

The value of combined skull and ventricular scanning in the initial investigation of infantile hydrocephalus is discussed and one case is described. Localized increase in activity on the skull scan, without evidence of a symmetrical communicating hydrocephalus on the ventricular scan, indicates the need for further neuroradiological investigations. (auth)

**55291** TANTALUM RADIOGRAPHY IN OTOLARYNGOLOGY. Pickard, Robert E. (Univ. of Miami, Fla.). Arch. Otolaryngol.; 94: No. 3, 202-7(Sep 1971).

More than 50 patients with various lesions of the upper respiratory tract and two healthy volunteers were studied roentgenographically using powdered tantalum (1$\mu$ to 5$\mu$) insufflated via catheter or intermittent positive pressure breathing apparatus, or both, after topical anesthesia with 5% cocaine and premedication with intramuscular atropine sulfate. Single frame and cineradiographic studies demonstrated details of airway mucosa and were of assistance in deciding the appropriate course of therapy in most patients. Powdered tantalum may be an ideal radioopaque contrast material in radiography of the upper respiratory tract and has potential as a research and clinical tool in otolaryngology. (auth)

**55292** IMMUNOFLUORESCENT TESTS IN THE COURSE OF $^{99m}$Tc SCINTISCANNING PROCEDURES IN CHILDREN AND ADOLESCENTS. Jeske, Wojciech; Gorowski, Tadeusz; Gajl-Peczalska,

XUM

Kazimiera; Chomicki, Oskar (Univ., Warsaw). Nucl. Med.; 10: No. 2, 146-9(15 Jul 1971).

A group of 18 girls and 2 boys scintiscanned with $^{99m}$Tc were tested for the presence of thyroid antibodies by the indirect Coons method and the passive hemagglutination test. Before the $^{99m}$Tc administration no antibodies were detected, but 6 to 14 weeks later antibodies directed against the second colloid antigen (CA-2) appeared in 9 cases. After 3 to 4 months, however, no antibodies could be found. (auth)

**55293** COMPARISON OF SCINTIGRAPHY AND ANGIOGRAPHY IN THE DIAGNOSIS OF INTRACRANIAL SPACE-OCCUPYING LESIONS. Kuba, J.; Klaus, E.; Sevcik, M. (Palacky-Univ., Olomouc, Czech.). Nucl.-Med.; 10: No. 2, 105-14(15 Jul 1971). (In German).

In 179 out of 573 patients in whom brain scintigraphy was performed, space-occupying lesions were demonstrated: 166 tumors, 7 abscesses, and 6 subdural hematomata. The diagnostic accuracy was 90%. Scintigraphy contributed decisively to the diagnosis in 55% of those cases in whom the angiographic findings were negative, in whom they provided only indirect evidence for the presence of a space-occupying lesions, or in whom angiography could be for several reasons not be done at all. Brain scanning did not only prove useful as an atraumatic screening test for the detection of intracranial focal lesions, but it also contributed considerably to the final diagnosis and the therapy plan. (auth)

**55294** SCINTIGRAPHIC EVALUATION OF THE ACTIVITY OF PAGET'S DISEASE (OSTEODYSTROPHIA DEFORMANS). Umek, H.; Imhof, H.; Czitober, H. (Medizinische Univ., Vienna). Nucl.-Med.; 10: No. 2, 115-21(15 Jul 1971). (In German).

In 19 patients with Paget's disease radiographic and biochemical findings were compared with the results of bone scintigraphy. The evaluation of the metabolic activity of the transformation processes in this slowly progressing and often remitting disease was so far only possible by using biochemical methods. It was demonstrated that scintigraphy may be used as an alternative. (auth)

**55295** $^{99m}$Tc TECHNETIUM SULFIDE AND THE SCINTILLATION CAMERA IN THE RAPID DIAGNOSIS OF PERICARDIAL EFFUSION. Weiss, E. (Wadsworth General Hospital, Los Angeles. Univ. of Southern California, Los Angeles); Blahd, W. H.; Winston, M. A.; Krishnamurthy, G. T.; Thomas, P. B. Nucl.-Med.; 10: No. 2, 122-8(15 Jul 1971).

Because of its speed, accuracy, and reproducibility, radioisotopic angiocardiography appears to be the method of choice for the diagnosis of pericardial effusion. Technetium-99m sulfide is preferable to $^{99m}$Tc sodium pertechnetate for the following reasons: its specific uptake by the liver aids both in patient positioning and in the accuracy of diagnosis; and studies can be repeated within 15 to 20 minutes should there be equipment or technical error. (auth)

**55296** LUNG SCANNING WITH THE GAMMA CAMERA, USING COMPLEXES OF $^{99m}$Tc–SULPHUR COLLOID AND MACROAGGREGATED HUMAN SERUM ALBUMIN. Weber, Theodor H.; Nordman, Clas T. (Maria Hospital, Helsinki. Minerva Foundation Inst. for Medical Research, Helsinki). Nucl.-Med.; 10: No. 2, 129-34(15 Jul 1971).

The results of lung scanning in suspected pulmonary embolism, using the gamma camera and complexes of $^{99m}$Tc sulfur colloid and macroaggregated human serum albumin are presented. In a series of 52 patients, excellent scanning images were obtained in each case without any adverse side effects. The preparation of the test substance takes about 20 minutes and can be performed routinely by a laboratory technician. The use of a gamma camera in connection with this test substance allows anterior, posterior, and lateral view scanning to be performed within 15 minutes, with minimal strain on the patients. Multiple-view scanning was found to be necessary in screening for pulmonary embolism. (auth)

**55297** EVALUATION OF THE LUNG SCINTIPHOTO AS A SCREENING TEST FOR PULMONARY DISEASE. Halpern, Sam; Golden, Melvin; Walsh, Carol (Wadsworth Veterans Hospital, Los Angeles). Nucl.-Med.; 10: No. 2, 135-45(15 Jul 1971).

A method is described for the manufacture of a $^{99m}$Tc lung scanning agent with sulfur colloid macroaggregates, which incorporates nearly 100% of the technetium eluate and can be made from bulk solutions in about sixteen minutes. These particles were used to study the value of the lung scintiphoto as a screening procedure for pulmonary disease. The method was compared with the posterior-anterior and left lateral chest roentgenogram, and the timed vital capacity. Many perfusion defects, sometimes multiple, were found to be present in lungs with normal chest roentgenograms. Perfusion abnormalities were noted in people with normal and near normal timed vital capacities. The lung scintiphoto is considered to be a useful adjunctive screening test for pulmonary disease. (auth)

**55298** SCINTIGRAPHIC PICTURE OF HYPERTROPHIC OSTEOARTHROPATHY. Bieler, E.; Albrecht, H. J. (Univ., Zurich). Nucl.-Med.; 10: No. 2, 196-200(15 Jul 1971). (In German).

Scintigraphic findings in hypertrophic osteoarthropathy are reported. Strontium-85 and $^{87m}$Sr were administered. Localization and distribution of the isotopes permitted differentiation between metastatic disease and hypertrophic changes. In the latter case, bone disturbances usually were symmetrical. (H.B.G.)

## *Radiotherapy*

*Refer also to abstracts 54852, 54902, 55209, 55211, 55212, 55218, 55222, 55244, 55338–55340, 55343–55345, 56581, and 56607.*

**55299** (LA-4490) PROPOSAL FOR A BIOMEDICAL ADDITION TO THE LOS ALAMOS SCIENTIFIC LABORATORY'S HIGH-FLUX MESON PHYSICS FACILITY. Langham, Wright H.; Groce, David E. (Los Alamos Scientific Lab., N. Mex.). Jul 1970. Contract W-7405-eng-36. 211p. Dep. NTIS.

Chapters are presented on the following topics: historical development and design of the Los Alamos meson physics facility; physical properties of Lampf particle beams; radiobiological properties of $\pi^-$ meson beams; clinical support program; clinical utilization and trials; organization and staff; and description of the biomedical addition. Design characteristics of the biomedical addition are outlined with regard to shielding, target vault, and exposure cell. Construction details, personnel requirements, and costs are discussed. The following appendices are included: AEC authorizing legislation for the fiscal year 1971: hearings before the joint committee; and the charter of the users group of the Los Alamos meson physics facility. (H.L.W.)

**55300** HIGH RADIOSENSITIVITY AND DIFFICULTY OF DIAGNOSIS OF SOLITARY METASTASES OF CANCER INTO THE LUNGS AND LYMPH NODES OF THE THORACIC CAVITY. Skotnikov, V. I.; Khazov, P. D.; Samsonova, L. A. Med. Radiol.; 16: No. 8, 14-19(Aug 1971). (In Russian).

Observations on nine patients with solitary metastases of cancer of the pancreas, prostate, ovaries, and hypernephroma into the lungs (3 persons) and lymph nodes of the mediastinum (6 cases) in whom the authors observed a reverse development of the tumor as the result of radiation treatment (telegammatherapy with a focal dose of 5000 to 6000 rad) are reported. The difficulty of the diagnosis is emphasized. (auth)

**55301** RADIATION TREATMENT OF LYMPHOGRANULOMATOSIS OF THE BONE. Pereslegin, I. A.; Fil'kova, E. M. (Moscow Medical Inst. Moscow Scientific Research Radiological Inst.). Med. Radiol.; 16: No. 8, 7-14(Aug 1971). (In Russian).

The experience gained with the treatment of 45 patients suffering from lymphogranulomatosis with solitary and multiple manifestations of the disease in the bones is summarized. Radiation and combined methods were employed. As the result of the treatment in 36 patients the authors achieved remission lasting from 2 months to 3 years. The advantages of telegammatherapy during irradiation of the bones and the technique of pendulum x-ray therapy in irradiation of the vertebrae are outlined. (auth)

**55302** APPLICATION OF THE OXYGEN FACTOR TO CLINICAL RADIOTHERAPY. Du Sault, Lucille A. (Henry Ford Hospital, Detroit). Radiology; 100: No. 3, 675-8(Sep 1971).

The oxygen-enhancing effects of air and carbogen atmospheres on tumor irradiation in mice are compared. Results indicate that the therapeutic effects are greatest in carbogen at one atmosphere, using large fractions and a long overall treatment time. The experimental data are discussed in relation to the clinical situation. (auth)

**55303** EFFECT OF NANDROLON-DECANOATE AND IRON PREPARATION ON THE HEMOGRAM OF IRRADIATED PATIENTS. Adam, Geza; Miltenyi, Laszlo; Molnar, Andreas (Univ., Debrecen, Hungary). Strahlentherapie; 141: No. 6, 696-8(Jun 1971). (In German).

The additional therapy of irradiated tumor patients, suffering from cancer, is important today. The rays from different sources can besides the therapeutic effect heavily damage the blood picture. To avoid side effects, the contemporary treatment with iron- and steroid preparations is successful. With the help of this method the hemogram of the patients can be normalized and the radiation dose can be further augmented. (auth)

**55304** PRIMARY CARCINOMA OF THE THYROGLOSSAL DUCT: REPORT ON A CASE TREATED BY RADIOIODINE. Zamrazil, V.; Nemec, J.; Proks, C.; (and others) (Research Inst. of Endocrinology, Prague. OUNZ Hospital, Pisek, Czech. Medical School, Prague. Motol Hospital, Prague). Neoplasma; 18: No. 4, 421-6(1971).

A patient with differentiated papillary cancer from thyroglossal duct is described in whom subtotal thyroidectomy disclosed no malignant changes in the thyroid gland. After thyroidectomy, radioiodine was accumulated in the tumor allowing thus treatment with $^{131}I$. Immediately after the radioiodine therapy, suppressive treatment with thyroid hormones was introduced. No recurrence was found within a year after the diagnosis. A short review of similar cases found in the literature is given. It is stressed that patients with differentiated cancer of thyroglossal duct should be treated the same way as those with primary differentiated thyroid cancer, namely by combination of surgical and radioisotope ablation of the tumor and of normal thyroid tissue, and with thyroid hormone suppression. (auth)

**55305** ENDOLYMPHATIC THERAPY WITH $^{131}I$-LIPIODOL. KINETICS, INDICATIONS, AND TECHNIQUE. Peters, Peter (Univ., Zurich). Nucl.-Med.; 10: No. 2, 150-66(15 Jul 1971). (In German).

The results of endolymphatic therapy with $^{131}I$-lipiodol in 34 patients with malignant melanomas or metastases are described. Using whole-body profile counting, the kinetics of the radioactive compound was studied for up to 4 weeks. Measurements of the effective half-life in the lymphatic system and in the lungs during two periods revealed differences that were the result of the transfer of part of the contrast medium from the lymphatic system to the lungs. The effects of the volume administered and of previous radiotherapy of the lymphatic system were studied. The most important indications for endolymphatic therapy are discussed. (auth)

**55306** RADIATION TREATMENT OF HUMAN TUMOURS FOLLOWING THE IN VIVO SYNCHRONIZATION OF THE CELL CYCLE. Nitze, H. R.; Vosteen, K.-H.; Ganzer, U. (Univ., Frankfurt am Main). Acta Oto-Laryngol.; 71: No. 2-3, 227-31 (Feb-Mar 1971).

An improvement of the method of radiation treatment of human tumours is presented. 5-fluor-uracil (FU) was used to inhibit the DNA-synthesis reversibly, so that the cells accumulated at the beginning of the S-phase of the cell cycle. Because of the rapid catabolism of FU the cells passed through the cell cycle after the blockage was terminated. The efficiency of the radiotherapy was improved by irradiating the cells at the most radiosensitive stage of the cell cycle. (Sweden)

### *Blast and Thermal Effects*

**55307** MORTALITY IN CHILDREN EXPOSED TO THE A-BOMBS WHILE IN-UTERO, 1945–1969. Kato, Hiroo (Atomic Bomb Casualty Commission, Hiroshima. Japanese National Inst. of Health, Hiroshima). Amer. J. Epidemiol.; 93: No. 6, 435-42(1971).

Mortality has been observed for 24 years from birth to 1969 in a cohort of 1,300 persons exposed to the A-bombs while in utero in Hiroshima and Nagasaki. Mortality for the whole period of 24 years increased with radiation dose. This increase of mortality with dose occurred during the first year of life. No increase in mortality was observed during the next 9 years of life, but mortality again increased with dose after 10 years of age. No particular cause of death was found to be especially related to radiation dose except for perinatal deaths. Only three deaths from malignant neoplasms, including one leukemia, occurred in the whole sample. The increase in mortality with dose was observed only for those exposed to the A-bombs in the third trimester. These increases in mortality with dose are not attributable to other concomitant variables such as parental age, birth order, socioeconomic factors and so on. (auth)

## Radiation Effects on Animals

*Refer also to abstracts 55127, 55205, and 55258.*

**55308** ALTERATION OF DNA BY SENSITIZED AND NON-SENSITIZED LONG-WAVE U. V. IRRADIATION. Zierenberg, B. E.; Kirste, R. G.; Geisert, M. G.; Kraemer, D. M. (Univ., Mainz). Strahlentherapie; 141: No. 6, 728-31(Jun 1971). (In German).

Two different types of photoreaction occur in DNA irradiated with longwave uv ($\lambda > 295$ nm), in aqueous systems, namely, thymine dimerization and single- and double-strand breakage of the sugar phosphate backbone; both reactions of which are not related to each other. The presence of acetophenone as a photosensitizer caused an increase in the first reaction by a factor of 16 and an increase of the second reaction by a factor of 4 related to the number of single strand breaks. The number of thymine dimers per single strand break was about 100 in the sensitized and 25 in the unsensitized reaction. The alteration of the radius of gyration of DNA molecules was in the order of magnitude that should be expected by the degradation observed. At the same time the change in hyperchromicity was very small. It was assumed that the gross conformation of the DNA double helix is stable against thymine dimerization. (auth)

**55309** SURVIVAL OF SYNCHRONIZED L CELLS IRRADIATED WITH 14 MeV NEUTRONS. Masuda, K. (Kyushu Univ., Fukuoka). Int. J. Radiat. Biol.; 20: No. 1, 85-6(1971).

Experiments were made to determine the fraction of L5 cells surviving reproductively after a dose of 260 rads of D–T neutrons administered at different times during the division cycle (dose rate of 12 rads/min at a room temperature of 22°C to 23°C). The surviving fraction was not so dependent on cell age as that of x irradiated cells. (UK)

**55310** CHANGE IN THE ELECTROPHORETIC BEHAVIOUR OF X-IRRADIATED LYMPHOCYTES BY PHYTOHAEMAGGLUTININ. Sato, C.; Kojima, K.; Matsuzawa, T. (Aichi Cancer Centre Research Inst., Nagoya, Japan). Int. J. Radiat. Biol.; 20: No. 1, 97-9(1971).

The electrophoretic mobility of human venous blood lymphocytes declined within 2 hrs of x irradiation with 500 R, and fell progressively with increasing time. The mobility of irradiated lymphocytes treated with phytohaemagglutinin (.02 ml to 1 ml of cell suspension) did not decrease. The addition of phytohaemagglutinin without irradiation gave a slight increase in mobility. The results suggested that treatment with phytohaemagglutinin prevented the loss of the lymphocytes' negative charge by irradiation. (UK)

**55311** DAUGHTER CELL REPAIR BY MAMMALIAN CELLS IN CULTURE AFTER POTENTIALLY LETHAL RADIATION DAMAGE. Belli, J. A. (Harvard Medical School, Boston). Nature (London) New Biol.; 233: No. 36, 47-8(8 Sep 1971).

Single cells from a cell line derived from lung cells of a female chinese hamster (V79-4) were x-irradiated with 800 R. They were allowed to grow to a multiplicity of 1.2 and then incubated in Puck's saline F for varying intervals before being refed with growth medium for colony formation. When the level of damage in the parent cell did not suppress the first or second post-irradiation division, but was great enough to make all resulting progeny nonviable, a significant proportion of progeny retained the capacity to repair the "inherited" damage. (UK)

**55312** RADIOBIOLOGICAL EFFECTS OF SOLELY NUCLEAR AND CYTOPLASMIC IRRADIATION WITH ULTRAVIOLET-MICROBEAM IN HeLa CELLS. Usui, Masahiko (Mie Prefectural Univ., Tsu, Japan). Mie Med. J.; 20: No. 1, 21-35(May 1970).

Mechanisms of radiation damage were investigated with HeLa cells exposed to the three modes of uv-microbeam irradiation, nuclear, cytoplasmic, and whole-cell irradiation; experiments on micrurgical cytoplasmic damage were used as a control. In typical cases of the nuclear irradiation, the cells were killed by a sudden shrinkage of the cytoplasm after they remained for several hours in a stationary state with or without morphological findings of a slight degeneration. The cytoplasmic irradiation induced vacuolar degeneration developing gradually and lethally in the cytoplasm. The whole cell irradiation induced either the former or the latter type. The lethal effect of the irradiations was induced rapidly and intensively in order of the whole-cell, cytoplasmic, and nuclear irradiation for 24 hours after irradiation. The inhibition of DNA and RNA synthesis was induced to the same degree but more rapidly by the whole-cell irradiation than by the nuclear irradiation, but the inhibition by the cytoplasmic irradiation was much less than that by the former two. The whole-cell irradiation inhibited the RNA transport only at high doses, but the partial irradiation of Golgi area had no effect at the same high doses. The micrurgical cytoplasmic damage was repairable for 24 hours when the cytoplasm did not exceed 40% of the reflected area of whole cell. Possible mechanisms of this discrepancy in the data on survival rates and inhibitory rates of nucleic acid syntheses between the nuclear and cytoplasmic irradiation were discussed. (auth) (Japan)

**55313** INACTIVATION OF CELLS BY HEAVY ION BOMBARDMENT. Katz, R.; Ackerson, B.; Homayoonfar, M.; Sharma, S. C. (Univ. of Nebraska, Lincoln). Radiat. Res.; 47: No. 2, 402-25 (Aug 1971).

XUM

The tracks formed in nuclear emulsion by energetic heavy ions are made up of grains sensitized by the passage of a single ion. Cells may also be inactivated by the passage of a single ion, in a mode called ion-kill. Emulsion tracks pass from the grain-count regime, where the track is a sequence of isolated grains, to the track-width regime, where the track is fully closed and has a cross-sectional area larger than that of an emulsion grain, with increasing values of $z^2/\beta^2$ for the charged particle causing the track. The measured value of the inactivation cross section for human kidney cells increases in a similar way. The response of cells is not the same as emulsion grains, because cells may also be inactivated by a gamma-kill mode, involving the cumulative effect of overlapping delta rays from several ions, in addition to the ion-kill mode present in both emulsion and cells. These considerations lead to the equations $P = \sigma/\sigma_0 = [1 - e^{-z^2/\kappa\beta^2}]^m$, and $N/N_0 = e^{-\sigma F}(1-[1-e^{-(1-P)E/E_0}]^m)$, where $E = FL$ is the dose deposited by a fluence F of particles of effective charge ze, speed $\beta c$, LET L. Cellular radiation response is described by the parameters $\sigma_0$, $E_0$, $\kappa$, and m, whose clear interpretation awaits further insight into cellular geometry and behavior. Parameters are determined for bacterial spores, haploid yeast, HeLa, Chinese hamster, and human kidney cells, by fitting these formulas to survival data. (auth)

## Invertebrates

*Refer also to abstracts 55170, 55176, 55185, and 55262.*

**55314** EFFECTS OF CHRONIC IRRADIATION ON LABORATORY POPULATIONS OF THE AQUATIC SNAIL PHYSA HETEROSTROPHA. Cooley, J. L.; Miller, F. L. Jr. (Oak Ridge National Lab., Tenn.). Radiat. Res.; 47: No. 3, 716-24(Sep 1971).

Effects of chronic gamma ($^{60}$Co) irradiation on population dynamics of snails (Physa heterostropha) were studied in the laboratory. Groups of snails of known age were exposed throughout their life span to dose rates of approximately 25, 10, and 1 rad/hr. Growth of snails was significantly increased by 10 and 25 rads/hr. A dose rate of 25 rads/hr eliminated reproduction and led to extinction of the population within one generation. Fecundity was reduced significantly by 10 rads/hr and probably would lead to extinction of the population in two generations. The dose rate of 1 rad/hr gave indications of reducing fecundity, but the effect was not definitive. The two higher dose rates significantly reduced egg hatchability and adult survival. (auth)

**55315** EFFECTS OF GAMMA RADIATION ON EPHESTIA CAUTELLA (Wlk.) (LEPIDOPTERA, PHYCITIDAE). I. EFFECTS ON ADULTS. Calderon, M.; Gonen, M. (Stored Products Research Lab., Jaffa, Israel). J. Stored Prod. Res.; 7: No. 2, 85-90(1971).

The effects of gamma rays, from a $^{60}$Co source on Ephestia cautella (Wlk.) adults, were investigated. The radiation affected longevity, caused reduced fecundity and a high degree of sterility. Male longevity was shortened only after a dose of 45 krad; female longevity was not affected by the same range of doses. Reduced fecundity was evident in irradiated females mated to normal males, after a dose of 20 krad and became more emphasized at higher doses; a dose of 40 krad reduced fecundity of irradiated females to one third. Normal females, mated to 45 krad irradiated males laid 55% of the normal number of eggs. Doses of 40 and 45 krad induced 99.9 and 99.25% sterility in females and males respectively. Only seven males out of sixty-two failed to transfer sperm after treatment with a dose of 45 krad. (auth)

**55316** EFFECTS OF GAMMA RADIATION ON EPHESTIA CAUTELLA (Wlk.) (LEPIDOPTERA, PHYCITIDAE). II. EFFECTS ON THE PROGENY OF IRRADIATED MALES. Gonen, M.; Calderon, M. (Stored Products Research Lab., Jaffa, Israel). J. Stored Prod. Res.; 7: No. 2, 91-6(1971).

Experiments were carried out to investigate the influence of gamma irradiation at doses of 20, 35, and 40 krad from a $^{60}$Co source on the progeny of adult males of Ephestia cautella (Wlk.). The findings showed a high mortality (90%) of immature stages of the $F_1$ at all doses used, and an increase in the proportion of males among adults of the $F_1$ with increasing radiation dose. A negative effect on the mating ability of offspring of irradiated males, which increased with rising doses to the male parents, was shown but the frequency of mating of male offspring whose mating ability was not affected rose. For male progeny of males irradiated at 35 krad a high frequency of transfer of empty spermatophores was noted (60% of all cases) even though sperm was present in their testes. A detrimental effect was noted on the oviposition resulting from the mating of both sexes of the $F_1$ with normal adults. This effect increased with increased doses. Irradiation of male parents at 35 krad induced complete sterility (apart from individual exceptions) of the progeny, whereas for males irradiated at 20 krad, the offspring could be grouped into different sterility levels ranging from complete sterility to normal fertility. (auth)

## Vertebrates

*Refer also to abstracts 55135, 55140, 55147, 55164, 55182, 55184, 55188, 55206, 55207, 55215, 55256, 55257, 55259, 55267, and 55268.*

**55317** (CEA-CONF-1744) RELATIVE BIOLOGICAL EFFECTIVENESS AS A FUNCTION OF LINEAR ENERGY TRANSFER FOR CATARACT CRITERION IN THE RABBIT. Legeay, G.; Haye, C. (Commissariat a l'Energie Atomique, Fontenay-aux-Roses (France). Centre d'Etudes Nucleaires); Drouet, J. (Commissariat a l'Energie Atomique, Saclay (France). Centre d'Etudes Nucleaires); Bazin, J. P. (Commissariat a l'Energie Atomique, Fontenay-aux-Roses (France). Centre d'Etudes Nucleaires). [1969]. 26p. (In French). (SM-145/29; CONF-710314-1). Dep. NTIS (U. S. Sales Only).

From symposium on biophysical aspects of radiation quality; Lucas Heights, Australia (8 Mar 1971).

Experimental studies on rabbits were made to determine the relative biological effectiveness for the cataractogenic criterion of $\gamma$ rays, neutrons at 14 and 2.5 MeV, and protons at 3 GeV. Response functions were obtained for the four irradiations. The RBE calculated from the response curves shows that the RBE is not a constant and that it increases when the administered doses decrease. The neutrons and $\gamma$ rays have RBE's in good correlation with the linear energy transfer. (J.S.R.)

**55318** (LB/G-2995) SOME PATHOMORPHOLOGICAL FINDINGS IN ACUTE RADIATION SICKNESS IN GOATS. Otoupal, P.; Pawel, O.; Dvorak, E. Translated by B. K. Bowes (Atomic Energy Research Establishment, Harwell, Eng.), from Vet. Med. (Prague); 12: 427-34(1967). 17p. Dep. NTIS (U. S. Sales Only).

Eleven goats aged 2 to 7 years were dissected and examined histologically. Of these, 5 animals had been irradiated with doses of 1200 or 1600 R and their death occurred between the 4th and 8th day after irradiation. Six goats had been irradiated with a dose of 700 R and they died or were killed between the 10th and 30th day after exposure. Irradiation was applied to the whole body by means of gamma rays from a $^{60}$Co source at a rate of 140 R per hour. The finding was characterized by a well-developed hemorrhagic diathesis with localization on serosas particularly in the thoracic cavity, and that especially in animals dissected after the eighth day after irradiation. A typical occurrence of hemorrhages was found in physiologically strained muscles — in intercostal muscles, in the diaphragm, and in the myocardium. No regressive changes in the form of ulcers in the digestive organs were found. Necrobiotic deposits in the livers were found macroscopically, and aggregations of bacteria were determined histologically in the centers of these deposits. A beginning of the regeneration of lymphoid tissue in the lymphatic nodes of goats that had been irradiated with a dose of 700 R was ascertained on the 10th day after exposure. In the adrenal cortex dystrophic changes in the epithelium of the efferent canals with an oedema were observed and a deposit of proteinic substances into Bowman's capsules. In the pathomorphological finding obtained in irradiated goats some deviations were obtained which were considered to be, to a certain extent, dependent on the species of the experimental animal. These are, in particular, the total intensity, extent, and localization of hemorrhages in the skin and muscles, and localization of regressive, and particularly of necrobiotic changes in intestinal mucous membranes and in the livers. (auth)

**55319** (UCD-472-118) ANNUAL REPORT, FISCAL YEAR 1971. (California Univ., Davis. Radiobiology Lab.). Jun 1971. Contract AT(04-3)-472. 143p. Dep. NTIS.

The research activities of the Radiobiology Laboratory during the fiscal year 1971 are reported. Both external irradiation studies and internal emitter studies are included. Fifty-five references to publications and presentations by the laboratory staff during the report period are cited. (E.R.B.)

**55320** GENETIC VARIATION IN IRRADIATED AND NONIRRADIATED POPULATIONS OF THE LIZARD, UTA STANSBURIANA. McKinney, Charles O. (Univ. of Texas, Austin); Turner, Frederick B. Contract AT(04-1)-Gen-12. Radiat. Res.; 47: No. 2, 530-6(Aug 1971).

Analysis of allelic variation in continuously irradiated and nonirradiated populations of the lizard, Uta stansburiana, in Rock Valley, Nevada, revealed no significant differences in relative allele frequencies at 19 loci controlling selected proteins. The

irradiated population did not differ significantly from control populations in three conventional measures of genetic variability. (auth)

**55321** FACTORS INFLUENCING CLASMATOSIS IN VIVO: OBSERVATIONS OF PERIODICITY OF CLASMATOSIS IN LYMPHOCYTES AND HEMATOPOIETIC RECOVERY AFTER IRRADIATION. Kabakov, Y. N. (Inst. of Medical Radiology, Obninsk, USSR). Radiat. Res.; 47: No. 2, 491-9(Aug 1971).

The relative content of clasmatocytes and cytoplasmic fragments which had detached themselves from them was determined in the smears from cell suspensions of the spleen, lymph nodes, and thymus of CBA mice 12, 24, 36, and 48 hours, and 4, 6, 9, 12, 18, 21, and 25 days after 150 R whole-body irradiation with $^{60}Co$ gamma rays. The behavior of the basic types of cells in the bone marrow and the total cellularity of the spleen was studied. It has been established that both clasmatosis indices have identical dynamics within each organ and common characteristic phases for all the three lymphoid organs; no clasmatosis was observed in the bone marrow. Three waves of clasmatosis activation with maximums in the 24th hour, 4th and 21st days were observed after irradiation. Comparison of clasmatosis with hemopoiesis has shown that its waves precede the activation of granulocytopoiesis in the bone marrow. These data have been discussed as indirect proof of the connection of phenomenon with the genesis of the early progenitors of blood cells. An assumption has been expressed that the cytoplasmic fragments or their products may be a feedback factor in the process of lymphocyte maturation in the centers of lymphopoiesis. (auth)

**55322** ALTERATION OF TASTE THRESHOLDS IN THE RAT FOLLOWING LOW DOSE X IRRADIATION. Shaber, Gary S. (Thomas Jefferson Univ., Philadelphia). Radiat. Res.; 47: No. 3, 689-703(Sep 1971).

The taste thresholds for saccharin (sweet), hydrochloric acid (sour), sodium chloride (salt), and quinine hydrochloride (bitter) were determined in 32 adult Wistar rats, 8 rats for each taste material, before and after a 50 R, 250-kVp x-ray exposure to the tongue. Taste thresholds were obtained using a behavioral technique employing lateral hypothalamic stimulation for the reward stimulus. The preirradiation taste threshold values for saccharin 0.001%, NaCl 0.002%, HCl 0.001%, and quinine hydrochloride 0.0001% were 3 to 6 times lower than previously reported values. Satiation for the reward stimulus (lateral hypothalamic stimulation) did not occur so that detection of the transient nature of the effect was accomplished with frequent daily taste threshold determinations. All animals experienced a 10-fold decrease in taste sensitivity within 24 hrs following the x-ray exposure and all threshold values returned to preirradiation levels within 72 hrs. The speed of onset and duration of the transient alteration in taste thresholds was dependent upon the particular taste substance under investigation. A study of the rate of tritiated thymidine incorporation into the taste bud confirmed the 10-day average life span for a taste bud cell and indicates that the immediate low dose radiation effect on taste is independent of taste bud cell renewal kinetics. Morphological study of the taste buds failed to reveal an anatomical explanation for the observed radiation change in taste acuity. (auth)

**55323** RADIATION EFFECTS ON WATER PERMEABILITY AND DISTRIBUTION IN FROG MUSCLE CELLS. Portela, Adolfo; Garfunkel, Marcelo; Vaccari, Jorge; (and others) (Universidad de Buenos Aires. Brown Univ., Providence). Radiat. Res.; 47: No. 3, 704-15(Sep 1971).

Radiation effects on cell water parameters were analyzed in 400 single muscle fibers from tibialis anticus muscles of the South American frog Leptodactylus occelatus. Cell volume was calculated from cell diameter measured photomicrographically at 10-sec intervals. Water permeability, $P_W$, and osmotically effective cell water, $W_{eff}$, were determined by cell volume changes between standard osmolarity Ringer (0.222 Osm/liter) and one-half standard osmolarity Ringer (0.111 Osm/liter). Cell volume in standard Ringer was not changed by 100 krads of x rays. Osmotically available cell water increased from 52% of cell volume without irradiation to 86% of cell volume after 100 krads. The water permeability coefficient increased by 100%, from 0.40 ± 0.02 to 0.80 ± 0.02 cm/sec/Osm/cm$^3$. In conjunction with data from earlier work, these results indicate that 100 krads alter the plasma membrane so as to increase its specific permeability to water and to sodium ions, but not to other solutes, and alter internal membranes of the cell so as to liberate normally unavailable solution from a not yet identified compartment within the cell to participate in osmotic effects. (auth)

**55324** MECHANISMS OF ACUTE INJURY IN THE γ-IRRADIATED CHICKEN: IN VIVO STUDIES OF DOSE PROTRACTION EFFECTS ON THE MICROVASCULATURE. Stearner, S. Phyllis; Christian, Emily J. B. (Argonne National Lab., Ill.). Radiat. Res.; 47: No. 3, 741-55(Sep 1971).

Early circulatory collapse in the lethally irradiated chicken, in which the vasculature is fully differentiated, is similar to that previously described in the chick embryo. Effects of whole-body $^{60}Co$ γ irradiation in the 3-week chick are considered in relation to quantitative difference in early mortality (<24 hrs) after short (15 min) and protracted (24 hr) exposures. The microcirculation in the wing skin was studied before and for several hours after irradiation and observations were recorded cinemicrographically. Intravenously injected colloidal carbon was used to indicate areas of vascular damage. Stasis and occlusion of smaller superficial vessels occurred within 1 or 2 hrs after a 15-min exposure to 1200 R. Swollen endothelial cells and carbon accumulation in disrupted vessel walls were demonstrated in localized regions, especially in capillaries and venules, within 3 or 4 hours after exposure. Mortality exceeded 80% within 24 hrs. When the radiation exposure was protracted over 24 hrs, a dose of 10,000 R resulted in stasis and lysis of relatively few vessels and fewer than 5% of the chicks died within 24 hrs after the exposure was completed. Radiation injury resulted in a random distribution of microvascular damage sufficient to cause carbon labeling, in contrast to the more uniform pattern that was observed after localized trauma (e.g., heat or crushing). (auth)

**55325** EFFECTIVENESS OF TRANQUILIZING DRUGS IN RATS EXPOSED TO MIXED GAMMA–NEUTRON RADIATIONS. Davis, Lawrence W.; Strike, Thomas A. (Armed Forces Radiobiology Research Inst., Bethesda, Md). Radiat. Res.; 47: No. 3, 725-30(Sep 1971).

Chlorpromazine, triflupromazine, and chlordiazepoxide were studied for their effect on a conditioned avoidance response in rats at selected times following 500, 1,000, and 10,000 rad whole-body doses of mixed gamma–neutron radiations. The $ED_{50}$ of the drugs increased in the rats receiving 1,000 rads and decreased in those receiving 10,000 rads when compared to unirradiated controls. Although the dose-response curve may be altered in irradiated rats, the three drugs studied remained effective even after radiation doses associated with central nervous system damage. (auth)

**55326** STATE OF HEMATOPOIESIS IN LOCAL FRACTIONAL IRRADIATION. II. THE HEMATOPOIESIS IN IRRADIATED AND NONIRRADIATED AREAS OF THE BONE MARROW. Pavlov, V. V.; Baisogolov, G. D. (Scientific Research Inst. of Medical Radiology, Obninsk, USSR). Med. Radiol.; 16: No. 9, 14-23 (Sep 1971). (In Russian).

It is shown that in local fractional irradiation of 15 to 20% of active bone marrow in irradiated areas aplasia develops and progresses with enlargement of the total dose of radiation. In the nonirradiated bone marrow there is seen an intensification of the proliferative activity, mainly among erythronormoblasts, and an increase of the bone marrow index of neutrophils as the result of accelerated production of mature granulocytes in the peripheral blood. The authors discuss the causes of reduction of the leukocyte count in the process of radiation treatment in oncological patients. An opinion is set forth that in patients with intoxication this reduction is largely associated with elimination of the myelotoxic action of the main process under the influence of radiation therapy. (auth)

**55327** ACUTE CHANGES IN PULMONARY ARTERIAL PERFUSION FOLLOWING IRRADIATION. Korsower, Jack M.; Skovron, Mary L.; Ghossein, Nemetallah A.; Goldman, Harold S. (Albert Einstein Coll. of Medicine, Bronx, N. Y.). Radiology; 100: No. 3, 691-3(Sep 1971).

Forty-four rabbits were given 3,000 rads to either hemithorax in a single dose. Lung scans demonstrated decreased perfusion in 52% of the animals at two hrs. Perfusion returned to normal by twenty-four hrs. Pulmonary angiograms showed decreased blood flow on the irradiated side, without demonstrable vascular occlusion. (auth)

**55328** LATE FUNCTIONAL AND CIRCULATORY CHANGES IN RATS AFTER LOCAL IRRADIATION. Keyeux, A.; Dunjic, A.; Royer, E.; Jovanovic, D.; Van de Merckt, J. (Catholic Univ., Louvain, Belgium). Int. J. Radiat. Biol.; 20: No. 1, 7-25(1971).

Late circulatory disturbances of the lungs, brain, liver and skin and late modifications of the respiratory and hepatic functions after local x-irradiation, were assessed by quantitative in vivo radiotracer tests in rats. Except for the central nervous system, which showed an increase of its blood flow, a decrease of the organic functions and their circulatory supply was observed. These late changes were statistically demonstrable above a dose-level of 1000 R. Tracers used were Xe-133, Tc-99m, Au-198, and I-131. (auth)

XUM

55329 EFFECTS OF IRRADIATION ON AVIAN LEUKOSIS. Loan, R. W.; Storm, Mary M.; Sloan, Kaaren C.; McCune, E. L. (Univ. of Missouri, Columbia, Mo.). Amer. J. Vet. Res.; 32: No. 6. 947-52(Jun 1971).

Whole body x-irradiation did not increase or decrease the frequency of death due to leukosis in chickens inoculated at 22 or 23 days of age or in ovo with RPL-12 virus. The levels of viremia in chickens inoculated in ovo were not increased by irradiation. Whole body irradiation (500 R) did not affect the frequency, progression, or regression of Rous sarcoma in adult chickens. More adult females developed Rous sarcoma (>3 cm. in diameter) and died than did males. More adult males developed Rous sarcoma (<3 cm. in diameter) and recovered than did females. Sex differences in susceptibility to Rous sarcoma were not found in sexually immature chickens. (auth)

55330 HISTOCHEMICAL AND HISTOLOGICAL INVESTIGATIONS IN BONE MARROW SECTIONS OF THE WISTAR RAT AFTER SINGLE WHOLE BODY-IRRADIATION WITH VARIOUS X-RAY DOSES. Jonecko, A.; Bartnikowa, W.; Schneiberg, K. (Inst. fuer Onkologie, Gliwice, Poland). Acta Histochem.; 39: No. 2, 257-67(1971). (In German).

Wistar rats were exposed to single whole body doses of 200, 400, 600, 800, 1000, 1200, 1400, 1600 or 1800 R x-rays. The bone-marrow was investigated after 48 hours and later. Using preparations that had been delimed with EDTA solution, the behavior of the histochemically detectable alkaline phosphatase, adenosine triphosphatase and acid phosphatase was studied. Preparations that had been delimed in Susa mixtures were morphologically stained and the PAS reaction was carried out. Intracellular activity of the alkaline phosphatase disappears after high radiation doses. Activity of the acid phosphatase strongly increases. An islandlike disappearance of the hematopoetic tissues can be observed in morphological preparations. Eosinophilic and lymphoid cells disappear at first. (auth)

55331 INVESTIGATIONS ON THE CALCIUM METABOLISM OF THE BONES FOLLOWING LOCAL IRRADIATION. XI. REPORT: SEX-CONDITIONED DIFFERENCES IN THE GENERAL RESPONSE OF TYPE AND INTENSITY OF THE DAMAGE. Babicky, A.; Kolar, J.; Bibr, B. (Tschechoslowakische Akademie der Wissenschaften, Prague. Karls-Univ., Prague). Strahlentherapie; 141: No. 6, 699-704(Jun 1971). (In German).

The general metabolic response of the skeleton of white rats to local radiation damage in the knee-joint region was explored in a parallel test with thermic injury in order to confirm the sex-conditioned differences. The more marked course of reaction in male animals is also seen in this kind of energy, caused by the regulatory influence of the sex hormones. Differences in the course of this reaction can be explained by various kinds of damage and producing energy doses. The common regularities in the course of the generalized oscillating reaction are discussed. Their course is similar to the undulating course, which is observed in the radiation erythema of the skin. This series of experiments is one of the steps of larger studies about the hormonal regulation of the general reactions in irradiated animals. (auth)

55332 INVESTIGATIONS OF INJURY INDUCED BY DIFFERENT CAUSES. Messerschmidt, Otfried; Kettermann, Karl-Bertold; Koslowski, Leo (Univ., Freiburg i. B. Chirurgische Univ., Tuebingen, Ger.). Strahlentherapie; 141: No. 6, 705-11 (Jun 1971). (In German).

Studies were made on the impairment of electrolyte metabolism in rats caused by whole-body irradiation, open skin lesions, or combinations of the two. Determinations in serum as well as in the 24 hour urine of Na, K, and Cl were carried out. Excretion of sodium and potassium in the urine was highest, if both injuries to the rats were combined. A marked chloride excretion was also noticed. It was also found that injuries induced by different means cause loss of water, electrolytes, and proteins through open skin lesions as well as weight loss in the animals. (auth)

55333 CONGENITAL CARDIOVASCULAR ANOMALIES IN CHICK EMBRYOS EXPOSED TO X-IRRADIATION AND HYPOTHERMIA. Gilani, Shamshad H.; Jaffee, Oscar C. (State Univ. of New York, Buffalo). Amer. J. Obstet. Gynecol.; 111: No. 1, 47-52(1 Sep 1971).

The effects of x-irradiation and hypothermia on cardiovascular development were analyzed in chick embryos. Cardiovascular anomalies produced by x-irradiation and hypothermia included aortic stenosis, common truncus arteriosus, ventricular and atrial septal defects, abnormal semilunar valves, thin ventricular wall, and inhibition of aortic arch development. Aortic stenosis was the most frequent finding at low dosages of radiation while common truncus arteriosus was the most frequent finding at higher levels of radiation. Exposure of the embryos to hypothermia before irradiation had a questionable effect upon radiosensitivity of the embryos (as determined by $LD_{50}$ values) or radiation damage to the developing heart (as determined by the incidence of cardiac defects). Exposure to cold after radiation appeared to exaggerate the effects of the radiation, as determined by an increased sensitivity and a greater incidence of cardiac anomalies. (auth)

55334 UNILATERAL AND BILATERAL EXPOSURE OF SWINE TO FISSION NEUTRONS. Brown, Daniel G. (UT-AEC Agricultural Research Lab., Oak Ridge, Tenn.); Johnson, Donald F.; Auxier, John A. Health Phys.; 21: No. 4, 537-45(Oct 1971).

Sixty swine, averaging 150 kg in body weight, were exposed unilaterally or bilaterally to fission neutrons and $\gamma$ rays from the Health Physics Research Reactor (HPRR) of the Oak Ridge National Laboratory for the purpose of evaluating effects of nonuniform exposures. Two modes of death were manifest. Deaths within 30 days postirradiation were primarily due to bone marrow damage; deaths after 30 days were presumably due to skin damage and infection. The skin was thus considered to be a critical organ relative to mortality. Due to the mortality pattern with deaths occurring from 6 to 117 days and because of high mortality in the unilaterally exposed animals at the lowest dose level, the number of animals used was insufficient to calculate 50% mortality on a time basis within a reasonable degree of confidence. The data, however, indicated the $LD_{50/30}$'s to be similar, but the $LD_{50/100}$'s were approximately 550 and 750 rad for unilateral and bilateral exposures, respectively. This difference was attributed to the more severe skin damage in the unilaterally exposed swine. (auth)

55335 STUDIES ON EXPERIMENTAL OSTEOGENIC SARCOMAS INDUCED BY RADIOISOTOPE $^{32}P$. Hayashi, Yasuo (Kumamoto Univ., Japan). Kumamoto Igakkai Zasshi; 44: No. 6, 534-70(Jun 1970). (In Japanese).

Experimental osteogenic sarcomas were produced in albino male rats of the C. F. Wistar strain by $^{32}P$ injected by the intraperitoneal route. Animals were sacrificed and the growing tumors were studied. Roentgenographically, some of the tumors were completely osteolytic, but most of the tumors exhibited a combination of osteolytic and osteoblastic figures. Cytologically, tumor cells exhibited the properties of malignant tumor cells. Histologically, these tumors revealed polymorph oval or fibroblast-like sarcoma cells and giant cells. Osteoid and bone formations were observed of the osteoblastic type in these osteogenic sarcomas. Many metastatic nodules in the lungs and within the lumen of pulmonary blood vessels were observed in one case. Although the original tumor had been non-osteoblastic, the transplanted tumors were osteoblastic. Histochemically, lipid, phospholipid, mucopolysaccharide and glycoprotein were observed in tumor cells and intercellular substances. Glycogenesis and glycogenolysis are considered not to be vigorous in these tumors, in that glycogen was slightly observed and that PR and UGT were inactive. Dehydrogenases without $\alpha$-GDH exhibited moderate activity in tumor cells. ALP, 5-N, ALPP and ATPase exhibited high activity in osteoblastic tumor cells, so they are considered to play an important role in tumorous bone formation as in normal bone formation. Electron-microscopically, tumor cells exhibited the properties of malignant tumor cells as in the cases of other experimental and human osteogenic sarcomas. (auth)

55336 CELL RESPONSE OF THE OLFACTORY BULB TO IONIZING RADIATION INJURY. AN ELECTRON MICROSCOPY STUDY. Estable-Puig, Rosita F.; Estable-Puig, Juan F. (Laval Univ., Quebec). Acta Neuropathol.; 17: 287-301(1971). (In French).

Effects of a single high dose of x-rays on the adult rat olfactory bulb were studied by electron microscopy. Several features of the cell response were described (neuronal pyknosis; glial response and glycogen accumulation; edema; phagocytic activity). Approaches towards understanding the mechanisms underlying these effects and their possible functional significance are discussed. The damage of the internal granule cells gave rise to synaptic degeneration at the level of the reciprocal mitro-granular contacts in the stratum plexiforme. The importance that this work may have when applied to the study of short axon neuron connections is stressed. (auth)

55337 DETERMINATION OF TESTES CONSISTENCY IN BULLS USING A TONOMETER TO TEST THE GERMINATIVE FUNCTIONS OF THE GONADS. Leidl, W.; Schefels, W. (Univ., Munich). Berlin Munchen. Tieraerztl. Worchenschr.; 84: 141-4(15 Apr 1971). (In German).

Tests were made to see how far a tonometer could be used to determine the consistency of the testes and the prognosis of these criteria for testes function. Six bulls were used which had been given local roentgen radiation of the testes with 500 R to produce reversible azoospermialike disturbances. Changes in the consistency of the testes were best seen by the values read directly from the tonometer. Tonometer values for non-disturbed testes dispersed rapidly, so that there was overlapping with findings on testes with degenerative processes. In the 6 test bulls, the tonometer values were significantly lower 5 to 6 weeks after radiation than in the period before ($P \leq 0.01$) and 7 to 8 weeks postirradiation reached their lowest values. Regeneration could be seen from the 11 to 12 week post irradiation by the higher tonometer values ($P \leq 0.01$). In the degeneration phase, the tonometer values were changed slightly earlier than the quality of the sperm, but the regeneration through changes in the consistency appeared as early as 8 weeks before that in sperm quality. The tonometer provided valuable information about the consistency of the testes which cannot be obtained through palpation. Because of individual differences in animals, the dispersal of the values in individual tests and phase distribution of testes consistency and condition of the sperm in regeneration, the method is more suitable for scientific research in groups than for routine use in fertility diagnosis on individual animals. (auth)

## Man

*Refer also to abstracts 55163, 55193, 55202, 55203, 55230, 55269, 55270, and 57099.*

**55338** CHANGES OF THE SKIN IN THE TREATMENT OF BONE SARCOMA WITH HIGH-ENERGY BREMSSTRAHLUNG. Savchenko, E. D.; Osipenkova-Vichtomova, T. K.; Zverev, M. P. (Moscow Scientific Research Radiological Inst.). Med. Radiol.; 16: No. 8, 25-32(Aug 1971). (In Russian).

The state of the skin after bremsstrahlung (25 MeV) treatment of sarcoma of long bones in 47 patients was studied. In 13 of them, a pathomorphological investigation according to isodose curves with the use of histological techniques was carried out. Irradiation was performed longitudinally with a daily single dose of 300 rad; for a period of 5 to 8 weeks the focal dose amounted to 6000 to 12000 rad. Bremsstrahlung therapy in a number of cases caused radiation injuries of the skin. Histochemical investigations revealed foci of metachromasia in the derm, as well as a disturbance of the enzymatic activity of acid phosphatase of epidermal cells. (auth)

**55339** ALTERATION OF THE FUNCTION OF EXTERNAL RESPIRATION IN PATIENTS WITH MALIGNANT TUMORS OF THE CHEST UNDER THE EFFECT OF RADIATION TREATMENT. Mityukhina, V. M.; Voznyuk, E. I.; Kesareva, N. S. (Moscow Scientific Research Inst., of Oncology). Med. Radiol.; 16: No. 9, 31-4(Sep 1971). (In Russian).

The function of the external respiration in 76 patients suffering from malignant neoplasms of the chest—the respiratory rate, respiratory volume, vital capacity of the lungs, minute volume, oxygen utilization, coefficient of oxygen utilization, maxillary pulmonary ventilation and residual air—was determined with the aid of a spirograph and evaluated in the process of radiation treatment. (auth)

**55340** CHANGES IN THE CONTENT OF ELECTROLYTES UNDER THE INFLUENCE OF RADIOIODINE TREATMENT IN PATIENTS SUFFERING FROM DIFFUSE TOXIC GOITER WITH A SEVERE FORM OF THYROTOXICOSIS. Lipets, A. I.; Dozorets, Yu. L. (Vitebsk Medical Inst., USSR). Med. Radiol.; 16: No. 9, 23-6(Sep 1971). (In Russian).

The sodium and potassium metabolism was studied in 64 patients suffering from diffuse toxic goiter with a severe form of thyrotoxicosis before and at different periods after radioiodine treatment. Before treatment, all the indices were disturbed: a reduction of sodium and potassium gradients, sodium/potassium coefficients of the plasma and urine, and an increase of the sodium/potassium coefficient of erythrocytes. After treatment, the indices of the electrolyte metabolism improved. For complete normalization, the authors recommend to treat thyrotoxicosis with due consideration of changes in the electrolyte metabolism. (auth)

**55341** VISUAL SENSATIONS PRODUCED BY COSMIC RAY MUONS. Charman, W. N.; Rowlands, C. M. (Univ. of Manchester, Eng.). Nature (London); 232: No. 5312, 574-5(20 Aug 1971).

Preliminary results are presented of a study which confirmed and extended earlier observations on this subject and which may have a bearing on reports by Apollo astronauts that they saw flashes of light while in translunar flight. Ten observers underwent four recording sessions in each of four body positions; the technique adopted and apparatus employed are described. When muons passed through the eye visual effects were observed, but not when the particles passed through the visual cortex. Results appeared to favor a direct retinal excitation process rather than the production of Cherenkov light in the eye media by relativistic singly charged particles. (UK)

**55342** FIZICHESKIE I RADIOBIOLOGICHESKIE ISSLEDOVANIYA NA ISKUSSTVENNYKH SPUTNIKAKH ZEMLI (K OTSENKE RADIATSIONNOI OPASNOSTI KOSMICHESKIKH POLETOV). (Physical and Radiobiological Investigations of Artificial Satellites of the Earth (With an Estimate of the Radiological Hazards to Interplanetary Flights)). Grigor'ev, Yu. G.; Kovalev, E. E. (eds.). Moscow; Atomizdat (1971). 200p.

The results of experiments obtained from the flights of satellites around the Earth, and from literature surveys of the physical and medical-biological studies made of interplanetary space are presented. Methods of calculating the permissible radiation dose from the radiological conditions that obtain in space are given, as well as estimating the physical shielding required for the space ships. The radiological hazards of cosmic radiation are evaluated for man and other forms of life. Data was gathered from various studies of the combined effect of radiation and other factors of space flight on animals, higher and lower plants, single-celled organisms, and models of biological systems. Each of the five chapters is provided with an extensive bibliography. (tr-auth)

**55343** THYROID CARCINOMA FOLLOWING $^{131}I$ THERAPY. REPORT OF A CASE AND REVIEW OF THE LITERATURE. McDougall, I. R.; Kennedy, J. S.; Thomson, J. A. (Royal Infirmary, Glasgow). J. Clin. Endocrinol. Metab.; 33: No. 2, 287-92(Aug 1971).

A 72-yr-old female presented with severe respiratory obstruction due to an infiltrating carcinoma of the thyroid. The patient had been subjected to radioiodine therapy ($^{131}I$) for thyrotoxicosis 13 yr prior to her present illness. The possible role of the $^{131}I$ therapy in the development of the thyroid tumor is discussed. (auth)

**55344** OSTEONECROSIS IN LOWER MANDIBLE AFTER POSTOPERATIVE RADIOTHERAPY ON MALIGNANT TUMOR IN THE ORAL CAVITY. Yamazaki, Hiroshi; Minamikawa, Yoshimasa; Nakanishi, Koichi; Furuta, Iwao (Kobe Univ., Japan). Kokobyogakkai Zasshi; 19: No. 3, 698-704(Jul 1970). (In Japanese).

A report is presented on a case of osteonecrosis in the lower mandible resulting from radiotherapy after surgery of malignant tumor in the oral field. In three cases operated for parotid tumor, malignant tumor in left lower mandible, and that in lower right mandible, two of them had a dentulous jaw with secondary infection, and one had an edentulous jaw. The doses of radiation given from $^{60}Co$ were 6500 to 7000, 7000, and 8000 R, and the periods required from radiotherapy to the appearance of osteonecrosis in the jaw were 1, 6, and 13 years in these three cases. (Japan)

**55345** CYTOLOGICAL CHANGES AND ITS EVALUATION AFTER TREATMENT OF ORAL CANCER. CYTOLOGICAL STUDIES DURING TREATMENT OF ORAL CANCER. 2. EFFECT OF EXFOLIATIVE CYTOLOGY DURING TREATMENT OF ORAL CANCER. Shimada, Keikichi (Tokyo Univ.). Kokobyogakkai Zasshi; 19: No. 3, 596-611(Jul 1970). (In Japanese).

In order to assess the therapeutic effect of radiation and 5-fluorouracil or 5-fluorouracil and Ametohepazon for the treatment of squamous epithelial cancer in the oral cavity, examinations were made on some clinical cases. Comparisons were made on the effects found through histopathological findings and morphological changes in desquamated cells during the same period, and assessment of therapuetic effect of exfoliative cytodiagnosis was attempted based on these comparative results. Radiotherapy was given with $^{60}Co$ (4,320–7,264 rads), radium (7,000–7,870 rads), and/or Betatron (4,500–9,500 rads), continuously or in divided doses. The total dose of 5-fluorouracil given was 1,250–5,250 mg and that of Ametohepazon, 12,250–2,050 mg. Morphological changes in the exfoliative normal epithelial cells, damaged by radiation and anticancer agent, were qualitatively the same as those of cancer cells. Observations on cell population in smear preparations, either cornified or noncornified type, indicated that cancer cells are more sensitive to treatment then the normal epithelial cells. Exfoliative cytology and histological effects of treatment seemed to have a parallel correlation, although in the range of therapeutic effect of degree II, the effect seemed to appear slightly earlier in histodiagnosis than in cytodiagnosis. From a total of 12 cases examined, 8 are alive (4 for more than 3 years, 4 for 2–3 years), 3 are dead, and fate of one is unknown. (Japan)

XUM

55346 INFLUENCE OF RADON INHALATION ON THE REACTIVITY OF LYMPHOCYTES. Wiktor, Zdzislaw; Szewczyk, Zenon. Pol. Tyg. Lek.; 25: No. 51, 1965-8(21 Dec 1970). (In Polish).

The effects of radon inhalation on blastic transformation in lymphocyte cultures stimulated with PHA in vitro were investigated. The material included patients with the following diseases: I, nephrotic syndrome; II, chronic glomerulonephritis; III, chronic renal failure; and IV, healthy subjects. Following 30 minute inhalation, statistically significant stimulation or inhibition of lymphocyte blastic transformation was not noted. After 20 radon inhalations a statistically significant decrease in blastic transformation in groups I, II, and IV was observed. In group III (chronic renal failure) an increase in blastic transformation after a single and after 20 radon inhalations was observed. The results indicate a biological effect of radon on immunologically competent lymphocytes. (auth)

55347 REACTORS, RADIATION, AND RISK: THE THREE Rs OF PUBLIC CONCERN. Corbit, C. D. (Douglas United Nuclear, Inc., Richland, Wash.). pp 676-715 of Health Physics Aspects of Nuclear Facility Siting. Vol. III. /Voilleque, Paul G. (comp.). Idaho Falls, Idaho; Burton R. Baldwin, Publications Chairman (1971).

From fifth annual midyear topical symposium on health physics aspects of nuclear facility siting; Idaho Falls, Idaho (3 Nov 1970).

Radioactive effluent releases reported from eleven operating U.S. power reactors are analyzed. Population exposure estimates are derived by assuming the relocation of these reactors to a common site. An extrapolation is made to show how many reactors, with similar effluent releases, could be operated at the selected site without exposing the general population to more than ten percent of the applicable Federal Radiation Council standards. The exposure results and the level of risk are quantitatively compared with other risks to which man is exposed. Perspective on risk is gained through in-depth evaluation of radioactive and nonradioactive wastes that are disposed of into man's biosphere. Additionally, comprehensive review of accident probabilities and the consequences of such accidents is needed. (auth)

## Radiation Effects on Plants

*Refer also to abstracts 55165, 55167–55169, 55172, 55175, 55177, 55180, 55181, 55183, 55205, 55206, 55260, 55261, and 55342.*

55348 ROOT RESPIRATION OF WHEAT PLANTS AS INFLUENCED BY AGE, TEMPERATURE, AND IRRADIATION OF SHOOTS. Osman, A. M. (Univ. of Nottingham, Loughborough, Eng.). Photosynthetica (Prague); 5: No. 2, 107-12(1971).

The respiration rates of wheat plants over a range of ages were measured at temperatures ranging between 10 and 30°C and with the shoots either irradiated or in darkness. A marked increase in root respiration was found within 12 min of exposing the shoot to photosynthetically active radiation (PhAR) and the fall in respiration after excluding PhAR was equally sharp. It is suggested that this is a direct consequence of the translocation of photosynthate from the leaves to the roots. Respiration rates during the day were about 50% higher than during darkness at the same temperature. A procedure is suggested for estimating respiratory losses from the roots of plants growing in the field. (auth)

55349 SENSITIVITY OF LIMA BEAN (PHASEOLUS LIMENSIS MACF.) YIELD TO $^{60}$Co GAMMA RADIATION GIVEN AT THREE REPRODUCTIVE STAGES. Bottino, P. J.; Sparrow, A. H. (Brookhaven National Lab., Upton, N. Y.). Crop Sci.; 11: No. 3, 436-7(May-Jun 1971).

Potted plants of lima beans (Phaseolus limensis Macf. "Fordhook 242") were given a series of 16-hour constant rate exposures to $^{60}$Co gamma radiation. The plants were at one of three stages of reproductive development: buds in early pollen development; flowers in anthesis or young pods after fertilization; and large pods containing small partially developed seeds. The decreasing order of sensitivity measured as seed yield was buds, flowers or young pods, large pods. The 50% yield reduction exposures were 0.42 ± 0.43 kR for buds, 1.47 ± 0.47 kR for flowers and young pods, and 6.34 ± 0.02 kR for large pods, indicating about a 15-fold difference between the most sensitive and most resistant stage. (auth)

55350 RELATIVE BIOLOGICAL EFFECTIVENESS OF X RAYS DELIVERED AT VERY HIGH DOSE RATES TO RADISH SEEDS (RAPHANUS SATIVUS). Kronenberg, Stanley; Lux, Robert; Nilson, Kristian (Army Electronics Command, Fort Monmouth, N. J.). Radiat. Res.; 47: No. 3, 589-97(Sep 1971).

It was hypothesized that direct radical–radical recombination reduces the relative biological effectiveness (RBE) of x rays delivered at sufficiently high dose rates. Order of magnitude calculations indicated the effect would be pronounced at rates of $10^{14}$ rad/sec. This hypothesis was tested experimentally using radish seeds (Raphanus sativus). To establish the behavior at low dose rates, the seeds were irradiated at a $^{60}$Co source at 10 rad/sec. High-rate exposures were made at the Air Force Weapons Laboratory flash x-ray generator at $5 \times 10^{11}$ rad/sec and the Rensselaer Polytechnic Institute LINAC at $6 \times 10^{10}$ rad/sec. Although these dose rates were three orders of magnitude lower than the estimate, a large increase in germination probability was seen for seeds irradiated at high rates. A dose 1.5 to 2.5 times greater was required at the high rates to produce the same reduction in germination probability as that following the low-rate irradiation. (auth)

55351 EFFECTS OF GAMMA IRRADIATION ON CHROMATIN ACTIVITY OF SUGAR BEET TISSUE. Dunham, V. L.; Jarvis, B. C.; Cherry, J. H.; Duda, C. T. (Purdue Univ., Lafayette, Ind.). Plant Physiol.; 47: No. 6, 771-4(Jun 1971).

Chromatin-associated RNA polymerase activity increases during washing of sugar beet tissue to a maximum by 20 hours. This increase was inhibited by dosages of gamma irradiation between 50 and 400 krad. Template availability, as measured by saturating levels of added Escherichia coli RNA polymerase, also increased with washing and was inhibited, although to a lesser extent, by the above irradiation dosages. Neither endogenous polymerase activity nor template availability was affected by high dosages (300 krad) in unwashed tissue. Exposure of tissue to irradiation (300 krad) at different times during a 20-hour washing period severely inhibited the development of RNA polymerase activity during the early stages of washing. The inhibition of template availability, however, was independent of time of irradiation. The data presented are discussed in relation to the mechanisms involved in the inhibitory effects of gamma irradiation on RNA production and subsequent protein synthesis. (auth)

55352 SPONTANEOUS REVERSION FREQUENCIES OF RADIOSENSITIVE STRAINS OF SACCHAROMYCES CEREVISIAE. Arman, I. P.; Dutova, T. A.; Devin, A. B. (Inst. of Atomic Energy, Moscow). Genetika; 7: No. 8, 186-8(Aug 1971). (In Russian).

The frequencies of spontaneous reversions towards adenine-independence were determined for six different radiosensitive and one insensitive (control) strains of Saccharomyces cerevisiae. The strains with mutations $uvs_2$ and $xrs_1$ revert to prototrophy more frequently (2 and 6 times respectively) than the insensitive strain and the other four sensitive strains. (auth)

55353 HIGH RESISTANCE TO X RAYS OF THE ACTIVITY AND LIGHT-INDUCED ACTIVATION OF NADP-DEPENDENT GLYCERALDEHYDE PHOSPHATE DEHYDROGENASE IN ANKISTRODESMUS BRAUNII. Seuberling, H.-B. (Univ., Wuerzburg, Ger.). Planta; 98: 270-3(1971). (In German).

In Ankistrodesmus braunii, a unicellular alga, the activity of NADP-dependent glyceraldehyde phosphate dehydrogenase (GPD) in darkness is very resistant to x-rays. The light-induced increase in the activity of this enzyme within one minute is also not affected by irradiation. Doses up to 1060 Krad had no inhibitory effect. The increase of GPD activity during the life cycle, however, is very sensitive to x-rays. (auth)

55354 EFFECTS OF GAMMA-RADIATION ON SPROUT-INHIBITION OF GARLIC BULBS AND THE CHANGES OF THEIR CHEMICAL CONTENTS. Park, Nou Pung; Choi, Eon Ho; Kim, Young Mu. J. Korean Agr. Chem. Soc.; 12: 83-8(1969).

In order to inhibit sprouting of garlic bulbs during the storage period, garlic bulbs were irradiated by gamma-rays ($^{60}$Co) and kept at room temperature. The effects of gamma radiation on sprouting inhibition, chemical contents during storage, and spoilage molds were investigated and the results are as follows: Garlic bulbs obtained from Muan showed a shorter dormancy period and sprouted earlier than those from Dangjin. Regarding the radioresistance, some differences were found between garlics from Muan and Dangjin. The sprouting of garlics from both areas was completely inhibited at 10 krad and a remarkable effect on sprouting was observed even with 5 krad in case of garlics from Dangjin. The rates of loss in moisture and weight were lower in irradiated lots than control. Change of sugar content was not observed with γ-irradiation under 300 krad. Spores of Aspergillus niger and Aspergillus alliaceus were little germinated at a level of 300 krad. (Korean Sci. Abstr.)

## Radiation Effects on Microorganisms

*Refer also to abstracts 55171, 55173, 55189, 55313, 55342, and 55365.*

**55355** RECOVERY FROM X-RAY AND NITROGEN MUSTARD INACTIVATION OF ESCHERICHIA COLI BY 2, 4-DINITROPHENOL TREATMENT. Lakchaura, Bala; Clark, J. B. (Univ. of Oklahoma, Norman). Radiat. Res.; 47: No. 3, 660-71(Sep 1971).

Nitrogen mustard-treated cells of Escherichia coli B show higher survival if preirradiated with near-ultraviolet radiation (photoprotection) or plated on a medium containing 2,4-dinitrophenol. These protection and recovery effects probably have a common mechanism, namely, inhibition of growth, which permits more time for the dark repair of damaged DNA. Recovery from nitrogen mustard lethal action appears similar to recovery from far-ultraviolet radiation (254 nm) lethal action. Damage caused by either agent is photoprotectable, can be reactivated by 2,4-dinitrophenol in the plating medium, and shows a liquid-holding recovery that is inhibited by 2,4-dinitrophenol. After x irradiation, however, 2,4-dinitrophenol treatment results in higher survival, but there is no photoprotection. This recovery cannot be accounted for by either inhibition of growth or inhibition of x-ray-induced DNA breakdown. (auth)

**55356** REPAIR OF ULTRAVIOLET-DAMAGES AFTER IRRADIATION OF BACTERIA IN THE VACUUM. Horneck, Gerda; Buecker, Horst (Univ., Frankfurt am Main). Strahlentherapie; 141: No. 6, 732-7(Jun 1971). (In German).

The sensitivity of bacteria (E. coli B/r, bacillus subtillis in vegetating and sporular forms) to ultraviolet rays, during irradiation in vacuum ($10^{-6}$ torr, $\lambda = 254$ nm) was higher in comparison to the controls which were irradiated at 760 torr in a suspension of phosphate-saline: The extent of the augmentation in the bacterial groups tested was comparable. The survival curves after irradiation in vacuum do not show a shoulder in contrast to the controls. The ultraviolet sensitivity of the mutant E. coli $B_{s-1}$, negative to dark reactivation, was only slightly augmented. It is assumed therefore that the uv-products, which led to inactivation during irradiation in the vacuum, were not approachable to the system of dark-repair. Moreover the uv-products, developing in the vacuum, were not repaired enzymatically (E. coli B/r). That is why the inactivation of ultraviolet rays in the vacuum probably cannot be explained by the formation of pyrimidine-dimers. Possibly it is a matter of DNA-protein-crosslinks or of the sporular product. (auth)

**55357** EFFECT OF DARK-REPAIR INHIBITORS ON THE SURVIVAL OF ESCHERICHIA COLI B UNDER DIFFERENT POST-IRRADIATION CONDITIONS. Vizdalova, M. (Biophysical Inst., Brno); Janovska, E.; Zhestyanikov, V. D. Int. J. Radiat. Biol.; 20: No. 1, 49-59(1971).

The effect was followed of dark-repair inhibitors (5-bromouracil, caffeine and acriflavine) on the survival of E. coli B bacteria under different cultivation conditions after u.v.- and x-irradiation. Increased survival of E. coli B bacteria at a raised cultivation temperature (44°C) and on minimal (M9) medium did not occur after incorporation of 5-BU into bacterial DNA. The radiosensitizing effect of 5-BU was characterized by sensitization factors at 50 percent to 1 percent survival levels, the values of which ranged in u.v.-irradiated bacteria between 3.0 and 2.2 (at 44°C) and 2.7 and 1.8(on M9 medium) and between 1.8 and 1.6 (at 44°C) and 2.4 and 1.6 (on M9) in bacteria irradiated with x-rays. During post-irradiation cultivation on complete medium at 19° and 37°C the radiosensitizing effect either did not occur or occurred only to a slight extent. The corresponding sensitization factors for u.v.-irradiated bacteria ranged between 1.0 and 0.8 (19°C) and 1.0 and 1.2 (37°C); and between 1.2 and 1.3 (19°C) and 1.7 and 1.5 (37°C) for those irradiated with x-rays. Post-irradiation cultivation in the presence of 0.3 percent caffeine partially removed the increased survival on complete medium at 44°C, but had almost no effect on survival on this medium at 19° and 37°C. The presence of acriflavine in the medium decreased the survival of u.v.- and x-irradiated bacteria cultivated under all the post-irradiation conditions investigated. The results show that the incorporation of 5-BU into DNA and the presence of caffeine in the culture medium inhibit the repair of the damaged mechanism of cell division taking place during cultivation of irradiated bacteria on complete medium at 44°C and on minimal medium. (auth)

**55358** EFFECT OF γ RADIATION ON THE DONOR ABILITY OF recA AND $recA^+$ STRAINS OF ESCHERICHIA COLI. Green, M. H. L.; Bridges, B. A.; Riazuddin, S. (Medical Research Council, Harwell, Eng. Univ. of Sussex, Brighton, Eng.). J. Gen. Microbiol.; 67: 63-8(Jul 1971).

The sensitivity to γ-radiation of the chromosome of a $recA^+$ Hfr strain of Escherichia coli was six times greater when assayed by donor ability in conjugation than when assayed by survival in unmated bacteria. With a recA Hfr strain sensitivities were comparable when assayed by the two methods, and were similar to the sensitivity of donor ability in the $recA^+$ strain. It is suggested that the greater resistance of survival in the $recA^+$ strain may be due to a post-replicational repair process which does not occur in the recA strain and which is prevented from occurring when a chromosome of either strain is involved in conjugation. When a recA Hfr and a recA $F^-$ strain were given 8.5 krads γ-radiation, enough to inhibit completely normal DNA synthesis, the DNA synthesis associated with conjugation still occurred. This suggests that the lesions which prevent recombinant formation may act not by inhibiting chromosome transfer, but by affecting a later stage in the process of integration. (auth)

**55359** EFFECT OF UV IRRADIATION AND $^{32}P$ DECAY ON THYMINELESS DEATH IN E. COLI 15. Mukherjee, P.; Mukherjee, Nati; Bhattacharjee, S. B. (Saha Inst. of Nuclear Physics, Calcutta). Mutat. Res.; 12: No. 4, 341-7(Aug 1971).

The sensitivity of thymine-requiring bacteria E. coli strain 15 to uv irradiation was not affected by previous incubation in the absence of thymine except for the decrease in the width of the shoulder in the survival curves. When uv-irradiated bacteria were held under conditions of thymineless death, a liquid holding type of recovery was observed. This recovery occurred only under conditions in which thymineless death would normally occur. However, thymineless incubation and the decay of incorporated radioactive phosphorus acted synergistically in killing the bacterial population. (auth)

**55360** TEMPERATURE-SENSITIVE RECOVERY OF A MUTANT OF ESCHERICHIA COLI K-12 IRRADIATED WITH ULTRAVIOLET LIGHT. Shimazu, Y.; Morimyo, M.; Suzuki, K. (National Inst. of Radiological Sciences, Chiba, Japan). J. Bacteriol.; 107: No. 3, 623-32(Sep 1971).

URT-43 is a mutant of Escherichia coli K-12 which gives a much larger number of survivors when ultraviolet (uv)-irradiated bacteria are incubated on agar medium at 30 C than when they are incubated on the medium at 41 C, although in both cases the number of survivors is fewer than that given by its wild-type ancestor. The uv sensitivity of this mutant was found to be markedly influenced by the presence of a high concentration of NaCl or sucrose in plating medium. Thus, when irradiated bacteria were plated on agar medium containing 2% NaCl or 0.5 M sucrose at 30 C, they exhibited a resistance similar to that of their wild-type ancestor. At 30 C, there was also an extensive recovery in liquid M9 medium supplemented with all of the nutrients required for growth and NaCl or sucrose. At 41 C, however, the recovery was greatly inhibited. Direct chemical analysis of thymine dimers has revealed that no significant amount of the dimer was released from deoxyribonucleic acid during the period of extensive recovery. It was concluded, therefore, that the temperature-sensitive recovery of URT-43 does not accompany excision of the bulk of pyrimidine dimers. To learn the gene function involved in the recovery, double mutants carrying an additional mutation either in a uvr or a rec gene have been investigated for their uv sensitivities and recovery in liquid medium. It was found that $recA^-$ and $recB^-$ derivatives retain the ability of undergoing an efficient recovery at a low temperature, whereas $uvrB^-$ and $uvrC^-$ derivatives have completely lost this ability. For these reasons, it was concluded that the mechanism responsible for the recovery of URT-43 involves the function controlled by the uvr genes. The results of photoreactivation suggested that most of the entities dealt with during recovery were pyrimidine dimers. (auth)

**55361** INACTIVATION OF ESCHERICHIA COLI, F' EPISOMES AT TRANSFER, AND BACTERIOPHAGE LAMBDA BY PSORALEN PLUS 360-nm LIGHT: SIGNIFICANCE OF DEOXYRIBONUCLEIC ACID CROSS-LINKS. Cole, Ronald S. (Yale Univ., New Haven). J. Bacteriol.; 107: No. 3, 846-52(Sep 1971).

Some biological consequences of light-induced psoralendeoxyribonucleic acid (DNA) adducts were investigated and it was found that for several Escherichia coli functions (killing of strain AB2480 recA13 uvrA6, inactivation of phage lambda plaque-forming ability in wild type and uvrA6 hosts, loss of ability to transmit intact $Flac^+$ episomes), a light exposure sufficient for production of a single crosslink per DNA molecule correlates well with the biological consequence. Although one cross-link per genome is apparently lethal to recA13 $uvr^-$ strains, mutants carrying the recA13 or uvrA6 markers survive light exposures producing 6.7 and 16 cross-links per genome, respectively, and wild-type cells recover from 65 psoralen cross-links. Evidently, the excision and recombinational repair systems complement one another in reconstructing an intact genome from cellular DNA containing psoralen photoproducts. The above bacterial and phage strains, in which DNA repair processes are minimized, are also extremely sensitive to pyrimidine dimer-forming 254-nm uv light (without psoralen), and were expected to respond similarly to formation of psoralen-pyrimidine base monoadducts in their DNA. Since

XUM

the biological inactivation by psoralen correlates well with cross-link formation, we suggest that the sensitizing action of this drug primarily derives from its ability to form DNA cross-links. (auth)

## Radiosterilization and Radiopreservation

*Refer also to abstracts 54837 and 55354.*

**55362** (LFEN-NI-56a) FREEZING AND IRRADIATING FISH. Simoes, Jose Henriques (Junta de Energia Nuclear, Sacavem (Portugal). Laboratorio de Fisica e Engenharia Nucleares). 1970. 75p. (In Portuguese). (CONF-670992-1). Dep. NTIS (U. S. Sales Only).

From Conference on frozen and irradiated fish and fishery products; Madrid, Spain (4 Sep 1967).

The 77 papers presented at the Congress in Madrid on the freezing and radiopreservation of fish are abstracted. The theme of these papers can be divided into four groupings: freezing at sea; freezing on land; distribution of frozen fish; and preservation of fish products by irradiation. (J.S.R.)

**55363** GAMMA IRRADIATION AS AN INDUSTRIAL PROCESS, AND BRITAIN'S ROLE IN ITS DEVELOPMENT. Longstaff, R. M. (Atomic Energy Research Establishment, Harwell, Eng.); Grant, J. J. Brit. Nucl. Energy Soc.; 10: No. 3, 229-36(Jul 1971).

The nature, effects, and uses of ionizing radiation for commercial processing are outlined, and a comparison is made between electron accelerators and radioactive materials as suitable radiation sources. The production of $^{60}Co$ is described, and the development of $\gamma$ irradiation facilities in the UK is traced from small experimental units at Harwell to a large automatic plant at Wantage, leading to the growth of commercial $\gamma$ ray processing in Britain and in British-designed plants overseas. Plant design criteria are discussed, and radiation dosimetry methods described. Current applications and possible developments of radiation processing in chemical and plastics manufacture, in food treatment, and in the sterilization of medical supplies are outlined. (auth)

**55364** EFFECT ON $\gamma$ IRRADIATION ON THE AMINO-ACID CONTENT OF PROTEINS. Chaudhry, M. T. N.; Evans, R. A. Biochem. J.; 124: No. 2, 29-30(Sep 1971).

Research has proved that foods rendered less susceptible to insect, bacterial and fungal attack by irradiation are safe to eat. However there is evidence that radiation can damage the free amino acids and amino acids contained in proteins. Reports vary as to the nature and extent of the damage caused due to variations in irradiation conditions. An investigation into the amino acid content of accelerated-freeze dried egg and wheat gluten before and after irradiation in the spent fuel rod assembly at AERE, Harwell is described. In egg, methionine and tryptophan were the only amino acids significantly damaged. In gluten, tryptophan in both batches, and threonine in the batch irradiated up to 5.0 Mrd and methionine in the batch irradiated at 10 Mrd were significantly diminished. (UK)

**55365** EFFECTS OF GAMMA IRRADIATION ON SALMONELLA SPP. IN SMOKED LAKE WHITEFISH (COREGONUS CLUPEAFORMIS). Ostovar, K. (Dept. of Fisheries and Forestry of Canada, Winnipeg); Pereira, R. R.; Gallop, R. A. J. Fish. Res. Board Can.; 28: 643-6(May 1971).

A dosage of 0.5 M rad was found sufficient to eliminate three species of Salmonella in smoked lake whitefish (Coregonus clupeaformis) regardless of the stage of processing at which steaks were inoculated with the bacteria. All three species survived smoking at temperatures up to 167°F. The dosages required for elimination of the bacteria when steaks were inoculated at various stages of processing were: before freezing at 0°F for 48 hr, 0.4 M rad for S. give, 0.3 for S. typhimurium, and 0.2 for S. java; before brining at 60 Salometer for 25 min, 0.4, 0.3, and 0.3; after smoking, 0.5, 0.4, and 0.35. Salmonella give was more resistant to heat than the other two species. (auth)

**55366** IRRADIATION OF PACIFIC COAST FISH AT SEA. Teeny, F. M.; Miyauchi, D. (Bureau of Commercial Fisheries, Seattle). J. Milk Food Technol.; 33: No. 8, 330-4(Aug 1970).

An experimental shipboard irradiator was installed aboard the Bureau Of Commercial Fisheries research vessel Miller Freeman and utilized to irradiate West Coast fish at sea. The optimum dose range for irradiating whole English sole (Parophrys vetulus), Dover sole (Microstomus pacificus), Pacific cod (Gadus macrocephalus), Pacific ocean perch (Sebastodes alutus), and black rockfish (Sebastodes melanops) is in the range of 50 to 100 kilorads. The shelf life (at a high level of quality) of the irradiated products was extended by one and one-half to two times that of the nonirradiated samples. Among the five species irradiated at various states of rigor, prerigor–rigor fish generally had better storage characteristics than postrigor fish. (auth)

**55367** EFFECT OF COOKED GAMMA-IRRADIATED BEEF ON WHITE RATS. Kamal'dinova, Z. M. (Inst. of Nutrition, Moscow). Vop. Pitan.; 29: 73-7([1970]). (In Russian).

The effect of gamma irradiated (0.8Mrad) beef on 110 rats of two generations was investigated. The beef was composed of 51% protein and 0.57% fat, which made up 25.6% of the caloric content. A study of the protein and lipid metabolism in experimental and control animals led to the conclusion that there was an unfavorable effect on metabolic processes. Therefore, gamma irradiated beef is not recommended for human consumption. (auth)

**55368** STERILIZATION OF THE SPOTTER BOLLWORM OF COTTON BY RADIATION. Anwar, M.; Arif, M. D. (Atomic Energy Agricultural Research Center, Tandojam, Pakistan). Int. J. Appl. Radiat. Isotop.; 22: No. 10, 625-7(Oct 1971).

To investigate the possibility of eradication of the spotted bollworm of cotton which is a destructive pest in Pakistan, larvae were collected and reared in the laboratory and the resulting pupae irradiated after 7 days at 0 to 40 kR as adult emergence started. Irradiated moths were caged with untreated virgin moths of opposite sex. Resulting mating frequency, fecundity, fertility, and percentage egg hatched were determined. Mating frequency after a 40 kR dose was unimpaired. Pupae irradiated at doses from 0 to 40 kR demonstrated a progressive increase in sterility with increasing dose. Germ cells of the female were more radiosensitive than those of the male but both sexes were completely sterilized at a dose of 35 kR. (UK)

# METALS, CERAMICS, AND OTHER MATERIALS

## Metals and Alloys

**55369** PLUTONIUM-DOKUMENTATION. Referate-Zeitschrift mit Anhang Transplutonium-Elemente. Band 5, Heft 1-3. 1. Vierteljahresregister 1971. (Plutonium-Documentation. Abstract Journal with Appendix on Transplutonium Elements. Vol. 5, No. 1-3, 1971. 1st Quarter Index). Karlsruhe, Ger.; Gesellschaft fuer Kernforschung m.b.H (1971). 70p. (In German and English).

### Corrosion and Erosion

*Refer also to abstracts 54587 and 57109.*

**55370** (BNWL-SA-2335) CORROSION AND DEPOSITION OF IRRADIATED STAINLESS STEEL IN SODIUM. Brehm, W. F.; Kovacevich, E. A.; Shannon, D. W. [Battelle-Northwest, Richland, Wash. Pacific Northwest Lab.]. [1968]. Contract AT(45-1)-1830. 18p. (CONF-690609-29). Dep. NTIS.

From fifteenth annual meeting of the American Nuclear Society; Seattle, Wash. (15 Jun 1969).

The effects of various FFTF operating variables such as temperature, system thermal gradients, coolant flow velocity, flow perturbations, and coolant impurity levels on transport and deposition of radioisotopes from irradiated stainless steel fuel cladding were investigated. Results show that FFTF heat removal systems must be designed for remote maintenance (core and probably closed loops) or else transport and deposition mechanisms must be identified so that preferential deposition sites can be established. The heat removal loops should be designed so that areas requiring maintenance would not be preferential deposition sites; and so that deposition could be enhanced in shielded low-maintenance areas. It was found that $^{54}Mn$ would be trapped just downstream of the heat exchanger, and in the cold trap, especially if high velocity, high turbulence flow conditions are present there. $^{51}Cr$ would probably be plated out on the top of the fuel pins just above the core, and may possibly have decayed away by the time the Cr atom is exchanged off the top of the fuel pin. The cobalt isotopes, $^{58}Co$ and $^{60}Co$, should be transported slowly to the hot leg in a similar manner to $^{51}Cr$, but the longer half-lives of the cobalt isotopes makes it unlikely that a buildup of cobalt activity in the hot leg will occur. (J.R.D.)

**55371** (CONF-690452) MEETING ON MECHANISMS OF CORROSION BY MOLTEN SALTS, APRIL 10, 1969, DUESSELDORF. (European Federation of Corrosion). 179p. (In several languages).

Nine papers were presented at the meeting. A separate abstract was prepared for each of five papers. The four papers presented at the meeting for which no abstracts were prepared are concerned with various aspects of corrosion, but are not in scope for NSA. (J.R.D.)

*For abstracts of individual papers see: 55372–55376.*

**55372** (CONF-690452–, Paper 5) CHEMICAL REACTION MECHANISMS FOR THE ATTACK OF HIGH-TEMPERATURE ALLOYS BY MOLTEN SULFATES. Umland, Fritz; Voigt, Hans-Peter (Muenster Univ. (West Germany). Institut fuer Anorganische Chemie). 12p. (In German).

From Meeting on mechanisms of corrosion by molten salts; Duesseldorf, Germany (10 Apr 1969).

The behavior of Cr-, Ni-, and Co-containing alloys and oxides in alkali sulfates at temperatures between 550 and 950°C under variable conditions has been studied. From the analysis of the reaction products a mechanism has been derived which gives a satisfactory explanation of the observations made. In a first step, chromate and small amounts of complex Co, Ni, and Fe sulfates are formed in contact action of oxide film and sulfate, which cause partial melting. The melt $O^{2-}$-ions migrate from outer to inner zones; the metal ions move the opposite way. Consequently the formation of complex sulfates increase. At saturation, non-protective porous oxides are precipitated from the melt. The transport of electrons from the metal to the surface of the melt is caused by redox systems especially by complex cobalt sulfates. In case of an oxygen deficiency, the sulfates are reduced to sulfides. Chromium in contact with sulfates is oxidized primarily by molecular oxygen and may be transported via vapor phase; the mechanism of this being different. (auth)

**55373** (CONF-690452–, Paper 6) ELECTROCHEMICAL INVESTIGATIONS ON THE CORROSION OF METALS IN ALKALI METAL SULFATE AND VANADIUM PENTOXIDE MELTS. Rahmel, A. (Dechema-Institut, Frankfurt am Main (West Germany)). 16p. (In German).

From Meeting on mechanisms of corrosion by molten salts; Duesseldorf, Germany (10 Apr 1969).

Results of electrochemical corrosion investigations involving eutectic alkali sulfate melts and $V_2O_5$ melts are reported. The behavior of the two melts is very different. In the alkali sulfate melt inert electrodes (Pt) may be polarized in a range covering about 2V without greater changes in the melt. The melt behaves like a redox-free electrolyte. For the anodic dissolution of Au, Ag, Cu, and Ni straight Tafel lines are obtained. On Fe, Ni, and, industrial heat-resistant alloys porous layers are formed having poor protective action. The corrosion-accelerating effect of $SO_3$ is primarily due to a promotion of the cathode process. The $V_2O_5$ melt behaves like a redox system having very high exchange current densities. The redox potential is high, so that all the metals exposed to a $V_2O_5$ melt are polarized to positive potentials. This fact serves to partially explain the strong reactivity of $V_2O_5$ melts. (auth)

**55374** (CONF-690452–, Paper 7) STUDY OF MECHANISM OF VANADIUM CORROSION USING THE ELECTROCHEMICAL METHOD. Balajka, J. 18p.

From Meeting on mechanisms of corrosion by molten salts; Duesseldorf, Germany (10 Apr 1969).

Results of studies on corrosion of Ni by $V_2O_5$ melts are presented which show that Fe, Ni electrodes and electrodes made of 15% Cr–18% Ni–1.5% Mn have a negative potential against Pt inert electrodes. Potentials of Ni electrodes decrease with the depth of submersion in the molten $V_2O_5$, which is perhaps caused by the lower ratio of $V_2O_5$ to $V_2O_4$ in the bottom of melt. In thin layers of molten $V_2O_5$, the value of emf of corrosion cell $(-Ni/V_2O_5/O_2/Pt/+)$ is almost linearly dependent on the log $P_{O_2}$. The dependence of corrosion reaction equilibrium on $P_{O_2}$ and the oxygen carrying capacity of molten $V_2O_5$ is thus proved. The equilibrium in thick layers of molten $V_2O_5$ during the experiment was not achieved. The emf value of corrosion cell $(-Ni/V_2O_5/O_2(Pt)+)$ decreases with the increase of concentration of corrosion products and therefore corrosiveness of molten $V_2O_5$ decreases. (auth)

**55375** (CONF-690452–, Paper 8) CORROSION OF GAS TURBINE ALLOYS IN MOLTEN SALTS OF HIGH $V_2O_5$ AND LOW SODIUM CONTENT. Moeller, W. (Brown, Boveri und Cie A. G., Mannheim (West Germany)). 25p. (In German).

From Meeting on mechanisms of corrosion by molten salts; Duesseldorf, Germany (10 Apr 1969).

Two commercial superalloys, a Ni-base alloy (NiCr20TiAl) and a complex alloy (X40CoCrNi 20–20–20), were exposed to molten salts at 700°C for 100 hr. The salts consisted of pure $V_2O_5$, $V_2O_5$ with additions of $Na_2O$, $Na_2SO_4$, NaCl, NaCl + $SO_4$ (molar ratio $V_2O_5 : Na_2O = 6 : 1$), and $Na_2SO_4$ + 25% NaCl. The evaluation was made using metallurgical methods (metallography, electron microprobe analysis, x-ray diffraction) along with analysis of specimens and chemical analysis of the residual melts. Generally a layer of corrosion products–primary vanadates–develops at the metal surface. The variation of these caused by the different sodium compounds is examined. In the sulfate-chloride melt, metal-oxides and -sulfides develop, which form no protective layer. (auth)

**55376** (CONF-690452–, Paper 9) TREATMENT OF NUCLEAR FUEL AND BREEDER MATERIALS IN OXIDIZING ALKALI METAL SALT MELTS. Riedel, H.-J. (Kernforschungsanlage, Juelich (West Germany). Institut fuer Chemische Technologie). 12p. (In German).

From Meeting on mechanisms of corrosion by molten salts; Duesseldorf, Germany (10 Apr 1969).

The fuel elements of high temperature gas-cooled reactors contain fissionable and fertile material such as spherical $(U,Th)C_2$ and $(U,Th)O_2$ particles, respectively, embedded in a graphite matrix. For better retention of the fission products, the particles are provided with dense shells of pyrocarbon and silicon carbide, respectively. The high chemical resistance of these coatings causes difficulties in the reprocessing of the spent nuclear fuel elements. All the carbon is removed in the so-called head-end step by burning it in a stream of oxygen, ending up in the case of pure pyrocarbon coatings with bare oxides, whereas the SiC layers stop the burning. For further treatment of these products a potassium pyrosulfate melt digestion at temperatures of 650 to 750°C may most successfully be employed for the bare oxides. SiC-coated particles have to be coarse ground prior to the salt-

XUM

melt processing. In this case, however, it seems to be more advantageous to apply an oxidizing alkali salt-melt digestion. The best results were obtained using NaOH in connection with the injection of gaseous $NO_2$ in the temperature range between 600 and 700°C. The use of reactive melts such as sodium hydroxide in combination with an $NO_2$ application as well as the pyrosulfate melts at temperatures of about 600 to 750°C increases corrosion. Among the most suitable materials for the reactor crucibles is platinum, which has proved superior for the pyrosulfate procedure. For sodium hydroxide salt-melt treatment, sintered aluminum oxide ceramics shows the lowest corrosion rates. (auth)

**55377** (N-71-26947) CORROSION RESISTANCE OF TANTALUM, T-111, AND Cb-1Zr TO MERCURY AT 1200 F. Engel, L. B. Jr.; Harrison, R. W. (General Electric Co., Cincinnati, Ohio). May 1971. Contract NAS3-10610. 25p. (NASA-CR-1811; GESP-199). NTIS.

Sheet specimens of tantalum, T-111, and Nb-1Zr were strained 5 and 20 percent by bending. Specimens representative of each strain level, and in the as-bent and the as-bent and annealed conditions, were tested at 1200°F for 1000 hours in sealed tantalum capsules containing liquid mercury. No changes were observed in any of the specimens as a result of the exposure to mercury. (auth) (STAR)

**55378** (SWRI-1228-P-7-40) INVESTIGATION OF SENSITIZATION OF TYPE 304 STAINLESS STEEL SAFE-ENDS. Burghard, H. C. Jr.; Lyle, Fred F. Jr. (Southwest Research Inst., San Antonio, Tex.). 12 Nov 1969. Contract AT(11-1)-1228. 29p. Dep. NTIS.

Results of investigations concerning sensitization of the stainless steel feedwater recirculating header inlet nozzle safe-ends in the LaCrosse Boiling Water Reactor are presented. It was found that the safe-end material is sensitized and is subject to failure if the environmental conditions are conducive to failure. Based on these tests and the service experience, it is recommended that consideration be given to replacing the LACBWR safe-ends. (J.R.D.)

**55379** (WARD-4210-T-1-2) SODIUM TECHNOLOGY PROGRAM PROGRESS REPORT FOR THE PERIOD ENDING MAY 31, 1971. Ray, W. E. (Westinghouse Electric Corp., Madison, Pa. Advanced Reactors Div.). Contract AT(30-1)-4210. 67p. Dep. NTIS.

Research progress on measuring the wear rates and friction coefficients of several material combinations in interface configurations simulating FFTF core components under prototypic operating conditions is described. The work is being done to provide reactor designers with the quantitative data and experience factors necessary to successfully design components or component interfaces which will experience sliding or rubbing contact while immersed in high-temperature sodium. Work devoted to obtaining experimental information and analytical relationships for design data is reported. This information is needed to predict the rate and direction of carbon and nitrogen transfer and associated mechanical property changes of structural materials within liquid metal systems, representative of primary and secondary circuits of an LMFBR. Research is also reported on the state-of-the-art liquid metal oxygen meters and provides the needed information on the performance characteristics of a standard electrochemical oxygen meter for FFTF and subsequent LMFBR applications. (auth)

**55380** EFFECT OF ALLOYING ON THE OXIDATION OF NIOBIUM AT LOW PRESSURES. Sokolova, G. V.; Yur'ev, S. F.; Mikhailov, S. K. Fiz. Metal. Metalloved.; 30: No. 6, 1157-61 (Dec 1970). (In Russian).

The effect of alloying with Mo, W, and/or Zr on the oxidation of Nb heated to 1600 to 2000°K at low pressures (i.e., on its interaction with the residual gases in an evacuated space at $10^{-5}$ torr) was studied by a gravimetric method. There was a clear correlation between the tensile strength of the alloys and the weight increment attributable to interaction with O. W and Mo increased this interaction while Zr reduced it. In ternary alloys of Nb with W and Zr or with Mo and Zr, the effect of the Zr tended to predominate. (Metals Abstr.)

**55381** INTERNAL OXIDATION OF Ag-Cd ALLOYS UNDER OXYGEN PRESSURE. Harmsen, U. (Metall-Laboratorium, Pforzheim, Ger.). Metall; 25: 133-7(Feb 1971). (In German).

The alloys AgCd 4.5, AgCd 9, AgCd 13.4, and AgCd 18 were prepared at 600, 700, and 800°C under various oxygen pressures. The oxidation constants were determined. With increasing oxygen pressure the oxidation rate increases but not proportionally with the oxygen pressure. The hardness, electrical conductivity, and cadmium oxide precipitation form of the sample internally oxidized under increased pressure were compared with these properties of the sample internally oxidized in air. (tr-auth)

**55382** INTERNAL OXIDATION IN Mg-Zr ALLOY IN CONTACT WITH CARBON DIOXIDE. Pegoud, J.; Guillaumin, J.; Millet, P. (Societe Industrielle de Combustible, Veurey, France). J. Nucl. Mater.; 41: No. 1, 51-71(Oct 1971). (In French).

A zone of internal oxidation was observed to develop in Mg-0.5% Zr alloy at temperatures above 400°C in the presence of high-pressure carbon dioxide. Details of the structure were examined by optical and electron microscopy, as were the growth kinetics of the zones and their influence on the creep behavior. Oxygen which penetrates into the alloy leads to the formation of zirconium dioxide, either direct from zirconium in solid solution or else via decomposition of zirconium hydride precipitates. At 500°C and 600°C the thickness of the internal oxidation zone increases slowly and irregularly. Frequent drops in oxygen concentration have a perturbing effect on the advance of the oxidation front, which is further influenced by the zirconium concentration, the physical state of the zirconium and by the nature of the atmosphere. Internal oxidation increases the creep resistance and reduces the ductility of Mg-Zr. Within the oxidized region, creep-rupture at high temperatures is intergranular and is the consequence of the growth of cavities along those grain-boundaries which are normal to the applied stress. (auth)

**55383** HOT-SALT STRESS-CORROSION OF TITANIUM: A REVIEW OF THE PROBLEM AND METHODS FOR IMPROVING THE RESISTANCE OF TITANIUM. Petersen, V. C. (Crucible Materials Research Center, Pittsburgh). J. Metals; 23: No. 4, 40-7(Apr 1971).

A review is given on the problem of hot-salt stress cracking of titanium which covers: steady-state threshold data, environmental effects, mechanism of attack, and preventive measures. The conditions to produce hot-salt cracking under static steady-state conditions are well defined. But, there is yet no rationale for the lack of a single part failure in aircraft flight. Effective preventive measures include: shot peening, metallic coatings, special heat treatments, and alloy selection. The Beta III alloy showed a high salt-cracking threshold even after heat treatment to high strength levels. The two alloys most extensively tested were Al-V-Ti and Al-Mo-V-Ti. (auth)

**55384** USE OF THE NUCLEAR REACTION $^{18}O(p,\alpha)^{15}N$ TO STUDY THE OXIDATION OF METALS. Skakun, N. A.; Klyucharev, A. P.; Khar'kov, O. N.; Zelenskii, V. P.; Kulakov, V. S. At. Energ. (USSR); 30: No. 5, 456-8(May 1971). (In Russian).

It is proposed that the reaction $^{18}O(p,\alpha)^{15}N$ be utilized to indicate the depth of an oxidized film on metals. The $^{18}O$ contained in the oxide layer is bombarded with monoenergetic protons, and the energy spectrum of the resulting alpha particles is recorded. Factors to be taken into account are the absorbing capability of the substance studied for protons and $\alpha$ particles and the cross section of the nuclear reaction. A synthetic standard was prepared by oxidizing a piece of Zr-2% Nb alloy at 500°C and 1.0 atm in steam containing 69% $^{18}O$. (K.S.W.)

**55385** OXIDATION OF TANTALUM-TUNGSTEN POLYCRYSTALS AND SINGLE CRYSTALS IN THE TEMPERATURE RANGE 850° TO 1100°C. Dooley, R. B.; Stringer, J. (Univ. of Liverpool). J. Less-Common Metals; 25: No. 1, 15-26(Sep 1971).

Single crystals and polycrystals of a Ta-3.9 at % W alloy were oxidized in the temperature range 850° to 1100°C in oxygen at approximately 740 torr. Recrystallized polycrystalline coupons exhibit cracking at the metal grain boundaries after oxidation at 950°C; this is believed to occur on cooling, and to be due to stresses imposed by the oxide growth process and the differential thermal contraction, and to the increase in resistance to fracture of the oxide and of the metal/oxide interface. However, cold-worked coupons show no sign of this effect. At 1050°C, recrystallized specimens ignited on admission of oxygen but cold-worked specimens oxidized without burning to produce compact, adherent scales. Single-crystal cylinders show similarly anisotropic scale-fracture morphologies to those observed in pure Ta, but the anisotropy in oxidation rate is much less marked. After oxidation at 1100°C the single crystals fractured along {100} planes on cooling; this appeared to be initiated again by the high stresses and to propagate along suboxide platelets. There are considerable intrusions of pentoxide along the suboxide platelets. However, unlike the intrusions observed in the oxidation of Nb below 600°C, they do not appear to lead to metal fragmentation and an increase in rate; instead they appear to improve the scale/metal adhesion. This amount of W reduces the oxidation rate of Ta throughout this temperature range. (auth)

**55386** EFFECT OF OXYGEN ON NIOBIUM–SODIUM COMPATIBILITY. Klueh, R. L. (Oak Ridge National Lab., Tenn.). Corrosion; 27: No. 8, 342-6(Aug 1971).

The effect of O on the compatibility of Nb and Na at 600°C was investigated. An increase in the O concentration of the Na leads to increased dissolution of the Nb. It was also observed that the experimentally determined O equilibrium distribution coefficient (i.e., the ratio of the O concentration in the refractory metal to that in the alkali metal at equilibrium) is much smaller than the theoretically calculated value. In the past, these observations have generally been explained by postulating the formation of a ternary oxide containing refractory metal, alkali metal, and O atoms. As an alternative to the ternary oxide hypothesis, it was proposed that at equilibrium, a liquid ternary solution exists and O affects the solubility of Nb by decreasing the activity coefficient of the Nb in the Na. The phase rule was used to check this hypothesis at 600°C. When the concentration of O in Nb exceeded a threshold level, the Nb was penetrated by Na. At low O concentrations, attack proceeds along grain boundaries, and as the O concentration is increased, the number of grain boundaries attacked and the depth of attack increases. (auth)

**55387** CYCLIC OXIDATION OF TD–NICKEL. Rhee, S. K.; Spencer, A. R. (Bendix Corp., Southfield, Mich.). Met. Trans.; 2: No. 8, 2285-7(Aug 1971).

The kinetics of oxidation of TD–Ni containing $ThO_2$ were investigated. The oxidation kinetics were found to obey the parabolic rate law up to 100 hr at 760 and 871°C and up to 64 hr at 982 and 1093°C. After these times, the oxidation rate varied irregularly. These results suggested that (1) the oxidation mechanism was controlled by the diffusion of $Ni^{2+}$ through the oxide layer, (2) the dispersoid $ThO_2$ did not influence the oxidation kinetics within the accuracy of these measurements, and (3) the cyclic oxidation did not significantly change the oxidation process up to ~50 to 100 hr, depending on the temperature. Values are tabulated for activation energies by both a nickel tracer method and the oxidation gain method. (B.L.M.)

**55388** CORROSION IN NUCLEAR APPLICATIONS. Berry, Warren E. Corrosion Monograph Series. New York; John Wiley and Sons, Inc. (1971). 592p. $24.95.

This book examines the corrosion problems that exist in nuclear reactors using water, liquid metals, gases, fused salts, organic coolants, or fluid fuels. Mining, refining, fuel reprocessing, and waste processing are also covered. A separate abstract was prepared for each of the seven chapters. A subject index is included. (D.L.C.)

*For abstracts of individual chapters see: 55389–55395.*

**55389** CORROSION IN MINING, REFINING, AND SEPARATION OF URANIUM. pp 1-21 of Corrosion in Nuclear Applications. /Berry, Warren E. New York; John Wiley and Sons, Inc. (1971).

After a brief description of the most commonly used steps in U production, consideration is given to corrosion in each of the environments: alkaline and acid leaching, solvent extraction, denitration, $UO_3$ reduction, $UF_4$ production. Data are given for corrosion of metals and alloys in HF, $F_2$, $UF_6$, $CCl_4$, phosgene, and $Cl_2$. (D.L.C.)

**55390** CORROSION PROBLEMS IN FUEL REPROCESSING AND WASTE HANDLING AND STORAGE. pp 23-87 of Corrosion in Nuclear Applications. /Berry, Warren E. New York; John Wiley and Sons, Inc. (1971).

A review is given of corrosion aspects of aqueous and nonaqueous processes that have been used or studied: Hf, Niflex, Zirflex, electrolytic disintegration, Sulfex, Darex, Perflex, Thorex, Redox, Purex, transuranium element reprocessing, fluoride volatility processes, and pyrometallurgical and pyrochemical processing. Corrosion problems with aqueous wastes and their solidification are also considered. (D.L.C.)

**55391** CORROSION IN WATER AND STEAM-COOLED REACTORS. pp 89-236 of Corrosion in Nuclear Applications. /Berry, Warren E. New York; John Wiley and Sons, Inc. (1971).

Corrosion problems in reactors of this type are reviewed under the following headings: core materials, cladding materials (Zr alloys, stainless steels and Ni alloys, Al alloys, SAP, Nb alloys, Be alloys, Mg alloys), structural materials (Fe alloys, oxides, crud, etc.), and control rod materials. (D.L.C.)

**55392** CORROSION BY LIQUID METALS. pp 237-356 of Corrosion in Nuclear Applications. /Berry, Warren E. New York; John Wiley and Sons, Inc. (1971).

After a general discussion of the several forms of attack by liquid metals, corrosion by the following metals are reviewed: Na and NaK, K, Li, Cs, Rb, Pb, Bi, Hg, and other metals (Sn, Zn, Al, Cd, Ga, and In). (D.L.C.)

**55393** CORROSION IN GAS-COOLED REACTORS. pp 357-431 of Corrosion in Nuclear Applications. /Berry, Warren E. New York; John Wiley and Sons, Inc. (1971).

A review is presented of the gas–metal reactions that could occur in gas-cooled reactors. The review is arranged according to structural materials, cladding materials, fuel materials, moderator materials, and ceramics, and the following gases are considered: air, $CO_2$, He, $N_2$, and $H_2$. (D.L.C.)

**55394** CORROSION IN ORGANIC-COOLED OR ORGANIC-MODERATED REACTORS. pp 433-57 of Corrosion in Nuclear Applications. /Berry, Warren E. New York; John Wiley and Sons, Inc. (1971).

After a description of the advantages and disadvantages of employing an organic coolant or moderator, the corrosion of the following materials in organics is reviewed: structural materials (Fe, Ni, Co, and Cu alloys), cladding materials (Al alloys, SAP, Be, Mg, refractory metals), fuel materials, and control rod materials. (D.L.C.)

**55395** CORROSION IN FLUID FUEL REACTORS. pp 459-520 of Corrosion in Nuclear Applications. /Berry, Warren E. New York; John Wiley and Sons, Inc. (1971).

Corrosion problems in each of the three fluid types used in homogeneous reactors are discussed: molten salts, liquid metals, and aqueous solutions or slurries. Metals, alloys, graphite, and ceramics are covered. The molten salts discussed include fluorides, chlorides, phosphates, and sodium hydroxide. Bi–U is considered among the liquid metal fuels. Emphasis in the aqueous slurry section is on uranyl sulfate. (D.L.C.)

**55396** SURFACE REACTION OF OXYGEN WITH TUNGSTEN. Dong, Wilbur Donald. Pullman, Wash.; Washington State Univ. (1971). 80p. University Microfilms Order No. 71-18,567. Thesis.

A steady-state nonequilibrium treatment of tungsten oxidation is proposed. The interaction of room-temperature low-pressure ($10^{-7}$ to 10 torr) oxygen gas with a hot (1250 to 3333°K) tungsten surface was studied. Evaporation rates for W, $O_2$, O, WO, $WO_2$, $WO_3$, $W_2O_6$, and $W_3O_9$ were obtained that agreed with experimental values. The treatment is divided into two problems: the scattering of oxygen from a tungsten surface, and the surface reaction of oxygen with tungsten. The first problem is concerned with how much of the incident oxygen remains on the surface in thermal equilibrium with the surface. The first problem was evaluated empirically using published experimental data. A model was constructed for the second problem of surface reaction. A central assumption of this model was that the adsorbed oxygen and the tungsten form a surface phase that is in thermal and chemical equilibrium with a set of activated complexes in the sense of absolute reaction rate theory. The oxides observed evaporating were regarded as evaporating from the corresponding activated complexes. Thermal and chemical equilibriums are maintained on the surface by requiring that the rate of evaporation from the activated complexes be slower than their rate for formation. The model predicts evaporation rates for the above species as a function of both oxygen pressure and tungsten temperature. The only data required for the model part are gas-phase molecular configurations and gas-phase heats of formation evaluated at 0°K. Total tungsten evaporation rates were also computed. This latter quantity corresponds to surface recession or weight loss of a tungsten sample in corrosion studies. The computations were carried out on a digital computer. (Diss. Abstr. Int., B)

**55397** OXIDATION OF TANTALUM–HAFNIUM POLYCRYSTALS AND SINGLE CRYSTALS IN THE TEMPERATURE RANGE 750° TO 1050°C. Dooley, R. B.; Stringer, J. (Univ. of Liverpool). J. Less-Common Metals; 25: No. 2, 115-22(Oct 1971).

Polycrystalline coupons of Ta–4.04 at.% Hf have been oxidized in the temperature range 850 to 1000°C in oxygen at approximately 760 torr. Hafnium increases the oxidation rate throughout this range, and above 1000°C the specimens ignite on admission of oxygen. The scale is finely laminated at all temperatures, and the decrease in lamination thickness is sufficient to mask any Wagner–Hauffe doping effect of the alloying element. There is some fine cracking in the scale formed at 950°C and above, which might be related to the original metal grain boundaries, but there is no evidence of penetration of pentoxide into the metal grain boundaries or of separation of the metal grains. Single crystal cylinders of Ta–1.2 at.% Hf with ⟨100⟩ axes have been oxidized in the range 750 to 1050°C. Fine suboxide platelets, which appear to

XUM

have been present at reaction temperature, are present beneath the metal/oxide interface in all cases, but only at the lowest temperatures do they lead to pores and pore-related failures in the scale. At 950°C the scale contains large aligned voids at about 60° over the {100} faces, and at higher temperatures there are cracks at the same angle. It has not been possible to determine the origin of these. The scale formed at 950°C exhibits a preferred orientation, but that formed at 1050°C is random. Microhardness indentations in the scale are surrounded by extensive cracking, suggesting that hafnium increases the brittleness of the oxide. (auth)

**55398** PROCESS FOR PROVIDING METAL COMPONENTS WITH COATINGS RESISTANT TO CORROSION. (to Ugine Kuhlmann). British Patent 1,246,306. 15 Sep 1971. Priority date 15 Nov 1967, France.

A process for deposition of protective coatings on metals such as Zr, Ti, Hf, Ta, Nb, and V is described. The process can also be used with alloys of these metals. The process involves Zn-plating an Al–Si alloy element and brazing this surface on the surface to be protected using Cu, Ag, Be, Ge, or Si or their alloys as braze filler. (J.R.D.)

## Preparation and Fabrication

*Refer also to abstracts 54906, 54928, and 57207.*

**55399** (N–71-27008) A STATE-OF-THE-ART LITERATURE SURVEY OF THORIA-DISPERSED NiCr FOR THE SPACE SHUTTLE THERMAL PROTECTION SYSTEMS. Hayes, W. L. (National Aeronautics and Space Administration, Huntsville, Ala. George C. Marshall Space Flight Center). 4 Mar 1971. 52p. (NASA-TM-X-64602). NTIS.

A literature survey is presented on the status of technology for processing and fabricating thoria-dispersed nickel chrome (TD-NiCr), a candidate material for space shuttle thermal protection systems. The literature indicates that TD-NiCr possesses the high-temperature strength (up to 1477°K) and other desirable characteristics. (auth) (STAR)

**55400** (NLCO–1077) SOLIDIFICATION MECHANISM OF URANIUM INGOTS. Eikenberry, H. M.; Graman, G. A. (National Lead Co. of Ohio, Cincinnati). Aug 1971. Contract AT-(30-1)-1156. 50p. Dep. NTIS.

Solidification of production size uranium ingots (8-inch, 9-inch, and 11-inch diameters) was studied by thermal analyses of experimental data. The temperature distribution in both the ingot and the mold, the progression of the solidification front, solidus isochrones, solidification rates in both the transverse and vertical direction, and volumetric percent of metal solidified with respect to time are shown. A method of correlating mold wall temperature data to ingot soundness by using a heat transfer mathematical model was developed and is discussed. (auth)

**55401** (RFP-Trans–87) PREPARATION OF RARE EARTH METAL ALLOYS WITH TRANSITION METALS OF THE 7th AND 8th GROUP OF THE PERIODIC SYSTEM AS WELL AS WITH COPPER, SILVER, AND GOLD USING AMALGAMS. Kirchmayer, H. R. Translated from Z. Metallk.; 56: No. 11, 767-70(1965). 10p. Dep. NTIS.

By a heat treatment of transition metals (Me) amalgams (Me = Mn, Fe, Co, Ni, Cu, Ag, Au) mercury free RE-Me-alloys can be prepared if the reaction between the components takes place in the absence of liquid mercury. The mercury, which is bound in the RE–Hg compounds, is set free. Although higher temperatures are required than in the amalgam process, nevertheless the advantages such as avoidance of the molten state and of reactions with the crucible remain. The range of application of the method is illustrated with the aid of RE (Y, Sm, Gd, Dy, Ho, Er)-Me-alloys. The compounds $REMn_2$, $REMn_{4-5}$, $REMn_{12}$, $YFe_2$, $YCo_5$, $YNi_5$, YCu, YAu have been identified. (auth)

**55402** (RMI-L–48) PRECISION EXTRUSION OF I AND E ELEMENTS. (Reactive Metals, Inc., Ashtabula, Ohio). Feb 1971. Contract AT(30-1)-1405. 21p. Dep. NTIS.

Results of investigations on the feasibility of precision extrusion of Hanford internally and externally cooled (I & E) fuel elements are presented. Experiments designed to determine optimum mandrel parameters are described along with extrusion methods. It was concluded that I & E precision extrusion is not a recommended method at present. (J.R.D.)

**55403** BEHAVIOR OF IMPURITIES IN NIOBIUM DURING VACUUM MELTING. Ivanova, M. I.; Elyutin, A. V. Tsvetn. Metal.; No. 11, 48-51(Nov 1970). (In Russian).

The behavior of impurities such as Si, Al, Ti, and Zr in Nb during vacuum remelting is discussed from the theoretical and experimental points of view, with special reference to the effect of Al on the behavior of the other three trace elements. In all cases the coefficient of separation of the other three impurities falls with increasing initial Al concentration. The practical importance of this effect in connection with the vacuum refining of Nb is considered. (Metals Abstr.)

**55404** VIEWPOINTS CONCERNING TECHNIQUES AND METALLOGRAPHY OF THE METALLURGY OF GRANULAR MATERIAL. Karsten, D.; Hiller, W. Metall; 25: 122-6(Feb 1971). (In German).

Granule metallurgy is compared and contrasted with powder metallurgy. The economic advantages of this technique are summarized. Alloys prepared by granule metallurgy are considered. These include alloys of Zn, Al, Mg, Pb, Cu, and Ti, composite materials, superconductors, and iron-base alloys. (J.S.R.)

**55405** PRODUCTION OF A COPPER/TUNGSTEN [MULTILAYER] COMPOSITE BY DIFFUSION WELDING. Budueva, V. G.; Fridman, Z. G.; Skazin, V. E.; Morozov, V. S.; Svirina, L. M. Fiz. Khim. Obrab. Mater.; No. 1, 107-11(Jan-Feb 1971). (In Russian).

The production of a Cu/W composite (alternate layers of Cu and W sheet or strip) by diffusion welding was studied, using the method of mathematical planning in order to determine the optimum conditions for the welding process. The factor chiefly influencing the quality of the welds was the temperature of the process; pressure, although important, was less critical. The time occupied by the process welding had hardly any effect on the quality of the result (within reasonable limits). The manner in which these composites fractured was similar to that characterizing fibrous compositions of the same type. (Metals Abstr.)

**55406** Zr Hf NEWSLETTER, MAY 1971. Akron, N. Y.; AMAX Specialty Metals Division (1971). 16p.

Development and new applications of Hf are reviewed. Similar information is included on Zr and Zr alloys. Information is also included on the physical properties of Zr, use of Zr as an alloying addition, and production of Zr. Information on oxides, borides, carbides, nitrides and silicides of Zr is summarized. 296 references are included. (J.R.D.)

**55407** PRODUCTION OF ZIRCONIUM DIOXIDE MICROBALLOONS BY MEANS OF NITROGEN PLASMA. Frolov, A. S.; Zakharov, B. M.; Umantseva, V. M.; Guseva, L. I. (All-Union Scientific-Research Inst. of Aviation Materials, Moscow). Sov. Powder Met. Metal Ceram. (Engl. Transl.); 10: No. 3, 204-6(Mar 1971).

Translated from Porosh. Met., Akad. Nauk Ukr. SSR; 10: No. 3, 41-4(Mar 1971).

Hollow spherical microparticles (microballoons) with controlled pore size can be made by subjecting refractory powders to the action of a $N_2$ plasma in a plasma torch. In order to study the microballoon formation process, experiments were carried out with a short-arc plasma torch, enabling the intermediate stages to be recorded. The molten particles were projected into water for quenching. In an attempt to increase the microballoon yield, ZrN was used in place of the starting dioxide. It was shown that some of the microballoons had a nitride sphere within their shells, and a description is given of the probable mechanism of microballoon formation. The product is monoclinic $ZrO_2$ when the starting material is the nitride, and cubic $ZrO_2$ with a small amount of monoclinic phase when stabilized $ZrO_2$ is used. (D.L.C.)

**55408** ELECTROREFINING OF VANADIUM PREPARED BY CARBOTHERMIC REDUCTION OF $V_2O_5$. Lei, K. P. V.; Sullivan, T. A. (Bureau of Mines, Boulder City, Nev.). Met. Trans.; 2: No. 8, 2312-14(Aug 1971).

High-purity V was prepared by molten salt electrorefining of a crude V feed material prepared by carbothermic reduction of $V_2O_5$. The electrolyte was prepared by the direct chlorination of V into the molten electrolyte of KCl–LiCl at 750°C to yield an electrolyte composed of 50 wt % KCl–39 wt % LiCl–11 wt % $VCl_2$ for the preparation of V that was 97.8 to 99.9% pure. The chief impurities were Cr, Fe, and O. (B.L.M.)

**55409** FRICTION WELDING OF TITANIUM ALLOYS. Nessler, C. G.; Rutz, D. A.; Eng, R. D.; Vozzella, P. A. (Pratt and Whitney Aircraft, East Hartford, Conn.). Weld. J. (N. Y.); 50: No. 9, 379s-85s(Sep 1971).

To determine the consistency of joint quality and the sensitivity of friction (inertia) welding in highly stressed gas turbine components, an extensive evaluation was made of the tensile, impact,

and fatigue properties of welded Ti–6Al–4V and Ti–6Al–2Sn–4Zr–2Mo. Properties were consistently good within a 10% range of parameter variation, as long as the upset exceeded a minimum level. Statistical analysis results showed that properties depended on the choice of parameters even when adequate upset was achieved. Therefore, degree of upset cannot be the sole criterion of acceptable properties. Tensile and fatigue test results showed that properties in reproducibly welded joints were consistent in level and scatter with the base metal. Additional evaluation assessing the inertia weldability of other titanium alloys also established that several alloys have slightly decreased but acceptable properties approximating base metal are usually achieved by welding followed by a 1000° (2 hr) stress relief. Inertia welded titanium joints were found to contain a narrow, highly worked heat-affected zone with an alpha prime structure at its center. Test specimen failures were consistently in the base metal. While ultrasonic inspection was found to be the only meaningful method of nondestructive testing, it could not detect slight residual contamination in low upset joints, indicating the necessity for close process control. (auth)

**55410** WELDABILITY OF TUNGSTEN AND ITS ALLOYS. Cole, N. C. (Oak Ridge National Lab., Tenn.); Gilliland, R. G.; Slaughter, G. M. Weld. J. (N. Y.); 50: No. 9, 419s-26s(Sep 1971).

The weldability of tungsten and a number of its alloys consolidated by arc casting, powder metallurgy, or chemical-vapor deposition (CVD) techniques was evaluated. Most of the materials used were nominally 0.060 in. thick sheet. The joining processes employed were (1) gas tungsten-arc welding, (2) gas tungsten-arc braze welding, (3) electron beam welding and (4) joining by CVD. Tungsten was successfully welded by all of these methods but the soundness of the welds was greatly influenced by the types of base and filler metals (i.e., powder or arc-cast products). For example, welds in arc-cast material were comparatively free of porosity whereas welds in powder metallurgy products were usually porous, particularly along the fusion line. For gas tungsten-arc (GTA) welds in $\frac{1}{16}$ in. unalloyed tungsten sheet, a minimum preheat of 150°C (which was found to be the ductile-to-brittle transition temperature of the base metal) produced welds free of cracks. As base metals, tungsten-rhenium alloys were weldable without preheat, but porosity was also a problem with tungsten alloy powder products. Preheating appeared not to affect weld porosity which was primarily a function of the type of base metal. The ductile-to-brittle transition temperatures (DBTT) for gas tungsten-arc welds in different types of powder metallurgy tungsten were 325 to 475°C, as compared to 150°C for the base metal and that of 425°C for electron beam-welded arc-cast tungsten. Braze welding of tungsten with dissimilar filler metals apparently did not produce better joint properties than did other joining methods. Nb, Ta, W-26% Re, Mo and Re were used as filler metals in the braze welds. The Nb and Mo caused severe cracking. Joining by CVD at 510 to 560°C eliminated all but a small amount of porosity and also eliminated the problems associated with the high temperatures necessary for welding (such as large grains in the weld and heat-affected zones). (auth)

**55411** MODERN DEVELOPMENTS IN POWDER METALLURGY. VOLUME 4. PROCESSES. Proceedings of the 1970 International Powder Metallurgy Conference, Held in New York, July 12–16, 1970. Hausner, Henry H. (ed.). New York; Plenum Publishing Corporation (1971). 603p. $29.50. (CONF-700709–(Vol.4)).

Forty-six articles are included; a separate abstract was prepared for each of seven. The remaining 39 articles contain information on: powders; powder consolidation; fundamentals of sintering; forging of P/M preforms; and P/M mill shapes. The keynote address is on new responsibilities in powder metallurgy. (P.C.H.)

*For abstracts of individual papers see: 55412–55415, 55480, 55642, and 55643.*

**55412** NEW TUNGSTEN POWDER FOR PRODUCING CARBIDES. Ramqvist, Lars (Axel Johnson Inst. for Industrial Research, Nynaeshamn, Sweden). pp 75–84 of Modern Developments in Powder Metallurgy. Vol. 4. /Hausner, Henry H. (ed.). New York; Plenum Publishing Corp. (1971).

From International powder metallurgy conference; New York, N. Y. (12 Jul 1970).

A new tungsten powder is described. Properties of the powder and especially its advantages for producing carbides are discussed. The powder is produced according to a method developed at the Axel Johnson Institute for Industrial Research. The method was developed in order to improve the properties of the W powder and the cemented carbides and to do it from an entirely different basis than from the APT method. The method is basically a chloride process, which can handle any type of raw material. (P.C.H.)

**55413** ELECTRICALLY ACTIVATED PRESSURE-SINTERING (SPARK SINTERING) OF TITANIUM–ALUMINUM–VANADIUM ALLOY POWDERS. Goetzel, C. G.; de Marchi, V. S. (Lockheed Palo Alto Research Lab., Calif.). pp 127-50 of Modern Developments in Powder Metallurgy. Vol. 4. /Hausner, Henry H. (ed.). New York; Plenum Publishing Corp. (1971).

From International powder metallurgy conference; New York, N. Y. (12 Jul 1970).

In the consolidation by spark sintering of Ti–6Al–4V, parts of about 10 in.$^3$ volume could be brought to nearly full density in 5 to 7 minutes. As the starting powders were low in interstitial elements, very good mechanical properties were obtained in the consolidated billets, and after heat treatment. Observed differences in ductility were mainly due to oxygen and nitrogen contamination of the outer regions, provided that full densification had previously been achieved. Adjustment of the heating cycle and argon purging generally controlled this problem. Embrittlement due to grain coarsening in areas adjacent to the punch faces should also be expected, but can be overcome by tooling modifications. All strength properties were found to equal those of wrought Ti–6Al–4V, but ductilities were lower. Based on experience with cold compacted and sintered Ti–6Al–4V, subsequent hot working can be expected to improve the ductilities. Particle shape and purity had some effect on consolidation rate and properties while no effect on properties could be observed for powder particle size distribution. Sintering and densification were greatly facilitated by the use of a clean particle powder, either of irregular shape, such as the hydride–dehydride type, or of spherical shape. The rapid rate of consolidation into parts of full density makes the spark sintering process economically attractive where high strength is more desirable than high ductility, and where cost savings become paramount consideration in chosing the powder metallurgy approach. The potential of using fully dense spark sintered and heat-treated titanium alloy parts in lieu of forged parts may ultimately be more rewarding than using these parts merely as forging performs. (auth)

**55414** POSSIBILITIES OF ACTIVATING SINTERING BY SPECIAL THERMAL TREATMENT. Labusca, Elena N. (Inst. for Atomic Physics, Bucharest). pp 241-53 of Modern Developments in Powder Metallurgy. Vol. 4. /Hausner, Henry H. (ed.). New York; Plenum Publishing Corp. (1971).

From International powder metallurgy conference; New York, N. Y. (12 Jul 1970).

A system of thermal treatments able to create conditions for delayed and decreased grain growth during sintering was conceived. The system consisted of systematic thermal fluctuations to which the powder compact was exposed during sintering (marked TZ). Experiments were made with a variety of materials, such as oxides ($Al_2O_3$, ferrites, etc.), metals (Fe, Ni, Cu, Zr) or alloys (Fe–Ni, Fe–Ni–Mo, etc.). The results showed that initial suppositions proved to be correct. The materials exposed to the TZ-treatment showed a finer crystalline structure than that of materials exposed to the more common type of sintering. Also, the grain structure of these materials was more homogeneous, which was reflected in some specific properties. Features pertaining to the fineness and isotropy of the crystalline structure were also modified. (P.C.H.)

**55415** TITANIUM P/M PREFORMS, PARTS, AND COMPOSITES. Abkowitz, S.; Siergiej, J. M.; Regan, R. D. (Dynamet Corp., Burlington, Mass.). pp 501-11 of Modern Developments in Powder Metallurgy. Vol. 4. /Hausner, Henry H. (ed.). New York; Plenum Publishing Corp. (1971).

From International powder metallurgy conference; New York, N. Y. (12 Jul 1970).

A new technology using powder metal techniques was developed for Ti and Ti alloy components. It extends throughout the broad areas of pressed and sintered parts, forging and extrusion preforms, and composites. These new materials have a wide variety of potential applications in the chemical processing, marine hardware, and aerospace industries. (P.C.H.)

**55416** NEW DEVELOPMENTS IN SUPERALLOY POWDERS. Reichman, S. H.; Smythe, J. W. pp 73-84 of Modern Developments in Powder Metallurgy. Vol. 5. /Hausner, Henry H. (ed.). New York; Plenum Publishing Corp. (1971).

From International powder metallurgy conference; New York, N. Y. (12 Jul 1970).

The advantages of a powder metallurgy (P/M) process for Ni-based superalloys are given in terms of better homogeneity than cast alloys. By using low interstitial-atomized powders densified by direct extrusion, superplastic structures were developed. The results of a thermomechanical process are presented through which large grained or even single crystal structures can be fabricated. Finally, an alloy series made specifically for P/M

XUM

processes is presented. These alloys have no carbon as atomized, densified, or formed. The resultant solution-annealed grain sizes were ASTM 1 to 0. These alloys were subsequently carburized to stabilize the grain boundaries. (auth)

**55417** MANUFACTURE AND PROPERTIES OF HIGH-CONDUCTIVITY HIGH-STRENGTH Cu–$ThO_2$. Scheithauer, W. Jr.; Cheney, R. F.; Kopatz, N. E. (Sylvania Electric Products Inc., Towanda, Pa.). pp 149-58 of Modern Developments in Powder Metallurgy. Vol. 5. /Hausner, Henry H. (ed.). New York; Plenum Publishing Corp. (1971).

From International powder metallurgy conference; New York, N. Y. (12 Jul 1970).

Methods are described for producing plate, sheet, rod, and wire of high-purity copper with dispersions of thorium oxide particles. Powders are first produced by spray drying, calcining, and selective hydrogen reduction. The reduced powders are isostatically compacted. Densification which cannot be accomplished by conventional sintering techniques is done either by hot forging, not rolling, or hot extrusion. After the thermomechanical densification step, the material can be further worked into wrought forms by somewhat conventional techniques. The primary problems encountered in the powder metallurgy approach were in obtaining low-oxygen consolidated forms and in obtaining dispersions with good spatial distributions. Low-oxygen consolidated forms were obtained by modifying the hot consolidation technique, the critical feature being that the porous billets be heated only in a hydrogen atmosphere until the resultant forms are 100% dense. The problem of improving the thoria spatial distribution was not solved and will require additional investigation. High purity permits attainment of conductivities in excess of 95% IACS. With the best $ThO_2$ dispersions, 600°C yield strengths to 20,000 psi were obtained with Cu–$1ThO_2$. Better dispersions should yield higher strengths. After annealing at temperatures as high as 1000°C, the room-temperature 0.2% yield strengths were still as high as 20,000 to 25,000 psi. (auth)

**55418** TZM MOLYBDENUM ALLOY VIA P/M. Clare, L. P. (Sylvania Electric Products Inc., Towanda, Pa.); Vazquez, A. J. pp 259-71 of Modern Developments in Powder Metallurgy. Vol. 5. /Hausner, Henry H. (ed.). New York; Plenum Publishing Corp. (1971).

From International powder metallurgy conference; New York, N. Y. (12 Jul 1970).

Studies were made on the properties of powder metallurgy fabricated TZM. The P/M TZM exhibited good forgeability in the forging temperature range from 1095°C to 1315°C; poor forgeability (hot-shortness characteristics) was encountered at forging temperatures above 1315°C; P/M TZM can be fully recrystallized by annealing for one hour at 1430°C. Partial recrystallization can occur at 1315°C; and the poor forgeability (hot-shortness) was attributed to unidentified precipitate(s) which formed at the grain boundaries at all forging temperatures studied. These precipitate(s) became severe and detrimental as the forging temperature exceeded 1315°C. (auth)

**55419** REDUCED MICROGELS: A NEW FORM OF POWDERED METALS AND METAL OXIDES. Lindquist, R. H. (Chevron Research Co., Richmond, Calif.). pp 289-98 of Modern Developments in Powder Metallurgy. Vol. 5. /Hausner, Henry H. (ed.). New York; Plenum Publishing Corp. (1971).

From International powder metallurgy conference; New York, N. Y. (12 Jul 1970).

For certain applications in electrical and microwave devices it is desirable to use extremely fine grain materials that behave as single magnetic domains. The Microgel process for making such materials is described. Single magnetic domain particles are produced by starting with the desired metal chlorides to make a given ferrite composition, such as $Mg_{.5}Mn_{1.5}Fe_2O_4$. After making a Microgel of such composition, the gel can be broken into micron size particles in a suspended fluid consisting of aluminum chloride in methanol using a colloid mill. When the colloid solution is gelled again by addition of more propylene oxide, the resultant material is a gel-coated gel, which upon drying and calcination produces submicron size ferrite particles coated with alumina. In effect, the small ferrite particles are insulated from each other by the alumina gel. Compaction and sintering yield a fine grain material processing high speed switching advantages for use in electronic applications. (auth)

**55420** DENSITY OF COEXTRUDED METAL CLADDED ROD CORE AS FUNCTION OF CARTRIDGE DENSITY AND CORE LENGTH. Rutkowski, W.; Szteke, W.; Wieczorkowski, M. (Inst. for Nuclear Research, Warsaw). pp 299-309 of Modern Developments in Powder Metallurgy. Vol. 5. /Hausner, Henry H. (ed.). New York; Plenum Publishing Corp. (1971).

From International powder metallurgy conference; New York, N. Y. (12 Jul 1970).

Studies were made on the coextrusion of metal powder and ceramic dispersions clad in alloyed aluminum. The results showed that visible differences in the behavior of core and clad physical characteristics, depending upon materials used and $Al_2O_3$ addition. The character of dimensional changes of the core and clad at the same $Al_2O_3$ addition depended on the matrix metal physical characteristics at given temperature and the core length. The $Al_2O_3$ content in the core acted in its volumetric ratio and changed the character of dimensional deviations of the core and clad on the core length very distinctly. The microhardness changed according to the core length and dimensional deviations. (P.C.H.)

**55421** NOVEL HIGH-STRENGTH TITANIUM ALLOY. Molinier, R.; Syre, R. Metall; 25: No. 5, 484-92(May 1971). (In German).

Steps in the development of a new high-strength Ti alloy Ti–6% Al–6% V–2% Sn–0.5% Cu–0.5% Fe are described. These include laboratory studies, semi-industrial studies on unworked material, evaluation of semi-processed material, and testing of finished material. (J.S.R.)

**55422** PC STEEL WIRES FOR REACTORS. Tomioka, Hiroyuki (Shinko Wire Co. Ltd., Amagasaki, Japan); Tani, Yoshio. R and D, Kobe Seiko Giho; 20: No. 3, 77-89(Jul 1970). (In Japanese).

A survey of prestressed concrete (PC) steel wires for reactors is reported. The present state of development of PC construction in various countries is outlined along with methods of manufacture of PC steel wires. It is noted that the wires should have high tensile strength and high elastic limit, small stress relaxation, stable mechanical properties, sufficient toughness, and corrosion-resistant surfaces as well as small coefficient friction. Emphasis is placed upon stress relaxation. In this regard, hot-stretching treatment should be used because hot-stretched wires exhibit extremely low stress relaxation. Descriptions of special tests for the PC wires for reactors are included. The wires were tested under neutron irradiation and stressed condition. A brief summary of typical PC construction techniques is included. (Japan)

**55423** DISPERSION-HARDENING OF AN IRON–COBALT–TUNGSTEN ALLOY. Ershova, L. S. Izv. Akad. Nauk SSSR, Metal.; No. 1, 151-6(Jan-Feb 1971). (In Russian).

The kinetics of dispersion-hardening in a maraging Fe–Co–W alloys were studied. Substantial changes took place in the structure of the $\alpha$-solid solution during aging. Dispersion-hardening was accompanied by a considerable reduction in the integral intensities of the x-ray lines of the corresponding lattice and an increase in the degree of microscopic distortion. The disorientation angles and the dimensions of the blocks remained relatively constant during isothermal annealing. There was a close correlation between the kinetics of the hardening process and the kinetics of the changes in x-ray intensity, suggesting that the hardening process was based on the formation of minute precipitates, coherent with the matrix, and an increase in the lattice defect density. (Metals Abstr.)

**55424** METHOD OF HOLDING MOLTEN METAL IN A SUSPENDED STATE: CHARACTERISTICS OF THE LODOCHKA INDUCTOR [LEVITATION MELTING]. Fogel, A. A.; Sidorova, T. A.; Mezdrogina, M. M. Izv. Akad. Nauk SSSR, Metal.; No. 1, 216-21(Jan-Feb 1971). (In Russian).

The construction of an inductor (the "Lodochka") for holding metals in a suspended state by virtue of an electromagnetic field during melting operations and other technological processing is described. The inductor in question is suitable for obtaining castings of Ti, Zr, Nb, and Mo in vacuum subject to the selection of an appropriate electromagnetic frequency in each case. Using a He atmosphere, Fe, Ni, and Co may be processed, and on adding a supplementary electron-beam system the same holds for Ru, Ta, Os, Re, and W. (Metals Abstr.)

**55425** BRAZING THE SHELL ASSEMBLY FOR THE BONUS SUPERHEATER FUEL ELEMENT. Tolson, G. M.; Williams, L. C.; Franco-Ferreira, E. A.; Kirstowsky, E. C. (Union Carbide Corp., Oak Ridge, Tenn.). Weld. J. (N. Y.); 50: No. 9, 641-6 (Sep 1971).

Methods used to braze eight shell subassemblies which house the superheater fuel rods for the BONUS reactor are described. Fixturing, welding, alloying, and braze cycle are also described. Techniques used to eliminate several defects found on the Core I subassemblies are discussed. A method of leak testing the subassemblies to a sensitivity of $1 \times 10^{-10}$ std cc/sec is covered. A prototype unit was pressure tested to failure. (auth)

XUM

**55426** EFFECT OF NICKEL ON THE SINTERING AND SELF DIFFUSION OF TUNGSTEN. Schintlmeister, W.; Richter, K. (Metallwerk Plansee AG, Reutte, Austria). Planseeber. Pulvermet.; 18: No. 1, 3-6(Mar 1970). (In German).

Tungsten powder was soaked in an alcoholic solution of nickel nitrate, dried, and reduced under hydrogen. The results showed that sintering activity increased with increasing nickel content up to a certain concentration beyond which no further activation occurred. In a second series of experiments, thin layers of tungsten-185 were electrically deposited on samples. After heat treatment, the samples were sectioned and studied by autoradiography. It was concluded that the effects of Ni on the sintering of tungsten depend not only on acceleration of diffusion at grain boundaries but also on other factors, not determined as yet. (H.B.G.)

## *Properties Evaluations*

*Refer also to abstracts 54583, 54929, 55626, 56346, 56349, 56351, 56386, and 57196.*

**55427** (BNWL-1567) EFFECT OF STRAIN RATE AND TEMPERATURE ON THE TENSILE PROPERTIES OF Pu-1 WT PERCENT Ga ALLOYS. Merz, M. D. (Battelle Pacific Northwest Labs., Richland, Wash.). Aug 1971. Contract AT(45-1)-1830. 23p. Dep. NTIS.

The tensile properties of a plutonium-1 wt % gallium alloy (fcc, delta stabilized) with two iron levels were determined at strain rates from $3.3 \times 10^{-4}$ to 20 $sec^{-1}$ and temperatures from 25 to 500°C. The yield stress and ultimate tensile strength increased with strain rate in proportion to log $\dot{\epsilon}$ at 25 and 100°C. At an intermediate temperature range, 150 to 200°C, the yield stress and ultimate strength were relatively insensitive to strain rate. At 300 and 500°C, both properties increased with strain rate at strain rates higher than 0.1 $sec^{-1}$. At 400°C, Pu-$Pu_6Fe$ melting occurred in the alloy containing 235 ppM iron. No melting occurred in the alloy containing 100 ppM iron. Pu-$Pu_6Fe$ melting caused embrittlement at 400°C at all testing rates. The ultimate tensile strength was relatively insensitive to strain rate at 400°C increasing from 4800 psi at 0.01 $sec^{-1}$ to 6600 psi at 18 $sec^{-1}$ Total elongation and reduction in area did not change significantly with strain rate and given temperature. However, as the test temperature was increased at a given rate, the elongation and reduction in area exhibited minima in the temperature interval of 100 to 200°C, increased at 300°C, and decreased to very low values at 400°C due to Pu-$Pu_6Fe$ melting. Recrystallization occurred during the tests at 400 and 500°C. (auth)

**55428** (BNWL-B-108) ON THE BERKELIUM-OXYGEN SYSTEM. Turcotte, R. P.; Chikalla, T. D. (Battelle Pacific Northwest Labs., Richland, Wash.); Eyring, L. (Arizona State Univ., Tempe). Mar 1971. Contract AT(45-1)-1830. 68p. Dep. NTIS.

A unique, highly sensitive system for the quantitative measurement of decomposition pressures of small samples has been used to obtain equilibrium oxygen decomposition pressures over a 1.22 milligram sample of nonstoichiometric berkelium-249 oxide. The temperature and pressure range investigated was 852 to 1150°C and from $10^{-7}$ to $10^{-20}$ atm $O_2$, respectively. These conditions were sufficient to enable examination of the entire compositional range between $BkO_2$ and $Bk_2O_3$. Partial thermodynamic quantities were derived and found to be a function of composition but independent of temperature. The shapes of the equilibrium decomposition pressure isotherms were used to deduce the possible condensed phase relationships in this oxide system. (auth)

**55429** (CEA-R-4177) MECHANICAL BEHAVIOR OF THE ALLOYS $UMo_{0.1}Al_{0.05}Sn_{0.05}$ AND SICRAL $F_1$ (ADJUSTED URANIUM) BETWEEN 20 AND 600°C. Khan, Tasadduq (Commissariat a l'Energie Atomique, Saclay (France). Centre d'Etudes Nucleaires). 1971. 120p. (In French). Dep. NTIS (U. S. Sales Only).

Thesis. Submitted to Paris Univ. (France). Faculte des Sciences.

The mechanical behavior in tension of two uranium alloys ($UMo_{1.1}Al_{0.05}Sn_{0.05}$ and Sicral $F_1$) was studied between room temperature and 600°C for four different tensile testing speeds. A large decrease in ductility (elongation to breaking) was observed for $UMo_{1.1}Al_{0.05}Sn_{0.05}$ alloys having undergone direct $\gamma \rightarrow (\alpha + \gamma)$ transformation, then tensile tested between 450 and 590°C. This ductility drop is shown to be connected with the development of cavities at the prior $\gamma$ grain boundaries, this cavity formation is greatest at 590°C, the temperature at which the ductility passes through a minimum is related to the rate of deformation. On the other hand, the behavior of Sicral $F_1$ (adjusted uranium) is comparable to that of technical uranium. The experimental results agree well with the hypothesis that the inherent resistance of the lattice plays an important role in the plastic deformation of Sicral $F_1$. Moreover the deformation rates have a strong effect on the modes of rupture, especially between 20 and 200°C. The results show that the cavities reported by other investigators are not produced to any great extent in the alloy Sicral $F_1$. (auth)

**55430** (IS-T-459) SMALL ANGLE TILT AND TWIST GRAIN BOUNDARY STRENGTHENING IN YTTRIUM. Carnahan, Thomas George (Ames Lab., Iowa). Sep 1971. Contract W-7405-eng-82. 129p. Dep. NTIS.

Thesis.

Bicrystals of yttrium containing pure $\langle 10\bar{1}0 \rangle$ twist or pure $\langle 11\bar{2}0 \rangle$ tilt grain boundaries were plastically deformed in uniaxial compression. The critical resolved yield stress was found to vary with the magnitude of the tilt or twist. It increased almost linearly until leveling off at about 5° misorientation. Tilt boundary samples were stronger. Their strength increased from a single crystal value of 0.34 kg/mm² to a plateau value of 0.70 kg/mm². This is compared with a plateau value of 0.58 kg/mm² for twist boundary samples. The strengthening mechanism in this region (<5°) appears to have been due to the formation of jogs in the glide and grain boundary dislocations when the glide dislocations passed through the grain boundary. The deformation modes of yttrium were determined for a variety of loading conditions. Slip was found to occur primarily on the $\{10\bar{1}0\}\langle 1\bar{2}10 \rangle$ system but $(0001)\langle 11\bar{2}0 \rangle$ slip was also found to occur. The primary twin mode was the $\{11\bar{2}1\}\langle \bar{1}126 \rangle$ mode and the secondary twin mode was the $\{10\bar{1}2\}\langle \bar{1}011 \rangle$ mode. No other twin modes were detected. Samples oriented for c-axis compression exhibited no operable deformation modes and failed by fracture along $\{11\bar{2}3\}$ planes at a resolved stress of 45 kg/mm². Thermal groove studies on twist grain boundaries provided relative grain boundary energies for yttrium. The energy in the small angle (<5°) region was shown to obey the Read-Shockley theory. A theoretical surface energy of 1460 erg/cm² was calculated from the grain boundary energy results. (auth)

**55431** (N-71-23110) EFFECT OF GRAIN SIZE ON CREEP PROPERTIES OF A TUNGSTEN-25 AT. PERCENT RHENIUM-30 AT. PERCENT MOLYBDENUM ALLOY FROM 1800 TO 4000°F. Buzzard, Robert J. (National Aeronautics and Space Administration, Cleveland, Ohio. Lewis Research Center). Apr 1971. 27p. (NASA-TN-D-6285). NTIS.

The stress to achieve 1% total creep strain at temperatures of 1800 to 4000°F was determined for powder metallurgy W-25 at. % Re-30 at. % Mo sheet. Grain sizes of 0.0014 and 0.0025 cm and a duplex structure of 0.0028 to 0.063 cm, resulted from 2-hr anneals at 2900, 3600, and 4000°F, respectively. For each annealing treatment, room temperature bend ductility also was determined. The 0.0025-cm grain size material offered the best creep resistance of the three at low temperatures (below 2400°F) and high stresses (4 ksi and above) and was ductile at room temperature. (auth) (STAR)

**55432** (N-71-23114) CREEP BEHAVIOR OF ELECTRON BEAM-MELTED RHENIUM. Witzke, Walter R.; Raffo, Peter L. (National Aeronautics and Space Administration, Cleveland, Ohio. Lewis Research Center). Apr 1971. 24p. (NASA-TN-D-6291). NTIS.

Creep deformation in electron beam-melted polycrystalline Re sheet was evaluated at 2200 to 4200°F and 4 to 40 ksi. Comparisons were made with powder-metallurgy Re under similar conditions. Changes in creep rupture behavior resulting from electron beam melting of Re were greater ductility, higher primary creep rate, and longer rupture life, especially at lower temperatures. The activation energy for creep was 72 kcal/mole for electron beam-melted Re and 64 kcal/mole for powder-metallurgy Re. (auth) (STAR)

**55433** (N-71-23982) MECHANICAL PROPERTIES OF A TUNGSTEN-23.4-PERCENT RHENIUM-0.27-PERCENT HAFNIUM-CARBON ALLOY. Klopp, William D.; Witzke, Walter R. (National Aeronautics and Space Administration, Cleveland, Ohio. Lewis Research Center). Apr 1971. 23p. (NASA-TN-D-6308). NTIS.

The alloy was arc-melted, fabricated, and evaluated to determine if particle strengthening by hafnium carbide could be achieved in a ductile, tungsten-high-rhenium matrix. The alloy was found to exhibit a good combination of tensile and creep strength to 3000°F with a ductile-brittle transition temperature near room temperature. (auth) (STAR)

**55434** (RLO-2221-T-7-3) ADSORPTION AND ABSORPTION OF HYDROGEN BY NIOBIUM. Johnson, L.; Dresser, M. J.;

XUM

Donaldson, E. E. (Washington State Univ., Pullman). [1970]. 13p. (CONF-711005-1). Dep. NTIS.

From International conference on solid surfaces; Boston, Mass. (11 Oct 1971).

Adsorption of hydrogen on a clean niobium surface and the absorption of hydrogen into the bulk were investigated. The sticking probability of hydrogen on a clean niobium surface was found to be about 0.13. Evidence for a precursor surface adsorption state and subsequent diffusion into the bulk was found; the sticking probability is independent of temperature when the surface is clean but becomes temperature dependent at higher coverage. The solubility study results indicate ideal interstitial solution obeying Sievert's law at concentrations of dissolved hydrogen below 0.1 atomic percent but show deviation from this ideal solution above 0.5 atomic percent. The heat of solution was found to vary from −16 to −10 kcal/mole. The resistivity of niobium depends on hydrogen concentration and also on temperature and time. The deviations from ideal solution agree with a hydrogen cluster model. (auth)

**55435** (RLO-2221-T-7-4) ELECTRON STIMULATED DESORPTION OF EXCITED NEUTRALS: CO ON W. Newsham, Ivor G.; Hogue, James V.; Sandstrom, Donald R. (Washington State Univ., Pullman. Dept. of Physics). [1970]. 14p. (CONF-711005-2). Dep. NTIS.

From International conference on solid surfaces; Boston, Mass. (11 Oct 1971).

A time-of-flight technique is used to study the release of excited neutrals and ions by electron-stimulated desorption for the system CO on W. The method ensures the detection of the excited neutral particles without interference from photons produced by the electron beam. Use of a channel electron multiplier allows the counting of individual particle arrivals, ensuring high sensitivity and allowing the use of low electron current densities. Energy distributions are obtained from the flight-time distributions for both kinds of particles, using a (100) single crystal sample. The release of excited neutrals for this system in the temperature range 130 to 270°K is demonstrated. (auth)

**55436** (SC-RR-710314) DYNAMIC MEASUREMENTS OF THE GRUENEISEN COEFFICIENTS OF TANTALUM, URANIUM, AND URANIUM-MOLYBDENUM ALLOYS. Gover, James E. (Sandia Labs., Albuquerque, N. Mex.). Aug 1971. 172p. Dep. NTIS.

Hooke's Law, Newton's Law, and the Grüneisen Equation of State were used to develop a nonhomogeneous displacement wave equation and the stress-displacement relationship for an isotropic solid. The Grüneisen coefficient in uranium alloys was measured by using the electron beam from the Febetron 705 to achieve a rapid change in the internal energy of uranium materials. The technique is also considered applicable to other metals. The study is relevant to development of fast-burst reactors in that stress magnitudes can be predicted that might occur in fuel mounting hardware of a nuclear assembly. (auth)

**55437** (TID-25784) QUANTITATIVE DETERMINATION OF THE STRUCTURE-PROPERTY RELATIONSHIPS IN NUCLEAR FUEL ELEMENT MATERIALS. Quarterly Progress Report, December 16, 1970–March 15, 1971. Rhines, F. N.; DeHoff, R. T.; Whitney, E. D. (Florida Univ., Gainesville). Apr 1971. Contract AT(38-1)-552. 34p. Dep. NTIS.

Continued experimental progress has been achieved in the areas of quantitative microstructural analysis, gas permeability studies, short-time mechanical properties, and high-temperature creep measurements in both sintered nickel and sintered uranium dioxide materials. In addition, distinct improvements have been realized in uranium dioxide specimen fabrication techniques and in the design of apparatus for creep measurements. Knowledge of the general dependence of mechanical properties upon geometric state has been extended and strengthened through studies of the anisotropy of metallographic properties. (auth)

**55438** METALLOVEDENIE SPLAVOV TUGOPLAVKIKH I REDKIKH METALLOV. (Physical Metallurgy of Refractory and Rare Metals). Savitskii, E. M.; Burkhanov, G. S. Moscow; Izdatel'stvo Nauka (1971). 355p.

This monograph is concerned with the structure and properties of refractory metals and their alloys and with fields of application. Interatomic bonds in alloys and basic physical properties, e.g., thermal, electrical, and mechanical, are considered. Some theories of alloys, and methods of constructing phase diagrams, are discussed. Topics such as the nature of cold brittleness and its prevention, growth and study of monocrystals, and interaction and compatibility of alloys with other materials, are presented. One chapter summarizes known data on the alloys of Cr, Mo, W, Re, V, Nb, and Ta. The effects of heat treatment and pressure and welding and soldering of refractory metal alloys are discussed. 1340 references. (tr-auth)

**55439** SURFACE LAYER OF SURFACE-HARDENED PARTS OF HEAT-RESISTING ALLOYS. Poloshkin, Yu. V.; Davykova, V. V. Metal Sci. Heat Treat. (USSR)(Engl. Transl.); 13: No. 1-2, 144-6(Jan-Feb 1971).

Translated from Metalloved. Term. Obrab. Metal.; 13: No. 2, 56-8(Feb 1971).

The effects of prolonged high temperatures on surface hardening and relaxation of residual stresses in two heat-resisting alloys were studied. The results showed that the effects of surface hardening by cold working depend mainly on the stability of residual compressive stresses. The residual stresses decreased greatly in the first hours at elevated temperature and then changed slowly. The time that the effect of surface hardening is retained in heat-resisting alloys can be determined approximately—from structural dislocations—by metallographic examination. (auth)

**55440** CHEMICAL VAPOR DEPOSITED TUNGSTEN: MECHANICAL EVALUATION AT HIGH TEMPERATURES. Chun, J. S. (Univ. of Utah, Salt Lake City); Nicholson, P. S.; Sosin, A.; Byrne, J. G. J. Electrochem. Soc.; 118: No. 9, 1492-8(Sep 1971).

A high-temperature hoop stress measurement apparatus has been developed for ring specimens of chemical vapor deposited (CVD) tungsten or other refractory metal alloys. This apparatus has the advantage of being adaptable for high-temperature tensile testing. Force is applied to a tapered cone which transmits force to eight equal segments which press uniformly on the inner surface of the ring specimen. The specimen is heated by induction in either vacuum or a protective atmosphere. Equations are developed for stress and strain from hoop stress parameters. Room temperature hoop and tensile tests on aluminum, copper, and brass specimens were compared to ascertain the role of friction in the hoop stress tests. For temperatures up to 1400°C, the effective friction coefficient, $\mu$, of the hoop testing apparatus was determined using CVD tungsten in a similar manner. Design details and the results of the elevated temperature tests on CVD tungsten are discussed. (auth)

**55441** CHEMISORPTION OF CARBON MONOXIDE ON TANTALUM. Ustinov, Yu. K. (Ioffe Inst. of Physics and Tech., Leningrad). Sov. Phys.-Tech. Phys. (Engl. Transl.); 16: No. 2, 311-14(Aug 1971).

Translated from Zh. Tekh. Fiz.; 41: No. 2, 411-16(Feb 1971).

The flash method was employed with a pulsed mass spectrometer to study the chemisorption of carbon monoxide molecules on polycrystalline tantalum strips. It has been established that some of the chemisorbed molecules are in the undissociated state, with a heat of adsorption of about 140 kcal/mole. The remainder of the molecules dissociate at the surface of the tantalum and diffuse into the interior of the adsorbent. The desorption of diffusing carbon monoxide in a flash is of interest: the amount of dissolved oxide varies with temperature, reaching a maximum at T ~ 1300°K. (auth)

**55442** THERMODYNAMIC PROPERTIES OF CERIUM IN MOLTEN ZINC. Lebedev, V. A.; Nichkov, I. F.; Raspopin, S. P.; Semenov, B. G. Izv. Akad. Nauk SSSR, Metal.; No. 5, 86-9(Sep-Oct 1970). (In Russian).

The thermodynamic characteristics of Ce in molten Zn were studied at 700 to 1000°K by the emf method using an electrolytic cell with a chloride electrolyte. The emf of the cell varied linearly with temperature. The activity coefficient of Ce in the solution differed markedly from the corresponding atomic proportions of the additive; the strong departure from the Raoult law in the negative direction indicated that the Ce formed strong groupings with the Zn atoms and that these were very slow in dissociating. (Metals Abstr.)

**55443** MECHANISM UNDERLYING THE DISPERSION HARDENING OF NIOBIUM ALLOYS. Savitskii, E. M.; Ivanova, K. N. Izv. Akad. Nauk SSSR, Metal.; No. 5, 149-56(Sep-Oct 1970). (In Russian).

Dispersion-hardening processes in Nb–Zr–C, Nb–Mo–C, and Nb–W–C alloys were studied by x-ray and electron-microscope methods together with measurements of electric resistance, mechanical strength, ductility, and creep strength. Dispersion hardening in association with quenching from high temperature (1750°C) greatly increases the creep strength at 1100 to 1200°C; in some alloys no softening occurs even after 1000 hr at these temperatures. The finely divided (Zr, Nb)C phase was particularly efficient in promoting dispersion hardening. On the basis of these results, improved methods of producing heat-resistant Nb alloys are considered. (Metals Abstr.)

XUM

**55444** DECOMPOSITION OF THE SOLID SOLUTION OF INTERSTITIAL IMPURITIES IN TUNGSTEN. Yudkovskii, S. I.; Shulepov, V. I.; Shvetsova, S. I.; (and others). Izv. Akad. Nauk SSSR, Metal.; No. 5, 157-63(Sep-Oct 1970). (In Russian).

The decomposition of the solid solutions formed by various interstitial impurities (N, O, H, etc.) in W was studied; the decomposition took place relatively slowly in the inside of the W grains. Alloying the metal with C and Zr and raising the annealing temperature intensified the decomposition of the solid solutions along the grain boundaries. For the annealing temperature of 2000°C, the solid solutions also decomposed in the inside of the grains. As a result of this effect, local internal stresses (phase hardening) developed at the grain boundaries, partly as a result of particle coagulation. (Metals Abstr.)

**55445** HEAT CONTENT OF METALLIC HAFNIUM. Golutvin, Yu. M.; Maslennikova, E. G. Izv. Akad. Nauk SSSR, Metal.; No. 5, 174-83(Sep-Oct 1970). (In Russian).

The heat content (relative enthalpy) of metallic Hf was studied by the method of mixing in massive calorimeters up to 1400°K. There was a sharp break in the heat content curve at 858°K, indicating the end point of a gradual phase transformation. This result was correlated with electrical-resistance measurements on the corresponding material and on Zr and Ti. The electrical resistance/temperature characteristics were interpreted in terms of the gradual collectivization of the d electrons with increasing temperature. (Metals Abstr.)

**55446** HEAT RESISTANCE AND ELASTIC PROPERTIES OF TITANIUM–TANTALUM ALLOYS. Nartova, T. T.; Andreev, O. N. Izv. Akad. Nauk SSSR, Metal.; No. 5, 194-6(Sep-Oct 1970). (In Russian).

The effects of composition and phase characteristics on the elastic properties, heat resistance, and density of Ti–Ta alloys were studied. The elastic and shear moduli of Ti–Ta alloys vary only slightly with composition, at least up to 30 at. % Ta. The heat resistance of the alloys at 400 to 600°C increases with increasing Ta content. The chemical interactions between the constituent metals correlate directly with the heat-resistance/composition diagram. (Metals Abstr.)

**55447** DETERMINATION OF THE LIMITS OF SOLUBILITY OF TUNGSTEN IN THE NICKEL–COPPER SOLID SOLUTION OF THE TUNGSTEN–NICKEL–COPPER SYSTEM. Chaporova, I. N.; Agababova, V. M. Izv. Akad. Nauk SSSR, Metal.; No. 5, 205-7 (Sep-Oct 1970). (In Russian).

The limiting solubility of W in the Ni–Cu solid solution of the W–Ni–Cu system was studied by x-ray diffraction supported by microstructural analysis and measurements of electrical resistance and microhardness. The results confirm that the limiting solubility of W in the $\gamma$ solid solution of Ni–Cu falls with increasing Cu content; for Ni–20% Cu the value is 21 and 19% at 1200 and 1100°C, respectively, and for Cu–40% Ni, 3 and 1% at the corresponding temperature. (Metals Abstr.)

**55448** KINETICS OF THE DECOMPOSITION OF BINARY AND TERNARY SOLID SOLUTIONS OF ALUMINUM WITH CHROMIUM OBTAINED BY QUENCHING THE ALLOYS FROM THE MOLTEN STATE. Polesya, A. F.; Stepina, A. I. (Dnepropetrovsk State Univ., USSR). Fiz. Metal. Metalloved.; 30: No. 5, 929-35(Nov 1970). (In Russian).

The kinetics of the decomposition of metastable binary and ternary solid solutions of the Al–Cr, Al–Mo, and Al–Cr–Mo obtained by quenching melts were studied. Al–4.0 wt. % Mo solid solutions did not decompose at all up to 600°C, but Al–Cr and Al–Cr–Mo decomposed at 475°C with the precipitation of Cr, and in some cases Mo. At 625°C the Mo precipitated from the alloys in two stages, accompanied by an anomalous rise in electrical resistance. At the same time spherical particles 100 Å in dia. were observed by electron microscopy. (Metals Abstr.)

**55449** CORRELATION EFFECT OF TRANSPORT PHENOMENA IN MOLTEN SOLUTIONS. Belashchenko, D. K.; Mityaev, V. V. Fiz. Metal. Metalloved.; 30: No. 5, 1007-13(Nov 1970). (In Russian).

The coefficient of mutual diffusion in molten alloys of the Sn–Zn system were studied at 500°C and those of molten Cd–Pb alloys at 300 to 400°C; the correlation factors, expressing the effects of the cataphoretic drag exerted on individual moving particles by the surrounding liquid atoms were determined in each case. By analyzing the experimental results, empirical equations relating the correlation factors of the binary systems to the viscosity of the corresponding melts were derived. From the physical point of view, the results indicated very substantial drag effects in both systems, i.e., a large number of atoms took part in every diffusion reaction. (Metals Abstr.)

**55450** NATURE OF THE EMBRITTLEMENT OF TWO-PHASE TITANIUM ALLOYS WITH COARSE LAMELLAR STRUCTURE. Pertsovskii, N. Z.; Brun, M. Ya.; Shakhanova, G. V. Fiz. Metal. Metalloved.; 30: No. 5, 1047-54(Nov 1970). (In Russian).

The nature of the mechanisms giving rise to brittleness in two-phase Ti alloys with coarse lamellar structure was studied by analyzing the microstructural characteristics of the deformation and rupture of a typical ($\alpha + \beta$) Ti–Al–Mo alloy (Al 6, Mo 2%) with various types of original structure. The main cause of the low ductility of coarse-lamellar alloys (contrasting with that of fine-grained and equiaxed samples of similar constitution) lay in their slip characteristics, which were conditioned by the "inheritance" of structure from the high-temperature $\beta$-phase. (Metals Abstr.)

**55451** FIELD-ION-MICROSCOPE STUDY OF TUNGSTEN DEFORMED BY AN ELECTROSTATIC FIELD AT 900 TO 1700°K. Afanas'ev, V. I.; Garber, R. I.; Dranova, Zh. I.; Mikhailovskii, I. M. (Kiev State Univ. Physical-Technical Inst., Moscow). Fiz. Metal. Metalloved.; 30: No. 5, 1070-1(Nov 1970). (In Russian).

The nature of the plastic deformation suffered by W microcrystals on being subjected to strong electrostatic fields at 900 to 1700°K was studied by analyzing field-ion-microscope photographs. The results showed that the stresses required to initiate plastic yield (flow) at the temperature in question were more than an order of magnitude lower than those initiating yield at liquid-N temperature, the latter being close to the theoretical tensile strength of the material. The difference was attributed to the thermal activation of surface dislocations. (Metals Abstr.)

**55452** MUTUAL DIFFUSION OF RUTHENIUM WITH NIOBIUM AND ZIRCONIUM. Ronami, G. N.; Gryzunov, V. I. (Moscow State Univ.). Fiz. Metal. Metalloved.; 30: No. 5, 1110-13(Nov 1970). (In Russian).

Mutual diffusion effects taking place between contiguous plates of Ru and Nb, Ru and Zr, Ru and Zr–Ru, and Ru and Nb–Ru alloys were studied by x-ray microanalysis. In each case the diffusion coefficient varied sharply with composition. For example, in the case of mutual diffusion between Ru and Nb, the activation energy fell with increasing Ru content for Nb-base solid solutions; this tendency was reversed in the case of Ru-base solid solutions. Similar though less marked effects occurred in the Zr–Ru system. (Metals Abstr.)

**55453** INFLUENCE OF ADDITIONS OF TRANSITION METALS ON THE SINTERING BEHAVIOUR OF TUNGSTEN. Samsonov, G. V.; Jakovlev, V. I. (Institut fuer Materialforschung, Kiev). Z. Metallk.; 62: No. 8, 621-6(Aug 1971). (In German).

The effects of additions of transition metals (Ti, Hf, Nb, Ta, Cr, Re, Fe, Co, Ni, Ru, Rh, Pd, Os, Ir, Pt) in concentrations of 0.005 to 1.0 wt % on the sintering behavior of tungsten in the temperature range between 1000 and 2000°C and on its properties were studied. The effects of transition metal additions on the sintering behavior of tungsten may be explained with an electron exchange between the alloy components. With an increase of the stable d-bonds in the system the free energy is lowered. The sintering process is activated. (auth)

**55454** ARC EROSION OF VARIOUS SINTERED AND INFILTRATED WCu-MATERIALS IN OIL AT HIGH CURRENTS. Haufe, Wolfgang; Reichel, Werner; Schreiner, Horst (Seimens AG, Erlangen, Ger. Technische Univ., Munich). Z. Metallk. ; 62: No. 8, 592-5(Aug 1971). (In German).

A testing apparatus for measuring arc-erosion in oil is described. The magnitude of the damped periodical discharging current is 90 kA at 3 kHz. Values of erosion for Cu, W, and Cu-infiltrated W-materials of various proportions are given. (auth)

**55455** THERMALLY ACTIVATED DEFORMATION MECHANISM IN MOLYBDENUM AND IN HIGH-TEMPERATURE MOLYBDENUM ALLOYS. Pink, Erwin (Oxford Univ.). Z. Metallk.; 62: No. 8, 616-21(Aug 1971). (In German).

The athermal component of the flow stress is different for molybdenum and its alloys Mo–0.5 wt % Ti, Mo–TZM, Mo–2 vol % $Al_2O_3$ and Mo–vol % MgO. A similar behavior, however, was observed for the temperature dependence of the effective stress. This together with comparable activation parameters suggests that the same deformation mechanism (probably initiated by dispersed particles) is operative in pure molybdenum as well as in the alloys between 100 and 600°C. (auth)

XUM

**55456** SOME OBSERVATIONS ON THE SUPERPLASTIC PROPERTIES OF A BISMUTH–INDIUM EUTECTIC ALLOY. Dasarathy, Cuppam (British Steel Corp., Port Talbot, Eng.). Z. Metallk.; 62: No. 8, 612-13(Aug 1971).

A Bi–In alloy of eutectic composition behaved superplastically when the as-cast alloy was initially rolled by ~85% at 20°C prior to tensile testing at 20°C, using slow crosshead speeds. (auth)

**55457** SOLID SOLUTION HARDENING IN TANTALUM ALLOYS. Braithwaite, Anthony A.; Mordike, Barry L.; Rogausch, Klaus-Dieter (Univ. of Liverpool). Z. Metallk.; 62: No. 8, 596-600(Aug 1971). (In German).

Solid-solution hardening was studied on single crystals of TaRe, TaW, TaMo, TaNb, TaHf, and TaRu over the temperature range 77 to 2000°K. At low temperatures alloying caused scavenging of interstitial impurities and modified the inherent lattice mechanism. In the plateau range solid-solution hardening is discussed in terms of elastic misfit parameters–atomic size misfit $\epsilon_b$ and the modulus defect $\epsilon_G$. The interaction is well described by the Labusch relationship. (auth)

**55458** DELAYED ELASTICITY RESULTING FROM PERIODIC STRESS-INDUCED ATOMIC DIFFUSION. Doremus, R. H. (General Electric Research and Development Center, Schenectady, N. Y.). J. Phys. Chem. Solids; 32: No. 9, 2211-15(Sep 1971).

The internal friction resulting from bulk redistribution of atoms in a periodic stress gradient is derived. The calculated internal friction peak agrees well with data on hydrogen in vanadium and niobium and deuterium in vanadium. The resulting diffusion parameters are different from these calculated previously with the assumption of a single relaxation time. (auth) (UK)

**55459** DEFORMATION DYNAMICS OF A B.C.C. TITANIUM ALLOY (15.2 AT.% Mo) BELOW 650°K (~0.4 $T_m$). Zeyfang, R.; Conrad, H. (Univ. of Kentucky, Lexington). Acta Met.; 19: No. 10, 985-90(Oct 1971).

The effects of temperature and strain rate on the flow stress of a bcc Ti–15.2 at.% Mo alloy with 0.5 at.% $O_{eq}$ interstitial solute content were investigated over the range of 77 to 824°K. Employing thermal activation analysis, the values of the activation parameters were: $H_0 \simeq 0.2\ \mu b^3$ and $v^*_{T_0} = 27\ b^3$. These values of $H_0$ and $v^*_{T_0}$ are in accord with those for unalloyed cph titanium of the same interstitial content. Also agreement was obtained for the force–distance curve and for the effects of interstitial content on $\tau^*_0$ (the effective stress at 0°K) and $v^*_{T_0}$. It is therefore concluded that the rate controlling mechanism in the bcc alloy is similar to that of unalloyed cph titanium, namely thermally activated overcoming of interstitial solute atoms. The increase in strength of titanium due to the molybdenum substitutional solute atoms is principally through the athermal component of the flow stress. (auth)

**55460** MECHANISMS OF GROWTH AND LOSS OF COHERENCY OF HfN PARTICLES IN MOLYBDENUM. Mitchell, J. B. (Univ. of California, Livermore). Acta Met.; 19: No. 10, 1063-77(Oct 1971).

Internal nitriding of a Mo–1 at.% solid-solution alloy produces a homogeneous dispersion of coherent plate-like HfN precipitates oriented on {001} planes of the Mo matrix. During nitriding, growth of HfN particles occurs principally at the advancing nitriding front by Ostwald ripening, which produces an increase in average particle size with increasing depth below the external surface. The high nitrogen activity in the alloy behind the nitriding front effectively inhibits dissociation and growth of the precipitates. The plate-like HfN particles grow in diameter in a coherent manner. Thickening of the particles occurs by the nucleation and growth of coherent ledges on the planar surfaces. This thickening process produces an increase in the coherency strain which is relaxed by the formation of intrinsic dislocation loops within the particles by the coalescence of vacancies. The large HfN particles developed by this growth mechanism retain substantial coherency strain. A severe particle-coarsening mechanism is operative at high temperatures in regions of the nitrided alloy containing a high density of small fully coherent precipitates. The coarsening occurs by the migration of grain boundaries which sweep up the small fully coherent precipitates, the components of which then feed large semicoherent particles growing behind the boundary. (auth)

**55461** DETERMINATION OF THE DIFFUSION PARAMETERS OF INTERSTITIAL ATOMS IN YTTRIUM BY REFERENCE TO THE DISLOCATION IMPURITY PEAKS OF INTERNAL FRICTION. Borisov, E. V.; Vedenyapin, G. A.; Smirnov, L. V.; Suganeev, Yu. S. Fiz. Khim. Obrab. Mater.; No. 1, 75-80(Jan-Feb 1971). (In Russian).

The relaxation spectrum of the internal friction of Y samples containing interstitial impurities of O, N, C, and other elements was measured at 20 to 300°C, and the results were interpreted in terms of the diffusion parameters of the impurity atoms and the interaction of the latter with dislocations, as revealed by the form of the impurity peaks in the internal-friction characteristic. The diffusion equations were as follows: $D_O = 1.14 \times 10^{-2} \exp [-21{,}500/RT]$, $D_N = 9 \times 10^{-2} \exp [-25{,}400/RT]$, $D_C = 1.8 \times 10^{-2} \exp [-28{,}000/RT]$. (Metals Abstr.)

**55462** DEVELOPMENT OF MICROPORES IN ALLOYS. Lyuttsau, V. G.; Belousov, N. N.; Rovinskii, B. M. Fiz. Khim. Obrab. Mater.; No. 1, 81-4(Jan-Feb 1971). (In Russian).

The microporosity of Al alloys containing Mg, Be, Ti, and Zr was studied by x-ray shadow microscopy. The size and shape of the micropores were sensitive to the conditions of crystallization (solidification) and heat treatment. Any increase in the cooling rate during solidification reduced the size and increased the concentration of the micropores. The pores tended to form in those places in which a second phase subsequently developed when the alloys were subjected to rapid heating and quenching. The mechanisms responsible for these effects are discussed. (Metals Abstr.)

**55463** ABSORPTION OF OXYGEN AND NITROGEN BY ZIRCONIUM AT LOW PRESSURES. Ryabchikov, L. N.; V'yugov, P. N. (Physical-Technical Inst., Kazan). Fiz. Khim. Obrab. Mater.; No. 1, 85-9(Jan-Feb 1971). (In Russian).

The interaction of Zr with O and N at pressures of $10^{-6}$ to $10^{-4}$ torr was studied at 900 to 1600°C. The absorption velocity constants varied from 5,000 to 10,000 cm/sec for O and from 150 to 1200 cm/sec for N over this range. The accommodation coefficients were respectively 0.47 to 0.94 and 0.013 to 0.1. The O absorption characteristic had an effective activation energy of 17 kJ/mole, suggesting that the limiting stage in the oxidation of Zr at low pressure was the formation of O ions on the surface. (Metals Abstr.)

**55464** SOLUBILITY AND SOLID-PHASE INTERACTION OF THE CARBIDES OF TRANSITION METALS WITH NICKEL AND COPPER. Samsonov, G. V.; Boiko, P. A.; Motyazhev, V. I.; Bondarenko, V. P.; Sleptsov, V. M. Fiz. Khim. Obrab. Mater.; No. 1, 112-19(Jan-Feb 1971). (In Russian).

The solubility characteristics and solid-state interaction of the carbides of transition metals of groups IV to VI (Ta, Nb, Zr, Hf, etc.) with Ni and Cu were studied up to 1250 and 1000°C, respectively. The solid-state interactions and solubilities increased on passing from the carbides of Group IV metals to the carbides of Group VI metals in the case of Ni; in the case of Cu there was very little interaction. These results were in accordance with the electron structures (stable electron configurations) of the corresponding elements. (Metals Abstr.)

**55465** X-RAY DIFFRACTION STUDY OF THE PHASE COMPOSITION OF ALUNDUM-SURFACED [TUNGSTEN–RHENIUM] ALLOYS VR-20 AND VA-3 AFTER VACUUM ANNEALING AT HIGH TEMPERATURES. Ivanova, R. S.; Ignatov, D. V.; Vinogradov, D. P. Fiz. Khim. Obrab. Mater.; No. 1, 127-31(Jan-Feb 1971). (In Russian).

The phase composition of alundum-surfaced W–Re alloys VR-20 and VA-3 annealed under vacuum ($10^{-2}$–$10^{-7}$ torr) at 1500 to 1900°C was studied by x-ray diffraction and compared with that of the same alloys in the absence of alundum. Annealing in a vacuum of $10^{-2}$–$10^{-3}$ torr led to the creation of a surface layer enriched with Re on the uncoated VR-20 alloy; the layer consisted of the $\sigma$ phase, and sometimes also the $\chi$ phase, of the W–Re system. In the case of the alundum-coated alloys, this effect rarely occurred. No such effect occurred in the case of VA-3 at all. The reasons for these differences are considered. (Metals Abstr.)

**55466** EFFECT OF CHANGES IN STRUCTURE ON MECHANICAL PROPERTIES OF STEEL FOR PRESSURE VESSELS OF NUCLEAR REACTORS. Bohusova, O. (Vitkovice Steel, Ostrava, Czech.). Strojirenstvi; 20: No. 12, 725-30(Dec 1970). (In Czech).

Results of studies are presented on the effects of heat treatment and multiple annealing on the structure and mechanical properties of a low-alloy, weldable steel. The steel contained 0.15% of C, 1.03% of Mn, 0.23% of Si, 0.89% of Ni, 0.35% of Cr, 0.35% of Mo, and 0.13% of Nb + Ta. Cooling from the austenitizing temperature of 880°C at a rate of 75 to 108°C/min, followed by tempering at 650°C, resulted in a fine-grain, predominantly bainitic structure and good mechanical properties (yield point exceeding 50 kg/mm², transition temperature of –14°C for 50% of brittle fracture). With a decreased cooling rate the structure changed to a mixture of ferrite and pearlite, and the mechanical properties were impaired. For subsequent multiple annealing, needed to relieve the stresses resulting from further treatment, a temperature of 620°C should be used, since temperatures exceeding 650°C bring about carbide

XUM

coagulation, grain growth, and impairment of mechanical properties. For the presumed operating temperature of the vessel of 250°C, the yield point was 42.9 kg/mm² after five-fold annealing at 620°C and the transition temperature was +6°C. (NSA of Czech)

**55467** PROPERTIES OF POWDERS PRODUCED BY PLASMA SPRAYING. Krasnov, A. N. (Inst. of Materials Science, Kiev). Sov. Powder Met. Metal Ceram. (Engl. Transl.); 10: No. 3, 173-6 (Mar 1971).

Translated from Porosh. Met., Akad. Nauk Ukr. SSR; 10: No. 3, 4-8(Mar 1971).

A determination was made of the technological properties of plasma-sprayed spherical W, Mo, Nb, and Cu powders. The properties determined were particle shape and surface condition, particle size distribution, density, structure, microhardness, and flowability. (D.L.C.)

**55468** THERMAL EXPANSION OF TUNGSTEN–COPPER PSEUDOALLOYS CONTAINING UP TO 25 TO 30 VOL. PERCENT COPPER. Ermolaev, B. I. Sov. Powder Met. Metal Ceram. (Engl. Transl.); 10: No. 3, 207-11(Mar 1971).

Translated from Porosh. Met., Akad. Nauk Ukr. SSR; 10: No. 3, 45-50(Mar 1971).

The thermal expansion up to 1500°C of W–Cu pseudo alloys prepared by infiltration of a porous W matrix was studied theoretically and experimentally. The law of additivity does not hold owing to the elastic deformation of the tungsten matrix (for matrix densities above 13 to 14 g/cm³), and the heating and cooling curves do not coincide. (D.L.C.)

**55469** LAWS GOVERNING THE SPREADING OF METALLIC MELTS OVER THE SURFACE OF BORON NITRIDE. ELEMENTS ADHESION-ACTIVE TOWARDS BORON NITRIDE. Naidich, Yu. V.; Kolesnichenko, G. A.; Drui, M. S.; Fel'dgun, L. I.; Chistyakov, E. M. Fiz. Khim. Obrab. Mater.; No. 1, 51-4(Jan-Feb 1971). (In Russian).

The contact behavior of molten Al, Si, B, and also Ti and Cr in alloys with surface-inactive metals (e.g., Ti–Sn), with respect to the surface of cubic and hexagonal BN was studied by the sessile-drop method. The Al wetted the surface of both types of BN intensely; the Si wetted the BN less intensely (having a lower chemical affinity for N). The B failed to wet the surface at all. The Ti and Cr spread rapidly over the surface of both types of BN. The interactions in question are discussed from the point of view of the stable electron configurations and chemical bonds of the corresponding compounds (e.g., CrB and NiB). (Metals Abstr.)

**55470** PROPERTIES OF WELDED JOINTS IN V92Ts ALLOY AFTER PROLONGED HEATING AT 70°C. Pospelov, K. S.; Chernyak, A. Ya.; Sverdlin, A. V. Metal Sci. Heat Treat. (USSR) (Engl. Transl.); No. 11-12, 930-4(Nov-Dec 1970).

Translated from Metalloved. Term. Obrab. Metal.; No. 11, 35-8; 43-4(Nov 1970).

The effects of heating at 1000 to 3000 hr on welded joints of Al–Zr–Mg alloys were studied. Data on property changes, toughness, strength, crack susceptibility, corrosion resistance, and delayed fracture are presented. (J.R.D.)

**55471** PROPERTIES OF Ti–V AND Ti–V–Al ALLOYS WITH OXYGEN. Maksimov, Yu. A.; Kornilov, I. I.; Vavilova, V. V. (Inst. of Metallurgy, Moscow). Metal Sci. Heat Treat. (USSR) (Engl. Transl.); No. 11-12, 922-4(Nov-Dec 1970).

Translated from Metalloved. Term. Obrab. Metal.; No. 11, 28-30(Nov 1970).

Results of investigations of the effects of oxygen on these alloys are presented which show that alloying with 0.2 to 0.35 wt % O increases the strength of Ti–V and Ti–V–Al alloys. The strengthening effect of oxygen is retained at elevated temperatures. The ductility of the alloys is satisfactory and changes little in impact tests at low temperature. The mechanical properties at room, elevated, and low temperatures are optimal for Ti–V–O and Ti–V–Al–O alloys with 0.3 to 0.35 wt % O (2.5% V and 3% Al). (J.R.D.)

**55472** CHANGE IN ELECTRICAL RESISTIVITY WITH DECOMPOSITION OF THE SUPERSATURATED SOLID SOLUTION IN ALLOY K30M18GSN. Nerodenko, M. M.; Nerodenko, L. M. (Inst. of Electric Welding, Kiev). Metal Sci. Heat Treat. (USSR) (Engl. Transl.); No. 11-12, 1039-40(Nov-Dec 1970).

Translated from Metalloved. Term. Obrab. Metal.; No. 12, 46-7(Dec 1970).

Components of the alloy are Fe, Co, and Mo. Results of the investigation showed that the anomalous change of the electrical resistivity during decomposition of the supersaturated solid solution in alloy K30M18GSN is due to structural changes such as the formation of precipitates of excess phase, impoverishment of the solid solution in alloying elements, the formation of coherent and stable particles of excess phase, and thermal vibration of atoms in the crystal lattice of the matrix. (J.R.D.)

**55473** EQUATIONS CORRELATING THE INFLAMMABILITY CHARACTERISTICS OF METAL POWDERS. Ioffe, V. G. (Moscow Inst. of Steel and Alloys). Sov. Powder Met. Metal Ceram. (Engl. Transl.); 10: No. 3, 252-3(Mar 1971).

Translated from Porosh. Met., Akad. Nauk Ukr. SSR; 10: No. 3, 103-5(Mar 1971).

The relation between L, the lower limiting inflammability concentration of the powder in air, and T, the inflammability temperature of a layer of the powder, was studied for the following alloys: Ti–Al, Ti–Mn, Zr–Si, Zr–Ti, and hydrided Zr–Ti. The relation between L and T is approximately linear, and the correlation equations are given. The plot for Zr–Si has an inflection at a point corresponding to $Zr_6Si_5$. (D.L.C.)

**55474** PLASTICITY AND STRENGTH OF NICKEL–MOLYBDENUM ALLOYS AT HIGH TEMPERATURE. Tikhonov, A. A.; Grigorovich, V. K.; Bulat, S. I. (Inst. of Metallurgy, Moscow). Metal Sci. Heat Treat. (USSR) (Engl. Transl.); No. 11-12, 968-9(Nov-Dec 1970).

Translated from Metalloved. Term. Obrab. Metal.; No. 11, 68-9(Nov 1970).

Properties of hot worked Ni–Mo alloys were investigated. The alloys contained from 1.96 to 47.25% Mo and other elements except Ni in trace quantities. Discussions and information are included on mechanical properties, phase transitions, plasticity, and microstructure. (J.R.D.)

**55475** SOLUBILITY OF NITROGEN IN ALPHA VANADIUM FROM 600° TO 1200°C. Henry, J. L.; O'Hare, S. A.; McCune, R. A.; Krug, M. P. (Bureau of Mines, Albany, Oreg.). J. Less-Common Metals; 25: No. 1, 39-47(Sep 1971).

Alloy specimens in the V-rich region of the V–N system were prepared by the reaction of high-purity V foil and $N_2$. Specimens were annealed, quenched, and examined by x-ray and metallographic techniques to determine the degree of N solubility in $\alpha$ V. Solubility was determined as a function of temperature at equilibrium pressure. Equilibrium pressures were not measured. Nitrogen solubility was found to be 1.15 wt % at 600°C, 1.65 wt % at 800°C, 2.20 wt % at 1000°C, and 2.95 wt % at 1200°C. A sluggish transformation was observed between 500° and 600°C for alloys having N contents above 1 wt %. It is likely that a peritectoid compound having a composition near $V_{13}N$ was formed. The composition range of the hexagonal $\beta$ phase could not be established accurately because of the small difference in lattice dimensions between the V-saturated and N-saturated compound. The range is narrow, probably lying between $VN_{0.32}$ and $VN_{0.36}$ and does not appear to vary within the temperature range 300° to 1000°C. (auth)

**55476** EFFECT OF STRESS ON MICROSEGREGATION OF HYDROGEN AT ELEVATED TEMPERATURES IN TITANIUM AND Ti–8Al–1Mo–1V. MacKay, T. L. (Douglas Aircraft Co., Long Beach, Calif.). Met. Trans.; 2: No. 8, 2299-2302(Aug 1971).

The distribution of H under a varying stress field in high-purity Ti and in an $\alpha$–$\beta$ Ti alloy, Ti–8Al–1Mo–1V, was studied in the temperature range of 450 to 600°F by an electron microautoradiography technique. A tritium tracer was used to show the distribution of the contained H. Large precipitates were noted in pure Ti stressed in the temperature range of 450 to 600°F with the H solubility considerably below the solubility limit. In the alloy, a high concentration of H was observed at the $\alpha$–$\beta$ phase boundary interfaces at all stress levels. Electron microautoradiographs are shown for variously stressed samples of metals and alloys, and the results are discussed in some detail. (B.L.M.)

**55477** BASIC PROPERTIES OF THIN-FILM DIFFUSION-BRAZED JOINTS IN Ti–6Al–4V. Freedman, Allan H. (Northrop Copr., Hawthorne, Calif.). Weld. J. (N. Y.); 50: No. 8, 343s-56s(Aug 1971).

Some of the basic metallurgical and mechanical properties of Ti–6Al–4V joints produced by thin-film diffusion-brazing with Cu were studied. Critical properties, which were determined, included tensile, fatigue, fracture toughness, stress corrosion, and corrosion-fatigue behavior of butt joints, shear strength of lap joints, and comparative properties of Ti–6Al–4V base metal. In addition, fracture modes of joints and base metal were determined from specimens exposed to tensile overload, fatigue, stress corrosion, and corrosion fatigue. The results of this study indicate that most of the properties of thin-film diffusion-brazed joints equal or exceed base metal properties. One property, plane-strain fracture toughness ($K_{IC}$), is lower for joints but the threshold stress-intensity factor for stress corrosion ($K_{ISCC}$) is somewhat higher for joints than for base metal. In addition, the

XUM

thin-film diffusion-brazing process offers much better versatility and substantial manufacturing advantages over solid-state diffusion bonding. Thus, the process offers very attractive potential for producing high-integrity joints under reasonable manufacturing conditions, and it should find wide use for joining Ti-alloy structures. (auth)

**55478** LOW-TEMPERATURE DEFORMATION AND FRACTURE OF IRON AND IRON–VANADIUM ALLOYS. Jellison, James Lee. Troy, N. Y.; Rensselaer Polytechnic Inst. (1971). 184p. University Microfilms Order No. 71-17,143.

Thesis.

The dependence of the mechanical properties of ferrite on temperature, solute content (vanadium), microstructure, and interstitial distribution was investigated. Slip character was evaluated by means of slip trace observation and transmission electron microscopy. The ductile-to-brittle transition (DBTT) of the iron-vanadium alloys, resulted from a change from wavy to planar glide at low temperatures, which is attributed to restricted cross slip. Vanadium also was observed to promote planar glide at higher concentrations and consequently raises the DBTT. A tensile cryostat was constructed to permit tests in the −269 (liquid helium) to −196°C (liquid nitrogen) range, since the DBTT of high-purity ferrite was known to be below −196°C. This investigation confirmed the importance of substitutional-interstitial solute interactions on strength and ductility. The mechanical properties of unalloyed iron were found to be markedly dependent on interstitial distribution, as influenced by heat-treatment, whereas identical heat-treatments had little or no influence on the Fe−V alloys. Highly stable vanadium carbides and nitrides are formed in the binary alloys; this prevents the interstitials from participating in low-temperature aging phenomena. The scavenging action of vanadium also resulted in alloy softening with additions of 1 or 5 at. % V. As demonstrated by earlier investigations, the aging phenomenon in unalloyed iron is related to the growth of coherent metastable carbide and nitride precipitates or their replacement by stable incoherent compounds at long times or high temperatures (above $\mu$ 200°C). It is postulated that small coherent interstitial precipitates embrittle ferrite as a consequence of a particle shearing mechanism which gives rise to large slip steps. The ductility of unalloyed iron at −196°C was observed to improve linearly with the cube root of time, $t^{\frac{1}{3}}$, upon aging at 100°C; this suggests a relation between ductility and the growth rate of spherical particles. As particles become larger, it is believed that particle shearing is replaced as a deformation mechanism by dislocation bowing, which does not lead to stress concentrations. Also, the low temperature ductility of unalloyed iron was markedly improved by furnace cooling rather than quenching from the annealing temperature (750°C). Aging of unalloyed iron containing 70 ppM carbon at 100°C caused precipitation hardening, as determined by room temperature tensile tests, with the peak strength occurring after about one week. (Diss. Abstr. Int., B)

**55479** THERMOMIGRATION OF CARBON IN METALS. Shaw, J. G.; Oates, W. A. (Univ. of Newcastle, New South Wales, Australia). Met. Trans.; 2: No. 8, 2127-34(Aug 1971).

An investigation of thermomigration in interstitial solid solutions of carbon in $\beta$−Ti, V, $\alpha$−Fe, Co, Ni, and Pd was carried out using a radioactive tracer technique. A substantial solute redistribution occurred towards the hotter regions in $\alpha$−Fe and V and towards the colder regions in Pd while for Co, Ni and $\beta$−Ti very little segregation was observed. The measured heats of transport were (in kcal per g-atom): $\alpha$−Fe, −14.1 ± 1.5; V, −4.9 ± 1.0; Pd, +8.4 ± 1.5; Co, +1.5 ± 1.5; Ni, −1.6 ± 1.4; $\beta$− Ti, −1.0 ± 1.0. An examination of the results obtained together with all of the published data for interstitial solute thermomigration suggests that electronic effects could be of major importance in determining the redistributions observed. (auth)

**55480** EFFECTS OF ATOMIZATION MEDIA AND CONSOLIDATION TECHNIQUES UPON PHYSICAL PROPERTIES OF A P/M COBALT-BASE ALLOY. Brandstedt, Sven B. pp 487-500 of Modern Developments in Powder Metallurgy. Vol. 4. /Hausner, Henry H. (ed.). New York; Plenum Publishing Corp. (1971).

From International powder metallurgy conference; New York, N. Y. (12 Jul 1970).

Water-atomization produced a powder with larger specific surface and higher oxygen content than gas-atomization, resulting in porosity and/or oxide-inclusions in the billet. The oxygen was mainly present as surface oxides on the powder particles. Physical properties were below those of cast material. Gas-atomization followed by coldstream processing yielded a powder with oxygen levels of 200 to 300 ppM in the 200 mesh size range. Argon as an atomization medium produced a powder with significantly lower nitrogen content than nitrogen atomization. This powder can be pressed at 40 tsi and sintered at 2300°F in hydrogen to a density of 96 percent with tensile strength of 118.000 psi. This is 10 to 15 percent higher than cast material. Canning and hot-extrusion of low oxygen containing powder produced 100 percent dense billets with satisfactory tensile strength and high ductility. It is believed that cold pressing and sintering as well as hot forging and extrusion of powders in the stellite family will expand the use of such alloy powders into areas other than castings, such as forgings, barstock, and rod as well as other applications that require freedom from alloy segregation. (auth)

**55481** MODERN DEVELOPMENTS IN POWDER METALLURGY. VOLUME 5. MATERIALS AND PROPERTIES. Proceedings of the 1970 International Powder Metallurgy Conference, Held in New York, July 12–16, 1970. Hausner, Henry H. (ed.). New York; Plenum Publishing Corporation (1971). 501p. $29.50. (CONF-700709-(Vol.5)).

Thirty-three articles are included; a separate abstract was prepared for each of 18. The remaining 15 papers contain information on: sintering of Al P/M parts; manufacture of Inconel Alloy 718 compressor rotor blades from metal powder preforms; hardening with dispersion of small holes; dispersion-hardened copper-base materials; dispersion strengthened ferritic heat-resisting steel; porous stainless steel; fabrication of two-phase alloys in Ru−Au−Pd system; electron microscopy of commercial metal powders; corrosion resistance of sintered iron and bronze parts; compaction behavior of metal powders; presintering effects on iron powder compacts; sintered and heat treated 4640 steel; point density measurement and flaw detection in P/M green compacts; microstructure of 4640 steel; and production of maraging steel P/M parts. (P.C.H.)

*For abstracts of individual papers see: 55067, 55416–55420, 55482–55487, 55603, and 55628–55632.*

**55482** PROPERTIES OF HOT PRESSED TITANIUM ALLOY POWDERS FOR CRYOGENIC APPLICATIONS. Friedman, Gerald I.; Kazaroff, John M. (Lewis Research Center, Cleveland). Contract NAS 3-10301. pp 3-18 of Modern Developments in Powder Metallurgy. Vol. 5. /Hausner, Henry H. (ed.). New York; Plenum Publishing Corp. (1971).

From International powder metallurgy conference; New York, N. Y. (12 Jul 1970).

It was found that of five titanium powder-making processes investigated, only the Rotating Electrode Process (REP) was capable of producing ELI grade titanium alloy powder. The oxygen content of compacted bodies made from the REP Ti−6Al−4V and Ti−5Al−2.5 Sn powders was 1000 ppM or less. In comparison, the compacts made from powder produced by the hydride–dehydride process, the mechanical attriting of chips, fluid-energy (gas) mill attriting of chips, and chemical reduction, had oxygen contents ranging from 1600 to over 8000 ppM. All powders, except those made by chemical reduction, could be compacted to full density at a temperature/pressure combination of 1650°F and 75 ton/in.$^2$. The chemically reduced powder could not be compacted to over 96.6 percent density at 1850°F and 1000 ton/in.$^2$, the highest temperature/pressure combination investigated. The as-compacted powder samples possessed only limited ductility, with elongation values ranging from 0 to 7.5 percent. The REP powder samples developed over 10 percent elongation and 40 percent reduction in area after a four-hour anneal at 1775°F. Blocks hot-pressed from the spherical REP powders had tensile properties equivalent to or better than those obtained from wrought bar. In particular, the powder Ti−6Al−4V block specimens were stronger and more ductile than the wrought bar samples at all test temperatures, in both longitudinal and transverse directions. The powder Ti−5Al−2.5Sn samples showed this same superiority in the transverse direction only. Longitudinal powder specimens of this alloy were either weaker or less ductile than corresponding wrought samples. (auth)

**55483** ELEVATED TEMPERATURE MECHANICAL PROPERTIES OF A DISPERSION STRENGTHENED SUPERALLOY. Benjamin, J. S.; Cairns, R. L. (International Nickel Co., Inc., Sterling Forrest, N. Y.). pp 47-71 of Modern Developments in Powder Metallurgy. Vol. 5. /Hausner, Henry H. (ed.). New York; Plenum Publishing Corp. (1971).

From International powder metallurgy conference; New York, N. Y. (12 Jul 1970).

A new process called mechanical alloying has been used to produce composite superalloy powders containing an intimate dispersion of refractory oxide particles. Consolidated materials made from these powders exhibit dispersion strengthening and gamma prime precipitation hardening. High temperature creep and stress rupture properties of a nickel-base alloy containing 19.7% Cr, 2.3% Ti, 0.88% Al, 0.067% Zr, 0.007% B, 0.06% C, 1.12% $Al_2O_3$ by weight with 2.25 volume % yttria dispersoid are pre-

XUM

sented. Two hardening mechanisms each influenced the high temperature mechanical properties of this material in a complex interaction. At lower temperatures the rupture strength behavior was similar to that of ordinary nickel base superalloys, while at high temperatures it corresponded to the behavior found in dispersion strengthened nickel. The apparent activation energy for creep was found to be 153 kcal/mole over the temperature range 0.55 to 0.6 Tm and 202 kcals/mole between 0.65 to 0.8 Tm. These energies were compared with values obtained for a dispersion-free, wrought superalloy of similar composition (103 kcals/mole between 0.55 to 0.6 Tm) and stress relief annealed TD Nickel bar (133 kcals/mole between 0.7 to 0.75 Tm). Although creep of the dispersion-strengthened superalloy clearly showed two regimes of behavior, the activation energy found below 0.6 Tm was still considerably higher than that for conventional hardened superalloys. This difference was also evident from the slopes of stress rupture plots, which were flatter for the dispersion-strengthened superalloy than for conventional alloys. High stress exponents were obtained over both temperature ranges. (auth)

**55484** CORRELATION OF MECHANICAL PROPERTIES OF SINTERED U-700 POWDER WITH PARTICLE BOUNDARY MORPHOLOGY. Moyer, Kenneth H. pp 85-94 of Modern Developments in Powder Metallurgy. Vol. 5. /Hausner, Henry H. (ed.). New York; Plenum Publishing Corp. (1971).

From International powder metallurgy conference; New York, N. Y. (12 Jul 1970).

Studies on hydropressed U-700 (Udimet 700) compacts showed that they can be sintered at 2300°F to a density of 93% of theoretical. The temperature range for sintering is narrow. At 2280°F, 93% theoretical density cannot be obtained; at 2330°F, incipient melting begins. Mechanical properties and fracture studies suggest a weakened particle boundary condition. It is thought that a continuous platelike MC carbide is responsible for the weakened condition. Further fabrication studies should be made to distribute the carbides more favorably in the particle boundaries. (auth)

**55485** STABILITY OF OXIDE DISPERSIONS IN IRON- AND NICKEL-BASED ALLOYS. Fischmeister, H.; Navara, E. (Chalmers Univ. of Tech., Goteborg). pp 97-107 of Modern Developments in Powder Metallurgy. Vol. 5. /Hausner, Henry H. (ed.). New York; Plenum Publishing Corp. (1971).

From International powder metallurgy conference; New York, N. Y. (12 Jul 1970).

The results showed that the structural stability of alumina dispersions in metal matrices can be strongly affected by the addition of alloying elements, both in the positive and in the negative direction. This opens up interesting possibilities for the design of stable dispersion-hardened alloys, which are not limited to materials with alumina dispersions only. The observed effects can be accounted for in a qualitative manner by the change in oxide stability and phase boundary energy that must be expected from the interaction of the alloying element with the oxide. To proceed to a quantitative understanding of these phenomena, more exact data on the solubility products of pure and contaminated oxide phases in alloyed matrices would be required. (auth)

**55486** HIGH-TEMPERATURE STRENGTH OF OXIDE-STRENGTHENED NICKEL ALLOYS. Cheney, R. F.; Scheithauer, W. Jr. (Sylvania Electric Products Inc., Towanda, Pa.). pp 137-48 of Modern Developments in Powder Metallurgy. Vol. 5. /Hausner, Henry H. (ed.). New York; Plenum Publishing Corp. (1971).

From International powder metallurgy conference; New York, N. Y. (12 Jul 1970).

Dispersion-strengthened Ni−$2ThO_2$ and Ni−15Mo−$ThO_2$ alloys were prepared by P/M methods and conditions affecting their tensile strengths at 1093°C (2000°F) were evaluated. Small $ThO_2$ and strongly developed crystallographic textures were both necessary for good strengths at 1093°C. Ni−15Mo−$ThO_2$ alloys having volume fractions, f, of 0, 0.0003, 0.003, 0.03, and 0.10 were made and evaluated. The 0.2% yield strengths at 1093°C increased in proportion to $f^{\frac{1}{3}}$, but only for sheet with mean $ThO_2$ diameters of about 150 Å and strong textures. The yield strengths of sheets without textures and with mean $ThO_2$ of 400 to 500 Å showed little dependence on volume fraction. Ni−$2ThO_2$ sheet with about 200 Å $ThO_2$ had strong texture and good strength at 1093°C while sheet with about 400 Å $ThO_2$ had little texture and poor strength. The thermomechanical processing of the alloys greatly influenced their strengths because of the affects on texture, grain structure, and the spatial distribution of the $ThO_2$. (auth)

**55487** MATRIX HARDENING IN DISPERSION STRENGTHENED POWDER PRODUCTS. Hansen, Niels; Lilholt, Hans (Danish Atomic Energy Commission Research Establishment, Risoe). pp 339-65 of Modern Developments in Powder Metallurgy. Vol. 5. /Hausner, Henry H. (ed.). New York; Plenum Publishing Corp. (1971).

From International powder metallurgy conference; New York, N. Y. (12 Jul 1970).

Experimental data for various dispersion-hardened systems have been examined in order to investigate whether it is possible to add the stress contributions from three different strengthening processes. The effects of dispersed particles have been accounted for by the Orowan-expression $\sigma_p = 2\ (G \cdot b/\Lambda)$. The effects of grain boundaries have been described by the Petch-expression $\sigma_{gb} = kD^{-\frac{1}{2}}$. The contribution from solid solution is entered as the empirically found value. Considering the flow stress values (0.2% offset) it has been determined to what extent the various contributions can be added independently, i.e., whether, $\sigma = \sigma_0 + \sigma_p + \sigma_{gb} + \sigma_{sol}$ is valid when inserting the stress values expected if the individual strengthening agents had occurred alone in the matrix. Data have been obtained from the following systems: Al−$Al_2O_3$, Ni−$ThO_2$, Zr−$Y_2O_3$, and Fe-carbides. The upper limit for the amount of dispersed phase has been about 10 vol %. The grain sizes have been in the range from 0.3 $\mu$ to the order of 1 mm (i.e., extruded, cold worked, and recrystallized materials). Within some limitations the strength data at room temperature indicate that the contributions from the various strengthening agents can be added, i.e., that each mechanism acts independently of the others. At higher temperatures in the range 0.5 to 0.8 $T_m$, the three strengthening processes may all contribute to the tensile strength and to the creep strength, but the use of the simple additive rule was inconclusive. At temperatures above 0.8 $T_m$ dispersion hardening is predominant. (auth)

**55488** LATTICE AND GRAIN BOUNDARY DIFFUSION OF CERIUM AND NEODYMIUM IN NICKEL. Paul, A. R.; Agarwala, R. P. (Bhabha Atomic Research Centre, Trombay, India). Met. Trans.; 2: No. 9, 2691-5(Sep 1971).

Diffusion of cerium and neodymium in nickel has been studied by the serial sectioning technique using radioactive tracers $^{141}Ce$ and $^{147}Nd$, in the temperature ranges 700 to 1100°C for volume and 500 to 875°C for grain-boundary diffusion respectively. Volume diffusivities can be expressed as: $D_{Ce/Ni} = (0.66 \pm 0.18)\ \exp\ [-(60{,}800 \pm 810/RT)]\ cm^2$ sec, and $D_{Nd/Ni} = (0.44 \pm 0.13)\ \exp\ [-(59{,}820 \pm 830/RT)]\ cm^2$/sec and grain boundary diffusivities by: $Ds_{Ce/Ni} = 0.11\ \exp\ [-(29{,}550/RT)]\ cm^2$/sec, and $Ds_{Nd/Ni} = 0.07\ \exp\ [-(28{,}580/RT)]\ cm^2$/sec. Results of volume diffusion have been compared with those calculated from the theories of diffusion based on size and charge difference between the solute and the solvent atoms. Whipple and Suzuoka methods have been used to evaluate the grain-boundary diffusion coefficients. Both the methods give similar results. (auth)

**55489** DETERMINATION OF THERMODYNAMIC INTERACTION PARAMETERS IN SOLID V−Ti ALLOYS USING THE MASS SPECTROMETER. Rolinski, Edmund J.; Hoch, Michael; Oblinger, Charles J. (Univ. of Cincinnati). Met. Trans.; 2: No. 9, 2613-18(Sep 1971).

The Knudsen effusion method was combined with a mass spectrometer sensing technique in order to measure thermodynamic quantities of solid-solution alloys of V−Ti binary system. The technique makes use of the regular solution model in order to treat the vaporization data in terms of ion current ratios obtained from the mass spectrometer. Within the experimental temperature range of 1500 to 1725°C and the composition range of $0.10 < N_{Ti} < 0.90$, the activity of titanium in the bcc ($\beta$) phase relative to pure titanium for the binary alloy is: $RT \ln a_{Ti} = RT \ln N_{Ti} + N_V^2\ (1.82 \pm 0.13)$ kcal per g-atom while the activity of vanadium is: $RT \ln a_V = RT \ln N_V + N_{Ti}^2\ (1.82 \pm 0.13)$ kcal per g-atom. The experimental result on the pairwise interaction parameter agrees well with the theoretically calculated value. (auth)

**55490** STRENGTH INCREASE IN Ti 35 WT. PERCENT Nb THROUGH STEP-AGING. Mendiratta, M. G.; Luetjering, G.; Weissman, S. (Rutgers–The State Univ., New Brunswick, N. J.). Met. Trans.; 2: No. 9, 2599-2605(Sep 1971).

The room temperature tensile properties of precipitation-hardened Ti−Nb alloys (35, 41, and 45 wt % Nb) were correlated to the microstructure obtained by aging in the ($\alpha + \beta$) phase field. Balanced strength properties with a flow stress of 100 ksi and an elongation to fracture of 4% were obtained by means of step aging. The distribution and size of the particles formed by step aging controlled the dislocation−particle interaction. The large $\alpha$ particles precipitated by first aging at 550°C imparted increased ductility while the smaller metastable particles precipitated by subsequent reaging at 400°C conferred a substantial increase in flow stress. (auth)

XUM

**55491** CREEP BEHAVIOR OF ELECTRON-BEAM-MELTED RHENIUM. Witzke, Walter R.; Raffo, Peter L. (Lewis Research Center, Cleveland). Met. Trans.; 2: No. 9, 2533-9(Sep 1971).

Creep deformation in electron-beam-melted polycrystalline rhenium sheet was evaluated at 2200 to 4200°F and 4 to 40 ksi. Comparisons were made with powder metallurgy rhenium under similar conditions. Changes in creep-rupture behavior resulting from electron-beam melting of rhenium were greater ductility, higher primary creep rate, and longer rupture life, especially at lower temperatures. The activation energy for creep was 72 kcal per mole for electron-beam-melted rhenium and 64 kcal per mole for powder-metallurgy rhenium. (auth)

**55492** SUBSTRUCTURE STRENGTHENING IN DISPERSION-STRENGTHENED NICKEL ALLOYS. Clegg, M. A.; Lund, J. A. (Univ. of British Columbia, Vancouver). Met. Trans.; 2: No. 9, 2495-2507(Sep 1971).

Pure nickel, 80% Ni–20% Cr, 98% Ni–2% $ThO_2$, and 78% Ni–20% Cr–2% $ThO_2$ were studied in a wide range of thermomechanical conditions to identify strengthening mechanisms in the dispersion-strengthened materials. An x-ray line profile technique was used to determine the distribution of lattice strain, the crystalline domain size, and the incidence of twins and stacking faults. Transmission electron microscopy was carried out, and tensile tests were done at room temperature and at an elevated temperature. It was found that cold deformation of Ni–$ThO_2$ did not produce lattice strains as large as was the case with pure nickel and Ni–Cr. However, deformation of Ni–Cr–$ThO_2$ did generate high lattice strains, due it is thought to the influence of chromium on cross-slip. The materials containing high lattice strains recrystallized more readily on annealing or testing at high temperature. It was concluded that room-temperature strength was related to domain size without regard to composition in the series investigated. Strengthening by particle–dislocation interaction was not thought to be applicable when the domain size was small compared to the interparticle spacing, or at elevated temperatures. High-temperature strength was determined primarily by the presence of a polygonized dislocation substructure which was stabilized by the thoria dispersion. (auth)

**55493** MEASUREMENT OF THERMAL EXPANSION OF SOLIDS AT HIGH TEMPERATURES. Chekhovskoi, V. Ya.; Petukhov, V. A. (Inst. for High Temperatures, Moscow). pp 366-72 of Proceedings of the Fifth Symposium on Thermophysical Properties. /Bonilla, C. F. (ed.). New York; American Society of Mechanical Engineers (1970).

From fifth symposium on thermophysical properties; Boston, Mass. (Sep–Oct 1970). See CONF-700901

Disclosure is made of the method of measurement and the design of experimental equipment used for an accurate investigation of thermal expansion of solids at temperatures of up to 2,500°C. The sample is heated in a furnace employing a tungsten heater. Elongation of the sample is measured by a special device with an accuracy of up to 1 $\mu$. Submitted below are results of the measurements of thermal elongation of molybdenum. (auth)

**55494** MEASUREMENT OF HEAT CAPACITY OF TANTALUM IN THE RANGE 1900 TO 3000 K BY A PULSE-HEATING METHOD. Cezairliyan, A.; McClure, J. L.; Morse, M. S.; Beckett, C. W. (National Bureau of Standards, Washington, D. C.). pp 385-90 of Proceedings of the Fifth Symposium on Thermophysical Properties. /Bonilla, C. F. (ed.). New York; American Society of Mechanical Engineers (1970).

From 5th symposium on thermophysical properties; Boston, Mass. (Sep-Oct 1970). See CONF-700901.

A technique is described for the high-speed (millisecond resolution) measurement of heat capacity of electrical conductors at high temperatures (above 1900°K). Measurements on heat capacity of tantalum in the temperature range 1900 to 3000°K are reported and are compared with those in the literature. Duration of an individual experiment in which the specimen was heated from room temperature to near its melting point is less than one second. Temperature measurements were made with a high-speed photoelectric pyrometer. Experimental quantities (voltage, current, temperature) were recorded with a high-speed digital data acquisition system, which has a time resolution of 0.4 msec. Estimated inaccuracy of heat capacity measurements in the above temperature range is 2 to 3 percent. (auth)

**55495** SPECTRAL EMISSIVITY OF TANTALUM. Lat'ev, L. N.; Chekhovskoi, V. Ya.; Shestakov, E. N. (Inst. of High Temperatures, Moscow). pp 436-42 of Proceedings of the Fifth Symposium on Thermophysical Properties. /Bonilla, C. F. (ed.). New York; American Society of Mechanical Engineers (1970).

From fifth symposium on thermophysical properties; Boston, Mass. (Sep–Oct 1970). See CONF-700901.

The direct method of investigation is used whereby the normal spectral emissivity was determined as the ratio of the signals of the radiation detector, corresponding to the spectral radiant intensity of the surface of the sample, i.e., a tantalum tube, to the black body spectral radiant intensity at the same temperature. The sample was placed into a high-vacuum chamber (the vacuum was 3 to $5 \times 10^{-7}$ mm Hg). The spectral apparatus used was made of a monochromator spectropyrometric comparator (visible region of the spectrum) and an infrared spectrometer (infrared region of the spectrum). The temperature under investigation was rather accurately measured. The method of investigation and the measuring apparatus made it possible to obtain rather accurate and reliable experimental data for the spectral region from 0.4 to 4 $\mu$ and in the 1,200 to 2,400°K temperature range. A temperature dependence was found of the X-point of tantalum. The results obtained by the authors were compared with those obtained by other investigators. (auth)

**55496** THERMODYNAMIC PROPERTIES OF LIQUID MOLYBDENUM BY LEVITATION CALORIMETRY. Treverton, J. A.; Margrave, J. L. (Rice Univ., Houston, Tex.). pp 489-94 of Proceedings of the Fifth Symposium on Thermophysical Properties. /Bonilla, C. F. (ed.). New York; American Society of Mechanical Engineers (1970).

From fifth symposium on thermophysical properties; Boston, Mass. (Sep–Oct 1970). See CONF-700901.

A new technique which combines electromagnetic levitation heating with conventional drop calorimetry was used in studies on the thermodynamic properties of liquid molybdenum. Values for the heat of fusion and specific heat were obtained and from observation of the melting point a new value of the emissivity of the liquid metal was derived. The values obtained were: $\Delta H_m = 8320 \pm 75$ cal/g-atom, $Cp = 8.19 \pm 0.48$ cal/deg K g-atom ($2690 < T$ deg K $< 3112$), and Emissivity $= 0.328 \pm 0.003$. (auth)

**55497** PURE COBALT ALLOYS WITH ADDITIVES OF CARBON, TUNGSTEN, AND TITANIUM. Hoffmann, A. (Krupp Forschungsinstitut, Essen). Metall; 25: No. 5, 493-500(May 1971). (In German).

The mechanical properties of ternary alloys of Co with C and W and of quarternary alloys with C, W, and Ti were determined. The alloys were heat treated at 850°C before the texture and tensile studies were made. The phases occurring in the alloys were determined by microscopic and x-ray analysis. (tr-auth)

**55498** ESTIMATE OF DIFFUSION COEFFICIENTS OF $\alpha$-RADIOACTIVE ELEMENTS IN THIN LAYERS. Pavlinov, L. V. Fiz. Metal. Metalloved.; 30: No. 2, 367-72(Aug 1970). (In Russian).

A method of experimentally determining the diffusion coefficient of $\alpha$-radioactive elements in thin metallic films is described; the method is applicable, in particular, to the case in which diffusion takes place from an instantaneous source into a medium of finite dimensions. The method was used to study the diffusion of U through $\beta$-Zr. The activation energy of 27 kcal/mole and the pre-exponential factor of $8 \times 10^{-5}$ cm$^2$/sec agree closely with the values obtained for thick samples. (Metals Abstr.)

**55499** THERMAL EXPANSION OF ALLOYS Al–Mo, Al–Zr, OBTAINED AT HIGHER COOLING RATES. Varich, N. I.; Sheiko, T. I. Fiz. Metal. Metalloved.; 30: No. 2, 443-5(Aug 1970). (In Russian).

The thermal expansion of a number of Al–Mo and Al–Zr alloys obtained by cooling very rapidly from the melt ($10^6$°C/sec) and thus having nonequilibrium structures was studied. Pure Al nearly doubles its thermal expansion coefficient on raising the temperature from 0 to 500°C, the thermal expansion coefficient of Al–3 wt.% Mo hardly changes at all over this range. Samples containing Zr exhibit an intermediate behavior. The reasons for these effects are considered. (Metals Abstr.)

**55500** ALLOYING OF THE SUPERCONDUCTING COMPOUND VANADIUM GALLIDE WITH GROUP III–VIII ELEMENTS. Svechnikov, V. N.; Pan, V. M.; Spektor, A. Ts. Izv. Akad. Nauk SSSR, Metal.; No. 1, 195-9(Jan-Feb 1971). (In Russian).

The properties of the ternary alloys formed by adding elements of Groups III–VIII to the superconducting compound $V_3Ga$ were studied. In the case of a large number of such elements phases of the $\beta$-$V_3Ga$-type were formed; in a few cases solid solutions and mixtures of $\alpha$ and $\beta$ phases were observed. After heat-treatment at 800 to 1400°C, mixtures of phases were obtained in nearly all cases. The temperature of the $\beta \rightarrow \alpha$ phase transformation

increased substantially on alloying $V_3Ga$ with Sn, Mo, Pt, or W; on alloying with Al, Si, Ge, or In it fell. (Metals Abstr.)

**55501** STUDY OF PHASE EQUILIBRIA AND PROPERTIES OF THE ALLOYS IN THE TITANIUM–ALUMINUM–IRON AND TITANIUM–ALUMINUM–VANADIUM SYSTEMS. Volkova, M. A.; Kornilov, I. I. Izv. Akad. Nauk SSSR, Metal.; No. 1, 200-5(Jan-Feb 1971). (In Russian).

The phase diagrams of the Ti–Al–Fe and Ti–Al–V systems were studied by thermal, microstructural, and x-ray analyses, together with measurements of electrical resistance and microhardness. The mechanical properties were also studied at 20 to 800°C. Isothermal sections were plotted at 550 to 1100°C. The following actions took place in the Ti corners of the two systems: $\beta \rightarrow (\alpha + \beta)$, $\beta \rightarrow (\alpha_2 + \beta)$, $(\beta + \alpha_2) \rightarrow \alpha$ in Ti–Al–V; $\beta \rightarrow (\alpha + \beta)$, $\beta \rightarrow (\alpha_2 + \beta)$, $(\beta + \alpha_2) \rightarrow \alpha$, and $\beta \rightarrow (\alpha + \text{TiFe})$, $\beta \rightarrow (\alpha_2 + \text{TiFe})$, $(\beta + \alpha_2) \rightarrow (\alpha + \text{TiFe})$ in Ti–Al–Fe (four-phase peritectoid process). A phase equilibrium between the compounds TiAl and $V_5Al_8$ occurred in the Ti–Al–V system. (Metals Abstr.)

**55502** DISTRIBUTION COEFFICIENTS OF TITANIUM AND IRON IN ZIRCONIUM. Sumin, V. V.; Kornilov, I. I.; Peizulaev, Sh. I. Tsvetn. Metal.; No. 7, 50(Jul 1971). (In Russian).

The behavior of Ti and Fe impurities was experimentally studied during the electric arc zone melting of Zr. The distribution coefficients measured were: for Ti, K = 0.48, and for Fe, K = 0.29 in Zr. (tr-auth)

**55503** RELATION BETWEEN $K_{Ic}$ AND MICROSCOPIC STRENGTH FOR LOW ALLOY STEELS. Malkin, J. (CEN, Saclay, France); Tetelman, A. S. Eng. Fracture Mech.; 3: No. 2, 151-67(Aug 1971).

A simple model was developed to determine $K_{Ic}$ in terms of the microscopic cleavage strength $\sigma_f^*$ and the tensile yield strength $\sigma_Y$ for low-temperature cleavage fracture in A302B and A533 reactor-grade quenched and tempered steels. The model applies at sufficiently low temperatures or in irradiated steels where $\sigma_f^* \leq 3.4\ \sigma_Y$. It was determined that $\sigma_f^*$ is independent of temperature below –150°F and then increases with increasing temperature. At this time, it appears that $\sigma^*$ is independent of irradiation. At temperatures above that at which $\sigma_f^* \leq 3.4\ \sigma_Y$, unstable fracture initiates when a critical plastic strain $\epsilon_f$ is achieved near to the crack tip. The critical local plastic strain for unstable fracture also increases with increasing temperature. (auth)

**55504** THERMAL STABILITY OF POWDER MAGNESIUM SYSTEM USED IN NUCLEAR TECHNOLOGY. Sokol, L. (Inst. of Nuclear Research, Rez, Czech.). Pokroky Praskove Met. VUPM; No. 2-3, 3-15(1970). (In Czech).

Causes of the thermal instability of sintered magnesium were investigated. The instability results from a surface reaction between metallic magnesium and air during storage when unstable nonmetallic components are formed on the phase boundary. During hot extrusion only part of nonmetallic inclusions is decomposed and the remaining part induces changes in the specific mass of the bars undergoing treatment at elevated temperature. The results indicate that the nonmetal layer on the surface of magnesium particles is formed by $H_2O$ and $CO_2$ molecules bound more firmly than would correspond to mere adsorption. In magnesium powder stored under air an increase in nitrogen content was found. (NSA of Czech.)

**55505** EFFECT OF VACUUM ON THE DIFFUSION MOBILITY OF NICKEL IN MOLYBDENUM. Makhlin, N. A.; Ivanov, L. I. Izv. Akad. Nauk SSSR, Metal.; No. 1, 222-3(Jan-Feb 1971). (In Russian).

The effect of the degree of vacuum surrounding the system on the diffusion mobility of Ni in Mo single crystals was studied at 1350°C, using a radioisotope method ($^{63}Ni$). Very little difference was observed. The actual values were $2.4 \times 10^{-12}$ cm$^2$/sec at $10^{-5}$ torr and $3.2 \times 10^{-12}$ cm$^2$/sec at $10^{-1}$ torr. This result contradicted certain published data. (Metals Abstr.)

**55506** INTRACRYSTALLITE LIQUATION IN NICKEL ALLOYS CONTAINING NIOBIUM. Burova, N. N.; Maslenkov, S. B. Izv. Akad. Nauk SSSR, Metal.; No. 1, 91-3(Jan-Feb 1971). (In Russian).

The tendency of Nb to undergo liquation of the intracrystallite type in Ni–Cr–Nb alloys was studied. In all cases Nb exhibited a very sharp tendency towards liquation. The non-uniformity in the Nb distribution was intensified in the presence of Cr; increasing the Nb content of Ni–Cr alloys also led to a marked change in the Cr liquation characteristics. Alloying elements exhibiting liquation tendencies in Ni–Cr alloys may be placed in the following order of increasing liquation tendency: Al, Cr, Fe, Mo, W, Ti, Nb. (Metals Abstr.)

**55507** ELECTROPHYSICAL PROPERTIES OF NIOBIUM FILMS PRODUCED AND ANNEALED IN A VERY HIGH VACUUM. Osipov, K. A.; Orlov, A. F.; Ivanovskaya, G. F.; Kafanova, T. A. Izv. Akad. Nauk SSSR, Metal.; No. 1, 144-50(Jan-Feb 1971). (In Russian).

The effect of the conditions of production and subsequent annealing on the electrophysical characteristics of thin Nb films was studied with special reference to the part played by a very high vacuum. Samples produced and annealed in a very high vacuum ($10^{-8}$ torr) contained few gaseous impurities and had a reasonably perfect structure. Changes in vacuum conditions resulted in corresponding changes of impurity content and structural perfection, and this reflected on the electrical properties. High-temperature annealing tended to break up the thin films into individual, electrically-insulated granules. An optimum combination of annealing temperature and pressure improved the superconducting properties of the resultant material. (Metals Abstr.)

**55508** THERMODYNAMIC PROPERTIES OF THE LAVES PHASE $TaFe_2$. Rezukhina, T. N.; Kravchenko, L. I. Izv. Akad. Nauk SSSR, Metal.; No. 1, 164-9(Jan-Feb 1971). (In Russian).

The thermodynamic characteristics of the Laves phase $TaFe_2$ were determined by the emf method, using a solid electrolyte containing $ThO_2$ and CaO, and the results were correlated with those relating to the oxidation of Ta to form $Ta_2O_5$. The incremental enthalpy corresponding to the reaction $Ta + 2Fe = TaFe_2$ at 300°K was 14 kcal/mole, the Gibbs energy 15 kcal/mole, and the incremental entropy 3 cal/°C. On the Fe side the range of homogeneity of $TaFe_2$ was only slight. (Metals Abstr.)

**55509** DIFFUSION DATA. NUMBER 2, 1971. Woehlbier, F. H. Diffus. Data; 5: No. 2, 271-430(1971).

Diffusion data and information are presented on metals, alloys, semiconductors, oxides, halides, ice, carbides, nitrides, nitrites, phosphates, and silicides. (J.R.D.)

**55510** STRUCTURE PROPERTY RELATIONS IN BERYLLIUM SHEET. Cooke, F. W. (Franklin Inst., Philadelphia); Damiano, V. V.; London, G. J.; Conrad, H.; Banerjee, B. R. J. Mater.; 6: No. 2, 403-21(Jun 1971).

Large strength and ductility changes are observed in unalloyed beryllium sheet with little change in optically measured grain size. Preferred orientation alone seems insufficient as a sheet property determinant; for example, sheets with a more random basal texture do not necessarily exhibit greater bend ductility. These changes appear to correlate with electron transmission microscopic observations on subgrain size as a function of heat treatment; for instance, at a constant grain size, tripling the subgrain diameter more than triples the plastic strain in bending. For a constant subgrain size, the dislocation density within the cells seems to correlate with sheet strength and ductility. In alloy sheet studies the best ductility was obtained with an optimally recovered microstructure rather than a recrystallized one. The results indicate that substructure analysis and control, along with minor texture components, must be considered carefully in any systematic attempt to improve sheet properties in beryllium. (auth)

**55511** MECHANISM AND KINETICS OF BUBBLE FORMATION IN DOPED TUNGSTEN. Moon, D. M. (Westinghouse Research and Development Center, Pittsburgh); Koo, R. C. Met. Trans.; 2: No. 8, 2115-22(Aug 1971).

The mechanisms and kinetics of bubble formation that occur during annealing of W doped with small amounts of K, Al, and Si compounds were investigated by electron microscopy. Bubbles were present in the sintered ingot due to volatilization of the dope during the sintering treatment. As the ingot is worked into wire, the bubbles present in the ingot become elongated. On annealing these elongated bubbles undergo shape changes which depend on the amount of working. Elongated bubbles with a length-to-width ratio of less than ten spheroidized while those with a length-to-width ratio greater than twenty are unstable and break up into a row of bubbles. If working was sufficient to close up the elongated bubbles, e.g., in ribbon, 0.125 mm thick rolled from 0.9 mm dia wire, bubble formation results from the diffusion of vacancies to the volatile dopant particles. (auth)

**55512** EFFECT OF MECHANICAL CONSTRAINT ON THE FRACTURE CHARACTERISTICS OF THICK-SECTION STEEL. Loss, F. J. (Naval Research Lab., Washington, D. C.). Nucl. Eng. Des.; 17: No. 1, 16-31(1971).

Operating limits for commercial reactor pressure vessels are often selected to take advantage of the brittle-to-ductile fracture toughness transition which has been observed to evolve above the nil ductility transaction (NDT) temperature for thin section, low alloy steels. Linear elastic fracture mechanics (LEFM) data obtained with thin sections and extrapolated to project thick section

XUM

fracture behavior have raised concern that this transition to high ductility may be severely depressed or eliminated near reactor operating temperatures. Research programs at NRL emphasizing thick section dynamic tear (DT) studies and those at Westinghouse relating to thick section LEFM investigations have resolved this issue. These studies have shown that thick section steels of shelf toughness and strength class similar to A533-B continue to exhibit a significant toughness transition within a relatively narrow temperature interval above NDT. Size-effect studies with the DT test indicate that the mechanical constraint associated with a 12-in. thick section elevates the corresponding FTE temperature approximately 70°F (39°C) above that for thin sections. For the steels investigated the DT energy curve may be divided into three toughness regimes, ranging from frangible to ductile, which are shown to indicate similar transition features for specimens of ⅝ in. to 12 in. thickness. (auth)

**55513** CRACK ARREST TOUGHNESS OF PRESSURE VESSEL STEELS. Crosley, P. B.; Ripling, E. J. (Materials Research Lab., Inc., Glenwood, Ill.). Nucl. Eng. Des.; 17: No. 1, 32-45 (1971).

Contoured double cantilever beam specimens were used to measure the crack arrest toughness, $K_{Ia}$, of A533 grade A steel and A533 grade B class 1 steel (HSST plate 02). The measurements were made at temperatures ranging from −70°F to above 100°F. For tests above room temperature a temperature gradient was imposed on the specimen so the crack could be initiated at a low temperature and arrested at a higher one. The arrest toughness was found to be independent of the preceding initiation toughness. At low temperatures the initiation and arrest toughness values were nearly equal; at higher temperatures the arrest toughness was significantly lower than the initiation toughness. The rapid increase of toughness with temperature, as shown by $K_{Ic}$ above the nil ductility transition (NDT) transition temperature, is not exhibited by $K_{Ia}$ values, at least up to NDT + 100°F. (auth)

**55514** GROSS STRAIN CRACK TOLERANCE OF STEELS. Randall, P. N. (TRW Systems Group, Redondo Beach, Calif.); Merkle, J. G. Nucl. Eng. Des.; 17: No. 1, 46-63(1971).

It is the intent of most structural designs that general yielding should always precede fracture, even in the presence of flaws. The objective of the gross strain approach is to make direct measurements of flaw tolerance, in terms of gross strain to maximum load, as a function of flaw size and temperature. Gross strain is defined as the strain at the crack location, normal to the crack plane, that would exist if the crack were not there. Gross strain is measured as the axial strain in a tensile specimen containing a fatigue sharpened part-through surface flaw. Measurements of critical gross strain and critical crack opening displacement have been made for A533-B pressure vessel steel. These values undergo an abrupt increase with temperature, at the temperature at which gross section yielding and fracture coincide. The transition temperature increased with flaw size, as expected. Specimen thickness and width criteria have been developed for ensuring adequate constraint at the crack tip. The gross strain approach showed definite promise of becoming a measure of toughness that can be used in a quantitative procedure for design against brittle fracture when the object is to insure yielding before fracture in the presence of the largest expected flaw. (auth)

**55515** PROGRESS IN THREE-DIMENSIONAL ELASTIC–PLASTIC STRESS ANALYSIS FOR FRACTURE MECHANICS. Levy, N.; Marcal, P. V.; Rice, J. R. (Brown Univ., Providence). Nucl. Eng. Des.; 17: No. 1, 64-75(1971).

Progress in the development of finite element methods for three-dimensional elastic-plastic stress analysis in fracture mechanics is summarized. The work is directed toward the study of stress states near flaws such as a part-through crack in a pressure vessel wall, and emphasis is placed on the large scale plastic yielding range. The development of a computer program with large computing capabilities is described. Special near crack tip elements and general isoparametric elements are used in problems with two crack configurations. Preliminary results are given for the elastic analysis of a through crack and for the elastic-plastic analysis of a part-through semi-elliptical crack in a plate. (auth)

**55516** FRACTURE TOUGHNESS PROPERTIES OF HEAVY SECTION A533, GRADE B, CLASS 1 STEEL PLATE AND SUBMERGED ARC WELDMENT. Mager, T. R. (Westinghouse Nuclear Energy Systems, Pittsburgh). Nucl. Eng. Des.; 17: No. 1, 76-90(1971).

The fracture toughness ($K_{Ic}$) properties generated for A533 grade B class 1 steel plate and submerged arc weldment material are reviewed and summarized. The materials for which the data are presented were specially evaluated in the Heavy Section Steel Technology Program. The fracture toughness of HSST plate and weldment material is presented as a function of loading rate, metallurgical condition and irradiation (fluence). The data indicate the fracture toughness properties to be highly temperature dependent. (auth)

**55517** FRACTURE TOUGHNESS $K_{Icd}$ VALUES AT TEMPERATURES UP TO 550°F FOR ASTM A 533 GRADE B, CLASS 1 STEEL. Witt, F. J. (Oak Ridge National Lab., Tenn.); Mager, T. R. Nucl. Eng. Des.; 17: No. 1, 91-102(1971).

An equivalent energy procedure has been proposed which uses a linear elastic fracture mechanics type formulation for predicting maximum load to fracture at any temperature. This formulation requires a knowledge of the fracture toughness parameter $K_{Icd}$ and the corresponding volumetric energy ratio. $K_{Icd}$ values as obtained from compact tension specimens are presented for ASTM A 533 grade B, class 1 steel at temperatures up to 550°F which cover the range of light water nuclear reactor vessel operating temperatures. Studies of impact energy ratios for the steel have indicated that $K_{Icd}$ values as determined from 1T compact tension specimens may be almost numerically equal to the $K_{Ic}$ values as determined from much larger specimens. This was found to be true at temperatures up to which $K_{Ic}$ values are known (50°F). These data indicate a very high resistance to fracture at higher temperatures even though a degradation is noted at 550°F. (auth)

**55518** RECRYSTALLIZATION OF A STRONGLY DEFORMED MONOCRYSTAL OF MOLYBDENUM. Kopetskii, Ch. V.; Kulesko, G. I.; Nasikanova, N. N. Fiz. Khim. Obrab. Mater.; No. 3, 73-8(May-Jun 1971). (In Russian).

The initial steps of recrystallization in a strongly deformed (total reduction by rolling = 99%) monocrystal were investigated by x-ray and electron microscopy with electron-beam-zone melting. The increase in dimensions of the block may be derived either as a result of collapse of unstable portions of the wall with consequent joining of adjacent blocks, or because of relatively high mobility of small-angled boundaries terminated by a dislocated interweaving. (tr-auth)

**55519** EFFECT OF GLOW DISCHARGE ON ELECTRICAL RESISTANCE OF Ta–N FILMS. Belevskii, V. P.; Gavrilyuk, O. Ya. Fiz. Khim. Obrab. Mater.; No. 3, 120-3(May-Jun 1971). (In Russian).

Films of the Ta−N system were obtained by seven-minute cathodic sputtering under various pressure of nitrogen gas in pure argon, in order to determine the effect of changing partial pressure. Ion bombardment of such films decreased the concentration of point defects in the film. Increase of the surface temperature also leads to a decrease of such defects. Several other factors (voltage, current, and distance) were investigated as a function of the film resistance. (K.S.W.)

**55520** MECHANICAL PROPERTIES OF POLYCRYSTALLINE SAMARIUM FROM 78 TO 600K. Owen, C. V.; Scott, T. E. (Ames Lab., Iowa). J. Less-Common Metals; 25: No. 2, 161-70 (Oct 1971).

The flow-stress temperature dependence, strain-hardening exponent, strain-rate sensitivity, and ductility of samarium were determined from 78 to 600°K at strain rates of 0.005, 0.01, 0.10, and 1.0 $min^{-1}$. The results are presented and similarities of some of the results to those obtained for other rare-earth metals are pointed out and discussed. (auth)

**55521** STRUCTURE AND TENSILE PROPERTIES OF Nb–4.6 Ti–O. Vercaemer, C.; Geschier, R.; Clauss, A. (Ecole National Superieure de Chimie, Strasbourg). J. Less-Common Metals; 25: No. 2, 187-97(Oct 1971). (In French).

The structure and tensile properties of a Nb−Ti alloy containing 4.6% titanium have been studied in relation to the concentration of oxygen. The solubility of oxygen in niobium is markedly reduced by titanium and the addition of oxygen results in the precipitation of titanium oxides. The presence of oxygen may improve the yield stress and the ultimate stress depending on oxygen concentration and heat treatment. However, the tensile properties of alloys aged over 1000°C are nearly independent of oxygen content. (auth)

**55522** STRUCTURE AND TENSILE PROPERTIES OF Nb–Zr–O ALLOYS RICH IN Nb. Vercaemer, C.; Geschier, R.; Clauss, A. (Ecole Nationale Superieure de Chimie, Strasbourg). J. Less-Common Metals; 25: No. 2, 199-213(Oct 1971). (In French).

The structures and tensile properties of three Nb−Zr alloys

containing respectively 2, 3.8, and 5.4 at.% zirconium have been studied in relation to the concentration of oxygen up to 2.5 at.%. Addition of oxygen results in the precipitation of two crystallographic forms of zirconium dioxide, the monoclinic form and the cubic form. The composition of the secondary phases depends on oxygen concentration and heat treatment. The presence of oxygen may improve the yield stress and the ultimate stress of aged alloys. However, the tensile properties over 1000°C are nearly independent of oxygen content. (auth)

**55523** TEMPERATURE DEPENDENCE OF THE ELECTRICAL AND THERMAL CONDUCTIVITY OF RHENIUM AND METALS OF THE PLATINUM SUBGROUP. L'vov, S. N.; Mal'ko, P. I.; Nemchenko, V. F. (Kherson Pedagogical Inst., USSR). Fiz. Metal. Metalloved.; 31: No. 1, 108-15(Jan 1971). (In Russian).

The electrical conductivity of Re, Os, Ir, and Pt was measured at 80 to 1900°K and the thermal conductivity at 80 to 1400°K. The electrical resistance of Re, for example, rose from an almost negligible value to 80 μΩ. cm over the range indicated, while that of the other metals rose rather less. The character of the temperature dependence also varied from metal to metal; this difference was attributed to differences in the corresponding Fermi levels. Similar effects characterized the thermal properties. These results are compared with analogous results for other metals. (Metals Abstr.)

## *Structure and Phase Studies*

*Refer also to abstracts 56108 and 56378.*

**55524** (COO-1707-11) SOLID-LIQUID PHASE EQUILIBRIA IN THE TERNARY SODIUM–POTASSIUM–RUBIDIUM ALLOY SYSTEM. Technical Progress Report, May 1, 1967–August 31, 1971. Ott, J. Bevan; Goates, J. Rex (Brigham Young Univ., Provo, Utah). 31 Aug 1971. Contract AT(11-1)-1707. 8p. Dep. NTIS.

Thermal methods were used to determine solid-liquid phase equilibria points for the ternary sodium-potassium-rubidium alloy system. Two temperature halts were observed for most of the compositions. The low temperature halt is a eutectic with a minimum value near 255.3°K. (auth)

**55525** (IS-T-462) THERMODYNAMICS OF FORMATION OF COMPOUNDS IN THE Ce–Mg, Nd–Mg, Gd–Mg, Dy–Mg, Er–Mg, AND Lu–Mg SYSTEMS FROM VAPOR PRESSURE MEASUREMENTS. Pahlman, John Edward (Ames Lab., Iowa). Sep 1971. Contract W-7405-eng-82. 130p. Dep. NTIS.

Thesis.

The vapor pressure of magnesium over a series of two-phase alloys of magnesium with cerium, neodymium, gadolinium, dysprosium, erbium, and lutetium have been measured by a Knudsen effusion technique in the temperature range 650 to 930°K. These vapor pressure measurements were combined with data concerning the terminal magnesium solubility in the rare earths and the vapor pressure of pure magnesium to evaluate the free energies for the formation of the compounds in the rare earth–magnesium systems from the pure solid elements. Because heat capacity data were not available, the $\Delta C_p$ values for the associated reactions were taken to be zero. The free energies of formation evaluated at the midpoint of the temperature range exhibit an asymmetric double-humped trend with increasing atomic number. Temperatures for the eutectoid decomposition of $LaMg_2$, $CeMg_2$ and $PrMg_2$ were estimated to be 616, 605, and 583°C, respectively. (auth)

**55526** SODIUM–BARIUM PHASE DIAGRAM. Addison, C. C.; Creffield, G. K.; Hubberstey, P.; Pulham, R. J. (Univ. of Nottingham, Eng.). J. Chem. Soc., A; No. 16, 2688-91(1971).

The phase diagram for solutions containing up to 44 at. % of barium in sodium was determined from breaks in resistivity–temperature curves. This technique is believed to be more sensitive than others employed previously, and details of the phase diagram obtained from resistivity measurements (e.g., the eutectic, peritectic, and peritectoid) are compared with published data. (auth)

**55527** ELECTRICAL RESISTIVITY OF LIQUID POTASSIUM AND OF SOLUTIONS OF SODIUM IN LIQUID POTASSIUM: THE POTASSIUM–SODIUM PHASE DIAGRAM. Addison, C. C.; Creffield, G. K.; Pulham, R. J. (Univ. of Nottingham, Eng.). J. Chem. Soc., A; No. 16, 2685-8(1971).

The electrical resistivity of liquid potassium and of solutions containing up to 30 at. % sodium in liquid potassium was determined from the liquidus to 300°C. Equations for the variation in the resistivity of the liquid metal with temperature and with composition are given. Resistivity-temperature curves at constant composition were extended into the solid phase to allow determination of part of the phase diagram. The resistivities and phase equilibria are compared with previously reported data. (auth)

**55528** TRANSFORMATIONS DURING QUENCHING OF ε-PHASE Pu–Zr ALLOYS. Perkins, A. J.; Goldberg, A.; Massalski, T. B. (Univ. of California, Livermore). J. Nucl. Mater.; 41: No. 1, 39-50(Oct 1971).

A study was made on the effects of cooling rate (1 to 18,500°C/sec) and composition (5 to 45 at. % Zr) on the transformation behavior of ε-phase Pu–Zr alloys in which the ε-Pu (bcc) phase can transform to the δ-Pu (fcc) phase during cooling. In all the alloys, it was found that the transformation mode gradually changed with cooling rate, with an oriented diffusional nucleation and growth mode (Widmanstätten growth) favored at low cooling rates, and a massive mode at high cooling rates. Relatively slow rates caused a lowering of the initial transformation temperature, but rates in excess of about 3000°C/sec caused either very little or no further depression of the ε → δ reaction-start temperature. Hence, a plateau behavior, typical of a massive transformation, was observed for all alloys. For the more highly alloyed samples a martensitic shear mode was obtained at cooling rates greater than about 10,000°C/sec. (auth)

**55529** CONSTRUCTION OF THE SOLIDUS VOLUME IN THE NIOBIUM–TUNGSTEN–TITANIUM–ZIRCONIUM SYSTEM BY THE SIMPLEX-LATTICE METHOD. Zakharov, A. M.; Novik, F. S.; Daneliya, E. P. Izv. Akad. Nauk SSSR, Metal.; No. 5, 212-21 (Sep-Oct 1970). (In Russian).

A method of constructing the solidus volume of a four-component intermetallic system by the simplex-lattice method is described with special reference to the case of Nb–Ti–W–Zr. Using a model based on the properties of 15 selected alloys, the solidus characteristics were predicted to a satisfactory accuracy, as determined by reference to the examination of an additional 16 control alloys. The model was then used without any further experiments to plot solidus temperature/composition relations for the constituent ternary systems. (Metals Abstr.)

**55530** EPITAXY OF VANADIUM ON SAPPHIRE. O'Neal, J. E.; Wyatt, R. L. (McDonnell Douglas Corp., St. Louis). Thin Films; 2: No. 1, 1-6(Jul 1971).

Vanadium thin films, deposited by electron–beam evaporation in an ultrahigh vacuum onto (00.1) and (10.2) sapphire substrates, were characterized by electron microscopy and reflection electron diffraction. Epitaxial growth, with triple positioning of the deposit, was found for the basal plane sapphires above 600°C. At lower substrate temperatures, the films deposited on the basal plane exhibited a [111] fiber texture. Single-crystal vanadium films were grown on (10.2) sapphires with substrate temperatures between 600 and 1000°C. Lower substrate temperatures yielded complex fiber textures for this substrate orientation. (auth)

**55531** HETERO-EPITAXIAL FILMS OF NIOBIUM ON SAPPHIRE. O'Neal, J. E.; Wyatt, R. L. (McDonnell Douglas Corp., St. Louis). Thin Films; 2: No. 1, 71-81(Jul 1971).

Niobium thin films were deposited by electron beam evaporation in an ultrahigh vacuum onto (00.1) and (10.2) sapphire substrates. A correlation was made between the structure of the deposited niobium films and the substrate orientation, the substrate temperature, and the deposition rate. The substrate temperature was varied between 25 and 1000°C and deposition rates of 500 and 1000 Å/min were used. Single-crystal niobium films were formed on both substrate orientations at temperatures between 700 and 1000°C. (auth)

**55532** LOW-TEMPERATURE X-RAY DIFFRACTION STUDIES OF NEAR-EQUIATOMIC V–RU ALLOYS. Marezio, M.; Dernier, P. D.; Chu, C. W. (Bell Telephone Labs., Inc., Murray Hill, N. J.). Phys. Rev., B; 4: No. 8, 2825-6(15 Oct 1971).

A crystallographic transition of the ordered near-equiatomic VRu alloys was observed between 360 and 110°K. This cubic-to-tetragonal distortion occurs over a temperature interval commensurate with the observed anomalies in electrical resistivity, magnetic susceptibility, and the Knight shift. The transition involves a 1.4% expansion in volume for $V_{0.50}Ru_{0.50}$. This expansion is very nearly temperature-independent between 300 and 110°K. The volume change for $V_{0.51}Ru_{0.49}$ at 110°K is 1.5%. For both compounds, the CsCl-type ordering is approximately 100%. (auth)

**55533** ISOTHERMAL HEAT OF EVAPORATION OF YTTERBIUM AND NEODYMIUM IONS ON A TUNGSTEN SURFACE. Ionov, N. I.; Marinova, Ts. S.; Fedchenko, M. A. (Leningrad State Univ.). Sov. Phys.-Tech. Phys. (Engl. Transl.); 16: No. 2, 345-6(Aug 1971).

XUM

Translated from Zh. Tekh. Fiz.; 41: No. 2, 449-50(Feb 1971).

From the equations for the rate of desorption of adsorbed atoms as ions and for the ion current density $j_+$, it is shown that a plot of $j_+$ versus 1/T should show a knee at $\Theta_0$ (degree of surface coverage) = $kT_0/a$ ($T_0$ = threshold temperature). The plots for various rates give a locus of knee points whose slope defines $l_{\phi+}$, the isothermal heat of desorption. Measurements were made using molecular beams of Yb and Nd directed on W wire, and the following $l_{\phi+}$ values were found: 3.7 ± 0.2 eV for $Yb^+$ and 4.2 ± 0.2 eV for $Nd^+$. (D.L.C.)

**55534** INTERACTION OF NIOBIUM WITH A ZINC MELT. Kozlova, I. R.; Korsukova, M. M.; Gurin, V. N.; Obukhov, A. P. Izv. Akad. Nauk SSSR, Metal.; No. 5, 83-5(Sep-Oct 1970). (In Russian).

The interaction of Nb with a Zn melt was studied by metallographic analysis and x-ray diffraction. A Zn melt containing ~2% Nb tended to form two phases on reaching equilibrium at 700 to 900°C: a solid phase of approximate composition $NbZn_3$, and a molten phase principally consisting of Zn. The formation of the intermetallic compound was readily confirmed by x-ray analysis. These and other results confirmed existing views to the effect that a wide range of two-phase products occurred in the Zn–Nb system, the intermetallic compound $NbZn_3$ undergoing a partial ordering process. (Metals Abstr.)

**55535** NON-EQUILIBRIUM SOLIDIFICATION AND STRUCTURAL TRANSFORMATIONS DURING HEATING IN ALUMINUM–MOLYBDENUM AND ALUMINUM–CHROMIUM ALLOYS. Vengrenovich, R. D.; Psarev, V. I. Izv. Akad. Nauk SSSR, Metal.; No. 5, 186-93(Sep-Oct 1970). (In Russian).

The nonequilibrium solidification of Al–Mo and Al–Cr alloys from temperatures corresponding to the one- and two-phase regions was studied and correlated with corresponding phase transformations taking place on heating the solidified material. Thus solidification took place in accordance with the metastable phase diagrams Al–$Al_3Mo$, Al–$Al_4Cr$, and Al–$Al_{11}Cr$ with the creation of metastable eutectics. Some of the metastable phases formed ($Al_3Mo$, $Cr_2Al_{11}$, and $Al_4Cr$) subsequently transformed into stable phases of the $Al_5Mo$ and $CrAl_7$ type. The associated mechanisms are discussed. (Metals Abstr.)

**55536** PHASE DIAGRAM OF THE MERCURY–INDIUM SYSTEM. Kozin, L. F.; Sudakov, V. A. Izv. Akad. Nauk SSSR, Metal.; No. 5, 197-201(Sep-Oct 1970). (In Russian).

The phase diagram of the Hg–In system was studied by thermographic methods. Two congruent melting compounds are formed: $InHg_6$ melting at −15° and InHg melting at −18.6°C. There are also two peritectically formed compounds, $InHg_4$ and $In_{11}Hg$, with mp of −21.5° and +105°C, respectively. In the Hg-rich region, there is an invariant reaction at a temperature close to the freezing point of pure Hg, the reaction being of the peritectic type. Thes' results are supported by x-ray diffraction and microhardness measurements. (Metals Abstr.)

**55537** PHASE EQUILIBRIA AND PROPERTIES OF ALLOYS IN THE TiAl–$V_5Al_8$ SECTION OF THE TITANIUM–ALUMINUM–VANADIUM SYSTEM. Volkova, M. A.; Kornilov, I. I. Izv. Akad. Nauk SSSR, Metal.; No. 5, 202-4(Sep-Oct 1970). (In Russian).

The phase diagram of the Ti–Al–V system was studied along the TiAl–$V_5Al_8$ section by thermal, microstructural, and x-ray analyses supported by measurements of microhardness and electrical resistance. In the solid state TiAl and $V_5Al_8$ exist in equilibrium and the section between them is quasi-binary. The compounds form a system with limited solubilities in the solid state. The solubility of V in TiAl is 19 at. % and that of Ti in $V_5Al_8$ 2 at. % at 1100°C. The hardness and electrical resistance increase with V content. (Metals Abstr.)

**55538** CROSS SECTION OF THE MOLYBDENUM–ZIRCONIUM–CHROMIUM SYSTEM AT 1150°C. Eremenko, V. N.; Prima, S. B.; Tret'yachenko, L. A. Izv. Akad. Nauk SSSR, Metal.; No. 5, 208-11(Sep-Oct 1970). (In Russian).

The structural characteristics of the Mo–Zr–Cr system were studied at 1150°C on the basis of x-ray diffraction and microstructural analysis. The following phase regions were distinguished: an $\alpha$ region constituting a solid solution of Zr in Mo–Cr, a $\beta$ region comprising a $\beta$–Zr base solid solution, a continuous series of solid solutions based on $Mo_2Zr$ and $Cr_2Zr$ with a cubic structure of the $MgCu_2$ type constituting the the $\gamma$ region, and extensive two-phase regions of the $\alpha + \gamma$ and $\beta + \gamma$ type. (Metals Abstr.)

**55539** CONDITIONS FOR THE FORMATION OF A PHASE WITH THE A15 STRUCTURE IN THE VANADIUM–GERMANIUM–ALUMINUM SYSTEM. Surikov, V. I.; Borzhitskaya, M. K.; Shtol'ts, A. K.; Zagryazhskii, V. L.; Gel'd, P. V. (Ural Polytechnic Inst., Sverdlovsk, USSR). Fiz. Metal. Metalloved.; 30: No. 6, 1167-72(Dec 1970). (In Russian).

The possibility of a phase with the A15 structure being formed in the V–Ge–Al system was studied by synthesizing a number of alloys of the $V_3Al_xGe_{1-x}$ type and studying these metallographically and by x-ray diffraction, as well as determining the temperature at which they passed into the superconducting state. A continuous series of solid solutions was found, although the preparation of true single-phase samples was impeded by kinetic processes taking place in these alloys. The ternary alloys synthesized at 1050°C had a structure of the same nature as the A15 structure of $V_3Al$. (Metals Abstr.)

**55540** INFLUENCE OF ORIENTATION OF ZIRCONIUM MONOCRYSTALS ON THE GROWTH STRUCTURES OF MONOCLINIC ZIRCONIA. Penelle, R.; Boisot, P.; Beranger, G.; Lacombe, P. (Centre de Recherches Metallurgiques, Paris). J. Nucl. Mater.; 38: 340-2(Mar 1971). (In French).

A monocrystal of Zr in parallelopiped form was oxidized in oxygen at atmospheric pressure at 850°C in order to determine the effect of the orientation of the Zr monocrystal on the growth texture of the oxide formed. The results obtained are tabulated and show that whatever the orientation of the Zr monocrystal, the zirconia formed is polycrystalline. The nature and intensity of the major components of the zirconia are functions of the orientation of the metal. There is only one major component on face A and its intensity decreases with increased oxidation time. Face B has 6 principal components and the evolution of each of these components is very different with the oxidation time. (J.S.R.)

**55541** RELATIONSHIPS BETWEEN THE REAL STRUCTURE OF ALLOYS AND THE MODEL REPRESENTATIONS OF HARD SUPERCONDUCTORS. Sudareva, S. V. (Inst. of Metal Physics, Moscow). Fiz. Metal. Metalloved.; 30: No. 5, 915-23(Nov 1971). (In Russian).

The relationship between the structure and superconducting properties of Zr–4% Nb and Ti–39% Nb alloys is discussed in the light of experimental data and existing models of hard superconductors. The high critical currents of the Zr–Nb alloy may be readily explained by the filament model; the concept of superconducting inclusions forming chains sometimes offered cannot explain the experimental facts. The experimental data obtained for the Ti–Nb alloy are in complete agreement with the Friedel model. (Metals Abstr.)

**55542** ELECTRON-MICROSCOPE AND X-RAY SPECTRAL STUDY OF THE SURFACE OF FRACTURES IN CAST TUNGSTEN. Gavrilyuk, M. I.; Vasenin, G. V.; Zherdev, A. M.; Tuzov, L. V. (Kirghiz State Univ., Frunze, USSR). Fiz. Metal. Metalloved.; 30: No. 5, 1035-40(Nov 1970). (In Russian).

The structure of the fracture surfaces of cast W subjected to various degrees of cold working and heat treatment was studied by electron microscopy, using the C-replica method, and the nature of the foreign inclusions removed from the W surface when detaching the C replicas was determined by x-ray spectral analysis. Both in the cold-worked state, and also after annealing, the rupture of the W at room temperature displayed a mixed (ductile/brittle) character. The foreign inclusions had a complex chemical composition, incorporating $SiO_2$ and $Al_2O$ particles. The brittleness of W at 20°C was attributed to its nonmetallic-inclusion content. (Metals Abstr.)

**55543** INFLUENCE OF PRIOR MECHANICAL AND THERMAL TREATMENTS ON SHOCK-INDUCED SUBSTRUCTURES IN MOLYBDENUM. Mahajan, S.; Bartlett, A. F. (Atomic Energy Research Establishment, Harwell, Eng.). Acta Met.; 19: No. 10, 1111-19(Oct 1971).

The effects of prior mechanical and thermal history on shock-induced substructures in polycrystalline molybdenum have been investigated by transmission electron microscopy. It was observed that annealed material deforms both by slip and twinning, but pre-staining suppresses the formation of twins. Arguments for rationalizing these observations have been developed. Small twins associated with "restricted slip bands" were observed, but twins formed in the absence of intersecting slip bands—contrary to the twin nucleation mechanism of Priestner and Leslie. It is suggested that these bands form to accommodate the strain of a twin which has stopped growing inside the crystal. The basic features of dislocation topologies observed in the 6% pre-strained or the 6% pre-strained and aged samples were retained after the passage of a 90 kbar shock-wave, but tangles became less dense and thus the dislocation density was reduced. This could occur if clear areas adjoining a tangle wall undergo shock-induced rotation. (auth)

XUM

**55544** METALLOGRAPHY OF THE 700°C PRECIPITATION IN A Fe–40% Ni ALLOY CONTAINING BERYLLIUM. Mazaud, J. C.; Vial, A. (Laboratoire de Metallurgie, Veurey-Voroize, France). Acta Met.; 19: No. 10, 1133-41(Oct 1971). (In French).

The 700°C precipitation in a Fe–40% Ni alloy containing beryllium was studied by transmission electron microscopy. Evidence of a new phase, $\beta'$, was made. This phase precipitates into discs or platelets situated in {100} planes of the matrix, with an ordered centered tetragonal structure, the parameters (calculated from microdiffraction patterns) being approximately a = 2.53 Å, c = 2.64 Å. The $\beta'$ orientation relationships in the matrix were determined. The $\beta'$ phase is a partially coherent phase: it is coherent in the basal plane but incoherent in the c$\beta'$ direction. The $\beta'$ coalescence was studied by measuring the mean length of the particle projection on {100} planes of the matrix, on dark field micrographies. The mean diameter of the particles increased as (time)$^{1/4}$. $\beta'$ was dissolved back again by discontinuous precipitation of ordered stable bcc $\beta$ NiBe phase (a = 2.61 – 2.62 Å). The $\beta'$ crystallographic characteristics were those of an intermediate phase, between the coherent metastable fcc $Ni_2Be$ phase, which was observed by others in a Ni–Be alloy, and the non-coherent stable $\beta$ NiBe phase. (auth)

**55545** NEUTRON SCATTERING STUDY OF THE LATTICE-DYNAMICAL PHASE TRANSITION IN $Nb_3Sn$. Shirane, G.; Axe, J. D. (Brookhaven National Lab., Upton, N. Y.). Phys. Rev., B; 4: No. 9, 2957-63(1 Nov 1971).

Neutron scattering experiments have been carried out on a single crystal of $Nb_3Sn$ through the lattice-dynamical phase transition at $T_m$ = 45°K. A small tetragonal lattice distortion, a/c = 1.0062 at 4°K, was previously established by x-ray studies, but sublattice displacements below $T_m$ have remained undetermined. The present study reveals that the tetragonal phase exhibits new Bragg reflections, which are forbidden by symmetry in the cubic phase. From the intensity distribution among these new reflections, the structure was determined uniquely as $D_{2h}^9$ with Nb displacements from the special positions of 0.016(3) Å at 4°K. Only the Nb sublattices shift, and in a pattern identical with the eigenvectors of the $\Gamma_{12}(+)q = 0$ optic-phonon mode in the cubic phase. Such a mode is linearly coupled with the soft [110] shear acoustic mode. This linear coupling requires, and the measurements confirm, that the intensities of new Bragg peaks are proportional to $(a/c - 1)^2$. An optic-phonon instability is not required to explain these internal displacements. (auth)

**55546** INTERRELATION BETWEEN THE PHASE DIAGRAM AND THE COMPOSITION–PROPERTY DIAGRAMS OF THE In–Sn SYSTEM. Dutchak, Ya. I.; Korsunskii, A. M.; Klym, N. M. (Lvov State Univ.). Izv. Vyssh. Ucheb. Zaved., Fiz.; No. 5, 36-41(1970). (In Russian).

The viscosity and electrical conductivity were determined in In–Sn alloy samples containing 0, 5, 10, 20, 26, 33, 40, 48, 55, 70, 90, and 100 at. % tin. The samples were prepared in ampules sealed under vacuum. The electrical conductivity measurement was carried out by a method employing a rotating magnetic field, and viscosity was determined by a rotational-oscillatory method at temperatures of 20 to 700°C. The composition–property plots show the existence of a sharp inflection at 40 to 55 at. % Sn. The experimental results show that beta- and gamma-phases are fixed at property–composition isotherms. From these results it is possible to propose that the beta phase has limits of 20 to 48 at. % Sn. A change in close-order structure is observed at temperatures above 500°C in alloys containing 20, 26, 33, and 40 at. % Sn. The results of x-ray studies of these changes will be published separately. (TTT)

**55547** COMPOSITION OF THE CARBIDE PHASE IN ALLOYS OF URANIUM WITH ZIRCONIUM AND NIOBIUM. Gomozov, L. I.; Lyutina, E. M.; Makhova, V. A.; Ivanov, O. S. At. Energ. (USSR); 31: No. 3, 279-81(Sep 1971). (In Russian).

The interaction of Zr and Nb with a basic U–C mixture was studied in which the C content was 1 at. % or more. Phase equilibrium diagrams were prepared for the ternary U–Zr–C system at 950 and 1000°C; at the latter temperature, a $\gamma$-phase which contains not more than 0.1 at. % carbon coexists with a solid solution (U, Zr) C. (K.S.W.)

**55548** STRUCTURAL CHANGE IN A SINTERED Mg–Zr ALLOY AFTER HOLDING AT HIGH TEMPERATURE. Pegoud, J.; Guillaumin, J.; Millet, P. (Societe Industrielle de Combustible Nucleaire, Veurey, France). J. Nucl. Mater.; 41: No. 1, 72-9(Oct 1971). (In French).

The structure of sintered Mg–0.5% Zr alloy was studied by optical and electron microscopy both in the as-fabricated condition and also after holding at 450°C or 600°C under $CO_2$. In the original condition the alloy consisted of a solid solution of zirconium in magnesium, zirconium hydride precipitates and particles of magnesium oxide and carbonate. During high-temperature anneals, these particles coalesce and partially dissolve; the oxygen thus liberated diffuses through the alloy and brings about internal oxidation of the zirconium. Up to the diffusion fronts, the hydride precipitates have decomposed and the zirconium in solid solution precipitated. In both cases, very fine zirconium oxide particles are formed. (auth)

**55549** EFFECT OF IMPURITIES, PARTICULARLY HYDROGEN, ON THE LATTICE PARAMETERS OF THE ABAB RARE EARTH METALS. Spedding, F. H.; Beaudry, B. J. (Ames Lab., Iowa). J. Less-Common Metals; 25: No. 1, 61-73(Sep 1971).

The common methods presently used to prepare samples of the heavy rare-earth metals for lattice parameter determinations were shown to give high results due to contamination by interstitial impurities, especially H. Two methods to produce fine-grained homogeneous samples in the form of wires were established. Both methods have the advantage of not requiring further heat treatment after preparation of the surface to be x-rayed. The lattice parameters of Gd, Tb, Dy, Ho, Er, Tm, Lu, Y, and Sc were determined on well-characterized samples. The density, mole atomic volume, atomic radius for $CN_{12}$, and c/a ratios were calculated based on the lattice parameters determined. The effect of hydrogen on the lattice parameters of these metals was determined. (auth)

**55550** EFFECTS OF COOLING RATE AND SUPERCOOLING DEGREE ON SOLIDIFIED STRUCTURES OF Al–Mn, Al–Cr, AND Al–Zr ALLOYS IN RAPID SOLIDIFICATION. Ichikawa, Riei; Ohashi, Teruo; Ikeda, Tetsuyuki (Nagoya Inst. of Tech., Japan). Trans. Jap. Inst. Metals; 12: No. 4, 280-4(Jul 1971).

Effects of supercooling and cooling rate on the solidified structures of Al–Mn, Al–Cr, and Al–Zr alloys, which had strong tendencies to form metastable solid solutions by rapid cooling of the molten alloys, were investigated by means of thermal analysis and microscopic observation. It was found that the square of the degree of supercooling was proportional to the cooling rate on the solidification of the alloys having a solute concentration up to the maximum solid solubility limit at equilibrium (Ce). At solute concentrations higher than Ce, this relation was satisfied under the conditions that the primary crystals were a supersaturated solid solution. The minimum cooling rate to form the super-saturated solid solutions containing more solute atoms than Ce was 115, 175 and 190°C/sec for Al–Mn, Al–Cr and Al–Zr respectively. Metastable phase diagrams were proposed under varying conditions of composition, temperature and cooling rate in the Al–Mn, Al–Cr,and Al–Zr systems. (auth)

**55551** RELATION BETWEEN THE KINETICS OF AGING AFTER DEFORMATION OF $\alpha$–ZIRCONIUM AND THE ANISOTROPIC DIFFUSION OF OXYGEN FOR A SHORT DISTANCE. de Paula E Silva, E.; Com-Nougue, J.; Beranger, G.; Lacombe, P. (Ecole des Mines, Paris). Scr. Met.; 5: No. 9, 795-800(Sep 1971). (In French).

The mechanisms of interstitial redistribution by aging after deformation of $\alpha$–Zr are analyzed as related to anisotropic oxygen diffusion. (J.R.D.)

**55552** KINETICS OF DISORDER–ORDER TRANSFORMATIONS. Ling, Fu-wen; Starke, E. A. Jr. (Georgia Inst. of Tech., Atlanta). Contract AT(40-1)-3908. Scr. Met.; 5: No. 9, 741-7 (Sep 1971).

Since most order-disorder transformations are diffusion controlled, the kinetics of the transformation should be treated by diffusion theory. However, they also involve changes in internal strain and gradient energy which become increasingly important as order progresses. In an equation, $1 - S = \exp(-Kt)$, which was derived in a previous paper, the later effects were ignored. That equation could also be derived by ignoring the strain and energy effects and treating the problem using a long-range-order wave instead of a domain wave, i.e., constant $\beta$. Most ordered alloys exhibit compositional fluctuations in the disordered state and this results in long-range diffusion playing a significant role in the late ordering stages. Consequently, it is necessary to consider both short-range diffusion (as described in changes in the long-range-order wave amplitude) and long-range diffusion (as described by changes in the domainwave amplitude). The equilibrium long-range order parameter depends on the temperature of ordering below the transformation temperature and may not be unity. Therefore equation should be $\ln(S_\infty - S) = -G_1(T)t^{(n-2)/n} - G_2(T)t^{(n-4)/n}$ where $S_\infty$ is the maximum long-range order parameter obtainable at the ordering temperature. (auth)

**55553** MICROSTRUCTURE OF 706, A NEW Fe–Ni-BASE SUPERALLOY. Moll, John H.; Maniar, Gunvant N.; Muzyka,

XUM

Donald R. (Carpenter Tech. Corp., Reading, Pa.). Met. Trans.; 2: No. 8, 2143-51(Aug 1971).

Alloy 706 is a precipitation-strengthened Fe–Ni-base superalloy, which has been reported to have improved machining characteristics over other similar alloys. The present work was conducted to document the phase relationships of the alloy in comparison with other Fe–Ni-base alloys. The precipitated phases identified in the alloy include $\gamma'$, $Ni_3Nb$, $Ni_3Ti$, $M_{23}C_6$, and MC. A small amount of Laves phase was also detected. The effects of some composition variations on solvus relationships for $\gamma'$ and $Ni_3Nb$/$Ni_3Ti$ are documented. Means to take advantage of the structural response of the alloy to develop desired properties are suggested. It is shown that on the basis of chemistry and microstructural response, 706 alloy can be considered to be intermediate to the well-known alloys, 718 and 901. (auth)

**55554** HEAT TREATMENT OF 706 ALLOY FOR OPTIMUM 1200°F STRESS-RUPTURE PROPERTIES. Moll, John H.; Maniar, Gunvant N.; Muzyka, Donald R. (Carpenter Tech. Corp., Reading, Pa.). Met. Trans.; 2: No. 8, 2153-60(Aug 1971).

Evaluation of a commercial heat treatment for 706 alloy indicated that it resulted in relatively low 1200°F stress rupture ductility. It was determined that this was caused by solution treatment, which dissolved all of the age-hardening phases in the alloy and caused a coarse grain size and supersaturated matrix condition. Based upon extensive fine structure study of the 706 alloy as well as previous experience with 718 alloy and other Fe–Ni-base superalloys, a heat treatment is developed which effectively optimizes the 1200°F stress-rupture properties of the alloy. The key to best properties was found to be the precipitation of globular to plate-like $Ni_3Nb$/$Ni_3Ti$ at the grain boundaries in conjunction with maintaining a fine as-forged grain structure. (auth)

**55555** POTENTIOSTATIC ETCHING AND POLISHING OF COPPER AND ITS ALLOYS. Mance, Amalija (Boris Kidric Inst. for Nuclear Sciences, Belgrade). Metallography; 4: No. 4, 287-96(Aug 1971).

An attempt to apply the potentiostatic method to the study of anodic dissolution of Cu and its alloys for metallographic purposes is reported. Copper and Cu–0.5% Be, Cu–1% Zr, and Cu–0.3% Be–2% Ni alloys were examined in 85% phosphoric acid, and the polarization curves were determined. A number of specimens were treated at potentials and current densities defined by polarization curves. The results indicate the relationship between the processes taking place on the anode at a given region of the polarization curves and the revealing of the microstructure components. Optimal conditions for revealing microstructure were determined. (auth)

**55556** FACTORS AFFECTING THE STRUCTURE OF CHROMIUM AND CHROMIUM–MOLYBDENUM WHITE IRONS. Maratray, F.; Usseglio-Nanot, R. Paris; Climax Molybdenum S.A. (1970). 32p.

Forty-two different alloys of the C–Cr–Mo system were studied. These alloys also contained small amounts of Mn, Si, S, and P. The study was aimed mainly at determining the factors involved in properly balancing chemical composition and thermal treatment to obtain the desired microstructure and hardenability. The following subjects are discussed in relation to the alloys: primary and eutectic carbides, matrix, decomposition mechanisms of the austenitic matrix, and transformation diagrams. Metallographic techniques, microprobe analysis of carbides and matrix, and determination of transformation curves are discussed in appendixes. (B.L.M.)

**55557** ISOTHERMAL OMEGA TRANSFORMATION IN ZIRCONIUM–BIOBIUM ALLOYS. Perkins, A. J. (Carnegie-Mellon Univ., Pittsburgh); Yaffe, P. E.; Hehemann, R. F. Metallography; 4: No. 4, 303-23(Aug 1971).

Transmission electron microscopy and diffraction were used to study the isothermal omega transformation in Zr–Nb alloys. A modulated structure of omega particles in a beta matrix is developed when alloys in the composition range 12 to 25% Nb are aged at appropriate temperatures. The omega particles are cuboidal, with $\{100\}_\beta$ faces, and are aligned in $\langle 100\rangle_\beta$ directions in a three-dimensional array. The average particle size is 1000 Å, and the interparticle spacing is a fraction of this value. Both the particle shape and the alignment can be interpreted in terms of the degree of precipitate–matrix lattice mismatch and elastic strain considerations. The critical factor is the elastic anisotropy of the beta matrix, having soft $\langle 100\rangle$ directions. The development of the modulated beta–omega microstructure involves selective nucleation and growth of particles at preferred locations with respect to existing particles. The growth kinetics during this selective nucleation and coarsening process obey a $t^{\frac{1}{3}}$ law. The effect of quenched omega phase formed prior to aging is important only in lean alloys. (auth)

**55558** DISLOCATION CELL FORMATION AND RECRYSTALLIZATION IN TUNGSTEN. Ostermann, F. (Air Force Materials Lab., Wright-Patterson Air Force Base, Ohio). Met. Trans.; 2: No. 9, 2737-40(Sep 1971).

A study was made of the effects of dislocation structures on the recrystallization resistance of polycrystalline W. Microstructures after deformation to ~4.8 and 9% strain at 400 and 200°C and annealing at 1400°C show that the lower temperature produces less dislocation cells. A plot of deformation temperature vs critical strain for recrystallization shows an inverse relationship. The results indicate that recrystallization depends on the distribution of dislocations, and that a homogeneous dislocation arrangement will lead to resistance to crystallization. (D.L.C.)

**55559** INFLUENCE OF DEFORMATION CONDITIONS ON POLYGONIZATION AND RECRYSTALLIZATION OF SINGLE-CRYSTAL MOLYBDENUM. Dubovitskaya, N. V.; Larikov, L. N.; Yakovenko, Yu. D. (Inst. of Metal Physics, Kiev). Fiz. Metal. Metalloved.; 30: No. 2, 400-5(Aug 1970). (In Russian).

The effect of the crystallographic conditions of deformation (direction of rolling) on the polygonization and recrystallization of Mo single crystals after subsequent heat treatment was studied by electron diffraction, x-ray diffraction, and microhardness measurements. Slight hardening developed when the original orientation coincided with the rolling texture; there was no serious distortion of the crystal lattice and the dislocations were uniformly distributed. In the case of other orientations, bending of the crystal lattice did occur, and this effect was subsequently relieved by polygonization. (Metals Abstr.)

**55560** LOW-TEMPERATURE ROLLING AND THE ANNEALING OF SINGLE-CRYSTAL NIOBIUM. Gindin, I. A.; Levikov, E. A.; Levikova, L. V.; (and others) (Physical-Technical Inst., Tashkent). Fiz. Metal. Metalloved.; 30: No. 2, 426-31(Aug 1970). (In Russian).

The structure of Nb single crystals was studied by x-ray diffraction before and after rolling at 20 to 300°K and again after annealing at 900 to 1800°K. The average scatter in local orientations after 60% rolling was <10%. Annealing at up to 1400°K led to fragmentation, the degree of scatter being preserved and no recrystallization occurring. The hardness and residual electrical resistance of samples so treated indicate a comparatively low level of lattice distortion in the material as a whole. (Metals Abstr.)

**55561** STUDY OF PHASE EQUILIBRIA IN THE ALUMINUM–COPPER–YTTRIUM SYSTEM. Drits, M. E.; Kadaner, E. S.; Nguyen Ting Shoa. Izv. Akad. Nauk SSSR, Metal.; No. 1, 181-5 (Jan-Feb 1971). (In Russian).

Isothermal cross-sections of the Al–Cu–Y phase diagram were plotted at 250 to 550°C on the basis of microstructural analysis and measurements of electric resistance and microhardness; the boundaries of the various phase regions in the Al-rich part of the diagram were established. There were two ternary phases in equilibrium with the Al-base solid solution, with the binary compounds $CuAl_2$ and $YAl_3$, and with each other. Both ternary phases had a tetragonal bc crystal structure. The addition of Y to the alloys substantially reduced the solubility of Cu in Al. (Metals Abstr.)

**55562** STUDY OF ALLOYS BELONGING TO THE $NiAl_3$–$VAl_3$ AND $Ni_2Al_3$–$V_5Al_8$ SECTIONS. Myasnikova, K. P.; Ponomareva, L. F.; Pryakhina, L. I.; Marshakov, I. K. Izv. Akad. Nauk SSSR, Metal.; No. 1, 186-9(Jan-Feb 1971). (In Russian).

Phase equilibria in alloys of the $NiAl_3$–$VAl_3$ and $Ni_2Al_3$–$V_5Al_8$ systems were studied, using microstructural, x-ray, and thermal analyses. In the solid state the alloys of both sections had a two-phase structure, the phase constituents of these being the original compounds. The polythermal section of the $NiAl_3$–$VAl_3$ system had three fields of primary crystallization. The melting of the compound $NiAl_3$ was incongruent in all cases studied. The combined solidification of $Ni_2Al_3$ and $V_5Al_8$ in the range $V_5Al_8$ 20 to 80 mol % took place in accordance with a eutectic law. The interchange of Ni and V atoms in the alloys had little effect on the hardness of the latter, owing to the similarity of the atomic radii. (Metals Abstr.)

**55563** NIOBIUM–HAFNIUM–CARBON SYSTEM IN THE NIOBIUM-RICH REGION. Zakharov, A. M.; Daneliya, E. P. Izv. Akad. Nauk SSSR, Metal.; No. 1, 190-4(Jan-Feb 1971). (In Russian).

The Nb corner of the Nb–Hf–C phase diagram was studied by microscopical and x-ray phase analysis together with thermal analysis and microhardness measurements; isothermal sections were plotted at 1200 to 2000°C and a polythermal section was derived for an Hf : C ratio of 17. The addition of Hf and C made little difference to the melting point of Nb. Only the carbide $Nb_2C$ was in equilibrium with the Nb-base solution at 1200 to 2000°C;

the solubility of C in Nb was ~0.03. There were no quasi-binary sections starting from the Nb corner in this system. (Metals Abstr.)

**55564** STUDY OF THE TITANIUM–ZIRCONIUM–NIOBIUM SYSTEM. Khegai, I. K.; Budberg, P. B. Izv. Akad. Nauk SSSR, Metal.; No. 1, 206-10(Jan-Feb 1971). (In Russian).

The phase diagram of the Ti–Zr–Nb system was studied by x-ray phase analysis and examination of the microstructure, supported by measurements of the physical properties (electric resistance, microhardness, etc.). Isothermal cross-sections were plotted at several points between 400 and 800°C, and a projection of the three-dimensional phase diagram was derived on the plane of the concentration triangle at 400°C. A number of non-variant and monovariant equilibria were established. The mechanisms responsible for the corresponding transformations are discussed. (Metals Abstr.)

**55565** STUDY OF PHASE EQUILIBRIA IN THE TITANIUM–TANTALUM–MOLYBDENUM SYSTEM IN THE TITANIUM CORNER. Nikitin, P. N.; Mikheev, V. S. Izv. Akad. Nauk SSSR, Metal.; No. 1, 211-15(Jan-Feb 1971). (In Russian).

The phase diagram of the Ti–Ta–Mo system was studied by microstructural analysis and x-ray diffraction aided by measurements of electric resistance and microhardness, with special reference to the Ti corner of the diagram. The electric resistance of alloys quenched from 900°C exhibited sharp maximum; these were attributed to the existence of ($\omega + \beta$) phases. The system contained a series of solid solutions based on $\beta$-Ti and a limited range of $\alpha$-Ti solid solutions. (Metals Abstr.)

**55566** EFFECT OF THE SIXTH PERIOD ELEMENTS ON THE MELTING AND TRANSFORMATION TEMPERATURES OF PRASEODYMIUM. PART II. THERMODYNAMIC ANALYSIS. Gschneidner, K. A. Jr.; Griffin, R. B. (Iowa State Univ., Ames). Met. Trans.; 2: No. 9, 2525-31(Sep 1971).

A thermodynamic analysis of the praseodymium-rich alloys containing Os, Ir, Pt, Au, Hg, Tl, Pb, and Bi indicated that most of the solutes dissolved in praseodymium follow ideal solution theory over a limited range of temperatures up to 40 to 135°C below the melting point of praseodymium (or concentrations out to 3 to 8 at. % solute). The activity coefficients, and excess partial free energies were calculated for liquid praseodymium at its melting point and for $\beta$-Pr at its $\alpha$ to $\beta$ transformation temperature. The so-called Q parameter has also been determined for these praseodymium systems, and it was found to exhibit the usual periodic dependence on the solute metal. As a result of these analyses a method has been developed which makes it possible to calculate phase boundaries for undetermined systems. This technique is shown to be especially valuable in calculating unknown phase boundaries for lanthanide-rich alloys, but for other metal solvents this method will probably be of a lesser utility. (auth)

**55567** EFFECT OF THE SIXTH PERIOD ELEMENTS ON THE MELTING AND TRANSFORMATION TEMPERATURES OF PRASEODYMIUM. PART I. EXPERIMENTAL. Griffin, R. B.; Gschneidner, K. A. Jr. (Iowa State Univ., Ames). Met. Trans.; 2: No. 9, 2517-24(Sep 1971).

The praseodymium-rich phase diagrams with the sixth period elements (Cs, Ba, Hf, and Re through Bi) have been determined by employing metallographic, thermal analysis, x-ray, and chemical analysis techniques. All of the solutes lower the melting point by at least 1°C to a maximum lowering of 316°C for gold. Monotectics are formed by cesium and barium and eutectics are formed by the other solvents when added to praseodymium. The $\alpha$ to $\beta$ transformation is also lowered by all of the solutes, but the lowering by Cs, Ba, Hf, and Re is 1°C or less. The maximum lowering is observed for mercury additions (281°C). The bcc $\beta$-Pr phase transforms to $\alpha$-Pr by means of an inverted peritectic reaction with Os, Ir, Pt, and Au, and by means of a eutectoid reaction for the remaining solutes. The largest solid solubility observed in $\beta$-Pr is 14.6 at. % Hg and that in $\alpha$-Pr is 2.5 at. % Tl. The praseodymium-rich compound in most of the systems was also determined. (auth)

**55568** SIMPLE METHOD OF DETERMINATION OF THE DISTRIBUTION AND SOLUBILITY LIMIT OF INTERSTITIALS IN SUBSTITUTIONAL SOLID SOLUTIONS. Liu, C. T.; Inouye, H.; Carpenter, R. W. (Oak Ridge National Lab., Tenn.). J. Less-Common Metals; 25: No. 2, 123-9(Oct 1971).

A simple method for the calculation of the solubility limit of certain interstitial species in solid solutions from a single lattice parameter measurement is described. The calculation is based on thermodynamic considerations, and the result allows qualitative conclusions to be made about the randomness of the solute distribution. The method is used to calculate oxygen solubility limits in Nb–Zr and Nb–Hf alloys and to explain previously reported, but apparently quite different, solubility limits in the two chemically similar alloys. (auth)

**55569** SAMARIUM–IRON SYSTEM. Buschow, K. H. J. (Phillips Research Labs., Eindhoven, Netherlands). J. Less-Common Metals; 25: No. 2, 131-4(Oct 1971).

The Sm–Fe system has been investigated by x-ray diffraction, thermoanalysis, and metallography. Three compounds have been observed: $SmFe_2$ ($MgCu_2$-type), $SmFe_3$ ($PuNi_3$-type), and $Sm_2Fe_{17}$ ($Th_2Zn_{17}$-type). Their lattice constants and Curie temperature have been determined. A tentative phase diagram has been constructed. (auth)

**55570** STOICHIOMETRY, CRYSTAL STRUCTURES, AND SOME MELTING POINTS OF THE LANTHANIDE–GOLD ALLOYS. McMasters, O. D. (Ames Lab., Iowa); Gschneidner, K. A. Jr.; Bruzzone, G.; Palenzona, A. J. Less-Common Metals; 25: No. 2, 135-60(Oct 1971).

The crystal structures of the intermetallic compounds in the trivalent lanthanide–gold systems were investigated using both powder- and single-crystal x-ray diffraction methods. Some of these alloys were studied by differential thermal analysis and metallographic evidence was used to confirm the stoichiometries. In the twelve R–Au systems (R = La, Ce, Pr, Nd, Sm, Gd, Tb, Dy, Ho, Er, Tm, Vb, and Lu), compounds exist at seven stoichiometries which involve twelve structure types and eighty phases. The $R_2Au$ phases represent the only complete isomorphic series. Depending upon R, the RAu (1 : 1) compounds exhibit two or three polymorphic forms. Three different structures occur as R is varied along the lanthanide series in the $RAu_2$ phases. For R = Gd–Lu, the $RAu_3$ compounds form and $RAu_{3.6}$ compounds exist for all the rare earths except Er, Tm, and Lu. $RAu_4$ phases exist only for R = Ho, Er, Tm, and Lu. A structural change occurs in the $RAu_6$ series between Nd and Sm and this phase does not form in the case of R = Er, Tm, and Lu. The crystallographic data for these compounds are presented and their structural relationships are discussed. The melting and transformation temperatures of some of the RAu (1 : 1) compounds have been determined. The melting points increase in a smooth fashion as a function of atomic number from 1325°C for LaAu to 1780°C for LuAu. (auth)

**55571** THORIUM–COPPER SYSTEM. Schiltz, R. J. Jr.; Stevens, E. R.; Carlson, O. N. (Ames Lab., Iowa). J. Less-Common Metals; 25: No. 2, 175-85(Oct 1971).

A binary phase diagram is proposed for the thorium–copper system based on thermal, microscopic, and x-ray analyses. Four compounds exist—$Th_2Cu$, $ThCu_2$, $ThCu_2$, "$ThCu_{3.6}$" and $ThCu_6$—which melt congruently at 1007, 1015, 1052, and 1055°C, respectively. Five eutectic reactions are found in this system; at 30 at.% Cu and 1000°C, at 51 at.% Cu and 880°C, at 74 at.% Cu and 980°C, at 82 at.% Cu and 1020°C and at 93 at.% Cu and 935°C. The terminal solid solubility of thorium in copper is negligible—less than 0.01 at.% Th. (auth)

## *Radiation Effects*

*Refer also to abstracts 54599, 55648, and 56313.*

**55572** (BLG-457) FAST NEUTRON IRRADIATION INDUCED SWELLING OF METALS AND ALLOYS. Stals, L. (Centre d'Etude de l'Energie Nucleaire, Mol (Belgium)). Dec 1970. 32p. Dep. NTIS (U. S. Sales Only).

A literature study of the experimental data on the swelling behavior of metals and alloys as observed after fast neutron irradiation is presented. The experimental data show that pure metals and alloys behave similarly as far as swelling is concerned. The threshold dose for swelling is for most metals a few orders of magnitude lower than for alloys. The temperature dependence of the swelling, however, is comparable. Theory predicts that in Types 304 and 316 austenitic stainless steel the swelling should saturate at $\Delta V/V \cong 12\%$. There is also some experimental evidence for saturation below $\Delta V/V \cong 20\%$. (auth)

**55573** (BNWL-SA-3962) SWELLING IN REFRACTORY METALS DURING HIGH TEMPERATURE ION BOMBARDMENT. Kulcinski, G. L.; Brimhall, J. L. (Battelle-Northwest, Richland, Wash. Pacific Northwest Lab.). Jun 1971. Contract AT(45-1)-1830. 7p. (CONF-711009-3). Dep. NTIS.

For Presentation at joint meeting of the American Nuclear Society; Miami, Fla. (17 Oct 1971).

Voids were found in Mo, TZM, and Nb after 5-MeV Ni ion bombardment (to 5 displacements per atom) at 800, 900, and 1000°C, but not at 650°C. The void size and shape are discussed. Voids were also found in V after 7.5-MeV Ta ion bombardment at 700 and 800°C, but not at 900°C. (D.L.C.)

XUM

**55574** (JAERI-Memo-4408) EFFECT OF ALPHA-RAY IRRADIATION ON CREEP-RUPTURE PROPERTIES OF AUSTENITIC STAINLESS STEEL. Furuta, Teruo; Ogawa, Yutaka; Nagasaki, Ryukichi (Japan Atomic Energy Research Inst., Tokyo). Apr 1971. 21p. (In Japanese and English). Dep. NTIS (U. S. Sales Only).

Mechanical properties of stainless steel are affected by neutron irradiation. Creep properties, of course, are largely reduced. It is deduced that this effect is principally caused by helium bubbles. It is important to study the effect of helium bubbles on the mechanical properties, especially creep-rupture, of stainless steel. There are two methods for injecting helium into stainless steel. One is by using a reactor, the other an accelerator. The use of an accelerator has some advantages over a reactor in that the activity of irradiated specimens is less and the irradiation time is shorter. Helium was injected into AISI Type 316 stainless steel using a cyclotron, then creep-rupture tests at 750°C were carried out. As a result, the presence of helium caused large reductions in rupture life and strain-to-rupture. Observing fractured surfaces with light and the scanning electron microscope, the effects of contained helium were clearly shown. (auth)

**55575** (LA-DC-12996) TRITIUM TRICK. Green, W. V.; Zukas, E. G.; Eash, D. T. (Los Alamos Scientific Lab., N. Mex.). [nd]. 2p. (CONF-710624-2). Dep. NTIS.

From International working session on fusion reactor technology conference; Oak Ridge, Tenn. (28 Jun 1971).

The use of tritium in accelerated damage rate studies on metals is discussed. Large controlled amounts of He in uniform concentration throughout thick samples can be readily obtained through radioactive decay of dissolved tritium gas to $^3He$. The name tritium trick was coined when helium added by this method was used to simulate $(n,\alpha)$ production of He in (simulated) hard flux radiation damage studies. As an example, Nb charged at 600°C under one atmosphere of tritium gas will collect 200 ppM He in only ten days. (P.C.H.)

**55576** (N-71-25034) NUCLEAR AND SPACE RADIATION EFFECTS ON MATERIALS: SPACE VEHICLE DESIGN CRITERIA. (National Aeronautics and Space Administration, Washington, D. C.). Jun 1970. 48p. (NASA-SP-8053). NTIS.

The results are presented of a study concerned with the identification of the significant property changes induced in structural materials by radiation from the nuclear reactor, the isotope power source, and from space, and the exposure levels at which these effects become important. Structural materials are defined as those that provide fundamental load-carrying capability or protection against the natural space environment while satisfying a functional requirement (e.g., viewing port for astronaut). Material properties affected by radiation are discussed in three categories: mechanical properties, including tensile strength, elasticity, elongation, impact properties, fatigue strength, hardness, shear strength, and dimensional stability; thermal properties, including thermal conductivity and stored energy; and optical properties including emissivity, absorptance, and reflectance. (auth) (STAR)

**55577** (NRL-7310) RESIDUAL ELEMENTS AND IRRADIATION EMBRITTLEMENT. Smidt, F. A. Jr.; Steele, L. E. (Naval Research Lab., Washington, D. C.). 25 May 1971. Contract AT(49-5)-2110. 22p.

Past work on the role of residual elements (particularly copper and phosphorus) in the enhanced irradiation embrittlement observed in pressure-vessel steels irradiated at 550°F is reviewed. Only three mechanisms for explaining the embrittlement are plausible—temper embrittlement, irradiation-enhanced diffusion to an interface, and enhanced nucleation of defect aggregates which produce hardening and embrittlement. Experiments employing scanning microscopy and Auger spectroscopy show that the embrittlement is not produced by segregation of copper or phosphorus at an interface. Microhardness recovery data indicate that the embrittlement in copper-containing alloys is accompanied by greater irradiation hardening. Transmission electron micrographs of special iron alloys doped with 0.3 at. % copper show a microstructure indicative of a higher concentration of defect aggregates than pure iron irradiated under the same conditions. These aggregates are believed to be vacancy in nature because vacancies are mobile during irradiation at 550°F and because no correlation between embrittlement and copper or phosphorus content is noted after irradiation at temperatures where vacancies are not mobile. (auth)

**55578** (RD/B/N-1990) APPLICATION OF SMALL ANGLE X-RAY SCATTERING TO THE STUDY OF IRRADIATION PRODUCED DEFECTS. Waterman, N. A. (Central Electricity Generating Board, Berkeley (England). Berkeley Nuclear Labs.). May 1971. 20p. Dep. NTIS (U. S. Sales Only).

The theoretical basis of the idea that x-ray small angle scattering may be used to study irradiation produced defects is presented and experimental difficulties are explored. Data are given which enable the feasibility of any projected experiment to be assessed. (auth)

**55579** (WAPD-TM-943) PHENOMENOLOGICAL MODEL OF IN-PILE STRESS RELAXATION (LWBR DEVELOPMENT PROGRAM). Wolfe, R. A. (Bettis Atomic Power Lab., Pittsburgh, Pa.). Aug 1971. Contract AT(11-1)-Gen-14. 21p. Dep. NTIS.

A phenomenological deformation model for the analysis of uniaxial in-pile stress relaxation is developed from a reference creep model that was proposed by Hesketh. The basis of this creep model is that the inelastic in-pile strain consists of two separate components, one of which is an exponential type of transient strain and the other a steady-state type of strain, with both components being linear functions of stress and fast neutron flux. The assumption of a mechanical equation of state, combined with these creep strain characteristics, gives the Maxwell-Kelvin linear viscoelastic model for the description of in-pile stress relaxation. Equations are derived for uniaxial stress relaxation and some implications of the deformation model are discussed. (auth)

**55580** RADIATION-INDUCED VOIDS IN HIGH-PURITY MAGNESIUM. Jostsons, A.; Farrell, K. (Oak Ridge National Lab., Tenn.). Radiat. Eff.; 8: No. 3-4, 287-8(Apr 1971).

Hcp magnesium was irradiated at ~0.36 to 0.4 Tm to a fast-neutron fluence of $2 \times 10^{21}$ n/cm$^2$ in the HFIR. The swelling amounted to 1.9%, and transmission-electron microscopy showed many voids arranged in layers parallel to the basal planes. Their shape is a hexagonal polygon squashed in (0001), with a maximum size of 2000 Å along the long axes. Stacking faults are also present on the basal planes. (D.L.C.)

**55581** RADIATION-INDUCED SWELLING OF STAINLESS STEEL. Shewmon, P. G. (Argonne National Lab., Ill.). Science; 173: No. 4001, 987-91(10 Sep 1971).

Significant swelling (1 to 10%) due to small voids has been found in stainless steel when it is exposed to fast neutron doses less than expected in commercial fast breeder reactors. The main features of this new effect are: the voids are formed by the precipitation of a small fraction of the radiation-produced vacancies; the voids form primarily in the temperature range 400 to 600°C (750 to 1100°F); and the volume increases with dose (fluence) at a rate between linear and parabolic. The limited temperature range of void formation can be explained, but the effects of fluence, microstructure, and composition are determined by a competition between several kinetic processes that are not well understood. This swelling does not affect the feasibility or safety of the breeder reactor, but will have a significant impact on the core design and economics of the breeder. Preliminary results indicate that one cannot eliminate the effect, but cold-working, heat treatment, or small changes in composition can reduce the swelling by a factor of 2 or more. Testing is hampered by the fact that several years in EBR-II are required to accumulate the fluence expected in demonstration plants. Heavy-ion accelerators, which allow damage rates corresponding to much higher fluxes than those found in EBR-II, hold great promise for short-term tests that will indicate the relative effect of the important variables. (auth)

**55582** THEORETICAL MODEL OF FAST-NEUTRON-INDUCED SWELLING IN METALS. Konobeev, Yu. V.; Subbotin, A. V. At. Energ. (USSR); 31: No. 3, 219-20(Sep 1971). (In Russian).

A simple theoretical model of fast neutron-induced swelling in metals is proposed. It is assumed that the swelling consists in the grain volume growth due to diffusion of interstitials and vacancies to the grain boundary. The difference of diffusional fluxes of point defects at grain boundaries is achieved by using the nonstationary diffusion equations for interstitials and vacancies. It is shown that the proposed model describes qualitatively the observed dependences of the swelling on the neutron fluence and the irradiation temperature. Alloying is proposed to be one of the means for reducing swelling. (auth)

**55583** EFFECTS OF NEUTRON IRRADIATION ON AGEING AND PRECIPITATION PHENOMENA IN COPPER-BERYLLIUM ALLOYS WITH OR WITHOUT ADDITIONAL ELEMENTS. Yoshida, Hiroyuki (Kyoto Univ.); Yamamoto, Satoru; Murakami, Yotaro; Kodaka, Hisao Trans. Jap. Inst. Metals; 12: No. 4, 229-37(Jul 1971).

In order to clarify the effects of neutron irradiation on the aging characteristics of copper-beryllium alloys with or without

small amounts of additional elements, the changes in electrical resistivities, Vickers microhardness tensile properties, electron microstructures, and selected area diffraction patterns were measured during aging after irradiation with about $1 \sim 4 \times 10^{17}$ nvt at reactor ambient temperature. It was found that the enhancement of Guinier–Preston (G.P.) zone formation during irradiation occurred in supersaturated alloys, and the dissolution of G. P. zones formed and the enhancement of $\gamma'$ precipitation occurred during subsequent aging. On the basis of the experimental results, the mechanism of these effects is discussed relating the interaction with the atoms of the third elements. (auth)

**55584** EFFECT OF NEUTRON IRRADIATION ON $Ni_3Cr$. Artsishevskii, M. A. (Inst. of Precision Alloys, Moscow). Fiz. Metal. Metalloved.; 31: No. 1, 202-4(Jan 1971). (In Russian).

The electrical resistance of $Ni_3Cr$ as a function of temperature was studied after fast neutron irradiation of the samples with $4.7 \times 10^{16}$ n/cm$^2$. Four irradiation temperatures were used: 190, 255, 305, and 353°C. At temperatures below 100°C, neutron bombardment causes a fall in the electrical resistance of $Ni_3Cr$ (1% for $10^{19}$ n/cm$^2$). At much higher temperatures radiation causes an increase in the resistance—as much as 5% in an extreme case. (K.S.W.)

**55585** RADIATION STRENGTHENING AND EMBRITTLEMENT IN HEAVY SECTION PLATE AND WELDS. Berggren, R. G.; Stelzman, W. J. (Oak Ridge National Lab., Tenn.). Nucl. Eng. Des.; 17: No. 1, 103-15(1971).

Fast neutron-induced changes in mechanical properties of a 12-in. thick manganese–molybdenum–nickel steel plate and notch-impact transition temperature and decreases in ductility are given for several temperatures of irradiation. Some observations using an instrumented Charpy testing machine are also presented. (auth)

**55586** POSTIRRADIATION DYNAMIC TEAR AND CHARPY-V PERFORMANCE OF 12-IN. THICK A533-B STEEL PLATES AND WELD METAL. Hawthorne, J. R. (Naval Research Lab., Washington, D. C.). Nucl. Eng. Des.; 17: No. 1, 116-30(1971).

Charpy-V ($C_V$) and dynamic tear (DT) test comparisons are developed for the irradiated condition of two 12 in. thick A533-B steel plates and a submerged arc weld deposit. Materials for the investigation were donated by the U. S. Atomic Energy Commission's Heavy Section Steel Technology (HSST) Program. Individual plates were identified as HSST plates 01 and 02; the weld was identified as weld 50. Low temperature (<300°F) and elevated temperature (550°F) irradiations were conducted. Fluences for the eight irradiation experiments ranged from 2.5 to $3.3 \times 10^{19}$ n/cm$^2$ (<1 MeV). Postirradiation $C_V$ and DT mid-energy transition temperature increases were found comparable for both plate and weld deposit (quarter thickness position evaluations). For the case of plate, percentage reductions in $C_V$ and DT shelf energy with irradiation also compared well. As a result, preirradiation DT to $C_V$ shelf energy ratios appeared to be retained with irradiation. Shelf observations are in agreement with recent findings for A543, A302-B, and other A533 steel plates which illustrate a DT to $C_V$ shelf energy ratio of 8.0 : 1 for pre- and postirradiation conditions. It was concluded that postirradiation DT properties of A533-B plate, including mid-energy transition and shelf level, can be calculated with reasonable accuracy from postirradiation $C_V$ results for use in fracture safety analyses. Assessments of shelf level toughness before and after irradiation were developed by ratio analysis diagram (RAD) procedures. Unlike observations for plate, a significant reduction in DT to $C_V$ shelf energy ratio by irradiation was found for the weld deposit. Weld metal fracture appearances suggest preferred paths for fracture within the duplex (layered) microstructure. Radiation embrittlement sensitivity at 550°F was found to increase with increasing copper content as expected; however, embrittlement sensitivities of all three materials exceeded expectations. An influence of nickel content on radiation embrittlement sensitivity development is proposed. (auth)

**55587** FRACTURE AND TENSILE BEHAVIOR OF NEUTRON-IRRADIATED A533-B PRESSURE VESSEL STEEL. Hunter, C. W.; Williams, J. A. (Hanford Engineering Development Lab., Richland, Wash.). Contract AT(45-1)-1830. Nucl. Eng. Des.; 17: No. 1, 131-48(1971).

The fracture potential of reactor pressure vessel materials can be evaluated in terms of critical fracture load-flaw size relationships by determining the linear elastic fracture mechanics $K_{Ic}$ toughness properties. Irradiation of 1-in. thick fracture mechanics specimens of A533 grade B class 1 steel to a fluence of $2 \times 10^{19}$ n/cm$^2$ (E > 1 MeV) at 540°F produced a shift of 230°F in the 50,000-psi$\sqrt{\text{in}}$ $K_{Ic}$-level. The measurement capability of small fracture mechanics specimens was limited to regions of lower toughness. The difficulty of irradiating large specimens will normally preclude $K_{Ic}$ determinations at higher toughness levels. Therefore, experimental correlations were needed between $K_{Ic}$ and impact energy behavior of materials that exhibit a degraded upper shelf toughness. Irradiation at fluence levels of $2 \times 10^{19}$ and $4.3 \times 10^{19}$ produced a 45 and 54% increase, respectively, in the room temperature yield strength. Post-irradiation annealing of tensile specimens revealed that reduction of irradiation hardening commenced above 540°F and was 70% complete at 650°F. (auth)

**55588** TRANSITION TEMPERATURE CONSIDERATIONS FOR THICK-WALL STEEL NUCLEAR PRESSURE VESSELS. Canonico, D. A. (Oak Ridge National Lab., Tenn.). Nucl. Eng. Des.; 17: No. 1, 149-60(1971).

The operation of nuclear power plants is limited by the properties of their steel pressure vessels. Of particular concern is the ductile-to-brittle transition temperature of the steel and how it is affected by irradiation. The current technique for assessing the effects of irradiation ignores two facts: the maximum fluence is imposed on the inner surface; and the thick-walled vessel is self-shielding. When these facts are considered, the predicted maximum 30 ft lb $C_V$ temperature of the pressure vessel is near 150°F for a fluence of $6 \times 10^{19}$ neutrons/cm$^2$ (>1 MeV). Further, the maximum 30 ft lb temperature occurs at a location about 2 in. below the inner surface. The weld metal, which does not exhibit the through-the-thickness variation in toughness, may have the highest 30 ft lb $C_V$ temperature, and this will be at the inner surface. (auth)

# Ceramics and Cermets

*Refer also to abstracts 55369 and 55509.*

## Corrosion and Erosion

*Refer also to abstracts 55371, 55372, 55374, 55540, and 57109.*

**55589** (JAERI-Memo-4438) KINETICS OF CARBON TRANSFER BETWEEN URANIUM CARBIDE FUEL AND STAINLESS STEEL BONDED WITH SODIUM. Nishio, Gunji; Shimokawa, Junichi (Japan Atomic Energy Research Inst., Tokyo). May 1971. 14p. Dep. NTIS (U. S. Sales Only).

The compatibility of carbide fuels and austenitic stainless steel was estimated by comparing experimental and calculated values of carbon transfer. Hyperstoichiometric uranium carbide containing $^{14}C$ (6.0 wt.% carbon) and stainless steel (AISI 304) specimen were enclosed in a nickel capsule with sodium and heated to 750°C. The degree of carburization of the steel was determined by monitoring $^{14}C$ using a $2\alpha$ gas-flow counter. The distribution profile of $^{14}C$ appeared to be nearly exponential, and the radioactivity on the surface of the stainless steel specimen increased with increase of the heating time. The kinetics of carbon transfer was interpreted by assuming that carbon atoms were leached out into sodium from $UC_2$ platelets which had been precipitated in the UC, and then diffused along the grain boundaries of stainless steel accompanied by the formation of new carbide such as $Cr_{23}C_6$. (auth)

## Preparation and Fabrication

*Refer also to abstracts 54711, 54716, 54717, 54841, 55411, 55412, 55414, and 55419.*

**55590** (EIR-192) PLUTONIUM FUEL PROGRAM. Annual Report, 1970. (Eidgenoessisches Institut fuer Reaktorforschung, Wuerenlingen (Switzerland)). May 1971. 133p. (In German). Dep. NTIS (U. S. Sales Only).

The status of the Pu fuel program of the Swiss institute for reactor research (EIR) is presented. Covered are production of $PuO_2$ sols, $UO_2$ sols, gel experiments in microcolumns, and gel extraction. Production of carbides and phase studies are discussed. Construction of the radiation facilities, special problems with the projected fuel elements, and the fuel for preliminary experiments are described. Installations for $\alpha$ measurements in hot cells and equipment for longitudinal scanning are also described. (H.B.G.)

**55591** (JUL-735-RW) ON THE FORMATION AND DEPOSITION OF PYROCARBON FROM METHANE IN THE TEMPERATURE RANGE OF 1650 TO 2150°C. Suetterlin, Lothar (Kernforschungsanlage, Juelich (West Germany). Institut fuer

XUM

Reaktorwerkstoffe). Feb 1971. 96p. (In German). Dep. NTIS (U. S. Sales Only).

The pyrolysis of methane was studied in the temperature range from 1650 to 2150°C at a gas pressure of 100 torr. During the pyrolysis the processes on the hot deposition surface were followed by measurement of the electrical resistance of the wire and the wattage used. Simultaneously the gases formed were determined quantitatively by mass spectrometric analysis. The experimental results showed that the precipitation of the pyrocarbon occurs only after a relatively long tempering phase. The pyrocarbon precipitation, which begins simultaneously with the occurrence of high acetylene in the gas phase, precedes the formation of ethane, ethene, propane, propene, butene, and butadiene. The pyrocarbon is precipitated on the hottest place in the reaction vessel, the heated W wire. The structure of the precipitated pyrocarbon is dependent on the temperature. Although the temperature drops to room temperature within a few minutes after shutting off the wire heating, alterations in the gas composition occur after some time. There was disagreement in the energy balance obtained on the basis of the quantitative determination of the gaseous pyrolysis products. A pyroaggregate concept was proposed to explain these results. (tr-auth)

**55592** (ORNL-4682, pp 144-59) SOL-GEL PROCESSES FOR THE URANIUM FUEL CYCLE. (Oak Ridge National Lab., Tenn.).

In Chemical Technology Division annual progress report.

Research progress is reported on: preparation of $UO_2$ sol by the CUSP process, development of the $UO_2-PuO_2$ sol-gel process, microsphere forming and preparation of $UO_2-PuO_2$ materials. (M.C.G.)

**55593** (ORNL-4682, pp 163-7) PREPARATION OF $^{233}UO_2$ FOR LIGHT-WATER BREEDER REACTORS. (Oak Ridge National Lab., Tenn.).

In Chemical Technology Division annual progress report.

Research progress is reported on: process development and flowsheets, plant modification, design of equipment for the $UO_2$ conversion line, receipt and storage of $^{233}U$ feed material, plant safety, and site preparation. (M.C.G.)

**55594** (ORNL-4682, pp 218-28) PREPARATION AND PROPERTIES OF ACTINIDE OXIDES. (Oak Ridge National Lab., Tenn.).

In Chemical Technology Division annual progress report.

Thoria desintering studies, adsorption of nitric acid on the surface of urania, and preparation of carbides and carbonitrides are discussed. (M.C.G.)

**55595** PREPARATION AND STRUCTURE OF ZIRCONIUM NITRIDE SPHERES. Streiff, R.; Smeltzer, W. W. (McMaster Univ., Hamilton, Ont.). J. Nucl. Mater.; 41: No. 1, 109-11(Oct 1971).

A method is described for the preparation of zirconium nitride spheres, 44 to 150 $\mu$ diameter, suitable for nitrogen diffusion studies. Approximately 80% of the spheres were single-phase zirconium nitride after one pass of the incompletely nitrided feed material through an arc. The remaining spheres exhibited varying amounts of a two-phase structure containing zirconium nitride and the metal-nitrogen solid solution. (P.C.H.)

**55596** SINTERED ZIRCONIA ELECTROLYTE FILMS IN HIGH-TEMPERATURE FUEL CELLS. Maskalick, N. J.; Sun, C. C. (Westinghouse Research Labs., Pittsburgh). J. Electrochem. Soc.; 118: No. 8, 1386-91(Aug 1971).

Thin-film fuel cells employing stabilized cubic zirconia as an oxygen anion-conducting electrolyte depend on an effective separation of fuel gas and air by the dense zirconia electrolyte layer. Fully stabilized solid-zirconia electrolyte films have been prepared by reactive sintering of zirconia, $ZrO_2$, and calcium zirconate, $CaZrO_3$. Such films are employed as the electrolyte in high-temperature fuel cells. Electrolyte film conductivity is at least 50% of that expected from the geometry of test cells. The films are sufficiently pure and gastight to allow near-theoretical open-circuit voltages to be displayed. (auth)

**55597** PREPARATION OF MIXED OXIDE NUCLEAR FUEL. Pawliw, J. (to Canadian General Electric Co. Ltd.). Canadian Patent 872,722. 8 Jun 1971.

An enriched mixed oxide nuclear fuel was prepared at reduced cost with enhanced safety by impregnating the shaped elements with a solution containing a salt of the enrichment material, which is then converted to the metallic oxide of Pu, $^{233}U$, or $^{235}U$ or mixture thereof. This method limits the number of glove box operations, thus enhancing safety and reducing cost, while the need to recover enrichment material from damaged pellets may be obviated. (F.S.A.) (Canada)

**55598** PREPARATION OF MIXTURES OF TUNGSTEN CARBIDE AND COBALT BY MEANS OF ULTRASONIC VIBRATIONS. Letunovskii, V. V.; Androsov, V. N.; Petrovskii, E. A. (Krasnoyarsk Engineering Inst., USSR). Sov. Powder Met. Metal Ceram. (Engl. Transl.); 10: No. 3, 244-6(Mar 1971).

Translated from Porosh. Met., Akad. Nauk Ukr. SSR; 10: No. 3, 93-6(Mar 1971).

The comminuting effects of ultrasonic vibrations were studied in WC-Co mixtures with initial particle sizes of 0.5 to 6 $\mu$, using ethyl alcohol as the working medium. The particle size distribution peak was rapidly reduced from 4 $\mu$ to 1 $\mu$. After 60 min, 96% of all the particles had a maximum size less than 2 $\mu$; for the same result, wet milling for 100 hr would be required. (D.L.C.)

**55599** PRODUCTION OF PARTS OF COMPLEX SHAPE IN LANTHANUM HEXABORIDE. Medvedev, O. G.; Trunov, G. V.; Chernyak, L. V.; Shlyuko, V. Ya. (Kiev Engineering Inst.). Sov. Powder Met. Metal Ceram. (Engl. Transl.); 10: No. 3, 250-1(Mar 1971).

Translated from Porosh. Met., Akad. Nauk Ukr. SSR; 10: No. 3, 101-2(Mar 1971).

A study was made of the hot casting under pressure of complex $LaB_6$ parts. The viscosity vs binder content relation showed that the optimum content of the 85% paraffin wax-15% beeswax in $LaB_6$ slips was 10.5 wt %. Sintering of the cast parts removed the binder traces and resulted in densities of 95 to 97%. (D.L.C.)

**55600** TECHNOLOGICAL CONDITIONS FOR HOT PRESSING OF ZIRCONIUM DIOXIDE. Kainarskii, I. S.; Alekseenko, L. S.; Degtyareva, E. V. Sb. Nauch. Tr., Ukr. Nauch.-Issled. Inst. Ogneuporov; No. 9, 125-38(1968). (In Russian).

Various factors which affect the hot pressing of $ZrO_2$ were investigated: the properties of the original powder, temperature, pressure, and its time of application. Optimal conditions were established for the preparation of dense pellets. Hot pressing of monoclinic $ZrO_2$ with 6% added CaO forms solid solutions with a cubic structure. Preliminary high-temperature treatment of monoclinic $ZrO_2$ diminishes its hot-pressing properties. Hot-pressing of $ZrO_2-6\%$ CaO at 150 kg.cm$^2$ achieved a density of 5.6 g/cm$^3$, or 98.4% of the theoretical density. (28 references) (K.S.W.)

**55601** PREPARATION AND NONSTOICHIOMETRY OF SAMARIUM HEXABORIDE. Niihara, Koichi (Tohoku Univ., Sendai). Bull. Chem. Soc. Jap.; 44: No. 4, 963-7(Apr 1971).

Samarium hexaboride was prepared by the borothermal reaction; $2\ Sm_2O_3 + (6 + 4x)B = 4\ SmB_x + 3\ B_2O_2$. The residual oxygen content amounted to less than 0.03 w/o under optimum reaction conditions heating at 1650°C for 2 hr under a high vacuum. It was found by x-ray intensity and density measurements that the samarium hexaboride stayed stable over a large nonstoichiometric region from $Sm_{0.68}B_6$ to $SmB_6$. These extensive nonstoichiometric properties of samarium hexaboride can be explained in terms of the required electron numbers of the $SmB_6$ network in hexaboride. (auth)

**55602** HYDROTHERMAL PREPARATION OF SOME OXIDES AND SOME OXIDE HYDROXIDES AT TEMPERATURES UP TO 900°C AND PRESSURES UP TO 80 KB. Christensen, A. Noerlund (CNRS, Grenoble, France). Mater. Res. Bull.; 6: No. 8, 691-7(Aug 1971).

Oxides and hydroxides of scandium, chromium, iron, nickel, zinc, gallium, indium, and bismuth were treated hydrothermally at temperatures up to 900°C and pressures up to 80 kb. ScOOH and CrOOH with the indium oxide hydroxide structure, and GaOOH with the diaspore structure were obtained. A new gallium hydroxide was found as well as the known forms of $\alpha-Fe_2O_3$, NiO, ZnO, and $\alpha-Bi_2O_3$. (auth)

**55603** INFLUENCE OF POWDER CHARACTERISTICS ON PROCESS AND PRODUCT PARAMETERS OF URANIUM DIOXIDE. Runfors, Ulf (Aktiebolaget Atomenergi, Stockholm). pp 311-38 of Modern Developments in Powder Metallurgy. Vol. 5. /Hausner, Henry H. (ed.). New York; Plenum Publishing Corp. (1971).

From International powder metallurgy conference; New York, N. Y. (12 Jul 1970).

A previously established production technique for $UO_2$ in Sweden is discussed. The efforts in Sweden were concentrated on finding correlations between the powder properties on the one hand and on the other hand the variables of the individual or partial processes such as pressing, sintering, etc. or intermediate product properties, which often introduce boundary limitations in the process. Next, six commercial $UO_2$ powders from UK, USA, and Canada are discussed. The object was to establish suitable pelletizing techniques. Data obtained from the six $UO_2$ powders were extracted and treated in the same way as in the case of the Swedish powder in order to test the generality of those findings. The results demonstrated that good correlations between powder prop-

erties on the one hand and process variables and product properties on the other can be established with certain provisions. The major conclusion was that powder metallurgy or pelletizing can be regarded as an optimization problem that could become quite valuable to the production man if supplemented by economic parameters. (P.C.H.)

**55604** DEPOSITION OF PYROLYTIC CARBON IN SILICA REACTORS. Cullis, C. F. (City Univ., London); Norris, A. C. Carbon; 9: No. 4, 517-20(Aug 1971).

When surface carbons are produced by the pyrolysis of gaseous hydrocarbons in a silica tube heated to about 1000°C, spectrographic analysis shows the presence of up to 1% silicon even when the carbon is deposited on a metal substrate. It seems likely that hydrocarbon radicals react with silica to produce volatile organo-silicon species. As a result, silicon eventually becomes incorporated in the solid carbon, although neither the free element nor silicon carbide appear to be formed. Consideration of the present and previous results indicates that the chemical reactivity of silica surfaces needs to be taken into account in studies of pyrolytic deposition and of catalysis at high temperatures. (auth)

**55605** PYROLYTIC TITANIUM AND ZIRCONIUM NITRIDES AND FIELDS OF THEIR USE. Emyashev, A. V.; Kilin, V. S.; Martynov, S. Z.; Sharova, A. V. Tsvetn. Metal.; No. 12, 30-2 (Dec 1970). (In Russian).

The chemical mechanisms responsible for the pyrolytic formation of TiN and ZrN from the corresponding tetrachlorides by interaction with N and H are discussed and the optimum constitution of the mixture for producing such reactions is considered. Examples of the microstructure of the refractory nitrides so obtained are presented. The materials in question are, for example, of particular value in creating refractory crucibles resistant to molten Fe. (Metals Abstr.)

**55606** SINTERING AND PROPERTIES OF YTTRIUM OXIDE CERAMICS. Borovkova, L. B.; Lukin, E. S.; Poluboyarinov, D. N.; Sapozhnikova, E. B. (Inst. of Chemical Tech., Moscow). Metal Sci. Heat Treat. (USSR) (Engl. Transl.); No. 11-12, 717-22 (Nov-Dec 1970).

Translated from Metalloved. Term. Obrab. Metal.; No. 11, 39-45(Nov 1970).

Preparation of dense ceramics from $Y_2O_3$ was investigated. It was found that high density of $Y_2O_3$ ceramics (approximately 95% of the theoretical) can be obtained by firing at 1750° in a furnace heated with kerosene. $Y_2O_3$ ceramics with a 96.5% theoretical density have a high strength at elevated temperatures, a low deformation rate, and a volatilization rate in vacuum that is less than that of corundum, and a relatively moderate electric conductivity. (auth)

## *Properties Evaluations*

*Refer also to abstracts 55428, 55469, 55481, 55500, 56087, 56346, 56355. 57053, and 57069.*

**55607** (JUL-739-PC) MASS-SPECTROSCOPIC DETERMINATION OF THE HEAT OF FORMATION AND THE INVESTIGATION OF THE EVAPORATION BEHAVIOR OF EuN, BN, AND AlN. Wu, Chung-Hsiung (Kernforschungsanlage, Juelich (West Germany). Institut fuer Physikalische Chemie). Mar 1971. 60p. (In German). Dep. NTIS (U. S. Sales Only).

The measurement of the heats of formation and the study of the evaporation behavior at high temperatures of AlN, BN, and EuN were made using a new mass-spectrographic arrangement and the Knudsen effusion method. The temperature was maintained within ±0.8°K constant in the temperature range from 1500 to 1800°K. The results showed that in the evaporation of AlN, BN, and EuN only nitrogen appeared in the gaseous phase and no gaseous metallic nitrides. With increasing evaporation time, the intensity of the nitrogen at a given temperature first decreased and then reached a constant value. Measurements made in the constant range gave the values: $\Delta H$ (AlN) = 62 ± 1.1 kcal/mol at 1615°K, $\Delta H$ (EuN) = 31.1 ± 0.25 kcal/mol at 1070°K, $\Delta H$ (BN) = 58.5 ± 0.5 kcal/mol at 1600°K. The evaporation temperature for AlN was increased to 1770°K. After extended evaporation time with decreasing nitrogen mol fraction to $AlN_{0.5}$ the metal Al was detected in the gas phase. The lattice constants were altered. For the study of EuN at increased temperature (1160°K) the same evaporation behavior was observed. During increasing nitrogen impoverishment of the sample, the spectrum of the metal in the gas phase was examined. The isotope distribution in the gaseous metal component was 47.8% for $^{151}Eu$ and 52.2% for $^{153}Eu$. Metallic Eu was detected in the sample in addition to the EuN. In the evaporation of BN at a temperature of 1770°K, only a low intensity of B in the gas phase was detected. The pressure of the gas phase at this order of magnitude is negligible. Because of the incongruent behavior of BN in its evaporation, it is assumed that the released B remains amorphous in the solid phase. (tr-auth)

**55608** (LB/G-3074) METAL-FIBRE-REINFORCED CERAMICS (A REVIEW). Busalov, Yu. E.; Kop'ev, I. M. Translated by J. A. Bartlett (Atomic Energy Research Establishment, Harwell, Eng.), from Fiz. Khim. Obrab. Mater.; No. 1, 57-69(1970). 22p. Dep. NTIS (U. S. Sales Only).

Data on ceramic-metal fiber composites are presented which show that it is possible, in principle, to fabricate quality ceramic-metal fiber composite systems. Continuous fibers, meshes or ribbons are the most suitable forms of reinforcing elements. The maximum fiber volume fraction which contributes to an effective increase in the mechanical properties is 30 to 40%. Reinforcement significantly improves the mechanical properties of the materials, particularly the impact strength and thermal shock resistance. Composites based on pure $Al_2O_3$, $SiO_2$, SiC, mullite, and mixtures of mullite and $Al_2O_3$(58.5% mullite and 41.5% $Al_2O_3$) reinforced with molybdenum and niobium are the most promising. (auth)

**55609** (ORNL-tr-2456) STUDY OF THE REACTIVITY OF $U_3O_8$-Al DISPERSIONS. Gentile, Erberto Francisco; Cintra, Sebastiao Hermano Leite; Tracanella, Roberto Barata. Translated by R. Gregg Mansfield (Oak Ridge National Lab., Tenn.), from Metalurgia (Sao Paulo); 26: No. 149, 305-9(1970). 10p. (CONF-690733-1). Dep. NTIS.

From twenty-fourth annual congress of ABM, Sao Paulo, Brazil (Jul 1969).

Studies made earlier on the process of fabrication of fuel plates based in $U_3O_8$-Al dispersions sheathed in aluminum alloys revealed the existence of phases other than $U_3O_8$ and aluminum in the core of the elements of this design. In order to determine the cause of the appearance of these other phases as well as to identify them, experiments were carried out at temperatures of 450°C, equivalent to the blister tests normally performed, as well as tests with heat fluctuating between temperatures of 83 ± 2°C and room temperature. For the identification of these phases a two-stage mechanism proposed by other investigators was used. The analysis of results obtained by metallographic examination led to the conclusion that the phases could be $UO_2$ or $UAl_4$, or a combination of the two in the case of the low temperatures at which the tests were made. The cause of their formation is probably a rupture of the protective barrier of $Al_2O_3$ owing to a process of deformation occurring during rolling as well as a shearing process resulting from expansion and contraction reactions between the ceramic and the metallic phase during the thermal fluctuation. (auth)

**55610** NATURE OF BRITTLE-TO-DUCTILE TRANSITION IN $UO_2$-20 wt. PERCENT $PuO_2$ NUCLEAR FUEL. Roberts, J. T. A.; Wrona, B. J. (Argonne National Lab., Ill.). J. Nucl. Mater.; 41: No. 1, 22-38(Oct 1971).

The four-point bend test was used to determine the brittle-to-ductile transition temperature $T_c$ in a mechanically blended $UO_2$-20 wt % $PuO_2$ fuel as a function of strain-rate $\dot{\epsilon}$ ($0.085-0.73\ hr^{-1}$), and volume-fraction porosity P ($0.034-0.12$). $T_c$ was located at about half the melting temperature on the absolute scale, and increased as the strain rate increased according to the relation $T_c(°C) = (5.5 \times 10^4)/(28.6 - \ln \dot{\epsilon}) - 273$, and decreased with an increase in porosity, according to the relation $T_c(°C) = 1487 - 1588$ P. Brittle fracture originated at existing surface flaws, and, therefore, crack propagation was the important process. A reduction in fracture toughness was achieved by increasing the strain rate. Pores can act as "crack blunting" agents, and the effects of blunting partly offset the reduction in strength due to a decrease in load-bearing surface. High-temperature deformation was described by the conventional Arrhenius expression, and the implication was that grain-boundary sliding was responsible for the enhanced ductility of the mixed oxide about 100°C above $T_c$. The results are discussed relative to an in-reactor fuel-cracking model. (auth)

**55611** DIFFUSION OF FISSION PRODUCT IONS IN GLASSES. Kahl, L.; Schiewer, E. (Hahn-Meitner-Institut fuer Kernforschung, Berlin). Atomwirt., Atomtech.; 16: No. 8-9, 434-5(Aug-Sep 1971). (In German).

The diffusion of radioactive Rb, Cs, and Sr in glass was studied and compared with that of sodium. The results showed that diffusion of the fission products consisted of ion exchange with the sodium ion of the glass. If the activation energy for sodium diffusion is known with sufficient accuracy, only a few experimental studies are necessary to assess the temperature dependency of diffusion for Rb, Cs, and Sr. (H.B.G.)

XUM

**55612** GAS PERMEABILITY OF EXTRUDED GRAPHITE. Jones, B. F.; Duncan, R. G. (Atomic Energy of Canada Ltd., Pinawa, Manitoba). Carbon; 9: No. 3, 229-36(May 1971).

The gas permeability of extruded graphite is extremely sensitive to the direction in which gas flow is measured. The technique of permeability measurement was used to study the variation of pore structure of an extruded graphite and the data showed that a distinct directional pore pattern is present in this material. The factors which affect the pore structure of extruded graphites are discussed. (auth) (UK)

**55613** VITROCERAMIC NUCLEAR FUEL COATING. II. COATINGS BASED ON ALUMINO-SILICATES. Maxim, I. V.; Apostol, D. (Comitelul de Stat Pentru Energia Nucleara, Bucharest). J. Nucl. Mater.; 41: No. 1, 80-6(Oct 1971).

The feasibility of coating vitroceramic nuclear fuel with an aluminosilicate glaze was investigated. Taking into account the requirements (neutron economy, thermal expansion, and physical, chemical, and irradiation stability), which restrict chemical composition, it was concluded that the glaze might contain only the following oxides: $SiO_2$, $Al_2O_3$, $Na_2O$, $K_2O$, MgO, CaO, BaO, ZnO, $SnO_2$, $ZrO_2$, $P_2O_5$. The characteristics of some glazes, obtained on the basis of these oxides, are reported and their ability to satisfy the required conditions is assessed. The best results were obtained with a zirconium-based glaze. The conditions for making such a glaze are described. (auth)

**55614** THERMODYNAMIC PROPERTIES OF TERNARY REFRACTORY CARBIDES. II. ZIRCONIUM–URANIUM–CARBON AND ZIRCONIUM–HAFNIUM–CARBON. Hoch, M.; Hapase, M. G.; Yamauchi, S. (Univ. of Cincinnati). J. Electrochem. Soc.; 118: No. 9, 1503-6(Sep 1971).

The thermodynamic properties of [ternary] zirconium–uranium–carbide $Zr_xU_{1-x}C_y$ and zirconium–hafnium–carbide $Zr_xHf_{1-x}C_y$ both with a sodium chloride type structure were studied using the time-of-flight mass spectrometer. The ratio of the activities of the components was measured as a function of composition at 2440°K, and from the variation of the ratio of activities with composition, the pairwise interaction energies were obtained. In the Zr–U–C system, the metal–metal interaction energy, $[E_{12} - (E_{11} + E_{22}/2)]$, was found to be 6.7 ± 0.6 kcal/mole, a value close to that obtained in the body-centered cubic, zirconium–uranium [metallic] system. The difference between the zirconium–carbon and uranium–carbon interaction energies, $E_{13} - E_{23}$ can be expressed as a function of composition by the equation $E_{13} - E_{23} = 8.5 \pm 0.05 - [23.6 \pm 0.2]x$ in kcal/mole. In the Zr–Hf–C system, the metal–metal interaction energy, $[E_{12} - (E_{11} + E_{22}/2)]$ was found to be 1.9 ± 0.3 kcal/mole, again a value close to that obtained in the body-centered cubic, zirconium–hafnium [metallic] system. The difference between the zirconium–carbon and hafnium–carbon interaction energies, $E_{13} - E_{23}$, can be expressed as a function of composition by the equation $E_{13} - E_{23} = 9.8 \pm 0.05 - [7.5 \pm 0.2]x$ in kcal/mole. (auth)

**55615** THERMODYNAMIC PROPERTIES OF TERNARY REFRACTORY CARBIDES. I. ZIRCONIUM–NIOBIUM–CARBON. Jun, C. K.; Hoch, M. (Univ. of Cincinnati). J. Electrochem. Soc.; 118: No. 9, 1498-1503(Sep 1971).

The nonstoichiometry of zirconium–niobium–carbide with the sodium chloride type structure, $Zr_xNb_{1-x}C_y$, was studied by measuring the activities of the components as a function of composition. Equations for the activities of the components as a function of composition were derived from statistical considerations, based on the pairwise interaction energies between various components. The energy terms, $(E_{12} - (E_{11} + E_{22})/2)$, $(E_{13} - E_{23})$, and $E_{33}$ were determined by measuring the variation with composition of the ratio of the activities of the various components. The ratio of activities of the various components at one composition was determined in one experiment; thus, the usual errors in temperature measurement were eliminated. A Bendix Time-of-Flight Mass Spectrometer was used. The samples were prepared by heating the required amounts of oxides and graphite in a high-vacuum induction furnace. The metal–metal interaction energy was not much different from that in the bcc metallic zirconium–niobium system. The difference between the zirconium–carbon and the niobium–carbon interaction energies $(E_{13} - E_{23})$ was linearly dependent on composition $(E_{13} - E_{23}) = (1.08 \pm 0.11) - (6.15 \pm 0.44)$ x kcal/mole whereas $E_{33}$, the carbon–carbon interaction energy, can be expressed as $E_{33} = 15.62 + 9.37x - 29.50x(1 - x)$ kcal/mole. (auth)

**55616** SURFACE ENERGY OF URANIUM DIOXIDE. Bratton, R. J.; Beck, C. W. (Westinghouse Research Labs., Pittsburgh). J. Amer. Ceram. Soc.; 54: No. 8, 379-81(Aug 1971).

Using the method of interfacial angle equilibrium in the system $UO_2$–Ni, a surface energy of 754 ± 150 ergs/cm$^2$ was determined for $UO_{2.01}$ at 1500°C in high-purity Ar. The absolute interfacial energies in the system $UO_2$–Ni at 1500°C were also determined. (auth)

**55617** PHASE EQUILIBRIA, VAPOR PRESSURE, AND KINETIC STUDIES IN THE URANIUM–NITROGEN SYSTEM. Hoenig, C. L. (Univ. of California, Livermore). J. Amer. Ceram. Soc.; 54: No. 8, 391-8(Aug 1971).

Uranium mononitride was studied in an automatic recording balance-furnace system capable of high vacuum or precisely controlled gas pressure. The decomposition pressure of $U_2N_3$, which was measured at 1483 and 1607°K, agreed with values in the literature. Uranium sesquinitride compositions were substoichiometric at the U-rich boundary, with compositions of $UN_{1.48 \pm 0.01}$ at 1483°K and 130 torr $N_2$ and $UN_{1.45 \pm 0.01}$ at 1607°K and 700 torr $N_2$. UN has very narrow composition limits ($UN_{0.995}$ to $UN_{0.997}$) from 1100 to 2450°K at $N_2$ pressures below 700 torr. In vacuum at 1538°K, the composition is $UN_{0.9954 \pm 0.0001}$. Vaporization rates for single-phase UN were studied by the Knudsen and Langmuir methods using temperatures from 1900 to 2860°K and $N_2$ pressures from $10^{-4}$ to 130 torr. The enthalpy of vaporization ($\Delta H^\circ_{298}$) for the reaction $UN(s) = U(g) + \frac{1}{2}N_2(g)$ was 199 ± 1 kcal/mol at $10^{-3}$ to 1.0 torr $N_2$. The Langmuir data indicated an evaporation coefficient of 0.3 for U from $10^{-4}$ to 1.0 torr $N_2$. A UN pellet (99.0% of theoretical density) was tested for spalling and cracking by repeated cycling between the UN and $U_2N_3$ phase regions at 130 torr $N_2$. At 1131°K, the nitriding rate to form $U_2N_3$ was $5.2 \times 10^{-3}$ mg/min-cm$^2$ in 130 torr $N_2$. After extensive nitriding and denitriding (19 cycles for times to 69 h), the bulk volume expansion of the pellet was 8.5%. The surface was not friable or powdery and the overall structural integrity was sound. (auth)

**55618** EFFECT OF SHOCK WAVES ON REFRACTORY COMPOUNDS. I. NIOBIUM, ZIRCONIUM, SILICON, CHROMIUM, AND GALLIUM NITRIDES. Adadurov, G. A.; Breusov, O. N.; Dremin, A. N.; Drobyshev, V. N. (Inst. of New Chemical Problems, Moscow). Sov. Powder Met. Metal Ceram. (Engl. Transl.); 10: No. 3, 227-8(Mar 1971).

Translated from Porosh. Met., Akad. Nauk Ukr. SSR; 10: No. 3, 71-3(Mar 1971).

An x-ray diffraction study was made of the shock compression of NbN, ZrN, $Si_3N_4$, $Cr_2N$, and GaN. After the shock compression, strong bars of high microporosity were formed from the starting powders. GaN decomposed with the formation of metallic Ga. The crystal lattice of CrN was changed, with line broadening, while ZrN, and $Si_3N_4$ had no structural changes. The hexagonal $\epsilon$ phase of NbN was transformed into the cubic $\delta$ phase. (D.L.C.)

**55619** WEAR RESISTANCE OF SURFACES FACED WITH BORIDES. Oreshkin, V. D.; Svetlopolyanskii, V. I.; Serebryakova, T. I. (Inst. of Materials Science, Kiev). Sov. Powder Met. Metal Ceram. (Engl. Transl.); 10: No. 3, 232-5(Mar 1971).

Translated from Porosh. Met., Akad. Nauk Ukr. SSR; 10: No. 3, 78-82(Mar 1971).

Facings of $TiB_2$, $CrB_2$, $TiB_2$–$CrB_2$, and $W_2B_5$ on steels and cast iron were made using an electroslag technique and a borax–KCl flux. The resulting deposited layers have a matrix-reinforced structure, whose binder is a solid solution of borides in a tough steel matrix. The depth distribution of the hardness was determined, and the composition through the depth was studied by x-ray diffraction. Wear tests show that the best facing is 50% (Ti, Cr)$B_2$ and 50% $W_2B_5$. (D.L.C.)

**55620** HIGH TEMPERATURE CERAMICS FROM SCANDIUM OXIDE. Popil'skii, R. Ya.; Smirnov, V. A. (Inst. of Chemical Tech., Moscow). Metal Sci. Heat Treat. (USSR) (Engl. Transl.); No. 11-12, 778-82(Nov-Dec 1970).

Translated from Metalloved. Term. Obrab. Metal.; No. 12, 31-5(Dec 1970).

Results of studies on the preparation and properties of scandium oxide ceramics are presented. It was found that ceramics based on scandium oxide should be considered as a favorable structural and electric insulating material. The combination of properties of scandium oxide is such that under certain operating conditions it has great advantages compared with the refractory oxides MgO, $ZrO_2$, $Al_2O_3$, and BeO. (J.R.D.)

**55621** THERMOMECHANICAL PROPERTIES OF SOME OXIDE REFRACTORIES. Karklit, A. K.; Tikhonova, L. A. Metal Sci. Heat Treat. (USSR) (Engl. Transl.); No. 11-12, 727-30(Nov-Dec 1970).

Translated from Metalloved. Term. Obrab. Metal.; No. 11, 49-52(Nov 1970).

Investigations are reported on preparation and properties of alumina, chromia, beryllia, zircon, synthetic corundum and Onotsk talc. The resulting data may be useful in evaluating the

resistance to mechanical and thermal stresses of these materials. (J.R.D.)

**55622** PHYSICAL PROPERTIES OF URANIUM DODECABORIDE. Odintsov, V. V.; Paderno, Yu. B. At. Energ. (USSR); 30: No. 5, 453 (May 1971). (In Russian).

Sintered samples of $UB_{12}$ had a porosity of 20 to 25%, a specific electrical resistance of 23 $\mu$ ohm·cm, a Hall coefficient of $-0.24 \times 10^{-4}$, and a coefficient of thermal expansion of 2.55 between −177 and +20°C. These data support the conclusion that $UB_{12}$ is a metallike compound with typically metallic properties. A graph is shown that illustrates the electrical resistance as a function of temperature. (K.S.W.)

**55623** SORPTION BEHAVIOR OF CESIUM–RUBIDIUM MIXTURES IN GRAPHITES AT HIGH TEMPERATURES. Haire, Marvin Jonathan. Raleigh, N. C.; North Carolina State Univ. (1970). 175p. University Microfilms Order No. 71-19,935. Thesis.

Results of research concerned with the quantitative thermodynamic aspects of the sorption of mixtures of fission product metals in graphite are summarized. Emphasis is placed on the equilibrium partial pressures versus concentration of metals in graphite. The metals of primary interest are those of the relatively volatile fission products of groups IA, IIA, and IIIB of the periodic table of elements which are known or expected to have a strong Freundlich isotherm type sorption interaction with graphite. Cesium and rubidium of group IA were chosen as being representative of this group of elements. The graphite materials studied were: 1. SP-1C graphite, a highly chemically pure and well-characterized graphite which was considered as a reference material, and 2. TS-688 graphite, a typical nuclear grade graphite. The experimental technique which was used to measure the equilibrium sorbate concentration for mixtures as a function of equilibrium partial vapor pressure is entitled the pseudo-isopiestic method. The method is described in detail and evaluated as to its performance relative to these studies. It was found that both cesium and rubidium exhibited unusually high heats of adsorption on the nuclear grade TS-688 graphite and the highly chemically pure SP-1C reference graphite. For example at a heat of absorption of 55 kcal/mole, the concentration of cesium was 3.5 $\mu$moles/m$^2$ and 0.33 $\mu$moles/m$^2$ and of rubidium 1.0 $\mu$moles/m$^2$ and 0.44 $\mu$moles/m$^2$ for TS-688 and SP-1C graphite respectively. By comparing the sorption behavior of the two graphite materials, it was concluded that the high heats of adsorption are characteristic of graphitic materials. It was concluded that the differences in the relative adsorptive capacity of the two graphites was the result of different densities of sorption sites. The primary objective was to obtain enough data on the vapor pressure of cesium and rubidium metals as a function of temperature and composition so that a model for the mixed sorption phenomenon could be developed and vapor pressures predicted. Three models were examined for their capability to predict binary sorption behavior. The previously developed Glueckauf model (32) was modified so that the enthalpy of adsorption had definite rather than infinite limits. The modified Glueckauf model is based upon Langmuir's adsorption equation for mixed gases. The second model is one which has found acceptance in industry (106, 107) and is called the FREVAP model. This model was originally proposed when no mixed adsorption data was available for sorbates which individually follow a Freundlich behavior with which to test the model. Now that data is available for the first time in this study, the model was tested for its accuracy and good agreement was found between predicted and experimental values. The third model is entitled the thermodynamic model which was formulated for gases that individually exhibit Freundlich behavior upon adsorption. This model has been rigorously derived from thermodynamic principles. On the basis of the results, the thermodynamic model is recommended as the best method of calculating volatile fission product metal partial pressures from reactor core fission product concentration levels. This research has shown at least for the case of cesium-rubidium mixtures that their equilibrium vapor pressures as a function of concentration can be predicted with fair accuracy from single component laboratory data. (Diss. Abstr. Int., B)

**55624** PROCEEDINGS OF THE FIFTH SYMPOSIUM ON THERMOPHYSICAL PROPERTIES, BOSTON, MASSACHUSETTS, SEPTEMBER 30–OCTOBER 2, 1970. Bonilla, C. F. (ed.). New York; American Society of Mechanical Engineers (1970). 513p. (CONF-700901).

A separate abstract was prepared for each of the 13 papers in scope for NSA. (M.O.W.)

*For abstracts of individual papers see: 55092, 55493–55496, 55625–55627, 56139, 56140, 56157, 56182, and 56183.*

**55625** THERMOPHYSICAL PROPERTIES OF MOLTEN BORON OXIDE. Spielrein, E. E.; Yakomovitch, R. A.; Tsytsarkin, A. F.; (and others) (Inst. for High Temperatures, Moscow). pp 96-106 of Proceedings of the Fifth Symposium on Thermophysical Properties. /Bonilla, C. F. (ed.). New York; American Society of Mechanical Engineers (1970).

From 5th symposium on thermophysical properties; Boston, Mass. (Sep-Oct 1970). See CONF-700901.

Results of experimental study up to 2000°C of density, enthalpy, viscosity of $B_2O_3$ are reported. Density is measured by a buoyancy technique, enthalpy by drop technique using a boiling calorimeter, and viscosity is determined in a rotation viscosimeter by relative reference technique. The techniques and equipment used are described and the results discussed. (auth)

**55626** HIGH-TEMPERATURE SPECIFIC HEAT OF METALS AND CERAMICS. Hoch, M. (Univ. of Cincinnati). pp 380-4 of Proceedings of the Fifth Symposium on Thermophysical Properties. /Bonilla, C. F. (ed.). New York; American Society of Mechanical Engineers (1970).

From fifth symposium on thermophysical properties; Boston, Mass. (Sep–Oct 1970). See CONF-700901.

The high temperature specific heat of lead, molybdenum, $UO_2$, US, UN, and UC were evaluated from room temperature up to within ten degrees of their melting points. It was found in all cases that the specific heat can be expressed as $C_p = 3RF(\theta_D/T) + bT + dT^3$. In this equation, the first term is due to the vibrational contribution, the second term contains the electronic contribution, and the third term is due to the anharmonicity of the vibrations. In the cases where no electronic contribution is present, such as in $UO_2$, b equals zero. The contribution of vacancies to the specific heat is quite negligible and within the experimental error of high temperature specific heat measurements. (auth)

**55627** THERMAL AND ELECTRICAL CONDUCTIVITIES OF SOME ELECTRICALLY CONDUCTING COMPOUNDS. Tye, R. P. (Dynatech R/D Co., Cambridge, Mass.); Clougherty, E. V. pp 396-401 of Proceedings of the Fifth Symposium on Thermophysical Properties. /Bonilla, C. F. (ed.). New York; American Society of Mechanical Engineers (1970).

From fifth symposium on thermophysical properties; Boston, Mass. (Sep-Oct 1970). See CONF-700901.

Measurements were made of the thermal conductivity and electrical resistivity of a variety of hot pressed polycrystalline powders of $ZrB_2$ and $HfB_2$ and their compounds containing SiC, C and combinations of both over the approximate temperature range 300 to 1300°K. Thermal conductivity determinations were made by the comparative cut-bar technique with Armco iron as the reference material. Electrical resistivity studies were carried out on small rod samples of the same stock. The results indicate that these materials retain their good thermal and electrical transport properties and have considerable lattice components of thermal conductivity. There was no indication that the thermal conductivity increased at the higher temperatures as was reported previously for some similar materials. (auth)

**55628** RELATIONS BETWEEN STEREOMETRIC MICROSTRUCTURE AND PROPERTIES OF CERMETS AND POROUS MATERIALS. Nazare, S.; Ondracek, G.; Thuemmler, F. (Kernforschungszentrum, Karlsruhe, Ger.). pp 171-86 of Modern Developments in Powder Metallurgy. Vol. 5. /Hausner, Henry H. (ed.). New York; Plenum Publishing Corp. (1971).

From International powder metallurgy conference; New York, N. Y. (12 Jul 1970).

The characteristic parameters of a dispersed phase in a matrix of another phase may strongly influence the properties of a two-phase material. This is especially true for cermets, which consist of a phase often having very different properties, because one phase is a ceramic, the other is a metal. In this sense, porous specimens, as achieved generally with powder metallurgical methods, are a special case of cermets. This is why the effects of several parameters of a dispersed phase in a matrix on some properties is now considered in a more general manner. At first theoretical considerations are discussed for the concentration function of the electrical conductivity of cermets. Some other properties like permeability and thermal conductivity are also mentioned. The limiting cases of the equations enable consideration of the influence of pores in single phase material as well as particle shape, distribution, and size of the dispersed phase on cermet properties. These considerations from a theoretical point of view are then compared with experimental results available. Conclusions are given concerning the relationship between the stereometric microstructure of cermets and porous materials and the properties mentioned. (52 references) (auth)

**55629** ABOUT NITRIDES AND CARBONITRIDES AND NITRIDE-BASED CEMENTED HARD ALLOYS. Kieffer, R.;

XUM

Ettmayer, P.; Freudhofmeier, M. (Technical Univ.Vienna). pp 201-14 of Modern Developments in Powder Metallurgy. Vol. 5. /Hausner, Henry H. (ed.). New York; Plenum Publishing Corp. (1971).

From International powder metallurgy conference; New York, N. Y. (12 Jul 1970).

After a short discussion on the physical properties of nitrides and carbonitrides of the transition metals some comments on the stability of carbides against high-pressure nitrogen are made. All carbides of the transition metals react with nitrogen by formation of carbonitrides with the exception of TaC and WC, which are stable against nitrogen even at 300 atm. Sintering experiments showed titanium nitride and carbonitrides to be suitable hard materials for cemented hard alloys. A 70 wt % nickel– 30 wt % molybdenum alloy binder phase gave optimum hardness and transverse rupture strength. Cobalt and iron were suitable binder metals, but were inferior to nickel–molybdenum alloys. Strength and hardness values of cemented titanium carbonitride were comparable to those of TiC/$Mo_2C$–Ni alloys. Cutting performance was excellent. Resistance to cratering is believed to be superior to analogous cemented carbides. (auth)

**55630** COMPOSITION AND PROPERTIES OF THE BINDER METAL IN COBALT BONDED TUNGSTEN CARBIDE. Ruediger, O.; Hirschfeld, D.; Hoffmann, A.; (and others) (Fried/Krupp GmbH, Essen). pp 215-24 of Modern Developments in Powder Metallurgy. Vol. 5. /Hausner, Henry H. (ed.). New York; Plenum Publishing Corp. (1971).

From International powder metallurgy conference; New York, N. Y. (12 Jul 1970).

For investigating the composition of the binder phase in WC–Co alloys, the carbide was removed electrolytically so that the remaining binder could be tested analytically and by x-ray diffraction. It was found that the tungsten content of the binder depends on the carbon content of the alloys, the grain size of the carbide used, the cobalt content, and the sintering and cooling conditions. The tungsten content of the binder increased as the carbon content of the alloys decreased, as the grain size of the carbide increased, as the sintering time increased, and as the Co-content of the alloy decreased. Additional heat treatment for 50 hr at 1250°C followed by water quenching almost eliminated the differences regardless of the initial grain size of the carbide, of the Co-content, and of the sintering time. The W-contents calculated for the binder of binary WC–Co alloys (free from other phases) from the total carbon contents of the alloys together with the C-values of the corresponding isolates, were in good agreement with the measured W-values for the coarse grained materials. However they differed for the fine grained alloys. In the range of composition studied, the tensile strength and the elongation of some melted, forged, and heat-treated model alloys of the Co–W–C system were determined. It was found that tensile strength of more than 120 kp/$mm^2$ at elongations of about 10% can be achieved. (auth)

**55631** HIGH STRENGTH TUNGSTEN CARBIDES. Moskowitz, D.; Ford, M. J.; Humenik, M. Jr. (Ford Motor Co., Dearborn, Mich.). pp 225-34 of Modern Developments in Powder Metallurgy. Vol. 5. /Hausner, Henry H. (ed.). New York; Plenum Publishing Corp. (1971).

From International powder metallurgy conference; New York, N. Y. (12 Jul 1970).

It was found that the formation of the detrimental $Fe_2W_3C$ phase in Fe–WC can be inhibited by proper control of the carbon content, resulting in mechanical properties for compositions in this system that are comparable to the Co–WC system. More significantly, it has been found that with alloying additions of nickel to iron, bend strength values can be obtained in the Fe/Ni–WC system that are substantially greater than comparable compositions in the Co–WC system. In addition, appropriate alloying additions of nickel to iron provide a means of producing pearlitic, austenitic, and martensitic-bonded WC, and further optimizing the properties of compositions in this system aimed for specific applications. (auth)

**55632** PHYSICAL PROPERTIES OF MONOCARBIDES OF ZIRCONIUM, NIOBIUM, AND THEIR ALLOYS IN HOMOGENEITY RANGE. Upadhyaya, G. S. (Univ. of Roorkee, India); Samsonov, G. V. pp 235-58 of Modern Developments in Powder Metallurgy. Vol. 5. /Hausner, Henry H. (ed.). New York; Plenum Publishing Corp. (1971).

From International powder metallurgy conference; New York, N. Y. (12 Jul 1970).

Attempts were made to measure the physical properties of monocarbides of Zr, Nb, and their alloys in the homogeneity range and also to explain the main relation of their electronic structure with the changes in compositions. (52 references) (P.C.H.)

**55633** DIFFUSION OF $^{133}Xe$ IN CESIUM IODIDE AND CALCIUM FLUORIDE SINGLE CRYSTALS. Ong, Andres Sy. Raleigh, N. C.; North Carolina State Univ. (1970). 162p. University Microfilms Order No. 71-18,619.

Thesis.

The diffusion of rare gases in solids may be affected by surface phenomena and trapping of the rare gas atoms at defects in the crystal lattice. The effect of surface properties and lattice on the diffusion release of fission-recoiled $^{133}Xe$ was studied for CsI and $CaF_2$ single crystals. CsI single crystals which were strained by mechanically polishing exhibited release behavior characterized by gas atom trapping near the surface while classical diffusion behavior was obtained from unstrained CsI crystals. Surface evaporation of $CaF_2$ at high temperatures increased the release rate of $^{133}Xe$ above the classical diffusion release rate and different evaporation characteristics were observed for different crystal orientations. Thin surface films were formed on the surface of $CaF_2$ single crystals as the result of unknown chemical reactions and produced lowered release behavior. Techniques for eliminating these anomalous surface effects were developed. Gas diffusion measurements with $CaF_2$ single crystals at different temperatures and $^{133}Xe$ concentrations were carried out and it was observed that gas atom trapping occurred at the higher gas concentrations. A trapping model was developed and series and integral form solutions were derived describing the trapping process. The available experimental data for $^{133}Xe$ diffusion in $CaF_2$ crystals were analyzed in terms of the model. It was shown that a quasi-equilibrium process existed where the $^{133}Xe$ gas atoms were repeatedly trapped and released from the traps, before they are released from the surface of the specimen. The nature of the traps became more complex as the amount of radiation damage was increased. (Diss. Abstr. Int., B)

**55634** PHYSICAL ADSORPTION OF CARBON DIOXIDE ON GRAPHON. Tyler, R. J.; Wouterlood, H. J. (Commonwealth Scientific and Industrial Research Organization, Chatswood. Australia). Carbon; 9: No. 4, 467-72(Aug 1971).

Adsorption isotherms of $CO_2$ on Graphon were determined at temperatures from –80 to +29°C and equilibrium pressures up to 30 atm. Plots of log (fugacity) against 1/T at constant amounts adsorbed are linear over the temperature range, showing no change in slope in the region of the triple point of bulk $CO_2$. With increasing amount adsorbed the isosteric heat of adsorption increases to a maximum of 4.5 kcal $mole^{-1}$ and then declines. Similar behaviour is shown by $CO_2$ adsorbed on partly combusted specimens of Graphon. Assuming that the maximum heat of adsorption occurs on completion of the first adsorbed layer, the average area of surface occupied by each $CO_2$ molecule at this point is 26 $Å^2$. The effect of O previously chemisorbed on the carbon surface is to increase the amount of $CO_2$ adsorbed at –80°C. This effect was studied gravimetrically and it was concluded that the extra amount adsorbed rises with increasing pressure of carbon dioxide to a value corresponding to the adsorption of an extra $CO_2$ molecule for each 3–5 O atoms on the surface. (auth) (UK)

**55635** EFFECT OF DOPING ON THE THERMAL CONDUCTIVITY OF POLYCRYSTALLINE GRAPHITE. Kelly, B. T. (United Kingdom Atomic Energy Authority, Culcheth, Eng.); Whittaker, A.; Tobin, D.; Wagner, P. Carbon; 9: No. 4, 447-55(Aug 1971).

Experimental data are presented on the changes of thermal conductivity of a number of polycrystalline graphites due to doping with B and $Br_2$ which respectively represent a substitutional and interstitial acceptor type defect. The results are compared with changes in thermal conductivity due to interstitial atoms and vacancies introduced by fast-neutron irradiation. It is found that a substitutional B atom in its ability to scatter phonons is roughly comparable to a lattice vacancy. The temperature dependence of the additional thermal resistance due to all four types of defects is found to be similarly increasing with decreasing temperature. A detailed attempt to fit a theoretical curve to the thermal conductivity results indicates that the mean free path for phonon scattering by point defects is independent of phonon frequency. (auth) (UK)

**55636** STABILIZATION OF ZIRCONIA WITH COMBINED ADDITIVES AND A STUDY OF THE SOLID SOLUTION STABILITY. Andreeva, A. B.; Keler, E. K.; Leonov, A. I. (Inst. of Silicate Chemistry, Moscow). Metal Sci. Heat Treat. (USSR) (Engl. Transl.); No. 11-12, 723-6(Nov-Dec 1970).

Translated from Metalloved. Term. Obrab. Metal.; No. 11, 45-8(Nov 1970).

The stability of solid solutions of $ZrO_2$–MgO and $ZrO_2$–CaO may be critically increased by incorporating small additions (1 to 2%) of yttrium oxide. Complete discontinuation of the decomposition of these solid solutions occurs with an addition of

3% $Y_2O_3$. Stabilization of zirconium dioxide by combined additions is achieved with a lower concentration of oxide-stabilizers compared with the required concentration of each of them separately. This permits a substantial reduction in the expenditure on costly and scarce additives, for instance, oxides of rare-earth elements, and yttrium. The synthesized ternary solid solutions possess valuable physicoengineering properties, such as high mechanical strength, and a lower average coefficient of thermal expansion than double solid solutions. (auth)

**55637** THERMAL CONDUCTIVITY OF SOME OXYGEN COMPOUNDS OF ZIRCONIUM AND HAFNIUM. Vishnevskii, I. I.; Skripak, V. N. (Scientific-Research Inst. of Refractories, Kiev). Metal Sci. Heat Treat. (USSR) (Engl. Transl.); No. 11-12, 693-4(Nov-Dec 1970).

Translated from Metalloved. Term. Obrab. Metal.; No. 11, 16-18(Nov 1970).

The thermal conductivities of $SrZrO_3$, $SrHfO_3$, $CaZrO_3$, solid solutions of $HfO_2-Y_2O_3$, and modifications of $ZrO_2$ and $HfO_2$ were measured. Resulting data are presented graphically and discussed. (J.R.D.)

## Structure and Phase Studies

*Refer also to abstracts 55455 and 56343.*

**55638** SUBSOLIDUS RELATIONS IN THE SYSTEM $ZrO_2-ThO_2-P_2O_5$. Laud, K. R. (Ford Motor Co., Dearborn, Mich.); Hummel, F. A. J. Amer. Ceram. Soc.; 54: No. 8, 407-9(Aug 1971).

Subsolidus phase equilibrium studies and linear thermal expansion data in the binary system $ZrP_2O_7-ThP_2O_7$ showed that a series of metastable, low-expansion cubic solid solutions can be obtained at room temperature by a process of mutual stabilization. These solid solutions are ordinarily stable only above the inversions of $ZrP_2O_7$ and $ThP_2O_7$ at 300° and 1294°, respectively. Compatibility relations in other areas of the ternary system are given in a diagram for equilibrium at 1400° and in another showing the influence of the metastable but very persistent form of $2ZrO_2 \cdot P_2O_5$. (auth)

**55639** CONGRUENT MELTING COMPOSITION OF LITHIUM METATANTALATE. Miyazawa, Shintaro; Iwasaki, Hiroshi (Nippon Telegraph and Telephone Public Corp., Tokyo). J. Cryst. Growth; 10: No. 3, 276-8(Aug 1971).

A tentative phase relation in the $Li_2O-Ta_2O_3$ system in the vicinity of $LiTaO_3$ is proposed, which was determined by measuring the Curie temperatures of the crystals from the melts with various ratios of $Ta_2O_5/Li_2O$. The congruent melting composition was determined as $Ta_2O_5/(Ta_2O_5 + Li_2O) = 51.25$ mol %. (auth)

**55640** TERNARY THORIUM–RUTHENIUM CARBIDE. Holleck, H. (Kernforschungszentrum, Karlsruhe, Ger.). J. Nucl. Mater.; 39: 226-8(May 1971). (In German).

In a study of the Th–Ru–C system three ternary compounds were detected and the three complex carbides coexist at the composition 20 at. % Th, 40 at. % Ru, and 40 at. % C. Metallographic and x-ray analysis of the sample gave the following compositions: Phase I, $Th_{3+x}Ru_{4-x}C_5$ ($x = 0.3$); Phase II, $ThRu_3C_{1-x}$ ($0 < x < 0.1$); and Phase III, $ThRu_3C_{1.5}$. The x-ray diagram of the sample with all three phases coexistent was evaluated. The $ThRu_3C_{1-x}$ phase was a cubic face-centered phase with the lattice constant $a = 4.21$ Å. (J.S.R.)

**55641** POLYMORPHIC TRANSFORMATION OF ZIRCONIUM DIOXIDE. Sukharevskii, B. Ya.; Gavrish, A. M.; Alapin, B. G. Sb. Nauch. Tr., Ukr. Nauch.-Issled. Inst. Ogneuporov; No. 9, 5-28(1968). (In Russian).

An extensive survey of the literature is presented, summarizing studies on the crystalline structure of $ZrO_2$. It is shown that the polymorphic transition of $ZrO_2$ resembles martensite. Isothermal kinetics were observed in the conversion $\alpha \rightarrow \beta$ $ZrO_2$, the velocity of which decreases with increase in the number of defects that arise from repeated conversions or other thermal treatment. An equation was developed that describes the isothermal kinetics. A mechanism was proposed for the formation of solid solutions of other oxide in the cubic structure of $ZrO_2$. This was experimentally tested with $ZrO_2/CaO$ and $ZrO_2/CaZrO_3$, for which a cubic phase emerges at 1200°C. Destabilization of the cubic phase may be caused by a eutectoid decomposition of the solid solutions, as corroborated by a phase diagram of the system $ZrO_2-CaO$. (57 references) (K.S.W.)

**55642** GRAIN GROWTH IN LIQUID-PHASE SINTERING OF CARBIDES. Exner, H. E. (Max-Planck-Institut fuer Metallforschung, Stuttgart); Santa Marta, E.; Petzow, G. pp 315-25 of Modern Developments in Powder Metallurgy. Vol. 4. /Hausner, Henry H. (ed.). New York; Plenum Publishing Corp. (1971).

From International powder metallurgy conference; New York, N. Y. (12 Jul 1970).

Studies were made on the effects of oxygen content and stoichiometry on the grain size and grain shape of TiC in TiC–Ni alloys, and the rate controlling mechanism in grain growth of VC and TaC grains during sintering in liquid Co and Ni. The results showed that oxide additions up to 2 wt % resulted in some rounding and grain growth. At 4 wt % $TiO_2$ reshaping and enhanced growth of the grains were observed. Pronounced grain growth and reshaping was obtained when the C content of the alloy was reduced by Ti corresponding to the reaction $(1-x)TiC + xTi \rightarrow TiC_{1-x}$. This implies that the effect of oxygen is, at least in part, caused by decarburization according to the reaction $(3-x)TiC + xTiO_2 \rightarrow 3TiC_{1-x} + xCo$. In practice, the carbon content of TiC–Ni alloys must be carefully controlled in order to achieve optimum mechanical properties. The rate controlling mechanism in growth of VC grains in liquid Ni and Co was found to be the solution reaction at the carbide-metal interface. The exponent in the grain size-time relationship and the apparent activation energy were usually not valid criteria for determining the rate controlling mechanism, but the size distributions must be considered as well. The growth rate of TaC grains was lower in Co than in Ni. The apparent activation energy was the same in both systems (about 55 kcal/mole). (P.C.H.)

**55643** ELECTRONIC STRUCTURE OF REFRACTORY CARBIDES AND ITS RELATION TO WETTING. Goretzki, H.; Exner, H. E.; Scheuermann, W. (Max-Planck-Institut fuer Metallforschung, Stuttgart). pp 327-37 of Modern Developments in Powder Metallurgy. Vol. 4. /Hausner, Henry H. (ed.). New York; Plenum Publishing Corp. (1971).

From International powder metallurgy conference; New York, N. Y. (12 Jul 1970).

Studies were made to correlate the adhesion energy computed from wetting experiments to the density of states at the Fermi level for carbide compounds showing a systematic variation in electronic configuration. Wetting by molten Cu in contact with transition metal carbides of different valence electron concentration (VEC) was considered. The results, especially for the carbides of the 4th group, showed that nonstoichiometry caused as unessential increase in the work of adhesion and a strong degradation of the mechanical properties. Exchange of the nonmetallic component caused a limited increase in wettability and a strong decrease in stability. The same effect would be expected for a solution of oxygen instead of nitrogen. The best influence on wetting was obtained by the exchange of the 4a metal for a transition metal of the 5th or 6th group. In all cases the stability of the solid compound decreased by alloying when wettability was improved. (P.C.H.)

**55644** THERMOCHEMISTRY OF THE HAFNIUM–SILICON SYSTEM. Golutvin, Yu. M.; Maslennikova, E. G. Izv. Akad. Nauk SSSR, Metal.; No. 1, 174-80(Jan 1971). (In Russian).

The thermochemical and thermophysical characteristics of a wide range of alloys belonging to the Hf–Si system were studied; these included the heats of formation from the elements at 300°K, the temperature coefficient of electrical resistance, the thermal-expansion coefficient, and the specific and molar volumes of the corresponding alloys. The results were compared with existing data relating to the Ti–Si and Zr–Si systems. A number of singularities appeared on the property/composition diagrams, particularly in the 40 to 60% region. These singularities are discussed on the basis of the electron structures of the alloys in question. (Metals Abstr.)

## Radiation Effects

*Refer also to abstracts 54531, 54599, 55101, 56282, and 56283.*

**55645** (CEA-CONF-1821) INFLUENCE OF SPEED OF GRAPHITIZATION OF CARBON PRODUCTS ON DIMENSIONAL VARIATIONS PRODUCED BY NEUTRON IRRADIATION. Rappeneau, J.; Yvars, M.; Mottet, P. (Commissariat a l'Energie Atomique, Saclay (France). Centre d'Etudes Nucleaires); Cornuault, P.; Lore, J.; Galy, A. (Compagnie Pechiney, Paris (France)). [Sep 1967]. 31p. (In French). (CONF-710612-5). Dep. NTIS (U. S. Sales Only).

From tenth biennial conference on carbon; Bethlehem, Pa. (27 Jun 1971).

Two types of baked carbon were graphitized by heat treatments at rates varying from 50 $hr^{-1}$ to 3300°C/$hr^{-1}$. For each type of

XUM

carbon it was observed that an increase in the heating rate led to considerable changes in the texture of the graphitized products particularly the apparent density, helium density, and microporosity. From these textural variations in graphitized products, various dimensional effects of neutron irradiation could be predicted. These effects were confirmed by a method of simulation using bromination. An irradiation experiment at 550°C to doses of about 3.5 $10^{21}$ n $cm^{-2}$ DEN (Dido equivalent nickel) corroborated the results obtained by bromination. (auth)

**55646** (EUR-4674) SIMPLIFIED VISCO-ELASTIC ANALYSIS OF GRAPHITIC BODIES SUBJECTED TO EXTERNAL LOADS, TEMPERATURE GRADIENTS AND NEUTRON IRRADIATION. Donea, J.; Giuliani, S. (European Atomic Energy Community, Ispra (Italy). Joint Nuclear Research Center). 13 Mar 1971. 28p. Dep. NTIS (U. S. Sales Only). EUR FF 4.45.

Within the frame of the finite-element method, the solution of viscoelastic problems governing the behavior of graphite structures under irradiation can be obtained by a conventional elastic analysis. Numerical examples are included to illustrate the method of analysis suggested. (auth)

**55647** (ORNL-4717, pp 83-90) CHEMICAL SUPPORT FOR HIGH TEMPERATURE GAS-COOLED REACTORS. (Oak Ridge National Lab., Tenn.).

In Reactor Chemistry Division annual progress for period May 31, 1971.

Studies are reported on cesium and strontium release from bonded beds of BISO-coated $UO_2$ particles during postirradiation annealing at 1250°C, cesium diffusion in BISO-coated fuel particles, and measurement of thermal conductivity of uranium dioxide during irradiation. (D.H.M.)

**55648** (RCN-144) POST-IRRADIATION EXAMINATION OF FUEL PINS R62-A01 AND -A02 IRRADIATED IN A SODIUM ENVIRONMENT UP TO 19 MWd/kg $UO_2$. Kwast, H. (Reactor Centrum Nederland, Petten). Apr 1971. 76p. Dep. NTIS (U. S. Sales Only).

Two fuel pins were irradiated in a sodium environment in the HFR Poolside Facility at Petten to a burnup of 6.9 and 19 MWd/kg $UO_2$ respectively. The fuel pins consisted of 50% enriched $UO_2$ pellets of 6 mm diameter, canned in an X-8 Cr-Ni-Nb 16-13 stainless steel tube with an outer diameter of 6.7 mm and a wall thickness of 0.3 mm. The dimensional changes of the fuel pins were measured as well as the amount of fission gas released. Metallographic examination revealed the occurrence of an interaction between fuel and canning. The irradiations are part of a program comprising stationary irradiations up to a burnup of 80 MWd/kg $UO_2$. (auth)

**55649** NUCLEATION OF BUBBLES AND RE-SOLUTION EFFECTS IN URANIUM DIOXIDE IRRADIATED AT ELEVATED TEMPERATURES. Cornell, R. M.; Turnbull, J. A. (Central Electricity Generating Board, Berkeley, Eng.). J. Nucl. Mater.; 41: No. 1, 87-90(Oct 1971).

Uranium dioxide samples have been irradiated at 1200°C to a variety of doses up to $3.2 \times 10^{25}$ fissions/$m^3$. Examination of these samples by transmission electron microscopy showed that there is a critical dose below which intragranular fission-gas bubbles are not observed to form. Above this critical dose these bubbles were found to nucleate heterogeneously upon fission-fragment tracks. Radioinduced re-solution was found to be effective in the removal of gas atoms from within the sintering pores of this material. (auth)

**55650** DEFECTS IN BORON CARBIDE BEFORE AND AFTER NEUTRON IRRADIATION. Ashbee, K. H. G. (Oak Ridge National Lab., Tenn.). Acta Met.; 19: No. 10, 1079-85(Oct 1971).

Many crystalline compounds contain regular geometrical arrangements of atoms which are so stable that the presence and motion of defects such as dislocations are expected to leave these units more or less intact. In boron and most of its compounds, the stable units are icosahedral groups of twelve boron atoms and in boron carbide, which is rhombohedral with rhombohedral angle 65°36′, the $B_{12}$ icosahedra are arranged in an array which is almost a fcc lattice, as a result of which, fault surfaces analogous to stacking faults in close-packed metals are observed. The small departure from cubic symmetry is, however, sufficient to impose a distinction between rhombohedral planes, which are hosts for translation twin boundaries created by the dissociation of glide dislocations, and the basal plane, which is believed to contain Frank partial dislocation loops resulting from the agglomeration of point defects introduced during neutron irradiation. Another important consequence of the rhombohedral distortion is that the atomic displacements produced by the leading and trailing partials in an extended dislocation are different. In physical terms, both refinements of the close-packed cubic case arise from the presence of the carbon atoms. The analogy to close-packed metals is carried over to the relationship between translation twins and orientation twins; the dissociation of a glide dislocation in boron carbide is accompanied by rotation of $C_3$ chains which thread the slip plane and this rotation both may and may not be sufficient to render the translation twin boundary region identical to a thin orientation twin. (auth)

**55651** DIMENSIONAL AND PHYSICAL PROPERTY CHANGES OF HIGH-TEMPERATURE REACTOR GRAPHITES, PYROCARBONS, AND FUEL BODIES IRRADIATED AT TEMPERATURES IN THE RANGE 600 TO 1200°C. Everett, M. R. (OECD, Winfrith, Eng.); Graham, L. W.; Manzel, R.; Blackstone, R. Carbon; 9: No. 4, 417-37(Aug 1971).

The 20 MW(t) experimental He-cooled reactor Dragon uses an all-graphite core with coated particle fuel embedded in a resin-bonded graphite powder matrix. The irradiation behaviour of the carbonaceous core components is described. Dimensional and physical property changes of extruded and pressed Gilsocarbon graphite irradiated to fast neutron doses of up to $5 \times 10^{21}$ n $cm^{-2}$ Ni DIDO equivalent were measured, and the results were compared with two earlier nuclear graphites. Differences in the shrinkage rates of the various Gilsocarbon graphites were related to their initial Young's Modulus and strength. The results indicated that for a given basic type of graphite (gilsonite) a higher strength material would shrink faster than a comparable low-strength material. Comparison of the volume changes of the graphites tested suggested that the expansion rate after the shrinkage maxima was more rapid for graphites irradiated at 900°C than at 1200°C. This rapid volume expansion at 900°C was accompanied by a loss of strength already shown by the fall in Young's Modulus of an earlier fine-grain nuclear graphite used in the Dragon Reactor. A range of pyrolytic carbon specimens having a range of densities was irradiated up to fast neutron doses of $3 \times 10^{21}$ n $cm^{-2}$ Ni DIDO equivalent. The results showed that the dimensional changes of these specimens depended primarily on their initial density. Measurements of the outer diameter and length changes of coated particle matrix-type fuel compacts irradiated at temperatures between 900°C to 1200°C, to a maximum fast neutron dose of $1.7 \times 10^{21}$ n $cm^{-2}$ Ni DIDO equivalent, revealed a relatively isotropic behaviour of these composite bodies. However they shrank more rapidly than most nuclear graphites. The influence of materials selection on some reactor design problems is briefly discussed. (auth)

**55652** IRRADIATION-INDUCED DIMENSIONAL CHANGES IN CO-DEPOSITED CARBON-SILICON COATINGS. Bokros, J. C.; Stevens, D. W.; Akins, R. J. (Gulf General Atomic Co., San Diego, Calif.). Carbon; 9: No. 4, 439-46(Aug 1971).

Irradiations of pure and silicon-alloyed isotropic carbons (deposited below 1500°C) at 910 to 1300°C to fast-neutron fluences in the range 1.4 to $1.8 \times 10^{21}$ n/$cm^2$ (E > 0.18 MeV) showed that silicon concentrations above about 18 wt % were effective in reducing the irradiation-induced dimensional changes, e.g., at 910°C the lineal shrinkages caused by irradiation were reduced by ~ a third by the addition of 34 wt % silicon. At 1250 to 1300°C, the corresponding reduction was ~ a half. At 910°C, irradiation creep strains as high as 5.5% per $10^{21}$ n/$cm^2$ were measured for the unalloyed carbons. At 1250 to 1300°C, total creep strains of 10% were observed for unalloyed carbons, and 8% were observed for the alloyed coatings. Since none of the creep specimens fractured, these were not limiting values. Comparison of data for isotropic carbons deposited below 1500°C (LTI carbons) with those for isotropic carbons deposited above 1500°C (HTI carbons) showed that at high fluences the LTI carbons expanded at a rate that is substantially less than the corresponding rate for HTI carbons. (auth) (UK)

**55653** INFLUENCE OF PITCH-BINDER COKE CONTENT ON THE PROPERTIES AND IRRADIATION BEHAVIOR OF MOLDED GRAPHITE. Engle, G. B. (Gulf General Atomic Co., San Diego, Calif.). Carbon; 9: No. 4, 383-90(Aug 1971).

Needle-coke graphites were prepared with various fractions of pitch-binder coke in the range 5.5 to 14.2 wt %. The specimens were irradiated to $9.70 \times 10^{21}$ n/$cm^2$ (E > 0.18 MeV) at 1225°C. Apparent bulk density and apparent crystallite size $L_c$ were dependent on the binder-coke content. Crystallite orientation and thermal expansivities were not affected. Dimensional and volumetric changes were sensitive to binder-coke content; specimens deficient in binder-coke showed volumetric turnaround at lower fluences and higher expansion rates at high fluences. Specimens of 5.5 wt % binder coke expanded 20 vol %, whereas those of 11.7 wt % binder coke expanded only 4 vol %. Thermal expansivity increases closely followed the volume changes and were large in specimens deficient in binder coke. Unbonded coke particles ex-

panded at three times the rate of coke particles bonded with pitch. The needle-coke particles were restrained by the binder coke during expansion at high fluences. Large cracks formed between filler particles during expansion and were responsible for the large volume expansions. (auth) (UK)

**55654** RADIOLYTIC REACTION BETWEEN GRAPHITE AND CARBON DIOXIDE. II. EFFECTS OF RANGE OF ACTIVE SPECIES AND OF WATER VAPOUR. Feates, F. S.; Poole, A. G. (Atomic Energy Research Establishment, Harwell, Eng.). Carbon; 9: No. 4, 499-509(Aug 1971).

Irradiations were conducted in sealed tubes at 2.5 $MNm^{-2}$ pressure and at 450°K to test the influence of active species range and water vapour on the radiolytic gasification of graphite in $CO_2$ or $CO/CO_2$ mixtures. A large effect of the free gas volume on G(CO) and G(–C) was observed which is related to a deactivation of active species within pores and interstices of the powder. No effect of water vapour was found. (auth) (UK)

**55655** RADIOLYTIC REACTION BETWEEN GRAPHITE AND $CO_2$. III. SURFACE COMPLEXES. Feates, F. S.; Fryer, J. R. (United Kingdom Atomic Energy Authority, Harwell, Eng.). Carbon; 9: No. 4, 511-16(Aug 1971).

Surface oxides form on graphite exposed to radiolysed $CO_2$ at 425°K by a process which is first order with respect to sites available for sorption. The oxide is formed radiolytically and is at least partially decomposed on heating the graphite to 775°K. Oxide formation appears to be an essential preliminary to gasification since negligible gasification takes place from an oxide free surface. A mechanism is proposed for the oxidation of graphite by radiolysed $CO_2$. (auth) (UK)

## Plastics and Other Materials

*Refer also to abstracts 54396, 54897, 55096, 55509, 56322, and 56882.*

**55656** (N–71-27736) EFFECTS OF CHARGED PARTICLE AND UV RADIATION ON THE STABILITY OF SILVERED AND ALUMINIZED FEP TEFLON SECOND SURFACE MIRRORS. Wappaus, Walter A. (National Aeronautics and Space Administration, Greenbelt, Md. Goddard Space Flight Center. Electro-Mechanical Research, Inc., College Park, Md.). May 1971. Contract NAS5-11326. 25p. (NASA-TM-X-65559). NTIS.

A series of tests were conducted on metallized 5-mil FEP teflon-film second-surface mirror thermal-control coatings to determine the solar absorptance stability as a function of electron, proton, and uv radiation dosage. Both silvered and aluminized FEP teflon coatings were irradiated with particle energies of 5 keV and 25 keV and with uv at an intensity of 5 solar constants. The combined effect of simultaneously irradiating these coatings with both uv and charged-particle radiation was also investigated. Results show that both silvered and aluminized coatings are more unstable to 25-keV protons than to 25-keV electrons. The combined effect of uv plus charged-particle radiation produces greater instability at higher dose levels than the effect of charged-particle radiation alone. The stability of the FEP teflon coatings are virtually unaffected by uv exposure in vacuum at 5 solar constants for 120 hours. The coatings are also stable to 5-keV electrons. (auth) (STAR)

**55657** IMPROVEMENTS IN AND RELATING TO NUCLEAR RADIATION ATTENUATING MEANS. Youell, Frederick Peter; Collins, Roy (to Nuclear Power Group Ltd.). British Patent 1,236,808. 23 Jun 1971. Filed 19 Nov 1968.

Reference is made to means for attenuating radiation streaming from radioactive material through gaps between structural members. The means described comprises compressible radiation attenuating members interposed between the structural members, each attenuating member comprising at least one layer of compressible material and at least one juxtaposed layer of solid radiation absorbing or moderating material. The compressible layer may be rubber and the solid layer, steel or lead. It is preferable to use rows of attenuating members, the members of adjacent rows being in inverted relationship, with alternate compressible and solid layers uppermost. Applications may include joints between fuel charging machines and reactor fuel loading faces. (UK)

**55658** RADIATION POLYMERISATION OF IMPREGNATED POROUS MATERIAL. Hills, P. R.; McGahan, D. J. (Atomic Energy Research Establishment, Harwell, Eng.). Atom (London); No. 176, 146-56(Jun 1971).

Desirable characteristics of monomer and polymer impregnants for use in improving cellulose mechanical properties are considered. Systems and costs of composite production using radiation techniques, and percentage property improvements are discussed. Wood floors, veneers, and fibreboard are at present the most commercially viable composites and their working techniques and production problems are considered. Treated and untreated cost comparisons are listed and commercial advantages of the former indicated. Concrete composites are considered similarly. (UK)

**55659** TRIAXIAL STATE OF STRESS OF CONCRETE STRUCTURES. Janda, L. (Technical Univ., Prague). pp H1/2.1-18 of Structural Mechanics in Reactor Technology. Vol. 3, Pt. H. /Jaeger, Thomas A. (comp). Luxemburg; Commission of the European Communities (1971).

From 1st International conference on structural mechanics in reactor technology; Berlin, Germany (20 Sep 1971).

The assessment of the state of stress and the safety margin against failure of triaxially stressed concrete structures is based on the actual concrete surface strength. According to the test results its form is not rotary. For analytical purposes a simplified form is introduced, suggested by Reimann, which is compared with the form deduced from the tests carried out by Launay, Gachon, and Poitevin. The application of Mohr's general theory according to Filonenko–Borodich makes it further possible, in the meaning of Mohr's failure hypothesis, to discern whether concrete under the given type of stress fails in shear (similarly as in the case of plain compression) or in tension (similarly as in the case of plain tension). In the case of the failure in tension, reinforcement is designed to transfer the tension. In this process a graduation of the permissible safety margin values is recommended in accordance with whether the structure is of plain, reinforced, or prestressed concrete. Use of the method makes it also possible to follow theoretically the states of overloading the structure to the point of failure. (16 references) (auth)

**55660** STRAIN AND ULTIMATE STRENGTH OF CONCRETE UNDER TRIAXIAL STRESS. Launay, P. (Compagnie Industrielle de Travaux, Paris); Gachon, H. pp H1/3.1-12 of Structural Mechanics in Reactor Technology. Vol. 3, Pt. H. /Jaeger, Thomas A. (comp). Luxemburg; Commission of the European Communities (1971).

From 1st International conference on structural mechanics in reactor technology; Berlin, Germany (20 Sep 1971).

An analysis of the measurements made on cubic specimens of concrete with a veiw to studying the deformability under service compression stresses and the failure strength of the thick concrete walls used in nuclear reactor vessels is presented. The deformability (Young's modulus, Poisson's ratio) was studied up to 500 bars in the three principal directions on cubes having 140 mm sides at 20, 40, and 60°C. The ultimate strength and the failure mechanism under multiaxial stresses were studied on cubes having 70 mm sides up to 2,000 bars in all three directions, with the same specially built testing machine. The specimens were concreted with the same materials as the two $\frac{1}{5}$ models of the BUGEY 1 caisson built of Chinon CPAC-325 cement. The silico-calcareous gravel used had a maximum grain size of 15 mm, but with two different batchings, the nominal strength at 28 days varying in the batches from 300 to 450 bars. (auth)

**55661** DEFORMATION AND CRACKING MECHANICS IN HARDENED CEMENT PASTE AND CONCRETE UNDER SHORT-TERM AND HIGH SUSTAINED LOADS. Wittmann, F. (Technische Univ., Munich); Zaitsev, Yu. pp H1/4.1-15 of Structural Mechanics in Reactor Technology. Vol. 3, Pt. H. /Jaeger, Thomas A. (comp). Luxemburg; Commission of the European Communities (1971). (In German).

From 1st International conference on structural mechanics in reactor technology; Berlin, Germany (20 Sep 1971).

The behavior of hardened cement paste and concrete under high sustained load was studied theoretically on the basis of fracture mechanics. In this connection it is necessary to use an idealized structure instead of the real structure of hardened cement paste. It could be shown that with a given pore size distribution the crack propagation becomes unstable beyond a certain load. This is the critical or ultimate load. In a viscoelastic material such as hardened cement paste, the critical mean crack length which is necessary for unstable crack propagation can be reached under a lower sustained load than the critical load in a short time test. To test the described theory, experiments have been carried out with hardened cement paste and concrete. The loss of strength has been measured as a function of time and as function of the age of the specimens. The experimental results are in good agreement with the theoretical predictions. Dried specimens of hardened cement paste show very little creep. As a consequence the loss of strength under sustained load is negligible for these specimens. (auth)

XUM

**55662** CONCRETE REINFORCED WITH STEEL MICRO-REINFORCEMENT. Komlos, K. (Inst. of Construction and Architecture, Bratislava). pp H1/7.1-14 of Structural Mechanics in Reactor Technology. Vol. 3, Pt. H. /Jaeger, Thomas A. (comp). Luxemburg; Commission of the European Communities (1971).

From 1st International conference on structural mechanics in reactor technology; Berlin, Germany (20 Sep 1971).

The role of short pieces of thin steel wire, used at appropriately small spacings, is in the arrest of cracks. As an internal tensile crack propagates, displacements perpendicular to the plane of the crack develop in the immediate vicinity of the crack tip as a result of the stress singularity in that region. The presence of a stiffening element in the immediate vicinity of the crack opposes these displacements by adhesive bond between the stiffening element and the matrix. Therefore, the cracks do not propagate rapidly, as would be the case with plain concrete, but expand more slowly with an increasing load. This is due to the energy required to strip the short wires free of their adhesion along the advancing crack front. Investigations have been carried out on concretes reinforced with 0.25, 0.50, 0.75, and 1.00 percent of steel wires, having a diameter of 0.3 mm and a length of 30 mm. The obtained results have shown that the increase of strength, due to the applied microreinforcement, varies slightly with the appropriate strength characteristic. The reinforcement seldom causes a higher increase of strength than 20 percent. The increase of strength in cement pastes and mortars, determined by other authors, was of a higher order. This is probably due to a higher percentage of microreinforcement applied in cement pastes and mortars, and the absence of coarse aggregates in the above mentioned materials, affecting negatively the bond strength between microreinforcement and matrix. (auth)

**55663** TIME-TEMPERATURE EXTRAPOLATION TECHNIQUES AS APPLIED TO CONCRETE CREEP STRAINS. Sullivan, P. J. E. (Imperial Coll. of Science and Tech., London). pp H2/2.1-14 of Structural Mechanics in Reactor Technology. Vol. 3, Pt. H. /Jaeger, Thomas A. (comp). Luxemburg; Commission of the European Communities (1971).

From 1st International conference on structural mechanics in reactor technology; Berlin, Germany (20 Sep 1971).

Results of experiments carried out on concrete beams in flexure at temperatures above 100°C indicate that creep strains follow a semilog law when plotted against temperature. In line with other materials it can be shown that diffusion processes are involved in the mechanism of creep and that diffusion equations can be used to describe these strains. A modified form of Arrhenius equation for creep rates is developed and the creep results of investigations on gravel concrete in compression and on limestone concrete in compression are shown to fit this equation. A technique similar to that developed by Dorn is used and found to give a fair representation of long term creep strains at low temperature from short term creep strains at higher temperature. This technique is used in two time-temperature extrapolation equations which are derived. (auth)

**55664** NUMERICALLY STABLE ALGORITHM WITH INCREASING TIME STEPS FOR INTEGRAL-TYPE AGING CREEP. Bazant, Z. P. (Northwestern Univ., Evanston, Ill.). pp H2/3.1-8 of Structural Mechanics in Reactor Technology. Vol. 3, Pt. H. /Jaeger, Thomas A. (comp). Luxemburg; Commission of the European Communities (1971).

From 1st International conference on structural mechanics in reactor technology; Berlin, Germany (20 Sep 1971).

The creep law of concrete is assumed to obey the principle of superposition and is expressed by hereditary integrals with nonconvolution type kernels, which are expanded in a degenerate form. For each material point, a set of certain additional hidden variables, fully characterizing the previous stress history, is defined and it is found that in a step-by-step integration in time these variables can be computed from simple recurrent formulas. This makes storage of the past stress history unnecessary and circumvents thus the main obstacle for creep analysis of large structures. Unlike the step-forward integration with a rate-type creep law, the method is found to be stable for any size of the time step. This enables the time steps in relaxation-type problems to be gradually increased and the asymptotic values of stresses to be closely approached. Results of a simple numerical example corroborate this conclusion. (auth)

**55665** MIGRATION OF MOISTURE AND PORE PRESSURES IN HEATED CONCRETE. England, G. L. (Kings Coll., London). pp H2/4.1-17 of Structural Mechanics in Reactor Technology. Vol. 3, Pt. H. /Jaeger, Thomas A. (comp). Luxemburg; Commission of the European Communities (1971).

From 1st International conference on structural mechanics in reactor technology; Berlin, Germany (20 Sep 1971).

The importance of water content on concrete properties is discussed in relation to ambient and moderately elevated temperatures. Methods of determining water contents in situ are cited and attempts to relate changes of moisture content to shrinkage in simple specimens are mentioned. Experimental results from tests performed under sustained non-uniform and elevated temperatures are included and reveal that drying is encountered in the hottest regions of the concrete mass in addition to boundary areas associated with free evaporation of water to the atmosphere. Simple diffusion theory based on concentration of water is incapable of predicting these moisture distributions and a method of prediction is sought which recognizes the pore air and vapor pressures as additional factors which cause moisture to migrate down the temperature gradient. Comparisons of experimental results and theoretical predictions are made for a concrete cylinder subjected to a longitudinal temperature crossfall of 110°C and a maximum temperature of 150°C. It is concluded that although simple diffusion theories may be adequate for specifying drying at ambient temperatures they do not provide adequate representation in regions of high temperature and recognition must be given to other more influential factors such as pore pressures in these regions. (auth)

**55666** EFFECT OF RADIATION ON THE ADHESIVE PROPERTIES OF EPOXY-METAL AND EPOXY-GLASS ADHINTS. Tilmans, A. (Univ. of Pittsburgh); Krokosky, E. M. J. Mater.; 6: No. 2, 482-99(Jun 1971).

A two-component shear specimen was designed to give bond strength values for an adhint (adhesive-joints) subject to various radiation levels. Overlap shear specimens were ruled out because of the stress concentrations induced and because of specimen size limitations. The two-component specimens used the following adherends: electrolytic tough pitch copper, Pyrex glass, Type 304 stainless steel, cold rolled SAE 1020 steel, and 6061-T6 aluminum. The surface treatments given to the above adherends consisted of the following: 2-μin. finish, 16-μin. finish, chromate conversion, sandblasting, silane coupling agent, and several combinations of the preceding. It was found, upon exposure of up to 5000 Mrad, that radiation had little effect on the interface bonding characteristics for all specimens of low bond strength; radiation affected only those two-component specimens that exhibited a bond strength approximating the bulk epoxy material shear strength; the surface treatments and finishes of adherends have more significant effects on the bond strength than does the type of adherend; and the bond strength of the epoxy-glass specimens was stronger than the tensile strength of the treated glass adherends used in the study. (auth)

**55667** EFFECT OF RADIATION ON SOME MECHANICAL PROPERTIES OF AN EPOXY SYSTEM. Tilmans, A. (Univ. of Pittsburgh); Krokosky, E. M. J. Mater.; 6: No. 2, 465-81(Jun 1971).

The effect of radiation on the mechanical properties of an epoxy adhesive was studied. Specimens were subjected to doses as high as 5000 Mrad. In addition to the tension and compression tests, a newly devised disk-type shear test was carried out. A new type of minispecimen for radiation testing also was proposed. From the tension, compression, and bulk shear specimens, it was found that the compressive shear stress was dependent on the dose, especially at low doses; radiation caused cross-linking in the epoxy system and this, in turn, resulted in an increase in the modulus of elasticity, an increase in the tensile strength, and embrittlement; the large scatter of the tension stress-strain curves at low doses of radiation was the result of nonuniform cross-linking density within the specimen; the minitension technique is an acceptable procedure for studying the effects of radiation on tensile properties; and the disk-type fixture is an acceptable apparatus for studying the effects of radiation on bulk shear properties. (auth)

XUM

# PHYSICS (GENERAL)

## Astrophysics and Cosmology

*Refer also to abstract 56685.*

**55668** RELATIVISTIC SHOCK WAVES. Lukas, George. Waltham, Mass.; Brandeis Univ. (1971). 121p. University Microfilms Order No. 71-20,338.

Thesis.

The interpretations of many phenomena in astrophysical situations depend on the existence of shock waves as a means of converting directed flow energy into other forms. A study of strong shocks, relevant to astrophysical situations, was made. Upon analysis of the underlying thermodynamics, it was found that there are three kinds of shock waves of particular interest. They are most easily classified by the state of the matter before and after passage of the shock. A careful study of the dissipation mechanisms in and the structure of such shocks was made. Also the possibility of these shocks acting to erase magnetic fields which they move into was explored. Finally, shocks propagating into degenerate electron gases were studied. It was found that neutrino emission provides an energy sink into which the flow energy can be drained across the shock without driving the temperature so high as to drive the gas into a completely nondegenerate regime. Suitable Hugoniot equations were written and solved. Then the possible neutrino production schemes were investigated and the structure equations derived. The solution of this complete set was not attempted, but it was found that with simplifying assumptions, it was easy to find the maximum temperature of any shock, in terms of the initial conditions. This was really the parameter of greatest interest. The velocity of sound was calculated and found to be compatible with mathematical stability arguments applied to such degenerate gas shocks. (TSS) (Diss. Abstr. Int., B)

### *Cosmic Ray Exposure Ages*

*Refer also to abstracts 54457, 54458, 54462, 54463, 54465, 54466, 54468, 54477, 54479, 54480, and 54484.*

**55669** (N-71-26344) NUCLEAR INTERACTION TRACKS IN MINERALS AND THEIR IMPLICATIONS FOR EXTRATERRESTRIAL MATERIALS. Crozaz, G.; Hair, M.; Maurette, M.; Walker, R. (Washington Univ., St. Louis, Mo. Lab. for Space Physics). May 1969. Contracts NAS9-8165; Z80058T. 19p. (NASA-CR-118658; SPP-17). NTIS.

The geometric characteristics and the thermal stability of the interaction tracks produced by protons and alpha particles in mica were studied. The tracks were also studied in minerals found in meteorites or that are likely to be found in lunar materials. The energy and the fluxes of the ion were chosen to simulate exposures of >1000 years in the light component of the solar-flare cosmic rays. (auth) (STAR)

**55670** NUCLEAR REACTION IN THE NUCLEOGENESIS OF XENON ISOTOPES IN SOLAR SYSTEM MATTER. Lavrukhina, A. K. Meteoritika; No. 29, 9-29(1969). (In Russian).

The nine stable isotopes of xenon and their distribution are briefly considered. Twelve possible Xe-producing nuclear reactions are listed and discussed from the viewpoints of neutron energies, availability of reactant nuclei, and relative abundance of Xe isotopes synthesized by slow and fast neutrons. Anomalies in the isotopic composition of Xe in 38 meteorites are summarized, noting that all carbonaceous chondrites found to date have the same Xe isotopic composition. Inferences about the meteoritic Xe anomalies are drawn from the four isotopic components: Primary Xe, radiogenic $^{129}Xe$, cosmogenic isotopes, and fission products of heavy elements. 75 references. (K.S.W.)

**55671** COSMOGENIC ISOTOPES IN 42 FRAGMENTS OF THE SIKHOTE-ALIN METEORITE. Levskii, L. K. (All-Union Scientific Research Inst. of Geology, Leningrad). Geokhimiya; No. 8, 932-7(Aug 1971). (In Russian).

The content of cosmogenic $He^3$, $Ne^{21}$, and $Ar^{38}$ isotopes was measured in 42 separate samples of the Sikhote-Alin meteorite. The data obtained were compared with calculated ones and the most probable r/R = 0.8 value was determined, where R and r are radii of pre-atmospheric and post-atmospheric bodies, respectively. In case of a lower r/R value, the number of samples with a low content of cosmogenic isotopes must be great, which does not agree with experimental data. Comparison of experimental data with results of iron target irradiation in accelerators showed a relative $He^3$ and $Ne^{21}$ excess in the meteoritic matter, previously noted for other meteorites. (auth)

**55672** DIFFUSION LOSSES OF RADIOGENIC ARGON FROM METEORITES. Brandt, S. B.; Volkova, N. V. (Inst. of Geochemistry, Irkutsk, USSR). Geokhimiya: No. 8, 1012-15(Aug 1971). (In Russian).

Solar heating causes loss of radiogenic argon by meteorites during perihelion. Since K-Ar dating is widely used, the question of error in age determination of lunar rocks, terrestrial rocks, and meteorites is discussed. Dissipation of radiogenic gaseous materials from the lunar surface might be the result of both diffusion losses through heating and radiation effects from cosmic radiation. The activation energy of argon diffusion is only 14 kcal/mole, and would not assure its retention during geologic time under terrestrial conditions. Radiation temperatures and diffusion coefficients were calculated for various points along an assumed orbit for purposes of discussion. Radiation age determinations may provide a scale for evaluating loss of radiogenic substances. (K.S.W.)

### *Stars*

**55673** MODELI ATMOSFER ZVEVZD KLASSOV O I B. (Model Atmospheres of Stars of Classes O and B). Kruusmaa, A. E.-V. Tartu; Tartu Astrofuusika Observatoorium (1970). 124p.

This book contains two separate articles: English abstracts are given for each. (K.S.W.)

**55674** METODY ISSLEDOVANIYA PEREMENNYKH ZVEZD. (Methods of Investigating Variable Stars). Nikonov, V. B. (ed.). Nestatsionarnye Zvezdy i Metody ikh Issledovaniya. Moscow; Izdatel'stvo Nauka Glavnaya Redaktsiya Fiziko-Matematicheskoi Literatury (1971). 336p.

The introductory chapter of this monograph focuses attention on the discovery of variable stars, with special reference to the probability aspects of discovery. Successive chapters are devoted to the various methods of evaluating stellar brightness: visual, photographic, and photoelectric. Other topics considered are methods of studying polarization of stellar light, photometric standards, and the determination of the period of a variable with the aid of a computer. (K.S.W.)

**55675** PERIOD OF TY PUPPIS. van Houten, C. J. (Leiden Observatory). Astron. Astrophys.; 14: No. 3, 487-8(Oct 1971).

The period derived by Campbell for the eclipsing variable TY Puppis is incorrect; the correct period is shown to be 0.819235 d. (auth)

**55676** NEW COMPUTATIONAL METHOD FOR X AND Y FUNCTIONS OF RADIATIVE TRANSFER. Shultis, J. K. (Kansas State Univ., Manhattan). Astron. Astrophys.; 14: No. 3, 463-7(Oct 1971).

The X and Y functions of radiative transfer are shown to satisfy a pair of Fredholm integral equations. The equations are derived by considering a particular problem of diffuse reflection and transmission whose emergent intensities are closely related to these functions. Application of the singular eigenfunction expansion technique of neutron transport theory to this particular problem yields the Fredholm equations for both nonconservative and conservative atmospheres. These integral equations can be approximated by a set of linear equations and very accurate numerical solutions for the X and Y functions can be obtained. (auth)

**55677** PRINCIPAL SPECTRUM OF NOVAE. Friedjung, M. (Institut d'Astrophysique, Paris). Astron. Astrophys.; 14: No. 3, 440-50(Oct 1971).

The excitation and ionization of the parts of a nova envelope producing the principal absorption system are discussed. It is shown for various novae that the regions considered were probably optically very thick for Lyman continuum radiation, but that ionization of hydrogen by Balmer continuum radiation was important. Deductions concerning the importance of the emission produced by these regions were also made. (auth)

**55678** MASS FORMULA AND PROPERTIES OF MATTER AT SUBNUCLEAR DENSITIES. Tondeur, F. (Univ., Brussels). Astron. Astrophys.; 14: No. 3, 451-62(Oct 1971). (In French).

To make a quantitative calculation of the composition and of the equation of state of matter at subnuclear densities, it is necessary to know the masses of the neutron-rich nuclei, which are highly unstable against $\beta^-$ decay on Earth. These masses are known through the extrapolation of the semi-empirical mass formulae.

XUM

However, the masses obtained using different mass formulae diverge far off the stability line. How the properties of superdense matter depend on the mass formula was studied, and these properties were calculated, using different sets of parameters for the mass formula; supplementary terms were included in the Bethe–Weizsäcker formula. The results showed that the composition of superdense matter depends on the mass formula; also, variations of the equation of state were found for densities $3 \times 10^{11} \lesssim \rho \lesssim 10^{13}$ g/cm$^3$. It appears that the classical description of the superdense matter in three phases (nuclei + free electrons, nuclei + free electrons and neutrons, free neutrons, protons, electrons, and other free elementary particles) is not adequate when the symmetry energy is too low (i.e. a low second-order symmetry term, or an important fourth-order or surface symmetry term). (auth)

**55679** CONVECTION AND METAL ABUNDANCE. Boehm-Vitense, Erika (Univ. of Washington, Seattle). Astron. Astrophys.; 14: No. 3, 390-5(Oct 1971).

The influence of the metal abundance Z on the structure of the convection zone is studied. The velocities in the convective zones decrease and the depths of the convection zones increase with decreasing metal abundance. For lower metal content the transition from radiative to convective atmospheres therefore occurs at higher effective temperatures. (auth)

**55680** DATA ON THREE NEW VV CEPHEI STARS: BD + 63°3, BD + 54°2698, BD + 61°219. Barbier, M. (Observatoires de Marseille). Astron. Astrophys.; 14: No. 3, 396–400(Oct 1971). (In French).

Three new VV Cephei stars to be added to the fifteen already known were studied at 40 Å/mm with the coudé spectrograph. Many [Fe II] emission lines were identified but [Ni II] [S II] and Fe II were also found. Except for BD + 63°3, the radial velocities of [Fe II] emission lines and metallic absorption lines were the same. An upper limit of absolute magnitude with the interstellar calcium radial velocity value was calculated. (auth)

**55681** BRIGHT CONDENSATION 3C 153.1 INSIDE THE H II REGION NGC 2175. Garnier, R.; Lortet-Zuckermann, M. C. (Observatoire de Haute Provence, France. Observatoire de Lyon. Institud d'Astrophysique de Paris). Astron. Astrophys.; 14: No. 3, 408-14(Oct 1971).

Physical parameters are derived for the bright knot inside NGC 2175 using optical dimensions 1′ × 2′. Photometry and spectrophotometry of the central star yield a spectral type 09-B0, a luminosity class IV–V, and a reddening E (B − V) = 0.69 ± 0.03. The central star is probably the source of excitation of the bright knot. (auth)

**55682** QUANTITAVE ANALYSIS OF THE O-SUBDWARF HD 49798. Richter, D. (Univ., Kiel). Astron. Astrophys.; 14: No. 3, 415-27(Oct 1971).

HD 49798, the brightest O-subdwarf known, was analyzed by evaluation of a blue plate (6.8 Å/mm), 25 image-tube spectra, scans and broad- and narrow-band colors. The spectrum showed helium- and nitrogen-lines enhanced relative to the hydrogen lines that still contribute most to the blends with the Pickering lines. The atmospheric parameters were derived by fitting the outer wings of typical lines to profiles computed with LTE models. First flux-constant unblanketed models were used for computing line widths. A better reproduction of the line centers was achieved by an approximately line-blanketed model and by an empirical model. The atmospheric parameters obtained in the three approximations differed slightly. As final parameters $T_e$ = 45,000°K, log g = 5.0, log $\epsilon_{He}$ = 11.8, log $\epsilon_N$ = 9.7 (one line only) (relative to log $\epsilon_n$ = 12.0) were adopted. From the interstellar lines Ca II K and Na D, an absolute visual magnitude $M_H \approx -0.2$m and a mass of about 2 $\mathfrak{M}_\odot$ were estimated. Considering also the close relation between O subdwarfs and static helium-star models as far as the mass–luminosity ratio and the position in the HR-diagram are concerned, an evolutionary track resembling that of a massive star losing a considerable fraction of its envelope while hydrogen is burning in a shell source is proposed. (auth)

**55683** TIDAL ACTIONS ON SMALL STAR CLUSTERS. Bouvier, P. (Observatoire de Geneva). Astron. Astrophys.; 14: No. 3, 341-50(Oct 1971).

The combined effect of the tidal action of the galactic field and that of passing interstellar clouds on a small star cluster containing, say, from one to three dozens of stars, is considered. The disruption time resulting from the sole influence of the clouds is calculated rigorously for spherical homogeneous clouds passing rapidly by the cluster; a reduction factor equal to $^4/_9$ should be applied to the usual value (Spitzer, 1958). The galactic field is introduced by ascribing a finite radius of stability to the cluster and after having defined the total energy of a cluster on the verge of disruption, the disruption time is calculated in the presence of the galactic field. A theoretical interpretation is given for the curve describing the energy increase with time obtained from previous numerical experiments (Bouvier and Janin, 1970). In the competition between both tidal actions it turns out that, for the small clusters of the type considered, the galactic field always outweighs the influence of the clouds. Finally, an investigation is carried out on the fluctuations of the gravitational field due to spherical homogeneous clouds moving randomly while keeping their concentration unchanged. (auth)

**55684** SCHOENBERG–CHANDRASEKHAR LIMIT AND ROTATION. Maeder, A. (Observatoire de Geneva). Astron. Astrophys.; 14: No. 3, 351-8(Oct 1971).

The effects of axial rotation on the Schoenberg–Chandrasekhar (S–C) limit are studied by means of a first-order analytic method. The virial theorem expressed for an isothermal rotating configuration permits the discussion of the effects of rotation on the stability of the stellar core and particularly on the maximum pressure which it can withstand. The expression of the S–C limit in presence of rotation is given. The S–C limit can increase or decrease according to the law of rotation in the stellar envelope. The physical reasons of these variations are given. The application of the given expressions shows that in case of uniform rotation the S–C limit does not change very much even for extreme rotation (max decrease ~3%). For nonuniform rotation, it is found that if stars have fast spinning cores, there is an appreciable increase of the S–C limit, which may lead to observable increases of the number of stars at the shell H-burning stage, in open star clusters for example. (auth)

**55685** STELLAR OPACITY. Carson, T. R. (Univ. Observatory, St. Andrews, Scotland). Progr. High Temp. Phys. Chem.; 4: 99-137(1971).

The subject is discussed in sections covering; stellar structure (energy transport in stars); radiative energy transport (radiative transport and opacity, the equation of transfer, and radiative flux); radiative processes (radiative processes in stars; absorption cross sections; bound–bound, bound–free, and free–free absorption; and scattering by free electrons); and opacity calculations (stellar mixtures, quantum statistical mechanics, monochromatic absorption coefficients, the radiative opacity, and the conductive opacity). (UK)

**55686** MILLIMETER OBSERVATIONS OF CO, CN, AND CS EMISSION FROM IRC + 10216. Wilson, R. W. (Bell Telephone Labs., Holmdel, N. J.); Solomon, P. M.; Penzias, A. A.; Jefferts, K. B. Astrophys. J.; 169: No. 1, L35-7(1 Oct 1971).

The discovery of three additional molecular lines is reported from an object in which was previously detected carbon monoxide. The data presented tend to support the model of a small expanding shell with high brightness temperature. (auth)

**55687** PERIOD–AGE DISTRIBUTION OF PULSARS. Sturrock, P. A. (Stanford Univ., Calif.). Astrophys. J.; 169: No. 1, L7-10(1 Oct 1971).

A recently proposed model of pulsars leads to a constraint on the values of period T and "age" $\tau$ [= $T(dT/dt)^{-1}$] of radio-emitting neutron stars and a similar constraint for optically emitting neutron stars. These constraints compare satisfactorily with available data. (auth)

**55688** NONLINEAR NUCLEAR-ENERGIZED STELLAR PULSATIONS. Ungar, Stephen Gene. New York; City Univ. of New York (1971). 302p. University Microfilms Order No. 71-20,946.

Thesis.

Nuclear-energized pulsations were investigated as a proposed mechanism for the observed variations in light and radial velocity curves of $\beta$ Cephei stars. In the past, such investigations were conducted by the construction of models utilizing linearized hydrodynamics. Although a linearized treatment yields useful information, it fails to provide many of the physical quantities necessary to adequately compare stellar models to observable stellar objects. To obviate this drawback, models were constructed using a fully nonlinear hydrodynamic computer code. For 15-$M_\odot$ main-sequence models with helium-enriched envelopes, it was found that pulsational instability induces mass loss at the rate of ~$5.10^{-5}$ $M_\odot$ per year in the form of ejected shells, each of which contains ~$5.10^{-7}$ $M_\odot$. The final shell velocities approach $10^3$ km/sec. These features are strongly reminiscent of recent Wolf–Rayet star observations by Underhill. Suppression of mass loss by computational techniques gives rise to models whose radial velocity curves display periods and structure similar to those of $\beta$ Cephei stars. Particularly characteristic of $\beta$ Cephei stars is the zero-phase displacement between the components of these radial velocity curves and the corresponding components of the computed light curves. The results lead to interesting speculations when con-

sidering that some Wolf–Rayet objects are found to form an extension of the $\beta$ Cephei instability strip when plotted on the H–R diagram. (Diss. Abstr. Int. B.)

**55689** PROPERTIES OF A SHORT-RANGE FIELD MODEL OF SUPERDENSE MATTER. Lai, Shu Tim. Waltham, Mass.; Brandeis Univ. (1971). 152p. University Microfilms Order No. 71-20,337.

Thesis.

An equation of state is obtained for ultrahigh-density matter of baryons interacting via a repulsive short-range vector field. Correlation effects are treated by means of a fluctuation–dissipation approach and also by the ring approximation of Ursell–Mayer cluster expansion. It is shown that in the domain of ultrahigh-density plasma, correlation effects cannot dominate over both kinetic and Hartree terms and sound speed is subluminal. For parameters continued beyond the plasma domain, correlations can dominate, possible phase transitions are present and sound speed approaches c, the velocity of light in vacuo, asymptotically from above c. Correlations beyond the ring approximation are calculated by summing melon-type cluster diagrams. Dispersion relations of the lattice model and the continuum model are compared. It is found that sound speed is subluminal and there are no unstable acoustic modes in the continuum model. Properties of ferromagnetic transitions of the short-range vector field model are obtained in Hartree–Fock approximation with plane wave states. It is found that in the nonrelativistic regime, ferromagnetic state is favored at intermediate densities, while in the relativistic regime with strong-interaction coupling strength, ferromagnetism is favored throughout the high-density domain. No van der Waals-type gas–liquid phase transition is associated with the ferromagnetic transitions. (Diss. Abstr. Int., B.)

**55690** EVOLUTION OF EARLY-TYPE CLOSE BINARY SYSTEMS. Benson, Robert Stanley. Berkeley, Calif.; Univ of California (1970). 94p. University Microfilms Order No. 71-20,773.

Thesis.

A modified version of the Berkeley evolutionary program was used to compute models approximating the nonspherical components of a close binary system, and to follow their evolution during mass exchange. Both components (initially 5 $M_\odot$ and 2.5 $M_\odot$) were assumed to always be in uniform rotation at a rate synchronous with their orbital motion. With an initial period of one day the (small) effects of rotational and tidal perturbations agreed well with those for models of rotating stars calculated by other investigators. The primary fills its Roche lobe after main-sequence hydrogen burning has reduced the central hydrogen content to about half its initial value. The rate of mass exchange was then determined by an iterative scheme such that the radius of the primary is equal to that of the Roche lobe to one part in $10^3$. All material leaving the primary flows isothermally to the surface of the secondary. After approximately $3.2 \times 10^4$ yr the rate of mass exchange reaches $10^{-5}$ $M_\odot$/yr; slightly more than 0.1 $M_\odot$ has been exchanged, and the secondary has rapidly increased in radius, forming a contact system. Discussion of structural changes during mass exchange reveals that the growth of the secondary's radius is directly related to the large difference in the Kelvin time scales for the two stars. (Diss. Abstr. Int. B)

**55691** EVOLUTIONARY MODELS OF STARS OF 15 AND 30 $M_\odot$. Simpson, Erik Elgar. Berkeley, Calif.; Univ. of California (1970). 53p. University Microfilms Order No. 71-20,909.

Thesis.

Evolutionary models were computed for stars of 15 and 30 $M_\odot$, with a composition given by the mass abundances X = 0.75, Y = 0.23, Z = 0.02. Parallel calculations were carried out with and without allowance for semi-convection or full convection in intermediate-mass shells. In the case of semiconvection the stability criterion adopted was $dT/dP = (dT/dP)_{ad}$. After the main-sequence phases the models with intermediate mixing develop fully convective shells that greatly alter the behavior of the models during helium burning. The models with the convective shells spend much of their helium-burning lifetimes as blue supergiants, while the models without convective shells rapidly become red supergiants. From an examination of the observations of h and $\chi$ Persei it was concluded that the convective shell models are more likely to be physically correct. (Diss. Abstr. Int., B)

**55692** SEARCH FOR DISCRETE CELESTIAL SOURCES OF FAR-INFRARED RADIATION. Joseph, Robert David. St. Louis; Washington Univ. (1971). 119p. University Microfilms Order No. 71-19,819.

Thesis.

After a brief indication of the astrophysical motivation for conducting a search for discrete sources of far-infrared radiation, there follow considerations pertinent to the experimental design of such an observation: detector calibration, spectral filtering, telescope optics, electronic signal handling, etc. Special complications attending the necessity for making these observations with telescope and detector lofted well into the stratosphere by balloon, such as determination of the celestial coordinates of the telescope beam throughout the flight, data recording on-board and via telemetry, and operation of the equipment in the hostile stratospheric environment, are also discussed. A gondola equipped with a Ge : Ga bolometer, cooled to the temperature of liquid helium, at the focus of an eight-inch Newtonian telescope is described. This instrument was flown at 28-km altitude for 12 hours on 21–22 January 1970, in an attempt to search the sky for discrete sources radiating strongly at wavelengths between 45 and 300 $\mu$. The data from this flight, and methods of its reduction, are presented. Four sources of apparent flux $\sim 10^{-13}$ watt $cm^{-2}$ were detected. Their celestial positions are not uniquely identifiable with sources prominent in other spectral regions. In conclusion, the prospects for future far-infrared sky surveys, as well as oriented observations, are indicated, both from an instrumental and an astrophysical point of view. (Diss. Abstr. Int., B)

**55693** STELLAR INTERFEROMETRY FOR FAINT ASTRONOMICAL OBJECTS. Davidson, Joseph Henry. Madison, Wis.; Univ. of Wisconsin (1971). 124p. University Microfilms Order No. 71-16,068.

Thesis.

Photoelectric detection of fringes from a Fizeau interferometer was used to measure the parameters of three visual binary systems: $\epsilon^1$ and $\epsilon^2$ Lyr, and $\epsilon$ Ari. Values for the angular separation and position angle agreed with the published measurements within the error limits of the eyepiece micrometer measurements. Values for $\Delta$m, the difference in magnitude between the two components, differ by about $0.2^m$ from the estimates made by visual observers; but it is difficult to say how accurate these estimates are. (TSS) (Diss. Abstr. Int. B)

**55694** ASYMPTOTIC SOLUTIONS IN NONLINEAR CONVECTION WITH FREE BOUNDARIES. Van der Borght, R. (Monash Univ., Clayton, Australia). Aust. J. Phys.; 24: 579-85(Aug 1971).

An investigation was made of the problem of nonlinear convection in an incompressible fluid at high Rayleigh number, using an asymptotic theory. An estimate is derived for the preferred horizontal wave number. (auth) (Australia)

**55695** NONLINEAR THERMAL CONVECTION WITH FREE BOUNDARIES. Murphy, J. O. (Monash Univ., Clayton, Australia). Aust. J. Phys.; 24: 587-92(Aug 1971).

The equations governing thermal convection in a horizontal fluid layer heated from below were solved by numerical integration when free boundary conditions apply. The computed forms for the vertical velocity, the mean temperature, and the temperature fluctuation are given for several values of the Rayleigh number in the range 900 to $0 \times 10^4$. Computational difficulties encountered in the step-by-step integration procedures set the upper limit of $2 \times 10^4$ for the Rayleigh number. For larger values of R comparison is made with the results predicted by an asymptotic theory. (auth)

**55696** APPLICATION OF TOLMAN'S SOLUTIONS OF FIELD EQUATIONS IN CASE OF VARIABLE-DENSITY CORES. Krori, K. D. (Cotton Coll., Gauhati, India). Indian J. Pure Appl. Phys.; 9: No. 1, 1-4(Jan 1971).

Tolman's solution V (Phys. Rev., 55: 364(1939)) of Einstein's field equations was applied in the case of stellar structures with a variable-density core with a finite density and pressure at the center of the body. Characteristics of Tolman's solution VI are discussed with reference to constant-density as well as variable-density cores. The astrophysical implications of the deductions are pointed out. (auth)

**55697** RADIAL VELOCITIES OF SOUTHERN B STARS DETERMINED AT THE RADCLIFFE OBSERVATORY. V. Hill, P. W. (University Observatory, St. Andrews, Scotland. Radcliffe Observatory, Pretoria). Mem. Roy. Astron. Soc.; 75: 1-20(1971).

Radial velocities are given for 85 O and B type stars at intermediate and high galactic latitudes. These include some brighter than $m_v = 6$ as well as some very distant stars fainter than $m_v = 10$. A number of high-velocity stars are noted, of which at least one is probably subluminous. (auth) (UK)

**55698** QUANTITATIVE INTERPRETATION OF THE INFRARED SPECTRA OF LATE-TYPE STARS. Price, Stephan Donald. Columbus, Ohio; Ohio State Univ. (1970). 150p. University Microfilms Order No. 71-18,068.

Thesis.

XUM

The effects on wide-bandpass infrared photometry of cool stars caused by blanketing due to molecular absorptions in the stellar atmosphere were investigated. Absorption by $H_2O$, CO, CN, $C_2$, TiO and VO, the most important absorbers in the infrared, was considered in the spectral region 0.7 to 6.3 $\mu$ for stellar temperatures of 1500 to 4000°K. Molecular absorption coefficients for $H_2O$ and CO are available from the literature, but the values for TiO, VO, CN, and $C_2$ were calculated. The results of the calculations of the absorption coefficients for the infrared transitions of CN and $C_2$ are presented in detail. The calculations show that while a set of wide-bandpass filters can be chosen in the infrared that will be relatively free of molecular absorptions and thus may be used to measure the continuum in cool stars, much narrower filters are needed to obtain useful quantitative indices of the abundance of each molecule. (TSS) (Diss. Abstr. Int., B)

**55699** HEAVY METAL ABUNDANCES IN S-STARS. Hackos, William Jr. Bloomington, Ind.; Indiana Univ. (1970). 151p. University Microfilms Order No. 71-17,445.

Thesis.

Two S stars, the long period variable R Cygni and the nonvarying S star HD 35155, were studied in the blue region of the spectrum in order to determine atomic abundances of the iron group metals and heavy metals. Of special interest were the abundances of technetium and niobium, which provide a time scale to estimate the age of the material in the atmosphere. Calibrated high-dispersion spectrograms (9 A/mm for R Cygni and 10 A/mm for HD 35155) were reduced to intensity profiles and compared with synthetic spectra calculated using a slab atmosphere and the Minnaert semi-empirical formula. As a check on the procedure, synthetic profiles were also compared with the spectrum of Arcturus which has well-known abundances. Excitation temperatures used were 2500°K for R Cygni, 2900°K for HD 35155, and 3500°K for Arcturus. The synthetic profiles were fitted to the observed profiles by iterating over the ionic abundances. Corrections were made for ionization to obtain atomic abundances. The resulting abundances were nearly the same as solar abundances for Arcturus. For both HD 35155 and R Cygni it was found that heavy element abundances were enhanced in a way consistent with neutron-capture theory. For both S stars the iron group elements were found to have abnormal abundances compared with solar abundances. The Nb and Tc abundances for HD 35155 suggest that material fresh from neutron exposure is no longer being brought to the surface. The Nb and Tc abundances for R Cyg yield ambiguous results. (Diss. Abstr. Int., B)

**55700** OBSERVATIONS OF INTERSTELLAR MOLECULAR HYDROGEN AND MEASUREMENTS OF HYDROGEN AND HELIUM FLUXES FROM PLANETARY NEBULAE. Gull, Theodore Raymond. Ithaca, N. Y.; Cornell Univ. (1971). 301p. University Microfilms Order No. 71-17,642.

Thesis.

An automated Fabry–Perot interferometer was developed for telescope use and was utilized in observations for several astrophysical problems. The search for interstellar molecular hydrogen begun by Werner (1968) was continued; the He $\lambda$10830 Å ($2^3P - 2^3S$) line fluxes and the P12 $\lambda$8750.36 Å (n = 12 to n = 3) line fluxes were measured in six planetary nebulae; upper limits to the sky background continuum in the near infrared were established. The major observing program was a search for lines in the 3–0 vibrational band of molecular hydrogen. No emission features attributed to $H_2$ were detected in any of many regions observed. (TSS) (Diss. Abstr. Int., B)

**55701** B-TYPE STARS WITH DISCREPANT COLORS. Molnar, Michael Robert. Madison, Wis.; Univ. of Wisconsin (1971). 92p. University Microfilms Order No. 71-14,156.

Thesis.

The color-spectrum discrepant stars, usually referred to as "weak helium-line" stars, have intrinsic colors too blue for the MK-type by at least two-tenths of a spectral type. The physical characteristics of this anomalous group were investigated by observing the stars' energy distributions, line profiles, and equivalent widths of prominent spectral lines. These data were used in a model atmosphere analysis and abundance determination. Another objective of this work was to better define the class and its members. (TSS) (Diss. Abstr. Int., B)

**55702** LIFE SPANS OF CONDENSATIONS IN PLANETARY NEBULAE. Holm, Albert Victor. Madison, Wis.; Univ. of Wisconsin (1971). 92p. University Microfilms Order No. 71-14,144.

Thesis.

It is shown that, under certain conditions, neutral condensations formed in a young planetary nebula and not held together by gravitational or magnetic forces can survive for a time span comparable with the ages of old planetaries in which condensations are observed. (TSS) (Diss. Abstr. Int., B)

**55703** PHOTODISINTEGRATION RATE OF $^{24}$Mg. Couch, R. G.; Shane, K. C. (California Inst. of Tech., Pasadena). Astrophys. J.; 169: No. 2, 413-19(15 Oct 1971).

The photodisintegration rate of $^{24}$Mg was investigated in the context of the silicon-burning process in stars. The results of a study of the $^{20}$Ne($\alpha,\gamma$)$^{24}$Mg reaction at low $\alpha$-particle energies are presented. The existing data for the $^{20}$Ne($\alpha,\gamma$)$^{24}$Mg and $^{23}$Na(p,$\gamma$)$^{24}$Mg reactions are summarized as tables of the two interaction rates. Multiparameter fits to the rates in the temperature range where the rates are well determined experimentally, and theoretical extrapolations to regions where the rates are not well determined, are provided. The photodisintegration rate of $^{24}$Mg is then calculated from these data. (auth)

**55704** STELLAR RATES FOR THE $^{28}$Si($\alpha,\gamma$)$^{32}$S AND $^{16}$O($\alpha,\gamma$)$^{20}$Ne REACTIONS. Toevs, James W.; Fowler, William A.; Barnes, C. A.; Lyons, Peter B. (California Inst. of Tech., Pasadena). Astrophys. J.; 169: No. 2, 421-4(15 Oct 1971).

The stellar interaction rate for the $^{28}$Si($\alpha,\gamma$)$^{32}$S reaction was calculated from new cross sections for this reaction for temperatures from 0.3 to $3 \times 10^{9}$°K. The astrophysical implications of new data for the $^{16}$O($\alpha,\gamma$)$^{20}$Ne reaction at low energy are also discussed. (auth)

**55705** SEARCH FOR LIGHT VARIATIONS IN SOME SUPERGIANTS IN THE LARGE MAGELLANIC CLOUD. Rosendhal, Jeffrey D. (Univ. of Wisconsin, Madison); Snowden, Michael S. Astrophys. J.; 169: No. 2, 281-8(15 Oct 1971).

A careful photometric study was made of five of the most luminous supergiants in the Large Magellanic Cloud. The results are (1) the maximum amplitude of variability on short time scales (minutes to hours) is less than ±0.015 mag in both the blue and visual wavelength ranges for all five program stars, and (2) all five stars appear to be variable when observed over a time interval of a month or more with the variability ranging from 0.02 to 0.07 mag in the visual and from 0.04 to 0.08 mag in the blue. Implications of these results for recent theoretical calculations of the stability of massive stars are briefly discussed. (auth)

**55706** IMPORTANCE OF THE INTERNAL VELOCITY FIELD IN STAR FORMATION. Arny, Thomas (Univ. of Massachusetts, Amherst). Astrophys. J.; 169: No. 2, 289-92(15 Oct 1971).

The assumption that opacity controls the mass of fragments in a collapsing cloud is shown to lead to results not in agreement with observation. It is shown that internal motions can set the mass of fragments, and that fragmentation at either constant angular-momentum density or kinetic-energy density reproduces the observed mass function. If the internal velocity field does not influence fragmentation, it is difficult to understand why there are any massive stars formed. (auth)

**55707** HYDRODYNAMICS OF THE CONVECTIVE ENVELOPES OF STARS. Mel'nikova, N. S.; Yavorskaya, I. M. Izv. Akad. Nauk SSSR, Mekh. Zhidk. Gaza; No. 2, 27-38(Mar-Apr 1971). (In Russian).

Using the methods of hydrodynamics the gas compressibility, rotation, gravitation, and anisotropic turbulent viscosity were investigated for large-scale movements in the convective envelopes of stars. Some dimensionless parameters that control the movements of the gaseous masses in the convective zone are evaluated, leading to a simplification of the equations of motion and to an approximate solution. It is suggested that the gas movements in the convective envelopes possess anisotropic turbulence. The Reynolds stress tensor depends on the velocity of deformation which, together with a coefficient of proportionality in a spherical system of coordinates, form a diagnonal tensor. The boundaries of the convective zone are considered free from turbulent stress. (tr-auth)

**55708** MASSES, LUMINOSITIES, AND COMPOSITIONS OF HORIZONTAL-BRANCH STARS. van Albada, T. S.; Baker, Norman (Columbia Univ., New York). Astrophys. J.; 169: No. 2, 311-26(15 Oct 1971).

For RR Lyrae stars in globular clusters, three different relations between mass and luminosity can be obtained from a combination of available observations and theoretical models. By requiring compatibility among these relations, the masses and luminosities of these stars can be inferred as functions of the composition parameters assumed for the models. This requirement also restricts the composition parameters. For the globular cluster M3, the helium abundance Y cannot be less than 0.15 and the abundance of heavier elements Z is probably not greater than $3 \times 10^{-4}$. Mass loss during pre-horizontal-branch evolution is neither required nor excluded. The ratio of horizontal-branch luminosity to that at the main-sequence turnoff is a sensitive function of Z; values of this function are given. The problem of deter-

XUM

mining Y in RR Lyrae stellar envelopes from the blue edge of the instability region is reexamined with the help of linear nonadiabatic models of pulsating stars. Y = 0.35 ± 0.10 was obtained for M3. The theoretical uncertainties and the consequent uncertainties in the inferred values of M, L, Y, and Z are emphasized. (auth)

**55709** MODELS FOR THE ENVELOPES OF Be STARS. III. POLE-ON STARS. Marlborough, J. M.; Roy, J.-Rene (Univ. of Western Ontario, London). Astrophys. J.; 169: No. 2, 327-31(15 Oct 1971).

Hα line profiles are presented for model envelopes for which the observer's line of sight is parallel to the rotation axis of the star. A comparison is made of these line profiles with the predicted Hα line profiles for the same model envelope when the observer's line of sight is perpendicular to the rotation axis. (auth)

**55710** RADIATIVE-TRANSFER MODEL OF A CEPHEID. Bendt, Janet E.; Davis, Cecil G. Jr. (Los Alamos Scientific Lab., N. Mex.). Astrophys. J.; 169: No. 2, 333-42(15 Oct 1971).

Extensive calculations were made on a nonlinear hydrodynamic model of a 10.78d Cepheid. It was first studied by using a gray diffusion approximation, and parameter studies were made of the effects of varying the zoning, the boundary conditions, and the artificial viscosity coefficient. Then a gray transport model was run by using a variable Eddington factor. This was followed by frequency-dependent radiative-transport calculations which used three different divisions of the spectrum, namely, divisions into 13, 19, and 28 frequency groups, respectively. Finally the latter calculation was compared with the V and B − V observational curves for XX Cen, a 10.96d Cepheid. Results of the gray calculation for a deep-envelope model were used to determine the most desirable values of the parameters to be used in the subsequent frequency-dependent calculations and also to obtain the inner (driving) boundary conditions for the thin-envelope models that followed. The procedure worked well, and good agreement was found in the V and B − V between the observational curves and the final curves of the radiative-transport model using 28-frequency groups. (auth)

**55711** ATMOSPHERIC ABUNDANCES IN THE BETA CEPHEI STARS. Watson, R. D. (Australian National Univ., Canberra). Astrophys. J.; 169: No. 2, 343-56(15 Oct 1971).

Extensive data on helium and metal line strengths are given for β Cephei stars. These data were used to determine atmospheric helium abundances for the β Cephei stars and relative metal abundances, the latter being obtained from a straightforward curve-of-growth procedure. A sample of other early B stars was used for comparison. The normality of the atmospheric composition of the β Cephei stars is the significant fact which emerges. No encouragement is given to Stothers and Simon's μ-mechanism hypothesis. (auth)

**55712** RADIATION PRESSURE AND ACCELERATING STELLAR WINDS. Marlborough, J. M. (Univ. of Western Ontario, London). Astrophys. J.; 169: No. 2, 441-2(15 Oct 1971).

It is shown that insofar as the hydrodynamics is concerned the conclusions of Marlborough and Roy concerning the effect of radiation pressure on stellar winds are completely consistent with the mechanism proposed by Lucy and Solomon regarding mass loss in hot stars. (auth)

**55713** ASTROPHYSICAL MODELS: A LOOK AT MODELS OF STELLAR ATMOSPHERES. Grant, I. P. (Oxford Univ. Atlas Computer Lab., Chilton, Eng.). pp E.0-16 of Computational Physics. Vols. I and II. London; Her Majesty's Stationery Office (1969).

From Conference on computational physics; Culham, England (28 Jul 1969). See CONF-690706-(Vols.1 and 2).

The interpretation of astrophysical observations requires the construction of theoretical models based on knowledge of laboratory physics. Preliminary investigations usually make use of simplifications in the physical assumptions and the mathematical treatment used, but it is often necessary to be more sophisticated if further progress is to be made. It is here that computers make their mark, as the rapid expansion in the last decade of their application to astrophysical problems shows. This pattern is exemplified by models of the internal structure of stars and of their atmospheres. Computations of stellar structure and evolution have illuminated many problems to an extent perhaps undreamed of ten or fifteen years ago. Models of the envelopes of pulsating stars have permitted a physical explanation of their existence and mechanisms. An attempt is made to illustrate the nature of the computations by examining the important field of model stellar atmospheres in some detail. (auth) (UK)

**55714** SUPERFLUID STATE IN NEUTRON STAR MATTER. II. PROPERTIES OF ANISOTROPIC ENERGY GAP OF $^3P_2$ PAIRING. Takatsuka, Tatsuyuki; Tamagaki, Ryozo (Kyoto Univ.). Progr. Theor. Phys. (Kyoto); 46: No. 1, 114-34(Jul 1971).

By applying the formulation developed in I and using several semiphenomenological two-nucleon potentials, properties of the $^3P_2$ pairing originating from spin-orbit forces were investigated at high density ($\rho \gtrsim 2 \times 10^{14}$ g cm$^{-3}$) in neutron-star matter. All the possible types of solutions were obtained by solving a coupled integral gap equation through an iterative procedure. Two of these five solutions represented axially symmetric energy gap. By a kind of self-consistency implied in the coupled gap equation the most general solution showed remarkable deviation from axial symmetry as a result of the mixing mainly of $m_j = \pm 2, 0$ components but the resulting gap was nodeless. The total energy shifts were very close for all the types of solutions. Although calculations showed the largest energy shift for the most general solution, this conclusion was a quantitative one. The $^3P_2$ gap at high densities depends critically on the effective mass and short-range behavior of nuclear forces, especially on the strong repulsive core of two-nucleon forces. In any case there exists neutron superfluidity due to the $^3P_2$ pairing at least in the density region $\rho \cong (2 \sim 5) \times 10^{14}$ g cm$^{-3}$. Consequences of the calculated results are discussed, and an argument is given to the connection between the mass of the pulsar and the strong density dependence of neutron superfluidity. (auth)

**55715** EQUATION OF STATE OF NEUTRON STAR MATTER AND NEUTRON STAR MODELS. Ikeuchi, Satoru (Kyoto Univ.); Nagata, Sinobu; Mizutani, Tetsuro; Nakazawa, Kiyoshi. Progr. Theor. Phys. (Kyoto); 46: No. 1, 95-113(Jul 1971).

The energy of neutron star matter was calculated by using the Brueckner theory for three different-type nuclear potentials in the range of densities $5 \times 10^{13} \lesssim \rho \lesssim 1.14 \times 10^{15}$ (g cm$^{-3}$). In this calculation, contributions from higher partial waves, three-body clusters, and mixture of protons were included. Contribution from three-body clusters became about 10% of the kinetic energy in a density region higher than $7 \times 10^{14}$ g cm$^{-3}$ in the case of a potential with strong hard core. The relative proton number was about $5 \sim 7$% of the neutron number, and energy gain by mixture of protons was about 10% of the total energy in higher densities. Using these results, equations of state were determined and extended by several methods to density regions higher than $1.14 \times 10^{15}$ g cm$^{-3}$. Neutron star models were constructed based on the derived equations of state. These models showed that the maximum mass of the stable neutron star lies between 1 and 3 $M_\odot$. The $^3P_2$-pairing superfluidity was investigated and the energy gap of half an MeV was obtained. Some physical effects of this superfluidity are discussed in relation to pulsars and the thermal history. (auth)

## *Quasi-Stellar, Radio, and X-Ray Sources*

*Refer also to abstract 55091.*

**55716** OH ABSORPTION IN THE DIRECTION OF W44. Goss, W. M.; Cadewell. J. L.; Robinson, B. J. (CSIRO, Sydney). Astron. Astrophys.; 14: No. 3, 481-6(Oct 1971).

Four 1667-MHz OH absorption components were seen in the direction of the supernova remnant W44 (G34.6 − 0.5) at velocities of 12.5, 22, 30, and 42 km s$^{-1}$. The distribution of the opacity of each component was determined by observations on a 24-point grid with basic spacing 6 arc min (half the half-power beamwidth). The opacity of the three low-velocity components at 12.5, 22, and 30 km s$^{-1}$ was essentially constant over the source with average optical depths of 0.045, 0.017, and 0.027, respectively. The +42 km s$^{-1}$ feature showed large variations of opacity with values ranging from 0.03 to 0.17. This feature had a velocity similar to that of the 1720-MHz OH emission lines, and maximum opacity near the position of 1720-MHz emission. It is suggested that the OH in emission and absorption at this velocity is physically associated with the supernova remnant. (auth)

**55717** DISTANCE DETERMINATION PROGRAM FOR SOME LOW-LATITUDE HIGH-VELOCITY NEUTRAL HYDROGEN CLOUDS AROUND LONGITUDE 125°. Hulsbosch, A. N. (Lieden Observatory). Astron. Astrophys.; 14: No. 3, 489-92(Oct 1971).

A list is given of 31 early-type stars down to magnitude 11.4 that are seen in projection against some low-latitude high-velocity H I clouds. These stars are very suitable to investigate cloud distances by studying interstellar absorption lines. The expected line strengths are also estimated. (auth)

**55718** INFRARED RADIATION FROM GRAINS IN ORION. Swamy, K. S. Krishna (Tata Inst. of Fundamental Research, Bombay). Astron. Astrophys.; 14: No. 3, 405-7(Oct 1971).

XUM

The calculated thermal emission from model grains is compared with some of the available infrared measurements for Orion. (auth)

**55719** POSSIBLE INTERPRETATION OF THE PRECURSOR PULSE IN NP 0532. Pacini, Franco (Laboratorio di Astrofisica Spaziale, Frascati, Italy. Cornell Univ., Ithaca, N. Y.). Astrophys. J.; 169: No. 1, L11-12(1 Oct 1971).

The properties of the precursor pulse of NP 0532 are consistent with the idea that it is emitted along the proton field lines. The sharp spectral cutoff above 430 MHz implies a cutoff in the proton energy spectrum around $2 \times 10^{11}$ eV. (auth)

**55720** X RAYS FROM A NEW VARIABLE SOURCE: GX 1 + 4. Lewin, Walter H. G.; Ricker, George R.; McClintock, Jeffrey E. (Massachusetts Inst. of Tech., Cambridge). Astrophys. J.; 169: No. 1, L17-21(1 Oct 1971).

On 1970 October 15–16 balloon x-ray observations were carried out from Australia (energies above 15 keV). A variable flux was detected from a source at $l^{II} = 1.4 \pm 0.7°$, $b^{II} = 3.9 \pm 0.8°$ (GX 1 + 4). The location of this source does not coincide with any of the accurately known locations of x-ray sources reported so far from rocket and satellite observations. During the ~40 minutes in which GX 1 + 4 was observed a series of flux changes by factors of 2 to 4 with rise and decay times of about 1 minute was detected. The data suggest that during the observations the flux changes may have been periodic with an approximate frequency of 1 cycle per 2.3 minutes. The integrated average energy from ~18 to 50 keV was ~1.5 keV $cm^{-2}$ $s^{-1}$. The average energy spectrum can be represented by an exponential form with values for kT of 28 ± 12 keV or by a power-law form with values for $\alpha$ of 1.4 ± 0.7. A high-energy x-ray flux was also detected from at least two more sources near the galactic center (quite likely GX 3 + 1 and GX 5 – 1). (auth)

**55721** PULSING X-RAY SOURCE IN CIRCINUS. Margon, Bruce; Lampton, Michael; Bowyer, Stuart; Cruddace, Ray (Univ. of California, Berkeley). Astrophys. J.; 169: No. 1, L23-5 (1 Oct 1971).

A pulsing x-ray source with period 685 ± 30 ms was observed in Circinus. Approximately 10% of the 1 to 10-keV x-ray emission of the source is contained in these pulses. A spectrum of the source is presented and may be fitted by a thermal bremsstrahlung emission mechanism with $T = 3.5 \times 10^7$ °K, or by a blackbody at $T = 1.1 \times 10^7$ °K, both subject to heavy absorption. (auth)

**55722** EMISSION NEBULAE IN THE MAGELLANIC CLOUDS AT 408 MHz. Mills, B. Y. (Univ. of Sydney); Aller, L. H. Aust. J. Phys.; 24: 609-15(Aug 1971).

Eleven emission complexes in the LMC and six in the SMC were observed at 408 MHz with a resolution of about 3′ arc. Electron densities and total masses were calculated, assuming uniform spherical models, and the values are compared with equivalent optical data. Although comparable, the optically derived values are significantly smaller than the radio results. (auth) (Australia)

**55723** OBSERVATIONS AT 408 MHz OF RADIO SOURCES FROM THE 4C CATALOGUE. II. DECLINATION RANGE $-3^0$ TO $0^0$. Munro, R. E. B. (Univ. of Sydney). Aust. J. Phys.; 24: 617-30(Aug 1971).

Radio positions and flux densities measured at 408 MHz with the Molonglo radio telescope are given for 235 sources from the Fourth Cambridge catalogue in the declination range –3° to 0°. Optical identifications are suggested for 70 of the sources. (auth) (Australia)

**55724** PULSAR JP 1933: 21-cm LINE ABSORPTION PROFILE AND INTERSTELLAR SCINTILLATION. Guelin, M.; Encrenaz, P.; Bonazzola, S. (Observatoire de Meudon, France). Astron. Astrophys.; 14: No. 3, 387-9(Oct 1971).

A lower limit of 6 kpc to the distance of JP 1933 is derived from the 21-cm-line absorption profile, using the galactic rotation model of Schmidt. The scintillation parameters observed at 1420 MHz for this source seem consistent with the mean parameters derived from low-frequency pulsar observations in the thin-screen model. (auth)

**55725** OPTICAL IDENTIFICATION OF SOUTHERN RADIO SOURCES. Hunstead, R. W. (Univ. of Sydney); Lasker, B. M.; Mintz, Betty; Smith, M. G. Aust. J. Phys.; 24: 601-7(Aug 1971).

The fields of 12 southern radio sources were photographed using a fiber-optics image tube at the 60-in. Cerro Tololo reflector. Identifications are suggested for 10 of the 12 sources on the basis of positional agreement with accurate 408-MHz radio positions. The remaining two fields contain faint galaxies within 10″ of the radio position. (auth) (Australia)

**55726** OPTICAL VARIABILITY OF A BRIGHT NEW QUASI-STELLAR SOURCE. Lucchetti, S. C.; Usher, P. D. (Pennsylvania State Univ., University Park). Nature (London); 232: No. 5313, 622-3(27 Aug 1971).

Reference is made to the radio source 1215 + 30, which was identified with a very bright quasar of magnitude ~14.5. The observations reported indicate that its optical flux is variable by more than two magnitudes, with discernible brightness changes over time scales of hours, as well as secular trends on a time scale of years. Data for the light curve are given in tabular form. The light curve is consistent with the interpretation that the optical output consists of long- and short-term variability known to be characteristic of compact galaxies and quasi-stellar radio sources. (UK)

**55727** UPPER LIMITS ON PULSATIONS FROM CYG X-1 IN HARD X RAYS. Manchandra, R. K. (Tata Inst. of Fundamental Research, Bombay). Nature (London) Phys. Sci.; 232: No. 35, 190-1(30 Aug 1971).

Reference is made to the communication of the authors (Nature, 232: 38(1971)) in which evidence was presented for short-term variations in the intensity of Cyg X-1 in the energy band 22.5 to 154 keV, based on observations with a balloon-borne oriented x-ray telescope in April, 1971. In the light of subsequent findings of the possible presence of pulsating components in the x-ray emission of Cyg X-1 at energies of a few keV, the data of April 1971 were analyzed to see whether similar pulsations occurred in the higher-energy band; it was found that there was no real evidence for such pulsations. The results indicated either that x-ray pulsations are confined to lower energies or that the intensity of the pulsating component falls considerably at higher energies; or that the phase or frequency of pulsation is not stable even for periods of a few minutes; or that Cyg X-1 pulsates only occasionally. The nature of pulsations of Cyg X-1 is thus very different from that of other pulsars, in which the relative intensity is higher at higher energies. (UK)

**55728** SEARCH FOR PULSED RADIO EMISSION FROM CYG X-1 AT 327 MHz. Mohanty, D. K.; Balasubramanian, V.; Swarup, G. (Tata Inst. of Fundamental Research, Bombay). Nature (London) Phys. Sci.; 232: No. 35, 191-2(30 Aug 1971).

The probable presence of an x-ray pulsar in the variable source Cygnus X-1 has been reported and also indications of a variable radio source with a flux density of $\sim 0.02 \times 10^{-26} W/m^2/Hz$ at 1415 MHz. The present authors describe an unsuccessful search for a pulsar in this region on two occasions (March 9 and May 5, 1971) using the large steerable radio telescope at Ootacamund. An upper limit of $\sim 1 \times 10^{-28}$ $J/m^2/Hz$ was found for the average energy per pulse at 327 MHz. (UK)

**55729** CRAB PULSAR RADIATION MECHANISM. Manchester, R. N.; Tademaru, E. (National Radio Astronomy Observatory, Green Bank, W. Va.). Nature (London) Phys. Sci.; 232: No. 34, 164-5(23 Aug 1971).

Reference is made to Smith (Nature Phys. Sci., 231: 191(1971)) who suggested an oblique rotator model for the Crab pulsar in which the magnetic axis is inclined at 45° to the rotation axis and the observer's line of sight is at a latitude of about 20°. This model is in conflict with that of other authors in which the magnetic axis is almost perpendicular to the rotation axis and the line of sight passes close to the magnetic axis (the magnetic pole model). It is argued that Smith's model, as presented, cannot explain the observations. A reply by Smith is given. (UK)

**55730** METER WAVELENGTH OBSERVATIONS OF GALACTIC RADIO SOURCES AND THE GALACTIC DISK RADIATION. Parrish, Alan deSchweinitz. Ithaca, N. Y.; Cornell Univ. (1971). 149p. University Microfilms Order No. 71-17,119.

Thesis.

The 1000-foot diameter radio telescope at the Arecibo Observatory was used to observe the continuum emission of galactic sources at low radio frequencies. The following sources were observed: W49, W51, W56, NGC 1499, IC 410, NGC 2175, NGC 2244, and Orion A. Observations were carried out at seven frequencies: 53, 65, 74, 89, 111, 196, and 318 MHz. Arrangements were made to obtain data on several of these frequencies simultaneously. Flux densities of the observed sources are presented at the low frequencies. The data was analyzed to obtain an estimate of the electron temperature of each thermal source, as well as the brightness temperature level of the nonthermal radiation in the line of sight to and beyond each source. The analysis procedure involved using models of the sources to generate theoretical spectra for various values of two free parameters: the electron temperature and the background brightness temperature level. In performing the analysis, convolution techniques were used to equalize the effects of different amounts of beam smoothing

XUM

at different frequencies. Such techniques were especially helpful in analyzing data containing contributions from nearby confusing sources. The derived electron temperature results were sufficiently accurate to be compared with the results of recombination line observations for Orion A and NGC 2244. A range of pairs of permissible electron temperatures and background brightness temperature levels was obtained for each of the other sources. Given this data, independent knowledge of the electron temperature of a source determines its associated background brightness temperature level, and the latter result may be used in estimating the spatial distribution of the galactic nonthermal radiation. (Diss. Abstr. Int., B)

**55731** DAILY AND HOURLY VARIATIONS IN FLUX DENSITY OF RADIO SOURCES. Wills, Beverley J. (Ohio State Univ., Columbus). Astrophys. J.; 169: No. 2, 221-33(15 Oct 1971).

Flux-density measurements with rms accuracy of ±1.6% were made in an attempt to detect day-to-day and hour-to-hour variations in flux density at a frequency of 2700 MHz, for radio sources selected from the Parkes Catalog. Day-to-day variations of about 2 to 4% detected for the sources PKS 0106 + 01, 0336 − 01 (CTA 26), 0440 − 00 (NRAO 190), and 1510 − 08 are probably significant, and their flux densities were compared with data at higher frequencies. If real, the variations do not preclude adiabatically expanding cloud models for these sources, provided the velocities of expansion are relativistic. Upper limits to variability are given for the other sources. (auth)

**55732** LABORATORY MEASUREMENT OF THE 6-CENTIMETER FORMALDEHYDE TRANSITIONS. Tucker, K. D. (Columbia Univ., New York); Tomasevich, G. R.; Thaddeus, P. Astrophys. J.; 169: No. 2, 429-40(15 Oct 1971).

The $1_{10}-1_{11}$ rotational transition of $H_2{}^{12}C^{16}O$ in its ground and first two excited vibrational states, and that of $H_2{}^{13}C^{16}O$, $H_2{}^{12}C^{18}O$, and $HD^{12}C^{16}O$ in their vibrational ground states, all of which lie at a wavelength of about 6 cm, were studied with a beam-maser spectrometer. Line widths in the range 1 to 3 kHz were attained, allowing the hyperfine structure of the transitions to be rather thoroughly resolved, and transition frequencies to be measured to an accuracy of the order of 100 Hz. All significant features of the observed spectra were successfully interpreted in terms of the current theory of molecular hyperfine structure, and the appropriate hyperfine coupling constants were determined. (auth)

## Solar Phenomena

*Refer also to abstracts 55909, 55940, 55992, 56000, 56126, and 56204.*

**55733** (N-71-23433) CURRENT SHEET MAGNETIC MODEL FOR THE SOLAR CORONA. Schatten, Kenneth H. (National Aeronautics and Space Administration, Greenbelt, Md. Goddard Space Flight Center). Mar 1971. 29p. (NASA-TM-X-65496). NTIS.

A new magnetic model is developed and compared with previous models and the observed solar corona. An attempt is made to more accurately compute the three-dimensional currents flowing in the solar corona. Physical reasons are given that require most of the large-scale currents flowing in the solar corona to lie near thin sheets. The current sheets are not constrained into any particular geometry or symmetry as in the previous models of Altschuler and Newkirk (1969) and Schatten et. al., (1969). A comparison with the axisymmetric, isothermal MHD solution of Pneuman and Kopp (1970) suggests that the model is able to simulate to high accuracy an isothermal corona. A comparison of the model with the May 30, 1965, solar eclipse and the November 12, 1966, solar eclipse shows the model is capable of computing many features, including the polar plume orientations as well as radial and nonradial streamers in the solar corona. (auth) (STAR)

**55734** (N-71-23434) EXPERIMENT TO MEASURE HARD SOLAR AND CELESTIAL X RAYS FROM THE FIFTH ORBITING SOLAR OBSERVATORY. Frost, K. J.; Dennis, B. R.; Lencho, R. J. (National Aeronautics and Space Administration, Greenbelt, Md. Goddard Space Flight Center). Dec 1970. 15p. (NASA-TM-X-65504). NTIS.

An experiment designed to measure solar and celestial x rays in the energy range 15 to 250 keV is described. The objectives for measuring solar x rays consist of: (1) measuring the spectrum of solar x-ray bursts as a function of time throughout the duration of the bursts; and (2) conducting a search for a weak, constantly present and/or activity-dependent component of solar x rays in the 15- to 250-keV range for successive solar rotations during the lifetime of the spacecraft. The objectives in measuring celestial x rays include: (1) measuring the intensity, spectrum, and spatial distribution of diffuse celestial x rays; and (2) measuring the intensity, spectrum, and possible temporal variations of those point sources that can be isolated with the rather broad field of view (40° FWHM) of the detector. (auth) (STAR)

**55735** (N-71-24166) REVERSE AND FORWARD SLOW SHOCKS IN THE SOLAR WIND. Burlaga, L. F.; Chao, J. K. (National Aeronautics and Space Administration, Greenbelt, Md. Goddard Space Flight Center). Mar 1971. 26p. (NASA-TM-X-65489). NTIS.

A reverse slow shock and a forward slow shock were found in plasma and magnetic field data from Pioneer 6. The shocks were oblique and weak (Mach ≈ 1.2). Numerous nonshock-like discontinuities were found with $B_1 \neq B_2$ and $N_1 \neq N_2$. Assuming pressure balance across them, an average electron temperature $T_e = (1.8 \pm 0.2) \times 10^5$ K was obtained. It was observed that discontinuities with $B_1 \pm B_2$, $n_1 = N_2$ seldom if ever occur. (auth) (STAR)

**55736** X-RAY AND RADIO EMISSIONS FROM THE SUN. Ghosh, S. N. (Univ. of Michigan, Ann Arbor). Indian J. Pure Appl. Phys.; 8: No. 12, 801-5(Dec 1970).

Assuming a Maxwell distribution of electron velocities in the solar corona, the x-ray fluxes at the Earth for temperatures $7 \times 10^5$, $1 \times 10^6$, $1 \times 10^7$, and $1 \times 10^8$ °K were calculated for free−free transitions. These temperatures correspond respectively to typical cases of completely quiet, quiet, active, and flare conditions of the Sun. The fluxes were compared with those for free−bound transitions and line emissions obtained by Elwert [Z. Naturf., 3a: 477(1948); 9a: 637(1954)] and Kawabata [Rep. Ionosph. Res. Japan, 14: 405(1960)]. It is shown that during flares, the radiations are emitted primarily by free−free transitions, and that coronal temperatures and electron densities during different types of flares can be precisely determined from observations of solar x-ray emissions. For other conditions of the Sun, line emissions predominate, and the spectrum becomes harder and the flux increases as the Sun passes from the quiet to active condition. The emissions of radio waves by free−free transitions for different conditions of the Sun were also calculated, and it is shown that the calculated flux for $T = 1 \times 10^6$ °K and $n_e = 10^9$ cm$^{-3}$ is the mean of the observed values for the quiet Sun. (auth)

**55737** STUDIES ON SOLAR X-RAY FLARES RECORDED BY SOLRAD-9 ON EXPLORER 37 SATELLITE. Das Gupta, M. K.; Sarkar, S. K. (Univ. of Calcutta). Indian J. Pure Appl. Phys.; 9: No. 4, 249-52(Apr 1971).

Solar x-ray flares (numbering about 1200) recorded by SOLRAD-9 on Explorer 37 at wavelength bands 0.5 to 3, 1 to 8, and 8 to 20 Å during the period December 1968 to November 1969 were examined. It was found that the majority of the x-ray flares occur within +2 min of the onsets of optical flares. Percentages of association of x-ray flares (0.5 to 3 Å) with optical flares, microwave bursts, and sudden ionospheric disturbances (SID) in general were determined. Percentage association values were found to increase with increasing intensity of the x-ray flares. The solar events appear to occur in general in the sequence: optical flares−microwave bursts−x-ray flares. It was further observed that the x-ray flares in the two wavelength bands 0.5 to 3 and 8 to 20 Å, though they start more or less simultaneously, attain their peaks at different times. In general, peaks are attained earlier by the x-ray flares in the lower-wavelength range. X-ray flares having smaller time separation between the peaks at the different wavelength ranges are associated more with the optical flares. (auth)

**55738** EFFECT OF THE SOLAR BOUNDARY CONDITION ON FLARE-PARTICLE PROPAGATION. Englade, Ronald C. (Air Force Cambridge Research Labs., Bedford, Mass.). J. Geophys. Res.; 76: No. 25, 6190-2(1 Sep 1971).

The effects of various solar boundary conditions on the interplanetary propagation of solar-flare particles for an anisotropic diffusion model were examined by J. R. Jokipii recently. The coefficient for diffusion perpendicular to the radial direction increases with the square of the heliocentric radius, and it is concluded that the proper boundary conditions are important. It is now shown that, for most times of interest in a flare event, the choice of the solar boundary condition should not significantly affect quantitative intensity versus time results in interplanetary space, aside from a constant factor. The radial-diffusion coefficient is taken to be independent of radius, and an absorbing boundary at $r_D$ is assumed to be equal to several AU and instantaneous injection at $r_s$, where $r_s$ is solar radius. It is concluded that the time behavior of flare particles in interplanetary space is independent of boundary conditions and the magnitude of the particle density does depend on the solar boundary condition. (J.C.W.)

**55739** SOLAR BRIGHTNESS MEASUREMENT BETWEEN 12 AND 24 MICRONS. Baluteau, J. P. (Laboratoire de Physique Stellaire et Planetaire, Verrieres-le-Buisson, France). Astron. Astrophys.; 14: No. 3, 428-36(Oct 1971).

XUM

The solar spectrum between 12 and 24 microns was obtained with a scanning grating spectrometer. A germanium bolometer, cooled with liquid helium, was used as detector. The experiment was carried on a balloon because of strong telluric absorption at ground level in this spectral range. Relative flux measurements were possible from calibration sequences during the flight. A continuous decrease of the solar brightness temperature was measured between 12 and 24 $\mu$. Temperatures as low as 4500°K above 20 $\mu$ were obtained. The measurements were not consistent with the predictions of the B.C.A. model (Gingerich and de Jager, 1968) but rather showed a good agreement with the model elaborated by Léna (1970). A slight deviation beyond 20 $\mu$ may indicate another source of opacity besides that of the $H^-$ ion. (auth)

**55740** HIGH-RESOLUTION EXTREME-ULTRAVIOLET SOLAR SPECTRUM RECORDED WITH A DIFFRACTION-FILTER SPECTROGRAPH. Schweizer, W.; Schmidtke, G. (Arbeitsgruppe fuer Physikalische Weltraumforschung, Freiburg i. B.). Astrophys. J.; 169: No. 1, L27-9(1 Oct 1971).

A diffraction filter for suppression of long-wavelength stray light was flown April 1971 in a grazing-incidence grating spectrograph. Although efficiency of the instrument was low, approximately 50 emission lines of the solar extreme-ultraviolet spectrum between 50 and 210 Å were recorded with a resolution of 0.05 Å. Preliminary analysis shows the strong iron emission near 188 Å as two lines 0.08 Å apart, which has been reported thus far as a single line. (auth)

**55741** NEUTRINO ASTRONOMY: PROBING THE SUN'S INTERIOR. Wick, Gerald L. Science; 173: No. 4001, 1011-12 (10 Sep 1971).

The experiments of Davis on detection of solar neutrinos are outlined and the various factors that possibly reconcile the experimentally and theoretically determined values are briefly discussed. (W.D.M.)

**55742** THE SOLAR CONSTANT: A COMPILATION OF RECENT MEASUREMENTS. Labs, Dietrich (Landessternwarte Heidelberg, Koenigstuhl, Ger.); Neckel, Heinz. Solar Phys.; 19: No. 1, 3-15(Aug 1971).

A detailed compilation of the most recent values of the solar constant is given (13 values published from 1967 to 1970). The most probable value seems to be 1.95 cal $cm^{-2}$ $min^{-1}$ or 1.36 kW $m^{-2}$ with a formal rms error of ±0.3%. The corresponding effective temperature is 5770 K. Systematic errors of the order of ±1%, but also a possible variability of the same order cannot be excluded. (auth)

**55743** ROTATION OF MAGNETIC LOOP SYSTEMS IN THE SOLAR ATMOSPHERE. Pneuman, G. W. (National Center for Atmospheric Research, Boulder, Colo.). Solar Phys.; 19: No. 1, 16-31(Aug 1971).

Eclipse photographs indicate that large regions of the inner solar corona are confined in various types of closed magnetic configurations and, as a result, do not participate in the general solar-wind expansion. The rotation of initially poloidal loop configurations of this type, as influenced by differential rotation of the footpoints, was investigated. The analysis was restricted to axially symmetric fields and it was assumed that the toroidal magnetic field induced by differential rotation is small as compared to the initial poloidal field. This restricted the validity of the analysis to times less than about one month. The most interesting physical situation was that of flux tubes existing in one solar hemisphere only, one end of the tube being fixed in the photosphere at a higher latitude than the other. As a consequence, the lower end of the tube rotates at a faster rate than the upper end. Solution of the pertinent equations revealed that the angular velocity measured along a field line increased monotonically from its value at the poleward footpoint to that at the lower footpoint. The variation of angular velocity along the field depends upon the field geometry only and is not directly related to the variation of angular velocity along the solar surface between the footpoints. Depending upon the field configuration, both outward radial increases and decreases are possible. Using the Newton and Nunn model for the surface differential rotation rate, the angular velocity distribution on two particularly simple types of closed magnetic loop systems was determined analytically. It is shown that the angular velocity increases outward in the polar regions but decreases outward near the equator—leading to a decrease in differential rotation with height. (auth)

**55744** rms INTENSITY FLUCTUATION OF SOLAR GRANULATION. Mehltretter, J. P. (Fraunhofer Institut, Freiburg i.B.). Solar Phys.; 19: No. 1, 32-9(Aug 1971).

Using a selected high-definition granulation photograph obtained with a 40-cm aperture telescope from the ground, a new determination of the rms intensity fluctuation was attempted. At λ5500 Å, a value of 0.058 was found without correction, 0.067 with correction for theoretical diffraction only, and 0.095 ± 0.015 as the most probable value, if the differences between the power spectrum and those given in the literature are interpreted as due to a residual seeing of $\sigma = 0.3''$ in the photograph. (auth)

**55745** METHOD FOR CONSTRUCTING STREAMLINES FOR THE SUN'S LARGE-SCALE FLOW FROM DOPPLER VELOCITIES. Gilman, Peter A. (National Center for Atmospheric Research, Boulder, Colo.). Solar Phys.; 19: No. 1, 40-3(Aug 1971).

It is shown that, if the large-scale departures from the mean differential rotation, measured by Howard and Harvey, represent nearly horizontal flow, one may under certain assumptions deduce a pattern of streamlines for these motions from the Doppler line of sight velocities. This can be done with data from a single day, without having to construct the total flow from different projections of the (assumed) same velocity vectors seen on different days. Mathematically, the method involves integrating a single first-order inhomogeneous partial differential equation along a set of characteristic curves that are circles concentric with the center of the solar disk. The structure of the resulting streamline pattern could be compared to large-scale magnetic patterns, and latitudinal transports of magnetic flux and momentum could be estimated. (auth)

**55746** HIGH-RESOLUTION PHOTOGRAPHY OF THE SOLAR CHROMOSPHERE. IX. LIMB OBSERVATIONS OF HIGH SPECTRAL PURITY. Loughhead, R. E.; Tappere, E. J. (CSIRO, Sydney). Solar Phys.; 19: No. 1, 44-51(Aug 1971).

High-quality photographs of the solar limb and neighboring regions of the disk at various wavelengths in the H$\alpha$ line were obtained through a tunable ⅛-Å filter used in tandem with a 1-Å Halle filter to eliminate parasitic light. The new observations throw further light on (a) the reappearance of the photospheric limb in the wings of H$\alpha$, and (b) the dark band lying immediately above the photospheric limb described by Loughhead (1969) and Nikolsky (1970). On the other hand, taken in isolation they add very little new information bearing on the question of the identification of spicules with disk structures. (auth)

**55747** OSCILLATIONS OF VISIBLE CHROMOSPHERE BOUNDARY AND REGULARITY IN POSITION OF SPICULE GROUPS ALONG THE LIMB. Platov, July V.; Shilova, Nataly S. (Inst. of Terrestrial Magnetism, Ionosphere, and Radio Wave Propagation, Moscow). Solar Phys.; 19: No. 1, 52-8(Aug 1971).

A series of H$\alpha$ filtergrams, covering about 42 min, was studied in order to obtain quantitative data on the oscillations of the visible chromosphere boundary and on the regularity in position of spicule groups along the limb. The results obtained reveal the existence of relatively slow vertical oscillations (a background) superimposed with those of ~5 min period. A horizontal dimension of a spicule group ≥400 km; a change of the chromosphere height within the latter occurs practically synchronously. A good correlation of height changes for groups of ~25,000 km apart was observed. (auth)

**55748** MORPHOLOGICAL RELATIONSHIPS IN CHROMOSPHERIC H$\alpha$ FINE STRUCTURE. Foukal, Peter (Carnegie Institution of Washington, D. C. California Inst. of Tech., Pasadena). Solar Phys.; 19: No. 1, 59-71(Aug 1971).

A continuous relationship is proposed between the basic elements of the dark fine structure of the quiet and active chromosphere. A progression from chromospheric bushes to fibrils, then to chromospheric threads and active region filaments, and finally to diffuse quiescent filaments, is described. It is shown that the horizontal component of the field on opposite sides of an active region quiescent filament can be in the same direction and closely parallel to the filament axis. Consequently, it is unnecessary to postulate twisted or otherwise complex field configurations to reconcile the support mechanism of filaments with the observed motion along their axis. (auth)

**55749** TOPOLOGY OF FILAMENTS AND CHROMOSPHERIC FIBRILS NEAR SUNSPOTS. Nakagawa, Y. (National Center for Atmospheric Research, Boulder, Colo.); Raadu, M. A.; Billings, D. E.; McNamara, D. Solar Phys.; 19: No. 1, 72-85(Aug 1971).

The similarity between the spiral topology of chromospheric fibrils and filaments observed in H$\alpha$ near sunspots and the configuration of an axisymmetric force-free magnetic field is examined. It is suggested that some of the observed features could be interpreted in terms of the configuration of lines of force of an axisymmetric force-free chromospheric magnetic field. Implications of the results of analysis to the possible interpretations of other observed topological features near a sunspot are discussed. (auth)

XUM

**55750** STUDIES OF THE ABUNDANCE OF ELEMENTS IN THE ATMOSPHERE OF A MAIN-SEQUENCE G2 V STAR: THE SUN. Grevesse, Nicolas (Univ., Liege). Acad. Roy. Belg., Cl. Sci., Mem., Collect. 8; 39: No. 3, 1-109(1969). (In French).

The abundance of elements in the atmosphere of the Sun was studied with a method based on the calculation of the line profiles by direct integration. This method is more precise and better adapted to the analysis of spectra with high resolution and low background than previous methods. A critical analysis is made of the different solar models. The deuterium abundance in the Sun was measured, and the results show that the upper limit is very small ($0 < D/H < 5 \times 10^{-6}$). The abundances of Li, Be, and B were determined to be lower than previously accepted. It appeared that there is no $^{6}Li$, but there is $^{10}B$ in the photosphere. The abundance of B (and perhaps the ratio $^{11}B/^{10}B$) can be deduced only from the study of the BH in the spectrum of sunspots. The consequences of these results on the theories on the formation and destruction of these elements were analyzed. The abundance of C, N, and O was determined and the consequences of the results are discussed. The abundance of the elements of the iron peak (Sc, Ti, V, Cr, Mn, Fe, Co, and Ni) was determined. The problem of the differences in the abundances of these elements in the photosphere, chromosphere, corona, and meteorites is considered in detail. (J.S.R.)

**55751** CALCULATION OF STELLAR STRUCTURE. II. DETERMINATION OF THE HELIUM ABUNDANCE OF THE SUN BY THE THEORETICAL PREDICTION OF LINE AND CONTINUUM RADIATION FROM SOLAR-MODEL PHOTOSPHERES. Rouse, Carl A. (Gulf General Atomic, Inc., San Diego, Calif.). Progr. High Temp. Phys. Chem.; 4: 139-91(1971).

The subject is covered in the following sections: calculations of a variable star, helium abundances of various astronomical objects, review of the present method for the determination of the helium abundance of the Sun (equation of state, solution of a standard Saha equation, screened Coulomb formation of the ionization equilibrium equation of state, opacity formulas, boundary conditions on the solar models and their photospheres, and radiative transfer in the model photosphere). Appendices are included considering the screened-Coulomb modified Saha or ionization equation, analytic expressions for the hydrogenic CSCP electronic partition function, limiting screening radii from numerical, perturbation and variational screened Coulomb solutions of the Schroedinger equation, and solar neutrinos. (UK)

**55752** THERMAL EFFECTS IN FORMATION OF LOOP PROMINENCES. Goldsmith, D. W. (Stanford Univ., Calif.). Solar Phys.; 19: No. 1, 86-91(Aug 1971).

Loop prominences that appear after some solar flares may owe their form and duration to the behavior of the cooling function of the material (Cox and Tucker, 1969) and to the magnetic field configuration. Computer simulation of a model event shows that small temperature contrasts in a medium of several million degrees temperature may be enhanced as the medium cools by line and recombination radiation, on a time scale of several minutes. The loop prominence systems could be the result of this process repeated through successively higher levels of the solar atmosphere. (auth)

**55753** SERIES OF RELATED ACTIVE REGIONS DURING JANUARY 14–JUNE 1, 1969. Prata, Stephen W. (California Inst. of Tech., Pasadena. Carnegie Inst. of Washington, D. C.). Solar Phys.; 19: No. 1, 92-109(Aug 1971).

The history of a series of active regions is traced for the first half of 1969. At least four active regions successively occupied positions near Carrington longitude 270. In some cases the emergence of new regions in the midst of old regions was observed. All the larger flares observed in the studied region were associated with inverted polarity. In some cases the fields emerged inverted; in other cases the inverted polarity appeared to result from the interaction of emerging flux with fields already present at the surface. (auth)

**55754** SOLAR CORONAL STREAMERS OBSERVED AT 169 MHz WITH THE NANCAY EAST–WEST RADIOHELIOGRAPH. Axisa, F. (Centre d'Etudes Nucleaires de Saclay, France); Avignon, Y.; Martres, M. J.; Pick, M.; Simon, P. Solar Phys.; 19: No. 1, 110-27(Aug 1971).

The slowly varying component of the Sun at 169 MHz for the period August 1962 to March 1966 was studied, using daily data from the east–west radioheliograph at Nançay. By relating these radio data to the optical features visible on the solar disc (calcium plages and filaments), this thermal radio emission can be satisfactorily interpreted as originating in both helmets and active streamers: The radio sources responsible for this emission are linked to the presence of filaments. Depending on the cases, these filaments are either very far from any calcium plage, or closely associated with them. The cross-sectional area of such sources is often far from having circular symmetry and seems to be closely related to the configuration of the underlying filament itself. In several cases, the altitude of the sources can be estimated, and a typical value of about 270,000 km is found. In this respect no significant difference is found between radio sources related to a filament closely associated with a calcium plage, and those which are related to a filament very far from such plages. At 169 MHz, coronal enhancements provide a relatively small contribution to the slowly varying component. Finally, the observations are used to derive a morphological model for streamers in the medium corona, and several implications of such a model are briefly discussed. (auth)

**55755** WAVE PROPAGATION IN WARM PLASMA AND SPECTRUM OF SOLAR RADIO BURSTS. Mollwo, L. (Heinrich-Hertz-Institut, Berlin). Solar Phys.; 19: No. 1, 128-48 (Aug 1971).

The frequency bands of noise storms and Type-I bursts as well as of Type-IV dm bursts are shown to be in accordance with the consequences of a recently proposed mechanism (Mollwo, 1970). An explanation results from the observed spectral minimum near 600 MHz and interpretations are proposed for some features of Type-III and of Type-IV mA bursts. The magnetic field strength over active regions in two coronal levels is deduced. The discussion leads to a conception of the coronal parameters in the level of Type-IV $\mu$ bursts which suggests an origin of these bursts by absolute instability of space-charge waves. (auth)

**55756** RESULTS OF NEW ABSOLUTE CALIBRATION OF SOLAR FLUX DENSITY AT 2980 MHz. Schmidt, G. K. (Heinrich-Hertz-Institut, Berlin). Solar Phys.; 19: No. 1, 149-51 (Aug 1971).

The solar flux density was measured absolutely at the frequency 2980 MHz and the results were compared with those of observers, working in the same frequency range. It was found, that the values are integrated well into a smooth spectral curve, whereas it seems that even the corrected values of Ottawa 2800 MHz are 4% too high. (auth)

**55757** SOLAR-MICROWAVE BURSTS AS INDICATORS OF OCCURRENCE OF SOLAR-PROTON EMISSION. Croom, David L. (Air Force Cambridge Research Labs., Bedford, Mass.). Solar Phys.; 19: No. 1, 152-70(Aug 1971).

A study was made of the relation of 19 GHz ($\lambda = 1.58$ cm) solar radio bursts to solar proton emission, with particular reference to the usefulness of relatively long duration bursts with intensities exceeding 50% of the quiet Sun flux (or exceeding $\approx 350 \times 10^{-22}$ W $m^{-2}Hz^{-1}$) as indicators of the occurrence of proton events during the four years from 1966–69. Seventy-six to 88% of such bursts are directly associated with solar protons and 60 to 85% of the moderate to large proton events in the four-year period could have been predicted from these bursts. The complete microwave spectra of the proton events were also studied and were used to extend the results obtained at 19 GHz to other frequencies, particularly in the 5 to 20-GHz band. The widely used frequency of 2.8 GHz is not the optimum frequency for this purpose since proton events have a minimum of emission in this region. Most of the radio energy of proton events is at frequencies above 10 GHz. The radio spectra of proton events tend to peak at higher frequencies than most non-proton events, the overall range being 5 to 70 GHz, with a median of 10 to 12 GHz and a mean of 17 GHz. (auth)

**55758** FORECASTING THE INTENSITY OF SOLAR-PROTON EVENTS FROM THE TIME CHARACTERISTICS OF SOLAR-MICROWAVE BURSTS. Croom, David L. (Air Force Cambridge Research Labs., Bedford, Mass.). Solar Phys.; 19: No. 1, 171-85(Aug 1971).

A survey of the main characteristics of solar microwave bursts in relation to their usefulness for indicating the intensity of associated solar proton emissions suggests that time parameters give much better results than intensity or spectrum parameters. In particular, best results are obtained by using the effective, or mean, burst duration defined by $T_M = 1/P_{max}\int_0^T P(t)dt$ where T is the overall burst duration, P is the power density at time t, and $P_{max}$ is the maximum power density. For proton energies >10 MeV the proton flux $N_p$ is given approximately by $N_p = 0.034\ T_M^3$ particles $ster^{-1}\ cm^{-2}\ s^{-1}$, where $T_M$ is in minutes, with a correlation factor of 0.8. Corresponding coefficients have been derived for a number of energy ranges. Using this parameter solar proton warnings and intensity estimates can be made with observations at only one frequency, preferably in the range 5 to 20 GHz. (auth)

**55759** STUDY OF CORRELATION OF HARD SOLAR X-RAY AND RADIO EMISSION. McKenzie, David Leroy. San Diego,

XUM

Calif.; Univ. of California (1971). 130p. University Microfilms Order No. 71-21,687.

Thesis.

The third Orbiting Solar Observatory (OSO III) carried an instrument that measured x rays from solar flares in the energy range 7.7 to 12.5 keV. Spectral and temporal properties of more than 300 solar x-ray bursts having accompanying microwave emission such that radio and X-ray burst peaked within four minutes of one another were studied. Two-point spectra taken during the decay of bursts were interpreted as arising from thermal free-free and free-bound emission. Start, peak, and end times of x-ray bursts were measured with respect to corresponding times of associated microwave bursts. Many x-ray bursts have, during their rising portions, transient periods with spectra extending to 38 keV or higher. These hard x-ray flashes correlate well with microwave emission. For 69 bursts the mean delay between the hard x-ray flash and the peak of associated microwave emission was .30 minutes with standard deviation .44 minutes. A model in which energy for heating of the soft X-ray source region is supplied by collisional energy transfer from nonthermal electrons was investigated. Correlation between Type-III radio burst and x-ray bursts was studied. Flashes appear to be well correlated in time with Type III bursts. (TSS) (Diss. Abstr. Int., B)

**55760** ACCELERATION OF ELECTRONS AND SOLAR FLARES DUE TO QUASI-STATIC ELECTRIC FIELD. Takakura Tatsuo (Tokyo Univ.). Solar Phys.; 19: No. 1, 186-201(Aug 1971).

The storage of flare energy, efficient acceleration of electrons, and the trigger of the flares are suggested to be attributed to a quasi-static electric field caused by a gas motion near the photosphere without satisfying the frozen condition. The primary cause of the onset of flares would be the acceleration of electrons due to the electric field above a critical strength. The electrons excite plasma waves which lower the conductivity by several orders in the lower corona, so that the electromagnetic energy $I^2L$ stored before the onset of the flare would be rapidly converted into heat due to the ohmic loss in about 10 s. (auth)

**55761** FLUX OF NEUTRONS FROM FLARES. Svestka, Z. (ESTEC, Noordwijk, Netherlands). Solar Phys.; 19: No. 1, 202-6(Aug 1971).

Under the assumption that white-light flares are caused by energetic particles penetrating into the photosphere (Švestka, 1970a; Najita and Orrall, 1970) the known number of protons needed for the white-light emission is used to obtain an estimate of the production of neutrons occurring at the same time. In the case of the white-light flare of May 23, 1967, the peak flux of neutrons at 1 AV had to exceed 3 neutrons/$cm^2$s, thus being detectable in space. This maximum neutron flux reached the Earth as early as the time of the maximum phase of the flare in the H$\alpha$ light. However, reasonable estimates show that flares associated with a detectable neutron flux should be fairly rare phenomena, maybe as rare as the white-light flares. (auth)

**55762** FLUX OF GAMMA RAYS FROM SOLAR FLARES. de Feiter, L. D. (Astronomical Inst., Utrecht). Solar Phys.; 19: No. 1, 207-8(Aug 1971).

Švestka (1971) presented the results of a computation of the neutron flux emitted by certain types of flares, namely those that show knots from which a weak continuum in the visual part of the spectrum is emitted. An attempt is made to extend his analyses by computing the fluxes of gamma rays produced by the same downward moving high-energy protons which give rise to the production of neutrons. (W.D.M.)

**55763** ANISOTROPY CHARACTERISTICS OF LOW-ENERGY COSMIC-RAY POPULATION OF SOLAR ORGIN. Rao, U. R. (Physical Research Lab., Ahmedabad, India); McCracke, K. G.; Allum, F. R.; (and others). Solar Phys.; 19: No. 1, 209-33(Aug 1971).

Comparison of Explorer 34 observations on solar protons in the energy range 0.7 to 55 MeV with similar observations from other spacecrafts show that the large field-aligned anisotropies which are observed during the rise time of a flare event change to an equilibrium anisotropy coming radially from the sunward direction due to the convective removal of the solar particles. At very late times during the decay ($T \geq 4$ days) the anisotropy is observed to be from a direction ~45°E of the satellite–Sun line which is interpreted as indicative of positive density gradient of solar cosmic-ray population. The dependence of both types of equilibrium anisotropies on the energy and the velocity of the particles and on plasma velocity are shown to be in agreement with the theoretical predictions. The amplitude of the large field-aligned anisotropies observed earlier in the event is found to be independent of the rise time of the event and to vary as $(V)^{-1}$. Interplanetary magnetic sector crossings during a flare event, cause abrupt changes in both the amplitude and phase of the nonequilibrium anisotropy whereas they have no significant effect on equilibrium anisotropy. The effect of azimuthal density gradients on the decay time constants of flare enhancements is also examined in an attempt to understand the complicated structures, often observed, in the time intensity profiles at low energies. (auth)

**55764** UNUSUAL ANISOTROPIC SOLAR-PARTICLE EVENT OF NOVEMBER 18, 1968. Duggal, S. P.; Guidi, I.; Pomerantz, M. A. (Bartol Research Foundation of The Franklin Inst., Swarthmore, Pa.). Solar Phys.; 19: No. 1, 234-46(Aug 1971).

The ground level event of November 18, 1968, was unusual in that pronounced anisotropy persisted essentially until the cessation of the arrival at the Earth of relativistic protons. Real and significant differences were observed in the intensity profiles at different neutron monitor stations. By a method of successive approximations, the geographical coordinates of the axis of symmetry were determined as : latitude $\lambda = -25 \pm 10°$ and longitude $\phi = -35 \pm 10°$. The exponent in a power law spectral representation over the narrow range covered by the nucleonic intensity measurements was $\gamma \approx 5$. The onset times of the GLE were related to the angular differences between the mean directions of viewing and the axis of symmetry. The event differed markedly from earlier isotropic events that were well described by diffusion theory, but was compatible with the predictions of a model envisaging diffusion only in the vicinity of the Sun (radius R of solar envelope ≈ 34 solar radii). The diffusion coefficient $D \approx 3 \times 10^{21}$ $cm^2/s$ is consistent with that deduced for earlier isotropic events, but the values of other parameters are smaller than those derived for the only previously observed event to which the model of diffusion in an inhomogeneous medium was applicable (May 4, 1960). It is concluded that the observed one hundred percent anisotropy was a direct consequence of the propagation mechanism rather than other postulated causes. Furthermore, the observed large pitch-angle distribution was produced by scattering from small-scale field irregularities. (auth)

**55765** ACTIVE SOLAR RADIO REGIONS AT METRIC FREQUENCIES AND THE INTERPLANETARY SECTOR STRUCTURES. Sakurai, Kunitomo; Stone, Robert G. (Goddard Space Flight Center, Greenbelt, Md.). Solar Phys.; 19: No. 1, 247-56(Aug 1971).

The possible relation between Type-I noise active regions and the polarity distribution of the interplanetary magnetic field was examined for the period from March 13 to August 21, 1968 (Solar Rotation Numbers 1842–1847) by using data from ground-based and satellite observations. In general four Type-I radio regions appeared during each solar rotation period except for Rotation No. 1842. The number of Type-I regions was the same as the number of sector boundaries. This result suggested that the configuration of the photospheric magnetic field extending into the interplanetary space may be related to the origin of the Type-I radio regions. Statistically the passage of the sector boundaries is delayed by approximately 5 days after the central meridian passage of the Type-I noise regions on the solar disk. The position of the source of the sector boundaries and its relation to the Type-I radio regions were investigated by taking into account the mean bulk velocity of solar winds as observed by space probes. A model of the large-scale structure of Type-I radio regions and their relation to the sector structure of the magnetic field as observed in the interplanetary space is briefly discussed. (auth)

**55766** SOLAR ACTIVITY AND PLANETARY LUMINOSITY. Balasubrahmanyan, V. K. (Goddard Space Flight Center, Greenbelt, Md.); Venkatesan, D. Solar Phys.; 19: No. 1, 257-63(Aug 1971).

The Chree superposition analysis of the luminosities of the planets Jupiter, Saturn, Uranus and Neptune indicates a correlation between solar activity and planetary luminosity. The variations of the solar constant in the visible range are considered to be too small to explain the observed changes in brightness. The interaction of solar extreme ultraviolet or solar-wind particles with the atmospheres of these planets is probably responsible for the increased albedo during periods of high solar activity. (auth)

**55767** IDENTIFICATION OF THE λ 417 LINE IN THE SOLAR EXTREME-ULTRAVIOLET SPECTRUM. Flower, D. R. (Observatoire de Paris); Jordan, Carole. Astron. Astrophys.; 14: No. 3, 473-6(Oct 1971).

Collision strengths for transitions between terms of the first four configurations of Fe xv were calculated in the distorted wave approximation and showed good agreement with Coulomb–Born results of Bely and Blaha (1968). The computed ratio of the intensity of the $3s^2\ ^1S_0 - 3s3p^3P_1^0$ transition to that of the $3s^2\ ^1S_0 - 3s3p\ ^1P_1^0$ transition agreed within a factor of two with the most recent observations by Hall and Hinteregger (1970) of the intensity ratio of the solar lines at 417 Å and 284 Å. The possibility of other contributors to the observed line at 417 Å is discussed. (auth)

XUM

**55768** SEARCH FOR $CH^+$ IN THE SOLAR PHOTOSPHERIC SPECTRUM. Grevesse, N. (Univ., Liege); Sauval, A. J. Astron. Astrophys.; 14: No. 3, 477-80(Oct 1971).

The results of a search for lines of $CH^+$ ($A^1\Pi - X^1\Sigma^+$ transition) in the solar photospheric spectrum are presented, and it is concluded that if $CH^+$ is present, the equivalent widths of the most intense lines cannot exceed 2 mÅ. An empirical solar $f_{00}$-value was derived and compared with a laboratory value and other available astrophysical values. Some possible reasons are given for explaining the large discrepancy between laboratory and astrophysical $f_{00}$-values. (auth)

**55769** SOLAR EXPLOSIONS. Wild, J. P. (CSIRO, Epping, Australia). Search; 2: No. 7, 229-(Jul 1971).

A description is given of the processes involved in the explosive ejection of solar flares and the means by which solar radio emission is used to interpret the various forms of corpuscular radiation from flares. Investigations into shock-fronted blasts of ionized gas acting as plasma emission mechanisms are outlined. Some ideas based on recent 80-MHz observations are presented on the subject of cosmic-ray generation. (Australia)

**55770** INVESTIGATION OF X-RAY FLARES ON THE SUN WITH THE COSMOS-230 SATELLITE. Beigman, I. L.; Vainshtein, L. A.; Vasil'ev, B. N.; (and others). Cosmic Res. (USSR) (Engl. Transl.); 9: No. 1, 106-16(Jan-Feb 1971).

Translated from Kosm. Issled.; 9: No. 1, 123-33(Jan-Feb 1971).

Results of studies of the flux, emission-spectrum composition, and structure of regions of x-ray flares on the Sun are presented: these were carried out with an x-ray photometer in the spectral regions <2.2; 1.4 to 2.2; 1.75 to 5; 2.1 to 5, and 8 to 14 Å and with an x-ray spectroheliograph with a spatial resolution of 15 to 20″, in the regions from 2 to 8 and from 8 to 12 Å. It was found that regions of x-ray flares have an elongated filamentary structure with lengths of 1 to 2′ and widths of 20″ and bright nodes that change rapidly in time. Short-lived periodic (0.05 sec) flareups in the x-ray intensity are observed in certain zones of the flare regions. The observed energy distribution over the spectrum is interpreted as emission from two regions — a colder region with a temperature of (7 to 9) $\times 10^6$ °K, an emission measure of 0.02 to 0.1 Baumbach units, and a density $N_e \sim$ (1 to 2) $\times 10^{10}$ $cm^{-3}$; and a hotter region with a temperature of (15 to 20) $\times 10^6$ °K and an emission measure $\frac{1}{5}$ to $\frac{1}{10}$ as large. It appears that this hotter region is not a concentrated nucleus, but is composed of isolated elements embedded throughout the entire volume of the flare region. (auth)

**55771** DETECTING THE POLARIZATION OF SOLAR-FLARE X-RAY EMISSION. Tindo, I. P.; Ivanov, V. D.; Mandel'shtam, S. L.; Shurygin, A. I.; Savel'ev, V. A. Cosmic Res. (USSR) (Engl. Transl.); 9: No. 1, 103-7(Jan-Feb 1971).

Translated from Kosm. Issled.; 9: No. 1, 116-22(Jan-Feb 1971).

The Intercosmos-1 satellite polarimeter, designed to use Thomson scattering, registered three x-ray flares at a wavelength of about 0.8 Å. A polarization $P \approx 0.4 \pm 0.2$ was detected with a certainty of 90% during the initial stages of the flares and at the second intensity maxima. (auth)

**55772** STUDY OF SOLAR FLARE HISTORY BY MEASUREMENT OF $^{22}Na$ AND $^{26}Al$ PRODUCTION PROFILES IN LUNAR ROCKS. Evans, John Charles Jr. San Diego, Calif.; Univ. of California (1971). 147p. University Microfilms Order No. 71-17,679.

Thesis.

Results are reported for the measurement of $^{26}Al$ and $^{22}Na$ in two lunar rocks and a sample of lunar soil. Crude depth samples were taken from Apollo 11 rock 10017 and more precise depth profiles were measured in rock 12002. A model was developed for the calculation of production of $^{22}Na$ and $^{26}Al$ in a lunar rock as a function of depth for bombardment by galactic and solar cosmic rays. Excitation function measurements for $^{26}Al$ and $^{22}Na$ from aluminum were carried out as an aid to the calculation. A comparison was made between observed production of $^{22}Na$ and that produced by observed flares from sunspot cycle 19 and 20. Agreement is not good at this time. From a comparison of the $^{22}Na$ and $^{26}Al$ measurements it was possible to conclude that solar activity has been relatively constant on a million-year time scale. Fluxes and spectral rigidities for solar cosmic rays at 1 A.U. were derived for a $10^6$-year time scale. The flux derived was 80 protons per $cm^2$ sec over $4\pi$ steradians with a spectral rigidity index of 80 MV. (Diss. Abstr. Int., B)

**55773** PROCESSES OF MAGNETIC-ENERGY CONVERSION AND SOLAR FLARES. Coppi, Bruno (International Center for Theoretical Physics, Trieste, Italy); Friedland, Allan B. Astrophys. J.; 169: No. 2, 379-404(15 Oct 1971).

A model is presented for the onset and development of solar flares which relies on the transformation of magnetic energy to kinetic energy in a plasma. A two-dimensional configuration in which plasma counterflows cross magnetic fields of opposite polarities is considered. The flow velocities are assumed to be both subsonic and sub-Alfvénic, and no shock-wave processes are considered. These velocities are taken sufficiently large to generate a relatively strong electric field and to set up a sequence of instabilities, the first of which is explosive in the region of zero magnetic field. As a result, generation of high-energy particles and onset of a strong turbulent electrical resistivity occur. Following this phase, conversion of magnetic energy into thermal and flow energy takes place as a consequence of a tearing-like mode set up around the same region. (auth)

**55774** CLASSIFICATION OF SOME HIGHLY IONIZED IRON AND NICKEL LINES IN THE 200- TO 400-A REGION OF THE SOLAR SPECTRUM. Widing, K. G. (Naval Research Lab., Washington, D. C.); Sandlin, G. D.; Cowan, Robert D. Astrophys. J.; 169: No. 2, 405-11(15 Oct 1971).

A number of previously unclassified multiplets of Fe XI–XIV produced by transitions of the type $3s^23p^n - 3s3p^{n+1}$ are identified in the extreme-ultraviolet spectrum of the Sun. The iron lines account for most of the previously unidentified strong lines between 330 and 370 Å. Other solar identifications include the resonance lines of Ni XVII and Ni XVIII, and one 3p–3d multiplet of Fe XIII. Oscillator strengths calculated in intermediate coupling for resonance transitions in Fe X–Fe XIV are tabulated. (auth)

**55775** CONVERSION OF MAGNETIC-FIELD ENERGY INTO KINETIC ENERGY IN THE SOLAR WIND. Whang, Y. C. (Catholic Univ. of America, Washington, D. C.). Astrophys. J.; 169: No. 2, 369-78(15 Oct 1971).

The conversion of magnetic-field energy into kinetic energy in the solar wind is identified as a source of energy which increases the velocity of the solar wind. The outflow of the energy of the interplanetary magnetic field (the radial component of the Poynting vector) per steradian is inversely proportional to the velocity of the solar wind. It is a decreasing function of the heliocentric distance. When the effect of the magnetic field is included in the numerical solution for a one-fluid model of the solar wind, the transformation of magnetic-field energy into kinetic energy during the expansion process increases the velocity of the solar wind at 1 A.U. by 17%. The predicted solar-wind conditions at 1 A.U. are u = 302 km $s^{-1}$, n = 5 protons $cm^{-3}$, T = $1.5 \times 10^5$°K, q = $0.85 \times 10^{-2}$ ergs $cm^{-2}$ $s^{-1}$, B = 5.8 gammas, $\phi = 129.5°$, and $\beta = 1.58$. The new results agree very well with the observed quiet solar wind. (auth)

**55776** OSCILLATOR STRENGTHS OF THE $3s^2S - 4p^2P$ AND $3d^2D - 4p^2P$ TRANSITIONS IN SODIUMLIKE IONS. Kunze, H.-J.; Datla, R. U. (Univ. of Maryland, College Park). Astrophys. J.; 169: No. 2, 425-7(15 Oct 1971).

The oscillator strength for the 3d–4p transition was derived from the measured intensity ratio of the 3d–4p and 3s–4p transitions emitted by Ar VIII ions in a theta-pinch plasma. Theoretical values along the isoelectronic sequence of sodium were computed by using a method of Burgess. (auth)

**55777** ANALOGUE OF THE PRIMARY SOLAR REACTION. Brolley, John E. (Los Alamos Scientific Lab., N. Mex.). Astrophys. J.; 169: No. 2, 443-4(15 Oct 1971).

Cross-sections for $n + n \rightarrow D + e^- + \bar{\nu}$ were calculated and compared with those of $p + p \rightarrow D + e^+ + \nu$. (auth)

**55778** INTERPLANETARY-PARTICLE ASSOCIATIONS WITH TYPE-III SOLAR BURSTS. Graedel, T. E. (Bell Telephone Labs., Whippany, N. J.); Lanzerotti, I. J. J. Geophys. Res.; 76: No. 28, 6932-8(1 Oct 1971).

Interplanetary proton (E ~ 0.6 and E ~ 1.2 MeV) and electron (E > 40 keV; E > 300 keV) data from May 28 to Nov. 30, 1967, are used to study the association of particle data with solar radio-burst data in the decametric band from Ogo 3 and with data reported in Solar Geophysical Data and the I.A.U. Quarterly Bulletin. By using reasonable particle- and radio-burst association criteria, it is concluded that the observed associations during this time period do not support the common belief that interplanetary-particle observations confirm the association of electrons with Type-III radio bursts. (auth)

**55779** NORTH–SOUTH COMPONENT OF INTERPLANETARY MAGNETIC FIELD: EXPLORER 33 AND 35 DATA. Rosenberg, R. L. (Univ. of California, Los Angeles); Coleman, P. J.; Colburn, D. S. J. Geophys. Res.; 76: No. 28, 6661-5(1 Oct 1971).

Measurements of the interplanetary magnetic field taken with Explorer 33 and 35 in 1967 and 1968 indicate that for a given polarity the north–south component or, more precisely, the $\theta$ com-

XUM

ponent in a spherical polar coordinate system (r, $\theta$, $\phi$) has, in general, a 27-day mean value that is significantly different from zero. The initial evidence for this effect was discovered in a study of magnetic-field records from Mariner 2, 4, and 5 recently published by Coleman and Rosenberg. For an interplanetary field directed outward from the Sun the mean value of $B_\theta$ is negative above the solar equatorial plane and positive below it, and vice versa for an inward field. Thus, for an outward field, the r$\theta$ component of a line of magnetic force above or below the equatorial plane is skewed relative to $\hat{r}$ in the direction away from the equatorial field. (auth)

**55780** OBSERVATIONS OF THE INTERPLANETARY MEDIUM: VELA 3 AND IMP 3, 1965–1967. Ness, N. F. (Goddard Space Flight Center, Greenbelt, Md.); Hundhausen, A. J.; Bame, S. J. J. Geophys. Res.; 76: No. 28, 6643-60(1 Oct 1971).

Simultaneous observations were made of the interplanetary plasma by the Vela-3 satellites and of the interplanetary magnetic field by the Imp-3 satellite from July 1965 to July 1967. Certain derived plasma properties are computed and statistically summarized. The quiet solar wind, defined by the velocity range $300 \leq V \leq 350$ km/sec, is found to be represented by an average field strength of 4.7 $\gamma$ at $\phi_{SE} = 137°$ (317°), $\theta_{SE} = -3.2°$, but having significant temporal departures from these averages. The ratio of plasma ion thermal energy density to magnetic-field energy density averages 1.2, with an average $\beta_p$ of 0.78. The average Alfvén speed is derived to be 36 km/sec, which yields a Mach number flow for the solar wind of 10.7. The solar-wind plasma most often is stable with respect to the firehose mode of instability. A nonstationary sector pattern does not destroy the sequence of correlated variations of plasma and field parameters observed within the sectors, although the distortion of sectors by propagating shock waves is suggested. (auth)

## Galaxies

**55781** RECENT DEVELOPMENTS IN THE HISTORY OF THE NUCLEOSYNTHESIS OF THE SOLAR SYSTEM. Reeves, H. (Institut d'Astrophysique, Paris. CEN, Saclay, France). pp 237-40 of Activation Analysis in Geochemistry and Cosmochemistry. /Brunfelt, Arild O. (ed.). Oslo; Universitetsforlaget (1971).

From Conference on activation analysis in geochemistry and cosmochemistry; Kjeller, Norway (7 Sep 1970). See CONF-700968.

The irradiation history of the Galaxy is briefly discussed. Meteorite studies show that the intensity of cosmic radiation has been constant, within a factor of two, for the last $10^9$ years. Spallation reactions leading to the formation of $^6$Li, $^9$Be, $^{10}$B and $^{11}$B and the relative abundance of these isotopes allow conclusions to be drawn as to the earlier galactic history. The $^7$Li/$^6$Li isotopic ratio is discussed and a tentative explanation proposed. A general history of nucleosynthesis in the Galaxy based on the long-lived radioactivities ($^{235}$U, $^{238}$U, $^{232}$Th) and fossil radioactivities ($^{129}$I and $^{244}$Pu, observed as Xe isotopes) is described. Finally the formation of a "solar" cluster of stars is discussed briefly. (Norway)

**55782** PHOTOGRAPHIC DETECTION OF INTERGALACTIC MATTER IN THE COMA CLUSTER. Welch, Gary A.; Sastry, G. N. (Van Vleck Observatory, Middletown, Conn.). Astrophys. J.; 169: No. 1, L3-5(1 Oct 1971).

Isodensitometry of deeply exposed plates of the Coma cluster of galaxies reveals the presence of diffuse luminous material at the center of the cluster. The material not only envelops the two supergiant galaxies NGC 4874 and NGC 4889 but extends outward to the southwest for at least 16 arc minutes. This extension may represent matter flowing out from NGC 4874. (auth)

**55783** ROCKET-INFRARED FOUR-COLOR PHOTOMETRY OF THE GALAXY'S CENTRAL REGIONS. Houck, J. R.; Soifer, B. T.; Pipher, Judith L.; Harwit, Martin (Cornell Univ., Ithaca, N. Y.). Astrophys. J.; 169: No. 1, L31-4(1 Oct 1971).

The central portion of the Galaxy was observed in the bandwidths 5 to 6, 12 to 14, 16 to 23, and 85 to 115 $\mu$ during an Aerobee 170 rocket flight launched on July 16, 1971. Measurements made during a 100-second time interval around 21:56 MST are reported. In addition to the galactic center, four new sources were also observed. (auth)

**55784** MICROWAVE DETECTION OF INTERSTELLAR FORMAMIDE. Rubin, R. H.; Swenson, G. W. Jr.; Benson, R. C.; Tigelaar, H. L.; Flygare, W. H. (Univ. of Illinois, Urbana). Astrophys. J.; 169: No. 1, L39-44(1 Oct 1971).

Formamide was detected by its microwave emission from the $2_{11} \rightarrow 2_{12}$ rotational transition at ~4620 MHz in the direction of Sgr B2 and possibly Sgr A. There is evidence that all three of the $\Delta F = 0$ hyperfine components are present. The astronomical rest frequencies are in good agreement with laboratory measurements. (auth)

**55785** CONDENSATION OF SOLID HYDROGEN IN CONTRACTING INTERSTELLAR CLOUDS. Nakano, Takenori (National Radio Astronomy Observatory, Green Bank, Va.). Progr. Theor. Phys. (Kyoto); 45: No. 6, 1737-46(Jun 1971).

Condensation of solid hydrogen was investigated for contracting interstellar clouds of various masses by taking into account the interaction between grains and gas particles (assuming different grain models) in determining the grain temperature. It was found that even with core–mantle grains with maximum possible impurity effect and with rather low saturation pressure used by Hoyle, Wickramasinghe, and Reddish, only 1.1% of hydrogen condenses in a cloud of $10^3 M_\odot$ and the contraction is not affected significantly by the condensation. About 11% of hydrogen condenses in a protostar of 1 $M_\odot$ with the same grain model and saturation pressure. The protostar becomes opaque to thermal radiation at rather low density; however, it contracts nearly freely until hydrogen is fully ionized. (auth)

**55786** RADIUS OF MAXIMUM ROTATIONAL VELOCITY IN SPIRAL GALAXIES. Noonan, Thomas W. (Brockport State Coll., N. Y.). Astron. Astrophys.; 14: No. 3, 437-9(Oct 1971).

An attempt to find a correlation between the radius R of maximum rotational velocity of spiral galaxies and other galaxian parameters gives negative results for the sparse data available, except for a possible increase in R (in steps in log R of ~0.3) with galaxy type a, b, c. Existing data is insufficient to distinguish between two cases: (i) Sb's have the same R; (ii) Sb's have a spread in R. In either case, our Galaxy has too large a value of R unless the Hubble constant is less than $H = 100$ km s$^{-1}$ Mpc$^{-1}$. For case (i), a value of $H = 50$ km s$^{-1}$ Mpc$^{-1}$ is indicated. More rotation curve data will allow a better determination of H. (auth)

**55787** SURVEY OF THE CONTINUUM RADIATION AT 820 MHz BETWEEN DECLINATIONS–7 AND +85°. II. A STUDY OF THE GALACTIC RADIATION AND THE DEGREE OF POLARIZATION WITH SPECIAL REFERENCE TO THE LOOPS AND SPURS. Berkhuijsen, Elly M. (Max-Planck-Institut fuer Radioastronomic, Bonn). Astron. Astrophys.; 14: No. 3, 359-86(Oct 1971).

The observations reported in paper I resulted in a map of contours of equal brightness temperature with a resolution of 1.2°. A discussion of the main features to be found on the map is given and comparisons with other observations are made. The temperature spectral index of the North Polar Spur between b = +15 and +45°, and of small parts of the other loops and spurs is derived. The survey was combined with a polarization survey at 820 mHz made with the same telescope. The resulting distribution of polarization percentages over the sky is discussed. Some aspects of the region of minimum brightness temperature around l = 190°, b = +50° are considered. (W.D.M.)

**55788** OB STARS AND GALACTIC STRUCTURE: THE PERSEUS SPIRAL ARM. Snyder, Glenn Alden. Cleveland; Case Western Reserve Univ. (1970). 112p. University Microfilms Order No. 71-19,058.

Thesis.

Photoelectric UBV photometry and MK spectral classifications were obtained for OB stars in region LF 5 (l = 129°, b = −2°). Investigation of absolute magnitudes and intrinsic colors revealed that there is a dependence of absolute magnitude on apparent magnitude, and a possible change in the classification system at B = 10.5, for the OB stars of the LS Catalogue in this region. To take this effect into account, new calibrations of $M_V$ and $(B-V)_0$ for OB stars, which include a photometric criterion, are given. The use of these calibrations on the OB stars in LF 5 and in six additional regions from l = 103 to 189°, and the addition of the MK data in LF 5, revealed that: (1) There is no evidence for an increase in interstellar absorption to be attributed to the Perseus spiral arm except at l = 142°. (2) The space density peaks of the OB stars generally agree with the space distribution of H II regions and galactic clusters containing early-type stars lying in the Perseus arm, including a sharp cutoff at l = 140°. (3) There is no evidence for a spiral feature lying beyond the Perseus arm in the OB star data. Analysis of radial velocities in and near LF 5 showed that the stars on the whole are following the Schmidt rotation model velocity characteristic of their region of peak density, but stars nearer and farther than the peak show motions indicating expansion or shearing along the arm. The H I in the region appears to lie about 750 pc farther than the stars, and to exhibit the same expansion or shearing motions. The resulting picture of the Perseus spiral arm is compared to the predictions of the density wave theory of spiral structure. (Diss. Abstr. Int., B)

XUM

**55789** RADIO INVESTIGATIONS OF CLUSTERS OF GALAXIES. Donivan, Frank Forbes Jr. Tallahassee; Univ. of Florida (1970). 121p. University Microfilms Order No. 71-16,778.

Thesis.

The mass discrepancy in clusters of galaxies arises when the number-mass (counts of galaxies on photographic plates) is compared to the mass derived by the virial theorem. The latter is usually one or two orders of magnitude larger than the observed or number-mass. If the clusters are stable systems, the "missing" mass may be present as intergalactic matter distributed throughout the cluster. If a weak ($10^{-7}$ gauss) intergalactic magnetic field exists, a distributed component of synchrotron-type radiation may be radiated by relativistic electrons in the intracluster medium. Detection of such emission would provide information on the quantity of intergalactic matter present. The results of radio-frequency observations of the Coma and Hercules clusters of galaxies (Abell Nos. 1656 and 2151) are presented. Antenna-temperature contour maps were constructed from observations made with the 1,000-foot Arecibo dish at frequencies of 195, 318, and 611 MHz. Analysis of the contour maps indicates the lack of a detectable distributed component of emission from the Coma cluster. The minimum detectable flux of the 195-MHz system can be set as the upper bound to the distributed component of radiation. Assuming the ratio of numbers of primary cosmic-ray particles to total interstellar particles in the Galaxy is the same in intergalactic space, the density of particles in the Coma cluster could be of the order of magnitude required by the virial theorem. Although the Hercules cluster is located in the galactic spur, the contour maps at 195 and 318 MHz both contain one contour interval which encloses the cluster. These contour intervals are much larger than the optical boundaries of the cluster, and may be the long-sought-after distributed component of emission. Assuming the intracluster matter is distributed over a region slightly smaller than that enclosed by the antenna temperature contour, and applying the same assumption regarding cosmic-ray to total-particle density as for the Coma cluster, the density of particles in the Hercules cluster is only a factor of three smaller than that required by the virial theorem. (Diss. Abstr. Int., B)

**55790** STELLAR DISTRIBUTION IN CYGNUS. Chartrand III, Mark Ray. Cleveland; Case Western Reserve Univ. (1970). 182p. University Microfilms Order No. 71-18,975.

Thesis.

Data from a catalogue of objective prism spectral types and photographic V magnitudes for approximately 5400 stars to V = 11.5 were used to study the distribution of common stars in the region l = 70 to 100° in a band 2° either side of the galactic equator. The surface distributions of several spectral groups are discussed in detail. The space density of stars as a function of distance was derived for several areas. A concentration of B7–A1 stars was found in a long ridge at l ≈ 75 to 80° extending from r ≈ 200 pc to r ≈ 800 pc. The surface distribution of early B stars and previous work by Nassau and MacRae (Astrophys. J., 110: 40(1949)) indicate that the B stars, too, are concentrated in this area. Another concentration of B7–A1 stars is at l ≈ 95°. The ratio of main-sequence A stars to giant K stars is derived as a function of distance in several areas. The value of this ratio over the entire region, when both types are taken to V = 10.0, is 2.2. Based on surface distributions, a very high value dA/gK = 9.0 is found at l = 89°. The maximum space density of early B and B7–A1 stars lies near and parallel to the inner edge (toward the galactic center) of the model Local Spiral Arm proposed by Dickel, Wendker, and Bieritz (I. A. U. Symp., No. 38, in press). (Diss. Abstr. Int., B)

**55791** STUDY OF 21 CM ABSORPTION BY NEUTRAL HYDROGEN IN THE GALAXY. Hughes, Michael Paul. Stanford, Calif.; Stanford Univ. (1970). 182p. University Microfilms Order No. 71-12,925.

Thesis.

This thesis is based upon the analysis of the hydrogen-line spectra of 105 small-diameter radio sources, most of which lie outside the Galaxy. The spectra, 73 of which are presented in an appendix, were measured with the two-element interferometer at the Owens Valley Radio Observatory. Most sources stronger than five flux units were observed. The frequency resolution was generally 4 kHz which corresponds to a velocity resolution of 0.81 km/sec. In contrast to previous findings published by other authors, who have found few cases of absorption at galactic latitudes greater than 30°, the spectra of many sources between 30 and 50° from the galactic plane contain clear evidence of absorption by neutral hydrogen in the Galaxy. A special series of observations of the relatively strong source 3C 274, at a galactic latitude of 74.5°, revealed the presence of a small absorption feature with an optical depth of 0.017. (TSS) (Diss. Abstr. Int., B)

**55792** ALIGNMENT OF INTERSTELLAR GRAINS. Goldstein, Mark Parnes. Pasadena, Calif.; California Inst. of Tech. (1971). 134p. University Microfilms Order No. 71-17,379.

Thesis.

The alignment of interstellar dust grains with respect to the magnetic field of the Galaxy is calculated. The alignment is found for several values of magnetic field strength, internal grain temperature, and grain shape. The following processes that affect the alignment are treated in detail: (i) a dissipative magnetic torque due to Davis and Greenstein; (ii) the collisions of the grain with interstellar hydrogen; and (iii) the nonzero internal temperature of the grain. A Fokker–Planck equation is obtained which takes account of these processes, and the solution of this equation provides the probability distribution of grain orientations. The equation is solved for these cases: (i) spherical grains in all fields; (ii) needles, prolate spheroidal grains, nearly spherical oblate grains, and disks in strong magnetic fields; (iii) needles and nearly spherical grains in weak fields. Using the distribution of orientations, the degrees of alignment are calculated. The results are in mixed agreement with those of Purcell and in good agreement with the weak-field calculation of Miller. It is found that for the relatively strong magnetic field of $10^{-5}$ gauss and grain temperature of 10°K, the measures of alignment are smaller than the values obtained from complete orientation of the grains. (Diss. Abstr. Int., B)

**55793** ENERGY DISTRIBUTIONS AND K CORRECTIONS FOR THE TOTAL LIGHT FROM GIANT ELLIPTICAL GALAXIES. Schild, R. (Smithsonian Astrophysical Observatory, Cambridge, Mass.); Oke, J. B. Astrophys. J.; 169: No. 2, 209-14(15 Oct 1971).

New absolute spectral-energy distributions of giant elliptical galaxies in the Virgo cluster are presented. Because the instrumental combination of a 4-inch telescope and the 200-inch prime-focus scanner permits apertures 6.2′ in diameter to be used without loss of spectral resolution, the energy distributions are expected to be comparable to those obtained when distant galaxies are observed in large telescopes. A comparison of the new energy distributions with those obtained previously for nuclei of elliptical galaxies shows little difference for λ > 4000 Å, but the nuclei are fainter by 0.3 mag below 4000 Å. New K-corrections are calculated for B, V, and $R_5$ magnitudes, and predicted color changes in B – V and V – $R_5$ are given to z = 0.28 and 0.60, respectively. The predicted run of B – V with z is within the accuracy of existing observations. Although entire elliptical galaxies are not so red as the elliptical-galaxy nuclei, they are redder than the star clusters M5, M67, and NGC 188. (auth)

**55794** ABSOLUTE ENERGY CURVES AND K CORRECTIONS FOR GIANT ELLIPTICAL GALAXIES. Whitford, A. E. (Univ. of California, Santa Cruz). Astrophys. J.; 169: No. 2, 215-20 (15 Oct 1971).

Scanner comparison of five typical giant elliptical galaxies with standard stars calibrated on the Hayes system was used to derive the absolute energy curve over the range 3400 < λ < 11000 Å. The mean aperture–diameter ratio A/D(0) = 0.6 was large enough to be insensitive to the aperture–color dependence found in broad-band photometry. The energy curve shows the galaxies to be bluer than found by Oke and Sandage; most of the difference is explained by the recalibration of standards and the aperture effect. The K corrections calculated from the curve are smaller than the Oke–Sandage values; in a typical case the resulting effect on the deceleration parameter would be $\Delta q_0 = -0.5$. The predicted apparent reddening of redshifted galaxies out to z = 0.20 is still within the range of uncertainty in Sandage's observed B – V colors. (auth)

**55795** KINEMATIC PROPERTIES OF SEVENTY-ONE H II REGIONS IN THE LARGE MAGELLANIC CLOUD. Smith, Malcolm G. (Cerro Tolodo Inter-American Observatory, La Serena, Chile); Weedman, Daniel W. Astrophys. J.; 169: No. 2, 271-80(15 Oct 1971).

Emission-line profiles and radial velocities for seventy-one H II regions in the Large Magellanic Cloud were observed with a pressure-scanned, Fabry–Perot interferometer having a spectral resolution of 11 km $s^{-1}$. The giant 30 Doradus Nebula was found to be kinematically unique, having much more rapid internal gas motions than any other nebula observed. The most probable velocities of internal gas motions vary little among the other seventy nebulae and average 15.1 km $s^{-1}$. Radial velocities accurate to 2.5 km $s^{-1}$ confirm Feast's rotation curve for the LMC and give a velocity dispersion perpendicular to the plane of 8.5 km $s^{-1}$. Comparison with 21-cm results shows that the average observed difference between H II and H I velocity in a particular region is only 4.6 km $s^{-1}$. If all regions for which H I and H II velocities were compared are taken together, the systematic difference (H I – H II) is 0.2 km $s^{-1}$. (auth)

XUM

**55796** 21-CENTIMETER STUDY OF THE SPIRAL GALAXY MESSIER 33. Gordon, Kurtiss J. (National Radio Astronomy Observatory, Green Bank, W. Va. Hampshire Coll., Amherst, Mass.). Astrophys. J.; 169: No. 2, 235-70(15 Oct 1971).

The distribution of neutral atomic hydrogen and the kinematic properties of the late-type spiral galaxy M33 are derived from observations obtained at 21-cm wavelength with a multichannel radiometer attached to the 300-foot paraboloidal transit telescope of the National Radio Astronomy Observatory. The effective half-power beam- and bandwidths of the telescope system are 10.0′ in $\delta$, 11.4′ in $\alpha$, and 21 km $s^{-1}$ in radial velocity. The assumed distance to M33 is 720 kpc. The galaxy contains $M_{H\,I} = 1.6 \times 10^9\ M_\odot$ of neutral hydrogen distributed in a broad ring of radius 18′ plus an underlying uniform distribution of radius ~35′ and two outlying "wings" or companions. The companions contain ~10% of the total hydrogen content. The centers of the H I ring and of the distributions of H II regions and luminous stars in M33 are offset by a few minutes of arc from the optical center of the galaxy. The systemic radial velocity is $S = -180$ km $s^{-1}$ (heliocentric). The rotation curve peaks at $V_r = S \pm \sim 85$ km $s^{-1}$, 30′ from the galactic center. For an inclination of 55°, this leads to a total mass of $M_t = 4.9 \times 10^{10}\ M_\odot$, of which $2.3 \times 10^{10}\ M_\odot$ is contained within 60′ of the center (roughly the extent of the observations). An asymmetry of the rotation curves for the two halves of the major axis leads to a mass ratio of $M_N/M_S = 1.2$. Noncircular motions are small in the main body of the galaxy. Velocities in the wings deviate by 40 to 50 km $s^{-1}$ from those predicted by the rotation curve. The data are consistent with a picture of the wings as stable gaseous companions of M33, gravitationally bound to the galaxy but not physically connected to the galactic plane. The global parameters of M33—$M_{H\,I}/M_t = 0.03$, $M_{H\,I}/L_\odot = 0.38$, and $M_t/L_\odot = 11.5$ (solar units)—are not significantly different from average values of the corresponding parameters for galaxies of similar structural type. (auth)

**55797** INTERPRETATION OF RECOMBINATION-LINE EMISSION FROM THE INTERSTELLAR MEDIUM. Cesarsky, Catherine J.; Cesarsky, Diego A. (Harvard Coll. Observatory, Cambridge, Mass.). Astrophys. J.; 169: No. 2, 293-8(15 Oct 1971).

The recombination-line emission detected by Gottesman and Gordon, which they attribute to a diffuse ionized component of the interstellar medium, can also be explained as resulting from a discrete distribution of cold and dense clouds. (auth)

## Cosmology

*Refer also to abstracts 54770, 55908, and 56570.*

**55798** SUPERMASSIVE OBJECTS IN ASTROPHYSICS. Trimble, V. (Cambridge Univ., Eng.). Nature (London); 232: No. 5313, 607-11(27 Aug 1971).

The scientific interests of W.A. Fowler in the fields of astrophysics are reviewed, with special reference to "black and white holes", supermassive stars and disks, and nucleosynthesis and reaction rates. It was the very large amounts of energy needed to explain radio sources and quasars that first led to the suggestion that single objects much more massive than stars might be important in astrophysics. Since then such supermassive objects have been "in and out of fashion" as energy sources and sites of nucleosynthesis. It is concluded that a number of problems remain concerning such objects, particularly regarding their mode of formation. In actual fact there is, so far, no really firm observational evidence for their existence. When supermassive stars were first proposed as a source of large amounts of energy they appeared to be pulsationally unstable, but subsequent studies have shown that this is probably not the case. 40 references. (UK)

**55799** NON-LINEAR THEORY OF GRAVITATIONAL INSTABILITY IN THE EXPANDING UNIVERSE. II. Tomita, Kenki (Hiroshima Univ.). Progr. Theor. Phys. (Kyoto); 45: No. 6, 1747-62(Jun 1971).

The general relativistic nonlinear theory of gravitational instability is reformulated in order to get a hydrodynamical system of equations which are applicable at any early stage of cosmic expansion. Nonlinearity is taken into account to the second-order smallness. On this basis, the second-order density perturbations associated with the first-order rotational and gravitational waves are derived, and the amplitudes of the density perturbations are shown to become comparable with the square of the amplitudes of the first-order waves. Moreover the second-order density perturbations corresponding to the first-order ones are derived and examined. (auth)

**55800** BRANS–DICKE COSMOLOGIES IN ARBITRARY UNITS: SOLUTIONS IN FLAT FRIEDMANN UNIVERSES. Morganstern, R. E. (Lunar Science Inst., Houston, Tex.). Phys. Rev., D; 4: No. 2, 278-82(15 Jul 1971).

Assuming a Robertson-Walker metric and an equation of state $p = \epsilon\rho$ ($0 \le \epsilon \le 1$), the Brans–Dicke (BD) field equations are found to yield a first integral of the form $a^{3(1+\epsilon)\lambda^{\frac{1}{2}}(2-\alpha)(1-\alpha)} = \text{const}$, where $\alpha$ is the parameter denoting the particular units in which the field equations are expressed. This first integral is employed in the remaining field equations to yield polynomial solutions for a, $\rho$, and $\lambda$. For $\epsilon = 0$, $\frac{1}{3}$, these solutions properly reduce to previously obtained pressure-free and radiation-filled universes, respectively. (auth)

**55801** EXACT SOLUTIONS TO RADIATION-FILLED BRANS–DICKE COSMOLOGIES. Morganstern, R. E. (Lunar Science Inst., Houston, Tex.). Phys. Rev., D; 4: No. 2, 282-6(15 Jul 1971).

Using the Robertson-Wal. r metric, exact general solutions to the Brans-Dicke cosmologies for $p = \frac{1}{3}\rho$ are found. The two first integrals which exist for this case reduce the problem to quadratures. In the case of flat space the quadratures may be integrated explicitly in terms of elementary functions, while in the curved spaces ($k = \pm 1$), the solutions may be expressed in terms of elliptic integrals. The limit as a approaches $\infty$ (or $a_{max}$ for a closed universe) may be evaluated for positive, negative, and zero curvature, and leads to the rather surprising result that the scalar field $\lambda$ approaches a constant. (auth)

**55802** TOPOLOGY AND COSMOLOGY. Ellis, G. F. R. (Cambridge Univ., Eng.). Gen. Relativity Gravitation; 2: No. 1, 7-21(1971).

Some topics concerning topology and cosmology are discussed. Firstly, topological properties that might be expected in any reasonable model of the Universe are considered, followed by consideration of some exact solutions that might serve as reasonable simple cosmological models. Finally some comments are made concerning properties that might be expected in more realistic universe models. It is stated that the essence of the study of cosmology is trying to determine not merely possible space–time structures, but those that probably exist in the Universe; this leads to the problem of attempting to verify the probable structure of the Universe. (UK)

**55803** EVENT HORIZONS AND GRAVITATIONAL COLLAPSE. Israel, W. (Univ. of Alberta, Edmonton). Gen. Relativity Gravitation; : No. 1, 53-9(1971).

A brief review is presented on the present status of the black hole concept and how it can be understood in physical terms. According to a widely held hypothesis every black hole should relax, after a transient period of the order of $2\ Gm/c^3$, to a Kerr black hole, and this, if correct, should be very useful in the construction of detailed models for astrophysical objects, such as galactic nuclei and certain x-ray sources, that might conceivably harbor black holes, it should also permit prediction of most of the parameters relating to the black hole itself. Both static and stationary event horizons are considered. (UK)

**55804** TOPOLOGY AND LOCAL PHYSICAL LAWS. Dautcourt, G. (Zentralinstitut fuer Astrophysik, Berlin). Gen. Relativity Gravitation; 2: No. 2, 97-103(1971).

In a closed universe, every physical system has a discrete infrastructure consisting of closely spaced ($\Delta E \approx \hbar^2/2mR^2$) energy eigenstates. Basic physical principles such as the uncertainty relation as well as semi-empirical facts like the finiteness of the world age seem to exclude a detection of this structure. (auth)

**55805** CONVERSION OF GRAVITATIONAL INTO ELECTROMAGNETIC WAVES. Boccaletti, D. (Univ., Ferrara, Italy. Istituto Nazionale di Fisica Nucleare, Bologna); Occhionero, F. Lett. Nuovo Cim.; 2: No. 11, 549-54(11 Sep 1971).

Under the assumed conditions of production and background, gravitational radiation will very likely behave as an active component of the Universe, being converted, although with very low efficiency, into other, more readily detectable forms of energy. For this reason, the conversion of gravitational into electromagnetic waves in a static magnetic field in vacuum is explored as a promising example, or phenomenon examined so far in connection with the possibility of building nonmechanical detectors and which might be of interest in its own right in astrophysics. (W.D.M.)

**55806** COMA CLUSTER AS AN X-RAY SOURCE: SOME COSMOLOGICAL IMPLICATIONS. Gott III, J. Richard (Princeton Univ., N. J.); Gunn, James E. Astrophys. J.; 169: No. 1, L13-15(1 Oct 1971).

Recent positive x-ray observations of the Coma Cluster make it possible to set firm upper limits on the mass of hot gas within the cluster. A theory of infall from the intergalactic medium relates this gas to the gas in intergalactic space and sets severe limits on the total gas density in the Universe; if most of the matter

in the Universe is gaseous, the Friedmann deceleration parameter $q_0$ must be less than about 0.1, corresponding to an open (''hyperbolic'') model. (auth)

**55807** LENSE-THIRRING TYPE GRAVITATIONAL FORCES BETWEEN DISKS AND CYLINDERS. O'Connell, R. F.; Rasband, S. N. (Louisiana State Univ., Baton Rouge. Montana State Univ., Bozeman). Nature (London) Phys. Sci.; 232: No. 35, 193-5(30 Aug 1971).

In view of the interest in measuring forces between spinning cylinders and disks, and the speculative nature of conclusions reached, a quantitative calculation of the magnitude of the forces was made, basing the approach on a weak-field low-velocity approximation to general relativity. Results are shown graphically for various configurations. (UK)

**55808** GRAVITATIONAL RED-SHIFT IN THE THEORY OF THE GENERALIZED GRAVITATIONAL POTENTIAL. Cherry, N. H. Lett. Nuovo Cim.; 2: No. 12, 619-20(18 Sep 1971).

Arp (1971) has recently pointed out that, in certain stellar systems of connected matter, different redshifts are obtained from different parts of the system, suggesting that more than Doppler redshift is present. In addition, the recent long-baseline interferometer results (Knight et al., 1971) on quasar 3C 279 imply mass separation exceeding the speed of light when Doppler redshift distances are used. Both of these effects suggest that at least some distances obtained from Doppler redshifts should be revalued. The application of a new physical proposition to these cosmological problems is suggested. (W.D.M.)

**55809** OBSERVATIONAL EFFECTS OF LOCAL INHOMOGENEITIES IN COSMOLOGICAL MODELS. Clark, Eugene Ellis. Tallahassee; Univ. of Florida (1970). 106p. University Microfilms Order No. 71-16,774.

Thesis.

Observational effects of the deflection of light caused by the gravitational field of a single cluster of galaxies are discussed. It is assumed that the cluster of galaxies is a transparent, homogeneous, spherical mass surrounded by a vacuum. (TSS) (Diss. Abstr. Int., B)

### *Planetary Phenomena*

*Refer also to abstracts 54459–54461, 54475, and 55983.*

**55810** ELECTRICAL CONDUCTIVITY AND TEMPERATURE OF THE LUNAR INTERIOR FROM MAGNETIC TRANSIENT-RESPONSE MEASUREMENTS. Dyal, Palmer; Parkin, Curtis W. (Ames Research Center, Moffett Field, Calif.). J. Geophys. Res.; 76: No. 25, 5947-69(1 Sep 1971).

The response of the Moon to magnetic-field step transients in the solar wind was investigated for over 100 events by using simultaneous data from the Apollo-12 lunar surface magnetometer and the lunar-orbiting Explorer-35 magnetometer. These transient events were all selected at times when the Moon was in the free-streaming solar wind and the Apollo-12 magnetometer was on the lunar dark side. The lunar-nighttime Apollo-12 magnetometer data consistently show a distinct difference between radial and tangential surface magnetic-field components for all step transients; this property strongly implies that the surface magnetometer is measuring a global rather than a local effect. The simplest model, although not unique, which qualitatively explains all the general aspects of the darkside transient-response data is a spherically symmetric three-layer model having a thin outer crust of very low electrical conductivity. The intermediate layer, of radial thickness $R_1-R_2$, where $0.95\ R_M \leq R_1 < R_M$ and $R_2 = 0.6 \pm 0.1\ R_M$, has an electrical conductivity $\sigma_1 \sim 10^{-4}$ mhos/meter; the inner core has radius $R_2 \sim 0.6\ R_M$ and conductivity $\sigma_2 \sim 10^{-2}$ mhos/meter. Temperatures are calculated from these conductivities for several possible lunar material compositions. For the example of an olivine moon, the temperatures of the layers are as follows: crust, <440°K; intermediate layer, ~810°K; core, ~1240°K. (auth)

**55811** ISOTOPES AND MOON ROCKS. Isotop. Radiat. Technol.; 9: No. 1, 64-5(Fall 1971).

A short review is given on some of the work presented at the Apollo 11 Lunar Science Conference, Houston, Jan. 1970. (W.D.M.)

**55812** MARINER 6 AND 7 ULTRAVIOLET SPECTROMETER EXPERIMENT: ANALYSIS OF HYDROGEN LYMAN-ALPHA DATA. Anderson, Donald E. Jr.; Hord, Charles W. (Univ. of Colorado, Boulder). J. Geophys. Res.; 76: No. 28, 6666-73 (1 Oct 1971).

Mariner 6 and 7 ultraviolet spectrometers that flew by Mars in 1969 observed the Lyman-$\alpha$ dayglow of atomic hydrogen. Data in the altitude range 200 to 24,000 km are analyzed to determine the structure of the Martian exosphere. The classical evaporative theory is applied to calculate a hydrogen density distribution. A spherical model of the dayglow Lyman-$\alpha$ emission, using radiative transfer theory, is used to produce theoretical intensities for comparison with the data in order to determine temperature and density in the exosphere. It is found that the exospheric temperature is 350 ± 100°K and that the number density at 250 km is $3 \pm 1 \times 10^4$ cm$^{-3}$. The existence of a Lyman-$\alpha$ corona implies a primary source of hydrogen on Mars, probably the photodissociation of water vapor. (auth)

## Atomic and Molecular Physics

*Refer also to abstract 56748.*

### *Atomic, Electron, Ion, and Molecular Beams and Their Reactions*

*Refer also to abstracts 56130, 56148, and 56218.*

**55813** (JINR–P4-5957) OPTICAL RADIATION EXCITED BY NONRELATIVISTIC CHARGED PARTICLES ON THE METAL SURFACE. Kobzev, A. P.; Mikhalyak, S.; Rutkovski, E.; Frank, I. M. (Joint Inst. for Nuclear Research, Dubna (USSR). Lab. of Neutron Physics). 1971. 22p. (In Russian). Dep. NTIS (U. S. Sales Only).

Polarization, angular distributions, and energy dependences are measured for the radiation (in the region of wave lengths of 3800 to 6500 Å) appearing on the surface of Ag, Al, W, and Ni targets when bombarding them with the 0.5- to 15-keV electrons and 1.5- to 4.5-MeV protons. The polarized component agrees well with the transition radiation theory. (auth)

**55814** (UCRL–73353) ION SOURCE TECHNOLOGY. Hamilton, Gordon W. (California Univ., Livermore. Lawrence Radiation Lab.). 18 Aug 1971. 7p. (CONF-711012-6). Dep. NTIS.

From Symposium on ion sources and formation of ion beams; Upton, N. Y. (19 Oct 1971).

A review is presented on technological areas involved in design and assembly of ion sources. Topics covered are electrode materials and designs, high-voltage and insulator techniques, and assembly and joining techniques. The intention is to describe technological problem areas usefully without attempting to be all-inclusive. (auth)

**55815** INSTRUMENTATION FOR THE STUDY OF ION REFLECTION AND SECONDARY ION EMISSION UPON ION BOMBARDMENT OF ATOMICALLY CLEAN AND SMOOTH MONOCRYSTALLINE METAL SURFACES. Suurmeijer, E. P. Th. M.; Boers, A. L. (State Univ.,Groningen, Netherlands). J. Phys., E (London); 4: 663-70(Sep 1971).

An apparatus was built for the study of energy distributions of reflected and secondary ions emitted from smooth and atomically clean monocrystalline metal surfaces upon bombardment with very-low-intensity noble gas ion beams (<10 nA cm$^{-2}$) in the energy range 0.5 to 10 keV. The construction of the apparatus is described and basic design features and operation principles discussed. Experimental procedures are described, among which those dealing with the generation and maintenance of ideal target conditions are considered to be especially important. The system performance is discussed on the basis of some preliminary experimental results. (auth) (UK)

**55816** CROSS BEAM NEUTRALIZER FOR ION BEAMS. Goodman, Ronald K.; Hunt, Angus L. (Univ. of California, Livermore). Rev. Sci. Instrum.; 42: No. 9, 1359-65(Sep 1971).

A cross-beam neutralizer that neutralizes ion beams by means of a directed gas flow from capillary arrays is described. The measurements given here show that such a neutralizer has an advantage over a uniform-density gas-cell neutralizer in that its contribution to beam line streaming is significantly less. Two versions of the cross-beam neutralizer that are suitable for injecting neutral hydrogen atoms into a plasma are described. (auth)

**55817** HIGH-FREQUENCY SOURCE OF HEAVY IONS. Komarov, V. L.; Tsepakin, S. G.; Chemyakin, G. V. (Scientific-Research Inst. of Electrophysical Equipment, Leningrad). Sov. Phys.-Tech. Phys. (Engl. Transl.); 16: No. 1, 150-2(Jul 1971).

Translated from Zh. Tekh. Fiz.; 41: No. 1, 198-200(Jan 1971).

A high-frequency ion source that operates in the continuous regime with vapors of low-melting elements (Sb and P), solid compounds (AgCl and $AlBr_3$), liquids ($BBr_3$, $SiCl_4$, $SbCl_5$, and $PCl_3$), and gases (Ar, $O_2$, He, and $N_2$) is described. The technique for using the source is described briefly and results are given. The source is intended for use in beam-type equipment for ion alloying of semiconductor elements and makes it possible to obtain beams of $P^+$, $Sb^+$, $Ag^+$, $Al^+$, $B^+$, $Si^+$, $Ar^+$, $O^+$, $O_2^+$, $He^+$, and

XUM

$N^+$ ions with currents of from 1 to 7 mA and a power consumption smaller than 1.5 kW. (auth)

**55818** SECONDARY ION EMISSION FROM METAL SURFACE IN COLLISIONS OF 30-keV $Ar^+$ IONS. Chida, Katsuhisa; Kaneko, Kumetaro; Iwata, Katsuhiko; Sakai, Mitsuo (Tokyo Univ.). Shitsuryo Bunseki; 19: No. 1, 49-74(Mar 1971).

Charge states and kinetic energies of scattered Ar ions and recoiled ions in collisions of 30-keV Ar ions with Mn, Fe, Co, Ni, Cu, Zn, Ge, Ag, Cd, Sb, Ta, Pt, Au, and Pb targets were measured at an angle of 70°. The targets were placed on the focal plane of the INS isotope separator. The spectra consisted of sharp peaks and a continuous background. It was confirmed from the peak positions that the collisions between the incident Ar ions and the target materials are of quasi-elastic character. However, an energy difference of about 500 eV, which can be interpreted as inelastic energy loss, was observed. Cross sections of scattered ions were measured and excitation curves are discussed. In the case of a $Nd_2O_3$ target, the collisions could be considered as independent collisions of Ar ions with individual Nd and O atoms formed by decomposition of the $Nd_2O_3$ molecule by ion impact. The shoulder, which was always observed in the high-energy side of the peak, could be explained quantitatively as a result of double scattering. The background is discussed in terms of multiple scattering and energy absorption in the target. (auth) (Japan)

**55819** SECONDARY EMISSION OF $W^+$ IONS DURING BOMBARDMENT OF TUNGSTEN BY IONS OF ALKALI METALS. Adylov, A. A.; Veksler, V. I.; Reznik, A. M. (Tashkent State Univ.). Dokl. Akad. Nauk Uzb. SSR; No. 12, 19-21(1971). (In Russian).

Data obtained on the secondary emission of $W^+$ ions during bombardment of polycrystalline tungsten by $Cs^+$, $Rb^+$, $K^+$, and $Na^+$ ions showed that the surface impurities, induced by the bombardment, strongly affected the temperature dependence of the sputtered ions. (R.V.J.)

## *Atomic and Molecular Properties*

*Refer also to abstracts 56156, 56398, and 56697.*

**55820** AUTOIONIZING STATES IN HELIUM-LIKE IONS. Balashov, V. V.;;Lipovetskii, S. S.; Pavlichenkov, A. V.; Polyudov, A. N.; Senashenko, V. S. (Moscow Univ.). Vestn. Mosk. Univ., Ser. III. Fiz. Astron.; 12: No. 1, 65-74(Jan-Feb 1971). (In Russian).

Using a diagonalized approximation, the positions and widths of some lower singlet and triplet $S^{(+)}$, $P^{(-)}$, and $D^{(+)}$ resonances for a series of helium-like ions from $Li^+$ to the quadruply charged carbon ion were calculated. The results obtained are compared with the available experimental and theoretical data. (tr-auth)

**55821** ISOTOPE SHIFTS IN ELECTRONIC AND MUONIC ATOMS, WITH APPLICATION TO NEODYMIUM. Stacey, D. N. (Clarendon Lab., Oxford). J. Phys., B (London); 4: No. 7, 969-75(Jul 1971).

The different dependence of optical and muonic isotope shifts on the nuclear charge distribution is discussed, with particular reference to the effects of nuclear deformation. This is shown to contribute proportionately less to muonic than to electronic shifts, and the effect is evaluated quantitatively as a function of proton number. It is shown that changes in the nuclear charge distribution can be studied in more detail than has previously been possible by combining optical and muonic results; the experimental data for neodymium are used to illustrate the analysis. This indicates that the use of data from Coulomb excitation experiments may give rise to serious errors in estimating the contribution of deformation effects to isotope shifts. (auth) (UK)

**55822** CHEMICAL SHIFTS OF $L_{III}$ X-RAY ABSORPTION EDGES OF Gd AND Dy. Agarwal, B. R. K. (M. M. H. Coll., Ghaziabad, India); Verma, L. P.; Agarwal, B. K. Lett. Nuovo Cim.; 2: No. 12, 581-2(18 Sep 1971).

Measurements on $L_{III}$ x-ray absorption edges of Gd and Dy metals are not available. Earlier measurements were made either on oxides or on salts. An attempt was made to measure (i) the positions of $L_{III}$ edges in Gd and Dy, and (ii) the chemical shifts of these edges in oxides and chlorides. The latter information is useful in view of the recent correlation established between the shifts and the ionicities. (W.D.M.)

**55823** L X-RAY TRANSITION PROBABILITIES IN ELEMENTS WITH $Z \geq 57$. Salem, S. I.; Tsutsui, R. T.; Rabbani, B. A. (California State Coll., Long Beach). Phys. Rev., A; 4: No. 5, 1728-35 (Nov 1971).

The $L\beta_3/L\beta_4$, $L\gamma_1/L\beta_1$, $L\alpha_2/L\alpha_1$, $L\beta_{2,15}/L\alpha_1$, and $L\beta_{2,15}/L\alpha_2$ transition probabilities were measured for 27 elements ranging in atomic number from La to U. Other L transitions were also measured for a smaller number of elements in the same range of atomic numbers. This was accomplished by bombarding these elements with a constant-energy electron beam and measuring their x-ray emission spectrum. The measured ratios are compared with the most recent calculation based on a relativistic Hartree–Fock–Slater (RHFS) potential and screened Coulomb potential. In general, the form of the dependence of these ratios on atomic number predicted by calculations based on a RHFS potential is favored, and the agreement between theory and experiment ranges from excellent for the $L\alpha_2/L\alpha_1$ ratio to a discrepancy of about 22% in the $L\beta_{2,15}/L\alpha_1$ ratio for elements of large atomic number. (auth)

**55824** GROUND-STATE ENERGIES OF THE He ATOM AND THE $Li^+$ ION IN THE FADDEEV APPROACH. Banerji, G.; Banerjee, S. N.; Sil, N. C. (Indian Association for the Cultivation of Science, Calcutta). Phys. Rev., A; 4: No. 5, 1705-8(Nov 1971).

The ground-state energies of the He atom and the $Li^+$ ion were calculated using the Faddeev formalism. For the off-shell two-body collision amplitude (t matrix), Sturmian-function (SF) as well as Coulomb-function representations were employed. For the He atom, calculations were performed retaining 1s, 1s and 2s, and 1s, 2s, and 3s states in the SF representation for the two-body t matrix, whereas only the 1s term was retained in the mixed-mode (MM) representation. For the $Li^+$ ion, computations were done after retaining terms up to 2s in the SF representation and only the 1s term in the MM representation. The results obtained by retaining only the 1s term are in marked disagreement with the experimental values in both representations. It is noticed that the results for the MM representation are almost as much below the experimental values as those for the SF representation are above. The results for the MM representation are slightly better than those for the SF representation. This is seen more clearly in the case of the $Li^+$ ion. The results in the SF representation are found to be in good agreement with the experimental findings after inclusion of the 2s term. (auth)

**55825** M-SUBSHELL FLUORESCENCE YIELDS AND THE $L_1-L_3$ RADIATIVE TRANSITION AT Z = 93 AND 96 FROM $^{241}Am$ AND $^{249}Cf$ DECAYS. Karttunen, E.; Freund, H. U.; Fink, R. W. (Georgia Inst. of Tech., Atlanta). Phys. Rev., A; 4: No. 5, 1695-1705(Nov 1971).

High-resolution Ge(Li) and Si(Li) x-ray spectrometers and a wall-less anticoincidence multiwire proportional counter were used for coincidence measurements between various K and L x rays and M x rays of Np (Z = 93) and Cm (Z = 96) following $\alpha$ decay of $^{241}Am$ and $^{249}Cf$, respectively. The effect of multiple vacancies in the M shell was taken into account in the determination of the following mean M-subshell fluorescence yields: $\nu_1^M = 0.065 \pm 0.014$, $\nu_2^M = 0.080 \pm 0.029$, $\nu_3^M = 0.062 \pm 0.005$, $\nu_{4,5}^M = 0.065 \pm 0.012 \approx \omega_2^M$ at Z = 93; and $\nu_1^M = 0.081 \pm 0.016$, $\nu_2^M = 0.068 \pm 0.023$, $\nu_3^M = 0.062 \pm 0.019$, $\nu_4^M = 0.080 \pm 0.006$, and $\nu_{4,5}^M = 0.075 \pm 0.012 \approx \omega_5^M$ at Z = 96. The close agreement of the various mean M-subshell fluorescence yields with that of the $M_{4,5}$ subshells for each element indicates that Coster–Kronig transitions are very strong in the M shell. Including earlier measurements of mean M-shell fluorescence yields at lower Z, corrected for multiple vacancies, and accepting Bhalla's theoretical calculations of radiative $M_{4,5}$-subshell widths, one concludes that the nonradiative widths of the $M_{4,5}$ subshells are essentially constant from Z = 76 to 96. Comparison of fluorescence yields of the K shell and the $L_3$ and $M_{4,5}$ subshells at the same energy of the principal radiative transition (i.e., at different values of Z) indicates that the ratio of radiative to Auger widths decreases from the $1s_{\frac{1}{2}}$ to $2p_{\frac{3}{2}}$ state, but remains constant from $2p_{\frac{3}{2}}$ to $3d_{\frac{5}{2}}$. The resolution of the Si(Li) detector was sufficient to separate the radiative transitions from fillings of the $M_{1,2}$- and $M_{3,4,5}$-subshell groups, so that from K and L x-ray coincidences with the $M_{1,2}$ group of x rays, it was possible to determine the following quantities: $\omega_1^M + f_{12}^M\omega_2^M = (2.0^{+0.3}_{-0.2}) \times 10^{-3}$ and $(7.5^{+0.7}_{-0.6}) \times 10^{-3}$ at Z = 93 and 96, respectively, and $\omega_2^M = (4.6^{+1.1}_{-1.0}) \times 10^{-3}$ at Z = 96. Thus, about 94% of $M_2$-subshell vacancies undergo Coster–Kronig shifts to higher subshells before filling from N and higher major shells occurs. Observation of the radiative $L_1-L_3$ transition was made for the first time in the high-Z region, and its intensity is in reasonable agreement with extrapolated theoretical predictions (6 to 7% of x rays filling $L_1$-subshell vacancies). The radiative fraction $\omega_{13}$ in the Coster–Kronig yield $f_{13}$ is found to be about 2% in the region of Z = 93 to 96, and $\omega_{13} = 0.011 \pm 0.005$ and $0.009 \pm 0.005$ at Z = 93 and 96, respectively. The absolute emission rate of M x rays from $^{241}Am$ was measured with multiwire and single-wire proportional counters, and values are found of $(6.35 \pm 0.60) \times 10^{-2}$ M x rays per $\alpha$ decay and $0.470 \pm 0.045$ M x rays per $L_\alpha$ x ray. These intensities were used in determinations of efficiency at 3.25 keV of the semiconductor x-ray detectors. (auth)

**55826** MOLECULAR-BEAM MAGNETIC-RESONANCE STUDIES OF HD AND $D_2$. Code, R. F.; Ramsey, N. F. (Harvard Univ., Cambridge, Mass.). Phys. Rev., A; 4: No. 5, 1945-59 (Nov 1971).

The results of some recent molecular-beam magnetic-resonance experiments on HD and $D_2$ are reported. A discussion is given of the shifts and distortions of the separated oscillatory field resonance pattern produced by inhomogeneities in the external magnetic field and by the Bloch–Siegert effect. The sign of the electron-coupled spin–spin interaction constant in HD was remeasured to be positive. Its magnitude was determined to be 47(7) Hz. The spectrum of the J = 1 state of $D_2$ was observed for external fields less than 160 G, and the spin-rotation and second-rank tensor interaction constants were determined to be $c_d = +8.768(3)$ and $d = +25.2414(14)$ kHz. Using the calculated value of $d'_M = +2.737(1)$ kHz for the magnetic spin–spin interaction constant, the value of the electric quadrupole interaction constant was determined from the observed value of d to be $eqQ/h = +225.044(24)$ kHz in the first rotational state of $D_2$. Hyperfine transitions were observed for the first time in the second rotational state of $D_2$. The hyperfine constants were determined from the transitions in the limit of zero external magnetic field to be $c_d = +8.723(20)$, $d'_M = 2.725(14)$, and $eqQ/h = +223.38(18)$ kHz in the second rotational state. The effects of isotopic substitution and nuclear motion on the hyperfine constants in molecular hydrogen are discussed. (auth)

**55827** K-FLUORESCENT-X-RAY RELATIVE-INTENSITY MEASUREMENTS. McCrary, J. H.; Singman, L. V.; Ziegler, L. H.; (and others) (EG and G, Inc., Las Vegas, Nev.). Phys. Rev., A; 4: No. 5, 1745-50(Nov 1971).

Measured values of the relative intensities of several K-fluorescent x rays are reported for 28 elements ranging from calcium through plutonium. Solid-state Si(Li) and Ge(Li) spectrometers and a Bragg-diffraction spectrometer were used in making the measurements. Fluorescence was excited in thin samples by higher-energy x rays. Corrections were made to the measured relative intensities for sample absorption, air absorption, and spectrometer efficiency. The accuracy of most of the measurements is ±2 to 5%. The results are compared with those of other experimenters and with the Schofield calculations. (auth)

**55828** ISOTOPIC SHIFT CONSTANT AND ELECTRIC QUADRUPOLE MOMENTS OF NEODYMIUM. Comaniciu, Nicolae (Institut de Physique Atomique, Bucarest). Rev. Roum. Phys.; 16: No. 5, 527-33(1971). (In French).

The isotopic constant for neodymium is calculated from the Nd I spectrum. The results are compared to the values of other authors. At the same time a method of estimating the electric nuclear quadrupole moments is given; the results turn out to be in good agreement with those obtained by nuclear-physics methods. (auth)

**55829** JAMES WAVE FUNCTION FOR THE GROUND STATE OF $H_2^+$. Jackson, M. (York Univ., Toronto); McEachran, R. P.; Cohen, M. Chem. Phys. Lett.; 10: No. 2, 143-5(15 Jul 1971).

The James function for the ground state of $H_2^+$ is determined variationally, and the electronic energy is calculated over a representative range of internuclear separations. The results are compared with other simple approximations. Although it decreases in accuracy as the internuclear separation increases, the James function is found to be comparable with the highly accurate Guillemin and Zener function for internuclear separations up to three times the equilibrium separation. (auth)

## Positronium, Muonium, and Mesic Atoms and Molecules

*Refer also to abstracts 56360 and 56705.*

**55830** MUONIC X-RAY MEASUREMENTS WITH A HIGH-PRESSURE GAS TARGET. Backenstoss, G.; Daniel, H.; Jentzsch, K.; (and others) (CERN, Geneva). Phys. Lett.; 36B: No. 4, 422-4(20 Sep 1971).

Muonic x rays from a high-pressure gas target were measured. Within a resolving time 0.03 μsec a transfer yield from hydrogen to argon of 0.36 ± 0.05 was obtained at an argon admixture of $1 \times 10^{-5}$ and 980 atmospheres. The rms radii of neon and argon were determined and found to be 3.07 ± 0.08 and 3.415 ± 0.005 fm, respectively. (auth)

**55831** MESON FINITE SIZE EFFECTS IN MESONIC ATOMS. Iachello, F. (Univ. of Copenhagen); Lande, A. Phys. Lett.; 35B: No. 3, 205-10(24 May 1971).

Meson finite size effects in mesonic atoms are considered. A limit on the q.e.d. cutoff mass Λ is set by present data on muonic $^{206}Pb$ at $\Lambda > 1.44$ GeV. This limit is comparable to recent high-energy estimates, and it can be improved upon. The importance of the pion form factor in extracting the strong π-nucleus optical potential is indicated. Finally, detection of a possible pion polarizability is discussed. (auth)

**55832** HYPERFINE STRUCTURE OF POSITRONIUM. Fulton, Thomas (CERN, Geneva); Owen, David A.; Repko, Wayne W. Phys. Rev., A; 4: No. 5, 1802-11(Nov 1971).

The details of a calculation of the $m\alpha^6 \ln\alpha^{-1}$ contributions to the triplet–singlet splitting of the positronium ground state are presented. The result $\Delta\nu(\alpha^6 \ln\alpha^{-1}) = \frac{3}{4}\alpha^4 R \infty \ln\alpha^{-1} = 34$ MHz places the theoretical value for the transition frequency $\nu$ approximately 1 standard deviation above the most recent experimental value. The calculation is performed using a perturbation theory based on the Bethe–Salpeter equation and on a wave function obtained by a single iteration from the nonrelativistic Pauli wave function. After a study of all relevant terms, it is concluded that the only diagrams that contribute to this order are those involving the exchange of one or two virtual transverse photons. These contributions are explicitly evaluated, and it is shown that other possible contributions actually vanish. (auth)

**55833** CONTRIBUTION ABSORPTION-REEMISSION PROCESS TO THE COMPLEX LEVEL SHIFT IN THE PIONIC ATOM. Nishimoto, Kazuya (Hiroshima Univ.); Ohtsubo, Hisao; Narumi, Hajime. Progr. Theor. Phys. (Kyoto); 46: No. 1, 135-47(Jul 1971).

Calling attention to the pion–nucleon interaction at low energy, an absorptive interaction including a rescattering process is derived on the basis of the dispersion relation. The cross section for the reaction $\pi^+ + d \rightarrow p + p$ is calculated for the s-wave pion at low energy in order to verify the approach, and the value is in good agreement with the recent experimental result. Then, it is shown that the real part of the two-nucleon amplitude associated with the absorption is attractive and about twice as large as the imaginary amplitude. From this consideration the pionic complex level shift is predicted for the deuteron. (auth)

**55834** LIFETIMES OF POSITRONS IN ALKALINE EARTH FLUORIDES. Singh, K. P.; Singru, R. M. (Indian Inst. of Tech., Kanpur). Chem. Phys. Lett.; 10: No. 3, 328-30(1 Aug 1971).

An empirical model is used to calculate the lifetimes $\tau_2$ in alkaline earth fluorides. The results are analyzed to bring out the importance of the ($e^+$–anion) system in the annihilation of positrons in ionic crystals. (auth)

**55835** POSITRON ANNIHILATION IN γ-IRRADIATED 10 M NaOH GLASSY ICE AT 85°K. Eldrup, M. (Danish Atomic Energy Establishment, Risoe); Mogensen, O.; Kevan, L. Chem. Phys. Lett.; 10: No. 4, 379-80(15 Aug. 1971).

Positron lifetime spectra in γ-irradiated 10M NaOH glass at 85°K show no significant effect due to the presence of 1.7 to 7.0 × $10^{18}$ trapped electrons $cm^{-3}$, i.e., positronium and positrons do not interact with trapped electrons in this matrix. (auth)

## Collision Phenomena

*Refer also to abstract 55094.*

**55836** (INR-P-1327) IONIZATION OF ATOMIC HYDROGEN BY ELECTRON IMPACT: NUMERICAL CALCULATIONS FOR THE "FREE-FALL" ATOMIC MODEL. Gryzinski, Michal; Kunc, Jozef; Zgorzelski, Maciej (Institute of Nuclear Research, Warsaw (Poland)). 1971. 10p. Dep. NTIS (U. S. Sales Only).

Numerical classical three-body calculations cross sections for ionization of atomic hydrogen by electron impact are presented. It is shown that for a classical free-fall (zero-angular-momentum) model of the ground-state hydrogen atom good agreement with experiment is obtained. (auth)

**55837** ELECTRON CAPTURE BY FAST PROTONS IN He AND $H_2$. Chatterjee, G.; McDowell, M. R. C. (London Univ.). J. Phys., B (London); 4: No. 7, 896-910(Jul 1971).

Single-center wave functions are used in evaluating the OBK approximation cross section for the capture process $H^+ + H_2(^1\Sigma_g) \rightarrow H(ns) + H_2^+(^2\Sigma_g^+)$ (n = 1, 2, 3) at energies up to 5 MeV. At low energies (≤500 keV) the results are in good agreement with those of two-center calculations, when the interaction with the passive electron is neglected. However it is shown that at high momentum transfers the dominant contributions to the matrix element arise from the interaction of the target proton with the passive electron. This is confirmed analytically for the reaction $H^+ + He \rightarrow H(1s) + He^+$. (auth) (UK)

**55838** EXCITATION OF HIGHLY EXCITED HYDROGENIC IONS AND ATOMS BY CHARGED PARTICLES. II. Percival, I. C.; Richards, D. (Univ. of Stirling, Scotland). J. Phys., B (London); 4: No. 7, 918-31(Jul 1971).

XUM

Heisenberg's form of the correspondence principle is used to study the excitation of hydrogen atoms and hydrogen-like ions by incident electrons or by incident ions. This principle and a generalization are used to show that there are at least four distinct ranges of the incident energy, in each of which the cross section has a different functional form. Classical perturbation theory, quantal perturbation theory (first Born), and the sudden approximation are compared, and regions of validity obtained. (auth) (UK)

**55839** EXCITATION OF HIGHLY EXCITED HYDROGENIC IONS AND ATOMS BY CHARGED PARTICLES. III. Percival, I. C.; Richards, D. (Univ. of Stirling, Scotland). J. Phys., B (London); 4: No. 7, 932-9(Jul 1971).

Heisenberg's form of the correspondence principle was used to calculate collisional excitation cross sections for transitions between two highly excited levels. An impact-parameter formulation of the sudden approximation and first-order perturbation theory was used. The range of incident energies for which the results are given, $2M/m_e\,|ZZ'|/n < E/Ryd < M/m_e\,Z'^2$, is determined by the condition that these approximations should have a common region of validity. Where possible these approximations were checked using a more general correspondence principle. The cross section is obtained in analytic form and is at worst in error by about 20%. (auth) (UK)

**55840** PROTON–HYDROGEN ATOM MOMENTUM TRANSFER CROSS SECTION AT ~5 eV. Brennan, M. H.; Morrow, R. (Flinders Univ. of South Australia, Bedford Park). J. Phys., B (London); 4: No. 7, L53-6(Jul 1971).

The momentum-transfer cross section for $H^+$–H collisions at ~5 eV was measured by observing the velocity and attenuation of compressional Alfven waves propagating in a partially ionized hydrogen plasma. The value obtained for the cross section is $6.0^{+2.0}_{-3.0} \times 10^{-15}$ cm$^2$. (auth) (UK)

**55841** EXCITATION OF THE HYDROGEN ATOM BY A FAST PROTON. Baye, D.; Binon, F.; Demeur, M. (Univ. Libre, Brussels). Bull. Cl. Sci., Acad. Roy. Belg.; 56: No. 11, 1238-73(1970). (In French).

The excitation of the hydrogen atom by a fast proton whose movement is described by a rectilinear trajectory was studied by the diagonalization method first introduced by Alder and Winther in the framework of the Coulomb excitation of collective states of atomic nuclei. The rough approximation, which is a particular case of this method, was not retained. The stability of the results as a function of the number of states retained was examined and judged to be good; the maximum number of states retained in this study of stability is 55 (shells $n < 5$). The energy region studied extends from 10 to 2500 keV. The results are good for the population of states that can be attained by an optically permitted transition. For the other transition the results are inferior to those obtained by resolution of the coupled equation system. The polarization of the de-excitation rays 2p–1s and 3d–2p was calculated. (tr-auth)

**55842** EXCITATION OF THE HELIUM ATOM BY A FAST PROTON. Baye, D. (Univ. Libre, Brussels). Bull. Cl. Sci., Acad. Roy. Belg.; 56: No. 11, 1274-90(1970). (In French).

The excitation of helium by a proton with energy higher than 25 keV was studied by the diagonalization method. The wave functions chosen contain at least 15 parameters in $r_1$, $\theta_1$, $\phi_1$, $r_2$, $\theta_2$, $\phi_2$ and form an orthonormal group up to $n = 5$. The populations of the state $n^1$ S are in disagreement with experience below 400 keV. The populations of the states $n^1$ P are in agreement with experience above 100 keV. Up to several MeV the populations of the states $n^1$ D and $4^1$ F are much greater than those given by the Born approximation and experimental values. The polarizations calculated for the $^1$D–$^1$P rays are in excellent agreement with experimental results. (tr-auth)

**55843** ELECTRON-IMPACT EXCITATION OF HELIUM ATOMS TO METASTABLE STATES: BORN–OPPENHEIMER APPROXIMATION. Kang, Ik-ju (Southern Illinois Univ., Edwardsville); Choi, Chan Kyoo. J. Korean Phys. Soc.; 4: No. 1, 1-8(Mar 1971).

The problem of excitation of helium atoms to metastable states by electron impact is formulated, treating all electrons on an equal footing in accordance with their indistinguishability. For a case of high-energy incident electrons, both direct and exchange amplitudes are evaluated, representing the Coulomb waves by the corresponding plane waves. An error made in the previous work is found and corrected. The results are then compared and found to be in disagreement with the forward peaking of the cross sections for the excitation of the triplet states observed by Vrien et al. (auth)

**55844** INTERFERENCE EFFECT IN THE CROSS SECTION FOR THE CHARGE EXCHANGE OF $Li^+$ IONS WITH He ATOMS. Latypov, Z. Z.; Shaporenko, A. A. (Ioffe Inst. of Physics and Tech., Leningrad). JETP Lett. (USSR) (Engl. Transl.); 13: No. 10, 375-6(20 May 1971).

Translated from Zh. Eksp. Teor. Fiz., Pis'ma Red.; 13: No. 10, 525-7(20 May 1971).

Cross sections of the charge-exchange process $Li^+ + He \rightarrow Li + He^+$ were measured in the collision-energy interval 600 to 2800 eV. Results show that the cross section oscillates regularly as a function of the collision velocity. Comparison with other results indicates that the oscillation is due to interaction of the term of the charge-exchange channel with the term of an excitation channel at an internuclear distance of about 9 au. (A.G.W.)

**55845** CHARGE-CHANGING PROCESSES FOR HELIUM BEAM INVOLVING METASTABLE ATOMS IN MOLECULAR HYDROGEN. Tawara, Hiroyuki (Kyushu Univ., Fukuoka). J. Phys. Soc. Jap.; 31: No. 3, 871-8(Sep 1971).

The cross sections for one-electron stripping from ground-state and metastable helium atoms in molecular hydrogen gas were measured in the energy range from 14 to 50 keV using the beam-attenuation technique developed by Gilbody et al. The fraction of the metastable atoms in the neutral helium beam after traversing a thin hydrogen gas was also determined; from this the cross sections for one-electron capture by singly charged helium ions resulting in ground-state and metastable helium atoms were estimated. The present results are in good agreement with previous experimental data and calculations by Bates et al. (auth)

**55846** APPROXIMATE EVALUATION OF THE RELATIVISTIC CORRECTION IN POTENTIAL SCATTERING OF CHARGED PARTICLES. Chraplyvy, Z. V. (St. Louis Univ.). J. Phys., B (London); 4: No. 8, 995-1007(Aug 1971).

In solving the relativistic scattering problem by the method of Sommerfeld and Maue (suitably iterated Dirac equation, expansion in powers of Z/137) an approximate scattering wave function in coordinate space is usually first obtained, from which the scattering amplitude is then extracted. An alternative method is based on the Sommerfeld–Maue Hamiltonian, but working in momentum space and aimed directly at the T-matrix. To the first order in the expansion parameter it yields simple formulae, which should prove useful for numerical computations. (auth) (UK)

**55847** ENERGY DISTRIBUTIONS OF ELECTRONS EJECTED IN IONIZING COLLISIONS OF ELECTRONS WITH HELIUM. Peterson, W. K.; Opal, C. B.; Beaty, E. C. (Univ. of Colorado, Boulder). J. Phys., B (London); 4: No. 8, 1020-5(Aug 1971).

Measurements of energy and angular distributions of electrons ejected from helium by 100- to 2000-eV electrons are reported. The results are integrated over angle to give secondary-electron energy distributions, which are compared with recent Born-approximation calculations. The Born exchange approximation represents the 100-eV data surprisingly well. (auth) (UK)

**55848** ROTATIONAL COUPLING EFFECTS ON DIFFERENTIAL ELASTIC AND INELASTIC CROSS SECTIONS IN $He^+$–He COLLISIONS. McCarroll, R.; Piacentini, R. D. (Observatoire de Paris, Meudon, France). J. Phys., B (London); 4: No. 8, 1026-39(Aug 1971).

The $He^+$–He collision is investigated using a molecular expansion that takes account of rotational coupling between the $^2\Sigma_u$ and $^2\Pi_u$ states and between the $^2\Sigma_g$, $^2\Pi_g$, and $^2\Delta_g$ states of the $He_2^+$ quasi molecule. Differential cross sections for elastic scattering, resonant charge transfer, and direct and exchange excitation of $He(1s,2p)^{1,3}P$, $He^+(2p)$ and of the autoionizing state $He(2p^2)^1S$, $^1D$ were computed for a range of energies from 300 eV to 1.5 keV and for a range of scattering angles from 0 to 24° (in center-of-mass system). The agreement with experiment is satisfactory. For $E\theta \gtrsim 3$ keV deg, it is seen that rotational coupling is the dominant mechanism for the excitation of inelastic transitions. The consequences with respect to the determination of potential energy curves from scattering data are briefly discussed. (auth) (UK)

**55849** A QUASI-DIABATIC REPRESENTATION FOR INELASTIC COLLISIONS. APPLICATION TO THE SCATTERING OF $He^+$ BY Ne. Sidis, V.; Lefebvre-Brion, H. (Centre de Mecanique Ondulatoire Appliquee, Paris). J. Phys., B (London); 4: No. 8, 1040-54(Aug 1971).

A "quasi-diabatic" representation based on LCAO–MO–SCF electronic wave functions, satisfying to a large extent Lichten's original suggestion and Smith's theoretical definition for diabatic states, is introduced. Potential-energy curves of the $HeNe^+$ molecular ion were obtained in this framework and subsequently used in computing differential cross sections for the inelastic scattering of $He^+$ by Ne in the Landau–Zener two-states approximation. The shape and the location of the crossings of the potential–energy curves agree with the experimental predictions of Coffey et al. (1969) and Baudon et al. (1970). The transition matrix element at

XUM

the outer crossing is calculated as an electrostatic interaction term and the value obtained is 0.26 eV. Some arguments are presented which suggest that the experimental values are overestimated. (auth) (UK)

**55850** COMPARISONS OF THE GLAUBER AND VAINSHTEIN APPROXIMATIONS FOR INELASTIC ELECTRON–HYDROGEN SCATTERING. Sheorey, V. B.; Gerjouy, E.; Thomas, B. K. (Univ. of Windsor, Ont.). J. Phys., B (London); 4: No. 8, L57-61(Aug 1971).

Total cross sections for the 1s–2p excitation of atomic hydrogen by electron impact, calculated in the Glauber approximation, are compared with the predictions of the various forms of the Vainshtein approximation. (auth)

**55851** RESONANCE PHENOMENA IN THE LOW-ENERGY-ELECTRON-IMPACT EXCITATION OF HELIUM BY A TRAPPED-ELECTRON METHOD. Reinhardt, J.; Hall, R. I.; Joyez, G.; Mazeau, J. (Univ., Paris). J. Phys., B (London); 4: No. 8, L61-5(Aug 1971).

A trapped-electron experiment is used to observe resonance phenomena in the electron-impact excitation of helium. For precise collision-chamber conditions, very sharp and complex structure is observed, which correlates well with the known series of resonances in the 19.8- to 22-eV energy range. (auth)

**55852** NONSPHERICAL POTENTIALS AND MOLECULAR SCATTERING AT THERMAL ENERGIES: NITROGEN AND THE NOBLE GASES. Cavillini, M.; Dondi, M. G.; Scoles, G.; Valbusa, U. (Univ., Genoa). Chem. Phys. Lett.; 10: No. 1, 22-4(1 Jul 1971).

High-resolution differential collision cross-section measurements for the systems $N_2$–Ar, $N_2$–Kr, and $N_2$–$N_2$ are presented and compared with equal resolution Ar–Ar data. The quenching of the amplitude of the rainbow oscillation in the cross section is consistent with theoretical predictions. (auth)

**55853** ELECTRON CAPTURE INTO THE n = 2 LEVELS OF HYDROGEN BY PROTONS PASSING THROUGH GAS TARGETS. Stokes, Everett Donald. Fayetteville, Ark.; Univ. of Arkansas (1971). 120p. University Microfilms Order No. 71-19,549.

Thesis.

Relative cross sections for electron capture into the n = 2 states of H were measured for 20- to 120-keV protons incident upon He, Ne, Ar, $N_2$, and $O_2$. Measurements were also made for capture into the 2s state using $H_2$ as the target gas. The cross sections were placed on an absolute basis by normalization to previous measurements. Above 50 keV the energy dependence of the 2s capture cross sections was found to be similar to the energy dependence of the 3s and 4s capture cross sections. At 100 keV the 2s cross sections averaged 5.6% higher than an $n^{-3}$ scaling of the 3s cross sections would indicate. Within experimental error the energy dependences for the 2p and 3p cross sections above 50 keV were the same for all gases except He. (Diss. Abstr. Int., B)

**55854** ALGEBRAIC CLOSE-COUPLING APPROACH TO ELECTRON–HYDROGEN SCATTERING. Seiler, George Joseph. Baton Rouge, La.; Louisiana State Univ. and Agricultural and Mechanical Coll. (1971). 131p. University Microfilms Order No. 71-20,623.

Thesis.

The algebraic close-coupling method is applied to slow collisions of electrons and positrons with atomic hydrogen. The wave function is assumed to be of the form appropriate for a 1s–2s–2p close-coupling calculation. The anomaly-free variational method proposed by Nesbet, essentially algebraic in nature, is used to calculate the appropriate phase shifts and cross sections. Excellent agreement with previously published results of Burke, Schey, Smith, and others is obtained for scattering below the n = 2 threshold. Valuable information concerning resonance structure for positrons, and for electrons in the singlet and triplet states, is also obtained. A 1s–2s approximation produces results in excellent agreement with the two-state approximation of Burke, Schey, and Smith for both the elastic and the inelastic cross sections. In the 3-state approximation above threshold, asymptotic forms of the type $j_l(1-e^{\gamma r})^{2l+1}$ and $n_l(1-e^{-\beta r})^{2l+1}$ are used, where $j_l$ and $n_l$ are spherical Bessel and Neumann functions, and $\beta$ and $\gamma$ are adjustable variational parameters. A solution is said to have converged when it is stable both with respect to variations of the parameters $\beta$ and $\gamma$ and with respect to an increase of the basis states. Because of the long-range effect of the $1/r^2$ potential that arises from the coupling of the degenerate 2s and 2p states, the spherical Bessel and Neumann functions are not the correct asymptotic solutions for the 2p channel. This effect is brought out in the 3-state calculation above the threshold and is fully discussed in this dissertation. Finally, the correct asymptotic forms are discussed. (Diss. Abstr. Int., B)

**55855** LOW ENERGY ELECTRON–MOLECULE SCATTERING EXPERIMENTS AND THE THEORY OF ROTATIONAL EXCITATION. Golden, D. E. (Univ. of Nebraska, Lincoln); Lane, Neal F.; Temkin, A.; Gerjuoy, E. Rev. Mod Phys.; 43: No. 4, 642-78 (Oct 1971).

The various experimental techniques used to obtain differential, total, and momentum-transfer electron–molecule scattering cross sections at low electron energies are reviewed, and observations are compared with theory, especially with theoretical calculations of rotational excitation cross sections for slow electrons incident on homonuclear diatomic molecules. A detailed discussion of the theory of rotational excitation by slow electrons is given, with particular attention to the merits and deficiencies of recent attempts to improve on the lowest-order Born approximation predictions, via the so-called rotational close coupling and adiabatic-nuclei approximations. (auth)

**55856** TOTAL ELECTRON–ATOM COLLISION CROSS SECTIONS AT LOW ENERGIES: A CRITICAL REVIEW. Bederson, Benjamin (New York Univ., N. Y.); Kieffer, L. J. Rev. Mod. Phys.; 43: No. 4, 601-41(Oct 1971).

Experiments relating to measurements of total and momentum-transfer cross sections for the scattering of low-energy electrons by atoms and diatomic molecules are critically reviewed. Principal emphasis is placed upon the Ramsauer method, dc swarms, and crossed-beams experiments, which account for the bulk of the reliable data in the literature although other techniques including differential measurements are also discussed. The theories of the various methods and possible sources of error are discussed. The case of low-energy electron scattering by helium is exhaustively reviewed since this system has been most intensively studied experimentally and is particularly amenable as well to theoretical calculations. The best available cross-section values, along with comments on individual experiments, are presented in several tables. (auth)

**55857** KINETIC ENERGIES OF PROTONS FORMED DURING THE COLLISION OF ELECTRONS WITH VIBRATIONALLY EXCITED HYDROGEN MOLECULES. Vinogradov, P. S.; Karachevtsev, G. V. (Physical-Technical Inst., Moscow). High Energy Chem. (USSR) (Engl. Transl.); 4: No. 5, 415-16(Sep-Oct 1970).

Translated from Khim. Vys. Energ.; 4: No. 5, 463-4(Sep-Oct 1970).

The reflection method was used for calculation of the kinetic-energy distribution of fragment ions formed as a result of collisions of an electron with a hydrogen molecule at various vibrational levels of the electronic ground state. Two processes were examined: $e^- + H_2 \rightarrow H + H^+ + 2e^-$ and $e^- + H_2 \rightarrow 2H^+ + 3e^-$. Figures show results for vibrational states v = 0 through 5 for the first process and for v = 1, 2, and 3 for the second process. (A.G.W.)

**55858** DISSOCIATION OF $D_2^+$ AND $H_2^+$ IONS WITH ENERGIES UP TO 100 eV IN COLLISIONS WITH $D_2$, He, AND Ne. Zhurkin, E. S.; Tikhomirov, M. V.; Tunitskii, N. N. (Inst. of Physical Chemistry, Moscow). Sov. Phys.-Tech. Phys. (Engl. Transl.); 16: No. 3, 495-6(Sep 1971).

Translated from Zh. Tekh. Fiz.; 41: No. 3, 636-8(Mar 1971).

The following processes were investigated for kinetic energies from threshold to 100 eV: (1) $D_2^+(D_2) + D_2 \rightarrow D^+ + D + D_2$, (2) $D_2^+(D_2) + He \rightarrow D^+ + D + He$, (3) $D_2^+(D_2) + Ne \rightarrow D^+ + D + Ne$, (4) $D_2^+(CD_4) + Ne \rightarrow D^+ + D + Ne$, (5) $H_2^+(H_2) + He \rightarrow H^+ + H + He$, and (6) $H_2^+(H_2) + Ne \rightarrow H^+ + H + Ne$, where the symbols in parentheses indicate the materials from which $D_2^+$ or $H_2^+$ ions were obtained by electron impact. The dissociation cross sections for $D_2^+$ were found to be independent of kinetic energy in the range 20 to 100 eV. In this region the cross sections for the $D_2^+$ processes were estimated to be $\sigma_1 = 0.66 \times 10^{-16}$ cm$^2$, $\sigma_2 = 0.47 \times 10^{-16}$ cm$^2$, $\sigma_3 = 0.61 \times 10^{-16}$ cm$^2$, and $\sigma_4 = 3.7 \times 10^{-16}$ cm$^2$. A direct-expulsion model proposed previously gives a qualitative explanation of the results for both ions. (A.G.W.)

**55859** CHARGE TRANSFER IN $Na^+$–$O^-$ COLLISIONS AT LOW RELATIVE ENERGY. Weiner, John; Peatman, William B.; Berry, R. Stephen (Univ. of Chicago). Phys. Rev., A; 4: No. 5, 1824-35(Nov 1971).

Total cross sections were measured for electron transfer from $O^-$ to $Na^+$, resulting in optically allowed transitions to $Na(^2S)$ ground state. A merged-beam technique was used to study the collisions in the energy range 0.1 to 7 eV. Structure in the curves of cross sections vs relative energy indicates that the excitation of oxygen plays an important role in the charge-transfer process. Cross sections for an endoergic process giving Na(4p) are of

XUM

order $10^{-14}$ cm$^2$; cross sections for the exoergic processes leading to production of Na(3d) and Na(3p) are of order $10^{-13}$ cm$^2$. Production of Na(3d) is nearly a resonant process; production of Na(3p) is apparently due to a cascade from Na(3d). (auth)

**55860** FURTHER CALCULATIONS OF s-WAVE ELASTIC e–H SCATTERING ABOVE THE IONIZATION THRESHOLD BY THE COMPLEX-ENERGY METHOD. McDonald, F. A. (Southern Methodist Univ., Dallas); Nuttall, J. Phys. Rev., A; 4: No. 5, 1821-4(Nov 1971).

The method of extrapolation from complex energies is used to calculated s-wave electron–hydrogen-atom elastic scattering from the ground state at energies in the region ranging from 1.21 to 2.25 Ry. (auth)

**55861** SEARCH PROCEDURE FOR MULTICHANNEL RESONANCES IN ELECTRON–ATOM SCATTERING. Nesbet, R. K.; Lyons, J. D. (IBM Research Lab., San Jose, Calif.). Phys. Rev., A; 4: No. 5, 1812-20(Nov 1971).

A general computational procedure is described for locating electron–atom scattering resonances and for computing accurate values of the resonance parameters (eigenchannel vector, energy, width, and background eigenphase). The procedure makes use of the anomaly-free multichannel variational method and of the hierarchical continuum Bethe–Goldstone formalism published previously. Eigenvalues of the electronic Hamiltonian in a variational Hilbert space are located by an accurate procedure that takes advantage of analytic properties of the matrices constructed in a variational phase-shift calculation. Without computing the Hilbert space eigenvector, effective bound–free matrix elements for a resonance are computed from residues of matrix elements that have poles at the Hilbert space eigenvalues. Each eigenvalue associated with a resonance defines an initial approximation to the resonance parameters, which are then refined by an iterative process that uses variational calculations of the eigenphases. The proposed method combines the ability of stabilization methods to locate narrow resonances with an accurate computation of phase shifts in the resonant region. Calculations of electron–hydrogen resonances are given as examples of the method. (auth)

**55862** ELECTRON CAPTURE BY 40-, 155-, AND 600-MeV PROTONS IN THIN FOILS OF MYLAR, Al, Ni, AND Ta. Raisbeck, G.; Yiou, F. (Centre National de la Recherche Scientifique, orsay, France). Phys. Rev., A; 4: No. 5, 1858-68(Nov 1971).

The charge-exchange process was studied at much higher energies than previously examined. Equilibrium charge distributions were measured in foils of Mylar, Al, Ni, and Ta for protons of 155 and 600 MeV and deuterons of 80 MeV. Estimates are made for the loss cross sections $\sigma_l$, and the resulting capture cross sections $\sigma_c$ are compared with theoretical expectations. Up to 155 MeV, $\sigma_c$ can be reasonably well accounted for by the nonradiative capture process. Above this energy there are significant departures from this simple behavior, which are consistent with the predicted onset of radiative capture. However, because of possible relativistic effects, such an interpretation is not certain. The present data suggest several interesting areas for future theoretical and experimental study. (auth)

**55863** QUANTUM THEORY OF (H,$H_2$) SCATTERING: APPROXIMATE TREATMENTS OF REACTIVE SCATTERING. Tang, K. T. (Columbia Univ., N. Y. Pacific Lutheran Univ., Tacoma, Wash.); Karplus, M. Phys. Rev., A; 4: No. 5, 1844-58(Nov 1971).

A quantum-mechanical study is made of reactive scattering in the (H, $H_2$) system. The problem is formulated in terms of a form of the distorted-wave Born approximation (DWBA) suitable for collisions in which all particles have finite mass. For certain incident energies, differential and total cross sections, as well as other attributes of the reactive collisions, (e.g., the reaction configuration) are determined. Two limiting models in the DWBA formulation are compared; in one, the molecule is unperturbed by the incoming atom, and in the other, the molecule adiabatically follows the incoming atom. For thermal incident energies and the semiempirical interaction potential employed, the adiabatic model seems to be more appropriate. Since the DWBA method is too complicated for a general study of the (H, $H_2$) reaction, a much simpler approximation method, the "linear model," is developed. This model is very different in concept from treatments in which the three atoms are constrained to move on a line throughout the collision. The present model includes the full three-dimensional aspect of the collision, and it is only the evaluation of the transition matrix element itself that is simplified. It is found that the linear model, when appropriately normalized, gives results in good agreement with that of the DWBA method. By application of this model, the energy dependence, rotational-state dependence, and other properties of the total and differential reaction cross sections are determined. These results of the quantum-mechanical treatment are compared with the classical calculation for the same potential surface. The most important result is that, in agreement with the classical treatment, the differential cross sections are strongly backward peaked at low energies and shift toward the forward direction as the energy increases. Finally, the implications of the present calculations for a theory of chemical kinetics are discussed. (auth)

**55864** ELECTRON-IMPACT EXCITATION OF LITHIUM. Tripathi, A. N.; Mathur, K. C.; Joshi, S. K. (Univ. of Roorkee, India). Phys. Rev., A; 4: No. 5, 1873-5(Nov 1971).

Electron-impact excitation cross sections for the resonant transition (2s–2p) in the lithium atom were calculated by use of the Born approximation for incident energies up to 60 eV. The polarization of the target atom caused by the incident charged particle is considered by modifying the target wave function. The exchange was also included via the Ochkur approximation. The cross sections obtained here are compared with the other theoretical calculations and the experimental data. (auth)

**55865** CLASSICAL LIMIT OF THE BINARY-COLLISION EXPANSION. Gibson, W. G. (Univ. of Sydney). Phys. Rev., A; 4: No. 5, 2108-9(Nov 1971).

It is shown that the classical form of the binary-collision expansion follows naturally from the multiple-scattering expansion for the T matrix. The limits of applicability of this classical expansion are discussed. (auth)

**55866** MULTIPLE-SCATTERING EXPANSIONS FOR NONRELATIVISTIC THREE-BODY COLLISION PROBLEMS. V. AN OFF-SHELL APPROACH TO THE FADDEEV–WATSON EXPANSIONS. Chen, Joseph C. Y. (Univ. of California, San Diego, La Jolla). Phys. Rev., A; 4: No. 5, 2012-19(Nov 1971).

Explicit relations between the on-shell three-body scattering and rearrangement-collision amplitudes are given. It is shown that the off-shell approach to the determination of the on-shell amplitudes is equivalent to the conventional method of taking on-shell matrix elements. As an example, the bare-potential term of the Faddeev–Watson multiple-scattering expansion for rearrangement collisions is evaluated using the two alternative approaches. (auth)

**55867** MULTIPLE-SCATTERING EXPANSIONS FOR NONRELATIVISTIC THREE-BODY COLLISION PROBLEMS. IV. APPLICATION OF THE FADDEEV–WATSON EXPANSION TO SCATTERING PROCESSES. Chen, Augustin C. (Univ. of California, San Diego, La Jolla); Chen, Joseph C. Y.; Sinfailam, A. -L.; Hambro, Lars. Phys. Rev., A; 4: No. 5, 1998-2012(Nov 1971).

The high-energy limit of the differential scattering cross section, according to the exact Born approximation, can have either an $E^{-2}$ or an $E^{-6}$ energy dependence, depending on the scattering angle and masses of the system. When the target is made of equal-mass particles having charges that are equal but opposite in sign, the first-order Born approximation predicts a zero for the elastic scattering amplitude. This anomalous behavior does not appear in the first-order Faddeev–Watson multiple-scattering approximation. An application of the first-order Faddeev–Watson multiple-scattering approximation to a three-body Coulomb system with arbitrary masses is considered. The three-body scattering amplitude is derived and expressed in terms of an integral consisting of contributions coming from (a) the two-body bound-state poles in the initial and final wave functions, (b) the branch-point singularities in the off-shell two-body Coulomb T matrices, and (c) the intermediate two-body bound- and antibound-state poles. (auth)

**55868** MULTIPLE-SCATTERING EXPANSIONS FOR NONRELATIVISTIC THREE-BODY COLLISION PROBLEMS. III. COMMENTS ON THE COULOMB T MATRIX AND THE APPLICATION OF THE FADDEEV–WATSON EXPANSION TO REARRANGEMENT COLLISION. Chen, Joseph C. Y.; Chen, Augustine C.; Kramer, Paul J. (Univ. of California, San Diego, La Jolla). Phys. Rev., A; 4: No. 5, 1982-98(Nov 1971).

An application of the Faddeev–Watson multiple-scattering expansion for rearrangement collision to an arbitrary three-body Coulomb system is presented. The importance of the Coulomb cuts on the energy shell is emphasized. A demonstration of how the second-order Born term and the truncated second-order multiple-scattering term considered by Carpenter and Tuan get canceled out in the second-order multiple-scattering term is given. It is then clear that considerable problems remain in the determination of the high-energy behavior of the cross section for rearrangement collisions. A number of errors that have recently appeared in the literature concerning the treatment of the branch-point singularities and the intermediate two-body bound- and antibound-state poles in the off-shell two-body Coulomb T matrix are rectified. Detailed expressions for the

XUM

three-body rearrangement-collision amplitude in the first-order multiple-scattering approximation are derived and expressed as a sum of three contributions coming from (a) the bound-state poles in the initial and final wave functions, (b) the intermediate two-body antibound-state poles, and (c) the branch-point singularities in the off-shell two-body Coulomb T matrix. (auth)

**55869** ELECTRON-CAPTURE PROCESSES OF 10- TO 40-MeV OXYGEN IONS IN HELIUM, NITROGEN, AND ARGON. Martin, F. W. (Univ. of Aarhus, Denmark); Macdonald, J. R. Phys. Rev., A; 4: No. 5, 1974-81(Nov 1971).

Experimental data on electron-capture cross sections are analyzed in order to obtain the cross sections for removal of n given atomic electrons, where n = 1, 2, or 3. Probabilities of capture averaged over certain regions of impact parameter are obtained from ratios of these cross sections. Maxima are found in the capture probabilities for +8 oxygen ions in helium and for +8 and +7 ions in nitrogen and argon. No maxima are found for ions of lower charge. The large cross sections at high velocities in nitrogen and argon are attributed to capture from the K shell of nitrogen and the L shell of argon, which contain electrons with momenta great enough to satisfy conservation requirements. The larger cross sections for +8 ions and the maxima in capture probability are attributed to exoergic capture from atomic energy levels into the deeply bound K shell of the oxygen +8 ion. A criterion based on an atomic-orbital theory is given for the velocity at which maxima due to exoergic capture should occur, and this is in rough agreement with the observed velocities. Electron-capture cross sections from atoms with tightly bound shells can generally be expected to be large for heavy ions even at velocities greater than $10^9$ cm/sec. (auth)

**55870** EXPERIMENTAL ELECTRON-TRANSFER CROSS SECTIONS FOR COLLISIONS OF OXYGEN IONS IN ARGON, NITROGEN, AND HELIUM AT ENERGIES OF 7 TO 40 MeV. Macdonald, J. R. (Niels Bohr Inst., Copenhagen); Martin, F. W. Phys. Rev., A; 4: No. 5, 1965-74(Nov 1971).

In the energy range 7 to 40 MeV, electron-capture and electron-loss cross sections were determined for incident oxygen ions of charges +2 to +8 passing through argon, nitrogen, and helium. Thin-target conditions were used in all cases. The analysis technique used to extract the cross sections allows relative cross sections to be obtained without consideration of the measurement of the gas target thickness. Multiple-transfer cross sections can thereby be determined reliably in the presence of cross sections three orders of magnitude greater. Double, triple, and quadruple transfers were observed. The electron-loss cross sections appear to pass through maxima when the velocity of the ion is in the vicinity of the velocity of the electron to be lost. Single-electron-capture cross sections have magnitudes as large as $10^{-17}$ cm$^2$ at 40 MeV in argon and depend on velocity approximately as $V^{-n}$, where n lies between 3 and 6 for the heavy gases. The importance of capture from inner shells of the heavy gases is inferred by comparison with helium, in which n is 8 or 9 and the cross sections are relatively small. The possibility of capture into the K shell of the oxygen ion is suggested by the systematic differences observed in capture by +7 and +8 oxygen ions from capture by ions of lower charge. (auth)

**55871** STUDY OF THE POLARIZED-ORBITAL METHOD AND ITS APPLICATION TO THE SCATTERING OF ELECTRONS BY HELIUM. Duxler, William M. (Univ. of California, Riverside); Poe, Robert T.; LaBahn, R. W. Phys. Rev., A; 4: No. 5, 1935-44(Nov 1971).

A study was made of the polarized-orbital method (POM) for electron–atom scattering. Within this framework, an exact calculation was carried out for the electron–helium–atom case. This study confirms the importance of the second-order distortion-exchange terms, which provide a nonadiabatic effect. A study is made of the much-criticized step function, and its inclusion within the POM framework is found to be not crucial. An attempt is made to clear up some of the present confusion in the literature by distinguishing between the POM and related methods. (auth)

**55872** DISSOCIATION CROSS SECTIONS FOR 0.5- TO 1-MeV $HeH^+$ IONS IN $H_2$, He, $N_2$, AND Ne GASES. Stearns, J. Warren (Univ. of California, Berkeley); Berkner, Klaus H.; Pyle, Robert V.; Briegleb, Bruce P.; Warren, M. Laird. Phys. Rev., A; 4: No. 5, 1960-4(Nov 1971).

The cross sections for the dissociation modes $^4He^1H^+ \rightarrow He^0 + H^0$, $He^0 + H^+$, $He^+ + H^0$, $He^+ + H^+$, $He^{++} + H^0$, or $He^{++} + H^+$ are reported for the $HeH^+$ energy range of 0.5 to 1 MeV in the target gases $H_2$, He, $N_2$, and Ne. Comparisons are made with available previous measurements. (auth)

**55873** ROTATIONALLY INDUCED TRANSITIONS IN ATOMIC COLLISIONS. Russek, A. (Univ. of Connecticut, Storrs). Phys. Rev., A; 4: No. 5, 1918-24(Nov 1971).

Excitation effects due to rotational motion of the internuclear line during an atomic collision are considered in the two-state approximation. These effects are governed by a pair of first-order differential equations coupling adiabatic levels of different angular momentum (e.g., $\sigma$ to $\pi$ transitions) that actually do cross. The equations are cast in such a form that the solution for rotational excitation may be expressed in terms of the well-known Landau–Zener solution. It is found, however, that application of these results to a real collision suffers from defects that are worse for the case of rotational excitation than for ordinary Landau–Zener transitions. The coupled differential equations are then solved numerically to document the shortcomings of the Landau–Zener approach to a real collision and to present cross-section results that are free from these defects. (auth)

**55874** EXCITATION OF ATOMIC HYDROGEN AND HELIUM IN THE EIKONAL APPROXIMATION. Byron, F. W. Jr. (Univ. of Massachusetts, Amherst). Phys. Rev., A; 4: No. 5, 1907-17(Nov 1971).

Some of the key approximations involved in the application of the eikonal method to atomic physics are analyzed, and the method is related to the close-coupling approach. The importance of an accurate treatment of kinematics is stressed, and a Monte Carlo integration technique is used to facilitate the application of eikonal equations without simplifying kinematical assumptions. Results are presented on the excitation of the $2^1P$ state of helium by electron impact, on the excitation of the 2p state of atomic hydrogen by electron impact, and on the excitation of the 2s state of hydrogen by electron and positron (or proton) impact. Detailed comparison with experiment is made wherever possible. (auth)

**55875** MULTIPHOTON PROCESSES IN A HYDROGEN ATOM. Gontier, Y.; Trahin, M. (CEN de Saclay, Gif-sur-Yvette, France). Phys. Rev., A; 4: No. 5, 1896-1906(Nov 1971).

Within the framework of time-dependent perturbation theory, general expressions are derived for the cross section of multiphoton processes induced by radiation acting on a hydrogen atom. Bound–bound transitions involving emission of a single quantum and bound–free transitions are calculated for a wide range of photon energies. In the case of resonance, the transition probability is also discussed. The procedure used to evaluate the sums over intermediate states is described. The numerical computation allows one to compare the results obtained for various competing processes. (auth)

**55876** UPPER AND LOWER BOUNDS FOR THREE-BODY SCATTERING. Payne, George (Wisconsin State Univ., Oshkosh). Phys. Rev., A; 4: No. 5, 1892-5(Nov 1971).

Upper and lower bounds for three-body scattering are studied using Hilbert-space results previously obtained. The evaluation of the bounds entails using a set of basis functions to approximate the exact wave function and requires a lower bound to an associated eigenvalue problem. The present Hilbert-space results yield the lower bound without additional calculations when the set of basis functions can adequately approximate the exact wave function. These bounds do not require knowledge of any bound state and indeed show how a trial bound-state wave function should be determined to minimize the error in a particle bound-state scattering process. Both one-channel and two-channel processes are treated. (auth)

**55877** FORCING CONSERVATION OF PARTICLE FLUX IN PERTURBATION-THEORY CALCULATIONS OF INELASTIC SCATTERING. Truhlar, Donald G. (Univ. of Minnesota, Minneapolis). Phys. Rev., A; 4: No. 5, 1886-91(Nov 1971).

Two approximations to Seaton's unitarization scheme are described which make it possible to impose the conservation-of-particle-flux requirements on an approximate calculation of inelastic scattering without making calculations of elastic scattering in the two channels that the transition connects. One approximation is based on the black-sphere model of Feshbach and Weisskopf. Another approximation corrects only for back coupling and can be equivalent to a method of Levine. The methods are illustrated by applying them to the Born approximation for the 1s–2s excitation of the hydrogen atom by electron impact. (auth)

**55878** QUASI-MINIMUM PRINCIPLE FOR MULTICHANNEL SCATTERING. Hahn, Yukap (Univ. of Connecticut, Storrs). Phys. Rev., A; 4: No. 5, 1881-6(Nov 1971).

A new variational principle for multichannel scattering is derived, which combines certain simplifying features of both Kohn and minimum principles. The rigorous bound property of the latter is relaxed slightly to gain simplifications and effi-

XUM

ciency, especially for collisions involving particle rearrangements. The approach is essentially equivalent to treating variationally the open-channel part of the wave function, rather than solving for it exactly as required by the minimum principle. However, variations of parameters for the open and closed channels are carried out separately using a double functional. (auth)

**55879** COLLISIONAL DISSOCIATIVE IONIZATION OF TlBr BY ACCELERATED Xe AND Kr ATOMS. Parks, E. K.; Wexler, S. (Argonne National Lab., Ill.). Chem. Phys. Lett.; 10: No. 3, 245-50(1 Aug 1971).

Ionization processes in collisions of thallium bromide and aerodynamically accelerated xenon and krypton were studied by the crossed-beam method. Absolute cross sections for positive-ion production were measured. Mass spectrometric analysis revealed that the positively charged products consisted of $Tl^+$, $TlXe^+$ (no $TlKr^+$ was observed), and $Tl_2Br^+$, whose relative yields varied with the relative energies of the colliding beams. (auth)

**55880** DEPENDENCE OF GENERALIZED OSCILLATOR STRENGTHS OF $H_2O$ ON MOMENTUM TRANSFER. Mielczarek, S. R. (National Bureau of Standards, Washington, D. C.); Miller, K. J. Chem. Phys. Lett.; 10: No. 4, 369-70(15 Aug 1971).

Experimental results on the dependence of generalized oscillator strengths of water on momentum transfer, showing the appearance of extrema and characteristic features in the electron scattering spectra, are reported and discussed. (auth)

**55881** FORCED COMMON TURNING-POINT PROCEDURE AND EXCITATION IN SLOW $H^+$–H(1s) COLLISIONS. Bates, D. R.; Sprevak, D. (Queen's Univ., Belfast). Chem. Phys. Lett.; 10: No. 4, 428-9(15 Aug 1971).

It is found that the forced common turning-point procedure is satisfactory for treating the excitation of hydrogen atoms by slow protons even at an energy of relative motion as low as 30 eV. (auth)

## Atomic Theory

*Refer also to abstracts 56387, 56397, and 56848.*

**55882** (NYO–1447-64) LIE GROUPS IN ATOMIC SPECTROSCOPY. Judd, B. R. (Johns Hopkins Univ., Baltimore, Md. Dept. of Physics). [1970]. 16p. (CONF-710914-1). Dep. NTIS.

From fifteenth Solvay conference; Brussels, Belgium (Sep 1971).

The role of Lie groups in atomic spectroscopy is surveyed in a general way. The actual usefulness of Lie groups in treating problems of direct physical significance and also those features whose main attraction seems to lie exclusively in the mathematics are described. (A.G.W.)

**55883** QUANTUM THEORY OF SPONTANEOUS EMISSION IN THE PRESENCE OF EXTERNAL RADIATION. Bose, R. (Univ. of Maryland, College Park); White, J. A. Nuovo Cim.; 5B: No. 1, 11-20(11 Sep 1971).

The theory of Weisskopf and Wigner is extended to describe the modifications of spontaneous emission that occur when atoms or molecules emit radiation spontaneously, while simultaneously undergoing stimulated emissions or absorptions. The theory is developed generally for radiation present initially at or off resonance. It is illustrated for the simple case that decay quanta are emitted spontaneously parallel or antiparallel to the direction of propagation of radiation causing stimulated transitions. Spectral-line profiles calculated for this case are shown in appropriate limits to agree with the results of previous theories and experiment. General theoretical procedures and explicit expressions are developed for a variety of more complex situations that might reasonably be encountered in future experiments. (auth)

**55884** ENERGIES OF "s" EIGENSTATES IN A STATIC SCREENED COULOMB POTENTIAL. Lam, C. S.; Varshni, Y. P. (Univ. of Ottawa). Phys. Rev., A; 4: No. 5, 1875-81 (Nov 1971).

Energies of the 1s, 2s, 3s, and 4s states are obtained by a perturbation calculation and by a one-parameter variational calculation for a two-particle system interacting through a static screened Coulomb potential. The variational results are practically identical with those recently obtained by Rogers, Graboske, and Harwood by the numerical integration of the wave equation, except in the region very close to the critical screening. (auth)

**55885** MASTER-EQUATION APPROACH TO SPONTANEOUS EMISSION. III. MANY-BODY ASPECTS OF EMISSION FROM TWO-LEVEL ATOMS AND THE EFFECT OF INHOMOGENEOUS BROADENING. Agarwal, G. S. (Univ. of Rochester, N. Y.). Phys. Rev., A; 4: No. 5, 1791-1801(Nov 1971).

A general theory of spontaneous emission was developed in Papers I and II of this series. In the present paper, the master equation describing spontaneous emission from N identical two-level atoms is investigated further. It is shown that the equation of motion for the p(<N)-atom density matrix is coupled to the (p + 1)-atom density matrix. The initial excitation of the system to state $|\theta_0, \varphi_0|$ ($\theta_0 < \pi$) is first considered, and the hierarchy of equations so obtained is solved in the "uncorrelated approximation." It is found that the presence of other atoms is equivalent to an external field, which is determined from a self-consistent analysis. It is also found that in this approximation the state of the atom at time t can be described by a single parameter $\theta(t)$ ($\theta < \pi$), with $\sin^2 \frac{1}{2}\theta$ giving the probability that the atom is to be found in the excited state. Next, some improvements over the uncorrelated approximation are given. This is done by decoupling the equation of motion for higher-order mean values. It is found that the fluctuation $[(S_i^x - \langle S_i^x \rangle)(S_j^x - \langle S_j^x \rangle)]$ for any pair of atoms is of the order of 1/N. The case when $\theta_0 = \pi$ is considered separately and an expression for the radiation rate is obtained by making a "Hartree–Fock" type of approximation on the two-particle mean values. In this case, the behavior of the radiation rate is found to differ markedly from the "sech" behavior. It is then shown that the entire dynamics of two-level atoms emitting spontaneously can be described by a set of 2N coupled first-order equations that clearly exhibit the type of nonlinearity (which is the analog of the van der Pol type of nonlinearity) for this problem and provide a better understanding of spontaneous emission. Finally in Sec. V, the theory is extended to include the effects of inhomogeneous broadening, and the functional dependence of the radiation rate on the atomic-line-shape factor is obtained. (auth)

**55886** THEORY OF DECAYING STATES. More, R. M. (Univ. of Pittsburgh). Phys. Rev., A; 4: No. 5, 1782-90(Nov 1971).

A special perturbation theory that directly describes the alteration of decaying states by an external perturbation is constructed. The complex energies of the decaying states appear in this theory. When lifetime effects are taken into account, it is found that the criteria for quantum degeneracy are slightly strengthened and sharpened. The smooth merger of the properties of decaying states and those of true eigenstates in the case of long lifetimes is also discussed. (auth)

**55887** ROTATING-WAVE APPROXIMATION AND SPONTANEOUS EMISSION. Agarwal, G. S. (Univ. of Rochester, N. Y.). Phys. Rev., A; 4: No. 5, 1778-81(Nov 1971).

Spontaneous emission from two systems, namely, N identical harmonic oscillators and N identical two-level atoms, is studied without the use of the rotating-wave approximation. Certain new features of spontaneous emission, for instance, the dependence of the radiation rate on the initial dipole-moment phase, are discussed. (auth)

**55888** THEORY OF THE RADIATIVE AUGER EFFECT. Aberg, T. (Univ. of Chicago). Phys. Rev., A; 4: No. 5, 1735-40(Nov 1971).

The probability of simultaneous emission of an x-ray photon and an electron is considered. It is shown that this process can occur as a consequence of the change in the average potential acting on the electrons when the x-ray hole is moving from an inner to an outer shell (shake-off) and as a consequence of interaction between single- and double-hole configurations in the final state. Relative shake-off probabilities of $K \rightarrow L^2$, $K \rightarrow M^2$, and $L_{2,3} \rightarrow M_1M_{2,3}$ transitions are calculated for $F^-$, Ne, $Na^+$, $Cl^-$, Ar, and $K^+$ from Bagus's self-consistent-field wave functions of single-hole x-ray states. The relative probability of $K \rightarrow L^2$ and $K \rightarrow M^2$ transitions is estimated for the rest of the atoms in the range $9 \leq Z \leq 22$. The estimated $K \rightarrow L^2$ and $K \rightarrow M^2$ probabilities are of the same order of magnitude as the observed probabilities. However, for low Z, they overestimate the observed probabilities, which may be because the shake-off calculations do not account properly for the interaction between single- and double-hole configurations in the final state. (auth)

**55889** ATOMIC AND MOLECULAR WAVE FUNCTIONS. Moser, C. (Centre de Mecanique Ondulatoire Appliquee, Paris). pp G.1-7 of Computational Physics. Vols. I and II. London; Her Majesty's Stationery Office (1969).

From Conference on computational physics; Culham, England (28 Jul 1969). See CONF-690706–(Vols.1 and 2).

A brief review of recent developments in the calculation of atomic and molecular wave functions is presented, and some suggestions as to where future efforts might be most useful are given. (auth) (UK)

**55890** STUDIES OF TWO METHODS FOR CALCULATING ELECTRONIC CORRELATION ENERGIES. Raas, Eugene

Richard. University Park, Pa.; Pennsylvania State Univ. (1970). 120p. University Microfilms Order No. 71-21,791.
Thesis.

A Coulomb hole is introduced into the two-electron potential of the Hartree–Fock equations to eliminate the majority of the correlation energy. Justification for this is based on arguments about the intra-atomic scattering of electrons among themselves. An equation is derived to give the size of the Coulomb hole for each electron in the system which is dependent on properties of the system. The multiconfigurational self-consistent-field equations derived by Adams are converted to a form suitable for computation and used for several closed- and open-shell atomic systems. (Diss. Abstr. Int., B)

**55891** ERROR BOUNDS FOR APPROXIMATE RAYLEIGH–SCHROEDINGER PERTURBATION ENERGIES AND WAVE FUNCTIONS. Ahlrichs, R. (Univ., Karlsruhe, Ger.). Chem. Phys. Lett.; 10: No. 2, 157-61(15 Jul 1971).

Error bounds for approximately calculated nth-order wave functions and energies of the Rayleigh–Schrödinger perturbation expansion are derived. An alternative to the Hylleraas–Knight–Scherr variation technique is proposed, which is designed to keep the accumulation of errors as small as possible. (auth)

**55892** COMMENTS ON CONFIGURATION INTERACTION COMBINED WITH A CORRELATION FACTOR FOR TWO-ELECTRON ATOMS. Hultgren, G. O. (Battelle Memorial Inst., Columbus, Ohio); Kern, C. W. Chem. Phys. Lett.; 10: No. 2, 233-5(15 Jul 1971).

Comments are made on the helium-atom calculations reported by Grein and Tseng (Chem. Phys. Lett., 7: 506(1970)). (auth)

## Cosmic Radiation

*Refer also to abstracts 55046, 56403, 56413, 56414, 56429, 56469, and 56643.*

**55893** (AECL–3971) COSMIC RAY NM-64 NEUTRON MONITOR DATA. XVIII. Monthly Graphs, January 1971–April 1971. Steljes, J. F. (Atomic Energy of Canada Ltd., Chalk River (Ontario). Chalk River Nuclear Labs.). Jun 1971. 77p. Dep. NTIS (U. S. Sales Only). AECL $2,00.

Uncorrected and barometer-corrected results from the cosmic-ray stations in Canada using equipment maintained by AECL are given in tabular form for the period from January to April 1971. Normalized graphs are given for the same period. Correction factors for the constant rates of drift of the barometers at each of the four stations are given. A small flare increase occurred on January 24, 1971. (auth)

**55894** (LUIP-CR-71-4) ISOTOPE ANALYSIS WITH NUCLEAR EMULSIONS. Kristiansson, K. (Lund Univ. (Sweden). Dept. of Physics). Apr 1971. 19p. (CONF-710331-1). Dep. NTIS (U. S. Sales Only).

From Isotopic composition of cosmic ray nuclei conference; Lyngby, Denmark (23 Mar 1971).

The mass resolution that can be expected in measurements of cosmic-ray heavy particles in nuclear emulsion is discussed. The estimates of the errors are based on accurate measurements with nuclear track photometers of the relations between track width and residual range in tracks of beryllium, carbon, oxygen, neon, magnesium, and iron. It is found that satisfactory isotope resolution can be reached for nuclei in the charge region $3 \leq Z \leq 8$. The error in a mass determination in this region is smaller than $\frac{1}{2}$ atomic mass unit. The error in the region $10 \leq Z$ 16 amounts to about $\frac{1}{2}$ atomic mass unit and some uncertainty will arise in estimates of isotopic abundances in this element interval. The accuracy is at present insufficient for isotope analyses in the iron region. (auth) (Sweden)

**55895** (N–71-24988) CONSIDERATIONS RELATED TO THE SUDDEN RELEASE OF A LARGE NUMBER OF COSMIC RAYS IN THE GALAXY. Fichtel, Carl E. (National Aeronautics and Space Administration, Greenbelt, Md. Goddard Space Flight Center). Oct 1970. 18p. (NASA-TM-X-65506). NTIS.

The implications of a sudden release of a large number of cosmic rays as in a supernova burst are considered in the light of the conditions for containment of cosmic rays in the galactic disk. Reasons are given to show that a significant portion of the cosmic rays could be lost quickly (<10,000 years) after a burst, and the question of whether most of the cosmic rays remaining in the Galaxy ultimately escape as the result of pressure effects rather than diffusion effects is considered. In considering the question of a possible cosmic-ray anisotropy, it is noted that the high degree of isotropy observed could be the result of cosmic rays existing at what is effectively their density-saturated limit with no easy escape. Finally, it is pointed out that cosmic rays could be supplied to intergalactic space at a level substantially above that deduced from diffusion theory; this explains what was previously considered a possible high intergalactic electron flux. (auth) (STAR)

**55896** (N–71-27639) ISOTROPY OF THE COSMIC $\gamma$-RAY FLUX BETWEEN 1 AND 6 MeV AND ITS IMPLICATIONS FOR FUTURE $\gamma$-RAY INVESTIGATIONS. Stecker, F. W.; Vette, J. I.; Trombka, J. I. (National Aeronautics and Space Administration, Greenbelt, Md. Goddard Space Flight Center). May 1971. 14p. (NASA-TM-X-65562). NTIS.

The alternative hypotheses of galactic and extragalactic origin of the observed cosmic gamma-ray flux between 1 and 6 MeV are examined in the light of the most-recent spectral information on cosmic rays above 50 MeV. It is concluded that the present data on cosmic gamma rays are not consistent with 1- to 6-MeV gamma-ray spectra generated by diffuse galactic production processes. Thus, the 1- to 6-MeV flux is, in all likelihood, extragalactic. It is, therefore, a strong background upon which both galactic and extragalactic point sources in this energy region will be superimposed. This necessitates the use of high-angular-resolution gamma-ray telescopes in order to study possible discrete sources in the 1- to 15-MeV energy region. (auth) (STAR)

**55897** MUON DECAYS UNDERGROUND AND THE UTAH EFFECT. Keuffel, J. W. (Univ. of Utah, Salt Lake City). Lett. Nuovo Cim.; 2: No. 13, 669-73(25 Sep 1971).

It was recently observed by the Turin group that the rate of underground muon decays was fifteen times higher than the expected number. It is shown that the long-standing discrepancy between deep-mine muon zenith-angle experiments using thin detectors and the thick-detector Utah experiment, if interpreted as a real effect due to low-energy particles, can be reasonably explained by the new component of slow muons or pions implied by the Turin discovery. A model is proposed that accounts for the slow particles in terms of a high multiplicity of slow pions associated with energetic hadronic cascades produced by fast muons. (L.B.S.)

**55898** SHORT-PERIOD TEMPERATURE EFFECT ON COSMIC RAYS. Attolini, M. R.; Cecchini, S.; Galli, M.; Guidi, I. (CNR, Bologna. Univ., Bologna). Lett. Nuovo Cim.; 2: No. 7, 329-36(14 Aug 1971).

The degree of precision and to what extent the temperature correction on the ionizing component of cosmic rays can be made was investigated. The following phenomena were examined: (a) cosmic-ray variations due to conspicuous atmospheric perturbations such as thunderstorms; and (b) the hourly variations of the ionizing component due to temperature effects. (W.D.M.)

**55899** STUDY OF THE CHEMICAL COMPOSITION OF PRIMARY COSMIC RAYS ON COSMOS 228. Volodichev, N. N.; Grigorov, N. L.; Nechaev, O. Yu.; (and others) (Moscow State Univ.). Geomagn. Aeron. (USSR) (Engl. Transl.); 11: No. 1, 114-15(1971).

Translated from Geomagn. Aeron.; 11: No. 1, 144(1971).

The chemical composition of primary cosmic rays was studied on Cosmos 228 with an SEZ-1 Cherenkov spectrometer which included an integral discriminator system and a linear-amplitude analyzer for measuring the nuclear component. The amplitude analyzer was used to measure the chemical component of cosmic rays in the ranges of nuclei charges $Z = 2$ to 5 and $Z = 12$ to 40. The Cherenkov spectrometer showed the amplitude distribution of pulses from nuclei with $Z = 2$ to 5. During the time of the measurements two nuclei with $Z = 30$ to 37 and 349 nuclei with $Z \geq 20$ were recorded. (J.C.W.)

**55900** ANNUAL VARIATIONS AND GRADIENT OF COSMIC-RAY INTENSITY IN THE MERIDIONAL PLANE. Chirkov, N. P.; Kuz'min, A. I.; Shafer, G. V. (Inst. of Cosmophysical Investigations and Aeronomy, Yakutsk, USSR). Geomagn. Aeron. (USSR) (Engl. Transl.); 11: No. 1, 119-21(1971).

Translated from Geomagn. Aeron.; 11: No. 1, 149-51(1971).

The annual variations in cosmic-ray intensity were studied using the average monthly values of the ASK-1 ionization chamber at Yakutsk and the neutron monitor at Ottawa for 1955–1969. The data were corrected for barometric pressure, and the ionization-chamber data were corrected for the temperature variations of the atmosphere using three temperature soundings over Yakutsk. Strong modulation and meteorological effects complicate the analysis, but a comparison of data from the two instruments agrees well. (J.C.W.)

**55901** DIMENSIONS OF THE GALACTIC COSMIC-RAY MODULATION REGION. Zusmanovich, A. G.; Kolomeets, E. V.; Chumbalova, R. A.; Shakhova, Yu. A. (Kazakh State Univ., Alma-

XUM

Ata, USSR). Geomagn. Aeron. (USSR) (Engl. Transl.); 11: No. 1, 42-5(1971).

Translated from Geomagn. Aeron.; 11: No. 1, 56-60(1971).

The dimensions of the modulation region are determined on the basis of experimental data on cosmic-ray modulation and on the radial cosmic-ray intensity gradient in interplanetary space. The dimensions obtained, 2 to 5 au at the solar-activity minimum and 6 to 8 au at its maximum, agree with estimates based on the determination of the lag of cosmic-ray intensity behind the solar-activity level, if coronal emission is taken as the solar-activity index. (auth)

**55902** MEASUREMENT OF TRITIUM AND $^3$He IN ALUMINUM TARGETS. Alimova, I. A.; Naidenov, V. O.; Boltenkov, B. S.; Gartmanov, V. N. Cosmic Res. (USSR) (Engl. Transl.); 9: No. 1, 137-8(Jan-Feb 1971).

Translated from Kosm. Issled.; 9: No. 1, 149-51(Jan-Feb 1971).

Measurements of helium-3 and tritium content in targets exposed in cosmic space aboard Soyuz-4 and Soyuz-5 were analyzed. Experiments aboard the craft were identical, but a considerable difference was observed in the content of the isotopes. An examination of solar and geophysical data during the concurrent flight of the two craft registers no reason for the difference. The difference cannot be explained by nuclear reactions in the target material; in fact, there is no satisfactory explanation at this time. (J.C.W.)

**55903** PROPAGATION OF COSMIC RAYS THROUGH THE GALAXY, AND THE PROBLEM OF DETERMINING THE PATH LENGTH TRAVERSED BY COSMIC RAYS FROM THEIR SOURCE TO THE EARTH. Kuzhevskii, B. M. Cosmic Res. (USSR) (Engl. Transl.); 9: No. 1, 129-32(Jan-Feb 1971).

Translated from Kosm. Issled.; 9: No. 1, 144-6(Jan-Feb 1971).

The motion of cosmic rays from the source, through the galaxy, to absorption on Earth is investigated. The composition of cosmic radiation observed on Earth gives the impression of different nuclear transformations occurring as particles of cosmic radiation interact with particles belonging to the interstellar medium. The conditions of the ratio of fluxes or concentration of two nuclides as an increasing function of the amount of matter traversed by cosmic rays in the interstellar medium are considered. In motion through the interstellar medium, a change in the flux of nuclei of the relativistic particles can be brought about by (a) the flux of nuclei decreasing as the nuclei are absorbed upon interacting with the particles of the interstellar medium, and (b) the flux increasing because of the appearance of those nuclides when heavier nuclides become fragmented. The condition is examined whereby a group of nuclei in cosmic radiation is in motion. The amount of matter that has to be traversed by cosmic radiation traveling through the local galaxy is determined. (J.C.W.)

**55904** INTERACTION OF GALACTIC COSMIC RAYS WITH THE INTERPLANETARY MAGNETIC FIELD (BASED ON THE DATA OF VENERA-4 SPACE PROBE). Gorchakov, E. V.; Ignat'ev, P. P.; Galach'ev, N. G. Cosmic Res. (USSR) (Engl. Transl.); 9: No. 1, 117-21(Jan-Feb 1971).

Translated from Kosm. Issled.; 9: No. 1, 134-8(Jan-Feb 1971).

Simultaneous measurements of the variations in the cosmic-ray intensity and magnetic-field intensity outside the Earth's magnetosphere were made aboard the Venera-4 space probe. Ground-based measurements reveal a reduction in cosmic-ray intensity during magnetic storms. Observations of the single cosmic-ray intensity decrease of March 31–April 1, 1960 showed that the magnetic-field intensity did not decrease as the cosmic-ray intensity decreased as observed in ground-based measurements. The relationship between the magnetic-field intensity and the particle density in interplanetary space was analyzed. No definite relationship was found. So, the change in the interplanetary-field intensity is probably not governed directly by the solar-wind velocity, but depends strongly on the phenomena shaping the field near the Sun and on the nature of the interaction of magnetic fields in the interplanetary medium. In the latter case, the difference between the plasma flow velocities plays a decisive role in the interaction of the magnetic fields carried by them. (J.C.W.)

**55905** AMBIGUITY IN THE DENSITY SPECTRUM OF COSMIC-RAY EXTENSIVE AIR SHOWERS. Hlavac, T. (Inst. of Experimental Physics, Kosice, Czech.). Fyz. Cas.; 19: No. 4, 229-31(1969). (In Slovak).

Density spectra of cosmic-ray extensive air showers were measured at an altitude of 3340 m. Results obtained with large-area scintillators were compared with those obtained with G–M counters and with results of other authors. With scintillators a smaller increase of exponent $\gamma$ with increasing density was found than with G–M counters. (NSA of Czech)

**55906** INCREASING HADRON–NUCLEUS CROSS SECTIONS AND COSMIC RAY MUON ZENITHAL VARIATIONS. Wayland, J. R.; Cantrell, W. G.; Duller, N. M.; Green, P. J. (Texas A and M Univ., College Station). Nucl. Phys.; B32: No. 2, 527-34(1971).

Ground-level muon intensities were calculated using both a constant and an energy-dependent inelastic cross section for hadron–nucleus interactions. The use of the energy-dependent cross section reduces the muon intensities significantly at high muon energies, but has very little effect on the zenithal enhancements. (auth)

**55907** LIFETIME OF COSMIC RAYS IN THE GALAXY IN PRESENCE OF ACCELERATION. Velinov, P. (Geophysical Inst., Sofia). Compt. Rend. Acad. Bulg. Sci.; 24: No. 4, 431-4(1971).

The lifetime of cosmic rays in the Galaxy was examined previously (Velinov, Compt. rend. Acad. Bulg. Sci., 23: 477 (1970)). However, the possible acceleration of particles in interstellar space was disregarded. This acceleration, which occurs when the particles collide with moving heterogeneities of the interstellar magnetic field, is considered. (W.D.M.)

**55908** ASTROPHYSICAL APPLICATIONS OF VARIOUS HIGH-ENERGY ELECTROMAGNETIC PHENOMENA. Blumenthal, George Ray. San Diego, Calif.; Univ. of California (1971). 154p. University Microfilms Order No. 71-18,671.

Thesis.

The problems of the effects of various energy-loss mechanisms on the distribution of relativistic electrons in various astrophysical circumstances are considered. It is shown that if the electron loses a small fraction of its energy in a single occurrence of a process, the electron distribution function satisfies a continuity equation which is a differential equation in energy space. For the more general case where the electron can lose energy in discrete amounts (as in bremsstrahlung and extreme Klein–Nishina Compton losses), the electron distribution function satisfies an integrodifferential equation. Some solutions to this equation are derived for certain special cases. Also considered is the energy loss of high-energy cosmic rays in pair-producing collisions with ambient photons. General and essentially exact formulas are derived for this process for high-energy cosmic ray nuclei traversing an isotropic radiation field of arbitrary energy spectrum. These formulas are obtained by integrating the appropriate differential cross section in the rest frame of the cosmic-ray particle. Results are then given for the case of a Planckian photon distribution at arbitrary temperature. The effect of this energy loss on a universal flux of cosmic rays is then investigated along with the possibility that the observed "knee" at high energies is due to pair production. Finally, the energy loss formula is applied to quasi-stellar objects, and it is shown that if these objects are at cosmological distances, they are opaque to particles above a certain energy which depends upon the size of the object. A calculation is also presented for the opacity of the Universe to high-energy cosmic photons. Compton scattering and pair-production in collisions with the intergalactic medium are considered. The effects of elastic scattering and pair-production in photon–photon collisions with the microwave background are calculated. Also considered is the opacity due to pair production in collisions with dilute optical and infrared radiation from galaxies. It is shown that the observation of cosmic photons above $3 \times 10^{10}$ eV from quasi-stellar objects at large redshift would be inconsistent with the hypothesis that they are at cosmological distances. Finally two processes through which cosmic-ray nuclei produce high-energy photons are considered. Exact expressions and useful approximations are derived for the spectrum of photons emitted in collisions of a cosmic ray with an electron at rest. Also considered are the effects of the electron-photon cascade that results from the electron–positron pair produced in collisions of high-energy cosmic rays and low-energy photons. (Diss. Abstr. Int., B)

**55909** SOLAR MODULATION OF THE VERY HEAVY ($20 \leq Z \leq 30$) COSMIC RAY NUCLEI. Cleghorn Timothy Fuller. Minneapolis; Univ. of Minnesota (1970). 128p. University Microfilms Order No. 71-18,703.

Thesis.

During a period of enhanced solar activity, (July, 1968), a large stack of nuclear emulsions was exposed at Fort Churchill. The intensity measured in this stack revealed the effects of solar modulation. The individual pellicles of the 1968 stack were scanned for VH nuclei entering within a prescribed opening angle. Approximately 475 tracks caused by VH nuclei were found and analyzed. The kinetic energy at the top of the atmosphere was determined for those nuclei entering the stack with less than ~800 MeV/nucleon. Integral intensities were calculated above 300 and 750 MeV/nucleon, as well as three differential values

between these limits. In order to determine whether the solar modulation is charge-dependent, the variation observed between 1964 and 1968 VH intensities was compared with the corresponding changes for the alpha particles. Within the limits of statistical accuracy, no difference between the two species was observed. In a separate analysis, weighted least square fits of power laws in total energy were made using the available VH and alpha particle data. It was found that an index of −1.49 describes both sets of data, contrary to previous results. Also at variance with earlier work, the mean free paths of fragment nuclei were found to be comparable to the values obtained for the primary nuclei. This indicates that possibly statistical fluctuations were responsible for the earlier results. (TSS) (Diss. Abstr. Int., B)

**55910** SEARCH FOR FRACTIONALLY CHARGED PARTICLES IN COSMIC RAYS AT MOUNTAIN ALTITUDE. Cox, Aaron J. Jr. Tucson, Ariz.; Univ. of Arizona (1971). 52p. University Microfilms Order No. 71-16,509.

Thesis.

A scintillation-counter telescope consisting of eight liquid scintillation counters and four wide-gap spark chambers was used to search for particles with electric charge ±1/3e and ±2/3e in cosmic rays at 9000 feet above sea level. No such particles were detected during the 1500-hour experimental run, establishing upper limits on the vertical fluxes of these particles of $8.3 \times 10^{-11}$ cm$^{-2}$ sec$^{-1}$ sr$^{-1}$ for charge ±1/3e and $9.6 \times 10^{-11}$ cm$^{-2}$ sec$^{-1}$ sr$^{-1}$ for charge ±2/3e at a 90% confidence level. (Diss. Abstr. Int., B)

**55911** ORIGIN OF FLUORINE, SODIUM, AND ALUMINUM IN THE GALACTIC COSMIC RADIATION. Cartwright, Brian G. (Univ. of Chicago). Astrophys. J.; 169: No. 2, 299-310(15 Oct 1971).

The abundances of F, Ne, Na, Mg, Al, and Si relative to oxygen in the galactic cosmic radiation in the 106- to 207-MeV kinetic energy per nucleon interval measured by the University of Chicago charged-particle telescope on board the IMP-5 satellite are reported, as well as the abundance ratio Γ(F/O) above 1 GeV per nucleon kinetic energy measured by the same experiment. The abundances of the odd-Z elements F, Na, and Al were investigated in the light of three models for their production: (1) production primarily as spallation fragments of even-Z nuclides during interstellar propagation; (2) production as spallation fragments both in an envelope surrounding the source(s) and in the interstellar medium during propagation; and (3) production primarily in the source(s) itself, followed by some modification of the source relative abundances during propagation. It is shown that only the latter possibility is consistent with the measured abundance ratios within the framework of the steady-state model for the propagation of cosmic rays. (auth)

**55912** STEPLIKE CHANGES IN THE LONG-TERM MODULATION OF COSMIC RAYS. Stoker, P. H. (Potchefstroom Univ., S. Afr.); Carmichael, Hugh. Astrophys. J.; 169: No. 2, 357-68 (15 Oct 1971).

An experimental investigation is reported of the rigidity dependence of the solar modulation of relativistic cosmic-ray particles at the orbit of Earth by comparison of the monthly averages of the neutron monitor at Deep River at geomagnetic cutoff rigidity 1 GV with those of the neutron monitor at Kula at cutoff 13 GV during the period of increasing solar activity which began in 1964–1965. The constancy with time of the efficiency of each monitor was confirmed to better than 0.5% by comparisons with other monitors near the same respective cutoffs. The regression curve expected between the monitor at Deep River and the monitor at Kula was calculated from the results of latitude survey by the method of coupling constants assuming that the modulating parameter $\eta(r,t)$ was independent of rigidity P and that the form of the modulation function was $f(P,\beta) = P^{\alpha}$. The monthly experimental points fitted the regression line calculated for $\alpha = 1$ until December 1966; but thereafter they suddenly (between successive months) formed, for periods varying from 6 to 18 months, new regression lines which appeared to have about the same slope as the $\alpha = 1$ line but were strongly displaced laterally. The $\alpha = 1$ slope of the separate successive segments of the regression is attributed to the local modulation in the vicinity of the Sun associated with Forbush decreases and 27-day variations. The steplike long-lasting changes between the successive segments of the regression are believed to be demonstrated for the first time. They are probably associated with the state of the interplanetary medium far beyond the orbit of Earth. Statements in the literature that the form of the modulation function is independent of time and that the modulating parameter is independent of rigidity appear to have been premature. (auth)

## Direct Energy Conversion

*Refer also to abstracts 55951 and 57134.*

**55913** ELECTRIC ENERGY TRANSMISSION BY MEANS OF MHD GENERATORS ACTING AS DIRECT VOLTAGE GENERATORS. (to Brown Boveri and Cie SA). French Patent 1,571,532. 12 May 1969. Priority date 17 May 1967, Switzerland. (In French).

A description and diagrams are given for an apparatus for electric energy transmission. In this device are included inverters, superconductors, an MHD generator, and a bridging switch for elements connected in series. (J.F.P.)

**55914** EXTERNAL CHARACTERISTICS OF MHD GENERATOR WITH SECTIONS CONNECTED IN SERIES. Gigauri, K. V. Magn. Gidrodin.; No. 3, 99-102(Jul-Sep 1970). (In Russian).

The external characteristics of a channel of variable cross section with the sections of electrodes connected in series were calculated for subsonic flow of plasma in thermal equilibrium. The effect on the strength and power value of the initial temperature and the velocity of plasma flow, magnetic induction, and the relations of section length to channel width are evaluated. (tr-auth)

**55915** CONTROL OF PROFILE OF ELECTRODYNAMIC FORCES IN CONDUCTING BODIES IN TRAVELING MAGNETIC FIELDS. Krumin, Yu. K. Magn. Gidrodin.; No. 3, 117-23 (Jul-Sep 1970). (In Russian).

The electromagnetic fields and electrodynamic forces acting on a conducting body, with the synchronous effect of several traveling magnetic fields, are examined. The spectrum of harmonic components of force, acting in the direction of field propagation, is calculated. The variation, constant in time, of the force component in the interior of the body is examined; it is found that, using fields with different characteristics, it is possible to obtain a different character of this variation. The case is examined in detail when it is required to obtain zero force on the surface of the body but nonzero in its interior. (tr-auth)

## Fluid Physics

**55916** DOUBLE CORRELATION EQUATIONS OF THE MAGNETIC FIELD AND VELOCITY IN AN ISOTROPIC CONDUCTING TURBULENT FLOW. Codreanu, Steliana. Stud. Univ. Babes-Bolyai, Ser. Phys.; 16: No. 1, 9-13(1971). (In Rumanian).

Equations are presented that govern the second-order correlation functions for the velocity and magnetic field. These equations are a hydromagnetic generalization of Smirnov's equation from hydrodynamic turbulence. (auth)

**55917** CHARACTER OF EQUILIBRIUM OF A HEAVY, VISCOUS, INCOMPRESSIBLE, INFINITELY CONDUCTING, ROTATING FLUID IN THE PRESENCE OF A VERTICAL MAGNETIC FIELD. Ariel, P. D. (Malaviya Regional Engineering Coll., Jaipur, India). Indian J. Pure Appl. Math.; 2: No. 2, 230-45(Apr 1971).

The character of equilibrium of a heavy, viscous, incompressible, infinitely conducting fluid in the presence of a vertical magnetic field and Coriolis forces is investigated. It is shown that the solution is characterized by a variational principle. Based on the variational principle, a dispersion relation is derived from the special case of a fluid of finite depth stratified in the vertical direction according to the exponential law of density. It is found that both the magnetic field and the Coriolis forces tend to stabilize the system separately. However, when they act together, the Coriolis forces cease to play any part in determination of the criterion of stability, though they considerably influence the mode of maximum instability in the unstable case. The solutions in the exact cases of zero viscosity and absence of buoyancy forces are treated at length, and the extreme cases of "low" and "high" rotation are also discussed. (auth)

**55918** NUMERICAL CALCULATION OF CONDUCTING FLUID FLOW IN A TRAVELING MAGNETIC FIELD. Panchuk, V. I.; Tkachenko, V. F. Bionika; No. 4, 111-16(1970). (In Russian).

The two-dimensional unsteady flow of a viscous, incompressible conducting fluid in an infinite duct was examined. A longitudinal fixed magnetic field surrounded the duct and fluid. Along one of the duct boundaries was assigned a longitudinal field in the form of a traveling wave. A solution was found for the equation for the magnetic field, assuming small magnetic Reynolds numbers. Magnetohydrodynamics furnished the initial equation of the development and described the movement of a viscous conducting fluid in a magnetic field. The relations developed suggest that it is possible to decrease the resistance to flow around a body by establishing on its surface an elastic traveling wave which induces a secondary cur-

XUM

rent. The character of fluid flow in the traveling magnetic field agrees qualitatively with the flow obtained from flow around an elastic surface, varying according to the law for a traveling wave. Consequently, in the conducting liquid, the creation of a secondary flow near the current around the body, and assuring the desired properties for the current, and inducing a lowering of the resistance of the body, it is easily possible to accomplish this with the aid of the traveling magnetic wave on the boundary of the body. (K.S.W.)

**55919** FLUID MOTION PRODUCED BY A TEMPERATURE GRADIENT PERPENDICULAR TO THE GRAVITATIONAL FIELD IN THE PRESENCE OF AN EXTERNAL MAGNETIC FIELD AND ROTATION. Zernyatko, V. G.; Tverskoi, B. A. (Moscow State Univ.). Geomagn. Aeron. (USSR) (Engl. Transl.); 11: No. 1, 46-9(1971).

Translated from Geomagn. Aeron.; 11: No. 1, 61-4(1971).

The motion of a rotating layer of a viscous, conductive fluid in an external magnetic field and a gravitational field that are both perpendicular to it under the effect of a temperature gradient parallel to this layer is analyzed. It is demonstrated that the magnetic field decelerates the fluid in the direction of the temperature gradient and that rotation produces a velocity component that is perpendicular to the initial direction. The behavior of the fluid in the near-wall region is investigated in detail for the limiting case of large and small values of the external magnetic field and of the angular velocity of rotation of the layer. (auth)

**55920** MAGNETOPLASMADYNAMIC EXPERIMENTS IN INDUCTIVE-HYDRODYNAMIC SHOCK WAVE TUBES. Rothhardt, L.; Jahn, G. (Zentralinstitut fuer Elektronenphysik, Berlin). Monatsber. Deut. Akad. Wiss. Berlin; 12: 958-60(1970). (In German).

The results of experiments in inductive hydrodynamic shock wave tubes in which magnetoplasmadynamic effects were investigated are reported. Experiments on one channel with ring cross section and radial magnetic field component are described. Studies on the plasma dynamics in a combined shock wave tube in which a plasma beam accelerator works opposite power operating in the inductive hydrodynamic shock wave tube are discussed. (J.S.R.)

**55921** MAGNETOHYDRODYNAMICS AT HIGH HARTMANN NUMBER. Hunt, J. C. R.; Shercliff, J. A. (Trinity Coll., Cambridge, Eng. Univ. of Warwick, Coventry, Eng.). Annu. Rev. Fluid Mech.; 3: 37-62(1971).

The field of steady, incompressible, rectilinear flow under transverse magnetic fields is reviewed. The review also briefly refers to three-dimensional, nonrectilinear flows, but concentrates throughout on cases where the Hartmann number M or $Bl(\sigma/\eta)^{1/2}$ is large. B, l, $\sigma$, and $\eta$ are imposed magnetic field, representative length scale, electric conductivity, and viscosity, respectively. (M.H.R.)

**55922** TURBULENT JETS OF CONDUCTING FLUIDS. II. RESULTS OF CALCULATIONS. Dzhaugashtin, K. E. Magn. Gidrodin.; No. 3, 3-15(Jul-Sep 1970). (In Russian).

A semi-empirical calculation scheme is used for solution of the problem of the average distribution and pulsation characteristics of velocity and temperature in turbulent jets of conducting fluid. For a longitudinal magnetic field, the equations of motion and energy reduce, by means of transformation of coordinates, to the corresponding equations for flow without field. The presence of the saturated flow regime, characterized by constant values of the momentum and the flow rate in the jet, is shown, and also the limiting values of velocity and jet widths are calculated for different types of jet stream. The effect of a transverse magnetic field is analyzed for the case of plane submerged jets. It was found that the magnetic field leads to the spreading of the jet in the transverse direction, yet the values of the momentum and the velocities of the jet are equal to zero, and the width infinite. The approximate solution of the problem is obtained without the calculation of the effect of the magnetic field on the eddy viscosity. The calculated average and pulsating characteristics of velocity and temperature are compared with the existing experimental data. (tr-auth)

**55923** GENERATION OF MAGNETOHYDRODYNAMIC WAVES IN NONHOMOGENEOUS PLASMA LOCATED IN INTENSE MAGNETIC FIELD. Zoler, D. I.; Deutsch, R. V.; Maxim-Gazi, R. G. (Centrul de Cercetari Technice si Fizice, Iasi). Magn. Gidrodin.; No. 3, 16-22(Jul-Sep 1970). (In Russian).

The phenomena of wave generation, originating in inhomogeneous plasma in a magnetic field, is considered. In weak fields these phenomena were studied previously using MHD equations; for the case of strong fields many aspects remain unexplained. In addition a number of interesting peculiarities occur, which deserve more thorough study as, for example, the tensor form of the pressure. The method used here is known in electrodynamics where it is used to study stratified media. Here the plasma is also assumed stratified. The coupling phenomena (generation, reflection) are studied for quasi-Alfven and acoustic waves. The conditions for formation of generated and reflected waves were clarified in relation to the plasma parameters. It turns out that the refractive indices for both waves depend on the pressures $p_\perp$ and $p_\parallel$. (tr-auth)

**55924** CLASSIFICATION OF INVARIANT SOLUTION OF EQUATIONS OF TWO-DIMENSIONAL UNSTEADY FLOW OF ELECTRICALLY CONDUCTING GASES IN MAGNETIC FIELDS. Gridnev, N. P. Magn. Gidrodin.; No. 3, 23-9(Jul-Sep 1970). (In Russian).

An attempt was made to find all of the invariant solutions of the system of equations of two-dimensional unsteady motion of compressed electric-conducting gas in a magnetic field. The calculation of viscosity and thermal conductivities reduces the class of invariant solutions. The examples given of invariant solutions of ranks 2 and 1 permit the study of both flow and asymmetric scattering. (tr-auth)

**55925** STABILIZATION OF MAGNETOHYDRODYNAMIC FLUTTER INSTABILITIES BY DISTRIBUTIVE CONTROL. Selezov, I. T. Magn. Gidrodin.; No. 3, 30-4(Jul-Sep 1970). (In Russian).

An infinite elastic panel is considered, which on the one hand is encircled by MHD flow and on the other is limited to a stationary nonconducting medium. Unstable traveling waves are excited by definite (critical) flow velocity in the system. It was found that by introduction of a controlling magnetic field it is possible to improve the stability of the system, i.e., to increase critical velocity. The realization of such a distributed control is possible due to the fact that mass-force-type terms enter in the magnetohydrodynamic equations, relating the hydrodynamic field with the electromagnetic. (tr-auth)

**55926** INFLUENCE OF TRANSVERSE MAGNETIC FIELD ON INTENSITY PROFILES OF TURBULENT VELOCITY FLUCTUATIONS IN PIPES OF RECTANGULAR CROSS SECTION. Branover, G. G.; Gel'fgat, Yu. M.; Kit, L. G.; Platnieks, I. A. Magn. Gidrodin.; No. 3, 41-9(Jul-Sep 1970). (In Russian).

Intensity profiles of the longitudinal component of velocity fluctuations along the axes of the transverse cross section of the pipe are presented at different distances from the flow intake in the electromagnet gap. Measurements were made with a two-electrode conduction anemometer. It was found that, according to the change of sign of the profile gradient of the intensity of the fluctuations, it is possible to judge the cessation of the production of turbulence. (tr-auth)

**55927** TRANSITION TO TURBULENCE IN MAGNETOHYDRODYNAMIC FLOW WITH FINITE PERTURBATIONS. Levin, V. B. Magn. Gidrodin.; No. 3, 50-6(Jul-Sep 1970). (In Russian).

On the basis of semi-empirical closure of the equations of conservation of the second moments of fluctuating velocities, an equation was obtained for the energy of turbulence in the flow of electro-conductive fluid in a magnetic field with $R_n \ll 1$. At Reynolds numbers greater than critical, the energy equation has two positive roots. The greater root corresponds to the regime of developed stationary turbulence, the lesser, however, determines the barrier of initial perturbation; if the perturbation is less than the barrier, then it dies out, and if greater, stationary turbulence evolves (hard excitation). The barrier of initial perturbation is increased sharply in a magnetic field; its increase is approximately equal to the cube of the increase of the local critical Reynolds number. (tr-auth)

**55928** TURBULENT JET OF CONDUCTING FLUID IN LONGITUDINAL MAGNETIC FIELD. Kuznetsov, A. P. Magn. Gidrodin.; No. 3, 57-66(Jul-Sep 1970). (In Russian).

The development of plane and axially symmetric turbulent jets of conducting fluid in a longitudinal magnetic field with an arbitrary change of magnetic induction along the axis of the jet is examined. Self-similar and non-self-similar flows in the main part of submerged jets of incompressible fluid are studied. The development of a jet in the main region with arbitrary assigned (average along the cross section) degrees of turbulence in the beginning of the main part was also examined. The main part here is understood to be the area of the jet where the general profile of the longitudinal component of average velocities exists. These problems are solved by the combined integration of the equations of motion and the fluctuating energy balances. (tr-auth)

**55929** FLOW OF NONVISCOUS PERFECTLY CONDUCTING FLUID PAST A THIN BODY IN PRESENCE OF TRANSVERSE MAGNETIC FIELD. Sher'yazdanov, G. B. Magn. Gidrodin.; No. 3, 67-73(Jul-Sep 1970). (In Russian).

Obscure functions are presented in the form of an asymptotic expansion by powers of a small parameter and, in the first approximation, the problem agrees with the approach of Sears and Resler (J. Fluid Mech., 5: 257(1959)). The determination of the vortex and vortex-free parts of the solution reduce to finding the obscure harmonic function. In contrast to Sears and Resler and other authors, a solution is obtained in a closed form which depends on the Alfven number for an arbitrarily thin profile. As an example, the flow of a three-parameter profile is examined; the coefficients of the aerodynamic forces and the distribution of the load are determined. In the case where the magnetic field is absent, the results obtained agree with the results of the usual hydrodynamic flow. (tr-auth)

**55930** DETERMINATION OF COEFFICIENT OF ELECTROMAGNETIC EJECTION OF SOLIDS FROM CONDUCTING FLUIDS DURING EXPERIMENT ON CONDITIONS OF VARIABLE ACCELERATION IN FORCE OF GRAVITY. Dobychin, E. I.; Popov, V. I. Magn. Gidrodin.; No. 3, 74-8(Jul-Sep 1970). (In Russian).

Results are cited of experiments on the coefficient of electromagnetic ejection, K, for conducting and dielectric solids, immersed in a conducting fluid in crossed homogeneous electric and magnetic fields. Under conditions of weak gravitation, a qualitative picture of the motion of solids with greater specific weight was obtained under the action of the electromagnetic field and a quantitative estimate of the ejection coefficient was given. The measurement of forces acting on solids in the liquid metal, mercury, permitted freedom from harmful electrochemical effects inherent in electrolytes, and the obtaining of K values with greater accuracy. It was found that for conducting solids immersed in liquid metal, the coefficient of electromagnetic injection is 2.6 to 2.9; in an electrolyte it is 1.9 to 2.3. For dielectric substances, in both cases, it is 0.85 to 1.0. (tr-auth)

**55931** EXPERIMENTAL INVESTIGATION OF DYNAMICS OF LIQUID-METAL DROPS IN ELECTROMAGNETIC FIELD IN CONDITIONS OF REDUCED GRAVITATION. Kirko, I. M.; Dobychin, E. I.; Popov, V. I. Magn. Gidrodin.; No. 3, 79-82(Jul-Sep 1970). (In Russian).

The results of experiments with mercury drops in a conducting liquid media in an electromagnetic field are presented. For a more accurate determination of electromagnetic force acting on the drop, the experiments were conducted with reduced gravitation. A series of photographs show the motion of the drop under the action of surface tension and also electric, magnetic, and crossed fields. The graphic treatment of the experimental results with the obtained approximation formulas allows the numerical estimate of the value of electromagnetic force acting on the conducting drop in the conducting media in the direction of the electromagnetic field and obtaining the value of the coefficient of electromagnetic expulsion. The coefficient obtained was 2.07 with an error of not more than 15%. (tr-auth)

**55932** MASS TRANSFER IN MAGNETOHYDRODYNAMIC FLOW CONSIDERING CHEMICAL KINETICS OF REACTIONS ON BOUNDARIES. Blum, E. Ya. Magn. Gidrodin.; No. 3, 83-90(Jul-Sep 1970). (In Russian).

Mass transfer is considered in MHD flows with mixed kinetics for reactions of half first and half second order. Its applicability in the integral method is illustrated by the reaction of the first order in Hartmann flow when an accurate solution was obtained using the Levich approach. Dimensionless coordinates were found in which mass exchange characteristics are described by general curve. The problem of MHD flow around the plate is complicated. The mass transfer intensity in this case is determined by two parameters: by a dimensionless complex from the relation of the rates of the chemical and diffusion processes and by the local parameter of MHD interaction. In all the cases studied the effect of the external magnetic field was directed to the increase of the transition value of the generalized Biot diffusion criterion, with which the deviation of mass transfer characteristics from diffusion kinetics begins. (tr-auth)

**55933** TEMPERATURE FIELD IN AXIALLY SYMMETRIC MAGNETOHYDRODYNAMIC FLOW IN VORTEX CHAMBER. Glazov, O. A. Magn. Gidrodin.; No. 3, 91-8(Jul-Sep 1970). (In Russian).

The temperature of the boundary layer on the end of the vortex chamber is considered in a nondissipative approach. The temperature distribution in the inlet of the chamber is considered homogeneous. The investigation was conducted over a wide range of Prandtl numbers and MHD interaction parameters. From the investigation presented it is observed that the magnetic field has an effect essentially on the heat transfer between the working fluid and the end, yet this effect is caused by the action of the magnetic field on secondary return flows at the end. (tr-auth)

**55934** POSSIBILITIES OF INFLUENCING THE BOUNDARY LAYER WITH CROSSED ELECTRIC AND MAGNETIC FIELDS. Shtern, A. G. Magn. Gidrodin.; No. 3, 124-8(Jul-Sep 1970). (In Russian).

Joule and viscous dissipation losses in the boundary layer, responsible for the delay of the transition to turbulent flow, are estimated. The major part of Joule losses is calculated on the basis of the solution of the problem of flowing of current between the electrodes of the system. The magnitude of these currents depends on the magnitude of the magnetic field, which according to estimate, has a value fully attainable for permanent magnet systems. A known integral solution of the boundary layer problem is used for the estimate of viscous dissipation. From the estimation results it follows that use of an MHD-engine can be energetically advantageous. The analysis of the effect on the turbulent boundary layer is based on use of the Karman hypothesis and the integral method of solution. In addition, a complete reconstruction of the layer structure is possible, which is expressed by the appearance of the asymptotic form, and which does not depend on the coordinate along the flow. (tr-auth)

**55935** CALCULATIONS OF MAGNETOGASDYNAMIC FLOW IN CHANNELS. Kolosnitsin, N. I.; Stanyukovich, K. P. Magn. Gidrodin.; No. 3, 138-40(Jul-Sep 1970). (In Russian).

A method of integration was developed for MHD equations for quasi-one-dimensional flow of viscous fluid allowing for dissipation of energy in a noninductive approximation. The method is illustrated by the calculation of an MHD channel with constant load parameters. (tr-auth)

**55936** DISCONTINUITY OF EQUATION OF OPTIMUM PROBLEMS OF MAGNETOGASDYNAMICS. Nazarov, E. V. Magn. Gidrodin.; No. 3, 140-2(Jul-Sep 1970). (In Russian).

It is shown, that formulated in a one-dimensional approximation at small magnetic Reynolds numbers, the problems of determination of optimum conversion regimes in MHD-generator channels do not always have a general solution. If the auxiliary function formulated by allowing for all couplings does not contain nonlinear terms derived from the required functions, the variational problem has only a partial solution, determined by the range of permissible boundary conditions. (tr-auth)

**55937** EXPERIMENTAL INVESTIGATION OF INFLUENCE OF LONGITUDINAL MAGNETIC FIELD ON HYDRAULIC RESISTANCE IN TURBULENT FLOW OF ELECTRICALLY CONDUCTING FLUIDS IN PIPES. Levin, V. B.; Chinenkov, I. A. Magn. Gidrodin.; No. 3, 145-6(Jul-Sep 1970). (In Russian).

An experimental investigation of the reduction of the coefficient of hydraulic resistance was conducted by superposition of a longitudinal magnetic field on the turbulent flow of gallium in a pipe. Experimental data were obtained in a wide range of Hartmann and Reynolds numbers. A significant increase of the Hartmann number in comparison with works from the literature permitted reducing the coefficient of hydraulic resistance by one order of magnitude. (tr-auth)

**55938** ROTATION OF ELECTRICALLY CONDUCTING FLUIDS IN CROSSED ELECTRIC AND MAGNETIC FIELDS. Gorbachev, L. P.; Potanin, E. P. Magn. Gidrodin.; No. 3, 146-9(Jul-Sep 1970). (In Russian).

Laminar axially symmetric rotary motion of electric-conducting fluids between two disks under the action of radial electric and axial magnetic fields is considered, assuming the existence of boundary layers. For a magnetic field, proportional to the square of the radius, in the case where the Hall current is neglected, a self-similar solution was obtained, constructed by the method of approximate calculation of inertial terms in the equations of motion. (tr-auth)

**55939** ELECTROMAGNETIC FIELDS IN AN INDUCTION MAGNETOHYDRODYNAMIC DEVICE WITH EXTENDABLE CHANNEL. Krishberg, R. R.; Sermons, G. Ya. Magn. Gidrodin.; No. 3, 149-52(Jul-Sep 1970). (In Russian).

In the model of the induction MHD device considered, in the active zone of nonmagnetic gap and channel the devices are extended vertically according to a linear law. Outside of the active zone, the channel cross section is constant. The channel width remains constant. It is assumed that the velocity of the conducting fluid has only one component $v = Q/S$, where Q is the fluid flow rate and S is the channel cross section. The presence of superconducting short-circuiting lateral busbars is assumed. A discrete system of exciting currents was specified for the surface of the magnetic circuit with $\mu = \infty$. Equations for the electromagnetic field in the nonmagnetic gap are solved. Certain special cases are considered. Calculated and experimental curves are given for a no-load operation field. (tr-auth)

XUM

**55940** IDEALLY CONDUCTING MAGNETOSTATIC EQUILIBRIA AND ASSOCIATED TIME-DEPENDENT RESISTIVE FLOWS. Stevenson, John C. (Post Coll., Greenvale, N. Y.). J. Plasma Phys.; 6: 125-36(Aug 1971).

Several types of two-dimensional solutions for the equations of magnetohydrodynamics are described. For all these solutions the magnetic field contains at least one hyperbolic neutral point. Two new magnetostatic equilibria are introduced for the ideally conducting case. The magnetic field associated with one of these is used to construct an exact time-dependent solution of the MHD equations where the fluid is necessarily at rest. In the case where the field lines are hyperbolae, it is demonstrated that retention of the energy equation (ordinarily decoupled for incompressible flows) implies that the flow beginning at rest, remains at rest. (auth) (UK)

**55941** FURTHER NOTE ON THE SLOW ROTATION OF AXISYMMETRIC SOLIDS IN MAGNETOHYDRODYNAMICS. Shail, R. (Univ. of Surrey, Guildford, Eng.). Proc. Cambridge Phil. Soc.; 70: 339-42(1971).

The slow steady rotation of an insulated axisymmetric solid in a bounded viscous fluid of finite conductivity, with a uniform magnetic field applied parallel to the axis of rotation, was previously considered (1967). Expressions were derived then for the frictional couple G on the solid in a number of different geometrical situations, the formulae obtained being in the form of power series in the Hartmann number M together with the lowest-order wall correction, the zero-order term in G being the frictional couple $G_0$ for the nonmagnetic infinite-fluid problem. Now, the problem of expressing the couple G in terms of $G_0$ is considered, and it is shown that, correct to $O(M^3)$ and the lowest-order wall correction, G may be calculated from the solution to the nonmagnetic problem for an infinite fluid and one further potential problem. This results in a considerable reduction in the amount of manipulation required to compute G, and the method is illustrated by reference to the case of a rotating prolate spheroid in a bounded fluid. (auth) (UK)

**55942** STUDY OF THE VELOCITY PROFILE IN THE ENTRANCE REGION OF A MAGNETOHYDRODYNAMIC CHANNEL. Flegal, William Malcolm. Atlanta; Georgia Inst. of Technology (1970). 139p. University Microfilms Order No. 71-17,334. Thesis.

The change in the velocity profile of a conducting fluid as it flows through a rectangular channel in the presence of electric and magnetic fields was investigated both analytically and experimentally for channels with height-to-width ratios of 6-to-1 and 4-to-1. The influence of the Hartmann number on the development of the velocity profile was studied also. The analytical investigation involved linearizing the differential equation of motion, expressing the velocity as a Fourier series in two variables, substituting this series in the differential equation, and solving for the Fourier constants. An experimental investigation was conducted for two rectangular channels, using potassium chloride solution as the working fluid. Tests were run at four different Hartmann numbers for each channel. The maximum Hartmann numbers attainable were 2.0 for the 6-to-1 channel and 2.9 for the 4-to-1 channel. The agreement of the experimental data with the analytical results was quite good, being within approximately 5 to 8% at all times. The influence of the Hartmann number and channel aspect ratio on the velocity profile development was observed. It was found that the rate of velocity development increases for a given channel with increasing Hartmann number. At a given Hartmann number, the velocity profile developed more slowly for the 4-to-1 channel than for the 6-to-1 channel. The electric field strength was found to have no measurable influence on the velocity profile or its development. (Diss. Abstr. Int., B)

**55943** ELECTRIC NETWORK CALCULATIONS IN PROBLEMS OF MAGNETOHYDRODYNAMICS. Popov, Yu. P. Zh. Vychisl. Mat. i Mat. Fiz.; 11: No. 2, 449-61(Mar-Apr 1971). (In Russian).

As an aid in solving problems concerning discharge in a plasma, an iteration-less numerical method was developed that involves an equation representing an external electric circuit. This method is utilized jointly with electromagnetic field equations on one-dimensional problems of magnetohydrodynamics. (tr-auth)

**55944** TRINITY: PROGRAMS FOR 3D MAGNETOHYDRODYNAMICS. Roberts, K. V.; Boris, J. P. (Culham Lab., Abingdon, Eng.). pp 44.1-5 of Computational Physics. Vols. I and II. London; Her Majesty's Stationery Office (1969).

From Conference on computational physics; Culham, England (28 Jul 1969). See CONF-690706-(Vols.1 and 2).

A step-by-step investigation of programming techniques for large MHD problems was undertaken. A method was devised for the efficient development, testing, and production of computer codes for complex sets of partial differential equations. This method was applied to a simple explicit 3D MHD difference scheme, generating a series of codes called TRINITY. The method is carried out in stages, starting from Stage 1 which is written in Symbolic Algol using a notation close to the language of classical vector analysis so that the program can be altered and improved very quickly. The second stage, TRINITY 2, was written in highly optimized Fortran implementing the same explicit difference scheme but executing 15 to 20 times faster than the Symbolic Algol version. Further stages of TRINITY are being developed to increase the permissible mesh size by using fully buffered backing storage and to increase the speed by using optimized assembly-language coding. A technique was developed whereby the Symbolic Algol version of a complex set of partial differential equations can be made to produce optimized source-language coding automatically, thereby greatly reducing the amount of time-consuming and error-prone hand coding required for optimization. A technique was also developed for coding implicit difference schemes using the same finite-difference operators appearing in the explicit formulation of the problem. (auth) (UK)

**55945** SUPPRESSION OF CONVECTION BY A MAGNETIC FLUID. Peckover, R. S. (United Kingdom Atomic Energy Authority, Abingdon, Eng.). pp 50.1-5 of Computational Physics. Vols. I and II. London; Her Majesty's Stationery Office (1969).

From Conference on computational physics; Culham, England (28 Jul 1969). See CONF-690706-(Vols.1 and 2).

As part of a study of the nonlinear behavior of fluids in the presence of magnetic fields, a simple configuration with motion restricted to two dimensions is discussed with its assumptions and boundary conditions. Three ranges of $\beta = (R_e R_m/Q)$, where $R_e$ = Reynolds number, $R_m$ = magnetic Reynolds number, and Q = Chandrasekhar number, are considered for Q small, intermediate and large. It is found that for the free decay of an eddy in the presence of a magnetic field, the stronger the magnetic field is the more rapidly the kinetic energy is dissipated. (UK)

**55946** BOUNDARY LAYER OF A COMPRESSED, ELECTRICALLY CONDUCTING GAS AT THE ELECTRODE OF A MAGNETOHYDRODYNAMIC DUCT IN THE ABSENCE OF IONIZATION EQUILIBRIUM. Ermolaeva, G. K.; Yuferev, V. S. Izv. Akad. Nauk SSSR, Mekh. Zhidk. Gaza; No. 3, 164-9(May-Jun 1971). (In Russian).

The laminar boundary layer of a compressed, conducting gas, formed on a conductive duct wall, is considered. It is assumed that the concentration of charged particles in the current is not at equilibrium. Attention is focused on a violation of the quasi-neutrality of the gas in a narrow layer adjacent to the wall. The Debye length is regarded as significantly greater than the free path of the charged particles. The case of sufficiently large emission currents is examined. Mathematical development demonstrates that the characteristic external current during supersonic flow is not at equilibrium. This is explained by a significant drop in temperature along the duct, and relatively large velocities of current at its center. Temperature profiles and charged particle profiles in the boundary layer at the anode and at the cathode some distance from the duct outlet are prepared in graphic form. A decrease in the concentration of charged particles at the wall for fixed values of certain parameters leads to an increase of thermal currents at the wall. This effect is explained by an increase in the Joule heat release. (K.S.W.)

**55947** HYDROMAGNETIC FLOW INDUCED BY THE IMPULSIVE ROTATION OF AN INFINITE DISC. Datta, Nanigopal; Biswas, Kalyan Kumar (Indian Inst. of Tech., Kharagpur, India). J. Phys. Soc. Jap.; 31: No. 4, 1259-65(Oct 1971).

The hydromagnetic flow due to the impulsive rotation of an infinite disc was studied. The equations of the problem were linearized by expanding the velocity components, pressure, and the magnetic field components in powers of the dimensionless angular rotation of the disc. It is observed that the velocity components are reduced by the increase of the magnetic field. The induced magnetic field components are of the order of the magnetic Prandtl number and is small for practical fluids. The boundary layer displacement thickness is decreased by the increase of the applied magnetic field. (auth)

**55948** CONVECTIVE MOVEMENT OF A CONDUCTING LIQUID WITH A CURRENT IN A TRANSVERSE MAGNETIC FIELD. Eismont, O. A. Izv. Akad. Nauk SSSR, Mekh. Zhidk. Gaza; No. 2, 20-6(Mar-Apr 1971). (In Russian).

The convective instability of a layer of conducting fluid is investigated under the conditions of a current passing through a magnetic field directed perpendicularly to the current. The prob-

lem is solved with a nonlinear approximation in a linear formulation. The dependence of the Rayleigh number on the Hartmann number is obtained, determining a neutral stability. The condition is analyzed in which an electric current passes through a fluid, the conductivity of which depends on the temperature, and which is located in the magnetic field directed perpendicular to the current. (tr-auth)

**55949** EFFECT OF MAGNETIC REYNOLDS'S NUMBERS ON DISTRIBUTION OF CURRENTS IN MAGNETOHYDRODYNAMIC DUCTS WITH CALCULATION OF THE HALL EFFECT. Levin, A. L. Izv. Akad. Nauk SSSR, Mekh. Zhidk. Gaza; No. 3, 148-52(May-Jun 1971). (In Russian).

A stationary plane flow of conducting gas across a magnetic field is examined in an MHD duct of constant cross section, formed by electrodes and insulators. The electromagnetic force is assumed to be small. It is shown that, with an increase in the magnetic Reynold's number, the current density rises near the outlet from the interelectrode distance. The mutual effect of the Hall parameter and magnetic Reynold's number is investigated with respect to the current distribution in the duct. (tr-auth)

**55950** ELECTRIC FIELD IN A MAGNETOHYDRODYNAMIC DUCT OF RECTANGULAR CROSS SECTION WITH END ELECTRODES. Kirillov, V. Kh. Izv. Vyssh. Ucheb. Zaved., Mat., No. 5, 38-45(May 1971). (In Russian).

The spatial distribution of a stationary electric field was found for an MHD channel of rectangular cross section and provided with terminal electrodes. The flow rate was chosen in the form of a "model" profile. Mathematical treatment was aided by a variant of the Wiener–Hopf approximation method. Long electrodes were considered in the calculation of duct characteristics. The equations produced show that the Joule loss, in addition to ordinary longitudinal losses, increases both on account of increase in the boundary layer, and also on account of the increase in electrode dimensions. (K.S.W.)

**55951** EXPERIMENTAL STUDY OF THE INTERACTION OF SHOCK WAVE WITH A MAGNETIC FIELD. Borisov, M. B.; Zaitsev, S. G.; Chebotareva, E. I.; Lazareva, E. V. Izv. Akad. Nauk SSSR, Mekh. Zhidk. Gaza; No. 3, 153-63(May-Jun 1971). (In Russian).

The propagation of a shock wave through a Faraday-type MHD duct was experimentally investigated. With short circuiting of the induced currents in the supersonic stream following the shock wave, the formation of a shock front was recorded. Duct cross section vs. time diagrams were prepared for the movements of the shock front and wave in the duct and behind it. For a series of fixed duct cross sections, the density and degree of ionization of the gas were measured as functions of time. Argon was used as a test gas, the ionizing shock wave being propagated at Mach 12 to 13. (tr-auth)

## Geophysics (Upper Atmosphere)

*Refer also to abstracts 55738, 55903, 55904, and 55919.*

**55952** (N-71-27604) MAGNETOSPHERIC FIELD DISTORTIONS OBSERVED BY OGO'S 3 AND 5. Sugiura, M.; Ledley, B. G.; Skillman, T. L.; Heppner, J. P. (National Aeronautics and Space Administration, Greenbelt, Md. Goddard Space Flight Center). May 1971. 44p. (NASA-TM-X-65563). NTIS.

Magnetospheric field distortions are studied using approximately 10,000 data points sampled from the rubidium magnetometer measurements on OGO 3 and 5. Analysis is made in terms of $\Delta B$ defined as the observed field magnitude minus the magnitude of a reference geomagnetic field. Average-contours of equal $\Delta B$ are shown in the geomagnetic noon–midnight and dawn–dusk meridian planes for magnetically quiet and slightly disturbed conditions. These $\Delta B$ contour maps show (a) a high-latitude + $\Delta B$ region on the night side and (b) an equatorial – $\Delta B$ region in the inner magnetosphere. The high-latitude +$\Delta B$ region extends toward the dayside magnetosphere beyond dawn and dusk with decreasing magnitude of $\Delta B$. Though the observations presented here do not cover southern high latitudes at appropriate geocentric distances to directly detect a southern counterpart of the +$\Delta B$ region, there is no indication in the available data to suggest absence of a similar region in the southern hemisphere. Region (b), also, the equatorial – $\Delta B$ region encircling the Earth, shows greater inflation of the inner magnetosphere during magnetically quiet periods than the inflation usually assumed. (auth) (STAR)

**55953** MULTIPLE CROSSINGS OF THE EARTH'S BOW SHOCK AT LARGE GEOCENTRIC DISTANCES. Bavassano, B.; Mariani, F.; Villante, U. (Univ., Rome). J. Geophys. Res.; 76: No. 25, 5970-7(1 Sep 1971).

A series of very distant crossings of the Earth's bow shock was identified by the magnetic-field experiment on board Pioneer 8 at geocentric distances between 120 and 200 $R_E$, during the period December 19 to 25, 1967. The normal to the shock is generally found lying in or very near the ecliptic plane, at an average angle of 68° with respect to the Earth–Sun line. The average ratio of field magnitudes on the interplanetary and the magnetosheath sides of the bow shock is nearly 2. The location of these crossings is consistent with that expected from the Dryer and Heckman computations of the distant bow-shock configuration, when the aberration of the solar wind is taken into account. The shock is also aligned with the configuration extrapolated from the Explorer 33 observations that extend only to 75 $R_E$. The conclusion is that a well-developed bow shock is still observed at these very large distances. The intermittent observations are interpreted as an effect of the sweeping back and forth of the shock across the spacecraft orbit, due to time variations of the solar wind. (auth)

**55954** MAGNETOSPHERIC CONVECTION PATTERN INFERRED FROM MAGNETIC DISTURBANCE AND AURORAL MOTIONS. Davis, T. N. (Univ. of Alaska, College). J. Geophys. Res.; 76: No. 25, 5978-84(1 Sep 1971).

The auroral display appearing over Alaska on the night of February 13–14, 1958 (LT), was characterized by a relatively uniform level of auroral and magnetic activity. Synoptic maps of auroral orientations and motions and of magnetic disturbance from this night are used to infer the steady-state magnetospheric convection during the display. The auroral motions imply an inward component to the convective motion during much of the display, westward motion at distances to 9 $R_E$ in evening and eastward motion beyond 9 $R_E$ in the evening hours and at radial distances 4 to 10 $R_E$ during the morning hours. (auth)

**55955** ASSOCIATION OF MAGNETOTAIL PHENOMENA WITH VISIBLE AURORAL FEATURES. Akasofu, S.-I.; Hones, E. W. Jr.; Montgomery, M. D.; Bame, S. J.; Singer, Sidney (Los Alamos Scientific Lab., N. Mex.). J. Geophys. Res.; 76: No. 25, 5985-6003(1 Sep 1971).

The behavior of the plasma sheet in the distant magnetotail ($r \sim 18\ R_E$) during auroral substorms is examined. In particular, the plasma-sheet variations associated with major features of auroral displays during auroral substorms are identified when Vela satellites were approximately in the field of view (along geomagnetic field lines) of all-sky cameras at Fort Yukon and College (Alaska). Data used were taken during a 1-week period in March 1968 when conjugate auroral flights were made by two airplanes. All-sky camera pictures taken from these airplanes are used to supplement those from the two ground stations. The results are summarized in which the variations of the cross section of the plasma sheet at $r \sim 18\ R_E$ at four different epochs of an auroral substorm are schematically illustrated. (auth)

**55956** LOW-ENERGY (≥0.3 MeV) SOLAR-PARTICLE OBSERVATIONS AT WIDELY SEPARATED POINTS (>0.1 AU) DURING 1967. Krimigis, S. M. (Johns Hopkins Univ., Silver Springs, Md.); Roelof, E. C.; Armstrong, T. P.; Van Allen, J. A. J. Geophys. Res.; 76: No. 25, 5921-46(1 Sep 1971).

Simultaneous observations of solar-particle events at low (<1 MeV) energies were obtained by using intercalibrated solid-state detectors on Mariner 5, Explorer 35, and Mariner 4 during days 200 to 271, 1967. An examination of the intensity–time profiles, anisotropies, intensity ratios of protons to $\alpha$ particles ($j_p/j_\alpha$), ratios of $\alpha$ particles to $Z \geq 3$ (M-nuclei) ($j_\alpha/j_M$), and the proton energy spectrums from several events led to the following results. (a) There are finite differences in particle intensity onsets following flares even when spacecrafts are located close to the same interplanetary magnetic-field line. (b) When particle fluxes have reached a quasi-stationary state, identifiable features in the intensity profile can often be observed to be convected by the solar wind past widely separated (>0.1 AU) spacecraft. (c) Several flare-associated and nonflare intensity peaks are found to corotate with the Sun. (d) Anisotropies are large during the onset phase of flare-associated events with the maximum intensity coming from the solar quadrant (±45° to the Sun-spacecraft line) and still larger for corotating events. (e) The proton spectrum hardens during event onsets and becomes softer as the event progresses at both spacecraft. (f) The $j_p/j_\alpha$ time profile generally follows the proton profile and varies considerably during events; also $j_p/j_\alpha$ decreases as the proton spectrum hardens in accordance with Schatzman's (1963) model. (g) The $j_\alpha/j_M$ ratio is relatively less variable than the $j_p/j_\alpha$ ratio. (h) Few intensity increases can be reliably associated with specific flares on the Sun. It is concluded that, in view of the observations, multi-spacecraft studies should allow the development of more sophisticated models for the understanding of low-energy solar-particle events. (auth)

**55957** FLUX PROFILE OF PROTONS MEASURED IN 1967 AT THE EQUATOR BETWEEN L = 1.15 AND 1.21. Achtermann,

XUM

E.; Paschmann, G.; Hovestadt, D. (Max-Planck-Institut fuer Physik und Astrophysik, Munich). J. Geophys. Res.; 76: No. 25, 6004-13(1 Sep 1971).

The flux-versus-L profiles of trapped protons measured on board a sounding rocket near the equator in 1967 are compared with calculations based on a neutron albedo source and atmospheric losses. The observed fluxes at two different energy channels (20 to 50 MeV > 100 MeV) exceed the fluxes calculated by assuming Lingenfelter's neutron spectrum by factors ranging from 15 to 40. The shapes of the profiles suggest that time variations in the atmospheric density with durations of 150 days preceding these measurements affect the fluxes of those protons with sufficiently short lifetimes. (auth)

**55958** DOUBLE-PROBE MEASUREMENTS OF CONVECTION ELECTRIC FIELDS WITH THE INJUN-5 SATELLITE. Cauffman, David P.; Gurnett, Donald A. (Univ. of Iowa, Iowa City). J. Geophys. Res.; 76: No. 25, 6014-27(1 Sep 1971).

The initial results of the double-probe direct-current electric-field experiment on the low-altitude polar-orbiting Injun-5 satellite are reported. With this experiment magnitudes of naturally occurring magnetospheric electric fields can be measured to an accuracy of ±30 mV/m, and under favorable conditions, to ±10 mV/m. At high latitudes, convection electric fields greater than 30 and sometimes greater than 100 mV/m are frequently observed in the auroral zone. A common feature of these high-latitude convection fields is the occurrence of abrupt reversals or discontinuities in the east–west convection velocity at auroral-zone latitudes. The reversals have been observed at both dawn and dusk local times and at magnetically conjugate points in both hemispheres. For dusk–dawn local times, these reversals correspond to an east–west flow away from the Sun on the high-latitude side of the reversal and toward the Sun on the low-latitude side. Over the polar region above the auroral zone the convection fields are usually not greater than ±30 mV/m, in contrast to the larger field magnitudes observed at the auroral zone. At the boundary of the plasmapause and the light ion trough small 10- to 20-mV/m electric-field perturbations are sometimes observed, corresponding to generally westward convection outside the plasmasphere. At high altitudes, above about 1500 km, over the auroral-zone and polar-cap regions, irregular electric-field noise with amplitudes from 10 to 30 mV/m is often observed. Among the possible explanations of the high-altitude electric-field noise is the presence of significant (>0.5 mV/m) electric fields parallel to the geomagnetic field. The results presented are consistent with measurements made by using the barium-cloud-drift technique. The observed convection is also compared with models of magnetospheric structure and with models of substorms and auroras. (auth)

**55959** ELECTRIC-FIELD MEASUREMENTS AND IDENTIFICATION OF CURRENTS CAUSING MAGNETIC DISTURBANCES IN POLAR CAP. Heppner, J. P.; Stolarik, J. D.; Wescott, E. M. (Goddard Space Flight Center, Greenbelt, Md.). J. Geophys. Res.; 76: No. 25, 6028-53(1 Sep 1971).

Twelve $Ba^+$ clouds were released at invariant latitudes 76 to 78° from three rockets launched from Cape Parry, Northwest Territories, Canada, for the study of polar-cap electric fields and their relationship to polar-cap magnetic-field disturbances. All flights occurred under conditions characterized by Kp ≈ 3. E was typically between 20 and 40 volts/km, directed roughly from dawn toward dusk, and was more uniform in space and time than E fields observed in the auroral belt. The measurements showed a large angular difference between the directions of E and ΔH, the horizontal polar-cap magnetic disturbance. This meant that ΔH could not be caused solely by ionospheric Hall currents in the form of a sheet across the polar cap; also the sign of the difference was opposite to that expected from other elements of the conductivity tensor. Various factors lead to the conclusion that ΔH is caused almost entirely by a source other than overhead ionospheric currents. This conclusion has the consequence that continuity for Hall-current auroral electrojets cannot be achieved by way of the polar-cap and midlatitude ionospheres as assumed in the past. A mutual solution for both the ΔH problem and the continuity problem was found in terms of a new model for continuity of the Hall-current auroral electrojets. Continuity by way of field-aligned currents is primarily a consequence of (grad N)/N being greater than (grad E)/E. N = electron density at 100 to 130 km. The large-scale properties of grad N/grad E appear to be compatible with the net distribution of field-aligned currents required to explain both the polar cap ΔH and the simultaneous disturbance observed on the low-latitude side of the auroral belt. The net field-aligned currents are equivalent to two sheet currents flowing out of and into the auroral-belt ionosphere, respectively, in the magnetic local time sectors 20 to 24 hr and 8 to 12 hr. Cause and effect between field-aligned currents and precipitating particles is implied, in that the distribution of grad N at 100 to 130 km depends on the distribution of the precipitation. (auth)

**55960** ELECTRIC FIELDS IN THE NIGHTTIME AND DAYTIME AURORAL ZONE. Kelley, M. C. (Univ. of California, Berkeley); Mozer, F. S.; Fahleson, U. V. J. Geophys. Res.; 76: No. 25, 6054-66(1 Sep 1971).

Two rockets were launched into the auroral-zone ionosphere to measure the vector electric field by the double Langmuir-probe technique. During part of a flight near magnetic midnight into an active auroral display, an electric-field component of about 20 mV/m was detected parallel to the magnetic-field direction, in agreement with results from a previous nighttime flight. The second flight, near local noon, detected no such parallel field. The parallel field measured at night is consistent with that which might be expected from laboratory measurements and theory. The nighttime electric-field component perpendicular to the magnetic-field direction was generally southerly with an amplitude in the range of 5 to 40 mV/m. The perpendicular electric field measured near local noon was generally northerly in the range of 0.5 to 8 mV/m. (auth)

**55961** ARTIFICIAL AURORA EXPERIMENT: EXPERIMENT AND PRINCIPAL RESULTS. Hess, W. N. (Environmental Research Labs., Boulder, Colo.); Trichel, M. C.; Davis, T. N.; (and others). J. Geophys. Res.; 76: No. 25, 6067-81(1 Sep 1971).

An electron accelerator was flown on an Aerobee-350 rocket from Wallops Island, Virginia, in January 1969. At appropriate altitude the accelerator put out a series of electron-beam pulses up to 1 sec long aimed downward along the magnetic-field line. Several electron energies up to a maximum of 9.5 keV were used. The beam current was also varied up to a maximum of 490 ma. The highest-power pulses were detected on the ground by sensitive optical systems. The vehicle neutralization was accomplished by collecting an ionospheric current equal to the beam current on a large aluminized mylar foil deployed perpendicular to the magnetic field. Attempts were made to measure electromagnetic waves that might be produced by the beam and also to measure with radar the ionization trail resulting from the beam interacting with the atmosphere. The artificial auroral rays produced by the electron beams appeared at the right place and time with about the right shape and intensity. The experiment demonstrates the feasibility of propagating electron beams long distances in space with relatively small alterations resulting from plasma instabilities or beam-propagation problems. (auth)

**55962** ARTIFICIAL AURORA EXPERIMENT: GROUND-BASED OPTICAL OBSERVATIONS. Davis, T. N. (Univ. of Alaska, College); Hallinan, T. J.; Mead, G. D.; (and others). J. Geophys. Res.; 76: No. 25, 6082-92(1 Sep 1971).

Ground-based image-orthicon television systems detected five ray-like artificial auroras produced by electron beams with maximum energy of 8.7 keV directed downward from a rocket-borne accelerator flown January 26, 1969, from Wallops Island, Virginia. Four rays produced by 1-sec 8.7-keV pulses were observed at two stations separated enough to enable the spatial coordinates of the rays to be determined by triangulation. The lower ends of the observed rays were located at altitudes of approximately 104 to 106 km; the upper ends, ranging from altitudes of 122 to 132 km, were not so well defined. Widths of the artificial auroral rays (130 ± 50 meters) and altitudes of the lower ends are in agreement with calculations of Berger et al. (1970), for which Coulomb scattering in a standard model atmosphere with a magnetic-dip angle of 69° is assumed. The observed ray positions were within 0.1° of arc, or approximately 400 meters, of the positions predicted from knowledge of the rocket trajectory and the direction of the local geomagnetic field. From the observed durations of three of these auroras and from other data, it is concluded that the ratio of $N_2^+$ first negative to O I 5577 emission was between 3 and 7. The observations show no delay in the arrival of the electron beams and indicate that most or all of the energy entered the atmosphere in a well-confined beam. (auth)

**55963** SIMULTANEOUS OBSERVATION OF PROTON PRECIPITATION AND AURORAL RADAR ECHOES. Hagfors, T. (Massachusetts Inst. of Tech., Lexington); Johnson, R. G.; Power, R. A. J. Geophys. Res.; 76: No. 25, 6093-8(1 Sep 1971).

Satellite data on precipitating auroral particle fluxes were acquired simultaneously with ground-based observations of auroral radar echoes. Measurements on the auroral-particle fluxes were in the energy range from about 0.5 to 50 keV, and the auroral radar observations were made at 23 cm with frequency spectra analysis to investigate the motion of the scattering region. The results for an afternoon event show that strong radar echoes occurred in the absence of observable electron precipitation but were in close time and spatial coincidence with proton precipitation, although the proton contribution to the ionization at the scattering height at 112 km was computed to be negligible compared with the solar ionization. The frequency spectra of the auroral radar echoes were not of the character expected from a two-stream instability. (auth)

XUM

**55964** POLAR IONOSPHERE: MEASURED ION DENSITY ENHANCEMENTS AND SOFT ELECTRON PRECIPITATION. Morse, Fred A.; Hilton, H. H.; Mizera, P. F. (Aerospace Corp., El Segundo, Calif.). J. Geophys. Res.; 76: No. 25, 6099-6111 (1 Sep 1971).

The experiment complement aboard a polar satellite having a perigee near 160 km and initial apogee near 1800 km included an ion trap and sensors for low-energy electrons and protons. The data from these two experiments were correlated for the period August 13–18, 1968, during which time the perigee invariant latitude was ≥70°. Results of these studies for the polar region are the following. (a) The large ion-density enhancements observed are correlated with simultaneously observed enhancements in the precipitating fluxes of low-energy electrons. (b) The trough and ionospheric enhancements are shown to occur below as well as above the F-region maximum density height. (c) It is concluded that the position of the midlatitude trough minimum should not be expected to show a simple relationship with magnetic indices since the shape depends on (1) the local precipitation (ionization) patterns; (2) the total energy input, its time and spatial extent; (3) diffusion rates of the ionized species; (4) universal time; and (5) altitude of the observation. (auth)

**55965** ELECTROSTATIC vlf WAVES OBSERVED IN THE POLAR MAGNETOSPHERE. McPherson, D. A.; Koons, H. C. (Aerospace Corp., El Segundo, Calif.). J. Geophys. Res.; 76: No. 25, 6112-21(1 Sep 1971).

Broadband electrostatic emissions are detected by a vlf receiver aboard the satellite OV3-3 (1966-70A). Enhancements of the electric-field intensity in 10 bandpass channels at frequencies between 400 and 14.5 kHz are observed when the spacecraft passes over the south polar region at altitudes between 2500 and 4500 km (satellite apogee). The power spectral density of these emissions decreases as approximately the inverse fourth power of the observed frequency. The most interesting feature of these emissions is the range of invariant magnetic latitudes (INVL) over which they are observed. The low-latitude limit at which they are detected is typically 72 to 76° INVL in local morning and 68° INVL near midnight. This dependence suggests that these emissions occur on magnetic-field lines along which the polar wind flows. During geomagnetically active periods, electrostatic waves with a high-frequency cutoff between 1.3 and 3.9 kHz are also observed in this altitude range. These emissions occur at latitudes below the low-latitude limit of the polar-electrostatic waves and above the latitude of the plasmapause. (auth)

**55966** ION-WAVE INSTABILITIES AT vlf IN THE POLAR WIND. Koons, H. C.; McPherson, D. A.; Schulz, Michael (Aerospace Corp., El Segundo, Calif.). J. Geophys. Res.; 76: No. 25, 6122-35(1 Sep 1971).

Considerations based on plasma kinetic theory suggest that a variety of ion waves in the elf and vlf bands can become unstable in the polar wind when the relative flow velocity between the hydrogen ions and oxygen ions enters the range 5 to 10 km/sec. Peak growth rates of ~100 $sec^{-1}$ seem achievable for wavelengths typically 10 times the Debye length (wavelengths of ~2 meters in the polar wind). The threshold flow velocity for instability generally decreases as altitude increases within the altitude range 2000 to 5000 km, where the waves are expected to appear. These numerical estimates are based on a heuristic calculation for a specific instability (ion-acoustic). Other ionic two-stream instabilities (e.g., ion-cyclotron) belonging to the more general class may be equally important in the Earth's polar wind. Electrostatic waves in the appropriate frequency range have been observed at altitudes 2500 to 4500 km over the polar regions by a vlf receiver on the OV3-3 satellite. These waves may be important in impeding the escape of polar-wind hydrogen and helium ions. (auth)

**55967** SOUNDING ROCKET OBSERVATION OF HELIUM 304- AND 584-A GLOW. Ogawa, Toshihiro (Tokyo, Univ.); Tohmatsu, Takao. J. Geophys. Res.; 76: No. 25, 6136-45 (1 Sep 1971).

The altitude distribution of the euv emissions of neutral helium (He 584 A) and singly ionized helium ($He^+$ 304 A) was measured by aluminum and bismuth thin-film photon counters aboard an exospheric sounding rocket flown from Uchinoura, Japan, on September 19, 1970, 2030 JST. On ascent the He 584-A intensity increased from 40 to 100 R between 250 to 720 km and then decreased gradually to 30 R at 1600 km. On the downleg the intensity remained nearly constant at 5 R between 1400 and 600 km and then decreased gradually to about 2 R at 440 km. The excitation mechanism of the He 584-A glow is ascribed to resonance fluorescence of atmospheric helium by solar 584-A radiation. The observed distribution is consistent with a diffusive equilibrium distribution of helium at a thermopause temperature of 1180 ± 50°K and having a base-line value of density of $(1.2 \pm 0.2) \times 10^6$ atoms/$cm^3$ at 720 km. The intensity of $He^+$ 304-A glow decreased from 12 to 4 R on ascent from 420 to 1200 km and then remained almost steady at 1.5 ± 0.5 R through the same altitude range on descent. The absolute intensity of the 304-A flow was at least 2.5 times greater than expected from resonance fluorescence by ionospheric helium ions of solar 304-A radiation. Evidence for the presence of extraterrestrial helium glow is discussed. (auth)

**55968** OGO-4 OBSERVATIONS OF LYMAN–BIRGE–HOPFIELD EMISSION IN DAY AIRGLOW. Prinz, D. K.; Meier, R. R. (Naval Research Lab., Washington, D. C.). J. Geophys. Res.; 76: No. 25, 6146-58(1 Sep 1971).

The results of measurements of the day airglow in the wavelength interval 1356 to 1600 A from detectors aboard the polar-orbiting satellite Ogo 4 are reported for the period Aug. 1967–July 1968. The columnar emission rates for the total Lyman–Birge–Hopfield system of molecular nitrogen (implied by assuming a relative spectral composition for the incident radiation) for a solar zenith angle 0° were of the order of 6.5 kR, with variations that tended to follow the 10.7-cm flux; however, the magnitudes of the variations of the two were not always the same. The emission rate at night has an upper limit of 25 R (determined by the data noise level). The dependence of the emission on solar zenith angle is shown to be approximately proportional to the reciprocal of the Chapman function; i.e., the local intensity can be expressed as the product of the reciprocal of the Chapman function, the subsolar point intensity, and a global distribution function that has a value close to one. This global distribution function is approximately related to the atmospheric composition and has a latitude and local-time dependence similar to that of the exospheric temperature. Using an expression for the diurnal variation of the exospheric temperature developed by Jacchia (1965), the relation implies that the global distribution function maximum (at 70° solar zenith angle) follows the latitude of the subsolar point with a lag of 5.3 hours. The magnitude of the observed columnar emission rate for the LBH band system agrees well with recent calculations that assume that the excitation mechanism is photoelectron impact. (auth)

**55969** TRANSPORT PROCESSES IN THE E REGION OF THE IONOSPHERE. Schunk, Robert W. (Univ. of Michigan, Ann Arbor); Walker, James C. G. J. Geophys. Res.; 76: No. 25, 6159-71(1 Sep 1971).

The role of plasma transport processes in the E region of the ionosphere is examined by using the method of moments to derive the transport equations up to and including the equation for the heat-flow vector of a weakly ionized, magnetized plasma containing a mixture of ion species. By using simple models of the midlatitude nocturnal ionosphere and the auroral ionosphere, the magnitudes of some of the terms in the transport equations are compared, including transport across the magnetic field as well as transport along it. In harmony with previous work, it is found that vertical diffusion can affect ion densities at night at altitudes above about 160 km. Diffusion velocities at altitudes below 200 km in the nocturnal midlatitude ionosphere can be influenced by field-aligned electric currents as small as $10^{-7}$ amp $m^{-2}$. The ion heating associated with vertical diffusion is negligible. The flow of heat associated with electrojet currents and with temperature gradients perpendicular to the magnetic field also has a negligibly small affect on ion temperatures. In the auroral oval the ion temperature is determined by a balance between Joule heating and ion-neutral cooling. (auth)

**55970** DETONATION-WAVE EFFECTS ON DECAMETER-WAVELENGTH RADIO WAVES IN THE LOWER IONOSPHERE. Davis, John R.; Uffelman, Donald R. (Naval Research Lab., Washington, D. C.). J. Geophys. Res.; 76: No. 25, 6172-84 (1 Sep 1971).

Three high-explosive charges were placed by rocket in the lower E layer to study the effects of detonation waves on this region of the ionosphere. Observations made by coherent-pulse-Doppler high-frequency radar and an ionosonde indicated that three types of radar targets were discerned. (1) Shock-wave excitation of atmospheric constituents and compression of existing ionization created an overdense reflecting surface, with a probable small additional contribution due to partial reflections, that traveled radially outward quite rapidly and was observed for a few tenths of a second. (2) Shock-induced ionization created as a result of the high temperatures achieved in the region between the first shock wave and the contact surface between the explosion products and the atmospheric fluid persisted as a nearly stationary radar target for several minutes. (3) Sonic waves propagating outward from the detonation were observed to perturb sky-wave transmission paths that passed through the ionosphere many tens of kilometers from the explosion. These effects were detected several minutes after the explosion. It is concluded that explosive

XUM

thermal excitation of the lower E layer is adequate to produce radar reflections of decameter wavelengths by compression of existing ionization and shock excitation of additional ionization and to deposit by this means long-lasting ionization, which may appear as an artificial sporadic-E layer of several minutes duration. (auth)

**55971** SIMULTANEOUS SPECTROGRAPHIC TRIANGULATION OF AN SAR ARC AND A HYDROGEN ARC. Hoch, R. J. (Battelle-Northwest, Richland, Wash.); Batishko, C. R.; Clark, K. C. J. Geophys. Res.; 76: No. 25, 6185-9(1 Sep 1971).

An SAR arc at about L = 2.8 and a hydrogen (H) arc between L = 3.4 and L = 4.0 were monitored from Richland and Banff throughout the night of March 23–24, 1969. The SAR arc remained stationary and during the night the 6300-A emission decreased steadily in intensity from about 1 kR to less than 300 rayleighs. In contrast, the H arc, in which Balmer-$\alpha$ emission reached an intensity of 1.7 kR, fluctuated by an order of magnitude in intensity, moved about vigorously, and split into two arcs in the morning. Spectrograms in the magnetic meridian display the monochromatic SAR-arc emission. The measurements show the SAR arc and H arc to be clearly separated by about 5° of latitude and apparently quite uncorrelated in behavior. (auth)

**55972** TIME-DEPENDENT PLASMAPAUSE MOTION. Grebowsky, J. M. (Goddard Space Flight Center, Greenbelt, Md.). J. Geophys. Res.; 76: No. 25, 6193-7(1 Sep 1971).

Time-dependent computations indicate that the configuration of the plasmapause can become quite complex and much different from the computed steady-state configurations when temporal variations in the thermal plasma flow across the magnetic-field lines are considered. An investigation is made of the plasmapause motion for the case in which the dayside electric field vanishes in the rest frame of the rotating ionosphere by using a simple convection model to describe the plasma flow, treating the Earth's magnetic field as dipolar, and ignoring the details of the plasma interaction at the magnetosphere boundary. It was assumed that the Earth's magnetic axis and the Earth's spin axis are coincident with one another. (J.C.W.)

**55973** TEMPORAL VARIATIONS OF THERMOSPHERIC HYDROGEN DERIVED FROM IN SITU MEASUREMENTS. Brinton, Henry C.; Mayr, Hans G. (Goddard Space Flight Center, Greenbelt, Md.). J. Geophys. Res.; 76: No. 25, 6198-6201(1 Sep 1971).

The first in situ determination of the temporal variations of thermospheric hydrogen is obtained from Explorer-32 data taken from June 1966 to Jan. 1967 at 280 to 450 km. Data are given on contributions to hydrogen concentration associated with exospheric temperature components related to 11-year solar cycle, 27-day solar rotation, and the diurnal variation. The increase in average solar activity ($F_{10.7}$) from 100 to 140 and resultant atmospheric temperature increase caused a factor of 2.5 decrease in hydrogen concentration. The 27-day variation in solar activity and the corresponding temperature component were correlated with an inverse variation of as much as a factor of 1.3. The concentration of hydrogen increased by approximately a factor of 2 between day and night, with a phase delay of about 3 hours between model exospheric temperature and n(H). (J.C.W.)

**55974** IONOSPHERIC STORM OF MARCH 8, 1970. Klobuchar, J. A. (Air Force Cambridge Research Lab., Bedford, Mass.); Mendillo, M.; Smith III, F. L.; (and others). J. Geophys. Res.; 76: No. 25, 6202-7(1 Sep 1971).

Data are reported from 10 stations during the Mar. 8, 1970 ionospheric storm that occurred following the total solar eclipse on Mar. 7, 1970. A morphological investigation is given in which the spatial and temporal variation of electron content occurred during the storm. Results show that the ionospheric effects observed for this storm depend on the location of the station. Very pronounced storm-associated east–west gradients in electron content were observed. (J.C.W.)

**55975** DEPENDENCE OF THE IONOSPHERIC ABSORPTION ON LUNAR PHASE. Mohan Rao, A. S.; Rao, B. Ramachandra (Andhra Univ., Waltair, India). J. Geophys. Res.; 76: No. 25, 6208-09(1 Sep 1971).

The dependence of the ionospheric absorption on the lunar phase for midlatitude and equatorial stations has been previously studied. These investigations have shown a perceptible lunar semidiurnal oscillation in the ionospheric absorption. A study of the lunar tidal effect on the ionospheric absorption measured at Waltair at noontime on two frequencies, 2.0 and 2.5 MHz, during Feb. 1963 to Feb. 1965 was made and the results are compared with those for other latitudes. (J.C.W.)

**55976** SIMULATION EXPERIMENTS ON SPACE PLASMA PHYSICS. Kawashima, Nobuki (Tokyo Univ.). Cho-Koon Kenkyu; 7: No. 3, 121-31(Oct 1970). (In Japanese).

Results of simulation experiments on space plasma physics is reviewed. The simulation experiment of solar wind–geomagnetic field interaction is discussed first. Local time (dawn–dusk) asymmetry of intruding plasma, with more plasma on the dawn side, was found. This was confirmed by recent satellite observation with Vela 2B. Effect of interplanetary magnetic field on the plasma intrusion was found both by simulation and by satellite observation. It was found that the effect of the external magnetic field parallel to the plasma stream appears in the north–south asymmetry. The structure of a comet tail was also simulated. Simulation of a solar flare was attempted. Accelerated plasma from neutral current sheet was detected. (Japan)

**55977** CALCULATIONS ON CURRENT SYSTEMS IN THE POLAR E REGION. Czechowsky, P. (Max-Planck-Institut fuer Aeronomie, Lindau, Ger.). Z. Geophys.; 36: 647-50(1970). (In German).

An exact calculation of the current systems registered in the ionosphere appeared impossible because of the number of parameters. However, with the assumption of a physically significant model, it is possible to find an equivalent current system which produces, at ground level in a given range, a corresponding perturbation field. A solution method is described with which nine parameters of a model current system can be determined. (J.S.R.)

**55978** MONOTONIC DECREASE OF THE INTENSITY OF ELECTRONS IN THE RADIATION BELTS OF THE EARTH. Kuznetsov, S. N.; Tverskoi, B. A. (Moscow State Univ.). Geomagn. Aeron. (USSR) (Engl. Transl.); 11: No. 1, 1-6(1971).

Translated from Geomagn. Aeron.; 11: No. 1, 3-10(1971).

The decrease in the intensity of electrons with E > 40 keV on the different shells of radiation belts in a magnetically quiet period is analyzed. This decrease is most frequently described by an exponential function. In some time intervals, when electron intensity is sufficiently high, a decrease may be observed that is described by a power function. It is demonstrated that when allowance is made for recombination processes in the ionosphere and when the electron intensity greatly exceeds the critical level, the decrease in the intensity of electrons with an energy less than several hundred keV can obey the power law. (auth)

**55979** SOME PATTERNS IN THE CORRELATION OF MAGNETIC ACTIVITY INDEXES WITH THE INTENSITY OF OUTER-BELT ELECTRONS. Vernov, S. N.; Kuznetsov, S. N.; Logachev, Yu. I.; (and others) (Moscow State Univ.). Geomagn. Aeron. (USSR) (Engl. Transl.); 11: No. 1, 7-11(1971).

Translated from Geomagn. Aeron.; 11: No. 1, 11-17(1971).

In comparing data on outer-belt electrons with $E_e \gtrsim 150$ keV with different geomagnetic activity indexes it was found that electron intensity is more closely associated with auroral activity characteristics than with $K_p$, and the highest negative coefficient of correlation was found to occur when a maximum decrease in the field near the equator is observed at 19 to 24 h LT. In the unstable radiation zone, the highest correlation coefficient is observed between electron intensity and the $K_p$ index. The possible mechanisms of the observed relationship between energetic electron fluxes in the magnetosphere and magnetic activity indexes are discussed. It is demonstrated that $K_p$ can be regarded as a measure of the electric field arising during magnetospheric disturbances. It is assumed that outer-belt electrons with E > 40 keV and electrons with E > 150 keV in the unstable radiation zone accelerate under the effect of a quasi-stationary field in the tail of the magnetosphere. Variations in the population of electrons with E > 150 keV in the outer belt are associated with the deformation of magnetic lines of force during auroral magnetic disturbances. An example of electron acceleration during the contraction of the lines of force from the tail into the core of the magnetosphere is discussed. (auth)

**55980** GLOBAL DISTRIBUTION OF ENERGETIC CHARGED-PARTICLE INTENSITY ABOVE THE ATMOSPHERE, ACCORDING TO COSMOS-208 AND COSMOS-228 DATA. Basilova, R. N.; Savenko, I. A. (Moscow State Univ.). Geomagn. Aeron. (USSR) (Engl. Transl.); 11: No. 1, 12-15(1971).

Translated from Geomagn. Aeron.; 11: No. 1, 18-22(1971).

The results of a study of the global distribution of primary cosmic rays and residual particles above the atmosphere are reported. The global distribution of primary cosmic rays is compared with that of vertical magnetic cutoff rigidities. (auth)

**55981** COORDINATED INTERNATIONAL MEASUREMENTS OF GEOPHYSICAL EFFECTS OF SOLAR ACTIVITY IN THE UPPER ATMOSPHERE. I. SYNCHRONOUS OBSERVATIONS BY THE GROUND-BASED NETWORK OF IONOSPHERIC STATIONS AND THE COSMOS-261 SATELLITE. Bentze, P. (Sopron Observatory, Hungary); Wernik, A.; Gal'perin, Yu. I.; (and others). Geomagn. Aeron. (USSR) (Engl. Transl.); 11: No. 1, 16-19(1971).

Translated from Geomagn. Aeron.; 11: No. 1, 23-8(1971).

XUM

Data from the Cosmos-261 satellite and the network of ground-based geophysical observatories in Bulgaria, Hungary, the German Democratic Republic, Poland, Rumania, the USSR, and Czechoslovakia are used to describe the experiment. The experiment was run from Dec. 20, 1968 through Feb. 12, 1969. Its purpose was to investigate the variations in the upper atmosphere produced by geophysically active particles. (auth)

**55982** COORDINATED INTERNATIONAL MEASUREMENTS OF GEOPHYSICAL EFFECTS OF SOLAR ACTIVITY IN THE UPPER ATMOSPHERE. II. MEASUREMENTS OF IONOSPHERIC EFFECTS OF THE DECEMBER 27, 1968, CHROMOSPHERIC FLARE BY COSMOS 261 AND GROUND-BASED OBSERVATORIES. Best, A. (Geomagnetic Inst., Potsdam, Ger.); Wernik, A.; Gal'perin, Yu. I.; (and others). Geomagn. Aeron. (USSR) (Engl. Transl.); 11: No. 1, 20-8(1971).

Translated from Geomagn. Aeron.; 11: No. 1, 29-39(1971).

SID and other effects accompanying the solar flare of December 27, 1968 are analyzed. The temporal variations of the lower boundary of the D region and of radio-wave absorption in the lf, mf, and hf ranges were measured and the variations in the state of ionization of the lower and middle ionosphere are estimated. A comparison of the observed increase in ionization rate with the results of simultaneous x-ray measurements on Explorer 37 shows that solar x radiation at $\lambda \leq 8$ Å contributed insignificantly to D-region ionization under quiet conditions. The data of 50 magnetic stations are used to construct an equivalent current system for the magnetic crochet effect associated with the flare. This system differs greatly from that of $S_q$ currents. Apparently it is produced mainly by solar x radiation in the interval 8 to 20 Å, which gives rise to additional ionization in the dynamo region. Measurements were made of the variations in the intensity of fresh photoelectrons with energies from 60 to 120 eV, which approximately reflect the intensity variations of solar uv radiation in the range $\lambda \lesssim 200$ and $\gtrsim 100$ Å, which ionizes the E region and the lower part of the F region of the ionosphere. Their intensity increased approximately 10 min before the increase in solar x radiation and before noticeable ionospheric and geomagnetic disturbances were observed. (auth)

**55983** IONIZATION OF A SUBSTANCE UNDER THE EFFECT OF CHARGED PARTICLES WITH ALLOWANCE FOR THEIR ENERGY AND SPACE DISTRIBUTIONS. Velinov, P. (Geophysical Inst., Sofia). Geomagn. Aeron. (USSR) (Engl. Transl.); 11: No. 1, 56-60(1971).

Translated from Geomagn. Aeron.; 11: No. 1, 72-8(1971).

Ionization produced by the penetration into a medium of energetic charged particles with a given spectrum and spatial distribution is analyzed. The solutions obtained can be used to compute the rate of electron production in the atmosphere of the Earth and planets as a result of their ionization by galactic and cosmic solar radiation and to determine the radiation absorbed dose during space flights. (auth)

**55984** NUMERICAL MODELS OF ELECTRON DENSITY DISTRIBUTION IN THE IONOSPHERIC F2 REGION. I. Fatkullin, M. N.; Muradov, A. (Inst. of Terrestrial Magnetism, Ionosphere, and Radio Wave Propagation, Moscow). Geomagn. Aeron. (USSR) (Engl. Transl.); 11: No. 1, 61-6(1971).

Translated from Geomagn. Aeron.; 11: No. 1, 79-85(1971).

The nonstationary continuity equation for the electron–ion gas in the F2 region has been integrated numerically with allowance for ionization–recombination processes, the absence of thermal equilibrium in the F region for ambipolar diffusion and other types of plasma motions, for diurnal temperature variations, and for the composition of the upper atmosphere. The approximations used are discussed. The selection of initial and boundary conditions and their effect on the $n_e$ distribution are examined. Preliminary results for the particular case of the diurnal equilibrium distribution of $n_e(h)$ are presented. (auth)

**55985** CHARACTERISTICS OF $\delta$ $f_0F2$ DISTRIBUTION CURVES. Vsekhsvyatskaya, I. S.; Sergeenko, N. P.; Yudovich, L. A. (Inst. of Terrestrial Magnetism, Ionosphere, and Radio Wave Propagation, Moscow). Geomagn. Aeron. (USSR) (Engl. Transl.); 11: No. 1, 67-70(1971).

Translated from Geomagn. Aeron.; 11: No. 1, 86-91(1971).

It is demonstrated on the basis of a statistical analysis of $\delta$ $f_0F2$ distribution curves, obtained from monthly samples of data from seven stations for three years, that the distribution law of the $\delta f_0F2$ population is far from normal. A method is proposed for interpreting the experimental curves of the probability density functions by means of a model with an excess and skew, based on a random Poisson process. (auth)

**55986** QUASI-LINEAR THEORY OF FORMATION OF INHOMOGENEITIES IN THE EQUATORIAL ELECTROJET. Kamenetskaya, G. Kh. (Gorky State Univ., USSR). Geomagn. Aeron. (USSR) (Engl. Transl.); 11: No. 1, 71-5(1971).

Translated from Geomagn. Aeron.; 11: No. 1, 92-6(1971).

The excitation of space-charge waves by an electric current perpendicular to the geomagnetic field is analyzed. Equations are obtained in the quasi-linear approximation that describe the change in the directional velocity of electrons u and the heating of the electrons and ions in the field of the generated waves. Estimates are made in the stationary case of the temperature of the electron and ion components of the plasma in the stream as a function of u. (auth)

**55987** DIURNAL VARIATIONS OF STRUCTURAL PARAMETERS OF THE ATMOSPHERE AT HEIGHTS OF 100 TO 220 KM. Starkova, A. G. (Inst. of Applied Geophysics, Moscow). Geomagn. Aeron. (USSR) (Engl. Transl.); 11: No. 1, 87-91(1971).

Translated from Geomagn. Aeron.; 11: No. 1, 110-14(1971).

The diurnal variations of the structural parameters of the atmosphere (temperature and concentrations of molecular nitrogen and molecular and atomic oxygen) in the height range 100 to 220 km obtained in rocket experiments are analyzed. The relationship between these parameters and the heating of the atmosphere by solar uv radiation is found. The minimum values of the structural parameters are observed near sunrise and the maximum values near sunset, both at low and moderate solar activity. (auth)

**55988** RELATIONSHIP BETWEEN MAGNETIC FIELDS OF SPACE AND OF THE EARTH. Mansurov, S. M.; Mansurova, L. G. (Inst. of Terrestrial Magnetism, Ionosphere, and Radio Wave Propagation, Moscow). Geomagn. Aeron. (USSR) (Engl. Transl.); 11: No. 1, 92-4(1971).

Translated from Geomagn. Aeron.; 11: No. 1, 115-18(1971).

The morphology of the effect produced in the geomagnetic field by the sector structure of the interplanetary magnetic field is described. Estimates are given of the diurnal and seasonal variations of this effect. It is shown that geomagnetic-field variations in the polar caps, associated with this effect, can be roughly approximated by zonal electric-current systems. The direction of the current is opposite in the Northern and Southern Hemispheres and depends on the direction of the interplanetary magnetic field. Two associated types of geomagnetic variations in the polar caps are found and their classification is given. (auth)

**55989** RAPIDLY VARYING GEOMAGNETIC FIELD DISTURBANCES PRODUCED BY A NONSTATIONARY SOURCE OF GAMMA QUANTA. Medvedev, Yu. A.; Stepanov, B. M.; Fedorovich, G. V. Geomagn. Aeron. (USSR) (Engl. Transl.); 11: No. 1, 95-100(1971).

Translated from Geomagn. Aeron.; 11: No. 1, 119-25(1971).

The fields and currents in the vicinity of a source of $\gamma$ quanta are examined and the developing phenomena are analyzed qualitatively. (auth)

**55990** METHOD FOR COMPUTING THE GEOMAGNETIC FIELD AT INTERMEDIATE IONOSPHERIC HEIGHTS. Fomin, B. V. Geomagn. Aeron. (USSR) (Engl. Transl.); 11: No. 1, 101-6(1971).

Translated from Geomagn. Aeron.; 11: No. 1, 126-32(1971).

A method is described for computing the total vector of the real magnetic field H at heights up to several hundred kilometers. The solution of the spherical Dirichlet problem is applied to each of the rectangular components of H, which are harmonic functions above the surface of the Earth. As a result, computation of any field component at some point above the Earth reduces to integration with definite weights of all three components of the known field at the surface of the Earth in some region under the given point. (auth)

**55991** MEASUREMENT OF SOLAR PROTONS FROM THE JULY 7, 1966 FLARE ON THE PROTON-3 SATELLITE. Zel'dovich, M. A.; Kovrizhnykh, O. M.; Madeev, M. O.; Savenko, I. A. (Moscow State Univ.). Geomagn. Aeron. (USSR) (Engl. Transl.); 11: No. 1, 115-17(1971).

Translated from Geomagn. Aeron.; 11: No. 1, 145-6(1971).

The Proton-3 satellite was launched on July 6, 1966 on a near-Earth orbit with an apogee of 630 km and a perigee of 190 km. The data obtained were the results of the operation of the equipment designed to search out quarks in primary cosmic radiation beyond the atmosphere. The class 2B chromospheric flare commenced on July 7, 1966 and after reaching a maximum, lasted two hours. The optical flare was accompanied by x-ray and radio-noise bursts in the centimeter range and types II and IV radio-noise bursts in the metric range. OGO-3 and IMP-3 satellites also recorded the July-7 flare and a comparison is made of the observations. (J.C.W.)

**55992** VARIATIONS OF INTERPLANETARY SPACE PARAMETERS DURING A SOLAR ACTIVITY CYCLE. Kovalevskii, I.

XUM

V. (Inst. of Terrestrial Magnetism, Ionosphere, and Radio Wave Propagation, Moscow). Geomagn. Aeron. (USSR) (Engl. Transl.); 11: No. 1, 118-19(1971).

Translated from Geomagn. Aeron.; 11: No. 1, 147-8(1971).

The behavior of interplanetary space at heliocentric distances of 0.7 to 1.4 AU is examined for 1959–1967. The data on proton density, temperature, velocity, and the intensity of the interplanetary magnetic field were averaged for each month and used to determine the intensity of the proton flux; dynamic, static, and magnetic pressure; the ratios $\beta' = p_1/2p_3$, $\beta = p_2/p_3$, and $\beta_T = p_2/p_1$; the intensities of the energy fluxes of directional and thermal motions and of electromagnetic energy; the acoustic, Alfvén, and magneto-acoustic velocities of propagation of weak disturbances; the corresponding Mach numbers $M_3 = v/v_3$, $M_A = v/v_A$, and $M_{ma} = v/v_{ma}$; the position of the zones of joint rotation of interplanetary space with the Sun; and the boundaries of the interplanetary cavity. The parameters are examined and correlations made. (J.C.W.)

55993 AVERAGE DIURNAL AND SEASONAL VARIATIONS OF ELECTRON DENSITY IN THE TOPSIDE IONOSPHERE AT MIDDLE LATITUDES. Fatkullin, M. N.; Legen'ka, A. D. (Inst. of Terrestrial Magnetism, Ionosphere, and Radio Wave Propagation, Moscow). Geomagn. Aeron. (USSR) (Engl. Transl.); 11: No. 1, 122-4(1971).

Translated from Geomagn. Aeron.; 11: No. 1, 152-3(1971).

Electron-density profiles obtained from Alouette 1 were used to study the average diurnal electron-density patterns in the topside ionosphere at 250 to 1000 km. The summer of May–July 1963 and winter of Nov.–Dec. 1963 and Jan. 1964 were considered. The vertical and temporal distributions of the seasonal electron-density anomaly in the topside ionosphere were investigated. The diurnal electron-density variations at fixed heights were compared with those at the F2-layer maximum by determining the diurnal variations of the critical frequency of the F2 layer at the same latitudes and longitudes used in the investigation of the topside ionosphere. The diurnal critical-frequency variations of the F2 layer were compared for Alouette and ground-based data. (J.C.W.)

55994 EFFECT OF UNIVERSAL TIME IN $f_0E$ VARIATIONS AT LARGE SOLAR ZENITH ANGLES. Korsunova, L. P. (Inst. of Terrestrial Magnetism, Ionosphere, and Radio Wave Propagation, Novosibirsk, USSR). Geomagn. Aeron. (USSR) (Engl. Transl.); 11: No. 1, 124-7(1971).

Translated from Geomagn. Aeron.; 11: No. 1, 154-6(1971).

A phenomenon found in the behavior of the critical frequency of the E layer associated with the evening–morning asymmetry variations at large solar zenith angles is discussed. A pattern is found in the variations with universal time, UT, if observations are made at stations located at close geomagnetic latitudes. The observational data are explained and it is concluded that the dependence of $f_0E$ on universal time makes it possible to explain the asymmetry, including the change in sign of the asymmetry for different stations located at different longitudes, the change in sign in the course of a year at Irkutsk and Sverdlovsk stations, and the preservation of the sign at Moscow. The results of ionospheric observations in 1963 at 8 midlatitude stations in the northern hemisphere during quiet geophysical conditions were analyzed to verify the phenomenon. (J.C.W.)

55995 COMPUTATION OF N(z) PROFILES IN THE UPPER IONOSPHERE FROM THE RESULTS OF GROUND-BASED VERTICAL SOUNDINGS. Slutsker, S. M. Geomagn. Aeron. (USSR) (Engl. Transl.); 11: No. 1, 127-9(1971).

Translated from Geomagn. Aeron.; 11: No. 1, 157-8(1971).

Ionization profiles obtained by vertical sounding from Alouette 1 in Oct.–Dec. 1962 are used to analyze the shape of the upper ionosphere. The model of the ionosphere for the new approximation method is given and the method is verified by comparing the computed profiles with the experimental profiles obtained by rockets. The main parameter of the upper ionosphere is the vertical gradient of the linear function of height. (J.C.W.)

55996 PROTON ANOMALIES IN PROPAGATION OF VERY LONG RADIO WAVES AT MIDDLE LATITUDES. Fedyakina, N. I. (Arctic and Antarctic Scientific Research Inst., Leningrad). Geomagn. Aeron. (USSR) (Engl. Transl.); 11: No. 1, 134-5(1971).

Translated from Geomagn. Aeron.; 11: No. 1, 164(1971).

Observations show that the behavior of very long waves on radio links that cross the polar cap or the auroral zone differs during auroral disturbances and PCA. The changes during magnetic disturbances or auroral anomalies are short and observed only during the disturbance, and not every magnetic-field disturbance is accompanied by auroral very-long-wave anomalies. Auroral anomalies have no significant effect on the diurnal pattern of very-long-wave signals but, during PCA events, the pattern changes significantly when the radio link crosses the polar cap. The behavior of very long waves associated with PCA is designated as proton anomalies. The anomalies are stable and persist for days. An analysis of this anomaly is given for midlatitude. (J.C.W.)

55997 SOME MORPHOLOGICAL CHARACTERISTICS OF WHISTLER SPECTRA AND THE NATURE OF IONIZATION IRREGULARITIES IN THE TOPSIDE IONOSPHERE. Likhter, Ya. I.; Sobolev, Ya. P. (Inst. of Terrestrial Magnetism, Ionosphere, and Radio Wave Propagation, Moscow). Geomagn. Aeron. (USSR) (Engl. Transl.); 11: No. 1, 136-7(1971).

Translated from Geomagn. Aeron.; 11: No. 1, 165-6(1971).

The whistlers recorded in Moscow between 1958 and 1962 and in Riga from 1965 and 1968 are analyzed to study the multicomponent and diffuse dynamic types. Both diffuse and multicomponent whistlers are recorded at night and the first predominate. Diffuse whistlers are not recorded during the daytime, generally. It is concluded that in the topside ionosphere there are two types of ionization irregularities that are oriented along the geomagnetic field, the discrete that leads to multicomponent whistlers and complex irregularities that lead to diffuse whistlers. Discrete ionization irregularities may exist during day and night. Irregularities responsible for diffuse whistlers occur only at night. The relationship found between ionospheric spread F and completely diffuse whistlers is discussed. (J.C.W.)

55998 SPECTRAL AND CORRELATION CHARACTERISTICS OF NOISE FROM THE LEADER STAGE OF A LIGHTNING DISCHARGE. Gladshteyn, N. D. (Inst. of Radio Engineering and Electronics, Moscow). Geomagn. Aeron. (USSR) (Engl. Transl.); 11: No. 1, 138-9(1971).

Translated from Geomagn. Aeron.; 11: No. 1, 167-8(1971).

A computer method is described for the correlation and spectral characteristics of pulses from the leader stage of a lightning discharge. The correlation characteristics were computed from photographs of the oscillograms of the process with an exposure of up to 200 μsec, recorded in the frequency band 0.5 to 150 kHz. The predischarge spectrum is vanishingly small at frequencies greater than 100 kHz. The recorded segments of the predischarge were not connected in any way with the beginning of the pulse from the main discharge. The main part of the energy of the predischarge is concentrated in the frequency range 8 to 40 kHz. The bipolar leader pulses, whose leading edges are properly approximated by exponential functions, have a spectrum that is shifted toward higher frequencies compared with the spectrum of ordinary pulses. The spectrum of the leader pulses recorded at night is more dissected than that of pulses recorded during the daytime. (J.C.W.)

55999 RELATIONSHIP BETWEEN VLF EMISSION AND COSMIC-NOISE ABSORPTION IN THE AURORAL ZONE. Osipov, K. K.; Osipov, N. K. (Radio Engineering Inst., Moscow). Geomagn. Aeron. (USSR) (Engl. Transl.); 11: No. 1, 139-41(1971).

Translated from Geomagn. Aeron.; 11: No. 1, 169-70(1971).

The study of the characteristics of electromagnetic vlf emission in the auroral zone in relation to other auroral substorm phenomena permits formulation of several requirements for the possible mechanisms of vlf generation and the physical conditions in the auroral ionosphere. Data have been analyzed by Vershinin and Ponomarev on the relationship between the intensities of two types of vlf emission, accompanying auroras, and absorption in the auroral ionosphere measured by riometer. According to these data, two characteristic situations are observed in the auroral zone that correspond to continuous vlf emission or to emission bursts. Various other experimental and observed data are analyzed, but the case presented allows for the variation of absorption produced mainly by a variation in electron flux, when the linear relationship is most simply realized if there is a linear relationship between the intensity of the vlf emission and the electron flux. (J.C.W.)

56000 IONOSPHERIC EFFECT OF THE SOLAR ECLIPSE OF SEPTEMBER 22, 1968, ACCORDING TO OBSERVATIONS AT TWO POINTS. Danilkin, N. P.; Kondratenko, S. G.; Fayer, Yu. N.; Shatkhin, Kh. Z. (Rostov State Univ., Rostov-on-Don, USSR). Geomagn. Aeron. (USSR) (Engl. Transl.); 11: No. 1, 141-3(1971).

Translated from Geomagn. Aeron.; 11: No. 1, 171-2(1971).

Observations of the Sept. 22, 1968 solar eclipse were made at Rostov from two stations 75 km apart. Generally, the course of the eclipse in the ionosphere was the same at both stations, but differences were noted in the interlayer region and the F2 region. The fact that $N_{max}F2$ increases in the first half of an eclipse against the background of a general decrease in N has been noted many times in previous eclipses. Two hypotheses have been presented, but the acceptable one explains the presence of motions in the ionosphere. Variations occurring in the first and second halves of the eclipse are noted. (J.C.W.)

XUM

**56001** MAGNETIC FIELD OF A LOCAL IONOSPHERIC CURRENT. Davydov, V. M.; Fedorov, A. N. (Inst. of Geology and Geophysics, Novosibirsk, USSR). Geomagn. Aeron. (USSR) (Engl. Transl.); 11: No. 1, 143-6(1971).

Translated from Geomagn. Aeron.; 11: No. 1, 173-5(1971).

Computer calculations are reported of the results of the components of the magnetic field under the ionosphere for the lf range of oscillations, including micropulsation frequencies. The calculation is confined to the case when the external magnetic field is oriented to the z axis. Boundary conditions are given fixing the position of the horizontal dipole with the current moment at the origin of the coordinates. The dipole is oriented along the x axis. A graphical representation of the spatial and frequency distribution of the field components is shown. (J.C.W.)

**56002** DEPRESSION OF THE GEOMAGNETIC FIELD DURING A MAGNETIC STORM. Shabanskii, V. P. (Moscow State Univ.). Geomagn. Aeron. (USSR) (Engl. Transl.); 11: No. 1, 148-50(1971).

Translated from Geomagn. Aeron.; 11: No. 1, 179-80(1971).

The main phase of a storm is characterized by a decrease of the horizontal field component in the equatorial region in three stages. These stages are rapid (several hours) decrease of the field from the increased level (by several tens of gammas) during the main storm phase; a slower stage of partial restoration; and slow (several days) final restoration to the undisturbed level. These stages are associated with characteristic periods of variations of the total magnetic energy and redistribution of this energy in the Earth, the Earth core, and the magnetotail. The energy is estimated in the three regions. The energy of the field in the three regions is redistributed during a storm and these calculations are made. (J.C.W.)

**56003** DIURNAL AND SEASONAL PATTERN IN FREQUENCY OF OCCURRENCE OF SUDDEN COMMENCEMENTS. Nesmyanovich, A. T.; Nesmyanovich, E. I. (Kiev State Univ. Inst. of Geophysics, Moscow). Geomagn. Aeron. (USSR) (Engl. Transl.); 11: No. 1, 150-2(1971).

Translated from Geomagn. Aeron.; 11: No. 1, 181-2(1971).

Global geomagnetic and solar data published for the years 1955 to 1969 are used to study the diurnal and seasonal pattern in frequency of occurrence of sudden commencements. The diurnal pattern in UT is the result of the superposition of the diurnal pattern in LT for magnetic stations unevenly distributed in longitude. The seasonal character is more pronounced in the variation of the diurnal pattern with the seasons. The results suggest that the presence or absence of SC in geomagnetic storms is determined not only by the nature of the corpuscular stream, but also partly by conditions on Earth. The classification of storm commencements as gradual or sudden is arbitrary. There are apparently no significant differences between the sources responsible for sporadic or recurrent storms. It is demonstrated that the maxima in geomagnetic disturbances are associated with the passage across the central meridian of the Sun of active regions where flares occur, rather than with the instant of the flare. (J.C.W.)

**56004** INVESTIGATION OF THE RELATIONSHIP BETWEEN THE PROPERTIES OF STEADY EARTH CURRENT PULSATIONS AND THE PARAMETERS OF THE MAGNETOSPHERE. Gorodnicheva, O. P. (Inst. of Terrestrial Magnetism, Ionosphere, and Radio Wave Propagation, Kiev). Geomagn. Aeron. (USSR) (Engl. Transl.); 11: No. 1, 155-7(1971).

Translated from Geomagn. Aeron.; 11: No. 1, 185-6(1971).

The possibility of using the properties of steady-Earth current pulsations to investigate the parameters of the magnetosphere and the solar wind is studied. It has been demonstrated that the Pc-type pulsations with periods from 10 to 150 sec continuously observed on the sunlit side of the Earth are a good indicator of the position of the day boundary of the magnetosphere. A comparison of the changes in the position of the magnetosphere boundary, observed on satellites, with ground-based observations of steady pulsations of the electromagnetic field of the Earth shows the relationship between the period of steady Pc and the distance to the magnetosphere boundary. A relationship is written for converting the observed period of steady pulsations $T_{Pc}$ to the computed distances to the daytime magnetosphere boundary. The computed and observed distances to the boundary of the subsolar magnetosphere were compared using Pleshchenitsa observations and the distance to the magnetosphere boundary from Pleshchenitsa data was compared with Explorer-12 data. (J.C.W.)

**56005** ENERGY DISSIPATION IN THE ATMOSPHERE AT PCA PHENOMENA. Velinov, P. (Geophysical Inst., Sofia). Compt. Rend. Acad. Bulg. Sci.; 24: No. 3, 307-10(1971).

Some generalizations of solutions for the energy losses of solar cosmic rays in the polar ionosphere, as presented by K. Maeda and S. Singer in 1962, are considered. The particles were assumed to be isotropically distributed in the upper hemisphere. (J.C.W.)

**56006** DAILY VARIATIONS IN HEIGHT OF THE SPORADIC-E LAYER. Serafimov, K.; Samardzhiev, D. (Inst. of Geophysics, Sofia). Compt. Rend. Acad. Bulg. Sci.; 24: No. 3, 311-14(1971).

The daily variations of the vertical spatial position of the sporadic-E layer are averaged for the monthly median values. Data from the ionospheric station at Dourbes for 1957–1968 are used. Great dispersions occur in sporadic E, but the variations resemble the changes in the simple Chapman layer. The known laws in the variations of the sporadic-E frequency parameters are correlated with law-governed variations of the initial height of the region, considering seasonal, cyclical, and geographic parameters. (J.C.W.)

**56007** CORRELATION BETWEEN GEOMAGNETIC ACTIVITY AND THE INTENSITY OF THE INTERPLANETARY MAGNETIC FIELD. Gorchakov, E. V.; Ignat'ev, P. P.; Galach'ev, N. G. Cosmic Res. (USSR) (Engl. Transl.); 9: No. 1, 122-4(Jan-Feb 1971).

Translated from Kosm. Issled.; 9: No. 1, 138-41(Jan-Feb 1971).

Results have been reported in recent years of the relationship between the geomagnetic activity and the total intensity of the interplanetary field measured outside the magnetosphere on both interplanetary probes and satellites. An analysis is made here of the data of measurements made on Venera-4 space probe in 1967. Corrections are made for the data of the magnetic-field intensities and geomagnetic activity. The solar-wind velocity was determined. The relationships between the indices $K_p$ and $A_p$, Bartels daily linear geomagnetic-activity index, and then between $K_p$ and the interplanetary-field intensity are examined; a correlation is implied, but not a functional dependence. This circumstance shows the importance and necessity of direct measurements of the interplanetary magnetic field outside the Earth's magnetosphere. (J.C.W.)

**56008** NATURE OF THE RADIATION BACKGROUND AT ALTITUDES OF 250 TO 500 KM. Kurnosova, L. V.; Logachev, V. I.; Razorenov, L. A.; (and others). Cosmic Res. (USSR) (Engl. Transl.); 9: No. 1, 94-102(Jan-Feb 1971).

Translated from Kosm. Issled.; 9: No. 1, 105-15(Jan-Feb 1971).

An analysis of the results of the experiments on recording electrons at altitudes of 200 to 300 km, which was carried out by the Cosmos-225 satellite, allowed the following hypothesis to be stated: the charged particles observed at these altitudes, whose flux noticeably exceeds the flux of cosmic-ray particles, are among the particles captured in the Earth's magnetic field and travel in the form of certain bunches. In particular, bunches may develop for the case in which accelerating mechanisms operate near the Earth, causing the formation of the radiation belts and fill them with particles. It is possible that the process of group acceleration of particles is generally characteristic for all regions of the radiation belt. (auth)

**56009** EXPERIMENTS WITH ARTIFICIAL SOLAR WIND. Podgornyi, I. M.; Dubinin, E. M.; Managadze, G. G. Cosmic Res. (USSR) (Engl. Transl.); 9: No. 1, 82-9(Jan-Feb 1971).

Translated from Kosm. Issled.; 9: No. 1, 91-9(Jan-Feb 1971).

Interaction of the artificial solar wind with a model of the Earth's magnetic dipole was investigated. Main attention was concentrated on an investigation of the shock waves. Results of magnetic measurements are given. Microfluctuations of the magnetic field on the front of the shock wave were revealed. The power spectrum of these microfluctuations was obtained. Correlation measurements by means of two probes provided the possibility of determining the characteristic scale of the microfluctuations. Data are given on the field configuration on the night side. It is proposed that the extension of the lines of force in the tail occurs due to the penetration of the plasma stream into the magnetosphere. (auth)

**56010** KINETICS OF IONS IN THE NIGHTTIME D REGION OF THE IONOSPHERE. Kozlov, S. I. Cosmic Res. (USSR) (Engl. Transl.); 9: No. 1, 73-81(Jan-Feb 1971).

Translated from Kosm. Issled.; 9: No. 1, 81-90(Jan-Feb 1971).

The kinetics of ions in the nighttime D region of the ionosphere is considered on the basis of experimental data obtained at the time of one of the American high-altitude nuclear explosions above the Pacific Ocean in 1962. The ionizing-radiation fluxes (fission-fragment $\beta$ electrons) and electron concentrations were measured simultaneously under quasi-equilibrium conditions. The general approach to this problem is analyzed, and the rate constants of the reactions $O_2^+ + N_2 \rightarrow NO^+ + NO$, $N_2 + O_2^- \rightarrow NO_2^- + NO$ and $e + O_3 \rightarrow O^- + O_2$ are estimated. The system of kinetic equations describing the time variation of the positive- and nega-

XUM

tive-ion concentrations is solved on the assumption that the rate constants of dissociative recombination and mutual neutralization are equal. It is concluded that the principal negative ion is $NO_2^-$. Definite identification of the principal positive ion is not possible, but it is indicated that it is probably $O_2^+$ in the upper part of the height range under consideration. (auth)

**56011** RELAXATION OF HIGH ENERGY PROTONS IN THE MAGNETOSPHERE OF THE EARTH UNDER THE EFFECT OF ALFVEN WAVES. Kovalenko, V. S.; Tuzova, S. I. (Physical-Technical Inst., Novosibirsk, USSR. Tomsk State Univ., USSR). Izv. Vyssh. Ucheb. Zaved., Fiz.; No. 5, 65-71(1971). (In Russian).

The basic results of a quantitative study of the interaction of protons with Alfven waves are presented. The solution to the problem intrinsically is determined by the spectrum of the Alfven waves, which is not known under the conditions of the magnetosphere. Therefore, certain approximations are necessary. (K.S.W.)

**56012** STEADY-STATE AND DYNAMIC PROBE CHARACTERISTICS IN A LOW-DENSITY PLASMA. Bunting, William David Jr. Denton, Tex.; North Texas State Univ. (1970). 120p. University Microfilms Order No. 71-18,650.

Thesis.

The problem with which this investigation is concerned is that of determining the steady-state and dynamic characteristics of the admittance of a metallic probe immersed in a laboratory plasma which has the low electron densities and low electron temperatures characteristic of the ionospheric plasma. The problem is separated into three related topics: the design and production of the laboratory plasma, the measurement of the steady-state properties of dc and vlf probe admittance, and the study of transient ion sheath effects on rf probe admittance. A method for producing a low-density, low-temperature plasma is described, and the resulting plasma is compared with the ionospheric plasma. The laboratory plasma, although differing in many details from the ionospheric plasma, is shown to be useful for studying probe characteristics. The measurement of dc and vlf current to a metallic probe immersed in the laboratory plasma is described. Good results were obtained when certain precautions were taken such as discharge cleaning of the probe and feedback control of plasma potential. Electron temperature measurements gave reasonable results and indicated a low electron temperature for most plasma conditions. The measurements of electron density gave reasonable results but were much more uncertain due to probable plasma disturbance effects and a lack of theory for probes immersed in collisional plasmas. An investigation of transient sheath effects on probe admittance is described. The transients were initiated by step-function changes in the probe potential; only negative potentials were used in order to minimize the disturbance to the ambient plasma. The ion sheath was detected through its effect on the complex admittance of the probe at two frequencies, 5 and 15 MHz. The plasma frequency was varied over the range 5 to 32 MHz. The admittance transients were usually too rapid to measure following the application of a large negative probe bias, but the return to a smaller negative bias produced a much slower transient due to the ambipolar diffusion back to a steady-state thin-sheath configuration. The transients were found to have distinctive shapes depending on the ratio of the operating frequency to the plasma frequency. An approximate theory for the transient sheath properties is described and numerical results are presented for a typical plasma condition. A few discrepancies are noted but, in general, there is agreement between the numerical results and the experiment. (Diss. Abstr. Int., B)

**56013** ELECTROSTATIC CONFINEMENT OF AN ALKALI-METAL PLASMA. Cataldo, Joseph C.; Jaffe, Morry; Jen, Norman C. (City Coll., N. Y.). Phys. Rev. Lett.; 27: No. 12, 786-89(20 Sep 1971).

The imposition of a hollow longitudinal beam of 2-kV electrons about a Q-machine potassium plasma column serves to deepen the radial potential well across that column. Transverse plasma flux is consequently decreased, while the peak ion density and endplate collector current rise an order of magnitude. A calculation is made of the transverse flux of ions in the plasma column with energy sufficient to surmount the potential well. (auth)

**56014** IONOSPHERIC DISTURBANCE BY A SATELLITE: BOUNDARY-VALUE PROBLEM FOR THE VLASOV-POISSON EQUATIONS. Taylor, J. C. (Univ. of Glasgow). pp 48.1-6 of Computational Physics. Vols. I and II. London; Her Majesty's Stationery Office (1969).

From Conference on computational physics; Culham, England (28 Jul 1969). See CONF-690706-(Vols.1 and 2).

The interaction of a conducting body and a rarefied plasma streaming supersonically is considered, and a boundary-value problem for the Vlasov–Poisson equations in a 4-dimensional phase-space is formulated. The electron density $n(x) = n_0 \exp(e\phi(x)/kT)$, where $\phi$ is the potential. The ion distribution function $F(x,v)$ and $\phi$ are connected by equations. This nonlinear system was tackled by two methods (Taylor 1967). The heuristic method given here is of iterative type. It is shown that an excellent zero approximation, $F_0$, is given by treating the ions as neutrals. $F_0$ being independent of $\phi$ can be written explicitly as can the approximate ion density and flux. The latter allows an approximation to $\phi_B$, the body potential to be found. The Poisson equation can be solved numerically and results for the zero-order potential $\phi_0(x)$ obtained, completing the zero-order calculation. The more complicated first-order solution $F^1$ is found by calculating ion paths in the field $\phi_0$. The ion density correct to zero and first order show striking differences. (auth) (UK)

**56015** SPORADIC E AND GEOMAGNETIC ACTIVITY. Closs, R. L. (Univ. of Otago, Dunedin, N. Z.). J. Geophys. Res.; 76: No. 28, 7000-2(1 Oct 1971).

Whitehead (1970) recently pointed out that there is evidence of changes in midlatitude sporadic E during periods of increased geomagnetic activity. The nature of these changes appears to depend on latitude with a reversal in the effect about the Sq current focus. A sporadic-E mechanism is suggested that is consistent with this reversal and yet not in conflict with other observed sporadic-E phenomena. The theory of the mechanism is based on the assumption that there are currents induced in the ionospheric E region by externally generated changes in the geomagnetic field. (W.D.M.)

**56016** ATMOSPHERIC GRAVITY WAVES INDUCED BY A SOLAR ECLIPSE. II. Chimonas, G. (Univ. of Colorado, Boulder); Hines, C. O. J. Geophys. Res.; 76: No. 28, 7003-5 (1 Oct 1971).

In a previous letter the authors drew attention to the fact that a solar eclipse would act as a generator of atmospheric gravity waves, which would interfere to produce a bow wave, and that this bow wave might be detectable at great distances from the eclipse path, both at ground level and at ionospheric heights. Davis and da Rosa (1970) reported the detection of a wave-like ionospheric disturbance at about the time predicted for the region of their observations and have interpreted it as a possible confirmation of the suggestion. Calculations are presented that appear to confirm beyond reasonable doubt that Davis and da Rosa did in fact observe the predicted low wave. (W.D.M.)

**56017** FREQUENCY TABLES OF THE GEOMAGNETIC INDEX Kp, 1932–1970. Zawalick, E. J.; Cage, A. L. (Air Force Cambridge Research Labs., Bedford, Mass.). J. Geophys. Res.; 76: No. 28, 7009-12(1 Oct 1971).

In order to demonstrate the persistent nature of $Kp_t$ a simple frequency table was generated that relates the Kp for a given 3-hr interval to the Kp in the succeeding 3-hr interval. Thirty-nine years of Kp data covering the period Jan. 1, 1932, through Dec. 31, 1970, a total of 113,960 three-hour Kp values were examined and tabular data are presented. (W.D.M.)

**56018** COMMENTS ON PAPER BY L. R. MEGILL, A. M. DESPAIN, D. J. BAKER, AND K. D. BAKER, "OXYGEN ATMOSPHERIC AND INFRARED ATMOSPHERIC BANDS IN THE AURORA". Evans, W. F. J.; Llewellyn, E. J. (Univ. of Saskatchewan, Saskatoon). J. Geophys. Res.; 76: No. 28, 7013-19 (1 Oct 1971).

Photometric results from two rocket flights under auroral conditions (Megill et al. (NSA 24: 47133)) were interpreted to mean that large enhancements of several megarayleigns in the ir atmospheric oxygen bands occurred during typical auroral displays. This comment attempts to demonstrate that the 1.27-$\mu$ data can be adequately explained as an observation of the nightglow layer, when the rocket aspect is considered, and that no large 1.27-$\mu$ auroral enhancement was observed. It is also suggested that: (1) Megill et al. have mistaken the intensity variation due to viewing the airglow layer edge-on for an auroral enhancement; (2) results do not support the conclusion that additional energy sources such as electric fields are required to explain the excitation of $O_2(^1\Delta_g)$, even though this conclusion may be correct; and (3) the apparent enhancement of 1.27-$\mu$ radiation was produced by geometrical effects encountered when viewing the airglow layer. A reply by Megill and the other authors is included. (J.C.W.)

**56019** NONTHERMAL ELECTRONS AND HIGH-FREQUENCY WAVES IN THE UPSTREAM SOLAR WIND. 2. ANALYSIS AND INTERPRETATION. Fredricks, R. W. (TRW Systems Group, Redondo Beach, Calif.); Scarf, F. L.; Frank, L. A. J. Geophys. Res.; 76: No. 28, 6691-9(1 Oct 1971).

A streaming instability caused by suprathermal electrons of bulk energy ~1 keV and random widths from ~60 to 4 keV is investigated

as a model to explain the Ogo-5 observations of electric-field fluctuations with frequencies at or near the local electron plasma frequency upstream from the Earth's bow shock. In Paper 1 (J. Geophys. Res., 76: 5162(1971)), it was shown that the waves appeared in direct correlation with enhanced anisotropic electron fluxes having $E_e \gtrsim 700$ eV. Here, it is shown that the streaming instability produced by this type of suprathermal electron beam leads to a wave frequency nearly equal to the local electron plasma frequency, whereas the growth rates are still significant even if the beam thermal speed becomes comparable to the bulk speed. (auth)

**56020** DETAILED DIRECTIONAL AND TEMPORAL PROPERTIES OF SOLAR ENERGETIC PARTICLES ASSOCIATED WITH PROPAGATING INTERPLANETARY SHOCK WAVES. Singer, Sidney; Montgomery, Michael D. (Los Alamos Scientific Lab., N. Mex.). J. Geophys. Res.; 76: No. 28, 6628-42(1 Oct 1971).

In the period May 1967 to May 1968, detailed Vela-4 observations of the properties of protons in the enhancements ("spikes") associated with propagating interplanetary shocks show that the proton energy spectrum does not extend beyond ~5 MeV; the protons often possess unusually large streaming anisotropies (e.g., a pitch-angle anisotropy of >1000 : 1 for the February 20, 1968, event), and the peak of the spike can occur as much as $3 \times 10^5$ km (~10 min) on the sunward side of the shock front. Neither the Axford–Reid nor the Fisk model satisfactorily explains the observations: shock spikes were observed to occur when the interplanetary-field line connecting the interplanetary shock and the observer probably did not intersect the bow shock, contrary to the prediction of the Axford–Reid model; and the prediction of Fisk concerning the shape of the proton energy spectrum at the shock front was not observed at energies above 0.5 MeV. In their published form, neither model can predict an extremely large streaming anisotropy, although a recent extension of Fisk's model may be able to explain anisotropy ratios as large as 10. A single-encounter model, where particles are accelerated in a single elastic collision with the interplanetary shock, is qualitatively examined and can explain large enhancements and anisotropies only if the magnetic field and the shock normal are inclined at an angle of $\gtrsim 85°$ to each other. (auth)

**56021** AVERAGE AND UNUSUAL LOCATIONS OF THE EARTH'S MAGNETOPAUSE AND BOW SHOCK. Fairfield, Donald H. (Goddard Space Flight Center, Greenbelt, Md.). J. Geophys. Res.; 76: No. 28, 6700-16(1 Oct 1971).

A best-fit ellipse and hyperbola were calculated to represent several hundred magnetopause and bow-shock positions observed by six Imp spacecraft. Average geocentric distances to the magnetopause and bow shock near the ecliptic plane are 11.0 and 14.6 $R_E$ in the sunward direction, 15.1 and 22.8 $R_E$ in the dawn meridian, and 15.8 and 27.6 $R_E$ in the dusk meridian. The bow-shock hyperbola is oriented in a direction consistent with that expected when the aberration of a radial solar wind is considered. Observed magnetopause crossings agree well with theoretical predictions in the noon meridian plane but fall outside the theoretical boundaries in the dawn–dusk meridian planes. Imp 4 plasma data are used to demonstrate that the solar-wind momentum flux is the prime factor controlling the orbit-to-orbit changes in the boundary positions. Data suggest that the interplanetary-field orientation also affects the distance to the magnetopause boundary, more earthward crossings corresponding to southward fields. Six unusual bow-shock locations up to 22 $R_E$ beyond the average position are found to be due to an enhanced standoff distance associated with a low Alfvén Mach number. The possibility that the solar wind may have become sub-Alfvénic on July 31, 1967, is suggested. (auth)

**56022** MAGNETOPAUSE STRUCTURE DURING THE MAGNETIC STORM OF SEPTEMBER 24, 1961. Sonnerup, Bengt U. O. (Dartmouth Coll., Hanover, N. H.). J. Geophys. Res.; 76: No. 28, 6717-35(1 Oct 1971).

Explorer-12 magnetic-field observations of the magnetopause current layer were made on the inbound pass of September 24, 1961, which occurred during the main phase of a moderately strong magnetic storm. The satellite was located near the subsolar point. The accuracy of the Explorer-12 data reported here was increased by use of an improved filtering procedure. Five magnetopause penetrations were observed in a time period of about 20 min and for each of these the data were used to calculate the vector normal to the current layer, the magnetic-field component along that vector, and the polarization of the current layer. Normal magnetic-field components significantly different from zero were obtained, and it is suggested that the observations during this pass in general are consistent with the so-called open magnetosphere model. In fact, it appears that the first and last of the boundary penetrations may have occurred on opposite sides of, but very near, the X-type magnetic null line, which is located on the front side of the open magnetosphere model. The direction of the normal magnetic-field component as well as the sense of rotation of the tangential magnetic-field component in the current layer were found to be opposite for these two boundaries. (auth)

**56023** MAGNETOPAUSE ATTITUDES DURING OGO 5 CROSSINGS. Ledley, B. G. (Goddard Space Flight Center, Greenbelt, Md.). J. Geophys. Res.; 76: No. 28, 6736-42(1 Oct 1971).

The attitude of the magnetopause current layer is determined for 31 Ogo-5 crossings located at subsatellite local times between 0430 and 1020 and solar magnetospheric latitudes between −8.5 and +40°. A consistent difference in this attitude is observed between crossings in which the satellite leaves the magnetosphere and crossings in which it enters. The magnitude of this difference appears to be independent of the Sun–Earth–satellite angle. The ratio of the component of the magnetic field normal to the magnetopause to the total adjacent magnetospheric field is computed for each crossing. Ratios ranging from +0.1 to −0.2 are obtained, where a plus sign signifies an outward directed component. The average ratio for those crossings in which the magnetosheath and magnetospheric fields subtended angles of greater than 90° is −0.03 ± 0.09. (auth)

**56024** OGO 5 OBSERVATIONS OF THE POLAR CUSP ON NOVEMBER 1, 1968. Russell, Christopher T. (Univ. of California, Los Angeles); Chappell, Charles R.; Montgomery, Michael D.; Neugebauer, Marcia; Scarf, Fredrick L. J. Geophys. Res.; 76: No. 28, 6743-64(1 Oct 1971).

During the large magnetic storm of November 1, 1968, the Ogo-5 spacecraft encountered the apparent direct penetration of magnetosheath plasma into the dayside magnetosphere at magnetic latitudes as low as 43°. Because this region of magnetosheath plasma occurred on magnetospheric field lines immediately adjacent to the zone of trapped energetic particles, it is interpreted to be the polar cusp. The temperature of the electrons in the polar cusp was 4 times greater than the electron temperature measured simultaneously by Vela 4B in the downstream magnetosheath at local dusk, and the electron energy distribution in the cusp was similar to the distribution observed later when Ogo 5 entered the magnetosheath. During the encounters with the polar cusp the amount of depression of the magnetic field implies the presence of magnetosheath protons together with the directly measured electrons. During this period of time the polar cusp was very turbulent at both ulf (magnetic) and vlf (electric) frequencies. Energetic (≥50-keV) electrons were also observed in the cusp. The cusp moved equatorward and poleward in response to changes in the north–south component of the interplanetary magnetic field. (auth)

**56025** MAGNETOSPHERIC SUBSTORMS ON SEPTEMBER 14, 1968. Hones, E. W. Jr. (Los Alamos Scientific Lab., N. Mex.); Karas, R. H.; Lanzerotti, L. J.; Akasofu, S.-I. J. Geophys. Res.; 76: No. 28, 6765-80(1 Oct 1971).

Several moderate magnetospheric substorms on September 14, 1968, were observed by two satellites (Vela 4A and ATS 1), balloon-borne x-ray detectors, and extensive arrays of ground-based instruments in Alaska. Combined results from those observations and their interpretations are described in detail. Several interesting aspects of magnetospheric substorms are suggested by the analysis. (a) Simultaneous with the brightening of an auroral arc that signals the onset of an auroral substorm, there can occur a sudden enhancement of energetic electron flux in a limited region of the distant magnetotail. The simultaneity of these two phenomena suggests a magnetic link between them. The region evidently contracts rapidly toward the Earth. A satellite appropriately situated in the magnetotail (e.g., a Vela satellite at 18 $R_E$) may be imbedded in the electron flux initially and then, after a short time, find itself outside it as the flux-containing region contracts earthward. This results in a brief impulsive flux of energetic electrons at the satellite starting at substorm onset. (b) The sharp enhancement of electron flux that, in the midnight sector of the geosynchronous orbit ($r = 6.6$ $R_E$), characterizes substorm onset and that is generally ascribed to a change of electron drift paths associated with earthward "collapse" of magnetic field may, in some substorms, be partly due to earthward motion of a nonadiabatic source region. (c) The westward drift motion of auroral patches results from that of a source or scattering region rather than from the drift of the individual precipitated electrons in a strong electric field. The number of substorms that can be studied with such a variety of simultaneous observations is obviously very limited, and thus the individual precipitated electrons in a strong electric field. The number of substorms that can be studied with such a variety of simultaneous observations is obviously very limited, and thus the generalization of our conclusions must be taken to be tentative. (auth)

**56026** STORM SUDDEN COMMENCEMENTS AND POLAR MAGNETIC SUBSTORMS. Kawasaki, K. (Univ. of Alaska,

XUM

College); Akasofu, S.-I.; Yasuhara, F.; Meng, C.-I. J. Geophys. Res.; 76: No. 28, 6781-9(1 Oct 1971).

IGY sudden commencements of magnitude greater than 20 gammas simultaneously (±3 min) triggered magnetospheric substorms with a very high probability (~90%). The magnitude dependence gives rise to a part of the large sunspot cycle variation of the probability of the occurrence of simultaneous events: 49% during the IGY and only 4% during the IQSY. Also, the degree of presubstorm disturbances measured in terms of $\Sigma K_p$, types of interplanetary discontinuities, and the direction of interplanetary magnetic field do not appear to be important parameters for ssc-triggered substorms. Therefore, these results may indicate that a sudden compression of the magnetosphere alone, if intense enough, can sometimes trigger substorms. (auth)

**56027** EQUATORIAL PROTON AND ELECTRON ANGULAR DISTRIBUTIONS IN THE LOSS CONE AND AT LARGE ANGLES. Bogott, F. H.; Mozer, F. S. (Univ. of California, Berkeley). J. Geophys. Res.; 76: No. 28, 6790-6805(1 Oct 1971).

Pitch-angle distributions have been obtained for protons and electrons of energy ~30 to 300 keV on the geostationary satellite ATS 5. Those obtained near and in the loss cone in Dec. 1969 and Jan. 1970 provide evidence for the existence of a depleted loss cone except during two active intervals when a "filled-in" loss cone was approached. The slopes of the proton and electron angular distributions outside the loss cone at small pitch angles (10 to 25°) remained unchanged as the loss cone filled in or became depleted, and the flux of particles in the loss cone at any energy did not necessarily depend on the intensity of particles outside of the loss cone at that energy. Data are also examined for 8 days in Aug. and Sept. 1969 when the detector sampled a wide range of pitch angles (usually 25 to 90°). The diurnal variations of these angular distributions are similar for protons and electrons and are in qualitative agreement with the predictions of a theory of drift-shell splitting, although the short lifetimes of the measured particles prevent the good quantitative agreement found by other experimenters at higher energies. Several substorm events are studied, with the result that both protons and electrons are introduced preferentially at large pitch angles near midnight and are introduced more uniformly with angle at other local times. (auth)

**56028** STRUCTURED VARIATIONS OF THE PLASMAPAUSE: EVIDENCE OF A COROTATING PLASMA TAIL. Taylor, Harry A. Jr. (Goddard Space Flight Center, Greenbelt, Md.); Grebowsky, Joseph M.; Walsh, William J. J. Geophys. Res.; 76: No. 28, 6806-14(1 Oct 1971).

Direct measurements of the pole-to-pole distributions of topside thermal protons obtained with the Ogo-4 ion composition experiment, near local midnight, reveal sharply structured variations of the plasmasphere boundary. With increasing L values the proton-density distributions may exhibit a pronounced inner trough, in which the ambient $H^+$ concentrations decrease by an order of magnitude near L = 2 and subsequently recover to mid-latitude concentration levels before a more pronounced and persistent trough is encountered at higher L positions. The time evolution of the trough boundaries observed during a sample of five consecutive satellite orbits following the peak of the magnetic storm on September 21, 1967, suggests that the observed structure results from a plasma tail or elongation of the plasmasphere that tends to corotate with the Earth. The empirical model deduced indicates that, at the time of these observations, the plasma tail has a width of about 0.8 L at the base, extending to an extremely thin region of 0.05 L or less near the tip, and with an azimuthal extent of approximately 85° longitude. The general features of the observed plasma tail structure are in accord with the time evolution of the plasmapause predicted theoretically, assuming that the magnitude of the thermal plasma convective flow from the magnetosphere tail varies directly with the magnetic index, $K_p$. (auth)

**56029** DEVELOPMENT OF THE POLAR ELECTROJET DURING POLAR MAGNETIC SUBSTORMS. Kisabeth, Jerry L.; Rostoker, Gordon (Univ. of Alberta, Edmonton). J. Geophys. Res.; 76: No. 28, 6815-28(1 Oct 1971).

Evidence is presented indicating that the structure of polar magnetic substorms is determined by the intensification of the current at the northern and/or southern borders of a small pre-existing westward electrojet. The substorm onset is characterized by the growth of the current at the southern border of the electrojet and further develops through quasi-periodic intensifications of the current at the northern border of the electrojet. The southern part of the electrojet varies only sporadically in intensity, and its strength and general stability make it the center of activity throughout the course of the substorm. The intensification of current at the northern border of the electrojet that occurs at roughly 15-min intervals is thought to be connected with the westward-traveling surge observed during auroral substorms and suggests a quasi-periodic input of energy from the magnetotail. (auth)

**56030** DISTRIBUTIONS OF PLASMAS AND ELECTRIC FIELDS OVER THE AURORAL ZONES AND POLAR CAPS. Frank, L. A.; Gurnett, D. A. (Univ. of Iowa, Iowa City). J. Geophys. Res.; 76: No. 28, 6829-46(1 Oct 1971).

Simultaneous observations of dc electric fields and low-energy charged particles at low altitudes over the auroral zones and polar caps were obtained with the satellite Injun 5. Results for several passes of the satellite through the evening and dawn local-time sectors are summarized. (1) The most prominent features of the convection electric fields are reversals located at high magnetic latitudes in the dawn and evening sectors. (2) The east–west convection velocity is usually antisunward at latitudes above the reversal boundary and sunward at latitudes below the reversal boundary. (3) The convection electric-field reversals in the dawn and evening sectors are coincident with the "trapping boundary" for energetic electrons E > 45 keV. (4) Over the polar caps the convection velocities are small or below the instrumental threshold of typically ~0.75 km $(sec)^{-1}$, relative to the convection velocities in the vicinity of the reversals. (5) The polar-cap region is characterized by an absence of measurable low-energy proton and electron intensities. (6) Inverted "V" precipitation events are located near or at the convection field reversals (and hence also the trapping boundaries) or within regions of measurable convection electric fields poleward of the trapping boundary. (7) Field-aligned electron angular distributions occur at and above the trapping boundary and within the inverted "V" precipitation events. (8) Diffuse precipitation zones of electron and proton intensities with spectrums similar to those observed in the near–Earth plasma sheet are located at latitudes below the trapping boundary and within the region of sunward convection velocities. (9) During a magnetic substorm the over-all configuration of the convection velocities and plasma regions remained similar to those observed during quiescent periods, except that convection velocities and particle intensities increased and the locations of these phenomena in magnetic latitude varied. These observations are interpreted in terms of a magnetospheric model as deduced from plasma observations in the distant magnetosphere and in terms of essential elements for any credible theory of auroral arcs, in particular those associated with inverted "V" precipitation bands. (auth)

**56031** SOUNDING-ROCKET OBSERVATIONS OF PARTICLE PRECIPITATION IN A POLAR-CAP ELECTRON AURORA. Whalen, B. A.; Miller, J. R.; McDiarmid, I. B. (National Research Council of Canada, Ottawa). J. Geophys. Res.; 76: No. 28, 6847-55(1 Oct 1971).

Results of low-energy particle measurements made from a sounding rocket launched from Resolute Bay, Northwest Territories (invariant latitude 84.5°), into a polar-cap aurora are presented. Soft electron fluxes were detected above a relatively stable 1-kR auroral arc that was aligned in the usual Earth–Sun direction. The electron precipitation, which was only slowly varying in time, was found to have an isotropic pitch–angle distribution and a differential energy spectrum that peaked in the 1.5- to 2.0-keV energy range with a peak intensity of $\sim 10^7$ $cm^{-2}$ $sec^{-1}$ $ster^{-1}$ $keV^{-1}$. Outside the arc, the electron energy flux fell below $10^{-2}$ erg $cm^{-2}$ $sec^{-1}$, as compared with 0.15 erg $cm^{-2}$ $sec^{-1}$ inside the arc. No positive-ion precipitation was detected, except that due to the remnant of a solar proton event. Upper limits of low-energy auroral proton fluxes were set near $10^5$ $cm^{-2}$ $sec^{-1}$ $ster^{-1}$ $keV^{-1}$ in the 0.6- to 6.0-keV energy interval. These data and previous measurements in the nightside and dayside auroral zones are compared, and current magnetospheric models, in particular the relationship between polar-cap auroras and such concepts as direct neutral-point entry and neutral-point acceleration mechanisms, are discussed. (auth)

**56032** PHOTOELECTRON EXCITATION OF ATOMIC-OXYGEN RESONANCE RADIATION IN THE TERRESTRIAL AIRGLOW. Zipf, E. C.; Stone, E. J. (Univ. of Pittsburgh). J. Geophys. Res.; 76: No. 28, 6865-74(1 Oct 1971).

Recent laboratory measurements of the absolute cross sections for the excitation of the O I ($^3S$) resonance state by electron impact on O and $O_2$ when combined with in situ measurements of the photoelectron energy distribution from 120 to 300 km show that photoelectron impact is the principal excitation mechanism for λ1304-A resonance radiation in the dayglow; dissociative excitation of $O_2$ is found to play a minor role. The laboratory measurements indicate that the $^3S$ state is strongly populated by cascade processes and imply that the O I($3p^3P \rightarrow 3s^3S$; λ8446 A) transition should be a prominent dayglow emission feature. These experiments also show that the excitation of atomic oxygen by low-energy electron impact cannot account for the λ1304- or 1356-A emission observed in the tropical ultraviolet airglow. (auth)

**56033** OBSERVATIONS OF STRIATION FORMATION IN A BARIUM ION CLOUD. Rosenberg, Norman W. (Air Force Research Labs., Bedford, Mass.). J. Geophys. Res.; 76: No. 28, 6856-64(1 Oct 1971).

The growth of a barium ion cloud released at 194 km has been documented. Within 930 sec after release, the cloud center had descended (at 27 m/sec) to 168 km with traces (~$10^{10}$/cm$^2$ column) visible at heights of 160 and 190 km along the Earth's magnetic field. During the same period, the cloud moved across (perpendicular to) field lines at a velocity of 35 m/sec relative to the neutral wind. For about 500 sec ambipolar diffusion perpendicular to the field lines led to a radial expansion with an effective diffusion rate of $6.10^3$ m$^2$/sec (about 10% of the neutral diffusion at that height). After 200 sec, the side facing the neutral cloud (the "downward" side of the ion cloud) steepened rather than decreased in brightness gradient; at 500 sec it had steepened to a Gaussian radius of 0.8 km, whereas the other side had grown to a 3.7-km Gaussian radius. At about 500 sec, an instability developed on the steep-gradient surface and grew into three vertical sheets, the edges of which moved much less rapidly (10 m/sec) with respect to the neutral wind than the 35-m/sec ion cloud from which they were being pulled. These sheets had dimensions about 10-km long, 30-km high, and 0.6-km wide at 930 sec after release. (auth)

**56034** COMPARISON OF THE NORTH- AND SOUTH-POLAR F LAYERS. Pike, C. P. (Air Force Cambridge Research Labs., Bedford, Mass.). J. Geophys. Res.; 76: No. 28, 6875-82 (1 Oct 1971).

Monthly median ionosonde data were used to investigate the north-polar F layer. The dependence of the north-polar F layer on universal time and on corrected geomagnetic latitude is clearly established, and the results are compared with the results of a previous study of the south-polar F layer so that similarities and differences between the F-layer features of the plasma ring and the polar cavity can be pointed out. The energy input into the zone of soft-electron precipitation is sufficient to produce the electron-density level of the plasma ring, whereas the energy input poleward of the soft zone is insufficient to produce the electron-density level that is observed in the polar F-layer cavity. Calculations, based on median levels of the wintertime polar F-layer peak electron density, indicate that an energy input of between 4 and $5 \times 10^{21}$ ergs day$^{-1}$ is required to produce the wintertime polar F layer. (auth)

**56035** ELECTRON DENSITY ENHANCEMENTS IN THE E AND F REGIONS OF THE IONOSPHERE DURING SOLAR FLARES. Thome, G. D.; Wagner, L. S. (Arecibo Ionospheric Observatory, Puerto Rico). J. Geophys. Res.; 76: No. 28, 6883-95(1 Oct 1971).

Using the method of Thomson scatter, it was possible to observe detailed ionospheric effects due to solar flares. Observations were limited to four 2B flares, and two of these events were examined intensively. The two events that were studied exhibit very similar characteristics, i.e., a strong and long-lasting E-region electron-density enhancement, a moderate and shorter duration F1-region enhancement, and a moderate F2-region enhancement characterized by a long-duration "tail". Flare x-ray data, available in the 2- to 12-angstrom band, show excellent agreement with electron-density fluctuations in the lower E region. The F1-region enhancement is believed to follow the time history of the euv ionizing radiations. The F2-region tail is attributed to the much smaller recombination rate at these heights. Plasma-line observations, permitting unequivocal measurement of electron density, were possible within a limited height range. Comparison of electron density, as deduced from the plasma lines, with backscattered power measurements corrected for the effects of absorption, resulted in estimates of flare-associated changes in the ratio of electron to ion temperature. (auth)

**56036** DIURNAL VARIATION OF THE GEOMAGNETIC FIELD. I. THE SOLAR VARIATION. Jackson, J. S. (Univ. of Ghana, Legon). J. Geophys. Res.; 76: No. 28, 6896-6908(1 Oct 1971).

The dynamo theory of the magnetic variations of the Earth's atmosphere is treated as a three-dimensional problem, considering the finite thickness of the ionospheric-current layer. The anisotropy of the conductivity of the ionosphere is also considered. By solving the basic equations of the problem, which are the equations of motion and Maxwell's equations, it is found that for both the diurnal and semidiurnal variations the horizontal magnetic field is greatest in the middle of the current layer and at that height it is about 7 times greater than at the ground. The pressure variations in the lower half of the layer are about 180° out of phase with those at ground level, for both variations. The diurnal velocities are much larger than the semidiurnal velocities. (auth)

**56037** DIURNAL VARIATION OF THE GEOMAGNETIC FIELD. II. THE LUNAR VARIATION. Jackson, J. S. (Univ. of Ghana, Legon). J. Geophys. Res.; 76: No. 28, 6909-14(1 Oct 1971).

The dynamo theory of the lunar magnetic variations is developed as a three-dimensional problem. The finite thickness of the ionospheric-current layer and the anisotropy of the conductivity are considered. The currents responsible for the lunar magnetic variations are assumed to flow in the same layer of the ionosphere as those responsible for the solar magnetic variations, i.e., from 100 to 120 km above the Earth's surface. The pattern of the results is similar to that for the solar variation, especially the magnetic-field results. The horizontal magnetic field is greatest in the middle of the current layer and at that height it is about 7 times as great as that at the ground. The pressure variation in the lower half of the layer is about 180° out of phase with that at the ground. (auth)

**56038** SOME STUDIES OF TRIGGERED WHISTLER EMISSIONS. Dysthe, K. B. (Stanford Univ., Calif.). J. Geophys. Res.; 76: No. 28, 6915-31(1 Oct 1971).

So-called triggered emissions of whistlers are considered. The effects of a nonlinear interaction between a whistler wave and the particles resonating with it are considered in some detail. The interaction gives rise to two closely related effects, namely, a change in the amplification or absorption by the plasma and a phase-bunching of the resonant and near-resonant particles, thus giving rise to a current. The current due to the phase-bunched particles has roughly the same structure (frequency and wave number) as the wave causing it, and will therefore give rise to emission of a new whistler wave, acting like an antenna. The possibility of having a self-sustained process of phase-bunching and emission is investigated. The structure of a region where this process can take place is proposed, and the corresponding conditions that must be met are stated. (auth)

**56039** ESTIMATE OF THE DEPENDENCE OF THE MAGNETOSPHERIC ELECTRIC FIELD ON THE VELOCITY OF THE SOLAR WIND. Mendillo, Michael; Papagiannis, Michael D. (Boston Univ.). J. Geophys. Res.; 76: No. 28, 6939-43(1 Oct 1971).

A model is developed that predicts that the magnetospheric dawn–dusk electric field varies as the square of the solar-wind speed, V. This relation is used to compute the radius of the plasmapause for given V at 1800 LT, where the dawn–dusk electric field cancels the electric field due to the rotation of the Earth. Using an empirical expression that relates V to $K_p$, we have found that the predictions of this model are in good agreement with plasmaspheric measurements in the dusk sector for different values of $K_p$. (auth)

**56040** LOCALIZED CHARACTER OF MAGNETOTAIL MAGMETIC FLUCTUATIONS DURING POLAR MAGNETIC SUBSTORMS. Rostoker, Gordon; Camidge, F. Paul (Univ. of Alberta, Edmonton). J. Geophys. Res.; 76: No. 28, 6944-51 (1 Oct 1971).

The magnetic fluctuations observed in the magnetotail in conjunction with polar magnetic substorms are discussed, and evidence is presented that only a confined portion of the magnetotail is affected during any given phase of a substorm. It is suggested that the magnetotail magnetic-field configuration may become even more tail-like, since a confined portion of the tail field is collapsing to a more dipolar configuration during periods of substorm activity. Caution is suggested in the correlation of magnetotail effects with specific aspects of a substorm if that substorm has a complex structure. (auth)

**56041** L PARAMETER: A NEW APPROXIMATION. Hilton, Henry H. (Aerospace Corp., El Segundo, Calif.). J. Geophys. Res.; 76: No. 28, 6952-4(1 Oct 1971).

McIlwain defined the magnetic-shell parameter L for a point in the Earth's magnetic field by the equation $L^3B/M = F(I^3B/M)$, where I is the integral invariant, B is the mirror-point field, M is the Earth's dipole moment, and F is a function calculated for a dipole field. A new approximation to F has been found: $L^3B/M = 1 + a_1X^{1/3} + a_2X^{2/3} + a_3X$, where $X = I^3B/M$, $a_1 = 1.35047$, $a_2 = 0.465376$, and $a_3 = 0.0475455$. The error in the determination of L is less than 0.01% for all L. The formula is asymptotically correct for $X \ll 1$ and $X \gg 1$. (auth)

**56042** NONPERIODIC IRREGULARITIES IN THE IONOSPHERE. Titheridge, J. E. (Univ. of Auckland, N. Z.). J. Geophys. Res.; 76: No. 28, 6955-60(1 Oct 1971).

Continuous records of the electron content of the ionosphere at latitudes of 34 and 42°S show both periodic and isolated (nonperiodic) fluctuations in approximately equal numbers. Both types have peaks of occurrence near noon and midnight, although the isolated

XUM

irregularities peak 2 hours before the periodic type. Periodic irregularities predominate in the relatively stable conditions from noon to 4 P.M. and 11 P.M. to 4 A.M., and show a large increase on winter days at high latitudes. Decreases in electron content account for about 16% of the nonperiodic irregularities; these negative irregularities are twice as common near 7 A.M., suggesting localized decreases in the production rate. (auth)

**56043** MAGNETIC DRIFT WAVES NEAR PROTON CYCLOTRON FREQUENCY. Wu, C. S. (Univ. of Maryland, College Park). J. Geophys. Res.; 76: No. 28, 6961-4(1 Oct 1971).

Discussion of magnetic drift waves with frequencies near proton cyclotron frequency is given. It is shown that in general two types of instability are possible. One is due to resonant proton-wave interaction and the other is not. The latter instability is much stronger than the former and occurs when the magnetic-field gradient is sufficiently small. (auth)

**56044** IMPULSIVE ENERGETIC ELECTRON FLUXES IN THE DISTANT MAGNETOTAIL ASSOCIATED WITH THE ONSET OF MAGNETOSPHERIC SUBSTORMS. Akasofu, S.-I.; Hones, E. W. Jr.; Singer, Sidney (Los Alamos Scientific Lab., N. Mex.). J. Geophys. Res.; 76: No. 28, 6976-9(1 Oct 1971).

A high flux of energetic electrons can occur far out in the magnetotail simultaneously with the onset of polar substorms. Vasyliunas (Eos Trans. AGU, 51, 814, 1970) showed that projection along geomagnetic-field lines of the earthward edge of the plasma sheet onto the polar cap coincides with the equatorward edge of the auroral oval. It is suggested, at the onset of the substorm, energetic electrons appear not only near the earthward edge of the plasma sheet but also in a limited region in the magnetotail. The electron flux tends to be impulsive and to disappear during an early epoch of the expansive phase of a substorm when auroras are moving poleward. It is concluded that possibly (1) the distant magnetotail region is connected magnetically to the auroral oval at the onset of some substorms and it then becomes disconnected as the substorm develops, or (2) the brightening of the equatorward edge of the oval is associated with discharge of electrons along the inner edge of the plasma sheet and at the same time the acceleration of electrons occurs elsewhere in the plasma sheet. (J.C.W.)

**56045** NEWLY OBSERVED PRE-MIDNIGHT ASYMMETRY IN THE 40-keV ELECTRON FLUX PROFILES. Rossberg, L. (Max-Planck-Institut fuer Aeronomie, Lindau, Ger.). J. Geophys. Res.; 76: No. 28, 6980-6(1 Oct 1971).

Measurements made aboard Azur satellite were used to study the sharp boundary of the pre-midnight asymmetry in the 40-keV electron-flux profiles of the low-altitude, high-latitude outer radiation zone. The occurrence of the sharp boundary is confined to a narrow MLT range before midnight, but in the midnight-to-dawn sector the electron flux decreases gradually with increasing latitude, accompanied by widespread precipitation. Relations of these observations to other auroral-zone phenomena that have asymmetric properties in the MLT range are discussed. A different definition of the "sharp" boundary is applied and called "chopped" because such electron-flux profiles appear equatorward compressed, or as if they were sliced or chopped, and part of the northern edge of the trapped radiation removed by some unknown mechanism. Electron-flux profiles from 27 selected Azur passes are studied. (J.C.W.)

**56046** $O_2$ HERZBERG I BANDS IN THE NIGHT AIRGLOW: COVARIATION WITH O I (5577). Deck, K. A. (Kitt Peak National Observatory, Tucson, Ariz.); Sivjee, G. G. J. Geophys. Res.; 76: No. 28, 6987-9(1 Oct 1971).

On the basis of measurements obtained during the NASA 1968 air-borne auroral expedition, the Herzberg I bands of $O_2$ and the 5577-A line of O I were found to covary in intensity under nonauroral conditions. This covariation appears independent of latitude and local time, and this independence is in contrast with the previously reported relationship between 5577 and OH, which exhibited local time effects. (auth)

**56047** COMBINED INCOHERENT-SCATTER F1-REGION OBSERVATIONS. Waldteufel, P. (Arecibo Observatory, Puerto Rico). J. Geophys. Res.; 76: No. 28, 6995-9(1 Oct 1971).

Wand (1970) used nearly simultaneous measurements of the ion and plasma line components throughout one day to obtain and compare two independent estimates of the temperature ratio $T_e/T_i$, one obtained by interpreting the ion spectrum with a model $T_i$ profile, the other by using the ratio of electron density given by the plasma line to power returned. The present work made use of similar data obtained over a period of about one year (May 1969 to March 1970) and analyzed a different point of view: the temperature ratio deduced from the plasma line measurement was used in the processing of the ion spectra to obtain the ion composition. (W.D.M.)

# Low-Temperature Physics and Cryogenic Equipment

## *Superfluidity*

**56048** VORTEX-FREE LANDAU STATE IN ROTATING SUPERFLUID HELIUM. Kojima, H.; Veith, W.; Putterman, S. J.; Guyon, E.; Rudnick, I. (Univ. of California, Los Angeles). Phys. Rev. Lett.; 27: No. 11, 714-18(13 Sep 1971).

Evidence is presented that, below a rather large angular velocity, $\omega_{c1}$, there is a vortex-free state in rotating locked helium, which is called the Landau state. This is similar to the Meissner state in superconductors. It is further shown that all the properties of the rotating helium have counterparts in irreversible type-II superconductors, and it is found that $\omega_{c2}$ (analogous to $H_{c2}$) greatly exceeds the high speeds of rotation. (auth)

**56049** POSSIBLE EXISTENCE OF BOSE-EINSTEIN CONDENSATION IN ONE AND TWO DIMENSIONS. Alexanian, Moorad (Instituto Politecnico Nacional, Mexico City). Phys. Rev., A; 4: No. 4, 1684-8(Oct 1971).

The proof of Jasnow and Fisher that no spontaneous ordering can occur in one- and two-dimensional systems with continuous symmetry is shown to fail for nonlocal potentials of sufficiently long range. The occurrence of Bose–Einstein condensation for finite temperature (in the infinite-volume limit) is, therefore, not forbidden for such potentials. This result also follows from the postulate of the completeness of the noninteracting equilibrium states. Thus, the completeness postulate represents a weaker assumption on the nature of an interacting equilibrium state (or, equivalently, on the basic interactions between particles) than is usually found in the literature. (auth)

**56050** GROUND-STATE ENERGY OF A MANY-PARTICLE BOSON SYSTEM. Lee, Deok Kyo (Univ. of Kansas, Lawrence). Phys. Rev., A; 4: No. 4, 1670-8(Oct 1971).

The ground state of a many-particle boson system is studied for two closely related limits: the uniform limit and the weak coupling limit. The former is defined by $\alpha = 1 - g(0) \ll 1$ and the latter by $\beta = (N - N_0)/N \ll 1$, where $g(r)$ is the radial distribution function and $N_0$ is the mean occupation number of the zero-momentum state. In the uniform limit the variation-perturbation approach based on (a) the method of correlated basis functions and (b) the series expansion in powers of $\alpha$ is found to be equivalent to the field-theoretic treatment given by Brueckner (for the charged-boson gas) in the weak coupling limit. In particular, it is shown that the variation-perturbation energy obtained for the uniform limit in the momentum representation is identical through second order to the ground-state energy evaluated for $\beta \ll 1$ by summing one- and two-ring diagrams in the Bogolyubov occupation-number representation. The charged-boson gas and the one-dimensional boson system with a $\delta$-function interaction are considered to examine some of the interesting features of the uniform limit procedure. (auth)

**56051** HYDRODYNAMICS OF A BOSE FLUID IN TERMS OF ACTION-ANGLE VARIABLES IN QUANTUM STATISTICS. Biswas, A. C.; Rama Rao, I. (Tata Inst. of Fundamental Research, Bombay). Physica; 53: No. 3, 493-7(15 Jun 1971).

Quantum hydrodynamic equations valid for any interacting Bose fluid at finite temperature are derived, using the action-angle variables in quantum statistics. (auth)

**56052** PHONON–PHONON INTERACTION IN LIQUID HELIUM. Zagrebnov, V. A. (Moscow Univ.). Vestn. Mosk. Univ., Ser. III. Fiz. Astron.; 12: No. 1, 75-81(Jan-Feb 1971). (In Russian).

The effect of the interaction of phonons in liquid helium at T = 0°K was evaluated with a cubic approximation at the natural phonon energy. It was shown that the renormalized ("dressed") spectrum of phonons is stable and that it has been assumed by Landau and Khalatnikov for the calculation of the viscosity of liquid helium. (tr-auth)

**56053** SIMPLE THEORETICAL MODELS OF THE BEHAVIOR OF SHEAR WAVES IN THE INTERACTION OF SUPERFLOW WITH THE VORTEX LATTICE. Le Ray, M.; Francois, M. (Faculte des Sciences, Orsay, France). Phys. Lett.; 36A: No. 5, 417-18(27 Sep 1971).

An explanation of the behavior of the vortex lattice in the presence of superflow is proposed, introducing a helicoidal deformation of the vortices and a new characteristic distance: the wavelength of the shear waves associated with the frequency of rotation. (auth)

**56054** VELOCITY OF SECOND SOUND IN ROTATING HELIUM II. Vidal, F.; Le Ray, M.; Francois, M. (Faculte

des Sciences, Orsay, France). Phys. Lett.; 36A: No. 5, 401-2(27 Sep 1971).

The velocity of second sound in rotating He II is found independent of the rotation in the direction parallel to the vortices and undergoes, when the propagation is normal to the vortices, a decrease much greater than that due to attenuation. (auth)

**56055** TEMPERATURE DEPENDENCE OF THE SOUND VELOCITY IN LIQUID $^4$He. Meier, P. F.; Beck, H. (Univ., Zurich). Phys. Lett.; 36A: No. 5, 397-8(27 Sep 1971).

By the use of the Hamiltonian for the hydrodynamical model, the self-energy of a long-wavelength phonon is calculated in lowest order of perturbation theory, starting from harmonic phonons with a linear spectrum. (auth)

**56056** SURFACE TENSION OF He II NEAR THE λ POINT AND THE BOUNDARY CONDITION OF THE ORDER PARAMETER ON THE FREE SURFACE. Sobyanin, A. A. (Inst. of Physics of High Pressures, Moscow). Zh. Eksp. Teor. Fiz.; 61: No. 1, 433-8(Jul 1971). (In Russian).

Thermodynamic considerations and the result of experiments on vapor dragging over the surface of superfluid helium under conditions of pure superfluid motion and of thermal counterflow of the normal and superfluid component are employed for substantiating the boundary condition $\Psi = 0$ for the order parameter in He II at the free surface. It is shown that, if $\Psi = 0$ at the surface with vapor, the surface tension of He II should contain an additional contribution that varies with temperature near the λ point as $\Delta\sigma = \Delta\sigma_0(T_\lambda - T)^{\frac{1}{2}}$. The result is in qualitative agreement with the experimental data. (auth)

**56057** IONS AND ROTONS IN SUPERFLUID HELIUM. Iguchi, Ienari. Stanford, Calif.; Stanford Univ. (1971). 146p. University Microfilms Order No. 71-19,706.

Thesis.

The excitations in liquid helium are studied. In particular, three different phenomena are treated: scattering of vortex waves by a trapped ion, vortex-wave creation, and roton scattering. For the problem of vortex-wave scattering, classical hydrodynamics is used, and the trapped ion is represented as a cylindrical or a spherical impurity located in the vortex core. To treat the problem of vortex-wave creation, it is assumed that there is an ac field perpendicular to the vortex line, as well as a dc field along the vortex axis. In this way, a trapped ion is perturbed and creates vortex waves. The analysis is also based on classical hydrodynamics, and a truncated Fourier expansion is used to obtain a solution valid for long wavelengths. Roton scattering is more interesting because there is at present no really satisfactory microscopic theory of rotons. Here, a linear Schroedinger equation with a hypothetical Hamiltonian describing a roton is postulated and both three- and two-dimensional problems are treated. The scattering formalism makes use of the Green's function satisfying appropriate boundary conditions, indicating the existence of two possible scattering channels. (TSS) (Diss. Abstr., Int., B)

**56058** QUANTUM LATTICE-GAS MODEL OF LIQUID $^4$He. Roy, Ranendra Kumar. Cleveland; Case Western Reserve Univ. (1970). 84p. University Microfilms Order No. 71-19,049.

Thesis.

The quantum lattice-gas model for a system of bosons with hard-core repulsion and nearest-neighbor attraction first introduced by Matsubara and Matsuda and further developed by Zilsel is applied to study the equilibrium properties of liquid $He^4$. Here an fcc lattice is considered rather than the sc lattice considered previously. The basic thing done is to include a zero-point energy term in the hamiltonian instead of Zilsel's static zero-point energy term which can be used only in the mean-field approximation. (TSS) (Diss. Abstr. Int., B)

**56059** EQUILIBRIUM PROPERTIES OF SUBMONOLAYER $^4$He FILMS. Wallace, John Longstreet. Pasadena, Calif.; Califronia Inst. of Tech. (1971). 192p. University Microfilms Order No. 71-17,387.

Thesis.

Isosteres were measured for submonolayer films of helium-four adsorbed on a sintered copper sponge precoated with each of the other noble gases. These measurements were carried out at temperatures between 3 and 4°K and at coverages between 0.5 and 1.0 monolayer; the pressures encountered were in the range from $10^{-7}$ to $10^{-1}$ torr. On the neon-coated substrate, the lower binding energy and higher lateral mobility made it feasible to take useful data at coverages as low as 0.025 monolayer. From the isosteres, information is derived about the partial molar entropy, entropy and heat capacity of the film. It appears that the submonolayer film is a well-defined entity whose qualitative properties remain unchanged as the substrate precoating is varied. These include a transition into a highly ordered state as the coverage is increased, a total heat capacity which is not monotonic with coverage, and significant lateral mobility. The transition into the ordered state is initiated at higher coverage as the temperature is lowered, and this anomaly is discussed in terms of a model in which two dimensional crystalline patches are broken up by thermal fluctuations. (Diss. Abstr. Int., B)

**56060** DISCREPANCIES IN CRITICAL-HEAT-FLUX DATA OBTAINED USING THIN-WIRE HEATERS IN SATURATED LIQUID HELIUM II. Leonard, A. C. (Royal Military Coll. of Canada, Kingston, Ont.); Lady, E. R. Advan. Cryog. Eng.; 16: 378-85(1971).

From Cryogenic engineering conference; Boulder, Colo. (17 Jun 1970). See CONF-700628.

The following topics are covered: the experimental apparatus and methods, the effect of dewar and specimen-holder geometry on the critical heat flux $q_{max}$, and the effect of specimen defects on $q_{max}$.(M.H.R.)

**56061** HIGH-SPEED MOTION-PICTURE STUDIES OF FILM BOILING IN LIQUID HELIUM II. Ebright, F. L.; Irey, R. K. (Univ. of Florida, Gainesville). Advan. Cryog. Eng.; 16: 386-92(1971).

From Cryogenic engineering conference; Boulder, Colo. (17 Jun 1970). See CONF-700628.

The properties, such as thickness, frequency, and wavelength, of the oscillating vapor film around small-diameter wires were characterized photographically for both the noise and no-noise conditions. This experimental evidence allows a check of the Rivers–McFadden (Trans. ASME, Sec. C, J. Heat Trans., 88(4): 343(1966)) explanation of the depth effect, and provides information on the noise phenomenon. (M.H.R.)

**56062** NEAR-ISOTHERMAL DISSIPATIVE FLOW OF LIQUID He II AT SUPERCRITICAL VELOCITIES. Vote, F. C.; Myers, J. E.; Chu, H. B.; Frederking, T.H. K. (Univ. of California, Los Angeles). Advan. Cryog. Eng.; 16: 393-401(1971).

From Cryogenic engineering conference; Boulder, Colo. (17 Jun 1970). See CONF-700628.

Flow resistance was measured in helium II under typical dewar insulation conditions. Data were taken with both rough and smooth channels. A generalized frame of phenomenological equations is considered from which pertinent dimensionless parameters become available. Helium-II hydrodynamics is outlined in sufficient detail to provide adequate background for a summary of the experimental details and findings. Generalized correlations are presented based on similarity parameters for superfluid helium. (M.H.R.)

## *Superconductivity*

*Refer also to abstracts 55086, 55541, 55545, 56359, and 56594.*

**56063** EFFECT OF MAGNETIC FIELDS ON STRESS RELAXATION IN THE MIXED-STATE SUPERCONDUCTING Pb-In ALLOYS. Suenaga, M.; Galligan, J. M. (Brookhaven National Lab., Upton, N. Y.). Phys. Rev. Lett.; 27: No. 11, 721-4(13 Sep 1971).

The magnetic field dependence of the stress changes associated with the normal-to-superconducting-state transition was measured for single crystals of Pb–5 at.% In and Pb–10 at.% In and was found to be in agreement with the magnetic field dependence of the ultrasonic-wave attenuation in type-II superconductors. (auth)

**56064** QUANTIZED FLUX STATES OF SUPERCONDUCTING CYLINDERS. Goodman, William L.; Willis, Wayne D.; Vincent, Daniel A.; Deaver, Bascom S. Jr. (Univ. of Virginia, Charlottesville). Phys. Rev., B; 4: No. 5, 1530-8(1 Sep 1971).

The magnetic flux trapped in hollow superconducting cylinders (14- to 56-μ ID, 0.1- to 5-μ walls, 0.5 to 2.5 cm long) was measured as a function of the applied magnetic field in which the cylinder was cooled through its transition temperature. For most applied fields, the entire cylinder is in the same quantum state; for some fields there is a mixed state with bands along the cylinder in states differing by one flux quantum. In cylinders with walls thick with respect to the penetration depth, the trapped flux is an integral multiple of $hc/2e \pm \frac{1}{2}\%$. The temperature dependence of the trapped flux in a cylinder containing a single flux quantum was measured, and a continuous reversible change by just the amount required to maintain the constancy of the fluxoid was found. (auth)

**56065** ANGULAR DEPENDENCE OF THE SUPERCONDUCTIVE NUCLEATION FIELD Hc4. van Gelder, A. P.; Hendriks, J. W.; Wyder, P. (Katholieke Univ., Nijmegen, Netherlands). Phys. Rev., B; 4: No. 9, 2950-7(1 Nov 1971).

The angular dependence of the superconducting nucleation field of a system with two intersecting vacuum faces is investigated. Within the framework of the simple Ginzburg–Landau theory using

XUM

a trial-function approach, it is shown that superconductivity can nucleate along the edge of a wedge-shaped geometry in fields $H_{c4}$ above $H_{c3}$. This nucleation field is calculated for different angles of the wedge and different directions of the field. The effect is studied experimentally on evaporated films with wedge-shaped edges produced with the use of a shadowing technique. It is shown that the experimental results can be explained on the basis of a $H_{c4}$ model. (auth)

**56066** SUPERCOOLING AND THERMAL CONDUCTIVITY IN SUPERCONDUCTING MOLYBDENUM. Waleh, A.; Zebouni, N. H. (Louisiana State Univ., Baton Route). Phys. Rev., B; 4: No. 9, 2977-87(1 Nov 1971).

The critical magnetic field and the associated supercooling are measured and analyzed in superconducting molybdenum. The coexistence of a superconducting surface sheath with a supercooled normal bulk is confirmed. Thermal-conductivity measurements are analyzed and the possible influence of s–d scattering close to $T_c$ is discussed. (auth)

**56067** INVESTIGATION OF SUPERCONDUCTING-ENERGY-GAP BEHAVIOR OF SINGLE-CRYSTAL RHENIUM BY TUNNELING. Ochiai, S. I. (Osaka Univ.); MacVicar, M. L. A.; Rose, R. M. Phys. Rev., B; 4: No. 9, 2988-96(1 Nov 1971).

A 15.7% anisotropy in the superconducting energy gap was measured by electron tunneling into single crystals of rhenium, using thin carbon films as the tunneling barrier to form Re/C/In sandwiches. The energy-gap behavior vs. temperature is BCS-like. The anisotropy agrees with ultrasonic measurements of other hcp metals and suggests that phonon dispersion plays a dominating role in the gap behavior. However, gap values determined from multiparticle tunneling data exhibited reduced gap magnitudes and a dissimilar crystallographic behavior. (auth)

**56068** SUPERCONDUCTIVITY AND MAGNETIC SCATTERING IN La–Ce. Wollan, J. J.; Finnemore, D. K. (Iowa State Univ., Ames). Phys. Rev., B; 4: No. 9, 2996-3002(1 Nov 1971).

Magnetic impurity scattering for La–Ce was studied for temperatures well below both the superconducting transition temperature and the Kondo temperature. Two different spin scattering times are involved in this problem. The spin scattering time associated with the breaking of Copper pairs is found to be approximately $5 \times 10^{-11}$ sec and to be nearly independent of temperature. The spin scattering time associated with the Kondo effect, however, is found to be on the order of $10^{-14}$ sec and to have a very strong temperature dependence. These two scattering times appear to be independent of one another. A thorough study of the negative magnetoresistance is presented for several values of impurity concentration to help unravel the effects of impurity–impurity interactions. (auth)

**56069** NORMALIZING CURRENT OF A TYPE-II SUPERCONDUCTOR. Walmsley, D. G. (New Univ. of Ulster, Eng.). Phys. Lett.; 36A: No. 5, 357-8(27 Sep 1971).

The theoretical maximum normalizing current of a type-II superconductor in a longitudinal field and current geometry is calculated. The influence of the Meissner state is included. (auth)

**56070** OSCILLATORY FLUX LINE PROFILES DERIVED FROM TEWORDT'S GENERALIZED GINZBURG–LANDAU FUNCTIONAL. Hubert, A. (MPI fuer Metallforschung, Stuttgart). Phys. Lett.; 36A: No. 5, 359-60(27 Sep 1971).

In an attempt to explain attractive forces between flux lines, Tewordt's extended Ginzburg–Landau functional is analyzed. Evaluating the full fourth-order equations, oscillatory flux line profiles are derived both numerically and from linearized equations. (auth)

**56071** LOCAL MOMENT RELAXATION IN A SUPERCONDUCTOR. Huefner, S.; Brinkman, J.; Crecelius, G. (Freie Univ., Berlin). Phys. Lett.; 36A: No. 5, 367-8(27 Sep 1971).

The linewidth of the 22-keV line of $^{151}$Eu was measured in Eu–La (1% Eu). Below the superconducting transition temperature it increases exponentially. (auth)

**56072** LOW-TEMPERATURE SPECIFIC HEAT MEASUREMENTS OF $ZrV_2$ AND $HfV_2$. Rapp, O. (Royal Inst. of Tech., Stockholm); Vieland, L. J. Phys. Lett.; 36A: No. 5, 369-71 (27 Sep 1971).

The C15 compounds $ZrV_2$ and $HfV_2$ show bulk superconductivity at 7.3 and 8.4°K, respectively, indicating a strong dependence of $T_c$ on the electron per atom number for C15 compounds. High electronic contributions to the specific heat are observed. (auth)

**56073** PHONON GENERATION BY THE AC JOSEPHSON EFFECT. Kinder, H. (Kernforschungsanlage, Juelich, Ger.). Phys. Lett.; 36A: No. 5, 379-80(27 Sep 1971).

Emission of phonons of energy $\hbar\omega \geq 2\Delta$ from a self-coupled Josephson tunneling junction into its substrate was observed. The quantum efficiency varies with the voltage applied to the junction and shows abrupt changes at the "subharmonic" voltages. (auth)

**56074** COMPENSATION OF EXTERNAL MAGNETIC FIELD BY AN INTERNAL FIELD IN A SUPERCONDUCTOR. Hillenbrand, B.; Schuster, K.; Wilhelm, M. (Forschungslaboratorien der Siemens, Erlangen, Ger.). Phys. Lett.; 36A: No. 5, 383-4 (27 Sep 1971).

The temperature dependence of the critical magnetic field $H_{c2}$ was measured for $CeRu_2$ and its solid solutions with other rare earth elements. Anomalies are interpreted as the combined influence of external and internal fields on the conduction electron spin. (auth)

**56075** PHONON SPECTRA OF DILUTE Pb–In ALLOYS OBSERVED BY SUPERCONDUCTING TUNNELING. Sood, B. R.; Chandrasekhar, B. S. (Case Western Reserve Univ., Cleveland). Phys. Lett.; 36A: No. 5, 385-6(27 Sep 1971).

The phonon spectra of dilute Pb–In alloys were studied to look for structure within the impurity band. For each alloy studied the impurity band was found to consist of two peaks. (auth)

**56076** STRONG-COUPLING PARAMETERS IN SUPERCONDUCTING In–Pb ALLOYS. Braendli, G.; Trofimenkoff, P. N. (Cornell Univ., Ithaca, N. Y.). Phys. Lett.; 36A: No. 5, 431-2 (27 Sep 1971).

Far-infrared measurements of the energy gap in In–Pb alloys were performed. The results indicate that neither of two proposed relationships between $2\Delta/kT_c$ and $T_c/\theta_D$ is adequate. (auth)

**56077** MICROWAVE OSCILLATIONS IN PARALLEL JOSEPHSON JUNCTIONS. Thomas, G.; Parthasarathy, L. (State Univ. of New York, Stony Brook). Physica; 53: No. 3, 351-63(15 Jun 1971).

It was found that when two Josephson junctions were connected in parallel, constant voltage–current steps appeared in the V–I characteristics for currents above the sum of the zero-field critical currents of the two junctions. These steps only occurred when the critical currents of the two junctions were different. The current steps were separated by voltages which corresponded fairly closely with the fundamental and 2nd and 6th harmonics of fundamental frequency determined by the length of the superconducting strips which connected the two junctions. When junctions that had the same critical currents were connected in parallel, no such steps were observed. An analysis, based on the equations derived by Ivanchenko and Stewart, is also presented. (auth)

**56078** ELECTRON TRANSPORT IN Nb/Nb OXIDE/Bi TUNNEL JUNCTIONS. Laibowitz, R. B. (IBM Thomas J. Watson Research Center, Yorktown Heights, N. Y.); Esaki, L.; Stiles, P. J. Phys. Lett.; 36A: No. 5, 529-30(27 Sep 1971).

Two stable conduction states were observed in tunnel junctions composed of Nb/Nb oxide/Bi. The conduction characteristics, including switching between the two states, are interpreted using a potential barrier model that is alterable by internal polarizations. (auth)

**56079** IMPROVEMENTS IN PROCESS FOR MAKING SUPERCONDUCTORS. (to General Electric Co.). British Patent 1,247,319. 22 Sep 1971. Priority date 29 Apr 1969, United States.

A process is described for producing a superconducting tape-like body of laminate construction. The process comprises the steps of providing a laminate composed of a material capable of being rendered superconducting, and integrally bonding to each side of the superconducting laminate an outer lamina which has a coefficient of thermal expansion greater than that of the superconducting laminate. The bonding is effected at an elevated temperature so that, upon cooling to room temperature, the superconducting laminate is in mechanical compression. The laminate composed of a material capable of being rendered superconducting is formed by passing a tape-like strip composed principally of niobium through a molten tin bath to form a coating of tin thereon, heating the tin-coated strip to react the tin and niobium at the tin/niobium interfaces to form the $Nb_3Sn$ intermetallic compound, and terminating the heating to preserve the elemental tin surfaces. (M.H.R.)

**56080** HEALING LENGTH OF THE SUPERCONDUCTING ORDER PARAMETER. Jacobs, A. E. (Univ. of Toronto). Phys. Rev., B; 4: No. 9, 3247-50(1 Nov 1971).

The healing length of the superconducting order parameter near $T = T_c$ is calculated by means of a variational method based on the Neumann–Tewordt expression for the free energy of an inhomogeneous superconductor. The result for the correction to the Ginzburg–Landau healing length near $T = T_c$ indicates

XUM

that the healing takes place over distances of the order of the coherence length at all temperatures, in disagreement with a recent calculation which predicts healing over atomic distances at low temperatures. (auth)

**56081** INTERACTION OF VORTICES IN TYPE-II SUPERCONDUCTORS NEAR $T = T_c$. Jacobs, A. E. (Univ. of Toronto). Phys. Rev., B; 4: No. 9, 3029-34(1 Nov 1971).

The theory of Mueller–Hartmann and Kramer for the interaction of widely separated vortices is extended to temperatures immediately below $T_c$. The interaction is found to be attractive below $T_c$ for type-II materials with $\kappa \approx 1/\sqrt{2}$ and not too small a mean free path, in agreement with experimental observations on such materials. The phenomenon of field reversal and the work of Eilenberger and Buettner are shown to be unrelated to an attractive interaction between vortices and the consequent first-order transition at the lower critical field, at least for temperatures near $T_c$; it is shown how field reversal, if it occurs in the mixed state, might result in an attractive interaction at lower temperatures. (auth)

**56082** FIRST-ORDER TRANSITIONS AT $H_{c1}$ AND $H_{c2}$ IN TYPE-II SUPERCONDUCTORS. Jacobs, A. E. (Univ. of Toronto). Phys. Rev., B; 4: No. 9, 3022-9(1 Nov 1971).

From a consideration of several different definitions of the critical value of $\kappa$ for type-II superconductivity at temperatures below $T_c$, it is proved that the initial flux penetration is not in the form of a singly quantized isolated vortex for pure or rather dirty materials with $\kappa$ values near $1/\sqrt{2}$ at temperatures below $T_c$. It is predicted that the initial flux penetration in such materials is in the form of a vortex lattice with finite spacing; the transition at the field of first flux penetration would be first order in such materials, with a discontinuity in the magnetization and a latent heat. Recent experimental evidence supporting this prediction is discussed. A similar analysis leads to the prediction that the transition from the mixed state to the normal state is first order for very dirty materials ($l \lesssim \xi_0/50$) with $\kappa$ values near $1/\sqrt{2}$, in qualitative agreement with the experimental results of Ehrat and Rinderer. Finally, it is shown by both qualitative and quantitative arguments that a negative normal–superconducting wall energy is only a sufficient condition for type-II superconductivity, and not a necessary one. (auth)

**56083** THEORY OF INHOMOGENEOUS SUPERCONDUCTORS NEAR $T = T_c$. Jacobs, A. E. (Univ. of Toronto). Phys. Rev., B; 4: No. 9, 3016-21(1 Nov 1971).

The work of Neumann and Tewordt is generalized to obtain the first-order correction (in $1 - T/T_c$) to the Ginzburg–Landau expression for the free energy of an inhomogeneous superconductor. From this expression, the generalized Neumann–Tewordt equations for the first-order corrections to the solutions of the Ginzburg–Landau equations are derived. For two important geometries, the normal–superconducting wall and the mixed state of type-II superconductors, it is shown that the free energy can be rewritten so that it involves only the solutions of the Ginzburg–Landau equations. This formalism is applied to the calculation of the N–S wall energy, where $\sigma_{NS}$ is calculated as a function of T and $\xi_0/l$ for $\kappa = 1/\sqrt{2}$, and to the mixed state of type-II superconductors, where $H_{c1}$ is calculated as a function of T, $\kappa$, and $\xi_0/l$ for singly and doubly quantized isolated vortices. (auth)

**56084** EFFECT OF CARBON ON THE CRITICAL CURRENT OF $Nb_3Sn$. Ziegler, G.; Blos, B.; Diepers, H.; Wohlleben, K. (Siemens AG, Erlangen, Ger.). Z. Angew. Phys.; 31: No. 4, 184-9(29 Jun 1971). (In German).

The addition of carbon during the deposition of the superconducting compound $Nb_3Sn$ from the vapor phase increases the critical current to a large extent. The critical current reaches a maximum value of about $1.6 \times 10^6$ A/cm$^2$ at 5 T at a carbon concentration of about 2 at. % and decreases slowly at higher concentrations. The addition of carbon has no influence on the lattice constant within the accuracy of the measurements, but reduces the critical temperature by a small amount. With the carbon-doped $Nb_3Sn$ there is no correlation between the grain size and the critical current; however, there is a correlation between the imperfections within the grains and the critical current. (auth)

**56085** MAGNETIZATION PROPERTIES OF NONIDEAL TYPE-II SUPERCONDUCTORS TRANSPORTING SINUSOIDAL ALTERNATING CURRENT IN A LONGITUDINAL MAGNETIC FIELD. Sugahara, M.; Kato, S. (Yokohama National Univ., Japan). Appl. Phys. Lett.; 19: No. 4, 111-13(15 Aug 1971).

Observations are presented on the ac magnetization of Nb–25% Zr and Nb–48% Ti wires in a longitudinal field $H_{z0}$. When $H_{z0}$ is higher than the field induced by the impressed ac conduction current, the magnetization data agree with the calculation based on a force-free model. The magnetization process of Nb–Zr shows a large deviation from the usual critical state behavior. (auth)

**56086** VISCOUS VORTEX FLOW IN SUPERCONDUCTORS WITH PARAMAGNETIC IMPURITIES. Gor'kov, L. P.; Kopnin, N. B. (Inst. of Theoretical Physics, Moscow). Zh. Eksp. Teor. Fiz.; 60: No. 6, 2331-43(Jun 1971). (In Russian).

An expression for the conductivity of a vortex lattice in fields such that $H \ll H_{c2}$ is obtained on basis of the nonstationary equations for superconductors with paramagnetic impurities. The case of high temperatures (small paramagnetic impurity concentrations) effectively leads to a greater conductivity compared to the conductivity in the low-temperature region. Qualitatively, this agrees with the experiments with ordinary alloys. Macroscopic electrodynamic equations are written down for vortex-structure superconductors. (auth)

**56087** SUPERCONDUCTIVITY OF MOLYBDENUM AND TUNGSTEN CARBIDES. Morton, N.; James, B. W.; Wostenholm, G. H.; (and others) (Univ. of Salford, Eng.). J. Less-Common Metals; 25: No. 1, 97-106(Sep 1971).

The superconducting critical temperatures of a total of 18 samples of $\alpha$–$Mo_2C$, $\beta$–$Mo_2C$, $\eta$–$MoC_{1-x}$ and $\alpha$–$W_2C$ were determined resistively. The critical temperatures lie within the ranges 6 to 7.3°, 5.1 to 7.2°, 7.4 to 8.9° and 2.95 to 3.05°K, respectively. The critical temperature for $\beta$–$Mo_2C$ is much higher than found previously and similar to that for $\alpha$–$Mo_2C$. (auth)

**56088** POLARIZATION OF CORE FERMION AND THE HEAT TRANSPORT OF FLUX LINE. Ohta, Tokio; Yamaguchi, Ken (Yokahama National Univ., Japan). J. Phys. Soc. Jap.; 31: No. 3, 636-40(Sep 1971).

The polarization energies of the bound fermion in the core of moving flux line by the core field are calculated. The contribution from around the core center is $10^{-2}$ to $10^{-3}$ times of the unperturbed energy, while the peripheral polarization makes ≥10% increment of the fermion energy. The polarization by core field may account for the fact that the transport heat exceeds the incremental heat under some conditions. (auth)

**56089** SOUND EXCITATION IN A JOSEPHSON JUNCTION. Ivanchenko, Yu. M.; Medvedev, Yu. V. (Donetsk Physical-Technical Inst., USSR). Zh. Eksp. Teor. Fiz.; 60: No. 6, 2274-85(Jun 1971). (In Russian).

A method, based on the Froehlich hamiltonian, which directly takes into account the electron–phonon interaction is developed for studying the Josephson transition. It is shown that long-wave lattice vibrations with Josephson frequency may arise as a result of the electron–phonon interaction. The effect of resonant sound generation on the shape of the junction volt–ampere characteristic is considered. (auth)

**56090** EFFECT OF EXTERNAL FLUCTUATIONS ON THE PROPERTIES OF SUPERCONDUCTING MICRO-JUNCTIONS NEAR CRITICAL TEMPERATURE. Zil'berman, L. A.; Ivanchenko, Yu. M. (Donetsk Physical-Technical Inst., USSR). Zh. Eksp. Teor. Fiz.; 60: No. 6, 2286-95(Jun 1971). (In Russian).

The effect of voltage fluctuations in the external circuit on the volt–ampere characteristic of a superconducting microjunction near $T_c$ is investigated. At temperatures exceeding the critical value, voltage fluctuations weaken superconductivity induced by fluctuation pairing. Stimulation of superconductivity should be possible on the negative part of the volt–ampere characteristic below $T_c$. It is shown that fluctuations introduced from the external circuit reduce the critical temperature of the microjunction. (auth)

**56091** INTERACTION BETWEEN A CAVITY AND VORTEX IN A TYPE II SUPERCONDUCTOR. Mkrtchyan, G. S.; Shmidt, V. V. (Inst. of Solid State Physics, Moscow). Zh. Eksp. Teor. Fiz.; 61: No. 1, 367-72(Jul 1971). (In Russian).

The free energy of a superconducting vortex in a Type-II superconductor interacting with a hollow cylindrical channel of radius $r \ll \delta_0$ parallel to it is calculated ($\delta_0$ is the penetration depth). It is shown that, on this assumption, capture of only a single vortex by the channel is energetically favorable. The pinning force is calculated to be $f_p = H_{ct}\xi(T)/2$, where $H_{ct}$ is the critical thermodynamic field strength. (auth)

**56092** CRITICAL CURRENT OF A PERFECT TYPE-II SUPERCONDUCTOR IN THE MIXED STATE. Shmidt, V. V. (Inst. of Solid State Physics, Moscow). Zh. Eksp. Teor. Fiz.; 61: No. 1, 398-413(Jul 1971). (In Russian).

A perfectly homogeneous film of a Type-II superconductor ($\kappa \gg 1$, $\xi \ll d \ll \delta_0$, d is the film thickness and $\delta_0$ the penetration depth) and a perfectly homogeneous plate ($d \gg \delta_0$) are considered. It is shown that, in both cases, when the external magnetic field $H_0$ is parallel

XUM

to the film or plate surface the mixed state is a vortex triangular lattice homogeneous in density and analogous to the lattice of the massive material. Stability of the vortex lattice with respect to small displacements (pinning) is ensured by interaction between the lattice and Meissner currents. The pinning force and critical transverse (with respect to the field) current violating stability of the vortex lattice are found. (auth)

**56093** KINETIC EQUATIONS FOR RELAXATION PROCESSES IN SUPERCONDUCTORS. Galaiko, V. P. (Physical-Technical Inst., Kharkov). Zh. Eksp. Teor. Fiz.; 61: No. 1, 382-97(Jul 1971). (In Russian).

A kinetic equation is obtained for the generalized electron density matrix of a superconductor. Relaxation of the system to an equilibrium state proceeds, according to this equation, in two stages. At first, a rapid quantum rearrangement of the system takes place; a self-consistent field of the superconducting condensate is formed and a quasi-particle description of excitations is valid. Later on, the quasi-particle distribution and superconducting ordering parameter slowly evolve as a result of collisions between excitations. (auth)

**56094** EXTERNALLY SHUNTED JOSEPHSON JUNCTIONS: GENERALIZED WEAK LINKS. Hansma, P. K. (Univ. of California, Berkeley); Rochlin, G. I.; Sweet, J. N. Phys. Rev., B; 4: No. 9, 3003-14(1 Nov 1971).

Using externally shunted thin-film Sn/I/Sn Josephson junctions, the Stewart–McCumber predictions were experimentally verified for the current–voltage (I–V) characteristics of a generalized weak link treated as a lumped circuit consisting of an ideal Josephson junction with critical current $i_c$, conductance G, and capacitance C. In addition, it was shown experimentally and theoretically that the predictions for the amount of hysteresis in the I–V characteristic as a function of the dimensionless circuit parameter $\beta_C = (2e/\hbar)\,(i_c C/G^2)$ can be generalized to include shunt inductance L by replacing the capacitance with an effective capacitance $C' = C - G^2L$. An externally shunted Josephson junction acts as a generalized weak link in that it can reproduce the behavior of other types of weak links. In fact, if the temperature of a single shunted junction is varied between 1.12 and 3.7°K, or the applied magnetic field is varied between 0 and 1 Oe, $\beta_C$ can be varied over two orders of magnitude while the junction is in the cryostat. Since $\beta_C$ determines the qualitative nature of the I–V characteristic, this variation of $\beta_C$ simulates widely different types of weak-link devices. Furthermore, the accessible range of $\beta_C$ for the single shunted junction can be changed while it is out of the cryostat by altering its external shunt conductance. Thus, externally shunted Josephson junctions are theoretically well-understood models of, and simulators for, the behavior of many weak-link junctions; they have the desirable property of adjustability both before and after cryostat installation. This versatility should find many significant applications. (auth)

**56095** FLUCTUATION EFFECTS ON THERMAL CONDUCTIVITY OF ONE-DIMENSIONAL SUPERCONDUCTORS. Wolf, S.; Chandrasekhar, B. S. (Case Western Reserve Univ., Cleveland). Phys. Rev., B; 4: No. 9, 3014-15(1 Nov 1971).

Thermal-conductivity measurements were made on wires of Pb–5 at. % In prepared by evaporation. The cross-sectional area of these wires determined in part by electron microscopy was less than $\xi^2$, where $\xi$ is the coherence length, and thus they can be considered "one-dimensional" superconductors. A well-defined peak in the thermal conductivity was found over a restricted range of temperature close to the bulk $T_c$ and this is attributed to fluctuation effects on the normal component of the electronic conduction effects on the normal component of the electronic conduction. The qualitative aspects of the results agree quite well with a recent prediction of Abrahams, Redi, and Woo. (auth)

**56096** SUPERCONDUCTIVITY IN NOBLE-METAL-RICH HEXAGONAL CLOSE-PACKED PHASES. Luo, H. L. (Univ. of California, San Diego, La Jolla); Andres, Klaus. Contract AT(11-1)-34. Phys. Rev., B; 1: 3002-6(1 Apr 1970).

The superconductivity of phases rich in the noble metals (Cu, Ag, Au) was investigated. All face-centered cubic solid solutions (with Zn, Cd, Al, In) remained normal down to 0.014°K; and all hexagonal close-packed phases (with Si, Ge, Sn, Sb, Al, In) became superconducting in the range of 0.019–0.61°K. The results are interpreted as due to the Fermi-surface–Brillouin-zone interaction. The first superconductor with a $DO_3$ structure was found in the alloy Cu–15.5 at. % Sb. (auth)

**56097** ELECTRON–PHONON INTERACTION IN NORMAL AND SUPERCONDUCTING STATES OF HIGH-PURITY RHENIUM. Robinson, David Allan. Los Angeles; Univ. of California (1971). 140p. University Microfilms Order No. 71-19,460.

Thesis.

The attenuation of transverse and longitudinal waves propagating along the c-axis in high-purity rhenium was measured in the normal and superconducting states. The transverse-wave-attenuation measurements were made at frequencies from 130 to 950 MHz and from about 0.45 to over 70°K. The longitudinal-wave attenuation was primarily studied at frequencies near 400 MHz over the same temperature range. Preliminary longitudinal attenuation measurements were also made from 15 to 195 MHz from about 1.2 to over 70°K. In the superconducting state the attenuation was compared with the simple BCS theory, using as adjustable parameters the gap parameter and the residual attenuation at $T_c$. Using transverse wave attenuation a gap parameter of 3.50 ± 0.10 was found, while the longitudinal attenuation gave a gap parameter of of 2.90 ± 0.10. The superconducting sharp drop in transverse attenuation near $T_c$ was investigated, using a mixed-mode transducer. It was found that, in the region of rapid fall, the attenuation is nonlinear in the sound-wave amplitude. The attenuation in the normal state was compared with a one-spherical-band theory of ultrasonic attenuation and a two-spherical-band theory which did not include interband scattering or deformation potential effects. It was concluded that the two-band theory was in reasonable agreement with the transverse data — in which a maximum in attenuation at 950 MHz appears to be due to both two-band effects and the screening breakdown predicted by Pippard. However, it also appears that interband scattering and possibly deformation potential effects will be needed for a complete description of the attenuation. (Diss. Abstr. Int., B)

**56098** STUDY OF THE NUCLEATION AND MOTION OF SINGLE FLUXONS IN SUPERCONDUCTORS. Burnette, Keith Thomas. Lafayette, Ind., Purdue Univ. (1971). 341p. University Microfilms Order No. 71-20,432.

Thesis.

What is believed to be the first direct observation of the drift of single fluxons through a superconductor is reported. This was achieved by using an ultrasensitive cryotron amplifier to sense the changes in persistent current that occur in a superconducting film loop when a fluxon is drifting into or out of the loop. Two unexpected results were observed. First, it was shown that fluxon nucleation is influenced not only by the nucleation-magnetic-field magnitude, but also by the time-rate-of-change of this field. Second, at applied field and current magnitudes too low to produce flux flow, transient single fluxon motion is observed, in response to long-duration pulsed-nucleation fields. The proposed explanation for the first of these results is that a localized reduction in the superconducting energy gap, in response to eddy-current-induced Joule heating, should result in fluxon nucleation at field magnitudes too low to produce fluxon nucleation in a steady magnetic field. The second result follows from the first in that the magnetic field magnitude present following the leading edge of the pulsed field is not sufficient to nucleate additional fluxons in the film once the nucleation field becomes constant. (TSS) (Diss. Abstr. Int., B)

**56099** EFFECT OF DEFORMATION ON THE SUPERCONDUCTING TRANSITION TEMPERATURE OF A NIOBIUM–32 PERCENT ZIRCONIUM ALLOY. Finlayson, T. R.; Milne, I. (Central Electricity Research Labs., Surry, Eng.). Solid State Commun.; 9: No. 15, 1339-41(1 Aug 1971).

An increase of $T_c$ by up to 0.5 K with a 93% area reduction of a Nb–32% Zr alloy is reported. Various possibilities for explaining this phenomenon are discussed. (auth)

**56100** PROPERTIES OF DEFORMED SUPERCONDUCTING ALLOYS OF VANADIUM–GALLIUM. Pan, V. M.; Beletskii, Yu. I.; Sudovtsov, A. I. Fiz. Khim. Obrab. Mater.; No. 3, 128-31 (May–Jun 1971). (In Russian).

A two-phase structure with the intermetallic compound $V_3Ga$ was detected in V-rich deformed samples of V–Ga alloys. Optimum thermo-mechanical working produced dispersed $V_3Ga$ in a matrix of body-centered-cubic solid solution with favorable superconductive properties. Transition into the superconducting state of such alloys was highly spread, in association with the dispersion of particles of the $V_3Ga$ phase, and occurred in the range 15 to 11.5°K. The critical temperature for the bcc solid solution matrix was about 2°K. (tr-auth)

**56101** CALCULATION OF HYSTERESIS LOSSES IN HARD SUPERCONDUCTORS: POLYGONAL-SECTION CONDUCTORS. Norris, W. T. (Central Electricity Research Labs., Leatherhead, Eng.). J. Phys., D (London); 4: No. 9, 1358-64(Sep 1971).

An approximate method of estimating hysteresis losses in hard superconductors of complex geometry is described. It is based on approximating contours of current penetration by polygons and adjusting the polygons so that the vector potential is the same at all the corners; this corresponds to zero flux crossing the contour

between corners. Two examples are worked: for a square-sectioned conductor and for a pair of closely spaced thick strips carrying antiparallel currents. (auth) (UK)

**56102** STRUCTURE OF THE CURRENT-INDUCED INTERMEDIATE STATE IN TYPE-I SUPERCONDUCTORS. Wiederick, H. D.; Mukherjee, B. K.; Baird, D. C. (Royal Military Coll. of Canada, Kingston, Ont.). J. Phys., D (London); 4: No. 9, 1365-9(Sep 1971).

Several models have been proposed for the intermediate state which occurs when superconductivity is destroyed in type-I wires by a current. Experimental testing of these models has, so far, only been possible through measurements of the resistance and the intermediate state core radius during the transition. An experiment is described in which a wire specimen is placed along the axis of a solenoid whose inductance is monitored as a steadily increasing direct current destroys superconductivity in the wire. The change in inductance of the solenoid is a function of the intermediate-state structure, and the experimental results are compared with theoretical values obtained on the basis of the various models. The results appear to favour the model presented by Baird and Mukherjee in 1971. (auth) (UK)

**56103** VOLUME DEPENDENCE OF TRANSITION TEMPERATURE AND EFFECTIVE INTERACTION STRENGTH IN TIN. Rajput, J. S. (Regional Coll. of Education, Bhubaneswar, India). J. Phys. Soc. Jap.; 31: No. 4, 1053-5(Oct 1971).

A method is presented to determine the variation of superconducting transition temperature for tin. The initial linear drop of $T_c$ when plotted against change in volume, an experimentally observed fact, is theoretically confirmed. (auth)

**56104** SUPERCONDUCTING PROPERTIES OF NIOBIUM–TITANIUM–ZIRCONIUM–HAFNIUM ALLOYS. Raevskii, I. I.; Stepanov, N. V.; Dubrovin, A. V.; Ivanov, O. S.; Alekseevskii, N. E. (Inst. of Metallurgy, Moscow). Fiz. Metal. Metalloved.; 31: No. 1, 72-8(Jan 1971). (In Russian).

Data are presented on the superconducting properties of several Nb–Ti–Zr–Hf alloys with 30 at.% Nb in each case. Critical current densities, field strength, critical magnetic field, and the temperature of transition from the superconducting state to the normal one were measured. Annealing of the alloys at 500°C for one hour increased the critical current density by two orders of magnitude. The largest values of the critical current density were associated with the Nb–Zr apex of the ternary diagram. An increase of the Hf content lowered the fundamental superconducting characteristics. (tr-auth)

**56105** SUPERCONDUCTIVE PROPERTIES OF NIOBIUM–ZIRCONIUM–HAFNIUM ALLOYS. Stepanov, N. V.; Raevskii, I. I.; Dubrovin, A. V.; Ivanov, O. S.; Alekseevskii, N. E. (Inst. of Metallurgy, Moscow). Fiz. Metal. Metalloved.; 31: No. 1, 64-71(Jan 1971). (In Russian).

Data are given on the superconductive properties of alloys containing 30, 50, and 70 atom percent niobium in alloys with zirconium and hafnium. Critical temperatures, the critical current, and the critical magnetic field were measured on samples of the ternary system corresponding to the three sections of constant niobium content. (K.S.W.)

**56106** MODEL CALCULATION OF THE ELECTRON–PHONON COUPLING PARAMETER λ. van Haeringen, W. (Philips Research Labs., Eindhoven, Netherlands); Junginger, H.-G. Z. Phys.; 246: 281-94(1971).

A simple model is described in which the influence of two parallel Brillouin zone faces on the electron–phonon coupling parameter λ can be studied. In this model it is observed that λ, considered as a function of the Fermi energy $E_F$, has a peculiar structure when the Fermi body just passes through the two Bragg planes. Both an enhancement as well as a reduction of the more familiar density of states effect on λ and, therefore, on the critical temperature $T_c$ of superconductors appear to be possible. In this respect approaching a Brillouin zone face turns out to be very favorable. The structure in λ is due to a combination of Umklapp, wave function mixing, and density of states effects. The calculations indicate that it is worthwhile to study these effects in detail in actual systems. (auth)

**56107** FINITE-VOLTAGE BEHAVIOR OF LEAD/COPPER/LEAD JUNCTIONS. Clarke, John (Univ. of California, Berkeley). Phys. Rev., B; 4: No. 9, 2963-77(1 Nov 1971).

Pb/Cu/Pb junctions were made by evaporating successively onto a glass substrate a strip of Pb, a disk of Cu, and a second strip of Pb at right angles to the first. Each Pb strip had a width w. At liquid-$^4$He temperatures, the junctions could sustain a dc Josephson supercurrent less than or equal to the critical current $i_c$. When $i_c$ was small enough so that the Josephson penetration depth $\lambda_J$ ($\propto i_c^{-1/2}$) was greater than $\frac{1}{4}$ w, the supercurrent flowed uniformly through the junction, which was said to be weak. When $i_c$ was higher so that $\lambda_J$ was less than $\frac{1}{4}$ w, the supercurrents were nonuniform, and the junction was said to be strong. At a current i greater than $i_c$, the voltage v across a weak junction was in reasonable agreement with the theoretical result $v = (i^2 - i_c^2)^{1/2} R$, where R is the normal-state resistance of the Cu film. For strong junctions, a dc supercurrent appeared at finite voltages, because the ac supercurrents had a nonzero time average. The experimental results are in good qualitative agreement with calculations on a one-dimensional model. When the current was fed into the junction asymmetrically, that is, when it was applied to one end of each Pb strip, the self-field of the current generated periodic structure on the i – v characteristic, the period being typically 3 mA. The structure vanished if the currents were applied symmetrically, that is, the input and output currents divided equally between the ends of each lead strip. The application to a junction of rf electromagnetic radiation of angular frequency Ω induced constant-voltage current steps at voltages $(n/m)\hbar\Omega/(2e)$, where n and m are integers. The amplitude of the steps was modulated by the amplitude of the rf power and by a magnetic field in approximately the manner observed in tunnel junctions with oxide barriers. The dynamic resistance of the steps was less than $1.7 \times 10^{-14}$ Ω. The electrochemical potential across the junction at which a given step appeared was not affected by either junction material or experimental conditions at a precision of 1 part in $10^8$. The highest frequency at which steps were induced was 2 MHz. At this frequency the skin depth of the copper was much less than w, and little radiation was coupled into the junction. The lowest frequency was 5 kHz, corresponding to a first-order-induced step at about $10^{-11}$ V. At this voltage the Johnson-noise broadening of the Josephson frequency was also about 5 kHz. At lower frequencies the noise completely destroyed the synchronization between the Josephson ac supercurrents and the rf radiation, so that no steps were observed. (auth)

**56108** SUPERCONDUCTIVITY AND CONSTITUTION OF TITANIUM BASE TRANSITION METAL ALLOYS. Luhman, Thomas Stewart. St. Louis; Univ. of Washington (1970). 168p. University Microfilms Order No. 71-16,976.

Thesis.

The decomposition of the metastable beta phase in titanium-base alloys was investigated by employing an impedance-measuring technique based on the superconducting phenomenon exhibited by these alloys. Experimental apparatus was constructed to measure, as a function of temperature, both the transition from the normal to the superconducting state, and the magnetic properties of alloy samples. A number of correlations were observed between the shapes of superconducting transition curves and the constitution of titanium base alloys. These correlations were used first to demonstrate the sensitivity of these temperature measurements to changes in alloy microstructure and then as a basis for investigating the mechanism by which the beta phase decomposed. It has been shown by step-quenching and aging experiments that a phase separation reaction occurs in Ti–Cr beta phase alloys. Examination of the superconducting temperature parameters revealed that the phase separation was manifested as a solvent clustering reaction. The effects of such a phase separation on omega phase precipitation and reversion were investigated using superconducting temperature measurements. The degree of prior compositional fluctuations, induced by step-quenching to a temperature above the range of thermal stability for the omega phase, did not affect subsequent omega phase precipitation at lower temperatures. However, it was shown that reversion during up-quenching occurred without appreciable solute redistribution, and that the remanent compositional inhomogeneities were stabilized by the tendency for solvent clustering to occur at the up-quenching temperature. Based on the superconducting transition measurements, a model was developed to describe the beta to omega phase transformation in titanium-base alloys. This transformation is described as a structural accommodation in titanium-rich clusters induced by the compressive stresses resulting from the imposed bulk constraints of the matrix. Superconducting magnetization measurements were made on Ti–V and Ti–Nb alloys. The results indicated that the magnetic parameters of these alloys are influenced by compositional as well as structural changes. More specifically, it was found that alterations in magnetic parameters could be detected in single-phase alloys that were heat-treated to produce compositional fluctuations. Thus these results indicate a potential use for such measurements in future metallurgical investigations. Previous discrepancies in the literature regarding the influence of specimen surface conditions on the magnetization parameters were resolved. For example, "peak effects" in alloy magnetization curves could be eliminated by chemical etching of the specimens. (Diss. Abstr. Int., B)

XUM

**56109** INCIPIENT ANTIFERROMAGNETISM IN SCANDIUM AND SUPERCONDUCTORS WITH MAGNETIC IMPURITIES IN A SINGLET GROUND STATE. Capellmann, Herbert. Philadelphia; Univ. of Pennsylvania (1970). 99p. University Microfilms Order No. 71-19,207.

Thesis.

The effect of magnetic impurities (Pr and Tm) on the superconductors Th, $LaPb_3$, $LaTl_3$ and $LaSn_3$ is discussed. Due to crystal field splitting, the impurities have a nonmagnetic ground state and low-lying excited states. In particular, the case of Pr in $LaPb_3$ is discussed. Interband mixing of 4f and conduction electrons leads to a dynamical electron–electron interaction due to exchange of virtual excitations of the impurities. This leads to a lowering of the superconducting transition temperature $T_c$. First, the influence of the magnetic properties of the elements on the left-hand side of the transition series on their superconducting transition temperature $T_c$ is discussed. In particular, the case of scandium is discussed. There is experimental evidence that scandium has strong antiferromagnetic spin fluctuations and it is shown that this leads to a repulsive effective electron–electron interaction. This possibility explains why Sc has not been found to be superconducting. (Diss. Abstr. Int., B)

## *Equipment and Devices*

*Refer also to abstracts 56361 and 56580.*

**56110** (LA-DC-12990) ENERGY STORAGE AND SWITCHING WITH SUPERCONDUCTORS. Laquer, H. L.; Ribe, F. L. (Los Alamos Scientific Lab., N. Mex.). 1971. 3p. (CONF-710624-3). Dep. NTIS.

From International working session on fusion reactor technology conference; Oak Ridge, Tenn. (28 Jun 1971).

Inductive magnetic energy storage with superconductors or cryogenic aluminum conductors is discussed in regard to its use in providing the magnetic fields needed in pulsed thermonuclear reactors and in some large-scale pulsed plasma physics experiments designed to demonstrate the scientific feasibility of controlled fusion. (M.H.R.)

**56111** SUPERCONDUCTIVE ENERGY TRANSMISSION LINE (CABLE) AND METHOD OF PRODUCING THE SAME. (to Licentia Patent-Verwaltungs GmbH). British Patent 1,246,578. 15 Sep 1971. Priority date 21 Mar 1968, Austria.

The superconducting cable described comprises a plurality of current conductors surrounded by a plurality of hollow cylindrical envelopes in the form of flexible, extensible, and corrugated tubes held apart by spacers having a low heat conductivity and that form between them at least one space that is evacuated or filled with liquefied gas. Each of the current conductors is encased by a prefabricated corrugated tube filled with a liquefied or gaseous coolant. The tubes are surrounded jointly by the cylindrical envelopes, which are concentric with one another and serve as insulation to prevent heat conduction from outside the cable. (M.H.R.)

**56112** THEORETICAL TREATMENT OF INTERNAL SHUNT PROTECTION FOR SUPERCONDUCTING MAGNETS. Atherton, D. L. (Ferranti-Packard Ltd., Toronto). J. Phys., E (London); 4: 653-9(Sep 1971).

The theory of internal protective shunts and switches used to limit the maximum temperature rise when a large high-current density superconducting magnet quenches, while operating in the persistent mode, is considered. The shunts can induce more even heating and dissipation, thus avoiding hotspots. The velocity of propagation of a normal spot in a composite superconductor is derived, and its variation is calculated for a particular conductor example. This is used to compute heat generation, temperature, resistivity and resistance increases, and current decay and voltage characteristics for a sample coil in order to determine the minimum number of shunts required to limit the maximum temperature rise to an acceptable value. (auth) (UK)

**56113** ADVANCES IN CRYOGENIC ENGINEERING. VOLUME 16. Proceedings of the 1970 Cryogenic Engineering Conference, Boulder, Colorado, June 17–19, 1970. Timmerhaus, K. D. (ed.). Cryogenic Engineering Conference Publication. New York; Plenum Publishing Corporation (1971). 518p. $30.00. (CONF-700628).

Sixty papers are included under the following topics: applied superconductivity, solid properties, thermodynamic properties, low-temperature insulation, low-temperature refrigeration, low-temperature instrumentation, low-temperature equipment, regenerative heat exchange, heat transfer in helium, film-boiling heat transfer, and heat transfer. Separate abstracts were prepared for thirteen papers. (M.H.R.)

*For abstracts of individual papers see: 56060–56062, 56114–56122, and 56361.*

**56114** APPLICATIONS OF SUPERCONDUCTIVITY AND CRYOGENICS IN ELECTRIC POWER SYSTEMS. Woodson, H. H. (Massachusetts Inst. of Tech., Cambridge). Advan. Cryog. Eng.; 16: 1-10(1971).

From Cryogenic engineering conference; Boulder, Colo. (17 Jun 1970). See CONF-700628.

Attention is focused on three applications of superconductivity and cryogenics in electric power systems that appear to have reasonable chances of success. They are: superconducting field windings in large synchronous machines, cryogenic resistive windings in transformers, and cryogenic resistive underground ac transmission lines. (M.H.R.)

**56115** BRITISH DEVELOPMENTS IN SUPERCONDUCTIVITY APPLICATIONS. Appleton, A. D. (International Research and Development Co., Ltd., Newcastle upon Tyne, Eng.). Advan. Cryog. Eng.; 16: 11-18(1971).

From Cryogenic engineering conference; Boulder, Colo. (17 Jun 1970). See CONF-700628.

The following conclusions were reached: The industrial application of superconductivity in the United Kingdom will be realized in the near future with the superconducting dc motors and generator developed at IRD. The continuing development towards practical superconducting ac transmission cables is assured through the large team working at CERL. Further work on superconducting transformers at any significant level is unlikely in the foreseeable future. The development of superconducting ac generators is expected to increase, although the many formidable problems that must be overcome will necessitate a substantial financial investment. The development of superconductors will continue, but as far as rotating machines are concerned, the order of priority is lower costs, improved techniques for fabricating windings, and improved performance. Improvements are required in the cryogenic field, particularly in the size and efficiency of helium-refrigerator components and in the cost of the refrigeration plant. There is no longer any doubt that superconductors will be employed increasingly in electrical power plants. (M.H.R.)

**56116** SUPERCONDUCTIVITY IN HIGH-ENERGY PHYSICS. Pewitt, E. G. (Argonne National Lab., Ill.). Advan. Cryog. Eng.; 16: 19-26(1971).

From Cryogenic engineering conference; Boulder, Colo. (17 Jun 1970). See CONF-700628.

The following topics are covered: detector magnets, beam transport, accelerator magnets, and rf-cavity applications. (M.H.R.)

**56117** LARGE-SCALE REFRIGERATION SYSTEMS FOR THE TEMPERATURE RANGE OF 1.0 TO 1.85°K. Ratliff, G.; St. Lorant, S. J. (Stanford Linear Accelerator Center, Calif.). Advan. Cryog. Eng.; 16: 154-62(1971).

From Cryogenic engineering conference; Boulder, Colo. (17 Jun 1970). See CONF-700628.

The following subjects are covered: refrigeration-system requirements, 1.85°K refrigeration systems, modified systems, a hybrid He-3–He-4 refrigerator, ejector expanders, cryogenic compressors, and 1.0 and 1.5°K refrigeration systems. (M.H.R.)

**56118** HELIUM-II REFRIGERATOR FOR 300 W AT 1.8°K. Baldus, W. (Linde Aktiengesellschaft, Munich). Advan. Cryog. Eng.; 16: 163-70(1971).

From Cryogenic engineering conference; Boulder, Colo. (17 Jun 1970). See CONF-700628.

A helium-II refrigerator for 300 W at a temperature of 1.80 ± 0.025°K is described in detail. (M.H.R.)

**56119** SUPERFLUID PLUG FOR SPACE. Selzer, P. M.; Fairbank, W. M.; Everitt, C. W. F. (Stanford Univ., Calif.). Advan. Cryog. Eng.; 16: 277-81(1971).

From Cryogenic engineering conference; Boulder, Colo. (17 Jun 1970). See CONF-700628.

In order to overcome the difficulties of containing liquid helium in space without spinning or using cumbersome electrostatic techniques, the use of a high thermal-conductivity porous plug is proposed which operates in the superfluid regime. Liquid flows through the plug in a controlled manner. The exit channel is evacuated in order to evaporate the liquid at its outer surface. With a plug of high thermal conductivity, the major portion of the heat needed to evaporate the liquid is conducted from inside the chamber, while the high effective thermal conductivity of the superfluid film, which coats all inner surfaces, establishes thermal equilibrium throughout the dewar. Preliminary calculations suggest that this film will be several orders of magnitude thicker in space than on earth, thereby conducting ample amounts of liquid to the plug and providing adequate liquid contact with the equipment. (M.H.R.)

**56120** APPLICATION OF A SUPERFLUID VALVE IN A VARIABLE-TEMPERATURE DEWAR. Kreitman, M. M. (Univ. of Dayton, Ohio). Advan. Cryog. Eng.; 16: 282-4(1971).

From Cryogenic engineering conference; Boulder, Colo. (17 Jun 1970). See CONF-700628.

The study of properties of materials at low temperatures is facilitated by an apparatus which can conveniently vary the temperature of an experimental sample. One simple method in common use is to suspend the sample from a cold finger in the vacuum or inner-wall space of a liquid-helium dewar. A modified version of this method is described. Two useful innovations are a demountable outer glass shell and the use of a superfluid valve for transferring helium from the dewar reservoir to a cold-finger reservoir. (M.H.R.)

**56121** CONTINUOUS-DISTILLATION APPARATUS FOR THE SEPARATION OF $^3$He FROM $^4$He. Wilkes, W. R. (Mound Lab., Miamisburg, Ohio). Advan. Cryog. Eng.; 16: 298-301(1971).

From Cryogenic engineering conference; Boulder, Colo. (17 Jun 1970). See CONF-700628.

The rapid improvement in cryogenic technology over the past decade made it desirable to investigate the possibility of separating $^3$He from $^4$He by means of distillation on a continuous basis. In order to gain practical information on the operation of a distillation column that might eventually handle the entire production of $^3$He, an experimental still was built and operated which has been quite successful in continuously separating moderate quantities of $^3$He. The design, development, apparatus, operation, and performance are summarized. (M.H.R.)

**56122** SUPERCRITICAL HELIUM COOLING OF HOLLOW SUPERCONDUCTORS. Bald, W. B. (Brookhaven National Lab., Upton, N. Y.). Advan. Cryog. Eng.; 16: 368-77(1971).

From Cryogenic engineering conference; Boulder, Colo. (17 Jun 1970). See CONF-700628.

A research program is currently in progress to examine the physical characteristics of hollow composite superconductors cooled by an internal flow of supercritical helium. This type of superconducting device has been proposed for producing the high magnetic field intensity in a large cryogenic bubble chamber. The first phase of the analytical work and the closed-loop arrangement presently under construction for testing various superconductor samples are described. (M.H.R.)

# Plasma and Thermonuclear Physics

## *Confinement and Heating*

*Refer also to abstract 56231.*

**56123** (ORO-4087-1) TEXAS TURBULENT TORUS EXPERIMENT. Progress Report. (Texas Univ., Austin. Center for Plasma Physics and Thermonuclear Research). May 1971. 23p. Dep. NTIS.

This investigation was undertaken to determine whether ohmic heating can be used to heat a tokamak plasma to thermonuclear temperature if the resistivity is artificially enhanced by the generation of strong turbulence in the plasma. The current status of the experiment is discussed. (M.O.W.)

**56124** RESONANCES OF ANOMALOUS MICROWAVE HEATING OF ELECTRONS IN A MAGNETIZED PLASMA. Batanov, G. M.; Sarksyan, K. A. (Lebedev Inst. of Physics, Moscow). JETP Lett. (USSR) (Engl. Transl.); 13: No. 10, 384-7(20 May 1971).

Translated from Zh. Eksp. Teor. Fiz., Pis'ma Red.; 13: No. 10, 539-43(20 May 1971).

The dependence of the effectiveness of microwave heating of electrons on the value of the magnetic field and the concentration of charged particles was studied. Plasma with $T_e = 6$ eV was generated by a spark gun and moved along a homogeneous magnetic field, flowing in and out through the narrow walls of the waveguide. A $TE_{10}$ wave was excited in the waveguide, with the electric field vector perpendicular to the constant magnetic field. The plasma density, the fast electron current, and their radial distributions in the plasma column were measured with a multigrid probe having an input diaphragm of 2 mm diameter.

**56125** COMPRESSION OF PLASMA BY A GROWING LONGITUDINAL MAGNETIC FIELD IN THE TOKAMAK. Dnestrovskii, Yu. N.; Kostomarov, D. P.; Pavlova, N. L. (Moscow State Univ.). JETP Lett. (USSR) (Engl. Transl.); 13: No. 12, 493-5(20 Jun 1971).

Translated from Zh. Eksp. Teor. Fiz., Pis'ma Red.; 13: No. 12, 697-9(20 Jun 1971).

A possible method for heating a plasma in Tokamak systems is to compress the plasma by increasing the main longitudinal field. A numerical integration is carried out for a system of equations for the balance of the particles and energy of the plasma for this condition. Density and temperature diagrams are given for various field strengths. (M.O.W.)

**56126** HEATING OF AN INHOMOGENEOUS COSMIC PLASMA. Platov, Yu. V. (Inst. of Terrestrial Magnetism, Ionosphere, and Radio Wave Propagation, Moscow). Geomagn. Aeron. (USSR) (Engl. Transl.); 11: No. 1, 38-41(1971).

Translated from Geomagn. Aeron.; 11: No. 1, 51-5(1971).

The heating by a homogeneous source of a plasma containing density inhomogeneities is investigated. It is demonstrated that the temperature of the individual parts of the heated region is either $\leq 10^5$ or $>10^7$°K, depending on density. If the temperature pattern with time is known, the characteristic dimensions of inhomogeneities can be estimated. A model of the high-temperature region is proposed, which is a conglomerate of relatively cold and hot filaments. (auth)

**56127** TURBULENT HEATING AND CONFINEMENT OF PLASMA IN A TOROIDAL MULTIPOLE TRAP. Demidov, B. A.; Fanchenko, S. D. At. Energ. (USSR); 30: No. 5, 468-70(May 1971). (In Russian).

The application of a strong electric field to change the method of heating a plasma from simple Joule heating to turbulent heating causes the resistance of the plasma to become abnormally large because of small-scale instabilities. Interferometric measurements of the plasma density under different conditions of operation made possible a comparison of: (1) plasma decay in a simple toroidal magnetic field, and (2) plasma decay with the turbulent heating. In the experiments described, a very substantial increase in the time of confinement of turbulently heated plasma was observed. (K.S.W.)

**56128** LASER HEATING OF A STATIONARY PLASMA. Steinhauer, Loren Clifford. Seattle; Univ. of Washington (1970). 242p. University Microfilms Order No. 71-17-002.

Thesis.

Some of the detailed phenomena in laser heating of a plasma to thermonuclear temperatures are examined. Analytic solutions are sought throughout because of the ease of interpretation and the wide range of conditions that can be examined with a single solution. The first study considers the simple case of a one-dimensional plasma. Very short laser pulses are used so that the plasma actually remains stationary during the heating. Maximum temperatures are thus achieved since none of the laser energy goes immediately into kinetic energy of plasma motion. The results of the study indicate that the heating falls into one of several regimes depending on the thickness of the plasma, and the energy and length of the laser pulse. Generally, only the electrons are heated during the pulse, the processes of equilibration with the ions having hardly begun. An interesting feature of one regime is the appearance of a "bleaching wave" whereby the beam bores its way into the plasma, heating as it proceeds. After the stationary heating, the plasma motion begins. The dynamics will appear in one of two regimes. In one of these regimes, the ions (reactants) do not equilibrate with the hot electrons before the motion dissipates and cools the plasma. Thus no thermonuclear energy would be released. Heating a three dimensional plasma was then studied. The cylindrical geometry is considered since it is appropriate for an available method of confinement (magnetic fields). For typical plasmas this geometry is characterized by major refraction problems, which greatly restrict the effectiveness of laser heating. However, it is possible to generate a plasma column that has favorable refracting characteristics. In this case, a laser beam propagated into the column is trapped and heats the plasma in a particularly effective manner. The next study considers the general idea of diffusion phenomena. The "bleaching wave" found in laser heating of a plasma is merely a form of diffusion—but in an extreme nonequilibrium limit. This is in contrast to the usual forms of diffusion which assume near equilibrium conditions. Generally, both equilibrium and nonequilibrium diffusion demonstrate a similar wave like character. There are many physical examples of both kinds of diffusion. (TSS) (Disser. Abstr.)

**56129** NUMERICAL SIMULATION OF TOROIDAL PLASMA CONFINEMENT WITH A FLUID MODEL. Johnson, John L.; Winsor, Niels K.; Dawson, John M.; Greene, John M. (Princeton Univ. Plasma Physics Lab., N. J.). pp 5.1-4 of Computational Physics. Vols. I and II. London; Her Majesty's Stationery Office (1969).

From Conference on computational physics; Culham, England (28 Jul 1969). See CONF-690706-(Vols.1 and 2).

A numerical program for studying confinement of low-pressure plasmas in simple axially symmetric configurations was developed and used to study bulk plasma motion, normal modes of oscilla-

XUM

tion, and the process of resistive diffusion. The fluid equations that describe the plasma include finite flow velocities, plasma inertia, resistivity, Hall currents, and electrostatic potentials along the magnetic field lines due to the electron-pressure term. In calculations with reasonable stellarator parameters and a constant rotational transform, the plasma loss times scale classically with the magnetic field, temperature, and rotational transform; however, the absolute value is about five times faster. The calculations require the presence of parallel velocities up to 10% of the ion thermal speed, a phenomenon which is not included in the classical treatment. (auth) (UK)

**56130** EQUILIBRIA AND STABILITY OF MAGNETICALLY CONFINED RELATIVISTIC ELECTRON CLOUDS. Hieronymus, James Lee. Ithaca, N. Y.; Cornell Univ. (1971). 192p. University Microfilms Order No. 71-17,097.

Thesis.

The equilibria and stability of electron clouds which stream relativistically parallel to an applied magnetic field were studied. The problem is of interest for understanding the propagation of intense relativistic electron beams and for electrostatic confinement of plasma in an electron beam potential well. Cylindrical and toroidal configurations were studied. Using the linearized relativistic Vlasov–Maxwell equations, the stability of the cylindrical equilibrium was studied. The Vlasov equation is solved by expanding the perturbed potentials to second order in the larmor radius and integrating along unperturbed orbits. A toroidal equilibrium was also found which reduces to the cylindrical equilibrium the limit of infinite major radius. The equilibrium is appropriate to an electron beam injected into a conducting torus which has a strong, toroidal magnetic field provided externally. (TSS) (Diss. Abstr. Int., B)

**56131** MEASUREMENT OF THE ION ENERGY DISTRIBUTION RESULTING FROM THE TURBULENT HEATING OF A PLASMA. Prono, Daniel Steve. Ithaca, N. Y.; Cornell Univ. (1971). 148p. University Microfilms Order No. 71-17,124.

Thesis.

Measurements were made of ion energy distributions resulting from the turbulent heating of a hydrogen plasma. A two-channel electrostatic energy analyzer was constructed and employed to determine energies of fast hydrogen neutrals resulting from a charge-exchange process involving hot plasma ions and a background gas. The hot plasma was created by passing a large pulsed current through a cold plasma contained in a mirror machine. This current created small-scale fluctuations whose decay was simultaneous to the heating of the plasma. When the level of the stored energy which drives the "turbulent heating" pulse was increased from 250 to 1000 joules, the percentage energy transfer to the plasma decreased from 4% to 3%. The turbulent heating mechanism was shown to simultaneously affect the ion population along the entire plasma length. Also, the heating mechanism only initiated after thresholds in drift velocity and temperature ratio ($\tau_e/\tau_i$) were exceeded. The resulting distribution which characterized the first few microseconds of the heated plasma was isotropic with a two-temperature nature. For the highest energy level, approximately 18% of the plasma energy is found in the ion population with approximately 95% of the ion energy in the low temperature bulk where $T_i \approx 320$ eV, while the heated tail displayed $T_i \approx 1400$ eV. For both ion temperature domains, the heating shows an $I^{\frac{1}{2}}$ relation to the current and an $\bar{E}^{<1}$ dependence on electric field strength. It was found experimentally that at the highest energy levels, the conductivity of the initially cold plasma affected the amount of energy accepted by the plasma, and influenced the thermal tail of the ion energy distribution. (Diss. Abstr. Int., B)

## Diagnostics

*Refer also to abstracts 56012 and 56216.*

**56132** (CEA-R-4079) CONTRIBUTION TO THE STUDY OF PLASMAS. AN ULTRA RAPID PHOTOMETRIC CAMERA. Alpern, Marc R. (Commissariat a l'Energie Atomique, Limeil-Brevannes (France). Centre d'Etudes). 1971. 79p. (In French). Dep. NTIS (U. S. Sales Only).

Thesis. Submitted to Paris Univ., Orsay (France). Faculte des Sciences.

The limitations of image converters in ultrarapid photography are discussed, after which an electronographic camera designed to make photometric measurements on plasmas is described. The electron optics and the performance attainable, particularly in dynamic operation, are then assessed. The experimental facts concerning the interaction between a laser beam and a thin layer of gold established by use of this camera are presented; the complexity of the mechanism involved in this interaction is shown. (France)

**56133** (INR-P-1322) UTILIZATION OF SELECTIVE CHANGE OF PLASMA OPTICAL THICKNESS TO DETERMINE THE ELECTRON DENSITY. Suckewer, Szymon (Institute of Nuclear Research, Warsaw (Poland)). 1971. 7p. Dep. NTIS (U. S. Sales Only).

A method is presented to determine the electron density in nonthermal plasma from the line-intensity ratios of neutrals or weakly ionized atoms. It is based on the utilization of selective change of plasma optical thickness. (auth)

**56134** (ORNL-TM-3582) REGULARIZATION METHOD OF UNFOLDING X-RAY SPECTRUM. Sen, A.; Clarke, John F. (Oak Ridge National Lab., Tenn.). Oct 1971. Contract W-7405-eng-26. 22p. Dep. NTIS.

Determination of the electron energy distribution function from x-ray spectrum involves the solution of a Fredhold Integral Equation of the first kind. The "regularization" technique for the solution of such an equation was investigated. A computer code was developed and tested for various arbitrary distributions. Some of the x-ray data of the INTEREM plasma are unfolded using this method. (auth)

**56135** EFFECT OF COLLISIONS ON COLD ION COLLECTION BY MEANS OF LANGMUIR PROBES. Shih, C. H.; Levi, E. (Polytechnic Inst., Brooklyn). AIAA (Amer. Inst. Aeronaut. Astronaut.) J.; 9: No. 9, 1673-80(Sep 1971).

Langmuir probes are extensively used to sample plasma densities. However, the interpretation of probe data is well established only for the limiting cases of collisionless and collision-dominated plasmas. A transitional regime prevails in some fluid-dynamic situations and electrical discharges in which the ions are colder than the electrons. A simple theory which accounts separately for the effects of collisions between charged particles and collisions with neutrals is presented. When the theory is applied to recent experimental data taken with cylindrical as well as spherical probes, the electron densities calculated from the probe measurements by using the present theory agree within 10% with those inferred from existing numerical solutions, an empirical formula, and microwave cavity data. (auth)

**56136** EXPERIMENTAL STUDY OF THE CYLINDRICAL LANGMUIR PROBE RESPONSE IN THE TRANSITION REGIME. Kirchhoff, R. H.; Peterson, E. W.; Talbot, L. (Univ. of California, Berkeley). AIAA (Amer. Inst. Aeronaut. Astronaut.) J.; 9: No. 9, 1686-94(Sep 1971).

A study of the response of cylindrical Langmuir probes in the transition regime was made. Experiments were performed in a highly expanded low-density flowing argon plasma using both single and double probes. Results are obtained in the near free-molecule regime over a wide range of ratios of Debye length to probe radius, probe length to probe radius, and probe radius to relevant mean free path. The effect of collisions on the ion-saturation current, the retarding field electron current, the floating potential, and the inferred electron temperature were investigated experimentally. An existing approximate analysis describing the collisional single-probe ion-saturation current and the retarding-field electron current was extended to describe the collisional double probe characteristic and magnitude of the single-probe floating potential. (auth)

**56137** PLANE ELECTROSTATIC ANALYZER FOR LASER PRODUCED PLASMA STUDIES. Allen, F. J. (Ballistic Research Labs., Aberdeen Proving Ground, Md.). Rev. Sci. Instrum.; 42: No. 10, 1423-7(Oct 1971).

The use of an electrostatic analyzer as a time-of-flight spectrometer for studying laser-produced plasmas is discussed. It is shown that a plane electrostatic analyzer, accommodating several detectors simultaneously, can be used to determine several points on the velocity distribution curve for the ions produced upon irradiation of a target with a single Q-switched laser pulse. This minimizes the problem of shot-to-shot reproducibility of the laser. It is shown also that with a 30° plane analyzer good energy and time resolution are obtainable in determining the time dependent ion velocity distribution for a laser-produced plasma. (auth)

**56138** EXPERIMENTAL DETERMINATION OF ENERGY DISTRIBUTION OF ELECTRONS IN A GAS-DISCHARGE PLASMA. Desai, S. K. (Indian Inst. of Tech., Bombay). Indian J. Pure Appl. Phys.; 9: No. 1, 50-5(Jan 1971).

Details of a method for the determination of energy distribution of electrons in a gas discharge plasma are reported. The method is based on the distribution function reported by M. J. Druyvesteyn (Z. Phys., 64: 781(1930)) for electrons in a uniform isotropic plasma. The merits and limitations of this method as compared to other existing methods are discussed. Results obtained in the case of a plasma caused by a hollow-cathode discharge through

helium–mercury mixtures are reported. Observations made indicate that optical properties of an electrical discharge can be predicted with reasonable accuracy based on the energy distribution values obtained by this method.

**56139** DETERMINATION OF PLASMA PROPERTIES AT VERY HIGH PRESSURES. Bauder, U. H. (Aerospace Research Labs. Wright Patterson AFB, Ohio); Bartelheimer, D. L. pp 219-22 of Proceedings of the Fifth Symposium on Thermophysical Properties. /Bonilla, C. F. (ed.). New York; American Society of Mechanical Engineers (1970).

From fifth symposium on thermophysical properties; Boston, Mass. (Sep-Oct 1970). See CONF-700901.

The knowledge of the transport properties of gases at high pressures and temperatures is necessary for the design and the optimization of application devices using electrical arcs. The properties of argon are presently being determined in the pressure range 1 to 130 atm from experiments using the cascade arc technique. Results of the spectroscopic temperature measurements are presented together with values of the electrical arc characteristic and of the measurable, i.e., unabsorbed part of the total radiation. Experimentally determined values of the electrical conductivity of argon at a pressure of 50 atm are compared to theoretical values by Devoto. (auth)

**56140** DETERMINATION OF THE TEMPERATURE DISTRIBUTION AND THE THERMAL CONDUCTIVITY IN AN ARGON PLASMA. Kroepelin, H.; Hoffmann, R.; Kalthoff, P. (Technische Univ., Brunswick). pp 347-57 of Proceedings of the Fifth Symposium on Thermophysical Properties. /Bonilla, C. F. (ed.). New York; American Society of Mechanical Engineers (1970).

From fifth symposium on thermophysical properties; Boston, Mass. (Sep-Oct 1970). See CONF-700901.

The temperature distribution in a cascade arc operated in argon was measured spectroscopically by the "plateau method" viz., with a wide slit of the spectrograph. The Ar I 4044.4 line and the electron continuum show different temperature distributions and no local thermodynamic equilibrium. In the center of the arc, both species have the same temperature. An observed instability of the arc at lower currents does not influence the results of the evaluation of the thermal conductivity. The maximum temperature is determined within ±2% . The evaluation of the over-all thermal conductivity following the method of ter Holst and Pflanz with respect to the measured radiation loss was made up to 14,500K. A form factor needed for the method determined by numerical integration of the measured data was found to be 0.6 ± 3%. (auth)

**56141** HOT-CATHODE IONIZATION GAUGES FOR USE IN A MAGNETIC FIELD. Hammond, D. P.; Riviere, A. C. (Culham Lab., Abingdon, Eng.). J. Phys., E (London); 4: 650-2 (Sep 1971).

The sensitivity of a hot-cathode ionization gauge in the presence of a magnetic field was measured and found to depend on the orientation of the grid support wires with respect to the field. A simple modification to a Bayard–Alpert gauge was made which gave it complete cylindrical symmetry. The sensitivity of this gauge was found to be essentially independent of the orientation of the field in the plane perpendicular to the gauge axis and within ±20° of this plane. The sensitivity of the modified gauge was also found to be only a slowly varying function of field strength up to a maximum applied value of 4 kG. (auth) (UK)

**56142** DETERMINATION OF TEMPERATURE AND ELECTRON DENSITY IN A SPARK PLASMA. Boettger, Peter; Krempl, Hans (Technische Univ., Munich). Spectrochim. Acta, Part B; 26: No. 8, 445-50(Aug 1971). (In German).

A spark plasma with an initial temperature of 30,000°K was created by a high-voltage discharge of 10 kV in a hydrogen atmosphere. The decrease in temperature was detected by the Larez norm-temperature-method in a time interval 1 to 4 μsec after ignition. By ohmic damping the hydrogen was prevented from being blown away during the ignition. The time-resolved profiles of the $H_\alpha$, $H_\beta$, and $H_\gamma$ lines were registered and compared with the broadening theory of Griem, Kolb, and Shen. Thus, the decrease in electron density could be determined by the half widths, that is by the distance of the two maxima of the $H_\beta$ line. The electron density of the two plasma components (electrode vapor-discharge gas) was calculated at various concentrations. A comparison with the measured values yielded a proportion of 1 : 9. (auth)

**56143** CONSTRUCTION OF ELECTRON DISTRIBUTION FUNCTIONS FROM LASER SCATTERING SPECTRA. Williamson, J. H. (United Kingdom Atomic Energy Authority, Abingdon, Eng.): Clarke. M. E. J. Plasma Phys.; 6: 211-21(Aug 1971).

The Thomson scattering spectrum for laser light scattered by a low-density plasma is determined by the Doppler shifts from the moving electrons. It is shown how the full three-dimensional distribution function may be constructed if spectra are observed in several directions. Calculations using a model loss-cone distribution show that four spectra are sufficient for a faithful reconstruction of f(v). Most of the complications that arise at relativistic electron velocities can be avoided by placing a diffraction grating in the scattered laser beam. (auth) (UK)

**56144** ELECTRICAL CONDUCTION FROM SHOCK HEATED ARGON TO CONICAL PROBES. Goodrich, Robert Warren. Cleveland; Case Western Reserve Univ. (1970). 179p. University Microfilms Order No. 71-18,993.

Thesis.

An experimental study was made of electrical conduction from shock heated argon plasmas to cold conical tungsten electrodes. The experiments consisted of obtaining probe V–I (voltage versus current) characteristics for several plasma and probe surface conditions. Ion saturation currents and apparent electron temperatures were obtained from the characteristics and compared to the calculations of Schwirian (where $T_{eapp} = 11600\ V_1 - V_2/\ln I_{e1} - \ln I_{e2}$). The plasmas used were generated by Mach 12 to 18 shocks into 1 torr argon and Mach 10 to 14 shocks into 10 torr argon. The plasma parameters were calculated from the shock speed and the initial argon pressure. A transient voltage technique was used to obtain a complete V–I characteristic from a single shock tube test. It was found that a) the measured and calculated ion saturation currents were within an order of magnitude of each other, b) the measured and calculated apparent electron temperatures were 20,000°K ± 15 percent for clean probes and c) the apparent electron temperatures for dirty probes are as high as 60,000°K. No simple relation was found between a probe V–I characteristic and the free stream plasma properties. Hence it was reconfirmed that a Langmuir-type probe is not useful as a diagnostic tool in dense flowing plasmas. It is also shown that the high apparent electron temperatures are probably due to a) the large electron heat flux to the probes and b) absorption of electron thermal energy by the surface layer of "dirty" probes. (Diss. Abstr. Int., B)

**56145** PROBING OF AN INHOMOGENEOUS PLASMA WITH ELECTROMAGNETIC WAVES. Ascoli-Bartoli, U.; Badiali, M.; De Marco, F.; Duscin, L.; Pieroni, L. (CNEN, Frascati, Italy). Riv. Nuovo Cim.; 1: No. 1, 79-156(Jan-Mar 1971). (In Italian).

The methods used for the probing of an inhomogeneous plasma with electromagnetic waves are examined and their advantages and disadvantages are evaluated. The indirect methods are based on the measurement of mean parameters and on the quality of the density profile. The direct methods give the local values of the plasma density and are therefore more precise. Optical methods for the measurement of correlations are also examined. (J.S.R.)

## *Kinetics (General)*

*Refer also to abstract 55816.*

**56146** (N-71-27023) RADIATION MEASUREMENTS AND LOW FREQUENCY AND HIGH-PRESSURE INVESTIGATIONS OF INDUCTION HEATED PLASMA. Vogel, Charles E.; Poole, John W.; Dundas, Peter H. (Humphreys Corp., Concord, N. H. TAFA Div.). May 1971. Contract NAS3-13225. 65p. (NASA-CR-1804). NTIS.

A number of induction-coupled plasma torches were operated under a variety of test conditions to simulate various requirements for the gas-core nuclear rocket. Specifically, tests were operated at 4 MHz, 9600 Hz, and 960 Hz. At 4 MHz, pressures up to 715 psia were obtained. Testing at 9600 and 960 Hz was performed up to 1 atm and 300 mm, respectively. In addition to obtaining radiation data, these tests provide operating techniques and design principles that will permit operating an induction-coupled plasma torch at extremely high powers and pressures, thereby more closely simulating the gas-core nuclear rocket. Plots are presented showing the relationship of frequency, pressure, gas type, torch diameter, minimum operating power, and coupling efficiency. (auth) (STAR)

**56147** COLLISIONLESS SHOCKS IN PLASMAS. Friedman, Herbert W.; Linson, Lewis M.; Patrick, Richard M.; Petschek, Harry E. (Avco Everett Research Lab., Everett, Mass.). Annu. Rev. Fluid Mech.; 3: 63-88(1971).

This review concentrates entirely on shocks in magnetized plasmas where the magnetic field plays a decisive role in determining the shock structure. Discussions are given of nonlinear wave theory, anomalous dissipation in a collisionless plasma, and critical Mach numbers. Laboratory experiments and their observations are described. 80 references. (M.O.W.)

XUM

**56148** ONE TYPE OF INSTABILITY OF THE EXIT CURRENT OF A PLASMA ELECTRON SOURCE. Gruzdev, V. A. (Tomsk Inst. of Radioelectrònics and Electronics, USSR). Izv. Vyssh. Ucheb. Zaved., Fiz.; No. 5, 136-8(1970). (In Russian).

A promising method of obtaining an electron beam in vacuum by means of an electric discharge is the extraction of electrons from the plasma of a Penning discharge through an opening in the anode of the discharge chamber. However, in some cases, the exit currents show a characteristic instability of the relaxation type. Experiments showed that the average, extracted beam current did not depend on the pressure in the discharge chamber, but was determined only by the extraction voltage and electron concentration in the region of the emission opening. The relaxation character of the exit current was observed up to a certain critical pressure $P_{cr}$ equal to $3.5 \times 10^{-3}$ mm Hg std. At a pressure greater than this critical pressure the exit current becomes continuous. This instability is caused by a "plasma torch" which rotates in the direction of the electron cyclotron rotation. It should be noted that the relaxation instability of the exit current of the electron source from a Penning discharge with hollow cathodes can be used in order to generate powerful electromagnetic oscillations and to obtain intense, pulsed electron beams with a small pulse duration. (TTT)

## Kinetics (Experimental)

*Refer also to abstract 55920.*

**56149** (IPP-1/108) RADIATION LOSSES OF A THETA PINCH PLASMA IN THE WAVELENGTH RANGE 100 TO 200 ANGSTROMS. Engelhardt, W. (Institut fuer Plasmaphysik, G,m,b,H., Garching (West Germany)). Jun 1971. 45p. Dep. NTIS (U. S. Sales Only).

In order to measure the radiation losses of a theta-pinch plasma (electron density 1 to $5 \times 10^{16}$ cm$^{-3}$, electron temperature 150 to 350 eV), a grazing incidence spectrograph is absolutely calibrated in the range 10 to 200 Å. This is done in two steps: First, the measured intensity ratios of lines emitted by hydrogen-like ions are compared with their calculated values, thus yielding the relative sensitivity of the instrument. The result is confirmed by incorporating well-known intensity ratios of lithium-like ions. Secondly, absolute calibration is possible by hanging the spectrograph on an absolutely calibrated monochromator via the branching-ratios of lithium-like ions. Radiation losses from the plasma turn out to be negligible compared to heat conduction losses and the whole energy radiated is found to be small compared to the energy content of the electrons, if the impurity concentration does not exceed 0.5%. The radiation is found to be predominantly emitted by the resonance lines of the oxygen and carbon ions O VI, O VII, O VIII, C V, and C VI, whereas continuum radiation and the contribution from other ions are negligibly small. However, in discharges where the oxygen concentration reaches 5%, radiation losses can exceed the losses by heat conduction during the early phase of the discharge; but the final electron temperature is not significantly influenced by the impurities (auth)

**56150** (LGI-70/14/E) TIME-SPACE RESOLVED SPECTROSCOPIC MEASUREMENTS ON A FAST Z-PINCH. Keller, R. (Comitato Nazionale per l'Energia Nucleare, Frascati (Italy). Laboratorio Gas Ionizzati). Oct 1970. 27p. Dep. NTIS (U. S. Sales Only).

The MIRAPINO experiment, a fast linear z pinch, is described. In order to study the mechanism of the collision near the axis, the pinch in noble gas is examined on varying the superposed axial magnetic field. A spectroscopic investigation was made of the visible electromagnetic radiation emitted by the plasma during and after the maximal contraction. The gas was neon in the pressure region of 100 $\mu$ HG. (M.O.W.)

**56151** (SC-T-713064) EXPERIMENTAL STUDY OF DESTRUCTION OF METASTABLE HELIUM ATOMS IN PLASMA AT LOW TEMPERATURES. Fugol, I. Ya.; Grigorashchenko, O. N.; Myshkis, D. A. Translated for Sandia Labs., Albuquerque, N. Mex., from Zh. Eksp. Teor. Fiz.; 60: No. 1, 423-40(1971). 34p. Dep. NTIS.

An abstract of this paper, prepared from the original language, appeared as NSA 25: 30512. (M.O.W.)

**56152** (SC-T-713065) EXPERIMENTAL STUDY OF THE DECAY OF CRYOGENIC HELIUM PLASMA. Fugol, I. Ya.; Samovarov, V. N.; Starkov, M. G. Translated for Sandia Labs., Albuquerque, N. Mex., from Sb. Nauch. Tr., Fiz.-Tekh. Inst. Nizk. Temp., Akad. Nauk Ukr. SSR; No. 11, 74-94(1971). 40p. Dep. NTIS.

The kinetics of recombination- and diffusion-controlled decay of the electron density n in helium plasma was measured by the resonator method over a wide temperature range from 293 to 10°K and in a pressure interval from 1- to 30-mm Hg. Room-temperature measurements of the coefficient of ambipolar diffusion of the diatomic $He_2^+$ ions gave $D_2P = 680$ cm$^2$sec$^{-1}$ mm Hg. The triatomic helium ion $He_3^+$ was observed at 100°K, with a coefficient $D_3P = (280 \pm 15)$ cm$^2$ sec$^{-1}$ mm Hg. These measurements were used for estimating the collision cross sections of multi-atomic helium ions with atoms. As the temperature is lowered, the region of recombination decay of the plasma is considerably broadened, and a linear $n^{-1}$ (t) law is observed over a large concentration interval. The coefficients $\alpha$ of the observed two-particle recombination are independent of pressure and are equal to $5.8 \times 10^{-8}$ cm$^3$ sec$^{-1}$ at 100°K and to $1.3 \times 10^{-7}$ cm$^3$ sec$^{-1}$ when the plasma is cooled by liquid helium. A very slow rate of electron cooling in helium plasma was observed at 10°K. Recombination mechanisms are discussed, and it is concluded that the main contribution to such large values of $\alpha$ is collisional–radiative recombination with dissociation, as well as purely dissociative recombination of triatomic $He_3^+$ ions with electrons. (auth)

**56153** ELECTRODE PHENOMENA AND THE ACCELERATION OF PLASMA. Babenko, A. N.; Kruglyakov, E. P.; Fedorov, V. M. Zh. Prikl. Mekh. Tekh. Fiz.; No. 3, 140-4(May-Jun 1971). (In Russian).

The acceleration of plasma was studied as a function of the electrode construction, using either of two methods: light measurement by an electron-optical converter, or with the aid of an optical Michelson interferometer. Three-electrode models were designed for the experimental testing of electrode processes in electron accelerators. One design provided smooth plasma acceleration, a second model was "profiled" with 8-mm-high ribs, 2 cm apart, and the third model used thin contact leaves and ceramic insulation, leaving only a small area of contact of plasma and electrode. The effects of these electrode designs on plasma acceleration are discussed. (K.S.W.)

**56154** IONIZATION WAVES AND WAKES EXCITED BY AN ACOUSTIC PULSE. Krejci, V. (Inst. of Physics, Prague). Czech. J. Phys.; 21: No. 8, 828-35(1971).

Any sudden change of plasma parameters in originally homogeneous positive columns of low-current discharges usually gives rise to a transient process, called stratification waves. Another form of ionization wave, a periodic wake, may be noticed in the neighborhood of a permanent local disturbance of plasma homogeneity. A third form of ionization wave which accompanies a pulse propagating with constant velocity through plasma is described. After a short description of the experimental techniques, a phenomenological theory of the phenomena observed is given. (auth)

**56155** DYNAMIC PRESSURE MEASUREMENT AT THE ANODE OF HIGH-CURRENT ELECTRIC ARCS. Kranz, Erich; Mueller, Harry (Technische Hochschule Ilmenau, Meiningen, Ger.). Beitr. Plasmaphys.; 11: No. 2, 149-57(1971). (In German).

A measuring method and system are described for determining the dynamic (stagnation) pressure in the anode spot of high-current arcs. For this use, a movable cooled or uncooled anode has a small bore hole of 1- to 1.5-mm diameter perpendicular to its surface. These holes are connected at a steel membrane by a short hose line. The membrane deflections caused by dynamic pressure are measured by means of an inductive-path measuring system and recorded by a storascope. The attained spatial resolution is 0.5 mm, the time resolution is 0.025 s, and the limiting sensitivity is lower than 0.1 torr. The method was applied to plasma welding arcs up to 700 A. It enabled the determination of dynamic pressures down to 0.3 torr, inertialess and free from distortions. (auth)

**56156** PRECISION MEASUREMENTS OF THE SPECTRA OF HYDROGEN PLASMAS. Behringer, Kurt (Technische Univ., Munich). Z. Phys.; 246: No. 4, 333-47(1971). (In German).

Detailed and precise investigations on the Balmer spectrum of a hydrogen arc were made in order to compare the measured absolute values of the spectral emission coefficients with the existing theories, the results being of special interest with respect to line-broadening calculations and to the lowering of the ionization energy. The plasma is generated in a stationary high-power cascade arc at atmospheric pressure. The experiment covers the temperature range between 12,000 and 20,000 K, where all emission coefficients show maxima in their temperature dependence. To keep self-absorption within the plasma as low as possible, the investigations were carried out in side-on observation. The extended gas layer of almost constant intensity surrounding the maxima ensures very accurate results of the side-on measurements. For the necessary precise calibration of the optical sys-

XUM

tem, both a standard carbon arc and tungsten strip lamps were used. As the intensity of these different radiation standards only shows a few percent deviation, a very high accuracy can also be established for the measured hydrogen emission coefficients. After evaluating an average radial temperature distribution, the absolute emission coefficients of five selected wavelengths are plotted vs. temperature and compared with theory; a very good agreement is found. The emission coefficients of the continuous radiation thus confirm the lowering of the ionization energy according to Griem. The spectral intensities for 16,250 K, i.e., the temperature in the neighborhood of which all the maxima occur, are represented vs. wavelength to investigate the spectral dependence of the emission coefficients; again, excellent agreement with theories of continuous radiation and line profiles is found. The experimental line shape of $H_\alpha$, however, is described much better by Vidal's "Unified Theory" than by Griem's standard profile. When the maxima of the emission coefficients appear approximately at half the tube radius, the side-on distributions of the intensity show a flat top in the center and their value is almost independent of the arc current. Because of these qualities and of the reliability of the theoretical calculations of the spectrum, the hydrogen arc is recommended for a radiation standard both for the visible and the uv region. (auth)

**56157** VORTICITY AND NEUTRONS IN THE PLASMA FOCUS. Bostick, W. H.; Grunberger, L.; Nardi, V.; Prior, W. (Stevens Inst. of Tech., Hoboken, N. J.). pp 495-502 of Proceedings of the Fifth Symposium on Thermophysical Properties. /Bonilla, C. F. (ed.). New York; American Society of Mechanical Engineers (1970).

From fifth symposium on thermophysical properties; Boston, Mass. (Sep-Oct 1970). See CONF-700901.

Plasma coaxial accelerators are used for studying the mechanism of heating processes by shock waves in deuterium and other gases at extremely high temperatures (up to $10^8$°K). At these temperatures, where the thermonuclear fusion reaction in deuterium produces neutrons, collective motion in the form of organized eddies plays a leading role in the heating process. It is shown experimentally that the achievement of the high deuteron velocities for the nuclear reaction involves first the storage of energy in organized hydromagnetic vortex filaments (~0.5 mm in diameter). This energy is then released during the decay of the magnetic structure of the filaments. This type of "induction heating" apparently involves the interaction of neighboring vortex filaments. (auth)

**56158** PHYSICAL AND ANALYTICAL PROPERTIES OF A MICROWAVE EXCITED PLASMA. Fallgatter, Karen. Tallahassee; Univ. of Florida (1970). 102p. University Microfilms Order No. 71-16,781.

Thesis.

A microwave generator with a maximum power output of 120 watts was used to sustain a discharge through flowing argon at atmospheric pressure, using a tapered rectangular cavity to couple the microwave power into the plasma discharge. A cell constructed from fused quartz tubing was used to contain the plasma, which was about 6 cm long and 0.05 cm in diameter. Excitation temperatures in the plasma were determined by applying the logarithmic plot method and the absolute radiance method to the measured radiances of argon atomic lines. At the center of the plasma, the logarithmic plot method gave a temperature of 6280°K, while a temperature of 8520°K was obtained using the absolute radiance method. The radiances of some rotational lines of the OH electronic band system were used to determine rotational temperatures by the logarithmic plot method. A rotational temperature of 2440°K was obtained at a point 0.08 mm from the center of the discharge. The width at half maximum of the Balmer $H\beta$ line was measured at several locations in the discharge. The Stark broadening of the hydrogen line was then used in the calculation of the electron density in the plasma. An electron density of $2.6 \times 10^{15}$ cm$^{-3}$ was obtained at the center of the plasma. The Abel transform was applied to the axial radiances from the nonhomogeneous plasma. The resulting radial radiances for argon lines yielded, using the absolute radiance method, a temperature of 9010°K at the center of the plasma. The transform shows that, in the center of the plasma, emission from OH is negligible. The plasma was examined as a source of excitation in atomic emission spectrometry. A dry aerosol, produced by a system consisting of a pneumatic sprayer which nebulized 1.1 ml/min of aqueous sample solution, a heated chamber and a specially constructed condenser could be introduced into the plasma. Analytical curves were obtained and detection limits estimated for cadmium, gallium, indium, mercury and zinc. Atomic lines of calcium, strontium, lead, and boron were observed, but no analytical curves were determined. A position in the plasma cell at a distance of about 0.3 mm from the center of the plasma was found to give the best analytical results for most of the elements examined. At this position, the absolute radiance of an argon line indicated a temperature of 4920°K and the two line method for lines of calcium and strontium yielded temperatures of 4980 and 5050°K, respectively. A value of $1.8 \times 10^{15}$ cm$^{-3}$ was obtained for the electron density in the analytical region. (Diss. Abstr. Int., B)

**56159** EXPERIMENTAL STUDY OF ANOMALOUS RESISTIVITY IN A POTASSIUM MAGNETOPLASMA. Gerdin, Glenn Andrew. Hanover, N. H.; Dartmouth Coll. (1971). 108p. University Microfilms Order No. 71-17,931.

This study is an attempt to determine experimentally the effect of collective interactions on the resistance along the magnetic field in a potassium magnetoplasma. When the fluctuations of the plasma, which are identified to be drift waves, are driven externally, the resistance of the plasma is found to be anomalous with respect to the Spitzer–Härm result after the sheath resistance has been substracted. A model for the anomalous resistance, based on the fluctuation–dissipation theorem, is derived and found to explain the driven data quite well. The model predicts for longitudinal transport that collective collision frequencies should be proportional to longitudinal wave numbers, and for perpendicular transport, collision frequencies should be proportional to longitudinal wave numbers, thus making the collision frequency a tensor quantity. The longitudinal wave numbers were measured for driven data only, so the wave numbers for the nondriven data have to be estimated from theoretical arguments. This is done on the basis of ion Landau damping and on the basis of an instability caused by gradients in density along the magnetic field derived here for the first time. Using the theoretical wave numbers, both the dominance of the sheath resistance and the frequency dependence of the nondriven resistances can be explained nicely. (Diss. Abstr. Int., B)

**56160** PARAMETERS OF IONIZED AIR IN FRONT OF A STRONG SHOCK WAVE. Gorelov, V. A.; Kil'dyushova, L. A. Izv. Akad. Nauk SSSR, Mekh. Zhidk. Gaza; No. 2, 147-51(Mar-Apr 1971). (In Russian).

The parameters of ionized air were experimentally measured in an electric discharge shock tube during an encounter with a shock wave proceeding at a speed of 11.3 km/sec. The initial pressure of air was 0.2 mm Hg, and the charged-particle concentration 10 to 100 cm in front of the shock front was $9 \times 10^{11}$ to $3 \times 10^{10}$ cm$^{-3}$. The electron temperature 20 cm in front of the shock front was 4000 to 6000°K. An oscillogram of the probe signal, and graphs of the ion and electron density in front of the shock wave are reproduced. The results compare favorably with those of previous experiments. (K.S.W.)

**56161** RECOMBINATION AND DETECTION OF THE THREE-ATOM ION IN A HELIUM PLASMA AT LOW TEMPERATURES. Reznikov, G. P.; Samovarov, V. N.; Fugol, I. Ya.; Shevchenko, Yu. F. (Physical-Technical Inst. of Low Temperatures, Kharkov). Dokl. Akad. Nauk SSSR; 197: No. 6, 1295-8(21 Apr 1971). (In Russian).

The late afterglow and electron concentration in a helium plasma were investigated at 77°K. Experiments testified to the prevalence of a three-atom ion $He_3^+$ at low temperatures and confirmed the recombination mechanism of this ion. At room temperatures $He_3^+$ is not observed. The afterglow was explained by the presence of atomic ions which rapidly changed to $He_2^+$ ions, which in turn became $He_3^+$. The three-atom ions predominated in the plasma and caused a concentration decrease in the ambipolar diffusion. The luminescence of the molecular band in the late afterglow was caused by a partial recombination of $He_3^+$ with subsequent dissociation. (K.S.W.)

## *Kinetics (Theoretical)*

*Refer also to abstract 55776.*

**56162** (CEA-CONF-1801) SPACE-TIME EVOLUTION OF A PLASMA SUBJECTED TO A DISCHARGE CURRENT. Mercier, C.; Soubbaramayer (Commissariat a l'Energie Atomique, Fontenay-aux-Roses (France). Centre d'Etudes Nucleaires). 1971. 2p. (In French). (CONF-710527-7). Dep. NTIS (U. S. Sales Only).

From Physics conference; Evian, France (25 May 1971).

A mathematical model simulates the evolution of a plasma subjected to a discharge current. An expression is proposed for the thermal electronic conductivity allowing the important experimental results on T-3 (Kurchatov) and S. T. (Princeton) to be explained. (France)

**56163** (LGI-70/16/E) BASIC STEADY STATE MAGNETIC "SCREW"-FIELD DISTRIBUTIONS IN PLASMA BETWEEN CONCENTRIC BOUNDARIES. Geiger, M. (Comitato Nazionale per

XUM

l'Energia Nucleare, Frascati (Italy). Laboratorio Gas Ionizzati). Oct 1970. 51p. Dep. NTIS (U. S. Sales Only).

The concentric field, and dilute plasma, structure extends between the surface of a (more dense) pinched plasma column as inner boundary ($r_0$) and an outer conducting shell ($r_1$). Particular consideration is given to pressure-determined distributions where the characteristic field inclination $\mu = B_\theta/(r\,B_z)$ begins from zero at $r_0$ and increases continuously with the radius. Model pressure functions are introduced which derive by a constant multiplicator from the special distributions determined by $B_{total}$ = constant over the radius r. The relation for the maximum permissible ratio $r_1/r_0$ with respect to Suydam's local stability criterion is analyzed. (auth)

**56164** (LGI-71/1/E) RADIATIVE RECOMBINATION OF HYDROGENIC IONS IN HIGH TEMPERATURE PLASMAS. Gratreau, P.; Robouch, B. V. (Comitato Nazionale per l'Energia Nucleare, Frascati (Italy). Laboratorio Gas Ionizzati). Jan 1971. 15p. Dep. NTIS (U. S. Sales Only).

The recombination rate and the mean kinetic energy loss of recombining electrons are calculated, using the expressions of Karzas and Latter, and compared with the values reported by Seaton. A higher accuracy (≲2%) is obtained for the high-temperature range. The results show that Seaton's estimate of the uncertainty of his results is pessimistic. (auth)

**56165** (N-71-27890) THEORY OF THOMSON SCATTERING FROM A WEAKLY-IONIZED PLASMA. Seasholtz, Richard G. (National Aeronautics and Space Administration, Cleveland, Ohio. Lewis Research Center). Jun 1971. 48p. (NASA-TN-D-6372). NTIS.

The theory of Thomson scattering from a weakly ionized plasma is extended to include the effects of unequal electron and ion temperatures, a constant magnetic field, and electron drift. The plasma is described by the two fluid continuum equations that are valid if the wavelength of the probing wave is longer than the ion-neutral mean free path. The spectrum and total scattered power are calculated. Collisions and a magnetic field are both shown to influence the scattered power for unequal electron and ion temperatures. (auth) (STAR)

**56166** (NP-19012) PROBLEMS OF INJECTION OF RELATIVISTIC ELECTRON BEAMS INTO PLASMA. Rosinskii, S. E.; Rukhadze, A. A. (Akademiya Nauk SSSR, Moscow. Institut Fiziki). 1971. 18p. (In Russian). Dep. NTIS (U. S. Sales Only).

Fields and currents induced in a dense plasma under injection of a relativistic electron beam are investigated. It is shown that in a time less than the collision time of plasma electrons the induced fields and currents represent the superposition of fields and currents accompanying the beam (static in a system of a beam at rest) and "transition" fields and currents, essentially caused by the very beginning of injection and disappearing over a time greater than the electron collision time. The nature and magnitude of this "transition" radiation are evaluated. It is shown in particular that "transition" fields have an almost potential character (the magnetic field is small in comparison with the electric). The problem is solved in two formulations: (1) injection of the beam with finite time $\tau$ and (2) injection of the beam in a finite interval of space between the points $z = 0$ and $z = l_0$. (JPRS)

**56167** RECOMBINATION DECAY OF PLASMA. Kapel'yan, S. N.; Perel'man, T. L. (Inst. of Textile and Light Industry, Minsk. Inst. of Heat and Mass Exchange, Minsk). Dokl. Akad. Nauk BSSR: 15: No. 3, 209-12(Mar 1971). (In Russian).

The diffusion equation for a singly ionized, two-component gas with sufficiently small mass values of the initial concentration is linearized. The residual number of particles not recombining at a given moment of time is calculated for the cases of plane, cylindrical, and spherical symmetry. (tr-auth)

**56168** RADIATION OF CHARGED-PARTICLE BEAMS IN PASSAGE THROUGH CUBIC NONLINEAR MEDIA. Demtchenko, V. V.; El-Siragy, N. M. (Atomic Energy Establishment, Cairo). Z. Phys.; 246: No. 3, 203-15(1971).

The interaction of charged-particle beams with nonlinear "cubic" type media was studied; the dielectric permeability of such media depends on the square strength of the electric field produced by the beam-excited wave. The processes of the Cherenkov excitation of the medium by a modulated definite current were investigated, as well as the polarization of longitudinal oscillations of the medium excited by the current. The equations are obtained to determine the dependence of fields excited by the current on the amplitude of the exciting current. It is found that under certain circumstances (near the radiation cutoff) the conditions of Cherenkov radiation may be violated due to nonlinearities of the medium and the particle radiation loss vanish. The amplification of longitudinal waves in an arbitrary isotropic medium with "cubic" nonlinearity by a monoenergetic particle beam is studied when the frequencies of amplified oscillations are close to the resonance frequencies of the medium. (auth)

**56169** DISPERSION IN BEAM-PLASMA SYSTEMS. II. EXTERNAL MAGNETIC FIELD. Verheest, Frank (State Univ., Ghent). Beitr. Plasmaphys.; 11: No. 2, 189-93(1971).

A treatment is given of linear waves in a homogeneous and infinite beam-plasma system in the presence of a uniform external magnetic field. A scalar pressure hypothesis is used to close the set of equations and enables the explicit derivation of the general dispersion formula. The dispersion relation shows a general coupling between all waves present in the system. This coupling is due, in principle, more to the external magnetic field than to the presence of stream velocities because part of that coupling disappears if and only if the external magnetic field vanishes or parallels the wave vector. (auth)

**56170** DISPERSION IN BEAM-PLASMA SYSTEMS. I. PRESSURE ANISOTROPY. Verheest, Frank (State Univ., Ghent). Beitr. Plasmaphys.; 11: No. 2, 133-9(1971).

A treatment is given of linear waves in a homogeneous and collisionless beam-plasma system of infinite extent. Two main features of the treatment are the arbitrariness of the composition of the system, even with regard to the direction of the beams, and the allowance of anisotropic pressure variation. The resulting dispersion equation is discussed in several forms. Generally, a coupling occurs between all waves usually present in a plasma, plus a modification of the frequencies due to parallel Doppler shifts. (auth)

**56171** ERRORS DUE TO AVERAGING SPECTRAL-LINE INTENSITIES IN THE PRESENCE OF ELECTRON-TEMPERATURE VARIATIONS. Weber, R. F.; Garscadden, A. (Aerospace Research Labs., Wright-Patterson AFB, Ohio). J. Opt. Soc. Amer.; 61: No. 10, 1330-4(Oct 1971).

An analysis is made of the errors that arise in line-intensity measurements due to the experimental averaging of the time-varying intensities caused by electron-temperature fluctuations in continuous-plasma sources. These calculations are made both for periodic and for random electron-temperature fluctuations. The errors are dependent on the method of measurement. The possible errors in the monochromator method are usually positive and significant for typical spectral lines and electron temperatures. An alternative method, which is shown to be subject to less error, is to use a polychromator and to measure the average of the instantaneous line-intensity ratio. In either method (but more applicable to the monochromator method) the additional measurement of the root-mean-square value of the intensity ratio gives another set of equations and allows the determination of both the mean electron temperature and the oscillation amplitude or standard deviation for gaussian-noise temperature fluctuations. (auth)

**56172** CANONICAL TRANSFORMATION METHOD IN THERMODYNAMICS OF PARTIALLY IONIZED PLASMA. Vorob'ev, V. S.; Khomkin, A. L. (Inst. of High Temperatures, Moscow). Teor. Mat. Fiz.; 8: No. 1, 109-18(Jul 1971). (In Russian).

The system of interacting fermions is considered in the conditions in which the formation of the paired bound states is possible. The canonical transformation for their description proposed includes the Fermi and Bose operators. After the transformation, the initial Hamiltonian is expressed in terms of these new operators. In the case of a rarefied gas, the transformed Hamiltonian describes the mixture of ideal gas of bosons and fermions, the interaction of which is described by a certain renormalized potential. As concerns the thermodynamics of partially ionized plasma, it is shown that taking into account this interaction leads to divergence-free expressions. The convergent expression for the statistical sum of atoms is obtained. (auth)

**56173** CONTRIBUTIONS TO THE THEORETICAL STUDY OF A LORENTZ PLASMA. Draganu, M. Mathematica; 12: No. 35, 39-68(1970). (In French).

Contrary to R. Jancel and Th. Kahan who tried to work out a solution to Boltzmann's equation for a weakly ionized plasma by an expansion of the electron distribution function in a series of normalized spherical functions, the authors develop the electron distribution function in the velocity space in a series of nonlinear spherical harmonics. (1) $f_e(\vec{x},\vec{v},t) = \Sigma_{l=0}^{+\infty}\ \Sigma_{m=\Lambda}^{+l}\ \alpha_\Lambda^m(\vec{x},v,t)\ Y_\Lambda^m(v,\theta,\varphi)$ where $Y_l^m = v_e^{\lim\varphi}\ \Theta_l^m$, $\Theta_l^m$ being normalized associate Legendre polynomials. Expressions are evolved in consequence of introducing the operators $\partial/\partial t$ and $\vec{v}\cdot\nabla_x$ into the expansion (1). The general equations for the coefficients $\alpha_l^m$, the expansion of the distribution function $f_e$ in terms of real tensors, and the first-order approximation of this distribution function are developed. (Nom. Sci. Abstr.)

**56174** NOTE ON THE FORMATION OF DEBYE POTENTIAL WELL IN CURRENT-CARRYING PLASMAS. Kan, J. R. (Dartmouth Coll., Hanover, N. H.). J. Plasma Phys.; 6: 223-8(Aug 1971).

It is shown that, in a collisionless current-carrying plasma, the potential profile along the radial direction parallel to the current changes from the Debye form to a potential well form, and causes a reversal of the electric field of the test charge. The formation of the Debye potential well is attributed to the resonant interaction between the particles and the waves stationary in the test charge frame when the net flux of charged particles is different from zero. This is the same type of resonant interaction which leads to the well-known Landau damping. (auth) (UK)

**56175** ELECTROSTATIC SHIELDING OF A TEST CHARGE IN A NON-NEUTRAL PLASMA. Davidson, R. C. (International Centre for Theoretical Physics, Trieste, Italy). J. Plasma Phys.; 6: 229-35(Aug 1971).

The electrostatic shielding of a test electron embedded in a magnetically confined pure electron gas column is investigated. For rigid-rotor equilibria with nearly uniform density in the column interior, it is shown that the shielding length is the local electron Debye length for the case that the test electron is at rest relative to the mean motion of the column. (auth) (UK)

**56176** TRANSONIC PLASMA FLOW PAST AN OBSTACLE. Stangeby, P. C.; Allen, J. E. (Oxford Univ.). J. Plasma Phys.; 6: 19-32(Aug 1971).

In many plasmas the ions are cold relative to the electrons but have a directed, subsonic velocity (the sonic velocity is $(kT_e/M)^{\frac{1}{2}}$). The behavior of this flow around an obstacle is considered and solutions obtained for cylindrical geometry. The results are of direct interest in the interpretation of probe characteristics, especially when relative density measurements are involved, as the effects of the flow are typically of the same order of magnitude as the relative variations expected. Plasma flow past an obstacle may be of interest in other contexts (e.g. the case of dust particles in a gas discharge). (auth) (UK)

**56177** RADIATION FROM CHARGED PARTICLES IN WEAKLY INHOMOGENEOUS MAGNETIC FIELDS. Cook, David M. (Lawrence Univ., Appleton, Wis.). J. Plasma Phys.; 6: 33-51(Aug 1971).

The spectral distribution of radiation emitted by a charged particle moving nonrelativistically in a prescribed electromagnetic field, consisting of a strong uniform magnetic induction on which is superimposed a weak inhomogeneity, is determined. The calculation is confined to trajectories characterized by small Larmor radii, and to the azimuthal average of the full angular distribution of the radiation, the azimuthal angle being measured in a coordinate system for which the uniform component of the field defines the polar axis. (UK)

**56178** FINITE-LARMOR-RADIUS EQUATIONS FOR COLLISIONLESS PLASMAS IN GENERAL MAGNETIC FIELDS. Bowers, E. (Princeton Univ., N. J.). J. Plasma Phys.; 6: 87-105(Aug 1971).

Expressing the Vlasov equation in a local system of co-ordinates defined by the magnetic field, the distribution function is expanded in terms of a small parameter $\epsilon$ (assumed <1), the ratio of the ion Larmor radius to a characteristic length of change perpendicular to the magnetic field. Since the finite-Larmor-radius (FLR) approximation restricts consideration to weakly unstable systems, the equations apply only to magnetic configurations in which the curvature of the lines of force is weak. In allowing for the effects of plasma pressure ($\beta \sim 1$) it is found that the FLR corrections to the stress tensor take their simplest form in the centre-of-mass frame, while the case of low $\beta$ yields equations best expressed in the guiding-centre frame. A comparison is made with magnetic viscosity terms derived using different ordering schemes. (UK)

**56179** COLLISION INTEGRAL BETWEEN PARTICLES OF DISPARATE MASS. Lo Surdo, C. (CNEN, Frascati, Italy). J. Plasma Phys.; 6: 107-17(Aug 1971).

Two alternative approaches to expanding the binary collision integral for particles of very different mass in powers of their small mass ratio m/M are examined in detail. One of them in particular is found to be suitable for a subsequent expansion of the above quantity in series of spherical harmonics. This reduces to a simple algebra the labor of determining the angular-moment form of the Boltzmann equation for Lorentzian mixtures. (auth) (UK)

**56180** EXPANSION OF A PLASMA FROM A SPHERICAL SOURCE INTO A VACUUM. PART I. FULLY-IONIZED FLOW. Goldfinch, Judith; Pack, D. C. (Univ. of Strathclyde, Glasgow). J. Plasma Phys.; 6: 137-52(Aug 1971).

An analytic treatment is applied to the expansion of a fully ionized plasma source, with the particles interacting according to the Coulomb law. The governing equations are derived from Poisson's equation and the full Boltzmann equation, with the assumption of an ellipsoidal distribution function, in order to close the moment equations and facilitate calculations of collision integrals. The investigation shows that the electrons and ions maintain equal isotropic temperatures, which fall adiabatically. In an appendix, a critical law of interaction for the freezing of the expansion is determined, accounting for the difference in behavior of a plasma and a binary mixture of Maxwell molecules. (auth) (UK)

**56181** EXPANSION OF A PLASMA FROM A SPHERICAL SOURCE INTO A VACUUM. PART 2. PARTIALLY IONIZED FLOW. Goldfinch, Judith (Univ. of Strathclyde, Glasgow). J. Plasma Phys.; 6: 153-67(Aug 1971).

The effects of partial ionization and recombination on the steady supersonic spherical source expansion of a plasma are discussed. An analytical solution for a problem previously solved only numerically is presented, using moment equations derived directly from the Boltzmann equation under the assumption of an ellipsoidal distribution function. The plasma is taken to be optically thick. The results show that, in a highly ionized plasma, the species maintain equal isotropic temperatures for the main part of the flow, with the degree of ionization tending to a finite limit. Recombinations, however, remain sufficiently frequent to keep the temperature above that in an expansion with no recombination. In a weakly ionized plasma the temperature of the heavy particles is almost unaffected by recombinations and falls adiabatically, although the electron temperature remains high. (auth) (UK)

**56182** ELECTRON–ION RECOMBINATION: CRITICAL REVIEW OF THEORIES AND EXPERIMENTAL RESULTS FOR AN ARGON PLASMA. Clark, K. J.; Incropera, F. P. (Purdue Univ., West Lafayette, Ind.). pp 331-41 of Proceedings of the Fifth Symposium on Thermophysical Properties. /Bonilla, C. F. (ed.). New York; American Society of Mechanical Engineers (1970).

From fifth symposium on thermophysical properties; Boston, Mass. (Sep-Oct 1970). See CONF-700901.

For the purpose of selecting a reliable method for calculating electron–ion recombination rate coefficients, available experimental results for recombination in an argon plasma are compared critically with corresponding predictions from four commonly used theoretical models. A high degree of scatter and experimental uncertainty is found to exist in the compilation of experimental results. Nevertheless, it is concluded that the theory that uses the principle of detailed balancing to relate the recombination rate coefficients to the inverse ionization rate coefficients gives the most satisfactory predictions for a wide range of conditions. (auth)

**56183** TRANSPORT PROPERTIES OF PARTIALLY IONIZED ARGON. Sandler, S. I. (Univ. of Delaware, Newark); Miller, E. J.; Mason, E. A. pp 342-6 of Proceedings of the Fifth Symposium on Thermophysical Properties. /Bonilla, C. F. (ed.). New York; American Society of Mechanical Engineers (1970).

From fifth symposium on thermophysical properties; Boston, Mass. (Sep-Oct 1970). See CONF-700901.

A new method of computing the transport coefficients of partially ionized gases from kinetic theory is applied to argon, for which the usual Chapman–Enskog procedure shows poor convergence. The basic idea of the method is that the velocity distribution function for the electrons is computed as a perturbation to the distribution function for a Lorentzian mixture. The new method is found to be much more rapidly convergent at low degrees of ionization. The present results and the Chapman–Enskog results appear to have the useful property of bracketing the actual values of the transport coefficients. (auth)

**56184** RELAXATION THEORY OF STARK BROADENING OF He II LINES IN PLASMAS. O'Brien, John Terrance. Tallahassee; Univ. of Florida (1970). 187p. University Microfilms Order No. 71-17,202.

Thesis.

The relaxation theory of plasma line broadening developed by Smith and Hooper, and extended by Smith, is applied to a charged radiator. The Lyman alpha line of He II is chosen as an example. The primary line broadening mechanism is the Stark effect. The perturbing electric field is due to the ions and electrons in the surrounding plasma. The effect of the ions is approximated by a static ion microfield. In addition to the static ion microfield, the radiator is perturbed by a rapidly fluctuating electron microfield. The power spectrum of the radiation, emitted by the $He^+$ ions in the plasma, is obtained by taking an ensemble average of the dipole–dipole correlation function over the states of the perturbing gas of electrons and two species of positive ions, as well as over the states of the excited radiator. It is shown that the en-

XUM

semble average over the ion states may be replaced by the familiar static ion microfield distribution function. No previous ion microfield distribution calculations consider the presence of more than one species of ion. Since a helium plasma may have significant percentages of $He^+$ and $He^{2+}$, a detailed calculation of a two-component ion microfield distribution function is included. The microfield distribution function calculation is an extension of the Hooper formalism. The fact that the radiator is charged complicates the treatment of electron perturbations. Two different approaches to this problem are included. The first approach neglects the effect of the charge of the radiator on the electron and assumes that the perturbing electrons can be represented by momentum wavefunctions. This approach corresponds to Smith's treatment of the electron perturbers. The second approach includes the effect of the charge of the radiator on the electrons; the perturbing electrons are represented by Coulomb wavefunctions. These two approaches can be compared with the classical path approach of Griem and Shen. Their treatment used straight line and hyperbolic trajectories which would correspond to the two approaches discussed in this dissertation. The calculation using Coulomb wavefunctions is shown to require evaluation of the free–free gaunt factors. An expression for the free–free gaunt factors which is more rapidly convergent than the Karzas and Latter formulation is included. Due to experimental difficulties, it was not possible to make a valid comparison between the resulting theoretical line shapes and the recent measurement of Greig et al. However, the theory does predict a blue asymmetry in the wings. If this asymmetry is interpreted as a shift it is of the same order as that observed in their experimental line shapes. Tables of line shapes and microfield distribution functions are included. (Diss. Abstr. Int., B)

**56185** TOPICS IN PLASMA THEORY. Lai, Hon-ming. Hanover, N. H.; Dartmouth Coll. (1971). 165p. University Microfilms Order No. 71-17,930.

Thesis.

The relativistic formalism of statistical mechanics (hereafter denoted as R.S.M.) with electromagnetic interactions developed by Balescu et al. is studied. The following sections are described: (1) Subsidiary conditions in R.S.M.: In a system of particles with electromagnetic interactions, it is proven that the subsidiary conditions restrict the phase space to a hypersurface which is invariant under the Poincare group of canonical transformations. (2) Pretensors in R.S.M.: In statistical mechanics, the average of a microscopic quantity is interpreted as the possible macroscopic observable. The explicit forms of those microscopic quantities (Pretensors) such that their averages transform as tensors in Minkowski space are obtained and classified. (3) Physical Quantities and Conservation Laws: It is shown that, with electromagnetic interactions, the mechanical momentum is a physical quantity while the canonical momentum is not. Forms of physical quantities have been found and those pretensors satisfying a continuity equation are classified. The well-known conserved quantities like mass, charge and energy-momentum are recovered. (4) As applications, the equations of state for a relativistic plasma have been obtained and the fundamental microscopic equation started by Klimantovich in his formalism was directly derived. The classical convergent kinetic equation, or the so-called "Balescu-Lenard-Guernsey" plus "Boltzmann" minus "Landau" kinetic equation was studied. This equation is applied to calculate the collisional part of the ac electrical conductivity of a magnetoplasma of any number of species to second order in the wave vector. Both dominate (Coulomb logarithmic) and sub-dominant terms are evaluated exactly to first order in the plasma parameter. The result is greatly simplified when only a two-component plasma is considered. Zero magnetic field limit is also discussed. (Diss. Abstr. Int., B)

**56186** VELOCITY DISTRIBUTION FUNCTION AND POWER BALANCE FOR ELECTRONS OF MEDIUM IONIZING POWER IN ARGON UNDER HOMOGENEOUS STATIONARY CONDITIONS. Winkler, R.; Wilhelm, J. (Rudolf Seeliger Institut, Greifswald, Ger.). Beitr. Plasmaphys.; 11: No. 2, 159-77(1971). (In German).

By means of an iteration method, the velocity distribution function was solved numerically for a homogeneous stationary argon plasma throughout a wide range of both electrical fields and decrease of ionization. The method is based on a combination of the Boltzmann and the Fokker–Planck equation describing elastic, excitation, and Coulomb interactions. Through the development of the Legendre polynomial an integro-differential difference equation is then obtained for the isotropic part of the velocity distribution function. Aside from computation of the isotropic distribution, the method simultaneously yields mean kinetic energy, diffusion coefficient, mobility, transport collision frequency, collision frequency for excitation of neutral atoms from the ground level and for step ionization of excited argon atoms. In addition, energy losses of electrons through elastic and excitation collisions are calculated and discussed. (tr-auth)

**56187** GALAXY: A SYSTEM FOR 2D MANY-BODY CALCULATIONS. Boris, J. P.; Roberts, K. V. (Culham Lab., Abingdon, Eng.). pp 4.1-7 of Computational Physics. Vols. I and II. London; Her Majesty's Stationery Office (1969).

From Conference on computational physics; Culham, England (28 Jul 1969). See CONF-690706-(Vols.1 and 2).

Three-dimensional many-body calculations following millions of interacting particles are now possible on suitably supported third-generation computers, provided that an appropriate blend of programming techniques can be used. A "vector-integration" technique was developed for solving the particle equations of motion in multidimensional problems, bringing savings of a factor 2 in storage requirements and about a factor 8 in execution speed over standard techniques. The test bed for this and related techniques is the GALAXY system, a 2D plasma or gravitational simulator with a doubly periodic fast Fourier-transforming Poisson solver and a set of diagnostic "analyzer" programs. GALAXY uses magnetic-tape backing store and a triple-buffer technique which overlaps tape and CPU operations, and problems were run with $10^6$ simulation particles to demonstrate the applicability of these techniques to moderately large computations. (auth) (UK)

**56188** EXPLICIT MAGNETOHYDRODYNAMIC CALCULATIONS IN THE R–Z PLANE. Potter, D. E. (Imperial Coll. of Science and Tech., London); Roberts, K. V. pp 6.1-6 of Computational Physics. Vols. I and II. London; Her Majesty's Stationery Office (1969).

From Conference on computational physics; Culham, England (28 Jul 1969). See CONF-690706-(Vols.1 and 2).

The physical model and numerical methods of a two-dimensional magnetohydrodynamic code applicable to the R–Z plane are described. Two cases are considered. If the magnetic field is perpendicular to the plane of the calculation, the problem is simplified since transport processes are isotropic and, in addition, the magnetic field is analytically known. The more general problem of arbitrary magnetic fields is discussed. The code was applied to the analysis of the dense plasma focus (Filippov et. al., 1962; Mather, 1965). Good agreement with experiment was reached in describing the high kinetic energy densities that occur, and a mechanism for the anomalously long duration of the pinch is suggested. (auth) (UK)

**56189** COMPARISON OF TWO COMPUTATIONAL MODELS FOR COLLISIONLESS PLASMA SHOCKS. Kilb, Ralph W. (General Electric Co., Santa Barbara, Calif.). pp 41.1-5 of Computational Physics. Vols. I and II. London; Her Majesty's Stationery Office (1969).

From Conference on computational physics; Culham, England (28 Jul 1969). See CONF-690706-(Vols.1 and 2).

Expanding collisionless cylindrical shocks in a magnetized plasma were simulated by a flux-conserving model and by a plasma model, including the electron inertia which requires the collisionless skin depth $c/\omega_{pe}$. The ion phase-space thermalization is found to be essentially the same in the two models and proceeds on the scales of the ion gyro diameter and period. (auth) (UK)

**56190** A LAMINAR KINETIC MODEL OF THE UNSTABLE EQUILIBRIUM UNDERLYING PERPENDICULAR SHOCK WAVES IN COLLISION-FREE MAGNETIZED PLASMAS. Buckley, R. (Radio and Space Research Station, Slough, Eng.). pp 42.1-7 of Computational Physics. Vols. I and II. London; Her Majesty's Stationery Office (1969).

From Conference on computational physics; Culham, England (28 Jul 1969). See CONF-690706-(Vols.1 and 2).

The structure of a laminar shock wave propagating perpendicular to the magnetic field in a collision-free plasma is described. The model is based on the time-independent Vlasov equations and extends some work by Morawetz (1961). The resulting downstream proton velocity distribution is hollow, and is thus subject to microinstabilities which, in practice, would provide the necessary thermalization. It was not possible to solve the equations completely either analytically or numerically. Instead, both mathematical and physical arguments are used to derive the shock structure and demonstrate its self-consistency. The numerical attempt failed because of the occurrence of looping protons, which give rise to two quite separate computational problems. (auth) (UK)

**56191** PARTICLE MODELS IN PLASMA PHYSICS. Hockney, R. W. (IBM Watson Research Center, Yorktown Heights, N. Y.). pp C.0-19 of Computational Physics. Vols. I and II. London; Her Majesty's Stationery Office (1969).

From Conference on computational physics; Culham, England (28 Jul 1969). See CONF-690706-(Vols.1 and 2).

Fundamental particle models of a low-density two-dimensional plasma are discussed, in which both the simulated electrons and simulated ions move according to Newton's laws of motion in their mutual electrostatic fields. Measurements of several relaxation times were made in such a model. It is found that the deflection time, the slowing-down time, and the thermalization time, $\tau$, can all be represented by the relation $\tau/\tau_{pe} = N_\lambda D/2$, $(10 \leq N_{\lambda D} \leq 1000)$ where $N_{\lambda D}$ is the number of simulated electrons or ions in a Debye square. In particular, it is found that smoothing techniques such as the Cloud In Cell (CIC) method have the same relaxation times as the quicker but noisier Nearest Grid Point (NGP) method. The stochastic heating of the plasma by computer errors was also measured. For sufficiently small time step and the same number of particles, the CIC method is found to heat up at only one-tenth the rate of the NGP method. A limited comparison of these measured rates with simple theoretical estimates is given. (auth) (UK)

**56192** MULTIDIMENSIONAL MAGNETOHYDRODYNAMIC SHOCK CALCULATIONS. Greene, J. S. Jr.; Nickel, G. H.; Allen, C. C. (Air Force Special Weapons Center, Kirtland AFB, N. Mex.). pp P.7-1 of Computational Physics. Vols. I and II. London; Her Majesty's Stationery Office (1969).

From Conference on computational physics; Culham, England (28 Jul 1969). See CONF-690706-(Vols.1 and 2).

A general Eulerian meshed computer code is being developed to solve any set of differential equations which may be written in flux conservative form. Equations are written relative to moving coordinates so that the mesh may expand with the problem and make calculation of strong shock formation and propagation easier. Use of the code to solve one-material magnetohydrodynamic equations for expansion of an infinite isothermal cylinder into a constant atmosphere is discussed, and results are compared with those of other methods. (UK)

## Production

*Refer also to abstract 56110.*

**56193** (IPP-4/82) NEODYMIUM GLASS LASER SYSTEM. Baumhacker, H. (Institut fuer Plasmaphysik, G.m.b.H., Garching (West Germany)). Mar 1971. 94p. (In German). Dep. NTIS (U. S. Sales Only).

A high-power neodymium glass laser system used mainly for plasma generation is described. Several oscillators with various types of Q switches were developed. Each oscillator can be operated in series with several amplifier stages. Presently, the most powerful system, which consists of an oscillator Q-switched by a rotating mirror and three subsequent amplifiers, delivers pulses with a peak power of 5 GW and 25 nsec half-width. (auth)

## Stability

*Refer also to abstract 56251.*

**56194** (EUR-CEA-FC-598) MHD STABILITY CRITERION IN A SHALLOW MAGNETIC WELL. APPLICATION TO DECA II B. Lecoustey, P. (Commissariat a l'Energie Atomique, Fontenay-aux-Roses (France). Centre d'Etudes Nucleaires). May 1971. 14p. (In French). Dep. NTIS (U. S. Sales Only).

A sufficient criterion of stability is given for all the particles confined in a shallow magnetic well. From the invariance of $\mu$ and J, the calculation gives the depth of the energy well for each particle. The critical $\beta$ of the configuration is deduced from this criterion. (France)

**56195** (JAERI-Memo-4483) TRAPPED-PARTICLE INSTABILITIES AND DIFFUSION RATES IN A TOKAMAK PLASMA. Sugawara, Tohru (Japan Atomic Energy Research Inst., Tokyo). Jun 1971. 9p. (In Japanese). Dep. NTIS (U. S. Sales Only).

Low-frequency dissipative trapped-particle instabilities in a tokamak plasma are investigated by using a simplified-model magnetic field. The cross-field particle diffusion due to these instabilities is estimated on the basis of nonlocal theory. The estimated particle-diffusion coefficients are rather small at low collision frequencies compared with the previous results of Kadomtsev and Pogutse. (auth)

**56196** (N-71-25028) INSTABILITIES AND TURBULENCE IN HIGHLY IONIZED PLASMAS IN A MAGNETIC FIELD. Semiannual Status Report, September 1, 1970-February 28, 1971. Noon, J. H.; Jennings, W. C. (Rensselaer Polytechnic Inst., Troy, N. Y. Plasma Dynamics Lab.). Apr 1971. 60p. (NASA-CR-118311). NTIS.

Further work was carried out on correlation length and time studies of the plasma turbulence spectrum in the highly ionized argon arc. New probe diagnostics were developed to allow improved measurements of radial, azimuthal, and axial parameters. The relation between wave growth in different frequency regions of the spectrum and the sense of energy cascade was studied both experimentally and theoretically. The technique used can also be applied to determine whether classical or anomalous diffusion across the magnetic field is dominant. An optical diagnostic method was developed for remote sensing of coherent instabilities and a feedback scheme was successfully applied to stabilize the plasma against the development of these coherent instabilities. A theoretical analysis shows promise in explaining the underlying mechanisms responsible for wave growth in different radial regions of the inhomogeneous plasma. (auth) (STAR)

**56197** EXPERIMENTS ON THE STABILIZATION OF FLUTE INSTABILITY WITH THE AID OF AN INTEGRATING FEEDBACK SYSTEM. Chuyanov, V. A. (Inst. of Atomic Energy, Moscow); Murphy, E. G. JETP Lett. (USSR) (Engl. Transl.); 13: No. 10, 395-7(20 May 1971).

Translated from Zh. Eksp. Teor. Fiz., Pis'ma Red.; 13: No. 10, 553-5(20 May 1971).

An integrating amplifier was used in the feedback system to stabilize the residual instability connected with the frequency characteristic of the feedback loop. Introduction of such a feedback system led to a significant change in the behavior of the plasma. (M.O.W.)

**56198** REVIEW OF TOKAMAK. Fujisawa, Noboru (Japan Atomic Energy Research Inst., Tokai). Cho-Koon Kenkyu; 7: No. 3, 142-54(Oct 1970). (In Japanese).

The Tokamak is composed of an iron core, primary windings and secondary windings. Energy of the primary windings is transferred to the plasma in the secondary windings through the iron core. Plasma current flows with this energy, and high-temperature plasma is obtained by resistance heating. The plasma is produced in a vacuum chamber which is composed of a shell, a liner, and a limiter. The shell provides for equilibrium and stabilization of the plasma. The plasma is made in the liner. The limiter determines radius of the plasma. Strong magnetic field is applied to stabilize the plasma. Equilibrium of the plasma was investigated for various dimensions of the shells, liners and limiters. Instability of Tokamak-type plasma was also studied. Stable plasma was obtained by application of a strong toroidal magnetic field. Characteristic oscillations were seen in wave forms of loop voltage and by magnetic probes. Two kinds of oscillations were observed. The first one was small and seen at an early stage of the discharge. The second one was a large-amplitude pulse oscillation at later stages of the discharge. The second one is called spike oscillations. Confinement of Tokamak-type plasma is also described. (Japan)

**56199** STABILIZATION OF MAGNETOHYDRODYNAMIC INSTABILITIES BY FORCE-FREE MAGNETIC FIELDS. I. PLANE PLASMA LAYER. Goedbloed, J. P. (FOM-Instituut voor Plasma-Fysica, Jutphaas, Netherlands). Physica; 53: No. 3, 412-44(15 Jun 1971).

A marginal-stability analysis is applied to the stability problem of a plane plasma layer under the influence of gravity. Complete stability criteria are derived from the marginal equation of motion and it is shown that this method is equivalent to the application of the energy principle. Ideal magnetohydrodynamic instabilities, as occurring in simple plasma-vacuum systems, can be suppressed by replacing the vacuum by a force-free magnetic field, that is a field satisfying the relation $\nabla \times B = \alpha B$. Force-free fields of constant $\alpha$ are investigated in particular. By proper choice of $\alpha$, the gravitational instabilities of nonlocal and of surface-layer type are absent in a plane plasma layer supported from below by a horizontal force-free magnetic field. An appendix is devoted to a rigorous treatment of the influence of singular points of the marginal equation of motion on the stability analysis. (auth)

**56200** STABILIZATION OF MAGNETOHYDRODYNAMIC INSTABILITIES BY FORCE-FREE MAGNETIC FIELDS. II. LINEAR PINCH. Goedbloed, J. P. (FOM-Instituut voor Plasma-Fysica, Jutphaas, Netherlands). Physica; 53: No. 4, 501-34(30 Jun 1971).

The marginal-stability analysis, developed in Part I is applied to the stability problem of a linear pinch with a distributed current. Complete stability criteria are derived from the marginal equation of motion, and it is shown that this method is equivalent to the application of the energy principle. For a sharp-pinch model of a dense plasma surrounded by a force-free magnetic field of constant $\alpha$ kinks, unstable modes of the surface-layer and of the force-free region are shown to be absent if $\alpha$ is properly chosen. Explicit expressions for the growth rates of unstable configurations

XUM

are derived. An appendix is devoted to the stability with respect to resistive tearing modes. (auth)

**56201** STABILIZATION OF MAGNETOHYDRODYNAMIC INSTABILITIES BY FORCE-FREE MAGNETIC FIELDS. III. SHEARLESS MAGNETIC FIELDS. Goedbloed, J. P. (FOM-Instituut voor Plasma-Fysica, Jutphaas, Netherlands). Physica; 53: No. 4, 535-70(30 Jun 1971).

The marginal-stability analysis, as given in Parts I and II, is further elaborated for magnetic fields of constant direction in the plane case and for magnetic fields of constant pitch in the cylindrical case. For these shearless magnetic fields, discontinuities arise in the stability criteria; the physical significance of these discontinuities is discussed. From the marginal-stability analysis the principle of exchange of stabilities is derived. This theory is applied to constant-pitch magnetic fields, which are shown to be necessarily unstable. Growth rates of the instabilities of these fields are calculated, correcting earlier results of Ware. Simple modifications of some constant-pitch models, namely Van der Laan's model of a constant-pitch force-free field and Alfvén's model of a constant-pitch field with parabolic pressure profile, prove to yield completely stable pinch configurations of a sharp or diffuse kind. An appendix is devoted to toroidal effects. (auth)

**56202** STABILITY OF A PLASMA STREAM IN A MAGNETIC FIELD. Lamont, A.; Taylor, J. C.; Laing, E. W. (Univ. of Glasgow). J. Plasma Phys.; 6: 169-86(Aug 1971).

The system studied is a plasma streaming parallel to a uniform magnetic field with a velocity that varies in a transverse direction. The flow is bounded at $y = \pm a$ by perfectly conducting planes. The Poisson–Vlasov equations are used to derive an integro-differential equation for $\phi$, the Fourier transform of the electrostatic potential. The kernel of this equation is expanded using a small Larmor radius expansion for $\phi$ and for the equilibrium distribution function $f_0$. This leads to an ordinary differential equation the order of which depends on the number of terms retained in the $\phi$ expansion. The application of the boundary conditions leads to an eigenvalue problem. It is found that an increase in the parameter A, which is a measure of the change in velocity across the stream, leads to a less-stable system, but, for any A, the system is stabilized by making the temperature or the magnetic field sufficiently large. (auth) (UK)

**56203** RESISTIVE INSTABILITY IN A UNIFORMLY ROTATING MAGNETOPLASMA. Lunn, A. D. (Mathematical Inst., Oxford). J. Plasma Phys.; 6: 73-85(Aug 1971).

A closed set of guiding-center equations, derived for a rotating plasma in a static magnetic field, is applied to the problem of the stability of a plasma in a sheared field. The rotation is found to have a stabilizing effect in the absence of resistivity. A pair of coupled, linear differential equations is derived for the rotating plasma in a weakly sheared field. Dispersion relations are obtained by phase integral methods and, in the absence of finite Larmor radius effects and rotation, instability growth rates proportional to $\eta^{\frac{1}{3}}$ are found which become proportional to $\eta$ when either is included. The inclusion of both finite Larmor radius and rotation gives growing instabilities proportional to $\eta$ which are stabilized by the rotation when the finite Larmor radius terms predominate. (auth) (UK)

**56204** ANALYSIS OF ELECTROMAGNETIC INSTABILITIES PARALLEL TO THE MAGNETIC FIELD. Pilipp, W.; Voelk, H. J. (Max-Planck-Institut fuer Physik und Astrophysik, Garching, Ger. Astrophysik, Institut fuer Extraterrestrische Physik, Garching, Ger.). J. Plasma Phys.; 6: 1-17(Aug 1971).

Transverse waves and instabilities propagating along the magnetic field in a homogeneous plasma are discussed analytically and numerically for frequencies of the order of the ion cyclotron frequency and below. The free energy driving the instabilities is assumed to be provided by thermal anisotropies, with the parallel temperature exceeding the perpendicular temperature, a situation appropriate to the solar wind near the earth and to the downstream conditions in collisionless shocks propagating approximately parallel to the magnetic field. Extensive discussions of the energy losses and gains of the ions and electrons are given for all unstable modes. (UK)

**56205** NUMERICAL EXPERIMENTS ON NONLINEAR PLASMA INSTABILITIES. McNamara, B.; Boris, J. P.; Cook, I.; Sykes, A. (Culham Lab., Abingdon, Eng.). pp 43.1-5 of Computational Physics. Vols. I and II. London; Her Majesty's Stationery Office (1969).

From Conference on computational physics; Culham, England (28 Jul 1969). See CONF-690706-(Vols.1 and 2).

The use of linear analysis of a simple electrostatic plasma instability to design a numerical experiment using the plasma simulation code, GALAXY, is shown. The numerical experiment computes the nonlinear behaviour of the instability, to which well-known nonlinear theory can be applied. An important feature of the GALAXY code is the production of a permanent record of the experiments which can be reprocessed many times for comparison with theory. A second code, THEORY, is under construction to solve the theoretical equations. This code will run at the parameters of the numerical experiment or, 1600 times faster, at the parameters of a real plasma. It should therefore be possible to check the theory against the numerical experiment and then apply it to a real experiment. (auth) (UK)

**56206** SIMULATION OF PLASMA MICROINSTABILITIES WITH SUPERPARTICLE COMPUTER MODELS. Byers, Jack A. (Univ. of California, Livermore). pp 45.1-5 of Computational Physics. Vols. I and II. London; Her Majesty's Stationery Office (1969).

From Conference on computational physics; Culham, England (28 Jul 1969). See CONF-690706-(Vols.1 and 2).

The use of superparticle computer models to simulate modes of plasma instability due to the loss-cone nature of the particle velocity distribution common to magnetic mirror confinement is discussed. An essential problem associated with the superparticle approach is the greatly enhanced noise due to the small number of particles per Debye length. For infinite-medium models, it was possible to create essentially noise-free starting conditions by loading the phase space in a precisely uniform way. For a $k_{||} = 0$ one-species mode, growth starting essentially from machine roundoff levels can be observed at precisely the linear Vlasov theory predictions up to the saturated level, many orders of magnitude above the starting point. A stable distribution remains at roundoff level with no tendency to establish a thermal fluctuation level. In addition, a nonlinear instability was observed. Also, other $k_{||} = 0$ unstable velocity distributions were examined, such as the combination of a stable loss cone plus a small amount of cold ions. The aim is the simulation of the finite-geometry mirror machine problem with a two-species, two-dimensional model encompassing density and magnetic field variations and with the attendant particle and wave reflection at the mirrors. One step now being taken to simulate finite-geometry effects is a one-species two-dimensional model to set up the ion bouncing motion between mirrors in a noise-free equilibrium. (auth) (UK)

**56207** NUMERICAL COMPUTATION OF PLASMA EQUILIBRIA. Killeen, John (Univ. of California, Livermore). pp 46.1-5 of Computational Physics. Vols. I and II. London; Her Majesty's Stationery Office (1969).

From Conference on computational physics; Culham, England (28 Jul 1969). See CONF-690706-(Vols.1 and 2).

A number of two-dimensional plasma equilibria problems are considered. In each case a confining vacuum magnetic field is given and the distortion of this field by the presence of the plasma, or the electron layer and plasma in the case of the Astron experiment, found. The magnetic field can be derived from a stream function $\psi(r,z)$ which satisfies a nonlinear, second-order, partial differential equation. The resulting boundary-value problem is solved by finite-difference methods. (auth) (UK)

## *Thermonuclear Processes*

**56208** (CONF-711012-9) ORNL MULTI-AMPERE ION SOURCE. Stirling, W. L.; Davis, R. C.; Morgan, O. B.; Stewart, L. D. (Oak Ridge National Lab., Tenn.). [nd]. 7p. Dep. NTIS.

From Symposium on ion sources and formation of ion beams; Upton, N. Y. (19 Oct 1971).

The multi-ampere ion source developed at ORNL called the "duoPIGatron" is described. The source is operated steady-state at 1 A output with ion energies from 1.5 to 5 keV. For 0.1-second pulses and 10% duty cycle, 4-ampere beams were achieved at ion energies from 20 to 40 keV. At 30 to 40 keV, about 60% of the beam is within a half-angular divergence of 1.2° with no magnetic lens. (auth)

**56209** (CTO-764) RESONANCE EFFECTS IN MAGNETIC CONFIGURATIONS HAVING A HELICAL MAGNETIC AXIS, WITH ALLOWANCE FOR TOROIDALITY. Aleksin, V. F.; Nemov, V. V.; Shishkin, A. A. ([Akademiya Nauk Ukrainskoi SSR, Kharkov. Fiziko-Tekhnicheskii Institut]). Translated by J. B. Sykes (Culham Lab., Abingdon, Eng.), from report KHFTI-70-72. 18p. Dep. NTIS (U. S. Sales Only).

Resonance effects are discussed with allowance for toroidality in magnetic configurations having a helical magnetic axis. Conditions for splitting of the magnetic axis are considered, and the order of magnitude of the distance between the new axes and that of the original linear system is stated. The appendix deals, for specific cases, with the possible use of a uniform transverse

external field to compensate the toroidal displacement of the magnetic axis in the nonresonance case. (auth)

**56210** (EUR-CEA-FC-603) MULTIPLY CHARGED ION SOURCE. DESIGN OF ELECTRON GYROMAGNETIC RESONANCE SOURCE. Bliman, S.; Geller, R. (Commissariat a l'Energie Atomique, Fontenay-aux-Roses (France). Centre d'Etudes Nucleaires). Jun 1971. 29p. (In French). Dep. NTIS (U. S. Sales Only).

The possibility of expanding the applications of Pleiade-type machines in order to obtain multiply charged heavy ion beams was studied. After a general review on the way in which heavy ion strippers are obtained, collisions in Pleiade-type electron cyclotron resonance sources (ionization, recombination, charge exchange) are studied. The properties of this type of plasma are described and the simplest way in which it is obtained is discussed; the problems arising within the plasma as a result of the extraction of an intense ion beam, the problems of transporting this type of beam, and the methods of obtaining $N^{7+}$ from the ion conglomeration drawn away were studied. (France)

**56211** (IPP-III-2) TOKAMAK WITH SUPERPOSED MULTIPOLE MAGNETIC FIELD. Feneberg, W. (Institut fuer Plasmaphysik, G.m.b.H., Garching (West Germany)). Jun 1971. 7p. Dep. NTIS (U. S. Sales Only).

It is proposed that multipole magnetic fields be superposed on the Tokamak to produce an equilibrium such that the plasma is separated from the wall by a magnetic separatrix. The equilibrium is calculated for a special configuration with four conductors in which small deviations from circular symmetry are assumed. (auth)

**56212** (LBL-35) LARGE-AREA HIGH-CURRENT ION SOURCE. Baker, W. R.; Ehlers, K. W.; Kunkel, W. B.; Lietzke, A. F. (California Univ., Berkeley. Lawrence Berkeley Lab.). Aug 1971. Contract W-7405-erg-48. 5p. (CONF-711012-10). Dep. NTIS.

From Symposium on ion sources and formation of ion beams; Upton, N. Y. (19 Oct 1971).

Neutral injection, a method of producing and heating plasmas in certain controlled-fusion experiments, requires the development of multiampere ion sources. A new type of ion source geometry capable of delivering a high ion current density over a large extraction area is reported. Probes used to determine the operating characteristics of the model tested indicate the availability of noise-free ion current densities in excess of 1 $A/cm^2$ and flat to ±15% over a 4-cm diameter. A larger version of the model tested is being designed to deliver a 30-msec 20-A, 20-keV deuterium ion beam for the Livermore 2X-II experiment. (auth)

**56213** (LBL-327) MULTIPLE APERTURE EXTRACTOR DESIGN FOR PRODUCING INTENSE ION AND NEUTRAL BEAMS. Berkner, K. H.; Cooper, W. B.; Pyle, R. V. (California Univ., Berkeley. Lawrence Berkeley Lab.). Aug 1971. Contract W-7405-eng-48. 2p. (CONF-711012-11). Dep. NTIS.

From Symposium on ion sources and formation of ion beams; Upton, N. Y. (19 Oct 1971).

A calculational and experimental program to optimize the extractor design of high-current multiple-aperture ion sources is in progress. In general, the computed and measured properties of extractors with circular apertures agree well. Very preliminary tests with a multiple slot extractor are encouraging. (auth)

**56214** (LGI-70/17/E) CALIBRATION OF THE SILVER ACTIVATED COUNTERS ON A PLASMA FOCUS EXPERIMENT. Luzzi, G.; Samuelli, M. (Comitato Nazionale per l'Energia Nucleare, Frascati (Italy). Laboratorio Gas Ionizzati). Oct 1970. 24p. Dep. NTIS (U. S. Sales Only).

The calibration of silver-activation counters was performed for measuring the anisotropy of the neutron emission of a plasma focus device. The characteristics and the limits of the measuring system were studied. (auth)

**56215** (N-71-25526) DEUTERIUM-$^3$He FUSION POWER BALANCE CALCULATIONS. Reinmann, John J.; Rayle, Warren D. (National Aeronautics and Space Administration, Cleveland, Ohio. Lewis Research Center). May 1971. 41p. (NASA-TM-X-2280). NTIS.

Steady-state operating parameters were calculated for the deuterium-helium-3 cycle. Energy equations were written for the electrons and the two ion species in the plasma. The effects of varying amounts of reflection and reabsorption of cyclotron radiation were studied by the inclusion of a variable cyclotron radiation parameter. Other parameters were varied to assess the effects of: (1) unequal confinement times of plasma electrons and ions, (2) plasma ion heating by fusion products at an enhanced rate, and (3) injection of fuel ions with varying amounts of initial energy. Results are presented in the form of equilibrium values of a containment parameter; the electron and ion temperatures; and a breakdown of the output power into bremsstrahlung, cyclotron radiation, and power carried out by escaping ions and electrons. Results are plotted as a function of plasma ion temperature. (auth) (STAR)

**56216** (NP-19014) TEMPERATURE PROFILE IN A THERMONUCLEAR REACTOR. Report 71-65. Verboom, G. K.; Rem, J. (Stichting voor Fundamenteel Onderzoek der Materie, Jutphaas (Netherlands). Instituut voor Plasma-Fysica). Apr 1971. 91p. Dep. NTIS (U. S. Sales Only).

The problem of a steady-state infinitely long plasma cylinder in which nuclear reactions take place is considered. The analysis is restricted to the fully ionized region, but the temperature at the "wall" is sufficiently low, so that nuclear energy is liberated only in the center. Of all possible nuclear reactions at axis temperature of $10^8$ to $10^9$ K, only the D-T reaction is considered (50/50 mixture). The energy is carried away by bremsstrahlung, reabsorption of which is neglected, and by heat conduction to the wall. An externally applied axial magnetic field (between 3 and 10 tesla at the "wall") perpendicular to the radial temperature gradient gives rise to a large diamagnetic azimuthal current, as a result of which the pressure at the boundary is much lower than in the center ($10^{-1}$ and 100 atm, respectively, for example). The fuel supply and the ash removal take place through classical diffusion to and from the "wall" through this low-pressure region. The macroscopic equations are solved for a number of values of the parameters involved. No acceptable solution exists if the helium density in the center is either too low or too high; but it must be higher than the deuterium-tritium density. Solutions with a power production up to 1 GW per meter length and a plasma radius up to a few meters are found. (auth)

**56217** (UCRL-73387) INTENSE 1-kV ION SOURCE FOR CONTROLLED FUSION RESEARCH. Osher, John E.; Hamilton, Gordon W. (California Univ., Livermore. Lawrence Radiation Lab.). 25 Aug 1971. 9p. (CONF-711012-7). Dep. NTIS.

From Symposium on ion sources and formation of ion beams; Upton, N. Y. (19 Oct 1971).

A multi-aperture source "MATS" was developed for steady-state 1-keV $H^+$ injection into the Baseball II controlled fusion experiment. This ion source utilizes a magnetically shaped reflex arc for plasma production over a large area array of aligned accel-decel apertures to yield the desired total output. The total ion current from the 6.35-cm-diam array of 331 apertures is 1 amp at 1 kV with a beam shape that can be fitted to a gaussian with a half-angle divergence (1/e) of 4 to 5°. The normalized beam emittance of .42 cm-mrad and lens magnet optics is given under typical operating conditions. The neutral beam yield with $H_2O$ vapor charge exchange medium varies nearly in proportion to $V^{\frac{1}{2}}$ to 3 kV with 47 mA $H^+$ equivalent at 1 keV into the Baseball II ± 1.4° acceptance angle. (auth)

**56218** (UCRL-73412) A REVIEW OF THE PRODUCTION OF INTENSE ION AND NEUTRAL BEAMS WITH ENERGIES BELOW 10 keV. Osher, John E. (California Univ., Livermore. Lawrence Radiation Lab.). 31 Aug 1971. 9p. (CONF-711012-8). Dep. NTIS.

From Symposium on ion sources and formation of ion beams; Upton, N. Y. (19 Oct 1971).

Intense ion and equivalent neutral beam production tends to depend directly on ion source output. At extracted ion energies below 10 keV, the space-charge problem becomes particularly severe with a corresponding tendency for the ion source to yield a decreased ion beam intensity and an increased beam divergence. This low-energy limitation is discussed in moderate detail. Examples of several ion sources yielding intense beams for the controlled fusion program are presented. The above approach is compared with several other different types of "sources." The principle and limitations of each type are given. A summary table is also presented with representative ion beam output data for each source type to better delineate the present state of the art. (auth)

**56219** GENERATION OF NEUTRONS IN A LASER $CD_2$ PLASMA HEATED BY PULSES OF NANOSECOND DURATION. Basov, N. G.; Boiko, V. A.; Zakharov, S. M.; Krokhin, O. N.; Sklizkov, G. V. (Lebedev Inst. of Physics, Moscow). JETP Lett. (USSR) (Engl. Transl.); 13: No. 12, 489-91(20 Jun 1971).

Translated from Zh. Eksp. Teor. Fiz., Pis'ma Red.; 13: No. 12, 691-4(20 Jun 1971).

Neutron measurements were made following irradiation of a deuterated polyethylene target by a pulsed neodymium laser beam. The experimental data were registered with a photomultiplier and a plastic scintillator. (M.O.W.)

XUM

**56220** SMALL COAXIAL GUN FOR PLASMA INJECTION STUDIES. de la Fuente, H.; Forsen, H. K. (Univ. of Wisconsin, Madison). Rev. Sci. Instrum.; 42: No. 10, 1453-5(Oct 1971).

Properties of plasmas produced by a 1.5 cm diam coaxial gun are investigated. Gas is provided from the center electrode material which is interchangeable. Materials such as lithium, titanium with occluded hydrogen, and carbon are used as the plasma source. Typically, a lithium plasma is produced which has equal ion and electron energies of 25 eV and $10^{17}$ to $10^{18}$ particles/pulse. (auth)

**56221** TOROIDAL TRAPS R-0 AND RT-2 WITH STEADY AND HIGH-FREQUENCY MAGNETIC FIELDS. Demirkhanov, R. A.; Kirov, A. G.; Baratov, D. G.; (and others). At. Energ. (USSR); 31: No. 3, 239-44(Sep 1971). (In Russian).

Two toroidal traps with quasi-static and rf magnetic fields are briefly described. They are intended for performing investigations on plasma confinement and dynamic stabilization. The trap diameters are 100 cm and 130 cm. Radiofrequency fields of the E-wave type with multipolarity m = 0 and m = 2 are generated by the system of helical conductors, which are the inductors of magnetically coupled oscillatory circuits. The rf magnetic field strength is 200 to 800 Oe and the field frequency is 0.2 to 5 Mc at a pulse duration 0.5 to 3 msec. Quasi-static magnetic fields of the trap have circular stellarator configurations with 1 to 2 or 1 to 3 helical windings, the spiral angles being close to the optimum ones for obtaining the highest values of the angle of torsion and the average shear. Magnetic systems of the equipment are made of single-turn demountable elements. The integral perturbation of the toroidal magnetic field $\Delta B/B$ does not exceed $1.5 \times 10^{-3}$. The highest confining fields of the traps are of the order of 10 kOe and 20 kOe, respectively, the field half-cycle duration being 15 msec. The condenser bank with the accumulated energy of 2.7 MJ serves as an energy source for the quasi-static magnetic fields. The equipment is designed for performing experiments in the plasma with the following parameters: $n = 10^{13}$ to $10^{15}$ cm$^{-3}$ and Te = 10 to 100 electron volts at $\beta = 8\pi nkT/\bar{H}^2 \ll 1$ and $\tilde{\beta} = 16\pi nkT/\bar{H}^2 \approx 1$. (auth)

**56222** POSSIBILITY OF STATIONARY REGIMES IN THERMONUCLEAR REACTIONS. Kolesnichenko, Ya. I. At. Energ. (USSR); 31: No. 3, 295-7(Sep 1971). (In Russian).

One of the essential conditions for a self-sustaining reaction is a predominating energy inflow in the plasma caused by those reactions associated with bremsstrahlung, synchrotron radiation, etc. Since, with increased temperature, the thermonuclear energy release also increases faster than the forms of energy loss mentioned, the plasma temperature must exceed some critical value of the temperature (given a transparent plasma). This leads to increased reaction velocities, evoking still higher temperatures, until the temperature function begins to change (40 to 50 keV for D–T mixtures). The question arises as to whether a stationary regime is possible, and a solution is obtained for the simplest mathematical model. (K.S.W.)

**56223** SPATIAL DETERMINATION OF THE DIRECTION OF THE MAGNETIC FIELD IN A TOKAMAK CONFIGURATION. Cano, R.; Fidone, I.; Schwartz, M. J. (EURATOM, Fontenay-aux-Roses, France). Phys. Rev. Lett.; 27: No. 12, 783-6(20 Sep 1971).

A method is suggested by which the local magnetic field direction can be determined in Tokamaks. A numerical application is made to the Princeton ST Tokamak. (auth)

## *Wave Phenomena*

**56224** (AEC-tr-7270) DETERMINATION OF THE BOUNDARY OF HIGH FREQUENCY WAVE ABSORPTION BETWEEN THE ELECTRON CYCLOTRON AND THE LOW HYBRID FREQUENCY. Galktinov, B. V.; Golant, V. E.; D'yachenko, V. D.; Shcherbinin, O. N. (Akademiya Nauk SSSR, Leningrad. Fiziko-Tekhnicheskii Institut). Translation of report FTI-295. 7p. Dep. NTIS.

An abstract of this paper, prepared from the original language, appeared as NSA 25: 11927. (M.O.W.)

**56225** (CEA-CONF-1802) COUPLING OF EM WAVES IN AN INHOMOGENEOUS PLASMA. Cano, R.; Schwartz, M.; Zanfagna, B. (Commissariat a l'Energie Atomique, Fontenay-aux-Roses (France). Centre d'Etudes Nucleaires). [1971]. 3p. (In French). (CONF-710527-2). Dep. NTIS (U. S. Sales Only).

From Physics conference; Evian, France (25 May 1971).

An experiment in which an extraordinary electromagnetic wave propagates through an inhomogeneous plasma in the presence of shear is discussed; under these conditions a coupling of the characteristic electromagnetic modes exists. (France)

**56226** (CEA-CONF-1804) SATURATION AND DAMPING OF ECHOES OF ELECTRON PLASMA WAVES. Guillemot, M.; Olivain, J.; Perceval, F.; Quemeneur, A. (Commissariat a l'Energie Atomique, Fontenay-aux-Roses (France). Centre d'Etudes Nucleaires); Matthieussent, G. (Paris Univ., Orsay (France). Laboratoire de Physique des Plasmas). [1970]. 3p. (In French). (CONF-710527-4). Dep. NTIS (U. S. Sales Only).

From Physics conference; Evian, France (25 May 1971).

When two strongly damped electron plasma waves are excited in two different points of a plasma, an electric field appears in a place where the mother waves have disappeared: this is the echo. Experimental results concerning the spatial behavior of the echo, the effect of Coulomb collisions, or the effect of an induced turbulence are in good agreement with theoretical predictions. (France)

**56227** (CEA-CONF-1805) INTERACTION OF A LARGE-AMPLITUDE WAVE WITH A PLASMA: TRAPPING. Guillemot, M.; Olivain, J.; Perceval, F.; Quemeneur, A. (Commissariat a l'Energie Atomique, Fontenay-aux-Roses (France). Centre d'Etudes Nucleaires). [1969]. 3p. (In French). (CONF-710527-5). Dep. NTIS (U. S. Sales Only).

From Physics conference; Evian, France (25 May 1971).

When an electron plasma wave propagates in a plasma, effects due to the trapping of particles in the wave well such as spatial oscillations of the wave and deformation of the distribution function appear. The experimental studies of the distribution function deformation are in good agreement with theoretical predictions obtained by solving exactly the Vlasov equation. (France)

**56228** (CEA-CONF-1806) ELECTROMAGNETIC INSTABILITIES IN A SLIGHTLY RELATIVISTIC PLASMA. Jacquinot, J.; Leloup, C. (Commissariat a l'Energie Atomique, Fontenay-aux-Roses (France). Centre d'Etudes Nucleaires). [1969]. 3p. (In French). (CONF-710527-6). Dep. NTIS (U. S. Sales Only).

From Physics conference; Evian, France (25 May 1971).

A solution of the relativistic dispersion relation for the electromagnetic modes with parallel propagation is given. The electron distribution function takes into account the presence of both a cold plasma and a hot anisotropic component with a loss cone. The relativistic contribution reduces strongly the growth rates for low-density cases even for rather low-energy plasmas. (France)

**56229** (EUR-CEA-FC-602) THEORETICAL AND EXPERIMENTAL STUDY OF NONLINEAR PROCESSES IN A PLASMA. Olivain, Jack (Commissariat a l'Energie Atomique, Fontenay-aux-Roses (France). Centre d'Etudes Nucleaires). May 1971. 167p. (In French). Dep. NTIS (U. S. Sales Only).

Thesis. Submitted to Paris Univ. (France). Faculte des Sciences.

High-frequency electrostatic oscillations in a plasma were studied by seeking a system of solution to the Vlasov equations. A perturbation technique was used, the magnitudes of the perturbations being expressed as a function of the amplitude of the electric potential. Under these conditions all oscillations may be represented by the superposition of Landau and Van Kampen solutions. A mechanism was studied in which two types of solution intervene in the oscillating current associated with the propagation of an electron plasma wave. Then, a process in which only the Landau mechanism intervenes, with a quasi-linear deformation of the distribution function is studied. Finally, the echo mechanism associated with the Van Kampen solution is considered. The three types of mechanism were studied experimentally in the plasma column of the EOS device; the results are compared with those obtained by theoretical analysis. (France)

**56230** (INR-1321) PENETRATION OF ELECTROMAGNETIC WAVE INTO THE PLASMA OF EXPONENTIAL DENSITY DISTRIBUTION. Legatowicz, Aleksander (Institute of Nuclear Research, Warsaw (Poland)). 1971. 10p. Dep. NTIS (U. S. Sales Only).

The problem of penetration of a plane electromagnetic wave into plasma of exponential density distribution is considered. The problem is investigated on the basis of the linearized Vlasov equation and the wave equation for the electric field. The solution has the form of a convergent exponential series in the variable $u = l^{(\omega/c)\mu x}$. The recurrence formulas for the series coefficients are given. (auth)

**56231** (N-71-25439) SOME LIMITATIONS ON ION-CYCLOTRON WAVE GENERATION AND SUBSEQUENT ION HEATING IN MAGNETIC BEACHES. Sigman, Donald R. (National Aeronautics and Space Administration, Cleveland, Ohio. Lewis Research Center). May 1971. 20p. (NASA-TM-X-2263). NTIS.

Thermal effects are included in the analysis of ion cyclotron

waves generated by a Stix coil. Peak-power coupling efficiency is reduced whenever ion or electron temperatures are sufficient for ion-cyclotron or Landau damping to occur. Because of the absorption of wave power under the coil, the wave power reaching an external magnetic beach is reduced. The effect of a Faraday shield on power coupling and wave damping, and the interference effects that arise when waves are reflected from the ends of the plasma column are also discussed. (auth) (STAR)

**56232** (NP-19020) EXCITATION OF LONGITUDINAL ELECTROMAGNETIC WAVES IN A BOUND PLASMA DURING INJECTION OF RELATIVISTIC ELECTRON BEAMS. Bogdankevich, L. S.; Rukhadze, A. A. (Akademiya Nauk SSSR, Moscow. Institut Fiziki). 1971. 24p. (In Russian). Dep. NTIS (U. S. Sales Only).

A detailed analysis is given of the character and conditions for excitation of longitudinal electromagnetic waves in a spatially bounded magneto-active plasma by a low-density relativistic electron beam. The increments of growth, the frequency spectra of plasma waves excited by the beam are determined. Nonlinear evaluations are given of the maximum amplitudes of steady-state oscillations. The results are discussed: (a) from the aspect of the possibility of using powerful relativistic electron beams to excite plasma waves of high amplitude and (b) using the example of probing the ionosphere of the earth with a relativistic electron beam of low density. (JPRS)

**56233** (ORO-3871-6) QUASISTATIC ION CYCLOTRON WAVE STUDIES. Progress Report. Swanson, D. G. (Texas Univ., Austin. Plasma Research Lab.). 31 Aug 1971. Contract AT(40-1)-3871. 15p. Dep. NTIS.

Theoretical progress was made in the study of damping of finite-amplitude waves. A technique was developed that is self-consistent and leads to an integral equation that was successfully solved by iteration on the CDC 6600 computer. Preliminary results show that the net damping is stronger than the original work indicated, but that there is still a finite amplitude steady-state solution for long times or far from the source. (M.O.W.)

**56234** OBSERVATIONS OF NONLINEAR LANDAU DAMPING OF ION-ACOUSTIC WAVES. Ikezi, H.; Kiwamoto, Y. (Nagoya Univ., Japan). Phys. Rev. Lett.; 27: No. 11, 718-21(13 Sep 1971).

Nonlinear Landau damping and growth were observed for ion-acoustic waves. The measured nonlinear wave–wave coupling coefficients are in reasonable agreement with theory. The forced beat oscillations between the two injected waves, which cause nonlinear Landau damping, were also observed. (auth)

**56235** EFFECT OF AN ELECTROMAGNETIC WAVE-FIELD PRESSURE ON THE PROPAGATION OF SLOW TM WAVES ALONG THE PLASMA LAYER. Demtchenko, V. V.; Hussein, A. M. (Atomic Energy Establishment, Cairo). Z. Phys.; 246: No. 3, 216-24(1971).

Slow electric-type waves are investigated when propagating along a plane plasma layer, taking into account the pressure of the high-frequency field of the wave. Expressions are obtained for the fields and the derived dispersion equations appreciably differ from those of linear theory. The high-frequency pressure is shown to ensure electromagnetic field penetration into the plasma, which is not brought about to a linear approximation (with no account of the high-frequency pressure) due to the skin effect. (auth)

**56236** PROPAGATION OF AN ELECTROMAGNETIC WAVE ACROSS A MAGNETIC FIELD IN A PARABOLIC PLASMA LAYER. Smilyanskii, V. R. Zh. Prikl. Mekh. Tekh. Fiz.; No. 3, 28-34 (May-Jun 1971). (In Russian).

The coefficients of reflection and penetration are obtained, as well as the coefficient of transformation of an electric wave into a plasma one. The selection of the "physical" path of the analytical continuation of the solution is examined in the case of a wave equation with two poles. (tr-auth)

**56237** PROPAGATION OF WEAK DISCONTINUITIES IN COLLISIONLESS PLASMA. Gopalakrishna, A. V. (Iowa State Univ., Ames). J. Math. Anal. Appl.; 35: No. 2, 349-60(Aug 1971).

A study was made of the growth characteristics of weak discontinuities propagating into a uniform collisionless plasma, at rest, on the basis of the full nonlinear equations using ray theory and singular surface theory. The growth equation governing the strength of the discontinuity is obtained and integrated completely in both the linear and nonlinear cases. (M.O.W.)

**56238** DAMPING OF LONGITUDINAL PLASMA OSCILLATIONS. Varma, N. L. (Univ. of Rajasthan, Jaipur, India); Khandpur, G. K. Z. Phys.; 246: No. 4, 295-301(1971).

Attenuation of electron oscillations in a fully ionized plasma is investigated by solving linearized equation without external fields. The general dispersion relation for longitudinal plasma oscillations is obtained using the BGK model. Damping due to electron ion collisions is obtained with a correction term. It is also observed that damping rate decreases as k increases, which is in agreement with McBride. (auth)

**56239** COORDINATE-INDEPENDENT DEFINITION OF POSITIVE AND NEGATIVE ENERGY WAVES IN PLASMA. Gratzl, H. (Univ., Innsbruck). Physica; 53: No. 3, 498-500(15 Jun 1971).

The conditions for positive or negative energy of plasma waves and for explosive instability are unchanged under Galilean transformations, if the wave energy is defined in accordance with the conservation laws. (auth)

**56240** PROPAGATION OF STRONG CYLINDRICAL AND SPHERICAL ELECTROMAGNETIC WAVES IN A PLASMA. Gurevich, Yu. G.; Pogrebnyak, V. A. (Kharkov State Univ.). Geomagn. Aeron. (USSR) (Engl. Transl.); 11: No. 1, 50-5(1971).
Translated from Geomagn. Aeron.; 11: No. 1, 65-71(1971).

Expressions are found for wave amplitude and electron temperature during propagation of strong cylindrical and spherical electromagnetic waves in a plasma. (auth)

**56241** CHERENKOV AND CYCLOTRON EXCITATION OF BERNSTEIN WAVES WITH ELECTRON BEAMS. Mizuno, K.; Sugaya, R.; Tanaka, S. (Kyoto Univ.). Phys. Lett.; 36A: No. 5, 441-2(27 Sep 1971).

Experimental results presented show the Cherenkov and cyclotron excitation of Bernstein waves coupled with the negative-energy modes of the spiraling electron beam. These waves are propagating obliquely to a static magnetic field and growing along the beam. (auth)

**56242** ELECTROSTATIC OSCILLATIONS IN COLD INHOMOGENEOUS PLASMA. PART 2. INTEGRAL EQUATION APPROACH. Sedlacek, Z. (Inst. of Plasma Physics, Prague). J. Plasma Phys.; 6: 187-99(Aug 1971).

Small-amplitude electrostatic oscillations in a cold plasma with continuously varying density were investigated. The treatment is based on an integro-differential equation for the transverse component of the electric field. This equation is very similar to the Vlasov equation, and this is shown to be the cause of the striking similarities between the two theories pointed out in Part 1. The normal-mode analysis utilizes the similarity of the integral equation for the eigenfunctions to the equation of anisotropic neutron transport. The continuum eigenfunctions are found in the form of a generalized van Kampen eigenmode, and their calculation is reduced to solving a nonsingular integral equation. Equivalence of the eigenfunctions found in this way and of those found by solving the equivalent differential equation is proved, and the question of orthogonality and normalization is discussed. (auth) (UK)

**56243** EFFECT OF IMPURITY IONS ON THE STABILITY OF DRIFT WAVES. Ong, R. S. B.; Yu, M. Y. (Univ. of Michigan, Ann Arbor). J. Plasma Phys.; 6: 201-9(Aug 1971).

The propagation and stability of ion and electron drift waves in a nonhomogeneous plasma containing impurity ions are considered. It is shown that the presence of impurities in the plasma may significantly affect the stability criteria of these low-frequency waves. Furthermore, perturbations at frequencies which are multiples of the impurity ion cyclotron frequency may also be unstable when $\frac{1}{2}k_y^2 R_I^2 > 1$. (auth) (UK)

**56244** EQUATIONS FOR NONLINEAR WAVE SOLUTIONS OF VLASOV AND POISSON EQUATIONS. Gribben, R. J. (Univ. of Strathclyde, Glasgow). J. Plasma Phys.; 6: 119-24(Aug 1971).

Butler and Gribben (1968) showed how to generalize nonlinear, uniform, wave-type solutions of the Vlasov–Poisson system of equations to allow for slow variations in the properties of the plasma. Here, one equation of the derived set (that obtained by ensuring that the appropriate solutions of the Poisson equation are non-secular) is rearranged (i) so as to bring out the physical importance of those particles, trapped and untrapped, travelling near the wave speed, and (ii) so as to yield a form particularly suited to the case when the electric field is small. (auth) (UK)

**56245** LAGRANGIAN APPROACH TO NONLINEAR WAVE INTERACTIONS IN A WARM PLASMA. Galloway, J. J.; Kim, H. (Stanford Univ., Calif.). J. Plasma Phys.; 6: 53-72(Aug 1971).

The coupled-mode equations and coupling coefficients for three-wave interactions are derived by a Lagrangian approach for a general medium. A derivation of the Low Lagrangian for a warm plasma is then given, which avoids certain problems associated with the original analysis. An application of the Lagrangian method is made to interaction between collinearly propagating electrostatic waves, and a coupling coefficient is derived which

XUM

agrees with a previous result obtained by direct expansion of the nonlinear equations. The paper serves primarily to present and demonstrate a conceptually useful and efficient theoretical approach to nonlinear wave interactions. (auth) (UK)

**56246** NONLINEAR COLLISIONLESS INTERACTION BETWEEN ELECTRON AND ION MODES IN INHOMOGENEOUS MAGNETOACTIVE PLASMAS. Booth, Newell Ormond. Los Angeles; Univ. of California (1971). 101p. University Microfilms Order No. 71-16,382.

Thesis.

A new method of excitation of electrostatic ion cyclotron (EIC) waves and drift waves by amplitude-modulating high-frequency waves in the quasi-transverse extraordinary (QTX) mode in an inhomogeneous magnetized plasma is presented. The QTX mode resonates at the upper hybrid frequency in the plasma and is cut off at the right-hand cutoff frequency. Excitation is observed at both frequencies. A theory of the excitation is proposed that contains coupling between electron and ion modes. The density gradient provides a localized excitation at the QTX resonance and cutoff which relaxes the usual $\bar{k}$ matching requirement of mode coupling. The other characteristic features of mode coupling are observed in the experiment. The density dependence of EIC wave excitation at the QTX resonance is measured and compares favorably with the theory. Feedback stabilization of the current-driven EIC wave by this method is reported. The inverse process is observed when an unstable EIC wave causes a modulation of the transmitted and reflected portion of an unmodulated microwave signal. This work is the first detailed study of coupling phenomena between electron and ion modes in a magnetized plasma. It essentially describes a new probeless technique for detecting, exciting, and stabilizing ion waves in fusion and space plasmas where the use of probes is not feasible. (Diss. Abstr. Int., B)

**56247** REFLECTION PROBLEMS IN KINETICALLY DESCRIBED PLASMA. Sakuda, Kyohei. New York, N. Y.; New York Univ. (1970). 173p. University Microfilms Order No. 71-18,535.

Thesis.

The reflection mechanism of the longitudinal wave in an inhomogeneous plasma due to an external static electric field is studied when an electron streaming beam is present and its direction is parallel with the external electric field. The reflection coefficient of the nonlocal effect is also calculated. The nonlocal reflection due to the presence of an electron streaming beam whose direction is perpendicular to the direction of the longitudinal wave is studied. It is obvious that the effect of an additional beam is very small, in other words, there is no synchronous region (or the resonant point) between the space charge wave and the plasma wave. The boundary problem at the interface between vacuum and plasma is studied. The plasma is one-component and homogeneous but anisotropic due to an external static magnetic field. Plasma is described by the linearized Vlasov equation. In order to obtain the field quantities, i.e., first-order electric field, magnetic field, and the velocity distribution function, the dyadic Green's function is first obtained, then by applying the completeness relationship, the complete set of eigenvectors is derived. Using the superposition, all first-order quantities are obtained in terms of the complete set of eigenvectors once the expansion coefficients are determined. The expansion coefficients are determined by the speculum assumption and the causality condition, or outgoing wave condition. (Diss. Abstr. Int., B)

**56248** KINETIC MODEL FOR AN INHOMOGENEOUS PLASMA. Heitowit, Ezra David. Ithaca, N. Y.; Cornell Univ. (1970). 150p. University Microfilms Order No. 71-17,643.

Thesis.

A consistent kinetic model is developed for investigating wave propagation in a fully ionized, inhomogeneous, low-pressure plasma with collisions. A Gross–Krook-type model is employed with arbitrary parameters determined by the method of Morse. The advantage of this kinetic model is that the collision terms satisfy conservation of energy as well as conservation of number density and momentum. (TSS) (Diss. Abstr. Int., B)

**56249** NOISE LEVELS OF LANGMUIR OSCILLATIONS IN A BEAM–PLASMA SYSTEM FROM STARK BROADENING OF HYDROGEN SPECTRAL LINES. Zakatov, L. P.; Plakhov, A. G.; Shapkin, V. V.; Sholin, G. V. (Inst. of Atomic Physics, Moscow). Dokl. Akad. Nauk SSSR: 198: No. 6, 1306-9(21 Jun 1971). (In Russian).

An experimental study was made of the Stark effect in a turbulent plasma with a high noise level of high-frequency Langmuir vibrations. The apparatus consisted of a vacuum chamber encased in coils that supplied the magnetic field and an electron beam and a plasma injector at opposite ends of the chamber. An interferometer and spectrograph were arranged to produce spectrochronograms of H$\alpha$ lines with a sweep time base of 200 $\mu$sec. Photometric measurements showed that H$\alpha$ line broadening was not observable in longitudinal observations; however, transverse observations revealed line broadening at Langmuir frequencies in the turbulent plasma. This is confirmation of the nonadiabatic character of the effect of the Langmuir vibrations on the radiating hydrogen atoms. (K.S.W.)

**56250** LINEAR TRANSFORMATION AND ABSORPTION OF A WAVE IN A PLASMA. Golant, V. E.; Piliya, A. D. (Physical-Technical Inst., Leningrad). Usp. Fiz. Nauk 104: No. 3, 413-57(Jul 1971). (In Russian).

Two linear mechanisms of collisionless absorption of a wave in a plasma exist — cyclotron attenuation and Landau damping — and are associated with radio waves in the ionosphere and emission from the Sun. Electromagnetic and plasma waves are theoretically examined, giving due attention to resonance excitation of plasma waves. Two sections are concerned with absorption in frequency bands between electron cyclotron and upper hybrid frequencies, and between electron cyclotron and lower hybrid frequencies, respectively. 115 references. (K.S.W.)

**56251** ION-ACOUSTIC INSTABILITY OF A TWO-TEMPERATURE, COLLISIONAL, FULLY IONIZED PLASMA. Rognlien, T. D.; Self, S. A. (Stanford Univ., Calif.). Phys. Rev. Lett.; 27: No. 12, 792-5(20 Sep 1971).

From a perturbation analysis of the fluid equations for a homogeneous, unmagnetized plasma it is shown that long-wavelength ion waves are unstable when $T_e \gtrsim T_i$. The additional destabilizing effect of a current is also investigated. (auth)

**56252** EFFECTS OF THE SHEATH AND THE DRIVING FIELD ON TONKS–DATTNER RESONANCE FREQUENCIES. Ramchandran, Shantakumari Thattat. College Station, Tex.; Texas A and M Univ. (1970). 76p. University Microfilms Order No. 71-17,830.

Thesis.

The results of a numerical experiment to study the effects of the sheath and the driving field on Tonks–Dattner resonance frequencies are presented. A one-dimensional, spatially-inhomogeneous plasma bounded by a sheath is numerically simulated and driven by an external oscillating electric field. The resulting currents are studied as a function of frequency. The results are compared with the previous investigations. Even though there is general agreement of the present results with that of the previous investigators, other significant observations are made. For example, oscillations can occur within the sheath depending on the strength of the driving field and several additional resonances are observed in the high frequency region. (Diss. Abstr. Int., B)

**56253** MAGNETOPLASMA WAVES IN STRONGLY CURVED CONFIGURATIONS. Martin, Jose Ginoris. Madison, Wis.; Univ. of Wisconsin (1971). 173p. University Microfilms Order No. 71-14,152.

Thesis.

For low-beta plasmas immersed in a magnetic field that has a purely transverse gradient, the conservation equations for particles or guiding centers yield a dispersion relation for electrostatic drift waves which explicitly includes the effect of curvature and "spread" in the plasma velocity spectrum. The analysis of this dispersion relation — which generates results obtained from other more complex models involving simultation under various limiting conditions — reveals the local stability of all configurations with very strong curvature and the peculiar behavior of the flute oscillations in the limit of infinite wavelength. For the interesting case of a plasma which is thermalized in the perpendicular component of velocity, the regions of temperature and density gradients that determine the behavior of the oscillations organize into a simple pattern. The pattern shows a region which is stable for plasmas with arbitrary dielectric constant, but strong temperature gradients may destabilize the plasma. Positive temperature gradients may lead to a single unstable mode which is not completely stabilized by finite gyroradius. For negative temperature gradients — unless the curvature is strong — there are two modes with phase velocities in the direction of the equilibrium drifts which do show the finite gyroradius stabilization effect. The stability criterion is in agreement with the minimum-B theorem, and some suggestive reports from the literature indicate that the behavior predicted by this analysis may have been observed since the earliest experiments. (Diss. Abstr. Int., B)

**56254** TRAVELLING WAVE ANTENNA FOR EXCITING WAVES IN A CYLINDRICAL, ANISOTROPIC PLASMA. Hipp, Jackie Ervin. Lubbock, Tex.; Texas Technological Univ. (1970). 79p. University Microfilms Order No. 71-17,898.

Thesis.

Several variations of a newly proposed device for exciting ion cyclotron waves in a magnetoplasma are analyzed theoretically and numerically. The results of this analysis are compared with those of a similar analysis of a Stix coil. The new coupler is composed of a set of identical helical straps driven by a multiphase rf source, and excites waves that vary asimuthally as $e^{jm\theta}$ where $m = \pm 1, \pm 2, \ldots$. The analysis reveals that the new coupler offers the following advantages over the Stix coil: (1) a certain degree of control over radial variations of accelerating fields, (2) a preferred direction of propagation, (3) more energy coupled into propagating waves (for a given input current), (4) maximum loading resistance at a higher plasma density, and (5) a slightly wider effective density range for propagating waves. (Diss. Abstr. Int., B)

## Shielding

*Refer also to abstracts 55233, 55676, 56362, 56617, 56618, 56621, 56625, 56845, 57026, 57133, 57153, and 57161.*

**56255** (AD–721388) RADIATION TRANSPORT STUDIES CARRIED OUT AT THE NATIONAL BUREAU OF STANDARDS WITH THE SUPPORT OF THE OFFICE OF NAVAL RESEARCH. Progress Report, July 1, 1970–February 15, 1971. Berger, M. J.; Eisenhauer, C. M.; Seltzer, S. M.; Simmons, G. L.; Spencer, L. V. (National Bureau of Standards, Washington, D. C.). 1 Mar 1971. Contract NAonr-4-71. 60p. (NBS–10550). NTIS.

Research on the following topics is described: on the accuracy of transport calculations using moment methods; improved moment-method calculations of gamma-ray transport: application to point isotropic sources in water; poly-series approximation of functions; neutron dose in air from a point-isotropic fission source; improvement in computer program to generate neutron flux moments; response of NaI detectors to high-energy gamma rays; and absorbed dose near an interface between two media. (auth) (USGRDR)

**56256** (AD–722012) SOME CALCULATIONS ON THE TRANSMISSION OF GAMMA RADIATION THROUGH HOMOGENEOUS SLABS. Final Report. Huddleston, Charles M. (Naval Ordnance Lab., White Oak, Md.). 1 Nov 1970. Contract DAHC20-70-C-0295. 57p. (NOLTR–70–222). NTIS.

An empirical formula was fitted to Monte Carlo values for the angular distribution of exposure due to gamma rays scattered through plane, concrete slabs of moderate thicknesses when one face of the slab is illuminated by a broad parallel beam of monochromatic radiation. (auth) (USGRDR)

**56257** (CO–2049–8) ORDERS-OF-SCATTERING CALCULATION FOR THE REFLECTION OF COLLIMATED, POLYENERGETIC FAST NEUTRONS FROM A SIX-INCH-THICK STEEL SLAB. Thiesing, James W.; Meyer, Walter (Kansas State Univ., Manhattan, Dept. of Nuclear Engineering). 1 Jun 1971. Contract AT(11-1)-2049. 21p. Dep. NTIS.

The orders-of-scattering approach to fast-neutron transport in slabs was evaluated for use in reflection calculations in the energy range 1 to 10 MeV. The geometry studied was that of a pencil beam of polyenergetic fast neutrons incident on an infinite slab with a detector located at a given position with respect to the incident beam and the slab orientation. Experiments and orders-of-scattering calculations (up to 2 scatterings) were carried out for normally incident beams on a 15.24 cm. thick steel slab with the detector located 167.64 cm from the point where the beam entered the slab. Two combinations of the angles determining the detector position were studied. The results of these calculations are discussed. A slab penetration experiment was carried out and compared with orders-of-scattering calculations to define precisely the number of neutrons incident on the slab and thus allow absolute comparison of experimental results and calculations. The cross sections used in the orders-of-scattering calculations were the DLC-2 grouped cross section set taken from the ENDF/B cross section library. (M.H.R.)

**56258** (COO–2049–9) ORDERS-OF-SCATTERING METHOD FOR FAST-NEUTRON TRANSPORT. Thiesing, J. W.; Meyer, Walter (Kansas State Univ., Manhattan, Dept. of Nuclear Engineering). 25 Aug 1971. Contract AT(11-1)-2049. 147p. Dep. NTIS.

The development of the orders-of-scattering technique for fast-neutron transport and an investigation into the utility of the orders-of-scattering technique for the prediction of the penetration and reflection of fast neutrons are reported. (M.H.R.)

**56259** (EGG–1183-1479) COHERENT AND INCOHERENT X-RAY SCATTERING FACTORS FOR THREE- AND FOUR-ELECTRON ATOMS. Tech. Report L-988. Brown, Robert T. (EG and G, Inc., Las Vegas, Nev.). 17 Apr 1970. 32p. Dep. NTIS.

Atomic form factors and incoherent scattering functions for the lithium and beryllium isoelectronic sequence through Z = 8 have been calculated with correlated ground-state wave functions. The form factors differ from Hartree–Fock values by one to two percent and differ from Hartree–Slater values by as much as ten percent. The incoherent scattering functions are much more dependent on correlation, with the values for neutral beryllium differing from the Hartree–Fock values by as much as thirty percent at very small values of the momentum transfer. (auth)

**56260** (EGG–1183-2284) MONTE CARLO TRANSPORT ANALYSIS FOR FINITE GROUND-DISTRIBUTED GAMMA SOURCES. O'Dell, A. A.; Harris, N. A. ([EG and G, Inc., Goleta, Calif.]). [nd]. 11p. (CONF-711009-7). Dep. NTIS.

From Joint meeting of the American Nuclear Society; Miami, Fla. (17 Oct 1971).

An outline for an oral presentation and the figures for it are presented. (M.H.R.)

**56261** (LA–4774) TWO-DIMENSIONAL AIR TRANSPORT CALCULATIONS. Lathrop, K. D. (Los Alamos Scientific Lab., N. Mex.). Sep 1971. Contract W-7405-eng-36. 4p. Dep. NTIS.

Modifications made to the TWOTRAN SPHERE discrete ordinates program and the ANDYMG3 Monte Carlo program to permit the calculation of the transport of particles from an anisotropic point source in air are described. Comparison of scalar fluxes calculated by the two programs is made in a production-type calculation involving 15 energy groups and P3 anisotropic scattering. Excellent agreement is obtained. (auth)

**56262** (N–71-22378) COHORT 2: A MONTE CARLO GENERAL PURPOSE SHIELDING COMPUTER CODE. Soffer, Leonard; Clemons, Lester Jr. (National Aeronautics and Space Administration, Cleveland, Ohio. Lewis Research Center). Apr 1971. 79p. (NASA-TN-D–6170). NTIS.

COHORT-2 is a Monte Carlo general purpose shielding computer program written completely in FORTRAN-4 for the IBM-7094 computer. In its present form, it represents a major revision and modernization of the original COHORT code. It has been integrated into a single package with more flexible geometry and biasing. The code method employed is the conventional one where individual particles are generated, tracked, and analyzed. The shielding geometry allowed is flexible with space divided into homogeneous regions bounded by surfaces describable by a general quadratic equation. Spherical, cylindrical, and rectangular parallelepipeds are allowed for the source particles from preferred locations energies and directions. The exponential transform can also be used during particle tracking. Secondary gammas can be generated and placed on tape during a neutron problem to be tracked during a subsequent computer run. Output includes number fluxes in energy bins at arbitrarily located point detectors and averaged over regions. Energy integrated quantities such as dose rates are also obtainable. (auth) (STAR)

**56263** (ORNL–4716) MORSEC: A REVISED CROSS-SECTION MODULE FOR THE MORSE MULTIGROUP MONTE CARLO CODE. Straker, E. A.; Emmett, M. B. (Oak Ridge National Lab., Tenn.). Aug 1971. Contract W-7405-eng-26. 42p. Dep. NTIS.

The cross-section module for the MORSE neutron and gamma-ray Monte Carlo transport code has been revised to treat upscattering, point total, scattering, and fission cross sections and to output a processed cross-section tape for use on subsequent problems. Several other minor changes in the logic have also been made to improve the overall capabilities of the code. (auth)

**56264** (ORNL-TM–3553) CONVERGENCE OF THE DISCRETE ORDINATES METHOD FOR ANISOTROPICALLY SCATTERING MULTIPLYING PARTICLES IN A SUBCRITICAL SLAB. Nelson, Paul Jr. (Oak Ridge National Lab., Tenn.). Sep 1971. Contract W-7405-eng-26. 11p. Dep. NTIS.

For steady-state transport of particles in a subcritical slab with arbitrary sources, it is shown that the continuous-space discrete ordinates approximation converges to the exact solution. This result is established for a spatially inhomogeneous slab and for a general class of scattering laws and quadrature rules. (auth)

**56265** (ORNL-tr–2518) SIMULATION OF AN ELECTRON AVALANCHE IN HELIUM BY A MONTE CARLO TYPE CALCULATION. Denes, Jean-Francois (Toulouse Univ. (France)). Translated for Oak Ridge National Lab., Tenn., from report NP–18798. 73p. Dep. NTIS.

XUM

An abstract of this paper, prepared from the original language, appeared as NSA 25: 30629. (M.O.W.)

**56266** (UCRL–51065) STIMULATED COMPTON ENERGY EXCHANGE RATE. Grasberger, William (California Univ., Livermore. Lawrence Radiation Lab.). 8 Jun 1971. Contract W-7405-eng-48. 30p. Dep. NTIS.

The stimulated Compton exchange rate between photons and free electrons with an isotropic velocity distribution is considered. Numerical results are obtained for electron temperatures between 0.1 and 10 keV and light beams with uniform intensities within cones of half-angles of 1, 5, 10, and 15° assuming square-shaped and Gaussian frequency profiles of various widths for a central frequency of 1.17 eV. Comparisons of these results with the inverse bremsstrahlung heating rate indicate the need for extremely high intensities for stimulated Compton to be competitive. (auth)

**56267** TABLITSY DLYA RASCHETA NESTATSIONARNYKH TEMPERATUR PLOSKIKH TEL PRI NAGREVE IZLUCHENIYAMI. (Tables for Calculating Nonstationary Temperatures of Plane Bodies During Heating by Irradiation). Grigor'ev, B. A.; Nuzhnyi, V. A.; Shibanov, B. V. Moscow; Izdatel'stvo Nauka (1971). 708p.

Tables are presented for the calculation of nonstationary temperatures of infinite plates and semi-finite bodies during pulsed and continuous heating by various radiations: photons, neutrons, or electrons. Dimensionless temperatures on the irradiated surface are tabulated for a long span of time and within the body at the moment the surface temperature reaches a maximum. An accuracy of four significant figures is claimed. The tables are suitable for internal and surface absorption calculations for the various radiations. Methods of interpolation and superposition are described in detail, and exemplary calculations are included. (K.S.W.)

**56268** MONTE CARLO METHOD OF CALCULATING THE GAMMA RADIATION FIELD IN A STATISTICALLY INHOMOGENEOUS MEDIUM. Kol'chuzhkin, A. M.; Uchaikin, V. V. (Tomsk Polytechnic Inst., USSR). Izv. Vyssh. Ucheb. Zaved., Fiz.; No. 3, 65-8(1971). (In Russian).

The Monte Carlo method is one of the most effective methods of calculating the gamma radiation field with a complex geometry. An example of the use of a Monte Carlo algorithm is worked out for the case of inhomogeneity, based on perturbation theory. (tr-auth)

**56269** RANGES OF RECOIL ATOMS FROM THE (n,γ) PROCESS. Pierson, William R.; Kummer, Joseph T.; Brachaczek, Wanda (Ford Motor Co., Dearborn, Mich.). Phys. Rev., B; 4: No. 9, 2846-53(1 Nov 1971).

Ranges of $^{198}$Au (estimated average energy 50 eV) recoiling from neutron capture in gold film surfaces have been estimated in deuterium, helium, neon, argon, and xenon by measuring the yield on a collector as a function of gas pressure. These ranges are 0.3, 0.54, 1.1, 0.8, and 1.2 μg/cm$^2$, respectively. From the shape of the curve of recoil yield vs pressure in helium, the range is inferred to be largely independent of energy; this contrasts with the strong dependence known to hold at higher energies. A simple model such as that used for neutron thermalization reproduces the magnitudes and trends of the ranges reasonably well. (auth)

**56270** ANALYTICALLY SOLVABLE PROBLEMS IN RADIATIVE TRANSFER. III. van Trigt, C. (Philips Research Labs., Eindhoven, Netherlands). Phys. Rev., A; 4: No. 3, 1303-16(Sep 1971).

The density of excited atoms and the diffusely re-emitted radiation is calculated for a homogeneous radiation field incident on a slab. The solutions of the Biberman–Holstein integral equation are used in the calculations. The optical thickness is assumed to be large. The line shapes of both the absorption line and the incident radiation are arbitrary. (auth)

**56271** SOLRF: A PROGRAM FOR APPROXIMATION COMPUTATION OF NEUTRON INTERACTION ACCORDING TO THE SOLID ANGLE METHOD OF SPACING. Thomas, W. (Laboratorium fuer Reaktorregelung und Anlagensicherung, Garching, Ger.). Atomwirt., Atomtech.; 16: No. 8-9, 435-6(Aug-Sep 1971). (In German).

The computer program SOLRF is applicable to the following container geometries: rectangular plates, circular plates, and cylinders in a Cartesian coordinate system as well as to spheres. Generally, the computer program yields conservative values as shown by numerous calculations of experimental criticality tests on uranium with various degrees of enrichment and configuration. In the important subcritical region, the program also leads to somewhat conservative results as shown by comparison with a Monte Carlo method. (H.B.G.)

**56272** ENERGY AND ANGULAR DISTRIBUTIONS OF $^{60}$Co GAMMA RAYS PENETRATING A CONCRETE SHIELD. Rubin, R. M.; Faw, R. E.; Coolbaugh, M. J.; Royer, J. M. (Kansas State Univ., Manhattan). Nucl. Eng. Des.; 16: No. 4, 429-43(1971).

The energy and angular spectra of gamma radiation penetrating a 48 ± 1 psf vertical slab bounding a simulated semi-infinite plane radiation source were measured. Representative results are given for the gamma-ray flux density $\Phi(E, \cos\theta, \phi)$ which is differential with respect to energy and direction, in units (cm$^{-2}$ sec$^{-1}$ sr$^{-1}$ keV$^{-1}$) normalized to a $^{60}$Co source strength of 1 Ci/ft$^2$. The exposure angular distribution, $D(\theta,\phi)$ in units (R hr$^{-1}$ sr$^{-1}$) normalized to a $^{60}$Co source strength of 1 Ci/ft$^2$ for each of 40 directions is also given. All measurements were made at a height of 3 ft above grade. (auth)

**56273** THREE-DIMENSIONAL STOCHASTIC GAMMA-RAY TRANSPORT METHOD FOR SHIELDING CALCULATIONS. Razani, Arsalan (Pahlavi Univ., Shiraz, Iran); Hungerford, H. E. Nucl. Sci. Eng.; 46: No. 1, 1-11(Oct 1971).

A new probabilistic formulation and development of a model for the investigation of three-dimensional gamma-ray transport problems are examined. This model assumes that gamma-ray motion may be sampled at predetermined points. A medium is considered to be filled with a cubic lattice whose unit distance between lattice points may be some fraction of the mean-free-path. The random walk of gamma rays from one point to another is constructed using the lattice framework as reference points. Using this model, a new type of stochastic gamma-ray transport code, PUGT I (Purdue University Gamma Ray Transport I), was developed, based on direct simulation of physical transport process. In another version of the code (PUGT II), capture of gamma rays is taken into account analytically by associating a weight factor to the gamma rays. The codes are used to calculate the transmission and reflection characteristics of gamma rays for different thicknesses of slabs of aluminum and iron. The contribution of annihilation radiation to reflection and transmission is investigated. The results of the calculations are in good agreement with other similar calculations and with experimental results. Gamma-ray streaming through two-legged rectangular concrete ducts was investigated. Results of these studies are in very good agreement with experimental results and demonstrate the ability of the codes and the power of the lattice model to calculate quickly and efficiently the transmission of gamma rays in three-dimensional complex shielding geometries. The method is several times faster than ordinary Monte Carlo. (auth)

**56274** MONTE CARLO CALCULATION OF THE EFFECT OF SUBTERRANEAN PERTURBATIONS ON REFLECTED X RAYS. Coleman, W. A. (Army Aberdeen Research and Development Center, Aberdeen Proving Ground, Md.). Nucl. Sci. Eng.; 46: No. 1, 12-21(Oct 1971).

Monte Carlo calculations for monoenergetic x rays (70 to 200 keV) normally incident on soil were performed to determine changes in the reflected radiation due to material perturbations at depths of 1 and 1.6 mean-free-paths. The accuracy of the calculations was achieved using a scheme of correlated sampling in which a complete correlation is maintained in the sense that identical sampled event sequences are used for the perturbed and unperturbed problem. A somewhat general discussion of correlated sampling is included with emphasis on the mathematical reasons for employing the method. It is shown for a special case that a naive use of correlated sampling may lead to results drastically inferior to those obtained by independent sampling. The Monte Carlo calculations are compared with two-dimensional discrete ordinates results and agreement is very good. Output quantities are reported in terms of energy-dependent fluence and current. The calculated results demonstrate the feasibility of the approach to albedo-sensitivity problems in general. (auth)

**56275** EXACT SCREENED CALCULATIONS OF ATOMIC-FIELD PAIR PRODUCTION AND LOW-ENERGY SCREENING. Tseng, H. K.; Pratt, R. H. (Univ. of Pittsburgh). Phys. Rev., A; 4: No. 5, 1835-43(Nov 1971).

A discussion of relativistic-pair-production cross sections is given for incident-photon energies in the range 1.073 to 2.615 MeV. Cross sections are obtained numerically for a screened potential, using an exact partial-wave formulation. Comparisons are made with previous results. For low photon energies the effect of atomic-electron screening on pair-production cross sections is significant. The screening increases the cross section, since the atomic electrons decrease the nuclear Coulomb repulsion of the positron. Comparisons of screened with unscreened results show that angular distributions are essentially unaffected in shape by the screening; cross sections are simply renormalized by replacing $|N_+N_-|^2$ in the point-Coulomb field by $|N_+N_-|^2$ in the screened field, where $N_\pm$ are the normalizations of the positron and electron wave functions at the origin. (auth)

**56276** RANGE–ENERGY RELATIONS FOR HELIUM IONS AND PROTONS IN Ar, $N_2$, $O_2$, AND AIR (0.2 TO 2.0 MeV). Langley, Robert A. (Sandia Labs., Albuquerque, N. Mex.). Phys. Rev., A; 4: No. 5, 1868-72(Nov 1971).

The ionization extrapolated ranges of $H^+$ and $He^+$ in Ar, $N_2$, $O_2$, and air were measured from 200 keV to 2.0 MeV with an accuracy of ±1%. A magnetically analyzed beam of ions was brought through a differential pumping system into a gas stopping cell. A single-grid ionization chamber, movable parallel to the beam axis, was used to obtain the data necessary to plot a Bragg curve. The observed range–energy relations are compared with previous data where possible. (auth)

**56277** SECONDARY GAMMA-RADIATION IN SHIELDING. Goryachev, I. V.; Kolevatov, Yu. I.; Kukhtevich, I. V. At. Energ. (USSR); 31: No. 3, 209-14(Sep 1971). (In Russian).

Spectral and angular characteristics of secondary gamma radiation from titanium, lead, water, concrete and iron were experimentally investigated. In these experiments the wide collimated initial neutron beam from a nuclear reactor bombarded the surfaces of barriers with various angles of incidence. (auth)

**56278** QUADRATURE VARIATIONS IN DISCRETE ORDINATES CALCULATIONS. Sullivan, Robert Emmett. Norman, Okla.; Univ. of Oklahoma (1971). 129p. University Microfilms Order No. 71-17,057.

Thesis.

Methods for circumventing certain limitations concerning application of the discrete-ordinates approximation to the linear Boltzmann transport equation are investigated. One method introduced is the decoupling of the discrete-ordinates angular quadratures in order to reduce preferential transmission along the ordinates (the ray effect). This technique is shown to be partially effective and the extent of the improvement is determined for both the homogeneous (eigenvalue) and inhomogeneous cases. Some features of other proposed methods for reducing or eliminating the ray effect are discussed, and the conclusion is reached that only the use of higher-order angular quadratures can yield acceptable accuracy in the general case. Several methods are then presented for reducing calculational effort and accelerating convergence in cases requiring higher-order quadratures. These methods may be used in conjunction with either the spatial or angular quadratures of the discrete-ordinates approximation. The principle involved is, in general, that of varying the quadrature orders during the course of the calculation. Some more general test cases are studied and the methods are shown to significantly reduce the effort required to obtain solutions identical to those of the standard approximation. The application of these quadrature variations is also studied to determine the optimum manner in which to approach convergency. Finally, a device for expanding scattering matrices is derived and some analytically soluble test cases are introduced. It is then shown that the discrete-ordinates approximation, using the methods developed, yields solutions which approach the analytic as the quadrature orders are increased. (Diss. Abstr. Int., B)

**56279** ENERGY LOSS AND STRAGGLING OF ALPHA PARTICLES IN A TISSUE-EQUIVALENT GAS. Haque, A. K. M. M. (Borough Polytechnic, London). pp 33.1-7 of Computational Physics. Vols. I and II. London; Her Majesty's Stationery Office (1969).

From Conference on computational physics; Culham, England (28 Jul 1969). See CONF-690706-(Vols.1 and 2).

A silicon detector was used to measure the residual alpha-particle energy after its passage through tissue-equivalent gas. From the pulse-height analysis, Gaussian energies and their polynomial fit were obtained. Straggling parameter I, $z^2_{eff}$ and $\Sigma(Ci/Z)$ were calculated from the computed stopping cross section. L(x) and $S_e$ of Lindhard and Scharff (1953) theories were also found. (auth) (UK)

**56280** DEPENDENCE OF BUILDUP FACTOR ON THE POSITION OF SHIELDING BETWEEN BREMSSTRAHLUNG SOURCE AND DETECTOR. Kovalev, V. P.; Kharin, V. P.; Gordeev, V. V.; Filipenok, S. P. At. Energ. (USSR); 30: No. 4, 396-7(Apr 1971). (In Russian).

A change of the position of the shield between the source and the detector results in changes in the incident scattered radiation and thus in the buildup factor. Results of the measurement of the dose on the position of the shield between a bremsstrahlung source and the detector are presented for electron energies of 12.5, 15.7, and 21.8 MeV. The experiment was carried out with a linear electron accelerator, using tungsten targets, aluminum, copper, and lead shields and an ionization chamber as detector placed at a distance of 1 m from the target. The highest buildup factor was obtained at the lowest electron energy of 12.5 MeV when the shield was placed against the target; the factor decreased as the electron energy increased. Increasing the diameter of the shield resulted in an increase of the buildup factor. Similar results were obtained with copper and lead shields; the buildup factor was not noticeably affected by the atomic number of the material of the shield. (TTT)

**56281** MEASUREMENT OF THE MEAN FREE PATH OF FAST ELECTRONS. Vlasov, A. N.; Kabanov, A. N.; Kurbatov, L. N.; (and others). Fiz. Khim. Obrab. Mater.; No. 3, 20-3 (May-Jun 1971). (In Russian).

The absorption in aluminum and Permalloy of 35- to 110-keV electrons was studied by the foil method under conditions resembling electron beam micro-working. The radiation intensity in these experiments reached 3 to $5 \times 10^{11}$ vt/m$^2$, and the pulse duration was 30 nsec. Path distribution data were obtained as well as maximum path of the electrons. The values of the latter satisfied W. F. Libby's formula. The maximum path might serve as a criterion for choosing the magnitude of the accelerating voltage for working thin films. (tr-auth)

# Solid-State Physics

## *Radiation Effects*

*Refer also to abstracts 55102 and 55103.*

**56282** (CEA-CONF-1822) ELECTRONIC AND MAGNETIC PROPERTIES OF CARBON FIBERS: DEVELOPMENT UNDER NEUTRON IRRADIATION. Rappeneau, J.; Micaud, G.; Drouet, A. (Commissariat a l'Energie Atomique, Saclay (France). Centre d'Etudes Nucleaires); Pacault, A.; Marchand, A.; Dupart, E. (Domaine Universitaire, Talence (France). Centre de Recherches Paul Pascal). [1970]. 22p. (In French). (CONF-710612-4). Dep. NTIS (U. S. Sales Only).

From tenth biennial conference on carbon; Bethlehem, Pa. (27 Jun 1971).

Methods were developed for the measurement of the electric resistivity and the diamagnetic anisotropy of carbon fibers, between 77 and 300°K. Two types of fibers were studied: the RIGILOR AC fibers treated at 1100°C and the RIGILOR AG fibers at 2500°C. The measurements of electric resistivity performed on single fibers show a correlation between this property and the section of the fiber. Those of diamagnetism carried out on bundles of fibers demonstrate a large anisotropy of the fibers. The effect of neutron irradiation on these fiber properties was studied at room temperature and at small irradiation doses. (auth)

**56283** (CEA-CONF-1823) THERMAL ANNEALING OF NEUTRON-IRRADIATED CARBON. DEVELOPMENT OF ELECTRONIC PROPERTIES. Pacault, A.; Marchand, A.; Amiell, J.; Dupart, E. (Domaine Universitaire, Talence (France). Centre de Recherches Paul Pascal); Rappeneau, J.; Micaud, G.; Wlodarsky, R. (Commissariat a l'Energie Atomique, Saclay (France). Centre d'Etudes Nucleaires). [1970]. 24p. (In French). (CONF-710612-3). Dep. NTIS (U. S. Sales Only).

From tenth biennial conference on carbon; Bethlehem, Pa. (27 Jun 1971).

Results of a study on the electronic properties of carbons after neutron irradiation are presented. The carbon specimens were thermally annealed and the resulting variation in their electronic properties (electrical resistivity, Hall effect, magnetoresistivity, magnetic susceptibility) were determined. Similar behavior found in oriented graphite and nuclear graphite have been observed. The pyrocarbon, which is damaged the most, recovers its initial properties with the most difficulty; however, the damage does not affect the eventual behavior during graphitization. (auth)

**56284** (JUL-731-FF) INFLUENCE OF FOREIGN ATOMS ON THE RECOVERY OF FRENKEL DEFECTS IN ELECTRON-IRRADIATED PLATINUM. Dibbert, Hans-Juergen (Kernforschungsanlage, Juelich (West Germany). Institut fuer Festkoerperforschung). Feb 1971. 66p. (In German). Dep. NTIS (U. S. Sales Only).

Pure platinum samples and samples doped with various concentrations of Au atoms were irradiated at 4.5°K with electrons at low doses and an isochronous recovery program was undertaken. The experimentally determined pattern of the recovery in the $I_D$ stage of the pure Pt samples was compared with the theoretical curves in which the time behavior of the correlated interstitial atom–vacancy recombination was calculated for various initial distributions of the interstitial atoms around the vacancy. A good agreement of the experimental results with that calculated for a $\delta$ distribution was found. It was observed that, with increasing Au doping, the total recovery in the $I_D$ stage

XUM

decreases. With increasing Au doping, these interstitial atoms were increasingly captured on the Au atoms, which were recombined in the pure material with their vacancies (correlated). The experimentally determined dependence of the total recovery in the $I_D$ stage of the gold concentration was compared with the Schroeder theory for one- and three-dimensional diffusion. The experimental results agree very well with the theory for three-dimensional diffusion. From the comparison with the theoretical recovery curve, the degrees of capture of the vacancy and of the Au atoms for freely diffusing interstitial atoms were determined. The model, which assumes a one-dimensional diffusion (crowdion diffusion) of the interstitial atoms, can not explain the experimental results on the gold-doped samples. (tr-auth)

**56285** (SC-RR-710424) ION IMPLANTATION DAMAGE STUDY USING LATERAL STRESS MEASUREMENTS. EerNisse, E. P. (Sandia Labs., Albuquerque, N. Mex.). Jul 1971. 43p. Dep. NTIS.

The stress set up lateral to the implanted surface by ion implantation lattice damage is measured for 220-keV $^{4}He$, $^{12}C$, $^{16}O$, $^{20}Ne$, $^{27}Al$, $^{40}Ar$, $^{84}Kr$, and Xe room-temperature implants into Si. It is found that the ions with atomic number greater than Si produce more damage per given energy density deposited into atomic processes $\epsilon$ than the lighter ions and produce damage almost linearly with $\epsilon$ up to a distinct maximum in the stress. The measurements from $^{4}He$, $^{12}C$, $^{16}O$, $^{20}Ne$, and $^{27}Al$ implants are indistinguishable from one another at low $\epsilon$ values where the damage depends linearly upon $\epsilon$. These lighter ions show a region at somewhat higher $\epsilon$ where damage is introduced sublinearly with $\epsilon$. The reactive ions $^{12}C$, $^{16}O$, and $^{27}Al$ apparently react strongly with lattice damage left from earlier arriving ions at high $\epsilon$ values and produce behavior quite different from that observed for the noble-ion implants at high $\epsilon$ values. The maximum in the stress versus $\epsilon$ results is taken as evidence for an elastic–plastic transition in the implanted layer. This elastic–plastic transition correlates with the beginning of the so-called crystalline-to-amorphous transition of the implanted layer as observed by other techniques. A dose rate dependence of the transition ion fluence is observed. (auth)

**56286** PHYSICAL PROPERTIES OF RADIATION-INDUCED AND GROWTH DEFECTS IN II–VI SEMICONDUCTORS. Williams, P. M.; Yoffe, A. D. (Cambridge Univ., Eng.). Radiat. Eff.; 9: No. 1-2, 139-44(May 1971). (CONF-700824-19).

From International conference on radiation effects and semiconductors; Albany, N. Y. (24 Aug 1970).

Defects in wurtzite single crystals of ZnS, ZnSe, and CdS were observed by means of both scanning and transmission electron microscopy. Application of the scanning technique to the observation of cathodoluminescence in these materials has demonstrated localized effects on the emission close to twin boundaries and stacking faults in the as-grown crystals, which may be interpreted in terms of changes in band gap at the defect. This method was also applied to heavy ion-bombarded crystals; in addition, transmission electron microscope studies were made of these irradiated samples and the annealing behavior of the radiation damage was observed. Finally, in-situ optical absorption experiments were carried out on samples irradiated at liquid nitrogen temperature, and effects on the characteristic exciton absorption were noted. (auth)

**56287** MEASUREMENT OF LATTICE DAMAGE CAUSED BY ION-IMPLANTATION DOPING OF SEMICONDUCTORS. Hunsperger, R. G.; Wolf, E. D.; Shifrin, G. A.; Marsh, O. J.; Jamba, D. M. (Hughes Research Labs., Malibu, Calif.). Radiat. Eff.; 9: No. 1-2, 133-8(May 1971). (CONF-700824-18).

From International conference on radiation effects and semiconductors; Albany, N. Y. (24 Aug 1970).

Two new techniques were used to measure the lattice damage produced in gallium arsenide by the implantation of 60-keV cadmium ions. In one of these methods, optical reflection spectra of the ion-implanted samples were measured in the wavelength range from 2000 to 4600 Å. The decrease in reflectivity resulting from ion implantation was used to determine the relative amount of lattice damage as a function of ion dose. The second technique employed the scanning electron microscope. Patterns very similar in appearance to Kikuchi electron-diffraction patterns are obtained when the secondary and/or backscattered electron intensity is displayed in the scanning electron microscope as a function of the angle of incidence of the electron beam on a single-crystal surface. The degradation of these "Coates–Kikuchi" patterns resulting from ion implantation was used to obtain a quantitative measure of the lattice damage caused by the implantation process. The results of measurements made by both of the methods described are compared with each other, and with data obtained by the more established method of measuring lattice damage by Rutherford scattering of 1-MeV helium ions. (auth)

**56288** ION IMPLANTATION OF SULFUR INTO GaAs, GaP, AND Ge MONOCRYSTALS. Whitton, J. L.; Bellavance, G. R. (Atomic Energy of Canada Ltd., Chalk River, Ont.). Radiat. Eff.; 9: No. 1-2, 127-31(May 1971). (CONF-700824-17).

From International conference on radiation effects and semiconductors; Albany, N. Y. (24 Aug 1970).

The possibility of using ion implantation to form high-concentration junctions in semiconductors was explored for the specific case of sulfur in GaAs, GaP, and Ge. The effects of ion dose, ion energy, crystal orientation, and target temperature were investigated by means of radio tracers and sectioning techniques. It is shown that high-concentration junctions can be formed using an incident ion having high electronic stopping cross section and implanted along the ⟨110⟩ channeling directions of the crystals. A large increase in junction concentration may be obtained when the GaAs and GaP crystals are maintained at 150°C during the implantation process, but this is not the case with Ge. Rutherford backscattering of 1-MeV $He^{+}$ ions was used to measure the ion-bombardment-induced damage in the crystals and to show how this damage can be annealed by heating the crystal during the implantation. The annealing, at temperatures up to 150°C, is most effective in GaAs and least effective in Ge. (auth)

**56289** LOW-TEMPERATURE CHANNELING MEASUREMENTS OF ION-IMPLANTATION LATTICE DISORDER IN GaAs. Weisenberger, W. H.; Picraux, S. T.; Vook, F. L. (Sandia Labs., Albuquerque, N. Mex.). Radiat. Eff.; 9: No. 1-2, 121-5(May 1971). (CONF-700824-16).

From International conference on radiation effects and semiconductors; Albany, N. Y. (24 Aug 1970).

Lattice disorder resulting from 140-keV Zn and 151-keV Xe implantations below 100°K was studied by channeling-effect analysis using 400-keV protons. Implantations and analyses were performed in the same system without warmup. Isochronal anneal curves show significant annealing of disorder below room temperature for low-temperature, low-fluence implants. The annealing is similar for both Zn and Xe implants and also is similar to previous measurements of the annealing of thermal conductivity following low-temperature electron irradiation. For 298°K implants, the disorder production is strongly dose-rate-dependent and increases significantly with increasing dose rate. For dose rates used in these measurements, the disorder production at 298°K was greatly reduced from that for the low-temperature implantations. (auth)

**56290** ELECTRON RADIATION DAMAGE AND EDGE EMISSION OF CADMIUM TELLURIDE. Bryant, F. J.; Totterdell, D. H. J. (Univ. of Hull, Eng.). Radiat. Eff.; 9: No. 1-2, 115-20(May 1971). (CONF-700824-15).

From International conference on radiation effects and semiconductors; Albany, N. Y. (24 Aug 1970).

The cathodoluminescence edge emission of cadmium telluride at 4.2°K was observed, (a) before and after displacement of cadmium atoms or displacement of cadmium and tellurium atoms by monoenergetic electrons, and (b) firing in vacuum or an overpressure of the cation. The intensities of emission bands occurring at 1.555, 1.572, and 1.588 eV are enhanced by cadmium displacement, and the defect centers responsible for these emissions are believed to involve the first charged state of the cadmium vacancy, the neutral cadmium vacancy, and an exciton bound to the neutral cadmium vacancy, respectively. The intensity of the emission band at 1.553 eV is enhanced by tellurium displacement or by firing the material in a high cadmium overpressure and is believed to be the double acceptor center already reported and involving a tellurium vacancy–halogen complex. (auth)

**56291** IRRADIATION EFFECTS IN II–VI COMPOUNDS. Watkins, G. D. (General Electric Research and Development Center, Schenectady, N. Y.). Radiat. Eff.; 9: No. 1-2, 105-13(May 1971). (CONF-700824-14).

From International conference on radiation effects and semiconductors; Albany, N. Y. (24 Aug 1970).

A summary of published results on electron energy threshold measurements in II–VI compounds, and their interpretation in terms of damage on the metal and chalcogenide sublattices, is given. EPR results in irradiated II–VI compounds are also reviewed. These include the $F^{+}$ center in ZnS, ZnO, and BeO and new results on the zinc vacancy (V) in ZnSe. For the zinc vacancy, optical absorption bands at 4680 and 8850 Å are identified with $V^{-}$ and a band at 5000 Å is tentatively assigned to $V^{2-}$. The activation energy for anneal of the vacancy is measured to be 1.26 ± 0.06 eV, and this is tentatively identified as the activation energy for vacancy motion. An EPR spectrum produced in a 20.4°K irradiation is tentatively identified as a zinc vacancy–interstitial pair. Complete annealing occurs for this defect in the range 60 to 100°K. 22 references. (auth)

**56292** ELECTRON IRRADIATION OF HEAVILY DOPED GaAs:Si AND GaAs:Te. Kahan, A.; Bouthillette, L.; DeAngelis, H. M. (Air Force Cambridge Research Labs., Bedford, Mass.). Radiat. Eff.; 9: No. 1-2, 99-103(May 1971). (CONF-700824-13).

From International conference on radiation effects and semiconductors; Albany, N. Y. (24 Aug 1970).

Infrared optical reflectivity measurement techniques are applied to determine the carrier removal rate, mobility changes, and annealing characteristics of heavily doped n-type silicon- or tellurium-doped gallium arsenide. 1-MeV room-temperature electron irradiation reduces both the carrier concentration and the mobility. Removal rates for GaAs:Te and GaAs:Si having initial carrier concentrations of $6 \times 10^{18}$ $cm^{-3}$ are approximately 3.4 and 3.0 $cm^{-1}$, respectively. The mobility degrades exponentially as a function of fluence. Isochronal anneal experiments show one major recovery stage between 170 and 230°C, and the results are in reasonable agreement with previous data obtained by electric measurements on more lightly doped n-type GaAs. (auth)

**56293** ANNEALING OF γ-IRRADIATED LITHIUM-COMPENSATED p-TYPE SILICON. Urli, N. B. (Rudjer Boskovic Inst., Zagreb). Radiat. Eff.; 9: No. 1-2, 93-7(May 1971). (CONF-700824-12).

From International conference on radiation effects and semiconductors; Albany, N. Y. (24 Aug 1970).

Floating-zone 100-ohm-cm boron-doped silicon, homogeneously compensated with lithium by the drift technique, was aged for several months at room temperature prior to irradiation in the $^{60}Co$ gamma source at 35°C. After aging, such a material became slightly undercompensated p-type. As a result of irradiation, there was a decrease in the concentration of free lithium ions directly proportional to the gamma fluence. Two deep donor levels, located at $E_v + 0.29$ eV and $E_v + 0.32$ eV were detected immediately after irradiation and attributed to the Li–V or Li–V–O complexes. A relatively fast precipitation of free lithium ions, with a time constant inversely proportional to the gamma fluence, was observed up to 30 to 40 days after irradiation. A short annealing at temperatures from 230 to 275°C almost restored the initial free-lithium-ion concentration. Heating at higher temperatures caused lithium outdiffusion to the surface. The results are compared with those already published and discussed in view of the probabilities for the formation of different defect complexes. (auth)

**56294** RECOMBINATION LUMINESCENCE IN IRRADIATED SILICON: EFFECTS OF THERMAL ANNEALING AND LITHIUM IMPURITY. Johnson, E. S.; Compton, W. D. (Univ. of Illinois, Urbana). Radiat. Eff.; 9: No. 1-2, 89-92(May 1971). (CONF-700824-11).

From International conference on radiation effects and semiconductors; Albany, N. Y. (24 Aug 1970).

Luminescence in irradiated silicon was used to determine the thermal stability of the defects responsible for the recombination. It was found that the defect responsible for the zero-phonon line at 0.97 eV has an annealing behavior similar to that of the divacancy, and the zero-phonon line at 0.79 eV anneals in a manner similar to the G-15 or K center. Annealing at temperatures up to 500°C generates other defects whose luminescence is distinct from that seen previously. Addition of lithium to the material produces defects with new characteristic luminescence. Of particular importance is a defect with a level of $E_g - 1.045$ eV. (auth)

**56295** RECOMBINATION LUMINESCENCE IN IRRADIATED SILICON: EFFECTS OF UNIAXIAL STRESS AND TEMPERATURE VARIATIONS. Jones, C. E.; Compton, W. D. (Univ. of Illinois, Urbana). Radiat. Eff.; 8: No. 1-2, 83-8(May 1971). (CONF-700824-38).

From International conference on radiation effects and semiconductors; Albany, N. Y. (24 Aug 1970).

Luminescence in irradiated silicon consists of a spectral group between 0.80 and 1.0 eV which seems to be independent of impurities while a lower-energy group between 0.60 and 0.80 eV is seen only in pulled crystals. The small halfwidth and temperature dependence of the sharp zero-phonon lines observed in these spectra indicates that the luminescence arises from a bound-to-bound transition. A model is proposed for the transition mechanism. Stress data taken on the 0.79-eV zero-phonon line in pulled crystals can be fit by either a tetragonal [100] defect symmetry or by conduction-band splitting effects. It is suggested that the 0.79-eV zero-phonon line and the 0.60- to 0.80-eV spectral group arise from the EPR G-15 center. Stress data on a zero-phonon line at 0.97 eV associated with the 0.80 to 1.0-eV spectral group can be explained by a trigonal [111] defect. The divacancy is tentatively suggested as responsible for this luminescence spectra. (auth)

**56296** PIEZO-SPECTROSCOPIC STUDY (78°K) OF RADIATION-PRODUCED ABSORPTION BANDS IN Si. Chen, C. S.; Corelli, J. C. (Rensselaer Polytechnic Inst., Troy, N. Y.). Radiat. Eff.; 9: No. 1-2, 75-9(May 1971). (CONF-700824-10).

From International conference on radiation effects and semiconductors; Albany, N. Y. (24 Aug 1970).

A detailed study has been made on two sharp sub-bands, 3.45 μ (2900 $cm^{-1}$) and 3.61 μ (2765 $cm^{-1}$) of the 3.3-μ broad defect absorption band in irradiated Si. The results indicate that the 3.45-μ and 3.61-μ bands are observed in all types of Si (n-, p-type, and intrinsic) subjected to fast-neutron reactor irradiation. Spectra were measured at 78°K under the effect of a variable uniaxial compressive stress with polarized light. A relatively large dichroism is observed for all three stress directions ⟨100⟩, ⟨110⟩, and ⟨111⟩. Both sharp bands exhibit splitting and energy shifts under the action of stress. The model of the divacancy defect given by Watkins and Corbett was utilized to explain the data. The dichroism can be accounted for by the effects of Jahn–Teller alignment, which arises from the strong bonding of nearest-neighbor atoms of the divacancy. The splittings of the bands are small, indicating that the Jahn–Teller distortion is little altered in the ground and excited states. The splittings appear to be most sensitive to stress along the vacancy–vacancy axis and a tentative model for the transitions is given. (auth)

**56297** INFRARED STUDIES OF LOW-TEMPERATURE ELECTRON-IRRADIATED SILICON CONTAINING GERMANIUM, OXYGEN, AND CARBON. Brelot, A.; Charlemagne, J. (Ecole Normale Superieure, Paris). Radiat. Eff.; 9: No. 1-2, 65-73(May 1971). (CONF-700824-9).

From International conference on radiation effects and semiconductors; Albany, N. Y. (24 Aug 1970).

Single-crystal silicon containing various concentrations of germanium, oxygen, and carbon was irradiated at 90°K with 2.8-MeV electrons and the ensuing defects studied by infrared-absorption measurements. It was found that, in n-type silicon containing $3 \times 10^{20}$ Ge atoms/$cm^3$, there is no 12-μ absorption line (A center) after a 90°K electron irradiation. The A centers appear only after annealing between 200°K and 280°K. It is therefore inferred that Ge in silicon acts as an efficient trap for vacancies at low temperatures, the trapped vacancies being released from the GeV centers by thermal activation in the 200 to 280°K range. These vacancies then migrate through the lattice and are trapped on oxygen atoms. On the other hand, the interaction between silicon interstitials and Ge atoms is very low. The 935 $cm^{-1}$ absorption line is unusually intense in these experiments. Results suggest that the defects ("B centers") which produce this absorption line are the result of the interaction of the silicon interstitials with oxygen atoms. The experimental results concerning the 921 $cm^{-1}$, 931 $cm^{-1}$, 959 $cm^{-1}$, and 966 $cm^{-1}$ absorption lines are studied. They are found to be associated with defect centers involving carbon atoms and are clearly found to be produced by silicon interstitials. On the other hand, experimental results suggest a fast diffusion of carbon, at 300°K, in interstitial sites aside from any irradiation effect. (auth)

**56298** ONE-VALLEY EPR SPECTRUM IN ELECTRON-IRRADIATED Sb-DOPED GERMANIUM. Hasiguti, R. R.; Nakanishi, T.; Funakoshi, N. (Tokyo Univ.). Radiat. Eff.; 9: No. 1-2, 57 (May 1971). (CONF-700824-8).

From International conference on radiation effects and semiconductors; Albany, N. Y. (24 Aug 1970).

Antimony-doped n-type Ge was irradiated by 2.5-MeV electrons and annealed at 485°C. The g-shifts in the one-valley EPR spectrum (Ge–T1) follow the equation $g^2 = g_{\parallel}^2 \cos^2\theta + g_{\perp}^2 \sin^2\theta$, where $g_{\parallel} = 0.82$ and $g_{\perp} = 1.93$. It is proposed that a divacancy–antimony atom complex causes the T1 spectrum, with the Sb atom situated at one end of $V_2$. (D.L.C.)

**56299** EPR IN ELECTRON-BOMBARDED PHOSPHORUS-DOPED N-TYPE GERMANIUM: AN ATTEMPT TO DETECT THE PRESENCE OF BOMBARDMENT-INDUCED INTERSTITIAL PHOSPHORUS. Hiraki, A. (Osaka Univ.). Radiat. Eff.; 9: No. 1-2, 51-5(May 1971). (CONF-700824-7).

From International conference on radiation effects and semiconductors; Albany, N. Y. (24 Aug 1970).

Effects of electron bombardment on phosphorus-doped N-type germanium were studied by EPR techniques in the hope of detecting the presence of interstitial phosphorus ($P_I$) which was ejected from the original substitutional sites through the interaction with the mobile interstitial Ge atoms produced by the bombardment. Bombardment induced the following two remarkable effects: (1) Extreme broadening of EPR linewidth of the normal substitutional phosphorus ($P_S$) donors which indicated that the bombardment produced large internal strains (~$10^{-3}$) at the sites of $P_S$; (2) occurrence of a new EPR line and study of its g-value showed that the corresponding impurities (i) had a symmetric wave function with the [001] axis and (ii) were located in the field of stronger

XUM

internal strain ($\sim 10^{-2}$) than that at $P_S$. A model of $P_I$ displaced into ⟨001⟩ directions from ordinary interstitial sites with tetrahedral symmetry due to Jahn–Teller effect was proposed to explain these effects. (auth)

**56300** 220 °K DEFECT IN ELECTRON-IRRADIATED p-TYPE GERMANIUM. Shimotomai, M.; Hasiguti, R. R. (Tokyo Univ.). Radiat. Eff.; 9: No. 1-2, 47-9(May 1971). (CONF-700824-6).

From International conference on radiation effects and semiconductors; Albany, N. Y. (24 Aug 1970).

Lattice defects introduced in p-type nondegenerate germanium by 1.5-MeV electron irradiation at liquid nitrogen temperature were investigated by means of electrical resistivity and Hall coefficient measurements. The annealing behavior of two kinds of defects, which anneal at about 220°K, was investigated in detail. Each of them has an electron trap. Making use of trap-filling and emptying processes, the 220°K defects are separated from other defects. (auth)

**56301** ELECTRON IRRADIATION OF LITHIUM-DOPED GERMANIUM AT COLD TEMPERATURES. Vavilov, V. S. (Lebedev Inst. of Physics, Moscow. Moscow State Univ.); Spitsyn, A. V.; Tchukitchev, M. V. Radiat. Eff.; 9: No. 1-2, 41-5(May 1971). (CONF-700824-5).

From International conference on radiation effects and semiconductors; Albany, N. Y. (24 Aug 1970).

Slices cut from antimony- or arsenic-doped n-type germanium ingots were additionally doped with various lithium-impurity concentrations. Samples, suited for Hall effect and minority-carrier diffusion-length measurements, were then irradiated by 1-MeV electrons at 78 or 125°K and after that, in some cases, were annealed isochronally. No differences in carrier removal or lifetime damage rates between lithium-doped and conventional n-type crystals were found up to 200 to 230°K. Hall mobility and lifetime in irradiated lithium-doped samples recovered substantially at the annealing temperature ranges of 240 to 320°K and 200 to 280°K, respectively, which is at much lower temperatures than in the crystals without lithium. No $E_c - 0.20$ eV acceptor level radiation defects were observed in the samples with large lithium impurity concentrations. (auth)

**56302** DEFECTS INDUCED BY ELECTRON IRRADIATION OF p-TYPE GERMANIUM. Matula, R. A.; Klontz, E. E. (Purdue Univ., Lafayette, Ind.). Radiat. Eff.; 9: No. 1-2, 37-40(May 1971). (CONF-700824-4).

From International conference on radiation effects and semiconductors; Albany, N. Y. (24 Aug 1970).

Illumination with filtered light after electron bombardment at ~8°K reveals defects produced in p-type germanium. During illumination, the carrier concentration decreases as the sum of two exponentials. Identification of the two time constants with two stages of thermal recovery at about 50 and 65°K indicates the short-time constant is associated with the low-temperature recovery and the long-time constant with the high-temperature recovery. Enhancement of the short-time component is accomplished by controlling the illumination time, and of the long-time component by heat treatment to 80°K prior to exposure by filtered light. Evidence is presented for nearly complete (98%) annealing of defects by white light illumination both before and after exposure to filtered light. This is in contrast to radiation annealing of the exposed defects by the 1-MeV electron beam which anneals only about 80% of the defects and converts the remainder to their neutral state. The rate of introduction of damage increases from very small values for low doses to ~0.1 to 0.2 $cm^{-1}$ for large doses of irradiation. It is believed that the low rate of damage together with the highly mobile effect constituents preclude the existence of isolated vacancies and interstitials. (auth)

**56303** REVIEW OF RADIATION EFFECTS IN GERMANIUM. MacKay, J. W.; Klontz, E. E. (Purdue Univ., Lafayette, Ind.). Radiat. Eff.; 9: No. 1-2, 27-36(May 1971). (CONF-700824-3).

From International conference on radiation effects and semiconductors; Albany, N. Y. (24 Aug 1970).

The review concentrates on low-temperature irradiation and annealing in germanium. Calculations are presented for the charge states to be expected for donor and acceptor centers during irradiation near 10°K. The calculations are applied to a discussion of the diffusion of an interstitial atom assuming it is mobile in various charge states during irradiation. The current experimental knowledge is reviewed, as are the various defect models that have been advanced to explain the behavior of germanium in recent years. Suggestions are made of certain experiments that might help in making a rational choice between the possible models. 26 references. (auth)

**56304** ION IMPLANTATION: LATTICE DISORDER. Mayer, J. W. (California Inst. of Tech., Pasadena). Radiat. Eff.; 8: No. 3-4, 269-77(Apr 1971). (CONF-700824-37).

From International conference on radiation effects and semiconductors; Albany, N. Y. (24 Aug 1970).

This review is directed toward some of the recent developments in the analysis of lattice disorder in ion-implanted silicon. Although the disorder picture has not been entirely clarified in silicon, many of the salient features have been identified. IR absorption and EPR measurements have been used to identify specific defects and correlation was found with anneal behavior in implanted and fast-neutron-irradiated samples. Analysis of low-temperature implants suggested that release of point defects (vacancies) played an important role in the growth of divacancies and the anneal of disorder. Depth distribution of defects has been investigated and compared with ion ranges and energy lost in atomic processes. Various models have been proposed for the nature of the disordered region around the ion track and the formation of an amorphous layer at high doses. The data indicates that the individual disordered regions are not primarily amorphous. The nature of ion-implanted layers in compound semiconductors has not yet been as thoroughly investigated as those in silicon. 49 references. (auth)

**56305** 14-MeV-NEUTRON IRRADIATION OF p-TYPE GERMANIUM AT 77°K. Wolf, D. (Univ., Kiel). Radiat. Eff.; 8: No. 3-4, 263-7(Apr 1971). (CONF-700824-36).

From International conference on radiation effects and semiconductors; Albany, N. Y. (24 Aug 1970).

P-type germanium was irradiated at 77°K by monoenergetic 14-MeV neutrons, and the changes of resistivity and Hall coefficient were measured. Subsequently, isochronal annealing experiments were performed. The results can be explained by the assumption that energetic neutrons create disordered regions that decay by annealing between 77 and 230°K, probably forming well-conducting zones. This decay is superposed on the annealing behavior of a type of defect, which is observed here as well after electron irradiation. (auth)

**56306** LOW-TEMPERATURE ELECTRON IRRADIATION OF TELLURIUM. Gmelin, E.; Stapf, R.; Klemt, P.; (and others) (Univ., Wurzburg, Ger.). Radiat. Eff.; 8: No. 3-4, 255-62(Apr 1971). (CONF-700824-35).

From International conference on radiation effects and semiconductors; Albany, N. Y. (24 Aug 1970).

Tellurium single crystal samples with a hole concentration of $3 \times 10^{14}/cm^3$ were irradiated at 10°K with electrons with an energy of 0.6 and 1 MeV. In the range investigated, resistivity and Hall coefficient $R_H$ both decreased linearly with the integrated electron flux. The hole generation rate was 0.09 $cm^{-1}$ and 0.47 $cm^{-1}$ for 0.6- and 1-MeV electrons, respectively. The Hall mobility $R_H/\rho$ increased with irradiation. Annealing of the radiation damage by raising the temperature clearly revealed three recovery stages in the resistivity and Hall data. At 180°K, $\rho$ and $R_H$ returned to their pre-irradiation values. The original Hall mobility was already restored close to 90°K. A more detailed study of the first recovery stage, which occurs at about 50°K, revealed an activation energy of 170 ± 40 MeV. It is most likely that the observed lattice defects are Frenkel defects. There are indications that the point defects interact with dislocations. (auth)

**56307** THERMAL NEUTRON DAMAGE IN CdS AND CdTe. Kikuchi, C. (Kyoto Univ.). Radiat. Eff.; 8: No. 3-4, 249-53 (Apr 1971). (CONF-700824-34).

From International conference on radiation effects and semiconductors; Albany, N. Y. (24 Aug 1970).

Photoluminescence and electrical resistivity changes in CdS and CdTe produced by thermal neutrons are discussed. The damage is produced principally by the neutron-capture reaction $^{113}Cd(n,\gamma)^{114}Cd$. Since the reaction product $^{114}Cd$ is stable, complications arising from impurity introduction are minimal. The cumulative recoil nuclear recoil energy is about 143 eV, but is not the recoil energy at the time atomic displacement occurs. Thermal and fast neutrons enhance the CdS luminescence band at 7200 Å in the ratio of 28 : 1, but the resistivity changes are in the ratio of 40 : 1. Cadmium interstitial is suggested as the luminescence center. Hall measurements on n-type CdTe suggest that only Cd defects are produced for low thermal-neutron doses. The acceptor introduction rate is about 1.0 to 0.6, compared to 0.098 for CdS. These are in good agreement with the values reported by R. O. Chester. The fast-neutron effects in high-resistivity CdS reported by Johnson indicate the need for further measurement. (auth)

**56308** LOW-TEMPERATURE PHOTOCONDUCTIVITY IN ELECTRON-IRRADIATED p-TYPE Si. Vajda, P.; Cheng, L. J.

(Chalk River Nuclear Labs., Ont.). Radiat. Eff.; 8: No. 3-4, 245-8(Apr 1971). (CONF-700824-33).

From International conference on radiation effects and semiconductors; Albany, N. Y. (24 Aug 1970).

The photoconductivity spectra of p-type silicon irradiated at ~15°K with 1.2 MeV electrons were studied in the wavelength range from 1.2 to 5.5 $\mu$ at temperatures from 23 to 80°K. The 3.9 $\mu$ photoconductivity band appears immediately after irradiation in all crystals already at low temperatures, giving further evidence that it is due to the divacancy formed directly during irradiation by electrons. Three main annealing stages of the photoconductivity have been observed: (a) below 160°K, (b) 160 to 250°K, and (c) 280 to 360°K. A radiation-induced deep level at $E_v + (0.12 \pm 0.02$ eV) disappears upon annealing at stage b. The annealing behavior of the spectra depends strongly on the measuring temperature. The dependence of the spectra on chopper speed was also investigated. (auth)

**56309** LITHIUM: AN IMPURITY OF INTEREST IN RADIATION EFFECTS OF SILICON. Naber, J. A.; Horiye, H.; Passenheim, B. C. (Gulf Radiation Tech., San Diego, Calif.). Radiat. Eff.; 8: No. 3-4, 239-44(Apr 1971). (CONF-700824-32).

From International conference on radiation effects and semiconductors; Albany, N. Y. (24 Aug 1970).

The introduction and annealing of defects produced in lithium-diffused float-zone n-type silicon by 30-MeV electrons and fission neutrons are studied. The introduction rate of recombination centers produced by electron irradiation is dependent on lithium concentration and, for neutron irradiation, is independent of lithium concentration. The introduction rate of Si-B1 centers also depends on the lithium concentration. The annealing of electron- and neutron-produced recombination centers, Si-B1, and Si-G7 centers in lithium-diffused silicon occurs at much lower temperatures than in nondiffused material. (auth)

**56310** LITHIUM-DEFECT INTERACTIONS IN ELECTRON-IRRADIATED n-TYPE SILICON BY EPR MEASUREMENTS. Goldstein, B. (RCA Labs., Princeton, N. J.). Radiat. Eff.; 8: No. 3-4, 229-37(Apr 1971). (CONF-700824-31).

From International conference on radiation effects and semiconductors; Albany, N. Y. (24 Aug 1970).

Single-crystal silicon, both with and without oxygen, was diffused with lithium to concentrations ~$10^{17}$/cm$^3$, irradiated with 1- to 1.5-MeV electrons, and the ensuing defects studied by EPR measurements. The presence of oxygen strongly affects the properties of these defects. Measurements indicated the presence of two new defects that involve Li—one in O-containing material and one in O-free material. The defects are observed in their electron-filled state, and indicate a net electron spin of 1/2. The defect spectra disappear (with time) at room temperature, and can be explained by the formation of other Li-involved defects which lie deeper in the energy bandgap and are not visible by EPR. Electron irradiation at 40°K followed by annealing at higher temperatures shows that both EPR defects described above begin to form at about 200°K and begin to decrease at about 275°K—just as does the 250°K reverse annealing observed generally for n-type Si. Based on these data, and the work of others, it is suggested that both defects form as a result of the motion of Si interstitials which produce a (Li-O-interstitial) complex in O-containing Si, and a (Li-interstitial) complex in O-free Si. (auth)

**56311** ABSORPTION MEASUREMENTS IN NEUTRON-IRRADIATED SILICON. Barnes, C. E. (Sandia Labs., Albuquerque, N. Mex.). Radiat. Eff.; 8: No. 3-4, 221-7(Apr 1971). (CONF-700824-30).

From International conference on radiation effects and semiconductors; Albany, N. Y. (24 Aug 1970).

Silicon samples were neutron-irradiated at 76°K with fluences sufficient to allow measurement of the 1.7-$\mu$ divacancy band at 76°K. The growth of the divacancy concentration and the recovery of the edge absorption were studied as a function of annealing temperature between 76 and 550°K. Immediately after irradiation the divacancy concentration is about 25% of its maximum value which is attained at 330°K, the temperature at which the divacancies begin to anneal out. Increases in the 1.7-$\mu$ band intensity and recovery of the edge absorption can also be achieved at 76°K by illuminating the sample with intense sub-bandgap light or white light. The experimental results suggest a neutron-induced cluster model in which the cluster is a vacancy-rich region whose annealing characteristics are controlled by the liberation and motion of vacancies. The injection effects can be explained by analogy to the charge state-dependent mobility of the Si vacancy. (auth)

**56312** STRUCTURE OF MULTIPLE-VACANCY (OXYGEN) CENTERS IN IRRADIATED SILICON. Brower, K. L. (Sandia Labs., Albuquerque, N. Mex.). Radiat. Eff.; 8: No. 3-4, 213-19(Apr 1971). (CONF-700824-29).

From International conference on radiation effects and semiconductors; Albany, N. Y. (24 Aug 1970).

Analysis of a new paramagnetic spin 1 spectrum, labeled Si-S1, indicates that it corresponds to the neutral charge state of the Si-B1 center in an excited spin-triplet state. An extension of this analysis to the Si-P1, -P2, -P3, -P4, and -P5 centers suggests that these centers comprise a family of defects that consist of a string of neighboring vacancies in a single (110) plane. In particular, it appears that the Si-P1 center is an odd (≥3)-vacancy defect; the Si-P2 center is a 2-vacancy, oxygen defect; the Si-P3 center is a 4-vacancy defect; the Si-P4 center is a 3-vacancy, oxygen defect of symmetry lower than $C_{2v}$; and the Si-P5 center is a 3 vacancy, oxygen defect having $C_{2v}$ symmetry. (auth)

**56313** PRODUCTION OF VACANCIES BY LASER BOMBARDMENT. Metz, S. A.; Smidt, F. A. Jr. (Naval Research Lab., Washington. D. C.). Appl. Phys. Lett.; 19: No. 6, 207-8 (15 Sep 1971).

Vacancy concentrations estimated to be as large as 1 at. % were induced in pure nickel and vanadium foils by bombardment with high-intensity laser pulses. Annealing bombarded foils at temperatures greater than $0.3T_m$(absolute melting point) allows vacancies to form into aggregates. Examples are shown of voids in nickel and faulted loops in vanadium. Possible mechanisms of vacancy generation are discussed. (auth)

**56314** LOW-TEMPERATURE PROTON RADIATION DAMAGE AND RECOVERY IN DISCONTINUOUS Ta FILMS. Hardy, W. R.; Pronko, P. P.; Shewchun, J. (McMaster Univ., Hamilton, Ont.). Appl. Phys. Lett.; 19: No. 6, 174-6(15 Sep 1971).

Tantalum films reactively sputtered in oxygen and nitrogen simultaneously were irradiated by 150-keV protons at 30°K. The observed conductance increase of these discontinuous films is ascribed to radiation-produced defect levels within the inter-island oxide regions. The nonlinearity of the conductance increase with fluence may be accounted for by a combination of close-pair thermal annealing and spontaneous recombination. Isochronal annealing experiments demonstrate that recovery occurs in two main stages. The first stage (34 to 120°K) is attributed to close-pair or correlated recombination, and the second stage (200 to 300°K) is attributed to uncorrelated migration of defects to the gap—island interface. (auth)

**56315** ELECTRONIC DEFECT STRUCTURE OF SINGLE-CRYSTAL $ThO_2$ BY THERMOLUMINESCENCE. Rodine, Elward T. (Systems Research Labs., Inc., Dayton, Ohio); Land, Peter L. Phys. Rev., B; 4: No. 8, 2701-24(15 Oct 1971).

Some electronic defects and the associated photoelectronic processes in $ThO_2$ are analyzed by utilizing the data from thermoluminescence (TL) and EPR measurements on a number of rare-earth-doped and undoped single crystals from various sources. (The EPR measurements were made by others.) Some fluorescence and absorption measurements are also ultilized. Some TL glow peaks in the undoped $ThO_2$ correlate with the annealing of EPR spectra which are associated with trapped electrons. The similarity of glow curves for different crystals, the lack of hyperfine EPR structure, and the dependence on rare-earth doping suggests that some of the major electron traps are associated with oxygen vacancies, which may be complexed. The TL and EPR were induced by uv excitation, which created electrons and holes which are trapped. Some of the hole traps are identified as rare-earth ions in cubic sites. The rare earths provide all of the TL and fluorescence observed in $Li_2O \cdot 2WO_3$ flux-grown $ThO_2$, and the total TL at saturation depends on the doping level. The TL excitation spectra and optical absorption measurements on $Li_2O \cdot 2WO_3$ flux-grown undoped thoria indicate a band gap of 5.75 eV which is larger than previously reported. The thermal activation energies are given for electron traps, and some indications of relative cross sections for electron or hole trapping or recombination processes are reported. (auth)

**56316** OSCILLATIONS OF THE PHOTOCURRENT IN Ge WITH RADIATION DEFECTS. Rubinova, E. E.; Novikov, S. R.; Konopleva, R. F. (Ioffe Inst. of Physics and Tech., Leningrad). Sov. Phys.-Semicond. (Engl. Transl.); 3: No. 10, 1294-6(Apr 1970).

Translated from Fiz. Tekh. Poluprov.; 3: No. 10, 1549-52(Oct 1969).

A study was made of slowly decaying low-frequency oscillations of the photocurrent in n-type Ge irradiated with either fast neutrons or 660-MeV protons. The oscillations appear only where the Fermi level was lowered near the forbidden band, and in the presence of an electric field of ~10 V/cm, and its frequency increases with exciting light intensity while its modulation depth decreases with intensity. The light probe method was used, and the resulting oscillograms show that the oscillations can be explained by the appearance of high-field domains moving in the electric field.

XUM

These domains are caused by the high-acceptor damage regions. (D.L.C.)

**56317** ANNEALING OF RADIATION DEFECTS AND THE ELECTRON MOBILITY IN INDIUM ANTIMONIDE IRRADIATED WITH FAST NEUTRONS. Kurdiani, N. I. Sov. Phys.-Semicond. (Engl. Transl.); 3: No. 11, 1415-17(May 1970).

Translated from Fiz. Tekh. Poluprov.; 3: No. 11, 1683-6(Nov 1969).

It is shown that the recovery of the original electron density in indium antimonide irradiated with fast neutrons at 50°C takes place in three stages. The recovery of the electron density is complete after annealing at 300°C. The electron mobility also increases as the isochronous annealing temperature is raised. However, a complete recovery of the electron mobility requires additionally several annealing cycles in the 300 to 360°C range. In order to obtain information on this effect, a study was made of the temperature dependence of the electron mobility in the irradiated and annealed (at 300°C) crystals of InSb. It was found that the electron mobility was independent of the temperature in the range 50 to 120°K. A similar relationship was observed also for heavily doped and heavily compensated crystals of InSb. It was concluded that oppositely charged radiation defects of the dipole type could be responsible for the scattering of electrons in the neutron-irradiated and annealed (at 300°C) crystals of indium antimonide. (auth)

**56318** TEMPERATURE OF THERMAL PEAKS DURING IRRADIATION OF IONIC CRYSTALS. Eremin, L. P.; Oblivantsev, A. N. (Tomsk Polytechnic Inst., USSR). Izv. Vyssh. Ucheb. Zaved., Fiz.; No. 3, 149-50(1971). (In Russian).

The effect of temperature on the dissociation of polycrystalline samples of sodium nitrate was studied by irradiating them in a cyclotron with 5-MeV protons and with 20-MeV $\alpha$ particles. In examining the dependency of log G upon reciprocal temperature, two distinct regions were observed, differing in the effective activation energy. The intersection of the two straight lines furnished the desired temperatures: 324°K for proton irradiation and 345°K for $\alpha$ particles. Such temperature peaks do not differ much from room temperature and are altered only slightly by the form of radiation. (K.S.W.)

**56319** STUDIES OF NEGATIVE MAGNETORESISTANCE IN NEUTRON-IRRADIATED POLYCRYSTALLINE GRAPHITE AND IN BORONATED KISH GRAPHITE. Hishiyama, Y.; Mrozowski, S.; Vagh, A. S. (State Univ. of New York, Buffalo). Carbon; 9: No. 4, 367-81(Aug 1971).

A study was made of the changes in magnetoresistance resulting from substitutional introduction of atoms into the lattice of a single crystal of graphite or from the introduction of vacancies, interstitial atoms and other defects into polycrystalline graphite by neutron irradiation. Measurements were performed at 300, 77, 4.2 and 1.6°K. Introduction of defects caused negative magnetoresistance to appear. The negative magnetoresistance of polycrystalline graphite showed in the process of gradual destruction of the graphitic lattice by neutron irradiation a quite different correlation with the Hall coefficient than was observed while the graphitic structure was formed in the original heat treatment process. The difference in behavior is believed to be related to the larger concentration of localized defects created and to the retention of some rudiments of the original structure in the case of irradiation. (auth) (UK)

**56320** MAGNETO-OPTICAL PROPERTIES OF THE $Cd^+$ ION IN X-IRRADIATED ALKALI HALIDES. Beaumont, J. H.; Hayes, W.; Laiho, R. T. S. (Oxford Univ.). J. Phys., C (London); 4: No. 12, 1505-9(Aug 1971).

Cadmium-doped alkali halide crystals were quenched, x-irradiated at room temperature, and subsequently investigated by magneto-optical methods. An optical absorption band of $Cd^+$ was identified at 342 nm in NaCl, 332 nm in KCl, 336 nm in KBr, and 345 nm in KI. This band was assigned to a transition of the type $^2S \rightarrow {}^2P$ and the spin–orbit coupling constant in the $^2P$ state of the transition was found by magnetic circular dichroism measurements to be 743 $cm^{-1}$ in NaCl, 845 $cm^{-1}$ in KCl, 513 $cm^{-1}$, in KBr and 263 $cm^{-1}$ in KI. The $Cd^+$ ion is created as a result of reduction of $Cd^{2+}$ by the irradiation. The interaction of the $Cd^+$ ion with the crystal environment is discussed. (auth) (UK)

**56321** ELECTRON TRAPS IN DEFORMED KCl. Clark, C. D.; Newman, D. H. (Univ. of Reading, Eng.). J. Phys., C (London); 4: No. 12, 1615-17(Aug 1971).

Deformation-induced and optically stimulated thermoluminescence peaks associated with new electron traps were observed from electron-irradiated KCl. It is suggested that the traps may be small anion–cation vacancy clusters produced by the jogged motion of dislocations during plastic deformation. (auth) (UK)

**56322** ELECTRON IRRADIATION AND EPITAXY ON ALKALI HALIDES. Lord, G. (Univ. of York, Heslington, Eng.). Thin Solid Films; 7: No. 6, R39-42(Jun 1971).

Surface damage studies on air-cleaned NaF after electron irradiation (0.5 keV, 1 $\mu A/cm^2$) show that small pits appear at low doses which tend to agglomerate into regular square-sided pits with increasing dose. The efficiency of the sputtering mechanism is extremely high, and this effect can be observed in KCl, NaCl, NaF, and LiF. Deposition of 10 A of Ag onto NaF before and after 1-keV electron irradiation shows that ordered metal growth occurs at the pitted areas in the irradiated specimens, in contrast to the random polycrystalline structure on unirradiated specimens. (D.L.C.)

**56323** THERMOLUMINESCENCE OF X-RAY-IRRADIATED KBr AND KBr:Cu CRYSTALS. Murti, Y. V. G. S.; Murthy, K. R. N.; Ramasastry, C. (Indian Inst. of Tech., Madras). J. Phys., C (London); 4: No. 12, 1606-14(Aug 1971).

The thermoluminescence of x-ray-irradiated KBr and KBr: Cu crystals was studied in the temperature range 300 to 510°K. Four glow peaks with first-order kinetics are observed at 359, 377, 392, and 409°K for a warming rate 40°K $min^{-1}$. The trap depths for the above peaks are respectively 0.86, 0.97, 1.00, and 1.05 eV. The 377°K peak is related to the presence of $Cu^+$ ions in the crystal. Based on the identification of the filled traps with F centres in different local environments, the thermal excitation energy of the F centres to the relaxed excited state is deduced to be 1.7 eV for KBr (and 2.0 eV for KCl). (auth) (UK)

**56324** EPR STUDY OF FAST-NEUTRON RADIATION DAMAGE IN SILICON. Daly, D. F.; Noffke, H. E. (Bell Telephone Labs., Inc., Whippany, N. J.). Radiat. Eff.; 8: No. 3-4, 203-11(Apr 1971). (CONF-700824-28).

From International conference on radiation effects and semiconductors; Albany, N. Y. (24 Aug 1970).

Using electron paramagnetic resonance (EPR), the identity of the point defects produced by fast-neutron irradiation of silicon at room temperature was determined and the concentration of each defect was measured. Irradiations were performed at an unmoderated fast burst reactor to assure that damage from gamma irradiation could be neglected and that all the observed damage could be attributed to displacements by fast neutrons. Total fast-neutron fluence between $1.2 \times 10^{15}$ n/$cm^2$ and $7 \times 10^{15}$ n/$cm^2$ was used. The initial rate of removal of the phosphorus donor agrees with the initial carrier removal. However, the production rate for the paramagnetic damage centers is approximately 10% of the carrier removal and less than 1% of the estimated number of displacements per neutron collision. For samples containing approximately $10^{16}$ phosphorus donors/$cm^3$, the neutral donor spectrum is observed simultaneously with the negative divacancy spectrum (Si–G7) in both crucible-grown and float-zone crystals. According to the energy level scheme determined for these spectra in electron-irradiated silicon, these spectra cannot appear simultaneously if the sample is in equilibrium and uniformly irradiated. From the observation of these spectra, it is concluded that the damage concentration and hence the depth of the Fermi level is nonuniform on a microscopic scale. These results are interpreted according to the cluster model for neutron damage. The cluster consists of a core of damaged silicon with the Fermi level at the center of the band gap and a surrounding space–charge region. Outside the space–charge region, the Fermi level is the same as in undamaged silicon. It is concluded that the low production rate of the point defects and the nonuniform Fermi level constitute microscopic evidence for the defect cluster model of fast-neutron damage in silicon. (auth)

**56325** IRRADIATION DAMAGE IN CARBON-DOPED SILICON IRRADIATED AT LOW TEMPERATURES BY 2-MeV ELECTRONS. Newman, R. C.; Bean, A. R. (J. J. Thomson Physical Lab., Reading, Eng.). Radiat. Eff.; 8: No. 3-4, 189-93(Apr 1971). (CONF-700824-26).

From International conference on radiation effects and semiconductors; Albany, N. Y. (24 Aug 1970).

Irradiation of silicon by 2-MeV electrons at 130°K leads to the removal of carbon from substitutional sites and the formation of centers with axial symmetry having vibrational modes at 921 and 930 $cm^{-1}$ for $^{12}C$; large isotope shifts are found in crystals containing $^{13}C$ and $^{14}C$. This center is considered to involve interstitial carbon atoms but not oxygen impurities. On annealing such irradiated crystals to room temperature, the concentration of these centers is reduced and a new transient center involving carbon was detected. Further annealing leads to the formation of the well-known 11.56-$\mu$m absorption band in pulled crystals, and it is shown that this may be correlated with another band at 1115.5 $cm^{-1}$. Again, large isotope effects are found in crystals containing $^{13}C$ and $^{14}C$

XUM

and this center is ascribed to a [O–C] complex involving an interstitial carbon atom. (auth)

**56326** NEUTRON IRRADIATIONS OF SILICON STUDIED BY $^{57}$Fe MOESSBAUER EFFECT. Matsui, K. (Univ. of Tohoku, Sendai); Hasiguti, R. R.; Onodera, H. Radiat. Eff.; 8: No. 3-4, 195-201(Apr 1971). (CONF-700824-27).

From International conference on radiation effects and semiconductors; Albany, N. Y. (24 Aug 1970).

Fast-neutron irradiations of silicon are studied through the cobalt-57 probe incorporated into the lattice. The cobalt substitutional atoms introduced by fast quenching from around 1100°C are found to be converted to interstitials by reactor irradiations at 80°C. The reverse effect in which the irradiations enhance the substitutional atoms also takes place. These conversion effects are accompanied by a marked dependence upon initial Fermi levels. Their efficiencies seem to be proportional to integrated neutron flux. A strong unstable spectrum best represented by 4 quadrupolar doublets arises before the interstitial-type conversion is observed. These doublets are tentatively assigned to the cobalt interstitials trapped by charged centers. The spectrum dies out with the decay of the induced radiation, suggesting that the pairs become unstable at thermal equilibrium at room temperatures. (auth)

**56327** RECOMBINATION PARAMETERS IN LOW-RESISTIVITY GAMMA-IRRADIATED n-TYPE GERMANIUM. Srour, J. R.; Curtis, O. L. Jr. (Northrop Corp. Labs., Hawthorne, Calif.). Radiat. Eff.; 8: No. 3-4, 183-8(Apr 1971). (CONF-700824-25).

From International conference on radiation effects and semiconductors; Albany, N. Y. (24 Aug 1970).

Studies of recombination in ~0.2 Ω-cm As- and Sb-doped $^{60}$Co γ-irradiated Ge which yield energy levels and the temperature dependence of the electron and hole capture probabilities are reported. For Sb-doped material at 323°K, the recombination center energy level position (neglecting statistical weight) was found to be 0.361 ± 0.005 eV above the valence band with a possible slight temperature dependence corresponding roughly to one-half the variation of band gap with temperature. The capture probability ratio at this same temperature was 740. For the As-doped case, two different levels appear to dominate the recombination process in annealed and unannealed low-resistivity material. The energy level positions relative to the valence band (neglecting statistical weight) are 0.327 ± 0.005 eV and 0.37 ± 0.01 eV at room temperature for the annealed and unannealed samples, respectively. The corresponding capture probability ratios are 650 and 810. As in the case of Sb doping, the energy level appears to shift with temperature at about one-half the rate of the shift in band-gap energy. (auth)

**56328** MOESSBAUER-TYPE PHOTOLUMINESCENCE SPECTRA OF IRRADIATED GERMANIUM. Spry, R. J. (Air Force Materials Lab., Wright-Patterson AFB, Ohio); Henes, J. D. Radiat. Eff.; 8: No. 3-4, 177-82(Apr 1971). (CONF-700824-24).

From International conference on radiation effects and semiconductors; Albany, N. Y. (24 Aug 1970).

A Moessbauer-type structure was observed in the 15°K spectra of germanium crystals irradiated at room temperature by $^{60}$Co γ rays and 700-keV electrons. The spectra consist of an intense band peaking at 0.688 eV accompanied by mainly TA-phonon-assisted lower-energy sidebands. The transition producing the luminescence is believed to be the annihilation of an exciton bound to a defect center by forces of shorter range than coulombic attraction. The dependence of the new spectra upon irradiation temperature and certain sample characteristics indicates that the center contains both primary defect(s) and an unknown impurity. (auth)

**56329** ANNEALING OF POINT DEFECTS IN p-TYPE GERMANIUM AFTER ELECTRON IRRADIATION AT LIQUID-NITROGEN TEMPERATURE. Saito, H.; Fukuoka, N.; Tatsumi, Y. (Osaka Univ.). Radiat. Eff.; 8: No. 3-4, 171-5(Apr 1971). (CONF-700824-23).

From International conference on radiation effects and semiconductors; Albany, N. Y. (24 Aug 1970).

Annealing of radiation-induced defects in p-type germanium was studied by measuring Hall coefficient and conductivity. The dopant was gallium or indium. It was concluded that the annealing stage between 80 and 140°K is caused by migration of the vacancy to the sink of an impurity atom. In this stage the vacancy migrates to a substitutional impurity atom and makes an association. The activation energy of the stage was found to be 0.1 eV and regarded to be that of the vacancy migration. The model for the annealing stage which occurs in the range 220 to 270°K is proposed as follows: an interstitial impurity atom migrates to a substitutional impurity atom and makes an association. From the activation energy of the stage, the migration energy of the interstitial impurity atom was concluded to be about 0.4 eV for gallium and 0.7 eV for indium atoms. (auth)

**56330** VACANCY–INTERSTITIAL PAIR IN ELECTRON-IRRADIATED GERMANIUM. Bourgoin, J.; Mollot, F. (Ecole Normale Superieure, Paris). Radiat. Eff.; 8: No. 3-4, 165-70 (Apr 1971). (CONF-700824-22).

From International conference on radiation effects and semiconductors; Albany, N. Y. (24 Aug 1970).

A study was made of the influence of the nature and concentration of donor impurity on the 65 and 35°K stages in electron-irradiated n-type germanium. Because the nature of the impurity does not influence the 65°K stage and because this stage is present alone in lightly doped samples, it is associated with the annihilation of a vacancy–interstitial pair. Because the 35°K stage is directly connected to the impurity concentration, and not to the free-electron concentration, it is associated with the annihilation of a vacancy and interstitial–impurity pair. It is shown that the annihilation of the vacancy–interstitial pair occurs through the interstitial mobility at 65, 27, and 4.5°K depending on its charge state, and that the interstitial–impurity mobility occurs at 35°K. The model explains easily the radiation annealing and the behavior of irradiated p-type germanium and can be extended to the case of indium antimonide and perhaps silicon. (auth)

**56331** IMPURITY DEPENDENCE OF THE LOW-TEMPERATURE ANNEALING IN n-TYPE GERMANIUM. Meese, J. M.; MacKay, J. W. (Purdue Univ., Lafayette, Ind.). Radiat. Eff.; 8: No. 3-4, 161-4(Apr 1971). (CONF-700824-21).

From International conference on radiation effects and semiconductors; Albany, N. Y. (24 Aug 1970).

Lightly doped n-type Ge, irradiated at liquid He temperatures with 1-MeV electrons, exhibits a large thermal recovery stage at 50 to 70°K. It was found that the rate at which this stage anneals depends on the type of group V impurity used to dope the sample. It is proposed that impurity complexes are involved in this annealing stage. The same impurity dependence was also observed when this annealing stage is destroyed by radiation annealing at liquid He temperatures. This suggests that one of the defects produced during irradiation is free to migrate at very low temperatures. (auth)

**56332** IMPORTANT UNANSWERED QUESTIONS, 1970: RADIATION EFFECTS IN SEMICONDUCTORS. Vook, F. L. (Sandia Labs., Albuquerque, N. Mex.). Radiat. Eff.; 8: No. 3-4, 155-60(Apr 1971). (CONF-700824-20).

From International conference on radiation effects and semiconductors; Albany, N. Y. (24 Aug 1970).

An attempt is made to establish a general overview of the field by concentrating on recent research developments and important unanswered questions. The continuing importance of impurity–defect interactions, of microscopic defect identification, and of the necessity for more theoretical calculations are emphasized. The rapid development of the field of ion implantation and its close relationship with radiation effects studies are pointed out. It is predicted that research in compound semiconductors will increase rapidly with close beneficial interaction with ion implantation studies. (auth)

**56333** KINETICS OF CROWDION REACTIONS. Frank, W. (Max-Planck Inst. fuer Metallforschung, Stuttgart. Univ., Stuttgart). Radiat. Eff.; 8: No. 3-4, 145-54(Apr 1971).

The basic equations that govern diffusion-controlled reactions of crowdions (crowdion–vacancy annihilation, conversion of crowdions to dumbbell interstitials by means of crowdion–crowdion collisions, as well as conversion of crowdions at dumbbells and at impurities) are derived. "Off-line" crowdions, which are unable to recombine with their "own" vacancies, as well as "on-line" crowdions, which anneal out preferentially in that way, are taken into account. Approaches to the solution of these equations are presented and compared with those found in the literature. In particular, an expression that was fitted successfully by Frank, Seeger, and Schottky to the Corbett–Smith–Walker annealing data in stage $I_E$ of electron-irradiated copper is rederived from the basic equations as an approximate solution for the regime of uncorrelated recovery. This means that the annealing kinetics in stage $I_E$ of electron-irradiated copper may be explained in terms of the conversion–two-interstitial model. (auth)

**56334** LINEAR HIGH FIELD MAGNETORESISTANCE IN ALUMINUM: DEPENDENCE ON DEFECT STRUCTURE AND CRYSTAL ORIENTATION. Kesternich, W.; Ullmaier, H. (Kernforschungsalage, Juelich, Ger.). Phys. Lett.; 36A: No. 5, 411-12(27 Sep 1971).

Defect production by electron irradiation and subsequent an-

XUM

nealing enables one to study the effects of different defect structures in the same sample. The results of such measurements show clearly that the linear increase of the high-field magnetoresistance in Al depends both on the type of defect structure and on the crystal orientation. (auth)

**56335** ELECTRONIC CONDUCTION IN YTTRIA-DOPED THORIA SOLID ELECTROLYTE. Rao, A. V. Ramana; Tare, V. B. (Banaras Hindu Univ., India). Scr. Met.; 5: No. 9, 813-19(Sep 1971).

Thoria doped with 15 mol % $YO_{1.5}$ was found to exhibit conductivities ranging from 0.221 at 1200 to 0.280 at 1448°K. From these values and assuming $p_{O_2}^{\frac{1}{4}}$ dependence of conductivity, the safe lower limits of oxygen pressure for the use of doped thoria as solid electrolyte are estimated to vary from $10^{-32.6}$ atmospheres at 1200 to $10^{-24.0}$ atmospheres at 1448°K. (auth)

**56336** FLASH X-RAY IRRADIATION OF P-N JUNCTIONS: A METHOD TO MEASURE MINORITY CARRIER LIFETIMES, DIFFUSION CONSTANTS, AND GENERATION CONSTANTS. Lindstroem, J. L. (Research Inst. of National Defence, Stockholm). Solid-State Electron.; 14: No. 9, 827-33(Sep 1971).

A method to measure the minority carrier lifetime in semiconductors was developed utilizing short flashes of x rays. The advantage with the use of x rays instead of light is that the generation of charge carriers can be made very homogenous and that the concentration of generated carriers can be varied within a wide range. The experiments were carried out on $p^+$–n silicon diodes and concerned measurements of the decay times for radiation-induced currents as function of reverse bias and width of the bulk regions of the diodes. It is shown that by plotting the decay rate as function of the inverse value of the square of the width of the bulk region (according to the theoretical model used) it is possible to obtain both the minority carrier lifetime and the diffusion constant of the n-material. Comparison with other methods confirms the usefulness of the method. By measuring the reverse bias dependence of the width of the depletion region and the corresponding variations in integrated radiation-induced current, it was possible to determine the generation constant. (auth) (UK)

**56337** LOCATION OF IMPURITIES IN ALKALI HALIDE CRYSTALS BY CHANNELING STUDIES. Tachibana, Kazuya; Morita, Kenji; Itoh, Noriaki (Nagoya Univ., Japan). Solid State Commun.; 9: No. 16, 1425-7(Aug 1971).

The axial channeling dips for the impurity ions in alkali halide crystals are measured and compared with the channeling dips for the host ions. Three typical profiles are presented. The atomic positions of the impurities in irradiated alkali halides are discussed. (auth) (UK)

**56338** COMMENTS ON SUPRALINEARITY AND SENSITIZATION OF THERMOLUMINESCENT PHOSPHOR LITHIUM FLUORIDE. De Werd, L. A.; Stoebe, T. G. (Univ. of Washington, Seattle). J. Phys., D (London); 4: No. 9, L31-3(Sep 1971).

Hwang (1971) presented data concerning two high-temperature thermoluminescent peaks and related optical absorption bands in LiF. Unfortunately, Hwang's analysis is based on certain misunderstanding of information in the literature. (auth) (UK)

**56339** IMPURITY PARAMAGNETIC CENTER APPEARANCE IN γ-IRRADIATED SALTS. Barsova, L. I.; Ershov, B. G.; Popova, G. Yu.; Spitsyn, I. (Inst. of Physical Chemistry, Moscow). Dokl. Akad. Nauk SSSR; 197: No. 6, 1355-7(21 Apr 1971). (In Russian).

Paramagnetic centers and thermal annealing were studied in γ-irradiated salts such as Ba and Sr sulfates and Sr phosphate with impurities of electron-donor and electron-acceptor materials: nitrite, formate, sulfite, or nitrate ions, and also $H_2O_2$ or methanol. The irradiation was conducted with a cobalt-60 source, with an absorbed dose of 0.3 to 0.5 mR. At 130 to 230°K, annealing of the hole centers took place, along with an accumulation of $NO_2^-$ radicals, for example, but the latter ceased above 230°K. In the presence of electron donor additives ($NO_2^-$, etc.), hole capture by the additives occurred with the formation of new paramagnetic centers. (K.S.W.)

## Physical Properties

*Refer also to abstracts 55445, 55472, 55527, 55532, 55622, 55627, 55633, and 56109.*

**56340** (AERE-Trans-1137) THE ZERO PLACZEK MOMENT AND THE n-PHONON CROSS SECTION. Eder, O. J. Translated by J. B. Sykes (Atomic Energy Research Establishment, Harwell, Eng.), from Acta Phys. Austr.; 30: No. 4, 334-45(1969). 11p. Dep. NTIS (U. S. Sales Only). UK 13p.

Use is made of the zero Placzek moment and the phonon expansion of the double differential scattering cross section for thermal neutrons scattered by a polycrystalline solid or a single crystal in order to calculate the contribution of the n-phonon term to the scattering intensity. This procedure can be extended to the case of liquids and anharmonic effects via a quasi-phonon expansion. (auth) (UK)

**56341** (NP-19010) TABLES OF MAGNETIC STRUCTURES DETERMINED BY NEUTRON DIFFRACTION. PART V. MONOCLINIC SYSTEM. Oles, A.; Bombik, A.; Kajzar, F.; Kucab, M. (Institute of Nuclear Techniques, Krakow (Poland)). May 1971. 28p. (INT-11). Dep. NTIS (U. S. Sales Only).

Compounds and alloys belonging to the monoclinic system at room temperature are covered. The tables include the space group, crystallographic data, cation distribution, temperatures of magnetic transitions, magnetic structure (including figures), magnetic moments, etc. Magnetic space groups for stoichiometric compounds are given. The references are arranged according to year. (D.L.C.)

**56342** PHONON SPECTRUM OF SCANDIUM METAL BY INELASTIC SCATTERING OF NEUTRONS. Wakabayashi, N.; Sinha, S. K.; Spedding, F. H. (Iowa State Univ., Ames). Phys. Rev., B; 4: No. 8, 2398-2406(15 Oct 1971).

The phonon dispersion relations along the principal symmetry axes of the hexagonal close-packed metal scandium were measured at room temperature by means of inelastic neutron scattering. The results were analyzed in terms of a sixth-neighbor modified axially symmetric force-constant model. Both the dispersion curves and the force-constant model are qualitatively similar to those obtained for yttrium metal and yield long-range interactions in the basal plane and interactions that decrease rapidly in the direction normal to the basal plane. A qualitative discussion is also given concerning the directional nature of the bonding in hcp metals from a consideration of the electron–phonon matrix elements. Evidence was found for an anomaly along the $\Delta_1$ branch reflecting the nesting feature of the Fermi surface along that direction. An unsuccessful search was made for paramagnon-type excitations in this metal down to 4.2°K. (auth)

**56343** STRUCTURE IN THE NEUTRON SCATTERING SPECTRA OF ZIRCONIUM HYDRIDE. Couch, J. G. (Southern Oregon Coll., Ashland); Harling, O. K.; Clune, Lavern C. Phys. Rev., B; 4: No. 8, 2675-81(15 Oct 1971).

Neutron double-differential cross sections of four polycrystalline samples of $ZrH_x$ with hydrogen-to-zirconium ratios (x) of 0.54, 1.03, 1.56, and 2.00 were measured with high-energy resolution by downscattering of neutrons from initial energies of 171.5 and 244.8 MeV. Clear evidence of structure in the one-phonon optical peak of $ZrH_2$ is observed for the first time. This structure consists of two maxima located at energy transfers of 137 and 143 MeV and a shoulder located at 154 MeV. Similar structure is indicated for the other hydride samples but it becomes less-well-defined as the hydrogen-to-zirconium ratio decreases. The observed structure is compared with predictions of a central-force model calculation by Slaggie, which includes the effects of interactions between hydrogen atoms. The widths of the hydrogen vibration peaks are found to depend upon the zirconium-to-hydrogen ratio as well as upon the momentum transferred in the scattering process. (auth)

**56344** THEORY OF LATTICE SOFTENING AND SPIN SUSCEPTIBILITY IN A 15 COMPOUNDS. Dieterich, W.; Klose, W. (Univ. of Saarland, Saarbruecken, Ger.). Z. Phys.; 246: No. 4, 323-32(1971).

The one-dimensional model of A15 compounds is used to calculate phonon frequencies $\omega_\lambda(q)$ from temperature-dependent screening properties of the electron system. The interrelationship between the magnetic susceptibility $\chi(q)$ and $\omega_\lambda(q)$ is derived, and both quantities are studied in the long-wavelength limit $|q| = 0$ and for $|q| = 2k_F$. Numerical values are obtained for $V_3Si$ and $Nb_3Sn$. (auth)

**56345** OPTICAL PROPERTIES OF URANIUM MONONITRIDE FROM 0 TO 74 eV. Arakawa, E. T. (Oak Ridge National Lab., Tenn.); Williams, M. W. J. Nucl. Mater.; 41: No. 1, 91-5(Oct 1971).

Optical constants were obtained for polycrystalline UN from 0 to 74 eV. The lower-energy data were compared with band-structure theory and higher-energy data with x-ray emission data. The P(III) level of U in UN has been set at –24 eV and the P(II) level at –32 eV relative to the Fermi energy by analysis of these data. The calculated energy loss functions $-\mathrm{Im}(\epsilon + 1)^{-1}$ and $-\mathrm{Im}(1/\epsilon)$ are interpreted in terms of a combination of single electron transitions and collective oscillations. (auth)

**56346** EMISSIONNYE SVOISTVA MATERIALOV. SPRAVOCHNIK. TRET'E DOPOLNENNOE I PERERABOTANNOE IZDANNE. (Emissive Properties of Materials. Handbook. Third Revised and Enlarged Edition). Fomenko, V. S. Kiev; Naukova Dumka (1970). 148p.

Primarily a manual in tabular form, the work functions of electrons and Richardson's constant are furnished for chemical elements and their compounds, and also for films, formed on given supports. The method of determination and the original publication are indicated for each value listed. 832 references. (K.S.W.)

**56347** EPITAXIAL GROWTH OF SILICON ASSISTED BY ION IMPLANTATION. Itoh, Tadatsugu; Nakamura, Tohru (Waseda Univ., Tokyo). Radiat. Eff.; 9: No. 1-2, 1-4(May 1971).

Epitaxial n-type silicon layers were grown on p-type silicon substrates by vacuum deposition combined with silicon ion implantation (PIVD). A dependency of electrical characteristics of Si epitaxial junction on acceleration energy of silicon ions was measured. A location of the interface and a distribution profile of defects were investigated by means of $He^+$ backscattering technique, and some distance shift of the interface occurred in the case of PIVD. (auth)

**56348** EXPERIMENTAL INVESTIGATION OF THE BAND STRUCTURE OF GRAPHITE. Willis, R. F.; Feuerbacher, B.; Fitton, B. (European Space Research and Technology Centre, Noordwijk, Holland). Phys. Rev., B; 4: No. 8, 2441-52(15 Oct 1971).

Photoemission and secondary electron emission (SEE) measurements were used to investigate the band structure of graphite. The energy distribution curves obtained from both types of measurements reveal identical features for those transitions to conduction-band states occurring up to 5 eV above the vacuum level. Two minima in the $\sigma_1$ conduction band, located at critical points $\Gamma_{3u}^+$ and $Q_{1u}^+$, have been observed at 7.5 and 8.6 eV above the Fermi level. Emission from these final states is observed for $\vec{E} \parallel c$ orientation due to the relaxation of electrons initially excited to $P_3^+$; this $\vec{E} \parallel c$ transition, which is observed at 14.5± 0.5 eV, is in good agreement with the predicted value of 13.5 eV assigned to transitions $P_3^- \rightarrow P_3^+$. The $\sigma$-band gap at the Brillouin-zone center has been measured for $\vec{E} \perp c$ to be 11.5 ± 0.1 eV and the separation of the $\sigma$ bands increases to 15.0 eV at Q in good agreement with the optical reflectivity data. The observation and assignment of interband transitions at higher SEE energies provide additional evidence in support of the two-dimensional band structure proposed by Painter and Ellis. The photoemission measurements give detailed information concerning the nature of the $\pi$-band structure at points along the three-dimensional Brillouin-zone face. The splitting of the $\pi$ bands at P and Q is observed to be 0.8 eV, which gives rise to $\vec{E} \perp c$ transitions at 4.76 and 4.82 eV associated with the saddle-point nature of the $\pi$ bands at Q, and a value of 0.42 eV for the Slonczewski and Weiss parameter $\gamma_1$. The SEE results locate $P_3^-$ below the Fermi level, which provides evidence for electron occupancy at the center of the Brillouin-zone edge in agreement with recent Fermi-surface studies. (auth)

**56349** ELECTRIC TRANSPORT OF TRACES OF TIN ISOTOPES IN THE TERNARY SYSTEM TIN–BISMUTH–CADMIUM AT 300°C. Belashchenko, D. K. Izv. Akad. Nauk SSSR, Metal.; No. 5, 90-6(Sep-Oct 1970). (In Russian).

The electric transport of Sn isotopes in the $^{113-123}$Sn range was studied in Sn–Bi–Cd melts at 300°C by a method based on establishing a stationary state in a vertical capillary. This method in fact measured the noncorrelated effective charge of the transported material; the transport characteristics were materially affected by statistical correlation. The relative electron-scattering cross sections of the Sn and Bi ions also depended substantially on the composition of the melt and were controlled by the degree of short-range ordering in the latter. (Metals Abstr.)

**56350** ELECTRON WORK FUNCTION OF TANTALUM–RUTHENIUM ALLOYS. Kultashev, O. K.; Makarov, A. P. Fiz. Metal. Metalloved.; 30: No. 5, 924-8(Nov 1970). (In Russian).

The work function of a wide range of Ta–Ru alloys was studied by analyzing the thermionic emission of electrons from the corresponding materials. There was a sharp rise in work function (from 4.1 to 4.9 eV) when the Ru concentration exceeded 5%. This effect was attributed to the formation of a monatomic film of Ru on the surface of the solid solution. The work function then remained constant up to 40% Ru (onset of the $\mu$ phase); it rose to a maximum of 5 eV at 57% Ru and then fell steadily to the normal Ru value (4.75 eV). (Metals Abstr.)

**56351** TEMPERATURE DEPENDENCE OF THE ABSOLUTE THERMO-E.M.F. COEFFICIENT OF CERTAIN TRANSITION METALS. Nemchenko, V. F.; L'vov, S. N.; Mal'ko, P. I.; Vereshchaka, N. P. Fiz. Metal. Metalloved.; 30: No. 5, 1088-90(Nov 1970). (In Russian).

The absolute thermo-emf coefficients of a number of transition metals (Ti, Zr, Hf, V, Cr, Fe) were measured at 0 to 1000°C and compared with the electron structure of the corresponding materials. The temperature dependence of the thermo-emf was of a complex nature in each case, exhibiting flat maximum and minima. Satisfactory explanations for the complex relationships demanded specific assumptions as to the structure of the d bands, which were arbitrarily divided into four subsidiary bands for this purpose. (Metals Abstr.)

**56352** OPTICAL CONSTANTS OF THE $\beta$-PHASES NiIn, PdAl, $NiGa_{1-y}Al_y$, AND (Ni,Cu)Ga. Best, Klaus-Juergen; Rodies, Heinz-Juergen; Jacobi, Hatto (Max-Planck-Institut fuer Metallforschung, Stuttgart). Z. Metallk.; 62: No. 8, 634-7(Aug 1971). (In German).

The absorption $\epsilon_2$ of several $\beta$-Hume-Rothery phases was measured for photon energies between 0.7 and 5.5 eV. The NiIn alloys with an excess of indium showed an absorption maximum at 3 eV and a shoulder at 3.7 eV. The spectra did not change with chemical composition as the number of electrons per unit cell remained constant due to the defect structure. The absorption spectrum of the $\beta$ phase PdAl deviated strongly from that of PdIn and was characterized by only one shoulder and a large free electron underground. This behavior, which is not typical for $\beta$ phases, is probably caused by a partial transformation during quenching of the alloy. (auth)

**56353** MAGNETIC PROPERTIES OF $LaSn_3$. Welsh, L. B. (Northwestern Univ., Evanston, Ill.); Toxen, A. M.; Gambino, R. J. Phys. Rev., B; 4: No. 9, 2921-31(1 Nov 1971).

The normal-state nuclear-magnetic-resonance (NMR) Knight shifts and spin–lattice relaxation times are reported for $^{139}$La and $^{119}$Sn in $LaSn_3$ from 1.6 to 300°K. New susceptibility data on higher-purity samples are reported for 4.2 to 700°K, which allow a more accurate determination of the susceptibility $\chi$ than previously reported. Above 100°K, $\chi$ is Curie–Weiss, but it increases by only 6% below 77°K. The $^{119}$Sn relaxation time ($T_1T$ = 0.033 sec°K) and isotropic Knight shift (+0.640%) are temperature-independent, while the anisotropic Knight shift is strongly temperature-dependent. The $^{139}$La Knight shift(+0.207% at 4.2°K) and relaxation time ($T_1T$ = 1.25 sec°K at 4.2°K) have a temperature dependence more than an order of magnitude smaller than expected in the case of a strong-exchange enhancement of the La d-spin susceptibility. Various partitions of the NMR and $\chi$ data are discussed using the customary approximations for transition metals. It was found that the assumption of a dominant La d-orbital susceptibility which has the same temperature dependence as the La d-spin susceptibility gives the most reasonable results, although with the large number of assumptions involved the fit is not unique. Finally, the nature of this orbital susceptibility is discussed and it is pointed out that paramagnetic contributions exist that usually are neglected and that may have the observed magnitude and temperature dependence. (auth)

**56354** NEUTRON ORBITAL CROSS SECTION FOR A TIGHT-BINDING MODEL OF PARAMAGNETIC NICKEL. Lovesey, S. W. (Oak Ridge National Lab., Tenn.); Windsor, C. G. Phys. Rev., B; 4: No. 9, 3048-54(1 Nov 1971).

The orbital contribution to the magnetic partial differential neutron cross section is calculated for a realistic band model of paramagnetic nickel within the tight-binding scheme. The orbital contribution is generally less than one-quarter that of the spin contribution in an energy range up to ~0.15 eV. At higher energies it exceeds the spin contribution and should be observable. (auth)

**56355** ELECTROLYTIC BEHAVIOR OF YTTRIA-STABILIZED HAFNIA. Schieltz, Jon D.; Patterson, John W.; Wilder, D. R. (Ames Lab., Iowa). J. Electrochem. Soc.; 118: No. 8, 1257-61(Aug 1971).

X-ray analysis and electrical conductivity measurements (800 to 1000°C) on yttria–hafnia solid solutions between 2 and 20 mole % $Y_2O_3$ were made to locate the cubic phase and to select the composition best suited as a solid electrolyte. The phase boundary is located near 7 mole % $Y_2O_3$. Total conductivities obtained from the cubic-phase solid solutions appear to be ionic. The 8 mole % $Y_2O_3$–$HfO_2$ composition showed the highest conductivity (log $\sigma_T$ = 1.57 at 1000°C), and lowest activation energy (16.9 kcal/mole), and was selected as the optimum composition for a solid electrolyte. Open-circuit emf, electrical conductivity, and Wagner d-c polarization measurements between 800 and 1000°C were made to determine the electrolytic domain of the 8 mole % $Y_2O_3$ composition. The electrolytic domain width at 1000°C extends from log $P_{O2}$ (atm) = –16.6 to +0.4. The 8 mole % yttria-stabilized hafnia composition does appear suitable as a solid electrolyte. Its electrical

XUM

properties are very similar to those of calcia-stabilized zirconia. (auth)

**56356** DE HAAS–VAN ALPHEN EFFECT IN VANADIUM. Phillips, R. A. (Ames Lab., Iowa). Phys. Lett.; 36A: No. 5, 361-2(27 Sep 1971).

De Haas–van Alphen oscillations in vanadium single crystals using large impulsive fields were investigated. The results are interpreted in terms of distorted ellipsoids located at the symmetry points N in the Brillouin zone. (auth)

**56357** THEORY OF THE ANOMALOUS HALL EFFECT IN THE RARE EARTHS. Giovannini, B. (Univ., Geneva). Phys. Lett.; 36A: No. 5, 381-2(27 Sep 1971).

A new contribution for the anomalous Hall resistivity in the rare earths is derived, which, together with the term calculated by Kondo and Maranzana, gives a very good fit with the experimental data. (auth)

**56358** SOME RECENT RESULTS ON MAGNETISM IN ALLOYS. Beck, Paul A. (Univ. of Illinois, Urbana). Met. Trans.; 2: No. 8, 2015-24(Aug 1971).

The effect of local atomic environment on the atomic moment of Fe in Fe–Al alloys and of V in Au–V alloys is re-evaluated, using improved methods of analysis and new magnetic data. Magnetic clusters with giant moments occur in many alloys in which one of the components has no magnetic moment. This is true for Fe–Al in spite of the presence of well-developed atomic long-range order, although the concentration of magnetic clusters does decrease with increasing long-range order. The phenomena of mictomagnetism are reviewed. Mictomagnetism occurs in many alloys having no long-range atomic order, and it is characterized by the freezing of the spin orientations at low temperatures but, in contrast to ferromagnetism and to antiferromagnetism, without long-range magnetic order. (auth)

**56359** CRYSTAL FIELD LEVELS AND SUPERCONDUCTIVITY IN $LaAl_2$–RARE EARTH ALLOYS. Cooper, J. R. (Imperial Coll. of Science and Tech., London). Solid State Commun.; 16: No. 9, 1429-32(Aug 1971).

The cubic crystal-field parameters for Tm impurities in a $LaAl_2$ host matrix were deduced from measurements of magnetic susceptibility and used to predict crystal-field-level schemes for the other $La_{1-n}R_nAl_2$ alloys. The effect of these splitting on the $T_c(n)$ curves and the values of the exchange parameter $J_{sf}$ derived from them is discussed. (auth)

**56360** POSITRON LIFETIME STUDIES IN SOME CRYSTALS. Sen, P. (Saha Inst. of Nuclear Physics, Calcutta). J. Phys., A (London); 4: No. 5, 744-7(Sep 1971).

Positron lifetime measurements in some single crystals were made with 0.200 nsec (fwhm) prompt time resolution and $4 \times 10^4$:1 peak-to-background ratio. In general, the decay spectra displayed essentially a single exponential. The intensity $I_2$ of the long component was found to be less than or equal to 1% in practically all cases and was assigned to source sample effects. No difference in lifetime was observed between n-type and p-type crystals. Measurements on x-ray-irradiated samples do not show any change in the $\tau_1$ lifetime values. (auth) (UK)

**56361** MAGNETIC PROPERTIES OF COMMERCIAL SOFT MAGNETIC ALLOYS AT CRYOGENIC TEMPERATURES. Ackermann, F. W. (Carpenter Tech. Corporation, Reading, Pa.); Klawitter, W. A.; Drautman, J. J. Advan. Cryog. Eng.; 16: 46-50(1971).

From Cryogenic engineering conference; Boulder, Colo. (17 Jun 1970). See CONF-700628.

Magnetic properties at cryogenic temperatures were investigated for the following alloys: 99.8% Fe, 2.5% Si–Fe, 49 Permalloy (49% Ni–Fe), 4 Mo–Permalloy (80% Ni–4% Mo–Fe), and 2 Vanadium–Permendur (2% V–49% Co–Fe). In certain commercial ferromagnetic alloys, the structure-sensitive magnetic properties such as permeability and coercive force are substantially poorer at low temperatures than at room temperature. However, saturation induction, which is structure-insensitive, is not influenced by low temperatures. It appears that the magnitude of the change in ferromagnetic properties is related to the difference between the test temperature and the Curie or magnetic-transformation temperature of the material. The change in magnetic properties with temperature is reversible. (M.H.R.)

**56362** MONTE CARLO METHODS IN ELECTRON TRANSPORT THEORY. Barker, J. R.; Hearn, C. J. (Univ. of Warwick, Coventry, Eng.). pp 34.1-5 of Computational Physics. Vols. I and II. London; Her Majesty's Stationery Office (1969).

From Conference on computational physics; Culham, England (28 Jul 1969). See CONF-690706-(Vols.1 and 2).

The recent application of Monte Carlo methods to highly non-equilibrium electron transport problems in solids is briefly reviewed. The complex nature of electron collisions with phonons and impurities in solids requires special handling of the time of flight sampling and collision channel selection. Generalizations of a self-scattering device to overcome these problems are presented, together with a proof of its validity. Application to studies of photo-excited electrons in semiconductors at low temperatures is mentioned. (auth) (UK)

## *Moessbauer Effects and NMR*

*Refer also to abstracts 55105 and 56071.*

**56363** NUCLEAR QUADRUPOLE INTERACTION IN CADMIUM METAL. Raghavan, P.; Raghavan, R. S. (Univ., Munich). Phys. Rev. Lett.; 27: No. 11, 724-6(13 Sep 1971).

The nuclear quadrupole interaction of the 247-keV level of $^{111}Cd$ in pure Cd metal was measured by the time-differential perturbed angular correlation method. The interaction frequency $\nu_Q = (e^2qQ/h) = 125(1)$ MHz at 298°K. A measurement at 77°K shows an increase of $\nu_Q$ by 10% instead of a decrease expected from the contraction of the unit lattice of Cd metal. (auth)

**56364** MOESSBAUER EFFECT METHODOLOGY. VOLUME 6. Proceedings of the Sixth Symposium, Chicago, January 25, 1970. Gruverman, Irwin J. (ed.). Boston; New England Nuclear Corporation (1971). 244p. (CONF-700114).

Fifteen papers are presented on the following topics: standards, Gol'danskii–Karyagin effect, frozen aqueous solutions, Ra compounds, comparison with time-differential perturbed angular correlations, $SnCl_2$ and $SnBr_2$ complexes of thiourea and tetramethylthiourea, spinodal decomposition in Fe–Cr, polarized $^{57}Fe$ source, coincidence Moessbauer spectroscopy, rf perturbation of hyperfine levels, recoil radiation damage following Coulomb excitation, and lunar sample investigations. Separate abstracts have been prepared for five of the papers. An index for Vol. 6 and a cumulative table of contents for Vols. 1 to 6 are included. (D.L.C.)

*For abstracts of individual papers see: 56365–56369.*

**56365** CURRENT STATUS OF MOESSBAUER SPECTROSCOPY STANDARDS. Herber, Rolfe H. (Rutgers–The State Univ., New Brunswick, N. J.). pp 3-15 of Moessbauer Effect Methodology. Vol. 6. /Gruverman, Irwin J. (ed.). Boston; New England Nuclear Corp. (1971).

From sixth symposium on Moessbauer effect methodology; Chicago, Ill. (25 Jan 1970).

Efforts to standardize the reporting of Moessbauer data are reviewed, including work on the velocity calibration of spectrometers and on isomer shift standards with respect to iron, tin, iodine, and other Moessbauer nuclides. Suggestions are made concerning nomenclature and conventions for reporting Moessbauer effect data. 43 references. (auth)

**56366** SIMPLE MONOCHROMATIC, POLARIZED $^{57}Fe$ MOESSBAUER SOURCE. Stampfel, John P.; Flinn, Paul A. (Carnegie-Mellon Univ., Pittsburgh). pp 95-107 of Moessbauer Effect Methodology. Vol. 6. /Gruverman, Irwin J. (ed.). Boston; New England Nuclear Corp. (1971).

From sixth symposium on Moessbauer effect methodology; Chicago, Ill. (25 Jan 1970).

The use of a polarized gamma-ray source in Moessbauer experiments leads to a significant simplification of complex spectra and the possibility of obtaining information not otherwise easily available. Previous attempts to produce a polarized source have been expensive or cumbersome and did not always produce a monochromatic beam. One technique is to use radiation scattered from a magnetized foil. This is wasteful of source intensity. A second is to magnetize the source, producing several lines of definite polarization. The most promising approach is to use a filter. Thus far, that has meant moving an absorber at a constant velocity with respect to the source such that one polarization is absorbed by it and the other is allowed to pass to the absorber sample of interest. Until now, this has required two driving systems. The recent availability of the source $^{57}CO$ in CoO for use in the Moessbauer spectroscopy of iron has made possible the following development. The isomer shift of this material is on the order of −1.0 mm/sec with respect to metallic iron, thus placing the right peak of the inner pair of the absorption spectrum of iron very nearly at zero velocity. Alloying iron with rhodium at a certain composition has produced a material one of whose absorption peaks is at zero velocity and is broad enough to cover the source line. When this material is attached to the source and suitably magnetized, a beam of monochromatic radiation of almost 100% linear, left or right circular, or elliptical polarization (de-

XUM

pending on the orientation of the magnetization) is produced. Several spectra have been taken as examples and are presented. (auth)

**56367** COINCIDENCE MOESSBAUER SPECTROSCOPY. Hoy, Gilbert R.; Hamill, Dennis W.; Wintersteiner, Peter P. (Boston Univ.). Contract AT(30-1)-3973. pp 109-21 of Moessbauer Effect Methodology. Vol. 6. /Gruverman, Irwin J. (ed.). Boston; New England Nuclear Corp. (1971).

From sixth symposium on Moessbauer effect methodology; Chicago, Ill. (25 Jan 1970).

Coincidence Moessbauer spectroscopy (CMS) is a technique that merges the methods of the Moessbauer effect and $\gamma-\gamma$ angular correlation. The ultimate goal is to obtain solid-state information that would otherwise be unavailable. The usual procedure is to observe two $\gamma$ rays in delayed coincidence. The first $\gamma$ ray signals the formation of the Moessbauer state, the second signals its decay. The Moessbauer absorption spectrum using a particular delay time T is, in the simplest cases, characteristic of T. This is called "time filtering". Experimental and computational techniques used in CMS are presented. Experimental data are shown that can be explained in terms of time filtering. Additional data indicate the improved resolution and increased percentage effect obtained using CMS. Numerical results are given so that one can estimate the necessary T needed to obtain a particular linewidth. Difficulties associated with interpreting multiline spectra are pointed out. A brief discussion of possible uses of CMS is also given. 25 references. (auth)

**56368** RADIOFREQUENCY PERTURBATION OF SELECTIVELY EXCITED NUCLEAR HYPERFINE LEVELS. Heiman, Neil D. (Johns Hopkins Univ., Baltimore); Walker, J. C.; Pfeiffer, Loren. pp 123-41 of Moessbauer Effect Methodology. Vol. 6. /Gruverman, Irwin J. (ed.). Boston; New England Nuclear Corp. (1971).

From sixth symposium on Moessbauer effect methodology; Chicago, Ill. (25 Jan 1970).

Many interesting experiments have been performed using optical resonance radiation. Similar types of experiments can, in some instances, be performed with nuclear resonance radiation. In the experiments described, the Moessbauer effect was used to selectively excite hyperfine sublevels, in direct analogy to the technique employed in optical pumping. Specifically, each of the four $m_j$ sublevels of the 14.4-keV state of $^{57}Fe$ were individually and exclusively populated, using a constant-velocity drive system, a single-line $^{57}Co$ source, and a metallic-iron scatterer arranged in 90° scattering geometry. The excited-state nuclear polarization was detected by analyzing the scattered radiation with a second spectrometer. This procedure was used to detect NMR transitions between the hyperfine sublevels of the 100-nsec state of $^{57}Fe$. This result is encouraging not only because it allows an accurate and velocity-independent determination of the $^{57}Fe$ hyperfine parameters, but, more importantly, the Moessbauer – NMR technique provides an unusually clear method for studying many fundamental physical problems associated with excited-state NMR. Results obtained thus far provide little evidence to support the predictions of Hack and Hammermesh, or Gabriel regarding the NMR-produced distortion of the gamma-ray line shape; however, the frequency dependence of the NMR transition probability is generally in accord with theory, although some anomalies result from the application of a static field. During the investigation of the NMR process, it was discovered that subjecting an iron absorbing foil to an rf magnetic field produced additional distinct lines in the Moessbauer absorption spectrum of $^{57}Fe$. These additional lines have been interpreted as frequency-modulated side bands caused by magnetostrictively produced vibrations. This sideband effect is the most likely explanation of the anomalous effects observed in earlier attempts to use the Moessbauer effect to observe excited-state NMR. (auth)

**56369** RECOIL RADIATION DAMAGE FOLLOWING COULOMB EXCITATION. Hershkowitz, N.; Jacobs, C. G. Jr. (Univ. of Iowa, Iowa City). pp 143-59 of Moessbauer Effect Methodology. Vol. 6. /Gruverman, Irwin J. (ed.). Boston; New England Nuclear Corp. (1971).

From sixth symposium on Moessbauer effect methodology; Chicago, Ill. (25 Jan 1970).

Coulomb excitation by 6-MeV alpha particles was used to produce excited states of $^{178}Hf$, $^{180}Hf$, $^{177}Hf$, $^{182}W$, $^{183}W$, $^{184}W$, and $^{186}W$. The Moessbauer effect of hafnium in several refractory hafnium compounds and of tungsten in tungsten metal was observed. In all experiments, anomalous hyperfine structure or line broadening was observed. Simultaneous measurements of the absorber thickness dependence of Moessbauer spectra of the even–even isotopes of tungsten yielded the narrowest sources yet reported for $^{184}W$ and $^{186}W$. Although the observed spectra for $^{186}W$ are narrower than what is expected from electronic lifetime measurements, it is likely that broadened lines have been observed. The anomalous hyperfine structure and line broadening are interpreted to be the result of radiation damage produced by replacement collisions made by excited nuclei. In all cases, the anomalous structure can be interpreted as electric quadrupole interactions. (auth)

**56370** PROBLEM OF CALIBRATION OF ISOMERIC SHIFTS IN GAMMA-RESONANCE SPECTROSCOPY. Ionov, S. P.; Kaipov, D. K.; Dautov, L. M. Izv. Akad. Nauk Kaz. SSR, Ser. Fiz.-Mat.; No. 4, 44-52(Jul-Aug 1970). (In Russian).

The problems of theoretical evaluation of electron density at the nucleus and of the scale multipliers in gamma-resonance spectroscopy are treated. The most important theoretical investigations are examined. Problems are considered, the solution of which can lead to the correct interpretation of isomer shifts in Moessbauer spectra. (tr-auth)

**56371** SPIN DYNAMICS IN NUCLEAR MAGNETIC RESONANCE. Schulenburg, H. (Freie Univ., Berlin). Z. Phys.; 246: No. 3, 189-202(1971). (In German).

The influence of frequency modulation of the rf field and modulation of the static magnetic field on NMR response is investigated. The mathematical treatment using density operator formalism results in a different dynamical behavior of the nuclei whether frequency- or field modulation is applied. Therefore a general equivalence of the two kinds of modulation does not exist. Explicit solutions for the nuclear magnetization with simultaneous frequency- and field modulation are evaluated for systems obeying Bloch equations. Resonance experiments were performed using different detection methods: i) rf spectrum analysis of the nuclear induction emf from a decoupled (zero-leakage) crossed-coil setup, and ii) conventional lock-in detection of the signal information from an NMR detector with single resonant circuit. (auth)

**56372** THEORY OF NUCLEAR MAGNETIC RESONANCE DETECTED BY NUCLEAR RADIATIONS. Matthias, E. (Univ. of California, Berkeley); Olsen, B.; Shirley, D. A.; Templeton, J. E.; Steffen, R. M. Phys. Rev., A; 4: No. 4, 1626-58(Oct 1971).

A comprehensive theoretical description is given for the effects of magnetic resonance on the angular distribution of radiation emitted from oriented nuclear states. The formulation is made in a general way. It may be applied to an ensemble of nuclei oriented by any method: for example, nuclear reactions, angular correlations, and low-temperature nuclear orientation may be treated. In fact, the theory can also be applied to optical–double-resonance experiments. Statistical tensors are defined to describe nuclear orientation in the "resonant" state. Interactions of the oriented ensemble with extranuclear fields are then considered, and the effect of a radio-frequency (rf) field on the angular distribution of radiation is given. Two formulations are given for the "pure magnetic" case, for which numerical calculations were done. One employs an angular correlation formalism, following the evolution of the density matrix in the laboratory frame S, while the other is more closely related to conventional NMR. In the latter approach the transformation into the frame S''', wherein the statistical tensors are time-invariant, is described in terms of a "generalized torque equation" governing the motion of a unit vector along the symmetry axis in S'''. Both formulations are exact. Time-dependent distribution functions are worked out in detail, with both fixed and random-phase angles between the rf field and the initial symmetry direction. Fast oscillations due to the constant magnetic field are modulated by slow oscillations due to the rf field. Time-integral curves were calculated. These show great sensitivity to the rank of the relevant statistical tensor, to geometry, and to the phase of the rf field. Multipole structure is predicted for certain geometries, with the resonance line showing a number of maxima equal to the rank of the statistical tensor. Under certain conditions two types of asymmetry are observable. A "transient" asymmetry appears for low-rf-field values: This asymmetry is sensitive to the sign of the nuclear moment, but it disappears in high-rf fields. Odd-rank statistical tensors can also give response functions with "persistent" asymmetry that remains at high-rf fields. This is a parity effect and is not sensitive to the sign of the nuclear moment. Effects of relaxation are also discussed briefly. (auth)

**56373** STUDY OF A SERIES OF $Nb_3X$ COMPOUNDS BY NUCLEAR MAGNETIC RESONANCE. Ehrenfreund, E.; Gossard, A. C.; Wernick, J. H. (Bell Telephone Labs., Murray Hill, N. J.). Phys. Rev., B; 4: No. 9, 2906-15(1 Nov 1971).

A series of $Nb_3X$ (X = Sn, Al, Au, Pt, Ir) compounds was studied by observation of nuclear magnetic resonances between 4.2 and 300°K. The full quadrupole structure of $^{93}Nb$ NMR was observed by

XUM

means of pulsed resonance techniques, while X-site resonances were also studied with steady-state techniques. Spin components of the magnetic susceptibility and Knight shift were deduced and found to be smaller and less temperature-dependent than in the case of the $V_3X$ compounds of comparable superconducting transition temperatures. The orbital term of the susceptibility (and the Knight shift) is found to be larger in compounds having higher density of states at the Fermi energy. An attempt is made to account for this correlation in terms of the Labbé–Friedel one-dimensional theory of the d-band structure. The linear relationship between the electric field gradient and the density of states at the Fermi energy found earlier in the $V_3X$ series is not fulfilled in the $Nb_3X$ series. An unusual increase in $1/(T_1T)$ slightly above the superconducting transition temperature is observed for $^{27}Al$ nuclei in $Nb_3Al$. The possibility that superconducting thermal fluctuations are the source of this effect is considered. (auth)

**56374** PROCEEDINGS OF THE CONFERENCE ON THE APPLICATION OF THE MOESSBAUER EFFECT, TIHANY, HUNGARY, 17th–21st JUNE 1969. Dezsi, I. (ed.). Budapest; Akademiai Kiado (1971). 808p. (CONF-690663).

Ninety papers and two abstracts are presented on the applications of the Moessbauer effect in solid-state physics, structural chemistry, and biology. They are arranged into the following sections: general problems, relaxation effects, Goldanskii–Karyagin effect, surface phenomena, alloys, oxides, frozen solutions, biology, chemistry, and miscellany. Separate abstracts were prepared for eight of the papers. (D.L.C.)

*For abstracts of individual papers see: 55105 and 56375–56381.*

**56375** HYPERFINE STRUCTURE OF $^{161}Dy$ IN $Gd_2O_3$ AT 300K. Moerup, S. (Technical Univ. of Denmark, Lyngby). pp 87-91 of Proceedings of the Conference on the Application of the Moessbauer Effect. /Dezsi, I. (ed.). Budapest; Akademiai Kiado (1971).

From Conference on the application of the Moessbauer effect; Tihany, Hungary (17 Jun 1969).

Moessbauer studies were performed with a source consisting of $^{161}Tb$ in a $Gd_2O_3$ lattice at room temperature and with ferromagnetic metallic Dy at 77°K as an absorber. The hyperfine splitting of the $^{161}Dy$, produced by the decay of $^{161}Tb$ in the source, was obtained. The results are interpreted as a pure quadrupole interaction and an upper limit for the electronic relaxation times is found. (auth)

**56376** REMARKS ON THE APPLICATION OF THE MOESSBAUER EFFECT IN THE INVESTIGATIONS OF CRYSTAL MICRODYNAMICS. Bara, J. J. (Jagellonian Univ., Krakow). pp 93-120 of Proceedings of the Conference on the Application of the Moessbauer Effect. /Dezsi, I. (ed.). Budapest; Akademiai Kiado (1971).

From Conference on the application of the Moessbauer effect; Tihany, Hungary (17 Jun 1969).

A short review of some theoretical and experimental aspects of the Moessbauer effect applications to crystal microdynamics is presented in the form of a selection of publications on the Moessbauer effect and a compilation of the numerical values of the Debye–Waller factors and Debye–Moessbauer characteristic temperatures calculated or derived from Moessbauer effect experiments. 295 references. (auth)

**56377** GOLDANSKII–KARYAGIN EFFECT IN MOESSBAUER PATTERNS AND THE ANISOTROPY OF ATOMIC VIBRATIONS IN CRYSTALS. Suzdalev, I. P.; Makarov, E. F. (Inst. of Chemical Physics, Moscow). pp 201-25 of Proceedings of the Conference on the Application of the Moessbauer Effect. /Dezsi, I. (ed.). Budapest; Akademiai Kiado (1971).

From Conference on the application of the Moessbauer effect; Tihany, Hungary (17 Jun 1969).

The experimental and theoretical results concerning the observations of the anisotropy of the atomic vibrations in single crystals and the appearance of the Goldanskii–Karyagin effect (GKE) in the spectra of polycrystalline samples are analyzed systematically. The appearance of GKE in the quadrupole-split spectra of samples without any magnetic field (and in an external magnetic field) and the contribution from the GKE to the magnetic hfs of Moessbauer patterns are investigated. (auth)

**56378** MOESSBAUER EFFECT IN THE SEGREGATING IRON–BERYLLIUM ALLOY. Dehtyar, I. Ya.; Nizin, P. S.; Nishchenko, M. M.; Chuistov, K. V. (Inst. of Metal Physics, Kiev). pp 435-40 of Proceedings of the Conference on the Application of the Moessbauer Effect. /Dezsi, I. (ed.). Budapest; Akademiai Kiado (1971).

From Conference on the application of the Moessbauer effect; Tihany, Hungary (17 Jun 1969).

Phase transitions are studied in quenched Fe–20 at.% Be alloys by isothermal annealing (T = 400°C) with the help of the Moessbauer effect. The analysis of the changes in the effective magnetic field at the nucleus, the isomer shift, and the magnitude in shift of the lines due to the quadrupole interaction made it possible to determine the character of the structural transitions occurring as a result of annealing the alloy. It is shown that after a short annealing of the Fe–Be alloy, these changes are connected with the formation of FeBe and $Fe_3Be$ regions with the structures of B2 and $DO_3$, respectively. A prolonged annealing results in the vanishing of the $DO_3$ structure, the formation of a three-dimensionally periodical modulation of the concentration of the alloy, and the change in the symmetry of the lattice from cubic to tetragonal in its enriched parts. The change of the effective magnetic fields at the nuclei after prolonged tempering is explained by the coagulation of the particles in the separated phase. (auth)

**56379** VALENCE STATES OF EUROPIUM AND DYSPROSIUM IN LAVES PHASES AND ISOMER SHIFTS IN THE MOESSBAUER SPECTRA. Efremov, E. N.; Babeshkin, A. M.; Nesmeyanov, A. N. (Moscow State Univ.). pp 459-64 of Proceedings of the Conference on the Application of the Moessbauer Effect. /Dezsi, I. (ed.). Budapest; Akademiai Kiado (1971).

From Conference on the application of the Moessbauer effect; Tihany, Hungary (17 Jun 1969).

Parameters of the gamma resonance absorption spectra of intermetallic compounds of europium and dysprosium are studied. It is shown that the electron density at the $^{151}Eu$ nucleus changes considerably less than that in the isostructural compounds of dysprosium. This is explained by the difference between the conduction-electron densities and the electron configurations of the ionic core of the rare earth metals. For europium in the Laves phase, the valence state changes periodically as a function of the electronic structure of the second component. (auth)

**56380** STRUCTURAL PROBLEMS IN SOLID-STATE CHEMISTRY. Johnson, C. E. (Univ. of Liverpool). pp 663-79 of Proceedings of the Conference on the Application of the Moessbauer Effect. /Dezsi, I. (ed.). Budapest; Akademiai Kiado (1971).

From Conference on the application of the Moessbauer effect; Tihany, Hungary (17 Jun 1969).

Applications of the Moessbauer Effect as a probe for chemical studies of iron and its environment in inorganic complexes and metallo-organic compounds are reviewed, especially with reference to structure. As with other spectroscopic techniques the interpretation of the data is often empirical, but if measurements can be made on series of similar compounds, reliable information may be obtained on the number, symmetry, and distortion of the ligands. The chemical shift is sensitive to the co-ordination number. The quadrupole splitting is a measure of the departure from cubic symmetry of the charge distribution around the iron site; the sign of the electric field gradient (efg) enables the sense (stretching or squashing) of the distortion to be determined, and the asymmetry of the efg tensor measures the rhombic component. Similar information may be obtained from the dipolar part of the magnetic hyperfine interaction, which is a measure of the distortion of the spin density from cubic symmetry. Experimental data are summarized and are discussed in terms of the stereochemistry of high-spin $Fe^{2+}$ ions in octahedral co-ordination, as well as in a square planar environment (gillespite) and in a series of tetrahedral complexes containing the tetrahaloferrate(II) ion. Intermediate-spin (ferrous phthalocyanine) and low-spin complexes are considered. Among the $Fe^{3+}$ complexes whose structures are discussed are a series of tetrahaloferrate(III) anions and the trisdialkyldithiocarbamates. 30 references. (auth)

**56381** INVESTIGATION OF LOCAL CHANGES IN VALENCE AND STRUCTURE CAUSED BY NUCLEAR TRANSFORMATION IN Co, Fe, I, AND Te COMPOUNDS BY GAMMA RESONANCE SPECTROSCOPIC METHOD. Babeshkin, A. M.; Perfilev, Yu. D.; Lebedev, V. A.; (and others) (Moscow State Univ.). pp 697-708 of Proceedings of the Conference on the Application of the Moessbauer Effect. /Dezsi, I. (ed.). Budapest; Akademiai Kiado (1971).

From Conference on the application of the Moessbauer effect; Tihany, Hungary (17 Jun 1969).

The consequences of the decay of $^{57}Co$, $^{125m}Te$, and $^{125}I$ in different compounds are studied by gamma resonance spectroscopy. The nuclear transformations are shown to induce valence as well as structural changes. The consequences of the decay of $^{57}Co$ in metallic oxides are interpreted by assuming the stability of the cluster structure. (auth)

**56382** MOESSBAUER STUDY OF DYSPROSIUM EQUIATOMIC COMPOUNDS WITH COPPER, SILVER, ZINC, AND RHODIUM. Belakhovskii, M. (CEN, Grenoble, France); Pierre, J. Solid State Commun.; 9: No. 16, 1409-15(Aug 1971).

XUM

Intermetallic cubic dysprosium compounds are studied by Moessbauer effect on $^{161}Dy$. The results are interpreted in terms of the ratio between crystalline field and exchange interactions. The influence of conduction electrons is discussed. (auth) (UK)

**56383** ELECTRON PARAMAGNETIC RESONANCE STUDIES OF TETRAVALENT NEPTUNIUM IN SINGLE CRYSTAL THORIUM OXIDE. Richardson, Riley Porter. Pullman, Wash.; Washington State Univ. (1971). 84p. University Microfilms Order No. 71-18,590.

Thesis.

The electron paramagnetic resonance spectrum of $Np^{4+}$ in single crystal $ThO_2$ was investigated at 7.5, 1.7, and 4.2°K in the 9-, 24-, and 34-GHz bands, respectively. Three basic Zeeman resonances (exclusive of hyperfine splittings) are found to be energetically isotropic about a particular [001] crystalline axis, with g values 2.02, 2.31, and 2.48. These resonances appear to come from three different sites where the $Np^{4+}$ ions are slightly axially displaced, along the [001] axis, from the usual $O_h$ point-group site. A final basic Zeeman resonance, found to be energetically isotropic about the [110] crystalline axis with g = 2.08, is thought to arise from a fourth site in which the $Np^{4+}$ ion is slightly displaced along the [110] axis. The zero-field splittings of the cubic-field ground Stark levels ($\Gamma_8$ quartets) that arise because of these four axial displacements must be between 5 $cm^{-1}$ and 20 $cm^{-1}$ in order to fit the EPR and optical data, respectively. The Lea, Leask and Wolf parameter $\chi$, relating the parameters of the cubic portion of the crystal-field Hamiltonian, is found to be $\chi = -0.667$, $\chi = -0.604$, and $\chi = -0.590$ for the four nearly cubic sites. Considerable hyperfine splitting due to the nuclear spin of $^{237}Np$ ($I = 5/2$) is observed, with $(390 \pm 30) \times 10^{-4}$ $cm^{-1}$ for the absolute value of the hyperfine coupling constant giving the best fit with the data. (Diss. Abstr. Int., B)

**56384** ELECTRON SPIN RESONANCE STUDY OF VANADIUM(II). PART IV. LATTICE SITES OF DIPOSITIVE IONS VANADIUM(II) AND MANGANESE(II) IN LITHIUM AND SODIUM FLUORIDE CRYSTALS, AND EFFECTS OF X IRRADIATION. Chan, K. K.; Shields, L.; Weston, G. J. (Univ. of Bradford, Eng.). J. Chem. Soc., A; No. 17, 2769-74(1971).

A numerical solution by complex Hermitian matrix diagonalisation is made for the spin eigenvalues and interpolated ESR transitions for an orthorhombically sited vanadium(II) ion in lithium fluoride crystal. It is concluded that vanadium(II) ions associate with a single cation vacancy in the nearest-neighbour cationic shells of lithium and sodium fluoride crystals as do manganese(II) ions in lithium fluoride crystals. Manganese(II) ions in sodium fluoride associate with cation vacancies in the next-nearest-neighbour cationic shell, and, in the presence of hydroxide anion, combine with the hydroxide anion in their first co-ordination shell. X rays induce vanadium(II) and manganese(II) migration by a triple process of oxidation by trapping $V_k$-centres ($F_2^-$), migration and then reduction back to their original oxidation state by combining with F-centres ($e^-$). The hydroxide anion in $NaF:OH^-:Mn^{2+}$ inhibits this process. Thermal annealing restores the doped crystals to their original condition. (auth) (UK)

### *Theory*

**56385** BINDING ENERGIES OF TRANSITION-METAL ATOMS ADSORBED ON A TRANSITION METAL. Cyrot-Lackmann, F. (Institut Laue-Langevin, Grenoble, France); Ducastelle, F. Phys. Rev., B; 4: No. 8, 2406-12(15 Oct 1971).

The binding energies of transition-metal atoms of the 5d series adsorbed on a 5d transition metal are calculated in the tight-binding approximation. The general features of the variation of the binding energy with the number of adatom 5d electrons are similar for all the substrates. It shows a parabolic behavior with a maximum of the order of the cohesive energy for the substrate, and a subsequent sharper decrease as the number of adatom 5d electrons is increased. The maximum is always located close to tungsten, as in the case of a tungsten substrate, where it is between tungsten and rhenium. (auth)

**56386** NATURE OF THE CHEMICAL-BOND FORCES IN COMPOUNDS FORMED BY d-TRANSITION METALS. Markhasev, B. I. Izv. Akad. Nauk SSSR, Metal.; No. 5, 170-3(Sep-Oct 1970). (In Russian).

Factors affecting the formation of chemical bonds between d-transition and other metals as in the phases $ZrV_2$, $ZrMo_2$, $HfW_2$, etc. are discussed. The main factor determining the chemical forces in such cases is the tendency for the d-shell electrons to be redistributed in accordance with the Hund "least-energy" rule (electron configurations with the maximum number of parallel spins). However, a number of Laves phases infringe this rule. Reasons for this anomaly are considered. (Metals Abstr.)

**56387** MODEL POTENTIAL FOR Zn, Cd, AND Hg. Shaw, R. W. Jr. (Bell Telephone Labs., Murray Hill, N. J.); Appapillai, M. Phys. Lett.; 36A: No. 5, 365-6(27 Sep 1971).

A simple procedure for modeling the l = 2 component of the potential in Zn, Cd, and Hg is suggested. The model accounts explicitly for the near resonant behavior of the d-states. (auth)

**56388** ELECTRONIC STRUCTURE OF THORIUM METAL: ROLE OF THE 5f ELECTRONS. Koelling, D. D. (Northwestern Univ., Evanston, Ill); Freeman, A. J. Solid State Commun.; 9: No. 16, 1369-72(Aug 1971).

Symmetrized Relativistic Augmented Plane Wave calculations for thorium, using Kohn–Sham–Gaspar exchange, demonstrate that the 5f states must be considered as band states, unlike the 4f states in the rare-earth metals which are localized states. (auth) (UK)

## Theoretical Physics

*Refer also to abstracts 55883, 56187, 56462, and 56575.*

**56389** (JINR-P4-5954) COHERENT RADIATION OF THE FAST ELECTRON IN MEDIUM. Frank, I. M. (Joint Inst. for Nuclear Research, Dubna (USSR). Lab. of Neutron Physics). 1971. 42p. (In Russian). Dep. NTIS (U. S. Sales Only).

The history of the work accounting for phenomena discovered by Vavilov and Cherenkov is given. Some problems related to this theory are considered. (auth)

**56390** (LYCEN-7104, S5.1-53) RESOLUTION OF THE N-BODY PROBLEM IN THE HYPERSPHERICAL FORMALISM. Fabre de la Ripelle, M. (Paris Univ., Orsay (France). Institut de Physique Nucleaire). (In French).

From Conference on some microscopic aspects of nuclear reactions; La Toussuire, France (15 Feb 1971).

The problem of N bodies is analyzed in a 3-N-dimensional coordinate system. Instead of studying the motion of N points in a 3-dimensional space, the system is solved by studying the motion of a point in a 3-N-dimensional space. The symmetry and invariance properties of the quantum states may be more easily determined. (France)

**56391** REDUCTION OF THE DIRAC EQUATION TO A NONRELATIVISTIC FORM. Moss, R. E. (Univ. of Southampton, Eng.). Amer. J. Phys.; 39: No. 10, 1169-72(Oct 1971).

The positive and negative energy solutions of the Dirac equation for a free electron are completely decoupled using the method of small components. It is shown that this separation is formally equivalent to that obtained with the Foldy–Wouthuysen transformation but that the separation is achieved much more economically with the method of small components. The method may also be used to relate operators in the relativistic and nonrelativistic representations. (auth)

**56392** PHENOMENOLOGICAL QUANTUM THEORY OF THE EXTERNAL CHERENKOV EFFECT. Agudin, J. L. (International Atomic Energy Agency, Vienna. International Center for Theoretical Physics, Trieste, Italy). Lett. Nuovo Cim.; 2: No. 12, 583-6(18 Sep 1971).

The emission of electromagnetic radiation from a charged particle that moves freely in vacuum and in close proximity to a dielectric surface—external Cherenkov effect—was observed by Danos et al. (1953). Although adequate classical explanations have been given, it was thought to be of interest to look at the experiment from a phenomenological point of view by considering the emission of evanescent photons by the charged particle. (W.D.M.)

**56393** MOTION OF CHARGED PARTICLES WITH RADIATION REACTION. Sen Gupta, N. D. (Tata Inst. of Fundamental Research, Bombay). Indian J. Pure Appl. Phys.; 9: No. 4, 201-3 (Apr 1971).

It is pointed out that the equation of motion with radiation reaction contains two parameters e/m and $e^2/mc^3$, and the physical solutions are those that admit the passage of the parameter $e^2/mc^3$ to the limit zero. It is shown that, in order to obtain the physical solutions of the equation of motion with radiation reaction, the initial acceleration has to be obtained from the equation of motion corresponding to the given initial velocity and position. (auth)

**56394** ELECTRONS IN A STRONG COULOMB FIELD. Sen Gupta, N. D. (Tata Inst. of Fundamental Research, Bombay). Indian J. Pure Appl. Phys.; 8: No. 12, 765-8(Dec 1970).

The nature of the Sommerfeld orbits is investigated for an electron in a strong Coulomb field when $\alpha Z > n_\varphi$. Further, it is shown that relativistic wave equations in a similar case lead

XUM

to non-steady decaying states. The decay time corresponds to the time of fall for the spiral inward orbit. The non-steady states lead to average radial current. This is shown to be the case with both the Klein-Gordon and the Dirac equations. (auth)

**56395** DYNAMICAL APPLICATIONS OF BARGMANN SPACE. III. ANGULAR MOMENTUM. Robinson, J. M.; Trubatch, S. L. (California State Coll., Long Beach). Amer. J. Phys.; 39: No. 10, 1190-4(Oct 1971).

The coherent state representation is developed for angular momentum operators. As an example, the one-boson Lee model is analyzed with its Fermi operators in Bargmann space. Finally, a synthesis is achieved by analyzing the three-level system with all operators in Bargmann space. (auth)

**56396** BOUND STATE AND CONTINUUM CONTRIBUTIONS TO THE TWO-BODY PARTITION FUNCTION. Gigson, W. G. (Univ. of Sydney). Phys. Lett.; 36A: No. 5, 403-4(27 Sep 1971).

The expression for the partition function in terms of the Jost function gives a unified description of bound state and continuum contributions. It demonstrates continuity as new bound states are introduced, and cancellation between bound state and continuum parts at high temperatures. (auth)

**56397** COLLECTIVE STATES AND STATISTICS OF SYSTEMS OF IDENTICAL ATOMS. Kruglik, G. S. (Inst. of Physics, Minsk). Teor. Mat. Fiz.; 8: No. 1, 130-9(Jul 1971). (In Russian).

Assuming the violation of the symmetrization postulate, the author suggests the generalization of the secondary quantization method in the quantum-mechanical approach and obtains the formula for the equilibrium distribution of atoms into the states (the formula of the generalized statistics). The well-known Bose, Fermi, and Boltzmann distributions follow from this formula as its particular cases. (auth)

**56398** REDUCTION OF THE MULTI-DIMENSIONAL SCHROEDINGER EQUATION TO A ONE-DIMENSIONAL INTEGRAL EQUATION. Rosenthal, C. M. (Univ. of Wisconsin, Madison). Chem. Phys. Lett.; 10: No. 4, 381-6(15 Aug 1971).

A method is proposed for reducing the multidimensional Schrödinger equation to a one-dimensional integral equation. The reduction is exact; the resulting integral equation, although complicated, may be treated for any of a number of numerical methods. Two 2-dimensional problems, the harmonic oscillator and the S-limit for helium, and one 3-dimensional problem, the helium ground state, are treated in this way. (auth)

**56399** METRIC EVALUATION IN THE SPACE OF EXPONENTIAL AND GAUSSIAN FUNCTIONS. Silver, D. M. (Johns Hopkins Univ., Silver Spring, Md.). Chem. Phys. Lett.; 10: No. 2, 227-9(15 Jul 1971).

A computational procedure is presented for the numerical evaluation of integrals having both gaussian and exponential functional dependence in the integrand: $\int_0^\infty dr\, r^k \exp(-\alpha r^2) \exp(-\beta r)$. On the basis of the parameter values, $\alpha$, $\beta$, and k, three ranges are distinguished, and in each one an appropriate evaluation method is suggested. (auth)

**56400** COMPUTATIONAL PHYSICS. VOLUMES I AND II. Proceedings of the Conference Held at Culham, England, July 1969. London; Her Majesty's Stationery Office (1969). 255p. £4. (CONF-690706-(Vols. 1 and 2)).

Sixty two papers were presented; twenty-eight were in NSA scope and separate abstracts were prepared. (UK)

*For abstracts of individual papers see: 55047–55050, 55093, 55094, 55713, 55889, 55944, 55945, 56014, 56129, 56187–56192, 56205–56207, 56279, 56362, 56401, 56612, 56865, 56866, and 57102.*

**56401** INVARIANTS IN THE MOTION OF A CHARGED PARTICLE IN A SPATIALLY MODULATED MAGNETIC FIELD. Dunnett, D. A. (Univ. of Liverpool); Laing, E. W.; Taylor, J. B. pp 49.1-8 of Computational Physics. Vols. I and II. London; Her Majesty's Stationery Office (1969).

From Conference on computational physics; Culham, England (28 Jul 1969). See CONF-690706-(Vols.1 and 2).

The effect of a spatial modulation in the magnetic field on invariants such as the magnetic moment $\mu = V^2/B$ is studied. Particular interest was taken as to whether an invariant still exists when the wavelength of the modulation is comparable to the gyro radius of the particle. In an axially symmetric magnetic field, with a square-wave modulation, the orbit equations reduce to algebraic relations convenient for numerical study. It is found from such studies that orbits are of two types: regular orbits that generate an invariant and orbits that are quasi-ergodic. An invariant was calculated by perturbation theory with the depth of modulation of the field as a small parameter. For this, a modified form of perturbation theory which overcomes the difficulty of infinities arising at resonance between the perturbation and the cyclotron period was developed. This difficulty in fact corresponds to a change in topology of the invariant curves. The invariant calculated from this theory shows very good agreement with the numerically computed orbits of the first type. The transition to quasi-ergodic behavior cannot be predicted analytically, but some indication of it may exist in the complex topology of the invariant curves in the ergodic regions. (auth) (UK)

**56402** MODIFICATION OF THE COULOMB LAW IN A STRONG MAGNETIC FIELD. Loskutov, Yu.; Skobelev, V. (Moscow State Univ.). Phys. Lett.; 36A: No. 5, 405-6(27 Sep 1971).

Corrections to the static field of a point electric charge in the presence of a constant and homogeneous magnetic field are found in the lowest-order perturbation theory. (auth)

XUM

# PHYSICS (HIGH ENERGY)

## Particle Interactions and Properties (Experimental)

*Refer also to abstracts 55050, 55093, 56443, 56444–56446, and 56600.*

**56403** SEARCH FOR 4e/3 CHARGED QUARKS IN THE COSMIC RADIATION AT 2750 METERS. Beauchamp, William Thomas. Tucson, Ariz.; Univ. of Arizona (1971). 65p. University Microfilms Order No. 71-18,116.

Thesis.

A scintillation counter telescope consisting of eight liquid scintillation counters and four wide-gap spark chambers was arranged to detect single particles with electric charge ±4e/3 which might be present in the cosmic radiation at 9000 feet above sea level. The apparatus was operated for a total running time of 1520 hours, and two events were found out of a total of 30,000 event triggers. This number of events is consistent with background and sets an upper limit on the vertical flux of 4e/3 charged quarks of $\varphi_q = 4.13 \times 10^{-10}$ cm$^{-2}$ sr$^{-1}$ sec$^{-1}$ if $M_q \gg 1$ GeV/c$^2$ or $\varphi_q = 6.45 \times 10^{-11}$ cm$^{-2}$ sr$^{-1}$ sec$^{-1}$ if $M_q \approx 0.4$ GeV/c$^2$ at the 90% confidence level. (Diss. Abstr. Int., B)

### *Electromagnetic*

*Refer also to abstracts 56643 and 56705.*

**56404** (CONF-701121-8) ELECTROPRODUCTION OF PIONS. Note No. 299. Amaldi, Edoardo (Rome Univ. (Italy). Istituto di Fisica). 11 Jan 1971. 53p. Dep. NTIS (U. S. Sales Only).

From Meeting on electron synchrotron; Frascati, Italy (5 Nov 1970).

The aim is to summarize the experimental and theoretical knowledge on electroproduction of positive and neutral pions at very low energy, in particular near threshold. After an introduction of kinematical nature, the general expression for the cross section—derived under the assumption of a single photon exchange—is given, and the main lines of the various theoretical approaches are summarized. The coincidence experiments made until now and the result of their analysis are considered. (auth)

**56405** (DESY-71/33) EXCITATION OF THE Δ (1236) RESONANCE ON BOUND STATE NEUTRONS. Bleckwenn, J.; Klein, H.; Moritz, J.; Schmidt, K. H.; Wegener, D. (Deutsches Elektronen-Synchrotron, Hamburg (West Germany)). Jun 1971. 18p. Dep. NTIS (U. S. Sales Only).

The cross sections for inelastic electron–deuteron scattering were measured for invariant masses $W \leq 1.4$ GeV of the final hadronic state and momentum transfers of $0.1(\text{GeV/c})^2 < q^2 < 0.5(\text{GeV/c})^2$. The cross section for inelastic electron–neutron scattering was obtained by subtracting the contribution of electron–proton scattering. The cross sections for inelastic electron–neutron and electron–proton scattering are shown to be equal. (auth)

**56406** (DESY-71/35) ELECTROPRODUCTION OF π-MESONS ON PROTONS ABOVE THE SECOND RESONANCE. Heinloth, K. (Deutsches Elektronen-Synchrotron, Hamburg (West Germany)). Jun 1971. 55p. Dep. NTIS (U. S. Sales Only).

Previous experiments on the electroproduction of pions on protons are discussed. Also future work on the electroproduction of pions is mentioned. (J.F.P.)

### *Weak*

**56407** FURTHER RESULTS ON THE INTERFERENCE BETWEEN THE $\pi^0\pi^0$ DECAY OF $K_L^0$ AND $K_S^0$. Wolff, B. (Laboratoire de l'Acclerateur Lineaire, Orsay, France); Chollet, J. C.; Repellin, J.-P.; (and others). Phys. Lett.; 36B: No. 5, 517-20(4 Oct 1971).

The experiment of Chollet et al. was continued with a similar set up. The analysis of these new data leads to 56 free decay events $K_L^0 \rightarrow \pi^0\pi^0$ and 1481 interference events $K_{S,L}^0 \rightarrow \pi^0\pi^0$ behind a 20 cm thick copper regenerator. The results are $\varphi_{00} = 38^0 \pm 25^0$ and $|\eta_{00}|/(|f\text{-}\bar{f}|/k) = (1.13 \pm 0.12) \times 10^{-3}$ where $|f\text{-}\bar{f}|/k$ is the regeneration amplitude for copper at 2 GeV/c in fm$^2$. (auth)

**56408** MEASUREMENT OF THE $K_L \rightarrow \pi e \nu$ FORM FACTOR. Bisi, V. (CERN, Aachen); Darriulat, P.; Ferrero, M. I.; (and others). Phys. Lett.; 36B: No. 5, 533-6(4 Oct 1971).

The $q^2$-dependence of the vector form factor $f_+$ was measured with a wire chamber magnetic spectrometer. Decays were identified by kinematics and gas Čerenkov counters. The vector form factor can be expressed as $f_+(q^2) = f_+(0)(1 + \lambda_+ q^2/m_\pi^2)$, with $\lambda_+ = 0.023 \pm 0.005$. (auth)

**56409** ANALYSIS OF $K_{e3}^+$ DECAY X2 COLLABORATION. Steiner, H. J. (Technischen Hochschule, Aachen); Natali, S.; Romano, F.; (and others). Phys. Lett.; 36B: No. 5, 521-4 (4 Oct 1971).

A study was made of 2700 decays of the type $K^+ \rightarrow \pi^0 e^+ \nu$ in the CERN 1.1 m$^3$ heavy liquid bubble chamber. The four-momentum transfer dependence of the form factor $f_+(q^2)$ was determined. The usual linear parametrization $f_+(q^2) = f_+(0)(1 + \lambda_+ q^2/m_\pi^2)$ gives $\lambda_+ = 0.027 \pm 0.010$. (auth)

**56410** ANALYSIS OF $K_{\mu 3}^+$ RADIATIVE DECAY. Romano, F. (Istituto di Fisica, Bari, Italy); Renton, P.; Aubert, B.; Burban-Lutz, A. M. Phys. Lett.; 36B: No. 5, 525-7(4 Oct 1971).

The branching ratio of $K^+ \rightarrow \pi^0 e^+ \nu\gamma / K^+ \rightarrow \pi^0 e^+ \nu$ was determined and is compared with theoretical predictions. (auth)

**56411** SPARK CHAMBER EXPERIMENT OF THE BETA DECAY OF $\Xi^-$ HYPERONS. Duclos, J.; Freytag, D.; Heintze, J.; (and others) (CERN, Geneva). Nucl. Phys.; B32: No. 2, 493-512 (1971).

A counter-spark chamber experiment to measure the β-decay rate of $\Xi^-$ hyperons is described. The $\Xi^-$ hyperons were produced by $K^-$ of 1.65 GeV/c in a polyethylene target, and their decay observed in an optical spark chamber. A focusing gas Čerenkov counter with cellular structure discriminated between π's and electrons from $\Xi^-$ decay. On the basis of $17 \pm {}^{5}_{4}$ observed β-decay events and 374 observed $\Xi^- \rightarrow \pi\Lambda^0$, $\Lambda^0 \rightarrow \pi^-$p decays representing 1% of the $\Xi^-$ decaying through this channel within the spark chamber during the run, a branching ratio $\Gamma(\Xi^- \rightarrow e\nu\Lambda^0 + e\nu\Sigma^0)/\Gamma(\Xi \rightarrow \pi\Lambda) = (6.8 \pm 2.2) \times 10^{-4}$ is obtained. From a Cabibbo fit to the other baryon leptonic decays, the branching ratio $R_{Cab} = 6.0 \times 10^{-4}$ is expected. As a test of the experimental method, the rate of $\Lambda \rightarrow e\nu p$ decay of Λ's originating from $\Xi \rightarrow \pi\Lambda$ decay is evaluated and found to be in agreement with published values. (auth)

### *Strong (Baryon-Induced)*

*Refer also to abstract 56438.*

**56412** (CEA-R-4193) POLARISATION PARAMETER MEASUREMENT IN THE PROTON–PROTON ELASTIC SCATTERING FROM 0,5 TO 1,2 GeV. Ducros, Yves (Commissariat a l'Energie Atomique, Saclay (France). Centre d'Etudes Nucleaires). 1971. 136p. (In French). Dep. NTIS (U. S. Sales Only).

Thesis. Submitted to Paris Univ., Orsay (France). Faculte des Sciences.

The angular distribution of the polarization parameter was measured in the proton-proton elastic–scattering at seven energies between 0.5 and 1.2 GeV. A polarized proton target was used. The results show a maximum of the polarization parameter of 0.6, at 0.73 GeV. This maximum is due to the important increase of the total cross section between 0.6 and 0.73 GeV. At 1.2 GeV the angular distribution of the polarization shows a minimum for a momentum transfer value of $-1$ (GeV/c)$^2$. A phase shift analysis was done at 0.66 GeV, using all available experimental data at this energy. There is no evidence of a dibaryonic resonance in the $^1D_2$ phase. (auth)

**56413** (INP-756) MEASUREMENTS OF ENERGY AND FLUX OF COSMIC RAY HADRONS USING AN IONIZATION SPECTROMETER. Massalski, J.; Mistygacz, Z.; Suszycki, L.; Warczewski, J. (Institute of Nuclear Physics, Krakow (Poland)). Feb 1971. 20p. Dep. NTIS (U. S. Sales Only).

A method for determining the energy of cosmic ray hadrons was elaborated. In this method besides the development of electromagnetic cascades, which is a dominating process, also other processes such as disintegrations of the nuclei of the absorber and charged π-meson ionization are taken into account. Particles escaping through the bottom of the apparatus, the transition effect: lead-brass (chamber wall), and the geometry of the absorber and detectors are also considered. The method is applied to the determination of energy and flux of cosmic-ray particles registered in an ionization spectrometer installed at the Mount Aragac Laboratory in Armenia (3250 m above sea level). (auth)

**56414** (INP-757) INELASTICITY COEFFICIENTS FOR PION–Fe AND NUCLEON–Fe COLLISIONS. Massalski, Jerzy;

XUM

Suszycki, Leszek; Warczewski, Jerzy (Institute of Nuclear Physics, Krakow (Poland)). Mar 1971. 22p. Dep. NTIS (U. S. Sales Only).

Nucleon-Fe interactions at energies above 1.5 TeV were studied, using the ionization spectrometer method. An analysis of 126 such events is presented. The average energy transferred to neutral pions in nucleon-Fe collisions is found to be 18.3% of the primary nucleon energy. The average total inelasticity for nucleons and $\pi^{\pm}$ mesons is 0.5 ± 0.6 and 0.8 ± 0.9, respectively. The main difficulties in determining inelasticity coefficients by the ionization spectrometer method are discussed. (auth)

**56415** (NP-18888) NEUTRON–PROTON CHARGE EXCHANGE AT 8 AND 19 GeV/c. Horn, Klaus (Kernforschungszentrum, Karlsruhe (West Germany). Institut fuer Experimentelle Kernphysik). Nov 1970. 93p. (In German). Dep. NTIS (U. S. Sales Only).

Thesis. Submitted to Univ. of Karlsruhe, Ger.

The differential effective cross sections for the neutron–proton charge exchange for primary momenta of 8 and 19 GeV/c were measured for scattering angles (in the laboratory system) from 0 to 48 mrad or 0 to 28 mrad (corresponding to a square of the momentum transfer $0 < |t| < 0.15$ or $0 < |t| < 0.27$ $(GeV/c)^2$). There were 3500 charge exchange events for 19 GeV/c and 2600 for 8 GeV/c taken in the wire spark chamber under the on-line control of a process computer. The differential effective cross section agrees in the t dependency for both primary momenta. It shows the characteristic sharp increase for $|t| < (m_\pi/c)^2 = 0.018$ $(GeV/c)^2$ and a flat pattern for $|t| > 0.05$ $(GeV/c)^2$. The results for 8 GeV/c agree with those of Manning et al. In the momentum spectrum of the forward-scattered protons the resonances Δ(1236) and N(1518) can be clearly detected. (tr-auth)

**56416** (USIP-71-1) ANNUAL REPORT, 1970 [ON] PARTICLE PHYSICS. (Stockholm Univ. (Sweden). Inst. of Physics). 44p. Dep. NTIS (U. S. Sales Only).

Research projects on particle physics at the Institute of Physics, University of Stockholm, are summarized. They consist of experiments using bubble chamber technique (proton–proton and proton–deuterium experiments), technical development of an on-line system for measuring machines, automatic registration for scanning tables, experiments at CERN, Geneva, using counter technique, and planning and preparations for experiments at the Intersecting Storage Rings (ISR) at CERN. A list of publications is included. (KK) (Sweden)

**56417** (USIP-71-4) TWO PRONG SAMPLE FROM PROTON–PROTON INTERACTIONS IN A HYDROGEN BUBBLE CHAMBER AT 19 GeV/c. Danielsson, O.; Granstroem, L. (Stockholm Univ. (Sweden). Inst. of Physics). Apr 1971. 52p. Dep. NTIS (U. S. Sales Only).

The scanning, measuring and hypothesis selection procedures of a sample of 12,500 two-prong proton-proton interactions at 19 GeV/c in the CERN 2m hydrogen bubble chamber are described. The total, elastic, $pp\pi^0$ and $pn\pi^+$ cross sections were determined. (auth)

**56418** (USIP-71-6) STUDY OF THE REACTION PROTON + PROTON → NUCLEON + NUCLEON + PION AT 19 GeV/c. Danielsson, Ove (Stockholm Univ. (Sweden). Inst. of Physics). Apr 1971. 69p. Dep. NTIS (U. S. Sales Only).

A bubble chamber experiment was performed to study inelastic three body reactions from proton–proton collisions at an incident momentum of 19 GeV/c. Scanning and measuring procedures and the program chain are described. Special attention is given to a method of automatic selection of kinematical hypotheses, which resulted in improvements in collecting the sample. An investigation of errors is made, and the error estimate of the Coulomb scattering is improved. The energy variation of the cross sections are shown for $pn\pi^+$, $pp\pi^0$ and $\Delta^{++}n$. Analysis of isospin states is done leading to information about the nature of exchangers. A method for distinguishing between the final state nucleons is presented. Finally longitudinal phase space analysis is given. (KK) (Sweden)

**56419** POLARIZATION IN PROTON–PROTON ELASTIC SCATTERING AT 10, 14, AND 17.5 GeV/c. Borghini, M. (CERN, Geneva); Dick, L.; Olivier, J. C.; (and others). Phys. Lett.; 36B: No. 5, 501-3(4 Oct 1971).

Data on the polarization parameter in pp elastic scattering in the $|t|$-range from ~0.1 to ~2.9 $(GeV/c)^2$ and at 10, 14 and 17.5 GeV/c are presented. (auth)

**56420** MEASUREMENTS OF SMALL ANGLE PROTON–PROTON ELASTIC SCATTERING AT THE CERN INTERSECTING STORAGE RINGS. Amaldi, U. (Istituto Superiore di Sanita, Rome. INFN, Rome); Biancastelli, R.; Bosio, C. Phys. Lett.; 36B: No. 5, 504-8(4 Oct 1971).

Proton–proton elastic scattering was measured over the angular range 7 to 16 mrad at center-of-mass energies of 31, 45 and 53 GeV using the CERN Intersecting Storage Rings. The results indicate that the diffraction peak has continued to shrink with increasing energy, but not as fast as suggested by the results at lower energies. (auth)

**56421** NEUTRON TOTAL CROSS SECTIONS ON PROTONS AND NUCLEI IN THe 10 TO 30 GeV/c MOMENTUM RANGE. Jones, L. W. (Univ. of Michigan, Ann Arbor); Longo, M. J.; McCorriston, T. P.; (and others). Phys. Lett.; 36B: No. 5, 509-12(4 Oct 1971).

The results of a recent AGS measurement of the total cross section for neutrons on protons, deuterons and other nuclei in the momentum range 10 to 30 GeV/c are presented. The standard good-geometry transmission technique was used with a total absorption spectrometer to detect the transmitted neutrons. Biasing the spectrometer towards high neutron momenta together with the strongly-peaked momentum spectrum of the beam gave relatively good momentum resolution. Measurements were made at mean momenta of 12, 13, 18 and 26.5 GeV/c. Results are presented and the cross sections for nuclei are compared with theoretical predictions. (auth)

## *Strong (Meson-Induced)*

*Refer also to abstracts 55048, 55049, 56588, and 56653.*

**56422** (CERN-71-14, pp 379-93) $\pi$P ELASTIC SCATTERING, 0 TO 300 MeV. Bugg, D. V. (Queen Mary Coll., London (England)). 4 Aug 1971.

In Spring school on pion interactions at low and medium energies.

The review of $\pi$p elastic scattering at 0 to 300 MeV covers the interest of measurements in this region, total cross sections, calculation of the Coulomb barrier effect, and the total charge-exchange cross section. (J.F.P.)

**56423** (COO-1195-217) A STUDY OF K-PLUS NEUTRON CHARGE EXCHANGE SCATTERING USING THE REACTION K-PLUS DEUTERON GOES TO PROTON PROTON K-ZERO AT 3.8 GeV/c. Moninger II, William Ringland (Illinois Univ., Urabana). 1971. Contract AT(11-1)-1195. 146p. Dep. NTIS.

Thesis.

Data are presented from 431 examples of the reaction $K^+d \to K^+pp_s$ at 3.8 GeV/c. The total and differential cross sections are presented. The total cross section is 498 ± 32 μb; the slope of the forward peak in the differential cross section is 4.1 ± 0.3 $(GeV/c)^{-2}$. The total cross section is compared to cross sections for this reaction at other energies. It is found that $\sigma(K^+d \to K^+pp_s) \sim P_{Lab}^{-2.09\pm0.04}$. The differential cross section for this reaction is compared to the prediction of Rarita and Schwarzschild and to $K^-p$ charge exchange. Total and differential cross sections $K^+n \to K^0p$ are inferred from the $K^+d$ data. The forward amplitude for $K^+n \to K^0p$ is found to be predominantly real. (auth)

**56424** (COO-1428-280) ANNUAL PROGRESS REPORT [ON HIGH ENERGY PHYSICS], TASK A, JUNE 1, 1970–MAY 31, 1971. (Purdue Univ., Lafayette, Ind. Dept. of Physics). Contract AT(11-1)-1428. 30p. Dep. NTIS.

Experimental research on strong interactions is summarized. A list of publications is included. (J.F.P.)

**56425** (COO-1428-294) DIFFRACTIVE $\pi\pi$ SCATTERING IN $\pi N \to \pi\pi N$ AT 13.1 (GeV/c). Gaidos, J. A.; Gutay, L. J.; Kramer, S. L.; Barton, H. R. Jr.; Miller, D. H.; Tebes, J. (Purdue Univ., Lafayette, Ind.). [1971]. 11p. Dep. NTIS.

Data on diffractive $\pi\pi$ scattering in the reactions $\pi^+p \to \pi^+\pi^0p$, $\pi^+p \to \pi^+\pi^+n$, and $\pi^+n \to \pi^+\pi^-p$ are presented and discussed in terms of a factorized double exchange model involving OPE and Pomeranchuk plus exchange-degenerate $\rho$, f contributions. The calculated relative diffractive cross sections, spectral distributions and Pomeranchuk-Regge pole interference terms are in excellent agreement with the data. (auth)

**56426** (FRNC-TH-53) INVESTIGATION OF THE STRANGE MESON RESONANCES PRODUCED IN ASSOCIATION WITH A NUCLEON IN 3 GeV $K^-$NUCLEON INTERACTIONS. Rouge, Andre (Paris Univ. (France). Faculte des Sciences). 1969. 123p. (In French). Dep. NTIS (U. S. Sales Only).

Thesis.

The strange meson resonances produced in 3-GeV $K^-N$ collisions were studied. The four-pronged events in a $K^-p$ experiment

were measured, and the results from a bubble chamber experiment on 3-GeV $K^-d$ collisions were analyzed. The mechanism of $K^*$ (890) production and the properties of $K^*$ (1400) (quantum numbers branching ratios) were studied. Some information was obtained about K pion pion systems with masses lower than 1.4 GeV and the K pion interaction in the S-wave. The upper limits for the production cross sections of possible K with $\frac{3}{2}$ isospin are given. (France)

**56427** (IFA-HE-73) ΛK PRODUCTION IN FOUR-PRONG $\pi^+p$ INTERACTIONS AT 8 GeV/c. Balea, E.; Balea, O.; Mihul, A.; Sabau, M. (Institutul de Fizica Atomica, Bucharest (Romania)). 1970. 14p. Dep. NTIS (U. S. Sales Only).

Investigations on five- and six-particle final states with ΛK production in $\pi^+p$ interactions at 8 GeV/c are reported. C.m.s. momentum and angular distributions of secondary particles are discussed. Results on invariant mass distributions and the cross sections for resonance production are presented. (auth)

**56428** (IFA-HE-75) $K\bar{K}$ PRODUCTION IN FOUR-PRONG $\pi^+p$ INTERACTIONS AT 8 GeV/c. Balea, E.; Balea, O.; Mihul, A.; Sabau, M. (Institutul de Fizica Atomica, Bucharest (Romania)). 1970. 17p. Dep. NTIS (U. S. Sales Only).

Results on five and six-body final states with $K\bar{K}$ production in four-prong $\pi^+p$ interactions at 8 GeV/c were presented. Cross sections for various channels are given. The kinematical behavior of secondary particles was discussed as well as the resonance production. (auth)

**56429** (INP-754) LOW-ENERGY PROTONS GENERATED IN NUCLEAR INTERACTIONS AT PRIMARY ENERGIES 60 GeV AND ~1000 GeV. Babecki, J.; Furmanska, B. (Institute of Nuclear Physics, Krakow (Poland)). 1971. 9p. (CONF-710437-1). Dep. NTIS (U. S. Sales Only).

From International symposium on high energy physics; Dresden, Germany (19 Apr 1971).

Taking into account the effect of secondary interactions in the nucleus and the effect of elastic scattering of the recoil proton on nucleons of the nucleus the fraction of the interactions with a single nucleon in the samples of jets from the Serpukhov accelerator and from cosmic rays selected by means of the criteria: $N_h \leq 5$, $n_s \leq 20$ was estimated as $(70 - 80)\%$. (auth)

**56430** GENERAL REMARKS ON EXPERIMENTS MEASURING PARTICLE WIDTHS AND THE WIDTH OF THE ω. Coyne, D. G.; Butler, W. R.; Fang-Landau, G.; MacNaughton, J. (Univ. of California, Berkeley). Nucl. Phys.; B32: No. 2, 333-65(1971).

The measurement of the width of a resonant state and the associated error depend in a complex way on the number of events, the resolution function and its error, and the background. Because of these dependences, the best result may not necessarily be from the experiment with the best resolution. Some simple approximation for these dependences, avoiding the errors of Gaussian formulae, are given. This enables the experimenter to determine where a more precise treatment is demanded and useful. Our application is to the problem of the width of the ω meson as seen in the reaction $\pi^+p \to \pi^+p\omega^0$. The data are taken from 180000 pictures in the LRL 72 inch hydrogen bubble chamber, incident momentum 3.7 GeV/c. The simple formulae indicate that for this experiment a precision in the ω width comparable to the world average value may be obtained. A near-optimal method of unfolding the true ω signal is described and justified. Application to these data yields $m_\omega = 784.7 \pm 1.0$ MeV, and $\Gamma_\omega = 9.5 \pm 1.0$ MeV. (auth)

**56431** STUDY OF $\pi^-p \to \pi^0n$ AND $\pi^-p \to \eta n$ REACTIONS IN NUCLEI AT 7.82 GeV/c. Guisan, O. (CEN, Saclay, France); Bonamy, P.; Le Du, P.; Paul, L. Nucl. Phys.; B32: No. 2, 681-90(1971).

$\pi^-p \to \pi^0n$ and $\pi^-p \to \eta n$ differential cross sections were measured in nine nuclei ranging from hydrogen to lead at a 7.82 GeV/c beam momentum and in a range of t going from 0 to $-2$ $(GeV/c)^2$. The results can be understood in the framework of the Glauber theory which allows in addition a determination of the $\pi^0$ and $\eta$ total cross sections on nucleons. (auth)

**56432** REGGE ANALYSES OF $\rho^0$ PRODUCTION IN πN CHARGE EXCHANGE CHANNELS AT 7 GeV/c. Matthews, J. A. J. (Univ. of Toronto, Ont.); Prentice, J. D.; Yoon, T. S.; (and others). Nucl. Phys.; B32: No. 2, 366-80(1971).

2380 events in the $\pi^+\pi^-$ mass interval $0.68 < m(\pi^+\pi^-) < 0.88$ GeV from $\pi^+d \to pp\pi^+\pi^-$ and $\pi^-p \to \pi^+\pi^-n$ experiments at 7 GeV/c have permitted an analysis of $\rho^0$ production to be made for momentum transfer, $|t| < 1.0$ $(GeV/c)^2$. The data were found to be in good agreement with a Regge $\pi + A_2$ model including absorption, but were not well described by a Regge $\pi$ model plus absorption. The data and the Regge analyses were consistent with the absence of a nonsense wrong signature zero in the pion Regge amplitude for $|t| < 1.0$ $(GeV/c)^2$. The $\pi + A_2$ Regge analysis of the $\rho^0$ data was compared with similar analyses used to describe $\pi^+$ photoproduction data, and was found to be in agreement with the predictions of vector dominance. (auth)

**56433** ENERGY DEPENDENCE OF $\pi^-$, $K^-$, AND $\bar{p}$ TOTAL CROSS SECTIONS ON PROTONS IN THE MOMENTUM RANGE UP TO 65 GeV/c. Denisov, S. P.; Dmitrevskii, Yu. P.; Donskov, S. V.; (and others). (Inst. for High Energy Physics, Serpukhov, USSR). Phys. Lett.; 36B: No. 5, 528-32(4 Oct 1971).

$\pi^-p$, $K^-p$ and $\bar{p}p$ total cross sections are measured at momenta up to 65 GeV/c with statistical accuracy 0.3 + 0.6% and systematical (scale) error ≈0.4%. (auth)

**56434** EVIDENCE FOR STRUCTURE IN THE Kπ MASS SYSTEM NEAR 1.85 GeV. Firestone, A.; Goldhaber, G.; Lissauer, D.; Trilling, G. H. (Univ. of California, Berkeley). Phys. Lett.; 36B: No. 5, 513-16(4 Oct 1971).

Evidence is presented for structure in the Kπ system at a mass near 1.85 GeV in the reaction $K^+n \to K^+\pi^-p$ at 12 GeV/c. One interpretation of the observations is the production by pion exchange of a $J^P = 3^-$ $K^*$ resonance at about this mass, which interferes strongly with other processes. (auth)

**56435** RESONANCES PRODUCED FROM $K^+p$ INTERACTIONS IN BUBBLE CHAMBER. Huq, S. S. (Univ. of Rajshahi, India). Nucleus (Karachi); 8: No. 1-2, 27-31(Jan-Jun 1971).

This review is concerned principally with the resonances produced from $K^+p$ interactions in liquid hydrogen bubble chamber. $K^*$ and $N^*$ resonances produced in the inelastic reactions are mainly discussed from the various $K^+p$ experiments carried out up to the incident K+ momentum of 10 GeV/c. (auth)

**56436** $A_2^-$ PRODUCTION IN THE CHANNEL $\pi^-$ + NEUTRALS NEAR THRESHOLD. Binnie, D. M. (Imperial Coll., Eng.); Camilleri, L.; Duane, A.; (and others). Phys. Lett.; 36B: No. 5, 537-40(4 Oct 1971).

The mass spectrum of the $A_2$ meson was studied in the reaction $\pi^- + p \to A_2^- + p$, $A_2^- \to \pi^-$ + neutrals near threshold. In contrast to a previous study of the channel $A_2^- \to \pi^+\pi^-\pi^-$ there is some evidence for structure within the resonance. (auth)

**56437** MEASUREMENT OF THE POLARIZATION PARAMETER IN $\pi^+p$ ELASTIC SCATTERING AT 10, 14, AND 17.5 GeV/c AND FOR $|t| \lesssim 2$ $(GeV/c)^2$. Borghini, M. (CERN, Geneva); Dick, L.; Olivier, J. C.; (and others). Phys. Lett.; 36B: No. 5, 493-6(4 Oct 1971).

Results on polarization in $\pi^-p$ and $\pi^+p$ forward elastic scattering at 10, 14 and 17.5 GeV/c are presented. (auth)

**56438** POLARIZATION PARAMETER IN $K^+p$ AND $\bar{p}p$ ELASTIC SCATTERING AT 10 AND 14 GeV/c. Borghini, M. (CERN, Geneva); Dick, L.; Olivier, J. C.; (and others). Phys. Lett.; 36B: No. 5, 497-500(4 Oct 1971).

Results on polarization in $K^-p$, $K^+p$ and $\bar{p}p$ forward elastic scattering at 10 and 14 GeV/c are presented. (auth)

**56439** ESTIMATION OF THE CROSS SECTION OF $\pi^- + {}^{12}C \to {}^{12}N + \pi^- + \pi^-$ REACTION AT Pc = 4 GeV. Abdullaeva, K. N.; Azimov, S. A.; Grishin, V. G.; (and others) (Inst. of Nuclear Physics, Tashkent). Dokl. Akad. Nauk Uzb. SSR; No. 12, 17-18(1971). (In Russian).

The cross section of the $\pi^- + {}^{12}C \to {}^{12}N + \pi^- + \pi^-$ reaction was estimated using a 24-liter propane ($C_3H_8$) bubble chamber irradiated with a π-meson beam at Pc = 4 GeV. The upper limit of the reaction cross section was found to be: $\sigma \leq (4 \pm 2.8)$ μ barn. (R.V.J.)

# Particle Interactions and Properties (Theoretical)

## General

*Refer also to abstract 56550.*

**56440** (COO-1428-276) ANNUAL PROGRESS REPORT [ON HIGH ENERGY PHYSICS], TASK B, JUNE 1, 1970–MAY 31, 1971. (Purdue Univ., Lafayette, Ind. Dept. of Physics). Contract AT(11-1)-1428. 33p. Dep. NTIS.

Research in theoretical high-high energy physics is summarized A list of publications is included. (J.F.P.)

**56441** (NP-18997) ANNUAL REPORT, 1970. (Chalmers Tekniska Hogskola, Goteborg (Sweden). Institutionen for Teoretisk Fysik). 56p. Dep. NTIS (U. S. Sales Only).

A summary is given of the current research projects at the Institute of Theoretical Physics in Gothenburg. Research on elementary particle physics, transport properties in anharmonic crystals, correlation effects in liquids and in ferromagnets, electronic structure of metals and mechanics of vibrations and fluid dynamics are described. A list of publications is included. (Sweden)

XUM

**56442** (PURC-4159-42) MULTIPERIPHERAL MODELS AND HIGH-ENERGY PROCESSES. Goldberger, M. L. (Princeton Univ., N. J. Joseph Henry Labs.). Jul 1971. Contract AT-(30-1)-4159. 77p. Dep. NTIS.

The lectures on the multiperipheral model cover the ABFST model, the variational principle for ABFST equations and applications, and the triple pomeron vertex and diffractive dissociation. Some material is new the rest is published elsewhere. (J.F.P.)

**56443** HIGH ENERGY PHYSICS INDEX. VOLUME 9, NO. 16, 1971. Frankfurt am Main; Zentralstelle fuer Atomkernenergie-Dokumentation (1971). 83p.

**56444** HIGH ENERGY PHYSICS INDEX. VOLUME 9, NO. 18, 1971. Frankfurt am Main; Zentralstelle fuer Atomkernenergie-Dokumentation (1971). 78p.

**56445** HIGH ENERGY PHYSICS INDEX. VOLUME 9, NO. 17, 1971. Frankfurt am Main; Zentralstelle fuer Atomkernenergie-Dokumentation (1971). 81p.

**56446** HIGH ENERGY PHYSICS INDEX. VOLUME 9, NO. 15, 1971. Frankfurt am Main; Zentralstelle fuer Atomkernenergie-Dokumentation (1971). 68p.

**56447** RELATIVISTIC WAVE EQUATIONS FOR MASSLESS PARTICLES OF SPIN ½. Simon, M. T. (Univ. of Madras). Lett. Nuovo Cim.; 2: No. 12, 616-18(18 Sep 1971).

It is pointed out that relativistic wave equations of the Dirac form can be derived by a uniform procedure developed by Mathews (Phys. Rev., 143: 978(1966)) for massless spin-½ particles. (L.B.S.)

**56448** PHASE SPACE, FIBRE BUNDLES, AND CURRENT ALGEBRAS. Hiley, Basil J. (London Univ.). Int. J. Theor. Phys.; 4: No. 4, 247-65(Aug 1971).

A previous cellular description is extended into phase space and it is shown how this may help to give an understanding of the current algebra approach to elementary particle phenomena. This cellular structure in phase space is investigated in some detail and it is shown how certain features of the structure may be described in terms of the mathematics of fiber bundle theory. The frame bundle is discussed and compared with the Yang-Mills theory. As a result of this discussion we are able to introduce generalized currents which are related to the duals of the curvature forms, and these are shown to span the Lie algebra of a subgroup of the structure group of the frame bundle. The implications of these results in terms of the cell structure are discussed. By assuming that the de Rham cohomology, defined by the curvature forms and their duals, reflects a cohomology on the integers defined on the original cell structure, it is shown that the currents and "curvature" can be given a meaning in terms of a discrete structure. In this case the currents only span a Lie algebra in some suitable limit, implying that a description using Lie algebras is only an approximation. (auth)

**56449** CURRENT AMPLITUDES IN THE DUAL RESONANCE MODEL. Sato, Hikaru (Tokyo Univ.). Progr. Theor. Phys. (Kyoto); 45: No. 5, 1592-1606(May 1971).

Current amplitudes satisfying the conditions of (1) duality, (2) factorization and (3) current algebra are constructed. As an application of our model, one-loop dual amplitudes including one or two currents are investigated. After renormalizing the one-loop function, finite expressions are obtained for the current loop amplitudes. It is shown that the form factor has a good high current mass behavior and that the Fubini-Dashen-Gel-Mann sum rule is satisfied by our current amplitude. (auth)

**56450** SEMI-CLASSICAL MODEL FOR ELEMENTARY PARTICLES. Bess, L. (Rutgers-The State Univ., New Brunswick, N. J.); Chandler, L. Progr. Theor. Phys. (Kyoto); 46: No. 1, 235-55(Jul 1971).

An elementary particle model is described which involves a point charge with a variable mass moving in quasi-circular orbits about the mass center. It is possible to derive a mean proton radius whose value compares well with the one measured by Hofstadter. (auth)

**56451** SOME PROPERTIES OF COHERENT SPIN STATES. Radcliffe, J. M. (Univ. of Sussex, Brighton, Eng.). J. Phys., A (London); 4: No. 3, 313-23(May 1971).

Spin states analogous to the coherent states of the linear harmonic oscillator are defined and their properties discussed. They are used to discuss some simple problems (a single spin in a field, a spin wave, two spin ½ particles with Heisenberg coupling) and it is shown that their use may often give increased physical insight. (auth) (UK)

## *Electromagnetic*

*Refer also to abstract 56404.*

**56452** (CALT-68-313) REGGE MODELS OF FORWARD PION AND ETA PHOTOPRODUCTION. Worden, Robert (California Inst. of Tech., Pasadena). [1971]. Contract AT(11-1)-68. 92p. (CONF-710816-1). Dep. NTIS.

From International symposium on electron and photon interactions; Ithaca, N. Y. (23 Aug 1971).

A Regge model of forward pion photoproduction should satisfy three separate criteria; it should fit the extensive high energy data, it should agree with all possible constraints on the Regge residues, and it should fit the finite energy sum rules. A Regge absorption model of pion and eta photoproduction is presented which satisfies all these conditions. The model uses poles with nonsense wrong-signature (NWS) zeroes, and uses a black disc form of absorption in which all low partial waves are completely absorbed and high partial waves are unabsorbed. The absorbed Regge amplitudes show remarkable $\rho-A_2$ and $\pi-B$ exchange degeneracy. The model agrees well with the FESR, which are given in terms of regularized s-channel helicity amplitudes, in order to examine their absorptive zero structure. Then models are examined using a conventional form of absorption, and models in which the poles do not have NWS zeroes. It is found that models without NWS zeroes are unable to fit the sum rules. Since Regge absorption models do not fit the distinctive large-t behavior of the cross sections, fixed-pole models are discussed as a possible explanation of these data, and it is shown that even in fixed pole models, some Regge cuts are necessary. The predictions of the various models for some new experimental quantities which can be measured using simultaneously polarized targets and beams are presented, and a test for $A_1$ exchange is suggested. (auth)

**56453** (ORO-3992-42) BLACK-BODY RADIATION AND GENERALIZED THEORY OF PHYSICAL DIMENSIONS. Recami, E. (Texas Univ., Austin. Center for Particle Theory). May 1971. Contract AT(40-1)-3992. 14p. (CPT-92). Dep. NTIS.

The Straneo's generalized theory of "physical dimensions" (valid for the whole classical physics) is used. In that theory, the "universal constants" have dimensions such that some linear relations hold, between the exponents of the fundamental quantities. For the physical laws obeying the conservation principles of thermodynamics, in those linear relations a variable n appears. The undulatory and the corpuscular aspects correspond to n = 1 and n - 2, respectively. This fact clarifies the classical dichotomy between these two theories. It is shown that: no "classical" law—besides the Wien's one—may be written for the black-body radiation density; the Rayleigh-Jeans formula is not consistent with classical physics, as it was derived in a wrong way; the previous statements are independent of any detail of the mathematical models (even recently explored). (auth)

**56454** THEORY OF REACTION BETWEEN POLARIZED PARTICLES AND GAMMA-QUANTA. Ritus, V. I. Tr. Fiz. Inst., Akad. Nauk SSSR; 53: 3-101(1971). (In Russian).

The structure of the scattering amplitude and of differential cross section was investigated for polarized particle-$\gamma$-quantum reactions, the latter being dependent upon invariance of interaction of rotation, repulsion, conversion of time and charge conjugation. The scattering amplitude was expanded by an invariant spin operator or angular operator, and the polarized structure of differential cross section and its simplification for invariance interaction of rotation, repulsion conversion of time and charge conjugation was accordingly found. The proposed method for the reaction with not too large a spin is simpler and more obvious than the previous fundamental methods. (tr-auth)

**56455** INTERACTION OF A SYSTEM OF PARTICLES WITH AN ELECTROMAGNETIC FIELD. II. Khokhlov, Yu. K. Tr. Fiz. Inst., Akad. Nauk SSSR; 53: 157-66(1971). (In Russian).

An advanced exposition is offered of an earlier proposed special calibration of potentials and a calculation of multipole moments. The special calibration is characterized by the fact that the effective scalar potential is expressed by electric field intensity whereas vector potential is expressed by magnetic field intensity. In the result the "relative" Hamiltonian of interaction is shown to be composed of two components-electric and magnetic- each of which has a closed form. A novel application of the theory is the field interaction with a free system and the scattering amplitude of a photon. The use of a special calibration avoids the appearance in the scattering amplitude of conventional unphysical components and permits immediate detection of the transition to Thompson limits. (tr-auth)

XUM

**56456** DISTURBANCE OF SECOND-ORDER COHERENCE BY INTERACTION. Bulla, Wolfgang (Technische Hochschule, Graz). Z. Phys.; 246: No. 4, 302-11(1971). (In German).

A definition of the disturbance of the second-order coherence of a photon field, scattered by an electron, is formulated within the framework of quantum electrodynamical coherence theory. As a special case forward scattering is considered, thus yielding a simple relation with the matrix element for one-photon-scattering. The scattering on a free polarized electron is treated as an example. (auth)

**56457** HIGH ENERGY PRODUCTION OF HADRONS IN THE COULOMB FIELD OF A NUCLEUS. Gourdin, M. (CERN, Geneva). Nucl. Phys.; B32: No. 2, 415-28(1971).

The one-photon exchange contribution to coherent production processes at high energy is computed. The Primakoff effect gives a measurement of total photo-absorption cross section and the integrated cross section is found to increase with energy like log s. Some discussion of inclusive reactions is given in particular for proton-proton colliding beam experiments. (auth)

**56458** COMPARISON OF THE HIGH ENERGY MODELS FOR NEUTRAL MESON PHOTOPRODUCTION AND THE RELATED HADRONIC PROCESSES. Gault, F. D. (Univ. of Durham, Eng.); Martin, A. D.; Kane, G. L. Nucl. Phys.; B32: No. 2, 429-52(1971).

To critically compare the Michigan and Argonne models simultaneous fits are made to the high-energy data for $\pi^0$ and $\eta$ photoproduction together with that for the related hadronic vector meson production reactions, in particular that for $\pi^+n \to \omega p$. Thus all constraints on these models are considered simultaneously. Particular attention is given to the strength of absorptive cuts in both models, and to the role of the B-meson exchange in filling dips in the Argonne model. It is found that the $\rho$-Pomeron cuts (i.e. cuts associated with large helicity flip at the $N\bar{N}$ vertex) are essential to introducing unnatural parity exchange in the Michigan model, and that the B-meson contribution is incapable of filling unwanted dips which appear in any model with nonsense wrong signature zeros as required by exchange degeneracy. The flip and non-flip $\rho$ and $\omega$ coupling strengths at the $N\bar{N}$ vertex are determined. Predictions are made for various polarization asymmetries for $\gamma p \to \pi^0 p$ and $\gamma p \to \eta p$. The differential cross section for $K_L^0 p \to K_S^0 p$ is calculated and compared with the existing data. (auth)

**56459** ANNIHILATION OF ELECTRON–POSITRON PAIRS TO PSEUDO-SCALAR MESONS. Yakh'yaev, R. Sh. (Azerbaidzhan State Univ., Baku). Izv. Vyssh. Ucheb. Zaved., Fiz.; No. 5, 48-52(1971). (In Russian).

The production of pseudoscalar mesons by the collision of polarized electron and positron beams, taking account of form factors of all participating particles is described. An equation was obtained for the angular and energy distributions of the produced pairs. Equations are also developed which give the angular and energy distribution of the mesons in a laboratory system. (tr-auth)

**56460** PRODUCTION OF PION PAIRS IN ELECTRON COLLIDING BEAMS. Cheng, Hung (Massachussetts Inst. of Tech., Cambridge); Wu, Tai Tsun. Nucl. Phys.; B32: No. 2, 461-85(1971).

Pionization in electron-electron (or electron-positron) colliding beams is studied in detail for the dominant case where the produced pions have nearly equal but opposite transverse momenta. Accurate measurements in this case, without detecting the outgoing electrons, can be used to determine all amplitudes and phases for $\gamma\gamma \to \pi^+\pi^-$. The results are obtained directly from Feynman diagrams and thus inaccuracies due to Weizsäcker-Williams approximation are avoided. All the formulas are equally applicable to the production of any pair of spinless bosons in electron-electron (or electron-positron) colliding beams. (auth)

**56461** GENERALIZED WEINBERG SUM RULES IN DEEP INELASTIC CURRENT–HADRON SCATTERINGS. Morita, K. (Nagoya Univ., Japan); Fukui, I. Lett. Nuovo Cim.; 2: No. 13, 661-4(25 Sep 1971).

A chiral symmetry on the light cone was previously proposed for the disconnected part of the matrix elements of the vector–vector and axial-vector–axial-vector current commutators, thereby obtaining the modified second Weinberg sum rule in addition to the first one. It was also remarked that the chiral symmetry on the like-cone applied to the connected matrix elements of the current commutators would lead to the equality of scaling functions for the vector and axial vector matrix elements. This is shown to be the case under certain assumptions. (L.B.S.)

**56462** RADIATION FROM AN ELECTRIC CHARGE MOVING ALONG A SPIRAL PATH IN A TRANSPARENT MEDIUM. Kukanov, A. B.; Lavrova, G. A.; Orisa, B. D. (Moscow Univ.). Vestn. Mosk. Univ., Ser. III. Fiz. Astron.; 12: No. 1, 111-13 (Jan-Feb 1971). (In Russian).

An attempt was made to adapt a general method of describing polarized properties of a light beam to the case of radiation by a charge moving on a spiral path. Such motion and radiation was investigated in a transparent isotropic medium with given dielectric and magnetic permeability. The formulas developed are in harmony with analogous studies by other authors. (K.S.W.)

**56463** FINITE-ENERGY SUM RULES AND THE REACTIONS $ee \to ee\epsilon$ (750) AND $ee \to eef$ (1260). Schrempp-Otto, B. (Univ., Hamburg); Schrempp, F.; Walsh, T. F. Phys. Lett.; 36B: No. 5, 463-6(4 Oct 1971).

The $\epsilon\gamma\gamma$ and $f\gamma\gamma$ coupling constants are calculated from finite-energy sum rules for $\gamma\pi \to \pi\gamma$. The cross sections for $\epsilon$ and f production in colliding electron beam reactions are found to be significant. There is reasonable agreement with the tensor meson dominance estimates for the $f\gamma\gamma$ couplings. (auth)

**56464** COMMENT ON SPIN ONE THEORY. Goldman, T.; Tsai, W. (Harvard Univ., Cambridge, Mass.). Phys. Lett.; 36B: No. 5, 467-9(4 Oct 1971).

A way to explain the inconsistency of the spin one theory with anomalous magnetic moment couplings observed by Tsai and Yildiz is proposed. By suitably adding infinitely many non-minimal coupling terms which are tensor functions of the field strength $F_{\mu\nu}$, the square of the energy eigenvalues can become positive definite. A particular model of replacing $\kappa$ by $\langle H^2 \rangle = \kappa'(1 + \frac{1}{4}\kappa'^2 e^2 H^2 m^{-4})^{-1}$, where no restriction is imposed on $\kappa'$, is discussed. (auth)

**56465** SCALE INVARIANCE AND RELATIVISTIC COMPOSITE NUCLEON. Sato, Atsushi; Fujii, Kanji; Kokuyama, Shigeru; Murota, Toshiyuki (Hokkaido Univ., Sapporo, Japan). Progr. Theor. Phys. (Kyoto); 46: No. 1, 341-3(Jul 1971).

The momentum distribution function for deep inelastic electron scattering is considered when the target nucleon is regarded as a composite state described by a relativistic wave function. The conditions for scale invariance are examined. (L.B.S.)

**56466** BHABHA SCATTERING ANOMALOUS INTERACTION OF MUON. Ng, S. H. (Dalhousie Univ., Halifax, Nova Scotia). Progr. Theor. Phys. (Kyoto); 46: No. 1, 211-19(Jul 1971).

It is suggested that high energy muon Bhabha scattering at large angles may distinguish the various forms of possible anomalous interaction of the muon. (auth)

**56467** DIRECT PAIR PRODUCTION BY CHARGED PARTICLE AT 4 GeV/c IN A PROPANE BUBBLE CHAMBER. Boehm, J.; Matlova, A.; Zacek, J.; Grishin, V. G. (Charles Univ., Prague). Nucl. Phys.; B32: No. 2, 632-44(1971).

The direct electron pair production by pions, muons and electrons at 4 GeV/c was investigated in a propane bubble chamber. The experimental results were found within the 30% in agreement with the cross sections calculated by Bhabha and Murota, Ueda and Tanaka. A special method of the background subtraction was developed. The method is very convenient for the investigation of the production of electron pairs by electrons in a hydrogen bubble chamber. (auth)

## Weak

*Refer also to abstracts 56547 and 56854.*

**56468** (FRNC-R-1) WEAK INTERACTIONS AND THE VECTOR DOMINANCE MODEL. Lopes, J. Leite (Centre National de la Recherche Scientifique, Paris (France)). Jun 1971. 12p. Dep. NTIS (U. S. Sales Only).

It is suggested that, in the same way that the electromagnetic form factors of hadrons are dominated by the neutral hadronic vector mesons in interaction with the photon, the weak reaction form factors of hadrons are correspondingly dominated by the hadronic charged vector and axial-vector mesons coupled to the intermediate W-bosons. A relation is obtained, between the coupling constants involved and Cabibbo's angle. A cancellation of dominant axial-vector pole terms in the matrix element of the nucleon axial current between neutron and proton states gives a better approximation for the Goldberger–Treiman relation. (France)

**56469** KOSMICHESKIE MYUONY I NEITRINO. (Cosmic Muons and Neutrinos). Bugaev, E. V.; Kotov, Yu. D.; Rozental, I. L. Moscow; Atomizdat (1970). 320p.

XUM

Contemporary knowledge of the characteristics and behavior of the muon and the neutrino is summarized. The electromagnetic-nuclear interaction of muons, electron-positron pair formation, and muon–muon pairs are discussed. The passage of muons through matter, the absorption and other losses of muons, and their mean free path are considered. Two chapters focus attention on high-energy muons and muons in atmospheric showers. The second half of the book introduces the neutrino, giving its theoretical implications, interaction cross sections, and its role in accelerator experiments. Recent research on origins of the neutrino in the Sun's interior, neutrino astrophysics, and experiments with the neutrino from cosmic rays are presented. 190 references. (K.S.W.)

**56470** URBARYON REARRANGEMENT DIAGRAM AND NONLEPTONIC HYPERON DECAYS. Noda, Hujio (Kyushu Univ., Fukuoka); Toyoda, Fumihiko. Progr. Theor. Phys. (Kyoto); 45: No. 5, 1634-45(May 1971).

Nonleptonic hyperon decays are investigated from the standpoint of urbaryon rearrangement diagram. It is shown that duality assures the Lee-Sugawara relation of both S-wave and P-wave amplitudes of nonleptonic hyperon decays under simple assumptions that the H-type diagram is dominant in S-wave decays and that the Z-type diagram is dominant in P-wave decays. The cluster model is discussed in connection with the assumptions for explaining the main dynamical properties of S-wave and P-wave decays. It is found that the characteristics of S-wave decays can be understood by setting a constraint to the t-channel and that those of the P-wave decays can be understood by setting the constraint to the s-channel. (auth)

**56471** IS THE LIGHTEST FRACTIONALLY-CHARGED PARTICLE STABLE? Verhaar, B. J. (Technische Hogeschool, Eindhoven, Netherlands). Progr. Theor. Phys. (Kyoto); 45: No. 5, 1689-90(May 1971).

It is suggested that quark-like particles have escaped observation because of their instability. It is also suggested that a certain type of violation of the conservation laws of electric charge and baryon number is not in contradiction with experimental facts, but that it yields the decay of the lightest fractionally charged particle. A specific form for a weak interaction incorporating nonconservation of B and Q is described for the decay of fractionally charged to integrally charged particles. (L.B.S.)

**56472** SECOND CLASS CURRENTS IN HIGH ENERGY NEUTRINO REACTIONS. Okamura, Hiroshi (Tokyo Univ.). Progr. Theor. Phys. (Kyoto); 45: No. 5, 1707-9(May 1971).

The existence of second-class currents is studied from polarization of the recoil proton in $\nu_\mu + n \rightarrow p + \mu^-$ interactions. (L.B.S.)

**56473** CROSS SECTION FOR THE PRODUCTION OF THE W BOSON BY HIGH-ENERGY NEUTRINOS IN THE ELECTROMAGNETIC FIELD OF A PROTON. Berkov, A. V.; Bunatyan, G. G.; Zhizhin, E. D.; Nikitin, Yu. P. (Moscow Engineering-Physics Inst.). Yadern. Fiz.; 13: No. 5, 1126-7(May 1971). (In Russian).

Calculation of the total cross section of formation of the W boson (the weak interaction vector quantum) at neutrino energies of E = 30 to 400 GeV and in the mass range from 3 to 10 GeV is of special interest for the current research at the Serpukhov accelerator and for work planned with the new large American accelerator. There is considerable divergence in the data published on this subject. Because of negligence, a previous work contained an exactly 10 times higher value than intended for the cross section of formation of W; even so, the value differs from that reported previously. Recalculation of the experimental data on a computer yielded results which agreed with previous data. It appears that the original data, as corrected subsequently, are reliable values, especially in the region far from threshold of generation of W bosons. (TTT)

## *Strong (General)*

**56474** (FRNC-TH-63) KINEMATIC STUDY OF A REACTION BETWEEN HADRONS (STABLE AND UNSTABLE). Keller, Jean-Pierre (Paris Univ., Orsay (France). Faculte des Sciences). 1970. 70p. (In French). Dep. NTIS (U. S. Sales Only).

Thesis.

Certain aspects of the construction of a space with states corresponding to one or several particles are considered, a problem of particular interest being the statistics of identical particles. The principles governing the definition of the collision operator are presented together with the main consequences of these principles. Unstable particles are also considered. (France)

**56475** (RPP/C-24) REGGE CUTS AND RELATED TOPICS. Phillips, R. J. N. (Rutherford High Energy Lab., Chilton (England)). Jul 1971. 59p. (CONF-710609-8). Dep. NTIS (U. S. Sales Only).

From International conference on elementary particles; Amsterdam, Netherlands (30 Jun 1971).

A review is given of Regge phenomenology particularly Regge cuts. The discussion covers the general properties of Regge cuts, duality and geometry, cut models and modifications, t-dependence, cuts, extensions of the empirical rule for cuts, selection rules for cuts, Pomeron couplings, FESR for poles alone, complex Regge poles, and new data. (J.F.P.)

**56476** INCLUSIVE REACTIONS IN DUAL MODELS WITH SECOND SHEET RESONANCES. Olesen, P. (CERN, Geneva). Nucl. Phys.; B32: No. 2, 609-31(1971).

The effects of unitarity-like features in inclusive reactions are investigated by means of two dual resonance models with second sheet resonance poles and Mandelstam analyticity. The first model has recently been proposed by Cohen-Tannoudjii, Henyey, Kane and Zakrzewski (CHKZ). The second model (a modification of the CHKZ model) has the additional feature that it approaches the Veneziano model in the zero-width limit. It turns out that the unitarity-like features contained in both models influence the transverse momentum spectrum strongly in the central region. The second model gives a transverse momentum cut-off of the form $\exp(-a_1 p_T - a_2 p_T^q)$, where $q > 1$ and where $a_1$ and $a_2$ are (not necessarily universal) constants. In the zero-width limit the spectrum decreases much faster [like $\exp(-a p_T^q)$]. In the fragmentation region the unitarity-like features of the models are of less importance. (auth)

**56477** EXISTENCE OF THE PSEUDOVECTOR ISOSPINOR HEAVY BOSON AND A NEW MODEL FOR HADRONS. Kushnirenko, A. N. (Inst. of Materials Research, Kiev). Izv. Vyssh. Ucheb. Zaved., Fiz.; No. 5, 40-7(1971). (In Russian).

The construction of the new hadron model, its charge and symmetry are discussed. With these equations, and the laws of momentum addition and isotopic spins, a set of 15 tables are assembled which are based on the new model. An approximation of SU(3)-symmetry is discussed, starting with the binding energy between the nucleon and the anti-nucleon, and their relation to the boson and antiboson. Mass relationships for baryons are mathematically developed, for which SU(3) symmetry is not realized. (K.S.W.)

**56478** DETERMINATION OF THE COUPLING STRENGTH FROM DUALITY AND UNITARITY. Igi, K.; Eguchi, T. (Tokyo Univ.). Phys. Lett.; 36B: No. 5, 486-8(4 Oct 1971).

A method is proposed to determine the absolute strength of the coupling. The crucial point consists in the use of duality and unitarity. The predicted values of the elastic and total widths of meson resonances are in reasonable agreement with experiments. (auth)

**56479** EXOTIC EXCHANGE PROCESSES AND URBARYON REARRANGEMENT DIAGRAMS. Ghoroku, Kazuo; Myozyo, Yasuo; Noda, Hujio (Kyushu Univ., Fukuoka). Progr. Theor. Phys. (Kyoto); 45: No. 5, 1694-6(May 1971).

The exotic quantum number exchange processes are classified into two groups in terms of urbaryon rearrangement diagrams (URD). It is pointed out that the s-dependence of URD is determined not only by the rearranged urbaryon lines but also by the spectator lines. It is shown that exotic mesons couple when the spectator lines exist on both sides in URD and that they lie on low-lying Regge trajectories. (L.B.S.)

**56480** CANONICAL QUANTIZATION OF THE PROPER TIME FORMALISM IN THE DUAL RESONANCE MODEL. Itoh, Chiaki (Meiji-Gakuin Univ., Tokyo); Kenmoku, Masakatsu; Minamikawa, Toshiyuki. Progr. Theor. Phys. (Kyoto); 45: No. 5, 1607-17 (May 1971).

The proper time formalism of the dual resonance model has been proposed. The proper time formalism is quantized to include diagrams of the general type such as loops, and diagrams of Feynman-like rule are obtained with a proper time propagator in place of the usual propagator. The minimal interaction in this formalism is discussed and currents and commutation relations among them are derived. (auth)

**56481** DUAL QUARK–PARTON MODEL AND HIGH ENERGY HADRONIC PROCESSES. Landshoff, P. V.; Polkinghorne, J. C. (Univ. of Cambridge, Eng.). Nucl. Phys.; B32: No. 2, 541-56 (1971).

The dual quark-parton model is extended to purely hadronic processes. An additional dynamical assumption then leads to the additive quark model for high energy cross sections, with naive quark model counting despite the more complicated character in fact possessed by the hadrons. Limiting fragmentation is also obtained. A further dynamical assumption leads to an approximation to the

differential cross section in terms of electromagnetic form factors of the form proposed by Wu and Yang. Conservation of s-channel helicity in pion-nucleon and nucleon-nucleon scattering is also deduced. (auth)

## *Strong (Baryon No. = 0)*

*Refer also to abstract 55833.*

**56482** (COO-1195-224) PARTIAL WAVE ANALYSIS OF THE $3\pi$ SYSTEM IN THE MASS REGION 1.0 TO 2.0 GeV. Eisenstein, Laura (Illinois Univ., Urbana). Aug 1971. Contract AT(11-1)-1195. 6p. (CONF-710819-1). Dep. NTIS.

From fourth topical conference; Honolulu, Hawaii (2 Aug 1971).

A new partial-wave analysis is described for the $3\pi$ system in the reactions $\pi^+ + p \to p + \pi^+ + \pi^+ + \pi^-$ and $\pi^- + p \to p + \pi^- + \pi^+ + \pi^-$ between 5 and 25 GeV/c. For each spin and parity state of the $3\pi$ system, decays into $\pi\epsilon$, $\pi\rho$, and $\pi f$ with all possible orbital angular momenta allowed by parity and angular momentum conservation are considered. The production and properties in the $A_1$, $A_2$, and $A_3$ regions are discussed. (J.F.P.)

**56483** (JINR-E$_2$-6017) LADDER APPROXIMATION FOR VERTEX FUNCTION IN NONRENORMALIZABLE THEORY OF $\omega\rho\pi$ INTERACTION. Flippov, A. T.; Epifanov, Yu. N. (Joint Inst. for Nuclear Research, Dubna (USSR). Lab. of Theoretical Physics). 1971. 14p. Dep. NTIS (U. S. Sales Only).

The method for solving ladder-type equations for the vertex function in nonrenormalizable theories previously suggested is extended to the case of nonvanishing 4-momenta of all three particles. An expansion of the vertex function in a series of powers of the coupling constant $g_{\omega\rho\pi}$ and in $g_{\omega\rho\pi}$ is obtained, with the example of the particularly interesting applications for the $\omega\rho\pi$ interaction. The first nonvanishing approximation is compared with the estimate obtained by use of the "unitary cut-off" in usual perturbation theory. (auth)

**56484** (ORO-3992-10) TWO VARIABLE CROSSING SYMMETRIC EXPANSION OF THE $\pi\pi$ SCATTERING AMPLITUDE AND LOW-ENERGY PARAMETER SUM RULES. Maiella, G. (Texas Univ., Austin. Center for Particle Theory). May 1970. Contract AT(40-1)-3992. 23p. (CPT-51). Dep. NTIS.

A two-variable crossing-symmetric expansion of the $\pi$-$\pi$ scattering amplitude in the interior of the Mandelstam triangle is obtained. From this expansion, sum rules are derived for the low-energy parameters, assuming the "weakness" of the threshold unitarity cut. Finally, these sum rules are compared with experimental data and theoretical predictions. (auth)

**56485** (ORO-3992-66) COMMENTS ON ANALYSES OF $\bar{p}n \to 3\pi$. Gleeson, A. M.; Meggs, W. J.; Parkinson, M. J. (Texas Univ., Austin. Center for Particle Theory). [1971]. Contract AT(30-1)-875. 7p. (CPT-116). Dep. NTIS.

The analysis of the reaction $\bar{p}n \to \pi^+\pi^-\pi^-$ using the rising phase shift model is compared with attempts to explain the data with the Veneziano model. The fact that daughter trajectories are not parallel to the leading trajectory is emphasized. (auth)

**56486** $K\pi$ SCATTERING PHASE SHIFTS DETERMINED FROM THE REACTIONS $K^+p \to K^+\pi^-\Delta^{++}$ AND $K^+p \to K^0\pi^0\Delta^{++}$. Mercer, R.; Antich, P.; Callahan, A.; (and others) (Johns Hopkins Univ., Baltimore). Nucl. Phys.; B32: No. 2, 381-414(1971).

The $K\pi$ scattering was studied from threshold to $m_{K\pi} = 1200$ MeV using the Chew-Low extrapolation method in the reactions $K^+p \to K^0\pi^0\Delta^{++}$. In addition to an analysis using only the data at 5.43 GeV/c incident momentum, the results using the world data compiled from experiments with momenta from 3.0 to 12.7 GeV/c are also presented. The extrapolated cross section for the elastic $K^+\pi^- \to K^+\pi^-$ scattering exceeds the p-wave isospin-$\frac{1}{2}$ unitarity limit in the $K^*(890)$ region. The phase shift $\delta_1^1$ (notation $\delta_1^{3/2}$) shows the expected Breit-Wigner behavior which suggests that $\delta_1^1 \simeq 0$ in the mass region studied. Solutions for the s-wave phase shifts $\delta_0^1$ and $\delta_0^0$ are obtained from the extrapolated differential cross sections. A unique set of solutions for $\delta_0^1$ and $\delta_0^0$ is obtained by requiring the calculated cross sections to agree with those extrapolated from $K^+\pi^-$ elastic scattering and with those for $K^-\pi^-$ scattering obtained in other experiments. $\delta_0^1$ was found to increase slowly from $0^0$ at threshold, approaching $80^\circ$ at $m_{K\pi} \simeq 1150$ MeV with no evidence of passing through $90^\circ$ in the mass range studied. The phase shift $\delta_0^0$ decreases slowly from $0^0$ at threshold to $\simeq -30^\circ$ at $m_{K\pi} \simeq 1200$ MeV. (auth)

**56487** SINGLE-AND DOUBLE-PION PRODUCTION IN PROTON-ANTIPROTON NONANNIHILATIONS AT 2.2 GeV/c. Stringer, T. A.; Kwak, N.; Mall, G. H.; Manweiler, J. E.; Stump, R. (Univ. of Kansas, Lawrence). Nucl. Phys.; B32: No. 2, 486-92(1971).

The final states $p\bar{p}\pi^0$ and $p\bar{p}\pi^+\pi^-$ appear to proceed predominantly through single- and double-isobar production respectively. However, in the $p\bar{n}\pi^-$ final state the data indicates another mechanism at work. Several OPE models are applied to the production angular distributions, and the density matrices are determined for the double-pion production reaction. (auth)

**56488** COUPLING CONSTANTS IN THE $(A_1\rho\pi)$ SYSTEM AND HELICITY CONSERVATION. Ahmed, K.; Razmi, M. S. K. (International Atomic Energy Agency, Vienna. International Centre for Theoretical Physics, Trieste, Italy). Lett. Nuovo Cim.; 2: No. 13, 657-60(25 Sep 1971).

The s-channel process $A_1A_1 \to \pi\pi$ is examined and, applying t-channel helicity conservation, it is found that the s-wave coupling for $A_1 \to \rho\pi$ decay vanishes. (L.B.S.)

**56489** DUFFIN-KEMMER-LIKE WAVE EQUATION FOR DUAL FREE MESONS. Casalbuoni, R. (Istituto Nazionale di Fisica Nucleare, Florence). Lett. Nuovo Cim.; 2: No. 13, 641-6 (25 Sep 1971).

The Ramond equation is generalized to a Duffin-Kemmer-type equation for mesons in such a way that the meson states transform like $q\bar{q}$, and it is shown that such an equation is equivalent to the Bargmann-Wigner equations for the field. The wave equation is modified to obtain a mass splitting which is suitable to reproduce the physical $\pi$ and $\rho$ trajectories. The possibility of constructing a conserved vector current for the case of the Klein-Gordon-like equation is discussed. (L.B.S.)

**56490** ANALYTIC, CROSSING-SYMMETRIC, UNITARITY $\pi\pi$ AMPLITUDES WHICH SATISFY I = 1 SUM RULES AND THE INEQUALITIES OF MARTIN. Tryon, E. P. (Columbia Univ., New York). Phys. Lett.; 36B: No. 5, 470-4(4 Oct 1971).

A model for analytic, crossing-symmetric $\pi\pi$ amplitudes is exhibited which satisfy I = 1 sum rules and the inequalities of Martin. The S-waves and P-wave are unitary to excellent approximation up to energies exceeding 1 GeV. The model enables a small number of experimentally accessible parameters to be converted into phase shifts reliable up to 1 GeV. Predictions are made for the S-waves which lend support to certain analyses of $\pi N \to \pi\pi N$ data. Solutions are displayed which constitute counter-examples to the claims of Le Guillou, Morel and Navelet that the S-waves must possess Adler-like zeroes, and that the $\epsilon$ resonance must be broad. (auth)

**56491** AVERAGE PROPERTIES OF DUAL RESONANCES. Green, M. B. (Princeton Univ., N. J.); Veneziano, G. Contract AT(30-1)-2098. Phys. Lett.; 36B: No. 5, 477-9(4 Oct 1971).

As a consequence of the strong interaction (A.F.S.) scaling of dual amplitudes, it is found that the average total width of a high mass resonance approaches a constant which is less than $1/\pi$ $(GeV)^2$. A logarithmic increase of the average multiplicity coming from the decay of dual resonances is also obtained. (auth)

**56492** STRUCTURE IN S-WAVE $\pi\pi$ SCATTERING. Bennett, G. W.; Johnson, R. C. (Durham Univ., Eng.). Phys. Lett.; 36B: No. 5, 483-5(4 Oct 1971).

Phenomenological phase shift data and crossing sum rules clearly indicate the presence of zeros below threshold in both S-wave $\pi\pi$ amplitudes, just as predicted by current algebra. Some preference for a resonant I = 0 amplitude emerges. (auth)

**56493** REGGE POLES AND THEIR RESIDUES IN THE VIRASORO MODEL. Kawai, Toshiharu (McMaster Univ., Hamilton, Ont.). Progr. Theor. Phys. (Kyoto); 45: No. 5, 1578-84(May 1971).

The complex l plane structure of the Virasoro model for $\eta^0\eta^0$ elastic scattering is investigated in detail. Explicit expressions for the residue functions and the positions of their poles and zeros are given for both moving and fixed Regge poles. Contrary to some statements in an earlier literature, it is shown that the poles of Regge residues do not show up as poles of the full signature amplitude and that they are not in conflict with unitarity. Besides, the fixed Regge poles are additive and not combined multiplicatively with moving Regge poles. (auth)

**56494** LORENTZ POLE STRUCTURE OF THE VIRASORO MODEL. Kawai, Toshiharu (McMaster Univ., Hamilton, Ont.). Progr. Theor. Phys. (Kyoto); 45: No. 5, 1585-91(May 1971).

The Virasoro amplitude for $\eta^0\eta^0$ elastic scattering is projected on the irreducible representations of the Lorentz group. An infinite sequence of moving Lorentz poles is found, but no fixed Lorentz poles at all. The relation between the Lorentz poles and the Regge poles is discussed. It is pointed out that fixed Regge poles come from a kinematical factor which relates the partial

XUM

wave amplitude to the Lorentz amplitude. The results are compared with those of the Veneziano model. (auth)

**56495** LOW ENERGY PION–PION SCATTERING. Kuehnelt, H. (Univ., Karlsruhe, Ger.). Z. Phys.; 246: No. 5, 447-58 (1971).

Pion–pion s- and p-wave amplitudes are investigated by means of dispersion relations for the inverse partial wave amplitudes. Possible low-energy zeros of the s waves are taken into account, and their positions as well as other parameters are determined by the imposition of the Balachandran–Nuyts crossing constraints and Martin's conditions and by postulating the existence of the $\rho$ meson. Very narrow bands of solutions are obtained, where the $I = J = 0$ phase shifts reach 90° and the s-wave scattering lengths $a_0$ vary between 0.13 and 0.23 $m_\pi^{-1}$ and the ratios $a_0/a_2$ vary between –1.8 and –3.5. It is shown that inelasticity or the passage through 180° of $\delta_0^0$ near 1 GeV does not change the predictions in the low-energy region much. (auth)

## Strong (Baryon No. = 1)

*Refer also to abstracts 56422 and 56807.*

**56496** (CERN–71-14, pp 101-54) PION–NUCLEON SCATTERING THEORY. Hamilton, J. (Nordisk Institut for Teoretisk Atomfysik, Copenhagen (Denmark)). 4 Aug 1971.

In Spring school on pion interactions at low and medium energies.

The discussion of pion–nucleon scattering covers the low-energy $\pi$N parameters, Coulomb corrections, the use of fixed-t dispersion relations, the dynamics of low-energy $\pi$N scattering, and information on $\sigma$. (J.F.P.)

**56497** (FRNC-TH-33) REGGE POLES AND $\pi-$N SCATTERING AT LOW AND INTERMEDIATE ENERGIES. Tounsi, Ahmed (Paris Univ. (France). Faculte des Sciences). 1970. 101p. (In French). Dep. NTIS (U. S. Sales Only).

Thesis.

The general $\pi-$N formalism is recalled and the form of the contributions of the Regge poles used is given. Recent ideas on overall and local duality and their applications to the dynamics of strong interactions are given. After describing the method used, it is applied to amplitudes recently used in the context of ideas on duality. The results obtained, both with respect to poles (resonances) and cross sections are compared with previous results obtained using the Argand diagram and also with experimental results. The unitarized Regge amplitudes are verified for medium and low energies. Problems concerning the introduction of inelasticity into this study and the asymptotic behavior of the modified Regge amplitudes are discussed. (auth)

**56498** (IFA-HE–76) CERENKOV MECHANISM AND RESONANCE PRODUCTION. Ion, D. B.; Nichitiu, F. Gh. (Institutul de Fizica Atomica, Bucharest (Romania)). 1971. 10p. Dep. NTIS (U. S. Sales Only).

The behavior of the cross sections for the reactions $\pi^- + p \to \pi^- + p(\Delta^{++}) + \rho^0(\pi^-)$ and $p + p \to p + \Delta^{++} + \pi^-$ interactions is analyzed using the Cherenkov mechanism. (J.F.P.)

**56499** (ORO–3992-8) INTERPRETATION OF ANGULAR DISTRIBUTION IN TERMS OF COMPLEX MASS PARTICLES. Gleeson, A. M.; Gundzik, M. G.; Sudarshan, E. C. G. (Texas Univ., Austin. Dept. of Physics); Pagnamenta, Antonio (Rutgers–The State Univ., New Brunswick, N. J. Dept. of Physics). Apr 1970. 14p. (CPT–47). Dep. NTIS.

The secondary maximum in the angular distribution of $\pi^-p \to \pi^0n$ is interpreted in terms of a negative mass squared resonance (NMSR). A consequence of the negative mass squared nature of this resonance is the natural appearance of a spin projection operator for a member of the principal series $j = -\frac{1}{2} + i\sigma$ of irreducible representations of the little group 0(2,1). A fit to the experimental data for laboratory momentum from 5.9 to 18.2 GeV/c requires an NMSR with $-m^2 = 1.0$ (GeV)$^2$, total width $\Gamma = 0.3$ GeV and $\sigma = 1.1$. (auth)

**56500** (ORO–3992-18) PHENOMENOLOGY OF COMPLEX SPIN TACHYONS. Gleeson, A. M.; Gundzik, M. G.; Sudarshan, E. C. G. (Texas Univ., Austin. Dept. of Physics); Pagnamenta, Antonio (Illinois Univ., Chicago. Dept. of Physics). Jun 1970. 14p. (CPT–65; CONF-700627–2). Dep. NTIS.

From fourth international conference on resonant particles; Athens, Ohio (15 Jun 1970).

A preliminary formulation of a phenomenology of negative mass squared resonances (NMSR) is described. The angular distribution of pion-nucleon charge exchange scattering is interpreted in terms of these objects. Negative mass squared resonances have as their spin projection operator a member of the principal series $j = -\frac{1}{2} + i\sigma$ of irreducible representations of the little group 0(2,1). A fit to the experimental data for laboratory momenta from 5.9 to 18.2 GeV/c requires a NMSR with $-m^2 = 1.0$ (GeV/c)$^2$, total width $\Gamma = 0.3$ GeV and $\sigma = 1.1$. (auth)

**56501** (RHEL/R-224) COEFFICIENTS FOR PARTIAL WAVE ANALYSIS OF THE REACTION $0^- + \frac{1}{2}^+ \to 1^- + \frac{1}{2}^+$. Brandstetter, A.; Deen, S. M.; Litchfield, P. J. (Rutherford High Energy Lab., Chilton (England)). Aug 1971. 91p. Dep. NTIS (U. S. Sales Only). UK Pound 1.00.

Coefficients for the Legendre polynomial expansion of differential cross sections and density matrices in terms of partial wave amplitudes are calculated. Tables for the reaction $0^- + \frac{1}{2}^+ \to 1^- + \frac{1}{2}^+$ are presented. (auth)

**56502** TOTAL EFFECTIVE CROSS SECTIONS FOR HIGH-ENERGY ACAUSAL PION–NUCLEON SCATTERING. Sekine, Matsuo (Kyoto Univ.). Progr. Theor. Phys. (Kyoto); 45: No. 1, 322-4(Jan 1971). (In German).

The possibility of the experimental observation of the nonlocality in microphenomena is investigated for the high-energy region. It is shown that in the high-energy range the total pion-nucleon scattering cross section is connected to the existence of an acausal length. (J.S.R.)

**56503** SOLUTION OF THE SU(3)-SYMMETRIC BARYON STRONG COUPLING BOOTSTRAP MODEL. Majewski, W. (Inst. of Physics, Warsaw). Bull. Acad. Pol. Sci., Ser. Sci., Math., Astron. Phys.; 19: No. 5, 407-14(1971).

The solutions have been obtained of equations on coupling constants between baryons and pseudoscalar mesons. These equations result from the algebraic formulation of the strong coupling model as well as from the static baryon bootstrap model. Both approaches lead to the dynamical noncompact group $G = K\square T$ for the one-baryon states spectrum, where K is the symmetry group. The solutions found in exact SU(3) symmetry case for mesons interacting with baryons in all partial waves are compared with experimental data on the low-energy baryon resonances. (auth)

**56504** BEHAVIOR OF THE DIFFRACTION MAXIMUM IN MESON–NUCLEON INELASTIC INTERACTIONS IN 2- TO 20-GeV/c RANGE. Andreescu, Ileana (Univ., Bucharest). Stud. Cercet. Fiz.; 23: No. 3, 249-85(1971). (In Rumanian).

The topics covered include the transfer distribution studies of recoil nucleons from the inelastic interactions up to 16 GeV, and at 20 GeV, transfer distribution analysis for two-body and quasi-two-body channels, analysis of theoretical hadron–hadron interaction models which could explain the diffraction maximum width behavior, and Regge-type models explaining the diffraction maximum width behavior. (J.F.P.)

**56505** REGGE CUTS AND HIGH ENERGY $\pi$N AND KN SCATTERING. Tuan, R. Hong; Kaplan, J. M. (Laboratoire de Physique Theorique et Hautes Energies, Orsay, France). Nucl. Phys.; B32: No. 2, 655-80(1971).

A phenomenological analysis of $\pi$N and KN elastic and charge exchange scattering is made in the framework of convolutions models. The pomeron trajectory is taken with a non-zero slope which allows one to describe high-energy total cross sections (without violating the Pomeranchuk conjecture) together with $d\sigma/dt$ and $P_0$. For the Regge contribution strong exchange degeneracy and Gell-Mann's ghost killing mechanism are used. A rather good fit to the data ($\sigma_T$, $d\sigma/dt$, $P_0$ for $|t| < 1.5$ GeV$^2$/c$^2$) is obtained. The slope of the pomeron is found to be the same as for pp scattering ($\alpha' p = 0.33$ GeV$^{-2}$/c$^{-2}$). In $\pi$p scattering no cut should be present in the helicity flip amplitude. (auth)

**56506** REGGE ANALYSIS OF THE REACTIONS $\pi^-p \to \eta n$ AND $K^- \to K\bar{K}^0n$ with $\rho$ and A2 DEGENERATE TRAJECTORIES. de Brion, J. P.; Derem, A.; Dronkers, J. (CEN, Saclay, France). Nucl. Phys.; B32: No. 2, 557-72(1971).

The results of a new analysis of the reactions $\pi^-p \to \eta n$, $K^-p \to \bar{K}^0n$ and $K^+n \to K^0p$ are reported. Data for the two first reactions range from 1.7 to 18.2 GeV/c, and the analysis extends to $t = -1.6$ GeV$^2$. It is found necessary to introduce four poles $\rho$, $\rho'$, A2 and A2', and a cut associated with the A2 pole. The Regge model is used when evaluating the spin correction to the reaction $K^+d \to K^0pp_s$ in order to obtain the charge-exchange distribution $K^+n \to K^0p$. The $\rho$ and A2 trajectories are practically degenerate, with a $t = 0$ intercept of 0.5. Polarizations expected from Regge models in $K^-p \to \bar{K}^0n$ and $K^+n \to K^0p$ are discussed. (auth)

**56507** HARMONIC OSCILLATOR ANALYSIS OF THE HYPERON SPECTRUM. Faiman, David (Department of

Theoretical Physics, Oxford). Nucl. Phys.; B32: No. 2, 573-608(1971).

By applying SU(3) symmetry to the quark-quark-meson vertex and ignoring any possible mass differences among the quarks, the harmonic oscillator quark model is generalized to include classification and decay properties of the hyperon resonances. This brings a very large number of two-body and quasi two-body decay processes within the scope of a basic two-parameter expression for partial widths. It is found that in situations for which configuration-mixing does not occur, nearly all measured rates (where these are available for comparison) fall within ±50% of the theoretically predicted values. For the low-lying negative-parity hyperons, configuration-mixing in threes is quantitatively discussed using an SU(6) formalism that could find useful application outside the quark model. (auth)

**56508** SECONDARY REGGE CONTRIBUTIONS IN CHARGE EXCHANGE REACTIONS AT t = O. Dronkers, J. (CEN, Saclay, France). Nucl. Phys.; B32: No. 2, 513-26(1971).

Second order contributions to Regge-pole exchange are analyzed in $\pi$N and KN charge-exchange reactions at zero angle, using recent experimental data. Models involving secondary trajectory exchange, contributions from cuts and complex Regge dipoles are compared. The breaking of the $\rho - A_2$ exchange degeneracy is found to be rather important for the residues; the second order corrections to pure $\rho$ and $A_2$ Regge-pole exchange are small, too small to account for the high-energy behavior of the total cross section $\Delta\sigma^{\pi} = \sigma_{tot}(\pi^-p) - \sigma_{tot}(\pi^+p)$ measured at the Serpukhov accelerator. It seems impossible to distinguish between second-order corrections from secondary trajectory exchange and cuts, at t = 0. The cut contribution to $\rho$ exchange predicted by a simple absorption model is very small in the forward direction; this is confirmed by the fit. (auth)

**56509** NOTE ON SURFACE (VOLUME) REACTIONS AND POLARIZATION IN $\pi^-$−p CHARGE-EXCHANGE SCATTERING AT HIGH ENERGY. Minami, S.; Tsujumura, T. (Osaka City Univ.). Lett. Nuovo Cim.; 2: No. 12, 587-91(18 Sep 1971).

In order to explain the characteristic features of high-energy $\pi^{\pm}$−p elastic polarization data, a model was suggested by Berlad et al. in which the scattering amplitude can be described in terms of the effects due to the surface and volume reactions corresponding to resonance scattering and diffraction scattering, respectively. A similar approach was suggested by Harari. The Harari model is discussed and the characteristic properties of the polarization of recoil nucleons in forward $\pi^-$p charge-exchange scattering at very high energy are predicted on the basis of the Berlad−Dar−Eilam model. (L.B.S.)

**56510** ADLER-WEISBERGER RELATION. Pajares, C.; Pascual, R. (Neuva Universidad Autonoma, Madrid). Lett. Nuovo Cim.; 2: No. 12, 598-600(18 Sep 1971).

A modification of the Adler−Weisberger relation using a once-subtracted dispersion relation is presented. The modified formula has two advantages over the usual relation: it is valid even if the Pomeranchuk theorem is violated, and it is much less dependent on the way in which the physical cross sections are extrapolated off the mass shell. (L.B.S.)

**56511** APPLICATION OF A VENEZIANO MODEL INCLUDING SPINS TO THE REACTION $K^+p \rightarrow K^{*+}(890)p$. Dibon, H.; Majerotto, W.; Markytan, M. (Institut fuer Hochenenergiephysik, Vienna). Lett. Nuovo Cim.; 2: No. 13, 621-6(25 Sep 1971).

A Veneziano-like model is applied to the reaction $K^+p \rightarrow K^{*+}(890)p$ by taking into account the spins of all the particles involved. For every invariant amplitude of this reaction a Veneziano four-point function is used in such a way that the whole amplitude has the correct Born terms and asymptotic behavior. The differential cross sections were fitted at 3.0, 3.5, 5.0, and 8.25 GeV/c. The spin-density matrix was calculated using the fitted parameters. The model was found to reproduce well the data. (L.B.S.)

**56512** MESONIC STRUCTURE IN THE NUCLEON. Galloway, K. F.; Mann, A.; Weiner, R. M. (Indiana Univ., Bloomington). Lett. Nuovo Cim.; 2: No. 13, 635-40(25 Sep 1971).

It is suggested that the concept of a mesonic cloud surrounding the nucleon should be considered along the lines similar to the problem of nucleons in nuclei. The essential point made is the assumption that mesons exist in nucleons, in the sense that the meson distribution manifests itself in scattering experiments on nucleons, in much the same way as the nucleon distribution appears in scattering on nuclei. Starting from the idea that the mesons in the nucleon can be characterized by the Bose−Einstein distribution, the momentum distribution is studied from one-pion production process on a nucleon. (L.B.S.)

**56513** U(6,6) ⊗ O(3,1) ABSORBED K-MATRIX MODEL FOR SPIN-2 EXCHANGE IN $\pi^-p \rightarrow \eta n$. III. Gujadhur, T. K. (International Centre for Theoretical Physics, Trieste, Italy); Moriarty, K. J. M.; Migneron, J. H. R. Lett. Nuovo Cim.; 2: No. 13, 652-6 (25 Sep 1971).

The process $\pi^-p \rightarrow \eta n$ with $A_2$ exchange is studied using a modified form of the absorption model within the U(6,6) ⊗ O(3,1) symmetry scheme. The model fails to predict the differential cross section. (L.B.S.)

**56514** INELASTICITY OF MULTIPION PRODUCTION FROM A QUARK MODEL. Erwin, A. R. (Univ. of Wisconsin, Madison). Contract AT(11-1)-881. Phys. Lett.; 36B: No. 5, 489-92(4 Oct 1971).

The maximum observed multiplicity in $\pi$p, pp and $\gamma$p interactions differs dramatically from what might reasonably be expected. The energy dependence of the maximum multiplicity suggests a quark model with near massless quarks which serve to partition the energy and momentum available for interaction in the incident particles. (auth)

**56515** SOME CONSEQUENCES OF EXCHANGE DEGENERACY AND THE TRIPLE-REGGE-HYPOTHESIS. Finkelstein, J. (Stanford Univ., Calif.); Rajaraman, R. Phys. Lett.; 36B: No. 5, 459-62(4 Oct 1971).

The proton-Reggeized rho total cross section is extracted from inclusive data for $K^+ + p \rightarrow K^0 +$ (anything) in the triple-Regge domain and it is found that it is of the same order as physical meson-proton cross-sections for a range of Reggeon mass. Other processes such as $pp \rightarrow pX$ and $K^+p \rightarrow K^+X$ to $K^+p \rightarrow K^0X$ are also related and good agreement with data is obtained. Methods for calculating baryon exchange processes as well are suggested. (auth)

**56516** DETERMINATION OF $|g_A|$ FROM VENEZIANO AMPLITUDE AND CURRENT ALGEBRA SUM RULE FOR $\pi$-N SCATTERING. Chowdhury, A. Roy; Banerjee, S. N. (Jadavpur Univ., Calcutta). Progr. Theor. Phys. (Kyoto); 45: No. 5, 1701-2 (May 1971).

An attempt is made to investigate the compatibility of current-algebraic sum rules with the Veneziano-type amplitude for $\pi$-N scattering, constructed mainly on the hypothesis of high-energy behavior, crossing symmetry, and duality. The investigation yields $|g_A|$ equal to 1.33, which compares favorably with the corresponding experimental value. (L.B.S.)

**56517** HELICITY CONSERVATION IN THE INELASTIC SCATTERING. Biyajima, Minoru (Tokyo Univ. of Education). Progr. Theor. Phys. (Kyoto); 45: No. 5, 1552-63(May 1971).

The helicity conservation in the inelastic channels is discussed: $\pi N \rightarrow VN$, $\pi N \rightarrow \sigma N$ and $\pi\pi \rightarrow \rho\rho$ scattering. Requiring the helicity conservation in $\pi N \rightarrow VN$ scattering, it is concluded that the coefficients of leading terms in Ball amplitudes $B_3$ and $B_5$ are zero. From these conditions, two relations can be derived. Further in $\pi N \rightarrow \sigma N$ scattering, it is concluded that the A invariant amplitude vanishes or $\beta_{\sigma \rightarrow 2\pi}(t) = 0$. The condition that the $C_2$ invariant amplitude must vanish in $\pi\pi \rightarrow \rho\rho$ scattering is obtained. Applying the factorization theorem to the $\pi$-meson pole, it is concluded that the existence of the $\pi$-meson pole is not compatible with helicity conservation hypothesis in inelastic scattering ($NN(N\bar{N})$ charge exchange, $\pi N \rightarrow VN$ and $\pi N \rightarrow \sigma N$ scattering. (auth)

**56518** PARTICLE EXCHANGE, REGGE-POLE EXCHANGE, AND THE VENEZIANO AMPLITUDE FOR KN SCATTERING. Kinoshita, Kisei; Shiga, Kunio (Kyushu Univ., Fukuoka). Progr. Theor. Phys. (Kyoto); 45: No. 5, 1564-77(May 1971).

Based on the observation that the (t,u)-Veneziano terms can be expressed as an infinite sum of one-particle exchange contributions in the physical region, contrary to the (s,t) and (s,u) terms where the particle exchange picture is divergent, the validity of the particle exchange picture and the transcendental mechanism to the Regge pole exchange picture is examined in a KN Veneziano amplitude consisting of (t,u) terms only. At threshold, the contribution of meson exchanges with the lowest mass almost saturates the KN Veneziano amplitude. The hyperon exchange contributions should be discarded there, because of the duality between meson exchange contributions and hyperon exchange contributions. As energy increases, the meson towers with various spin states and degenerate mass begin to contribute one by one. Regge behavior is obtained as a result of a detailed cancellation among the contributions of meson exchangers with various masses and spins. Here, Regge behavior in a limited energy region is given by a finite sum of one-meson exchange terms. On the other hand, the hyperon exchange picture with finite terms does not approximate well the amplitude in the low energy region, even at threshold. These situations are understood through the study of the condition for an approximate truncation of infinite series of poles in the

XUM

(t,u)-terms. The low energy interpolations of Regge asymptotic forms are studied, and the meson Regge pole exchange is also confirmed to give the gross features of the amplitude down to the threshold. The problem of double counting between the t- and u-Regge poles in low energy is noted. (auth)

**56519** $P_{11}\pi N$ SCATTERING IN THE THREE-CHANNEL MODEL. Hori, Setsuko (Osaka Univ.). Progr. Theor. Phys. (Kyoto); 45: No. 5, 1703-4(May 1971).

Bootstrap calculations for the $P_{11}\pi N$ scattering are carried out in the three-channel model, taking into account only the $\rho N$ and $\pi N^*$ inelastic channels. Coupling constants for $\pi NN$, $\rho NN$, and $\pi NN^*$ are obtained. It is found that the Roper resonance could not be produced dynamically in the three-channel model. (L.B.S.)

## *Strong (Baryon No. ≥ 2)*

*Refer also to abstract 56810.*

**56520** (IC-71/106) MULTIPLE SCATTERING EFFECTS IN QUASIFREE SCATTERING. Abul-Magd, A. Y.; Guardiola, R. (International Centre for Theoretical Physics, Trieste (Italy)). Sep 1971. 18p. (CONF-710911-9). Dep. NTIS (U. S. Sales Only).

From fourth international conference on high energy physics and nuclear structure; Dubna, USSR (7 Sep 1971).

The Glauber multiple scattering theory is applied to the study of quasi-free scattering of high-energy protons by nuclei. The multiple scattering of the knocked-out nucleon is not considered. The differential cross section is written as a sum of different terms corresponding to single, double, ..., incoherent scattering of the incident nucleon inside the target nucleus. It is shown that the single scattering term is similar to the outcome of the distorted wave impulse approximation. The theory is compared with the experimental cross section of the quasi-free scattering of 1 GeV protons from $^{12}C$ and the agreement is satisfactory at forward angles. The contribution from double scattering terms appears to be rather important. (auth)

**56521** (JINR-P1-5975) ANALYSIS OF THE REACTION $np \rightarrow pp\pi^-$ FROM THE POINT OF VIEW OF REGGEIZED OPE MODEL. Boreskov, K. G.; Gasparyan, A. P.; Kaidalov, A. B.; Nikitin, A. V.; Ponomarev, L. A.; Troyan, Yu. A. (Joint Inst. for Nuclear Research, Dubna (USSR). Lab. of High Energy). 1971. 18p. (In Russian). Dep. NTIS (U.S. Sales Only).

In the framework of the Reggeized OPE model the handling was performed of the available experimental data on the $np \rightarrow pp\pi^-$ reaction in the energy range from 2 to 30 GeV. It is shown that side by side with the $\pi$-meson exchange, beginning from the energy of 4 GeV the mechanism of diffraction production of $N^*(1470)\,1/2(1/2)+$ and $N^*(1690)1/2(5/2)+$ isobars is revealed which contribution is of (30 to 40)% from the value of the total reaction cross section. (auth)

**56522** (ORNL-tr-2520) CLASSIFICATION OF INELASTIC INTERACTIONS OF HIGH-ENERGY PROTONS AND NUCLEI. II. CHARACTERISTICS OF LOW-ENERGY NUCLEI. Barashenkov, V. S.; Il'inov, A. S.; Sobolevskii, N. M.; Toneev, V. D. (Joint Inst. for Nuclear Research, Dubna (USSR). Lab. of Theoretical Physics). Translated for Oak Ridge National Lab., Tenn., from report JINR-P2-5549. 26p. Dep. NTIS.

A detailed calculation and discussion is given of the properties of the low-energy secondary particle component produced in proton reactions with nuclei from aluminum to lead at 0.010 to 5 GeV. The stage is investigated in which the characteristics of these particles depend on the cascade stage of the process. The evaporation model description of the experiments in this case is discussed. The results in conjunction with previous data on cascade particle characteristics allow one to determine essentially all characteristics of an inelastic proton reaction with a nucleus for any nucleus and for energy values in the studied region as a function of energy. (J.F.P.)

**56523** (USIP-71-3) AUTOMATIC SELECTION OF KINEMATICAL HYPOTHESES FROM TWO PRONG PROTON-PROTON INTERACTIONS IN A HYDROGEN BUBBLE CHAMBER AT 19 GeV/c. Danielsson, O.; Granstroem, L.; Ronne, B. E. (Stockholm Univ. (Sweden). Inst. of Physics). Apr 1971. 63p. Dep. NTIS (U. S. Sales Only).

A program, ALICE, is described which automatically selects hypotheses accepted by a kinematics program applied to two-prong reactions from proton-proton interactions at 19 GeV/c. It is demonstrated to be both much faster and more accurate than manual selection. (auth)

**56524** Λ-EXCITED STATES OF HYPERNUCLEI. Deloff, A; Pniewski, J. (Inst. for Nuclear Research, Warsaw Univ., Warsaw). Nucl. Phys.; B32: No. 2, 453-60(1971).

Excited Λ-states of hypernuclei are considered by means of the optical potential model. A realistic Saxon-Woods potential is simulated by an equivalent square well potential. The positions of the levels are calculated in terms of the mass number A of the core nucleus. The spread in binding energies due to uncertainties in the value of parameters characterizing the optical potential is discussed.

**56525** EVIDENCE FOR BOSON PRODUCTION VIA ISOBAR DECAY. Dubal, L. (Conseil National de Recherches du Canada, Ottawa); Brown, D. J. Nucl. Phys.; B32: No. 2, 535-40(1971).

Boson production in processes of type $NA' \rightarrow AX$, where A(A') is a light nucleus of atomic number a (a' = a − 1), and X a boson, is probably mediated by the formation of intermediate nucleon-isobars. All available experimental data including the results of the Saclay experiment on $np \rightarrow d\sigma(310)$ and $dp \rightarrow {}^3He\sigma(310)$ strongly support the model proposed based on the Selleri OPE triangle diagram. (auth)

**56526** RADIATIVE NEUTRON-PROTON SCATTERING AT LOW ENERGY. Baier, R. (Univ., Graz); Kuehnelt, H. Acta Phys. Austr.; 32: No. 1, 60-4(1970).

Neutron-proton bremsstrahlung cross sections were calculated for a laboratory energy of 14.4 MeV with the help of two relativistically covariant models. Results are given for coplanar (symmetric and nonsymmetric) as well as for noncoplanar symmetric geometries. (auth)

**56527** MULTI-PION EXCHANGE CONTRIBUTION TO NUCLEON-NUCLEON BINDING AND THE ELECTRODISINTEGRATION OF DEUTERONS. Bebel, D.; Biebl, K. J.; Otto, H. J. (Humboldt-Univ., Berlin. Institut fuer Hochenergiephysik, Berlin). Monatsber. Deut. Akad. Wiss. Berlin; 12: 876-83(1970). (In German).

The results of a dispersion theoretical calculation of the deuteron-nucleon vertex function, which represents the relativistic analog to the deuteron wave function, are reported. The question of its experimental detection in the electrodisintegration of deuterons is considered. This calculation includes one-, two-, and three-pion exchange effect in the abnormal and part of the normal spectral range of the vertex function. (tr-auth)

**56528** BREAKS OF $d\delta/dt$ IN HIGH-ENERGY PROTON-PROTON SCATTERING. Sawada, T. (Univ., Sao Paulo, Brazil). Lett. Nuovo Cim.; 2: No. 13, 647-51(25 Sep 1971).

It is pointed out that in the high-energy limit breaks occur in the differential cross sections of proton-proton scattering at $t = t_{Bj}$, which satisfies $\alpha(t_{Bj}) = \alpha_j(0)$, where $\alpha_j(0)$ are values of lower Regge trajectories at $t = 0$ and $\alpha(t)$ is the leading Regge trajectory, and that discontinuity of $(d/dt)\ln(d\delta/dt)$ at these break points can be computed from the known Regge parameters. (L.B.S.)

**56529** COMMENT ON THE $^1S_0$ NUCLEON-NUCLEON EFFECTIVE-RANGE EXPANSION PARAMETERS. Noyes, H. Pierre; Lipinski, Hubert M. (Stanford Univ., Calif.). Phys. Rev., C; 4: No. 3, 995-1002(Sep 1971).

The most accurate nucleon-nucleon scattering experiments below 10 MeV are now consistent with the following values and uncertainties for the $^1S_0$ scattering lengths and effective ranges: $a_{pp}^c = -7.823 \pm 0.01$ F, $r_{pp}^c = 2.794 \pm 0.015$ F; $a_{nn} = -17 \pm 1$ F, $r_{nn} = 2.84 \pm 0.03$ F; $a_{np} = -23.715 \pm 0.015$ F, $r_{np} = 273 \pm 0.03$ F. Unless strong theoretical arguments can be advanced that all charge-dependent corrections to the parameters can be calculated accurately enough to prove that the values $a_{nn}$, $r_{nn}$, or $r_{np}$ must be moved outside these limits, or strong experimental reasons given to believe that experiments leading to these results were significantly in error, it is argued that new calculations or experiments aimed at changing these values are likely to fail. This argument is supported by an analysis of the latest p-p experiments of Jarmie, Jett, Detch, and Hutson at 9.918 MeV, which reconfirm the one-pion-exchange shape effect and give $G^2_{\pi^0 p} = 15.3 \pm 2.4$ for the pion-nucleon coupling constant. (auth)

**56530** PION PRODUCTION AND NUCLEAR SURFACE. Lombard, R. J. (Institut de Physique Nucleaire, Orsay, France); Auger, J. P.; Basile, R. Phys. Lett.; 36B: No. 5, 480-2(4 Oct 1971).

The pion production by high energy protons on nuclei is calculated within the framework of an isobar model using realistic nu-

clear proton and neutron distributions. The sensitivity of the pion production to nuclear surface properties is discussed. (auth)

**56531** SEPARABLE POTENTIALS. Oberhummer, H.; Zingl, H. F. K. (Univ., Graz). Acta Phys. Austr.; 31: No. 4, 373-6(1970).

The Schroedinger equation is used to obtain a separable potential. The case of low-energy p + p scattering is considered. (J.F.P.)

**56532** ONE-BOSON-EXCHANGE MODEL OF NUCLEON–NUCLEON SCATTERING FOR THE 0 TO 3 GeV ENERGY RANGE. Ueda, Tamotsu (Osaka Univ.). Progr. Theor. Phys. (Kyoto); 45: No. 5, 1527-51(May 1971).

With the technique of dispersion relation, one-boson-exchange models involving $\pi$, $\rho$, $\omega$, $\eta_V$, f and $\sigma(0^+, I = 0, 416$ MeV) are studied for the nucleon–nucleon interaction below 3 GeV. The models give qualitatively good fits to all observables of proton–proton scattering at 670, 970, and 1400 MeV, in addition to nucleon–nucleon elastic data. Effects of absorption on phase shifts, nucleon–meson form factor and high-energy cutoff of the one-boson-exchange amplitudes are discussed. Nucleon–nucleon scattering amplitudes in which a meson with an arbitrary spin is exchanged are formulated. (auth)

# Particle Invariance Principles and Symmetries

## General

*Refer also to abstracts 56542, 56549, and 56558.*

**56533** (IFA-FT–85) SYMMETRY BREAKING OF CHIRAL SU(3) x SU(3) IN PHENOMENOLOGICAL LAGRANGIANS. Marculescu, Sorin (Institutul de Fizica Atomica, Bucharest (Romania)). 1971. 8p. Dep. NTIS (U. S. Sales Only).

The symmetry breaking model of Gell–Mann, Oakes and Renner is considered using nonlinear realizations. The value of the breaking parameter can be found in principle without any saturation assumption. (auth)

**56534** (KFKI–71-38) REPRESENTATIONS OF THE POINCARE GROUP AS FUNCTIONS OF THE EIGENVALUES OF CASIMIR OPERATORS. Szego, K.; Toth, K. (Magyar Tudomanyos Akademia Kozponti Fizikai Kutato Intezete, Budapest). [1971]. 19p. Dep. NTIS (U. S. Sales Only).

Explicit basis functions are defined for the Poincaré group. Both these functions and the representation matrix elements are continuous functions of the momentum variables for the whole real $p^2$ spectrum, including the $p^2 = 0$ point. The essence of the method is to enlarge the previously obtained SL(2,C) basis and representations of similar nature. (auth)

**56535** (ORO–3992-7) SYMMETRY BREAKING IN THE HARD-MESON CURRENT ALGEBRAIC TREE-GRAPH THEORY. Pande, L. K. (Ohio State Univ., Columbus. Dept. of Physics. Texas Univ., Austin. Center for Particle Theory). [nd]. 10p. (CPT–45). Dep. NTIS.

A formula is derived for the symmetry breaking parameter C using the hard-meson current algebraic tree-graph theory which possesses $(3^*,3) \oplus (3,3^*)$ broken chiral SU(3) $\otimes$ SU(3). A discussion of the formula as well as a numerical evaluation is presented. $C = \sqrt{2}$ (0.8) is obtained. (auth)

**56536** PARA-FERMI OPERATORS AND SPECIAL UNITARY ALGEBRAS. Ramakrishnan, Alladi; Vasudevan, R.; Chandrasekaran, P. S. (Inst. of Mathematical Sciences, Madras). J. Math. Anal. Appl.; 35: No. 2, 249-54(Aug 1971).

It is shown that the generators of the special unitary group SU(n) can be constructed from para-Fermi operators of order n. (J.F.P.)

## Applications (Electromagnetic and Weak)

*Refer also to abstract 56855.*

(JINR–E2-5996) THE $K_{l3}$ DECAYS AND CHIRAL SYMMETRY-BREAKING. Eliashvili, M. A.; Magradze, B. A.; Tugulea, M. N. (Joint Inst. for Nuclear Research, Dubna (USSR). Lab. of Theoretical Physics). 1971. 9p. Dep. NTIS (U. S. Sales Only).

An effective Lagrangian model with SU(3) x SU(3) symmetry-breaking terms transforming as $(3.3^*) + (3^*,3)$ and $(1.8) + (8.1)$ representations is considered. It is shown that such a model gives a realistic description of the $K_{l3}$ form factors. (auth)

## Applications (Strong)

*Refer also to abstract 56503.*

**56538** (ORO–3992-2) GAUGE INVARIANT CHIRAL LAGRANGIAN AND $\bar{P}P$ ANNIHILATIONS. Chiang, C. C. (Syracuse Univ., N. Y. Dept. of Physics. Texas Univ., Austin. Center for Particle Theory). Dec 1969. Contracts AT(30-1)-3399; AT(40-1)-3992. 38p. Dep. NTIS.

Two-meson production processes in $\bar{p}p$ annihilation at rest are investigated using a gauge invariant, chiral SU(3) x SU(3) symmetric Lagrangian model. The gauge field is identified as the massive vector field which is decomposed into $\rho$ octet and $\rho'$ octet. Both S-wave and P-wave annihilations are computed. The result is compatible with most recent experimental data. The possible contribution from higher-integer spin dominance is also discussed. (auth)

**56539** (ORO–3992-11) SCALAR MESONS IN BROKEN CHIRAL SYMMETRY. Pande, L. K. (Texas Univ., Austin. Center for Particle Theory). May 1970. 10p. (CPT–52). Dep. NTIS.

A discussion of the masses of scalar mesons within the broken chiral symmetry framework is presented. (auth)

**56540** MASS FORMULAS SU(3) AND CLASSIFICATION OF HEAVY HYPERONS. Zamiralov, V. S. (Moscow State Univ.). Vestn. Mosk. Univ., Ser. III. Fiz. Astron.; 12: No. 1, 109-10 (Jan-Feb 1971). (In Russian).

In this inquiry into the characteristics of SU(3) mass formulas restriction is made to baryon octets and an attempt was made to predict the quantum numbers of cascade hyperons. A relation was derived from the Gell-Mann formula, and it was shown that good agreement was obtained with all eight baryon octets. (K.S.W.)

# Field Theories

## General

**56541** LAGRANGIAN FORMALISM FOR FREE MAXWELL FIELD IN SPINOR NOTATION. Srivastava, C. M. (Indian Inst. of Tech., Bombay). Indian J. Pure Appl. Phys.; 9: No. 1, 5-7 (Jan 1971).

The conventional Lagrangian formalism for the free Maxwell field in the spinor notation leads to conservation laws which are not in agreement with the classical conservation laws. A new Lagrangian formalism in spinor notation was developed which leads to the correct conservation laws. (auth)

## Quantum Field Theory

*Refer also to abstracts 56571 and 56839.*

**56542** (CNRS-CPT-71/P-378) DIVERGENCES OF MASSIVE YANG–MILLS THEORIES: HIGHER GROUPS. Glashow, S. L.; Iliopoulos, J.; Yao, Andrew (Centre National de la Recherche Scientifique, Marseilles (France). Centre de Physique Theorique). Jun 1971. 5p. Dep. NTIS (U. S. Sales Only).

An analysis is made of massive Yang–Mills theories based on semi-simple groups other than SO(3). The multiplet of vector mesons may have arbitrary Yukawa couplings to fermions. It is shown that the naive degree of divergence of any Feynman amplitude is not worse than for the same theory without the meson self-couplings: the worst divergences are like $(g \Lambda)^{2n}$. (France)

**56543** (DESY–71/39) SMALL-DISTANCE-BEHAVIOUR ANALYSIS AND WILSON EXPANSIONS. Symanzik, K. (Deutsches Elektronen-Synchrotron, Hamburg (West Germany)). Jul 1971. 85p. Dep. NTIS (U. S. Sales Only).

A previously described method to obtain the asymptotic forms of vertex functions at large momenta is, with the help of Wilson operator product expansion formulas, extended to momenta where the vertex functions of the zero-mass theory underlying the asymptotic forms are infrared singular. To obtain from asymptotic forms information on asymptotic behavior requires assumptions on the behavior of the zero-mass theory in the limit of infinite dilatation. One particular set of assumptions is discussed and found to pass a simple consistency test; this set of assumptions leads to power laws, or slight modifications thereof, with coupling-constant-independent exponents. The detailed discussion is given for the $\varphi^4$ model. (auth)

XUM

**56544** (IC-71/71) FORMULATION OF QUANTUM FIELD THEORY IN TERMS OF TEMPERED DISTRIBUTIONS AND A POSSIBLE DEPARTURE FROM THE PRINCIPLE OF SUPERPOSITION. Rayski, J. (International Centre for Theoretical Physics, Trieste (Italy)). Jul 1971. 9p. Dep. NTIS (U. S. Sales Only)

A new type of representations related to complete sets of square integrable functions is introduced. The Green's functions of the theory become tempered distributions. Normal ordering of creation and annihilation operators related to such representations yields Hamiltonians which are no longer positive definite. This difficulty is circumvented by introducing suitable supplementary conditions. The principle of superposition of states breaks down under such supplementary conditions but a probabilistic interpretation in terms of conditioned probabilities is still possible. The difficulties with an infinite volume are avoided. The cases of massive and massless particles may be treated on an equal footing. The old difficulty with securing the Lorentz condition is avoided without having to introduce a nondefinite metric. A large class of nonpolynomial (e.g. square root) lagrangians becomes quantizable along these lines. (auth)

**56545** (IC-71/108) FINITE FIELD THEORIES. Salam, Abdus (International Centre for Theoretical Physics, Trieste (Italy)). Sep 1971. 27p. (CONF-710810-3). Dep. NTIS (U. S. Sales Only).

From Meeting on particles and fields; Rochester, N. Y. (30 Aug 1971).

Developments in finite field theories are reviewed nonrigorously. Exponential Lagrangian theories as good field theories, and inbuilt cut-offs in some currently accepted field theories are discussed. (J.F.P.)

**56546** (JINR-P2-5998) NONPOLYNOMIAL LAGRANGIANS (HIGHEST PERTURBATION ORDERS). Volkov, M. K. (Joint Inst. for Nuclear Research, Dubna (USSR). Lab. of Theoretical Physics). 1971. 21p. (In Russian). Dep. NTIS (U. S. Sales Only).

It is proved that the theory with nonpolynomial Lagrangians is finite and unitary in highest perturbation orders. The order of increase of amplitudes in an arbitrary perturbation order is found. (auth)

**56547** (NYO-1932(2)-200) SOME NEW APPLICATIONS OF INDEFINITE METRIC TO QUANTUM ELECTRODYNAMICS AND WEAK INTERACTIONS. Lee, T. D. (Columbia Univ., New York). [1971]. Contract AT(30-1)-1932. 19p. (CONF-710609-9). Dep. NTIS.

From International conference on elementary particles; Amsterdam, Netherlands (30 Jun 1971).

Several topics related to possible physical applications of indefinite metric are discussed; among these are the neutron–proton mass difference, the production cross section of the heavy photon and the possible existence of the spin-0 charged intermediate boson. (auth)

**56548** (ORO-3992-1) LAGRANGIAN FORMALISM FOR NEUTRAL MASSIVE SPIN 3 FIELDS. Chiang, C. C. (Syracuse Univ., N. Y. Dept. of Physics. Texas Univ., Austin. Center for Particle Theory). Sep 1969. Contracts AT(30-1)-3399; AT(40-1)-3992. 22p. (CPT-26). Dep. NTIS.

The Lagrangian formalism for massive neutral spin-3 fields is investigated without introducing an auxiliary field. The field variables are assumed a priori to be symmetric. By using the Takahashi–Umezawa method, the relativistic quantization is also carried out for this field. It is shown that both Lagrangian and field equations are parameter dependent. However, these parameters do not have any real physical significance as far as the free field is concerned. In the presence of an interaction, the Green's function is also parameter dependent. The determination of the parameters should be based on the high-energy behavior of the Green's function from experimental results. (auth)

**56549** (ORO-3992-9) BREAKING OF CONFORMAL SYMMETRY AND RENORMALIZATION OF NONPOLYNOMIAL THEORIES. Salam, A. (Texas Univ., Austin. Center for Particle Theory). May 1970. 25p. (CPT-50; CONF-700424-2). Dep. NTIS.

From Symposium on the past decade in particle theory; Austin, Tex. (14 Apr 1970).

Nonlinear realizations of the conformal group and the group of general relativity and nonpolynomial Lagrangians in general are considered, including nonlinear realizations. The problem of the kind of field theories such nonlinear nonpolynomial Lagrangians define is discussed. In particular it is shown that these theories do not appear to suffer from the ultraviolet infinities of usual polynomial Lagrangian theories. It is shown that explicit calculations give the result that in quantized general relativity theory all infinities still surviving in renormalized theories like quantum electrodynamics disappear. (J.F.P.)

**56550** (ORO-3992-14) ACTION-AT-A-DISTANCE. Sudarshan, E. C. G. (Texas Univ., Austin. Center for Particle Theory). Sep 1970. 41p. (CPT-55). Dep. NTIS.

The historical development of "action-at-a-distance" theories is reviewed. The formulation of classical action-at-a-distance theories is reviewed, and the relevant conserved quantities are identified. This theory is compared with a corresponding classical field theory. The lessons of this classical theory are applied to the formulation of a quantum theory of action-at-a-distance. The problems of unitarity and physical interpretation are described. The relation with indefinite metric theories of elementary particles is clarified and finally a theory of interactions which includes self interaction but contains only finite computations is formulated. (auth)

**56551** BOUNDARIES OF THE SINGULARITY MANIFOLDS ASSOCIATED WITH A FIVE POINT FUNCTION. Berkmen, Haluk (Middle East Technical Univ., Ankara). Nucl. Phys.; B32: No. 2, 645-54(1971).

The Feynman graph of a five point function and its singularity manifolds are investigated. (auth)

**56552** TWO-COMPONENT THEORY OF FERMIONS. Volkovyskii, R. Yu. (Leningrad Inst. of Railway Transport Engineers). Izv. Vyssh. Ucheb. Zaved., Fiz.; No. 5, 53-8(1971). (In Russian).

A variant of the theory of the Fermi-particle is given which is described by two-component spinors, conforming to a relativistic equation of the second order. In order to positively determine the probability density of the particles with a spin of $\frac{1}{2}$, a procedure is proposed, in which a complex conjugation of a function and Hermitian conjugation of operators are followed by an operation of spatial reflection. A single-particle theory is developed in Hamiltonian form. The Lagrange formalism is suggested for a free, two-component field and second quantization. For quantum-electrodynamic calculations there is proposed the Hamiltonian related to the Hamiltonian interaction of spinless particles with an electromagnetic field, but containing a spin contribution. (tr-auth)

**56553** UNIFIED TREATMENT OF THE $V-\theta$, $V-2\theta$ SECTORS OF THE LEE MODEL. Uliu, Florea (Univ., Craiova, Rumania). Stud. Cercet. Fiz.; 23: No. 3, 287–309(1971). (In Rumanian).

The treatment covers field operators, S-matrices, bound states, scattering states, the $V-\theta$ and $V-2\theta$ sectors, and $\tau(W)$ functions. (J.F.P.)

**56554** EQUIVALENCE OF LORENTZ TRANSFORMATIONS AND FOLDY–WOUTHUYSEN TRANSFORMATIONS FOR FREE SPINOR FIELDS. Tiomno, J. (International Centre for Theoretical Physics, Trieste, Italy). Physica; 53: No. 4, 581-601 (30 Jun 1971).

Generalized Lorentz and Foldy–Wouthuysen transformations are introduced. They lead to parametrized forms of the Dirac equation which include, besides the previously known representations, other simple ones which are explicitly given. Equivalence of generalized Lorentz and Foldy–Wouthuysen transformations is proved. It is shown that this is a consequence of the invariance of the Dirac equation under $D_1 \otimes O(4,1)$, where $D_1$ is a one-parameter dilatation group and O(4,1) is a De Sitter group. It is also shown that the referred equivalence is connected to the fact that $i\partial/\partial t$ must be used as a hermitian operator. (auth)

**56555** CANONICAL PROPER-TIME FORMALISM. Bakri, M. M. (Cairo Univ.). Lett. Nuovo Cim.; 2: No. 12, 603-7 (18 Sep 1971).

An attempt is made to develop a five-dimensional manifestly covariant canonical formalism, which leads automatically to a self-consistent proper-time formalism, and, at the same time, to a Lorentz-covariant set of Hamilton's equations. The results hold for any n-dimensional space. (L.B.S.)

**56556** SUBSIDIARY CONDITIONS FOR GENERATING FUNCTIONALS. Graff, P. (Max-Planck-Institut fuer Plasmaphysik, Garching, Ger.). Lett. Nuovo Cim.; 2: No. 12, 611-15 (18 Sep 1971).

It is pointed out that the functional equation of the dynamics can be used to describe a statistical ensemble; the conditions for various possible ensembles in terms of the functionals are con-

sidered. The equal-time formalism is discussed, starting with one degree of freedom. The connection between von Neumann formulation of statistical mechanics, the Wigner distribution function in phase space, and the Schwinger formalism in its simplest version is established. An attempt is made to extend the results to infinitely many degrees of freedom. (L.B.S.)

**56557** GEOMETRIC STRUCTURE OF A PARITY-CONSERVING RELATIVISTIC QUANTUM FIELD THEORY. Westenholz, C. v. (Rhodes Univ., Grahamstown, South Africa). Int. J. Theor. Phys.; 4: No. 4, 305-20(Aug 1971).

Wheeler's conjecture that there might exist a "principle" which rules out parity-nonconserving spaces was analyzed. The following result was obtained: A local relativistic quantum field theory is parity-conserving if the following conditions hold: (a) The fields are derived from geometry, i.e. they are represented by quantized currents (in the sense of de Rham); and (b) The theory may be defined on a connected and, under certain restrictions, on a disconnected orientable space-time continuum $M^4$. (auth)

**56558** REMARK ON GENERAL LORENTZ COVARIANCE. Braeuer, Hans-Juergen (Zentralinstitut fuer Astrophysik, Berlin). Int. J. Theor. Phys.; 4: No. 4, 243-6(Aug 1971).

A mathematical comment is made on previous work. The metric tensor g reduces the tangent bundle T of a space-time to the tangent Lorentz bundle L. The Levi-Civita connection in T induces in a natural way connections in L, and in the tensor product bundles of T, L, and the spinor bundle S. These connections are "the general Lorentz-covariant connection" by Treder. It is possible to treat the local tetrad field components as local components of a global cross-section of $L \otimes T$, with vanishing general Lorentz-covariant derivative. (auth)

**56559** TWO-COMPONENT SPHERICAL FACTORIZATION OF THE KLEIN-GORDON AND KRAMERS EQUATIONS. Biedenharn, L. C.; Han, M. Y. (Duke Univ., Durham, N. C.). Phys. Lett.; 36B: No. 5, 475-6(4 Oct 1971).

An alternative to Dirac's factorization of the K-G equation is presented, and a two-component, first-order wave equation for $m \neq 0$ spin-$\frac{1}{2}$ particles is obtained. Applied to the Coulomb potential it reproduces precisely the Dirac-Coulomb energies. (auth)

**56560** COMMENTS ON QUANTUM FIELD THEORY OF TACHYONS. Kamoi, Koichi; Kamefuchi, Susumu (Tokyo Univ. of Education). Progr. Theor. Phys. (Kyoto); 45: No. 5, 1646-61 (May 1971).

The problem of tachyons is investigated within the framework of quantum field theory. The quantization methods for a free scalar tachyon field, which have so far been proposed by various authors, are critically reviewed. Among them the Arons-Sudarshan method is found to be most satisfactory, which guarantees at least the relativistic covariance of the theory at the expense of locality and reasonable energy spectrum. On the basis of this method, interactions of a tachyon field are investigated. It is found that causal S-matrices do not exist as far as interaction terms are restricted to the ordinary, local-polynomial type. A model S-matrix, which is unitary but not causal, is then assumed, and the reinterpretation principle is applied to it in order to remove states of negative-energy tachyons. It is found that the reinterpreted S-matrix thus obtained is not consistent with unitarity. (auth)

**56561** SCHWINGER EQUATIONS FOR THE YANG-MILLS AND THE GRAVITATIONAL FIELDS. Maheshwari, Amar (Tokyo Univ.). Progr. Theor. Phys. (Kyoto); 45: No. 5, 1662-72(May 1971).

It is established that the nonlinear gauge formulation of non-Abelian gauge fields is equivalent to the path-dependent and gauge-independent field-theoretic formalism of Mandelstam. This is proved by showing that the generating functionals for the Yang-Mills and the gravitational fields in the functional integral form, derived using the method of nonlinear gauge, are solutions of Mandelstam's equations for the auxiliary Green's functions of the Yang-Mills and the gravitational field, respectively. Schwinger equations for the gravitational field in the harmonic gauge are also obtained. (auth)

**56562** AXIOMATIC FOUNDATIONS OF SPECIAL RELATIVITY. Bosch, Jorge (Facultad de Ciencias Exactas, La Plata). Progr. Theor. Phys. (Kyoto); 45: No. 5, 1673-88(May 1971).

A mathematical axiom system for general affine kinematics is proposed, and then the relativistic case is separated from the classical one by means of a single axiom. A "characteristic" k is introduced, which allows to classify naturally three distinct types of affine kinematics. It is shown that, once the classical point of view is abandoned, there are essentially two types of relativistic affine kinematics: one of them is characterised by the existence of a limit velocity, and the other by the existence of time reversal. Physical axioms are later introduced and the concept of model is studied in connection with transformation groups. A general epistemological discussion is given. (L.B.S.)

**56563** QUANTIZED FIELDS ASSOCIATED WITH THE ANNULUS-TYPE MEDIUM. Minami, Masatsugu (Kyoto Univ.); Sughimoto, Hiroshi. Progr. Theor. Phys. (Kyoto); 45: No. 5, 1618-33(May 1971).

The boundary-value problem is stated for the position (the potential) and the dual position (the stream function) associated with the "one-loop" medium which is a continuous version of a planar Feynman graph. The solutions are obtained as convolutions of the external momentum and a Green function which is a commutator of the quantized fields. A canonical formalism is exploited to quantize the fields. The Koba-Nielsen kernel is presented also for the non-planar orientable case. (auth)

**56564** LORENTZ INVARIANCE AND FINITE SELF-MASS IN LOCAL FIELD THEORY. Taguchi, Yukio (Univ. of Osaka Prefecture); Yamamoto, Kunio. Progr. Theor. Phys. (Kyoto); 45: No. 5, 1692-4(May 1971).

It is shown that the self-energy divergent terms have incorrect transformation properties under the Lorentz group; then the Lorentz invariant theory has no divergent terms. The quadratic divergence of the pion mass of the $\pi N$ system is considered to order $g^2$ in renormalization theory. (L.B.S.)

## *Gravitation and General Relativity*

*Refer also to abstracts 55807 and 56577.*

**56565** PHENOMENOLOGICAL ENERGY TENSOR IN THE FRAMEWORK OF LINEAR FIELD THEORY. Scherrer, Willy. Helv. Phys. Acta; 44: No. 4, 530-44(7 Jan 1971). (In German).

The phenomenological energy tensor of Einstein's theory of gravitation can be incorporated covariantly into the linear field theory. Application to a resting homogenous and incompressible liquid sphere yields a solution that differs from the corresponding Schwarzschild solution only by the fact that the total energy tensor appears in absolute covariant form. Through calculation of the total energy, equivalence of energy and mass is confirmed at a high degree of accuracy. It is demonstrated that Einstein's gravitation tensor is contained exactly in the linear field theory. (tr-auth)

**56566** EXCITATION OF ULTRASONIC WAVES BY PASSAGE OF FAST ELECTRONS THROUGH A METAL. Borshkovskii, I. A.; Volovik, V. D.; Grishaev, I. A.; (and others) (Kharkov State Univ.). JETP Lett. (USSR) (Engl. Transl.); 13: No. 10, 390-2(20 May 1971).

Translated from Zh. Eksp. Teor. Fiz., Pis'ma Red.; 13: No. 10, 546-9(20 May 1971).

Data from experiments performed on the excitation of ultrasonic waves by the passage of fast electrons through a metal were used to estimate the level of the signal excited by muon showers in Weber experiments. It is concluded that the random coincidences of the pulses from two Weber detectors of muons from extensive air showers with $E_0 > 5 \times 10^{14}$ eV have a frequency not higher than $10^{-3}$/year. (J.F.P.)

**56567** LORENTZ TRANSFORMATIONS WHICH DO NOT CHANGE THE MAGNITUDE OF THE ELECTRIC TENSION VECTOR AND MOTION OF ELECTRIC CHARGES IN STATIONARY, HOMOGENEOUS ELECTROMAGNETIC FIELDS. Tarnovskii, A. S. (Kubyshev State Teacher's Inst., USSR). Izv. Vyssh. Ucheb. Zaved., Fiz.; No. 5, 109-10(1970). (In Russian).

Assume that an electromagnetic field is given in an inertial system O, and let a system O' move translationally with respect to the system O. What should its velocity be in order that the electric field vector E have the same value in both systems? With the use of Lorentz transformations for the field vectors, an expression is obtained for the velocity vector. It is found that the electric charge in a stationary homogeneous electromagnetic field moves in such a fashion that the electric tension vector does not change in magnitude. Thus these vectors are reduced to rotating at a constant angular velocity. A charge moving in such a field radiates energy at a constant rate. (TTT)

**56568** REFERENCE SYSTEMS AND GRAVITATION. Treder, Hans-Juergen; Borzeszkowski, Horst-Heino V. (Zentralinstitut fuer Astrophysik, Berlin). Int. J. Theor. Phys.; 4: No. 4, 295-303(Aug 1971).

It is shown how the formalism of the tetrad theory of gravitation

XUM

used previously follows from the more general fiber bundle formalism. This is of interest in the study of the relations between tetrad theories and the general theory of relativity. In particular, the breaking of the principle of general relativity and the interpretation of tetrad fields as reference systems are considered in greater detail. (auth)

**56569** SCALAR-TENSOR THEORIES AND THE PRINCIPLE OF EQUIVALENCE. Ohanian, H. C. (Rensselaer Polytechnic Inst., Troy, N. Y.). Int. J. Theor. Phys.; 4: No. 4, 273-80 (Aug 1971).

The restrictions on scalar-tensor theories of gravitation implied by the assumptions: the field equations are derivable from an action principle, units of mass length and time are defined by atomic standards, and the principle of equivalence holds whenever gravitational self-energy can be neglected are investigated. It is shown that in all these theories the presence of gravitational energy in a system leads to violations of the principle of equivalence. (auth)

**56570** GRAVITATIONAL WAVES IN CLOSED UNIVERSES. Gowdy, Robert H. (Univ. of Maryland, College Park, Md.). Phys. Rev. Lett.; 27: No. 12, 826-9(20 Sep 1971).

New boundary conditions on the Einstein–Rosen–Bondi gravitational-wave metrics yield closed inhomogeneous universes which solve Einstein's vacuum field equations exactly. Space sections of these universes have either the three-sphere topology $S^3$ or the wormhole (hypertorus) topology $S^1 \otimes S^2$. (auth)

## Scattering Theory

**56571** (CERN–71-14, pp 229-87) BASIC NOTIONS OF RELATIVISTIC SCATTERING THEORY. Steinmann, O. (Schweizerisches Institut fuer Nuklearforschung, Zurich). 4 Aug 1971.

In Spring school on pion interactions at low and medium energies.

The phenomenology of elementary particle interactions is placed in the general theoretical context of quantum field theory. The postulates of relativistic quantum field theory, the LSZ formalism, the S-matrix, analyticity, and analyticity of the scattering amplitude are covered. (J.F.P.)

**56572** SCATTERING PROBLEM UNDER A NON-MONOTONIC POTENTIAL FOR THE CLASSICAL CASE. Kochetov, I. I.; Rakhmatulina, A. Kh. Zh. Vychisl. Mat. i Mat. Fiz.; 11: No. 2, 525-8(Mar-Apr 1971). (In Russian).

The dependence of the scattering angle $\theta$ on the impact parameter $\rho$ was investigated for non-monotonic potentials. It is apparent that for a non-monotonic potential U(r), the function $\theta(\rho)$ as well is non-monotonic, provided that the energy of the scattering particle is sufficiently great. The function $\theta(\rho)$ may be non-monotonic if U(r) is monotonic, but has recurvature. A sufficient indication of monotony in $\theta(\rho)$ was obtained for a monotonic U(r). (tr-auth)

**56573** POLARIZATION FORCES IN ELASTIC NUCLEAR COULOMB SCATTERING. Beck, Rainer; Kleber, Manfred (Technische Univ., Munich). Z. Phys.; 246: No. 5, 383-95 (1971).

The polarization potential is determined for the adiabatic sub-Coulomb scattering of two nuclei. No collective coordinates are used. The relevant nuclear polarizabilities are evaluated by means of sum rules. The departure from the pure Rutherford scattering law is calculated for various nuclei. For adiabatic heavy-ion collisions, the differential cross section is found to be reduced below the Coulomb scattering by 1% at backward angles. (auth)

**56574** PROPERTIES OF THE AMPLITUDE OF ELASTIC SCATTERING AT EXTREMELY HIGH ENERGIES. Vernov, Yu. S. Tr. Fiz. Inst., Akad. Nauk SSSR; 53: 102-56(1971). (In Russian).

Proceeding from general quantum field theory, the association was studied between the behavior of the amplitude of elastic scattering and the ratio of its real and imaginary parts for extremely high (asymptotic) energies. It is shown that the use of this association permits one to obtain a series of new scattering amplitudes, limited by asymptotic behavior, and dependent upon the behavior of the ratio of its real and imaginary parts. The reverse of this problem was undertaken in order to establish the connection between asymptotic behavior of the amplitude of elastic scattering of a particle and an antiparticle. Both the amplitude of scattering and the amplitude of elastic scattering were calculated for an arbitrary, fixed, momentum transfer. (tr-auth)

**56575** MULTIPLE-SCATTERING EXPANSIONS FOR NON-RELATIVISTIC THREE-BODY COLLISION PROBLEMS. Chen, J. C. Y. (Univ. of California, San Diego, La Jolla); Joachain, C. J. Physica; 53: No. 3, 333-50(15 Jun 1971).

A simple derivation of the three-body multiple-scattering expansions from the Faddeev equations is given for non-relativistic elastic, inelastic, rearrangement, and break-up processes. The Faddeev approach to the multiple scatterings is compared with the Watson multiple-scattering theory and is shown to be equivalent to a symmetric version of the Watson multiple-scattering theory, treating all three particles on the same footing. The significance of the Faddeev–Watson expansion is interpreted diagrammatically. The advantages of these expansions lie in the fact that there is no disconnected diagram, suggesting a better convergence behavior. The modifications required by the inclusion of an intrinsic three-body interaction are investigated. (auth)

**56576** ADDITIVITY OF PHASE SHIFTS FOR SCATTERING IN ONE DIMENSION. Kujawski, E. (Univ. of Maryland, College Park). Amer. J. Phys.; 39: No. 10, 1248-54(Oct 1971).

Scattering by two delta-function potentials in one dimension is solved using the "one-dimensional partial wave" analysis developed by Eberly. Despite its simplicity, the above example exhibits a wide range of multiple scattering effects and is quite useful for illustrating some of the difficulties associated with scattering by a many-body system. This example is used to investigate the validity of additivity of phase shifts, which is one of the basic assumptions in Glauber's multiple scattering formalism. (auth)

**56577** SOME RELATIVISTIC EXPANSIONS. Desimirov, G.; Krapchev, V. (Inst. of Physics, Sofia). Compt. Rend. Acad. Bulg. Sci.; 24: No. 3, 289-92(1971).

The problem of expansion in relativistic invariant functions of a scalar function defined in a pseudoeuclidean space is investigated. This is a generalization of previous work in which formulas for the expansion of the scattering amplitude on the mass shell are given. The purpose is to go off the mass shell. (J.F.P.)

**56578** ANALYTIC FORM OF MULTIPLE SCATTERING AMPLITUDES IN THE REGGE POLE MODEL. Sakai, Sunao (Tokyo Univ. of Education). Progr. Theor. Phys. (Kyoto); 45: No. 5, 1699-1700(May 1971).

It is shown that the contribution of multiple scattering amplitudes in high energy scattering can be obtained without making use of eikonal approximation; the integration over the intermediate momentum is carried out analytically. (L.B.S.)

**56579** CONDITION FOR REGGE ASYMPTOTIC BEHAVIOUR. Kobayashi, Masanori (Kyoto Univ.). Progr. Theor. Phys. (Kyoto); 45: No. 5, 1711-13(May 1971).

A condition for the infinite one-particle-exchange type model imposed from the requirement of Regge asymptotic behavior is given. (L.B.S.)

## Particle Accelerators

*Refer also to abstracts 55044, 55299, 56116, 56390, 56688, and 56752.*

**56580** (BNL–16026) RECENT DEVELOPMENTS IN PULSED MAGNET MULTIFILAMENT SUPERCONDUCTING WIRES. McInturff, A. D.; Dahl, P. F.; Sampson, W. B.; Robins, K. E. (Brookhaven National Lab., Upton, N. Y.). 30 Jun 1971. 23p. (CONF-710625–1). Dep. NTIS.

From Thermonuclear information meeting; Oak Ridge, Tenn. (Jun 1971).

It has been noted that the introduction of a metallic or intermetallic insulator to bond the individual multifilamentary wires into a fully transposed or partially transposed conductor, e.g., braid, greatly enhances the performance of the magnets constructed with them. The wires in these conductors tend to be coupled at low dB/dt, thus leading to high losses. Data are presented showing a metallic and intermetallic insulated braid with excellent magnet performance while maintaining losses comparable to that of an organically insulated braid (wire to wire) for rise times of $dB/dt \leq 5$ kG/sec. (auth)

**56581** (BNL-tr–442) PROTON BEAM OF THE ITEP ACCELERATOR FOR RADIUM [RADIATION] THERAPY. Khoroshkov, V. S.; Barabash, L. Z.; Barkhudaryan, A. V.; Gol'din, L. L.; Lomanov, M. F.; Onosovskii, K. K.; Plyashkevich, L. N. Translated by S. J. Amoretty (Brookhaven National Lab., Upton, N. Y.), from Med. Radiol.; 14: No. 4, 58-62(1969). 11p. Dep. NTIS.

The design features of the ITEP proton synchrotron are described, with emphasis on beam extraction at the proper energy.

The advantages of proton beams for therapy of human neoplasms are reviewed. Preliminary tests indicate that the proton beam extracted from the ITEP accelerator has a small diameter, small angular divergence, adequate intensity, and a highly uniform energy. (C.H.)

**56582** (CEA-R-4188) SHIELDING PROBLEMS SET BY THE USE OF A NATURAL URANIUM TARGET WITH A LINEAR ELECTRON ACCELERATOR. SHIELDING AND SAFETY SYSTEMS NECESSARY. Vialettes, Henry; Rocchesani, Jean; Lemure, Pierre (Commissariat a l'Energie Atomique, Saclay (France). Centre d'Etudes Nucleaires). 1971. 32p. (In French). Dep. NTIS (U. S. Sales Only).

The use of a natural uranium target for neutron production with a linear electron accelerator sets special shielding problems due to the fact that, to standard photonuclear reactions, are added photoneutron-induced photofission reactions giving rise to fission products, of which the untimely liberation could cause very serious contamination problems. On the occasion of a recent accident on the target used with the Saclay 60-MeV linear accelerator, activity measurements were carried out on a certain number of samples taken. This revealed the presence of some twenty radionuclides of half-lives between 30 minutes and 30 years and of activities such that the combustion of 1 g of target would release about 30 mCi of fission products of medium and short half-life (over 1 hour). This figure shows the magnitude of a contamination accident on a unit of this type, which is why the present report describes the systems to be employed in order, on the one hand, to detect the appearance of contamination as quickly as possible and, on the other hand, to channel and retain this contamination so as to avoid a personnel contamination accident and/or the spread of contamination toward the outside. (auth)

**56583** (IAE-1980) PULSE GENERATOR OF MEGAVOLT CAPACITY. Mikhailov, V. I. (Institut Atomnoi Energii, Moscow (USSR)). 1970. 11p. (In Russian). Dep. NTIS (U. S. Sales Only).

A transformer with a sectioned core and a special commutated circuit was used as a generator of high voltage for accelerator tubes. Such an arrangement provides semisinusoidal voltage pulses with an amplitude of several megavolts. Experimental and calculated results are introduced and discussed. (tr-auth)

**56584** (JINR-P6-5888) COLLECTOR SYSTEM OF AN ISOTOPE SEPARATOR FOR INVESTIGATING SHORT-LIVED ISOTOPES. Vasilenko, A. T.; Makhunka, I.; Mate, Z.; Nad, J.; Soroko, V. M.; Stancheva, N. S.; Stanchev, S. M.; Utkin, V. A.; Fenyes, T. (Joint Inst. for Nuclear Research, Dubna (USSR). Lab. of Nuclear Problems). Jul 1971. 19p. (In Russian). Dep. NTIS (U. S. Sales Only).

The investigated isotopes are collected on a tape near the focal plane and then transported to the detectors in 2 to 3 sec with an accuracy of ±1 mm. There is a possibility for $\alpha$-, $\beta^{\pm}$-, $e^{-}$-, and $\gamma$-ray spectrum measurements with surface barrier Si, Si(Li), and Ge(Li) detectors. The characteristic properties of the mass marker beam are measured during separation with a Faraday chamber and a vibrational scanner. A formula is given for the calculation of the collection place of the investigated mass. (auth)

**56585** (JINR-P9-5945) DEPENDENCE OF THE BEAM SHAPE IN THE CENTRE OF THE SYNCHROCYCLOTRON ON THE ACCELERATING VOLTAGE AND MAGNETIC FIELD DECAY. Danilov, V. I.; Poluboyarova, P. A.; Safonov, A. N.; Feoktistov, B. V. (Joint Inst. for Nuclear Research, Dubna (USSR)). 1971. 12p. (In Russian). Dep. NTIS (U. S. Sales Only).

The dependence of the beam shape on the accelerating voltage, by proportional decrease of the modulation frequency, and on the decay of the magnetic field at different radii is cleared up by means of computer calculations for radial-phase motion of particles in the center of the synchrocyclotron. The process of the beam formation during the capture is considered taking into account the changes of the range of the captured phases. (auth)

**56586** (JINR-P9-5956) DEBUNCHER OF THE JINR SYNCHROPHASOTRON INJECTOR WITH MODULATION OF THE ACCELERATED BEAM ENERGY. Beznogikh, Yu. D.; Zinov'ev, L. P.; Kadyrov, R. B.; Karyagin, Yu. K.; Plyashkevich, N. N.; Popov, V. A.; Semenyushkin, I. N.; Stepanyuk, V. L. (Joint Inst. for Nuclear Research, Dubna (USSR). Lab. of High Energy). 1971. 9p. (In Russian). Dep. NTIS (U. S. Sales Only).

The main results of calculation of the injection efficiency for the JINR proton synchrotron at the modulation of the energy and narrowing of the energy spread of the injector beam are given as well as a brief description of the debuncher and the experimental results obtained in the process of its adjustment and testing in the synchrotron. (auth)

**56587** (JUL-748-PP) QUANTITATIVE COMPARISON OF THE CONTINUUM RADIATION OF HIGH-TEMPERATURE PLASMAS WITH SYNCHROTRON RADIATION IN THE WAVELENGTH RANGE 500 TO 9000 A. I. INVESTIGATION WITH THE SYNCHROTRON OF THE BONN UNIV. 2.5-GeV ELECTRON SYNCHROTRON. Thimm, Klaus (Kernforschungsanlage, Juelich (West Germany). Institut fuer Plasmaphysik). Apr 1971. 89p. (In German). Dep. NTIS (U. S. Sales Only).

The synchrotron radiation from the Bonn synchrotron was measured for wave lengths ranging from 450 to 9000 Å. For various electron energies, calculations yielded spectral distribution, angular distribution, and polarization. A method for calibrating the synchrotron beam was developed which is based on a carbon-arc standard. With the calibrated beam, a series of wavelengths was measured in the radiation continuum of a carbon V-plasma. Spectral distribution of the radiation also was calculated by means of the bremsstrahlung theory. After corrections according to Gaunt, Inglis, Teller, and Griem, theoretical and experimental results showed good agreement. (H.B.G.)

**56588** (LA-4535) A PROPOSAL FOR $P^3$: A VERSATILE HIGH-ENERGY PION BEAM FACILITY. Gram, Peter A. M.; (and others) (Los Alamos Scientific Lab., N. Mex.). Sep 1970. Contract W-7405-eng-36. 76p. Dep. NTIS.

A proposal for a versatile, high-energy (100 to 600 MeV), high-intensity ($10^{10}$ $\pi$/sec) pion beam for LAMPF is presented. Experimental proposals are described including the pion beta-decay experiment, ratio of $\pi_{e2}$ to $\pi_{\mu 2}$ decay rates, complete study of the reaction $\pi^- p \rightarrow n\gamma$, radiative pion scattering on protons, discussion of radiative scattering experiments, muon g-2 experiment at LAMPF, single pion production in pion-nucleon scattering, measurement of threshold pion production cross section ($\pi^{\pm} p \rightarrow \pi^{\pm}\pi^{+}n$) at LAMPF, comments on $\pi N \rightarrow \pi\pi N$, mechanisms of simple pion-induced reactions on complex nuclei, comments on experiments detecting prompt gammas, and nuclear chemistry studies with energetic pions. (W.H.K.)

**56589** (LA-DC-12730) LAMPF LOW-ENERGY PION LINE. Amato, J.; Burman, R. L. (Los Alamos Scientific Lab., N. Mex.); Jakobson, M. (Montana Univ., Missoula. Dept. of Physics). [1971]. 4p. (CONF-710911-2). Dep. NTIS.

From fourth international conference on high energy physics and nuclear structure; Dubna, USSR (7 Sep 1971).

The proposed LAMPF low-energy pion line is designed to provide charged-pion beams of 20 to 300 MeV. The design parameters and expected performance of the channel are described, and electron and neutron contamination of the pion beam is estimated. (R.W.R.)

**56590** (LA-tr-71-46) CHARGE-EXCHANGE METHOD OF PROTON INJECTION INTO ACCELERATORS AND ACCUMULATORS. Dimov, G. I. (Akademiya Nauk SSSR, Novosibirsk. Institut Yadernoi Fiziki). Translated by Helen Dahlby (Los Alamos Scientific Lab., N. Mex.), from report IIF-304. 28p. Dep. NTIS.

Features of a charge-exchange target for proton injection, development of sources of negative hydrogen ions, regions of application, comparison with the usual injection methods, and the density of protons in the phase space are discussed. Also, the status of the charge-exchange method of proton injection is outlined. (62 references) (W.H.K.)

**56591** (LAL-RT-42-70) STATUS REPORT ON ACO. Le Duff, J. (Paris Univ., Orsay (France). Laboratoire de l'Accelerateur Lineaire). 10 Sep 1970. 13p. Dep. NTIS (U. S. Sales Only).

During the first half of 1969, the ACO has been prepared and run for the study of the $\varphi$ decay into $K^+K^-$. An integrated luminosity of $7 \times 10^{33}$ $cm^{-2}$ was obtained with an average of $4.5 \times 10^{31}$ $cm^{-2}$ per hour of data taking. For the similar period during 1970 it was run with a new apparatus for the study of the $\varphi$ decay into neutrals. Owing to its large size and its complicated structure, the setting-up of this equipment involved a major effort of the laboratory. The most significant results concern the transverse instabilities and the study of a new structure for reaching higher luminosities. (French)

**56592** (LAL-RT-43-70) SPACE CHARGE EFFECTS IN BEAM-BEAM CROSSING. Augustin, J. E. (Paris Univ., Orsay (France). Laboratoire de l'Accelerateur Lineaire). 10 Sep 1970. 7p. Dep. NTIS (U. S. Sales Only).

Results concerned with space charge effects between two colliding beams, in head-on collisions and in crossing at an angle in the Orsay storage ring are given. (France)

**56593** (LYCEN-7104, S7.1-2) PROJECT OF NUCLEAR SPECTROMETRY AT THE SATURNE SYNCHROTRON (1 GeV).

XUM

Birien, P.; Saudinos, J.; Thirion, J. (Commissariat a l'Energie Atomique, Saclay (France). Centre d'Etudes Nucleaires). (In French).

From Conference on some microscopic aspects of nuclear reactions; La Toussuire, France (15 Feb 1971).

A nuclear spectrometry device to be used in conjunction with the Saturne synchrotron at Saclay is briefly described. (France)

**56594** (NP-18998) DEFLECTION OF ELECTRONS IN A SUPERCONDUCTING $HEM_{11}$ RESONATOR. Bauer, W. (Kernforschungszentrum, Karlsruhe (West Germany). Institut fuer Experimentelle Kernphysik). May 1971. 22p. (In German). Dep. NTIS (U. S. Sales Only).

A deflection test measurement of a lead-plated, superconducting deflecting cavity of about 0.5-m length using 1-MeV electrons from a radioactive beta source is described. The measurement yielded a transverse interaction parameter $R_t/Q = (0.46 \pm 0.07)$ kΩ/m which is about 16% below the theoretical value of 0.55 kΩ/m. Reasons for this difference and possible improvements of the experimental setup are given. (auth)

**56595** (NP-19007) MAGNETIC FIELD TOLERANCE AND SELF FIELD EFFECTS OF AN ELECTRON RING ACCELERATOR. Kappe, P. (Kernforschungszentrum, Karlsruhe (West Germany). Institut fuer Experimentelle Kernphysik). May 1971. 105p. (In German). Dep. NTIS (U. S. Sales Only).

In connection with the project of an electron ring accelerator the kinematics of electron rings in a magnetic field is studied. The single particle dynamics during the compression of the electron ring inside a set of pulsed Helmholtz coils is investigated. The magnetic field tolerances of such a setup which are important for betatron resonances are calculated, and a procedure for the compensation of certain field errors is given. Also, the influence of the ring self fields on the kinematics during the axial acceleration in an axially decreasing magnetic field (expansion) is calculated. It is shown, that the relative blow up of the large ring radius due to collective effects is a constant of the motion, and the influence of the self fields on the axial motion is calculated. (auth)

**56596** (SC-RR-710436) IMPLICATIONS OF A MODEL OF CHARGE-NEUTRALIZED, HIGH-CURRENT RELATIVISTIC ELECTRON BEAMS WITHIN CONDUCTING BOUNDARIES ON DIODE AND TRANSPORT SYSTEM DESIGN. Kelly, John G. (Sandia Labs., Albuquerque, N. Mex.). Jul 1971. 94p. Dep. NTIS.

A careful analysis is given to the implications of the behavior of idealized, high-current electron beams within conducting boundaries. Complete space charge neutralization and weak z dependence are assumed for line currents in cylinders and cylindrical sheet beams between coaxial cylinders. The forces on these beams are determined and the equations of motion found. The solutions to these problems can be used as Green's functions for more general current distributions. The results have been used as an aid in the design of a new converging annular diode that injects a beam between concentric cones. The central cone then conducts current back through the cathode in order to prevent diode pinch. The important physics involved in using conductors such as cones to compress high-current relativistic electron beams is identified and discussed. (auth)

**56597** (SJC-A-71-3) COMPUTER CONTROL OF AN ACCELERATOR. Hidechika, Takahashi; Kazuhiro, Ishii; Hideyo, Kodama (Tokyo Univ. (Japan). Inst. for Nuclear Study). Mar 1971. 18p. (In Japanese). Dep. NTIS (U. S. Sales Only).

A fundamental experiment was performed to study the computer control of a proton synchrotron. The control of the voltage of the power source was examined. Two systems were employed. In one method the reference voltage was given by rotation of a helipot driven by a servomotor. The other method was based on the principle that the reference voltage of a stabilized power source, which was controllable from outside of system, was given through a DAC of the computer. When the servomotor was used the final value was within ±1 digit of the set voltage. The voltage was within ±3 digit of the set voltage when the stabilized power source was used. (Japan)

**56598** (SLAC-75(Rev.2)) FIRST- AND SECOND-ORDER MATRIX THEORY FOR THE DESIGN OF BEAM TRANSPORT SYSTEMS AND CHARGED PARTICLE SPECTROMETERS. Brown, Karl L. (Stanford Linear Accelerator Center, Calif.). Aug 1971. Contract AT(04-3)-515. 117p. Dep. NTIS.

A matrix algebra formalism is used to develop the essential principles governing the design of charged particle beam transport systems, with particular emphasis on the design of high energy magnetic spectrometers. (W.H.K.)

**56599** (SLAC-136) TWO-MILE ACCELERATOR PROJECT. Quarterly Status Report, April 1-June 30, 1971. (Stanford Linear Accelerator Center, Calif.). Sep 1971. Contracts AT(04-3)-400; AT(04-3)-515. 60p. Dep. NTIS.

A status report on the Stanford Linear Accelerator Project covering the period April 1, 1971 to June 30, 1971 is presented. Topics included are accelerator and research area operations, accelerator and research area equipment development, and physics research equipment development. (auth)

**56600** (TID-25781) 1970 ANNUAL REPORT OF THE STANFORD LINEAR ACCELERATOR CENTER. (Stanford Linear Accelerator Center, Calif.). 123p. Dep. NTIS.

Highlights in the development and operation of the Stanford Linear Accelerator in 1970 are discussed. High-energy research projects are described, and publications are listed. (W.H.K.)

**56601** SECTOR CYCLOTRON AT 300 keV WITH EXTERNAL INJECTION. Gladyshev, V. A. Tr. Fiz. Inst., Akad. Nauk SSSR; 53: 187-225(1971). (In Russian).

The construction and startup are described for a sector cyclotron designed for deuteron acceleration up to 300 keV. The cyclotron design incorporates a number of special features: the magnet was completed in the form of three separate C-shaped magnets; the vacuum chamber was assembled from a large number of components with an original seal design; and the power supply of the dee is implemented by a four-wave spiral line. The magnetic field has a good depth of azimuthal variation which assures adequate focusing at all orbits. External injection, using ion drift along the sector edge, brings the beam to the accelerating interval of the dees without loss. (tr-auth)

**56602** FOCUSING OF AN ION BEAM DRIFTING IN A NONUNIFORM MAGNETIC FIELD. Gladyshev, V. A.; Katsaurov, L. N.; Moroz, E. M.; Nechaeva, L. P. Tr. Fiz. Inst., Akad. Nauk SSSR; 53: 226-38(1971). (In Russian).

In the presence of ion drift along a magnet edge, the vertical focusing of a beam occurs over a broad range of initial conditions. In the median plane the beam size increases during drift. An appropriate selection of initial conditions, however, permits a few dozen turns without substantial increase in beam size. (tr-auth)

**56603** IMPROVEMENTS IN OR RELATING TO PARTICLE ACCELERATORS. (to KEV Electronics Corp.). British Patent 1,241,407. 4 Aug 1971. Priority date 4 Jun 1969, United States.

Shielding means for a high-voltage electrostatic accelerator is described. The shielding surrounds the accelerating tube, and consists of a high-Z element supported in a semi-insulating matrix, e.g., black rubber filled with lead oxide. (R.W.R.)

**56604** ABERRATIONS OF ASYMMETRIZED QUADRUPOLE LENSES. Ovsyannikova, L. P. (Physical-Technical Inst., Leningrad); Szabo, Gy. ATOMKI (At. Kut. Intez.) Kozlem.; 13: No. 1-2, 1-16(May 1971). (In Russian).

An investigation of the third order geometric aberrations of combined electrostatic and magnetic quadrupole lenses with asymmetrized field, giving the aberration coefficients valid for an arbitrary longitudinal distribution of the field, and related to a point object located on the axis is described. Analytically obtained third order trajectory equations are presented for electrostatic lenses, assuming a rectangular model. Aberration curves are reported as calculated by the help of the above formulae for lenses, of given configurations singlets and doublets. (auth)

**56605** IMPROVEMENTS IN OR RELATING TO SUPPLY CIRCUITS FOR ION ACCELERATORS. Wood, James David London Hedley (to National Research Development Corp.). British Patent 1,243,056. 18 Aug 1971. Filed 2 Feb 1968.

Reference is made, in particular, to supply circuits for neutron generators in which D and/or T ions are extracted from a plasma and accelerated onto a target containing D and/or T. Optimum operation requires that the ion beam shall pass through the extractor aperture with minimum interception, to prevent undue heating or sputtering of the extractor electrode. If there is too much interception, adsorbed gas may also be released into the accelerator tube and cause an unstable condition which can result in destruction of the tube; this is particularly liable to occur under start-up conditions. The object of the system described is to alleviate such problems. The system includes a negative feedback loop connected so as to cause the extractor electrode current to control the ion source energizing supply output in a sense to maintain the extractor current constant. The energizing supply may be a radiofrequency supply adapted to energize a plasma ion source. (UK)

**56606** CHARGED PARTICLE ANALYZER OF MAGNETIC AND ELECTROSTATIC SECTOR TYPE. Matsuda, Hisashi (Osaka Univ.). Cho-Koon Kenkyu; 7: No. 3, 132-41(Oct 1970). (In Japanese).

A magnetic and electrostatic sector field is discussed, and the effect of fringing fields is described. Barber's law that the ion source and the top of the field boundary and image are on a straight line is satisfied in the case of a uniform field. This law is extended for an inhomogeneous field by replacement of the opening angle of a sector field $\phi$ with $k\phi$ and the radius a of the orbit with $a/k$. The k is defined in relation to the inhomogeneity factor. Dispersion and resolving power are explained. The matrix representation of the orbit of a charged particle is also described. The effect of the fringing field is analyzed with a proper transform matrix. The effect is treated as follows. (1) An ideal field extends up to normal boundary. (2) Optic axis shifts at the boundary. (3) The charged particle advances straight up to the boundary, and here it is subjected to a change of position and direction, and this phenomena is described by a transform matrix. (4) The particle moves in the ideal field thereafter. The image and secondary aberration are also analyzed by the matrix representation. (Japan)

**56607** EXPERIMENTAL RESEARCH ON DESIGN CRITERIA OF FACILITIES FOR PARTICLE ACCELERATORS FOR MEDICAL USE. Okajima, Nobuo; Yamamoto, Moriyuki; Mizushina, Tomoyuki; Maeda, Hidenori; Kitamura, Takeshi (Taisei Construction Co. Ltd., Tokyo). Taisei Kensetsu Gijutsu Kenkyusho-Ho; No. 3, 67-91(Oct 1970). (In Japanese).

The research project was sponsored by the research fund for peaceful uses of atomic energy established by the Science and Technology Agency. A Specialist Committee was organized to carry on this research program, and many meetings were held to discuss the methodologies of experimental research to make the tests useful, and some criteria were derived from them. Examples of facilities are described according to these criteria derived. (auth) (Japan)

**56608** FOCUSING OF HIGH-CURRENT ELECTRON BEAMS IN LINEAR INDUCTION ACCELERATORS. Vakhrushin, Yu. P.; Kuznetsov, V. S.; Komarov, O. L.; Bogdanova, V. I.; Ivanova, N. I. At. Energ. (USSR); 31: No. 3, 294-5(Sep 1971). (In Russian).

Linear induction accelerators are used for accelerating electron beams in currents of hundreds of amperes. Focusing such beams is discussed relative to their deviation from equilibrium, and an equation describing a high-current relativistic beam of electrons is presented. Criteria for stability were obtained for the motion of beams of charged particles in discrete focussed systems, valid for arbitrary values of the accelerating field. (K.S.W.)

**56609** PROCESS FOR MEASURING ENERGY. Tyapkin, A. A. (to Joint Inst for Nuclear Research). Russian Patent 265,301. 9 Mar 1970. Filed 24 Mar 1969. (In Russian).

A method for measuring electron and gamma energies above 5 GeV is described. A converter, the thickness of which corresponds to the maximum of the electron and photon cascade curve, is placed in the beam trajectory; from the intensity of the secondary electrons the energy of the electrons or gamma rays measured is determined. (R.W.R.)

**56610** ISTOCHNIKI POLYARIZOVANNYKH CHASTITS. (Polarized Particle Sources). Pucherov, N. N.; Romanovskii, S. V.; Tarasov, G. P.; Chernievskii, V. K. Kiev; Izdatel'stvo Naukova Dumka (1968). 116p.

This survey describes the basic methods of producing polarized particle sources which are widely used today in contemporary experimental nuclear physics. Polarized particle beams, their parameters, and source construction are examined. Multipole magnets, separating magnets, and the motion of charged particles in a magnetic field are studied. Vacuum systems, dissociation of hydrogen and deuterium, and the ionization of atom beams are also treated. 103 references. (K.S.W.)

**56611** MEASUREMENT OF THE EMITTANCE OF AN ION-OPTICAL SYSTEM. Marghitu, S. (Institut de Physique Atomique, Bucharest). Rev. Roum. Phys.; 16: No. 4, 461-6(1971). (In French).

An apparatus for the measurement of emittance, used with particle accelerators for the study of ion sources and formation systems for beam acceleration and ion-optical transport is presented. The idea of emittance as a unit of measurement used in the phase plane is discussed, and the principle of emittance measurements with the help of a baffle with an opening and the method of plotting the form of emittance are presented. A description of a realized apparatus and its operation with an ion source is given. (tr-auth)

**56612** DIRECT-ACCESS MULTI-USER COMPUTER SYSTEM FOR THE HARWELL SYNCHROCYCLOTRON. Jarvis, O. N.; Langsford, A.; Whitehead, C. (Atomic Energy Research Establishment, Harwell, Eng.). pp 53.1-2 of Computational Physics. Vols. I and II. London; Her Majesty's Stationery Office (1969).

From Conference on computational physics; Culham, England (28 Jul 1969). See CONF-690706-(Vols.1 and 2).

A Honeywell DDP-516 computer system and its real time executive system (OLERT) were chosen for future experimental work on the Harwell Synchrocyclotron on the following grounds; experiments change frequently, a high-level real-time programming language is necessary for visiting experimentalists, and off-line data analysis, assemblies, compilations and other utility programs should run as background jobs. The hardware is configured as follows. The CPU has an extended arithmetic unit and the 16-bit, 32K word store has full memory protection. There are four ASR 33 teletypes, high speed paper tape equipment, 3 seven-track magnetic tape units and an incremental plotter. Data from experiments and CRT display units are driven through CAMAC. The basic OLERT operating system was augmented to provide the software to drive the CAMAC units both for autonomous data transfer and I/O-bus operations so that all communication with experiments could take place through simple INPUT/OUTPUT statements. The present operating system takes one third of the available core store and it is hoped to purchase a high capacity fixed head disc and install some degree of peripheral processing in the CAMAC system to ease the demands on core store. (auth) (UK)

XUM

# PHYSICS (NUCLEAR)

## Neutron Interactions with Matter

*Refer also to abstracts 54444, 56258, 56271, 56340, 56342, 56343, 56354, 56605, 56733, 57165, and 57173–57177.*

**56613** (AD-715563) NEUTRON TRANSPORT FROM A POINT SOURCE IN A SLAB; A COMPARISON BETWEEN DIFFUSION THEORY AND TRANSPORT THEORY. Shimerda, John Henry (Naval Postgraduate School, Monterey, Calif.). Sep 1970. 53p. NTIS.

Thesis.

The one-speed, steady state, diffusion equation was solved for a point source and for a normal pencil beam in a homogeneous, isotropically scattering slab. Numerical results obtained using diffusion theory were compared to available transport theory results for two slab thickness. This comparison demonstrated that the diffusion theory approximation to the transport equation will yield accurate results except within about one-half mean free path of a boundary and except within about three mean free paths of a source. The best agreement between diffusion theory and transport theory is obtained if the first radial buckling constant in the diffusion solution is chosen equal to the radial buckling computed using transport theory. (auth) (USGRDR)

**56614** (ANL-7714) ARC SYSTEM CROSS-SECTION HOMOGENIZATION AND MODIFICATION CAPABILITIES. Kovalsky, E. A.; Zapatka, J.; Henryson II, H.; Hoover, J.; Walker, P. M. (Argonne National Lab., Ill.). Jun 1971. Contract W-31-109-eng-38. 455p. Dep. NTIS.

This document presents the documentation of the ARC System modules INHOMG (NUI001), HOMOG (NUC001), HHOMOG (NUC007) MICCOL (AJC007), MACCOL (AJC008), and MODXSISO (NUI006). NUI001 reads and processes BCD card images which define isotope to material and material to composition assignments for the various reactor regions. NUC001 generates the material and composition level macroscopic cross sections using the mixture information processed by NUI001 and a specified microscopic cross-section data set, XS.ISO or XS.ISO2. NUC007 is a restricted version of NUC001 in that it generates only composition level cross sections based on a homogenization of existing material level cross sections. AJC007 performs a group collapse for microscopic cross sections using a specified multigroup spectrum. AJC008 performs a group collapse for macroscopic cross sections using a specified multigroup spectrum. NUI006 processes the type 20 cards in the BCD data set A.NIP to provide run-time modification of an XS.ISO2 microscopic cross-section data set. (auth)

**56615** (FMRB-37/71) THEORETICAL INVESTIGATION ON DIFFRACTION OF SLOW NEUTRONS. Heintz, W. (Physikalisch-Technische Bundesanstalt, Brunswick (West Germany)). Jun 1971. 25p. (In German). Dep. NTIS (U. S. Sales Only).

It was previously observed that the interference in a neutron-interferometer disappeared, when two samples of the same material, only separated by a narrow cut, were placed into the neutron beam. An attempt was made to explain this by waves originating from the cut between the two samples. The gradual disappearance of the interference by moving both samples is described by splitting the neutron wave in two components with a phase difference. It is attempted to explain the existence of a phase difference symmetric to the plane of the cut by means of Sommerfeld's theory of diffraction. The result is unsatisfactory. Therefore a simple calculation, based on quantum mechanics is made with the assumption that the cut is splitting the incident neutron beam into two components. The result is that with small angles of incidence the reflection is very strong and the ratio of the reflected to the transmitted intensity oscillates sensitively with the cross section of the cut. (auth)

**56616** (JUL-764-RG) NUMERICAL METHOD FOR THE SOLUTION OF THE TIME INDEPENDENT TRANSPORT EQUATION FOR NEUTRONS. Lindenmayr, Georg (Kernforschungsanlage, Juelich (West Germany). Institut fuer Reaktorentwicklung). May 1971. 60p. (In German). Dep. NTIS (U. S. Sales Only).

A discrete form of the stationary, one-dimensional multigroup transport equation for neutrons is solved. Sphere geometry and isotropic scattering cross sections are assumed. Starting with the integral form of the neutron transport equation a system of difference equations is derived. An existence theorem independent of the mesh size chosen can be proved: There exists a single positive eigenvalue ($k_{eff}$) which is larger than the absolute value of any other eigenvalue and a corresponding unique positive eigenvector (neutron flux). The eigenvalue and the corresponding eigenvector can be calculated by the power method. In any iteration step a high-order system of simultaneous equations must be solved. Four iteration methods are defined and the convergence is proved: a point iteration method (PI), a block iteration method (BI), a combination of the two which can be interpreted as an ADI (alternating direction implicit) —method for the special case $\omega = 0$, and the block-SOR (successive overrelaxation) —method. Convergence properties of the methods are studied by some numerical examples. It is demonstrated that the PI method is fast only for small mesh sizes and small values $s = \sigma^s/\sigma^t$. The BI method has opposite convergence property: it is very fast for large mesh sizes and large s. The ADI ($\omega = 0$) and SOR ($\omega = 1$) are well convergent methods in any case, the ADI being somewhat superior over SOR. Difference scheme and iteration methods are well suited for calculating neutron flux and $k_{eff}$ of large thermal assemblies with voids ($\sigma^t = 0$) and strong absorbers. (auth)

**56617** (JUL-765-RG) METHOD FOR THE NUMERICAL SOLUTION OF THE LINEAR POSITION DEPENDENT BOLTZMAN EQUATION IN SPHERICAL GEOMETRY AND SPHERICAL SYMMETRY. Wolf, Lothar (Kernforschungsanlage, Juelich (West Germany). Institut fuer Reaktorentwicklung). May 1971. 52p. (In German). Dep. NTIS (U. S. Sales Only).

In its integral form and by means of Green's functions with a $P_1$ method, the neutron transport equation is solved with respect to position, angle, and energy. An analytical calculation successfully yielded the moment of Green functions for spherical geometry and spherical symmetry. A well-convergent iteration method is developed for the inversion of the transport matrix, which is diagonal with respect to energy. (H.B.G.)

**56618** (RPI-328-230) EXPERIMENTAL AND ANALYTICAL STUDIES OF FAST NEUTRON TRANSPORT IN IRON. Malaviya, B. K.; Kaushal, N. N.; Becker, M.; Burns, E. T.; Ginsberg, A.; Gaerttner, E. R. (Rensselaer Polytechnic Inst., Troy, N. Y. Dept. of Nuclear Science). [1971]. Contract AT(30-1)-328. 58p. Dep. NTIS.

As part of a comprehensive program devoted to the integral checks of differential microscopic cross section data pertinent to the LMFBR program, the experimental and analytical investigations of fast-neutron transport in bulk assemblies of iron are described. Time-of-flight-measured fast-neutron angular flux spectra at different positions in a simple, clean, homogeneous assembly are analyzed using ENDF/B data as input, the $MC^2$ code system, and $S_N$ transport calculations. In addition, continuous slowing-down theory was developed to complement precise calculations by indicating direct relationships between cross-section uncertainties and spectra; this approach permits integrating, in the analysis, other non-ENDF/B data. The well-defined integral experiment permits clear-cut interpretation, leading to definitive conclusions with respect to input data and also checks of standard analytical codes. The Karlsruhe (KEDAK) data set and the ENDF/B-I and ENDF/B-II files for iron have been assessed. On the basis of cross section uncertainties in iron and of their influence on spectra, it is possible to recommend not only preferred data but also a redirection in emphasis in differential measurements and evaluation. (auth)

**56619** (RT/FI-(70)49) NEUTRON THERMALIZATION IN POLYCRYSTALLINE MATERIAL BY MONTE CARLO METHOD. Ardente, V.; Cupini, E.; Molinari, V. G. (Comitato Nazionale per l'Energia Nucleare, Rome (Italy)). 20 Nov 1970. 27p. Dep. NTIS (U. S. Sales Only).

The thermalization phenomena of neutron population in finite and infinite samples of beryllium are studied by using the Monte Carlo method. The preliminary analysis presented intends to show the reliability of the Monte Carlo method in the field of the time-dependent neutron thermalization for different geometrical situations, and represents a basis for a detailed investigation of the problems of the equilibrium approach in small samples of beryllium. The scattering kernel from polycrystalline beryllium is calculated at room temperature. For the contribution to the scattering from inelastic processes the incoherent approximation was used. Interference effects were taken into account by evaluating the elastic (zero-phonon) term of the polycrystalline coherent scattering cross section for a hexagonal lattice. (auth)

**56620** (RT/FI-(70)53) ANALYSIS BY A SIMULATED MEASUREMENT OF NEUTRON SPECTRA. Giovannini, R.; Menapace,

E. (Comitato Nazionale per l'Energia Nucleare, Bologna (Italy). Centro di Calcolo). 16 Dec 1970. 36p. (In Italian). Dep. NTIS (U. S. Sales Only).

A neutron spectrum measurement performed with a proton recoil proportional counter is analyzed. The unfolding method here adopted utilizes the "a priori" information of spectrum nonnegativity. By means of the linear programming technique the confidence intervals of integral quantities of the unknown spectrum are obtained. (auth)

**56621** NONHOMOGENEOUS BOUNDARY-VALUE PROBLEM FOR THE LINEAR TRANSPORT EQUATION FOR A SLAB GEOMETRY. Hintz, Gerald R. (California Inst. of Tech., Pasadena). J. Math. Phys. (N. Y.); 12: No. 7, 1100-12(Jul 1971).

A nonhomogeneous boundary-value problem for the infinite slab of finite thickness is considered. In this problem, the slab receives radiation from a time-dependent source on one of its surfaces. The intensity of this radiation increases from zero at time zero until a later time $t_0'$, after which the intensity is a function of direction only. This problem is solved in the strong sense. The asymptotic behavior of the solution is determined and related to results for steady-state problems in neutron transport theory and radiative transfer. (auth)

**56622** FUNCTIONS OF THE TRANSITION REGION FOR BERYLLIUM AND SOME EXAMPLES OF ITS USE. Bogomolov, V. N.; Chernov, L. A. At. Energ. (USSR); 30: No. 6, 543-5(Jun 1971). (In Russian).

The mathematical relation which describes the energy distribution of neutrons contains the expression $\Delta(E/kT)$ which is the transition region function, calculable from a single experimental spectrum. The authors obtained $\Delta(E/kT)$ for Be, and thence the Maxwellian distribution $M(E/kT)$. It was noted that the function $\Delta(E/kT)$ for Be was graphically quite similar to that for C(graphite). If the function $\Delta(E/kT)$ for Be was obtained from an equation by Bekurts and Virtts, an error of ~50°K was inherent in the neutron temperature. (K.S.W.)

**56623** SCATTERING CROSS-SECTION AT SUBTHERMAL ENERGIES AND GENERALIZED PHONON FREQUENCY SPECTRUM OF ZIRCONIUM HYDRIDE. Saastamoinen, J.; Palmgren, A. (Helsinki Univ. of Tech., Otaniemi, Finland). J. Nucl. Energy; 25: No. 5, 189-202(May 1971).

Total neutron cross section for $ZrH_2$ was measured at the subthermal wavelength range from 7 Å to 17.5 Å, the sample temperature ranging from 20°C to 270°C. From the measured values the slope of the scattering cross section vs. wavelength was determined. The measured slope values were compared with theoretical values to determine the weight of the acoustical part in the generalized phonon frequency spectrum of zirconium hydride. An acoustical weight factor of about 1/150 gave the best fit to the measurements. A calculation method based on the phonon expansion method was developed to determine the coefficients of the first terms in the presentation of the scattering cross section as a power series in neutron wavelength. The question of existence of a discrete thermalization time constant in zirconium hydride is discussed. (auth) (UK)

**56624** INTENSE THERMAL-NEUTRON GENERATING APPARATUS. (to Atomic Energy of Canada Ltd.). British Patent 1,246,235. 15 Sep 1971. Priority date 16 May 1969, United States.

An intense thermal neutron generator is described which is based on proton reactions with liquid metal targets. (W.H.K.)

**56625** SPECTRAL FUNCTION REPRESENTATION OF TIME- AND ENERGY-DEPENDENT NEUTRON DENSITY IN FAST MEDIA. PART 2. MEDIA WITH MULTIPLICATION. Collatz, S. (Zentralinstitut fuer Kernforschung, Rossendorf, Ger.). Kernenergie; 14: No. 5, 148-52(May 1971).

A representation with the spectral functions of the time-independent part of the transport operator without fission for the energy and the time dependent neutron density in multiplying media in the buckling approximation is found in two ways. According to this method, the pulse experiment in subcritical systems is studied. (auth)

**56626** IMPROVEMENTS IN OR RELATING TO NEUTRON TARGETS. Stark, Donald Sutherland (to National Research Development Corp.). British Patent 1,243,262. 18 Aug 1971. Filed 12 Feb 1969.

Reference is made to neutron generator targets consisting of D and/or T absorbed in a film of Sc, Y or a lanthanon supported on a metal substrate. With such targets disintegration may occur owing to trihydride formation; the target described is claimed to show a reduced tendency to such disintegration. A film of a second metal is interposed between the substrate and the first film. This second metal is selected so as to diffuse readily into the metal of the first film under solid state conditions to form a solid solution or compound therewith, and also to adhere well to the substrate. The thickness of the intermediate film is made much less than that of the hydrogen-absorbing film in order to limit dilution of the latter by diffusion when the solid solution or compound is formed, but is sufficient to increase its adhesion to the substrate. Production methods are described both for the targets and for sealed neutron generators using them, and examples are given. Metals suitable for the intermediate film include Be, Au, Ag, Ni, Co, and Cu, and Mo is suitable as substrate. Erbium is suitable as hydrogen-absorbing film. (UK)

**56627** SUPPRESSION OF (n,γ) REACTION IN RESONANT SCATTERING OF NEUTRONS BY A PERFECT CdS CRYSTAL. Shil'shtein, S. Sh.; Somenkov, V. A.; Dokashenko, V. P. JETP Lett. (USSR) (Engl. Transl.); 13: No. 6, 214-17(20 Mar 1971).

Translated from Zh. Eksp. Teor. Fiz., Pis'ma Red.; 13: No. 6, 301-5(20 Mar 1971).

A search was made for the suppression of the inelastic channels for neutrons at resonant energies in transmission experiments. Reflection and transmission curves in CdS were measured for neutron wavelengths of 0.81 and 1.06 Å (0.123 and 0.08 eV). The results show that anomalous transmission occurs in resonant neutron scattering, i.e., the (n,γ) reaction is suppressed when a neutron interacts with a perfect crystal in the Bragg position. (D.L.C.)

**56628** MULTIPLE SCATTERING OF NEUTRONS IN GASEOUS AND LIQUID METHANE. Agrawal, Ashok K. (Argonne National Lab., Ill.). Phys. Rev., A; 4: No. 4, 1560-7(Oct 1971).

A "factor method" of evaluating the double-scattering correction for inelastic-neutron-scattering experiments with an infinite-plane-slab specimen was developed. Using appropriate dynamical models, calculations have been made both for highly compressed room-temperature gaseous methane and for liquid methane at 98°K. As a result, the agreement between analytical results with measurements is remarkably improved. In addition, the model sensitivity of the correction and the advantages of reflection-type experimental geometry over transmission-type are investigated. (auth)

**56629** MEASUREMENTS OF TIME-DEPENDENT THERMAL NEUTRON SPECTRA IN PULSED MODERATORS USING A TIME-FOCUSSED CRYSTAL SPECTROMETER. Graham, Kingsley F. Ann Arbor, Mich.; Univ. of Michigan (1970). 197p. University Microfilms Order No. 71-15,160.

Thesis.

A technique is described for measuring the joint time and energy dependence of the rate of emission of slow neutrons emerging from the surface of a moderator following the injection of a short pulse of fast neutrons into the moderator. A crystal spectrometer is used to select neutrons of a given energy. The leakage current at that energy is examined as a function of time. The crystal spectrometer is arranged to be time-focussed; time resolution is decoupled from energy, spatial and angular resolution. The time-focussing feature enables measurements to be performed with much less intense neutron sources ($\sim 10^{11}$ neutrons/sec peak) than used by previous workers. Adequate statistical precision in a reasonable length of time is obtained by sampling the leakage current from most of the moderator surface with a relatively large angular and energy resolution ($\Delta E/E \simeq 20\%$). Good time resolution (<5 μsec at 0.025 eV) is maintained by time focussing. A second set of measurements using standard time-of-flight techniques is used to determine the absolute time-integrated leakage current per incident 14.7 MeV neutron as a function of energy. This result is used to normalize the time dependent spectra measured with the time focussed crystal spectrometer. Measurements were performed on rectangular moderator blocks of nominal lateral dimensions of 10 cm × 10 cm and various thicknesses from 2.55 cm to 7.65 cm. Many of the moderators had a cadmium or gadolinium filter (heterogeneous poison) placed in a plane parallel to the viewed 10 cm × 10 cm face and various depths beneath it. Polyethylene moderators were studied at both 296°K and 77°K. Solid methane and solid anhydrous ammonia moderators were studied at 77°K. For most moderators, both a measurement of the absolute energy dependent leakage spectrum per incident neutron and a measurement of the time dependent leakage spectrum were performed. No one moderator appeared superior giving both high yield and narrow time width. Significant differences were apparent at 0.025 eV, while at 0.1 eV and above the difference between moderators was less pronounced. Both solid methane and solid ammonia at 77°K appear to be good moderator materials with ammonia better at 0.025 eV and above. Methane may be superior be-

XUM

low about 0.01 eV. It was further found that heterogeneous poisoning can be used to decrease the time width without severely reducing the slow neutron peak yield rate, although the time integrated yield is strongly reduced. Decreasing the moderator temperature also produces narrower time widths while not significantly changing the peak yield rate for neutrons above 0.025 eV. Below about 0.025 eV the time integrated yield is increased by cooling the moderator. (Diss. Abstr. Int., B)

**56630** DEGENERATE KERNEL TECHNIQUE IN NEUTRON THERMALIZATION THEORY. Turinsky, Paul Josef. Ann Arbor, Mich.; Univ. of Michigan (1970). 259p. University Microfilms Order No. 71-15,328.

Thesis.

The degenerate kernel technique (DKT) has been developed to improve the computational efficiency of treating the speed dependence in neutron thermalization calculations. The only approximation employed in the DKT is that the scattering kernel can be accurately represented in the thermal range by a degenerate kernel expansion (DKE). Using the DKE in the inscattering term encountered in neutron thermalization theory is found to recast the initial Fredholm integral equation in speed into a speed-independent matrix operator equation of size K, the DKE size. To render equivalent accuracy, K has been found to be considerably smaller than the number of mesh points employed in a discrete speed mesh treatment (multigroup). Hence the matrix operator equations that the DKT give rise to are solved more readily on a digital computer due to reduced matrix size. To minimize K (therefore computational costs), the DKE was so constructed such that it: converged rapidly pointwise to the true scattering kernel; preserved the total scattering cross section; and yielded the correct speed dependence to known analytic solutions to several infinite media neutron thermalization problems when employed in the inscattering term. The DKT was employed to numerically solve the infinite media thermal neutron steady state, time moment, time eigenvalue, and time dependent problems. These same problems were resolved within the spatial modal expansion of the diffusion equation for finite media for various values of $B^2$. The use of the DKT in the linear transport equation for the isotropic scattering slab geometry problem is studied and found to also yield a (K X K) speed-independent matrix integral equation. The DKT is also applied within the invariant-imbedding transport formalism for obtaining the reflection (R) and transmission (T) probabilities of thermal neutrons impinging on an isotropic scattering slab system. The DKT is found to mathematically decouple the initial and final neutron states, resulting in considerable computational storage and CPU time reductions as has been confirmed by computational studies. The DKT and the numerical methods employed were also confirmed to yield accurate results for R and T. (Diss. Abstr. Int., B)

**56631** CALCULATION OF THERMAL NEUTRON PARAMETERS IN HYDROGENOUS LIQUID MODERATORS. Ben Ahmed, Ali. Morgantown, W. Va.; West Virginia Univ. (1970). 88p. University Microfilms Order No. 71-15,477.

Thesis.

Adapting the Brown and St. John cross section formalism for low energy neutron scattering in $D_2O$, a modified classical monatomic gas model is presented for light water and benzene. This is accomplished by the computation of different sets of BSJ parameters over three specified energy regions encompassed by the total thermal scattering cross section, $\sigma_s(E)$, to a more accurately match experimental and gas model calculated values of $\sigma_s(E)$. In addition, a new temperature-dependent closed form expression has been derived for the second energy transfer moment, $M_2$. These theoretical developments are applied to temperature-dependent calculations of the thermal diffusion constant, $D_0$, and the thermal diffusion cooling coefficient, C, in heavy water, light water, and benzene. Also computed are the average cosine of neutron scattering angle, $\bar{\mu}_0$, in $H_2O$ and $C_6H_6$ plus the thermal diffusion length, $\bar{L}_T$, in $H_2O$ at different levels of boron poisoning. Good agreement between this work and the results of other investigators is noted for $D_0$ and $\bar{L}_T$. The values of $M_2$ used to obtain C, however, are approximately 15 to 40% higher than quantum model calculations, suggesting that the monatomic gas model underestimates the chemical binding effects of atoms in liquid moderators. Inconsistencies in the average cosine of the scattering angle, $\bar{\mu}_0$, are noted since it is higher for light water but lower for benzene than the experimentally obtained values at low neutron energies. This indicates that refinements on gas model scattering cross sections are still needed. (Diss. Abstr. Int., B)

**56632** ENERGY-DEPENDENT NEUTRON TRANSPORT CALCULATIONS IN THICK AND THIN SLABS. Larson, Howard Allen. Seattle; Univ. of Washington (1970). 199p. University Microfilms Order No. 71-16,970.

Thesis.

An efficient method for the calculation of transmission and reflection functions for the albedo problem in a thick slab has been developed. The results, continuous in angle and energy, depend upon the expansion of the scattering kernel in a nonisotropic degenerate form. The mathematical procedure utilizes principles of invariance to express the collision density in the slab in terms of a generalized Milne collision density and the transmitted or reflected collision density. Neutron angular collision densities, obtained from the reflection and transmission functions, are expressed in terms of normal modes using the singular eigenfunction technique. In order to demonstrate the feasibility of the numerical method, calculations are performed on model problems using the isotropic form of the thermalization scattering kernel for the heavy gas. Numerical results illustrate the effects of kernels for different gases on the eigenvalue spectrum, emergent Milne distribution, and half-space and slab collision densities. In order to solve the thin slab albedo problem with a minimum of computational effort, an exact solution is also developed for the angle- and energy-dependent transmission and reflection functions of the slab using the separable kernel for neutrons in thermal equilibrium with a non-multiplying medium. This is accomplished by a method which relates the functions to the endpoint values of the solution of a non-homogeneous Fredholm integral equation. This method is most efficient for thin slab calculations where the optical path for transmission is small. Model calculations are performed for reflection and transmission functions of neutrons incident upon a slab of free gas; the effects of varying the mass number, the slab width, the amount of absorption and absorption law, and the angle and energy of the incident beam are illustrated. (Diss. Abstr. Int., B)

**56633** SPIN POLARIZATION EFFECTS ON NEUTRON TRANSPORT. Cardito, Joseph Michael. University Park, Pa.; Pennsylvania State Univ. (1970). 55p. University Microfilms Order No. 71-16,578.

Thesis.

The effects of spin polarization on neutron transport are quantitatively investigated. Azimuthal asymmetries of differential scattering cross sections are considered for transport in non-multiplying and multiplying systems. Consequences of considering polarization in calculations of the neutron flux are determined for both the monoenergetic and the polyenergetic case. Specific attention is given to the dependence of these effects on neutron energy and system size. For a non-multiplying medium the scalar flux penetrating a finite slab is decreased by polarization. Maximum effects of 3.1% were found for a seventeen mean free path slab. For a multiplying medium the scalar flux of neutrons escaping from the system is decreased by less than one percent. These maximum effects occur in the energy range 0.25 to 1.0 MeV. In all cases the effects of polarization on the neutron flux increase with system size. Uncertainties in neutron cross sections of two percent or less produce errors in computed neutron fluxes comparable to polarization effects. (Diss. Abstr. Int., B)

**56634** DIFFUSIVE MOTIONS IN NEUTRON COHERENT SCATTERING BY LIQUIDS BY FILTER TIME-OF-FLIGHT SPECTROMETRY. Teutsch, Heinz (Inst. of Atomic Physics, Bucharest). Stud. Cercet. Fiz.; 23: No. 5, 517-33(1971). (In Rumanian).

Topics include information on the diffusive motion in liquids that can be obtained by neutron scattering, the time-of-flight neutron spectrometer, determination of the scattering law and the $1 + \tau(K)$ function for liquid nitrogen and liquid bismuth, convolution of Gaussian and Lorentzian functions, and conclusions. (W.H.K.)

**56635** CALCULATION OF CONSTANT RELAXATION OF AN AVERAGE NEUTRON FLUX IN A NONUNIFORM MEDIUM WITH ANISOTROPIC SCATTERING. Stepanov, A. V.; Shelagin, A. V. Tr. Fiz. Inst., Akad. Nauk SSSR; 53: 181-6(1971). (In Russian).

Green's function was employed in an examination of a steady-state transport of monoenergetic neutrons in a nonuniform medium with weakly anisotropic scattering. An expression was obtained for constant relaxation of an average neutron flux. (tr-auth)

**56636** USE OF GREEN'S FUNCTION IN THE THEORY OF NEUTRON DIFFUSION IN A HETEROGENEOUS MEDIUM WITH SLUGS OF SMALL DIMENSIONS. Stepanov, A. V. Tr. Fiz. Inst., Akad. Nauk SSSR; 53: 167-80(1971). (In Russian).

The passage of neutrons through a nonuniform medium is considered, with an expression for a constant relaxation for an average neutron current in a diffuse medium with an arbitrary absorber being obtained. A coefficient of loss was calculated

for thermal neutrons for a system with small slug effect. (tr-auth)

**56637** CONTRIBUTIONS TO THE SUNAKAWA MODEL OF ELASTIC MULTIPLE NEUTRON SCATTERING: DETERMINATION AND INTERPRETATION OF MANY-PARTICLE DISTRIBUTION FUNCTIONS. Weil, Juergen W. (Univ. of Innsbruck). Rev. Roum. Phys.; 16: No. 1, 19-29(1971).

The connection between the Van Hove and the Sunakawa pair distribution functions is reviewed; the Sunakawa functions are interpreted as to their physical content and their connection with the two-particle distribution function. The free Sunakawa functions are calculated up to the fifth order; a graphical method for setting up such functions of any order is presented. (auth)

**56638** SCAT: CODE FOR COMPUTING SCATTERING CROSS SECTION OF LIGHT AND HEAVY WATER. Rapeanu, S.; Stefan, H.; Gheorghe, D. (Inst. of Atomic Physics, Bucharest). Rev. Roum. Phys.; 16: No. 2, 241-3(1971).

A computer program was written for the analysis of thermal neutron scattering in light and heavy water using the Koppel-Young model. The computing algorithm used is described. (J.W.R.)

**56639** USE OF $^{252}$Cf AS A RANDOMLY PULSED NEUTRON SOURCE FOR PROMPT NEUTRON DECAY MEASUREMENTS. Mihalczo, John Thomas. Knoxville, Tenn.; Univ. of Tennessee (1970). 115p. University Microfilms Order No. 71-17,760.

Thesis.

Cross correlation measurements were performed for unmoderated and polyethylene-moderated uranium (~93 wt % $^{235}$U) assemblies with prompt neutron decay constants varying from $3 \times 10^3$ to $10^5$ sec$^{-1}$. One of the detectors was an ionization chamber containing $^{252}$Cf which triggered the time analysis equipment every time a spontaneous fission of $^{252}$Cf occurred. The other was a proton recoil scintillator which measured the response of the multiplying assembly to the neutrons emitted in the $^{252}$Cf fission. These measurements used $^{252}$Cf as a randomly pulsed neutron source but had the simplicity of the Rossi-$\alpha$ technique. The randomly pulsed neutron method allowed the measurement of the prompt neutron decay without the use of a complicated pulsed neutron source where Rossi-$\alpha$ measurements were not practical. In assemblies for which Rossi-$\alpha$ measurements were also made, the prompt neutron decay constant agreed within the precision of the measurements with those obtained by this technique. The ratio of the correlated count rate in a randomly pulsed neutron measurement to that in a Rossi-$\alpha$ measurement was inversely proportional to the detector efficiency. This ratio was quite large for some assemblies; for example, it was 7,900 for a cylindrical assembly of 38.09-diam, 0.303-cm-thick uranium discs with 38.07-cm-diam, 0.628-cm-thick polyethylene discs between the uranium discs. The mass of uranium in this assembly was approximately one half of the critical mass. This type of source provided a good simple way to determine the characteristics of detection systems since the time at which the neutrons or gamma rays from fission enter the detector was known. It was used to determine detector efficiency, time resolution and to evaluate in a quantitative way the performance of a gamma discrimination method. (Diss. Abstr. Int., B)

## Nuclear Properties and Reactions, A≤5

*Refer also to abstracts 56421, 56654, 56851, 56852, and 56859.*

**56640** (FRNC-CONF-8) QUASI FREE SCATTERING IN THE $^2$H(p,2p) AND $^2$H(p,pn) REACTION FROM 21.5 TO 56.4 MeV. Durand, J. L.; Arvieux, J.; Durand, M.; Fiore, A.; Perrin, C. (Grenoble Univ. (France). Institut des Sciences Nucleaires). 8 Jul 1971. 2p. (CONF-710708-3). Dep. NTIS (U. S. Sales Only).

From Symposium on the nuclear three body problem and related topics; Budapest, Hungary (7 Jul 1971).

Quasi free scattering was studied as function of energy using the spectator model. The absolute cross section was measured for incident energies from 21.5 MeV to 56.4 MeV. Data for the two reactions $^2$H(p,2p) and $^2$H(p,pn) were obtained from the same experiment. The experimental results show an important enhancement at minimum energy of the spectator. The absolute peak cross section for the (p,pn) reaction is 2.5 times greater than that corresponding to the (p,2p) enhancement. This ratio is almost independent of the incident energy. (France)

**56641** (JINR-P4-5986) NEUTRON-CHANNEL IN MUON CAPTURE AND SHORT RANGE NUCLEON-NUCLEON CORRELATIONS. REACTION $\mu^- + {}^4\mathrm{He} \rightarrow {}^3\mathrm{He} + n + \nu$. Salganic, Yu. A.; Eramzhyan, R. A. (Joint Inst. for Nuclear Research, Dubna (USSR). Lab. of Theoretical Physics). 1971. 13p. (In Russian). Dep. NTIS (U. S. Sales Only)

The neutron channel in muon capture by complex nuclei is investigated in the example of the reaction $\mu^- + {}^4\mathrm{He} \rightarrow {}^3\mathrm{H} + n + \nu$. The effect of the short-range nucleon-nucleon correlations on the energy spectrum and asymmetry of the angular distribution is investigated. The final state interaction and relativistic terms of the muon-nucleon Hamiltonian is taken into account. It is shown, that the short range correlations influence significantly the high energy part of the spectrum and the asymmetry, too, although their form remains about the same. (auth)

**56642** (LYCEN-7104, C5,1-15) SEPARABLE NONLOCAL POTENTIALS AND THEIR EQUIVALENT LOCAL POTENTIALS IN ELASTIC SCATTERING STUDIES. El Baz, E.; Barguil, J.; Pigeon, J.; Fayard, C.; Lamot, G.-H. (Lyon Univ. (France). Institut de Physique Nucleaire). (In French).

From Conference on some microscopic aspects of nuclear reactions; La Toussuire, France (15 Feb 1971).

Separable nonlocal potentials have been widely used for describing two body interactions in scattering problems and bound state studies. The general formalism leading to the scattering amplitude analytical expression was studied. When Coulomb effects are introduced, the separable nonlocal potential is expanded in a Coulomb representation rather than in configuration spaces of phase spaces. The choice of the separable nonlocal potential is discussed. This formalism is applied to neutron-alpha and proton-alpha elastic scattering. The method used by Coz et al to obtain local potentials equivalent to separable nonlocal potentials in elastic scattering is described. (France)

**56643** (NP-19018) ANNUAL REPORT, 1970. (Lund Univ. (Sweden)). Jan 1971. 112p. Dep. NTIS (U. S. Sales Only).

The research carried out at the departments of cosmic high energy physics, elementary particle physics and nuclear physics of the University of Lund and the Institute of Technology is reviewed. The equipment is dominated by three accelerators: a 1.2-GeV electron synchrotron, a 3-MeV Van de Graaff generator and a 0.4-MeV neutron generator. (K.K.) (Sweden)

**56644** EXPERIMENTAL DETERMINATION OF THE DIFFERENTIAL CROSS SECTION FOR THE REACTION d(p,2p)n. Burns, James Martin Jr. College Station, Tex.; Texas A and M Univ. (1970). 139p. University Microfilms Order No. 71-17,797.

Thesis

A kinematically complete experiment for the reaction d(p,2p)n has been performed for an incident proton energy of 28.61 MeV. Simultaneous detection of the two protons was made by two systems of 96 scintillation detectors each (9216 detector pairs), located uniformly over a 1.22 m diameter spherical scattering chamber. Use of an IBM 7094 computer for on-line data acquisition allowed accumulation of approximately 300,000 three-nucleon break-up events during an eight hour period. The differential cross section as a function of the proton center-of-momentum energies and the total break-up cross section are presented. Comparison of the total break-up cross section with a value suggested by other experiments shows fairly good agreement. (Diss. Abstr. Int., B)

**56645** RADIATIVE PROTON CAPTURE IN DEUTERIUM. Vos, Robert. Philadelphia; Univ. of Pennsylvania (1970). 158p. University Microfilms Order No. 71-19,295.

Thesis.

The d(p,$\gamma$)He$^3$ differential cross section at 90° has been measured for proton energies from 0.82 to 3.24 MeV, and a gamma ray angular distribution measurement carried out at 3.24 MeV. The gamma rays were detected by 3'' × 4'' Na-I counters, whose spectra were analyzed for absolute or relative photon flux per run, using spectrum shape Monte Carlo calculations. A deuterium gas target was used. The results of the angular distribution measurement, as well as absolute cross section measurements are compared with other data on the d(p,$\gamma$)He$^3$, d(n,$\gamma$)H$^3$, He$^3$($\gamma$,p)d and $^3$H($\gamma$,n)d reactions, with brief mention of the $^3$He($\gamma$,n)pp and $^3$H($\gamma$,p)nn reaction data. A survey of theoretical $^3$He and $^3$H photodisintegration cross section calculations is also made, and theoretical results are compared with experimental data. A modified Dalitz-Thacker type ground state $^3$H, $^3$He wave function is suggested, which includes t = ½ $^4$D and $^2$S mixed symmetry states and has correct asymptotic structure. (Diss. Abstr. Int., B)

**56646** STUDY OF THE REACTION T($^3$He,$\gamma$)$^6$Li FROM 0.5 TO 20 MeV. Young, Alan Morris. Columbus, Ohio; Ohio State Univ. (1970). 102p. University Microfilms Order No. 71-18,110.

Thesis.

Gamma-ray spectra from the T($^3$He,$\gamma$)$^6$Li reaction have been

XUM

obtained over a range of $^3$He bombarding energies from 0.5 to 20 MeV. The anticoincidence-shielded NaI(Tl) detection systems employed are capable of providing better than 7% energy resolution (FWHM) for 20 MeV gamma radiation, and reject cosmic rays in the ratio of 1000 to 1. The detectors are gain stabilized and utilize pulse-pileup rejection logic. Strong $\gamma$-ray transitions were seen to the ground and first two excited states of $^6$Li. Evidence was also found for a transition to the second T = 1 state in $^6$Li. Angular distributions for the three strong transitions were recorded at 1.0, 2.7, 5.0, and 8.25 MeV. The observed $\sin^2\theta$ angular dependence for the ground state transition is apparently independent of bombarding energy. The capture cross sections for transitions to the ground and first two excited states were found to vary smoothly with energy with an apparent lack of resonant behavior. The integrated cross section for the inverse reaction $^6$Li($\gamma_0$,t)$^3$He up to $E_\gamma$ = 25.8 MeV was found to be 10.1 ± 1.6 MeV-mb in good agreement with the phototriton sum rule prediction for $^6$Li. The angular distributions and energy dependence of the capture cross sections for the three strong transitions can be most easily understood within the framework of the direct capture model. The energy dependence of the calculated ground state capture cross section agrees quite well with that observed experimentally over the entire range studied. T + $^3$He resonating-group wave functions, which describe T + $^3$He elastic scattering well, were employed in the direct-capture calculation. Coefficients of fractional parentage, $\theta^2_{T+^3He}$, were obtained for the ground state and for the first, second and fourth excited states of $^6$Li. Substantial T + $^3$He clustering in these four low lying $^6$Li states is evident. (Diss. Abstr. Int., B)

**56647** COMMENTS ON CENTER-OF-MASS MOTION AND THE $^4$He CHARGE FORM FACTOR. Friar, J. L. (Massachusetts Inst. of Tech., Cambridge). Nucl. Phys.; A173: No. 2, 257-64(1971).

Various methods of removing the cm coordinate from single-particle wave functions are discussed. A nonunitary generalization of the Gartenhaus–Schwartz transformation is shown to incorporate both of the common methods for constructing translation-invariant wave functions as limiting cases. By using a simple single-particle model density for $^4$He, a family of charge form factor curves is generated. It is shown that two-body correlations may be sensitive to the procedure used to remove the cm coordinate from the problem. (auth)

**56648** SPIN-ORBIT COUPLING FOR $\Lambda$-$^4$He SCATTERING USING A ONE-BOSON-EXCHANGE MODEL FOR THE $\Lambda N$ INTERACTION. Londergan, J. T. (Oxford Univ. Case Western Reserve Univ., Cleveland); Dalitz, R. H. Phys. Rev., C; 4: No. 3, 747-64(Sep 1971).

The polarization and cross sections for $\Lambda$-$^4$He elastic scattering are calculated for $\Lambda$ incident energies 1–20 MeV. A $\Lambda$-$^4$He potential is constructed using a phenomenological $\Lambda N$ Gaussian central potential and the empirical shape for $^4$He, and a spin-orbit potential obtained from a one-boson-exchange (OBE) model for the $\Lambda N$ interaction. As indicated recently by Downs, the OBE model for $\Lambda N$ forces leads to strong antisymmetric spin-orbit terms due to vector-meson exchange. This means that the $\Lambda$-$^4$He potential depends only on part of the $\Lambda N$ spin-orbit interaction, since it results from summing the latter interaction over the nucleon spin states. Parameters from three quite different OBE calculations are used to predict the $\Lambda$-$^4$He scattering, and these three sets of OBE parameters lead to remarkably similar predictions concerning the cross sections and polarization properties for this energy range. However, no $\Lambda$-$^4$He resonances are predicted, in contrast to recent Hartree–Fock calculations of $\Lambda$-$^4$He scattering. The polarization effects predicted are large, and experimental data concerning them would have interesting consequences for our knowledge of the origin of spin-orbit forces in the baryon-baryon system. (auth)

**56649** PHOTONEUTRON CROSS SECTION FOR $^4$He UP TO 31 MeV. Berman, B. L.; Fultz, S. C.; Kelly, M. A. (Univ. of California, Livermore). Phys. Rev., C; 4: No. 3, 723-32(Sep 1971).

The photoneutron cross section for $^4$He has been measured with monoenergetic photons from threshold to 31 MeV. The cross section reaches its maximum value of 1.0 mb from 24.3 to 27.3 MeV and appears to be split into two broad peaks. The integrated cross section is 7.9 MeV mb. The fore-aft asymmetry of the photoneutrons also was measured. This quantity, which is a measure of the interference between the E1 amplitude and the underlying positive-parity contribution, changes from forward to backward peaking at about 27 MeV. The E2-to-E1 amplitude ratio deduced from these data is of the order of 0.04. A comparison of the cross-section results with the considerably larger values for the $^4$He($\gamma$,p) reaction measured elsewhere shows appreciable (≳15%) isospin mixing throughout the energy region studied, with indications that this mixing might be increasing with energy above 28 MeV. (auth)

## Nuclear Properties and Reactions, 6 ≤ A ≤ 19

*Refer also to abstracts 55384, 55704, 56643, 56695, 56706, 56711, 56713, 56716, 56717, 56724, 56752, 56780, 56832, 56833, 56847, and 56868.*

**56650** (COO–2049–5) EVALUATION OF MINIMA IN TOTAL NEUTRON CROSS SECTION BY TRANSMISSION OF FISSION SPECTRA THROUGH THICK SAMPLES. Miller, William H.; Meyer, Walter (Kansas State Univ., Manhattan. Dept. of Nuclear Engineering). 30 Jul 1971. Contract AT(11-1)-2049. 97p. Dep. NTIS.

An evaluation of minima in total neutron cross sections was performed for several materials by comparing an experimentally measured transmitted spectrum with the corresponding calculated result. Published cross section data were evaluated for iron, lead, liquid oxygen, and solid and liquid sodium. Since thick samples (three or more mean free paths thick) were used, the analysis was very sensitive to minima in the cross-section. The incident neutron spectrum was obtained from the Triga Mark II reactor and was detected using an NE-213 liquid scintillator spectrometer system. Computer codes were used to unfold the raw data and to calculate the transmitted spectrum (which was a function of published cross section data, the measured incident flux on the sample and the resolution of the detector). The results of this study demonstrate the usefulness of this technique in evaluating total neutron cross section. Several experimental geometry conditions were used in this work to obtain valid results and to study the effects of forward scattering and multiple scattering in the thick samples. The results showed that there is a question as to the accuracy of published angular-dependent cross section data near the zero scattering angle. (auth)

**56651** (INSJ–127) TABLE OF BANDS IN EVEN–EVEN NUCLEI. Sakai, Mitsuo (Tokyo Univ. (Japan). Inst. for Nuclear Study). 2 Jun 1971. 35p. Dep. NTIS (U. S. Sales Only).

For even-even nuclei, a list is presented of the probable members of quasi-ground, quasi-beta and quasi-gamma bands of the spherical regions and the corresponding ground, beta and gamma bands of the deformed region. For simplicity the term "quasi" is used for both regions. References are given to the experimental data basic to the level assignments. The literature was covered up to the middle of May, 1971. (auth)

**56652** (LYCEN–7104, S2,1-2) SUBSTRUCTURES IN $^{12}$C AND $^{14}$N BY STUDYING VISUAL INTERACTIONS OF PROTONS AND ALPHA PARTICLES OF INTERMEDIATE ENERGY (70 TO 150 MeV). Jacquot, C.; Sakamoto, Y.; Braun, H. (Centre National de la Recherche Scientifique, Strasbourg (France). Laboratoire de Physique Corpusculaire). (In French).

From Conference on some microscopic aspects of nuclear reactions; La Toussuire, France (15 Feb 1971).

All the interactions of $\alpha$ particles with $^{12}$C and $^{14}$N at 70 and 90 MeV were studied and a table of the structures knocked out and the cross sections was drawn up. (France)

**56653** (LYCEN–7104, S4.1-10) $\pi$ AND K MESONS USED FOR INVESTIGATING LIGHT NUCLEI STRUCTURES FROM THE ANALYSIS OF THEIR INTERACTIONS (IN FLIGHT AND STOPPING ABSORPTION, DOUBLE CHARGE EXCHANGE). Massue, J. P.; Kurtz, N.; Sakamoto, Y.; Batusov, I.; Souslenko, V.; Sidorov (Centre National de la Recherche Scientifique, Strasbourg (France). Laboratorie de Physique Corpusculaire). (In French).

From Conference on some microscopic aspects of nuclear reactions; La Toussuire, France (15 Feb 1971).

The absorption of $\pi^-$, $\pi^+$, and $K^-$ mesons by $^{12}$C, $^{14}$N, and $^{16}$O nuclei of the ionographic emulsion was studied. The most important primary mechanisms involved are the absorption by one or two nucleons in the case of $K^-$ and by two nucleons in the case of $\pi^-$. Clusters of more than two nucleons, especially the alpha cluster, contribute to the absorption process; this was verified by the double charge exchange of $\pi$ mesons. (auth)

**56654** (LYCEN–7104, S13,1-11) MICROSCOPIC DESCRIPTION AND CLUSTER STRUCTURE OF LIGHT NUCLEI. Leclercq-Willain, C. (Brussels Univ. (Belgium)). (In French).

From Conference on some microscopic aspects of nuclear reactions; La Toussuire, France (15 Feb 1971).

The energy states of light nuclei which can be described by a cluster model ($\alpha$ or other clusters) were studied. Quasi molecular systems where one or several nucleons describe "molecular" orbits and the remaining nucleons are in "atomic" orbits were investigated. This study was restricted to two-cluster states in $^{8}$Be, $^{4}$He, $^{9}$Be, and $^{5}$He. (France)

**56655** (ORNL-TM-3379) keV NEUTRON CAPTURE GAMMA RAY SPECTRA. Bird, J. R.; Bergqvist, I.; Biggerstaff, J. A.; Gibbons, J. H.; Good, W. M. (Oak Ridge National Lab., Tenn.). Apr 1971. 78p. Dep. NTIS.

Techniques are described for using a 9'' × 12'' NaI detector to measure pulse height spectra for gamma rays from the capture of 10 to 100-keV neutrons generated by a pulsed Van de Graaff beam. Pulse height spectra are given for capture in 36 elements or separated isotopes. In many cases, tabulated gamma ray intensities are compared with results for thermal neutron capture. In a few cases the excitation functions for particular gamma rays are included. The experimental work described was carried out at ORNL during the period 1961 to 1963 and some of the results have been presented previously. This compilation summarizes all the spectra and intensities measured during that period. (auth)

**56656** ISOSPIN FORBIDDEN $^{12}$C(d,$\alpha_2$)$^{10}$B(1.74) REACTION. Smith, Horace Vernon Jr. Madison, Wis.; Univ. of Wisconsin (1971). 113p. University Microfilms Order No. 71-14,166.

Thesis.

Extensive new data on the isospin forbidden $^{12}$C(d,$\alpha_2$)$^{10}$B(1.74) reaction for 7.2 MeV ≤ $E_d$ ≤ 14.0 MeV are reported. A multi-detector array in a differentially pumped gas scattering chamber ($CH_4$ target) allows simultaneous measurement of eight to fourteen excitation functions in $E_d$ steps of 40 keV. The cross sections exhibit resonant behavior indicative of compound nucleus formation. No evidence for appreciable direct or semi-direct contribution to the reaction cross sections was found. The cross sections are expanded according to the following: $(d\sigma/d\Omega) = (\lambda^2/12) \mid \Sigma_l [2l+1\ l(l+1)]S[dP_l(\cos\theta)/d\theta]\mid^2$ where $S_l$ is the complex amplitude for the $l^{th}$ partial wave. Partial waves up to l = 5 are necessary for satisfactory fits to the data. This expansion uniquely determines the $J^\pi$ of an isolated resonant state of $^{14}$N. Extensive data are reported for the isospin allowed $^{12}$C(d,$\alpha$)$^{10}$B reactions leaving $^{10}$B in its ground, first, and third excited states. The total cross section ratios of the $\alpha_2$ group to the $\alpha_0$, $\alpha_1$, and $\alpha_3$ groups are determined to obtain lower limits to the isospin impurities present in $^{14}$N. The lower limit to the average isospin impurities in $^{14}$N(17.1 MeV < $E_x$ < 22.3 MeV) is ~4%. The lower limit to the isospin impurity at some individual resonances is 9%. (Diss. Abstr. Int., B)

**56657** $^{16}$O + $^{16}$O REACTION. Spinka, Harold. Pasadena, Calif.; California Inst. of Tech. (1971). 237p. University Microfilms Order No. 71-17,386.

Thesis.

The $^{16}$O + $^{16}$O total reaction cross section was measured at six energies between $E_{cm}$ = 6.80 to 11.85 MeV near the astrophysical region of interest. Angular distributions and cross sections for the production of protons, alphas and deuterons were obtained with counter telescopes in a differentially pumped gas target. No $^{3}$He or $^{3}$H was observed. Cross sections for the formation of $^{31}$S and $^{30}$P were measured by detecting the betas from their radioactive decays. The angular distribution and cross section for production of neutrons was obtained with a "long counter" at $E_{cm}$ = 12 MeV, demonstrating that the $^{16}$O ($^{16}$O,pn) process accounts for over 90% of the $^{30}$P formed at this energy. The presence of such three body breakup reactions made the experimental determination of the total cross section difficult. Finally, the $^{16}$O + $^{16}$O → $^{12}$C(g.s.) + $^{20}$Ne(g.s.) reaction was studied with a coincidence technique at $E_{cm}$ = 12 MeV. Gamma spectra were taken at several energies for a number of targets using Ge(Li) counters. Gamma lines from nuclei produced in both two and three body exit channels from $^{16}$O + $^{16}$O reactions were observed. In addition, the gamma yield as a function of bombarding energy was measured in 50 keV (C.M.) steps for both $^{16}$O + $^{16}$O and $^{12}$C + $^{12}$C. The $^{16}$O + $^{16}$O gamma yield is smoothly varying, indicating that the $^{16}$O + $^{16}$O reaction cross section does not have large fluctuations with energy similar to the structure seen in $^{12}$C + $^{12}$C reactions. Nearly all cross sections were measured relative to the $^{16}$O + $^{16}$O elastic scattering at $\theta_{lab}$ = 45° to avoid the problems with direct current integration of heavy ion beams in gas targets. A new, more precise determination of the elastic scattering cross section at $\theta_{cm}$ = 90° was made for $E_{cm}$ = 7.3 to 14.4 MeV in steps of 100 keV (C.M.). A previously unknown anomaly was observed near $E_{cm}$ = 10 MeV. Elastic scattering cross sections were also obtained for $^{12}$C + $^{12}$C in steps of 60 keV C.M. energy from $E_{cm}$ = 3.9 to 8.0 MeV at $\theta_{cm}$ = 90°. In both cases, gas mixtures were used in the differentially pumped system as the target. (Diss. Abstr. Int., B)

**56658** MEASUREMENT OF THE HALF-LIFE OF $^{16}$N DECAY. Karlik, Berta. Oesterr. Akad. Wiss., Math.-Naturwiss. Kl., Anz.; No. 10, 1-4(1967). (In German).

The half-life of $^{16}$N was remeasured with special attention to correct statistical evaluation and interferring activities. A measurement device consisting of a NaI(Tl) crystal and a 100-channel analyser was used. A value of $t_{\frac{1}{2}}$ = 7.090 ± 0.016 sec was obtained. (J.S.R.)

**56659** HEAVY ION EMISSION FROM LIGHT NUCLEI. Rudy, Clifford Robert Jr. Seattle; Univ. of Washington (1970). 104p. University Microfilms Order No. 71-16,994.

Thesis.

Reactions involving the emission of heavy ions leading to low-lying states of the residual nucleus have been studied using 42 MeV alpha particles incident on light target nuclei. The heavy ions resulting from these reactions were identified by mass number using the time of flight technique. With this method products with a mass number as high as A = 14 could generally be separated from neighboring isobars. Reactions leading to different particle masses from a particular target were studied simultaneously. Angular distributions and total cross sections were obtained for the reactions $^{12}$C($\alpha$,$^{6}$Li(g.s.))$^{10}$B(g.s.), $^{12}$C($\alpha$,$^{6}$Li(g.s.))$^{10}$B(0.717 MeV), $^{12}$C($\alpha$,$^{7}$Be(g.s.))$^{9}$Be(g.s.), $^{12}$C($\alpha$,$^{7}$Be(0.431 MeV))$^{9}$Be(g.s.), $^{16}$O($\alpha$,$^{6}$Li(g.s.))$^{14}$N(g.s.) and $^{16}$O($\alpha$,$^{7}$Be(g.s. + 0.431 MeV))$^{13}$C(g.s.). In addition to these reactions, others leading to different states of excitation of the above-mentioned products and to different masses were studied over a limited angular range for the $^{12}$C and $^{16}$O targets. Fragmentary angular distributions were obtained for the reactions $^{24}$Mg($\alpha$,$^{6}$Li(g.s.))$^{22}$Na(g.s.) and $^{24}$Mg($\alpha$,$^{12}$C(g.s.))$^{16}$O (g.s.). The reactions $^{28}$Si($\alpha$,$^{16}$O(g.s.))$^{16}$O(g.s.), $^{28}$Si($\alpha$,$^{16}$O(g.s.))$^{16}$O(6-7 MeV), $^{28}$Si($\alpha$,$^{12}$C(g.s.))$^{20}$Ne(g.s.) and $^{28}$Si($\alpha$,$^{12}$C(g.s.))$^{20}$Ne (1.63 MeV) were also observed. The $^{28}$Si($\alpha$,$^{12}$C(g.s.))$^{20}$Ne(g.s.) cross sections were several times larger than the $^{28}$Si($\alpha$,$^{16}$O (g.s.))$^{16}$O(g.s.) reactions. A comparison of the experimental angular distributions and cross sections with statistical model calculations was carried out. It is shown that as the mass of the emitted heavy ions increases for a particular reaction, the amount of compound nuclear contribution increases. Considerable compound nuclear contributions to all the reactions studied are indicated. Contrary to previous suggestions, comparison of the calculated and experimental results for the $^{16}$O($\alpha$,$^{7}$Be)$^{13}$C and $^{16}$O ($\alpha$,$^{7}$Li)$^{13}$N reactions with those for the reaction $^{16}$O($\alpha$,$^{8}$Be)$^{12}$C indicate that there is no enhancement of this reaction due to alpha clustering relative to the ($\alpha$,$^{7}$Li) and ($\alpha$,$^{7}$Be) reactions. Evidence is given for the conservation of isotopic spin in complex reactions proceeding through a short-lived compound nucleus. (Diss. Abstr. Int., B)

**56660** REALISTIC SHELL MODEL CALCULATIONS FOR $^{14}$C AND $^{14}$N. Ostrander, Peter Erling. University Park, Pa.; Pennsylvania State Univ. (1970). 81p. University Microfilms Order No. 71-16,648.

Thesis.

The low-lying energy level structure of $^{14}$C and $^{14}$N and the $^{14}$C → $^{14}$N ground state beta decay are investigated in a shell model calculation employing the nonlocal interaction of Tabakin and the realistic matrix elements of Elliott as the residual interactions. In this calculation, second-Born terms are taken into account and lowest order core polarization processes are evaluated in a microscopic approach for both interactions. Two approaches are used for the mass-14 calculations; in the first, the $0^+1$ ground state of $^{14}$C and the ground and first excited $1^+0$ levels of $^{14}$N are assumed to arise from p-2 configurations in a $^{16}$O core. In the second, a $^{12}$C core is chosen and the residual interactions are diagonalized in 2s-1d shell configurations. In addition, a similar investigation of the energy levels of $^{18}$O and $^{18}$F is carried out for purposes of comparison with other realistic calculations. The results obtained indicate that although these realistic interactions are able to predict the mass-18 spectra with considerable accuracy, the same methods do not properly give the $1^+0$ ground state of $^{14}$N and the ground state beta decay. This is probably due to the significance of higher order core-polarization processes for the mass-14 nuclei. Other levels are predicted in fair agreement with experimental results. (Diss. Abstr. Int., B)

**56661** PHOTONUCLEAR REACTIONS IN LIGHT NUCLEI. Mustafa, Mohammed Golam. New Haven; Yale Univ. (1970). 163p. University Microfilms Order No. 71-17,013.

Thesis.

Photonucleon emission in $^{16}$O and $^{12}$C has been studied up to

XUM

excitation energy of 50 MeV. The giant resonance and the high energy ($E_\gamma$ > 30 MeV) emissions are described from a reaction theory point of view. For the high energy emission, this theory is compatible with the standard direct reaction model and, therefore, the high energy photonucleon yield was studied using (a) the standard direct reaction model and (b) the standard direct reaction model modified to incorporate the ground state correlation. Electric dipole (E1), electric quadrupole (E2), and magnetic dipole (M1) transitions are considered. The calculation has been made for the 90° differential cross section, integrated cross section, angular distributions at a few energies, and polarizations at 45° and at 90°. The results are compared with the available experimental data. In the giant resonance region, the theory is compatible with an intermediate coupling model; the giant dipole region was studied in that context. The calculation has been made for the electric dipole transition strength in $^{16}O$ and compared with one particle-one hold and other calculations. The following conclusions are made: (1) The high energy ($E_\gamma$ = 30-50 MeV) photonucleon emission in light nuclei is a dominant direct process with E1, E2, and M1 transitions participating. There is substantial direct reaction amplitude even in the giant resonance region. (2) The magnitude of the cross section is reduced by the ground state correlation. The amount of reduction sensitively depends on the degree of correlation. (3) The intermediate coupling model calculation of dipole strength produces a distribution of strength different from one particle-one hole calculation and can be brought in accord with experimental observation. Thus the structure seen in $^{16}O$ is likely to be actual resonances. (Diss. Abstr. Int., B)

**56662** STUDY OF $^{17}N$ LEVELS AND T = 3/2 MULTIPLETS IN MASS 17 NUCLEI. Hartwig, D. (Kernforschungszentrum, Karlsruhe, Ger.). Z. Phys.; 246: No. 5,418-23(1971).

Ten states of $^{17}N$ were excited via the $^{18}O(d,^3He)^{17}N$ reaction at $E_d$ = 52 MeV. The l-transfer values are presented for eight of these states. Based on the subsequent spin and parity assignments, proposals for several T = 3/2 isobaric multiplets are made. (auth)

**56663** INVESTIGATION OF THE LEVEL STRUCTURE OF $^{17}O$. Schmidt-Boecking, H.; Brommundt, G.; Bethge, K. (Univ., Heidelberg). Z. Phys.; 246: No. 5, 431-46(1971).

The reactions $^{12}C(^7Li,d)$ and $^{13}C(^7Li,t)$ were studied at $E_{C.M.}$ = 13.3 MeV. Spin assignments are extracted from the integrated cross sections of the first reaction. The latter reaction is analyzed in terms of a modified-DWBA code. (auth)

**56664** $^3H(^3He,\gamma)^6Li$ CAPTURE REACTION AND THE STRUCTURE OF $^6Li$. Ventura, E.; Chang, C. C.; Meyerhof, W. F. (Stanford Univ., Calif.). Nucl. Phys.; A173: No. 1, 1-16(1971).

The capture reaction $^3H(^3He,\gamma)^6Li$ has been studied for $^3He$ bombarding energies from 9 to 26 MeV. Transitions to the ground and first four excited states in $^6Li$ are observed. The 90° differential cross section for the ground state transition decreases smoothly from 9 to 26 MeV. The 90° differential cross section for the first excited state transition shows a broad maximum centered at $E_{^3He}$ = 20.6 ± 0.4 MeV, indicating a possible resonance in $^6Li$ at $E_x$ = 26.2 ± 0.2 MeV. The excitation function for the transition to the third excited state also shows a broad maximum centered at $E_x$ = 26.6 ± 0.4 MeV. The excitation functions for the transitions to the second ($T = 1,0^+$) and fourth ($T = 1,2^+$) excited states have also been measured. The former does not show any resonance structure, while the latter shows a broad maximum indicating a possible resonance in $^6Li$ at $E_x$ = 26.7 ± 0.4 MeV. These results are compared with theoretical predictions. (auth)

**56665** STUDY OF THE ($^4He,^6He$) REACTION ON s–d SHELL NUCLEI. Arnold, Jeffrey Mark. Cleveland; Case Western Reserve Univ. (1970). 64p. University Microfilms Order No. 71-18,966.

Thesis.

The ($^4He,^6He$) reaction has been studied using targets of $^{18}O$, $^{22}Ne$, and $^{26}Mg$ at an incident energy of 42 MeV. Solid state detectors and the Goulding double particle identification technique have been used. Angular distributions have been obtained over the range from 15° to 70° (lab) for transitions to the ground states of all the nuclei, to the excited states of 6.052-6.131 MeV (unresolved) and 6.916-7.115 MeV (unresolved) in $^{16}O$, to the excited states at 1.63 and 4.25 MeV in $^{20}Ne$, and to the excited states at 1.37 and 4.123-4.23 MeV (unresolved) in $^{24}Mg$. Diffraction-like patterns are observed for most transitions, indicating that the reactions may be predominantly direct in nature. All levels in the final nuclei are populated with comparable intensity in contrast to the enhancement of the ground state transitions in (p,t) reactions. A zero-range two-nucleon transfer DWBA analysis of the $^{18}O(^4He,^6He)^{16}O$ g.s. transition was attempted with unsatisfactory results. (Diss. Abstr. Int., B)

**56666** SHELL MODEL WITH REACTION MATRICES AND PAIRING CORRELATIONS. Mercier, Roch Edouard. Pittsburgh; Univ. of Pittsburgh (1970). 151p. University Microfilms Order No. 71-18,139.

Thesis.

In light nuclei, the calculation of Kuo and Brown in $^{18}O$-$^{18}F$ was repeated with important modifications. The reference spectrum approximation with harmonic oscillator intermediate states, coupled with the Köhler–McCarthy matrix inversion technique gives an accurate treatment of the Pauli operator and the long range part of the tensor force. Various intermediate spectra are used to test the sensitivity of the calculation. In heavy nuclei the spectrum of the antimony isotopes was studied with the smooth Tabakin interaction. The wave function representing the states of antimony consist of an admixture of |IP > and |2QP IP > wave functions with the proton one-particle (IP) and the neutron quasiparticle (QP) states restricted to the 5 filling levels. Following the work of the Trieste group it was found that it is necessary to renormalize the model space in order to obtain reasonable agreement with the odd-even mass difference data in the Tin isotopes. The effective G-matrix elements include the 2p, 2h and 3plh diagrams of Kuo and Brown. The single QP energies were taken from experiment. It was found that the weak coupling approximation is very good in this region. The antimony wave function corresponding to the lowest part of the spectrum is well represented by a phonon state (in even tin) plus a proton. The crossing of the $d_{5/2}$ and $g_{7/2}$ levels is fairly well reproduced by this method. The spectroscopic factors and BE2 transition rates are in reasonable agreement with experiment. However one difficulty arises for the 2QP IP states. If the coupling is really weak these states should occur at an energy of about 1 MeV above the ground state. They were found much higher. This is because the energy shift produced by the matrix element connecting the 4QP IP subspace to the 2QP IP subspace was neglected. When this is taken into consideration reasonable agreement with experiment is obtained. (Diss. Abstr. Int., B)

**56667** ISOSPIN FORBIDDEN $^{16}O(d,\alpha_1)^{14}N$ REACTION FOR 2 < $E_d$ < 14 MeV. Jolivette, Peter Lauson. Madison, Wis.; Univ. of Wisconsin (1971). 103p. University Microfilms Order No. 71-14,146.

Thesis.

Data is presented for the isospin forbidden $^{16}O(d,\alpha_1)^{14}N$ reaction in 10–30 keV steps at 12 to 18 angles for 1.8 < $E_d$ < 14 MeV. The data is expanded in partial waves: $(d\sigma/d\Omega) = (\lambda^2/12)|\Sigma_l[2l + 1/\sqrt{l(l+1)}]Sl\ e^{i\Phi}(dPl/d\theta)(\cos\theta)|^2$. There are $2^l$ sets of S-matrix elements that give identical angular distributions as calculated from the above equation. The "physical" solution is selected on the basis of simplicity and the lack of correlation between the partial waves. The S-matrix elements are parameterized as a coherent sum of Breit–Wigner resonances for each partial wave and the level parameters for about a hundred states in $^{18}F$ are presented. A number of levels have been identified as the analogs of T = 1 states in $^{18}O$. No evidence was found for a direct reaction contribution to the isospin forbidden $^{16}O(d,\alpha_1)^{14}N$ reaction even near $E_d$ = 14 MeV ($E_x(^{18}F) \simeq 20$ MeV). The allowed $^{16}O(d,\alpha_0)^{14}N$ reaction also appears to be primarily compound nuclear at all energies studied. The isospin violating reaction does not show the expected decrease in cross section relative to the allowed reactions at high energy and the average magnitudes of the S-matrix elements do not show a strong J dependence even at 20 MeV excitation in $^{18}F$. The isospin allowed $^{16}O(d,\alpha_0)^{14}N$ data taken simultaneously with the forbidden data has been expanded in Legendre polynomials and the coefficients are presented for the entire energy range. The total cross section for $^{16}O(d,\alpha_2)^{14}N$ is shown for 7 < $E_d$ < 14 MeV. (Diss. Abstr. Int., B)

**56668** QUADRUPOLE SURFACE OSCILLATIONS AND THE ELASTIC FORM FACTOR OF $^{16}O$ AND $^{12}C$. Friar, J. L. (Univ. of Washington, Seattle). Nucl. Phys.; A173: No. 2, 248-56(1971).

By using a volume-conserving liquid-drop model for quadrupole surface oscillations, the elastic form factors for $^{16}O$ and $^{12}C$ are calculated. It is shown that zero-point oscillations of the quantized drop produce an effective charge density which differs from that of the uniform, unquantized drop by having a reasonable skin thickness. The resulting elastic form factors are in reasonable agreement with recent experimental data. The transition density for exciting the lowest quadrupole state in this model is shown to be the same as that of Tassie's hydrodynamical model [Aust. J. Phys., 9: 407(1956)]. (auth)

**56669** PROPERTIES OF THE 12,50 AND 12,52 MeV LEVELS OF $^{15}N$. Young, F. C.; Figuera, A. S.; Steerman, C. E. (Univ.

of Maryland, College Park). Nucl. Phys.; A173: No. 2, 239-47 (1971).

Simultaneous $\gamma$-ray and neutron excitation functions were measured for the bombardment of $^{14}C$ with 2.3- to 2.6-MeV protons to identify a $^{15}N$ level at $E_p$ = 2.452 MeV ($E_x$ = 12.50 MeV, $\Gamma$ = 44 keV), which is observed by neutron decay, and a level at $E_p$ = 2.482 MeV ($E_x$ = 12.52 MeV, $\Gamma$ = 58 keV), which is observed by $\gamma$ decay. Absolute cross sections were used to determine $\gamma$-ray partial widths. Transition strengths are compared with results based on shell-model and weak-coupling-model calculations. The absolute (p,n) cross section for the 2.452-MeV resonance indicates J = $^5/_2$ or $^7/_2$. Spin $^7/_2$ is suggested based on the lack of evidence for isospin mixing of these levels. (auth)

**56670** ELASTIC SCATTERING OF DEUTERONS BY $^6Li$ AND $^7Li$ AT 8.0 TO 12.0 MeV. Bingham, H. G.; Zander, A. R.; Kemper, K. W.; Fletcher, N. R. (Florida State Univ., Tallahassee). Nucl. Phys.; A173: No. 2, 265-72(1971).

Absolute differential cross sections for the elastic scattering of protons and deuterons by $^6Li$ and $^7Li$ were measured with an error of ≈2% at selected angles and bombarding energies. The optical model is used to describe the angular distributions of the deuteron scattering at $E_d$ = 8.0, 10.0, and 12.0 MeV. The model parameters found for a real potential radius between 3 F and 4 F are more nearly constant with changes in bombarding energy than are those obtained using a value ≈2 F. The two sets of parameters represent a phase equivalent ambiguity. (auth)

**56671** MEASUREMENT AND DIRECT REACTION ANALYSIS OF THE REACTIONS $^7Li(d,t)^6Li$ AND $^7Li(\tau,\alpha)^6Li$. Zander, A. R.; Kemper, K. W.; Fletcher, N. R. (Florida State Univ., Tallahassee). Nucl. Phys.; A173: No. 2, 273-85(1971).

Angular distributions for the reactions $^7Li(d,t)^6Li$ and $^7Li(^3He,\alpha)^6Li$ were measured and analyzed in an energy region shown to be relatively free of compound-nucleus resonance structure. Both front and back angle maxima in the measured angular distributions are reproduced by the conventional DWBA without the inclusion of exchange effects. The zero-range DWBA calculation is a factor of 25 smaller than the $^7Li(^3He,\alpha)^6Li$ cross section and a factor of 2.5 to 4.5 smaller than the $^7Li(d,t)^6Li$ cross section. In a true finite-range calculation the large renormalization of the DWBA calculation is no longer necessary. (auth)

**56672** NUCLEAR SPECTROSCOPIC STUDIES ON $^{18}O$. Berant, Z.; Goldberg, M. B.; Popp, M.; (and others) (Weizmann Inst. of Science, Rehovot, Israel). Nucl. Phys.; A173: No. 2, 401-13(1971).

Nuclear spectroscopic studies of $^{18}O$ were made by $\alpha$-bombardment of enriched self-supporting $Al_2{}^{18}O_3$ targets at energies between 13.5 and 17 MeV. Alpha–gamma angular correlation measurements were performed on decay transitions from levels at 3.92, 4.45, 5.09, 5.25, 5.33, 6.19, and 6.39 MeV. Spins of levels up to 5.33 MeV excitation were confirmed, and levels at 6.19 and 6.39 MeV are assigned $I^\pi = 1^-$ and $3^-$, respectively. The 1.94-MeV transition from the 3.92-MeV level and the 3.27-MeV transition from the 5.25-MeV level are found to be almost pure M1 in character. Decay branching ratios of all investigated levels were determined. (auth)

**56673** REACTION MECHANISMS OF $^{10}B(d,\alpha)^8Be_{2.9}(\alpha)^4He$ FOR $E_d$ = 0.4, 1.0, AND 1.5 MeV. Lambert, J. M.; Treado, P. A.; Haddad, D.; Moyle, R. A.; Sessler, J. C. (Georgetown Univ., Washington, D. C.). Phys. Rev. Lett.; 27: No. 12, 820-2 (20 Sep 1971).

The angular correlation of the first-emitted $\alpha$ and an $\alpha$ from the sequential decay of the $^8Be_{2.9}$ state in the reaction $^{10}B(d,\alpha)^8Be_{2.9}(\alpha)^4He$ strongly suggests that this reaction proceeds by compound-nucleus formation at $E_d$ = 0.4 MeV and by a deuteron-pickup direct interaction at $E_d$ = 1.0 and 1.5 MeV. The observed symmetry axis for the $^8Be_{2.9}$ breakup distribution in its own center of mass is compared to the momentum-transfer and recoil directions associated with various possible mechanisms and appears to provide the necessary information to select the mechanism. (auth)

**56674** $(\alpha,2\alpha)$ REACTION ON $^9Be$ AT 42.8 AND 49.2 MeV AND ON $^{16}O$ AT 49.2 AND 52.5 MeV. Guichard, A.; Chevallier, M.; Gaillard, O.; (and others) (Univ. Claude Bernard, Lyon). Phys. Rev., C; 4: No. 3, 700-3(Sep 1971).

The $(\alpha,2\alpha)$ reactions on $^9Be$ at 42.8 and 49.2 MeV and $^{16}O$ at 46.0 and 52.5 MeV have been studied in order to test the validity of the impulse approximation. The experimental data are consistent with this approximation, but the over-all agreement is much worse than in the case of the $(\alpha,2\alpha)$ reaction on $^6Li$. (auth)

**56675** STUDIES OF THE REACTION $^{12}C(\alpha p_0)^{15}N$. Zelenskaya, N. S.; Tarov, K. G.; Teplov, I. B.; Fateeva, L. N. Izv. Akad. Nauk SSSR, Ser. Fiz.; 35: No. 1, 193-8(Jan 1971). (In Russian).

Excitation functions and angular distributions of protons from the reactor $^{12}C(\alpha p_0)^{15}N$ were measured of $\alpha$-particle energies from 11.3 to 17.9 MeV. Data obtained were combined with data obtained previously for the $\alpha$-partical energy range from 16 to 26 MeV and were used for determining the cross sections as functions of energy in the range from 11.3 to 26.3 MeV. (R.V.J.)

**56676** VERIFICATION OF CERTAIN REGULARITIES OF PHOTONUCLEAR REACTIONS BY PROPERTIES OF FEYNMAN TRIANGLE DIAGRAMS. Dubovoi, E. I. Izv. Akad. Nauk SSSR, Ser. Fiz.; 35: No. 1, 199-202(Jan 1971). (In Russian).

A method of polar and triangle skeletal diagrams for elementary calculations of fine-structure peaks for heavy magic nuclei and also for a large number of light nuclei is described. Photospallation of $^{12}C$, $^{16}O$, $^{19}F$, $^{40}Ca$, and $^{208}Pb$ nuclei is analyzed. Energy behavior of the cross section for $\gamma$,n reactions and the peculiarities of cross sections in the presence of amplitudes in the triangle-type diagrams are studied. Tabulated data are given of the fine structure of the giant resonance in $^{12}C$, $^{16}O$, $^{19}F$, $^{40}Ca$, and $^{208}Pb$ in $(\gamma,n)$ reactions and absorption cross sections. The positions of the radical extrema in $^{12}C(\gamma,n)^{11}C$ and $^{16}O(\gamma,n)^{15}O$ reactions coincide completely with the fine structure of the giant resonance in $^{12}C$ and $^{16}O$. For $^{19}F$ and $^{208}Pb$ the theoretical and experimental data were in good agreement. (R.V.J.)

**56677** METHOD OF DISTORTED WAVES IN CALCULATIONS OF ANGULAR DISTRIBUTION IN THE STRIPPING PROCESS FOR $(\alpha,p)$ AND $(\alpha,d)$ REACTIONS ON CERTAIN LIGHT NUCLEI. Burymov, E. M.; Gridnev, K. A.; Karabanov, N. V. Izv. Akad. Nauk SSSR, Ser. Fiz.; 35: No. 1, 159-64(Jan 1971). (In Russian).

Experimental data on $(\alpha,p)$ and $(\alpha,d)$ reactions with light nuclei at $E_\alpha$ = 25 were analyzed by the method of distorted waves for the multinucleon stripping process. The relation of the shape of the angular distributions in the $(\alpha,p)$ and $(\alpha,d)$ reactions and the optical parameters of the incident $\alpha$ particles and transferred particles was studied. Reactions of $^{14}N(\alpha,p)^{17}O$, $^{10}B(\alpha,d)^{12}C$, and $^{14}N(\alpha,d)^{16}O$ were calculated for various radii of the $\alpha$ particles and the transferred particles at a 4-Fermi stripping radius. Theoretical and experimental angular distributions for the $(\alpha,p)$ reactions with $^{10}B$, $^{11}B$, $^{12}C$, $^{14}N$, $^{27}Al$, and $^{28}Si$ and for $(\alpha,d)$ reactions with $^{6,7}Li$, $^9Be$, $^{10}B$, $^{11}B$, $^{14}N$, $^{12}C$, and $^{13}C$ nuclei were compared. It was concluded that the distorted-wave calculations do not produce any correct results in the case of $\alpha$ reactions with light nuclei because the true mechanism of these reactions is unknown and the correctness of the optical model for $\alpha$-particle scattering by light nuclei is doubtful. (R.V.J.)

**56678** POLARIZATION OF PROTONS ELASTICALLY SCATTERED ON NUCLEI WITH A ZERO SPIN. Klyucharev, A. P.; Slabospitskii, R. P. Izv. Akad. Nauk SSSR, Ser. Fiz.; 35: No. 1, 71-80(Jan 1971). (In Russian).

Polarization effects appearing during resonance elastic scattering of protons by nuclei with a zero spin were studied. Polarization of protons as a function of their energy in elastic scattering by $^{40}Ca$ at $\theta_{cm}$ = 60°, $^{28}Si$ at $\theta_{cm}$ = 90°, $^{12}C$ at $\theta_{cm}$ = 120° and 150°, and $^{16}O$ at $\theta_{cm}$ = 100° was established. Results of the theoretical and experimental studies showed that the polarization studies produced unambiguous data for complete spin–parity assignments for the excited states of nuclei, permitted determination of the parameters of overlapping nuclear levels, and revealed a set of phase shifts which were used for reproducing the scattering matrix. (R.V.J.)

**56679** T = $^3/_2$ STATES IN $^{11}C$. Watson, B. A.; Chang, C. C.; Hasinoff, M. (Stanford Univ., Calif.). Nucl. Phys.; A173: No. 3, 634-40(1971).

The $^{11}B(\tau,t)$ $^9Be(\tau,n)$ and $^{10}B(p,p')$ reactions have been employed to investigate T = $^3/_2$ states in $^{11}C$. States are observed at 12.17 ± 0.05, 12.57 ± 0.07 and 13.92 ± 0.05 MeV excitation having widths of 250 ± 50, 350 ± 100 and 250 ± 50 keV, respectively. The strength with which these states are populated in the $^{11}B(\tau,t)$ reaction are compared to the population of the T = $^3/_2$ states in $^{11}B(\tau,\tau')$ reaction. The first two of these states in $^{11}C$ are observed to decay predominantly by proton emission to the T = 1 state in $^{10}B$ at 1.74 MeV. These states are, thus, tentatively identified as the first three T = $^3/_2$ states in $^{11}C$. (auth)

**56680** STUDY OF THE REACTION $^{14}N(n,2\alpha)^7Li$. Schmidt, Guenter; Moesner, Juergen; Schintlmeister, Josef (Zentralinstitut fuer Kernforschung, Rossendorf, Ger.). Nucl. Phys.; A173: No. 3, 449-55(1971).

The reaction $^{14}N(n,2\alpha)^7Li$ was analyzed at an energy of 14.1 MeV. A cloud chamber was employed. About 1400 events were evaluated and interpreted as decay cascades via various excited levels of $^{11}B$ or via the ground state of $^8Be$. In both cases, the $^7Li$ nucleus is produced in the ground state or the first excited state.

XUM

Branching ratios for the various types of decay are given. The measured total cross section was 58 ± 12 mb. The spin of the energy levels 9.19 MeV ($^1/_2$) and 9.277 MeV ($^5/_2$) of $^{11}$B was confirmed. (auth)

**56681** ENERGY LEVELS OF $^{16}$O IN THE REGION OF EXCITATION BETWEEN 13.5 AND 15.0 MeV. Ophel, T. R.; Martin, Ph.; Cloud, S. D.; Morris, J. M. (Australian National Univ., Canberra). Nucl. Phys.; A173: No. 3, 609-33(1971).

Measurements have been made of the $^{12}C(\alpha,\alpha_0)$, $^{12}C(\alpha,\alpha'\gamma)$ and $^{12}C(\alpha,p)$ reactions for bombarding energies between $E_\alpha$ = 8.5 and 10.5 MeV. Phase-shift analysis of the elastic scattering angular distributions and excitation functions complemented by particle and γ-ray angular distributions and Doppler-broadened profile measurements of the $^{12}C(\alpha,\alpha'\gamma)$ reaction, enabled level assignments in $^{16}$O. A complete description of the levels in the region of excitation studied was not possible because of the strong interference effects which were present. (auth)

**56682** STUDY OF $^{14}$N USING THE $^{12}C(^3He,p)^{14}N$ AND $^{12}C(^3He,2p)$–$^{13}C$(g.s.) REACTIONS. Focht, William Laurie. Philadelphia; Univ. of Pennsylvania (1970). 150p. University Microfilms Order No. 71-19,222.

Thesis.

The levels of $^{14}$N populated in the reactions $^{12}C(^3He,p)^{14}N$ and $^{12}C(^3He,2p)^{13}C$(g.s.) have been studied using a 15 MeV $He^{3+}$ beam from the University of Pennsylvania Tandem Accelerator. In the $^{12}C(^3He,p)^{14}N$ study, performed on a single-gap Browne-Beuchner magnetic spectrograph, $^{14}$N excited states up to 13 MeV excitation energy were observed. The 8.96–8.98 MeV doublet was resolved, and a new doublet was discovered at 10.06–10.10 MeV, which has previously been listed as a singlet ($1^+$) 0 level. The angular distributions of protons for $^{14}$N states between 0 and 13 MeV were measured over a range of laboratory angles of at least 10° to 60°, and were analyzed employing the DWBA computer code "JULIE" using the optical-model parameters of Mangelson. Dominant (NLSJ) values were successfully assigned, particularly to $^{14}$N states of low excitation energy. Good agreement was shown between these assignments and the dominant configurations predicted by True's shell-model analysis of $^{14}$N. In the $^{12}C(^3He,2p)$ $^{13}C$(g.s.) reaction study at 15 MeV, proton-proton events were measured in coincidence between a silicon surface-barrier detector fixed at a lab angle of 30° and any one of an array of four similar detectors placed at other angles covering the full 180° range in the $^{14*}$N intermediate state center-of-mass system. In this reaction study, the sequential mechanism (through excited states of $^{14}$N) was observed to dominate over the direct mechanism. Angular correlations corresponding to populating intermediate $^{14}$N states of 8.49, 8.91 + 8.96 + 8.98, 9.18, 9.39, 9.70, 10.06 + 10.10, 10.44, and 10.81 MeV excitation energy were measured. Two methods of predicting these angular correlations were employed. A simple "plane-wave" theory prediction of the $^{14}$N substate populations is characterized by stronger 0° and 180° peaking for higher $J_f$ values, and symmetry about 90° in the $^{14}$N center-of-mass system. A more complex "distorted-wave" theory based on the DWBA code "JULIE" analysis of the first step of the sequential reaction does not in general maintain this symmetry. A comparison of these two methods of correlation prediction was made. On the basis of the "plane-wave" theory predictions, a spin-parity assignment of $5^+$ for the 10.81 T = 0 intermediate $^{14}$N state is noted to be more likely than Mangelson's choice of $4^+$. This viewpoint is supported by the work of Zurmühle, Noé and Balamuth studying the same reaction with the first proton detected at 0°. A comparison of their results and the present work was made for several intermediate $^{14}$N states. (Diss. Abstr. Int., B)

## Nuclear Properties and Reactions, 20 ≤ A ≤ 89

*Refer also to abstracts 55040, 55089, 55704, 55828, 56368, 56421, 56643, 56650, 56651, 56655, 56659, 56665, 56676–56678, 56752, 56776, 56778, 56780, 56782, 56789, 56806, 56827, 56832, 56847, 56857, and 56868.*

**56683** (FEI–205) GAMMA-RADIATION DURING THERMAL NEUTRON CAPTURE ON CHROMIUM AND IRON ISOTOPES. Broder, D. L.; Gamalii, A. F.; Zemtsev, B. V.; Nesterov, B. V.; Kham'yapov, L. P. (Gosudarstvennyi Komitet po Ispol'zovaniyu Atomnoi Energii SSSR, Obninsk, Fiziko-Energeticheskii Institut). 1970. 29p. (In Russian). Dep. NTIS (U. S. Sales Only).

Gamma radiation resulting from thermal-neutron capture by the isotopes $^{50}$Cr, $^{52}$Cr, $^{53}$Cr, $^{54}$Fe, and $^{56}$Fe was examined by means of a Ge(Li) gamma spectrometer. The gamma line yield per 100 captured neutrons was determined for each isotope, and energy-level diagrams were prepared. The results are compared with those of other authors. (tr-auth)

**56684** (FEI–216) INTERACTION BETWEEN 14-MeV NEUTRONS AND THE NUCLEI OF IRON, COPPER, AND NIOBIUM. Sal'nikov, O. A.; Lovchikova, G. N.; Kotel'nikova, G. V.; Nesterenko, V. S.; Fetisov, N. I.; Trufanov, A. M. (Gosudarstvennyi Komitet po Ispol'zovaniyu Atomnoi Energii SSSR, Obninsk, Fiziko-Energeticheskii Institut). 1970. 49p. (In Russian). Dep. NTIS (U. S. Sales Only).

This is a study of the spectra and differential inelastic scattering cross sections of neutrons as well as of (n,2n) reactions on nuclei of Fe, Cu, and Nb in the presence of initial neutron energies amounting to 14.4 MeV. The differential cross sections were measured at angles of 30 to 150° through every 30°. The measurements were performed by the method of transit time in cylindrical geometry. A correction for multiple scattering of neutrons in the specimen, calculated by the Monte Carlo method, was introduced. In this study the differential inelastic scattering cross sections of neutrons as well as the differential cross-sections of the (n,2n) reaction are derived, as are the spectra of sound neutrons for this reaction. The nuclear-level density parameters are calculated taking the nucleus model to be a Fermi gas with allowance for residual interaction in the form of vaporization energy, and the contribution of direct processes to the inelastic scattering cross section in the presence of that energy is estimated. The findings are compared with the data of other studies, praticularly studies of the nuclear-level density parameter by other methods. It is established that a Fermi gas model allowing for residual interaction makes it possible to calculate with sufficient accuracy the nuclear-level density parameter. (JPRS)

**56685** (FRNC-TH–48) STUDY OF NUCLEAR REACTIONS INDUCED BY ALPHA PARTICLES WITH ENERGIES BETWEEN 70 AND 160 MeV IN VARIOUS LIGHT NUCLEI, PARTICULARLY ALUMINUM AND SILICON. POSSIBILITY OF A FISSION MECHANISM. Tirard, Michele (Paris Univ., Orsay (France). Faculte des Sciences). 1971. 101p. (In French). Dep. NTIS (U. S. Sales Only).

Thesis.

Al and Si targets were bombarded with α particles with energies between 70 and 160 MeV. Measurements were made on the formation of some nearly stable nuclei and others deficient in neutrons ($^7$Be, $^{11}$C, $^{13}$N, $^{15}$O, $^{18}$F). At 160 MeV the cross sections for the formation of the highly neutron enriched nuclei $^9$Li, $^{16}$C and $^{17}$N, detected by their delayed neutron emission, were determined. In order to explain these results, the usual mechanisms involved in spallation reactions are considered. The simple case is envisaged, in which the compound nuclei formed ($^{31}$P or $^{32}$S) de-excite emitting a neutron, proton, deuteron, triton, $^3$He, or alpha particles, and leave at the end of the evaporation chain, a residual cold nucleus. This process was studied using a computer and the Monte Carlo method with the EVA 67 program. A comparison between the calculated results and the experimental results demonstrated that the formation of certain nuclei might be difficult to explain by the de-excitation by particle evaporation process; the fission mechanism is envisaged as the reaction process. Applications of this experimental study to activation analysis and astrophysics are presented. (France)

**56686** (JINR–P3-5875) SEARCH FOR THE (n,α) REACTION IN THE RESONANCES OF THE ZINC AND HAFNIUM ISOTOPES. Popov, Yu. P.; Semenov, V. G.; Florek, M. (Joint Inst. for Nuclear Research, Dubna (USSR). Lab. of Neutron Physics). Jul 1971. 11p. (In Russian). Dep. NTIS (U. S. Sales Only).

The results of the search for the (n,α) reactions in the nuclei-targets $^{64}$Zn, $^{67}$Zn and $^{177}$Hf are presented. The α-decay is observed in the resonance states appearing in the capture of neutrons with the energies 281 and 2637 eV by $^{64}$Zn nuclei, with the energy 1548 eV by $^{67}$Zn nuclei and with the energies 1.09; 2.38; 5.89; 6.57; 8.87 eV by $^{177}$Hf nuclei. The α-widths ($\Gamma_\alpha$) of the mentioned levels are given. (auth)

**56687** (KFK–1397) INVESTIGATION OF THE DEFORMATION OF LIGHT NUCLEI WITH THE HELP OF SCATTERING OF 104-MeV ALPHA PARTICLES. Rebel, H. (Kernforschungszentrum, Karlsruhe (West Germany). Zyklotron-Laboratorium). Apr 1971. 78p. (In German). Dep. NTIS (U. S. Sales Only).

The differential cross sections for the elastic and inelastic scattering of 104-MeV α-particles from low-lying states of $^{20}$Ne, $^{22}$Ne, $^{24}$Mg, $^{26}$Mg and $^{28}$Si are measured. The experimental results are analyzed in terms of coupled channels on the basis of the rotational model. The method and formalism of the analysis are

described in detail. The sensitivity of the analyzing technique for magnitude and sign of possible hexadecapole deformation are studied. The results show a systematic trend of the $\beta_4$ deformation parameter through the region A = 20–28 and confirm the oblate shape of $^{28}$Si known from reorientation measurements. The $(\alpha,\alpha')$-scattering results are compared to results of other experimental and theoretical investigations. (auth)

**56688** (LYCEN–7104, S6,1-2) REACTIONS PERFORMED WITH POLARIZED PROTONS AT SACLAY. Thirion, J. (Commissariat a l'Energie Atomique, Saclay (France). Centre d'Etudes Nucleaires). (In French).

From Conference on some microscopic aspects of nuclear reactions; La Toussuire, France (15 Feb 1971).

The experimental aspects of the reactions performed at Saclay with polarized protons are described (beams, injection, acceleration). The reactions actually studied or planned are mentioned. (France)

**56689** (RLO–1062-711) LOW ENERGY NUCLEAR RESEARCH. Final Report. Schecter, Larry (Oregon State Univ., Corvallis. Dept. of Physics). Jul 1971. Contract AT(45-1)-1062. 45p. Dep. NTIS.

Research progress in nuclear spectroscopy and nuclear interactions at Oregon State University for the contract period ending July 1971 is briefly reported. (J.W.R.)

**56690** (RT/FI–(70)47) METHOD OF ANALYSIS OF NEUTRON CAPTURE GAMMA-RAY SPECTRA. Fubini, A.; Napoli, A.; Prosperi, D.; Terrasi, F. (Comitato Nazionale per l'Energia Nucleare, Rome (Italy)). 19 Nov 1970. 28p. Dep. NTIS (U. S. Sales Only).

The method used to calibrate the neutron capture gamma-ray spectra of a Ge(Li) detector is described in detail. The procedure used to obtain from the gamma-ray energy a decay scheme is reported. The method is applied to the $^{35}$Cl(n, $\gamma$) reaction. (auth)

**56691** MEASUREMENT OF THE THERMAL NEUTRON CAPTURE CROSS SECTION AND RESONANCE CAPTURE CROSS SECTION OF $^{80}$Kr. Bradley, James Garrison. Minneapolis; Univ. of Minnesota (1970). 66p. University Microfilms Order No. 71-18,691.

Thesis.

The thermal neutron capture cross section and resonance capture cross section of krypton-80 were measured by mass spectroscopy methods. A tandem double focusing mass spectrometer of high abundance sensitivity was used to measure the $^{81}$Kr/$^{80}$Kr isotopic ratios produced in thermal neutron irradiations of about $10^{19}$ neutrons/cm$^2$. One krypton sample was irradiated uncovered and one sample was irradiated inside a cylindrical cadmium cover with 0.020 inch thick walls. The reactor flux reaching the sample was monitored during each irradiation with National Bureau of Standards aluminum-1% cobalt wire. The resulting cobalt-20 activities were determined by the Nuclear Science Group at the University of Missouri reactor facility used for the irradiations. Three measurements of the uncovered sample isotopic ratio yielded a mean value of $^{81}$Kr/$^{80}$Kr = $146.2 \times 10^{-6}$ with a range of 2% in the three measurements. Three measurements of the cadmium covered sample isotopic ratio yielded a mean value of $^{81}$Kr/$^{80}$Kr = $16.0 \times 10^{-6}$ with a range of 4% in the three measurements. From the spectrometer measurements and the flux monitor cobalt-60 activities, it is deduced that the 2200 m/s neutron cross section for $^{80}$Kr(n,$\gamma$)$^{81}$Kr is $g\sigma_0 = 11.5 \pm 0.6$ barns and $s_0/g = 5.04 \pm 0.40$ with respect to $\sigma_0 = 37.2$ barns and $s_0 = 1.77$ for cobalt. The 0.5 eV epicadmium resonance absorption integral for krypton-80 is deduced to be $56.6 \pm 4.5$ barns with respect to 75 barns for cobalt. (Diss. Abstr. Int., B)

**56692** PARTICLE–GAMMA ANGULAR CORRELATIONS IN THE $^{50}$Cr($^3$He,$\alpha\gamma$)$^{49}$Cr REACTION. Blumenthal, David Alan. Philadelphia; Univ. of Pennsylvania (1970). 116p. University Microfilms Order No. 71-19,204.

Thesis.

Alpha-gamma angular correlations have been measured in the $^{50}$Cr($^3$He,$\alpha\gamma$)$^{49}$Cr reaction to study excited levels in $^{49}$Cr. A $^{50}$Cr target of 200 $\mu$g/cm$^2$ was bombarded with 15 MeV $^3$He$^{++}$ ions from the University of Pennsylvania Tandem Accelerator. The emerging $\alpha$ particles were detected at 0° using a position sensitive detector located in the focal plane of a double focusing magnetic spectrometer. Coincident $\gamma$-rays were detected at four angles simultaneously using 7.6 cm × 10.2 cm NaI(Tl) crystals. The angular distributions of the $\alpha$ particles from the $^{50}$Cr($^3$He,$\alpha$)$^{49}$Cr reaction were measured using the University of Pennsylvania multi-angle magnetic spectrograph. l-values extracted from these measurements were used together with the alpha-gamma correlation measurements to determine the spins and parities of excited levels. The results are: 0.27 MeV $^1/_2^-$, 1.07 MeV ($^5/_2^-$, $^9/_2^-$), 1.57 MeV($^5/_2^-$,$^7/_2^-$,$^{11}/_2^-$), 1.71 MeV ($^1/_2^-$,$^3/_2^-$), 1.74 MeV $^3/_2^-$, 1.98 MeV $^3/_2^+$, 2.43 MeV $^5/_2^-$, 2.58 MeV $^1/_2^+$, 2.61 MeV $^3/_2^-$, 3.24 MeV $^5/_2^-$, 3.51 MeV ($^5/_2^-$,$^7/_2^-$), 3.93 MeV $^1/_2^-$, 4.76 MeV $^7/_2^-$, 6.43 MeV $^1/_2^+$, 6.47 MeV $^1/_2^+$, 6.76 MeV $^1/_2^+$. Branching ratios of the decay $\gamma$ radiations are presented along with multipole mixing ratios for the stronger transitions. (Diss. Abstr. Int., B)

**56693** K = $^3/_2^+$ ROTATIONAL BAND IN $^{45}$Ti. Blasi, P. (Max-Planck-Institut fuer Kernphysik, Heidelberg); Morando, M.; Maurenzig, P. R.; Taccetti, N. Lett. Nuovo Cim.; 2: No. 2, 63-7 (10 Jul 1971).

Internal conversion coefficients for some transitions in $^{45}$Ti were determined from a study of the $\gamma$ and conversion electron spectra following the $^{45}$Sc(p,n$\gamma$) reaction at proton energies of 3.5 to 5.5 MeV. Lifetimes and transition probabilities for the same levels were determined from a recoil distance study of the $^{31}$P($^{16}$O,pn$\gamma$) reaction at 34 and 36 MeV. The data support the existence of a K = $^3/_2^+$ rotational band in $^{45}$Ti. (J.W.R.)

**56694** ANALYSIS OF PROTON SCATTERING ON $^{32}$S. Berinde, A.; Neamu, I.; Vladuca, G. (Inst. of Atomic Physics, Bucharest). Rev. Roum. Phys.; 16: No. 3, 341-8(1971).

The competition of the direct interaction and of the compound nucleus mechanism in the $p_0$ and $p_1$ angular distributions on $^{32}$S is analyzed in the energy range $E_p = 5.05$ to 14.00 MeV. The direct interaction contribution was calculated for elastic and inelastic distributions in terms of the optical model and DWBA, respectively. The compound nucleus component was calculated in terms of Hauser–Feshbach theory, with fluctuation correction included. All the disintegration channels of the compound nucleus were taken into account; at the energies of 11.00 and 14.00 MeV, the Gilbert–Cameron level density formula was also used. A good agreement between theory and experimental data was obtained using Perey's average optical parameters for a theoretical estimation of both mechanisms. (auth)

**56695** CALCULATION PROGRAM FOR DETERMINATION OF HALF-LIVES AND INTENSITIES OF TOTAL DECAY CURVES OF RADIOACTIVITY. Karlik, B. Oesterr. Akad. Wiss., Math.-Naturwiss. Kl., Anz.; No. 3, 1-7(1968). (In German).

A computer program in Fortran II-D for the IBM-1620 for the determination of the half-lives and intensity of total decay curves is described. The program is applicable to all decays with interferring reactions. The program was tested on half-life determination of $^{79m}$Br, $^{89m}$Y, $^{197m}$Au, $^{20}$F, and $^{11}$Be. (J.S.R.)

**56696** MEASUREMENT OF SOME CAPTURE CROSS SECTIONS FOR FAST NEUTRONS. Karlik, B. Oesterr. Akad. Wiss., Math.-Naturwiss. Kl., Anz.; No. 10, 1-6(1968). (In German).

At a neutron energy of $2.9 \pm 0.2$ MeV, the following (n,$\gamma$) effective cross sections were determined: $^{26}$Mg (n,$\gamma$) = $0.21 \pm 0.03$ mb; $^{27}$Al (n,$\gamma$) = $0.30 \pm 0.05$ mb; $^{37}$Cl (n,$\gamma$) = $0.59 \pm 0.09$ mb; $^{51}$V (n,$\gamma$) = $1.4 \pm 0.2$ mb; $^{55}$Mn (n,$\gamma$) = $2.2 \pm 0.2$ mb; $^{65}$Cu (n,$\gamma$) = $6.2 \pm 0.8$ mb; $^{68}$Zn (n,$\gamma$) = $2.6 \pm 0.4$ mb; $^{75}$As (n,$\gamma$) = $14.0 \pm 1.4$ mb; $^{115}$In (n,$\gamma$) = $68 \pm 11$ mb; $^{127}$I (n,$\gamma$) = $42.8 \pm 5.0$ mb; $^{138}$Ba (n,$\gamma$) = $3.0 \pm 0.4$ mb. All effective cross section measurements were made by the activation method relative to the cross section $\sigma^{115}$/n(n,n'$\gamma$)$^{115}$m/n = 360 mb. Various materials were investigated on their suitability as deuterium self-targets for the production of fast neutrons. (tr-auth)

**56697** DECAY OF $^{84}$Rb AND THE FLUORESCENCE YIELD OF KRYPTON. Gehrling, Volker; Hammer, J. Wolfgang; Hoffmann, Klaus-Werner (Univ., Stuttgart). Z. Phys.; 246: No. 5, 376-82(1971). (In German).

The electron-capture decay and the positron decay of $^{84}$Rb were investigated using NaI(Tl) detectors and a Ge(Li) detector. Measurements of all intensities and of some informative double and triple coincidences were performed. From coincidence measurements between K X radiation and the subsequent $\gamma$ radiation the K-fluorescence yield of krypton was found to be $\omega_K = 0.653 \pm 0.004$. Consideration of former measurements [Grotheer et al., Z. Phys., 225: 293(1969)] indicates a continuous behaviour of $\omega_K$ (Z) for Z = 36, 37, and 38 within an uncertainty of 1%. Branching ratios of the decay of $^{84}$Rb were obtained. The half-life of $^{84}$Rb was determined to be $T_{\frac{1}{2}} = (34.5 \pm 0.2)$d. (auth)

**56698** ENERGY LEVELS OF $^{79}$Br AND $^{81}$Br. Barnard, E.; de Villiers, J. A. M.; Coetzee, N.; Reitmann, D.; van der Merwe, P. (Atomic Energy Board, Pretoria). Z. Phys.; 246: No. 5, 424-30(1971).

XUM

The low-lying energy-level and decay schemes of the stable bromine isotopes were studied by observing the γ rays from the (n,n'γ) reactions in a natural bromine sample with the aid of a Ge(Li) detector. A pulsed neutron source and time-of-flight methods were used to reduce background due to neutron events in the detector. Most of the γ rays observed could be assigned to transitions in either $^{79}$Br or $^{81}$Br. In addition to those levels previously known from γ-decay or Coulomb-excitation experiments, several new levels were excited in each isotope. (auth)

**56699** NUCLEON DENSITY DISTRIBUTION IN NUCLEI $^{54,56}$Fe. Shilyaev, B. A.; Shlyakhov, N. A.; Golavnya, B. Ya.; (and others) (Physical-Technical Inst., Kazan). Yadern. Fiz.; 13: No. 5, 918-22(May 1971). (In Russian).

Angular distributions of elastically scattered protons with energy of 9.6 MeV were measured on $^{54}$Fe and $^{56}$Fe, and were analyzed by means of the modified optical model. Values of the r.m.s. radii of the nuclear matter distribution are obtained from the analysis of the data. (auth)

**56700** DETERMINATION OF ANGULAR CORRELATIONS AND MEAN LIFETIMES IN $^{57}$Co. Dayras, R.; Toulemonde, M.; Cujec, B.; (and others) (Laval Univ., Quebec). Nucl. Phys.; A173: No. 1, 49-72(1971). (In French).

The reaction $^{54}$Fe(α,p)$^{57}$Co at 9.86, 10.02 and 10.40 MeV incident energies was used to measure the proton-gamma angular correlations in the Litherland–Ferguson geometry and to measure the mean lifetimes by the Doppler-shift attenuation method. The mixing ratios have been obtained for levels at 1.897, 2.134, 2.311 and 2.879 MeV. The mean lifetimes have been determined for 14 levels up to 2.9 MeV. The spins have been unambiguously assigned to all levels up to 2.311 MeV and to the 2.879($\frac{3}{2}^-$) and 2.981($\frac{1}{2}^+$) MeV levels. The partial radiative widths have been determined for all levels, except 1.505 MeV, up to 2.311 MeV. (auth)

**56701** ELASTIC SCATTERING OF 60 TO 120 MeV ELECTRONS FROM $^{46,48,50}$Ti. Romberg, E. F. (Univ. of Maryland, College Park); Wall, N. S.; Blum, D.; Lightbody, J. W. Jr.; Penner, S. Nucl. Phys.; A173: No. 1, 124-8(1971).

The elastic electron scattering from the isotopes of $^{46,48,50}$Ti has been measured at an angle of 127.5°. The ratios of the cross sections were analyzed with a partial-wave analysis for a Fermi-shaped charge distribution and the parameter variations were deduced. Some consequences of these results are discussed. (auth)

**56702** THRESHOLD PHOTONEUTRON CROSS SECTIONS FOR MEDIUM AND HEAVY NUCLEI. Baglan, Robert Joseph. Berkeley, Calif.; Univ. of California (1970). 142p. University Microfilms Order No. 71-15,710.

Thesis.

The following (γ,n) cross sections were measured with very high resolution in the energy range from threshold to ~1 MeV above threshold: $^{25}$Mg, $^{52,53}$Cr, $^{56,57}$Fe, and $^{206,207,208}$Pb. Many individual compound nucleus resonances were resolved and area analyzed to give $\Gamma_{\gamma 0}$, from which El-strength functions, $\langle\Gamma_{\gamma 0}/D\rangle$, were obtained. In addition, the cross sections were investigated for the occurrence of three distinct nuclear phenomenon: (1) nonresonant neutron capture; (2) doorway states; and (3) analog states. Nonresonant neutron-capture cross sections of 0.5 mb/sr for $^{207}$Pb, and 4.2 μb/sr for $^{56}$Fe were determined by measuring the asymmetry of resonances. In $^{207}$Pb, additional evidence, in the form of an envelope of γ-ray widths, was found for the previously reported $\frac{1}{2}^+$ doorway state at 500 keV. A correlation analysis for the γ-ray and neutron widths of the fine structure of the doorway state determined its ground-state γ-ray width to be 36.5 eV. Evidence was found for a $\frac{3}{2}^+$ doorway state near 125 keV in $^{207}$Pb. The analogs of the ground and first excited states of $^{25}$Na were seen in $^{25}$Mg and the following lower limits were determined for their $\Gamma_n$'s: 0.25 and 1.8 eV, respectively. Five analog states of $^{56}$Mn may have been excited in $^{56}$Fe, and lower limits for their $\Gamma_{\gamma 0}$'s were determined. (Diss. Abstr. Int., B)

**56703** SEARCH FOR GAMMA-RAY EMISSION FROM UNBOUND PARTICLE STATES IN $^{87}$K AND THE DECAY SCHEME OF $^{87}$Kr TO LEVELS IN $^{87}$Rb. Shihab-Eldin, Adnan Ahmed. Berkeley, Calif.; Univ. of California (1970). 246p. University Microfilms Order No. 71-15,883.

Thesis.

A chemical system was built for the rapid separation of bromine isotopes from fission products. Bromine sources with varying $^{86}$Br/$^{87}$Br yield ratios were prepared and studied with a Ge(Li) γ-ray spectrometer. The stripping of the resulting composite γ-ray spectra to $^{86}$Br and $^{87}$Br yield ratios was partially successful. Out of a total of 316 γ-ray lines found in these composite γ-ray spectra, 13 γ-ray lines had energies above 5.5 MeV, which is the neutron binding energy in $^{87}$Kr. Three of these high-energy γ-ray lines were tentatively assigned to the decay of $^{87}$Br. The significance of the presence of such high-energy γ-ray transitions in $^{87}$Kr in competition with delayed neutron competition is discussed and compared to the predictions of a "semi-theoretical" approach to delayed neutron emission. As a preliminary work, the gamma-ray transitions following β-decay of 78-minute $^{87}$Kr have been studied with Ge(Li) spectrometers. Thirty-three transitions between levels in $^{87}$Rb have been observed and γ–γ coincidence relations have been obtained for the prominent lines. A level scheme is presented that incorporates 28 of these transitions between thirteen levels in $^{87}$Rb. The level scheme is qualitatively interpreted according to the predictions of a simple weak-coupling model for excited states in $^{87}$Rb. Also, the results from an exact diagonalization of the seniority-one pairing force Hamiltonian matrix are compared with the proposed experimental single-particle energy levels in $^{87}$Rb and $^{89}$Y. (Diss. Abstr. Int., B)

**56704** STUDY OF THE ISOTOPES OF NEON WITH PROTON REACTIONS AT 40 MeV. Madland, David George. Minneapolis; Univ. of Minnesota (1970). 180p. University Microfilms Order No. 71-18,772.

Thesis.

The (p,p), (p,p'), and (p,d) reactions on the isotopes of neon have been studied with 40-MeV protons produced by the University of Minnesota Linear Accelerator. Differential scattering cross sections are presented for the elastic scattering by $^{20}$Ne and $^{22}$Ne, for the inelastic scattering by $^{20}$Ne, $^{21}$Ne, and $^{22}$Ne, and for the (p,d) reaction leading to states in $^{19}$Ne, $^{20}$Ne, and $^{21}$Ne. The elastic data has been analyzed in terms of the regular optical-model. The resultant optical potentials are utilized in both DWBA and coupled-channels analysis of the inelastic data, and in a DWBA analysis of the (p,d) reactions. Particular emphasis has been placed on the inelastic transitions within the ground state rotational bands of $^{20}$Ne and $^{22}$Ne. Permanent quadrupole ($\beta_2$) and hexadecapole ($\beta_4$) deformations in the intrinsic ground states are found necessary to reproduce the data in a collective form factor, coupled-channels, analysis. The data is sensitive to the signs as well as the magnitudes of the deformations. The values of the deformations are: $\beta_2(^{20}\text{Ne}) = 0.42 \pm 0.5$, $\beta_4(^{20}\text{Ne}) = 0.22 \pm 0.5$, $\beta_2(^{22}\text{Ne}) = 0.44 \pm .05$, and $\beta_4(^{22}\text{Ne}) = 0.08 \pm .05$, all with positive signs. The present determinations together with others in the (2s-1d) shell indicates the $\beta_2$ and $\beta_4$ deformations to be changing in a fashion not dissimilar to those in the heavy deformed region. A DWBA analysis is found inadequate because of the existence of multiple step processes and because the collective form factor is treated only to first order in the deformations. Spectroscopic factors have been extracted from a DWBA analysis of the observed transitions in the (p,d) reactions. The experimental spectroscopic factors are compared with those obtained from a Nilsson type calculation in the strong coupling collective model. The calculations utilized a deformed Woods–Saxon potential characterized by quadrupole deformations obtained from the inelastic scattering analysis. The results have shown that the measured spectroscopic factors are not inconsistent with the measured quadrupole deformations. Further interpretations are limited by the uncertainties associated with DWBA extracted spectroscopic factors. (Diss. Abstr. Int., B)

**56705** PHOTON ASYMMETRY FOR RADIATIVE μ CAPTURE IN CALCIUM. DiLella, L.; Hammerman, I.; Rosenstein, L. M. (Columbia Univ., New York). Phys. Rev. Lett.; 27: No. 12, 830-3(20 Sep 1971).

The photon asymmetry parameter for radiative μ capture in $^{40}$Ca was measured for photon energies from 57 to 75 MeV. The result obtained seems inconsistent with predictions based on the V–A theory. (auth)

**56706** SEPARATION ENERGY FOR SOME INTERMEDIATE-MASS NUCLEI IN THE (p,2p) REACTIONS AT 600 MeV. Landaud, G.; Yonnet, J.; Kullander, S.; (and others) (CERN, Geneva). Nucl. Phys.; A173: No. 2, 337-56(1971). (In French).

The separation-energy spectra obtained in a 600-MeV (p,2p) experiment are presented for the nuclei $^{12}$C, $^{28}$Si, $^{40}$Ca, $^{51}$V, and $^{90}$Zr. The structure above 25 MeV separation energy is assumed to originate from the 1p and 1s shells. The momentum distributions of the residual nuclei are used to separate a peak characteristic for the 1s shell from the rest of the spectrum. This peak lies at 35 MeV for $^{12}$C and at around 50 MeV for the other nuclei. (auth)

**56707** SCATTERING OF 14-MeV NEUTRONS BY IRON. Gurtovoi, M. E.; Kadkin, E. P.; Kukhlenko, A. C.; (and others). At. Energ. (USSR); 30: No. 5, 455-6(May 1971). (In Russian).

Inelastic neutron scattering to the excited state of $^{56}$Fe at 0.85 MeV was studied using a time-of-flight spectrometer with pulsed neutrons, generated by the reaction T(d,n)$^4$He. The data obtained

XUM

show that a vibrating model satisfactorily describes the cross sections of elastic and inelastic neutron scattering by $^{56}$Fe nuclei. A deformation parameter $\beta_2$ was estimated to be 0.21 ± 0.03, in agreement with the results of other investigators. (K.S.W.)

**56708** INTERNAL-CONVERSION COEFFICIENTS IN THE DECAY OF $^{83m}$Kr. Ruby, S. L.; Clark, R. G.; Glendenin, L. E. (Argonne National Lab., Ill.). Phys. Lett.; 36A: No. 4, 321-2 (13 Sep 1971).

The radiations from the decay of $^{83m}$Kr were measured with a high-resolution Si(Li) detector. The results are $T_{\frac{1}{2}}(^{83m}Kr)$ = 1.83 ± 0.02h, $E_{32}$ = 32.16 ± 0.02 keV, $E_9$ = 9.40 ± 0.02 keV, $\alpha_T(9)$ = 17.5 ± 1.4, and $\alpha_K(32)$ = 454 ± 15. (auth)

**56709** INVESTIGATION OF THE $^{27}$Al(d,p)$^{28}$Al REACTION AT $E_d$ = 12 MeV. Carola, T. P. G.; Van der Baan, J. G. (Rijksuniversteit, Utrecht). Nucl. Phys.; A173: No. 2, 414-26(1971).

The $^{27}$Al(d,p)$^{28}$Al reaction was investigated with a split-pole magnetic spectrograph at a bombarding energy of 12 MeV. The angular distributions of 41 proton groups were measured. One new state was found in $^{28}$Al at an excitation energy of 3762 ± 5 keV. Absolute spectroscopic factors were determined by DWBA analysis. Some new $l_n$ values are reported. The results are discussed within the framework of the shell model, and comparison is made with recent many-particle calculations. (auth)

**56710** DECAY OF $^{58}$Mn. Dyer, N. C.; Hamilton, J. H. (Vanderbilt Univ., Nashville). Nucl. Phys.; A173: No. 2, 393-400 (1971).

Gamma-ray singles spectra in the decay of $^{58}$Mn to $^{58}$Fe were measured with a Ge(Li) detector. Beta groups of 3.8 ± 0.1 (63.5%/decay) and 5.9 ± 0.1 (11.5%/decay) MeV were measured with a plastic scintillator. Sixteen γ transitions were observed, 10 for the first time. Twelve were fitted into levels (in keV) at 810.73, $2^+$; 1674.71, $2^+$; 2134.0, $3^+$; 2600.7; 3399.7; 3442.9; and 3634, $2^+$. The half-life was found to be 65.3 ± 0.7 s. (auth)

**56711** (p,2p) REACTIONS AT 600 MeV AND THE DISTORTED-WAVE IMPULSE APPROXIMATION. Kullander, S.; Lemeilleur, F.; Renberg, P. U.; (and others) (CERN, Geneva). Nucl. Phys.; A173: No. 2, 357-82(1971).

The summed-energy spectra obtained in a 600-MeV (p,2p) experiment on $^{12}$C, $^{28}$Si, and $^{40}$Ca were analyzed so that a large amount of the information from a nonsymmetric coplanar experiment is utilized. The experimental cross section is integrated over a selected interval in the summed-energy spectrum and presented as a function of the polar angle, $\theta_R$, and of the momentum, $p_R$, of the residual nucleus. By comparing the distributions of the experimental cross sections to $p_R$ and $\theta_R$ distributions calculated in the distorted-wave impulse approximation (DWIA), information is obtained on distortion effects and on rms radii for the various shell-model states contained in the summed-energy spectra. The DWIA calculations reproduce quite well the experimental distributions for the outer shells, while for the 1s shell in $^{28}$Si and $^{40}$Ca values of the proton occupation numbers that are too large are found. (auth)

**56712** ANGULAR CORRELATION STUDIES IN $^{32}$S($^3$He,pγ)$^{34}$Cl. DeLuca, P. M.; Lawson, J. C.; Berners, E. D.; Chagnon, P. R. (Univ. of Notre Dame, Ind.). Nucl. Phys.; A173: No. 2, 307-20 (1971).

The levels of $^{34}$Cl were investigated by means of the $^{32}$S($^3$He,pγ) reaction at 8 to 9 MeV bombarding energy. Ge(Li) detectors were employed to determine these excitation energies: 146.4 ± 0.3, 461.0 ± 0.1, 665.6 ± 0.1, 1230.3 ± 0.2, 1887.7 ± 0.9, 2158.6 ± 0.4, 2181.5 ± 0.8, 2376.5 ± 0.5, and 2721.7 ± 0.8 keV. In an axially symmetric geometry, p−γ angular correlations were measured for most levels below 3.2 MeV in excitation. All previous spin assignments are confirmed, and new assignments of J = 1 to the 2581 keV and 3126 keV levels and J = 2 to the 2722 keV levels are made. From the p−γ coincidence data, branching ratios are deduced. Multipole mixing ratios, determined from the correlation analysis, are compared with those predicted by a recent calculation based upon the shell model. (auth)

**56713** $^{28}$Si($^6$He,2p) AND $^{12}$C($^6$He,2p) REACTIONS AT 40 MeV. Stupin, D. M. (Univ. of Colorado, Boulder); Ristinen, R. A.; Schwandt, P. Nucl. Phys.; A173: No. 2, 286-306(1971).

Kinematically complete two-detector coincidence experiments were performed in which the angular distributions of the cross sections and the proton−proton relative energy distributions of the triple differential cross sections $d^3\sigma/d\Omega_1 d\Omega_2 dT_1$ were measured for $^{12}$C($^3$He,2p) and $^{28}$Si($^3$He,2p) reactions. Five states in $^{29}$Si and two states in $^{13}$C were studied at an incident $^3$He energy of 40 MeV. Angular distributions for the ($^3$He,2p) cross sections are compared to corresponding measurements for ($^3$He,d) reactions and to angular distributions predicted by distorted-wave calculations. The shapes of the ($^3$He,2p) and ($^3$He,d) distributions are similar, and distorted-wave calculations that use deuteron-like optical potentials for the 2p cluster are reasonable representations of the ($^3$He,2p) data. Enhancements in the measured cross sections due to final-state proton−proton interactions were also observed. (auth)

**56714** IS THE FIRST EXCITED $0^+$ STATE IN $^{44}$Ca of 6p-2h CHARACTER? Fortune, H. T.; Powers, J. R. (Univ. of Pennsylvania, Philadelphia). Phys. Rev., C; 4: No. 3, 776-8(Sep 1971).

The $^{40}$Ar($^6$Li,d) reaction has been used to investigate the structure of the low-lying states of $^{44}$Ca. Cross sections are small (a few μb/sr) but angular-distribution shapes are consistent with a direct process. The results suggest considerable mixing between low-lying four-particle and six-particle−two-hole states in $^{44}$Ca. (auth)

**56715** $^{31}$P($^3$He,pγ)$^{33}$S AND $^{39}$K($^3$He,pγ)$^{41}$Ca REACTIONS AND THE γ DECAY OF ANALOG STATES IN $^{33}$S AND $^{41}$Ca. Knoepfle, K. T. (Max-Planck-Institut fuer Kernphysik, Heidelberg. Kernforschungsanlage, Juelich, Ger.); Rogge, M.; Mayer-Boericke, C.; (and others). Phys. Rev., C; 4: No. 3, 818-35(Sep 1971).

Proton-γ-ray coincidence measurements have been made on the reactions $^{31}$P($^3$He,pγ)$^{33}$S and $^{39}$K($^3$He,pγ)$^{41}$Ca at incident $^3$He energies of 12 and 13 MeV. The protons were detected at 0° to the beam direction, thereby preferentially selecting L = 0 transfers of neutron−proton pairs. A Ge(Li) detector at 90° detected the γ rays with good energy resolution. Angular distributions for the $^{31}$P($^3$He,p)$^{33}$S reaction were measured with a magnetic spectrograph. These, together with previous results on the $^{39}$K($^3$He,p)$^{41}$Ca reaction, gave precise information on the intensities of the states excited, as well as their energies. The main purpose of the experiments was to measure the γ decay of the lowest-lying isobaric analog states in $^{33}$S and $^{41}$Ca. The analog state in $^{33}$S was found to decay primarily (85%) to the 842-keV level and secondarily (15%) to the ground state. The analog state in $^{41}$Ca decays in a more complex fashion to several states. The strongest transition (55%) is to the 4091-keV state. γ-ray decay schemes for several other low-lying even-parity levels in $^{33}$S and $^{41}$Ca were also measured. The observation that the 4091-keV level of $^{41}$Ca decays (34%) to the $\frac{7}{2}^-$ ground state and (58%) to the $\frac{3}{2}^+$ level at 2009 keV suggests a $\frac{5}{2}^+$ assignment. The implications of the measurements are discussed, particularly with reference to the structure of low-lying two-particle−one-hole states in these nuclei. (auth)

**56716** SPIN ASSIGNMENTS IN $^{20}$F. Fortune, H. T.; Garrett, J. D.; Powers, J. R.; Middleton, R. (Univ. of Pennsylvania, Philadelphia). Phys. Rev., C; 4: No. 3, 850-4(Sep 1971).

Comparison of the results of the $^{18}$O($^3$He,p), $^{19}$F(d,p), and $^{22}$Ne(d,α) reactions leads to an assignment of $J^\pi = 1^+$ for the state at $E_x$ = 3.489 MeV in $^{20}$F. These results, together with previous information, lead to the identification of the 3.531-MeV state as the only $0^+$ state predicted below 6 MeV. Recent information for the low-lying levels of $^{20}$F is reviewed and compared with predictions of recent shell-model calculations. (auth)

**56717** REACTIONS OF $^{20}$Ne WITH 14.3-MeV NEUTRONS. Kardonsky, Stanley; Finston, Harmon L.; Williams, Evan T. (Brooklyn Coll.). Phys. Rev., C; 4: No. 3, 846-50(Sep 1971).

Energy levels in $^{17}$O and $^{20}$F have been observed in the $^{20}$Ne(n,α) and $^{20}$Ne(n,p) reactions using a gridded ionization chamber. In the reaction $^{20}$Ne(n,α)$^{17}$O, cross sections to the ground state and four excited states in $^{17}$O at 0.83, 3.18, 3.90, and 4.63 MeV were determined to be 6.6 ± 2.5, 1.0 ± 0.4, 1.5 ± 0.4, 2.0 ± 0.4, and 1.3 ± 0.3 mb, respectively. The total cross section for the $^{20}$Ne(n,α) reaction is 12.4 ± 4 mb. The $^{20}$Ne(n,2α)$^{13}$C reaction was observed and the Q value and cross section to the ground state of $^{13}$C were found to be −7.00 ± 0.02 MeV and 41.8 ± 8.1 mb, respectively. (auth)

**56718** $^{40}$Ar(n,α)$^{37}$S REACTION AT 14.4 MeV. Kardonsky, Stanley; Finston, Harmon L.; Williams, Evan T. (Brooklyn Coll.). Contract AT(30-1)-3417. Phys. Rev., C; 4: No. 3, 840-6(Sep 1971).

A gridded ionization chamber was used to detect charged particles produced when $^{40}$Ar was bombarded with 14.4-MeV neutrons. The energies of the α particles so produced yielded levels in $^{37}$S of 0.59 ± 0.10, 1.39 ± 0.09, 2.20 ± 0.05, and 2.83 ± 0.09 MeV. The Q value for the $^{40}$Ar(n,α)$^{37}$S reaction was determined to be −2.41 MeV. Cross sections calculated for the reaction to the ground state and the four excited states are 2.1 ± 0.4, 0.3 ± 0.1, 3.1 ± 0.6, 3.5 ± 0.7, and approximately 0.3 mb. The total cross section for the $^{40}$Ar(n,α)$^{37}$S reaction was determined to be 9.4 ± 1.0 mb. Comparisons between the results herein reported, other work, and theoretical predictions are made. (auth)

XUM

**56719** $^{86}Kr(d,n)^{87}Rb^{A}$ THRESHOLD CUSP AND THE SYSTEMATIC APPEARANCE OF CHARGE-EXCHANGE CUSPS. Coker, W. R.; Hollas, C. L.; Riley, P. J.; Sen, S. (Univ. of Texas, Austin). Phys. Rev., C; 4: No. 3, 836-9(Sep 1971).

The $^{86}Kr(d,p)^{87}Kr$ reaction leading to three strong low-lying states in $^{87}Kr$($d_{\frac{5}{2}}$ g.s., 0.53 MeV $s_{\frac{1}{2}}$, and 1.47 MeV $d_{\frac{3}{2}}$) has been studied as a function of energy from 5.0 to 10.5 MeV at 100, 120, 140, and 160° laboratory angles. The strong, unusually shaped threshold cusp observed in the $^{86}Kr(d,p)^{87}Kr$($d_{\frac{5}{2}}$ g.s.) excitation curve near 7.56 MeV, threshold of the $^{86}Kr(d,n)^{87}Rb^{A}$ ($d_{\frac{5}{2}}$ isobaric analog resonance) reaction, is discussed in terms of its position in a systematic study and classification of such threshold effects, using simple quantitative physical considerations. The $^{86}Kr$ data are fit with coupled-channel Born-approximation calculations. (auth)

**56720** SELF-CONSISTENT STUDY OF EVEN Zn AND Ge ISOTOPES. Chandra, Harish; Rustgi, M. L. (State Univ. of New York, Buffalo). Phys. Rev., C; 4: No. 3, 874-86(Sep 1971).

Employing the central Yukawa and Kuo-Brown renormalized matrix elements for the Hamada-Johnston interaction, a self-consistent study of even Zn and Ge isotopes is made within the framework of Hartree-Fock (HF), Hartree-Fock-Bogoliubov (HFB), and spherical BCS approximations. It is found that both the interactions yield either oblate or spherical shapes for these isotopes except for $^{60}Zn$ for which a prolate shape is favored. Isotopes having 20 neutrons outside the $^{40}Ca$ core favor spherical BCS shapes. The agreement of the calculated binding energy per particle with the experimental ones is quite good. It is pointed out that for Zn isotopes, both the interactions do not exhibit the saturation in binding energy with the increase in neutron numbers which is observed experimentally. It is also found that for some of the solutions the HFB multipole moments acquire larger values as compared to the HF ones, though the cranking model moment of inertia is always decreased. The pickup strengths for neutrons and protons are also compared for the minimum energy solutions. (auth)

**56721** $^{40}Ca(^{20}Ne,^{16}O)^{44}Ti$ REACTION. Siemssen, R. H. (Argonne National Lab., Ill.); Halbert, M. L.; Saltmarsh, M.; van der Woude, A. Phys. Rev., C; 4: No. 3, 1004-5(Sep 1971).

The reaction $^{40}Ca(^{20}Ne,^{16}O)^{44}Ti$ has been studied at 63.0 and 73.7 MeV. The reaction is found to populate the same final states as the reaction $^{40}Ca(^{16}O,^{12}C)^{44}Ti$ and with comparable cross sections. (auth)

**56722** DECAY OF $^{85}Y$ (5 hr), $^{85}Y$ (2.68 hr), AND $^{85}Sr$. MULTIPLE THREE-PARTICLE LEVELS IN $^{85}Sr$. Arl't, R.; Zaitseva, N. G.; Kratsik, B.; (and others). Izv. Akad. Nauk SSSR, Ser. Fiz.; 35: No. 1, 48-55(Jan 1971). (In Russian).

Decay schemes of the isomers $^{85}Y$ and $^{85}Sr^{*}$ were studied using Ge(Li) spectrometers with sensitive volumes of 6.3 and 10 $cm^3$ and resolution of 3.5 to 5 keV for $^{60}Co$ $\gamma$ transitions. A 4096-channel analyzer was used for the amplitude analysis. In addition to the $^{85}Y$ source there were present also isotopes of $^{84}Y$(39 min), $^{86}Y$(14.6 hr), $^{87}Y$(80 hr), $^{87}Y^{*}$(12.5 hr) and $^{88}Y$(105 days). Energies and intensities of gamma rays from decay of $^{85}Y$($T_{\frac{1}{2}}$ = 2.68 hr) and $^{85}Sr^{*}$($T_{\frac{1}{2}}$ = 70 min) are tabulated and data on observed levels are correlated with published data. (R.V.J.)

**56723** DECAY OF $^{89}Zr$ AND $^{87}Zr$. Arl't, R.; Zaitseva, N. G.; Kratsik, B.; (and others). Izv. Akad. Nauk SSSR, Ser. Fiz.; 35: No. 1, 56-64(Jan 1971). (In Russian).

Studies were made on the decay of the $^{89}Zr$($T_{\frac{1}{2}}$ = 4.18 min) and $^{89}Zr^{*}$($T_{\frac{1}{2}}$ = 78.4 hr) isomers using $\gamma$-spectrometers with Ge(Li) detectors. The data obtained added to and verified the schemes of excited levels for $^{89}Y$. A decay scheme for $^{87}Zr$ was also constructed using the same methods. (C.E.S.)

**56724** STUDIES OF THE $^{14}N(d,p)^{15}N$, $^{28}Si(d,p)^{29}Si$, AND $^{32}S(d,p)^{33}S$ REACTIONS WITH POLARIZED DEUTERONS. Egoshin, V. G.; Igolkin, V. V.; Saltykov, L. S.; (and others) (Inst. of Physics, Moscow). Izv. Akad. Nauk SSSR, Ser. Fiz.; 35: No. 1, 205-6(Jan 1971). (In Russian).

The vector analyzing power was measured in the stripping reactions $^{14}N(d,p)^{15}N$, $^{28}Si(d,p)^{29}Si$, and $^{32}S(d,p)^{33}S$. The polarized deuteron beam was produced by elastic scattering of the primary 13.8-MeV deuteron beam by carbon at $\theta = 25°$. At such an angle scattered deuterons possess a considerable vector polarization. Results of the measurements are tabulated. Previously, it was observed that in (d,p) reactions with polarized deuterons, the vector analyzing power is connected with $j_n$. In the case of the reaction $^{14}N(d,p)^{15}N$, the angular and total momenta of the captured neutron are equal to 1 and $\frac{1}{2}$, respectively. However, the shape of the measured vector analyzing power was different from that observed for the reactions with $l_n = 1$ and $j_n = \frac{1}{2}$ with intermediate nuclei. For the reactions $^{28}Si(d,p)^{29}Si$ (the 1.28-MeV level) and $^{32}S(d,p)^{33}S$ neutron capture was observed with angular momentum $l_n = 2$ and total angular momentum $j_n = \frac{3}{2}$. The values $P^{D}$ for $^{28}Si(d,p)^{29}Si$ and $^{32}S(d,p)^{33}S$ in the angular range corresponding to the principal maximum of the proton angular distribution had negative values; this result is in agreement with the regularities observed in other intermediate-weight nuclei. (R.V.J.)

**56725** LIMITATIONS IMPOSED BY THE DISTORTED-WAVE METHOD ON THE SELECTION OF OPTICAL POTENTIALS OF DEUTERON INTERACTIONS WITH NUCLEI. Terenetskii, K. O.; Tokarevskii, V. V. (Inst. of Physics, Kiev). Izv. Akad. Nauk SSSR, Ser. Fiz.; 35: No. 1, 100-6(Jan 1971). (In Russian).

Properties of the optical potential for interactions of 13.6-MeV deuterons with $^{48}Ti$ and $^{50,52}Cr$ isotopes were studied by means of detailed analysis of experimental data. Elastic scattering of deuterons was analyzed using the optical model, and the optical potentials obtained were used for calculating the angular distributions of the protons from the stripping reactions $^{48}Ti(d,p)^{49}$ and $^{50,52}Cr(d,p)^{51,53}Cr$. An attempt was made to limit the number of optical-potential parameters varied by fixing certain processes without disturbing the theoretical and experimental correlation. The results of the combined analysis of the elastic scattering of deuterons and of the (d,p) stripping reactions showed that it was possible to limit the number of free optical-potential parameters varied for deuterons; consideration of spin-orbit interactions in the deuteron optical parameters improved the description of elastic scattering differential cross sections and did not interfere with calculations of stripping reaction cross sections. Calculations of cross sections for stripping reactions by the distorted-wave method were independent of optical potential with parameters $V \approx 30$ and 65 MeV. (R.V.J.)

**56726** INELASTIC SCATTERING OF $\alpha$ PARTICLES BY Zn ISOTOPES. Alekseev, V. V.; Gonchar, V. G.; Polyanskii, V. N.; (and others). Izv. Akad. Nauk SSSR, Ser. Fiz.; 35: No. 1, 107-11 (Jan 1971). (In Russian).

Inelastic scattering of $\alpha$ particles was analyzed as a means for obtaining spectroscopic information on collective nuclear levels. Inelastic scattering of $\alpha$ particles by the even-parity isotopes $^{64,66,70}Zn$ was studied in order to determine the possibility of using the distorted-wave method for imposing certain limitations on the parameters of optical potentials and finding out the influence of the selection of parameters on the reliability of the calculation of B(El)'s within the framework of the distorted-wave method. (R.V.J.)

**56727** INELASTIC PROTON SCATTERING IN INTERMEDIATE-WEIGHT NUCLEI. Pasechnik, M. V.; Prokopenko, V. S.; Tokarevskii, V. V ; (and others). Izv. Akad. Nauk SSSR, Ser. Fiz.; 35: No. 1, 81-5(Jan 1971). (In Russian).

Differential cross sections for inelastic scattering of 6.9-MeV protons by $^{50,52}Cr$, $^{56}Fe$, $^{58,60}Ni$, and $^{64,66}Zn$ were measured; subsequently, the results were analyzed by the distorted-wave method. Data obtained were correlated with the values obtained by other experiments (for Coulomb excitation and inelastic scattering of electrons, deuterons, and $\alpha$ particles). Tabulated data on excited states of nuclei and their respective integrated cross sections for proton scattering showed that the processes during the formation of the compound nuclei play an important role during inelastic scattering of 6.9-MeV protons by $^{52}Cr$, $^{60}Ni$, $^{64}Zn$, and $^{66}Zr$; however, their role is less significant during scattering by $^{50}Cr$, $^{56}Fe$, and $^{58}Ni$. (R.V.J.)

**56728** EXAMINATION OF COUPLED-CHANNEL CALCULATIONS FOR THE REACTION $^{24}Mg(d,p)^{25}Mg$. Hofmann, A.; Vogler, F. (Univ., Erlangen, Ger.). Lett. Nuovo Cim.; 2: No. 4, 133-4(24 Jul 1971).

The cross sections for the $^{24}Mg(d,p)$ reaction leading to the $^{25}Mg$ ground and first-excited states were measured at a deuteron energy of 10 MeV. The protons were detected in a multicounter arrangement using surface barrier detectors. The measured cross sections were compared with coupled channel calculations. (J.W.R.)

**56729** GAMMA-RAY SPECTRA FOLLOWING THE CAPTURE OF 14 MeV NEUTRONS BY $^{59}Co$, $^{93}Nb$, AND $^{103}Rh$. Rigaud, F. (CEN de Bordeaux, Gradignan, France); Irigaray, J. L.; Petit, G. Y.; Longo, G.; Saporetti, F. Nucl. Phys.; A173: No. 3, 551-60(1971).

Gamma-ray spectra from the radiative capture of 14.06 MeV neutrons in $^{59}Co$, $^{93}Nb$ and $^{103}Rh$ are measured by means of a time-of-flight spectrometer. The $(n,\gamma)$ cross sections, deduced from the integration of measured spectra, are very similar for

XUM

the three nuclei considered. The value of the $^{103}Rh(n,\gamma)$ cross section obtained here is lower by about a factor of 20 than that previously obtained from activation analysis. Comparisons of the measured cross sections with calculations based on the direct and collective capture models, including the contribution of interference between them, show a satisfactory agreement with the present experimental data. (auth)

**56730** INVESTIGATION OF THE $^{33}S(d,p)^{34}S$ REACTION. Van der Baan, J. G.; Sikora, B. R. (Rijksuniversiteit, Utrecht). Nucl. Phys.; A173: No. 3, 456-64(1971).

Angular distributions have been measured of proton groups, corresponding to $^{34}S$ states up to $E_x = 6.63$ MeV excited in the reaction $^{33}S(d,p)^{34}S$ at $E_d = 12$ MeV, with the use of a split-pole magnetic spectrograph. The ground state Q-value has been measured as $Q_0 = 9195 \pm 6$ keV. A DWBA analysis yields $l_n$ values and spectroscopic factors. The results of many-particle shell-model calculations for $^{34}S$ positive-parity are found to agree well with experiment. (auth)

**56731** QUADRUPOLE VIBRATIONS IN THE NICKEL REGION: STRUCTURE OF ODD-MASS Cu ISOTOPES. Gomez, Jose M. G. (Univ., Valencia). Nucl. Phys.; A173: No. 3, 537-50(1971).

The low-lying levels of the odd-mass copper isotopes are described as a proton in the $2p_{\frac{3}{2}}$, $1f_{\frac{5}{2}}$ and $2p_{\frac{1}{2}}$ orbits coupled to a quadrupole vibrator. The calculated and observed excitation energies, spectroscopic factors, static moments, B(E2) values, mixing ratios and branching ratios of $\gamma$-rays are discussed in detail. Some spin and parity assignments are proposed on the basis of a reasonable agreement of theory and experiments. (auth)

**56732** IN-BEAM STUDY OF PROMPT $\gamma$-RAYS EMITTED IN THE $^{66}Zn(p,n\gamma)^{66}Ga$ REACTION. Najam, M. R.; Davidson, W. F.; Zuk, W. M.; Carlson, L. E.; Awal, M. A. (Australian National Univ., Canberra). Nucl. Phys.; A173: No. 3, 577-94(1971).

The level structure of the nucleus $^{66}Ga$ has been studied by means of the $^{66}Zn(p,n\gamma)^{66}Ga$ reaction ($Q = -5.957$ MeV). Levels in $^{66}Ga$ up to 730 keV in excitation were selectively populated by varying the proton bombarding energy in the range of 6.00 to 6.82 MeV. The $\gamma$-rays associated with these levels were identified both in singles spectra, from a study of their threshold behavior, and in $\gamma\gamma$-coincidence measurements. Altogether 24 levels in $^{66}Ga$ were identified, of which 10 are known from previous studies of the $\beta^+$ decay of $^{66}Ge$ to $^{66}Ga$, and the remaining 14 are reported here for the first time. Gamma-ray branching ratios for these new levels have been determined and a decay scheme comprising 68 $\gamma$-transitions is presented. Angular distributions of de-excitation $\gamma$-rays have been measured at proton bombarding energies close to threshold for the levels studied. Comparison of these distributions with the theoretical predictions of the compound nucleus statistical model has led to spin and parity assignments for the levels studied. (auth)

# Nuclear Properties and Reactions, A ≥ 90

*Refer also to abstracts 54672, 54696, 55038–55041, 55089, 55369, 56269, 56421, 56643, 56650, 56651, 56655, 56666, 56676, 56686, 56695, 56696, 56702, 56706, 56729, 56816, 56832, 56847, 56856, and 56982.*

**56733** (AECL-3912) PHYSICS DIVISION PROGRESS REPORT, JANUARY 1–MARCH 31, 1971. (Atomic Energy of Canada Ltd., Chalk River (Ontario). Chalk River Nuclear Labs.). 105p. (PR-P-89). Dep. NTIS (U. S. Sales Only). AECL $2.00.

Research progress by the Physics Division at Chalk River Nuclear Laboratories in the period January 1 through March 31, 1971 is briefly reported. (J.W.R.)

**56734** (BNL-tr-446) MEASUREMENT OF THE RATIO OF THE RADIATIVE CAPTURE TO FISSION CROSS SECTIONS ($\alpha$) FOR $^{239}Pu$ IN THE NEUTRON ENERGY RANGE 0.1 TO 30 keV. Kurov, M. A.; Ryabov, Yu. V.; Sik, So Don; Chikov, N.; Kononov, V. N.; Poletaev, E. D.; Prokopets, Yu. S.; Stavisskii, Yu. Ya. Translated by S. J. Amoretty (Brookhaven National Lab., Upton, N. Y.), from At. Energ. (USSR); 30: No. 4, 362-9(1971). 16p. Dep. NTIS

Because of the unsatisfactory state of the experimental data on $\alpha(E)$, this quantity was measured for plutonium-239 in the energy range 0.1 to 30 keV. (J.F.P.)

**56735** (FEI-202) PROBABILITY OF ELECTROMAGNETIC QUADRUPOLE TRANSITIONS IN THE PHENOMENOLOGICAL NUCLEAR THEORY. Rabotnov, N. S.; Seregin, A. A. (Gosudarstvennyi Komitet po Ispol'zovaniyu Atomnoi Energii SSSR, Obninsk. Fiziko-Energeticheskii Institut). 1970. 11p. (In Russian). Dep. NTIS (U. S. Sales Only).

Within the framework of a phenomenological collective model of a nucleus with a potential dependent on the internal variables $\beta$ and $\gamma$ and corresponding to nuclei of the deformed transition region, the probability of an electric quadrupole transition between $2^+$ states, and from a $2^+$ state to a $0^+$ state is calculated. In comparison with theories that use an adiabatic approximate separation of variables, the probability depends nonmonotonically on the stiffness parameters of the potential, in particular for the binding energy of the second and third $2^+$ states. A sharp minimum is observed in the probability of the $2_2^+ \rightarrow 0_0^+$ transition. This may be the source of the anomalously low value of this probability for some medium-weight nuclei. (tr-auth)

**56736** (FEI-233) ANGULAR ANISOTROPY AND THE EFFECTS OF NUCLEON PAIRING IN $^{239}Pu$ FISSION BY NEUTRONS. Shpak, D. L.; Ostapenko, Yu. B.; Smirenkin, G. N. (Gosudarstvennyi Komitet po Ispol'zovaniyu Atomnoi Energii SSSR, Obninsk. Fiziko-Energeticheskii Institut). 1970. 25p. (In Russian). Dep. NTIS (U. S. Sales Only).

The angular anisotropy of $^{239}Pu$ fission (n,f) was studied as a function of neutron energy in the range 0.05 to 7.20 MeV using glass detectors. The considerable effect of pair correlations of nucleons of the superconducting type on the spectrum of transition states of the $^{240}Pu$ nucleus was shown. The critical energy of the phase transition $E_{kr}^* = 12.0 \pm 2.5$ MeV and the energy slot $2\Delta_0^f = 1.7 \pm 0.2$ MeV were determined. Several conclusions relative to the structure of the fission barrier are deduced. (JPRS)

**56737** (JINR-E4-5877) $\Delta N = \pm 2$ MIXING IN ODD-N DEFORMED NUCLEI. Gareev, F. A.; Fedotov, S. I.; Solov'ev, V. G. (Joint Inst. for Nuclear Research, Dubna (USSR). Lab. of Theoretical Physics). 1971. 20p. Dep. NTIS (U. S. Sales Only).

The $\Delta N = \pm 2$ mixing in a number of the Sm, Gd and Dy isotopes is studied in the framework of the model taking into account the superconducting pairing correlations and the quasiparticle-phonon interaction and using the Saxon–Woods single-particle energies and wave functions. It is shown that at deformations $\beta_{20} = 0.30 - 0.33$ and $\beta_{40} = 0.04$ there occurs a strong mixing of the following pairs of states: $\frac{1}{2}^+$ [400], $\frac{1}{2}^+$ [600] and $\frac{3}{2}^+$ [402], $\frac{3}{2}^+$ [651]. The results of calculations of the energies of these states and the wave function N = 4 and N = 6 components are in rather good agreement with the corresponding experimental data. It is shown that the quasiparticle-phonon interactions lead to an essential increase of the $\Delta\beta_{20}$ interval in which the $\Delta N = \pm 2$ mixing occurs as compared with the single-particle model. (auth)

**56738** (JINR-P-15-5959) EXCITATION OF THE SPONTANEOUSLY FISSIONING ISOMERIC STATES OF $^{239}Pu$ AND $^{243}Am$ IN INELASTIC $\gamma$-QUANTUM SCATTERING. Gangrskii, Yu. P.; Markov, B. N.; Kharisov, I. F.; Tsipenyuk, Yu. M. (Joint Inst. for Nuclear Research, Dubna (USSR). Lab. of Nuclear Reactions). 1971. 7p. (In Russian). Dep. NTIS (U. S. Sales Only).

The production of the spontaneously fissioning isomers of $^{239}Pu$ and $^{243}Am$ in inelastic $\gamma$-quantum scattering was investigated. Based on the isomeric excitation function the possibilities of the isomeric level population are analyzed. (auth)

**56739** (JINR-P1-6006) PROBABILITY OF THE $(\mu^-,\nu)$ PROCESS ON $^{139}La$ AND $^{208}Pb$ NUCLEI. Bunatyan, G. G.; Wilhelmova, V. S.; Evseev, V. S.; Nikityuk, L. N.; Pokrovskii, V. N.; Rybakov, V. N.; Yutlandov, I. A. (Joint Inst. for Nuclear Research, Dubna (USSR). Lab. of Nuclear Problems). 1971. 9p. (In Russian). Dep. NTIS (U. S. Sales Only).

With the finite Fermi-system methods proved to be successful in calculating the total muon capture rates in nuclei, the comparison of the theoretical and experimental values of certain partial capture rates, e.g., those of the $(\mu^-,\nu)$ process probabilities, appeared to be appropriate for a further investigation of the suitability of these methods. For the $^{27}Al$, $^{28}Si$, $^{51}V$ and $^{56}Fe$ nuclei the theoretical $W_{\mu^-,\nu}$ estimates gave qualitative account for the experimental values while the quantitative agreement turned out to be worse than for the total capture rates. This discrepancy supposed being smaller for heavier nuclei, the $W_{\mu^-,\nu}$ value is now determined for the $^{139}La$ and $^{208}Pb$ nuclei. The determinations were carried out by the activation technique, the experimental layout and conditions described earlier. The activities of the $(\mu^-,\nu)$ reaction products were measured on scintillation $\gamma$-spectrometers, the $^{139}Ba$ activity determined after the radiochemical separation while that of $^{208}Tl$ measured without separation. The main results are presented. The targets and the experimental results are indicated. The value of the probability of muon cap-

XUM

ture without subsequent neutron emission for natural Pb (evaluated from previous data) is given. The reasons for the evident disagreement are unclear; for the $^{27}Al$, $^{28}Si$ and $^{56}Fe$ nuclei the agreement was quite satisfactory. The experimental and theoretical total capture rates are quoted. The theoretical $W_{\mu^-,\nu}$ estimates, $\Lambda'$ denoting the muon capture rate on the levels placed below the threshold of particle emission, are presented. It may be worth noting that in the case of $^{208}Pb$ the dipole transitions yield is negligible and the major yield results from the quadrupole transitions due to axial and induced pseudoscalar interactions: $\Lambda_2^{GT} = 9.64 \cdot 10^5$ sec$^{-1}$ while total $\Lambda' = 12.7 \cdot 10^5$ sec$^{-1}$. (auth)

**56740** (JINR–P7–5884) ELASTIC SCATTERING OF HEAVY IONS BY NUCLEI. Karamyan, S. A.; Oganesyan, Yu. Ts.; Penionzhkevich, Yu. E.; Pustyinik, B. I. (Joint Inst. for Nuclear Research, Dubna (USSR). Lab. of Nuclear Reactions). 1971. 18p. (In Russian). Dep. NTIS (U. S. Sales Only).

Elastic scattering of $^{12}C$, $^{14}N$, $^{16}O$, $^{20,22}Ne$, $^{40}Ar$ ions by $^{108}Ag$, $^{141}Pr$, $^{159}Tb$, $^{165}Ho$, $^{197}Au$, $^{209}Bi$, $^{236}V$ nuclei in various combinations is studied in a wide range of energies of incident particles. The phase shift analysis of the angular distributions was performed and values $\langle l^2 \rangle$, $l_{cp}$ and $l_{max}$ were obtained. (auth)

**56741** (KFKI–71–35) REMARKS ON THE EXISTENCE OF RETARDED NEUTRONS IN FISSION. Jeki, L.; Kluge, Gy.; Lajtai, A. (Magyar Tudomanyos Akademia Kozponti Fizikai Kutato Intezete, Budapest). [1971]. 8p. Dep. NTIS (U. S. Sales Only).

New measurements on "retarded" fission neutrons are critically discussed. (auth)

**56742** (LYCEN–7101) INSTITUTE OF NUCLEAR PHYSICS ANNUAL PROGRESS REPORT, JANUARY 1971. (Lyon Univ. (France). Institut de Physique Nucleaire). 144p. (In French). Dep. NTIS (U. S. Sales Only).

The annual progress report of the Lyon Nuclear Physics Institute (Lycen) for 1970 is presented. The fields covered are: nuclear structures and spectrometry, nuclear reactions, and radiochemistry (theoretical and experimental studies), and nuclear instrumentation. A list of the published work is given. (France)

**56743** (NP–18966) EXPERIMENTAL INVESTIGATION OF FISSION. Boldeman, J. W. ([Australian Atomic Energy Commission Research Establishment, Lucas Heights]). May 1970. 196p. Dep. NTIS (U. S. Sales Only).

Thesis. Submitted to Wollongong Univ. Coll., Australia.

Accurate measurements have been made of the average number of prompt neutrons, $\bar{\nu}_p$, emitted per fission for thermal neutron fission of $^{233}U$, $^{235}U$, $^{239}Pu$ and $^{241}Pu$ and spontaneous fission of $^{240}Pu$ and $^{242}Pu$. The large liquid scintillator method has been used and sources of error in this method have been closely examined. In addition, precise measurements have been made of the probability distribution of neutron emission for each of the six cases above and the spontaneous fission of $^{252}Cf$. The data have been compared with the neutron emission distribution calculated from fragment kinetic energy data. It is noted that the existing discrepancy between experiment and calculation may be due to gamma ray competition. The variation of $\bar{\nu}_p$ with compound excitation has been determined for neutron fission of $^{233}U$ and $^{235}U$. The $\bar{\nu}_p(E_n)$ dependence was found to be linear and the claim of fine structure in some previous experiments has not been substantiated. The variation of the correlated parameter, the average total kinetic energy of the fission fragments ($\bar{E}_K$) with compound excitation for neutron fission of $^{235}U$ has also been examined. $\bar{E}_K$ was found to be constant in the range measured (0–1 MeV) and the lack of structure in $\bar{E}_K(E_n)$ confirmed the linear data for $\bar{\nu}_p(E_n)$. From an evaluation of the present and existing $\bar{\nu}_p$ data for $^{233}U$, $^{235}U$ and $^{239}Pu$, it is observed that the $\bar{\nu}_p(E_n)$ dependence, although linear, is characterized by a change in slope at the pairing energy. The nature of the dependence has been explained in terms of the double humped fission barrier with the adiabatic assumption of weak coupling of the collective saddle point energy to the nuclear degrees of freedom at scission. The change in the character of the $\bar{\nu}_p(E_n)$ dependence between $^{233}U$ and $^{235}U$ is associated with the change in the relative heights of the two humps of the fission barrier. It is noted that gamma ray competition has a slight effect on the $\bar{\nu}_p(E_n)$ dependence. Measurements have been made of the average neutron emission from fission fragments of specific mass for values of the total fragment kinetic energy in the thermal neutron fission of $^{235}U$. The well known sawtooth curve has been observed and the data confirm the most recent previous investigation. (auth) (Australia)

**56744** (NP-tr–1936) DELAYED FISSION OF SOME NEUTRON-DEFICIENT ATOMIC NUCLEI. Skobelev, N. K. (Joint Inst. for Nuclear Research, Dubna (USSR). Lab. of Nuclear Reactions). Translation of report JINR–P7–5584. 8p.

This item was previously abstracted from the original language and appeared in NSA as 25: 20371. (auth)

**56745** (ORNL–4691) TOTAL GAMMA-RAY ENERGY SPECTRUM ABOVE 1 MeV FROM NEUTRON INTERACTIONS IN $^{235}U$ AND $^{238}U$. Booth, R. S.; Muckenthaler, F. J. (Oak Ridge National Lab., Tenn.). Aug 1971. Contract W-7405-eng-26. 34p. Dep. NTIS.

The total gamma-ray energy spectra above 1 MeV from neutron interactions in $^{235}U$ and $^{238}U$ were measured to test the accuracy of model calculations and to improve the accuracy of shielding calculations by reducing the uncertainty in the source term. The general structure of the gamma-ray energy spectrum above 1 MeV from fission was independent of the isotope where the fission occurred and the energy of the neutron that caused the fission. This total fission spectrum was approximated to an accuracy of 20% by a simple empirical expression which, between 1 and 5.12 MeV, is twice the spectrum from prompt fission. The gamma-ray energy spectrum from all neutron interactions in $^{235}U$ was dominated by the total fission spectrum. The photon spectrum obtained as a result of reactor neutrons striking $^{235}U$ had the same shape as the proton spectrum obtained from the same neutron beam filtered with cadmium. When the reactor spectrum was filtered with $^{10}B$, a photon spectrum due to interactions other than fission was evident for photon energies between 1 and 3 MeV. The measured photon spectrum from thermal neutron interactions in $^{235}U$ was compatible with previous estimates and measurements. The photon energy spectra from $^{238}U$ were isolated from the measurements and presented on an absolute basis for three situations: (1) capture of thermal neutrons, (2) interactions with a 1/E spectrum of intermediate energy neutrons, and (3) interactions with a fission spectrum of neutrons. The first two spectra were used to determine parameters in model calculations of differential yield data which were compared to measured differential yield data. The relative photon spectra from neutron interactions in $^{233}U$ and $^{239}Pu$ were measured in preliminary experiments. The shapes of these spectra were quite similar to spectra obtained with $^{235}U$. (auth)

**56746** (ORNL–4707) MEASUREMENTS OF THE NEUTRON FISSION AND ABSORPTION CROSS SECTIONS OF $^{239}Pu$ OVER THE ENERGY REGION 0.02 eV TO 30 keV, PART II. Gwin, R.; Weston, L. W.; de Saussure, G.; Ingle, R. W.; Todd, J. H.; Gillespie, F. E.; Hockenbury, R. W.; Block, R. C. (Oak Ridge National Lab., Tenn.). Jul 1971. Contract W-7405-eng-26. 43p. Dep. NTIS.

The neutron absorption and fission cross sections for $^{239}Pu$ were measured simultaneously over the neutron energy range from 0.02 eV to 30 keV. These cross sections were measured using an ionization chamber containing $^{239}Pu$. The differential cross sections derived from these measurements are presented along with a multilevel analysis of the data up to 100 eV. A re-evaluation of data obtained using a metal foil of $^{239}Pu$ was also made. Average values of the neutron capture and fission cross sections are presented for $^{239}Pu$ as obtained using the ionization chamber as well as with the metal foil. A detailed comparison of the present data is made with the results of the ENDF/B evaluation for $^{239}Pu$ (material 1104). The neutron cross sections presented supersede the results previously reported. (auth)

**56747** (ORNL-tr–2531) STUDY OF THE $\gamma$ RADIATION ACCOMPANYING THE DECAY OF Ms Th(II) ($^{228}Ac$). Dalmasso, Josette; Maria, Henriette. Translated by David C. West (Oak Ridge National Lab., Tenn.), from Compt. Rend., Ser. B; 272 905-8(1971). 8p. Dep. NTIS.

The $\gamma$ radiation of $^{228}Ra$ and its daughters was studied using a coaxial Ge(Li) detector of very high resolution. The intensities of more than 156 transitions were determined; 32 transitions were observed for the first time. (auth)

**56748** (ORO–2408-45) PROGRESS REPORT, APRIL 1, 1971–JUNE 30, 1971. (North Carolina Univ., Chapel Hill). Contract AT(40-1)-2408. 10p. Dep. NTIS.

The activities of the atomic and nuclear physics groups at the University of North Carolina in the period April 1 to June 30, 1971, are briefly outlined. A list of publications is included. (J.W.R.)

**56749** (RCN–142) FISSION OF ORIENTED NUCLEI BY LOW ENERGY NEUTRONS. Kuiken, R. (Reactor Centrum Nederland,

XUM

Petten). Jun 1971. 171p. Dep. NTIS (U. S. Sales Only). Thesis. Submitted to Leiden Rijksuniversiteit (Netherlands).

The angular distribution of $\alpha$-particles and of fission fragments originating from neutron capture in heavy nuclei, which are aligned at low temperatures by the method of hyperfine interaction, are reported. The results of the measurements with the target nucleus $^{233}U$ with neutrons in the energy range from 0 to 2000 eV can be interpreted with the Bohr-theory of transition states at the deformation barrier for nuclear fission. The relatively invariant behavior of the anisotropy in the angular distribution of fission fragments as a function of neutron energy indicates that the available fission channels are strongly mixed. For neutron resonances with spin and parity $2^+$ 2 to 3 channels are open and for $3^+$ resonances 1 to 2. The group structure in the subthreshold fission cross section of $^{237}Np$ has been explained by the double-humped deformation barrier proposed by Strutinsky. The implication of this interpretation is that all the resonances in one group have the same spin. The resonances in the first group at 40 eV agree consistently with the fission channel $(2^+,2)$. The groups at higher neutron energies up to 2000 eV correspond mainly with the channels $(2^+,2)$ and $(3^+,2)$. (auth)

**56750** (RLO-1759-25) FISSION STUDIES ON ELEMENTS BELOW POLONIUM. Progress Report, July 1, 1970–June 30, 1971. Neuzil, Edward F. (Western Washington State Coll., Bellingham). Contract AT(45-1)-1759. 15p. Dep. NTIS.

Research on fission reactions producing the same compound nucleus at the same excitation energy but induced by different particles and tantalum fission at 65 and 41 MeV is summarized. (J.F.P.)

**56751** (RT/FI-(70)55) SPIN-DEPENDENCE OF LEVEL DENSITY IN $^{178}Hf$ AND $^{180}Hf$ BY RESONANCE NEUTRON CAPTURE EXPERIMENTS. Coceva, C.; Corvi, F.; Giacobbe, P.; Stefanon, M. (Comitato Nazionale per l'Energia Nucleare, Rome (Italy)). 23 Dec 1970. 19p. Dep. NTIS (U. S. Sales Only).

Measurement of gamma-rays from s-wave resonance neutron capture allowed the spin assignment to 97 resonances of $^{177}Hf$ below 300 eV and to 44 resonances of $^{179}Hf$ below 200 eV. Values of the spin cut-off parameter were deduced. (auth)

**56752** (SUNI-14) ANNUAL RESEARCH REPORT FOR THE YEAR ENDING DECEMBER 1970. McMurray, W. R. (comp.) (Southern Universities Nuclear Inst., Faure (South Africa)). 67p. Dep. NTIS (U. S. Sales Only).

ARSENIC-75—energy levels and transitions from neutron inelastic scattering, (E)
BORON-10—deuteron reactions (d,n$\gamma$) at 3 MeV, n-$\gamma$ coincidence spectra from, (E)
CARBON-12—deuteron reactions (d,n$\gamma$) at 5 MeV, n-$\gamma$ coincidence spectra from, (E)
—neutron inelastic scattering at 22 MeV with subsequent $\gamma$ decay, n-$\gamma$ coincidence spectra from, (E)
CHARGED PARTICLES—energy losses in unknown materials, technique for determination of
CHLORINE-35—proton inelastic scattering at 5.47 to 5.61 MeV, excitation function for, (E)
CHLORINE-35—energy levels from proton inelastic scattering, lifetimes of, (E)
ELEMENTS—determination of light, by coincident measurement of complementary particles from nuclear reactions
GALLIUM-70—energy levels from gallium-69 (d,p) reactions, (E)
GLASS—analysis for aluminum, boron, and sodium in, by simultaneous measurement of scattered $\alpha$ particles and prompt protons
—analysis for boron in, by measurement of prompt proton spectra from (d,p) reactions
INDIUM-115—energy-level scheme from neutron inelastic scattering, (E)
LITHIUM-7—proton reactions (p,n) at 2 to 5.5 MeV, excitation function for, (E)
NIOBIUM-93—energy-level scheme from neutron inelastic scattering, (E)
SAMARIUM-154—neutron inelastic scattering at 1.5 MeV, $\gamma$ spectra from, (E)
—energy-level scheme from neutron inelastic scattering, (E)
SCANDIUM-48—energy-level scheme from calcium-48 (p,n) reactions, (E)
SILICON-29—alpha reactions ($\alpha$,n) at 2.8 to 4.1 MeV, excitation function for, (E)
SODIUM-23—energy levels from neon-22 (p,$\gamma$) reactions, $\gamma$ branching ratios for, (E)
SULFUR ISOTOPES—determination of abundance of, in sulfur compounds
SULFUR-33—energy levels from resonance in silicon-29 ($\alpha$,n) reactions, spin assignments for, (E)
TOURMALINES—analysis for boron in, by measurement of prompt proton spectra from (d,p) reactions
—analysis for aluminum, calcium, iron, lithium, magnesium, manganese, and sodium by deuteron activation analysis and $\gamma$ counting
URANIUM-235—neutron fission at 30 keV, time analysis of compound-nucleus decays in, (E)
VAN de GRAAFF ACCELERATORS—research and development at SUNI 5.5 MV (J.W.R.)

**56753** (UCRL-51087) GAMMA-RAY ENERGIES AND ABSOLUTE BRANCHING INTENSITIES FOR $^{238,239,240,241}Pu$ AND $^{241}Am$. Gunnink, R.; Morrow, R. J. (California Univ., Livermore. Lawrence Radiation Lab.). 22 Jul 1971. Contract W-7405-eng-48. 26p. Dep. NTIS.

Using sources of very high isotopic purity, precise values were obtained for the energies and absolute branching intensities of the gamma rays following the alpha-decay of $^{238,239,240,241}Pu$ and $^{241}Am$. (auth)

**56754** (UCRL-Trans-10541) ALPHA WIDTHS OF NEUTRON RESONANCES. Popov, Yu. P.; Pshitula, M.; Rumi, R. F.; Stempinskii, M.; Florek, M.; Furman, V. I. (Joint Inst. for Nuclear Research, Dubna (USSR)). Translated by T. Watt for Univ. of California, Lawrence Radiation Lab., Livermore, from pp 669-78 of report STI/PUB-259(Vol.1). 18p. (CONF-700605-12). Dep. NTIS.

From second international conference on nuclear data for reactors; Helsinki, Finland (15 Jun 1970).

An abstract of this paper, prepared from the original language, appeared as NSA 25: 15097.

**56755** GAMMA X-RAY ANGULAR CORRELATION. Gelberg, A.; Piticu, I. (Inst. of Atomic Physics, Bucharest). Rev. Roum. Phys.; 16: No. 2, 153-6(1971).

The directional correlation between X-rays following electron conversion and gamma rays in $^{191}Ir$ has been measured. The X rays were detected by a high-resolution lithium drifted silicon detector, so as to separate photons originating from the $L_{III}(2p_{\frac{3}{2}})$ subshell. An asymmetry of $-(6.2 \pm 1.8)\%$ has been found, thus confirming Dolginov's theory. (auth)

**56756** NUCLEAR STRUCTURE EFFECTS IN THE INTERNAL CONVERSION OF SOME MAGNETIC DIPOLE TRANSITIONS IN DEFORMED NUCLEI. Protop, C. (Inst. of Atomic Physics, Bucharest). Rev. Roum. Phys.; 16: No. 3, 367-9(1971).

Penetration parameters for the effects of nuclear structure on the internal conversion of M1 transitions were extracted from experimental data on L-subshell internal conversion ratios for some heavy deformed nuclei. Results are presented for transitions in $^{153}Eu$, $^{165}Ho$, $^{175}Lu$, $^{187}Re$, and $^{249}Bk$. It was found that nuclear structure effects may be significant even for enhanced transitions when the penetration matrix element is large. (J.W.R.)

**56757** YIELDS AND CHARGE DISPERSION OF ANTIMONY PRODUCED IN URANIUM FISSION BY MEDIUM-ENERGY PROTONS. Miller, Larry Day. Montreal; McGill Univ. (1970). National Library of Canada, Ottawa. Thesis.

The independent formation cross sections of $^{120}Sb^m$, $^{124}Sb$, $^{125}Sb$, $^{126}Sb$, $^{127}Sb$, and $^{128}Sb^g$ and the cumulative cross sections of $^{125}Sb$, $^{127}Sb$, $^{129}Sb$, and $^{131}Sb$ produced in the fission of uranium by protons of energies 30–160 MeV have been measured radiochemically. Excitation functions were constructed whose maxima decrease monotonically with proton energy when compared to the increasing neutron-to-proton ratio of the products. Charge-dispersion curves were constructed at each energy from the cross sections as a function of neutron-to-proton ratio. These curves were observed to broaden and the most probable charge moved toward beta-stability with increased bombarding energy. The magnitude of these widths compared to those determined by other workers suggests a mass region dependence. The formation cross sections of fifteen fission products ranging in mass from A = 95 to A = 144 were determined by gamma-ray spectroscopy at a bombarding energy of 75 MeV without previous chemical separation. (Diss. Abstr. Int., B)

**56758** NUCLEAR STRUCTURE OF $^{92}Nb$. Bagne, Farideh. Philadelphia; Univ. of Pennsylvania (1970). 190p. University

XUM

Microfilms Order No. 71-19,201.
Thesis.

The study of the reactions $^{90}Zr(^3He,p)^{92}Nb$ and $^{94}Mo(d,\alpha)^{92}Nb$ was undertaken to clarify the structure of $^{92}Nb$ by confirming the properties of the known levels, identifying new states, and establishing quantum numbers and obtaining information on the wave functions of several levels. The reactions $^{90}Zr(^3He,p)^{92}Nb$ and $^{94}Mo(d,\alpha)^{92}Nb$ have been studied respectively with 16.5 and 18 MeV $^3He^{++}$ ions and 10 MeV deuterons from the University of Pennsylvania Tandem Van de Graaff accelerator. The $(^3He,p)$ reaction products were analyzed with a multiangle magnetic spectrograph. The deuterons in the $(d,\alpha)$ reaction were detected in a scattering chamber using solid state detectors. The new states up to 4.5 MeV were identified in the above reactions and the proton angular distributions for several states were measured and compared with the DWBA predictions codes "DWUC2" and "DWUCK". L-values were extracted, and spins, parities and dominant configurations were suggested. Shell model calculations based on pure configuration assumption were used to obtain the energy values for the coupling of a proton–neutron pair, in the (sgd) shell, outside the "closed" core of 90. The energies, L-values and possible spins and parities of the levels of $^{92}Nb$ found in this study are: 0.00 MeV (L = 6, $J^\pi = 7^+$); 0.136 (L = 2, $J^\pi = 2^+$); 0.224 (L = 1 + 3, $J^\pi = 2^+$); 0.283 (L = 2 + 4, $J^\pi = 3^+$); 0.350; 0.386; 0.492* (L = 4 + 6); 1.080 (L = 0 + 2, $J^\pi = 1^+$); 1.362; 1.488 (L = 0 + 2, $J^\pi = 1^+$); 1.615; 1.647; 1.792 (L = 2, $J^\pi = 2^+$); (1.90); 2.001 (L = 0, $J^\pi = (0,1)^+$); 2.209; 2.270; 2.355; (2.51); 2.602 (L = 2, $J^\pi = (2,3)^+$); 2.698; 2.770; 2.81; 2.895; (3.00); 3.030; 3.106 (L = 0, $J^\pi = (0,1)^+$); 3.276 (L = 0 + 2, $J^\pi = 1^+$); 3.375 (L = 0 + 2, $J^\pi = 1^+$); 3.475 (L = 0 + 2, $J^\pi = 1^+$); 3.536, 3.550 (L = 0 + 2, $J^\pi = 1^+$); 3.753; 3.818; 3.884; 4.07; 4.45; 4.58. (Diss. Abstr. Int., B)

**56759** STUDY OF $^{107}Cd$ EXCITED LEVELS. Rivier, Janine; Moret, Roger (Univ., Grenoble, France). Compt. Rend., Ser. B; 272: No. 21, 1215-7(24 May 1971). (In French).

The study of the $^{107}Indium \rightarrow {}^{107}Cd$ decay allowed the determination of 41 excited levels of cadmium 107 between 0 and 3 MeV. (France)

**56760** ELECTROMAGNETIC TRANSITIONS IN $^{190}Pt$. Husson, Jean-Pierre (Paris Univ., Orsay, France); Macias-Marques, Maria-Ines; Dionisio, Jose Sant'Ana; Vieu, Charles. Compt. Rend., Ser. B; 272: No. 20, 1189-92(17 May 1971). (In French).

The spectra of the internal conversion electrons of some electromagnetic transitions associated with the $^{190}Au \rightarrow {}^{190}Pt$ transmutation, are analyzed with a $\pi\sqrt{2}$ double focusing spectrometer. (France)

**56761** $^{139}Sm$, A NEW NUCLIDE OF RELEVANCE FOR THE SYSTEMATICS OF THE N = 77 ISOMERS. van Klinken, J.; Goering, S.; Habs, D.; (and others) (Kernforschungszentrum, Karlsruhe, Ger. Univ., Heidelberg). Z. Phys.; 246: No. 5, 369-75(1971).

The ground state and an isomeric state of $^{139}Sm$ were identified with $t_{1/2}^{m} = 9.5 \pm 1.0$ s and $t_{1/2}^{g} = 2.6 \pm 0.3$ min. The isomeric decay scheme is presented. It extends the chain of isomers with N = 77. The distance between the $d_{5/2}$ and $h_{11/2}$ levels reaches a maximum for Z = 60. This maximum is much more pronounced than expected from previous theoretical considerations and from systematic trends in the N = 81 and 79 chains. (auth)

**56762** LEVEL SCHEME OF $^{177}Lu$ IN THE REACTION $(n,\gamma)$. Manfrass, P. (Zentralinstitut fuer Kernforschung, Rossendorf, Ger.); Prade, H.; Beitinis, M. R.; (and others). Nucl. Phys.; A172: No. 2, 298-322(1971). (In German).

The level scheme of $^{177}Lu$ has been studied in the $(n,\gamma)$ reaction up to excitation energies of about 2.2 MeV. The singles $\gamma$-ray spectrum and $\gamma\gamma$ coincidences have been measured using Ge(Li) detectors, and conversion electrons have been measured up to 2.2 MeV with a $\beta$-spectrograph. Many levels above 1.2 MeV were found to be excited directly from the capture state at 7070.8 keV. The de-excitation of these levels to lower rotational bands was investigated. The positions of the Nilsson orbitals $1/2^-[541]$, $1/2^-[523]$ and the $\gamma$-vibrational state $(K_0 - 2)$ associated with the $1/2^+[404]$ state are discussed. The rotational bands of the states $1/2^+[404]$, $9/2^-[514]$, $5/2^+[402]$ and $1/2^+[411]$ are discussed in terms of a rotational formula. The quantities $Q_0$, g and $(g_K - g_R)^2/Q_0^2$ have been deduced. (auth)

**56763** NON-NORMAL PARITY STATES OF $^{209}Bi$ AND $^{207}Pb$. Arita, K.; Horie, H. (Tokyo Inst. of Tech.). Nucl. Phys.; A173: No. 1, 97-123(1971).

The low-lying nonnormal parity states of $^{209}Bi$ and $^{207}Pb$ are studied by means of the shell model, assuming 1h-2p and 2h-1p configurations, respectively. The observed energy spectra are well reproduced. The wave functions obtained are analysed in comparison with those defined in the weak-coupling model and existence of the octupole multiplet and the mixing with other states are discussed in detail. The conditions for the existence of the weak-coupling states are also discussed. (auth)

**56764** PROTON DIFFERENTIAL ELASTIC SCATTERING CROSS SECTIONS FOR THE EVEN ISOTOPES OF TIN AT 30.4 MeV. Hardacre, A. G.; Turner, J. F.; Kerr, J. C.; (and others) (Atomic Energy Research Establishment, Harwell, Eng.). Nucl. Phys.; A173: No. 2, 436-48(1971).

Differential cross sections for the elastic scattering of 30.4-MeV protons were measured for the isotopes $^{112}Sn$, $^{114}Sn$, $^{116}Sn$, $^{118}Sn$, $^{122}Sn$, and $^{124}Sn$. With an experimental angular resolution of 0.94° (FWHM) and relative error assignments mostly in the range 1 to 2.5%, results were obtained over the angular range 6° to 88° in 2° intervals, and 90° to 144° in 4° intervals. These measurements are intended as an extension to existing data that already incorporate a similar measurement for $^{120}Sn$. (auth)

**56765** ISOMERIC CROSS-SECTION RATIOS ANALYSIS OF THE $^{134}Ba(\alpha,n)^{137}Ce$ REACTION IN THE SUPERCONDUCTIVITY MODEL. Ribansky, I.; Oblozinsky, P. (Inst. of Physics, Bratislava). Nucl. Phys.; A173: No. 2, 427-35(1971).

The isomeric cross-section ratios of the $^{134}Ba(\alpha,n)^{137}Ce$ reaction at $\alpha$-particle energies between 15 and 28 MeV are analyzed in the statistical-model theory of nuclear reactions by using the superconductivity model of the level density. The results are compared with the experimental data of Swanson and Porile [Nucl. Phys., A144: 344, 355(1970)]. The direct-process contribution is estimated to be ≈7% well above the $(\alpha,2n)$ threshold. Conventional odd-even corrections are found to be inadequate to reproduce the experimental data. (auth)

**56766** SPECTROSCOPY OF $^{93,95}Tc$ BY MEANS OF $^{92,94}Mo(d,n)$. Bommer, J.; Fuchs, H.; Grabisch, K.; Kluge, H.; Roeschert, G. (Hahn-Meitner-Institut fuer Kernforschung, Berlin). Nucl. Phys.; A173: No. 2, 383-92(1971).

The reactions $^{92,94}Mo(d,n)$ were investigated with the time-of-flight method at 6.25 and 7.0 MeV bombarding energy. Ten levels in $^{93}Tc$ and 16 levels in $^{95}Tc$ were observed. Excitation energies and angular distributions were obtained. Analysis with DWBA yielded l values and transition strengths. Spin and parity of three levels in $^{93}Tc$ and ten levels in $^{95}Tc$ are found to be $1/2^+$ because they are populated by l = 0 transfer. Shell-model orbit occupation probabilities of the target ground states are derived by means of sum rules. (auth)

**56767** RADIOACTIVE DECAY OF $^{168}Ho$ AND $^{169}Ho$. Haustein, P. E.; Tucker, A. B. (Ames Lab., Iowa). Nucl. Phys.; A173: No. 2, 321-36(1971).

Gamma rays accompanying the $\beta$ decay of $^{168}Ho$ (3.3 min) and $^{169}Ho$ (4.8 min) were investigated using Ge(Li) detectors. Sources were prepared by the reactions $^{170}Er(\gamma,np)^{168}Ho$ and $^{170}Er(\gamma,p)^{169}Ho$ from targets of isotopically enriched $^{170}Er_2O_3$ and from erbium metal of natural isotopic distribution. Energies and relative intensities are reported for 9 $\gamma$-ray transitions in $^{168}Ho$ decay and 23 transitions in $^{169}Ho$ decay. The decay of $^{168}Ho$ populates primarily the $2^+$, $3^+$, and $4^+$ members of the K = 2, $\gamma$-vibrational band of $^{168}Er$. The spin and parity of doubly odd $^{168}Ho$ are deduced to be $3^+$, in agreement with the theory of Gallagher and Moszkowski. The decay of the $^{169}Ho$ ground state, assigned to the $7/2^-(523)$ Nilsson state, occurs primarily to the first two members of the $5/2^-(523)$ rotational band in $^{169}Er$. The $\gamma$-ray decay pattern to $1/2^-(521)$, $5/2^-(512)$, and $7/2^+(633)$ bands is analyzed. (auth)

**56768** PARITY NONCONSERVATION IN HEAVY NUCLEI AND THE STRUCTURE OF WEAK-INTERACTION HAMILTONIANS. Eman, B.; Tadic, D. (Inst. Rudjer Boskovic, Zagreb. Univ., Zagreb). Phys. Rev., C; 4: No. 3, 661-72(Sep 1971).

Circular $\gamma$ polarization in heavy nuclei ($^{181}Ta$, $^{175}Lu$) has been calculated using the two-body parity-nonconserving potential deduced on the basis of several weak-interaction Hamiltonians. Gauge invariance was elucidated by the Feynman-diagram analysis. The relative contributions from various nuclear single-particle states have been analyzed in detail. Short-range correlations have been approximately taken into account. Our calculation is compared with earlier calculations. According to the calculations, the Cabibbo conventional weak-Hamiltonian model seems to disagree with the $^{181}Ta$ experiment. Other models allowing for extra neutron currents, such as d'Espagnat and the Lee model, might agree with experimental results. This conclusion depends

on the sign of the theoretical result, which cannot be fixed with absolute certainty. The Oakes model seems to give absolute values which are too large. (auth)

**56769** QUANTITATIVE STUDIES OF NUCLEAR STRUCTURE THROUGH ISOBARIC ANALOG RESONANCES. Darmodjo, S.; Alders, R. D.; Martin, D. G.; (and others) (Univ. of Texas, Austin). Phys. Rev., C; 4: No. 3, 672-83(Sep 1971).

Isobaric analog resonances (IAR) observed in the elastic scattering of protons from $^{208}$Pb, $^{138}$Ba, $^{124}$Sn, and $^{120}$Sn are analyzed in the framework of the shell-model theory of reactions. Parametrization of the energy-averaged S matrix elements given by the shell-model theory is discussed, and the dependence of the spectroscopic factors upon the various optical-model parameters is exhibited. The resonance mixing phases for most of the IAR analyzed here cannot be distinguished from zero. Damping of the single-particle wave functions arising from the nonlocality of the optical potentials is consistently incorporated. The nonlocality length of 0.85 F employed in this analysis leads to an attenuation of the single-particle wave functions by about 15% inside the nucleus. Neutron spectroscopic factors obtained here compare favorably with corresponding results from the study of (d,p) and (t,d) reactions. (auth)

**56770** NEUTRON-HOLE-STATE STRUCTURE IN N = 81 NUCLEI. I. $^{144}$Sm AND $^{142}$Nd (p,d). Jolly, R. K.; Kashy, E. (Michigan State Univ., East Lansing). Phys. Rev., C; 4: No. 3, 887-900(Sep 1971).

Angular distributions of deuterons from the (p,d) reaction (energy resolution ~35 keV) on $^{144}$Sm and $^{142}$Nd at E = 35 MeV have been measured and compared with distorted-wave Born-approximation (DWBA) calculations. The DWBA calculations were performed both with and without the finite-range and nonlocality corrections. In some typical cases corrections were also included for the nuclear density dependence of the effective pn interaction. The DWBA cross sections for l = 5 show an enhanced sensitivity to the inclusion of these corrections. Calculations including both the nonlocality and finite-range corrections yield acceptable spectroscopic factors. Considerable fractionation of the $(2d_{\frac{5}{2}})^{-1}_{\nu}$ and the $(1g_{\frac{9}{2}})^{-1}_{\nu}$ states is observed. No measurable population of neutron states in the 82 < N≤ 126 major shell was observed. The single-neutron-hole energies (in MeV) are as follows: $d_{\frac{5}{2}}$, 0.0; $s_{\frac{1}{2}}$, 0.45; $h_{\frac{11}{2}}$, 1.22; $d_{\frac{3}{2}}$, 1.52; and $g_{\frac{7}{2}}$, 2.12 for $^{143}$Sm; and $d_{\frac{5}{2}}$, 0.0; $s_{\frac{1}{2}}$, 0.43; $h_{\frac{11}{2}}$ 1.07; $d_{\frac{3}{2}}$, 1.47; and $g_{\frac{7}{2}}$, 2.20 for $^{141}$Nd. Data on the systematics of splitting and movement of these single-neutron-hole states as a function of the proton number (Z) in $^{143}$Sm, $^{141}$Nd, $^{139}$Ce, and $^{137}$Ba shall be presented in a subsequent paper. (auth)

**56771** INTERNAL-CONVERSION AND $\gamma$-$\gamma$ DIRECTIONAL-CORRELATION STUDIES IN THE DECAY OF $^{103}$Ru. Avignone III, F. T.; Frey, G. D. (Univ. of South Carolina, Columbia). Phys. Rev., C; 4: No. 3, 912-18(Sep 1971).

Internal-conversion coefficients, $\gamma$-ray intensities of weak $\gamma$ rays, and two $\gamma$-$\gamma$ directional correlations in the transitions of $^{103}$Rh, after the $\beta^-$ decay of $^{103}$Ru, were measured. The conversion coefficients are: $\alpha_K(53) = 2.47 \pm 0.14$, $\alpha_K(444) = (6.4 \pm 2.7) \times 10^{-3}$, $\alpha_K(497) = (4.4 \pm 0.4) \times 10^{-3}$, $\alpha_K(557) = (3.7 \pm 0.7) \times 10^{-3}$, $\alpha_K(610) = (2.7 \pm 0.3) \times 10^{-3}$, and $K/L + M + (497) = 8.43 \pm 0.40$. The $\gamma$-$\gamma$ directional correlations of the 557-53 and 444-53-keV cascades were measured with a 33-cm$^3$ Ge(Li) detector and a 2 × 2-in. NaI(Tl) detector on an automatic cycling correlation apparatus. The results are $A_2(557\text{-}53) = -0.130 \pm 0.008$ and $A_2(444\text{-}53) = -0.23 \pm 0.02$. The data imply that the 444-keV transition is pure E2 while the 53-keV transition is mixed M1 + E2 with $\delta(53) = -0.13 \pm 0.03$. The data allow unambiguous spin and parity assignments of $\frac{9}{2}^+$, $\frac{5}{2}^+$, and $\frac{7}{2}^+$ for the 93-, 537-, and 650-keV levels, respectively. The above data imply that the 557-keV transition is a multipole mixed transition with $\delta(557) = -0.32 \pm 0.03$. (auth)

**56772** DECAY OF $^{152}$Nd AND THE ISOMERS OF $^{152}$Pm. Daniels, William R.; Hoffman, Darleane C. (Los Alamos Scientific Lab., N. Mex.). Phys. Rev., C; 4: No. 3, 919-30(Sep 1971).

The radiations associated with the decay of 11.4-min $^{152}$Nd and its 4.1-min $^{152}$Pm daughter have been studied with Ge(Li), NaI(Tl), and anthracene detectors in both singles and coincidence configurations. A tentative decay scheme for $^{152}$Nd involving allowed $\beta$ decay to the 4.1-min isomer of $^{152}$Pm ($1^+$) (log ft = 4.8) and to an excited $1^+$ level 294.6-keV higher (log ft = 4.2) is presented. The 4.1-min level undergoes $\beta$ decay to 10 levels in $^{152}$Sm which have been previously established in decay studies of $^{152}$Eu, and from Coulomb excitation and reaction studies. A new level in $^{152}$Sm has been placed at ≈1081 keV. The total $\beta$-decay energy is nearly the same as the measured $\beta$ end-point energy, 3.6 ± 0.2 MeV. Evidence is presented for the existence of two previously unreported high-spin isomers of $^{152}$Pm having half-lives of 7.5 ± 1.0 min and ≈18 min. A decay scheme is proposed for the 7.5-min isomer ($4^\pm$) of $^{152}$Pm including 16 known $^{152}$Sm levels and new levels at 1081, 1804, and possible 1941 keV. At least 40% of the $\beta$ transitions decay to the 1804-keV level with a log ft of ≈5.7 which suggests hindered allowed or first-forbidden decay. The observation of a 1.8-MeV $\beta$ group in coincidence with an intense 1437-keV $\gamma$ transition which deexcites the 1804-keV level establishes the total $\beta$-decay energy for 7.5-min $^{152}$Pm as 3.6 ± 0.1 MeV. The ≈18-min isomer ($\geq 6^\pm$) of $^{152}$Pm appears to populate a new level at 2172 keV and possibly the 1941-keV level in $^{152}$Sm. (auth)

**56773** COMPARISON OF THE NUCLEAR-REACTION ENERGY SCALE WITH THE GAMMA-RAY ENERGY SCALE. Stocker, H.; Rollefson, A. A.; Hrejsa, A. F.; Browne, C. P. (Univ. of Notre Dame, Dame, Ind.). Phys. Rev., C; 4: No. 3, 930-3(Sep 1971).

The excitation energy of the first excited state of $^{24}$Mg was measured with inelastic deuteron scattering using the energy of $\alpha$ particles from $^{210}$Po as a standard. The result is 1368.2 ± 0.5 keV. The average of recent measurements of the energy of $\gamma$ rays emitted by this state gives an excitation energy of 1368.67 keV based on the electron rest-mass energy. Thus the widely used polonium calibration energy is found to be consistent with the $\gamma$-ray energy standard to within 0.04%. (auth)

**56774** PROTON INELASTIC SCATTERING FROM THE FIVE STABLE, EVEN-MASS ISOTOPES OF MOLYBDENUM. Lutz, H. F.; Heikkinen, D. W.; Bartolini, W. (Univ. of California, Livermore). Phys. Rev., C; 4: No. 3, 934-44(Sep 1971).

Elastic and inelastic scattering of 15-MeV protons, accelerated by the 90-in. cyclotron at Lawrence Radiation Laboratory, Livermore, from isotopically enriched targets of $^{92,94,96,98,100}$Mo was studied with an over-all resolution of 50 keV (full width at half maximum). The experimental angular distributions were analyzed using a coupled-channel calculation. The collective vibrational model was employed to describe the states of the nucleus. Fifty angular distributions of scattered particles were measured and all but three were fitted with theoretical curves. The results for $^{92}$Mo, which has a closed neutron shell associated with the magic number N = 50, are discussed separately. All the inelastic scattering to levels in $^{92}$Mo was fitted with single-step processes. The other even-mass isotopes of molybdenum were analyzed first by considering the main quadrupole and octupole vibrational states and then considering the states that can be described as possible mixtures of one- and two-quadrupole phonons. A high degree of single-phonon admixture was found to be present. Finally the weaker states were considered with the simple $0^+$-$I^\pi$ coupling scheme. Electromagnetic transition rates were inferred from the deformabilities deduced in the present experiment. The results are compared with other experiments. (auth)

**56775** MASS-YIELD CURVE OF FIRST-CHANCE FISSION FROM PROTON- AND DEUTERON-INDUCED FISSION OF $^{226}$Ra. Perry, D. G.; Fairhall, A. W. (Univ. of Washington, Seattle). Phys. Rev., C; 4: No. 3, 977-89(Sep 1971).

Information has been obtained on the mass distribution and kinetic energy release for fission of $^{226}$Ra induced by protons and deuterons at moderate bombarding energies (<20 MeV). The mass distribution, which is triple peaked, has previously been interpreted in terms of two separate fission "modes:" a single symmetric peak, characteristic of symmetric fission, associated with higher excitation energies; and a double-peaked distribution, characteristic of asymmetric fission, associated with lower excitation energies. It is shown that by a proper choice of proton and deuteron bombarding energies, and by a proper weighting of their respective mass-yield curves, the mass distribution for the fission of a single species, $^{228}$Ac, can be determined for a single excitation energy. At excitation energies near 25 MeV this mass distribution for $^{228}$Ac is shown to be a single symmetric peak, in agreement with the hypothesis of two fission components. It is shown further that the measured kinetic energy distributions can also be interpreted in terms of the two-component hypothesis. (auth)

**56776** BETA-GAMMA CORRELATIONS AND MATRIX ELEMENTS FOR SOME FIRST FORBIDDEN NONUNIQUE BETA TRANSITIONS. Manthuruthil, J. C. (Aerospace Research Labs., Wright-Patterson Air Force Base, Ohio); Poirier, C. P.; Sastry, K. S. R.; (and others). Phys. Rev., C; 4: No. 3, 960-76(Sep 1971).

Results of $\beta$-$\gamma$ directional-correlation measurements in the nonunique first-forbidden $\beta$ decay of the ground states of several odd-odd nuclei ($^{124}$Sb, $^{152}$Eu, $^{186}$Re, $^{170}$Tm, $^{84}$Rb) to the first $2^+$ levels in the even-even daughter nuclei are presented. These measurements were made as a function of the $\beta$-ray energy using

XUM

a small shaped-field magnetic spectrometer. The results, in combination with all other available experimental data on each $\beta$ transition, have been analyzed to obtain the nuclear matrix element parameters. The analysis is based on the theoretical expressions given by Morita and Morita using exact electron radial wave functions which include finite nuclear size corrections. In addition, all available experimental data for the nonunique first-forbidden $\beta$ decay of $^{183}$Re and $^{86}$Rb were analyzed. A unique set of parameters was found for $^{186}$Re, $^{189}$Re, and $^{170}$Tm although the set for $^{170}$Tm suffers from a lack of adequate experimental information. For $^{86}$Rb, the matrix element sets depend on whether the shape of the $\beta$ spectrum is statistical or not. For $^{84}$Rb, five distinct sets of parameters were found which fit all available data equally well. For both $^{124}$Sb and $^{152}$Eu, two sets of parameters were found that fit the data equally well; however, it is shown that a measurement of the $\beta$-circularly-polarized $\gamma$ correlation as a function of energy can eliminate one set in each case. Appropriate discussions based on nuclear models are given. (auth)

**56777** DIRECTIONAL CORRELATIONS OF GAMMA RAYS IN $^{152}$Sm MEASURED BY GATING ON THE 244.66-keV TRANSITION. Barrette, J. (Univ. of Montreal); Barrette, M.; Haroutunian, R.; (and others). Phys. Rev., C; 4: No. 3, 991-5(Sep 1971).

Directional-correlation measurements have been performed with two high-resolution and high-efficiency Ge(Li) counters on several $\gamma$ rays in coincidence with the 244.66-keV transition which deexcites the 366.44-keV ($4^+$) state to the 121.78-keV ($2^+$) level in $^{152}$Sm. It was determined that the 1005.15-keV transition deexciting the $4^+$ level of the $\gamma$ band to the $4^+$ level of the ground-state rotational band has 93.3% E2 mixing. Furthermore, the existence of a new level in $^{152}$Sm at 1681.5 keV has been established. (auth)

**56778** DISTORTED-WAVE BORN-APPROXIMATION ANALYSIS OF THE $^{90}$Zr(d,$\gamma$)$^{88}$Y AND $^{89}$Y($^3$He,$\alpha$)$^{88}$Y REACTIONS. Park, Yong Sook; Jones, H. D.; Bainum, D. E. (Army Ballistic Research Labs., Aberdeen Proving Ground, Md.). Phys. Rev., C; 4: No. 3, 778-802(Sep 1971).

The levels of $^{88}$Y have been studied with the $^{90}$Zr(d,$\alpha$) and $^{89}$Y($^3$He,$\alpha$) reactions with 30- to 40-keV resolution at 15-MeV incident energy. The (d,$\alpha$) angular distributions for transitions to eight prominent levels below 2.2 MeV have been measured over $15° \leq \theta \leq 150°$. The reliability of parameters entering distorted-wave Born-approximation calculations was checked in detail. The (d,$\alpha$) calculations include the finite-range correction of Chant and Mangelson. The two-nucleon form factors (f.f.) were generated by the oscillator-expansion technique of Drisko and Rybicki, and the effect of residual interaction on the f.f. and angular distributions was studied. An attempt has been made to determine the (d,$\alpha$) absolute normalization constant based on local zero-range calculations, and limits of $20 \leq D_0^2 \leq 30$ have been set. Two-nucleon f.f. generated by the Bayman-Kallio method were compared with the Drisko-Rybicki f.f. The ($^3$He,$\alpha$) angular distributions for eight strongly populated levels below 1.7 MeV were measured $20° \leq \theta \leq 125°$. Spectroscopic factors and $l_n$ transfers have been extracted with both local zero-range and nonlocal finite-range calculations. The ($^3$He,$\alpha$) results were compared with (d,$\alpha$) results to determine unique parities and narrow $J^\pi$ limits for the levels studied. $^3$He and $\alpha$ elastic scattering on $^{89}$Y has also been measured and optical-model potentials have been determined. Good agreement between this work and the recently reported $^{85}$Rb($\alpha$,n$\gamma$)$^{88}$Y results is seen for the level energy and $J^\pi$ assignments made. (auth)

**56779** PARTICLE-HOLE MULTIPLETS IN $^{88}$Y AND THE MECHANISM OF THE ($^3$He,t) REACTION. Comfort, J. R. (Argonne National Lab., Ill.); Schiffer, J. P. Phys. Rev., C; 4: No. 3, 803-17(Sep 1971).

The reactions $^{87}$Sr($^3$He,d)$^{88}$Y, $^{87}$Sr($\alpha$,t)$^{88}$Y, $^{88}$Sr($^3$He,t)$^{88}$Y, and $^{89}$Y($^3$He,$\alpha$)$^{88}$Y were studied and the data were used to construct a level scheme of $^{88}$Y. Spin and parity assignments are suggested for many new states below 2.5 MeV. The principal components of their wave functions are interpreted in terms of particle-hole multiplets. The angular distributions from the ($^3$He,t) reaction are not well fitted by distorted-wave calculations. Some systematic patterns of the ($^3$He,t) reaction mechanism are noted, but the exceptions indicate that the conventional treatment of the ($^3$He,t) reaction may be far from adequate. (auth)

**56780** ANALYSIS OF THE INELASTIC SCATTERING OF DEUTERONS WITH EXCITED COLLECTIVE STATES IN A MODEL OF STRONG CHANNEL BONDS. Korbetskii, E. V.; Nemets, O. F.; Sokolov, L. S. (Kiev State Univ.). Izv. Akad. Nauk SSSR, Ser. Fiz.; 35: No. 1, 187-92(Jan 1971). (In Russian).

It is shown that the method of [strong channel bond] can be used for spectroscopic analysis of even-even nuclei by means of elastic and inelastic deuteron scattering. Used in scattering through single-phonon excitation states, it does not differ much from the distorted-wave method. The method was used for describing the elastic and inelastic scattering of 13.6-MeV deuterons by $^{12}$C, $^{48}$Ti, $^{60}$Ni, $^{117}$Cd, and $^{118}$Sn nuclei. (R.V.J.)

**56781** NEW $0^+$ STATES IN $^{124}$Te AND $^{126}$Te. Zhelev, Zh. T.; Zaitseva, N. G.; Sabirov, S. S. Izv. Akad. Nauk SSSR, Ser. Fiz.; 35: No. 1, 43-7(Jan 1971). (In Russian).

Excited states in Te populated by the $\beta$-decay of $^{120m,g}$I, $^{120}$I, $^{120*}$I, $^{122}$I, $^{124}$I, and $^{126}$ I were studied using two Ge(Li) detectors with 4.0-keV and 6.0-keV resolution for the 1333-keV $\gamma$-line of $^{60}$Co. Electron internal conversion spectra were studied using a double-focusing $2\pi\sqrt{2}$ $\beta$ spectrometer (R = 0.20%, $\Omega$ = 0.1%). Samples for examination of the $\gamma$-$\gamma$-coincidences were prepared six days following the irradiation of the target. In $^{124}$Te new levels were found at 1156 keV (from 602.5-554 gamma coincidences) and at 2020 keV (from 602.5-1418 and 722.5-695 gamma coincidences). New levels in $^{126}$Te were found at 1396 and 1685 keV by study of coincidences between 389-, 491-, 666-, 730-, and 754-keV gamma rays from the decay of $^{126}$I. (R.V.J.)

**56782** RESONANCE SCATTERING OF $\gamma$ RAYS OF RADIATIVE THERMAL NEUTRON CAPTURE ON CERTAIN NUCLEI. Begzhanov, R. V.; Akharov, S. M. Izv. Akad. Nauk SSSR, Ser. Fiz.; 35: No. 1, 131-4(Jan 1971). (In Russian).

Resonance scattering of capture $\gamma$ rays was studied in a horizontal channel of the VVR-S reactor. A detector with a 70 × 70 mm NaI(Tl) crystal and an FEU-52 photomultiplier connected to a multichannel pulse analyzer were used in the studies of the scattered radiation. In order to determine the partial width of radiation transition to the ground state, $\Gamma_\gamma^0$, total widths, $\Gamma_\gamma$, the energy difference between the lines of emission and absorption, $\delta = |E_\gamma - E_p|$, and the statistical factor, $g = (2I + 1)\ (2I_0 + 1)$, measurements were made of the effective transverse cross section according to the intensity of resonance scattering, resonance absorption using self-absorber, effective cross section of resonance scattering at various temperatures of the diffuser, and the angular $\gamma$-ray distribution during resonance scattering. Parameters of resonance levels from various diffuser-sources are tabulated. (R.V.J.)

**56783** PROPERTIES OF CERTAIN MULTIPARTICLE STATES WITH LARGE SPINS. Kharitonov, Yu. I.; Peker, L. K.; Sliv, L. A. Izv. Akad. Nauk SSSR, Ser. Fiz.; 35: No. 1, 94-9(Jan 1971). (In Russian).

Highly excited energy levels with excitations ranging from 3 to 5 MeV and high spins are considered; production is by spallation induced by residual interactions of three-particle $(j^3)$ and four-particle $(j^3, j_1 = 1/2)$ configurations. The studies are limited to the diagonal approximation. Cascades of the E2 transitions in $^{92}$Mo, $^{209}$Po, and $^{210}$Po are shown and analyzed. (R.V.J.)

**56784** CERTAIN STATES OF $^{134}$Cs. Rozantsev, I. N. Izv. Akad. Nauk SSSR, Ser. Fiz.; 35: No. 1, 112-17(Jan 1971). (In Russian).

Relative intensities of delayed gamma coincidences and multipole transitions following the decay of $^{134}$Cs with $T_{1/2}$ = 53 nsec were studied. The decay scheme is given, and the intensities of $\gamma$-ray cascade transitions for $^{134}$Cs were measured and correlated with published data. (R.V.J.)

**56785** EXCITED STATES OF ODD NONAXIAL NUCLEI. Begzhanov, R. B.; Belen'kii, V. M.; Sharipov, Sh. Izv. Akad. Nauk SSSR, Ser. Fiz.; 35: No. 1, 141-5(Jan 1971). (In Russian).

Energies of excited states and probabilities of electric quadrupole transitions for the odd nonaxial atomic nuclei with the ground-state spin 9/2 are calculated on the basis of the A. S. Davydov model (Excited States of Atomic Nuclei, Atomizdat, 1967), in which it is assumed that the angular momentum j of the external nucleon is retained and the equilibrium shape of the core is approximated by a triaxial ellipoid. Experimental and theoretical data on spins and energies of the excited states of $^{115}$In and $^{249}$Cf and the ratios of the E2 transition probabilities in $^{115}$In are tabulated. (R.V.J.)

**56786** STUDIES OF THE FISSION PROCESS IN ATOMIC NUCLEI IN THE TRANSITION REGION NEAR X = 0.7. Bochagov, B. A.; Kassirov, S. A.; Solyakin, G. E.; Semenchuk, G. G. Izv.

XUM

Akad. Nauk SSSR, Ser. Fiz.; 35: No. 1, 175-9(Jan 1971). (In Russian).

Experimental studies were made of the liquid-drop simulation of light and heavy nuclei in order to determine the differences in the fission of nuclei with identical values of $Z^2/A$ but with a different nucleon composition. The fission was studied with $^{221}$Ac and $^{236}$U with $Z^2/A = 35.84$ and 35.86, respectively; for these nuclei A differed by 15 nucleons (12 n and 3 p). Surface-barrier detectors were used for measuring the energies of paired fission fragments. Experiments with $^{221}$Ac fission were carried out in a multicharged-ion accelerator with a $^{209}$Bi target irradiated by $^{12}$C ions with 82 and 62 MeV energy, and $^{236}$U fission was studied in a cyclotron with a target of $^{232}$Th nuclei irradiated by $^{4}$He ions with 26.4 MeV energy. The results verified the concept of two types of fission—the symmetric and the asymmetric. In the cases in which the distribution p(u) has one maximum during the rupture of the fissioning nucleus at an arbitrary point of the potential barrier (i.e., at arbitrary fixed magnitude E*), the fission is symmetric; the fission is asymmetric when the distribution has two maxima. An intermediate case in which the p(u) has three maxima with one value of E* and one or two maxima with other E* values is also possible. (R.V.J.)

**56787** DROP NUCLEAR MODEL OF FISSION AND KINETIC ENERGY OF FRAGMENTS OF $^{238}$U AND $^{232}$Th FISSION BY NEUTRONS AND $\gamma$ QUANTA. Bochagov, B. A.; Fadeev, V. I. Izv. Akad. Nauk SSSR, Ser. Fiz.; 35: No. 1, 169-74(Jan 1971). (In Russian).

The physical concept of the parameter E* was studied, and the results obtained on the $^{232}$Th and $^{238}$U fission by $\gamma$ quanta and neutrons (at 14 MeV) were analyzed using the parameter E*. The contour of $^{238}$U fission by 14-MeV neutrons is constructed, and the $\overline{M}_H$ (heavy-fragment mass) as a function of E* for $^{238}$U fission by 14-MeV neutrons and 35-MeV $\gamma$ quanta and for $^{232}$Th fission by 14-MeV neutrons and 90-MeV $\gamma$ quanta is given in graphical form. The $\overline{M}_H$ as a function of E* is also given for $^{233}$U, $^{235}$U, and $^{239}$Pu fission by thermal neutrons. It was observed that during fission by 14-MeV neutrons and photons the most probable value of the heavy-fragment mass drops with an increase of E*; i.e., that a symmetrization of fission takes place with the drop from the apex of the barrier. (R.V.J.)

**56788** NUCLEI OF LIGHT ELEMENTS WITH LARGER NEUTRON EXCESS. Artyukh, A. G.; Avdeichikov, V. V.; Vil'chinski, Ya.; (and others) (Joint Inst. for Nuclear Research, Dubna, USSR. Inst. of Physics and Tech., Leningrad). Izv. Akad. Nauk SSSR, Ser. Fiz.; 35: No. 1, 2-17 (Jan 1971). (In Russian).

An attempt was made to produce neutron-rich light elements using the methods of spontaneous fission of $^{252}$Cf and fission of $^{235}$U, $^{233}$U, and $^{239}$Pu by thermal neutrons; deep nuclear spallation reactions induced by high-energy protons; $\pi$-meson capture; and transfer reactions with heavy ions. Graphical data are given of the yield of light-element isotopes during uranium irradiation by 5.5-GeV protons, two-dimensional spectra obtained during irradiation of $^{232}$Th by $^{22}$Ne ions with an energy of 174 MeV, and the yield of O, N, C, B, and Be isotopes during irradiation of $^{232}$Th by $^{15}$N, $^{22}$Ne, and $^{18}$O ions. The search for $^{10}$He as a neutron-rich nucleus and determination of its nuclear stability is described. (R.V.J.)

**56789** DIFFERENTIAL CROSS SECTIONS FOR ELASTIC SCATTERING OF NUCLEONS CONSIDERING EXCITATION LEVELS OF THE COMPOUND NUCLEUS. Sirotkin, V. K.; Chesnokova, V. D. Izv. Akad. Nauk SSSR, Ser. Fiz.; 35: No. 1, 118-24(Jan 1971). (In Russian).

Cross sections for reactions and differential cross sections for elastic scattering of 7-MeV neutrons by $^{90}$Zr, $^{120}$Sn, and $^{181}$Ta; 9.6-MeV protons by $^{120}$Sn; and 11-MeV protons by $^{60}$Ni were analyzed using the method suggested by D. F. Zaretskii et al., (Yader. Fiz. 11: 361(1970)). (R.V.J.)

**56790** DISTRIBUTION OF PARTIAL RADIATION WIDTHS IN $^{238}$U(n,$\gamma$)$^{239}$U. Wasson, O. A. (Brookhaven National Lab., Upton, N. Y.); Chrien, R. E.; Slaughter, G. G.; Harvey, J. A. Phys. Rev., C; 4: No. 3, 900-12(Sep 1971).

The resonant-neutron-capture $\gamma$-ray spectra for 28 resonances below 600-eV neutron energy are measured in $^{238}$U(n,$\gamma$)$^{239}$U with improved neutron and $\gamma$-ray energy resolution to allow an accurate test of the predictions of the statistical model of neutron capture. No convincing departures from these predictions are observed. The variation over 23 S-wave neutron resonances of the $\gamma$-ray transition probabilities to 15 final states is consistent with the Porter-Thomas distribution for both E1 and M1 multipoles. There is also no statistically significant correlation between the different decay modes of the neutron resonances. A large correlation coefficient of +0.81 is observed between the partial radiative widths of the 3991- and 3982-keV $\gamma$ rays. This result, however, is not in violation of statistical independence for a sample size of 15 $\gamma$ rays. The E1 and M1 $\gamma$-ray strength functions are $(2.6 \pm 0.4) \times 10^{-3}$ and $(8.1 \pm 1.6) \times 10^{-3}$, respectively, compared to $3 \times 10^{-3}$ and $4 \times 10^{-3}$ listed by Bartholomew as the median values of all nuclei. Three of the weaker resonances at 10.2, 89.5, and 263 eV are assigned to P-wave capture. The neutron binding energy is measured to be 4806.7 ± 2.0 keV, which is 5.0 keV higher than the previously accepted value. Previously unobserved $\gamma$-ray transitions are reported. (auth)

**56791** DECAY OF $^{90}$Nb. HIGH-EXCITATION STATES IN THE MAGIC NUCLEUS $^{90}$Zr. Zaitseva, N. G.; Kratsik, B.; Muziol, G.; (and others). Izv. Akad. Nauk SSSR, Ser. Fiz.; 35: No. 1, 35-42(Jan 1971). (In Russian).

Measurements were made of $\gamma$ spectra and $\gamma\gamma$-coincidence spectra in $^{90}$Nb decay. The data obtained were used for developing a series of new levels for $^{90}$Zr and studying the properties of these levels. Preparation of the radioactive sources and measuring instrumentation are described, and the energies and intensities of $\gamma$ rays in $^{90}$Nb decay and K-shell internal conversion coefficients for transitions in $^{90}$Zr are tabulated. (R.V.J.)

**56792** DECAY OF $^{238}$Am. Post, J. C.; Aten, A. H. W. Jr. (Instituut voor Kernphysisch Onderzock, Amsterdam. Univ., Amsterdam). Radiochim. Acta; 15: No. 4, 205-6(Jun 1971).

Neutron deficient isotopes of americium were produced in $^{237}$Np($\alpha$,xn) reactions at $\alpha$ energies of 38 to 46 MeV. The $\gamma$ activity of the americium isotopes was studied with a germanium detector. The $\gamma$ lines corresponding to the decay of $^{238}$Am were identified and placed in a decay scheme. (J.W.R.)

**56793** STUDY OF THE $^{236mf}$U ISOMERIC FISSION THROUGH THE $^{235}$U(n,$\gamma$) REACTION IN THE ENERGY RANGE 0.25 TO 4 MeV. Boca, I.; Sezon, M.; Vilcov, I.; Vilcov, N. (Inst. of Atomic Physics, Bucharest). Rev. Roum. Phys.; 16: No. 4, 473-8(1971).

The excitation function for the $^{235}$U(n,$\gamma$) reaction with excitation of the $^{236}$U fission isomer was measured for neutron energies of 0.25 to 4 MeV. A half-life of 80 ± 20 ns was found for the $^{236}$U fission isomer. The measurements were compared with theoretical predictions. (J.W.R.)

**56794** QUASI-PARTICLE DESCRIPTION FOR INDIUM. Alzetta, R. (Nuclear Research Inst., Rez, Czech.); Gmitro, M.; Gambhir, Y. K. Czech. J. Phys.; 21: No. 7, 768-84(1971).

The quasiparticle model has been applied for the description of the nuclear properties of the low-lying states of In isotopes. The Hamiltonian is diagonalized in the space obtained by coupling zero- and two-quasineutron configurations with the proton-hole states in N = Z = 50 core, using the renormalized Tabakin interaction. The inclusion of two-hole one-particle proton configurations, consistent with the experimental findings in $^{114}$Cd($^{3}$He,d)$^{115}$In reaction, in a weak coupling approximation in which the quasineutron excitation modes are first generated independently, and then coupled to the proton hole excitations to obtain the configuration space for the diagonalization work, is also studied quantitatively. The energy spectrum of $^{115}$In is calculated and discussed. (auth)

**56795** NEUTRON RESONANCE CROSS SECTION ANALYSIS IN FILTERED NEUTRON BEAMS. Bohl, William Raymond. Madison, Wis.; Univ. of Wisconsin (1971). 197p. University Microfilms Order No. 71-14,128.

Thesis.

A novel technique to verify low keV cross sections has been developed at the National Reactor Testing Station. The technique follows from the prominent interference minimums in the cross sections of scandium and iron. Beams of 2 and 24.5 keV based on scandium- and iron-filtered neutrons have been developed. The problem treated here is the analysis of filtered beam measurements on materials containing unresolved resonance cross sections. For accuracy in treating resonance overlap and interference, a ladder approach is used. Stratification procedures are investigated to obtain statistical mean values utilizing only a few ladders such that computer time is minimized. The use of individual resonance test statistics closely correlated to predictions of possible measurable quantities is found to possess good stratification properties if self-shielding is significant and resonance overlap is small. If self-shielding is small and resonance overlap is significant, the optimum approach is to sample without replacement from a pool initially containing all resonances for the ladder. An integral transport theory (ITT) treatment is applied to correct for multiple scattering and self-shielding effects in analyzing activation measurements. The ITT technique forms the basis of the computer code FACE, written in FORTRAN IV for

XUM

the UNIVAC 1108 and IBM 360/75. The code treats a one-dimensional homogeneous slab with up to 5 isotopes, 20 spatial regions, and an arbitrary number of energy groups. The savings in time over Monte Carlo is estimated to be at least a factor of 10. Activation in gold and indium using the iron-filtered beam are the principle measurements analyzed. The cross section stratification approach is coupled with the FACE code. Parametric studies indicate that multiple scattering and self-shielding effects are relatively insensitive to the average resonance parameter set used. The shape of curves of activation as a function of thickness determined from a stack of foils compare reasonably well with FACE predictions. A slight low-energy flux component at the present irradiation position is probably present. Further, present reproducibility of measurements is found to be poor. However, it is believed that with a systematic experimental approach in a high flux reactor, scandium- and iron-filtered neutron beams could produce useful and rather precise cross section information. (Diss. Abstr. Int., B)

**56796** HIGH-SPIN ROTATIONAL EXCITATION IN $^{173}$Hf. Birattari, C.; Grassi Strini, A. M.; Strini, G.; Tagliaferri, G. (Univ., Milan. Istituto Nazionale di Fisica Nucleare, Milan). Lett. Nuovo Cim.; 2: No. 4, 187-92(24 Jul 1971).

The high-spin rotational states of $^{173}$Hf were excited in the reaction $^{175}$Lu(p,3n) using a natural Lu target. The proton energy was varied from 20 to 40 MeV in 2 MeV steps. Transitions in $^{173}$Hf were studied by in-beam $\gamma$-ray spectroscopy. Gamma spectra and excitation functions are presented. A level scheme for the K = 112$^-$ rotational band in $^{173}$Hf is proposed. (J.W.R.)

**56797** ANOMALOUS INTERNAL CONVERSION OF E1 TRANSITIONS IN OUTER ATOMIC SHELLS. Dragoun, O. (Nuclear Research Inst., Rez, Czech.); Blumberg, H. Czech. J. Phys.; 21: No. 7, 785-93(1971).

The experimental N and O shell conversion coefficients of highly hindered E1 transitions were found to be anomalous. The discrepancies as well as those for the L and M shells were removed by using the following values of the nuclear current parameter $\eta$: 9.2 ± 0.1 for the 6.21 keV transition in $^{181}$Ta, 8.5 ± 0.5 or −7.5 ± 0.5 for the 84.20 keV transition in $^{231}$Pa and 1.9 ± 0.2 for the 26.38 keV one in $^{237}$Np. (auth)

**56798** LEVEL STRUCTURE OF THE NEAR $^{208}$Pb NUCLEI (NEUTRON-DEFICIENT Pb AND Bi ISOTOPES). Kusch, Wlodzimierz (Instytut Badan Jadrowych, Swierk, Poland). Nukleonika; 16: No. 3-4, 97-124(1971). (In Polish).

The structure of the low-lying levels of the near $^{208}$Pb nuclei, especially of neutron-deficient Pb and Bi isotopes is discussed. Both experimental and theoretical works concerned with the determination of the energy of excited states by the shell model are discussed. The regularity of the level structure revealed by the existence of isomeric states among these nuclei as well as to the effects of the particle-vibration coupling have been observed. Special attention has been concentrated on the results concerning the $^{204}$Po decay to the excited states of $^{204}$Bi, recently obtained by the author. A tentative level scheme of $^{204}$Bi is proposed on the basis of measurements of the $\gamma$-spectra, coincidence spectra, and electron conversion spectra. (auth)

**56799** RECOIL STUDY OF THE $^{209}$Bi($\alpha$,p)$^{212m,g}$Po REACTION MECHANISM. Chulick, E. T.; Natowitz, J. B. (Texas A and M Univ., College Station). Nucl. Phys.; A173: No. 3, 487-96(1971).

Recoil techniques have been used to determine excitation functions, recoil ranges and angular distributions of the product nuclei in the reaction $^{209}$Bi($\alpha$,p)$^{212m,g}$Po. The production of both states is found to occur by a direct reaction mechanism. A comparison of experimental recoil angular distributions with DWBA calculations of the angular distributions expected from triton transfers of varying orbital angular momentum suggests that the $^{212m}$Po state is populated primarily by l = 11 transfer reactions. (auth)

**56800** CALCULATION OF THE GIANT DIPOLE RESONANCE IN A 1p–1h CONTINUUM SHELL-MODEL APPROXIMATION FOR $^{208}$Pb. Barrett, R. F. (Univ., Frankfurt am Main); Delsanto, P. P. Nucl. Phys.; A173: No. 3, 641-64(1971).

The results of a continuum shell-model calculation for $^{208}$Pb are presented and discussed. A method of locating the bound states embedded in the continuum is described which enables the accurate location and identification of resonances in the total photo-absorption cross section. The final cross section is then calculated using the eigenchannel reaction theory. The partial photo cross sections and the angular distribution of the reaction products are also calculated. Results of the calculations are compared with those of experiment and of earlier bound-state calculations. (auth)

**56801** SEARCH FOR BREMSSTRAHLUNG-INDUCED FISSION ISOMERS OF $^{238}$U AND $^{239}$Pu. Tamain, B. (Univ., Clermont, France); Pfeiffer, B.; Wollnik, H.; Konecny, E. Nucl. Phys.; A173: No. 3, 465-76(1971).

Delayed fission of $^{238}$U and $^{239}$Pu induced by bremsstrahlung has been measured using the Giessen linear electron accelerator at an electron energy of 53 MeV. The half-lives found are about 200 ns for $^{238}$U and about 500 ns for $^{239}$Pu. For both nuclei the delayed to prompt fission ratio is about $10^{-5}$. (auth)

**56802** RESONANCE NEUTRON CAPTURE BY $^{170}$Yb AND $^{172}$Yb. Ritter, J. C.; Namenson, A. I. (Naval Research Lab., Washington, D. C.). Nucl. Phys.; A173: No. 3, 477-86(1971).

Primary $\gamma$-ray spectra following resonance neutron capture by $^{170}$Yb and $^{172}$Yb were observed using the NRL linac neutron time-of-flight facility. Spectra from the first four resonances in $^{170}$Yb and the first three resonances in $^{172}$Yb were studied with a 30 cm$^3$ Ge(Li) detector using natural and separated isotope targets. The intensity of $\gamma$-ray transitions to particular Nilsson bands in $^{171}$Yb and $^{173}$Yb was examined for non-statistical effects. Possible regularities similar to those observed in thermal capture are discussed. (auth)

**56803** DELAYED NEUTRONS FROM THE $\tau$- AND $\alpha$ INDUCED FISSION OF $^{238}$U, $^{232}$Th, AND $^{209}$Bi. Chulick, Eugene T.; Reeder, Paul L. (Washington Univ., St. Louis). Nucl. Phys.; A173: No. 3, 497-519(1971).

The production of delayed neutrons from fission of $^{238}$U, $^{232}$Th and $^{209}$Bi with 20–34 MeV $\tau$- and $\alpha$-particles has been studied. For $^{238}$U and $^{232}$Th, delayed-neutron decay curves were analyzed into 7 components, three of which correspond to the particular precursors $^{87}$Br, $^{88}$Br and $^{137}$I. The cross sections for delayed-neutron production increase up to about 30 MeV due to the increase in fission cross section, but then decrease with 34 MeV $\tau$-particles. The number of delayed neutrons per fission as a function of excitation energy shows structure attributed to enhanced chain yields for certain light masses. For $\tau$-fission of $^{209}$Bi, four components were sufficient to fit the observed delayed-neutron decay curves. Half-lives of 55, 16.2 ± 1.5, 3.2 ± 0.7 and 1.4 ± 0.8 s were obtained corresponding to the half-lives of known Br precursors. Heavy-mass precursors in the iodine mass region are noticeably absent as expected from the symmetric mass-yield curve for Bi. (auth)

**56804** ANGULAR DISTRIBUTIONS OF FRAGMENTS IN THE FISSION OF URANIUM AND THORIUM NEAR THE (n,2n'f) THRESHOLD. Barutcugil, E.; Juhasz, S.; Varnagy, M.; Nagy, S.; Csikai, J. (Kossuth Univ., Debreccen, Hungary). Nucl. Phys.; A173: No. 3, 571-6(1971).

The angular distributions of fragments from the neutron-induced fission of $^{236}$U and $^{232}$Th were measured by polycarbonate track detectors at the energy $E_n$ = 14.1 MeV. The effect of the (n,2n'f) threshold has been observed. (auth)

**56805** NUCLEAR CHARGE DISPERSION OF LIGHT-MASS ELEMENTS IN THE FISSION OF $^{232}$Th BY PROTONS OF MEDIUM ENERGY. McGee, T.; Rao, C. L.; Yaffe, L. (McGill Univ., Montreal). Nucl. Phys.; A173: No. 3, 595-608(1971).

The fission of $^{232}$Th by protons of energies 20–85 MeV has been studied. Independent formation cross sections of $^{90m}$Y, $^{90m+g}$Y, $^{91m}$Y, $^{91m+g}$Y, $^{92}$Y, $^{95m+g}$Nb, $^{96}$Nb, $^{97}$Nb and $^{98}$Nb, and cumulative formation cross sections for $^{91}$Sr, $^{92}$Sr, $^{93}$Y, and $^{97}$Zr were measured. Charge dispersion curves were obtained. The full-width at half-maximum remains sensibly constant over this energy range, unlike products studied in the heavy-mass region. The value of $Z_A - Z_p$ decreases, but does not show the same sensitivity to the N/Z value of the target, as found in the heavy-mass region. Calculation shows that the data for $Z_p$ lie closer to the unchanged charge distribution than that suggested by the equal charge displacement hypothesis. An estimate was made of the number of neutrons emitted in fission. The light fragment was found to emit half the number of neutrons as the heavy fragment. (auth)

**56806** FISSION OF MEDIUM MASS NUCLEI INDUCED BY 167 MeV ALPHA PARTICLES. Pate, Brian D.; Peter, J. (Laboratoire de Chimie Nucleaire, Orsay, France). Nucl. Phys.; A173: No. 3, 520-36(1971).

Mica track detectors have been employed to measure the intensity, angular distribution and track-length distribution of fission fragments from eleven target nucleides from Cu to Ho, bombarded with 167 MeV $\alpha$-particles. Calibration of the mica detectors was effected with known projectiles, energies and intensities. Fissilities have been found to decrease monotonically with decreasing target mass, and no abrupt change in the fission mass-division mode was detectable in the series of systems studied, in conflict with theo-

retical expectations. The total fission fragment kinetic energy was, however, found to decrease with target mass in accordance with model calculations. (auth)

## Nuclear Theory

*Refer also to abstracts 56529, 56530, 56741, and 56768.*

**56807** (CERN–71-14) SPRING SCHOOL ON PION INTERACTIONS AT LOW AND MEDIUM ENERGIES, LYCEUM ALPINUM, ZUOZ, ENGADIN, SWITZERLAND, 29 MARCH–8 APRIL 1971. PROCEEDINGS. (Schweizerisches Institut fuer Nuklearforschung, Zurich. European Organization for Nuclear Research, Geneva (Switzerland)). 4 Aug 1971. 396p. Dep. NTIS (U. S. Sales Only).

Separate abstracts were prepared for the seven lectures presented. (J.F.P.)

*For abstracts of individual lectures see: 56422, 56496, 56571, and 56808–56811.*

**56808** (CERN–71-14, pp 1-65) SOFT AND HARD PIONS IN NUCLEI. Ericson, M. (Lyon Univ. (France). European Organization for Nuclear Research, Geneva (Switzerland)). 4 Aug 1971.

In Spring school on pion interactions at low and medium energies.

The applications of the soft pion theorems to pion reactions with nuclei are discussed. Examples of soft pion theorems, applications of soft pion results, the elastic scattering charge antisymmetric amplitude, the charge symmetric amplitude, and radiative capture are covered. (J.F.P.)

**56809** (CERN–71-14, pp 67-99) NUCLEAR MODELS. Green, A. M. (Eidgenoessische Technische Hochschule, Zurich (Switzerland)). 4 Aug 1971.

In Spring school on pion interactions at low and medium energies.

The aim is to illustrate ways in which the nuclear physics aspects of various middle-energy phenomena are treated. Wherever possible, the same phenomena will be discussed, as the nuclear physics approximations employed become more and more realistic. Firstly, the use of the so-called elementary particle method is discussed in the particular case of the partial capture rate $\mu^- + O^{16}(g.s) \rightarrow N^{16}(g.s.) + \nu_\mu$. Then we shall look at the corresponding total capture rate to illustrate the use of the Fermi gas model, Migdal theory, and the standard shell model. (auth)

**56810** (CERN–71-14, pp 155-228) PRODUCTION AND ABSORPTION OF PIONS ON NUCLEI, AND DISPERSION RELATIONS FOR ELASTIC NUCLEAR SCATTERING. Locher, M. P. (Schweizerisches Institut fuer Nuklearforschung, Zurich). 4 Aug 1971.

In Spring school on pion interactions at low and medium energies.

These review lectures cover the $NN \rightarrow NN\pi$ interaction, pion absorption on light nuclei, forward dispersion relations for nd and $n^4He$ scattering and for incident pions on nuclei, and partial-wave dispersion relations for $\pi d$ and nd elastic scattering. (J.F.P.)

**56811** (CERN–71-14, pp 289-378) SCATTERING OF PIONS FROM NUCLEI. Wilkin, C. (University Coll., London (England)). 4 Aug 1971.

In Spring school on pion interactions at low and medium energies.

A review is given of pion scattering from nuclei in processes where the pion does not vanish. The phase shift analysis, the impact parameter representation, simple collective models, the single scattering approximation, the optical potential including correlations, Glauber theory, the influence of spin and isospin, Coulomb distortion of the optical potential, inelastic scattering to discrete levels, and other inelastic scatterings are covered. (J.F.P.)

**56812** (COO–1120-124) COLLECTIVE MODEL OF ODD-ODD DEFORMED NUCLEI. Sharma, S. D. (Kansas Univ., Lawrence. Nuclear Structure Lab.). [1970]. Contract AT(11-1)-1120. 134p. Dep. NTIS.

Thesis.

A model of odd-odd nuclei, in which two odd nucleons are attached to a rotating core, is described. The Hamiltonian consists of $H_R$, the rotational part, $H_p$ and $H_n$, the Hamiltonians for proton and neutron moving in harmonic oscillator potential wells with l.s and $l^2$ terms, $V_{pn}$, the residual neutron-proton interaction which has a Gaussian radial dependence with a Serber exchange mixture. The model is applied to all the main odd-odd nuclei whose energy spectra are experimentally known. The present investigation deals with all the main odd-odd nuclei on the basis of symmetric and asymmetric core models. The important feature of the model spectrum is found to be the constancy of basis in the symmetric core formulation which is shown to be related with core-rotation. The concept of state-gradient is introduced and the modification of the rotational features of the spectra by the particle states is explained in terms of state-gradient. The magnetic moments and quadrupole moments of ground states are calculated and compared with the experimental values, wherever possible. The general conclusions from this study are discussed and the suggestions for improvements are made. (auth)

**56813** (COO–1746-57) MARISCOTTI DESCRIPTION OF GROUND STATE BANDS OF EVEN–EVEN NUCLEI. Harris, Samuel M. (Purdue Univ., Lafayette, Ind. Dept. of Physics). [1970]. Contract AT(11-1)-1746. 8p. Dep. NTIS.

Mariscotti has shown that almost all ground-state bands in even-even nuclei may be fit within the framework of the higher-order-cranking model. Three types of bands are observed; some follow the $\gamma$ trajectory ($\vartheta_0 > 0$, $C > 0$), others the $\alpha$ and $\alpha$–$\beta$ trajectories ($\vartheta_0 < 0$, $C > 0$). It is shown that the first two trajectories are unique in that they yield bands with no upper cut-off for which the angular momenta and angular velocities are parallel, whereas the $2^+$ state of the $\alpha$–$\beta$ trajectory has its angular momentum opposite to its angular velocity. (auth)

**56814** (COO–2022-7) CODILLI II: A FORTRAN IV PROGRAM FOR THE ANALYSIS OF NEUTRON RESONANCE WITH PROGRAM SCORE. Technical Report No. 3. Adler, D. B.; Adler, F. T. (Illinois Univ., Urbana. Dept. of Physics). Jan 1971. Contract AT(11-1)-2022. 29p. Dep. NTIS.

This FORTRAN IV version of Program CODILLI was made compatible with Program SCORE so that it can be used in the interactive analysis of neutron resonance data with Program SCORE. The batchmode version of CODILLI II can be used independently. CODILLI II utilizes the multilevel expansion in a form which is applicable to the analysis of neutron resonance data of fissile as well as of nonfissile nuclides. Options are included which permit one to treat selected resonances as symmetrical, so that nonfissile nuclides can readily be analyzed. The program allows one either to use a least-squares data ditting procedure, or to calculate cross section curves from prescribed resonance parameters. In either case, the cross section curve may include contributions of several (at present four) nuclides. Different spin states may also be treated as separate isotopes. Tests were implemented which allow one to display the quality of fit of individual lines or of the entire cross section curve. Provisions are made to treat experimental resolution effects in a flexible manner, with particular attention to the use of the program in analyzing LINAC data. The option of calculating with CODILLI II cross section curves from prescribed parameters is of particular relevance for the anticipated use with Program SCORE. The "conversational mode" of this program will allow for a rapid adjustment of parameters which enter the trial function in a nonlinear form, and thus eliminate the need for nonlinear fitting procedures which were contained in the older version of CODILLI. (auth)

**56815** (INP–741) OPTICAL MODEL PROGRAMME WITH THE AUTOMATIC SEARCH ROUTINE EXTENDED TO INCLUDE THE SPIN-ORBIT TERM. "OMAS." Ziemkiewicz, Miroslaw (Institute of Nuclear Physics, Krakow (Poland)). Jan 1971. 41p. Dep. NTIS (U. S. Sales Only).

The OMAS program written in the ODRA–ALGOL autocode calculates the differential cross sections and polarizations for particles with spin 0, $\frac{1}{2}$ and 1 elastically scattered on atomic nuclei. The program permits an automatic search over the space of the nuclear optical model parameters, yielding optimum fits to experimental cross sections. (auth)

**56816** (JAERI-Memo-4383) METHOD FOR CALCULATING ENERGY DEPENDENCE OF MASS CHAIN YIELD OF FISSION. Tasaka, Kanji; Seki, Yasushi (Japan Atomic Energy Research Inst., Tokyo). Mar 1971. 39p. (In Japanese). Dep. NTIS (U. S. Sales Only).

An attempt to give a phenomenological explanation for the energy dependence of the mass chain yield of nuclear fission, using the energy dependence of the penetration factor through the potential barrier for nuclear fission is presented. The mass chain yield of nuclear fission is defined as the sum of the fission yields of the nuclides with the same mass number. The mass chain yield of $^{235}U$ fission by the neutrons with kinetic energies, 1.95 and 15 MeV was calculated utilizing the experimental mass chain yield data for thermal neutrons. The calculated values are compared with the experimental values in ENDF/B. As the result, it is concluded that the calculated values coincide with the experimental

XUM

values fairly well, if appropriate parameters are chosen. Using this method, the mass chain yield of $^{235}U$ fission by a neutron of any desired energy can be calculated from the mass chain yield data by a thermal neutron. It is planned to apply this method to calculate the mass chain yield of other nuclides, especially fertile nuclides, and through comparison with the experimental data to investigate the application limit of the method more thoroughly. This method is programmed for computer calculation. The programme list of the code "TUNNEL-FY" is given in Appendix 1. (auth)

**56817** (JINR-E4-5836) MULTI-CHANNEL ASPECTS IN STRIPPING REACTIONS ON SPHERICAL AND DEFORMED NUCLEI. Luk'yanov, V. K. (Joint Inst. for Nuclear Research, Dubna (USSR). Lab. of Theoretical Physics). 1971. 12p. (CONF-710708-2). Dep. NTIS (U. S. Sales Only).

From Symposium on the nuclear three body problem and related topics; Budapest, Hungary (7 Jul 1971).

The main multi-channel features of A(d,p)B stripping reactions, connected with low-lying collective state virtual excitations in the nuclei A and B are analyzed. In deriving the reaction amplitude the generalized distorted wave method is used where the multi-channel aspects of the problem are taken into account by the coupled channel calculations of the corresponding distorted waves. Using the so-called double adiabatic approach it is possible to obtain the cross section in a very simple and obvious form. The reaction turns out to be a multistep one where each step characterizes the transfer of a neutron via one of the excited levels of the nuclei A and B. The multistep effects are analyzed in the case of the spherical (with phonon states) and deformed (with rotational states) nuclei. (auth)

**56818** (JINR-E4-5880) ON CORRELATIONS BETWEEN REDUCED NEUTRON AND RADIATIVE WIDTHS IN NEUTRON RESONANCES OF COMPOUND ODD-N NUCLEI. Solov'ev, V. G. (Joint Inst. for Nuclear Research, Dubna (USSR). Lab. of Theoretical Physics). 1971. 5p. Dep. NTIS (U. S. Sales Only).

The cases are considered which are the most favorable for experimental studies of correlations between reduced neutron and radiative widths in s- and p-neutron resonances of compound odd-N nuclei. (auth)

**56819** (JINR-P4-5889) COLLECTIVE $1^+$ STATES IN EVEN-EVEN DEFORMED NUCLEI. Gabrakov, S. I.; Kuliev, A. A.; Pyatov, N. I.; Salamov, D. I.; Schulz, H. (Joint Inst. for Nuclear Research, Dubna (USSR). Lab. of Theoretical Physics). Jul 1971. 17p. (In Russian). Dep. NTIS (U. S. Sales Only).

In the framework of Tamm-Dankov and RPA methods the properties of collective states with $I^\pi = 1^+$ (K = 0 or 1) in even-even deformed nuclei were studied. The pairing interactions and spin-spin correlations are taken into account in the model. The strength of the spin-spin force is deduced from the calculation of magnetic moments in odd-mass nuclei. The calculation of $B(M1, 0 \rightarrow 1^+)$ values, dipole sum rule and M1-transition strength function showed that in rare-earth nuclei the spin-spin correlations concentrate the main M1-transition strength in the high-energy region (≈10 MeV), where the coherent $1^+$ states (magnetic dipole resonance) can be formed. The structure of these states is investigated. (auth)

**56820** (JINR-P1-5997) SPECTRUM AND ASYMMETRY OF HIGH ENERGY NEUTRONS IN THE REACTION $\mu^- + {}^{16}O \rightarrow {}^{15}N + n + \nu$. Salganik, Yu. A.; Eramzhyan, R. A. (Joint Inst. for Nuclear Research, Dubna (USSR). Lab. of Theoretical Physics). 1971. 14p. (In Russian). Dep. NTIS (U. S. Sales Only).

The spectrum and asymmetry of angular distribution in the $\mu^- + {}^{16}O \rightarrow {}^{15}N + n + \nu$ is calculated in the framework of the direct reaction mechanism. The dependence of above mentioned characteristics on the final state interaction is investigated. The effect of the exchange terms in the matrix elements is discussed. The relativistic terms of the muon-nucleon Hamiltonian are taken into account. (auth)

**56821** (LYCEN-7104) SOME MICROSCOPIC ASPECTS OF NUCLEAR REACTIONS. A Conference Held at La Toussuire, France, February 15-19, 1971. (Lyon Univ. (France). Institut de Physique Nucleaire). 1971. 284p. (In French and English). (CONF-710216).

Twenty-five papers were presented at the conference. Eight of them are presented in abstract form. Separate abstracts were prepared for the remaining 17. (France)

*For abstracts of individual papers see: 56390, 56593, 56642, 56652-56654, 56688, and 56822-56831.*

**56822** (LYCEN-7104, C1,1-13) MICROSCOPIC THEORY OF NUCLEON-NUCLEUS SCATTERING AND OPTICAL POTENTIAL. Vinh Mau, N. (Paris Univ., Orsay (France). Institut de Physique Nucleaire). (In French).

From Conference on some microscopic aspects of nuclear reactions; La Toussuire, France (15 Feb 1971).

To describe the nucleon-nucleus scattering in a microscopic theory, a system composed of a nucleon and a set of nucleons interacting in a given bound state was studied. The principle of the optical potential calculation and the approximation made are recalled. (France)

**56823** (LYCEN-7104, C3,1-40) METHODS FOR ANALYZING TRANSFER REACTIONS. Becker, Francois (Centre National de la Recherche Scientifique, Strasbourg (France). Laboratoire de Physique Theorique). (In French).

From Conference on some microscopic aspects of nuclear reactions; La Toussuire, France (15 Feb 1971).

The properties of the scattering amplitude in direct reactions or compound nuclei reactions are discussed and a separation method is deduced from them. The different factors involved in a transfer reaction are analyzed and the physical bases of most of the classical theories are shown. The methods for analyzing direct transfer reactions (particularly distorted wave methods) are presented. (France)

**56824** (LYCEN-7104, C4,1-17) SHORT-RANGE CORRELATIONS. Do Dang, G.; Longuemare, C. (Paris Univ., Orsay (France). Laboratoire de Physique Theorique et Hautes Energies). (In French).

From Conference on some microscopic aspects of nuclear reactions; La Toussuire, France (15 Feb 1971).

The existence of a strong repulsion or a hard core leads to short range correlations. Methods used for studying these correlations (Jastrow wave function and Villars formalism) are described. The effect of correlations in electron-nucleus scattering and $\mu$ capture is recalled and an example of the direct investigation of correlations is given. (France)

**56825** (LYCEN-7104, C6,1-12) GENERATING COORDINATES IN CONTINUUM STATES. Giraud, B.; Hocquenghem, J. C.; Lumbroso, A. (Commissariat a l'Energie Atomique, Saclay (France). Centre d'Etudes Nucleaires). (In French).

From Conference on some microscopic aspects of nuclear reactions; La Toussuire, France (15 Feb 1971).

The generator coordinate formalism leads to a microscopic description of nuclear collisions and might be able to describe fission and heavy nuclei collisions. An example which can be solved exactly and a numerical application in the case of the elastic collision between two very light nuclei are given. This theory was shown to be equivalent to the resonating group formalism for clusters. (auth)

**56826** (LYCEN-7104, C7,1-36) SPIN-ORBIT INTERACTION IN NUCLEON INELASTIC SCATTERING. Raynal, J. (Commissariat a l'Energie Atomique, Saclay (France). Centre d'Etudes Nucleaires). (In French).

From Conference on some microscopic aspects of nuclear reactions; La Toussuire, France (15 Feb 1971).

Spin-orbit coupling was introduced into the optical model to describe the elastic scattering polarization of particles with spin and inelastic scattering. A macroscopic description of the target nucleus was made without taking into account the orbits of the nucleons. Then the scattering amplitude of particles of spin ½, and the deformed spin-orbit coupling were calculated; this coupling was introduced into a coupled equation program using the sequential interaction method (ECIS). The microscopic description takes into account the different nucleons. The helicity formalism was presented and nuclear reactions were studied using either a finite interacting distance neglecting the incident nucleon antisymmetrization with nucleons, or a zero interacting distance interaction. It is thus possible to understand why the spin-orbit coupling deformation is more important for some targets. (France)

**56827** (LYCEN-7104, S8,1-10) ISOVECTOR EXCITATIONS IN PHOTONUCLEAR REACTIONS. Goulard, B. (Laval Univ. (Quebec)). (In French).

From Conference on some microscopic aspects of nuclear reactions; La Toussuire, France (15 Feb 1971).

Some simple properties of isovector nuclear excitations are given. The total strength excitation (that is to say the sum of the intensities leading to all the possible states) was studied and these excitations and their energy spectra were analyzed

in the framework of the shell model. A complete calculation was made for $^{88}Sr$. The experimental results concern essentially isospin in photonuclear reactions. (France)

**56828** (LYCEN–7104, S9.1–7) DEFORMATIONS IN THE s–d SHELL AND INELASTIC SCATTERING OF POLARIZED PROTONS. de Swiniarski, R. (Grenoble Univ. (France). Laboratoire de Physique Nucleaire); Raynal, J. (Commissariat a l'Energie Atomique, Saclay (France). Centre d'Etudes Nucleaires). (In French).

From Conference on some microscopic aspects of nuclear reactions; La Toussuire, France (15 Feb 1971).

The deformations determined by calculations on cross sections only are not modified when polarizations are taken into account unless the complete Thomas form is used for the spin-orbit coupling. Therefore, the complete Thomas form must be used in all inelastic scattering calculations with polarized protons. (France)

**56829** (LYCEN–7104, S12.1–4) PAULI PRINCIPLE IN THE THEORY OF REACTIONS BETWEEN LIGHT NUCLEI. Zaikine, D. A. (Commissariat a l'Energie Atomique, Saclay (France). Centre d'Etudes Nucleaires). (In French).

From Conference on some microscopic aspects of nuclear reactions; La Toussuire, France (15 Feb 1971).

The influence of the Pauli principle is studied in the framework of the generator coordinate principle, and is applied to collisions between two light fragments. (auth) (France)

**56830** (LYCEN–7104, S14.1–18) QUASI-ELASTIC SCATTERING BY SUBSTRUCTURE OF LIGHT NUCLEI. Gaillard, Paul (Lyon Univ. (France). Institut de Physique Nucleaire). (In French).

From Conference on some microscopic aspects of nuclear reactions; La Toussuire, France (15 Feb 1971).

The formalism used to obtain the quasielastic scattering cross section in the P.W.I.A. is recalled. The spectroscopic data related to the nuclear clusters are given. Information about reaction mechanisms and spectroscopy obtained from the study of these reactions is presented. (France)

**56831** (LYCEN–7104, S18.1–18) DIFFERENTIAL METHOD AND FEYNMAN NUCLEAR GRAPHS. Giffon, M. (Lyon Univ. (France). Institut de Physique Nucleaire).

From Conference on some microscopic aspects of nuclear reactions; La Toussuire, France (15 Feb 1971).

The differential method introduced in the relativistic theory is used as a first step in a unified treatment of the nonrelativistic Feynman amplitudes (NRFA) describing direct nuclear reactions. Only single loop graphs (triangular and box diagrams) were studied. (France)

**56832** (NYO–3525–67) STUDIES OF ELECTROMAGNETIC PROPERTIES OF EXCITED STATES OF NUCLEI. Final Report, March 15, 1965–March 14, 1971. Metzger, F. R. (Bartol Research Foundation, Swarthmore, Pa.). 31 Mar 1971. 27p. Dep. NTIS.

Research on the electromagnetic properties of nuclear excited states is summarized and covers experimental work using the high-speed rotor and the gaseous source methods, the method using nuclear reaction gamma rays, and the bremsstrahlung method. The theoretical research includes isobaric analog states, shell model calculations, and boson exchange potentials. A list of publications is given. (J.F.P.)

**56833** (ORO–3765–31) PAULI BREAK-UP IN DEUTERON REACTIONS. Technical Report No. 71–116. Gambhir, B. L.; Griffin, James J. (Maryland Univ., College Park. Dept. of Physics and Astronomy). May 1971. 13p. Dep. NTIS.

An approximate method for including effects of Pauli Exclusion Principle in deuteron break-up on heavier nuclei is described. A Hilber-Schmidt Integral equation is obtained for the break-up amplitude, in which the Pauli term is isolated. This term is estimated for a model $^{16}O$ target. Interesting features of energy and angular correlations are discussed. The large magnitude (10 Mb/$Sr^2$MeV at peak) of the cross section guarantees the importance of Pauli break-up in nuclear reactions involving deuterons. (auth)

**56834** (ORO–3765–32) BRUECKNER–HARTREE–FOCK CALCULATIONS USING DENSITY-DEPENDENT EFFECTIVE INTERACTIONS. APPLICATION TO $^{16}O$. Technical Report No. 71–123. Reid, Neal E.; Banerjee, Manoj K.; Stephenson, G. J. Jr. (Maryland Univ., College Park. Dept. of Physics and Astronomy). Jun 1971. 42p. Dep. NTIS.

The effects of allowing variations in the radial orbital wave functions, or major shell mixing, were investigated within the framework of Brueckner-Hartree-Fock theory for $^{16}O$. The calculation is carried out in the matrix representation using harmonic oscillator wave functions as a basis. Effective G-matrix elements are calculated through the use of a density-dependent, two-body operator following a prescription of Bethe. Two possible parameterizations, the local density approximation and an average density approximation are compared. A consideration of the rearrangement energy shows that it is an important contribution to the binding energy. The problem is formulated in a way which facilitates the application of BHF theory to deformed as well as spherical nuclei. (auth)

**56835** (UCRL-Trans–10540) DENSITY OF THE EXCITED STATES OF ATOMIC NUCLEI. Ignatyuk, A. V.; Stavinskii, V. S.; Shubin, Yu. N. (Gosudarstvennyi Komitet po Ispol'zovaniyu Atomnoi Energii SSSR, Obninsk. Fiziko-Energeticheskii Institut). Translated by T. Watt for Univ. of California, Lawrence Radiation Lab., Livermore, from pp 885–907 of report STI/PUB–259(Vol.2). 41p. (CONF-700605–11). Dep. NTIS.

From second international conference on nuclear data for reactors; Helsinki, Finland (15 Jun 1970).

This item was previously abstracted from the original language and appeared in NSA as 25: 15208. (auth)

**56836** (UCRL-Trans–10542) MEAN RADIATION WIDTHS AT EXCITATION ENERGIES OF THE ORDER OF THE NEUTRON BINDING ENERGY. Zakharova, S. M.; Stavinskii, V. S.; Shubin, Yu. N. (Gosudarstvennyi Komitet po Ispol'zovaniyu Atomnoi Energii SSSR, Obninsk. Fiziko-Energeticheskii Institut). Translated by T. Watt for Univ. of California, Lawrence Radiation Lab., Livermore, from pp 909–16 of report STI/PUB–259(Vol.2). 15p. (CONF-700605–13). Dep. NTIS.

From second international conference on nuclear data for reactors; Helsinki, Finland (15 Jun 1970).

This item was previously abstracted from the original language and appeared in NSA as 25: 15209. (auth)

**56837** (UCRL-Trans–10544) SINGLE PARTICLE STATES IN A DEFORMED ENERGY-DIFFERENT NUCLEUS POTENTIAL. Roeper, Peter. Translated for Univ. of California Lawrence Radiation Lab., Livermore, from Z. Phys.; 195: 316-42(1966). 32p. Dep. NTIS.

The nucleon wave functions and energy eigenvalues in a spheroidal potential well of Woods–Saxon type are calculated approximately by diagonalizing the Hamiltonian in a finite subspace of Hilbertspace. The depth of the potential well is made energy dependent to account for the nonlocality of nucleon–nucleus interaction. With the pairing theory of residual interaction taken into consideration these results are used to determine nuclear deformation, energy of single-particle excited states, and an estimate of magnetic moments of nuclei with mass number about 177. Several methods are applied to calculate the equilibrium deformation. They all yield nearly identical results. The experimentally given low-energy spectra of odd-A nuclei however, could not be reproduced satisfactorily. Some pronounced discrepancy between calculated and measured magnetic moments as already observed by Mottelson and Nilsson could not be reduced, either, though in other cases there is considerable improvement to their results. When comparing the structure of the calculated single particle scheme with the observed sequence of nuclear levels one is led to the conclusion that better agreement will be found for a somewhat different deformation: the nuclear shape will be given by a spheroid necked in to some degree by the equator and thickened at the ends. (auth)

**56838** (UR–875–350) LECTURES ON GROUP SYMMETRIES IN NUCLEAR STRUCTURE. Parikh, J. C. (Rochester Univ., N. Y. Dept. of Physics and Astronomy). 24 Jun 1971. Contract AT(30-1)-875. 217p. Dep. NTIS.

The lectures cover abstract group theory, group representations, representation theory and the symmetric group, continuous groups and Lie groups, irreducible tensors, the unitary group and its subgroups, and spectral distribution methods. Also discussed are isospin distributions, the space symmetry group Wigner supermultiplet scheme, SU(3) symmetry and rotational features in light nuclei, and seniority and symplectic symmetry. (J.F.P.)

**56839** STUDY OF THE ISOSPIN FORM OF THE ELECTROMAGNETIC OPERATOR. Divon, Baruch. Ithaca, N. Y.; Cornell Univ. (1971). 133p. University Microfilms Order No. 71-15,623.

Thesis.

Two alternative methods are devised for a low-energy nuclear

XUM

physics test of the existence of an isotensor component in the electromagnetic operator. The methods allow extraction of the relative magnitude of the isovector and isotensor γ-matrix elements, and also suggest the phase of the isotensor matrix element. The first method is an extended Blin–Stoyle's method, in which isospin mixing effect is considered explicitly. Measured decay widths ($\Gamma_\gamma$) of $T = 3/2 \rightarrow T = 1/2$ transitions in $Tz = \pm 1/2$ mirror nuclei are compared, and the difference in widths attributed to both electromagnetic isotensor and nuclear isospin mixing effects. It is demonstrated that the isospin mixing effect can inhibit the isotensor effect in the expression for $\Gamma_\gamma$, since both are expected to be of the same order of magnitude but may be of opposite phase. A method is suggested for the experimental measurement of the isospin mixing effect, assuming that the dominant mixing is due to the antianalog state. This method is applied to the ground state transition of the lowest $T = 3/2$ level in mass-13. It is demonstrated that the introduction of isospin mixing changes the phase of the isotensor matrix element, determined without isospin mixing, although the upper limit for the relative magnitude remains 10%. This method is found to be of limited usefulness due to the small number of cases to which it can be applied. In order to apply the test to more cases a second method is suggested. According to this method the measured γ-decay width of a $T = 3/2 \rightarrow T = 1/2$ transition in the $Tz = -1/2$ nuclei is compared to the mirror decay width, as obtained from the measured log ft values of the analogous $\beta^-$ decay. This method is again applied to the lowest $T = 3/2$ states in mass-13, and the results for the isotensor matrix element are found to be equivalent to those obtained using the first method. Accordingly, this method is applied to the γ-decay of the lowest $T = 3/2$ states in mass-29, mass-25, and mass-21. It is concluded that the isotensor matrix element is about 4%, but no more than 15%, of the isovector matrix element. In most of the cases the phase of the isotensor matrix element is found to be positive. The isotensor effect also is found to be roughly independent of the mass number A. The second method also suggests the experimental measurement of the isospin mixing amplitude ($\alpha_A$) of the antianalog state in the analog state. The application of this method to mass-13 yields an upper limit of $4.5 \times 10^{-3}$ for $\alpha_A^2$, which is in good agreement with previous shell model calculations for adjacent even nuclei. (Diss. Abstr. Int., B)

**56840** GROUND STATE PROPERTIES OF SPHERICALLY SYMMETRIC NUCLEI USING THE MODIFIED DELTA INTERACTION. Ehlers, Jerry William. Los Angeles; Univ. of California (1970). 92p. University Microfilms Order No. 71-13,994.

Thesis.

Calculations of ground state properties of spherically symmetric nuclei (especially double closed shell nuclei) were made using the Modified Delta Interaction. Preliminary studies were done using first the Harmonic Oscillator approximation, then the more realistic Woods–Saxon potential. In using the latter potential, variational calculations were made. Finally, Hartree–Fock calculations were performed taking into consideration the center-of-mass corrections, proton size corrections, Coulomb energy, rearrangement potential, and adding a spin-orbit splitting. With only 3 parameters in the Modified Delta Interaction, good agreement with experimental ground state energies and charge radii was obtained, while moderate agreement was reached for single particle energies. (Diss. Abstr. Int., B)

**56841** NEW STATISTICAL THEORY OF THE NUCLEAR SURFACE. Siemens, Philip John. Ithaca, N. Y.; Cornell Univ. (1970). 67p. University Microfilms Order No. 71-14,595.

Thesis.

The Thomas–Fermi integral theory of the nuclear surface is shown to have singular solutions for the nuclear density. This failure is traced to its inadequate representation of the behavior of wave functions in a potential. A new theory based on approximate wave functions is developed and shown to be asymptotic to the Thomas–Fermi theory in the interior of the nucleus. An improved treatment of exchange forces is shown to be essential to obtaining realistic solutions. (Diss. Abstr. Int., B)

**56842** ANHARMONIC EFFECTS IN SPHERICAL NUCLEI. Almoney, Stanley Richard. Bethlehem, Pa.; Lehigh Univ. (1971). 211p. University Microfilms Order No. 71-17,074.

Thesis.

The method of Bal'butsev and Jolos (Yad. Fiz, 7: p. 738(1968)) to include anharmonic effects in even–even spherical nuclei is extended to include both neutrons and protons. These anharmonicities are introduced in order to explain the large experimental values for the static quadrupole moment of the first excited $2^+$ state, $Q_{2+}$, that have been observed in several spherical nuclei. The pairing plus quadrupole · quadrupole Hamiltonian is used and the anharmonic effects are produced by retaining the quasi-particle scattering terms in the quadrupole interaction. The even–even nucleus is first described by harmonic quadrupole phonon states, and the anharmonic terms are considered as a perturbation which admixes these harmonic phonon states. The matrix elements of the quadrupole operator between these admixed anharmonic states are then calculated and the results are non-zero values for both the static $Q_{2+}$ moment and the reduced cross-over $B(E2; Q_1^+ - 2_2^+)$. Calculations that included up to three phonon states are performed on spherical nuclei throughout the periodic table and the theory is found to provide qualitative estimates in all nuclei investigated. The energy spectra for several neighboring odd mass spherical nuclei are also calculated as a check of the description of the even–even nucleus. The method used for calculating the odd nucleus is the equations of motion developed in such a manner that the input parameters include the matrix elements of the quadrupole operator between states of the even–even nucleus. Again the pairing plus quadrupole · quadrupole Hamiltonian is used and the quasi-particle scattering term is again retained. The introduction of "backward-going" amplitudes provides a technique for including the total quadrupole· quadrupole interaction, but it also introduces spurious states that are in addition to those states that are spurious because of the disregard of the Pauli Principle. It is found that the anharmonic effects are larger than previously anticipated and that the theory can only provide qualitative estimates for the static $Q_{2+}$ moments, the B(E2) values, and the energy spectra for large regions of neighboring spherical nuclei. For the odd nucleus the extreme sensitivity of the calculations to the input parameters and the spurious states severely limits its applicability. (Diss. Abstr. Int., B)

**56843** BOSON EXPANSION METHOD IN NUCLEAR PHYSICS. Li, Shou-yung. Philadelphia; Univ. of Pennsylvania (1970). 117p. University Microfilms Order No. 71-19,252.

Thesis.

A method of constructing boson expansions of fermion pair and multipole operators, which correctly includes the effect of the Pauli principle to all orders and gives convergent expansions within some well-defined subspaces of the boson representation space is presented. In this way it is shown explicitly how the Pauli principle limits the boson degrees of freedom in any attempt to approximate fermion pairs by bosons. The expansions are constructed in a basis in which the total angular momentum is a good quantum number. Therefore the expansion is especially suitable for practical applications. The expansion methods are described for both even and odd systems in single-shell or multishell problems. An interesting application of the method would be the calculation of energy levels of the pairing-plus-quadrupole Hamiltonian in a single j-shell, with large $\Omega = (2j + 1)/2$ and N nucleons, but $N \ll 2\Omega$. For given j and N, one can construct a subspace in which the boson expansions are convergent. In this subspace it is therefore legitimate to neglect the higher order terms in the boson expansion of the Hamiltonian. It is then easy to diagonalize this approximated Hamiltonian and compare its low-lying states with those obtained from the exact diagonalization. If the agreement is reasonably good, then one can probably expect to get fairly good results in using this method as an approximate shell model calculation for heavy spherical nuclei, where an exact shell model calculation would be impossible. (Diss. Abstr. Int., B)

**56844** STUDIES IN HIGH ENERGY PARTICLE PRODUCTION IN NUCLEI. Tang, Chi-li. Montreal; McGill Univ. (1970). National Library of Canada, Ottawa.

Thesis.

Methods for calculating high energy particle production in nuclei for the cases of diffractive production including multi-step processes, non-diffractive reactions and Coulomb production are presented. The formalism for multi-step processes is used to calculate the photon-nucleus total cross section with the vector mesons, $\rho^0$, $\omega$ and $\varphi$, as intermediate particles according to the vector dominance assumption for the photon. The agreement with experiment is good. Effects on the production cross section due to nuclear correlations, nuclear spin and the finite range of the interactions between the projectile particles and the nucleon are studied. Absorption of the projectile particles by the nucleus in non-diffractive coherent reactions is found to be less than in diffractive reactions. Such a difference is observed in the $\gamma + A \rightarrow \pi^0 + A$ reaction. (Diss. Abstr. Int., B)

**56845** YADERNAYA FIZIKA. TOM II. VZAIMODEISTVIE IZLUCHENII S VESHCHESTVOM. KNIGA 2. (Nuclear Physics. Volume 2. Interactions of Radiation and Matter. Book 2).

Starodubtsev, S. V. Polnoe Sobranie Nauchnykh Trudov. V Shesti Tomakh. Tashkent; Izdatel'stvo Fan Uzbekskoi SSR (1970). 380p.

This book is written in three distinct parts, the first and most extensive portion being concerned with the passage of charged particles through matter. This includes topics such as elastic collisions and elastic scatter of particles by matter, energy loss theory for inelastic collisions, experimental tests of deceleration theory, and the relationship between the mean/range free path of fast neutrons and their energy. Vavilov–Cherenkov radiation is discussed, with an application to the energy measurement of ultrafast neutrons. Loss of energy through ionization, and radiation during the passage of heavy charged particles through a substance is considered, 520 references are appended. The second part of this book constitutes a survey of beta-decay problems, accompanied by discussions of the neutrino, beta-interaction, beta-neutrino correlation, spectra and forbidden transitions, and concludes with beta-decay and models of the nucleus and nuclear shells, with 56 references. The final section of the book examines atom recoil during beta-conversion. Source requirements—gaseous and film sources and their uses—are treated. Results are summarized for experimental studies of atom recoil during beta conversion, with reference to the law of conservation of energy, and studies of K-capture for a number of isotopes. (71 references) (K.S.W.)

**56846** IMPROVED THEORY OF NUCLEAR COMPRESSIBILITY AND ITS APPLICATION TO THE ISOTOPE SHIFT PROBLEM. Ionescu-Pallas, N. J. (Inst. of Atomic Physics, Bucharest). Rev. Roum. Phys.; 16: No. 1, 3-10(1971).

The problem of the nuclear compressibility and of its role in defining the radii of heavy nuclei is investigated from a phenomenological standpoint, accounting for all the terms which enter the nuclear binding energy formula. The expression of the nuclear radius, so obtained, exhibits a dependence in terms of neutron number N and proton number Z, respectively, different from that taking place through the agency of the sum N + Z. (auth)

**56847** DIFFRACTION ANALYSIS OF TRANSFER REACTIONS. Gonchar, V. Yu.; Yushkov, A. V. Izv. Akad. Nauk Kaz. SSR, Ser. Fiz.-Mat.; No. 4, 67-72(Jul-Aug 1970). (In Russian).

Diffraction analysis of the angular distributions from stripping reactions was conducted for ten nuclei from $^{10}B$ to $^{91}Zr$ for deuteron energies from 7 to 21.4 MeV. The following results were obtained: diffraction theory describes the angular distribution well, in some cases better than the distorted wave method (DWM); the interaction radii found from the diffraction theory agree with values derived from the DWM and plane-wave method; reduced widths coincide with the quantities from the DWM; the deuteron interaction radii are increased 1 F, on the average, for a unit increase of angular momentum transfer. From the optimization of theoretical parameters the domain of applicability of the theory is carefully determined. (tr-auth)

**56848** HIGHLY RESTRICTED PARTITIONS AND ANGULAR-MOMENTUM STATES OF EQUIVALENT PARTICLE CONFIGURATIONS. Bose, A. K.; Patera, J. (Univ. of Montreal). Can. J. Phys.; 49: 1919-23(15 Jul 1971).

A simple method is given for determining the angular-momentum multiplets of equivalent particle configurations of symmetry [λ]. The number of times a multiplet occurs in a configuration can be found directly without doing a complete analysis. The problem is reduced to the evaluation of certain partition functions $P^{(c)}(J)$. As an example the $k^4$ configuration (j = 7) is analyzed. First, the frequency of one multiplet in $k^4$ of any symmetry [λ] is determined and then a complete angular-momentum analysis is made. (auth) (Canada)

**56849** CROSS SECTIONS FOR SUMMED QUASI-ELASTIC AND INELASTIC SCATTERING. Jackson, Daphne F. (Univ. of Surrey, Guildford, Eng.). Nucl. Phys.; A173: No. 2, 225-38(1971).

Recent studies of the energy spectra of medium- and high-energy protons and electrons inelastically scattered from nuclei have used a variety of assumptions concerning the mechanism of the scattering process. By using the impulse approximation and a single-particle model, the connection between the description in terms of quasi-elastic knockout, in which the struck nucleon is ejected from the nucleus, and a description that includes the excitation of bound and quasi-bound states of the target nucleus is examined. Some problems arising from the formalism are discussed, with particular reference to the results for inelastic proton scattering at 160 MeV and 1014 MeV. (auth)

**56850** CLUSTER EXPANSIONS FOR CORRELATED WAVE FUNCTIONS IN NUCLEAR PHYSICS. Shakin, C. M. (Case Western Reserve Univ., Cleveland). Phys. Rev., C; 4: No. 3, 684-92(Sep 1971).

The cluster expansion for the energy for a system with Bijl–Dingle–Jastrow (BDJ) correlation structure is derived in a new form. It is shown how the theory may be related to the Brueckner–Bethe–Goldstone theory with a particular choice for the correlation operator (or wave matrix) appearing in the BDJ wave function. The three-body cluster terms are discussed. It is shown that these clusters contain a limited class of dispersive terms which may be included in the analysis of the two-body clusters. The three-body clusters are also shown to contain terms which correct for violations of the Pauli principle in the correlation operator. (auth)

**56851** EXTRAPOLATION TO THE LIMIT OF SINGULAR-CORE INTERACTIONS IN THE THREE-BODY PROBLEM. Kim, Y. E.; Tubis, A. (Purdue Univ., Lafayette, Ind.). Phys. Rev., C; 4: No. 3, 693-9(Sep 1971).

Several aspects of the three-body problem with singular-core interactions given by the boundary-condition model (BCM), are studied. The kernel of the Faddeev equations for these interactions is shown to have an infinite Schmidt norm even if the two-body interactions are confined to a single partial wave. This does not necessarily imply that the Faddeev kernel is noncompact. A proof of the compactness (or noncompactness) of the kernel has not been found. A family of two-body interactions, with square repulsions of strength V for particle separation $r < r_0$, which become the BCM in the limit $V_0 \to \infty$ is considered. For finite $V_0$, the Faddeev kernel has a finite Schmidt norm (and is hence compact) and standard numerical matrix techniques may be used for solving the three-body equations. Simplified calculations of the triton binding energy, using two-body s-wave interactions of this type, are carried out for a number of choices of $V_0$. The two-body potentials for $r > r_0$ are not varied. It is found that the three-particle binding energy has a simple dependence on $V_0$. The value of the binding energy extrapolated to the limit $V_0 = \infty$ is found to be in excellent agreement with the result of a previous calculation based on BCM two-particle interactions and numerical methods predicted on the assumed validity of standard matrix-inversion techniques. Some implications of these results for more realistic calculations on three-body systems with two-body singular-core interactions are discussed. (auth)

**56852** DESCRIPTION OF ELASTIC SCATTERING PROCESSES WITH THE USE OF NONLOCAL SEPARABLE POTENTIALS. Pigeon, J.; Barguil, J.; Fayard, C.; Lamot, G.-H.; El Baz, E. (Univ., Lyon). Phys. Rev., C; 4: No. 3, 704-22(Sep 1971).

Elastic scattering processes are studied with the use of nonlocal separable interactions. An explicit and general expression for the transition amplitude has been given which includes Coulomb effects and possible excitation of the particles involved. As a first application of the formalism it is shown that a striking improvement of Mongan's results can be obtained in p-p elastic scattering just by including Coulomb effects at low energy. The nucleon-$\alpha$ elastic scattering below 50 MeV and the $\alpha-\alpha$ elastic scattering below 100 MeV are studied, and the results obtained are in very good agreement with experimental data. (auth)

**56853** MASS FORMULA CONSISTENT WITH NUCLEAR-MATTER CALCULATIONS VS CONVENTIONAL MASS-LAW EXTRAPOLATIONS. Brueckner, K. A.; Chirico, J. H.; Meldner, H. W. (Univ. of California, San Diego, La Jolla). Contract AT(11-1)-Gen-10. Phys. Rev., C; 4: No. 3, 732-40(Sep 1971).

The energy-density functional proposed by Brueckner et al. is used to calculate the average nuclear-binding-energy surface on the N-Z plane at $\beta$ stability ± about 40 units. The equibinding contours are compared with those predicted by recent liquid-droplet models. Normally, some disagreement begins about 15 units away from the region of known nuclei. The deviations toward lower binding are significant for neutron-rich transuranium (superheavy) nuclei. This would seem to indicate a physically important uncertainty in conventional mass-law extrapolations. The semiempirical dependence on neutron excess cannot be established very well, because of the narrowness of the region of known isotopes. The energy-density functional, on the other hand, incorporates the present knowledge about nuclear matter—including recent neutron-matter results. The disagreement with other extrapolations, therefore, questions the validity of stability and formation (e.g., r-process) calculations based on conventional mass formulas. (auth)

XUM

**56854** SECOND-CLASS CURRENTS AND ANALOG PROCESSES. Holstein, Barry H. (Princeton Univ., N. J.). Phys. Rev., C; 4: No. 3, 764-75(Sep 1971).

Semileptonic processes between members of a common isotopic multiplet provide a nearly model-independent test for currents with anomalous or "second-class" G-parity properties. For such processes the implications of the presence of second-class currents are discussed for $\beta$ decay, muon capture, and elastic neutrino scattering. (auth)

**56855** PARITY-INVARIANCE TESTS ORIGINATING WITH NUCLEAR BETA DECAY. Walker, James F. (Univ. of Massachusetts, Amherst). Phys. Rev., C; 4: No. 3, 951-60(Sep 1971).

Most of the experiments to date which have indicated the presence of a parity-nonconversing component to the nuclear force have used $\beta$ decays to populate states which in turn decay electromagnetically. This report analyzes the degree to which parity nonconservation, present in the $\beta$ decay, affects the experimentally observed circular polarization of the electromagnetic radiation. A background contribution is found which has no monochromatic component, provided the electromagnetic and $\beta$-decay interactions are time-reversal invariant. A crude estimate of the effect of this background on specific experiments indicates that it should be much smaller than presently observed effects. A second more elaborate estimate comparing this background effect with the effect expected using theories of the parity-nonconserving forces confirms this. (auth)

**56856** NEUTRON EMISSION FROM PROMPT FRAGMENTS IN THE FISSION OF EXCITED NUCLEI. Sarkar, Ratna (Saha Inst. of Nculear Physics, Calcutta); Chatterjee, Aparesh. Phys. Rev., C; 4: No. 3, 944-51(Sep 1971).

An improved approach combining the renormalized Fermi-gas model (RGM) with the use of an average collective potential energy surface (PES) has been used to estimate the energy release in prompt fission phenomena from fission of excited nuclei. The role of excess excitation $\Delta U_I$ on top of the fission barrier, under several assumed constraints, is discussed. The partition of $\Delta U_I$ into the conjugate prompt fragments has been calculated from a simple RGM saturation condition. The practical limits of $\Delta U_I$ have been discussed from the viewpoint of the statistical model of nuclear reactions. The number of evaporated neutrons from the prompt fragments $\nu_F$ has been estimated from LeCouteur and Lang's approximation using Wing and Varley's neutron binding-energy tables. Fairly satisfactory agreement for the number $\nu_F$ has been obtained with the experimental work on fission of $^{230}$Th by 25.7- and 29.5-MeV $^4$He ions and of $^{226}$Ra by 13.0-MeV protons. A linear relationship of the average number of prompt neutrons $\bar{\nu}$ with $\Delta U_I$ is predicted from the model. (auth)

**56857** REACTION MATRIX ELEMENTS AND STRUCTURE CALCULATIONS WITH THE YALE AND REID POTENTIALS FOR THE Ni REGION. Rustgi, M. L.; Kung, H. W.; Raj, R.; Nisley, R. A.; Hull, M. H. Jr. (State Univ. of New York, Buffalo). Phys. Rev., C; 4: No. 3, 854-73(Sep 1971).

Employing the Yale and soft-core Reid free nucleon-nucleon potentials, the shell-model reaction matrix elements are calculated and tabulated for the Ni region. The matrix elements consist of the bare part and the renormalization effects due to the core polarization. The bare matrix elements are evaluated following the unitary-model approach of Shakin, Waghmare, Tomaselli, and Hull and the renormalization corrections are calculated in the same manner as by Kuo and Brown for a $^{56}$Ni core. As a test of these matrix elemits, spherical shell-model spectra of $^{58}$Ni, $^{58}$Cu, $^{59}$Ni, $^{59}$Cu, $^{60}$Ni, $^{60}$Zn, and $^{60}$Cu are calculated. Quasiparticle calculations for the odd and even Ni isotopes are also performed. In general the calculated results are in good agreement with each other as well as with the observed data. It is concluded that different potentials which fit the same nucleon–nucleon scattering data give essentially the same results for effective-interaction and nuclear-structure calculations for the Ni region of the Periodic Table. (auth)

**56858** EFFECT OF HEXADECAPOLE DEFORMATION ON THE $\Delta N = 2$ CROSSING OF THE NILSSON ORBITALS. Mukherjee, P.; Ramakrishna, G. (Saha Inst. of Nuclear Physics, Calcutta). Phys. Rev., C; 4: No. 3, 990-1(Sep 1971).

The effect of $Y_{40}$ deformation on the $\Delta N = 2$ orbital crossing is found to yield the observed splitting of the levels. (auth)

**56859** REDETERMINATION OF THE SINGLET EFFECTIVE-RANGE PARAMETERS OF THE MONGAN SEPARABLE POTENTIALS. Serduke, Franklin, J. D. (Argonne National Lab., Ill. Univ. of California, Davis); Afnan, I. R. Phys. Rev., C; 4: No. 3, 1002-3(Sep 1971).

The singlet effective-range parameters for the Mongan separable potentials are shown to be more than trivially in error. The implications of this result on triton calculations using these potentials are discussed. (auth)

**56860** STATIC QUADRUPOLE MOMENTS OF VIBRATIONAL STATES OF SPHERICAL NUCLEI IN THE SELF-CONSISTENT CRANKING APPROXIMATION. Marshalek, E. R.; Sabato, M. (Univ. of Notre Dame, Ind.). Phys. Rev., C; 4: No. 3, 1006-9 (Sep 1971).

A simple microscopic expression is derived for static quadrupole moments of vibrational states by means of the self-consistent cranking model. The result sums together the effects of all relevant cubic anharmonicities of the Beliaev–Zelevinsky boson expansion taken in perturbation theory. (auth)

**56861** INDUCED TENSOR IN ALLOWED NUCLEAR BETA DECAY. Holstein, Barry R. (Princeton Univ., N. J.). Phys. Rev., C; 4: No. 3, 740-6(Sep 1971).

The contribution of the "induced-tensor" term in allowed nuclear $\beta$ decays is predicted in the impulse approximation. Current experimental results are compared with these predictions and additional experiments are suggested which could verify the existence of such an effect. (auth)

**56862** INFLUENCE OF STRUCTURE OF NUCLEUS WITH ELECTROMAGNETIC MULTIPOLE MOMENTS ON THE BREMSSTRAHLUNG OF NONPOLARIZED AND LONGITUDINALLY POLARIZED ELECTRONS. Kerimov, B. K.; Sokolov, A. A.; El Gavkhari, A. Izv. Akad. Nauk SSSR, Ser. Fiz.; 35: No. 1, 125-30 (Jan 1971). (In Russian).

The Born approximation was used for calculating differential cross sections for bremsstrahlung of nonpolarized and longitudinally polarized electrons in a nuclear field with electric quadrupole moment Q, magnetic dipole moment $\mu_I$, and octopole moment $\Omega$, with the distribution of electric and magnetic multipole moments in the nuclei taken into account. The process can be written symbolically as $e^- + (Ze, Q, \mu_I, \Omega) \rightarrow (Ze, Q, \mu_I, \Omega) + e^{-\prime} + \gamma$. Effects of finite dimensions were calculated by means of form factors $F_i(q^2)$, where i = C, Q, M1, and M3, obtained in experiments with high-energy electron scattering on nuclei in the 1p shell. It is shown that, at high energies and large angles of radiation ($\theta \rightarrow 180°$), the form factors of nuclear magnetic multipole moments influence the electron bremsstrahlung significantly. (R.V.J.)

**56863** SOME PECULIARITIES OF THE HEAVY-PARTICLE STRIPPING PROCESS. Teplov, I. B. Izv. Akad. Nauk SSSR, Ser. Fiz.; 35: No. 1, 154-8(Jan 1971). (In Russian).

Differential cross sections for the heavy-particle stripping process are calculated in the plane-wave Born approximation with the assumption that the heavy-particle stripping corresponds to the interaction V(x,C). The $\alpha$-induced reactions $^{12}C(\alpha,\alpha_0)^{12}C$, $^{12}(\alpha,\alpha_1)^{12}C$, where $E_\alpha$ = 25 MeV, $^{15}N(\alpha,\alpha_0)^{15}N$, $^{16}O(\alpha,\alpha_0)^{16}O$, $N(\alpha,d_0)^{16}O$, where $E_\alpha$ = 25 MeV, $^{12}C(\alpha,p_0)^{15}N$, where $E_\alpha$ = 25 MeV, and $^{12}C(\alpha,n_0)^{16}O$, where $E_\alpha$ = 20 MeV were studied; results of the analysis are presented graphically. (R.V.J.)

**56864** POSSIBILITY OF IDENTIFICATION OF THE MECHANISM OF DIRECT NUCLEAR REACTIONS ACCORDING TO THE EXTREMES OF DIAGRAM ORIGIN IN THE SPECTRUM OF INTERNAL BREMSSTRAHLUNG $\gamma$ QUANTA. Dubovoi, E. I. Izv. Akad. Nauk SSSR, Ser. Fiz.; 35: No. 1, 203-4(Jan 1971). (In Russian).

Arbitrary triangle diagrams for multiparticle and binary (n = 0) nuclear reactions are analyzed. (R.V.J.)

**56865** LANCZOS METHOD FOR NUCLEAR SHELL MODEL CALCULATIONS. Whitehead, R. R. (Univ. of Glasgow). pp 32.1-4 of Computational Physics. Vols. I and II. London; Her Majesty's Stationery Office (1969).

From Conference on computational physics; Culham, England (28 Jul 1969). See CONF-690706-(Vols.1 and 2).

A new scheme for nuclear shell model calculations is described which makes use of a novel application of the Lanczos method of tridiagonalizing matrices. The scheme appears to have several advantages over conventional approaches particularly where one is interested in systematic studies of a shell rather than in one particular nucleus. (auth) (UK)

**56866** SYSTEMS APPROACH TO THE NUCLEAR SHELL MODEL. Cohen, S. (Argonne National Lab., Ill.). pp H.1-

XUM

12 of Computational Physics. Vols. I and II. London; Her Majesty's Stationery Office (1969).

From Conference on computational physics; Culham, England (28 Jul 1969). See CONF-690706-(Vols.1 and 2).

Theoretical studies of nuclear structure rely heavily on calculations using an independent-particle model similar to the shell model of atomic structure. A typical nuclear shell-model calculation involves several different steps. First a complete set of basis states is constructed. The matrices of the model Hamiltonian in this basis are then constructed and diagonalized. Finally the resultant eigenvalues and eigenvectors are used to make theoretical predictions of experimentally measured quantities. In a systematic approach to the problem, an open-ended evolutionary system called DELPHI was designed and constructed to cater to the needs of scientists relatively unskilled in the use of computers. The facilities provided range from documentation techniques and large libraries of coherently designed algorithmic subroutines to automatic means of managing the dynamic storage of data. They also include a user-oriented language called SPEAKEASY, designed to make short investigations even more direct. In all cases the design specifications are such as to aid the scientist in obtaining answers to his problems quickly. The growth capability led to the use of the system in ways not originally contemplated; extensions of the system to allied fields of study in nuclear physics are already under way. (auth) (UK)

**56867** NEUTRON MATTER COMPUTATIONS IN BRUECKNER AND VARIATIONAL THEORIES. Siemens, P. J. (Niels Bohr Inst., Copenhagen); Pandharipande, V. R. Nucl. Phys.; A173: No. 3, 561-70(1971).

The binding energy of dense neutron gas is calculated in lowest-order Brueckner theory, and in Jastrow variational theory using the lowest-order cluster expansion of the energy, with a Reid soft-core potential. Subsidiary healing conditions are imposed on the Jastrow correlation function to simulate the Pauli exclusion effects. Due to the soft-core nature of the potential, the defect parameter $\kappa$ is small even at high densities and hence the lowest-order calculation could be a fair approximation. Up to $\rho = 0.5$ fm$^{-3}$ the Brueckner and variational calculations give comparable results. Technical complications in applying the Brueckner theory for $\rho >$ 0.5 fm$^{-3}$ are discussed and the results of only the variational calculation are presented for $0.5 < \rho < 4.5$ fm$^{-3}$. These may be useful in astrophysical studies. (auth)

**56868** ISOTENSOR DIPOLE SUM RULES IN NUCLEAR ELECTROEXCITATION. Cannata, F. (Scuola Normale Superiore, Pisa, Italy. Scuola di Perfezionamento in Fisica, Bologna); Leonardi; R. Nucl. Phys.; A173: No. 3, 665-72 (1971).

Electric dipole sum rules are analyzed in electron-nucleus scattering for different isotensor components, in the limit $q^2 \to 0$. As an application, the giant resonance form factor of several nuclei is studied. In particular the relation between the dip at 60 MeV/c and the existence of the $(\Sigma_i \mathbf{l}_i \cdot \mathbf{s}_i)$ $SU_4$ symmetry-breaking term is analyzed. (auth)

**56869** SHELL EFFECTS IN (n,p) AND (n,$\alpha$) CROSS-SECTIONS AT ABOUT 14 MeV. Cuzzocrea, P. (Instituto di Fisica Nucleare, Naples. Univ., Naples); Notarrigo, S. Nuovo Cim.; 4A: No. 2, 251-98(21 Jul 1971).

A comprehensive compilation of the available data on (n,p) and (n,$\alpha$) reaction cross sections, up to December 1969, for about 14 MeV neutrons is given. These data, suitably averaged, have been used in a search for shell effects by standard statistical methods. The analysis shows that the evaporation model is able to explain the experimental data when shell effects are included in the excitation energy in analogy with pairing corrections. This simple model gives the absolute value of a cross-section with a relative standard error of about 40% to be compared with an expectation value of about 10% as deduced from the errors (systematic plus random) with which the cross sections have been measured. The most critical parameter in this model is that which takes roughly into account quantum penetration, while other approximations, i.e., neglecting secondary emission, considering independence of the temperature parameter on excitation energy and mass number, and so on, prove to be quite reasonable. However the temperature parameter mentioned above does not correspond to the nuclear temperature because it includes shell and Coulomb barrier effects; its value is about 2.1 MeV. (auth)

**56870** CROSS SECTIONS IN THE UNRESOLVED RESONANCE REGION: METHODS AND EVALUATION OF APPROXIMATIONS. Heenan, T. F.; Adkins, C. R. (Carnegie-Mellon Univ., Pittsburgh). Nucl. Sci. Eng.; 45: No. 3, 279-96(Sep 1971).

A method is presented for calculating pointwise average cross sections in the unresolved region. This method can assess the effects of interference and overlap up to the fourth decimal place in cross-section calculations, having the capability of considering the effects of interference among sequences of resonances and of overlap between resonances in a sequence up to third order in each. Thus, the method, while more sophisticated than justified in view of current cross-section data uncertainties, can be used to evaluate the validity of various approximations currently made in the determination of cross sections for use in Doppler calculations. The effects of the level of approximation on cross-section calculations are given, Hwang's method for calculating the overlap in a single sequence is assessed, and the range of validity of Hwang's method and the approximations used in it are evaluated. Results of studies to determine the relative speed and accuracy of methods for calculating the J integral, performing the statistical average, and computing the complex probability integral, W, are also presented. The effects of interference among sequences are shown to be small for the calculation of cross sections and the Doppler change in cross sections over a wide range of composition. The effects of resonance overlap within one sequence, however, may be significant for the calculation of both cross sections and Doppler changes in cross sections in some critical assemblies. (auth)

**56871** ADVANCES IN NUCLEAR PHYSICS. VOLUME 3. Baranger, Michel; Vogt, Erich (eds.). New York; Plenum Publishing Corporation (1969). 491p. $22.50.

Articles are included on the nuclear three-body problem, the interactions of pions with nuclei, complex spectroscopy, single nucleon transfer in deformed nuclei, and isoscaler transition rates in nuclei from the ($\alpha$,$\alpha'$) reaction. Separate abstracts were prepared for each of the articles. (J.W.R.)

*For abstracts of individual chapters see: 56872–56876.*

**56872** NUCLEAR THREE-BODY PROBLEM. Mitra, A. N. (Univ. of Delhi). Advan. Nucl. Phys.; 3: 1-70(1969).

The treatment of the nuclear three-body problem is discussed from the point of view of potentials. Three-body techniques using separable potentials which are applicable to few-nucleon problems and light nuclei are described. Topics examined in detail include separable potentials, the model three-body problem, a model stripping problem, the three-nucleon formalism, numerical results for PN systems, and unequal mass three-body systems. (127 references) (J.W.R.)

**56873** INTERACTION OF PIONS WITH NUCLEI. Koltun, Daniel S. (Univ. of Rochester, N. Y.). Advan. Nucl. Phys.; 3: 71-191(1969).

A survey of experimental and theoretical research on the interaction of pions with nuclei is presented. Some of the inadequacies of currently available data are discussed. Some particularly useful experiments for the understanding of $\pi$-nuclear interactions are suggested. A thorough list of references is included. (J.W.R.)

**56874** COMPLEX SPECTROSCOPY. French, J. B. (Univ. of Rochester, N. Y.); Halbert, E. C.; McGrory, J. B.; Wong, S. S. M. Advan. Nucl. Phys.; 3: 193-257(1969).

The application of a formalism for treating large spectroscopic calculations is described and illustrated. The discussion includes notation and formalism, structure of the Hamiltonian matrix, multishell programs, and methods for checking spectroscopic calculations. Some studies making use of the system are reviewed, and some suggestions for future extension of the system are made. (J.W.R.)

**56875** SINGLE NUCLEON TRANSFER IN DEFORMED NUCLEI. Elbek, Bent (Univ. of Copenhagen); Tjoem, Per Olav. Advan. Nucl. Phys.; 3: 259-323(1969).

The properties of single-nucleon transfer reactions are surveyed from an experimental and theoretical point of view. The theory of single-nucleon excitations in deformed nuclei is reviewed. Experimental methods used in the study of transfer reactions are described. The available experimental data is discussed. Some problems which deserve further study are pointed out. (53 references) (J.W.R.)

**56876** ISOSCALAR TRANSITION RATES IN NUCLEI FROM THE ($\alpha$,$\alpha'$) REACTION. Bernstein, Aron M. (Massachusetts Inst. of Tech., Cambridge). Advan. Nucl. Phys.; 3: 325-476 (1969).

The role of the isoscalar transition operator in alpha inelastic scattering by nuclei is examined. Treatments of alpha scattering using diffraction, optical, and DWBA models are compared. The experimental data on isoscaler transition rates are reviewed. Tables for calculating transition rates and sum rules using a Fermi distribution are presented in an appendix. An extensive bibliography is also included. (J.W.R.)

XUM

# REACTOR TECHNOLOGY

## Commercial Power Reactors

*Refer also to abstracts 54934 and 55378.*

**56877** (CONF-700438) REACTOR CONFERENCE, BERLIN, APRIL 20–22, 1970. (Deutsches Atomforum e. V., Bonn (West Germany). Kerntechnische Gesellschaft (West Germany)). Jun 1970. 715p. (In German and English).

In 1970, the nuclear technological society of the German Atomic Forum arranged the second annual meeting in Berlin, where a survey was given about the development and present status of reactor technology in Germany. Also presented was the international status of reactor technology. Presentations were arranged under the following topics: reactor analysis; development and technology of structural reactor elements and components; construction and operation experiences with nuclear power plants; fuel cycle; and reactor concepts and economic problems. (H.B.G.)

**56878** (CONF-710302–(Vol.1), pp 199-214) APPLICATIONS SOFTWARE FOR A FAST REACTOR MALFUNCTION DETECTOR ANALYZER. Masters, S. M.; Cox, T. H. (Atomic Power Development Associates, Inc., Detroit, Mich.).

From Meeting on new development in reactor mathematics and applications; Idaho Falls, Idaho (29 Mar 1971).

A digital data acquisition and analysis system is operational at the Enrico Fermi Atomic Power Plant. Known as the malfunction detection analyzer (MDA), the system compares measured data with results predicted by calculational models and initiates alarms to plant operations personnel if the comparisons exceed prescribed limits. The implementation and operation of the MDA from a system programming point of view are described. (auth)

**56879** (EUR–4638) EXPERIMENTAL AND THEORETICAL DETERMINATION OF BURNUP AND HEAVY ISOTOPE CONTENT IN A FUEL ASSEMBLY IRRADIATED IN THE GARIGLIANO BOILING WATER REACTOR. Ariemma, A.; Bramati, L.; Galliani, M.; Gualandi, M. Paoletti; Zaffiro, B.; Cricchio, A.; Koch, L. (Ente Nazionale per l'Energia Elettrica, Rome (Italy)). Jul 1971. 120p. Dep. NTIS (U. S. Sales Only). EUR F,Fr. 18.35.

Under the joint ENEL-EURATOM program for the utilization of Pu in thermal reactors, post-irradiation analyses were carried out on an enriched-uranium assembly irradiated at about 10,000 MWd/MTU in the Garigliano boiling water reactor. The objective was the determination of burn-up and U and Pu concentration in order to supplement the experimental data to be used for the verification of the calculation method on irradiated fuel. Burn-up was measured non-destructively by means of a high-resolution solid-state detector and destructively through $^{148}Nd$ determination, whereas heavy isotope concentrations by mass spectrometry combined with isotopic dilution techniques. The measurements compare favorably with the five-group BURSQUID calculation; the burn-up values agree within ±1.5%, whereas the concentrations of $^{235}U$, $^{239}Pu$, and $^{240}Pu$ are within less than 4%. Several correlations of general interest that were found among different isotope ratios or between isotopic abundances and burn-up parameters are discussed. The correlations were used only to check the consistency of experimental results, although their validity to determine also burn-up and isotopic abundances is recognized. 27 references. (auth)

**56880** (ZJE–104) RESEARCH OF THE HYDRODYNAMICS OF A ROD FUEL ASSEMBLY. Stepanek, K. (Skoda Works, Pilsen (Czechoslovakia). Nuclear Power Construction Dept.). 1971. 28p. Dep. NTIS (U. S. Sales Only).

The results of experimental work performed in connection with the development of the rod type fuel assembly for the heavy water reactors A–1 and A–2 are summarized. Main attention is given to tasks directly associated with the fuel assembly for A–1 which consists of a bundle of finned rods provided with spacers. The results presented were obtained by a measurement on a low pressure air loop. (auth)

**56881** CAN ALL LIQUID RADWASTE DISCHARGES BE ELIMINATED? Wilson, R. L.; Lee, J. (Sacramento Municipal Utility District, Calif.). Elec. Light Power (Boston); 49: No. 7, 40-2(May 1971).

The Rancho Seco power reactor site is described, and the reasons for selecting a "dry site" are discussed. The operation of the liquid radwaste system to eliminate liquid effluent discharges is described. (H.D.R.)

**56882** STRUCTURAL MECHANICS IN REACTOR TECHNOLOGY. VOL. 3. REACTOR PRESSURE VESSELS. PART H. PRESTRESSED CONCRETE PRESSURE VESSELS. Preprints of the First International Conference, Berlin, Germany, 20–24 September 1971. Jaeger, Thomas A. (comp.). Luxemburg; Commission of the European Communities (1971). 492p. (In several languages). (CONF-710903–(Vol.3)(Pt.H)).

Twenty-six conference papers are presented in Part H. A separate abstract was prepared for each paper. (J.R.D.)

*For abstracts of individual papers see: 55659–55665, 56883–56890, and 56985–56995.*

**56883** PRESTRESSING AND PROOF PRESSURE TESTING OF THE WYLFA PRESTRESSED CONCRETE PRESSURE VESSELS AND COMPARISON OF MEASURED DATA WITH PREDICTED PERFORMANCE. Carlton, D. (Taylor Woodrow Construction Ltd., Southall, Eng.); Smith, J. R.; Bellwood, G. N. pp H4/1.1-33 of Structural Mechanics in Reactor Technology. Vol. 3, Pt. H. /Jaeger, Thomas A. (comp). Luxemburg; Commission of the European Communities (1971).

From 1st International conference on structural mechanics in reactor technology; Berlin, Germany (20 Sep 1971).

The analytical approaches adopted for the Wylfa vessel design and the background experimental work undertaken to establish the necessary basic parameters of the concrete and prestress system are described. Brief details are also given of the in situ tests which confirmed the design values of the parameters. Each of the vessels was provided with extensive instrumentation to observe strains, deformations and temperatures, and these were monitored during prestressing and the cold proof pressure tests. The results of all this work in comparing the behaviors of both vessels with each other and with the analytical predictions are examined. Sources of error are identified and discussed. General conclusions are drawn on the overall degree of correlation achieved. (auth)

**56884** PRESTRESSED CONCRETE PRESSURE VESSEL OF THE THTR-300-MW(e) PROTOTYPE NUCLEAR POWER PLANT. Lotz, H.; Schwiers, H.-G.; Schoenig, J. (Brown Boveri/Krupp Reaktorbau GmbH, Mannheim, Ger.). pp H4/3.1-15 of Structural Mechanics in Reactor Technology. Vol. 3, Pt. H. /Jaeger, Thomas A. (comp). Luxemburg; Commission of the European Communities (1971). (In German).

From 1st International conference on structural mechanics in reactor technology; Berlin, Germany (20 Sep 1971).

The first prestressed concrete pressure vessel for a nuclear plant in Germany will be constructed for the THTR-300 MW(e)-power plant. Information on the design and the calculations of the vessel and its components, the liner, the cooling system, and the insulation is presented. (auth)

**56885** DESIGN OF POD BOILER PRESSURE VESSELS WITH PARTICULAR REFERENCE TO HARTLEPOOL NUCLEAR POWER STATION. Langan, D.; O'Flynn, M.; Welch, A. K. (Taylor Woodrow Construction Ltd., Southall, Eng.). pp H4/4.1-39 of Structural Mechanics in Reactor Technology. Vol. 3, Pt. H. /Jaeger, Thomas A. (comp). Luxemburg; Commission of the European Communities (1971).

From 1st International conference on structural mechanics in reactor technology; Berlin, Germany (20 Sep 1971).

The design and development of the podded boiler type of prestressed concrete pressure vessel now being constructed for both the Hartlepool and Heycham Nuclear Power Stations in the United Kingdom are described. In this form of vessel two features of the reactor layout govern the vessel design: (1) The adoption of a single channel fueling arrangement with interstitial control rods and consequent close spacing of standpipes through the top cap of the vessel. (2) The housing of the boilers in the wall of the vessel. Prestressing of the top cap, therefore, has to be accomplished by circumferential tendons located outside the perforated zone. The second feature restricts the space available for internal hoop tendons and therefore external wire winding was adopted. The principal method used in analyzing the Hartlepool vessel and model, based on dynamic relaxation, is described. Various programs were developed in which plane stress and strain solutions were expressed in Cartesian and polar coordinates. Additional programs using axisymmetric and three-dimensional cylindrical coordinates were derived. An ultimate load analysis is introduced which shows the response of the vessel to overload pressures which would cause progressive cracking and rotation. The method is based on finding the collapse mechanism associated with the minimum potential energy in the vessel. The experimental pro-

XUM

gram which has been conducted on a $^1/_{10}$th scale model concrete vessel of the Hartlepool design is described. The essential experimental details, together with the degree of simulation achieved, are presented. The elastic response, overload, and ultimate load behavior of the model are then correlated with two methods of analysis described. (auth)

**56886** SIMULATION OF THE PRESSURE VESSEL OF THE BUGEY REACTOR. Boisserie, J. M. (Electricite de France, Chatou). pp H5/2.1-12 of Structural Mechanics in Reactor Technology. Vol. 3, Pt. H. /Jaeger, Thomas A. (comp). Luxemburg; Commission of the European Communities (1971). (In French).

From 1st International conference on structural mechanics in reactor technology; Berlin, Germany (20 Sep 1971).

The first phase in the testing of the prestressed concrete pressure vessel in the summer of 1971 is described. During this phase and in the future, results of careful stain measurements "in situ" will be compared to these of mathematical models. The thermal properties and the creep of concrete were simulated. Initial results are presented. (auth)

**56887** THREE-DIMENSIONAL ELASTIC STRESS CONDITIONS IN THE AREA OF THE OPENINGS OF THE THTR PRESTRESSED CONCRETE VESSEL: A COMPARISON BETWEEN NUMERICAL CALCULATION AND MEASURING RESULTS OF AN ELASTIC MODEL. Hansson, V. (Ruhr-Univ., Bochum, Ger.). pp H5/4.1-16 of Structural Mechanics in Reactor Technology. Vol. 3, Pt. H. /Jaeger, Thomas A. (comp). Luxemburg; Commission of the European Communities (1971). (In German).

From 1st International conference on structural mechanics in reactor technology; Berlin, Germany (20 Sep 1971).

Stresses were determined at the surfaces and inside the wall and plates of a model of the THTR-vessel made of epoxy resin. With this experimental investigation results of three-dimensional calculations were checked. The region with large horizontal and vertical openings near the junction of wall and plate was of greatest interest. The computation with the dynamic relaxation method and the model test are described. Both results show good agreement and are discussed. (auth)

**56888** MODEL EXPERIMENTS ON THE CARRYING CAPACITY OF THE PRESTRESSED CONCRETE PRESSURE VESSEL FOR THE THTR-300-MW(e) PROTOTYPE NUCLEAR POWER STATION. Lotz, H.; Meerwald, K. (Brown Boveri/Krupp Reaktorbau GmbH, Mannheim, Ger.). pp H5/5.1-18 of Structural Mechanics in Reactor Technology. Vol. 3, Pt. H. /Jaeger, Thomas A. (comp). Luxemburg; Commission of the European Communities (1971). (In German).

From 1st International conference on structural mechanics in reactor technology; Berlin, Germany (20 Sep 1971).

Three model tests for the prestressed concrete pressure vessel for the THTR 300 MW(e) power plant are described. The top slab of the vessel has numerous penetrations. It was tested as a partial model at a scale of 1:20. The vessel will be tested as a full scale model at a scale of 1:5 consisting of concrete and also as a model consisting of casting resin at a scale of 1:47. (auth)

**56889** INVESTIGATION INTO STRUCTURAL BEHAVIOUR OF INSULATION OF THE PRESTRESSED CONCRETE PRESSURE VESSELS OF WYLFA NUCLEAR POWER STATION. Williams, A. J. (British Nuclear Design and Construction Ltd., Whetstone, Eng.). pp H6/5.1-10 of Structural Mechanics in Reactor Technology. Vol. 3, Pt. H. /Jaeger, Thomas A. (comp). Luxemburg; Commission of the European Communities (1971).

From 1st International conference on structural mechanics in reactor technology; Berlin, Germany (20 Sep 1971).

Experience at Wylfa has shown that under some conditions, and particularly where highly turbulent flow occurs, the stresses induced in the studs retaining insulation cover plates may be sufficiently high to cause fatigue failure. The course of events related to this situation are outlined, stress data obtained by measurement under reactor conditions are presented, tentative conclusions are drawn from the available data. (auth)

**56890** EXPERIMENTS ON THE BEHAVIOR OF METALLIC INSULATIONS IN HELIUM. von der Weyden, H. D. (Brown Boveri/Krupp Reaktorbau GmbH, Mannheim, Ger.). pp H6/6.1-18 of Structural Mechanics in Reactor Technology. Vol. 3, Pt. H. /Jaeger, Thomas A. (comp). Luxemburg; Commission of the European Communities (1971). (In German).

From 1st International conference on structural mechanics in reactor technology; Berlin, Germany (20 Sep 1971).

In order to find a safe design for the insulation of the THTR-300, the behavior of the insulation modified for application in helium was investigated by testing in helium atmosphere. The tests were carried out under the operating conditions of THTR-300. The total and local heat fluxes in the insulation were regularly repeated after temperature cycles, depressurizations, and pressurizations with regard to the expected operating conditions of THTR-300. The tests confirm that the modifications carried out on the original insulation system to achieve the adaptation to helium were appropriate. (auth)

**56891** FAST-NEUTRON FLUX MEASUREMENT IN AES NOVO-VORONEZHSKII REACTORS. Lomakin, S. S.; Morozov, A. G.; Petrov, V. I.; (and others). At. Energ. (USSR); 31: No. 1, 54-6(Jul 1971). (In Russian).

Neutron spectra of reactors in the first and second units of the Novo-Voronezh nuclear power station were determined with threshold detectors. The characteristics of threshold detectors and gamma-sources are tabulated and discussed. Eight threshold nuclear reactions were investigated, and for each the fast neutron spectra were measured at the core center, behind the thermal shield, and outside of the reactor vessel. (K.S.W.)

**56892** RESULTS OF ULTRA-SOUND TESTS ON THE REACTOR PRESSURE VESSEL OF THE NUCLEAR POWER STATION OBRIGHEIM. Schenk, H.; Mayr, A.; Pickel, E. (Kernkraftwerk Obrigheim GmbH, Stuttgart). Atomwirt., Atomtech.; 16: No. 8-9, 453-4(Aug-Sep 1971). (In German).

Experience with ultrasound testing on the reactor pressure vessel of the nuclear power station Obrigheim leads to the conclusion that remote controlled nondestructive testing is possible in water depths of 11 meters. The test equipment can be handled with ease and results are reproducible. The present state of development, however, does not permit establishment of a definite relationship between echo and type as well as size of defect. To achieve a reliable coordination, testing should be performed before the start of operation; the cause of equivocal echo could be determined directly. (tr-auth)

## *Operation and Economics*

**56893** (70-CNA-631) OPERATING EXPERIENCE WITH OTHER REACTORS. Foulkes, F. M. (Canatom Ltd., Montreal (Quebec)). 1970. 11p. (CONF-700564-5). Dep. NTIS (U. S. Sales Only).

From tenth annual international conference of the Canadian Nuclear Association; Toronto, Canada (24 May 1970).

Operating experiences with Magnox and water cooled power reactors are reviewed and compared. Capacity and availability factors are listed. (D.C.C.)

**56894** (DLCS-5000271) SHIPPINGPORT ATOMIC POWER STATION QUARTERLY OPERATING REPORT. Second Quarter, 1971. (Duquesne Light Co., Shippingport, Pa.). Contract AT(11-1)-292. 23p. Dep. NTIS.

During the second quarter of 1971, the Shippingport Atomic Power Station was operated for Duquesne Light Company system load demand, training, testing, and maintenance. The Heat Dissipation System remained shutdown throughout the period. Three operational incidents occurred during the quarter. On April 7, during the quarterly flush of the condensate surge header, the six inch rubber hose attached to the flush connection ruptured causing approximately 25,000 gallons of condensate to be inadvertently discharged to the river. On April 16, a full Reactor scram occurred during the performance of weekly Nuclear Protection System checks when test leads were erroneously plugged into incorrect test points on the 1A Nuclear Channel. The cause was determined to be a grounding of the power range signal causing a spurious scram signal from the 1A Nuclear Channel. Chemistry results on May 17 indicated the Reactor Coolant System to contain above limit total gas concentration and low coolant pH. The BD purification loop was removed from service and the AC purification loop returned to service, which restored normal RCS chemistry conditions. The resin charge was changed in the BD demineralizer and the demineralizer was returned to service on May 21 without further problems. The cause is undetermined. During the second quarter period, there were two shipments made for off-site disposal of solid radioactive waste for a total of 1,422 millicuries of radioactivity contained in 300 drums weighing 63,486 pounds. (auth)

**56895** (DOCKET-1155-135) LA CROSSE BOILING WATER REACTOR. Environmental Monitoring Associated with Radioactive Discharges, January 1, 1969-June 30, 1971. (Dairyland Power Cooperative, La Crosse, Wis.). 16 Sep 1971. 46p. (DPC-851-31). Dep. NTIS.

**56896** (DOCKET-50010-95) DRESDEN NUCLEAR POWER STATION, UNIT 1. Unplanned Release of Radioactive Liquid.

XUM

(Commonwealth Edison Co., Chicago, Ill.). 22 Sep 1971. 2p. Dep. NTIS.

Safety aspects are presented concerning an unplanned release of radioactive liquid to the Illinois River from a tube leak in the 1B unloading heat exchanger. Corrective actions are described. (D.C.C.)

**56897** (DOCKET-50029-158) YANKEE NUCLEAR POWER STATION. Operation Report No. 128, August 1971. (Yankee Atomic Electric Co., Westboro, Mass.). 21 Sep 1971. 8p. Dep. NTIS.

**56898** (DOCKET-50206-124) SAN ONOFRE NUCLEAR GENERATING STATION, UNIT 1. Technical Specifications, Proposed Change No. 7. (Southern California Edison Co., Los Angeles). 22 Sep 1971. 12p. Dep. NTIS.

Revised technical specifications are presented concerning the core burnup limit for Cycle 2 operation. The present burnup limit of 17000 MWD/MTM is changed to 18000 MWD/MTM. (D.C.C.)

**56899** (DOCKET-50219-146) OYSTER CREEK NUCLEAR POWER PLANT, UNIT NO. 1. Semiannual Report No. 4, January 1, 1971-June 30, 1971. (Jersey Central Power and Light Co., Morristown, N. J.). 22 Sep 1971. 36p. Dep. NTIS.

**56900** (DOCKET-50219-147) OYSTER CREEK NUCLEAR POWER PLANT, UNIT NO. 1. Technical Specifications, Change Request No. 8. (Jersey Central Power and Light Co., Morristown, N. J.). 28 Sep 1971. 4p. Dep. NTIS.

Revised technical specifications are presented concerning the replacement procedures for a local power range monitor. (D.C.C.)

**56901** (DOCKET-50220-73) NINE MILE POINT NUCLEAR STATION. Semiannual Operation Reports for 1970 Corrections. (Niagara Mohawk Power Corp., Syracuse, N. Y.). 14 Sep 1971. 2p. Dep. NTIS.

Revised data on radioactive effluents from the Nine Mile Point Power Reactor during January to December 1970 are presented. (D.C.C.)

**56902** (DOCKET-50220-74) NINE MILE POINT NUCLEAR STATION. Broken Pins in Turbine Wheel. (Niagara Mohawk Power Corp., Syracuse, N. Y.). 25 Sep 1971. 2p. Dep. NTIS.

Inspection and maintenance requirements for cracked and broken attachment pins of last stage turbine bucket shanks are described. (D.C.C.)

**56903** (DOCKET-50244-80) ROBERT EMMETT GINNA NUCLEAR POWER PLANT. $^{131}I$ Release. (Rochester Gas and Electric Corp., N. Y.). 6 Oct 1971. 3p. Dep. NTIS.

The excessive release of $^{131}I$ from the plant vent during September 27 and September 28, 1971, is described. Revised sampling and operating procedures are studied to prevent reoccurrence of the incident. (D.C.C.)

**56904** (DOCKET-50245-89) MILLSTONE NUCLEAR POWER STATION, UNIT NO. 1. Failure of Motor Operators (A0-71-9 and A0-71-10) Found in Control Circuit of Automatic Valves. (Millstone Point Co., Hartford, Conn.). 7 Sep 1971. 4p. Dep. NTIS.

The failure of electric motors used to actuate the emergency core cooling system valves is described. The failures were initiated by control circuit set conditions. Corrective actions are described. (D.C.C.)

**56905** (DOCKET-50245-90) MILLSTONE NUCLEAR POWER STATION, UNIT NO. 1. Reevaluation of Number of Curies of Liquid Waste Activity Discharged During 1970. (Millstone Point Co., Hartford, Conn.). 28 Sep 1971. 1p. Dep. NTIS.

**56906** (DOCKET-50245-91) MILLSTONE NUCLEAR POWER STATION, UNIT NO. 1. Abnormal Occurrence No. A0-71-15 and A0-71-16. (Millstone Point Co., Hartford, Conn.). 28 Sep 1971. 2p. Dep. NTIS.

On September 17, 1971, the loop pressure coolant injection valve on the B loop and the torus spray valve on the A loop failed to operate. Both actuating motors had burned out. Replacement of the motors is described. On September 18, 1971, the low pressure coolant injection outboard containment spray valve failed to operate. The operation failure was due to disengaged drive unit. Worn pins allowed the drive unit to become disengaged. Corrective actions are described. (D.C.C.)

**56907** (DOCKET-50245-92) MILLSTONE NUCLEAR POWER STATION, UNIT NO. 1. Abnormal Occurrence No. A0-71-17. (Millstone Point Co., Hartford, Conn.). 30 Sep 1971. 1p. Dep. NTIS.

The failure of the emergency service water pumps to reach their specified pumping pressure at 2500 gallons per minute during a surveillance test is described. (D.C.C.)

**56908** (DOCKET-50245-93) MILLSTONE NUCLEAR POWER STATION, UNIT 1. Abnormal Occurrence A0-71-18, September 23, 1971. (Millstone Point Co., Hartford, Conn.). 4 Oct 1971. 1p. Dep. NTIS.

Failure of the turbine steam bypass valves to open during a plant shutdown is described. The failure resulted from a fractured stud on one of the six bypass valve linkages. Corrective actions are described. (D.C.C.)

**56909** (DOCKET-50249-101) DRESDEN NUCLEAR POWER STATION. Facility License DPR-25, Proposed Change No. 7 to Appendix A. (Commonwealth Edison Co., Chicago, Ill.). 24 Sep 1971. 7p. Dep. NTIS.

Revised technical specifications are presented concerning the substitution of the steam jet air ejector off-gas monitors to perform the monitoring function of the plant chimney monitoring system. The substitution is effective during steady state operation or during testing to determine the plateout of iodine and particulates in the chimney off-gas monitoring system piping. A description of the chimney sample line plateout test is included. (D.C.C.)

**56910** (DOCKET-50255-53) PALISADES PLANT. Incident Involving the Primary Cooling System. (Consumers Power Co., Jackson, Mich.). 16 Sep 1971. 5p. Dep. NTIS.

On September 8, 1971, a technician de-energized the breakers to the reactor protective system to install a minor modification. This action de-energized the feed to the electromatic relief valve pilot valve solenoids allowing the valves to open. The primary system pressure decreased to a low point of 1280 psia over a period of 2 to 3 minutes until the blowdown was terminated by closure of the motor operated valves used to isolate the open relief valves. The incident occurred due to non-standard designation of contacts in the control circuit to the power operated relief valves. Corrective actions are described. (D.C.C.)

**56911** (DOCKET-50255-54) PALISADES PLANT. Two Incidents Involving Control Rod Drive System. (Consumers Power Co., Jackson, Mich.). 24 Sep 1971. 2p. Dep. NTIS.

The failure of control rod drive mechanisms numbers 4 and 31 to drop control rods when tested is described. The cause of drop failure is attributed to excessive epoxy deposits on the clutch surfaces of the control rod drives. Corrective actions are described. (D.C.C.)

**56912** (DOCKET-50263-82) MONTICELLO NUCLEAR GENERATING PLANT, UNIT 1. Inoperability of the High Pressure Coolant Injection System. (Northern States Power Co., Minneapolis, Minn.). 15 Sep 1971. 2p. Dep. NTIS.

**56913** (DOCKET-50263-84) MONTICELLO NUCLEAR GENERATING PLANT, UNIT 1. Inoperability of the High Pressure Coolant Injection System. (Northern States Power Co., Minneapolis, Minn.). 28 Sep 1971. 2p. Dep. NTIS.

**56914** (DOCKET-50263-85) MONTICELLO NUCLEAR GENERATING PLANT, UNIT NO. 1. Unusual Occurrences, September 5, 1971 and September 9, 1971. (Northern States Power Co., Minneapolis, Minn.). 5 Oct 1971. 2p. Dep. NTIS.

On September 5, 1971, a reactor scram resulted from a low pressure condition in the plant compressed air system. A failed compressor control combined with operator action of improperly placing the standby air compressor controls in the "OFF" position caused the scram. On September 9, 1971, a shorted switch during surveillance testing caused emergency core cooling system initiation. The shorted switch was the "low-low" reactor water level switch. Also, on September 9, 1971, a failed mercury wetted, magnetic switch in a low-low water level instrument was discovered and replaced. (D.C.C.)

**56915** (DOCKET-50269-37) OCONEE NUCLEAR STATION, UNIT NO. 1. Description of Cause and Correction of Damage to Control Rod Drive Mechanisms During Preoperational Testing. (Duke Power Co., Charlotte, N. C.). 29 Sep 1971. 51p. Dep. NTIS.

**56916** (TID-25791) GUNDREMMINGEN NUCLEAR POWER PLANT. Monthly Report, May 1971. (Kernkraftwerk RWE-Bayernwerk G.m.b.H., Gundremmingen (West Germany)). 23 Jun 1971. 53p. (In German). Dep. NTIS.

The plant was run at full load throughout the month. To check the efficiency of all the units necessary for load switching and to train the personnel, the plant was disconnected from the grid for a short

XUM

time on 23 May and the load was reduced briefly to 65 MWe on 30 May. Both load reductions went according to plan. The activity in the reactor water and the waste gas rose appreciably, but not dangerously, so that it was possible to repair leaks caused by load switching at various weak points in the fuel element cans. Preparations are in hand for work during the overhaul shut-down beginning on 12 June. (auth)

**56917** (TID-25805) SENA NUCLEAR POWER PLANT. Report for November 1970. (Societe d'Energie Nucleaire Franco-Belge des Ardennes, Chooz-lez-Givet (France)). 21p. Dep. NTIS.

The SENA power reactor operated throughout November 1970 at an average power level of 245 MW(e). There were four unscheduled scrams and a scheduled shutdown for maintenance. The operating statistics and equipment and systems performance are summarized. (H.D.R.)

**56918** (TID-25806) SENA NUCLEAR POWER PLANT. Report for December 1970. (Societe d'Energie Nucleaire Franco-Belge des Ardennes, Chooz-lez-Givet (France)). 21p. Dep. NTIS.

Operations and maintenance requirements are described. Fuel inventory is itemized. (J.M.J.)

**56919** (TID-25807) SENA NUCLEAR POWER PLANT. Report for January 1971. (Societe d'Energie Nucleaire Franco-Belge des Ardennes, Chooz-lez-Givet (France)). 22p. Dep. NTIS.

Operations and maintenance requirements are described. Fuel inventory is itemized. (J.M.J.)

**56920** (TID-25808) SENA NUCLEAR POWER PLANT. Monthly Report for February 1971. (Societe d'Energie Nucleaire Franco-Belge des Ardennes, Chooz-lez-Givet (France)). 20p. Dep. NTIS.

Operations and maintenance requirements are described. Fuel inventory is itemized. (J.M.J.)

**56921** (TID-25809) SENA NUCLEAR POWER PLANT. Monthly Report for March 1971. (Societe d'Energie Nucleaire Franco-Belge des Ardennes, Chooz-lez-Givet (France)). 19p. Dep. NTIS.

Operation and maintenance requirements are described. Fuel inventory is itemized. (J.M.J.)

**56922** (TID-25810) SENA NUCLEAR POWER PLANT. Monthly Report for May 1971. (Societe d'Energie Nucleaire Franco-Belge des Ardennes, Chooz-lez-Givet (France)). 19p. Dep. NTIS.

Operations and maintenance requirements are described. Fuel inventory is itemized. (J.M.J.)

**56923** (TID-25811) SENA NUCLEAR POWER PLANT. Report for June 1971. (Societe d'Energie Nucleaire Franco-Belge des Ardennes, Chooz-lez-Givet (France)). 21p. Dep. NTIS.

Operations and maintenance requirements are described. Fuel inventory is itemized. (J.M.J.)

**56924** (TID-25812) GUNDREMMINGEN NUCLEAR POWER PLANT. Monthly Report, June 1971. (Kernkraftwerk RWE-Bayernwerk G.m.b.H., Gundremmingen (West Germany)). 27 Jul 1971. 56p. (In German). Dep. NTIS.

After 10½ months of trouble-free operation the plant was shut down on 12 June 1971 for a scheduled overhaul and refueling. The tasks featured in the flow chart were carried out according to plan and the plant was restarted on 17 July 1971. All fuel elements were examined for burst clads, and 38 of them were found to be defective. Of these, 22 had in any case attained their rated burn-up. Of the remaining 16 fuel elements, four had been loaded into the reactor in 1966, six in 1969 and six in 1970. Altogether, 88 new and three partly spent, repaired elements were charged. The HP and IP turbine sections were entered and visually inspected. The last-row blading appeared to be in good condition. In the HP casing and at various extraction points corroded spots were found, some of which had to be repaired. It was possible to carry out all the repair and maintenance jobs despite the sometimes considerable hindrances caused by high local dose rates. (auth)

## *Safety and Siting*

*Refer also to abstracts 54980, 55157, 55193, 55242, 55347, and 57103.*

**56925** (DOCKET-1155-134) LA CROSSE BOILING WATER REACTOR. Provisional Operating Authorization No. DPRA-6, Amendment No. 4, Quality Assurance Program. (Dairyland Power Cooperative, La Crosse, Wis.). 2 Sep 1971. 28p. Dep. NTIS.

**56926** (DOCKET-50003-89) INDIAN POINT STATION, UNIT NO. 1. Reply to Inquiry Relative to Adequacy of Emergency Core Cooling System. (Consolidated Edison Co. of New York, Inc., New York). 27 Sep 1971. 3p. Dep. NTIS.

**56927** (DOCKET-50003-90) INDIAN POINT STATION, UNIT NO. 1. Technical Specifications, Proposed Augmented In-Service Inspection Program. (Consolidated Edison Co. of New York, Inc., New York). 28 Sep 1971. 29p. Dep. NTIS.

**56928** (DOCKET-50003-91) INDIAN POINT STATION, UNIT NO. 1. Technical Specifications, Proposed Change Limiting Allowable Rates of Leakage. (Consolidated Edison Co. of New York, Inc., New York). 29 Sep 1971. 7p. Dep. NTIS.

**56929** (DOCKET-50016-127) ENRICO FERMI ATOMIC POWER PLANT. Amended Change Request No. 15, Supplement No. 1. (Power Reactor Development Co., Detroit, Mich.). 13 Sep 1971. 10p. Dep. NTIS.

Revised technical specifications are presented concerning operating limits for the irradiated fuel transfer tank. (D.C.C.)

**56930** (DOCKET-50016-128) ENRICO FERMI ATOMIC POWER PLANT. Amended Change Request No. 16, Supplement No. 1. (Power Reactor Development Co., Detroit, Mich.). 10 Sep 1971. 16p. Dep. NTIS.

Revised technical specifications are presented concerning operating limits for the irradiated fuel transfer tank. (D.C.C.)

**56931** (DOCKET-50016-129) ENRICO FERMI ATOMIC POWER PLANT. Technical Specifications, Change No. 30. (Division of Reactor Licensing (AEC), Washington, D. C.). 6 Oct 1971. 2p. Dep. NTIS.

Revised technical specifications are presented concerning the installation of secondary containment on two runs of primary Na piping located outside the reactor containment building. (D.C.C.)

**56932** (DOCKET-50133-68) HUMBOLDT BAY POWER PLANT, UNIT NO. 3. Technical Specifications, Proposed Change No. 36. (Pacific Gas and Electric Co., San Francisco, Calif.). 29 Sep 1971. 8p. Dep. NTIS.

Additional technical specifications are presented concerning a leak rate limit for the primary cooling system. (D.C.C.)

**56933** (DOCKET-50146-91) SAXTON NUCLEAR EXPERIMENT. Technical Specifications, Change No. 41 Allowed. (Division of Reactor Licensing (AEC), Washington, D. C.). 8 Sep 1971. 2p. Dep. NTIS.

Revised technical specifications are presented concerning modifications of $PuO_2-UO_2$ fuel assemblies arrangements in the loose lattice and peripheral regions of the core. (D.C.C.)

**56934** (DOCKET-50146-92) SAXTON REACTOR. Information Requested on Saxton Coolant System. (Saxton Nuclear Experimental Corp., Pa.). 5 Oct 1971. 4p. Dep. NTIS.

Requested additional information is presented concerning inspection and leak detection procedures for the primary cooling system. (D.C.C.)

**56935** (DOCKET-50155-92) BIG ROCK POINT NUCLEAR PLANT. Emergency Core Cooling System Performance and Core Spray System Modifications. (Consumers Power Co., Jackson, Mich.). 29 Sep 1971. 17p. Dep. NTIS.

**56936** (DOCKET-50206-125) SAN ONOFRE NUCLEAR GENERATING STATION, UNIT 1. Interim Measures for Improvements in ECCS Performance and Reliability. (Southern California Edison Co., Los Angeles). 30 Sep 1971. 12p. Dep. NTIS.

**56937** (DOCKET-50219-145) OYSTER CREEK NUCLEAR POWER PLANT, UNIT NO. 1. Facility Change Request No. 1, Supplement No. 1. (Jersey Central Power and Light Co., Morristown, N. J.). 13 Sep 1971. 8p. Dep. NTIS.

The effects of possible loading errors for fuel rods on emergency core cooling system performance calculations are analyzed. (D.C.C.)

**56938** (DOCKET-50237-200) DRESDEN NUCLEAR POWER STATION, UNIT 2. Technical Specifications, Change No. 15 Allowed. (Division of Reactor Licensing (AEC), Washington, D. C.). 17 Sep 1971. 3p. Dep. NTIS.

Revised technical specifications and limiting conditions are

XUM

presented to allow the steam jet air ejector offgas monitor to perform the monitoring function of the plant chimney monitoring system during testing operations. (D.C.C.)

**56939** (DOCKET-50237-201) DRESDEN NUCLEAR POWER STATION, UNIT 2. Technical Specifications, Proposed Change No. 16. (Commonwealth Edison Co., Chicago, Ill.). 27 Sep 1971. 14p. Dep. NTIS.

Revised technical specifications are presented concerning the turbine control valve fast closure scram, surveillance of the intermediate range monitors, and the addition of a rod block for the average power range monitors and intermediate range monitors. (D.C.C.)

**56940** (DOCKET-50244-78) ROBERT EMMETT GINNA NUCLEAR POWER PLANT, UNIT NO. 1. A Review of Fuel Rod Integrity at the Ginna Facility. (Westinghouse Electric Corp., Pittsburgh, Pa.). 27 Aug 1971. 35p. (WCAP-7703). Dep. NTIS.

For Rochester Gas and Electric Corp., N. Y.

Early in the operation of the first cycle at the Ginna reactor, increases in primary coolant activity indicated the development of fuel leaks. During a recent shutdown, many fuel assemblies were visually examined and leak tested. Leaks were confirmed as being distributed within, and limited to, Region 3 fuel assemblies. The source of the leaks has been determined to be moisture contained in the fuel resulting in local hydriding. Twelve of these assemblies were removed and replaced with new assemblies. The new fuel incorporates later engineering/manufacturing changes and should not be subject to this defect mechanism. Although some leaks remain in the core, a thorough review of the causes and effects of these leaks leads to the conclusion that the reactor can be operated safely without any additional technical or administrative restrictions. (auth)

**56941** (DOCKET-50244-79) ROBERT EMMETT GINNA NUCLEAR POWER PLANT, UNIT NO. 1. Technical Supplement Accompanying Application to Increase Power, Amendment No. 2. (Rochester Gas and Electric Corp., N. Y.). 1 Oct 1971. 57p. Dep. NTIS.

**56942** (DOCKET-50249-102) DRESDEN NUCLEAR POWER STATION, UNIT 3. Technical Specifications, Proposed Change No. 8. (Commonwealth Edison Co., Chicago, Ill.). 27 Sep 1971. 14p. Dep. NTIS.

Revised technical specifications are presented concerning the turbine control valve fast closure scram, surveillance of the intermediate range monitors, and the addition of a rod block for the average power range monitor and the intermediate range monitor. (D.C.C.)

**56943** (DOCKET-50249-103) DRESDEN NUCLEAR POWER STATION, UNIT 3. Technical Specifications, Change No. 7. (Division of Reactor Licensing (AEC), Washington, D. C.). 7 Oct 1971. 3p. Dep. NTIS.

Revised technical specifications are presented to allow the steam jet air ejector offgas monitor to perform the monitoring function of the plant chimney monitoring system with the plant operating at steady state. (D.C.C.)

**56944** (DOCKET-50254-52) QUAD-CITIES STATION, UNIT 1. Facility Operating License No. DPR-29 with Appendix A, Technical Specifications. (Division of Reactor Licensing (AEC), Washington, D. C.). 1 Oct 1971. 269p. (DOCKET-50265-44). Dep. NTIS.

**56945** (DOCKET-50261-73) H. B. ROBINSON UNIT NO. 2. Emergency Core Cooling Performance. (Carolina Power and Light Co., Raleigh, N. C.). 29 Sep 1971. 80p. Dep. NTIS.

**56946** (DOCKET-50263-83) MONTICELLO NUCLEAR GENERATING PLANT, UNIT 1. Emergency Core Cooling System to New AEC Interim Acceptance Criteria. (Northern States Power Co., Minneapolis, Minn.). 20 Aug 1971. 37p. Dep. NTIS.

**56947** (DOCKET-50266-55) POINT BEACH NUCLEAR PLANT, UNIT NO. 1. Environmental Studies, Report No. PBR-2, (Wisconsin Electric Power Co., Milwaukee). Apr 1971. 90p. (DOCKET-50301-40). Dep. NTIS.

Information concerning radioactive and thermal discharges from the reactor is presented. The effects of reactor operations on the environment are analyzed. Radiation and temperature monitoring data are presented for the reactor site during April to November 1970. (D.C.C.)

**56948** (DOCKET-50280-45) SURRY POWER STATION, UNIT 1. Report on Metallurgical Examination of Weld Samples. (Division of Compliance (AEC), Washington, D. C.). 10 Sep 1971. 25p. Dep. NTIS.

Inspection and test results of Type 304 and Type 316 stainless steel weld joints in the Surry Power Reactor Unit 1 cooling system are presented. (D.C.C.)

**56949** (DOCKET-50280-46) SURRY POWER STATION, UNITS 1 AND 2. Final Safety Analysis Report, Amendment 25. (Virginia Electric and Power Co., Richmond). 30 Sep 1971. 277p. (DOCKET-50281-44). Dep. NTIS.

Additional information is presented concerning earthquake stresses on structures and piping systems, loss of coolant accident conditions, and qualification test of prototype vertical induction motor for containment recirculation spray pump. (D.C.C.)

**56950** (DOCKET-50280-47) SURRY POWER STATION, UNITS NO. 1 AND NO. 2. Additional Information Concerning the Quality Assurance Program. (Virginia Electric and Power Co., Richmond). 6 Aug 1971. 251p. (DOCKET-50281-45). Dep. NTIS.

Requested additional information is presented concerning the performance of stainless steel welds in cooling system piping. (D.C.C.)

**56951** (DOCKET-50280-48) SURRY POWER STATION, UNITS 1 AND 2. Preliminary Safety Analysis Report, Amendment 2. (Virginia Electric and Power Co., Richmond). 5 Jul 1967. 84p. (DOCKET-50281-46). Dep. NTIS.

Additional information is presented concerning reactor response characteristics during various operations incidents. (D.C.C.)

**56952** (DOCKET-50280-49) SURRY POWER STATION, UNITS 1 AND 2. Reasons Why the Construction Permits Should Not Be Suspended Pending Environmental Review. (Virginia Electric and Power Co., Richmond). 11 Oct 1971. 42p. (DOCKET-50281-47). Dep. NTIS.

**56953** (DOCKET-50282-40) PRAIRIE ISLAND NUCLEAR GENERATING PLANT, UNITS 1 AND 2. Final Safety Analysis Report, Amendment No. 11. (Northern States Power Co., Minneapolis, Minn.). 20 Sep 1971. 547p. (DOCKET-50306-39). Dep. NTIS.

Revised design parameters of the Prairie Island Power Reactor Units 1 and 2 are presented. Included also are additional data on the reactor requested by the Division of Reactor Licensing. (D.C.C.)

**56954** (DOCKET-50295-30) ZION STATION, UNITS 1 AND 2. Final Safety Analysis Report, Amendment No. 15. (Commonwealth Edison Co., Chicago, Ill.). 13 Sep 1971. 110p. (DOCKET-50304-29). Dep. NTIS.

Revised design parameters of the Zion Power Reactor Units 1 and 2 are presented. Included also are additional data on the reactor requested by the Division of Reactor Licensing. (D.C.C.)

**56955** (DOCKET-50298-22) COOPER NUCLEAR STATION. Environmental Report, Operating License Stage. (Nebraska Public Power District, Columbus). 17 Sep 1971. 343p. Dep. NTIS.

Information concerning chemical, radioactive, and thermal discharge from the reactor is presented. The effects of reactor operations on the environment are analyzed. (D.C.C.)

**56956** (DOCKET-50302-25) CRYSTAL RIVER NUCLEAR GENERATING PLANT, UNIT 3. Application for Licenses, Amendment No. 13. (Florida Power Corp., St. Petersburg). 20 Sep 1971. 103p. Dep. NTIS.

**56957** (DOCKET-50305-25) KEWAUNEE NUCLEAR POWER PLANT. Final Safety Analysis Report, Amendment 10. (Wisconsin Public Service Corp., Green Bay). 15 Sep 1971. 298p. Dep. NTIS.

Revised design parameters of the Kewaunee Power Reactor are presented. Included also are additional data on the reactor requested by the Division of Reactor Licensing. (D.C.C.)

**56958** (DOCKET-50309-41) MAINE YANKEE ATOMIC POWER STATION. Final Safety Analysis Report, Amendment No. 30. (Maine Yankee Atomic Power Co., Westboro, Mass.). 17 Sep 1971. 127p. Dep. NTIS.

Weld metal was removed from nine Type 316 stainless steel pipe-to-valve joints in the Maine Yankee reactor coolant system

XUM

and sent to Battelle's Columbus Laboratories for evaluation. The examinations made on each sample follow: liquid-penetrant inspection of the top surface and the major surfaces cut during removal of the sample from the pipe joint; metallographic examination of a cross section of each sample cut perpendicular to the major axis at the location of greatest width of the weld sample; and determination of the delta ferrite content for each sample. The procedures used to process the nine weld metal samples submitted are described. The observations made during the studies are presented. (7 references) (auth)

**56959** (DOCKET-50313-31) ARKANSAS NUCLEAR ONE, UNIT NO. 1. Final Safety Analysis Report, Amendment No. 21. (Arkansas Power and Light Co., Little Rock). 6 Oct 1971. 133p. Dep. NTIS.

Revised and additional data on design parameters and operations aspects of the reactor are presented. Technical qualifications of operating personnel are included. (D.C.C.)

**56960** (DOCKET-50324-22) BRUNSWICK STEAM ELECTRIC PLANT, UNITS NO. 1 AND NO. 2. ECCS Conformance to New AEC Adopted Interim Acceptance Criteria. (Carolina Power and Light Co., Raleigh, N. C.). 30 Sep 1971. 45p. (DOCKET-50325-22). Dep. NTIS.

**56961** (DOCKET-50333-30) JAMES A. FITZPATRICK NUCLEAR POWER PLANT. Final Safety Analysis Report, Supplement No. 1. (Power Authority of the State of New York). 17 Sep 1971. 645p. Dep. NTIS.

Revised and additional data on the design and operations aspects of the reactor are presented. The containment system is described. Technical specifications are included. (D.C.C.)

**56962** (DOCKET-50334-25) BEAVER VALLEY POWER STATION, UNIT NO. 1. Environmental Report, Operating License Stage. (Duquesne Light Co., Pittsburgh, Pa.). 24 Sep 1971. 356p. Dep. NTIS.

Information concerning chemical, radioactive, and thermal discharges from the reactor is presented. The effects of reactor operations on the environment are analyzed. Geological, hydrological, and meteorological data for the reactor site are included. (D.C.C.)

**56963** (DOCKET-50344-22) TROJAN NUCLEAR PLANT, Interim Statement of General Policy and Procedure: Implementation of the National Environmental Policy Act of 1969. (Portland General Electric Co., Oreg.). 27 Sep 1971. 43p. Dep. NTIS.

The effects of reactor construction and operations on the environment are analyzed. (D.C.C.)

**56964** (DOCKET-50348-24) JOSEPH M. FARLEY NUCLEAR PLANT, UNITS NO. 1 AND NO. 2. Preliminary Safety Analysis Report, Amendment No. 20. (Alabama Power Co., Birmingham). 13 Sep 1971. 12p. (DOCKET-50364-18). Dep. NTIS.

Revised and additional data are presented for the applications for construction permit and operating license. (D.C.C.)

**56965** (DOCKET-50348-25) JOSEPH M. FARLEY NUCLEAR PLANTS, UNITS 1 AND 2. Preliminary Safety Analysis Report, Amendment 21. (Alabama Power Co., Birmingham). 10 Sep 1971. 100p. (DOCKET-50364-19). Dep. NTIS.

Revised design parameters of the Joseph M. Farley Power Reactor Units 1 and 2 are presented. Included also are additional data on the reactor requested by the Division of Reactor Licensing. (D.C.C.)

**56966** (DOCKET-50348-26) JOSEPH M. FARLEY NUCLEAR PLANT, UNITS NO. 1 AND NO. 2. Preliminary Safety Analysis Report, Amendment No. 22. (Alabama Power Co., Birmingham). 30 Sep 1971. 6p. (DOCKET-50364-20). Dep. NTIS.

Revised information is presented concerning control system wiring requirements. (D.C.C.)

**56967** (DOCKET-50352-19) LIMERICK GENERATING STATION, UNITS 1 AND 2. Preliminary Safety Analysis Report, Amendment No. 11. (Philadelphia Electric Co., Pa.). 16 Sep 1971. 210p. (DOCKET-50353-19). Dep. NTIS.

Revised design parameters of the Limerick Power Reactor Units 1 and 2 are presented. Included also are additional data on the reactor requested by the Division of Reactor Licensing. (D.C.C.)

**56968** (DOCKET-50352-20) LIMERICK GENERATING STATION, UNITS 1 AND 2. Preliminary Safety Analysis Report, Amendment No. 12. (Philadelphia Electric Co., Pa.). 22 Sep 1971. 22p. (DOCKET-50353-20). Dep. NTIS.

Revised and additional data on the emergency core cooling system, classification requirements for nuclear storage tank joints, cooling system equipment, and piping systems, and quality assurance program organization chart are presented. (D.C.C.)

**56969** (DOCKET-50366-15) EDWIN I. HATCH NUCLEAR PLANT, UNIT 2. Preliminary Safety Analysis Report, Amendment 9. (Georgia Power Co., Atlanta). 24 Sep 1971. 136p. Dep. NTIS.

Revised design parameters of the Edwin I. Hatch Power Reactor Unit 2 are presented. Included also are additional data on the reactor requested by the Division of Reactor Licensing. (D.C.C.)

**56970** (DOCKET-50367-21) BAILLY GENERATING STATION, NUCLEAR I. Preliminary Safety Analysis Report, Amendment 13. (Northern Indiana Public Service Co., Hammond). 17 Sep 1971. 351p. Dep. NTIS.

Revised design parameters of the Bailly Power Reactor Unit 1 are presented. Included also are additional data on the reactor requested by the Division of Reactor Licensing. (D.C.C.)

**56971** (DOCKET-50367-22) BAILLY GENERATING STATION, NUCLEAR I. Preliminary Safety Analysis Report, Amendment No. 14. (Northern Indiana Public Service Co., Hammond). 17 Sep 1971. 33p. Dep. NTIS.

Additional data on the design parameters and operations aspects of the reactor requested by the Division of Reactor Licensing are presented. (D.C.C.)

**56972** (DOCKET-50376-21) AGUIRRE NUCLEAR PLANT, UNIT NO. 1. Preliminary Facility Description and Safety Analysis Report, Amendment 10. (Puerto Rico Water Resources Authority, San Juan). 30 Sep 1971. 640p. Dep. NTIS.

Revised design parameters of the Aguirre Power Reactor Unit 1 are presented. Included also are additional data on the reactor requested by the Division of Reactor Licensing. (D.C.C.)

**56973** (DOCKET-50398-8) MENDOCINO POWER PLANT, UNITS 1 AND 2. Environmental Report, Construction Permit Stage. (Pacific Gas and Electric Co., San Francisco, Calif.). 28 Sep 1971. 120p. (DOCKET-50399-8). Dep. NTIS.

Information concerning chemical, radioactive, and thermal discharges from the reactor is presented. The effects of reactor operations on the environment are analyzed. (D.C.C.)

**56974** (DOCKET-50400-1) SHEARON HARRIS NUCLEAR POWER PLANT, UNITS 1, 2, 3, AND 4. License Application. (Carolina Power and Light Co., Raleigh, N. C.). 7 Sep 1971. 36p. (DOCKET-50401-1; DOCKET-50402-1; DOCKET-50403-1). Dep. NTIS.

Applications for construction permits and operating licenses for Shearon Harris Power Reactor Units 1, 2, 3, and 4 are presented. The 1970 Annual Report for the Carolina Power and Light Company is included. (D.C.C.)

**56975** CONSISTENCY IN SITING PRACTICES REGARDING NUCLEAR PLANTS. Ergen, William K. (Oak Ridge National Lab., Tenn.). pp 1-9 of Health Physics Aspects of Nuclear Facility Siting. Vol. I. /Voilleque, Paul G. (comp.). Idaho Falls, Idaho; Burton R. Baldwin, Publications Chairman (1971).

From fifth annual midyear topical symposium on health physics aspects of nuclear facility siting; Idaho Falls, Idaho (3 Nov 1970).

Experience shows that various methods of evaluating nuclear-power-plant sites with respect to the surrounding population yield rather similar results, though the methods may be quite different. The methods all use certain fundamental facts, such as Sutton's equation for atmospheric diffusion; they have to be consistent with previous practice; they have to be reasonably simple; demographic facts put limits on the variation in the population distributions likely to be encountered; and economic considerations militate against certain types of sites. As an example, for 12 representative sites, "characteristics" are derived by weighting the population by $r^{-n}$ (r distance from the reactor) and by integrating the weighted population over r. Drastic variations are introduced by varying n between 1.5 and 3, but nevertheless, when the sites are ordered according to their characteristics, the result depends only very little on n. 12 references. (auth)

**56976** NUCLEAR FACILITY SITING IN THE UNITED STATES. Goldman, Morton I. pp 10-16 of Health Physics Aspects of Nuclear Facility Siting. Vol. I. /Voilleque, Paul G. (comp.). Idaho Falls, Idaho; Burton R. Baldwin, Publications Chairman (1971).

From fifth annual midyear topical symposium on health physics aspects of nuclear facility siting; Idaho Falls, Idaho (3 Nov 1970).

XUM

Problems concerning the selection of appropriate sites for power reactors are described. The effects of public opinion on the site selection are discussed. (D.C.C.)

**56977** ENVIRONMENTAL CONSEQUENCES FROM THE NORMAL OPERATION OF AN URBAN NUCLEAR POWER PLANT. Bergstroem, Stig O. W. (Aktiebolaget Atomenergi, Studsvik, Sweden). pp 29-55 of Health Physics Aspects of Nuclear Facility Siting. Vol. I. /Voilleque, Paul G. (comp.). Idaho Falls, Idaho; Burton R. Baldwin, Publications Chairman (1971).

From fifth annual midyear topical symposium on health physics aspects of nuclear facility siting; Idaho Falls, Idaho (3 Nov 1970).

An official Swedish study on the economical and hygienic consequences of urban siting has been started. It was triggered by a license application for the construction of a combined district heating and power producing plant close to the center of Stockholm. Plans for similar plants exist in the cities of Gothenburg, Malmö, Norrköping and Gävle. The study has been limited to two main designs, both of roughly 500 MW(e) capacity, one BWR and one PWR, with two alternative containment systems, rock cavern and surface building. A final report is to be delivered in the summer of 1971, but a continuation is foreseen, covering the problems of very large plants and of advanced reactor designs sited in industrial areas. The work has started with a general study of how the environment is affected by normal releases and by standardized accidental releases as the site is moved towards the center of a simple standard population distribution. Later on the effect of more complex population distribution assumptions will be studied. Different kinds of radiological dose criteria will be discussed and a comparison with the corresponding criteria for pollutants from conventional power plants will be attempted. The environmental impact of normal operations is described. Normal is then defined as all states where proper authorities permit the plant to operate. Health effects of such releases as are judged permissible and probable, respectively, will be discussed. 8 references. (auth)

**56978** RADIOIODINE DISTRIBUTION IN THE TARAPUR POWER REACTOR ENVIRONMENT DURING COMMISSIONING AND INITIAL OPERATIONS. Bhat, I. S.; Osinski, J.; Chandramouli, S.; Kamath, P. R. (TAPS Colony, Boisar, India). pp 361-71 of Health Physics Aspects of Nuclear Facility Siting. Vol. II. /Voilleque, Paul G. (comp.). Idaho Falls, Idaho; Burton R. Baldwin, Publications Chairman (1971).

From fifth annual midyear topical symposium on health physics aspects of nuclear facility siting; Idaho Falls, Idaho (3 Nov 1970).

The liquid radioactive wastes from the Tarapur Power Reactor are discharged to the sea along with the hot condenser coolant seawater. The gaseous wastes are released through the 113 m tall stack. It has been observed that 70 to 90% of the total activity in the radwaste is due to radioiodines. The radioiodine levels in various environmental samples both from the sea and from deposition on land are presented. 3 references. (D.C.C.)

**56979** RADIOLOGICAL SURVEILLANCE STUDIES AT A BWR NUCLEAR POWER STATION: ESTIMATED DOSE RATES. Blanchard, R. L.; Krieger, H. L.; Kolde, H. E.; Kahn, B. (Bureau of Radiological Health, Cincinnati). pp 372-84 of Health Physics Aspects of Nuclear Facility Siting. Vol. II. /Voilleque, Paul G. (comp.). Idaho Falls, Idaho; Burton R. Baldwin, Publications Chairman (1971).

From fifth annual midyear topical symposium on health physics aspects of nuclear facility siting; Idaho Falls, Idaho (3 Nov 1970).

Techniques for estimating off-site dose rates are presented using effluent data from an operating nuclear power plant. The critical exposure pathway appears to be, as expected, via external radiation from fission-produced radioactive noble gases that are released from the stack. This exposure was measured directly in the environment with a sensitive tissue-equivalent ionization chamber. Exposures via other paths could not be measured directly, but were estimated by measuring radionuclide concentrations in airborne and liquid effluents from the station. The following exposure routes were considered: drinking milk from cows that grazed in the vicinity; eating leafy vegetables grown in the vicinity; eating beef from steer that grazed in the vicinity; inhalation of radioactive gases and particles; eating fish from the river below the point of liquid waste discharge; and drinking water from the river below the point of liquid waste discharge. The dose rate attributable to external radiation from the noble gases was a fraction of the background value, and all the other estimated dose rates were considerably lower. 18 references. (auth)

**56980** DERIVATION OF GASEOUS RELEASE LIMITS FOR THE BROWNS FERRY NUCLEAR PLANT. Belvin, E. A.; Smith, J. M.; Montgomery, T. L.; Oppold, J. A. (Tennessee Valley Authority, Muscle Shoals, Ala.). pp 385-408 of Health Physics Aspects of Nuclear Facility Siting. Vol. II. /Voilleque, Paul G. (comp.). Idaho Falls, Idaho; Burton R. Baldwin, Publications Chairman (1971).

From fifth annual midyear topical symposium on health physics aspects of nuclear facility siting; Idaho Falls, Idaho (3 Nov 1970).

The methods used for calculation of the radioactive gaseous release limits for the Browns Ferry Power Reactor are described. Operational limits are determined for normal releases of low-level radiogases from three 1,098-MW(e) boiling water reactors. The methods employed in these calculations are expanded from those used in the past for calculation of release limits from boiling water reactors. Release limits are derived for both radioactive noble gases and radioiodine. In deriving the noble gas limits, both the external whole body gamma exposure from the noble gases and the internal exposure from the particulate daughters are considered. Since ventilation air is discharged through reactor building and turbine building roof ventilators during normal operation, it is necessary to compute release limits for the noble gases and radioiodines for both the plant stack (assuming a point, elevated release) and the reactor building complex (using a ground level, volume release). Consequently, the overall site release limit is presented in the form of an equation which assures exposures to the general population which will not exceed the AEC guidelines. The Browns Ferry Nuclear Plant Technical Specifications for gaseous releases were prepared using the information presented. 12 references. (auth)

**56981** PUBLIC HEALTH SERVICE ROLE IN PROVIDING INFORMATION RELATIVE TO THE NUCLEAR POWER CONTROVERSY. Martin, J. E.; Harward, E. D.; Weaver, C. L. (Bureau of Radiological Health, Rockville, Md.). pp 724-35 of Health Physics Aspects of Nuclear Facility Siting. Vol. III. /Voilleque, Paul G. (comp.). Idaho Falls, Idaho; Burton R. Baldwin, Publications Chairman (1971).

From fifth annual midyear topical symposium on health physics aspects of nuclear facility siting; Idaho Falls, Idaho (3 Nov 1970).

The results of several extensive studies of the effects of radioactivity discharges from nuclear facilities on the environment and the dose to the population are summarized. Also discussed are the impact that this information has had on the current debate over nuclear power and the types of studies and programs that will be conducted in the future to provide data on this subject. Public Health Service studies have been of value because a polarization of viewpoints on nuclear power has made the credibility of information furnished by either side suspect by the other. One major conclusion reached is that the success or failure of nuclear power may well depend on the availability of credible, non-biased, reliable data such as that provided by health agency programs. 26 references. (auth)

## Power Reactor Development

*Refer also to abstracts 55651 and 56882.*

**56982** (ANL-7791) INTEGRAL MEASUREMENTS IN EBR-II OF CAPTURE RATES, FISSION RATES, AND ALPHA FOR $^{233}U$, $^{235}U$, $^{238}U$, $^{239}Pu$, $^{240}Pu$, AND $^{242}Pu$. Heinrich, R. R.; Williams, J.; Madson, A. A.; Dudey, N. D. (Argonne National Lab., Ill.). Jul 1971. Contract W-31-109-eng-38. 32p. Dep. NTIS.

Integral capture rates, fission rates, and their ratio, alpha, were determined for $^{233}U$, $^{235}U$, $^{238}U$, $^{239}Pu$, $^{240}Pu$, and $^{242}Pu$ as a function of position in EBR-II. A total of 64 samples were irradiated in EBR-II over a period of 6 to 12 months for accumulated exposures ranging from 2000 to 10,000 MWd. Fission rates were determined by assaying the fission product $^{137}Cs$, and capture rates were determined by mass-spectrometric and alpha-spectrometric analysis. Breeding potentials for the six isotopes were calculated from the alpha values determined in the core and blanket of EBR-II. 14 references. (auth)

**56983** (NP-18992) LECTURES HELD BY THE NORWEGIAN ATOMIC ENERGY ASSOCIATION, AUTUMN 1970, AND SPRING 1971, NORSK ATOMENERGIFORENING, POLYTEKNISK FORENING, OSLO (NORWAY) 1971. (Institutt for Atomenergi, [Kjeller] (Norway)). 65p. Dep. NTIS (U. S. Sales Only).

The texts of four lectures, two in English and two in Swedish, are presented. The first is a lecture by F. R. Farmer on the safety of nuclear power plants. The second, by S. O. W. Bergstroem (in Swedish), is on environmental aspects of nuclear power. The third, by S. Eklund (in Swedish), is on international cooperation in nuclear power. The fourth, by J. C. Charlton, is on trends in the use of radioisotopes, especially in medicine. (Norway)

**56984** (STI/PUB-194/4) POWER AND RESEARCH REACTORS IN MEMBER STATES. 1971 Edition. (International Atomic Energy Agency, Vienna (Austria)). 1971. 85p. IAEA $2.00.

XUM

A comprehensive list of land-based nuclear power and research reactors in the Member States of the International Atomic Energy Agency is presented. The list includes data on all reactors in operation, under construction, and planned. The cumulative electric power generated up to December 1970 is given for operating plants, and the growth of installed capacities of power reactors and the increase in the number of research reactors are illustrated. A reactor name index is included. (H.D.R.)

**56985** TWO-DIMENSIONAL TIME-DEPENDENT ANALYSIS OF PERFORATED END CAPS FOR NUCLEAR REACTOR PRESSURE VESSELS BY THE FINITE ELEMENT METHOD. Stefanou, G. D. (City Univ., London); Yu, C. W.; England, G. L. pp H3/3.1-16 of Structural Mechanics in Reactor Technology. Vol. 3, Pt. H. /Jaeger, Thomas A. (comp). Luxemburg; Commission of the European Communities (1971).

From 1st International conference on structural mechanics in reactor technology; Berlin, Germany (20 Sep 1971).

The design of prestressed concrete pressure vessels for nuclear reactors, and in particular, the design of the end caps to the cylinders increasingly call for more sophisticated and better analytical techniques. A method is proposed to analyze the mode of action of the end slabs, assuming constant elevated temperature and radial compression. These simplified assumptions represent reasonably realistic operating conditions. If required, more complex operating conditions can be incorporated. A special feature of the proposed analysis is the method by which an elastic solution can be modified to take account of the time-dependent effects such as creep and shrinkage at ambient and under elevated temperatures. The elastic solution is based on the two-dimensional finite element formulation using triangular plate elements. After obtaining the initial elastic state of stress, a complete elastic, thermoelastic and time-dependent solution is achieved in a step-by-step manner, based on the "Rate of Creep" approach, and using small time intervals during which the stresses are assumed constant. The technique was used to analyze slab models tested and reported elsewhere. It was shown that the proposed method estimates the deformational behavior of the models with an acceptable degree of accuracy. The redistribution of stress as a result of thermal creep predicted by the method also agreed well with the cracking pattern of the models. It is also seen that the proposed method, which is quite general, takes into account loading history. In addition, it has the advantage of economizing in computer time. (auth)

**56986** BEHAVIOR OF END SLABS IN CYLINDRICAL PRESTRESSED CONCRETE PRESSURE VESSELS. Langan, D.; Garas, F. K. (Taylor Woodrow Construction Ltd., Southall, Eng.). pp H3/4.1-40 of Structural Mechanics in Reactor Technology. Vol. 3, Pt. H. /Jaeger, Thomas A. (comp). Luxemburg; Commission of the European Communities (1971).

From 1st International conference on structural mechanics in reactor technology; Berlin, Germany (20 Sep 1971).

The general behavior and shear failure mechanism of restrained thick slabs which form the end closures of cylindrical prestressed concrete pressure vessels are examined. Typical results from a five year parametric study of over 20 model pilecaps are presented. The effects of bonded reinforcement, lined and unlined penetrations, span to depth ratio, concrete strength, level of hoop prestress and boundary conditions were investigated. The factors which may influence the representivity of end slab tests and the effect of the significant parameters on the overload and ultimate load behavior of the full scale structures are discussed. The components of internal shear resistance which balance the total shear force along the failure plane are described. Simplified design methods for determining the ultimate shear strength of end slabs are considered and related to the available test data. 18 references. (auth)

**56987** GENERAL CALCULATION OF PRESTRESSED CONCRETE REACTOR PRESSURE VESSELS WITH CONSIDERATION OF NON-LINEAR STRESS-EXPANSION LAWS BY THE METHOD OF DYNAMIC RELAXATION. Schnellenbach, G. (Ruhr-Univ., Bochum, Ger.). pp H3/7.1-20 of Structural Mechanics in Reactor Technology. Vol. 3, Pt. H. /Jaeger, Thomas A. (comp). Luxemburg; Commission of the European Communities (1971). (In German).

From 1st International conference on structural mechanics in reactor technology; Berlin, Germany (20 Sep 1971).

The dynamic relaxation method is applied for three-dimensional calculations of prestressed concrete pressure vessels. The theory for elastic solutions with the dynamic relaxation method described only as far as necessary to understand computation processes with constitutive laws different from linear elasticity. Some remarks are made on the computation of three-dimensional temperature distributions and the calculation of resulting stresses. Assumptions and the computation process for the creep calculation are outlined. An elasto-plastic calculation with the dynamic relaxation method is described with an example of a plane problem using a nonlinear constitutive law basing on Prandtl–Reusz theory. Assumptions for calculations of prestressed concrete pressure vessels with cracked zones are outlined. 10 references. (auth)

**56988** CALCULATION OF TIME-DEPENDENT STRESSES IN PCPVS BY AN APPROXIMATE METHOD. England, G. L. (Kings Coll., London); Allen, S. J. pp H3/8.1-25 of Structural Mechanics in Reactor Technology. vVol. 3, Pt. H. /Jaeger, Thomas A. (comp). Luxemburg; Commission of the European Communities (1971).

From 1st International conference on structural mechanics in reactor technology; Berlin, Germany (20 Sep 1971).

The calculation of time-varying stresses in materials subject to nonhomogeneous creep is discussed. Economic solutions are sought using a general theory based on a power variational principle. This permits approximate solutions to the time-varying stresses, in real and complex structures, to be obtained with little effort from a minimum of input data. It is shown that conventional finite element stiffness analyses may be used to provide the necessary input data to the creep problem; these take the form of a set of independent stress distributions throughout the structure. Then, using a flexibility approach these stress distributions are optimized to achieve the best possible fit to the true solutions during the time-dependent phase of the problem. Finally, the theory is applied to two problems and solutions are presented for (a) a thin plate subject to in-plane edge loading and nonuniform temperature distribution, (b) a short cylindrical prestressed concrete reactor pressure vessel, with end caps, subjected to internal pressure and temperature crossfall through the walls and caps. (auth)

**56989** NOTE ON A PRESTRESSED CONCRETE PRESSURE VESSEL FOR THE INSTITUTO DE PESQUISAS RADIOACTIVAS. de Souza e Silva, R.; Pinheiro, R. B. (Instituto de Pesquisas Radioactivas, Belo-Horizonte, Brazil). pp H4/5.1-12 of Structural Mechanics in Reactor Technology. Vol. 3, Pt. H. /Jaeger, Thomas A. (comp). Luxemburg; Commission of the European Communities (1971).

From 1st International conference on structural mechanics in reactor technology; Berlin, Germany (20 Sep 1971).

The studies concerning the prestressed concrete pressure vessel for a natural uranium heavy water moderated and cooled power reactor are described. For circumferential prestress, the method of exterior high strength steel strips was adopted. A modified system of the Swedish approach for the top removable lid and the thermal insulation was adopted. The stress analysis was performed by a finite elements program which uses TRIA-3 axisymmetric elements. Creep and shrinkage were also investigated. 17 references. (auth)

**56990** DESIGN CONCEPT AND ANALYSIS OF CYLINDRICAL PRESTRESSED CONCRETE REACTOR PRESSURE VESSELS WITH AXIAL RIBS. Sebock, F. (Hungarian Academy of Sciences, Budapest). pp H4/7.1-25 of Structural Mechanics in Reactor Technology. Vol. 3, Pt. H. /Jaeger, Thomas A. (comp). Luxemburg; Commission of the European Communities (1971). (In German).

From 1st International conference on structural mechanics in reactor technology; Berlin, Germany (20 Sep 1971).

Research work is reported on circular cylindrical shells with axial ribs. Rib interstices are filled out with a good shielding and heat insulating material without inherent strength. Prestress is due to axial wires led in ducts in the ribs and tangential ones wound around rib crests. For the vessel a structural analysis was worked out based on the conventional energy method. As primary members, the hinged short circular cylindrical shell and the beam supported elastically on the tangential prestressing wires are chosen. All loads are expanded in Fourier series. Equality of displacements yields for each wave period a system of linear equations. (auth)

**56991** SCANDINAVIAN PCRV MODEL PROJECT: STRESS CALCULATION AND EXPERIMENTAL VERIFICATION. Andersen, S. I. (Danish Atomic Energy Commission, Copenhagen); Hamre, E.; Tarandi, T. pp H5/3.1-16 of Structural Mechanics in Reactor Technology. Vol. 3, Pt. H. /Jaeger, Thomas A. (comp). Luxemburg; Commission of the European Communities (1971).

From 1st International conference on structural mechanics in reactor technology; Berlin, Germany (20 Sep 1971).

Part of a joint development program by Denmark, Finland, Norway, and Sweden in the field of prestressed concrete vessels for water reactors is described. PCRV's for water reactors are characterized by their relatively high ratio of wall thickness to radius

XUM

and, to the Scandinavian design, by a removable top closure that permits refueling to be done in the traditional LWR manner. The results of the theoretical and experimental structural analysis obtained during testing of the Scandinavian PCRV model vessel are presented. Testing of the model vessel showed good agreement with theoretical predictions. 8 references. (auth)

**56992** INVESTIGATION ON A PRESTRESSED CONCRETE REACTOR VESSEL UNDER INTERNAL GAS PRESSURE. MODE OF RUPTURE. Lenschow, R. (Norges Tekniske Hoegskole, Trondheim, Norway). pp H5/7.1-17 of Structural Mechanics in Reactor Technology. Vol. 3, Pt. H. /Jaeger, Thomas A. (comp). Luxemburg; Commission of the European Communities (1971).

From 1st International conference on structural mechanics in reactor technology; Berlin, Germany (20 Sep 1971).

Tests to rupture were performed on 2 models of prestressed concrete pressure vessels. The mode of rupture of the vessels loaded by internal gas-pressure was studied. Model No. 1 was a model in a scale 1:3.6, of the Scandinavian PCRV-model, except for the removable lid. The vessel had an inside diameter of 55 cm and an inside height of 111 cm. The cylindrical wall thickness was 30 cm and the top and bottom slabs were 33 cm. The reference pressure was 85 bar. Model No. 2 was equal to No. 1, but had no bonded reinforcement in the cylindrical wall. The models were instrumented with vibrating wire strain gauges in the concrete and electrical resistance strain gauges on the reinforcement and on the lining and thermocouples registered concrete temperature. Both models were loaded with an internal gas-pressure to failure. Model No. 1 failed by an extensive leakage at 270 kp/cm$^2$, model No. 2, however, exploded at 267 kp/cm$^2$ internal overpressure. Both models had a significant deformations and cracks before failure. The maximum measured deflections were about 25 times the deflections by the reference pressure. The test results are interpreted and compared with computed values. Calculation of ultimate load is discussed. (auth)

**56993** THEORETICAL AND EXPERIMENTAL INVESTIGATIONS ON THE STRESS-STRAIN BEHAVIOR OF PRESTRESSED CONCRETE REACTOR PRESSURE VESSELS. Servit, R. (Technical Univ., Prague). pp H5/8.1-10 of Structural Mechanics in Reactor Technology. Vol. 3, Pt. H. /Jaeger, Thomas A. (comp). Luxemburg; Commission of the European Communities (1971).

From 1st International conference on structural mechanics in reactor technology; Berlin, Germany (20 Sep 1971).

The stress–strain behavior of a thick-walled cylindrical prestressed concrete pressure vessel with originally designed secantial cable arrangement was investigated. Using the finite difference method with displacements expressed as curvilinear, cylindrical coordinates are derived and computed taking into account geometric irregularities. The experimental solution by photoelasticity verified the computed stress field in the environs of the holes. (auth)

**56994** MATRIX DISPLACEMENT METHOD ON PRE- AND POST-BUCKLING ANALYSIS OF LINERS FOR REACTOR VESSELS. Yang, T. Y. (Purdue Univ., Lafayette, Ind.). pp H6/2.1-22 of Structural Mechanics in Reactor Technology. Vol. 3, Pt. H. /Jaeger, Thomas A. (comp). Luxemburg; Commission of the European Communities (1971).

From 1st International conference on structural mechanics in reactor technology; Berlin, Germany (20 Sep 1971).

A matrix displacement method is suggested for the solution of instability problems for liners of nuclear containment vessels. The method uses the incremental stiffness formulations for the plate and shell discrete elements to predict the pre- and post-buckling behavior by either an iterative or an incremental procedure. The inclusion of initial displacement terms in the element formulations allows the method to account for the possible initial displacement of the liner caused by constructional inaccuracies. Applications are illustrated by using the formulation for a doubly curved shell discrete element. 12 references. (auth)

**56995** LINER PLATE BUCKLING AND BEHAVIOR OF STUD AND RIB TYPE ANCHORS. Doyle, J. M. (Univ. of Chicago); Chu, S. L. pp H6/3.1-14 of Structural Mechanics in Reactor Technology. Vol. 3, Pt. H. /Jaeger, Thomas A. (comp). Luxemburg; Commission of the European Communities (1971).

From 1st International conference on structural mechanics in reactor technology; Berlin, Germany (20 Sep 1971).

The evaluation of forces and deformations of liner plate anchors in containment structures is studied. These forces and deformations are due to buckling, and hence, reduction in load carrying capacity of a panel of the liner plate. Specifically, the behavior of headed studs and of continuous rib type anchors is investigated. The stiffness characteristics of the anchors are based on experimental evidence, and are nonlinear. Parameters which are varied include the plate thickness, yield stress and anchor spacing. The results of several representative configurations are presented from which behavior trends can be observed. It is found that an increase in yield stress of an amount often encountered in practice causes a large increase in anchor force and deformation. On the other hand, a plate thickness increase of 15% results in a much smaller increase of anchor force and displacement. (auth)

**56996** DETECTION OF BOILING IN NUCLEAR REACTORS. Saxe, R. F.; Sides, W. H. Jr.; Foster, R. G. Jr. (North Carolina State Univ., Raleigh). J. Nucl. Energy; 25: 139-53(Apr 1971).

The relative sensitivities of two possible methods for the detection of boiling in reactors were measured, under near ideal conditions, and it was shown that the acoustical method is more sensitive than the neutron-flux noise method by a factor of at least $10^3$ or $10^4$. An upper limit for the amount of boiling void was measured as 0.4 ml and the neutron-flux noise measurements were calibrated in terms of reactivity fluctuations so that these results could be applied to other reactors. (auth) (UK)

**56997** RAPSODIE AS AN IRRADIATION REACTOR. Bull. Inform. Sci. Tech. (Paris); No. 153-154, 118-29(Nov-Dec 1970).

The Rapsodie irradiation characteristics obtained were: fission and capture cross sections and specific power of $^{235}U$, $^{238}U$, $^{239}Pu$, and $^{240}Pu$; thermal and hydraulic characteristics. The ICN 3 irradiation assembly of fissile pins was developed which has a geometry different to that of the fuel pins. The fissile device of type ICN 1 with a movable capsule is intended for the long term irradiation of samples in the core. The IRZ 4 device was developed from the preceding one for irradiation in the nickel reflector. The ICN2 and IFZ3 devices allow various materials to be irradiated. Structural materials were irradiated between 400 and 700°C in an IVZ3 type device. An in-pile creep device was also studied. (France)

**56998** CONSTRUCTION AND ENGINEERING OF PFR. Cambell, R. H. Nucl. Eng. Int.; 16: No. 183, 636-40(Aug 1971).

The system of control under which the PFR was designed, developed, and constructed is outlined. The method of construction is described and construction progress to mid 1971 is recorded. The work still to be done in completing and commissioning the reactor is reviewed. (auth) (UK)

**56999** NUCLEAR POWER AND INTERNATIONAL COOPERATION. Eklund, S. (International Atomic Energy Agency, Vienna). Tek. Ukebl.; 118: No. 35, 17-20(26 Aug 1971). (In Norwegian).

Following a general consideration of the world's energy resources and their rational exploitation, their different effects on the environment are considered. The short term and long term demand for uranium is analyzed and the known reserves estimated. Based on these figures, and on recent results of new prospecting it is found unlikely that any dramatic increase in price will occur within the foreseeable future. Brief reviews of reprocessing and enrichment capacities and plans are given, also mentioning European enrichment cooperation. A consideration of the reactor field leads to the conclusion that nuclear power will become increasingly attractive. The possibility of enormous reactor-based agro-industrial complexes in coastal desert areas, based on nuclear power and desalination is mentioned. The economic potential of peaceful nuclear explosions is examined. Finally a realist opinion that reactor development will increase the technological gap between developed and developing countries is expressed. (Norway)

**57000** LEIDI; A COMPUTER PROGRAM FOR THE POWER DISTRIBUTION WITH RESPECT TO MATERIALS AND PROCESSES WITHIN A REACTOR. Faber, C. (INTERATOM, Bensberg, Ger.). Atomwirt., Atomtech.; 16: No. 6, 304-5(Jun 1971). (In German).

The computer program LEIDI is based on a one-dimensional model. It permits the calculation of local power densities for various materials. In addition, it allows the breakdown of local power density with regard to nuclear processes. Neutron flux is based on a diffusion calculation. Since the one-dimensional model permits only rough estimates, a two-dimensional computer program is under development. (H.B.G.)

**57001** HIGH LEVEL OR LOW LEVEL IT'S A ROCKY ROAD FOR RADWASTES. Owens, Ken. Elec. Light Power (Boston); 49: No. 7, 29-38(May 1971).

The controversy over radioactive waste discharges to the environment from nuclear power plants is examined. Licensing procedures and regulations governing effluent discharge levels and waste handling and disposal are discussed. The anticipated growth in waste production is indicated, and waste management services performed by private companies are tabulated. (H.D.R.)

XUM

**57002** CONVENTIONAL AND NUCLEAR THERMAL ENERGY. Hannothiaux, Andre (Electricite de France, Paris). Rev. Fr. Energ.; No. 230, 246-53(Mar-Apr 1971). (In French).

The evolution of the nuclear policies of the EDF (Electricite de France) during the past 25 years is presented. The initial motivations in 1946 and the resulting experimental program are recalled. After being associated with Marcoule in the recovering of energy from the plutonium producing reactors G1, G2, and G3, EDF undertook the construction at Chinon of the first nuclear power stations. Their expertise extended into both the classical and nuclear aspects of the projects, the CEA acting in an advisory capacity. The economic criteria which led to the adopting by the EDF of the American light water (PWR and BWR) systems for power stations envisaged under the VI plan are discussed. This decision was taken in spite of the technical success of the St. Laurent 1 project. Investigations envisaged or presently being carried out with heavy water or fast reactors are also enumerated. (France)

**57003** HOW SHOULD FUTURE NUCLEAR ENERGY BE SUPPORTED BY THE FEDERAL REPUBLIC OF GERMANY? Schuster, G. (Bundesministerium fuer Bildung und Wissenschaft, Bonn). Atomwirt., Atomtech.; 16: No. 8-9, 410-12(Aug-Sep 1971). (In German).

At the present time, light water reactors are established for power plants, and the fast breeder, probably cooled by sodium, claims priority for the future. Whether or not the high-temperature gas-cooled reactor should be developed as an intermediate step is discussed. Because of previous experiences with gas turbines in the primary circuit and with helium in the production of gas from coal as well as in metallurgy, Germany possesses a promising position. Analysis of cost and risk, however, practically prohibits any single European nation or industrial company to support the necessary research and development. Therefore, international cooperation becomes mandatory for West-European countries. Examples for the beginning of such collective efforts are given. (H.B.G.)

**57004** APPLICATION OF NUCLEAR ENERGY FROM THE STANDPOINT OF THE REACTOR CONSTRUCTION INDUSTRY. Goeschel, H. (Siemens AG, Erlangen, Ger.). Atomwirt., Atomtech.; 16: No. 8-9, 412-13(Aug-Sep 1971). (In German).

The positive aspects of nuclear energy application are discussed. It serves as a substitute for fossil fuel and plants can be located close to population centers. It permits an increase of plant unit size from 600 MW for fossil fuel to at least 1200 MW for nuclear energy. Nuclear plant safety requirements far exceed those of conventional plants. It requires close cooperation between West European nations as to further research and development. (H.B.G.)

**57005** ELECTRICITY IN THE MODERN INDUSTRIAL SOCIETY. Kletsch, E. (Nordwestdeutsche Kraftwerke AG, Hamburg). Atomwirt., Atomtech.; 16: No. 8-9, 414-17(Aug-Sep 1971). (In German).

Within an industrial society, electric energy must be doubled every decade. An analysis shows that West Germany will soon become unable to build the necessary installations because of lack of personnel and equipment. Projections show that energy demand should be supplied at the base level by nuclear energy; up to a medium level by coal; and peaks by natural gas. The ease and safety of storing sufficient nuclear energy is emphasized. In addition, discussed are the market for nuclear power plants, large scale distribution system for energy, safety, environment, and economy. (H.B.G.)

**57006** POSSIBILITIES FOR INTERNATIONAL COOPERATION IN THE AREA OF NUCLEAR ENERGY. Mandel, H. (Rheinisch-Westfaelisches Elektrizitaetswerk AG, Essen). Atomwirt., Atomtech.; 16: No. 8-9, 418-26(Aug-Sep 1971). (In German).

Efforts to lower the cost of nuclear energy should concentrate on construction and operation of nuclear power plants including all parts of the fuel cycle. Also included must be research and development of new reactor types. Rising costs of development as well as the rapidly growing market for nuclear power plants necessitate an analysis of possibilities for the lowering of costs through international cooperation. Such a cooperation should extend to reactor construction, fuel element industry, electricity supply systems, and research centers and administrative agencies. (tr-auth)

**57007** ADVANCED COMPUTER GRAPHICS. ECONOMICS, TECHNIQUES, AND APPLICATIONS. International Symposium Held at London, England, April 14-16, 1970. Parslow, R. D.; Green, R. Elliot (eds.). New York; Plenum Publishing Corporation (1971). 1242p. $47.50. (CONF-700445).

A separate abstract is included for one of the 62 papers presented. The paper describes the use of graphic display computer systems for power reactor design and information retrieval. (D.C.C.)

*For an abstract of an individual paper see: 57008.*

**57008** APPLICATION OF COMPUTER GENERATED GRAPHS AND DIAGRAMS TO THE DEVELOPMENT OF ADVANCED NUCLEAR REACTORS. Cardwell, D. W. (Oak Ridge National Lab., Tenn.). pp 555-73 of Advanced Computer Graphics. /Parslow, R. D. (ed.). New York; Plenum Publishing Corp. (1971).

From International symposium on computer graphics; London, England (14 Apr 1970).

The use of computer systems with graphic displays for the design of advanced power reactors is described. Data acquisition and processing systems with graphic displays are also described for information retrieval systems. 7 references. (D.C.C.)

**57009** TRANSACTIONS OF THE INTERNATIONAL ASSOCIATION FOR HYDRAULIC RESEARCH. PART 2. Symposium Held in Stockholm, August 23-26, 1970. Vaellingby, Sweden; Svenska Centralkommitten foer Internationella Ingenjoerskongresser (1970). 315p. (In English and French). (CONF-700846-(Pt.2)).

A separate abstract is included for one of the 11 sessions discussed. The session presented discusses flow characteristics of pumps for power reactors. (D.C.C.)

*For an abstract of an individual section see: 57039.*

**57010** NUCLEAR REACTOR. (to English Electric Co. Ltd.). French Patent 1,568,881. 21 Apr 1969. Filed 6 Feb 1968. (In French).

A nuclear reactor is described consisting of graphite moderator pilings and a lateral restraint structure encircling the pilings. In the graphite columns there are fuel channels. The structure is supported inside a pressurized concrete vessel. The support is circumferentially positioned by pins. (J.S.R.)

**57011** PFR COMPONENTS. Scott, R. W. (British Nuclear Forum, London). Nucl. Eng. Int.; 16: No. 183, 646-50(Aug 1971).

Special features of design, materials, fabrication, and assembly of PFR components to ensure reliable operation in Na are described. Among the components considered are those for the core, heat-exchanger systems, fuel-handling, shielding, control and coolant purification. (UK)

**57012** PLACE OF FAST REACTORS IN THE UK POWER PROGRAMME. Grieves, J. O. (Central Electricity Generating Board, London). Nucl. Eng. Int.; 16: No. 183, 630-1(Aug 1971).

A program for the introduction of the first commercial fast breeder reactor into the CEGB system, in relation to the completion of the Prototype Fast Reactor at Dounreay, is outlined. This envisages site selection in 1972 and commercial operation in 1979. The problems and decisions involved are discussed. (UK)

**57013** TECHNICAL DESCRIPTION OF PFR. Henry, K. J. (United Kingdom Atomic Energy Authority, Risley, Eng.). Nucl. Eng. Int.; 16: No. 183, 632-6(Aug 1971).

Descriptions, accompanied by detailed illustrations, are presented for the core, primary circuit, fuel handling system, sodium purity control, secondary and steam circuits, turbine generator plant, instrumentation and plant control of the PFR reactor. Brief outlines are given of the method of assembly of the reactor vessel and of commissioning plans. (UK)

**57014** ORGANIZATION AND FINANCING OF NUCLEAR RESEARCH AND TECHNOLOGY IN THE FEDERAL REPUBLIC OF GERMANY. Weber, A. Atomwirt., Atomtech.; 16: No. 8-9, 444-6(Aug-Sep 1971). (In German).

The Ministry for Education and Science absorbed the previously existing Ministry for Atomic Energy. Of the 4 billion DM budget, 1.3 billion was allocated for nuclear energy. The nuclear energy allocations for 1971 are detailed in regard to large nuclear research installations, reactor development, advisory organizations, and international cooperation. (H.B.G.)

**57015** HETEROGENEOUS NUCLEAR REACTOR. (to Brown Boveri/Krupp Reaktorbau GmbH). French Patent 1,567,592. 8 Apr 1969. Priority date 2 Jun 1967, Germany. (In French).

A heterogeneous reactor is described in which the different fuel elements contribute a high reactivity and have eventually excess reactivity in the cold state. The control of the power is done with absorbing rods. The specific reactors considered are high temperature reactors with fertile elements and reactive elements. The

XUM

sliding absorbing rods are in the shape of crossed clads and cap the elements with high associated reactivity. (J.S.R.)

**57016** GERMAN-BENELUX FAST BREEDER PROJECT AND FUTURE DEVELOPMENTS IN EUROPEAN FAST BREEDER REACTORS. Haefele, W. (Inst. for Applied Reactor Physics, Karlsruhe, Ger.). J. Brit. Nucl. Energy Soc.; 10: No. 3, 169-75(Jul 1971).

The philosophy behind the development of the German fast reactor project is briefly summarized. Main objectives of the SNR 300 prototype reactor and the more important features of its design are described. Other aspects discussed include safety, siting, sodium component development, international cooperation, fuel cycles and costs. (UK)

## *Kinetics and Dynamics*

**57017** (BAW-3647-22) PHYSICS VERIFICATION PROGRAM PART III, TASK 5. Quarterly Technical Report, April-June 1971. Baldwin, M. N. (Babcock and Wilcox Co., Lynchburg, Va. Research and Development Div.). Sep 1971. Contract AT(30-1)-3647. 26p. Dep. NTIS.

An experimental program to correlate the response of all-solid, self-powered, in-core neutron flux detectors to power density profiles of a critical assembly is described. The experimental assembly, a water-moderated, slightly enriched, $UO_2$ lattice, perturbed by Ag-In-Cd poison pins and dissolved boric acid, is arranged to mock up fuel elements of a commercial pressurized water reactor. Results obtained during the second calendar quarter are presented. They will serve to check analytical techniques for relating detector signals and power profiles in commercial power reactors. (auth)

**57018** (CONF-710302-(Vol.1), pp 452-63) WORK OF THE COMMITTEE ON COMPUTER CODE COORDINATION. Hannum, W. H.; Lewellen, J. W. (Division of Reactor Development and Technology (AEC), Washington, D. C. Reactor Physics Branch).
From Meeting on new development in reactor mathematics and applications; Idaho Falls, Idaho (29 Mar 1971).

A committee was assembled in March 1969 at the request of the Advisory Committee for Reactor Physics to consider the general question of how the development of neutronic coding could be better coordinated with the fast reactor community. The factual history of the committee in its various forms and its charter, conclusions, and general working arrangements are given. Orientation toward the purpose for the committee, the significant recommendations from the committee, and suggestions as to the future course in co ordinated computer code development are presented. (auth)

**57019** (CONF-710302-(Vol.2), pp 1065-85) COMPARISON CALCULATIONS FOR A LWR BENCHMARK PACKAGE USING ENDF/B-I AND -II DATA. Olhoeft, J. E. (Westinghouse Electric Corp., Pittsburgh, Pa. Nuclear Energy Systems Div.).
From Meeting on new development in reactor mathematics and applications; Idaho Falls, Idaho (29 Mar 1971).

A package of benchmark problems was generated to test modifications to production nuclear codes for light water reactors. The selected benchmark problems fall into three general classes: (1) critical experiments to evaluate fundamental integral quantities in static calculations; (2) single pellet depletion calculations to evaluate irradiated fuel isotopics; and (3) depletion sequence calculations to evaluate key parameters of importance for PWR reactors. This set of benchmark problems is useful to test the effects on thermal reactors of cross section differences between the version I and version II library tapes of ENDF/B. The results of this test for classes (1) and (3) are discussed. 5 references. (auth)

**57020** (EUR-4709) TRACE: FUEL CYCLE COMPUTER CODE FOR FAST REACTOR ANALYSIS. Graziani, G. (European Atomic Energy Community, Ispra (Italy). Joint Nuclear Research Center). Aug 1971. 34p. Dep. NTIS (U. S. Sales Only). EUR F.Fr. 5.60.

A two-dimensional computer program written for the IBM 360/65 which calculates the fuel input requirements and the neutron physics behavior of the equilibrium fuel cycle of a fast reactor using a partial refuelling scheme is described. (auth)

**57021** (JAERI-Memo-4449) DELIGHT: THE POINT REACTIVITY BURNUP CODE FOR HTGR LATTICES. Shindo, Ryuichi; Hirano, Mitsumasa; Aruga, Takeo (Japan Atomic Energy Research Inst., Tokyo). May 1971. 55p. (In Japanese and English). Dep. NTIS (U. S. Sales Only).

The code, DELIGHT, was developed to analyze the burnup characteristics of the lattices with fuel matrices composed of coated fuel particles. The lattice is assumed to be homogeneous. The number of neutron energy groups is 61 for fast neutrons (10 MeV ~ 2.38 eV) and 50 for thermal neutrons (2.38 eV ~ 0 eV). The slowing down of fast neutrons is treated by the discontinuous slowing-down model, while the scattering of thermal neutrons by graphite and/or other moderator nuclides is dealt with scattering law for free gas. The calculations of criticality and burnup are based on few energy groups (maximum 10 for fast or thermal neutrons) and the nuclide chains of thorium-uranium and uranium-plutonium are taken in for burnup calculation. The space shielding effect of coated fuel particles for fast neutrons is considered for the calculation of resonance absorptions. Few group constants of the lattice can also be processed by the code for the use of reactor-physics analyses of HTGR cores. 9 references. (auth) (Japan)

**57022** (MRR-73) SIMULATION OF THE HYDRODYNAMICS OF BOILING WATER REACTORS. Wagner, H. (Technische Hochschule, Munich (West Germany). Institut fuer Mess- und Regelungstechnik). Jul 1970. 87p. (In German). Dep. NTIS (U. S. Sales Only).

The one-dimension non-linear dynamics of a boiling water reactor with natural or forced circulation, limited to pure hydrodynamic processes, were studied. Feedbacks of the reactor power by means of neutron kinetics were not considered. By means of a separation expression for the site and time dependence of the pressure, a dynamic pressure feedback to the hydrodynamics in the reactor perturbations could be obtained. The coolant values were reduced to pure time functions. The special advantage of this method lies in the elimination of pressure wave propagation effects with the concomitant high computation time because of the great propagation velocity of pressure perturbations. The feedback of water level changes to the system dynamics was considered. The equations for site and time variable two-phase backlash were treated in the two-phase perturbation range. In order to simulate as well as possible the natural circulation behavior of boiling water reactors, the incorporation of the driving force determining the coolant circulation because of the density variation of the coolant is necessary. In the present model this was accomplished by consideration of the coolant density corresponding to the prevailing coolant enthalpy in the return pipes and in the uncooled zone of the reactor core. The formulation of time-changing dead-time terms in the subcooled return flow yields the feedback of enthalpy changes (which can originate by perturbations in the heat exchanger of disturbances in the coolant feed) to the reactor inlet enthalpy. The consideration of pressure and water level feedback permits the complete application of the model both to the direct circuits of the boiling water and to the indirect circuits. 45 references. (tr-auth)

**57023** POWER REACTOR STATISTICAL DIAGNOSTIC TECHNIQUES. Kemeny, L. G. (Univ. of New South Wales, Kensington). At. Energy Aust.; 14: No. 2, 8-13(Apr 1971).

Aspects of a program involving analysis of stochastic models for reactor signal sources are discussed. Power reactor dynamics studies using HIFAR involve measurement of many system fluctuating parameters from reactor noise sources, which are analysed statistically. Techniques involved in out-of-pile simulation and experiment are briefly described. An outline is given of the work of a joint noise analysis laboratory utilizing ISAC and SNEDAC data acquisition systems for analysis of fluctuating signals. (Australia)

**57024** ATTEMPT TO USE STEADY-STATE DATA FOR DETERMINING CRITICAL HEAT FLUX IN TRANSIENT CONDITIONS. Hassid, A. (CISE, Milan); Rychlicki, R. Energ. Nucl. (Milan); 18: No. 6, 333-45(Jun 1971).

The way to use steady-state data together with the MATRA code for predicting critical heat flux in transient conditions resulting from a loss of flow and/or power surge accidents for nuclear reactor safety assessment is described. MATRA code was developed in connection with safety studies for a CIRENE type reactor, to simulate the voiding of a constant area channel in which a steam-water mixture flows. A systematic comparison was made with a set of data obtained in different conditions (round tube with axial uniform and non uniform power distribution, 36 rod cluster with uniform axial power distribution). To derive critical heat flux in transient conditions, the experimental data obtained in steady-state conditions were used. The results of calculations are in satisfactory agreement with experimental data, except in some special cases. 10 references. (auth)

## *Control Systems*

**57025** DEVELOPMENT OF REACTOR IN-CORE NEUTRON MONITOR. Yokota, Mitsuo (Japan Atomic Energy Research

Inst., Tokai); Shirayama, Shinpei; Kasai, Makoto. Keisoku To Seigyo; 10: No. 1, 50-7(Jan 1971). (In Japanese).

For the core of Japan Power Demonstration Reactor (JPDR), application of in-core neutron monitor was planned at beginning of construction, and development of their domestic production has been pursued because they are considered to be expendables. The detector is composed of a sensor, mineral-oxide insulated cables to transmit signal, and connectors to connect with external cables. The sensor is an ionization chamber internally coated with natural boron and filled with 1 atm argon. As pre-test prior to in-core test in a power reactor, performance test of the sensor, treatment of the mineral-oxide insulated cables and check up of thermal characteristics of the detector were conducted. Practical test was carried out in the JPDR of BWR type and 45 MW(t), and saturation current characteristics, linearity, frequency response and sensitivity were checked. The results are summarized. (Japan)

## Shielding

*Refer also to abstract 57153.*

**57026** (RCN–146) RAGA: A MONTE CARLO PROGRAM FOR CALCULATION OF GAMMA-RAY TRANSPORT IN A REACTOR SHIELD FOR MULTI-REGION SLAB GEOMETRY, USING EXPONENTIAL TRANSFORMATION. Verschuur, K. A.; Molenaar, J.; den Houting, A. W. (Reactor Centrum Nederland, Petten). Apr 1971. 25p. Dep. NTIS (U. S. Sales Only).

The ALGOL program RAGA is a Monte Carlo program which calculates the gamma ray flux-, energy absorption- and dose rate distribution in a reactor shield with multiregion slab geometry. Importance sampling is performed by exponential transformation of the track length distribution function and of the source distribution, by splitting, and Russian Roulette. The program is in operation on a 48K Philips Electrologica X8 computer. The calculation time for a reactor shield with a thickness of the order of 250 cm is about 10 minutes. (auth)

**57027** (RCN–147) EXPERIMENTAL STUDY OF THE NEUTRON ATTENUATION IN CONCRETE SHIELDS FOR FAST AND THERMAL REACTORS, WITH THE AID OF SIMULATED CONCRETE CONFIGURATIONS. Verschuur, K. A.; Quaadvliet, W. H. J. (Reactor Centrum Nederland, Petten). Apr 1971. 59p. Dep. NTIS (U. S. Sales Only).

Fundamental measurements were done on the shielding properties of concrete with various iron contents in a thermal and a fast reactor spectrum. The purpose of the experiments was to get insight in the influence of the iron on the shielding properties of concrete and to prepare a set of well defined measurements to test shielding programs. The concrete was simulated by layers of glass, polythene and iron. The "fast reactor spectrum" was attained with an iron filter. The measurements were carried out in a lid tank shielding facility with a fission plate, placed in an Argonaut type reactor. 4 references. (auth)

## Cooling Systems

*Refer also to abstracts 54583 and 55069.*

**57028** (ANL/EBR–27) OPERATING EXPERIENCE WITH SODIUM PUMPS AT EBR-II. EBR-II PROJECT. Davis, J. R.; Deegan, G. E.; Leman, J. D.; Perry, W. H. (Argonne National Lab., Idaho Falls, Idaho). Oct 1970. Contract W-31-109-eng-38. 53p. Dep. NTIS.

Several types and sizes of sodium pumps have been used at EBR-II since initial operation of the primary sodium system in April 1963. Two 4500-gpm centrifugal pumps provide flow in the primary sodium system, and one 6500-gpm linear-induction electromagnetic (EM) pump provides the main flow in the secondary sodium system. A 500-gpm permanent-magnet dc EM pump operates continuously in the primary system to ensure removal of decay heat from the reactor if both primary pumps are lost. Smaller pumps in sodium use are two 100-gpm dc EM pumps, a 100-gpm ac EM pump (for NaK), two ac linear-induction EM pumps, and several EM sampling pumps. The measured hydraulic performance of all pumps has been adequate for their applications at EBR-II. Modification of the main primary-sodium pumps eliminated binding of both pumps which occurred during initial testing. Repair of the main secondary pump and an increase in differential pressure across the pump duct resulted in successful operation to flow rates needed for 62.5-MW(t) operation. Several auxiliary pumps have operated trouble-free since they were installed. Others have had to be replaced or repaired because they failed in service. (auth)

**57029** (RDT-E–5-1-T) PRESSURIZER FOR PRESSURIZED WATER REACTORS. (Division of Reactor Development and Technology (AEC), Washington, D. C.). Dec 1970. 45p. RSO.

The requirements for design, fabrication, testing, and inspection of an electrically heated pressurizer for pressurized water nuclear reactors using either direct immersion or non-immersion type heaters are presented. (auth)

**57030** (RDT-E–5-2-T) ELECTRIC HEATER AND CONNECTOR ASSEMBLY FOR PRESSURIZER FOR PRESSURIZED WATER REACTOR. (Division of Reactor Development and Technology (AEC), Washington, D. C.). Dec 1970. 25p. RSO.

The requirements for design, fabrication, testing and inspection of a single electric heater and connector assembly for pressurizers for pressurized water nuclear reactors are presented. (auth)

**57031** (WCAP–7755) TOPICAL REPORT: INTERCHANNEL THERMAL MIXING WITH MIXING VANE GRIDS. Cadek, F. F. (Westinghouse Electric Corp., Pittsburgh, Pa.). Sep 1971. 38p.

The experimental results and data analysis of a series of mixing tests using top, split mixing vane grids on 20 inch axial spacing are presented. These tests were conducted in pressurized water loops at Reynolds numbers similar to that of a PWR core under single and two phase (subcooled boiling) flow conditions. The thermal diffusion coefficient, TDC, is determined by comparing the THINC code predictions with the measured subchannel exit temperatures. TDC is found to be independent of Reynolds number, mass velocity, pressure and quality over the ranges tested. The two phase runs (local, subcooled boiling) fell within the scatter of the single phase runs. A conservative value of TDC = 0.038 is recommended for current design use. This represents a lower limit value of all the test runs. 11 references. (auth)

**57032** DENSITY MEASUREMENTS OF STEAM–WATER MIXTURES FLOWING IN A TUBULAR CHANNEL UNDER ADIABATIC AND HEATED CONDITIONS. Agostini, G.; Era, A.; Premoli, A. (CISE, Milan). Energ. Nucl. (Milan); 18: No. 5, 295-310(May 1971).

The experimental results of a systematic investigation concerning the density of steam-water mixtures flowing under adiabatic and heated conditions are presented. Measurements were carried out by means of the quick closing valve technique, in the following conditions: (1) Test section: vertical tube ID 0.91 cm; (2) Pressure: 30; 50; 70 kg/cm$^2$; (3) Specific mass flowrate: 40 ÷ 350 g/cm$^2$s; (4) Adiabatic conditions: channel length: 414 cm; quality: 0 ÷ 0.80; (5) Heated conditions: heated length: 100 ÷ 410 cm; inlet quality: −0.15; −0.02; +0.10; exit quality: up to heat transfer crisis; heat flux: 0 ÷ 300 W/cm$^2$. A preliminary analysis is also given of data and of main parameters affecting two-phase mixture density. 10 references. (auth)

**57033** SYSTEM OF RADIOACTIVE PRODUCTS CONTROL IN GAS COOLANT OF NUCLEAR REACTORS. Moravek, J.; Pietrik, I.; Hladky, E.; Vespalec, R. Jad. Energ.; 17: No. 5, 150-7(May 1971). (In Czech).

A dosimetric control system for the coolant in gas cooled nuclear reactors is described. Main attention is devoted to the control of gas fission products by detection of delayed neutrons and by gas chromatography. These controls provide information about contamination of the reactor core by fissionable material and information about conditions of fuel elements. These data ensure timely determination of risk in operation of a nuclear power plant. (auth)

**57034** HEAT AND MASS TRANSFER AS RELATED TO CORROSION PRODUCT DEPOSITION. Kabanov, L. (CISE, Milan). Energ. Nucl. (Milan); 18: No. 5, 285-94(May 1971).

The main factors affecting the formation of corrosion product (crud) deposits are discussed, and the significance of boiling and heat flux for this process is underlined. The available experimental results and correlations for determining the amount of deposit are presented, as well as the connection between crud deposition and thermal performance of heating elements. Special consideration is given to subcooled boiling, where the heat flux, supplied by latent heat on dependence of subcooling, is fairly important for determining the amount of crud deposits. The peculiarity of deposition relevant to very high and temporary increases in crud concentration is pointed out as well. Finally the thermal effects of deposits are considered, taking into account both the intensification of heat transfer and the addition of thermal resistance. 22 references. (auth)

**57035** TRANSACTIONS OF THE INTERNATIONAL ASSOCIATION FOR HYDRAULIC RESEARCH. PART 1. Symposium Held in Stockholm, August 23–26, 1970. Vaellingby, Sweden;

XUM

Svenska Centralkommitten foer Internationella Ingenjoerskongresser (1970). 575p. (In English and French). (CONF-700846-(Pt.1)).

Separate abstracts are included for 3 of the 48 papers presented on flow characteristics and performance of power plant equipment. (D.C.C.)

*For abstracts of individual papers see: 57036–57038.*

**57036** SURGE AND WATER HAMMER PROBLEMS IN THE COOLING WATER SYSTEM OF LARGE THERMAL POWER PLANTS. Jansa, B. (Vattenbyggnadsbyraan, Goteborg). pp J.1.1-8 of Transactions of the International Association for Hydraulic Research. Part 1. Vaellingby, Sweden; Svenska Centralkommitten foer Internationella Ingenjoerskongresser (1970).

From fifth symposium of the International Association for Hydraulic Research; Stockholm, Sweden (23 Aug 1970). See CONF-700846-(Pt.1).

Design criteria for calculating cooling water flow through condensers are stated in respect of level-conditions, surges, and vacuum risks. The influence of rotating parts in the axial flow pumps at the moment of power failure is discussed and the method of calculating cooling water flow through a system of tunnels and shafts including the effect of pump characteristics is described. The criteria have been used for design work at Oskarshamn nuclear power station and two other new Swedish thermal oil fired power stations. (auth)

**57037** WATER JET PUMPS FOR REACTORS. Geijerstam, E. af (Aktiebolaget Atomenergi, Studsvik, Sweden). pp J.3.1-12 of Transactions of the International Association for Hydraulic Research. Part 1. Vaellingby, Sweden; Svenska Centralkommitten foer Internationella Ingenjoerskongresser (1970).

From fifth symposium of the International Association for Hydraulic Research; Stockholm, Sweden (23 Aug 1970). See CONF-700846-(Pt.1).

Efficiency for water jet pumps is derived theoretically and tests made at about 30°C and 210°C are described. Small differences in momentum efficiency were obtained, indicating that the friction losses are low. Best efficiencies are 35% at flow ratio 2 decreasing to 26% at flow ratio 4. Phenomena in the mixing chamber and in the diffuser are discussed. (auth)

**57038** PROBLEMS OF REACTOR CIRCULATING PUMPS. Florjancic, D.; Brun, J.; Frei, A. (Sulzer Bros. Ltd., Winterthur, Switzerland). pp J.4.1-12 of Transactions of the International Association for Hydraulic Research. Part 1. Vaellingby, Sweden; Svenska Centralkommitten foer Internationella Ingenjoerskongresser (1970).

From fifth symposium of the International Association for Hydraulic Research; Stockholm, Sweden (23 Aug 1970). See CONF-700846-(Pt.1).

A semi-sphere was chosen as pump casing for larger reactor circulating pumps in order to keep the bending stresses to a minimum. The stress distribution due to the forces on the inlet, outlet and cover was tested. To this casing form the hydraulic parts were tested as regards efficiency and suction characteristic for the questionable specific speed range. Comparison of the results of analytical calculating methods, photoelastic experiments and strain gauge measurements on a model casing gave a design value for prototypes. The shaft seal, which is the most sensitive part of the pump, was developed in long term tests under operating conditions. Design was developed for hydrostatic and hydrodynamic shaft seals, which offers a reliable solution in operation of circulating pumps. 2 references. (auth)

**57039** PUMPS AND PUMP SCHEMES. pp 237-46 of Transactions of the International Association for Hydraulic Research. Part 2. Vaellingby, Sweden; Svenska Centralkommitten foer Internationella Ingenjoerskongresser (1970). (In French and English).

From fifth symposium of the International Association for Hydraulic Research; Stockholm, Sweden (23 Aug 1970). See CONF-700846-(Pt.2).

Technical discussions during one session of the symposium are covered. The papers discussed were: Surge and Waterhammer Problems in the Cooling Water Systems of Large Thermal Power Plants (B. Jansa, Sweden) and Problems of Reactor Circulating Pumps (D. Florjancic et. al., Switzerland). To the paper Water Jet Pumps for Reactors (E. af Geijerstam, Sweden) a correction is given. (auth)

**57040** STATE OF HELIUM TECHNOLOGY FOR HIGH TEMPERATURE REACTORS. von der Decken, C.-B. (Kernforschungsanlage, Juelich, Ger.); Mueller, H.-W.; Muser, W. H. Atomwirt., Atomtech.; 16: No. 8-9, 468-72(Aug-Sep 1971). (In German).

Selection of a cooling gas for high temperature reactors necessarily leads to helium from the standpoint of neutron physics, heat technology, and corrosion chemistry. Helium technology comprises experiences with Peach Bottom, Dragon, and AVR. These experiences especially focus on chemical impurities, friction values, heat transfer, heat shielding, acoustical oscillations, leak proofing of valves, and the design of gas compressors. For the concept of the spherical-pile reactor, general problems of helium technology can be considered solved. (tr-auth)

**57041** IMPROVEMENTS TO GAS COOLED NUCLEAR REACTORS. (to Atomic Power Constructions Ltd.). French Patent 1,567,560. 8 Apr 1969. Priority date 31 May 1967, Great Britain. (In French).

An improved gas-cooled reactor is described. The reactor consists of a core, a pressurized vessel around the core, at least one coolant flow line across the core, and a coolant chamber. This chamber has at least one inlet and at least two outlets for the coolant. It has a control device to regulate the coolant flow across one of the outlets. (J.S.R.)

**57042** GAS ELUTION IN A WATER-COOLED REACTOR PRIMARY CIRCUIT WITH GASEOUS PRESSURIZER. Bodnar, Yu. F. At. Energ. (USSR); 31: No. 2, 150-1(Aug 1971). (In Russian).

The conditions are examined for gas elution in the primary loop of a water-cooled reactor with a gaseous pressurizer. The temperature in the pressurizer should be maintained below the temperature of the heat exchange fluid in the primary loop. Temperature conditions should be selected so as to ensure absence of local boiling of the water. In order to dissolve bubbles it is essential to lower the temperature in the loop to a value below $T_K$. Here $T_K$ is the maximum temperature for an equilibrium state of a heterogeneous system at a given nitrogen concentration in the water. (K.S.W.)

**57043** LEAK PROOF MECHANICAL DEVICE FOR NUCLEAR REACTOR PRESSURE VESSELS. Serafini, A. (to SNAM Progetti S.p.A.). French Patent 2,003,480. 7 Nov 1969. Priority date 8 Mar 1968, Italy. (In French).

A leak proof mechanical device to produce coolant barriers circulating at the interior of the pressure vessel of liquid sodium reactors is described. This device is characterized by the fact that it contains a series of metallic piston segments of a special type. The piston segments alternate with spacing segments. The piston segments are placed between the internal wall of the pressure vessel and the external wall of the cylinder, and between the inlet and outlet coolant pipes. (J.S.R.)

**57044** METHANE DIFFUSION: AN EXAMINATION OF THE COMMERCIAL ADVANCED GAS COOLED REACTORS. Hawtin, P.; Klaschka, J. T.; Huber, R. A. (Atomic Energy Research Establishment, Harwell, Eng.). J. Brit. Nucl. Energy Soc.; 10: No. 3, 237-47(Jul 1971).

The addition of a mixture of $CH_4$ and CO to the $CO_2$ coolant of a commercial advanced gas cooled reactor is one suggested method for inhibiting the rate of radiolytic corrosion of the graphite moderator. However, under certain circumstances, in-pore mass transport effects can lead to a marked reduction of $CH_4$ concentration within the pores of a graphite moderator block in a commercial AGR. A mathematical model based on an earlier model used in safety studies in MAGNOX reactors is developed to estimate these effects quantitatively. The basic model assumes cylindrical symmetry and is slightly non-linear due to the nature of the radiolytic destruction term. Results computed from this model are presented for a typical commercial AGR. These results are compared with values obtained from a linear approximation and the validity of the approximation is demonstrated. The degree of nonlinearity of the model is dependent on the values of parameters in the radiolytic destruction term. A series of graphs are given which enable the validity of the linear approximation to be tested without the need to solve the non-linear equation. Calculations carried out on the linear model are described. Results are presented in a generalized form which enables the user to specify reactor operating parameters without reference to the basic differential equation. Results calculated from the cylindrical model involve the assumption of an inner and an outer radius. They are therefore specific to a particular reactor. A further simplification is introduced into the theory which enables the effect of variations in the graphite thickness to be readily determined. The range of graphite thickness over which this approximation is valid is described. (auth) (UK)

## *Fuels*

**57045** (GEAP-10385) HIGH BURNUP PERFORMANCE OF POWDER AND PELLET MIXED-OXIDE FUEL. Perry, K. J.; Baily, W. E. (General Electric Co., Sunnyvale, Calif. Breeder

Reactor Dept.). Jul 1971. Contract AT(04-3)-189. 60p. Dep. NTIS.

The performance at high burnup (~148,000 MWd/Te) of powder and pellet mixed-oxide fuel was investigated. Fuel-cladding reaction resulted in the uniform loss of 0.003 to 0.004 inch of 347 stainless steel from the inside surface of the cladding at inside surface temperatures in excess of 1300°F for both types of fuel. Nonuniform cladding attack of 0.005 inch was observed in the pellet pin. 20 references. (auth)

**57046** (GEAP-13722) PERFORMANCE TESTS OF SODIUM-FILLED POWDER AND PELLET OXIDE FUEL UNDER TRANSIENT OVERPOWER. Hikido, T.; Field, J. H. (General Electric Co., San Jose, Calif. Breeder Reactor Dept.). Jul 1971. Contract AT(04-3)-189. 56p. Dep. NTIS.

The performance of sodium-filled fuel pins in power transients was investigated using two experimental capsules in the TREAT (transient) facility. Each capsule contained three slightly enriched 0.250-inch o.d., stainless steel clad $UO_2$ fuel specimens. The three specimens (reference gas-bonded pellet, sodium-filled pellet, and sodium-filled powder) arranged side-by-side, were compared with regard to fuel temperatures, mechanical deformations, and post-irradiation appearance. There were no failures even though over fifty area percent of the gas-bonded pellet fuel specimen melted. The increased heat transfer afforded by the sodium resulted in significantly lower fuel temperatures in those two fuel pins. 12 references. (auth)

**57047** (JAERI-Memo-4157, pp 2-22) JPDR IRRADIATION EXPERIMENT OF ARTIFICIALLY PIN-HOLED NUCLEAR FUEL RODS. Ishiwatari, Nasumi (Japan Atomic Energy Research Inst., Tokyo). (In Japanese and English).

From Fuel failure detection symposium; Tokyo, Japan (31 Jan 1969).

From operating experience with LWR power plants, it comes to be recognized that failure of loaded fuel rods is a matter of probability, and that the consequential release of fission products is inevitable. The experiment is aimed to get coefficients of release rate of the fission products into primary circuit water and into off gas system, and also to confirm detection method by isolating a fuel assembly likely to contain failed fuel rods into a container. The experiment was executed by loading of a failed fuel rod into the BWR type JPDR core. The fuel rod was designed to be a replica of other fuel rods consisted of $UO_2$ pellets and clad with Zircaloy-2. Two pin-holes of 0.5 mm dia. were made artificially at diametrical positions in plenum of the rod. The release of fission products was measured under light burnup, thermal flux where the failed fuel rod was located was (1 to 3) $\times 10^{13}$ n/cm$^3$. sec. The acquired release rate coefficients of the fission products were as follows: $^{131}I : 3 \times 10^{-11}$, $^{133}Xe : 1 \times 10^{-9}$, $^{137}Cs : 8 \times 10^{-9}$ and so on. These values are conditional as the released quantity was measured from reactor water for I and Cs and from the off gas system for Kr and Xe. The method to detect the likely fuel assembly to contain failed fuel rods was confirmed with the same artificially failed fuel rod. In this case, both $^{131}I$ and $^{137}Cs$ were measured, and proved to be useful signals. 12 references. (Japan)

**57048** (ORNL-TM-3359) ROD: A NUCLEAR AND FUEL-CYCLE ANALYSIS CODE FOR CIRCULATING-FUEL REACTORS. Bauman, H. F.; Cunningham III, G. W.; Lucius, J. L.; Kerr, H. T.; Craven, C. W. Jr. (Oak Ridge National Lab., Tenn.). Sep 1971. Contract W-7405-eng-26. 244p. Dep. NTIS.

ROD (Reactor Optimum Design) is a computer code for simultaneously optimizing the core design and performing the fuel-cycle analysis for circulating-fuel reactors. It consists of a multigroup diffusion calculation, including multiple thermal groups with neutron upscatter, in one-dimension or in two-dimensional synthesis, combined with an equilibrium fuel-cycle calculation. Cross sections in the CITATION format are required. The equilibrium calculation is a detailed model of the fuel cycle, including the effects of processing and of nuclear transmutation and decay. Fuel-cycle costs and fission-product concentrations are calculated, the fission products by an independent calculation from internally stored two-group cross sections. Special features of ROD are an optimization routine based on the gradient-projection method, a flux-plotting option, and a subprogram for simple time-dependent calculations based on reaction rates from the main program. (6 references) (auth)

**57049** (RDT-E-13-15-T) FUEL ASSEMBLIES FOR PRESSURIZED WATER REACTORS. (Division of Reactor Development and Technology (AEC), Washington, D. C.). Jul 1971. 47p. RSO.

The requirements for fuel assemblies for pressurized water reactors typical of those (including associated clustered control rod assemblies or burnable poison rod assemblies) in commercial electric power utility service are presented. Specifically, these requirements cover design, materials, process and personnel qualification, fabrication, assembly, quality assurance, test, inspection and examination, cleaning, packaging, and shipping. A fuel assembly is defined as a fabricated assembly of fuel rod support structures (skeletons). Only Zircaloy clad fuel rods containing sintered uranium dioxide pellets are covered. (auth)

**57050** (UJV-2551-RT) RADIATION EXPERIMENT ON TUBULAR FUEL ELEMENT WITH FINNED SURFACE. II. EXPERIMENTAL RESULTS. Derian, L.; Kadlec, J. (Ceskoslovenska Akademie Ved, Rez. Ustav Jaderneho Vyzkumu). 1971. 45p. (In Czech). Dep. NTIS (U. S. Sales Only).

The second irradiation experiment with a test model of the fuel tube for the heavy-water moderated gas-cooled KS type reactor is described and the results of this experiment are given. The aim of this experiment was to check the shape stability of the fuel tube and the stage of its technological development during the irradiation and after thermal cycling. The experiment was carried out in the reactor loop of the Nuclear Research Institute at Rez and the element tested was irradiated during 594 hours at reactor power of 4 MW. The test element was operated at average thermal fuel load of 13.4 kW/kg and at maximum surface temperature of 400°C. Total radiation stability of the test element and long-term canning tightness were confirmed. The element was inspected and cut, and metallographical analysis was carried out after the irradiation. No changes due to radiation were found in examining the element. High grade joints of uranium with the can were confirmed after element cutting and metallographical examination. Experimental measurements were compared to proposed values calculated in the evaluation. 10 references. (auth)

**57051** CALCULATION OF STRESSES IN THE GRAPHITE-FUEL TUBES OF A HIGH TEMPERATURE REACTOR. Jezernik, A.; Head, J. L. (Imperial Coll. of Science and Tech., London). Atomkernenergie; 18: No. 1, 51-60(Aug 1971).

The calculation of the time-dependent stresses in a graphite fuel tube of a High Temperature Gas-Cooled Reactor (HTGCR) is presented using a CDC 6600 computer. By way of an example, the analysis is presented of a fuel tube made from a particular graphite (Dragon-Pechiney G5) during a life of approximately 600 days in the research reactor Dragon, a 20 MW(t) reactor. The results of the computer calculation are compared with experimental results. A flow chart and the bulk of the main computer program are presented. It should be noted that the method is applicable to some other mechanical engineering problems. With some changes, it is possible, for example, to calculate the time-dependent stresses in steel tubes under internal or external pressure and with a radial temperature gradient. The thermal creep of steel must of course be calculated using a different creep law. 11 references. (auth)

**57052** COATED PARTICLE FUELS. Rose, K. S. B. (Atomic Energy Research Establishment, Harwell, Eng.). J. Inst. Nucl. Eng.; 12: No. 4, 101-5(Jul-Aug 1971).

The fuels and coatings described were developed for use in High Temperature Gas Cooled Reactors. Their small size gives the advantage that high reactor ratings can be achieved without the high center temperatures which would occur with fuel pins. The composition and purpose of the materials used, fuel kernel (fuel is $UO_2$, 800 $\mu$m diameter), buffer layer, seal layer, silicon carbide and pyrocarbon layers, are described and the differences between coated particle performance in British, American and German reactors are tabulated. Fabrication of the particles is noted. Initially irradiation causes a decrease in the kernel size of porous fuels, but at higher burnups, accommodation of the fission products causes it to swell slowly. The proportion of fission products leaving the kernel depends on its temperature; at the highest temperatures, most of the Xe, Kr, Cs, Sr, and Ba migrate. Some of the problems posed by internal CO pressure are discussed. Properties of the pyrocarbon are described, in particular its density as related to porosity, polished sections under the optical microscope, x ray measurements, mechanical properties and irradiation effects. Silicon carbide is more stable under irradiation and less variable in properties than pyrocarbon. Possible uses for the coated particle fuels are discussed. (UK)

**57053** STUDIES ABOUT USE OF DIRECTLY-COOLED COATED-PARTICLE AGGREGATES AS FUEL ELEMENTS. Barthels, A.; Boettcher, A.; Gyarmati, E.; (and others) (Kernforschungsanlage, Juelich, Ger.). Atomwirt. Atomtech.; 16: No. 4, 187-8(Apr 1971). (In German).

Temperature behavior of coated-particle fuel elements was determined mathematically and studied experimentally. Results show that coated particles can be used for gas-cooled and also for water-cooled research reactors. To maintain porosity between the coated particles for sufficient cooling, they were covered by a SiC layer. Following irradiation in the Oak Ridge HFIR at 850°C and $6 \times 10^{21}$

XUM

$n/cm^2$, the particles maintained a stable configuration. The SiC cover was not damaged. (H.B.G.)

## Auxiliary and Emergency Systems

*Refer also to abstract 55078.*

**57054** (ANL/EBR-30) EQUIPMENT FOR REMOTE MEASUREMENT OF BOW, LENGTH, AND WEIGHT OF IRRADIATED EXPERIMENTAL CAPSULES AND ELEMENTS AT EBR-II. EBR-II PROJECT. Rizzie, J. W. (Argonne National Lab., Idaho Falls, Idaho). Jun 1970. Contract W-31-109-eng-38. 25p. Dep. NTIS.

The measurement equipment is used in the air-cell complex of the Fuels and Examination Facility at the EBR-II site to support the irradiation program of the EBR-II Project. The device for measuring bow and length and the remotely controlled balance provide physical data from irradiated experimental elements or capsules that can be used to determine the experiment integrity and help evaluate the results of the irradiation cycle. A gross change in weight of an irradiated capsule or element before and after irradiation is a definite indication of a defected capsule or element cladding. Bow and length measurements are used to qualify capsules or elements for reconstitution (for continued irradiation in EBR-II subassembly form) and to analytically determine the stress exerted on the subassembly hexagonal tube by the enclosed elements or capsules. The bow of the irradiated element or capsule is measured vertically by mechanically locating the centerline of the subject and comparing this location with the centerline of a known straight standard. Bow is mechanically encoded in X and Y coordinates and later converted to an angle and radius from a fixed position on the capsule or element. Lengths of capsules and elements are measured with a dial indicator, which is calibrated with a standard-length Invar rod. Capsule and element weights are measured remotely using an electromechanical balance with digital readout. (auth)

**57055** (JAERI-Memo-4157, pp 84-8) RESEARCH AND DEVELOPMENT PROGRAM OF FUEL FAILURE DETECTION FOR FAST BREEDER REACTOR IN JAERI. Sakai, Eiji (Japan Atomic Energy Research Inst., Tokyo). (In Japanese and English).

From Fuel failure detection symposium; Tokyo, Japan (31 Jan 1969).

A research and development program of fuel failure detection for LMFBR is described. Graphite is used for a neutron moderating system for delayed neutron method, while neutron detection efficiency and effect of $\gamma$ background are checked. FFD in LMFBR is carried out under high $\gamma$-ray background by measurement of fission products leached in coolant sodium or cover gas. Improvement of S/N ratio of $BF_3$ and $^{10}B$ neutron detectors is undertaken with pulse shape discrimination between those of $\gamma$-ray and neutrons. As for $\gamma$-ray measurement of fission products double diode Compton suppression spectrometers seem to be hopeful. It is planned to check effectiveness of the spectrometer by measuring actual $\gamma$-ray from the fission products in the coolant and the cover gas and being applied to precipitator detection. 7 references. (Japan)

**57056** (JAERI-Memo-4157, pp 89-100) PRESENT STATUS OF FUEL FAILURE DETECTION AND LOCATION METHOD IN VARIOUS COUNTRIES IN THE WORLD. Mochizuki, Keiichi (Japan Atomic Energy Research Inst., Tokyo). (In Japanese and English).

From Fuel failure detection symposium; Tokyo, Japan (31 Jan 1969).

Present state of fuel failure detection and location method in various foreign countries is reviewed in relation to its application for Na-cooled fast breeder reactors. Associated problems, sensitivity and required research and development work are described. Definition of sensitivity, the fuel failure detectors equipped in foreign Na-cooled fast reactors, and further research and development work are discussed. 74 references. (Japan)

**57057** (NEDO-10320(Suppl.1)) GENERAL ELECTRIC PRESSURE SUPPRESSION CONTAINMENT ANALYTICAL MODEL. Licensing Topical Report. (General Electric Co., San Jose, Calif. Atomic Power Equipment Dept.). May 1971. 24p.

Clarification of analytical modeling methods used to simulate the short term transient in a pressure suppression type containment following a loss of coolant accident in boiling water reactors is presented. Models discussed include: vessel blowdown model; drywell model; vent clearing model; vent flow model; and suppression chamber model. (D.C.C.)

**57058** FAST REACTOR TOP ACTING AS A SAFETY VALVE IN CASE OF A SUDDEN PRESSURE INCREASE. (to Commissariat a l'Energie Atomique). French Patent 1,572,466. 19 May 1969. Filed 6 May 1968. (In French).

A fast reactor top acting as a safety valve in case of sudden pressure increase is described. The top itself consists of thin material covered by a heat insulator. It has good ductility and very good resilience. Beams of a material with the same coefficient of expansion as the head itself are sunk in the heat insulator and kept against the head by clamps. The beams have very low resilience. (J.S.R.)

## Operation and Economics

*Refer also to abstracts 54711 and 57135.*

**57059** (70-CNA-628) PROBLEMS OF COMPARING POWER REACTORS FOR SPECIFIC APPLICATION. Guard, Robin F. W. (Canatom Ltd., Montreal (Quebec)). 1970. 18p. (CONF-700564-7). Dep. NTIS (U. S. Sales Only).

From tenth annual international conference of the Canadian Nuclear Association; Toronto, Canada (24 May 1970).

Financial aspects associated with the construction and operation of power reactors are discussed. Effects of reactor types and fuel cycles on the costs of power reactors are compared. 8 references. (D.C.C.)

**57060** (JUL-736-RG) OPTIMIZATION OF THE FUEL CYCLE AND CORE SECTIONING OF A 2500-MW(th) THORIUM HIGH-TEMPERATURE REACTOR WITH MULTIZONE LOADING. Markowski, Baldur (Kernforschungsanlage, Juelich (West Germany). Institut fuer Reaktorentwicklung). Feb 1971. 84p. (In German). Dep. NTIS (U. S. Sales Only).

For a pebble-bed reactor of 2500 MW(t) used also for the production of process heat, the possibilities for an optimization were investigated with respect to the fuel cycle costs and to the thermodynamic properties. These properties are dependent on the zone sectioning and design. It was shown that the most important results of the single zone optimization can be transferred to the multizone core. The power flattening was obtained best by reduction of the thorium input to the exterior zone. In order to attain a satisfactory temperature and power distribution a core sectioning into two zones of suitable design was used. The flattening of the radial power density distribution has a rise of the specific fuel cycle costs of about 0.02 Dpf/kWhr in comparison with the single zone calculation. 18 references. (auth)

**57061** (MLM-1851) TECHNICAL AND ECONOMIC PARAMETERS AFFECTING FAST BREEDER REACTOR DEPLOYMENT. O'Hara, F. A. (Mound Lab., Miamisburg, Ohio). 13 Sep 1971. Contract AT(33-1)-Gen-53. 198p. Dep. NTIS.

The effects of various technical and economic parameters on LMFBR deployment plans were studied to assess the best future "mix" of light water reactors and fast breeder reactors which will result in minimum cumulative nuclear generating costs discounted to the year 1985. Projected growth in domestic nuclear generating capacity was taken from various predictions and the future domestic nuclear generating capacity was assumed to consist only of light water reactors and liquid metal cooled fast breeder reactors. Technical characteristics representing the two reactor types were taken as fixed, typical values. The light water reactor characteristics represent a composite between PWRs and BWRs, whereas a recent follow-on design was used as the reference for LMFBRs. Annual domestic power generation costs are calculated as a function of the installed capacity of both light water and fast breeder reactors in each particular year, the unit costs of each reactor type, the load factor, plutonium requirements, plutonium price and discount rate, and other factors. The cumulative nuclear generating costs are then computed as the sum of the discounted annual costs. (auth)

**57062** (ORNL-4682, pp 240-1) REACTOR EVALUATION STUDIES. (Oak Ridge National Lab., Tenn.).

In Chemical Technology Division annual progress report.

Computer program analysis of nuclear power plant fuel cycle economics is reviewed. The optimum economic schedule for introducing nuclear power plants into existing power systems is discussed. (D.C.C.)

**57063** (ORNL-TM-3276) CONCEPT: COMPUTERIZED CONCEPTUAL COST ESTIMATES FOR STEAM-ELECTRIC POWER PLANTS. Phase I User's Manual. DeLozier, R. C.; Reynolds, L. D.; Bowers, H. I. (Oak Ridge National Lab., Tenn.). Oct 1971. Contract W-7405-eng-26. 140p. Dep. NTIS.

The computer code CONCEPT was developed to provide con-

ceptual capital cost estimates for single-unit nuclear and fossil-fueled power plants. Cost estimates can be made with this code as a function of plant type, size, location, and date of operation. Output from the code includes a detailed breakdown of the estimate into direct and indirect costs according to the USAEC accounting system. The cost model presented is for PWR plants only. 9 references. (auth)

**57064** FUEL AND FUEL CYCLE FOR PFR. Bishop, J. F. W.; Kemp, E. F. Nucl. Eng. Int.; 16: No. 183, 643-5 (Aug 1971).

High burn-up and the ability for failed fuel to remain in the reactor pending a convenient discharge are the salient requirements for fast reactor fuel. Valuable irradiation experience was obtained in DFR and it is now possible to characterize events leading to pin failure in PFR oxide pins. Operation of PFR will provide adequate statistical guidance on the low failure rates expected in the fuel and will also provide the high flux facility required for complete clarification of the phenomenon of decreasing density of metal components subjected to an intense fast neutron flux. Consideration is given to reprocessing requirements of PFR fuel. (auth) (UK)

**57065** GAS-BREEDER MEMORANDUM. Dalle Donne, M. (Kernforschungszentrum, Karlsruhe, Ger.). Atomwirt., Atomtech.; 16: No. 8-9, 430(Aug-Sep 1971). (In German).

The nuclear research centers in Karlsruhe and Juelich, in cooperation with several German industrial firms, conducted a preliminary study of various types of gas-cooled fast breeder reactors. Following a survey of all reported reactor types, a closer analysis was restricted to three only. For these three types, the main characteristics were calculated and compared with data applying to an advanced sodium-cooled breeder reactor. It was concluded that gas-cooled fast breeders do not represent a goal of the distant future but a concept that is competitive with the first generation of sodium-cooled reactors. (H.B.G.)

**57066** NUCLEAR POWER REACTORS: THE PROBLEMS OF ACCESSIBILITY FOR TESTING AND REPAIR AND THE INFLUENCE OF EXPERIENCE ON THE DESIGN. Fletcher, P. T. (Atomic Power Constructions Ltd., Surrey, Eng.). Proc. Inst. Mech. Eng. (London); 184: 1179-1200(1969-70).

Experiences in dealing with engineering problems in Magnox reactors by performing remote operations under radiation conditions are discussed. Detailed descriptions are given of the procedures adopted after the following incidents: a fuel melt failure in one channel of a Chapelcross reactor, occurring during start up after off-load refuelling; failure of the charge machine grab to secure a fuel element when load changing in Tokai-Mura during a maintenance shutdown; dislodgement of a charge pan, and the jamming of a charge tube in Trawsfynydd-2 reactor; dislodgement of part of cover plates and damage to exposed insulation of two main gas ducts of Tokai-Mura, discovered during routine boiler inspection. The lessons learned from these and other incidents, and ways in which new advances in design of reactors and components will preclude such incidents, are briefly discussed. (UK)

**57067** INFLUENCE OF IRRADIATION CONDITIONS ON CALIFORNIUM FORMATION IN NUCLEAR REACTORS. Eberle, S. H.; Bleyl, H.-J. (Univ., Karlsruhe, Ger. Kernforschungszentrum, Karlsruhe, Ger.). Radiochim. Acta; 15: No. 4, 180-7 (Jun 1971). (In German).

The yields of nuclides obtained on irradiation of $^{242}$Pu, $^{243}$Am, and $^{244}$Cm in a nuclear reactor are calculated as a function of the absolute value of thermal flux, relative epithermal flux, and on/off schedule as parameters. At constant thermal neutron dose, the $^{252}$Cf production rate increases exponentially with increasing epithermal flux; hence, the yield may differ by several powers of ten, depending on this factor. The absolute value of the thermal flux has only a small effect, an increase by a factor of ten (from $2.5 \times 10^{14}$ to $2.5 \times 10^{15}$ $N_{th}/cm^2 \cdot sec$) results in only about 30% more Californium at the same neutron dose. The on/off-schedule of the reactor has no practical importance if the down-time is not more than half the on-time. The numerical results of the calculations are given as yield curves of the nuclides. (auth)

## *Safety and Siting*

*Refer also to abstracts 54545, 54547, and 54777.*

**57068** (AI-AEC-13006) LMFBR SAFETY PROGRAMS. Annual Technical Progress Report, GFY 1971. (Atomics International, Canoga Park, Calif.). 15 Sep 1971. Contract AT(04-3)-701. 59p. Dep. NTIS.

LIQUID METAL FAST BREEDER REACTOR — safety research on, summary of fiscal year 1971
— coolant combustion accidents in, release and transport of aerosols and energy from sodium, (E/T)
— coolant boiling in, initiation and thermal hydraulics aspects of sodium, (E/T)
REACTOR FUEL ELEMENTS — explosion in liquid sodium of uranium oxide ($UO_2$), mechanical energy conversion efficiency and particle size distribution from, (E/T)
REACTOR SAFETY — programs for LMFBR, summary for fiscal year 1971
SODIUM — combustion in reactor accidents, release and transport of aerosols and energy from, (E/T)
— boiling in reactor cores, initiation and thermal hydraulics aspects of, (E/T) (H.D.R.)

**57069** (ANL-7800) LMFBR NUCLEAR SAFETY PROGRAM. Annual Report, July 1, 1969-June 30, 1970. (Argonne National Lab., Ill.). Jul 1971. Contract W-31-109-eng-38. 462p. Dep. NTIS.

Program activities for July 1969 to June 1970 are described. Areas of research and development include: LMFBR accident analysis and safety evaluation; reactor control and stability; coolant dynamics; core structural safety; fuel element failure propagation; fuel dynamics studies in TREAT; materials behavior and energy transfer; fast reactor safety test facility study; fuel-coolant interactions; postaccident heat removal; 1000 MW(e) safety study contract management, technical review, and evaluation; 1000 MW(e) safety study subcontracts; reactor system and containment structural dynamic response; thermal-plume dispersion studies; plant dynamics and control analysis; and 1000 MW(e) plant study contract management, technical review, and evaluation. (D.C.C.)

**57070** (CEA-CONF-1796) PROBLEMS OF EXPLOSIONS INSIDE CONTAINMENT VESSELS. [Sep 1970]. 23p. (In French). (CONF-710903-3). Dep. NTIS (U. S. Sales Only).

From first international conference on structural mechanics in reactor technology; Berlin, Germany (20 Sep 1971).

Some elementary ideas about explosions and pressure waves are presented in the aim of identifying the simpler tests to be performed for finding elementary laws of explosion containment. The scale effect is discussed for production, propagation and containment of pressure waves; it appears necessary to conduct simulated tests at various scales. The low pressure explosions with gas mixtures appear useful for simulating nuclear core explosions. Some unpublished CEA results on structural behaviors under explosion are summarized. A correlation law is given for published American results on open tubes. (auth)

**57071** (CONF-710302-(Vol.1)) PROCEEDINGS OF CONFERENCE ON NEW DEVELOPMENTS IN REACTOR MATHEMATICS AND APPLICATIONS, IDAHO FALLS, IDAHO, MARCH 29-31, 1971. (American Nuclear Society, Hinsdale, Ill. American Nuclear Society. Eastern Idaho Section). 569p. Dep. NTIS.

Included are 35 papers on mathematical methods used in reactor safety calculations and the development of modular programming systems. A separate abstract was prepared for each of 26 papers. Nine papers were previously abstracted for Nuclear Science Abstracts and may be located under CEA-CONF-1772 and CONF-710302 in the Report Number Index. (H.D.R.)

*For abstracts of individual papers see: 56878, 57018, 57072-57087, 57110, and 57140-57146.*

**57072** (CONF-710302-(Vol.1), pp 1-24) LIQUID METAL FAST REACTOR ACCIDENTS. Wolfe, B. (Hanford Engineering Development Lab., Richland, Wash.).

From Meeting on new development in reactor mathematics and applications; Idaho Falls, Idaho (29 Mar 1971).

Hypothetical accidents considered in the safety evaluation of sodium cooled fast reactors are discussed. Reactivity excursions, core voiding, sodium fuel interactions, and after heat removal are described, and phenomena which significantly decrease the effects of such accidents are examined. 9 references. (H.D.R.)

**57073** (CONF-710302-(Vol.1), pp 25-49) PRESSURE GENERATION BY MOLTEN FUEL-COOLANT INTERACTIONS UNDER LMFBR ACCIDENT CONDITIONS. Cho, D. H.; Ivins, R. O.; Wright, R. W. (Argonne National Lab., Ill.).

From Meeting on new development in reactor mathematics and applications; Idaho Falls, Idaho (29 Mar 1971).

A comprehensive analysis of pressure generation by molten fuel-coolant interactions is presented, incorporating various limiting rate processes. Pressure-time histories are calculated considering a 35 cm long molten zone in an FFTF subassembly, and parametric effects are discussed. 10 references. (auth)

XUM

**57074** (CONF-710302-(Vol.1), pp 50-78) AN EVALUATION OF FUEL-COOLANT INTERACTIONS DURING DISASSEMBLY OF AN LMFBR. Lorenzini, P. G.; Flanagan, G. F. (Atomics International, Canoga Park, Calif.).

From Meeting on new development in reactor mathematics and applications; Idaho Falls, Idaho (29 Mar 1971).

A model which calculates the feedback from fuel-coolant interactions during the disassembly of the core is presented. The model is incorporated in the computer code, FISFAX. The FISFAX code does not use the Bethe-Tait disassembly model, and therefore it is no longer necessary to assume that the core is homogeneous. By calculating the FCI feedback during the core disassembly, the reactivity feedback can be time dependent. Calculations presented show that this feedback is a rapidly varying function of time, and can provide a negative reactivity feedback as well as the customary positive feedback. The negative reactivity feedback resulting from the FCI was the principal mechanism for terminating the excursion in the cases presented. The FISFAX model is described first, followed by some results of analyses using the code. 16 references. (auth)

**57075** (CONF-710302-(Vol.1), pp 79-96) FISSION GAS AND MOLTEN FUEL EJECTION FROM FAILED FUEL RODS IN AN LMFBR. Carelli, Mario D. (Westinghouse Electric Corp., Madison, Pa. Advanced Reactors Div.).

From Meeting on new development in reactor mathematics and applications; Idaho Falls, Idaho (29 Mar 1971).

Two computer codes are described for use in analyzing the effects of fuel rod failure in a Liquid Metal Fast Breeder Reactor (LMFBR). The code FIGAFRO investigates the characteristics of fission gas ejection, while the code FIDES studies a molten fuel ejection. Their applicability to the possible accidents occurring during the fuel rod lifetime is discussed, and the main features of the physical models employed and of the solution methods adopted are described. Typical results of the ejection characteristics, which constitute the necessary basis to investigate the consequences of the failure and the possibility of its propagation, are also illustrated. (auth)

**57076** (CONF-710302-(Vol.1), pp 102-19) LOCAL FLOW BLOCKAGE EFFECTS IN AN LMFBR FUEL PIN BUNDLE. Moore, R. W. (Babcock and Wilcox Co., Lynchburg, Va.).

From Meeting on new development in reactor mathematics and applications; Idaho Falls, Idaho (29 Mar 1971).

The determination of the effects of a localized blockage within a fuel pin bundle requires (1) a knowledge of the blockage geometry and (2) a method to calculate the coolant velocity and temperature distributions in the affected channels. A calculational tool was developed to determine the coolant velocity and temperature distributions resulting from a blockage. This computer program (BLOCKO) was written in Fortran for the CDC 6600. Application was made to numerous types of hypothetical blockages described by the number of blocked coolant channels, the axial blockage length, the flow area reduction in each channel and the hydraulic diameter reduction in each channel. (auth)

**57077** (CONF-710302-(Vol.1), pp 120-7) SAS2A LMFBR ACCIDENT ANALYSIS CODE. Dunn, F. E.; Heames, T. J.; Pizzica, P. A.; Fischer, G. (Argonne National Lab., Ill.).

From Meeting on new development in reactor mathematics and applications; Idaho Falls, Idaho (29 Mar 1971).

The SAS2A accident analysis code is an upgraded multi-channel version of the SAS1A code. It predicts accident behavior, starting from an unfaulted normal operating condition, through a transient caused by a coolant flow perturbation or a reactivity insertion, and through any resulting core disassembly. SAS2A uses physically meaningful models to explicitly calculate accident behavior. The models are verified by comparison with in-pile and out-of-pile experiments. 9 references. (auth)

**57078** (CONF-710302-(Vol.1), pp 128-51) TWO-DIMENSIONAL FAST-REACTOR DISASSEMBLY ANALYSIS WITH SPACE-TIME KINETICS. Sha, W. T.; Daly, T. A.; Lindeman, A. J.; Fuller, E. L.; Meneley, D. A.; Leaf, G. K. (Argonne National Lab., Ill.).

From Meeting on new development in reactor mathematics and applications; Idaho Falls, Idaho (29 Mar 1971).

A two-dimensional (r-z), space-time-energy-dependent computational method was developed for use in LMFBR disassembly analyses. The model consists of multigroup neutronics based on a flux factorization technique, hydrodynamics, energy balance, and an energy-density-dependent equation of state. Reactivity feedbacks due to Doppler broadening and material motion are taken into account. The Eulerian coordinate system is used in the neutronics; the hydrodynamics, energy balance, and equations of state are formulated based on the Lagrangian coordinate frame. An algorithm transformation of temperature and reactor material contents from the Lagrangian (deformed mesh) to Eulerian (fixed mesh), or vice versa, was also developed. A unique feature of this model is the ability to account for large reactor material motion during a disassembly accident. For most accident conditions, this model predicts a higher energy yield than would be computed by using point neutron kinetics. 6 references. (auth)

**57079** (CONF-710302-(Vol.1), pp 152-66) NUMERICAL STABILITY PROBLEMS IN THE VENUS DISASSEMBLY CODE. Jackson, J. F.; Nicholson, R. B.; Sha, W. T. (Argonne National Lab., Idaho Falls, Idaho).

From Meeting on new development in reactor mathematics and applications; Idaho Falls, Idaho (29 Mar 1971).

The VENUS computer program calculates the behavior of an LMFBR during a disassembly accident. The power and energy release are determined using a standard point kinetics model that accounts for reactivity feedback due to Doppler broadening and material motion. The disassembly motion is calculated by a direct finite difference solution of a set of two-dimensional (r-z) hydrodynamics equations. This allows the use of a density dependent energy-pressure relationship (equation of state) to link the kinetics and hydrodynamics equations. Temporal and spatial oscillations in the calculated pressures were observed in applying the code to various types of excursions. An example of such oscillations is shown. The total energy release is often not greatly affected by these pressure spikes, unless they become extremely large. Although the energy is usually the primary result, in some instances one is interested in actual physical pressure oscillations, and is therefore faced with the difficulty of eliminating possible numerical instabilities in order to see the true oscillations. In some cases, using a time step that is too large will cause the pressure calculations to become completely unstable, causing the calculation to terminate in a computer overflow. A time step selection criterion that has been found to give good results for a broad range of accidents is presented. 7 references. (auth)

**57080** (CONF-710302-(Vol.1), pp 167-79) AN AXIAL KINETICS MODEL FOR FAST REACTOR DISASSEMBLY ACCIDENTS. Mills, Joseph C.; Kastenberg, William E. (California Univ., Los Angeles).

From Meeting on new development in reactor mathematics and applications; Idaho Falls, Idaho (29 Mar 1971).

A physical model describing the transient behavior of moderate accidents in fast liquid metal cooled reactors is postulated. The physical model was transformed into a preliminary computational tool used for analyzing accidents with sodium-fuel interactions during the nuclear power transient. Calculations performed for typical 1,000 MW(e) LMFBR's indicate reasonable results and yield an accurate representation of the physics. 17 references. (auth)

**57081** (CONF-710302-(Vol.1), pp 180-98) COMPARISON BETWEEN MOMENTUM INTEGRAL AND COMPRESSIBLE MODELS FOR SODIUM VOIDING CALCULATIONS IN LMFBR's. MacFarlane, D. R.; Siegmann, E. R. (Argonne National Lab., Ill.); Eggen, D. T. (Northwestern Univ., Evanston, Ill.).

From Meeting on new development in reactor mathematics and applications; Idaho Falls, Idaho (29 Mar 1971).

Some results obtained with a new compressible sodium voiding model which was developed for calculating the two-phase flow in LMFBR coolant channels are presented and compared with similar calculations performed using the older momentum integral model. It was recognized that computer calculations using a compressible model would probably be considerably more costly due to the much reduced time steps which are generally required in practical computing algorithms using such models. Accordingly, a secondary purpose of the work was to investigate how severe restrictions of this type would be in limiting the use of the compressible model in place of the momentum integral model in a large computer code such as SAS1A. The describing equations and assumptions for the two models, a brief description of the methods of solving the equations for each, and finally, a comparison of results obtained for some typical bench mark-type problems each using each of the two calculational schemes are presented. 6 references. (auth)

**57082** (CONF-710302-(Vol.1), pp 215-40) COOLANT VOIDING TRANSIENTS IN LMFBR's. Tilbrook, R. W. (Westinghouse Electric Corp., Madison, Pa. Advanced Reactors Div.).

From Meeting on new development in reactor mathematics and applications; Idaho Falls, Idaho (29 Mar 1971).

A code, PASET, is described for use in studying sodium voiding in a LMFBR due to either loss of coolant or fuel/sodium interaction incidents. Its range of validity is discussed and its application to accident scoping studies and the identification of data requirements is illustrated. 13 references. (auth)

XUM

**57083** (CONF-710302-(Vol.1), pp 241-58) CONSEQUENCES OF MOLTEN FUEL EJECTION IN A LMFBR. Graham, John; Versteeg, Joost (Westinghouse Electric Corp., Madison, Pa. Advanced Reactors Div.).

From Meeting on new development in reactor mathematics and applications; Idaho Falls, Idaho (29 Mar 1971).

The possibility of a progressive failure of fuel rods starting from a single failed rod and leading to gross core damage has been postulated as an initiator for a LMFBR accident. In order to scope the magnitude of potential damage effects and calculate the effective time-scale of the several events, the case of the failure of an over-enriched fuel rod was examined. The objective of the work was to study the consequences of the possible ejection of molten fuel into the sodium coolant and to determine whether a serious potential for a propagation of the failure existed. 12 references. (auth)

**57084** (CONF-710302-(Vol.1), pp 259-81) MODELING AND APPLICATION OF THE ADIABATIC APPROXIMATION FOR ANALYZING ROD DROP EXCURSIONS. Stirn, R. C.; Woolley, J. A.; Cheng, H. S. (General Electric Co., San Jose, Calif.).

From Meeting on new development in reactor mathematics and applications; Idaho Falls, Idaho (29 Mar 1971).

The modeling and application of an adiabatic model to analyze control rod drop excursions are presented. A description of the solution of the neutron kinetics equations in two space dimensions using the adiabatic approximations is given, and a comparison between a one-dimensional space-time and adiabatic solution to a rod drop transient is also presented. In addition, a control rod drop excursion for a large boiling water reactor (BWR) is analyzed in RZ-coordinates using linear and non-linear reactivity feedback mechanisms. It is demonstrated that the adiabatic model is accurate for analyzing prompt critical rod drop excursions in the startup power range. Furthermore, it is also shown that the spatial effects of non-linear reactivity feedback mechanisms must be properly accounted for in calculating these prompt critical transients, or large errors in the analysis could result. 13 references. (auth)

**57085** (CONF-710302-(Vol.1), pp 282-95) SAFETY ANALYSES OF PRESSURIZED WATER REACTORS. Margolis, Stephen G. (State Univ. of New York, Buffalo).

From Meeting on new development in reactor mathematics and applications; Idaho Falls, Idaho (29 Mar 1971).

Numerical methods for dealing with hydrodynamic problems involving the propagation of pressure waves are reviewed. Difficulties associated with solving pressurized water reactor loss-of-coolant problems using these methods are discussed. (H.D.R.)

**57086** (CONF-710302-(Vol.1), pp 356-9) STABILITY CALCULATIONAL PROCEDURE FOR FLOW-INDUCED VIBRATIONS OF REACTOR INTERNALS IN PARALLEL FLOW. Lowe, P. A. (Combustion Engineering, Inc., [Windsor, Conn.]); Zanoni, E. A. (Bettis Atomic Power Lab., Pittsburgh, Pa.).

From Meeting on new development in reactor mathematics and applications; Idaho Falls, Idaho (29 Mar 1971).

An analysis method designed to calculate and predict the presence of dynamic instabilities of a structure which is acted upon by a fluid flowing parallel to the principal axis of the structure is presented. In modeling the physical situation, it is assumed that the structural displacements are small and that the fluid velocity is composed of a steady-state component and a small time varying perturbation component. These assumptions allow the transient fluid conservation equations for the flow channels contiguous to the structure to be linearized about a steady-state operating condition. The linearized equations are then solved to establish the fluid-induced forces and moments which act upon the structure. These forces and moments are introduced into the differential equations which govern the dynamics of the structure. The dynamic equations, coupled with a boundary constraint which describes the fluid conditions at the downstream end of the structure, represent the system's characteristic equation. They are manipulated into a convenient form with standard matrix techniques, and then analyzed by numerically evaluating the system's complex eigenvalues. 7 references. (auth)

**57087** (CONF-710302-(Vol.1), pp 436-51) PRESCON: A DIGITAL COMPUTER PROGRAM FOR CONTAINMENT PRESSURE TRANSIENTS. Elliott, J. N.; Odlozinski, G. (Atomic Energy of Canada Ltd., Chalk River (Ontario)); D'Arcy, D. F. (Atomic Energy of Canada Ltd., Chalk River (Ontario). Chalk River Nuclear Labs.).

From Meeting on new development in reactor mathematics and applications; Idaho Falls, Idaho (29 Mar 1971).

The simple explicit numerical method used in the PRESCON code for calculating transient pressures in CANDU reactor containment systems following a major failure of the heat transport system is described. Results obtained with the PRESCON code are compared to results obtained with the method of characteristics for a subsonic flow problem. (H.D.R.)

**57088** (GEAP-13639-1) CORE DESIGN DEVELOPMENT NEEDS IN RELATION TO FUEL FAILURE PROPAGATION, SODIUM BOILING, AND CLAD/FUEL-SODIUM THERMAL INTERACTION. McWethy, L. M.; Pluta, P. R.; Sherer, D. B. (comps.) (General Electric Co., Sunnyvale, Calif. Breeder Reactor Dept.). Oct 1970. Contract AT(04-3)-189. 133p. Dep. NTIS.

A comprehensive assessment of LMFBR safety-related core design information needs was conducted. A basic hypothesis was that core performance under off-design and accident conditions will affect the choice of core design parameters. The economic consequences of fuel failure effects and random accidents were compared with fault tree results based on a "mean-annual-cost" concept. It is concluded that fuel failure effects dominate the expected cost penalties. Principal development recommendations are for integral tests of: (1) fuel failure propagation; and (2) loss-of-cooling consequences. 35 references. (auth)

**57089** (GEAP-13639-2) CORE DESIGN DEVELOPMENT NEEDS IN RELATION TO FUEL FAILURE PROPAGATION, SODIUM BOILING, AND CLAD/FUEL-SODIUM THERMAL INTERACTION. McWethy, L. M.; Pluta, P. R.; Sherer, D. B. (comps.) (General Electric Co., Sunnyvale, Calif. Breeder Reactor Dept.). Oct 1970. Contract AT(04-3)-189. 382p. Dep. NTIS.

Details of the review and analysis of specific phenomena identified by a fault tree analysis as having a major impact on LMFBR safety and core design are presented. Fuel failure propagation effects dominate the events which most affect core performance under off-design or accident conditions. (H.D.R.)

**57090** (ORNL-4717, pp 91-107) NUCLEAR SAFETY. (Oak Ridge National Lab., Tenn.).

In Reactor Chemistry Division annual progress for period May 31, 1971.

The status of projects on the effects of chemical processes and properties on reactor safety is reported. Brief summaries are included on fuel coating properties, fission product removal from reactor systems, fuel element failure mechanisms, and steam-graphite reactions. (H.D.R.)

**57091** (ORNL-NSIC-94) COMPILATION OF NATIONAL AND INTERNATIONAL NUCLEAR STANDARDS (EXCLUDING U.S. ACTIVITIES). 7th Edition, 1971. Information Gathered to Dec. 31, 1970. (Oak Ridge National Lab., Tenn.). Sep 1971. Contract W-7405-eng-26. 129p. Dep. NTIS.

All known national and international nuclear standards activities are tabulated. Standards activities of all national organizations, technical societies and government agencies are listed alphabetically by country. Standards activities are included for: Australia, Austria, Belgium, Canada, Denmark, France, Germany, Hungary, India, Israel, Italy, Japan, Netherlands, Norway, Pakistan, Republic of South Africa, Sweden, United Kingdom, and Yugoslavia. International organizations activities include: Bureau Venitas, European Organization for Nuclear Research, European Atomic Energy Community, International Air Transport Association, IAEA, International Commission on Radiological Protection, International Commission on Radiation Units and Measurements, International Electrotechnical Commission, Intergovernmental Maritime Consulative Organization, International Organization for Standardization, Floyds, Organization for Economic Cooperation and Development, European Nuclear Energy Agency, and United Nations. 18 references. (D.C.C.)

**57092** (ORNL-TM-3483) ORNL NUCLEAR SAFETY RESEARCH AND DEVELOPMENT PROGRAM BIMONTHLY REPORT FOR MAY-JUNE 1971. Cottrell, Wm. B. (Oak Ridge National Lab., Tenn.). Sep 1971. Contract W-7405-eng-26. 112p. Dep. NTIS.

The accomplishments during the months of May and June in the research and development program on nuclear safety are summarized. Much of this work is in general support of water-cooled power reactor technology, including LOFT and industry programs, and reflects current safety problems, such as measurements of prompt fuel element failure phenomena and the problems associated with the long-term operation of containment spray systems. Several projects are also conducted in support of the high-temperature gas-cooled reactor (HTGR) and liquid-metal fast breeder reactor (LMFBR) programs. Other major projects are those on primary piping and steel pressure-vessel technology. They also include experimental investigations of the attachment of nozzles to shells and the implementation of joint AEC-PVRC programs on heavy-section steel technology and nuclear piping, pumps, and valves. Seismic considerations of particular significance in nuclear plant design are being evaluated in the seismic program.

XUM

Several of the above projects are also directly related to the AEC's standards program, which entails development of engineering safeguards and the establishment of codes and standards for government-owned or -sponsored reactor facilities. The recent activities of NSIC and the Nuclear Safety journal in behalf of the nuclear community are also discussed. Of particular interest in both of these activities is the recent emphasis on environmental effects. (auth)

**57093** (ORNL-TM-3504) CORE MELT-THROUGH IN LMFBR'S: A CONDENSED REVIEW. Fontana, M. H. (Oak Ridge National Lab., Tenn.). Sep 1971. Contract W-7405-eng-26. 30p. (CONF-701102-24). Dep. NTIS.

From Meeting of the American Nuclear Society; Washington, D. C. (15 Nov 1970).

The problem of postaccident heat removal and core melt-through in liquid-metal fast breeder reactors must be considered in the context of the particular reactor design, and in light of a realistic sequence of events leading to the melt-through accident. If the integrity of the ultimate Na containment vessel and stand-by decay-heat removal systems could be assured for the energy release that might accompany the core disassembly accident, it should be possible to control further melt-through of the structure by core debris. If it must be assumed that Na cooling would not be available then a much more difficult situation occurs. The mixture of molten fuel and structural materials would melt through the primary vessel and fall upon the structure below. The interaction of molten fuel with the structural materials must be known to evaluate the dispersion and dilution of the molten mass. Unless proved otherwise by experiment, contact with concrete should be avoided because of the possibility of violent spalling due to steam generation from the water of hydration. Also, concrete made with limestone aggregate would generate enough $CO_2$ to overpressurize the containment in a few hours. Both of these effects would cause violent mixing of the molten pool, thereby increasing transfer of the heat and fission products to the surface. The radiant heat load on structures above the melt could cause failure if additional cooling is not available. Internal convection circulation greatly enhances heat and mass transfer and must be considered. There have been several methods mentioned to contain the core melt-through accident. Zivi has proposed a bed of depleted $UO_2$ which would suffer sacrificial melting as the molten mass of $UO_2$-steel progresses downward. Jansen et al. have calculated 24 ft to be the maximum depth to which the FFTF core could penetrate in a deep layer of basaltic concrete, considering the effects of solution of contiguous materials in the molten mass. Gilby has suggested a core catching system in which troughs are spaced and staggered to catch molten core material; cooling being maintained by the "sea of sodium" used in the pot-type PFR design. The ultimate heat dump would be the emergency decay-heat removal systems. These and other designs are reviewed, and recommendations made on experimental data required to ensure the validity of the designs. 30 references. (auth)

**57094** (RISO-M-1391) HEATING IN A REACTOR FUEL ELEMENT ROD UNDER TRANSIENT CONDITIONS. PART I. HEAT CONDUCTION PROGRAM. Abel-Larsen, H.; Larsen, M. Lolk (Danish Atomic Energy Commission, Risoe, Research Establishment). 1 Jul 1971. 57p. Dep. NTIS (U. S. Sales Only).

A computer program to solve the transient and steady-state heat conduction equation in a two dimensional cylindrical geometry by the finite difference method is described. The program uses the alternating directional implicit (ADI) method, which is always stable i.e., the integration is independent of time steps. The resulting three-diagonal matrix can be solved directly by a simple algorithm. Complicated heat conduction problems, as those in reactor fuel elements, can be solved. The program takes into account materials with different conductivities, heat conduction and radiation in gaps between materials and heat transfer to coolants and radiation between cooling surfaces. This is achieved by calculating effective conductivities between adjacent mesh points. The program does not treat coolants with phase changes. The program has an operational status at the Burroughs B6500 computer. Computer time requirements are moderate. A complete listing of the program is presented. (auth)

**57095** (WCAP-7422) TOPICAL REPORT: WESTINGHOUSE PWR CORE BEHAVIOR FOLLOWING A LOSS OF COOLANT ACCIDENT. (Westinghouse Electric Corp., Pittsburgh, Pa. PWR Systems Div.). Aug 1971. 174p.

A complete description is presented of the behavior of a PWR core during a loss of coolant accident. Detailed discussions of the codes and assumptions used in the analysis are discussed as well as the experimental verification of the codes or correlations used in the code. The improved analytical techniques that have been developed to analyze the loss of coolant accident are described. These are the BLODWN-2 code which replaces the BLODWN-1 code for the core internals analysis, and the SATAN V code which replaces the FLASH-R code for evaluating the pertinent parameters for the core cooling analysis such as core flow and pressure. A transition boiling heat transfer correlation for evaluating the heat removal from the fuel rod after DNB has also been incorporated. A parameter study is presented that shows the sensitivity to the various important core cooling phenomenon. (31 references) (auth)

**57096** (WCAP-7722) TOPICAL REPORT: SAFETY RELATED RESEARCH AND DEVELOPMENT FOR WESTINGHOUSE PRESSURIZED WATER REACTORS. PROGRAM SUMMARIES, SPRING 1971. Boyer, G. D. (comp.) (Westinghouse Electric Corp., Pittsburgh, Pa.). 1971. 67p.

The status of pressurized water reactor safety related research and development programs is summarized. The programs summarized include: (1) core stability evaluation; (2) ice condenser containment; (3) high power density fuel development; (4) in-core detector program; (5) gross failed fuel program; (6) full length emergency cooling heat transfer test; (7) blowdown forces program; (8) reactor vessel thermal shock program; (9) reactor containment fan cooler components tests; and (10) testing of engineered safeguards equipment. (H.D.R.)

**57097** (WCAP-7744) TOPICAL REPORT: ENVIRONMENTAL TESTING OF ENGINEERED SAFETY FEATURES RELATED EQUIPMENT (NSSS: STANDARD SCOPE). Locante, J.; Igne, E. G. (Westinghouse Electric Corp., Pittsburgh, Pa.). Aug 1971. 39p.

A program was undertaken in order to ensure the continued operability of the reactor safety related equipment in the post accident environments of temperature, pressure, chemistry, and radiation. The objectives of this program were met by measuring the performance or characteristics of the safety related equipment during or after exposure to the anticipated post accident containment conditions. The results of the overall test program on process instrumentation and control equipment and on valve motor operators indicate that the safeguards equipment will operate satisfactorily during and following exposure to the containment post accident environments of temperature, pressure, chemistry, and radiation. Discussions of the testing performed and results obtained and on the post accident containment conditions selected for the environmental testing program are included. (auth)

**57098** ENERGY PRODUCTION AND ENVIRONMENT. AN ANALYSIS WITH SPECIAL CONSIDERATION OF NUCLEAR ENERGY. Gruemm, H. (Oesterreichische Studiengesellschaft fuer Atomenergie GmbH., Seibersdorf, Austria). Atomwirt., Atomtech.; 16: No. 6, 278-88(Jun 1971). (In German).

Discussed are the hazards resulting from energy production at the present time and in the future. The following factors are analyzed: available energy deposits; necessity of nuclear energy to cover future requirements; environmental burden caused by burning of fossil fuels; comparison of environmental burden between fossil fuel and nuclear power production; environmental burden in case of reactor incidents; and proposals for further studies about protection of the environment. 38 references. (tr-auth)

**57099** RADIATION INJURIES AND RADIATION PROTECTION. Hug, O. (Univ., Munich). Atomwirt., Atomtech.; 16: No. 6, 294-300(Jun 1971). (In German).

Unrealistic exaggeration of radiation hazards is as damaging as underestimation of the problem. Radiations that are associated with nuclear power plants require constant monitoring. When the existing standards and regulations are properly applied in health physics, reduction of permissible doses by a factor of 10, as suggested by several agencies, appears unwarranted. Under such conditions, radiation burden is significantly lower than variations in the level of background radiation. The conclusions are derived from an analysis of the following factors: dose-effect relationship, late injuries, leukemia risk, malignant tumors, time factor in radiocarcinogenesis, special susceptibility of developing organisms, and genetic effects. (H.B.G.)

**57100** RADIOIODINE IN NUCLEAR POWER REACTORS. Hladky, E. Bull. EGU; 12: No. 3-4, 39-47(Mar 1971). (In Czech).

The experience is summarized with the problems of radioiodine in nuclear power plants operating in the world. The subject is divided into the following parts: the mechanism of radioiodine release and forms of its existence, its adsorption on structural materials, radioiodine removal, and its detection. (INIS)

**57101** BEHAVIOR OF LIGHT WATER REACTORS UNDER LOSS OF COOLING MEDIUM. Agemar, F.; Hartl, R.; Hicken, E.

XUM

(AEG-Telefunken, Frankfurt am Main). Atomwirt., Atomtech.; 16: No. 6, 302-4(Jun 1971). (In German).

An experimental research program is outlined for the determination of thermohydraulic processes in reactor cores. The program comprises four phases. The first one concerns preliminary theoretical and experimental studies of the primary cooling system after sudden rupture. Methods are developed for the measurement of two-phase flow and fast transients of pressure as well as temperature. The second phase, planned for spring 1972, comprises studies of tubes and fuel elements with interior cooling flow as to initial current, pressure, heat production, flow resistance, and heat conduction. In the third phase, the expected transients will be examined with test fuel elements of original size. Geometry effects will be excluded to obtain reliable data about tube temperatures and heat transfer coefficients. The last phase studies not only transients in the primary circuit but also effects of the low-pressure emergency cooling system. (H.B.G.)

**57102** USE OF COMPUTERS IN INVESTIGATIONS ON HYDRODYNAMIC ASPECTS OF REACTOR SAFETY PROBLEMS. Hoskin, N. E. (Atomic Weapons Research Establishment, Aldermaston, Eng.). pp 12.1-5 of Computational Physics. Vols. I and II. London; Her Majesty's Stationery Office (1969).

From Conference on computational physics; Culham, England (28 Jul 1969). See CONF-690706-(Vols.1 and 2).

In order to assess the damage potential of various hypothetical accident conditions in reactors much experimental work has been carried out. The study of explosion containment has included observation of the dynamic response of scale models in which the energy release in the core was simulated by detonation of high explosive. Investigation of fuel-coolant interaction has involved experiments on the pressure generation by water impact upon molten aluminum. The use of large computer codes in the analysis of these experiments is demonstrated and the relative advantages of such direct calculations are discussed. (auth) (UK)

**57103** HEALTH PHYSICS ASPECTS OF NUCLEAR FACILITY SITING. VOLUME I. Proceedings of the Fifth Annual Health Physics Society Midyear Topical Symposium, Idaho Falls, Idaho, November 3-6, 1970. Voilleque, Paul G.; Baldwin, Burton R. (comps.). Idaho Falls, Idaho; Burton R. Baldwin, Publications Chairman (1971). 259p. (CONF-701106-(Vol.1)).

Sixteen articles are included; separate abstracts were prepared for 14. The remaining two articles on power reactor siting in various countries and possible contamination of groundwater systems near a 300 GeV proton accelerator were previously published in NSA as 25: 31482 and 7778, respectively. (P.C.H.)

*For abstracts of individual papers see: 54545, 54546, 54753, 54754, 54777, 54793, 55199, 55237, 56975-56977, and 57104-57106.*

**57104** FISSION PRODUCT RELEASE DURING A LOCA. Walker, D. H. (Idaho Nuclear Corp., Idaho Falls). pp 113-29 of Health Physics Aspects of Nuclear Facility Siting. Vol. I. /Voilleque, Paul G. (comp.). Idaho Falls, Idaho; Burton R. Baldwin, Publications Chairman (1971).

From fifth annual midyear topical symposium on health physics aspects of nuclear facility siting; Idaho Falls, Idaho (3 Nov 1970).

In determining the site boundary distances required to meet the loss-of-coolant accident dose limits for water cooled power reactors, potential doses to the thyroid from inhalation of released iodine are generally the limiting consideration. One useful method of representing the fraction of the core iodine inventory that might reach the environment for various conditions is an iodine attenuation diagram. The fraction of the iodine removed in each of the processes in the transport of iodine from the core, through the reactor system to the containment, and through the containment to the environment can be represented on the diagram. Various assumptions regarding radioiodine removal by a particular process of the transport chain can be evaluated quickly through use of the diagram. The attenuation diagrams presented show that application of the guidelines of 10 CFR-100 and TID-14844 to a 1000 MW(e) water-cooled reactor leads to a potential release of $10^4$ to $10^5$ curies of I-131 in the event of an MHA. A second attenuation diagram shows I-131 releases to the environment following an MHA may be as low as 10 curies if current indications regarding the release and transport of radioactivity are correct. Additional definitive analytical and experimental studies are required before the conservatism in current reactor licensing practices can be relaxed. Information presented indicates that noble gases and iodines are the principal fission product species present in the containment atmosphere and available for leakage following a loss-of-coolant accident. Containment designs for current reactor plants incorporate systems for fission product removal. These systems will remove most of the radioiodine from the containment atmosphere in the first few minutes following an accident. However, some small fraction (0.1 to 10%) of the iodine will be present for substantially longer times as persistent iodine species that are not easily removed by the containment removal systems and thus are available for leakage for longer times. Current information indicates these species are principally methyl iodide ($CH_3I$) and hypoiodous acid (HIO). Methyl iodide probably retains its chemical form in leaking from the containment to the environment. Little is known concerning the behavior of hypoiodous acid once it reaches the environment. However, available information indicates it likely decomposes to other chemical forms of iodine. 16 references. (auth)

**57105** EFFECTS OF AEROSOL AGGLOMERATION ON REACTOR DOSE EVALUATIONS. Koontz, R.; Baurmash, L.; Morewitz, H. (Atomics International, Canoga Park, Calif.). Contract AT(04-3)-701. pp 130-50 of Health Physics Aspects of Nuclear Facility Siting. Vol. I. /Voilleque, Paul G. (comp.). Idaho Falls, Idaho; Burton R. Baldwin, Publications Chairman (1971).

From fifth annual midyear topical symposium on health physics aspects of nuclear facility siting; Idaho Falls, Idaho (3 Nov 1970).

Equations have been written and solved numerically which predict the behavior of aerosols including time dependent size distribution of the mass leaked from a containment system after various hypothetical Liquid Metal Fast Breeder Reactor accidents. The results show that high concentration, small diameter aerosols are not stable and agglomerate to form larger particles with increased settling velocities. The mass and particle concentration in the primary containment vessel is reduced rapidly, decreasing the amount of material and the number of particles which leak to the secondary containment system, where dilution and fallout further reduce the material available for leakage to the environs. The amount of material which leaks is shown to be a function of the released mass concentration. The distribution of particles and the mass leaking from the outer containment vessel are computed and from these data the number of particles which contribute to the dose at the site boundaries can be estimated. These data can be used in conjunction with the size dependent efficiency of retention in the lung as specified by the ICRP Task Group on Lung Dynamics to estimate the dose. 7 references. (auth)

**57106** LEAKAGE FROM A RUPTURED CONTAINMENT AFTER ACCIDENTAL DEPRESSURISATION OF A GAS COOLED REACTOR. Charlesworth, F. R.; Mercer, A.; Jackson, E. W. pp 151-70 of Health Physics Aspects of Nuclear Facility Siting. Vol. I. /Voilleque, Paul G. (comp.). Idaho Falls, Idaho; Burton R. Baldwin, Publications Chairman (1971).

From fifth annual midyear topical symposium on health physics aspects of nuclear facility siting; Idaho Falls, Idaho (3 Nov 1970).

Gas cooled reactors in the U.K. have typically a single pressure containment system. In the event of a depressurization accident it is not expected that any significant emission of fission products will occur during the rundown of pressure. However, if a fuel fire ensues or significant fuel cladding rupture occurs fission products will be released to the primary reactor containment and would have direct access to atmosphere through the breach. Leakage of gaseous and volatile fission products outwards through the breach would be accompanied by the inleakage of air. The reaction of hot graphite with oxygen increases with temperature and becomes exothermic. This reaction poses long term fuel integrity problems for metallic uranium fuel elements and for uranium dioxide fuels. It is of considerable importance to determine the possible modes of gaseous exchange that may obtain with breached primary pressure circuits. The mechanics of exchange processes through such breaches are being investigated and models devised to assist in the assessment of hazard from escaping fission products. The time scale and magnitude of events are discussed and the consequences of leakage examined. The experiments are being extended to determine possible modes of inert gas feed to the breached pressure circuit, together with the operation of high efficiency gas filters, to minimize the escape of fission products through the breach and to keep the graphite/oxygen reaction to a minimum. As a longer term aim the design of ducts and closures will be studied to optimize advantageous factors which may influence gaseous exchange flows. The application of the analysis to other situations (e.g., openings in secondary containment systems, fires involving radioactive materials) is discussed. 6 references. (auth)

**57107** INFLUENCE OF $PuO_2$ PARTICLE SIZE OF MIXED OXIDE FUEL IN RELATION TO FAST REACTOR SAFETY. Takahashi, Ryoichi; Matsuoka, Yoshinori; Shindo, Masuo (Tokyo Inst. of Tech.). Bull. Tokyo Inst. Technol. (Engl. Ed.); No. 102, 33-43(Mar 1971).

An elementary heat transport process is considered in order to study the influence of $PuO_2$ particle size on power transients. It

XUM

is shown that the particle size limit of $PuO_2$ is about 80 $\mu$ for a very severe accident. (auth) (Japan)

57108 EARTHQUAKE FORCES ON EQUIPMENT IN NUCLEAR POWER PLANTS. Hadjian, Asadour H. (Bechtel Corp., Vernon, Calif.). J. Power Div., Amer. Soc. Civil Eng.; 97: No. PO3, 649-65(Jul 1971).

Earthquake stress resisting design requirements for Class 1 structures and equipment of power reactors are described. Methods of analyzing earthquake stress characteristics and stress effects on reactor structures and equipment are presented. 14 references. (D.C.C.)

### Power Conversion Systems

*Refer also to abstracts 57035 and 57039.*

## Research and Test Reactors

*Refer also to abstracts 56984, 57053, 57069, and 57073.*

57109 (ANL-7771) MATERIALS-COOLANT INTERACTIONS RELEVANT TO EBR-II. Ruther, W. E.; Claar, T. D.; Greenberg, S.; Strain, R. V. (Argonne National Lab., Ill.). Apr 1971. Contract W-31-109-eng-38. 43p. Dep. NTIS.

Investigations of six bellows that had failed in Na service indicated that Na penetration of inclusion stringers led to perforation in three of them. Excessive travel of the valve stem was probably the cause of failure of two others. The sixth failure, the only one causing a reactor shutdown, was ascribed to a defect introduced in the manufacturing process. Investigations of failures in a Na sampler and in a tool for in-reactor cutting of sensor leads of an instrumented subassembly showed that the presence of Na was not deleterious. Type 304L stainless steel fuel cladding and Type 304 stainless steel hexagonal cans exposed to EBR-II primary coolant showed no selective attack or microstructural change that could be attributed to the Na or to the procedure for postirradiation removal of Na. Slow migration of carbon was observed from Type 304 stainless steel foils (C > 0.04%) into Type 304L stainless steel foils (C < 0.02%) immersed in the EBR-II primary Na. During this experiment, the measured concentration of carbon in the primary Na varied from 0.4 to 1.3 ppM. Corrosion of nickel exposed for 380 days to ~920°F primary Na was 0.08 mg/cm$^2$. Deliberately defected mixed-oxide fuel elements exhibited only minor dimensional changes when exposed to 700°F Na. In other ex-reactor Na exposures: free-machining stainless steels were unsuitable for reactor use; modified Belloseal valves were not affected by 5000 cycles in 700°F Na; brazed joints retained their shear strength in a 2-month test at 850°C; dissolved tin (1500 ppM) in the Na did not penetrate stainless steel in 1-month tests at 1020 and 1200°F; and nitridation of Type 304 stainless steel was insignificant under simulated conditions of the EBR-II gas/liquid interface. 12 references. (auth)

57110 (CONF-710302-(Vol.1), pp 97-101) ANALYSIS OF FUEL FAILURE EXPERIMENTS WITH TREAT. Agrawal, A. K.; Dickerman, C. E.; Rothman, A. B. (Argonne National Lab., Ill.).

From Meeting on new development in reactor mathematics and applications; Idaho Falls, Idaho (29 Mar 1971).

An outline of a method employing the SAS1A-A5H code for prediction of fuel pin failure is presented. Analytical results are compared with data from two experiments conducted in the Mark-II flowing sodium coolant loop in the TREAT reactor. (H.D.R.)

57111 (GEAP-10010-29) SOUTHWEST EXPERIMENTAL FAST OXIDE REACTOR DEVELOPMENT PROGRAM. Twenty-Ninth Quarterly Report, May-July 1971. Pflasterer, G. R.; Becker, R. A. (comps.) (General Electric Co., Sunnyvale, Calif. Breeder Reactor Development Operation). Aug 1971. Contract AT(04-3)-540. 74p. Dep. NTIS.

REACTOR FUEL ELEMENTS — repair of instrumented plutonium oxide ($PuO_2$)-uranium oxide ($UO_2$) rod type
— inspection of plutonium oxide ($PuO_2$)-uranium oxide ($UO_2$) rod type

SOUTHWEST EXPERIMENTAL FAST OXIDE REACTOR — fuel elements for, inspection of plutonium oxide ($PuO_2$)-uranium oxide ($UO_2$) rod type
— fuel elements for, repair of instrumented
— startup testing of plutonium oxide ($PuO_2$)-uranium oxide ($UO_2$) fueled
— physics measurements for plutonium oxide ($PuO_2$)-uranium oxide ($UO_2$) fueled, (E/T)
— pressure vessel for, installation of backup seal for head of
— maintenance during May to July 1971
— operations during May to July 1971 (D.C.C.)

57112 (HEDL-TME-71-31) SODIUM FIRES ANALYSES FOR THE FAST FLUX TEST FACILITY. Hale, J. P.; Shire, P. R. (Hanford Engineering Development Lab., Richland, Wash.). 12 Feb 1971. Contract AT(45-1)-2170. 52p. Dep. NTIS.

Summaries of sodium fire cases of practical value for sodium cooled reactor plant safety are reviewed. Sodium pool fire calculations are reported in depth. Surveys of pool and spray fire calculation methods and experimental progress are summarized where applicable to the present plant design parameters. For the pool fire calculations various accident conditions are investigated: two-cell configuration in air atmosphere, release of sodium and fission products due to fuel handling, and closed cells with low oxygen atmosphere. Time history curves display the thermal transients to near ambient conditions at the end of 20 to 100 hours. Spray fires are treated for low oxygen conditions. 20 references. (auth)

57113 (HEDL-TME-71-33) RADIOLOGICAL EVALUATION OF A HYPOTHETICAL CORE DISRUPTIVE ACCIDENT. Fies, C. L. (Hanford Engineering Development Lab., Richland, Wash.). Feb 1971. Contract AT(45-1)-2170. 37p. Dep. NTIS.

A mechanistic analysis of the radiological consequences of the hypothetical core disruptive accident for the FTR indicate that the containment structures, together with the isolation characteristics of the site, are more than adequate to protect the general public from excessive radiation exposure. The potential radiation exposure resulting from a hypothetical core disruptive accident is analyzed. 23 references. (auth)

57114 (HEDL-TME-71-58) PRELIMINARY OUTLINE OF FTR NUCLEAR SYSTEMS START-UP TESTS. Fleischman, R. M. (Hanford Engineering Development Lab., Richland, Wash.). Aug 1971. Contract AT(45-1)-2170. 31p. Dep. NTIS.

Preliminary outlines of anticipated FFTF startup tests related to Nuclear Systems are presented. For each test brief sections on Purpose, Test Description, Plant Status, and Special Equipment are provided. The test outlines, as given, are intended to serve as a "working" outline for the development of a more detailed FFTF startup testing program. (auth)

57115 (HEDL-TME-71-65) CROSS SECTIONS FOR PRELIMINARY DESIGN OF FTR, FTR SET NO. 200. Nelson, J. V. (Hanford Engineering Development Lab., Richland, Wash.). Aug 1971. Contract AT(45-1)-2170. 19p. Dep. NTIS.

A 26 group cross section library, designated FTR Set #200, which has been used in Fast Test Reactor (FTR) design calculations and in the analyses of critical experiments in support of the design of FTR is presented. (auth)

57116 (INR-1303) REACTOR EWA-10 INFORMATION. (Institute of Nuclear Research, Warsaw (Poland)). 1971. 74p. (In Polish). Dep. NTIS (U. S. Sales Only).

The main parameters and characteristics of the EWA-10 reactor are presented. The technical and formal requirements to be fulfilled in the case of irradiations and research in reactor EWA-10 are also included. (auth)

57117 (JAERI-Memo-4157, pp 23-43) FUEL FAILURE DETECTOR IN JRR-3. Tsunoda, Junsaku (Japan Atomic Energy Research Inst., Tokyo). (In Japanese and English).

From Fuel failure detection symposium; Tokyo, Japan (31 Jan 1969).

A fuel failure detecting equipment, with which the JRR (Japanese Research Reactor)-3 is equipped, is called Failed Fuel Detector, and detects fuel failure by monitoring of gaseous fission products released into primary coolant. It is capable of identifying individual failed fuel rods out of 246 fuel rods loaded into the JRR-3 core, using a matrix method. The failed fuel detector system is described. (Japan)

57118 (JAERI-Memo-4157, pp 44-50) GAMMA-RAY SPECTROSCOPY OF HEAVY WATER AND He-GAS IN JRR-3 FUEL FAILURE. Nemoto, Tsuyoshi (Japan Atomic Energy Research Inst., Tokyo). (In Japanese and English).

From Fuel failure detection symposium; Tokyo, Japan (31 Jan 1969).

Measurement was carried out with a previously failed fuel by loading it again into the Japan Research Reactor (JRR)-3 core, a heavy water moderated and cooled natural uranium type reactor. The aim was to assess basic data to predict fuel failure with $\gamma$-ray spectrum. Separated gas in FFD gas water separators, separated heavy water, coolant heavy water and cover gas were measured

for their γ-ray spectra, and contained nuclides were detected. Certain fission product nuclides were measured for their concentration. Iodine in the coolant was separated with ion exchange resin, and was measured. In the separated gas, Kr-85m, 87, 88, 89, 90; Xe-135, 137, 138, 139; Cs-138, 139; Rb-89, 90 and A-41 were detected. A-41 comes from A-40 existed in He gas as impurity and is made radioactive by neutrons. In comparison with γ measurements for the cover gas and the separated gas, it was found that significant gaseous fission products remained still in the water. From the γ spectrograph of the heavy water contaminated but not by the failed fuel, it was found that initial detection of fuel failure is difficult from the coolant because of high radiation from Na-24 mostly, and Mn-56 and Mg-27 partly. Iodine detection was unsuccessful. Ge(Li activated) γ detectors with high energy resolution were confirmed to be more useful means to detect fuel failure than GM counters of FFD measuring β ray. (Japan)

**57119** (JAERI-Memo-4157, pp 51-65) STUDY ON JRR-4 DELAYED NEUTRON-TYPE FUEL FAILURE DETECTOR. Onishi, Nobuaki (Japan Atomic Energy Research Inst., Tokyo). (In Japanese and English).

From Fuel failure detection symposium; Tokyo, Japan (31 Jan 1969).

Japan Research Reactor-4 is a swimming pool type light water cooled reactor with MTR type fuel of 90% enriched uranium. Equipment to detect fuel failure is designed for measurement of delayed neutrons from failed fuels. The failed fuel detector intakes 10 l/min from primary cooling water. Delay time is 60 sec from core to measuring tank. Present counting rate is 500 cpm, and the experiment is aimed to know origin of the counting rate. Pulse height of 5 $BF_3$ counters was analyzed, and discrimination level was set at the value at which the counting rate was not affected from pile-up of γ-ray. Correlation between counting rate for delayed neutrons and coolant mass flow was measured. The experiment revealed lack of evaluation method to estimate bare $^{235}U$ quantity in pile from the counting rate, and equipment optimization for the failed fuel detection is necessary. (Japan)

**57120** (ORNL-TM-3569) HIGH FLUX ISOTOPE REACTOR QUARTERLY REPORT: APRIL, MAY, AND JUNE OF 1971. McCord, R. V.; Corbett, B. L. (Oak Ridge National Lab., Tenn.). 3 Sep 1971. 26p. Dep. NTIS.

Operation of the HFIR was routine with an on-stream time of 96.1%. An unusual amount of maintenance was required on the pneumatic instrumentation. This has been attributed to debris from the air dryers caused by the increase in pressure and duty cycle required to supply air to the TRU facility. Special filters were installed in the air system and this is expected to reduce the maintenance required on the pneumatic instrumentation. About 5 mg of plutonia–thoria microspheres were released in an activation analysis irradiation tube. The system was successfully decontaminated with very little radiation exposure to personnel. (auth)

**57121** (RCN-145) PRESSURIZED WATER LOOP IN THE HIGH FLUX REACTOR AT PETTEN. van der Kleij, N.; Vader, D. C.; Visser, J. F. J. (Reactor Centrum Nederland, Petten). Jun 1971. 20p. Dep. NTIS (U. S. Sales Only).

A description is given of an in-pile loop for the irradiation of fuel pins under similar working conditions as in Pressurized Water Reactors. The working pressure of the loop is 140 bar and the water temperature at the inlet of the in-pile section is 280°C. The water flow is approx. 15 $m^3$/hr, depending on the hydraulic characteristics of the experiments. The in-pile section of the loop can be loaded with two fuel bundles. A great number of irradiations have been carried out with different linear powers and burnup. The maximum linear power and burnup have been 1200 W/cm and 16,000 MWD/tonne resp. A short survey of the operational experience and irradiation programmes up to the end of 1970 is presented. The working conditions, flowsheet and lay-out of the loop are discussed to some detail, with emphasis on the in-pile part of the loop. (auth)

**57122** TECHNICAL SURVEY NO. 5: REACTOR IRRADIATION SERVICES. Nucl. Eng. Int.; 16: 469-92(Jun 1971).

The survey comprises 5 articles describing the irradiation facilities of major organizations, a folding chart which lists the parameters of irradiation facilities throughout the world, and a tabulated guide giving addresses, availability etc. of these facilities. The following services are described: testing of fuels in the Halden reactor, which is based on extensive use of in-core instrumentation; commercial irradiation activities of the UKAEA, including planning, preirradiation and postirradiation examination, and special facilities in DFR, SGHWR, and AGR; irradiation rigs and loops used in CEA reactors, Triton, Melusine, Siloe, Pegase and Osiris; and facilities supplied with TRIGA reactor systems for isotope production, in-core irradiation, neutron radiography, use of dry irradiation facilities, thermal columns and neutron beams. Finally the development and progress of the Fast Flux Test Facility are discussed. Descriptions are given of the isolated test loops, the reactor and cooling system, and the fuel cycle. (UK)

**57123** SPECTROCALORIMETRIC MEASUREMENTS IN THE CORE OF THE HEAVY WATER REACTOR RA AT VINCA. Kott, J. (ŠKODA Works, Pilsen, Czech.); Jirousek, V.; Nemec, J.; Dach, K.; Radak, B. Bull. Boris Kidric Inst. Nucl. Sci., Chem.; 21: No. 2, 7-19(May 1970).

The measurements of the photon field in the RA reactor with the ŠKODA reactor spectrocalorimeters are described. The design of calorimeters and the basic spectrocalorimetric theory are given briefly. Results obtained in the VK-1 and VK-5 experimental holes of the RA reactor are presented and compared to the ones (for graphite) obtained at the same place. The intercomparison of the RA results with the values for other reactors (VVR-S and EWA-10) obtained by the calorimeters of the same design is also given and discussed. (auth)

**57124** MEASUREMENT OF REACTOR POWER BY DETERMINATION OF $^{17}N$ NEUTRONS IN THE COOLING MEDIUM WITH TRACK DETECTORS. Nedelik, A.; Gruenwald, H. (ASTRA-Reaktor Institut, Seibersdorf, Austria). Atomwirt., Atomtech.; 16: No. 6, 301(Jun 1971). (In German).

The power of ASTRA, a 5 MW pool reactor, was measured with a special track detector. Several pellets of highly enriched uranium oxide were attached to glass slides and placed on the outlet of the primary cooling system. Moderation of the $^{17}N$ neutrons from the $^{17}O(n,p)^{17}N$ reaction produced sufficient thermal neutrons to cause fission in the uranium pellets. Following etching, fission product tracks in the glass could be easily counted under the microscope. The dosimeter yielded 70 tracks/$cm^2$/MWh. The simple inexpensive dosimeter proved suitable for assessment of reactor power. (H.B.G.)

**57125** SPECTRAL DISTRIBUTION OF NEUTRONS FROM THE REACTOR HORIZONTAL CHANNEL OF THE INSTITUTE OF NUCLEAR RESEARCH, REZ, MEASURED BY MEANS OF THE CRYSTAL SPECTROMETER KSN-2. Vratislav, S. (Faculty of Applied and Nuclear Physics, Prague). Jad. Energ.; 17: No. 6, 191-4(Jun 1971). (In Czech).

The spectral distribution of neutrons from the reactor horizontal channel of the Institute of Nuclear Research, Řež, was measured by the crystal spectrometer KSN-2. The Cu crystal was employed as monochromator. The mosaic spread of the single crystal as well as the correction factors to be applied to the measured value obtained, are given. The neutron spectral distribution was approximated by a Maxwellian distribution in the range of energy 0.01 to 0.1 eV.with the value $E_0 = 0.031$ eV, which corresponds to the neutron gas temperature $T = (361 \pm 11)°K$. (auth)

**57126** DETERMINATION OF INTERMEDIATE NEUTRON ENERGY SPECTRUM FOR A POOL-TYPE REACTOR. Weng, Pao-shan; Lee, Ming-huei (National Tsing Hua Univ., Hsinchu, Taiwan). Atomkernenergie; 18: No. 1, 25-9(Aug 1971).

The quadruple foil technique was used for the determination of intermediate neutron energy spectrum in the core center of THOR. The relationship between the differential resonance flux and the activities of resonance detectors was derived. A comparison between the quadruple foil technique and the cadmium ratio method is given. The correction factors involved such as self-shielding, reactor startup, perturbation, power level, and cadmium transmission are discussed in detail. A full description of resonance detectors and the associated parameters are given. The analysis of the intermediate neutron spectrum indicates that the spectrum in the core center of THOR is very close to a 1/E spectrum. 17 references. (auth)

**57127** ISOTOPES AND RADIATION TECHNOLOGY. VOLUME 9, NUMBER 1. Baker, P. S.; Lafferty, R. H. Jr.; Gerrard, Martha; (and others) (eds.). One of Four Quarterly Technical Progress Reviews Published for the Division of Technical Information, USAEC. Oak Ridge, Tenn.; Oak Ridge National Laboratory (1971). 132p. GPO $0.70.

Current literature reviews and special review articles are presented on isotope production, development, and applications, process radiation development, and radiation preservation and sterilization. A separate abstract was prepared for each of 11 reviews. (H.D.R.)

*For abstracts of individual papers see: 54443, 54506, 54507, 54739, 54906–54908, 55065, 55107, 55811, and 57128.*

**57128** ATOMICS INTERNATIONAL'S L-88 NUCLEAR REACTOR FOR NEUTRON RADIOGRAPHY. Henrie, J. O. (Atomics

XUM

International, Canoga Park, Calif.). Isotop. Radiat. Technol.; 9: No. 1, 41-4(Fall 1971).

The L-88 reactor is designed expressly for neutron radiography. The reactor core provides a maximum ratio of collimated-neutron-beam strength to reactor thermal power. The low thermal-power requirements result in system simplicity and compactness, which in turn hold the initial costs and subsequent operating and maintenance costs to a minimum and allow the use of a sealed reactor system, since no refueling is required in its lifetime of 20 years or more. The complete reactor system is shipped in three preassembled packages (reactor, console, and cooler) designed for rapid, minimum-effort installation. The reactor can be moved to a new location with comparatively little difficulty. The L-88 reactor can be provided with highly flexible experimental facilities for other nondestructive testing as well as for research in physics, chemistry, and biology. The characteristics of the L-88 reactor are summarized. (auth)

**57129** HIGH-POWER RADIATION LOOP IN THE IRT NUCLEAR REACTOR AT TBILISI. Kiknadze, G. I.; Andronikashvili, E. L.; Bedbenov, V. C.; (and others). At. Energ. (USSR); 31: No. 2, 143-5(Aug 1971). (In Russian).

A high-power loop is described for use in the IRT research reactor at Tiblisi which utilizes 2.6 liters of the eutectic alloy of indium-gallium as the gamma-carrier. The maximum radiation power of this loop amounted to 300,000 gram-equivalents of radium during a thermal power level of the reactor of 5,000 MW. Compactness and simplicity distinguish this loop from its predecessors of 1963 and 1969. (K.S.W.)

**57130** PNEUMATIC LOADING AND UNLOADING OF CHANNELS FOR IRRADIATION IN THE IRT-M REACTOR. Ambardanishvili, T. C.; Zakomornyi, G. V.; Kiasashvili, G. D.; (and others). At. Energ. (USSR); 31: No. 2, 147-50(Aug 1971). (In Russian).

The system designed for pneumatic loading/unloading of vertical channels in the IRT-M reactor in Tiblisi is described. The channel for sample irradiation may be located in the core or reflector and consists of two coaxial steel tubes. A working gas is used to move samples to some location determined by a sensor. A distributing device equipped with microswitches gives direction to the pneumatic rabbit. A loading unit is provided with a valve mechanism for admitting the working gas to the system. The complete operation of the system is explained in some detail. (K.S.W.)

**57131** EXPERIENCE OF LEGAL PROCEEDINGS FOR SITING A RESEARCH REACTOR IN AN URBAN AREA. Lorio, Philip M. (Columbia Univ., New York). pp 716-23 of Health Physics Aspects of Nuclear Facility Siting. Vol. III. /Voilleque, Paul G. (comp.). Idaho Falls, Idaho; Burton R. Baldwin, Publications Chairman (1971).

From fifth annual midyear topical symposium on health physics aspects of nuclear facility siting; Idaho Falls, Idaho (3 Nov 1970).

Procedures for licensing a U. S. research reactor located in an urban area are listed and discussed. (D.C.C.)

## Rocket and Space Reactors

*Refer also to abstract 56146.*

**57132** (AI-AEC-Memo-12715(Del.)) REFERENCE ZIRCONIUM HYDRIDE REACTOR. Maki, L. M.; Donovan, E. J. Jr. (Atomics International, Canoga Park, Calif.). 15 Jun 1969. Contract AT-(04-3)-701. 66p. Dep. NTIS.

A conceptual design of a reference zirconium hydride (ZrH) nuclear reactor suitable for relatively high power, long duration space applications is presented. The design is based on the technology of the zirconium hydride moderated, $^{235}U$ fueled, NaK-cooled reactor type as typified by the SNAP 8 reactor. The design evolved has a minimum performance capability of 600 kW(t) for 20,000 hours at 1300°F, is suitable for use with a number of candidate power conversion systems, and can be operated with either a shadow shield or within a fully enclosed ($4\pi$) radiation shield. 12 references. (auth)

**57133** (ORNL-TM-3366) MORSE MONTE CARLO SHIELDING CALCULATIONS FOR THE ZIRCONIUM HYDRIDE REFERENCE REACTOR. Burgart, C. E. (Oak Ridge National Lab., Tenn.). 26 Aug 1971. 23p. (CONF-710304-13). Dep. NTIS.

From Symposium on natural and manmade radiation in space; Las Vegas, Nev. (1 Mar 1971).

DOT-SPACETRAN transport calculations and MORSE Monte Carlo calculations of a lithium-hydride and tungsten shield for a SNAP reactor were compared. Transport of both neutrons and gamma rays was considered. Several forms of importance sampling were utilized in the MORSE calculations. Quantities internal to the shield, as well as dose at several points outside of the configuration, were in satisfactory agreement with similar DOT calculations. 9 references. (auth)

**57134** DESIGN AND OPTIMIZATION OF A FAST HEAT PIPE THERMIONIC REACTOR. Hanke, H. (Univ., Stuttgart). Atomkernenergie; 18: No. 1, 61-9(Aug 1971). (In German).

The concept of an energy supply plant for space vehicles, consisting of a fast reactor has heat source and out-of-core thermionic converters heated and cooled by heat pipes, is designed and optimized. The criterion for optimization is the cost-to-power-ratio. The costs are given by the price of the fissile material and the expense for the transport of the device into orbit. The reactor power is limited by the maximum tolerable values for the temperature at the free surface of a cell and for the output current of a single converter. If the composition of core and reflector, and the converter output is given, it is possible, applying the reflector saving concept, to construct an analytical correlation between the geometric parameters as well as between these and the reactor power output. Therefore it is possible to optimize these parameters with a very small effort for calculation. 33 references. (auth)

## Process Heat and Desalination Reactors

**57135** TECHNICAL-ECONOMIC CONSIDERATIONS OF HEAT SUPPLY FROM POWER STATIONS WITH LIGHT WATER REACTORS. Hromek, R. (Federal Ministry of Fuel and Power, Prague). Jad. Energ.; 17: No. 6, 181-4(Jun 1971). (In Czech).

Problems related to nuclear central heating stations and the calculation system for economic expenses (costs) for heat and electric power in power stations with light water pressure reactors are discussed. The basic effectivity criterion is mentioned for heat supply from nuclear power stations for public purposes. The detailed calculation system is suitable also for the solution of problems having a general character in other sectors of nuclear economics. (auth)

## Marine and Portable Power Reactors

**57136** (DOCKET-50238-83) N. S. SAVANNAH. Supplement No. 1 to Safety Analysis Report Fuel Shuffle with Core II. (Maritime Administration, Washington, D. C.). 20 Sep 1971. 126p. Dep. NTIS.

Operating limits for the reactor following fuel shuffle procedures with Core 2 are presented. (D.C.C.)

**57137** (DOCKET-50238-84) N. S. SAVANNAH. Dropping of Fuel Element. (Maritime Administration, Washington, D. C.). 29 Sep 1971. 3p. Dep. NTIS.

The accidental dropping of a fuel element into the spent fuel pool is described. Recovery and repair procedures are discussed. Possible causes for the fuel element drop incident are listed. (D.C.C.)

**57138** NUCLEAR POWER VERSUS CONVENTIONAL SYSTEMS FOR NUCLEAR SHIPS. Motor Ship; 52: No. 613, 124-5(Aug 1971).

A comparative study is made of building and operating costs for nuclear and conventional container ships with speeds of 23-29 knots and a capacity of 1800 standard 20 ft containers. It is concluded that nuclear power is not yet economically viable for this application. (UK)

**57139** OPERATIONAL RESULTS FOR 1970 OF THE NUCLEAR SHIP OTTO HAHN. Atomwirt., Atomtech.; 16: No. 8-9, 452(Aug-Sep 1971). (In German).

In 1970, the nuclear ship Otto Hahn obtained permission for the first time to enter foreign ports. During the year, 15 voyages were undertaken; of these, 10 involved commercial transportation of phosphate, two were devoted to research, and the other two to testing. The ship performed satisfactorily. Two minor problems were encountered which involved a pump and the filter system. To reduce corrosion in the primary circuit, the addition of hydrazine/levoxin was found most effective. (H.B.G.)

XUM

## Production Reactors

*Refer also to abstract 55402.*

## Reactor Theory

*Refer also to abstracts 57019 and 57071.*

**57140** (CONF-710302–(Vol.1), pp 464-71) CONVERSION OF THE ARGONNE REACTOR COMPUTATION (ARC) SYSTEM TO CONTROL DATA 6000 AND 7000 SERIES EQUIPMENT. Lindeman, A. J.; Just, L. C. (Argonne National Lab., Ill.); Lee, R. H. (Control Data Corp., Oak Brook, Ill.).

From Meeting on new development in reactor mathematics and applications; Idaho Falls, Idaho (29 Mar 1971).

The Argonne Reactor Computation (ARC) System is a collection of computational programs embedded in a modular environment so as to facilitate reactor physics calculations that involve many independent computations. The ARC System was designed for and implemented on the IBM System/360 computer with the MVT (multiprogramming with a variable number of tasks) Operating System. Project EXODUS was launched to examine the practicability of producing a version of the ARC System operable on CDC machinery. The system requirements, both hardware and software, as well as the ARC System's dependencies on the System/360 and the capability of the 6000 and 7000 series to support the ARC System were determined. (auth)

**57141** (CONF-710302–(Vol.1), pp 472-7) USER EXPERIENCE WITH DATATRAN AT LASL. McGirt, Frank; Alcouffe, Raymond E. (Los Alamos Scientific Lab., N. Mex.).

From Meeting on new development in reactor mathematics and applications; Idaho Falls, Idaho (29 Mar 1971).

Los Alamos Scientific Laboratory (LASL) assessed the problems involved in adapting existing modular programming systems to the LASL CDC-6600 computers. Of the modular systems available, the DATATRAN system was chosen for investigation first since there seemed to be no extreme demands made on computer hardware or software by DATATRAN. In addition, DATATRAN was designed for the CDC-6600 computer. 8 references. (auth)

**57142** (CONF-710302–(Vol.1), pp 478-93) USER EXPERIENCE WITH THE ARC SYSTEM. Henryson II, H.; Toppel, B. J. (Argonne National Lab., Ill.).

From Meeting on new development in reactor mathematics and applications; Idaho Falls, Idaho (29 Mar 1971).

The capabilities of the Argonne Reactor Computation (ARC) system are briefly described. The performance of the system in meeting the needs of both standard and non-standard uses is reviewed. 8 references. (H.D.R.)

**57143** (CONF-710302–(Vol.1), pp 494-504) EXPERIENCE WITH THE MODULARIZATION OF ITERATION PROCEDURES IN ENGINEERING APPLICATIONS. Schmidt, Reiner (Westinghouse Electric Corp., Pittsburgh, Pa. PWR Systems Div.).

From Meeting on new development in reactor mathematics and applications; Idaho Falls, Idaho (29 Mar 1971).

The convergence module U4 for solving engineering problems requiring iteration procedures is described. The performance of U4 is compared to that of other methods. (H.D.R.)

**57144** (CONF-710302–(Vol.1), pp 505-7) PSKIT: A CDC-6600 COMPUTER PROGRAMMING PACKAGE PROVIDING EASY USE OF FINK/PANTRY. Bohl, H. Jr. (Bettis Atomic Power Lab., Pittsburgh, Pa.).

From Meeting on new development in reactor mathematics and applications; Idaho Falls, Idaho (29 Mar 1971).

The programming package PSKIT is described as a FORTRAN IV service program that makes the use of the dynamic storage allocators FINK and PANTRY quite simple. PSKIT provides input functions to read files from File Manager store and to read CARDS-type cards and provides output functions to write files into File Manager store. Sandwiched in between these functions are one or more compute functions. All of the functions are controlled through built-in directive paths or directive paths input on cards. 5 references. (auth)

**57145** (CONF-710302–(Vol.1), pp 508-15) JOSHUA TERMINAL SYSTEM. Jensen, J. C.; Boyce, R. L.; Suich, J. E.; Haywood, R. C. (Du Pont de Nemours (E. I.) and Co., Aiken, S. C. Savannah River Lab.).

From Meeting on new development in reactor mathematics and applications; Idaho Falls, Idaho (29 Mar 1971).

A major design goal of the JOSHUA system is to enable users to execute modules and access the extensive data base with remote display terminals. The JOSHUA Terminal System (JTS) was developed to provide the terminal facilities required for module execution and data base manipulation. The capabilities of the JTS, implementation, and some experience with the system are described. (auth)

**57146** (CONF-710302–(Vol.1), pp 516-30) NETWORK ORGANIZATION OF AN AUTOMATED NUCLEAR DESIGN SYSTEM. O'Shea, D. M.; Lee, R. R.; Ancona, A.; Rohan, P. E. (Combustion Engineering, Inc., Windsor, Conn.).

From Meeting on new development in reactor mathematics and applications; Idaho Falls, Idaho (29 Mar 1971).

The design of nuclear reactors for power generation places increasing emphasis on the sophisticated use of large and complex computer calculations. Efficient use of the third generation computers being employed for these calculations requires a heavy emphasis on the development of computer code systems to provide the flexibility and accuracy required. These needs can be satisfied by an automated design system that provides a means to sequentially execute a number of distinct calculations and for manipulation of the data used in the calculation. A new structure for an automated design system called a network organization is described that offers several advantages over existing systems. (auth)

**57147** (CONF-710302–(Vol.2)) PROCEEDINGS OF CONFERENCE ON NEW DEVELOPMENTS IN REACTOR MATHEMATICS AND APPLICATIONS, IDAHO FALLS, IDAHO, MARCH 29–31, 1971. (American Nuclear Society, Hinsdale, Ill. American Nuclear Society. Eastern Idaho Section). 566p. Dep. NTIS.

Included are 43 papers on transport theory calculations, the Monte Carlo method, reactor physics codes, and ENDF/B and associated processing codes. A separate abstract was prepared for each of 33 papers. Five papers were previously abstracted for Nuclear Science Abstracts. They may be located under CONF-710302, CEA-CONF-1755, CEA-CONF-1762, and DP-MS-70-78 in the Report Number Index. (H.D.R.)

*For abstracts of individual papers see: 57019, 57148–57178, and 57191.*

**57148** (CONF-710302–(Vol.2), pp 557-60) $S_n$ PROGRAMMING TECHNIQUES. Pfeifer, C. J. (Bettis Atomic Power Lab., Pittsburgh, Pa.).

From Meeting on new development in reactor mathematics and applications; Idaho Falls, Idaho (29 Mar 1971).

The desire for greater accuracy in the calculation of neutron flux distributions in a reactor has led to the development of computer programs to solve the two-dimensional neutron transport equation using the $S_n$ method. Some programming methods are discussed which can be used to solve the problems encountered in the implementation of such a program, especially if that program is to provide the capability to solve very large problems. A large problem is defined as one consisting of fifty or sixty thousand mesh elements and perhaps two or three hundred angles per quadrant, thus requiring a solution for approximately fifty million unknowns per energy group. These large problems occur in shielding calculations requiring many mesh elements to cover very large distances and in core "truth" calculations when extreme geometric detail is desired. It is assumed that the mathematics of the solution of the finite difference approximation to both the diffusion and transport equations is well known and only the programming of these solutions is discussed. (auth)

**57149** (CONF-710302–(Vol.2), pp 561-4) NEW FORM OF THE $P_3$ APPROXIMATION. Selengut, D. S. (Knolls Atomic Power Lab., Schenectady, N. Y.).

From Meeting on new development in reactor mathematics and applications; Idaho Falls, Idaho (29 Mar 1971).

The $P_3$ approximation to the transport equation in three dimensions involves a total of 16 first-order differential equations to determine the 16 moments of the neutron angular distribution. The complexity has apparently precluded the writing of any computer program, in spite of the potentially significant improvement over diffusion theory. A widely used alternative is the simplified $P_3$ approximation due to Gelbard, which involves the neglect of the tensor character of the higher angular flux moments, but permits the flux calculation to be put in the form of a pair of coupled diffusion equations. The complete $P_3$ equations are developed in a form which retains the computational advantage of the simplified theory. Isotropic scattering and sources are assumed, and cross sections are taken to be constant within each region. (auth)

**57150** (CONF-710302–(Vol.2), pp 565-76) CONVERGENCE OF THE WEIGHTED DIAMOND DIFFERENCE APPROXIMATIONS TO THE DISCRETE ORDINATE EQUATIONS. Madsen, N. K. (Bettis Atomic Power Lab., Pittsburgh, Pa.).

XUM

From Meeting on new development in reactor mathematics and applications; Idaho Falls, Idaho (29 Mar 1971).

The class of difference methods commonly known as the weighted diamond difference approximations is examined. These approximations are considered for vacuum, reflecting, and periodic boundary conditions in x-y geometry. It is shown that all of the difference schemes considered (with several exceptions) lead to nonsingular systems of algebraic equations. This guarantees the existence of a unique solution to each set of difference equations. The exceptional cases yield singular systems of difference equations. It is also shown that for any of the above boundary conditions the solution of a weighted diamond difference scheme converges to the solution of the discrete ordinate equations. The convergence is shown in a discrete $L_2$ norm and convergence rates are established. (auth)

**57151** (CONF-710302-(Vol.2), pp 577-607) ELIMINATION OF RAY EFFECTS BY CONVERTING DISCRETE ORDINATE EQUATIONS TO SPHERICAL HARMONIC-LIKE EQUATIONS. Lathrop, K. D. (Los Alamos Scientific Lab., N. Mex.).

From Meeting on new development in reactor mathematics and applications; Idaho Falls, Idaho (29 Mar 1971).

Remedies are considered for the ray effect which is a flux distortion producing defect of the discrete ordinates approximation to the transport equation. It is shown how to formulate multidimensional discrete ordinate equations equivalent to spherical harmonic equations and relate the order of the equivalent spherical harmonic equations to the degree of precision of the numerical quadrature. Numerical results for this kind of remedy are given in three test problems, including a problem with material discontinuities. The use of orthonormal polynomials is shown to permit the formulation of discrete ordinates approximations which have properties "like" those of the highest order spherical harmonic equations consistent with the number of directions in the discrete ordinates approximation. These formulations also eliminate ray effects. It is concluded that the partially effective remedy of using more, specially chosen, directions is the most practical remedy for most applications, but that for especially difficult situations or for reference calculations, the defect-eliminating spherical harmonic-like formulations should be available for use. 15 references. (auth)

**57152** (CONF-710302-(Vol.2), pp 608-16) DP-O METHOD ACCORDING TO A VARIATIONAL TREATMENT THAT EXTENDS ITS APPLICABILITY TO ALL GEOMETRIES. Amster, Harvey; Paveri-Fontana, Stefano L. (California Univ., Berkeley. Dept. of Nuclear Engineering).

From Meeting on new development in reactor mathematics and applications; Idaho Falls, Idaho (29 Mar 1971).

DP-O equations for neutron flux calculations for general three-dimensional geometries are derived from the variational principle that yields the standard P-1 equations. The DP-O approximation for the leakage term in the transport equation is examined. 8 references. (H.D.R.)

**57153** (CONF-710302-(Vol.2), pp 617-24) ARRANGEMENT OF ORDINATES IN DEEP-PENETRATION CYLINDRICAL AND X-Y $S_n$ CALCULATIONS. Gelbard, E. M. (Bettis Atomic Power Lab., Pittsburgh, Pa.).

From Meeting on new development in reactor mathematics and applications; Idaho Falls, Idaho (29 Mar 1971).

A broad class of problems are selected and ordinate arrays for routine use in problems which belong to this broad class are developed. Specifically the problems dealt with are deep-penetration (i.e., shielding) neutron transport problems in one-dimensional cylindrical configurations, or in X-Y configurations without significant voids. (auth)

**57154** (CONF-710302-(Vol.2), pp 625-43) SYNTHETIC TRANSPORT THEORY METHOD. Crawford, Bruce W.; Friedman, Jack P. (Knolls Atomic Power Lab., Schenectady, N. Y.).

From Meeting on new development in reactor mathematics and applications; Idaho Falls, Idaho (29 Mar 1971).

The synthetic transport theory method is extended to two-dimensional XY and RZ geometries with either a multigroup or few group energy structure. The method is verified through several benchmark problem solutions and comparisons. 12 references. (H.D.R.)

**57155** (CONF-710302-(Vol.2), pp 644-54) MODIFIED COLLISION PROBABILITY METHOD FOR NON-UNIFORM LATTICES. Leonard, A.; McDaniel, C. T.; Petrick, W. P. (General Electric Co., San Jose, Calif.).

From Meeting on new development in reactor mathematics and applications; Idaho Falls, Idaho (29 Mar 1971).

A new method for the determination of multigroup, two-dimensional neutron distributions in non-uniform lattices is described. The method is similar to the usual collision probability approach except for two important differences. First, the only first-flight probabilities that are required are those for paths within homogeneous components of the lattice, e.g., a fuel rod or the water region in the bundle interior. The second modification is that multiple scatterings within each "mesh" region are precalculated by a successive generation technique which accounts for the spatial distribution of each scattering generation in the fuel rod and energy transfer in the moderator by use of matrix algebra. (auth)

**57156** (CONF-710302-(Vol.2), pp 655-78) NODAL INTEGRAL TRANSPORT METHOD FOR CALCULATION OF TWO-DIMENSIONAL POWER DISTRIBUTIONS IN NON-UNIFORM LATTICES. Cheng, H. S.; McDaniel, C. T.; Leonard, A. (General Electric Co., San Jose, Calif.).

From Meeting on new development in reactor mathematics and applications; Idaho Falls, Idaho (29 Mar 1971).

A nodal integral transport method for the solution of the two-dimensional steady-state multigroup integral transport equations with linearly anisotropic scattering for heterogeneous systems in cartesian geometry is presented. The method consists of the division of a system of interest into subregions or "nodes" and the specification of neutronic coupling between nodes by means of a variant of collision probability method. Instead of using a set of formal node-to-node transport kernels to describe integral neutron transport, one assigns a set of partial currents and first-collision sources (direct fission or external sources plus indirect scattering sources) to each node and precalculates a set of escape and transmission probabilities for each node, with provisions for a linear spatial variation and $P_1$ angular distribution of the partial currents and collision sources. The coupling between nodes is then specified by applying the law of neutron conservation to each node and adjacent neighbors in terms of the set of partial currents, collision sources, and escape and transmission probabilities. It is also shown that the conventional integral transport equations may be reduced to equivalent partial current equations in an integral sense. Thus, the solution of the multigroup partial current equations is equivalent to the solution of the conventional multigroup integral transport equations. Comparisons against a series of available critical experiments and Gundremmingen (KRB) gamma-scan data illustrate the accuracy of the method. 12 references. (auth)

**57157** (CONF-710302-(Vol.2), pp 679-700) NON-ITERATIVE METHOD FOR TIME DEPENDENT TRANSPORT. Reed, Wm. H. (Los Alamos Scientific Lab., N. Mex.).

From Meeting on new development in reactor mathematics and applications; Idaho Falls, Idaho (29 Mar 1971).

A numerical method for time dependent transport theory is presented. This method is explicit in the sense that no iterative matrix inversions need be performed over a time step. It is unconditionally stable but relatively inaccurate. Two acceleration devices designed to improve the accuracy of this and other methods are presented. The effectiveness of this method and these acceleration devices is illustrated by a set of test problems in one space dimension. (auth)

**57158** (CONF-710302-(Vol.2), pp 701-22) TIME DISCRETIZATION OF THE NEUTRON TRANSPORT EQUATION. Morante, Aldo Belleni (Florence Univ. (Italy). Istituto Matematico).

From Meeting on new development in reactor mathematics and applications; Idaho Falls, Idaho (29 Mar 1971).

It is shown that, if only the time variable of the transport equation is discretized, the neutron density at $t = k\tau$ ($k = 1, 2, \ldots$; $\tau$ = time step) can be given explicitly as a function of the initial neutron distribution. By using the theory of semigroups the method is proved to be convergent and the error is evaluated. 14 references. (auth)

**57159** (CONF-710302-(Vol.2), pp 723-38) APPLICATION OF FINITE ELEMENT SOLUTION TECHNIQUE TO NEUTRON DIFFUSION AND TRANSPORT EQUATIONS. Ohnishi, T. (Hitachi Ltd., Kawasaki (Japan). Atomic Energy Research Lab.).

From Meeting on new development in reactor mathematics and applications; Idaho Falls, Idaho (29 Mar 1971).

A finite element method was applied to the solution of neutron diffusion and transport equations. The finite element method is one of the variational approximations. The essence of the method is the division of the domain under consideration into a number of nonoverlapping small subregions of known geometric shape (which are called "finite elements") and the use of the unique base functions which are constructed in each finite element. The finite element approximation is also considered as an extension of Ritz finite difference approximation. Two-dimensional x-y geometry and the triangular finite element are examined. Other multidimensional geometries, however, are also objects of the application of the finite element method and various kinds of finite elements are considered. (auth)

**57160** (CONF-710302-(Vol.2), pp 771-81) MACHINE GENERATION OF MONTE CARLO SAMPLING FUNCTIONS. Steinberg, Herbert A.; Troubetzkoy, Eugene S. (Mathematical Applications Group, Inc., White Plains, N. Y.); Kalos, Malvin H. (Mathematical Applications Group, Inc., White Plains, N. Y. New York Univ., N. Y. Courant Inst. of Mathematical Sciences).

From Meeting on new development in reactor mathematics and applications; Idaho Falls, Idaho (29 Mar 1971).

A scheme for the automatic generation of importance functions for three-dimensional Monte Carlo problems is described. The procedure involves generation of a sequence of closed surfaces, starting at the detector, on which the importance functions are estimated to be independent of position. Using a recursive Monte Carlo, the adjoint function is estimated sequentially from surface to surface. (H.D.R.)

**57161** (CONF-710302-(Vol.2), pp 794-7) NON-LINEAR MONTE CARLO. Brooks, Joan; Kalos, M. H.; Steinberg, H. A.; Troubetzkoy, E. S. (Mathematical Applications Group, Inc., White Plains, N. Y.).

From Meeting on new development in reactor mathematics and applications; Idaho Falls, Idaho (29 Mar 1971).

A Monte Carlo solution to the photon transport equation was developed and programmed for a pure scattering medium which exhibits both ordinary and stimulated Compton scattering. This latter phenomenon is a property of Bose particles, namely that the differential scattering probability is a linear function of intensity at the scattered momentum. (auth)

**57162** (CONF-710302-(Vol.2), pp 803-32) SOME APPLICATIONS OF THE MONTE CARLO METHOD AT THE EURATOM RESEARCH CENTER, ISPRA. Matthes, W. (European Atomic Energy Community, Ispra (Italy). Joint Nuclear Reserch Center).

From Meeting on new development in reactor mathematics and applications; Idaho Falls, Idaho (29 Mar 1971).

Two independent games of two different kinds of particles are considered with the condition that the expectation value of some estimator in the two games should be equal. This leads directly to the Monte Carlo game for the adjoint flux and provides a large arbitrariness for the adjoint game. This arbitrariness can be used to find "adjoint games" with smaller variances. This method is applied to the calculation of the neutron flux in an annular air gap in the water shield of a reactor. (auth)

**57163** (CONF-710302-(Vol.2), pp 857-70) COMPARISON OF 3 METHODS TO CONTROL THE LEAKAGE OF PARTICLES IN A MONTE CARLO GAME. Borgwaldt, H. (Kernforschungszentrum, Karlsruhe (West Germany). Institut fuer Neutronenphysik und Reaktortechnik).

From Meeting on new development in reactor mathematics and applications; Idaho Falls, Idaho (29 Mar 1971).

Estimating with a Monte Carlo code quantities which depend primarily on neutrons which have performed many collisions in a system becomes difficult when a high probability for neutron leakage has to be faced. This may necessitate the use of track length truncation as a non-analogue method for treating neutron leakage, in order to improve the statistics for neutrons with high numbers of collisions. Kschwendt and Rief have shown the advantage of track length truncation (Expected Leakage Probability method, ELP) in estimating time-dependent neutron leakage from bare spheres. The same type of test problem was investigated. It is demonstrated that a considerable improvement over the ELP method can be achieved by combining track length truncation with a technique of angular biassing which promotes inward scattering in the immediate vicinity of all outer boundaries. (auth)

**57164** (CONF-710302-(Vol.2), pp 871-6) MONTE CARLO SAMPLING WITH CONTINUOUSLY VARYING CROSS SECTIONS ALONG FLIGHT PATHS. Carter, L. L.; Cashwell, E. D.; Taylor, W. M. (Los Alamos Scientific Lab., N. Mex.).

From Meeting on new development in reactor mathematics and applications; Idaho Falls, Idaho (29 Mar 1971).

In systems where the total cross section is continuously changing along the flight path of a particle, the straightforward sampling approach is to compute the number of mean free paths to each collision point numerically. The numerical computation generally requires a considerable amount of computation time. An alternative sampling scheme which avoids the numerical integration altogether is investigated. (auth)

**57165** (CONF-710302-(Vol.2), pp 877-86) CURRENT STATUS OF ENDF/B PROCESSING CODES. Dannels, R. A. (Westinghouse Electric Corp., Pittsburgh, Pa. Nuclear Energy Systems Div.).

From Meeting on new development in reactor mathematics and applications; Idaho Falls, Idaho (29 Mar 1971).

The history and development philosophy of the Evaluated Nuclear Data File are presented. The ENDF/B data manipulation and library preparation codes are discussed. (H.D.R.)

**57166** (CONF-710302-(Vol.2), pp 887-900) DANISH MONTE CARLO WORK IN REACTOR PHYSICS AND RELATED AREAS. Kirkegaard, Peter (Danish Atomic Energy Commission, Risoe. Research Establishment).

From Meeting on new development in reactor mathematics and applications; Idaho Falls, Idaho (29 Mar 1971).

A survey of the application of Monte Carlo methods in Denmark is presented. Attention is focused on problems in reactor physics, but also related topics are discussed. 10 references. (auth)

**57167** (CONF-710302-(Vol.2), pp 901-12) COMPUTER PERFORMANCE MEASUREMENTS USING THE ARGONNE BENCHMARK PROBLEM COLLECTION: A STATUS REPORT. Butler, M. K. (Argonne National Lab., Ill.).

From Meeting on new development in reactor mathematics and applications; Idaho Falls, Idaho (29 Mar 1971).

Argonne has in the past undertaken "crash" benchmark problem collection efforts in conjunction with each proposed computer system acquisition. It was decided to initiate a small continuing benchmark research project in conjunction with the ongoing development of software monitoring techniques and the design and construction of a hardware monitor. Development of the benchmark collection was initiated in two separate but related sections. The first consists of those problems representative of and essential to the Laboratory's discipline-oriented research programs and reactor development activities. The second consists of a sample job stream simulating the Laboratory's computing workload. 8 references. (auth)

**57168** (CONF-710302-(Vol.2), pp 920-38) ALTERNATIVE APPROACH TO CORE CALCULATIONS FOR BOILING WATER REACTORS. Jonsson, A. (Vattenbyggnadsbyran, Stockholm (Sweden)).

From Meeting on new development in reactor mathematics and applications; Idaho Falls, Idaho (29 Mar 1971).

The coarse mesh (or nodal) method is widely accepted as an inexpensive and practical tool for core calculations. However, the simplifications made in this approach lead to a situation where a number of parameters have to be determined by reference either to empirical relationships or to a more or less complete range of situations studied with a more exact means of solving the diffusion equation. This situation may well have a bearing on the accuracy that can be achieved in predicted power distributions and reactivity. An approach is described that can claim accuracies similar to conventional difference solutions and yet be as economic to execute as the coarse mesh method. 8 references. (auth)

**57169** (CONF-710302-(Vol.2), pp 939-52) DISCUSSION ABOUT THE NUCLEAR REACTOR CORE ANALYSIS CODE CITATION. Vondy, D. R.; Fowler, T. B.; Cunningham III, G. W. (Oak Ridge National Lab., Tenn.).

From Meeting on new development in reactor mathematics and applications; Idaho Falls, Idaho (29 Mar 1971).

The CITATION computer code was developed for analysis of nuclear reactor cores. Emphasis was placed on rapid solution of finite-difference diffusion theory neutronics problems of reasonable size in up to three geometric dimensions. Development effort added fuel management capability for fuel cycle analysis. Techniques of calculation which have been implemented are discussed and results of calculations are presented. 8 references. (auth)

**57170** (CONF-710302-(Vol.2), pp 953-67) APPLICATIONS OF SPACE-ENERGY FACTORIZATION TO THE SOLUTION OF STATIC FAST-REACTOR NEUTRONICS PROBLEMS. Stacey, W. M. Jr.; Henryson II, H. (Argonne National Lab., Ill.).

From Meeting on new development in reactor mathematics and applications; Idaho Falls, Idaho (29 Mar 1971).

The space-energy factorization method, in which the neutron flux is factored into a spectral and a spatial function and equations for each are solved iteratively, was extended and applied to a number of problems of interest in fast-reactor physics. An extension which uses several spectral functions, rather than a single spectral function as in the original method, was examined. Applications to many-group and two-dimensional neutron diffusion theory problems were investigated. Numerical results are presented which indicate the potential of the space-energy factorization method in fast-reactor analysis. (auth)

**57171** (CONF-710302-(Vol.2), pp 968-82) NEW MULTIGROUP CROSS SECTION CODE, MC$^2$-2. Toppel, B. J. (Argonne National Lab., Ill.).

From Meeting on new development in reactor mathematics and applications; Idaho Falls, Idaho (29 Mar 1971).

XUM

The $MC^2$-2 code is intended to provide multigroup cross sections for critical experiment analysis, core calculations, and shielding applications. The code is planned so that approximate cross sections may be rapidly generated by relaxing the rigor of the basic algorithms. The $MC^2$-2 code is described by means of comparisons with $MC^2$ algorithms. 21 references. (H.D.R.)

**57172** (CONF-710302–(Vol.2), pp 983-90) AUTOMATED MODULAR LIGHT WATER REACTOR CALCULATION CODE PACKAGE. Karin, S.; Meyer, P. E.; Steinke, R. G. (ESZ Associates, Inc., Ann Arbor, Mich.).

From Meeting on new development in reactor mathematics and applications; Idaho Falls, Idaho (29 Mar 1971).

The POWER-B Code Package is a lifetime calculational tool for light water reactors. It is designed to be used in scoping studies for bid evaluation, fuel cycle analysis, and analysis of day to day reactor operation. It is modular in form; the modules are automatically linked by a driver program so that no module manipulation by the user is required. The input to the code consists of a physical description of the reactor to be analyzed and a small set of parameters describing the calculational options to be used. This input is checked internally to insure that it is logically consistent and physically reasonable. All of the input is edited and processed into a common form to be used by individual modules. The important output can be divided into three types: (1) the lifetime of the reactor with the current fuel loading; (2) the thermal hydraulic performance limits throughout the lifetime of the reactor; and (3) the isotopic composition on an assembly basis throughout the lifetime of the reactor. 15 references. (auth)

**57173** (CONF-710302–(Vol.2), pp 991-1003) ENDF/B LIBRARY: A CURRENT STATUS REPORT. Drake, Marvin K. (Brookhaven National Lab., Upton, N. Y.).

From Meeting on new development in reactor mathematics and applications; Idaho Falls, Idaho (29 Mar 1971).

The development of the Evaluated Nuclear Data File (ENDF) library is reviewed. The formats and contents of ENDF/A and ENDF/B sections of the library are described, and the data included in ENDF/B-II are discussed. (H.D.R.)

**57174** (CONF-710302–(Vol.2), pp 1004-15) PSYCHE: PHYSICS CHECKING OF THE ENDF/B EVALUATED NUCLEAR DATA FILE. Raymund, Mahlon (Brookhaven National Lab., Upton, N. Y.).

From Meeting on new development in reactor mathematics and applications; Idaho Falls, Idaho (29 Mar 1971).

The CHECKER Code checks formats, smoothness of tabulated curves, and some order-of-magnitude properties of ENDF/B data. PSYCHE is programmed to do physics tests on data which has already passed the CHECKER tests. The standard nuclide data used for many of the simple tests is presented. The most important tests performed and details on information printouts are described. Some of the programming philosophy is discussed, with a summary of actual achievement in the development of the working code. 14 references. (auth)

**57175** (CONF-710302–(Vol.2), pp 1016-23) GENERATING MOMENTS OF THE PHOTON PRODUCTION MATRICES AND SOURCES FROM ENDF DATA: THE LAPHAN CODE. Dudziak, Donald J.; Seamon, Robert E. (Los Alamos Scientific Lab., N. Mex.).

From Meeting on new development in reactor mathematics and applications; Idaho Falls, Idaho (29 Mar 1971).

The function of the LAPHAN code is to obtain pointwise cross sections from the data given in ENDF Files 12, 13, 14, and 15; to apply suitable weighting functions over specified photon and neutron groups; and to construct microscopic photon production matrices. For each material considered, the number of matrices is $L + 1$, where $L \leq 4$ is the order of the Legendre expansion required. As an option, the code will combine the microscopic matrices with the appropriate atom-number densities and will operate with the resulting macroscopic matrices on the corresponding moments of the flux density vectors, in order to provide spatially dependent moments of the photon source terms for transport calculations. 5 references. (auth)

**57176** (CONF-710302–(Vol.2), pp 1024-30) ENDF/B CROSS SECTION PREPARATION AND TESTING IN THE JOSHUA SYSTEM. Finch, D. R.; Honeck, H. C.; Stewart II, J. W.; Baxter, W. V. (Du Pont de Nemours (E. I.) and Co., Aiken, S. C. Savannah River Lab.).

From Meeting on new development in reactor mathematics and applications; Idaho Falls, Idaho (29 Mar 1971).

The features of the JOSHUA Cross Section Subsystem and the communication features that enable the subsystem to function smoothly are described. An example taken from ENDF/B-II data testing is followed through the Cross Section Subsystem to demonstrate the methods available. (auth)

**57177** (CONF-710302–(Vol.2), pp 1031-46) ETOG-2 AND ETOT–ENDF/B DATA PROCESSOR PROGRAMS TO PRODUCE EPITHERMAL AND THERMAL MULTIGROUP LIBRARIES. Kusner, Daniel E.; Beard, Charles L. Jr. (Westinghouse Electric Corp., Pittsburgh, Pa. Nuclear Energy Systems Div.).

From Meeting on new development in reactor mathematics and applications; Idaho Falls, Idaho (29 Mar 1971).

To use data in the various multigroup spectrum codes required for reactor analysis, additional linking codes are necessary. These linking codes process the ENDF data files and prepare data necessary for the generation of the required multigroup libraries. ETOG and ETOT are two such linking programs. ETOG produces data necessary for the generation of fast libraries while ETOT produces data necessary for the generation of thermal libraries. 19 references. (auth)

**57178** (CONF-710302–(Vol.2), pp 1053-64) STATUS OF DATA TESTING USING THE ENDF/B LIBRARY. Alter, Harry; Hubner, Robert S. (Atomics International, Canoga Park, Calif.).

From Meeting on new development in reactor mathematics and applications; Idaho Falls, Idaho (29 Mar 1971).

With the distribution of the second version of the ENDF/B data files, the comprehensive data testing program, which began with the Version 1 files, was continued. The term "data testing" is understood to relate comparisons of specific integral parameters measured in a reactor or shielding environment with values calculated using the ENDF/B data files. Specific reactors or shield systems for which sets of well established experimental data had been defined and compiled were designated as "benchmarks." A report on the status of testing the ENDF/B-2 data files with a set of ten benchmark fast critical assemblies is presented. (auth)

**57179** MOMENTS OF THE DISTRIBUTION FUNCTION OF THE NEUTRON DENSITY. Zima, T. E.; Kostritsa, A. A.; Neimotin, E. I. At. Energ. (USSR); 31: No. 2, 154-6(Aug 1971). (In Russian).

The determination of moments of the distribution function of the neutron density by Marshak's equation does not require a knowledge of the function or its Fourier-form. It is sufficient to know the value of the Fourier-form and its derivative at the coordinate origin. The mathematical development involves the kinetic equation for a distribution function, in the case of a plane geometry with a local pulsed neutron source. (K.S.W.)

**57180** RECENT STUDY OF NUCLEAR REACTOR OPTIMIZATION. Hara, Fumio (Tokyo Univ.). Seisan Kenkyu; 22: No. 10, 425-36(Oct 1970). (In Japanese).

Methodology for optimization of nuclear reactor design is examined. The fluctuation of neutron flux, caused by the statistic property of neutron transport and the fluctuation of reactor parameters, is estimated on the basis of theories of probability and statistics. Moreover, the problem of statistic optimization of nuclear reactor design in steady state operation is dealt with by application of the following methods: mode variation method or more generalized mode optimization method; semi-linear, nonlinear programming and phase plane method. Methods for maximizing heat output, flattening neutron flux distribution, maximizing fuel conversion rate and minimizing output protrusion are discussed. Constituent parameters of the optimum reactor are calculated by application of the mode optimization method and the phase plane method. Especially the mode optimization method enables optimization of a reactor statistically. (Japan)

## *Kinetics*

*Refer also to abstracts 56614 and 57021.*

**57181** (BNWL–1609) BNW PROGRAM NOISE. Seybold, G. D. (Battelle Pacific Northwest Labs., Richland, Wash.). Jul 1971. Contract AT(45-1)-1830. 54p. Dep. NTIS.

A computer code, NOISE, is presented which serves as an aid in determining reactor parameters from data obtained in zero-power reactor noise experiments. The code uses a nonlinear least-squares fitting package to provide the best estimate of these reactor parameters. Special options are available which allow for specification of the theoretical model, modifications of the experimental data in order to put them in units describable by the theory, and plotting features which illustrate the experimental measurements along with the best least-squares fit to the measurements. (auth)

**57182** (JAERI-Memo-4481) SDRC: THE ULTRA-FINE SPECTRUM CALCULATION CODE IN RESONANCE ENERGY REGION. Suzuki, Tomoo (Japan Atomic Energy Research Inst., Tokyo). Jun 1971. 30p. (In Japanese and English). Dep. NTIS (U. S. Sales Only).

For the detailed study of heterogeneity effects in hexagonal lattices of pin-typed fuels and coolant, the ultra-fine spectrum calculation code SDRC has been developed. For heavy nuclides, the ultrahigh resolution data are used on which the JAERI-fast set was based. The code was developed from the U.K.'s code SDR, so that it could treat the two-region hexagonal lattices. Though it deals only with the resonance region, the heterogeneity effects in the lattices can be examined in detail, in all the energy region, when used with the fine spectrum code ESELEM-3 mainly for the fission spectrum region. From the calculations, it was confirmed that the ratio of the flux in fuel region to the total flux in a cell does not change much with the energy. From these results, a simple method was developed for obtaining the effective cross sections for the heterogeneous systems in few group structures. This method was incorporated in the criticality calculation code EXPANDA-5 with one-dimensional diffusion model for less than 30 energy groups. To prepare the microscopic cross sections as the input data for SDRC, the auxiliary codes LTSDR, COMPLETION and PRESDRJ were also made. The subprogram BINPUT originally developed by D.C. Bindon to accept the data cards punched in free-format was introduced in the SDRC. IBM-360/J75 is used because the temporary memory storages of direct access type are necessary for SDRC. (auth) (Japan)

**57183** (ORNL-TM-2496(Rev.2)) NUCLEAR REACTOR CORE ANALYSIS CODE: CITATION. Fowler, T. B.; Vondy, D. R.; Cunningham, G. W. (Oak Ridge National Lab., Tenn.). Jul 1971. Contract W-7405-eng-26. 251p. Dep. NTIS.

The CITATION code is used for solving problems involving the finite-difference diffusion-theory representation of neutron transport theory. The code is designed to solve depletion problems with or without elaborate refueling treatment for multi-cycle analysis. Macroscopic cross sections may be used to solve usual eigenvalue problems. The adjoint flux may be determined and extensive first-order perturbation results obtained. The code will treat point, one, two or three space dimensions. Data storage is allocated for solution of neutronics problems with minimum input/output of data during the iterative process. Only relatively small problems (few space-energy points) may be solved on a computer having a small memory. Moderately large problems in two or three space dimensions are solved with an IBM-360/75 having directly addressible extended core storage and with an IBM-360/91 having a large memory (375,000 short words). Instructions to the user about input data requirements, information about using the code, as details of local implementation, a list of the input data for a simple problem and selected results obtained for it, and the mathematical formulations which are programmed are presented. (auth)

**57184** CONSIDERATIONS ON THE HETEROGENEOUS METHODS FOR CORE PHYSICS AFTER THE SECOND EACRP MEETING IN PARIS. Bonalumi, R.; Bozzola, S. (CISE, Milan). Energ. Nucl. (Milan); 18: No. 5, 271-84(May 1971).

The major achievements in the heterogeneous theory of nuclear reactors are summarized. The calculation of dipolar heterogeneous parameters is discussed, along with the closely related subject of the homogenized cell diffusion coefficients, for which corrections to Benoist's practical formulas are proposed. A new theory by Berna is outlined and the comparison of heterogeneous calculations with experiments is presented. 10 references. (auth)

**57185** INVESTIGATION OF THE AREA-RATIO METHOD OF PULSED REACTIVITY DETERMINATION. Kosaly, G.; Valko, J. (Central Research Inst. for Physics, Budapest). J. Nucl. Energy; 25: No. 7, 297-315(Jul 1971).

The theoretical interpretation of the area-ratio method of pulsed reactivity determination starting from transport theory is given. It is shown that the removal of prompt harmonics does not necessarily improve the method unless the reactor is bare and homogeneous. Reviewing the theory of the extrapolated area-ratio method, several difficulties are pointed out that are encountered in the application of this method to heavily reflected systems. Numerical experiments were performed simulating the above measuring methods in two-group diffusion approximation. Results indicate that the simple area-ratio method is superior to its extrapolated version in the case of heavily reflected reactors. (auth) (UK)

**57186** RELATION BETWEEN SOLUTIONS OF NON-STATIONARY AND QUASI-CRITICAL TRANSPORT EQUATIONS. Abramov, B. D. At. Energ. (USSR); 31: No. 2, 153-4(Aug 1971). (In Russian).

Noncritical reactors in a single-velocity approximation may be described by equations of two types: nonstationary transport equations allowing for delayed neutrons, or a quasi-critical equation involving the $k_{eff}$. The mathematical development shows that the true neutron distribution in a nonstationary reactor may be determined from a solution of the quasi-critical equation. (K.S.W.)

## Dynamics

**57187** (EUR-4673) COSTANZA (R,Z). Vincenti, E.; Clusaz, A. (European Atomic Energy Community, Ispra (Italy). Joint Nuclear Research Center). 15 Mar 1971. 78p. Dep. NTIS (U. S. Sales Only). EUR F,Fr. 13.08.

The code COSTANZA (R, Z) written in FORTRAN for IBM 360/65 solves the kinetic diffusion equations in two groups and two dimensions (radial and axial for a cylindrical reactor). The neutronic calculation is coupled with the calculation of the heat transmission from the fuel to the cladding and to the coolant, and with the thermohydraulics of channels with forced circulation of a single phase coolant. Fuel elements of prismatic shape are considered. Up to 6 groups of delayed neutrons are allowed. Temperature feedback of fuel and coolant are considered independently and affect the nuclear constants. Control rod movement or diffused poison concentrations are simulated by externally imposed variations of the thermal absorption cross section in the different regions of the reactors. Inlet temperatures and mass flow in the coolant channels may be varied according to any externally given time table. Before starting the transient, initial calculations put the reactor in criticality conditions at a given power level in equilibrium with the temperature feedback. (auth)

**57188** SUFFICIENT AND NECESSARY CONDITIONS OF ASYMPTOTIC STABILITY OF NONLINEAR SPACE–TIME REACTOR DYNAMICS. Yu, Dahsoong (Univ. of Oklahoma, Norman). Atomkernenergie; 18: No. 1, 1-10(Aug 1971).

For the nonlinear space-time reactor dynamics with positive feedback, a computational method is developed for the determination of the domain asymptotic stability (DAS) in the state space. A new derivation of the coupling coefficients is presented to reduce the nonlinear space-time reactor dynamics equation to a finite set of nonlinear ordinary differential equations. Zubov's method of constructing the Lyapunov functions and an optimum search technique are then used to determine and improve the extent of the DAS of the nonlinear space-time reactor dynamics problem. The influence of the coupling coefficient on the size of the DAS is also explicitly determined. Criteria of stability of the multiple equilibrium solutions are also obtained by the perturbation method. 22 references. (auth)

## Experimental Applications

**57189** PULSED-SOURCE INVESTIGATIONS. I. THE EFFECT OF VOIDS ON THE NEUTRON TRANSPORT IN A DIFFUSING MEDIUM. Dance, K. D.; Connolly, T. J. (Stanford Univ., Calif.). J. Nucl. Energy; 25: 155-77(Apr 1971).

Pulsed-source measurements were conducted on rectangular graphite systems containing a transverse void gap. The principal objectives were to obtain experimental measurements of neutron transport in a void-containing medium of simple configuration, to provide a basis for comparison with analytical methods, and also to provide a sensitive test of the validity of the steps in transforming the time-dependent, pulsed-source measurements to time-independent neutron transport parameters. The measurements were conducted in graphite assemblies formed of two identical parallel slabs with an intervening gap. Slab widths were 29.21 and 43.82 cm; the gap widths were 2.54, 5.08, 7.62 and 10.16 cm. It was found that the pulsed-source measurements of time-dependent leakage could not be used directly to predict steady-state leakage and a theory was developed to interpret pulsed-source measurements in terms of diffusion coefficients appropriate for steady-state leakage calculations. Specifically, a "time delay" correction was developed and applied to the experimental decay constants so that they could be used for determining diffusion coefficients. The results of the experiments and the theoretical treatment are in good agreement, but the theory showed that pulsed-source measurements in systems with voids will not yield rigorously discrete eigenvalues and cannot be extended to achieve results to any arbitrarily high degree of accuracy. (auth) (UK)

**57190** PULSED-SOURCE INVESTIGATIONS. II. THE EFFECT OF CYLINDRICAL VOID CHANNELS IN A NEUTRON DIFFUSING MEDIUM. Bull, S. R.; Connolly, T. J. (Stanford Univ., Calif.). J. Nucl. Energy; 25: 179-87(Apr 1971).

Consistent experimental measurements of the neutron leakage

XUM

from cavity-containing media were made and interpreted in terms of effective diffusion parameters. The technique employed was the pulsed-source method, in which the diffusion coefficient is inferred from the asymptotic decay constant curve. The ranges of pertinent variables (e.g., size and shape of the medium, cavity size, cavity spacing) were made large enough to afford a sound basis for checking the adequacy of various theoretical treatments of the problem. The graphite assembly used enabled construction of solid graphite systems or lattices of cylindrical void channels with seven different combinations of channel spacing and diameter (void fractions ranging from 0.0371 to 0.3801). The experimental results are compared with other analytical results and discussed in the light of the recent measurements. (auth) (UK)

## Reactor Components, Fuels, and Accessories

*Refer also to abstracts 54396, 54842, 54848, 54856, 54857, 54880, 54926, 54935, 55068, 55077, 55088, 55379, 55391–55395, 55420, 55422, 55429, 55579, and 55609.*

**57191** (CONF-710302–(Vol.2), pp 1086-1101) FUTURE PROSPECTS IN COMPUTER TECHNOLOGY. Worlton, William J. (Los Alamos Scientific Lab., N. Mex.).

From Meeting on new development in reactor mathematics and applications; Idaho Falls, Idaho (29 Mar 1971).

Since the early 1950's, improvements in computer circuits, storage elements, and logical design have contributed to an increase of about an order of magnitude in computing speed every five years. Whether or not this same exponential growth rate can be maintained indefinitely in the future was the subject of several reviews during the 1960's. These papers considered the question of ultimate bounds on computing speed imposed by the laws of physics, as well as the more immediate problems of technology. These results are summarized. Trends and prospects in the areas of storage, architecture, and input–output are reviewed. Some industry-wide trends are noted. 31 references. (auth)

**57192** (JAERI-Memo–4157) PROCEEDINGS OF FUEL FAILURE DETECTION SYMPOSIUM. Sakai, Eiji; Kitahara, Tanemichi (eds.) (Japan Atomic Energy Research Inst., Tokyo). Oct 1970. 113p. (In Japanese and English). (CONF-690128).

Separate abstracts are included for each of the 7 papers presented on the development and performance of fuel element failure detection systems. (D.C.C.)

*For abstracts of individual papers see: 57047, 57055, 57056, 57117–57119, and 57193.*

**57193** (JAERI-Memo–4157, pp 66-83) FUEL FAILURE DETECTOR EXPERIMENT IN A He GAS INPILE LOOP, USE OF PRECIPITATOR AND GAS-CHROMATOGRAPH. Kitahara, Tanemichi (Japan Atomic Energy Research Inst., Tokyo). (In Japanese and English).

From Fuel failure detection symposium; Tokyo, Japan (31 Jan 1969).

Characteristics of failed fuel detectors with a preciptitator and gas chromatography were measured and checked in a He-gas loop called TLG-1 inpile gas loop. A foil of 19.3% enriched uranium and aluminum alloy was irradiated in the loop, and elapsed time for gas arrival from an irradiation point to a sampling point was 10 to 20 seconds. Saturation voltages of the precipitator with different diameter cylinders were measured, and found to be two places as large as calculated values by Long et al. Half-life was 18 ± 2 minutes, and γ-ray spectrography showed that main nuclides are $^{88}$Rb (half-life 17.7 min), $^{89}$Rb (half-life, 15.4 min) and $^{138}$Cs (half-life : 33 min). The nuclides were as expected. Precipitation efficiency obtained was between 10 and 50%. The gas chromatogram FFD with cycles of 4 minutes gave good separation between Kr and $^{138}$Xe. $^{135}$Xe concentration in sample gas was $8.2 \times 10^{-4}$ μci/cc i.e., $2.4 \times 10^{-16}$ mol%, and was detected satisfactorily. The associated problem is small amount of sampled gas, and therefore small counting rate. The counting rates were 12,000 cpm with the precipitator detection and 800 cpm with the gas chromatograph detection. But reduction in short lived nuclides gives better response to the gas chromatograph detection. Hereafter it is planned that response of each FFD is studied when fuels with different behaviors of fission product release are irradiated. Besides, simulation experiment will be carried out for the case of application to Na-cooled fast reactor. 7 references. (Japan)

**57194** TEMPERATURE DISTRIBUTION IN IRRADIATED OXIDE FUEL WITH DISPERSED BURNABLE POISON. Flipot, A. J.; Delbrassine, A.; Gilissen, R. (CEN/SCK, Mol, Belgium). Nucl. Eng. Int.; 16: 329-33(Apr 1971).

The temperature distribution in an irradiated pellet can be calculated from data such as linear power, thermal conductivity and, in particular, the determination of a specific isothermal line. Such lines can be detected using the method of dispersed monitors. The influence of some irradiation parameters and the characteristics of alumina as a monitor are discussed. Some comments regarding the $UO_2$–$Dy_2O_3$–$Al_2O_3$ system and especially about the eutectic temperature (1915°C) are mentioned. The liquid phase, formed from 1915°C onwards, increases the formation rate of the columnar structure, which allows one to detect the 1915°C eutectic isotherm to within about 0.1 mm. (au h) (UK)

**57195** INSULATING DEVICE FOR A FUEL ELEMENT. Droussent, Roger; Houyvet, Alain (to Commissariat a l'Energie Atomique). French Patent 1,528,864. 21 Mar 1970. Filed 22 Feb 1968. (In French).

A metallic joint capable of maintaining the tightness of a fuel element during a 500°C rise or fall of temperature is described. The joint consists of a hard metal circular knife working with a soft metal circular gate. (J.S.R.)

**57196** STUDIES ON THE SELF-SHIELDING OF HIGHLY DILUTED RESONANCE ABSORBERS. Huettel, G. (Zentralinstitut fuer Kernforschung, Rossendorf, Ger.). Kernenergie; 14: No. 3, 73-9(Mar 1971). (In German).

The self-shielding of the resonance absorption of highly diluted absorbers was measured by a reactivity technique using a pile oscillator in an annular zero-power reactor. The reactivities of the materials were determined by the two-spectra method with a sensitivity of $\Delta\delta \approx 5 \times 10^{6}$ and an accuracy of $\Delta(\Sigma_a V) = 0.04$ mm². The results indicate a substantial change even in the regions of smallest concentration. The courses of self-shielding determined experimentally were found in a good agreement with perturbation theoretical multigroup calculations. (auth)

**57197** DEVICE FOR THE REFUELLING OF A NUCLEAR REACTOR. (to English Electric Co. Ltd.). French Patent 1,569,263. 21 Apr 1969. Priority date 16 Jun 1967, Great Britian. (In French).

Refueling devices which consists of access wells penetrating the biological shield of the reactor are described. The refueling device is arranged to communicate with the core at the interior of the biological shield. Each of the access wells is cooled by liquid coolant when the reloading machine is in contact with the access wells. The access wells also have removable protection plugs which are the access for electrical cables. (J.S.R.)

**57198** FUEL CARTRIDGE WITH HELICAL CROSS-PIECES. Andersson, H. O.; Ekwall, P. A. (to Allmanna Svenska Elektriska AB). French Patent 1,579,744. 21 Jul 1969. Priority date 4 Sep 1967, Sweden. (In French).

A fuel cartridge is described in which there are two types of fuel rods. The first type of rod has a helical cross piece and the second does not. Arrangement in the cartridge is such that each type of rod is surrounded by the other type. (J.S.R.)

**57199** RADIATION PROTECTING SHIELD FOR NUCLEAR REACTORS. (to English Electric Co. Ltd.). French Patent 1,567,656. 8 Apr 1969. Priority date 6 Jun 1967, Great Britian. (In French).

A movable radiation shield to be used above access wells is described. The shield is composed of alternating square and round slabs. The square slabs have arc indentations to receive the circular slabs. (J.S.R.)

**57200** UNIFORM MOTION HYDRAULIC CONTROL DEVICE IN PARTICULAR FOR CONTROLLING CONTROL RODS IN NUCLEAR REACTORS. (to Gesellschaft fuer Kernforschung mbH). French Patent 1,568,335. 14 Apr 1969. Priority date 3 Mar 1967, Germany. (In French).

A uniform-motion hydraulic device for the control of reactor control rods is described. The pistons with the corresponding guide cylinders are set up as hydraulic potentiometers arranged in parallel. The intermediate intakes are connected to the regulator which maintains the differential pressure at a constant ratio. (J.S.R.)

**57201** NONDESTRUCTIVE DETERMINATION OF AVERAGE BURNUP FOR IRRADIATED FUEL RODS. Takayanagi, Hiroshi; Adachi, Mamoru (Japan Atomic Energy Research Inst., Tokai). Nippon Genshiryoku Gakkaishi; 13: No. 7, 374-9(Jul 1971). (In Japanese).

A nondestructive measurement on average burnup of irradiated fuel rods with use of a Ge(Li) detector is described. In order to obtain the average burnup directly and to simplify measurement

and analysis, the γ-ray spectrum from the irradiated fuel rod was measured by scanning along the whole length of the rod. The total absorption peaks for the 0.662 MeV ($^{137}$Cs) and the 2.18 MeV ($^{144}$Pr) γ-rays were used in the analysis, and the peak areas were estimated by Covell's method. The absolute value of average burnup was determined by comparison of the peak area with that of a standard fuel rod. The accuracy of the nondestructive measurement is discussed on the basis of an accurate value from destructive analysis. The result shows that it is possible to give the average burnup with good accuracy when the ratio of the peak height for $^{137}$Cs to the Compton background is larger than about 1.5, that is, after about 1 year of cooling. 14 references. (auth)

**57202** PLUTONIUM RECYCLE DEVELOPMENTS. **Astley, Wayne C. (Philadelphia Electric Co.); Walke, Gerald J.; Ladesich, John. Nucl. News; 14: No. 8, 29-32(Aug 1971).**

This status report represents the viewpoint of the Committee on Nuclear Fuels of the Edison Electric Institute. Plutonium utilization in the HTGR, BWR's, and PWR's is discussed. (M.C.G.)

**57203** PRESTRESSED CONCRETE PRESSURE VESSEL. **Margen, P. H. E. (to AB Atomenergi). French Patent 1,577,543. 30 Jun 1969. Priority date 1 Jul 1967, Germany. (In French).**

A pressurized prestressed concrete vessel for reactors is described. The vessel consists of a relatively thin lining of steel surrounded by pressure container. The steel lining is surrounded by concrete blocks. These blocks are held in place by prestressed steel stays. (J.S.R.)

**57204** TRAVEL END COMMUTATOR DEVICE AND POSITION INDICATORS FOR CONTROLLING THE RODS OF NUCLEAR REACTORS. **(to Licentia Patent Verwaltungs GmbH). French Patent 1,567,270. 8 Apr 1969. Priority date 14 Mar 1967, Germany. (In French).**

A position indicator and a travel end commutator device for controlling reactor rods are described. The apparatus have a reproducer mechanism for the transmission of the rod movement to the travel end commutator device and/or to position indicators. The reproducer mechanism is a measurement gear consisting of a threaded rod which is mobile in an integral screw support. The gear is connected to a cogged wheel movable axially. (J.S.R.)

**57205** STUDY OF INTERFERENCE OF "BLACK" ABSORBERS IN A MODERATING MEDIUM USING PULSED-NEUTRON METHOD. **Yurova, L. N.; Romodanov, V. L.; Fedorovich, V. A. At. Energ. (USSR); 31: No. 1, 67-8(Jul 1971). (In Russian).**

Individual Cd rods were successively moved along the radius of a cylinder, measuring the decay constant of thermal neutrons at various positions. The interaction between two rods was investigated when positioned in the center and shifted along the radius. The coefficient of interference for all positions of the absorbers was calculated. (K.S.W.)

**57206** MEASUREMENT OF "BLACK" ABSORBERS OF EQUIVALENT SIZES AND IDENTICAL EFFICIENCY IN A MODERATING MEDIUM BY A PULSED-SOURCE TECHNIQUE. **Yurova, L. N.; Romodanov, V. L.; Fedorovich, V. A. At. Energ. (USSR); 31: No. 1, 65-7(Jul 1971). (In Russian).**

Nuclear reactor regulating rods may be cylindrical, cruciform, Y-form, or other shape in cross section. A comparison was made of the effectiveness of neutron interaction with control rods ("black" absorbers) of various shapes. (K.S.W.)

**57207** NUCLEAR MATERIALS AND SOME ASPECTS OF MACHINING. **Datta, D. K.; Ratnam, V. V. (BARC, Bombay). Mach. Build. Ind.; 7: No. 5, 74-81(1968).**

The criteria of selection of various nuclear materials such as fissile, fertile, canning, structural, moderator, reflector, control, shielding materials, and coolants are given. The hazards involved in handling these materials are classified. A few aspects of the machining of some of the materials being handled at Trombay are discussed. (Indian Sci. Abstr.)

**57208** IMPROVEMENTS TO THE CORES OF NEUTRON SLOWING DOWN NUCLEAR REACTORS. **(to Atomic Power Constructions Ltd.). French Patent 1,569,730. 28 Apr 1969. Priority date 8 Mar 1967, Great Britian. (In French).**

A neutron moderating core for a nuclear reactor is described which consists of columns of blocks of a neutron moderating material. The distance between adjacent columns is kept constant by pins set in grooves in the blocks. The grooves extend the length of a block wall. Its length is less than that of the blocks between its ends. Each pin has a length less than that of the corresponding pin groove. (J.S.R.)

**57209** DEVICE WITH PROTECTING SHIELDS FOR A NUCLEAR REACTOR. **(to English Electric Co. Ltd.). French Patent 1,567,688. 8 Apr 1969. Priority date 6 Jun 1967, Great Britian. (In French).**

A supplementary shield in the shape of a ring is proposed for use during the refueling of a reactor. The ring shield is at the base of the refueling device and its use reduces significantly the thickness of the shielding slabs. (J.S.R.)

**57210** LOADING AND UNLOADING MACHINE. **de Temple, Bernhard (to Gesellschaft fuer Kernforschung mbH). German Patent 1,464,988. 17 Jul 1969. Filed 31 Dec 1964. (In German).**

A method for the insertion and removal of fuel elements from reactor cores is described. Lifting, lowering, and grasping of the elements are controlled by a guidance plate. The guidance plate can be located outside of the reactor containment vessel and can be mechanically coupled with the lifting and lowering mechanism of the reactor. (H.B.G.)

XUM

# GENERAL

57211 (70-CNA-657) INDUSTRY REPORTS: CANADIAN CONSULTANTS AND THE CANADIAN NUCLEAR INDUSTRY. Hueton, J. W. (Canatom Ltd., Montreal (Quebec)). 1970. 6p. (CONF-700564-10). Dep. NTIS (U. S. Sales Only).
From tenth annual international conference of the Canadian Nuclear Association; Toronto, Canada (24 May 1970).

57212 (AAEC/E-219(Pt.1)) POTENTIAL-pH DIAGRAMS AT TEMPERATURES ABOVE 298.16°K. PART 1. THEORETICAL BACKGROUND. Lowson, R. T. (Australian Atomic Energy Commission Research Establishment, Lucas Heights). Jul 1971. 29p. Dep. NTIS (U. S. Sales Only).

57213 (AECL-3793) EFFECT OF TEMPERATURE, PRESSURE AND CONCENTRATION GRADIENTS ON DIFFUSION. Stevens, R. N.; Dutton, R. (Atomic Energy of Canada Ltd., Pinawa (Manitoba). Whiteshell Nuclear Research Establishment). Jul 1971. 25p. Dep. NTIS (U. S. Sales Only). AECL $1.00.

57214 (AWRE-O-77/70) FIBRE REINFORCED MATERIALS. A PRELIMINARY SURVEY OF DESIGN ASPECTS. Dunbar, J. L. (Atomic Weapons Research Establishment, Aldermaston (England)). Dec 1970. 125p. Dep. NTIS (U. S. Sales Only). UK 85p.

57215 (CEA-Bib-198) INDEX OF RADIATIVE LIFETIMES. Schmidt, Michel (Commissariat a l'Energie Atomique, Saclay (France). Centre d'Etudes Nucleaires). Jun 1971. 27p. (In French). Dep. NTIS (U. S. Sales Only).
The radiative lifetimes of the various fluorescent states of many ions, molecules, and molecular radicals were listed on punched cards with a view to the electronic sorting out of the informations. The present compilation is an output listing, classified accordingly to the chemical species. (auth)

57216 (COO-1456-16) HIGH TEMPERATURE ANNEALS OF DEFECTS QUENCHED IN METALS. Final Report. Emrick, Roy M. (Arizona Univ., Tucson. Dept. of Physics). [1971]. Contract AT(11-1)-1456. 17p. Dep. NTIS.

57217 (COO-1469-187) GRASS: SYSTEM OVERVIEW. Report No. 465. Michel, M. J. (Illinois Univ., Urbana. Dept. of Computer Science). Jul 1971. Contract AT(11-1)-1469. 27p. Dep. NTIS.

57218 (COO-1469-190) GRASS: SYSTEM SOFTWARE DESCRIPTION. Report No. 468. Michel, M. J. (Illinois Univ., Urbana. Dept. of Computer Science). Aug 1971. Contract AT(11-1)-1469. 139p. Dep. NTIS.

57219 (COO-1469-193) QUARTERLY TECHNICAL PROGRESS REPORT, APRIL-JUNE 1971. (Illinois Univ., Urbana. Dept. of Computer Science). Contracts AT(11-1)-1469; AT-(11-1)-2118. 164p. (COO-2118-15). Dep. NTIS.

57220 (COO-1533-15) SOFT SPHERE MODEL FOR NUCLEAR QUADRUPOLE RESONANCE IN RARE EARTH TRICHLORIDES UNDER HYDROSTATIC PRESSURE. Current, David Harlan (Michigan State Univ., East Lansing. Dept. of Physics). 1971. 88p. Dep. NTIS.
Thesis.

57221 (COO-1707-12) ELECTROCHEMICAL CELLS USING ALKALI METALS AND CHARGE TRANSFER COMPLEXES. Technical Progress Report, May 1, 1967-August 31, 1971. Ott, J. Bevan; Goates, J. Rex (Brigham Young Univ., Provo, Utah). 31 Aug 1971. Contract AT(11-1)-1707. 11p. Dep. NTIS.

57222 (COO-2013-19) CONGENITAL MALFORMATIONS: THE INFLUENCE OF GENETIC AND NONGENETIC FACTORS. Progress Report, January 1-December 31, 1971. Woolf, Charles M. (Arizona State Univ., Tempe. Dept. of Zoology). 1 Sep 1971. Contract AT(11-1)-2013. 53p. Dep. NTIS.

57223 (COO-2118-13) GEOMETRICAL MODEL FOR THE SYNTHESIS OF INTERVAL COVERS. Report No. 461. Michalski, R. S. (Illinois Univ., Urbana. Dept. of Computer Science). 24 Jun 1971. Contract AT(11-1)-2118. 39p. Dep. NTIS.

57224 (COO-2118-14) CONTROL POINT DESIGN USING MODULAR LOGIC. Report No. 463. Rey, Christian A. (Illinois Univ., Urbana. Dept. of Computer Science). Jun 1971. Contract AT(11-1)-2118. 35p. Dep. NTIS.

57225 (COO-2118-17) IBAL MANUAL. THE ILLIAC III BASIC ASSEMBLER LANGUAGE. Report No. 469. Masumi, Ahmad E. (Illinois Univ., Urbana. Dept. of Computer Science). Jul 1971. Contract AT(11-1)-2118. 87p. Dep. NTIS.

57226 (COO-2118-19) ILLIAC III REFERENCE MANUAL. VOLUME IV. SUPERVISOR ORGANIZATION. Report No. 472. McCormick, B. H.; Nordmann, B. J. Jr. (eds.) (Illinois Univ., Urbana. Dept. of Computer Science). 12 Aug 1971. Contracts AT(11-1)-1018; AT(11-1)-2118. 55p. Dep. NTIS.

57227 (COO-2118-21) ILLIAC III REFERENCE MANUAL. VOLUME III. INPUT/OUTPUT. Report No. 473. McCormick, B. H.; Nordmann, B. J. Jr. (eds.) (Illinois Univ., Urbana. Dept. of Computer Science). 13 Aug 1971. Contracts AT(11-1)-1018; AT(11-1)-2118. 127p. Dep. NTIS.

57228 (DP-929(Rev.1)(Suppl.3)) PUBLICATIONS, 1970. Hilborn, H. S. (comp.) (Du Pont de Nemours (E.I.) and Co., Aiken, S. C. Savannah River Lab.). Aug 1971. Contract AT(07-2)-1. 23p. Dep. NTIS.

57229 (EUR-4483) CHEMOTHERAPY OF LEUKEMIA AND CHEMICAL PROTECTION AGAINST IONIZING RADIATIONS. Final Report. Garattini, S.; Donelli, M. G.; Franchi, G.; Guaitani, A.; (and others) [European Atomic Energy Community, Ispra (Italy). Joint Nuclear Research Center]. 1970. 66p. NTIS (U. S. Sales Only).

57230 (HEDL-TME-71-108) TGO, A LINEAR PROGRAMMING MODEL FOR OPTIMIZING A POWER TRANSMISSION GRID. Omberg, R. P. (Hanford Engineering Development Lab., Richland, Wash.). Jul 1971. Contract AT(45-1)-2170. 90p. Dep. NTIS.

57231 (IS-2305) USE OF SIMPLOTTER: A HIGH-LEVEL PLOTTING SYSTEM. Scranton, D. G.; Manchester, E. G. (Ames Lab., Iowa). Jun 1971. Contract W-7405-eng-82. 103p. Dep. NTIS.

57232 (IS-T-494) AN OPTICAL MIXING SPECTROSCOPIC STUDY OF INTERFACIAL FLUCTUATIONS. Dechow, Frederick John (Ames Lab., Iowa). Aug 1971. Contract W-7405-eng-82. 120p. Dep. NTIS.
Thesis.

57233 (LA-4545) USE OF A MAGNETIC FIELD TO MEASURE PARTICLE VELOCITY. I. BASIC CONCEPTS AND EXPLORATORY EXPERIMENTS. Fritz, J. N.; Caird, R. S.; McQueen, R. G. (Los Alamos Scientific Lab., N. Mex.). Oct 1970. Contract W-7405-eng-36. 14p. Dep. NTIS.

57234 (LA-4721) DYNAMIC BUFFER ALLOCATION ON THE CDC 6600: THE DYNBUF PROGRAM. Vigil, John C. (Los Alamos Scientific Lab., N. Mex.). Sep 1971. Contract W-7405-eng-36. 9p. Dep. NTIS.

57235 (LA-4728) SUBROUTINE PACKAGE FOR CALCULATING WITH B-SPLINES. de Boor, Carl (Los Alamos Scientific Lab., N. Mex.). Aug 1971. Contract W-7405-eng-36. 12p. Dep. NTIS.

57236 (LA-tr-71-73) DECOLORING CYANOPHYCENE ALGAE BY EXTRACTION OF THEIR PIGMENTS. Clement, Genevieve; Meyer, Colette; Rebeller, Michel. Translated for Los Alamos Scientific Lab., N. Mex., from French Patent 1,591,570. 6p. Dep. NTIS.

57237 (LBL-133) REACTIVE SCATTERING OF $N_2O$ MOLECULAR BEAMS FROM CLEAN AND CARBON COVERED (100) PLATINUM SINGLE CRYSTAL SURFACES. West, L. A.; Somorjai, G. A. (California Univ., Berkeley. Lawrence Berkeley Lab.). Jul 1971. Contract W-7405-eng-48. 17p. (CONF-711005-3). Dep. NTIS.
From International conference on solid surfaces; Boston, Mass. (11 Oct 1971).

**57238** (MLM-OP-71003) REACTION DIFFUSION IN THE SILVER-ZINC AND SILVER-ALUMINUM SYSTEMS. Braun, Japnell D.; Powell, Gordon W. (Mound Lab., Miamisburg, Ohio). [1968]. Contract AT(33-1)-Gen-53. 9p. (CONF-710902-2). Dep. NTIS.
From fourth annual meeting of the International Metallographic Society; Denver, Colo. (21 Sep 1971).

**57239** (MLM-OP-71004) TECHNIQUE FOR THE METALLOGRAPHIC PREPARATION OF LEAD. Downs, Gene L.; Jones, V. Dean (Mound Lab., Miamisburg, Ohio). [nd]. Contract AT(33-1)-Gen-53. 13p. (CONF-710902-3). Dep. NTIS.
From fourth annual meeting of the International Metallographic Society; Denver, Colo. (21 Sep 1971).

**57240** (MLM-OP-71007) EVALUATION OF THE USE OF A QUANTITATIVE IMAGE ANALYZER TO DETERMINE MICROHARDNESS VALUES. Teaney, P. E.; Selle, J. E. (Mound Lab., Miamisburg, Ohio). [nd]. Contract AT(33-1)-Gen-53. 20p. (CONF-710902-6). Dep. NTIS.
From fourth annual meeting of the International Metallographic Society; Denver, Colo. (21 Sep 1971).

**57241** (NYO-1480-179) SIZE EFFECTS IN THE THREE DIMENSIONAL ISING LATTICE. Jennette, Robert L.; Kalos, Malvin; Percus, Jerome (New York Univ., N. Y. AEC Computing and Applied Mathematics Center). Jun 1971. Contract AT(30-1)-1480. 75p. Dep. NTIS.

**57242** (NYO-3406-20) PHOTON STATISTICS OF LINEAR COHERENT AMPLIFICATION OF SPONTANEOUSLY EMITTED LIGHT. Technical Report No. 11. Cantrell, C. D. (Princeton Univ., N. J. Dept. of Physics). 1 Aug 1971. Contract AT(30-1)-3406. 29p. Dep. NTIS.

**57243** (NYO-3406-22) RESEARCH PROGRESS AT THE MARINE BIOLOGICAL LABORATORY, SUMMER 1971. Technical Report No. 12. Reynolds, Geo. T. (Princeton Univ., N. J. Elementary Particles Lab.). 18 Sep 1971. Contract AT(30-1)-3406. 36p. Dep. NTIS.

**57244** (NYO-3489-22) CELLULAR BASIS OF MAMMALIAN CALCIUM HOMEOSTASIS. Rasmussen, Howard (Pennsylvania Univ., Philadelphia. Dept. of Biochemistry). [1971]. Contract AT(30-1)-3489. 44p. Dep. NTIS.

**57245** (ORNL-4685) ANALYSIS OF ROUND, TURBULENT, BUOYANT JETS DISCHARGED TO FLOWING STRATIFIED AMBIENTS. Hirst, E. A. (Oak Ridge National Lab., Tenn.). Jun 1971. Contract W-7405-eng-26. 37p. Dep. NTIS.

**57246** (ORNL-NSF-EP-8) OAK RIDGE AIR QUALITY INDEX. Thomas, W. A.; Babcock, L. R. Jr.; Shults, W. D. (Oak Ridge National Lab., Tenn.). Sep 1971. Contract W-7405-eng-26. 10p. Dep. NTIS.

**57247** (ORNL-TM-2713(Rev.1)) TUBE IDENTIFIER: A PHYSICAL DESCRIPTION OF TUBES TESTED IN THE OSW PROGRAM ON IMPROVED HEAT-TRANSFER SYSTEM FOR EVAPORATORS: ADVANCED LTV HEAT-TRANSFER SURFACES. Hoffman, H. W.; Alexander, L. G. (Oak Ridge National Lab., Tenn.). Oct 1971. Contract W-7405-eng-26. 36p. Dep. NTIS.

**57248** (ORNL-TM-2933) DIGITAL COMPUTER CODE FOR SIMULATING LARGE MULTISTAGE FLASH EVAPORATOR DESALTING PLANT DYNAMICS. Delene, J. G.; Ball, S. J. (Oak Ridge National Lab., Tenn.). Sep 1971. Contract W-7405-eng-26. 98p. Dep. NTIS.

**57249** (ORNL-TM-3536) CYTOFLUOROGRAPH SYSTEM. East, J. K.; Harris, W. W.; Moore, E. C.; Bell, P. R. (Oak Ridge National Lab., Tenn.). Oct 1971. Contract W-7405-eng-26. 9p. Dep. NTIS.

**57250** (ORNL-TM-3547) FOURIER ANALYSIS OF UNEQUALLY SPACED DATA. Patterson, M. R.; Hammerling, F. D. (Oak Ridge National Lab., Tenn.). 20 Sep 1971. 19p. Dep. NTIS.

**57251** (ORNL-tr-2509) FREEZE ETCHING OF CORRESPONDING FRACTURE MOIETIES: A NEW APPROACH TO MEMBRANE STRUCTURES. Sleytr, Uwe. Translated by R. Gregg Mansfield (Oak Ridge National Lab., Tenn.), from Protoplasma; 70: 101-17(1970). 16p. Dep. NTIS.

**57252** (ORNL-tr-2525) PLANNING AND EXECUTION OF THE MT. ENASAN TUNNEL. Esaki, Kenichiro; Nagatomo, Seiki. Translated for Oak Ridge National Lab., Tenn., from Doboku Gakkaishi; 54: 2-9(1969). 17p. Dep. NTIS.

**57253** (ORO-3195-41) SEQUENTIAL ADSORPTION ANALYSIS OF RADIOIODINATED PSEUDOGLOBULINS AS ILLUSTRATED BY THE IMMUNOLOGICAL DISTINCTION BETWEEN BRAIN AND LIVER MITOCHONDRIA. Day, Eugene D.; McMillan, Paul N.; Mickey, Don D. (Duke Univ., Durham, N. C. Dept. of Microbiology and Immunology). [1971]. Contract AT(40-1)-3195. 19p. Dep. NTIS.

**57254** (ORO-3195-42) SPECIFICITY AND CROSS-REACTIVITY OF ANTISYNAPTOSOME ANTIBODIES AS DETERMINED BY SEQUENTIAL ADSORPTION ANALYSIS. Mickey, Don D.; McMillan, Paul N.; Appel, Stanley H.; Day, Eugene D. (Duke Univ., Durham, N. C. Dept. of Microbiology and Immunology). [1971]. Contract AT(40-1)-3195. 26p. Dep. NTIS.

**57255** (ORO-3195-43) SPECIFICITY AND CROSS-REACTIVITY OF ANTIMYELIN ANTIBODIES AS DETERMINED BY SEQUENTIAL ADSORPTION ANALYSIS. McMillan, Paul N.; Mickey, Don D.; Kaufman, Bernard; Day, Eugene D. (Duke Univ., Durham, N. C. Medical Center). [1971]. Contract AT(40-1)-3195. 21p. Dep. NTIS.

**57256** (ORO-3195-44) ZONAL CENTRIFUGE PROFILE ANALYSIS OF MSD MUTANT MOUSE BRAIN. THE LOSS OF THE THREE-PEAK MYELIN PROFILE WITH THE ONSET OF SYMPTOMS. Day, Eugene D.; Mickey, Don D.; McMillan, Paul N.; Meier, Hans (Duke Univ., Durham, N. C. Dept. of Microbiology and Immunology. Jackson Lab., Bar Harbor, Maine). [1971]. Contract AT(40-1)-3195. 29p. Dep. NTIS.

**57257** (ORO-3195-45) FLOTATION-FRACTIONATION OF LATE FETAL, NEONATAL, AND ADULT RAT BRAIN IN ISO-OSMOTIC FICOLL-SUCROSE DENSITY-GRADIENTS. A PRELIMINARY REPORT ON THE PROBABLE ISOLATION OF GLIAL CELL MEMBRANES. Mickey, Don D.; McMillan, Paul N.; Day, Eugene D. (Duke Univ., Durham, N. C. Dept. of Microbiology and Immunology). [1971]. Contract AT(40-1)-3195. 16p. Dep. NTIS.

**57258** (ORO-3195-46) ISOLATION AND BIOCHEMICAL CHARACTERIZATION OF THREE SUBFRACTIONS OF ADULT RAT CENTRAL NERVOUS TISSUE MYELIN. McMillan, Paul N.; Mickey, Don D.; Kaufman, Bernard; Day, Eugene D. (Duke Univ., Durham, N. C. Medical Center). [1971]. Contract AT(40-1)-3195. 21p. Dep. NTIS.

**57259** (ORO-3195-47) CELLULAR AND SUBCELLULAR FRACTIONATION OF BRAIN TISSUE. Appel, Stanley H.; Day, Eugene D.; Mickey, Don D. (Duke Univ., Durham, N. C. Medical Center). [1971]. Contract AT(40-1)-3195. 51p. Dep. NTIS.

**57260** (ORO-3195-48) INCORPORATION OF [$^{14}$C]-GLUCOSAMINE INTO SYNAPTOSOMES IN VITRO. Festoff, B. W.; Appel, Stanley H.; Day, Eugene (Duke Univ., Durham, N. C. Medical Center). [1971]. Contract AT(40-1)-3195. 39p. Dep. NTIS.

**57261** (ORO-3195-49) HETEROGENEITY OF CENTRAL NERVOUS SYSTEM MYELIN AS DISCERNED BY ISOTOPIC LABELING AND CHEMICAL ANALYSIS. Daniel, Amiram; Day, Eugene D.; Kaufman, Bernard (Duke Univ., Durham, N. C. Dept. of Microbiology and Immunology). [1971]. Contract AT(40-1)-3195. 32p. Dep. NTIS.

**57262** (ORO-3195-50) VIRUS-CELL RELATIONSHIPS IN DOG BRAIN TUMORS INDUCED WITH SCHMIDT-RUPPIN ROUS SARCOMA VIRUS. Bigner, Darell D.; Vick, Nicholas A.; Kvedar, John P.; Mahaley, M. S. Jr.; Day, Eugene D. [Duke Univ., Durham, N. C. Medical Center]. [1971]. 27p. Dep. NTIS.

**57263** (ORO-3195-51) IN VITRO DEMONSTRATION OF CELL-MEDIATED IMMUNITY TO HUMAN BRAIN TUMORS. Levy, Nelson L.; Mahaley, M. S. Jr.; Day, Eugene D. (Duke Univ., Durham, N. C. Medical Center). [1971]. Contract AT(40-1)-3195. 28p. Dep. NTIS.

XUM

**57264** (ORO-3553-17) FLUORESCENCE PROPERTIES OF PYRIDOXAL-5-PHOSPHATE ENZYMES. Progress Report, June 1, 1970–May 1, 1971. (Tennessee Univ., Knoxville). 25 May 1971. Contract AT(40-1)-3553. 19p. Dep. NTIS.

**57265** (ORO-3883-3) [STUDIES ON THE BIOCHEMISTRY OF DEVELOPMENT IN THE DIPTERA.] Comprehensive Progress Report, January 1, 1969–September 15, 1971. Dobrogosz, Walter J. (North Carolina State Univ., Raleigh. Dept. of Microbiology). Contract AT(40-1)-3883. 7p. Dep. NTIS.

**57266** (RLO-1929-16) TRACKING AND TELEMETRY SYSTEM FOR WILDLIFE RESEARCH. Varney, Joel R. (Montana Cooperative Wildlife Research Unit, Missoula). [1971]. 6p. (CONF-710438-1). Dep. NTIS.
From National telemetering conference; Washington, D. C. (12 Apr 1971).

**57267** (SC-DR-710438) DEVELOPMENT OF PROCESSES FOR THE HOT PRESSING OF SILICON–GERMANIUM THERMOELECTRIC ELEMENTS. Dungan, R. H.; Smith, J. C. (Sandia Labs., Albuquerque, N. Mex.). Aug 1971. 30p. Dep. NTIS.

**57268** (SC-DR-710463) CURRENT SHAPING TECHNIQUES FOR HIGH-VOLTAGE CAPACITOR BANKS. Tucker, William K. (Sandia Labs., Albuquerque, N. Mex.). Aug 1971. 19p. Dep. NTIS.

**57269** (SC-DR-710472) FREQUENCY-FILTERING THEORY FOR THE PROPAGATION OF STRESS PULSES IN COMPOSITE MATERIALS. Drumheller, D. S. (Sandia Labs., Albuquerque, N. Mex.). Jul 1971. 25p. Dep. NTIS.

**57270** (SC-M-710527) EDIT PROGRAM OPERATING MANUAL FOR THE PLAYBACK EXECUTIVE SYSTEM. Fienning, William C. (Sandia Labs., Albuquerque, N. Mex.). Sep 1971. 30p. Dep. NTIS.

**57271** (SC-RR-710475) RECEIVING PROPERTIES OF AN ASYMMETRIC CYLINDRICAL ANTENNA. Licking, L. D. (Sandia Labs., Albuquerque, N. Mex.). Sep 1971. 18p. Dep. NTIS.

**57272** (SC-RR-710483) EFFECTS OF RF ACTIVATED INERT GAS PLASMAS ON CRITICAL SURFACE TENSION AND BONDABILITY OF POLYDIMETHYL SILICONES AND POLYETHYLENE. Sowell, R. R.; DeLollis, N. J.; Gregory, H. J.; Montoya, O. (Sandia Labs., Albuquerque, N. Mex.). Sep 1971. 12p. Dep. NTIS.

**57273** (SC-RR-710519) RESPONSE OF A SHORT MONOPOLE ANTENNA MOUNTED ON THE SKIN OF A FINITE-LENGTH CYLINDER. Licking, L. D. (Sandia Labs., Albuquerque, N. Mex.). Sep 1971. 14p. Dep. NTIS.

**57274** (SC-RR-710541) DENSITY OF THE NEUTRAL ATMOSPHERE ABOVE 100 km, KAUAI, MAY–JUNE 1970. Woods, R. O. (Sandia Labs., Albuquerque, N. Mex.). Sep 1971. 18p. Dep. NTIS.

**57275** (SC-T-713060) INTERACTIONS AMONG VARIOUS CARBONS IN THE COURSE OF HEAT TREATMENT. Cornualt, P.; Du Chaffaut, F.; Rappeneau, J.; Yvars, M.; Fillatre, A. Translated for Sandia Labs., Albuquerque, N. Mex., from Carbon; 6: 857-76(1968). 38p. Dep. NTIS.

**57276** (SC-T-713061) DIFFUSION-CONTROLLED GROWTH OF TWO-PHASE COVERING LAYERS IN BINARY SYSTEMS. Fromm, Eckehard. Translated for Sandia Labs., Albuquerque, N. Mex., from Z. Metallk.; 57: 60-5(1966). 20p. Dep. NTIS.

**57277** (SC-T-713063) TRANSMISSION LINE CONSTANTS OF COUPLED MICROSTRIP. Braeckelmann, Walter. Translated by R. J. Erlandson (Sandia Labs., Albuquerque, N. Mex.), from NTZ-Nachrtech. Z.; 24: No. 3, 157-60(Mar 1971). 10p. Dep. NTIS.

**57278** (SC-T-713066) CARBON BLACK FORMATION IN THE THERMAL DECOMPOSITION OF HYDROCARBONS. Rafal'kes, I. S.; Tesner, P. A. Translated by Pat Newman (Sandia Labs., Albuquerque, N. Mex.), from Tr., Vses. Nauch.-Issled. Inst. Prir. Gazov; No. 3, 3-33(1958). 54p. Dep. NTIS.

**57279** (SC-T-713067) MEASUREMENT PROGRAM AND CALIBRATION STANDARDS FOR MICROSTRIP MEASUREMENTS WITH AN AUTOMATIC NETWORK ANALYZER. Reich, Volker. Translated by Pat Newman (Sandia Labs., Albuquerque, N. Mex.), from NTZ-Nachrtech. Z.; 24: No. 5, 255-9(1971). 20p. Dep. NTIS.

**57280** (SCL-DR-69-155) PNEUMATIC HAMMER DEVELOPMENT. Barr, V. C. (Sandia Labs., Livermore, Calif.). Sep 1971. Contract AT(29-1)-789. 74p. Dep. NTIS.

**57281** (SRO-641-2) RADIOACTIVE TRACER STUDIES OF SOIL AND LITTER ARTHROPOD FOOD CHAINS. Summary Report, November 1, 1968–October 31, 1971. Crossley, D. A. Jr. (Georgia Univ., Athens). 10 Aug 1971. Contract AT(38-1)-641. 87p. Dep. NTIS.

**57282** (TID-25789) ANNUAL TECHNICAL PROGRESS REPORT, OCTOBER 1, 1970–JUNE 1, 1971. PART 1. (Illinois Univ., Urbana. Dept. of Computer Science). 3 Jun 1971. Contract AT(11-1)-2118. 46p. Dep. NTIS.

**57283** (TID-25790) PLANETARY QUARANTINE PROGRAM. Twenty-First Quarterly Report of Progress for Period Ending June 30, 1971. (Sandia Labs., Albuquerque, N. Mex.). Contract W-12,853. 85p. Dep. NTIS.

**57284** (TID-25802) CONTROL OF LYMPHOCYTE GROWTH IN RESPONSE TO PHYTOHEMAGGLUTININ STIMULATION. Rubin, Arnold D. (Mount Sinai School of Medicine, New York). [1970]. Contract AT(30-1)-3833. 14p. Dep. NTIS.

**57285** (TRG-Report-1813) TRESS: A FINITE ELEMENT CODE FOR STRESS ANALYSIS PROBLEMS. Collier, W. D.; Ellington, J. P.; Rees, P. M. (United Kingdom Atomic Energy Authority, Risley (England). Reactor Group). 1971. 77p. Dep. NTIS (U. S. Sales Only). UK 50p.

**57286** (UCLA-12-832) ISOLATION OF HIGH MOLECULAR WEIGHT RNAs FROM CULTURED NEURAL TUMOR CELLS. Edwards, Ross B.; de Vellis, Jean (California Univ., Los Angeles. Lab. of Nuclear Medicine and Radiation Biology). [1971]. Contract AT(40-1)-Gen-12. 6p. Dep. NTIS.

**57287** (UCRL-51075) NUMERICAL CALCULATION (SOC) vs EXPERIMENTAL DATA FOR WESTERLY GRANITE. Brown, Stephen R. (California Univ., Livermore. Lawrence Radiation Lab.). 22 Jun 1971. 55p. Dep. NTIS.

**57288** (UCRL-51088) DYE LASER PERFORMANCE ENHANCEMENT BY CHEMICAL QUENCHING OF THE TRIPLET STATE. Marling, John B. (California Univ., Livermore. Lawrence Radiation Lab.). 6 Jul 1971. Contract W-7405-eng-48. 101p. Dep. NTIS.
Thesis.

**57289** (UCRL-51098) LOW-VELOCITY AIR GUN AND HOPKINSON SPLIT-BAR FACILITY. Wasley, Richard J.; Cast, John C.; Hoge, Kenneth G.; Breithaupt, R. Don (California Univ., Livermore. Lawrence Radiation Lab.). 16 Jul 1971. Contract W-7405-eng-48. 16p. Dep. NTIS.

**57290** (UCRL-Trans-10539) APPROXIMATIVE METHOD OF CALCULATING PHYSICAL QUANTITIES BEHIND A SHOCK-WAVE FRONT. Kuropatenko, V. R. Translated by T. Watt for Univ. of California, Lawrence Radiation Lab., Livermore, from Chislennye Metody Mekh. Sploshnoi Sredy; 1: No. 5, 77-83(1970). 17p. Dep. NTIS.

**57291** (UR-49-1515) DETERMINATION BY X-RAY DIFFRACTION OF CRYSTAL STRUCTURES OF SILVER DIETHYLPHOSPHATE AND POTASSIUM O, O-DIBENZYLPHOSPHORODITHIOATE. Hazel, John P. (Rochester Univ., N. Y. Dept. of Radiation Biology and Biophysics). 1971. 50p. Dep. NTIS.
Thesis.

**57292** (UR-49-1516) THERMODYNAMIC AND CONFORMATIONAL ASPECTS OF THE NOVOBIOCIN–SERUM ALBUMIN COMPLEX. Brand III, Joseph G. (Rochester Univ., N. Y. Dept. of Radiation Biology and Biophysics). 1971. 133p. Dep. NTIS.
Thesis.

**57293** (UR-49-1517) INTERACTIONS OF SULFATE AND PHOSPHATE ANIONS WITH ALKALINE EARTH CATIONS IN

CRYSTALS. Murfitt, Robert Roscoe (Rochester Univ., N. Y. Dept. of Radiation Biology and Biophysics). 1971. 116p. Dep. NTIS.
Thesis.

**57294** (WASH–1132) SCIENCE AND SOCIETY. A Bibliography. Voress, Hugh E. (comp.) (Division of Headquarters Services (AEC), Washington, D. C.). Jul 1971. 21p. (TID–3916(Suppl.1)). GPO $0.35.

**57295** (Y–1790) PROPERTIES OF CARBON DERIVED FROM INDENE COMPOUNDS. Smith, W. E.; Horne, O. J. Jr.; Napier, B. Jr.; Larson, E. A.; Harper, W. L. (Union Carbide Corp., Oak Ridge, Tenn. Y-12 Plant). 15 Sep 1971. Contract W-7405-eng-26. 134p. Dep. NTIS.

**57296** (Y-IA–92) PRIMARY FREQUENCY STANDARDS IN THE Y-12 PHYSICAL AND ELECTRICAL STANDARDS LABORATORY. Wolny, R. F. (Union Carbide Corp., Oak Ridge, Tenn. Y-12 Plant). 20 Sep 1971. Contract W-7405-eng-26. 13p. Dep. NTIS.

XUM

# CORPORATE AUTHOR INDEX

In the Corporate Author Index, technical report literature is indexed by the organization or institution responsible for issuing the report. Entries are given for all report literature and for published literature for which a corporate author approach is especially desirable, e.g., symposium and conference proceedings.

Each entry under a corporate author gives the publication title and the *NSA* volume and abstract numbers. Report numbers, where applicable, are given in parentheses at the end of the entry.

## A


AKADEMIYA NAUK SSSR, LENINGRAD. FIZIKO-TEKHNICHESKII INSTITUT.
Determination of the boundary of high frequency wave absorption between the electron cyclotron and the low hybrid frequency, 25:56224 (AEC-tr-7270)

AKADEMIYA NAUK SSSR, MOSCOW. INSTITUT FIZICHESKOI KHIMII.
Nature and properties of trapped electrons in polar substances, 25:54593 (CONF-700652-(Vol.2), pp 261-93)

AKADEMIYA NAUK SSSR, MOSCOW. INSTITUT FIZIKI.
Excitation of longitudinal electromagnetic waves in a bound plasma during injection of relativistic electron beams, 25:56232 (NP-19020)
Problems of injection of relativistic electron beams into plasma, 25:56166 (NP-19012)

AKADEMIYA NAUK SSSR, NOVOSIBIRSK. INSTITUT YADERNOI FIZIKI.
Charge-exchange method of proton injection into accelerators and accumulators, 25:56590 (LA-tr-71-46)

AKADEMIYA NAUK UKRAINSKOI SSR, KHARKOV. FIZIKO-TEKHNICHESKII INSTITUT.
Resonance effects in magnetic configurations having a helical magnetic axis, with allowance for toroidality, 25:56209 (CTO-764)

ALABAMA POWER CO., BIRMINGHAM.
Joseph M. Farley Nuclear Plant, Units No. 1 and No. 2. Preliminary safety analysis report, amendment No. 20, 25:56964 (DOCKET-50348-24)
Joseph M. Farley Nuclear Plant, Units No. 1 and No. 2. Preliminary safety analysis report, amendment No. 22, 25:56966 (DOCKET-50348-26)
Joseph M. Farley Nuclear Plants, Units 1 and 2. Preliminary safety analysis report, amendment 21, 25:56965 (DOCKET-50348-25)

ALBERTA UNIV., EDMONTON. DEPT. OF CHEMISTRY.
Progress and problems in the radiolysis of alcohols, 25:54629 (CONF-700652-(Vol.3), pp 479-521)

AMERICAN NUCLEAR SOCIETY, HINSDALE, ILL.
Conference on new developments in reactor mathematics and applications, Idaho Falls, Idaho, 3/71, 25:57147 (CONF-710302-(Vol.2))
Conference on new developments in reactor mathematics and applications, Idaho Falls, Idaho, 3/71, 25:57071 (CONF-710302-(Vol.1))

AMERICAN NUCLEAR SOCIETY. EASTERN IDAHO SECTION.
Conference on new developments in reactor mathematics and applications, Idaho Falls, Idaho, 3/71, 25:57147 (CONF-710302-(Vol.2))
Conference on new developments in reactor mathematics and applications, Idaho Falls, Idaho, 3/71, 25:57071 (CONF-710302-(Vol.1))

AMES LAB., IOWA.
An optical mixing spectroscopic study of interfacial fluctuations, 25:57232 (IS-T-494)
Small angle tilt and twist grain boundary strengthening in yttrium, 25:55430 (IS-T-459)
Survey of environmental radioactivity, 1--6/71, 25:55152 (IS-2658)
Thermodynamics of formation of compounds in the Ce--Mg, Nd--Mg, Gd--Mg, Dy--Mg, Er--Mg, and Lu--Mg systems from vapor pressure measurements, 25:55525 (IS-T-462)
Use of simplotter: a high-level plotting system, 25:57231 (IS-2305)

ARGONNE NATIONAL LAB., IDAHO FALLS, IDAHO.
Equipment for remote measurement of bow, length, and weight of irradiated experimental capsules and elements at EBR-II. EBR-II Project, 25:57054 (ANL-EBR-30)
Numerical stability problems in the VENUS disassembly code, 25:57079 (CONF-710302-(Vol.1), pp 152-66)
Operating experience with sodium pumps at EBR-II. EBR-II Project, 25:57028 (ANL-EBR-27)

ARGONNE NATIONAL LAB., ILL.
Analysis of fuel failure experiments with TREAT, 25:57110 (CONF-710302-(Vol.1), pp 97-101)
Applications of space-energy factorization to the solution of static fast-reactor neutronics problems, 25:57170 (CONF-710302-(Vol.2), pp 953-67)
ARC system cross-section homogenization and modification capabilities, 25:56614 (ANL-7714)
Behavior and calibration of devices for monitoring impurities in sodium, 25:55069 (ANL-7804)
Comparison between momentum integral and compressible models for sodium voiding calculations in LMFBR, 25:57081 (CONF-710302-(Vol.1), pp 180-98)
Computer performance measurements using the Argonne benchmark problem collection: a status report, 25:57167 (CONF-710302-(Vol.2), pp 901-12)
Conversion of the Argonne Reactor Computation (ARC) System to control data 6000 and 7000 series equipment, 25:57140 (CONF-710302-(Vol.1), pp 464-71)
Engineering relationships for turbulent forced-convection heat transfer in ducts with flux transients, 25:54864 (ANL-7754)
Inert atmosphere management and surveillance at the Argonne National Laboratory Fuels Technology Center, 25:54945 (CONF-710401-, pp 98-105)
Integral measurements in EBR-II of capture rates, fission rates, and $\alpha$ for $^{233}U$, $^{235}U$, $^{238}U$, $^{239}Pu$, $^{240}Pu$, and $^{242}Pu$, 25:56982 (ANL-7791)
LMFBR Nuclear Safety Program. Annual report, July 1, 1969--June 30, 1970, 25:57069 (ANL-7800)
Materials-coolant interactions relevant to EBR-II, 25:57109 (ANL-7771)
New multigroup cross section code, MC$^2$--2, 25:57171 (CONF-710302-(Vol.2), pp 968-82)
Plume rise calculations using selected functional forms and the tabulation prediction technique, 25:54780 (CONF-710505-6)
Pressure generation by molten fuel-coolant interactions under LMFBR accident conditions, 25:57073 (CONF-710302-(Vol.1), pp 25-49)
Proposal for P$^3$: versatile high-energy pion beam facility, 25:56588 (LA-4535)
Reactions of the hydrated electron with organic compounds, 25:54631 (CONF-700652-(Vol.3), pp 601-48)
SAS2A LMFBR accident analysis code, 25:57077 (CONF-710302-(Vol.1), pp 120-7)
Two-dimensional fast-reactor disassembly analysis with space-time kinetics, 25:57078 (CONF-710302-(Vol.1), pp 128-51)
Users experience with the ARC system, 25:57142 (CONF-710302-(Vol.1), pp 478-93)

ARIZONA STATE UNIV., TEMPE.
Berkelium--oxygen system, 25:55428 (BNWL-B-108)

ARIZONA STATE UNIV., TEMPE. DEPT. OF ZOOLOGY.
Prog. rpt. on congenital malformations, 1--12/71, 25:57222 (COO-2013-19)

ARIZONA UNIV., TUCSON. DEPT. OF PHYSICS.
Prog. rpt. on high temperature anneals of defects quenched in metals, final, 1971, 25:57216 (COO-1456-16)

ARKANSAS POWER AND LIGHT CO., LITTLE ROCK.
Arkansas Nuclear One, Unit No. 1. Final safety analysis report, amendment No. 21, 25:56959 (DOCKET-50313-31)

ARMY TEST AND EVALUATION COMMAND, ABERDEEN PROVING GROUND, MD.
Nuclear yield measuring devices, 25:54993 (AD-720974)

ATLANTIC RICHFIELD HANFORD CO., RICHLAND, WASH.
Administrative procedures for criticality prevention in plutonium operations, 25:54966 (CONF-710401-, pp 430-7)
Description of ARHCO's new compact plutonium storage facility, 25:54942 (CONF-710401-, pp 56-67)
Fire protection test facility for cells and caves, 25:54956 (CONF-710401-, pp 237-47)
Human element design considerations with gloveboxes at the Atlantic Richfield Hanford Company, 25:54938 (CONF-710401-, pp 4-16)
Problems associated with $^{238}Pu$ processing, 25:54707




XUM

(CONF-710401-, pp 300-6)
ATOMIC ENERGY COMMISSION, WASHINGTON, D. C.
Compaction of radioactive solid waste, 25:54975 (WASH-1167)
ATOMIC ENERGY ESTABLISHMENT, WINFRITH (ENGLAND).
Boiling on surfaces overlayed with a porous deposit: heat transfer rates obtainable by capillary action, 25:54862 (AEEW-R-711)
Investigation into effect of ''crud'' deposits on surface temperature, dry-out and pressure drop, with forced convection boiling of water at 69 bar in annular test section, 25:54861 (AEEW-R-705)
ATOMIC ENERGY OF CANADA LTD., CHALK RIVER (ONTARIO).
Biological significance of radioactive releases to the environment, 25:55194 (70-CNA-641)
PRESCON: a digital computer program for containment pressure transients, 25:57087 (CONF-710302-(Vol.1), pp 436-51)
ATOMIC ENERGY OF CANADA LTD., CHALK RIVER (ONTARIO). CHALK RIVER NUCLEAR LABS.
Cosmic ray NM-64 neutron monitor data. XVIII, 25:55893 (AECL-3971)
PRESCON: a digital computer program for containment pressure transients, 25:57087 (CONF-710302-(Vol.1), pp 436-51)
Prog. rpt. on chemistry and materials, 1--3/71, 25:54587 (AECL-3909)
Prog. rpt. on physics, 1--3/71, 25:56733 (AECL-3912)
ATOMIC ENERGY OF CANADA LTD., PINAWA (MANITOBA). WHITESHELL NUCLEAR RESEARCH ESTABLISHMENT.
Effect of temperature, pressure and concentration gradients on diffusion, 25:57213 (AECL-3793)
ATOMIC POWER DEVELOPMENT ASSOCIATES, INC., DETROIT, MICH.
Applications software for a fast reactor malfunction detector analyzer, 25:56878 (CONF-710302-(Vol.1), pp 199-214)
ATOMIC WEAPONS RESEARCH ESTABLISHMENT, ALDERMASTON (ENGLAND).
Fibre reinforced materials, 25:57214 (AWRE-O-77/70)
ATOMICS INTERNATIONAL, CANOGA PARK, CALIF.
Evaluation of fuel-coolant interactions during disassembly of an LMFBR, 25:57074 (CONF-710302-(Vol.1), pp 50-78)
Forced-flow sodium boiling in multiple channels, 25:54863 (AI-AEC-13010)
LMFBR safety programs. Annual technical progress report, GFY 1971, 25:57068 (AI-AEC-13006)
Reference zirconium hydride reactor, 25:57132 (AI-AEC-Memo-12715(Del.))
Status of data testing using the ENDF/B library, 25:57178 (CONF-710302-(Vol.2), pp 1053-64)
AUSTRAL OIL CO., INC., HOUSTON, TEX.
Project Rulison. Post-Shot Test Data, 25:54817 (PNE-R-52)
AUSTRALIAN ATOMIC ENERGY COMMISSION RESEARCH ESTABLISHMENT, LUCAS HEIGHTS.
Experimental investigation of fission, 25:56743 (NP-18966)
Potential--pH diagrams at temperatures above 298.16°K. I, 25:57212 (AAEC/E-219(Pt.1))

## B

BABCOCK AND WILCOX CO., LYNCHBURG, VA.
Local flow blockage effects in an LMFBR fuel pin bundle, 25:57076 (CONF-710302-(Vol.1), pp 102-19)
BABCOCK AND WILCOX CO., LYNCHBURG, VA. RESEARCH AND DEVELOPMENT DIV.
Prog. rpt. on physics verification program, Pt. III, Task 5, 4--6/71, 25:57017 (BAW-3647-22)
Safety considerations at the Babcock and Wilcox Plutonium Development Laboratory, 25:54958 (CONF-710401-, pp 258-66)
BARTOL RESEARCH FOUNDATION, SWARTHMORE, PA.
Studies of electromagnetic properties of excited states of nuclei. Final report, March 15, 1965--March 14, 1971, 25:56832 (NYC-3525-67)
BATTELLE MEMORIAL INST., COLUMBUS, OHIO.
Battelle's research plutonium facility environmental control and safety, 25:54959 (CONF-710401-, pp 280-92)
BATTELLE-NORTHWEST, RICHLAND, WASH. PACIFIC NORTHWEST LAB.
Comparative metabolism of intravenously injected prosethium in swine and humans, 25:55108 (BNWL-SA-3747)
Comparison of maximum exposures at ground level resulting from simultaneous release of tracers from elevations of 2 and 26 meters, 25:56395 (BNWL-1551(Vol.2)(Pt.1), pp 108-12)
Corrosion and deposition of irradiated stainless steel in sodium, 25:55370 (BNWL-SA-2335)
Integrated lanthanide--actinide solvent extraction process, 25:54706 (BNWL-SA-3345)
Prog. rpt. on isotope development, 2--4/71, 25:54887 (BNWL-1308-6)
Swelling in refractory metals during high temperature ion bombardment, 25:55573 (BNWL-SA-3962)
BATTELLE PACIFIC NORTHWEST LABS., RICHLAND, WASH.
Berkelium--oxygen system, 25:55428 (BNWL-B-108)
BNW program noise, 25:57181 (BNWL-1609)
Effect of strain rate and temperature on the tensile properties of Pu--1 wt percent Ga alloys, 25:55427 (BNWL-1567)
Influence of the physico-chemical forms of radionuclides and stable trace elements in seawater in relation to uptake by the marine biosphere, 25:55149 (BNWL-SA-4048)
Nuclear power plant in the nuclear material safeguards accounting system, 25:54934 (BNWL-1598)
Status of burnup calculational technology as applied to the nuclear materials safeguards accounting system, 25:54935 (BNWL-1599)
BETTIS ATOMIC POWER LAB., PITTSBURGH, PA.
Arrangement of ordinates in deep-penetration cylindrical and X--Y S/sub n/ calculations, 25:57153 (CONF-710302-(Vol.2), pp 617-24)
Bibliography on electrical discharge machining and electrochemical machining, 25:54834 (WAPD-331)
Convergence of the weighted diamond difference approximations to the discrete ordinate equations, 25:57150 (CONF-710302-(Vol.2), pp 565-76)
Phenomenological model of in-pile stress relaxation (LWBR Development Program), 25:55579 (WAPD-TM-943)
PSKIT: CDC-6600 computer programming package providing easy use of FINK/PANTRY, 25:57144 (CONF-710302-(Vol.1), pp 505-7)
S/sub n/ programming techniques, 25:57148 (CONF-710302-(Vol.2), pp 557-60)
Stability calculational procedure for flow-induced vibrations of reactor internals in parallel flow, 25:57086 (CONF-710302-(Vol.1), pp 356-9)
BRIGHAM YOUNG UNIV., PROVO, UTAH.
Prog. rpt. on electrochemical cells using alkali metals and charge transfer complexes, 5/67--8/71, 25:57221 (COO-1707-12)
Prog. rpt. on solid-liquid phase equilibria in the ternary sodium--potassium--rubidium alloy system, 5/67--8/71, 25:55524 (COO-1707-11)
BROOKHAVEN NATIONAL LAB., UPTON, N. Y.
ENDF/B library: a current status report, 25:57173 (CONF-710302-(Vol.2), pp 991-1003)
PSYCHE: physics checking of the ENDF/B evaluated nuclear data file, 25:57174 (CONF-710302-(Vol.2), pp 1004-15)
Recent developments in pulsed magnet multifilament superconducting wires, 25:56580 (BNL-16026)
BROOKLYN COLL., N. Y. DEPT. OF CHEMISTRY.
Prog. rpt., 6/70--5/71, 25:54692 (NYO-3417-15)
BROWN, BOVERI UND CIE A. G., MANNHEIM (WEST GERMANY).
Corrosion of gas turbine alloys in molten salts of high $V_2O_5$ and low Na content, 25:55375 (CONF-690452-, Paper 8)
BRUSSELS UNIV. (BELGIUM).
Microscopic description and cluster structure of light nuclei, 25:56654 (LYCEN-7104, S13.1-11)
BUREAU OF RADIOLOGICAL HEALTH, MONTGOMERY, ALA. DIV. OF MEDICAL RADIATION EXPOSURE.
Storage and handling devices for radium, 25:54936 (BRH/DMRE-71-3)

## C

CALIFORNIA INST. OF TECH., PASADENA.
Regge models of forward pion and eta photoproduction, 25:56452 (CALT-68-313)
CALIFORNIA UNIV., BERKELEY. DEPT. OF NUCLEAR ENGINEERING.
DP-O method according to a variational treatment that extends its applicability to all geometries, 25:57152 (CONF-710302-(Vol.2), pp 608-16)
CALIFORNIA UNIV., BERKELEY. LAWRENCE BERKELEY LAB.
Large-area high-current ion source, 25:56212 (LBL-35)
Multiple aperture extractor design for producing intense ion and neutral beams, 25:56213 (LBL-327)
Reactive scattering of $N_2O$ molecular beams from clean and carbon covered (100) platinum single crystal surfaces, 25:57237 (LBL-133)
CALIFORNIA UNIV., DAVIS. RADIOBIOLOGY LAB.
Prog. rpt. on radiobiology, annual, 1971, 25:55319 (UCD-472-118)
CALIFORNIA UNIV., LIVERMORE. LAWRENCE LIVERMORE LAB.
Numerical calculation vs experimental data for Westerly granite, 25:57287 (UCRL-51075)
CALIFORNIA UNIV., LIVERMORE. LAWRENCE RADIATION LAB.
Comparison of U.S. and U.S.S.R. methods of calculating the transport, diffusion, and deposition of radioactivity, 25:54782 (UCRL-51054)
Dye laser performance enhancement by chemical quenching of the triplet state, 25:57288 (UCRL-51088)
Engineering fire-suppression systems for large volumes using Halon 1301, 25:54957 (CONF-710401-, pp 248-56)
Facility for the determination of low-level tritium in biological and environmental samples, 25:55003 (UCRL-73128)
Gamma-ray energies and absolute branching intensities for $^{238}$ $^{239}$ $^{240}$ $^{241}$Pu and $^{241}$Am, 25:56753 (UCRL-51087)
In-residence health and safety support in a plutonium facility, 25:55204 (CONF-710401-, pp 267-79)
Intense 1-kV ion source for controlled fusion research, 25:56217 (UCRL-73387)
Ion source technology, 25:55814 (UCRL-73353)
Low-velocity air gun and Hopkinson split-bar facility, 25:57289 (UCRL-51098)
Production of intense ion and neutral beams with energies

below 10 keV, 25:56218 (UCRL-73412)
Stimulated Compton energy exchange rate, 25:56266 (UCRL-51065)

CALIFORNIA UNIV., LOS ANGELES.
Axial kinetics model for fast reactor disassembly accidents, 25:57080 (CONF-710302-(Vol.1), pp 167-79)

CALIFORNIA UNIV., LOS ANGELES. DEPT. OF CHEMISTRY.
Prog. rpt. on intra- and inter-molecular energy transfer studies, 5/70--5/71, 25:54600 (UCLA-34-P-88-32)

CALIFORNIA UNIV., LOS ANGELES. LAB. OF NUCLEAR MEDICINE AND RADIATION BIOLOGY.
Isolation of high molecular weight RNAs from cultured neural tumor cells, 25:57286 (UCLA-12-832)

CANATOM LTD., MONTREAL (QUEBEC).
Industry reports: Canadian consultants and the Canadian nuclear industry, 25:57211 (70-CNA-657)
Operating experience with other reactors, 25:56893 (70-CNA-631)
Problems of comparing power reactors for specific application, 25:57059 (70-CNA-628)

CAROLINA POWER AND LIGHT CO., RALEIGH, N.C.
Brunswick Steam Electric Plant, Units No. 1 and No. 2. ECCS conformance to new AEC adopted interim acceptance criteria, 25:56960 (DOCKET-50324-22)
H. B. Robinson Unit No. 2. Emergency core cooling performance, 25:56945 (DOCKET-50261-73)
Shearon Harris Nuclear Power Plant, Units 1, 2, 3, and 4. License application, 25:56974 (DOCKET-50400-1)

CENTRAL ELECTRICITY GENERATING BOARD, BERKELEY (ENGLAND). BERKELEY NUCLEAR LABS.
Application of small angle x-ray scattering to the study of irradiation produced defects, 25:55578 (RD/B/N-1990)
Delta spectrometer results on water reactor shields, 25:55043 (RD/B/N-2034)
Heat transfer and pressure drop performance of roughened surfaces, 25:54874 (RD/B/N-1980)
MIMUSA: a FORTRAN IV subroutine for unfolding spectra. II, 25:55042 (RD/B/N-1963)

CENTRAL ELECTRICITY GENERATING BOARD, BRISTOL (ENGLAND). BERKELEY NUCLEAR LABS.
Estimation of friction factor of rough surfaces from the pressure distribution around a roughness element, 25:54873 (RD/B/N-1967)

CENTRE D'ETUDE DE L'ENERGIE NUCLEAIRE, MOL (BELGIUM).
Fast neutron irradiation induced swelling of metals and alloys, 25:55572 (BLG-457)

CENTRE NATIONAL DE LA RECHERCHE SCIENTIFIQUE, MARSEILLES (FRANCE). CENTRE DE PHYSIQUE THEORIQUE.
Divergences of massive Yang--Mills theories: higher groups, 25:56542 (CNRS-CPT-71/P-378)

CENTRE NATIONAL DE LA RECHERCHE SCIENTIFIQUE, PARIS (FRANCE).
Weak interactions and the vector dominance model, 25:56468 (FRNC-R-1)

CENTRE NATIONAL DE LA RECHERCHE SCIENTIFIQUE, STRASBOURG (FRANCE). LABORATOIRE DE PHYSIQUE CORPUSCULAIRE.
π and K mesons used for investigating light nuclei structures, 25:56653 (LYCEN-7104, S4.1-10)
Substructures in $^{12}C$ and $^{14}N$, 25:56652 (LYCEN-7104, S2.1-2)

CENTRE NATIONAL DE LA RECHERCHE SCIENTIFIQUE, STRASBOURG (FRANCE). LABORATOIRE DE PHYSIQUE DES RAYONNEMENTS ET D'ELECTRONIQUE NUCLEAIRE.
Comments on the activated species in irradiated organic media, 25:54626 (CONF-700652-(Vol.1), pp 139-219)

CENTRE NATIONAL DE LA RECHERCHE SCIENTIFIQUE, STRASBOURG (FRANCE). LABORATOIRE DE PHYSIQUE THEORIQUE.
Methods for analyzing transfer reactions, 25:56823 (LYCEN-7104, C3.1-40)

CESKOSLOVENSKA AKADEMIE VED, REZ. USTAV JADERNEHO VYZKUMU.
Calculation of the sorption kinetics of radioactive microcomponent on a cation exchanger in the presence of competing ions in a batch arrangement, 25:54720 (UJV-2550-Ch)
Conference on progress and problems in contemporary radiation chemistry, Marianske Lazne, Czechoslovakia, 6/70, 25:54588 (CONF-700652-(Vol.1))
Conference on progress and problems in contemporary radiation chemistry, Marianske Lazne, Czechoslovakia, 6/70, 25:54592 (CONF-700652-(Vol.2))
Conference on progress and problems in contemporary radiation chemistry, Marianske Lazne, Czechoslovakia, 6/70, 25:54595 (CONF-700652-(Vol.3))
Current state of a priori yield predictions, 25:54590 (CONF-700652-(Vol.1), pp 51-136)
Hydrogen atoms as studied by ESR, 25:54628 (CONF-700652-(Vol.2), pp 367-420)
Radiation experiment on tubular fuel element with finned surface. II, 25:57050 (UJV-2551-RT)

CHALMERS TEKNISKA HOGSKOLA, GOTEBORG (SWEDEN). INSTITUTIONEN FOR TEORETISK FYSIK.
Prog. rpt., annual, 1970, 25:56441 (NP-18997)

CHEMTREE CORP., CENTRAL VALLEY, N.Y.
Materials for shielding nuclear radiations from plutonium processing, 25:54962 (CONF-710401-, pp 307-10)

COLORADO STATE DEPT. OF PUBLIC HEALTH, DENVER.
Environmental sampling. A critical look at common procedures, 25:54779 (CONF-710401-, pp 347-51)

COLORADO STATE UNIV., FORT COLLINS. DEPT. OF RADIOLOGY AND RADIATION BIOLOGY.
Plutonium movement in aquatic systems: a review, 25:55150 (CONF-710401-, pp 407-10)

COLUMBIA UNIV., NEW YORK.
Some new applications of indefinite metric to quantum electrodynamics and weak interactions, 25:56547 (NYO-1932(2)-200)

COLUMBIA UNIV., NEW YORK. RADIOLOGICAL RESEARCH LAB.
Biophysics, 25:55206 (NYO-2740-8, pp 147-219)
Prog. rpt. on research project, annual, 7/71, 25:55205 (NYO-2740-8)
Radiobiology, 25:55207 (NYO-2740-8, pp 220-59)
Radiological physics, 25:55002 (NYO-2740-8, pp 7-146)

COMBUSTION ENGINEERING, INC., WINDSOR, CONN.
Network organization of an automated nuclear design system, 25:57146 (CONF-710302-(Vol.1), pp 516-30)
Stability calculational procedure for flow-induced vibrations of reactor internals in parallel flow, 25:57086 (CONF-710302-(Vol.1), pp 356-9)

COMITATO NAZIONALE PER L'ENERGIA NUCLEARE, BOLOGNA (ITALY). CENTRO DI CALCOLO.
Analysis by a simulated measurement of neutron spectra, 25:56620 (RT/FI-(70)53)

COMITATO NAZIONALE PER L'ENERGIA NUCLEARE, FRASCATI (ITALY). LABORATORIO GAS IONIZZATI.
Basic steady state magnetic screw-field distributions in plasma between concentric boundaries, 25:56163 (LGI-70/16/E)
Calibration of the silver activated counters on a plasma focus experiment, 25:56214 (LGI-70/17/E)
Radiative recombination of hydrogenic ions in high temperature plasmas, 25:56164 (LGI-71/1/E)
Time-space resolved spectroscopic measurements on a fast z-pinch, 25:56150 (LGI-70/14/E)

COMITATO NAZIONALE PER L'ENERGIA NUCLEARE, ROME (ITALY).
Health protection analysis of transportation of radioactive substances through tunnels, 25:54973 (RT/PROT-(71)11)
Method of analysis of neutron capture gamma-ray spectra, 25:56690 (RT/FI-(70)47)
Neutron thermalization in polycrystalline material by Monte Carlo method, 25:56619 (RT/FI-(70)49)
Photographic study of two-phase highly dispersed flows, 25:54875 (RT/ING-(71)8)
Space time temperature distribution in a semi infinite medium under particular conditions of thermal transient, 25:54876 (RT/ING-(71)11)
Spin-dependence of level density in $^{178}Hf$ and $^{180}Hf$ by resonance neutron capture experiments, 25:56751 (RT/FI-(70)55)

COMMISSARIAT A L'ENERGIE ATOMIQUE, FONTENAY-AUX-ROSES (FRANCE). CENTRE D'ETUDES NUCLEAIRES.
Analysis of the safety problems due to fluorine and fluorine compounds, 25:55246 (CEA-Bib-200)
Coupling of EM waves in an inhomogeneous plasma, 25:56225 (CEA-CONF-1802)
Electrical equipment for measuring small currents. Applications to dosimetry using classical ionization chambers, liquid dielectric ionization chambers, and electric charge measurements in connection with aerosol studies, 25:55071 (CEA-N-1433)
Electromagnetic instabilities in a slightly relativistic plasma, 25:56228 (CEA-CONF-1806)
Interaction of a large-amplitude wave with a plasma: trapping, 25:56227 (CEA-CONF-1805)
MHD stability criterion in shallow magnetic well, 25:56194 (EUR-CEA-FC-598)
Multiply charged ion source. Design of electron gyromagnetic resonance source, 25:56210 (EUR-CEA-FC-603)
Prog. rpt. from neutron working group, 3/69--12/70, 25:55203 (CEA-N-1449)
Relative biological effectiveness as a function of linear energy transfer for cataract criterion in the rabbit, 25:55317 (CEA-CONF-1744)
Saturation and damping of echoes of electron plasma waves, 25:56226 (CEA-CONF-1804)
Space--time evolution of a plasma subjected to a discharge current, 25:56162 (CEA-CONF-1801)
Theoretical and experimental study of nonlinear processes in a plasma, 25:56229 (EUR-CEA-FC-602)

COMMISSARIAT A L'ENERGIE ATOMIQUE, GRENOBLE (FRANCE). CENTRE D'ETUDES NUCLEAIRES.
Nuclear thermal studies in France and their applications to other fields, 25:54865 (CEA-CONF-1758)

COMMISSARIAT A L'ENERGIE ATOMIQUE, LIMEIL-BREVANNES (FRANCE). CENTRE D'ETUDES.
Contribution to study of plasmas. An ultra rapid photometric camera, 25:56132 (CEA-R-4079)

COMMISSARIAT A L'ENERGIE ATOMIQUE, PARIS (FRANCE).
Nuclear explosions for peaceful purposes, 25:54819 (UCRL-Trans-10543, pp 1-3)

COMMISSARIAT A L'ENERGIE ATOMIQUE, SACLAY (FRANCE). CENTRE D'ETUDES NUCLEAIRES.
Deformations in the s--d shell and inelastic scattering of polarized protons, 25:56828 (LYCEN-7104, S9.1-7)
Electronic and magnetic properties of carbon fibers: development under neutron irradiation, 25:56282 (CEA-CONF-1822)
Generating coordinates in continuum states, 25:56825 (LYCEN-7104, C6.1-12)
Index of radiative lifetimes, 25:57215 (CEA-Bib-198)
Influence of speed of graphitization of carbon products


XUM

on dimensional variations produced by neutron irradiation, 25:55645 (CEA-CONF-1821)
Mechanical behavior of alloys $UMo_{1-x}Al_{0.05}Sn_{0.05}$ and Sicral $F_1$ (adjusted uranium) between 20 and 600°C, 25:55429 (CEA-R-4177)
Nuclear spectrometry at Saturne synchrotron, 25:56593 (LYCEN-7104, S7.1-2)
Pauli principle in the theory of reactions between light nuclei, 25:56829 (LYCEN-7104, S12.1-4)
Polarization parameter measurement in proton--proton elastic scattering from 0.5 to 1.2 GeV, 25:56412 (CEA-R-4193)
Reactions performed with polarized protons at Saclay, 25:56688 (LYCEN-7104, S6.1-2)
Relative biological effectiveness as a function of linear energy transfer for cataract criterion in the rabbit, 25:55317 (CEA-CONF-1744)
Shielding problems set by use of natural U target with linear electron accelerator. Shielding and safety systems necessary, 25:56582 (CEA-R-4188)
Spin--orbit interaction in nucleon inelastic scattering, 25:56826 (LYCEN-7104, C7.1-36)
Thermal annealing of neutron-irradiated carbon, 25:56283 (CEA-CONF-1823)
COMMONWEALTH EDISON CO., CHICAGO, ILL.
Dresden Nuclear Power Station. Facility license DPR-25, proposed change No. 7 to appendix A, 25:56909 (DOCKET-50249-101)
Dresden Nuclear Power Station, Unit 1. Unplanned release of radioactive liquid, 25:56896 (DOCKET-50010-95)
Dresden Nuclear Power Station, Unit 2. Technical specifications, Proposed Change No. 16, 25:56939 (DOCKET-50237-201)
Dresden Nuclear Power Station, Unit 3. Technical specifications, Proposed Change No. 8, 25:56942 (DOCKET-50249-102)
Zion Station, Units 1 and 2. Final safety analysis report, amendent No. 15, 25:56954 (DOCKET-50295-30)
COMPAGNIE PECHINEY, PARIS (FRANCE).
Influence of speed of graphitization of carbon products on dimensional variations produced by neutron irradiation, 25:55645 (CEA-CONF-1821)
CONSOLIDATED EDISON CO. OF NEW YORK, INC., NEW YORK.
Indian Point Station, Unit No. 1. Reply to inquiry relative to adequacy of Emergency Core Cooling System, 25:56926 (DOCKET-50003-89)
Indian Point Station, Unit No. 1. Technical specifications, proposed augmented in-service inspection program, 25:56927 (DOCKET-50003-90)
Indian Point Station, Unit No. 1. Technical specifications, proposed change limiting allowable rates of leakage, 25:56928 (DOCKET-50003-91)
CONSUMERS POWER CO., JACKSON, MICH.
Big Rock Point Nuclear Plant. Emergency core cooling system performance and core spray system modifications, 25:56935 (DOCKET-50155-92)
Palisades Plant. Incident involving the primary cooling system, 25:56910 (DOCKET-50255-53)
Palisades Plant. Two incidents involving control rod drive system, 25:56911 (DOCKET-50255-54)
CONSUMERS PUBLIC POWER DISTRICT, COLUMBUS, NEBR.
Cooper Nuclear Station. Environmental report, operating license stage, 25:56955 (DOCKET-50298-22)
CONTROL DATA CORP., OAK BROOK, ILL.
Conversion of the Argonne Reactor Computation (ARC) System to control data 6000 and 7000 series equipment, 25:57140 (CONF-710302-(Vol.1), pp 464-71)
CORNELL UNIV., ITHACA, N. Y. DEPT. OF CHEMISTRY.
Electrons in non-polar solids, 25:54594 (CONF-700652-(Vol.2), pp 331-64)

## D

DAIRYLAND POWER COOPERATIVE, LA CROSSE, WIS.
La Crosse Boiling Water Reactor. Environmental montoring associated with radioactive discharges, January 1, 1969--June 30, 1971, 25:56895 (DOCKET-1155-135)
La Crosse Boiling Water Reactor. Provisional operating authorization No. DPRA-6, amendment No. 4, quality assurance program, 25:56925 (DOCKET-1155-134)
DANISH ATOMIC ENERGY COMMISSION, RISOE. RESEARCH ESTABLISHMENT.
Danish Monte Carlo work in reactor physics and related areas, 25:57166 (CONF-710302-(Vol.2), pp 887-900)
Heating in a reactor fuel element rod under transient conditions. I, 25:57094 (RISO-M-1391)
DECHEMA-INSTITUT, FRANKFURT AM MAIN (WEST GERMANY).
Electrochemical investigations on the corrosion of metals in alkali metal sulfate and vanadium pentoxide melts, 25:55373 (CONF-690452-, Paper 6)
DEUTSCHE FORSCHUNGS- UND VERSUCHSANSTALT FUER LUFT- UND RAUMFAHRT E.V., PORZ-WAHN (WEST GERMANY).
Kinetic theory of flow between rotating cylinders: the gas centrifuge, 25:54888 (CONF-700557-5)
DEUTSCHES ATOMFORUM E. V., BONN (WEST GERMANY).
Conference on reactor, Berlin, 4/1970, 25:56877 (CONF-700438)
DEUTSCHES ELEKTRONEN-SYNCHROTRON, HAMBURG (WEST GERMANY).
Electroproduction of π-mesons on protons above the second resonance, 25:56406 (DESY-71/35)
Excitation of Δ(1236) resonance on bound state neutrons, 25:56405 (DESY-71/33)
Small-distance-behavior analysis and Wilson expansions, 25:56543 (DESY-71/39)
DIVISION OF COMPLIANCE (AEC), WASHINGTON, D.C.
Surry Power Station, Unit 1. Report on metallurgical examination of weld samples, 25:56948 (DOCKET-50280-45)
DIVISION OF HEADQUARTERS SERVICES (AEC), WASHINGTON, D.C.
Science and society, 25:57294 (WASH-1182)
DIVISION OF OPERATIONAL SAFETY (AEC), WASHINGTON, D. C.
Safety criteria for the design of facilities processing plutonium, 25:54967 (CONF-710401-, pp 438-53)
DIVISION OF REACTOR DEVELOPMENT AND TECHNOLOGY (AEC), WASHINGTON, D. C.
Air-cooled heat exchanger for nuclear steam-supplied systems, 25:54833 (RDT-E-4-18-T)
Electric heater and connector assembly for pressurizer for pressurized water reactor, 25:57030 (RDT-E-5-2-T)
Fuel assemblies for pressurized water reactors, 25:57049 (RDT-E-13-15-T)
Heat exchanger, Class 2, water-to-water, straight, or U-tube, 25:54832 (RDT-E-4-17-T)
Pressurizer for pressurized water reactors, 25:57029 (RDT-E-5-1-T)
Vertical, shaft-sealed, motor drive, single-stage centrifugal pump, 25:54831 (RDT-E-3-3-T)
DIVISION OF REACTOR DEVELOPMENT AND TECHNOLOGY (AEC), WASHINGTON, D. C. REACTOR PHYSICS BRANCH.
Work of the Committee on Computer Code Coordination, 25:57018 (CONF-710302-(Vol.1), pp 452-63)
DIVISION OF REACTOR LICENSING (AEC), WASHINGTON, D. C.
Dresden Nuclear Power Station, Unit 2. Technical specifications, change No. 15 allowed, 25:56938 (DOCKET-50237-200)
Dresden Nuclear Power Station, Unit 3. Technical specifications, change No. 7, 25:56943 (DOCKET-50249-103)
Enrico Fermi Atomic Power Plant. Technical specifications, change No. 30, 25:56931 (DOCKET-50016-129)
Quad-Cities Station, Unit 1. Facility operating license No. DPR-29 with appendix A, technical specifications, 25:56944 (DOCKET-50254-52)
Saxton Nuclear Experiment. Technical specifications, change No. 41 allowed, 25:56933 (DOCKET-50146-91)
DOMAINE UNIVERSITAIRE, TALENCE (FRANCE). CENTRE DE RECHERCHES PAUL PASCAL.
Electronic and magnetic properties of carbon fibers: development under neutron irradiation, 25:56282 (CEA-CONF-1822)
Thermal annealing of neutron-irradiated carbon, 25:56283 (CEA-CONF-1823)
DOW CHEMICAL CO., GOLDEN, COLO. ROCKY FLATS DIV.
Administrative procedures and controls in plutonium production areas, 25:54960 (CONF-710401-, pp 293-6)
Air leakage into plutonium gloveboxes and its effect on inert operations, 25:54944 (CONF-710401-, pp 83-97)
Application of an inert atmosphere to a plutonium processing system, 25:54943 (CONF-710401-, pp 69-82)
Conference on safety in plutonium handling facilities, Rocky Flats, 4/71, 25:54937 (CONF-710401)
Design of filter plenum heat exchangers, 25:54950 (CONF-710401-, pp 162-80)
Glovebox design and operation. Glovebox materials studies, 25:54940 (CONF-710401-, pp 26-43)
Glovebox gloves, 25:54941 (CONF-710401-, pp 44-55)
Performance of high efficiency particulate air filter for fume from burning plutonium metal, 25:54951 (CONF-710401-, pp 181-202)
Plutonium ignition in inert atmospheres, 25:54946 (CONF-710401-, pp 106-17)
Rocky Flats environmental research, 25:54964 (CONF-710401-, pp 316-19)
Safety considerations in the new Rocky Flats Plutonium Recovery Plant, 25:54961 (CONF-710401-, pp 297-9)
Waste reduction studies, 25:54709 (CONF-710401-, pp 386-91)
DU PONT DE NEMOURS (E.I.) AND CO., AIKEN, S. C. SAVANNAH RIVER LAB.
ENDF/B cross section preparation and testing in the JOSHUA system, 25:57176 (CONF-710302-(Vol.2), pp 1024-30)
Fire detection and suppression in glove box systems, 25:54954 (CONF-710401-, pp 212-20)
GELI2 and SPAN2: programs to calculate nuclide abundances from multichannel γ ray spectra, 25:55035 (DP-1275)
JOSHUA terminal system, 25:57145 (CONF-710302-(Vol.1), pp 508-15)
Publications, 1970, 25:57228 (DP-929(Rev.1)(Suppl.3))
DUKE POWER CO., CHARLOTTE, N.C.
Oconee Nuclear Station, Unit No. 1. Description of cause and correction of damage to control rod drive mechanisms during preoperational testing, 25:56915 (DOCKET-50269-37)
DUKE UNIV., DURHAM, N. C. DEPT. OF MICROBIOLOGY AND IMMUNOLOGY.
Flotation-fractionation of late fetal, neonatal, and adult rat brain in iso-osmotic Ficoll-sucrose density-

XUM

gradients, 25:57257 (ORO-3195-45)
Heterogeneity of central nervous system myelin, 25:57261 (ORO-3195-49)
Sequential adsorption analysis of antisynaptosome antibodies, 25:57254 (ORO-3195-42)
Sequential adsorption analysis of radioantibodies, 25:57253 (ORO-3195-41)
Zonal centrifuge profile analysis of msd mutant mouse brain, 25:57256 (ORO-3195-44)
DUKE UNIV., DURHAM, N. C. MEDICAL CENTER.
Cellular and subcellular fractionation of brain tissue, 25:57259 (ORO-3195-47)
Immunity to human brain tumors, 25:57263 (ORO-3195-51)
Incorporation of [$^{14}$C]-glucosamine into synaptosomes, 25:57260 (ORO-3195-48)
Isolation and biochemical characterization of subfractions of rat central nervous tissue myelin, 25:57258 (ORO-3195-46)
Sequential adsorption analysis of antimyelin antibodies, 25:57255 (ORO-3195-43)
Virus-cell relationships in dog brain tumors, 25:57262 (ORO-3195-50)
DUQUESNE LIGHT CO., PITTSBURGH, PA.
Beaver Valley Power Station, Unit No. 1. Environmental report, operating license stage, 25:56962 (DOCKET-50334-25)
DUQUESNE LIGHT CO., SHIPPINGPORT, PA.
Shippingport Atomic Power Station operating report, 4--6/71, 25:56894 (DLCS-5000271)

## E

EG AND G, INC., GOLETA, CALIF.
Monte Carlo calculation of sodium iodide scintillation detector response function, 25:54994 (EGG-1183-2283)
Monte Carlo transport analysis for finite ground-distributed γ sources, 25:56260 (EGG-1183-2284)
EG AND G, INC., LAS VEGAS, NEV.
Coherent and incoherent x-ray scattering factors for three- and four-electron atoms, 25:56259 (EGG-1183-1479)
EIDGENOESSISCHE TECHNISCHE HOCHSCHULE, ZURICH (SWITZERLAND).
Nuclear models, 25:56809 (CERN-71-14, pp 67-99)
EIDGENOESSISCHES INSTITUT FUER REAKTORFORSCHUNG, WUERENLINGEN (SWITZERLAND).
Convective heat transfer in longitudinal flow through tubes and rod bundles, 25:54866 (EIR-198)
Prog. rpt. on plutonium fuel program, annual, 1970, 25:55590 (EIR-192)
ELECTRO-MECHANICAL RESEARCH, INC., COLLEGE PARK, MD.
Effects of charged particle and uv radiation on stability of silvered and aluminized FEP teflon second surface mirrors, 25:55656 (N-71-27736)
ENTE NAZIONALE PER L'ENERGIA ELETTRICA, ROME (ITALY).
Experimental and theoretical determination of burnup and heavy isotope content in a fuel assembly irradiated in the Garigliano boiling water reactor, 25:56879 (EUR-4638)
ENVIRONMENTAL PROTECTION AGENCY, CINCINNATI, OHIO.
Rulison ground motions recorded at the TOSCO Mine and Tower Stations, 25:54813 (PNE-R-51)
ENVIRONMENTAL RESEARCH CORP., LAS VEGAS, NEV.
Predicted San Fernando earthquake spectra: Glendale area, 25:54812 (NVO-1163-TM-30)
ESZ ASSOCIATES, INC., ANN ARBOR, MICH.
Automated modular light water reactor calculation code package, 25:57172 (CONF-710302-(Vol.2), pp 983-90)
EUROPEAN ATOMIC ENERGY COMMUNITY.
Experimental study of incipient boiling superheat of sodium on artificial surface roughnesses, 25:54868 (EURFNR-897)
EUROPEAN ATOMIC ENERGY COMMUNITY, ISPRA (ITALY). JOINT NUCLEAR RESEARCH CENTER.
Chemotherapy of leukemia and chemical protection against ionizing radiations, 25:57229 (EUR-4483)
COSTANZA (R,Z), 25:57187 (EUR-4673)
Neutron coincidences counting system, 25:54995 (EUR-4611)
Pressurized and boiling water loop of the Technology Division at Ispra, 25:54867 (EUR-4683)
Simplified visco-elastic analysis of graphitic bodies subjected to external loads, temperature gradients and neutron irradiation, 25:55646 (EUR-4674)
Some applications of the Monte Carlo method at the Euratom Research Center, Ispra, 25:57162 (CONF-710302-(Vol.2), pp 803-32)
TRACE: fuel cycle computer code for fast reactor analysis, 25:57020 (EUR-4709)
EUROPEAN FEDERATION OF CORROSION.
Conference on mechanisms of corrosion by molten salts, Duesseldorf, 4/69, 25:55371 (CONF-690452)
EUROPEAN ORGANIZATION FOR NUCLEAR RESEARCH, GENEVA (SWITZERLAND).
Pion interactions at low and medium energies, 25:56807 (CERN-71-14)
Soft and hard pions in nuclei, 25:56808 (CERN-71-14, pp 1-65)

## F

FACTORY INSURANCE ASSOCIATION, CHICAGO, ILL.
Organization and planning for fire control, 25:54952 (CONF-710401-, pp 204-7)
FLORENCE UNIV. (ITALY). ISTITUTO MATEMATICO.
Time discretization of the neutron transport equation, 25:57158 (CONF-710302-(Vol.2), pp 701-22)
FLORIDA POWER CORP., ST. PETERSBURG.
Crystal River Nuclear Generating Plant, Unit 3. Application for licenses, amendment No. 13, 25:56956 (DOCKET-50302-25)
FLORIDA UNIV., GAINESVILLE.
Prog. rpt. on quantitative determination of structure-property relationships in nuclear fuel element materials, 12/16/70--3/15/71, 25:55437 (TID-25784)
FRANKFURT UNIV. (WEST GERMANY). INSTITUT FUER KERNPHYSIK.
Growing and investigation of silver chloride crystals: a contribution to the development of a precipitation detector for tracks of ionizing particles, 25:54996 (IKF-28)

## G

GENERAL ELECTRIC CO., CINCINNATI, OHIO.
Corrosion resistance of tantalum, T-111, and Nb--1Zr to Hg at 1200 F, 25:55377 (N-71-26947)
GENERAL ELECTRIC CO., SAN JOSE, CALIF.
Modeling and application of the adiabatic approximation for analyzing rod drop excursions, 25:57084 (CONF-710302-(Vol.1), pp 259-81)
Modified collision probability method for non-uniform lattices, 25:57155 (CONF-710302-(Vol.2), pp 644-54)
Nodal integral transport method for calculation of two-dimensional power distributions in non-uniform lattices, 25:57156 (CONF-710302-(Vol.2), pp 655-78)
GENERAL ELECTRIC CO., SAN JOSE, CALIF. ATOMIC POWER EQUIPMENT DEPT.
General Electric pressure suppression containment analytical model, 25:57057 (NEDO-10320(Suppl.1))
Two-phase flow and heat transfer in multirod geometries. Final report, 25:54870 (GEAP-10347)
GENERAL ELECTRIC CO., SAN JOSE, CALIF. BREEDER REACTOR DEPT.
Performance tests of sodium-filled powder and pellet oxide fuel under transient overpower, 25:57046 (GEAP-13722)
GENERAL ELECTRIC CO., SUNNYVALE, CALIF. BREEDER REACTOR DEPT.
Core design development needs in relation to fuel failure propagation, sodium boiling, and clad/fuel--sodium thermal interaction, 25:57088 (GEAP-13639-1)
Core design development needs in relation to fuel failure propagation, sodium boiling, and clad/fuel--sodium thermal interaction, 25:57089 (GEAP-13639-2)
High burnup performance of powder and pellet mixed-oxide fuel, 25:57045 (GEAP-10385)
GENERAL ELECTRIC CO., SUNNYVALE, CALIF. BREEDER REACTOR DEVELOPMENT OPERATION.
Prog. rpt. on fast oxide reactor program, 5--7/71, 25:57111 (GEAP-10010-29)
GEORGIA POWER CO., ATLANTA.
Edwin I. Hatch Nuclear Plant, Unit 2. Preliminary safety analysis report, Amendment 9, 25:56969 (DOCKET-50366-15)
GEORGIA UNIV., ATHENS.
Radioactive tracer studies of soil and litter arthropod food chains, 25:57281 (SRO-641-2)
GEORGIA UNIV., ATHENS. DEPT. OF PHYSICS.
Mean radiation widths at excitation energies of the order of the neutron binding energy, 25:56836 (UCRL-Trans-10542)
GESELLSCHAFT FUER KERNFORSCHUNG m.b.H., KARLSRUHE (WEST GERMANY).
Plutonium-documentation, Vol. 5, No. 1-3, 1971, 25:55369
GOLDWATER MEMORIAL HOSPITAL, NEW YORK.
Prog. rpt. on effects of $^{3}$H-thymidine as a DNA label in rat liver, 25:55110 (TID-25801)
GOSUDARSTVENNYI KOMITET PO ISPOL'ZOVANIYU ATOMNOI ENERGII SSSR, OBNINSK. FIZIKO-ENERGETICHESKII INSTITUT.
Angular anisotropy and effects of nucleon pairing in $^{239}$Pu fission by neutrons, 25:56736 (FEI-233)
Crisis of heat transfer in pipes, 25:54869 (FEI-217)
Density of the excited states of atomic nuclei, 25:56835 (UCRL-Trans-10540)
Gamma-radiation during thermal neutron capture on chromium and iron isotopes, 25:56683 (FEI-205)
Interaction between 14-MeV neutrons and nuclei of Fe, Cu, and Nb, 25:56684 (FEI-216)
Probability of electromagnetic quadrupole transitions in the phenomenological nuclear theory, 25:56735 (FEI-202)
GRENOBLE UNIV. (FRANCE). INSTITUT DES SCIENCES NUCLEAIRES.
Quasi free scattering in $^{2}$H(p,2p) and $^{2}$H(p,pn) reaction from 21.5 to 56.4 MeV, 25:56640 (FRNC-CONF-8)

XUM

GRENOBLE UNIV. (FRANCE). LABORATOIRE DE PHYSIQUE NUCLEAIRE.
Deformations in the s--d shell and inelastic scattering of polarized protons, 25:56828 (LYCEN-7104, S9.1-7)

## H

HAHN-MEITNER-INSTITUT FUER KERNFORSCHUNG, BERLIN (WEST GERMANY).
Pulse radiolysis of organic compounds in aqueous solutions, 25:54632 (CONF-700652-(Vol.3), pp 649-92)
HANFORD ENGINEERING DEVELOPMENT LAB., RICHLAND, WASH.
Categorization and posting of nuclear facilities for fire protection purposes at WADCO, 25:54953 (CONF-710401-, pp 208-11)
Cross sections for preliminary design of FTR, FTR Set No. 200, 25:57115 (HEDL-TME-71-65)
Liquid metal fast reactor accidents, 25:57072 (CONF-710302-(Vol.1), pp 1-24)
Preliminary outline of FTR nuclear systems start-up tests, 25:57114 (HEDL-TME-71-58)
Radiological evaluation of a hypothetical core disruptive accident, 25:57113 (HEDL-TME-71-33)
Sodium fires analyses for the Fast Flux Test Facility, 25:57112 (HEDL-TME-71-31)
TGO, a Linear Programming model for optimizing power transmission grid, 25:57230 (HEDL-TME-71-108)
HITACHI LTD., KAWASAKI (JAPAN). ATOMIC ENERGY RESEARCH LAB.
Application of finite element solution technique to neutron diffusion and transport equations, 25:57159 (CONF-710302-(Vol.2), pp 723-38)
HUGHES AIRCRAFT CO., EL SEGUNDO, CALIF. SPACE SYSTEMS DIV.
Prog. rpt. on solar cell radiation damage experiment, 12/28/70--3/27/71, 25:55098 (N-71-26389)
HUMPHREYS CORP., CONCORD, N.H. TAFA DIV.
Radiation measurements and low frequency and high-pressure investigations of induction heated plasma, 25:56146 (N-71-27023)

## I

IDAHO NUCLEAR CORP., IDAHO FALLS.
Operation of a transuranic storage area at NRTS, 25:54965 (CONF-710401-, pp 365-8)
IDAHO OPERATIONS OFFICE (AEC), IDAHO FALLS. HEALTH SERVICES LAB.
Solubility of plutonium in soil/water environments. A theoretical study, 25:54756 (CONF-710401-, pp 411-29)
ILLINOIS UNIV., CHICAGO. DEPT. OF PHYSICS.
Phenomenology of complex spin tachyons, 25:56500 (ORO-3992-18)
ILLINOIS UNIV., URBANA.
K-plus neutron charge exchange scattering, 25:56423 (COO-1195-217)
Partial wave analysis of 3π system in mass region 1.0 to 2.0 GeV, 25:56482 (COO-1195-224)
ILLINOIS UNIV., URBANA. DEPT. OF COMPUTER SCIENCE.
Control point design using modular logic, 25:57224 (COO-2118-14)
Geometrical model for the synthesis of interval covers, 25:57223 (COO-2118-13)
GRASS: system overview, 25:57217 (COO-1469-187)
GRASS: system software description, 25:57218 (COO-1469-190)
IBAL manual. The Illiac III basic assembler language, 25:57225 (COO-2118-17)
ILLIAC III reference manual. III, 25:57227 (COO-2118-21)
ILLIAC III reference manual. IV, 25:57226 (COO-2118-19)
Prog. rpt., 4--6/71, 25:57219 (COO-1469-193)
Prog. rpt., annual, Pt. 1, 10/70--6/71, 25:57282 (TID-25789)
ILLINOIS UNIV., URBANA. DEPT. OF PHYSICS.
CODILLI II: a FORTRAN IV Program for the analysis of neutron resonance with Program SCORE, 25:56814 (COO-2022-7)
INSTITUT ATOMNOI ENERGII, MOSCOW (USSR).
Pulse generator of megavolt capacity, 25:56583 (IAE-1980)
INSTITUT DE DROIT COMPARE DE PARIS (FRANCE).
Notebook of atomic energy law. II, 25:55252 (NP-18752)
INSTITUT FUER PLASMAPHYSIK, G.M.B.H. GARCHING (WEST GERMANY).
Neodymium glass laser system, 25:56193 (IPP-4/82)
Radiation losses of a theta pinch plasma in the wavelength range 100 to 200 Angstroms, 25:56149 (IPP-1/108)
Tokamak with superposed multipole magnetic field, 25:56211 (IPP-III-2)
INSTITUTE OF CANCER RESEARCH, SUTTON (ENGLAND). SURREY BRANCH.
Approaches to track structure, 25:54589 (CONF-700652-(Vol.1), pp 19-49)
INSTITUTE OF EXPERIMENTAL METEOROLOGY, OBNINSK (USSR).
Global contamination of the atmosphere by $^{85}Kr$ from worldwide nuclear power plants and the radiation danger, 25:54781 (JPRS-53174)
INSTITUTE OF NUCLEAR PHYSICS, KRAKOW (POLAND).
Inelasticity coefficients for pion--Fe and nucleon--Fe collisions, 25:56414 (INP-757)
Low-energy protons generated in nuclear interactions at primary energies 60 GeV and approximately 1000 GeV, 25:56429 (INP-754)
Measurements of energy and flux of cosmic ray hadrons using an ionization spectrometer, 25:56413 (INP-756)
Optical model program with the automatic search routine extended to include the spin-orbit term. OMAS, 25:56815 (INP-741)
INSTISUTE OF NUBLEAR RESEERCH, WARSEW (POLAND).
Integral discriminator for amplitude analyzers, 25:55073 (INR-1315)
Ionization of atomic H by electron impact: numerical calculations for free-fall atomic model, 25:55836 (INR-P-1327)
Penetration of electromagnetic wave into the plasma of exponential density distribution, 25:56230 (INR-1321)
Preparation of high purity carrier-free $^{131}Cs$ source for spectroscopic measurements, 25:54889 (INR-P-1325)
Reactor EWA-10 information, 25:57116 (INR-1303)
Utilization of selective change of plasma optical thickness to determine the electron density, 25:56133 (INR-P-1322)
INSTITUTE OF NUCLEAR TECHNIQUES, KRAKOW (POLAND).
Tables of magnetic structures determined by neutron diffraction. V, 25:56341 (NP-19010)
INSTITUTT FOR ATOMENERGI, KJELLER (NORWAY).
Lectures held by the Norwegian Atomic Energy Association, autumn 1970, and spring 1971, Norsk Atomenergiforening, Polyteknisk Forening, Oslo (Norway) 1971, 25:56983 (NP-18992)
INSTITUTUL DE FIZICA ATOMICA, BUCHAREST (ROMANIA).
Burn-out heat fluxes at subcooled boiling, 25:54871 (IFA-TR-58)
Cerenkov mechanism and resonance production, 25:56498 (IFA-HE-76)
FORTRAN programs for Ge(Li) detector time characteristics, 25:55001 (NP-19011)
K anti K production in four-prong π⁺p interactions at GeV/c, 25:56428 (IFA-HE-75)
Λ K production in four-prong π⁺p interactions at 8 GeV/c, 25:56427 (IFA-HE-73)
Symmetry breaking of chiral SU(3) x SU(3) in phenomenological Lagrangians, 25:56533 (IFA-FT-85)
INTERNATIONAL ATOMIC ENERGY AGENCY, VIENNA (AUSTRIA).
Power and research reactors in member states, 25:56984 (STI/PUB-194/4)
INTERNATIONAL CENTRE FOR THEORETICAL PHYSICS, TRIESTE (ITALY).
Finite field theories, 25:56545 (IC-71/108)
Formulation of quantum field theory in terms of tempered distributions and a possible departure from the principle of superposition, 25:56544 (IC-71/71)
Multiple scattering effects in quasifree scattering, 25:56520 (IC-71/106)

## J

JACKSON LAB., BAR HARBOR, MAINE.
Zonal centrifuge profile analysis of msd mutant mouse brain, 25:57256 (ORO-3195-44)
JAPAN ATOMIC ENERGY RESEARCH INST., TOKYO.
DELIGHT: the point reactivity burnup code for HTGR lattices, 25:57021 (JAERI-Memo-4449)
Effect of alpha-ray irradiation on creep-rupture properties of austenitic stainless steel, 25:55574 (JAERI-Memo-4408)
Fuel failure detection for fast breeder reactor, 25:57055 (JAERI-Memo-4157, pp 84-8)
Fuel failure detector experiment in a He gas inpile loop, 25:57193 (JAERI-Memo-4157, pp 66-83)
Fuel failure detector in JRR-3, 25:57117 (JAERI-Memo-4157, pp 23-43)
Gamma-ray spectroscopy of heavy water and He-gas in JRR-3 fuel failure, 25:57118 (JAERI-Memo-4157, pp 44-50)
Health and safety at Oarai Research Establishment, 10--12/70, 25:55247 (JAERI-Memo-4353)
JPDR irradiation experiment of artificially pin-holed nuclear fuel rods, 25:57047 (JAERI-Memo-4157, pp 2-22)
Kinetics of carbon transfer between uranium carbide fuel and stainless steel bonded with sodium, 25:55589 (JAERI-Memo-4438)
Method for calculating energy dependence of mass chain yield of fission, 25:56816 (JAERI-Memo-4383)
Present status of fuel failure detection and location method in various countries in the world, 25:57056 (JAERI-Memo-4157, pp 89-100)
Proceedings of fuel failure detection symposium, 25:57192 (JAERI-Memo-4157)
SDRC: the ultra-fine spectrum calculation code in resonance energy region, 25:57182 (JAERI-Memo-4481)
Study on JRR-4 delayed neutron-type fuel failure detector, 25:57119 (JAERI-Memo-4157, pp 51-65)
Trapped-particle instabilities and diffusion rates in Tokamak plasma, 25:56195 (JAERI-Memo-4483)
JERSEY CENTRAL POWER AND LIGHT CO., MORRISTOWN, N. J.
Oyster Creek Nuclear Power Plant, Unit No. 1. Facility change request No. 1, supplement No. 1, 25:56937 (DOCKET-50219-145)

Oyster Creek Nuclear Power Plant, Unit No. 1. Semiannual report No. 4, January 1, 1971--June 30, 1971, 25:56899 (DOCKET-50219-146)
Oyster Creek Nuclear Power Plant, Unit No. 1. Technical specifications, Change Request No. 8, 25:56900 (DOCKET-50219-147)

JOHNS HOPKINS UNIV., BALTIMORE, MD. DEPT. OF PHYSICS.
Lie groups in atomic spectroscopy, 25:55882 (NYO-1447-64)

JOINT INST. FOR NUCLEAR RESEARCH, DUBNA (USSR).
Alpha widths of neutron resonances, 25:56754 (UCRL-Trans-10541)
Dependence of the beam shape in the centre of the synchrocyclotron on the accelerating voltage and magnetic field decay, 25:56585 (JINR-P9-5945)

JOINT INST. FOR NUCLEAR RESEARCH, DUBNA (USSR). LAB. OF HIGH ENERGY.
Analysis of the reaction np → pp $\pi^-$ from the point of view of Reggeized OPE model, 25:56521 (JINR-P1-5975)
Debuncher of the JINR synchrophasotron injector with modulation of the accelerated beam energy, 25:56586 (JINR-P9-5956)
Readout electronics for $\pi$--e experiment at 50 GeV, 25:55044 (JINR-E1-5818)

JOINT INST. FOR NUCLEAR RESEARCH, DUBNA (USSR). LAB. OF NEUTRON PHYSICS.
Coherent radiation of the fast electron in medium, 25:56389 (JINR-P4-5954)
Optical radiation excited by nonrelativistic charged particles on the metal surface, 25:55813 (JINR-P4-5957)
Search for the (n,$\alpha$) reaction in the resonances of the zinc and hafnium isotopes, 25:56686 (JINR-P3-5875)
Technique of average $\nu$ measurement with the neutron time-of-flight spectrometer, 25:55039 (LB/G-3040)

JOINT INST. FOR NUCLEAR RESEARCH, DUBNA (USSR). LAB. OF NUCLEAR PROBLEMS.
Collector system of an isotope separator for investigating short-lived isotopes, 25:56584 (JINR-P6-5888)
Probability of the ($\mu^-$, $\nu$) process of $^{139}$La and $^{208}$Pb nuclei, 25:56739 (JINR-P1-6006)

JOINT INST. FOR NUCLEAR RESEARCH, DUBNA (USSR). LAB. OF NUCLEAR REACTIONS.
Delayed fission of some neutron-deficient atomic nuclei, 25:56744 (NP-tr-1936)
Elastic scattering of heavy ions by nuclei, 25:56740 (JINR-P7-5884)
Excitation of spontaneously fissioning isomeric states of $^{239}$Pu and $^{243}$Am at inelastic $\gamma$-quantum scattering, 25:56738 (JINR-P15-5959)
Investigation of the silicon surface-Barrier $\Delta$ E-detector characteristics for the nuclear reaction studying, 25:54998 (JINR-P13-5970)

JOINT INST. FOR NUCLEAR RESEARCH, DUBNA (USSR). LAB. OF THEORETICAL PHYSICS.
Classification of inelastic interactions of high-energy protons and nuclei. II, 25:56522 (ORNL-tr-2520)
Collective $1^+$ states in even--even deformed nuclei, 25:56819 (JINR-P4-5889)
Correlations between reduced neutron and radiative widths in neutron resonances of compound odd-N nuclei, 25:56818 (JINR-E4-5880)
$\Delta$ N = +- 2 mixing in odd-N deformed nuclei, 25:56737 (JINR-E4-5877)
K/sub 13/ decays and chiral symmetry-breaking, 25:56537 (JINR-E2-5996)
Ladder approximation for vertex function in non renormalizable theory of w rho $\pi$ interaction, 25:56483 (JINR-E2-6017)
Multi-channel aspects in stripping reactions on spherical and deformed nuclei, 25:56817 (JINR-E4-5836)
Neutron-channel in muon capture and short range nucleon--nucleon correlations, 25:56641 (JINR-P4-5986)
Nonpolynomial Lagrangians (highest perturbation orders), 25:56546 (JINR-P2-5998)
Spectrum and asymmetry of high energy neutrons in the reaction $\mu^-$ + $^{16}$O → $^{15}$N + n + $\nu$, 25:56820 (JINR-P4-5997)

JUNTA DE ENERGIA NUCLEAR, SACAVEM (PORTUGAL). LABORATORIO DE FISICA E ENGENHARIA NUCLEARES.
Freezing and irradiating fish, 25:55362 (LFEN-NI.-56a)

## K

KANSAS STATE UNIV., MANHATTAN. DEPT. OF NUCLEAR ENGINEERING.
Development of an NE-213 fast-neutron TAC spectrometer system utilizing off-line gamma-ray discrimination, 25:55033 (COO-2049-6)
Evaluation of minima in total neutron cross section by transmission of fission spectra through thick samples, 25:56650 (COO-2049-5)
Fast neutron spectroscopy in aqueous media using an NE-213 proton-recoil neutron spectrometer system, 25:55034 (COO-2049-7)
Orders-of-scattering calculation for the reflection of collimated, polyenergetic fast neutrons from a six-inch-thick steel slab, 25:56257 (COO-2049-8)
Orders-of-scattering method for fast-neutron transport, 25:56258 (COO-2049-9)

KANSAS UNIV., LAWRENCE. NUCLEAR STRUCTURE LAB.
Collective model of odd--odd deformed nuclei, 25:56812 (COO-1120-124)

KARLSRUHE UNIV. (WEST GERMANY).
Neutron--proton charge exchange at 8 and 19 GeV/c, 25:56415 (NP-18888)

KERNFORSCHUNGSANLAGE, JUELICH (WEST GERMANY).
Conference on siemens process calculator utilization, 6/70, Juelich, 25:55074 (JUL-Conf-5)

KERNFORSCHUNGSANLAGE, JUELICH (WEST GERMANY). INSTITUT FUER CHEMISCHE TECHNOLOGIE.
Energy accumulation in solid bodies through nuclear radiation by storage of highly radioactive scrap, 25:54969 (JUL-766-CT)
Treatment of nuclear fuel and breeder materials in oxidizing alkali metal salt melts, 25:55376 (CONF-690452-, Paper 9)

KERNFORSCHUNGSANLAGE, JUELICH (WEST GERMANY). INSTITUT FUER FESTKOERPERFORSCHUNG.
Influence of foreign atoms on recovery of Frenkel defects in electron-irradiated platinum, 25:56284 (JUL-731-FF)
Optimization of the resolving power and the intensity of particle spectrometers using as the example the parabolic spectrographs, 25:55037 (JUL-737-FF)

KERNFORSCHUNGSANLAGE, JUELICH (WEST GERMANY). INSTITUT FUER PHYSIKALISCHE CHEMIE.
Mass-spectroscopic determination of the heat of formation and the investigation of the evaporation behavior of EuN, BN, and AlN, 25:55607 (JUL-739-PC)

KERNFORSCHUNGSANLAGE, JUELICH (WEST GERMANY). INSTITUT FUER PLASMAPHYSIK.
Comparison of continuum radiation of high-temperature plasmas with synchrotron radiation in range 500 to 9000 A. I, 25:56587 (JUL-748-PP)

KERNFORSCHUNGSANLAGE, JUELICH (WEST GERMANY). INSTITUT FUER REAKTORBAUELEMENTE.
Measurement of heat transfer in the bubble boiling of water in metallic tubes, 25:54872 (JUL-740-RB)

KERNFORSCHUNGSANLAGE, JUELICH (WEST GERMANY). INSTITUT FUER REAKTORENTWICKLUNG.
Method for the numerical solution of the linear position dependent Boltzman equation in spherical geometry and spherical symmetry, 25:56617 (JUL-765-RG)
Numerical method for the solution of the time independent transport equation for neutrons, 25:56616 (JUL-764-RG)
Optimization of fuel cycle and core sectioning of a 2500-MW(th) thorium high-temperature reactor with multizone loading, 25:57060 (JUL-736-RG)
Temperature measurement based on thermal noise, 25:55077 (LA-tr-71-71)

KERNFORSCHUNGSANLAGE, JUELICH (WEST GERMANY). INSTITUT FUER REAKTORWERKSTOFFE.
Formation and deposition of pyrocarbon from methane in temperature range of 1650 to 2150°C, 25:55591 (JUL-735-RW)

KERNFORSCHUNGSZENTRUM, KARLSRUHE (WEST GERMANY). INSTITUT FUER ANGEWANDTE KERNPHYSIK.
Proposal for installation of a versatile $e^-$ - $e^+$ - $\gamma$ spectrometer for neutron capture spectroscopy, 25:55040 (NP-18994)

KERNFORSCHUNGSZENTRUM, KARLSRUHE (WEST GERMANY). INSTITUT FUER EXPERIMENTELLE KERNPHYSIK.
Deflection of electrons in a superconducting $HEM_{11}$ resonator, 25:56594 (NP-18998)
Magnetic field tolerance and self field effects of an electron ring accelerator, 25:56595 (NP-19007)
Neutron--proton charge exchange at 8 and 19 GeV/c, 25:56415 (NP-18888)

KERNFORSCHUNGSZENTRUM, KARLSRUHE (WEST GERMANY). INSTITUT FUER NEUTRONENPHYSIK UND REAKTORTECHNIK.
Comparison of 3 methods to control the leakage of particles in a Monte Carlo game, 25:57163 (CONF-710302-(Vol.2), pp 857-70)

KERNFORSCHUNGSZENTRUM, KARLSRUHE (WEST GERMANY). INSTITUT FUER REAKTORENTWICKLUNG.
Experimental study of incipient boiling superheat of sodium on artificial surface roughnesses, 25:54868 (EURFNR-897)

KERNFORSCHUNGSZENTRUM, KARLSRUHE (WEST GERMANY). SCHULE FUER KERNTECHNIK.
Investigation of the deformation of light nuclei with the help of scattering of 104-MeV, 25:56687 (KFK-1397)

KERNKRAFTWERK RWE-BAYERNWERK G.M.B.H., GUNDREMMINGEN (WEST GERMANY).
Gundremmingen Nuclear Power Plant operations report, 5/71, 25:56916 (TID-25791)
Gundremmingen Nuclear Power Plant operations report, 6/71, 25:56924 (TID-25812)

KERNTECHNISCHE GESELLSCHAFT (WEST GERMANY).
Conference on reactor, Berlin, 4/1970, 25:56877 (CONF-700438)

KNOLLS ATOMIC POWER LAB., SCHENECTADY, N. Y.
New form of the $P_3$ approximation, 25:57149 (CONF-710302-(Vol.2), pp 561-4)
Synthetic transport theory method, 25:57154 (CONF-710302-(Vol.2), pp 625-43)

KUNGLIGA TEKNISKA HOGSKOLAN, STOCKHOLM (SWEDEN).
Investigation into some properties and applications of semiconductor nuclear radiation detectors, 25:55000 (NP-19008)

# L


LAVAL UNIV. (QUEBEC).
Isovector excitations in photonuclear reactions, 25:56827 (LYCEN-7104, S8.1-10)
LEEDS UNIV. (ENGLAND).
Recent experiments on steady state and pulse radiolysis of alkaline aqueous systems, 25:54627 (CONF-700652-(Vol.2), pp 295-330)
LEIDEN RIJKSUNIVERSITEIT (NETHERLANDS).
Fission of oriented nuclei by low energy neutrons, 25:56749 (RCN-142)
LOS ALAMOS SCIENTIFIC LAB., N. MEX.
Approach to plutonium surface contamination levels, 25:55195 (CONF-710401-, pp 352-64)
Dynamic Buffer allocation on the CDC 600: the DYNBUF program, 25:57234 (LA-4721)
Electrochemical reduction of europium at a porous carbon cathode with flowing electrolyte, 25:54530 (LA-DC-12469)
Elimination of ray effects by converting discrete ordinate equations to spherical harmonic-like equations, 25:57151 (CONF-710302-(Vol.2), pp 577-607)
Energy storage and switching with superconductors, 25:56110 (LA-DC-12990)
Evaluation of respirator performance by DOP man test, 25:55243 (CONF-710401-, pp 392-406)
Fully interactive graphics data retrieval system, 25:55076 (LA-DC-12576)
Future prospects in computer technology, 25:57191 (CONF-710302-(Vol.2), pp 1086-1101)
Generating moments of the photon production matrices and sources from ENDF data: the LAPHAN code, 25:57175 (CONF-710302-(Vol.2), pp 1016-23)
Instituting a neutron spectrum unfolding capability, 25:55038 (LA-DC-12314)
LAMPF low-energy pion line, 25:56589 (LA-DC-12730)
Monte Carlo sampling with continuously varying cross section along flight paths, 25:57164 (CONF-710302-(Vol.2), pp 871-6)
Non-iterative method for time dependent transport, 25:57157 (CONF-710302-(Vol.2), pp 679-700)
Processing of plutonium-contaminated liquid wastes at Los Alamos, 25:54708 (CONF-710401-, pp 369-85)
Proposal for a biomedical addition to Los Alamos Scientific Laboratory's High-Flux Meson Physics Facility, 25:55299 (LA-4490)
Study of a thermal neutron calibrator, 25:54892 (LA-4745)
Subroutine package for calculating with B-splines, 25:57235 (LA-4728)
Surface contamination: decision levels, 25:55196 (LA-4558)
Tritium trick, 25:55575 (LA-DC-12996)
Two-dimensional air transport calculations, 25:56261 (LA-4774)
Use of a magnetic field to measure particle velocity. I, 25:57233 (LA-4545)
User experience with DATATRAN at LASL, 25:57141 (CONF-710302-(Vol.1), pp 472-7)
LUND UNIV. (SWEDEN).
Prog. rpt., annual, 1970, 25:56643 (NP-19018)
LUND UNIV. (SWEDEN). DEPT. OF PHYSICS.
Description of the logic unit of the photometer system SFIL 70, 25:55045 (LUIP-CR-71-2)
Isotope analysis with nuclear emulsions, 25:55894 (LUIP-CR-71-4)
LYON UNIV. (FRANCE).
Soft and hard pions in nuclei, 25:56808 (CERN-71-14, pp 1-65)
LYON UNIV. (FRANCE). INSTITUT DE PHYSIQUE NUCLEAIRE.
Conference on microscopic aspects of nuclear reactions, La Toussuire, France, 2/71, 25:56821 (LYCEN-7104)
Differential method and Feynman nuclear graphs, 25:56831 (LYCEN-7104, S18.1-18)
Prog. rpt., annual, 1/71, 25:56742 (LYCEN-7101)
Quasi-elastic scattering by substructure of light nuclei, 25:56830 (LYCEN-7104, S14.1-18)
Separable nonlocal potentials and their equivalent local potentials in elastic scattering studies, 25:56642 (LYCEN-7104, C5.1-15)


# M


MAGYAR TUDOMANYOS AKADEMIA KOZPONTI FIZIKAI KUTATO INTEZETE, BUDAPEST.
Remarks on the existence of retarded neutrons in fission, 25:56741 (KFKI-71-35)
Representations of Poincare group as functions of eigenvalues of Casimir operators, 25:56534 (KFKI-71-38)
Some problems of ion-electron recombination, 25:54591 (CONF-700652-(Vol.1), pp 221-58)
MAINE YANKEE ATOMIC POWER CO., WESTBORO, MASS.
Maine Yankee Atomic Power Station. Final safety analysis report, amendment No. 30, 25:56958 (DOCKET-50309-41)
MARITIME ADMINISTRATION, WASHINGTON, D. C.
N. S. Savannah. Dropping of fuel element, 25:57137 (DOCKET-50238-84)
N. S. Savannah. Supplement No. 1 to safety analysis report fuel shuffle with Core II, 25:57136 (DOCKET-50238-83)
MARYLAND UNIV., COLLEGE PARK. DEPT. OF CHEMICAL ENGINEERING.
Prog. rpt. on radiation induced decomposition of inorganic molecular ions, 1970, 25:54633 (ORO-3660-4)
MARYLAND UNIV., COLLEGE PARK. DEPT. OF PHYSICS AND ASTRONOMY.
Brueckner--Hartree--Fock calculations using density-dependent effective interactions, 25:56834 (ORO-3765-32)
Pauli breakup in deuteron reactions. Technical Report No. 71-116, 25:56833 (ORO-3765-31)
MASSACHUSETTS INST. OF TECH., CAMBRIDGE. DEPT. OF EARTH AND PLANETARY SCIENCES.
Variations in isotopic abundances of strontium, calcium, and argon and related topics. Eighteenth annual progress report for 1970, 25:54757 (MIT-1381-18)
MATHEMATICAL APPLICATIONS GROUP, INC., WHITE PLAINS, N.Y.
Machine generation of monte carlo sampling functions, 25:57160 (CONF-710302-(Vol.2), pp 771-81)
Non-linear Monte Carlo, 25:57161 (CONF-710302-(Vol.2), pp 794-7)
MICHIGAN STATE UNIV., EAST LANSING. DEPT. OF PHYSICS.
Soft sphere model for nuclear quadrupole resonance in rare earth trichlorides, 25:57220 (COO-1533-15)
MILLSTONE POINT CO., HARTFORD, CONN.
Millstone Nuclear Power Station, Unit 1. Abnormal occurrence A0-71-18, September 23, 1971, 25:56908 (DOCKET-50245-93)
Millstone Nuclear Power Station, Unit No. 1. Abnormal occurrence No. A0-71-15 and A0-71-16, 25:56906 (DOCKET-50245-91)
Millstone Nuclear Power Station, Unit No. 1. Abnormal occurrence No. A0-71-17, 25:56907 (DOCKET-50245-92)
Millstone Nuclear Power Station, Unit No. 1. Failure of motor operators (A0-71-9 and A0-71-10) found in control circuit of automatic valves, 25:56904 (DOCKET-50245-89)
Millstone Nuclear Power Station, Unit No. 1. Reevaluation of number of curies of liquid waste activity discharged during 1970, 25:56905 (DOCKET-50245-90)
MISSOURI UNIV., ROLLA. SPACE SCIENCES RESEARCH CENTER.
Prog. rpt. on nuclear radiation effects on silicon p--n junctions, 25:55095 (COO-1624-41)
MONTANA COOPERATIVE WILDLIFE RESEARCH UNIT, MISSOULA.
Tracking and telemetry system for wildlife research, 25:57266 (RLO-1929-16)
MONTANA UNIV., MISSOULA. DEPT. OF PHYSICS.
LAMPF low-energy pion line, 25:56589 (LA-DC-12730)
MOUND LAB., MIAMISBURG, OHIO.
Design features of Mound Laboratory's Medical Decontamination facility, 25:54963 (CONF-710401-, pp 311-15)
Different type glovebox filters used for $^{238}Pu$ work at Mound Laboratory, 25:54949 (CONF-710401-, pp 149-61)
Evaluation of the use of a quantitative image analyzer to determine microhardness values, 25:57240 (MLM-OP-71007)
Reaction diffusion in the silver--zinc and silver--aluminum systems, 25:57238 (MLM-OP-71003)
Supplement to summary report on SNAP-19B (IRHS) program, 25:54893 (MLM-1736)
Technical and economic parameters affecting fast breeder reactor deployment, 25:57061 (MLM-1851)
Technique for the metallographic preparation of lead, 25:57239 (MLM-OP-71004)
Ventilation systems at Mound Laboratory ''PP'' Building, 25:54948 (CONF-710401-, pp 133-48)
MOUNT SINAI SCHOOL OF MEDICINE, NEW YORK.
Control of lymphocyte growth in response to phytohemagglutinin stimulation, 25:57284 (TID-25802)
MUENSTER UNIV. (WEST GERMANY). INSTITUT FUER ANORGANISCHE CHEMIE.
Chemical reaction mechanisms for the attack of high-temperature alloys by molten sulfates, 25:55372 (CONF-690452-, Paper 5)


# N


NATIONAL AERONAUTICS AND SPACE ADMINISTRATION, CLEVELAND, OHIO. LEWIS RESEARCH CENTER.
COHORT-2: Monte Carlo general purpose shielding computer code, 25:56262 (N-71-22378)
Creep behavior of electron beam-melted rhenium, 25:55432 (N-71-23114)
Deuterium--$^{3}He$ fusion power balance calculations, 25:56215 (N-71-25526)
Effect of grain size on creep properties of a W--25 at. percent Re--30 at. percent Mo alloy from 1800 to 4000°F, 25:55431 (N-71-23110)
Effects of nuclear radiation on high-reliability silicon power diode. III, 25:55097 (N-71-25389)
Mechanical properties of a W--23.4-percent Re--0.27-percent Hf--C alloy, 25:55433 (N-71-23982)
Reactor irradiation of thermionic sheath insulators, 25:55096 (N-71-24635)


XUM

Some limitations on ion-cyclotron wave generation and subsequent ion heating in magnetic beaches, 25:56231 (N-71-25439)
Theory of Thomson scattering from a weakly ionized plasma, 25:56165 (N-71-27890)

NATIONAL AERONAUTICS AND SPACE ADMINISTRATION, GREENBELT, MD. GODDARD SPACE FLIGHT CENTER.
Calibration of NASA--GSFC High Energy Cosmic Ray Experiment, 25:55046 (N-71-16750)
Considerations related to the sudden release of a large number of cosmic rays in the galaxy, 25:55895 (N-71-24988)
Current sheet magnetic model for the solar corona, 25:55733 (N-71-23433)
Effects of charged particle and uv radiation on stability of silvered and aluminized FEP teflon second surface mirrors, 25:55656 (N-71-27736)
Experiment to measure hard solar and celestial x rays, 25:55734 (N-71-23434)
Isotropy of cosmic γ-ray flux, 25:55896 (N-71-27639)
Magnetospheric field distortions observed by OGO's 3 and 5, 25:55952 (N-71-27604)
Reverse and forward slow shocks in the solar wind, 25:55735 (N-71-24166)

NATIONAL AERONAUTICS AND SPACE ADMINISTRATION, HUNTSVILLE, ALA. GEORGE C. MARSHALL SPACE FLIGHT CENTER.
State-of-the-art literature survey of thoria-dispersed NiCr for space shuttle thermal protection systems, 25:55399 (N-71-27008)

NATIONAL AERONAUTICS AND SPACE ADMINISTRATION, WASHINGTON, D. C.
Nuclear and space radiation effects on materials: space vehicle design criteria, 25:55576 (N-71-25034)

NATIONAL BUREAU OF STANDARDS, WASHINGTON, D. C.
Conference on accurate characterization of the high-pressure environment, Gaithersburg, Md., 10/68, 25:54878
Prog. rpt. on radiation transport studies, 7/70--2/71, 25:56255 (AD-721388)

NATIONAL LEAD CO. OF OHIO, CINCINNATI.
Solidification mechanism of uranium ingots, 25:55400 (NLCO-1077)

NAVAL ORDNANCE LAB., WHITE OAK, MD.
Calculations on transmission of gamma radiation through homogeneous slabs, 25:56256 (AD-722012)

NAVAL POSTGRADUATE SCHOOL, MONTEREY, CALIF.
Neutron transport from a point source in a slab, 25:56613 (AD-715563)

NAVAL RESEARCH LAB., WASHINGTON, D. C.
Residual elements and irradiation embrittlement, 25:55577 (NRL-7310)

NEW YORK OPERATIONS OFFICE (AEC), N. Y. HEALTH AND SAFETY LAB.
User's guide to SWIFT, Monte Carlo technique for unfolding neutron spectra, 25:55036 (HASL-244)

NEW YORK UNIV., N. Y. AEC COMPUTING AND APPLIED MATHEMATICS CENTER.
Size effects in three dimensional Ising lattice, 25:57241 (NYO-1480-179)

NEW YORK UNIV., N. Y. COURANT INST. OF MATHEMATICAL SCIENCES.
Machine generation of monte carlo sampling functions, 25:57160 (CONF-710302-(Vol.2), pp 771-81)

NEW YORK UNIV., N.Y. SCHOOL OF MEDICINE.
Prog. rpt. on effects of $^{3}H$-thymidine as a DNA label in rat liver, 25:55110 (TID-25801)

NIAGARA MOHAWK POWER CORP., SYRACUSE, N. Y.
Nine Mile Point Nuclear Station. Broken pins in turbine wheel, 25:56902 (DOCKET-50220-74)
Nine Mile Point Nuclear Station. Semiannual operation reports for 1970 corrections, 25:56901 (DOCKET-50220-73)

NORDISK INSTITUT FOR TEORETISK ATOMFYSIK, COPENHAGEN (DENMARK).
Pion--nucleon scattering theory, 25:56496 (CERN-71-14, pp 101-54)

NORTH CAROLINA STATE UNIV., RALEIGH. DEPT. OF MICROBIOLOGY.
Prog. rpt. on biochemistry of development in the diptera, 1/1/69--9/15/71, 25:57265 (ORO-3883-3)

NORTH CAROLINA UNIV., CHAPEL HILL.
Prog. rpt., 4--6/71, 25:56748 (ORO-2408-45)

NORTHERN INDIANA PUBLIC SERVICE CO., HAMMOND.
Bailly Generating Station, Nuclear I. Preliminary safety analysis report, Amendment 13, 25:56970 (DOCKET-50367-21)
Bailly Generating Station, Nuclear I. Preliminary safety analysis report, amendment No. 14, 25:56971 (DOCKET-50367-22)

NORTHERN STATES POWER CO., MINNEAPOLIS, MINN.
Monticello Nuclear Generating Plant, Unit 1. Emergency core cooling system to new AEC interim acceptance criteria, 25:56946 (DOCKET-50263-83)
Monticello Nuclear Generating Plant, Unit 1. Inoperability of the high pressure coolant injection system, 25:56912 (DOCKET-50263-82)
Monticello Nuclear Generating Plant, Unit 1. Inoperability of the High Pressure Coolant Injection System, 25:56913 (DOCKET-50263-84)
Monticello Nuclear Generating Plant, Unit No. 1. Unusual occurrences, September 5, 1971 and September 9, 1971, 25:56914 (DOCKET-50263-85)
Prairie Island Nuclear Generating Plant, Units 1 and 2. Final safety analysis report, Amendment No. 11, 25:56953 (DOCKET-50282-40)

NORTHWESTERN UNIV., EVANSTON, ILL.
Comparison between momentum integral and compressible models for sodium voiding calculations in LMFBR, 25:57081 (CONF-710302-(Vol.1), pp 180-98)

NUCLEAR AUDIT AND TESTING CO., WASHINGTON, D.C.
Analysis of the safeguards capabilities of material balance accounting systems in selected uranium and plutonium scrap processing, 25:54968 (IAEA-R-878-F)

NUCLEAR FUEL SERVICES, INC., WEST VALLEY, N.Y.
West Valley Reprocessing Plant. Addendum, site environmental studies, 25:54710 (DOCKET-50201-86)

NUCLEAR MATERIALS AND EQUIPMENT CORP., APOLLO, PA.
Glovebox fire-resistant materials and fire suppression tests, 25:54939 (CONF-710401-, pp 17-25)


## O


OAK RIDGE GASEOUS DIFFUSION PLANT, TENN.
Solid-state automatic beam positioner for mass spectrometers, 25:55075 (K-1817)

OAK RIDGE NATIONAL LAB., TENN.
Analysis of round, turbulent, buoyant jets discharged to flowing stratified ambients, 25:57245 (ORNL-4685)
Aqueous studies, 25:54535 (ORNL-4717, pp 57-82)
Chemical applications of nuclear explosives, 25:54816 (ORNL-4682, pp 182-6)
Chemical behavior salt reactor experiment, 25:54533 (ORNL-4717, pp 29-41)
Chemical Engineering Research, 25:54719 (ORNL-4682, pp 229-39)
Chemical support for high temperature gas-cooled reactors, 25:55647 (ORNL-4717, pp 83-90)
Chemical Technology Division annual progress report for the period ending March 31, 1971, 25:54711 (ORNL-4682)
Compilation of national and international nuclear standards (excluding U.S. activities). 7th Edition, 1971. Information gathered to Dec. 31, 1970, 25:57091 (ORNL-NSIC-94)
Computer code for simulating large MSF evaporator desalting plant dynamics, 25:57248 (ORNL-TM-2933)
CONCEPT: computerized conceptual cost estimates for steam--electric power plants. Phase I user's manual, 25:57063 (ORNL-TM-3276)
Convergence of the discrete ordinates method for anisotropically scattering multiplying particles in a subcritical slab, 25:56264 (ORNL-TM-3553)
Conversion studies in the LMFBR fuel cycle, 25:54717 (ORNL-4682, pp 160-2)
Core melt-through in LMFBR's: a condensed review, 25:57093 (ORNL-TM-3504)
Cytofluorograph system, 25:57249 (ORNL-TM-3536)
Development of aqueous processes for LMFBR fuels, 25:54713 (ORNL-4682, pp 39-79)
Development of methods for reprocessing HTGR fuels, 25:54714 (ORNL-4682, pp 80-94)
Development of the thorium fuel cycle, 25:54716 (ORNL-4682, pp 133-43)
Discussion about the nuclear reactor core analysis code citation, 25:57169 (CONF-710302-(Vol.2), pp 939-52)
Energies and intensities of gamma rays emitted by a $^{226}Ra$ source, 25:55041 (ORNL-TM-3509)
Engineering evaluation of LMFBR fuel shipment, 25:54972 (ORNL-TM-2723)
Fourier analysis of unequally spaced data, 25:57250 (ORNL-TM-3547)
Isotopes and radiation technology, Vol. 9, No. 1, 1971, 25:57127
keV neutron capture γ ray spectra, 25:56655 (ORNL-TM-3379)
Measurements of the neutron fission and absorption cross sections of $^{239}Pu$ over the energy region 0.02 eV to 30 keV, Part II, 25:56746 (ORNL-4707)
Miscellaneous programs, 25:54396 (ORNL-4682, pp 242-9)
Molten salt breeder studies, 25:54534 (ORNL-4717, pp 43-56)
Molten salt chemistry, 25:54532 (ORNL-4717, pp 1-27)
Molten-salt reactor processing, 25:54712 (ORNL-4682, pp 1-38)
MORSE Monte Carlo shielding calculations for the zirconium hydride reference reactor, 25:57133 (ORNL-TM-3366)
MORSEC: revised cross-section module for MORSE multigroup Monte Carlo code, 25:56263 (ORNL-4716)
Nuclear reactor core analysis code: CITATION, 25:57183 (ORNL-TM-2496(Rev.2))
Nuclear safety, 25:57090 (ORNL-4717, pp 91-107)
Oak Ridge Air Quality Index, 25:57246 (ORNL-NSF-EP-8)
ORNL multi-ampere ion source, 25:56208 (CONF-711012-9)
ORNL nuclear safety research and development program bimonthly report for May--June 1971, 25:57092 (ORNL-TM-3483)
Preparation and properties of actinide oxides, 25:55594 (ORNL-4682, pp 218-28)
Preparation of $^{233}UO_2$ for Light-Water Breeder Reactors, 25:55593 (ORNL-4682, pp 163-7)
Prog. rpt. on chemistry, annual, 5/31/71, 25:54531 (ORNL-4717)


XUM

Prog. rpt. on high flux isotope reactor, 4--6/71, 25:57120 (ORNL-TM-3569)
Reactor evaluation studies, 25:57062 (ORNL-4682, pp 240-1)
Regularization method of unfolding x-ray spectrum, 25:56134 (ORNL-TM-3582)
ROD: a nuclear and fuel-cycle analysis code for circulating-fuel reactors, 25:57048 (ORNL-TM-3359)
Safety analysis of waste disposal by hydraulic fracturing at Oak Ridge, 25:54971 (ORNL-4665)
Salt mine repository, 25:54758 (ORNL-4717, pp 109-15)
Selected abstracts of world literature on production and industrial uses of radioisotopes, 25:54894 (ORNL-IIC-37(Pt.2))
Separations chemistry research, 25:54718 (ORNL-4682, pp 168-81)
Sol-gel processes for the uranium fuel cycle, 25:55592 (ORNL-4682, pp 144-59)
Special researches, 25:54599 (ORNL-4717, p 117-24)
Spectrophotometric studies of solutions of lanthanides and actinides, 25:54578 (ORNL-4682, pp 215-17)
Techniques used at Oak Ridge National Laboratory for unfolding neutron and gamma-ray pulse-height spectra, 25:54436 (ORNL-TM-3463)
Total gamma-ray energy spectrum above 1 MeV from neutron interactions in $^{233}U$ and $^{235}U$, 25:56745 (ORNL-4691)
Transuranium-element processing, 25:54671 (ORNL-4682, pp 114-32)
Tube identifier: physical description of tubes tested in OSW program on improved heat-transfer system for evaporators, 25:57247 (ORNL-TM-2713(Rev.1))
Waste treatment and disposal, 25:54715 (ORNL-4682, pp 95-113)

OESTERREICHISCHE STUDIENGESELLSCHAFT FUER ATOMENERGIE G.M.B.H., SEIBERSDORF. INSTITUT FUER REAKTORTECHNIK.
Investigations of the dynamics of heat transfer. II, 25:54877 (SGAE-RT-38/1971)

OHIO STATE UNIV., COLUMBUS. DEPT. OF PHYSICS.
Symmetry breaking in the hard-meson current algebraic tree-graph theory, 25:56535 (ORO-3992-7)

OREGON STATE UNIV., CORVALLIS. DEPT. OF PHYSICS.
Low energy nuclear research, 25:56689 (RLO-1062-711)

## P

PACIFIC GAS AND ELECTRIC CO., SAN FRANCISCO, CALIF.
Humboldt Bay Power Plant, Unit No. 3. Technical specifications proposed change No. 36, 25:56932 (DOCKET-50133-68)
Mendocino Power Plant, Units 1 and 2. Environmental report, construction permit stage, 25:56973 (DOCKET-50398-8)

PADUCAH GASEOUS DIFFUSION PLANT, KY.
Additional testing of ten-ton uranium hexafluoride cylinders, 25:54970 (KY-631)

PANAMETRICS, INC., WALTHAM, MASS.
Prog. rpt. on ultrasonic thermometry in LMFBR systems, 12/68, 25:55078 (NYO-3906-5)

PARIS UNIV. (FRANCE). FACULTE DES SCIENCES.
Improvements to the planar electrostatic analyzer for slow electrons, 25:55072 (FRNC-TH-54)
Investigation of strange meson resonances produced in association with nucleon in 3 GeV K-nucleon interactions, 25:56426 (FRNC-TH-53)
Mechanical behavior of alloys $UMo_{1.5}Al_{0.05}Sn_{0.05}$ and Sicral $F_5$ (adjusted uranium) between 20 and 600°C, 25:55429 (CEA-R-4177)
Regge poles and $\pi$--N scattering at low and intermediate energies, 25:56497 (FRNC-TH-33)
Theoretical and experimental study of nonlinear processes in a plasma, 25:56229 (EUR-CEA-FC-602)

PARIS UNIV., ORSAY (FRANCE). FACULTE DES SCIENCES.
Contribution to study of plasmas. An ultra rapid photometric camera, 25:56132 (CEA-R-4079)
Kinematic study of reaction between hadrons (stable and unstable), 25:56474 (FRNC-TH-63)
Nuclear reactions induced by $\alpha$ particles with energies between 70 and 160 MeV in light nuclei, 25:56685 (FRNC-TH-48)
Polarization parameter measurement in proton--proton elastic scattering from 0.5 to 1.2 GeV, 25:56412 (CEA-R-4193)

PARIS UNIV., ORSAY (FRANCE). LABORATOIRE DE PHYSICO-CHIMIE DES RAYONNEMENTS.
Postluminescence of organic solid solutions, 25:54598 (CONF-700652-(Vol.2), pp 423-75)

PARIS UNIV., ORSAY (FRANCE). INSTITUT DE PHYSIQUE NUCLEAIRE.
Microscopic theory of nucleon--nucleus scattering and optical potential, 25:56822 (LYCEN-7104, C1.1-13)
Resolution of the N-body problem in the hyperspherical formalism, 25:56390 (LYCEN-7104, S5.1-53)

PARIS UNIV., ORSAY (FRANCE). LABORATOIRE DE L'ACCELERATEUR LINEAIRE.
Space charge effects in beam--beam crossing, 25:56592 (LAL-RT-43-70)
Status report on ACO, 25:56591 (LAL-RT-42-70)

PARIS UNIV., ORSAY (FRANCE). LABORATOIRE DE PHYSIQUE DES PLASMAS.
Saturation and damping of echoes of electron plasma waves, 25:56226 (CEA-CONF-1804)

PARIS UNIV., ORSAY (FRANCE). LABORATOIRE DE PHYSIQUE THEORIQUE ET HAUTES ENERGIES.
Short-range correlations, 25:56824 (LYCEN-7104, C4.1-17)

PENNSYLVANIA UNIV., PHILADELPHIA. DEPT. OF BIOCHEMISTRY.
Cellular basis of mammalian calcium homeostasis, 25:57244 (NYO-3489-22)

PHILADELPHIA ELECTRIC CO., PA.
Limerick Generating Station, Units 1 and 2, 25:56968 (DOCKET-50352-20)
Limerick Generating Station, Units 1 and 2. Preliminary safety analysis report, Amendment No. 11, 25:56967 (DOCKET-50352-19)

PHYSIKALISCH-TECHNISCHE BUNDESANSTALT, BRUNSWICK (WEST GERMANY).
Theoretical investigation on diffraction of slow neutrons, 25:56615 (FMRB-37/71)

PORTLAND GENERAL ELECTRIC CO., OREG.
Trojan Nuclear Plant. Interim statement of general policy and procedure: Implementation of the national environmental policy act of 1969, 25:56963 (DOCKET-50344-22)

POWER AUTHORITY OF THE STATE OF NEW YORK.
James A. Fitzpatrick Nuclear Power Plant. Final safety analysis report, Supplement No. 1, 25:56961 (DOCKET-50333-30)

POWER REACTOR DEVELOPMENT CO., DETROIT, MICH.
Enrico Fermi Atomic Power Plant. Amended change request No. 16, supplement No. 1, 25:56930 (DOCKET-50016-128)
Enrico Fermi Atomic Power Plant. Amended change request No. 15, supplement No. 1, 25:56929 (DOCKET-50016-127)

PRINCETON UNIV., N.J. DEPT. OF PHYSICS.
Photon statistics of linear coherent amplification of spontaneously emitted light, 25:57242 (NYO-3406-20)

PRINCETON UNIV., N. J. ELEMENTARY PARTICLES LAB.
Prog. rpt., 1971, 25:57243 (NYO-3406-22)

PRINCETON UNIV., N.J. JOSEPH HENRY LABS.
Multiperipheral models and high-energy processes, 25:56442 (PURC-4159-42)

PUERTO RICO WATER RESOURCES AUTHORITY, SAN JUAN.
Aguirre Nuclear Plant, Unit No. 1. Preliminary facility description and safety analysis report, Amendment 10, 25:56972 (DOCKET-50376-21)

PURDUE UNIV., LAFAYETTE, IND.
Diffractive $\nu\nu$ scattering in $\nu N \rightarrow \nu\nu N$ at 13.1 GeV/c, 25:56425 (COO-1428-294)

PURDUE UNIV., LAFAYETTE, IND. DEPT. OF PHYSICS.
Mariscotti description of ground state bands of even--even nuclei, 25:56813 (COO-1746-57)
Prog. rpt. on high energy physics, Task A, annual, 6/70--5/71, 25:56424 (COO-1428-280)
Prog. rpt. on high energy physics, Task B, annual, 6/70--5/71, 25:56440 (COO-1428-276)

## Q

QUEEN MARY COLL., LONDON (ENGLAND).
$\nu P$ elastic scattering, 0 to 300 MeV, 25:56422 (CERN-71-14, pp 379-93)

## R

RAND CORP., SANTA MONICA, CALIF.
Possible effects of atmospheric particles on fireball emissions, 25:54815 (AD-722031)

REACTIVE METALS, INC., ASHTABULA, OHIO.
Precision extrusion of I and E elements, 25:55402 (RMI-L-48)

REACTOR CENTRUM NEDERLAND, PETTEN.
Experimental study of the neutron attenuation in concrete shields for fast and thermal reactors, with the aid of simulated concrete configurations, 25:57027 (RCN-147)
Fission of oriented nuclei by low energy neutrons, 25:56749 (RCN-142)
Post-irradiation examination of fuel pins R62-A01 and -A02 irradiated in a sodium environment up to 19 MWd/kg $UO_2$, 25:55648 (RCN-144)
Pressurized water loop in the high flux reactor at Petten, 25:57121 (RCN-145)
RAGA: a Monte Carlo program for calculation of gamma-ray transport in a reactor shield for multi-region slab geometry, using exponential transformation, 25:57026 (RCN-146)

RENSSELAER POLYTECHNIC INST., TROY, N.Y. DEPT. OF NUCLEAR SCIENCE.
Experimental and analytical studies of fast neutron transport in iron, 25:56618 (RPI-328-230)

RENSSELAER POLYTECHNIC INST., TROY, N.Y. PLASMA DYNAMICS LAB.
Prog. rpt. on instabilities and turbulence in highly ionized plasmas in a magnetic field, semiannual, 9/70--2/71, 25:56196 (N-71-25028)

ROCHESTER GAS AND ELECTRIC CORP., N. Y.
Robert Emmett Ginna Nuclear Power Plant. $^{131}I$ release, 25:56903 (DOCKET-50244-80)
Robert Emmett Ginna Nuclear Power Plant, Unit No. 1. A review of fuel rod integrity at the Ginna facility, 25:56940 (DOCKET-50244-78)

XUM

Robert Emmett Ginna Nuclear Power Plant, Unit No. 1. Technical supplement accompanying application to increase power, amendment No. 2, 25:56941 (DOCKET-50244-79)
ROCHESTER UNIV., N. Y. DEPT. OF PHYSICS AND ASTRONOMY.
Lectures on group symmetries in nuclear structure, 25:56838 (UR-875-350)
ROCHESTER UNIV., N. Y. DEPT. OF RADIATION BIOLOGY AND BIOPHYSICS.
Determination by x-ray diffraction of crystal structures of silver diethylphosphate and potassium O, O-dibenzylphosphorodithioate, 25:57291 (UR-49-1515)
Interactions of sulfate and phosphate anions with alkaline earth cations in crystals, 25:57293 (UR-49-1517)
Thermodynamic and conformational aspects of Novobiocin--serum albumin complex, 25:57292 (UR-49-1516)
ROME UNIV. (ITALY). ISTITUTO DI FISICA.
Electroproduction of pions, 25:56404 (CONF-701121-8)
RUTGERS--THE STATE UNIV., NEW BRUNSWICK, N. J. DEPT. OF PHYSICS.
Interpretation of angular distribution in terms of complex mass particles, 25:56499 (ORO-3992-8)
RUTHERFORD HIGH ENERGY LAB., CHILTON (ENGLAND).
Coefficients for partial wave analysis of the reaction $0^- + {}^1/_2{}^+ \to 1^- + {}^1/_2{}^+$, 25:56501 (RHEL/R-224)
Regge cuts and related topics, 25:56475 (RPP/C-24)

## S

SANDIA LABS., ALBUQUERQUE, N. MEX.
Current shaping techniques for high-voltage capacitor banks, 25:57268 (SC-DR-710463)
Density of the neutral atmosphere above 100 km, Kauai, May--June 1970, 25:57274 (SC-RR-710541)
Development of processes for the hot pressing of silicon--germanium thermoelectric elements, 25:57267 (SC-DR-710438)
Dynamic measurements of the Grueneisen coefficients of tantalum, uranium, and uranium--molybdenum alloys, 25:55436 (SC-RR-710314)
EDIT program operating manual for the Playback Executive System, 25:57270 (SC-M-710527)
Effects of rf activated inert gas plasmas on critical surface tension and bondability of polydimethyl silicones and polyethylene, 25:57272 (SC-RR-710483)
Environment experienced by cargo during normal rail and truck transport, 25:54974 (SC-M-710241)
Frequency-filtering theory for the propagation of stress pulses in composite materials, 25:57269 (SC-DR-710472)
Implications of a model of charge-neutralized, high-current relativistic electron beams within conducting boundaries on diode and transport system design, 25:56596 (SC-RR-710436)
Ion implantation damage study using lateral stress measurements, 25:56285 (SC-RR-710424)
Method for the routine measurement of dielectric photoconductivity, 25:55079 (SC-DC-713696)
Neutron radiography at Sandia Laboratories: its techniques and instrumentation, 25:54924 (SC-DR-710178)
Prog. rpt. on planetary quarantine program, 6/71, 25:57283 (TID-25790)
Receiving properties of an asymmetric cylindrical antenna, 25:57271 (SC-RR-710475)
Thermal analysis of the intact SNAP-19/NIMBUS B/AGENA system, 25:54895 (SC-RR-710353)
SANDIA LABS., LIVERMORE, CALIF.
Pneumatic hammer development, 25:57280 (SCL-DR-69-155)
Response of a short monopole antenna mounted on the skin of a finite-length cylinder, 25:57273 (SC-RR-710519)
SAXTON NUCLEAR EXPERIMENTAL CORP., PA.
Saxton Reactor. Information requested on Saxton coolant system, 25:56934 (DOCKET-50146-92)
SCHWEIZERISCHES INSTITUT FUER NUKLEARFORSCHUNG, ZURICH.
Basic notions of relativistic scattering theory, 25:56571 (CERN-71-14, pp 229-87)
Pion interactions at low and medium energies, 25:56807 (CERN-71-14)
Production and absorption of pions on nuclei, and dispersion relations for elastic nuclear scattering, 25:56810 (CERN-71-14, pp 155-228)
SCRIPPS INSTITUTION OF OCEANOGRAPHY, LA JOLLA, CALIF.
Concentrations of plutonium, cobalt, and silver radionuclides in selected Pacific seaweeds, 25:55151 (CONF-710817-1)
SCRIPPS INSTITUTION OF OCEANOGRAPHY, LA JOLLA, CALIF. SOLEDAD LAB.
Nonmetallic tools for sampling frozen tissues for trace metal analyses, 25:54450 (TID-25773)
SKODA WORKS, PILSEN (CZECHOSLOVAKIA). NUCLEAR POWER CONSTRUCTION DEPT.
Research of the hydrodynamics of a rod fuel assembly, 25:56880 (ZJE-104)
SLOAN-KETTERING INST. FOR CANCER RESEARCH, NEW YORK.
Prog. rpt. on biological and clinical dosimetry, annual, 7/70--6/71, 25:55208 (NYO-3510-18)
SOCIETE D'ENERGIE NUCLEAIRE FRANCO-BELGE DES ARDENNES, CHOOZ-LEZ-GIVET (FRANCE).
SENA Nuclear Power Plant operations report, 1/71, 25:56919 (TID-25807)
SENA Nuclear Power Plant operations report, 11/70, 25:56917 (TID-25805)
SENA Nuclear Power Plant operations report, 12/70, 25:56918 (TID-25806)
SENA Nuclear Power Plant operations report, 2/71, 25:56920 (TID-25808)
SENA Nuclear Power Plant operations report, 3/71, 25:56921 (TID-25809)
SENA Nuclear Power Plant operations report, 5/71, 25:56922 (TID-25810)
SENA Nuclear Power Plant operations report, 6/71, 25:56923 (TID-25811)
SOUTHERN CALIFORNIA EDISON CO., LOS ANGELES.
San Onofre Nuclear Generating Station, Unit 1. Interim measures for improvements in ECCS performance and reliability, 25:56936 (DOCKET-50206-125)
San Onofre Nuclear Generating Station, Unit 1. Technical specifications, proposed change No. 7, 25:56898 (DOCKET-50206-124)
SOUTHERN UNIVERSITIES NUCLEAR INST., FAURE (SOUTH AFRICA).
Prog. rpt., annual, 1970, 25:56752 (SUNI-14)
SOUTHWEST RESEARCH INST., SAN ANTONIO, TEX.
Investigation of sensitization of type 304 stainless steel safe-ends, 25:55378 (SWRI-1228-P-7-40)
SOUTHWESTERN RADIOLOGICAL HEALTH LAB., LAS VEGAS, NEV.
Measurement of plutonium in soil around the Nevada Test Site, 25:54755 (CONF-710401-, pp 320-7)
STANFORD LINEAR ACCELERATOR CENTER, CALIF.
First- and second-order matrix theory for the design of beam transport systems and charged particle spectrometers, 25:56598 (SLAC-75(Rev.2))
Prog. rpt. on two-mile accelerator project, 4--6/71, 25:56599 (SLAC-136)
Prog. rpt., annual, 1970, 25:56600 (TID-25781)
STATE UNIV. OF NEW YORK, BUFFALO.
Safety analyses of pressurized water reactors, 25:57085 (CONF-710302-(Vol.1), pp 282-95)
STICHTING VOOR FUNDAMENTEEL ONDERZOEK DER MATERIE, JUTPHAAS (NETHERLANDS). INSTITUUT VOOR PLASMA-FYSICA.
Temperature profile in thermonuclear reactor, 25:56216 (NP-19014)
STOCKHOLM UNIV. (SWEDEN). INST. OF PHYSICS.
Automatic selection of kinematical hypotheses from two prong proton--proton interactions in a hydrogen bubble chamber at 19 GeV/c, 25:56523 (USIP-71-3)
Prog. rpt. on particle physics, annual, 1970, 25:56416 (USIP-71-1)
Study of the reaction proton + proton → nucleon + nucleon + pion at 19 GeV/c, 25:56418 (USIP-71-6)
Two prong sample from proton--proton interactions in a hydrogen bubble chamber at 19 GeV/c, 25:56417 (USIP-71-4)
SYRACUSE UNIV., N. Y. DEPT. OF PHYSICS.
Gauge invariant chiral Lagrangian and anti pp annihilations, 25:56538 (ORO-3992-2)
Lagrangian formalism for neutral massive spin 3 fields, 25:56548 (ORO-3992-1)

## T

TECHNICAL UNIV., LODZ (POLAND). INST. OF RADIATION CHEMISTRY.
Role of ions in the radiolysis of hydrocarbons, 25:54630 (CONF-700652-(Vol.3), pp 523-98)
TECHNISCHE HOCHSCHULE, MUNICH (WEST GERMANY). INSTITUT FUER MESS- UND REGELUNGSTECHNIK.
Simulation of the hydrodynamics of boiling water reactors, 25:57022 (MRR-73)
TENNESSEE UNIV., KNOXVILLE.
Prog. rpt. on fluorescence properties of pyridoxal-5-phosphate enzymes, annual, 6/1/70--5/1/71, 25:57264 (ORO-3553-17)
TEXAS UNIV., AUSTIN. CENTER FOR PARTICLE THEORY.
Action-at-a-distance, 25:56550 (ORO-3992-14)
Black-body radiation and generalized theory of physical dimensions, 25:56453 (ORO-3992-42)
Breaking of conformal symmetry and renormalization of nonpolynomial theories, 25:56549 (ORO-3992-9)
Comments on analyses of anti pn → 3π, 25:56485 (ORO-3992-66)
Gauge invariant chiral Lagrangian and anti pp annihilations, 25:56538 (ORO-3992-2)
Lagrangian formalism for neutral massive spin 3 fields, 25:56548 (ORO-3992-1)
Scalar mesons in broken chiral symmetry, 25:56539 (ORO-3992-11)
Symmetry breaking in the hard-meson current algebraic tree-graph theory, 25:56535 (ORO-3992-7)
Two variable crossing symmetric expansion of the ππ scattering amplitude and low-energy parameter sum rules, 25:56484 (ORO-3992-10)
TEXAS UNIV., AUSTIN. CENTER FOR PLASMA PHYSICS AND THERMONUCLEAR RESEARCH.
Prog. rpt. on Texas Turbulent Torus Experiment, annual, 5/71, 25:56123 (ORO-4087-1)
TEXAS UNIV., AUSTIN. DEPT. OF PHYSICS.
Interpretation of angular distribution in terms of complex mass particles, 25:56499 (ORO-3992-8)
Phenomenology of complex spin tachyons, 25:56500 (ORO-3992-18)

XUM

TEXAS UNIV., AUSTIN. PLASMA RESEARCH LAB.
Prog. rpt. on quasistatic ion cyclotron wave studies, 8/71, 25:56233 (ORO-3871-6)
TOKYO UNIV. (JAPAN). INST. FOR NUCLEAR STUDY.
Computer control of an accelerator, 25:56597 (SJC-A-71-3)
Method of correction on a spectrum distorted by accidental coincidence in an address-matrix of a counter array, 25:54997 (INSJ-128)
Table of bands in even--even nuclei, 25:56651 (INSJ-127)
TOULOUSE UNIV. (FRANCE).
Simulation of electron avalanche in He by Monte Carlo type calculation, 25:56265 (ORNL-tr-2518)

## U

UNION CARBIDE CORP., OAK RIDGE, TENN. Y-12 PLANT.
Primary frequency standards in the Y-12 Physical and Electrical Standards Laboratory, 25:57296 (Y-IA-92)
Properties of carbon derived from indene compounds, 25:57295 (Y-1790)
UNITED KINGDOM ATOMIC ENERGY AUTHORITY, DOUNREAY (SCOTLAND). REACTOR GROUP.
Remote-readout balance for use in a highly radioactive environment, 25:55080 (TRG-Report-2086)
UNITED KINGDOM ATOMIC ENERGY AUTHORITY, RISLEY (ENGLAND). REACTOR GROUP.
TRESS: a finite element code for stress analysis problems, 25:57285 (TRG-Report-1813)
UNITED NUCLEAR CORP., NEW HAVEN, CONN. COMMERCIAL PRODUCTS DIV.
Prog. rpt. on fabrication and evaluation of isotopic source assay system, 7--10/70, 25:55070 (BHO-67-2)
UNIVERSITY COLL., LONDON (ENGLAND).
Scattering of pions from nuclei, 25:56811 (CERN-71-14, pp 289-378)

## V

VATTENBYGGNADSBYRAN, STOCKHOLM (SWEDEN).
Alternative approach to core calculations for boiling water reactors, 25:57168 (CONF-710302-(Vol.2), pp 920-38)
VETERANS ADMINISTRATION HOSPITAL, HINES, ILL.
Metabolism and removal of radiostrontium in man, 25:55109 (COO-1231-67)
VIRGINIA ELECTRIC AND POWER CO., RICHMOND.
Surry Power Station, Units 1 and 2. Final safety analysis report, Amendment 25, 25:56949 (DOCKET-50280-46)
Surry Power Station, Units 1 and 2. Preliminary safety analysis report, Amendment 2, 25:56951 (DOCKET-50280-48)
Surry Power Station, Units 1 and 2. Reasons why the construction permits should not be suspended pending environmental review, 25:56952 (DOCKET-50280-49)
Surry Power Station, Units No. 1 and No. 2. Additional information concerning the quality assurance program, 25:56950 (DOCKET-50280-47)
VITRO/HANFORD ENGINEERING SERVICES, RICHLAND, WASH.
Filtration for the exhaust ventilation of plutonium recovery facilities, 25:54947 (CONF-710401-, pp 118-32)
Fire detection systems in gloveboxes, 25:54955 (CONF-710401-, pp 221-36)

## W

WASHINGTON STATE UNIV., PULLMAN.
Adsorption and absorption of hydrogen by niobium, 25:55434 (RLO-2221-T-7-3)
WASHINGTON STATE UNIV., PULLMAN. DEPT. OF PHYSICS.
Electron stimulated desorption of excited neutrals: CO on W, 25:55435 (RLO-2221-T-7-4)
WASHINGTON UNIV., ST. LOUIS, MO. LAB. FOR SPACE PHYSICS.
Comments of a paper on elastically scattered recoil nuclei in solid state detectors, 25:54999 (N-71-26447)
Nuclear interaction tracks in minerals and their implications for extraterrestrial materials, 25:55669 (N-71-26344)
WESTERN WASHINGTON STATE COLL., BELLINGHAM.
Prog. rpt. on fission studies on elements below Po, 7/70--6/71, 25:56750 (RLO-1759-25)
WESTINGHOUSE ELECTRIC CORP., MADISON, PA. ADVANCED REACTORS DIV.
Consequences of molten fuel ejection in a LMFBR, 25:57083 (CONF-710302-(Vol.1), pp 241-58)
Coolant voiding transients in LMFBR's, 25:57082 (CONF-710302-(Vol.1), pp 215-40)
Fission gas and molten fuel ejection from failed fuel rods in an LMFBR, 25:57075 (CONF-710302-(Vol.1), pp 79-96)
Sodium technology program progress report for the period ending May 31, 1971, 25:55379 (WARD-4210-T-1-2)
WESTINGHOUSE ELECTRIC CORP., PITTSBURGH, PA.
Environmental testing of engineered safety features related equipment, 25:57097 (WCAP-7744)
Interchannel thermal mixing with mixing vane grids, 25:57031 (WCAP-7755)
Plant Instrumentation Program. Final quarterly progress report for the period ending March 31, 1971, 25:55004 (WCAP-7562-4)
Robert Emmett Ginna Nuclear Power Plant, Unit No. 1. A review of fuel rod integrity at the Ginna facility, 25:56940 (DOCKET-50244-78)
Safety related research and development for pressurized water reactors, 25:57096 (WCAP-7722)
WESTINGHOUSE ELECTRIC CORP., PITTSBURGH, PA. NUCLEAR ENERGY SYSTEMS DIV.
Comparison calculations for a LWR benchmark package using ENDF/B-1 and -II data, 25:57019 (CONF-710302-(Vol.2), pp 1065-85)
Current status of ENDF/B processing codes, 25:57165 (CONF-710302-(Vol.2), pp 877-86)
ETOG-2 and ETOT--ENDF/B data processor programs to produce epithermal and thermal multigroup libraries, 25:57177 (CONF-710302-(Vol.2), pp 1031-46)
WESTINGHOUSE ELECTRIC CORP., PITTSBURGH, PA. PWR SYSTEMS DIV.
Experience with the modularization of iteration procedures in engineering applications, 25:57143 (CONF-710302-(Vol.1), pp 494-504)
Topical report: Westinghouse PWR core behavior following a loss of coolant accident, 25:57095 (WCAP-7422)
WISCONSIN ELECTRIC POWER CO., MILWAUKEE.
Point Beach Nuclear Plant, Unit No. 1. Environmental studies, report No. PBR-2, 25:56947 (DOCKET-50266-55)
WISCONSIN PUBLIC SERVICE CORP., GREEN BAY.
Kewaunee Nuclear Power Plant. Final safety analysis report, Amendment 10, 25:56957 (DOCKET-50305-25)
WOLLONGONG UNIV. COLL. (AUSTRALIA).
Experimental investigation of fission, 25:56743 (NP-18966)

## Y

YANKEE ATOMIC ELECTRIC CO., WESTBORO, MASS.
Yankee Nuclear Power Station. Operation report No. 128, August 1971, 25:56897 (DOCKET-50029-158)

## Z

ZENTRALSTELLE FUER ATOMKERNENERGIE-DOKUMENTATION, FRANKFURT AM MAIN (WEST GERMANY).
High energy physics index. Vol. 9, No. 16, 1971, 25:56443
High energy physics index, Vol. 9, No. 10, 1971, 25:56446
High energy physics index, Vol. 9, No. 17, 1971, 25:56445
High energy physics index, Vol. 9, No. 18, 1971, 25:56444

XUM

# PERSONAL AUTHOR INDEX

Authors' names are indexed in the form appearing in the abstracted publication. Each entry under an author's name gives the publication title and the *NSA* volume and abstract numbers. Report numbers, where applicable, are given in parentheses at the end of the entry.

Because of problems involved in the mechanical preparation of this index, all accent marks are omitted. The following changes in spelling have been introduced to reduce some of the confusion which might result from omitting the accents:

| | | |
|---|---|---|
| Germanic | ä | appears as ae |
| Germanic | ö | oe |
| Germanic | ü | ue |
| Scandinavian | ϕ | oe |

## A


ABDULLAEVA, K. N., Cross section of $\pi^-$ + $^{12}C$ + $^{12}N$ + $\pi^-$ + $\pi^-$ reaction, 25:56439

ABEL-LARSEN, H., Heating in a reactor fuel element rod under transient conditions. I, 25:57094 (RISO-M-1391)

ABERG, T., Theory of radiative Auger effect, 25:55888

ABKOWITZ, S., Titanium P/M preforms, parts, and composites, 25:55415

ABRAHAMS, C. J., Ultrasonic examination of thin wall tube to tube butt welds using assisted hand scanning methods, 25:54928

ABRAMOV, B. D., Relation between solutions of non-stationary and quasi-critical transport equations, 25:57186

ABSEL-RASSOUL, A. A., Improved techniques for separation and determination of rare-earth elements in extraterrestrial material, 25:54475

ABUL-MAGD, A. Y., Multiple scattering effects in quasifree scattering, 25:56520 (IC-71/106)

ACHTERMANN, E., Flux profile of protons measured in 1967 at equator, 25:55957

ACKERMANN, F. W., Magnetic properties of commercial soft magnetic alloys at cryogenic temperatures, 25:56361

ACKERSON, B., Inactivation of cells by heavy ion bombardment, 25:55313

ADACHI, Mamoru, Nondestructive determination of average burnup for irradiated fuel rods, 25:57201

ADADUROV, G. A., Effect of shock waves on refractory compounds. I, 25:55618

ADAM, Geza, Effect of nandrolon-decanoate and iron preparation on the hemogram of irradiated patients, 25:55303

ADAMS, F., Computer-assisted qualitative analysis of gamma-ray spectra, 25:54523

ADDISON, C. C., Electrical resistivity of liquid K and of solutions of Na liquid K, 25:55527

Equilibrium between sodium hydrogen acetylide and disodium acetylide, 25:54537

Sodium--barium phase diagram, 25:55526

ADKINS, C. R., Cross sections in the unresolved resonance region: methods and evaluation of approximations, 25:56870

ADLER, D. B., CODILLI II: a FORTRAN IV Program for the analysis of neutron resonance with Program SCORE, 25:56814 (COO-2022-7)

ADLER, F. T., CODILLI II: a FORTRAN IV Program for the analysis of neutron resonance with Program SCORE, 25:56814 (COO-2022-7)

ADYLOV, A. A., Secondary emission of $W^+$ ions during bombardment of W by ions of alkali metals, 25:55819

AFANAS'EV, V. I., Field-ion-microscope study of W deformed by an electrostatic field at 900 to 1700°K, 25:55451

AFNAN, I. R., Redetermination of the singlet effective-range parameters of the Hongan separable potentials, 25:56859

AGABABOVA, V. M., Determination of the limits of solubility of tungsten in the nickel--copper solid solution of the tungsten--nickel--copper system, 25:55447

AGARWAL, B. K., Chemical shifts of L/sub III/ x-ray absorption edges of Gd and Dy, 25:55822

AGARWAL, B. R. K., Chemical shifts of L/sub III/ x-ray absorption edges of Gd and Dy, 25:55822

AGARWAL, G. S., Master-equation approach to spontaneous emission. III, 25:55885

Rotating-wave approximation and spontaneous emission, 25:55887

AGARWALA, R. P., Lattice and grain boundary diffusion of cerium and neodymium in nickel, 25:55488

AGEMAR, F., Behavior of light water reactors under loss of cooling medium, 25:57101

AGOSTINI, G., Density measurements of steam--water mixtures flowing in a tubular channel under adiabatic and heated conditions, 25:57032

AGRAWAL, A. K., Analysis of fuel failure experiments with TREAT, 25:57110 (CONF-710302-(Vol.1), pp 97-101)

AGRAWAL, Ashok K., Multiple scattering of neutrons in gaseous and liquid methane, 25:56628

AGUDIN, J. L., Phenomenological quantum theory of external Cherenkov effect, 25:56392

AHLRICHS, R., Error bounds for approximate Rayleigh--Schroedinger perturbation energies and wave functions, 25:55891

AHMED, K., Coupling constants in ($A_1$rhov) system and helicity conservation, 25:56488

AKABOSHI, Sanya, Effect of tetrahydrofolic acid x-irradiated mice, 25:55268

AKALAEV, G. G., Model simulation of a radioactive process with a computer, 25:54441

AKASOFU, S.-I., Association of magnetotail phenomena with visible auroral features, 25:55955

Energetic electron fluxes in magnetotail associated with onset of magnetospheric substorms, 25:56044

Magnetospheric substorms on Sept. 14, 1968, 25:56025

Storm sudden commencements and polar magnetic substorms, 25:56026

AKATSU, Eiko, Radiochemical studies on solvent extraction of several elements in $Mn(NO_3)_2.6\ H_2O$-- and $CaCl_2.6\ H_2O$--TBP, 25:54740

AKHAROV, S. M., Resonance scattering of γ rays of radiative thermal neutron capture on certain nuclei, 25:56782

AKHTAR, S. M. S., γ radiolysis of liquid ethanol. Yields of hydrogen and free ions. Solvated electron rate constants, 25:54660

AKIBA, K., Extraction of uranyl thenoyltrifluoroacetonate into solvents, 25:54751

AKINS, R. J., Irradiation-induced dimensional changes in co-deposited carbon--silicon coatings, 25:55652

AKTIPIS, Stelios, Ultraviolet light-induced changes in ribonuclease conformation, 25:55137

ALAPIN, B. G., Polymorphic transformation of zirconium dioxide, 25:55641

ALBRECHT, A. C., Electrons in non-polar solids, 25:54594 (CONF-700652-(Vol.2), pp 331-64)

ALBRECHT, H. J., Scintigraphic picture of hypertrophic osteoarthropathy, 25:55298

ALCOUFFE, Raymond E., User experience with DATATRAN at LASL, 25:57141 (CONF-710302-(Vol.1), pp 472-7)

ALDERS, R. D., Quantitative studies of nuclear structure through isobaric analog resonances, 25:56769

ALEKSANDROVA, G. I., Radioactive determination of oxygen in germanium and silicon, 25:54502

ALEKSEENKO, L. S., Technological conditions for hot pressing of zirconium dioxide, 25:55600

ALEKSEEV, V. V., Inelastic scattering of γ particles on Zn isotopes, 25:56726

ALEKSEEVSKII, N. E., Superconducting properties of niobium--titanium--zirconium hafnium alloys, 25:56104

Superconductive properties of niobium--zirconium--hafnium alloys, 25:56105

ALEKSIN, V. F., Resonance effects in magnetic configurations having a helical magnetic axis, with allowance for toroidality, 25:56209 (CTO-764)

ALET, I., Measurement of mobility and mass of atmospheric ions, 25:54800

ALEXANDER, L. G., Tube identifier: physical description of tubes tested in OSW program on improved heat-transfer system for evaporators, 25:57247 (ORNL-TM-2713(Rev.1))

ALEXANIAN, Moorad, Possible existence of Bose--Einstein condensation in one and two dimensions, 25:56049

ALFASSI, Zeev B., Efficacy of various scavengers in the study of hot chlorine reactions, 25:54681




XUM

ALIMOVA, . A., Measurement of t [illegible] and $^{3}$He in Al targets, 25:55902
ALLARD, P., Electrostatic spectrometer. II, 25:55083
ALLEMAND, R., Use of liquefied noble gases, 25:55028
ALLEN, C. C., Multidimensional magnetohydrodynamic shock calculations, 25:56192
ALLEN, F. J., Plane electrostatic analyzer for laser produced plasma studies, 25:56137
ALLEN, J. E., Transonic plasma flow past an obstacle, 25:56176
ALLEN, S. J., Calculation of time-dependent stresses in PCPVS, 25:56988
ALLER, L. H., Emission nebulae in Magellanic Clouds at 408 MHz, 25:55722
ALLEWAERT, J., Battery-operated universal dosimeter, 25:55052
ALLUM, F. R., Anosotropy characteristics of low-energy cosmic-ray population of solar orgin, 25:55763
ALMONEY, Stanley Richard, Anharmonic effects in spherical nuclei, 25:56842
ALPERN, Marc R., Contribution to study of plasmas. An ultra rapid photometric camera, 25:56132 (CEA-R-4079)
ALTER, Harry, Status of data testing using the ENDF/B library, 25:57178 (CONF-710302-(Vol.2), pp 1053-64)
ALZETTA, R., Quasi-particle description for indium, 25:56794
AMADESI, P., Determination of the activity of fission products, 25:54699
AMALDI, Edoardo, Electroproduction of pions, 25:56404 (CONF-701121-8)
AMALDI, U., Small angle proton--proton elastic scattering, 25:56420
AMATO, J., LAMPF low-energy pion line, 25:56589 (LA-DC-12730)
AMBARDANISHVILI, T. C., Pneumatic loading and unloading of channels for irradiation in IRT-M reactor, 25:57130
AMIEL, Saadia, Efficacy of various scavengers in the study of hot chlorine reactions, 25:54681
AMIELL, J., Thermal annealing of neutron-irradiated carbon, 25:56283 (CEA-CONF-1823)
AMSTER, Harvey, DP-O method according to a variational treatment that extends its applicability to all geometries, 25:57152 (CONF-710302-(Vol.2), pp 608-16)
ANAN'EV, L. L., Quality factor of superconducting lumped-parameter circuits, 25:55086
ANASTASIU, Gh., Mitotic aberrations induced in rat by single dose of 800 R, 25:55192
ANCONA, A., Network organization of an automated nuclear design system, 25:57146 (CONF-710302-(Vol.1), pp 516-30)
ANDERBERG, Dane H., Rotated mercury cell for controlled potential coulometry. Elimination of background current by digital normalization, 25:54427
ANDERSEN, S. I., Scandinavian PCRV model protect, 25:56991
ANDERSON, Donald E. Jr., Mariner 6 and 7 hydrogen Lyman-alpha data, 25:55812
ANDERSON, H. F., Different type glovebox filters used for $^{238}$Pu work at Mound Laboratory, 25:54949 (CONF-710401-, pp 149-61)
ANDERSON, R. D., Human element design considerations with gloveboxes at the Atlantic Richfield Hanford Company, 25:54938 (CONF-710401-, pp 4-16)
ANDERSSON, H. O., Fuel cartridge with helical cross-pieces, 25:57198
ANDO, Yoshiaki, Radiocontamination in Hokkaido. IX, 25:54789
ANDREESCU, Ileana, Behavior of diffraction maximum in meson--nucleon inelastic interactions in 2- to 20-GeV/c range, 25:56504
ANDREEV, B. M., Investigation of the kinetics of oxygen isotopic exchange between water and carbon dioxide in the presence of soluble additives, 25:54549
ANDREEV, O. N., Heat resistance and elastic properties of titanium--tantalum alloys, 25:55446
ANDREEVA, A. B., Stabilization of zirconia with combined additives and a study of the solid solution stability, 25:55636
ANDRES, Klaus, Superconductivity in noble-metal-rich hexagonal close-packed phases, 25:56096
ANDRONIKASHVILI, E. L., High-power radiation loop in IRT nuclear reactor at Tbilisi, 25:57129
ANDROSOV, V. N., Preparation of mixtures of tungsten carbide and cobalt by means of ultrasonic vibrations, 25:55598
ANGUS, N. S., Determination of trace elements in igneous rocks by nuclear techniques, 25:54462
ANISHCHENKO, Yu. V., Preparation and operation of silicon and germanium semiconductor counters, 25:55013
ANTICH, P., Kπ scattering phase shifts determined from the reactions K$^{+}$p → K$^{+}$π$^{-}$Δ and K$^{+}$p → K$^{0}$π$^{0}$Δ, 25:56486
ANTIPOV, V. V., Study of reactivity of the organism exposed to transverse accelerations and radioprotectants, 25:55264
ANWAR, M., Sterilization of the spotted bollworm of cotton by radiation, 25:55368
APIDIANAKIS, J., Liquid waste effluents from a nuclear fuel reprocessing plant, 25:54753
APOSTOL, D., Vitroceramic nuclear fuel coating. II, 25:55613
APPAPILLAI, M., Model potential for Zn, Cd, and Hg, 25:56387
APPEL, Stanley H., Cellular and subcellular fractionation of brain tissue, 25:57259 (ORO-3195-47)
Incorporation of [$^{14}$C]-glucosamine into synaptosomes, 25:57260 (ORO-3195-48)
Sequential adsorption analysis of antisynaptosome antibodies, 25:57254 (ORO-3195-42)
APPLETON, A. D., British developments in superconductivity applications, 25:56115
ARAKAWA, E. T., Optical properties of UN from 0 to 74 eV, 25:56345
ARCE QUINTERO, Rafael Angel, Reactions and identification of radicals produced by photochemical methods and gamma irradiation in branched alkane glasses, 25:54648
ARDENTE, V., Neutron thermalization in polycrystalline material by Monte Carlo method, 25:56619 (RT/FI-(70)49)
ARDOUIN, B., Balance of $^{90}$Sr over Antarctica, 25:54788
ARIEL, P. D., Equilibrium of heavy, viscous, incompressible, infinitely conducting, rotating fluid in vertical magnetic field, 25:55917
ARIEMMA, A., Experimental and theoretical determination of burnup and heavy isotope content in a fuel assembly irradiated in the Garigliano boiling water reactor, 25:56879 (EUR-4638)
ARIF, M. D., Sterilization of the spotted bollworm of cotton by radiation, 25:55368
ARITA, K., Non-normal parity states of $^{209}$Bi and $^{207}$Pb, 25:56763
ARLMAN, Jan Jacob, Radioisotope generator of the mother-daughter type having quick-detachable members, 25:54909
ARL'T, R., Decay of $^{85}$Y (5 hr), $^{85}$Y (2.68 hr), and $^{85}$Sr, 25:56722
Decay of $^{89}$Zr and $^{97}$Zr, 25:56723
ARMAN, I. P., Spontaneous reversion frequencies of radiosensitive strains of Saccharomyces cerevisiae, 25:55352
ARMSTRONG, T. P., Low-energy (greater than or equal to 0.3 MeV) solar-particle observations, 25:55956
ARMSTRONG, T. W., Calculation of the absorbed dose and dose equivalent induced by medium-energy neutrons and protons and comparison with experiment, 25:55216
ARNOLD, James R., Radon emanation from the lunar surface, 25:54440
ARNOLD, Jeffrey Mark, Study of the ($^{3}$He,$^{6}$He) reaction on s-d shell nuclei, 25:56665
ARNY, Thomas, Importance of the internal velocity field in star formation, 25:55706
ARTSISHEVSKII, M. A., Effect of neutron irradiation on $Ni_3Cr$, 25:55584
ARTYUKH, A. G., Nuclei of light elements with larger neutron excess, 25:56788
ARUGA, Takeo, DELIGHT: the point reactivity burnup code for HTGR lattices, 25:57021 (JAERI-Memo-4449)
ARVIEUX, J., Quasi free scattering in $^{2}$H(p,2p) and $^{2}$H(p,pn) reaction from 21.5 to 56.4 MeV, 25:56640 (FRNC-CONF-8)
ASANO, H., Extraction of uranyl thenoyltrifluoroacetonate into solvents, 25:54751
ASANO, Masaharu, Radiochemical studies on solvent extraction of several elements in $Mn(NO_3)_2.6\ H_2O$-- and $CaCl_2.6\ H_2O$--TBP, 25:54740
ASCOLI-BARTOLI, U., Probing of an inhomogeneous plasma with electromagnetic waves, 25:56145
ASHBEE, K. H. G., Defects in boron carbide before and after neutron irradiation, 25:55650
ASHBURN, W. L., Health physics aspects of $^{133}$Xe lung studies, 25:55248
ASPILA, K. I., Solvent isotope effects on decomposition of N,N-dialkyldithiocarbamic acids, 25:54560
ASTLEY, Wayne C., Plutonium recycle developments, 25:57202
ATEN, A. H. W. Jr., Decay of $^{238}$Am, 25:56792
ATHERTON, D. L., Theoretical treatment of internal shunt protection for superconducting magnets, 25:56112
ATTOLINI, M. R., Short-period temperature effect on cosmic rays, 25:55898
AUBERT, B., Analysis of K+/sub e3/ radiative decay, 25:56410
AUGER, J. P., Pion production and nuclear surface, 25:56530
AUGUSTIN, J. E., Space charge effects in beam--beam crossing, 25:56592 (LAL-RT-43-70)
AUXIER, John A., Unilateral and bilateral exposure of swine to fission neutrons, 25:55334
AVDEICHIKOV, V. V., Nuclei of light elements with larger neutron excess, 25:56788
AVDONINA, E. N., Mechanism of formation of $C_1$--$C_6$ alkanes in action of recoil tritium atoms on cyclohexane, 25:54685
AVIGNON, Y., Solar coronal streamers observed at 169 MHz, 25:55754
AVIGNONE III, F. T., Internal-conversion and γ--γ directional-correlation studies in the decay of $^{103}$Ru, 25:56771
AVRAM, Magdalena, Device for measuring the thermal conductivity of U dioxide, 25:55088
AWAL, M. A., In-beam study of prompt γ-rays emitted in $^{66}$Zn(p,nγ)$^{66}$Ga reaction, 25:56732
AXE, J. D., Neutron scattering study of the lattice-dynamical phase transition in $Nb_3Sn$, 25:55545
AXISA, F., Solar coronal streamers observed at 169 MHz, 25:55754
AYRES, R. L., Reactions of iodine with olefins. II.

Radiative neutron capture induced reactions of $^{128}I$ with various $C_5$ isomers: evidence for a mechanism other than autoradiolysis in the condensed state, 25:54705
AZHIGALIEV, N. A., Dose distribution of high-energy electrons in tissue-equivalent media, 25:55214
AZIMOV, S. A., Cross section of $\pi^- + {}^{12}C + {}^{12}N + \pi^- + \pi^-$ reaction, 25:56439

## B

BABA, Riichi, Utilization of pegmatitic ores, 25:54752
BABCOCK, L. R. Jr., Oak Ridge Air Quality Index, 25:57246 (ORNL-NSF-EP-8)
BABECKI, J., Low-energy protons generated in nuclear interactions at primary energies 60 GeV and approximately 1000 GeV, 25:56429 (INP-754)
BABENKO, A. N., Electrode phenomena and the acceleration of plasma, 25:56153
BABESHKIN, A. M., Local changes in valence and structure caused by nuclear transformation in Co, Fe, I, and Te compounds, 25:56381
Valence states of Eu and Dy in Laves phases and isomer shifts in Moessbauer spectra, 25:56379
BABICKY, A., Investigations on calcium metabolism of bones following local irradiation. XI, 25:55331
BACKENSTOSS, G., Muonic x-ray measurements with a high-pressure gas target, 25:55830
BADIALI, M., Probing of an inhomogeneous plasma with electromagnetic waves, 25:56145
BAECHMANN, K., Chemical problems in the production of superheavy elements by nuclear reactions, 25:54672
BAEDECKER, P. A., Digital methods of photo peak integration in activation analysis, 25:54473
BAERTSCH, Richard D., Schottky barrier atomic particle and x-ray detector, 25:55007
BAGLAN, Robert Joseph, Threshold photoneutron cross sections for medium and heavy nuclei, 25:56702
BAGNALL, K. W., N-substituted urea complexes of thorium and uranium tetrahalides, 25:54536
BAGNE, Farideh, Nuclear structure of $^{92}Nb$, 25:56758
BAIER, R., Radiative neutron--proton scattering at low energy, 25:56526
BAILY, W. E., High burnup performance of powder and pellet mixed-oxide fuel, 25:57045 (GEAP-10385)
BAINUM, D. E., Distorted-wave Born-approximation analysis of the $^{90}Zr(d,\alpha)^{88}Y$ and $^{89}Y(^3He,\alpha)^{88}Y$ reactions, 25:56778
BAIRD, D. C., Structure of current-induced intermediate state in Type-I superconductors, 25:56102
BAIRD, M. B., X-ray induced life-shortening mutations in Habrobracon: a genetic approach to senescence and duration of life, 25:55185
BAISOGOLOV, G. D., State of hematopoiesis in local fractional irradiation. II, 25:55326
BAKER, H. M., Performance of high efficiency particulate air filter for fume from burning plutonium metal, 25:54951 (CONF-710401-, pp 181-202)
BAKER, Norman, Masses, luminosities, and compositions of horizontal-branch stars, 25:55708
BAKER, P. S., Isotopes and radiation technology, Vol. 9, No. 1, 1971, 25:57127
Selected abstracts of world literature on production and industrial uses of radioisotopes, 25:54894 (ORNL-IIC-37(Pt.2))
BAKER, R. J., System for routine production of concentrated /sup 99m/Tc by solvent extraction of $^{99}Mo$, 25:54675
BAKER, W. R., Large-area high-current ion source, 25:56212 (LBL-35)
BAKRI, M. M., Canonical proper-time formalism, 25:56555
BALAJKA, J., Study of mechanism of vanadium corrosion using the electrochemical method, 25:55374 (CONF-690452-, Paper 7)
BALANCA, Pierre, Methods of and apparatus for irradiation of articles by radioactive panels, 25:54849
BALASHOV, V. V., Autoionizing states in helium-like ions, 25:55820
BALASUBRAHMANYAN, V. K., Solar activity and planetary luminosity, 25:55766
BALASUBRAMANIAN, V., Search for pulsed radio emission from CYG X-1 at 327 MHz, 25:55728
BALD, W. B., Supercritical helium cooling of hollow superconductors, 25:56122
BALDUS, W., Helium-II refrigerator for 300 W at 1.8°K, 25:56118
BALDWIN, Burton R., Health physics aspects of nuclear facility siting. Volume I. Proceedings of the fifth annual health physics society midyear topical symposium, Idaho Falls, Idaho, November 3--6, 1970, 25:55157
Health physics aspects of nuclear facility siting. Volume I. Proceedings of the fifth annual health physics society midyear topical symposium, Idaho Falls, Idaho, November 3--6, 1970, 25:57103
Health physics aspects of nuclear facility siting. Volume I. Proceedings of the fifth annual health physics society midyear topical symposium, Idaho Falls, Idaho, November 3--6, 1970, 25:55193
BALDWIN, M. N., Prog. rpt. on physics verification program, Pt. III, Task 5, 4--6/71, 25:57017 (BAW-3647-22)
BALEA, E., K anti K production in four-prong $\pi^+p$ interactions at GeV/c, 25:56428 (IFA-HE-75)
Λ K production in four-prong $\pi^+p$ interactions at 8 GeV/c, 25:56427 (IFA-HE-73)
BALEA, O., K anti K production in four-prong $\pi^+p$ interactions at GeV/c, 25:56428 (IFA-HE-75)
Λ K production in four-prong $\pi^+p$ interactions at 8 GeV/c, 25:56427 (IFA-HE-73)
BALES, Barney L., Multiple $Ag^0$ trapping sites in gamma-irradiated $AgNO_3$ ices, 25:54666
BALL, S. J., Computer code for simulating large MSF evaporator desalting plant dynamics, 25:57248 (ORNL-TM-2933)
BALUTEAU, J. P., Solar brightness measurement between 12 and 24 microns, 25:55739
BAME, S. J., Association of magnetotail phenomena with visible auroral features, 25:55955
Observations of the interplanetary medium: Vela 3 and Imp 3, 1965--1967, 25:55780
BANERJEE, B. R., Structure property relations in beryllium sheet, 25:55510
BANERJEE, Manoj K., Brueckner--Hartree--Fock calculations using density-dependent effective interactions, 25:56834 (ORO-3765-32)
BANERJEE, S. N., Determination of absolute value g/sub A/ from Veneziano amplitude and current algebra sum rule for $\pi$--N scattering, 25:56516
Ground-state energies of He atom and $Li^+$ ion in Faddeev approach, 25:55824
BANERJI, G., Ground-state energies of He atom and $Li^+$ ion in Faddeev approach, 25:55824
BARA, J. J., Application of Moessbauer effect in investigations of crystal microdynamics, 25:56376
BARABASH, L. Z., Proton beam of the ITEP accelerator for radium therapy, 25:56581 (BNL-tr-442)
BARANGER, Michel, Advances in nuclear physics. III, 25:56871
BARASHENKOV, V. S., Classification of inelastic interactions of high-energy protons and nuclei. II, 25:56522 (ORNL-tr-2520)
BARATOV, D. G., Toroidal traps R-0 and RT-2 with steady and high-frequency magnetic fields, 25:56221
BARBER, S. A., Differential Sr--Ca bonding on soil as influenced by bonding site, 25:54778
BARBIER, M., Data on three new VV Cephei stars, 25:55680
BARBIER, Marcel, Radioactivity induced in materials, 25:54987
BARCLAY, T. R., Miniaturized probe for detecting radioactivity at thyroid surgery, 25:55018
BARGUIL, J., Description of elastic scattering processes with the use of nonlocal separable potentials, 25:56852
Separable nonlocal potentials and their equivalent local potentials in elastic scattering studies, 25:56642 (LYCEN-7104, C5.1-15)
BARKER, J. R., Monte Carlo methods in electron transport theory, 25:56362
BARKHUDARYAN, A. V., Proton beam of the ITEP accelerator for radium therapy, 25:56581 (BNL-tr-442)
BARNARD, A. J. Jr., Practical analysis of high-purity chemicals. VI. Emission spectrographic analysis of high-purity acids, 25:54431
BARNARD, E., Energy levels of $^{79}Br$ and $^{81}Br$, 25:56698
BARNES, C. A., Stellar rates for $^{28}Si(\alpha,\gamma)^{32}S$ and $^{16}O(\alpha,\gamma)^{20}Ne$ reactions, 25:55704
BARNES, C. E., Absorption measurements in neutron-irradiated silicon, 25:56311
BARNOV, V. A., Automation of chromatography of radioactive substances, 25:54727
BAROCZY, C. J., Forced-flow sodium boiling in multiple channels, 25:54863 (AI-AEC-13010)
BARONE, Gregory J., Dose distribution for single- and three-phase x-ray equipment, 25:55227
BARR, V. C., Pneumatic hammer development, 25:57280 (SCL-DR-69-155)
BARRETT, R. F., Giant dipole resonance in 1p--1h continuum shell-model approximation for $^{208}Pb$, 25:56800
BARRETTE, J., Directional correlations of gamma rays in $^{152}Sm$ measured by gating on the 244.66-keV transition, 25:56777
BARRETTE, M., Directional correlations of gamma rays in $^{152}Sm$ measured by gating on the 244.66-keV transition, 25:56777
BARSOVA, L. I., Impurity paramagnetic center in $\gamma$-irradiated salts, 25:56339
BARTEL, A. J., Neutron activation analysis for osmium, ruthenium, and iridium in some silicate rocks and rock-forming minerals, 25:54486
BARTELHEIMER, D. L., Determination of plasma properties at very high pressures, 25:56139
BARTELL, A. J., Neutron activation analysis procedure for the determination of the noble metals in geological samples, 25:54485
BARTHELS, A., Studies about use of directly-cooled coated-particle aggregates as fuel elements, 25:57053
BARTLETT, A. F., Influence of prior mechanical and thermal treatments on shock-induced substructures in molybdenum, 25:55543
BARTNIKOWA, W., Bone marrow sections of rat after whole body-irradiation, 25:55330
BARTOLINI, W., Proton inelastic scattering from the five stable, even-mass isotopes of molybdenum, 25:56774

XUM

BARTON, H. R. Jr., Diffractive ππ scattering in πN → ππN at 13.1 GeV/c, 25:56425 (COO-1428-294)
BARUTCUGIL, E., Angular distributions of fragments in fission of U and Th near (n,2n'f) threshold, 25:56804
BASILE, R., Pion production and nuclear surface, 25:56530
BASILOVA, R. N., Global distribution of energetic charged-particle intensity above atmosphere, 25:55980
BASKOVA, K. A., Use of accelerated charged particles for determination of concentration of light elements, 25:54528
BASOV, N. G., Generation of neutrons in laser $CD_2$ plasma heated by pulses of nanosecond duration, 25:56219
BATAEV, K. G., Distribution of radioactivity in rocks and petroleum from contained nuclear explosions, 25:54826 (UCRL-Trans-10543, pp 99-116)
BATANOV, G. M., Resonances of anomalous microwave heating of electrons in a magnetized plasma, 25:56124
BATES, D. R., Forced common turning-point procedure and excitation in slow $H^+$--H(2s) collisions, 25:55881
BATISHKO, C. R., Simultaneous spectrographic triangulation of an SAR arc and a hydrogen arc, 25:55971
BATTAERD, Hendrik Adriaan Jacobus, Manufacture of aliphatic aldehydes by radiolysis, 25:54625
BATTIST, Lewis, Determination of the maximum permissible body burdens using the methods of the medical internal radiation dose (MIRD) committee of the Society of Nuclear Medicine, 25:55201
BATUSOV, I., π and K mesons used for investigating light nuclei structures, 25:56653 (LYCEN-7104, S4.1-10)
BAUDER, U. H., Determination of plasma properties at very high pressures, 25:56139
BAUER, W., Deflection of electrons in a superconducting $HEM_{11}$ resonator, 25:56594 (NP-18998)
BAUMAN, H. F., ROD: a nuclear and fuel-cycle analysis code for circulating-fuel reactors, 25:57048 (ORNL-TM-3359)
BAUMHACKER, H., Neodymium glass laser system, 25:56193 (IPP-4/82)
BAURMASH, L., Effects of aerosol agglomeration on reactor dose evaluations, 25:57105
BAVASSANO, B., Multiple crossings of the Earth's bow shock at large geocentric distances, 25:55953
BAXTER, W. V., ENDF/B cross section preparation and testing in the JOSHUA system, 25:57176 (CONF-710302-(Vol.2), pp 1024-30)
BAYE, D., Excitation of the helium atom by a fast proton, 25:55842
  Excitation of the hydrogen atom by a fast proton, 25:55841
BAZANT, Z. P., Numerically stable algorithm with increasing time steps for integral-type aging creep, 25:55664
BAZIN, J. P., Relative biological effectiveness as a function of linear energy transfer for cataract criterion in the rabbit, 25:55317 (CEA-CONF-1744)
BEAN, A. R., Irradiation damage in carbon-doped silicon, 25:56325
BEARD, Charles L. Jr., ETOG-2 and ETOT--ENDF/B data processor programs to produce epithermal and thermal multigroup libraries, 25:57177 (CONF-710302-(Vol.2), pp 1031-46)
BEARDWELL, C. G., Radioimmunoassay of arginine vasopressin in human plasma, 25:55142
BEATY, E. C., Energy distributions of electrons ejected in ionizing collisions of electrons with helium, 25:55847
BEAUCHAMP, William Thomas, Search for 4e/3 charged quarks in cosmic radiation at 2750 meters, 25:56403
BEAUDRY, B. J., Effect of impurities on lattice parameters of ABAB rare earth metals, 25:55549
BEAUMONT, J. H., Magneto-optical properties of $Cd^+$ in x-irradiated alkali halides, 25:56320
BEBEL, D., Multi-pion exchange contribution to nucleon--nucleon binding and the electrodisintegration of deuterons, 25:56527
BECK, C. W., Surface energy of uranium dioxide, 25:55616
BECK, Gerald, Use of a styrofoam block cutter to make tissue-equivalent compensators, 25:55244
BECK, H., Temperature dependence of the sound velocity in liquid $^3He$, 25:56055
BECK, Paul A., Some recent results on magnetism in alloys, 25:56358
BECK, Rainer, Polarization forces in elastic nuclear Coulomb scattering, 25:56573
BECKER, Francois, Methods for analyzing transfer reactions, 25:56823 (LYCEN-7104, C3.1-40)
BECKER, M., Experimental and analytical studies of fast neutron transport in iron, 25:56618 (RPI-328-230)
BECKER, R., Neutron activation analysis of standardized Al--Si alloy. II, 25:54455
BECKER, R. A., Prog. rpt. on fast oxide reactor program, 5--7/71, 25:57111 (GEAP-10010-29)
BECKETT, C. W., Heat capacity of tantalum in range 1900 to 3100 K, 25:55494
BEDBENOV, V. C., High-power radiation loop in IRT nuclear reactor at Tbilisi, 25:57129
BEDERSON, Benjamin, Total electron--atom collision cross sections at low energies: a critical review, 25:55856
BEECHEY, C. V., Induction of translocations in mouse spermatogonia. IV, 25:55182
BEEN, Julian F., Effects of nuclear radiation on high-reliability silicon power diode. III, 25:55097 (N-71-25389)
BEGZHANOV, R. B., Excited states of odd nonaxial nuclei, 25:56785
  Resonance scattering of γ rays of radiative thermal neutron capture on certain nuclei, 25:56782
BEHNE, D., Multi-element separation for activation analysis using countercurrent electrolysis, 25:54493
BEHRINGER, Kurt, Precision measurements of the spectra of hydrogen plasmas, 25:56156
BEHRNETZ, S., Description of the logic unit of the photometer system SFIL 70, 25:55045 (LUIP-CR-71-2)
BEIGMAN, I. L., Investigation of x-ray flares on Sun with Cosmos-230, 25:55770
BEITINIS, M. R., Level scheme of $^{177}Lu$ in reaction (n,γ), 25:56762
BELAKHOVSKII, M., Moessbauer study of Dy equiatomic compounds with Cu, Ag, Zn, and Rh, 25:56382
BELASHCHENKO, D. K., Correlation effect of transport phenomena in molten solutions, 25:55449
  Electric transport of traces of tin isotopes in ternary system Sn--Bi--Cd at 300°C, 25:56349
BELEKHOVA, N. G., Stationary vertical profiles of radon and thoron decay product concentrations in the surface layer of the atmosphere, 25:54787
BELEN'KII, V. M., Excited states of odd nonaxial nuclei, 25:56785
BELETSKII, Yu. I., Properties of deformed superconducting alloys of vanadium--gallium, 25:56100
BELEVSKII, V. P., Effect of glow discharge on electrical resistance of Ta--N films, 25:55519
BELKIN, I. L., Preparation and operation of silicon and germanium semiconductor counters, 25:55013
BELL, P. R., Cytofluorograph system, 25:57249 (ORNL-TM-3536)
BELLAVANCE, G. R., Ion implantation of S into GaAs, GaP, and Ge monocrystals, 25:56288
BELLI, J. A., Daughter cell repair by mammalian cells in culture after potentially lethal radiation damage, 25:55311
BELLONI, J., Kinetic study of species formed during the pulsed radiolysis of ammonia, 25:54661
BELLWOOD, G. N., Prestressing and proof pressure testing of Wylfa prestressed concrete pressure vessels, 25:56883
BELOUSOV, N. N., Development of micropores in alloys, 25:55462
BELVIN, E. A., Derivation of gaseous release limits for the Browns Ferry Nuclear Plant, 25:56980
BELYAKOVA, L. D., Gas-chromatographic study of the effect of radioactive radiation and heat treatment on the adsorptive properties of magnesium sulfate, 25:54603
BEN AHMED, Ali, Calculation of thermal neutron parameters in hydrogenous liquid moderators, 25:56631
BENDT, Janet E., Radiative-transfer model of a Cepheid, 25:55710
BENJAMIN, J. S., Elevated temperature mechanical properties of a dispersion strengthened superalloy, 25:55483
BENNETT, G. W., Structure in S-wave ππ scattering, 25:56492
BENSON, R. C., Microwave detection of interstellar formamide, 25:55784
BENSON, Robert Stanley, Evolution of early-type close binary systems, 25:55690
BENTZE, P., Geophysical effects of solar activity in upper atmosphere. I, 25:55981
BERANGER, G., Influence of orientation of zirconium monocrystals on the growth structures of monoclinic zirconia, 25:55540
  Relation between the kinetics of aging after deformation of α-zirconium and the anisotropic diffusion of oxygen for a short distance, 25:55551
BERANT, Z., Nuclear spectroscopic studies on $^{18}O$, 25:56672
BERGER, G. W., Determination of geological time with a nuclear reactor and a mass spectrometer, 25:54765
BERGER, Harold, Neutron radiography for nondestructive testing, 25:54930
BERGER, M. J., Prog. rpt. on radiation transport studies, 7/70--2/71, 25:56255 (AD-721388)
BERGGREN, R. G., Radiation strengthening and embrittlement in heavy section plate and welds, 25:55585
BERGQVIST, I., keV neutron capture γ ray spectra, 25:56655 (ORNL-TM-3379)
BERGSTROEM, Stig O. W., Environmental consequences from the normal operation of an urban nuclear power plant, 25:56977
BERGSTROEM, Sug. O. W., Strontium levels in Swedish fish, 25:55156
BERINDE, A., Analysis of proton scattering on $^{32}S$, 25:56694
BERKHUIJSEN, Elly M., Survey of continuum radiation at 820 MHz between declinations -7 and +85°. II, 25:55787
BERKMEN, Haluk, Boundaries of the singularity manifolds associated with a five point function, 25:56551
BERKNER, K. H., Multiple aperture extractor design for producing intense ion and neutral beams, 25:56213 (LBL-327)
BERKNER, Klaus H., Dissociation cross sections for 0.5- to 1-MeV $HeH^+$ ions in $H_2$, He, $N_2$, and Ne gases, 25:55872
BERKOV, A. V., Cross section for production of W boson by high-energy neutrinos in the electromagnetic field of a proton, 25:56473
BERLIN, L. B., Some principles of evaluating the effectiveness of radioprotective agents in man, 25:55256
BERLIN, Yu. A., Concentration dependence in binary systems

in the case of indirect action via an ion-pair mechanism, 25:54670
BERMAN, B. L., Photoneutron cross section for $^{4}$He up to 31 MeV, 25:56649
BERNERS, E. D., Angular correlations studies in $^{32}$S($^{3}$He,pγ)$^{34}$Cl, 25:56712
BERNSTEIN, Aron M., Isoscalar transition rates in nuclei from the (α,α') reaction, 25:56876
BERNSTEIN, S., Additional testing of ten-ton uranium hexafluoride cylinders, 25:54970 (KY-631)
BERRY, R. Stephen, Charge transfer in Na$^{+}$--O$^{-}$ collisions at low relative energy, 25:55859
BERRY, Warren E., Corrosion in nuclear applications, 25:55388
BESNARD, Madeleine, Radiochemical study of stability of selenomethionine $^{75}$Se, 25:54698
BESS, L., Semi-classical model for elementary particles, 25:56450
BEST, A., Geophysical effects of solar activity in upper atmosphere. II, 25:55982
BEST, Klaus-Juergen, Optical constants of β-phases NiIn, PdAl, NiGa/sub 1-y/Al/sub y/, and (Ni,Cu)Ga, 25:56352
BETHGE, K., Investigation of level structure of $^{17}$O, 25:56663
BEZNOGIKH, Yu. D., Debuncher of the JINR synchrophasotron injector with modulation of the accelerated beam energy, 25:56586 (JINR-P9-5956)
BHAT, I. S., Radioiodine distribution in the Tarapur power reactor environment during commissioning and initial operations, 25:56978
BHATTACHARJEE, S. B., Effect of uv irradiation and $^{32}$P decay on thymineless death in E. coli, 25:55359
BHATTACHARYYA, Chitta R., Reverse phase partition chromatography on paper impregnated with 2-thenoyltrifluoroacetone, 25:54746
BIANCASTELLI, R., Small angle proton--proton elastic scattering, 25:56420
BIBR, B., Investigations on calcium metabolism of bones following local irradiation. XI, 25:55331
BICHSEL, Hans, In-phantom microdosimetry with 14.6 MeV neutrons, 25:55232
BIEBL, K. J., Multi-pion exchange contribution to nucleon--nucleon binding and the electrodisintegration of deuterons, 25:56527
BIEDENHARN, L. C., Two-component spherical factorization of Klein--Gordon and Kramers equations, 25:56559
BIELER, E., Scintigraphic picture of hypertrophic osteoarthropathy, 25:55298
BIGGERSTAFF, J. A., keV neutron capture γ ray spectra, 25:56655 (ORNL-TM-3379)
BIGNER, Darell D., Virus-cell relationships in dog brain tumors, 25:57262 (ORO-3195-50)
BILAL, B. A., Countercurrent electrophoresis, 25:54742
BILES, M. B., Safety criteria for the design of facilities processing plutonium, 25:54967 (CONF-710401-, pp 438-53)
BILKIEWICZ, J., Incorporation of $^{239}$Pu into hair, 25:55116
BILLINGS, D. E., Topology of filaments and chromospheric fibrils near sunspots, 25:55749
BINFORD, F. T., Safety analysis of waste disposal by hydraulic fracturing at Oak Ridge, 25:54971 (ORNL-4665)
BINGHAM, H. G., Elastic scattering of deuterons by $^{6}$Li and $^{7}$Li at 8.0 to 12.0 MeV, 25:56670
BINKERT, Thomas, Absolute measurement of the radioactivity of pure β emitters with liquid scintillators, 25:54697
BINNIE, D. M., $A_2^-$ production in channel $\pi^-$+ neutrals near threshold, 25:56436
BINON, F., Excitation of the hydrogen atom by a fast proton, 25:55841
BIRATTARI, C., High-spin rotational excitation in $^{173}$Hf, 25:56796
BIRD, J. R., keV neutron capture γ ray spectra, 25:56655 (ORNL-TM-3379)
BIRIEN, P., Nuclear spectrometry at Saturne synchrotron, 25:56593 (LYCEN-7104, S7.1-2)
BISHOP, B. L., Calculation of the absorbed dose and dose equivalent induced by medium-energy neutrons and protons and comparison with experiment, 25:55216
BISHOP, J. F. W., Fuel and fuel cycle for PFR, 25:57064
BISI, V., Measurement of K/sub L/ + νeV form factor, 25:56408
BISWAS, A. C., Hydrodynamics of Bose fluid in terms of action-angle variables in quantum statistics, 25:56051
BISWAS, Kalyan Kumar, Hydromagnetic flow induced by the impulsive rotation of an infinite disc, 25:55947
BITTEL, Robert, Analysis of the safety problems due to fluorine and fluorine compounds, 25:55246 (CEA-Bib-200)
BIYAJIMA, Minoru, Helicity conservation in the inelastic scattering, 25:56517
BIZER, V. A., Neutron-activation analysis of Ca, P, and Na in bones, 25:55106
BLACKSTONE, R., Dimensional and physical property changes of graphites, pyrocarbons, and fuel bodies, 25:55651
BLAHD, W. H., /sup 99m/Tc technetium sulfide and scintillation camera in rapid diagnosis of pericardial effusion, 25:55295
BLANCHARD, R. L., Body burden, distribution, and internal dose of $^{210}$Pb and $^{210}$Po in a U miner population, 25:55117
Radiological surveillance studies at a BWR nuclear power station: estimated dose rates, 25:56979
BLASI, P., K = 3/2$^{+}$ rotational band in $^{45}$Ti, 25:56693
BLECKWENN, J., Excitation of Δ(1236) resonance on bound state neutrons, 25:56405 (DESY-71/33)
BLEYL, H.-J., Influence of irradiation conditions on californium formation in nuclear reactors, 25:57067
BLIMAN, S., Multiply charged ion source. Design of electron gyromagnetic resonance source, 25:56210 (EUR-CEA-FC-603)
BLINOV, A. P., Determination of $^{239}$Pu and enriched U in the urine in their combined presence, 25:55197
BLISS, Wayne, Measurement of plutonium in soil around the Nevada Test Site, 25:54755 (CONF-710401-, pp 320-7)
BLOCK, Arthur D., Radiometric method and apparatus for measuring and controlling foundry sand moisture, 25:55064
BLOCK, R. C., Measurements of the neutron fission and absorption cross sections of $^{239}$Pu over the energy region 0.02 eV to 30 keV, Part II, 25:56746 (ORNL-4707)
BLOMSTRAND, C., Subcellular distribution of radioactivity in neuronal and glial-enriched fractions after incorporation of [$^{3}$H]leucine in vivo and in vitro, 25:55119
BLOS, B., Effect of C on critical current of $Nb_3Sn$, 25:56084
BLUM, D., Elastic scattering of 60 to 120 MeV electrons from $^{46}$ $^{48}$ $^{50}$Ti, 25:56701
BLUM, E. Ya., Mass transfer in magnetohydrodynamic flow considering chemical kinetics of reactions on boundaries, 25:55932
BLUMBERG, H., Anomalous internal conversion of E1 transitions in outer atomic shells, 25:56797
BLUMENTHAL, David Alan, Particle--gamma angular correlations in the $^{50}$Cr($^{3}$He,αγ)$^{49}$Cr reaction, 25:56692
BLUMENTHAL, George Ray, Astrophysical applications of various high-energy electromagnetic phenomena, 25:55908
BOAG, John W., Approaches to track structure, 25:54589 (CONF-700652-(Vol.1), pp 19-49)
BOCA, I., Study of /sup 236mf/U isomeric fission through $^{235}$U(n,γ) reaction, 25:56793
BOCCALETTI, D., Conversion of gravitational into electromagnetic waves, 25:55805
BOCHAGOV, B. A., Fission process in atomic nuclei in transition region, 25:56786
Kinetic energy of fragments of $^{238}$U and $^{232}$Th fission, 25:56787
BOCHARD, Camille, Improved container for radioactive substances, 25:54977
BOCHIN, V. P., Reparation of stable isotopes for scientific research purposes, 25:54899
BOCK, Rudolf, Separation of mercury from solutions by means of mercuration reactions, 25:54499
Separation of selenium and tellurium by means of Bismuthiol II, 25:54724
BOCOLA, W., Conditioning of high activity liquid wastes, 25:54726
BODNAR, Yu. F., Gas elution in a water-cooled reactor primary circuit with gaseous pressurizer, 25:57042
BOECK, F., Ventricular scintigraphy for diagnosis of cerebral tumors in early childhood, 25:55290
BOEHM, J., Direct pair production by charged particles at 4 GeV/c in a propane bubble chamber, 25:56467
BOEHM-VITENSE, Erika, Convection and metal abundance, 25:55679
BOENZI, D., Conditioning of high activity liquid wastes, 25:54726
BOERS, A. L., Instrumentation for study of ion reflection and secondary ion emission, 25:55815
BOETTCHER, A., Studies about use of directly-cooled coated-particle aggregates as fuel elements, 25:57053
BOETTGER, Peter, Determination of temperature and electron density in a spark plasma, 25:56142
BOGARD, C. F., Application of an inert atmosphere to a plutonium processing system, 25:54943 (CONF-710401-, pp 69-82)
BOGART, Ralph, Genetics lectures. Volume 2, 25:55179
BOGDANKEVICH, L. S., Excitation of longitudinal electromagnetic waves in a bound plasma during injection of relativistic electron beams, 25:56232 (NP-19020)
BOGDANOV, Yu. Yu., Determination of the rate of movement of the charge in rotary kilns by means of radioative isotopes, 25:54898
BOGDANOVA, V. I., Focusing of high-current electron beams in linear induction accelerators, 25:56608
BOGDANOVICH, L. I., Ruthenium and osmium separate spectrophotometric determination by use of 4-(2-pyridylazo)-resorcinol, 25:54412
BOGOMOLOV, V. N., Functions of the transition region for beryllium and some examples of its use, 25:56622
BOGOTT, F. H., Equatorial proton and electron angular distributions in the loss cone and at large angles, 25:56027
BOHL, H. Jr., PSKIT: CDC-6600 computer programming package providing easy use of FINK/PANTRY, 25:57144 (CONF-710302-(Vol.1), pp 505-7)
BOHL, William Raymond, Neutron resonance cross section analysis in filtered neutron beams, 25:56795

XUM

BOHNING, D. E., Urinary excretion of $^{241}Am$ under DTPA therapy, 25:55118
BOHUSOVA, O., Effect of changes in structure on mechanical properties of steel for pressure vessels of nuclear reactors, 25:55466
BOIKO, P. A., Solubility and solid-phase interaction of the carbides of transition metals with nickel and copper, 25:55464
BOIKO, V. A., Generation of neutrons in laser $CD_2$ plasma heated by pulses of nanosecond duration, 25:56219
BOISOT, P., Influence of orientation of zirconium monocrystals on the growth structures of monoclinic zirconia, 25:55540
BOISSERIE, J. M., Simulation of pressure vessel of Bugey reactor, 25:56886
BOKROS, J. C., Irradiation-induced dimensional changes in co-deposited carbon--silicon coatings, 25:55652
BOLCH, W. E., Ecological approach to environmental surveillance, 25:55238
BOLDEMAN, J. W., Experimental investigation of fission, 25:56743 (NP-18966)
BOLDYREV, V. V., Radiolysis of crystalline alkaline azides, bromates, and nitrates, 25:54638
BOLTENKOV, B. S., Measurement of tritium and $^3He$ in Al targets, 25:55902
BOLTZ, D. F., Ultraviolet spectrophotometric determination of tellurium, 25:54400
BOMBIK, A., Tables of magnetic structures determined by neutron diffraction. V, 25:56341 (NP-19010)
BOMMER, J., Spectroscopy of $^{93}$ $^{95}Tc$, 25:56766
BONALUMI, R., Considerations on heterogeneous methods for core physics after second EACRP meeting in Paris, 25:57184
BONAMY, P., Study of $\pi^-p \to \pi^0 n$ and $\pi^-p \to eta$ reactions in nuclei at 7.82 GeV/c, 25:56432
BONAZZOLA, S., Pulsar JP 1933: 21-cm line absorption profile and interstellar scintillation, 25:55724
BONDARENKO, V. P., Solubility and solid-phase interaction of the carbides of transition metals with nickel and copper, 25:55464
BONILLA, C. F., Proceedings of the fifth symposium on thermophysical properties, Boston, Massachusetts, September 30--October 2, 1970, 25:55624
BONNEVILLE, Jacques M., Heat-rejection radiator mass and its influence in space power systems, 25:54916
BOOTH, Newell Ormond, Nonlinear collisionless interaction between electron and ion modes in inhomogeneous magnetoactive plasmas, 25:56246
BOOTH, R. S., Total gamma-ray energy spectrum above 1 MeV from neutron interactions in $^{235}U$ and $^{238}U$, 25:56745 (ORNL-4691)
BOPP, A., Radiation-induced breaks in DNA, 25:55133
BORCHARDT, G. A., Trace element correlation of volcanic ash soils, 25:54513
BORCHERT, I., Coulomb fragmentation in InI and $InI_3$, 25:54696
BORESKOV, G. K., Isotope exchange in system $H_2$--$H_2O$ on some oxide catalysts, 25:54554
BORESKOV, K. G., Analysis of the reaction $np \to pp\pi^-$ from the point of view of Reggeized OPE model, 25:56521 (JINR-P1-5975)
BORGHINI, M., Polarization in proton--proton elastic scattering at 10, 14, and 17.5 GeV/c, 25:56419
Polarization parameter in $K^+$-p and anti pp elastic scattering at 10 and 14 GeV/c, 25:56438
Polarization parameter in $\pi^+p$ elastic scattering at 10, 14, and 17.5 GeV/c, 25:56437
BORGWALDT, H., Comparison of 3 methods to control the leakage of particles in a Monte Carlo game, 25:57163 (CONF-710302-(Vol.2), pp 857-70)
BORIS, J. P., GALAXY: a system for 2D many-body calculations, 25:56187
Numerical experiments on nonlinear plasma instabilities, 25:56205
TRINITY: programs for 3D magnetohydrodynamics, 25:55944
BORISEVICH, V. A., Large γ facility UGU-200, 25:54844
BORISOV, E. A., Feasibility of the thermal decomposition of methyl alcohol in fission fragment tracks, 25:54645
BORISOV, E. V., Determination of the diffusion parameters of interstitial atoms in yttrium by reference to the dislocation impurity peaks of internal friction, 25:55461
BORISOV, M. B., Interaction of a shock wave with a magnetic field, 25:55951
BORN, H.-J., Determination of beryllium in rocks by activation analysis, using the $^9Be(\alpha,n\gamma)^{12}C$ reaction with $^{210}Po$, 25:54467
BOROVKOVA, L. B., Sintering and properties of yttrium oxide ceramics, 25:55606
BORSHKOVSKII, I. A., Excitation of ultrasonic waves by passage of fast electrons through a metal, 25:56566
BORZESZKOWSKI, Horst-Heino V., Reference systems and gravitation, 25:56568
BORZHITSKAYA, M. K., Conditions for formation of phase with A15 structure in V--Ge--Al system, 25:55539
BOSCH, Jorge, Axiomatic foundations of special relativity, 25:56562
BOSE, A. K., Highly restricted partitions and angular-momentum states of equivalent particle configurations, 25:56848
BOSE, R., Quantum theory of spontaneous emission in the presence of external radiation, 25:55883
BOSIO, C., Small angle proton--proton elastic scattering, 25:56420
BOSTICK, W. H., Vorticity and neutrons in the plasma focus, 25:56157
BOTTINO, P. J., Sensitivity of lima bean to gamma radiation, 25:55349
BOUET, Joseph, Electrical equipment for measuring small currents. Applications to dosimetry using classical ionization chambers, liquid dielectric ionization chambers, and electric charge measurements in connection with aerosol studies, 25:55071 (CEA-N-1433)
BOURGOIN, J., Vacancy--interstitial pair in electron-irradiated germanium, 25:56330
BOUTHILLETTE, L., Electron irradiation of heavily doped GaAs:Si and GaAs:Te, 25:56292
BOUVIER, P., Tidal actions on small star clusters, 25:55683
BOWDEN, P., Determination of trace elements in igneous rocks by nuclear techniques, 25:54462
BOWEN, V. T., Plutonium concentration in organisms of the Atlantic Ocean, 25:55161
BOWERS, E., Finite-Larmor-radius equations for collisionless plasmas in general magnetic fields, 25:56178
BOWERS, H. I., CONCEPT: computerized conceptual cost estimates for steam--electric power plants. Phase I user's manual, 25:57063 (ORNL-TM-3276)
BOWMAN, Worth B., Production of gases of known specific activity in a reactor for calibrating gaseous effluent monitors, 25:54986
BOWYER, Stuart, Pulsing x-ray source in Circinus, 25:55721
BOX, Harold C., Effects of ionizing radiation on potassium hydrogen malonate, 25:54654
Oxidation and reduction of organic compounds by ionizing radiation: L-penicillamine hydrochloride, 25:54605
BOYCE, R. L., JOSHUA terminal system, 25:57145 (CONF-710302-(Vol.1), pp 508-15)
BOYER, G. D., Safety related research and development for pressurized water reactors, 25:57096 (WCAP-7722)
BOYKO, Stephen, Method and means for changing radioactive sources, 25:54983
BOZZOLA, S., Considerations on heterogeneous methods for core physics after second EACRP meeting in Paris, 25:57184
BRACHACZEK, Wanda, Ranges of recoil atoms from the (n,γ) process, 25:56269
BRADLEY, A. E., Facility for the determination of low-level tritium in biological and environmental samples, 25:55003 (UCRL-73128)
BRADLEY, James Garrison, Measurement of the thermal neutron capture cross section and resonance capture cross section of $^{80}Kr$, 25:56691
BRADNA, F., Detection of alpha-radionuclides in the bone--marrow and blood of miners by the method of nuclear emulsions, 25:55236
Influence of stopping power on threshold sensitivity of nuclear emulsions for measurement of spectra and dosimetry of fast neutrons, 25:55022
Television monitor for dosimetric and spectrometric measurement by method of nuclear-track emulsions, 25:55021
Utilization of polymer-gelatin nuclear emulsions for fast neutron dosimetry, 25:55057
BRAECKELMANN, Walter, Transmission line constants of coupled microstrip, 25:57277 (SC-T-713063)
BRAENDLI, G., Strong-coupling parameters in superconducting In--Pb alloys, 25:56076
BRAETTER, P., Determination of the trace element distribution in coexisting calcite and dolomite by neutron activation analysis, 25:54497
BRAEUER, Hans-Juergen, Remark on general Lorentz covariance, 25:56558
BRAITHWAITE, Anthony A., Solid solution hardening in tantalum alloys, 25:55457
BRAMATI, L., Experimental and theoretical determination of burnup and heavy isotope content in a fuel assembly irradiated in the Garigliano boiling water reactor, 25:56879 (EUR-4638)
BRAND III, Joseph G., Thermodynamic and conformational aspects of Novobiocin--serum albumin complex, 25:57292 (UR-49-1516)
BRANDSTEDT, Sven B., Effects of atomization media and consolidation techniques upon physical properties of a P/M cobalt-base alloy, 25:55480
BRANDSTETTER, A., Coefficients for partial wave analysis of the reaction $0^- + 1/2^+ \to 1^- + 1/2^+$, 25:56501 (RHEL/R-224)
BRANDT, S. B., Diffusion losses of radiogenic argon from meteorites, 25:55672
BRANOVER, G. G., Influence of transverse magnetic field on intensity profiles of turbulent velocity fluctuations in pipes of rectangular cross section, 25:55926
BRASE, A., Scintigraphy of inflammations using silver isotopes, 25:55286
BRATTON, R. J., Surface energy of uranium dioxide, 25:55616
BRAUN, H., Substructures in $^{12}C$ and $^{14}N$, 25:56652 (LYCEN-7104, S2.1-2)
BRAUN, Japnell D., Reaction diffusion in the silver--zinc and silver--aluminum systems, 25:57238 (MLM-OP-71003)
BRAUNSTEIN, P., $^{167}Tm$: a new bone scanning agent,

25:55279
BREGER, A. Kh., Gamma radiation dose rate in the emitter of a radiation-chemistry device provided with a uranium-based radiation circuit, 25:54914
Method for calculation of field dose of uranium radiation loop linear source of γ-radiation, 25:54991
BREHM, W. F., Corrosion and deposition of irradiated stainless steel in sodium, 25:55370 (BNWL-SA-2335)
BREITHAUPT, R. Don, Low-velocity air gun and Hopkinson split-bar facility, 25:57289 (UCRL-51098)
BRELOT, A., Infrared studies of low-temperature electron-irradiated Si, 25:56297
BRENNAN, M. H., Proton--hydrogen atom momentum transfer cross section at approximately 5 eV, 25:55840
BRETIN, Lucien, Introduction of hydrogen isotopes in metals by means of a miniaturized cathode loading cell, 25:54858
BREUSOV, O. N., Effect of shock waves on refractory compounds. I, 25:55618
BRICARD, J., Study of the mobility of ions in air, 25:54801
BRICHET, E., Balance of $^{90}Sr$ over Antarctica, 25:54788
BRIDGES, B. A., Effect of γ radiation on donor ability of Escherichia coli, 25:55358
BRIEGLEB, Bruce P., Dissociation cross sections for 0.5- to 1-MeV $HeH^+$ ions in $H_2$, He, $N_2$, and Ne gases, 25:55872
BRIERE, Michel, Radioactivity measurements, 25:55020
BRIGHT, W. C., Rocky Flats environmental research, 25:54964 (CONF-710401-, pp 316-19)
BRIMHALL, J. L., Swelling in refractory metals during high temperature ion bombardment, 25:55573 (BNWL-SA-3962)
BRINKLOEV, Morten, Glomerular filtration rate determined by $^{51}Cr$-EDTA, 25:55122
BRINKMAN, J., Local moment relaxation in a superconductor, 25:56071
BRINTON, Henry C., Temporal variations of thermospheric hydrogen derived from in situ measurements, 25:55973
BRIXY, Heinz G., Temperature measurement based on thermal noise, 25:55077 (LA-tr-71-71)
BROCK, William A., Radioimmunoassay of the F prostaglandins, 25:55144
BRODER, D. L., Gamma-radiation during thermal neutron capture on chromium and iron isotopes, 25:56683 (FEI-205)
BRODSKII, A. M., Kinetic isotope effect of reactions of hot atoms in gaseous mixtures, 25:54684
BRODSKY, A., Urinary excretion of $^{241}Am$ under DTPA therapy, 25:55118
BROLLEY, John E., Analogue of the primary solar reaction, 25:55777
BROMMUNDT, G., Investigation of level structure of $^{170}$, 25:56663
BROOKS, A. L., Comparison of the relative biological effectiveness of $^{241}Am$ and $^{144}Ce$ on the production of chromosome aberrations in the Chinese hamster liver, 25:55188
BROOKS, Joan, Non-linear Monte Carlo, 25:57161 (CONF-710302-(Vol.2), pp 794-7)
BROUDEUR, Robert, Introduction of hydrogen isotopes in metals by means of a miniaturized cathode loading cell, 25:54858
BROWER, J. H., Method of dosimetry for a bulk-grain irradiator, 25:55234
BROWER, K. L., Structure of multiple-vacancy (oxygen) centers in irradiated silicon, 25:56312
BROWN, B. P., Safety criteria for the design of facilities processing plutonium, 25:54967 (CONF-710401-, pp 438-53)
BROWN, D. J., Evidence for boson production via isobar decay, 25:56525
BROWN, Daniel G., Unilateral and bilateral exposure of swine to fission neutrons, 25:55334
BROWN, J. K., Biological dosimetry in an industrial radiography accident, 25:55228
BROWN, Karl L., First- and second-order matrix theory for the design of beam transport systems and charged particle spectrometers, 25:56598 (SLAC-75(Rev.2))
BROWN, Mark, Neutron radiography of the dental pulp, 25:55277
BROWN, Robert T., Coherent and incoherent x-ray scattering factors for three- and four-electron atoms, 25:56259 (EGG-1183-1479)
BROWN, Stephen R., Numerical calculation vs experimental data for Westerly granite, 25:57287 (UCRL-51075)
BROWNE, C. P., Comparison of the nuclear-reaction energy scale with the gamma-ray energy scale, 25:56773
BRUECKNER, K. A., Mass formula consistent with nuclear-matter calculations vs conventional mass-law extrapolations, 25:56853
BRUN, J., Problems of reactor circulating pumps, 25:57038
BRUN, M. Ya., Nature of the embrittlement of two-phase titanium alloys with coarse lamellar structure, 25:55450
BRUNFELT, A. O., Rare earth abundances in mesozoic dolerite dikes from eastern United States, 25:54476
BRUNFELT, Arild O., Conference on activation analysis in geochemistry and cosmochemistry, Kjeller, Norway, 9/70, 25:54457
BRUZZONE, G., Stoichiometry, crystal structures, and some melting points of the La--Au alloys, 25:55570
BRYANT, D. T. W., Removal of cationic fission products from milk, 25:54722
BRYANT, F. J., Electron radiation damage and edge emission of cadmium telluride, 25:56290
BRYANT, Pamela M., Derivation and application of limits and reference levels for environmental radioactivity in the United Kingdom, 25:55241
BRYANTSEV, I. N., Radiation telomerization of ethylene by propionic acid, 25:54612
BUCKLEY, R., Unstable equilibrium underlying perpendicular shock waves in collision-free plasmas, 25:56190
BUCKMEIER, F. J., Comparison of airborne spectral gamma radiation data with field verification measurements, 25:54768
BUDASHKINA, E. B., Content of $^{90}Sr$, Ca, and Sr units in seeds of wheat hybrids, 25:55223
BUDBERG, P. B., Study of the titanium--zirconium--niobium system, 25:55564
BUDUEVA, V. G., Production of Cu/W composite by diffusion welding, 25:55405
BUDZINSKI, Edwin E., Effects of ionizing radiation on potassium hydrogen malonate, 25:54654
Oxidation and reduction of organic compounds by ionizing radiation: L-penicillamine hydrochloride, 25:54605
BUECKER, Horst, Repair of ultraviolet-damages after irradiation of bacteria in the vacuum, 25:55356
BUELTMANN, F.-J., Profilography of sacroiliac joints in ankylosing spondylitis, 25:55287
BUGAEV, E. V., Cosmic muons and neutrinos, 25:56469
BUGG, D. V., πP elastic scattering, 0 to 300 MeV, 25:56422 (CERN-71-14, pp 379-93)
BUHL, David, Microwave receivers for molecular line radio astronomy, 25:55091
BULANOV, L. A., Feasibility of the thermal decomposition of methyl alcohol in fission fragment tracks, 25:54645
BULAT, S. I., Plasticity and strength of nickel--molybdenum alloys at high temperature, 25:55474
BULL, S. R., Pulsed-source investigations. II, 25:57190
BULLA, Wolfgang, Disturbance of second-order coherence by interaction, 25:56456
BUNATYAN, G. G., Cross section for production of W boson by high-energy neutrinos in the electromagnetic field of a proton, 25:56473
Probability of the ($\mu^-$, ν) process of $^{139}La$ and $^{208}Pb$ nuclei, 25:56739 (JINR-P1-6006)
BUNNEY, Leland R., Exposure rates from products of thermal-neutron fission of $^{235}U$ at selected times after fission, 25:55231
BUNTING, William David Jr., Steady-state and dynamic probe characteristics in a low-density plasma, 25:56012
BURBAN-LUTZ, A. M., Analysis of $K^+$/sub e3/ radiative decay, 25:56410
BURGART, C. E., MORSE Monte Carlo shielding calculations for the zirconium hydride reference reactor, 25:57133 (ORNL-TM-3366)
BURGHARD, H. C. Jr., Investigation of sensitization of type 304 stainless steel safe-ends, 25:55378 (SWRI-1228-P-7-40)
BURKE, J. C., Plutonium concentration in organisms of the Atlantic Ocean, 25:55161
BURKHANOV, G. S., Physical metallurgy of refractory and rare metals, 25:55438
BURLAGA, L. F., Reverse and forward slow shocks in the solar wind, 25:55735 (N-71-24166)
BURLIN, T. E., Radiation quantities in health physics, 25:55251
BURMAN, R. L., LAMPF low-energy pion line, 25:56589 (LA-DC-12730)
BURNETTE, Keith Thomas, Nucleation and motion of single fluxons in superconductors, 25:56098
BURNS, E. T., Experimental and analytical studies of fast neutron transport in iron, 25:56618 (RPI-328-230)
BURNS, James Martin Jr., Experimental determination of the differential cross section for the reaction d(p,2p)n, 25:56644
BUROVA, N. N., Intracrystallite liquation in nickel alloys containing niobium, 25:55506
BURREN, J. W., Automatic measurement of film from high-energy physics experiments, 25:55047
BURSTEIN, Sumner, Radioimmunoassay of the F prostaglandins, 25:55144
BURYMOV, E. M., Stripping process for (α,p) and (α,d) reactions on light nuclei, 25:56677
BUSALOV, Yu. E., Metal-fibre-reinforced ceramics, 25:55608 (LB/G-3074)
BUSCHOW, K. H. J., Samarium--iron system, 25:55569
BUSEV, A. I., Ruthenium and osmium separate spectrophotometric determination by use of 4-(2-pyridylazo)-resorcinol, 25:54412
BUSI, Fabio, Effect of olefins on the reactions of nitrous oxide in γ-irradiated liquid cyclopentane, 25:54655
BUTLER, J. K., Remote-readout balance for use in a highly radioactive environment, 25:55080 (TRG-Report-2086)
BUTLER, M. K., Computer performance measurements using the Argonne benchmark problem collection: a status report, 25:57167 (CONF-710302-(Vol.2), pp 901-12)
BUTLER, M. M., Hydrogen isotope effect in the reaction of trityl radicals with thiophenol, 25:54570
BUTLER, W. R., Experiments measuring particle widths and the width of the ω, 25:56430
BUXTON, G. V., Recent experiments on steady state and pulse radiolysis of alkaline aqueous systems, 25:54627 (CONF-700652-(Vol.2), pp 295-330)

XUM

BUZZARD, Robert J., Effect of grain size on creep properties of a W--25 at. percent Re--30 at. percent Mo alloy from 1800 to 4000°F, 25:55431 (N-71-23110)
BYAKOV, V. M., Reactivity of $Ce^{4+}$ ions in irradiated aqueous solutions of sulfuric acid, 25:54647
BYERS, Jack A., Simulation of plasma microinstabilities with superparticle computer models, 25:56206
BYRNE, J. G., Chemical vapor deposited tungsten: mechanical evaluation at high temperatures, 25:55440
BYRON, F. W. Jr., Excitation of atomic hydrogen and helium in the eikonal approximation, 25:56874

## C

CABANE, M., Study of the mobility of ions in air, 25:54801
CABASSA, M., Uses of computer in radiotherapy. III, 25:55218
CADEK, F. F., Interchannel thermal mixing with mixing vane grids, 25:57031 (WCAP-7755)
CADEWELL, J. L., OH absorption in the direction of W44, 25:55716
CAFASSO, Fred A., Solubility of helium and argon in liquid sodium, 25:54583
CAGE, A. L., Frequency tables of the geomagnetic index Kp, 1932--1970, 25:56017
CAGNETTI, P., Atmospheric diffusion parameters by smoke plume photography, 25:54783
Conditioning of high activity liquid wastes, 25:54726
CAIRD, R. S., Use of a magnetic field to measure particle velocity. I, 25:57233 (LA-4545)
CAIRNS, R. L., Elevated temperature mechanical properties of a dispersion strengthened superalloy, 25:55483
CALDERON, M., Effects of gamma radiation on moths. I, 25:55315
Effects of gamma radiation on moths. II, 25:55316
CALDWELL, Burton V., Radioimmunoassay of the F prostaglandins, 25:55144
CALKINS, K. W., Application of an inert atmosphere to a plutonium processing system, 25:54943 (CONF-710401-, pp 69-82)
CALLAHAN, A., Kπ scattering phase shifts determined from the reactions $K^+p \to K^+\pi^-\Delta$ and $K^+p \to K^0\pi^0\Delta$, 25:56486
CAMBELL, R. H., Construction and engineering of PFR, 25:56998
CAMIDGE, F. Paul, Localized character of magnetotail magnetic fluctuations during polar magnetic substorms, 25:56040
CAMILLERI, L., $A_2^-$ production in channel $\pi^-+$ neutrals near threshold, 25:56436
CANDES, P., Irradiation and calibration devices, 25:54851
CANNATA, F., Isotensor dipole sum rules in nuclear electroexcitation, 25:56868
CANO, R., Coupling of EM waves in an inhomogeneous plasma, 25:56225 (CEA-CONF-1802)
Spatial determination of direction of magnetic field in Tokamak configuration, 25:56223
CANONICO, D. A., Transition temperature considerations for thick-wall steel nuclear pressure vessels, 25:55588
CANT, Noel W., Catalytic oxidation. IV. Ethylene and propylene oxidation over gold, 25:54569
CANTRELL, C. D., Photon statistics of linear coherent amplification of spontaneously emitted light, 25:57242 (NYO-3406-20)
CANTRELL, W. G., Increasing hadron--nucleus cross sections and cosmic ray muon zenithal variations, 25:55906
CAPELLMANN, Herbert, Incipient antiferromagnetism in scandium and superconductors with magnetic impurities in a singlet ground state, 25:56109
CARDITO, Joseph Michael, Spin polarization effects on neutron transport, 25:56633
CARDWELL, D. W., Application of computer generated graphs and diagrams to the development of advanced nuclear reactors, 25:57008
CARELLI, Mario D., Fission gas and molten fuel ejection from failed fuel rods in an LMFBR, 25:57075 (CONF-710302-(Vol.1), pp 79-96)
CARETTE, J.-D., Electrostatic spectrometer. I, 25:55082
Electrostatic spectrometer. II, 25:55083
Electrostatic spectrometer. III, 25:55084
CARLSON, L. E., In-beam study of prompt γ-rays emitted in $^{66}Zn(p,n\gamma)^{66}Ga$ reaction, 25:56732
CARLSON, O. N., Thorium--copper system, 25:55571
CARLSON, R. V., Safety considerations at the Babcock and Wilcox Plutonium Development Laboratory, 25:54958 (CONF-710401-, pp 258-66)
CARLTON, D., Prestressing and proof pressure testing of Wylfa prestressed concrete pressure vessels, 25:56883
CARMICHAEL, Hugh, Steplike changes in the long-term modulation of cosmic rays, 25:55912
CARNAHAN, Thomas George, Small angle tilt and twist grain boundary strengthening in yttrium, 25:55430 (IS-T-459)
CARNEVALE, E. H., Prog. rpt. on ultrasonic thermometry in LMFBR systems, 12/68, 25:55078 (NYO-3906-5)
CAROLA, T. P. G., $^{27}Al(d,p)^{28}Al$ reaction at E/sub d/ = 12 MeV, 25:56709
CARPENTER, J. D., Safety considerations in the new Rocky Flats Plutonium Recovery Plant, 25:54961 (CONF-710401-, pp 297-9)
CARPENTER, R. W., Simple method of determination of the distribution and solubility limit of interstitials in substitutional solid solutions, 25:55568
CARPENTIER, Serge, Thermal luminescent material for ionizing radiation dosimetry, 25:55055
CARROLL, William R., Oxidative decarboxylation of polyaminocarboxylic acids. II, 25:54422
CARSON, T. R., Stellar opacity, 25:55685
CARTER, L. L., Monte Carlo sampling with continuously varying cross section along flight paths, 25:57164 (CONF-710302-(Vol.2), pp 871-6)
CARTER, Melvin W., Off-site medical planning and management for an experimental underground nuclear detonation, 25:55249
CARTWRIGHT, Brian G., Origin of F, Na, and Al in galactic cosmic radiation, 25:55911
CARUTHERS, L. T., Production of gases of known specific activity in a reactor for calibrating gaseous effluent monitors, 25:54986
CASALBUONI, R., Duffin--Kemmer-like wave equation for dual free mesons, 25:56489
CASE, A. H., Problems associated with $^{238}Pu$ processing, 25:54707 (CONF-710401-, pp 300-6)
CASEY, E. J., Reply to electron spin resonance of atomic silver on porous glass and silica gel surfaces, 25:54607
CASHWELL, E. D., Monte Carlo sampling with continuously varying cross section along flight paths, 25:57164 (CONF-710302-(Vol.2), pp 871-6)
CAST, John C., Low-velocity air gun and Hopkinson split-bar facility, 25:57289 (UCRL-51098)
CASTIGLIONI, M., Hot tritium reactions in $CH_4$ + $SiH_4$ system, 25:54678
CATALDO, Joseph C., Electrostatic confinement of an alkali-metal plasma, 25:56013
CATTELL, F. C., Recent experiments on steady state and pulse radiolysis of alkaline aqueous systems, 25:54627 (CONF-700652-(Vol.2), pp 295-330)
CAUFFMAN, David P., Double-probe measurements of convection electric fields with Injun-5, 25:55958
CAVILLINI, M., Nonspherical potentials and molecular scattering at thermal energies, 25:55852
CAZZOLI, S., Determination of the activity of fission products, 25:54699
CECCHINI, S., Short-period temperature effect on cosmic rays, 25:55898
CELONI, A. M., In-residence health and safety support in a plutonium facility, 25:55204 (CONF-710401-, pp 267-79)
CEMBER, Herman, Effect of temperature upon the uptake of $^{144}Ce$ by Chlamydomonas, 25:55162
CERNATESCU, C., Activity of hexokinase in rats, 25:55140
CESARSKY, Catherine J., Interpretation of recombination-line emission from the interstellar medium, 25:55797
CESARSKY, Diego A., Interpretation of recombination-line emission from the interstellar medium, 25:55797
CEZAIRLIYAN, A., Heat capacity of tantalum in range 1900 to 3000 K, 25:55494
CHAGNON, P. R., Angular correlations studies in $^{32}S(^3He,p\gamma)^{34}Cl$, 25:56712
CHAKRABARTI, C. L., Solvent isotope effects on decomposition of N,N-dialkyldithiocarbamic acids, 25:54560
CHAN, K. K., Electron spin resonance study of V(II). IV, 25:56384
CHAN, L. H., Marine geochemistry of uranium isotopes $^{230}Th$ and $^{231}Pa$, 25:54810
CHANDLER, L., Semi-classical model for elementary particles, 25:56450
CHANDRA, Harish, Self-consistent study of even Zn and Ge isotopes, 25:56720
CHANDRA, R., $^{167}Tm$: a new bone scanning agent, 25:55279
CHANDRAMOULI, S., Radioiodine distribution in the Tarapur power reactor environment during commissioning and initial operations, 25:56978
CHANDRASEKARAN, P. S., Para-Fermi operators and special unitary algebras, 25:56536
CHANDRASEKHAR, B. S., Fluctuation effects on thermal conductivity of one-dimensional superconductors, 25:56095
Phonon spectra of dilute Pb--In alloys observed by superconducting tunneling, 25:56075
CHANG, C. C., $^3H(^3He,\gamma)^6Li$ capture reaction and the structure of $^6Li$, 25:56664
T = 3/2 states in $^{11}C$, 25:56679
CHANG, Chau-ting, Behaviors of neptunium in aqueous solutions. I, 25:54733
CHANG, Shu-ting, Dome morphological mutant linked to the B incompatibility factor of Schizophyllum commune, 25:55186
CHAO, J. K., Reverse and forward slow shocks in the solar wind, 25:55735 (N-71-24166)
CHAPOROVA, I. N., Determination of the limits of solubility of tungsten in the nickel--copper solid solution of the tungsten--nickel--copper system, 25:55447
CHAPPELL, Charles R., Ogo 5 observations of polar cusp on Nov. 1, 1968, 25:56024
CHAPRON, Yves, Electrochemical process for detecting microporous zones in film material such as insulating films, 25:54859
CHAPUIS, Anne-Marie, Electrochemical process for detecting microporous zones in film material such as insulating films, 25:54859
CHARLEMAGNE, J., Infrared studies of low-temperature electron-irradiated Si, 25:56297

CHARLESWORTH, F. R., Leakage from a ruptured containment after accidental depressurisation of a gas cooled reactor, 25:57106
CHARMAN, W. N., Visual sensations produced by cosmic ray muons, 25:55341
CHARTRAND III, Mark Ray, Stellar distributions in Cygnus, 25:55790
CHASSAGNE, Daniel, Projector for radioactive sources used in plesiotherapy for nonradioactive preparation technique, 25:54902
CHATTERJEE, Aparesh, Neutron emission from prompt fragments in the fission of excited nuclei, 25:56856
CHATTERJEE, G., Electron capture by fast protons in He and $H_2$, 25:55837
CHAU, A. Y., Use of interactive computer graphics in high-energy physics, 25:55093
CHAUDHRY, M. T. N., Effect of γ irradiation on amino-acid content of proteins, 25:55364
CHAUDHURI, N. K., Spectrophotometric determination of uranium(VI) with benzoylacetanilide, 25:54423
CHEBOTAREVA, E. I., Interaction of a shock wave with a magnetic field, 25:55951
CHEEMA, M. N., Simultaneous determination of Sb, As, and Cu by neutron activation, 25:54515
CHEKHOVSKOI, V. Ya., Spectral emissivity of tantalum, 25:55495
CHEKHOVSKOYI, V. Ya., Measurement of thermal expansion of solids at high temperatures, 25:55493
CHEMYAKIN, G. V., High-frequency source of heavy ions, 25:55817
CHEN, Augustin C., Multiple-scattering expansions for nonrelativistic three-body collision problems. IV, 25:55867
CHEN, Augustine C., Multiple-scattering expansions for nonrelativistic three-body collision problems. III, 25:55868
CHEN, C. S., Piezo-spectroscopic study of radiation-produced absorption bands in Si, 25:56296
CHEN, H., Raman spectral study of bisulfate--sulfate systems. II. Constitution, equilibria, and ultrafast proton transfer in sulfuric acid, 25:54564
CHEN, J. C. Y., Multiple-scattering expansions for non-relativistic three-body collision problems, 25:56575
CHEN, Joseph C. Y., Multiple-scattering expansions for nonrelativistic three-body collision problems. V, 25:55866
Multiple-scattering expansions for nonrelativistic three-body collision problems. IV, 25:55867
Multiple-scattering expansions for nonrelativistic three-body collision problems. III, 25:55868
CHENEY, R. F., High-temperature strength of oxide-strengthened nickel alloys, 25:55486
Manufacture and properties of high-conductivity high-strength Cu--$ThO_2$, 25:55417
CHENG, H. S., Modeling and application of the adiabatic approximation for analyzing rod drop excursions, 25:57084 (CONF-710302-(Vol.1), pp 259-81)
Nodal integral transport method for calculation of two-dimensional power distributions in non-uniform lattices, 25:57156 (CONF-710302-(Vol.2), pp 655-78)
CHENG, Hung, Production of pion pairs in electron colliding beams, 25:56460
CHENG, L. J., Low-temperature photoconductivity in electron irradiated p-type Si, 25:56308
CHEREL, Guy, Improvements to shears used with irradiated fuel elements, 25:54838
CHEREPIVSKII, A. A., Determination of the rate of movement of the charge in rotary kilns by means of radioative isotopes, 25:54898
CHERNIEVSKII, V. K., Polarized particle sources, 25:56610
CHERNOV, L. A., Functions of the transition region for beryllium and some examples of its use, 25:56622
CHERNYAK, A. Ya., Properties of welded joints in V92Ts alloy, 25:55470
CHERNYAK, L. V., Production of parts of complex shape in lanthanum hexaboride, 25:55599
CHERNYSHOV, A. M., Effect of neutron irradiation on hydrogen electrode in fuel cell, 25:54602
CHERRY, J. H., Effects of gamma irradiation on chromatin of sugar beet, 25:55351
CHERRY, N. H., Gravitational red-shift in the theory of the generalized gravitational potential, 25:55808
CHERRY, R. D., $^{226}Ra$ in marine phytoplankton, 25:55155
CHERTOK, Robert J., Retention and excretion by pigs of radionuclides produced by the Plowshare Event Schooner, 25:55124
CHESNOKOVA, V. D., Differential cross sections for elastic scattering of nucleons, 25:56789
CHEVALLIER, M., (α, 2α) reaction on $^{9}Be$ at 42.8 and 49.2 MeV and on $^{16}O$ at 49.2 and 52.5 MeV, 25:56674
CHIANG, C. C., Gauge invariant chiral Lagrangian and anti pp annihilations, 25:56538 (ORO-3992-2)
Lagrangian formalism for neutral massive spin 3 fields, 25:56548 (ORO-3992-1)
CHIBOWSKI, D., Application of γ irradiated heterogenic bovine fascia in filling brain defects in dogs, 25:55148
CHIDA, Katsuhisa, Secondary ion emission from metal surface in collisions of 30-keV $Ar^+$ ions, 25:55818
CHIKALLA, T. D., Berkelium--oxygen system, 25:55428 (BNWL-B-108)
CHIKOV, N., Measurement of the ratio of the radiative capture to fission cross sections (α) for $^{239}Pu$ in the neutron energy range 0.1 to 30 keV, 25:56734 (BNL-tr-446)
Technique of average ν measurement with the neutron time-of-flight spectrometer, 25:55039 (LB/G-3040)
CHIMONAS, G., Atmospheric gravity waves induced by solar eclipse. II, 25:56016
CHINENKOV, I. A., Influence of longitudinal magnetic field on hydraulic resistance in turbulent flow of fluids in pipes, 25:55937
CHIOLA, Vincent, Process for removing cerium and thorium from the other rare earth metals, 25:54749
CHIRICO, J. H., Mass formula consistent with nuclear-matter calculations vs conventional mass-law extrapolations, 25:56853
CHIRKOV, N. P., Annual variations and gradient of cosmic-ray intensity in the meridional plane, 25:55900
CHISTOV, E. D., Accidental dosage estimation at large gamma-irradiation facilities, 25:55235
CHISTYAKOV, E. M., Laws governing spreading of metallic melts over surface of boron nitride, 25:55469
CHMUTOV, K. V., Isolation of promethium by displacement chromatography due to complex formation, 25:54723
CHO, D. H., Pressure generation by molten fuel-coolant interactions under LMFBR accident conditions, 25:57073 (CONF-710302-(Vol.1), pp 25-49)
CHOI, Chan Kyoo, Electron-impact excitation of helium atoms to metastable states, 25:55843
CHOI, Eon Ho, Effects of gamma-radiation on sprout-inhibition of garlic bulbs and the changes of their chemical contents, 25:55354
CHOLLET, J. C., Interference between $\pi^0\pi^0$ decay of K/sub L/$^0$ and K/sub S/$^0$, 25:56407
CHOMICKI, Oskar, Immunofluorescent tests in course of /sup 99m/Tc scintiscanning, 25:55292
CHOWDHURY, A. Roy, Determination of absolute value g/sub A/ from Veneziano amplitude and current algebra sum rule for π--N scattering, 25:56516
CHRAPLYVY, Z. V., Approximate evaluation of the relativistic correction in potential scattering of charged particles, 25:55846
CHRIEN, R. E., Distribution of partial radiation widths in $^{238}U(n,\gamma)^{239}U$, 25:56790
CHRISTENSEN, A. Noerlund, Hydrothermal preparation of some oxides and some oxide hydroxides at temperatures up to 900°C and pressures up to 80 kb, 25:55602
CHRISTENSON, C. W., Processing of plutonium-contaminated liquid wastes at Los Alamos, 25:54708 (CONF-710401-, pp 369-85)
CHRISTIAN, Emily J. B., Mechanisms of acute injury in the γ-irradiated chicken: in vivo studies of dose protraction effects on the microvasculature, 25:55324
CHRYSOCHOOS, John, Reactivity of hydrogen atoms and hydrated electrons toward aqueous erythrosin. X-radiolysis, 25:54664
X-radiolysis of aqueous erythrosin, 25:55139
CHU, C. W., Low-temperature x-ray diffraction studies of near-equiatomic V--Ru alloys, 25:55532
CHU, H. B., Near-isothermal dissipative flow of liquid He II at supercritical velocities, 25:56062
CHU, S. L., Liner plate buckling and behavior of stud and rib type anchors, 25:56995
CHUISTOV, K. V., Moessbauer effect in the segregating iron--beryllium alloy, 25:56378
CHULICK, E. T., Recoil study of $^{209}Bi(\alpha,p)$/sup 212m,g/Po reaction mechanism, 25:56799
CHULICK, Eugene T., Delayed neutrons from tau- and α-induced fission of $^{238}U$, $^{232}Th$, and $^{209}Bi$, 25:56803
CHUMBALOVA, R. A., Dimensions of the galactic cosmic-ray modulation region, 25:55901
CHUN, Hee Young, Gamma-irradiation effect on electrical properties of B-type insulator, 25:55101
CHUN, J. S., Chemical vapor deposited tungsten: mechanical evaluation at high temperatures, 25:55440
CHUYANOV, V. A., Stabilization of flute instability with integrating feedback system, 25:56197
CILIEVICI, O., Mitotic aberrations induced in rat by single dose of 800 R, 25:55192
CINTRA, Sebastiao Hermano Leite, Reactivity of $U_3O_8$--Al dispersions, 25:55609 (ORNL-tr-2456)
CLAAR, T. D., Materials-coolant interactions relevant to EBR-II, 25:57109 (ANL-7771)
CLARE, L. P., TZM molybdenum alloy via P/M, 25:55418
CLARK, A. M., X-ray induced life-shortening mutations in Habrobracon: a genetic approach to senescence and duration of life, 25:55185
CLARK, C. D., Electron traps in deformed KCl, 25:56321
CLARK, Eugene Ellis, Observational effects of local inhomogeneities in cosmological models, 25:55809
CLARK, J. B., Recovery from x-ray and nitrogen mustard inactivation of Escherichia coli by 2, 4-dinitrophenol treatment, 25:55355
CLARK, K. C., Simultaneous spectrographic triangulation of an SAR arc and a hydrogen arc, 25:55971
CLARK, K. J., Electron--ion recombination: critical review of theories and experimental results for an argon plasma, 25:56182
CLARK, R. G., Internal-conversion coefficients in decay of /sup 83m/Kr, 25:56708
Nuclear power plant in the nuclear material safeguards accounting system, 25:54934 (BNWL-1598)

XUM

Status of burnup calculational technology as applied to the nuclear materials safeguards accounting system, 25:54935 (BNWL-1599)
CLARKE, John, Finite-voltage behavior of lead/copper/lead junctions, 25:56107
CLARKE, John F., Regularization method of unfolding x-ray spectrum, 25:56134 (ORNL-TM-3582)
CLARKE, M. E., Construction of electron distribution functions from laser scattering spectra, 25:56143
CLAUSS, A., Structure and tensile properties of Nb--4.6 Ti--O, 25:55521
Structure and tensile properties of Nb--Zr--O alloys rich in Nb, 25:55522
CLEGG, M. A., Substructure strengthening in dispersion-strengthened nickel alloys, 25:55492
CLEGHORN, Timothy Fuller, Solar modulation of the very heavy (Z0 less than or equal to Z less than or equal to 30) cosmic ray nuclei, 25:55909
CLEM, Ray G., Rotated mercury cell for controlled potential coulometry. Elimination of background current by digital normalization, 25:54427
CLEMENT, Genevieve, Decoloring Cyanophycene algae by extraction of their pigments, 25:57236 (LA-tr-71-73)
CLEMONS, Lester Jr., COHORT-2: Monte Carlo general purpose shielding computer code, 25:56262 (N-71-22378)
CLERC, M., Kinetic study of species formed during the pulsed radiolysis of ammonia, 25:54661
CLOSS, R. L., Sporadic E and geomagnetic activity, 25:56015
CLOUD, S. D., Energy levels of $^{16}O$ in region of excitation between 13.5 and 15.0 MeV, 25:56681
CLOUGHERTY, E. V., Thermal and electrical conductivities of some electrically conducting compounds, 25:55627
CLOUT, P. N., Computer control of experiments in atomic physics, 25:55094
CLUNE, Lavern C., Structure in the neutron scattering spectra of zirconium hydride, 25:56343
CLUSAZ, A., COSTANZA (R,Z), 25:57187 (EUR-4673)
COCEVA, C., Spin-dependence of level density in $^{178}Hf$ and $^{180}Hf$ by resonance neutron capture experiments, 25:56751 (RT/FI-(70)55)
CODE, R. F., Molecular-beam magnetic-resonance studies of HD and $D_2$, 25:55826
CODREANU, Steliana, Double correlation equations of the magnetic field and velocity in an isotropic conducting turbulent flow, 25:55916
COETZEE, N., Energy levels of $^{79}Br$ and $^{81}Br$, 25:56698
COGBURN, R. R., Method of dosimetry for a bulk-grain irradiator, 25:55234
COHEN, D., Reaction of Re and Tc metals with molten Li perchlorate and the Raman spectra of corresponding melts, 25:54538
COHEN, H., Oxidation of benzoatopentaamminecobalt(III) by hydroxyl radicals, 25:54669
COHEN, M., James wave function for the ground state of $H_2^+$, 25:55829
COHEN, S., Systems approach to the nuclear shell model, 25:56866
COHEN, Theodore, Isotope effects after the rate-determining step. The role of rotational isomerism in a hydrogen transfer, 25:54577
COHEN, Y., Radiochemical study of stability of selenomethionine $^{75}Se$, 25:54698
COJOCARU, V., Instrumental neutron activation analysis of some new standard rocks, 25:54464
COKER, W. R., $^{86}Kr(d,n)^{87}Rb$/sup A/ threshold cusp and the systematic appearance of charge-exchange cusps, 25:56719
COLBURN, D. S., North--south component of interplanetary magnetic field: Explorer 33 and 35 data, 25:55779
COLE, C. R., Comparative metabolism of intravenously injected promethium in swine and humans, 25:55108 (BNWL-SA-3747)
COLE, N. C., Weldability of tungsten and its alloys, 25:55410
COLE, Ronald S., Inactivation of Escherichia coli, F' episomes at transfer, and bacteriophage lambda by psoralen plus 360-nm light: significance of deoxyribonucleic acid cross-links, 25:55361
COLEMAN, P. J., North--south component of interplanetary magnetic field: Explorer 33 and 35 data, 25:55779
COLEMAN, W. A., Monte Carlo calculation of the effect of subterranean perturbations on reflected x rays, 25:56274
COLLATZ, S., Spectral function representation of time- and energy-dependent neutron density in fast media. II, 25:56625
COLLIER, W. D., TRESS: a finite element code for stress analysis problems, 25:57285 (TRG-Report-1813)
COLLINS, C. H., Influence of ionising radiation on thermal annealing in the crossover region of potassium chromate, 25:54679
COLLINS, K. E., Influence of ionising radiation on thermal annealing in the crossover region of potassium chromate, 25:54679
COLLINS, Roy, Improvements in and relating to nuclear radiation attenuating means, 25:55657
COLUCCI, John, Radioimmunoassay of triiodothyronine in unextracted human serum, 25:55146
COLUCCIA, S., Infrared study of surface properties of α-chromia. I. Preparation and adsorption of water, heavy water, and carbon monoxide, 25:54565
COMANICIU, Nicolae, Isotopic shift constant and electric quadrupole moments of neodymium, 25:55828
COMFORT, J. R., Particle-hole multiplets in $^{88}Y$ and the mechanism of ($^3He$,t) reaction, 25:56779
COM-NOUGUE, J., Relation between the kinetics of aging after deformation of α-zirconium and the anisotropic diffusion of oxygen for a short distance, 25:55551
COMPTON, W. D., Recombination luminescence in irradiated silicon, 25:56294
Recombination luminescence in irradiated silicon, 25:56295
CONDON, J. B., Instrument for measuring the hydrogen content of metals, 25:54424
CONNOLLY, T. J., Pulsed-source investigations. I, 25:57189
Pulsed-source investigations. II, 25:57190
CONRAD, H., Deformation dynamics of a b.c.c. titanium alloy (15.2 at. percent Mo) below 650°K (approximately or proportional to 0.4 T/sub m/), 25:55459
Structure property relations in beryllium sheet, 25:55510
COOK, David M., Radiation from charged particles in weakly inhomogeneous magnetic fields, 25:56177
COOK, E. M., Radioactivity released from a liquid metal fast breeder reactor fuel recycle complex, 25:54754
COOK, I., Numerical experiments on nonlinear plasma instabilities, 25:56205
COOKE, F. W., Structure property relations in beryllium sheet, 25:55510
COOLBAUGH, M. J., Energy and angular distributions of $^{60}Co$ gamma rays penetrating a concrete shield, 25:56272
Fast neutron spectroscopy in aqueous media using an NE-213 proton-recoil neutron spectrometer system, 25:55034 (COO-2049-7)
COOLEY, J. L., Effects of chronic irradiation on laboratory populations of the quatic snail physa heterostropha, 25:55314
COOPER, J. R., Crystal field levels and superconductivity in $LaAl_2$--rare earth alloys, 25:56359
COOPER, W. B., Multiple aperture extractor design for producing intense ion and neutral beams, 25:56213 (LBL-327)
COPPI, Bruno, Processes of magnetic-energy conversion and solar flares, 25:55773
CORAOR, G. R., Flash photolysis of a substituted hexaarylbiimidazole and reactions of the imidazolyl radical, 25:54561
CORBETT, B. L., Prog. rpt. on high flux isotope reactor, 4--6/71, 25:57120 (ORNL-TM-3569)
CORBIT, C. D., Reactors, radiation, and risk: the three Rs of public concern, 25:55347
CORELLI, J. C., Piezo-spectroscopic study of radiation-produced absorption bands in Si, 25:56296
CORNELL, R. M., Nucleation of bubbles and re-solution effects in uranium dioxide irradiated at elevated temperatures, 25:55649
CORNUALT, P., Interactions among various carbons in the course of heat treatment, 25:57275 (SC-T-713060)
CORNUAULT, P., Influence of speed of graphitization of carbon products on dimensional variations produced by neutron irradiation, 25:55645 (CEA-CONF-1821)
CORVI, F., Spin-dependence of level density in $^{178}Hf$ and $^{180}Hf$ by resonance neutron capture experiments, 25:56751 (RT/FI-(70)55)
COTTRELL, Wm. B., ORNL nuclear safety research and development program bimonthly report for May--June 1971, 25:57092 (ORNL-TM-3483)
COUCH, J. G., Structure in the neutron scattering spectra of zirconium hydride, 25:56343
COUCH, R. G., Photodisintegration rate of $^{24}Mg$, 25:55703
COULTER, H. W., Geologic and seismic consideratıcns affecting nuclear power plant site selection, 25:54777
COULTER, J. R., Electronic particle counting and dispensing device for use in animal injection experiments, 25:55090
COWAN, Robert D., Highly ionized Fe and Ni lines in 200- to 400-A of solar spectrum, 25:55774
COX, Aaron J. Jr., Search for fractionally charged particles in cosmic rays at mountain altitude, 25:55910
COX, T. H., Applications software for a fast reactor malfunction detector analyzer, 25:56878 (CONF-710302-(Vol.1), pp 199-214)
COYNE, D. G., Experiments measuring particle widths and the width of the ω, 25:56430
CRANDALL, W. K., Comparison of U.S. and U.S.S.R. methods of calculating the transport, diffusion, and deposition of radioactivity, 25:54782 (UCRL-51054)
CRANNELL, C. J., Calibration of NASA--GSFC High Energy Cosmic Ray Experiment, 25:55046 (N-71-16750)
CRASTAN, Valentin, Use of an element method program for solution of temperature distribution problems, 25:54882
CRAVEN, C. W. Jr., ROD: a nuclear and fuel-cycle analysis code for circulating-fuel reactors, 25:57048 (ORNL-TM-3359)
CRAWFORD, Bruce W., Synthetic transport theory method, 25:57154 (CONF-710302-(Vol.2), pp 625-43)
CRAWFORD, T. V., Comparison of U.S. and U.S.S.R. methods of calculating the transport, diffusion, and deposition of radioactivity, 25:54782 (UCRL-51054)

CRAWFORD, Wayne Thomas, Track registration process, 25:55010
CRAWLEY, D. T., Administrative procedures for criticality prevention in plutonium operations, 25:54966 (CONF-710401-, pp 430-7)
CRECELIUS, G., Local moment relaxation in a superconductor, 25:56071
CREFFIELD, G. K., Electrical resistivity of liquid K and of solutions of Na liquid K, 25:55527
Sodium--barium phase diagram, 25:55526
CRICCHIO, A., Experimental and theoretical determination of burnup and heavy isotope content in a fuel assembly irradiated in the Garigliano boiling water reactor, 25:56879 (EUR-4638)
CROCKET, J. H., Neutron activaton analysis for noble metals in geochemistry, 25:54484
CROOM, David L., Forecasting solar-proton events from time characteristics of solar-microwave bursts, 25:55758
Solar-microwave bursts as indicators of occurrence of solar-proton emission, 25:55757
CROSLEY, P. B., Crack arrest toughness of pressure vessel steels, 25:55513
CROSSLEY, D. A. Jr., Radioactive tracer studies of soil and litter arthropod food chains, 25:57281 (SRO-641-2)
CROZAZ, G., Nuclear interection tracks in minerals and their implications for extraterrestrial materials, 25:55669 (N-71-26344)
CRUDDACE, Ray, Pulsing x-ray source in Circinus, 25:55721
CRUSHA, Kenneth L., Record-keeping in a radiation safety office by timesharing digital computer, 25:54984
CSATH, G., Neutron activation analysis of impurities in Th and Zr, 25:54518
CSIKAI, J., Angular distributions of fragments in fission of U and Th near (n,2n'f) threshold, 25:56804
CUCCHI, G., Determination of the activity of fission products, 25:54699
CUJEC, B., Determination of angular correlations and mean lifetimes in $^{57}$Co, 25:56700
CULLIS, C. F., Deposition of pyrolytic carbon in silica reactors, 25:55604
CUMO, M., Photographic study of two-phase highly dispersed flows, 25:54875 (RT/ING-(71)8)
CUNNINGHAM, G. W., Nuclear reactor core analysis code: CITATION, 25:57183 (ORNL-TM-2496(Rev.2))
CUNNINGHAM III, G. W., Discussion about the nuclear reactor core analysis code citation, 25:57169 (CONF-710302-(Vol.2), pp 939-52)
ROD: a nuclear and fuel-cycle analysis code for circulating-fuel reactors, 25:57048 (ORNL-TM-3359)
CUPINI, E., Neutron thermalization in polycrystalline material by Monte Carlo method, 25:56619 (RT/FI-(70)49)
CURRENT, David Harlan, Soft sphere model for nuclear quadrupole resonance in rare earth trichlorides, 25:57220 (COO-1533-15)
CURTIS, O. L. Jr., Recombination parameters in low-resistivity gamma-irradiated n-type germanium, 25:56327
CUZZOCREA, P., Shell effects in (n,p) and (n,α) cross-sections at about 14 MeV, 25:56869
CYGANSKI, Andrzej, Analytical uses of lanthanide nitrite complexes. II, 25:54415
CYROT-LACKMANN, F., Binding energies of transition-metal atoms adsorbed on a transition metal, 25:56385
CYVIN, B. N., Infrared spectra of $LiAlF_4$ and $NaAlF_4$, 25:54563
CYVIN, S. J., Infrared spectra of $LiAlF_4$ and $NaAlF_4$, 25:54563
CZAPSKI, Gideon, Electron spin resonance studies of short-lived radicals generated by fast flow techniques in aqueous solutions, 25:54662
CZECHOWSKY, P., Calculations on current systems in the polar E region, 25:55977
CZITOBER, H., Scintigraphic evaluation of activity of Paget's disease, 25:55294
CZOCHRA, M., Application of γ irradiated heterogenic bovine fascia in filling brain defects in dogs, 25:55148

## D

DACH, K., Spectrocalorimetric measurements in core of heavy water reactor, 25:57123
D'ADAMO, D., Sampling of $^{3}$H-water vapor and measurement with a liquid scintillator, 25:54798
DAFFORN, Geoffrey Alan, Solvolysis of sulfonate esters in solvents of low nucleophilicity, 25:54559
DAHL, P. F., Recent developments in pulsed magnet multifilament superconducting wires, 25:56580 (BNL-16026)
DAINTON, F. S., Recent experiments on steady state and pulse radiolysis of alkaline aqueous systems, 25:54627 (CONF-700652-(Vol.2), pp 295-330)
DAJLEVIC, Radovan, Thermal luminescent material for ionizing radiation dosimetry, 25:55055
DALITZ, R. H., Spin-orbit coupling for Λ-$^{4}$He scattering using a one-boson-exchange model for the ΛN interaction, 25:56648
DALLE DONNE, M., Gas-breeder memorandum, 25:57065
DALMASSO, Josette, Study of the γ radiation accompanying the decay of Ms Th(II) ($^{228}$Ac), 25:56747 (ORNL-tr-2531)
DALU, G., Automatic counter for direct measurements of radon concentration, 25:55032
Experimental check on the removal of radon, 25:54802
DALU, G. A., Automatic counter for direct measurements of radon concentration, 25:55032
Experimental check on the removal of radon, 25:54802
DALY, D. F., EPR study of fast-neutron radiation damage in silicon, 25:56324
DALY, T. A., Two-dimensional fast-reactor disassembly analysis with space-time kinetics, 25:57078 (CONF-710302-(Vol.1), pp 128-51)
DAMIANO, V. V., Structure property relations in beryllium sheet, 25:55510
DAMS, R., Computer-assisted qualitative analysis of gamma-ray spectra, 25:54523
DANCE, K. D., Pulsed-source investigations. I, 25:57189
DANCHEVSKAYA, M. N., Catalysis by metal vapors. IV, 25:54552
DANELIYA, E. P., Construction of the solidus volume in the niobium--tungsten--titanium--zirconium system by the simplex-lattice method, 25:55529
Niobium--hafnium--carbon system in the niobium-rich region, 25:55563
DANETSKAYA, E. V., Effectiveness of a number of chemical substances in poisoning with a mixture of radioisotopes of cesium and strontium, 25:55113
DANIEL, Amiram, Heterogeneity of central nervous system myelin, 25:57261 (ORO-3195-49)
DANIEL, H., Muonic x-ray measurements with a high-pressure gas target, 25:55830
DANIELS, William R., Decay of $^{152}$Nd and the isomers of $^{152}$Pm, 25:56772
DANIELSON, B. G., Hepatic blood flow measured by $^{133}$Xe clearance, 25:55123
DANIELSSON, O., Automatic selection of kinematical hypotheses from two prong proton--proton interactions in a hydrogen bubble chamber at 19 GeV/c, 25:56523 (USIP-71-3)
Two prong sample from proton--proton interactions in a hydrogen bubble chamber at 19 GeV/c, 25:56417 (USIP-71-4)
DANIELSSON, Ove, Study of the reaction proton + proton + nucleon + nucleon + pion at 19 GeV/c, 25:56418 (USIP-71-6)
DANILKIN, N. P., Ionospheric effect of solar eclipse of Sep 22, 1968, 25:56000
DANILOV, V. I., Dependence of the beam shape in the centre of the synchrocyclotron on the accelerating voltage and magnetic field decay, 25:56585 (JINR-P9-5945)
DANNELS, R. A., Current status of ENDF/B processing codes, 25:57165 (CONF-710302-(Vol.2), pp 877-86)
DARASELIYA, G. Ya., Variability of Mycobacterium phlei in pigment formation induced by different mutagens, 25:55171
D'ARCY, D. F., PRESCON: a digital computer program for containment pressure transients, 25:57087 (CONF-710302-(Vol.1), pp 436-51)
DARMODJO, S., Quantitative studies of nuclear structure through isobaric analog resonances, 25:56769
DARNAULT, J., Effects in vivo of ionizing radiations on human chromosomes, 25:55178
DARRIULAT, P., Measurement of K/sub L/ + xeV form factor, 25:56408
DAS, H. A., Determination by neutron activation analysis of alkali and other trace elements in ultramafic rocks, 25:54496
Practical aspects of activation analysis with fast neutrons and photons, 25:54470
Routine determinations on rocks and sediments by activation analysis, 25:54463
DAS, J., Spectrophotometric determination of uranium(VI) with benzoylacetanilide, 25:54423
DASARATHY, Cuppam, Superplastic properties of Bi--In eutectic alloy, 25:55456
DAS GUPTA, M. K., Studies on solar x-ray flares recorded by SOLRAD-9 on Explorer 37 satellite, 25:55737
DATLA, R. U., Oscillator strengths of sodiumlike ions, 25:55776
DATTA, D. K., Nuclear materials and some aspects of machining, 25:57207
DATTA, Nanigopal, Hydromagnetic flow induced by the impulsive rotation of an infinite disc, 25:55947
DAUTCOURT, G., Topology and local physical laws, 25:55804
DAUTOV, L. M., Problem of calibration of isomeric shifts in gamma-resonance spectroscopy, 25:56370
DAVENPORT, C. H., Supplement to summary report on SNAP-19B (IRHS) program, 25:54893 (MLM-1736)
DAVIDSON, Joseph Henry, Stellar interferometry for faint astronomical objects, 25:55693
DAVIDSON, R. C., Electrostatic shielding of a test charge in a non-neutral plasma, 25:56175
DAVIDSON, W. F., In-beam study of prompt γ-rays emitted in $^{66}$Zn(p,nγ)$^{66}$Ga reaction, 25:56732
DAVIDSON, William Henry Thomas, Apparatus for irradiating materials with electrons, 25:54835
DAVIES, B. W., Use of interactive computer graphics in high-energy physics, 25:55093
DAVIS, Cecil G. Jr., Radiative-transfer model of a Cepheid, 25:55710
DAVIS, J. R., Operating experience with sodium pumps at EBR-II. EBR-II Project, 25:57028 (ANL-EBR-27)

XUM

DAVIS, John R., Detonation-wave effects on decameter-wavelength radio waves in the lower ionosphere, 25:55970
DAVIS, Lawrence W., Effectiveness of tranquilizing drugs in rats exposed to mixed gamma--neutron radiations, 25:55325
DAVIS, R. C., ORNL multi-ampere ion source, 25:56208 (CONF-711012-9)
DAVIS, T. N., Artificial aurora experiment: experiment and principal results, 25:55961
Artificial aurora experiment: ground-based optical observations, 25:55962
Magnetospheric convection pattern inferred from magnetic disturbance and auroral motions, 25:55954
DAVYDOV, B. I., Study of reactivity of the organism exposed to transverse accelerations and radioprotectants, 25:55264
DAVYDOV, V. M., Magnetic field of a local ionospheric current, 25:56001
DAVYDOV, Yu. P., Solubility products and colloid formation of radioelements, 25:54695
DAVYKOVA, V. V., Surface layer of surface-hardened parts of heat-resisting alloys, 25:55439
DAWSON, John M., Numerical simulation of toroidal plasma confinement with a fluid model, 25:56129
DAY, Eugene, Incorporation of [$^{14}$C]-glucosamine into synaptosomes, 25:57260 (ORO-3195-48)
DAY, Eugene D., Cellular and subcellular fractionation of brain tissue, 25:57259 (ORO-3195-47)
Flotation-fractionation of late fetal, neonatal, and adult rat brain in iso-osmotic Ficoll-sucrose density-gradients, 25:57257 (ORO-3195-45)
Heterogeneity of central nervous system myelin, 25:57261 (ORO-3195-49)
Immunity to human brain tumors, 25:57263 (ORO-3195-51)
Isolation and biochemical characterization of subfractions of rat central nervous tissue myelin, 25:57258 (ORO-3195-46)
Sequential adsorption analysis of antisynaptosome antibodies, 25:57254 (ORO-3195-42)
Sequential adsorption analysis of antimyelin antibodies, 25:57255 (ORO-3195-43)
Sequential adsorption analysis of radioantibodies, 25:57253 (ORO-3195-41)
Virus-cell relationships in dog brain tumors, 25:57262 (ORO-3195-50)
Zonal centrifuge profile analysis of msd mutant mouse brain, 25:57256 (ORO-3195-44)
DAYRAS, R., Determination of angular correlations and mean lifetimes in $^{57}$Co, 25:56700
DE, Anil K., Reverse phase partition chromatography on paper impregnated with 2-thenoyltrifluoroacetone, 25:54746
DEANGELIS, H. M., Electron irradiation of heavily doped GaAs:Si and GaAs:Te, 25:56292
DEAVER, Bascom S. Jr., Quantized flux states of superconducting cylinders, 25:56064
DE BOOR, Carl, Subroutine package for calculating with B-splines, 25:57235 (LA-4728)
DE BORTOLI, M., Sampling of $^{3}$H-water vapor and measurement with a liquid scintillator, 25:54798
DE BRION, J. P., Regge analysis of the reactions $\pi^-$p → etan and K$^-$p → KantiK$^0$n with rho and A2 degenerate trajectories, 25:56506
DECHOW, Frederick John, An optical mixing spectroscopic study of interfacial fluctuations, 25:57232 (IS-T-494)
DECK, K. A., $O_2$ Herzberg I bands in the night airglow, 25:56046
DEDENKOV, A. N., $^{103}$Pd distribution in the animal organism, 25:55112
DEEGAN, G. E., Operating experience with sodium pumps at EBR-II. EBR-II Project, 25:57028 (ANL-EBR-27)
DEEN, S. M., Coefficients for partial wave analysis of the reaction $0^- + 1/2^+ \rightarrow 1^- + 1/2^+$, 25:56501 (RHEL/R-224)
DE FEITER, L. D., Flux of gamma rays from solar flares, 25:55762
DEGTYAREVA, E. V., Technological conditions for hot pressing of zirconium dioxide, 25:55600
DEHOFF, R. T., Prog. rpt. on quantitative determination of structure-property relationships in nuclear fuel element materials, 12/16/70--3/15/71, 25:55437 (TID-25784)
DEHTYAR, I. Ya., Moessbauer effect in the segregating iron--beryllium alloy, 25:56378
DEISENHAMMER, E., Angiographic and angioscintigraphic comparisons in cerebral vascular processes, 25:55289
DE LA FUENTE, H., Small coaxial gun for plasma injection studies, 25:56220
DELAGE, Y., Electrostatic spectrometer. I, 25:55082
DE LAGUNA, W., Safety analysis of waste disposal by hydraulic fracturing at Oak Ridge, 25:54971 (ORNL-4665)
DELARUE, Roger, Thermal luminescent material for ionizing radiation dosimetry, 25:55055
DELBRASSINE, A., Temperature distribution in irradiated oxide fuel with dispersed burnable poison, 25:57194
DELENE, J. G., Computer code for simulating large MSF evaporator desalting plant dynamics, 25:57248 (ORNL-TM-2933)
DELOFF, A., Λ-excited states of hypernuclei, 25:56524
DELOLLIS, N. J., Effects of rf activated inert gas plasmas on critical surface tension and bondability of polydimethyl silicones and polyethylene, 25:57272 (SC-RR-710483)
DELOUCHE, Gilles, Projector for radioactive sources used in plesiotherapy for nonradioactive preparation technique, 25:54902
DELOZIER, R. C., CONCEPT: computerized conceptual cost estimates for steam--electric power plants. Phase I user's manual, 25:57063 (ORNL-TM-3276)
DELSANTO, P. P., Giant dipole resonance in 1p--1h continuum shell-model approximation for $^{208}$Pb, 25:56800
DELUCA, P. M., Angular correlations studies in $^{32}$S($^{3}$He,pγ)$^{34}$Cl, 25:56712
DE MARCHI, V. S., Electrically activated pressure-sintering (spark sintering) of titanium--aluminum--vanadium alloy powders, 25:55413
DE MARCO, F., Probing of an inhomogeneous plasma with electromagnetic waves, 25:56145
DEMEUR, M., Excitation of the hydrogen atom by a fast proton, 25:55841
DEMIDOV, B. A., Turbulent heating and confinement of plasma in a toroidal multipole trap, 25:56127
DEMIRKHANOV, R. A., Toroidal traps R-0 and RT-2 with steady and high-frequency magnetic fields, 25:56221
DEMTCHENKO, V. V., Effect of electromagnetic wave-field pressure on the propagation of slow TM waves, 25:56235
Radiation of charged-particle beams in passage through cubic nonlinear media, 25:56168
DENES, Jean-Francois, Simulation of electron avalanche in He by Monte Carlo type calculation, 25:56265 (ORNL-tr-2518)
DEN HOUTING, A. W., RAGA: a Monte Carlo program for calculation of gamma-ray transport in a reactor shield for multi-region slab geometry, using exponential transformation, 25:57026 (RCN-146)
DENISOV, S. P., Energy dependence of $\pi^-$, K$^-$, and a anti p total cross sections on protons in momentum range up to 65 GeV/c, 25:56433
DENNIS, B. R., Experiment to measure hard solar and celestial x rays, 25:55734 (N-71-23434)
DE PAULA E SILVA, E., Relation between the kinetics of aging after deformation of α-zirconium and the anisotropic diffusion of oxygen for a short distance, 25:55551
DEREM, A., Regge analysis of the reactions $\pi^-$p → etan and K$^-$p → KantiK$^0$n with rho and A2 degenerate trajectories, 25:56506
DERIAN, L., Radiation experiment on tubular fuel element with finned surface. II, 25:57050 (UJV-2551-RT)
DERNIER, P. D., Low-temperature x-ray diffraction studies of near-equiatomic V--Ru alloys, 25:55532
DERUSSIT, Richard, Substantially fluid tight closure device between two coaxial walls, 25:54860
DESAI, S. K., Energy distribution of electrons in gas-discharge plasma, 25:56138
DE SAUSSURE, G., Measurements of the neutron fission and absorption cross sections of $^{239}$Pu over the energy region 0.02 eV to 30 keV, Part II, 25:56746 (ORNL-4707)
DESBOROUGH, G. A., Neutron activation analysis for osmium, ruthenium, and iridium in some silicate rocks and rock-forming minerals, 25:54486
DESHPANDE, Y. H., Studies on yttrium, thorium, and uranium salicylaldehyde complexes, 25:54539
DESIMIROV, G., Relativistic expansions, 25:56577
DE SOUZA E SILVA, R., Note on prestressed concrete pressure vessel, 25:56989
DESREUX, V., Automatic dilatometer for radiation polymerizations, 25:54616
DE SWINIARSKI, R., Deformations in the s--d shell and inelastic scattering of polarized protons, 25:56828 (LYCEN-7104, S9.1-7)
DE TEMPLE, Bernhard, Loading and unloading machine, 25:57210
DEUTSCH, R. V., Generation of magnetohydrodynamic waves in nonhomogeneous plasma located in intense magnetic field, 25:55923
DE VELLIS, Jean, Isolation of high molecular weight RNAs from cultured neural tumor cells, 25:57286 (UCLA-12-832)
DE VILLIERS, J. A. M., Energy levels of $^{79}$Br and $^{81}$Br, 25:56698
DEVIN, A. B., Spontaneous reversion frequencies of radiosensitive strains of Saccharomyces cerevisiae, 25:55352
DE VRIES, D. P., Compact mutants induced by x-ray treatment in apple and pear, 25:55174
DE WERD, L. A., Comments on supralinearity and sensitization of thermoluminescent phosphor lithium fluoride, 25:56338
DE WET, W. J., Direct determination of the noble metals by activation analysis utilizing high-resolution gamma spectrometry, 25:54487
DEWEY, W. C., Radiosensitization with 5-bromodeoxyuridine of Chinese hamster cells x-irradiated during different phases of the cell cycle, 25:55258
DE WINTER, H., Isotopic renogram by patients suffering from cervical carcinoma, 25:55275
DEZSI, I., Conference on the application of the Moessbauer effect, Tihany, Hungary, 6/69, 25:56374
DHAR, Sanat K., Solubility of helium and argon in liquid sodium, 25:54583

DIAMOND, I., Uptake and release of $^{45}Ca$ by brain microsomes, synaptosomes, and synaptic vesicles, 25:55120
DIBBERT, Hans-Juergen, Influence of foreign atoms on recovery of Frenkel defects in electron-irradiated platinum, 25:56284 (JUL-731-FF)
DIBON, H., Application of Veneziano model including spins to reaction $k^+p \to K^{*+}(890)p$, 25:56511
DICK, L., Polarization in proton--proton elastic scattering at 10, 14, and 17.5 GeV/c, 25:56419
Polarization parameter in $K^+$-p and anti pp elastic scattering at 10 and 14 GeV/c, 25:56438
Polarization parameter in $\pi^+p$ elastic scattering at 10, 14, and 17.5 GeV/c, 25:56437
DICKENS, J. K., Energies and intensities of gamma rays emitted by a $^{226}Ra$ source, 25:55041 (ORNL-TM-3509)
DICKERMAN, C. E., Analysis of fuel failure experiments with TREAT, 25:57110 (CONF-710302-(Vol.1), pp 97-101)
DIEPERS, H., Effect of C on critical current of $Nb_3Sn$, 25:56084
DIETERICH, W., Theory of lattice softening and spin susceptibility in A 15 compounds, 25:56344
DIHLMANN, W., Profilography of sacroiliac joints in ankylosing spondylitis, 25:55287
DILELLA, L., Photon asymmetry for radiative $\mu$ capture in Ca, 25:56705
DILLINGER, Pavel, Determination of boron in boric glasses by the neutron absorption method, 25:54437 (RFP-Trans-82)
DIMOV, G. I., Charge-exchange method of proton injection into accelerators and accumulators, 25:56590 (LA-tr-71-46)
DIONISIO, Jose Sant'Ana, Electromagnetic transitions in $^{190}Pt$, 25:56760
DITZEL, Joern, Glomerular filtration rate determined by $^{51}Cr$-EDTA, 25:55122
DIVON, Baruch, Study of the isospin form of the electromagnetic operator, 25:56839
DJORDJEVIC, Cirila, Spectrophotometric determination of niobium with 4-(2-pyridylazo)resorcinol and colored complexes separated from oxalic and tartaric acid systems, 25:54425
DLUGACH, R. E., Determination of the association constants of ions from the rate of oxygen exchange between anions and water, 25:54553
DMITREVSKII, Yu. P., Energy dependence of $\pi^-$, $K^-$, and a anti p total cross sections on protons in momentum range up to 65 GeV/c, 25:56433
DMITRIEV, P. P., $^{48}V$ in nuclear reactions on cyclotron, 25:54677
$^{51}Cr$ on cyclotron, 25:54691
DNESTROVSKII, Yu. N., Compression of plasma by growing longitudinal magnetic field in Tokamak, 25:56125
DOBRESCU, C., Burn-out heat fluxes at subcooled boiling, 25:54871 (IFA-TR-58)
DOBROGOSZ, Walter J., Prog. rpt. on biochemistry of development in the diptera, 1/1/69--9/15/71, 25:57265 (ORO-3883-3)
DOBROWOLSKI, Jan, Determination of impurities in high purity tellurium. III, 25:54414
DOBYCHIN, E. I., Coefficient of electromagnetic ejection of solids from conducting fluids, 25:55930
Dynamics of liquid-metal drops in electromagnetic field in conditions of reduced gravitation, 25:55931
DO DANG, G., Short-range correlations, 25:56824 (LYCEN-7104, C4.1-17)
DODDS, Phyllis R., Separation of yttrium and cerium, 25:54750
DODELET, J.-P., Kinetics of charge scavenging in $\gamma$-irradiated liquid cyclohexane, 25:54668
DOERING, George I., Radiation gauge calibration, 25:55060
DOGADKIN, N. N., Radioactivation determination of impurities in the epitaxial films of gallium arsenide, 25:54512
DOKASHENKO, V. P., Suppression of $(n,\gamma)$ reaction in resonant scattering of neutrons by a perfect CdS crystal, 25:56627
DOMINICI, G., Sampling of $^3H$-water vapor and measurement with a liquid scintillator, 25:54798
DOMNING, W. E., Design of filter plenum heat exchangers, 25:54950 (CONF-710401-, pp 162-80)
DONALDSON, E. E., Adsorption and absorption of hydrogen by niobium, 25:55434 (RLO-2221-T-7-3)
DONDI, M. G., Nonspherical potentials and molecular scattering at thermal energies, 25:55852
DONEA, J., Simplified visco-elastic analysis of graphitic bodies subjected to external loads, temperature gradients and neutron irradiation, 25:55646 (EUR-4674)
DONELLI, M. G., Chemotherapy of leukemia and chemical protection against ionizing radiations, 25:57229 (EUR-4483)
DONG, Wilbur Donald, Surface reaction of oxygen with tungsten, 25:55396
DONIVAN, Frank Forbes Jr., Radio investigations of clusters of galaxies, 25:55789
DONOVAN, E. J. Jr., Reference zirconium hydride reactor, 25:57132 (AI-AEC-Memo-12715(Del.))
DONSKOV, S. V., Energy dependence of $\pi^-$, $K^-$, and a anti p total cross sections on protons in momentum range up to 65 GeV/c, 25:56433
DOOLEY, R. B., Oxidation of Ta--Hf polycrystals and single crystals, 25:55397
Oxidation of Ta--W polycrystals and single crystals, 25:55385
DOREMUS, R. H., Delayed elasticity resulting from periodic stress-induced atomic diffusion, 25:55458
DORONIN, V. T., Estimation of the single-stage isotope separation factor in the electromigration of isotopic ions through an ion-exchange membrane, 25:54729
DOSE, Klaus, Effect of ionizing radiation and uv light on N-acetylglycine, 25:54650
DOSHCHECHKIN, V. P., Possibility of gamma spectroscopy in well logging in the presence of radon, 25:54759
DOWD, M., Experimental approach to the determination of radiographic technique for light alloy specimens of 3-30 mm thickness, 25:54929
DOWNS, Gene L., Technique for the metallographic preparation of lead, 25:57239 (MLM-OP-71004)
DOWNS, W. E., Neutron activation and on-stream analysis in mineral industries using SHERLOCK III, 25:54506
DOYLE, J. M., Liner plate buckling and behavior of stud and rib type anchors, 25:56995
DOZORETS, Yu. L., Changes in the content of electrolytes under the influence of radioiodine treatment in patients suffering from diffuse toxic goiter with a severe form of thyrotoxicosis, 25:55340
DRAGANU, M., Theoretical study of Lorentz plasma, 25:56173
DRAGOUN, O., Anomalous internal conversion of E1 transitions in outer atomic shells, 25:56797
DRAKE, Marvin K., ENDF/B library: a current status report, 25:57173 (CONF-710302-(Vol.2), pp 991-1003)
DRANOVA, Zh. I., Field-ion-microscope study of W deformed by an electrostatic field at 900 to 1700°K, 25:55451
DRAUTMAN, J. J., Magnetic properties of commercial soft magnetic alloys at cryogenic temperatures, 25:56361
DREMIN, A. N., Effect of shock waves on refractory compounds. I, 25:55618
DRESSER, M. J., Adsorption and absorption of hydrogen by niobium, 25:55434 (RLO-2221-T-7-3)
DRITS, M. E., Study of phase equilibria in the aluminum--copper--yttrium system, 25:55561
DROBYSHEV, V. N., Effect of shock waves on refractory compounds. I, 25:55618
DRONKERS, J., Regge analysis of the reactions $\pi^-p \to \eta n$ and $K^-p \to Kant\bar{K}^0n$ with rho and A2 degenerate trajectories, 25:56506
Secondary Regge contributions in charge exchange reactions at $t = 0$, 25:56508
DROUET, A., Electronic and magnetic properties of carbon fibers: development under neutron irradiation, 25:56282 (CEA-CONF-1822)
DROUET, J., Relative biological effectiveness as a function of linear energy transfer for cataract criterion in the rabbit, 25:55317 (CEA-CONF-1744)
DROUSSENT, Roger, Insulating device for a fuel element, 25:57195
DRUI, M. S., Laws governing spreading of metallic melts over surface of boron nitride, 25:55469
DRUMHELLER, D. S., Frequency-filtering theory for the propagation of stress pulses in composite materials, 25:57269 (SC-DR-710472)
DRYNKIN, V. I., Cupel assay of gold by an activation method, 25:54521
D'SILVA, Arthur P., Analytical applications of x-ray excited optical fluorescence. Direct determinations of rare earth nuclear poisons in uranium at the part per giga (1 in $10^9$) level, 25:54428
DUANE, A., $A_2^-$ production in channel $\pi^-+$ neutrals near threshold, 25:56436
DUBAL, L., Evidence for boson production via isobar decay, 25:56525
DUBININ, E. M., Experiments with artificial solar wind, 25:56009
DUBININ, N. P., Potential changes of chromosomes as a result of interaction of radiation and alkylating compounds, 25:55260
DUBOVITSKAYA, N. V., Influence of deformation conditions on polygonization and recrystallization of single-crystal molybdenum, 25:55559
DUBOVOI, E. I., Mechanism of direct nuclear reactions, 25:56864
Regularities of photonuclear reactions, 25:56676
DUBROVIN, A. V., Superconducting properties of niobium--titanium--zirconium hafnium alloys, 25:56104
Superconductive properties of niobium--zirconium--hafnium alloys, 25:56105
DUCASTELLE, F., Binding energies of transition-metal atoms adsorbed on a transition metal, 25:56385
DUCE, F. A., Iodine chemistry in steam air atmospheres, 25:54547
DU CHAFFAUT, F., Interactions among various carbons in the course of heat treatment, 25:57275 (SC-T-713060)
DUCLOS, J., Spark chamber experiment on the beta decay of $\Xi^-$ hyperons, 25:56411
DUCROS, Yves, Polarization parameter measurement in proton--proton elastic scattering from 0.5 to 1.2 GeV, 25:56412 (CEA-R-4193)
DUDA, C. T., Effects of gamma irradiation on chromatin of sugar beet, 25:55351
DUDEY, N. D., Integral measurements in EBR-II of capture rates, fission rates, and $\alpha$ for $^{233}U$, $^{235}U$, $^{238}U$, $^{239}Pu$, $^{240}Pu$, and $^{242}Pu$, 25:56982 (ANL-7791)
DUDZIAK, Donald J., Generating moments of the photon

XUM

production matrices and sources from ENDF data: the LAPHAN code, 25:57175 (CONF-710302-(Vol.2), pp 1016-23)
DUFFA, G., Measurement of mobility and mass of atmospheric ions, 25:54800
DUGGAL, S. P., Unusual anisotropic solar-particle event of November 18, 1968, 25:55764
DULCIC, Antonije, Crystal structure dependence of radiation-induced radicals in thymine: an esr study, 25:55130
DULLER, N. M., Increasing hadron--nucleus cross sections and cosmic ray muon zenithal variations, 25:55906
DUMONT, G., Chemical decanning of fuel elements by means of $HF/O_2$ mixtures, 25:54747
DUNAEVA, K. M., Investigation of U(IV) complexing with acetate and formate ions, 25:54581
DUNBAR, J. L., Fibre reinforced materials, 25:57214 (AWRE-O-77/70)
DUNCAN, R. G., Gas permeability of extruded graphite, 25:55612
DUNDAS, Peter H., Radiation measurements and low frequency and high-pressure investigations of induction heated plasma, 25:56146 (N-71-27023)
DUNGAN, R. H., Development of processes for the hot pressing of silicon--germanium thermoelectric elements, 25:57267 (SC-DR-710438)
DUNHAM, V. L., Effects of gamma irradiation on chromatin of sugar beet, 25:55351
DUNJIC, A., Functional and circulatory changes in rats after local irradiation, 25:55328
DUNLAP, J. H., Battelle's research plutonium facility environmental control and safety, 25:54959 (CONF-710401-, pp 280-92)
DUNN, F. E., SAS2A LMFBR accident analysis code, 25:57077 (CONF-710302-(Vol.1), pp 120-7)
DUNN, Leslie, Measurement of plutonium in soil around the Nevada Test Site, 25:54755 (CONF-710401-, pp 320-7)
DUNNETT, D. A., Invariants in the motion of a charged particle in a spatially modulated magnetic field, 25:56401
DUPART, E., Electronic and magnetic properties of carbon fibers: development under neutron irradiation, 25:56282 (CEA-CONF-1822)
Thermal annealing of neutron-irradiated carbon, 25:56283 (CEA-CONF-1823)
DU PREEZ, J. G. H., N-substituted urea complexes of thorium and uranium tetrahalides, 25:54536
DURAND, J. L., Quasi free scattering in $^2H(p,2p)$ and $^2H(p,pn)$ reaction from 21.5 to 56.4 MeV, 25:56640 (FRNC-CONF-8)
DURAND, M., Quasi free scattering in $^2H(p,2p)$ and $^2H(p,pn)$ reaction from 21.5 to 56.4 MeV, 25:56640 (FRNC-CONF-8)
DU SAULT, Lucille A., Application of the oxygen factor to clinical radiotherapy, 25:55302
DUSCIN, L., Probing of an inhomogeneous plasma with electromagnetic waves, 25:56145
DUTCHAK, Ya. I., Interrelation between phase diagram and composition--property diagrams of In--Sn system, 25:55546
DUTOVA, T. A., Spontaneous reversion frequencies of radiosensitive strains of Saccharomyces cerevisiae, 25:55352
DUTT, V. V. S. Eswara, Triphenylmethane dyes as redox indicators in dichrometry, 25:54410
DUTTON, R., Effect of temperature, pressure and concentration gradients on diffusion, 25:57213 (AECL-3793)
DUXLER, William M., Polarized-orbital method and application to scattering of electrons by He, 25:55871
DVORAK, E., Some pathomorphological findings in acute radiation sickness in goats, 25:55318 (LB/G-2995)
D'YACHENKO, V. D., Determination of the boundary of high frequency wave absorption between the electron cyclotron and the low hybrid frequency, 25:56224 (AEC-tr-7270)
DYAL, Palmer, Electrical conductivity and temperature of lunar interior, 25:55810
DYER, N. C., Decay of $^{58}Mn$, 25:56710
DYSTHE, K. B., Triggered whistler emissions, 25:56038
DZHARAK'YAN, T. K., Some principles of evaluating the effectiveness of radioprotective agents in man, 25:55256
DZHAUGASHTIN, K. E., Turbulent jets of conducting fluids. II, 25:55922
DZHEMARD'YAN, Yu. A., Use of accelerated charged particles for determination of concentration of light elements, 25:54528

## E

EARGLE, D. Hoye, Uranium in Texas, 25:54804
EASH, D. T., Tritium trick, 25:55575 (LA-DC-12996)
EAST, J. K., Cytofluorograph system, 25:57249 (ORNL-TM-3536)
EBERLE, S. H., Influence of irradiation conditions on californium formation in nuclear reactors, 25:57067
EBRIGHT, F. L., High-speed motion-picture studies of film boiling in liquid helium II, 25:56061
EBSTEIN, B. S., Respiration of brain slices in heavy water, 25:55121
EDER, O. J., Zero Placzek moment and the n-phonon cross section, 25:56340 (AERE-Trans-1137)
EDISS, C., Some aspects of measurement of $^{32}P$ Cherenkov radiation in water by liquid scintillation spectrometer, 25:54438
EDWARDS, Ross B., Isolation of high molecular weight RNAs from cultured neural tumor cells, 25:57286 (UCLA-12-832)
EERNISSE, E. P., Ion implantation damage study using lateral stress measurements, 25:56285 (SC-RR-710424)
EFREMOV, E. N., Valence states of Eu and Dy in Laves phases and isomer shifts in Moessbauer spectra, 25:56379
EGGEN, D. T., Comparison between momentum integral and compressible models for sodium voiding calculations in LMFBR, 25:57081 (CONF-710302-(Vol.1), pp 180-98)
EGOSHIN, V. G., $^{14}N(d,p)^{15}N$, $^{28}Si(d,p)^{29}Si$, and $^{32}S(d,p)^{33}S$ reactions with polarized deuterons, 25:56724
EGUCHI, T., Determination of the coupling strength from duality and unitarity, 25:56478
EHLERS, Jerry William, Ground state properties of spherically symmetric nuclei using the modified delta interaction, 25:56840
EHLERS, K. W., Large-area high-current ion source, 25:56212 (LBL-35)
EHMANN, W. D., 14 MeV neutron activation analysis of rocks and meteorites, 25:54465
Coincidence counting applied to the activation analysis of meteorites and rocks, 25:54479
Elemental abundance trends in the australite strewn field by non-destructive neutron activation, 25:54478
EHRENFREUND, E., Study of a series of $Nb_3X$ compounds by nuclear magnetic resonance, 25:56373
EICHHORN, Hans-Juergen, Standardization of 2- and 4-axial $^{60}Co$ pendulum irradiation of small pelvis, 25:55222
EIKENBERRY, H. M., Solidification mechanism of uranium ingots, 25:55400 (NLCO-1077)
EISENBUD, Merril, Manmade radionuclides in the Hudson River estuary, 25:55160
EISENHAUER, C. M., Prog. rpt. on radiation transport studies, 7/70--2/71, 25:56255 (AD-721388)
EISENHAUER, P., Quantitative evaluation of thyroid scintigrams by computer, 25:55282
EISENSTEIN, Laura, Partial wave analysis of 3π system in mass region 1.0 to 2.0 GeV, 25:56482 (COO-1195-224)
EISMONT, O. A., Convective movement of a conducting liquid with a current in a transverse magnetic field, 25:55948
EKLUND, S., Nuclear power and international cooperation, 25:56999
EKWALL, P. A., Fuel cartridge with helical cross-pieces, 25:57198
EL BAZ, E., Description of elastic scattering processes with the use of nonlocal separable potentials, 25:56852
Separable nonlocal potentials and their equivalent local potentials in elastic scattering studies, 25:56642 (LYCEN-7104, C5.1-15)
ELBEK, Bent, Single nucleon transfer in deformed nuclei, 25:56875
ELDRUP, M., Positron annihilation in γ-irradiated 10 M NaOH glassy ice, 25:55835
EL GAWHARY, A., Bremsstrahlung of nonpolarized and longitudinally polarized electrons, 25:56862
ELGAWHARY, S. M., Differential Sr--Ca bonding on soil as influenced by bonding site, 25:54778
ELIASHVILI, M. A., K/sub 13/ decays and chiral symmetry-breaking, 25:56537 (JINR-E2-5996)
ELLINGTON, J. P., TRESS: a finite element code for stress analysis problems, 25:57285 (TRG-Report-1813)
ELLIOTT, J. N., PRESCON: a digital computer program for containment pressure transients, 25:57087 (CONF-710302-(Vol.1), pp 436-51)
ELLIS, G. F. R., Topology and cosmology, 25:55802
ELLIS, R., Least-squares fitting of wire spark chamber events, 25:55049
ELLIS, R. J., Track finding in wire spark chamber data, 25:55048
EL-SIRAGY, N. M., Radiation of charged-particle beams in passage through cubic nonlinear media, 25:56168
ELYUTIN, A. V., Behavior of impurities in niobium during vacuum melting, 25:55403
EMAN, B., Parity nonconservation in heavy nuclei and the structure of weak-interaction Hamiltonians, 25:56768
EMELITY, L. A., Processing of plutonium-contaminated liquid wastes at Los Alamos, 25:54708 (CONF-710401-, pp 369-85)
EMMETT, M. B., MORSEC: revised cross-section module for MORSE multigroup Monte Carlo code, 25:56263 (ORNL-4716)
EMRICK, Roy M., Prog. rpt. on high temperature anneals of defects quenched in metals, final, 1971, 25:57216 (COO-1456-16)
EMYASHEV, A. V., Pyrolytic titanium and zirconium nitrides and fields of their use, 25:55605
ENCRENAZ, P., Pulsar JP 1933: 21-cm line absorption profile and interstellar scintillation, 25:55724
ENG, R. D., Friction welding of titanium alloys, 25:55409
ENGEL, L. B. Jr., Corrosion resistance of tantalum, T-111, and Nb--1Zr to Hg at 1200 F, 25:55377 (N-71-26947)
ENGELHARDT, W., Radiation losses of a theta pinch plasma in the wavelength range 100 to 200 Angstroms, 25:56149 (IPP-1/108)

ENGELMANN, Ch., Determination of Be, B, C, N, O, and F by p, d, $^{3}$He, and α activation. II, 25:54520
ENGLADE, Ronald C., Effect of the solar boundary condition on flare-particle propagation, 25:55738
ENGLAND, G. L., Analysis of perforated end caps for pressure vessels by finite element method, 25:56985
Calculation of time-dependent stresses in PCPVS, 25:56988
Migration of moisture and pore pressures in heated concrete, 25:55665
ENGLE, G. B., Influence of pitch-binder coke content on the properties and irradiation behavior of molded graphite, 25:55653
EPIFANOV, Yu. N., Ladder approximation for vertex function in non renormalizable theory of ω rho π interaction, 25:56483 (JINR-E2-6017)
ERA, A., Density measurements of steam--water mixtures flowing in a tubular channel under adiabatic and heated conditions, 25:57032
ERAMZHYAN, R. A., Neutron-channel in muon capture and short range nucleon--nucleon correlations, 25:56641 (JINR-P4-5986)
Spectrum and asymmetry of high energy neutrons in the reaction $\mu^- + {}^{16}O \rightarrow {}^{15}N + n + \nu$, 25:56820 (JINR-P4-5997)
ERDTMANN, G., Combined peaksearch and peakfit in data processing of γ-spectra, 25:54472
EREMENKO, V. N., Cross section of Mo--Zr--Cr system at 1150°C, 25:55538
EREMIN, L. P., Temperature of thermal peaks during irradiation of ionic crystals, 25:56318
ERGEN, William K., Consistency in siting practices regarding nuclear plants, 25:56975
ERICSON, M., Soft and hard pions in nuclei, 25:56808 (CERN-71-14, pp 1-65)
ERIKSSON, Goesta, Radiosensitivity and dose-effect relation in low dose region, 25:55190
ERMOLAEV, B. I., Thermal expansion of W--Cu pseudoalloys, 25:55468
ERMOLAEVA, G. K., Boundary layer at electrode of an MHD duct in absence of ionization equilibrium, 25:55946
ERNST, H., Perfusion lung scintigraphy in primary vascular pulmonary hypertension, 25:55284
ERNST, O., Photometric determination of small amounts of chloride in selenium, tellurium, gallium, and bismuth, 25:54407
ERSHOV, B. G., Impurity paramagnetic center in γ-irradiated salts, 25:56339
Nature and properties of trapped electrons in polar substances, 25:54593 (CONF-700652-(Vol.2), pp 261-93)
ERSHOVA, L. S., Dispersion-hardening of an iron--cobalt--tungsten alloy, 25:55423
ERWIN, A. R., Inelasticity of multipion production from a quark model, 25:56514
ERWIN, Wallace, Hot-atom chemistry of $^{14}C$ in solid benzene at kinetic energies between 5 and 100 electron volts, 25:54703
ESAKI, Kenichiro, Planning and execution of the Mt. Enasan Tunnel, 25:57252 (ORNL-tr-2525)
ESAKI, L., Electron transport in Nb/Nb oxide/Bi tunnel junctions, 25:56078
ESTABLE-PUIG, Juan F., Cell response of the olfactory bulb to ionizing radiation injury, 25:55336
ESTABLE-PUIG, Rosita F., Cell response of the olfactory bulb to ionizing radiation injury, 25:55336
ETTMAYER, P., About nitrides and carbonitrides and nitride-based cemented hard alloys, 25:55629
EVANS, D. J. R., Neutron activation analysis of intact drill core, 25:54469
EVANS, E. P., Induction of translocations in mouse spermatogonia. IV, 25:55182
EVANS, John C. Jr., Radon emanation from the lunar surface, 25:54440
EVANS, John Charles Jr., Study of solar flare history by measurement of $^{22}Na$ and $^{26}Al$ production profiles in lunar rocks, 25:55772
EVANS, R. A., Effect of γ irradiation on amino-acid content of proteins, 25:55364
EVANS, Rudolph, Mechanism of the radiation-induced dechlorination of 1,1,1-trichloro-2,2-bis(p-chlorophenyl)ethane in alcholic solution, 25:54620
EVANS, W. F. J., Comments on paper 'oxygen atmospheric and infrared atmospheric bands in the aurora', 25:56018
EVDOKIMOV, Yu. D., Gamma--gamma method in mining geology, 25:55066
EVERETT, M. R., Dimensional and physical property changes of graphites, pyrocarbons, and fuel bodies, 25:55651
EVERITT, C. W. F., Superfluid plug for space, 25:56119
EVSEEV, V. S., Probability of the ($\mu^-$, ν) process of $^{139}La$ and $^{208}Pb$ nuclei, 25:56739 (JINR-P1-6006)
EWING, R. L., Method for the routine measurement of dielectric photoconductivity, 25:55079 (SC-DC-713696)
EXNER, H. E., Electronic structure of refractory carbides and its relation to wetting, 25:55643
Grain growth in liquid-phase sintering of carbides, 25:55642
EYRING, L., Berkelium--oxygen system, 25:55428 (BNWL-B-108)
EZAKI, Y., Circulation pumps for nuclear use, 25:54857

# F

FABER, C., LEIDI: computer program for power distribution with respect to materials and processes within a reactor, 25:57000
FABRE DE LA RIPELLE, M., Resolution of the N-body problem in the hyperspherical formalism, 25:56390 (LYCEN-7104, S5.1-53)
FADEEV, V. I., Kinetic energy of fragments of $^{238}U$ and $^{232}Th$ fission, 25:56787
FAHLESON, U. V., Electric fields in the nighttime and daytime auroral zone, 25:55960
FAHR, Egon, Physical, chemical, and molecular biological processes in ultraviolet irradiation of biological objects, 25:55136
FAIMAN, David, Harmonic oscillator analysis of the hyperon spectrum, 25:56507
FAIRBANK, W. M., Superfluid plug for space, 25:56119
FAIRFIELD, Donald H., Average and unusual locations of the Earth's magnetopause and bow shock, 25:56021
FAIRHALL, A. W., Mass-yield curve of first-chance fission from proton- and deuteron-induced fission of $^{226}Ra$, 25:56775
FALLGATTER, Karen, Physical and analytical properties of a microwave excited plasma, 25:56158
FALOCI, C., Health protection analysis of transportation of radioactive substances through tunnels, 25:54973 (RT/PROT-(71)11)
FAM, S., Prog. rpt. on ultrasonic thermometry in LMFBR systems, 12/68, 25:55078 (NYO-3906-5)
FANCHENKO, S. D., Turbulent heating and confinement of plasma in a toroidal multipole trap, 25:56127
FANGER, U., Proposal for installation of a versatile $e^- - e^+ - \gamma$ spectrometer for neutron capture spectroscopy, 25:55040 (NP-18994)
FANG-LANDAU, G., Experiments measuring particle widths and the width of the ω, 25:56430
FANTOLA-LAZZARINI, A. L., Correlated annealings of $^{60}Co$ recoiled atoms in cationic and anionic sites of neutron-irradiated crystals of cis-[Co en$_2$($NO_2$) CNS][Co EDTA]$2H_2O$, 25:54682
FARACH, Horacio A., Influence of nuclear Zeeman term on anisotropic hyperfine patterns in electron spin resonance, 25:54641
FARELLO, G. E., Photographic study of two-phase highly dispersed flows, 25:54875 (RT/ING-(71)8)
FARRELL, K., Radiation-induced voids in high-purity magnesium, 25:55580
FARRER, P. A., Production of $^{52}Fe$ by $^{55}Mn(p,4n)^{52}Fe$ reaction for medical use, 25:54676
FASISKA, Barbara C., Urinary excretion of $^{241}Am$ under DTPA therapy, 25:55118
FASSEL, Velmer A., Analytical applications of x-ray excited optical fluorescence. Direct determinations of rare earth nuclear poisons in uranium at the part per giga (1 in $10^9$) level, 25:54428
FATEEVA, L. N., Reaction $^{12}C(\alpha p_0)^{15}N$, 25:56675
FATKULLIN, M. N., Models of electron density distribution in F2 region. I, 25:55984
Variations of electron density in topside ionosphere at middle latitudes, 25:55993
FAW, R. E., Energy and angular distributions of $^{60}Co$ gamma rays penetrating a concrete shield, 25:56272
Fast neutron spectroscopy in aqueous media using an NE-213 proton-recoil neutron spectrometer system, 25:55034 (COO-2049-7)
FAY, K., Radioprotective action of endotoxin, 25:55267
FAYARD, C., Description of elastic scattering processes with the use of nonlocal separable potentials, 25:56852
Separable nonlocal potentials and their equivalent local potentials in elastic scattering studies, 25:56642 (LYCEN-7104, C5.1-15)
FAYER, Yu. N., Ionospheric effect of solar eclipse of Sep 22, 1968, 25:56000
FEATES, F. S., Radiolytic reaction between graphite and $CO_2$. II, 25:55654
Radiolytic reaction between graphite and $CO_2$. III, 25:55655
FEDCHENKO, M. A., Isothermal heat of evaporation of ytterbium and neodymium ions on a tungsten surface, 25:55533
FEDDERS, Heinrich, Measurement of heat transfer in the bubble boiling of water in metallic tubes, 25:54872 (JUL-740-RB)
FEDER, Harold M., Solubility of helium and argon in liquid sodium, 25:54583
FEDOROV, A. N., Magnetic field of a local ionospheric current, 25:56001
FEDOROV, M. I., Effect of the dimensions of the fuel element of the heat transfer at supercritical pressures, 25:54880
FEDOROV, V. M., Electrode phenomena and the acceleration of plasma, 25:56153
FEDOROVICH, G. V., Rapidly varying geomagnetic field disturbances produced by a nonstationary source of gamma quanta, 25:55989
FEDOROVICH, V. A., Interference of ''black'' absorbers in

XUM

moderating medium, 25:57205
Measurement of ''black'' absorbers of equivalent sizes and identical efficiency in a moderating medium by a pulsed-source technique, 25:57206
FEDOTOV, S. I., Δ N = +- 2 mixing in odd-N deformed nuclei, 25:56737 (JINR-E4-5877)
FEDYAKINA, N. I., Proton anomalies in propagation of very long radio waves at middle latitudes, 25:55996
FEHRENTZ, Dieter, Ratio tissue and maximum for 42 and 25 MV x-rays of 42 MeV betatron, 25:55219
FEIGE, Yehuda, Passive moisture meter, 25:55061
FELBER, G., Non-contact thread velocity measurement through point labelling, 25:54900
FEL'DGUN, L. I., Laws governing spreading of metallic melts over surface of boron nitride, 25:55469
FENEBERG, W., Tokamak with superposed multipole magnetic field, 25:56211 (IPP-III-2)
FENYES, T., Collector system of an isotope separator for investigating short-lived isotopes, 25:56584 (JINR-P6-5888)
FEOKTISTOV, B. V., Dependence of the beam shape in the centre of the synchrocyclotron on the accelerating voltage and magnetic field decay, 25:56585 (JINR-P9-5945)
FERRARI, G., Photographic study of two-phase highly dispersed flows, 25:54875 (RT/ING-(71)8)
FERRERO, M. I., Measurement of K/sub L/ + neV form factor, 25:56408
FERRIEUX, H., Mechanical effects of a contained nuclear explosion, 25:54820 (UCRL-Trans-10543, pp 4-35)
FESENKO, V. V., Mass-spectrometric ion source for high-temperature investigations, 25:55081
FESTOFF, B. W., Incorporation of [$^{14}$C]-glucosamine into synaptosomes, 25:57260 (ORO-3195-48)
FETISOV, N. I., Interaction between 14-MeV neutrons and nuclei of Fe, Cu, and Nb, 25:56684 (FEI-216)
FEUERBACHER, B., Experimental investigation of the band structure of graphite, 25:56348
FICHTEL, Carl E., Considerations related to the sudden release of a large number of cosmic rays in the galaxy, 25:55895 (N-71-24988)
FIDELLE, Jean-Pierre, Introduction of hydrogen isotopes in metals by means of a miniaturized cathode loading cell, 25:54858
FIDONE, I., Spatial determination of direction of magnetic field in Tokamak configuration, 25:56223
FIEBIG, Guenter, Optimization of the resolving power and the intensity of particle spectrometers using as the example the parabolic spectrographs, 25:55037 (JUL-737-FF)
FIELD, J. H., Performance tests of sodium-filled powder and pellet oxide fuel under transient overpower, 25:57046 (GEAP-13722)
FIENNING, William C., EDIT program operating manual for the Playback Executive System, 25:57270 (SC-M-710527)
FIES, C. L., Radiological evaluation of a hypothetical core disruptive accident, 25:57113 (HEDL-TME-71-33)
FIGUERA, A. S., Properties of 12.50 and 12.52 MeV levels of $^{15}$N, 25:56669
FILEWICZ, E. C., Behavior and calibration of devices for monitoring impurities in sodium, 25:55069 (ANL-7804)
FILIPENOK, S. P., Dependence of buildup factor on the position of shielding between bremsstrahlung source and detector, 25:56280
FILIPPOV, A. T., Ladder approximation for vertex function in non renormalizable theory of w rho w interaction, 25:56483 (JINR-E2-6017)
FIL'KOVA, E. M., Radiation treatment of lymphogranulomatosis of the bone, 25:55301
FILLATRE, A., Interactions among various carbons in the course of heat treatment, 25:57275 (SC-T-713060)
FINCH, D. R., ENDF/B cross section preparation and testing in the JOSHUA system, 25:57176 (CONF-710302-(Vol.2), pp 1024-30)
FINK, R. W., M-subshell fluorescence yields and $L_1$--$L_3$ radiative transition at Z = 93 and 96, 25:55825
FINKEL, Robert C., Radon emanation from the lunar surface, 25:54440
FINKELSTEIN, J., Some consequences of exchange degeneracy and tripe-Regge-hypothesis, 25:56515
FINLAYSON, T. R., Effect of deformation on transition temperature of Nb--32 percent Zr, 25:56099
FINNEMORE, D. K., Superconductivity and magnetic scattering in La--Ce, 25:56068
FINSTON, Harmon L., $^{40}$Ar(n,α)$^{37}$S reaction at 14.4 MeV, 25:56718
Prog. rpt., 6/70--5/71, 25:54692 (NYO-3417-15)
Reactions of $^{20}$Ne with 14.3-MeV neutrons, 25:56717
FIORE, A., Quasi free scattering in $^{2}$H(p,2p) and $^{2}$H(p,pn) reaction from 21.5 to 56.4 MeV, 25:56640 (FRNC-CONF-8)
FIRESTONE, A., Evidence for structure in Kr mass system near 1.85 GeV, 25:56434
FISCHER, G., SAS2A LMFBR accident analysis code, 25:57077 (CONF-710302-(Vol.1), pp 120-7)
FISCHMEISTER, H., Stability of oxide dispersions in iron- and nickel-based alloys, 25:55485
FISHER, F. D., Glovebox fire-resistant materials and fire suppression tests, 25:54939 (CONF-710401-, pp 17-25)
FITTON, B., Experimental investigation of the band structure of graphite, 25:56348
FLAKUS, F. N., Determination of beryllium in rocks by activation analysis, using the $^{9}$Be(α,nγ)$^{12}$C reaction with $^{210}$Po, 25:54467
FLANAGAN, G. F., Evaluation of fuel-coolant interactions during disassembly of an LMFBR, 25:57074 (CONF-710302-(Vol.1), pp 50-78)
FLEGAL, William Malcolm, Study of the velocity profile in the entrance region of a magnetohydrodynamic channel, 25:55942
FLEISCHMAN, R. M., Preliminary outline of FTR nuclear systems start-up tests, 25:57114 (HEDL-TME-71-58)
FLEMING, S. J., Thermoluminescent dating principles and application, 25:54764
FLETCHER, N. R., Direct reaction analysis of reactions $^{7}$Li(d,t)$^{6}$Li and $^{7}$Li(tau,α)$^{6}$Li, 25:56671
Elastic scattering of deuterons by $^{6}$Li and $^{7}$Li at 8.0 to 12.0 MeV, 25:56670
FLETCHER, P. T., Nuclear power reactors, 25:57066
FLINN, Paul A., Simple monochromatic, polarized $^{57}$Fe Moessbauer source, 25:56366
FLIPOT, A. J., Temperature distribution in irradiated oxide fuel with dispersed burnable poison, 25:57194
FLOREK, M., Alpha widths of neutron resonances, 25:56754 (UCRL-Trans-10541)
Search for the (n,α) reaction in the resonances of the zinc and hafnium isotopes, 25:56686 (JINR-P3-5875)
FLORJANCIC, D., Problems of reactor circulating pumps, 25:57038
FLOWER, D. R., Identification of the lambda 417 line in the solar extreme-ultraviolet spectrum, 25:55767
FLYGARE, W. H., Microwave detection of interstellar formamide, 25:55784
FOCHT, William Laurie, Study of $^{14}$N using the $^{12}$C($^{3}$He,p)$^{14}$N and $^{12}$C($^{3}$He,2p)--$^{13}$C(g.s.) reactions, 25:56682
FOGEL, A. A., Method of holding molten metal in suspended state: characteristics of Lodochka inductor, 25:55424
FOLEY, J. T., Environment experienced by cargo during normal rail and truck transport, 25:54974 (SC-M-710241)
FOLSOM, T. R., Concentrations of plutonium, cobalt, and silver radionuclides in selected Pacific seaweeds, 25:55151 (CONF-710817-1)
Nonmetallic tools for sampling frozen tissues for trace metal analyses, 25:54450 (TID-25773)
FOMENKO, V. S., Emissive properties of materials, 25:56346
FOMIN, B. V., Computing geomagnetic field at intermediate ionospheric heights, 25:55990
FONTAN, J., Measurement of mobility and mass of atmospheric ions, 25:54800
FONTANA, M. H., Core melt-through in LMFBR's: a condensed review, 25:57093 (ORNL-TM-3504)
FORD, C. E., Induction of translocations in mouse spermatogonia. IV, 25:55182
FORD, M. J., High strength tungsten carbides, 25:55631
FORIS, Gabriella, Radioprotective action of endotoxin, 25:55267
FORSEN, H. K., Small coaxial gun for plasma injection studies, 25:56220
FORTUNE, H. T., Is the first excited 0$^{+}$ state in $^{44}$Ca of 6p-2h character, 25:56714
Spin assignments in $^{20}$F, 25:56716
FOSTER, R. G. Jr., Detection of boiling in nuclear reactors, 25:56996
FOUKAL, Peter, Morphological relationships in chromospheric Hα fine structure, 25:55748
FOULKES, F. M., Operating experience with other reactors, 25:56893 (70-CNA-631)
FOWLER, T. B., Discussion about the nuclear reactor core analysis code citation, 25:57169 (CONF-710302-(Vol.2), pp 939-52)
Nuclear reactor core analysis code: CITATION, 25:57183 (ORNL-TM-2496(Rev.2))
FOWLER, William A., Stellar rates for $^{28}$Si(α,γ)$^{32}$S and $^{16}$O(α,γ)$^{20}$Ne reactions, 25:55704
FRADIN, Jean, Projector for radioactive sources used in plesiotherapy for nonradioactive preparation technique, 25:54902
FRANCHI, G., Chemotherapy of leukemia and chemical protection against ionizing radiations, 25:57229 (EUR-4483)
FRANCO-FERREIRA, E. A., Brazing the shell assembly for the BONUS superheater fuel element, 25:55425
FRANCOIS, Henri, Electrochemical process for detecting microporous zones in film material such as insulating films, 25:54859
FRANCOIS, M., Behavior of shear waves in interaction of superflow with the vortex lattice, 25:56053
Velocity of second sound in rotating helium II, 25:56054
FRANK, I. M., Coherent radiation of the fast electron in medium, 25:56389 (JINR-P4-5954)
Optical radiation excited by nonrelativistic charged particles on the metal surface, 25:55813 (JINR-P4-5957)
FRANK, L. A., Distributions of plasmas and electric fields over the auroral zones and polar caps, 25:56030
Nonthermal electrons and high-frequency waves in upstream solar wind. II, 25:56019
FRANK, W., Kinetics of crowdion reactions, 25:56333
FRAPART, P., Radiochemical study of stability of selenomethionine $^{75}$Se, 25:54698
FREAS, D. G., Battelle's research plutonium facility environmental control and safety, 25:54959 (CONF-710401-, pp 280-92)

FREDERKING, T. H. K., Near-isothermal dissipative flow of liquid He II at supercritical velocities, 25:56062
FREDRICKS, R. W., Nonthermal electrons and high-frequency waves in upstream solar wind. II, 25:56019
FREEDMAN, Allan H., Basic properties of thin-film diffusion-brazed joints in Ti--6Al--4V, 25:55477
FREEMAN, A. J., Electronic structure of Th metal, 25:56388
FREEMAN, G. R., γ radiolysis of liquid ethanol. Yields of hydrogen and free ions. Solvated electron rate constants, 25:54660
Kinetics of charge scavenging in γ-irradiated liquid cyclohexane, 25:54668
FREEMAN, Gordon R., Effect of olefins on the reactions of nitrous oxide in γ-irradiated liquid cyclopentane, 25:54655
Progress and problems in the radiolysis of alcohols, 25:54629 (CONF-700652-(Vol.3), pp 479-521)
FREI, A., Problems of reactor circulating pumps, 25:57038
FREIBURG, C., Combined peaksearch and peakfit in data processing of γ-spectra, 25:54472
FREIDLINA, R. Kh., Radiation telomerization of ethylene by propionic acid, 25:54612
FRENCH, J. B., Complex spectroscopy, 25:56874
FREUDHOFMEIER, M., About nitrides and carbonitrides and nitride-based cemented hard alloys, 25:55629
FREUND, H. U., M-subshell fluorescence yields and $L_1$--$L_3$ radiative transition at Z = 93 and 96, 25:55825
FREY, G. D., Internal-conversion and γ--γ directional-correlation studies in the decay of $^{103}$Ru, 25:56771
FREYER, H. D., Countercurrent electrophoresis, 25:54742
FREYTAG, D., Spark chamber experiment on the beta decay of Ξ⁻ hyperons, 25:56411
FRIAR, J. L., Center-of-mass motion and $^6$He charge form factor, 25:56647
Quadrupole surface oscillations and elastic form factor of $^{16}$O and $^{12}$C, 25:56668
FRIDMAN, Z. G., Production of Cu/W composite by diffusion welding, 25:55405
FRIED, S., Reaction of Re and Tc metals with molten Li perchlorate and the Raman spectra of corresponding melts, 25:54538
FRIEDJUNG, M., Principal spectrum of novae, 25:55677
FRIEDLAND, Allan B., Processes of magnetic-energy conversion and solar flares, 25:55773
FRIEDMAN, Gerald I., Properties of hot pressed titanium alloy powders for cryogenic applications, 25:55482
FRIEDMAN, Herbert W., Collisionless shocks in plasmas, 25:56147
FRIEDMAN, Jack P., Synthetic transport theory method, 25:57154 (CONF-710302-(Vol.2), pp 625-43)
FRIGNET, Georges, Methods of and apparatus for irradiation of articles by radioactive panels, 25:54849
FRITZ, J. N., Use of a magnetic field to measure particle velocity. I, 25:57233 (LA-4545)
FRITZE, K., Neutron activation analysis for aluminum in animal tissue, 25:54514
FROLOV, A. S., Production of zirconium dioxide microballoons by means of nitrogen plasma, 25:55407
FROLOVA, A. V., Tissue equivalent scintillators in radiometry of long wave x radiation, 25:55213
FROMM, Eckehard, Diffusion-controlled growth of two-phase covering layers in binary systems, 25:57276 (SC-T-713061)
FROST, K. J., Experiment to measure hard solar and celestial x rays, 25:55734 (N-71-23434)
FRYER, J. R., Radiolytic reaction between graphite and $CO_2$. III, 25:55655
FUBINI, A., Method of analysis of neutron capture gamma-ray spectra, 25:56690 (RT/FI-(70)47)
FUCHS, H., Spectroscopy of $^{93}$ $^{95}$Tc, 25:56766
FUGOL, I. Ya., Experimental study of destruction of metastable helium atoms in plasma at low temperatures, 25:56151 (SC-T-713064)
Experimental study of the decay of cryogenic helium plasma, 25:56152 (SC-T-713065)
Recombination and detection of the three-atom ion in a helium plasma at low temperatures, 25:56161
FUJII, Kanji, Scale invariance and relativistic composite nucleon, 25:56465
FUJIMOTO, M., Electron spin resonance and relaxation studies of internal motion in $CH_2CO_2^-$ radicals trapped in γ-irradiated Na acetate crystals, 25:54652
FUJISAKI, Noboru, Radiolysis of liquid n-butane, 25:54659
FUJISAWA, Noboru, Review of Tokamak, 25:56198
FUKUI, I., Generalized Weinberg sum rules in deep inelastic current--hadron scatterings, 25:56461
FUKUOKA, N., Annealing of point defects in p-type germanium after electron irradiation at liquid-nitrogen temperature, 25:56329
FUKUTOMI, Hiroshi, Kinetic study of the photosensitized electron exchange reaction between U(IV) and U(VI) in hydrochloric acid, 25:54618
Preparation and the absorption spectra of U(III) in various acid solutions, 25:54540
FULLER, E. L., Two-dimensional fast-reactor disassembly analysis with space-time kinetics, 25:57078 (CONF-710302-(Vol.1), pp 128-51)
FULLWOOD, R. R., Instituting a neutron spectrum unfolding capability, 25:55038 (LA-DC-12314)
FULTON, Thomas, Hyperfine structure of positronium, 25:55832
FULTZ, S. C., Photoneutron cross section for $^6$He up to 31 MeV, 25:56649
FUNAKOSHI, N., One-valley EPR spectrum in electron-irradiated Sb-doped Ge, 25:56298
FURMAN, V. I., Alpha widths of neutron resonances, 25:56754 (UCRL-Trans-10541)
FURMANSKA, B., Low-energy protons generated in nuclear interactions at primary energies 60 GeV and approximately 1000 GeV, 25:56429 (INP-754)
FURUTA, Iwao, Osteonecrosis in lower mandible after postoperative radiotherapy, 25:55344
FURUTA, Teruo, Effect of alpha-ray irradiation on creep-rupture properties of austenitic stainless steel, 25:55574 (JAERI-Memo-4408)
FUTAMURA, Yoshiaki, Ultrasonic flaw testing method for a reactor pressure vessel using a mockup, 25:54925
FYHRQUIST, F., Radioimmunoassay of plasma angiotensin II in patients with hypertension, in renal transplant recipients, and in anephric patients, 25:55141

## G

GABRAKOV, S. I., Collective 1⁺ states in even--even deformed nuclei, 25:56819 (JINR-P4-5889)
GABUNIYA, R. I., Distribution of $^{59}$Fe in man, 25:55111
GACHON, H., Strain and ultimate strength of concrete under triaxial stress, 25:55660
GADEKEN, O. C., Reactions of iodine with olefins. II. Radiative neutron capture induced reactions of $^{128}$I with various $C_8$ isomers: evidence for a mechanism other than autoradiolysis in the condensed state, 25:54705
GAERTTNER, E. R., Experimental and analytical studies of fast neutron transport in iron, 25:56618 (RPI-328-230)
GAFFEY, C. T., Radiation between RBE and LET to inhibit neutral impulse conduction, 25:55215
GAIDOS, J. A., Diffractive νN scattering in νN + νN at 13.1 GeV/c, 25:56425 (COO-1428-294)
GAILLARD, O., (α, 2α) reaction on $^9$Be at 42.8 and 49.2 MeV and on $^{16}$O at 49.2 and 52.5 MeV, 25:56674
GAILLARD, Paul, Quasi-elastic scattering by substructure of light nuclei, 25:56830 (LYCEN-7104, S14.1-18)
GAINES, Thomas B., γ irradiation of DDT: radiation products and their toxicity, 25:55135
GAJL-PECZALSKA, Kazimiera, Immunofluorescent tests in course of /sup 99m/Tc scintiscanning, 25:55292
GALACH'EV, N. G., Correlation between geomagnetic activity and the intensity of the interplanetary magnetic field, 25:56007
Interaction of galactic cosmic rays with interplanetary magnetic field, 25:55904
GALAIKO, V. P., Kinetic equations for relaxation processes in superconductors, 25:56093
GALE, N. H., Distribution of uranium in some basic igneous cumulates and its petrological significance, 25:54809
GALIMOV, E. M., Mass-spectrometric analysis of the isotopic composition of iron in the gas phase, 25:54404
GALKTINOV, B. V., Determination of the boundary of high frequency wave absorption between the electron cyclotron and the low hybrid frequency, 25:56224 (AEC-tr-7270)
GALLAGHER, W. J., Prog. rpt. on fabrication and evaluation of isotopic source assay system, 7--10/70, 25:55070 (BHO-67-2)
GALLEGOS, A. F., Accumulation of radiocesium in rainbow trout via a non-foodchain pathway, 25:55159
GALLI, M., Short-period temperature effect on cosmic rays, 25:55898
GALLIANI, M., Experimental and theoretical determination of burnup and heavy isotope content in a fuel assembly irradiated in the Garigliano boiling water reactor, 25:56879 (EUR-4638)
GALLIGAN, J. M., Effect of magnetic fields on stress relaxation in mixed-state superconducting Pb--In alloys, 25:56063
GALLOP, R. A., Effects of gamma irradiation on Salmonella in smoked lake whitefish, 25:55365
GALLOWAY, J. J., Lagrangian approach to nonlinear wave interactions in a warm plasma, 25:56245
GALLOWAY, K. F., Mesonic structure in the nucleon, 25:56512
GAL'PERIN, Yu. I., Geophysical effects of solar activity in upper atmosphere. I, 25:55981
Geophysical effects of solar activity in upper atmosphere. II, 25:55982
GALY, A., Influence of speed of graphitization of carbon products on dimensional variations produced by neutron irradiation, 25:55645 (CEA-CONF-1821)
GAMALII, A. F., Gamma-radiation during thermal neutron capture on chromium and iron isotopes, 25:56683 (FEI-205)
GAMBHIR, B. L., Pauli breakup in deuteron reactions. Technical Report No. 71-116, 25:56833 (ORO-3765-31)
GAMBHIR, Y. K., Quasi-particle description for indium, 25:56794
GAMBINO, R. J., Magnetic properties of $LaSn_3$, 25:56353
GAMBLE, J. F., Ecological approach to environmental surveillance, 25:55238
GANGRSKII, Yu. P., Excitation of spontaneously fissioning isomeric states of $^{239}$Pu and $^{243}$Am at inelastic γ-quantum scattering, 25:56738 (JINR-P15-5959)

XUM

GANZER, U., Radiation treatment of human tumours, 25:55306
GARAS, F. K., Behavior of end slabs in cylindrical prestressed concrete pressure vessels, 25:56986
GARATTINI, S., Chemotherapy of leukemia and chemical protection against ionizing radiations, 25:57229 (EUR-4483)
GARBER, R. I., Field-ion-microscope study of W deformed by an electrostatic field at 900 to 1700°K, 25:55451
GARDNER, C. L., Reply to electron spin resonance of atomic silver on porous glass and silica gel surfaces, 25:54607
GAREEV, F. A., Δ N = +- 2 mixing in odd-N deformed nuclei, 25:56737 (JINR-E4-5877)
GARFUNKEL, Marcelo, Radiation effects on water permeability and distribution in frog muscle cells, 25:55323
GARNIER, R., Bright condensation 3C 153.1 inside the H II region NGC 2175, 25:55681
GARRETT, J. D., Spin assignments in $^{20}$F, 25:56716
GARSCADDEN, A., Errors due to averaging spectral-line intensities in the presence of electron-temperature variations, 25:56171
GARSON, Lorrin R., Organosilicon entities as prophylactic and therapeutic agents, 25:55263
GARTMANOV, V. N., Measurement of tritium and $^{3}$He in Al targets, 25:55902
GASKILL, J. R., Engineering fire-suppression systems for large volumes using Halon 1301, 25:54957 (CONF-710401-, pp 248-56)
GASPARYAN, A. P., Analysis of the reaction np → pp π⁻ from the point of view of Reggeized OPE model, 25:56521 (JINR-P1-5975)
GAULT, F. D., Comparison of the high energy models for neutral meson photoproduction and the related hadronic processes, 25:56458
GAVRILYUK, M. I., Electron-microscope and x-ray spectral study of the surface of fractures in cast tungsten, 25:55542
GAVRILYUK, O. Ya., Effect of glow discharge on electrical resistance of Ta--N films, 25:55519
GAVRISH, A. M., Polymorphic transformation of zirconium dioxide, 25:55641
GAWLOWSKI, Janusz, Effect of some oxygen-containing compounds on the radiolysis of gaseous ethylene, 25:54643
GEHRLING, Volker, Decay of $^{84}$Rb and fluorescence yield of Kr, 25:56697
GEIGER, M., Basic steady state magnetic screw-field distributions in plasma between concentric boundaries, 25:56163 (LGI-70/16/E)
GEIJERSTAM, E. af, Water jet pumps for reactors, 25:57037
GEISERT, M. G., Alteration of DNA by sensitized and non-sensitized long-wave uv irradiation, 25:55308
GELBARD, E. M., Arrangement of ordinates in deep-penetration cylindrical and X--Y S/sub n/ calculations, 25:57153 (CONF-710302-(Vol.2), pp 617-24)
GELBERG, A., Gamma x-ray angular correlation, 25:56755
GEL'D, P. V., Conditions for formation of phase with A15 structure in V--Ge--Al system, 25:55539
GEL'FGAT, Yu. M., Influence of transverse magnetic field on intensity profiles of turbulent velocity fluctuations in pipes of rectangular cross section, 25:55926
GELLER, R., Multiply charged ion source. Design of electron gyromagnetic resonance source, 25:56210 (EUR-CEA-FC-603)
GELSKEY, Dale E., In situ measurements of environmental radioactivity, 25:55239
GENKOV, D., Yearly course of radon and thoron inductions and long lasting radioactivity of aerosols in Plovdiv, 25:54792
GENS, M. B., Environment experienced by cargo during normal rail and truck transport, 25:54974 (SC-M-710241)
GENSHO, Reisuke, Measurements of the isotopic ratio of boron, 25:54432
GENTILE, Erberto Francisco, Reactivity of $U_3O_8$--Al dispersions, 25:55609 (ORNL-tr-2456)
GERASIMOV, N. P., Quality factor of superconducting lumped-parameter circuits, 25:55086
GERDIN, Glenn Andrew, Experimental study of anomalous resistivity in a potassium magnetoplasma, 25:56159
GERJOUY, E., Comparisons of Glauber and Vainshtein approximations for inelastic e--H scattering, 25:55850
GERJUOY, E., Low energy electron--molecule scattering experiments and the theory of rotational excitation, 25:55855
GERRARD, Martha, Isotopes and radiation technology, Vol. 9, No. 1, 1971, 25:57127
Recent DID radiometric-technique developments, 25:55065
Selected abstracts of world literature on production and industrial uses of radioisotopes, 25:54894 (ORNL-IIC-37(Pt.2))
GERSHENGORN, Marvin, Radioimmunoassay of triiodothyronine in unextracted human serum, 25:55146
GERUSKY, Thomas M., Radiation incidents registry: Pennsylvania experience, 25:55250
GESCHIER, R., Structure and tensile properties of Nb--4.6 Ti--O, 25:55521
Structure and tensile properties of Nb--Zr--O alloys rich in Nb, 25:55522
GHEORGHE, D., SCAT: code for computing scattering cross section of light and heavy water, 25:56638
GHIOTTI, G., Infrared study of surface properties of α-chromia. I. Preparation and adsorption of water, heavy water, and carbon monoxide, 25:54565
GHOROKU, Kazuo, Exotic exchange processes and urbaryon rearrangement diagrams, 25:56479
GHOSH, S. N., X-ray and radio emissions from the Sun, 25:55736
GHOSSEIN, Nemetallah A., Acute changes in pulmonary arterial perfusion following irradiation, 25:55327
GIACOBBE, P., Spin-dependence of level density in $^{178}$Hf and $^{180}$Hf by resonance neutron capture experiments, 25:56751 (RT/FI-(70)55)
GIBBONS, J. H., keV neutron capture γ ray spectra, 25:56655 (ORNL-TM-3379)
GIBLAK, R. E., Radiosensitization with 5-bromodeoxyuridine of Chinese hamster cells x-irradiated during different phases of the cell cycle, 25:55258
GIBSON, M. L., N-substituted urea complexes of thorium and uranium tetrahalides, 25:54536
GIBSON, W. G., Classical limit of the binary-collision expansion, 25:55865
GIEBEL, R. E., Glovebox gloves, 25:54941 (CONF-710401-, pp 44-55)
GIFFON, M., Differential method and Feynman nuclear graphs, 25:56831 (LYCEN-7104, S18.1-18)
GIGAURI, K. V., External characteristics of MHD generator with sections connected in series, 25:55914
GIGSON, W. G., Bound state and continuum contributions to the two-body partition function, 25:56396
GIJBELS, R., Neutron activation analysis for osmium, ruthenium, and iridium in some silicate rocks and rock-forming minerals, 25:54486
GILANI, Shamshad H., Congenital cardiovascular anomalies in chick embryos exposed to x-irradiation and hypothermia, 25:55333
GILISSEN, R., Temperature distribution in irradiated oxide fuel with dispersed burnable poison, 25:57194
GILLBRO, T., ESR single-crystal study of radical and radical-pair formation in some γ-irradiated vinyl monomers, 25:54634
GILLESPIE, F. E., Measurements of the neutron fission and absorption cross sections of $^{239}$Pu over the energy region 0.02 eV to 30 keV, Part II, 25:56746 (ORNL-4707)
GILLET, R., Liquid scintillation applications in radioprotection, 25:55217
GILLILAND, R. G., Weldability of tungsten and its alloys, 25:55410
GILLY, C., Effects in vivo of ionizing radiations on human chromosomes, 25:55178
GILMAN, Peter A., Constructing streamlines for Sun's large-scale flow from Doppler velocities, 25:55745
GILMORE, Forrest R., Possible effects of atmospheric particles on fireball emissions, 25:54815 (AD-722031)
GIMESI, O., Acid determination with the help of radioiodine, 25:54439
GINDIN, I. A., Low-temperature rolling and the annealing of single-crystal niobium, 25:55560
GINSBERG, A., Experimental and analytical studies of fast neutron transport in iron, 25:56618 (RPI-328-230)
GINSBURG, Theo, Peaceful application of nuclear explosions, 25:54830
GIOVANNINI, B., Anomalous Hall effect in the rare earths, 25:56357
GIOVANNINI, R., Analysis by a simulated measurement of neutron spectra, 25:56620 (RT/FI-(70)53)
GIRAUD, B., Generating coordinates in continuum states, 25:56825 (LYCEN-7104, C6.1-12)
GIULIANI, S., Simplified visco-elastic analysis of graphitic bodies subjected to external loads, temperature gradients and neutron irradiation, 25:55646 (EUR-4674)
GLADSHTEYN, N. D., Spectral and correlation characteristics of noise from the leader stage of a lightning discharge, 25:55998
GLADYSHEV, V. A., Focusing of an ion beam drifting in a nonuniform magnetic field, 25:56602
Sector cyclotron at 300 keV with external injection, 25:56601
GLASCOCK, R. F., Removal of cationic fission products from milk, 25:54722
GLASHOW, S. L., Divergences of massive Yang--Mills theories: higher groups, 25:56542 (CNRS-CPT-71/P-378)
GLAZA, Donald D., Radiometric method and apparatus for measuring and controlling foundry sand moisture, 25:55064
GLAZOV, O. A., Temperature field in axially symmetric magnetohydrodynamic flow in vortex chamber, 25:55933
GLEESON, A. M., Comments on analyses of anti pn → 3π, 25:56485 (ORO-3992-66)
Interpretation of angular distribution in terms of complex mass particles, 25:56499 (ORO-3992-8)
Phenomenology of complex spin tachyons, 25:56500 (ORO-3992-18)
GLENDENIN, L. E., Internal-conversion coefficients in decay of /sup 83m/Kr, 25:56708
GMELIN, E., Low-temperature electron irradiation of tellurium, 25:56306
GMITRO, M., Quasi-particle description for indium, 25:56794
GNANAPURANI, M., Induction of heteroallelic reversions and lethality in Saccharomyces cerevisiae exposed to radiation of various LET ($^{60}$Co γ rays, heavy ions, and

π- mesons) in air and nitrogen atmospheres, 25:55165
GOATES, J. Rex, Prog. rpt. on electrochemical cells using alkali metals and charge transfer complexes, 5/67--8/71, 25:57221 (COO-1707-12)
Prog. rpt. on solid-liquid phase equilibria in the ternary sodium--potassium--rubidium alloy system, 5/67--8/71, 25:55524 (COO-1707-11)
GOBEN, Charles A., Prog. rpt. on nuclear radiation effects on silicon p--n junctions, 25:55095 (COO-1624-41)
GODART, Michel, Device for the leak-tight transfer of objects to a container through an enclosure wall, 25:54988
GODFREY, K. V., Neutron activation and on-stream analysis in mineral industries using SHERLOCK III, 25:54506
GODLEWSKI, Michael P., Effects of nuclear radiation on high-reliability silicon power diode. III, 25:55097 (N-71-25389)
GOEDBLOED, J. P., Stabilization of MHD instabilities by force-free magnetic fields. III, 25:56201
Stabilization of MHD instabilities by force-free magnetic fields. II, 25:56200
Stabilization of MHD instabilities by force-free magnetic fields. I, 25:56199
GOERING, S., $^{139}$Sm, new nuclide of relevance for systematics of N = 77 isomers, 25:56761
GOERLICH, W., Measurementof isotope abundance shifts by means of neutron activation analysis, 25:54492
GOESCHEL, H., Application of nuclear energy from the standpoint of the reactor construction industry, 25:57004
GOETZEL, C. G., Electrically activated pressure-sintering (spark sintering) of titanium--aluminum--vanadium alloy powders, 25:55413
GOLANT, V. E., Determination of the boundary of high frequency wave absorption between the electron cyclotron and the low hybrid frequency, 25:56224 (AEC-tr-7270)
Linear transformation and absorption of a wave in a plasma, 25:56250
GOLAVNYA, B. Ya., Nucleon density distribution in nuclei $^{54}$ $^{56}$Fe, 25:56699
GOLDBERG, A., Transformations during quenching of epsilon-phase Pu--Zr alloys, 25:55528
GOLDBERG, A. L., Uptake and release of $^{45}$Ca by brain microsomes, synaptosomes, and synaptic vesicles, 25:55120
GOLDBERG, M. B., Nuclear spectroscopic studies on $^{18}$O, 25:56672
GOLDBERGER, M. L., Multiperipheral models and high-energy processes, 25:56442 (PURC-4159-42)
GOLDEN, D. E., Low energy electron--molecule scattering experiments and the theory of rotational excitation, 25:55855
GOLDEN, John C. Jr., Use of stable element concentrations in pre-operational environmental monitoring, 25:55240
GOLDEN, Melvin, Evaluation of the lung scintiphoto as a screening test for pulmonary disease, 25:55297
GOLDFINCH, Judith, Expansion of plasma from spherical source into vacuum. I, 25:56180
Expansion of plasma from spherical source into vacuum. II, 25:56181
GOLDHABER, G., Evidence for structure in Kπ mass system near 1.85 GeV, 25:56434
GOL'DIN, L. L., Proton beam of the ITEP accelerator for radium therapy, 25:56581 (BNL-tr-442)
GOLDMAN, Harold S., Acute changes in pulmonary arterial perfusion following irradiation, 25:55327
GOLDMAN, Morton I., Nuclear facility siting in the United States, 25:56976
GOLDMAN, T., Spin one theory, 25:56464
GOLDSMITH, D. W., Thermal effects in formation of loop prominences, 25:55752
GOLDSTEIN, B., Lithium-defect interactions in electron-irradiated n-type silicon, 25:56310
GOLDSTEIN, Mark Parnes, Alignment of interstellar grains, 25:55792
GOLEB, Joseph A., Determination of mercury in small terrestrial and nonterrestrial rock samples by atomic-absorption spectroscopy, and the study of mercury release at elevated temperatures, 25:54511
GOLES, G. G., Instrumental activation analysis of Columbia River, 25:54460
GOLUBENTSEV, D. A., Some principles of evaluating the effectiveness of radioprotective agents in man, 25:55256
GOLUTVIN, Yu. M., Heat content of metallic hafnium, 25:55445
Thermochemistry of the hafnium--silicon system, 25:55644
GOLUTVINA, M. M., Determination of $^{239}$Pu and enriched U in the urine in their combined presence, 25:55197
GOMEZ, Jose M. G., Quadrupole vibrations in Ni region: structure of odd-mass Cu isotopes, 25:56731
GOMOZOV, L. I., Composition of the carbide phase in alloys of uranium with zirconium and niobium, 25:55547
GONCHAR, V. G., Inelastic scattering of γ particles on Zn isotopes, 25:56726
GONCHAR, V. Yu., Diffraction analysis of transfer reactions, 25:56847
GONEN, M., Effects of gamma radiation on moths. II, 25:55316
Effects of gamma radiation on moths. I, 25:55315
GONTIER, Y., Multiphoton processes in a hydrogen atom, 25:55875
GOOD, W. M., keV neutron capture γ ray spectra, 25:56655 (ORNL-TM-3379)
GOODINGS, Anthony, Neutron counters, 25:55014
GOODMAN, Ronald K., Cross beam neutralizer for ion beams, 25:55816
GOODMAN, W. K., Safety considerations at the Babcock and Wilcox Plutonium Development Laboratory, 25:54958 (CONF-710401-, pp 258-66)
GOODMAN, William L., Quantized flux states of superconducting cylinders, 25:56064
GOODRICH, Robert Warren, Electrical conduction from shock heated argon to conical probes, 25:56144
GOOSMAN, D. R., Technique for efficiently converting $^{13}CH_4$ into pyrolytic $^{13}C$, 25:54542
GOOSSENS, W., Chemical decanning of fuel elements by means of $HF/O_2$ mixtures, 25:54747
GOPALAKRISHNA, A. V., Propagation of weak discontinuities in collisionless plasma, 25:56237
GORANSON, Richard B., Implantable radioisotope-fueled stirling engine, 25:54910
GORBACHEV, L. P., Rotation of electrically conducting fluids in crossed electric and magnetic fields, 25:55938
GORCHAKOV, E. V., Correlation between geomagnetic activity and the intensity of the interplanetary magnetic field, 25:56007
Interaction of galactic cosmic rays with interplanetary magnetic field, 25:55904
GORDEEV, V. V., Dependence of buildup factor on the position of shielding between bremsstrahlung source and detector, 25:56280
GORDIENKO, S. P., Mass-spectrometric ion source for high-temperature investigations, 25:55081
GORDON, John Albert, Mechanical surface aerator evaluation using radio-krypton as a standard indicator of mass transfer, 25:54903
GORDON, Kurtiss J., 21-cm study of the spiral galaxy Messier 33, 25:55796
GORELOV, V. A., Parameters of ionized air in front of a strong shock wave, 25:56160
GORETZKI, H., Electronic structure of refractory carbides and its relation to wetting, 25:55643
GOR'KOV, L. P., Viscous vortex flow in superconductors with paramagnetic impurities, 25:56086
GOROBETS, V. F., Distribution of $^{59}$Fe in man, 25:55111
GORODNICHEVA, O. P., Relationship between steady earth current pulsations and parameters of magnetosphere, 25:56004
GOROWSKI, Tadeusz, Immunofluorescent tests in course of /sup 99m/Tc scintiscanning, 25:55292
GORYACHEV, A. N., Infrared investigation of the action of ionizing radiation on carbon-chain polymers, 25:54604
GORYACHEV, I. V., Secondary γ-radiation in shielding, 25:56277
GOSS, W. M., OH absorption in the direction of W44, 25:55716
GOSSARD, A. C., Study of a series of $Nb_3X$ compounds by nuclear magnetic resonance, 25:56373
GOTT III, J. Richard, Coma Cluster as x-ray source, 25:55806
GOTTSCHALK, Alexander, Pancreas imaging: is it worth it, 25:55280
GOUGH, R. M., Categorization and posting of nuclear facilities for fire protection purposes at WADCO, 25:54953 (CONF-710401-, pp 208-11)
GOULARD, B., Isovector excitations in photonuclear reactions, 25:56827 (LYCEN-7104, S8.1-10)
GOURDIN, M., High energy production of hadrons in the Coulomb field of a nucleus, 25:56457
GOVER, James E., Dynamic measurements of the Grueneisen coefficients of tantalum, uranium, and uranium--molybdenum alloys, 25:55436 (SC-RR-710314)
GOWDY, Robert H., Gravitational waves in closed universes, 25:56570
GRABISCH, K., Spectroscopy of $^{93}$ $^{95}$Tc, 25:56766
GRAEDEL, T. E., Interplanetary-particle associations with Type-III solar bursts, 25:55778
GRAFF, P., Subsidiary conditions for generating functionals, 25:56556
GRAHAM, John, Consequences of molten fuel ejection in a LMFBR, 25:57083 (CONF-710302-(Vol.1), pp 241-58)
GRAHAM, Kingsley F., Measurements of time-dependent thermal neutron spectra in pulsed moderators using a time-focussed crystal spectrometer, 25:56629
GRAHAM, L. W., Dimensional and physical property changes of graphites, pyrocarbons, and fuel bodies, 25:55651
GRAHAM, W. A. G., Silicon--transition metal chemistry. VI. Kinetics and mechanism of the replacement of triphenylsilane by triphenylphosphine in hydridotriphenylsilyl(π-cyclopentadienyl)dicarbonylmanganese, 25:54567
GRAM, Peter A. M., Proposal for P$^3$: versatile high-energy pion beam facility, 25:56588 (LA-4535)
GRAMAN, G. A., Solidification mechanism of uranium ingots, 25:55400 (NLCO-1077)
GRANSTROEM, L., Automatic selection of kinematical hypotheses from two prong proton--proton interactions in a hydrogen bubble chamber at 19 GeV/c, 25:56523 (USIP-71-3)
Two prong sample from proton--proton interactions in a


XUM

hydrogen bubble chamber at 19 GeV/c, 25:56417 (USIP-71-4)
GRANT, C. W. M., Reply to electron spin resonance of atomic silver on porous glass and silica gel surfaces, 25:54607
GRANT, I. P., Astrophysical models: a look at models of stellar atmospheres, 25:55713
GRANT, J., Gamma irradiation as industrial process, 25:55363
GRASBERGER, William, Stimulated Compton energy exchange rate, 25:56266 (UCRL-51065)
GRASSI STRINI, A. M., High-spin rotational excitation in $^{173}$Hf, 25:56796
GRATREAU, P., Radiative recombination of hydrogenic ions in high temperature plasmas, 25:56164 (LGI-71/1/E)
GRATZL, H., Coordinate-independent definition of positive and negative energy waves in plasma, 25:56239
GRAZIANI, G., TRACE: fuel cycle computer code for fast reactor analysis, 25:57020 (EUR-4709)
GREBOWSKY, J. M., Time-dependent plasmapause motion, 25:55972
GREBOWSKY, Joseph M., Structured variations of the plasmapause: evidence of a corotating plasma tail, 25:56028
GREEN, A. M., Nuclear models, 25:56809 (CERN-71-14, pp 67-99)
GREEN, M. B., Average properties of dual resonances, 25:56491
GREEN, M. H. L., Effect of $\gamma$ radiation on donor ability of Escherichia coli, 25:55358
GREEN, P. J., Increasing hadron--nucleus cross sections and cosmic ray muon zenithal variations, 25:55906
GREEN, R. Elliot, Conference on advanced computer graphics, London, 4/70, 25:57007
GREEN, W. V., Tritium trick, 25:55575 (LA-DC-12996)
GREENBERG, S., Behavior and calibration of devices for monitoring impurities in sodium, 25:55069 (ANL-7804)
Materials-coolant interactions relevant to EBR-II, 25:57109 (ANL-7771)
GREENE, J. S. Jr., Multidimensional magnetohydrodynamic shock calculations, 25:56192
GREENE, John M., Numerical simulation of toroidal plasma confinement with a fluid model, 25:56129
GREGORY, H. J., Effects of rf activated inert gas plasmas on critical surface tension and bondability of polydimethyl silicones and polyethylene, 25:57272 (SC-RR-710483)
GREGORY, Walton C., Mutations and biological improvement, 25:55181
GREVESSE, N., Search for CH$^+$ in the solar photospheric spectrum, 25:55768
GREVESSE, Nicolas, Elements in atmosphere of main-sequence G2 V star, 25:55750
GRIBBEN, R. J., Nonlinear wave solutions of Vlasov and Poisson equations, 25:56244
GRIDNEV, K. A., Stripping process for ($\alpha$,p) and ($\alpha$,d) reactions on light nuclei, 25:56677
GRIDNEV, N. P., Two-dimensional unsteady flow of electrically conducting gases in magnetic fields, 25:55924
GRIEVES, J. O., Place of fast reactors in UK power programme, 25:57012
GRIFFIN, James J., Pauli breakup in deuteron reactions. Technical Report No. 71-116, 25:56833 (ORO-3765-31)
GRIFFIN, R. B., Effect of the sixth period elements on the melting and transformation temperatures of praseodymium. Part II. Thermodynamic analysis, 25:55566
Effect of the sixth period elements on the melting and transformation temperatures of praseodymium. Part I. Experimental, 25:55567
GRIFFITH, James M., Improved detector for video systems used in radionuclide studies, 25:55278
GRIGORASHCHENKO, O. N., Experimental study of destruction of metastable helium atoms in plasma at low temperatures, 25:56151 (SC-T-713064)
GRIGOR'EV, B. A., Tables for calculating nonstationary temperatures of plane bodies during heating by irradiation, 25:56267
GRIGOR'EV, Yu. G., Investigations of artificial satellites of the Earth, 25:55342
GRIGOROV, N. L., Chemical composition of primary cosmic rays, 25:55899
GRIGOROVICH, V. K., Plasticity and strength of nickel--molybdenum alloys at high temperature, 25:55474
GRISHAEV, I. A., Excitation of ultrasonic waves by passage of fast electrons through a metal, 25:56566
GRISHIN, V. G., Cross section of $\pi^- + {}^{12}C \to {}^{12}N + \pi^- + \pi^-$ reaction, 25:56439
Direct pair production by charged particles at 4 GeV/c in a propane bubble chamber, 25:56467
GROCE, David E., Proposal for a biomedical addition to Los Alamos Scientific Laboratory's High-Flux Meson Physics Facility, 25:55299 (LA-4490)
GRUEMM, H., Energy production and environment, 25:57098
GRUENWALD, H., Measurement of reactor power by determination of $^{17}$N neutrons in the cooling medium with track detectors, 25:57124
GRUNBERGER, L., Vorticity and neutrons in the plasma focus, 25:56157
GRUNERT, V., Ventricular scintigraphy for diagnosis of cerebral tumors in early childhood, 25:55290
GRUVERMAN, Irwin J., Conference on Moessbauer effect methodology, Chicago, 1/70. VI, 25:56364
GRUZDEV, V. A., One type of instability of the exit current of a plasma electron source, 25:56148
GRYZINSKI, Michal, Ionization of atomic H by electron impact: numerical calculations for free-fall atomic model, 25:55836 (INR-P-1327)
GRYZUNOV, V. I., Mutual diffusion of ruthenium with niobium and zirconium, 25:55452
GSCHNEIDNER, K. A. Jr., Effect of the sixth period elements on the melting and transformation temperatures of praseodymium. Part II. Thermodynamic analysis, 25:55566
Effect of the sixth period elements on the melting and transformation temperatures of praseodymium. Part I. Experimental, 25:55567
Stoichiometry, crystal structures, and some melting points of the La--Au alloys, 25:55570
GUAITANI, A., Chemotherapy of leukemia and chemical protection against ionizing radiations, 25:57229 (EUR-4483)
GUALANDI, M. Paoletti, Experimental and theoretical determination of burnup and heavy isotope content in a fuel assembly irradiated in the Garigliano boiling water reactor, 25:56879 (EUR-4638)
GUARD, Robin F. W., Problems of comparing power reactors for specific application, 25:57059 (70-CNA-628)
GUARDIOLA, R., Multiple scattering effects in quasifree scattering, 25:56520 (IC-71/106)
GUDKOV, A. N., Global contamination of the atmosphere by $^{85}$Kr from worldwide nuclear power plants and the radiation danger, 25:54781 (JPRS-53174)
GUELIN, M., Pulsar JP 1933: 21-cm line absorption profile and interstellar scintillation, 25:55724
GUERRINI, C., Mechanical effects of a contained nuclear explosion, 25:54820 (UCRL-Trans-10543, pp 4-35)
GUGLIELMINOTTI, E., Infrared study of surface properties of $\alpha$-chromia. I. Preparation and adsorption of water, heavy water, and carbon monoxide, 25:54565
GUICHARD, A., ($\alpha$, 2$\alpha$) reaction on $^9$Be at 42.8 and 49.2 MeV and on $^{16}$O at 49.2 and 52.5 MeV, 25:56674
GUIDI, I., Short-period temperature effect on cosmic rays, 25:55898
Unusual anisotropic solar-particle event of November 18, 1968, 25:55764
GUILLAUMIN, J., Internal oxidation in Mg--Zr alloy in contact with carbon dioxide, 25:55382
Structural change in sintered Mg--Zr alloy after holding at high temperature, 25:55548
GUILLEMOT, M., Interaction of a large-amplitude wave with a plasma: trapping, 25:56227 (CEA-CONF-1805)
Saturation and damping of echoes of electron plasma waves, 25:56226 (CEA-CONF-1804)
GUISAN, O., Study of $\pi^- p \to \pi^0 n$ and $\pi^- p \to$ eta reactions in nuclei at 7.82 GeV/c, 25:56432
GUJADHUR, T. K., U(6,6) x O(3,1) absorbed K-matrix model for spin-2 exchange in $\pi^- p \to$ etan. III, 25:56513
GULL, Theodore Raymond, Observations of interstellar molecular hydrogen and measurements of hydrogen and helium fluxes from planetary nebulae, 25:55700
GUMANSKII, G. A., Isodose distribution of a beam of positrons with an energy of 5 to 15 MeV, 25:55210
GUMENYUK, T. D., Investigation of the kinetics of oxygen isotopic exchange between water and carbon dioxide in the presence of soluble additives, 25:54549
GUNDZIK, M. G., Interpretation of angular distribution in terms of complex mass particles, 25:56499 (ORO-3992-8)
Phenomenology of complex spin tachyons, 25:56500 (ORO-3992-18)
GUNN, James E., Coma Cluster as x-ray source, 25:55806
GUNNINK, R., Gamma-ray energies and absolute branching intensities for $^{238}$ $^{239}$ $^{240}$ $^{241}$Pu and $^{241}$Am, 25:56753 (UCRL-51087)
GUREVICH, Yu. G., Propagation of strong cylindrical and spherical electromagnetic waves in a plasma, 25:56240
GURIN, V. N., Interaction of niobium with a zinc melt, 25:55534
GURNETT, D. A., Distributions of plasmas and electric fields over the auroral zones and polar caps, 25:56030
GURNETT, Donald A., Double-probe measurements of convection electric fields with Injun-5, 25:55958
GURTOVOI, M. E., Scattering of 14-MeV neutrons by Fe, 25:56707
GUSEVA, L. I., Production of zirconium dioxide microballoons by means of nitrogen plasma, 25:55407
GUTAY, L. J., Diffractive $\pi\pi$ scattering in $\pi N \to \pi\pi N$ at 13.1 GeV/c, 25:56425 (COO-1428-294)
GUTSCHE, Brigitte, Iodine-specific detector for a gas chromatograph, 25:54406
GUYON, E., Vortex-free Landau state in rotating superfluid helium, 25:56048
GUZIK, Z., Readout electronics for $\nu_\mu$--e experiment at 50 GeV, 25:55044 (JINR-E1-5818)
GWIN, R., Measurements of the neutron fission and absorption cross sections of $^{239}$Pu over the energy region 0.02 eV to 30 keV, Part II, 25:56746 (ORNL-4707)
GYARMATI, E., Studies about use of directly-cooled coated-particle aggregates as fuel elements, 25:57053

# H


HABERMEHL, A., Quantitative evaluation of thyroid scintigrams by computer, 25:55282
HABS, D., $^{139}$Sm, new nuclide of relevance for systematics of N = 77 isomers, 25:56761
HACKOS, William Jr., Heavy metal abundances in S-stars, 25:55699
HADDAD, D., Reaction mechanisms of $^{10}$B(d,α)$^{8}$Be$_{2}$ ,(α)$^{4}$He for E/sub d/ = 0.4, 1.0, and 1.5 MeV, 25:56673
HADJIAN, Asadour H., Earthquake forces on equipment in nuclear power plants, 25:57108
HAEBLER, Dietrich V., Apparatus for measuring and evaluating the activity of measuring probes irradiated in a nuclear reactor, 25:55008
HAEFELE, W., German-beneflux fast breeder project and future developments in European Fast Breeder Reactors, 25:57016
HAFT, Jacob, Radiation exposure to personnel during cardiac catheterization, 25:55226
HAGEGE-TEMMAN, J., Kinetic study of species formed during the pulsed radiolysis of ammonia, 25:54661
HAGEN, U., Radiation-induced breaks in DNA, 25:55133
HAGFORS, T., Simultaneous observation of proton precipitation and auroral radar echoes, 25:55963
HAHN, Paul B., Public health aspects of $^{129}$I from the nuclear power industry, 25:55199
HAHN, Yukap, Quasi-minimum principle for multichannel scattering, 25:55878
HAIR, M., Nuclear interaction tracks in minerals and their implications for extraterrestrial materials, 25:55669 (N-71-26344)
HAIRE, Marvin Jonathan, Sorption behavior of cesium--rubidium mixtures in graphites at high temperatures, 25:55623
HAKONSON, T. E., Accumulation of radiocesium in rainbow trout via a non-foodchain pathway, 25:55159
HALBERT, E. C., Complex spectroscopy, 25:56874
HALBERT, M. L., $^{40}$Ca($^{20}$Ne,$^{16}$O)$^{44}$Ti reaction, 25:56721
HALE, J. P., Sodium fires analyses for the Fast Flux Test Facility, 25:57112 (HEDL-TME-71-31)
HALL, G. Richard, Record-keeping in a radiation safety office by timesharing digital computer, 25:54984
HALL, R. I., Resonance phenomena in low-energy-electron-impact excitation of He, 25:55851
HALL, W. Keith, Catalytic oxidation. IV. Ethylene and propylene oxidation over gold, 25:54569
HALL, Wm. Cornelius, Materials for shielding nuclear radiations from plutonium processing, 25:54962 (CONF-710401-, pp 307-10)
HALLINAN, T. J., Artificial aurora experiment: ground-based optical observations, 25:55962
HALPERN, Sam, Evaluation of the lung scintiphoto as a screening test for pulmonary disease, 25:55297
HALTER, J., Thirteenth report of federal commission on monitoring of radioactivity for year 1969 delivered to federal council, 25:54791
HAMBERGER, A., Subcellular distribution of radioactivity in neuronal and glial-enriched fractions after incorporation of [$^{3}$H]leucine in vivo and in vitro, 25:55119
HAMBRO, Lars, Multiple-scattering expansions for nonrelativistic three-body collision problems. IV, 25:55867
HAMILL, Dennis W., Coincidence Moessbauer spectroscopy, 25:56367
HAMILTON, E. I., Concentration and distribution of Pb in materials, 25:54452
HAMILTON, Gordon W., Intense 1-kV ion source for controlled fusion research, 25:56217 (UCRL-73387)
Ion source technology, 25:55814 (UCRL-73353)
HAMILTON, J., Pion--nucleon scattering theory, 25:56496 (CERN-71-14, pp 101-54)
HAMILTON, J. H., Decay of $^{58}$Mn, 25:56710
HAMMER, B., Angiographic and angioscintigraphic comparisons in cerebral vascular processes, 25:55289
HAMMER, J. Wolfgang, Decay of $^{83}$Rb and fluorescence yield of Kr, 25:56697
HAMMERLING, F. D., Fourier analysis of unequally spaced data, 25:57250 (ORNL-TM-3547)
HAMMERMAN, I., Photon asymmetry for radiative μ capture in Ca, 25:56705
HAMMOND, D. P., Hot-cathode ionization gauges for use in a magnetic field, 25:56141
HAMMONS, Anna S., Recovery of the antigen retention mechanism after sublethal x-irradiation in mice receiving cells from various sources, 25:55147
HAMRE, E., Scandinavian PCRV model project, 25:56991
HAN, M. Y., Two-component spherical factorization of Klein--Gordon and Kramers equations, 25:56559
HANKE, H., Design and optimization of a fast heat pipe thermionic reactor, 25:57134
HANKINS, Dale E., Study of a thermal neutron calibrator, 25:54892 (LA-4745)
HANNA, Samir B., Oxidative decarboxylation of polyaminocarboxylic acids. II, 25:54422
HANNOTHIAUX, Andre, Conventional and nuclear thermal energy, 25:57002
HANNUM, W. H., Work of the Committee on Computer Code Coordination, 25:57018 (CONF-710302-(Vol.1), pp 452-63)
HANSEN, J. E., Prog. rpt. on isotope development, 2--4/71, 25:54887 (BNWL-1308-6)
HANSEN, Niels, Matrix hardening in dispersion strengthened powder products, 25:55487
HANSLIK, E., Study of natural radionuclides in waste and surface waters, 25:54774
HANSMA, P. K., Externally shunted Josephson junctions: generalized weak links, 25:56094
HANSSON, V., Three-dimensional elastic stress conditions in area of openings of THTR prestressed concrete vessel, 25:56887
HAPASE, M. G., Thermodynamic properties of ternary refractory carbides. II. Zirconium--uranium--carbon and zirconium--hafnium--carbon, 25:55614
HAQUE, A. K. M. M., Energy loss and straggling of alpha particles in a tissue-equivalent gas, 25:56279
HARA, Fumio, Nuclear reactor optimization, 25:57180
HARDACRE, A. G., Proton differential elastic scattering cross sections for even isotopes of tin at 30.4 MeV, 25:56764
HARDER, C. A., Engineering fire-suppression systems for large volumes using Halon 1301, 25:54957 (CONF-710401-, pp 248-56)
HARDWICK, E. R., Prog. rpt. on intra- and inter-molecular energy transfer studies, 5/70--5/71, 25:54600 (UCLA-34-P-88-32)
HARDY, W. R., Proton radiation damage and recovery in Ta films, 25:56314
HARLING, O. K., Structure in the neutron scattering spectra of zirconium hydride, 25:56343
HARMAN, Randall W., Method and apparatus for detecting gas leaks using radioactive techniques, 25:55063
HARMSEN, U., Internal oxidation of Ag--Cd alloys under oxygen pressure, 25:55381
HAROUTUNIAN, R., Directional correlations of gamma rays in $^{152}$Sm measured by gating on the 244.66-keV transition, 25:56777
HARPER, W. L., Properties of carbon derived from indene compounds, 25:57295 (Y-1790)
HARRIS, N. A., Monte Carlo transport analysis for finite ground-distributed γ sources, 25:56260 (EGG-1183-2284)
HARRIS, Samuel M., Mariscotti description of ground state bands of even--even nuclei, 25:56813 (COO-1746-57)
HARRIS, W. W., Cytofluorograph system, 25:57249 (ORNL-TM-3536)
HARRISON, R. W., Corrosion resistance of tantalum, T-111, and Nb--1Zr to Hg at 1200 F, 25:55377 (N-71-26947)
HART, Edwin J., Absorption spectrum of e/sub aq/- in the temperature range -4 to 390°, 25:54658
Reactions of the hydrated electron with organic compounds, 25:54631 (CONF-700652-(Vol.3), pp 601-48)
HART-DAVIS, A. J., Silicon--transition metal chemistry. VI. Kinetics and mechanism of the replacement of triphenylsilane by triphenylphosphine in hydridotriphenylsilyl(π-cyclopentadienyl)dicarbonylmanganese, 25:54567
HARTL, R., Behavior of light water reactors under loss of cooling medium, 25:57101
HARTWIG, D., Study of $^{17}$N levels and T = $^{3}/_{2}$ multiplets in mass 17 nuclei, 25:56662
HARVEY, J. A., Distribution of partial radiation widths in $^{238}$U(n,γ)$^{239}$U, 25:56790
HARWARD, E. D., Public Health Service role in providing information relative to the nuclear power controversy, 25:56981
HARWARD, M. E., Trace element correlation of volcanic ash soils, 25:54513
HARWIT, Martin, Rocket-infrared four-color photometry of Galaxy's central regions, 25:55783
HASHIMOTO, Shoji, Effect of dose rate on the radiation graft polymerization of acrylonitrile onto poly(vinyl chloride) fiber, 25:54613
HASHIZUME, Tadashi, Estimation of genetically significant dose equivalent from occupational exposure to external sources of radiation in Japan, 25:55230
HASIGUTI, R. R., 2200°K defect in electron-irradiated p-type germanium, 25:56300
Neutron irradiations of silicon studied by $^{57}$Fe Moessbauer effect, 25:56326
One-valley EPR spectrum in electron-irradiated Sb-doped Ge, 25:56298
HASINOFF, M., T = $^{3}/_{2}$ states in $^{11}$C, 25:56679
HASSID, A., Attempt to use steady-state data for determining critical heat flux in transient conditions, 25:57024
HATANO, Yoshihiko, Radiolysis of liquid n-butane, 25:54659
HAUFE, Wolfgang, Arc erosion of various sintered and infiltrated WCu-materials in oil, 25:55454
HAULICA, A., Activity of hexokinase in rats, 25:55140
HAUSCHILDT, W. H., Administrative procedures and controls in plutonium production areas, 25:54960 (CONF-710401-, pp 293-6)
HAUSNER, Henry H., Modern developments in powder metallurgy. Volume 5. Materials and properties. Proceedings of the 1970 international powder metallurgy conference, held in New York, July 12--16, 1970, 25:55481
Modern developments in powder metallurgy. Volume 4. Processes. Proceedings of the 1970 international powder metallurgy conference, held in New York, July


XUM

12--16, 1970, 25:55411
HAUSTEIN, P. E., Radioactive decay of $^{169}$Ho and $^{149}$Ho, 25:56767
HAVELKOVA, V., Detection of alpha-radionuclides in the bone--marrow and blood of miners by the method of nuclear emulsions, 25:55236
Influence of stopping power on threshold sensitivity of nuclear emulsions for measurement of spectra and dosimetry of fast neutrons, 25:55022
Television monitor for dosimetric and spectrometric measurement by method of nuclear-track emulsions, 25:55021
HAWTHORNE, J. R., Postirradiation dynamic tear and Charpy-V performance of steel plates and weld metal, 25:55586
HAWTIN, P., Methane diffusion: an examination of commercial advanced gas cooled reactors, 25:57044
HAYASHI, Yasuo, Experimental osteogenic sarcomas induced by radioisotope $^{32}$P, 25:55335
HAYE, C., Relative biological effectiveness as a function of linear energy transfer for cataract criterion in the rabbit, 25:55317 (CEA-CONF-1744)
HAYES, W., Magneto-optical properties of $Cd^+$ in x-irradiated alkali halides, 25:56320
HAYES, W. L., State-of-the-art literature survey of thoria-dispersed NiCr for space shuttle thermal protection systems, 25:55399 (N-71-27008)
HAYNES, R., Dependence of isotope separation factor of the H-evolution reaction upon potential, 25:54721
HAYS, Walter W., Rulison ground motions recorded at the TOSCO Mine and Tower Stations, 25:54813 (PNE-R-51)
HAYWARD, C. C., Activation analysis applied to non-aqueous flowing system, 25:54524
HAYWOOD, R. C., JOSHUA terminal system, 25:57145 (CONF-710302-(Vol.1), pp 508-15)
HAZEL, John P., Determination by x-ray diffraction of crystal structures of silver diethylphosphate and potassium O, O-dibenzylphosphorodithioate, 25:57291 (UR-49-1515)
HAZLE, A. J., Environmental sampling. A critical look at common procedures, 25:54779 (CONF-710401-, pp 347-51)
HEAD, J. L., Calculation of stresses in graphite-fuel tubes, 25:57051
HEALY, J. W., Surface contamination: decision levels, 25:55196 (LA-4558)
HEALY, John W., Approach to plutonium surface contamination levels, 25:55195 (CONF-710401-, pp 352-64)
HEAMES, T. J., SAS2A LMFBR accident analysis code, 25:57077 (CONF-710302-(Vol.1), pp 120-7)
HEARLD, Albert B., Radioactive isotope distillation system for recovering water from waste in a spacecraft, 25:54911
HEARN, C. J., Monte Carlo methods in electron transport theory, 25:56362
HECHT, F., Determination of trace elements by neutron activation in meteorites, 25:54517
HEDDLE, D. W. O., Computer control of experiments in atomic physics, 25:55094
HEENAN, T. F., Cross sections in the unresolved resonance region: methods and evaluation of approximations, 25:56870
HEGEDUS, Andras J., Determination of small amounts of impurities in molybdenum and its compounds, 25:54399
HEHEMANN, R. F., Isothermal omega transformation in zirconium--niobium alloys, 25:55557
HEIDENREICH, P., Investigations on tumor localization using $^{67}$Ga, 25:55283
HEIJINK, A., Radiometric titration method based on separation by ion-exchange. IV, 25:54448
HEIKKINEN, D. W., Proton inelastic scattering from the five stable, even-mass isotopes of molybdenum, 25:56774
HEIMAN, Neil D., Radiofrequency perturbation of selectively excited nuclear hyperfine levels, 25:56368
HEINLOTH, K., Electroproduction of $\pi$-mesons on protons above the second resonance, 25:56406 (DESY-71/35)
HEINRICH, R. R., Integral measurements in EBR-II of capture rates, fission rates, and $\alpha$ for $^{233}$U, $^{235}$U, $^{238}$U, $^{239}$Pu, $^{240}$Pu, and $^{242}$Pu, 25:56982 (ANL-7791)
HEINTZ, Philip H., In-phantom microdosimetry with 14.6 MeV neutrons, 25:55232
HEINTZ, W., Theoretical investigation on diffraction of slow neutrons, 25:56615 (FMRB-37/71)
HEINTZE, J., Spark chamber experiment on the beta decay of $\Xi^-$ hyperons, 25:56411
HEITOWIT, Ezra David, Kinetic model for an inhomogeneous plasma, 25:56248
HELLMANN, H., Determination of metals in river sludge by means of x-ray fluorescence and its application in actual practice, 25:54408
HELLNER, Lucette, Reactions of H and deuterium formed in photolysis of methane and perdeuterated methane, 25:54573
HENDEE, William R., Record-keeping in a radiation safety office by timesharing digital computer, 25:54984
HENDERSON, P., Distribution of uranium in some basic igneous cumulates and its petrological significance, 25:54809
HENDRIKS, J. W., Angular dependence of the superconductive nucleation field Hc4, 25:56065
HENES, J. D., Moessbauer-type photoluminescence spectra of irradiated germanium, 25:56328
HENGLEIN, Arnim, Pulse radiolysis of organic compounds in aqueous solutions, 25:54632 (CONF-700652-(Vol.3), pp 649-92)
HENKELMANN, R., Analytical evaluation of prompt gamma radiation after neutron capture, 25:54451
HENRIE, J. O., Atomics International's L-88 nuclear reactor for neutron radiography, 25:57128
HENRION, P. N., Kinetics of reaction of $UO_2$, $NpO_2$, and $(U,Pu)O_2$ with F, 25:54736
HENRY, J. L., Solubility of nitrogen in alpha vanadium, 25:55475
HENRY, K. J., Technical description of PFR, 25:57013
HENRY, Patrick M., Palladium(II)-catalyzed exchange and isomerization reactions. I. The exchange of enol acetates with acetic acid catalyzed by palladium(II) chloride, 25:54557
HENRYSON II, H., Applications of space-energy factorization to the solution of static fast-reactor neutronics problems, 25:57170 (CONF-710302-(Vol.2), pp 953-67)
ARC system cross-section homogenization and modification capabilities, 25:56614 (ANL-7714)
Users experience with the ARC system, 25:57142 (CONF-710302-(Vol.1), pp 478-93)
HEPPNER, J. P., Electric-field measurements and identification of currents causing magnetic disturbances in polar cap, 25:55959
Magnetospheric field distortions observed by OGO's 3 and 5, 25:55952 (N-71-27604)
HERAGE, T. I., Neutron activation analysis of intact drill core, 25:54469
HERAK, Janko N., Crystal structure dependence of radiation-induced radicals in thymine: an esr study, 25:55130
HERAK, M. J., Solvent extraction study of lanthanum and europium by acidic esters of aminophosphonic acids, 25:54732
HERBER, Rolfe H., Current status of Moessbauer spectroscopy standards, 25:56365
HERBIG, Wolfgang, Ratio tissue and maximum for 42 and 25 MV x-rays of 42 MeV betatron, 25:55219
HERKENRATH, H., Pressurized and boiling water loop of the Technology Division at Ispra, 25:54867 (EUR-4683)
HERMANOWICZ, Ryszard, Separation of the alkaline earth metal ions by ionophoresis on filter paper and poly(vinyl alcohol), 25:54725
HERMANUTZ, K. D., Quantitative analysis of lung perfusion following bronchography, 25:55285
HERNBERG, J., $^{167}$Tm: a new bone scanning agent, 25:55279
HERPERS, U., Improved techniques for separation and determination of rare-earth elements in extraterrestrial material, 25:54475
HERR, W., Improved techniques for separation and determination of rare-earth elements in extraterrestrial material, 25:54475
HERRMANN, D. B., New measurement of radon content of waters at Bad Brambach, 25:54766
HERRMANN, Roland, Iodine-specific detector for a gas chromatograph, 25:54406
HERSHKOWITZ, N., Recoil radiation damage following coulomb excitation, 25:56369
HESS, W. N., Artificial aurora experiment: experiment and principal results, 25:55961
HESSLEY, Rita, Oxidative decarboxylation of polyaminocarboxylic acids. II, 25:54422
HEURTEBISE, M., Semi-automated determination of iodine in biological fluids by activation analysis, 25:54516
HEURTEBISE, Michel, Application of an iodide-specific resin to the determination of iodine in biological fluids by activation analysis, 25:54509
HICKEN, E., Behavior of light water reactors under loss of cooling medium, 25:57101
HIDECHIKA, Takahashi, Computer control of an accelerator, 25:56597 (SJC-A-71-3)
HIDEYO, Kodama, Computer control of an accelerator, 25:56597 (SJC-A-71-3)
HIEDA, Kotaro, Effects of dehydration on the sensitivity of yeast to ultraviolet light, 25:55183
HIERONYMUS, James Lee, Equilibria and stability of magnetically confined relativistic electron clouds, 25:56130
HIKIDO, T., Performance tests of sodium-filled powder and pellet oxide fuel under transient overpower, 25:57046 (GEAP-13722)
HILBORN, H. S., Publications, 1970, 25:57228 (DP-929(Rev.1)(Suppl.3))
HILEY, Basil J., Phase space, fibre bundles, and current algebras, 25:56448
HILL, A. J., Fire detection and suppression in glove box systems, 25:54954 (CONF-710401-, pp 212-20)
HILL, P. W., Radial velocities of southern B stars. V, 25:55697
HILLENBRAND, B., Compensation of external magnetic field by an internal field in a superconductor, 25:56074
HILLER, W., Viewpoints concerning techniques and metallography of the metallurgy of granular material, 25:55404
HILLS, P. R., Radiation polymerisation of impregnated porous material, 25:55658
HILTON, H. H., Polar ionosphere: measured ion density enhancements and soft electron precipitation, 25:55964
HILTON, Henry H., L parameter: a new approximation, 25:56041
HINES, C. O., Atmospheric gravity waves induced by solar eclipse. II, 25:56016

HINTZ, Gerald R., Nonhomogeneous boundary-value problem for the linear transport equation for a slab geometry, 25:56621
HIPP, Jackie Ervin, Travelling wave antenna for exciting waves in a cylindrical, anisotropic plasma, 25:56254
HIRAKI, A., EPR in electron-bombarded phosphorus-doped N-type germanium, 25:56299
HIRANO, Mitsumasa, DELIGHT: the point reactivity burnup code for HTGR lattices, 25:57021 (JAERI-Memo-4449)
HIRASAWA, Tomowo, Radiation patterns of S waves from underground nuclear explosions, 25:54814
HIRSCHEL, E. H., Radial flow through a one-dimensional gas centrifuge, 25:54890 (K-Trans-61-3)
HIRSCHFELD, D., Composition and properties of the binder metal in cobalt bonded tungsten carbide, 25:55630
HIRST, E. A., Analysis of round, turbulent, buoyant jets discharged to flowing stratified ambients, 25:57245 (ORNL-4685)
HISHIYAMA, Y., Negative magnetoresistance in neutron-irradiated graphite, 25:56319
HLADKY, E., Radioiodine in nuclear power reactors, 25:57100
System of radioactive products control in gas coolant of nuclear reactors, 25:57033
HLAVAC, T., Ambiguity in the density spectrum of cosmic-ray extensive air showers, 25:55905
HOBDELL, M. R., Equilibrium between sodium hydrogen acetylide and disodium acetylide, 25:54537
HOCH, M., High-temperature specific heat of metals and ceramics, 25:55626
Thermodynamic properties of ternary refractory carbides. II. Zirconium--uranium--carbon and zirconium--hafnium--carbon, 25:55614
Thermodynamic properties of ternary refractory carbides. I. Zirconium--niobium--carbon, 25:55615
HOCH, Michael, Determination of thermodynamic interaction parameters in solid V--Ti alloys using the mass spectrometer, 25:55489
HOCH, R. J., Simultaneous spectrographic triangulation of an SAR arc and a hydrogen arc, 25:55971
HOCKENBURY, R. W., Measurements of the neutron fission and absorption cross sections of $^{239}$Pu over the energy region 0.02 eV to 30 keV, Part II, 25:56746 (ORNL-4707)
HOCKNEY, R. W., Particle models in plasma physics, 25:56191
HOCQUENGHEM, J. C., Generating coordinates in continuum states, 25:56825 (LYCEN-7104, C6.1-12)
HODGE, V. F., Concentrations of plutonium, cobalt, and silver radionuclides in selected Pacific seaweeds, 25:55151 (CONF-710817-1)
HOEGDAHL, O., Reveiw of the application of activation analysis in oceanography, 25:54481
HOEHNDORF, A., Tritium fractionation in water-carbide to benzene reaction, 25:54735
HOEL, John E., Gamma ray density gauging, 25:55067
HOENIG, C. L., Phase equilibria, vapor pressure, and kinetic studies in the uranium--nitrogen system, 25:55617
HOFFMAN, B. W., Analysis of oceanographic samples from the glomar challenger voyage, 25:54482
HOFFMAN, Darleane C., Decay of $^{152}$Nd and the isomers of $^{152}$Pm, 25:56772
HOFFMAN, H. W., Tube identifier: physical description of tubes tested in OSW program on improved heat-transfer system for evaporators, 25:57247 (ORNL-TM-2713(Rev.1))
HOFFMANN, A., Composition and properties of the binder metal in cobalt bonded tungsten carbide, 25:55630
Pure Co alloys with additives of C, W, and Ti, 25:55497
HOFFMANN, G., Conference on radioisotopes in pharmacological and clinical biochemistry, Wiesbaden, Ger., 9/68, 25:55255
HOFFMANN, Klaus-Werner, Decay of $^{84}$Rb and fluorescence yield of Kr, 25:56697
HOFFMANN, P., Chemical problems in the production of superheavy elements by nuclear reactions, 25:54672
HOFFMANN, R., Temperature distribution and thermal conductivity in an argon plasma, 25:56140
HOFMANN, A., Examination of coupled-channel calculations for reaction $^{24}$Mg(d,p)$^{25}$Mg, 25:56728
HOGE, Kenneth G., Low-velocity air gun and Hopkinson split-bar facility, 25:57289 (UCRL-51098)
HOGUE, James V., Electron stimulated desorption of excited neutrals: CO on W, 25:55435 (RLO-2221-T-7-4)
HOLLANDER, Charles S., Radioimmunoassay of triiodothyronine in unextracted human serum, 25:55146
HOLLAS, C. L., $^{86}$Kr(d,n)$^{87}$Rb/sup A/ threshold cusp and the systematic appearance of charge-exchange cusps, 25:56719
HOLLECK, H., Ternary thorium--ruthenium carbide, 25:55640
HOLM, Albert Victor, Life spans of condensations in planetary nebulae, 25:55702
HOLSTEIN, Barry H., Second-class currents and analog processes, 25:56854
HOLSTEIN, Barry R., Induced tensor in allowed nuclear beta decay, 25:56861
HOMAYOONFAR, M., Inactivation of cells by heavy ion bombardment, 25:55313
HONDA, Masatake, Measurements of the isotopic ratio of boron, 25:54432
HONECK, H. C., ENDF/B cross section preparation and testing in the JOSHUA system, 25:57176 (CONF-710302-(Vol.2), pp 1024-30)
HONES, E. W. Jr., Association of magnetotail phenomena with visible auroral features, 25:55955
Energetic electron fluxes in magnetotail associated with onset of magnetospheric substorms, 25:56044
Magnetospheric substorms on Sept. 14, 1968, 25:56025
HONIG, Milton L., Deuterium isotope effects on thermal cyclobutene isomerizations. An investigation of competitive conrotatory ring openings, 25:54568
HONMA, Takashi, Simultaneous determination of O, F, and Al in Al electrolytic bath by fast-neutron activation, 25:54503
HOOD, D. W., Determination of gold in geological materials by neutron activation analysis, 25:54488
HOOVER, J., ARC system cross-section homogenization and modification capabilities, 25:56614 (ANL-7714)
HORD, Charles W., Mariner 6 and 7 hydrogen Lyman-alpha data, 25:55812
HORI, Setsuko, $P_{11}$ $\pi$N scattering in three-channel model, 25:56519
HORIE, H., Non-normal parity states of $^{209}$Bi and $^{207}$Pb, 25:56763
HORIYE, H., Lithium: an impurity of interest in radiation effects of silicon, 25:56309
HORKAY-BORSOS, Klara, Determination of small amounts of impurities in molybdenum and its compounds, 25:54399
HORM, J., Urinary excretion of $^{241}$Am under DTPA therapy, 25:55118
HORN, Klaus, Neutron--proton charge exchange at 8 and 19 GeV/c, 25:56415 (NP-18888)
HORNE, O. J. Jr., Properties of carbon derived from indene compounds, 25:57295 (Y-1790)
HORNECK, Gerda, Repair of ultraviolet-damages after irradiation of bacteria in the vacuum, 25:55356
HOSKIN, N. E., Use of computers in investigations on hydrodynamic aspects of reactor safety problems, 25:57102
HOUCK, J. R., Rocket-infrared four-color photometry of Galaxy's central regions, 25:55783
HOUYVET, Alain, Insulating device for a fuel element, 25:57195
HOVESTADT, D., Flux profile of protons measured in 1967 at equator, 25:55957
HOWER, C. O., Replacement reactions of hot chlorine atoms in chlorofluoromethanes, 25:54688
HOY, Gilbert R., Coincidence Moessbauer spectroscopy, 25:56367
HREJSA, A. F., Comparison of the nuclear-reaction energy scale with the gamma-ray energy scale, 25:56773
HROMEK, R., Technical-economic considerations of heat supply from power stations with light water reactors, 25:57135
HUBBARD, S. A., Cation-exchange separation of uranium in dimethylsulphoxide medium, 25:54728
HUBBERSTEY, P., Sodium--barium phase diagram, 25:55526
HUBER, P., Thirteenth report of federal commission on monitoring of radioactivity for year 1969 delivered to federal council, 25:54791
HUBER, R. A., Methane diffusion: an examination of commercial advanced gas cooled reactors, 25:57044
HUBERT, A., Oscillatory flux line profiles from generalized Ginzburg--Landau functional, 25:56070
HUBNER, Robert S., Status of data testing using the ENDF/B library, 25:57178 (CONF-710302-(Vol.2), pp 1053-64)
HUDDLESTON, Charles M., Calculations on transmission of gamma radiation through homogeneous slabs, 25:56256 (AD-722012)
HUEFNER, S., Local moment relaxation in a superconductor, 25:56071
HUENERMANN, B., Quantitative analysis of lung perfusion following bronchography, 25:55285
HUERTAS, M. L., Measurement of mobility and mass of atmospheric ions, 25:54800
HUETON, J. W., Industry reports: Canadian consultants and the Canadian nuclear industry, 25:57211 (70-CNA-657)
HUETTEL, G., Studies on the self-shielding of highly diluted resonance absorbers, 25:57196
HUG, O., Radiation injuries and radiation protection, 25:57099
HUGHES, Michael Paul, Study of 21 cm absorption by neutral H in Galaxy, 25:55791
HULL, Andrew P., Recapitulation of effluent releases and related changes in background radiation levels at Brookhaven National Laboratory, and some comparisons with those associated with nuclear power reactor plants, 25:55200
HULL, M. H. Jr., Reaction matrix elements and structure calculations with the Yale and Reid potentials for the Ni region, 25:56857
HULSBOSCH, A. N., Distance determination for high-velocity H I clouds around longitude 125°, 25:55717
HULTGREN, G. O., Comments on configuration interaction combined with a correlation factor for two-electron atoms, 25:55892
HUMENIK, M. Jr., High strength tungsten carbides, 25:55631
HUMMEL, F. A., Subsolidus relations in the system $ZrO_2$--$ThO_2$--$P_2O_5$, 25:55638
HUMPHREY, Joseph Stevenson Jr., Track registration process, 25:55010
HUMPHREYS, J. Ross Jr., Behavior and calibration of devices for monitoring impurities in sodium, 25:55069 (ANL-

XUM

7804)
HUNDHAUSEN, A. J., Observations of the interplanetary medium: Vela 3 and Imp 3, 1965--1967, 25:55780
HUNGERFORD, H. E., Three-dimensional stochastic gamma-ray transport method for shielding calculations, 25:56273
HUNG LAM THANH, Method for preparing molecules labeled with tritium, 25:54693
HUNSPERGER, R. G., Measurement of lattice damage caused by ion-implantation doping of semiconductors, 25:56287
HUNSTEAD, R. W., Optical identification of southern radio sources, 25:55725
HUNT, Angus L., Cross beam neutralizer for ion beams, 25:55816
HUNT, J. C. R., Magnetohydrodynamics at high Hartmann number, 25:55921
HUNT, J. W., Factors affecting the rate of hydrated electron attach on polynucleotides, 25:55131
HUNTER, C. W., Fracture and tensile behavior of neutron-irradiated A533-B pressure vessel steel, 25:55587
HUQ, S. S., Resonances produced from K⁺p interactions in bubble chamber, 25:56435
HUSAK, V., Choice of an optimum detector and an optimum adjustment of the apparatus for the detection of very low gamma activities, 25:55024
HUSSEIN, A. M., Effect of electromagnetic wave-field pressure on the propagation of slow TM waves, 25:56235
HUSSON, Jean-Pierre, Electromagnetic transitions in $^{190}$Pt, 25:56760
HUTCHIN, W. H., Facility for the determination of low-level tritium in biological and environmental samples, 25:55003 (UCRL-73128)
HUTCHINS, Robert R., Photoelectron-induced decomposition of ethane, 25:54597
HYATT, D., Influence of rotational energy on ion--molecule cross sections, 25:54550
HYATT, E. C., Evaluation of respirator performance by DOP man test, 25:55243 (CONF-710401-, pp 392-406)
HYCHE, Carolyn M., Determination of mercury in biological and environmental samples by neutron activation analysis, 25:54508

## I

IACHELLO, F., Meson finite size effects in mesonic atoms, 25:55831
IANMARTINO, Albert J., Ultraviolet light-induced changes in ribonuclease conformation, 25:55137
IBBOTT, Geoffrey S., Record-keeping in a radiation safety office by timesharing digital computer, 25:54984
ICHIKAWA, Riei, Effects of cooling rate and supercooling degree on Al--Mn, Al--Cr, and Al--Zr alloys, 25:55550
ICHINOSE, Norio, Extraction and determination of metal salts with methylisobutyl ketone. XV, 25:54420
IGI, K., Determination of the coupling strength from duality and unitarity, 25:56478
IGNAT'EV, P. P., Correlation between geomagnetic activity and the intensity of the interplanetary magnetic field, 25:56007
Interaction of galactic cosmic rays with interplanetary magnetic field, 25:55904
IGNATOV, D. V., X-ray diffraction study of phase composition of alundum-surfaced alloys VR-20 and VA-3 after vacuum annealing at high temperatures, 25:55465
IGNATYUK, A. V., Density of the excited states of atomic nuclei, 25:56835 (UCRL-Trans-10540)
IGNE, E. G., Environmental testing of engineered safety features related equipment, 25:57097 (WCAP-7744)
IGOLKIN, V. V., $^{14}$N(d,p)$^{15}$N, $^{28}$Si(d,p)$^{29}$Si, and $^{32}$S(d,p)$^{33}$S reactions with polarized deuterons, 25:56724
IGUCHI, Ienari, Ions and rotons in superfluid helium, 25:56057
IKEDA, Nagao, New method for radiochemical analysis of iodide and iodate in environmental water, 25:54442
IKEDA, Tetsuyuki, Effects of cooling rate and supercooling degree on Al--Mn, Al--Cr, and Al--Zr alloys, 25:55550
IKEUCHI, Satoru, Equation of state of neutron star matter and neutron star models, 25:55715
IKEZI, H., Observations of nonlinear Landau damping of ion-acoustic waves, 25:56234
ILIC-POPOVIC, J., Applicability of a solid-state Bragg--Gray cavity chamber for luminescence degradation dosimetry, 25:55056
IL'INOV, A. S., Classification of inelastic interactions of high-energy protons and nuclei. II, 25:56522 (ORNL-tr-2520)
ILIOPOULOS, J., Divergences of massive Yang--Mills theories: higher groups, 25:56542 (CNRS-CPT-71/P-378)
IMAGAWA, Koji, Utilization of pegmatitic ores, 25:54752
IMHOF, H., Scintigraphic evaluation of activity of Paget's disease, 25:55294
INCLAN-SUAREZ, Manuel, Critical review of the assumptions involved in establishing the MPD and MPC's in air and water, 25:55254
INCROPERA, F. P., Electron--ion recombination: critical review of theories and experimental results for an argon plasma, 25:56182
INGLE, R. W., Measurements of the neutron fission and absorption cross sections of $^{239}$Pu over the energy region 0.02 eV to 30 keV, Part II, 25:56746 (ORNL-4707)
INOUYE, H., Simple method of determination of the distribution and solubility limit of interstitials in substitutional solid solutions, 25:55568
IOFFE, V. G., Equations correlating the inflammability characteristics of metal powders, 25:55473
ION, D. B., Cerenkov mechanism and resonance production, 25:56498 (IFA-HE-76)
IONESCU-PALLAS, N. J., Theory of nuclear compressibility and application to isotope shift problem, 25:56846
IONOV, N. I., Isothermal heat of evaporation of ytterbium and neodymium ions on a tungsten surface, 25:55533
IONOV, S. P., Problem of calibration of isomeric shifts in gamma-resonance spectroscopy, 25:56370
IORGULESCU, Adriana, Study of $^{37}$Ar disintegration with various types of organic scintillators, 25:55030
IPPOLITOVA, E. A., Investigation of U(IV) complexing with acetate and formate ions, 25:54581
IREY, R. K., High-speed motion-picture studies of film boiling in liquid helium II, 25:56061
IRIGARAY, J. L., Gamma-ray spectra following capture of 14 MeV neutrons by $^{59}$Co, $^{93}$Nb, and $^{103}$Rh, 25:56729
IRISH, D. E., Raman spectral study of bisulfate--sulfate systems. II. Constitution, equilibria, and ultrafast proton transfer in sulfuric acid, 25:54564
IRKOV, V. I., Determination of diffusion coefficients in liquid metals by isotope exchange through the gas phase, 25:54556
IRVINE, A. R., Engineering evaluation of LMFBR fuel shipment, 25:54972 (ORNL-TM-2723)
ISHIWATARI, Nasumi, JPDR irradiation experiment of artificially pin-holed nuclear fuel rods, 25:57047 (JAERI-Memo-4157, pp 2-22)
ISPAS, M., Instrumental neutron activation analysis of some new standard rocks, 25:54464
ISRAEL, W., Event horizons and gravitational collapse, 25:55803
ITOH, Chiaki, Canonical quantization of the proper time formalism in the dual resonance model, 25:56480
ITOH, Noriaki, Location of impurities in alkali halide crystals by channeling studies, 25:56337
ITOH, Tadatsugu, Epitaxial growth of silicon assisted by ion implantation, 25:56347
IVANCHENKO, Yu. M., Effect of external fluctuations on the properties of superconducting micro-junctions near critical temperature, 25:56090
Sound excitation in a Josephson junction, 25:56089
IVANOV, L. I., Effect of vacuum on the diffusion mobility of nickel in molybdenum, 25:55505
IVANOV, O. S., Composition of the carbide phase in alloys of uranium with zirconium and niobium, 25:55547
Superconducting properties of niobium--titanium--zirconium hafnium alloys, 25:56104
Superconductive properties of niobium--zirconium--hafnium alloys, 25:56105
IVANOV, V. D., Detecting the polarization of solar-flare x-ray emission, 25:55771
IVANOV, V. M., Global contamination of the atmosphere by $^{85}$Kr from worldwide nuclear power plants and the radiation danger, 25:54781 (JPRS-53174)
Ruthenium and osmium separate spectrophotometric determination by use of 4-(2-pyridylazo)-resorcinol, 25:54412
IVANOV, V. N., Local irregularity of doses in neutron-capture therapy, 25:55212
Study of the absorbing surface of the suspensions in sea water by means of radioisotopes, 25:54811
IVANOVA, K. N., Mechanism underlying the dispersion hardening of niobium alloys, 25:55443
IVANOVA, M. I., Behavior of impurities in niobium during vacuum melting, 25:55403
IVANOVA, N. I., Focusing of high-current electron beams in linear induction accelerators, 25:56608
IVANOVA, R. S., X-ray diffraction study of phase composition of alundum-surfaced alloys VR-20 and VA-3 after vacuum annealing at high temperatures, 25:55465
IVANOVSKAYA, G. F., Electrophysical properties of niobium films produced and annealed in a very high vacuum, 25:55507
IVINS, R. O., Pressure generation by molten fuel-coolant interactions under LMFBR accident conditions, 25:57073 (CONF-710302-(Vol.1), pp 25-49)
IVLEV, A. A., Mass-spectrometric analysis of the isotopic composition of iron in the gas phase, 25:54404
IWAKI, I., Optimum planning for radiation facilities, 25:54852
IWASAKI, Hiroshi, Congruent melting composition of lithium metatantalate, 25:55639
IWASAKI, Machio, Radical pair from primary ionic species produced by ionizing radiation, 25:54665
IWASAKI, Tamiko, Sensitivity of Artemia eggs to γ irradiation. IX, 25:55262
IWATA, Katsuhiko, Secondary ion emission from metal surface in collisions of 30-keV Ar⁺ ions, 25:55818
IZRAEL, Yu. A., Distribution of radioactivity in rocks and petroleum from contained nuclear explosions, 25:54826 (UCRL-Trans-10543, pp 99-116)

## J

JACKSON, Daphne F., Cross sections for summed quasi-elastic and inelastic scattering, 25:56849

JACKSON, E. W., Leakage from a ruptured containment after accidental depressurisation of a gas cooled reactor, 25:57106
JACKSON, J. F., Numerical stability problems in the VENUS disassembly code, 25:57079 (CONF-710302-(Vol.1), pp 152-66)
JACKSON, J. S., Diurnal variation of the geomagnetic field. II, 25:56037
Diurnal variation of the geomagnetic field. I, 25:56036
JACKSON, M., James wave function for the ground state of $H_2^+$, 25:55829
JACOBI, Hatto, Optical constants of β-phases NiIn, PdAl, NiGa/sub 1-y/Al/sub y/, and (Ni,Cu)Ga, 25:56352
JACOBS, A. E., First-order transistion at H/sub c1/ and H/sub c2/ in type-II superconductors, 25:56082
Healing length of the superconducting order parameter, 25:56080
Interaction of vortices in Type-II superconductors near T = T/sub c/, 25:56081
Theory of inhomogeneous superconductors near T = T/sub c/, 25:56083
JACOBS, C. G. Jr., Recoil radiation damage following coulomb excitation, 25:56369
JACOBS, H. S., Mathematical analysis of kinetics of radioligand assays: improved sensitivity obtained by delayed addition of labeled ligand, 25:55145
JACOBSON, A. P., In situ measurements of environmental radioactivity, 25:55239
JACOBSON, Arnold F., Effect of temperature upon the uptake of $^{144}$Ce by Chlamydomonas, 25:55162
JACQUINOT, J., Electromagnetic instabilities in a slightly relativistic plasma, 25:56228 (CEA-CONF-1806)
JACQUOT, C., Substructures in $^{12}$C and $^{14}$N, 25:56652 (LYCEN-7104, S2.1-2)
JAEGER, Thomas A., Conference on structural mechanics in reactor technology, Berlin, 9/71. Vol. 3, Pt. H, 25:56882
JAFFE, Morry, Electrostatic confinement of an alkali-metal plasma, 25:56013
JAFFEE, Oscar C., Congenital cardiovascular anomalies in chick embryos exposed to x-irradiation and hypothermia, 25:55333
JAGODIC, V., Solvent extraction study of lanthanum and europium by acidic esters of aminophosphonic acids, 25:54732
JAHN, G., Magnetoplasmadynamic experiments in inductive-hydrodynamic shock wave tubes, 25:55920
JAHN, Gunther, Apparatus for measuring and evaluating the activity of measuring probes irradiated in a nuclear reactor, 25:55008
JAHNS, E., Scintigraphy of inflammations using silver isotopes, 25:55286
JAKOB, Fredi, Rotated mercury cell for controlled potential coulometry. Elimination of background current by digital normalization, 25:54427
JAKOBSON, M., LAMPF low-energy pion line, 25:56589 (LA-DC-12730)
JAKOVLEV, V. I., Influence of additions of transition metals on the sintering behaviour of tungsten, 25:55453
JAMBA, D. M., Measurement of lattice damage caused by ion-implantation doping of semiconductors, 25:56287
JAMES, B. W., Superconductivity of molybdenum and tungsten carbides, 25:56087
JAMES, R. W., Recoil synthesis of high specific activity $^{11}$C-cyanide, 25:54683
JANAUER, Gilbert E., Cation-exchange separation of uranium in dimethylsulphoxide medium, 25:54728
JANDA, L., Triaxial state of stress of concrete structures, 25:55659
JANECKA, J., Electron spin resonance and relaxation studies of internal motion in $CH_2CO_2^-$ radicals trapped in γ-irradiated Na acetate crystals, 25:54652
JANOVSKA, E., Survival of E. coli B under different post-irradiation conditions, 25:55357
JANSA, B., Surge and water hammer problems in the cooling water system of large thermal power plants, 25:57036
JANSSEN, E., Two-phase flow and heat transfer in multirod geometries. Final report, 25:54870 (GEAP-10347)
JARVIS, B. C., Effects of gamma irradiation on chromatin of sugar beet, 25:55351
JARVIS, O. N., Direct-access multi-user computer system for the Harwell synchrocyclotron, 25:56612
JAWOROWSKI, Z., Incorporation of $^{239}$Pu into hair, 25:55116
JEFFERTS, K. B., CO, CN, and CS emission from IRC + 10216, 25:55686
JEFFREY, Paul G., Chemical methods of rock analysis, 25:54403
JEKI, L., Remarks on the existence of retarded neutrons in fission, 25:56741 (KFKI-71-35)
JELLISON, James Lee, Low-temperature deformation and fracture of iron and iron--vanadium alloys, 25:55478
JEN, Norman C., Electrostatic confinement of an alkali-metal plasma, 25:56013
JENCKS, William P., Equilibrium deuterium isotope effects on the ionization of thiol acids, 25:54566
JENKINS, J. L., $^{237}$Pu production by $^{235}$U(γ,2n) reaction, 25:54674
JENNETTE, Robert L., Size effects in three dimensional Ising lattice, 25:57241 (NYO-1480-179)
JENNINGS, R. L., Recoil bromine reaction. The isomerization of excited cyclopropyl bromide, 25:54690
JENNINGS, W. C., Prog. rpt. on instabilities and turbulence in highly ionized plasmas in a magnetic field, semiannual, 9/70--2/71, 25:56196 (N-71-25028)
JENSEN, J. C., JOSHUA terminal system, 25:57145 (CONF-710302-(Vol.1), pp 508-15)
JENTZSCH, K., Muonic x-ray measurements with a high-pressure gas target, 25:55830
JERGER, E. W., Environmental problems of fallout shelters, 25:54933
JESKE, Wojciech, Immunofluorescent tests in course of /sup 99m/Tc scintiscanning, 25:55292
JEZERNIK, A., Calculation of stresses in graphite-fuel tubes, 25:57051
JIROUSEK, V., Spectrocalorimetric measurements in core of heavy water reactor, 25:57123
JOACHAIN, C. J., Multiple-scattering expansions for non-relativistic three-body collision problems, 25:56575
JOHN, W., Diurnal variation of aerosol trace element concentrations in Livermore, Calif, 25:54456
JOHNSON, C. E., Structural problems in solid-state chemistry, 25:56380
JOHNSON, Donald F., Unilateral and bilateral exposure of swine to fission neutrons, 25:55334
JOHNSON, E. R., Analysis of the safeguards capabilities of material balance accounting systems in selected uranium and plutonium scrap processing, 25:54968 (IAEA-R-878-F)
JOHNSON, E. S., Recombination luminescence in irradiated silicon, 25:56294
JOHNSON, Everett R., Prog. rpt. on radiation induced decomposition of inorganic molecular ions, 1970, 25:54633 (ORO-3660-4)
JOHNSON, G. W., Peaceful nuclear explosions, 25:54828
JOHNSON, J. E., Plutonium movement in aquatic systems: a review, 25:55150 (CONF-710401-, pp 407-10)
JOHNSON, John L., Numerical simulation of toroidal plasma confinement with a fluid model, 25:56129
JOHNSON, L., Adsorption and absorption of hydrogen by niobium, 25:55434 (RLO-2221-T-7-3)
JOHNSON, R. C., Structure in S-wave νν scattering, 25:56492
JOHNSON, R. G., Simultaneous observation of proton precipitation and auroral radar echoes, 25:55963
JOHNSON, T. C., Air leakage into plutonium gloveboxes and its effect on inert operations, 25:54944 (CONF-710401-, pp 83-97)
JOHNSON, Walter H., Method for constructing a lined underground cavity by underreaming, grouting, and boring through the grouting, 25:54854
JOHNSTON, Richard P., Implantable radioisotope-fueled stirling engine, 25:54910
JOLIVETTE, Peter Lauson, Isospin forbidden $^{16}$O(d,$\alpha_1$)$^{14}$N reaction for 2 < E/sub d/ < 14 MeV, 25:56667
JOLLY, R. K., Neutron-hole-state structure in N = 81 nuclei. I. $^{144}$Sm and $^{142}$Nd (p,d), 25:56770
JONECKO, A., Bone marrow sections of rat after whole body-irradiation, 25:55330
JONES, B. F., Gas permeability of extruded graphite, 25:55612
JONES, C. E., Recombination luminescence in irradiated silicon, 25:56295
JONES, C. H. W., $^{129}$I Moessbauer studies of the chemical effects of nuclear transformations in compounds of tellurium, 25:54704
JONES, G. R., Health physics aspects of $^{133}$Xe lung studies, 25:55248
JONES, H. C., Solid-state automatic beam positioner for mass spectrometers, 25:55075 (K-1817)
JONES, H. D., Distorted-wave Born-approximation analysis of the $^{90}$Zr(d,α)$^{88}$Y and $^{89}$Y($^3$He,α)$^{88}$Y reactions, 25:56778
JONES, L. W., Neutron total cross sections on protons and nuclei in 10 to 30 GeV/c momentum range, 25:56421
JONES, T. D., Dose and LET in a rabbit and a rat, 25:55229
JONES, V. Dean, Technique for the metallographic preparation of lead, 25:57239 (MLM-OP-71004)
JONSSON, A., Alternative approach to core calculations for boiling water reactors, 25:57168 (CONF-710302-(Vol.2), pp 920-38)
JORDAN, Carole, Identification of the lambda 417 line in the solar extreme-ultraviolet spectrum, 25:55767
JORDANA, R., Effect of ionizing radiation on rat liver, 25:55128
JORIS, S. J., Solvent isotope effects on decomposition of N,N-dialkyldithiocarbamic acids, 25:54560
JOSEPH, K., Quantitative evaluation of thyroid scintigrams by computer, 25:55282
JOSEPH, Robert David, Search for discrete celestial sources of far-infrared radiation, 25:55692
JOSHI, S. K., Electron-impact excitation of lithium, 25:55864
JOSTSONS, A., Radiation-induced voids in high-purity magnesium, 25:55580
JOUVE, Bernard, Radioactivity measurements, 25:55020
JOVANOVIC, D., Functional and circulatory changes in rats after local irradiation, 25:55328
JOY, E. F., Practical analysis of high-purity chemicals. VI. Emission spectrographic analysis of high-purity acids, 25:54431
JOYEZ, G., Resonance phenomena in low-energy-electron-impact excitation of He, 25:55851

XUM

JUDD, B. R., Lie groups in atomic spectroscopy, 25:55882 (NYO-1447-64)
JUHASZ, S., Angular distributions of fragments in fission of U and Th near (n,2n'f) threshold, 25:56804
JUN, C. K., Thermodynamic properties of ternary refractory carbides. I. Zirconium--niobium--carbon, 25:55615
JUNG, E., Determination of the temperature and flow relationships in the interior of a gas centrifuge rotor, 25:54891 (K-Trans-61-5)
JUNGINGER, H.-G., Model calculation of the electron--phonon coupling parameter lambda, 25:56106
JUST, L. C., Conversion of the Argonne Reactor Computation (ARC) System to control data 6000 and 7000 series equipment, 25:57140 (CONF-710302-(Vol.1), pp 464-71)

# K

KABAKCHI, A. M., Kinetics of the low-dose radiolysis of concentrated aqueous acidic solutions of sodium nitrate, 25:54657
KABAKOV, Y. N., Factors influencing clasmatosis in vivo: observations of periodicity of clasmatosis in lymphocytes and hematopoietic recovery after irradiation, 25:55321
KABANOV, A. N., Measurement of the mean free path of fast electrons, 25:56281
KABANOV, L., Heat and mass transfer as related to corrosion product deposition, 25:57034
KACKER, S. C., Estimation of friction factor of rough surfaces from the pressure distribution around a roughness element, 25:54873 (RD/B/N-1967)
KADANER, E. S., Study of phase equilibria in the aluminum--copper--yttrium system, 25:55561
KADKIN, E. P., Scattering of 14-MeV neutrons by Fe, 25:56707
KADLEC, J., Radiation experiment on tubular fuel element with finned surface. II, 25:57050 (UJV-2551-RT)
KADYROV, R. B., Debuncher of the JINR synchrophasotron injector with modulation of the accelerated beam energy, 25:565 6 (JINR-P9-5956)
KAFANOVA, T. A., Electrophysical properties of niobium films produced and annealed in a very high vacuum, 25:55507
KAFENGAUZ, N. L., Effect of the dimensions of the fuel element of the heat transfer at supercritical pressures, 25:54880
KAGEYAMA, Eiichi, Effect of dose rate on the radiation graft polymerization of acrylonitrile onto poly(vinyl chloride) fiber, 25:54613
KAGEYAMA, Misao, Heavy-particle ray damage to a Si solar battery, 25:55099
KAHAN, A., Electron irradiation of heavily doped GaAs:Si and GaAs:Te, 25:56292
KAHL, L., Diffusion of fission product ions in glasses, 25:55611
KAHN, B., Radiological surveillance studies at a BWR nuclear power station: estimated dose rates, 25:56979
KAIDALOV, A. B., Analysis of the reaction np + pp $\pi^-$ from the point of view of Reggeized OPE model, 25:56521 (JINR-P1-5975)
KAINARSKII, I. S., Technological conditions for hot pressing of zirconium dioxide, 25:55600
KAIPOV, D. K., Problem of calibration of isomeric shifts in gamma-resonance spectroscopy, 25:56370
KAJZAR, F., Tables of magnetic structures determined by neutron diffraction. V, 25:56341 (NP-19010)
KAKKAR, L. R., Separation of rhenium from molybdenum and other heavy metals by solvent extraction, 25:54401
KAL'CHENKO, V. A., Content of $^{90}$Sr, Ca, and Sr units in seeds of wheat hybrids, 25:55223
KALOS, M. H., Non-linear Monte Carlo, 25:57161 (CONF-710302-(Vol.2), pp 794-7)
KALOS, Malvin, Size effects in three dimensional Ising lattice, 25:57241 (NYO-1480-179)
KALOS, Malvin H., Machine generation of monte carlo sampling functions, 25:57160 (CONF-710302-(Vol.2), pp 771-81)
KALTHOFF, P., Temperature distribution and thermal conductivity in an argon plasma, 25:56140
KAMAL'DINOVA, Z. M., Effect of cooked gamma-irradiated beef on rats, 25:55367
KAMATH, P. R., Radioiodine distribution in the Tarapur power reactor environment during commissioning and initial operations, 25:56978
KAMEFUCHI, Susumu, Quantum field theory of tachyons, 25:56560
KAMENETSKAYA, G. Kh., Quasi-linear theory of formation of inhomogeneities in the equatorial electrojet, 25:55986
KAMIN, George J., Process for removing cerium and thorium from the other rare earth metals, 25:54749
KAMINSKI, S., Application of $\gamma$ irradiated heterogenic bovine fascia in filling brain defects in dogs, 25:55148
KAMOI, Koichi, Quantum field theory of tachyons, 25:56560
KAN, J. R., Formation of Debye potential well in current-carrying plasmas, 25:56174
KANAPILLY, G. M., Physical and chemical characteristics of aerosols produced from solutions of polyvalent metallic nuclides, 25:54545
KANASHIN, Yu. P., Precipitation of uranium from a melt of fused halides with a molten zinc cathode, 25:54580
KANE, G. L., Comparison of the high energy models for neutral meson photoproduction and the related hadronic processes, 25:56458
KANEKO, Kumetaro, Secondary ion emission from metal surface in collisions of 30-keV $Ar^+$ ions, 25:55818
KANG, Ik-ju, Electron-impact excitation of helium atoms to metastable states, 25:55843
KANNO, T., Extraction of uranyl thenoyltrifluoroacetonate into solvents, 25:54751
KAPEL'YAN, S. N., Recombination decay of plasma, 25:56167
KAPLAN, J. M., Regge cuts and high energy $\pi$N and KN scattering, 25:56505
KAPPE, P., Magnetic field tolerance and self field effects of an electron ring accelerator, 25:56595 (NP-19007)
KARABANOV, N. V., Stripping process for ($\alpha$,p) and ($\alpha$,d) reactions on light nuclei, 25:56677
KARACHEVTSEV, G. V., Kinetic energies of protons formed during collision of electrons with excited $H_2$, 25:55857
KARAMYAN, S. A., Elastic scattering of heavy ions by nuclei, 25:56740 (JINR-P7-5884)
KARAS, R. H., Magnetospheric substorms on Sept. 14, 1968, 25:56025
KARDONSKY, Stanley, $^{40}$Ar(n,$\alpha$)$^{37}$S reaction at 14.4 MeV, 25:56718
Reactions of $^{20}$Ne with 14.3-MeV neutrons, 25:56717
KARIN, S., Automated modular light water reactor calculation code package, 25:57172 (CONF-710302-(Vol.2), pp 983-90)
KARKLIT, A. K., Thermomechanical properties of some oxide refractories, 25:55621
KARLIK, B., Calculation program for determination of half-lives and intensities of total decay curves of radioactivity, 25:56695
Measurement of some capture cross sections for fast neutrons, 25:56696
KARLIK, Berta, Measurement of half-life of $^{16}$N decay, 25:56658
KARLMARK, B., Hepatic blood flow measured by $^{133}$Xe clearance, 25:55123
KAROL, I. L., Global contamination of the atmosphere by $^{85}$Kr from worldwide nuclear power plants and the radiation danger, 25:54781 (JPRS-53174)
KAROL, P. J., Method for calculating cross-contamination in column chromatographic separation of radioactive parent--daughter pairs, 25:54701
KARPLUS, M., Quantum theory of ($H,H_2$) scattering: approximate treatments of reactive scattering, 25:55863
KARPUKHIN, V. I., Use of irradiated diamonds for temperature measurement, 25:55104
KARSTEN, D., Viewpoints concerning techniques and metallography of the metallurgy of granular material, 25:55404
KARTTUNEN, E., M-subshell fluorescence yields and $L_1$--$L_3$ radiative transition at Z = 93 and 96, 25:55825
KARYAGIN, Yu. K., Debuncher of the JINR synchrophasotron injector with modulation of the accelerated beam energy, 25:56586 (JINR-P9-5956)
KASAI, Makoto, Development of reactor in-core neutron monitor, 25:57025
KASHUKEEV, N., Gamma-radiation-induced desorption of gas from SiC varistors, 25:55102
KASHY, E., Neutron-hole-state structure in N = 81 nuclei. I. $^{146}$Sm and $^{142}$Nd (p,d), 25:56770
KASSIROV, S. A., Fission process in atomic nuclei in transition region, 25:56786
KASTENBERG, William E., Axial kinetics model for fast reactor disassembly accidents, 25:57080 (CONF-710302-(Vol.1), pp 167-79)
KASTERKA, Barbara, Determination of impurities in high purity tellurium. III, 25:54414
KASTNER, Jacob, Passive moisture meter, 25:55061
KATAYOSE, K., Gamma-logging method in coal field, 25:54772
KATO, A., Emission-spectrometric determination of trace non-rare earth elements in yttrium oxide, 25:54419
KATO, Hiroo, Mortality in children exposed to the A-bombs while in-utero, 1945--1969, 25:55307
KATO, S., Magnetization properties of nonideal Type-II superconductors transporting sinusoidal alternating current in a longitudinal magnetic field, 25:56085
KATO, Shin'ichi, Oxidation of alcohols by Fenton's reagent. The effect of copper ion, 25:54576
KATO, Yasuyoshi, Kinetic study of the photosensitized electron exchange reaction between U(IV) and U(VI) in hydrochloric acid, 25:54618
KATSAUROV, L. N., Focusing of an ion beam drifting in a nonuniform magnetic field, 25:56602
KATZ, R., Inactivation of cells by heavy ion bombardment, 25:55313
KAUFMAN, Bernard, Heterogeneity of central nervous system myelin, 25:57261 (ORO-3195-49)
Isolation and biochemical characterization of subfractions of rat central nervous tissue myelin, 25:57258 (ORO-3195-46)
Sequential adsorption analysis of antimyelin antibodies, 25:57255 (ORO-3195-43)
KAUSHAL, N. N., Experimental and analytical studies of fast neutron transport in iron, 25:56618 (RPI-328-230)
KAUSHANSKII, D. A., Gamma-ray irradiation equipment, 25:54837

KAWAHARA, Hosaku, Radiocontamination in Hokkaido. IX, 25:54789
KAWAI, Toshiharu, Lorentz pole structure of the Virasoro model, 25:56494
Regge poles and their residues in the Virasoro model, 25:56493
KAWAMORI, Asako, X-ray irradiated crystals of Cu acetate monohydrate, 25:54610
KAWANO, Minoru, Vertical distribution of the intensity of ionization due to terrestrial gamma-radiation, 25:54790
KAWASAKI, K., Storm sudden commencements and polar magnetic substorms, 25:56026
KAWASHIMA, Nobuki, Simulation experiments on space plasma physics, 25:55976
KAZAROFF, John M., Properties of hot pressed titanium alloy powders for cryogenic applications, 25:55482
KAZIMIERCZYK, Stefania, Determination of strontium in barium minerals by atomic absorption spectroscopy, 25:54413
KAZUHIRO, Ishii, Computer control of an accelerator, 25:56597 (SJC-A-71-3)
KEDROVSKII, O. L., Making contained nuclear explosions radiation-safe, 25:54823 (UCRL-Trans-10543, pp 56-69)
Status report on the program of contained nuclear explosions for use in industry, 25:54821 (UCRL-Trans-10543, pp 36-41)
Use of contained nuclear explosions to stop runaway oil and gas wells, 25:54825 (UCRL-Trans-10543, pp 81-98)
Use of contained nuclear explosions to stimulate petroleum output, 25:54822 (UCRL-Trans-10543, pp 42-55)
KELER, E. K., Stabilization of zirconia with combined additives and a study of the solid solution stability, 25:55636
KELLER, J. H., Iodine chemistry in steam air atmospheres, 25:54547
KELLER, Jean-Pierre, Kinematic study of reaction between hadrons (stable and unstable), 25:56474 (FRNC-TH-63)
KELLER, R., Time-space resolved spectroscopic measurements on a fast z-pinch, 25:56150 (LGI-70/14/E)
KELLERER, Albrecht M., Assessment of wall effects in microdosimetric measurements, 25:55058
KELLEY, M. C., Electric fields in the nighttime and daytime auroral zone, 25:55960
KELLY, B. T., Effect of doping on the thermal conductivity of polycrystalline graphite, 25:55635
KELLY, John G., Implications of a model of charge-neutralized, high-current relativistic electron beams within conducting boundaries on diode and transport system design, 25:56596 (SC-RR-710436)
KELLY, M. A., Photoneutron cross section for $^{4}$He up to 31 MeV, 25:56649
KEMENY, L. G., Power reactor statistical diagnostic techniques, 25:57023
KEMP, E. F., Fuel and fuel cycle for PFR, 25:57064
KEMP, J. L., Description of ARHCO's new compact plutonium storage facility, 25:54942 (CONF-710401-, pp 56-67)
KEMPER, K. W., Direct reaction analysis of reactions $^{7}$Li(d,t)$^{6}$Li and $^{7}$Li(tau,$\alpha$)$^{6}$Li, 25:56671
Elastic scattering of deuterons by $^{6}$Li and $^{7}$Li at 8.0 to 12.0 MeV, 25:56670
KEMPKEN, K., Investigations on tumor localization using $^{67}$Ga, 25:55283
KENMOKU, Masakatsu, Canonical quantization of the proper time formalism in the dual resonance model, 25:56480
KENNEDY, J. S., Thyroid carcinoma following $^{131}$I therapy. Report of a case and review of the literature, 25:55343
KENNEDY, Joseph P., Molecular weights and molecular weight distributions of polyisobutylenes produced by $\gamma$-irradiation, 25:54621
KERIMOV, B. K., Bremsstrahlung of nonpolarized and longitudinally polarized electrons, 25:56862
KERN, C. W., Comments on configuration interaction combined with a correlation factor for two-electron atoms, 25:55892
KERN, R. D., Dynamic sampling of the deuterium hydride self-exchange behind reflected shock waves, 25:54562
KERR, Carolyn M. L., Electron spin resonance spectrum and structure of the radical anion of phosphorus oxychloride, 25:54667
KERR, H. T., ROD: a nuclear and fuel-cycle analysis code for circulating-fuel reactors, 25:57048 (ORNL-TM-3359)
KERR, J. C., Proton differential elastic scattering cross sections for even isotopes of tin at 30.4 MeV, 25:56764
KERSHNER, N. A., Practical analysis of high-purity chemicals. VI. Emission spectrographic analysis of high-purity acids, 25:54431
KERTAI, P., Radioprotective action of endotoxin, 25:55267
KESAREVA, N. S., Alteration of the function of external respiration in patients with malignant tumors of the chest under the effect of radiation treatment, 25:55339
KESSLER, B., Radiation-induced breaks in DNA, 25:55133
KESTERNICH, W., Linear high field magnetoresistance in aluminum, 25:56334
KETCHUM, Lynn D., Management of radionecrosis, 25:55270
KETTERMANN, Karl-Bertold, Investigations of injury induced by different causes, 25:55332
KEUFFEL, J. W., Muon decays underground and the Utah effect, 25:55897
KEVAN, L., Positron annihilation in $\gamma$-irradiated 10 M NaOH glassy ice, 25:55835
KEVAN, Larry, Multiple Ag$^{0}$ trapping sites in gamma-irradiated $AgNO_3$ ices, 25:54666
KEYEUX, A., Functional and circulatory changes in rats after local irradiation, 25:55328
KHAM'YAPOV, L. P., Gamma-radiation during thermal neutron capture on chromium and iron isotopes, 25:56683 (FEI-205)
KHAN, Fahmida, Quantitative separation of magnesium and palladium from numerous metal ions on titanium tungstate papers by electrochromatography, 25:54744
KHAN, Tasadduq, Mechanical behavior of alloys $UMo_{0.1}Al_{0.05}Sn_{0.05}$ and Sicral $F_1$ (adjusted uranium) between 20 and 600°C, 25:55429 (CEA-R-4177)
KHANDPUR, G. K., Damping of longitudinal plasma oscillations, 25:56238
KHARIN, V. P., Dependence of buildup factor on the position of shielding between bremsstrahlung source and detector, 25:56280
KHARISOV, I. F., Excitation of spontaneously fissioning isomeric states of $^{239}$Pu and $^{243}$Am at inelastic $\gamma$-quantum scattering, 25:56738 (JINR-P15-5959)
KHARITONOV, Yu. I., Properties of certain multiparticle states with large spins, 25:56783
KHAR'KOV, O. N., Use of reaction $^{18}$O(p,$\alpha$)$^{15}$N to study oxidation of metals, 25:55384
KHAZOV, P. D., Radiosensitivity and diagnosis of metastases into lungs and lymph nodes, 25:55300
KHEGAI, I. K., Study of the titanium--zirconium--niobium system, 25:55564
KHOKHLOV, Yu. K., Interaction of system of particles with electromagnetic field. I, 25:56455
KHOMKIN, A. L., Canonical transformation method in thermodynamics of partially ionized plasma, 25:56172
KHOROSHKOV, V. S., Proton beam of the ITEP accelerator for radium therapy, 25:56581 (BNL-tr-442)
KHOVANOVICH, A. I., Photoelectric colorimeter for counting charged particle tracks on surface of glass detectors, 25:55029
KHRUSHCHEV, V. G., Gamma-ray irradiation equipment, 25:54837
KHVAN, G. V., Dose distribution of high-energy electrons in tissue-equivalent media, 25:55214
KHVOSTOVA, V. V., Content of $^{90}$Sr, Ca, and Sr units in seeds of wheat hybrids, 25:55223
Metaphase analysis of chromosome rearrangements in barley, 25:55175
KIASASHVILI, G. D., Pneumatic loading and unloading of channels for irradiation in IRT-M reactor, 25:57130
KIEFFER, L. J., Total electron--atom collision cross sections at low energies: a critical review, 25:55856
KIEFFER, R., About nitrides and carbonitrides and nitride-based cemented hard alloys, 25:55629
KIESL, W., Determination of trace elements by neutron activation in meteorites, 25:54517
Determination of trace elements in meteoritic phases by neutron activation analysis, 25:54477
KIKNADZE, G. I., High-power radiation loop in IRT nuclear reactor at Tbilisi, 25:57129
KIKUCHI, C., Thermal neutron damage in CdS and CdTe, 25:56307
KIKUKAWA, Hiroji, Solidification of radioactive wastes with cement, 25:54979
KILB, Ralph W., Comparison of two computational models for collisionless plasma shocks, 25:56189
KIL'DYUSHOVA, L. A., Parameters of ionized air in front of a strong shock wave, 25:56160
KILIN, V. S., Pyrolytic titanium and zirconium nitrides and fields of their use, 25:55605
KILLEEN, John, Numerical computation of plasma equilibria, 25:56207
KIM, H., Lagrangian approach to nonlinear wave interactions in a warm plasma, 25:56245
KIM, H. S., Isolation of auxotrophic mutants of subtilis and E. coli, 25:55189
KIM, J. I., Determination of beryllium in rocks by activation analysis, using the $^{9}$Be($\alpha$,n$\gamma$)$^{12}$C reaction with $^{210}$Po, 25:54467
Monostandard activation analysis and its application to geological samples, 25:54490
KIM, Y. E., Extrapolation to the limit of singular-core interactions in the three-body problem, 25:56851
KIM, Young Mu., Effects of gamma-radiation on sprout-inhibition of garlic bulbs and the changes of their chemical contents, 25:55354
KIM, Young S., Rapid adsorbing colloid flotation method for the separation of molybdenum from seawater, 25:54743
Separation of uranium from seawater by adsorbing colloid flotation, 25:54738
KIMBROUGH, Raymond D. Jr., $\gamma$ irradiation of DDT: radiation products and their toxicity, 25:55135
KIMURA, Kan, New method for radiochemical analysis of iodide and iodate in environmental water, 25:54442
KINDER, H., Phonon generation by the ac Josephson effect, 25:56073
KINELL, P.-O., ESR single-crystal study of radical and radical-pair formation in some $\gamma$-irradiated vinyl monomers, 25:54634
KINELL, Per-Olof, Electron spin resonance studies of

XUM

primary processes in radiation-induced reactions. I, 25:54640
Electron spin resonance studies of primary processes in radiation-induced reactions. II, 25:54639
KING, Franklin D. R., Sealed container with pressure relief for hazardous material, 25:54989
KINOSHITA, Kisei, Particle exchange, Regge-pole exchange, and the Veneziano amplitude for KN scattering, 25:56518
KIRCHHOFF, R. H., Experimental study of the cylindrical Langmuir probe response in the transition regime, 25:56136
KIRCHMAYER, H. R., Preparation of rare earth metal alloys, 25:55401 (RFP-Trans-87)
KIRCHNER, Lucille K., Organosilicon entities as prophylactic and therapeutic agents, 25:55263
KIRILLOV, V. Kh., Electric field in an MHD duct of rectangular cross section with end electrodes, 25:55950
KIRKEGAARD, Peter, Danish Monte Carlo work in reactor physics and related areas, 25:57166 (CONF-710302-(Vol.2), pp 887-900)
KIRKO, I. M., Dynamics of liquid-metal drops in electromagnetic field in conditions of reduced gravitation, 25:55931
KIROV, A. G., Toroidal traps R-0 and RT-2 with steady and high-frequency magnetic fields, 25:56221
KIRSTE, R. G., Alteration of DNA by sensitized and non-sensitized long-wave uv irradiation, 25:55308
KIRSTOWSKY, E. C., Brazing the shell assembly for the BONUS superheater fuel element, 25:55425
KIR'YAKOV, M. A., $^{103}$Pd distribution in the animal organism, 25:55112
KIRZHNER, M. A., Tricomponent activity induced by competing reaction, 25:54498
KISABETH, Jerry L., Development of the polar electrojet during polar magnetic substorms, 25:56029
KISELEV, A. V., Gas-chromatographic study of the effect of radioactive radiation and heat treatment on the adsorptive properties of magnesium sulfate, 25:54603
KIST, A. A., Tricomponent activity induced by competing reaction, 25:54498
KIT, L. G., Influence of transverse magnetic field on intensity profiles of turbulent velocity fluctuations in pipes of rectangular cross section, 25:55926
KITAHARA, Tamemichi, Fuel failure detector experiment in a He gas inpile loop, 25:57193 (JAERI-Memo-4157, pp 66-83)
Proceedings of fuel failure detection symposium, 25:57192 (JAERI-Memo-4157)
KITAMURA, Takeshi, Facilities for accelerators for medical use, 25:56607
KIWAMOTO, Y., Observations of nonlinear Landau damping of ion-acoustic waves, 25:56234
KLASCHKA, J. T., Methane diffusion: an examination of commercial advanced gas cooled reactors, 25:57044
KLAUS, E., Comparison of scintigraphy and angiography in the diagnosis of intracranial space-occupying lesions, 25:55293
KLAWITTER, W. A., Magnetic properties of commercial soft magnetic alloys at cryogenic temperatures, 25:56361
KLEBER, Manfred, Polarization forces in elastic nuclear Coulomb scattering, 25:56573
KLEHR, Edwin H., Radiometric method for sulfate determination, 25:54443
KLEIN, H., Excitation of Δ(1236) resonance on bound state neutrons, 25:56405 (DESY-71/33)
KLEINE, P. J., Ventilation systems at Mound Laboratory ''PP'' Building, 25:54948 (CONF-710401-, pp 133-48)
KLEMM, C., Profilography of sacroiliac joints in ankylosing spondylitis, 25:55287
KLEMT, P., Low-temperature electron irradiation of tellurium, 25:56306
KLETSCH, E., Electricity in the modern industrial society, 25:57005
KLETT, R. D., Thermal analysis of the intact SNAP-19/NIMBUS B/AGENA system, 25:54895 (SC-RR-710353)
KLOBUCHAR, J. A., Ionospheric storm of March 8, 1970, 25:55974
KLONTZ, E. E., Defects induced by electron irradiation of p-type germanium, 25:56302
Review of radiation effects in germanium, 25:56303
KLOPP, William D., Mechanical properties of a W--23.4-percent Re--0.27-percent Hf--C alloy, 25:55433 (N-71-23982)
KLOSE, M., Analysis comparisons of thermal and surface waters, 25:54409
KLOSE, W., Theory of lattice softening and spin susceptibility in A 15 compounds, 25:56344
KLUEH, R. L., Determination of O in liquid alkali metals by Zr gettering, 25:54418
Effect of oxygen on niobium--sodium compatibility, 25:55386
KLUGE, Gy., Remarks on the existence of retarded neutrons in fission, 25:56741 (KFKI-71-35)
KLUGE, H., Spectroscopy of $^{93}$ $^{95}$Tc, 25:56766
KLUGER, F., Determination of trace elements by neutron activation in meteorites, 25:54517
KLYM, N. M., Interrelation between phase diagram and composition--property diagrams of In--Sn system, 25:55546
KLYUCHAREV, A. P., Polarization of protons elastically scattered on nuclei with a zero spin, 25:56678
Use of reaction $^{18}O(p,\alpha)^{15}N$ to study oxidation of metals, 25:55384
KLYUKIN, L. P., Individual dosimeter, 25:55051
KNAIFL, Josef, Recognition of the fragment nuclides $^{90}$Sr and $^{89}$Sr on the basis of radioactivity. II, 25:54803
KNEIP, Theodore J., Manmade radionuclides in the Hudson River estuary, 25:55160
KNOEPFLE, K. T., $^{31}P(^{3}He,p\gamma)^{33}S$ and $^{39}K(^{3}He,p\gamma)^{41}Ca$ reactions and the γ decay of analog states in $^{33}$S and $^{41}$Ca, 25:56715
KNOX, J. B., Comparison of U.S. and U.S.S.R. methods of calculating the transport, diffusion, and deposition of radioactivity, 25:54782 (UCRL-51054)
KNUFELMANN, Manfred, Apparatus for continuously measuring the cross-section of wire, 25:55062
KNYAZEV, D. A., Mass-spectrometric analysis of the isotopic composition of iron in the gas phase, 25:54404
KOBAYASHI, Masanori, Condition for Regge asymptotic behavior, 25:56579
KOBOZEV, N. I., Catalysis by metal vapors. IV, 25:54552
KOBZEV, A. P., Optical radiation excited by nonrelativistic charged particles on the metal surface, 25:55813 (JINR-P4-5957)
KOCH, L., Experimental and theoretical determination of burnup and heavy isotope content in a fuel assembly irradiated in the Garigliano boiling water reactor, 25:56879 (EUR-4638)
KOCHETOV, I. I., Scattering problem under a non-monotonic potential for the classical case, 25:56572
KODAKA, Hisao, Effects of neutron irradiation on Cu--Be alloys, 25:55583
KOELLING, D. D., Electronic structure of Th metal, 25:56388
KOHRI, Masaharu, Radioactive waste disposal at PWR power plant, 25:54980
KOJIMA, H., Vortex-free Landau state in rotating superfluid helium, 25:56048
KOJIMA, K., Electrophoretic behavior of x-irradiated lymphocytes, 25:55310
KOKAME, Jun, Method of correction on a spectrum distorted by accidental coincidence in an address-matrix of a counter array, 25:54997 (INSJ-128)
KOKOREV, L. S., Calculation of stable heat transfer from rod bundles in longitudinal flow, 25:54883
Hydraulic drag and heat transfer in turbulent flow of liquids in triangular channels, 25:54884
KOKUYAMA, Shigeru, Scale invariance and relativistic composite nucleon, 25:56465
KOLAR, J., Investigations on calcium metabolism of bones following local irradiation. XI, 25:55331
KOLB, W., $^{181}$W and other short lived fission products in ground-level air in north Germany and north Norway, 25:54785
KOL'CHUZHKIN, A. M., Monte Carlo method of calculating gamma radiation field in a statistically inhomogeneous medium, 25:56268
KOLDE, H. E., Radiological surveillance studies at a BWR nuclear power station: estimated dose rates, 25:56979
KOLESNICHENKO, G. A., Laws governing spreading of metallic melts over surface of boron nitride, 25:55469
KOLESNICHENKO, Ya. I., Possibility of stationary regimes in thermonuclear reactions, 25:56222
KOLEVATOV, Yu. I., Secondary γ-radiation in shielding, 25:56277
KOLOBASHKIN, V. M., Global contamination of the atmosphere by $^{85}$Kr from worldwide nuclear power plants and the radiation danger, 25:54781 (JPRS-53174)
KOLOKOL'TSOV, N. A., Theory of asymmetric separation cascades with an arbitrary enrichment in the separation element, 25:54917
KOLOMEETS, E. V., Dimensions of the galactic cosmic-ray modulation region, 25:55901
KOLOSNITSIN, N. I., Calculations of magnetogasdynamic flow in channels, 25:55935
KOLOTILOVA, V. G., Tissue equivalent scintillators in radiometry of long wave x radiation, 25:55213
KOLTUN, Daniel S., Interaction of pions with nuclei, 25:56873
KOMAROV, O. L., Focusing of high-current electron beams in linear induction accelerators, 25:56608
KOMAROV, V. L., High-frequency source of heavy ions, 25:55817
KOMAROVA, I. V., Calculation and optimization of the demineralization of water for reactors by ion exchange, 25:54737
KOMLOS, K., Concrete reinforced with steel micro-reinforcement, 25:55662
KOMURA, Kohjiro, Uraniferous bed in Mizusawa area, 25:54806
KONDRATENKO, S. G., Ionospheric effect of solar eclipse of Sep 22, 1968, 25:56000
KONECNY, E., Search for bremsstrahlung-induced fission isomers of $^{238}$U and $^{239}$Pu, 25:56801
KONISHI, Kenji, Evaluation of apparent ionium ages of some hermatypic corals, 25:54776
KONOBEEV, Yu. V., Theoretical model of fast-neutron-induced swelling in metals, 25:55582
KONONOV, V. N., Measurement of the ratio of the radiative capture to fission cross sections (α) for $^{239}$Pu in the neutron energy range 0.1 to 30 keV, 25:56734 (BNL-tr-

446)
KONOPLEVA, R. F., Oscillations of photocurrent in Ge with radiation defects, 25:56316
KONSTANTINOV, I. O., $^{60}$V in nuclear reactions on cyclotron, 25:54677
$^{51}$Cr on cyclotron, 25:54691
KOO, R. C., Mechanism and kinetics of bubble formation in doped tungsten, 25:55511
KOONS, H. C., Electrostatic vlf waves observed in the polar magnetosphere, 25:55965
Ion-wave instabilities at vlf in the polar wind, 25:55966
KOONTZ, R., Effects of aerosol agglomeration on reactor dose evaluations, 25:57105
KOPATZ, N. E., Manufacture and properties of high-conductivity high-strength Cu--$ThO_2$, 25:55417
KOPETSKII, Ch. V., Recrystallization of a strongly deformed monocrystal of molybdenum, 25:55518
KOP'EV, I. M., Metal-fibre-reinforced ceramics, 25:55608 (LB/G-3074)
KOPNIN, N. B., Viscous vortex flow in superconductors with paramagnetic impurities, 25:56086
KOPPENHAGEN, K., Perfusion lung scintigraphy in primary vascular pulmonary hypertension, 25:55284
KORBETSKII, E. V., Inelastic scattering of deuterons, 25:56780
KORENKOV, I. P., Accidental dosage estimation at large gamma-irradiation facilities, 25:55235
KORKISCH, J., Cation-exchange separation of uranium in dimethylsulphoxide medium, 25:54728
KORNEV, I. I., Parameters of betatron B-30 bremsstrahlung, 25:55209
KORNILOV, I. I., Distribution coefficients of titanium and iron in zirconium, 25:55502
Phase equilibria and properties of alloys in TiAl--$V_3Al_2$ section of Ti--Al--V system, 25:55537
Properties of Ti--V and Ti--V--Al alloys with O, 25:55471
Study of phase equilibria and properties of the alloys in the titanium--aluminum--iron and titanium--aluminum--vanadium systems, 25:55501
KOROTIN, B. A., Neutron scintillation detector, 25:55012
KORSHUNOV, F. P., Some regularities in measurement of characteristics of silicon diodes under the action of radiation, 25:55100
KORSOWER, Jack M., Acute changes in pulmonary arterial perfusion following irradiation, 25:55327
KORSUKOVA, M. M., Interaction of niobium with a zinc melt, 25:55534
KORSUN, A. S., Calculation of stable heat transfer from rod bundles in longitudinal flow, 25:54883
Hydraulic drag and heat transfer in turbulent flow of liquids in triangular channels, 25:54884
KORSUNOVA, L. P., Effect of universal time in $f_0E$ variations at large solar zenith angles, 25:55994
KORSUNSKII, A. M., Interrelation between phase diagram and composition--property diagrams of In--Sn system, 25:55546
KORYCHANEK, Ya., Critical heat fluxes encountered in the case of boiling of organic heat transfer agents with a high boiling point, 25:54879
KORYTOVA, A. I., Potential changes of chromosomes as a result of interaction of radiation and alkylating compounds, 25:55260
KORZUN, V. N., Effectiveness of a number of chemical substances in poisoning with a mixture of radioisotopes of cesium and strontium, 25:55113
KOSALY, G., Investigation of the area-ratio method of pulsed reactivity determination, 25:57185
KOSLOWSKI, Leo, Investigations of injury induced by different causes, 25:55332
KOSTOMAROV, D. P., Compression of plasma by growing longitudinal magnetic field in Tokamak, 25:56125
KOSTRITSA, A. A., Moments of the distribution function of the neutron density, 25:57179
KOSTYUNIN, B. N., Hydraulic drag and heat transfer in turbulent flow of liquids in triangular channels, 25:54884
KOTEL'NIKOV, G. A., Study of development of leaks in fuel element cladding by means of $^{85}$Kr, 25:54904
KOTEL'NIKOVA, G. V., Interaction between 14-MeV neutrons and nuclei of Fe, Cu, and Nb, 25:56684 (FEI-216)
KOTLINSKA-FILIPEK, Barbara, Preparation of high purity carrier-free $^{131}$Cs source for spectroscopic measurements, 25:54889 (INR-P-1325)
KOTOV, Yu. D., Cosmic muons and neutrinos, 25:56469
KOTRAPPA, P., Production of relatively monodisperse aerosols for inhalation experiments by aerosol centrifugation, 25:54982
KOTT, J., Spectrocalorimetric measurements in core of heavy water reactor, 25:57123
KOVACEVICH, E. A., Corrosion and deposition of irradiated stainless steel in sodium, 25:55370 (BNWL-SA-2335)
KOVALENKO, V. S., Relaxation of high energy protons in magnetosphere of Earth under effect of Alfven waves, 25:56011
KOVALEV, E. E., Investigations of artificial satellites of the Earth, 25:55342
KOVALEV, V. P., Dependence of buildup factor on the position of shielding between bremsstrahlung source and detector, 25:56280
KOVALEVSKII, I. V., Variations of interplanetary space parameters during a solar activity cycle, 25:55992
KOVALSKY, E. A., ARC system cross-section homogenization and modification capabilities, 25:56614 (ANL-7714)
KOVRIZHNYKH, O. M., Measurement of solar protons from July 7, 1966 flare, 25:55991
KOZHEVNIKOV, I. V., Broensted type equation for solvolysis of tert-butyl halides under action of metal ions, 25:54548
KOZIN, L. F., Phase diagram of the mercury--indium system, 25:55536
KOZLOV, S. I., Kinetics of ions in nighttime D region of ionosphere, 25:56010
KOZLOV, Stanislav Fedorovich, Neutron detector, 25:55009
KOZLOVA, I. R., Interaction of niobium with a zinc melt, 25:55534
KOZODAEVA, N. M., Neutron scintillation detector, 25:55012
KRAEMER, D. M., Alteration of DNA by sensitized and non-sensitized long-wave uv irradiation, 25:55308
KRAIMER, Martin R., Plume rise calculations using selected functional forms and the tabulation prediction technique, 25:54780 (CONF-710505-6)
KRAMER, Lois, Metabolism and removal of radiostrontium in man, 25:55109 (COO-1231-67)
KRAMER, Paul J., Multiple-scattering expansions for nonrelativistic three-body collision problems. III, 25:55868
KRAMER, S. L., Diffractive $\nu\nu$ scattering in $\nu N \to \nu\nu N$ at 13.1 GeV/c, 25:56425 (COO-1428-294)
KRANE, K. S., Ultralow temperature rotating polarization system, 25:55089
KRANZ, Erich, Dynamic pressure measurement at the anode of high-current electric arcs, 25:56155
KRAPCHEV, V., Relativistic expansions, 25:56577
KRASIN, A. K., Large $\gamma$ facility UGU-200, 25:54844
KRASNOPEVTSEV, Yu. V., Estimate of the influence of the natural radioactivity on the ion balance in the atmosphere, 25:54786
KRASNOV, A. N., Properties of powders produced by plasma spraying, 25:55467
KRASNOV, N. N., $^{60}$V in nuclear reactions on cyclotron, 25:54677
$^{51}$Cr on cyclotron, 25:54691
KRATSIK, B., Decay of $^{85}$Y (5 hr), $^{85}$Y (2.68 hr), and $^{85}$Sr, 25:56722
Decay of $^{89}$Zr and $^{97}$Zr, 25:56723
Decay of $^{90}$Nb, 25:56791
KRAVCHENKO, L. I., Thermodynamic properties of laves phase $TaFe_2$, 25:55508
KREITMAN, M. M., Application of a superfluid valve in a variable-temperature dewar, 25:56120
KREJCI, V., Ionization waves and wakes excited by an acoustic pulse, 25:56154
KREMPL, Hans, Determination of temperature and electron density in a spark plasma, 25:56142
KREZHOV, K., Gamma-radiation-induced desorption of gas from SiC varistors, 25:55102
KRICK, Merlyn S., Development of an NE-213 fast-neutron TAC spectrometer system utilizing off-line gamma-ray discrimination, 25:55033 (COO-2049-6)
KRIEGER, H. L., Radiological surveillance studies at a BWR nuclear power station: estimated dose rates, 25:56979
KRIMIGIS, S. M., Low-energy (greater than or equal to 0.3 MeV) solar-particle observations, 25:55956
KRISHBERG, R. R., Electromagnetic fields in an induction magnetohydrodynamic device with extendable channel, 25:55939
KRISHNAMURTHY, G. T., /sup 99m/Tc technetium sulfide and scintillation camera in rapid diagnosis of pericardial effusion, 25:55295
KRISTIANSSON, K., Isotope analysis with nuclear emulsions, 25:55894 (LUIP-CR-71-4)
KROEPELIN, H., Temperature distribution and thermal conductivity in an argon plasma, 25:56140
KROH, Jerzy, Role of ions in the radiolysis of hydrocarbons, 25:54630 (CONF-700652-(Vol.3), pp 523-98)
KROKHIN, O. N., Generation of neutrons in laser $CD_2$ plasma heated by pulses of nanosecond duration, 25:56219
KROKOSKY, E. M., Effect of radiation on some mechanical properties of an epoxy system, 25:55667
Effect of radiation on the adhesive properties of epoxy-metal and epoxy-glass adhints, 25:55666
KRONENBERG, Stanley, Relative biological effectiveness of x rays delivered at very high dose rates to radish seeds (raphanus sativus), 25:55350
KRONGAUZ, A. N., Tissue equivalent scintillators in radiommetry of long wave x radiation, 25:55213
KRORI, K. D., Application of Tolman's solutions of field equations in case of variable-density cores, 25:55696
KRUG, M. P., Solubility of nitrogen in alpha vanadium, 25:55475
KRUGER, O. L., Battelle's research plutonium facility environmental control and safety, 25:54959 (CONF-710401-, pp 280-92)
KRUGLIK, G. S., Collective states and statistics of systems of identical atoms, 25:56397
KRUGLYAKOV, E. P., Electrode phenomena and the acceleration of plasma, 25:56153
KRUMIN, Yu. K., Control of profile of electrodynamic forces in conducting bodies in traveling magnetic fields, 25:55915

KRUPKOWSKI, A., Standard potential and enthalpy values of metals and their compounds based on electrode potentials, 25:54586
KRUUSMAA, A. E.-V., Model atmospheres of stars of classes O and B, 25:55673
KRYUKOV, S. N., Determination of diffusion coefficients in liquid metals by isotope exchange through the gas phase, 25:54556
KRYVOKRYSENKO, I. F., Photoelectric colorimeter for counting charged particle tracks on surface of glass detectors, 25:55029
KRYZHENKOVA, N. A., Tricomponent activity induced by competing reaction, 25:54498
KUBA, J., Comparison of scintigraphy and angiography in the diagnosis of intracranial space-occupying lesions, 25:55293
KUBYSHEV, N. N., Determination of the rate of movement of the charge in rotary kilns by means of radioactive isotopes, 25:54898
KUCAB, M., Tables of magnetic structures determined by neutron diffraction. V, 25:56341 (NP-19010)
KUDINOV, B. S., Development of a fast-neutron activation method for determination of N in Nb, Ta, and Ti, 25:54501
KUDO, Hiroshi, Observation of neutron dose dependence of the apparent initial retention in chloroindium chlorophthalocyanine, 25:54680
KUEHN, K., Radioactive waste, 25:54985
KUEHNELT, H., Low energy pion--pion scattering, 25:56495
Radiative neutron--proton scattering at low energy, 25:56526
KUEPER, K. D., Computer program for the dynamic calculation of pressure over time duration in coupled volumes, 25:54886
KUGAI, L. N., Chemical stability of diborides of transition metals, 25:54543
KUIKEN, R., Fission of oriented nuclei by low energy neutrons, 25:56749 (RCN-142)
KUJAWSKI, E., Additivity of phase shifts for scattering in one dimension, 25:56576
KUKANOV, A. B., Radiation from an electric charge moving along a spiral path in a transparent medium, 25:56462
KUKHLENKO, A. C., Scattering of 14-MeV neutrons by Fe, 25:56707
KUKHTEVICH, I. V., Secondary γ-radiation in shielding, 25:56277
KULAKOV, V. S., Use of reaction $^{18}O(p,\alpha)^{15}N$ to study oxidation of metals, 25:55384
KULCINSKI, G. L., Swelling in refractory metals during high temperature ion bombardment, 25:55573 (BNWL-SA-3962)
KULES, Inna, Radiation chemistry of supercooled water, 25:54663
KULESKO, G. I., Recrystallization of a strongly deformed monocrystal of molybdenum, 25:55518
KULIEV, A. A., Collective $1^+$ states in even--even deformed nuclei, 25:56819 (JINR-P4-5889)
KULKA, Zbigniew, Integral discriminator for amplitude analyzers, 25:55073 (INR-1315)
KULLANDER, S., (p,2p) reactions at 600 MeV, 25:56711
Energy of separation for some nuclei of medium mass in the reaction (p,2p) at 600 MeV, 25:56706
KULTASHEV, O. K., Electron work function of tantalum--ruthenium alloys, 25:56350
KULUS, E., Concentration and determination of rare earth impurities in an yttrium matrix, 25:54525
KUMAMOTO, Yoshikazu, Estimation of genetically significant dose equivalent from occupational exposure to external sources of radiation in Japan, 25:55230
KUMMER, Joseph T., Ranges of recoil atoms from the (n,γ) process, 25:56269
KUNC, Jozef, Ionization of atomic H by electron impact: numerical calculations for free-fall atomic model, 25:55836 (INR-P-1327)
KUNCOVA, Vlasta, Recognition of the fragment nuclides $^{90}Sr$ and $^{89}Sr$ on the basis of radioactivity. II, 25:54803
KUNG, H. W., Reaction matrix elements and structure calculations with the Yale and Reid potentials for the Ni region, 25:56857
KUNKEL, W. B., Large-area high-current ion source, 25:56212 (LBL-35)
KUNTZ, Robert R., Photoelectron-induced decomposition of ethane, 25:54597
KUNZE, H.-J., Oscillator strengths of sodiumlike ions, 25:55776
KURANZ, John L., Twenty-five years of isotopes in life sciences, 25:55107
KURATOVA, T. S., Determination of the association constants of ions from the rate of oxygen exchange between anions and water, 25:54553
KURBATOV, L. N., Measurement of the mean free path of fast electrons, 25:56281
KURDIANI, N. I., Annealing of radiation defects and the electron mobility in indium antimonide irradiated with fast neutrons, 25:56317
KURIN, M. N., Determination of the relative difference between the mobilities of isotopic lithium ions in an ion-exchange resin--solution system, 25:54730
KURNOSOVA, L. V., Nature of the radiation background at altitudes of 250 to 500 km, 25:56008
KUROPATENKO, V. F., Approximative method of calculating physical quantities behind a shock-wave front, 25:57290 (UCRL-Trans-10539)
KUROV, M. A., Measurement of the ratio of the radiative capture to fission cross sections (α) for $^{239}Pu$ in the neutron energy range 0.1 to 30 keV, 25:56734 (BNL-tr-446)
KURTZ, N., π and K mesons used for investigating light nuclei structures, 25:56653 (LYCEN-7104, S4.1-10)
KUSAMA, Yasuo, Effect of dose rate on the radiation graft polymerization of acrylonitrile onto poly(vinyl chloride) fiber, 25:54613
KUSCH, Wlodzimierz, Level structure of near $^{208}Pb$ nuclei (neutron-deficient Pb and Bi isotopes), 25:56798
KUSHNIRENKO, A. N., Existence of the pseudovector isospinor heavy boson and a new model for hadrons, 25:56477
KUSHNIRUK, V. F., Investigation of the silicon surface-Barrier Δ E-detector characteristics for the nuclear reaction studying, 25:54998 (JINR-P13-5970)
KUSNER, Daniel E., ETOG-2 and ETOT--ENDF/B data processor programs to produce epithermal and thermal multigroup libraries, 25:57177 (CONF-710302-(Vol.2), pp 1031-46)
KUUSI, J., Use of radioisotopic neutron sources for process-control activation analysis, 25:54507
KUYKENDALL, W. E. Jr., Analysis of oceanographic samples from the glomar challenger voyage, 25:54482
KUZHEVSKII, B. M., Propagation of cosmic rays through galaxy, 25:55903
KUZ'MIN, A. I., Annual variations and gradient of cosmic-ray intensity in the meridional plane, 25:55900
KUZNETSOV, A. P., Turbulent jet of conducting fluid in longitudinal magnetic field, 25:55928
KUZNETSOV, S. N., Correlation of magnetic activity indexes with intensity of outer-belt electrons, 25:55979
Monotonic decrease of intensity of electrons in radiation belts, 25:55978
KUZNETSOV, V. S., Focusing of high-current electron beams in linear induction accelerators, 25:56608
KVAPIL, Jiri, Growth and structure of $RbUO_2(NO_3)_3$ crystals, 25:54579
KVAPIL, Josef, Growth and structure of $RbUO_2(NO_3)_3$ crystals, 25:54579
KVEDAR, John P., Virus-cell relationships in dog brain tumors, 25:57262 (ORO-3195-50)
KWAK, N., Single- and double-pion production in proton--antiproton nonannihilations at 2.2 GeV/c, 25:56487
KWAST, H., Post-irradiation examination of fuel pins R62-A01 and -A02 irradiated in a sodium environment up to 19 MWd/kg $UO_2$, 25:55648 (RCN-144)

## L

LABAHN, R. W., Polarized-orbital method and application to scattering of electrons by He, 25:55871
LABELLA, Frank S., Classic bioassay statistical procedures applied to radioimmunoassay of bovine thyrotropin, growth hormone and prolactin, 25:55143
LABS, Dietrich, The solar constant, 25:55742
LABUSCA, Elena N., Possibilities of activating sintering by special thermal treatment, 25:55414
LACHMANN, D., Ventricular scintigraphy for diagnosis of cerebral tumors in early childhood, 25:55290
LACOMBE, P., Influence of orientation of zirconium monocrystals on the growth structures of monoclinic zirconia, 25:55540
Relation between the kinetics of aging after deformation of α-zirconium and the anisotropic diffusion of oxygen for a short distance, 25:55551
LADESICH, John, Plutonium recycle developments, 25:57202
LADNER, H.-A., Conference on radioisotopes in pharmacological and clinical biochemistry, Wiesbaden, Ger., 9/68, 25:55255
LADY, E. R., Discrepancies in critical-heat-flux data obtained using thin-wire heaters in saturated liquid helium II, 25:56060
LAFFERTY, R. H. Jr., Isotopes and radiation technology, Vol. 9, No. 1, 1971, 25:57127
LAFFON, Jean-Louis, Process for the measurement of a displacement and device for its use, 25:55068 (AEC-tr-7240)
LAGUNTSOV, N. I., Theory of asymmetric separation cascades with an arbitrary enrichment in the separation element, 25:54917
LAI, Hon-ming, Topics in plasma theory, 25:56185
LAI, Shu Tim, Properties of a short-range field model of superdense matter, 25:55689
LAIBOWITZ, R. B., Electron transport in Nb/Nb oxide/Bi tunnel junctions, 25:56078
LAIHO, R. T. S., Magneto-optical properties of $Cd^+$ in x-irradiated alkali halides, 25:56320
LAING, E. W., Invariants in the motion of a charged particle in a spatially modulated magnetic field, 25:56401
Stability of a plasma stream in a magnetic field, 25:56202
LAIZIER, Jacques, Treatment of elastomers, 25:54619
LAJTAI, A., Remarks on the existence of retarded neutrons in fission, 25:56741 (KFKI-71-35)
LAKCHAURA, Bala, Recovery from x-ray and nitrogen mustard inactivation of Escherichia coli by 2, 4-dinitrophenol treatment, 25:55355
LAKE, Suzanne, Retention and excretion by pigs of radionuclides produced by the Plowshare Event Schooner,

XUM

25:55124
LAM, C. S., Energies of ''s'' eigenstates in a static screened Coulomb potential, 25:55884
LAMB, J. F., Recoil synthesis of high specific activity $^{11}$C-cyanide, 25:54683
LAMBERT, G., Balance of $^{90}$Sr over Antarctica, 25:54788
LAMBERT, J. M., Reaction mechanisms of $^{10}B(d,\alpha)^{8}Be_{g.s.}(\alpha)^{5}He$ for E/sub d/ = 0.4, 1.0, and 1.5 MeV, 25:56673
LAMONT, A., Stability of a plasma stream in a magnetic field, 25:56202
LAMOT, G.-H., Description of elastic scattering processes with the use of nonlocal separable potentials, 25:56852
Separable nonlocal potentials and their equivalent local potentials in elastic scattering studies, 25:56642 (LYCEN-7104, C5.1-15)
LAMPTON, Michael, Pulsing x-ray source in Circinus, 25:55721
LAMSFUS, Carmen, Effect of ionizing radiation on rat liver, 25:55128
LAND, Peter L., Electronic defect structure of single-crystal $ThO_2$ by thermoluminescence, 25:56315
LANDAUD, G., Energy of separation for some nuclei of medium mass in the reaction (p,2p) at 600 MeV, 25:56706
LANDE, A., Meson finite size effects in mesonic atoms, 25:55831
LANDMAN, Silviu, Pancreas imaging: is it worth it, 25:55280
LANDSHOFF, P. V., Dual quark--parton model and high energy hadronic processes, 25:56481
LANE, Neal F., Low energy electron--molecule scattering experiments and the theory of rotational excitation, 25:55855
LANG, G., Application of the Moessbauer effect in biology, 25:55105
LANG, Gerhard, Optimization of a heavy-water enrichment plant based on $H_2/NH_3$ exchange, 25:54748
LANGAN, D., Behavior of end slabs in cylindrical prestressed concrete pressure vessels, 25:56986
Design of pod boiler pressure vessels, 25:56885
LANGENDORFF, H., Radiobiological investigations with fast neutrons. II, 25:55266
LANGENDORFF, M., Radiobiological investigations with fast neutrons. II, 25:55266
LANGHAM, Wright H., Proposal for a biomedical addition to Los Alamos Scientific Laboratory's High-Flux Meson Physics Facility, 25:55299 (LA-4490)
LANGHANS, J., Computer program for the dynamic calculation of pressure over time duration in coupled volumes, 25:54886
LANGHOFF, H., Coulomb fragmentation in InI and $InI_3$, 25:54696
LANGLEY, Robert A., Range--energy relations for He ions and protons in Ar, $N_2$, $O_2$, and air (0.2 to 2.0 MeV), 25:56276
LANGSFORD, A., Direct-access multi-user computer system for the Harwell synchrocyclotron, 25:56612
LANTZ, T. E., Recent experiments on steady state and pulse radiolysis of alkaline aqueous systems, 25:54627 (CONF-700652-(Vol.2), pp 295-330)
LANZEROTTI, I. J., Interplanetary-particle associations with Type-III solar bursts, 25:55778
LANZEROTTI, L. J., Magnetospheric substorms on Sept. 14, 1968, 25:56025
LAQUER, H. L., Energy storage and switching with superconductors, 25:56110 (LA-DC-12990)
LARIKOV, L. N., Influence of deformation conditions on polygonization and recrystallization of single-crystal molybdenum, 25:55559
LARIONOV, V. V., Estimation of the single-stage isotope separation factor in the electromigration of isotopic ions through an ion-exchange membrane, 25:54729
LARSEN, M. Lolk, Heating in a reactor fuel element rod under transient conditions. I, 25:57094 (RISO-M-1391)
LARSON, E. A., Properties of carbon derived from indene compounds, 25:57295 (Y-1790)
LARSON, Howard Allen, Energy-dependent neutron transport calculations in thick and thin slabs, 25:56632
LARSON, Steven M., Improved detector for video systems used in radionuclide studies, 25:55278
LASER, M., Energy accumulation in solid bodies through nuclear radiation by storage of highly radioactive scrap, 25:54969 (JUL-766-CT)
LASKER, B. M., Optical identification of southern radio sources, 25:55725
LASSNER, E., Determination of O, H, and N in high-melting metals. VI, 25:54426
LAT'EV, L. N., Spectral emissivity of tantalum, 25:55495
LATHROP, K. D., Elimination of ray effects by converting discrete ordinate equations to spherical harmonic-like equations, 25:57151 (CONF-710302-(Vol.2), pp 577-607)
Two-dimensional air transport calculations, 25:56261 (LA-4774)
LATYPOV, Z. Z., Interference effect in cross section for charge exchange of $Li^+$ ions with He atoms, 25:55844
LAUBER, Alexander, Investigation into some properties and applications of semiconductor nuclear radiation detectors, 25:55000 (NP-19008)
LAUD, K. R., Subsolidus relations in the system $ZrO_2$--$ThO_2$--$P_2O_5$, 25:55638
LAUGHLIN, John S., Prog. rpt. on biological and clinical dosimetry, annual, 7/70--6/71, 25:55208 (NYO-3510-18)
LAUNAY, P., Strain and ultimate strength of concrete under triaxial stress, 25:55660
LAVAL, M., Use of liquefied noble gases, 25:55028
LAVROVA, G. A., Radiation from an electric charge moving along a spiral path in a transparent medium, 25:56462
LAVRUKHINA, A. K., Nuclear reaction in the nucleogenesis of xenon isotopes in solar system matter, 25:55670
LAWN, C. J., Heat transfer and pressure drop performance of roughened surfaces, 25:54874 (RD/B/N-1980)
LAWSON, J. C., Angular correlations studies in $^{32}S(^3He,p\gamma)^{34}Cl$, 25:56712
LAZAREVA, E. V., Interaction of a shock wave with a magnetic field, 25:55951
LAZZARINI, E., Correlated annealings of $^{60}$Co recoiled atoms in cationic and anionic sites of neutron-irradiated crystals of cis-[Co $en_2(NO_2)$ CNS][Co EDTA]$2H_2O$, 25:54682
LEAF, G. K., Two-dimensional fast-reactor disassembly analysis with space-time kinetics, 25:57078 (CONF-710302-(Vol.1), pp 128-51)
LEAKE, John Walgate, Neutron counters, 25:55014
LEBEDEV, V. A., Local changes in valence and structure caused by nuclear transformation in Co, Fe, I, and Te compounds, 25:56381
Thermodynamic properties of cerium in molten zinc, 25:55442
LEBOULEUX, Ph., Real time treatment of information provided by atmospheric contamination detectors, 25:55006
LECLERCQ-WILLAIN, C., Microscopic description and cluster structure of light nuclei, 25:56654 (LYCEN-7104, S13.1-11)
LECOUSTEY, P., MHD stability criterion in shallow magnetic well, 25:56194 (EUR-CEA-FC-598)
LEDLEY, B. G., Magnetopause attitudes during Ogo 5 crossings, 25:56023
Magnetospheric field distortions observed by OGO's 3 and 5, 25:55952 (N-71-27604)
LE DU, P., Study of $\pi^-p \to \pi^0n$ and $\pi^-p \to eta$ reactions in nuclei at 7.82 GeV/c, 25:56432
LE DUFF, J., Status report on ACO, 25:56591 (LAL-RT-42-70)
LEE, C. Y., Isolation of auxotrophic mutants of subtilis and E. coli, 25:55189
LEE, Deok Kyo, Ground-state energy of a many-particle boson system, 25:56050
LEE, Duck Chool, Gamma-irradiation effect on electrical properties of B-type insulator, 25:55101
LEE, H. A., Fire protection test facility for cells and caves, 25:54956 (CONF-710401-, pp 237-47)
LEE, J., Can all liquid radwaste discharges be eliminated, 25:56881
LEE, K. H., Isolation of auxotrophic mutants of subtilis and E. coli, 25:55189
LEE, Ming-huei, Determination of intermediate neutron energy spectrum, 25:57126
LEE, R. H., Conversion of the Argonne Reactor Computation (ARC) System to control data 6000 and 7000 series equipment, 25:57140 (CONF-710302-(Vol.1), pp 464-71)
LEE, R. R., Network organization of an automated nuclear design system, 25:57146 (CONF-710302-(Vol.1), pp 516-30)
LEE, S. C., Replacement reactions of hot chlorine atoms in chlorofluoromethanes, 25:54688
LEE, T. D., Some new applications of indefinite metric to quantum electrodynamics and weak interactions, 25:56547 (NYO-1932(2)-200)
LEETZ, Hans-Karl, Program for computation of dose distributions in teletherapy with $^{60}$Co gamma radiation. II, 25:55220
Program used for calculation of dose distributions for teletherapy with $^{60}$Co-gamma rays. III, 25:55221
LEFEBVRE-BRION, H., Quasi-diabatic representation for inelastic collisions, 25:55849
LEFEVRE, Ultra high vacuum metrology, description of a calibration bench and associated measuring equipment, 25:54992
LEGATOWICZ, Aleksander, Penetration of electromagnetic wave into the plasma of exponential density distribution, 25:56230 (INR-1321)
LEGEAY, G., Relative biological effectiveness as a function of linear energy transfer for cataract criterion in the rabbit, 25:55317 (CEA-CONF-1744)
LEGEN'KA, A. D., Variations of electron density in topside ionosphere at middle latitudes, 25:55993
LEHNERG, B., Partially ionized plasma centrifuge, 25:54912
LEI, K. P. V., Electrorefining of V prepared by carbothermic reduction of $V_2O_5$, 25:55408
LEIDL, W., Determination of testes consistency in bulls, 25:55337
LEIPUNSKAYA, D. I., Cupel assay of gold by an activation method, 25:54521
LELOUP, C., Electromagnetic instabilities in a slightly relativistic plasma, 25:56228 (CEA-CONF-1806)
LEMAN, J. D., Operating experience with sodium pumps at EBR-II. EBR-II Project, 25:57028 (ANL-EBR-27)
LEMBO, G., Measuring of artificial $\alpha$-emitters in presence of natural $\alpha$ activity, 25:54762
LEMEILLEUR, F., (p,2p) reactions at 600 MeV, 25:56711
LEMMON, Richard M., Hot-atom chemistry of $^{14}$C in solid benzene at kinetic energies between 5 and 100 electron volts, 25:54703

XUM

Partial degradation of 1,3,5-cycloheptatriene-$^{14}$C obtained from hot-atom, photolytic, and thermal reactions, 25:54702
LEMONTT, Jeffrey F., Mutants of yeast defective in mutation induced by ultraviolet light, 25:55187
LEMURE, Pierre, Shielding problems set by use of natural U target with linear electron accelerator. Shielding and safety systems necessary, 25:56582 (CEA-R-4188)
LENCHO, R. J., Experiment to measure hard solar and celestial x rays, 25:55734 (N-71-23434)
LENSCHOW, R., Investigation on prestressed concrete reactor vessel under internal gas pressure, 25:56992
LENTSCH, Jack W., Manmade radionuclides in the Hudson River estuary, 25:55160
LEONARD, A., Modified collision probability method for non-uniform lattices, 25:57155 (CONF-710302-(Vol.2), pp 644-54)
Nodal integral transport method for calculation of two-dimensional power distributions in non-uniform lattices, 25:57156 (CONF-710302-(Vol.2), pp 655-78)
LEONARD, A. C., Discrepancies in critical-heat-flux data obtained using thin-wire heaters in saturated liquid helium II, 25:56060
LEONARDI, R., Isotensor dipole sum rules in nuclear electroexcitation, 25:56868
LEONOV, A. I., Stabilization of zirconia with combined additives and a study of the solid solution stability, 25:55636
LEONOV, V. F., Study of development of leaks in fuel element cladding by means of $^{85}$Kr, 25:54904
LE RAY, M., Behavior of shear waves in interaction of superflow with the vortex lattice, 25:56053
Velocity of second sound in rotating helium II, 25:56054
LETUNOVSKII, V. V., Preparation of mixtures of tungsten carbide and cobalt by means of ultrasonic vibrations, 25:55598
LEURS, A., Kinetics of reaction of $UO_2$, $NpO_2$, and $(U,Pu)O_2$ with F, 25:54736
LEVEDAHL, William J., Nuclear-thermionic lunar base power supply, 25:54905
LEVI, E., Effect of collisions on cold ion collection by means of Langmuir probes, 25:56135
LEVIKOV, E. A., Low-temperature rolling and the annealing of single-crystal niobium, 25:55560
LEVIKOVA, L. V., Low-temperature rolling and the annealing of single-crystal niobium, 25:55560
LEVIN, A. L., Effect of magnetic Reynolds's numbers on distribution of currents in MHD ducts, 25:55949
LEVIN, V. B., Influence of longitudinal magnetic field on hydraulic resistance in turbulent flow of fluids in pipes, 25:55937
Transition to turbulence in magnetohydrodynamic flow with finite perturbations, 25:55927
LEVIN, V. I., $^{103}$Pd distribution in the animal organism, 25:55112
LEVSKII, L. K., Cosmogenic isotopes in 42 fragments of Sikhote--Alin meteorite, 25:55671
LEVY, N., Progress in three-dimensional elastic--plastic stress analysis for fracture mechanics, 25:55515
LEVY, Nelson L., Immunity to human brain tumors, 25:57263 (ORO-3195-51)
LEWELLEN, J. W., Work of the Committee on Computer Code Coordination, 25:57018 (CONF-710302-(Vol.1), pp 452-63)
LEWIN, Walter H. G., X rays from new variable source: GX 1 + 4, 25:55720
LEWIS, E. S., Hydrogen isotope effect in the reaction of trityl radicals with thiophenol, 25:54570
LEYPUNSKII, O. I., Global contamination of the atmosphere by $^{85}$Kr from worldwide nuclear power plants and the radiation danger, 25:54781 (JPRS-53174)
LI, Shou-yung, Boson expansion method in nuclear physics, 25:56843
LIAW, Chiu-fong, Behaviors of neptunium in aqueous solutions. I, 25:54733
LICKING, L. D., Receiving properties of an asymmetric cylindrical antenna, 25:57271 (SC-RR-710475)
Response of a short monopole antenna mounted on the skin of a finite-length cylinder, 25:57273 (SC-RR-710519)
LIEBENSCHUETZ, H. W., Perfusion lung scintigraphy in primary vascular pulmonary hypertension, 25:55284
LIETZKE, A. F., Large-area high-current ion source, 25:56212 (LBL-35)
LIGHTBODY, J. W. Jr., Elastic scattering of 60 to 120 MeV electrons from $^{46}$ $^{48}$ $^{50}$Ti, 25:56701
LIKHTER, Ya. I., Morphological characteristics of whistler spectra and ionization irregularities in topside ionosphere, 25:55997
LILHOLT, Hans, Matrix hardening in dispersion strengthened powder products, 25:55487
LIMPERT, J. C., Plant Instrumentation Program. Final quarterly progress report for the period ending March 31, 1971, 25:55004 (WCAP-7562-4)
LIN, Tz-hong, Hot-atom chemistry of $^{14}$C in solid benzene at kinetic energies between 5 and 100 electron volts, 25:54703
LINDEMAN, A. J., Conversion of the Argonne Reactor Computation (ARC) System to control data 6000 and 7000 series equipment, 25:57140 (CONF-710302-(Vol.1), pp 464-71)
Two-dimensional fast-reactor disassembly analysis with space-time kinetics, 25:57078 (CONF-710302-(Vol.1), pp 128-51)
LINDENMAYR, Georg, Numerical method for the solution of the time independent transport equation for neutrons, 25:56616 (JUL-764-RG)
LINDQUIST, R. H., Reduced microgels: a new form of powdered metals and metal oxides, 25:55419
LINDSAY, John W., Glovebox design and operation. Glovebox materials studies, 25:54940 (CONF-710401-, pp 26-43)
LINDSTAM, S., Description of the logic unit of the photometer system SFIL 70, 25:55045 (LUIP-CR-71-2)
LINDSTROEM, J. L., Flash x-ray irradiation of P--N junctions, 25:56336
LINDSTROM, R. E., Liquid--liquid chromatographic separation of neodymium, samarium, and gadolinium, 25:54745
LINDSTROM, Richard M., Radon emanation from the lunar surface, 25:54440
LING, Fu-wen, Kinetics of disorder--order transformations, 25:55552
LINSON, Lewis M., Collisionless shocks in plasmas, 25:56147
LIPETS, A. I., Changes in the content of electrolytes under the influence of radioiodine treatment in patients suffering from diffuse toxic goiter with a severe form of thyrotoxicosis, 25:55340
LIPINSKI, Hubert M., Comment on the $^1S_0$ nucleon--nucleon effective-range expansion parameters, 25:56529
LIPOVETSKII, S. S., Autoionizing states in helium-like ions, 25:55820
LISSAUER, D., Evidence for structure in Kπ mass system near 1.85 GeV, 25:56434
LITCHFIELD, P. J., Coefficients for partial wave analysis of the reaction $0^- + {}^1/_2{}^+ \to 1^- + {}^1/_2{}^+$, 25:56501 (RHEL/R-224)
LIU, C. T., Simple method of determination of the distribution and solubility limit of interstitials in substitutional solid solutions, 25:55568
LIVERNASH, William H., Inert atmosphere management and surveillance at the Argonne National Laboratory Fuels Technology Center, 25:54945 (CONF-710401-, pp 98-105)
LLEWELLYN, E. J., Comments on paper 'oxygen atmospheric and infrared atmospheric bands in the aurora', 25:56018
LLOYD, Edward C., Conference on accurate characterization of the high-pressure environment, Gaithersburg, Md., 10/68, 25:54878
LOAN, R. W., Effects of irradiation on avian leukosis, 25:55329
LOBANOVA, T. S., Investigation of U(IV) complexing with acetate and formate ions, 25:54581
LOCANTE, J., Environmental testing of engineered safety features related equipment, 25:57097 (WCAP-7744)
LOCHER, M. P., Production and absorption of pions on nuclei, and dispersion relations for elastic nuclear scattering, 25:56810 (CERN-71-14, pp 155-228)
LOGACHEV, V. I., Nature of the radiation background at altitudes of 250 to 500 km, 25:56008
LOGACHEV, Yu. I., Correlation of magnetic activity indexes with intensity of outer-belt electrons, 25:55979
LOGAN, D., Forced-flow sodium boiling in multiple channels, 25:54863 (AI-AEC-13010)
LOMAKIN, S. S., Fast-neutron flux measurement in AES Novo-Voronezhskii reactors, 25:56891
LOMANOV, M. F., Proton beam of the ITEP accelerator for radium therapy, 25:56581 (BNL-tr-442)
LOMBARD, R. J., Pion production and nuclear surface, 25:56530
LOMBERSKA, Ljuba, Thermal resistance and dependence of scintillation detectors at elevated temperatures, 25:55025
LONDERGAN, J. T., Spin-orbit coupling for A-$^4$He scattering using a one-boson-exchange model for the ΛN interaction, 25:56648
LONDON, G. J., Structure property relations in beryllium sheet, 25:55510
LONGO, G., Gamma-ray spectra following capture of 14 MeV neutrons by $^{59}$Co, $^{93}$Nb, and $^{103}$Rh, 25:56729
LONGO, M. J., Neutron total cross sections on protons and nuclei in 10 to 30 GeV/c momentum range, 25:56421
LONGSTAFF, R. M., Gamma irradiation as industrial process. 25:55363
LONGUEMARE, C., Short-range correlations, 25:56824 (LYCEN-7104, C4.1-17)
LONGWORTH, J. P., Delta spectrometer results on water reactor shields, 25:55043 (RD/B/N-2034)
MIMUSA: a FORTRAN IV subroutine for unfolding spectra. II, 25:55042 (RD/B/N-1963)
LOOYENGA, Robert W., Ultraviolet spectrophotometric determination of tellurium, 25:54400
LOPES, J. Leite, Weak interactions and the vector dominance model, 25:56468 (FRNC-R-1)
LORD, G., Electron irradiation and epitaxy on alkali halides, 25:56322
LORE, J., Influence of speed of graphitization of carbon products on dimensional variations produced by neutron irradiation, 25:55645 (CEA-CONF-1821)
LORENZINI, P. G., Evaluation of fuel-coolant interactions during disassembly of an LMFBR, 25:57074 (CONF-710302-(Vol.1), pp 50-78)
LORIO, Philip M., Experience of legal proceedings for siting a research reactor in an urban area, 25:57131
LORIUS, C., Balance of $^{90}$Sr over Antarctica, 25:54788
LORTET-ZUCKERMANN, M. C., Bright condensation 3C 153.1

inside the H II region NGC 2175, 25:55681
LOSKUTOV, Yu., Modification of the Coulomb law in a strong magnetic field, 25:56402
LOSS, F. J., Effect of mechanical constraint on the fracture characteristics of thick-section steel, 25:55512
LO SURDO, C., Collision integral between particles of disparate mass, 25:56179
LOTZ, H., Carrying capacity of prestressed concrete pressure vessel for THTR-300-MW(e) prototype nuclear power station, 25:56888
Prestressed concrete pressure vessel of the THTR-300-MW(e) prototype nuclear power plant, 25:56884
LOUGHHEAD, R. E., High-resolution photography of the solar chromosphere. IX, 25:55746
LOVCHIKOVA, G. N., Interaction between 14-MeV neutrons and nuclei of Fe, Cu, and Nb, 25:56684 (FEI-216)
LOVERING, J. F., Uranium and thorium in some basic and ultra basic rocks of possible deep-seated origin, 25:54495
LOVESEY, S. W., Neutron orbital cross section for a tight-binding model of paramagnetic nickel, 25:56354
LOWE, P. A., Stability calculational procedure for flow-induced vibrations of reactor internals in parallel flow, 25:57086 (CONF-710302-(Vol.1), pp 356-9)
LOWSON, R. T., Potential--pH diagrams at temperatures above 298.16°K. I, 25:57212 (AAEC/E-219(Pt.1))
LOYER, D. E., Supplement to summary report on SNAP-19B (IRHS) program, 25:54893 (MLM-1736)
LUBENAU, Joel O., Radiation incidents registry: Pennsylvania experience, 25:55250
LUBYANSKII, Ye. M., Nomogram for determining the number of separators in the combination of radiometric lump and batch separation of radioactive ores, 25:54847
LUCA, L., Burn-out heat fluxes at subcooled boiling, 25:54871 (IFA-TR-58)
LUCCHETTI, S. C., Optical variability of a bright new quasi-stellar source, 25:55726
LUCCI, F., Health protection analysis of transportation of radioactive substances through tunnels, 25:54973 (RT/PROT-(71)11)
LUCIUS, J. L., ROD: a nuclear and fuel-cycle analysis code for circulating-fuel reactors, 25:57048 (ORNL-TM-3359)
LUDWICK, J. D., Atmospheric tracer technique employing $^{85}Kr$ and use of this technique in defining puff dimensions and transport speed, 25:54908
LUETJERING, G., Strength increase in Ti 35 wt. percent Nb through step-aging, 25:55490
LUHMAN, Thomas Stewart, Superconductivity and constitution of titanium base transition metal alloys, 25:56108
LUKAS, George, Relativistic shock waves, 25:55668
LUKIN, E. S., Sintering and properties of yttrium oxide ceramics, 25:55606
LUK'YANOV, V. K., Multi-channel aspects in stripping reactions on spherical and deformed nuclei, 25:56817 (JINR-E4-5836)
LUMBROSO, A., Generating coordinates in continuum states, 25:56825 (LYCEN-7104, C6.1-12)
LUND, A., ESR single-crystal study of radical and radical-pair formation in some γ-irradiated vinyl monomers, 25:54634
LUND, Anders, Electron spin resonance studies of primary processes in radiation-induced reactions. II, 25:54639
Electron spin resonance studies of primary processes in radiation-induced reactions. I, 25:54640
LUND, J. A., Substructure strengthening in dispersion-strengthened nickel alloys, 25:55492
LUNN, A. D., Resistive instability in a uniformly rotating magnetoplasma, 25:56203
LUNTZ, Myron, Track-effect theory of scintillation efficiency, 25:55016
LUO, H. L., Superconductivity in noble-metal-rich hexagonal close-packed phases, 25:56096
LUR'E, L. S., Gamma-ray irradiation equipment, 25:54837
LUTZ, H. F., Proton inelastic scattering from the five stable, even-mass isotopes of molybdenum, 25:56774
LUX, Robert, Relative biological effectiveness of x rays delivered at very high dose rates to radish seeds (raphanus sativus), 25:55350
LUZZI, G., Calibration of the silver activated counters on a plasma focus experiment, 25:56214 (LGI-70/17/E)
L'VOV, S. N., Temperature dependence of absolute thermo-EMF coefficient of certain transition metals, 25:56351
Temperature dependence of the electrical and thermal conductivity of rhenium and metals of the platinum subgroup, 25:55523
LYKHIN, V. M., Effect of water on radiation chemical stability of crystalline $NaNO_3$, 25:54649
LYLE, Fred F. Jr., Investigation of sensitization of type 304 stainless steel safe-ends, 25:55378 (SWRI-1228-P-7-40)
LYNCH, R. D., Predicted San Fernando earthquake spectra: Glendale area, 25:54812 (NVO-1163-TM-30)
LYNNWORTH, L. C., Prog. rpt. on ultrasonic thermometry in LMFBR systems, 12/68, 25:55078 (NYO-3906-5)
LYONS, J. D., Search procedure for multichannel resonances in electron--atom scattering, 25:55861
LYONS, Peter B., Stellar rates for $^{28}Si(\alpha,\gamma)^{32}S$ and $^{16}O(\alpha,\gamma)^{20}Ne$ reactions, 25:55704
LYSENKO, A. A., Mass-spectrometric ion source for high-temperature investigations, 25:55081
LYSYKH, A. P., Topography of the evolution of the radiolysis products of lead azide ($PbN_6$), 25:54642
LYTLE, William O., Statistical relationship of brain scans, cervicocranial dynamic studies, and cerebral arteriograms, 25:55281
LYUTINA, E. M., Composition of the carbide phase in alloys of uranium with zirconium and niobium, 25:55547
LYUTTSAU, V. G., Development of micropores in alloys, 25:55462

# M

MACBETH, R. V., Boiling on surfaces overlayed with a porous deposit: heat transfer rates obtainable by capillary action, 25:54862 (AEEW-R-711)
Investigation into effect of "crud" deposits on surface temperature, dry-out and pressure drop, with forced convection boiling of water at 69 bar in annular test section, 25:54861 (AEEW-R-705)
MACDONALD, J. R., Electron-capture processes 10- to 40-MeV O ions in He, N, and Ar, 25:55869
Electron-transfer cross sections for O ions in Ar, N, and He at 7 to 40 MeV, 25:55870
MACFARLANE, D. R., Comparison between momentum integral and compressible models for sodium voiding calculations in LMFBR, 25:57081 (CONF-710302-(Vol.1), pp 180-98)
MACIAS-MARQUES, Maria-Ines, Electromagnetic transitions in $^{190}Pt$, 25:56760
MACKAY, J. W., Impurity dependence of the low-temperature annealing in n-type germanium, 25:56331
Review of radiation effects in germanium, 25:56303
MACKAY, T. L., Effect of stress on microsegregation of H in Ti and Ti--8Al--1Mo--1V, 25:55476
MACKINNON, A., Distribution of uranium in some basic igneous cumulates and its petrological significance, 25:54809
MACLACHLAN, A., Flash photolysis of a substituted hexaarylbiimidazole and reactions of the imidazolyl radical, 25:54561
MACLEOD, A. C., High-temperature thermodynamic properties of uranium monosulphide, 25:54584
MACLEOD, G. R., Computers and computation in experimental high-energy physics, 25:55050
MACNAUGHTON, J., Experiments measuring particle widths and the width of the ω, 25:56430
MACPHEE, J. Anthony, Bell-shaped pH-rate profile for an oxidation. The reaction of permanganate with hydroxycyclohexanecarboxylic acids, 25:54575
MACVICAR, M. L. A., Investigation of superconducting-energy-gap behavior of single-crystal rhenium by tunneling, 25:56067
MADEEV, M. O., Measurement of solar protons from July 7, 1966 flare, 25:55991
MADELAINE, G., Study of the mobility of ions in air, 25:54801
MADLAND, David George, Study of the isotopes of neon with proton reactions at 40 MeV, 25:56704
MADSEN, N. K., Convergence of the weighted diamond difference approximations to the discrete ordinate equations, 25:57150 (CONF-710302-(Vol.2), pp 565-76)
MADSON, A. A., Integral measurements in EBR-II of capture rates, fission rates, and α for $^{233}U$, $^{235}U$, $^{238}U$, $^{239}Pu$, $^{240}Pu$, and $^{242}Pu$, 25:56982 (ANL-7791)
MAECK, W. J., Iodine chemistry in steam air atmospheres, 25:54547
MAEDA, Hidenori, Facilities for accelerators for medical use, 25:56607
MAEDER, A., Shoenberg--Chandrasekhar limit and rotation, 25:55684
MAGAT, Michel, Postluminescence of organic solid solutions, 25:54598 (CONF-700652-(Vol.2), pp 423-75)
MAGER, T. R., Fracture toughness K/sub Icd/ values for ASTM A533 grade B, class 1 steel, 25:55517
Fracture toughness properties of steel plate and submerged arc weldment, 25:55516
MAGNO, P., Liquid waste effluents from a nuclear fuel reprocessing plant, 25:54753
MAGRADZE, B. A., K/sub 13/ decays and chiral symmetry-breaking, 25:56537 (JINR-E2-5996)
MAHAJAN, S., Influence of prior mechanical and thermal treatments on shock-induced substructures in molybdenum, 25:55543
MAHALEY, M. S. Jr., Immunity to human brain tumors, 25:57263 (ORO-3195-51)
Virus-cell relationships in dog brain tumors, 25:57262 (ORO-3195-50)
MAHESHWARI, Amar, Schwinger equations for Yang--Mills and gravitational fields, 25:56561
MAIELLA, G., Two variable crossing symmetric expansion of the ππ scattering amplitude and low-energy parameter sum rules, 25:56484 (ORO-3992-10)
MAIER, Mary Louise, Investigation of a $U^{+5}$ system: $(C_5H_5N)_2UOCl_3$, 25:54541
MAJEROTTO, W., Application of Veneziano model including spins to reaction $k^+p \to K^{*+}(890)p$, 25:56511
MAJEWSKI, W., Solution of SU(3)-symmetric baryon strong coupling bootstrap model, 25:56503
MAJOR, G., Misuse of threshold limit values, 25:55198
MAKAROV, A. P., Electron work function of tantalum--ruthenium alloys, 25:56350

XUM

MAKAROV, S. F., Goldanskii--Karyagin effect in Moessbauer patterns and the anisotropy of atomic vibrations in crystals, 25:56377
MAKHLIN, M. A., Effect of vacuum on the diffusion mobility of nickel in molybdenum, 25:55505
MAKHOVA, V. A., Composition of the carbide phase in alloys of uranium with zirconium and niobium, 25:55547
MAKHUNKA, I., Collector system of an isotope separator for investigating short-lived isotopes, 25:56584 (JINR-P6-5888)
MAKI, L. M., Reference zirconium hydride reactor, 25:57132 (AI-AEC-Memo-12715(Del.))
MAKSIMOV, Yu. A., Properties of Ti--V and Ti--V--Al alloys with O, 25:55471
MALAKHOV, S. S., Nomogram for determining the number of separators in the combination of radiometric lump and batch separation of radioactive ores, 25:54847
MALAVIYA, B. K., Experimental and analytical studies of fast neutron transport in iron, 25:56618 (RPI-328-230)
MALKIN, J., Relation between K/sub Ic/ and microscopic strength for low alloy steels, 25:55503
MAL'KO, P. I., Temperature dependence of absolute thermo-EMF coefficient of certain transition metals, 25:56351
Temperature dependence of the electrical and thermal conductivity of rhenium and metals of the platinum subgroup, 25:55523
MALL, G. H., Single- and double-pion production in proton--antiproton nonannihilations at 2.2 GeV/c, 25:56487
MALLIARIS, Angelos, Influence of sample size on radiation damage of polyethylene, 25:54623
MALSKY, Stanley J., Radiation exposure to personnel during cardiac catheterization, 25:55226
MALYSHEV, V. V., Experimental study of the equation of state of uranium hexafluoride, 25:54582
MANAGADZE, G. G., Experiments with artificial solar wind, 25:56009
MANCE, Amalija, Potentiostatic etching and polishing of copper and its alloys, 25:55555
MANCHANDRA, R. K., Upper limits on pulsations from CYG X-1 in hard x rays, 25:55727
MANCHESTER, E. G., Use of simplotter: a high-level plotting system, 25:57231 (IS-2305)
MANCHESTER, R. N., Crab pulsar radiation mechanism, 25:55729
MANDEL, H., Possibilities for international cooperation in the area of nuclear energy, 25:57006
MANDEL'SHTAM, S. L., Detecting the polarization of solar-flare x-ray emission, 25:55771
MANDEL'TSVAIG, Yu. B., Performance in recording of x- and gamma-rays by combined detectors, 25:55005
MANFRASS, P., Level scheme of $^{177}$Lu in reaction (n,γ), 25:56762
MANIAR, Gunvant N., Heat treatment of 706 Alloy, 25:55554
Microstructure of 706, a new Fe--Ni-base superalloy, 25:55553
MANN, A., Mesonic structure in the nucleon, 25:56512
MANN, Bruce J., Examination of the emergency radiation doses used for nuclear power plant siting evaluations, 25:55242
MANRI, Teruo, Determination of chlorobiphenyl in rat adipose tissue by neutron activation analysis, 25:54500
MANSFELD, A., Study of natural radionuclides in waste and surface waters, 25:54774
MANSUROV, S. M., Relationship between magnetic fields of space and of Earth, 25:55988
MANSUROVA, L. G., Relationship between magnetic fields of space and of Earth, 25:55988
MANTHURUTHIL, J. C., Beta--gamma correlations and matrix elements for some first-forbidden nonunique beta transitions, 25:56776
MANWEILER, J. E., Single- and double-pion production in proton--antiproton nonannihilations at 2.2 GeV/c, 25:56487
MANZEL, R., Dimensional and physical property changes of graphites, pyrocarbons, and fuel bodies, 25:55651
MARANS, Nelson Samuel, Irradiation process for reducing the molecular weight of polyoxymethylene and thereby increasing thermal stability, 25:54611
MARATRAY, F., Factors affecting the structure of chromium and chromium--molybdenum white irons, 25:55556
MARCAL, P. V., Progress in three-dimensional elastic--plastic stress analysis for fracture mechanics, 25:55515
MARCHAND, A., Electronic and magnetic properties of carbon fibers: development under neutron irradiation, 25:56282 (CEA-CONF-1822)
Thermal annealing of neutron-irradiated carbon, 25:56283 (CEA-CONF-1823)
MARCULESCU, Sorin, Symmetry breaking of chiral SU(3) x SU(3) in phenomenological Lagrangians, 25:56533 (IFA-FT-85)
MAREZIO, M., Low-temperature x-ray diffraction studies of near-equiatomic V--Ru alloys, 25:55532
MARGEN, P. H. E., Prestressed concrete pressure vessel, 25:57203
MARGHITU, S., Measurement of the emittance of an ion-optical system, 25:56611
MARGOLIS, Stephen G., Safety analyses of pressurized water reactors, 25:57085 (CONF-710302-(Vol.1), pp 282-95)
MARGON, Bruce, Pulsing x-ray source in Circinus, 25:55721
MARGRAVE, J. L., Thermodynamic properties of liquid molybdenum by levitation calorimetry, 25:55496
MARIA, Henriette, Study of the γ radiation accompanying the decay of Ms Th(II) ($^{228}$Ac), 25:56747 (ORNL-tr-2531)
MARIANI, F., Multiple crossings of the Earth's bow shock at large geocentric distances, 25:55953
MARINOVA, Ts. S., Isothermal heat of evaporation of ytterbium and neodymium ions on a tungsten surface, 25:55533
MARKHASEV, B. I., Nature of the chemical-bond forces in compounds formed by d-transition metals, 25:56386
MARKO, A. M., Biological significance of radioactive releases to the environment, 25:55194 (70-CNA-641)
MARKOCZY, G., Convective heat transfer in longitudinal flow through tubes and rod bundles, 25:54866 (EIR-198)
MARKOV, B. N., Excitation of spontaneously fissioning isomeric states of $^{239}$Pu and $^{243}$Am at inelastic γ-quantum scattering, 25:56738 (JINR-P15-5959)
MARKOV, G. S., Quaternary ammonium bases as analytical reagents. II, 25:54434
MARKOWSKI, Baldur, Optimization of fuel cycle and core sectioning of a 2500-MW(th) thorium high-temperature reactor with multizone loading, 25:57060 (JUL-736-RG)
MARKYTAN, M., Application of Veneziano model including spins to reaction k⁺p → K*⁺(890)p, 25:56511
MARLBOROUGH, J. M., Models for envelopes of Be stars. III, 25:55709
Radiation pressure and accelerating stellar winds, 25:55712
MARLING, John B., Dye laser performance enhancement by chemical quenching of the triplet state, 25:57288 (UCRL-51088)
MAROWSKY, G., Sensitivity ranges in neutron activation analysis of some rare trace elements (Cd, Hg, Tl, Bi) in silicate samples, 25:54489
MAROWSKY, Gerd, Determination of cadmium, mercury, thallium, and bismuth in terrestrial rocks by neutron activation analysis, 25:54454
MARSH, O. J., Measurement of lattice damage caused by ion-implantation doping of semiconductors, 25:56287
MARSHAKOV, I. K., Study of alloys belonging to $NiAl_3$--$VAl_3$ and $Ni_2Al_3$--$V_5Al_8$ sections, 25:55562
MARSHALEK, E. R., Static quadrupole moments of vibrational states of spherical nuclei in the self-consistent cranking approximation, 25:56860
MARSHALL, A. L., In-residence health and safety support in a plutonium facility, 25:55204 (CONF-710401-, pp 267-79)
MARTENSSON, M., Swedish studies on the economics of uranium enrichment, 25:54921
MARTIN, A. D., Comparison of the high energy models for neutral meson photoproduction and the related hadronic processes, 25:56458
MARTIN, D. G., Quantitative studies of nuclear structure through isobaric analog resonances, 25:56769
MARTIN, F. W., Electron-capture processes 10- to 40-MeV O ions in He, N, and Ar, 25:55869
Electron-transfer cross sections for O ions in Ar, N, and He at 7 to 40 MeV, 25:55870
MARTIN, J. E., Public Health Service role in providing information relative to the nuclear power controversy, 25:56981
MARTIN, Jose Ginoris, Magnetoplasma waves in strongly curved configurations, 25:56253
MARTIN, Ph., Energy levels of $^{14}$O in region of excitation between 13.5 and 15.0 MeV, 25:56681
MARTINI, William R., Implantable radioisotope-fueled stirling engine, 25:54910
MARTRES, M. J., Solar coronal streamers observed at 169 MHz, 25:55754
MARTY, A. M., Measurement of mobility and mass of atmospheric ions, 25:54800
MARTYNOV, S. Z., Pyrolytic titanium and zirconium nitrides and fields of their use, 25:55605
MARUYAMA, Takashi, Estimation of genetically significant dose equivalent from occupational exposure to external sources of radiation in Japan, 25:55230
MARYGINA, A. B., $^{103}$Pd distribution in the animal organism, 25:55112
MASANET, Jeannine, Reactions of H and deuterium formed in photolysis of methane and perdeuterated methane, 25:54573
MASKALICK, N. J., Sintered zirconia electrolyte films in high-temperature fuel cells, 25:55596
MASLENKOV, S. B., Intracrystallite liquation in nickel alloys containing niobium, 25:55506
MASLENNIKOVA, E. G., Heat content of metallic hafnium, 25:55445
Thermochemistry of the hafnium--silicon system, 25:55644
MASLOWSKA, Joanna, Separation of the alkaline earth metal ions by ionophoresis on filter paper and poly(vinyl alcohol), 25:54725
MASON, E. A., Transport properties of partially ionized argon, 25:56183
MASSALSKI, J., Measurements of energy and flux of cosmic ray hadrons using an ionization spectrometer, 25:56413 (INP-756)
MASSALSKI, Jerzy, Inelasticity coefficients for pion--Fe and nucleon--Fe collisions, 25:56414 (INP-757)
MASSALSKI, T. B., Transformations during quenching of epsilon-phase Pu--Zr alloys, 25:55528
MASSLOVA, G. B., Isolation of promethium by displacement

chromatography due to complex formation, 25:54723
MASSON, Maurice, Process for the measurement of a displacement and device for its use, 25:55068 (AEC-tr-7240)
MASSUE, J. P., π and K mesons used for investigating light nuclei structures, 25:56653 (LYCEN-7104, S4.1-10)
MASTERS, Frank W., Management of radionecrosis, 25:55270
MASTERS, S. M., Applications software for a fast reactor malfunction detector analyzer, 25:56878 (CONF-710302-(Vol.1), pp 199-214)
MASUDA, K., Survival of synchronized L cells irradiated with 14 MeV neutrons, 25:55309
MASUMI, Ahmad E., IBAL manual. The Illiac III basic assembler language, 25:57225 (COO-2118-17)
MATE, Z., Collector system of an isotope separator for investigating short-lived isotopes, 25:56584 (JINR-P6-5888)
MATHESON, L. A., Air leakage into plutonium gloveboxes and its effect on inert operations, 25:54944 (CONF-710401-, pp 83-97)
MATHIESEN, O., Description of the logic unit of the photometer system SFIL 70, 25:55045 (LUIP-CR-71-2)
MATHUR, K. C., Electron-impact excitation of lithium, 25:55864
MATLOVA, A., Direct pair production by charged particles at 4 GeV/c in a propane bubble chamber, 25:56467
MATSUDA, Hisashi, Charged particle analyzer of magnetic and electrostatic sector type, 25:56606
MATSUI, K., Neutron irradiations of silicon studied by $^{57}$Fe Moessbauer effect, 25:56326
MATSUOKA, Yoshinori, Influence of $PuO_2$ particle size of mixed oxide fuel in relation to fast reactor safety, 25:57107
MATSUZAKI, Kei, Triad tacticity of polyacrylonitrile, 25:54622
MATSUZAWA, T., Electrophoretic behavior of x-irradiated lymphocytes, 25:55310
MATTHES, W., Some applications of the Monte Carlo method at the Euratom Research Center, Ispra, 25:57162 (CONF-710302-(Vol.2), pp 803-32)
MATTHEWS, J. A. J., Regge analyses of rho$^0$ production in πN charge exchange channels at 7 GeV/c, 25:56431
MATTHIAS, E., Theory of nuclear magnetic resonance detected by nuclear radiations, 25:56372
MATTHIEUSSENT, G., Saturation and damping of echoes of electron plasma waves, 25:56226 (CEA-CONF-1804)
MATULA, R. A., Defects induced by electron irradiation of p-type germanium, 25:56302
MATVIENKO, N. I., Target of recombination in crosses of different mutants of phage T4, 25:55173
MAURENZIG, P. R., Dose distribution surrounding a sealed linear radium source, 25:54923
K = 3/2$^+$ rotational band in $^{45}$Ti, 25:56693
MAURETTE, M., Comments of a paper on elastically scattered recoil nuclei in solid state detectors, 25:54999 (N-71-26447)
Nuclear interaction tracks in minerals and their implicatcns for extraterrestrial materials, 25:55669 (N-71-26344)
MAXIM, I. V., Vitroceramic nuclear fuel coating. II, 25:55613
MAXIM-GAZI, R. G., Generation of magnetohydrodynamic waves in nonhomogeneous plasma located in intense magnetic field, 25:55923
MAXWELL, Ronald B., Production of gases of known specific activity in a reactor for calibrating gaseous effluent monitors, 25:54986
MAYER, J. W., Ion implantation: lattice disorder, 25:56304
MAYER, John T., Reactor irradiation of thermionic sheath insulators, 25:55096 (N-71-24635)
MAYER-BOERICKE, C., $^{31}$P($^3$He,pγ)$^{33}$S and $^{39}$K($^3$He, pγ)$^{41}$Ca reactions and the γ decay of analog states in $^{33}$S and $^{41}$Ca, 25:56715
MAYNARD, C. Douglas, Statistical relationship of brain scans, cervicocranial dynamic studies, and cerebral arteriograms, 25:55281
MAYR, A., Results of ultra-sound tests on reactor pressure vessel of nuclear power station Obrigheim, 25:56892
MAYR, Hans G., Temporal variations of thermospheric hydrogen derived from in situ measurements, 25:55973
MAZAUD, J. C., Metallography of the 700°C precipitation in a Fe--40 percent Ni alloy containing beryllium, 25:55544
MAZEAU, J., Resonance phenomena in low-energy-electron-impact excitation of He, 25:55851
MCCARROLL, R., Rotational coupling effects on differential elastic and inelastic cross sections in He$^+$--He collisions, 25:55848
MCCLELLAN, R. O., Comparison of the relative biological effectiveness of $^{241}$Am and $^{144}$Ce on the production of chromosome aberrations in the Chinese hamster liver, 25:55188
Relative hazards from $^{95}$Zr and $^{95}$Nb based upon inhalation of particles formed under various thermal conditions, 25:55125
MCCLENAHAN, C. R., Electrochemical reduction of europium at a porous carbon cathode with flowing electrolyte, 25:54530 (LA-DC-12469)
MCCLINTOCK, Jeffrey E., X rays from new variable source: GX 1 + 4, 25:55720
MCCLURE, J. L., Heat capacity of tantalum in range 1900 to 3000 K, 25:55494
MCCONNON, D., Comparative metabolism of intravenously injected promethium in swine and humans, 25:55108 (BNWL-SA-3747)
MCCORD, R. V., Prog. rpt. on high flux isotope reactor, 4--6/71, 25:57120 (ORNL-TM-3569)
MCCORMICK, B. H., ILLIAC III reference manual. III, 25:57227 (COO-2118-21)
ILLIAC III reference manual. IV, 25:57226 (COO-2118-19)
MCCORRISTON, T. P., Neutron total cross sections on protons and nuclei in 10 to 30 GeV/c momentum range, 25:56421
MCCRACKE, K. G., Anosotropy characteristics of low-energy cosmic-ray population of solar orgin, 25:55763
MCCRARY, J. H., K-fluorescent-x-ray relative-intensity measurements, 25:55827
MCCUNE, E. L., Effects of irradiation on avian leukosis, 25:55329
MCCUNE, R. A., Solubility of nitrogen in alpha vanadium, 25:55475
MCDANIEL, C. T., Modified collision probability method for non-uniform lattices, 25:57155 (CONF-710302-(Vol.2), pp 644-54)
Nodal integral transport method for calculation of two-dimensional power distributions in non-uniform lattices, 25:57156 (CONF-710302-(Vol.2), pp 655-78)
MCDIARMID, I. B., Sounding-rocket observations of particle precipitation in a polar-cap electron aurora, 25:56031
MCDILL, William H., Implantable radioisotope-fueled stirling engine, 25:54910
MCDONALD, F. A., s-wave elastic e--H scattering above ionization threshold, 25:55860
MCDOUGALL, I. R., Thyroid carcinoma following $^{131}$I therapy. Report of a case and review of the literature, 25:55343
MCDOWELL, M. R. C., Electron capture by fast protons in He and $H_2$, 25:55837
MCEACHRAN, R. P., James wave function for the ground state of $H_2^+$, 25:55829
MCGAHAN, D. J., Radiation polymerisation of impregnated porous material, 25:55658
MCGEE, T., Nuclear charge dispersion of light-mass elements in fission of $^{232}$Th, 25:56805
MCGIRT, Frank, User experience with DATATRAN at LASL, 25:57141 (CONF-710302-(Vol.1), pp 472-7)
MCGONNAGLE, Warren J., Use of a styrofoam block cutter to make tissue-equivalent compensators, 25:55244
MCGREGOR, John F., Persistence of heritable changes in an irradiated rat population after cessation of the exposures, 25:55164
MCGRORY, J. B., Complex spectroscopy, 25:56874
MCINTURFF, A. D., Recent developments in pulsed magnet multifilament superconducting wires, 25:56580 (BNL-16026)
MCKAY, L. R., Comparison of the relative biological effectiveness of $^{241}$Am and $^{144}$Ce on the production of chromosome aberrations in the Chinese hamster liver, 25:55188
MCKENZIE, David Leroy, Correlation of hard solar x-ray and radio emission, 25:55759
MCKINNEY, Charles O., Genetic variation in irradiated and nonirradiated populations of the lizard, Uta stansburiana, 25:55320
MCKOWN, D. M., Coincidence counting applied to the activation analysis of meteorites and rocks, 25:54479
MCMANNON, R. U., Design features of Mound Laboratory's Medical Decontamination facility, 25:54963 (CONF-710401-, pp 311-15)
MCMASTERS, O. D., Stoichiometry, crystal structures, and some melting points of the La--Au alloys, 25:55570
MCMILLAN, Paul N., Flotation-fractionation of late fetal, neonatal, and adult rat brain in iso-osmotic Ficoll-sucrose density-gradients, 25:57257 (ORO-3195-45)
Isolation and biochemical characterization of subfractions of rat central nervous tissue myelin, 25:57258 (ORO-3195-46)
Sequential adsorption analysis of antisynaptosome antibodies, 25:57254 (ORO-3195-42)
Sequential adsorption analysis of antimyelin antibodies, 25:57255 (ORO-3195-43)
Sequential adsorption analysis of radioantibodies, 25:57253 (ORO-3195-41)
Zonal centrifuge profile analysis of msd mutant mouse brain, 25:57256 (ORO-3195-44)
MCMILLAN, W. G., Prog. rpt. on intra- and inter-molecular energy transfer studies, 5/70--5/71, 25:54600 (UCLA-34-P-88-32)
MCMURRAY, W. R., Prog. rpt., annual, 1970, 25:56752 (SUNI-14)
MCNAMARA, B., Numerical experiments on nonlinear plasma instabilities, 25:56205
MCNAMARA, D., Topology of filaments and chromospheric fibrils near sunspots, 25:55749
MCNEILL, J. R., Biological dosimetry in an industrial radiography accident, 25:55228
MCPHERSON, D. A., Electrostatic vlf waves observed in the polar magnetosphere, 25:55965
Ion-wave instabilities at vlf in the polar wind, 25:55966
MCQUEEN, R. G., Use of a magnetic field to measure particle velocity. I, 25:57233 (LA-4545)

XUM

MCWETHY, L. M., Core design development needs in relation to fuel failure propagation, sodium boiling, and clad/fuel--sodium thermal interaction, 25:57088 (GEAP-13639-1)
Core design development needs in relation to fuel failure propagation, sodium boiling, and clad/fuel--sodium thermal interaction, 25:57089 (GEAP-13639-2)
MEAD, G. D., Artificial aurora experiment: ground-based optical observations, 25:55962
MEDNIS, I. V., Calculations of induced activity in the case of intermittent irradiation, 25:54527
MEDVEDEV, O. G., Production of parts of complex shape in lanthanum hexaboride, 25:55599
MEDVEDEV, Yu. A., Rapidly varying geomagnetic field disturbances produced by a nonstationary source of gamma quanta, 25:55989
MEDVEDEV, Yu. V., Sound excitation in a Josephson junction, 25:56089
MEERWALD, K., Carrying capacity of prestressed concrete pressure vessel for THTR-300-MW(e) prototype nuclear power station, 25:56888
MEESE, J. M., Impurity dependence of the low-temperature annealing in n-type germanium, 25:56331
MEGGS, W. J., Comments on analyses of anti pn → 3π, 25:56485 (ORO-3992-66)
MEHLTRETTER, J. P., rms intensity fluctuation of solar granulation, 25:55744
MEIER, Hans, Zonal centrifuge profile analysis of msd mutant mouse brain, 25:57256 (ORO-3195-44)
MEIER, P. F., Temperature dependence of the sound velocity in liquid $^4$He, 25:56055
MEIER, R. R., Ogo-4 observations of Lyman--Birge--Hopfield emission in day airglow, 25:55968
MEINHOLD, H., Perfusion lung scintigraphy in primary vascular pulmonary hypertension, 25:55284
MELDNER, H. W., Mass formula consistent with nuclear-matter calculations vs conventional mass-law extrapolations, 25:56853
MEL'NIK, A. D., Neutron-activation analysis of Ca, P, and Na in bones, 25:55106
MEL'NIKOVA, N. S., Hydrodynamics of the convective envelopes of stars, 25:55707
MENAPACE, E., Analysis by a simulated measurement of neutron spectra, 25:56620 (RT/FI-(70)53)
MENDILLO, M., Ionospheric storm of March 8, 1970, 25:55974
MENDILLO, Michael, Dependence of magnetospheric electric field on velocity of solar wind, 25:56039
MENDIRATTA, M. G., Strength increase in Ti 35 wt. percent Nb through step-aging, 25:55490
MENELEY, D. A., Two-dimensional fast-reactor disassembly analysis with space-time kinetics, 25:57078 (CONF-710302-(Vol.1), pp 128-51)
MENG, C.-I., Storm sudden commencements and polar magnetic substorms, 25:56026
MERCER, A., Leakage from a ruptured containment after accidental depressurisation of a gas cooled reactor, 25:57106
MERCER, R., Kπ scattering phase shifts determined from the reactions $K^+p \to K^+\pi^-\Delta$ and $K^+p \to K^0\pi^0\Delta$, 25:56486
MERCIER, C., Space--time evolution of a plasma subjected to a discharge current, 25:56162 (CEA-CONF-1801)
MERCIER, Roch Edouard, Shell model with reaction matrices and pairing correlations, 25:56666
MERETSKII, A. M., Investigation of the kinetics of oxygen isotopic exchange between water and carbon dioxide in the presence of soluble additives, 25:54549
MERKLE, J. G., Gross strain crack tolerance of steels, 25:55514
MERKOVA, M. A., Radiation reactions of the nervous system in irradiation of tumors of the head, 25:55269
MERZ, E., Energy accumulation in solid bodies through nuclear radiation by storage of highly radioactive scrap, 25:54969 (JUL-766-CT)
MERZ, M. D., Effect of strain rate and temperature on the tensile properties of Pu--1 wt percent Ga alloys, 25:55427 (BNWL-1567)
MESCHAN, I., Statistical relationship of brain scans, cervicocranial dynamic studies, and cerebral arteriograms, 25:55281
MESSERSCHMIDT, Otfried, Investigations of injury induced by different causes, 25:55332
METZ, S. A., Production of vacancies by laser bombardment, 25:56313
METZGER, Courtney A., Radioactive isotope distillation system for recovering water from waste in a spacecraft, 25:54911
METZGER, F. R., Studies of electromagnetic properties of excited states of nuclei. Final report, March 15, 1965--March 14, 1971, 25:56832 (NYO-3525-67)
METZNER, R., Radiobiological investigations with fast neutrons. II, 25:55266
MEYER, Colette, Decoloring Cyanophycene algae by extraction of their pigments, 25:57236 (LA-tr-71-73)
MEYER, M. L., Conference on experimental stress analysis and its influence on design, Cambridge, Eng., 4/70, 25:54846
MEYER, P. E., Automated modular light water reactor calculation code package, 25:57172 (CONF-710302-(Vol.2), pp 983-90)
MEYER, Walter, Development of an NE-213 fast-neutron TAC spectrometer system utilizing off-line gamma-ray discrimination, 25:55033 (COO-2049-6)
Evaluation of minima in total neutron cross section by transmission of fission spectra through thick samples, 25:56650 (COO-2049-5)
Fast neutron spectroscopy in aqueous media using an NE-213 proton-recoil neutron spectrometer system, 25:55034 (COO-2049-7)
Orders-of-scattering calculation for the reflection of collimated, polyenergetic fast neutrons from a six-inch-thick steel slab, 25:56257 (COO-2049-8)
Orders-of-scattering method for fast-neutron transport, 25:56258 (COO-2049-9)
MEYER-BURG, J., Scintigraphic investigations of parasternal lymph nodes with $^{198}$Au, 25:55288
MEYERHOF, W. F., $^3$H($^3$He,γ)$^6$Li capture reaction and the structure of $^6$Li, 25:56664
MEYERSTEIN, D., Oxidation of benzoatopentaamminecobalt(III) by hydroxyl radicals, 25:54669
MEZDROGINA, M. M., Method of holding molten metal in suspended state: characteristics of Lodochka inductor, 25:55424
MGLINETS, V. A., Radiation-induced crossovers in males of Drosophila melanogaster, 25:55170
MICAUD, G., Electronic and magnetic properties of carbon fibers: development under neutron irradiation, 25:56282 (CEA-CONF-1822)
Thermal annealing of neutron-irradiated carbon, 25:56283 (CEA-CONF-1823)
MICHAEL, B. D., Absorption spectrum of e/sub aq/$^-$ in the temperature range -4 to 390°, 25:54658
MICHAELIS, W., Proposal for installation of a versatile $e^- - e^+ - \gamma$ spectrometer for neutron capture spectroscopy, 25:55040 (NP-18994)
MICHAELS, H. B., Factors affecting the rate of hydrated electron attach on polynucleotides, 25:55131
MICHALEWSKA, Malgorzata, Determination of strontium in barium minerals by atomic absorption spectroscopy, 25:54413
MICHALSKI, R. S., Geometrical model for the synthesis of interval covers, 25:57223 (COO-2118-13)
MICHEL, M. J., GRASS: system overview, 25:57217 (COO-1469-187)
GRASS: system software description, 25:57218 (COO-1469-190)
MICHEL, Rupprecht, Forced-flow steam generator to be heated by pressurized coolant of a nuclear reactor, 25:54836
MICKEY, Don D., Cellular and subcellular fractionation of brain tissue, 25:57259 (ORO-3195-47)
Flotation-fractionation of late fetal, neonatal, and adult rat brain in iso-osmotic Ficoll-sucrose density-gradients, 25:57257 (ORO-3195-45)
Isolation and biochemical characterization of subfractions of rat central nervous tissue myelin, 25:57258 (ORO-3195-46)
Sequential adsorption analysis of antimyelin antibodies, 25:57255 (ORO-3195-43)
Sequential adsorption analysis of antisynaptosome antibodies, 25:57254 (ORO-3195-42)
Sequential adsorption analysis of radioantibodies, 25:57253 (ORO-3195-41)
Zonal centrifuge profile analysis of msd mutant mouse brain, 25:57256 (ORO-3195-44)
MIDDLETON, R., Spin assignments in $^{20}$F, 25:56716
MIELCZAREK, S. R., Dependence of generalized oscillator strengths of $H_2O$ on momentum transfer, 25:55880
MIHAILA, A., Burn-out heat fluxes at subcooled boiling, 25:54871 (IFA-TR-58)
MIHALCZO, John Thomas, Use of $^{252}$Cf as a randomly pulsed neutron source for prompt neutron decay measurements, 25:56639
MIHUL, A., K anti K production in four-prong π$^+$p interactions at GeV/c, 25:56428 (IFA-HE-75)
Λ K production in four-prong π$^+$p interactions at 8 GeV/c, 25:56427 (IFA-HE-73)
MIKADO, Tomohisa, Ionization chamber response for pulsed radiation and drift velocity distribution of filling gas, 25:55015
MIKHAILENKO, I. E., Gas-chromatographic study of the effect of radioactive radiation and heat treatment on the adsorptive properties of magnesium sulfate, 25:54603
MIKHAILOV, A. I., Potential role of the tunnel effect in postradiation reactions in solid organic materials, 25:54596
MIKHAILOV, O. F., Potential changes of chromosomes as a result of interaction of radiation and alkylating compounds, 25:55260
MIKHAILOV, S. K., Effect of alloying on the oxidation of niobium at low pressures, 25:55380
MIKHAILOV, V. I., Pulse generator of megavolt capacity, 25:56583 (IAE-1980)
MIKHAILOVSKII, I. M., Field-ion-microscope study of W deformed by an electrostatic field at 900 to 1700°K, 25:55451
MIKHALYAK, S., Optical radiation excited by nonrelativistic charged particles on the metal surface, 25:55813 (JINR-P4-5957)
MIKHEEV, V. S., Study of phase equilibria in the titanium--tantalum--molybdenum system in the titanium corner, 25:55565
MILANESI, R., Uses of computer in radiotherapy. III, 25:55218
MILLARD, H. T. Jr., Neutron activation analysis for osmium,

XUM

ruthenium, and iridium in some silicate rocks and rock-forming minerals, 25:54486
Neutron activation analysis procedure for the determination of the noble metals in geological samples, 25:54485
MILLER, Carl R., Critical review of the assumptions involved in establishing the MPD and MPC's in air and water, 25:55254
MILLER, D. H., Diffractive $\pi\pi$ scattering in $\pi N \rightarrow \pi\pi N$ at 13.1 GeV/c, 25:56425 (COO-1428-294)
MILLER, E. J., Transport properties of partially ionized argon, 25:56183
MILLER, F. L. Jr., Effects of chronic irradiation on laboratory populations of the quatic snail physa heterostropha, 25:55314
MILLER, H. H., Radiosensitization with 5-bromodeoxyuridine of Chinese hamster cells x-irradiated during different phases of the cell cycle, 25:55258
MILLER, J. R., Sounding-rocket observations of particle precipitation in a polar-cap electron aurora, 25:56031
MILLER, K. J., Dependence of generalized oscillator strengths of $H_2O$ on momentum transfer, 25:55880
MILLER, Larry Day, Yields and charge dispersion of antimony produced in uranium fission by medium-energy protons, 25:56757
MILLER, William H., Evaluation of minima in total neutron cross section by transmission of fission spectra through thick samples, 25:56650 (COO-2049-5)
MILLET, P., Internal oxidation in Mg--Zr alloy in contact with carbon dioxide, 25:55382
Structural change in sintered Mg--Zr alloy after holding at high temperature, 25:55548
MILLS, B. Y., Emission nebulae in Magellanic Clouds at 408 MHz, 25:55722
MILLS, Joseph C., Axial kinetics model for fast reactor disassembly accidents, 25:57080 (CONF-710302-(Vol.1), pp 167-79)
MILNE, I., Effect of deformation on transition temperature of Nb--32 percent Zr, 25:56099
MIL'SHTEIN, R. S., Parameters of betatron B-30 bremsstrahlung, 25:55209
MILTENYI, Laszlo, Effect of nandrolon-decanoate and iron preparation on the hemogram of irradiated patients, 25:55303
MINAKATA, Kayoko, Radical pair from primary ionic species produced by ionizing radiation, 25:54665
MINAMI, Masatsugu, Quantized fields associated with the annulus-type medium, 25:56563
MINAMI, S., Surface (volume) reactions and polarization in $\pi^-$--p charge-exchange scattering at high energy, 25:56509
MINAMIKAWA, Toshiyuki, Canonical quantization of the proper time formalism in the dual resonance model, 25:56480
MINAMIKAWA, Yoshimasa, Osteonecrosis in lower mandible after postoperative radiotherapy, 25:55344
MINATO, Susumu, Vertical distribution of the intensity of ionization due to terrestrial gamma-radiation, 25:54790
MINTZ, Betty, Optical identification of southern radio sources, 25:55725
MISHIMA, J., Amount and characteristics of plutonium made airborne under thermal stress, 25:54546
MISIUNA, P., Application of $\gamma$ irradiated heterogenic bovine fascia in filling brain defects in dogs, 25:55148
MISTYGACZ, Z., Measurements of energy and flux of cosmic ray hadrons using an ionization spectrometer, 25:56413 (INP-756)
MITCHELL, J. B., Mechanisms of growth and loss of coherency of HfN particles in molybdenum, 25:55460
MITRA, A. N., Nuclear three-body problem, 25:56872
MITRA, Ved, Fractional burnup in a thermonuclear explosion, 25:54827
MITROFANOV, Yu. A., Combined treatment of barley and wheat seeds with ionizing radiation and ethylene-imine for the induction of mutations, 25:55261
MITSUMA, Terunori, Radioimmunoassay of triiodothyronine in unextracted human serum, 25:55146
MITTEL'MAN, V. A., Use of EDTA preparations labelled with $^{51}Cr$ and $^{169}Yb$ in radioisotope diagnosis, 25:55272
MITYAEV, V. V., Correlation effect of transport phenomena in molten solutions, 25:55449
MITYUKHINA, V. M., Alteration of the function of external respiration in patients with malignant tumors of the chest under the effect of radiation treatment, 25:55339
MIYAGAWA, Ichiro, X-ray irradiated crystals of Cu acetate monohydrate, 25:54610
MIYAKE, Y., Emission-spectrometric determination of trace non-rare earth elements in yttrium oxide, 25:54419
MIYAUCHI, D., Irradiation of Pacific Coast fish at sea, 25:55366
MIYAZAWA, Shintaro, Congruent melting composition of lithium metatantalate, 25:55639
MIZERA, P. F., Polar ionosphere: measured ion density enhancements and soft electron precipitation, 25:55964
MIZUNO, K., Cherenkov and cyclotron excitation of Bernstein waves with electron beams, 25:56241
MIZUSHINA, Tomoyuki, Facilities for accelerators for medical use, 25:56607
MIZUTANI, Tetsuro, Equation of state of neutron star matter and neutron star models, 25:55715
MKRTCHYAN, G. S., Interaction between a cavity and vortex in a type ii superconductor, 25:56091
MOCHIZUKI, Keiichi, Present status of fuel failure detection and location method in various countries in the world, 25:57056 (JAERI-Memo-4157, pp 89-100)
MOCHIZUKI, Yoshio, Determination of chlorobiphenyl in rat adipose tissue by neutron activation analysis, 25:54500
MOELLER, P., Determination of the trace element distribution in coexisting calcite and dolomite by neutron activation analysis, 25:54497
Measurementof isotope abundance shifts by means of neutron activation analysis, 25:54492
MOELLER, W., Corrosion of gas turbine alloys in molten salts of high $V_2O_5$ and low Na content, 25:55375 (CONF-690452-, Paper 8)
MOERK-MOERKENSTEIN, P., Pressurized and boiling water loop of the Technology Division at Ispra, 25:54867 (EUR-4683)
MOERUP, S., Hyperfine structure of $^{161}Dy$ in $Gd_2O_3$ at 300K, 25:56375
MOESNER, Juergen, Study of reaction $^{14}N(n,2\alpha)^7Li$, 25:56680
MOGENSEN, O., Positron annihilation in $\gamma$-irradiated 10 M NaOH glassy ice, 25:55835
MOHAN RAO, A. S., Dependence of the ionospheric absorption on lunar phase, 25:55975
MOHANTY, D. K., Search for pulsed radio emission from CYG X-1 at 327 MHz, 25:55728
MOLENAAR, J., RAGA: a Monte Carlo program for calculation of gamma-ray transport in a reactor shield for multi-region slab geometry, using exponential transformation, 25:57026 (RCN-146)
MOLINARI, V. G., Neutron thermalization in polycrystalline material by Monte Carlo method, 25:56619 (RT/FI-(70)49)
MOLINIER, R., Novel high-strength titanium alloy, 25:55421
MOLL, John H., Heat treatment of 706 Alloy, 25:55554
Microstructure of 706, a new Fe--Ni-base superalloy, 25:55553
MOLLOT, F., Vacancy--interstitial pair in electron-irradiated germanium, 25:56330
MOLLWO, L., Wave propagation in warm plasma and spectrum of solar radio bursts, 25:55755
MOLNAR, Andreas, Effect of nandrolon-decanoate and iron preparation on the hemogram of irradiated patients, 25:55303
MOLNAR, F., Concentration and determination of rare earth impurities in an yttrium matrix, 25:54525
MOLNAR, Michael Robert, B-type stars with discrepant colors, 25:55701
MONDIN, Henri, Nuclear thermal studies in France and their applications to other fields, 25:54865 (CEA-CONF-1758)
MONINGER II, William Ringland, K-plus neutron charge exchange scattering, 25:56423 (COO-1195-217)
MONTGOMERY, M. D., Association of magnetotail phenomena with visible auroral features, 25:55955
MONTGOMERY, Michael D., Ogo 5 observations of polar cusp on Nov. 1, 1968, 25:56024
Properties of solar energetic particles associated with propagating interplanetary shock waves, 25:56020
MONTGOMERY, T. L., Derivation of gaseous release limits for the Browns Ferry Nuclear Plant, 25:56980
MONTOYA, O., Effects of rf activated inert gas plasmas on critical surface tension and bondability of polydimethyl silicones and polyethylene, 25:57272 (SC-RR-710483)
MOODY, H. D., Neutron radiography at Sandia Laboratories: its techniques and instrumentation, 25:54924 (SC-DR-710178)
MOON, D. M., Mechanism and kinetics of bubble formation in doped tungsten, 25:55511
MOORE, E. C., Cytofluorograph system, 25:57249 (ORNL-TM-3536)
MOORE, J. B., Body burden, distribution, and internal dose of $^{210}Pb$ and $^{210}Po$ in a U miner population, 25:55117
MOORE, R. W., Local flow blockage effects in an LMFBR fuel pin bundle, 25:57076 (CONF-710302-(Vol.1), pp 102-19)
MOORE, Raymond T., Off-site medical planning and management for an experimental underground nuclear detonation, 25:55249
MORANDO, M., K = 3/2$^+$ rotational band in $^{45}Ti$, 25:56693
MORANTE, Aldo Belleni, Time discretization of the neutron transport equation, 25:57158 (CONF-710302-(Vol.2), pp 701-22)
MORAVEK, J., System of radioactive products control in gas coolant of nuclear reactors, 25:57033
MORDIKE, Barry L., Solid solution hardening in tantalum alloys, 25:55457
MORE, R. M., Theory of decaying states, 25:55886
MORET, Roger, $^{107}Cd$ excited levels, 25:56759
MOREWITZ, H., Effects of aerosol agglomeration on reactor dose evaluations, 25:57105
MOREWITZ, H. A., Forced-flow sodium boiling in multiple channels, 25:54863 (AI-AEC-13010)
MORGAN, J. W., 14 MeV neutron activation analysis of rocks and meteorites, 25:54465
Coincidence counting applied to the activation analysis of meteorites and rocks, 25:54479
Electrodeposition of Th, U, and Np from ammonium sulphate solutions, 25:54673
Uranium and thorium in some basic and ultra basic rocks of possible deep-seated origin, 25:54495

XUM

MORGAN, O. B., ORNL multi-ampere ion source, 25:56208 (CONF-711012-9)
MORGANSTERN, R. E., Brans--Dicke cosmologies in arbitrary units: solutions in flat Friedmann universes, 25:55800
Exact solutions to radiation-filled Brans--Dicke cosmologies, 25:55801
MORGAT, Jean-Louis, Method for preparing molecules labeled with tritium, 25:54693
MORIMOTO, E. M., Facility for the determination of low-level tritium in biological and environmental samples, 25:55003 (UCRL-73128)
MORIMYO, M., Temperature-sensitive recovery of a mutant of Escherichia coli K-12 irradiated with ultraviolet light, 25:55360
MORITA, K., Generalized Weinberg sum rules in deep inelastic current--hadron scatterings, 25:56461
MORITA, Kenji, Location of impurities in alkali halide crystals by channeling studies, 25:56337
MORITZ, J., Excitation of Δ(1236) resonance on bound state neutrons, 25:56405 (DESY-71/33)
MOROZ, E. M., Focusing of an ion beam drifting in a nonuniform magnetic field, 25:56602
MOROZOV, A. G., Fast-neutron flux measurement in AES Novo-Voronezhskii reactors, 25:56891
MOROZOV, V. S., Production of Cu/W composite by diffusion welding, 25:55405
MORRIS, A. C. Jr., Miniaturized probe for detecting radioactivity at thyroid surgery, 25:55018
MORRIS, J. M., Energy levels of $^{16}O$ in region of excitation between 13.5 and 15.0 MeV, 25:56681
MORRISON, G. H., Multielement neutron activation analysis of geological and lunar material using chemical group separations and high resolution gamma spectrometry, 25:54461
MORROW, R., Proton--hydrogen atom momentum transfer cross section at approximately 3 eV, 25:55840
MORROW, R. J., Gamma-ray energies and absolute branching intensities for $^{238}$ $^{239}$ $^{240}$ $^{241}$Pu and $^{241}$Am, 25:56753 (UCRL-51087)
MORSE, Fred A., Polar ionosphere: measured ion density enhancements and soft electron precipitation, 25:55964
MORSE, J. L., In-residence health and safety support in a plutonium facility, 25:55204 (CONF-710401-, pp 267-79)
MORSE, M. S., Heat capacity of tantalum in range 1900 to 3000 K, 25:55494
MORSE, T. F., Kinetic theory of flow between rotating cylinders: the gas centrifuge, 25:54888 (CONF-700557-5)
MORTON, N., Superconductivity of molybdenum and tungsten carbides, 25:56087
MOSER, C., Atomic and molecular wave functions, 25:55889
MOSES, Harry, Plume rise calculations using selected functional forms and the tabulation prediction technique, 25:54780 (CONF-710505-6)
MOSKOWITZ, D., High strength tungsten carbides, 25:55631
MOSS, Owen R., Production of relatively monodisperse aerosols for inhalation experiments by aerosol centrifugation, 25:54982
MOSS, R. E., Reduction of Dirac equation to nonrelativistic form, 25:56391
MOTTET, P., Influence of speed of graphitization of carbon products on dimensional variations produced by neutron irradiation, 25:55645 (CEA-CONF-1821)
MOTYAZHEV, V. I., Solubility and solid-phase interaction of the carbides of transition metals with nickel and copper, 25:55464
MOULTHROP, H. A., Description of ARHCO's new compact plutonium storage facility, 25:54942 (CONF-710401-, pp 56-67)
MOURIQUAND, C., Effects in vivo of ionizing radiations on human chromosomes, 25:55178
MOYER, Kenneth H., Correlation of mechanical properties of sintered U-700 powder with particle boundary morphology, 25:55484
MOYLE, R. A., Reaction mechanisms of $^{10}B(d,\alpha)^8Be_{2.9}(\alpha)^4He$ for E/sub d/ = 0.4, 1.0, and 1.5 MeV, 25:56673
MOZER, F. S., Electric fields in the nighttime and daytime auroral zone, 25:55960
Equatorial proton and electron angular distributions in the loss cone and at large angles, 25:56027
MROZOWSKI, S., Negative magnetoresistance in neutron-irradiated graphite, 25:56319
MUCKENTHALER, F. J., Total gamma-ray energy spectrum above 1 MeV from neutron interactions in $^{235}$U and $^{238}$U, 25:56745 (ORNL-4691)
MUELLER, H.-W., State of helium technology for high temperature reactors, 25:57040
MUELLER, Harry, Dynamic pressure measurement at the anode of high-current electric arcs, 25:56155
MUELLER, K., Determination of triiodothyronine and thyroxine in blood serum by activation analysis, 25:54453
MUELLER, Klaus-Dieter, Conference on siemens process calculator utilization, 6/70, Juelich, 25:55074 (JUL-Conf-5)
MUELLER, Walter A., Short-lived internal α-emitters in mice and rats. I, 25:55115
MUKHERJEE, B. K., Structure of current-induced intermediate state in Type-I superconductors, 25:56102
MUKHERJEE, Nati, Effect of uv irradiation and $^{32}P$ decay on thymineless death in E. coli, 25:55359
MUKHERJEE, P., Effect of hexadecapole deformation on the ΔN = 2 crossing of the Nilsson orbitals, 25:56858
Effect of uv irradiation and $^{32}P$ decay on thymineless death in E. coli, 25:55359
MUKHIN, G. I., Individual dosimeter, 25:55051
MULLANEY, P. F., Electronic particle counting and dispensing device for use in animal injection experiments, 25:55090
MULVANEY, J. E., Ring-opening reactions of triphenylcyclopropyllithium compounds, 25:54571
MUNDSCHENK, H., Mechanism of β recoil, 25:54694
MUNRO, R. E. B., Observations at 408 MHz of radio sources from 4C catalogue, 25:55723
MURADOV, A., Models of electron density distribution in F2 region. I, 25:55984
MURAKAMI, Yotaro, Effects of neutron irradiation on Cu--Be alloys, 25:55583
MURAKAWA, Shoichiro, Determination of chlorobiphenyl in rat adipose tissue by neutron activation analysis, 25:54500
MURATA, Jiro, Solidification of radioactive wastes with cement, 25:54979
MURFITT, Robert Roscoe, Interactions of sulfate and phosphate anions with alkaline earth cations in crystals, 25:57293 (UR-49-1517)
MURMANN, R. Kent, $ReO_4^-$---$H_2O$ exchange kinetics in methanol using $^{18}O$, 25:54574
MUROTA, Toshiyuki, Scale invariance and relativistic composite nucleon, 25:56465
MURPHY, E. G., Stabilization of flute instability with integrating feedback system, 25:56197
MURPHY, J. O., Nonlinear thermal convection with free boundaries, 25:55695
MURPHY, J. R., Predicted San Fernando earthquake spectra: Glendale area, 25:54812 (NVO-1163-TM-30)
MURTHY, K. R. N., Thermoluminescence of x-ray-irradiated KBr and KBr:Cu crystals, 25:56323
MURTI, Y. V. G. S., Thermoluminescence of x-ray-irradiated KBr and KBr:Cu crystals, 25:56323
MUSEN, L. G., Design features of Mound Laboratory's Medical Decontamination facility, 25:54963 (CONF-710401-, pp 311-15)
MUSER, W. H., State of helium technology for high temperature reactors, 25:57040
MUSGRAVE, L. E., Plutonium ignition in inert atmospheres, 25:54946 (CONF-710401-, pp 106-17)
MUSSO, B., Space time temperature distribution in a semi infinite medium under particular conditions of thermal transient, 25:54876 (RT/ING-(71)11)
MUSTAFA, Mohammed Golam, Photonuclear reactions in light nuclei, 25:56661
MUZIOL, G., Decay of $^{90}$Nb, 25:56791
MUZYKA, Donald R., Heat treatment of 706 Alloy, 25:55554
Microstructure of 706, a new Fe--Ni-base superalloy, 25:55553
MYASNIKOV, K. V., Creating underground storage cavities with contained nuclear explosions detonated in rock salt, 25:54824 (UCRL-Trans-10543, pp 70-80)
MYASNIKOVA, K. P., Study of alloys belonging to $NiAl_3$--$VAl_3$ and $Ni_2Al_3$--$V_2Al_3$ sections, 25:55562
MYERS, D. K., Initial effect of x radiation of thymidine incorporation into DNA in thymus cells, 25:55127
MYERS, Ira T., Effects of nuclear radiation on high-reliability silicon power diode. III, 25:55097 (N-71-25389)
MYERS, J. E., Near-isothermal dissipative flow of liquid He II at supercritical velocities, 25:56062
MYOZYO, Yasuo, Exotic exchange processes and urbaryon rearrangement diagrams, 25:56479
MYSHKIS, D. A., Experimental study of destruction of metastable helium atoms in plasma at low temperatures, 25:56151 (SC-T-713064)
MYSLEK, Bogumila, Preparation of high purity carrier-free $^{131}$Cs source for spectroscopic measurements, 25:54889 (INR-P-1325)

# N

NABER, J. A., Lithium: an impurity of interest in radiation effects of silicon, 25:56309
NAD, J., Collector system of an isotope separator for investigating short-lived isotopes, 25:56584 (JINR-P6-5888)
NADJO, L., Disproportionation and ECE mechanisms. III, 25:54585
NAGASAKI, Ryukichi, Effect of alpha-ray irradiation on creep-rupture properties of austenitic stainless steel, 25:55574 (JAERI-Memo-4408)
NAGATA, Sinobu, Equation of state of neutron star matter and neutron star models, 25:55715
NAGATOMO, Seiki, Planning and execution of the Mt. Enasan Tunnel, 25:57252 (ORNL-tr-2525)
NAGATSUKA, Sumiko, Activation analysis of lanthanide elements in natural water, 25:54504
NAGENDRA, H. R., Onset of free convection in annuli, 25:54881
NAGI, F. I., Simultaneous determination of Sb, As, and Cu by neutron activation, 25:54515
NAGLE, Constance, Steadiness of the wind during stable conditions, 25:54794

NAGY, S., Angular distributions of fragments in fission of U and Th near (n,2n'f) threshold, 25:56804
NAIDENOV, V. O., Measurement of tritium and $^{3}$He in Al targets, 25:55902
NAIDICH, Yu. V., Laws governing spreading of metallic melts over surface of boron nitride, 25:55469
NAIR, G. M., Indirect potentiometric method for the determination of plutonium, 25:54411
NAJAM, M. R., In-beam study of prompt γ-rays emitted in $^{66}$Zn(p,nγ)$^{66}$Ga reaction, 25:56732
NAKAGAWA, Isamu, Spectrographical analysis of $^{235}$U with a hollow cathode discharge tube, 25:54435
NAKAGAWA, Y., Topology of filaments and chromospheric fibrils near sunspots, 25:55749
NAKAJIMA, Kiyoshi, Activation analysis of lanthanide elements in natural water, 25:54504
NAKAMURA, Shigeru, Preparation and the absorption spectra of U(III) in various acid solutions, 25:54540
NAKAMURA, Tohru, Epitaxial growth of silicon assisted by ion implantation, 25:56347
NAKAMURA, Yutaka, Simultaneous determination of O, F, and Al in Al electrolytic bath by fast-neutron activation, 25:54503
NAKANISHI, Koichi, Osteonecrosis in lower mandible after postoperative radiotherapy, 25:55344
NAKANISHI, T., One-valley EPR spectrum in electron-irradiated Sb-doped Ge, 25:56298
NAKANO, Takenori, Condensation of solid hydrogen in contracting interstellar clouds, 25:55785
NAKAZAWA, Kiyoshi, Equation of state of neutron star matter and neutron star models, 25:55715
NAMENSON, A. I., Resonance neutron capture by $^{170}$Yb and $^{172}$Yb, 25:56802
NAPIER, B. Jr., Properties of carbon derived from indene compounds, 25:57295 (Y-1790)
NAPOLI, A., Method of analysis of neutron capture gamma-ray spectra, 25:56690 (RT/FI-(70)47)
NAPRAVNIK, J., Plant project for fixation of radioactive wastes into bitumen, 25:54981
NARDI, V., Vorticity and neutrons in the plasma focus, 25:56157
NARTOVA, T. T., Heat resistance and elastic properties of titanium--tantalum alloys, 25:55446
NARUMI, Hajime, Contribution absorption-reemission process to the complex level shift in the pionic atom, 25:55833
NASHIYAMA, Isamu, Heavy-particle ray damage to a Si solar battery, 25:55099
NASIKANOVA, N. N., Recrystallization of a strongly deformed monocrystal of molybdenum, 25:55518
NASRA, M., Simultaneous determination of Sb, As, and Cu by neutron activation, 25:54515
NATALI, S., Analysis of K+/sub e3/ decay X2, 25:56409
NATORI, Hiroo, Uraniferous bed in Mizusawa area, 25:54806
NATOWITZ, J. B., Recoil study of $^{209}$Bi(α,p)/sup 212m,g/Po reaction mechanism, 25:56799
NATSUME, H., Systematic radiochemical analysis of fission products, 25:54449
NAUMENKO, Yu. I., Use of EDTA preparations labelled with $^{51}$Cr and $^{169}$Yb in radioisotope diagnosis, 25:55272
NAVARA, E., Stability of oxide dispersions in iron- and nickel-based alloys, 25:55485
NAZARCHUK, T. N., Chemical stability of diborides of transition metals, 25:54543
NAZARE, S., Relations between stereometric microstructure and properties of cermets and porous materials, 25:55628
NAZAROV, E. V., Discontinuity of equation of optimum problems of magnetogasdynamics, 25:55936
NAZAROV, P. P., Isolation of promethium by displacement chromatography due to complex formation, 25:54723
NAZHAT, N. B., Reply to formation of ozonide ions in γ-irradiated aqueous solutions of alkali hydroxides, 25:54609
NAZZER, D. B., Low pressure stripping, 25:54918
NEAMU, I., Analysis of proton scattering on $^{32}$S, 25:56694
NECHAEV, O. Yu., Chemical composition of primary cosmic rays, 25:55899
NECHAEVA, L. P., Focusing of an ion beam drifting in a nonuniform magnetic field, 25:56602
NECKEL, Heinz, The solar constant, 25:55742
NEDELIK, A., Measurement of reactor power by determination of $^{17}$N neutrons in the cooling medium with track detectors, 25:57124
NEIMOTIN, E. I., Moments of the distribution function of the neutron density, 25:57179
NEKRASOV, V. I., Global contamination of the atmosphere by $^{85}$Kr from worldwide nuclear power plants and the radiation danger, 25:54781 (JPRS-53174)
NELLIGAN, William B., Method and apparatus for measuring neutron characteristics of a material surrounding a well bore, 25:54769
NELSON, G. O., Engineering fire-suppression systems for large volumes using Halon 1301, 25:54957 (CONF-710401-, pp 248-56)
NELSON, J. V., Cross sections for preliminary design of FTR, FTR Set No. 200, 25:57115 (HEDL-TME-71-65)
NELSON, Paul Jr., Convergence of the discrete ordinates method for anisotropically scattering multiplying particles in a subcritical slab, 25:56264 (ORNL-TM-3553)
NEMCEK, J. V., Miniaturized probe for detecting radioactivity at thyroid surgery, 25:55018
NEMCHENKO, V. F., Temperature dependence of absolute thermo-EMF coefficient of certain transition metals, 25:56351
Temperature dependence of the electrical and thermal conductivity of rhenium and metals of the platinum subgroup, 25:55523
NEMEC, J., Primary carcinoma of thyroglossal duct, 25:55304
Spectrocalorimetric measurements in core of heavy water reactor, 25:57123
NEMETS, O. F., Inelastic scattering of deuterons, 25:56780
NEMIROVSKII, B. V., Neutron scintillation detector, 25:55012
NEMOTO, Tsuyoshi, Gamma-ray spectroscopy of heavy water and He-gas in JRR-3 fuel failure, 25:57118 (JAERI-Memo-4157, pp 44-50)
NEMOV, V. V., Resonance effects in magnetic configurations having a helical magnetic axis, with allowance for toroidality, 25:56209 (CTO-764)
NEMTSEVA, L. S., Protracted mutagenesis induced by ionizing irradiation and its dependence on the water content of a biosystem, 25:55167
NERODENKO, L. M., Change in electrical resistivity with decomposition of supersaturated solid solution in alloy K30M18GSN, 25:55472
NERODENKO, M. M., Change in electrical resistivity with decomposition of supersaturated solid solution in alloy K30M18GSN, 25:55472
NESBET, R. K., Search procedure for multichannel resonances in electron--atom scattering, 25:55861
NESMEYANOV, A. N., Valence states of Eu and Dy in Laves phases and isomer shifts in Moessbauer spectra, 25:56379
NESMYANOVICH, A. T., Diurnal and seasonal pattern in frequency of occurrence of sudden commencements, 25:56003
NESMYANOVICH, E. I., Diurnal and seasonal pattern in frequency of occurrence of sudden commencements, 25:56003
NESS, N. F., Observations of the interplanetary medium: Vela 3 and Imp 3, 1965--1967, 25:55780
NESSLER, C. G., Friction welding of titanium alloys, 25:55409
NESTERENKO, V. S., Interaction between 14-MeV neutrons and nuclei of Fe, Cu, and Nb, 25:56684 (FEI-216)
NESTEROV, B. V., Gamma-radiation during thermal neutron capture on chromium and iron isotopes, 25:56683 (FEI-205)
NESYTO, Edwin, Mechanism of the radiation-induced dechlorination of 1,1,1-trichloro-2,2-bis(p-chlorophenyl)ethane in alcholic solution, 25:54620
NETA, P., Electron spin resonance study of irradiated aqueous solutions of fumarate ion. The use of fumarate for radical trapping, 25:54656
Rate constants for reaction of hydrogen atoms with compounds of biochemical interest, 25:55132
NETTESHEIM, P., Recovery of the antigen retention mechanism after sublethal x-irradiation in mice receiving cells from various sources, 25:55147
NEUGEBAUER, Marcia, Ogo 5 observations of polar cusp on Nov. 1, 1968, 25:56024
NEUHAUS, Otto W., In vitro uptake of model amino acids by rat liver following whole-body γ-irradiation, 25:55126
NEUZIL, Edward F., Prog. rpt. on fission studies on elements below Po, 7/70--6/71, 25:56750 (RLO-1759-25)
NEWCOMBE, Howard B., Persistence of heritable changes in an irradiated rat population after cessation of the exposures, 25:55164
NEWMAN, D. H., Electron traps in deformed KCl, 25:56321
NEWMAN, R. C., Irradiation damage in carbon-doped silicon, 25:56325
NEWSHAM, Ivor G., Electron stimulated desorption of excited neutrals: CO on W, 25:55435 (RLO-2221-T-7-4)
NEWTON, G. J., Physical and chemical characteristics of aerosols produced from solutions of polyvalent metallic nuclides, 25:54545
NG, S. H., Bhabha scattering anomalous interaction of muon, 25:56466
NGUYEN TING SHOA, Study of phase equilibria in the aluminum--copper--yttrium system, 25:55561
NICHIPOROV, F. G., Reactivity of $Ce^{4+}$ ions in irradiated aqueous solutions of sulfuric acid, 25:54647
Yields of hydrogen peroxide in aqueous solutions of thallium sulfate, 25:54646
NICHITIU, F. Gh., Cerenkov mechanism and resonance production, 25:56498 (IFA-HE-76)
NICHKOV, I. F., Precipitation of uranium from a melt of fused halides with a molten zinc cathode, 25:54580
Thermodynamic properties of cerium in molten zinc, 25:55442
NICHOLS, C. E., Operation of a transuranic storage area at NRTS, 25:54965 (CONF-710401-, pp 365-8)
NICHOLSON, P. S., Chemical vapor deposited tungsten: mechanical evaluation at high temperatures, 25:55440
NICHOLSON, R. B., Numerical stability problems in the VENUS disassembly code, 25:57079 (CONF-710302-(Vol.1), pp 152-66)
NICKEL, G. H., Multidimensional magnetohydrodynamic shock calculations, 25:56192
NICKOLA, P. W., Atmospheric tracer technique employing $^{85}$Kr


XUM

and use of this technique in defining puff dimensions and transport speed, 25:54908
Comparison of maximum exposures at ground level resulting from simultaneous release of tracers from elevations of 2 and 26 meters, 25:56395 (BNWL-1551(Vol.2)(Pt.1), pp 108-12)
NICOL, M. F., Prog. rpt. on intra- and inter-molecular energy transfer studies, 5/70--5/71, 25:54600 (UCLA-34-P-88-32)
NIEDERKORN, I., Determination of the concentration of U in different materials by measurement of alpha, beta, and gamma radiations, 25:54445
NIEDZIELSKI, Jan, Effect of some oxygen-containing compounds on the radiolysis of gaseous ethylene, 25:54643
NIEZETTE, J., Automatic dilatometer for radiation polymerizations, 25:54616
NIFONG, Gordon Dale, Particle size distributions of trace elements in pollution aerosols, 25:54505
NIIHARA, Koichi, Preparation and nonstoichiometry of samarium hexaboride, 25:55601
NIKA, G. G., Dynamic sampling of the deuterium hydride self-exchange behind reflected shock waves, 25:54562
NIKASHINA, V. A., Calculation and optimization of the demineralization of water for reactors by ion exchange, 25:54737
NIKITIN, A. V., Analysis of the reaction np → pp $\pi^-$ from the point of view of Reggeized OPE model, 25:56521 (JINR-P1-5975)
NIKITIN, P. N., Study of phase equilibria in the titanium--tantalum--molybdenum system in the titanium corner, 25:55565
NIKITIN, Yu. P., Cross section for production of W boson by high-energy neutrinos in the electromagnetic field of a proton, 25:56473
NIKITYUK, L. N., Probability of the ($\mu^-$, $\nu$) process of $^{139}$La and $^{208}$Pb nuclei, 25:56739 (JINR-P1-6006)
NIKODEMOVA, D., Utilization of polymer-gelatin nuclear emulsions for fast neutron dosimetry, 25:55057
NIKOLAENKO, V. A., Use of irradiated diamonds for temperature measurement, 25:55104
NIKOL'SKII, B. P., Quaternary ammonium bases as analytical reagents. II, 25:54434
NIKONOV, V. B., Methods of investigating variable stars, 25:55674
NILSON, Kristian, Relative biological effectiveness of x rays delivered at very high dose rates to radish seeds (raphanus sativus), 25:55350
NISHCHENKO, M. M., Moessbauer effect in the segregating iron--beryllium alloy, 25:56378
NISHIHARA, Kiyokado, Spectrographical analysis of $^{235}$U with a hollow cathode discharge tube, 25:54435
NISHIMOTO, Kazuya, Contribution absorption-reemission process to the complex level shift in the pionic atom, 25:55833
NISHIMURA, Akihisa, Estimation of genetically significant dose equivalent from occupational exposure to external sources of radiation in Japan, 25:55230
NISHIMURA, Susumu, Study of age determination method on some minerals and glasses by fission-track registration, 25:54760
NISHIO, Gunji, Kinetics of carbon transfer between uranium carbide fuel and stainless steel bonded with sodium, 25:55589 (JAERI-Memo-4438)
NISLEY, R. A., Reaction matrix elements and structure calculations with the Yale and Reid potentials for the Ni region, 25:56857
NISSEN, H.-U., Feldspar analysis by neutron activation, 25:54494
NITZE, H. R., Radiation treatment of human tumours, 25:55306
NIZIN, P. S., Moessbauer effect in the segregating iron--beryllium alloy, 25:56378
NOBLE, Jack E., Implantable radioisotope-fueled stirling engine, 25:54910
NODA, Hujio, Exotic exchange processes and urbaryon rearrangement diagrams, 25:56479
Urbaryon rearrangement diagram and nonleptonic hyperon decays, 25:56470
NOEL, Marie-Therese, Treatment of elastomers, 25:54619
NOFFKE, H. E., EPR study of fast-neutron radiation damage in silicon, 25:56324
NOLTINGK, Bernard Edward, Apparatus for irradiating materials with electrons, 25:54835
NONNEBEL, Dirk, Radioisotope generator of the mother-daughter type having quick-detachable members, 25:54909
NOON, J. H., Prog. rpt. on instabilities and turbulence in highly ionized plasmas in a magnetic field, semiannual, 9/70--2/71, 25:56196 (N-71-25028)
NOONAN, Thomas W., Radius of maximum rotational velocity in spiral galaxies, 25:55786
NORDMAN, Clas T., Lung scanning with gamma cameras, 25:55296
NORDMAN, Eeva, Reliability of liver scanning with $^{198}$Au, 25:55276
NORDMANN, B. J. Jr., ILLIAC III reference manual. III, 25:57227 (COO-2118-21)
ILLIAC III reference manual. IV, 25:57226 (COO-2118-19)
NORKUS, P. K., Use of $OsO_4$ as catalyst in titrimetry. XI, 25:54433
NORRIS, A. C., Deposition of pyrolytic carbon in silica reactors, 25:55604
NORRIS, W. T., Calculation of hysteresis losses in hard superconductors, 25:56101
NOTARRIGO, S., Shell effects in (n,p) and (n,$\alpha$) cross-sections at about 14 MeV, 25:56869
NOUJAIM, A. A., Some aspects of measurement of $^{32}$P Cherenkov radiation in water by liquid scintillation spectrometer, 25:54438
NOVIK, F. S., Construction of the solidus volume in the niobium--tungsten--titanium--zirconium system by the simplex-lattice method, 25:55529
NOVIKOV, S. R., Oscillations of photocurrent in Ge with radiation defects, 25:56316
NOVITSKY, Thomas W., Gamma ray density gauging, 25:55067
NOVOTNY, J., Alpha dosimetry and spectrometry by solid-state nuclear track detector, 25:55026
NOWAK, E. S., Calorimeter to investigate saturation behavior of heavy water and other fluids, 25:55092
NOWAK, Teresa, Gravimetric determination of tellurium in silicon--magnesium master alloys, 25:54416
NOWAK, Zofia, Radiolysis of diluent--TBP--$HNO_3$ systems, 25:54644
NOYES, H. Pierre, Comment on the $^1S_0$ nucleon--nucleon effective-range expansion parameters, 25:56529
NUTTALL, J., s-wave elastic e--H scattering above ionization threshold, 25:55860
NUZHNYI, V. A., Tables for calculating nonstationary temperatures of plane bodies during heating by irradiation, 25:56267

## O

OATES, W. A., Thermomigration of carbon in metals, 25:55479
OBERHUMMER, H., Separable potentials, 25:56531
OBLINGER, Charles J., Determination of thermodynamic interaction parameters in solid V--Ti alloys using the mass spectrometer, 25:55489
OBLIVANTSEV, A. N., Temperature of thermal peaks during irradiation of ionic crystals, 25:56318
OBLOZINSKY, P., Isomeric cross-section ratios analysis of $^{136}$Ba($\alpha$,n)$^{137}$Ce reaction, 25:56765
O'BRIEN, John Terrance, Relaxation theory of Stark broadening of He II lines in plasmas, 25:56184
O'BRIEN, L. J., Predicted San Fernando earthquake spectra: Glendale area, 25:54812 (NVO-1163-TM-30)
OBUKHOV, A. P., Interaction of niobium with a zinc melt, 25:55534
OCCHIONERO, F., Conversion of gravitational into electromagnetic waves, 25:55805
OCHIAI, S. I., Investigation of superconducting-energy-gap behavior of single-crystal rhenium by tunneling, 25:56067
O'CONNELL, R. F., Lense-Thirring type gravitational forces between disks and cylinders, 25:55807
O'DELL, A. A., Monte Carlo calculation of sodium iodide scintillation detector response function, 25:54994 (EGG-1183-2283)
Monte Carlo transport analysis for finite ground-distributed $\gamma$ sources, 25:56260 (EGG-1183-2284)
ODINTSOV, V. V., Physical properties of uranium dodecaboride, 25:55622
ODLOZINSKI, G., PRESCON: a digital computer program for containment pressure transients, 25:57087 (CONF-710302-(Vol.1), pp 436-51)
OERDOEGH, M., Neutron activation analysis of impurities in Th and Zr, 25:54518
O'FLYNN, M., Design of pod boiler pressure vessels, 25:56885
OGANESYAN, Yu. Ts., Elastic scattering of heavy ions by nuclei, 25:56740 (JINR-P7-5884)
OGAWA, Toshihiro, Sounding rocket observation of helium 304- and 584-A glow, 25:55967
OGAWA, Yutaka, Effect of alpha-ray irradiation on creep-rupture properties of austenitic stainless steel, 25:55574 (JAERI-Memo-4408)
OHANIAN, H. C., Scalar-tensor theories and the principle of equivalence, 25:56569
O'HARA, F. A., Technical and economic parameters affecting fast breeder reactor deployment, 25:57061 (MLM-1851)
O'HARE, S. A., Solubility of nitrogen in alpha vanadium, 25:55475
OHASHI, Teruo, Effects of cooling rate and supercooling degree on Al--Mn, Al--Cr, and Al--Zr alloys, 25:55550
OHNISHI, T., Application of finite element solution technique to neutron diffusion and transport equations, 25:57159 (CONF-710302-(Vol.2), pp 723-38)
OHTA, Tokio, Polarization of core fermion and the heat transport of flux line, 25:56088
OHTSUBO, Hisao, Contribution absorption-reemission process to the complex level shift in the pionic atom, 25:55833
OHTSUKA, Shigeo, Solidification of radioactive wastes with cement, 25:54979
OKADA, Munehisa, Triad tacticity of polyacrylonitrile, 25:54622
OKAJIMA, Nobuo, Facilities for accelerators for medical use, 25:56607
OKAMURA, Hiroshi, Second class currents in high energy

neutrino reactions, 25:56472
OKAZAKI, Masahiko, Effect of tetrahydrofolic acid x-irradiated mice, 25:55268
OKE, J. B., Energy distributions and K corrections for light from giant elliptical galaxies, 25:55793
OLDHAM, G., Activation analysis applied to non-aqueous flowing system, 25:54524
OLES, A., Tables of magnetic structures determined by neutron diffraction. V, 25:56341 (NP-19010)
OLESEN, P., Inclusive reactions in dual models with second sheet resonances, 25:56476
OLHOEFT, J. E., Comparison calculations for a LWR benchmark package using ENDF/B-1 and -II data, 25:57019 (CONF-710302-(Vol.2), pp 1065-85)
OLIMPIENKO, G. S., Combined treatment of barley and wheat seeds with ionizing radiation and ethylene-imine for the induction of mutations, 25:55261
OLIVAIN, J., Interaction of a large-amplitude wave with a plasma: trapping, 25:56227 (CEA-CONF-1805)
Saturation and damping of echoes of electron plasma waves, 25:56226 (CEA-CONF-1804)
OLIVAIN, Jack, Theoretical and experimental study of nonlinear processes in a plasma, 25:56229 (EUR-CEA-FC-602)
OLIVER, A. J., Air leakage into plutonium gloveboxes and its effect on inert operations, 25:54944 (CONF-710401-, pp 83-97)
OLIVIER, J. C, Polarization parameter in K+-p and anti pp elastic scattering at 10 and 14 GeV/c, 25:56438
OLIVIER, J. C., Polarization in proton--proton elastic scattering at 10, 14, and 17.5 GeV/c, 25:56419
Polarization parameter in π+p elastic scattering at 10, 14, and 17.5 GeV/c, 25:56437
OLSEN, B., Theory of nuclear magnetic resonance detected by nuclear radiations, 25:56372
OLSON, R. E., Human element design considerations with gloveboxes at the Atlantic Richfield Hanford Company, 25:54938 (CONF-710401-, pp 4-16)
OLTMAN, Billie G., Passive moisture meter, 25:55061
OMBERG, R. P., TGO, a Linear Programming model for optimizing power transmission grid, 25:57230 (HEDL-TME-71-108)
OMORI, Takashi, Thermal annealing behavior of recoil $^{57}$Co formed by decay of $^{57}$Ni-labeled hexamminenickel(II) complexes, 25:54689
ONURA, Akio, Evaluation of apparent ionium ages of some hermatypic corals, 25:54776
ONDRACEK, G., Relations between stereometric microstructure and properties of cermets and porous materials, 25:55628
O'NEAL, J. E., Epitaxy of vanadium on sapphire, 25:55530
Hetero-epitaxial films of niobium on sapphire, 25:55531
ONG, Andres Sy., Diffusion of $^{133}$Xe in cesium iodide and calcium fluoride single crystals, 25:55633
ONG, R. S. B., Effect of impurity ions on the stability of drift waves, 25:56243
ONISHI, Nobuaki, Study on JRR-4 delayed neutron-type fuel failure detector, 25:57119 (JAERI-Memo-4157, pp 51-65)
ONODERA, H., Neutron irradiations of silicon studied by $^{57}$Fe Moessbauer effect, 25:56326
ONOSOVSKII, K. K., Proton beam of the ITEP accelerator for radium therapy, 25:56581 (BNL-tr-442)
ONSTOTT, E. I., Electrochemical reduction of europium at a porous carbon cathode with flowing electrolyte, 25:54530 (LA-DC-12469)
OOSTEROM, M. G., Determination by neutron activation analysis of alkali and other trace elements in ultramafic rocks, 25:54496
OOTSUKA, Ryoichi, Ultrasonic flaw testing method for a reactor pressure vessel using a mockup, 25:54925
OPAL, C. B., Energy distributions of electrons ejected in ionizing collisions of electrons with helium, 25:55847
OPHEL, T. R., Energy levels of $^{18}$O in region of excitation between 13.5 and 15.0 MeV, 25:56681
OPPOLD, J. A., Derivation of gaseous release limits for the Browns Ferry Nuclear Plant, 25:56980
OREKHOV, V. D., Kinetics of the low-dose radiolysis of concentrated aqueous acidic solutions of sodium nitrate, 25:54657
ORESHKIN, V. D., Wear resistance of surfaces faced with borides, 25:55619
ORIHOOD, Glenn M., Fire detection systems in gloveboxes, 25:54955 (CONF-710401-, pp 221-36)
ORISA, B. D., Radiation from an electric charge moving along a spiral path in a transparent medium, 25:56462
ORLOV, A. F., Electrophysical properties of niobium films produced and annealed in a very high vacuum, 25:55507
ORMES, J. F., Calibration of NASA--GSFC High Energy Cosmic Ray Experiment, 25:55046 (N-71-16750)
ORNELAS, Lawrence D., Rotated mercury cell for controlled potential coulometry. Elimination of background current by digital normalization, 25:54427
ORO, F., Tritium fractionation in water-carbide to benzene reaction, 25:54735
ORY, Hai A., Possible effects of atmospheric particles on fireball emissions, 25:54815 (AD-722031)
OSANOV, D. P., Dose function of a plane infinitely thin source situated on the dividing boundary between two media, 25:55233
O'SHEA, D. M., Network organization of an automated nuclear design system, 25:57146 (CONF-710302-(Vol.1), pp 516-30)
OSHER, John E., Intense 1-kV ion source for controlled fusion research, 25:56217 (UCRL-73387)
Production of intense ion and neutral beams with energies below 10 keV, 25:56218 (UCRL-73412)
OSINSKI, J., Radioiodine distribution in the Tarapur power reactor environment during commissioning and initial operations, 25:56978
OSIPENKOVA-VICHTOMOVA, T. K., Treatment of bone sarcoma with high-energy bremsstrahlung, 25:55338
OSIPOV, K. A., Electrophysical properties of niobium films produced and annealed in a very high vacuum, 25:55507
OSIPOV, K. K., Relationship between vlf emission and cosmic-noise absorption in the auroral zone, 25:55999
OSIPOV, N. K., Relationship between vlf emission and cosmic-noise absorption in the auroral zone, 25:55999
OSMAN, A. M., Root respiration of wheat plants as influenced by age, temperature, and irradiation of shoots, 25:55348
OSTAPENKO, Yu. B., Angular anisotropy and effects of nucleon pairing in $^{239}$Pu fission by neutrons, 25:56736 (FEI-233)
OSTERMANN, F., Dislocation cell formation and recrystallization in tungsten, 25:55558
OSTOVAR, K., Effects of gamma irradiation on Salmonella in smoked lake whitefish, 25:55365
OSTRANDER, Peter Erling, Realistic shell model calculations for $^{14}$C and $^{14}$N, 25:56660
OSUMI, Y., Emission-spectrometric determination of trace non-rare earth elements in yttrium oxide, 25:54419
OTOUPAL, P., Some pathomorphological findings in acute radiation sickness in goats, 25:55318 (LB/G-2995)
OTT, J. Bevan, Prog. rpt. on electrochemical cells using alkali metals and charge transfer complexes, 5/67--8/71, 25:57221 (COO-1707-12)
Prog. rpt. on solid-liquid phase equilibria in the ternary sodium--potassium--rubidium alloy system, 5/67--8/71, 25:55524 (COO-1707-11)
OTTMAN, R. J., Battelle's research plutonium facility environmental control and safety, 25:54959 (CONF-710401-, pp 280-92)
OTTO, H. J., Multi-pion exchange contribution to nucleon--nucleon binding and the electrodisintegration of deuterons, 25:56527
OVSYANNIKOVA, L. P., Aberrations of asymmetrized quadrupole lenses, 25:56604
OWEN, C. V., Mechanical properties of polycrystalline Sm, 25:55520
OWEN, David A., Hyperfine structure of positronium, 25:55832
OWENS, Ken, High level or low level it's a rocky road for radwastes, 25:57001
OZOL, A. A., Uv-sensitive mutants of Chlorella vulgaris, 25:55172

## P

PACAULT, A., Electronic and magnetic properties of carbon fibers: development under neutron irradiation, 25:56282 (CEA-CONF-1822)
Thermal annealing of neutron-irradiated carbon, 25:56283 (CEA-CONF-1823)
PACINI, Franco, Possible interpretation of precursor pulse in NP 0532, 25:55719
PACK, D. C., Expansion of plasma from spherical source into vacuum. I, 25:56180
PADERNO, Yu. B., Physical properties of uranium dodecaboride, 25:55622
PAEPRER, H., Perfusion lung scintigraphy in primary vascular pulmonary hypertension, 25:55284
PAGNAMENTA, Antonio, Interpretation of angular distribution in terms of complex mass particles, 25:56499 (ORO-3992-8)
Phenomenology of complex spin tachyons, 25:56500 (ORO-3992-18)
PAHLMAN, John Edward, Thermodynamics of formation of compounds in the Ce--Mg, Nd--Mg, Gd--Mg, Dy--Mg, Er--Mg, and Lu--Mg systems from vapor pressure measurements, 25:55525 (IS-T-462)
PAINE, D., Plutonium movement in aquatic systems: a review, 25:55150 (CONF-710401-, pp 407-10)
PAJARES, C., Adler--Weisberger relation, 25:56510
PALENZONA, A., Stoichiometry, crystal structures, and some melting points of the La--Au alloys, 25:55570
PALMGREN, A., Scattering cross-section and phonon spectrum of Zr hydride, 25:56623
PAN, V. M., Alloying of superconducting compounds vanadium gallide with group III--VIII elements, 25:55500
Properties of deformed superconducting alloys of vanadium--gallium, 25:56100
PANA, M., Burn-out heat fluxes at subcooled boiling, 25:54871 (IFA-TR-58)
PANCHENKOVA, E. F., Study of reactivity of the organism exposed to transverse accelerations and radioprotectants, 25:55264
PANCHUK, V. I., Numerical calculation of conducting fluid flow in a traveling magnetic field, 25:55918
PANDE, L. K., Scalar mesons in broken chiral symmetry, 25:56539 (ORO-3992-11)
Symmetry breaking in the hard-meson current algebraic tree-graph theory, 25:56535 (ORO-3992-7)

XUM

PANDHARIPANDE, V. R., Neutron matter computations in Brueckner and variational theories, 25:56867
PANKRATOVA, L. N., Infrared investigation of the action of ionizing radiation on carbon-chain polymers, 25:54604
PANTA, P. P., Electronic properties of anodized Al electrode, 25:54601
PAPAGIANNIS, Michael D., Dependence of magnetospheric electric field on velocity of solar wind, 25:56039
PAPWORTH, D. G., Induction of translocations in mouse spermatogonia. IV, 25:55182
PARIKH, J. C., Lectures on group symmetries in nuclear structure, 25:56838 (UR-875-350)
PARK, Nou Pung, Effects of gamma-radiation on sprout-inhibition of garlic bulbs and the changes of their chemical contents, 25:55354
PARK, Yong Sook, Distorted-wave Born-approximation analysis of the $^{90}$Zr(d,α)$^{89}$Y and $^{89}$Y($^{3}$He,α)$^{88}$Y reactions, 25:56778
PARKIN, Curtis W., Electrical conductivity and temperature of lunar interior, 25:55810
PARKINSON, M. J., Comments on analyses of anti pn + 3π, 25:56485 (ORO-3992-66)
PARKS, E. K., Collisional dissociative ionization of TlBr by accelerated Xe and Kr atoms, 25:55879
PARRISH, Alan de Schweinitz, Meter wavelength observations of galactic radio sources and the galactic disk radiation, 25:55730
PARSLOW, R. D., Conference on advanced computer graphics, London, 4/70, 25:57007
PARTHASARATHY, L., Microwave oscillations in parallel Josephson junctions, 25:56077
PASCHMANN, G., Flux profile of protons measured in 1967 at equator, 25:55957
PASCUAL, R., Adler--Weisberger relation, 25:56510
PASECHNIK, M. V., Inelastic proton scattering by intermediate-weight nuclei, 25:56727
PASOLI, A., Uses of computer in radiotherapy. III, 25:55218
PASSENHEIM, B. C., Lithium: an impurity of interest in radiation effects of silicon, 25:56309
PATE, Brian D., Fission of medium mass nuclei induced by 167 MeV alpha particles, 25:56806
PATERA, J., Highly restricted partitions and angular-momentum states of equivalent particle configurations, 25:56848
PATET, J., Effects in vivo of ionizing radiations on human chromosomes, 25:55178
PATRICK, Richard M., Collisionless shocks in plasmas, 25:56147
PATTERSON, D. E., Safety criteria for the design of facilities processing plutonium, 25:54967 (CONF-710401-, pp 438-53)
PATTERSON, John W., Electrolytic behavior of yttria-stabilized hafnia, 25:56355
PATTERSON, M. R., Fourier analysis of unequally spaced data, 25:57250 (ORNL-TM-3547)
PAUL, A. R., Lattice and grain boundary diffusion of cerium and neodymium in nickel, 25:55488
PAUL, L., Study of π$^{-}$p + π$^{0}$n and π$^{-}$p + ηn reactions in nuclei at 7.82 GeV/c, 25:56432
PAULIN, Robert, Radioactivity measurements, 25:55020
PAVERI--FONTANA, Stefano L., DP-0 method according to a variational treatment that extends its applicability to all geometries, 25:57152 (CONF-710302-(Vol.2), pp 608-16)
PAVLICHENKOV, A. V., Autoionizing states in helium-like ions, 25:55820
PAVLIK, W. R., Radioisotopes in blast-furnace ironmaking operations, 25:54906
PAVLINOV, L. V., Estimate of diffusion coefficients of α-radioactive elements in thin layers, 25:55498
PAVLOV, V. V., State of hematopoiesis in local fractional irradiation. II, 25:55326
PAVLOVA, N. L., Compression of plasma by growing longitudinal magnetic field in Tokamak, 25:56125
PAWEL, O., Some pathomorphological findings in acute radiation sickness in goats, 25:55318 (LB/G-2995)
PAWLIW, J., Preparation of mixed oxide nuclear fuel, 25:55597
PAYNE, George, Upper and lower bounds for three-body scattering, 25:55876
PEATMAN, William B., Charge transfer in Na$^{+}$--O$^{-}$ collisions at low relative energy, 25:55859
PECKOVER, R. S., Suppression of convection by a magnetic fluid, 25:55945
PEDROLI, G., Neutron coincidences counting system, 25:54995 (EUR-4611)
PEELLE, R. W., Techniques used at Oak Ridge National Laboratory for unfolding neutron and gamma-ray pulse-height spectra, 25:54436 (ORNL-TM-3463)
PEGOUD, J., Internal oxidation in Mg--Zr alloy in contact with carbon dioxide, 25:55382
Structural change in sintered Mg--Zr alloy after holding at high temperature, 25:55548
PEIZULAEV, Sh. I., Distribution coefficients of titanium and iron in zirconium, 25:55502
PEKER, L. K., Properties of certain multiparticle states with large spins, 25:56783
PENCE, D. T., Iodine chemistry in steam air atmospheres, 25:54547
PENELLE, R., Influence of orientation of zirconium monocrystals on the growth structures of monoclinic zirconia, 25:55540
PENIONZHKEVICH, Yu. E., Elastic scattering of heavy ions by nuclei, 25:56740 (JINR-P7-5884)
PENNER, S., Elastic scattering of 60 to 120 MeV electrons from $^{46}$ $^{48}$ $^{50}$Ti, 25:56701
PENZIAS, A. A., CO, CN, and CS emission from IRC + 10216, 25:55686
PEPELNIK, R., Proposal for installation of a versatile e$^{-}$ - e$^{+}$ - γ spectrometer for neutron capture spectroscopy, 25:55040 (NP-18994)
PERCEVAL, F., Interaction of a large-amplitude wave with a plasma: trapping, 25:56227 (CEA-CONF-1805)
Saturation and damping of echoes of electron plasma waves, 25:56226 (CEA-CONF-1804)
PERCIVAL, I. C., Excitation of highly excited hydrogenic ions and atoms by charged particles. III, 25:55839
Excitation of highly excited hydrogenic ions and atoms by charged particles. II, 25:55838
PERCUS, Jerome, Size effects in three dimensional Ising lattice, 25:57241 (NYO-1480-179)
PEREIRA, R. R., Effects of gamma irradiation on Salmonella in smoked lake whitefish, 25:55365
PEREL'MAN, T. L., Recombination decay of plasma, 25:56167
PERESLEGIN, I. A., Radiation treatment of lymphogranulomatosis of the bone, 25:55301
PERETYAKA, A. R., Catalysis by metal vapors. IV, 25:54552
PEREZ-BUSTAMANTE, J. A., Anomalous ion-exchange behavior exhibited by aged acid-free uranyl nitrate solutions, 25:54402
PERFILEV, Yu. D., Local changes in valence and structure caused by nuclear transformation in Co, Fe, I, and Te compounds, 25:56381
PERKINS, A. J., Transformations during quenching of epsilon-phase Pu--Zr alloys, 25:55528
PERRIN, C., Quasi free scattering in $^{2}$H(p,2p) and $^{2}$H(p,pn) reaction from 21.5 to 56.4 MeV, 25:56640 (FRNC-CONF-8)
PERRY, D. G., Mass-yield curve of first-chance fission from proton- and deuteron-induced fission of $^{226}$Ra, 25:56775
PERRY, K. J., High burnup performance of powder and pellet mixed-oxide fuel, 25:57045 (GEAP-10385)
PERRY, W. H., Operating experience with sodium pumps at EBR-II. EBR-II Project, 25:57028 (ANL-EBR-27)
PERTSOVSKII, N. Z., Nature of the embrittlement of two-phase titanium alloys with coarse lamellar structure, 25:55450
PESKOV, O. L., Crisis of heat transfer in pipes, 25:54869 (FEI-217)
PETER, J., Fission of medium mass nuclei induced by 167 MeV alpha particles, 25:56806
PETERS, Peter, Endolymphatic therapy with $^{131}$I-lipiodol, 25:55305
PETERSEN, V. C., Hot-salt stress-corrosion of titanium, 25:55383
PETERSON, E. W., Experimental study of the cylindrical Langmuir probe response in the transition regime, 25:56136
PETERSON, Harold T. Jr., Stable element and radionuclide reconcentration in aquatic ecosystems. I. Stable element effects in the equilibrium situation, 25:55158
PETERSON, J. Merriam, Materials for shielding nuclear radiations from plutonium processing, 25:54962 (CONF-710401-, pp 307-10)
PETERSON, K. R., Comparison of U.S. and U.S.S.R. methods of calculating the transport, diffusion, and deposition of radioactivity, 25:54782 (UCRL-51054)
PETERSON, W. K., Energy distributions of electrons ejected in ionizing collisions of electrons with helium, 25:55847
PETIT, G. Y., Gamma-ray spectra following capture of 14 MeV neutrons by $^{59}$Co, $^{93}$Nb, and $^{103}$Rh, 25:56729
PETRI, H., Combined peaksearch and peakfit in data processing of γ-spectra, 25:54472
PETRICK, W. P., Modified collision probability method for non-uniform lattices, 25:57155 (CONF-710302-(Vol.2), pp 644-54)
PETROV, V. I., Fast-neutron flux measurement in AES Novo-Voronezhskii reactors, 25:56891
PETROVICHEV, V. I., Calculation of stable heat transfer from rod bundles in longitudinal flow, 25:54883
Hydraulic drag and heat transfer in turbulent flow of liquids in triangular channels, 25:54884
PETROVSKII, E. A., Preparation of mixtures of tungsten carbide and cobalt by means of ultrasonic vibrations, 25:55598
PETSCHEK, Harry E., Collisionless shocks in plasmas, 25:56147
PETTINGER, Donald Stanley, Fluid sealing devices, 25:54845
PETUKHOV, V. A., Measurement of thermal expansion of solids at high temperatures, 25:55493
PETUSHKOV, A. A., Si(Li)-detectors for diagnosis of neoplasm of the skin, 25:55273
PETZOW, G., Grain growth in liquid-phase sintering of carbides, 25:55642
PEWITT, E. G., Superconductivity in high-energy physics, 25:56116
PFEIFER, C. J., S/sub n/ programming techniques, 25:57148 (CONF-710302-(Vol.2), pp 557-60)
PFEIFFER, B., Search for bremsstrahlung-induced fission isomers of $^{238}$U and $^{239}$Pu, 25:56801

PFEIFFER, Loren, Radiofrequency perturbation of selectively excited nuclear hyperfine levels, 25:56368
PFLASTERER, G. R., Prog. rpt. on fast oxide reactor program, 5--7/71, 25:57111 (GEAP-10010-29)
PHILLIPS, R. A., De Haas--van Alphen effect in vanadium, 25:56356
PHILLIPS, R. J. N., Regge cuts and related topics, 25:56475 (RPP/C-24)
PHILLIPS, Richard Busbee, Studies of lignin--cellulose--styrene graft copolymerization reactions, 25:54614
PIACENTINI, R. D., Rotational coupling effects on differential elastic and inelastic cross sections in $He^+$--He collisions, 25:55848
PICK, M., Solar coronal streamers observed at 169 MHz, 25:55754
PICKARD, Robert E., Tantalum radiography in otolaryngology, 25:55291
PICKEL, E., Results of ultra-sound tests on reactor pressure vessel of nuclear power station Obrigheim, 25:56892
PICRAUX, S. T., Low-temperature channeling measurements of ion-implantation lattice disorder in GaAs, 25:56289
PIERLAS, Rene, Methods of and apparatus for irradiation of articles by radioactive panels, 25:54849
PIERONI, L., Probing of an inhomogeneous plasma with electromagnetic waves, 25:56145
PIERRE, J., Moessbauer study of Dy equiatomic compounds with Cu, Ag, Zn, and Rh, 25:56382
PIERSON, William R., Ranges of recoil atoms from the (n,γ) process, 25:56269
PIETRIK, I., System of radioactive products control in gas coolant of nuclear reactors, 25:57033
PIGEON, J., Description of elastic scattering processes with the use of nonlocal separable potentials, 25:56852
  Separable nonlocal potentials and their equivalent local potentials in elastic scattering studies, 25:56642 (LYCEN-7104, C5.1-15)
PIKALOV, G. L., Photoelectric colorimeter for counting charged particle tracks on surface of glass detectors, 25:55029
PIKE, C. P., Comparison of north- and south-polar F layers, 25:56034
PILIPP, W., Analysis of electromagnetic instabilities parallel to the magnetic field, 25:56204
PILIYA, A. D., Linear transformation and absorption of a wave in a plasma, 25:56250
PILLAY, K. K. Sivasankara, Determination of mercury in biological and environmental samples by neutron activation analysis, 25:54508
PILYAVETS, V. I., Isodose distribution of a beam of positrons with an energy of 5 to 15 MeV, 25:55210
PINHEIRO, R. B., Note on prestressed concrete pressure vessel, 25:56989
PINK, Erwin, Thermally activated deformation mechanism in molybdenum and in high-temperature molybdenum alloys, 25:55455
PINKERTON, D. M., Effects of nitrous oxide and ethylene on gas yields and gel formation from γ-irradiated polypropylene, 25:54637
PIPHER, Judith L., Rocket-infrared four-color photometry of Galaxy's central regions, 25:55783
PITICU, I., Gamma x-ray angular correlation, 25:56755
PIZZICA, P. A., SAS2A LMFBR accident analysis code, 25:57077 (CONF-710302-(Vol.1), pp 120-7)
PLAKHOV, A. G., Noise levels of Langmuir oscillations in beam--plasma system, 25:56249
PLANTA, R. J., Size and location of ribosomal RNA segments in ribosomal precursor RNA of yeast, 25:55138
PLATNIEKS, I. A., Influence of transverse magnetic field on intensity profiles of turbulent velocity fluctuations in pipes of rectangular cross section, 25:55926
PLATO, Phillip, In situ measurements of environmental radioactivity, 25:55239
PLATOV, July V., Oscillations of visible chromosphere boundary and regularity in position of spicule groups along the limb, 25:55747
PLATOV, Yu. V., Heating of an inhomogeneous cosmic plasma, 25:56126
PLATOVSKIKH, Yu. A., Asymptotic behavior of neutron pulses in a hard multiplying system, 25:55017
PLESHAKOVA, G. P., Radioactive determination of oxygen in germanium and silicon, 25:54502
PLETNEV, V. P., Effect of neutron irradiation on hydrogen electrode in fuel cell, 25:54602
PLUTA, P. R., Core design development needs in relation to fuel failure propagation, sodium boiling, and clad/fuel--sodium thermal interaction, 25:57089 (GEAP-13639-2)
  Core design development needs in relation to fuel failure propagation, sodium boiling, and clad/fuel--sodium thermal interaction, 25:57088 (GEAP-13639-1)
PLYASHKEVICH, L. N., Proton beam of the ITEP accelerator for radium therapy, 25:56581 (BNL-tr-442)
PLYASHKEVICH, N. N., Debuncher of the JINR synchrophasotron injector with modulation of the accelerated beam energy, 25:56586 (JINR-P9-5956)
PNEUMAN, G. W., Rotation of magnetic loop systems in the solar atmosphere, 25:55743
PNIEWSKI, J., Λ-excited states of hypernuclei, 25:56524
PODGORNYI, I. M., Experiments with artificial solar wind, 25:56009
PODGORNYI, V. N., Performance in recording of x- and gamma-rays by combined detectors, 25:55005
PODSEVALOV, Yu. N., Dose function of a plane infinitely thin source situated on the dividing boundary between two media, 25:55233
PODZOROVA, E. A., Kinetics of the low-dose radiolysis of concentrated aqueous acidic solutions of sodium nitrate, 25:54657
POE, Robert T., Polarized-orbital method and application to scattering of electrons by He, 25:55871
POENARU, D. N., FORTRAN programs for Ge(Li) detector time characteristics, 25:55001 (NP-19011)
POGREBNYAK, V. A., Propagation of strong cylindrical and spherical electromagnetic waves in a plasma, 25:56240
POHLIT, Helmut M., Hot-atom chemistry of $^{14}C$ in solid benzene at kinetic energies between 5 and 100 electron volts, 25:54703
  Partial degradation of 1,3,5-cycloheptatriene-$^{14}C$ obtained from hot-atom, photolytic, and thermal reactions, 25:54702
POIRIER, C. P., Beta--gamma correlations and matrix elements for some first-forbidden nonunique beta transitions, 25:56776
POKROVSKII, V. N., Probability of the ($\mu^-$, $\nu$) process of $^{139}La$ and $^{208}Pb$ nuclei, 25:56739 (JINR-P1-6006)
POLAK, H. L., Radiometric titration method based on separation by ion-exchange. IV, 25:54448
POLCYN, Robert E., Pancreas imaging: is it worth it, 25:55280
POLESYA, A. F., Kinetics of the decomposition of binary and ternary solid solutions of aluminum with chromium obtained by quenching the alloys from the molten state, 25:55448
POLETAEV, E. D., Measurement of the ratio of the radiative capture to fission cross sections (α) for $^{239}Pu$ in the neutron energy range 0.1 to 30 keV, 25:56734 (BNL-tr-446)
POLKINGHORNE, J. C., Dual quark--parton model and high energy hadronic processes, 25:56481
POLOSHKIN, Yu. V., Surface layer of surface-hardened parts of heat-resisting alloys, 25:55439
POLUBOYARINOV, D. N., Sintering and properties of yttrium oxide ceramics, 25:55606
POLUBOYAROVA, P. A., Dependence of the beam shape in the centre of the synchrocyclotron on the accelerating voltage and magnetic field decay, 25:56585 (JINR-P9-5945)
POLYANSKII, V. N., Inelastic scattering of γ particles on Zn isotopes, 25:56726
POLYUDOV, A. N., Autoionizing states in helium-like ions, 25:55820
POLZER, W. L., Solubility of plutonium in soil/water environments. A theoretical study, 25:54756 (CONF-710401-, pp 411-29)
POMERANTZ, M. A., Unusual anisotropic solar-particle event of November 18, 1968, 25:55764
PONNAMPERUMA, Cyril, Effect of ionizing radiation and uv light on N-acetylglycine, 25:54650
PONOMAREV, L. A., Analysis of the reaction np → pp $\pi^-$ from the point of view of Reggeized OPE model, 25:56521 (JINR-P1-5975)
PONOMAREVA, L. F., Study of alloys belonging to $NiAl_3$--$VAl_3$ and $Ni_2Al_3$--$V_5Al_8$ sections, 25:55562
POOLE, A. G., Radiolytic reaction between graphite and $CO_2$. II, 25:55654
POOLE, Charles P. Jr., Influence of nuclear Zeeman term on anisotropic hyperfine patterns in electron spin resonance, 25:54641
POOLE, John W., Radiation measurements and low frequency and high-pressure investigations of induction heated plasma, 25:56146 (N-71-27023)
POPESCU, H. I., Cytogenetic investigation of industrial workers occupationally exposed to gamma rays, 25:55163
POPIELSKA, E., Readout electronics for $\pi^-$e experiment at 50 GeV, 25:55044 (JINR-E1-5818)
POPIELSKI, W., Readout electronics for $\pi^-$e experiment at 50 GeV, 25:55044 (JINR-E1-5818)
POPIL'SKII, R. Ya., High temperature ceramics from scandium oxide, 25:55620
POPOV, V. A., Debuncher of the JINR synchrophasotron injector with modulation of the accelerated beam energy, 25:56586 (JINR-P9-5956)
POPOV, V. I., Coefficient of electromagnetic ejection of solids from conducting fluids, 25:55930
  Dynamics of liquid-metal drops in electromagnetic field in conditions of reduced gravitation, 25:55931
POPOV, Yu. P., Alpha widths of neutron resonances, 25:56754 (UCRL-Trans-10541)
  Electric network calculations in problems of magnetohydrodynamics, 25:55943
  Search for the (n,α) reaction in the resonances of the zinc and hafnium isotopes, 25:56686 (JINR-P3-5875)
POPOVA, G. Yu., Impurity paramagnetic center in γ-irradiated salts, 25:56339
POPP, M., Nuclear spectroscopic studies on $^{18}O$, 25:56672
PORDES, Maurice, Treatment of elastomers, 25:54619
PORTELA, Adolfo, Radiation effects on water permeability and distribution in frog muscle cells, 25:55323
POSPELOV, K. S., Properties of welded joints in V92Ts alloy, 25:55470
POST, J. C., Decay of $^{238}Am$, 25:56792

XUM

POST, Joseph, Prog. rpt. on effects of $^{3}H$-thymidine as a DNA label in rat liver, 25:55110 (TID-25801)
POSVOL'SKII, M. V., Quaternary ammonium bases as analytical reagents. II, 25:54434
POTANIN, E. P., Rotation of electrically conducting fluids in crossed electric and magnetic fields, 25:55938
POTTER, D. E., Explicit magnetohydrodynamic calculations in the R--Z plane, 25:56188
POTTER, William, Effects of ionizing radiation on potassium hydrogen malonate, 25:54654
POWELL, G. L., Instrument for measuring the hydrogen content of metals, 25:54424
POWELL, Gordon W., Reaction diffusion in the silver--zinc and silver--aluminum systems, 25:57238 (MLM-OP-71003)
POWER, R. A., Simultaneous observation of proton precipitation and auroral radar echoes, 25:55963
POWERS, J. R., Is the first excited $0^{+}$ state in $^{44}Ca$ of 6p-2h character, 25:56714
Spin assignments in $^{20}F$, 25:56716
PRADE, H., Level scheme of $^{177}Lu$ in reaction (n,$\gamma$), 25:56762
PRATA, Stephen W., Series of related active regions during January 14--June 1, 1969, 25:55753
PRATT, R. H., Exact screened calculations of atomic-field pair production and low-energy screening, 25:56275
PREMOLI, A., Density measurements of steam--water mixtures flowing in a tubular channel under adiabatic and heated conditions, 25:57032
PRENTICE, J. D., Regge analyses of rho$^{0}$ production in $\pi N$ charge exchange channels at 7 GeV/c, 25:56431
PRESSMAN, A. Ya., Distribution of radioactivity in rocks and petroleum from contained nuclear explosions, 25:54826 (UCRL-Trans-10543, pp 99-116)
PRETORIUS, R., Alpha activation of calcium and its possible use for analysis, 25:54522
PRICE, Stephan Donald, Quantitative interpretation of the infrared spectra of late-type stars, 25:55698
PRIGENT, Raymond, Electrical equipment for measuring small currents. Applications to dosimetry using classical ionization chambers, liquid dielectric ionization chambers, and electric charge measurements in connection with aerosol studies, 25:55071 (CEA-N-1433)
PRIKHOD'KO, V. A., Determination of the relative difference between the mobilities of isotopic lithium ions in an ion-exchange resin--solution system, 25:54730
PRIKHOZHENKO, E. Ya., Cytogenetic effect of repeated x-irradiation and storage of wheat seeds, 25:55169
PRIMA, S. B., Cross section of Mo--Zr--Cr system at 1150°C, 25:55538
PRINZ, D. K., Ogo-4 observations of Lyman--Birge--Hopfield emission in day airglow, 25:55968
PRIOR, W., Vorticity and neutrons in the plasma focus, 25:56157
PRITCHARD, J. A., Evaluation of respirator performance by DOP man test, 25:55243 (CONF-710401-, pp 392-406)
PRITCHIN, B. P., Interpreting $\gamma$-measurements of exogenous epigenetic U deposit, 25:54808
PROKOPEC, J., Detection of alpha-radionuclides in the bone--marrow and blood of miners by the method of nuclear emulsions, 25:55236
PROKOPENKO, V. S., Inelastic proton scattering by intermediate-weight nuclei, 25:56727
PROKOPETS, Yu. S., Measurement of the ratio of the radiative capture to fission cross sections ($\alpha$) for $^{239}Pu$ in the neutron energy range 0.1 to 30 keV, 25:56734 (BNL-tr-446)
PROKS, C., Primary carcinoma of thyroglossal duct, 25:55304
PROKSCH, E., Dosimetry by means of formation of radiolytic gases from fluorocarbons, 25:55053
PRONKO, P. P., Proton radiation damage and recovery in Ta films, 25:56314
PRONMAN, I. M., Development of a fast-neutron activation method for determination of N in Nb, Ta, and Ti, 25:54501
PRONO, Daniel Steve, Measurement of the ion energy distribution resulting from the turbulent heating of a plasma, 25:56131
PROSHIN, V. V., Neutron-activation analysis of Ca, P, and Na in bones, 25:55106
PROSPERI, D., Method of analysis of neutron capture gamma-ray spectra, 25:56690 (RT/FI-(70)47)
PROTOP, C., Nuclear structure effects in the internal conversion of some magnetic dipole transitions in deformed nuclei, 25:56756
PROTOPOPOVA, E. M., Premutational oxygen-sensitive changes of chromosomes induced by irradiation of seeds, 25:55168
PRUCHNIK, Florian, Radioisotopic exchange of ligands in chloro- and thio-cyanatomolybdates(III), 25:54558
PRUNIER, J. F., Use of liquefied noble gases, 25:55028
PRYAKHIN, Yu. F., Si(Li)-detectors for diagnosis of neoplasm of the skin, 25:55273
PRYAKHINA, L. I., Study of alloys belonging to $NiAl_3$--$VAl_3$ and $Ni_2Al_3$--$V_5Al_8$ sections, 25:55562
PSAREV, V. I., Non-equilibrium solidification and structural transformations during heating in aluminum-molybdenum and aluminum--chromium alloys, 25:55535
PSHITULA, M., Alpha widths of neutron resonances, 25:56754 (UCRL-Trans-10541)
PUCHEROV, N. N., Polarized particle sources, 25:56610
PUFF, Hans-Juergen, Separation of mercury from solutions by means of mercuration reactions, 25:54499
PULHAM, R. J., Electrical resistivity of liquid K and of solutions of Na liquid K, 25:55527
Equilibrium between sodium hydrogen acetylide and disodium acetylide, 25:54537
Sodium--barium phase diagram, 25:55526
PUPPINI, G., Uses of computer in radiotherapy. III, 25:55218
PURI, B. K., Polarographic determination of Cd, Pb, Ni, Tl, and U(VI) in isoquinoline formate, 25:54421
PURVIS, A. E., Comparison of airborne spectral gamma radiation data with field verification measurements, 25:54768
PUSTYINIK, B. I., Elastic scattering of heavy ions by nuclei, 25:56740 (JINR-P7-5884)
PUTTERMAN, S. J., Vortex-free Landau state in rotating superfluid helium, 25:56048
PYATOV, N. I., Collective $1^{+}$ states in even--even deformed nuclei, 25:56819 (JINR-P4-5889)
PYLE, R. V., Multiple aperture extractor design for producing intense ion and neutral beams, 25:56213 (LBL-327)
PYLE, Robert V., Dissociation cross sections for 0.5- to 1-MeV $HeH^{+}$ ions in $H_2$, He, $N_2$, and Ne gases, 25:55872

## Q

QUAADVLIET, W. H. J., Experimental study of the neutron attenuation in concrete shields for fast and thermal reactors, with the aid of simulated concrete configurations, 25:57027 (RCN-147)
QUEMENEUR, A., Interaction of a large-amplitude wave with a plasma: trapping, 25:56227 (CEA-CONF-1805)
Saturation and damping of echoes of electron plasma waves, 25:56226 (CEA-CONF-1804)
QURESHI, I. H., Simultaneous determination of Sb, As, and Cu by neutron activation, 25:54515
QURESHI, Mohsin, Quantitative separation of magnesium and palladium from numerous metal ions on titanium tungstate papers by electrochromatography, 25:54744

## R

RAABE, O. G., Physical and chemical characteristics of aerosols produced from solutions of polyvalent metallic nuclides, 25:54545
RAABE, Otto G., Estimation of the relative inhalation hazard of reactor inventory radionuclides, 25:55202
RAADU, M. A., Topology of filaments and chromospheric fibrils near sunspots, 25:55749
RAAS, Eugene Richard, Two methods for calculating electronic correlation energies, 25:55890
RABBANI, B. A., L x-ray transition probabilities in elements with Z greater than or equal to 57, 25:55823
RABOTNOV, N. S., Probability of electromagnetic quadrupole transitions in the phenomenological nuclear theory, 25:56735 (FEI-202)
RACHKOVSKII, E. E., Isotope exchange in system $H_2$--$H_2O$ on some oxide catalysts, 25:54554
RACK, E. P., Reactions of iodine with olefins. II. Radiative neutron capture induced reactions of $^{128}I$ with various $C_5$ isomers: evidence for a mechanism other than autoradiolysis in the condensed state, 25:54705
RADAK, B., Spectrocalorimetric measurements in core of heavy water reactor, 25:57123
RADCLIFFE, J. M., Some properties of coherent spin states, 25:56451
RADLOWSKI, Cecilia, Mechanism of the radiation-induced dechlorination of 1,1,1-trichloro-2,2-bis(p-chlorophenyl)ethane in alcholic solution, 25:54620
RADOSEVIC, J., Solvent extraction study of lanthanum and europium by acidic esters of aminophosphonic acids, 25:54732
RAEVSKII, I. I., Superconducting properties of niobium--titanium--zirconium hafnium alloys, 25:56104
Superconductive properties of niobium--zirconium--hafnium alloys, 25:56105
RAFAL'KES, I. S., Carbon black formation in the thermal decomposition of hydrocarbons, 25:57278 (SC-T-713066)
RAFFO, Peter L., Creep behavior of electron beam-melted rhenium, 25:55432 (N-71-23114)
Creep behavior of electron-beam-melted rhenium, 25:55491
RAGHAVAN, P., Nuclear quadrupole interaction in cadmium metal, 25:56363
RAGHAVAN, R. S., Nuclear quadrupole interaction in cadmium metal, 25:56363
RAGLAND, P. C., Rare earth abundances in mesozoic dolerite dikes from eastern United States, 25:54476
RAHMEL, A., Electrochemical investigations on the corrosion of metals in alkali metal sulfate and vanadium pentoxide melts, 25:55373 (CONF-690452-, Paper 6)
RAHN, K., Diurnal variation of aerosol trace element concentrations in Livermore, Calif, 25:54456
RAISBECK, G., Electron capture by 40-, 155-, and 600-MeV protons in thin foils of Mylar, Al, Ni, and Ta, 25:55862
RAJ, R., Reaction matrix elements and structure calculations with the Yale and Reid potentials for the

Ni region, 25:56857
RAJARAMAN, R., Some consequences of exchange degeneracy and tripe-Regge-hypothesis, 25:56515
RAJPUT, J. S., Volume dependence of transition temperature and effective interaction strength in tin, 25:56103
RAJU, M. R., Induction of heteroallelic reversions and lethality in Saccharomyces cerevisiae exposed to radiation of various LET ($^{60}$Co γ rays, heavy ions, and π⁻ mesons) in air and nitrogen atmospheres, 25:55165
RAKHMATULINA, A. Kh., Scattering problem under a non-monotonic potential for the classical case, 25:56572
RALKOVA, J., Plant project for fixation of radioactive wastes into bitumen, 25:54981
RALSTON, H. R., Diurnal variation of aerosol trace element concentrations in Livermore, Calif, 25:54456
RAMACHANDRAN, A., Onset of free convection in annuli, 25:54881
RAMAKRISHNA, G., Effect of hexadecapole deformation on the ΔN = 2 crossing of the Nilsson orbitals, 25:56858
RAMAKRISHNAN, Alladi, Para-Fermi operators and special unitary algebras, 25:56536
RAMANIAH, M. V., Indirect potentiometric method for the determination of plutonium, 25:54411
RAMA RAO, I., Hydrodynamics of Bose fluid in terms of action-angle variables in quantum statistics, 25:56051
RAMASASTRY, C., Thermoluminescence of x-ray-irradiated KBr and KBr:Cu crystals, 25:56323
RAMCHANDRAN, Shantakumari Thattat, Effects of sheath and driving field on Tonks--Dattner resonance frequencies, 25:56252
RAMONDA, G., Hot tritium reactions in $CH_4$ + $SiH_4$ system, 25:54678
RAMQVIST, Lars, New tungsten powder for producing carbides, 25:55412
RAMSDELL, J. V. Jr., Atmospheric tracer technique employing $^{85}$Kr and use of this technique in defining puff dimensions and transport speed, 25:54908
RAMSEY, N. F., Molecular-beam magnetic-resonance studies of HD and $D_2$, 25:55826
RAMZAEV, P. V., Effectiveness of a number of chemical substances in poisoning with a mixture of radioisotopes of cesium and strontium, 25:55113
RANDALL, P. N., Gross strain crack tolerance of steels, 25:55514
RAO, A. L. J., Polarographic determination of Cd, Pb, Ni, Tl, and U(VI) in isoquinoline formate, 25:54421
RAO, A. V. Ramana, Electronic conduction in yttria-doped thoria solid electrolyte, 25:56335
RAO, B. Ramachandra, Dependence of the ionospheric absorption on lunar phase, 25:55975
RAO, C. L., Indirect potentiometric method for the determination of plutonium, 25:54411
Nuclear charge dispersion of light-mass elements in fission of $^{232}$Th, 25:56805
RAO, K. V. S., Formation of ozonide ions in γ-irradiated aqueous solutions of alkali hydroxides, 25:54608
RAO, N. Venkateswara, Triphenylmethane dyes as redox indicators in dichrometry, 25:54410
RAO, U. R., Anosotropy characteristics of low-energy cosmic-ray population of solar orgin, 25:55763
RAO, V. Ramachandra, Studies on yttrium, thorium, and uranium salicylaldehyde complexes, 25:54539
RAPEANU, S., SCAT: code for computing scattering cross section of light and heavy water, 25:56638
RAPP, O., Low-temperature specific heat measurements of $ZrV_2$ and $HfV_2$, 25:56072
RAPPENEAU, J., Electronic and magnetic properties of carbon fibers: development under neutron irradiation, 25:56282 (CEA-CONF-1822)
Influence of speed of graphitization of carbon products on dimensional variations produced by neutron irradiation, 25:55645 (CEA-CONF-1821)
Interactions among various carbons in the course of heat treatment, 25:57275 (SC-T-713060)
Thermal annealing of neutron-irradiated carbon, 25:56283 (CEA-CONF-1823)
RASBAND, S. N., Lense-Thirring type gravitational forces between disks and cylinders, 25:55807
RASMUSSEN, Howard, Cellular basis of mammalian calcium homeostasis, 25:57244 (NYO-3489-22)
RASPOPIN, S. P., Precipitation of uranium from a melt of fused halides with a molten zinc cathode, 25:54580
Thermodynamic properties of cerium in molten zinc, 25:55442
RATLIFF, G., Large-scale refrigeration systems for 1.0 to 1.85°K, 25:56117
RATNAM, V. V., Nuclear materials and some aspects of machining, 25:57207
RAY, W. E., Sodium technology program progress report for the period ending May 31, 1971, 25:55379 (WARD-4210-T-1-2)
RAYLE, Warren D., Deuterium--$^3$He fusion power balance calculations, 25:56215 (N-71-25526)
RAYMUND, Mahlon, PSYCHE: physics checking of the ENDF/B evaluated nuclear data file, 25:57174 (CONF-710302-(Vol.2), pp 1004-15)
RAYNAL, J., Deformations in the s--d shell and inelastic scattering of polarized protons, 25:56828 (LYCEN-7104, S9.1-7)
Spin--orbit interaction in nucleon inelastic scattering, 25:56826 (LYCEN-7104, C7.1-36)
RAYSKI, J., Formulation of quantum field theory in terms of tempered distributions and a possible departure from the principle of superposition, 25:56544 (IC-71/71)
RAZANI, Arsalan, Three-dimensional stochastic gamma-ray transport method for shielding calculations, 25:56273
RAZMI, M. S. K., Coupling constants in (A,rhow) system and helicity conservation, 25:56488
RAZORENOV, L. A., Nature of the radiation background at altitudes of 250 to 500 km, 25:56008
REAVEY, T., Liquid waste effluents from a nuclear fuel reprocessing plant, 25:54753
REBEL, H., Investigation of the deformation of light nuclei with the help of scattering of 104-MeV, 25:56687 (KFK-1397)
REBELLER, Michel, Decoloring Cyanophycene algae by extraction of their pigments, 25:57236 (LA-tr-71-73)
RECAMI, E., Black-body radiation and generalized theory of physical dimensions, 25:56453 (ORO-3992-42)
REED, Wm. H., Non-iterative method for time dependent transport, 25:57157 (CONF-710302-(Vol.2), pp 679-700)
REEDER, Paul L., Delayed neutrons from tau- and α-induced fission of $^{238}$U, $^{232}$Th, and $^{209}$Bi, 25:56803
REES, P. M., TRESS: a finite element code for stress analysis problems, 25:57285 (TRG-Report-1813)
REEVES, H., Recent developments in the history of the nucleosynthesis of the solar system, 25:55781
REGAN, R. D., Titanium P/M preforms, parts, and composites, 25:55415
REGIBEAU, A., Liquid scintillation applications in radioprotection, 25:55217
REGNAUT, Christian, Improvements to the planar electrostatic analyzer for slow electrons, 25:55072 (FRNC-TH-54)
REICH, Volker, Measurement program and calibration standards for microstrip measurements with an automatic network analyzer, 25:57279 (SC-T-713067)
REICHEL, Werner, Arc erosion of various sintered and infiltrated WCu-materials in oil, 25:55454
REICHMAN, S. H., New developments in superalloy powders, 25:55416
REID, Cyprian B., Radiation exposure to personnel during cardiac catheterization, 25:55226
REID, Neal E., Brueckner--Hartree--Fock calculations using density-dependent effective interactions, 25:56834 (ORO-3765-32)
REINHARDT, J., Resonance phenomena in low-energy-electron-impact excitation of He, 25:55851
REINMANN, John J., Deuterium--$^3$He fusion power balance calculations, 25:56215 (N-71-25526)
REINOV, N. M., Quality factor of superconducting lumped-parameter circuits, 25:55086
REITMANN, D., Energy levels of $^{79}$Br and $^{81}$Br, 25:56698
REKHKOLAINEN, G. I., X-ray spectral determination of La, Ce, Pr, and Nd in intermediate products of rare earth production, 25:54417
REM, J., Temperature profile in thermonuclear reactor, 25:56216 (NP-19014)
REMPLIK, V., Investigations on tumor localization using $^{67}$Ga, 25:55283
RENBERG, P. U., (p,2p) reactions at 600 MeV, 25:56711
RENTON, P., Analysis of K+/sub e3/ radiative decay, 25:56410
RENZI, R., Dose distribution surrounding a sealed linear radium source, 25:54923
Dosimetry of fast electron beams, 25:55224
REPELLIN, P.-P., Interference between π⁰π⁰ decay of K/sub L/⁰ and K/sub S/⁰, 25:56407
REPKO, Wayne W., Hyperfine structure of positronium, 25:55832
RETEL, J., Size and location of ribosomal RNA segments in ribosomal precursor RNA of yeast, 25:55138
REY, Christian A., Control point design using modular logic, 25:57224 (COO-2118-14)
REYNOLDS, Geo. T., Prog. rpt., 1971, 25:57243 (NYO-3406-22)
REYNOLDS, L. D., CONCEPT: computerized conceptual cost estimates for steam--electric power plants. Phase I user's manual, 25:57063 (ORNL-TM-3276)
REZNIK, A. M., Secondary emission of W+ ions during bombardment of W by ions of alkali metals, 25:55819
REZNIKOV, G. P., Recombination and detection of the three-atom ion in a helium plasma at low temperatures, 25:56161
REZUKHINA, T. N., Thermodynamic properties of laves phase $TaFe_2$, 25:55508
RHEE, S. K., Cyclic oxidation of TD--Ni, 25:55387
RHINES, F. N., Prog. rpt. on quantitative determination of structure-property relationships in nuclear fuel element materials, 12/16/70--3/15/71, 25:55437 (TID-25784)
RIAZUDDIN, S., Effect of γ radiation on donor ability of Escherichia coli, 25:55358
RIBANSKY, I., Isomeric cross-section ratios analysis of $^{136}$Ba(α,n)$^{137}$Ce reaction, 25:56765
RIBAROV, S., Effect of reactor-neutron irradiation of SiC varistors, 25:55103
Gamma-radiation-induced desorption of gas from SiC varistors, 25:55102
RIBE, F. L., Energy storage and switching with superconductors, 25:56110 (LA-DC-12990)
RICE, J. R., Progress in three-dimensional elastic--plastic stress analysis for fracture mechanics, 25:55515

XUM

RICHARDS, C. P., Evaluation of respirator performance by DOP man test, 25:55243 (CONF-710401-, pp 392-406)
RICHARDS, D., Excitation of highly excited hydrogenic ions and atoms by charged particles. II, 25:55838
Excitation of highly excited hydrogenic ions and atoms by charged particles. III, 25:55839
RICHARDSON, E. W., Additional testing of ten-ton uranium hexafluoride cylinders, 25:54970 (KY-631)
RICHARDSON, Gerald L., Integrated lanthanide--actinide solvent extraction process, 25:54706 (BNWL-SA-3345)
RICHARDSON, Riley Porter, Electron paramagnetic resonance studies of tetravalent neptunium in single crystal thorium oxide, 25:56383
RICHMOND, P. M., Use of interactive computer graphics in high-energy physics, 25:55093
RICHTER, D., Quantitative analysis of the Q-subdwarf HD 49798, 25:55682
RICHTER, K., Effect of nickel on the sintering and self diffusion of tungsten, 25:55426
RICHTER, Malgorzata, Analytical uses of lanthanide nitrite complexes. II, 25:54415
RICKER, George R., X rays from new variable source: GX 1 + 4, 25:55720
RIDGWAY, K. R., Administrative procedures for criticality prevention in plutonium operations, 25:54966 (CONF-710401-, pp 430-7)
RIDOUT, Edmund Umfreville, Improvements in or relating to hopper feeders, 25:54841
RIEDEL, H.-J., Treatment of nuclear fuel and breeder materials in oxidizing alkali metal salt melts, 25:55376 (CONF-690452-, Paper 9)
RIEM, R. H., Flash photolysis of a substituted hexaarylbiimidazole and reactions of the imidazolyl radical, 25:54561
RIEMAN III, William, Ion exchange in analytical chemistry, 25:54397
RIGAUD, F., Gamma-ray spectra following capture of 14 MeV neutrons by $^{59}$Co, $^{93}$Nb, and $^{103}$Rh, 25:56729
RILEY, P. J., $^{86}$Kr(d,n)$^{87}$Rb/sup A/ threshold cusp and the systematic appearance of charge-exchange cusps, 25:56719
RIPLING, E. J., Crack arrest toughness of pressure vessel steels, 25:55513
RISTINEN, R. A., $^{28}$Si($^{3}$He,2p) and $^{12}$C($^{3}$He,2p) reactions at 40 MeV, 25:56713
RITTER, J. C., Resonance neutron capture by $^{170}$Yb and $^{172}$Yb, 25:56802
RITUS, V. I., Theory of reaction between polarized particles and gamma-quanta, 25:56454
RIVIER, Janine, $^{107}$Cd excited levels, 25:56759
RIVIERE, A. C., Hot-cathode ionization gauges for use in a magnetic field, 25:56141
RIZZIE, J. W., Equipment for remote measurement of bow, length, and weight of irradiated experimental capsules and elements at EBR-II. EBR-II Project, 25:57054 (ANL-EBR-30)
ROBBA, A. A., Instituting a neutron spectrum unfolding capability, 25:55038 (LA-DC-12314)
ROBERTS, J. T. A., Brittle-to-ductile transition in $UO_2$--20 wt. percent $PuO_2$ nuclear fuel, 25:55610
ROBERTS, K. V., Explicit magnetohydrodynamic calculations in the R--Z plane, 25:56188
GALAXY: a system for 2D many-body calculations, 25:56187
TRINITY: programs for 3D magnetohydrodynamics, 25:55944
ROBERTS, Thomas G., Simple solid-electrolyte gamma-ray and relativistic-charged particle dosimeter, 25:55054
ROBERTSON, A., Remote-readout balance for use in a highly radioactive environment, 25:55080 (TRG-Report-2086)
ROBERTSON, D. E., Influence of the physico-chemical forms of radionuclides and stable trace elements in seawater in relation to uptake by the marine biosphere, 25:55149 (BNWL-SA-4048)
ROBERTSON, R., Neutron activation analysis for aluminum in animal tissue, 25:54514
ROBINS, K. E., Recent developments in pulsed magnet multifilament superconducting wires, 25:56580 (BNL-16026)
ROBINSON, B. J., OH absorption in the direction of W44, 25:55716
ROBINSON, David Allan, Electron--phonon interaction in normal and superconducting states of high-purity rhenium, 25:56097
ROBINSON, David W., Management of radionecrosis, 25:55270
ROBINSON, H. N., Performance of high efficiency particulate air filter for fume from burning plutonium metal, 25:54951 (CONF-710401-, pp 181-202)
ROBKIN, M. A., In-phantom microdosimetry with 14.6 MeV neutrons, 25:55232
ROBOUCH, B. V., Radiative recombination of hydrogenic ions in high temperature plasmas, 25:56164 (LGI-71/1/E)
ROCCHESANI, Jean, Shielding problems set by use of natural U target with linear electron accelerator. Shielding and safety systems necessary, 25:56582 (CEA-R-4188)
ROCHLIN, G. I., Externally shunted Josephson junctions: generalized weak links, 25:56094
ROCOPLAN, Jean Antoine, Projector for radioactive sources used in plesiotherapy for nonradioactive preparation technique, 25:54902
RODBARD, David, Mathematical analysis of kinetics of radioligand assays: improved sensitivity obtained by delayed addition of labeled ligand, 25:55145
RODIES, Heinz-Juergen, Optical constants of β-phases NiIn, PdAl, NiGa/sub 1-y/Al/sub y/, and (Ni,Cu)Ga, 25:56352
RODINE, Elward T., Electronic defect structure of single-crystal $ThO_2$ by thermoluminescence, 25:56315
ROELOF, E. C., Low-energy (greater than or equal to 0.3 MeV) solar-particle observations, 25:55956
ROEPER, Peter, Single particle states in a deformed energy-different nucleus potential, 25:56837 (UCRL-Trans-10544)
ROESCHERT, G., Spectroscopy of $^{93}$ $^{95}$Tc, 25:56766
ROESICK, U., Determination of the trace element distribution in coexisting calcite and dolomite by neutron activation analysis, 25:54497
ROESSLER, C. E., Ecological approach to environmental surveillance, 25:55238
ROGAUSCH, Klaus-Dieter, Solid solution hardening in tantalum alloys, 25:55457
ROGGE, M., $^{31}$P($^{3}$He,pγ)$^{33}$S and $^{39}$K($^{3}$He, pγ)$^{41}$Ca reactions and the γ decay of analog states in $^{33}$S and $^{41}$Ca, 25:56715
ROGNLIEN, T. D., Ion-acoustic instability of two-temperature, collisional, fully ionized plasma, 25:56251
ROHAN, P. E., Network organization of an automated nuclear design system, 25:57146 (CONF-710302-(Vol.1), pp 516-30)
ROKITSKII, P. F., Problems in radiobiology, 25:55134
ROLINSKI, Edmund J., Determination of thermodynamic interaction parameters in solid V--Ti alloys using the mass spectrometer, 25:55489
ROLLAR, H.-G., Infrared spectra and vapor pressure isotope effect of crystallized ammonia and its deuterium derivatives, 25:54572
ROLLEFSON, A. A., Comparison of the nuclear-reaction energy scale with the gamma-ray energy scale, 25:56773
ROMAN, Herschel, Induced recombination in mitotic diploid cells of Saccharomyces, 25:55180
ROMANINI, A., Radioisotope scanning with $^{75}$Se-selenomethionine in the morphological and functional study of the pancreas, 25:55271 (LB/G-3059)
ROMANO, F., Analysis of K$^{+}$/sub e3/ decay X2, 25:56409
Analysis of K$^{+}$/sub e3/ radiative decay, 25:56410
ROMANOV, V. S., Reparation of stable isotopes for scientific research purposes, 25:54899
ROMANOVSKII, S. V., Polarized particle sources, 25:56610
ROMBERG, E. F., Elastic scattering of 60 to 120 MeV electrons from $^{46}$ $^{48}$ $^{50}$Ti, 25:56701
ROMERIL, M. G., Uptake and distribution of $^{65}$Zn in oysters, 25:55153
ROMODANOV, V. L., Interference of ''black'' absorbers in moderating medium, 25:57205
Measurement of ''black'' absorbers of equivalent sizes and identical efficiency in a moderating medium by a pulsed-source technique, 25:57206
RONAMI, G. N., Mutual diffusion of ruthenium with niobium and zirconium, 25:55452
RONNE, B. E., Automatic selection of kinematical hypotheses from two prong proton--proton interactions in a hydrogen bubble chamber at 19 GeV/c, 25:56523 (USIP-71-3)
ROSE, K. S. B., Coated particle fuels, 25:57052
ROSE, R. M., Investigation of superconducting-energy-gap behavior of single-crystal rhenium by tunneling, 25:56067
ROSENBERG, Norman W., Observations of striation formation in a barium ion cloud, 25:56033
ROSENBERG, R. L., North--south component of interplanetary magnetic field: Explorer 33 and 35 data, 25:55779
ROSENDHAL, Jeffrey D., Light variations in supergiants in LMC, 25:55705
ROSENFELD, W., $^{167}$Tm: a new bone scanning agent, 25:55279
ROSENSTEIN, L. M., Photon asymmetry for radiative μ capture in Ca, 25:56705
ROSENTHAL, C. M., Reduction of multi-dimensional Schroedinger equation to one-dimensional integral equation, 25:56398
ROSINSKII, S. E., Problems of injection of relativistic electron beams into plasma, 25:56166 (NP-19012)
ROSS, W. J., Application of an iodide-specific resin to the determination of iodine in biological fluids by activation analysis, 25:54509
ROSSBERG, L., Pre-midnight asymmetry in 40-keV electron flux profiles, 25:56045
ROSTOKER, Gordon, Development of the polar electrojet during polar magnetic substorms, 25:56029
Localized character of magnetotail magnetic fluctuations during polar magnetic substorms, 25:56040
ROSWIT, Bernard, Radiation exposure to personnel during cardiac catheterization, 25:55226
ROTHHARDT, L., Magnetoplasmadynamic experiments in inductive-hydrodynamic shock wave tubes, 25:55920
ROTHMAN, A. B., Analysis of fuel failure experiments with TREAT, 25:57110 (CONF-710302-(Vol.1), pp 97-101)
ROUGE, Andre, Investigation of strange meson resonances produced in association with nucleon in 3 GeV K-nucleon interactions, 25:56426 (FRNC-TH-53)
ROUSE, Carl A., Calculation of stellar structure. II, 25:55751
ROVINSKII, B. M., Development of micropores in alloys, 25:55462
ROWLAND, F. S., Relative rates of hydrogen atom abstraction

by near-thermal $^{18}F$ atoms, 25:54686
ROWLANDS, C. M., Visual sensations produced by cosmic ray muons, 25:55341
ROY, D., Electrostatic spectrometer. III, 25:55084
ROY, J.-Rene, Models for envelopes of Be stars. III, 25:55709
ROY, Ranendra Kumar, Quantum lattice-gas model of liquid $^3He$, 25:56058
ROYER, E., Functional and circulatory changes in rats after local irradiation, 25:55328
ROYER, J. M., Energy and angular distributions of $^{60}Co$ gamma rays penetrating a concrete shield, 25:56272
ROZANTSEV, I. N., Certain states of $^{134}Cs$, 25:56784
ROZENTAL, I. L., Cosmic muons and neutrinos, 25:56469
RUBIN, Arnold D., Control of lymphocyte growth in response to phytohemagglutinin stimulation, 25:57284 (TID-25802)
RUBIN, Philip, Comment: radiosensitization and the selective effect, 25:55265
RUBIN, R. H., Microwave detection of interstellar formamide, 25:55784
RUBIN, R. M., Energy and angular distributions of $^{60}Co$ gamma rays penetrating a concrete shield, 25:56272
RUBINOVA, E. E., Oscillations of photocurrent in Ge with radiation defects, 25:56316
RUBINSHTEIN, R. N., Calculation and optimization of the demineralization of water for reactors by ion exchange, 25:54737
RUBY, S. L., Internal-conversion coefficients in decay of /sup 83m/Kr, 25:56708
RUDAKOV, E. S., Broensted type equation for solvolysis of tert-butyl halides under action of metal ions, 25:54548
RUDER, H. J., Mathematical analysis of kinetics of radioligand assays: improved sensitivity obtained by delayed addition of labeled ligand, 25:55145
RUDNICK, I., Vortex-free Landau state in rotating superfluid helium, 25:56048
RUDY, Clifford Robert Jr., Heavy ion emission from light nuclei, 25:56659
RUEDIGER, D., Composition and properties of the binder metal in cobalt bonded tungsten carbide, 25:55630
RUKHADZE, A. A., Excitation of longitudinal electromagnetic waves in a bound plasma during injection of relativistic electron beams, 25:56232 (NP-19020)
Problems of injection of relativistic electron beams into plasma, 25:56166 (NP-19012)
RUMI, R. F., Alpha widths of neutron resonances, 25:56754 (UCRL-Trans-10541)
RUMMERFIELD, P. S., Health physics aspects of $^{133}Xe$ lung studies, 25:55248
RUNFORS, Ulf, Influence of powder characteristics on process and product parameters of uranium dioxide, 25:55603
RUSCH, Roger J., Method and apparatus for detecting gas leaks using radioactive techniques, 25:55063
RUSSEK, A., Rotationally induced transitions in atomic collisions, 25:55873
RUSSELL, Christopher T., Ogo 5 observations of polar cusp on Nov. 1, 1968, 25:56024
RUSSELL, John L., Public health aspects of $^{129}I$ from the nuclear power industry, 25:55199
RUST, Charles M., Simple solid-electrolyte gamma-ray and relativistic-charged particle dosimeter, 25:55054
RUSTGI, M. L., Reaction matrix elements and structure calculations with the Yale and Reid potentials for the Ni region, 25:56857
Self-consistent study of even Zn and Ge isotopes, 25:56720
RUTHER, W. E., Materials-coolant interactions relevant to EBR-II, 25:57109 (ANL-7771)
RUTKAUSKAS, Vincent J., Combination linear lifting and translation mechanism, 25:54853
RUTKOVSKI, E., Optical radiation excited by nonrelativistic charged particles on the metal surface, 25:55813 (JINR-P4-5957)
RUTKOWSKI, W., Density of coextruded metal cladded rod core as function of cartridge density and core length, 25:55420
RUTZ, D. A., Friction welding of titanium alloys, 25:55409
RUZICKA, J., Study of natural radionuclides in waste and surface waters, 25:54774
RYABCHIKOV, L. N., Absorption of oxygen and nitrogen by zirconium at low pressures, 25:55463
RYABOV, Yu. V., Measurement of the ratio of the radiative capture to fission cross sections ($\alpha$) for $^{239}Pu$ in the neutron energy range 0.1 to 30 keV, 25:56734 (BNL-tr-446)
Technique of average $\nu$ measurement with the neutron time-of-flight spectrometer, 25:55039 (LB/G-3040)
RYABUKHIN, Yu. S., Local irregularity of doses in neutron-capture therapy, 25:55212
Neutron-activation analysis of Ca, P, and Na in bones, 25:55106
RYABYKH, S. M., Topography of the evolution of the radiolysis products of lead azide ($PbN_6$), 25:54642
RYAN, M. J., Calibration of NASA--GSFC High Energy Cosmic Ray Experiment, 25:55046 (N-71-16750)
RYBACH, L., Feldspar analysis by neutron activation, 25:54494
RYBAKOV, V. N., Probability of the ($\mu^-$, $\nu$) process of $^{139}La$ and $^{208}Pb$ nuclei, 25:56739 (JINR-P1-6006)
RYCHLICKI, R., Attempt to use steady-state data for determining critical heat flux in transient conditions, 25:57024

# S

SAASTAMOINEN, J., Scattering cross-section and phonon spectrum of Zr hydride, 25:56623
SABAN, J., Reluctance motor for driving control rods of nuclear reactors, 25:54848
SABATO, M., Static quadrupole moments of vibrational states of spherical nuclei in the self-consistent cranking approximation, 25:56860
SABAU, M., K anti K production in four-prong $\pi^+p$ interactions at GeV/c, 25:56428 (IFA-HE-75)
$\Lambda$ K production in four-prong $\pi^+p$ interactions at 8 GeV/c, 25:56427 (IFA-HE-73)
SABIROV, S. S., New $0^+$ states in $^{126}Te$ and $^{128}Te$, 25:56781
SADIKOVA, N. M., Determination of $^{239}Pu$ and enriched U in the urine in their combined presence, 25:55197
SAFONOV, A. N., Dependence of the beam shape in the centre of the synchrocyclotron on the accelerating voltage and magnetic field decay, 25:56585 (JINR-P9-5945)
SAHA, G. B., Production of $^{52}Fe$ by $^{55}Mn(p,4n)^{52}Fe$ reaction for medical use, 25:54676
SAINIO, M., Finnish radiological bibliography, 25:55274
SAITO, H., Annealing of point defects in p-type germanium after electron irradiation at liquid-nitrogen temperature, 25:56329
SAITO, Yasutoshi, Thermal decomposition of thorium oxalate, 25:54544
SAKAI, Eiji, Fuel failure detection for fast breeder reactor, 25:57055 (JAERI-Memo-4157, pp 84-8)
Proceedings of fuel failure detection symposium, 25:57192 (JAERI-Memo-4157)
SAKAI, Mitsuo, Secondary ion emission from metal surface in collisions of 30-keV $Ar^+$ ions, 25:55818
Table of bands in even--even nuclei, 25:56651 (INSJ-127)
SAKAI, Sunao, Analytic form of multiple scattering amplitudes in the Regge pole model, 25:56578
SAKAMOTO, Y., $\pi$ and K mesons used for investigating light nuclei structures, 25:56653 (LYCEN-7104, S4.1-10)
Substructures in $^{12}C$ and $^{14}N$, 25:56652 (LYCEN-7104, S2.1-2)
SAKANUSHI, Katsuhiro, Charge removal from powder using $\beta$-radiation. I, 25:54897
SAKUDA, Kyohei, Reflection problems in kinetically described plasma, 25:56247
SAKURAI, Kunitomo, Active solar radio regions at metric frequencies and the interplanetary sector structures, 25:55765
SALAM, A., Breaking of conformal symmetry and renormalization of nonpolynomial theories, 25:56549 (ORO-3992-9)
SALAM, Abdus, Finite field theories, 25:56545 (IC-71/108)
SALAMATOV, I. I., Large $\gamma$ facility UGU-200, 25:54844
SALAMOV, D. I., Collective $1^+$ states in even--even deformed nuclei, 25:56819 (JINR-P4-5889)
SALEM, S. I., L x-ray transition probabilities in elements with Z greater than or equal to 57, 25:55823
SALGANIC, Yu. A., Neutron-channel in muon capture and short range nucleon--nucleon correlations, 25:56641 (JINR-P4-5986)
SALGANIK, Yu. A., Spectrum and asymmetry of high energy neutrons in the reaction $\mu^- + {}^{16}O \rightarrow {}^{15}N + n + \nu$, 25:56820 (JINR-P4-5997)
SAL'NIKOV, O. A., Interaction between 14-MeV neutrons and nuclei of Fe, Cu, and Nb, 25:56684 (FEI-216)
SALTMARSH, M., $^{40}Ca(^{20}Ne,^{16}O)^{44}Ti$ reaction, 25:56721
SALTYKOV, L. S., $^{14}N(d,p)^{15}N$, $^{28}Si(d,p)^{29}Si$, and $^{32}S(d,p)^{33}S$ reactions with polarized deuterons, 25:56724
SALVESEN, Karin, Equilibrium deuterium isotope effects on the ionization of thiol acids, 25:54566
SAM, Daniel, Exposure rates from products of thermal-neutron fission of $^{235}U$ at selected times after fission, 25:55231
SAMACHSON, Joseph, Metabolism and removal of radiostrontium in man, 25:55109 (COO-1231-67)
SAMARDZHIEV, D., Daily variations in height of sporadic-E layer, 25:56006
SAMOVAROV, V. N., Experimental study of the decay of cryogenic helium plasma, 25:56152 (SC-T-713065)
Recombination and detection of the three-atom ion in a helium plasma at low temperatures, 25:56161
SAMPSON, W. B., Recent developments in pulsed magnet multifilament superconducting wires, 25:56580 (BNL-16026)
SAMSONOV, G. V., Influence of additions of transition metals on the sintering behaviour of tungsten, 25:55453
Physical properties of monocarbides of zirconium, niobium, and their alloys in homogeneity range, 25:55632
Solubility and solid-phase interaction of the carbides of transition metals with nickel and copper, 25:55464
SAMSONOVA, L. A., Radiosensitivity and diagnosis of metastases into lungs and lymph nodes, 25:55300
SAMUEL, D., Respiration of brain slices in heavy water, 25:55121

XUM

SAMUELLI, M., Calibration of the silver activated counters on a plasma focus experiment, 25:56214 (LGI-70/17/E)
SANDLER, S. I., Transport properties of partially ionized argon, 25:56183
SANDLIN, G. D., Highly ionized Fe and Ni lines in 200- to 400-A of solar spectrum, 25:55774
SANDS, Donald E., Synergistic solvent extraction of rare earths by mixtures of thenoyltrifluoroacetone and acetylacetone, 25:54731
SANDSTROM, Donald R., Electron stimulated desorption of excited neutrals: CO on W, 25:55435 (RLO-2221-T-7-4)
SANNA, Robert S., User's guide to SWIFT, Monte Carlo technique for unfolding neutron spectra, 25:55036 (HASL-244)
SANTA MARTA, E., Grain growth in liquid-phase sintering of carbides, 25:55642
SANTAR, Ivan, Current state of a priori yield predictions, 25:54590 (CONF-700652-(Vol.1), pp 51-136)
SANTHOLZER, Vilem, Recognition of the fragment nuclides $^{90}Sr$ and $^{89}Sr$ on the basis of radioactivity. II, 25:54803
SANTNER, E., Activation analysis of Si in steel, 25:54519
SANTORO, Michael P., Method and means for changing radioactive sources, 25:54983
SANTOS, G. G. Jr., Activation analysis of Philippine magnetite sands, 25:54483
SAPANKEVICH, A. P., Crisis of heat transfer in pipes, 25:54869 (FEI-217)
SAPORETTI, F., Gamma-ray spectra following capture of 14 MeV neutrons by $^{59}Co$, $^{93}Nb$, and $^{103}Rh$, 25:56729
SAPOZHNIKOVA, E. B., Sintering and properties of yttrium oxide ceramics, 25:55606
SARGENT, F. P., Recent experiments on steady state and pulse radiolysis of alkaline aqueous systems, 25:54627 (CONF-700652-(Vol.2), pp 295-330)
SARKAR, Ratna, Neutron emission from prompt fragments in the fission of excited nuclei, 25:56856
SARKAR, S. K., Studies on solar x-ray flares recorded by SOLRAD-9 on Explorer 37 satellite, 25:55737
SARKSYAN, K. A., Resonances of anomalous microwave heating of electrons in a magnetized plasma, 25:56124
SASTRY, G. N., Photographic detection of intragalactic matter in Coma Cluster, 25:55782
SASTRY, K. S. R., Beta--gamma correlations and matrix elements for some first-forbidden nonunique beta transitions, 25:56776
SATO, Atsushi, Scale invariance and relativistic composite nucleon, 25:56465
SATO, C., Electrophoretic behavior of x-irradiated lymphocytes, 25:55310
SATO, Fumiko, Effect of tetrahydrofolic acid x-irradiated mice, 25:55268
SATO, Hikaru, Current amplitudes in the dual resonance model, 25:56449
SATTAROV, M. G., Tricomponent activity induced by competing reaction, 25:54498
SAUDINOS, J., Nuclear spectrometry at Saturne synchrotron, 25:56593 (LYCEN-7104, S7.1-2)
SAUVAL, A. J., Search for $CH^+$ in the solar photospheric spectrum, 25:55768
SAVAGE, Dennis, Ring-opening reactions of triphenylcyclopropyllithium compounds, 25:54571
SAVCHENKO, E. D., Treatment of bone sarcoma with high-energy bremsstrahlung, 25:55338
SAVEANT, J. M., Disproportionation and ECE mechanisms. III, 25:54585
SAVEL'EV, V. A., Detecting the polarization of solar-flare x-ray emission, 25:55771
SAVENKO, I. A., Global distribution of energetic charged-particle intensity above atmosphere, 25:55980
Measurement of solar protons from July 7, 1966 flare, 25:55991
SAVITSKII, E. M., Mechanism underlying the dispersion hardening of niobium alloys, 25:55443
Physical metallurgy of refractory and rare metals, 25:55438
SAVOSIN, S. I., Cupel assay of gold by an activation method, 25:54521
SAWADA, T., Breaks of ddelta/dt in high-energy proton--proton scattering, 25:56528
SAXE, R. F., Detection of boiling in nuclear reactors, 25:56996
SAXONOV, P. P., Study of reactivity of the organism exposed to transverse accelerations and radioprotectants, 25:55264
SCARF, F. L., Nonthermal electrons and high-frequency waves in upstream solar wind. II, 25:56019
SCARF, Fredrick L., Ogo 5 observations of polar cusp on Nov. 1, 1968, 25:56024
SCHADT, Warren W., Determination of the maximum permissible body burdens using the methods of the medical internal radiation dose (MIRD) committee of the Society of Nuclear Medicine, 25:55201
SCHALL, Gerald L., Improved detector for video systems used in radionuclide studies, 25:55278
SCHATTEN, Kenneth H., Current sheet magnetic model for the solar corona, 25:55733 (N-71-23433)
SCHECTER, Larry, Low energy nuclear research, 25:56689 (RLO-1062-711)
SCHEDLE, H., Determination of O, H, and N in high-melting metals. VI, 25:54426
SCHEFELS, W., Determination of testes consistency in bulls, 25:55337
SCHEITHAUER, W. Jr., High-temperature strength of oxide-strengthened nickel alloys, 25:55486
Manufacture and properties of high-conductivity high-strength Cu--$ThO_2$, 25:55417
SCHENK, H., Results of ultra-sound tests on reactor pressure vessel of nuclear power station Übrigheim, 25:56892
SCHERRER, Willy, Phenomenological energy tensor in the framework of linear field theory, 25:56565
SCHEUBECK, E., Photometric determination of small amounts of chloride in selenium, tellurium, gallium, and bismuth, 25:54407
SCHEUERMANN, W., Electronic structure of refractory carbides and its relation to wetting, 25:55643
SCHIELTZ, Jon D., Electrolytic behavior of yttria-stabilized hafnia, 25:56355
SCHIEWER, E., Diffusion of fission product ions in glasses, 25:55611
SCHIFFER, J. P., Particle-hole multiplets in $^{88}Y$ and the mechanism of ($^3He$,t) reaction, 25:56779
SCHILD, R., Energy distributions and K corrections for light from giant elliptical galaxies, 25:55793
SCHILLER, Robert, Radiation chemistry of supercooled water, 25:54663
Some problems of ion-electron recombination, 25:54591 (CONF-700652-(Vol.1), pp 221-58)
SCHILTZ, R. J. Jr., Thorium--copper system, 25:55571
SCHINDEWOLF, Ulrich, Optimization of a heavy-water enrichment plant based on $H_2/NH_3$ exchange, 25:54748
SCHINTLMEISTER, Josef, Study of reaction $^{14}N(n,2\alpha)^7Li$, 25:56680
SCHINTLMEISTER, W., Effect of nickel on the sintering and self diffusion of tungsten, 25:55426
SCHMIDL, H., Investigations of the dynamics of heat transfer. II, 25:54877 (SGAE-RT-38/1971)
SCHMIDT, D., Neutron activation analysis of tin in geochemical and cosmochemical material, using 40 minute $^{123}Sn$, 25:54480
SCHMIDT, G. K., Results of new absolute calibration of solar flux density at 2980 MHz, 25:55756
SCHMIDT, Guenter, Study of reaction $^{14}N(n,2\alpha)^7Li$, 25:56680
SCHMIDT, K. H., Excitation of Δ(1236) resonance on bound state neutrons, 25:56405 (DESY-71/33)
SCHMIDT, Klaus H., Absorption spectrum of e/sub aq/$^-$ in the temperature range -4 to 390°, 25:54658
SCHMIDT, M., Kinetic study of species formed during the pulsed radiolysis of ammonia, 25:54661
SCHMIDT, Michel, Index of radiative lifetimes, 25:57215 (CEA-Bib-198)
SCHMIDT, Reiner, Experience with the modularization of iteration procedures in engineering applications, 25:57143 (CONF-710302-(Vol.1), pp 494-504)
SCHMIDT-BOECKING, H., Investigation of level structure of $^{17}O$, 25:56663
SCHMIDTKE, G., High-resolution extreme-ultraviolet solar spectrum recorded with a diffraction-filter spectrograph, 25:55740
SCHMIER, H., Effectiveness of measurements made with the human whole-body γ counter, 25:55225
SCHMOELZER, G., Determination of triiodothyronine and thyroxine in blood serum by activation analysis, 25:54453
SCHNEEWEISS, F., Measurementof isotope abundance shifts by means of neutron activation analysis, 25:54492
SCHNEIBERG, K., Bone marrow sections of rat after whole body-irradiation, 25:55330
SCHNELLENBACH, G., General calculation of prestressed concrete reactor pressure vessels, 25:56987
SCHNIPPERING, H. G., Whole body radioactivity counter for multipurpose use in clinical diagnosis and research, 25:55023
SCHOENIG, J., Prestressed concrete pressure vessel of the THTR-300-MW(e) prototype nuclear power plant, 25:56884
SCHREINER, Horst, Arc erosion of various sintered and infiltrated WCu-materials in oil, 25:55454
SCHREMPP, F., Finite-energy sum rules and reactions ee + eeepsilon(750) and ee + eef(1260), 25:56463
SCHREMPP-OTTO, B., Finite-energy sum rules and reactions ee + eeepsilon(750) and ee + eef(1260), 25:56463
SCHROEDER, Johannes Horst, Search for radiation-induced recessive sex-linked lethal and detrimental mutations in immature germ cells of the house mouse (Mus musculus), 25:55184
SCHULENBURG, H., Spin dynamics in nuclear magnetic resonance, 25:56371
SCHULER, Robert H., Rate constants for reaction of hydrogen atoms with compounds of biochemical interest, 25:55132
SCHULTHEISS, G. F., Experimental study of incipient boiling superheat of sodium on artificial surface roughnesses, 25:54868 (EURFNR-897)
SCHULTZ, H., Collective $1^+$ states in even--even deformed nuclei, 25:56819 (JINR-P4-5889)
SCHULZ, Michael, Ion-wave instabilities at v1f in the polar wind, 25:55966
SCHULZ, Wallace W., Integrated lanthanide--actinide solvent extraction process, 25:54706 (BNWL-SA-3345)
SCHUMACHER, M., Coulomb fragmentation in InI and $InI_3$, 25:54696
SCHUMANN, Frederick A., Nuclear-thermionic lunar base power supply, 25:54905

SCHUNK, Robert W., Transport processes in E region of ionosphere, 25:55969
SCHUSTER, G., How should future nuclear energy be supported by Federal Republic of Germany, 25:57003
SCHUSTER, K., Compensation of external magnetic field by an internal field in a superconductor, 25:56074
SCHWABE, H., Quantitative analysis of lung perfusion following bronchography, 25:55285
SCHWANDT, P., $^{28}Si(^{3}He,2p)$ and $^{12}C(^{3}He,2p)$ reactions at 40 MeV, 25:56713
SCHWARTZ, M., Coupling of EM waves in an inhomogeneous plasma, 25:56225 (CEA-CONF-1802)
SCHWARTZ, M. J., Spatial determination of direction of magnetic field in Tokamak configuration, 25:56223
SCHWEIKERT, E. A., Alpha activation of calcium and its possible use for analysis, 25:54522
SCHWEIZER, W., High-resolution extreme-ultraviolet solar spectrum recorded with a diffraction-filter spectrograph, 25:55740
SCHWENDIMAN, L. C., Amount and characteristics of plutonium made airborne under thermal stress, 25:54546
SCHWIERS, H.-G., Prestressed concrete pressure vessel of the THTR-300-MW(e) prototype nuclear power plant, 25:56884
SCICCHITANO, Edward A., Nuclear-thermionic lunar base power supply, 25:54905
SCOLES, G., Nonspherical potentials and molecular scattering at thermal energies, 25:55852
SCOTT, R. W., PFR components, 25:57011
SCOTT, T. E., Mechanical properties of polycrystalline Sm, 25:55520
SCRANTON, D. G., Use of simplotter: a high-level plotting system, 25:57231 (IS-2305)
SEAMON, Robert E., Generating moments of the photon production matrices and sources from ENDF data: the LAPHAN code, 25:57175 (CONF-710302-(Vol.2), pp 1016-23)
SEARLE, A. G., Induction of translocations in mouse spermatogonia. IV, 25:55182
SEASHOLTZ, Richard G., Theory of Thomson scattering from a weakly ionized plasma, 25:56165 (N-71-27890)
SEBOEK, F., Design concept and analysis of cylindrical prestressed concrete reactor pressure vessels with axial ribs, 25:56990
SECK, Richard E., Development of an NE-213 fast-neutron TAC spectrometer system utilizing off-line gamma-ray discrimination, 25:55033 (COO-2049-6)
SEDLACEK, Z., Electrostatic oscillations in cold inhomogeneous plasma. II, 25:56242
SEDOV, A. V., Accidental dosage estimation at large gamma-irradiation facilities, 25:55235
SEETHARAM, A., Inheritance of gamma ray induced chlorophyll mutation in linseed, 25:55177
SEIDEL, Ingo, Apparatus for continuously measuring the cross-section of wire, 25:55062
SEILER, George Joseph, Algebraic close-coupling approach to electron--hydrogen scattering, 25:55854
SEITNER, H., Determination of trace elements by neutron activation in meteorites, 25:54517
SEKI, Humitake, Bioaccumulation of radioisotopes by microorganisms in the sea, 25:55154
SEKI, Yasushi, Method for calculating energy dependence of mass chain yield of fission, 25:56816 (JAERI-Memo-4383)
SEKIGUCHI, Hiroyoshi, Heavy-particle ray damage to a Si solar battery, 25:55099
SEKINE, Matsuo, Total effective cross sections for high-energy acausal pion--nucleon scattering, 25:56502
SELENGUT, D. S., New form of the $P_3$ approximation, 25:57149 (CONF-710302-(Vol.2), pp 561-4)
SELEZOV, I. T., Stabilization of magnetohydrodynamic flutter instabilities by distributive control, 25:55925
SELF, S. A., Ion-acoustic instability of two-temperature, collisional, fully ionized plasma, 25:56251
SELIG, H., Reaction of Re and Tc metals with molten Li perchlorate and the Raman spectra of corresponding melts, 25:54538
SELLE, J. E., Evaluation of the use of a quantitative image analyzer to determine microhardness values, 25:57240 (MLM-OP-71007)
SELTZER, S. M., Prog. rpt. on radiation transport studies, 7/70--2/71, 25:56255 (AD-721388)
SEL'VENSKII, Ya. D., Investigation of the kinetics of oxygen isotopic exchange between water and carbon dioxide in the presence of soluble additives, 25:54549
SELZER, P. M., Superfluid plug for space, 25:56119
SEMENCHUK, G. G., Fission process in atomic nuclei in transition region, 25:56786
SEMENOV, B. G., Thermodynamic properties of cerium in molten zinc, 25:55442
SEMENOV, V. G., Search for the (n,$\alpha$) reaction in the resonances of the zinc and hafnium isotopes, 25:56686 (JINR-P3-5875)
SEMENYUSHKIN, I. N., Debuncher of the JINR synchrophasotron injector with modulation of the accelerated beam energy, 25:56586 (JINR-P9-5956)
SEN, A., Regularization method of unfolding x-ray spectrum, 25:56134 (ORNL-TM-3582)
SEN, P., Positron lifetime studies in some crystals, 25:56360
SEN, S., $^{84}Kr(d,n)^{87}Rb/sup A/$ threshold cusp and the systematic appearance of charge-exchange cusps, 25:56719
SENASHENKO, V. S., Autoionizing states in helium-like ions, 25:55820
SEN GUPTA, N. D., Electrons in strong Coulomb field, 25:56394
Motion of charged particles with radiation reaction, 25:56393
SENYAVIN, M. M., Calculation and optimization of the demineralization of water for reactors by ion exchange, 25:54737
SERAFIMOV, K., Daily variations in height of sporadic-E layer, 25:56006
SERAFINI, A., Leak proof mechanical device for nuclear reactor pressure vessels, 25:57043
SERDUKE, Franklin, J. D., Redetermination of the singlet effective-range parameters of the Hongan separable potentials, 25:56859
SERDYUKOVA, A. S., Possibility of gamma spectroscopy in well logging in the presence of radon, 25:54759
SEREBRYAKOVA, T. I., Wear resistance of surfaces faced with borides, 25:55619
SEREDA, M. G., Distribution of $^{59}Fe$ in man, 25:55111
SEREGIN, A. A., Probability of electromagnetic quadrupole transitions in the phenomenological nuclear theory, 25:56735 (FEI-202)
SERGEENKO, N. P., Characteristics of delta $f_0F2$ distribution curves, 25:55985
SERGEEV, I. V., Asymptotic behavior of neutron pulses in a hard multiplying system, 25:55017
SERMONS, G. Ya., Electromagnetic fields in an induction magnetohydrodynamic device with extendable channel, 25:55939
SERVIT, R., Theoretical and experimental investigations on the stress-strain behavior of prestressed concrete reactor pressure vessels, 25:56993
SESSLER, J. C., Reaction mechanisms of $^{10}B(d,\alpha)^{8}Be_{2}$ $_{g}(\alpha)^{4}He$ for E/sub d/ = 0.4, 1.0, and 1.5 MeV, 25:56673
SEUBERLING, H.-B., High resistance to rays of NADP-dependent glyceraldehyde phosphate dehydrogenase in alga, 25:55353
SEVCIK, M., Comparison of scintigraphy and angiography in the diagnosis of intracranial space-occupying lesions, 25:55293
SEYBOLD, G. D., BNW program noise, 25:57181 (BNWL-1609)
SEZON, M., Study of /sup 236mf/U isomeric fission through $^{235}U(n,\gamma)$ reaction, 25:56793
SHA, W. T., Numerical stability problems in the VENUS disassembly code, 25:57079 (CONF-710302-(Vol.1), pp 152-66)
Two-dimensional fast-reactor disassembly analysis with space-time kinetics, 25:57078 (CONF-710302-(Vol.1), pp 128-51)
SHABANSKII, V. P., Depression of the geomagnetic field during a magnetic storm, 25:56002
SHABER, Gary S., Alteration of taste thresholds in the rat following low dose x irradiation, 25:55322
SHAFER, G. V., Annual variations and gradient of cosmic-ray intensity in the meridional plane, 25:55900
SHAGIMARDANOV, N. Sh., Tissue equivalent scintillators in radiometry of long wave x radiation, 25:55213
SHAIL, R., Slow rotation of axisymmetric solids in magnetohydrodynamics, 25:55941
SHAKHANOVA, G. V., Nature of the embrittlement of two-phase titanium alloys with coarse lamellar structure, 25:55450
SHAKHOVA, Yu. A., Dimensions of the galactic cosmic-ray modulation region, 25:55901
SHAKIN, C. M., Cluster expansions for correlated wave functions in nuclear physics, 25:56850
SHANE, K. C., Photodisintegration rate of $^{24}Mg$, 25:55703
SHANNON, D. W., Corrosion and deposition of irradiated stainless steel in sodium, 25:55370 (BNWL-SA-2335)
SHANNON, L. V., $^{226}Ra$ in marine phytoplankton, 25:55155
SHAPIRO, N. I., Premutational oxygen-sensitive changes of chromosomes induced by irradiation of seeds, 25:55168
SHAPKIN, V. V., Noise levels of Langmuir oscillations in beam--plasma system, 25:56249
SHAPORENKO, A. A., Interference effect in cross section for charge exchange of $Li^{+}$ ions with He atoms, 25:55844
SHARIPOV, Sh., Excited states of odd nonaxial nuclei, 25:56785
SHARKOV, Yu. V., Prospecting for U deposits in mountainous Taiga, 25:54805
SHARMA, S. C., Inactivation of cells by heavy ion bombardment, 25:55313
SHARMA, S. D., Collective model of odd--odd deformed nuclei, 25:56812 (COO-1120-124)
SHAROVA, A. V., Pyrolytic titanium and zirconium nitrides and fields of their use, 25:55605
SHATKHIN, Kh. Z., Ionospheric effect of solar eclipse of Sep 22, 1968, 25:56000
SHAW, J. G., Thermomigration of carbon in metals, 25:55479
SHAW, R. W. Jr., Model potential for Zn, Cd, and Hg, 25:56387
SHCHERBAKOV, D. I., Essays on the geology and geochemistry of ore deposits, 25:54763
SHCHERBININ, O. N., Determination of the boundary of high frequency wave absorption between the electron cyclotron and the low hybrid frequency, 25:56224 (AEC-tr-7270)

XUM

SHCHULEPNIKOV, M. N., Development of a fast-neutron activation method for determination of N in Nb, Ta, and Ti, 25:54501
SHEIKO, T. I., Thermal expansion of alloys Al--Mo, Al--Zr, obtained at higher cooling rates, 25:55499
SHELAGIN, A. V., Calculation of constant relaxation of an average neutron flux in a nonuniform medium with anisotropic scattering, 25:56635
SHEOREY, V. B., Comparisons of Glauber and Vainshtein approximations for inelastic e--H scattering, 25:55850
SHEPTUNOV, V. N., Isolation of promethium by displacement chromatography due to complex formation, 25:54723
SHERCLIFF, J. A., Magnetohydrodynamics at high Hartmann number, 25:55921
SHERER, D. B., Core design development needs in relation to fuel failure propagation, sodium boiling, and clad/fuel--sodium thermal interaction, 25:57088 (GEAP-13639-1)
Core design development needs in relation to fuel failure propagation, sodium boiling, and clad/fuel--sodium thermal interaction, 25:57089 (GEAP-13639-2)
SHERIDAN, Michael Eugene, Mechanism of radiolytic hydrocarbons formation from methane in dilute solutions in liquid argon, 25:54615
SHERMAN, H., Least-squares fitting of wire spark chamber events, 25:55049
Track finding in wire spark chamber data, 25:55048
SHERMAN, Warren V., Mechanism of the radiation-induced dechlorination of 1,1,1-trichloro-2,2-bis(p-chlorophenyl)ethane in alcholic solution, 25:54620
SHER'YAZDANOV, G. B., Flow of nonviscous perfectly conducting fluid past a thin body in presence of transverse magnetic field, 25:55929
SHESTAKOV, E. N., Spectral emissivity of tantalum, 25:55495
SHEVCHENKO, Yu. F., Recombination and detection of the three-atom ion in a helium plasma at low temperatures, 25:56161
SHEVTSOV, B. I., Determination of the rate of movement of the charge in rotary kilns by means of radioative isotopes, 25:54898
SHEWCHUN, J., Proton radiation damage and recovery in Ta films, 25:56314
SHEWMON, P. G., Radiation-induced swelling of stainless steel, 25:55581
SHIBANOV, B. V., Tables for calculating nonstationary temperatures of plane bodies during heating by irradiation, 25:56267
SHIDA, Shoji, Radiolysis of liquid n-butane, 25:54659
SHIELDS, L., Electron spin resonance study of V(II). IV, 25:56384
SHIFRIN, G. A., Measurement of lattice damage caused by ion-implantation doping of semiconductors, 25:56287
SHIGA, Kunio, Particle exchange, Regge-pole exchange, and the Veneziano amplitude for KN scattering, 25:56518
SHIGA, Tetsuo, Electron spin resonance studies of primary processes in radiation-induced reactions. II, 25:54639
Electron spin resonance studies of primary processes in radiation-induced reactions. I, 25:54640
SHIH, C. H., Effect of collisions on cold ion collection by means of Langmuir probes, 25:56135
SHIHAB-ELDIN, Adnan Ahmed, Particle states and decay scheme of $^{87}$Kr, 25:56703
SHIHABI, David S., Reactivity of hydrogen atoms and hydrated electrons toward aqueous erythrosin. X-radiolysis, 25:54664
X-radiolysis of aqueous erythrosin, 25:55139
SHIKITA, Mikio, Effect of tetrahydrofolic acid x-irradiated mice, 25:55268
SHILOVA, Nataly S., Oscillations of visible chromosphere boundary and regularity in position of spicule groups along the limb, 25:55747
SHIL'SHTEIN, S. Sh., Suppression of (n,γ) reaction in resonant scattering of neutrons by a perfect CdS crystal, 25:56627
SHILYAEV, B. A., Nucleon density distribution in nuclei $^{54}$-$^{56}$Fe, 25:56699
SHIMA, Makoto, Fission track and alpha-particle recoil track dating, 25:54771
Fission track dating of ancient glasses, 25:54761
SHIMADA, Keikichi, Cytological studies during treatment of oral cancer. II, 25:55345
SHIMAZU, Y., Temperature-sensitive recovery of a mutant of Escherichia coli K-12 irradiated with ultraviolet light, 25:55360
SHIMERDA, John Henry, Neutron transport from a point source in a slab, 25:56613 (AD-715563)
SHIMKYAVICHYUTE, G. S., Use of $Os0_4$ as catalyst in titrimetry. XI, 25:54433
SHIMOKAWA, Junichi, Kinetics of carbon transfer between uranium carbide fuel and stainless steel bonded with sodium, 25:55589 (JAERI-Memo-4438)
SHIMOTOMAI, M., 220°K defect in electron-irradiated p-type germanium, 25:56300
SHIN, H. K., Vibration--rotation--translation energy transfer in HF--HF and DF--DF, 25:54551
SHINBORI, Yoshio, Determination of chlorobiphenyl in rat adipose tissue by neutron activation analysis, 25:54500
SHINDO, Masuo, Influence of $PuO_2$ particle size of mixed oxide fuel in relation to fast reactor safety, 25:57107
SHINDO, Ryuichi, DELIGHT: the point reactivity burnup code for HTGR lattices, 25:57021 (JAERI-Memo-4449)
SHINKAWA, Akihiro, Molecular weights and molecular weight distributions of polyisobutylenes produced by γ-irradiation, 25:54621
SHIOKAWA, Takanobu, Thermal annealing behavior of recoil $^{57}$Co formed by decay of $^{57}$Ni-labeled hexamminenickel(II) complexes, 25:54689
SHIRAIWA, Toshio, Ultrasonic testing of nuclear fuel cladding tubes, 25:54926
SHIRANE, G., Neutron scattering study of the lattice-dynamical phase transition in $Nb_3Sn$, 25:55545
SHIRAYAMA, Shinpei, Development of reactor in-core neutron monitor, 25:57025
SHIRE, P. R., Sodium fires analyses for the Fast Flux Test Facility, 25:57112 (HEDL-TME-71-31)
SHIRLEY, D. A., Theory of nuclear magnetic resonance detected by nuclear radiations, 25:56372
SHISHKIN, A. A., Resonance effects in magnetic configurations having a helical magnetic axis, with allowance for toroidality, 25:56209 (CTO-764)
SHLEIEN, B., Estimate of radiation doses received by individuals living in the vicinity of a nuclear fuel reprocessing plant in 1968, 25:55237
SHLYAKHOV, N. A., Nucleon density distribution in nuclei $^{54}$-$^{56}$Fe, 25:56699
SHLYUKO, V. Ya., Production of parts of complex shape in lanthanum hexaboride, 25:55599
SHMANENKOVA, G. I., Radioactivation determination of impurities in the epitaxial films of gallium arsenide, 25:54512
SHMIDT, V. V., Critical current of a perfect type-II superconductor in the mixed state, 25:56092
Interaction between a cavity and vortex in a type II superconductor, 25:56091
SHOEMAKER, David J., Linearization of radiation gauges for measuring the quantity of fluidic materials in containers, 25:55059
SHOLIN, G. V., Noise levels of Langmuir oscillations in beam--plasma system, 25:56249
SHOWALTER, D. L., Elemental abundance trends in the australite strewn field by non-destructive neutron activation, 25:54478
SHPAK, D. L., Angular anisotropy and effects of nucleon pairing in $^{239}$Pu fission by neutrons, 25:56736 (FEI-233)
SHRABSHTEIN, S. A., Automation of chromatography of radioactive substances, 25:54727
SHRAGGE, P. C., Factors affecting the rate of hydrated electron attach on polynucleotides, 25:55131
SHTERN, A. G., Possibilities of influencing the boundary layer with crossed electric and magnetic fields, 25:55934
SHTOL'TS, A. K., Conditions for formation of phase with A15 structure in V--Ge--Al system, 25:55539
SHUBIN, Yu. N., Density of the excited states of atomic nuclei, 25:56835 (UCRL-Trans-10540)
Mean radiation widths at excitation energies of the order of the neutron binding energy, 25:56836 (UCRL-Trans-10542)
SHULEPNIKOV, M. N., Radioactivation determination of impurities in the epitaxial films of gallium arsenide, 25:54512
SHULEPOV, V. I., Decomposition of the solid solution of interstitial impurities in tungsten, 25:55444
SHULTIS, J. K., New computational method for X and Y functions of radiative transfer, 25:55676
SHULTS, W. D., Oak Ridge Air Quality Index, 25:57246 (ORNL-NSF-EP-8)
SHURYGIN, A. I., Detecting the polarization of solar-flare x-ray emission, 25:55771
SHVETSOVA, S. I., Decomposition of the solid solution of interstitial impurities in tungsten, 25:55444
SIDES, W. H. Jr., Detection of boiling in nuclear reactors, 25:56996
SIDIS, V., Quasi-diabatic representation for inelastic collisions, 25:55849
SIDOROV, π and K mesons used for investigating light nuclei structures, 25:56653 (LYCEN-7104, S4.1-10)
SIDOROVA, T. A., Method of holding molten metal in suspended state: characteristics of Lodochka inductor, 25:55424
SIEGMANN, E. R., Comparison between momentum integral and compressible models for sodium voiding calculations in LMFBR, 25:57081 (CONF-710302-(Vol.1), pp 180-98)
SIEK, R. D., Environmental sampling. A critical look at common procedures, 25:54779 (CONF-710401-, pp 347-51)
SIEMENS, P. J., Neutron matter computations in Brueckner and variational theories, 25:56867
SIEMENS, Philip John, New statistical theory of the nuclear surface, 25:56841
SIEMSSEN, R. H., $^{40}$Ca($^{20}$Ne,$^{16}$O)$^{44}$Ti reaction, 25:56721
SIERGIEJ, J. M., Titanium P/M preforms, parts, and composites, 25:55415
SIGMAN, Donald R., Some limitations on ion-cyclotron wave generation and subsequent ion heating in magnetic beaches, 25:56231 (N-71-25439)
SIK, So Don, Measurement of the ratio of the radiative capture to fission cross sections (α) for $^{239}$Pu in the neutron energy range 0.1 to 30 keV, 25:56734 (BNL-tr-

446)
SIKORA, B. R., Investigation of $^{33}S(d,p)^{34}S$ reaction, 25:56730
SIL, N. C., Ground-state energies of He atom and $Li^+$ ion in Faddeev approach, 25:55824
SILAR, Josef, Cherenkov detectors for beta radiation detection in water and their present applications, 25:55031
Thermal resistance and dependence of scintillation detectors at elevated temperatures, 25:55025
SILVER, D. M., Metric evaluation in the space of exponential and gaussian functions, 25:56399
SIMMONS, G. L., Prog. rpt. on radiation transport studies, 7/70--2/71, 25:56255 (AD-721388)
SIMOES, Jose Henriques, Freezing and irradiating fish, 25:55362 (LFEN-NI.-56a)
SIMON, M. T., Relativistic wave equations for massless particles of spin $^1/_2$, 25:56447
SIMON, P., Solar coronal streamers observed at 169 MHz, 25:55754
SIMPSON, Erik Elgar, Evolutionary models of stars of 15 and 30 M/sub sun mass/, 25:55691
SIMS, J., Luxembourg sodium test facility, 25:54839
SINCLAIR, James, ESR study of irradiated glycine at low temperatures, 25:54653
SINFAILAM, A.-L., Multiple-scattering expansions for nonrelativistic three-body collision problems. IV, 25:55867
SINGER, Irving A., Steadiness of the wind during stable conditions, 25:54794
SINGER, Sidney, Association of magnetotail phenomena with visible auroral features, 25:55955
Energetic electron fluxes in magnetotail associated with onset of magnetospheric substorms, 25:56044
Properties of solar energetic particles associated with propagating interplanetary shock waves, 25:56020
SINGH, K. P., Lifetimes of positrons in alkaline earth fluorides, 25:55834
SINGH, N. P., Indirect potentiometric method for the determination of plutonium, 25:54411
SINGMAN, L. V., K-fluorescent-x-ray relative-intensity measurements, 25:55827
SINGRU, R. M., Lifetimes of positrons in alkaline earth fluorides, 25:55834
SINHA, S. K., Phonon spectrum of scandium metal by inelastic scattering of neutrons, 25:56342
SIPALO, B., Solvent extraction study of lanthanum and europium by acidic esters of aminophosphonic acids, 25:54732
SIRLIBAEV, T., Physico-chemical properties of polyvinyl fluoride obtained by γ-irradiation, 25:54624
SIROKI, Marija, Spectrophotometric determination of niobium with 4-(2-pyridylazo)resorcinol and colored complexes separated from oxalic and tartaric acid systems, 25:54425
SIROTKIN, V. K., Differential cross sections for elastic scattering of nucleons, 25:56789
SITES, James R., Ultralow temperature rotating polarization system, 25:55089
SIVJEE, G. G., $O_2$ Herzberg I bands in the night airglow, 25:56046
SIVOSHINSKII, D. S., Si(Li)-detectors for diagnosis of neoplasm of the skin, 25:55273
SJOEDIN, Jan, Translocations in Vicia faba L, 25:55191
SKAKUN, N. A., Use of reaction $^{18}O(p,\alpha)^{15}N$ to study oxidation of metals, 25:55384
SKAZIN, V. E., Production of Cu/W composite by diffusion welding, 25:55405
SKILLMAN, T. L., Magnetospheric field distortions observed by OGO's 3 and 5, 25:55952 (N-71-27604)
SKLADZIEN, S. B., Behavior and calibration of devices for monitoring impurities in sodium, 25:55069 (ANL-7804)
SKLIZKOV, G. V., Generation of neutrons in laser $CD_2$ plasma heated by pulses of nanosecond duration, 25:56219
SKOBELEV, N. K., Delayed fission of some neutron-deficient atomic nuclei, 25:56744 (NP-tr-1936)
SKOBELEV, V., Modification of the Coulomb law in a strong magnetic field, 25:56402
SKOTNIKOV, V. I., Radiosensitivity and diagnosis of metastases into lungs and lymph nodes, 25:55300
SKOVRON, Mary L., Acute changes in pulmonary arterial perfusion following irradiation, 25:55327
SKRIPAK, V. N., Thermal conductivity of some oxygen compounds of zirconium and hafnium, 25:55637
SLABOSPITSKII, R. P., Polarization of protons elastically scattered on nuclei with a zero spin, 25:56678
SLADE, David H., Meteorological questions concerning plant siting, 25:54793
SLATES, R. V., GELI2 and SPAN2: programs to calculate nuclide abundances from multichannel γ ray spectra, 25:55035 (DP-1275)
SLAUGHTER, G. G., Distribution of partial radiation widths in $^{238}U(n,\gamma)^{239}U$, 25:56790
SLAUGHTER, G. M., Weldability of tungsten and its alloys, 25:55410
SLEPTSOV, V. M., Solubility and solid-phase interaction of the carbides of transition metals with nickel and copper, 25:55464
SLEYTR, Uwe, Freeze etching of corresponding fracture moieties: a new approach to membrane structures, 25:57251 (ORNL-tr-2509)
SLIV, L. A., Properties of certain multiparticle states with large spins, 25:56783
SLOAN, Kaaren C., Effects of irradiation on avian leukosis, 25:55329
SLUTSKER, S. M., Computation of N(z) profiles in upper ionosphere, 25:55595
SMALES, A. A., Place of activation analysis in geochemistry and cosmochemistry, 25:54458
SMEETS, J., Effectiveness of measurements made with the human whole-body γ counter, 25:55225
SMELTZER, W. W., Preparation and structure of zirconium nitride spheres, 25:55595
SMIDT, F. A. Jr., Production of vacancies by laser bombardment, 25:56313
Residual elements and irradiation embrittlement, 25:55577 (NRL-7310)
SMILYANSKII, V. R., Propagation of an electromagnetic wave across a magnetic field in a parabolic plasma layer, 25:56236
SMIRENKIN, G. N., Angular anisotropy and effects of nucleon pairing in $^{239}Pu$ fission by neutrons, 25:56736 (FEI-233)
SMIRNOV, A. D., Some principles of evaluating the effectiveness of radioprotective agents in man, 25:55256
SMIRNOV, L. V., Determination of the diffusion parameters of interstitial atoms in yttrium by reference to the dislocation impurity peaks of internal friction, 25:55461
SMIRNOV, V. A., High temperature ceramics from scandium oxide, 25:55620
SMITH, Horace Vernon Jr., Isospin forbidden $^{12}C(d,\alpha_2)^{10}B(1.74)$ reaction, 25:56656
SMITH, J. C., Development of processes for the hot pressing of silicon--germanium thermoelectric elements, 25:57267 (SC-DR-710438)
SMITH, J. M., Derivation of gaseous release limits for the Browns Ferry Nuclear Plant, 25:56980
SMITH, J. R., Prestressing and proof pressure testing of Wylfa prestressed concrete pressure vessels, 25:56883
SMITH, Katherine W., Isotope effects after the rate-determining step. The role of rotational isomerism in a hydrogen transfer, 25:54577
SMITH, M. G., Optical identification of southern radio sources, 25:55725
SMITH, Malcolm G., Kinematic properties of 71 H II regions in LMC, 25:55795
SMITH, V. H., Comparative metabolism of intravenously injected promethium in swine and humans, 25:55108 (BNWL-SA-3747)
SMITH, W. E., Properties of carbon derived from indene compounds, 25:57295 (Y-1790)
SMITH III, F. L., Ionospheric storm of March 8, 1970, 25:55974
SMYTHE, J. W., New developments in superalloy powders, 25:55416
SNELSON, A., Infrared spectra of $LiAlF_4$ and $NaAlF_4$, 25:54563
SNOWDEN, Michael S., Light variations in supergiants in LMC, 25:55705
SNYDER, Glenn Alden, OB stars and galactic structure: the perseus spiral arm, 25:55788
SNYDER, Lewis E., Microwave receivers for molecular line radio astronomy, 25:55091
SOBBE, A., Quantitative analysis of lung perfusion following bronchography, 25:55285
SOBOLEV, Ya. P., Morphological characteristics of whistler spectra and ionization irregularities in topside ionosphere, 25:55997
SOBOLEVSKII, N. M., Classification of inelastic interactions of high-energy protons and nuclei. II, 25:56522 (ORNL-tr-2520)
SOBOTOVICH, E. V., Lead isotopes in geochemistry and cosmochemistry, 25:54770
SOBYANIN, A. A., Surface tension of He II near lambda point and boundary condition of order parameter on the free surface, 25:56056
SOEDERSTROEM, K., Description of the logic unit of the photometer system SFIL 70, 25:55045 (LUIP-CR-71-2)
SOFFER, Leonard, COHORT-2: Monte Carlo general purpose shielding computer code, 25:56262 (N-71-22378)
SOIFER, B. T., Rocket-infrared four-color photometry of Galaxy's central regions, 25:55783
SOKOL, L., Thermal stability of powder magnesium system used in nuclear technology, 25:55504
SOKOLOV, A. A., Bremsstrahlung of nonpolarized and longitudinally polarized electrons, 25:56862
SOKOLOV, L. S., Inelastic scattering of deuterons, 25:56780
SOKOLOV, V. A., Metaphase analysis of chromosome rearrangements in barley, 25:55175
SOKOLOVA, G. V., Effect of alloying on the oxidation of niobium at low pressures, 25:55380
SOLDATOV, E. A., Determination of diffusion coefficients in liquid metals by isotope exchange through the gas phase, 25:54556
SOLOMON, P. M., CO, CN, and CS emission from IRC + 10216, 25:55686
SOLOV'EV, V. G., Correlations between reduced neutron and radiative widths in neutron resonances of compound odd-N nuclei, 25:56818 (JINR-E4-5880)
Δ N = +- 2 mixing in odd-N deformed nuclei, 25:56737

XUM

(JINR-E4-5877)
SOLOYAN, G. A., Gas-chromatographic study of the effect of radioactive radiation and heat treatment on the adsorptive properties of magnesium sulfate, 25:54603
SOLYAKIN, G. E., Fission process in atomic nuclei in transition region, 25:56786
SOMENKOV, V. A., Suppression of (n,γ) reaction in resonant scattering of neutrons by a perfect CdS crystal, 25:56627
SOMORJAI, G. A., Reactive scattering of $N_2O$ molecular beams from clean and carbon covered (100) platinum single crystal surfaces, 25:57237 (LBL-133)
SONDEL, James A., Determination of mercury in biological and environmental samples by neutron activation analysis, 25:54508
SONNERUP, Bengt U. O., Magnetopause structure during magnetic storm of Sept. 24, 1961, 25:56022
SONODA, Takenori, Spectrographical analysis of $^{235}U$ with a hollow cathode discharge tube, 25:54435
SOOD, B. R., Phonon spectra of dilute Pb--In alloys observed by superconducting tunneling, 25:56075
SORANTIN, H., Neutron activation analysis of standardized Al--Si alloy. II, 25:54455
SOROKO, V. M., Collector system of an isotope separator for investigating short-lived isotopes, 25:56584 (JINR-P6-5888)
SOSIN, A., Chemical vapor deposited tungsten: mechanical evaluation at high temperatures, 25:55440
SOUBBARAMAYER, Space--time evolution of a plasma subjected to a discharge current, 25:56162 (CEA-CONF-1801)
SOULE, Harvey F., Radiation standards and radioactive waste, 25:55253
SOUSLENKO, V., π and K mesons used for investigating light nuclei structures, 25:56653 (LYCEN-7104, 54.1-10)
SOWELL, R. R., Effects of rf activated inert gas plasmas on critical surface tension and bondability of polydimethyl silicones and polyethylene, 25:57272 (SC-RR-710483)
SPAHR, Juerg, Absolute measurement of the radioactivity of pure β emitters with liquid scintillators, 25:54697
SPALEK, Ursula, Separation of selenium and tellurium by means of Bismuthiol II, 25:54724
SPARROW, A. H., Sensitivity of lima bean to gamma radiation, 25:55349
SPEDDING, F. H., Effect of impurities on lattice parameters of ABAB rare earth metals, 25:55549
Phonon spectrum of scandium metal by inelastic scattering of neutrons, 25:56342
SPEKTOR, A. Ts., Alloying of superconducting compounds vanadium gallide with group III--VIII elements, 25:55500
SPENCER, A. R., Cyclic oxidation of TD--Ni, 25:55387
SPENCER, Herta, Metabolism and removal of radiostrontium in man, 25:55109 (COO-1231-67)
SPENCER, L. V., Prog. rpt. on radiation transport studies, 7/70--2/71, 25:56255 (AD-721388)
SPENCER, R. I., Organization and planning for fire control, 25:54952 (CONF-710401-, pp 204-7)
SPEROFF, Leon, Radioimmunoassay of the F prostaglandins, 25:55144
SPIELREIN, E. E., Thermophysical properties of molten boron oxide, 25:55625
SPINKA, Harold, $^{16}O$ + $^{16}O$ reaction, 25:56657
SPITSYN, A. V., Electron irradiation of lithium-doped germanium at cold temperatures, 25:56301
SPITSYN, I., Impurity paramagnetic center in γ-irradiated salts, 25:56339
SPITSYN, V. I., Gas-chromatographic study of the effect of radioactive radiation and heat treatment on the adsorptive properties of magnesium sulfate, 25:54603
SPREVAK, D., Forced common turning-point procedure and excitation in slow $H^+$--H(2s) collisions, 25:55881
SPRINGBORN, Richard L., Chemical effects of the nuclear reaction $^{14}N(n,p)^{14}C$ in potassium azide, 25:54687
SPRY, R. J., Moessbauer-type photoluminescence spectra of irradiated germanium, 25:56328
SPRYGAEV, I. F., Accidental dosage estimation at large gamma-irradiation facilities, 25:55235
SRAPENYANTS, R. A., Gamma-ray irradiation equipment, 25:54837
SRINIVASAN, N., Indirect potentiometric method for the determination of plutonium, 25:54411
SRIVASTAVA, C. M., Lagrangian formalism for free Maxwell field in spinor notation, 25:56541
SROUR, J. R., Recombination parameters in low-resistivity gamma-irradiated n-type germanium, 25:56327
ST. LORANT, S. J., Large-scale refrigeration systems for 1.0 to 1.85°K, 25:56117
STACEY, D. N., Isotope shifts in electronic and muonic atoms, with application to neodymium, 25:55821
STACEY, W. M. Jr., Applications of space-energy factorization to the solution of static fast-reactor neutronics problems, 25:57170 (CONF-710302-(Vol.2), pp 953-67)
STACKLER, B., Induction of heteroallelic reversions and lethality in Saccharomyces cerevisiae exposed to radiation of various LET ($^{60}Co$ γ rays, heavy ions, and π⁻ mesons) in air and nitrogen atmospheres, 25:55165
STAERK, H., Monostandard activation analysis and its application to geological samples, 25:54490
STALS, L., Fast neutron irradiation induced swelling of metals and alloys, 25:55572 (BLG-457)
STAMPFEL, John P., Simple monochromatic, polarized $^{57}Fe$ Moessbauer source, 25:56366
STANCHEV, S. M., Collector system of an isotope separator for investigating short-lived isotopes, 25:56584 (JINR-P6-5888)
STANCHEVA, N. S., Collector system of an isotope separator for investigating short-lived isotopes, 25:56584 (JINR-P6-5888)
STANGEBY, P. C., Transonic plasma flow past an obstacle, 25:56176
STANTON, L., Influence of rotational energy on ion--molecule cross sections, 25:54550
STANYUKOVICH, K. P., Calculations of magnetogasdynamic flow in channels, 25:55935
STAPF, R., Low-temperature electron irradiation of tellurium, 25:56306
STARCHENKO, B. M., Readout electronics for π--e experiment at 50 GeV, 25:55044 (JINR-E1-5818)
STARIZNYI, E. S., Gamma radiation dose rate in the emitter of a radiation-chemistry device provided with a uranium-based radiation circuit, 25:54914
Method for calculation of field dose of uranium radiation loop linear source of γ-radiation, 25:54991
STARK, Donald Sutherland, Improvements in or relating to neutron targets, 25:56626
STARKE, E. A. Jr., Kinetics of disorder--order transformations, 25:55552
STARKIE, H. C., Electron spin resonance of atomic silver on porous glass and silica gel surfaces, 25:54606
STARKOV, M. G., Experimental study of the decay of cryogenic helium plasma, 25:56152 (SC-T-713065)
STARKOVA, A. G., Diurnal variations of structural parameters of the atmosphere at heights of 100 to 220 km, 25:55987
STARODUBTSEV, S. V., Nuclear physics. II, 25:56845
STARODUBTSEVA, E. V., Feasibility of the thermal decomposition of methyl alcohol in fission fragment tracks, 25:54645
START, G. E., Comparative diffusion and deposition of uranin dye, molecular iodine gas, and methyl iodide gas, 25:54795
STAVINSKII, V. S., Density of the excited states of atomic nuclei, 25:56835 (UCRL-Trans-10540)
Mean radiation widths at excitation energies of the order of the neutron binding energy, 25:56836 (UCRL-Trans-10542)
STAVISSKII, Yu. Ya., Measurement of the ratio of the radiative capture to fission cross sections (α) for $^{239}Pu$ in the neutron energy range 0.1 to 30 keV, 25:56734 (BNL-tr-446)
STEARNER, S. Phyllis, Mechanisms of acute injury in the γ-irradiated chicken: in vivo studies of dose protraction effects on the microvasculature, 25:55324
STEARNS, J. Warren, Dissociation cross sections for 0.5- to 1-MeV $HeH^+$ ions in $H_2$, He, $N_2$, and Ne gases, 25:55872
STECKER, F. W., Isotropy of cosmic γ-ray flux, 25:55896 (N-71-27639)
STEELE, L. E., Residual elements and irradiation embrittlement, 25:55577 (NRL-7310)
STEERMAN, C. E., Properties of 12.50 and 12.52 MeV levels of $^{15}N$, 25:56669
STEFAN, H., SCAT: code for computing scattering cross section of light and heavy water, 25:56638
STEFANESCU, D. T., Cytogenetic investigation of industrial workers occupationally exposed to gamma rays, 25:55163
STEFANON, M., Spin-dependence of level density in $^{179}Hf$ and $^{180}Hf$ by resonance neutron capture experiments, 25:56751 (RT/FI-(70)55)
STEFANOU, G. D., Analysis of perforated end caps for pressure vessels by finite element method, 25:56985
STEFANOVA, M., Yearly course of radon and thoron inductions and long lasting radioactivity of aerosols in Plovdiv, 25:54792
STEFFEN, R. M., Theory of nuclear magnetic resonance detected by nuclear radiations, 25:56372
STEIN, Ralph P., Engineering relationships for turbulent forced-convection heat transfer in ducts with flux transients, 25:54864 (ANL-7754)
STEINBERG, H. A., Non-linear Monte Carlo, 25:57161 (CONF-710302-(Vol.2), pp 794-7)
STEINBERG, Herbert A., Machine generation of monte carlo sampling functions, 25:57160 (CONF-710302-(Vol.2), pp 771-81)
STEINER, H. J., Analysis of K+/sub e3/ decay X2, 25:56409
STEINHAUER, Loren Clifford, Laser heating of a stationary plasma, 25:56128
STEINKE, R. G., Automated modular light water reactor calculation code package, 25:57172 (CONF-710302-(Vol.2), pp 983-90)
STEINMANN, O., Basic notions of relativistic scattering theory, 25:56571 (CERN-71-14, pp 229-87)
STEINNES, E., Epithermal neutron activation analysis of geological material, 25:54468
STEINNES, Eiliv, Conference on activation analysis in geochemistry and cosmochemistry, Kjeller, Norway, 9/70, 25:54457
STELJES, J. F., Cosmic ray NM-64 neutron monitor data. XVIII, 25:55893 (AECL-3971)
STELZMAN, W. J., Radiation strengthening and embrittlement in heavy section plate and welds, 25:55585
STEMPINSKII, M., Alpha widths of neutron resonances,

25:56754 (UCRL-Trans-10541)
STEPANEK, K., Research of the hydrodynamics of a rod fuel assembly, 25:56880 (ZJE-104)
STEPANOV, A. P., Determination of $^{239}$Pu and enriched U in the urine in their combined presence, 25:55197
STEPANOV, A. V., Calculation of constant relaxation of an average neutron flux in a nonuniform medium with anisotropic scattering, 25:56635
Use of Green's function in theory of neutron diffusion in heterogeneous medium with slugs of small dimensions, 25:56636
STEPANOV, B. M., Rapidly varying geomagnetic field disturbances produced by a nonstationary source of gamma quanta, 25:55989
STEPANOV, N. V., Superconducting properties of niobium--titanium--zirconium hafnium alloys, 25:56104
Superconductive properties of niobium--zirconium--hafnium alloys, 25:56105
STEPANYUK, V. L., Debuncher of the JINR synchrophasotron injector with modulation of the accelerated beam energy, 25:56586 (JINR-P9-5956)
STEPHENSON, Dwight L., Fully interactive graphics data retrieval system, 25:55076 (LA-DC-12576)
STEPHENSON, G. J. Jr., Brueckner--Hartree--Fock calculations using density-dependent effective interactions, 25:56834 (ORO-3765-32)
STEPINA, A. I., Kinetics of the decomposition of binary and ternary solid solutions of aluminum with chromium obtained by quenching the alloys from the molten state, 25:55448
STERLINSKI, S., Dependence of activation upon the pulse form in a pulsed neutron generator, 25:54526
STERMAN, L. S., Critical heat fluxes encountered in the case of boiling of organic heat transfer agents with a high boiling point, 25:54879
STEVENS, D. W., Irradiation-induced dimensional changes in co-deposited carbon--silicon coatings, 25:55652
STEVENS, E. R., Thorium--copper system, 25:55571
STEVENS, R. N., Effect of temperature, pressure and concentration gradients on diffusion, 25:57213 (AECL-3793)
STEVENSON, John C., Ideally conducting magnetostatic equilibria and associated time-dependent resistive flows, 25:55940
STEWART, L. D., ORNL multi-ampere ion source, 25:56208 (CONF-711012-9)
STEWART, Ross, Bell-shaped pH-rate profile for an oxidation. The reaction of permanganate with hydroxycyclohexanecarboxylic acids, 25:54575
STEWART II, J. W., ENDF/B cross section preparation and testing in the JOSHUA system, 25:57176 (CONF-710302-(Vol.2), pp 1024-30)
STEYERT, W. A., Ultralow temperature rotating polarization system, 25:55089
STILES, P. J., Electron transport in Nb/Nb oxide/Bi tunnel junctions, 25:56078
STIRLING, W. L., ORNL multi-ampere ion source, 25:56208 (CONF-711012-9)
STIRN, R. C., Modeling and application of the adiabatic approximation for analyzing rod drop excursions, 25:57084 (CONF-710302-(Vol.1), pp 259-81)
STOCKBERG, H., Profilography of sacroiliac joints in ankylosing spondylitis, 25:55287
STOCKER, H., Comparison of the nuclear-reaction energy scale with the gamma-ray energy scale, 25:56773
STODDART, P. G., Radioactivity released from a liquid metal fast breeder reactor fuel recycle complex, 25:54754
STOEBE, T. G., Comments on supralinearity and sensitization of thermoluminescent phosphor lithium fluoride, 25:56338
STOKER, P. H., Steplike changes in the long-term modulation of cosmic rays, 25:55912
STOKES, Everett Donald, Electron capture into the n = 2 levels of hydrogen by protons passing through gas targets, 25:55853
STOLARIK, J. D., Electric-field measurements and identification of currents causing magnetic disturbances in polar cap, 25:55959
STONE, E. J., Photoelectron excitation of atomic-oxygen resonance radiation in the terrestrial airglow, 25:56032
STONE, L. E., Radiosensitization with 5-bromodeoxyuridine of Chinese hamster cells x-irradiated during different phases of the cell cycle, 25:55258
STONE, Robert G., Active solar radio regions at metric frequencies and the interplanetary sector structures, 25:55765
STORER, John B., Chemical protection of the mouse against radiation-induced life shortening, 25:55257
STORM, Mary M., Effects of irradiation on avian leukosis, 25:55329
STRAIN, R. V., Materials-coolant interactions relevant to EBR-II, 25:57109 (ANL-7771)
STRAKER, E. A., MORSEC: revised cross-section module for MORSE multigroup Monte Carlo code, 25:56263 (ORNL-4716)
STRANSKY, Pravoslav, Recognition of the fragment nuclides $^{90}$Sr and $^{89}$Sr on the basis of radioactivity. II, 25:54803
STREHLOW, R. A., Instrument for measuring the hydrogen content of metals, 25:54424
STREIFF, R., Preparation and structure of zirconium nitride spheres, 25:55595
STRIKE, Thomas A., Effectiveness of tranquilizing drugs in rats exposed to mixed gamma--neutron radiations, 25:55325
STRINGER, J., Oxidation of Ta--Hf polycrystals and single crystals, 25:55397
Oxidation of Ta--W polycrystals and single crystals, 25:55385
STRINGER, T. A., Single- and double-pion production in proton--antiproton nonannihilations at 2.2 GeV/c, 25:56487
STRINI, G., High-spin rotational excitation in $^{173}$Hf, 25:56796
STRUXNESS, E. G., Safety analysis of waste disposal by hydraulic fracturing at Oak Ridge, 25:54971 (ORNL-4665)
STRYCZNIEWICZ, Kamila, Preparation of high purity carrier-free $^{131}$Cs source for spectroscopic measurements, 25:54889 (INR-P-1325)
STUKIN, E. D., Distribution of radioactivity in rocks and petroleum from contained nuclear explosions, 25:54826 (UCRL-Trans-10543, pp 99-116)
STUMP, R., Single- and double-pion production in proton--antiproton nonannihilations at 2.2 GeV/c, 25:56487
STUPIN, D. M., $^{28}$Si($^{3}$He,2p) and $^{12}$C($^{3}$He,2p) reactions at 40 MeV, 25:56713
STURROCK, P. A., Period--age distribution of pulsars, 25:55687
STUSSI, Jean-Marc, Uranium and Th geochemistry of volcanic rocks, 25:54807
SUBBOTIN, A. V., Theoretical model of fast-neutron-induced swelling in metals, 25:55582
SUCKEWER, Szymon, Utilization of selective change of plasma optical thickness to determine the electron density, 25:56133 (INR-P-1322)
SUDAKOV, V. A., Phase diagram of the mercury--indium system, 25:55536
SUDAREVA, S. V., Relationships between the real structure of alloys and the model representations of hard superconductors, 25:55541
SUDARSHAN, E. C. G., Action-at-a-distance, 25:56550 (ORO-3992-14)
Interpretation of angular distribution in terms of complex mass particles, 25:56499 (ORO-3992-8)
Phenomenology of complex spin tachyons, 25:56500 (ORO-3992-18)
SUDOVTSOV, A. I., Properties of deformed superconducting alloys of vanadium--gallium, 25:56100
SUENAGA, M., Effect of magnetic fields on stress relaxation in mixed-state superconducting Pb--In alloys, 25:56063
SUETTERLIN, Lothar, Formation and deposition of pyrocarbon from methane in temperature range of 1650 to 2150°C, 25:55591 (JUL-735-RW)
SUGAHARA, M., Magnetization properties of nonideal Type-II superconductors transporting sinusoidal alternating current in a longitudinal magnetic field, 25:56085
SUGANEEV, Yu. S., Determination of the diffusion parameters of interstitial atoms in yttrium by reference to the dislocation impurity peaks of internal friction, 25:55461
SUGAWARA, Tohru, Trapped-particle instabilities and diffusion rates in Tokamak plasma, 25:56195 (JAERI-Memo-4483)
SUGAYA, R., Cherenkov and cyclotron excitation of Bernstein waves with electron beams, 25:56241
SUGHIMOTO, Hiroshi, Quantized fields associated with the annulus-type medium, 25:56563
SUGIURA, M., Magnetospheric field distortions observed by OGO's 3 and 5, 25:55952 (N-71-27604)
SUICH, J. E., JOSHUA terminal system, 25:57145 (CONF-710302-(Vol.1), pp 508-15)
SUKHAREVSKII, B. Ya., Polymorphic transformation of zirconium dioxide, 25:55641
SUKHOV, G. V., Radioactive determination of oxygen in germanium and silicon, 25:54502
SULLIVAN, Carole A., Use of a styrofoam block cutter to make tissue-equivalent compensators, 25:55244
SULLIVAN, P. J. E., Time-temperature extrapolation techniques as applied to concrete creep strains, 25:55663
SULLIVAN, Robert Emmett, Quadrature variations in discrete ordinates calculations, 25:56278
SULLIVAN, T. A., Electrorefining of V prepared by carbothermic reduction of $V_2O_5$, 25:55408
SULLIVAN, W. H., Method for the routine measurement of dielectric photoconductivity, 25:55079 (SC-DC-713696)
SUMIN, V. V., Distribution coefficients of titanium and iron in zirconium, 25:55502
SUN, C. C., Sintered zirconia electrolyte films in high-temperature fuel cells, 25:55596
SUNDER-PLASSMANN, M., Ventricular scintigraphy for diagnosis of cerebral tumors in early childhood, 25:55290
SUNG, Young Kwon, Gamma-irradiation effect on electrical properties of B-type insulator, 25:55101
SURIKOV, V. I., Conditions for formation of phase with A15 structure in V--Ge--Al system, 25:55539
SUSANNA, A., Health protection analysis of transportation of radioactive substances through tunnels, 25:54973 (RT/PROT-(71)11)
SUSZYCKI, L., Measurements of energy and flux of cosmic ray

hadrons using an ionization spectrometer, 25:56413 (INP-756)
SUSZYCKI, Leszek, Inelasticity coefficients for pion--Fe and nucleon--Fe collisions, 25:56414 (INP-757)
SUTER, Peter, Gas turbine plant, 25:54856
SUURMEIJER, E. P. Th. M., Instrumentation for study of ion reflection and secondary ion emission, 25:55815
SUZDALEV, I. P., Goldanskii--Karyagin effect in Moessbauer patterns and the anisotropy of atomic vibrations in crystals, 25:56377
SUZUKI, Hameji, Activation analysis of lanthanide elements in natural water, 25:54504
SUZUKI, K., Temperature-sensitive recovery of a mutant of Escherichia coli K-12 irradiated with ultraviolet light, 25:55360
SUZUKI, Kazunori, Preparation and the absorption spectra of U(III) in various acid solutions, 25:54540
SUZUKI, Masao, Fission track dating and U contents of obsidian. II, 25:54773
SUZUKI, N., Extraction of uranyl thenoyltrifluoroacetonate into solvents, 25:54751
SUZUKI, T., Systematic radiochemical analysis of fission products, 25:54449
SUZUKI, Tomoo, SDRC: the ultra-fine spectrum calculation code in resonance energy region, 25:57182 (JAERI-Memo-4481)
SVECHNIKOV, V. N., Alloying of superconducting compounds vanadium gallide with group III--VIII elements, 25:55500
SVERDLIN, A. V., Properties of welded joints in V92Ts alloy, 25:55470
SVESTKA, Z., Flux of neutrons from flares, 25:55761
SVETLOPOLYANSKII, V. I., Wear resistance of surfaces faced with borides, 25:55619
SVIRINA, L. M., Production of Cu/W composite by diffusion welding, 25:55405
SVOBODA, H. J., Nuclear power plant in the nuclear material safeguards accounting system, 25:54934 (BNWL-1598)
Status of burnup calculational technology as applied to the nuclear materials safeguards accounting system, 25:54935 (BNWL-1599)
SWAMY, K. S. Krishna, Infrared radiation from grains in Orion, 25:55718
SWANSON, D. G., Prog. rpt. on quasistatic ion cyclotron wave studies, 8/71, 25:56233 (ORO-3871-6)
SWARUP, G., Search for pulsed radio emission from CYG X-1 at 327 MHz, 25:55728
SWEET, J. N., Externally shunted Josephson junctions: generalized weak links, 25:56094
SWENSON, G. W. Jr., Microwave detection of interstellar formamide, 25:55784
SWERDLOFF, Michael D., Isotope effects after the rate-determining step. The role of rotational isomerism in a hydrogen transfer, 25:54577
SYDER, P., Angular dependence of the superconductive nucleation field Hc4, 25:56065
SYKES, A., Numerical experiments on nonlinear plasma instabilities, 25:56205
SYMANZIK, K., Small-distance-behavior analysis and Wilson expansions, 25:56543 (DESY-71/39)
SYMONS, M. C. R., Electron spin resonance of atomic silver on porous glass and silica gel surfaces, 25:54606
Formation of ozonide ions in γ-irradiated aqueous solutions of alkali hydroxides, 25:54608
SYRE, R., Novel high-strength titanium alloy, 25:55421
SZABADVARY, F., Acid determination with the help of radioiodine, 25:54439
SZABO, E., Concentration and determination of rare earth impurities in an yttrium matrix, 25:54525
Neutron activation analysis of impurities in Th and Zr, 25:54518
SZABO, Gy., Aberrations of asymmetrized quadrupole lenses, 25:56604
SZEGO, K., Representations of Poincare group as functions of eigenvalues of Casimir operators, 25:56534 (KFKI-71-38)
SZEWCZYK, Zenon, Influence of radon inhalation on lymphocytes, 25:55346
SZTEKE, W., Density of coextruded metal cladded rod core as function of cartridge density and core length, 25:55420

# T

TACCETTI, N., K = 3/2+ rotational band in $^{45}$Ti, 25:56693
TACHIBANA, Kazuya, Location of impurities in alkali halide crystals by channeling studies, 25:56337
TADEMARU, E., Crab pulsar radiation mechanism, 25:55729
TADIC, D., Parity nonconservation in heavy nuclei and the structure of weak-interaction Hamiltonians, 25:56768
TAFEL, Linda L., Bibliography on electrical discharge machining and electrochemical machining, 25:54834 (WAPD-331)
TAGLIAFERRI, G., High-spin rotational excitation in $^{173}$Hf, 25:56796
TAGUCHI, Yukio, Lorentz invariance and finite self-mass in local field theory, 25:56564
TAIRA, Shigenobu, Simultaneous determination of O, F, and Al in Al electrolytic bath by fast-neutron activation, 25:54503
TAKAHASHI, Ryoichi, Influence of $PuO_2$ particle size of mixed oxide fuel in relation to fast reactor safety, 25:57107
TAKAHASHI, Yasuko, New method for radiochemical analysis of iodide and iodate in environmental water, 25:54442
TAKAKURA, Tatsuo, Acceleration of electrons and solar flares due to quasi-static electric field, 25:55760
TAKATSUKA, Tatsuyuki, Superfluid state in neutron star matter. II, 25:55714
TAKATSUNA, Toshio, Simultaneous determination of O, F, and Al in Al electrolytic bath by fast-neutron activation, 25:54503
TAKAYANAGI, Hiroshi, Nondestructive determination of average burnup for irradiated fuel rods, 25:57201
TAKEUCHI, Kunito, Ultrasonic flaw testing method for a reactor pressure vessel using a mockup, 25:54925
TALBOT, L., Experimental study of the cylindrical Langmuir probe response in the transition regime, 25:56136
TALROZE, V. L., Concentration dependence in binary systems in the case of indirect action via an ion-pair mechanism, 25:54670
TAMAGAKI, Ryozo, Superfluid state in neutron star matter. II, 25:55714
TAMAIN, B., Search for bremsstrahlung-induced fission isomers of $^{238}$U and $^{239}$Pu, 25:56801
TAMURA, Mituhisa, Simultaneous determination of O, F, and Al in Al electrolytic bath by fast-neutron activation, 25:54503
TANAKA, Kiriko, New method for radiochemical analysis of iodide and iodate in environmental water, 25:54442
TANAKA, S., Cherenkov and cyclotron excitation of Bernstein waves with electron beams, 25:56241
TANG, Chi-li., Studies in high energy particle production in nuclei, 25:56844
TANG, K. T., Quantum theory of ($H_2$,$H_2$) scattering: approximate treatments of reactive scattering, 25:55863
TANI, Yoshio, PC steel wires for reactors, 25:55422
TANIDA, R., Miniaturized probe for detecting radioactivity at thyroid surgery, 25:55018
TANNO, Kuniyasu, Radiolysis of liquid n-butane, 25:54659
TAPPERE, E. J., High-resolution photography of the solar chromosphere. IX, 25:55746
TARANDI, T., Scandinavian PCRV model project, 25:56991
TARASOV, G. P., Polarized particle sources, 25:56610
TARASOVA, T. B., Finishing of crude pyrochlore concentrates, 25:54741
TARE, V. B., Electronic conduction in yttria-doped thoria solid electrolyte, 25:56335
TARNOVSKII, A. S., Lorentz transformations and motion of electric charges in stationary, homogeneous electromagnetic fields, 25:56567
TAROV, K. G., Reaction $^{12}C(\alpha p_0)^{15}N$, 25:56675
TARUTIN, I. G., Isodose distribution of a beam of positrons with an energy of 5 to 15 MeV, 25:55210
TASAKA, Kanji, Method for calculating energy dependence of mass chain yield of fission, 25:56816 (JAERI-Memo-4383)
TATSUMI, Y., Annealing of point defects in p-type germanium after electron irradiation at liquid-nitrogen temperature, 25:56329
TAWARA, Hiroyuki, Charge-changing processes for helium beam involving metastable atoms in molecular hydrogen, 25:55845
TAYLOR, Charles L., Filtration for the exhaust ventilation of plutonium recovery facilities, 25:54947 (CONF-710401-, pp 118-32)
TAYLOR, Harry A. Jr., Structured variations of the plasmapause: evidence of a corotating plasma tail, 25:56028
TAYLOR, J. B., Invariants in the motion of a charged particle in a spatially modulated magnetic field, 25:56401
TAYLOR, J. C., Ionospheric disturbance by a satellite: boundary-value problem for the Vlasov-Poisson equations, 25:56014
Stability of a plasma stream in a magnetic field, 25:56202
TAYLOR, W. M., Monte Carlo sampling with continuously varying cross section along flight paths, 25:57164 (CONF-710302-(Vol.2), pp 871-6)
TCHUKITCHEV, M. V., Electron irradiation of lithium-doped germanium at cold temperatures, 25:56301
TEANEY, P. E., Evaluation of the use of a quantitative image analyzer to determine microhardness values, 25:57240 (MLM-OP-71007)
TEBES, J., Diffractive νν scattering in νN → ννN at 13.1 GeV/c, 25:56425 (COO-1428-294)
TEENY, F. M., Irradiation of Pacific Coast fish at sea, 25:55366
TEMKIN, A., Low energy electron--molecule scattering experiments and the theory of rotational excitation, 25:55855
TEMKIN, A. Ya., Kinetic isotope effect of reactions of hot atoms in gaseous mixtures, 25:54684
TEMPLETON, J. E., Theory of nuclear magnetic resonance detected by nuclear radiations, 25:56372
TENTEN, Walter, Conference on siemens process calculator utilization, 6/70, Juelich, 25:55074 (JUL-Conf-5)
TEPLOV, I. B., Reaction $^{12}C(\alpha p_0)^{15}N$, 25:56675
Some pecularities of the heavy-particle stripping process, 25:56863

TEPLY, J., Conference on progress and problems in contemporary radiation chemistry, Marianske Lazne, Czechoslovakia, 6/70, 25:54588 (CONF-700652-(Vol.1))
Conference on progress and problems in contemporary radiation chemistry, Marianske Lazne, Czechoslovakia, 6/70, 25:54592 (CONF-700652-(Vol.2))
Conference on progress and problems in contemporary radiation chemistry, Marianske Lazne, Czechoslovakia, 6/70, 25:54595 (CONF-700652-(Vol.3))
TERANISHI, Eizo, Heavy-particle ray damage to a Si solar battery, 25:55099
TERENETSKII, K. O., Optical potentials of deuteron interactions with nuclei, 25:56725
TERENT'EV, A. B., Radiation telomerization of ethylene by propionic acid, 25:54612
TERESHKEVICH, M. O., Determination of the association constants of ions from the rate of oxygen exchange between anions and water, 25:54553
TERMAN, A. V., Accidental dosage estimation at large gamma-irradiation facilities, 25:55235
TERRASI, F., Method of analysis of neutron capture gamma-ray spectra, 25:56690 (RT/FI-(70)47)
TESNER, P. A., Carbon black formation in the thermal decomposition of hydrocarbons, 25:57278 (SC-T-713066)
TETELMAN, A. S., Relation between K/sub Ic/ and microscopic strength for low alloy steels, 25:55503
TETHAL, Tomas, Growth and structure of $RbUO_2(NO_3)_3$ crystals, 25:54579
TEUTSCH, Heinz, Diffusive motions in neutron coherent scattering by liquids by filter time-of-flight spectrometry, 25:56634
THADDEUS, P., Laboratory measurement of the 6-centimeter formaldehyde transitions, 25:55732
THAYER, V. R., Low pressure stripping, 25:54918
THERENE, P., Nuclear explosions for peaceful purposes, 25:54819 (UCRL-Trans-10543, pp 1-3)
THIESING, J. W., Orders-of-scattering method for fast-neutron transport, 25:56258 (COO-2049-9)
THIESING, James W., Orders-of-scattering calculation for the reflection of collimated, polyenergetic fast neutrons from a six-inch-thick steel slab, 25:56257 (COO-2049-8)
THIMM, Klaus, Comparison of continuum radiation of high-temperature plasmas with synchrotron radiation in range 500 to 9000 A. I, 25:56587 (JUL-748-PP)
THIRION, J., Nuclear spectrometry at Saturne synchrotron, 25:56593 (LYCEN-7104, S7.1-2)
Reactions performed with polarized protons at Saclay, 25:56688 (LYCEN-7104, S6.1-2)
THOMAS, B. K., Comparisons of Glauber and Vainshtein approximations for inelastic e--H scattering, 25:55850
THOMAS, Bernard, Substantially fluid tight closure device between two coaxial walls, 25:54860
THOMAS, Charles C. Jr., Determination of mercury in biological and environmental samples by neutron activation analysis, 25:54508
THOMAS, G., Microwave oscillations in parallel Josephson junctions, 25:56077
THOMAS, P. B., /sup 99m/Tc technetium sulfide and scintillation camera in rapid diagnosis of pericardial effusion, 25:55295
THOMAS, R. G., Relative hazards from $^{95}Zr$ and $^{95}Nb$ based upon inhalation of particles formed under various thermal conditions, 25:55125
THOMAS, W., SOLRF: program for approximation computation of neutron interaction according to solid angle method of spacing, 25:56271
THOMAS, W. A., Oak Ridge Air Quality Index, 25:57246 (ORNL-NSF-EP-8)
THOME, G. D., Electron density enhancements in E and F regions during solar flares, 25:56035
THOMSON, J. A., Thyroid carcinoma following $^{131}I$ therapy. Report of a case and review of the literature, 25:55343
THUEMMLER, F., Relations between stereometric microstructure and properties of cermets and porous materials, 25:55628
TIGELAAR, H. L., Microwave detection of interstellar formamide, 25:55784
TIKHOMIROV, I. A., Determination of the relative difference between the mobilities of isotopic lithium ions in an ion-exchange resin--solution system, 25:54730
Estimation of the single-stage isotope separation factor in the electromigration of isotopic ions through an ion-exchange membrane, 25:54729
TIKHOMIROV, M. V., Dissociation of $D_2^+$ and $H_2^+$ ions in collisions with $D_2$, He, and Ne, 25:55858
TIKHONOV, A. A., Plasticity and strength of nickel--molybdenum alloys at high temperature, 25:55474
TIKHONOVA, L. A., Thermomechanical properties of some oxide refractories, 25:55621
TILBROOK, R. W., Coolant voiding transients in LMFBR's, 25:57082 (CONF-710302-(Vol.1), pp 215-40)
TILMANS, A., Effect of radiation on some mechanical properties of an epoxy system, 25:55667
Effect of radiation on the adhesive properties of epoxy-metal and epoxy-glass adhints, 25:55666
TILTON, E. W., Method of dosimetry for a bulk-grain irradiator, 25:55234
TIMMERHAUS, K. D., Advances in cryogenic engineering. Volume 16. Proceedings of the 1970 cryogenic engineering conference, Boulder, Colorado, June 17--19, 1970, 25:56113
TINDALE, John Basil, Improvements in or relating to hopper feeders, 25:54841
TINDO, I. P., Detecting the polarization of solar-flare x-ray emission, 25:55771
TIOMNO, J., Equivalence of Lorentz transformations and Foldy--Wouthuysen transformations for free spinor fields, 25:56554
TIRARD, Michele, Nuclear reactions induced by α particles with energies between 70 and 160 MeV in light nuclei, 25:56685 (FRNC-TH-48)
TIRUNARAYANAN, M. A., Onset of free convection in annuli, 25:54881
TITHERIDGE, J. E., Nonperiodic irregularities in the ionosphere, 25:56042
TJOEM, Per Olav, Single nucleon transfer in deformed nuclei, 25:56875
TKACHENKO, V. F., Numerical calculation of conducting fluid flow in a traveling magnetic field, 25:55918
TOBIN, D., Effect of doping on the thermal conductivity of polycrystalline graphite, 25:55635
TODD, J. H., Measurements of the neutron fission and absorption cross sections of $^{239}Pu$ over the energy region 0.02 eV to 30 keV, Part II, 25:56746 (ORNL-4707)
TOERIEN, F. V. S., Direct determination of the noble metals by activation analysis utilizing high-resolution gamma spectrometry, 25:54487
TOEVS, James W., Stellar rates for $^{28}Si(\alpha,\gamma)^{32}S$ and $^{16}O(\alpha,\gamma)^{20}Ne$ reactions, 25:55704
TOHMATSU, Takao, Sounding rocket observation of helium 304- and 584-A glow, 25:55967
TOKAREVSKII, V. V., Inelastic proton scattering by intermediate-weight nuclei, 25:56727
Optical potentials of deuteron interactions with nuclei, 25:56725
TOLGYESSY, Juraj, Determination of boron in boric glasses by the neutron absorption method, 25:54437 (RFP-Trans-82)
TOLSON, G. M., Brazing the shell assembly for the BONUS superheater fuel element, 25:55425
TOMASEVICH, G. R., Laboratory measurement of the 6-centimeter formaldehyde transitions, 25:55732
TOMIMASU, Takio, Ionization chamber response for pulsed radiation and drift velocity distribution of filling gas, 25:55015
TOMIOKA, Hiroyuki, PC steel wires for reactors, 25:55422
TOMITA, Kenki, Non-linear theory of gravitational instability in the expanding universe. II, 25:55799
TONDEUR, F., Mass formula and properties of matter at subnuclear densities, 25:55678
TONEEV, V. D., Classification of inelastic interactions of high-energy protons and nuclei. II, 25:56522 (ORNL-tr-2520)
TOPPEL, B. J., New multigroup cross section code, MC²--2, 25:57171 (CONF-710302-(Vol.2), pp 968-82)
Users experience with the ARC system, 25:57142 (CONF-710302-(Vol.1), pp 478-93)
TORIYAMA, Kazumi, Radical pair from primary ionic species produced by ionizing radiation, 25:54665
TOTH, K., Representations of Poincare group as functions of eigenvalues of Casimir operators, 25:56534 (KFKI-71-38)
TOTTERDELL, D. H. J., Electron radiation damage and edge emission of cadmium telluride, 25:56290
TOULEMONDE, M., Determination of angular correlations and mean lifetimes in $^{57}Co$, 25:56700
TOUNSI, Ahmed, Regge poles and π--N scattering at low and intermediate energies, 25:56497 (FRNC-TH-33)
TOXEN, A. M., Magnetic properties of $LaSn_3$, 25:56353
TOYODA, Fumihiko, Urbaryon rearrangement diagram and nonleptonic hyperon decays, 25:56470
TRACANELLA, Roberto Barata, Reactivity of $U_3O_8$--Al dispersions, 25:55609 (ORNL-tr-2456)
TRAHIN, M., Multiphoton processes in a hydrogen atom, 25:55875
TRANDAFIRESCU, M., Activity of hexokinase in rats, 25:55140
TREADO, P. A., Reaction mechanisms of $^{10}B(d,\alpha)^8Be_{g.s.}(\alpha)^4He$ for E/sub d/ = 0.4, 1.0, and 1.5 MeV, 25:56673
TREDER, Hans-Juergen, Reference systems and gravitation, 25:56568
TRENBERTH, R., Investigation into effect of ''crud'' deposits on surface temperature, dry-out and pressure drop, with forced convection boiling of water at 69 bar in annular test section, 25:54861 (AEEW-R-705)
TRET'YACHENKO, L. A., Cross section of Mo--Zr--Cr system at 1150°C, 25:55538
TREVERTON, J. A., Thermodynamic properties of liquid molybdenum by levitation calorimetry, 25:55496
TRICHEL, M. C., Artificial aurora experiment: experiment and principal results, 25:55961
TRILLING, G. H., Evidence for structure in Kπ mass system near 1.85 GeV, 25:56434
TRIMBLE, V., Supermassive objects in astrophysics, 25:55798
TRIPATHI, A. N., Electron-impact excitation of lithium, 25:55864
TROFIMENKOFF, P. N., Strong-coupling parameters in superconducting In--Pb alloys, 25:56076
TROMBKA, J. I., Isotropy of cosmic γ-ray flux, 25:55896

XUM

(N-71-27639)
TRONCONE, L., Radioisotope scanning with $^{75}$Se-selenomethionine in the morphological and functional study of the pancreas, 25:55271 (LB/G-3059)
TROUBETZKOY, E. S., Non-linear Monte Carlo, 25:57161 (CONF-710302-(Vol.2), pp 794-7)
TROUBETZKOY, Eugene S., Machine generation of monte carlo sampling functions, 25:57160 (CONF-710302-(Vol.2), pp 771-81)
TROUT, E. Dale, Dose distribution for single- and three-phase x-ray equipment, 25:55227
TROYAN, Yu. A., Analysis of the reaction np + pp $\pi^-$ from the point of view of Reggeized OPE model, 25:56521 (JINR-P1-5975)
TRUFANOV, A. M., Interaction between 14-MeV neutrons and nuclei of Fe, Cu, and Nb, 25:56684 (FEI-216)
TRUHLAR, Donald G., Forcing conservation of particle flux in perturbation-theory calculations of inelastic scattering, 25:55877
TRUNOV, G. V., Production of parts of complex shape in lanthanum hexaboride, 25:55599
TRYON, E. P., Analytic, crossing-symmetric, unitarity $\pi\pi$ amplitudes which satisfy I = 1 sum rules and the inequalities of Martin, 25:56490
TSAI, W., Spin one theory, 25:56464
TSENG, H. K., Exact screened calculations of atomic-field pair production and low-energy screening, 25:56275
TSEPAKIN, S. G., High-frequency source of heavy ions, 25:55817
TSETSKHLADZE, T. V., Automation of chromatography of radioactive substances, 25:54727
TSIPENYUK, Yu. M., Excitation of spontaneously fissioning isomeric states of $^{239}$Pu and $^{243}$Am at inelastic $\gamma$-quantum scattering, 25:56738 (JINR-P15-5959)
TSUCHIYA, Yoshio, Ionization chamber response for pulsed radiation and drift velocity distribution of filling gas, 25:55015
TSUJIMURA, T., Surface (volume) reactions and polarization in $\pi$---p charge-exchange scattering at high energy, 25:56509
TSUNODA, Junsaku, Fuel failure detector in JRR-3, 25:57117 (JAERI-Memo-4157, pp 23-43)
TSUTSUI, R. T., L x-ray transition probabilities in elements with Z greater than or equal to 57, 25:55823
TSYGANOV, E. N., Readout electronics for $\pi$--e experiment at 50 GeV, 25:55044 (JINR-E1-5818)
TSYTSARKIN, A. F., Thermophysical properties of molten boron oxide, 25:55625
TUAN, R. Hong, Regge cuts and high energy $\pi$N and KN scattering, 25:56505
TUBIS, A., Extrapolation to the limit of singular-core interactions in the three-body problem, 25:56851
TUCKER, A. B., Radioactive decay of $^{169}$Ho and $^{169}$Ho, 25:56767
TUCKER, K. D., Laboratory measurement of the 6-centimeter formaldehyde transitions, 25:55732
TUCKER, William K., Current shaping techniques for high-voltage capacitor banks, 25:57268 (SC-DR-710463)
TUGULEA, M. N., K/sub 13/ decays and chiral symmetry-breaking, 25:56537 (JINR-E2-5996)
TUNITSKII, N. N., Dissociation of $D_2^+$ and $H_2^+$ ions in collisions with $D_2$, He, and Ne, 25:55858
TURALA, M., Readout electronics for $\pi$--e experiment at 50 GeV, 25:55044 (JINR-E1-5818)
TURCOTTE, R. P., Berkelium--oxygen system, 25:55428 (BNWL-B-108)
TUREKIAN, K. K., Marine geochemistry of uranium isotopes $^{230}$Th and $^{231}$Pa, 25:54810
TURILINA, E. S., Calculation of heat transfer in slender bodies, 25:54885
TURINSKY, Paul Josef, Degenerate kernel technique in neutron thermalization theory, 25:56630
TURKEVICH, A., In-situ chemical analysis of extra-terrestrial objects such as the Moon and Mars by use of alpha particles, 25:54459
TURKSTRA, J., Direct determination of the noble metals by activation analysis utilizing high-resolution gamma spectrometry, 25:54487
TURNBULL, J. A., Nucleation of bubbles and re-solution effects in uranium dioxide irradiated at elevated temperatures, 25:55649
TURNER, D. T., Influence of sample size on radiation damage of polyethylene, 25:54623
TURNER, Frederick B., Genetic variation in irradiated and nonirradiated populations of the lizard, Uta stansburiana, 25:55320
TURNER, J. F., Proton differential elastic scattering cross sections for even isotopes of tin at 30.4 MeV, 25:56764
TUZOV, L. V., Electron-microscope and x-ray spectral study of the surface of fractures in cast tungsten, 25:55542
TUZOVA, S. I., Relaxation of high energy protons in magnetosphere of Earth under effect of Alfven waves, 25:56011
TVERSKOI, B. A., Fluid motion produced by temperature gradient perpendicular to gravitational field in presence of magnetic field, 25:55919
Monotonic decrease of intensity of electrons in radiation belts, 25:55978
TYAPKIN, A. A., Process for measuring energy, 25:56609
TYE, R. P., Thermal and electrical conductivities of some electrically conducting compounds, 25:55627
TYLER, R. J., Physical adsorption of carbon dioxide on graphon, 25:55634
TYMINSKII, V. G., Role of radiohydrochemical indexes in the study of regional tectonic activity, 25:54775

## U

UCHAIKIN, V. V., Monte Carlo method of calculating gamma radiation field in a statistically inhomogeneous medium, 25:56268
UCHIYAMA, Yuichi, Stress calculation for the piping systems in a nuclear reactor plant, 25:54850
UDAGAWA, Akira, Effect of dose rate on the radiation graft polymerization of acrylonitrile onto poly(vinyl chloride) fiber, 25:54613
UEDA, Tamotsu, One-boson-exchange model of nucleon--nucleon scattering for the 0 to 3 GeV energy range, 25:56532
UFFELMAN, Donald R., Detonation-wave effects on decameter-wavelength radio waves in the lower ionosphere, 25:55970
UHER, E., Calculation of the sorption kinetics of radioactive microcomponent on a cation exchanger in the presence of competing ions in a batch arrangement, 25:54720 (UJV-2550-Ch)
UJHELYI, K., Radioprotective action of endotoxin, 25:55267
ULIU, Florea, Unified treatment of the V--theta, V--2theta sectors of the Lee model, 25:56553
ULLMAIER, H., Linear high field magnetoresistance in aluminum, 25:56334
UMANTSEVA, V. M., Production of zirconium dioxide microballoons by means of nitrogen plasma, 25:55407
UMEDA, Minoru, Ultrasonic flaw testing method for a reactor pressure vessel using a mockup, 25:54925
UMEK, H., Scintigraphic evaluation of activity of Paget's disease, 25:55294
UMEZAWA, H., Systematic radiochemical analysis of fission products, 25:54449
UMLAND, Fritz, Chemical reaction mechanisms for the attack of high-temperature alloys by molten sulfates, 25:55372 (CONF-690452-, Paper 5)
UNGAR, Stephen Gene, Nonlinear nuclear-energized stellar pulsations, 25:55688
UNNERUS, C. E., Finnish radiological bibliography, 25:55274
UOTINEN, V. O., Nuclear power plant in the nuclear material safeguards accounting system, 25:54934 (BNWL-1598)
Status of burnup calculational technology as applied to the nuclear materials safeguards accounting system, 25:54935 (BNWL-1599)
UPADHYAYA, G. S., Physical properties of monocarbides of zirconium, niobium, and their alloys in homogeneity range, 25:55632
UPOR, Endre, Separation of the trace elements by precipitation and extraction, 25:54734
URBAN, E. J., Flash photolysis of a substituted hexaarylbiimidazole and reactions of the imidazolyl radical, 25:54561
URLI, N. B., Annealing of $\gamma$-irradiated lithium-compensated p-type silicon, 25:56293
URYU, Toshiyuki, Triad tacticity of polyacrylonitrile, 25:54622
USHAKOVA, N. P., Global contamination of the atmosphere by $^{85}$Kr from worldwide nuclear power plants and the radiation danger, 25:54781 (JPRS-53174)
USHER, P. D., Optical variability of a bright new quasi-stellar source, 25:55726
USMANOV, Kh. U., Physico-chemical properties of polyvinyl fluoride obtained by $\gamma$-irradiation, 25:54624
USSEGLIO-NANOT, R., Factors affecting the structure of chromium and chromium--molybdenum white irons, 25:55556
USTINOV, Yu. K., Chemisorption of carbon monoxide on tantalum, 25:55441
USUI, Masahiko, Radiobiological effects of ultraviolet-microbeam in HeLa cells, 25:55312
UTKIN, V. A., Collector system of an isotope separator for investigating short-lived isotopes, 25:56584 (JINR-P6-5888)

## V

VACCARI, Jorge, Radiation effects on water permeability and distribution in frog muscle cells, 25:55323
VACEK, Karel, Hydrogen atoms as studied by ESR, 25:54628 (CONF-700652-(Vol.2), pp 367-420)
VADER, D. C., Pressurized water loop in the high flux reactor at Petten, 25:57121 (RCN-145)
VAGH, A. S., Negative magnetoresistance in neutron-irradiated graphite, 25:56319
VAINBERG, M. Sh., Programming of irradiation and description of the dose field, 25:55211
VAINSHTEIN, L. A., Investigation of x-ray flares on Sun with Cosmos-230, 25:55770
VAITUKAITIS, J., Mathematical analysis of kinetics of radioligand assays: improved sensitivity obtained by delayed addition of labeled ligand, 25:55145
VAJDA, P., Low-temperature photoconductivity in electron irradiated p-type Si, 25:56308
VAKHRUSHIN, Yu. P., Focusing of high-current electron beams

in linear induction accelerators, 25:56608
VALBUSA, U., Nonspherical potentials and molecular scattering at thermal energies, 25:55852
VALKO, J., Investigation of the area-ratio method of pulsed reactivity determination, 25:57185
VAN ALBADA, T. S., Masses, luminosities, and compositions of horizontal-branch stars, 25:55708
VAN ALLEN, J. A., Low-energy (greater than or equal to 0.3 MeV) solar-particle observations, 25:55956
VAN DE MERCKT, J., Functional and circulatory changes in rats after local irradiation, 25:55328
VAN DEN BOS, R. C., Size and location of ribosomal RNA segments in ribosomal precursor RNA of yeast, 25:55138
VAN DER BAAN, J. G., $^{27}Al(d,p)^{28}Al$ reaction at E/sub d/ = 12 MeV, 25:56709
Investigation of $^{33}S(d,p)^{34}S$ reaction, 25:56730
VAN DER BORGHT, R., Asymptotic solutions in nonlinear convection with free boundaries, 25:55694
VAN DER KLEIJ, N., Pressurized water loop in the high flux reactor at Petten, 25:57121 (RCN-145)
VAN DER MERWE, P., Energy levels of $^{79}Br$ and $^{81}Br$, 25:56698
VAN DER WOUDE, A., $^{40}Ca(^{20}Ne,^{16}O)^{44}Ti$ reaction, 25:56721
VAN DE VORST, Albert, Effects of ionizing radiations on matter in the solid state. II, 25:54636
Effects of ionizing radiations on matter in the solid state. I, 25:54635
VAN GELDER, A. P., Angular dependence of the superconductive nucleation field Hc4, 25:56065
VAN HAERINGEN, W., Model calculation of the electron--phonon coupling parameter lambda, 25:56106
VAN HOUTEN, C. J., Period of TY Puppis, 25:55675
VAN KLINKEN, J., $^{139}Sm$, new nuclide of relevance for systematics of N = 77 isomers, 25:56761
VAN TRIGT, C., Analytically solvable problems in radiative transfer. III, 25:56270
VAN VAERENBERGH, P. M., Isotopic renogram by patients suffering from cervical carcinoma, 25:55275
VAN ZELST, L., Non-destructive activation analysis of some elements in stony meteorites by proton and bremsstrahlung-irradiation, 25:54466
VARICH, N. I., Thermal expansion of alloys Al--Mo, Al--Zr, obtained at higher cooling rates, 25:55499
VARMA, N. L., Damping of longitudinal plasma oscillations, 25:56238
VARNAGY, M., Angular distributions of fragments in fission of U and Th near (n,2n'f) threshold, 25:56804
VARNEY, Joel R., Tracking and telemetry system for wildlife research, 25:57266 (RLO-1929-16)
VARSHNEY, K. G., Quantitative separation of magnesium and palladium from numerous metal ions on titanium tungstate papers by electrochromatography, 25:54744
VARSHNI, Y. P., Energies of ''s'' eigenstates in a static screened Coulomb potential, 25:55884
VASENIN, G. V., Electron-microscope and x-ray spectral study of the surface of fractures in cast tungsten, 25:55542
VASILENKO, A. T., Collector system of an isotope separator for investigating short-lived isotopes, 25:56584 (JINR-P6-5888)
VASIL'EV, B. N., Investigation of x-ray flares on Sun with Cosmos-230, 25:55770
VASIL'EV, S. S., Use of accelerated charged particles for determination of concentration of light elements, 25:54528
VASIN, M. V., Study of reactivity of the organism exposed to transverse accelerations and radioprotectants, 25:55264
VASUDEV, P., $^{129}I$ Moessbauer studies of the chemical effects of nuclear transformations in compounds of tellurium, 25:54704
VASUDEVAN, R., Para-Fermi operators and special unitary algebras, 25:56536
VAUBERT, Bernadette, Analysis of the safety problems due to fluorine and fluorine compounds, 25:55246 (CEA-Bib-200)
VAUGHAN, John D., Chemical effects of the nuclear reaction $^{14}N(n,p)^{14}C$ in potassium azide, 25:54687
VAUGHAN, Virginia L., Chemical effects of the nuclear reaction $^{14}N(n,p)^{14}C$ in potassium azide, 25:54687
VAVILOV, V. S., Electron irradiation of lithium-doped germanium at cold temperatures, 25:56301
VAVILOVA, V. V., Properties of Ti--V and Ti--V--Al alloys with O, 25:55471
VAZQUEZ, A. J., TZM molybdenum alloy via P/M, 25:55418
VEBER, Andre, Treatment of elastomers, 25:54619
VEDENYAPIN, G. A., Determination of the diffusion parameters of interstitial atoms in yttrium by reference to the dislocation impurity peaks of internal friction, 25:55461
VEESER, L. R., Instituting a neutron spectrum unfolding capability, 25:55038 (LA-DC-12314)
VEITH, W., Vortex-free Landau state in rotating superfluid helium, 25:56048
VEKSLER, V. I., Secondary emission of $W^+$ ions during bombardment of W by ions of alkali metals, 25:55819
VELECKIS, Ewald, Solubility of helium and argon in liquid sodium, 25:54583
VELINOV, P., Energy dissipation in atmosphere at PCA phenomena, 25:56005
Ionization of substance under effect of charged particles, 25:55983
Lifetime of cosmic rays in Galaxy in presence of acceleration, 25:55907
VENERABLE II, G. D., Reactivity trend seen in the reduction of transition metal complexes by outer-sphere reactants verified for hydrated electron reactions; pulse radiolysis studies of cobalt(III) complexes, 25:54651
VENEZIANO, G., Average properties of dual resonances, 25:56491
VENGRENOVICH, R. D., Non-equilibrium solidification and structural transformations during heating in aluminum-molybdenum and aluminum--chromium alloys, 25:55535
VENKATESAN, D., Solar activity and planetary luminosity, 25:55766
VENTURA, E., $^3H(^3He,\gamma)^6Li$ capture reaction and the structure of $^6Li$, 25:56664
VERBOOM, G. K., Temperature profile in thermonuclear reactor, 25:56216 (NP-19014)
VERCAEMER, C., Structure and tensile properties of Nb--4.6 Ti--O, 25:55521
Structure and tensile properties of Nb--Zr--O alloys rich in Nb, 25:55522
VERESHCHAKA, N. P., Temperature dependence of absolute thermo-EMF coefficient of certain transition metals, 25:56351
VERESHCHINSKII, I. V., Kinetics of the low-dose radiolysis of concentrated aqueous acidic solutions of sodium nitrate, 25:54657
Radiation chemical synthesis of organic compounds in liquid nonaqueous systems (survey), 25:54617
VERGUN, A. P., Determination of the relative difference between the mobilities of isotopic lithium ions in an ion-exchange resin--solution system, 25:54730
Estimation of the single-stage isotope separation factor in the electromigration of isotopic ions through an ion-exchange membrane, 25:54729
VERHAAR, B. J., Is the lightest fractionally-charged particle stable, 25:56471
VERHAEGH, J. J., Compact mutants induced by x-ray treatment in apple and pear, 25:55174
VERHEEST, Frank, Dispersion in beam--plasma systems. II, 25:56169
Dispersion in beam--plasma systems. I, 25:56170
VERMA, L. P., Chemical shifts of L/sub III/ x-ray absorption edges of Gd and Dy, 25:55822
VERMEIL, Catherine, Reactions of H and deuterium formed in photolysis of methane and perdeuterated methane, 25:54573
VERNOV, S. N., Correlation of magnetic activity indexes with intensity of outer-belt electrons, 25:55979
VERNOV, Yu. S., Properties of the amplitude of elastic scattering at extremely high energies, 25:56574
VERSCHUUR, K. A., Experimental study of the neutron attenuation in concrete shields for fast and thermal reactors, with the aid of simulated concrete configurations, 25:57027 (RCN-147)
RAGA: a Monte Carlo program for calculation of gamma-ray transport in a reactor shield for multi-region slab geometry, using exponential transformation, 25:57026 (RCN-146)
VERSTEEG, Joost, Consequences of molten fuel ejection in a LMFBR, 25:57083 (CONF-710302-(Vol.1), pp 241-58)
VESPALEC, R., System of radioactive products control in gas coolant of nuclear reactors, 25:57033
VESTERGAARD, Per, Glomerular filtration rate determined by $^{51}Cr$-EDTA, 25:55122
VETTE, J. I., Isotropy of cosmic $\gamma$-ray flux, 25:55896 (N-71-27639)
VIAL, A., Metallography of the 700°C precipitation in a Fe--40 percent Ni alloy containing beryllium, 25:55544
VIALETTES, Henry, Shielding problems set by use of natural U target with linear electron accelerator. Shielding and safety systems necessary, 25:56582 (CEA-R-4188)
VICK, Nicholas A., Virus-cell relationships in dog brain tumors, 25:57262 (ORO-3195-50)
VIDAL, F., Velocity of second sound in rotating helium II, 25:56054
VIELAND, L. J., Low-temperature specific heat measurements of $ZrV_2$ and $HfV_2$, 25:56072
VIEU, Charles, Electromagnetic transitions in $^{190}Pt$, 25:56760
VIGIL, John C., Dynamic Buffer allocation on the CDC 600: the DYNBUF program, 25:57234 (LA-4721)
VIGLA, D., Study of the mobility of ions in air, 25:54801
VIL'CHINSKI, Ya., Nuclei of light elements with larger neutron excess, 25:56788
VILCOV, I., Study of /sup 236mf/U isomeric fission through $^{235}U(n,\gamma)$ reaction, 25:56793
VILCOV, N., Study of /sup 236mf/U isomeric fission through $^{235}U(n,\gamma)$ reaction, 25:56793
VILINSKAS, P., Behavior and calibration of devices for monitoring impurities in sodium, 25:55069 (ANL-7804)
VILLANTE, U., Multiple crossings of the Earth's bow shock at large geocentric distances, 25:55953
VINCENT, Daniel A., Quantized flux states of superconducting cylinders, 25:56064
VINCENTI, E., COSTANZA (R,Z), 25:57187 (EUR-4673)
VINH MAU, N., Microscopic theory of nucleon--nucleus scattering and optical potential, 25:56822 (LYCEN-7104, Cl.1-13)
VINOGRADOV, D. P., X-ray diffraction study of phase composition of alundum-surfaced alloys VR-20 and VA-3

XUM

after vacuum annealing at high temperatures, 25:55465
VINOGRADOV, P. S., Kinetic energies of protons formed during collision of electrons with excited $H_2$, 25:55857
VISHNEVSKII, I. I., Thermal conductivity of some oxygen compounds of zirconium and hafnium, 25:55637
VISSER, J. F. J., Pressurized water loop in the high flux reactor at Petten, 25:57121 (RCN-145)
VISSER, T., Compact mutants induced by x-ray treatment in apple and pear, 25:55174
VIVIAN, Stanley R., Classic bioassay statistical procedures applied to radioimmunoassay of bovine thyrotropin, growth hormone and prolactin, 25:55143
VIZDALOVA, M., Survival of E. coli B under different post-irradiation conditions, 25:55357
VLADIMIROV, V. G., Some principles of evaluating the effectiveness of radioprotective agents in man, 25:55256
VLADUCA, G., Analysis of proton scattering on $^{32}S$, 25:56694
VLASOV, A. N., Measurement of the mean free path of fast electrons, 25:56281
VOELK, H. J., Analysis of electromagnetic instabilities parallel to the magnetic field, 25:56204
VOGEL, Charles E., Radiation measurements and low frequency and high-pressure investigations of induction heated plasma, 25:56146 (N-71-27023)
VOGLER, F., Examination of coupled-channel calculations for reaction $^{24}Mg(d,p)^{25}Mg$, 25:56728
VOGT, Erich, Advances in nuclear physics. III, 25:56871
VOIGT, Hans-Peter, Chemical reaction mechanisms for the attack of high-temperature alloys by molten sulfates, 25:55372 (CONF-690452-, Paper 5)
VOILLEQUE, Paul G., Health physics aspects of nuclear facility siting. Volume I. Proceedings of the fifth annual health physics society midyear topical symposium, Idaho Falls, Idaho, November 3--6, 1970, 25:55157
Health physics aspects of nuclear facility siting. Volume I. Proceedings of the fifth annual health physics society midyear topical symposium, Idaho Falls, Idaho, November 3--6, 1970, 25:57103
Health physics aspects of nuclear facility siting. Volume I. Proceedings of the fifth annual health physics society midyear topical symposium, Idaho Falls, Idaho, November 3--6, 1970, 25:55193
VOLDET, Pia, Non-destructive analysis of hafnium in zircons by neutron activation and gamma spectrometry of /sup 179m/Hf, 25:54491
VOLKOV, A. N., Preparation and operation of silicon and germanium semiconductor counters, 25:55013
VOLKOV, M. K., Nonpolynomial Lagrangians (highest perturbation orders), 25:56546 (JINR-P2-5998)
VOLKOVA, M. A., Phase equilibria and properties of alloys in TiAl--$V_3Al_3$ section of Ti--Al--V system, 25:55537
Study of phase equilibria and properties of the alloys in the titanium--aluminum--iron and titanium--aluminum--vanadium systems, 25:55501
VOLKOVA, N. V., Diffusion losses of radiogenic argon from meteorites, 25:55672
VOLKOVA, S. A., Determination of the association constants of ions from the rate of oxygen exchange between anions and water, 25:54553
VOLKOVICH, A. V., Precipitation of uranium from a melt of fused halides with a molten zinc cathode, 25:54580
VOLKOVYSKII, R. Yu., Two-component theory of fermions, 25:56552
VOLODICHEV, N. N., Chemical composition of primary cosmic rays, 25:55899
VOLOVIK, V. D., Excitation of ultrasonic waves by passage of fast electrons through a metal, 25:56566
VOLPE, P., Hot tritium reactions in $CH_4$ + $SiH_4$ system, 25:54678
VOLTZ, Rene, Comments on the activated species in irradiated organic media, 25:54626 (CONF-700652-(Vol.1), pp 139-219)
VON DER DECKEN, C.-B., State of helium technology for high temperature reactors, 25:57040
VON DER WEYDEN, H. D., Experiments on the behavior of metallic insulations in helium, 25:56890
VONDY, D. R., Discussion about the nuclear reactor core analysis code citation, 25:57169 (CONF-710302-(Vol.2), pp 939-52)
Nuclear reactor core analysis code: CITATION, 25:57183 (ORNL-TM-2496(Rev.2))
VOOK, F. L., Important unanswered questions, 1970, 25:56332
Low-temperature channeling measurements of ion-implantation lattice disorder in GaAs, 25:56289
VORESS, Hugh E., Science and society, 25:57294 (WASH-1182)
VOROB'EV, N. I., Si(Li)-detectors for diagnosis of neoplasm of the skin, 25:55273
VOROB'EV, V. S., Canonical transformation method in thermodynamics of partially ionized plasma, 25:56172
VOROB'EVA, E. A., Combined treatment of barley and wheat seeds with ionizing radiation and ethylene-imine for the induction of mutations, 25:55261
VOROPAEV, Yu. V., Gamma-ray irradiation equipment, 25:54837
VOS, Robert, Radiative proton capture in deuterium, 25:56645
VOSKRESENSKII, K. D., Calculation of heat transfer in slender bodies, 25:54885
VOSS, Milo D., Survey of environmental radioactivity, 1--6/71, 25:55152 (IS-2658)
VOSTEEN, K.-H., Radiation treatment of human tumours, 25:55306
VOTE, F. C., Near-isothermal dissipative flow of liquid He II at supercritical velocities, 25:56062
VOZNYUK, E. I., Alteration of the function of external respiration in patients with malignant tumors of the chest under the effect of radiation treatment, 25:55339
VOZZELLA, P. A., Friction welding of titanium alloys, 25:55409
VRATISLAV, S., Spectral distribution of neutrons from the reactor horizontal channel, 25:57125
VSEKHSVYATSKAYA, I. S., Characteristics of delta $f_0F2$ distribution curves, 25:55985
VUKMIROVICH, Z., Isotope effect upon hydrogen exchange of m-carborane with bases, 25:54555
V'YUGOV, P. N., Absorption of oxygen and nitrogen by zirconium at low pressures, 25:55463

# W

WADA, Susumu, Design of the valves for nuclear power generation, 25:54842
WADLEIGH, W., Facility for the determination of low-level tritium in biological and environmental samples, 25:55003 (UCRL-73128)
WAGENER, K., Countercurrent electrophoresis, 25:54742
WAGNER, H., Simulation of the hydrodynamics of boiling water reactors, 25:57022 (MRR-73)
WAGNER, L. S., Electron density enhancements in E and F regions during solar flares, 25:56035
WAGNER, P., Effect of doping on the thermal conductivity of polycrystalline graphite, 25:55635
WAGNER, William F., Synergistic solvent extraction of rare earths by mixtures of thenoyltrifluoroacetone and acetylacetone, 25:54731
WAHL, W. C., Bibliography on electrical discharge machining and electrochemical machining, 25:54834 (WAPD-331)
WAI, C. M., Recoil bromine reaction. The isomerization of excited cyclopropyl bromide, 25:54690
WAI, Chun-chung, Dome morphological mutant linked to the B incompatibility factor of Schizophyllum commune, 25:55186
WAIN, A. G., $^{237}Pu$ production by $^{235}U(\gamma,2n)$ reaction, 25:54674
WAINERDI, R. E., Analysis of oceanographic samples from the glomar challenger voyage, 25:54482
WAJDA, Stanislaw, Radioisotopic exchange of ligands in chloro- and thio-cyanatomolybdates(III), 25:54558
WAKABAYASHI, N., Phonon spectrum of scandium metal by inelastic scattering of neutrons, 25:56342
WAKEMAN, James F., Method and apparatus for detecting gas leaks using radioactive techniques, 25:55063
WALDRON, H. H., Geologic and seismic considerations affecting nuclear power plant site selection, 25:54777
WALDTEUFEL, P., Combined incoherent-scatter F1-region observations, 25:56047
WALEH, A., Supercooling and thermal conductivity in superconducting molybdenum, 25:56066
WALKE, Gerald J., Plutonium recycle developments, 25:57202
WALKER, D. H., Fission product release during a LOCA, 25:57104
WALKER, J. C., Radiofrequency perturbation of selectively excited nuclear hyperfine levels, 25:56368
WALKER, James C. G., Transport processes in E region of ionosphere, 25:55969
WALKER, James F., Parity-invariance tests originating with nuclear beta decay, 25:56855
WALKER, P. M., ARC system cross-section homogenization and modification capabilities, 25:56614 (ANL-7714)
WALKER, R., Nuclear interaction tracks in minerals and their implications for extraterrestrial materials, 25:55669 (N-71-26344)
WALKER, R. M., Comments of a paper on elastically scattered recoil nuclei in solid state detectors, 25:54999 (N-71-26447)
WALKER, S. A., Relative hazards from $^{95}Zr$ and $^{95}Nb$ based upon inhalation of particles formed under various thermal conditions, 25:55125
WALL, N. S., Elastic scattering of 60 to 120 MeV electrons from $^{46}$ $^{48}$ $^{50}Ti$, 25:56701
WALLACE, John Longstreet, Equilibrium properties of submonolayer $^4He$ films, 25:56059
WALLING, Cheves, Oxidation of alcohols by Fenton's reagent. The effect of copper ion, 25:54576
WALMSLEY, D. G., Normalizing current of a Type-II superconductor, 25:56069
WALSH, Carol, Evaluation of the lung scintiphoto as a screening test for pulmonary disease, 25:55297
WALSH, T. F., Finite-energy sum rules and reactions ee + eeepsilon(750) and ee + eef(1260), 25:56463
WALSH, William J., Structured variations of the plasmapause: evidence of a corotating plasma tail, 25:56028
WALTERS, L. J. Jr., Activation analysis of Philippine magnetite sands, 25:54483
WALTON, Harold F., Ion exchange in analytical chemistry,

25:54397
WAPPAUS, Walter A., Effects of charged particle and uv radiation on stability of silvered and aluminized FEP teflon second surface mirrors, 25:55656 (N-71-27736)
WARCZEWSKI, J., Measurements of energy and flux of cosmic ray hadrons using an ionization spectrometer, 25:56413 (INP-756)
WARCZEWSKI, Jerzy, Inelasticity coefficients for pion--Fe and nucleon--Fe collisions, 25:56414 (INP-757)
WARE, A. R., Activation analysis applied to non-aqueous flowing system, 25:54524
WARREN, J. L., $^{129}$I Moessbauer studies of the chemical effects of nuclear transformations in compounds of tellurium, 25:54704
WARREN, M. Laird, Dissociation cross sections for 0.5- to 1-MeV HeH$^+$ ions in $H_2$, He, $N_2$, and Ne gases, 25:55872
WASLEY, Richard J., Low-velocity air gun and Hopkinson split-bar facility, 25:57289 (UCRL-51098)
WASSON, O. A., Distribution of partial radiation widths in $^{238}$U(n,$\gamma$)$^{239}$U, 25:56790
WATANABE, Kiyokazu, Nondestructive inspection of jet engines with radioisotopes, 25:54927
WATERMAN, N. A., Application of small angle x-ray scattering to the study of irradiation produced defects, 25:55578 (RD/B/N-1990)
WATKINS, G. D., Irradiation effects in II--VI compounds, 25:56291
WATKINS, R. D., Computer control of experiments in atomic physics, 25:55094
WATSON, B. A., T = $^3/_2$ states in $^{11}$C, 25:56679
WATSON, R. D., Atmospheric abundances in the beta Cephei stars, 25:55711
WATTERS, R. L., Plutonium movement in aquatic systems: a review, 25:55150 (CONF-710401-, pp 407-10)
WAYLAND, J. R., Increasing hadron--nucleus cross sections and cosmic ray muon zenithal variations, 25:55906
WEAVER, C. L., Public Health Service role in providing information relative to the nuclear power controversy, 25:56981
WEBB, William H., Oxidative decarboxylation of polyaminocarboxylic acids. II, 25:54422
WEBER, A., Organization and financing of nuclear research and technology in Federal Republic of Germany, 25:57014
WEBER, O., Acid determination with the help of radioiodine, 25:54439
WEBER, R. F., Errors due to averaging spectral-line intensities in the presence of electron-temperature variations, 25:56171
WEBER, Theodor H., Lung scanning with gamma camera, 25:55296
WEBSTER, R. K., On-line computers for gamma spectrometry and activation analysis, 25:54474
WEEDMAN, Daniel W., Kinematic properties of 71 H II regions in LMC, 25:55795
WEEREN, H. O., Safety analysis of waste disposal by hydraulic fracturing at Oak Ridge, 25:54971 (ORNL-4665)
WEGENER, D., Excitation of $\Delta$(1236) resonance on bound state neutrons, 25:56405 (DESY-71/33)
WEIGAND, P. W., Rare earth abundances in mesozoic dolerite dikes from eastern United States, 25:54476
WEIL, Juergen W., Contributions to the Sunakawa model of elastic multiple neutron scattering, 25:56637
WEINER, John, Charge transfer in $Na^+$--$O^-$ collisions at low relative energy, 25:55859
WEINER, R. M., Mesonic structure in the nucleon, 25:56512
WEISENBERGER, W. H., Low-temperature channeling measurements of ion-implantation lattice disorder in GaAs, 25:56289
WEISMAN, Manuel I., Neutron radiography of the dental pulp, 25:55277
WEISS, E., /sup 99m/Tc technetium sulfide and scintillation camera in rapid diagnosis of pericardial effusion, 25:55295
WEISS, J. J., Reply to formation of ozonide ions in $\gamma$-irradiated aqueous solutions of alkali hydroxides, 25:54609
WEISSMAN, S., Strength increase in Ti 35 wt. percent Nb through step-aging, 25:55490
WELCH, A. K., Design of pod boiler pressure vessels, 25:56885
WELCH, Gary A., Photographic detection of intragalactic matter in Coma Cluster, 25:55782
WELKER, Klaus, Standardization of 2- and 4-axial $^{60}$Co pendulum irradiation of small pelvis, 25:55222
WELSH, L. B., Magnetic properties of $LaSn_3$, 25:56353
WENG, Pao-shan, Determination of intermediate neutron energy spectrum, 25:57126
WENZEL, D. R., Cloud gamma calculations, 25:54797
WERNICK, J. H., Study of a series of $Nb_3X$ compounds by nuclear magnetic resonance, 25:56373
WERNIK, A., Geophysical effects of solar activity in upper atmosphere. I, 25:55981
Geophysical effects of solar activity in upper atmosphere. II, 25:55982
WESCOTT, E. M., Electric-field measurements and identification of currents causing magnetic disturbances in polar cap, 25:55959
WESOLOWSKI, J. J., Diurnal variation of aerosol trace element concentrations in Livermore, Calif, 25:54456
WEST, L. A., Reactive scattering of $N_2O$ molecular beams from clean and carbon covered (100) platinum single crystal surfaces, 25:57237 (LBL-133)
WESTENHOLZ, C. v., Geometric structure of a parity-conserving relativistic quantum field theory, 25:56557
WESTERMAN, M., Effect of x irradiation on Chorthippus brunneus, 25:55176
WESTON, G. J., Electron spin resonance study of V(II). IV, 25:56384
WESTON, L. W., Measurements of the neutron fission and absorption cross sections of $^{239}$Pu over the energy region 0.02 eV to 30 keV, Part II, 25:56746 (ORNL-4707)
WEXLER, S., Collisional dissociative ionization of TlBr by accelerated Xe and Kr atoms, 25:55879
WHALEN, B. A., Sounding-rocket observations of particle precipitation in a polar-cap electron aurora, 25:56031
WHANG, Y. C., Conversion of magnetic-field energy into kinetic energy in the solar wind, 25:55775
WHEATLEY, B. M., Radiation quantities in health physics, 25:55251
WHEELER, Jamie K., Off-site medical planning and management for an experimental underground nuclear detonation, 25:55249
WHICKER, F. W., Accumulation of radiocesium in rainbow trout via a non-foodchain pathway, 25:55159
WHIPPLE, G. Hoyt, Use of stable element concentrations in pre-operational environmental monitoring, 25:55240
WHITE, J. A., Quantum theory of spontaneous emission in the presence of external radiation, 25:55883
WHITE, Maurice A., Implantable radioisotope-fueled stirling engine, 25:54910
WHITEHEAD, C., Direct-access multi-user computer system for the Harwell synchrocyclotron, 25:56612
WHITEHEAD, R. R., Lanczos method for nuclear shell model calculations, 25:56865
WHITEHEAD, Thomas Wilson Jr., Ion optics of a three-stage inhomogeneous magnetic field isotope separator, 25:54920
WHITESIDE, H., Calibration of NASA--GSFC High Energy Cosmic Ray Experiment, 25:55046 (N-71-16750)
WHITFORD, A. E., Absolute energy curves and K corrections for giant elliptical galaxies, 25:55794
WHITLEY, J. E., Determination of trace elements in igneous rocks by nuclear techniques, 25:54462
WHITNEY, E. D., Prog. rpt. on quantitative determination of structure-property relationships in nuclear fuel element materials, 12/16/70--3/15/71, 25:55437 (TID-25784)
WHITTAKER, A., Effect of doping on the thermal conductivity of polycrystalline graphite, 25:55635
WHITTON, J. L., Ion implantation of S into GaAs, GaP, and Ge monocrystals, 25:56288
WICK, Gerald, New vistas for isotope separation, 25:54919
WICK, Gerald L., Neutrino astronomy: probing the sun's interior, 25:55741
WIDING, K. G., Highly ionized Fe and Ni lines in 200- to 400-A of solar spectrum, 25:55774
WIEBE, L. I., Some aspects of measurement of $^{32}$P Cherenkov radiation in water by liquid scintillation spectrometer, 25:54438
WIECZORKOWSKI, M., Density of coextruded metal cladded rod core as function of cartridge density and core length, 25:55420
WIEDERICK, H. D., Structure of current-induced intermediate state in Type-I superconductors, 25:56102
WIGGINS, Peter Frederick, Neutron capture gamma ray studies of metals, mixtures, ores, and marine samples using $^{252}$Cf, 25:54913
WIKTOR, Zdzislaw, Influence of radon inhalation on lymphocytes, 25:55346
WILD, J. P., Solar explosions, 25:55769
WILDER, D. R., Electrolytic behavior of yttria-stabilized hafnia, 25:56355
WILHELM, J., Velocity distribution function for electrons of medium ionizing power in Ar, 25:56186
WILHELM, M., Compensation of external magnetic field by an internal field in a superconductor, 25:56074
WILHELMI, U., Scintigraphic investigations of parasternal lymph nodes with $^{198}$Au, 25:55288
WILHELMOVA, V. S., Probability of the ($\mu^-$, $\nu$) process of $^{139}$La and $^{208}$Pb nuclei, 25:56739 (JINR-P1-6006)
WILKES, W. R., Continuous-distillation apparatus for the separation of $^3$He from $^4$He, 25:56121
WILKIN, C., Scattering of pions from nuclei, 25:56811 (CERN-71-14, pp 289-378)
WILKINS, Charles A., Sealed container with pressure relief for hazardous material, 25:54989
WILLES, E., Facility for the determination of low-level tritium in biological and environmental samples, 25:55003 (UCRL-73128)
WILLIAMS, A. J., Structural behaviour of insulation of prestressed concrete pressure vessels, 25:56889
WILLIAMS, Evan T., $^{40}$Ar(n,$\alpha$)$^{37}$S reaction at 14.4 MeV, 25:56718
Reactions of $^{20}$Ne with 14.3-MeV neutrons, 25:56717
WILLIAMS, Ffrancon, Electron spin resonance spectrum and structure of the radical anion of phosphorus oxychloride, 25:54667
Molecular weights and molecular weight distributions of polyisobutylenes produced by $\gamma$-irradiation, 25:54621
WILLIAMS, J., Integral measurements in EBR-II of capture

XUM

rates, fission rates, and α for $^{233}U$, $^{235}U$, $^{238}U$, $^{239}Pu$, $^{240}Pu$, and $^{242}Pu$, 25:56982 (ANL-7791)
WILLIAMS, J. A., Fracture and tensile behavior of neutron-irradiated A533-B pressure vessel steel, 25:55587
WILLIAMS, L. C., Brazing the shell assembly for the BONUS superheater fuel element, 25:55425
WILLIAMS, M. W., Optical properties of UN from 0 to 74 eV, 25:56345
WILLIAMS, P. M., Physical properties of radiation-induced and growth defects in II--VI semiconductors, 25:56286
WILLIAMS, Ronald L., Relative rates of hydrogen atom abstraction by near-thermal $^{18}F$ atoms, 25:54686
WILLIAMSON, J. H., Construction of electron distribution functions from laser scattering spectra, 25:56143
WILLIS, C. A., Photon energy and air shielding in cloud gamma dose calculations, 25:54796
WILLIS, R. F., Experimental investigation of the band structure of graphite, 25:56348
WILLIS, Wayne D., Quantized flux states of superconducting cylinders, 25:56064
WILLS, Beverley J., Daily and hourly variations in flux density of radio sources, 25:55731
WILSON, R. L., Can all liquid radwaste discharges be eliminated, 25:56881
WILSON, R. W., CO, CN, and CS emission from IRC + 10216, 25:55686
WINCHELL, H. S., Recoil synthesis of high specific activity $^{11}C$-cyanide, 25:54683
WINDSOR, C. G., Neutron orbital cross section for a tight-binding model of paramagnetic nickel, 25:56354
WINGET, J. O., Liquid--liquid chromatographic separation of neodymium, samarium, and gadolinium, 25:54745
WINKLER, R., Velocity distribution function for electrons of medium ionizing power in Ar, 25:56186
WINSOR, Niels K., Numerical simulation of toroidal plasma confinement with a fluid model, 25:56129
WINSTON, M. A., /sup 99m/Tc technetium sulfide and scintillation camera in rapid diagnosis of pericardial effusion, 25:55295
WINTER, Rudolph Ernest K., Deuterium isotope effects on thermal cyclobutene isomerizations. An investigation of competitive conrotatory ring openings, 25:54568
WINTERSTEINER, Peter P., Coincidence Moessbauer spectroscopy, 25:56367
WITKOWSKI, E. J., Safety analysis of waste disposal by hydraulic fracturing at Oak Ridge, 25:54971 (ORNL-4665)
WITT, F. J., Fracture toughness K/sub Icd/ values for ASTM A533 grade B, class 1 steel, 25:55517
WITTMANN, F., Deformation and cracking mechanics in hardened cement paste and concrete under short-term and high sustained loads, 25:55661
WITZKE, Walter R., Creep behavior of electron beam-melted rhenium, 25:55432 (N-71-23114)
Creep behavior of electron-beam-melted rhenium, 25:55491
Mechanical properties of a W--23.4-percent Re--0.27-percent Hf--C alloy, 25:55433 (N-71-23982)
WLODARSKY, R., Thermal annealing of neutron-irradiated carbon, 25:56283 (CEA-CONF-1823)
WOEHLBIER, F. H., Diffusion data. Number 2, 1971, 25:55509
WOHLLEBEN, K., Effect of C on critical current of $Nb_3Sn$, 25:56084
WOLF, D., 14-MeV-neutron irradiation of p-type germanium, 25:56305
WOLF, E. D., Measurement of lattice damage caused by ion-implantation doping of semiconductors, 25:56287
WOLF, Lothar, Method for the numerical solution of the linear position dependent Boltzman equation in spherical geometry and spherical symmetry, 25:56617 (JUL-765-RG)
WOLF, S., Fluctuation effects on thermal conductivity of one-dimensional superconductors, 25:56095
WOLFE, B., Liquid metal fast reactor accidents, 25:57072 (CONF-710302-(Vol.1), pp 1-24)
WOLFE, R. A., Phenomenological model of in-pile stress relaxation (LWBR Development Program), 25:55579 (WAPD-TM-943)
WOLFF, B., Interference between $\pi^0\pi^0$ decay of K/sub L/$^0$ and K/sub S/$^0$, 25:56407
WOLFF, Ch., Effects in vivo of ionizing radiations on human chromosomes, 25:55178
WOLFF, E., Infrared spectra and vapor pressure isotope effect of crystallized ammonia and its deuterium derivatives, 25:54572
WOLFF, H., Infrared spectra and vapor pressure isotope effect of crystallized ammonia and its deuterium derivatives, 25:54572
WOLKENHAUER, W. C., Nuclear power plant in the nuclear material safeguards accounting system, 25:54934 (BNWL-1598)
Status of burnup calculational technology as applied to the nuclear materials safeguards accounting system, 25:54935 (BNWL-1599)
WOLLAN, J. J., Superconductivity and magnetic scattering in La--Ce, 25:56068
WOLLNIK, H., Search for bremsstrahlung-induced fission isomers of $^{238}U$ and $^{239}Pu$, 25:56801
WOLNY, R. F., Primary frequency standards in the Y-12 Physical and Electrical Standards Laboratory, 25:57296 (Y-IA-92)
WONG, K. M., Concentrations of plutonium, cobalt, and silver radionuclides in selected Pacific seaweeds, 25:55151 (CONF-710817-1)
Plutonium concentration in organisms of the Atlantic Ocean, 25:55161
WONG, S. S. M., Complex spectroscopy, 25:56874
WOO, Ching, Synergistic solvent extraction of rare earths by mixtures of thenoyltrifluoroacetone and acetylacetone, 25:54731
WOOD, E. D., Determination of gold in geological materials by neutron activation analysis, 25:54488
WOOD, James David London Hedley, Improvements in or relating to supply circuits for ion accelerators, 25:56605
WOOD, R. W., Investigation into effect of ''crud'' deposits on surface temperature, dry-out and pressure drop, with forced convection boiling of water at 69 bar in annular test section, 25:54861 (AEEW-R-705)
WOODARD, R. W., Performance of high efficiency particulate air filter for fume from burning plutonium metal, 25:54951 (CONF-710401-, pp 181-202)
WOODS, R. D., Density of the neutral atmosphere above 100 km, Kauai, May--June 1970, 25:57274 (SC-RR-710541)
WOODSON, H. H., Applications of superconductivity and cryogenics in electric power systems, 25:56114
WOOLF, Charles M., Prog. rpt. on congenital malformations, 1--12/71, 25:57222 (COO-2013-19)
WOOLLEY, J. A., Modeling and application of the adiabatic approximation for analyzing rod drop excursions, 25:57084 (CONF-710302-(Vol.1), pp 259-81)
WOOTTON, Peter, In-phantom microdosimetry with 14.6 MeV neutrons, 25:55232
WORDEN, Robert, Regge models of forward pion and eta photoproduction, 25:56452 (CALT-68-313)
WORLTON, William J., Future prospects in computer technology, 25:57191 (CONF-710302-(Vol.2), pp 1086-1101)
WOSTENHOLM, G. H., Superconductivity of molybdenum and tungsten carbides, 25:56087
WOUTERLOOD, H. J., Physical adsorption of carbon dioxide on graphon, 25:55634
WRENN, McDonald E., Manmade radionuclides in the Hudson River estuary, 25:55160
WRIGHT, R. W., Pressure generation by molten fuel-coolant interactions under LMFBR accident conditions, 25:57073 (CONF-710302-(Vol.1), pp 25-49)
WRONA, B. J., Brittle-to-ductile transition in $UO_2$--20 wt. percent $PuO_2$ nuclear fuel, 25:55610
WU, C. S., Magnetic drift waves near proton cyclotron frequency, 25:56043
WU, Chung-Hsiung, Mass-spectroscopic determination of the heat of formation and the investigation of the evaporation behavior of EuN, BN, and AlN, 25:55607 (JUL-739-PC)
WU, Shaw-chii, Thermal annealing behavior of recoil $^{57}Co$ formed by decay of $^{57}Ni$-labeled hexammine nickel(II) complexes, 25:54689
WU, Tai Tsun, Production of pion pairs in electron colliding beams, 25:56460
WUTHRICH, Paul, Horological movement utilizing a radioactivity detector and source, 25:55085
WYATT, R. L., Epitaxy of vanadium on sapphire, 25:55530
Hetero-epitaxial films of niobium on sapphire, 25:55531
WYKOFF, M. H., Distribution of $^{134}Cs$ in the conceptus of the pregnant rat, 25:55114

## Y

YAFFE, L., Nuclear charge dispersion of light-mass elements in fission of $^{232}Th$, 25:56805
YAKH'YAEV, R. Sh., Annihilation of electron--positron pairs to pseudo-scalar mesons, 25:56459
YAKOMOVITCH, R. A., Thermophysical properties of molten boron oxide, 25:55625
YAKOVENKO, Yu. D., Influence of deformation conditions on polygonization and recrystallization of single-crystal molybdenum, 25:55559
YAKOVLEV, Yu. V., Radioactivation determination of impurities in the epitaxial films of gallium arsenide, 25:54512
YAKOVLEVA, E. A., Isotope effect upon hydrogen exchange of m-carborane with bases, 25:54555
YAKUSHIN, F. S., Isotope effect upon hydrogen exchange of m-carborane with bases, 25:54555
YAMAGUCHI, Hisao, Ultrasonic testing of nuclear fuel cladding tubes, 25:54926
YAMAGUCHI, Ken, Polarization of core fermion and the heat transport of flux line, 25:56088
YAMAMOTO, Kunio, Lorentz invariance and finite self-mass in local field theory, 25:56564
YAMAMOTO, Moriyuki, Facilities for accelerators for medical use, 25:56607
YAMAMOTO, Satoru, Effects of neutron irradiation on Cu--Be alloys, 25:55583
YAMAUCHI, S., Thermodynamic properties of ternary refractory carbides. II. Zirconium--uranium--carbon and zirconium--hafnium--carbon, 25:55614
YAMAZAKI, Hiroshi, Osteonecrosis in lower mandible after postoperative radiotherapy, 25:55344
YANAGIHARA, T., Subcellular distribution of radioactivity in neuronal and glial-enriched fractions after

incorporation of [$^{3}$H]leucine in vivo and in vitro, 25:55119
YANASE, Y., Determination of geological time with a nuclear reactor and a mass spectrometer, 25:54765
YANG, Kuo-pao, In vitro uptake of model amino acids by rat liver following whole-body γ-irradiation, 25:55126
YANG, T. Y., Matrix displacement method on pre- and post-buckling analysis of liners for reactor vessels, 25:56994
YAO, Andrew, Divergences of massive Yang--Mills theories: higher groups, 25:56542 (CNRS-CPT-71/P-378)
YASUBUCHI, Shiro, Estimation of genetically significant dose equivalent from occupational exposure to external sources of radiation in Japan, 25:55230
YASUHARA, F., Storm sudden commencements and polar magnetic substorms, 25:56026
YATIRAJAM, V., Separation of rhenium from molybdenum and other heavy metals by solvent extraction, 25:54401
YAVORSKAYA, I. M., Hydrodynamics of the convective envelopes of stars, 25:55707
YIOU, F., Electron capture by 40-, 155-, and 600-MeV protons in thin foils of Mylar, Al, Ni, and Ta, 25:55862
YOFFE, A. D., Physical properties of radiation-induced and growth defects in II--VI semiconductors, 25:56286
YOKOTA, Mitsuo, Development of reactor in-core neutron monitor, 25:57025
YONNET, J., Energy of separation for some nuclei of medium mass in the reaction (p,2p) at 600 MeV, 25:56706
YOON, T. S., Regge analyses of rho$^{0}$ production in πN charge exchange channels at 7 GeV/c, 25:56431
YORK, D., Determination of geological time with a nuclear reactor and a mass spectrometer, 25:54765
YOSHIDA, Hiroyuki, Effects of neutron irradiation on Cu--Be alloys, 25:55583
YOSHIHARA, Kenji, Observation of neutron dose dependence of the apparent initial retention in chloroindium chlorophthalocyanine, 25:54680
YOSHIKURA, H., Radiation effects on macromolecular synthesis in contact inhibition-sensitive cells synchronized by medium change, 25:55129
YOSHIMURA, R. H., Neutron radiography at Sandia Laboratories: its techniques and instrumentation, 25:54924 (SC-DR-710178)
YOUELL, Frederick Peter, Improvements in and relating to nuclear radiation attenuating means, 25:55657
YOUNG, Alan Morris, Study of the reaction T($^{3}$He,γ)$^{6}$Li from 0.5 to 20 MeV, 25:56646
YOUNG, F. C., Properties of 12.50 and 12.52 MeV levels of $^{15}$N, 25:56669
YU, C. W., Analysis of perforated end caps for pressure vessels by finite element method, 25:56985
YU, Dahsoong, Conditions of asymptotic stability of nonlinear space--time reactor dynamics, 25:57188
YU, M. Y., Effect of impurity ions on the stability of drift waves, 25:56243
YUDKOVSKII, S. I., Decomposition of the solid solution of interstitial impurities in tungsten, 25:55444
YUDOVICH, L. A., Characteristics of delta $f_0$F2 distribution curves, 25:55985
YUFEREV, V. S., Boundary layer at electrode of an MHD duct in absence of ionization equilibrium, 25:55946
YUHAS, John M., Biological factors affecting the radioprotective efficiency of S-2-[3-aminopropylamino]ethylphosphorothioic acid (WR-2721): LD/sub 50(7)/ doses, 25:55259
YULCHIBAEV, A. A., Physico-chemical properties of polyvinyl fluoride obtained by γ-irradiation, 25:54624
YULE, H. P., Computer data reduction in activation analysis, 25:54471
YURA, Osamu, Disintegration rate determination of $^{241}$Am by liquid scintillation counting, 25:54700
YUR'EV, S. F., Effect of alloying on the oxidation of niobium at low pressures, 25:55380
YUROVA, L. N., Interference of ''black'' absorbers in moderating medium, 25:57205
Measurement of ''black'' absorbers of equivalent sizes and identical efficiency in a moderating medium by a pulsed-source technique, 25:57206
YUSHKOV, A. V., Diffraction analysis of transfer reactions, 25:56847
YUTLANDOV, I. A., Probability of the ($\mu^{-}$, ν) process of $^{139}$La and $^{208}$Pb nuclei, 25:56739 (JINR-P1-6006)
YVARS, M., Influence of speed of graphitization of carbon products on dimensional variations produced by neutron irradiation, 25:55645 (CEA-CONF-1821)
Interactions among various carbons in the course of heat treatment, 25:57275 (SC-T-713060)

## Z

ZACEK, J., Direct pair production by charged particles at 4 GeV/c in a propane bubble chamber, 25:56467
ZACHAROV, B., Use of interactive computer graphics in high-energy physics, 25:55093
ZACKOVA, H., Detection of alpha-radionuclides in the bone--marrow and blood of miners by the method of nuclear emulsions, 25:55236
ZADUBAN, M., Use of $^{40}$K and $^{87}$Rb in radionuclide metrology, 25:54901
ZADUBAN, Milan, Naturally unstable nuclides, their radiometric determination and possibilities of their utilization, 25:54446
ZAFFIRO, B., Experimental and theoretical determination of burnup and heavy isotope content in a fuel assembly irradiated in the Garigliano boiling water reactor, 25:56879 (EUR-4638)
ZAGORETS, P. A., Radiation telomerization of ethylene by propionic acid, 25:54612
ZAGORSKI, Z. P., Electronic properties of anodized Al electrode, 25:54601
ZAGREBNOV, V. A., Phonon--phonon interaction in liquid helium, 25:56052
ZAGRYAZHSKII, V. L., Conditions for formation of phase with A15 structure in V--Ge--Al system, 25:55539
ZAICHIK, V. E., Local irregularity of doses in neutron-capture therapy, 25:55212
ZAIKINE, D. A., Pauli principle in the theory of reactions between light nuclei, 25:56829 (LYCEN-7104, S12.1-4)
ZAITSEV, S. G., Interaction of a shock wave with a magnetic field, 25:55951
ZAITSEV, Yu., Deformation and cracking mechanics in hardened cement paste and concrete under short-term and high sustained loads, 25:55661
ZAITSEVA, N. G., Decay of $^{85}$Y (5 hr), $^{85}$Y (2.68 hr), and $^{85}$Sr, 25:56722
Decay of $^{89}$Zr and $^{87}$Zr, 25:56723
Decay of $^{90}$Nb, 25:56791
New 0$^{+}$ states in $^{124}$Te and $^{126}$Te, 25:56781
ZAKATOV, L. P., Noise levels of Langmuir oscillations in beam--plasma system, 25:56249
ZAKHAROV, A. M., Construction of the solidus volume in the niobium--tungsten--titanium--zirconium system by the simplex-lattice method, 25:55529
Niobium--hafnium--carbon system in the niobium-rich region, 25:55563
ZAKHAROV, B. M., Production of zirconium dioxide microballoons by means of nitrogen plasma, 25:55407
ZAKHAROV, S. M., Generation of neutrons in laser $CD_2$ plasma heated by pulses of nanosecond duration, 25:56219
ZAKHAROV, Yu. A., Topography of the evolution of the radiolysis products of lead azide ($PbN_6$), 25:54642
ZAKHAROVA, S. M., Mean radiation widths at excitation energies of the order of the neutron binding energy, 25:56836 (UCRL-Trans-10542)
ZAKOMORNYI, G. V., Pneumatic loading and unloading of channels for irradiation in IRT-M reactor, 25:57130
ZAMIRALOV, V. S., Mass formulas SU(3) and classification of heavy hyperons, 25:56540
ZAMRAZIL, V., Primary carcinoma of thyroglossal duct, 25:55304
ZANDER, A. R., Direct reaction analysis of reactions $^{7}$Li(d,t)$^{6}$Li and $^{7}$Li(tau,α)$^{6}$Li, 25:56671
Elastic scattering of deuterons by $^{6}$Li and $^{7}$Li at 8.0 to 12.0 MeV, 25:56670
ZANFAGNA, B., Coupling of EM waves in an inhomogeneous plasma, 25:56225 (CEA-CONF-1802)
ZANONI, E. A., Stability calculational procedure for flow-induced vibrations of reactor internals in parallel flow, 25:57086 (CONF-710302-(Vol.1), pp 356-9)
ZAPATKA, J., ARC system cross-section homogenization and modification capabilities, 25:56614 (ANL-7714)
ZARZECZNY, August, Radioisotopic exchange of ligands in chloro- and thio-cyanatomolybdates(III), 25:54558
ZAWALICK, E. J., Frequency tables of the geomagnetic index Kp, 1932--1970, 25:56017
ZEBOUNI, N. H., Supercooling and thermal conductivity in superconducting molybdenum, 25:56066
ZECCHINA, A., Infrared study of surface properties of α-chromia. I. Preparation and adsorption of water, heavy water, and carbon monoxide, 25:54565
ZEIDLER, H., Non-contact thread velocity measurement through point labelling, 25:54900
ZEITLIN, Harry, Rapid adsorbing colloid flotation method for the separation of molybdenum from seawater, 25:54743
Separation of uranium from seawater by adsorbing colloid flotation, 25:54738
ZEL'DOVICH, M. A., Measurement of solar protons from July 7, 1966 flare, 25:55991
ZELENSKAYA, N. S., Reaction $^{12}$C(αp$_0$)$^{15}$N, 25:56675
ZELENSKII, V. P., Use of reaction $^{18}$O(p,α)$^{15}$N to study oxidation of metals, 25:55384
ZELENTSOVA, M. V., Si(Li)-detectors for diagnosis of neoplasm of the skin, 25:55273
ZEMTSEV, B. V., Gamma-radiation during thermal neutron capture on chromium and iron isotopes, 25:56683 (FEI-205)
ZENKEVICH, B. A., Crisis of heat transfer in pipes, 25:54869 (FEI-217)
ZERNYATKO, V. G., Fluid motion produced by temperature gradient perpendicular to gravitational field in presence of magnetic field, 25:55919
ZEYFANG, R., Deformation dynamics of a b.c.c. titanium alloy (15.2 at. percent Mo) below 650°K (approximately or proportional to 0.4 T/sub m/), 25:55459
ZGORZELSKI, Maciej, Ionization of atomic H by electron impact: numerical calculations for free-fall atomic model, 25:55836 (INR-P-1327)
ZHELEV, Zh. T., New 0$^{+}$ states in $^{124}$Te and $^{126}$Te, 25:56781
ZHELEZNYAKOVA, N. Yu., Uv-sensitive mutants of Chlorella vulgaris, 25:55172

XUM

ZHERDEV, A. M., Electron-microscope and x-ray spectral study of the surface of fractures in cast tungsten, 25:55542
ZHESTYANIKOV, V. D., Survival of E. coli B under different post-irradiation conditions, 25:55357
ZHIZHIN, E. D., Cross section for production of W boson by high-energy neutrinos in the electromagnetic field of a proton, 25:56473
ZHUK, L. I., Tricomponent activity induced by competing reaction, 25:54498
ZHURKIN, E. S., Dissociation of $D_2^+$ and $H_2^+$ ions in collisions with $D_2$, He, and Ne, 25:55858
ZIEGLER, D. L., Waste reduction studies, 25:54709 (CONF-710401-, pp 386-91)
ZIEGLER, G., Effect of C on critical current of $Nb_3Sn$, 25:56084
ZIEGLER, L. H., K-fluorescent-x-ray relative-intensity measurements, 25:55827
ZIEMKIEWICZ, Miroslaw, Optical model program with the automatic search routine extended to include the spin-orbit term. OMAS, 25:56815 (INP-741)
ZIERENBERG, B. E., Alteration of DNA by sensitized and non-sensitized long-wave uv irradiation, 25:55308
ZIL'BERMAN, L. A., Effect of external fluctuations on the properties of superconducting micro-junctions near critical temperature, 25:56090
ZIMA, T. E., Moments of the distribution function of the neutron density, 25:57179
ZIMAKOV, I. E., Effect of neutron irradiation on hydrogen electrode in fuel cell, 25:54602
ZINGL, H. F. K., Separable potentials, 25:56531
ZINOV'EV, L. P., Debuncher of the JINR synchrophasotron injector with modulation of the accelerated beam energy, 25:56586 (JINR-P9-5956)
ZIPF, E. C., Photoelectron excitation of atomic-oxygen resonance radiation in the terrestrial airglow, 25:56032
ZOERGIEBEL, Friedrich, Growing and investigation of silver chloride crystals: a contribution to the development of a precipitation detector for tracks of ionizing particles, 25:54996 (IKF-28)
ZOLER, D. I., Generation of magnetohydrodynamic waves in nonhomogeneous plasma located in intense magnetic field, 25:55923
ZOLOTAREV, V. S., Reparation of stable isotopes for scientific research purposes, 25:54899
ZONA, R., Space time temperature distribution in a semi infinite medium under particular conditions of thermal transient, 25:54876 (RT/ING-(71)11)
ZONDERHUIS, J., Practical aspects of activation analysis with fast neutrons and photons, 25:54470
Routine determinations on rocks and sediments by activation analysis, 25:54463
ZORIN, G. N., Investigation of the silicon surface-Barrier Δ E-detector characteristics for the nuclear reaction studying, 25:54998 (JINR-P13-5970)
ZUBOVSKII, G. A., Use of EDTA preparations labelled with $^{51}Cr$ and $^{169}Yb$ in radioisotope diagnosis, 25:55272
ZUK, W. M., In-beam study of prompt γ-rays emitted in $^{66}Zn(p,n\gamma)^{66}Ga$ reaction, 25:56732
ZUKAS, E. G., Tritium trick, 25:55575 (LA-DC-12996)
ZUSMANOVICH, A. G., Dimensions of the galactic cosmic-ray modulation region, 25:55901
ZVEREV, M. P., Treatment of bone sarcoma with high-energy bremsstrahlung, 25:55338
ZYLICZ, E., Incorporation of $^{239}Pu$ into hair, 25:55116

XUM

# SUBJECT INDEX

Cross references are included in cumulative subject indexes and in *Subject Headings Used by the USAEC Division of Technical Information* (USAEC report TID-5001).

The reader is also referred to *Guide to Abstracting and Indexing for Nuclear Science Abstracts* (USAEC report TID-4576).

Most headings in the subject index are specific materials, things, and processes. The headings are followed by modifiers that describe the properties of, or processes applied to, the headings.

All index entries cite *NSA* volume and abstract numbers; volume number precedes the colon and the abstract number follows it. The designation (R) following the abstract number indicates a progress report; (P) indicates a patent; and (T) indicates a translation. Abstracts for reports other than progress reports carry no letter designation. Report numbers, where applicable, are included in parentheses after the abstract number of the citation. Published literature (journal article or book) can be identified by the absence of a report number.

Ideas presented in the original literature, rather than key words, have been indexed. The indexers have selected what seemed the most probable and logical place to look for typical information. Since it is not always possible to anticipate where a user would look for information, the cumulative indexes include numerous cross references. Consideration of synonymous or closely related terms will prove valuable.

Information is indexed for the greatest use to the greatest number of users. This requires that a topic be indexed to headings that most specifically describe it and not ordinarily to the headings that describe its ultimate use or to the general class headings that include the specific headings. For example, information on boiler design for the Fermi Fast Breeder Reactor would be indexed under the headings BOILERS and FERMI FAST BREEDER REACTOR but not necessarily under the headings REACTORS, FAST or REACTORS, BREEDER.

General or broad headings are reserved for general summaries, reviews, comprehensive reports, and similar literature.

## Subject Heading Styles

Generally, the direct form of subject entry is used rather than inverted headings; e.g., AMINO ACIDS rather than ACIDS, AMINO; HELIUM ISOTOPES He-4 rather than HELIUM—ISOTOPES He-4 or HELIUM—He-4 ISOTOPES. Note, however, that in some cases parenthetic modifying terms or inverted headings such as NEUTRONS, FAST, are used where the alphabetical arrangement of a direct entry would cause information to be scattered. In addition, organic compounds are usually entered in the index in the inverted form to facilitate grouping like or related compounds with the parent compounds; e.g., BENZENE, BROMO- rather than BROMOBENZENE. In general, the nomenclature used is that of the subject indexes to *Chemical Abstracts*.

## Alphabetization

Subject headings are alphabetized word by word. Parenthetic qualifiers, numbers, and Greek letters within subject headings are disregarded in alphabetizing unless there are two or more headings that are otherwise identical, in which case the qualifier, numerical progression, or spelled names for the Greek letters determine the order.

Examples:

M-Capture
  see ELECTRON CAPTURE
MAGNESIUM
MAGNESIUM ALLOYS AND SYSTEMS
MANGANESE FLUORIDES
MANGANESE FLUORIDES $MnF_2$
MESONS
MESONS ($\pi$)
MESONS ($\rho$)
1-PENTANOL
2-PENTANOL

## Modifying Phrases

The modifiers appearing under a subject heading are written specifically to show the relation between the item being indexed and the heading. The modifier therefore contains a maximum of useful information. Although the modifier begins with the word judged to be of greatest use to the greatest number of users, there is still need for the searcher to consider all modifiers under the heading(s) of interest.

Modifiers usually form meaningful phrases when combined with the subject heading. Some are intended to be read following the subject heading, e.g., the entry HYDROGEN—sorption by charcoal should be read "hydrogen sorption by charcoal." As a result of placing the important word first, however, many modifiers must be rearranged for smooth reading, e.g., FORMALDEHYDE—yields in radiolysis of ethyl ether, effects of deuterium on, should be read "effects of deuterium on formaldehyde yields in radiolysis of ethyl ether" and URANIUM—crystal structure of, effect of cooling rate on allotropic transformations in, should be read "effect of cooling rate on allotropic transformations in crystal structure of uranium."

Special characters are added to modifiers in the fields of physics and reactor technology; if the modifier does not establish the experimental or theoretical character of a reference, a symbol (E), (T), or (E/T) is placed immediately after the modifying phrase and before the abstract number.



XUM

### Physical States and Configurations of Materials

The specific physical state, if other than normal, or the geometric configuration of the material is included in the modifying phrase; e.g., information on liquid metals is indexed under the specific metal with "liquid" in the modifier and carbon crucibles is indexed under CARBON with "crucibles" appropriately placed in the modifier. The information on carbon crucibles is also indexed under CRUCIBLES.

### Nomenclature of Inorganic Compounds

Inorganic compounds are indexed to subject headings in the direct form. Cations are listed in the order of increasing valence for polycationic salts of varying valence and in alphabetic order for polycationic salts in which all cations have the same valence; e.g., SODIUM ALUMINUM SILICATES and POTASSIUM SODIUM SULFATES. If more than one anionic species is presented in a compound, the anions are arranged alphabetically, e.g., BERYLLIUM FLUORIDE HYDROXIDES.

### Nomenclature of Organic Compounds

Organic compounds are indexed by subject headings based on the indexes to *Chemical Abstracts* except in the area of enzymes, in which specific enzymes, named according to the 1964 recommendations of the International Union of Biochemistry, are used. In many cases nonproprietary names for drugs are used as subject headings, and cross references are made from the systematic chemical names. Subject headings for hormones appear in the inverted style at HORMONES.

### Nomenclature of Life Sciences

Subject headings for plants are names of phyla with one exception: members of the Phylum Tracheophyta are indexed under class or subclass names. Scientific names (genus and species) are used as the initial, or file, word in the modifying phrase. Scientific names are omitted only when the name is not available in the literature or cannot be found in available references.

Subject headings for animals are the names of phyla with the following exceptions: (1) members of Phylum Arthropoda and Phylum Chordata are indexed under appropriate class name, and (2) common names are used for members of Class Mammalia.

Subject headings are entered for various classes of commodities, and specific products are identified in the file-word position of the modifier. In the following examples, approved subject headings are capitalized and typical modifier file words are listed in lower case.

| Example 1 | Example 2 |
|---|---|
| CEREALS | MEATS |
| bread | beef |
| flour | fish |
| oats | mutton |
| rice | pork |
| rye | poultry |
| wheat | seafood |

Diseases, pathological conditions, and in vitro studies of atypical cells and tissues are indexed under subject headings for the organism affected, under the appropriate anatomical structure of physiological phenomenon affected, and under the appropriate disease heading. Subject headings for diseases (defined as any deviation from the norm) are DISEASES; DISEASES, INFECTIOUS; DISEASES, NEOPLASTIC; DISEASES, PHYSIOLOGICAL; DISEASES, PLANT; and DISEASES, TRAUMATIC.

Diseases of mixed etiology are treated in the following manner: neoplastic diseases that are also classified as infectious or physiological are indexed under DISEASES, NEOPLASTIC; diseases in which a microorganism is the etiologic agent are classified under DISEASES, INFECTIOUS; physiological anomalies that are neither neoplastic nor infectious are indexed under DISEASES, PHYSIOLOGICAL; the acute radiation syndrome, nonspecific radiation injuries, trauma, and wounds or incisions inflicted mechanically are indexed under DISEASES, TRAUMATIC.

Specific diseases or pathological conditions are named in the file-word position of the modifier, in the author's terminology, and are set off from the remainder of the modifier by commas. Neoplasms are designated as benign or malignant in the file-word position when more specific information is not available.

### Multicomponent Alloys and Other Systems

Multicomponent alloys and systems, except well-known trade names, are indexed under a subject heading for each component in the form "element systems" for nonmetals or "element alloys and systems" for metals. The modifier begins with element symbols for each component arranged alphabetically. In addition, if significance is placed on the base metal of the alloy, this is indicated by adding "-base" to the element symbol.

Example: A 1.5C, 12Cr, 0.25V, 0.8Mo, bal Fe alloy is indexed as

```
CARBON SYSTEMS
  C--Cr--Fe-base--Mo--V, ...
CHROMIUM ALLOYS AND SYSTEMS
  C--Cr--Fe-base--Mo--V,...
IRON ALLOYS AND SYSTEMS
  C--Cr--Fe-base--Mo--V, ...
MOLYBDENUM ALLOYS AND SYSTEMS
  C--Cr--Fe-base--Mo--V, ...
VANADIUM ALLOYS AND SYSTEMS
  C--Cr--Fe-base--Mo--V, ...
```

Well-known alloys, such as ZIRCALOY-2, are indexed under the trade name; cross references from each component of the alloy to the trade name appear in cumulative indexes.

Multicomponent systems in which nonmetallic elements are present in large percentage and which are commonly referred to as systems or mixtures are indexed in a manner similar to alloys.

Example: A tungsten–silicon preparation is indexed as

```
TUNGSTEN ALLOYS AND SYSTEMS
  Si--W, ...
SILICON SYSTEMS
  Si--W, ...
```

Multicompound systems and mixtures of inorganic compounds are indexed under the subject heading for each component compound; the modifiers begin with an alphabetical listing of compound formulas.

Example: A lead titanate–lead zirconate mixture is indexed as

```
LEAD TITANATES
  PbTiO3--PbZrO3
LEAD ZIRCONATES
  PbTiO3--PbZrO3
```

XUM

A mixed system of compounds and elements is indexed by a combined form of the preceding conventions; e.g., a dispersion of copper and alumina would be indexed as

ALUMINUM OXIDES
  $Al_2O_3$—Cu, ...
COPPER ALLOYS AND SYSTEMS
  $Al_2O_3$—Cu, ...

Mixtures of organic compounds are indexed under subject headings for each component of the mixture; the modifiers begin with an alphabetical listing of compound names.

Example:

ACETIC ACID
  acetic acid—$BF_3$, ...
BORON FLUORIDES
  acetic acid—$BF_3$, ...

Example:

BENZENE, CHLORO-
  bromophenol—chlorobenzene, ...
PHENOL, BROMO-
  bromophenol—chlorobenzene, ...

If modifiers for alloys and systems are included with other modifiers under the same subject heading, they are filed last.

Example:

CARBON SYSTEMS
  deposition on nuclear fuel particles
  molecular structure of
  neutron total cross section for
  sorptive properties for xenon
  Young's modulus for
  Al—C—Cr, superconductivity in
  B—C, phase studies for
  C—U—Zr, fabrication and physical properties of

## Nomenclature of High Energy Physics

Information on particle-particle events is indexed under subject headings for the specific particles involved. The modifier file word *interactions* is followed by the specific interaction written in symbolic form. Particle nomenclature and symbols follow that of Rosenfeld, et al. *Data on Particles and Resonant States,* UCRL-8030 (latest revision). For consistency the incident particle is always written first. The mass (in MeV) of a resonance state is included in parentheses after the symbol to avoid ambiguity. Hyperfragments are indicated in modifiers as in the following examples: $\Lambda$-$He^5$, $\Sigma$-$H^3$, $\Lambda\Lambda$-$Be^{10}$. The superscript on the right indicates the total number of baryons in the composite system.

Examples:

MESONS ($\pi^-$)
  interactions $\pi^- + p \rightarrow \Lambda + K^+ + \pi^-$ at 6 GeV/c in hydrogen bubble chamber, $\Lambda$K(1700) enhancement in, (E)
BARYONS, RESONANCE (N*)
  production of $\Delta^{++}(1236)$ and $\Delta^0(1236)$ from $K^- + p \rightarrow K^- + p + \pi^+ + \pi^-$ interactions at 2.63 and 2.70 GeV/c, (E)
HYPERFRAGMENTS
  binding energy of $\Lambda\Lambda$-$He^6$, three-body $\alpha$—$\Lambda$—$\Lambda$ model for

Subject headings are also provided for specific models and theories.

Examples:

ELEMENTARY PARTICLE MODELS (TRIPLET)
  hadron total cross sections in quark, numerical analysis of
CURRENT ALGEBRA
  PCAC hypothesis for $A_1$ and rho dominance in $\pi \rightarrow e + \nu + \gamma$ decay
REGGE POLE THEORY
  predictions for polarization in $K^- + p \rightarrow$ anti $K^0 + n$, $\pi^- + p \rightarrow \pi^0 + n$, and $\pi^- + p \rightarrow$ eta + n interactions at high energies
SYMMETRY GROUPS
  SU(2) × SU(4) intermediate-coupling model for nucleon and hyperon isobars

## Nomenclature of Reactor Technology

Subject headings for reactors are of three types:

(1) Specific reactors, e.g., ARGONNE RESEARCH REACTOR, SAXTON POWER REACTOR

(2) Reactors having a common physics or engineering characteristic, e.g., REACTORS, FAST; REACTORS, ORGANIC-COOLED; REACTORS, PRESSURIZED-WATER

(3) Reactors having a common purpose, e.g., REACTORS, POWER; REACTORS, RESEARCH

Information on specific reactors, type (1), is indexed under the one specific subject heading. Information on classes or types of reactors, types (2) (characteristics) and (3) (purpose), is indexed under all applicable headings. For example, information on a heavy-water-moderated organic-cooled power reactor is indexed under REACTORS, HEAVY WATER-MODERATED; REACTORS, ORGANIC-COOLED; and REACTORS, POWER.

Subject headings exist for selected reactor components, e.g., REACTOR FUEL ELEMENTS. When applicable, headings for components are indexed even though they may have been included in a modifier under a type (1) or (2) heading. The materials in reactor components are indexed when the information is peculiar to the material.

Modifier file words under reactor headings are of two primary types: one type expresses reactor characteristics, e.g., reactivity; the other, components, e.g., control rod. If no subject heading appears for a reactor component, the heading REACTORS is used, and the component is used as the modifier file word.

XUM

# A


ACCELERATION
effects on guinea pigs and mice, effects of radioprotective compounds on sensitivity to transverse, 25:55264
ACCELERATOR TUBES
pulse generator for, design of megavolt, 25:56583 (IAE-1980)
shielding material for, x-ray, 25:56603(P)
ACCELERATORS
beam emittance of, device for measuring, 25:56611
beam injection into, charge-exchange method for proton, 25:56590(T) (LA-tr-71-46)
experimental facilities for medical use, design criteria for, 25:56607
ACCIDENTS
legal aspects of radiological, in France, 25:55252 (NP-18752)
radiation, proposed USA registry for, 25:55250
ACETIC ACID
reactions with tetravalent uranium in aqueous benzene solutions, stability constants for complex ions produced by, 25:54581
ACETIC ACID, [(CARBOXYMETHYLIMINO)BIS(ETHYLENENITRILO)]TETRA-
effects on excretion of americium-241 in urine of man following inhalation as oxide, 25:55118
oxidation by cerium(IV) in sulfuric acid solutions, 25:54422
ACETIC ACID, (1,2-CYCLOHEXYLENEDINITRILO)TETRA-
oxidation by cerium(IV) in sulfuric acid solutions, 25:54422
ACETIC ACID, (ETHYLENEDINITRILO)TETRA-
oxidation by cerium(IV) in sulfuric acid solutions, 25:54422
use of chromium-51- or ytterbium-169-labeled, for brain and kidney scanning, 25:55272
ACETIC ACID, NITRILOTRI-
oxidation by cerium(IV) in sulfuric acid solutions, 25:54422
ACETYLENE
reactions with liquid sodium, 25:54537
ACID PHOSPHATASE
radiation effects on activity of rat bone marrow, effects of dose on x, 25:55330
ACIDS
analysis of high-purity, for trace impurities by emission spectrography, 25:54431
determination of free, in uranyl nitrate, effects of solution age on, 25:54402
determination using iodine-131, radiometric, 25:54439
ACRIFLAVINE
radiosensitizing effects on Escherichia coli, effects of temperature on uv and x, 25:55357
ACROLEIN
radiolysis of single crystals of, at 77°K, ESR study of radicals and radical pairs from γ, 25:54634
ACRYLIC ACID, METHYL ESTER
radiolysis of single crystals of, at 77°K, ESR study of radicals and radical pairs from γ, 25:54634
ACRYLONITRILE
radioinduced grafting on poly(vinyl chloride), effects of dose on γ, 25:54613
radioinduced polymerization of, comparison of structure of products of chemically initiated and γ, 25:54622
ACTINIDE BROMIDES
formation of, estimation of free energies of, 25:54712 (ORNL-4682, pp 1-38)
ACTINIDE CHLORIDES
formation of, estimation of free energies of, 25:54712 (ORNL-4682, pp 1-38)
ACTINIDE HYDROXIDES
basicities of, 25:54718 (ORNL-4682, pp 168-81)
ACTINIDE OXIDES
preparation for HFIR targets, 25:54671 (ORNL-4682, pp 114-32)
ACTINIDES
chemical properties of aqueous solutions of, spectrophotometric studies on, 25:54578 (ORNL-4682, pp 215-17)
complexes of, research progress on, 25:54671 (ORNL-4682, pp 114-32)
compounds, electron microscopic and thermal analysis of, 25:54671 (ORNL-4682, pp 114-32)
concentration by (n,γ) reactions in molecular sieves, 25:54718 (ORNL-4682, pp 168-81)
determination by extraction and scintillation counting, 25:54718 (ORNL-4682, pp 168-81)
distribution between liquid bismuth and molten lithium halides, 25:54712 (ORNL-4682, pp 1-38)
separation by ion exchange chromatography using aminopolyacetic acids, 25:54718 (ORNL-4682, pp 168-81)
separation from molten manganese nitrate hexahydrate or calcium chloride hexahydrate by solvent extraction using TBP, 25:54740
ACTINIUM ISOTOPES Ac-228
beta decay of, gamma ray intensities from, (E), 25:56747(T) (ORNL-tr-2531)
energy level transitions from radon-228 beta decay, (E), 25:56747(T) (ORNL-tr-2531)
ACTIVATION ANALYSIS
activity induction by intermittent irradiation in, calculation of, 25:54527
conference on, in geochemistry and cosmochemistry, Kjeller, Norway, September, 1970, 25:54457
development of epithermal neutron, of geological materials, 25:54468
development of fast neutron and photon, 25:54470
development of monostandard, using lithium-drifted germanium gamma spectrometer, 25:54490
development of, on-line computer used as spectrometer in, 25:54474
gamma coincidence spectrometry in instrumental, 25:54479
gamma spectra analysis in neutron, computer program for, 25:54523
gamma spectra analysis in, combined peaksearch and peakfit in data processing for, 25:54472
gamma spectra analysis in, computer data reduction technique for, 25:54471
gamma spectra for, digital methods of photopeak integration for, 25:54473
method for pool type reactor intermediate neutron spectrum, quadruple foil, 25:57126
methods and uses of neutron, in forensic science, 25:55065
methods for determination of light elements in metals, alpha reactions with aluminum and silicon at 70 to 160 MeV for, 25:56685 (FRNC-TH-48)
neutron detectors for, standard for selection of materials for, 25:54510
neutron pulse form in, dependence of induced activity on, 25:54526
reactions in, rational methods for deciphering tricomponent activity induced by competing, 25:54498
sensitivity evaluation of neutron capture-prompt γ, 25:54451
sensitivity of charged particle, for light elements, 25:54528
sensitivity of neutron, for nonaqueous flowing systems, 25:54524
separation processes in, countercurrent electrolytic, 25:54493
use in oceanography, review of, 25:54481
ADENOSINE 5'-TRIPHOSPHATE
effects on calcium-45 uptake and release by rat brain microsomes, 25:55120
AEROSOLS
analysis of pollution, for trace amounts of 29 elements by neutron activation and γ spectroscopy, 25:54505
conference on chemical and physical properties of, Fontenay-aux-Roses, France, Sept. 24 to 25, 1970, 25:54799
distribution characteristics in liquid metal cooled fast breeder reactor systems, effects of accident conditions on, (E/T), 25:57105
production in liquid metal cooled fast breeder reactor systems, effects of accident conditions on, (E/T), 25:57105
production of monodisperse transuranic oxide, for inhalation studies in dogs, 25:54982
properties of, produced from solutions of polyvalent metallic nuclides, chemical and physical, 25:54545
AET
effects on sensitivity of guinea pigs and mice to transverse acceleration, 25:55264
radioprotective effects on mice, effects of dose, sex, and strain on x, 25:55257
AGE
effects on respiration rate in wheat seedlings, 25:55348
AGE ESTIMATION
argon/potassium method for, using neutron activation and mass spectrometry, 25:54765
book: Lead Isotopes in Geochemistry and Cosmochemistry, 25:54770
methods for Quaternary materials, development of alpha-particle recoil and fission track, 25:54771
thorium-230/uranium-234 method for, of corals, accuracy of, 25:54776
AGUIRRE POWER REACTOR, UNIT 1
design parameters of, revised and additional data on, 25:56972 (DOCKET-50376-21)
operations aspects of, revised and additional data on, 25:56972 (DOCKET-50376-21)
AIR
analysis of aerosol particles in, for trace elements by neutron activation and γ spectrometry, 25:54456
corrosive effects on reactor materials, review of, 25:55393
helium-ion range at 0.2 to 2.0 MeV in, as function of energy, (E), 25:56276
ion mobility in, spectra of alpha particle-induced, 25:54801
ionization in front of strong shock wave, parameter, 25:56160
leakage into glove boxes, empirical method for determining, 25:54944 (CONF-710401-, pp 83-97)
particle transport calculations from anisotropic point sources in, modifications to TWOTRAN SPHERE and ANDYMG3 programs for, 25:56261 (LA-4774)
proton range at 0.2 to 2.0 MeV in, as function of energy,


XUM

(E), 25:56276
reactions with powdered magnesium, effects of temperature on, 25:55504
sampling for tritiated water vapor, use of molecular sieves in, 25:54798
air--$CO_2$, plutonium ignition in, effects of oxygen content on, 25:54946 (CONF-710401-, pp 106-17)
air--N, plutonium ignition in, effects of oxygen content on, 25:54946 (CONF-710401-, pp 106-17)
AIR SAMPLERS
data processing system for, 25:55006
design with electrostatic precipitation for radon monitoring, 25:55032
AIRCRAFT
lift indicator for helicopters, development of radiometric, 25:55065
AIRGLOW
oxygen (O I) 1304-A resonance radiation in day, photoelectron-impact excitation of, (E), 25:56032
oxygen spectral intensity in night, covariation of nonauroral Herzberg I band and O I 5577-A, (E), 25:56046
spectral emission of daytime, Lyman--Birge--Hopfield nitrogen system from Aug. 1967 to July 1968, (E), 25:55968
ALBUMINS
complexes of serum, with novobiocin, thermodynamic and conformational aspects of, 25:57292 (UR-49-1516)
ALCOHOLS
radiolysis of gaseous, liquid, and solid, review on, 25:54629 (CONF-700652-(Vol.3), pp 479-521)
radiolysis of, production of aliphatic aldehydes by γ, 25:54625(P)
ALDEHYDES
radioinduced production of aliphatic, from alcohols, γ, 25:54625(P)
ALGINIC ACID
sodium salt, effects on distribution of mixed cesium and strontium radioisotopes in man following ingestion, 25:55113
ALKALI METAL BROMATES
radiolysis of crystalline, effects of additives on yields from proton and γ, 25:54638
ALKALI METAL HALIDES
impurity location in crystals of, by axial channeling of helium ions and protons, 25:56337
ALKALI METAL HYDROXIDES
radiation effects on aqueous solutions of, reply to paper on formation of ozonide ions from γ, 25:54609
ALKALI METAL NITRATES
radiolysis of crystalline, effects of additives on yields from proton and γ, 25:54638
ALKALI METAL SULFATES
corrosive effects on transition metals, relations with polarization, 25:55373 (CONF-690452-, Paper 6)
reactions with alloys and oxides containing chromium, nickel, and cobalt at 550 to 950°C, 25:55372 (CONF-690452-, Paper 5)
ALKALI METALS
corrosive effects of liquid, on reactor components, review of, 25:55392
determination in fission product mixtures by ion exchange and β counting, 25:54449
ALKALINE EARTH IONS
reactions with phosphate and sulfate ions in crystals, 25:57293 (UR-49-1517)
ALKALINE EARTH METALS
determination in fission product mixtures by ion exchange and β counting, 25:54449
ALKALINE PHOSPHATASE
effectiveness in comparison with gold-198 scanning for diagnosis of human liver cancer, 25:55276
radiation effects on activity of rat bone marrow, effects of dose on x, 25:55330
ALLOYS
book: Corrosion in Nuclear Applications, 25:55388
book: Emissive Properties of Materials (Handbook), 25:56346
crystal disorder--order transformation in, kinetics of, 25:55552
diffusion in, data tabulations on, 25:55509
properties and structure of, produced by sintering using systematic thermal fluctuations, 25:55414
radiation effects on stress relaxation in, model for fast neutron, 25:55579 (WAPD-TM-943)
ALPHA PARTICLES
detection and measurement of artificial, in presence of natural alpha radiation, sensitive method for, 25:54762
dosimetry of, triacetate cellulose track detectors for, 25:55026
effects on creep in Type 316 stainless steel at 750°C, relations with injected helium content, 25:55574 (JAERI-Memo-4408)
effects on crystals and polymeric solutions of anthracene, 25:54600(R) (UCLA-34-P-88-32)
effects on hafnium compounds and tungsten at 6 MeV, Moessbauer-effect evidence for radiation damage from Coulomb-excitation, 25:56369
effects on sodium nitrate at 20 MeV, 25:56318
effects on survival of hamster cells, effects of dose on RBE for, 25:55207 (NYO-2740-8, pp 220-59)
energy scale for, comparison with γ-ray energy scale, 25:56773
energy-loss measurement in tissue-equivalent gas, calculation of straggling parameters from, 25:56279
interaction tracks in mica and extraterrestrial materials, (E), 25:55669 (N-71-26344)
observations of solar 0.5-MeV/nucleon, during 1967 at widely separated locations, (E), 25:55956
reactions (α, He-6) with magnesium-26, neon-22, and oxygen-18 at 42 MeV, angular distributions for, (E), 25:56665
reactions (α,2α) with beryllium-9 at 42.8 and 49.2 MeV, analysis using impulse approximation, (E), 25:56674
reactions (α,2α) with oxygen-16 at 46 and 52.5 MeV, analysis using impulse approximation, (E), 25:56674
reactions (α,2n) with uranium-235, production of plutonium-237 by, 25:54674
reactions (α,Be-7) and (α,Li-6) with carbon-12 and oxygen-16 at 42 MeV, cross sections for, (E), 25:56659
reactions (α,C-12) and (α,Li-6) with magnesium-24 at 42 MeV, cross sections for, (E), 25:56659
reactions (α,C-12) and (α,O-16) with silicon-28 at 42 MeV, cross sections for, (E), 25:56659
reactions (α,d) and (α,p) with light nuclei at 25 MeV, distorted-wave analysis of differential cross sections for, (T), 25:56677
reactions (α,d) with strontium-87 at 25 MeV, angular distributions for, (E), 25:56779
reactions (α,f) with bismuth-209, thorium-232, and uranium-238 at 20 to 34 MeV, cross sections and delayed neutron yields for, (E), 25:56803
reactions (α,f) with thorium-230 at 25.7 and 29.5 MeV, analysis using renormalized Fermi gas model and collective potential energy surface, (T), 25:56856
reactions (α,f) with thorium-232 at 26.4 MeV, liquid-drop analysis of, (E/T), 25:56786
reactions (α,f) with Z = 29 to 67 nuclei at 167 MeV, angular distributions and particle track lengths for, (E), 25:56806
reactions (α,γ) on neon-20, magnesium-24 photodisintegration rates from, 25:55703
reactions (α,γ) with silicon-28 and oxygen-16; rates for, (E), 25:55704
reactions (α,n) with barium-134 at 15 to 28 MeV, superconductivity model calculations of isomeric-cross-section ratios for, (T), 25:56765
reactions (α,n) with silicon-29 at 2.8 to 4.1 MeV, excitation function for, (E), 25:56752(R) (SUNI-14)
reactions (α,p) with bismuth-209 at 26.5 to 60 MeV, angular distributions, excitation functions, and recoil ranges for, (E), 25:56799
reactions (α,p) with carbon-12 at 11.3 to 26.3 MeV, angular distributions and excitation functions for, (E), 25:56675
reactions (α,p) with carbon-12 at 8.5 to 10.5 MeV, angular distributions for, (E), 25:56681
reactions (α,p) with iron-54 at 9.86, 10.02, and 10.40 MeV, p--γ angular correlations from, (E), 25:56700
reactions (α,xnypzα) with neodymium-142 at 104 MeV, gamma spectra from, (E), 25:56761
reactions with air, mobility of ions from, 25:54801
reactions with aluminum and silicon at 160 MeV, cross sections and fission mechanism for lithium-9, carbon-16, and nitrogen-17 production in, (E/T), 25:56685 (FRNC-TH-48)
reactions with aluminum and silicon at 70 to 160 MeV, cross sections and fission mechanism for production of stable and neutron-deficient nuclei in, (E/T), 25:56685 (FRNC-TH-48)
reactions with carbon-12 and nitrogen-14 at 70 and 90 MeV, cross sections for, (E), 25:56652 (LYCEN-7104, S2.1-2)
reactions with chromium and titanium, production of chromium-51 by, 25:54691
reactions with scandium and titanium, production of vanadium-48 by, 25:54677
scattering by carbon-12 at 8.5 to 10.5 MeV, angular distributions for elastic and inelastic, (E), 25:56681
scattering by helium-4 below 100 MeV, analysis using nonlocal separable potential, (T), 25:56852
scattering by light nuclei at 104 MeV, nuclear deformation study from differential cross sections for elastic and inelastic, (E), 25:56687 (KFK-1397)
scattering by nuclei, role of isoscalar transition operator in inelastic, (T), 25:56876
scattering by oxygen-18 at 13.5 to 17.0 MeV, alpha and gamma spectra and α--γ angular correlations in inelastic, (E), 25:56672
scattering by yttrium-89 at 20 MeV, angular distribution for elastic, (E), 25:56778
scattering by zinc-64, -66, and -70 at 27.2 MeV, distorted-wave analysis of differential cross sections for elastic and inelastic, (T), 25:56726
spectra measurements of, triacetate cellulose track detectors for, 25:55026
ALPHA SOURCES
calibration of polonium-210, with γ-ray energy scale, 25:56773
detection in blood and bone marrow of miners using nuclear emulsions, 25:55236
preparation of neptunium, thorium, or uranium, by

XUM

electrodeposition, 25:54673
ALUMINUM
abundance in primary cosmic radiation, (E), 25:55911
alpha reactions at 160 MeV, cross sections and fission mechanism for lithium-9, carbon-16, and nitrogen-17 production in, (E/T), 25:56685 (FRNC-TH-48)
alpha reactions at 70 to 160 MeV, cross sections and fission mechanism for production of stable and neutron deficient nuclei in, (E/T), 25:56685 (FRNC-TH-48)
analysis of pure, for calcium by nondestructive alpha activation, 25:54522
bremsstrahlung buildup factor for, dependence on position of shielding between source and detector, 25:56280
cracks in, optimization of radiographic method for detection of, 25:54929
determination in aluminum electrolytic bath by 14-MeV neutron activation simultaneously with oxygen and fluorine, 25:54503
determination in animal tissues and plants by separation and neutron activation, 25:54514
determination in glass, by simultaneous measurement of scattered α particles and prompt protons, 25:56752(R) (SUNI-14)
determination in tourmaline, by deuteron activation analysis and γ counting, 25:56752(R) (SUNI-14)
determination in yttrium oxide by emission spectrometry, 25:54419
determination of trace amounts of, in air by neutron activation and γ spectrometry, 25:54456
determination of trace amounts of, in ultramafic rocks by thermal neutron activation and γ spectrometry, 25:54496
deuteron reactions at 80 MeV with foils of, cross sections for electron capture in, (E), 25:55862
effects of compounds of, on bubble formation during annealing of doped tungsten, 25:55511
effects on separation of impurities from niobium by vacuum melting, 25:55403
effects on solvolysis of tert-butyl halides, Broensted correlation for, 25:54548
electron mean free path in foils of, fast, (E), 25:56281
electron reactions at 0.5 to 15 keV, optical radiation from, (E), 25:55813 (JINR-P4-5957)
mechanical properties of chemical vapor deposited rings of, design of apparatus for testing, 25:55440
neutron reactions at 10 to 30 GeV/c, total cross sections for, (E), 25:56421
proton reactions at 1.5 to 4.5 MeV, optical radiation from, (E), 25:55813 (JINR-P4-5957)
proton reactions at 155 and 600 MeV with foils of, cross sections for electron capture in, (E), 25:55862
radiation effects on adhesion of epoxy cemented specimen couples of, gamma, 25:55666
radiation effects on electronic properties of anodized electrode of, 25:54601
radiation effects on magnetoresistance of single crystals of, orientation dependence and annealing of 3-MeV electron, (E/T), 25:56334
radiation effects on, fast neutron, 25:54599 (ORNL-4717, p 117-24)
reactions with uranium oxides at 450°C, identification of phases in, 25:55609(T) (ORNL-tr-2456)
separation of uranium from, in methyl sulfoxide by cation exchange chromatography, 25:54728
surface wetting of molten, on boron nitride, mechanisms of, 25:55469
thermal expansion of quenched, 25:55499
ALUMINUM ALLOYS AND SYSTEMS
porosity of, effects of annealing and crystallization on micro-, 25:55462
preparation by granule metallurgy, evaluation of, 25:55404
Ag--Al, diffusion in, 25:57238 (MLM-OP-71003)
Ag--Al, superconductivity in hcp phases of, (E), 25:56096
Al--$Al_2O_3$, strength of powder shapes of, effects of dispersion-, grain boundary-, and solid solution-hardening on, 25:55487
Al--Co--Cr--Mo--Ni-base--Ti, fabrication of powdered, powder metallurgy and thermomechanical processes for, 25:55416
Al--Co--Cr--Mo--Ti--W, stress relaxation and surface hardening in, effects of high temperatures on, 25:55439
Al--Cr, crystal structure of solidified, effects of cooling rate and supercooling on, 25:55550
Al--Cr, solidification and phase transformations in, nonequilibrium, 25:55535
Al--Cr, thermal decomposition of solid solutions of, kinetics of, 25:55448
Al--Cr--Mo, thermal decomposition of solid solutions of, kinetics of, 25:55448
Al--Cr--Mo--Ni-base--W, fabrication of powdered, powder metallurgy and thermomechanical processes for, 25:55416
Al--Cr--Ni-base--Ti, corrosion by molten vanadium oxide, effects of chlorides, oxides, and sulfides of sodium on, 25:55375 (CONF-690452-, Paper 8)
Al--Cr--Ni-base--Ti, mechanical properties of dispersion-strengthened, at high temperatures, 25:55483
Al--Cu--Fe--Sn--Ti-base--V, development and evaluation of high-strength, 25:55421
Al--Cu--Y, phase studies of, 25:55561
Al--Fe, magnetic properties of, 25:56358
Al--Fe--Ti, mechanical properties at 550 to 1100°C, 25:55501
Al--Fe--Ti, phase studies of, 25:55501
Al--Ga--Ni, optical constants for β-phase NiGa/sub 1-y/Al/sub y/ intermetallic compound in, 25:56352
Al--Ge--V, phase formation in $V_3Al_{sub\ x}Ge_{sub\ 1-x}$ with A15 structure, 25:55539
Al--La--rare earths, crystal field levels, superconducting transition temperature, and exchange parameters of, (T), 25:56359
Al--La--Tm, crystal field levels of La/sub 1-x/Tm/sub x/$Al_2$, (E), 25:56359
Al--Mg--Zr, cracking and mechanical properties of welded joints of, effects of long-term heating at 70°C on, 25:55470
Al--Mn, crystal structure of solidified, effects of cooling rate and supercooling on, 25:55550
Al--Mo, solidification and phase transformations in, nonequilibrium, 25:55535
Al--Mo, thermal decomposition of solid solutions of, kinetics of, 25:55448
Al--Mo--Sn--Ti-base--Zr, welding of, properties of joints produced by friction, 25:55409
Al--Mo--Sn--U-base, tensile properties of dilute, at 23 to 600°C, 25:55429 (CEA-R-4177)
Al--Mo--Ti--V, corrosion cracking of, review on methods and problem of hot-salt stress, 25:55383
Al--Mo--Ti--V, diffusion of hydrogen in, at 450 to 600°F, effects of stress on, 25:55476
Al--Mo--Ti-base, embrittlement of two-phase, mechanisms of, 25:55450
Al--Nb, niobium-93 NMR in $Nb_3Al$, 25:56373
Al--Ni--V, phase equilibria in intermetallic compounds of, 25:55562
Al--Pd, optical constants for β-phase PdAl intermetallic compound in, 25:56352
Al--Si, analysis of standard, by neutron activation, 25:54455
Al--Sn--Ti, mechanical properties of hot pressed powders of, for cryogenic uses, 25:55482
Al--Ti, inflammability correlation of powdered, 25:55473
Al--Ti--V, corrosion cracking of, review on methods and problem of hot-salt stress, 25:55383
Al--Ti--V, fabrication and tensile properties of composites, parts, and preforms of powder metallurgy, 25:55415
Al--Ti--V, mechanical properties at 550 to 1100°C, 25:55501
Al--Ti--V, mechanical properties of hot pressed powders of, for cryogenic uses, 25:55482
Al--Ti--V, microstructure and properties of pressure-sintered powders of, 25:55413
Al--Ti--V, phase equilibria and properties along TiAl--$V_3Al$, section, 25:55537
Al--Ti--V, phase studies of, 25:55501
Al--Ti--V, properties of thin-film diffusion brazed joints in, corrosion, mechanical, and metallurgical, 25:55477
Al--Ti--V, sintering of powdered, electrically-activated pressure method for, 25:55413
Al--Ti-base--V, tensile properties of, effects of oxygen additions on, 25:55471
Al--Ti-base--V, welding of, properties of joints produced by friction, 25:55409
Al--Zr, crystal structure of solidified, effects of cooling rate and supercooling on, 25:55550
Al-base--Mn, binding energy and entropy of vacancies in, 25:54587(R) (AECL-3909)
Al-base--Mo, thermal expansion of quenched, 25:55499
Al-base--Zr, thermal expansion of quenched, 25:55499
Au--Al, search for superconductivity in fcc phases of, (E), 25:56096
ALUMINUM IONS
effects on silicon at 220 keV, lateral-stress study of damage produced in, 25:56285 (SC-RR-710424)
ALUMINUM ISOTOPES Al-26
abundance in lunar materials, (E), 25:55772
ALUMINUM ISOTOPES Al-27
deuteron reactions (d,p) at 12 MeV, l values, spectra, and DWBA analysis of differential cross sections for, (E), 25:56709
neutron capture at 2.9 MeV, cross section for, (E), 25:56696
proton reactions at high energies, isobar model for analysis of meson (π) production in, 25:56530
ALUMINUM ISOTOPES Al-28
energy levels from aluminum-27 (d,p) reactions, spectroscopic factors and spin--parity assignments for, (E), 25:56709
ALUMINUM NITRIDES
evaporation behavior at 1500 to 1800°K, 25:55607 (JUL-739-PC)
formation heat of, 25:55607 (JUL-739-PC)
ALUMINUM OXIDES
decomposition oxygen pressures over test samples of, at high temperatures and low pressures, 25:55428 (BNWL-B-108)
effects of surface coating of, on phase composition of rhenium--tungsten alloys at 1500 to 1900°C, 25:55465

XUM

fabrication of small grains of, for thermoluminescent dosimetry, 25:55055(P)
properties and structure of, produced by sintering using systematic thermal fluctuations, 25:55414
properties of container materials of, for sodium hydroxide--nitrogen oxide processing of carbide fuels, 25:55376 (CONF-690452-, Paper 9)
properties of cordierite-strengthened refractories of, mechanical and thermal, 25:55621
properties of metal fiber reinforced composites of, review on, 25:55608(T) (LB/G-3074)
$Al_2O_3$--Cu, production of fine powders of, Microgel process for, 25:55419
$Al_2O_3$--$Dy_2O_3$--$UO_2$, temperature distribution in irradiated fuels of, use of eutectic isotherm for monitoring, (E), 25:57194
$Al_2O_3$--$Fe_2O_3$, production of fine powders of, Microgel process for, 25:55419
$Al_2O_3$--Mo, deformation mechanisms in, effects of temperature on, 25:55455
$Al_2O_3$--Ni, production of fine powders of, Microgel process for, 25:55419
Al--$Al_2O_3$, strength of powder shapes of, effects of dispersion-, grain boundary-, and solid solution-hardening on, 25:55487

ALUMINUM PHOSPHATES
effects on strontium-85 sorption by man, 25:55109 (COO-1231-67)

ALUMINUM SILICIDES
deposition of zinc-plated, on refractory metals for corrosion protection, method for, 25:55398(P)

AMERICIUM
separation from irradiated LMFBR fuel by solvent extraction using dibutyl butylphosphonate, 25:54706 (BNWL-SA-3345)
spectra of trivalent, in calcium tungstate, 25:54578 (ORNL-4682, pp 215-17)

AMERICIUM ISOTOPES Am-232
electron capture decay of, plutonium-232 delayed fission from, (E), 25:56744(T) (NP-tr-1936)

AMERICIUM ISOTOPES Am-234
electron capture decay of, plutonium-234 delayed fission from, (E), 25:56744(T) (NP-tr-1936)

AMERICIUM ISOTOPES Am-238
electron-capture decay scheme, (E), 25:56792

AMERICIUM ISOTOPES Am-241
alpha decay of, gamma energies and absolute branching intensities for, (E), 25:56753 (UCRL-51087)
decay of, efficiency of scintillation counting measurement of, 25:54700
effects on chromosomes in liver of hamsters following injection, RBE for aberrant, 25:55188
excretion in urine of man following inhalation as oxide, effects of DTPA on, 25:55118
production of aerosols of oxides of, for inhalation studies in dogs, 25:54982
toxicity to hamsters following intraperitoneal injection, 25:55188

AMERICIUM ISOTOPES Am-243
energy levels from gamma inelastic scattering, (E), 25:56738 (JINR-P15-5959)
photon inelastic scattering by, production of spontaneously fissioning isomers in, (E), 25:56738 (JINR-P15-5959)
production of spontaneously fissioning isomers in gamma inelastic scattering, (E), 25:56738 (JINR-P15-5959)

AMES RESEARCH REACTOR
radiation monitoring of environs of, during 1971, 25:55152 (IS-2658)

AMINO ACIDS
radiation effects on content of, in proteins of processed food, 25:55364
radiolysis of, rate constants for hydrogen atom reactions following electron, 25:55132

AMINOPTERIN
effects on mutation induction in uv irradiated Bacillus subtilis, 25:55189

AMMETERS
design of d-c, for weak currents, 25:55071 (CEA-N-1433)

AMMONIA
complexes with benzoic acid and cobalt perchlorate, radiolysis of, oxidation by hydroxyl radical of benzoatopentaamminecobalt(III) from $\gamma$ and electron pulse, 25:54669
effects on radiolysis of N-acetylglycine, 25:54650
neutron spectra in solid anhydrous, time dependence following fast pulses, 25:56629
radiolysis at 0.1 to 760 Torr, kinetic study of species formed during electron pulse, 25:54661

AMPHIBIA
Leptodactylus occelatus, radiation effects on water distribution and permeability in muscle cells of, x, 25:55323

AMPLIFIERS
design of d-c, for weak currents, 25:55071 (CEA-N-1433)

ANALYTICAL CHEMISTRY
book: Ion Exchange in Analytical Chemistry, 25:54397

ANGIOSPERMIDAE
Allium sp., radiation effects on sprouting, spoilage molds, and sugar content of bulbs of, $\gamma$, 25:55354
Arachis hypogaea, radioinduced mutations for improved yield of, x, 25:55181
Beta sp., radiation effects on chromatin and RNA polymerase activity in, effects of dose and washing on $\gamma$, 25:55351
Citrus sp., radioinduced mutations for increased resistance to low temperature, x, 25:55181
Crepis capillaris, radioinduced chromosome aberrations in seeds of, effects of time of administration on additive or protective effects of ethylenimine on x, 25:55260
Crepis capillaris, radioinduced mutations in seeds of, effects of water content on $\gamma$ and x, 25:55167
Crepis capillaris, radioinduced premutational oxygen-sensitive changes in chromosomes of seeds of, $\gamma$, 25:55168
Hordeum distichon, radioinduced mutations in seeds of, effects of ethylenimine on x, 25:55261
Hordeum sp., radioinduced chromosome aberrations in seeds of, method for metaphase analysis of x, 25:55175
Hordeum sp., radioinduced mutations in, effects of developmental stage and dose on, 25:55190
Linum sp., radioinduced mutations for chlorophyll in, dose dependence of $\gamma$, 25:55177
Phaseolus limensis, radiation effects on yield of, effects of developmental stage on $\gamma$, 25:55349
Pyrus sp., selection of compact x-radioinduced mutants of, for grafting on rootstocks, 25:55174
Raphanus sativus, radioinduced inhibition of seed germination in, effects of very high dose rate on RBE for x, 25:55350
Tradescantia sp., radiation effects on pollen and stamen hairs of, RBE for neutron, 25:55206 (NYO-2740-8, pp 147-219)
Triticum aestivum, radioinduced mutations in seeds of, effects of ethylenimine on x, 25:55261
Triticum aestivum, respiration rate in seedlings of, effects of age, light, radiation, and temperature on, 25:55348
Triticum durum, radioinduced chromosome aberrations in seeds of, effects of prolonged storage on repeated-exposure x, 25:55169
Triticum sp., strontium-90 content of seeds of hybrid, in relation to phenotype, 25:55223
Vicia faba, chromosome translocation induction in, comparison of effectiveness of ionizing radiation and chemicals for, 25:55191
Zea mays, radioinduced mutations in, effects of developmental stage and dose on, 25:55190

ANGIOTENSINS
radioimmunoassay in blood plasma of man with hypertension and with renal transplants, 25:55141

ANIMALS
strontium-90 toxicity to, extrapolation to man of data for long-term, 25:55319 (UCD-472-118)

ANTARCTIC REGION
strontium-90 content of snow in, 1955 and 1964 measurements of, 25:54788

ANTENNAS
receiving properties of asymmetric cylindrical, 25:57271 (SC-RR-710475)
response of short monopole, on skin of finite cylinders, 25:57273 (SC-RR-710519)

ANTHRACENE
radiation effects on crystals and polymeric solutions of, $\alpha$, 25:54600(R) (UCLA-34-P-88-32)

ANTIBODIES
cross reactivity of antimyelin, sequential absorption analysis of, 25:57255 (ORO-3195-43)
cross reactivity of antisynaptosome, sequential absorption analysis of, 25:57254 (ORO-3195-42)
production of human thyroid, following technetium-99m scintiscanning, immunofluorescent tests on, 25:55292

ANTIMONY
argon-ion reactions at 30 keV with surfaces of, charge states and kinetic energies of scattered and recoil ions from, (E), 25:55818
determination by x-ray counting after neutron activation, 25:54692(R) (NYO-3417-15)
determination in lead-base alloys by neutron activation and radiochemical separation, 25:54515
determination of trace amounts of, in air by neutron activation and $\gamma$ spectrometry, 25:54456
properties of aerosols of, produced from solutions at high temperatures, chemical and physical, 25:54545
separation simultaneously with arsenic from aqueous solutions by solvent extraction using tribenzylamine, 25:54515

ANTIMONY ALLOYS AND SYSTEMS
Ag--Sb, superconductivity in hcp phases of, (E), 25:56096
Cu--Sb, superconductivity in, with $DO_3$ structure, (E), 25:56096
In--Sb, radioinduced defects and electron mobility changes in InSb single crystals, annealing of fast-neutron, 25:56317

ANTIMONY ISOTOPES
energy levels of, shell-model calculations with Tabakin potential, (T), 25:56666
yields from uranium proton fission, (E), 25:56757

ANTIMONY ISOTOPES Sb-121
energy levels from tin-120 proton elastic scattering, spectroscopic factors for isobaric analog, (E), 25:56769


XUM

ANTIMONY ISOTOPES Sb-124
beta decay of, β-γ angular correlations and matrix elements for nonunique first-forbidden, (E), 25:56776
ANTIMONY ISOTOPES Sb-125
energy levels from tin-124 proton elastic scattering, spectroscopic factors for isobaric analog, (E), 25:56769
ARCHAEOLOGICAL SPECIMENS
age of, effects of geophysical variables on fission track method for estimation, 25:54760
ARCTIC REGION
radio-wave propagation across polar cap during PCA, proton anomaly of very long, (E), 25:55996
ARGON
electric conductivity of, at pressure of 50 atm, (E/T), 25:56139
gold-198 ranges in, from gold-197(n,γ) recoil, 25:56269
helium-ion range at 0.2 to 2.0 MeV in, as function of energy, (E), 25:56276
meson (μ⁻) reactions with, x-ray emission from, (E), 25:55830
nuclear charge radius of, determination from x-ray emission in argon--meson (μ⁻) reactions, 25:55830
oxygen-ion reactions at 10 to 40 MeV with, cross sections for electron capture in, 25:55869
oxygen-ion reactions at 7 to 40 MeV with, cross sections for electron capture and loss in, (E), 25:55870
plasma of, analytical and physical properties of microwave-excited, (E), 25:56158
plasma of, electron velocity distribution function for homogeneous, (T), 25:56186
plasma of, electron--ion recombination rate coefficients for, (T), 25:56182
plasma of, instabilities and turbulence in arcs in magnetic fields, (E/T), 25:56196(R) (N-71-25028)
plasma of, Langmuir probe performance for diagnostics of shock-heated, (E/T), 25:56144
plasma of, spectroscopic diagnostics of arc, (E/T), 25:56139
plasma of, temperature distribution and thermal conductivity in arc, (E), 25:56140
plasma of, transport properties of partially ionized, (T), 25:56183
proton range at 0.2 to 2.0 MeV in, as function of energy, (E), 25:56276
proton reactions at 20 to 120 keV with, cross sections for electron capture into n = 2 states of hydrogen in, (E), 25:55853
scattering by nitrogen molecules, rainbow oscillations in differential cross sections for, (E), 25:55852
solubility in liquid sodium at 330 to 550°C, 25:54583
ARGON IONS
atomic oscillator strength for Ar VIII, 3d--4p transition, (E/T), 25:55776
effects on silicon at 220 keV, lateral-stress study of damage produced in, 25:56285 (SC-RR-710424)
reactions with metal surfaces and neodymium oxides at 30 keV, charge states and kinetic energies of scattered and recoil ions from, (E), 25:55818
ARGON ISOTOPES Ar-38
abundance in Sikhote--Alin meteorite, (E), 25:55671
ARGON ISOTOPES Ar-40
diffusion from meteorites, lunar materials, and terrestrial rocks, (E), 25:55672
lithium-6 reactions (Li-6,d) at 22 MeV, angular distributions for, (E), 25:56714
neutron reactions (n,α) at 14.4 MeV, α spectra, cross sections, and Q-value for, (E), 25:56718
scattering by nuclei in wide energy range, phase shift analysis of angular distributions for elastic, (E), 25:56740 (JINR-P7-5884)
ARGON SYSTEMS
Ar--H, meson(μ⁻) reactions with, meson transfer from hydrogen to argon and x-ray emission in, (E), 25:55830
ARKANSAS NUCLEAR ONE POWER REACTOR
design parameters of, revised and additional data on, 25:56959 (DOCKET-50313-31)
operations aspects of, revised and additional data on, 25:56959 (DOCKET-50313-31)
personnel for, technical qualifications of operating, 25:56959 (DOCKET-50313-31)
ARSENIC
determination by x-ray counting after neutron activation, 25:54692(R) (NYO-3417-15)
determination in lead-base alloys by neutron activation and radiochemical separation, 25:54515
determination in meteorites and meteoritic phases by neutron activation and γ spectrometry, 25:54477
determination in yttrium oxide by emission spectrometry, 25:54419
separation simultaneously with antimony from aqueous solutions by solvent extraction using tribenzylamine, 25:54515
ARSENIC ISOTOPES As-75
energy levels and transitions from neutron inelastic scattering, (E), 25:56752(R) (SUNI-14)
neutron capture at 2.9 MeV, cross section for, (E), 25:56696
ASPHALT
density of highway surface, tabulation of US state highway departments' uses of radiometric gages for measuring, 25:54907
ASTRON DEVICE
plasma equilibrium calculational methods for, 25:56207
ASTRONAUTS
radioinduced light flashes in eyes of, following exposure to cosmic mesons (μ), 25:55341
ASTROPHYSICS
supermassive objects in, (T), 25:55798
ATLANTIC OCEAN
plutonium-239 content of organisms of, 25:55161
ATMOSPHERE
density of neutral, above 100 km, 25:57274 (SC-RR-710541)
diffusion and deposition of iodomethane gas, molecular iodine gas, and uranin dye in, 25:54795
diffusion in Casaccia, Italy, smoke plume photography studies of, 25:54783
diffusion of plumes and puffs in, krypton-85 tracer studies of, 25:54908
fallout monitoring in Swiss, following Dec. 1968 and Sept. 1969 Chinese nuclear explosions, 25:54791
fallout monitoring of ground-level, in north Germany and north Norway during 1970 and 1971, 25:54785
gravity-wave generation in, by solar eclipse, (E/T), 25:56016
ion balance in, effects of natural radioactive products on, 25:54786
ion mass and mobility in, methods for measuring, 25:54800
ionization by terrestrial gamma radiation, vertical distribution of, 25:54790
ionization in, produced by penetration of energetic charged particles, (T), 25:55983
krypton-85 content of global, forecasts to year 2000 of, 25:54781(T) (JPRS-53174)
plutonium particle release to, effects of thermal stress on nature and quantity of, 25:54546
quality index for, 25:57246 (ORNL-NSF-EP-8)
radioactivity in, measurements for determining strontium-89/strontium-90 fractionation factor in fallout, 25:54803
radioactivity monitoring in, data processing system for, 25:55006
radioactivity monitoring in, review of current methods for, 25:54784
radon concentration in, electrostatic sampler and detector system for measuring, 25:55032
radon content of Plovdiv, Bulgaria, during 1966 to 1969, 25:54792
radon decay products in ground-level, model for propagation of, 25:54787
radon washout from, method for measuring, 25:54802
ATMOSPHERES
management and surveillance of inert-gas, for ANL fuels center, 25:54945 (CONF-710401-, pp 98-105)
ATMOSPHERIC PRECIPITATION
radiation monitoring in environs of Ames Research Reactor during 1971, 25:55152 (IS-2658)
ATOMIC BEAMS
detection of, surface-barrier detector for, 25:55007(P)
ATOMIC ENERGY
engineering consultants in, Canadian, 25:57211 (70-CNA-657)
ATOMIC ENERGY, LEGAL ASPECTS
handbook on nuclear law in Latin America, 25:55252 (NP-18752)
legislation for biomedical addition to Los Alamos Meson Physics Facility, 25:55299 (LA-4490)
regulations for medical irradiation facilities, review of Japanese, 25:54852
regulations for overland shipping of sealed gamma sources, description of French, 25:54976
treaties for control of nuclear weapons, history and principles of, 25:54829
ATOMIC PHYSICS
energy states and statistics of atomic systems, 25:56397
quantum theory of spontaneous emission in presence of external radiation, 25:55883
research at University of North Carolina April 1 to June 30, 1971, 25:56748(R) (ORO-2408-45)
wave functions for, calculation of, 25:55889
ATOMIC STRUCTURE
theory of, survey of use of Lie groups in, 25:55882 (NYO-1447-64)
ATOMS
electron configurations in, highly restricted partitions and angular-momentum states of equivalent-particle, (T), 25:56848
electron correlation energies in, methods for calculation of, 25:55890
electron reactions at low energies with, review of total and momentum-transfer cross sections for, (E), 25:55856
electron reactions with, computer control system for studying, 25:55094
electron scattering by, computational procedures for multichannel resonances in, 25:55861
electron scattering by, polarized-orbital method for, 25:55871
energies of s eigenstates of, calculation using static screened Coulomb potential, 25:55884
energy levels of, perturbation theory for decaying,

25:55886
energy-level transitions in, probability of radiative Auger-type, (T), 25:55888
energy-level transitions of Z = 57 through 92, probabilities of L x-ray, (E), 25:55823
neutron elastic scattering by, analysis of many-particle distribution functions in Sunakawa model for multiple, (T), 25:56637
nuclear charge distribution of electronic and muonic, relation of isotope shifts to, 25:55821
perturbation energies and wave functions for, error bounds for nth-order Rayleigh--Schroedinger, 25:55891
photon emission from systems of N identical two-level, rotating-wave approximation and spontaneous, (T), 25:55887
photon emission from systems of N identical two-level, many-body aspects and inhomogeneous broadening in master-equation approach to spontaneous, 25:55885
photon emission in presence of external radiation, spontaneous, (T), 25:55883
spectra of Z = 20 through 94, relative intensities of K x-ray emission lines of, (E), 25:55827
ATPase
radiation effects on activity of rat bone marrow, effects of dose on x, 25:55330
AURORAE
activity in, correlation patterns with radiation-belt electron intensity, (E/T), 25:55979
arcs in nighttime, simultaneous spectrographic triangulation on Mar. 23-24, 1969 of SAR and hydrogen, (E), 25:55971
charged-particle density and precipitation in polar-cap, sounding-rocket observations of, (E), 25:56031
creation of elecron-beam-produced artifial, magnetospheric magnetic-field configuration from, (E), 25:55961
occurrence over Alaska, Feb. 14-15, 1958, form-position, orientation, and motion plots of, (E), 25:55954
production of artificial, ground-based optical observations of electron-beam, 25:55962
spectra in, enhancement and excitation mechanisms of oxygen infrared, (E/T), 25:56018
AURORAL ZONE
electric field in nighttime and daytime, Langmuir-probe measurement of vector, 25:55960
electromagnetic-wave emission in relation to auroral cosmic-noise absorption, vlf, (E/T), 25:55999
magnetic substorm in, over Alaska associated with plasma-sheet behavior, (E), 25:55955
magnetic substorm structure in, effect of intensification of westward electrojet current on, (E/T), 25:56029
magnetic substorms in, relation to generation of magnetospheric sudden commencements, (E/T), 25:56026
proton precipitation in and radar echoes from, simultaneous observations of, (E), 25:55963
radio-wave propagation across, anomaly of very long, (E), 25:55996
AVES
Gallus sp., radiation effects on blood vessels in, in relation to mechanisms of acute injury, whole-body γ, 25:55324
Gallus sp., radiation effects on leukosis and Rous sarcoma frequency in, effects of sex on x, 25:55329
Gallus sp., radioinduced cardiovascular anomalies in embryos of, additive effects of hypothermia on x, 25:55333

## B

BACKGROUND RADIATION
levels in environment of nuclear power plants, effects of long-term release of radioactivity on, 25:55200
BACTERIOPHAGES
lambda, radioinduced inactivation of, role of DNA cross-links in sensitizing effects of psoralen on uv, 25:55361
T4, radioinduced mutations in, recombination in mutant crosses following uv, 25:55173
BAILLY POWER REACTOR, UNIT 1
design parameters of, requested additional information on, 25:56971 (DOCKET-50367-22)
design parameters of, revised and additional data on, 25:56970 (DOCKET-50367-21)
operations aspects of, requested additional information on, 25:56971 (DOCKET-50367-22)
operations aspects of, revised and additional data on, 25:56970 (DOCKET-50367-21)
BALANCES
readout device for use in radioactive environments, design of remote-, 25:55080 (TRG-Report-2086)
BARIUM
analysis of minerals containing, for strontium by atomic absorption spectroscopy, 25:54413
determination in feldspar by neutron activation and γ spectrometry, 25:54494
determination in fission product mixtures by ion exchange and β counting, 25:54449
determination in volcanic ash by neutron activation and γ spectrometry, 25:54513
determination of trace amounts of, in air by neutron activation and γ spectrometry, 25:54456
distribution between bismuth--lead eutectic and MSBR fuel solvent, reductive extraction, 25:54534 (ORNL-4717, pp 43-56)
separation from other alkaline earths by ionophoresis on filter paper and poly(vinyl alcohol), 25:54725
separation of uranium from, in methyl sulfoxide by cation exchange chromatography, 25:54728
BARIUM ALLOYS AND SYSTEMS
Ba--Na, phase diagram of, 25:55526
Ba--Pr-base, phase diagram of, 25:55567
BARIUM FLUORIDES
positron lifetimes in, empirical model for calculation of, 25:55834
BARIUM ISOTOPES Ba-134
alpha reactions (α,n) at 15 to 28 MeV, superconductivity-model calculations of isomeric-cross-section ratios for, (T), 25:56765
BARIUM ISOTOPES Ba-138
neutron capture at 2.9 MeV, cross section for, (E), 25:56696
proton elastic scattering with isobaric analog excitation, shell-model analysis of, (E/T), 25:56769
BARIUM ISOTOPES Ba-140
determination as measure of fast neutron flux, standard for, 25:54444
BARIUM SULFATES
radioinduced paramagnetic centers in doped crystals of, EPR and annealing of gamma, 25:56339
BARYONS
coupling constants between pseudoscalar mesons and, in SU(3) strong coupling baryon bootstrap model, 25:56503
equation of state for ultradense matter of, (T), 25:55689
interactions with pseudoscalar mesons, tables of coefficients for partial-wave analysis of vector meson and 1/2+ baryon production in, (T), 25:56501 (RHEL/R-224)
mass relations in broken SU(3) symmetry, 25:56477
model for, pseudovector isospinor heavy-boson, 25:56477
BARYONS, RESONANCE
reactions with stable and unstable hadrons, kinematic study of, (T), 25:56474 (FRNC-TH-63)
BARYONS, RESONANCE (N*)
mass and width of complex-spin negative-mass-squared tachyon, in angular distributions of π + N charge-exchange interactions at 5.9 to 18.2 GeV/c, (T), 25:56500 (ORO-3992-18)
mass and width of N(1470) in four-prong π+ + p interactions at 8 GeV/c in hydrogen bubble chamber, (E), 25:56428 (IFA-HE-75)
mass and width of negative-mass-squared, in π− + p → π0 + n interactions at 5.9 to 18.2 GeV/c, (T), 25:56499 (ORO-3992-8)
production in K+ + p interactions at 10 GeV/c in hydrogen bubble chamber, review of, (E), 25:56435
production of complex-spin negative-mass-squared tachyon, in angular distributions of π + N charge-exchange interactions at 5.9 to 18.2 GeV/c, (T), 25:56500 (ORO-3992-18)
production of Δ(1236) and N(1518) in n + p → p + n interactions at 8 and 19 GeV/c, spark chamber study of, (E), 25:56415 (NP-18888)
production of Δ(1236) in e + n interactions in e + d interactions at high energies, cross sections for, (E), 25:56405 (DESY-71/33)
production of Δ(1236), Δ(1640), N(1470) in four-prong π+ + p interactions at 8 GeV/c in hydrogen bubble chamber, (E), 25:56428 (IFA-HE-75)
production of Δ++ in π− + p → π− + Δ++ + π− and p + p → p + Δ++ + π− interactions, Cherenkov mechanism for cross section behavior for, (T), 25:56498 (IFA-HE-76)
production of N(1470) and N(1688) in n + p → 2p + π− interactions at 2 to 30 GeV, Reggeized one-pion-exchange model for diffraction, (T), 25:56521 (JINR-P1-5975)
production of negative-mass-squared, in π− + p → π0 + n interactions at 5.9 to 18.2 GeV/c, interpretation of angular distribution for, (T), 25:56499 (ORO-3992-8)
BARYONS, RESONANCE (Y*)
mass and width of Λπ+(2000) enhancement in π+ + p interactions at 8 GeV/c in hydrogen bubble chamber, (E), 25:56427 (IFA-HE-73)
production of Σ+(1385), Σ-(1385), and Λπ+(2000) and ΛK(1800) enhancements in π+ + p interactions at 8 GeV/c in hydrogen bubble chamber, cross sections for, (E), 25:56427 (IFA-HE-73)
spectra of, harmonic oscillator quark model for, 25:56507
BASALT
age of, use of neutron activation in argon--potassium method of estimation of, 25:54765
analysis of Columbia River, by activation and γ spectrometry, 25:54460
thorium content in Australian and Hawaiian, 25:54495
uranium content in Australian and Hawaiian, 25:54495
BEAVER VALLEY POWER REACTOR, UNIT 1
effluents from, effects on environment of chemical, radioactive, and thermal, 25:56962 (DOCKET-50334-25)
site for, geological, hydrological, and meteorological data for, 25:56962 (DOCKET-50334-25)

XUM

BELLOWS
corrosion by liquid sodium of stainless steel, 25:57109 (ANL-7771)
BENZENE
neutron diffusion constant and cooling coefficient for, calculation using modified classical monatomic gas model, (T), 25:56631
radiation effects on sorption on magnesium sulfate incorporating sulfur-35, gas chromatographic studies of, 25:54603
radiolysis of aqueous solutions of, 25:54631 (CONF-700652-(Vol.3), pp 601-48)
reactions of solid, with carbon-14 ions at 5 to 100 eV, hydrocarbon yields from, 25:54703
reactions of solid, with carbon-14 ions at 5, 31, and 100 eV, partial degradation of carbon-14-labeled 1,3,5-cycloheptatriene from, 25:54702
BENZOIC ACID
complexes with ammonia and cobalt perchlorates, radiolysis of, oxidation by hydroxyl radical of benzoatopentaamminecobalt(III) from γ and electron pulse, 25:54669
BERKELIUM
purification by oxidation and solvent extraction, 25:54671 (ORNL-4682, pp 114-32)
BERKELIUM ISOTOPES Bk-249
energy-level transitions in, nuclear structure effects on internal conversion of M1, 25:56756
BERKELIUM OXIDES
decomposition oxygen pressures over nonstoichiometric samples of, at 852 to 1150°C and $10^{-7}$ to $10^{-20}$ atm, 25:55428 (BNWL-B-108)
BERYLLIUM
abundance in solar atmosphere, (E/T), 25:55750
determination by charged particle activation methods, optimum irradiation conditions and nuclear interferences for, 25:54520
determination in rocks by alpha activation and prompt γ counting, 25:54467
mechanical properties of sheets of, relations with microstructure, 25:55510
neutron reactions at 10 to 30 GeV/c, total cross sections for, (E), 25:56421
separation of uranium from, in methyl sulfoxide by cation exchange chromatography, 25:54728
stopping of nuclei of, in nuclear emulsion, mass resolution of, (E/T), 25:55894 (LUIP-CR-71-4)
x-ray scattering by, form factors and scattering functions for coherent and incoherent, 25:56259 (EGG-1183-1479)
BERYLLIUM ALLOYS AND SYSTEMS
porosity of, effects of annealing and crystallization on micro-, 25:55462
Be--Cu-base, microstructure of, potentiostatic studies on, 25:55555
Be--Cu-base, radiation effects on aging and precipitation in, neutron, 25:55583
Be--Cu-base--Ni, microstructure of, potentiostatic studies on, 25:55555
Be--Fe-base, phase transitions in 400°C annealing of, Moessbauer-effect study of, 25:56378
BERYLLIUM FLUORIDES
$BeF_2$--$CeF_3$--LiF, phase equilibria in, 25:54532 (ORNL-4717, pp 1-27)
$BeF_2$--LiF, thermodynamics of mixing in molten, electrochemical measurements of, 25:54532 (ORNL-4717, pp 1-27)
$BeF_2$--LiF--$ThF_4$, liquidus temperature of, 25:54534 (ORNL-4717, pp 43-56)
$BeF_2$--LiF--$ThF_4$, plutonium trifluoride solubility and absorption spectra in molten, effects of oxide on, 25:54532 (ORNL-4717, pp 1-27)
$BeF_2$--LiF--$ThF_4$--$UF_4$, separation of protactinium from molten, by oxide precipitation, 25:54712 (ORNL-4682, pp 1-38)
$BeF_2$--LiF--$ThF_4$--$UF_4$, separation of uranium from molten, by oxide precipitation, 25:54712 (ORNL-4682, pp 1-38)
$BeF_2$--NaF, electric conductivity of molten, 25:54532 (ORNL-4717, pp 1-27)
$BeF_2$--NaF, glass transition temperatures of molten, 25:54532 (ORNL-4717, pp 1-27)
BERYLLIUM IONS
energy levels of $Be^{2+}$, positions and widths of autoionizing, (T), 25:55820
x-ray scattering by Be II, form factors and scattering functions for coherent and incoherent, 25:56259 (EGG-1183-1479)
BERYLLIUM ISOTOPES Be-7
production in alpha reactions with aluminum and silicon at 70 to 160 MeV, cross sections and fission mechanism for, (E/T), 25:56685 (FRNC-TH-48)
separation from rainwater by countercurrent electrophoresis, 25:54742
BERYLLIUM ISOTOPES Be-8
energy levels of, microscopic description using cluster model, 25:56654 (LYCEN-7104, S13.1-11)
BERYLLIUM ISOTOPES Be-9
abundance in Galaxy, (T), 25:55781
alpha reactions (α,2α) at 42.8 and 49.2 MeV, analysis using impulse approximation, (E/T), 25:56674
energy levels of, microscopic description using cluster model, 25:56654 (LYCEN-7104, S13.1-11)
helium-3 reactions (He-3,n) at 8 MeV, neutron spectra from, (E), 25:56679
neutron energy distribution in, transition region function for, (T), 25:56622
neutron thermalization in polycrystalline, Monte Carlo method for calculating, (T), 25:56619 (RT/FI-(70)49)
BERYLLIUM OXIDES
properties of oxide-strengthened refractories of, mechanical and thermal, 25:55621
BETA DECAY
induced tensor contribution in allowed, calculation using impulse approximation, (T), 25:56861
parity nonconservation in, effect on γ circular polarization, 25:56855
second-class currents in, G-parity properties of, (T), 25:56854
BETA PARTICLES
detection in water, development of Cherenkov detectors for, 25:55031
dose distribution in bones of beagle dogs following strontium-90--yttrium-90 ingestion, 25:55319 (UCD-472-118)
dose to organs of mice following inhalation of niobium-95 and zirconium-95, effects of chemical form of inhaled particles on, 25:55125
effectiveness for therapy of squamous epithelial cancer of mouth in comparison with ametohepazon, gamma radiation, 5-fluorouracil, and radium, 25:55345
monitoring in atmosphere at Plovdiv, Bulgaria during 1966 to 1969, 25:54792
BETA SOURCES
activity of pure, liquid scintillators for absolute measurement of, 25:54697
BETA SPECTROMETERS
design of electron--positron pair, for neutron capture spectroscopy, 25:55040 (NP-18994)
energy distributions in electrostatic, calculations of, 25:55084
performance and testing of electrostatic, 25:55083
spectra from electrostatic, method for evaluation of, 25:55082
BIBLIOGRAPHIES
on electrical discharge machining and electrochemical machining, 25:54834 (WAPD-331)
on Finnish radiology, 25:55274
on national and international nuclear standards, 25:57091 (ORNL-NSIC-94)
on production and industrial uses of radioisotopes, April through June 1971, 25:54894 (ORNL-IIC-37(Pt.2))
on radiative lifetimes, 25:57215 (CEA-Bib-198)
on science and society, 25:57294 (WASH-1182)
BIG ROCK POINT POWER REACTOR
emergency core cooling system for, performance evaluation and design modifications for, 25:56935 (DOCKET-50155-92)
BINDING ENERGY
calculation of nuclear, using energy-density functional, 25:56853
BIOCHEMISTRY
tracer techniques in, 25 year summary of, 25:55107
BIOLOGICAL MATERIALS
analysis for lead by irradiation with 30-MeV α particles and track registration of α particles from decay of resulting polonium, 25:54452
analysis for trace mercury by neutron activation and radiochemical separation, 25:54508
analysis of fluid, for iodine by neutron activation, ion exchange, and γ spectrometry, semi-automated, 25:54516
BIOLOGICAL MODELS
development for promethium-147 metabolism in man and swine, 25:55108 (BNWL-SA-3747)
use of mathematical, for analysis of kinetics of radioligand assays, 25:55145
BIOLOGY
research program on marine, Princeton Univ, 25:57243(R) (NYO-3406-22)
tracer techniques in, 25 year summary of, 25:55107
BIOPHYSICS
research at Columbia Univ., July 1, 1971, 25:55205(R) (NYO-2740-8)
BIPHENYL, CHLORO-
determination in rat adipose tissue by neutron activation and radiochemical separation, 25:54500
BISMUTH
analysis for chlorides, photometric, 25:54407
determination in standard rocks and quartzes by neutron activation and radiochemical separation, 25:54454
determination in yttrium oxide by emission spectrometry, 25:54419
determination of trace amounts of, in silicate rocks by neutron activation and radiochemical separations, 25:54489
effects on solvolysis of tert-butyl halides, Broensted correlation for, 25:54548
separation of uranium from, in methyl sulfoxide by cation exchange chromatography, 25:54728
solute distribution in, on crystallization in reductive extraction of metals from molten fluoride mixtures, 25:54534 (ORNL-4717, pp 43-56)
solvent properties for actinides and lanthanides, 25:54712 (ORNL-4682, pp 1-38)

XUM

BISMUTH ALLOYS AND SYSTEMS
Bi--Cd--Sn, electric transport of tin isotopes in 300°C melts of, 25:56349
Bi--In, superplastic properties of eutectic, 25:55456
Bi--Li, solvent properties for rare earths and thorium, 25:54712 (ORNL-4682, pp 1-38)
Bi--Mn, properties as extractant for rare earths from MSBR fuel solvent, 25:54534 (ORNL-4717, pp 43-56)
Bi--Pr-base, phase diagram of, 25:55567
Bi--Pr-base, phase diagram of, thermodynamic analysis of, 25:55566
BISMUTH ISOTOPES
energy levels of neutron-deficient, survey of data on low-lying, 25:56798
BISMUTH ISOTOPES Bi-204
energy-level scheme from polonium-204 decay, 25:56798
BISMUTH ISOTOPES Bi-209
alpha fission at 20 to 34 MeV, cross section and delayed neutron yields for, (E), 25:56803
alpha reactions (α,p) at 26.5 to 60 MeV, angular distributions, excitation functions, and recoil ranges for, (E), 25:56799
carbon-12 fission at 62 and 82 MeV, liquid-drop analysis of, (E/T), 25:56786
energy levels from lead-208 proton elastic scattering, spectroscopic factors for isobaric analog, (E), 25:56769
energy levels of, shell-model analysis of nonnormal, (T), 25:56763
helium-3 fission at 20 to 34 MeV, cross section and delayed neutron yields for, (E), 25:56803
ion elastic scattering in wide energy range, phase shift analysis of angular distributions for, (E), 25:56740 (JINR-P7-5884)
BISMUTH ISOTOPES Bi-214
content in sand and clay soils, performance of airborne gamma spectrometer system for measuring, 25:54768
effects on ion balance in atmosphere, 25:54786
BITUMINOUS MATERIALS
radioactive waste fixation in, mixer-evaporator and plant design for, 25:54981
BLACK BODY RADIATION
theory for, physical dimensions in generalized, (T), 25:56453 (ORO-3992-42)
BLACK HOLES
parameters of, (T), 25:55803
relaxation of, (T), 25:55803
BLOOD
alpha detection in, of miners using nuclear emulsions, 25:55236
flow in liver of dogs, use of xenon-133 clearance technique in measurement of, 25:55123
radiation effects on human, use of additional treatment with iron and steroid preparations for reducing therapeutic, 25:55303
radiation effects on pulmonary circulation in rabbits, acute x, 25:55327
BLOOD PLASMA
angiotensin radioimmunoassay in human, effects of hypertension and renal transplants on, 25:55141
radioimmunoassay of arginine vasopressin in human, use of double antibody technique for, 25:55142
strontium-90 content of, in beagle dogs following prolonged ingestion, 25:55319 (UCD-472-118)
BLOOD SERUM
analysis for iodine by neutron activation and radiochemical separation, 25:54509
analysis for thyroxine and triiodothyronine by activation and ion exchange, 25:54453
triiodothyronine radioimmunoassay in human, effects of hyperthyroidism and hypothyroidism on, 25:55146
BLOOD VESSELS
radiation effects on, in chickens in relation to mechanisms of acute injury, whole-body γ, 25:55324
radioinduced anomalies in chick embryo, additive effects of hypothermia on x, 25:55333
scanning of cerebral, comparison of angiography with iodine-131 for, 25:55289
scanning of human pulmonary, for diagnosis of pulmonary hypertension, effectiveness of two-phase scintigraphy method with iodine-131-labeled albumen and technetium-99m-labeled albumen for, 25:55284
BODY FLUIDS
analysis for iodine by neutron activation and radiochemical separation, 25:54509
BOHUNICE POWER REACTOR, UNIT 1
fuel assemblies for, hydrodynamics of rod type, (E), 25:56880 (ZJE-104)
fuel elements for, irradiation testing of tubular finned, 25:57050 (UJV-2551-RT)
BOHUNICE POWER REACTOR, UNIT 2
fuel assemblies for, hydrodynamics of rod type, (E), 25:56880 (ZJE-104)
BOILERS
design of forced flow steam, heated by pressurized water from nuclear reactors, 25:54836(P)
heat transfer in forced-convection water, effects of surface crud deposits on, (E), 25:54861 (AEEW-R-705)
BOILING
detection in reactors, sensitivity of methods for, (E), 25:56996
effects on crud deposition, 25:57034
heat transfer during subcooled, measurement of burnout, 25:54871 (IFA-TR-58)
initiation in superheated sodium, effects of heating surface material and roughness on, (E), 25:54868(T) (EURFNR-897)
model for wick-, in porous magnetite deposits on heating surfaces, (T), 25:54862 (AEEW-R-711)
occurrence of film, on surfaces immersed in boiling high-boiling-point organic compounds, 25:54879
BONE MARROW
alpha detection in, of miners using nuclear emulsions, 25:55236
radiation effects on enzyme activity and hematopoietic tissues in rat, effects of dose on x, 25:55330
radiation effects on hematopoiesis in active, effects of dose fractionation on, 25:55326
BONES
analysis for lead by irradiation with 30-MeV α particles and track registration of α particles from decay of resulting polonium, 25:54452
analysis of diseased and normal human, for calcium, phosphorus, and sodium by neutron activation methods, 25:55106
radiation dose distribution in beagle dog, strontium-90--yttrium-90 β, 25:55319 (UCD-472-118)
radiation effects on beagle dog, estimation of hazards to man from model for long-term low dose radium-226, 25:55319 (UCD-472-118)
radiation effects on calcium metabolism in rat, effects of sex on, 25:55331
radiotherapy of lymphogranulomatosis of, effectiveness of γ and x, 25:55301
scanning of human, use of thulium-167 for, 25:55279
BORATES
borates--boric acid, equilibria at high temperatures, 25:54535 (ORNL-4717, pp 57-82)
BORIC ACID
borates--boric acid, equilibria at high temperatures, 25:54535 (ORNL-4717, pp 57-82)
BORON
abundance in solar atmosphere, (E/T), 25:55750
determination by charged particle activation methods, optimum irradiation conditions and nuclear interferences for, 25:54520
determination by neutron capture γ spectroscopy, 25:54462
determination by spectroscopy of prompt γ radiation following neutron capture, 25:54451
determination in borate glasses by neutron absorption method, 25:54437(T) (RFP-Trans-82)
determination in glass and tourmaline, by measuresent of prompt proton spectra from (d,p) reactions, 25:56752(R) (SUNI-14)
determination in glass, by simultaneous measurement of scattered α particles and prompt protons, 25:56752(R) (SUNI-14)
determination in semiconductor silicon by alpha or proton activation, 25:54528
determination in yttrium oxide by emission spectrometry, 25:54419
effects on magnetoresistance in graphite, 25:56319
effects on thermal conductivity of polycrystalline graphite, 25:55635
surface wetting of molten, on boron nitride, mechanisms of, 25:55469
BORON CARBIDES
radioinduced defects in polycrystalline, neutron, 25:55650
radioinduced swelling of, development of gas pycnometer for measuring, 25:54599 (ORNL-4717, p 117-24)
BORON FLUORIDES
solubility of gaseous, in fluoride melts, 25:54532 (ORNL-4717, pp 1-27)
BORON IONS
energy levels of $B^{3+}$, positions and widths of autoionizing, (T), 25:55820
x-ray scattering by three- and four-electron, form factors and scattering functions for coherent and incoherent, 25:56259 (EGG-1183-1479)
BORON ISOTOPES B-10
abundance in Galaxy, (T), 25:55781
abundance in solar atmosphere, (E/T), 25:55750
determination of abundance relative to boron-11, by method using $Rb_2BO_2^+$ ion, 25:54432
deuteron reactions (d,α) at 0.4 to 1.5 MeV with subsequent alpha decay, reaction mechanisms of, (E), 25:56673
deuteron reactions (d,nγ) at 3 MeV, n-γ coincidence spectra from, (E), 25:56752(R) (SUNI-14)
proton inelastic scattering at 3.5 to 5 MeV, excitation functions for, (E), 25:56679
BORON ISOTOPES B-11
abundance in Galaxy, (T), 25:55781
abundance in solar atmosphere, (E/T), 25:55750
determination of abundance relative to boron-10 by method using $Rb_2BO_2^+$ ion, 25:54432
energy levels from intermediate resonances in nitrogen-14 ($n,2\alpha$) reactions, spin assignments for, (E), 25:56680
helium-3 inelastic scattering at 26 MeV, helium-3 spectra from, (E), 25:56679
helium-3 reactions (He-3,t) at 26 MeV, triton spectra


XUM

from, (E), 25:56679
BORON NITRIDES
evaporation behavior at 1500 to 1800°K, 25:55607 (JUL-739-PC)
formation heat of, 25:55607 (JUL-739-PC)
wetting of surfaces of, by molten aluminum, boron, chromium, silicon, and titanium, mechanisms of, 25:55469
BORON OXIDES
density, enthalpy, and viscosity of molten $B_2O_3$, to 2000°C, 25:55625
BOSONS
Bose--Einstein condensation in one and two dimensions, possible existence of, 25:56049
existence of pseudovector isospinor heavy, 25:56477
ground-state energy of many-particle system of, 25:56050
hydrodynamics of Bose fluid in terms of action-angle variables in quantum statistics, 25:56051
production from intermediate nucleon isobar decay in nucleon reactions with light nuclei, model for, 25:56525
BOSONS, INTERMEDIATE-VECTOR
existence of spin-0 charged, indefinite metric for, (T), 25:56547 (NYO-1932(2)-200)
production in ν + p interactions in proton electromagnetic field at 30 to 400 GeV, total cross sections for, (T), 25:56473
BRAIN
calcium-45 uptake by microsomes, synaptosomes, and synaptic vesicles of rat, 25:55120
fractionation of, cellular and subcellular, 25:57259 (ORO-3195-47)
radiation effects on olfactory bulb cells of rat, electron microscopy of x, 25:55336
radioactivity distribution in neuronal and glial-enriched fractions of, following in vitro and in vivo administration of tritium-labeled leucine, 25:55119
respiratory rate of slices of rat, in $D_2O$, 25:55121
scanning of blood vessels in human, comparison of angiography with iodine-131 for, 25:55289
scanning of human, for diagnosis of neurological disorders, role of prescanning cerebral angiography and pneumography in, 25:55281
scanning of human, using chromium-51 or ytterbium-169-labeled EDTA, 25:55272
transplantation of γ-irradiated bovine fascia in dogs, for filling dura mater defects, 25:55148
BRASS
mechanical properties of chemical vapor deposited rings of, design of apparatus for testing, 25:55440
BREMSSTRAHLUNG
buildup factor dependence on position of shielding between source and detector, 25:56280
dose field parameters for high energy, effects of electron component of beam on, 25:55209
effects on human skin following therapy of bone sarcomas, pathological, 25:55338
production in n + p interactions at 14.1 MeV, relativistically covariant models for cross sections for, (T), 25:56526
production in polarized and unpolarized electron scattering by nuclei with multipole moments, effects of nuclear structure on, (T), 25:56862
reactions (γ,f) with plutonium-239 and uranium-238, delay time for isomeric fission in, (E), 25:56801
BROMINE
determination of trace amounts of, in air by neutron activation and γ spectrometry, 25:54456
effects on reactions of recoil chlorine-38 in neutron-irradiated chloromethane, 25:54681
effects on thermal conductivity of polycrystalline graphite, 25:55635
BROMINE ISOTOPES Br-79
energy levels from neutron inelastic scattering, spin--parity assignments for, (E), 25:56698
energy-level transitions from neutron inelastic scattering, branching ratios for, (E), 25:56698
BROMINE ISOTOPES Br-80
reactions of recoil isomeric, with bromocyclopropane, formation of allyl bromide from isomerization, 25:54690
BROMINE ISOTOPES Br-81
energy levels from neutron inelastic scattering, spin--parity assignments for, (E), 25:56698
energy-level transitions from neutron inelastic scattering, branching ratios for, (E), 25:56698
BROMINE ISOTOPES Br-87
beta decay of, high-energy γ transitions from neutron-unbound states in, (E), 25:56703
BROMINE SYSTEMS
Br--cyclopropane, neutron reactions (n,γ) with, products from reactions of recoil bromine-80m from, 25:54690
BROWNS FERRY POWER REACTOR, UNIT 1
radioactive effluents from, release limits for gaseous, 25:56980
BROWNS FERRY POWER REACTOR, UNIT 2
radioactive effluents from, release limits for gaseous, 25:56980
BROWNS FERRY POWER REACTOR, UNIT 3
radioactive effluents from, release limits for gaseous, 25:56980
BRUNSWICK POWER REACTOR, UNIT 1
emergency core cooling system for, performance requirements for, 25:56960 (DOCKET-50324-22)
BRUNSWICK POWER REACTOR, UNIT 2
emergency core cooling system for, performance requirements for, 25:56960 (DOCKET-50324-22)
BUGEY REACTORS (EDF-5)
pressure vessel for, testing of model of, 25:56886
BUILDING MATERIALS
book: Corrosion in Nuclear Applications, 25:55388
radiation effects on space-vehicle, studies of nuclear and space, 25:55576 (N-71-25034)
BULGARIA
radiation monitoring of atmosphere at Plovdiv, during 1966 to 1969, 25:54792
BUTADIENE
effects on reactions of recoil chlorine-38 in neutron-irradiated chloromethane, 25:54681
1,3-BUTADIENE
radiation effects on single crystals of, ESR studies of radicals from γ, 25:54639
radiation effects on, adsorbed on silica gel, ESR studies of radicals from γ, 25:54640
BUTANE
radiolysis of liquid, effects of oxygen and sulfur hexafluoride on yields from γ, 25:54659
radiolysis of mixtures of normal and deuterated, effects of oxygen on yields from γ, 25:54659
butane--$N_2O$, radiolysis of, effects of oxygen on yields of nitrogen from γ, 25:54659
1,3-BUTANEDIONE, 4,4,4-TRIFLUORO-1-(2-THIENYL)-
complexes with iron, spectrophotometric study of, 25:54692(R) (NYO-3417-15)
solvent properties for rare earths, synergistic effects of 2,4-pentanedione on, 25:54731
solvent properties for uranium, 25:54751
BUTYRIC ACID, AMINO-
radiation effects on in vitro rat liver uptake of, γ, 25:55126
BUTYRIC ACID, 2-AMINO-4-(METHYLSELENYL)-
effectiveness of selenium-75-labeled, for scintiscanning of human pancreas, 25:55271(T) (LB/G-3059)
radiochemical purity and stability of selenium-75-labeled, 25:54698

## C

CABLES
design of superconducting energy transmission, 25:56111(P)
production of superconducting energy transmission, method for, 25:56111(P)
CADARACHE REACTORS
loop for Pegase, description of high-temperature in-pile, 25:54840
CADARACHE REACTORS (RAPSODIE)
radiation effects testing in, facilities and equipment for, 25:56997
CADMIUM
argon-ion reactions at 30 keV with surfaces of, charge states and kinetic energies of scattered and recoil ions from, (E), 25:55818
association equilibria with bromide or chloride in molten calcium nitrate hydrate, 25:54535 (ORNL-4717, pp 57-82)
determination by controlled potential coulometry using rotated mercury cell, 25:54427
determination in fission product mixtures by ion exchange and polarography or β counting, 25:54449
determination in isoquinoline formate by polarography, 25:54421
determination in standard rocks and quartzes by neutron activation and radiochemical separation, 25:54454
determination in yttrium oxide by emission spectrometry, 25:54419
determination of trace amounts of, in silicate rocks by neutron activation and radiochemical separations, 25:54489
determination of trace amounts of, in thorium and zirconium compounds by neutron activation, separation processes, and γ spectrometry, 25:54518
effects of vapors of, on hydrogen isotope exchange at 300 to 500°C, 25:54552
effects on radiolysis of crystalline silver oxalate, 25:54638
effects on solvolysis of tert-butyl halides, Broensted correlation for, 25:54548
neutron reactions at 10 to 30 GeV/c, total cross sections for, (E), 25:56421
nuclear quadrupole interaction of cadmium-111 247-keV level in, 25:56363
potential for, method for modeling l = 2 component of, 25:56387
separation of uranium from, in methyl sulfoxide by cation exchange chromatography, 25:54728
CADMIUM ALLOYS AND SYSTEMS
Ag--Cd, oxidation at 600 to 800°C, mechanisms of internal, 25:55381
Ag--Cd, search for superconductivity in fcc phases of, (E), 25:56096
Au--Cd, search for superconductivity in fcc phases of,

(E), 25:56096
Bi--Cd--Sn, electric transport of tin isotopes in 300°C melts of, 25:56349
Cd--Pb, diffusion in molten, kinetics of mutual, 25:55449
CADMIUM IONS
implantation in gallium arsenide at 60 keV, lattice damage induced in, 25:56287
radioinduced reduction in doped alkali-metal halide crystals, magneto-optical study of x-,, 25:56320
CADMIUM ISOTOPES Cd-107
energy levels from indium-107 decay, (E), 25:56759
CADMIUM ISOTOPES Cd-111
nuclear quadrupole interaction of 247-keV level in pure cadmium metal, 25:56363
CADMIUM ISOTOPES Cd-114
deuteron elastic and inelastic scattering at 13.6 MeV, strong-coupling analysis of, (T), 25:56780
energy-level transitions from indium-114 electron-capture decay, effects of Coulomb fragmentation in indium iodides on line profiles of, (E), 25:54696
CADMIUM SULFIDES
defects in wurtzite single crystals of, studies of growth and radioinduced, 25:56286
neutron scattering by crystals of, anomalous transmission from suppression of (n,γ) reaction in resonant, 25:56627
radiation damage in, luminescence and electric resistivity study of thermal-neutron, 25:56307
CADMIUM TELLURIDES
radiation damage in, luminescence and electric resistivity study of thermal-neutron, 25:56307
radiation effects on cathodoluminescence spectrum of, electron, 25:56290
CAFFEINE
radiosensitizing effects on Escherichia coli, effects of temperature on uv and x, 25:55357
CALCITES
analysis for trace elements in sample coexisting with dolomite by neutron activation and γ spectrometry, 25:54497
CALCIUM
analysis for calcium-44/calcium-40 by neutron activation, 25:54492
content of diseased and normal human bones, neutron activation determination of, 25:55106
determination by nondestructive alpha activation, 25:54522
determination in stony meteorites by proton and bremsstrahlung activation, 25:54466
determination in tourmaline, by deuteron activation analysis and γ counting, 25:56752(R) (SUNI-14)
determination in yttrium oxide by emission spectrometry, 25:54419
radiation effects on rat bone metabolism of, effects of hormonal mechanism and sex on, 25:55331
separation from other alkaline earths by ionophoresis on filter paper and poly(vinyl alcohol), 25:54725
separation of uranium from, in methyl sulfoxide by cation exchange chromatography, 25:54728
sorption by soils, effects of soil exchange sites on differential, 25:54778
CALCIUM ALLOYS AND SYSTEMS
C--Ca--Ce--Mg--Si, analysis for tellurium by gravimetry, 25:54416
CALCIUM CARBONATES
decomposition oxygen pressures over test samples of, at high temperatures and low pressures, 25:55428 (BNWL-B-108)
CALCIUM FLUORIDES
positron lifetimes in, empirical model for calculation of, 25:55834
CALCIUM ISOTOPES Ca-40
determination of abundance of, relative to calcium-44 by neutron activation, 25:54492
meson ($\mu^-$) capture by, photon asymmetry for radiative, (E), 25:56705
neon-20 reactions (Ne-20,O-16) at 63 and 73.7 MeV, cross sections for, (E), 25:56721
photon reactions (γ,n) with, analysis by Feynman triangle diagrams of fine-structure peaks in cross sections for, (T), 25:56676
proton elastic scattering by, phase-shift analysis of polarization effects in, (T), 25:56678
proton reactions (p,2p) at 600 MeV, distorted-wave impulse-approximation analysis of cross sections from, (E/T), 25:56711
proton reactions (p,2p) at 600 MeV, separation-energy spectra and momentum distributions of residual nuclei from, (E), 25:56706
CALCIUM ISOTOPES Ca-41
energy levels from potassium-39 (He-3,p) reaction, γ decay properties of isobaric analog, (E), 25:56715
CALCIUM ISOTOPES Ca-44
determination of abundance of, relative to calcium-40 by neutron activation, 25:54492
energy levels from argon-40 (Li-6,d) reactions, configurations of low-lying, (E), 25:56714
CALCIUM ISOTOPES Ca-45
radioactivity of, liquid scintillators for absolute measurement of, 25:54697
uptake by brain microsomes, synaptosomes, and synaptic vesicles, 25:55120
CALCIUM OXIDES
CaO--$Y_2O_3$--$ZrO_2$-base, thermal stability of solid solutions of, effects of yttrium oxide content on, 25:55636
CaO--$ZrO_2$, crystal structure of, polymorphic transformations in, 25:55641
CaO--$ZrO_2$, densification by hot pressing, 25:55600
CALCIUM PHOSPHATES
effects on distribution of mixed cesium and strontium radioisotopes in man following ingestion, 25:55113
CALCIUM ZIRCONATES
thermal conductivity at high temperatures, 25:55637
$CaZrO_3$--$ZrO_2$, crystal structure of, polymorphic transformations in, 25:55641
CALIFORNIUM
purification by oxidation and solvent extraction, 25:54671 (ORNL-4682, pp 114-32)
CALIFORNIUM ISOTOPES Cf-249
energy levels of, Davydov-model calculations of spins for, (T), 25:56785
CALIFORNIUM ISOTOPES Cf-252
effects on survival of hamster cells, RBE of, 25:55207 (NYO-2740-8, pp 220-59)
fission of, prompt neutron yield for spontaneous, (E), 25:56743 (NP-18966)
performance of neutron source of, in seabed mineral prospecting, 25:54913
production in reactors, effects of irradiation conditions on, 25:57067
use as neutron source in nuclear methods for seabed mineral exploration, 25:54887(R) (BNWL-1308-6)
use as source for low-flux neutron radiography, 25:54887(R) (BNWL-1308-6)
uses of, 25:54396 (ORNL-4682, pp 242-9)
CALIFORNIUM OXIDES
preparation and identification of, 25:54671 (ORNL-4682, pp 114-32)
CALORIMETERS
design and performance of adiabatic, for studying thermal behavior of saturated heavy water, 25:55092
CAMERAS
performance of ultrarapid photometric, for plasma diagnostics, 25:56132 (CEA-R-4079)
CANADA
radioactive contamination of environment by nuclear industry in, biological significance of, 25:55194 (70-CNA-641)
CARBIDES
diffusion in, data tabulations on, 25:55509
preparation by sol-gel process, 25:55594 (ORNL-4682, pp 218-28)
carbides--Fe, strength of powder shapes of, effects of dispersion-, grain boundary-, and solid solution-hardening on, 25:55487
CARBON
abundance in B-type stars, (E), 25:55701
abundance in solar atmosphere, (E/T), 25:55750
abundance of molecular, in atmospheres of late-type stars, (E/T), 25:55698
deposition of pyrolytic, on silicon oxides, effects of chemical reactivity on, 25:55604
determination by charged particle activation methods, optimum irradiation conditions and nuclear interferences for, 25:54520
determination in liquid sodium, development of meter for, 25:55379(R) (WARD-4210-T-1-2)
diffusion in solid solutions of cobalt, alpha-iron, nickel, palladium, beta-titanium, and vanadium, 25:55479
diffusion in yttrium at 20 to 300°C, effects of dislocations on, 25:55461
mass transfer in reactor materials exposed to sodium, measurement of, 25:55379(R) (WARD-4210-T-1-2)
neutron reactions at 10 to 30 GeV/c, total cross sections for, (E), 25:56421
production of highly isotopically enriched pyrolytic, 25:54542
production of pyrolytic, from methane at 1650 to 2150°C, mechanisms of, 25:55591 (JUL-735-RW)
properties of, derived from indene compounds, 25:57295 (Y-1790)
radiation effects on Dragon pyrolytic, 25:55651
radiation effects on electric conductivity and diamagnetic anisotropy of fibers of, neutron, 25:56282 (CEA-CONF-1822)
radiation effects on electronic properties of, relations of annealing with neutron, 25:56283 (CEA-CONF-1823)
radioinduced dimensional changes in deposited coatings of isotropic, fast neutron, 25:55652
radioinduced dimensional changes in, relations of graphitization with neutron, 25:55645 (CEA-CONF-1821)
reactions between forms of, during heat treatment, 25:57275(T) (SC-T-713060)
stopping of nuclei of, in nuclear emulsion, mass resolution of, (E/T), 25:55894 (LUIP-CR-71-4)
transfer between stainless steel and uranium carbide, carbon-14 tracer measurements of, 25:55589 (JAERI-Memo-4438)
CARBON BLACK
formation in hydrocarbon thermal decomposition,

XUM

25:57278(T) (SC-T-713066)
sorptive properties of graphitized, for carbon dioxide, 25:55634
CARBON DIOXIDES
corrosive effects on reactor materials, review of, 25:55393
radioinduced reactions with graphite, effects of active species range and water vapor on, 25:55654
radioinduced reactions with graphite, surface oxide formation in, 25:55655
sorption on Graphon, effects of oxygen on, 25:55634
air--$CO_2$, plutonium ignition in, effects of oxygen content on, 25:54946 (CONF-710401-, pp 106-17)
CARBON IONS
effects on diploid yeast cells, OER and RBE for mutagenic and lethal, 25:55165
effects on silicon at 220 keV, lateral-stress study of damage produced in, 25:56285 (SC-RR-710424)
energy levels of $C^{++}$, positions and widths of autoionizing, (T), 25:55820
x-ray scattering by three- and four-electron, form factors and scattering functions for coherent and incoherent, 25:56259 (EGG-1183-1479)
CARBON ISOTOPES C-11
energy levels of, widths for T = 3/2, (E), 25:56679
production in alpha reactions with aluminum and silicon at 70 to 160 MeV, cross sections and fission mechanism for, (E/T), 25:56685 (FRNC-TH-48)
CARBON ISOTOPES C-12
alpha elastic and inelastic scattering at 8.5 to 10.5 MeV, angular distributions for, (E), 25:56681
alpha reactions (α,Be-7) and (α,Li-6) at 42 MeV, cross sections for, (E), 25:56659
alpha reactions (α,p) at 11.3 to 26.3 MeV, angular distributions and excitation functions for, (E), 25:56675
alpha reactions (α,p) at 8.5 to 10.5 MeV, angular distributions for, (E), 25:56681
alpha reactions at 70 and 90 MeV, cross sections for, (E), 25:56652 (LYCEN-7104, S2.1-2)
deuteron elastic and inelastic scattering at 13.6 MeV, strong-coupling analysis of, (T), 25:56780
deuteron reactions (d,α) at 7.2 to 14 MeV, excitation functions for isospin forbidden, (E), 25:56656
deuteron reactions (d,nγ) at 5 MeV, n-γ coincidence spectra from, (E), 25:56752(R) (SUNI-14)
electron inelastic scattering by, form-factor calculations using isotensor dipole sum rules, (T), 25:56868
form factor of, liquid-drop-model calculation including quadrupole surface oscillations of elastic, (T), 25:56668
helium-3 reactions (He-3,2p) and (He-3,d) at 40 MeV, DWBA analysis of angular distributions and spectra from, (E), 25:56713
helium-3 reactions (He-3,p) and (He-3,2p) at 15 MeV, angular distributions and p-p angular correlations for, (E), 25:56682
lithium-7 elastic scattering at 21 MeV, optical-model analysis of, (E), 25:56663
lithium-7 reactions (Li-7,d) at 21.1 MeV, Hauser--Feshbach analysis of differential cross sections and spectra from, (E), 25:56663
meson ($K^-$) absorption in, analysis of mechanism in, 25:56653 (LYCEN-7104, S4.1-10)
meson ($\pi^-$) absorption by, analysis of mechanism in, 25:56653 (LYCEN-7104, S4.1-10)
meson reactions ($\pi^-$,2$\pi^-$) at 4 GeV in propane bubble chamber, upper limit of cross sections for, (E), 25:56439
neutron inelastic scattering at 22 MeV with subsequent α decay, n-α coincidence spectra from, (E), 25:56752(R) (SUNI-14)
photon reactions (γ,n) with, analysis by Feynman triangle diagrams of fine-structure peaks in cross sections for, (T), 25:56676
photon reactions with, model analysis of, (T), 25:56661
proton elastic scattering by, phase-shift analysis of polarization effects in, (T), 25:56678
proton reactions (p,2p) at 1 GeV, Glauber multiple scattering theory for differential cross sections for quasi-free, (T), 25:56520 (IC-71/106)
proton reactions (p,2p) at 600 MeV, distorted-wave impulse-approximation analysis of cross sections from, (E/T), 25:56711
proton reactions (p,2p) at 600 MeV, separation-energy spectra and momentum distributions of residual nuclei from, (E), 25:56706
reactions (C-12,f) with bismuth-209 at 62 and 82 MeV, liquid-drop analysis of, (E/T), 25:56786
scattering by nuclei in wide energy range, phase shift analysis of angular distributions for elastic, (E), 25:56740 (JINR-P7-5884)
CARBON ISOTOPES C-13
effects on infrared absorption spectra of irradiated carbon-doped silicon, 25:56325
lithium-7 elastic scattering at 21 MeV, optical-model analysis of, (E), 25:56663
lithium-7 reactions (Li-7,t) at 20.5 MeV, DWBA and Hauser--Feshbach analyses of differential cross sections and spectra from, (E), 25:56663
production of dense cylinders of, 25:54542
CARBON ISOTOPES C-14
accumulation by marine phytoplankton, mechanisms of, 25:55154
distribution of recoil, from neutron reactions with nitrogen-14 in potassium azide, 25:54687
effects on infrared absorption spectra of irradiated carbon-doped silicon, 25:56325
energy levels of, shell-model calculation using Fabakin potential, (T), 25:56660
proton reactions (p,γ) and (p,n) at 2.3 to 2.6 MeV, excitation functions and gamma spectra from, (E), 25:56669
reactions of ions of, with solid benzene at 5 to 100 eV, hydrocarbon yields from, 25:54703
reactions of ions of, with solid benzene at 5, 31, and 100 eV, partial degradation of carbon-14-labeled-1,3,5-cycloheptatriene from, 25:54702
CARBON ISOTOPES C-16
production in alpha reactions with aluminum and silicon at 160 MeV, cross sections and fission mechanism for, (E/T), 25:56685 (FRNC-TH-48)
CARBON MONOXIDES
abundance in atmospheres of late-type stars, (E/T), 25:55698
desorption from tungsten, time-of-flight study of electron-stimulated, 25:55435 (RLO-2221-T-7-4)
sorption by tantalum, flash--mass spectrometric study of chemi-, 25:55441
spectral lives due to, in IRC + 10216, (E), 25:55686
CO--O, radiolysis of, electron pulse, 25:54587(R) (AECL-3909)
CARBON SULFIDES
spectral lives due to, in IRC + 10216, (E), 25:55686
CARBON SYSTEMS
C--Ca--Ce--Mg--Si, analysis for tellurium by gravimetry, 25:54416
C--Co-base--Ti--W, mechanical properties of heat-treated, 25:55497
C--Co-base--W, mechanical properties of heat-treated, 25:55497
C--Cr--Mo, microstructure of white irons of, 25:55556
C--Hf--Nb, phase diagram of niobium--rich corner of, 25:55563
C--Hf--Re--W, mechanical properties of, 25:55433 (N-71-23982)
C--Hf--Zr, thermodynamic properties of, 25:55614
C--$HfB_2$, electric and thermal conductivity at 300 to 1300°K, 25:55627
C--$HfB_2$--SiC, electric and thermal conductivity at 300 to 1300°K, 25:55627
C--Mo, superconductivity of phases of, 25:56087
C--N--O--Pu--U, preparation of carbides, carbonitrides, and hypostoichiometric oxides in, 25:55594 (ORNL-4682, pp 218-28)
C--Nb--U, phase diagram at 1000°C, carbide composition in, 25:55547
C--Nb--Zr, thermodynamic properties of, relations with composition, 25:55615
C--Ru--Th, phase studies of, 25:55640
C--Si, radioinduced dimensional changes in codeposited coatings of isotropic, fast neutron, 25:55652
C--SiC--$ZrB_2$, electric and thermal conductivity at 300 to 1300°K, 25:55627
C--U--Zr, phase diagram at 950°C, carbide composition in, 25:55547
C--U--Zr, thermodynamic properties of, 25:55614
C--W, superconductivity of phases of, 25:56087
C--$ZrB_2$, electric and thermal conductivity at 300 to 1300°K, 25:55627
CARBON TETRACHLORIDE
effects on radiolysis of cyclohexane, 25:54670
effects on separation of europium or lanthanum from acid solutions by solvent extraction using acidic esters of aminophosphonic acids, 25:54732
neutron reactions with, replacement reactions of recoil chlorine-38 in, 25:54688
CARBON TETRAFLUORIDE
neutron reactions with, replacement reactions of recoil chlorine-38 in, 25:54688
CARBONITRIDES
preparation by sol-gel process, 25:55594 (ORNL-4682, pp 218-28)
CATHODES
design for injecting hydrogen isotopes into metals, 25:54858
CATTLE
radiation effects on function of testes in male, tonometer measurements on x, 25:55337
CAVITIES
construction of lined underground, method for, 25:54854(P)
excavation of storage, in salt deposits, feasibility study of nuclear methods for, (E), 25:54824(T) (UCRL-Trans-10543, pp 70-80)
CAVITY RESONATORS
design for in-core displacement measurements, 25:55068(T) (AEC-tr-7240)
electron deflection in superconducting $HEM_{11}$, 25:56594 (NP-18998)
CELLS
cycle synchronization in tumor, using 5-fluorouracil,

25:55306
density bands of isolated membranes of rat brain glial, 25:57257 (ORO-3195-45)
density bands of membranes from glial, of mutant and normal mice, 25:57256 (ORO-3195-44)
effects of injections of bone marrow, peritoneal exudate, spleen, or thymus, on recovery of antigen retention system in x-irradiated mice, 25:55147
properties of radioinduced osteosarcoma, in rats, 25:55335
radiation effects on DNA and RNA synthesis in mouse kidney, γ and uv, 25:55129
radiation effects on hamster, sensitizing effects of isoniazid on x, 25:55207 (NYO-2740-8, pp 220-59)
radiation effects on morphology of normal and neoplastic oral cavity, comparison of β, γ, and radium, 25:55345
radiation effects on rat olfactory bulb nerve, electron microscopy of x, 25:55336
radiation effects on renewal patterns of rat liver, tritium-labeled thymidine, 25:55110(R) (TID-25801)
radiation effects on survival of hamster, RBE of californium-252 and radium, 25:55207 (NYO-2740-8, pp 220-59)
radiation effects on water distribution and permeability in frog muscle, x, 25:55323
radiation effects on, theorems for dose--effect relations in, 25:55206 (NYO-2740-8, pp 147-219)
radioactivity distribution in organelles of brain, following administration of tritium-labeled leucine, 25:55119

CELLS, CULTURED
radiation effects on hamster lung, daughter cell repair of lethal x, 25:55311
radiation effects on survival of Chinese hamster and human kidney, parameters for heavy ion, 25:55313
radiation effects on thymidine incorporation into DNA of rat thymus, factors affecting x, 25:55127
radiosensitivity of synchronized Chinese hamster, effects of 5-bromodeoxyuridine on x, 25:55258

CELLS, HeLa
labeling with tritium-labeled thymidine, correlation between radioactivity levels and degree of, 25:55110(R) (TID-25801)
radiation effects on survival of, parameters for heavy ion, 25:55313
radiation effects on survival of, protective effects of tetrahydrofolic acid against x, 25:55268
radiation effects on, following exposure of cytoplasm, nucleus, and whole cells, comparison of uv, 25:55312

CELLS, L
radiation effects on survival of synchronized, effects of age on 14-MeV neutron and x, 25:55309

CELLULOSE
radioinduced polymerization of monomer and polymer impregnants in, mechanical properties of products of, 25:55658

CEMENTS
radioactive waste solidification in, for disposal in seawater, 25:54979

CEREALS
flour, charge removal from, using promethium-147 and strontium-90 beta sources, 25:54897

CERIUM
determination in fission product mixtures by ion exchange and β counting, 25:54449
determination in intermediate products of rare earth production by x-ray spectroscopy, 25:54417
determination in river water and seawater by neutron activation and radiochemical separation, 25:54504
determination in volcanic ash by neutron activation and γ spectrometry, 25:54513
determination using N-benzylquinolinium nitrate, gravimetric, 25:54434
diffusion in nickel at 500 to 1100°C, volume and grain-boundary, 25:55488
effects on radiolysis of crystalline potassium nitrate, 25:54638
properties of aerosols of, produced from solutions at high temperatures, chemical and physical, 25:54545
reactions of tetravalent, in γ-irradiated aqueous solutions of sulfuric acid, 25:54647
reduction of, evaluation of various chelating agents for, 25:54422
separation from aqueous Savannah River fuel reprocessing wastes by batch solvent extraction, 25:54739
separation from lanthanum on titanium tungstate papers by electrochromatography, 25:54744
separation from lanthanum, niobium, thorium, and zirconium, by reverse phase partition chromatography on TTA-impregnated paper, 25:54746
separation from rare earth phosphors by precipitation as iodates, 25:54749(P)
separation of yttrium from, by extraction with bis(2-ethylhexyl) phosphate, 25:54750(P)

CERIUM ALLOYS AND SYSTEMS
Au--Ce, crystal structures and melting points of intermetallic, 25:55570
C--Ca--Ce--Mg--Si, analysis for tellurium by gravimetry, 25:54416
Ce--Gd--Ru, critical magnetic field in superconducting, (E), 25:56074
Ce--La, magnetic impurity scattering and superconductivity in, 25:56068
Ce--Mg, compound formation in, vapor pressure measurements for studies of thermodynamics of, 25:55525 (IS-T-462)
Ce--Nd--Ru, critical magnetic field in superconducting, (E), 25:56074
Ce--Ru, critical magnetic field in superconducting intermetallic $CeRu_2$, (E/T), 25:56074
Ce--Ru--Y, critical magnetic field in superconducting, (E), 25:56074
Ce--Zn-base, thermodynamics of molten, at 700 to 1000°K, emf studies of, 25:55442

CERIUM FLUORIDES
$BeF_2$--$CeF_3$--LiF, phase equilibria in, 25:54532 (ORNL-4717, pp 1-27)
$CeF_3$--$ThF_4$, phase studies in, 25:54532 (ORNL-4717, pp 1-27)

CERIUM ISOTOPES Ce-135
energy-level transitions in, branching ratios, internal conversion coefficients, and multipolarities for, (E), 25:56761

CERIUM ISOTOPES Ce-140
proton reactions at high energies, isobar model for analysis of meson (π) production in, 25:56530

CERIUM ISOTOPES Ce-144
content in seawater, role of adsorption processes in, 25:54811
effects on chromosomes in liver of hamsters following injection, RBE for aberrant, 25:55188
toxicity to hamsters following intraperitoneal injection, 25:55188
uptake by Chlamydomonas, statistical analysis of factors affecting, 25:55162

CERIUM OXIDES
decomposition oxygen pressures over test samples of, at high temperatures and low pressures, 25:55428 (BNWL-B-108)

CERIUM SULFATES
radiolysis of sulfuric acid solutions of, reactivity of tetravalent cerium from γ, 25:54647

CERMETS
properties of, effects of stereometric microstructure on, 25:55628

CESIUM
determination as silver hexanitritocerite complex, indirect titrimetric, 25:54415
determination in Australian tektites by neutron activation and gamma spectrometry, 25:54478
determination in fission product mixtures by ion exchange and β counting, 25:54449
determination in volcanic ash by neutron activation and γ spectrometry, 25:54513
diffusion in BISO-coated fuel particles, 25:55647 (ORNL-4717, pp 83-90)
diffusion in glass, effects of temperature on, 25:55611
release from bonded beds of BISO-coated uranium dioxide particles during post irradiation annealing at 1250°C, 25:55647 (ORNL-4717, pp 83-90)
separation from milk, double-bed ion exchange process for, 25:54722
separation from MSBR fuel solvent by extraction into bismuth by reduction with lithium at 650°C, 25:54534 (ORNL-4717, pp 43-56)
sorption of fission-product, by graphite at high temperatures, 25:55623

CESIUM ALLOYS AND SYSTEMS
Cs--Pr-base, phase diagram of, 25:55567

CESIUM AZIDES
radiolysis of crystalline, effects of additives on yields from proton and γ, 25:54638

CESIUM FLUORIDES
diffusion of xenon-133 in single crystals of, effects of surface properties and structure on, 25:55633

CESIUM IODIDES
diffusion of xenon-133 in single crystals of, effects of surface properties and structure on, 25:55633

CESIUM IONS
reactions with tungsten, sputtering of secondary tungsten ions from, 25:55819

CESIUM ISOTOPES Cs-131
preparation of high-purity carrier-free sources of, for spectroscopic measurements, 25:54889 (INR-P-1325)

CESIUM ISOTOPES Cs-134
content in liquid radioactive waste effluents from Nuclear Fuel Services West Valley reprocessing plant, 25:54753
distribution in conceptus of pregnant rats following injection, 25:55114
distribution in man following ingestion, effects of calcium phosphate, methionine, Prussian blue, and sodium alginate on, 25:55113
energy levels from cesium-133 neutron capture, lifetimes for, (E), 25:56784
energy-level transitions from cesium-133 neutron capture, intensities and multipolarities for, (E), 25:56784

CESIUM ISOTOPES Cs-137
content in liquid radioactive waste effluents from Nuclear Fuel Services West Valley reprocessing plant, 25:54753
content in petroleum, following production stimulation by contained nuclear explosion, (E/T), 25:54826(T) (UCRL-

Trans-10543, pp 99-116)
content of man, comparison of whole-body counter measurements of, 25:55225
distribution in man following ingestion, effects of calcium phosphate, methionine, Prussian blue, and sodium alginate on, 25:55113
release from failed water cooled Zircaloy 2 clad uranium oxide ($UO_2$) fuel rods, 25:57047 (JAERI-Memo-4157, pp 2-22)
uptake by organisms of marine food chain, effects of physico-chemical form on, 25:55149 (BNWL-SA-4048)
uptake by rainbow trout in mountain lake ecosystem, role of bottom sediment in pathway for, 25:55159
uses as radiation source, development of market for, 25:54887(R) (BNWL-1308-6)
CESIUM PERCHLORATES
radiolysis of crystalline, effects of additives on yields from proton and γ, 25:54638
CESIUM URANIUM FLUORIDES
crystal structure of $CsU_6F_{25}$, 25:54532 (ORNL-4717, pp 1-27)
CHARGED-PARTICLE BEAMS
interactions in Orsay storage ring, space charge effects in, 25:56592 (LAL-RT-43-70)
interactions with nonlinear media, radiations from, (T), 25:56168
radiations from passage through cubic nonlinear media, (T), 25:56168
transport systems for, first- and second-order matrix theory for, 25:56598 (SLAC-75(Rev.2))
CHARGED PARTICLES
Coulomb field corrections for, in strong magnetic fields, 25:56402
dosimetry of relativistic, design of solid-electrolyte dosimeter for, 25:55054(P)
dosimetry using tissue-equivalent wall-less proportional detectors, 25:55002 (NYO-2740-8, pp 7-146)
energy losses in unknown materials, technique for determination of, 25:56752(R) (SUNI-14)
flux of bunches of, at 250 to 500 km in ionosphere, (E/T), 25:56008
intensity at 200 to 300 km of primary cosmic, global distribution of, (E), 25:55980
intensity observations at low altitudes over auroral zones and polar caps, simultaneous electric-field observations and, 25:56030
interactions of system with electromagnetic field, potentials and multipole moments for, (T), 25:56455
motion along spiral path in transparent media, radiations from, (T), 25:56462
motion in electromagnetic fields, radiation corrections for, (T), 25:56393
motion in spatially modulated magnetic fields, invariants in, 25:56401
penetration into Earth and other planetary atmospheres, energy- and space-distribution-related, (T), 25:55983
photon emission in vacuum by, evanescent, (T), 25:56392
reactions with hydrogen atoms and hydrogen-like ions, cross sections for transitions between highly excited levels in, (T), 25:55838
reactions with hydrogen atoms and hydrogen-like ions, cross sections for transitions between highly excited levels in, (T), 25:55839
scattering by electrostatic fields, approximate evaluation of relativistic correction in, 25:55846
trajectories in 1/r electrostatic fields, second-order approximation for calculating, (T), 25:55082
CHEMISTRY
potential--pH diagrams for temperatures above 298.16°K, (T), 25:57212 (AAEC/E-219(Pt.1))
research progress on, April 1, 1970 to March 31, 1971, 25:54711(R) (ORNL-4682)
CHERENKOV RADIATION
discovery of, review of, 25:56389 (JINR-P4-5954)
quantum theory of external, phenomenological, (T), 25:56392
theoretical problems of, 25:56389 (JINR-P4-5954)
CHLORDIAZEPOXIDE
effects on whole-body mixed gamma and neutron irradiated rats, 25:55325
CHLORIDES
thermodynamic potentials and enthalpies of, calculations of standard, 25:54586
CHLORINE
determination as chloride in bismuth, gallium, selenium, and thallium, photometric, 25:54407
determination of trace amounts of, in air by neutron activation and γ spectrometry, 25:54456
radiation effects on excretion of, in rat urine, combined effects of open skin lesions and, 25:55332
CHLORINE FLUORIDES
reactions with neptunium dioxide, plutonium dioxide--uranium dioxide, and uranium dioxide, kinetics of, 25:54736
CHLORINE ISOTOPES Cl-34
energy levels from sulfur-32 (He-3,pγ) reactions, spin--parity assignments for, (E), 25:56712
energy-level transitions from sulfur-32 (He-3,pγ) reactions, branching and mixing ratios for, (E), 25:56712
CHLORINE ISOTOPES Cl-35
energy levels from proton inelastic scattering, lifetimes of, (E), 25:56752(R) (SUNI-14)
neutron capture by, γ spectra from, (E), 25:56690 (RT/FI-(70)47)
proton inelastic scattering at 5.47 to 5.61 MeV, excitation function for, (E), 25:56752(R) (SUNI-14)
CHLORINE ISOTOPES Cl-36
energy levels from chlorine-35 neutron capture, (E), 25:56690 (RT/FI-(70)47)
exchange between chloride and chloromolybdate(III), 25:54558
CHLORINE ISOTOPES Cl-37
neutron capture at 2.9 MeV, cross section for, (E), 25:56696
CHLORINE ISOTOPES Cl-38
reactions of recoil, in chlorofluoromethanes, replacement, 25:54688
reactions of recoil, with chloromethane, effects of scavengers on, 25:54681
CHLOROFORM
effects on separation of europium or lanthanum from acid solutions by solvent extraction using acidic esters of aminophosphonic acids, 25:54732
CHLOROPHYTA
Ankistrodesmus braunii, radiation effects on activity of NADP-dependent glyceraldehyde phosphate dehydrogenase in, effects of light on x, 25:55353
Chlamydomonas sp., cerium-144 uptake by, statistical analysis of factors affecting, 25:55162
Chlorella vulgaris, radioinduced mutations in, photoreactivation capacity following uv, 25:55172
CHLORPROMAZINE
effects on whole-body mixed gamma and neutron irradiated rats, 25:55325
CHOLINE
effects on calcium-45 uptake and release by rat brain microsomes, 25:55120
CHROMATIN
radiation effects on activity of sugar beet, effects of dose on γ, 25:55351
CHROMATOGRAPHY
automation of, punched tape and computer processes for, 25:54727
conference on, Russian--Italian, Thilisi, USSR, Oct. 26-29, 1970, 25:54398
development of electro-, using titanium tungstate papers, 25:54744
CHROMIUM
abundance in solar atmosphere, (E/T), 25:55750
alpha reactions with, production of chromium-51 by, 25:54691
determination in Australian tektites by neutron activation and gamma spectrometry, 25:54478
determination in epitaxial films of gallium arsenide by neutron activation and radiochemical separation, 25:54512
determination in process and quality control during ore beneficiation by neutron activation, 25:54507
determination in standard aluminum--silicon system by neutron activation, 25:54455
determination in stony meteorites by proton and bremsstrahlung activation, 25:54466
determination in volcanic ash by neutron activation and γ spectrometry, 25:54513
determination of trace amounts of, in air by neutron activation and γ spectrometry, 25:54456
determination of trace amounts of, in thorium and zirconium compounds by neutron activation, separation processes, and γ spectrometry, 25:54518
deuteron reactions with, production of chromium-51 by, 25:54691
deuteron reactions with, production of vanadium-48 by, 25:54677
effects on properties and sintering of tungsten at 1000 to 2000°C, 25:55453
proton reactions with, production of chromium-51 by, 25:54691
separation of uranium from, in methyl sulfoxide by cation exchange chromatography, 25:54728
surface wetting of molten, on boron nitride, mechanisms of, 25:55469
CHROMIUM ALLOYS AND SYSTEMS
reactions with alkali metal sulfates at 550 to 950°C, 25:55372 (CONF-690452-, Paper 5)
thermoelectric properties of, at 0 to 1000°C, 25:56351
Al--Co--Cr--Mo--Ni-base--Ti, fabrication of powdered, powder metallurgy and thermomechanical processes for, 25:55416
Al--Co--Cr--Mo--Ti--W, stress relaxation and surface hardening in, effects of high temperatures on, 25:55439
Al--Cr, crystal structure of solidified, effects of cooling rate and supercooling on, 25:55550
Al--Cr, solidification and phase transformations in, nonequilibrium, 25:55535
Al--Cr, thermal decomposition of solid solutions of, kinetics of, 25:55448
Al--Cr--Mo, thermal decomposition of solid solutions of, kinetics of, 25:55448
Al--Cr--Mo--Ni-base--W, fabrication of powdered, powder metallurgy and thermomechanical processes for, 25:55416

Al--Cr--Ni-base--Ti, corrosion by molten vanadium oxide, effects of chlorides, oxides, and sulfides of sodium on, 25:55375 (CONF-690452-, Paper 8)
Al--Cr--Ni-base--Ti, mechanical properties of dispersion-strengthened, at high temperatures, 25:55483
C--Cr--Mo, microstructure of white irons of, 25:55556
Co--Cr--Ni--W, physical properties of, effects of atomization media and consolidation methods on, 25:55480
Co-base--Cr--Mo--Nb--Ni--W, corrosion by molten vanadium oxide, effects of chlorides, oxides, and sulfides of sodium on, 25:55375 (CONF-690452-, Paper 8)
Cr--Fe, iron-57 Moessbauer spectra using polarized cobalt oxide source, 25:56366
Cr--Fe-base, stability of aluminum oxide dispersions in, at high temperatures, 25:55485
Cr--Fe-base--Ni, stability of aluminum oxide dispersions in, at high temperatures, 25:55485
Cr--Mo--Zr, phase diagram at 1150°C, 25:55538
Cr--Nb--Ni, liquation of, mechanism of intracrystallite, 25:55506
Cr--Ni, radiation effects on electric conductivity of $Ni_3Cr$, neutron, 25:55584
Cr--Ni-base, stability of aluminum oxide dispersions in, at high temperatures, 25:55485
Cr--Ni-base, strengthening of, effects of substructure domain on dispersion, 25:55492
Cr--Ti-base, superconductivity and constitution of, 25:56108

CHROMIUM BORIDES
wear resistance of deposited, on steels, 25:55619

CHROMIUM HYDROXIDES
preparation of CrOOH, high-pressure hydrothermal method for, 25:55602

CHROMIUM ISOTOPES Cr-49
energy levels from chromium-50 (He-3,$\alpha\gamma$) reactions, spin-parity assignments for, (E), 25:56692
energy-level transitions from chromium-50 (He-3,$\alpha\gamma$) reactions, branching and multipole mixing ratios for, 25:56692

CHROMIUM ISOTOPES Cr-50
deuteron elastic scattering at 13.6 MeV, optical-model analysis of angular distributions from, (T), 25:56725
deuteron reactions (d,p) at 13.6 MeV, distorted-wave analysis of differential cross sections for, (T), 25:56725
helium-3 reactions (He-3,$\alpha\gamma$) at 15 MeV, $\alpha$-$\gamma$ angular correlations from, (E), 25:56692
neutron capture by, gamma spectra from thermal, (E), 25:56683 (FEI-205)
proton inelastic scattering at 6.9 MeV, distorted-wave analysis of differential and integrated cross sections for, (E), 25:56727

CHROMIUM ISOTOPES Cr-51
deposition and transport in FFTF cooling system, 25:55370 (BNWL-SA-2335)
energy levels from chromium-50 (d,p) reactions, spectroscopic factors for, (T), 25:56725
energy levels from chromium-50 neutron capture, spin--parity assignments for, (E), 25:56683 (FEI-205)
production in cyclotron by $\alpha$, deuteron, and proton reactions with chromium, titanium, and vanadium, 25:54691
use of EDTA-incorporated, for brain and kidney scanning, 25:55272
use of EDTA-incorporated, for measuring glomerular filtration rate of human kidneys, 25:55122

CHROMIUM ISOTOPES Cr-52
deuteron elastic scattering at 13.6 MeV, optical-model analysis of angular distributions from, (T), 25:56725
deuteron reactions (d,p) at 13.6 MeV, distorted-wave analysis of differential cross sections for, (T), 25:56725
neutron capture by, gamma spectra from thermal, (E), 25:56683 (FEI-205)
photon reactions ($\gamma$,n) near threshold energy, cross section for, (E), 25:56702
proton inelastic scattering at 6.9 MeV, distorted-wave analysis of differential and integrated cross sections for, (E), 25:56727

CHROMIUM ISOTOPES Cr-53
energy levels from chromium-52 (d,p) reactions, spectroscopic factors for, (T), 25:56725
energy levels from chromium-52 neutron capture, spin--parity assignments for, (E), 25:56683 (FEI-205)
neutron capture by, gamma spectra from thermal, (E), 25:56683 (FEI-205)
photon reactions ($\gamma$,n) near threshold energy, cross section for, (E), 25:56702

CHROMIUM ISOTOPES Cr-54
energy levels from chromium-53 neutron capture, spin--parity assignments for, (E), 25:56683 (FEI-205)

CHROMIUM NITRIDES
shock compression effects on powdered, x-ray-diffraction study of, 25:55618

CHROMIUM OXIDES
reactions with alkali metal sulfates at 550 to 950°C, 25:55372 (CONF-690452-, Paper 5)
spectra of, after adsorption of water, effects of deuterium on, 25:54565

CHROMOSOMES
radiation effects on chiasma frequency of grasshopper, x, 25:55176
radiation effects on human, bibliography on ionizing, 25:55178
radiation effects on mouse fetus, 25:55207 (NYO-2740-8, pp 220-59)
radiation effects on spontaneous recombination frequency of diploid yeast, uv, 25:55180
radioinduced aberrations in human blood cell, following occupational exposure, $\gamma$, 25:55163
radioinduced aberrations in rat bone marrow, x, 25:55192
radioinduced aberrations of barley seed, method for metaphase analysis of x, 25:55175
radioinduced aberrations of Crepis capillaris seed, effects of time of administration on additive or protective effects of ethylenimine on x, 25:55260
radioinduced aberrations of hamster liver, comparison of RBE for americium-241 $\alpha$ and cerium-144 $\beta$, 25:55188
radioinduced aberrations of male Drosophila, cytological analysis of $\gamma$, 25:55170
radioinduced aberrations of mouse blood, extrapolation to man of protective effects of cystamine against $\gamma$, 25:55256
radioinduced aberrations of peripheral human blood, biological dosimetry using, 25:55228
radioinduced aberrations of wheat seed, effects of prolonged storage on repeated-exposure x, 25:55169
radioinduced premutational oxygen-sensitive changes in Crepis capillaris seed, $\gamma$, 25:55168
radioinduced translocations in Drosophila, effects of dose on neutron and x, 25:55206 (NYO-2740-8, pp 147-219)
radioinduced translocations in mouse spermatogonia, RBE for gamma, 25:55182
translocation induction in Vicia, comparison of effectiveness of ionizing radiation and chemicals for, 25:55191

CHROMOSPHERE
boundary of oscillations of visible, (E), 25:55747
element abundances in, (E/T), 25:55750
fibrils near sunspots, topology of filaments and, (E), 25:55749
limb observations at high-spectral purity, (E), 25:55746
solar-flare emission from, Proton-3 measurement of proton flux from July 7, 1966, (E), 25:55991
spectral fine structure in, morphological relations in H$\alpha$, (E), 25:55748

CHRONOMETERS
design with oscillator time base using radioisotope source, 25:55085(P)

CIRCUITS
calibration of microstrip, using automatic network analyzer, 25:57279(T) (SC-T-713067)

CIVIL ENGINEERING
uses of radiometric gages in, for highway construction and maintenance in US, tabulation of, 25:54907

CLAYS
age of ancient pottery, thermoluminescence method for estimation of, 25:54764

CLOTHING
radioisotope contamination of, derivation of decision levels for control of, 25:55196 (LA-4558)

CLOUDS
gamma radiation dose from radioactive, air attenuation and photon energy in calculation of, 25:54796
gamma radiation doses from radioactive, calculation of, 25:54797

CNIDARIA
corals, age of fossil, accuracy of thorium-230/uranium-234 method for estimating, 25:54776
corals, uranium-238 content in fossil, effects on accuracy of thorium-230/uranium-234 method for age estimation, 25:54776
thorium-232 content in fossil, effects on accuracy of thorium-230/uranium-234 method for age estimation, 25:54776

COAL DEPOSITS
prospecting for, gamma logging method for, (E), 25:54772

COATINGS
growth of binary two-phase, diffusion-controlled, 25:57276(T) (SC-T-713061)
radiation effects on stability of silvered and aluminized FEP teflon-film thermal-control, electron, proton, and uv, 25:55656 (N-71-27736)

COBALT
abundance in solar atmosphere, (E/T), 25:55750
argon-ion reactions at 30 keV with surfaces of, charge states and kinetic energies of scattered and recoil ions from, (E), 25:55818
casting by levitation melting using magnetic field, 25:55424
complexes, radiation effects on cis-$[Co(en)_2(NO_2)CNS][CoEDTA].2H_2O$, correlated annealing of recoil cobalt-60 in cationic and anionic sites from neutron, 25:54682
deposition on surfaces, basic chemistry in, 25:54587(R) (AECL-3909)
determination in Australian tektites by neutron activation and gamma spectrometry, 25:54478
determination in epitaxial films of gallium arsenide by neutron activation and radiochemical separation, 25:54512


XUM

determination in standard aluminum--silicon system by neutron activation, 25:54455
determination in volcanic ash by neutron activation and γ spectrometry, 25:54513
determination in yttrium oxide by emission spectrometry, 25:54419
determination of trace amounts of, in thorium and zirconium compounds by neutron activation, separation processes, and γ spectrometry, 25:54518
determination of trace amounts of, in ultramafic rocks by thermal neutron activation and γ spectrometry, 25:54496
diffusion of carbon in solid solutions of, 25:55479
effects on properties and sintering of tungsten at 1000 to 2000°C, 25:55453
effects on solvolysis of tert-butyl halides, Broensted correlation for, 25:54548
neutron resonance absorption in, self-shielding of, (E/T), 25:57196
properties of aerosols of, produced from solutions at high temperatures, chemical and physical, 25:54545
separation of uranium from, in methyl sulfoxide by cation exchange chromatography, 25:54728
COBALT ALLOYS AND SYSTEMS
Co--WC, composition and tensile properties of binder phase in, 25:55630
reactions with alkali metal sulfates at 550 to 950°C, 25:55372 (CONF-690452-, Paper 5)
Al--Co--Cr--Mo--Ni-base--Ti, fabrication of powdered, powder metallurgy and thermomechanical processes for, 25:55416
Al--Co--Cr--Mo--Ti--W, stress relaxation and surface hardening in, effects of high temperatures on, 25:55439
C--Co-base--Ti--W, mechanical properties of heat-treated, 25:55497
C--Co-base--W, mechanical properties of heat-treated, 25:55497
Co--Cr--Ni--W, physical properties of, effects of atomization media and consolidation methods on, 25:55480
Co--Fe--Mo, electric conductivity of supersaturated solid solutions of, effects of phase decomposition on, 25:55472
Co--Fe--V, magnetic properties at cryogenic temperatures, 25:56361
Co--Fe--W, hardening of, kinetics of dispersion, 25:55423
Co--Fe-base, stability of aluminum oxide dispersions in, at high temperatures, 25:55485
Co--WC, preparation of fine powdered mixtures of, using ultrasonic vibrations, 25:55598
Co-base--Cr--Mo--Nb--Ni--W, corrosion by molten vanadium oxide, effects of chlorides, oxides, and sulfides of sodium on, 25:55375 (CONF-690452-, Paper 8)
COBALT ISOTOPES Co-57
decay in iron compounds, Moessbauer spectral studies of valence and structural changes from, 25:56381
distribution of recoil, from beta decay and electron capture of nickel-57 in nickel complexes, thermal annealing effects on, 25:54689
energy levels from iron-54 (α,p) reactions, γ branching, spin, mixing ratios, and mean lifetimes of, (E), 25:56700
COBALT ISOTOPES Co-58
content of Pacific seaweeds in environs of reactors in comparison to other locations, 25:55151 (CONF-710817-1)
deposition and transport in FFTF cooling system, 25:55370 (BNWL-SA-2335)
COBALT ISOTOPES Co-59
neutron capture at 14 MeV, γ spectra and cross section for, (E), 25:56729
COBALT ISOTOPES Co-60
annealing of recoil, in cationic and anionic sites of neutron-irradiated crystals of cis-$[Co(en)_2(NO_2)CNS][CoEDTA].2H_2O$, 25:54682
content of Pacific seaweeds in environs of reactors in comparison to other locations, 25:55151 (CONF-710817-1)
deposition and transport in FFTF cooling system, 25:55370 (BNWL-SA-2335)
uptake by organisms of marine food chain, effects of physico-chemical form on, 25:55149 (BNWL-SA-4048)
use as radiation source to determine charge residence time in rotary kilns, 25:54898
COBALT OXIDES
reactions with alkali metal sulfates at 550 to 950°C, 25:55372 (CONF-690452-, Paper 5)
use of CoO as polarized iron-57 Moessbauer source, 25:56366
CoO--MgO, fabrication for in-core neutron flux monitoring, 25:55019(P)
COBALT PERCHLORATES
complexes with ammonia and benzoic acid, radiolysis of, oxidation by hydroxyl radical of benzoatopentaamminecobalt(III) from γ and electron pulse, 25:54669
COINCIDENCE CIRCUITS
design for detection and discrimination of fission neutrons, 25:54995 (EUR-4611)
COINCIDENCE MEASUREMENTS
use of delayed γ--γ, in Moessbauer spectroscopy, 25:56367
COLLISION PROCESSES
classical binary-collision expansion for, limits of applicability of, 25:55865
Coulomb T matrix for nonrelativistic three-body rearrangement, 25:55868
excitation due to rotational motion in atomic, two-state approximation for, 25:55873
Faddeev--Watson multiple-scattering expansion for nonrelativistic three-body, 25:55867
Faddeev--Watson multiple-scattering expansion for nonrelativistic three-body, off-shell approach to, 25:55866
Faddeev--Watson multiple-scattering expansion for nonrelativistic three-body rearrangement, 25:55868
theory of inelastic, quasi-diabatic representation for, 25:55849
COMPOSITE MATERIALS
design aspects of fibre reinforced, survey of, 25:57214 (AWRE-O-77/70)
preparation by granule metallurgy, evaluation of, 25:55404
properties of metal fiber-reinforced ceramic, review on, 25:55608(T) (LB/G-3074)
stress pulse propagation in, frequency-filtering theory for, 25:57269 (SC-DR-710472)
COMPUTER PROGRAMS
ALICE, for automatic selection of kinematical hypotheses for two-prong p + p interactions at 19 GeV/c in hydrogen bubble chamber, 25:56523 (USIP-71-3)
ANDYMG3, modifications for two-dimensional air transport calculations, 25:56261 (LA-4774)
CITATION, for reactor fuel depletion and management calculations, FORTRAN IV for IBM 360, 25:57183 (ORNL-TM-2496(Rev.2))
CODILLI, for neutron resonance analysis, in FORTRAN IV for IBM 360, 25:56814 (COO-2022-7)
COHORT-2, Monte Carlo general purpose shielding, 25:56262 (N-71-22378)
CONCEPT, for conceptual cost estimates for single unit pressurized water power reactors, FORTRAN 4 for IBM 360, 25:57063 (ORNL-TM-3276)
COSTANZA (R,Z), for dynamics analysis of cylindrical reactors during transients, FORTRAN for IBM 360/65, 25:57187 (EUR-4673)
DELIGHT, for high temperature gas cooled reactor coated particle fuel burnup, 25:57021 (JAERI-Memo-4449)
DYNBUF, for dynamic buffer allocation on CDC 6600, 25:57234 (LA-4721)
EDIT, for Playback Executive System, 25:57270 (SC-M-710527)
for calculating half-lives and intensity of total decay curves, 25:56695
for calculating time characteristics of lithium-drifted germanium detectors, in FORTRAN, 25:55001 (NP-19011)
for calculation of pressure over time duration in coupled volumes, 25:54886
for gamma spectra analysis in FORTRAN IV for PDP-9, 25:54523
for heat conduction in reactor fuel rods during coolant loss accidents, ALGOL for Burroughs B6500, 25:57094 (RISO-M-1391)
GELI2 and SPAN2, for calculating nuclide abundances from multichannel gamma spectra, in FORTRAN, 25:55035 (DP-1275)
GRASS, for remote access support systems, 25:57218 (COO-1469-190)
MIMUSA, for unfolding spectra, in FORTRAN IV, 25:55042 (RD/B/N-1963)
modular logic for control point design, 25:57224 (COO-2118-14)
MORSEC, revised cross-section module for MORSE multigroup Monte Carlo code, 25:56263 (ORNL-4716)
NOISE, for determining reactor transfer function from noise measurements, 25:57181 (BNWL-1609)
OMAS, for optical-model analysis of nuclear elastic scattering, 25:56815 (INP-741)
RAGA, for calcuation of γ-ray transport in reactor shields with multiregion slab geometry, ALGOL for Philips X8, 25:57026 (RCN-146)
ROD, for core design and fuel cycle calculations for fluid fueled reactors, FORTRAN 4 for IBM 360, 25:57048 (ORNL-TM-3359)
SDRC, for heterogeneous reactor resonance energy neutron spectra, IBM 360, 25:57182 (JAERI-Memo-4481)
SIMPLOTTER, for plotting graphs, 25:57231 (IS-2305)
SOLRF, for approximation computation of neutron interaction by solid-angle spacing method, 25:56271
SWIFT, for unfolding neutron spectra, in FORTRAN IV for CDC-6600, 25:55036 (HASL-244)
TESTY, for unfolding spectra, in FORTRAN IV, 25:55042 (RD/B/N-1963)
TGO, for design optimization of power transmission grid, 25:57230 (HEDL-TME-71-108)
TRACE, for fast reactor fuel cycle analysis, for IBM 360/65, 25:57020 (EUR-4709)
TRESS, for finite element stress analysis, 25:57285 (TRG-Report-1813)
TRINITY, for three-dimensional magnetohydrodynamics calculations, 25:55944

TWOTRAN SPHERE, modifications for two-dimensional air transport calculations, 25:56261 (LA-4774)
COMPUTERS
basic assembler language manual for Illiac III, 25:57225 (COO-2118-17)
conference on, June 29--July 1, 1970, Juelich, Germany, 25:55074 (JUL-Conf-5)
development at Illinois Univ, 25:57219(R) (COO-1469-193)
development at Illinois Univ., Oct. 1970 to June 1971, 25:57282(R) (TID-25789)
development of, review of trends in, 25:57191 (CONF-710302-(Vol.2), pp 1086-1101)
performance of IBM 1130, for calculation of opposed fixed-field irradiation plans in telecobalt therapy, 25:55218
performance of timesharing, for maintaining and updating radioactive materials inventories at University of Colorado Medical Center, 25:54984
performance of, Argonne benchmark problem collection for evaluation of, 25:57167 (CONF-710302-(Vol.2), pp 901-12)
reference manual for Illiac III, input--output, 25:57227 (COO-2118-21)
reference manual for Illiac III, supervisor organization, 25:57226 (COO-2118-19)
system description for powerful low-cost timeshared, 25:57217 (COO-1469-187)
use in experimental high-energy physics, 25:55050
use of graphic display, for design of advanced nuclear reactors, 25:57007
CONCRETES
cracking and deformation under high sustained loads, mechanics of, 25:55661
creep of prestressed, algorithm for integral-type aging, 25:55664
creep strains in beams of, time-temperature extrapolation analysis of, 25:55663
diffusion of moisture in heated, effects of pore pressure on, 25:55665
gamma penetration of shield of, energy and angular distributions of cobalt-60, (E), 25:56272
gamma transmission through homogeneous slabs, (T), 25:56256 (AD-722012)
neutron attenuation in, effects of iron contents on fast and thermal, (E), 25:57027 (RCN-147)
neutron reactions with, secondary gamma radiation in shielding from, 25:56277
properties of prestressed, for use in pressure vessels, 25:56882
radioinduced polymerization of monomer and polymer impregnants in, mechanical properties of products of, 25:55658
tensile properties of steel wire-reinforced, 25:55662
tensile properties of test cubes of, under triaxial stress, 25:55660
testing of triaxially stressed structures of, for safety margins, 25:55659
vapor pressures in pores of heated, effects on moisture diffusion, 25:55665
CONDENSERS
surge in nuclear power plant cooling system, calculations of, 25:57036
water hammer in nuclear power plant cooling system, calculations of, 25:57036
CONVEYERS
design of hopper-type, for fuel pellets, 25:54841(P)
design of tape-type, for leak-tight transfer of radioactive materials in and out of containers, 25:54988(P)
COOPER POWER REACTOR
effluents from, effects on environment of chemical, radioactive, and thermal, 25:56955 (DOCKET-50298-22)
site for, geological, hydrological, and meteorological data for, 25:56955 (DOCKET-50298-22)
COPPER
alpha fission at 167 MeV, angular distributions and particle track lengths for, (E), 25:56806
argon-ion reactions at 30 keV with surfaces of, charge states and kinetic energies of scattered and recoil ions from, (E), 25:55818
bremsstrahlung buildup factor for, dependence on position of shielding between source and detector, 25:56280
determination in drill core by neutron activation and γ spectrometry, 25:54469
determination in epitaxial films of gallium arsenide by neutron activation and radiochemical separation, 25:54512
determination in lead-base alloys by neutron activation and radiochemical separation, 25:54515
determination in meteorites and meteoritic phases by neutron activation and γ spectrometry, 25:54477
determination in sediments of Rhine River basin by x-ray fluorescence, 25:54408
determination in yttrium oxide by emission spectrometry, 25:54419
determination of trace amounts of, in tellurium by complexing with Bengal Rose and phenanthroline, spectrophotometric, 25:54414
determination of trace amounts of, in thorium and zirconium compounds by neutron activation, separation processes, and γ spectrometry, 25:54518
determination of trace amounts of, in ultramafic rocks by thermal neutron activation and γ spectrometry, 25:54496
effects of residual, on neutron embrittlement of Types A302B and A533B steel, 25:55577 (NRL-7310)
effects on solvolysis of tert-butyl halides, Broensted correlation for, 25:54548
erosion of sintered, in oil, design of equipment for measuring arc, 25:55454
mechanical properties of chemical vapor deposited rings of, design of apparatus for testing, 25:55440
microstructure of, potentiostatic studies on, 25:55555
neutron inelastic scattering at 14.4 MeV, differential cross sections, nuclear-level density parameters, and contribution of direct processes for, (E), 25:56684 (FEI-216)
neutron reactions (n,2n) at 14.4 MeV, differential cross sections, second-neutron spectra, and nuclear-level density parameters for, (E), 25:56684 (FEI-216)
neutron reactions at 10 to 30 GeV/c, total cross sections for, (E), 25:56421
physical properties of plasma-sprayed spherical powders of, 25:55467
radiation damage in, kinetics of crowdion reactions in annealing stage I/sub E/ of electron, (T), 25:56333
radiation effects on adhesion of epoxy cemented specimen couples of, gamma, 25:55666
reactions with Groups IV and VI transition metal carbides at 1000 to 1200°C, solid-phase, 25:55464
separation from ores by solvent extraction, 25:54816 (ORNL-4682, pp 182-6)
separation of uranium from, in methyl sulfoxide by cation exchange chromatography, 25:54728
solvent properties for Groups IV and VI transition metal carbides at 1000 to 1200°C, 25:55464
wetting of refractory carbides as function of electronic structure, 25:55643
COPPER ACETATES
radiation effects on single crystals of monohydrates of, at 80 and 290°K, ESR studies on x, 25:54610
COPPER ALLOYS AND SYSTEMS
preparation by granule metallurgy, evaluation of, 25:55404
$Al_2O_3$--Cu, production of fine powders of, Microgel process for, 25:55419
Al--Cu--Fe--Sn--Ti-base--V, development and evaluation of high-strength, 25:55421
Al--Cu--Y, phase studies of, 25:55561
Be--Cu-base, microstructure of, potentiostatic studies on, 25:55555
Be--Cu-base, radiation effects on aging and precipitation in, neutron, 25:55583
Be--Cu-base--Ni, microstructure of, potentiostatic studies on, 25:55555
Cu--Dy, hyperfine parameters in DyCu, Moessbauer-effect study of, 25:56382
Cu--Ga--Ni, optical constants for β-phase in, 25:56352
Cu--Ge, superconductivity in hcp phases of, (E), 25:56096
Cu--Ni, solvent properties of solid solutions of, for tungsten in copper--nickel--tungsten alloys, 25:55447
Cu--Ni--W, tungsten solubility in copper--nickel solid solutions of, limits of, 25:55447
Cu--Sb, superconductivity in, with $DO_3$ structure, (E), 25:56096
Cu--Si, superconductivity in hcp phases of, (E), 25:56096
Cu--Th, phase diagram and intermetallic compounds, 25:55571
Cu--$ThO_2$, production of plates, rods, sheets, and wires of high-conductivity high-strength, description of process for, 25:55417
Cu--$UO_2$, properties of, effects of stereometric microstructure on, 25:55628
Cu--W, preparation of composites of, by diffusion welding, 25:55405
Cu--W, thermal expansion of infiltrated pseudoalloys of, up to 1500°C, (E/T), 25:55468
Cu--Zn, search for superconductivity in fcc phases of, (E), 25:56096
Cu-base--Zr, microstructure of, potentiostatic studies on, 25:55555
COPPER ISOTOPES Cu-58
energy levels of, shell-model calculation with Reid and Yale potentials, 25:56857
COPPER ISOTOPES Cu-59
energy levels of, calculation of properties using proton-quadrupole vibration coupling, (T), 25:56731
energy levels of, shell-model calculation with Reid and Yale potentials, 25:56857
COPPER ISOTOPES Cu-60
energy levels of, shell-model calculation with Reid and Yale potentials, 25:56857
COPPER ISOTOPES Cu-61
energy levels of, calculation of properties using proton-quadrupole vibration coupling, (T), 25:56731
COPPER ISOTOPES Cu-63
energy levels of, calculation of properties using proton-quadrupole vibration coupling, (T), 25:56731
COPPER ISOTOPES Cu-65
energy levels of, calculation of properties using proton-quadrupole vibration coupling, (T), 25:56731


XUM

neutron capture at 2.9 MeV, cross section for, (E), 25:56696
COPPER ORES
fracturing deposits of, using nuclear explosions, 25:54816 (ORNL-4682, pp 182-6)
CORROSION
book: Corrosion in Nuclear Applications, 25:55388
conference on mechanisms of molten salt, Duesseldorf, April 10, 1969, 25:55371 (CONF-690452)
research progress on, 25:54587(R) (AECL-3909)
CORROSION FILMS
deposition of, effects of heat flux and boiling on, 25:57034
heat transfer effects of, 25:57034
COSMIC PARTICLES
acceleration of, in Milky Way, (T), 25:55907
book; Cosmic Muons and Neutrinos, 25:56469
composition of primary Z = 2 to 5 and Z = 12 to 40, Cosmos-228 observations of, (E), 25:55899
composition of primary, chemical, (E), 25:55911
density in intergalactic space in clusters of galaxies, (E), 25:55789
energy of hadron, at 3250 m above sea level, ionization spectrometer determination of, (E), 25:56413 (INP-756)
flux measurements of muon, discrepancy between underground, 25:55897
flux of 4e/3-charged quarks at 2750 m above sea level, scintillation counter telescope study of upper limit for vertical, (E), 25:56403
flux of hadron, at 3250 m above sea level, ionization spectrometer determination of, (E), 25:56413 (INP-756)
intensity distribution at 200 to 300 km of primary, global, (E), 25:55980
interactions with ambient photons, energy losses in, (T), 25:55908
lifetime of, in Milky Way, (T), 25:55907
modulation of primary Z = 20 to 30, solar, (E), 25:55909
monitoring of neutrons, data from Canadian stations for Jan.--Apr. 1971, (E), 25:55893 (AECL-3971)
proton reactions with iron above 1.5 TeV, ionization spectrometer study of inelasticity coefficients for, (E), 25:56414 (INP-757)
reactions with nuclei above 100 GeV in emulsions, production of low-energy protons in, (E), 25:56429 (INP-754)
research at Lund Univ., 1970, (E), 25:56643(R) (NP-19018)
stopping in nuclear emulsion, mass resolution of tracks from, (E/T), 25:55894 (LUIP-CR-71-4)
COSMIC RADIATION
containment of sudden burst of, in the galactic disk, (T), 25:55895 (N-71-24988)
effects on eyes of astronauts, 25:55341
electron ionization by solar, in Earth and other planetary atmospheres, (T), 25:55983
flux at 250 to 500 km in ionosphere, nature of, (E/T), 25:56008
flux of quarks in, upper limits for, (E), 25:55910
intensity in meridional plane, annual variations and gradient of, (E), 25:55900
intensity of, for last $10^9$ years, (E/T), 25:55781
interaction of galactic, with interplanetary magnetic field, (E), 25:55904
isotropy and origin of 1- to 6-MeV background gamma, (E/T), 25:55896 (N-71-27639)
modulation of primary, step-like changes in long-term, (E), 25:55912
modulation region of galactic, solar-activity-dependent dimensions of, (E/T), 25:55901
propagation through interstellar space and Earth atmosphere, path-length determination for, (E/T), 25:55903
temperature effects on ionizing component of primary, short-period, (E), 25:55898
COSMIC RADIO SOURCES
brightness temperature level of galactic, (E), 25:55730
electron temperatures of galactic, (E), 25:55730
energy sources for, supermassive objects as, (T), 25:55798
identification of 12 small-diameter southern, optical, (E), 25:55725
identification of 70 4C, between -3 and 0°, optical, (E), 25:55723
observations of 3C 153.1, optical, (E), 25:55681
radio positions and flux densities of 235 4C, between -3 and 0°, (E), 25:55723
spectra of 105 small-diameter, absorption, (E), 25:55791
COSMIC RAY TELESCOPES
calibration of satellite-borne NASA--GSFC, 25:55046 (N-71-16750)
COSMIC SHOWERS
density spectra of extensive, ambiguity in, (E), 25:55905
COSMIC X-RAY SOURCES
Cir XR-1, pulsations and spectra from, (E), 25:55721
Cyg X-1, search for pulsed radio emission from, (E), 25:55728
Cyg X-1, upper limits on hard x-ray pulsations from, (E), 25:55727
GX 1 + 4, flux and spectrum from, (E), 25:55720
GX 3 + 1, flux from, (E), 25:55720
GX 5 - 1, flux from, (E), 25:55720
models for, containing black holes, (T), 25:55803
spectra of, OSO-V experiment for, (E), 25:55734 (N-71-23434)
COSMOLOGY
book: Lead Isotopes in Geochemistry and Cosmochemistry, 25:54770
Brans--Dicke field equations in, solutions in flat Friedmann universes, (T), 25:55800
gravitational redshift in theory of generalized gravitational potential, (T), 25:55808
models of, observational effects of local inhomogeneities in, (T), 25:55809
models of, topological properties of, (T), 25:55802
radiation-filled Brans--Dicke, exact solutions to, (T), 25:55801
CREEP
model for in-pile deformation of materials, 25:55579 (WAPD-TM-943)
CROLOY
reactions with sodium at 1000 to 1300°F, carbon and nitrogen mass transfer in, 25:55379(R) (WARD-4210-T-1-2)
CRUSTACEA
Artemia sp., radiation effects on hatchability of eggs of, relation between production of free radicals and protective effects of MEA against γ, 25:55262
CRYOGENICS
conference on cryogenic engineering, Boulder, Colorado, June 17-19, 1970, 25:56113
uses in electric power systems, 25:56114
CRYSTAL RIVER POWER REACTOR, UNIT 3
construction of, revised permit application for, 25:56956 (DOCKET-50302-25)
operation of, revised license application for, 25:56956 (DOCKET-50302-25)
CRYSTAL STRUCTURE
model for order--disorder transformations in alloys and metals, 25:55552
size effects in three-dimensional Ising, 25:57241 (NYO-1480-179)
CRYSTALLOGRAPHY
method for freeze etching corresponding fracture moieties in, 25:57251(T) (ORNL-tr-2509)
CRYSTALS
Debye--Waller factors and Debye--Moessbauer temperatures of, tables of, 25:56376
diffusion in, effects of concentration gradients, pressure, and temperature on, 25:57213 (AECL-3793)
neutron scattering by, use of zero Placzek moment to calculate n-phonon cross section in thermal, (T), 25:56340(T) (AERE-Trans-1137)
CURIUM
energy-level transitions of, following californium-249 decay, (E), 25:55825
separation from irradiated LMFBR fuel by solvent extraction using dibutyl butylphosphonate, 25:54706 (BNWL-SA-3345)
x-ray yields from, following californium-249 decay, M-subshell, (E), 25:55825
CURIUM ISOTOPES Cm-244
production of aerosols of oxides of, for inhalation studies in dogs, 25:54982
CURIUM OXIDES
preparation for HFIR targets, 25:54671 (ORNL-4682, pp 114-32)
CURRENT ALGEBRA
amplitudes in dual resonance model, 25:56449
elementary particles in, cellular structure in phase space in fibre bundle theory for, 25:56448
SU(3) x SU(3) chiral symmetry breaking parameter in hard-meson tree-graph theory in, 25:56535 (ORO-3992-7)
sum rules in, use of once-subtracted dispersion relation for modification of Adler--Weisberger, 25:56510
CUTTING TOOLS
description of shear-type, for fuel element cutting, 25:54838(P)
CYANIDES
preparation of carbon-11-labeled, by recoil reactions following proton bombardment of lithium amide or nitrogen--hydrogen mixtures, 25:54683
CYANOCOBALTATES
radiolysis of aqueous solutions of, kinetics of reactions of hydrated electrons in electron pulse, 25:54651
CYANOGEN
abundance in atmospheres of late-type stars, (E/T), 25:55698
spectral lives due to, in IRC + 10216, (E), 25:55686
CYCLOHEPTATRIENE
decomposition of carbon-14-labeled, from reactions of solid benzene with carbon-14 ions at 5, 31, and 100 eV, 25:54702
photoinduced decomposition of carbon-14-labeled, 25:54702
CYCLOHEXANE
radiolysis of liquid, kinetics of charge scavenging in γ, 25:54668
radiolysis of, scavenging effects of carbon tetrachloride and nitrous oxide on, 25:54670
reactions with recoil tritium, yields of alkanes from, 25:54685

CYCLOPENTANE
cyclopentane--$N_2O$, radiolysis of, effects of cyclopentene and propene on nitrogen yields from γ, 25:54655
CYCLOPENTENE
effects on reactions of nitrous oxide in γ-irradiated liquid cyclopentane, 25:54655
CYCLOPROPANE
Br--cyclopropane, neutron reactions (n,γ) with, products from reactions of recoil bromine-80m from, 25:54690
CYCLOPROPANE, BROMO-
neutron reactions (n,γ) with, formation of allyl bromide by reaction of recoil bromine-80m from, 25:54690
CYCLOTRON RADIATION
emission by charged particles moving along spiral path in transparent media, 25:56462
CYCLOTRONS
beam injection into sector, ion focusing in drift space for external, 25:56602
design of 300-keV separated-sector, for deuterons, 25:56601
CYSTAMINE
effects on sensitivity of guinea pigs and mice to transverse acceleration, 25:55264
radioprotective effects of, on mice, fast neutron and x, 25:55266
radioprotective effects on mice, extrapolation to man of γ, 25:55256
CYSTEAMINE
radioprotective effects of silicon-substituted thiophene derivatives of, uv, 25:55263
radioprotective effects on Artemia eggs, relation between radioinduced free radicals and γ, 25:55262
radioprotective effects on mice, effects of dose, sex, and strain on x, 25:55257
CZECHOSLOVAKIA
radioisotope content in river waters of, 25:54774


## D


DATA ACQUISITION SYSTEMS
computer systems for, description of graphic display, 25:57008
development of noise analysis, for power reactor dynamics, 25:57023
use of FINK and PANTRY, PSKIT programming package for simplification of, 25:57144 (CONF-710302-(Vol.1), pp 505-7)
use of JOSHUA Terminal System, review of, 25:57145 (CONF-710302-(Vol.1), pp 508-15)
DATA PROCESSING SYSTEMS
computer systems for, description of graphic display, 25:57008
description of interactive graphics data retrieval system, 25:55076 (LA-DC-12576)
use of interactive computer graphics in high energy physics, 25:55093
DATA RECORDING SYSTEMS
description of cytofluorograph, 25:57249 (ORNL-TM-3536)
DATA TABULATIONS
coefficients for partial-wave analysis of vector meson and $1/2^+$ baryon production in pseudoscalar meson interactions with $1/2^+$ baryons, 25:56501 (RHEL/R-224)
DECONTAMINATION
facility for, design of Mound Laboratory medical, 25:54963 (CONF-710401-, pp 311-15)
DEHYDROGENASES
activity in cells of radioinduced osteosarcomas of rats, 25:55335
DENSIMETERS
design and operation of gamma radiometric, for pressed powdered metals, 25:55067
design and operation of in situ gamma radiometric, for ores, 25:55066
development of airborne radiometric, for snow, 25:55065
uses of radiometric, in highway construction and maintenance in US, tabulation of, 25:54907
DESALTING
plant for, digital computer program for simulating dynamics of large multistage flash evaporator, 25:57248 (ORNL-TM-2933)
DEUTERIUM
abundance in solar atmosphere, (E/T), 25:55750
concentration in water by exchange with ammonia, 25:54748
determination of, evaluation of methods for, 25:54587(R) (AECL-3909)
deuterium-ion reactions up to 100 eV with molecular, cross sections for dissociation in, (E), 25:55858
diffusion and internal friction in vanadium, calculation from redistribution in periodic stress gradient, 25:55458
effects of rotational energy of, on cross sections of reactions of argon ions with hydrogen, 25:54550
effects on absorption spectra of water, 25:54578 (ORNL-4682, pp 215-17)
effects on catalytic oxidation of ethylene and propylene over gold, 25:54569
effects on decomposition of dialkyldithiocarbamic acids, 25:54560
effects on ionization of thiol acids, solvent, 25:54566
effects on ir spectra and vapor pressure of crystalline ammonia, 25:54572
effects on ir spectra of α-chromia after adsorption of water, 25:54565
effects on kinetics of reactions of 2-(o-chlorophenyl)-4,5-diphenylimidazolyl radicals with amines and hydroquinone, 25:54561
effects on oxidation of 2-propanol by Fenton's reagent, 25:54576
effects on permanganate oxidation of hydroxycyclohexanecarboxylic acids, 25:54575
effects on photolysis of methane, 25:54573
effects on proton transfer in aqueous sulfuric acid solutions, 25:54564
effects on rate of hydrogen abstraction reactions of hydrogen and methane with moderated recoil fluorine-18 atoms, 25:54686
effects on reaction of thiophenol with trityl radicals, 25:54570
effects on reaction of triphenylphosphine with hydridotriphenylsilyl(π-cyclopentadienyl)dicarbonylmanganese, 25:54567
effects on reactions of radiolytic hydrated electrons in aqueous solutions of cobalt(III) cyanide complexes, 25:54651
effects on reactions of recoil tritium atoms in a gaseous mixture of ethane, methane, and neon, 25:54684
effects on solvolysis of sulfonate esters in solvents of low nucleophilicity, 25:54559
effects on thermal isomerization of 1,2-bis(trimethylsiloxy)cyclobutene, 25:54568
effects on vibrational relaxation times of hydrofluoric acid at 400 to 4000°K, 25:54551
effects on x radiolysis of glycine, ESR studies on, 25:54653
exchange between acetic acid and enol acetates catalyzed by palladium(II) chloride, kinetics of, 25:54557
exchange between ammonia and hydrogen in production of heavy water, 25:54748
exchange between water-d and hydrogen, catalytic effects of platinum on, 25:54587(R) (AECL-3909)
exchange in hydrogen--water system on chromium oxide, iron oxide, and copper chromite catalysts, kinetics of, 25:54554
exchange with hydrogen in cis- and trans-1,1,3,-triphenylcyclopropane and water, 25:54571
exchange with tritium between m-carborane and tert-butanol, ethanol, or liquid ammonia in metal alkoxide-catalyzed reactions, primary kinetic isotope effects in, 25:54555
gold-198 ranges in, from gold-197(n,γ) recoil, 25:56269
injection into metals, design of cathode for, 25:54858
meson (π⁻) absorption in, energy level shift in π-mesic deuterium from, 25:55833
neutron reactions at 10 to 30 GeV/c, total cross sections for, (E), 25:56421
properties of molecular, molecular-beam magnetic-resonance measurements of, 25:55826
proton reactions (p,2p) and (p,pn) at 21.5 to 56.4 MeV, absolute cross sections for quasi-free scattering in, (E), 25:56640 (FRNC-CONF-8)
proton reactions (p,2p) at 28.6 MeV, differential cross section for, (E), 25:56644
proton reactions (p,γ) at 0.8 to 3.2 MeV, angular distribution and cross section for, (E), 25:56645
separation from hydrogen, electrochemical, 25:54587(R) (AECL-3909)
DEUTERIUM HYDRIDES
exchange reactions in neon at 1800 to 2800°K, self, 25:54562
properties of, molecular-beam magnetic-resonance measurements of, 25:55826
DEUTERIUM IONS
reactions with deuterium molecules, helium, and neon up to 100 eV, dissociation cross sections for, (E), 25:55858
DEUTERIUM SYSTEMS
D--He-3, energy balance calculations for use in thermonuclear reactors, 25:56215 (N-71-25526)
D--T, burnup in thermonuclear explosions, fractional, 25:54827
D--T, energy balance calculations for fusion reactor conditions, 25:56222
DEUTERONS
interactions e + d → e + p + n, multi-pion exchange contribution to nucleon-nucleon binding in, (T), 25:56527
interactions e + d at high energies, cross sections, Δ(1236) production in e + n interactions, and cross sections for inelastic e + n and e + p interactions from inelastic, (E), 25:56405 (DESY-71/33)
interactions $K^+ + d \rightarrow K^0 + 2p$ at 3.8 GeV/c in deuterium bubble chamber, total and differential cross sections for $K^+ + n \rightarrow K^0 + p$ interactions and total and differential cross sections for, (E), 25:56423 (COO-1195-217)
interactions n + d → n + d, lectures on forward and partial-wave dispersion relations for, (T), 25:56810 (CERN-71-14, pp 155-228)
interactions N + d, dispersion theoretical calculation of vertex function for, (T), 25:56527
interactions p + d → $^3$He + γ, model of intermediate


XUM

nucleon isobar for, 25:56525
interactions p + d → $^3$He + sigma(310), model of intermediate nucleon isobar for, 25:56525
interactions π + d → π + d, lectures on partial-wave dispersion relations for, (T), 25:56810 (CERN-71-14, pp 155-228)
interactions π⁺ + d → p + p + π⁺ + π⁻ at 7 GeV/c, Regge analysis of rho⁰ production in, (E/T), 25:56431
interactions π⁺ + d → p + p, lectures on partial-wave dispersion relations for, (T), 25:56810 (CERN-71-14, pp 155-228)
production in n + n reactions, cross sections for, (T), 25:55777
reactions (d,α) with boron-10 at 0.4 to 1.5 MeV with subsequent alpha decay, reaction mechanisms of, (E), 25:56673
reactions (d,α) with carbon-12 at 7.2 to 14 MeV, excitation functions for isospin forbidden, (E), 25:56656
reactions (d,α) with molybdenum-94 at 10 MeV, α spectra from, (E), 25:56758
reactions (d,α) with neon-22 at 10 MeV, angular distributions for, (E), 25:56716
reactions (d,α) with oxygen-16 at 1.8 to 14 MeV, analysis for reaction mechanism in isospin-forbidden, (E/T), 25:56667
reactions (d,α) with zirconium-90 at 15 MeV, DWBA analysis of, (E), 25:56778
reactions (d,f) with radium-226 at 16 to 19 MeV, mass-yield curve for, (E), 25:56775
reactions (d,He-3) with oxygen-18 at 52 MeV, differential cross sections and spectra from, (E), 25:56662
reactions (d,n) with molybdenum-92 and -94 at 6.25 and 7.0 MeV, time-of-flight spectra and DWBA analysis of differential cross sections for, (E), 25:56766
reactions (d,nγ) with boron-10 at 3 MeV, n-γ coincidence spectra from, (E), 25:56752(R) (SUNI-14)
reactions (d,nγ) with carbon-12 at 5 MeV, n-γ coincidence spectra from, (E), 25:56752(R) (SUNI-14)
reactions (d,p) at 7 to 21.4 MeV with A = 10 to 91 nuclei, diffraction analysis of angular distributions from, (T), 25:56847
reactions (d,p) with aluminum-27 at 12 MeV, l values, spectra, and DWBA analysis of differential cross sections for, (E), 25:56709
reactions (d,p) with chromium-50 and -52 and titanium-48 at 13.6 MeV, distorted-wave analysis of differential cross sections for, (T), 25:56725
reactions (d,p) with fluorine-19 at 10 MeV, angular distributions for, (E), 25:56716
reactions (d,p) with krypton-86 at 5 to 10.5 MeV, analysis of (d,n) threshold cusp using coupled-channel Born approximation, (E/T), 25:56719
reactions (d,p) with magnesium-24 at 10 MeV, cross sections for, (E), 25:56728
reactions (d,p) with nitrogen-14, silicon-28, and sulfur-32 at 13.8 MeV, vector analyzing power from polarized, (E), 25:56724
reactions (d,p) with nuclei, analysis of multi-channel features of, (T), 25:56817 (JINR-E4-5836)
reactions (d,p) with sulfur-33 at 12 MeV, angular distributions and Q-value for, (E), 25:56730
reactions (d,t) with lithium-7 at 10 to 12 MeV, excitation function, spectrum, and DWBA analysis of angular distributions from, (E), 25:56671
reactions with aluminum, Mylar, nickel, and tantalum foils at 80 MeV, cross sections for electron capture in, (E), 25:55862
reactions with chromium and titanium, production of vanadium-48 by, 25:54677
reactions with chromium and vanadium, production of chromium-51 by, 25:54691
reactions with nuclei, method for treatment of Pauli principle in breakup, (T), 25:56833 (ORO-3765-31)
reactions with oxygen-16, Pauli breakup cross section for, (T), 25:56833 (ORO-3765-31)
scattering by cadmium-114, carbon-12, nickel-60, tin-118, and titanium-48 at 13.6 MeV, strong-coupling analysis of elastic and inelastic, (T), 25:56780
scattering by chromium-50 and -52 and titanium-48 at 13.6 MeV, optical-model analysis of angular distributions from elastic, (T), 25:56725
scattering by lithium-6 at 8.0 to 12.0 MeV, optical-model analysis of differential cross sections and excitation functions for elastic, (E), 25:56670
scattering by lithium-7 at 10.0 to 12.0 MeV, optical-model analysis of differential cross sections and excitation function for elastic, (E), 25:56670

DEWAR VESSELS
design of variable-temperature, using superfluid valve, 25:56120

DIAMONDS
use of irradiated, for temperature measurements based on defect annealing using x-ray diffraction readout, 25:55104

DIAZO COMPOUNDS
effects on γ radiolysis of acetic acid solutions of sodium nitrate, 25:54657

DIFFERENTIAL EQUATIONS
solution of, computer subroutines for, 25:57235 (LA-4728)

DIFFERENTIAL THERMAL ANALYSIS
apparatus for use with sealed specimens to 1500°C, 25:54532 (ORNL-4717, pp 1-27)

DIFFUSION
research progress on, in solids, 25:54587(R) (AECL-3909)

DILATOMETERS
design of automatic, for radiation polymerization studies, 25:54616

DIODES
radiation effects on volt--ampere characteristics of silicon, neutron, 25:55100

DISEASES
radiodiagnosis of neurological, role of prescanning cerebral angiography and pneumography in, 25:55281

DISEASES, INFECTIOUS
leukosis, radiation effects on frequency in chickens, x, 25:55329

DISEASES, NEOPLASTIC
adenocarcinomas, radiotherapy of mouse mammary, comparison of effects of air and carbogen atmosphere on cure rate during, 25:55302
cancer, diagnosis of human liver, effectiveness of gold-198 in comparison with alkaline phosphatase evaluation for, 25:55276
carcinomas, radiodiagnosis of human bronchial and thyroid, effectiveness of gallium-67 for, 25:55283
carcinomas, radiodiagnosis of human cervical, effectiveness of renography for, 25:55275
carcinomas, radioinduced thyroid, in man following iodine-131 therapy, 25:55343
carcinomas, radiotherapy of thyroglossal duct, role of surgery and thyroid hormone suppression in iodine-131, 25:55304
carcinomas, scanning of parasternal lymph nodes in patients with mammary, effectiveness of gold-198 for, 25:55288
carcinomas, screening compounds for prevention and therapy of, 25:57229 (EUR-4483)
lymphogranulomatosis, radiotherapy of, effectiveness of γ and x, 25:55301
malignant, radiodiagnosis of skin, use of phosphorus-32 and Si(Li) detectors for, 25:55273
melanomas, endolymphatic therapy for human malignant, effectiveness of iodine-131-labeled lipiodol for, 25:55305
metastases, endolymphatic therapy for human, effectiveness of iodine-131-labeled lipiodol for, 25:55305
metastases, radiodiagnosis of lymph node, in patients with mammary carcinomas, effectiveness of gold-198 for, 25:55288
metastases, radiotherapy of solitary lung and thoracic lymph node, γ, 25:55300
osteosarcomas, radioinduced, in rats following injection of phosphorus-32, cytology and histology of, 25:55335
Rous sarcoma, radiation effects on frequency in chickens, x, 25:55329
sarcomas, cell cycle kinetics for, tritium-labeled thymidine tracer studies on, 25:55110(R) (TID-25801)
sarcomas, radiodiagnosis of human reticulum cell, effectiveness of gallium-67 for, 25:55283
tumors, diagnosis of human brain, comparison of effectiveness of radioisotope scanning and angiography for, 25:55293
tumors, in vitro demonstration of immunity to human brain, 25:57263 (ORO-3195-51)
tumors, radioinduced, in mice following chronic ingestion of strontium-89, 25:55319 (UCD-472-118)
tumors, radiotherapy of deep, preparation of Styrofoam compensators to correct for surface irregularities during x, 25:55244
tumors, radiotherapy of human, effectiveness of iron and steroid treatment for reducing dose and side effects in, 25:55303
tumors, radiotherapy of human, synchronization of cell cycle for improvement of, 25:55306
tumors, tritium-labeled thymidine incorporation in human, method for in vivo, 25:55110(R) (TID-25801)
tumors, virus--cell relations in dog brain, 25:57262 (ORO-3195-50)

DISEASES, PHYSIOLOGICAL
abscesses, diagnosis of human brain, comparison of effectiveness of radioisotope scanning and angiography for, 25:55293
cataracts, radioinduced, in eyes of rabbits, effects of dose and LET on RBE for cobalt-60 γ, 2.5 and 14 MeV neutron, and 3 GeV proton, 25:55317 (CEA-CONF-1744)
effects of human kidney, on lymphocyte changes following radon inhalation, 25:55346
effusions, radiodiagnosis of human pericardial, effectiveness of technetium-99m-labeled sulfide for, 25:55295
embolism, radiodiagnosis of human lung, effectiveness of technetium-99m-labeled human serum albumin and sulfur colloid in combination with gamma camera for, 25:55296
hematoma, diagnosis of human brain, comparison of effectiveness of radioisotope scanning and angiography for, 25:55293
hemorrhages, radioinduced, in muscles of goats, γ, 25:55318(T) (LB/G-2995)
hydrocephalus, radiodiagnosis of infantile, by combined skull and ventricular scanning, 25:55290


XUM

hypertension, radiodiagnosis of human pulmonary, effectiveness of two-phase scintigraphy method with iodine-131-labeled albumen and technetium-99m-labeled albumen for, 25:55284
inflammations, radiodiagnosis of human, effectiveness of silver-105 for, 25:55286
osteoarthropathy, radiodiagnosis of human hypertrophic, effectiveness of strontium-85 and strontium-87m for, 25:55298
osteodystrophia deformans, diagnosis of human, comparison of effectiveness of radioisotope scanning with biochemical methods or radiography for, 25:55294
osteonecrosis, radioinduced in human jaw following malignant tumor therapy, γ, 25:55344
osteonecrosis, treatment of radioinduced human, following therapy of carcinomas, 25:55270
radiodiagnosis of human lung, effectiveness of technetium-99m-labeled sulfur colloid macroaggregates for, 25:55297
spondylitis, scanning of sacroiliac joints in patients with ankylosing, effectiveness of strontium-85 for, 25:55287

DISEASES, TRAUMATIC
radiation injuries, prophylaxis and treatment of human nervous system, following therapy of head tumors, 25:55269
radiation sickness, pathomorphological findings in goats on γ, 25:55318(T) (LB/G-2995)
wounds, effects on electrolyte metabolism in rats, combined effects of radiation and, 25:55332

DISPERSION RELATIONS
sum rule compatible with violation of Pomeranchuk theorem, modified Adler--Weisberger, 25:56510

DISPLACEMENT GAGES
design characteristics of reactor control rod, description of, 25:57204(P)
design of resonance cavity, for in-core use, 25:55068(T) (AEC-tr-7240)

DISTILLATION APPARATUS
design and operation of radioisotope-heated, for recovering potable water from urine, 25:54911(P)
development of continuous-, for separation of helium-3 from helium-4, 25:56121

DODECANE
dodecane--TBP, radiolysis of, effects of nitric acid on reactor, 25:54644

DOGS
blood flow in liver of, xenon-133 clearance method for measurement of, 25:55123
radiation dose distribution in bones of beagle, strontium-90--yttrium-90 β, 25:55319 (UCD-472-118)
radiation dosimetry in lens of beagle, methods for proton, 25:55319 (UCD-472-118)
radiation effects on bones of beagle, estimation of hazards to man from model for long-term low dose radium-226, 25:55319 (UCD-472-118)
radiation effects on erythrocytes of beagle, protective effects of hydrogen peroxide against strontium-90 β, 25:55319 (UCD-472-118)
radiation effects on eyes of beagle, effects of dose on proton, 25:55319 (UCD-472-118)
radioinduced sterility in developing ovaries of beagle, following exposure in utero, effects of dose fractionation on x, 25:55319 (UCD-472-118)
radium-226 content of uveal tissue in eyes of beagle, use of autoradiography to measure, 25:55319 (UCD-472-118)
strontium-90 content of blood plasma in beagle, following prolonged ingestion, 25:55319 (UCD-472-118)
transplantation of γ-irradiated bovine fascia in brain of, for filling dura mater defects, 25:55148

DOLOMITES
analysis for trace elements in sample coexisting with calcite by neutron activation and γ spectrometry, 25:54497

DRESDEN POWER REACTOR, UNIT 1
radioactive liquid release from, safety analysis of unloading heat exchanger tube leak, 25:56896 (DOCKET-50010-95)

DRESDEN POWER REACTOR, UNIT 2
instrumentation for, rod block for average power range and intermediate power range monitoring, 25:56939 (DOCKET-50237-201)
radiation monitoring system for, use of steam jet air ejector offgas monitor to substitute plant chimney, 25:56938 (DOCKET-50237-200)
radiation monitors for, substitution of stacks monitors by steam jet air ejector off-gas, 25:56909 (DOCKET-50249-101)
stack sample line for, plateout test procedures for, 25:56909 (DOCKET-50249-101)
turbine control valve for, fast closure scram for, 25:56939 (DOCKET-50237-201)

DRESDEN POWER REACTOR, UNIT 3
instrumentation for, modification of rod block functions for intermediate range and average power range monitors, 25:56942 (DOCKET-50249-102)
radiation detectors for, temporary substitution of steam jet air ejector off-gas monitor for plant chimney monitoring, 25:56943 (DOCKET-50249-103)
radiation monitors for, substitution of stacks monitors by steam jet air ejector off-gas, 25:56909 (DOCKET-50249-101)
stack sample line for, plateout test procedures for, 25:56909 (DOCKET-50249-101)
turbine control valve for, fast closure scram modification for, 25:56942 (DOCKET-50249-102)

DRILL CORES
analysis of intact, for copper by neutron activation, 25:54469

DYSPROSIUM
determination in river water and seawater by neutron activation and radiochemical separation, 25:54504
determination of trace amounts of, in nuclear grade uranium by x-ray excited optical fluorescence, 25:54428
lattice parameters of, effects of hydrogen on, 25:55549
neutron resonance absorption in, self-shielding of, (E/T), 25:57196
separation from aqueous solutions by solvent extraction using TTA, synergistic effects of 2,4-pentanedione on, 25:54731
x-ray absorption edges of, positions of L/sub III/, (E), 25:55822

DYSPROSIUM ALLOYS AND SYSTEMS
Ag--Dy, hyperfine parameters in DyAg, Moessbauer-effect study of, 25:56382
Au--Dy, crystal structures and melting points of intermetallic, 25:55570
Cu--Dy, hyperfine parameters in DyCu, Moessbauer-effect study of, 25:56382
Dy--Mg, compound formation in, vapor pressure measurements for studies of thermodynamics of, 25:55525 (IS-T-462)
Dy--Rh, hyperfine parameters of DyRh, Moessbauer-effect study of, 25:56382
Dy--Zn, hyperfine parameters of DyZn, Moessbauer-effect study of, 25:56382

DYSPROSIUM CHLORIDES
x-ray absorption edges of, chemical shifts of, (E), 25:55822

DYSPROSIUM ISOTOPES Dy-157
energy levels of, model analysis for ΔN = 2 mixing in, (T), 25:56737 (JINR-E4-5877)

DYSPROSIUM ISOTOPES Dy-159
energy levels of, model analysis for ΔN = 2 mixing in, (T), 25:56737 (JINR-E4-5877)

DYSPROSIUM ISOTOPES Dy-161
energy levels of, model analysis for ΔN = 2 mjxing in, (T), 25:56737 (JINR-E4-5877)
Moessbauer effect in DyCu, DyAg, DyZn, and DyRh, 25:56382
Moessbauer effect in dysprosium intermetallic compounds, 25:56379
Moessbauer spectrum in gadolinium oxide, hyperfine structure in, 25:56375
valence states of dysprosium in intermetallic compounds, Moessbauer-effect study of, 25:56379

DYSPROSIUM ISOTOPES Dy-163
energy levels of, model analysis for ΔN = 2 mixing in, (T), 25:56737 (JINR-E4-5877)

DYSPROSIUM OXIDES
x-ray absorption edges of, chemical shifts of, (E), 25:55822
$Al_2O_3$--$Dy_2O_3$--$UO_2$, temperature distribution in irradiated fuels of, use of eutectic isotherm for monitoring, (E), 25:57194


## E


EARTH
book: Physical and Radiobiological Investigations of Artificial Satellites of the Earth, 25:55342
surface lunar variations of diurnal magnetic fields and pressure, out-of-phase phenomena with ionosphere solar variations, (E/T), 25:56037
surface solar variations of diurnal magnetic fields and pressure, out-of-phase phenomena with ionosphere solar variations, (E/T), 25:56036

EARTHQUAKES
effects on design requirements of power reactor Class 1 equipment and structures, 25:57108
effects on radioisotope content of ground waters in USSR, (E), 25:54775
ground motion from San Fernando, predictions for Glendale area, 25:54812 (NVO-1163-TM-30)
occurrence following underground nuclear explosions, effects of shear wave polarization on, 25:54814

ECOSYSTEMS
plutonium movement in aquatic, 25:55150 (CONF-710401-, pp 407-10)
radioisotope accumulation by organisms in aquatic, effects of stable element content on, 25:55158

EDWIN I. HATCH POWER REACTOR, UNIT 2
design parameters of, revised and additional data on, 25:56969 (DOCKET-50366-15)
operations aspects of, revised and additional data on, 25:56969 (DOCKET-50366-15)

EGGS
radiation processing effects on amino acid content of, 25:55364

ELASTOMERS
radiation processing of, 25:54619(P)


XUM

ELECTRIC ARCS
plasma diagnostics in, spectroscopic, (E/T), 25:56139
plasma instabilities and turbulence in argon, (E/T), 25:56196(R) (N-71-25028)
plasma temperature and electron density in spark, hydrogen, (E), 25:56142
plasma temperature distribution and thermal conductivity in argon, spectral measurements of, (E), 25:56140
pressure measurement near anode of high-current, 25:56155
ELECTRIC CAPACITORS
current shaping techniques for high voltage, 25:57268 (SC-DR-710463)
ELECTRIC CELLS
design of promethium-147-powered, 25:54922(P)
properties of, using alkali metals and charge transfer complexes, 25:57221(R) (COO-1707-12)
ELECTRIC CHARGES
motion in electromagnetic field, Lorentz transformation for invariant electric tension vector, 25:56567
ELECTRIC CONDUCTORS
transmission line constants for coupled microstrip, 25:57277(T) (SC-T-713063)
ELECTRIC DISCHARGE
electron avalanche in helium, simulation by Monte Carlo calculations, 25:56265(T) (ORNL-tr-2518)
electron energy distribution measurement in, (E), 25:56138
electron extraction from Penning, instabilities in, 25:56148
ionization wave excitation in positive columns by acoustic pulses, (E), 25:56154
shock waves in, parameters of ionized air in front of, (E), 25:56160
ELECTRIC FIELDS
electron acceleration of quasi-static, as trigger mechanism for solar flares, (T), 25:55760
intensity observations at low altitudes over auroral zones and polar caps, simultaneous charged-particle observations and, 25:56030
ELECTRIC INSULATORS
development of radiation-resistant, 25:54599 (ORNL-4717, p 117-24)
radiation effects on properties of B-kind, γ, 25:55101
radiation effects on thermionic sheath trilayer, fast-neutron, 25:55096 (N-71-24635)
radiation effects on, fast neutron, 25:54599 (ORNL-4717, p 117-24)
ELECTRIC POWER
superconductivity and cryogenics in, uses of, 25:56114
ELECTRIC PROBES
performance of conical Langmuir, for diagnostics of shock-heated plasmas, (E/T), 25:56144
performance of Langmuir, collisional effects on, 25:56135
properties of electrostatic, in ionospheric plasmas, (E), 25:56012
response of cylindrical Langmuir, in plasma transition regime, (E/T), 25:56136
ELECTROJETS
development of polar, during polar magnetic substorms, (E/T), 25:56029
ion motion in auroral, characterization of auroral electric fields from artificial, (E/T), 25:55959
plasma inhomogeneity formation in equatorial, quasi-linear equations of electron and ion, (T), 25:55986
ELECTROLYSIS
use of countercurrent, in activation analysis, 25:54493
ELECTROLYTES
isopiestic studies of very concentrated aqueous, 25:54535 (ORNL-4717, pp 57-82)
mass transfer in systems of, multicomponent, 25:54719 (ORNL-4682, pp 229-39)
ELECTROLYTIC CELLS
calibration for impurity monitoring in liquid sodium, 25:55069 (ANL-7804)
ELECTROMAGNETIC FIELDS
charged particle motion in, radiation corrections for, (T), 25:56393
charged-particle system interactions with, potentials and multipole moments for, (T), 25:56455
Lagrangian formalism for free Maxwell, in spinor notation, (T), 25:56541
Lorentz transformations for invariant electric tension vector for motion of electric charges in, 25:56567
ELECTROMAGNETIC LENSES
aberrations of asymmetrized quadrupole, 25:56604
ELECTROMAGNETIC SEPARATION
equipment for isotope, collector system for, 25:56584 (JINR-P6-5888)
ion optics system for, design of, 25:54920
ELECTROMAGNETIC WAVES
absorption and transformation in plasma, (T), 25:56250
coupling in inhomogeneous plasma, (E), 25:56225 (CEA-CONF-1802)
emission of auroral vlf, relation to auroral cosmic-noise absorption, (E/T), 25:55999
interactions with inhomogeneous plasma, diagnostic use of, 25:56145
interactions with plasma with exponential density distribution, (T), 25:56230 (INR-1321)
production of high-frequency, by electron beams in solar-wind region upstream from bow shock, (E/T), 25:56019
propagation across magnetic field in parabolic plasma layer, (T), 25:56236
propagation along plasma layers, effect of field pressure on, (T), 25:56235
propagation in slightly relativistic plasma, (T), 25:56228 (CEA-CONF-1806)
propagation of strong cylindrical and spherical, from infinitely weakly ionized plasma, (T), 25:56240
radiation conversion into, in static magnetic fields in vacuum, gravitational, (T), 25:55805
ELECTRON BEAMS
dosimetry of fast, calibrations and controls for, 25:55224
energy determination above 5 GeV, method for, 25:56609(P)
equilibrium and stability of magnetically confined relativistic, (T), 25:56130
focusing and transport of high-current charge-neutralized, in conducting boundaries, 25:56596 (SC-RR-710436)
interactions with collisionless plasma, dispersion relations for linear waves from, 25:56170
interactions with dense plasmas, self fields and currents from relativistic, (T), 25:56166 (NP-19012)
interactions with homogeneous plasma, dispersion relations for linear waves from, (T), 25:56169
interactions with plasma, Bernstein wave excitation in, (E), 25:56241
interactions with plasma, longitudinal wave excitation in, (T), 25:56232 (NP-19020)
interactions with plasma, longitudinal wave reflection in, (T), 25:56247
interactions with plasma, noise levels of Langmuir oscillations from, (E), 25:56249
production of artificial aurorae with, ground-based optical observations of, 25:55962
reactions with solar-wind region upstream from bow shock, high-frequency electromagnetic waves from, (E/T), 25:56019
ELECTRON MICROSCOPES
lens of, spatial frequency of, 25:54587(R) (AECL-3909)
ELECTRON-RING ACCELERATORS
beam dynamics during axial acceleration in, effects of self fields on, 25:56595 (NP-19007)
ring compression in, magnetic field tolerances during, 25:56595 (NP-19007)
ELECTRONIC EQUIPMENT
performance for measuring nuclear yields, tests for determining, 25:54993 (AD-720974)
ELECTRONS
accelertion in solar flares due to quasistatic electric fields, (T), 25:55760
angular distributions of equatorial 30 to 300 keV, in loss cone and at large angles, (E), 25:56027
book: Emissive Properties of Materials (Handbook), 25:56346
distribution of relativistic cosmic, effects of energy-loss mechanisms on, (T), 25:55908
dose distribution in tissue-equivalent phantoms, (T), 25:55214
effects of pulsed, on ammonia at 0.1 to 750 Torr, kinetic study of species formed from, 25:54661
effects of pulsed, on aqueous solutions of cobalt(III) cyanide complexes, kinetics of reactions of hydrated electrons in, 25:54651
effects of pulsed, on benzoatopentaamminecobalt perchlorate, oxidation of benzoatopentaamminecobalt(III) by hydroxyl radical from, 25:54669
effects of pulsed, on carbon monoxide--oxygen mixtures, 25:54587(R) (AECL-3909)
effects of pulsed, on heavy water--water systems, 25:54587(R) (AECL-3909)
effects on antimony-doped germanium at 2.5 MeV, one-valley EPR spectrum of, 25:56298
effects on aqueous solutions of fumarates, ESR studies of radicals from, 25:54656
effects on aqueous solutions of organic compounds, rate constants for hydrogen atom reactions following lytic, 25:55132
effects on carbon-doped silicon at 2 MeV and 130°K, infrared absorption spectral study of, 25:56325
effects on cathodoluminescence spectrum of cadmium telluride, 25:56290
effects on copper, kinetics of crowdion reactions in annealing stage I/sub E/ of, (T), 25:56333
effects on germanium at 700 keV, luminescence spectra from defects induced in, 25:56328
effects on gold-doped platinum at 4.5°K, annealing of Frenkel defects induced in, 25:56284 (JUL-731-FF)
effects on heating of plane bodies, tables for transient temperatures from, 25:56267
effects on lithium-diffused n-type silicon at 30 MeV, defects induced in, 25:56309
effects on lithium-doped n-type germanium at 1 MeV, 25:56301
effects on lithium-doped n-type silicon at 1 to 1.5 MeV, lithium--defect interactions in, 25:56310
effects on luminescence spectra of silicon at 2.5 MeV, effects of uniaxial stress and temperature on,

XUM

25:56295
effects on luminescence spectra of silicon at 3 MeV, effects of annealing and lithium impurity on, 25:56294
effects on magnetoresistance of aluminum single crystals at 3 MeV, (E/T), 25:56334
effects on N-acetylglycine in the presence of ammonia at 7.5 MeV, 25:54650
effects on n-type germanium at 1 MeV, effects of impurities on 65°K annealing stage, 25:56331
effects on n-type germanium, effects of donor impurity on 35 and 65°K stages in annealing of, 25:56330
effects on p-type germanium at 1 MeV and 8°K, defects induced in, 25:56302
effects on p-type germanium at 1.5 MeV and 77°K, annealing of defects induced in, 25:56329
effects on p-type germanium at 1.5 MeV, 220°K defects induced in, 25:56300
effects on p-type silicon at 1.2 MeV, photoconductivity spectral study of, 25:56308
effects on phosphorus-doped n-type germanium at 1.5 MeV, EPR study of, 25:56299
effects on potassium chloride at 2 MeV, thermoluminescence induced by deformation and light after, 25:56321
effects on silicon doped with germanium, oxygen, and carbon at 2.8 MeV and 90°K, infrared absorption spectral study of, 25:56297
effects on silicon- and tellurium-doped n-type gallium arsenide at 1 MeV, 25:56292
effects on stability of silvered and aluminized FEP teflon second-surface mirrors, 25:55656 (N-71-27736)
effects on surfaces and deposit epitaxy of sodium fluoride substrates at 0.2 to 1 keV, 25:56322
effects on tellurium at 0.6 and 1 MeV and 10°K, annealing recovery of, 25:56306
effects on water, effects of temperature on absorption spectrum of hydrated electrons from, 25:54658
emission from materials, manual of tables on, 25:56346
interactions e + d → e + p + n, multi-pion exchange contribution to nucleon-nucleon binding in, (T), 25:56527
interactions e + d at high energies, cross sections, Δ(1236) production in e + n interactions, and cross sections for inelastic e + n and e + p interactions from inelastic, (E), 25:56405 (DESY-71/33)
interactions e + e → e + e + epsilon(750), cross sections for, (T), 25:56463
interactions e + e → e + e + f(1260), cross sections for, (T), 25:56463
interactions e + e → e + e + $\pi^+ + \pi^-$, Feynman diagram model of, 25:56460
interactions e + N at very low energies, review of $\pi^+$ and $\pi^0$ production in, (E/T), 25:56404 (CONF-701121-8)
interactions e + n in e + d interactions at high energies, cross sections for inelastic, (E), 25:56405 (DESY-71/33)
interactions e + n in e + d interactions at high energies, cross sections for Δ(1236) production in, (E), 25:56405 (DESY-71/33)
interactions e + p above second resonance, review of $\pi$ production in, (E), 25:56406 (DESY-71/35)
interactions e + p in composite model, scale invariance of structure function for deep inelastic, 25:56465
interactions e + p in e + d interactions at high energies, cross sections for inelastic, (E), 25:56405 (DESY-71/33)
interactions $e^+ + e^- \rightarrow e^+ + e^- + \pi^+ + \pi^-$, Feynman diagram model of, 25:56460
interactions $e^+ + e^- \rightarrow \pi^+ + \pi^-$ angular and energy distributions for, (T), 25:56459
interactions $e^+ + e^-$, production of pseudoscalar mesons in, 25:56459
interactions γ + e, disturbance of second-order coherence of photon field in quantum electrodynamics for forward, (T), 25:56456
interactions with electromagnetic field at 4 GeV/c in propane bubble chamber, direct electron pair production in, 25:56467
laser beam interactions with, stimulated Compton energy exchange rate in, (T), 25:56266 (UCRL-51065)
mean free path in aluminum and Permalloy foils, (E), 25:56281
motion in strong Coulomb field, Sommerfeld orbits in, (T), 25:56394
photodissociation of complex hydrated, 25:54595 (CONF-700652-(Vol.3))
production and properties of trapped radiolytic, in polar substances, 25:54593 (CONF-700652-(Vol.2), pp 261-93)
production of $e^+e^-$ in electron interactions with electromagnetic field at 4 GeV/c in propane bubble chamber, direct, 25:56467
properties of trapped radiolytic, in alkaline aqueous glasses, 25:54627 (CONF-700652-(Vol.2), pp 295-330)
properties of trapped, in nonpolar solids, 25:54594 (CONF-700652-(Vol.2), pp 331-64)
reactions of hydrated radiolytic, in aqueous solutions of organic compounds, 25:54632 (CONF-700652-(Vol.3), pp 649-92)
reactions of hydrated, chemical reaction kinetic studies using, 25:54631 (CONF-700652-(Vol.3), pp 601-48)
reactions of hydrated, with organic compounds, 25:54631 (CONF-700652-(Vol.3), pp 601-48)
reactions of hydrated, with polynucleotides, effects of secondary structure on, 25:55131
reactions of radiolytic hydrated, in aqueous solutions of cobalt(III) cyanide complexes, kinetics of, 25:54651
reactions of radiolytic, with ion, 25:54591 (CONF-700652-(Vol.1), pp 221-58)
reactions with atoms and diatomic molecules at low energies, review of total and momentum-transfer cross sections for, (E), 25:55856
reactions with atoms and molecules, computer control system for studying, 25:55094
reactions with helium at 100 to 2000 eV, angular and energy distributions of electrons from ionization in, (E), 25:55847
reactions with helium, Born--Oppenheimer approximation for excitation to metastable states in, 25:55843
reactions with helium, eikonal approximation for excitation of $2^1P$ state in, 25:55874
reactions with helium, trapped-electron study of resonances in excitation in, 25:55851
reactions with hydrogen atoms at low energies, use of free-fall atomic model in three-body calculations of ionization cross sections for, 25:55836 (INR-P-1327)
reactions with hydrogen atoms, eikonal approximation for excitation of 2p and 2s states in, 25:55874
reactions with hydrogen atoms, Glauber and Vainshtein approximations for total cross sections for 1s--2p excitation in, 25:55850
reactions with hydrogen atoms, perturbation-theory calculations of 1s--2s excitation in, 25:55877
reactions with hydrogen molecules, effects of vibrational level on kinetic-energy distribution of protons from, (T), 25:55857
reactions with lithium up to 60 eV, Born-approximation calculations of excitation cross sections for, 25:55864
reactions with metal targets at 0.5 to 15 keV, optical radiation from, (E), 25:55813 (JINR-P4-5957)
reactions with molecules at low energies, review of theory of rotational excitation in, 25:55855
reactions with molecules at low energies, review of methods of measurement of cross sections for, 25:55855
reactions with water molecules, dependence of generalized oscillator strengths on momentum transfer in, (E), 25:55880
scattering by atoms, computational procedure for multichannel resonances in, 25:55861
scattering by atoms, polarized-orbital method for, 25:55871
scattering by carbon-12, oxygen-16, and silicon-28, form-factor calculations using isotensor dipole sum rules, (T), 25:56868
scattering by hydrogen atoms at 1.21 to 2.25 rydbergs, complex-energy calculations of s-wave elastic, 25:55860
scattering by hydrogen atoms, algebraic close-coupling approach to, 25:55854
scattering by hydrogen atoms, parameters for multichannel resonances in, (T), 25:55861
scattering by nuclei at medium and high energies, cross sections for summed inelastic and quasi-elastic, (T), 25:56849
scattering by nuclei with multipole moments, effects of nuclear structure on bremsstrahlung produced in polarized and unpolarized, (T), 25:56862
scattering by nuclei, analysis for isotensor components in dipole sum rules for, (T), 25:56868
scattering by nuclei, effect of short-range correlations in, (T), 25:56824 (LYCEN-7104, C4.1-17)
spectra of hydrated, effects of temperature on, 25:54658
transport in solids, Monte Carlo calculations for, 25:56362

ELECTROPHORESIS
review of countercurrent, 25:54742

ELECTROSTATIC ANALYZERS
calculations for a sector field magnetic and, 25:56606
design improvement of planar, for slow electrons, 25:55072 (FRNC-TH-54)
electron energy distributions of, calculations of, 25:55084
performance as time-of-flight spectrometer for plasma diagnostics, (E), 25:56137
performance for electron spectrometry, 25:55083
spectra from charged-particle, method for evaluation of, 25:55082

ELECTROSTATIC FIELDS
charged-particle trajectories in 1/r, second-order approximation for calculating, (T), 25:55082
Coulomb field corrections for, in strong magnetic fields, 25:56402
electron motion in strong Coulomb, Sommerfeld orbits in, (T), 25:56394

ELECTROSTATIC GENERATORS
shielding material for, x-ray, 25:56603(P)

ELECTROSTATIC LENSES
aberrations of asymmetrized quadrupole, 25:56604

ELEMENTARY PARTICLE MODELS
classical stochastic, formulation of Bohr-like, 25:56450
dual quark--parton, for hadron interactions, 25:56481
dual resonance, canonical quantization of proper time formalism in, 25:56480

XUM

dual resonance, current amplitudes in, 25:56449
dual resonance, with second sheet resonances, effects of unitarity-like features in inclusive interactions in, 25:56476
harmonic oscillator quark, for hyperon resonance spectra, 25:56507
Lee, unified treatment of V--theta and V--2theta sectors of, 25:56553
multiperipheral, lectures on interactions at high energies in, 25:56442 (PURC-4159-42)
Regge absorption, $\pi$ and eta production in forward $\gamma$ + N + $\pi$(eta) + N interactions in, 25:56452 (CALT-68-313)
Reggeized one-pion-exchange, diffraction production of N(1470) and N(1688)in n + p + 2p + $\pi^-$ interactions at 2 to 30 GeV in, 25:56521 (JINR-P1-5975)
rising phase shift, mass and width of rho' in anti p + n + $\pi^+$ + 2$\pi^-$ interactions in, 25:56485 (ORO-3992-66)
strong coupling baryon bootstrap, coupling constants between baryons and pseudoscalar mesons in SU(3), 25:56503
vector dominance, hadron weak interaction form factors in, 25:56468 (FRNC-R-1)
ELEMENTARY PARTICLE MODELS (BOOTSTRAP)
theory of SU(3) strong coupling baryon, for coupling constants between baryons and pseudoscalar mesons, 25:56503
ELEMENTARY PARTICLES
current algebra for, cellular structure in phase space in fibre bundle theory in, (T), 25:56448
electromagnetic interactions of, indefinite metric for cross sections of production of heavy photon in, (T), 25:56547 (NYO-1932(2)-200)
inteactions with photons, structure of amplitude and differential cross sections for, (T), 25:56454
interactions at high energies, lectures on multiperipheral models for, (T), 25:56442 (PURC-4159-42)
interactions in dual resonance models with second sheet resonances, effects of unitarity-like features in inclusive, 25:56476
interactions of, formulation of action-at-distance field theory for, (T), 25:56550 (ORO-3992-14)
interactions of, lectures on quantum field theory for relativistic, (T), 25:56571 (CERN-71-14, pp 229-87)
interactions with particles and antiparticles at extremely high energies, asymptotic behavior of amplitudes of elastic, (T), 25:56574
interactions with photons, research at Lund Univ., 1970, (E), 25:56643(R) (NP-19018)
magnetic moment of spin-1/2, in Bohr-like model, 25:56450
mass spectra of spin-1/2, in Bohr-like model, 25:56450
research at Institute of Theoretical Physics, Gothenburg, Sweden, 1970, (T), 25:56441(R) (NP-18997)
research at Purdue Univ., June 1970 to May 1971, (T), 25:56440(R) (COO-1428-276)
spin states of, properties of coherent, (T), 25:56451
strong interactions at high energies, research at Purdue Univ., June 1970 to May 1971, (E), 25:56424(R) (COO-1428-280)
strong interactions of, research at Stockholm Univ., 1970, (E), 25:56416(R) (USIP-71-1)
strong interactions of, review of Regge cuts for, (T), 25:56475 (RPP/C-24)
theory for, anomalous magnetic moment couplings in spin-one, 25:56464
wave equations for massive spin-1/2, two-component, 25:56559
wave equations for massless spin-$^1/_2$, relativistic, 25:56447
widths of, use of resolution functions in experimental measurement of, 25:56430
ELEMENTARY PARTICLES (TRIPLET)
decay of quark-like, weak interaction with nonconservation of baryon number and electric charge for, 25:56471
flux in cosmic rays, upper limits for, (E), 25:55910
flux of 4e/3-charged quarks in cosmic radiation at 2750 m above sea level, scintillation counter telescope study of upper limit for vertical, (E), 25:56403
ELEMENTS
book: Emissive Properties of Materials (Handbook), 25:56346
determination of light, by coincident measurement of complementary particles from nuclear reactions, 25:56752(R) (SUNI-14)
determination of light, in metals, alpha reactions with aluminum and silicon at 70 to 160 MeV for activation analysis methods for, 25:56685 (FRNC-TH-48)
determination of trace amounts of, in particle size fractions of pollution aerosols by neutron activation and gamma spectrometry, 25:54505
energy-level transitions of Z = 57 through 92, probabilities of L x-ray, (E), 25:55823
production of superheavy, by nuclear reactions, chemical problems in, 25:54672
spectra of Z = 20 through 94, relative intensities of K x-ray emission lines of, (E), 25:55827
EMBRYOS
radiation effects on mammalian, 25:55207 (NYO-2740-8, pp 220-59)
radioinduced cardiovascular anomalies in chick, additive effects of hypothermia on x, 25:55333
ENDOTOXINS
radioprotective effects of, use of immune reactions of rats to Trypanosoma in studies of, 25:55267
ENGINEERING TEST REACTOR
experimental capabilities of, liquid metal cooled fast breeder reactor safety programs, 25:57069(R) (ANL-7800)
ENVIRONMENT
conference on remote sensing of, Sixth International, Ann Arbor, Mich., Oct. 13 to 16, 1969, 25:54767
conference on sciences of, 1970 Annual, Boston, April 12 to 16, 1970, 25:54932
contamination by radioactive waste disposal, review on, 25:54784
contamination of, economic aspects of, 25:54599 (ORNL-4717, p 117-24)
fluorine release to, hazards to man following, 25:55246 (CEA-Bib-200)
iodine-129 content of nuclear fuel reprocessing plant, public health hazards from, 25:55199
radiation monitoring of nuclear power plant, design and performance of amphibious detection system for in situ $\gamma$, 25:55239
radioactive contamination of, by nuclear industry in Canada, biological significance of, 25:55194 (70-CNA-641)
radioactivity monitoring in aquatic, role of stable element content measurements in pre-operational, 25:55240
radioactivity monitoring in United Kingdom, derivation and use of reference levels and working limits as standards for, 25:55241
radioactivity monitoring in, consideration of ecological factors in developing program for, 25:55238
radioactivity release to, estimation of effects on background radiation levels of long-term nuclear power plant, 25:55200
sampling for radioactive or toxic materials, evaluation of methods for, 25:54779 (CONF-710401-, pp 347-51)
thermal energy utilization in, 25:54396 (ORNL-4682, pp 242-9)
EPISOMES
radioinduced inactivation of F', role of DNA cross-links in sensitizing effects of psoralen on uv, 25:55361
EPOXY RESINS
radiation effects on adhesive properties in glass--glass and metal--metal joints, gamma, 25:55666
radiation effects on mechanical properties of cured, gamma, 25:55667
EQUIPMENT AND PROCEDURES
development for compacting solid radioactive wastes, 25:54975 (WASH-1167)
ERBIUM
lattice parameters of, effects of hydrogen on, 25:55549
separation from aqueous solutions by solvent extraction using TTA, synergistic effects of 2,4-pentanedione on, 25:54731
ERBIUM ALLOYS AND SYSTEMS
Au--Er, crystal structures and melting points of intermetallic, 25:55570
Er--Mg, compound formation in, vapor pressure measurements for studies of thermodynamics of, 25:55525 (IS-T-462)
ERBIUM ISOTOPES Er-168
energy levels from holmium-168 beta decay, spin--parity assignments for, (E), 25:56767
energy-level transitions from holmium-168 beta decay, branching ratios and relative intensities for, (E), 25:56767
ERBIUM ISOTOPES Er-169
energy levels from holmium-169 beta decay, spin--parity assignments for, (E), 25:56767
ERBIUM OXALATES
crystal structure of trihydrate of, 25:54532 (ORNL-4717, pp 1-27)
ERYTHROCYTES
radiation effects on beagle dog, protective effects of hydrogen peroxide against strontium-90 $\beta$, 25:55319 (UCD-472-118)
ESTUARIES
radioisotope content and distribution of Hudson River, analysis of fallout, natural, and reactor produced, 25:55160
ETHANE
effects on reactions of recoil tritium with deuterated methane, 25:54684
photoelectron-induced decomposition of, duplication of excitation mechanism in radiation chemistry by, 25:54597
radiation effects on exchange reactions of, with tritium, 25:54727
radioinduced polymerization in dilute solutions in liquid argon, yields from $\gamma$, 25:54615
reactions with moderated recoil fluorine-18 atoms, rate of hydrogen abstraction, 25:54686
ETHANE, 1,1,1-TRICHLORO-2,2-BIS(p-CHLOROPHENYL)-
radioinduced dechlorination in alcoholic solution, mechanism of $\gamma$, 25:54620
radiolysis of, toxicity to rats of products formed following $\gamma$, 25:55135

ETHANE, TRIFLUORO-
reactions with moderated recoil fluorine-18 atoms, rate of hydrogen abstraction, 25:54686
ETHANOL
effects on radiolysis of gaseous ethylene, 25:54643
radiolysis of liquid, yields of hydrogen and free ions in γ, 25:54660
ETHYL ETHER
effects on radiolysis of gaseous ethylene, 25:54643
ETHYLENE
effects on γ radiolysis of propene polymers, 25:54637
effects on reactions of recoil chlorine-38 in neutron-irradiated chloromethane, 25:54681
oxidation over gold, effects of deuterium on, 25:54569
radioinduced polymerization in dilute solutions in liquid argon, yields from γ, 25:54615
radioinduced telomerization by propionic acid, γ, 25:54612
radiolysis of gaseous, effects of ethanol, ethyl ether, and methyl ether on γ, 25:54643
ETHYLENE, CHLORO-, POLYMERS
radioinduced grafting of acrylonitrile on, effects of dose on γ, 25:54613
ETHYLENE, 1,1-DICHLORO-
effects on reactions of recoil chlorine-38 in neutron-irradiated chloromethane, 25:54681
ETHYLENE, FLUORO-
radioinduced polymerization of gaseous and liquid, comparison of properties of products of chemically initiated and γ, 25:54624
ETHYLENE POLYMERS
neutron emission from laser-irradiated deuterated polyethylene, 25:56219
neutron spectra in, time dependence following fast pulses, 25:56629
radiation effects on cuttings and powders of crystals of, effects of dose and sample size on γ, 25:54623
radiation effects on low- and high-pressure films of, comparison of γ and proton, 25:54604
radioactive waste incorporation in, 25:54715 (ORNL-4682, pp 95-113)
ETHYLENE, TETRAFLUORO-, POLYMERS
photoconductivity during ionizing radiation pulses, analysis of dielectric, 25:55079 (SC-DC-713696)
ETHYLENIMINE
effects on mutations in x-irradiated seeds of barley and wheat, 25:55261
effects on x-irradiated seeds of Crepis capillaris, effects of time of administration on additive or radioprotective, 25:55260
EUMYCOTA
Aspergillus sp., radiation effects on germination of, in processed garlic, γ, 25:55354
Saccharomyces carlsbergensis, radiation effects on synthesis of ribosomal precursor RNA in, uv, 25:55138
Saccharomyces cerevisiae, radiation effects on genetics and survival of, effects of dehydration and vapor pressure on, 25:55183
Saccharomyces cerevisiae, radiation effects on survival of, effects of LET on OER and RBE for heavy ion, meson ($\pi^-$), and x, 25:55165
Saccharomyces cerevisiae, radioinduced mutations in, gene control of uv, 25:55187
Saccharomyces cerevisiae, radioinduced mutations in, effects of LET on OER and RBE for γ, heavy ion, and meson ($\pi^-$), 25:55165
Saccharomyces cerevisiae, radiosensitivity of mutants of, correlation between spontaneous reversion frequency and, 25:55352
Saccharomyces sp., rdioinduced chromosome recombination in diploid, uv, 25:55180
Schizophyllum commune (mushroom), radioinduced dome mutants of, morphology of uv, 25:55186
yeasts, radiation effects on survival of haploid, parameters for heavy ion, 25:55313
EUROPE
research programs of EURATOM, 25:55252 (NP-18752)
EUROPIUM
determination in Australian tektites by neutron activation and gamma spectrometry, 25:54478
determination in fission product mixtures by ion exchange and β counting, 25:54449
determination in river water and seawater by neutron activation and radiochemical separation, 25:54504
determination in volcanic ash by neutron activation and γ spectrometry, 25:54513
determination of trace amounts of, in nuclear grade uranium by x-ray excited optical fluorescence, 25:54428
reduction at porous carbon cathode with flowing electrolyte, electrochemical, 25:54530 (LA-DC-12469)
separation from acid solutions by solvent extraction using acidic esters of aminophosphonic acids, 25:54732
EUROPIUM ALLOYS AND SYSTEMS
valence states of europium in intermetallic compounds, Moessbauer-effect study of, 25:56379
Eu--La-base, local moment relaxation in superconducting, (E), 25:56071
EUROPIUM ISOTOPES Eu-151
Moessbauer effect in europium intermetallic compounds, 25:56379
EUROPIUM ISOTOPES Eu-152
beta and electron-capture decay of, γ-γ directional correlation from, (E), 25:56777
beta decay of, β-γ angular correlations and matrix elements for nonunique first-forbidden, (E), 25:56776
EUROPIUM ISOTOPES Eu-153
energy-level transitions in, nuclear structure effects on internal conversion of M1, 25:56756
EUROPIUM NITRIDES
evaporation behavior at 1500 to 1800°K, 25:55607 (JUL-739-PC)
formation heat of, 25:55607 (JUL-739-PC)
EXHAUST SYSTEMS
design for Battelle plutonium facility, 25:54959 (CONF-710401-, pp 280-92)
filters for plutonium recovery plant, design of HEPA, 25:54947 (CONF-710401-, pp 118-32)
heat exchangers for radioactive processing building, design of filter plenum, 25:54950 (CONF-710401-, pp 162-80)
operation of plutonium processing building, 25:54948 (CONF-710401-, pp 133-48)
EXOSPHERE
ultraviolet radiation emission in, altitude distribution of neutral helium He 584-A and $He^+$ 304-A extreme-, (E), 25:55967
EXPERIMENTAL BREEDER REACTOR-II
coolant for, corrosive effects on core components and cooling system of liquid sodium, 25:57109 (ANL-7771)
coolant pumps for, summary of operating performance of sodium, 25:57028 (ANL-EBR-27)
cooling system for, corrosive effects of liquid sodium on, 25:57109 (ANL-7771)
core components for, corrosive effects of liquid sodium on, 25:57109 (ANL-7771)
hot cell facility for, equipment for remote measurements on irradiated components in, 25:57054 (ANL-EBR-30)
EXPLOSIONS
effect on radar reflected-produced decameter-wavelength radio waves in ionospheric E region, E-region-detonated, (E/T), 25:55970
EXPONENTIAL PILES
neutron decay constants for uranium, measurements using californium-252 neutron source, 25:56639
EYES
radiation effects on beagle dog, effects of dose on proton, 25:55319 (UCD-472-118)
radioinduced cataracts in rabbit, effects of dose and LET on RBE for cobalt-60 γ, 2.5 and 14 MeV neutron, and 3 GeV proton, 25:55317 (CEA-CONF-1744)
radioinduced light flashes in astronaut, following exposure to cosmic mesons (μ), 25:55341
radium-226 content of uveal tissue of beagle dog, use of autoradiography to measure, 25:55319 (UCD-472-118)

## F

FALLOUT
content in rainwater at Hokkaido, Japan following Sept. 1969 Chinese nuclear explosion, (E), 25:54789
fractionation of, method for determining strontium-89/strontium-90, 25:54803
monitoring in ground-level atmosphere in north Germany and north Norway, 1970 and 1971, 25:54785
monitoring in Swiss atmosphere following Dec. 1968 and Sept. 1969 Chinese nuclear explosions, 25:54791
radiation dose rates from, calculation of, 25:55231
FAST FLUX TEST FACILITY
coolant combustion in, analysis of liquid sodium, (E/T), 25:57112 (HEDL-TME-71-31)
cooling system for, design for safe handling of coolant radioisotopes, 25:55370 (BNWL-SA-2335)
core components for, wear testing in sodium, 25:55379(R) (WARD-4210-T-1-2)
materials for, research progress on development of, 25:55379(R) (WARD-4210-T-1-2)
FAST TEST REACTOR
coolant interaction with molten fuel in, pressure generation by, (T), 25:57073 (CONF-710302-(Vol.1), pp 25-49)
core failure accident in, analysis of radiation hazards from, 25:57113 (HEDL-TME-71-33)
physics calculation for, listing of 26 group cross section set for, 25:57115 (HEDL-TME-71-65)
startup tests of, preliminary outline of, 25:57114 (HEDL-TME-71-58)
FEDERAL REPUBLIC OF GERMANY
fallout monitoring in ground-level atmosphere of north, 1970 and 1971, 25:54785
nuclear power development in, planning for, 25:57003
nuclear power plant requirements in, projections of, 25:57005
nuclear research in, organization and financing of, 25:57014
power reactor development and operation in, review of, 25:56877 (CONF-700438)
FELDSPARS
analysis for barium, potassium, and sodium by neutron activation and γ spectometry, 25:54494
FERMI FAST BREEDER REACTOR
cooling system for, secondary containment requirements

XUM

for external liquid sodium primary piping of, 25:56931 (DOCKET-50016-129)
data acquisition and analysis in, malfunction detection analyzer system for, 25:56878 (CONF-710302-(Vol.1), pp 199-214)
fuel element transfer tank for, operating limits for irradiated, 25:56929 (DOCKET-50016-127)
fuel element transfer tank for, operating limits for irradiated, 25:56930 (DOCKET-50016-128)
FERMIONS
spinor theory of, two-component, 25:56552
theory for two spin-1/2, with Heisenberg coupling, properties of coherent spin states in, (T), 25:56451
wave equations for massive spin-1/2, two-component, 25:56559
wave equations for massless spin-$^1/_2$, relativistic, 25:56447
FERREDOXINS
Moessbauer-spectra studies of, review, 25:55105
FERROCYANIDES
determination by dichrometric titration using triphenylmethane dyes as redox indicators, 25:54410
FETUSES
radiation effects on chromosomes of mouse, 25:55207 (NYO-2740-8, pp 220-59)
FIBERS
radiation effects on electric conductivity and diamagnetic anisotropy of carbon, neutron, 25:56282 (CEA-CONF-1822)
FILMS
book: Emissive Properties of Materials (Handbook), 25:56346
microporous areas in, method of detecting, 25:54859(P)
FILTERS
description of glove box, for plutonium-238 handling, 25:54949 (CONF-710401-, pp 149-61)
description of HEPA, for plutonium processing building, 25:54948 (CONF-710401-, pp 133-48)
installation and performance of HEPA, for radioactive effluents, 25:54947 (CONF-710401-, pp 118-32)
performance of HEPA, in retaining plutonium combustion aerosols, 25:54951 (CONF-710401-, pp 181-202)
FIRES
control and prevention at WADCO, categorization of nuclear facilities for, 25:54953 (CONF-710401-, pp 208-11)
control and prevention in hot cells, design and performance of test facility for, 25:54956 (CONF-710401-, pp 237-47)
control in large volumes using Halon 1301 suppressing agent, 25:54957 (CONF-710401-, pp 248-56)
control of nuclear plant, organization and planning for, 25:54952 (CONF-710401-, pp 204-7)
detection and suppression in glove boxes, design of automatic system for, 25:54954 (CONF-710401-, pp 212-20)
detection and suppression in glove boxes, development of systems for, 25:54939 (CONF-710401-, pp 17-25)
detection in glove boxes, development of reliable system for, 25:54955 (CONF-710401-, pp 221-36)
effects on radioactive processing building exhaust systems, use of filter plenum heat exchangers for minimizing, 25:54950 (CONF-710401-, pp 162-80)
FISSION
energy release in, calculation using renormalized Fermi gas model and collective potential energy surface, (T), 25:56856
mass chain yields in, method for calculation of energy dependence of, (T), 25:56816 (JAERI-Memo-4383)
neutron emission in, analysis of data on retarded, 25:56741 (KFKI-71-35)
neutron yield in, time-of-flight spectrometer for measuring average prompt, 25:55039(T) (LB/G-3040)
FISSION FRAGMENTS
effects on methanol, 25:54645
FISSION PRODUCTS
activity of, formalism for calculation of, 25:54699
deposition of noble metal, on samples from MSRE, 25:54533 (ORNL-4717, pp 29-41)
deposition on samples from MSRE pump bowl, 25:54533 (ORNL-4717, pp 29-41)
detection in failed water cooled Zircaloy 2 clad uranium oxide ($UO_2$) fuel rods, 25:57047 (JAERI-Memo-4157, pp 2-22)
distribution in high temperature gas cooled reactor cooling systems, 25:57092(R) (ORNL-TM-3483)
distribution in MSRE moderator graphite, 25:54533 (ORNL-4717, pp 29-41)
monitoring of stack-disposed gaseous, from reactors, production of gases of known specific activity for calibrating detectors for, 25:54986
production and uses of, research progress on, 25:54887(R) (BNWL-1308-6)
production of iodine, power reactor safety problems from, 25:57100
radiation dose rates from uranium-235, at selected times after fission, 25:55231
release during coolant loss accident in water cooled and moderated power reactors, 25:57104
release from failed water cooled Zircaloy 2 clad uranium oxide ($UO_2$) fuel rods, 25:57047 (JAERI-Memo-4157, pp 2-22)
release from fast reactors following core failure accident, 25:57113 (HEDL-TME-71-33)
release from gas cooled reactor pressure loss accidents, 25:57106
separation by ion exchange, 25:54449
separation from milk, double-bed ion exchange process for, 25:54722
separation from molten manganese nitrate hexahydrate or calcium chloride hexahydrate by solvent extraction using TBP, 25:54740
separation from MSBR fuel solvent by metal transfer process, distribution of sodium and potassium in, 25:54534 (ORNL-4717, pp 43-56)
separation from plutonium and uranium by fluorination process, 25:54736
separation of short-lived, beta recoil mechanism for, 25:54694
separation of volatile, from LMFBR fuels, 25:54713 (ORNL-4682, pp 39-79)
volatility of oxides of, effects of water vapor on, 25:54758 (ORNL-4717, pp 109-15)
FLOWMETERS
development of radioisotope tracer, for measuring turbine and pump discharge, 25:55065
FLUID FLOW
heat transfer and velocity distribution in turbulent, in triangular channels, calculations of, 25:54884
heat transfer coefficients for turbulent, in ducts with flux transients, derivation of forced-convection, 25:54864 (ANL-7754)
heat transfer in axial turbulent, through tubes and rod bundles, 25:54866 (EIR-198)
heat transfer in incompressible turbulent, through tubes, model for axial, (T), 25:54877 (SGAE-RT-38/1971)
heat transfer in longitudinal turbulent, containing heated rod bundles, equations for calculating stable, 25:54883
heat transfer in two-phase annular, in heated pipes, effects of diffusion and film formation on critical, (E), 25:54869 (FEI-217)
heat transfer in two-phase, in multirod coolant channels, (E), 25:54870(R) (GEAP-10347)
heat transfer in, through vertical annular space, onset of free convection, (E/T), 25:54881
heat transfer to, at supercritical pressures, effects of fuel element dimensions on, 25:54880
magnetohydrodynamic channel, velocity profile in entrance region of, (E/T), 25:55942
magnetohydrodynamic conducting, numerical calculation in traveling magnetic field, 25:55918
magnetohydrodynamic duct, effect of magnetic Reynold's number and Hall effect on current distribution in, (T), 25:55949
magnetohydrodynamic duct, shock-wave propagation in, (E), 25:55951
magnetohydrodynamic extendable channel, electromagnetic fields in induction, 25:55939
magnetohydrodynamic heavy viscous incompressible, infinitely conducting, rotating, equilibrium in vertical magnetic field of, 25:55917
magnetohydrodynamic inviscid perfectly conducting, past thin body in transverse magnetic field, (T), 25:55929
magnetohydrodynamic turbulent, double correlation equations of magnetic field and velocity in isotropic conducting, 25:55916
magnetohydrodynamic turbulent, effect of longitudinal magnetic field on hydraulic resistance in pipes on, (E/T), 25:55937
magnetohydrodynamic, at high Hartmann number, review of, 25:55921
magnetohydrodynamic, coefficient of electromagnetic ejection of solids from, (E/T), 25:55930
magnetohydrodynamic, convective motion in transverse magnetic field in, (T), 25:55948
magnetohydrodynamic, dynamics of liquid-metal drops in conditions of reduced gravitation, 25:55931
magnetohydrodynamic, effect of transverse magnetic field on intensity profiles in turbulent velocity fluctuations in rectangular pipes, (E/T), 25:55926
magnetohydrodynamic, effects of crossed electric and magnetic fields on boundary layer in, (T), 25:55934
magnetohydrodynamic, electric field in rectangular duct with end electrodes, (T), 25:55950
magnetohydrodynamic, equations for magnetostatic equilibria and associated time-dependent resistive flows, 25:55940
magnetohydrodynamic, induced by impulsive rotation of infinite disc, (T), 25:55947
magnetohydrodynamic, mass transfer considering chemical reaction kinetics at boundaries, (T), 25:55932
magnetohydrodynamic, rotation in crossed fields of electrically conducting, (T), 25:55938
magnetohydrodynamic, slow rotation of axisymmetric solids in, (T), 25:55941
magnetohydrodynamic, stabilization of flutter instabilities by distributive control, (T), 25:55925
magnetohydrodynamic, suppression of convection in, (T), 25:55945
magnetohydrodynamic, temperature field in vortex chamber in axially symmetric, (T), 25:55933
magnetohydrodynamic, transition to turbulence with finite

perturbations, (T), 25:55927
magnetohydrodynamic, turbulent jet in longitudinal magnetic field, (T), 25:55928
magnetohydrodynamic, turbulent jets of conducting, (T), 25:55922
pressure distribution in, around roughness element, estimation of rough surface friction factor from measurements of, 25:54873 (RD/B/N-1967)
study of post-burnout two-phase, high-speed photographic method for, 25:54875 (RT/ING-(71)8)
temperature and velocity distribution in turbulent, in annular channel with roughened core rods, calculations of, 25:54874 (RD/B/N-1980)
velocity distribution in cylindrical Couette, method for calculating, 25:54888 (CONF-700557-5)
FLUIDIC DEVICES
design for sealing pressurized tubes in reactor steam generators, 25:54845(P)
FLUIDS
containment between two coaxial walls, design of fluid-tight device for, 25:54860(P)
motion of rotating, produced by temperature gradient perpendicular to gravitational and magnetic fields, (T), 25:55919
temperature distribution in moving, finite element method for calculation of, 25:54882
FLUORESCEIN
sodium salt, diffusion and deposition of, in atmosphere, 25:54795
FLUORESCEIN, TETRAIODO-
radiolysis of aqueous, absorption spectra studies of x, 25:54664
radiolysis of aqueous, reaction mechanisms for x, 25:55139
FLUORIDES
electrode for molten, development of nickel--nickel oxide reference, 25:54532 (ORNL-4717, pp 1-27)
separation from molten lithium chloride by reactions with boron trichloride, 25:54534 (ORNL-4717, pp 43-56)
solvent properties of molten, for boron trifluoride gas, 25:54532 (ORNL-4717, pp 1-27)
solvent properties of molten, for hydrogen, 25:54534 (ORNL-4717, pp 43-56)
sonic velocity of molten, estimation from absolute entropy of, 25:54532 (ORNL-4717, pp 1-27)
FLUORINATION
equipment for continuous, axial dispersion in, 25:54712 (ORNL-4682, pp 1-38)
equipment for continuous, development of frozen-wall, 25:54712 (ORNL-4682, pp 1-38)
FLUORINE
abundance in primary cosmic radiation, (E), 25:55911
determination by charged particle activation methods, optimum irradiation conditions and nuclear interferences for, 25:54520
determination in aluminum electrolytic bath by 14-MeV neutron activation simultaneously with aluminum and oxygen, 25:54503
hazards to man following release to environment, 25:55246 (CEA-Bib-200)
reactions with neptunium dioxide, plutonium dioxide--uranium dioxide, and uranium dioxide, kinetics of, 25:54736
FLUORINE ISOTOPES F-18
energy levels from resonances in oxygen-16 (d,α) reactions, (E), 25:56667
energy levels of, shell-model calculation with reaction matrices and pairing correlations, (T), 25:56666
production in alpha reactions with aluminum and silicon at 70 to 160 MeV, cross sections and fission mechanism for, (E/T), 25:56685 (FRNC-TH-48)
reactions of moderated recoil, with deuterium, hydrogen, deuterated methane, ethane, and trifluoroethane, rate of hydrogen abstraction, 25:54686
FLUORINE ISOTOPES F-19
deuteron reactions (d,p) at 10 MeV, angular distributions for, (E), 25:56716
photon reactions (γ,n) with, analysis by Feynman triangle diagrams of fine-structure peaks in cross sections for, (T), 25:56676
FLUORINE ISOTOPES F-20
energy levels from neon-20 (n,p) reactions, (E), 25:56717
energy levels of, spin--parity assignments for, (E), 25:56716
FLUOROBORATES
thermal decomposition of, mass spectrometric studies of, 25:54532 (ORNL-4717, pp 1-27)
tritium exchange in molten, 25:54534 (ORNL-4717, pp 43-56)
FLUOROCARBONS
radiolysis of, for gamma dosimetry, 25:55053
FOOD
radiation processing in United Kingdom, development of facilities for, 25:55363
FOOD CHAINS
radioisotope transport in marine, effects of physico-chemical form on, 25:55149 (BNWL-SA-4048)
tracer studies of soil and litter arthropod, 25:57281 (SRO-641-2)
FOOD IRRADIATION FACILITIES
design of gamma, for potatoes, 25:54837(P)
FORMALDEHYDE
transitions of normal and isotopic-species, 6-cm rotational, (E), 25:55732
FORMAMIDE
microwave emission from interstellar, detection of, (E), 25:55784
FORMIC ACID
reactions with tetravalent uranium in aqueous benzene solutions, stability constants for complex ions produced by, 25:54581
FRACTURE TESTS
stress analysis for, developments in three-dimensional elastic--plastic, 25:55515
FRANCE
neutron research at CEA in, during October 1969 to December 1970, 25:55203(R) (CEA-N-1449)
nuclear explosions in, program for peaceful uses of, 25:54819(T) (UCRL-Trans-10543, pp 1-3)
radiological accidents in, legal aspects of, 25:55252 (NP-18752)
regulations for overland shipping of sealed gamma sources for radiography, 25:54976
research on heat transfer in, for nuclear programs, 25:54865 (CEA-CONF-1758)
thorium deposits in Vosges Mountains of, effects of thorite and zircon on geochemistry of, 25:54807
uranium deposits in Vosges Mountains of, effects of thorite and zircon on geochemistry of, 25:54807
FREE RADICALS
production of radiolytic, by fast reaction flow systems in aqueous solutions, ESR studies of, 25:54662
radioinduced production in deuterated and normal glycine monocrystals, ESR studies on x, 25:54653
radioinduced production in potassium hydrogen malonate monocrystals at 4.2°K, ESR spectral studies on x, 25:54654
radioinduced production in single crystals of thymine, γ, 25:55130
radioinduced production in vinyl monomers, ESR study of gamma, 25:54634
reactions in photolysis and radiolysis of branched alkane glasses, 25:54648
FREQUENCY STANDARDS
calibration of primary, 25:57296 (Y-IA-92)
FUEL CAPSULES
design and fabrication of SNAP-19B, 25:54893 (MLM-1736)
FUEL CELLS
performance of thin-film, using calcium oxide-stabilized zirconium dioxide, 25:55596
FUMARIC ACID
potassium salt, radiolysis of, radical pair formation in, 25:54665
salts of, radiolysis of aqueous solutions of, ESR studies of radicals from electron, 25:54656
FURNACES
ironmaking in blast, uses of radioisotopes for process studies of, 25:54906
FUSED SALTS
corrosive effects on reactor materials, conference on, 25:55371 (CONF-690452)
production of, for MSR program, 25:54534 (ORNL-4717, pp 43-56)
purification of, equipment and methods for continuous, 25:54712 (ORNL-4682, pp 1-38)

## G

GADOLINIUM
determination of trace amounts of, in nuclear grade uranium by x-ray excited optical fluorescence, 25:54428
lattice parameters of, effects of hydrogen on, 25:55549
separation from aqueous solutions by solvent extraction using TTA, synergistic effects of 2,4-pentanedione on, 25:54731
separation from neodymium and samarium by liquid--liquid chromatography using bis(2-ethylhexyl) phosphate and sulfuric acid, 25:54745
x-ray absorption edges of, positions of L/sub III/, (E), 25:55822
GADOLINIUM ALLOYS AND SYSTEMS
Au--Gd, crystal structures and melting points of intermetallic, 25:55570
Ce--Gd--Ru, critical magnetic field in superconducting, (E), 25:56074
Gd--Mg, compound formation in, vapor pressure measurements for studies of thermodynamics of, 25:55525 (IS-T-462)
GADOLINIUM CHLORIDES
x-ray absorption edges of, chemical shifts of, (E), 25:55822
GADOLINIUM ISOTOPES Gd-157
energy levels of, model analysis for ΔN = 2 mixing in, (T), 25:56737 (JINR-E4-5877)
GADOLINIUM ISOTOPES Gd-159
energy levels of, model analysis for ΔN = 2 mixing in, (T), 25:56737 (JINR-E4-5877)
GADOLINIUM ISOTOPES Gd-161
energy levels of, model analysis for ΔN = 2 mixing in,

XUM

(T), 25:56737 (JINR-E4-5877)
GADOLINIUM OXIDES
dysprosium-161 Moessbauer spectrum in, hyperfine structure in, 25:56375
x-ray absorption edges of, chemical shifts of, (E), 25:55822
GALAXIES
energy curves and K corrections for giant elliptical, absolute, (E), 25:55794
H II regions in LMC, kinematic properties of 71, (E), 25:55795
hydrogen distribution in M33, (E), 25:55796
infrared emission from, (T), 25:55908
light deflection by gravitational field of cluster of, (T), 25:55809
light from giant elliptical, energy distributions and K-corrections for total, (E), 25:55793
mass of M33, (E), 25:55796
matter in Coma Cluster of, intergalactic, (E), 25:55782
models for nuclei of, containing black holes, (T), 25:55803
particle densities in clusters of, (E), 25:55789
radio emission from nebulae in Magellanic Clouds at 408 MHz, (E), 25:55722
radio observations of Coma and Hercules clusters of, (E), 25:55789
rotational velocity in spiral, radius of maximum, (T), 25:55786
stars in LMC, light variations of supergiant, (E), 25:55705
x-ray emission from Coma Cluster of, cosmological implications of, (E/T), 25:55806
GALLIUM
analysis for chlorides, photometric, 25:54407
determination in meteorites and meteoritic phases by neutron activation and γ spectrometry, 25:54477
effects on solvolysis of tert-butyl halides, Broensted correlation for, 25:54548
separation of uranium from, in methyl sulfoxide by cation exchange chromatography, 25:54728
GALLIUM ALLOYS AND SYSTEMS
Al--Ga--Ni, optical constants for β-phase NiGa/sub 1-y/Al/sub y/ intermetallic compound in, 25:56352
Cu--Ga--Ni, optical constants for β-phase in, 25:56352
Ga--Pu-base, tensile properties of, at 25 to 500°C, effects of strain rate and temperature on, 25:55427 (BNWL-1567)
Ga--transition metals--V, properties of ternary phases of, 25:55500
Ga--V-base, properties of deformed superconducting, 25:56100
GALLIUM ARSENIDES
analysis of epitaxial films of, for impurities by neutron activation and radiochemical separation, 25:54512
ion implantation in, 40-keV sulfur, 25:56288
ion-implantation lattice damage in, reflectivity and scanning electron microscopic studies of 60-keV cadmium, 25:56287
ion-implantation-induced lattice disorder in, proton-channeling study of 140-keV-zinc and 151-keV xenon, 25:56289
radiation effects on carrier properties of heavily doped silicon- and tellurium-doped n-type, 1-MeV-electron, 25:56292
GALLIUM HYDROXIDES
preparation of α-GaOOH, high-pressure hydrothermal method for, 25:55602
GALLIUM ISOTOPES Ga-66
energy levels from zinc-66 (p,nγ) reactions, spin--parity assignments for, (E), 25:56732
energy-level transitions from zinc-66 (p,nγ) multipolarities and branching ratios for reactions, (E), 25:56732
GALLIUM ISOTOPES Ga-67
effectiveness for diagnosis of human bronchial and thyroid carcinomas and reticulum cell sarcomas, 25:55283
GALLIUM ISOTOPES Ga-70
energy levels from gallium-69 (d,p) reactions, (E), 25:56752(R) (SUNI-14)
GALLIUM NITRIDES
shock compression effects on powdered, x-ray-diffraction study of, 25:55618
GALLIUM PHOSPHIDES
ion implantation in, 40-keV sulfur, 25:56288
GAMMA CAMERAS
development using liquefied noble gases in ionization detectors, possibilities for, 25:55028
GAMMA RADIATION
angular distribution from polarized nuclei, system for measuring, 25:55089
detection of, design and construction of self-powered detector for, 25:55011(P)
detection of, design and performance of combined solar battery--scintillation detector for, 25:55005
dose distribution calculations for therapeutic, development of computer program for cobalt-60, 25:55220
dose distribution for teletherapy, development of digital computer method for cobalt-60, 25:55221
dose distributions in rabbit and rat phantoms following exposure to monoenergetic neutron beams, correlation of LET distributions and, 25:55229
dose from radioactive clouds, air attenuation and photon energy in calculation of, 25:54796
dose from radioactive clouds, calculation of, 25:54797
dose rates in uranium radiation loops, calculation of, 25:54991
dose to man following accidental exposure to iridium-192, use of chromosome aberration frequency in biological dosimetry of, 25:55228
dose to man from irradiation facilities, use of aluminum phosphate dosimeter data in calculations of, 25:55235
dose to man in Japan from external occupational exposures, estimation of genetically significant equivalent, 25:55230
dose to organs of mice following inhalation of niobium-95 and zirconium-95, effects of chemical form of inhaled particles on, 25:55125
dosimetry for standardization of pendular pelvic therapy, 25:55222
dosimetry in bulk grain irradiator, performance of encapsulated LiF dosimeter for, 25:55234
dosimetry of, design of solid-electrolyte dosimeter for, 25:55054(P)
dosimetry using tissue-equivalent wall-less proportional detectors, 25:55002 (NYO-2740-8, pp 7-146)
effectiveness for therapy of squamous epithelial cancer of mouth in comparison with ametohepazon, beta particles, 5-fluorouracil, and radium, 25:55345
effects of terrestrial, on vertical distribution of ionization in atmosphere, 25:54790
effects on 1,3-butadiene adsorbed on silica gel, ESR studies of radicals from, 25:54640
effects on 1,3-butadiene single crystals, ESR studies of radicals from, 25:54639
effects on acetic acid solutions of sodium nitrate, effects of diazo reagents on, 25:54657
effects on adhesive properties of epoxy resin in glass--glass and metal--metal joints, 25:55666
effects on alcohols, production of aliphatic aldehydes by, 25:54625(P)
effects on alkaline aqueous glasses, 25:54627 (CONF-700652-(Vol.2), pp 295-330)
effects on aqueous solutions of alkali hydroxides, ESR studies of ozonide ion formation from, 25:54608
effects on aqueous solutions of alkali hydroxides, reply to paper on formation of ozonide ions from, 25:54609
effects on aqueous solutions of sulfuric acid and cerium sulfate, reactivity of tetravalent cerium from, 25:54647
effects on benzoatopentaamminecobalt perchlorate, oxidation of benzoatopentaamminecobalt(III) of hydroxyl radical from, 25:54669
effects on black silicon-carbide varistors, gas desorption in, 25:55102
effects on blood cell chromosomes of industrial personnel following occupational exposure, 25:55163
effects on blood vessels in chickens in relation to mechanisms of acute injury, whole-body exposure, 25:55324
effects on bovine fascia for transplantation in dog brains for filling of defects in dura mater, 25:55148
effects on branched alkane glasses, identification of free radicals from, 25:54648
effects on chromosomes in blood of mice, extrapolation to man of protective effects of cystamine against aberrant, 25:55256
effects on chromosomes of Crepis capillaris seeds, incidence of premutational oxygen-sensitive changes following, 25:55168
effects on chromosomes of Drosophila males, cytological analysis of aberrant, 25:55170
effects on clasmatocyte count in lymph nodes, spleen, and thymus of mice, 25:55321
effects on crystalline alkali metal azides, bromates, and nitrates, 25:54638
effects on crystalline sodium nitrate, 25:54649
effects on cuttings and powders of crystalline polyethylene, effects of dose and sample size on, 25:54623
effects on cyclopentane--nitrous oxide solutions, effects of cyclopentene and propene on yields from, 25:54655
effects on DDT, toxicity to rats of products formed following, 25:55135
effects on dechlorination of 1,1,1-trichloro-2,2-bis(p-chlorophenyl)ethane, 25:54620
effects on dielectric properties of mica insulators, 25:55101
effects on diploid yeast cells, mutagenic, 25:55165
effects on DNA and RNA synthesis in mouse kidney cells synchronized by medium change, 25:55129
effects on donor ability of recA and recA+ strains of Escherichia coli, 25:55358
effects on electronic properties of anodized aluminum electrode, 25:54601
effects on external respiration in man following therapy of malignant chest tumors, 25:55339
effects on eyes of rabbits, effects of dose and LET on RBE for, 25:55317 (CEA-CONF-1744)
effects on gaseous ethylene, effects of ethanol, ethyl ether, and methyl ether on, 25:54643
effects on genetic variation in lizard populations in

Nevada, 25:55320
effects on germanium, luminescence spectra from defects induced in, 25:56328
effects on graft copolymerization of lignin and styrene, 25:54614
effects on grafting of acrylonitrile on poly(vinyl chloride), effects of dose on, 25:54613
effects on hatchability of Artemia eggs, relation between production of free radicals and protective effects of MEA against, 25:55262
effects on human nervous system following therapy of head tumors, prophylaxis and treatment of pathological, 25:55269
effects on in vitro uptake of α-aminoisobutyric acid and cycloleucine by rat liver, 25:55126
effects on incidence of chromosome translocations in mouse spermatogonia, RBE for, 25:55182
effects on incidence of osteonecrosis in human jaw following tumor therapy, 25:55344
effects on incidence of single-strand breaks in double-stranded circular DNA, effects of dose on, 25:55133
effects on linseed, dose dependence of mutagenic, 25:55177
effects on liquid butane and deuterated butane--butane mixtures, effects of scavengers on yields from, 25:54659
effects on liquid cyclohexane, kinetics of charge scavenging in, 25:54668
effects on liquid ethanol, yields of hydrogen and free ions from, 25:54660
effects on lithium-compensated boron-doped silicon, annealing of defects induced in, 25:56293
effects on longevity and reproduction of grain moths, effects of dose on, 25:55315
effects on low- and high-pressure polyethylene films, 25:54604
effects on low-resistivity n-type germanium, recombination of defects induced in, 25:56327
effects on mechanical properties of cured epoxy resins, 25:55667
effects on N-acetylglycine in the presence of ammonia, 25:54650
effects on nutritive properties of beef, 25:55367
effects on phosphorus oxychloride, ESR spectra of radical anion from, 25:54667
effects on polymerization of 2-methylpropene compounds, comparison of molecular weight distribution of products produced by, with that of chemically initiated products, 25:54621
effects on polymerization of acrylonitrile, comparison of structure of products produced by, and chemically initiated products, 25:54622
effects on polymerization of gaseous and liquid fluoroethylene, comparison of properties of products produced by, and those of chemically initiated products, 25:54624
effects on polymerization of methane, ethane, and ethylene, 25:54615
effects on population dynamics of freshwater snails following chronic low dose rate exposure, 25:55314
effects on potassium fluoride--silver nitrate and silver nitrate ices, EPR studies of neutral silver trapping sites from, 25:54666
effects on propene polymers, effects of ethylene and nitrous oxide on, 25:54637
effects on pupae of cotton spotted bollworm, 25:55368
effects on reproduction and survival of progeny of adult male grain moths, effects of dose on, 25:55316
effects on response of rats to tranquilizers following whole-body exposure in mixed neutron fields, 25:55325
effects on RNA polymerase activity in sugar beets, effects of dose and washing on, 25:55351
effects on salts, impurity paramagnetic center appearance in, 25:56339
effects on seed yield of lima beans, effects of developmental stage on, 25:55349
effects on seeds of Crepis capillaris, effects of water content on mutagenic, 25:55167
effects on shelf life of Pacific Coast fish following shipboard exposure, 25:55366
effects on silicon p--n junctions, (E/T), 25:55095(R) (COO-1624-41)
effects on silver nitrate on porous glass or silica gel surfaces, ESR studies of, 25:54606
effects on silver nitrate on porous glass or silica gel surfaces, ESR studies of, 25:54607
effects on single crystals of thymine, 25:55130
effects on sodium acetate crystals, ESR studies on trapped $CH_2CO^-$ radicals produced by, 25:54652
effects on sprouting, spoilage molds, and sugar content of garlic bulbs, 25:55354
effects on supercooled water, yields from, 25:54663
effects on survival of hamster cells, effects of dose on RBE for, 25:55207 (NYO-2740-8, pp 220-59)
effects on survival of Salmonella species in smoked lake whitefish, effects of dose on, 25:55365
effects on swine following bilateral and unilateral exposures, LD-50 for lethal, 25:55334
effects on telomerization of ethylene by propionic acid, 25:54612
effects on thallium sulfate, yields of hydrogen peroxide from, 25:54646
effects on tissues of goats, pathology of, 25:55318(T)
(LB/G-2995)
effects on vinyl monomers at 77°K, ESR study of radicals induced in, 25:54634
energy scale for, comparison with α-particle energy scale, 25:56773
flux in statistically inhomogeneous medium, Monte Carlo method of calculating, 25:56268
flux of, from solar flares, (T), 25:55762
isotropy of cosmic background, between 1 and 6 MeV, (E/T), 25:55896 (N-71-27639)
monitoring for heavy water moderated research reactor fuel element failure detection system, 25:57118 (JAERI-Memo-4157, pp 44-50)
monitoring in environment of nuclear power plant, design and performance of amphibious detection system for in situ, 25:55239
penetration of concrete shield, energy and angular distributions of cobalt-60, (E), 25:56272
properties of secondary, produced by neutron reactions with shielding, 25:56277
reactions (γ,n) with helium-4 at threshold to 31 MeV, cross section for, (E), 25:56649
reactions with intermediate nuclei, cross sections for, (E), 25:56782
scattering by americium-243, production of spontaneously fissioning isomers in inelastic, (E), 25:56738 (JINR-P15-5959)
scattering by plutonium-239, production of spontaneously fissioning isomers in inelastic, (E), 25:56738 (JINR-P15-5959)
transmission through homogeneous concrete slabs, (T), 25:56256 (AD-722012)
transport code for, revised cross-section module for Monte Carlo multigroup, 25:56263 (ORNL-4716)
transport method for shielding calculations, three-dimensional stochastic, (T), 25:56273
transport studies, (E/T), 25:56255(R) (AD-721388)
use for therapy of lung and thoracic lymph node metastases, 25:55300
use for therapy of lymphogranulomatosis of bones, 25:55301

**GAMMA SOURCES**
activity measurements of low-level, crystal scintillation detector design optimization for, 25:55024
development of economical high-intensity, for industrial irradiation plant, 25:54914
dose distribution around sealed linear radium, electronic calculations for, 25:54923
gamma energies and intensities for radium-226, for efficiency calibration of lithium-drifted germanium detectors, 25:55041 (ORNL-TM-3509)
Monte Carlo transport analysis for finite ground-distributed, 25:56260 (EGG-1183-2284)
shipping of sealed, for radiography, French regulations for overland, 25:54976
use of cobalt-60, for commercial processing in United Kingdom, 25:55363

**GAMMA SPECTROMETERS**
data acquisition and processing system for, on-line computer, 25:54474
data processing system for, combined computer peaksearch and peakfit in, 25:54472
design of electron--positron pair, for neutron capture spectroscopy, 25:55040 (NP-18994)
performance of airborne, for measuring radioisotope content of soils, 25:54768

**GAMMA SPECTROSCOPY**
isomer shifts in Moessbauer, calibration of, (T), 25:56370
pulse-height spectra unfolding techniques for, 25:54436 (ORNL-TM-3463)
spectra analysis for calculating nuclide abundances, computer program for, 25:55035 (DP-1275)
use for well logging in presence of radon, (E), 25:54759

**GARIGLIANO POWER REACTOR**
fuel assemblies for, burnup and heavy isotope content of irradiated, (E/T), 25:56879 (EUR-4638)

**GAS CENTRIFUGES**
economic aspects of uranium enrichment using, Swedish studies on, 25:54921
efficiency of partially ionized plasma, method for improvement of, 25:54912
flow and temperature in, calculations of, 25:54891(T) (K-Trans-61-5)
flow in, method for calculating velocity distribution in, 25:54888 (CONF-700557-5)
flow through one-dimensional, calculation of radial, 25:54890(T) (K-Trans-61-3)

**GAS CHROMATOGRAPHY**
method for fuel element failure detection system, development of, 25:57193 (JAERI-Memo-4157, pp 66-83)

**GAS FLOW**
magnetohydrodynamic channel, calculations of, 25:55935
magnetohydrodynamic duct, boundary layer in absence of ionization equilibrium in, 25:55946
magnetohydrodynamic two-dimensional unsteady, classification of invariant solutions of equations of, 25:55924
magnetohydrodynamic wave generation in nonhomogeneous plasma in strong magnetic field, (T), 25:55923


XUM

magnetohydrodynamic, discontinuity in solution of optimum problems in, (T), 25:55936
magnetohydrodynamic, in inductive shock wave tubes, (E), 25:55920
GASEOUS DIFFUSION PROCESS
economic aspects of uranium enrichment using, Swedish studies on, 25:54921
GASES
alpha-particle energy loss and straggling in tissue-equivalent, (E/T), 25:56279
collision integral for particles of disparate mass, 25:56179
neutrino emission from, due to propagation of relativistic shock waves, (T), 25:55668
GENES
effects on uv radioinduced site reversion in yeast mutants, 25:55187
radiation effects on order of, in chromosomes of Schizophyllum mutants, uv, 25:55186
GENETICS
abstracts of papers presented at 1971 meeting of Genetics Society of America, 25:55166
book: Genetics Lectures, Volume 2, 25:55179
GEOCHEMISTRY
activation analysis in, development of epithermal neutron, 25:54468
activation analysis in, review of routine, 25:54463
book: Essays on the Geology and Geochemistry of Ore Deposits, 25:54763
book: Lead Isotopes in Geochemistry and Cosmochemistry, 25:54770
conference on activation analysis in cosmochemistry and, Kjeller, Norway, September, 1970, 25:54457
GEOLOGY
book: Essays on the Geology and Geochemistry of Ore Deposits, 25:54763
GEOMAGNETIC FIELDS
activity index for 1932--70, frequency tables for Kp, 25:56017
activity of, correlation patterns with radiation-belt electron intensity, (E/T), 25:55979
activity of, correlation with intensity of interplanetary magnetic field, (E), 25:56007
depression in Earth core and Earth surface and in magnetotail, during magnetic storms, (E/T), 25:56002
disturbances in, produced by nonstationary source of γ quanta, rapidly varying, (T), 25:55989
effects on midlatitude sporadic E, (E/T), 25:56015
intensity at 100 to 500 km in ionosphere, computation of total vector of real, 25:55990
magnetic-shell parameter L for point in, new approximation of, (T), 25:56041
pulsations in, relationship of Pc-type steady Earth-current, with magnetosphere and solar-wind parameters, (E/T), 25:56004
relation with magnetospheric field deformation, (E), 25:55952 (N-71-27604)
solar-wind interaction with dipole model of, 25:56009
variations at Earth surface and in ionosphere, out-of-phase phenomena of solar diurnal, (E/T), 25:56036
variations at Earth surface and in ionosphere, out-of-phase phenomena of lunar diurnal, (E/T), 25:56037
variations of, effect of sector structure of interplanetary magnetic fields on, (E/T), 25:55988
GERMANIUM
alpha fission at 167 MeV, angular distributions and particle track lengths for, (E), 25:56806
analysis for oxygen by helium-3 activation and radiochemical separations, 25:54502
argon-ion reactions at 30 keV with surfaces of, charge states and kinetic energies of scattered and recoil ions from, (E), 25:55818
determination in meteorites and meteoritic phases by neutron activation and γ spectrometry, 25:54477
ion implantation in, 40-keV sulfur, 25:56288
radiation damage in lithium-doped n-type, 1-MeV-electron, 25:56301
radiation damage in n-type, effects of donor impurity on 35 and 65°K stages in annealing of electron, 25:56330
radiation damage in n-type, effects of impurities on annealing of 65°K in 1-MeV-electron, 25:56331
radiation effects on p-type, annealing of 77°K 14-MeV-neutron, 25:56305
radioinduced defects in low-resistivity n-type, study of recombination of γ-, 25:56327
radioinduced defects in p-type, 220°K stage in annealing of 1.5-MeV-electron, 25:56300
radioinduced defects in p-type, annealing at 77°K of 1.5-MeV-electron, 25:56329
radioinduced defects in p-type, electric properties and annealing of 8°K 1-MeV-electron, 25:56302
radioinduced defects in, Moessbauer-type structure in luminescence spectra of electron- and γ-, 25:56328
radioinduced defects in, review of studies of low-temperature, 25:56303
radioinduced interstitial phosphorus in phosphorus-doped n-type, EPR study of 1.5-MeV-electron, 25:56299
radioinduced one-valley EPR spectrum in antimony-doped, 2.5-MeV-electron, 25:56298
radioinduced photocurrent oscillations in n-type, fast-neutron and proton, 25:56316
GERMANIUM ALLOYS AND SYSTEMS
Al--Ge--V, phase formation in $V_3Al/sub\ x/Ge/sub\ 1-x/$ with A15 structure, 25:55539
Cu--Ge, superconductivity in hcp phases of, (E), 25:56096
Ge--Si, fabrication of thermoelements of, hot pressing method for, 25:57267 (SC-DR-710438)
GERMANIUM ISOTOPES Ge-64
binding energy, deformation, and single-particle spectra for, self-consistent calculation using Yukawa and Kuo-Brown matrix elements, (T), 25:56720
GERMANIUM ISOTOPES Ge-66
binding energy, deformation, and single-particle spectra for, self-consistent calculation using Yukawa and Kuo-Brown matrix elements, (T), 25:56720
GERMANIUM ISOTOPES Ge-68
binding energy, deformation, and single-particle spectra for, self-consistent calculation using Yukawa and Kuo-Brown matrix elements, (T), 25:56720
GERMANIUM ISOTOPES Ge-70
binding energy, deformation, and single-particle spectra for, self-consistent calculation using Yukawa and Kuo-Brown matrix elements, (T), 25:56720
GERMANIUM ISOTOPES Ge-72
binding energy, deformation, and single-particle spectra for, self-consistent calculation using Yukawa and Kuo-Brown matrix elements, (T), 25:56720
GLASS
age of ancient, fission track method for estimation of, 25:54761
age of man-made and volcanic, fission track method for estimation of, 25:54771
analysis for aluminum, boron, and sodium in, by simultaneous measurement of scattered α particles and prompt protons, 25:56752(R) (SUNI-14)
analysis for boron in, by measurement of prompt proton spectra from (d,p) reactions, 25:56752(R) (SUNI-14)
analysis of borate, for boron by neutron absorption method, 25:54437(T) (RFP-Trans-82)
analysis of natural, for tin by neutron activation using 40-min tin-123, 25:54480
diffusion in, data tabulations on, 25:55509
diffusion of radioactive cesium, rubidium, sodium, and strontium in, effects of temperature on, 25:55611
radiation effects on adhesion of epoxy cemented specimen couples of, gamma, 25:55666
radioactive waste storage in, safety of high-level, 25:54969 (JUL-766-CT)
GLAZES
composition, deposition, and properties of aluminosilicate, for vitroceramic fuel elements, 25:55613
GLOVE BOXES
air leakage into, effects on plutonium inert gas atmosphere processing, 25:54944 (CONF-710401-, pp 83-97)
atmosphere control in Battelle plutonium facility, 25:54959 (CONF-710401-, pp 280-92)
atmosphere system for, surveillance of inert argon--nitrogen, 25:54945 (CONF-710401-, pp 98-105)
design for use at HAPO, personnel considerations in, 25:54938 (CONF-710401-, pp 4-16)
filter changes in, description of contamination control valve for minimizing, 25:54958 (CONF-710401-, pp 258-66)
filters for plutonium-238 handling, description of, 25:54949 (CONF-710401-, pp 149-61)
fire detection system for, development of, 25:54955 (CONF-710401-, pp 221-36)
fire extinguishing system for nonmetals in, design of automatic, 25:54954 (CONF-710401-, pp 212-20)
fire protection in plutonium, description of system for, 25:54948 (CONF-710401-, pp 133-48)
gloves for, evaluation of properties of, 25:54941 (CONF-710401-, pp 44-55)
materials for construction of, evaluation of, 25:54940 (CONF-710401-, pp 26-43)
materials for fire-resistant, equipment and methods for testing, 25:54939 (CONF-710401-, pp 17-25)
operation of, design and construction material selection for safe, 25:54940 (CONF-710401-, pp 26-43)
protection from overpressure, description of manometer for, 25:54958 (CONF-710401-, pp 258-66)
GLUCOSE, 2-AMINO-2-DEOXY-
incorporation of carbon-14-labeled, into synaptosomes in vitro, 25:57260 (ORO-3195-48)
GLUTEN
radiation effects on amino acid content of processed wheat, 25:55364
GLYCERALDEHYDEPHOSPHATE DEHYDROGENASE
radiation effects on activity of algae, x, 25:55353
GLYCINE
radiolysis of single crystals of deuterated and normal, at low temperature, ESR studies on free radicals produced by x, 25:54653
GLYCINE, N-ACETYL-
radiolysis of aqueous solutions of, in presence of ammonia, electron, γ, and uv, 25:54650
GLYCOGEN
metabolism in radioinduced osteosarcomas in rats, 25:55335

GOATS
radiation injuries to tissues of, pathology of gamma, 25:55318(T) (LB/G-2995)
GOLD
argon-ion reactions at 30 keV with surfaces of, charge states and kinetic energies of scattered and recoil ions from, (E), 25:55818
determination in Australian tektites by thermal neutron activation and radiochemical separations, 25:54478
determination in geochemical samples by neutron activation, 25:54484
determination in geological materials by neutron activation, 25:54488
determination in geological sample by neutron activation and radiochemical separations, 25:54485
determination in meteorites and meteoritic phases by neutron activation and γ spectrometry, 25:54477
determination in ores and rocks by neutron activation of lead alloy obtained in cupel assay, 25:54521
effects on annealing of Frenkel defects in irradiated platinum, 25:56284 (JUL-731-FF)
separation from aqueous solutions by solvent extraction using tribenzylamine, 25:54515
GOLD ALLOYS AND SYSTEMS
Au--Al, search for superconductivity in fcc phases of, (E), 25:56096
Au--Cd, search for superconductivity in fcc phases of, (E), 25:56096
Au--Ce, crystal structures and melting points of intermetallic, 25:55570
Au--Dy, crystal structures and melting points of intermetallic, 25:55570
Au--Er, crystal structures and melting points of intermetallic, 25:55570
Au--Gd, crystal structures and melting points of intermetallic, 25:55570
Au--Ho, crystal structures and melting points of intermetallic, 25:55570
Au--In, search for superconductivity in fcc phases of, (E), 25:56096
Au--In, superconductivity in hcp phases of, (E), 25:56096
Au--La, crystal structures and melting points of intermetallic, 25:55570
Au--Lu, crystal structures and melting points of intermetallic, 25:55570
Au--Nb, niobium-93 NMR in $Nb_3Au$, 25:56373
Au--Nd, crystal structures and melting points of intermetallic, 25:55570
Au--Pr, crystal structures and melting points of intermetallic, 25:55570
Au--Pr-base, phase diagram of, 25:55567
Au--Pr-base, phase diagram of, thermodynamic analysis of, 25:55566
Au--Sm, crystal structures and melting points of intermetallic, 25:55570
Au--Sn, superconductivity in hcp phases of, (E), 25:56096
Au--Tb, crystal structures and melting points of intermetallic, 25:55570
Au--Tm, crystal structures and melting points of intermetallic, 25:55570
Au--V, magnetic properties of, 25:56358
Au--Yb, crystal structures and melting points of intermetallic, 25:55570
Au--Zn, search for superconductivity in fcc phases of, (E), 25:56096
GOLD ISOTOPES Au-190
beta and electron-capture decay of, conversion electron spectra from, (E), 25:56760
GOLD ISOTOPES Au-197
ion elastic scattering in wide energy range, phase shift analysis of angular distributions for, (E), 25:56740 (JINR-P7-5884)
neutron capture by, range of recoil atoms from, 25:56269
neutron reactions using iron-filtered beams, analysis of resonance cross sections for, 25:56795
GOLD ISOTOPES Au-198
effectiveness for human liver scanning in comparison to alkaline phosphatase evaluation and histological studies, 25:55276
effectiveness for scanning parasternal lymph nodes in patients with mammary carcinomas, 25:55288
recoil from gold-197(n,γ) reaction, ranges of, 25:56269
use for estimating late x radiation effects on circulation in brain, liver, lungs, and skin of rats, 25:55328
GRANITES
damage to surrounding Sahara, from Monique nuclear explosion, evaluation of mechanical, 25:54820(T) (UCRL-Trans-10543, pp 4-35)
seismic shock propagation in, comparison of experimental and calculated data on, 25:57287 (UCRL-51075)
GRAPHITE
corrosion by high temperature steam, 25:57092(R) (ORNL-TM-3483)
development for molten salt reactor, use of high-temperature centrifugation in, 25:54534 (ORNL-4717, pp 43-56)
diffusion of methane in moderator, mathematical model of, 25:57044
electron band structure of, electron-emission study of, (E), 25:56348
fission product distribution in MSRE moderator, 25:54533 (ORNL-4717, pp 29-41)
gas diffusion in MSRE moderator, 25:54533 (ORNL-4717, pp 29-41)
magnetoresistance in boronated and neutron-irradiated, 25:56319
permeability of extruded, gas flow method for measurement of, 25:55612
radiation effects on Dragon high-temperature, 25:55651
radiation effects on mechanical properties of, viscoelastic analysis of neutron, 25:55646 (EUR-4674)
radiation effects on properties of needle-coke, relation of pitch-binder content with fast neutron, 25:55653
radioinduced surface oxidation in carbon dioxide, 25:55655
radiolytic gasification in carbon dioxide, effects of active species range and water vapor on, 25:55654
sorption reaction with fission-product cesium-rubidium mixtures at high temperatures, 25:55623
stresses in high temperature gas cooled reactor fuel tubes, (E/T), 25:57051
thermal conductivity of polycrystalline, effects of boron and bromine doping on, 25:55635
GRAVITATION
forces between disks and cylinders, Lense--Thirring, (T), 25:55807
formalism of tetrad theory of, reference systems in, 25:56568
redshift in theory of generalized gravitational potential, (T), 25:55808
theories of, principle of equivalence in scalar--tensor, 25:56569
GRAVITATIONAL FIELDS
energy tensor of Einstein linear, resting liquid sphere in phenomenological, (T), 25:56565
fluid motion produced by perpendicular temperature gradient of, in magnetic field, rotating, (T), 25:55919
light deflection by, associated with clusters of galaxies, (T), 25:55809
Schwinger equations for, 25:56561
GRAVITATIONAL RADIATION
conversion to electromagnetic waves in static magnetic fields in vacuum, (T), 25:55805
density waves associated with first-order, second-order, (T), 25:55799
detection of, experiments for estimation of upper limit for muon shower signal in background in Weber detector for, (E), 25:56566
waves in closed universe, (T), 25:56570
GRAVITY WAVES
generation of atmospheric, by solar eclipse, (E/T), 25:56016
GROUND
motion at Tosco mine and tower stations from Rulison Event, (E), 25:54813 (PNE-R-51)
motion from San Fernando earthquake, predictions for Glendale area, 25:54812 (NVO-1163-TM-30)
GROUND WATERS
radioisotope content of USSR, effects of earthquakes on, 25:54775
GROUP THEORY
conformal, nonlinear realizations for breaking of, 25:56549 (ORO-3992-9)
Lie groups in, survey of use in atomic spectroscopy, 25:55882 (NYO-1447-64)
Lorentz covariance in, general, 25:56558
nuclear structure in, lectures on, 25:56838 (UR-875-350)
Poincare group in, representations as functions of eigenvalues of Casimir operators in, 25:56534 (KFKI-71-38)
GUANIDINE, NITROSO-
effects on spontaneous recombination frequency of chromosomes of diploid yeast, 25:55180
GUINEA PIGS
sensitivity to transverse acceleration, effects of radioprotective compounds on, 25:55264
GUNDREMMINGEN POWER REACTOR
fuel element failure in, effects of $10^1/_2$ month operation on, 25:56924 (TID-25812)
inspection after $10^1/_2$ months of operation, findings of, 25:56924 (TID-25812)
maintenance during June 1971, 25:56924 (TID-25812)
maintenance during May 1971, 25:56916 (TID-25791)
operations during June 1971, 25:56924 (TID-25812)
operations during May 1971, 25:56916 (TID-25791)

## H

H.B. ROBINSON POWER REACTOR, UNIT 2
emergency core cooling system for, performance evaluation for, 25:56945 (DOCKET-50261-73)
HI REGIONS
distance to low-latitude high-velocity, method for determining, (E), 25:55717
distribution in M33, (E), 25:55796
distribution in Milky Way, 21-cm absorption study of, (E), 25:55791

XUM

HII REGIONS
distribution in M33, (E), 25:55796
infrared emission from dust grains in, (T), 25:55718
observations in NGC 2175, of bright condensation 3C 153.1, (E), 25:55681
properties of 71, in LMC, (E), 25:55795
HADRONS
energy of cosmic, at 3250 m above sea level, ionization spectrometer determination of, (E), 25:56413 (INP-756)
flux of cosmic, at 3250 m above sea level, ionization spectrometer determination of, (E), 25:56413 (INP-756)
form factors of, vector dominance model for weak interaction, (T), 25:56468 (FRNC-R-1)
interactions of, dual quark--parton model for, 25:56481
interactions with hadrons at high energies, research at Purdue Univ., June 1970 to May 1971, (E), 25:56424(R) (COO-1428-280)
interactions with hadrons, research at Stockholm Univ., 1970, (E), 25:56416(R) (USIP-71-1)
interactions with hadrons, review of Regge cuts for, (T), 25:56475 (RPP/C-24)
interactions with leptons, generalized Weinberg sum rules in deep inelastic, 25:56461
model for, pseudovector isospinor heavy-boson, 25:56477
production in photon reactions in Coulomb field of nuclei at high energies, 25:56457
reactions with stable and unstable hadrons, kinematic study of, (T), 25:56474 (FRNC-TH-63)
HAFNIUM
coating with zinc-plated aluminum silicide, corrosion protection by, 25:55398(P)
determination in Australian tektites by neutron activation and gamma spectrometry, 25:54478
determination in standard aluminum--silicon system by neutron activation, 25:54455
determination in volcanic ash by neutron activation and $\gamma$ spectrometry, 25:54513
determination in zircons by neutron activation and $\gamma$ spectrometry of hafnium-179m, 25:54491
effects on properties and sintering of tungsten at 1000 to 2000°C, 25:55453
electric conductivity of, temperature dependence of, 25:55445
enthalpy to 1400°K, 25:55445
preparation and uses of, newsletter on, 25:55406
HAFNIUM ALLOYS AND SYSTEMS
coating with zinc-plated aluminum silicide, corrosion protection by, 25:55398(P)
thermoelectric properties of, at 0 to 1000°C, 25:56351
C--Hf--Nb, phase diagram of niobium--rich corner of, 25:55563
C--Hf--Re--W, mechanical properties of, 25:55433 (N-71-23982)
C--Hf--Zr, thermodynamic properties of, 25:55614
Hf--Mo, nitriding of, mechanism of growth and loss of coherency of hafnium nitride precipitates during internal, 25:55460
Hf--Nb--Ti--Zr, superconducting properties of, with, 25:56104
Hf--Nb--Zr, superconducting properties of, 25:56105
Hf--Nb-base, oxygen solubility limits in, lattice parameter measurements of, 25:55568
Hf--Pr-base, phase diagram of, 25:55567
Hf--Si, properties of, thermochemical and thermophysical, 25:55644
Hf--Ta, hardening in monocrystals of, at 77 to 2000°K, solid-solution, 25:55457
Hf--Ta-base, oxidation behavior of polycrystals and single crystals of, at 750 to 1050°C, 25:55397
Hf--V, thermal capacity of superconducting intermetallic $HfV_2$, (E), 25:56072
HAFNIUM BORIDES
hafnium-isotope Moessbauer effect following Coulomb excitation by alpha particles, 25:56369
stability in acids, 25:54543
C--$HfB_2$, electric and thermal conductivity at 300 to 1300°K, 25:55627
C--$HfB_2$--SiC, electric and thermal conductivity at 300 to 1300°K, 25:55627
SiC--$HfB_2$, electric and thermal conductivity at 300 to 1300°K, 25:55627
HAFNIUM CARBIDES
hafnium-isotope Moessbauer effect following Coulomb excitation by alpha particles, 25:56369
physical properties and stability to nitrogen, 25:55629
HAFNIUM ISOTOPES Hf-173
energy levels from lutetium-175 (p,3n) reactions, high-spin rotational, (E), 25:56796
HAFNIUM ISOTOPES Hf-177
neutron capture up to 300 eV, $\gamma$ spectra and resonance spin assignments for, (E), 25:56751 (RT/FI-(70)55)
neutron reactions (n,$\alpha$) at 1.09 to 8.87 eV, $\alpha$ widths of levels in search for, (E), 25:56686 (JINR-P3-5875)
HAFNIUM ISOTOPES Hf-178
Moessbauer effect in hafnium compounds following Coulomb excitation by alpha particles, 25:56369
HAFNIUM ISOTOPES Hf-179
neutron capture up to 200 eV, $\gamma$ spectra and resonance spin assignments for, (E), 25:56751 (RT/FI-(70)55)
HAFNIUM ISOTOPES Hf-180
Moessbauer effect in hafnium compounds following Coulomb excitation by alpha particles, 25:56369
HAFNIUM NITRIDES
growth and loss of coherency of precipitates of, in hafnium--molybdenum alloy during internal nitriding, 25:55460
hafnium-isotope Moessbauer effect following Coulomb excitation by alpha particles, 25:56369
physical properties of, 25:55629
HAFNIUM OXIDES
thermal conductivity at high temperatures, 25:55637
$HfO_2$--$Y_2O_3$, thermal conductivity of solid solutions of, at high temperatures, 25:55637
$HfO_2$-base--$Y_2O_3$, properties as electrolyte, 25:56355
HAIR
plutonium-239 incorporation in rabbit, effects of dose on rate of, 25:55116
HALIDES
diffusion in, data tabulations on, 25:55509
uranium precipitation from molten, using molten zinc cathode, 25:54580
HAMSTERS
radioinduced chromosome aberrations in liver of Chinese, comparison of RBE for americium-241 $\alpha$ and cerium-144 $\beta$, 25:55188
radioisotope toxicity to Chinese, following intraperitoneal injection, comparison of americium-241 and cerium-144, 25:55188
HANDLING AND STORAGE
facility for plutonium, design of safe shielded, 25:54942 (CONF-710401-, pp 56-67)
HANFORD PRODUCTION REACTORS
fuel elements for, development of method for extrusion of internally and externally cooled, 25:55402 (RMI-L-48)
HARDNESS
determination of micro-, evaluation of quantitative image analyzer for, 25:57240 (MLM-OP-71007)
HARMONIC ANALYSIS
coefficients from unequally spaced data, 25:57250 (ORNL-TM-3547)
HARTLEPOOL POWER REACTORS
pressure vessels for, design of podded boiler type, (E/T), 25:56885
HEALTH PHYSICS
personnel qualifications for, in plutonium facility, 25:55204 (CONF-710401-, pp 267-79)
programs at Oarai Research Establishment in Japan during October through December 1970, 25:55247(R) (JAERI-Memo-4353)
reactor siting problems in, conference on, Vol. I, Idaho Falls, Idaho, Nov. 3 to 6, 1970, 25:57103
reactor siting problems in, conference on, Vol. III, Idaho Falls, Idaho, Nov. 3 to 6, 1970, 25:55193
reactor siting problems in, conference on, Vol. II, Idaho Falls, Idaho, Nov. 3 to 6, 1970, 25:55157
HEART
radiation effects on monkey fetus, 25:55207 (NYO-2740-8, pp 220-59)
radioinduced anomalies in chick embryo, additive effects of hypothermia on x, 25:55333
HEART, MECHANICAL
power system for, design of plutonium-238-fueled Stirling cycle, 25:54910(P)
HEAT
effects on respiration rate in wheat seedlings, 25:55348
HEAT EXCHANGERS
design of filter plenum, for radioactive processing buildings, 25:54950 (CONF-710401-, pp 162-80)
sodium boiling on surfaces of, effects of heating surface material and roughness on incipient, 25:54868(T) (EURFNR-897)
standard for design and performance of air-cooled, for nuclear steam-supplied systems, 25:54833 (RDT-E-4-18-T)
HEAT EXCHANGERS (LIQUID-LIQUID)
standard for fabrication and acceptance of shell and tube, 25:54832 (RDT-E-4-17-T)
HEAT-RESISTING ALLOYS AND METALS
book: Physical Metallurgy of Refractory and Rare Metals, 25:55438
corrosion by molten salts, conference on, 25:55371 (CONF-690452)
stress relaxation and surface hardening in, effects of high temperatures on, 25:55439
testing for friction and wear in high-temperature sodium, plans for, 25:55379(R) (WARD-4210-T-1-2)
HEAT SOURCES
use of radioisotope, in distillation system for recovering potable water from urine in spacecraft, 25:54911(P)
HEAT TRANSFER
burnout during subcooled boiling, measurement of, 25:54871 (IFA-TR-58)
calculation and measurement of critical, on surfaces immersed in boiling high-boiling-point organic compounds, 25:54879
calculation of stable, from rod bundles in longitudinal turbulent flow, equations for, 25:54883
calculations for heating surfaces with porous magnetite deposits, model for, 25:54862 (AEEW-R-711)
calculations for slender bodies, equations for, 25:54885
calculations for turbulent flow in annular channel with

XUM

roughened core rods, eddy viscosity model for, 25:54874 (RD/B/N-1980)
calculations for turbulent liquid flow in triangular channels, 25:54884
coefficients for forced-convection, in ducts with flux transients, derivation of, 25:54864 (ANL-7754)
effects of crud deposits, 25:57034
effects of transient, on space--time temperature distribution in semi-finite medium, 25:54876 (RT/ING-(71)11)
measurement of critical, for two-phase annular flow in heated pipes, effects of diffusion and film formation on, 25:54869 (FEI-217)
mechanisms of boiling, in two-phase flow in multirod coolant channels, (E), 25:54870(R) (GEAP-10347)
mechanisms of free convection, in fluid contained in vertical annular space, (E/T), 25:54881
model for axial, with incompressible turbulent flow through tubes, (T), 25:54877 (SGAE-RT-38/1971)
research for French nuclear programs, review of, 25:54865 (CEA-CONF-1758)
HEAT TRANSFER SYSTEMS
design and operation of, for measuring heat transfer to high-pressure boiling water, 25:54867 (EUR-4683)
HEATED EFFLUENTS
effects on environment of liquid metal cooled fast breeder reactor, 25:57069(R) (ANL-7800)
physical properties of round, turbulent, buoyant jet, 25:57245 (ORNL-4685)
HELIUM
abundance in atmospheres of beta Cephei stars, (E/T), 25:55711
abundance in B-type stars, (E), 25:55701
abundance in horizontal-branch stars, (E/T), 25:55708
abundance in interstellar gas, alpha reactions with aluminum and silicon at 70 to 160 MeV for determining, 25:56685 (FRNC-TH-48)
abundance in Sun, (E/T), 25:55751
burning in 15- and 30-solar-mass stars, (T), 25:55691
corrosive effects on reactor materials, review of, 25:55393
deuterium-ion reactions up to 100 eV with, cross sections for dissociation in, (E), 25:55858
distribution of solar neutral 584-A euv, observations of glow from exospheric, (E), 25:55967
electric discharges in, simulation of electron avalanche by Monte Carlo calculations, 25:56265(T) (ORNL-tr-2518)
electron reactions at 100 to 2000 eV with, angular and energy distributions of electrons from ionization in, (E), 25:55847
electron reactions at low energies with, review of total and momentum-transfer cross sections for, (E), 25:55856
electron reactions with, Born--Oppenheimer approximation for excitation to metastable states in, 25:55843
electron reactions with, eikonal approximation for excitation of $2^1P$ state in, 25:55874
electron reactions with, trapped-electron study of resonances in excitation in, 25:55851
electron scattering by, polarized-orbital calculations of, 25:55871
energy levels of, positions and widths of autoionizing, (T), 25:55820
energy of ground state of, calculation using configuration-interaction wave functions and correlation factor, 25:55892
energy of ground-state atom of, calculation using Faddeev formalism, 25:55824
gold-198 ranges in, from gold-197(n,γ) recoil, 25:56269
helium-hydride-ion reactions at 0.5 to 1 MeV with, cross sections for dissociation in, (E), 25:55872
helium-ion elastic and inelastic scattering at 300 eV to 1.5 keV, by rotational coupling effects on differential cross sections for, (T), 25:55848
hydrogen-ion ($H_2^+$) reactions up to 100 eV with, cross sections for dissociation in, (E), 25:55858
lithium-ion reactions at 600 to 2800 eV with, interference effects in charge-exchange cross sections for, 25:55844
oxygen-ion reactions at 10 to 40 MeV with, cross sections for electron capture in, 25:55869
oxygen-ion reactions at 7 to 40 MeV with, cross sections for electron capture and loss in, (E), 25:55870
phonon--phonon interaction in liquid, below 1°K, (T), 25:56052
plasma of, destruction of metastable states in, (E), 25:56151(T) (SC-T-713064)
plasma of, electron--ion recombination at low temperatures in, (E), 25:56161
plasma of, electron--ion recombination in cryogenic, (E), 25:56152(T) (SC-T-713065)
plasma of, relaxation theory of Stark broadening of spectral lines in, 25:56184
properties as high temperature gas cooled reactor coolant, 25:57040
properties of, calculation using one-dimensional integral equation obtained by reduction of multidimensional Schroedinger equation, 25:56398
proton reactions above 25 keV with, excitation in, (T), 25:55842
proton reactions at 20 to 120 keV with, cross sections for electron capture into n = 2 states of hydrogen in, (E), 25:55853
proton reactions up to 5 MeV with, cross sections for electron capture in, (T), 25:55837
reactions with hydrogen molecules at 14 to 50 keV, cross sections for one-electron stripping from ground-state and metastable helium atoms in, (E), 25:55845
release from irradiated boron carbide, research progress on, 25:54599 (ORNL-4717, p 117-24)
solubility in liquid sodium at 330 to 550°C, 25:54583
spectral lines of, in planetary nebulae, (E), 25:55700
HELIUM HYDRIDES
reactions with gases at 0.5 to 1 MeV of ions of, cross sections for dissociation in, (E), 25:55872
HELIUM IONS
distribution of $He^+$ 304-A euv, observations of glow from exospheric, (E), 25:55967
effects on diploid yeast cells, OER and RBE for mutagenic and lethal, 25:55165
effects on silicon at 220 keV, lateral-stress study of damage produced in, 25:56285 (SC-RR-710424)
range in air, argon, nitrogen, and oxygen at 0.2 to 2.0 MeV as function of energy, (E), 25:56276
reactions with hydrogen molecules, cross sections for one-electron capture in, 25:55845
scattering by helium at 300 eV to 1.5 keV, rotational coupling effects on differential cross sections for elastic and inelastic, (T), 25:55848
scattering by neon, quasi-diabatic calculation of differential cross sections for inelastic, 25:55849
scattering by sodium chloride crystals, channeling in, 25:54587(R) (AECL-3909)
HELIUM ISOTOPES
content in USSR ground waters, effects of earthquakes on, 25:54775
HELIUM ISOTOPES He-3
abundance in Sikhote--Alin meteorite, (E), 25:55671
abundance in targets aboard Soyuz space probes, (E), 25:55902
reactions (He-3,2p) and (He-3,d) with carbon-12 and silicon-28 at 40 MeV, DWBA analysis of angular distributions and spectra from, (E), 25:56713
reactions (He-3,α) with lithium-7 at 16 to 18 MeV, excitation functions, spectrum, and zero- and finite-range DWBA analyses of angular distributions from, (E), 25:56671
reactions (He-3,α) with yttrium-89 at 15 MeV, DWBA analysis of, (E), 25:56778
reactions (He-3,α) with yttrium-89 at 25 MeV, angular distributions for, (E), 25:56779
reactions (He-3,αγ) with chromium-50 at 15 MeV, α-γ angular correlations from, (E), 25:56692
reactions (He-3,d) with strontium-87 at 18 MeV, angular distributions for, (E), 25:56779
reactions (He-3,f) with bismuth-209, thorium-232, and uranium-238 at 20 to 34 MeV, cross sections at delayed neutron yields for, (E), 25:56803
reactions (He-3,γ) with tritium at 0.5 to 20 MeV, angular distributions for, (E), 25:56646
reactions (He-3,γ) with tritium at 9 to 26 MeV, differential cross section for, (E), 25:56664
reactions (He-3,n) with beryllium-9 at 8 MeV, neutron spectra from, (E), 25:56679
reactions (He-3,p) and (He-3,2p) with carbon-12 at 15 MeV, angular distribution and p-p angular correlations for, (E), 25:56682
reactions (He-3,p) with oxygen-18 at 18 MeV, angular distributions for, (E), 25:56716
reactions (He-3,p) with phosphorus-31 and potassium-39 at 12 and 13 MeV, p-γ coincidence spectra from, (E), 25:56715
reactions (He-3,p) with zirconium-90 at 16.5 and 18 MeV, proton spectra and angular distributions for, (E), 25:56758
reactions (He-3,pγ) with sulfur-32 at 8.00 to 9.00 MeV, proton spectrum and p--γ angular correlations in, (E), 25:56712
reactions (He-3,t) with boron-11 at 26 MeV, triton spectra from, (E), 25:56679
reactions (He-3,t) with strontium-88 at 23 MeV, analysis for reaction mechanism in, (E), 25:56779
scattering by boron-11 at 26 MeV, helium-3 spectra from inelastic, (E), 25:56679
scattering by yttrium-89 at 15 and 20 MeV, angular distributions for elastic, (E), 25:56778
separation from helium-4, continuous-distillation apparatus for, 25:56121
D--He-3, energy balance calculations for use in thermonuclear reactors, 25:56215 (N-71-25526)
HELIUM ISOTOPES He-4
alpha elastic scattering below 100 MeV, analysis using nonlocal separable potential, (T), 25:56852
charge form factor of, effects of cms motion on calculation of, (T), 25:56647
containment of liquid, by superfluid plug in space, 25:56119
critical-heat flux in saturated liquid II, discrepancies using thin-wire-heaters for, 25:56060
energy levels of, microscopic description using cluster model, 25:56654 (LYCEN-7104, S13.1-11)
equilibrium properties of submonolayer films of, (E/T),

XUM

25:56659
excitations in superfluid, ion and roton, 25:56057
film boiling in liquid II, high-speed motion-picture studies of, 25:56061
flow of liquid II at supercritical velocities, near-isothermal dissipative, 25:56062
hyperons (Λ) elastic scattering at 1 to 20 MeV, calculation of polarization and cross sections using OBE model, (T), 25:56648
meson reactions ($\mu^-$,nν) with, short-range nucleon--nucleon correlation effects on energy spectrum and angular distribution asymmetry of neutrons from, (T), 25:56641 (JINR-P4-5986)
neutron elastic scattering below 50 MeV, analysis using nonlocal separable potential, (T), 25:56852
neutron elastic scattering by, analysis using separable nonlocal potential, (T), 25:56642 (LYCEN-7104, C5.1-15)
neutron elastic scattering by, lectures on forward dispersion relations for, (T), 25:56810 (CERN-71-14, pp 155-228)
order parameter on free surface of liquid II, boundary condition of, (T), 25:56056
phonon--phonon interaction in liquid, below 1°K, (T), 25:56052
photon reactions (γ,n) at threshold to 31 MeV, cross section for, (E), 25:56649
proton elastic scattering below 50 MeV, analysis using nonlocal separable potential, (T), 25:56852
proton elastic scattering by, analysis using separable nonlocal potential, (T), 25:56642 (LYCEN-7104, C5.1-15)
quantum lattice-gas model of equilibrium properties of liquid, 25:56058
second sound velocity in rotating liquid II, (E), 25:56054
sound velocity in liquid, (T), 25:56055
superflow interaction with vortex lattice in, theoretical models of behavior of shear waves in, 25:56053
surface tension of liquid II, near lambda point, (T), 25:56056
vortex-free Landau state in rotating superfluid, 25:56048

HELIUM ISOTOPES He-5
energy levels of, microscopic description using cluster model, 25:56654 (LYCEN-7104, S13.1-11)

HELIUM ISOTOPES He-10
production in neutron fission of uranium-235, yields for, (E), 25:56788

HELIUM SYSTEMS
He--methane--$SiH_4$, radiation effects on, reactions of recoil tritium from neutron, 25:54678

HEMATOPOIESIS
radiation effects on, in active bone marrow, effects of dose fractionation on, 25:55326
radiation effects on, in mice in comparison to effects on clasmatosis, γ, 25:55321

HEMOPROTEINS
Moessbauer-spectra studies of, review, 25:55105

HEXANE
hexane--naphthalene, radiation effects on, products from, 25:54599 (ORNL-4717, p 117-24)

HEXOKINASE
radiation effects on activity of, in brain, erythrocytes, and liver of tumor-bearing rats, x, 25:55140

HIGH-ENERGY PHYSICS
High Energy Physics Index. Vol. 9, No. 15, 25:56446
High Energy Physics Index, Vol. 9, No. 16, 25:56443
High Energy Physics Index. Vol. 9, No. 17, 25:56445
High Energy Physics Index. Vol. 9, No. 18, 25:56444
research at Institute of Theoretical Physics, Gothenburg, Sweden, 1970, (T), 25:56441(R) (NP-18997)
research at Purdue Univ., June 1970 to May 1971, (T), 25:56440(R) (COO-1428-276)

HIGH-TEMPERATURE GAS-COOLED REACTOR EXPERIMENT
core components for, radiation effects on carbonaceous, 25:55651
fuel reprocessing for, development of head-end methods in, 25:54714 (ORNL-4682, pp 80-94)
fuel tubes for, calculation of stresses in graphite, (E/T), 25:57051

HIROSHIMA
atomic bombing of, radiation effects on mortality of man exposed in utero to, 25:55307

HOLMIUM
lattice parameters of, effects of hydrogen on, 25:55549

HOLMIUM ALLOYS AND SYSTEMS
Au--Ho, crystal structures and melting points of intermetallic, 25:55570

HOLMIUM ISOTOPES Ho-165
alpha fission at 167 MeV, angular distributions and particle track lengths for, (E), 25:56806
energy-level transitions in, nuclear structure effects on internal conversion of M1, 25:56756
ion elastic scattering in wide energy range, phase shift analysis of angular distributions for, (E), 25:56740 (JINR-P7-5884)

HOLMIUM ISOTOPES Ho-168
beta decay of, branching ratios, gamma spectra, and log-ft values for, (E), 25:56767

HOLMIUM ISOTOPES Ho-169
beta decay of, gamma spectra and log-ft values for, (E), 25:56767

HORMONES, ADRENAL
hydrocortisone, effects on renewal patterns of normal and tumor cells, 25:55110(R) (TID-25801)

HORMONES, PARATHYROID
effects on strontium-85 sorption by man, 25:55109 (COO-1231-67)

HORMONES, PITUITARY
growth hormone, radioimmunoassay in anterior pituitary medium, application of statistical procedures to double antibody technique for, 25:55143
growth hormone, radioimmunoassay in man, mathematical analysis of, 25:55145
luteinizing, radioimmunoassay in man, mathematical analysis of, 25:55145
prolactin, radioimmunoassay in anterior pituitary medium, application of statistical procedures to double antibody technique for, 25:55143
thyrotropin, radioimmunoassay in anterior pituitary medium, application of statistical procedures to double antibody technique for, 25:55143
vasopressin, radioimmunoassay in human blood plasma, use of double antibody technique for, 25:55142

HORMONES, SEX
chlorotrianisine, radioprotective effects of, on mice, fast neutron and x, 25:55266
estradiol, estimation in man using radioligand assay, (T), 25:55145
prostaglandins, radioimmunoassay in blood plasma of rabbits, 25:55144

HORMONES, THYROID
thyroxine, determination in blood serum by activation and ion exchange, 25:54453
triiodothyronine, determination in blood serum by activation and ion exchange, 25:54453
triiodothyronine, radioimmunoassay in human serum, effects of hyperthyroidism and hypothyroidism on, 25:55146

HOT CELLS
atmosphere system for, surveillance of inert argon--nitrogen, 25:54945 (CONF-710401-, pp 98-105)
design for α radiation measurements, 25:55590(R) (EIR-192)
design of box-type, for poisonous or radioactive materials, 25:54978(P)
equipment for remote measurements in irradiated components in, description of, 25:57054 (ANL-EBR-30)
fire protection test facility for, design and performance of, 25:54956 (CONF-710401-, pp 237-47)

HUMBOLDT BAY POWER REACTOR
cooling system for leak rate limit for primary, 25:56932 (DOCKET-50133-68)

HYDROAROMATIC COMPOUNDS
radioinduced hydrogenation and alkylation of, 25:54599 (ORNL-4717, p 117-24)

HYDROCARBONS
radiolysis of, excited states and intermediates in, 25:54626 (CONF-700652-(Vol.1), pp 139-219)
radiolysis of, review on ionic processes in, 25:54630 (CONF-700652-(Vol.3), pp 523-98)
mepasine--TBP, radiolysis of, effects of nitric acid on reactor, 25:54644

HYDROCHLORIC ACID
dissociation at high temperatures using flowing cell, potentiometric determination of, 25:54535 (ORNL-4717, pp 57-82)

HYDROFLUORIC ACID
solubility in sodium fluoroborate--sodium fluoride eutectic, 25:54532 (ORNL-4717, pp 1-27)

HYDROGEN
abundance in M33, (E), 25:55796
abundance in solar atmosphere, (E/T), 25:55750
charged-particle reactions with atomic, cross sections for transitions between highly excited levels in, (T), 25:55838
charged-particle reactions with atomic, cross sections for transitions between highly excited levels in, (T), 25:55839
condensation of solid, in contracting interstellar clouds and protostars, (T), 25:55785
content in thermosphere from June 1966 to Jan. 1967, temporal variations from in situ, (E), 25:55973
corrosive effects on reactor materials, review of, 25:55393
detection of interstellar molecular, (E), 25:55700
determination in metals, design of instrument for, 25:54424
diffusion and internal friction in niobium and vanadium, calculation from redistribution in periodic stress gradient, 25:55458
diffusion in titanium and titanium alloy at 450 to 600°F, effects of stress on, 25:55476
diffusion through metals, effects of hydrogen pressure on rate of, 25:54534 (ORNL-4717, pp 43-56)
diffusion through oxide-coated metals, effects of water vapor on rate of, 25:54534 (ORNL-4717, pp 43-56)
effects on lattice parameters of rare earth metals, scandium, and yttrium, 25:55549
electron elastic scattering at 1.21 to 2.25 rydbergs by atomic, complex-energy calculations of s-wave, 25:55860

electron reactions at low energies with atomic, use of free-fall atomic model in three-body calculations of ionization cross sections for, 25:55836 (INR-P-1327)
electron reactions with atomic, eikonal approximation for excitation of 2p and 2s states in, 25:55874
electron reactions with atomic, Glauber and Vainshtein approximations for total cross sections for 1s--2p excitation in, 25:55850
electron reactions with atomic, perturbation-theory calculations of 1s--2s excitation in, 25:55877
electron reactions with molecular, effects of vibrational level on kinetic-energy distribution of protons from, (T), 25:55857
electron scattering by atomic, algebraic close-coupling approach to, 25:55854
electron scattering by, parameters for multichannel resonances in, (T), 25:55861
helium-atom reactions at 14 to 50 keV with molecular, cross sections for one-electron stripping in, (E), 25:55845
helium-hydride-ion reactions at 0.5 to 1 MeV with molecular, cross sections for dissociation in, (E), 25:55872
helium-ion reactions with molecular, cross sections for one-electron capture into ground-state and metastable atoms in, 25:55845
injection into metals, design of cathode for, 25:54858
photon reactions with atomic, perturbation-theory calculations of bound--bound and bound--free transitions in multi-, 25:55875
plasma of, ion energy distribution during turbulent heating of, (E), 25:56131
plasma of, precision measurements of spectra of, (E), 25:56156
plasma of, temperature and electron density determination in spark, (E), 25:56142
positron reactions with atomic, eikonal approximation for excitation of 2s state in, 25:55874
positron scattering by atomic, algebraic close-coupling approach to, 25:55854
proton reactions at 10 to 2500 keV with atomic, excitation in, (T), 25:55841
proton reactions at 20 to 120 keV with molecular, cross sections for electron capture into 2s state of hydrogen in, (E), 25:55853
proton reactions at 30 and 50 eV with atomic, forced common turning-point treatment of excitation in, 25:55881
proton reactions at 5 eV with atomic, cross sections for momentum transfer in, (E), 25:55840
proton reactions up to 5 MeV with molecular, cross sections for electron capture in, (T), 25:55837
proton reactions with atomic, eikonal approximation for excitation of 2s state in, 25:55874
radiation effects on catalytic properties of electrodes of, neutron, 25:54602
reactions between atoms and molecules of, quantum mechanical treatment of, 25:55863
reactions of radiolytic, ESR studies on, 25:54628 (CONF-700652-(Vol.2), pp 367-420)
reactions with biochemicals, rate constants for, 25:55132
reactions with moderated recoil fluorine-18 atoms, effects of deuterium on rate of hydrogen abstraction, 25:54686
solubility in molten fluorides, 25:54534 (ORNL-4717, pp 43-56)
sorption by niobium, bulk and surface, 25:55434 (RLO-2221-T-7-3)
spectral 6300-A emission in nighttime auroral ionosphere on Mar. 23-24, 1969, simultaneous triangulation with SAR arc, (E), 25:55971
spectral lines of, in planetary nebulae, (E), 25:55700
spectral Lyman-α dayglow analysis of Martian exosphere, (E), 25:55812
yields from γ radiolysis of supercooled water, 25:54663
yields from radiolysis of liquid ethanol, 25:54660

HYDROGEN IONS
scattering by sodium chloride crystals, channeling in, 25:54587(R) (AECL-3909)

HYDROGEN IONS ($H_2^+$)
energy of ground-state, calculation from James wave functions, 25:55829
reactions with helium and neon up to 100 eV, dissociation in, (E), 25:55858

HYDROGEN ISOTOPES
determination in heavy water by specific gravity measurements, standard for, 25:54430
exchange at 300 to 500°C, catalytic effects of cadmium, thallium, or zinc vapors on homomolecular, 25:54552
fractionation in synthesis of benzene from calcium carbide--water reaction, 25:54735
separation of, effects of overpotential on electrochemical, 25:54721

HYDROGEN PEROXIDES
radioprotective effects on erythrocytes of beagle dogs, strontium-90 β, 25:55319 (UCD-472-118)
yields from γ radiolysis of supercooled water, 25:54663
yields from γ radiolysis of thallium sulfate, 25:54646

HYDROGEN SULFIDES
separation from heavy water plant effluents for recycle in incoming water, 25:54918(P)

HYDROGEN SYSTEMS
Ar--H, meson(μ⁻) reactions with, meson transfer from hydrogen to argon and x-ray emission in, (E), 25:55830
H--N, radiation effects on, production of carbon-11-labeled cyanides by recoils from proton, 25:54683
H--Ti--Zr, inflammability correlation of powdered, 25:55473

HYDROMAGNETIC WAVES
effects on high-energy proton relaxation in magnetosphere, (T), 25:56011

HYDROQUINONE
determination by dichrometric titration using triphenylmethane dyes as redox indicators, 25:54410

HYDROXIDES
radiolysis of aqueous glasses of, electron trapping in γ, 25:54627 (CONF-700652-(Vol.2), pp 295-330)

HYDROXYL (HO)
radio-wave absorption due to, in direction of W44, (E), 25:55716
reactions of radiolytic, in aqueous solutions of organic compounds, 25:54632 (CONF-700652-(Vol.3), pp 649-92)
reactions with benzoatopentaamminecobalt(III) from radiolysis of benzoatopentaamminecobalt perchlorate, 25:54669
yields from γ radiolysis of supercooled water, 25:54663

HYPERFRAGMENTS
energy levels of, optical potential model for excited, 25:56524
hyperon (Λ) binding energy of excited, 25:56524

HYPERONS
classification of heavy octet, SU(3) mass formulas for, (T), 25:56540
decays of, urbaryon rearrangement diagram for nonleptonic, 25:56470
spectra of, harmonic oscillator quark model for, 25:56507

HYPERONS (Λ)
production in $\pi^+ + p$ interactions at 8 GeV/c in hydrogen bubble chamber, momentum and angular distributions for, (E), 25:56427 (IFA-HE-73)
scattering by helium-4 at 1 to 20 MeV, calculation of polarization and cross sections using OBE model, (T), 25:56648

HYPERONS (Ξ)
properties of, SU(3) mass formulas for prediction of, (T), 25:56540

HYPERONS ($\Xi^-$)
decay $\Xi^- \rightarrow e + \nu + \Lambda^0$ relative to $\Xi^- \rightarrow \pi + \Lambda$, counter--spark chamber measurement of branching ratio for, 25:56411
decays of, counter--spark chamber measurement of beta, 25:56411

HYPOIODOUS ACID
production by reactions of fission product iodine in steam--air mixtures, 25:54547

HYPOXIA
effects of cyanide-induced, on hexokinase activity in brain, erythrocytes, and liver of rats, 25:55140


## I


ICE
diffusion in, data tabulations on, 25:55509

IGNEOUS ROCKS
age of, effects of geophysical variables on fission track method for estimation, 25:54760
analysis for trace elements by nuclear techniques, 25:54462
analysis of Mesozoic dolerite, for rare earths, 25:54476
uranium distribution in Skaergaard, Rhum, and Bushveld cumulates, use as indicator of mesostasis, 25:54809

IMIDE POLYMERS
photoconductivity during ionizing radiation pulses of H-film, analysis of dielectric, 25:55079 (SC-DC-713696)

IMMUNE REACTIONS
radiation effects on mouse, effects of injections of bone marrow, peritoneal exudate, spleen, or thymus cells on recovery from x, 25:55147

IN-PILE LOOPS
description of Osiris and Pegase high-temperature, for irradiation testing, 25:54840
design of high-power gamma rdiation, for IRT Tbilisi, 25:57129
design parameters of high flux research reactor pressurized water, 25:57121 (RCN-145)
operations of high flux research reactor pressurized water, 25:57121 (RCN-145)

INCOLOY 800
reactions with sodium at 1000 to 1300°F, carbon and nitrogen mass transfer in, 25:55379(R) (WARD-4210-T-1-2)

INDIAN POINT POWER REACTOR, UNIT 1
coolant leakage rates for, limits for allowable, 25:56928 (DOCKET-50003-91)
emergency core cooling system for, performance evaluation for, 25:56926 (DOCKET-50003-89)
inspection program for, proposed augmented in-service, 25:56927 (DOCKET-50003-90)


XUM

INDIUM
alpha fission at 167 MeV, angular distributions and particle track lengths for, (E), 25:56806
determination by neutron activation, use of ion exchange in, 25:54397
effects on solvolysis of tert-butyl halides, Broensted correlation for, 25:54548
magnetic flux states of superconducting cylinders of, quantized, (E), 25:56064
neutron reactions using iron-filtered beams, analysis of resonance cross sections for, 25:56795
neutron resonance absorption in, self-shielding of, (E/T), 25:57196
separation of uranium from, in methyl sulfoxide by cation exchange chromatography, 25:54728
superconducting transition temperature of, effects of compression deformation on, 25:54587(R) (AECL-3909)
INDIUM ALLOYS AND SYSTEMS
Ag--In, search for superconductivity in fcc phases of, (E), 25:56096
Au--In, search for superconductivity in fcc phases of, (E), 25:56096
Au--In, superconductivity in hcp phases of, (E), 25:56096
Bi--In, superplastic properties of eutectic, 25:55456
Hg--In, phase diagram of, 25:55536
In--Ni, optical constants for β-phase NiIn intermetallic compound in, 25:56352
In--Pb, phonon spectra of dilute, superconducting tunneling study of, 25:56075
In--Pb, stress relaxation in mixed-state superconductivity, effect of magnetic fields on, 25:56063
In--Pb, strong-coupling parameters in superconducting, (E), 25:56076
In--Pb-base, thermal conductivity of one-dimensional superconducting, fluctuation effects on, (E/T), 25:56095
In--Sb, radioinduced defects and electron mobility changes in InSb single crystals, annealing of fast-neutron, 25:56317
In--Sn, phase diagrams of, relations with property--composition diagrams, 25:55546
INDIUM CHLORIDES
complexes with phthalocyanine, radiation effects on, Szilard--Chalmers process from neutron, 25:54680
INDIUM HYDROXIDES
preparation of InOOH, high-pressure hydrothermal method for, 25:55602
INDIUM IODIDES
indium-114m electron capture decay in, Coulomb fragmentation from, 25:54696
INDIUM ISOTOPES
energy levels of, quasiparticle description of low-lying, (T), 25:56794
INDIUM ISOTOPES In-107
beta and electron-capture decay of, γ spectra from, (E), 25:56759
INDIUM ISOTOPES In-114
electron capture decay of metastable, in indium iodides, Coulomb fragmentation from, 25:54696
INDIUM ISOTOPES In-115
energy levels of, Davydov-model calculations of spins for, (T), 25:56785
energy-level scheme from neutron inelastic scattering, (E), 25:56752(R) (SUNI-14)
energy-level transitions in, Davydov-model calculations of probabilities for E2, (T), 25:56785
neutron capture at 2.9 MeV, cross section for, (E), 25:56696
INDOLE, 3-(2-AMINOETHYL)-5-METHOXY-
effects on sensitivity of guinea pigs and mice to transverse acceleration, 25:55264
INFORMATION CENTERS
operation of Nuclear Safety, during May and June 1971, 25:57092(R) (ORNL-TM-3483)
INFORMATION RETRIEVAL SYSTEMS
computer systems for, use of graphic display, 25:57007
computer systems for, use of graphic display, 25:57008
INFRARED RADIATION
detection of discrete celestial sources of far-, (E), 25:55692
emission from central region of Milky Way, 4-color photometry of, (E), 25:55783
solar spectrum between 12 and 24 μ, (E), 25:55739
INORGANIC COMPOUNDS
entropies of, use of molar volumes in method for estimating, 25:54532 (ORNL-4717, pp 1-27)
INSECTA
Chorthippus brunneus, radiation effects on chiasma frequency in, x, 25:55176
Drosophila melanogaster, radioinduced chromosome aberrations in male, cytological analysis of γ, 25:55170
Drosophila melanogaster, radioinduced translocations in chromosomes of, effects of dose on neutron and x, 25:55206 (NYO-2740-8, pp 147-219)
Earias vittella, radioinduced sterilization of, γ, 25:55368
Ephestia cautella, radiation effects on longevity and reproduction of, effects of dose on γ, 25:55315
Ephestia cautella, radiation effects on reproduction and survival of progeny of, effects of dose to male parents on γ, 25:55316
Habrobracon sp., radioinduced mutations for life-shortening in, x, 25:55185
Phorma regina, biochemistry of development of, 25:57265(R) (ORO-3883-3)
INTERSTELLAR MATERIAL
alignment of grains of, with respect to the magnetic field, (T), 25:55792
condensation of solid hydrogen in contracting clouds of, (T), 25:55785
detection of molecular hydrogen in, (E), 25:55700
helium abundance in, alpha reactions with aluminum and silicon at 70 to 160 MeV for determining, 25:56685 (FRNC-TH-48)
infrared emission from dust grains in H II regions, (T), 25:55718
microwave emission from formamide in, detection of, (E), 25:55784
INTESTINES
strontium-85 sorption by human, effects of aluminum phosphate gel on, 25:55109 (COO-1231-67)
INVARIANCE PRINCIPLES
parity-conserving relativistic quantum field theory, geometric structure of, (T), 25:56557
INVERTEBRATES
plutonium-239 content of Atlantic Ocean, 25:55161
IODINE
determination as iodate, iodine monochloride, or periodate by potentiometric titration, 25:54433
determination by gas chromatography and photometry, in-flame detector for, 25:54406
determination by radioactive, in rainwater and seawater by isotope exchange and scintillation counting, 25:54442
determination in biological fluids by neutron activation, ion exchange, and γ spectrometry, semi-automated, 25:54516
determination in biological fluids by neutron activation and radiochemical separation, 25:54509
diffusion and deposition of gaseous, in atmosphere, 25:54795
effects on reactions of recoil chlorine-38 in neutron-irradiated chloromethane, 25:54681
production in power reactors, safety problems from, 25:57100
reactions of fission product, in steam--air mixtures, 25:54547
separation of fission product, from off-gases from reprocessing of LMFBR fuels, 25:54713 (ORNL-4682, pp 39-79)
IODINE ISOTOPES I-124
beta and electron-capture decay of, gamma energies and intensities from, (E), 25:56781
IODINE ISOTOPES I-125
decay in iodine compounds, Moessbauer spectral study of effects of, 25:56381
transport across placenta in pregnant sheep, 25:55319 (UCD-472-118)
IODINE ISOTOPES I-126
beta and electron-capture decay of, gamma energies and intensities from, (E), 25:56781
IODINE ISOTOPES I-127
neutron capture at 2.9 MeV, cross section for, (E), 25:56696
IODINE ISOTOPES I-128
yields from neutron reactions (n,γ) with iodine-127 in pentane or pentenes, 25:54705
IODINE ISOTOPES I-129
abundance in Galaxy, (T), 25:55781
content of environment of nuclear fuel reprocessing plant, public health hazards from, 25:55199
IODINE ISOTOPES I-131
determination of, use of ion exchange in methods for, 25:54397
effectiveness for lung scanning for evaluating perfusion changes following bronchography, 25:55285
effectiveness for scanning cerebral blood vessels in comparison with angiography, 25:55289
effectiveness in combination with surgery and thyroid hormone suppression for therapy of thyroglossal duct carcinomas, 25:55304
effectiveness of albumen-incorporated, for scanning pulmonary arteries in patients with pulmonary hypertension, 25:55284
effectiveness of lipiodol-incorporated, for endolymphatic therapy in patients with malignant melanomas or metastases, 25:55305
effects on potassium and sodium metabolism in man following therapy of diffuse toxic goiter, 25:55340
release during coolant loss accident in water cooled and moderated power reactors, 25:57104
release from failed water cooled Zircaloy 2 clad uranium oxide ($UO_2$) fuel rods, 25:57047 (JAERI-Memo-4157, pp 2-22)
release of liquid and gaseous effluents from power reactors, 25:56978
transport across placenta in pregnant sheep, 25:55319 (UCD-472-118)
use for estimating late x radiation effects on circulation in brain, liver, lungs, and skin of rats,

25:55328
use for therapy, development of thyroid carcinoma following, 25:55343
IODINE ISOTOPES I-132
release from failed water cooled Zircaloy 2 clad uranium oxide ($UO_2$) fuel rods, 25:57047 (JAERI-Memo-4157, pp 2-22)
IODINE ISOTOPES I-133
release from failed water cooled Zircaloy 2 clad uranium oxide ($UO_2$) fuel rods, 25:57047 (JAERI-Memo-4157, pp 2-22)
IODINE ISOTOPES I-134
release from failed water cooled Zircaloy 2 clad uranium oxide ($UO_2$) fuel rods, 25:57047 (JAERI-Memo-4157, pp 2-22)
IODINE ISOTOPES I-135
release from failed water cooled Zircaloy 2 clad uranium oxide ($UO_2$) fuel rods, 25:57047 (JAERI-Memo-4157, pp 2-22)
IODINE SYSTEMS
I--1-pentene, neutron reactions (n,γ) with iodine-127 in, yields and product distribution from, 25:54705
I--1-pentene, radiolysis of, distribution of iodine-131-labeled products from, 25:54705
I--2-pentene, neutron reactions (n,γ) with iodine-127 in, yields and product distribution from, 25:54705
I--2-pentene, radiolysis of, distribution of iodine-131-labeled products from, 25:54705
I--pentane, neutron reactions (n,γ) with iodine-127 in, yields and product distribution from, 25:54705
I--pentane, radiolysis of, distribution of iodine-131-labeled products from, 25:54705
ION-ACOUSTIC WAVES
damping and growth in plasma, nonlinear Landau, (T), 25:56234
excitation in polar regions by streaming instability in polar wind, v1f, (E/T), 25:55966
propagation in fully ionized collisional plasma, instabilities from, (T), 25:56251
ION BEAMS
charge neutralization in, cross-beam technique for, 25:55816
focusing in magnetic field isotope separators, design of optical system for, 25:54920
focusing of drifting, in non-uniform magnetic field, 25:56602
ION EXCHANGE
book: Ion Exchange in Analytical Chemistry, 25:54397
ION EXCHANGE MATERIALS
isotope separation factors for electromigration through, single-stage, 25:54729
ION SOURCES
aperture extractor design for high-current, 25:56213 (LBL-327)
control circuit for deuterium--tritium, for neutron generators, 25:56605(P)
description of high-temperature molecular-stream, for MI-1305 mass spectrometer, 25:55081
design and operation of polarized, review on, 25:56610
design of duoPIGatron, for plasma injection experiments, 25:56208 (CONF-711012-9)
design of high-frequency heavy-, 25:55817
design of large-area high-current, for plasma injection experiments, 25:56212 (LBL-35)
design of multi-aperture 1-keV hydrogen, for injection into magnetic mirror machines, 25:56217 (UCRL-73387)
design of multiply charged heavy, using electron resonance plasmas, 25:56210 (EUR-CEA-FC-603)
development for plasma injection studies, review of, 25:56218 (UCRL-73412)
development of, review of, 25:55814 (UCRL-73353)
emittance of, device for measuring, 25:56611
IONOSPHERE
charged-particle density and precipitation in polar-cap auroral, sounding-rocket observations of, (E), 25:56031
charged-particle flux at 250 to 500 km in, acceleration mechanism of bunches of, (E/T), 25:56008
charged-particle intensity at low altitudes over auroral zones and polar caps, relation of simultaneous electric-field observations to, (E), 25:56030
charged-particle intensity distribution at 200 to 300 km in, global primary cosmic rays and residual, (E), 25:55980
cosmic-ray propagation from source to, path-length determination for, (E/T), 25:55903
creation of electron-beam-produced artificial aurorae, magnetospheric magnetic-field configuration from, (E), 25:55961
D region, effect on parameters of Dec. 27, 1968 chromospheric flare, (E/T), 25:55982
D region, ion kinetics in nighttime, nuclear-explosion-associated, (E), 25:56010
diagnostics using electrostatic probes, probe properties in, (E), 25:56012
E region, critical-frequency variations at large solar zenith angles, universal-time-dependent, (E), 25:55994
E region, current systems in polar, ground-level perturbation-field model of, (T), 25:55977
E region, detonation-wave effects on decameter-wavelength radio waves in, (E/T), 25:55970
E region, effect on parameters of Dec. 27, 1968 chromospheric flare, (E/T), 25:55982
E region, electron density enhancements during 2B solar flares, (E/T), 25:56035
E region, plasma transport processes in, theoretical formulation for, 25:55969
electric field in nighttime and daytime auroral, Langmuir-probe measurement of vector, 25:55960
electric fields in polar, correlation with magnetic disturbances in polar regions, (E/T), 25:55959
electric-field intensity at low altitudes over auroral zones and polar caps, relation of simultaneous charged-particle observations to, (E), 25:56030
electron content during Mar. 8, 1970 magnetic storm, spatial and temporal variations of, (E), 25:55974
electron density in topside, ground-based and topside-sounding diurnal and seasonal variations of midlatitude, (E), 25:55993
electron density irregularities in, nonperiodic, (E), 25:56042
electron precipitation in polar, during Aug. 13-18, 1968 magnetic storm, soft-, (E), 25:55964
F region, effect on parameters of Dec. 27, 1968 chromospheric flare, (E/T), 25:55982
F region, plasma ring and polar cavity in, comparison of north- and south-polar, (E), 25:56034
F region, striation formation in barium clouds released at 157 and 194 km, (E), 25:56033
F1 layer, electron and ion temperatures and densities in, (E), 25:56047
F1 layer, electron density enhancements during 2B solar flares, (E/T), 25:56035
F2 layer, characteristics of critical frequency distribution curves, statistical analysis of, (E/T), 25:55985
F2 layer, electron density enhancements during 2B solar flares, (E/T), 25:56035
F2 layer, electron-density distribution in, numerical models of, (T), 25:55984
F2 layer, ground-based and topside-sounding diurnal and seasonal variations of electron density in, (E), 25:55993
geomagnetic-field intensity at 100 to 500 km, computation of total vector of real, 25:55990
ion-density enhancements in polar, during Aug. 13-18, 1968 magnetic storm, positive-, (E), 25:55964
ionization irregularities in geomagnetic-field-oriented topside, whistler-associated, (E), 25:55997
ionization profile in upper, computation from ground-based vertical soundings, (E/T), 25:55995
lightning discharge pulses in, correlation and spectral characteristics from leader stage of, (E/T), 25:55998
magnetic field of 1f oscillations under, computer calculations of, (T), 25:56001
magnetic-field and pressure variations in, compared to Earth surface, solar diurnal, (E/T), 25:56036
magnetic-field and pressure variations in, compared to Earth surface, lunar diurnal, (E/T), 25:56037
parameters of, ground-based and satellite observations of solar-activity effects on geophysical, (E), 25:55981
plasma disturbances by satellite in, boundary-value problem for Vlasov--Poisson equation, 25:56014
plasma inhomogeneity formation in equatorial electrojets, quasi-linear equations of electron and ion, (T), 25:55986
proton precipitation in and radar echoes from auroral, simultaneous observations of, (E), 25:55963
radio-wave absorption in, latitudinal dependence of lunar-phase effect on, (E), 25:55975
radio-wave propagation at midlatitude across polar cap during PCA, proton anomaly of very long, (E), 25:55996
solar particles in polar, energy dissipation of PCA-associated, (T), 25:56005
solar-eclipse effect on, observations from two stations of Sept. 22, 1968, (E), 25:56000
sporadic E, daily variation in height of, (E/T), 25:56006
sporadic E, detonation-wave effects on decameter-wavelength radio waves in, (E/T), 25:55970
sporadic E, effects of geomagnetic activity on, (E/T), 25:56015
spread F, relation to whistler characteristics, (E), 25:55997
variations of temperature and molecular nitrogen and atomic and molecular oxygen concentrations at 100 to 200 km, diurnal, (E), 25:55987
IONS
atomic oscillator strengths for sodium-like, (T), 25:55776
charged-particle reactions with hydrogen-like, cross sections for transitions between highly excited levels in, (T), 25:55839
charged-particle reactions with hydrogen-like, cross sections for transitions between highly excited levels in, (T), 25:55838
detection of heavy, efficiency of scintillation counters for, 25:55016
effects of beams of heavy, on survival of bacterial spores and cultured cells, 25:55313
energy level lifetimes for fluorescent states, compilation of, 25:57215 (CEA-Bib-198)
implantation in semiconductors, review of analysis of

XUM

lattice disorder in, 25:56304
mass and mobility of atmospheric, methods for measuring, 25:54800
mobility of alpha particle-induced, in air, spectra of, 25:54801
reactions of radiolytic, with electrons, 25:54591 (CONF-700652-(Vol.1), pp 221-58)
reactions with monocrystalline metal surfaces at 0.5 to 10 keV, equipment for study of reflection and secondary emission from, 25:55815
reactions with thorium-232, light-element yields from heavy, (E), 25:56788

IRIDIUM
conductivity at 80 to 1900°K, electric and thermal, 25:55523
determination in geochemical samples by neutron activation, 25:54484
determination in geological sample by neutron activation and radiochemical separations, 25:54485
determination in silicate rocks and rock-forming minerals by neutron activation and radiochemical separations, 25:54486
effects on properties and sintering of tungsten at 1000 to 2000°C, 25:55453

IRIDIUM ALLOYS AND SYSTEMS
Ir--Nb, niobium-93 NMR in $Nb_3Ir$, 25:56373
Ir--Pr-base, phase diagram of, 25:55567
Ir--Pr-base, phase diagram of, thermodynamic analysis of, 25:55566

IRIDIUM ISOTOPES Ir-192
uses as gamma source for jet engine inspection, 25:54927

IRON
abundance in solar atmosphere, (E/T), 25:55750
argon-ion reactions at 30 keV with surfaces of, charge states and kinetic energies of scattered and recoil ions from, (E), 25:55818
casting by levitation melting using magnetic field, 25:55424
complexes with TTA, spectrophotometric study of, 25:54692(R) (NYO-3417-15)
compounds, effectiveness for treatment of human tumors combined with radiation for normalization of blood picture, 25:55303
deformation and fracture at low temperatures, effects of vanadium on, 25:55478
determination by dichrometric titration using triphenylmethane dyes as redox indicators, 25:54410
determination in Australian tektites by neutron activation and gamma spectrometry, 25:54478
determination in standard aluminum--silicon system by neutron activation, 25:54455
determination in stony meteorites by proton and bremsstrahlung activation, 25:54466
determination in tourmaline, by deuteron activation analysis and $\gamma$ counting, 25:56752(R) (SUNI-14)
determination in volcanic ash by neutron activation and $\gamma$ spectrometry, 25:54513
determination in yttrium oxide by emission spectrometry, 25:54419
determination of trace amounts of, in air by neutron activation and $\gamma$ spectrometry, 25:54456
determination of trace amounts of, in ultramafic rocks by thermal neutron activation and $\gamma$ spectrometry, 25:54496
diffusion of carbon in solid solutions of alpha, 25:55479
distribution coefficient of impurity of, in zirconium, measurement of, 25:55502
effects on properties and sintering of tungsten at 1000 to 2000°C, 25:55453
effects on solvolysis of tert-butyl halides, Broensted correlation for, 25:54548
effects on sorption of strontium on cation exchanger from strong acid, 25:54720 (UJV-2550-Ch)
iron-57 Moessbauer spectra using polarized cobalt oxide source, 25:56366
magnetic properties of, at cryogenic temperatures, 25:56361
neutron cross sections for, transmission of fission spectra through thick samples for evaluation of minima in total, (E), 25:56650 (COO-2049-5)
neutron inelastic scattering at 14.4 MeV, differential cross sections, nuclear-level density parameters, and contribution of direct processes for, (E), 25:56684 (FEI-216)
neutron reactions (n,2n) at 14.4 MeV, differential cross sections, second-neutron spectra, and nuclear-level density parameters for, (E), 25:56684 (FEI-216)
neutron reactions with, secondary gamma radiation in shielding from, 25:56277
neutron transport in, fast, (E/T), 25:56618 (RPI-328-230)
production in blast furnaces, uses of radioisotopes for studying operations in, 25:54906
properties and structure of, produced by sintering using systematic thermal fluctuations, 25:55414
proton reactions above 1.5 TeV, ionization spectrometer study of inelasticity coefficients for, (E), 25:56414 (INP-757)
reactions with sodium at 1000 to 1300°F, carbon and nitrogen mass transfer in, 25:55379(R) (WARD-4210-T-1-2)
separation of ferric, by solvent extraction using TTA, effects of TOPO on, 25:54692(R) (NYO-3417-15)
separation of uranium from, in methyl sulfoxide by cation exchange chromatography, 25:54728
stopping of nuclei of, in nuclear emulsion, mass resolution of, (E/T), 25:55894 (LUIP-CR-71-4)

IRON ALLOYS AND SYSTEMS
preparation by granule metallurgy, evaluation of, 25:55404
stability of aluminum oxide dispersions in, at high temperatures, 25:55485
thermoelectric properties of, at 0 to 1000°C, 25:56351
Al--Cu--Fe--Sn--Ti-base--V, development and evaluation of high-strength, 25:55421
Al--Fe, magnetic properties of, 25:56358
Al--Fe--Ti, mechanical properties at 550 to 1100°C, 25:55501
Al--Fe--Ti, phase studies of, 25:55501
Be--Fe-base, phase transitions in 400°C annealing of, Moessbauer-effect study of, 25:56378
carbides--Fe, strength of powder shapes of, effects of dispersion-, grain boundary-, and solid solution-hardening on, 25:55487
Co--Fe--Mo, electric conductivity of supersaturated solid solutions of, effects of phase decomposition on, 25:55472
Co--Fe--V, magnetic properties at cryogenic temperatures, 25:56361
Co--Fe--W, hardening of, kinetics of dispersion, 25:55423
Co--Fe-base, stability of aluminum oxide dispersions in, at high temperatures, 25:55485
Cr--Fe, iron-57 Moessbauer spectra using polarized cobalt oxide source, 25:56366
Cr--Fe-base, stability of aluminum oxide dispersions in, at high temperatures, 25:55485
Cr--Fe-base--Ni, stability of aluminum oxide dispersions in, at high temperatures, 25:55485
Fe--Mo--Ni, properties and structure of, produced by sintering using systematic thermal fluctuations, 25:55414
Fe--Mo--Ni-base, magnetic properties at cryogenic temperatures, 25:56361
Fe--Ni, electron mean free path in Permalloy foils, fast, (E), 25:56281
Fe--Ni, magnetic properties at cryogenic temperatures, 25:56361
Fe--Ni, precipitation in beryllium-containing, metallography of 700°C, 25:55544
Fe--Ni, properties and structure of, produced by sintering using systematic thermal fluctuations, 25:554..
Fe--Ni--WC, phase relations and tensile properties of sintered, 25:55631
Fe--Ni-base, microstructure of Type 706, 25:55553
Fe--Ni-base, microstructure of Type 706, effects of heat treatment on, 25:55554
Fe--Sm, phase diagram and intermetallic compounds, 25:55569
Fe--Ta, thermodynamic properties of intermetallic $TaFe_2$, 25:55508
Fe--WC, phase relations and tensile properties of sintered, 25:55631
Fe-base--Mn--Ni, stability of aluminum oxide dispersions in, at high temperatures, 25:55485
Fe-base--Mo, stability of aluminum oxide dispersions in, at high temperatures, 25:55485
Fe-base--Mo--Ni, stability of aluminum oxide dispersions in, at high temperatures, 25:55485
Fe-base--Ni, stability of aluminum oxide dispersions in, at high temperatures, 25:55485
Fe-base--Ni--Rh, use as filter in polarized iron-57 Moessbauer source, 25:56366
Fe-base--Si, magnetic properties at cryogenic temperatures, 25:56361
Fe-base--Ti, stability of aluminum oxide dispersions in, at high temperatures, 25:55485
Fe-base--V, deformation and fracture at low temperatures, effects of vanadium content on, 25:55478

IRON BROMIDES
Moessbauer-spectral study of cobalt-57 decay effects on valence and structure of, 25:56381

IRON CHLORIDES $FeCl_2$
Moessbauer-spectral study of cobalt-57 decay effects on valence and structure of, 25:56381

IRON IODIDES
Moessbauer-spectral study of cobalt-57 decay effects on valence and structure of, 25:56381

IRON IONS
Moessbauer-effect studies of structure of inorganic complexes and organometallic compounds of, review, 25:56380
spectra of Fe XV in solar corona, extreme-ultraviolet, (E), 25:55767
spectral lines due to, in solar euV spectrum, (E), 25:55774

IRON ISOTOPES
determination of, gas-phase mass spectrometric, 25:54404

IRON ISOTOPES Fe-52
nuclear properties of, for medical use, 25:54676
production by proton reactions with manganese and ion

exchange, 25:54676
IRON ISOTOPES Fe-54
alpha reactions (α,p) at 9.86, 10.02, and 10.40 MeV, p--γ angular correlations from, (E), 25:56700
neutron capture by, gamma spectra from thermal, (E), 25:56683 (FEI-205)
proton elastic scattering at 9.6 MeV, optical-model analysis of, (E/T), 25:56699
IRON ISOTOPES Fe-55
uptake by organisms of marine food chain, effects of physico-chemical form on, 25:55149 (BNWL-SA-4048)
IRON ISOTOPES Fe-56
energy level 0.85 MeV from neutron inelastic scattering, deformation parameter for, (E), 25:56707
energy levels from resonances in (γ,n) reactions, isobaric analog, (E), 25:56702
neutron capture by, cross section for nonresonant, (E), 25:56702
neutron capture by, gamma spectra from thermal, (E), 25:56683 (FEI-205)
neutron elastic and inelastic scattering at 14 MeV, vibrating-model analysis of differential cross sections for, (E), 25:56707
photon reactions (γ,n) near threshold energy, cross section for, (E), 25:56702
proton elastic scattering at 9.6 MeV, optical-model analysis of, (E/T), 25:56699
proton inelastic scattering at 6.9 MeV, distorted-wave analysis of differential and integrated cross sections for, (E), 25:56727
IRON ISOTOPES Fe-57
Moessbauer effect in fast-neutron-irradiated cobalt-doped silicon, 25:56326
Moessbauer effect in iron inorganic complexes and organometallic compounds, review, 25:56380
Moessbauer source, preparation of polarized, 25:56366
Moessbauer technique, delayed-coincidence, 25:56367
Moessbauer--NMR study of rf-perturbed hyperfine levels of, 25:56368
photon reactions (γ,n) near threshold energy, cross section for, (E), 25:56702
IRON ISOTOPES Fe-58
energy levels from manganese-58 beta decay, spin--parity assignments for, (E), 25:56710
IRON ISOTOPES Fe-59
distribution in man, whole-body radiometric method for studies of, 25:55111
IRON OXIDES
properties and structure of, produced by sintering using systematic thermal fluctuations, 25:55414
IRON OXIDES FeO
Moessbauer-spectral study of cobalt-57 decay effects on valence and structure of, 25:56381
IRON OXIDES $Fe_2O_3$
Moessbauer-spectral study of cobalt-57 decay effects on valence and structure of, 25:56381
$Al_2O_3$--$Fe_2O_3$, production of fine powders of, Microgel process for, 25:55419
IRRADIATION FACILITIES
accidents at, methods of estimating gamma radiation dose to man following, 25:55235
description of alpha, for irradiating mammalian cells, 25:55002 (NYO-2740-8, pp 7-146)
description of SHERLOCK III neutron, 25:54506
description of STIRCA, at Cadarache, France, 25:54851
description of USSR UGU-200 gamma, 25:54844
design and operation of safe, for medical use in Japan, 25:54852
design of, 25:54855(P)
design of dual compartment portable, with panel-type radiation source, 25:54849(P)
design of electron, for industrial materials, 25:54835(P)
design proposal for biomedical, at Los Alamos Meson Physics Facility, 25:55299 (LA-4490)
development of gamma, in United Kingdom for commercial processing, 25:55363
dosimetry in 380-Ci cobalt-60 dual, 25:55319 (UCD-472-118)
gamma sources for, development of economical high-intensity, 25:54914
radiation dose in uranium loop-type, calculation of gamma, 25:54991
radiation dosimetry in bulk grain, performance of encapsulated LiF dosimeter for γ, 25:55234
ISONIAZID
radiosensitizing effects on hamster cells, x, 25:55207 (NYO-2740-8, pp 220-59)
ISOTOPE EFFECTS
use of, after rate-determining step to study behavior of bonds during hydrogen transfer, 25:54577
ISOTOPE EXCHANGE
processes in gaseous phase for measurement of diffusion coefficients of liquid metals, 25:54556
radiation effects on, chromatographic studies on, 25:54727
ISOTOPE GENERATORS
design of mother--daughter-type, with quick coupling mechanism, 25:54909(P)
development of, using countercurrent electrophoresis, 25:54742
ISOTOPE SEPARATION METHODS
cascades for large arbitrary enrichment, design of asymmetric, 25:54917
development of countercurrent electrophoresis, 25:54742
review of new, for uranium isotopes, 25:54919
ISOTOPES
separation factors for, in electromigration through ion exchange membranes, single stage, 25:54729
ITALY
reform of C.N.E. in, 25:55252 (NP-18752)


## J


JAMES A. FITZPATRICK POWER REACTOR
containment system for, design parameters of, 25:56961 (DOCKET-50333-30)
design parameters for, revised and additional data on, 25:56961 (DOCKET-50333-30)
operations aspects for, revised and additional data on, 25:56961 (DOCKET-50333-30)
technical specifications for, 25:56961 (DOCKET-50333-30)
JAPAN
health and safety at Oarai Research Establishment in, during October through December 1970, 25:55247(R) (JAERI-Memo-4353)
radiation dose to man in, from external occupational exposures, estimation of genetically significant equivalent γ, neutron, and x, 25:55230
JAPANESE POWER DEMONSTRATION REACTOR
fuel rods of, fission product release and detection of failed Zircaloy 2 clad uranium oxide ($UO_2$), 25:57047 (JAERI-Memo-4157, pp 2-22)
neutron monitor for, development of in-core boron coated ionization chamber, 25:57025
JET ENGINES
inspection of, use of iridium-192 gamma sources for radiographic, 25:54927
JOINTS
scanning of sacroiliac, in ankylosing spondylitis patients, effectiveness of strontium-85 for, 25:55287
JOSEPH M. FARLEY POWER REACTOR, UNIT 1
construction of, revised and additional data for permit application for, 25:56964 (DOCKET-50348-24)
control system for, wiring requirements for, 25:56966 (DOCKET-50348-26)
design parameters of, revised and additional data on, 25:56965 (DOCKET-50348-25)
operation of, revised and additional data for license application for, 25:56964 (DOCKET-50348-24)
operations aspects of, revised and additional data on, 25:56965 (DOCKET-50348-25)
JOSEPH M. FARLEY POWER REACTOR, UNIT 2
construction of, revised and additional data for permit application for, 25:56964 (DOCKET-50348-24)
control system for, wiring requirements for, 25:56966 (DOCKET-50348-26)
design parameters of, revised and additional data on, 25:56965 (DOCKET-50348-25)
operation of, revised and additional data for license application for, 25:56964 (DOCKET-50348-24)
operations aspects of, revised and additional data on, 25:56965 (DOCKET-50348-25)
JUPITER (PLANET)
luminosity of, relation to solar activity, (T), 25:55766


## K


KEROSENE
kerosene--TBP, radiolysis of, effects of nitric acid on reactor, 25:54644
KEWAUNEE POWER REACTOR
design parameters of, revised and additional data on, 25:56957 (DOCKET-50305-25)
operations aspects of, revised and additional data on, 25:56957 (DOCKET-50305-25)
KIDNEYS
glomerular filtration rate of human, use of chromium-51-labeled EDTA for measurement of, 25:55122
scanning in patients with cervical carcinomas for course control and prognosis, 25:55275
scanning of human, using chromium-51 or ytterbium-169-labeled EDTA, 25:55272
KILNS
charge residence time in rotary, use of cobalt-60 source for determination of, 25:54898
KIMBERLITES
thorium content in African, 25:54495
uranium content in African, 25:54495
KRYPTON
reactions with thallium bromides, crossed-beam measurements of cross sections for dissociative ionization in, 25:55879
release from liquid metal fast breeder reactor fuel recycle complex, 25:54754
scattering by nitrogen molecules, rainbow oscillations in differential cross sections for, (E), 25:55852
x-ray fluorescence yield of, K, (E), 25:56697
KRYPTON IONS
effects on silicon at 220 keV, lateral-stress study of damage produced in, 25:56285 (SC-RR-710424)


XUM

KRYPTON ISOTOPES
uses of radioactive, as indicator of oxygen mass transfer in aqueous solutions and slurries, 25:54903
KRYPTON ISOTOPES Kr-80
neutron capture by, cross sections for thermal and resonance, (E), 25:56691
KRYPTON ISOTOPES Kr-83
energy-level transitions in isomeric, energies and internal conversion coefficients for, (E), 25:56708
isomeric transition in, gamma and x-ray spectra and half-life for, (E), 25:56708
KRYPTON ISOTOPES Kr-85
content in global atmosphere, forecasts to year 2000 of, 25:54781(T) (JPRS-53174)
release from failed water cooled Zircaloy 2 clad uranium oxide ($UO_2$) fuel rods, 25:57047 (JAERI-Memo-4157, pp 2-22)
uses as tracer for studying atmospheric diffusion of plumes and puffs, 25:54908
KRYPTON ISOTOPES Kr-86
deuteron reactions (d,p) at 5 to 10.5 MeV, analysis of (d,n) threshold cusp using coupled-channel Born approximation, (E/T), 25:56719
KRYPTON ISOTOPES Kr-87
beta decay scheme, (E), 25:56703
release from failed water cooled Zircaloy 2 clad uranium oxide ($UO_2$) fuel rods, 25:57047 (JAERI-Memo-4157, pp 2-22)
KRYPTON ISOTOPES Kr-88
release from failed water cooled Zircaloy 2 clad uranium oxide ($UO_2$) fuel rods, 25:57047 (JAERI-Memo-4157, pp 2-22)
uses in detection of leaks in reactor fuel cans, 25:54904

# L

LA CROSSE BOILING-WATER REACTOR
cooling system for, stainless steel intergranular sensitization and failure probability in, 25:55378 (SWRI-1228-P-7-40)
quality assurance program for, 25:56925 (DOCKET-1155-134)
site of, environmental radiation survey during January 1969 to June 1971, 25:56895 (DOCKET-1155-135)
LABORATORIES
design and operational safety of Battelle plutonium, at West Jefferson, Ohio, 25:54959 (CONF-710401-, pp 280-92)
safety organization and procedures for plutonium development, 25:54958 (CONF-710401-, pp 258-66)
LABORATORY EQUIPMENT
design for measuring arc erosion of sintered copper and tungsten in oil, 25:55454
LACTOSE
effects on strontium-85 sorption by man, 25:55109 (COO-1231-67)
LANTHANUM
alpha fission at 167 MeV, angular distributions and particle track lengths for, (E), 25:56806
determination in Australian tektites by neutron activation and gamma spectrometry, 25:54478
determination in fission product mixtures by ion exchange and β counting, 25:54449
determination in intermediate products of rare earth production by x-ray spectroscopy, 25:54417
determination in river water and seawater by neutron activation and radiochemical separation, 25:54504
determination in volcanic ash by neutron activation and γ spectrometry, 25:54513
determination of trace amounts of, in air by neutron activation and γ spectrometry, 25:54456
effects on radiolysis of crystalline potassium nitrate, 25:54638
properties of aerosols of, produced from solutions at high temperatures, chemical and physical, 25:54545
separation from acid solutions by solvent extraction using acidic esters of aminophosphonic acids, 25:54732
separation from cerium and niobium by reverse-phase partition chromatography on TTA-impregnated paper, 25:54746
separation from cerium on titanium tungstate papers by electrochromatography, 25:54744
LANTHANUM ALLOYS AND SYSTEMS
Al--La--rare earths, crystal field levels, superconducting transition temperature, and exchange parameters of, (T), 25:56359
Al--La--Tm, crystal field levels of La/sub 1-x/Tm/sub x/$Al_2$, (E), 25:56359
Au--La, crystal structures and melting points of intermetallic, 25:55570
Ce--La, magnetic impurity scattering and superconductivity in, 25:56068
Eu--La-base, local moment relaxation in superconducting, (E), 25:56071
La--Pb, magnetic impurities effect on superconducting intermetallic $LaPb_3$, 25:56109
La--Sn, magnetic impurities effect on superconducting intermetallic $LaSn_3$, 25:56109
La--Sn, magnetic properties of $LaSn_3$, NMR and susceptibility, 25:56353
La--Tl, magnetic impurities effect on superconducting intermetallic $LaTl_3$, 25:56109
LANTHANUM BORIDES
production of complex $LaB_6$ shapes by hot casting under pressure, 25:55599
LANTHANUM ISOTOPES La-139
energy levels from barium-138 proton elastic scattering, spectroscopic factors for isobaric analog, (E), 25:56769
meson reactions ($\mu^-,\nu$) with, probability for, (E), 25:56739 (JINR-P1-6006)
nuclear magnetic resonance in $LaSn_3$, 25:56353
LASER RADIATION
effects on vanadium and nickel of pulsed, vacancy formation of, 25:56313
interactions with electrons, stimulated Compton energy exchange rate in, (T), 25:56266 (UCRL-51065)
scattering on plasma, electron distribution functions from Thomson, (E/T), 25:56143
LASERS
design of neodymium, for plasma production, 25:56193 (IPP-4/82)
performance of dye, effects of chemical quenching of triplet state on, 25:57288 (UCRL-51088)
quantum theory of spontaneous emission in presence of external radiation, 25:55883
use for plasma heating, prospects for, 25:56128
LAVA
analysis of peralkaline, by nuclear methods, 25:54462
LEAD
analysis of beads of, for noble metals by neutron activation and γ spectrometry, 25:54487
argon-ion reactions at 30 keV with surfaces of, charge states and kinetic energies of scattered and recoil ions from, (E), 25:55818
bremsstrahlung buildup factor for, dependence on position of shielding between source and detector, 25:56280
determination by controlled potential coulometry using rotated mercury cell, 25:54427
determination by x-ray counting after neutron activation, 25:54692(R) (NYO-3417-15)
determination in biological materials by irradiation with 30-MeV α particles and track registration of α particles from decay of resulting polonium, 25:54452
determination in isoquinoline formate by polarography, 25:54421
determination in sediments of Rhine River basin by x-ray fluorescence, 25:54408
determination in yttrium oxide by emission spectrometry, 25:54419
effects on radiolysis of crystalline potassium nitrate, 25:54638
effects on solvolysis of tert-butyl halides, Broensted correlation for, 25:54548
metallography of, sample preparation for, 25:57239 (MLM-OP-71004)
microwave oscillations in parallel superconducting Josephson junctions, 25:56077
neutron cross sections for, transmission of fission spectra through thick samples for evaluation of minima in total, (E), 25:56650 (COO-2049-5)
neutron reactions at 10 to 30 GeV/c, total cross sections for, (E), 25:56421
neutron reactions with, secondary gamma radiation in shielding from, 25:56277
separation of uranium from, in methyl sulfoxide by cation exchange chromatography, 25:54728
superconducting junctions of, finite-voltage behavior of Pb/Cu/Pb, (E), 25:56107
thermal capacity at 25 to 317°C, 25:55626
LEAD ALLOYS AND SYSTEMS
analysis for antimony, arsenic, and copper by neutron activation and radiochemical separation, 25:54515
preparation by granule metallurgy, evaluation of, 25:55404
Cd--Pb, diffusion in molten, kinetics of mutual, 25:55449
In--Pb, phonon spectra of dilute, superconducting tunneling study of, 25:56075
In--Pb, stress relaxation in mixed-state superconductivity, effect of magnetic fields on, 25:56063
In--Pb, strong-coupling parameters in superconducting, (E), 25:56076
In--Pb-base, thermal conductivity of one-dimensional superconducting, fluctuation effects on, (E/T), 25:56095
La--Pb, magnetic impurities effect on superconducting intermetallic $LaPb_3$, 25:56109
Pb--Pr-base, phase diagram of, 25:55567
Pb--Pr-base, phase diagram of, thermodynamic analysis of, 25:55566
LEAD AZIDES
radiolysis of crystalline, effects of additives on yields from proton and γ, 25:54638
radiolysis of, topography of evolution of products from x, 25:54642
LEAD ISOTOPES
book: Lead Isotopes in Geochemistry and Cosmochemistry, 25:54770
energy levels of neutron-deficient, survey of data on

low-lying, 25:56798
LEAD ISOTOPES Pb-206
photon reactions (γ,n) near threshold energy, cross section for, (E), 25:56702
LEAD ISOTOPES Pb-207
energy levels from resonances in (γ,n) reactions, doorway-state, (E), 25:56702
energy levels of, shell-model analysis of nonnormal, (T), 25:56763
neutron capture by, cross section for nonresonant, (E), 25:56702
photon reactions (γ,n) near threshold energy, cross section for, (E), 25:56702
LEAD ISOTOPES Pb-208
energy levels of, continuum shell-model calculation for giant dipole resonance, (T), 25:56800
meson reactions ($\mu^-,\nu$) with, probability for, (E), 25:56739 (JINR-P1-6006)
photon reactions (γ,n) near threshold energy, cross section for, (E), 25:56702
photon reactions (γ,n) with, analysis by Feynman triangle diagrams of fine-structure peaks in cross sections for, (T), 25:56676
photonuclear reactions of, analysis using eigenchannel reaction theory and continuum shell model, (T), 25:56800
proton elastic scattering with isobaric analog excitation, shell-model analysis of, (E/T), 25:56769
proton reactions at high energies, isobar model for analysis of meson (π) production in, 25:56530
LEAD ISOTOPES Pb-210
content in river waters in Czechoslovakia, (E), 25:54774
determination in lunar rocks and soils by β scintillation counting of bismuth-210, 25:54440
distribution in tissues of uranium mining personnel, 25:55117
LEAD ISOTOPES Pb-212
beta decay of, effects of chemical binding on recoil yields from, 25:54694
LEAD ISOTOPES Pb-214
beta decay of, effects of chemical binding on recoil yields from, 25:54694
LEAK DETECTORS
design for detecting gas leaks using radioisotope tracers, 25:55063(P)
LEPTONS
interactions with hadrons, generalized Weinberg sum rules in deep inelastic, 25:56461
LEUCINE
radiation effects on in vitro rat liver uptake of, γ, 25:55126
LEVEL INDICATORS
design of linearized radiometric, for measuring quantities of fluidic materials in containers, 25:55059(P)
LIGHT
amplification of spontaneously emitted, photon statistics of linear coherent, 25:57242 (NYO-3406-20)
deflection by gravitational field of cluster of galaxies, (T), 25:55809
effects on respiration rate in wheat seedlings, 25:55348
scattering by random surface ripples, optical mixing spectroscopic study of, 25:57232 (IS-T-494)
scattering by weakly ionized plasma, theory of Thomson, 25:56165 (N-71-27890)
LIGHT SOURCES
design of encapsulated radioactivated, 25:54915(P)
LIGHTNING
discharge pulses in ionosphere, correlation and spectral characteristics of leader stage of, (E/T), 25:55998
LIGNIN
radioinduced graft polymerization with polystyrene, γ, 25:54614
LIGROINE
effects on separation of europium or lanthanum from acid solutions by solvent extraction using acidic esters of aminophosphonic acids, 25:54732
LIMERICK POWER REACTOR, UNIT 1
cooling system equipment for, classification requirements for, 25:56968 (DOCKET-50352-20)
design parameters of, revised and additional data on, 25:56967 (DOCKET-50352-19)
emergency core cooling system for, revised and additional data on, 25:56968 (DOCKET-50352-20)
operations aspects of, revised and additional data on, 25:56967 (DOCKET-50352-19)
piping systems for, classification requirements for, 25:56968 (DOCKET-50352-20)
quality assurance program for, organization chart for, 25:56968 (DOCKET-50352-20)
LIMERICK POWER REACTOR, UNIT 2
cooling system equipment for, classification requirements for, 25:56968 (DOCKET-50352-20)
design parameters of, revised and additional data on, 25:56967 (DOCKET-50352-19)
emergency core cooling system for, revised and additional data on, 25:56968 (DOCKET-50352-20)
operations aspects of, revised and additional data on, 25:56967 (DOCKET-50352-19)
piping systems for, classification requirements for, 25:56968 (DOCKET-50352-20)
quality assurance program for, organization chart for, 25:56968 (DOCKET-50352-20)
LINEAR ACCELERATORS
beam focusing in high-current electron induction, 25:56608
target failure at electron, contamination and radioprotection problems resulting from natural uranium, 25:56582 (CEA-R-4188)
LINEAR ENERGY TRANSFER
analysis of, algorithm for, 25:55002 (NYO-2740-8, pp 7-146)
distributions in rabbit and rat phantoms following exposure to monoenergetic neutron beams, correlation of γ, neutron, and recoil ion dose distributions with, 25:55229
effects on RBE for effects of protons on impulse transmission in frog sciatic nerve, 25:55215
LIPIODOL
effectiveness of iodine-131-labeled, for human endolymphatic therapy, 25:55305
LIPOPOLYSACCHARIDES
radioprotective effects of, on mice, fast neutron and x, 25:55266
LIQUID METAL FAST BREEDER REACTOR
accidents in, analysis of aerosol production and distribution characteristics following, (E/T), 25:57105
accidents in, analysis of molten uranium oxide ($UO_2$) reaction with liquid sodium during, 25:57069(R) (ANL-7800)
containment structures for, effects of accidents on dynamic response of, 25:57069(R) (ANL-7800)
control system for 1000 MW(e), design requirements and simulation studies for, 25:57069(R) (ANL-7800)
coolant boiling in, detection and stability analysis of, 25:57069(R) (ANL-7800)
coolant boiling in, initiation and thermal hydraulics aspects of sodium, (E/T), 25:57068(R) (AI-AEC-13006)
coolant combustion accidents in, release and transport of aerosols and energy from sodium, (E/T), 25:57068(R) (AI-AEC-13006)
coolant interaction with molten fuel in, fuel rod failure propagation from, (T), 25:57083 (CONF-710302-(Vol.1), pp 241-58)
coolant interaction with molten fuel in, pressure generation by, (T), 25:57073 (CONF-710302-(Vol.1), pp 25-49)
coolant interaction with molten fuel in, reactivity feedback from, (T), 25:57074 (CONF-710302-(Vol.1), pp 50-78)
coolant voiding accidents in, PASET code for analysis of, 25:57082 (CONF-710302-(Vol.1), pp 215-40)
coolant voiding analysis in, comparison of momentum integral and compressible models for, 25:57081 (CONF-710302-(Vol.1), pp 180-98)
core disassembly accidents in, axial kinetics model for analysis of, 25:57080 (CONF-710302-(Vol.1), pp 167-79)
core disassembly accidents in, numerical instabilities in VENUS code for analysis of, 25:57079 (CONF-710302-(Vol.1), pp 152-66)
core disassembly accidents in, use of SAS2A code for analysis of, 25:57077 (CONF-710302-(Vol.1), pp 120-7)
core disassembly accidents in, two-dimensional space-time kinetics method for analysis of, 25:57078 (CONF-710302-(Vol.1), pp 128-51)
core for, effects of fuel failure propagation on safety and economic performance of, (E/T), 25:57089 (GEAP-13639-2)
core for, effects of fuel failure propagation on safety and economic performance of, (E/T), 25:57088 (GEAP-13639-1)
core melt-through accident in, safety aspects and containment methods for, 25:57093 (ORNL-TM-3504)
core structures for, effects of accident initiated stresses on plastic deformation of, 25:57069(R) (ANL-7800)
fuel cycle for, research progress on, 25:54717 (ORNL-4682, pp 160-2)
fuel element failure in, effects of fission gas and molten fuel ejection from, (T), 25:57075 (CONF-710302-(Vol.1), pp 79-96)
fuel elements for, Failed Fuel Mockup facility for testing, 25:57092(R) (ORNL-TM-3483)
fuel elements for, failure propagation characteristics of bundle arranged pin type, 25:57069(R) (ANL-7800)
fuel elements for, safety evaluation of equipment and methods for shipping spent, 25:54972 (ORNL-TM-2723)
fuel pin bundles for, effects of coolant flow blockage on, (T), 25:57076 (CONF-710302-(Vol.1), pp 102-19)
fuel pins for, effects of high temperature and burnup on performance of Type 347 stainless steel clad plutonium oxide ($PuO_2$)--uranium oxide ($UO_2$), 25:57045 (GEAP-10385)
fuel pins for, effects of overpower transients on performance of stainless steel clad uranium oxide ($UO_2$), 25:57046 (GEAP-13722)
fuel reprocessing for, development of aqueous methods for, 25:54713 (ORNL-4682, pp 39-79)
fuels for, radiation properties and shielding requirements of, 25:54713 (ORNL-4682, pp 39-79)
safety aspects of, research and development program during July 1969 to June 1970, 25:57069(R) (ANL-7800)


XUM

safety research on, summary of fiscal year 1971, 25:57068(R) (AI-AEC-13006)
safety studies for 1000 MW(e), review of, 25:57069(R) (ANL-7800)
stability of, analytical methods and transfer function techniques for, 25:57069(R) (ANL-7800)
standards for, development of engineering, 25:57092(R) (ORNL-TM-3483)
temperature measurement in, program for testing ultrasonic/thermocouple probe for, 25:55078(R) (NYO-3906-5)
thermal effluents from, effects on environment of, 25:57069(R) (ANL-7800)
LIQUIDS
containers for hazardous, design of pressure-relief plugged sealed, 25:54989(P)
diffusive motion in, time-of-flight neutron scattering method for studying, 25:56634
LITHIUM
abundance in solar atmosphere, (E/T), 25:55750
determination in tourmaline, by deuteron activation analysis and γ counting, 25:56752(R) (SUNI-14)
electron reactions up to 60 eV with, Born-approximation calculations of excitation cross sections for, 25:55864
reaction with defects in electron-irradiated n-type silicon, 25:56310
separation from salt solutions by solvent extraction using fluorinated β-diketones, 25:54718 (ORNL-4682, pp 168-81)
x-ray scattering by, form factors and scattering functions for coherent and incoherent, 25:56259 (EGG-1183-1479)
LITHIUM ALLOYS AND SYSTEMS
Bi--Li, solvent properties for rare earths and thorium, 25:54712 (ORNL-4682, pp 1-38)
LITHIUM ALUMINUM FLUORIDES
spectra of, effects of lithium-6 on ir, 25:54563
LITHIUM AMIDES
radiation effects on, production of carbon-11-labeled cyanides by recoils from proton, 25:54683
LITHIUM CHLORIDES
separation of fluoride from molten, by reactions with boron trichloride, 25:54534 (ORNL-4717, pp 43-56)
LITHIUM FLUORIDES
lattice sites of vanadium and manganese ions in crystals of, calculation and x-irradiation effects on, 25:56384
radioinduced thermoluminescence peaks and absorption bands of, error in analysis of, 25:56338
$BeF_2$--$CeF_3$--LiF, phase equilibria in, 25:54532 (ORNL-4717, pp 1-27)
$BeF_2$--LiF, thermodynamics of mixing in molten, electrochemical measurements of, 25:54532 (ORNL-4717, pp 1-27)
$BeF_2$--LiF--$ThF_4$, liquidus temperature of, 25:54534 (ORNL-4717, pp 43-56)
$BeF_2$--LiF--$ThF_4$, plutonium trifluoride solubility and absorption spectra in molten, effects of oxide on, 25:54532 (ORNL-4717, pp 1-27)
$BeF_2$--LiF--$ThF_4$--$UF_4$, separation of protactinium from molten, by oxide precipitation, 25:54712 (ORNL-4682, pp 1-38)
$BeF_2$--LiF--$ThF_4$--$UF_4$, separation of uranium from molten, by oxide precipitation, 25:54712 (ORNL-4682, pp 1-38)
LiF--NaF--$ThF_4$, phase equilibria in, high-temperature, 25:54532 (ORNL-4717, pp 1-27)
LITHIUM HALIDES
solvent properties of molten, for actinides and lanthanides, 25:54712 (ORNL-4682, pp 1-38)
LITHIUM HYDRIDES
LiH--W, shielding properties of, calculation of, 25:57133 (ORNL-TM-3366)
LITHIUM HYDROXIDES
radiation effects on aqueous solutions of, ESR studies of ozonide ion formation from γ, 25:54608
LITHIUM IONS
energy levels of $Li^+$, positions and widths of autoionizing, (T), 25:55820
energy of ground-state $Li^+$, calculation using Faddeev formalism, 25:55824
reactions with helium at 600 to 2800 eV, interference effects in charge-exchange cross sections for, 25:55844
LITHIUM ISOTOPES
separation in ion exchange resin--lithium salt solution system, 25:54730
LITHIUM ISOTOPES Li-6
abundance in Galaxy, (T), 25:55781
abundance in solar atmosphere, (E/T), 25:55750
deuteron elastic scattering at 8.0 to 12.0 MeV, optical-model analysis of differential cross sections and excitation functions for, (E), 25:56670
effects on ir spectra of lithium aluminum fluoride, 25:54563
energy levels from tritium (He-3,γ) reactions, resonance, (E), 25:56664
proton elastic scattering at 6.868 MeV, absolute cross section for, (E), 25:56670
reactions (Li-6,d) with argon-40 at 22 MeV, angular distributions for, (E), 25:56714
LITHIUM ISOTOPES Li-7
abundance in Galaxy, (T), 25:55781
deuteron elastic scattering at 10.0 to 12.0 MeV, optical-model analysis of differential cross sections and excitation function for, (E), 25:56670
deuteron reactions (d,t) at 10 to 12 MeV, excitation function, spectrum, and DWBA analysis of angular distributions from, (E), 25:56671
helium-3 reactions (He-3,α) at 16 to 18 MeV, excitation functions, spectrum, and zero- and finite-range DWBA analyses of angular distributions from, (E), 25:56671
proton elastic scattering at 6.868 MeV, absolute cross section for, (E), 25:56670
proton reactions (p,n) at 2 to 5.5 MeV, excitation function for, (E), 25:56752(R) (SUNI-14)
reactions (Li-7,d) with carbon-12 at 21.1 MeV, Hauser--Feshbach analysis of differential cross sections and spectra from, (E), 25:56663
reactions (Li-7,t) with carbon-13 at 20.5 MeV, DWBA and Hauser--Feshbach analyses of differential cross sections and spectra from, (E), 25:56663
scattering by carbon-12 and -13 at 21 MeV, optical-model analysis of, (E), 25:56663
LITHIUM ISOTOPES Li-9
production in alpha reactions with aluminum and silicon at 160 MeV, cross sections and fission mechanism for, (E/T), 25:56685 (FRNC-TH-48)
LITHIUM PERCHLORATES
reactions of molten, with rhenium or technetium, Raman spectral studies on compounds produced by, 25:54538
LITHIUM TANTALATES
congruent melting composition of $LiTaO_3$, from Curie temperatures, 25:55639
LITHIUM YTTERBIUM FLUORIDES
crystal structure of $LiYbF_4$, 25:54532 (ORNL-4717, pp 1-27)
LIVER
radiation effects on in vitro uptake of α-aminoisobutyric acid and cycloleucine by, γ, 25:55126
radiation effects on succinate dehydrogenase activity in rat in vitro, x, 25:55128
scanning of human, comparison of alkaline phosphatase evaluation and histological studies with gold-198, 25:55276
LOOPS
description of Luxembourg sodium test, 25:54839
design of sodium, for reactor material self-welding tests, 25:55379(R) (WARD-4210-T-1-2)
operation of sodium, for measurement of carbon and nitrogen mass transfer, 25:55379(R) (WARD-4210-T-1-2)
LOS ALAMOS MESON PHYSICS FACILITY
experimental facilities at, description of low-energy meson (π), 25:56589 (LA-DC-12730)
experimental facilities of, proposal for biomedical, 25:55299 (LA-4490)
meson (π) beam facility for, proposal for, 25:56588 (LA-4535)
LUNAR MATERIALS
aluminum-26 abundance in, (E), 25:55772
analysis by instrumental neutron activation and neutron activation with radiochemical separations, 25:54461
analysis for lead-210 by β scintillation counting of bismuth-210, 25:54440
analysis of fines No. 10084 from Apollo 11 for rare earths by ion exchange chromatography on high-voltage electrophoresis and neutron activation, 25:54475
analysis of rock, by activation and γ spectrometry, 25:54460
argon-40 diffusion from, (E), 25:55672
diffusion of radon in, 25:54440
isotope studies of Apollo 11 samples, (T), 25:55811
particle tracks in, characteristics of proton and alpha, (E), 25:55669 (N-71-26344)
sodium-22 abundance in, (E), 25:55772
LUNGS
radiation effects on blood circulation in rabbit, acute x, 25:55327
radiotherapy of metastases into, γ, 25:55300
scanning of human, effectiveness of technetium-99m-labeled sulfur colloid macroaggregates for, 25:55297
scanning of human, for diagnosis of embolism, effectiveness of technetium-99m-labeled human serum albumin and sulfur colloids in combination with gamma camera for, 25:55296
scanning of human, for evaluating perfusion changes following bronchography, use of iodine-131 for, 25:55285
scanning of human, health physics aspects of xenon-133, 25:55248
LUTETIUM
determination in river water and seawater by neutron activation and radiochemical separation, 25:54504
determination in volcanic ash by neutron activation and γ spectrometry, 25:54513
lattice parameters of, effects of hydrogen on, 25:55549
LUTETIUM ALLOYS AND SYSTEMS
Au--Lu, crystal structures and melting points of intermetallic, 25:55570
Lu--Mg, compound formation in, vapor pressure measurements for studies of thermodynamics of, 25:55525 (IS-T-462)
LUTETIUM ISOTOPES Lu-175
energy-level transition in, calculation of γ circular

polarization using parity-nonconserving potential, (T), 25:56768
energy-level transitions in, nuclear structure effects on internal conversion of M1, 25:56756
proton reactions (p,3nγ) at 20 to 40 MeV, γ spectra and excitation functions for, (E), 25:56796
LUTETIUM ISOTOPES Lu-176
neutron capture by, gamma and conversion-electron spectra from thermal, (E), 25:56762
LUTETIUM ISOTOPES Lu-177
energy levels from thermal neutron capture by lutetium-176, (E), 25:56762
LYMPH NODES
radiotherapy of metastases into thoracic, γ, 25:55300
scanning of parasternal, in patients with mammary carcinomas, effectiveness of gold-198 for, 25:55288
LYMPHOCYTES
growth following phytohemagglutinin stimulation, control of, 25:57284 (TID-25802)
radiation effects on clasmatosis periodicity in mouse, in relation hematopoietic recovery, γ, 25:55321
radiation effects on electrophoretic mobility of, effects of phytohemagglutinin on x, 25:56310
radiation effects on reactivity of human, following radon inhalation, effects of kidney disease type on, 25:55346
radiation effects on renewal patterns of rat spleen, tritium-labeled-thymidine, 25:55110(R) (TID-25801)
radiation effects on response of rat spleen, to sheep erythrocytes, tritium-labeled thymidine, 25:55110(R) (TID-25801)
LYSINE
effects on strontium-85 sorption by man, 25:55109 (COO-1231-67)


# M


MACHINING
methods for electrical discharge and electrochemical, bibliography on, 25:54834 (WAPD-331)
MAGNESIUM
abundance in B-type stars, (E), 25:55701
abundance in primary cosmic radiation, (E), 25:55911
analysis for calcium by nondestructive alpha activation, 25:54522
determination in tourmaline, by deuteron activation analysis and γ counting, 25:56752(R) (SUNI-14)
determination in yttrium oxide by emission spectrometry, 25:54419
effects on solvolysis of tert-butyl halides, Broensted correlation for, 25:54548
radioinduced void production in high-purity, fast neutron, 25:55580
separation from other alkaline earths by ionophoresis on filter paper and poly(vinyl alcohol), 25:54725
separation from other metal ions on titanium tungstate papers by electrochromatography, 25:54744
separation of uranium from, in methyl sulfoxide by cation exchange chromatography, 25:54728
stopping of nuclei of, in nuclear emulsion, mass resolution of, (E/T), 25:55894 (LUIP-CR-71-4)
thermal stability of powdered, in air, 25:55504
MAGNESIUM ALLOYS AND SYSTEMS
porosity of, effects of annealing and crystallization on micro-, 25:55462
preparation by granule metallurgy, evaluation of, 25:55404
Al--Mg--Zr, cracking and mechanical properties of welded joints of, effects of long-term heating at 70°C on, 25:55470
C--Ca--Ce--Mg--Si, analysis for tellurium by gravimetry, 25:54416
Ce--Mg, compound formation in, vapor pressure measurements for studies of thermodynamics of, 25:55525 (IS-T-462)
Dy--Mg, compound formation in, vapor pressure measurements for studies of thermodynamics of, 25:55525 (IS-T-462)
Er--Mg, compound formation in, vapor pressure measurements for studies of thermodynamics of, 25:55525 (IS-T-462)
Gd--Mg, compound formation in, vapor pressure measurements for studies of thermodynamics of, 25:55525 (IS-T-462)
Lu--Mg, compound formation in, vapor pressure measurements for studies of thermodynamics of, 25:55525 (IS-T-462)
Mg--Nd, compound formation in, vapor pressure measurements for studies of thermodynamics of, 25:55525 (IS-T-462)
Mg-base--Zr, oxidation above 400°C in presence of carbon dioxide, mechanisms of internal, 25:55382
Mg-base--Zr, structure of sintered, following high-temperature annealing, optical and electron microscopy studies of changes in, 25:55548
MAGNESIUM FLUORIDES
positron lifetimes in, empirical model for calculation of, 25:55834
MAGNESIUM ISOTOPES Mg-24
alpha elastic and inelastic scattering at 104 MeV, nuclear deformation study from differential cross sections for, (E), 25:56687 (KFK-1397)
alpha reactions (α,C-12) and (α,Li-6) at 42 MeV, cross sections for, (E), 25:56659
deuteron reactions (d,p) at 10 MeV, cross sections for, (E), 25:56728
nuclear deformation of, differential cross sections for alpha elastic and inelastic scattering by magnesium-24 for determining, (E), 25:56687 (KFK-1397)
photodisintegration rate of, relation to silicon burning in stars, 25:55703
MAGNESIUM ISOTOPES Mg-25
energy levels from resonances in (γ,n) reactions, isobaric analog, (E), 25:56702
photon reactions (γ,n) near threshold energy, cross section for, (E), 25:56702
MAGNESIUM ISOTOPES Mg-26
alpha elastic and inelastic scattering at 104 MeV, nuclear deformation study from differential cross sections for, (E), 25:56687 (KFK-1397)
alpha reactions (α, He-6) at 42 MeV, angular distributions for, (E), 25:56665
neutron capture at 2.9 MeV, cross section for, (E), 25:56696
nuclear deformation of, differential cross sections for alpha elastic and inelastic scattering by magnesium-26 for determining, (E), 25:56687 (KFK-1397)
MAGNESIUM OXIDES
CoO--MgO, fabrication for in-core neutron flux monitoring, 25:55019(P)
MgO--Mo, deformation mechanisms in, effects of temperature on, 25:55455
MgO--NiO, fabrication for in-core neutron flux monitoring, 25:55019(P)
MgO--$Y_2O_3$--$ZrO_2$-base, thermal stability of solid solutions of, effects of yttrium oxide content on, 25:55636
MAGNESIUM SULFATES
radiation effects from incorporated sulfur-35 on sorptive properties for hydrocarbons, gas chromatographic studies of, 25:54603
MAGNET COILS
developments in pulsed multifilament superconducting, 25:56580 (BNL-16026)
MAGNETIC ANALYZERS
calculations for a sector field electrostatic and, 25:56606
MAGNETIC FIELDS
cosmic-ray interactions with interplanetary, galactic, (E), 25:55904
currents under ionosphere, computer calculations of If, (T), 25:56001
effect on fluid motion produced by temperature gradient perpendicular to gravitational field, (T), 25:55919
energy conversion processes in solar, (T), 25:55773
magnetic drift waves near proton cyclotron frequency, (E/T), 25:56043
measurements of interplanetary, north--south component, (E), 25:55779
rotation of loop systems in solar atmosphere, (E/T), 25:55743
structure of interplanetary, effects on geomagnetic fields of sector, (E/T), 25:55988
structure of interplanetry, sector, (E/T), 25:55765
tidal effects of galactic, on small star clusters, (T), 25:55683
MAGNETIC MATERIALS
structures of compounds and alloys in monoclinic system, tables of neutron-diffraction, 25:56341 (NP-19010)
MAGNETIC MIRROR MACHINES
ion extraction from Pleiade-type, multiply charged heavy, 25:56210 (EUR-CEA-FC-603)
plasma injection into 2X II, large-area high-current ion source for, 25:56212 (LBL-35)
plasma injection into Baseball II, source for, 25:56217 (UCRL-73387)
plasma stability criteria for DECA II B, MHD, (T), 25:56194 (EUR-CEA-FC-598)
plasma stabilization in Phoenix II, using integrity feedback system, (E), 25:56197
x-ray spectra from INTEREM plasma, regularization technique for electron energy, distribution function for, 25:56134 (ORNL-TM-3582)
MAGNETIC RESONANCE
hyperfine structure of electron, effects of nuclear Zeeman term on, 25:54641
MAGNETIC STORMS
effect of Mar. 8, 1970, on ionospheric spatial and temporal electron content variations, (E), 25:55974
effect of polar, on localized characteristics of magnetotail magnetic fluctuations, (E), 25:56040
effect on geomagnetic fields in Earth core and on Earth surface and in magnetotail, (E/T), 25:56002
effect on interaction of galactic cosmic rays with interplanetary magnetic fields, (E), 25:55904
effect on magnetopause structure, Explorer-12 observations of Sept. 24, 1961, (E), 25:56022
effect on relation of positive ion-density enhancements to soft electron precipitation in polar ionosphere, Aug. 13-18, 1968, (E), 25:55964
observations of magnetospheric substorms on Sept. 14, 1968, balloon and satellite, (E), 25:56025


XUM

occurrence of substorm onset in magnetosphere, association with impulsive energetic electron flux in distant magnetotail, (E/T), 25:56044
production of magnetospheric sudden commencements, relation to polar magnetic substorms, (E/T), 25:56026
structure of polar, effect of intensification of westward electrojet current on, (E/T), 25:56029
sudden commencements of, diurnal and seasonal pattern in occurrence frequency from 1955--1969 of, (E/T), 25:56003
MAGNETITES
analysis for vanadium by activation method, 25:54483
effects of surface deposits of, on wick-boiling on heating surfaces, 25:54862 (AEEW-R-711)
MAGNETOHYDRODYNAMIC GENERATORS
electric energy transmission by, acting as direct voltage generators, 25:55913(P)
electrodynamic force profile control in conducting bodies in traveling magnetic field, (T), 25:55915
external characteristics of, with sections connected in series, (T), 25:55914
shock wave interactions in Faraday-type, (E), 25:55951
MAGNETOHYDRODYNAMICS
calculational method for n--z plane,, 25:56188
calculational programs for three-dimensional, 25:55944
electric circuit calculations in problems of, 25:55943
MAGNETOPAUSE
current-layer attitudes in, during Ogo-5 crossings, (E), 25:56023
position of, Imp spacecraft tabulations of averge and unusual, (E), 25:56021
structure during Sept. 24, 1961 magnetic storm, Explorer-12 data of, (E), 25:56022
MAGNETOSHEATH
plasma penetration from, into dayside magnetosphere forming polar cusp, (E), 25:56024
MAGNETOSPHERE
boundary parameters of, relation with Pc-type steady Earth-current pulsations, (E/T), 25:56004
bow-shock crossings at geocentric distances between 120 and 200 R/sub E/, Pioneer 8, (E/T), 25:55953
bow-shock position in, Imp spacecraft tabulations of average and unusual, (E), 25:56021
characteristics of polar cusp during magnetic storm, Nov. 1, 1968, (E), 25:56024
convection pattern from magnetic disturbance and auroral motion during Feb. 14-15, 1958, aurorae over Alaska, (E), 25:55954
current source and conductivity in equatorial, field-aligned, (E/T), 25:55959
deformation of, OGO 3 and 5 observations of magnetic-activity-related and time-dependent, (E), 25:55952 (N-71-27604)
electric field in, estimate of solar-wind-velocity-dependent, (T), 25:56039
electric fields in, satellite-borne double-probe dc measurements of convection, 25:55958
electron-flux profiles of pre-midnight asymmetry in outer radiation zones, 40-keV, (E), 25:56045
electrostatic-wave emissions in polar, satellite observations of vlf, (E), 25:55965
electrostatic-wave excitation in polar regions by streaming instability in polar wind, vlf, (E/T), 25:55966
magnetic drift waves near proton cyclotron frequency, (E/T), 25:56043
magnetic storm sudden commencements in, relation to polar magnetic substorms, (E/T), 25:56026
magnetic storms on Sept. 14, 1968 in, balloon and satellite observations of, (E), 25:56025
magnetic-field configuration from controlled injection of electron beams on magnetic-field lines, (E), 25:55961
magnetic-shell parameter L for point in magnetic field, new approximation of, (T), 25:56041
particle angular distribution near loss cone, equatorial 30 to 300 keV electrons and protons, (E), 25:56027
plasma-sheet behavior in, associated with visible auroral substorms over Alaska, (E), 25:55955
proton interactions with Alfven waves in, (T), 25:56011
solar wind interactions with, simulation of, 25:55976
whistler emission in, effect of whistler-wave interaction with related resonating particles on triggered, (E/T), 25:56038
MAGNETOTAIL
electron flux in distant, association with magnetic substorm onset in magnetosphere, (E/T), 25:56044
geomagnetic-field depression in, during magnetic storm, (T), 25:56002
magnetic-field fluctuations during polar magnetic substorms, localized characteristics of, (E), 25:56040
plasma-sheet behavior in, associated with visible auroral substorms over Alaska, (E), 25:55955
MAGNETS
shunt protection for superconducting, internal, (T), 25:56112
MAINE YANKEE POWER REACTOR
cooling system for, inspection of Type 316 stainless steel welds in pipe-to-valve joints of, 25:56958 (DOCKET-50309-41)
MALONIC ACID
potassium salt, radiation effects on monocrystals of, at 4.2°K, ESR spectral studies on production of radicals by x, 25:54654
MAMMALIA
calcium homeostasis in, cellular basis for, 25:57244 (NYO-3489-22)
MAN
americium-241 excretion in urine of, following inhalation as oxide, effects of DTPA on, 25:55118
cesium-137 content of, comparison of whole-body counter measurements of, 25:55225
congenital malformations in, genetic and nongenetic factors in, 25:57222(R) (COO-2013-19)
fluorine hazards to, following release to environment, 25:55246 (CEA-Bib-200)
glomerular filtration rate of kidneys of, use of chromium-51-labeled EDTA for measurement of, 25:55122
iron-59 distribution in, whole-body radiometric method for studies of, 25:55111
promethium-147 metabolism in, use of data from swine experiments in development of model for studies on, 25:55108 (BNWL-SA-3747)
radiation dose distribution in, during radiography using single- and three-phase equipment, comparison of x, 25:55227
radiation dose field in, standardization of isodose charts for expressing therapeutic, 25:55211
radiation dose to organs of, terminology for expressing, 25:55251
radiation dose to, during therapy, use of IBM 1130 computer for calculation of treatment fields in planning γ, 25:55218
radiation dose to, following accidental exposure to iridium-192, use of chromosome aberration frequency in biological dosimetry of γ, 25:55228
radiation dose to, following accidents at gamma irradiation facilities, use of aluminum phosphate dosimeters and phantom for estimating, 25:55235
radiation dose to, from external occupational exposures, estimation of genetically significant equivalent γ, neutron, and x, 25:55230
radiation dose to, from iodine-129 in environment of nuclear fuel reprocessing plant, 25:55199
radiation dose to, in vicinity of nuclear fuel reprocessing plant, estimation of, 25:55237
radiation dose to, interpretation of emergency, used in nuclear power plant site evaluations, 25:55242
radiation dose to, plutonium surface contamination levels for, 25:55195 (CONF-710401-, pp 352-64)
radiation effects on external respiration in, following therapy of malignant chest tumors, γ, 25:55339
radiation effects on mortality of, exposed in utero to atomic bombing in Hiroshima and Nagasaki, effects of dose on, 25:55307
radiation effects on potassium and sodium metabolism in, following iodine-131 therapy of diffuse toxic goiter, 25:55340
radiation effects on skin of, following therapy of bone sarcomas, high energy bremsstrahlung, 25:55338
radiation hazards to, from inhalation of reactor radioisotopes following accidental release, estimation of relative, 25:55202
radiation hazards to, from nuclear power plant effluent, evaluation of, 25:55347
radiation hazards to, use of model for effects on dogs to estimate long-term low dose radium-226, 25:55319 (UCD-472-118)
radiation protection of, dioctyl phthalate tests on respirators for, 25:55243 (CONF-710401-, pp 392-406)
radioimmunoassay of angiotensins in blood plasma of, effects of hypertension and renal transplants on, 25:55141
radioinduced injuries to nervous system of, following therapy of head tumors, prophylaxis and treatment of γ, 25:55269
radioinduced osteonecrosis in jaw of, following therapy of malignant tumor, γ, 25:55344
radioinduced osteonecrosis treatment in, following therapy of carcinomas, 25:55270
radioinduced thyroid carcinoma in, following iodine-131 therapy, 25:55343
radioisotope contamination of clothing and skin of, derivation of decision levels for control of, 25:55196 (LA-4558)
radioisotope content of, comparison of ICRP and MIRD methods for calculating maximum permissible, 25:55201
radioisotope distribution in, effects of calcium phosphate, methionine, Prussian blue, and sodium alginate on mixed cesium and strontium, 25:55113
radioprotection using cystamine, extrapolation of data on mice to γ, 25:55256
radiotherapy in, digital computer method for dose distribution calculations during cobalt-60 γ, 25:55221
radiotherapy of lung and thoracic lymph node metastases in, γ, 25:55300
radiotherapy of lymphogranulomatosis of bones in, effectiveness of γ and x, 25:55301
radiotherapy of malignant melanomas or metastases in, effectiveness of iodine-131-labeled lipiodol for endolymphatic, 25:55305
radiotherapy of small pelvis in, dosimetry for standardization of pendular cobalt-60 γ, 25:55222

radiotherapy of thyroglossal duct carcinomas in, role of surgery and thyroid hormone suppression in iodine-131, 25:55304
scanning of kidneys in, for course control and prognosis of cervical carcinomas, 25:55275
scanning of lungs in, for evaluating perfusion changes following bronchography, 25:55285
scanning of thyroid of children, immunofluorescent tests on antibody production following, 25:55292
strontium-85 metabolism following intravenous and oral administration, effects of calcium intake on, 25:55109 (COO-1231-67)
strontium-90 toxicity to, extrapolation of data on animals to determine long-term, 25:55319 (UCD-472-118)

MANGANESE
abundance in solar atmosphere, (E/T), 25:55750
argon-ion reactions at 30 keV with surfaces of, charge states and kinetic energies of scattered and recoil ions from, (E), 25:55818
determination in epitaxial films of gallium arsenide by neutron activation and radiochemical separation, 25:54512
determination in tourmaline, by deuteron activation analysis and γ counting, 25:56752(R) (SUNI-14)
determination in yttrium oxide by emission spectrometry, 25:54419
determination of trace amounts of, in air by neutron activation and γ spectrometry, 25:54456
determination of trace amounts of, in thorium and zirconium compounds by neutron activation, separation processes, and γ spectrometry, 25:54518
determination of trace amounts of, in ultramafic rocks by thermal neutron activation and γ spectrometry, 25:54496
effects on solvolysis of tert-butyl halides, Broensted correlation for, 25:54548
separation of uranium from, in methyl sulfoxide by cation exchange chromatography, 25:54728

MANGANESE ALLOYS AND SYSTEMS
Al--Mn, crystal structure of solidified, effects of cooling rate and supercooling on, 25:55550
Al-base--Mn, binding energy and entropy of vacancies in, 25:54587(R) (AECL-3909)
Bi--Mn, properties as extractant for rare earths from MSBR fuel solvent, 25:54534 (ORNL-4717, pp 43-56)
Fe-base--Mn--Ni, stability of aluminum oxide dispersions in, at high temperatures, 25:55485
Mn--Mo--Ni--steel, radiation effects on brittleness and strength of heavy-section plates and welds of, fast neutron, 25:55585
Mn--Ni-base, stability of aluminum oxide dispersions in, at high temperatures, 25:55485
Mn--Ti, inflammability correlation of powdered, 25:55473

MANGANESE IONS
lattice sites in lithium fluoride and sodium fluoride crystals, calculation and x-irradiation effects, 25:56384

MANGANESE ISOTOPES Mn-54
deposition and transport in FFTF cooling system, 25:55370 (BNWL-SA-2335)
uptake by organisms of marine food chain, effects of physico-chemical form on, 25:55149 (BNWL-SA-4048)

MANGANESE ISOTOPES Mn-55
neutron capture at 2.9 MeV, cross section for, (E), 25:56696
proton reactions (p,4n) at 65 MeV, production of iron-52 by, 25:54676

MANGANESE ISOTOPES Mn-58
beta decay of, gamma spectra, half-life, Kurie plots, and log-ft and Q values for, (E), 25:56710

MANOMETERS
design for prevention of glove box overpressure, 25:54958 (CONF-710401-, pp 258-66)
design of capacitance, for measuring oxygen pressures over dissociating oxides, 25:55428 (BNWL-B-108)
performance of molecular, for calibrating instruments for ultrahigh vacuum, 25:54992

MANY BODY PROBLEM
analysis using hyperspherical formalism, 25:56390 (LYCEN-7104, S5.1-53)
calculational system for two-dimensional, 25:56187
theory for nonrelativistic three-body, Faddeev approach for, 25:56575
treatment of nuclear three-body, using potential concept, 25:56872

MARITIME PRESSURIZED-WATER REACTOR
fuel element dropping incident for, recovery and repair procedures for, 25:57137 (DOCKET-50238-84)
operating limits for, safety analysis for Core 2 fuel shuffle, 25:57136 (DOCKET-50238-83)

MARS (PLANET)
exosphere structure of, from hydrogen Lyman-α dayglow analysis, (E), 25:55812
surface analysis by alpha scattering, 25:54459

MASS SPECTROGRAPHY
research progress on, 25:54587(R) (AECL-3909)

MASS SPECTROMETERS
beam positioner for, solid-state automatic, 25:55075 (K-1817)
ion source for MI-1305, high-temperature molecular-stream, 25:55081
performance for isotopic analysis of rocks, 25:54757(R) (MIT-1381-18)

MATHEMATICS
conference on reactor, 25:57071 (CONF-710302-(Vol.1))
conference on reactor, 25:57147 (CONF-710302-(Vol.2))
integrals having both exponential and gaussian functions in, evaluation of, 25:56399
synthesis of interval covers, geometrical model for, 25:57223 (COO-2118-13)

MATTER
detection of intergalactic, in Coma Cluster, (E), 25:55782
equation of state of, in neutron stars, (T), 25:55715
mass formula and properties of, at subnuclear densities, (T), 25:55678
model of superdense, properties of short-range field, (T), 25:55689
superfluid state in neutron-star, (T), 25:55714

MEATS
beef, effects of gamma irradiated, on lipid and protein metabolism of rats, 25:55367
fish, preservation by freezing, conference on, 25:55362 (LFEN-NI.-56a)
fish, radiation processing effects on survival of Salmonella species in smoked lake whitefish, γ, 25:55365
fish, radiation processing of Pacific Coast, effectiveness of shipboard γ, 25:55366
fish, radiation processing of, conference on, 25:55362 (LFEN-NI.-56a)
fish, strontium-90 content of, calculation of, 25:55156

MECHANICAL ENGINEERING
book: Experimental Stress Analysis and its Influence on Design, 25:54846

MEDICAL PERSONNEL
radiation dose to, during cardiac catheterization procedure, x, 25:55226
requirements of Los Alamos Meson Physics Facility, 25:55299 (LA-4490)

MEDICAL SUPPLIES
radiosterilization in United Kingdom, development of facilities for, 25:55363

MEDICINE
radioisotope uses in clinical, conference on, pharmacodynamic and pharmacokinetics of, 25:55255

MEMBRANE FILTERS
efficiency of molecular sieve-type, for sampling tritiated water vapor in air, 25:54798

MENDOCINO POWER REACTOR, UNIT 1
effluents from, effects on environment of chemical, radioactive, and thermal, 25:56973 (DOCKET-50398-8)

MENDOCINO POWER REACTOR, UNIT 2
effluents from, effects on environment of chemical, radioactive, and thermal, 25:56973 (DOCKET-50398-8)

MERCHANT VESSELS
economics of nuclear versus diesel powered, (T), 25:57138

MERCURY
corrosive effects on niobium--zirconium and T-111 alloys at 1200°F, 25:55377 (N-71-26947)
determination by neutron activation or photometry following solvent extraction, 25:54499
determination in Australian tektites by thermal neutron activation and radiochemical separations, 25:54478
determination in biological and environmental samples by neutron activation and radiochemical separation, 25:54508
determination in standard rocks and quartzes by neutron activation and radiochemical separation, 25:54454
determination in terrestrial and nonterrestrial rocks by atomic absorption spectroscopy, comparison of neutron activation analysis results with those from, 25:54511
determination of trace amounts of, in silicate rocks by neutron activation and radiochemical separations, 25:54489
potential for, method for modeling 1 + 2 component of, 25:56387
separation of uranium from, in methyl sulfoxide by cation exchange chromatography, 25:54728

MERCURY ALLOYS AND SYSTEMS
Hg--In, phase diagram of, 25:55536
Hg--Pr-base, phase diagram of, 25:55567
Hg--Pr-base, phase diagram of, thermodynamic analysis of, 25:55566

MESIC ATOMS
energy level shift in deuterium π-, contribution of absorption--re-emission process to, 25:55833
energy levels of μ- and π-, effects of meson finite size on, (T), 25:55831
meson (π) polarizability in, possibility of detection of, 25:55831
spectra of μ-, relation of nuclear charge distribution to isotope shifts in, 25:55821
x-ray emission from argon and neon μ-, (E), 25:55830

MESONS
coupling constants between baryons and pseudoscalar, in SU(3) strong coupling baryon bootstrap model, 25:56503
interactions of, symmetry breaking of chiral SU(3) x SU(3) in phenomenological Lagrangians for, (T), 25:56533 (IFA-FT-85)
interactions with 1/2+ baryons, tables of coefficients for partial-wave analysis of vector meson and 1/2+


XUM

baryon production in, (T), 25:56501 (RHEL/R-224)
masses of scalar, in broken chiral SU(3) x SU(3), (T), 25:56539 (ORO-3992-11)
model for, pseudovector isospinor heavy-boson, 25:56477
production from intermediate nucleon isobar decay in nucleon reactions with light nuclei, 25:56525
production of two, in anti p + p s- and p-wave interactions at rest, gauge-invariant chiral SU(3) x SU(3) symmetric Lagrangian model for, (T), 25:56538 (ORO-3992-2)
wave equation for dual free, Duffin--Kemmer, 25:56489

MESONS (eta)
interactions eta + eta, Lorentz pole structure of Virasoro model for, 25:56494
interactions eta + eta, Regge poles and residues in Virasoro model for elastic, 25:56493
production in forward γ + N → eta + N interactions, Regge absorption model for, (T), 25:56452 (CALT-68-313)

MESONS (f)
production in e + e → e + e + f(1260) interactions, cross sections for, (T), 25:56463

MESONS (K)
decay K → π + l + ν, effective Lagrangian model with SU(3) x SU(3) chiral symmetry-breaking terms for form factors of, (E), 25:56537 (JINR-E2-5996)
interactions K + N at 2 to 20 GeV/c, behavior of diffraction maximum in inelastic, (T), 25:56504
interactions K + N, particle exchange and Regge-pole exchange in Veneziano model for, 25:56518
interactions K + p and p + p, triple-Regge hypothesis for relations between cross sections for inclusive, 25:56515
interactions K + π from Chew--Low extrapolation of K+ + p interactions, phase shifts for, 25:56486
interactions K + π in K- + p and K- + n interactions at 3 GeV in bubble chamber, s-wave, (E), 25:56426 (FRNC-TH-53)
production in four-prong π+ + p interactions at 8 GeV/c in hydrogen bubble chamber, angular and momentum distributions for, (E), 25:56428 (IFA-HE-75)
production in π+ + p interactions at 8 GeV/c in hydrogen bubble chamber, momentum and angular distributions for, (E), 25:56427 (IFA-HE-73)
production of anti K - K pairs in four-prong π+ + p interactions at 8 GeV/c in hydrogen bubble chamber, (E), 25:56428 (IFA-HE-75)

MESONS (K-)
absorption by carbon-12, nitrogen-14, and oxygen-16, analysis of mechanism in, 25:56653 (LYCEN-7104, S4.1-10)
interactions K- + n at 3 GeV in deuterium bubble chamber, production of K(890), K(1400), and Kππ systems, upper limits for production cross sections of isospin-3/2 K*, and K + π s-wave interactions in, (E), 25:56426 (FRNC-TH-53)
interactions K- + p → anti K0 + n at 1.7 to 18.2 GeV/c, Regge analysis of, (E/T), 25:56506
interactions K- + p → anti K0 + n at high energies, Regge pole--cut model for analysis of, 25:56505
interactions K- + p → anti K0 + n, secondary Regge contributions in, 25:56508
interactions K- + p → K- + p at high energies, Regge pole--cut model for analysis of, 25:56505
interactions K- + p at 10 and 14 GeV/c, polarization parameter in forward elastic, (E), 25:56438
interactions K- + p at 20 to 65 GeV/c, energy dependence of total cross sections for, (E), 25:56433
interactions K- + p at 3 GeV in hydrogen bubble chamber, production of K(890), K(1400) and Kππ systems, upper limits for production cross sections of isospin-3/2 K*, and K + π s-wave interactions in, (E), 25:56426 (FRNC-TH-53)

MESONS (K0)
decay K0 → π0 + π0, K1^0 and K2^0 interference in, (E), 25:56407
decay K2^0 → π + e + ν, q²-dependence of vector form factor for, (E), 25:56408

MESONS (K+)
decay K+ → π0 + e+ + ν + γ, branching ratio for, (E), 25:56410
decay K+ → π0 + e+ + ν in heavy-liquid bubble chamber, form factor in, (E), 25:56409
interactions K+ + d → K0 + 2p at 3.8 GeV/c in deuterium bubble chamber, total and differential cross sections for K+ + n → K0 + p interactions and total and differential cross sections for, (E), 25:56423 (COO-1195-217)
interactions K+ + n → K0 + p at 5.5 GeV/c, Regge analysis of, (E/T), 25:56506
interactions K+ + n → K0 + p in K+ + d → K0 + 2p interactions at 3.8 GeV/c in deuterium bubble chamber, total and differential cross sections and forward amplitude for, (E), 25:56423 (COO-1195-217)
interactions K+ + n → K0 + p, secondary Regge contributions in, 25:56508
interactions K+ + n → K+ + π- + p at 12 GeV/c, structure in Kπ mass spectra near 1.85 GeV from, (E), 25:56434
interactions K+ + p → K*+(890) + p at 3.0 to 8.25 GeV/c, Veneziano model for, 25:56511
interactions K+ + p → K0 + π0 + Δ++, Kπ phase shifts from Chew--Low extrapolation of, 25:56486
interactions K+ + p → K0 + X (anything), triple-Regge hypothesis for p-Reggeon total cross section from inclusive, 25:56515
interactions K+ + p → K+ + p at high energies, Regge pole--cut model for analysis of, 25:56505
interactions K+ + p → K+ + π- + Δ++, Kπ phase shifts from Chew--Low extrapolation of, 25:56486
interactions K+ + p at 10 and 14 GeV/c, polarization parameter in forward elastic, (E), 25:56438
interactions K+ + p at 10 GeV/c in hydrogen bubble chamber, review of K* and N* production in, (E), 25:56435

MESONS (μ)
book; Cosmic Muons and Neutrinos, 25:56469
capture by nuclei, second-class G-parity properties in, (T), 25:56854
effects of cosmic, on eyes of astronauts, 25:55341
flux measurements underground using thin detectors and thick Utah detector, discrepancy between cosmic, 25:55897
intensity variations of cosmic, use of energy-dependent hadron--nucleus cross sections for calculation of ground level, 25:55906

MESONS (μ-)
capture by calcium-40, photon asymmetry for radiative, (E), 25:56705
capture by nuclei, effect of short-range correlations in, (T), 25:56824 (LYCEN-7104, C4.1-17)
capture by nuclei, lectures on models for, (T), 25:56809 (CERN-71-14, pp 67-99)
interactions μ+ + μ- at high energies, cross sections for Bhabha, 25:56466
interactions with electromagnetic field at 4 GeV/c in propane bubble chamber, direct electron pair production in, 25:56467
reactions (μ-,nν) with helium-4, short-range nucleon--nucleon correlation effects on energy spectrum and angular distribution asymmetry of neutrons from, (T), 25:56641 (JINR-P4-5986)
reactions (μ-,nν) with oxygen-16, neutron spectrum and angular distribution asymmetry in, (T), 25:56820 (JINR-P4-5997)
reactions (μ-,ν) with lanthanum-139 and lead-208, probability for, (E), 25:56739 (JINR-P1-6006)
reactions (μ-,ν) with oxygen-16, lectures on elementary particle method for partial capture rate for, (T), 25:56809 (CERN-71-14, pp 67-99)
reactions with argon and neon at high pressures, x-ray emission from, (E), 25:55830
reactions with argon--hydrogen mixtures, meson transfer from hydrogen to argon and x-ray emission in, (E), 25:55830

MESONS (μ+)
interactions μ+ + μ- at high energies, cross sections for Bhabha, 25:56466

MESONS (ω)
mass and width from π+ + p → π+ + p + ω0 interactions at 3.7 GeV/c, (E), 25:56430
vertex function in nonrenormalizable theory of ωrhoπ interactions, ladder approximation for, (T), 25:56483 (JINR-E2-6017)

MESONS (π)
absorption by carbon-12, nitrogen-14, and oxygen-16, analysis of mechanism in, 25:56653 (LYCEN-7104, S4.1-10)
absorption by light nuclei, lectures on, (T), 25:56810 (CERN-71-14, pp 155-228)
exchange contribution to nucleon-nucleon binding in e + d → e + p + n interactions, (T), 25:56527
exchange in n + p → 2p + π- interactions at 2 to 30 GeV, Reggeized one-pion-exchange model for, (T), 25:56521 (JINR-P1-5975)
interactions γ + π → π + γ, epsilonγγ and fγγ coupling constants from finite-energy sum rules for, (T), 25:56463
interactions K + π from Chew--Low extrapolation of K+ + p interactions, phase shifts for, 25:56486
interactions K + π in K- + p and K- + n interactions at 3 GeV in bubble chamber, s-wave, (E), 25:56426 (FRNC-TH-53)
interactions π + d → π + d, lectures on partial-wave dispersion relations for, (T), 25:56810 (CERN-71-14, pp 155-228)
interactions π + N → sigma + N, helicity conservation in, 25:56517
interactions π + N → vector meson + N, helicity conservation in, 25:56517
interactions π + N at 2 to 20 GeV/c, behavior of diffraction maximum in inelastic, (T), 25:56504
interactions π + N at 5.9 to 18.2 GeV/c, phenomenology of complex-spin negative-mass-squared resonance tachyons in angular distributions of charge-exchange, (T), 25:56500 (ORO-3992-18)
interactions π + N at high energies, total effective cross sections for acausal, (T), 25:56502
interactions π + N at low and intermediate energies, Regge poles for, (T), 25:56497 (FRNC-TH-33)
interactions π + N at low and medium energies, lectures on, (T), 25:56807 (CERN-71-14)
interactions π + N at low energies, lectures on, (T), 25:56496 (CERN-71-14, pp 101-54)
interactions π + N, coupling constant from current-

algebra sum rules and Veneziano amplitude for, 25:56516
interactions π + N, dual quark--parton model for, 25:56481
interactions π + N, three-channel model for $P_{11}$, 25:56519
interactions π + p → π + p at 0 to 300 MeV, review lectures on, (E/T), 25:56422 (CERN-71-14, pp 379-93)
interactions π + p at 4 to 36 GeV, quark model for multiple π production in, 25:56514
interactions π + π → rho + rho, helicity conservation in, 25:56517
interactions π + π at low energies, dispersion-relation calculations of amplitudes, phase shifts, and scattering lengths for, (T), 25:56495
interactions π + π in $\pi^+ + p \to \pi^+ + \pi^0(\pi^+) + p(n)$ and $\pi^+ + n \to \pi^+ + \pi^- + p$ interactions at 13.1 GeV/c in bubble chamber, diffractive, (E), 25:56425 (COO-1428-294)
interactions π + π, low-energy-parameter sum rules from two-variable crossing-symmetric expansion of amplitude of, (T), 25:56484 (ORO-3992-10)
interactions π + π, model for analytic, crossing-symmetric amplitudes of, 25:56490
interactions π + π, resonant structure in S-wave amplitudes of, 25:56492
interactions with nuclei, survey of research on, 25:56873
mass in renormalization theory, quadratic divergence of, 25:56564
production in e + p interactions above second resonance, review of, (E), 25:56406 (DESY-71/35)
production in forward γ + N → π + N interactions, Regge absorption model for, (T), 25:56452 (CALT-68-313)
production in four-prong $\pi^+$ + p interactions at 8 GeV/c in hydrogen bubble chamber, angular and momentum distributions for, (E), 25:56428 (IFA-HE-75)
production in γ + p, π + p, and p + p interactions at 4 to 36 GeV, quark model for multiple, 25:56514
production in $\pi^+$ + p interactions at 8 GeV/c in hydrogen bubble chamber, momentum and angular distributions for, (E), 25:56427 (IFA-HE-73)
radiobiological properties of, 25:55299 (LA-4490)
reactions with nuclei at 60 GeV in emulsions, production of low-energy protons in, (E), 25:56429 (INP-754)
reactions with nuclei at low and medium energies, lectures on, (T), 25:56807 (CERN-71-14)
reactions with nuclei, lectures on soft pion theorems for, (T), 25:56808 (CERN-71-14, pp 1-65)
scattering by nuclei, lectures on forward dispersion relations for elastic, (T), 25:56810 (CERN-71-14, pp 155-228)
scattering by nuclei, review lectures on nonvanishing pions in, (T), 25:56811 (CERN-71-14, pp 289-378)
vertex function in nonrenormalizable theory of πrhoπ interactions, ladder approximation for, (T), 25:56483 (JINR-E2-6017)

MESONS ($\pi^-$)
absorption in deuterium, energy level shift in π-mesic atom from, 25:55833
effects on diploid yeast cells, OER and RBE for mutagenic, 25:55165
interactions $\pi^- + p \to A_2^- + p$, $A_2^- \to \pi^- +$ neutrals near threshold energy, mass spectra of $A_2$ in, (E), 25:56436
interactions $\pi^- + p \to eta + n$ at 1.7 to 18.2 GeV/c, Regge analysis of (E/T), 25:56506
interactions $\pi^- + p \to eta + n$ in nuclei at 7.82 GeV/c, differential cross sections for, (E), 25:56432
interactions $\pi^- + p \to eta + n$ with $A_2$ exchange, K-matrix absorption model in U(6,6) x O(3,1) for, 25:56513
interactions $\pi^- + p \to eta + n$, secondary Regge contributions in, 25:56508
interactions $\pi^- + p \to K^+ + \Sigma^-$, spark chamber study of $\pi^-$, $K^+$, and $\Sigma^-$ decay products in, (E), 25:55048
interactions $\pi^- + p \to K^+ + \Sigma^-$, $\Sigma^- \to n + \pi^-$, spark chamber study of, (E), 25:55049
interactions $\pi^- + p \to n + \pi^+ + \pi^-$ at 7 GeV/c, Regge analysis of $rho^0$ production in, (E/T), 25:56431
interactions $\pi^- + p \to p + 2\pi^- + \pi^+$ at 5 to 25 GeV/c, partial-wave analysis for 3π system in mass region 1.0 to 2.0 GeV, (T), 25:56482 (COO-1195-224)
interactions $\pi^- + p \to \pi^0 + n$ at 5.9 to 18.2 GeV/c, negative-mass-squared resonance interpretation of angular distribution for, (T), 25:56499 (ORO-3992-8)
interactions $\pi^- + p \to \pi^0 + n$ at high energies, Regge pole--cut model for analysis of, 25:56505
interactions $\pi^- + p \to \pi^0 + n$ at very high energies, polarization in, 25:56509
interactions $\pi^- + p \to \pi^0 + n$ in nuclei at 7.82 GeV/c, differential cross sections for, (E), 25:56432
interactions $\pi^- + p \to \pi^0 + n$, secondary Regge contributions in, 25:56508
interactions $\pi^- + p \to \pi^- + p$ at high energies, Regge pole--cut model for analysis of, 25:56505
interactions $\pi^- + p \to \pi^- + p(\Delta^{++}) + rho^0(\pi^-)$, Cherenkov mechanism for cross section behavior of, (T), 25:56498 (IFA-HE-76)
interactions $\pi^-$ + p at 10 to 17.5 GeV/c, polarization parameter in forward elastic, (E), 25:56437
interactions $\pi^-$ + p at 20 to 65 GeV/c, energy dependence of total cross sections for, (E), 25:56433
interactions with electromagnetic field at 4 GeV/c in propane bubble chamber, direct electron pair production in, 25:56467
production in e + e → $\pi^+ + \pi^-$ interactions, Feynman diagram model for, 25:56460
production in proton reactions with nuclei at high energies, isobar model for analysis of nuclear surface effects on, 25:56530
reactions ($\pi^-$,2$\pi^-$) with carbon-12 at 4 GeV in propane bubble chamber, upper limit of cross sections for, (E), 25:56439
reactions ($\pi^-$,eta) with nuclei at 7.82 Gev/c, differential cross sections for, (E), 25:56432
reactions ($\pi^-$,$\pi^0$) with nuclei at 7.82 GeV/c, differential cross sections for, (E), 25:56432

MESONS ($\pi^0$)
interactions $\pi^0 + p \to \omega + p$, Reggeized absorption model fits to, 25:56458
interactions $\pi^0 + p \to rho^0 + p$, Reggeized absoption model fits to, 25:56458
production in e + N interactions at very low energies, review of, (E/T), 25:56404 (CONF-701121-8)

MESONS ($\pi^+$)
interactions $\pi^+ + d \to p + p + \pi^+ + \pi^-$ at 7 GeV/c, Regge analysis of $rho^0$ production in, (E/T), 25:56431
interactions $\pi^+ + d \to p + p$, lectures on partial-wave dispersion relations for, (T), 25:56810 (CERN-71-14, pp 155-228)
interactions $\pi^+ + n \to \pi^+ + \pi^- + p$ at 13.1 GeV/c in deuterium bubble chamber, diffractive π + π interactions in, (E), 25:56425 (COO-1428-294)
interactions $\pi^+ + p \to p + 2\pi^+ + \pi^-$ at 5 to 25 GeV/c, partial-wave analysis for 3π system in mass region 1.0 to 2.0 GeV, (T), 25:56482 (COO-1195-224)
interactions $\pi^+ + p \to \pi^+ + p + \omega^0$ at 3.7 GeV/c, mass and width of ω from, (E), 25:56430
interactions $\pi^+ + p \to \pi^+ + p$ at high energies, Regge pole--cut model for analysis of, 25:56505
interactions $\pi^+ + p \to \pi^+ + \pi^0(\pi^+) + p(n)$ at 13.1 GeV/c in hydrogen bubble chamber, diffractive π + π interactions in, (E), 25:56425 (COO-1428-294)
interactions $\pi^+ + p$ at 10 to 17.5 GeV/c, polarization parameter in forward elastic, (E), 25:56437
interactions $\pi^+ + p$ at 8 GeV/c in hydrogen bubble chamber, cross sections, kinematical behavior of secondaries, and K--anti K pairs and resonance production in four-prong, (E), 25:56428 (IFA-HE-75)
interactions $\pi^+ + p$ at 8 GeV/c in hydrogen bubble chamber, mass distributions and cross sections for resonance production and momentum and angular distributions for, (E), 25:56427 (IFA-HE-73)
production in e + e → $\pi^+ + \pi^-$ interactions, Feynman diagram model for, 25:56460
production in e + N interactions at very low energies, review of, (E/T), 25:56404 (CONF-701121-8)
production in proton reactions with nuclei at high energies, isobar model for analysis of nuclear surface effects on, 25:56530

MESONS (rho)
mass and width of rho' in anti p + n → $\pi^+ + 2\pi^-$ interactions in rising phase shift model, (T), 25:56485 (ORO-3992-66)
production in $\pi^+ + d \to p + p + \pi^+ + \pi^-$ interactions at 7 GeV/c, Regge analysis of (E/T), 25:56431
production in $\pi^- + p \to \pi^+ + \pi^- + n$ interactions at 7 GeV/c, Regge analysis of, 25:56431
production in $\pi^+ + p$ interactions at 8 GeV/c in hydrogen bubble chamber, (E), 25:56427 (IFA-HE-73)
production of $rho^0$ in $\pi^- + p \to \pi^- + p + rho^0$ interactions, Cherenkov mechanism for cross section behavior for, (T), 25:56498 (IFA-HE-76)
vertex function in nonrenormalizable theory of πrhoπ interactions, ladder approximation for, (T), 25:56483 (JINR-E2-6017)

MESONS, RESONANCE
coupling constants for epsilonγγ and fγγ from finite-energy sum rles for γ + π → π + γ interactions, (T), 25:56463
coupling strength from duality and unitarity, absolute, 25:56478
decay 3π → π + epsilon, partial-wave analysis for, (T), 25:56482 (COO-1195-224)
decay 3π → π + rho(f), partial-wave analysis for, (T), 25:56482 (COO-1195-224)
decay $A_1 \to \pi$ + rho, partial-wave analysis for s-wave, (T), 25:56482 (COO-1195-224)
decay $A_1 \to rho + \pi$, zero S-wave coupling from t-channel helicity conservation in $A_1 + A_1 \to \pi + \pi$ interactions, 25:56488
decay $A_2 \to \pi + f^0$, partial-wave analysis for s-wave, (T), 25:56482 (COO-1195-224)
decay of high-mass, dual resonance model for multiplicity in, 25:56491
decay of K(890) and K(1400) in bubble chamber, branching ratios for, (E), 25:56426 (FRNC-TH-53)
exchange of exotic, urbaryon rearrangement diagrams for two-body reactions with, 25:56479
interactions $A_1 + A_1 \to \pi + \pi$, zero S-wave coupling in $A_1$ rho π from t-channel helicity conservation in, 25:56488
production in $A_1$, $A_2$, and $A_3$ in 3π system in mass region 1.0 to 2.0 GeV in $\pi^+ + p \to p + 2\pi^+ + \pi^-$ and $\pi^- + p \to p + 2\pi^- + \pi^+$ interactions at 5 to 25 GeV, partial-wave


XUM

analysis for, (T), 25:56482 (COO-1195-224)
production of 3π system in mass region 1.0 to 2.0 GeV in $\pi^- + p \rightarrow 2\pi^- + \pi^+ + p$ and $\pi^+ + p \rightarrow p + 2\pi^+ + \pi^-$ interactions at 5 to 25 GeV/c, partial-wave analysis for, (T), 25:56482 (COO-1195-224)
production of $A_2$ in $\pi^- + p \rightarrow A_2^- + p$, $A_2^- \rightarrow \pi^- +$ neutrals near threshold energy, (E), 25:56436
production of anti K(890), K(890), and KantiK(1150), and KantiK(1325) enhancements in four-prong $\pi^+ + p$ interactions at 8 GeV/c in hydrogen bubble chamber, (E), 25:56428 (IFA-HE-75)
production of epsilon(750) in $e + e \rightarrow e + e +$ epsilon interactions, cross sections for, (T), 25:56463
production of isospin-3/2 $K^*$ in $K^- + p$ and $K^- + n$ interactions at 3 GeV in bubble chamber, upper limits for cross sections for, (E), 25:56426 (FRNC-TH-53)
production of $K^*$ in $K^+ + p$ interactions at 10 GeV/c in hydrogen bubble chamber, review of, (E), 25:56435
production of K(890) in $\pi^+ + p$ interactions at 8 GeV/c in hydrogen bubble chamber, cross sections for, (E), 25:56427 (IFA-HE-73)
production of K(890), K(1400), and K$\pi\pi$ systems in $K^- + p$ and $K^- + n$ interactions at 3 GeV in bubble chamber, (E), 25:56426 (FRNC-TH-53)
production of K$\pi$(1850) in $K^+ + n \rightarrow K^+ + \pi^- + p$ interactions at 12 GeV/c, (E), 25:56434
properties of $A_1$, $A_2$, and $A_3$ in 3π system in mass region 1.0 to 2.0 GeV in $\pi^+ + p \rightarrow p + 2\pi^+ + \pi^-$ and $\pi^- + p \rightarrow p + 2\pi^- + \pi^+$ interactions at 5 to 25 GeV, partial-wave analysis for, (T), 25:56482 (COO-1195-224)
properties of K(890) and K(1400) in $K^- + p$ and $K^- + n$ interactions at 3 GeV in bubble chamber, (E), 25:56426 (FRNC-TH-53)
reactions with stable and unstable hadrons, kinematic study of, (T), 25:56474 (FRNC-TH-63)
widths from duality and unitarity, elastic and total, 25:56478
widths of high-mass, in dual resonance model, 25:56491
METALLURGICAL EQUIPMENT
design for high-temperature stress measurement in chemical vapor deposited tungsten rings, 25:55440
METALLURGY
book: Physical Metallurgy of Refractory and Rare Metals, 25:55438
METALS
abundance in atmospheres of beta Cephei stars, (E/T), 25:55711
abundance in R Cyg and HD 35155, (E), 25:55699
abundance in stars, effects on structure of convection zone, (T), 25:55679
analysis for hydrogen, design of instrument for, 25:54424
analysis for light elements, alpha reactions with aluminum and silicon at 70 to 160 MeV for activation, 25:56685 (FRNC-TH-48)
book: Corrosion in Nuclear Applications, 25:55388
book: Emissive Properties of Materials (Handbook), 25:56346
book: Physical Metallurgy of Refractory and Rare Metals, 25:55438
corrosion by vanadium pentoxide melts, effects of polarization on, 25:55373 (CONF-690452-, Paper 6)
corrosive effects of liquid, on reactor components, review of, 25:55392
crystal disorder--order transformation in, kinetics of, 25:55552
defects in, high temperature annealing of quenched, 25:57216(R) (COO-1456-16)
density of pressed powdered, gamma radiometric measurement of, 25:55067
diffusion coefficients for liquid, use of isotope exchange in gaseous phase for measurement of, 25:54556
diffusion in, data tabulations on, 25:55509
ion reactions at 0.5 to 10 keV with monocrystalline surfaces of, equipment for study of reflection and secondary emission from, 25:55815
oxidation of, use of oxygen-18 (p,α) reaction for studying depth of, 25:55384
properties and structure of, produced by sintering using systematic thermal fluctuations, 25:55414
radiation effects on, tritium decay to helium for studies of, 25:55575 (LA-DC-12996)
radioinduced defects in, small angle x-ray scattering method for studies of, 25:55578 (RD/B/N-1990)
radioinduced swelling of pure, relations of dose and temperature with fast neutron, 25:55572 (BLG-457)
radioinduced swelling of, theoretical model for fast neutron, 25:55582
surface relaxations in cubic, 25:54587(R) (AECL-3909)
thermodynamic potentials and enthalpies during chlorination and oxidation, calculations of standard, 25:54586
METEORITES
analysis by 14-MeV neutron activation and γ spectrometry, review of, 25:54465
analysis by activation, comparison of other methods with, 25:54458
analysis by instrumental activation, gamma--gamma coincidence spectrometry in, 25:54479
analysis by instrumental neutron activation and neutron activation with radiochemical separations, 25:54461
analysis for tin by neutron activation using 40-min tin-123, 25:54480
analysis for trace amounts of elements by neutron activation, 25:54517
analysis for trace elements by neutron activation, 25:54477
analysis of stony, for calcium, chromium, iron, nickel, and titanium by proton and bremsstrahlung activation, 25:54466
analysis of terrestrial, for noble metals by neutron activation, 25:54484
argon-40 diffusion from, (E), 25:55672
element abundances in, (E/T), 25:55750
isotope abundance in Sikhote--Alin, helium-3, neon-21, and argon-38, (E), 25:55671
particle tracks in, characteristics of proton and alpha, (E), 25:55669 (N-71-26344)
xenon-isotope abundances in, (E/T), 25:55670
METHACRYLIC ACID, METHYL ESTER
radiolysis of single crystals of, at 77°K, ESR study of radicals and radical pairs from γ, 25:54634
METHANE
diffusion in graphite moderator, mathematical model of, 25:57044
neutron inelastic scattering by gaseous and liquid, calculation of second-order corrections for, 25:56628
neutron spectra in solid, time dependence following fast pulses, 25:56629
photolysis of, effects of deuterium on, 25:54573
pyrolysis at 1650 to 2150°C to produce carbon, mechanisms of, 25:55591 (JUL-735-RW)
pyrolysis of carbon-13-labeled, production of dense cylinders of carbon-13 by, 25:54542
radioinduced polymerization in dilute solutions in liquid argon, yields from γ, 25:54615
reactions with moderated recoil fluorine-18 atoms, effects of deuterium on rate of hydrogen abstraction, 25:54686
reactions with recoil tritium, kinetics of, 25:54684
He--methane--$SiH_4$, radiation effects on, reactions of recoil tritium from neutron, 25:54678
METHANE, BROMOTRIFLUORO-
properties for use in control of fires in large volumes, 25:54957 (CONF-710401-, pp 248-56)
properties for use in suppression of fires in glove boxes, 25:54954 (CONF-710401-, pp 212-20)
METHANE, CHLORO-
radiation effects on, effects of scavengers on reactions of recoil chlorine-38 from neutron, 25:54681
METHANE, CHLOROTRIFLUORO-
neutron reactions with, replacement reactions of recoil chlorine-38 in, 25:54688
METHANE, DICHLORODIFLUORO-
flow of highly dispersed, photographic study of post-burnout two-phase, 25:54875 (RT/ING-(71)8)
neutron reactions with, replacement reactions of recoil chlorine-38 in, 25:54688
METHANE, IODO-
diffusion and deposition of gaseous, in atmosphere, 25:54795
production in sodium hydroxide sprays, effects of organic materials on, 25:57092(R) (ORNL-TM-3483)
removal from reactor containment systems, effectiveness of sprays for, 25:57092(R) (ORNL-TM-3483)
METHANE, TRICHLOROFLUORO-
neutron reactions with, replacement reactions of recoil chlorine-38 in, 25:54688
METHANOL
radiolysis by fission fragments, thermal decomposition processes in, 25:54645
METHIONINE
effects on distribution of mixed cesium and strontium radioisotopes in man following ingestion, 25:55113
METHOTREXATE
effects on renewal patterns of normal and tumor cells, 25:55110(R) (TID-25801)
METHYL ETHER
effects on radiolysis of gaseous ethylene, 25:54643
METHYLIDYNE
detection of ionized, in photospheric spectrum, (E), 25:55768
METROLOGY
book: Accurate Characterization of the High-Pressure Environment, 25:54878
standards for nuclear, use of potassium-40 and rubidium-87 as, 25:54901
MICA
age of, effects of partial pressure on fission track estimation of, 25:54760
particle tracks in, characteristics of proton and alpha, (E), 25:55669 (N-71-26344)
radiation effects on dielectric properties of, γ, 25:55101
MICE
radiation dose to organs of, effects of chemical form of inhaled particles on niobium-95 and zirconium-95, β and γ, 25:55125
radiation effects on antigen retention system of, effects of cell inspection on recovery from x, 25:55147
radiation effects on clasmatocyte count in lymph nodes, spleen, and thymus of, γ, 25:55321
radiation effects on gastrointestinal tract of,

protective effects of S-2-[3-aminopropylamino]ethylphosphorothioic acid against x, 25:55259
radiation effects on growth and survival of, protective effects of tetrahydrofolic acid against x, 25:55268
radioinduced chromosome aberrations in blood of, extrapolation to man of protective effects of cystamine against γ, 25:55256
radioinduced chromosome translocations in spermatogonia of, RBE for gamma, 25:55182
radioinduced life shortening in, effects of dose, sex, and strain on protective effects of AET, cysteamine, PAPP, and serotonin against x, 25:55257
radioinduced recessive sex-linked lethal mutations in, three-generation test for frequency of x, 25:55184
radioinduced tumors in, following chronic ingestion of strontium-89, 25:55319 (UCD-472-118)
radioisotope distribution in, following inhalation, effects of chemical form on niobium-95 and zirconium-95, 25:55125
radiosensitivity of male, effects of radioprotective compounds on neutron and x, 25:55266
radiotherapy of mammary adenocarcinomas in, comparison of effects of air and carbogen atmosphere on cure rate during, 25:55302
radium-224 distribution in tissues of, following intraperitoneal injection, dose relation for radium-226 and, 25:55115
sensitivity to transverse acceleration, effects of radioprotective compounds on, 25:55264

MICROORGANISMS
radiation effects on DNA in, mechanism for mutagenic uv, 25:55136
radioisotope accumulation by marine, mechanisms of, 25:55154

MICROSOMES
calcium-45 uptake and release by rat brain, effects of ATP, choline, KCl, NaCl, and sucrose on, 25:55120

MICROWAVES
cosmic background, effects of elastic scattering and pair production in photon--photon collisions, 25:55908
use for heating of magnetized plasmas, resonances in anomalous, (E), 25:56124

MILK
separation of fission products from, double-bed ion exchange process for, 25:54722

MILKY WAY
cosmic-particle lifetimes in, (T), 25:55907
cosmic-ray containment in disk of, (T), 25:55895 (N-71-24988)
cosmic-ray history of, (T), 25:55781
hydrogen in, distribution of neutral, (E), 25:55791
infrared emission from central region of, 4-color photometry of, (E), 25:55783
interstellar grain alignment in, (T), 25:55792
nucleosynthesis in, (T), 25:55781
radio recombination-line emission from interstellar medium, (T), 25:55797
radio-wave polarization in loops and spurs between -7 and +85°, (E), 25:55787
rotational velocity of, radius of maximum, (T), 25:55786
stellar distribution in Cygnus, (E), 25:55790
structure of, from study of OB stars, (E), 25:55788
synchrotron radiation in, spatial distribution of, (E), 25:55730

MILLSTONE POINT POWER REACTOR, UNIT 1
emergency core cooling system for, effects of control circuit set conditions on failure of motor activated valves for, 25:56904 (DOCKET-50245-89)
emergency core cooling system for, failure of low pressure injection outboard containment spray valve for, 25:56906 (DOCKET-50245-91)
emergency core cooling system for, replacement of burned out actuating motors for low pressure injection valve and torus spray valve for, 25:56906 (DOCKET-50245-91)
emergency service water pumps for, failure to reach specified pumping pressure during surveillance test of, 25:56907 (DOCKET-50245-92)
radioactive effluents from, revised curie number for 1970, 25:56905 (DOCKET-50245-90)
turbine steam bypass valves for, failure of, 25:56908 (DOCKET-50245-93)

MINERALS
analysis of rock-forming, for iridium, osmium, and ruthenium by neutron activation and radiochemical separation, 25:54486
prospecting for seabed, using californium-252 neutron source, 25:54913

MIRRORS
radiation effects on stability of silvered and aluminized FEP teflon second-surface, electron, proton, and uv, 25:55656 (N-71-27736)

MITOCHONDRIA
immunological distinction of rat brain and liver, by sequential absorption analysis, 25:57253 (ORO-3195-41)
radiation effects on permeability and structure of membranes of rat liver, x, 25:55128

MITOSIS
radioinduced aberrations in rat bone marrow, x, 25:55192

MIXER-SETTLERS
design for radioactive waste fixation in bitumen, 25:54981

MOESSBAUER EFFECT
coincidence technique, delayed, 25:56367
conference on application of, Tihany, Hungary, June 17 to 21, 1969, 25:56374
conference on methodology of, sixth, Chicago, Jan. 25, 1970, 25:56364
gamma source for, preparation of polarized iron-57, 25:56366
Goldanskii--Karyagin effect of atomic vibration anisotropy in polycrystals, review, 25:56377
spectral shifts in, scale multipliers and calibration of isomer, (T), 25:56370
standards for, review of, 25:56365
use in studies of biological materials, review, 25:55105

MOESSBAUER SPECTROMETERS
velocity calibration of, review of, 25:56365

MOISTURE GAGES
design of passive radiometric, using cosmic ray neutrons, for soils, 25:55061(P)
design of radiometric, for sand, 25:55064(P)

MOLECULES
electron reactions at low energies with diatomic, review of total and momentum-transfer cross sections for, (E), 25:55856
electron reactions at low energies with, review of methods of measurement of cross sections for, 25:55855
electron reactions at low energies with, review of theory of rotational excitation in, 25:55855
electron reactions with, computer control system for studying, 25:55094
energy level lifetimes for fluorescent states, compilation of, 25:57215 (CEA-Bib-198)
energy transfer in systems of, research progress on, 25:54600(R) (UCLA-34-P-88-32)
photon emission in presence of external radiation, spontaneous, (T), 25:55883

MOLLUSCA
Aplysia californica, radioisotope content of Pacific Ocean, in environs of reactors, 25:55151 (CONF-710817-1)
Crassostrea angulata, zinc-65 uptake by shell and soft tissues of, effects of cobalt and iron on, 25:55153
Ostrea edulis, zinc-65 uptake by shell and soft tissues of, effects of cobalt and iron on, 25:55153
Physa heterostropha, radiation effects on population dynamics of, chronic low dose rate γ, 25:55314

MOLTEN SALT BREEDER REACTOR
fuel reprocessing for, by reductive extraction, 25:54534 (ORNL-4717, pp 43-56)
fuel reprocessing for, flow sheet analysis for, 25:54712 (ORNL-4682, pp 1-38)

MOLTEN SALT REACTOR EXPERIMENT
chemistry of coolant, fuel, and moderator in, 25:54533 (ORNL-4717, pp 29-41)
metal transfer studies in, 25:54533 (ORNL-4717, pp 29-41)

MOLYBDENUM
alpha fission at 167 MeV, angular distributions and particle track lengths for, (E), 25:56806
analysis for oxygen using exhalograph EAO-201, 25:54426
analysis for trace impurities, review on methods for, 25:54399
crystallization and polygonization of single crystals of, effects of rolling direction on, 25:55559
crystallization in strongly deformed monocrystal of, 25:55518
deformation mechanisms in, effects of temperature on, 25:55455
determination by dichrometric titration using triphenylmethane dyes as redox indicators, 25:54410
determination in fission product mixtures by ion exchange and polarography or β counting, 25:54449
determination in rocks, chemical methods for, 25:54403
determination of trace amounts of, in high-purity acids by emission spectrography, 25:54431
determination of, solvent extraction methods in, 25:54401
diffusion of nickel in monocrystalline, effects of vacuum on, 25:55505
effects on oxidation of niobium at 1500 to 2000°C and low pressures, 25:55380
microstructure of, effects of prior mechanical and thermal treatments on shock-induced, 25:55543
physical properties of plasma-sprayed spherical powders of, 25:55467
properties of aerosols of, produced from solutions at high temperatures, chemical and physical, 25:54545
properties of fibers of, for use in preparation of ceramic composites, 25:55608(T) (LB/G-3074)
radioinduced void production in, 5-MeV nickel ion, 25:55573 (BNWL-SA-3962)
separation from chromium, tungsten, and uranium by reverse-phase partition chromatography on TTA-impregnated paper, 25:54746
separation from other metal ions on titanium tungstate papers by electrochromatography, 25:54744
separation from rhenium by solvent extraction, 25:54401
separation from seawater by rapid adsorbing colloid flotation method, 25:54743
separation of uranium from, in methyl sulfoxide by cation


XUM

exchange chromatography, 25:54728
supercooling and thermal conductivity in superconducting, (E/T), 25:56066
thermal capacity at 25 to 2600°C, 25:55626
thermal expansion to 2000°C, 25:55493
thermodynamic properties of liquid, levitation calorimetry method for studies of, 25:55496
MOLYBDENUM ALLOYS AND SYSTEMS
$Al_2O_3$--Mo, deformation mechanisms in, effects of temperature on, 25:55455
Al--Co--Cr--Mo--Ni-base--Ti, fabrication of powdered, powder metallurgy and thermomechanical processes for, 25:55416
Al--Co--Cr--Mo--Ti--W, stress relaxation and surface hardening in, effects of high temperatures on, 25:55439
Al--Cr--Mo, thermal decomposition of solid solutions of, kinetics of, 25:55448
Al--Cr--Mo--Ni-base--W, fabrication of powdered, powder metallurgy and thermomechanical processes for, 25:55416
Al--Mo, solidification and phase transformations in, nonequilibrium, 25:55535
Al--Mo, thermal decomposition of solid solutions of, kinetics of, 25:55448
Al--Mo--Sn--Ti-base--Zr, welding of, properties of joints produced by friction, 25:55409
Al--Mo--Sn--U-base, tensile properties of dilute, at 23 to 600°C, 25:55429 (CEA-R-4177)
Al--Mo--Ti--V, corrosion cracking of, review on methods and problem of hot-salt stress, 25:55383
Al--Mo--Ti--V, diffusion of hydrogen in, at 450 to 600°F, effects of stress on, 25:55476
Al--Mo--Ti-base, embrittlement of two-phase, mechanisms of, 25:55450
Al-base--Mo, thermal expansion of quenched, 25:55499
C--Cr--Mo, microstructure of white irons of, 25:55556
C--Mo, superconductivity of phases of, 25:56087
Co--Fe--Mo, electric conductivity of supersaturated solid solutions of, effects of phase decomposition on, 25:55472
Co-base--Cr--Mo--Nb--Ni--W, corrosion by molten vanadium oxide, effects of chlorides, oxides, and sulfides of sodium on, 25:55375 (CONF-690452-, Paper 8)
Cr--Mo--Zr, phase diagram at 1150°C, 25:55538
Fe--Mo--Ni, properties and structure of, produced by sintering using systematic thermal fluctuations, 25:55414
Fe--Mo--Ni-base, magnetic properties at cryogenic temperatures, 25:56361
Fe-base--Mo, stability of aluminum oxide dispersions in, at high temperatures, 25:55485
Fe-base--Mo--Ni, stability of aluminum oxide dispersions in, at high temperatures, 25:55485
Hf--Mo, nitriding of, mechanism of growth and loss of coherency of hafnium nitride precipitates during internal, 25:55460
MgO--Mo, deformation mechanisms in, effects of temperature on, 25:55455
Mn--Mo--Ni--steel, radiation effects on brittleness and strength of heavy-section plates and welds of, fast neutron, 25:55585
Mo--Ni, mechanical properties at high temperatures, effects of molybdenum content on, 25:55474
Mo--Ni-base, stability of aluminum oxide dispersions in, at high temperatures, 25:55485
Mo--Ni-base--$ThO_2$, tensile strength at 1093°C, effects of thermomechanical processing on, 25:55486
Mo--Re--W, creep properties of, at 1800 to 4000°F, effects of grain size on, 25:55431 (N-71-23110)
Mo--Ta, hardening in monocrystals of, at 77 to 2000°K, solid-solution, 25:55457
Mo--Ta--Ti, phase studies of, 25:55565
Mo--Ti, deformation mechanisms in, effects of temperature on, 25:55455
Mo--Ti-base, deformation of, effects of strain rate and temperature on, 25:55459
Mo--TZM, deformation mechanisms in, effects of temperature on, 25:55455
Mo--U, thermoelastic response of, Grueneisen coefficient for, 25:55436 (SC-RR-710314)
MOLYBDENUM CARBIDES
wetting by copper, effects of electronic structure on, 25:55643
MOLYBDENUM FLUORIDES
stability in molten lithium beryllium fluoride solution, 25:54532 (ORNL-4717, pp 1-27)
MOLYBDENUM ISOTOPES Mo-92
deuteron reactions (d,n) at 6.25 and 7.0 MeV, time-of-flight spectra and DWBA analysis of differential cross sections for, (E), 25:56766
energy levels from proton inelastic scattering, transition probabilities for, (E), 25:56774
energy levels of, properties of multiparticle, (T), 25:56783
energy-level transitions in, analysis of E2, (T), 25:56783
proton elastic and inelastic scattering at 15 MeV, coupled-channel analysis of, (E/T), 25:56774
MOLYBDENUM ISOTOPES Mo-94
deuteron reactions (d,α) at 10 MeV, α spectra from, (E), 25:56758
deuteron reactions (d,n) at 6.25 and 7.0 MeV, time-of-flight spectra and DWBA analysis of differential cross sections for, (E), 25:56766
energy levels from proton inelastic scattering, transition probabilities for, (E), 25:56774
proton elastic and inelastic scattering at 15 MeV, coupled-channel analysis of, (E/T), 25:56774
MOLYBDENUM ISOTOPES Mo-95
neutron reactions (n,α) at resonance energies, α widths and resonance spin assignments for, (E/T), 25:56754(T) (UCRL-Trans-10541)
MOLYBDENUM ISOTOPES Mo-96
energy levels from proton inelastic scattering, transition probabilities for, (E), 25:56774
proton elastic and inelastic scattering at 15 MeV, coupled-channel analysis of, (E/T), 25:56774
MOLYBDENUM ISOTOPES Mo-98
energy levels from proton inelastic scattering, transition probabilities for, (E), 25:56774
proton elastic and inelastic scattering at 15 MeV, coupled-channel analysis of, (E/T), 25:56774
MOLYBDENUM ISOTOPES Mo-99
beta decay of, routine separation by solvent extraction of technetium-99m from, 25:54675
MOLYBDENUM ISOTOPES Mo-100
energy levels from proton inelastic scattering, transition probabilities for, (E), 25:56774
proton elastic and inelastic scattering at 15 MeV, coupled-channel analysis of, (E/T), 25:56774
MONKEYS
radioinduced sterility in developing ovaries of, following exposure in utero, effects of dose fractionation on x, 25:55319 (UCD-472-118)
MONTICELLO POWER REACTOR, UNIT 1
compressed air system for, scram initiation from failed loading controls for, 25:56914 (DOCKET-50263-85)
emergency core cooling system for, inoperability of high pressure coolant injection, 25:56912 (DOCKET-50263-82)
emergency core cooling system for, inoperability of high pressure coolant injection, 25:56913 (DOCKET-50263-84)
emergency core cooling system for, performance evaluation of, 25:56946 (DOCKET-50263-83)
instrumentation for, failure of mercury wetted magnetic switch in low-low water level, 25:56914 (DOCKET-50263-85)
MOON
electric conductivity and temperature of interior of, magnetic transient-response measurements of, 25:55810
magnetic field on surface of, magnetic transient-response measurements of, 25:55810
phase of, latitudinal dependence of ionospheric absorption on, (E), 25:55975
solar-wind interactions with, (E), 25:55810
surface analysis by alpha scattering, 25:54459
MOTORS
description and use of reluctance, for driving reactor control rods, 25:54848
MULLITES
properties of metal fiber-reinforced composites of, review on, 25:55608(T) (LB/G-3074)
properties of refractories of, mechanical and thermal, 25:55621
MUSCOVITES
age of, use of neutron activation in argon--potassium method of estimation of, 25:54765
MUTAGENS
effectiveness for inducing chromosome translocations in Vicia, 25:55191
MUTATIONS
induction in Mycobacterium phlei by 1-methyl-1-nitrosourea, 25:55171
radiation effects on survival of Escherichia coli, temperature dependence of recovery from uv, 25:55360
radioinduced adenine auxotrophic, in Bacillus subtilis, effects of aminopterin on uv, 25:55189
radioinduced adenine auxotrophic, in Escherichia coli, effects of streptomycin on uv, 25:55189
radioinduced dome, in Schizophyllum, linkage with B incompatibility factor of uv, 25:55186
radioinduced recessive sex-linked lethal, in germ cells of mice, three-generation test for frequency of x, 25:55184
radioinduced, in apples and pears for grafting on rootstocks, selection of, 25:55174
radioinduced, in bacteriophage T4, recombination in mutant crosses following uv, 25:55173
radioinduced, in barley and maize, effects of developmental stage and dose on, 25:55190
radioinduced, in barley and wheat seeds, effects of ethylenimine on x, 25:55261
radioinduced, in Chlorella vulgaris, photoreactivation capacity following uv, 25:55172
radioinduced, in diploid yeast cells, effects of LET on OER and RBE for γ, heavy ion, and meson ($\pi^-$), 25:55165
radioinduced, in Habrobracon for life-shortening, 25:55185
radioinduced, in lens of mice, effects of dose fractionation on x, 25:55206 (NYO-2740-8, pp 147-219)
radioinduced, in linseed for chlorophyll, dose dependence of γ, 25:55177

radioinduced, in linseed for chlorophyll, mechanisms of inheritance of γ, 25:55177
radioinduced, in Mycobacterium phlei for pigment formation, uv, 25:55171
radioinduced, in plants for improved agricultural qualities, review of, 25:55181
radioinduced, in plants for improved agricultural qualities, review of, 25:55179
radioinduced, in seeds of Crepis capillaris, effects of water content on γ and x, 25:55167
radioinduced, in yeast, gene control of uv, 25:55187
MYELIN
heterogeneity of central nervous system, 25:57261 (ORO-3195-49)
subfractions of rat central nervous tissue, isolation and biochemical characterization of, 25:57258 (ORO-3195-46)
MYLAR
deuteron reactions at 80 MeV with foils of, cross sections for electron capture in, (E), 25:55862
proton reactions at 155 and 600 MeV with foils of, cross sections for electron capture in, (E), 25:55862


# N


NAGASAKI
atomic bombing of, radiation effects on mortality of man exposed in utero to, 25:55307
NAPHTHALENE
hexane--naphthalene, radiation effects on, products from, 25:54599 (ORNL-4717, p 117-24)
NATURAL BACKGROUND RADIATION
effects on ion balance in atmosphere, 25:54786
NATURAL GAS
analysis of Rulison Event-stimulated, results of chemical and radiochemical, 25:54817 (PNE-R-52)
flow and pressure in wells following Rulison Event, data tabulation on, 25:54817 (PNE-R-52)
flow from runaway gas field wells, use of contained nuclear explosions for stopping, 25:54825(T) (UCRL-Trans-10543, pp 81-98)
production by underground nuclear explosions, consequences of using products from, 25:54599 (ORNL-4717, p 117-24)
production stimulation using underground nuclear explosions, radiation hazards from, 25:54823(T) (UCRL-Trans-10543, pp 56-69)
radioisotope content of, use of threshold limit values in establishing standards for, 25:55198
storage of, use of nuclear explosions to prepare reservoirs for, 25:54816 (ORNL-4682, pp 182-6)
NATURAL WATERS
radon content of Bad Brambach, Germany, dual ionization chamber measurements of, 25:54766
NEBULAE
infrared emission from dust grains in Orion, (T), 25:55718
radio emission from, in Magellanic Clouds at 408 MHz, (E), 25:55722
NEODYMIUM
desorption from tungsten, heat of, 25:55533
determination in intermediate products of rare earth production by x-ray spectroscopy, 25:54417
determination in volcanic ash by neutron activation and γ spectrometry, 25:54513
diffusion in nickel at 500 to 1100°C, volume and grain-boundary, 25:55488
effects on radiolysis of crystalline potassium nitrate, 25:54638
separation from aqueous solutions by solvent extraction using TTA, synergistic effects of 2,4-pentanedione on, 25:54731
separation from gadolinium and samarium by liquid--liquid chromatography using bis(2-ethylhexyl) phosphate and sulfuric acid, 25:54745
separation from promethium by displacement chromatography using [(carboxymethylimino)bis(ethylenenitrilo)]tetraacetic acid, EDTA, and nitrilotriacetic acid, 25:54723
solubility in liquid bismuth--lithium systems, 25:54712 (ORNL-4682, pp 1-38)
NEODYMIUM ALLOYS AND SYSTEMS
Au--Nd, crystal structures and melting points of intermetallic, 25:55570
Ce--Nd--Ru, critical magnetic field in superconducting, (E), 25:56074
Mg--Nd, compound formation in, vapor pressure measurements for studies of thermodynamics of, 25:55525 (IS-T-462)
NEODYMIUM ISOTOPES
nuclear electric quadrupole moments of, (E), 25:55828
spectra of electronic and muonic, relation of nuclear charge distribution to isotope shifts in, 25:55821
spectra of, isotopic shift in, (E), 25:55828
NEODYMIUM ISOTOPES Nd-137
energy-level transitions in, branching ratios, internal conversion coefficients, and multipolarities for, (E), 25:56761
NEODYMIUM ISOTOPES Nd-141
energy levels from neodymium-142 (p,d) reactions, neutron-hole structure of, (E), 25:56770
NEODYMIUM ISOTOPES Nd-142
alpha reactions (α,xnypzα) at 104 MeV, gamma spectra from, (E), 25:56761
proton reactions (p,α) at 35 MeV, DWBA analysis of, (E), 25:56770
NEODYMIUM ISOTOPES Nd-143
neutron reactions (n,α) at resonance energies, α widths and resonance spin assignments for, (E/T), 25:56754(T) (UCRL-Trans-10541)
NEODYMIUM ISOTOPES Nd-145
neutron reactions (n,α) at resonance energies, α widths and resonance spin assignments for, (E/T), 25:56754(T) (UCRL-Trans-10541)
NEODYMIUM ISOTOPES Nd-152
beta decay of, β and γ singles and coincidence spectra from, (E), 25:56772
NEODYMIUM OXIDES
argon-ion reactions at 30 keV with, charge states and kinetic energies of scattered and recoil ions of, (E), 25:55818
NEON
abundance in primary cosmic radiation, (E), 25:55911
deuterium-ion reactions up to 100 eV with, cross sections for dissociation in, (E), 25:55858
effects on yields from reactions of recoil tritium with ethane and methane, 25:54684
gold-198 ranges in, from gold-197(n,γ) recoil, 25:56269
helium-hydride-ion reactions at 0.5 to 1 MeV with, cross sections for dissociation in, (E), 25:55872
helium-ion inelastic scattering by, quasi-diabatic calculation of differential cross sections for, 25:55849
hydrogen-ion ($H_2^+$) reactions up to 100 eV with, cross sections for dissociation in, (E), 25:55858
meson ($\mu^-$) reactions with, x-ray emission from, (E), 25:55830
nuclear charge radius of, determination from x-ray emission in neon--meson ($\mu^-$) reactions, 25:55830
proton reactions at 20 to 120 keV with, cross sections for electron capture into n = 2 states of hydrogen in, (E), 25:55853
stopping of nuclei of, in nuclear emulsion, mass resolution of, (E/T), 25:55894 (LUIP-CR-71-4)
NEON IONS
effects on diploid yeast cells, OER and RBE for mutagenic and lethal, 25:55165
effects on silicon at 220 keV, lateral-stress study of damage produced in, 25:56285 (SC-RR-710424)
NEON ISOTOPES Ne-19
energy levels from neon-20 (p,d) reactions, spectroscopic factors for, (E), 25:56704
NEON ISOTOPES Ne-20
alpha elastic and inelastic scattering at 104 MeV, nuclear deformation study from differential cross sections for, (E), 25:56687 (KFK-1397)
alpha reactions (α,γ), magnesium-24 photodisintegration rates from, 25:55703
energy levels from neon-21 (p,d) reactions, spectroscopic factors for, (E), 25:56704
energy levels from proton inelastic scattering, deformation parameters for, (E), 25:56704
neutron reactions (n,2α) at 14.3 MeV, Q-value and cross section for, (E), 25:56717
neutron reactions (n,α) and (n,p) at 14.3 MeV, spectra and cross sections for, (E), 25:56717
nuclear deformation of, differential cross sections for alpha elastic and inelastic scattering by neon-20 for determining, (E), 25:56687 (KFK-1397)
proton elastic scattering at 40 MeV, differential cross sections for, (E), 25:56704
proton inelastic scattering at 40 MeV, differential cross sections for, (E), 25:56704
proton reactions (p,d) at 40 MeV, differential cross sections for, (E), 25:56704
reactions (Ne-20,O-16) with calcium-40 at 63 and 73.7 MeV, cross sections for, (E), 25:56721
scattering by nuclei in wide energy range, phase shift analysis of angular distributions for elastic, (E), 25:56740 (JINR-P7-5884)
NEON ISOTOPES Ne-21
abundance in Sikhote--Alin meteorite, (E), 25:55671
energy levels from neon-22 (p,d) reactions, spectroscopic factors for, (E), 25:56704
proton inelastic scattering at 40 MeV, differential cross sections for, (E), 25:56704
proton reactions (p,d) at 40 MeV, differential cross sections for, (E), 25:56704
NEON ISOTOPES Ne-22
alpha elastic and inelastic scattering at 104 MeV, nuclear deformation study from differential cross sections for, (E), 25:56687 (KFK-1397)
alpha reactions (α, He-6) at 42 MeV, angular distributions for, (E), 25:56665
deuteron reactions (d,α) at 10 MeV, angular distributions for, (E), 25:56716
energy levels from proton inelastic scattering, deformation parameters for, (E), 25:56704
nuclear deformation of, differential cross sections for alpha elastic and inelastic scattering by neon-22 for determining, (E), 25:56687 (KFK-1397)


XUM

proton elastic scattering at 40 MeV, differential cross sections for, (E), 25:56704
proton inelastic scattering at 40 MeV, differential cross sections for, (E), 25:56704
proton reactions (p,d) at 40 MeV, differential cross sections for, (E), 25:56704
scattering by nuclei in wide energy range, phase shift analysis of angular distributions for elastic, (E), 25:56740 (JINR-P7-5884)
NEPHELINE
age of, use of neutron activation in argon--potassium method of estimation of, 25:54765
NEPTUNE (PLANET)
luminosity of, relation to solar activity, (T), 25:55766
NEPTUNIUM
deposition on stainless steel from ammonium sulfate solutions, 25:54673
energy-level transitions of, following americium-241 decay, (E), 25:55825
preparation of sources of, for alpha spectrometry, 25:54673
separation from irradiated LMFBR fuel by solvent extraction using dibutyl butylphosphonate, 25:54706 (BNWL-SA-3345)
separation from nitric acid solutions by solvent extraction using benzene--EDTA--TTA, kinetics of reactions in, 25:54733
x-ray yields from, following americium-241 decay, M-subshell, (E), 25:55825
NEPTUNIUM IONS
electron paramagnetic resonance spectrum in thoria single crystals, 25:56383
NEPTUNIUM ISOTOPES Np-228
electron capture decay of, uranium-238 delayed fission from, (E), 25:56744(T) (NP-tr-1936)
NEPTUNIUM ISOTOPES Np-237
alpha decay of aligned, analysis of α angular distributions for, (E/T), 25:56749 (RCN-142)
energy levels from americium-241 alpha decay, (E), 25:56753 (UCRL-51087)
energy-level transition in, nuclear current parameter for internal conversion of 26.38-keV, 25:56797
neutron fission of aligned, analysis of angular distributions for slow, (E/T), 25:56749 (RCN-142)
NEPTUNIUM OXIDES
reactions with fluorine and fluorine chlorides, kinetics of, 25:54736
NERVES
radiation effects on impulse transmission in frog sciatic, effects of LET on RBE for proton, 25:55215
NERVOUS SYSTEM
radioinduced injuries to human, following therapy of head tumors, prophylaxis and treatment of γ, 25:55269
NEUTRINOS
book; Cosmic Muons and Neutrinos, 25:56469
detection of solar, (E/T), 25:55741
emission from relativistic shock-wave propagation in gases, (T), 25:55668
emission from Sun, discrepancy between experimental and theoretical values, (E/T), 25:55741
interactions ν + N, second-class G-parity properties in elastic scattering, (T), 25:56854
interactions ν + p in proton electromagnetic field at 30 to 400 GeV, total cross sections for W production from, (T), 25:56473
NEUTRINOS (ν/sub μ/)
interactions ν + n → p + μ⁻, evidence for second-class currents from proton polarization in, (T), 25:56472
NEUTRON CAPTURE THERAPY
dose irregularities during, local, 25:55212
NEUTRON CROSS SECTIONS
computation system for, homogenization and modification capabilities of ARC, 25:56614 (ANL-7714)
evaluation of ENDF/B data on, PSYCHE code for, 25:57174 (CONF-710302-(Vol.2), pp 1004-15)
evaluation of ENDF/B-I and ENDF/B-II data, water moderated reactor benchmark problems for, 25:57019 (CONF-710302-(Vol.2), pp 1065-85)
evaluation of ENDF/B-II data files, status of benchmark testing for, 25:57178 (CONF-710302-(Vol.2), pp 1053-64)
evaluation of ENDF/B-II, JOSHUA system for, 25:57176 (CONF-710302-(Vol.2), pp 1024-30)
evaluation of, status of ENDF/B processing codes for, 25:57173 (CONF-710302-(Vol.2), pp 991-1003)
evaluation of, status of ENDF/B processing codes for, 25:57165 (CONF-710302-(Vol.2), pp 877-86)
listing of 26 group set for fast test reactor physics calculations, 25:57115 (HEDL-TME-71-65)
preparation of moment of ENDF/B photon production matrices and sources, LAPHAN code for, 25:57175 (CONF-710302-(Vol.2), pp 1016-23)
preparation of multigroup, MC²--2 code for, 25:57171 (CONF-710302-(Vol.2), pp 968-82)
production of multigroup libraries from ENDF/B data, ETOG-2 and ETOT codes for, 25:57177 (CONF-710302-(Vol.2), pp 1031-46)
NEUTRON SOURCES
description of paraffin-moderated radioisotope thermal, for detector calibration, 25:54892 (LA-4745)
design of intense thermal, based on proton reactions with liquid metals, 25:56624(P)
fabrication of californium-252, 25:54671 (ORNL-4682, pp 114-32)
ion source for deuterium--tritium, control circuit for, 25:56605(P)
isodose curves for californium-252, 25:55002 (NYO-2740-8, pp 7-146)
properties of radioisotope, review on, 25:54507
targets for, design of absorbed deuterium--tritium, 25:56626(P)
use of californium-252, as randomly pulsed source for prompt neutron decay measurements, 25:56639
NEUTRON SPECTROMETERS
data processing for, computer program for, 25:55036 (HASL-244)
data unfolding technique for, 25:55038 (LA-DC-12314)
description of time-focused crystal, for measuring time-dependent spectra in pulsed moderators, 25:56629
design of cadmium-loaded liquid scintillation time-of-flight, for measuring average number of neutrons per fission, 25:55039(T) (LB/G-3040)
development of NE-213 scintillation, 25:55002 (NYO-2740-8, pp 7-146)
development of NE-213 scintillation, for operation in aqueous media, 25:55034 (COO-2049-7)
development of NE-213 scintillation, using off-line gamma-ray discrimination, 25:55033 (COO-2049-6)
performance of lithium fluoride, 25:55043 (RD/B/N-2034)
NEUTRON SPECTROSCOPY
pulse-height spectra unfolding techniques for, 25:54436 (ORNL-TM-3463)
NEUTRON STARS
equation of state of matter in, (T), 25:55715
gravitational redshifts in, (T), 25:55808
matter in, mass formula and properties of, (T), 25:55678
models for, (T), 25:55715
period--age distribution of, (E/T), 25:55687
superfluid state in, (T), 25:55714
superfluidity in, (T), 25:55715
NEUTRONS
capture by chlorine-35, γ spectra from, (E), 25:56690 (RT/FI-(70)47)
capture by gold-197, range of recoil atoms from, 25:56269
capture by hafnium-177 up to 200 eV, γ spectra and resonance spin assignments for, (E), 25:56751 (RT/FI-(70)55)
capture by hafnium-177 up to 300 eV, γ spectra and resonance spin assignments for, (E), 25:56751 (RT/FI-(70)55)
capture by iron-56 and lead-207, cross sections for nonresonant, (E), 25:56702
capture by krypton-80, cross section for resonance, (E), 25:56691
capture by nuclei at 10 to 100 keV, compilation of gamma spectra and intensities for, (E), 25:56655 (ORNL-TM-3379)
capture by nuclei, correlation between reduced neutron and radiative widths for resonance, 25:56818 (JINR-E4-5880)
capture by plutonium-239 at 0.02 to 30 keV, cross sections for, (E), 25:56746 (ORNL-4707)
capture by plutonium-239 at 0.1 to 30 keV, ratio of cross sections for fission and radiative, (E), 25:56734(T) (BNL-tr-446)
capture by uranium-233, uranium-235, uranium-238, plutonium-239, plutonium-240, and plutonium-242, EBR-II integral measurements of, 25:56982 (ANL-7791)
capture by uranium-238 below 600 eV, γ spectra and distribution of partial radiation widths in, (E), 25:56790
capture by ytterbium-170 at 8.1 to 73 eV, γ spectra from resonance, (E), 25:56802
capture by ytterbium-172 at 140 to 202 eV, γ spectra from resonance, (E), 25:56802
capture-to-fission ratios for uranium-233, uranium-235, uranium-238, plutonium-239, plutonium-240, and plutonium-242, EBR-II integral measurements of, 25:56982 (ANL-7791)
collisions along flight paths with continuously varying cross sections, Monte Carlo sampling method for, 25:57164 (CONF-710302-(Vol.2), pp 871-6)
density in multiplying media, spectral function representation of time- and energy-dependent, 25:56625
detection of, design of boron trifluoride ionization chamber for, 25:55014(P)
detection of, design of scintillation detector for, 25:55012(P)
detection of, radiator foil converter with diamond crystal detector for, 25:55009(P)
diffusion in benzene, heavy water, and light water, diffusion constant and cooling coefficients for, (T), 25:56631
diffusion in heterogeneous medium with slugs of small dimensions, Green function in, (T), 25:56636
dose distributions in rabbit and rat phantoms following exposure to monoenergetic beams, correlation of LET distributions and, 25:55229
dose to man in Japan from external occupational exposures, estimation of genetically significant equivalent, 25:55230
dose to tissue equivalent phantoms, Monte Carlo

calculations of absorbed and equivalent 580-MeV, 25:55216
dosimetry for irradiation of biological materials, 25:55002 (NYO-2740-8, pp 7-146)
dosimetry using tissue-equivalent wall-less proportional detectors, 25:55002 (NYO-2740-8, pp 7-146)
effects on aging and precipitation in beryllium--copper alloys, 25:55583
effects on black silicon-carbide varistors, 25:55103
effects on catalytic properties of hydrogen electrodes, 25:54602
effects on cells, effects of absorbed dose on RBE for, 25:55206 (NYO-2740-8, pp 147-219)
effects on Charpy-V performance and dynamic tear of ASTM A533B steel plates and weld deposits, 25:55586
effects on chloroindium chlorophthalocyanine, Szilard--Chalmers process from, 25:54680
effects on chloromethane, reactions of recoil chlorine-38 from, 25:54681
effects on cobalt complexes, annealing of recoil cobalt-60 from, 25:54682
effects on defect production in polycrystalline boron carbide, 25:55650
effects on dimensional changes in carbon, relations with graphitization, 25:55645 (CEA-CONF-1821)
effects on ductile-to-brittle transition temperature of thick-wall pressure vessel steels, 25:55588
effects on electric conductivity and diamagnetic anisotropy of carbon fibers, 25:56282 (CEA-CONF-1822)
effects on electronic properties of graphite, relations with annealing, 25:56283 (CEA-CONF-1823)
effects on embrittlement of Types A302B and A533B steel, relations with impurity copper and phosphorus content, 25:55577 (NRL-7310)
effects on heating of plane bodies, tables for transient temperatures from, 25:56267
effects on helium--methane--silane system, reactions of recoil tritium from, 25:54678
effects on incidence of dominant lethal mutations in Drosophila, 25:55206 (NYO-2740-8, pp 147-219)
effects on magnetoresistance in graphite, 25:56319
effects on mechanical properties of graphite, viscoelastic analysis of, 25:55646 (EUR-4674)
effects on opacity of lens of mice, effects of dose fractionation on, 25:55206 (NYO-2740-8, pp 147-219)
effects on pollen and stamen hairs of Tradescantia, RBE for, 25:55206 (NYO-2740-8, pp 147-219)
effects on potassium chromates, role of recoil reactions in "Crossover reaction" on thermal annealing of, 25:54679
effects on response of rats to tranquilizers following whole-body exposure in mixed γ fields, 25:55325
effects on silicon at 76°K, growth and annealing of divacancies induced in, 25:56311
effects on silicon p--n junctions, (E/T), 25:55095(R) (COO-1624-41)
effects on survival of hamster cells, effects of dose on RBE for, 25:55207 (NYO-2740-8, pp 220-59)
effects on volt--ampere characteristics of silicon diodes, 25:55100
energy distribution in beryllium, transition region function for, (T), 25:56622
flux distribution in non-uniform lattices, nodal integral transport method for calculation of, 25:57156 (CONF-710302-(Vol.2), pp 655-78)
flux distribution in non-uniform reactor lattices, modified collision probability method for calculation of, 25:57155 (CONF-710302-(Vol.2), pp 644-54)
flux distribution in reactors, determination of function moments of, (T), 25:57179
flux distribution in reactors, finite element solution of diffusion and transport equations for calculation of, 25:57159 (CONF-710302-(Vol.2), pp 723-38)
flux distribution in reactors, Monte Carlo calculation of adjoint, 25:57162 (CONF-710302-(Vol.2), pp 803-32)
flux distribution in reactors, non-iterative method for calculation of time dependent, 25:57157 (CONF-710302-(Vol.2), pp 679-700)
flux distribution in reactors, S/sub n/ programming techniques for calculation of, 25:57148 (CONF-710302-(Vol.2), pp 557-60)
flux distribution in reactors, solution of non-stationary and quasi-critical transport equations for, 25:57186
flux distribution in reactors, spherical harmonic equations for elimination of ray effects in, 25:57151 (CONF-710302-(Vol.2), pp 577-607)
flux distribution in reactors, synthetic transport theory method for calculation of, 25:57154 (CONF-710302-(Vol.2), pp 625-43)
flux distribution in reactors, time discretization of transport equation for calculation of, 25:57158 (CONF-710302-(Vol.2), pp 701-22)
flux distribution in reactors, variational treatment of DP-0 method for calculation of, 25:57152 (CONF-710302-(Vol.2), pp 608-16)
flux distribution in reactors, weighted diamond difference approximations for calculation of, 25:57150 (CONF-710302-(Vol.2), pp 565-76)
flux distributions in reactors, $P_3$ approximation for calculation of, 25:57149 (CONF-710302-(Vol.2), pp 561-4)
flux from solar flares, (T), 25:55761
flux measurements, handling and readout system for activation detectors for in-core, 25:55008(P)
flux monitoring, fabrication of MgO--NiO and MgO--CoO activation detectors for in-core, 25:55019(P)
interactions anti p + n → $\pi^+ + 2\pi^-$, mass and width of rho' in rising phase shift model for, (T), 25:56485 (ORO-3992-66)
interactions e + n in e + d interactions at high energies, cross sections for Δ(1236) production in, (E), 25:56405 (DESY-71/33)
interactions e + n in e + d interactions at high energies, cross sections for inelastic, (E), 25:56405 (DESY-71/33)
interactions γ + n in e + d interactions at high energies, cross sections for particle production in, (E), 25:56405 (DESY-71/33)
interactions $K^+ + n \rightarrow K^0 + p$ at 5.5 GeV/c, Regge analysis of, (E/T), 25:56506
interactions $K^+ + n \rightarrow K^0 + p$, secondary Regge contributions in, 25:56508
interactions $K^+ + n \rightarrow K^+ + \pi^- + p$ at 12 GeV/c, structure in $K\pi$ mass spectra near 1.85 GeV from, (E), 25:56434
interactions $K^-$ + n at 3 GeV in deuterium bubble chamber, production of K(890), K(1400), and $K\pi\pi$ systems, upper limits for production cross sections of isospin-3/2 K*, and K + π s-wave interactions in, (E), 25:56426 (FRNC-TH-53)
interactions n + d → n + d, lectures on forward and partial-wave dispersion relations for, (T), 25:56810 (CERN-71-14, pp 155-228)
interactions n + n, cross sections for, and comparison with p + p interactions, (T), 25:55777
interactions n + p → 2p + $\pi^-$ at 2 to 30 GeV, Reggeized one-pion-exchange model for π exchange and diffraction production of N(1470) and N(1688) in, (T), 25:56521 (JINR-P1-5975)
interactions n + p → d + γ, model of intermediate nucleon isobar for, 25:56525
interactions n + p → d + π, model of intermediate nucleon isobar for, 25:56525
interactions n + p → d + rho, model of intermediate nucleon isobar for, 25:56525
interactions n + p → d + sigma(310), model of intermediate nucleon isobar for, 25:56525
interactions n + p → p + n at 8 and 19 GeV/c; spark chamber study of differential cross sections and Δ(1236) and N(1518) production in, (E), 25:56415 (NP-18888)
interactions n + p at 10 to 30 GeV/c, total cross sections for, (E), 25:56421
interactions n + p at 14.1 MeV, relativistically covariant models for bremsstrahlung cross sections for, (T), 25:56526
interactions $\nu + n \rightarrow p + \mu^-$, evidence for second-class currents from proton polarization in, (T), 25:56472
interactions $\pi^+ + n \rightarrow \pi^+ + \pi^- + p$ at 13.1 GeV/c in deuterium bubble chamber, diffractive π + π interactions in, (E), 25:56425 (COO-1428-294)
interactions, SOLRF program for computation of, according to solid-angle method of spacing, 25:56271
leakage from graphite systems with cylindrical voids, pulsed source measurements on, (E/T), 25:57190
leakage from small multiplying assemblies, Monte Carlo method for calculation of, 25:57163 (CONF-710302-(Vol.2), pp 857-70)
mass difference (n - p), indefinite metric for electromagnetic, (T), 25:56547 (NYO-1932(2)-200)
monitoring of cosmic, data from Canadian stations for Jan.--Apr. 1971, (E), 25:55893 (AECL-3971)
production in meson reactions ($\mu^-$,nν) with helium-4, short-range nucleon--nucleon correlation effects on energy spectrum and angular distribution asymmetry in, (T), 25:56641 (JINR-P4-5986)
production in meson reactions ($\mu^-$,nν) with oxygen-16, spectrum and angular distribution asymmetry in, (T), 25:56820 (JINR-P4-5997)
reactions (n,2n) with copper, iron, and niobium at 14.4 MeV, differential cross sections, second-neutron spectra, and nuclear-level density parameters for, (E), 25:56684 (FEI-216)
reactions (n,α) with hafnium-177 at 1.09 to 8.87 eV, α widths of levels in search for, (E), 25:56686 (JINR-P3-5875)
reactions (n,α) with molybdenum-99, neodymium-143, neodymium-145, samarium-147, samarium-149, and tellurium-123 at resonance energies, α widths and resonance spin assignments for, (E/T), 25:56754(T) (UCRL-Trans-10541)
reactions (n,α) with zinc-64 at 281 and 2637 eV, α widths of levels in search for, (E), 25:56686 (JINR-P3-5875)
reactions (n,α) with zinc-67 at 1548 eV, α widths of levels in search for, (E), 25:56686 (JINR-P3-5875)
reactions (n,f) with neptunium-237, uranium-233, and uranium-235 using oriented targets, analysis of angular distributions for slow, 25:56749 (RCN-142)
reactions (n,f) with plutonium-239 at 0.02 to 30 keV, cross sections for, (E), 25:56746 (ORNL-4707)
reactions (N,f) with plutonium-239 at 0.05 to 7.20 MeV, angular anisotropy and nucleon-pairing effects in, (E), 25:56736 (FEI-233)
reactions (n,f) with plutonium-239 at 0.1 to 30 keV,

XUM

ratio of cross sections for radiative capture and, (E), 25:56734(T) (BNL-tr-446)
reactions (n,f) with plutonium-239, plutonium-241, uranium-233, and uranium-235, prompt neutron yield from, (E), 25:56743 (NP-18966)
reactions (n,f) with uranium-233, uranium-235, uranium-238, plutonium-239, plutonium-240, and plutonium-242, EBR-II integral measurements of, 25:56982 (ANL-7791)
reactions (n,γ) with actinide isotopes in molecular sieves, isotope enrichment by, 25:54718 (ORNL-4682, pp 168-81)
reactions with aluminum at 10 to 30 GeV/c, total cross sections for, (E), 25:56421
reactions with beryllium at 10 to 30 GeV/c, total cross sections for, (E), 25:56421
reactions with bromocyclopropane and bromine--cyclopropane, reactions of recoil bromine-80m from, 25:54690
reactions with cadmium at 10 to 30 GeV/c, total cross sections for, (E), 25:56421
reactions with carbon at 10 to 30 GeV/c, total cross sections for, (E), 25:56421
reactions with chlorofluoromethanes, replacement reactions of recoil chlorine-38 from, 25:54688
reactions with copper at 10 to 30 GeV/c, total cross sections for, (E), 25:56421
reactions with deuterium at 10 to 30 GeV/c, total cross sections for, (E), 25:56421
reactions with gold-197 and indium using iron-filtered beams, analysis of resonance cross sections for, 25:56795
reactions with iodine-127 in pentane and pentenes, yields and product distribution from, 25:54705
reactions with iron, lead, oxygen, and sodium, transmission of fission spectra through thick samples for evaluation of minima in total cross sections for, (E), 25:56650 (COO-2049-5)
reactions with lead at 10 to 30 GeV/c, total cross sections for, (E), 25:56421
reactions with nitrogen-14 in potassium azide, distribution of recoil carbon-14 from, 25:54687
reactions with nuclei at low energies, computer program for cross sections of resonance, (T), 25:56814 (COO-2022-7)
reactions with nuclei in unresolved resonance region, method for calculation of cross sections for, (T), 25:56870
reactions with shielding, secondary gamma radiation from, 25:56277
reactions with tellurium-128 in tellurium--oxygen compounds, iodine-129 Moessbauer studies of recoil tellurium-129 reactions from, 25:54704
reactions with tungsten at 10 to 30 GeV/c, total cross sections for, (E), 25:56421
reactions with uranium-235 and -238, total γ spectrum above 1 MeV from, (E), 25:56745 (ORNL-4691)
research at CEA in France during October 1969 to December 1970, 25:55203(R) (CEA-N-1449)
scattering by atoms, analysis of many-particle distribution functions in Sunakawa model for elastic multiple, (T), 25:56637
scattering by cadmium sulfide crystals, anomalous transmission from suppression of (n,γ) reaction in resonant, 25:56627
scattering by copper, iron, and niobium at 14.4 MeV, differential cross sections, nuclear-level density parameters, and contribution of direct processes for inelastic, (E), 25:56684 (FEI-216)
scattering by gaseous and liquid methane, calculation of second-order corrections for inelastic, 25:56628
scattering by helium-4 below 50 MeV, analysis using nonlocal separable potential, (T), 25:56852
scattering by helium-4, analysis using separable nonlocal potential, (T), 25:56642 (LYCEN-7104, C5.1-15)
scattering by helium-4, lectures on forward dispersion relations for elastic, (T), 25:56810 (CERN-71-14, pp 155-228)
scattering by liquids, time-of-flight method for studying diffusive motion by, 25:56634
scattering by paramagnetic nickel, orbital contribution to magnetic cross section for, (T), 25:56354
scattering by zirconium hydride, effects of stoichiometry on structure in down-, 25:56343
shielding of, properties of Chemtree products for, 25:54962 (CONF-710401-, pp 307-10)
spectra from proton reactions (p,xn) with uranium-238 at 750 MeV, unfolding capability for, (E), 25:55038 (LA-DC-12314)
spectra in polyethylene, solid anhydrous ammonia, and solid methane following fast pulses, time-dependent, 25:56629
spectra of, method for analysis of, 25:56620 (RT/FI-(70)53)
thermalization in polycrystalline beryllium, Monte Carlo method for calculating, (T), 25:56619 (RT/FI-(70)49)
thermalization of, degenerate kernel technique for calculation of, 25:56630
transport code for, revised cross-section module for Monte Carlo multigroup, 25:56263 (ORNL-4716)
transport equation for, numerical method for solution of time-independent, (T), 25:56616 (JUL-764-RG)
transport equation for, solution of Boltzmann, with respect to position, angle, and energy, 25:56617 (JUL-765-RG)
transport equations for slab geometry, nonhomogeneous boundary-value problem for linear, (T), 25:56621
transport in graphite systems with voids, pulsed-source measurements on, (E/T), 25:57189
transport in homogeneous slabs, comparison of diffusion and transport theory for, 25:56613 (AD-715563)
transport in nonuniform medium with anisotropic scattering, constant relaxation of average flux, (T), 25:56635
transport in shielding, S/sub n/ discrete ordinate sets for deep-penetration, 25:57153 (CONF-710302-(Vol.2), pp 617-24)
transport in thick and thin slabs, calculation of energy-dependent, (T), 25:56632
transport in three-dimensional geometries, computer generation of Monte Carlo sampling functions for, 25:57160 (CONF-710302-(Vol.2), pp 771-81)
transport of, spin polarization effects in, (T), 25:56633
transport studies, (E/T), 25:56255(R) (AD-721388)
uses in radiography, design of equipment for, 25:54931(P)

NEUTRONS, COLD
scattering by zirconium hydride, total cross section for, (E), 25:56623

NEUTRONS, DELAYED
monitoring for liquid metal cooled fast breeder reactor fuel element failure detection system, 25:57055 (JAERI-Memo-4157, pp 84-8)
monitoring for water cooled research reactor fuel element failure detection system, 25:57119 (JAERI-Memo-4157, pp 51-65)

NEUTRONS, FAST
attenuation in concrete shielding, effects of iron contents on, (E), 25:57027 (RCN-147)
capture by A = 26 through 136 nuclei at 2.9 MeV, cross sections for, (E), 25:56696
capture by cobalt-59, niobium-93, and rhodium-103 at 14 MeV, γ spectra and cross sections for, (E), 25:56729
capture by uranium-235 at 0.25 to 4 MeV with fission isomer excitation, excitation function for, (E), 25:56793
detection of, effect of stopping power on threshold sensitivity of nuclear emulsions for, 25:55022
dosimetry in lucite phantoms using thermoluminescent dosimeters, 25:55319 (UCD-472-118)
dosimetry in tissue-equivalent phantoms, effects of energy spectra and location of dosimeters on, 25:55232
dosimetry of, performance of polymer gelatin nuclear emulsions for, 25:55057
effects on brittleness and strength of manganese--molybdenum--nickel steel plates and welds, 25:55585
effects on dimensions of codeposited isotropic carbon--silicon coatings, 25:55652
effects on electric conductivity of $CrNi_3$, 25:55584
effects on eyes of rabbits, effects of dose and LET on RBE for, 25:55317 (CEA-CONF-1744)
effects on fracture and tensile properties of A533B pressure vessel steel, 25:55587
effects on graphite properties, relations with pitch-binder content, 25:55653
effects on graphites, pyrocarbons, and fuel bodies in Dragon reactor at 600 to 1200°C, 25:55651
effects on indium antimonide at 50°C, annealing of, 25:56317
effects on junction capacitance of silicon $n^+ - p - p^+$ power diode, 25:55097 (N-71-25389)
effects on mice, effects of radioprotective compounds on, 25:55266
effects on p-type germanium at 14 MeV and 77°K, annealing of, 25:56305
effects on photocurrent of n-type germanium, 25:56316
effects on silicon at 78°K, infrared absorption bands induced in, 25:56296
effects on silicon doped with cobalt, $^{57}Fe$ Moessbauer-effect study of, 25:56326
effects on silicon, EPR study of defects induced in, 25:56324
effects on stress relaxation in alloys, model for, 25:55579 (WAPD-TM-943)
effects on survival of synchronized L cells, effects of age on, 25:55309
effects on swelling of metals, theoretical model for, 25:55582
effects on swelling of pure metals and Types 304 and 316 stainless steel, relations with dose and temperature, 25:55572 (BLG-457)
effects on swelling of stainless steel for use in fast breeder reactors, 25:55581
effects on thermionic sheath trilayer insulators, 25:55096 (N-71-24635)
effects on void production in high-purity magnesium, 25:55580
flux measurements on, by uranium-238 fission and determination of barium-140, standard for, 25:54444
reactions (n,2α) with neon-20 at 14.3 MeV, cross section and Q-value for, (E), 25:56717
reactions (n,2α) with nitrogen-14 at 14.1 MeV, intermediate structure in cross section for, (E),

25:56680
reactions (n,α) and (n,p) with neon-20 at 14.3 MeV, spectra and cross sections for, (E), 25:56717
reactions (n,α) with argon-40 at 14.4 MeV, α spectra, cross sections, and Q-value for, (E), 25:56718
reactions (n,f) with thorium-232 and uranium-238 at 14 MeV, liquid-drop-model calculations of heavy-fragment masses in, (T), 25:56787
reactions (n,f) with thorium-232 and uranium-238 at 14.1 MeV, angular distributions for, (E), 25:56804
reactions (n,f) with uranium-235 at 2 and 15 MeV, mass chain yield for, (T), 25:56816 (JAERI-Memo-4383)
reactions with nuclei near 14 MeV, statistical analysis of shell effects in, (T), 25:56869
reflection by steel slab, orders-of-scattering calculation for collimated polyenergetic, 25:56257 (COO-2049-8)
scattering by carbon-12 at 22 MeV with subsequent α decay, n-α coincidence spectra from inelastic, (E), 25:56752(R) (SUNI-14)
scattering by iron-56 at 14 MeV, vibrating-model analysis of differential cross sections for elastic and inelastic, (E), 25:56707
scattering by samarium-154 at 1.5 MeV, γ spectra from inelastic, 25:56752(R) (SUNI-14)
scattering by tantalum-181, tin-120, and zirconium-90 at 7 MeV, S-matrix analysis of differential cross sections for elastic, (T), 25:56789
transport in iron, (E/T), 25:56618 (RPI-328-230)
transport in shielding slabs, orders-of-scattering method for, 25:56258 (COO-2049-9)
NEUTRONS, FISSION
detection and discrimination of, coincidence system for, 25:54995 (EUR-4611)
effects on bubble nucleation and re-solution in uranium dioxide at high temperatures, 25:55649
effects on lithium-diffused n-type silicon, defects induced in, 25:56309
effects on swine following bilateral and unilateral exposures, LD-50 for lethal, 25:55334
NEUTRONS, FUSION
emission from laser irradiated deuterated polyethylene, 25:56219
NEUTRONS, INTERMEDIATE
reactions (n,f) with uranium-235 at 30 keV, time analysis of compound-nucleus decays in, (E), 25:56752(R) (SUNI-14)
spectra for heterogeneous reactors, computer program calculation of, 25:57182 (JAERI-Memo-4481)
spectrum in pool type reactors, quadruple foil method for measurement of, 25:57126
NEUTRONS, THERMAL
attenuation in concrete shielding, effects of iron contents on, (E), 25:57027 (RCN-147)
capture by chromium-50, -52, and -53 and iron-54 and -56, gamma spectra from, (E), 25:56683 (FEI-205)
capture by krypton-80, cross section for, (E), 25:56691
capture by lutetium-176, gamma and conversion-electron spectra from, (E), 25:56762
diffraction of, quantum mechanical calculation for, (T), 25:56615 (FMRB-37/71)
effects on bubble nucleation and re-solution in uranium dioxide at high temperatures, 25:55649
effects on cadmium sulfide and telluride, luminescence and electric resistivity study of, 25:56307
reactions (n,f) with plutonium-239 and uranium-233 and -235, liquid-drop-model calculations of heavy-fragment masses in, (T), 25:56787
reactions (n,f) with uranium-235, yields of light elements in, (E), 25:56788
scattering by crystals, use of zero Placzek moment to calculate n-phonon cross section in, (T), 25:56340(T) (AERE-Trans-1137)
scattering in light and heavy water, computer program for analysis of, 25:56638
NEVADA TEST SITE
soils around, plutonium content of, 25:54755 (CONF-710401-, pp 320-7)
NICKEL
abundance in solar atmosphere, (E/T), 25:55750
argon-ion reactions at 30 keV with surfaces of, charge states and kinetic energies of scattered and recoil ions from, (E), 25:55818
casting by levitation melting using magnetic field, 25:55424
corrosion by vanadium oxide melts, mechanisms of, 25:55374 (CONF-690452-, Paper 7)
determination in epitaxial films of gallium arsenide by neutron activation and radiochemical separation, 25:54512
determination in isoquinoline formate by polarography, 25:54421
determination in standard aluminum--silicon system by neutron activation, 25:54455
determination in stony meteorites by proton and bremsstrahlung activation, 25:54466
deuteron reactions at 80 MeV with foils of, cross sections for electron capture in, (E), 25:55862
diffusion in molybdenum single crystals, effects of vacuum on, 25:55505
diffusion of carbon in solid solutions of, 25:55479
diffusion of cerium and neodymium in, at 500 to 1100°C, volume and grain-boundary, 25:55488
effects on properties and sintering of tungsten at 1000 to 2000°C, 25:55453
electron reactions at 0.5 to 15 keV, optical radiation from, (E), 25:55813 (JINR-P4-5957)
mechanical properties of sintered, at room temperature, 25:55437(R) (TID-25784)
microstructure of sintered, 25:55437(R) (TID-25784)
neutron cross section in tight-binding model of paramagnetic, calculation of orbital contribution to magnetic, (T), 25:56354
proton reactions at 1.5 to 4.5 MeV, optical radiation from, (E), 25:55813 (JINR-P4-5957)
proton reactions at 155 and 600 MeV with foils of, cross sections for electron capture in, (E), 25:55862
radioinduced vacancies in, aggregate formation from laser-beam, 25:56313
reactions with Groups IV and VI transition metal carbides at 1000 to 1200°C, solid-phase, 25:55464
separation of uranium from, in methyl sulfoxide by cation exchange chromatography, 25:54728
solvent properties for Groups IV and VI transition metal carbides at 1000 to 1200°C, 25:55464
sorptive properties for tellurium, 25:54587(R) (AECL-3909)
strengthening of, effects of substructure domain on dispersion, 25:55492
NICKEL ALLOYS AND SYSTEMS
reactions with alkali metal sulfates at 550 to 950°C, 25:55372 (CONF-690452-, Paper 5)
stability of aluminum oxide dispersions in, at high temperatures, 25:55485
$Al_2O_3$--Ni, production of fine powders of, Microgel process for, 25:55419
Al--Co--Cr--Mo--Ni-base--Ti, fabrication of powdered, powder metallurgy and thermomechanical processes for, 25:55416
Al--Cr--Mo--Ni-base--W, fabrication of powdered, powder metallurgy and thermomechanical processes for, 25:55416
Al--Cr--Ni-base--Ti, corrosion by molten vanadium oxide, effects of chlorides, oxides, and sulfides of sodium on, 25:55375 (CONF-690452-, Paper 8)
Al--Cr--Ni-base--Ti, mechanical properties of dispersion-strengthened, at high temperatures, 25:55483
Al--Ga--Ni, optical constants for β-phase NiGa/sub 1-y/Al/sub y/ intermetallic compound in, 25:56352
Al--Ni--V, phase equilibria in intermetallic compounds of, 25:55562
Be--Cu-base--Ni, microstructure of, potentiostatic studies on, 25:55555
Co--Cr--Ni--W, physical properties of, effects of atomization media and consolidation methods on, 25:55480
Co-base--Cr--Mo--Nb--Ni--W, corrosion by molten vanadium oxide, effects of chlorides, oxides, and sulfides of sodium on, 25:55375 (CONF-690452-, Paper 8)
Cr--Fe-base--Ni, stability of aluminum oxide dispersions in, at high temperatures, 25:55485
Cr--Nb--Ni, liquation of, mechanism of intracrystallite, 25:55506
Cr--Ni, radiation effects on electric conductivity of $Ni_3Cr$, neutron, 25:55584
Cr--Ni-base, stability of aluminum oxide dispersions in, at high temperatures, 25:55485
Cr--Ni-base, strengthening of, effects of substructure domain on dispersion, 25:55492
Cu--Ga--Ni, optical constants for β-phase in, 25:56352
Cu--Ni, solvent properties of solid solutions of, for tungsten in copper--nickel--tungsten alloys, 25:55447
Cu--Ni--W, tungsten solubility in copper--nickel solid solutions of, limits of, 25:55447
Fe--Mo--Ni, properties and structure of, produced by sintering using systematic thermal fluctuations, 25:55414
Fe--Mo--Ni-base, magnetic properties at cryogenic temperatures, 25:56361
Fe--Ni, electron mean free path in Permalloy foils, fast, (E), 25:56281
Fe--Ni, magnetic properties at cryogenic temperatures, 25:56361
Fe--Ni, precipitation in beryllium-containing, metallography of 700°C, 25:55544
Fe--Ni, properties and structure of, produced by sintering using systematic thermal fluctuations, 25:55414
Fe--Ni--WC, phase relations and tensile properties of sintered, 25:55631
Fe--Ni-base, microstructure of Type 706, 25:55553
Fe--Ni-base, microstructure of Type 706, effects of heat treatment on, 25:55554
Fe-base--Mn--Ni, stability of aluminum oxide dispersions in, at high temperatures, 25:55485
Fe-base--Mo--Ni, stability of aluminum oxide dispersions in, at high temperatures, 25:55485
Fe-base--Ni, stability of aluminum oxide dispersions in, at high temperatures, 25:55485
Fe-base--Ni--Rh, use as filter in polarized iron-57 Moessbauer source, 25:56366
In--Ni, optical constants for β-phase NiIn intermetallic compound in, 25:56352

XUM

Mn--Mo--Ni--steel, radiation effects on brittleness and strength of heavy-section plates and welds of, fast neutron, 25:55585
Mn--Ni-base, stability of aluminum oxide dispersions in, at high temperatures, 25:55485
Mo--Ni, mechanical properties at high temperatures, effects of molybdenum content on, 25:55474
Mo--Ni-base, stability of aluminum oxide dispersions in, at high temperatures, 25:55485
Mo--Ni-base--$ThO_2$, tensile strength at 1093°C, effects of thermomechanical processing on, 25:55486
Ni--NiO, development of reference electrode of, for molten fluorides, 25:54532 (ORNL-4717, pp 1-27)
Ni--$ThO_2$, production of fine powders of, Microgel process for, 25:55419
Ni--TiC, grain growth in liquid-phase sintering of, 25:55642
Ni--$UO_2$, surface energy of, at 1500°C, 25:55616
Ni--W-base, sintering of powdered dilute, effects of nickel content on, 25:55426
NICKEL IONS
effects on void production in refractory metals at 5 MeV, 25:55573 (BNWL-SA-3962)
spectral lines due to, in solar euV spectrum, (E), 25:55774
NICKEL ISOTOPES Ni-57
beta decay and electron capture of, in hexaamminenickel(II) complexes, behavior of cobalt-57 from, thermal annealing effects on, 25:54689
NICKEL ISOTOPES Ni-58
energy levels of, shell-model calculation with Reid and Yale potentials, 25:56857
proton inelastic scattering at 6.9 MeV, distorted-wave analysis of differential and integrated cross sections for, (E), 25:56727
NICKEL ISOTOPES Ni-59
energy levels of, shell-model calculation with Reid and Yale potentials, 25:56857
NICKEL ISOTOPES Ni-60
deuteron elastic and inelastic scattering at 13.6 MeV, strong-coupling analysis of, (T), 25:56780
energy levels of, shell-model calculation with Reid and Yale potentials, 25:56857
proton elastic scattering at 11 MeV, differential cross sections for, (T), 25:56789
proton inelastic scattering at 6.9 MeV, distorted-wave analysis of differential and integrated cross sections for, (E), 25:56727
NICKEL ISOTOPES Ni-63
uses as tracer in measuring diffusion of nickel in molybdenum, 25:55505
NICKEL OXIDES
preparation of uniform particles of, for fission product deposition studies, 25:54587(R) (AECL-3909)
reactions with alkali metal sulfates at 550 to 950°C, 25:55372 (CONF-690452-, Paper 5)
MgO--NiO, fabrication for in-core neutron flux monitoring, 25:55019(P)
Ni--NiO, development of reference electrode of, for molten fluorides, 25:54532 (ORNL-4717, pp 1-27)
NINE MILE POINT POWER REACTOR
radioactive effluents from, corrections for January to December 1970, 25:56901 (DOCKET-50220-73)
turbine for, inspection and repair of broken attachment pins for last stage bucket shanks of, 25:56902 (DOCKET-50220-74)
NIOBIUM
abundance in R Cyg and HD 35155, (E), 25:55699
analysis for nitrogen by fast neutron activation, 25:54501
casting by levitation melting using magnetic field, 25:55424
coating with zinc-plated aluminum silicide, corrosion protection by, 25:55398(P)
corrosion by sodium at 600°C, effects of oxygen on, 25:55386
determination of trace amounts of, in high-purity acids by emission spectrography, 25:54431
determination of, study of complexes with 4-(2-pyridylazo)resorcinol in oxalic and tartaric acid systems in spectrophotometric, 25:54425
diffusion and internal friction of hydrogen in, calculation from redistribution in periodic stress gradient, 25:55458
effects on properties and sintering of tungsten at 1000 to 2000°C, 25:55453
electron transport in superconducting Nb/Nb oxide/Bi tunnel junctions, (E/T), 25:56078
melting of, behavior of impurities during vacuum, 25:55403
oxidation at 1500 to 2000°C and low pressures, effects of zirconium, molybdenum, and tungsten on, 25:55380
performance in superconducting lumped-parameter oscillator circuit, 25:55086
physical properties of plasma-sprayed spherical powders of, 25:55467
properties of fibers of, for use in preparation of ceramic composites, 25:55608(T) (LB/G-3074)
properties of vacuum electrodeposited thin films of, electric and physical, 25:55507
radiation effects on beryllia- and alumina-bonded trilayer sheath insulators, fast-neutron, 25:55096 (N-71-24635)
radioinduced void production in, 5-MeV nickel ion, 25:55573 (BNWL-SA-3962)
separation from cerium and lanthanum by reverse-phase partition chromatography on TTA-impregnated paper, 25:54746
separation from pegmatitic ores, leaching studies for, 25:54752
separation from pyrochlore concentrates as oxide, 25:54741
sorptive properties for hydrogen, bulk and surface, 25:55434 (RLO-2221-T-7-3)
structure of single crystals of, effects of low-temperature rolling and annealing on, 25:55560
structure of thin films of, deposited on sapphire, epitaxy in, 25:55531
NIOBIUM ALLOYS AND SYSTEMS
coating with zinc-plated aluminum silicide, corrosion protection by, 25:55398(P)
hardening mechanisms of, electron microscope and x-ray studies of dispersion, 25:55443
Al--Nb, niobium-93 NMR in $Nb_3Al$, 25:56373
Au--Nb, niobium-93 NMR in $Nb_3Au$, 25:56373
C--Hf--Nb, phase diagram of niobium--rich corner of, 25:55563
C--Nb--U, phase diagram at 1000°C, carbide composition in, 25:55547
C--Nb--Zr, thermodynamic properties of, relations with composition, 25:55615
Co-base--Cr--Mo--Nb--Ni--W, corrosion by molten vanadium oxide, effects of chlorides, oxides, and sulfides of sodium on, 25:55375 (CONF-690452-, Paper 8)
Cr--Nb--Ni, liquation of, mechanism of intracrystallite, 25:55506
Hf--Nb--Ti--Zr, superconducting properties of, with, 25:56104
Hf--Nb--Zr, superconducting properties of, 25:56105
Hf--Nb-base, oxygen solubility limits in, lattice parameter measurements of, 25:55568
Ir--Nb, niobium-93 NMR in $Nb_3Ir$, 25:56373
Nb--Pt, niobium-93 NMR in $Nb_3Pt$, 25:56373
Nb--Ru, diffusion in, effects of composition on mutual, 25:55452
Nb--Sn, fabrication of laminated superconducting $Nb_3Sn$, 25:56079(P)
Nb--Sn, niobium-93 in $Nb_3Sn$, 25:56373
Nb--Sn, phase transition in $Nb_3Sn$, neutron-scattering study of lattice-dynamical, 25:55545
Nb--Sn, phonon frequencies and susceptibility of $Nb_3Sn$, (T), 25:56344
Nb--Sn, superconducting critical current of intermetallic $Nb_3Sn$, effect of carbon on, 25:56084
Nb--Ta, hardening in monocrystals of, at 77 to 2000°K, solid-solution, 25:55457
Nb--Ti, strengthening by step-aging, relations with microstructure, 25:55490
Nb--Ti--W--Zr, solidus volume of, simplex-lattice method for prediction of, 25:55529
Nb--Ti--Zr, phase studies of, 25:55564
Nb--Ti-base, superconductivity and constitution of, 25:56108
Nb--Ti-base, superconductivity of, relations with crystal structure, 25:55541
Nb--Zn, phase and intermetallic compound formation in, 25:55534
Nb--Zr, microstructure of, isothermal omega transformation in, 25:55557
Nb--Zr-base, superconductivity of, relations with crystal structure, 25:55541
Nb-base--O--Ti, structure and tensile properties of, 25:55521
Nb-base--O--Zr, structure and tensile properties of, 25:55522
Nb-base--Ti, magnetization properties of superconducting, transporting sinusoidal alternating current in longitudinal magnetic field, (E/T), 25:56085
Nb-base--Zr, corrosion by mercury at 1200°F, 25:55377 (N-71-26947)
Nb-base--Zr, magnetization properties of superconducting, transporting sinusoidal alternating current in longitudinal magnetic field, (E/T), 25:56085
Nb-base--Zr, oxygen solubility limits in, lattice parameter measurements of, 25:55568
Nb-base--Zr, superconducting transition temperature of, effect of deformation on, (E/T), 25:56099
NIOBIUM BORIDES
stability in acids, 25:54543
NIOBIUM CARBIDES
physical properties and stability to nitrogen, 25:55629
physical properties and structure of, review on effects of composition on, 25:55632
wetting by copper, effects of electronic structure on, 25:55643
NbC--ZrC, physical properties and structure of, review on effects of composition on, 25:55632
NbC--ZrC, wetting by copper at 1100°C, effects of electronic structure on, 25:55643
NIOBIUM FLUORIDES
disproportionation of $NbF_4$, at 350°C, 25:54532 (ORNL-4717, pp 1-27)
mass spectrometric studies of, 25:54532 (ORNL-4717, pp

XUM

1-27)
preparation of $NbF_4$, by reduction of excess niobium pentafluoride with niobium metal, 25:54532 (ORNL-4717, pp 1-27)
stability in molten lithium beryllium fluoride solution, 25:54532 (ORNL-4717, pp 1-27)
NIOBIUM ISOTOPES Nb-90
beta and electron-capture decay of, branching ratios, gamma energies and intensities and log-ft values from, (E), 25:56791
NIOBIUM ISOTOPES Nb-92
energy levels from molybdenum-94 (d,α) and zirconium-90 (He-3,p) reactions, spin-parity assignments for, (E), 25:56758
NIOBIUM ISOTOPES Nb-93
energy-level scheme from neutron inelastic scattering, (E), 25:56752(R) (SUNI-14)
neutron capture at 14 MeV, γ spectra and cross section for, (E), 25:56729
neutron inelastic scattering at 14.4 MeV, differential cross sections, nuclear-level density parameters, and contribution of direct processes for, (E), 25:56684 (FEI-216)
neutron reactions (n,2n) at 14.4 MeV, differential cross sections, second-neutron spectra, and nuclear-level density parameters for, (E), 25:56684 (FEI-216)
nuclear magnetic resonance in $Nb_3Al$, $Nb_3Sn$, $Nb_3Ir$, $Nb_3Pt$, and $Nb_3Au$ at 4.2 to 300°K, 25:56373
NIOBIUM ISOTOPES Nb-95
content in atmosphere during 1969, (E), 25:54803
distribution in mice following inhalation, effects of chemical form on, 25:55125
NIOBIUM NITRIDES
physical properties of, 25:55629
shock compression effects on powdered, x-ray-diffraction study of, 25:55618
NIOBIUM OXYFLUORIDES
mass spectrometric studies of, 25:54532 (ORNL-4717, pp 1-27)
NITRIC ACID
density of aqueous solutions of, 25:54578 (ORNL-4682, pp 215-17)
effects on radiolysis of hydrocarbon TBP mixtures, 25:54644
sorption on uranium dioxide, 25:55594 (ORNL-4682, pp 218-28)
NITRIDES
diffusion in, data tabulations on, 25:55509
NITRITES
diffusion in, data tabulations on, 25:55509
yields from radiolysis of sodium nitrate, comparison of Ceric and Shinn methods for determining, 25:54633(R) (ORO-3660-4)
NITROGEN
abundance in solar atmosphere, (E/T), 25:55750
content at 100 to 200 km of molecular, diurnal variations of, (E), 25:55987
corrosive effects on reactor materials, review of, 25:55393
determination by charged particle activation methods, optimum irradiation conditions and nuclear interferences for, 25:54520
determination in niobium, tantalum, and titanium by fast neutron activation, 25:54501
diffusion in yttrium at 20 to 300°C, effects of dislocations on, 25:55461
helium-hydride-ion reactions at 0.5 to 1 MeV with molecular, cross sections for dissociation in, (E), 25:55872
helium-ion range at 0.2 to 2.0 MeV in, as function of energy, (E), 25:56276
mass transfer in reactor materials exposed to sodium, measurement of, 25:55379(R) (WARD-4210-T-1-2)
oxygen-ion reactions at 10 to 40 MeV with molecular, cross sections for electron capture in, 25:55869
oxygen-ion reactions at 7 to 40 MeV with molecular, cross sections for electron capture and loss in, (E), 25:55870
proton range at 0.2 to 2.0 MeV in, as function of energy, (E), 25:56276
proton reactions at 20 to 120 keV with molecular, cross sections for electron capture into n = 2 states of hydrogen in, (E), 25:55853
scattering by argon, krypton, and nitrogen molecules of molecular, rainbow oscillations in differential cross sections for, (E), 25:55852
solubility in alpha-vanadium at 300 to 1000°C, 25:55475
sorption by zirconium at low pressures and high temperatures, 25:55463
spectral emission of Lyman--Birge--Hopfield system of molecular, in day airglow from Aug. 1967 to July 1968, (E), 25:55968
NITROGEN IONS
x-ray scattering by three- and four-electron, form factors and scattering functions for coherent and incoherent, 25:56259 (EGG-1183-1479)
NITROGEN ISOTOPES N-13
production in alpha reactions with aluminum and silicon at 70 to 160 MeV, cross sections and fission mechanism for, (E/T), 25:56685 (FRNC-TH-48)
NITROGEN ISOTOPES N-14
alpha reactions at 70 and 90 MeV, cross sections for, (E), 25:56652 (LYCEN-7104, S2.1-2)
deuteron reactions (d,p) at 13.8 MeV, vector analyzing power for polarized, (E), 25:56724
energy levels from carbon-12 (He-3,p) and (He-3,2p) reactions, spin-parity assignments for, (E), 25:56682
energy levels of, shell-model calculation using Fabakin potential, (T), 25:56660
exchange between thiocyanate and thiocyanatomolybdate(III), 25:54558
meson (K-) absorption in, analysis of mechanism in, 25:56653 (LYCEN-7104, S4.1-10)
meson (π) absorption by, analysis of mechanism in, 25:56653 (LYCEN-7104, S4.1-10)
neutron reactions (n,2α) at 14.1 MeV, intermediate structure in cross section for, (E), 25:56680
neutron reactions (n,p) in potassium azide, distribution of recoil carbon-14 from, 25:54687
scattering by nuclei in wide energy range, phase shift analysis of angular distributions for elastic, (E), 25:56740 (JINR-P7-5884)
NITROGEN ISOTOPES N-15
energy levels at 12.50 and 12.52 MeV from carbon-14 (p,γ) and (p,n) reactions, spin--parity assignments and widths for, (E), 25:56669
energy-level transitions from carbon-14 (p,γ) and (p,n) reactions, branching and mixing ratios and multipolarities for, (E), 25:56669
NITROGEN ISOTOPES N-16
beta decay of, half-life for, (E), 25:56658
NITROGEN ISOTOPES N-17
energy levels from oxygen-18 (d,He-3) reactions, l-transfer values and spin--parity assignments for, (E), 25:56662
production in alpha reactions with aluminum and silicon at 160 MeV, cross sections and fission mechanism for, (E/T), 25:56685 (FRNC-TH-48)
NITROGEN MUSTARDS
effects on Escherichia coli, effects of 2,4-dinitrophenol on recovery from lethal, 25:55355
effects on renewal patterns of normal and tumor cells, 25:55110(R) (TID-25801)
NITROGEN OXIDES $N_2O$
effects on γ radiolysis of propane polymers, 25:54637
effects on radiolysis of cyclohexane, 25:54670
butane--$N_2O$, radiolysis of, effects of oxygen on yields of nitrogen from γ, 25:54659
cyclopentane--$N_2O$, radiolysis of, effects of cyclopentene and propene on nitrogen yields from γ, 25:54655
NITROGEN SYSTEMS
air--N, plutonium ignition in, effects of oxygen content on, 25:54946 (CONF-710401--, pp 106-17)
C--N--O--Pu--U, preparation of carbides, carbonitrides, and hypostoichiometric oxides in, 25:55594 (ORNL-4682, pp 218-28)
H--N, radiation effects on, production of carbon-11-labeled cyanides by recoils from proton, 25:54683
N--Ta, electric conductivity of films of, effects of glow discharge on, 25:55519
NONANE
radiation effects on sorption on magnesium sulfate incorporating sulfur-35, gas chromatographic studies of, 25:54603
NORWAY
fallout monitoring in ground-level atmosphere of north, 1970 and 1971, 25:54785
NOVAE
spectra of, principal absorption, (E/T), 25:55677
NOVO VORONEZH POWER REACTOR, UNIT 1
neutron flux in, threshold detector measurement of fast, 25:56891
NOVO VORONEZH POWER REACTOR, UNIT 2
neutron flux in, threshold detector measurement of fast, 25:56891
NOZZLES
stresses in reactor pressure vessel, effects of attachment configuration on, 25:57092(R) (ORNL-TM-3483)
testing of pressure vessel, ultrasonic method for, 25:54925
NUCLEAR AUXILIARY POWER SYSTEMS
design of plutonium-238-fueled, for implantable circulatory support system, 25:54910(P)
design parameters of heat pipe cooled thermionic fast reactor, calculations for optimum economic, 25:57134
mass of space, effects of radiator mass on, 25:54916
NUCLEAR CHEMISTRY
research progress in, 25:54587(R) (AECL-3909)
NUCLEAR EMULSIONS
cosmic particle reactions with nuclei above 100 GeV in, production of low-energy protons in, (E), 25:56429 (INP-754)
cosmic-ray tracks in, mass resolution of, (E/T), 25:55894 (LUIP-CR-71-4)
development of doped silver chloride, for detection of ionizing particles, 25:54996 (IKF-28)
meson (π) reactions with nuclei at 60 GeV in, production of low-energy protons in, (E), 25:56429 (INP-754)
particle tracks in, logic unit of PFIL 70 photometer for measuring, 25:55045 (LUIP-CR-71-2)
particle tracks in, television system for scanning, 25:55021

XUM

performance of polymer gelatin, for fast neutron dosimetry, 25:55057
sensitivity for fast neutrons, effect of stopping power on threshold, 25:55022
use for detection of alpha particles in bone marrow and blood of miners, 25:55236
NUCLEAR EXPLOSIONS
effects of, tests for determining performance of equipment for measuring, 25:54993 (AD-720974)
peaceful uses of, review of research on, 25:54830
uses of, review on industrial, 25:54816 (ORNL-4682, pp 182-6)
NUCLEAR EXPLOSIONS, ATMOSPHERIC
effect on kinetics of ions in nighttime ionospheric D region, (E), 25:56010
effects on mortality of man exposed in utero in Hiroshima and Nagasaki, long-term, 25:55307
fireballs from, effects of atmospheric particles on, (T), 25:54815 (AD-722031)
NUCLEAR EXPLOSIONS, UNDERGROUND
conference on peaceful uses of, Vienna, Austria, Jan. 18 to 22, 1971, 25:54818(T) (UCRL-Trans-10543)
effects of Nonique, on surrounding granite, studies of mechanical, 25:54820(T) (UCRL-Trans-10543, pp 4-35)
engineering and scientific uses of, review of, 25:54828
medical planning for experimental, off-site, 25:55249
peaceful uses of contained, USSR program on, 25:54821(T) (UCRL-Trans-10543, pp 36-41)
peaceful uses of, French program on, 25:54819(T) (UCRL-Trans-10543, pp 1-3)
radiation hazards from contained, evaluation of, 25:54823(T) (UCRL-Trans-10543, pp 56-69)
radioactivity from, comparison of US and USSR methods for calculating deposition, diffusion, and transport of, 25:54782 (UCRL-51054)
radiological safety for, off-site planning of, 25:55249
seismic wave propagation from Nonique, in Sahara granite, measurement of, 25:54820(T) (UCRL-Trans-10543, pp 4-35)
seismic waves from, determination of earthquake focal mechanisms from polarization angles of S, 25:54814
uses for petroleum production stimulation, USSR studies on, 25:54822(T) (UCRL-Trans-10543, pp 42-55)
uses of contained, for creating storage cavities in salt deposits, feasibility study of, (E), 25:54824(T) (UCRL-Trans-10543, pp 70-80)
uses of contained, for production stimulation of petroleum, 25:54826(T) (UCRL-Trans-10543, pp 99-116)
uses of contained, for stopping runaway gas and oil wells, 25:54825(T) (UCRL-Trans-10543, pp 81-98)
NUCLEAR MAGNETIC RESONANCE
modulation effects on, study of frequency- and field-, (E/T), 25:56371
theory of radiation detection and double-resonance techniques, 25:56372
NUCLEAR MATERIALS MANAGEMENT
equipment and methods for fuel rods and fabrication waste, nondestructive, 25:55004(R) (WCAP-7562-4)
safeguards system for, at nuclear power plants, role of reactor in, 25:54934 (BNWL-1598)
safeguards systems for, role of burnup calculation technology in, 25:54935 (BNWL-1599)
NUCLEAR MATTER
binding energy of neutron, calculations using Brueckner and variational theories, (T), 25:56867
NUCLEAR MODELS
collective, formulation for odd--odd deformed nuclei, 25:56812 (COO-1120-124)
Fermi gas, lectures on μ capture by nuclei in, (T), 25:56809 (CERN-71-14, pp 67-99)
Nilsson, effect of hexadecapole deformation on ΔN = 2 crossing in, (T), 25:56858
shell, Lanczos method for calculations in, (T), 25:56865
shell, lectures on μ capture by nuclei in, (T), 25:56809 (CERN-71-14, pp 67-99)
shell, systems approach to, 25:56866
NUCLEAR PARTICLES
detection of, development of doped silver chloride detectors for, 25:54996 (IKF-28)
NUCLEAR PHYSICS
book: Advances in Nuclear Physics. Volume 3, 25:56871
book: Nuclear Physics. Volume II. Interactions of Radiation and Matter Book 2, 25:56845
research at Oregon State University, 25:56689 (RLO-1062-711)
research at University of North Carolina April 1 to June 30, 1971, 25:56748(R) (ORO-2408-45)
NUCLEAR POWER PLANTS
development in France, review of, 25:57002
development in U. S., analysis of optimum economic, 25:57062 (ORNL-4682, pp 240-1)
development of, international cooperation in, 25:57006
development of, international cooperation in, 25:56983 (NP-18992)
effects on krypton-85 content in global atmosphere, 25:54781(T) (JPRS-53174)
environmental effects of, 25:56983 (NP-18992)
environmental effects of, estimate of potential, 25:57098
piping systems for, analysis of earthquake- and thermal-induced stresses in, (E/T), 25:54850
radiation monitoring in environment of, design and performance of amphibious detection system for in situ γ, 25:55239
radioactive effluent from, evaluation of hazards to human population from, 25:55347
radioactivity monitoring in environment of, consideration of ecological factors in developing program for, 25:55239
radioactivity release to environment from, estimation of effects on background radiation levels of long-term, 25:55200
requirements in Germany, projections of, 25:57005
siting of, geologic and seismic factors in, 25:54777
siting of, interpretation of emergency radiation doses to man used as guidelines for, 25:55242
systems analysis of, 25:54396 (ORNL-4682, pp 242-9)
NUCLEAR REACTIONS
conference on, 25:56821 (LYCEN-7104)
description of quasielastic scattering, on light nuclei, 25:56830 (LYCEN-7104, S14.1-18)
isovector excitations in photon-induced, (T), 25:56827 (LYCEN-7104, S8.1-10)
particle production in, methods for calculation of high-energy, (T), 25:56844
properties of single-nucleon transfer, on deformed nuclei, 25:56875
properties of transfer, methods for analysis of, 25:56823 (LYCEN-7104, C3.1-40)
research at Lyon Institute of Nuclear Physics in 1970, 25:56742(R) (LYCEN-7101)
research on polarized proton-induced, at Saclay, 25:56688 (LYCEN-7104, S6.1-2)
theory of nucleus--nucleus, Pauli principle in, 25:56829 (LYCEN-7104, S12.1-4)
NUCLEAR REACTIONS (DIRECT)
cross sections for summed inelastic and quasi-elastic scattering of medium- and high-energy electrons and protons, (T), 25:56849
Feynman diagrams for, unified treatment of nonrelativistic, (T), 25:56831 (LYCEN-7104, S18.1-18)
heavy-particle stripping in, PWBA calculations of differential cross sections for, (T), 25:56863
mechanisms in, use of triangle diagrams for internal bremsstrahlung for identification of, (T), 25:56864
stripping, diffraction analysis of angular distributions from (d,p), (T), 25:56847
NUCLEAR STRUCTURE
calculation for ground state properties of spherically symmetric nuclei using modified delta interaction, 25:56840
calculation of shell-model reaction matrix elements in Z = 28 region, using Reid and Yale potentials, (T), 25:56857
calculations for single-particle states in A =177 region using Woods--Saxon potential, (T), 25:56837(T) (UCRL-Trans-10544)
calculations for spherical even--even nuclei including anharmonic effects, 25:56842
configurations in, symmetry for highly restricted partitions and angular-momentum states of equivalent-particle, 25:56848
group symmetries for, lectures on, (T), 25:56838 (UR-875-350)
vibrational states of spherical nuclei, description of static quadrupole moments using self-consistent cranking approximation, 25:56860
NUCLEAR THEORY
boson expansion method in, treatment including Pauli principle, 25:56843
cluster expansion method for correlated wave functions, 25:56850
electromagnetic operator in, test for isotensor component of, 25:56839
generator coordinate formalism in, application to nuclear collisions, (T), 25:56825 (LYCEN-7104, C6.1-12)
Hamiltonian function for heavy nuclei in, structure of weak-interaction, 25:56768
mass formula in, energy-density functional form for, 25:56853
nuclear compressibility in, phenomenological description for, 25:56846
nucleon--nucleon correlations in, analysis of short-range, 25:56824 (LYCEN-7104, C4.1-17)
spectroscopic calculations in, formalism for, 25:56874
statistical description of nuclear surface, 25:56841
three-body problem in, analysis of singular-core interactions in boundary-condition model, 25:56851
three-body problem in, treatment using potential concept, 25:56872
NUCLEAR WEAPONS
control of, history and principles of treaties for, 25:54829
NUCLEI
alpha inelastic scattering by, role of isoscalar transition operator in, (T), 25:56876
alpha reactions (α,d) and (α,p) at 25 MeV with light, distorted-wave analysis of differential cross sections for, (T), 25:56677
cosmic particle reactions above 100 GeV in emulsions, production of low-energy protons in, (E), 25:56429 (INP-754)
deuteron reactions (d,p) at 7 to 21.4 MeV with A = 10 to


XUM

91, diffraction analysis of angular distributions from, (T), 25:56847
deuteron reactions (d,p) with, analysis of multi-channel features of, (T), 25:56817 (JINR-E4-5836)
deuteron reactions with, method for treatment of Pauli principle in breakup, (T), 25:56833 (ORO-3765-31)
electron density near, evaluation of, (T), 25:56370
electron scattering by, analysis for isotensor components in dipole sum rules for, (T), 25:56868
electron scattering by, effect of short-range correlations in, (T), 25:56824 (LYCEN-7104, C4.1-17)
electron scattering by, effects of nuclear structure on bremsstrahlung produced in polarized and unpolarized, (T), 25:56862
energy level radiation widths at excitation energies of the order of neutron binding energy, mean, (T), 25:56836(T) (UCRL-Trans-10542)
energy level transitions in, pair spectrometer for measuring multipolarities for, 25:55040 (NP-18994)
energy levels from gamma resonance scattering, resonance parameters for, (E), 25:56782
energy levels of even--even deformed, collective $1^+$, (T), 25:56819 (JINR-P4-5889)
energy levels of even--even, Mariscotti description of ground-state, (T), 25:56813 (COO-1746-57)
energy levels of even--even, table of quasi-ground, quasi-$\beta$, and quasi-$\gamma$ bands for, (E), 25:56651 (INSJ-127)
energy levels of nonaxial, Davydov-model calculations of 9/2, (T), 25:56785
energy levels of, method for calculating energy and spin dependence of density of excited, (T), 25:56835(T) (UCRL-Trans-10540)
energy levels of, reseach on electromagnetic properties of excited, (E/T), 25:56832(R) (NYO-3525-67)
energy-level transitions in deformed, probabilities for E2, (T), 25:56735 (FEI-202)
energy-level transitions in nonaxial, Davydov-model calculations of probabilities for E2, (T), 25:56785
fission of $Z < 84$, research at Western Washington State College, 1970 to 1971, (E), 25:56750(R) (RLO-1759-25)
masses of neutron-rich, (T), 25:55678
meson ($\mu^-$) capture by, effect of short-range correlation in, (T), 25:56824 (LYCEN-7104, C4.1-17)
meson ($\mu^-$) capture by, lectures on models for, (T), 25:56809 (CERN-71-14, pp 67-99)
meson ($\pi$) absorption by light, lectures on, (T), 25:56810 (CERN-71-14, pp 155-228)
meson ($\pi$) elastic scattering by, lectures on forward dispersion relations for, (T), 25:56810 (CERN-71-14, pp 155-228)
meson ($\pi$) reactions at 60 GeV in emulsions, production of low-energy protons in, (E), 25:56429 (INP-754)
meson ($\pi$) reactions at low and medium energies, lectures on, (T), 25:56807 (CERN-71-14)
meson ($\pi$) reactions with, lectures on soft pion theorems for, (T), 25:56808 (CERN-71-14, pp 1-65)
meson ($\pi$) scattering by, review lectures on nonvanishing pions in, (T), 25:56811 (CERN-71-14, pp 289-378)
meson ($\pi^-$) reactions ($\pi^-$,eta) at 7.82 GeV/c, differential cross sections for, (E), 25:56432
meson ($\pi^-$) reactions ($\pi^-$,$\pi^0$) at 7.82 GeV/c, differential cross sections for, (E), 25:56432
meson($\pi$) interactions with, survey of research on, 25:56873
mesons ($\mu$) capture by, second-class G-parity properties in, (T), 25:56854
neutron capture at 10 to 100 keV, compilation of gamma spectra and intensities for, (E), 25:56655 (ORNL-TM-3379)
neutron capture by, correlation between reduced neutron and radiative widths for resonance, 25:56818 (JINR-E4-5880)
neutron reactions (n,$\alpha$) and (n,p) near 14 MeV, statistical analysis of shell effects in, (T), 25:56869
neutron reactions in unresolved resonance region, method for calculation of cross sections for, (T), 25:56870
neutron resonance cross sections at low energies, computer program for, (T), 25:56814 (COO-2022-7)
nucleon elastic scattering by, computer program for optical-model analysis of, 25:56815 (INP-741)
nucleon inelastic scattering by, analysis using spin-orbit interaction, (T), 25:56826 (LYCEN-7104, C7.1-36)
nucleon scattering by, microscopic description using optical model, (T), 25:56822 (LYCEN-7104, C1.1-13)
observations of solar low-energy, during 1967 at widely separated locations, (E), 25:55956
photon reactions in Coulomb field at high energies, hadron production in, 25:56457
photon reactions with intermediate, cross sections for, (E), 25:56782
production and properties of low-energy, from proton inelastic reactions with $12 < Z < 83$ nuclei at 0.010 to 5 GeV, (T), 25:56522(T) (ORNL-tr-2520)
proton inelastic scattering by s-d shell, analysis of deformation in polarized, (T), 25:56828 (LYCEN-7104, S9.1-7)
proton reactions with $12 < Z < 83$, at 0.010 to 5 GeV, properties of low-energy nuclei from, (T), 25:56522(T) (ORNL-tr-2520)
research at Lund Univ., 1970, (E), 25:56643(R) (NP-19018)
scattering by light nuclei, analysis using generator coordinate formalism, (T), 25:56825 (LYCEN-7104, C6.1-12)

NUCLEIC ACID
radiolysis of solid, effects of electron dislocation and molecular weight on resistance to, 25:54636

NUCLEIC ACID, DEOXYRIBO-
isolation of high molecular weight, from cultured neural tumor cells, 25:57286 (UCLA-12-832)
labeling rat liver cell and spleen lymphocyte, with tritium-labeled thymidine, 25:55110(R) (TID-25801)
radiation effects on chemical, molecular biology, and physical processes in, mechanism of uv, 25:55136
radiation effects on single- and double-strand breaks in, mechanism of uv, 25:55308
radiation effects on structure of yeast, in relation to genetic damage, uv, 25:55183
radiation effects on synthesis of mouse kidney cell, $\gamma$ and uv, 25:55129
radiation effects on thymidine incorporation in cultured rat thymus cell, factors affecting x, 25:55127
radioinduced single-strand breaks in double-stranded circular, effects of dose on, 25:55133
radiolysis of solid, effects of electron dislocation and molecular weight on resistance to, 25:54636
role of cross links of, in inactivation of bacteriophage lambda, F' episomes, and Escherichia coli by combined psoralen and uv radiation, 25:55361

NUCLEIC ACID, RIBO-
radiation effects on synthesis of mouse kidney cell, $\gamma$ and uv, 25:55129
radiation effects on synthesis of ribosomal precursor of, in yeast, uv, 25:55138

NUCLEOGENESIS
history of galactic, (T), 25:55781
xenon isotope production in solar system, (E/T), 25:55670

NUCLEONS
binding to nucleons in e + d + e + p + n interactions, multi-pion exchange contribution to, (T), 25:56527
interactions e + N at very low energies, review of $\pi^+$ and $\pi^0$ production in, (E/T), 25:56404 (CONF-701121-8)
interactions $\gamma$ + N + $\pi$(eta) + N, Regge absorption model for forward, (T), 25:56452 (CALT-68-313)
interactions K + N at 2 to 20 GeV/c, behavior of diffraction maximum in inelastic, (T), 25:56504
interactions K + N, particle exchange and Regge-pole exchange in Veneziano model for, 25:56518
interactions N + d, dispersion theoretical calculation of vertex function for, (T), 25:56527
interactions N + N + d + boson, model of intermediate nucleon-isobar decay for, 25:56525
interactions N + N + N + N + $\pi$, lectures on kinematics and phenomenological and dynamical models for, (T), 25:56810 (CERN-71-14, pp 155-228)
interactions N + N at low energy, analysis of $^1S_0$ scattering lengths and effective ranges for, 25:56529
interactions N + N below 3 GeV, one-boson-exchange models for, 25:56532
interactions N + N, dual quark--parton model for, 25:56481
interactions N + N, singlet effective-range parameters of Mongan separable potential for, (T), 25:56859
interactions $\nu$ + N, second-class G-parity properties in elastic scattering, (T), 25:56854
interactions $\pi$ + N + sigma + N, helicity conservation in, 25:56517
interactions $\pi$ + N + vector meson + N, helicity conservation in, 25:56517
interactions $\pi$ + N at 2 to 20 GeV/c, behavior of diffraction maximum in inelastic, (T), 25:56504
interactions $\pi$ + N at 5.9 to 18.2 GeV/c, phenomenology of complex-spin negative-mass-squared resonance tachyons in angular distributions of charge-exchange, (T), 25:56500 (ORO-3992-18)
interactions $\pi$ + N at high energies, total effective cross sections for acausal, (T), 25:56502
interactions $\pi$ + N at low and intermediate energies, Regge poles for, (T), 25:56497 (FRNC-TH-33)
interactions $\pi$ + N at low and medium energies, lectures on, (T), 25:56807 (CERN-71-14)
interactions $\pi$ + N at low energies, lectures on, (T), 25:56496 (CERN-71-14, pp 101-54)
interactions $\pi$ + N, coupling constant from current-algebra sum rules and Veneziano amplitude for, 25:56516
interactions $\pi$ + N, dual quark--parton model for, 25:56481
interactions $\pi$ + N, three-channel model for $P_{11}$, 25:56519
production in four-prong $\pi^+$ + p interactions at 8 GeV/c in hydrogen bubble chamber, angular and momentum distributions for, (E), 25:56428 (IFA-HE-75)
scattering by nuclei, analysis using spin-orbit interaction, (T), 25:56826 (LYCEN-7104, C7.1-36)
scattering by nuclei, computer program for optical-model analysis of elastic, 25:56815 (INP-741)
scattering by nuclei, microscopic description using optical model, (T), 25:56822 (LYCEN-7104, C1.1-13)
structure of, meson momentum distribution in, 25:56512


XUM

NUCLEOTIDES
electron reactions with poly-, effects of secondary structure on hydrated, 25:55131

O

OBRIGHEIM POWER REACTOR (GERMANY)
pressure vessel for, ultrasonic testing for defects in, 25:56892
OBSIDIAN
age of Japanese, fission track method for estimation of, 25:54773
uranium content of Japanese, measurement of, 25:54773
OCEANOGRAPHY
activation analysis in, review of, 25:54481
OCONEE POWER REACTOR, UNIT 1
control rod drive for, preoperational testing damage repair for, 25:56915 (DOCKET-50269-37)
OCTANE
radiation effects on sorption on magnesium sulfate incorporating sulfur-35, gas chromatographic studies of, 25:54603
OIL SHALES
fracture by nuclear explosions, 25:54816 (ORNL-4682, pp 182-6)
ORES
analysis for chromium for process and quality control during beneficiation by neutron activation, 25:54507
analysis for gold by neutron activation of lead alloy obtained in cupel assay, 25:54521
analysis of platinum-bearing, for noble metals by neutron activation and γ spectrometry, 25:54487
analysis of slurries of, by neutron activation, irradiator for on-stream, 25:54506
analysis of terrestrial, for noble metals by neutron activation, 25:54484
analysis of, gamma radiometric equipment for field, 25:55066
density measurement of, gamma radiometric equipment for field, 25:55066
ORGANIC ACIDS
radiolysis of, rate constants for hydrogen atom reactions following electron, 25:55132
ORGANIC COMPOUNDS
radiation effects on luminescence of, 25:54598 (CONF-700652-(Vol.2), pp 423-75)
radioinduced preparation of, in liquid nonaqueous systems, review of, 25:54617
radiolysis of aqueous solutions of, reactions of hydrated electrons and hydroxyl radicals in pulse, 25:54632 (CONF-700652-(Vol.3), pp 649-92)
radiolysis of single crystals of, effects of Zeeman terms on hyperfine structure of ESR spectra following, 25:54641
radiolysis of solid, effects of electron dislocation and molecular dimensions on, 25:54635
radiolysis of solid, role of tunnel effects in reactions after, 25:54596
radiolysis of sulfur-containing, rate constants for hydrogen atom reactions following electron, 25:55132
radiolysis of, excited states and intermediates in, 25:54626 (CONF-700652-(Vol.1), pp 139-219)
reactions with hydrated electrons, 25:54631 (CONF-700652-(Vol.3), pp 601-48)
ORGANISMS
radioisotope accumulation by aquatic, effects of stable element content on, 25:55158
radioisotope uptake by marine, effects of physico-chemical form on, 25:55149 (BNWL-SA-4048)
ORGANS
radiation dose to human, terminology for expressing, 25:55251
ORNL HIGH-FLUX ISOTOPE REACTOR
maintenance during April through June 1971, 25:57120(R) (ORNL-TM-3569)
operation during April through June 1971, 25:57120(R) (ORNL-TM-3569)
OSMIUM
casting by levitation melting using magnetic field, 25:55424
conductivity at 80 to 1900°K, electric and thermal, 25:55523
determination in geochemical samples by neutron activation, 25:54484
determination in geological sample by neutron activation and radiochemical separations, 25:54485
determination in presence of ruthenium, spectrophotometric, 25:54412
determination in silicate rocks and rock-forming minerals by neutron activation and radiochemical separations, 25:54486
effects on properties and sintering of tungsten at 1000 to 2000°C, 25:55453
separation from rhenium by solvent extraction, 25:54401
OSMIUM ALLOYS AND SYSTEMS
Os--Pr-base, phase diagram of, 25:55567
Os--Pr-base, phase diagram of, thermodynamic analysis of, 25:55566
Os--Re-base, sound velocity at room temperature in, 25:55078(R) (NYO-3906-5)
OSMIUM ISOTOPES Os-191
beta decay of, gamma--x-ray angular correlation from, (E), 25:56755
OSTEICHTHYES
plutonium-239 content of Atlantic Ocean, 25:55161
Salmo gairdneri, cesium-137 uptake by mountain lake, role of bottom sediment in pathway for, 25:55159
OTTO HAHN REACTOR
operation during 1970, 25:57139
OVARIES
radioinduced sterility of developing beagle dog and monkey, following exposure in utero, effects of dose fractionation on x, 25:55319 (UCD-472-118)
OXIDES
diffusion in, data tabulations on, 25:55509
diffusion on sodium chloride surface, 25:54758 (ORNL-4717, pp 109-15)
properties and structure of, produced by sintering using systematic thermal fluctuations, 25:55414
thermodynamic potentials and enthalpies of, calculations of standard, 25:54586
OXYCHLORODURANATES
properties of pyridinium, 25:54541
OXYGEN
abundance in primary cosmic radiation, (E), 25:55911
abundance in solar atmosphere, (E/T), 25:55750
content at 100 to 200 km of atomic and molecular, diurnal variations of, (E), 25:55987
determination by charged particle activation methods, optimum irradiation conditions and nuclear interferences for, 25:54520
determination in aluminum electrolytic bath by 14-MeV neutron activation simultaneously with aluminum and fluorine, 25:54503
determination in germanium and silicon by helium-3 activation, 25:54502
determination in liquid potassium or sodium by zirconium gettering-vacuum-fusion method, 25:54418
determination in liquid sodium, development of meter for, 25:55379(R) (WARD-4210-T-1-2)
determination in molybdenum using exhalograph EAO-201, 25:54426
determination in semiconductor silicon by alpha or proton activation, 25:54528
diffusion in alpha-phase zirconium following deformation, mechanisms of, 25:55551
diffusion in yttrium at 20 to 300°C, effects of dislocations on, 25:55461
effects of additions of, on tensile properties of titanium--vanadium and aluminum--titanium--vanadium alloys, 25:55471
effects on carbon dioxide sorption on graphite, 25:55634
effects on corrosion of niobium by sodium at 600°C, 25:55386
effects on ignition of plutonium in inert atmospheres, 25:54946 (CONF-710401-, pp 106-17)
effects on lithium--defect interactions in electron-irradiated silicon, 25:56310
effects on reactions of recoil chlorine-38 in neutron-irradiated chloromethane, 25:54681
effects on yields from radiolysis of butane, 25:54659
helium-ion range at 0.2 to 2.0 MeV in, as function of energy, (E), 25:56276
infrared spectra in aurora, enhancement and excitation mechanisms of 1.27-μ, (E/T), 25:56018
mass transfer in aqueous solutions and slurries, use of radiokrypton as indicator for, 25:54903
neutron cross sections for, transmission of fission spectra through thick samples for evaluation of minima in total, (E), 25:56650 (COO-2049-5)
proton range at 0.2 to 2.0 MeV in, as function of energy, (E), 25:56276
proton reactions at 20 to 120 keV with molecular, cross sections for electron capture into n = 2 states of hydrogen in, (E), 25:55853
reactions with single and polycrystals of tantalum--tungsten alloys at 850 to 1100°C, 25:55385
reactions with tungsten surfaces at low pressures and high temperatures, (T), 25:55396
solubility limits in niobium--zirconium and niobium--hafnium alloys, lattice parameter measurements of, 25:55568
sorption by zirconium at low pressures and high temperatures, 25:55463
spectral excitation of 1304-A resonance radiation in dayglow, photoelectron-impact, (E), 25:56032
spectral intensity in night airglow, covariation of nonauroral O II Herzberg I band and O I 5577-A, (E), 25:56046
stopping of nuclei of, in nuclear emulsion, mass resolution of, (E/T), 25:55894 (LUIP-CR-71-4)
OXYGEN IONS
effects on silicon at 220 keV, lateral-stress study of damage produced in, 25:56285 (SC-RR-710424)
reactions with argon, helium, and nitrogen at 10 to 40 MeV, cross sections for electron capture in, 25:55869
reactions with argon, helium, and nitrogen at 7 to 40 MeV, cross sections for electron capture and loss in, (E), 25:55870
x-ray scattering by three- and four-electron, form factors and scattering functions for coherent and incoherent, 25:56259 (EGG-1183-1479)

XUM

OXYGEN IONS (O⁻)
reactions with sodium ions ($Na^+$) at 0.1 to 7 eV, merged-beam measurement of total cross sections for charge exchange in, 25:55859
OXYGEN ISOTOPES O-15
production in alpha reactions with aluminum and silicon at 70 to 160 MeV, cross sections and fission mechanism for, (E/T), 25:56685 (FRNC-TH-48)
OXYGEN ISOTOPES O-16
alpha reactions (α,2α) at 46 and 52.5 MeV, analysis using impulse approximation, (E/T), 25:56674
alpha reactions (α,Be-7) and (α,Li-6) at 42 MeV, cross sections for, (E), 25:56659
alpha reactions (α,γ) at 850 to 2490 keV, astrophysical implications of, (E/T), 25:55704
deuteron reactions (d,α) at 1.8 to 14 MeV, analysis for reaction mechanism in isospin-forbidden, (E/T), 25:56667
deuteron reactions with, Pauli breakup cross section for, (T), 25:56833 (ORO-3765-31)
electron inelastic scattering by, form-factor calculations using isotensor dipole sum rules, (T), 25:56868
energy levels from alpha resonances in carbon-12, partial and total widths for, (E), 25:56675
energy levels from carbon-12 alpha resonances, spin--parity assignments and widths for, (E), 25:56681
energy levels of, Brueckner--Hartree--Fock calculations using density-dependent effective interactions in, (T), 25:56834 (ORO-3765-32)
exchange between carbon dioxide and water, effects of amines and inorganic salts on kinetics of, 25:54549
form factor of, liquid-drop-model calculation including quadrupole surface oscillations of elastic, (T), 25:56668
meson ($K^-$) absorption in, analysis of mechanism in, 25:56653 (LYCEN-7104, S4.1-10)
meson (π) absorption by, analysis of mechanism in, 25:56653 (LYCEN-7104, S4.1-10)
meson reactions ($\mu^-,n\nu$) with, neutron spectrum and angular distribution asymmetry in, (T), 25:56820 (JINR-P4-5997)
meson reactions ($\mu^-,\nu$) with, lectures on elementary particle method for partial capture rate for, (T), 25:56809 (CERN-71-14, pp 67-99)
oxygen-16 elastic scattering at 13.6 to 23.7 MeV, cross section for, (E), 25:56657
oxygen-16 reactions at 13.6 to 23.7 MeV, cross sections, γ spectra, and particle angular distributions for, (E), 25:56657
photon reactions (γ,n) with, analysis by Feynman triangle diagrams of fine-structure peaks in cross sections for, (T), 25:56676
photon reactions with, model analysis of, (T), 25:56661
proton elastic scattering by, phase-shift analysis of polarization effects in, (T), 25:56678
reactions (O-16, pnγ) with phosphorus-31 at 34 and 36 MeV, p-γ and γ-γ coincidence spectra from, (E), 25:56693
scattering by nuclei in wide energy range, phase shift analysis of angular distributions for elastic, (E), 25:56740 (JINR-P7-5884)
OXYGEN ISOTOPES O-17
energy levels from carbon-12 (Li-7,d) reactions, spin assignments for, (E), 25:56663
energy levels from neon-20 (n,α) reactions, (E), 25:56717
OXYGEN ISOTOPES O-18
alpha inelastic scattering at 13.5 to 17.0 MeV, alpha and gamma spectra and α--γ angular correlations in, (E), 25:56672
alpha reactions (α, He-6) at 42 MeV, angular distributions for, (E), 25:56665
deuteron reactions (d,He-3) at 52 MeV, differential cross sections and spectra from, (E), 25:56662
energy levels from alpha inelastic scattering, spin--parity assignments for, (E), 25:56672
energy levels of, shell-model calculation with reaction matrices and pairing correlations, (T), 25:56666
energy-level transitions from alpha inelastic scattering, branching and multipole mixing ratios for, (E), 25:56672
exchange between carbon dioxide and water, effects of amines and inorganic salts on kinetics of, 25:54549
exchange between perrhenate and water in methanol, kinetics of, 25:54574
exchange between water and lithium bromates, nickel nitrates, or sodium selenates at 100 to 170°C, 25:54553
helium-3 reactions (He-3,p) at 18 MeV, angular distributions for, (E), 25:56716
proton reactions (p,α) at 500 to 750 keV, excitation function for, (E), 25:55384
radiation effects on potassium salts in presence of, production of oxygen-18-labeled products from, 25:54633(R) (ORO-3660-4)
OXYGEN SYSTEMS
C--N--O--Pu--U, preparation of carbides, carbonitrides, and hypostoichiometric oxides in, 25:55594 (ORNL-4682, pp 218-28)
CO--O, radiolysis of, electron pulse, 25:54587(R) (AECL-3909)
Nb-base--O--Ti, structure and tensile properties of, 25:55521
Nb-base--O--Zr, structure and tensile properties of, 25:55522
OYSTER CREEK POWER REACTOR, UNIT 1
emergency core cooling system for, effects of fuel element loading errors on performance calculations for, 25:56937 (DOCKET-50219-145)
instrumentation for, replacement procedures for local power range monitor, 25:56900 (DOCKET-50219-147)
operations during January to June 1971, 25:56899 (DOCKET-50219-146)


## P


PACIFIC OCEAN
protactinium-231 distribution in, 25:54810
thorium-230 distribution in, 25:54810
PACKED COLUMNS
dispersion in, for contacting liquids with high density difference, axial, 25:54719 (ORNL-4682, pp 229-39)
PAINTS
radiation resistance of selected, evaluation of, 25:54396 (ORNL-4682, pp 242-9)
PAIR PRODUCTION
cross sections for incident photons of 1.073 to 2.615 MeV, effects of atomic-electron screening on, (T), 25:56275
PALISADES POWER REACTOR
control rod drives for, effects of epoxy deposits on test failure of, 25:56911 (DOCKET-50255-54)
cooling system for, description of unintentional pressure reduction in, 25:56910 (DOCKET-50255-53)
PALLADIUM
determination in fission product mixtures by ion exchange and polarography or β counting, 25:54449
determination in geochemical samples by neutron activation, 25:54484
determination in geological sample by neutron activation and radiochemical separations, 25:54485
determination in lead beads, matte, and platinum-bearing ores by neutron activation and γ spectrometry, 25:54487
diffusion of carbon in solid solutions of, 25:55479
effects on properties and sintering of tungsten at 1000 to 2000°C, 25:55453
separation from other metal ions on titanium tungstate papers by electrochromatography, 25:54744
separation from rhenium by solvent extraction, 25:54401
separation of uranium from, in methyl sulfoxide by cation exchange chromatography, 25:54728
PALLADIUM ALLOYS AND SYSTEMS
Al--Pd, optical constants for β-phase PdAl intermetallic compound in, 25:56352
PALLADIUM ISOTOPES Pd-103
distribution in rats following introduction into thigh muscle, effects of carrier on, 25:55112
PALLADIUM ISOTOPES Pd-107
hazards from, evaluation of radiological, 25:54887(R) (BNWL-1308-6)
PANCREAS
scanning of human, diagnostic value of, 25:55280
scintiscanning of human, effectiveness of selenium-75-labeled selenomethionine for, 25:55271(T) (LB/G-3059)
PARTICLE TRACKS
analysis of spark chamber, stringing method for, 25:55048
measurement of bubble and spark chamber, automatic, 25:55047
structure in liquids and solids, models for, 25:54589 (CONF-700652-(Vol.1), pp 19-49)
PARTICLES
counting of radioisotope-labeled 10 μ diameter, Coulter type instrument for, 25:55090
effects of atmospheric meteoritic and sulfate, on nuclear fireball emissions, (T), 25:54815 (AD-722031)
PEGMATITES
processing of, leaching studies for, 25:54752
PENICILLAMINE
hydrochloride, radiation effects on single crystals of, ESR studies of x, 25:54605
PENTANE
I--pentane, neutron reactions (n,γ) with iodine-127 in, yields and product distribution from, 25:54705
I--pentane, radiolysis of, distribution of iodine-131-labeled products from, 25:54705
PENTANE, 3-METHYL-
radiation effects on glasses of, reactions and identification of free radicals produced by γ and uv, 25:54648
2,4-PENTANEDIONE
effects on separation of rare earths from aqueous solutions by solvent extraction using TTA, synergistic, 25:54731
1-PENTENE
I--1-pentene, neutron reactions (n,γ) with iodine-127 in, yields and product distribution from, 25:54705
I--1-pentene, radiolysis of, distribution of iodine-131-labeled products from, 25:54705


XUM

2-PENTENE
I--2-pentene, neutron reactions (n,γ) with iodine-127 in, yields and product distribution from, 25:54705
I--2-pentene, radiolysis of, distribution of iodine-131-labeled products from, 25:54705
PEPTIDES
preparation of tritium-labeled, development of catalytic method for, 25:54693(P)
PERCHLORIC ACID
reactions with uranyl ions, disproportionation and ECE kinetics in reduction, 25:54585
PERSONNEL
alpha detection in blood and bone marrow of mining, using nuclear emulsions, 25:55236
decontamination of, design of Mound Laboratory facility for medical, 25:54963 (CONF-710401-, pp 311-15)
qualifications for health and safety support in plutonium facility, 25:55204 (CONF-710401-, pp 267-79)
radiation dose to, from radioactive objects, method for estimation of, 25:54987
radioinduced chromosome aberrations in blood cells of industrial, γ, 25:55163
radioisotope distribution in tissues of uranium mining, lead-210 and polonium-210, 25:55117
PERTURBATION THEORY
error bounds for nth-order energies and wave functions in Rayleigh--Schroedinger, 25:55891
five-point function and singularity manifolds in, Feynman graph of, 25:56551
PETROLEUM
cesium-137 content of, following production stimulation by contained nuclear explosion, (E/T), 25:54826(T) (UCRL-Trans-10543, pp 99-116)
flow from runaway oil field wells, use of contained nuclear explosions for stopping, 25:54825(T) (UCRL-Trans-10543, pp 81-98)
production stimulation by contained nuclear explosion, calculation of contamination from, 25:54826(T) (UCRL-Trans-10543, pp 99-116)
production stimulation using underground nuclear explosions, radiation hazards from, 25:54823(T) (UCRL-Trans-10543, pp 56-69)
production stimulation using underground nuclear explosions, USSR studies on, 25:54822(T) (UCRL-Trans-10543, pp 42-55)
recovery by fracturing oil shales by nuclear explosions, 25:54816 (ORNL-4682, pp 182-6)
strontium-89 content of, following production stimulation by contained nuclear explosion, (E/T), 25:54826(T) (UCRL-Trans-10543, pp 99-116)
PHAEOPHYTA
radioisotope content of Pacific, in environs of reactors, 25:55151 (CONF-710817-1)
PHANTOMS
radiation dose distribution in tissue-equivalent, calculation of high energy electron, 25:55214
radiation dose distribution in water, isodose curves for 5 to 15 MeV positron, 25:55210
radiation dose distributions in rabbit and rat, following exposure to monoenergetic neutron beams, correlation of LET distributions with γ, neutron, and recoil ion, 25:55229
radiation dose to bone and muscle, use of tissue-equivalent organic scintillators in measurement of x, 25:55213
radiation dose to tissue equivalent, Monte Carlo calculations of absorbed and equivalent 592-MeV proton, 25:55216
radiation dose to tissue equivalent, Monte Carlo calculations of absorbed and equivalent 580-MeV neutron, 25:55216
radiation dosimetry in lucite, performance of thermoluminescent dosimeters for fast neutron, 25:55319 (UCD-472-118)
radiation dosimetry in tissue-equivalent, effects of energy spectra and dosimeter location on fast neutron, 25:55232
use with aluminum phosphate dosimeters for evaluation of gamma dose to man accidentally exposed at irradiation facilities, 25:55235
PHARMACEUTICALS
production of radioisotope-labeled, conference on, 25:55255
PHENOL, 2,4-DINITRO-
effects on recovery of Escherichia coli following uv or x irradiation or nitrogen mustard treatment, 25:55355
PHONONS
cross section in thermal neutron scattering by crystal of n-, use of zero Placzek moment to calculate, (T), 25:56340(T) (AERE-Trans-1137)
PHOSPHATES
diffusion in, data tabulations on, 25:55509
PHOSPHONIC ACID, BUTYL-, DIBUTYL ESTER
solvent properties for actinides and lanthanides in reprocessing of LMFBR fuel, 25:54706 (BNWL-SA-3345)
PHOSPHORIC ACID, DIETHYL ESTER
silver salt, crystal structure of, x-ray diffraction studies of, 25:57291 (UR-49-1515)
PHOSPHORIC ACID, TRIBUTYL ESTER
solvent properties for plutonium, 25:54713 (ORNL-4682, pp 39-79)
dodecane--TBP, radiolysis of, effects of nitric acid on reactor, 25:54644
kerosene--TBP, radiolysis of, effects of nitric acid on reactor, 25:54644
mepasine--TBP, radiolysis of, effects of nitric acid on reactor, 25:54644
PHOSPHORODITHIOIC ACID, DIBENZYL ESTER
potassium salt, crystal structure of, x-ray diffraction studies of, 25:57291 (UR-49-1515)
PHOSPHOROTHIOIC ACID, S-(2-AMINOETHYL) ESTER
effects on sensitivity of guinea pigs and mice to transverse acceleration, 25:55264
PHOSPHOROTHIOIC ACID, S-2-(3-AMINOPROPYLAMINO)ETHYL ESTER
radioprotective effects on gastrointestinal tract of mice, effects of strain on x, 25:55259
PHOSPHORS
purification of rare earth, by precipitation of cerium and thorium impurities as iodates, 25:54749(P)
use of tissue-equivalent organic, in measurement of x radiation absorbed dose to bones and muscles, 25:55213
PHOSPHORUS
content of diseased and normal human bones, neutron activation determination of, 25:55106
determination in calcite and dolomite by neutron activation and γ spectrometry, 25:54497
effects of residual, on neutron embrittlement of Types A302B and A533B steel, 25:55577 (NRL-7310)
PHOSPHORUS ISOTOPES P-31
helium-3 reactions (He-3,pγ) at 12 and 13 MeV, p-γ coincidence spectra from, (E), 25:56715
oxygen-16 reactions (O-16,pnγ) at 34 and 36 MeV, p-γ and γ-γ coincidence spectra from, (E), 25:56693
PHOSPHORUS ISOTOPES P-32
accumulation by marine phytoplankton, mechanisms of, 25:55154
determination in water by Cherenkov radiation counting using liquid scintillation spectrometer, 25:54438
effects on incidence of osteosarcomas in rats following intraperitoneal injection, 25:55335
effects on thymineless death and liquid holding recovery in Escherichia coli, synergistic effects of uv radiation on, 25:55359
use as tracer for measuring velocity of moving thread, 25:54900
use with Si(Li) detectors for diagnosis of skin neoplasms, 25:55273
PHOSPHORUS OXIDES
$P_2O_5$--$ThO_2$--$ZrO_2$, phase studies on subsolidus equilibrium in, 25:55638
PHOSPHORYL CHLORIDES
radiolysis of, ESR spectra of $POCl_3^-$ radical anion from γ, 25:54667
PHOTOCONDUCTIVITY
measurement during and after ionizing radiation pulses, technique for routine, 25:55079 (SC-DC-713696)
PHOTOGRAPHY
method for high-speed, for studying post-burnout two-phase flow, 25:54875 (RT/ING-(71)8)
PHOTOMETERS
circuits for PFIL 70, for nuclear emulsion particle track analysis, logic, 25:55045 (LUIP-CR-71-2)
PHOTOMULTIPLIER TUBES
temperature effects on scintillation detector, at 20 to 70°C, 25:55025
PHOTON BEAMS
energy determination above 5 GeV, method for, 25:56609(P)
PHOTONS
effects on heating of plane bodies, tables for transient temperatures from, 25:56267
emission of evanescent, by charged particles in vacuum, (T), 25:56392
emission of high-energy, from quasars, (T), 25:55908
interactions γ + e, disturbance of second-order coherence of photon field in quantum electrodynamics for forward, (T), 25:56456
interactions γ + N → π(eta) + N, Regge absorption model for forward, (T), 25:56452 (CALT-68-313)
interactions γ + n → $\pi^0$ + n, Reggeized absorption model fits to, 25:56458
interactions γ + n in e + d interactions at high energies, cross sections for particle production in, (E), 25:56405 (DESY-71/33)
interactions γ + p → eta + p, Reggeized absorption model fits to, 25:56458
interactions γ + p → $\pi^0$ + p, Reggeized absorption model fits to, 25:56458
interactions γ + p at 4 to 36 GeV, quark model for multiple π production in, 25:56514
interactions γ + p in e + d interactions at high energies, cross sections for particle production in, (E), 25:56405 (DESY-71/33)
interactions γ + π → π + γ, epsilonγγ and fγγ coupling constants from finite-energy sum rules for, (T), 25:56463
interactions of, potentials and multipole moments for amplitudes of, (T), 25:56455
interactions of, research at Lund Univ., 1970, (E), 25:56643(R) (NP-19018)
interactions with high-energy cosmic rays, energy-loss mechanisms in, (T), 25:55908
interactions with polarized particles, structure of

amplitude and differential cross sections for, (T), 25:56454
production in n + p interactions at 14.1 MeV, relativistically covariant models for cross sections for, (T), 25:56526
production of heavy, in electromagnetic interactions, indefinite metric for cross sections of, (T), 25:56547 (NYO-1932(2)-200)
reactions (γ,f) with thorium-232 at 90 MeV, liquid-drop-model calculations of heavy-fragment masses in, (T), 25:56787
reactions (γ,f) with uranium-238 at 35 MeV, liquid-drop-model calculations of heavy-fragment masses in, (T), 25:56787
reactions (γ,r) with A = 25 to 208 nuclei near threshold energies, cross sections for, (E), 25:56702
reactions (γ,n) with calcium-40, carbon-12, fluorine-19, lead-208, and oxygen-16, analysis by Feynman triangle diagrams of fine-structure peaks in cross sections for, (T), 25:56676
reactions with atoms at 1.073 to 2.615 MeV, effects of atomic-electron screening on cross sections for pair production in, (T), 25:56275
reactions with carbon-12 and oxygen-16, model analysis of, (T), 25:56661
reactions with hydrogen atoms, perturbation-theory calculations of bound--bound and bound--free transitions in multi-, 25:55875
reactions with lead-208, analysis using eigenchannel reaction theory and continuum shell model, (T), 25:56800
reactions with nuclei in Coulomb field at high energies, hadron production in coherent, 25:56457
reactions with UN at 0 to 74 eV, optical constants from, (E/T), 25:56345
scattering by plutonium-239, production of spontaneously fissioning isomers in inelastic, (E), 25:56738 (JINR-P15-5959)
transport equation for, non-linear Monte Carlo solution of, 25:57161 (CONF-710302-(Vol.2), pp 794-7)

PHOTOSPHERE
element abundances in, (E/T), 25:55750
spectra of, search for CH+ in, (E), 25:55768

PHTHALOCYANINE
complexes with indium chloride, radiation effects on, Szilard--Chalmers process from neutron, 25:54680

PHYSICS
conference on computational, Culham, England, 7/69, 25:56400
research at Chalk River January 1 to March 31, 1971, 25:56733(R) (AECL-3912)

PHYTOHEMAGGLUTININ
effects on electrophoretic mobility of x-irradiated human lymphocytes, 25:55310

PIGMENTS
extraction from Cyanophycene algae, decolaration by, 25:57236(T) (LA-tr-71-73)

PINCH DEVICES
radiation from fast z-, time--space resolved spectroscopic measurements of, (E), 25:56150 (LGI-70/14/E)
radiation losses from theta, at 100 to 200 A, (E), 25:56149 (IPP-1/108)

PINCH EFFECT
plasma stabilization by force-free magnetic fields in linear, magnetohydrodynamic, (T), 25:56200

PIPES
design criteria for nuclear service, development program for, 25:57092(R) (ORNL-TM-3483)
heat transfer from heated, to two-phase annular flow, effects of diffusion and film formation on critical, (E), 25:54869 (FEI-217)
stresses in nuclear power plant, analysis of earthquake- and thermal-induced, 25:54850
tees for nuclear service, elastic response and fatigue testing of, 25:57092(R) (ORNL-TM-3483)

PLACENTA
iodine-125 and -131 transport across, in pregnant sheep, 25:55319 (UCD-472-118)

PLANETARY NEBULAE
condensations in, life spans of neutral, (T), 25:55702
model for IRC + 10216, (E), 25:55686
spectra of, helium and hydrogen lines in, (E), 25:55700

PLANETS
atmospheres of, ionization by penetration of energetic charged particles, (T), 25:55983

PLANKTON
plutonium-239 content of Atlantic Ocean, 25:55161
radioisotope accumulation by marine, mechanisms of, 25:55154
radium-226 content of marine phyto-, off coast of South Africa, 25:55155

PLANTS
analysis for aluminum by separation and neutron activation, 25:54514
radiation monitoring in environs of Ames Research Reactor during 1971, 25:55152 (IS-2658)

PLASMA
charged particle beam interactions with nonlinear, radiations from, (T), 25:56168
charged-particle motion in, formation of Debye potential well in, (T), 25:56174
collision integral for particles of disparate mass, 25:56179
collisions in low-temperature helium, destruction of metastables in, (E), 25:56151(T) (SC-T-713064)
collisions in, system for two-dimensional many body calculations, 25:56187
conductivity in T-3 and ST Tokamak, mathematical model for, 25:56162 (CEA-CONF-1801)
conductivity of magnetized potassium, anomalous, (E), 25:56159
confinement and turbulent heating in toroidal magnetic traps, (E), 25:56127
confinement in Q devices, electrostatic, (T), 25:56013
confinement in toroidal devices, numerical simulation with fluid model, 25:56129
diagnostics in spark discharges, temperature and electron density, (E), 25:56142
diagnostics in thermonuclear devices, temperature profile in, 25:56216 (NP-19014)
diagnostics of argon arc, spectroscopic, (E/T), 25:56139
diagnostics of argon arc, temperature distribution and thermal conductivity in, (E), 25:56140
diagnostics of discharge, electron energy distribution, (E), 25:56138
diagnostics of inhomogeneous, using electromagnetic wave probes, 25:56145
diagnostics of ionospheric, steady-state and dynamic probe characteristics in, (E), 25:56012
diagnostics of laser-produced, plane electrostatic analyzer for, (E), 25:56137
diagnostics of shock-heated, use of conical probes for, (E/T), 25:56144
diagnostics of, using ultrarapid photometric camera, 25:56132 (CEA-R-4079)
diagnostics using cylindrical Langmuir probes, response in transition regime, (E/T), 25:56136
diagnostics using Langmuir probes, effects of collisions on, 25:56135
diagnostics using selective change of optical thickness, electron density, (E), 25:56133 (INR-P-1322)
diagnostics using Thomson scattering of laser light, construction of electron distribution, 25:56143
effects of rf-activated inert gas, on bondability and critical surface tension of polydimethyl silicones and polyethylene, 25:57272 (SC-RR-710483)
electron beam injection into dense, self fields and currents from relativistic, (T), 25:56166 (NP-19012)
electron beam interactions with collisionless, dispersion relations for linear waves from, 25:56170
electron beam interactions with homogeneous, dispersion relations for linear waves from, (T), 25:56169
electron beam interactions with, Bernstein wave excitation in, (E), 25:56241
electron beam interactions with, longitudinal wave reflection in, (T), 25:56247
electron beam interactions with, longitudinal wave excitation in, (T), 25:56232 (NP-19020)
electron beam interactions with, noise levels of Langmuir oscillations from, (E), 25:56249
electron distribution function for Lorentz, (T), 25:56173
electron shielding in non-neutral, test-particle, (T), 25:56175
electron velocity distribution function for homogeneous argon, (T), 25:56186
electron--ion recombination calculations for two-component, (T), 25:56167
electron--ion recombination in cryogenic helium, (E), 25:56152(T) (SC-T-713065)
electron--ion recombination in helium, at low temperatures, (E), 25:56161
electron--ion recombination in high-temperature hydrogenic, (T), 25:56164 (LGI-71/1/E)
electron--ion recombination rate coefficients for argon, (T), 25:56182
equilibrium calculations for confining vacuum magnetic field, two-dimensional, 25:56207
expansion from spherical source into vacuum, (T), 25:56180
expansion from spherical source into vacuum, effect of partial ionization and recombination on, (T), 25:56181
flow in shock tubes, dynamics of, (E), 25:55920
heating and confinement in toroidal magnetic traps, turbulent, (E), 25:56127
heating by ion cyclotron waves in magnetic beaches, (E), 25:56231 (N-71-25439)
heating by turbulence in tokamak devices, ohmic, (E), 25:56123(R) (ORO-4087-1)
heating in tokamaks by increasing longitudinal magnetic field, (T), 25:56125
heating of electrons in magnetized, resonances in anomalous microwave, (E), 25:56124
heating of hydrogen, ion energy distribution in turbulent, (E), 25:56131
heating of inhomogeneous cosmic, density-dependent, (T), 25:56126
heating using lasers, prospects for, 25:56128
injection into 2X mirror machine, large-area high-current ion source for, 25:56212 (LBL-35)
injection into Baseball II, multi-aperture 1-kV ion source for, (E), 25:56217 (UCRL-73387)


XUM

injection into mirror machines, ion source development for, 25:56213 (LBL-327)
injection into thermonuclear devices, duoPIGatron source for, 25:56208 (CONF-711012-9)
injection of, development of intense ion and neutral sources for, 25:56218 (UCRL-73412)
ionization wave excitation in positive columns by acoustic pulses, (E), 25:56154
kinetic theory of collisionless, finite-Larmor-radius equations for, 25:56178
kinetic theory of, statistical, 25:56185
light scattering by weakly ionized, theory of Thomson, 25:56165 (N-71-27890)
magnetic field distribution in, between concentric boundaries, (T), 25:56163 (LGI-70/16/E)
models for two-dimensional, properties of Cloud-in-Cell and Nearest-Grid-Point, 25:56191
neutron emission from laser irradiated deuterated polyethylene, 25:56219
oscillations in beam--plasma system, noise levels from Stark broadening analysis, (E), 25:56249
oscillations in cold inhomogeneous, electrostatic, (T), 25:56242
oscillations in, nonlinear processes in, (E/T), 25:56229 (EUR-CEA-FC-602)
properties of microwave-excited argon, analytical and physical, (E), 25:56158
radiation in weakly inhomogeneous magnetic fields, spectral distribution of, (T), 25:56177
radiations from fast z-pinch, time--space resolved spectroscopic measurements of, (E), 25:56150 (LGI-70/14/E)
radiations from theta pinch, at 100 to 200 A, (E), 25:56149 (IPP-1/108)
shock wave formation and propagation in, multi-dimensional magnetohydrodynamic calculations for, 25:56192
shock wave propagation in collisionless magnetized, kinetic model for unstable equilibrium in, 25:56190
shock wave propagation in, models for collisionless, 25:56189
shock wave propagation in, review of collisionless, (E/T), 25:56147
simulation of microinstabilities in, using superparticle computer models, 25:56206
simulation of toroidal confinement using fluid model, 25:56129
spectra measurements of hydrogen, precision, (E), 25:56156
spectra of helium, relaxation theory of Stark broadening in, 25:56184
spectral line intensities in, effect of electron temperature variations on, 25:56171
stability in argon arcs in magnetic fields, (E/T), 25:56196(R) (N-71-25028)
stability in shallow magnetic wells as in DECA II B, MHD criteria for, (T), 25:56194 (EUR-CEA-FC-598)
stability in tokamak devices, trapped-particle, (T), 25:56195 (JAERI-Memo-4483)
stability in tokamaks, review of, 25:56198
stability of streaming, in parallel uniform magnetic fields, (T), 25:56202
stability of uniformly rotating magnetized, resistive, (T), 25:56203
stability of, electromagnetic instabilities parallel to magnetic fields, (T), 25:56204
stability of, numerical experiments on nonlinear, 25:56205
stability of, simulation of microinstabilities using superparticle computer models, 25:56206
stabilization of flute instabilities in, using integrating feedback system, (E), 25:56197
stabilization of MHD instabilities by force-free magnetic fields in cylindrical geometries, (E), 25:56201
stabilization of MHD instabilities by force-free magnetic fields, (T), 25:56199
stabilization of MHD instabilities in force-free magnetic fields in linear pinches, (E), 25:56200
thermodynamics of partially ionized, canonical transformation method in, 25:56172
transport properties of partially ionized argon, (T), 25:56183
turbulence in argon arcs in magnetic fields, (E/T), 25:56196(R) (N-71-25028)
wave absorption by, boundary for electron cyclotron and low hybrid frequency, 25:56224(T) (AEC-tr-7270)
wave coupling in inhomogeneous, electromagnetic, (E), 25:56225 (CEA-CONF-1802)
wave coupling in warm, Lagrange solutions for three nonlinear, (T), 25:56245
wave damping and growth in, nonlinear Landau, (T), 25:56234
wave damping in fully ionized, dispersion relations for electron, (T), 25:56238
wave damping in, echoes from, (E), 25:56226 (CEA-CONF-1804)
wave damping in, research on quasi-static ion cyclotron, (E), 25:56233(R) (ORO-3871-6)
wave excitation and ion heating in magnetic beaches, ion cyclotron, (E), 25:56231 (N-71-25439)
wave excitation by Cherenkov and cyclotron coupling in beam--plasma system, Bernstein, (E), 25:56241
wave excitation in beam--plasma system, longitudinal, (T), 25:56232 (NP-19020)
wave excitation in cylindrical anisotropic, traveling wave antenna for, 25:56254
wave generation in inhomogeneous, in strong magnetic field, (T), 25:55923
wave interactions in inhomogeneous magnetized, nonlinear electron and ion, (E/T), 25:56246
wave interactions with exponential density distribution, electromagnetic, (T), 25:56230 (INR-1321)
wave propagation across magnetic field in parabolic layer of, electromagnetic, (T), 25:56236
wave propagation along layer of, effect of electromagnetic field pressure on, (T), 25:56235
wave propagation and stability, effect of impurity ions on drift, (T), 25:56243
wave propagation in collisionless, weak discontinuities, (T), 25:56237
wave propagation in fully ionized collisional, ion acoustic, (T), 25:56251
wave propagation in inhomogeneous collisional, kinetic model for, 25:56248
wave propagation in slightly relativistic, electromagnetic, (T), 25:56228 (CEA-CONF-1806)
wave propagation in strongly curved configurations of, dispersion relations for, 25:56253
wave propagation in weakly ionized, strong cylindrical and spherical electromagnetic-, (T), 25:56240
wave propagation in, effects on Tonks--Dattner resonant frequencies, (T), 25:56252
wave propagation in, nonlinear solutions of Vlasov and Poisson equations for, 25:56244
wave propagation in, particle trapping in large-amplitude, (T), 25:56227 (CEA-CONF-1805)
wave reflection in beam--plasma system, longitudinal, (T), 25:56247
wave transformation and absorption in, linear, (T), 25:56250
wave-propagation in, definition of positive and negative energy, (T), 25:56239
x-ray spectra from, regularization technique for electron energy distribution function for, 25:56134 (ORNL-TM-3582)

PLASMA ACCELERATORS
current sheath structure in dense focus, (E), 25:56157
design and performance for plasma injection into toroidal octupoles, 25:56220
electrode effects on performance of, (E), 25:56153
magnetohydrodynamic calculations for dense focus, 25:56188
neutron emission from dense focus, calibration of silver activated counters for measuring, 25:56214 (LGI-70/17/E)

PLASMA JETS
flow past obstacles, transonic, (T), 25:56176
properties of induction-heated, for simulation of gas-core nuclear rockets, 25:56146 (N-71-27023)
stability in parallel uniform magnetic fields, (T), 25:56202

PLASMAPAUSE
motion of, calculations of time-dependent, 25:55972
radius determination of, from relation of magnetospheric electric-field dependence on solar-wind velocity, (T), 25:56039
structure in boundary of, evidence of corotating tail-like, (E/T), 25:56028
structure on boundary of, evidence of corotating tail-like, (E/T), 25:56028

PLATES
book:Tables for Calculating Nonstationary Temperatures of Plane Bodies During Heating by Irradiation, 25:56267
fracture mechanics of, developments in three-dimensional elastic--plastic stress analysis for, 25:55515
heating by irradiation, tables for transient temperatures from, 25:56267

PLATINUM
argon-ion reactions at 30 keV with surfaces of, charge states and kinetic energies of scattered and recoil ions from, (E), 25:55818
compounds with electropositive metals, formation of intermetallic, 25:54534 (ORNL-4717, pp 43-56)
conductivity at 80 to 1900°K, electric and thermal, 25:55523
determination in geochemical samples by neutron activation, 25:54484
determination in geological sample by neutron activation and radiochemical separations, 25:54485
determination in lead beads, matte, and platinum-bearing ores by neutron activation and γ spectrometry, 25:54487
effects on properties and sintering of tungsten at 1000 to 2000°C, 25:55453
nitrogen oxide molecular beam scattering from clean and carbon coated single crystals of, 25:57237 (LBL-133)
properties for container material in alkali pyrosulfate processing of carbide fuels, 25:55376 (CONF-690452-, Paper 9)
radioinduced Frenkel defects in, effects of gold dopant on annealing of electron, 25:56284 (JUL-731-FF)
separation from rhenium by solvent extraction, 25:54401

XUM

PLATINUM ALLOYS AND SYSTEMS
Nb--Pt, niobium-93 NMR in $Nb_3Pt$, 25:56373
Pr-base--Pt, phase diagram of, 25:55567
Pr-base--Pt, phase diagram of, thermodynamic analysis of, 25:55566
PLATINUM ISOTOPES Pt-190
energy-level transitions from gold-197 decay, internal conversion coefficients for, (E), 25:56760
PLOWSHARE PROJECT
debris from Schooner Event of, radioisotope retention and excretion by peccaries following ingestion of, 25:55124
developments in, review of, 25:54828
ground motion from Rulison Event, at Tosco mine and tower stations, pseudorelative velocity spectra for, 25:54813 (PNE-R-51)
natural gas production stimulation by Rulison Event in, post-shot well test data for, 25:54817 (PNE-R-52)
research programs in, review of, 25:54830
research progress on, 25:54816 (ORNL-4682, pp 182-6)
PLUMES
diffusion in atmosphere, krypton-85 tracer studies of, 25:54908
rise of stack-released, method for calculating, (E/T), 25:54780 (CONF-710505-6)
PLUTONIUM
bibliography on, First Quarter 1971 index to, 25:55369
combustion aerosols from, retention efficiency of particulate air filters for, 25:54951 (CONF-710401-, pp 181-202)
compounds, heating of dry, fractional release during, 25:54546
content and distribution in desert soils around Nevada Test Site, 25:54755 (CONF-710401-, pp 320-7)
content on surfaces based on radiation dose to humans, decision levels for establishing, 25:55195 (CONF-710401-, pp 352-64)
determination by indirect potentiometry, 25:54411
development for nuclear uses, operation of inert atmosphere system in, 25:54945 (CONF-710401-, pp 98-105)
diffusion in sodium chloride, solid-state, 25:54758 (ORNL-4717, pp 109-15)
handling of, conference on safety in facilities for, Rocky Flats, Colo., April 13 to 16, 1971, 25:54937 (CONF-710401)
ignition in air--carbon dioxide mixtures, effects of oxygen content on, 25:54946 (CONF-710401-, pp 106-17)
ignition in air--nitrogen mixtures, effects of oxygen content on, 25:54946 (CONF-710401-, pp 106-17)
metallurgy of, health and safety support in facility for studying, 25:55204 (CONF-710401-, pp 267-79)
movement in aquatic systems, 25:55150 (CONF-710401-, pp 407-10)
oxidation of ignited, in air stream, fractional release during, 25:54546
processing facilities for, installation and performance of HEPA filters for, 25:54947 (CONF-710401-, pp 118-32)
processing facility for, administrative procedures for Rocky Flats, 25:54960 (CONF-710401-, pp 293-6)
processing in inert gas atmosphere glove boxes, effects of air in-leakage on, 25:54944 (CONF-710401-, pp 83-97)
processing of liquid waste materials of, methods and safety at Los Alamos plant for, 25:54708 (CONF-710401-, pp 369-85)
processing of scrap, safeguards capabilities of materials accounting systems in facilities for, 25:54968 (IAEA-R-878-F)
processing of, administrative methods for criticality control in, 25:54966 (CONF-710401-, pp 430-7)
processing of, design of plant using nitrogen atmosphere for, 25:54943 (CONF-710401-, pp 69-82)
processing of, effects of thermal stress on airborne particle release during, 25:54546
processing of, evaluation of shielding materials for use in, 25:54962 (CONF-710401-, pp 307-10)
processing of, operation of building ventilation system for, 25:54948 (CONF-710401-, pp 133-48)
processing of, safety criteria for design of facilities for, 25:54967 (CONF-710401-, pp 438-53)
recycle of, review on developments in, 25:57202
separation from aqueous Savannah River fuel reprocessing wastes by batch solvent extraction, 25:54739
separation from fission products by fluorination process, 25:54736
separation from irradiated LMFBR fuel by solvent extraction using dibutyl butylphosphonate, 25:54706 (BNWL-SA-3345)
separation from LMFBR fuels by solvent extraction using TBP, 25:54713 (ORNL-4682, pp 39-79)
solubility in soil--water environments, theoretical studies of, 25:54756 (CONF-710401-, pp 411-29)
storage of, design of safe shielded facility for, 25:54942 (CONF-710401-, pp 56-67)
PLUTONIUM ALLOYS AND SYSTEMS
C--N--O--Pu--U, preparation of carbides, carbonitrides, and hypostoichiometric oxides in, 25:55594 (ORNL-4682, pp 218-28)
Ga--Pu-base, tensile properties of, at 25 to 500°C, effects of strain rate and temperature on, 25:55427 (BNWL-1567)
Pu--Zr, phase transformations in, during quenching, effects of composition and cooling rate on epsilon, 25:55528
PLUTONIUM CARBIDES
PuC--UC, production of fuels of, development of process for, 25:55590(R) (EIR-192)
PLUTONIUM FLUORIDES $PuF_3$
solubility in molten beryllium fluoride--lithium fluoride--thorium fluoride, effects of oxide on, 25:54532 (ORNL-4717, pp 1-27)
spectra in molten beryllium fluoride--lithium fluoride--thorium fluoride, effects of oxide on, 25:54532 (ORNL-4717, pp 1-27)
PLUTONIUM ISOTOPES Pu-232
fission of, delayed, (E), 25:56744(T) (NP-tr-1936)
PLUTONIUM ISOTOPES Pu-234
fission of, delayed, (E), 25:56744(T) (NP-tr-1936)
PLUTONIUM ISOTOPES Pu-237
production by alpha reactions (α,2n) with uranium-235, 25:54674
PLUTONIUM ISOTOPES Pu-238
alpha decay of, gamma energies and absolute branching intensities for, (E), 25:56753 (UCRL-51087)
fabrication and properties of heat sources of, for SNAP-19B, 25:54893 (MLM-1736)
processing of, description of filters for glove boxes for, 25:54949 (CONF-710401-, pp 149-61)
processing of, methods and safety precautions for, 25:54707 (CONF-710401-, pp 300-6)
production of aerosols of oxides of, for inhalation studies in dogs, 25:54982
radiation dose from heat source of, in circulatory support system, (E), 25:54887(R) (BNWL-1308-6)
uptake by organisms of marine food chain, effects of physico-chemical form on, 25:55149 (BNWL-SA-4048)
use as heat source in Stirling cycle power system for implantable circulatory support system, 25:54910(P)
PLUTONIUM ISOTOPES Pu-239
alpha decay of, gamma energies and absolute branching intensities for, (E), 25:56753 (UCRL-51087)
content of marine organisms of Atlantic Ocean, 25:55161
content of Pacific seaweeds in environs of reactors in comparison to other locations, 25:55151 (CONF-710817-1)
determination in human urine in presence of enriched uranium, radiochemical method for, 25:55197
energy levels from gamma inelastic scattering, (E), 25:56738 (JINR-P15-5959)
fission of isomeric, half-life for spontaneous, (E), 25:56801
incorporation in hair of rabbits, effects of dose on rate of, 25:55116
neutron capture at 0.1 to 30 keV, ratio of cross sections for fission and radiative, (E), 25:56734(T) (BNL-tr-446)
neutron capture cross sections at 0.02 to 30 keV, (E), 25:56746 (ORNL-4707)
neutron capture-to-fission ratios for, effects of EBR-II core position on, (E), 25:56982 (ANL-7791)
neutron fission at 0.05 to 7.20 MeV, angular anisotropy and nucleon-pairing effects in, (E), 25:56736 (FEI-233)
neutron fission at 0.1 to 30 keV, ratio of cross sections for radiative capture and, (E), 25:56734(T) (BNL-tr-446)
neutron fission cross sections at 0.02 to 30 keV, (E), 25:56746 (ORNL-4707)
neutron fission of, liquid-drop-model calculations of heavy-fragment masses in thermal, (T), 25:56787
neutron fission of, prompt neutron yield from, (E), 25:56743 (NP-18966)
neutron fission of, yields from thermal, 25:54587(R) (AECL-3909)
photofission at 53 MeV, delay time for isomeric fission in, (E), 25:56801
photon inelastic scattering by, production of spontaneously fissioning isomers in, (E), 25:56738 (JINR-P15-5959)
production of aerosols of oxides of, for inhalation studies in dogs, 25:54982
production of spontaneously fissioning isomers in gamma inelastic scattering, (E), 25:56738 (JINR-P15-5959)
uptake by organisms of marine food chain, effects of physico-chemical form on, 25:55149 (BNWL-SA-4048)
PLUTONIUM ISOTOPES Pu-240
alpha decay of, gamma energies and absolute branching intensities for, (E), 25:56753 (UCRL-51087)
energy-level transitions from neutron fission of plutonium-239 at 0.05 to 7.20 MeV, nucleon-pairing effects on, (E), 25:56736 (FEI-233)
fission of, prompt neutron yield for spontaneous, (E), 25:56743 (NP-18966)
neutron capture-to-fission ratios for, effects of EBR-II core position on, (E), 25:56982 (ANL-7791)
uptake by organisms of marine food chain, effects of physico-chemical form on, 25:55149 (BNWL-SA-4048)
PLUTONIUM ISOTOPES Pu-241
alpha decay of, gamma energies and absolute branching intensities for, (E), 25:56753 (UCRL-51087)
neutron fission of, prompt neutron yield from, (E),


XUM

25:56743 (NP-18966)
PLUTONIUM ISOTOPES Pu-242
fission of, prompt neutron yield for spontaneous, (E), 25:56743 (NP-18966)
neutron capture-to-fission ratios for, effects of EBR-II core position on, (E), 25:56982 (ANL-7791)
PLUTONIUM ISOTOPES Pu-244
abundance in Galaxy, (T), 25:55781
PLUTONIUM NITRATES
conversion of plutonium-238-containing, to oxide, methods and safety precautions for, 25:54707 (CONF-710401-, pp 300-6)
heating of sand-bearing dried, fractional release during, 25:54546
heating of solutions of, fractional release during, 25:54546
PLUTONIUM OXIDES $PuO_2$
effects of particle size on fast reactor power transients, 25:57107
production of plutonium-238-containing, from nitrate, methods and safety precautions for, 25:54707 (CONF-710401-, pp 300-6)
production of sols of, method for, 25:55590(R) (EIR-192)
$PuO_2$--$UO_2$, brittle-to-ductile transition temperature in blended fuels of, bend tests on, 25:55610
$PuO_2$--$UO_2$, dissolution rate of pellets of, 25:54713 (ORNL-4682, pp 39-79)
$PuO_2$--$UO_2$, physical properties of solid, measurement of high temperature, 25:57069(R) (ANL-7800)
$PuO_2$--$UO_2$, preparation by sol-gel process, 25:55592 (ORNL-4682, pp 144-59)
$PuO_2$--$UO_2$, preparation of enriched fuels of, method for safe and economical, 25:55597(P)
$PuO_2$--$UO_2$, preparation of powders of, 25:54717 (ORNL-4682, pp 160-2)
$PuO_2$--$UO_2$, radiation effects on fuel spheres of, at high burnups, 25:55590(R) (EIR-192)
$PuO_2$--$UO_2$, reactions of solid solutions of, with fluorine and fluorine chlorides, kinetics of, 25:54736
PNEUMATIC SYSTEMS
design of gas gun, 25:57280 (SCL-DR-69-155)
design of low-velocity air gun, 25:57289 (UCRL-51098)
POINT BEACH POWER REACTOR, UNIT 1
effluents from, effects on environment of radioactive and thermal, 25:56947 (DOCKET-50266-55)
site for, environmental radiation and temperature survey during April to November 1970, 25:56947 (DOCKET-50266-55)
POLONIUM ISOTOPES Po-209
energy levels of, properties of multiparticle, (T), 25:56783
energy-level transitions in, analysis of E2, (T), 25:56783
POLONIUM ISOTOPES Po-210
content in river waters in Czechoslovakia, (E), 25:54774
distribution in tissues of uranium mining personnel, 25:55117
energy levels of, properties of multiparticle, (T), 25:56783
energy-level transitions in, analysis of E2, (T), 25:56783
POLONIUM ISOTOPES Po-218
effects on ion balance in atmosphere, 25:54786
POLYCRYSTALS
Moessbauer spectra of, Goldanskii--Karyagin effect of vibration anisotropy in, 25:56377
POLYMERIZATION
radioinduced, dilatometer for determination of rate in, 25:54616
POLYOXYMETHYLENE
radiation effects on, reduction of molecular weight and increase in thermal stability from, 25:54611(P)
POLYPHENYLS
corrosive effects on reactor materials, review of, 25:55394
POROSITY
evaluation of film, electrochemical method for, 25:54859(P)
POSITRONIUM
hyperfine structure of ground-state, (T), 25:55832
POSITRONS
annihilation in sodium hydroxide glassy ice, effects of radioinduced trapped electrons on, (E), 25:55835
dose distribution in water phantoms, isodose curves for 5 to 15 MeV, 25:55210
interactions $e^+ + e^- \rightarrow e^+ + e^- + \mu^+ + \mu^-$, Feynman diagram model of, 25:56460
interactions $e^+ + e^- \rightarrow \mu^+ + \mu^-$ angular and energy distributions for, (T), 25:56459
interactions $e^+ + e^-$, production of pseudoscalar mesons in, 25:56459
lifetime measurements in semiconductor single crystals, 25:56360
lifetimes in alkaline earth fluorides, empirical model for calculation of, 25:55834
production of $e^+e^-$ in electron interactions with electromagnetic field at 4 GeV/c in propane bubble chamber, direct, 25:56467
reactions with hydrogen atoms, eikonal approximation for excitation of 2s state in, 25:55874
scattering by hydrogen atoms, algebraic close-coupling approach to, 25:55854
POTASSIUM
analysis for potassium-39/potassium-41 by neutron activation, 25:54492
analysis of liquid, for oxygen by zirconium gettering-vacuum-fusion method, 25:54418
determination in feldspar by neutron activation and $\gamma$ spectrometry, 25:54494
determination of trace amounts of, in air by neutron activation and $\gamma$ spectrometry, 25:54456
determination of trace amounts of, in ultramafic rocks by thermal neutron activation and $\gamma$ spectrometry, 25:54496
distribution in metal transfer process for fission product removal from MSBR fuel solvent, 25:54534 (ORNL-4717, pp 43-56)
effects of compounds of, on bubble formation during annealing of doped tungsten, 25:55511
effects on determination of calcium by nondestructive alpha activation, 25:54522
electric conductivity of liquid, to 300°C, 25:55527
plasma of, anomalous resistivity of magnetized, (E), 25:56159
radiation effects on excretion of, in rat urine, combined effects of open skin lesions and, 25:55332
radiation effects on metabolism of, in man following therapy of diffuse toxic goiter, iodine-131, 25:55340
POTASSIUM ALLOYS AND SYSTEMS
K--Na, electric conductivity of, to 300°C, 25:55527
K--Na, phase diagram of, 25:55527
K--Na--Rb, phase studies of, thermal methods for, 25:55524(R) (COO-1707-11)
POTASSIUM AZIDES
neutron reactions (n,p) with nitrogen-14 in, distribution of recoil carbon-14 from, 25:54687
radiolysis of crystalline, effects of additives on yields from proton and $\gamma$, 25:54638
POTASSIUM BROMATES
radiation effects on, in presence of oxygen-18, production of oxygen-18-labeled products from, 25:54633(R) (ORO-3660-4)
POTASSIUM BROMIDES
radioinduced reduction of cadmium ions in crystals of, magneto-optical study of x-,, 25:56320
radioinduced thermoluminescence of crystals of undoped and copper-doped, x-,, 25:56323
radiolysis in air, mechanism of formation of nitrate ion on crystal surface from, 25:54633(R) (ORO-3660-4)
POTASSIUM CHLORATES
radiation effects on, in presence of oxygen-18, production of oxygen-18-labeled products from, 25:54633(R) (ORO-3660-4)
POTASSIUM CHLORIDES
effects on calcium-45 uptake and release by rat brain microsomes, 25:55120
impurity location in crystals of, by axial channeling of helium ions and protons, 25:56337
radiation effects on, thermoluminescence induced by deformation and light after 2-MeV-electron, 25:56321
radioinduced reduction of cadmium ions in crystals of, magneto-optical study of x-,, 25:56320
POTASSIUM CHROMATES
radiation effects on, role of recoil reactions in ''Crossover reaction'' on thermal annealing of neutron, 25:54679
POTASSIUM FLUORIDES
$AgNO_3$--KF, radiolysis of, EPR studies on neutral silver trapping sites from $\gamma$, 25:54666
POTASSIUM HYDROXIDES
dissociation at high temperatures using flowing cell, potentiometric determination of, 25:54535 (ORNL-4717, pp 57-82)
radiation effects on aqueous solutions of, ESR studies of ozonide ion formation from $\gamma$, 25:54608
POTASSIUM IODATES
radiation effects on, in presence of oxygen-18, production of oxygen-18-labeled products from, 25:54633(R) (ORO-3660-4)
POTASSIUM IODIDES
radioinduced reduction of cadmium ions in crystals of, magneto-optical study of x-,, 25:56320
POTASSIUM IONS
reactions with tungsten, sputtering of secondary tungsten ions from, 25:55819
POTASSIUM IRON OXALATES
Moessbauer-spectral study of cobalt-57 decay effects on valence and structure of, 25:56381
POTASSIUM ISOTOPES K-39
determination of abundance of, relative to potassium-41 by neutron activation, 25:54492
helium-3 reactions (He-3,p$\gamma$) at 12 and 13 MeV, p-$\gamma$ coincidence spectra from, (E), 25:56715
POTASSIUM ISOTOPES K-40
content in sand and clay soils, performance of airborne gamma spectrometer system for measuring, 25:54768
use as standard in nuclear metrology, 25:54901
POTASSIUM ISOTOPES K-41
determination of abundance of, relative to potassium-39 by neutron activation, 25:54492
POTASSIUM NITRATES
radiation effects on, in presence of oxygen-18, production of oxygen-18-labeled products from,

XUM

25:54633(R) (ORO-3660-4)
radiolysis of crystalline, effects of additives on yields from proton and γ, 25:54638
POTASSIUM PERCHLORATES
radiation effects on, in presence of oxygen-18, production of oxygen-18-labeled products from, 25:54633(R) (ORO-3660-4)
radiolysis of crystalline, effects of additives on yields from proton and γ, 25:54638
POWDER METALLURGY
comparison with granule metallurgy, 25:55404
conference on modern developments in, New York, July 12 to 16, 1970, 25:55411
conference on modern developments in, New York, July 12 to 16, 1970, 25:55481
POWDERS
production of fine metal--metal oxide, Microgel process for, 25:55419
POWER BURST FACILITY
experimental capabilities of, liquid metal cooled fast breeder reactor safety programs, 25:57069(R) (ANL-7800)
POWER CYCLES
development of Stirling, for powering implantable plutonium-238-fueled circulatory support system, 25:54910(P)
PRAIRIE ISLAND POWER REACTOR, UNIT 1
design parameters of, revised and additional data on, 25:56953 (DOCKET-50282-40)
operations aspects of, revised and additional data on, 25:56953 (DOCKET-50282-40)
PRAIRIE ISLAND POWER REACTOR, UNIT 2
design parameters of, revised and additional data on, 25:56953 (DOCKET-50282-40)
operations aspects of, revised and additional data on, 25:56953 (DOCKET-50282-40)
PRASEODYMIUM
determination in fission product mixtures by ion exchange and β counting, 25:54449
determination in intermediate products of rare earth production by x-ray spectroscopy, 25:54417
determination of trace amounts of, in nuclear grade uranium by x-ray excited optical fluorescence, 25:54428
effects on radiolysis of crystalline potassium nitrate, 25:54638
PRASEODYMIUM ALLOYS AND SYSTEMS
Au--Pr, crystal structures and melting points of intermetallic, 25:55570
Au--Pr-base, phase diagram of, 25:55567
Au--Pr-base, phase diagram of, thermodynamic analysis of, 25:55566
Ba--Pr-base, phase diagram of, 25:55567
Bi--Pr-base, phase diagram of, 25:55567
Bi--Pr-base, phase diagram of, thermodynamic analysis of, 25:55566
Cs--Pr-base, phase diagram of, 25:55567
Hf--Pr-base, phase diagram of, 25:55567
Hg--Pr-base, phase diagram of, 25:55567
Hg--Pr-base, phase diagram of, thermodynamic analysis of, 25:55566
Ir--Pr-base, phase diagram of, 25:55567
Ir--Pr-base, phase diagram of, thermodynamic analysis of, 25:55566
Os--Pr-base, phase diagram of, 25:55567
Os--Pr-base, phase diagram of, thermodynamic analysis of, 25:55566
Pb--Pr-base, phase diagram of, 25:55567
Pb--Pr-base, phase diagram of, thermodynamic analysis of, 25:55566
Pr-base--Pt, phase diagram of, 25:55567
Pr-base--Pt, phase diagram of, thermodynamic analysis of, 25:55566
Pr-base--Re, phase diagram of, 25:55567
Pr-base--Tl, phase diagram of, 25:55567
Pr-base--Tl, phase diagram of, thermodynamic analysis of, 25:55566
PRASEODYMIUM ISOTOPES Pr-141
alpha fission at 167 MeV, angular distributions and particle track lengths for, (E), 25:56806
ion elastic scattering in wide energy range, phase shift analysis of angular distributions for, (E), 25:56740 (JINR-P7-5884)
PRESSURE
calculation of time-dependent, for coupled volumes, computer program for, 25:54886
PRESSURE VESSELS
cover for fast reactor, design characteristics of thermal insulated ductile pressure relieving, 25:57058(P)
design characteristics of prestressed concrete, with steel lines, 25:57203(P)
design of podded boiler types prestressed concrete, for nuclear power plants, (E/T), 25:56885
design of prestressed concrete, for heavy water moderated and cooled power reactor, 25:56989
end caps for reactor prestressed concrete, two-dimensional time-dependent deformation analysis of perforated, (E/T), 25:56985
end slabs for reactor prestressed concrete, overload and ultimate load behavior of, (E/T), 25:56986
failure testing of reactor prestressed concrete, under internal gas pressure, 25:56992
fracture in walls of, developments in three-dimensional elastic--plastic stress analysis for mechanics of, 25:55515
fracture of heavy section steel, effects of flow growth and propagation on, 25:57092(R) (ORNL-TM-3483)
mechanical properties of steel for, effects of microstructure changes on, 25:55466
nozzles for, effects of attachment configuration on stresses in, 25:57092(R) (ORNL-TM-3483)
prestressing wires for concrete reactor, fabrication and properties of steel, 25:55422
seals for liquid metal cooled reactor, design of coolant, 25:57043(P)
stress analysis in reactor prestressed concrete, (E/T), 25:56993
stress analysis of prestressed concrete, 25:56884
stress analysis of prestressed concrete, for water cooled reactors, (E/T), 25:56991
stress analysis of reactor prestressed concrete, with axial ribs, (T), 25:56990
stress calculations for reactor prestressed concrete, dynamic relaxation method for, 25:56987
stress calculations for reactor prestressed concrete, approximate method for time dependent, 25:56988
structural mechanics of prestressed concrete, 25:56882
tensile properties of concretes for, under triaxial stress, 25:55660
PRESSURIZERS
electric heater and connector assembly for, standards for, 25:57030 (RDT-E-5-2-T)
standards for electrically heated, for pressurized water reactors, 25:57029 (RDT-E-5-1-T)
PROMETHIUM
separation from aqueous Savannah River fuel reprocessing wastes by batch solvent extraction, 25:54739
separation from neodymium and samarium by displacement chromatography using [(carboxymethylimino)bis(ethylenenitrilo)]tetraacetic acid, EDTA, and nitrilotriacetic acid, 25:54723
PROMETHIUM ISOTOPES Pm-146
burnout of, (E/T), 25:54887(R) (BNWL-1308-6)
PROMETHIUM ISOTOPES Pm-147
deposition of thin films of, for use as beta source, 25:54896(P)
half-life in human bone, comparison of ICRP value and experimental data for biological, 25:55108 (BNWL-SA-3747)
metabolism in man and swine following intravenous injection, comparison of, 25:55108 (BNWL-SA-3747)
performance as beta source for neutralization of electrically charged flour, 25:54897
recovery from aqueous Savannah River fuel reprocessing wastes by batch solvent extraction, 25:54739
use as power source for electric cells, 25:54922(P)
PROMETHIUM ISOTOPES Pm-152
beta decay of isomers of, half-lives and β and γ singles and coincidence spectra from, (E), 25:56772
energy levels from neodymium-152 decay, (E), 25:56772
PROMETHIUM OXIDES
decomposition oxygen pressures over test samples of, at high temperatures and low pressures, 25:55428 (BNWL-B-108)
PROPANE, 2-BROMO-2-METHYL-
solvolysis of, Broensted correlation for effects of metal ions on, 25:54548
PROPANE, 2-CHLORO-2-METHYL-
solvolysis of, Broensted correlation for effects of metal ions on, 25:54548
PROPANE, 2-FLUORO-2-METHYL-
solvolysis of, Broensted correlation for effects of metal ions on, 25:54548
2-PROPANOL
oxidation by Fenton's reagent, effects of deuterium on, 25:54576
PROPENE
effects on reactions of nitrous oxide in γ-irradiated liquid cyclopentane, 25:54655
oxidation over gold, effects of deuterium on, 25:54569
PROPENE, 2-METHYL-
radioinduced polymerization of, comparison of molecular weight distribution of products of catalytically initiated and γ, 25:54621
PROPENE POLYMERS
radiolysis of atactic and isotactic, effects of ethylene and nitrous oxide on γ, 25:54637
PROPIONIC ACID
radioinduced telomerization of ethylene by, γ, 25:54612
PROPIOPHENONE, p-AMINO-
radioprotective effects of, on mice, fast neutron and x, 25:55266
radioprotective effects on mice, effects of dose, sex, and strain on x, 25:55257
PROTACTINIUM
precipitation of pentavalent or tetravalent, as oxide from molten beryllium fluoride--lithium fluoride--thorium fluoride, 25:54532 (ORNL-4717, pp 1-27)
separation from molten salt fuel, flow sheet for, 25:54712 (ORNL-4682, pp 1-38)
separation from MSBR fuel by oxide precipitation, 25:54712 (ORNL-4682, pp 1-38)
stability of tetravalent, in molten beryllium fluoride--

XUM

lithium fluoride--thorium fluoride, 25:54532 (ORNL-4717, pp 1-27)
PROTACTINIUM ISOTOPES Pa-231
distribution in Pacific Ocean, 25:54810
energy-level transition in, nuclear current parameter for internal conversion of 84.2-keV, 25:56797
PROTEINS
radiation effects on amino acid content of, in processed foods, 25:55364
PROTON BEAMS
charge neutralization in, cross-beam technique for, 25:55816
PROTON SOURCES
development of charge-exchange, for injection into accelerators and storage rings, 25:56590(T) (LA-tr-71-46)
PROTONS
angular distributions of equatorial 30 to 300 keV, in loss cone and at large angles, (E), 25:56027
anisotropy of solar, in event of Nov. 18, 1968, (E), 25:55764
dose to tissue equivalent phantoms, Monte Carlo calculations of absorbed and equivalent 592-MeV, 25:55216
dosimetry in lens of beagle dogs, methods for, 25:55319 (UCD-472-118)
effects on crystalline alkali metal azides, bromates, and nitrates, 25:54638
effects on discontinuous tantalum films at 150 keV and 30°K, annealing of, 25:56314
effects on eyes of beagle dogs, effects of dose on pathological, 25:55319 (UCD-472-118)
effects on eyes of rabbits, effects of dose and LET on RBE for, 25:55317 (CEA-CONF-1744)
effects on impulse transmission in frog sciatic nerve, effects of LET on RBE for, 25:55215
effects on lithium amide or hydrogen--nitrogen mixtures, production of carbon-11-labeled cyanides by, 25:54683
effects on low- and high-pressure polyethylene films at 6.3 MeV, 25:54604
effects on photocurrent of n-type germanium, 25:56316
effects on silicon solar batteries at high energies, 25:55099
effects on sodium nitrate at 5 MeV, 25:56318
effects on stability of silvered and aluminized FEP teflon second-surface mirrors, 25:55656 (N-71-27736)
emission of solar, relation to microwave bursts, (E), 25:55758
emission of solar, relation to microwave bursts, (E), 25:55757
flux profiles of near-equatorial 20 to 50, and greater than 100 MeV trapped, at L = 1.15 to 1.21 in 1967, (E), 25:55957
interaction tracks in mica and extraterrestrial materials, (E), 25:55669 (N-71-26344)
interactions anti p + p → anti p + p + $\pi^0$ at 2.2 GeV/c, OPE models for, 25:56487
interactions anti p + p → anti p + p + $\pi^+$ + $\pi^-$ at 2.2 GeV/c, OPE models for, 25:56487
interactions anti p + p at rest, gauge-invariant chiral SU(3) x SU(3) symmetric Lagrangian model for two-meson production in s- and p-wave, (T), 25:56538 (ORO-3992-2)
interactions anti p + p at 10 and 14 GeV/c, polarization parameter in forward elastic, (E), 25:56438
interactions anti p + p at 20 to 65 GeV/c, energy dependence of total cross sections for, (E), 25:56433
interactions e + p above second resonance, review of $\pi$ production in, (E), 25:56406 (DESY-71/35)
interactions e + p in composite model, scale invariance of structure function for deep inelastic, 25:56465
interactions e + p in e + d interactions at high energies, cross sections for inelastic, (E), 25:56405 (DESY-71/33)
interactions $\gamma$ + p → $\pi^0$ + n, Reggeized absorption model fits to, 25:56458
interactions $\gamma$ + p → $\pi^0$ + p, Reggeized absorption model fits to, 25:56458
interactions $\gamma$ + p at 4 to 36 GeV, quark model for multiple $\pi$ production in, 25:56514
interactions $\gamma$ + p in e + d interactions at high energies, cross sections for particle production in, (E), 25:56405 (DESY-71/33)
interactions K⁻ + p → anti $K^0$ + n at 1.7 to 18.2 GeV/c, Regge analysis of, (E/T), 25:56506
interactions K⁻ + p → anti $K^0$ + n at high energies, Regge pole--cut model for analysis of, 25:56505
interactions K⁻ + p → anti $K^0$ + n, secondary Regge contributions in, 25:56508
interactions K⁺ + p → $K^{*0}$(890) + p at 3.0 to 8.25 GeV/c, Veneziano model for, 25:56511
interactions K⁺ + p → $K^0$ + $\pi^0$ + $\Delta^{++}$, K$\pi$ phase shifts from Chew--Low extrapolation of, 25:56486
interactions K⁺ + p → $K^0$ + X (anything), triple-Regge hypothesis for p-Reggeon total cross section from inclusive, 25:56515
interactions K⁻ + p → K⁻ + p at high energies, Regge pole--cut model for analysis of, 25:56505
interactions K⁺ + p → K⁺ + $\pi^-$ + $\Delta^{++}$, K$\pi$ phase shifts from Chew--Low extrapolation of, 25:56486
interactions K⁻ + p at 10 and 14 GeV/c, polarization parameter in forward elastic, (E), 25:56438
interactions K⁺ + p at 10 and 14 GeV/c, polarization parameter in forward elastic, (E), 25:56438
interactions K⁺ + p at 10 GeV/c in hydrogen bubble chamber, review of K* and N* production in, (E), 25:56435
interactions K⁻ + p at 20 to 65 GeV/c, energy dependence of total cross sections for, (E), 25:56433
interactions K⁻ + p at 3 GeV in hydrogen bubble chamber, production of K(890), K(1400) and K$\pi$ systems, upper limits for production cross sections of isospin-3/2 K*, and K + $\pi$ s-wave interactions in, (E), 25:56426 (FRNC-TH-53)
interactions n + p → 2p + $\pi^-$ at 2 to 30 GeV, Reggeized one-pion-exchange model for $\pi$ exchange and diffraction production of N(1470) and N(1688) in, (T), 25:56521 (JINR-P1-5975)
interactions n + p → d + $\gamma$, model of intermediate nucleon isobar for, 25:56525
interactions n + p → d + $\pi$, model of intermediate nucleon isobar for, 25:56525
interactions n + p → d + rho, model of intermediate nucleon isobar for, 25:56525
interactions n + p → d + sigma(310), model of intermediate nucleon isobar for, 25:56525
interactions n + p → p + n at 8 and 19 GeV/c, spark chamber study of differential cross sections and $\Delta$(1236) and N(1518) production in, (E), 25:56415 (NP-18888)
interactions n + p at 10 to 30 GeV/c, total cross sections for, (E), 25:56421
interactions n + p at 14.1 MeV, relativistically covariant models for bremsstrahlung cross sections for, (T), 25:56526
interactions $\nu$ + p in proton electromagnetic field at 30 to 400 GeV, total cross sections for W production from, (T), 25:56473
interactions p + d → $^3$He + $\gamma$, model of intermediate nucleon isobar for, 25:56525
interactions p + d → $^3$He + sigma(310), model of intermediate nucleon isobar for, 25:56525
interactions p + p → $\Delta^{++}$ + n at 19 GeV/c in hydrogen bubble chamber, energy dependence of cross sections for, (E), 25:56418 (USIP-71-6)
interactions p + p → p + $\Delta^{++}$ + $\pi^-$, Cherenkov mechanism for cross section behavior of, (T), 25:56498 (IFA-HE-76)
interactions p + p → p + hadrons, one-photon exchange contribution to, 25:56457
interactions p + p → p + n(p) + $\pi^+$($\pi^0$) at 19 GeV/c in hydrogen bubble chamber, energy dependence of cross sections for, (E), 25:56418 (USIP-71-6)
interactions p + p → p + p at 0.5 to 1.2 GeV, polarization parameter angular distribution and phase shift analysis for, (E), 25:56412 (CEA-R-4193)
interactions p + p → p + p at 19 GeV/c in hydrogen bubble chamber, cross sections for, (E), 25:56417 (USIP-71-4)
interactions p + p → p + p(n) + $\pi^0$($\pi^+$) at 19 GeV/c in hydrogen bubble chamber, cross sections for, (E), 25:56417 (USIP-71-4)
interactions p + p and K + p, triple-Regge hypothesis for relations between cross sections for inclusive, 25:56515
interactions p + p at 10 to 17.5 GeV, polarization parameter in elastic, (E), 25:56419
interactions p + p at 19 GeV/c in hydrogen bubble chamber, total cross sections for two-prong, (E), 25:56417 (USIP-71-4)
interactions p + p at 19 GeV/c in hydrogen bubble chamber, computer program for automatic selection of kinematical hypotheses for two-prong, (T), 25:56523 (USIP-71-3)
interactions p + p at 19.20 GeV/c, breaks in differential cross sections for, 25:56528
interactions p + p at 31 to 53 GeV, slope parameter for colliding-beam elastic, (E), 25:56420
interactions p + p at 4 to 36 GeV, quark model for multiple $\pi$ production in, 25:56514
interactions p + p at 670 to 1400 MeV, one-boson-exchange models for, 25:56532
interactions p + p at low energies, separable potentials for, (T), 25:56531
interactions $\pi$ + p → $\pi$ + p at 0 to 300 MeV, review lectures on, (E/T), 25:56422 (CERN-71-14, pp 379-93)
interactions $\pi$ + p at 4 to 36 GeV, quark model for multiple $\pi$ production in, 25:56514
interactions $\pi^0$ + p → $\omega$ + p, Reggeized absorption model fits to, 25:56458
interactions $\pi^0$ + p → rho$^0$ + p, Reggeized absoption model fits to, 25:56458
interactions $\pi^-$ + p → $A_2^-$ + p, $A_2^-$ → $\pi^-$ + neutrals near threshold energy, mass spectra of $A_2$ in, (E), 25:56436
interactions $\pi^-$ + p → eta + n at 1.7 to 18.2 GeV/c, Regge analysis of (E/T), 25:56506
interactions $\pi^-$ + p → eta + n in nuclei at 7.82 GeV/c, differential cross sections for, (E), 25:56432
interactions $\pi^-$ + p → eta + n with $A_2$ exchange, K-matrix absorption model in U(6,6) x O(3,1) for, 25:56513
interactions $\pi^-$ + p → eta + n, secondary Regge contributions in, 25:56508
interactions $\pi^-$ + p → K⁺ + $\Sigma^-$, spark chamber study of $\pi^-$, K⁺, and $\Sigma^-$ decay products in, (E), 25:55048

interactions $\pi^-$ + p → $K^+$ + $\Sigma^-$, $\Sigma^-$ → n + $\pi^-$, spark chamber study of, (E), 25:55049
interactions $\pi^-$ + p → n + $\pi^+$ + $\pi^-$ at 7 GeV/c, Regge analysis of $rho^0$ production in, (E/T), 25:56431
interactions $\pi^+$ + p → p + 2$\pi^+$ + $\pi^-$ at 5 to 25 GeV/c, partial-wave analysis for 3$\pi$ system in mass region 1.0 to 2.0 GeV, (T), 25:56482 (COO-1195-224)
interactions $\pi^-$ + p → p + 2$\pi^-$ + $\pi^+$ at 5 to 25 GeV/c, partial-wave analysis for 3$\pi$ system in mass region 1.0 to 2.0 GeV, (T), 25:56482 (COO-1195-224)
interactions $\pi^-$ + p → $\pi^0$ + n at 5.9 to 18.2 GeV/c, negative-mass-squared resonance interpretation of angular distribution for, (T), 25:56499 (ORO-3992-8)
interactions $\pi^-$ + p → $\pi^0$ + n at high energies, Regge pole--cut model for analysis of, 25:56505
interactions $\pi^-$ + p → $\pi^0$ + n at very high energies, polarization in, 25:56509
interactions $\pi^-$ + p → $\pi^0$ + n in nuclei at 7.82 GeV/c, differential cross sections for, (E), 25:56432
interactions $\pi^-$ + p → $\pi^0$ + n, secondary Regge contributions in, 25:56508
interactions $\pi^+$ + p → $\pi^+$ + p + $\omega^0$ at 3.7 GeV/c, mass and width of $\omega$ from, (E), 25:56430
interactions $\pi^-$ + p → $\pi^-$ + p at high energies, Regge pole--cut model for analysis of, 25:56505
interactions $\pi^+$ + p → $\pi^+$ + p at high energies, Regge pole--cut model for analysis of, 25:56505
interactions $\pi^-$ + p → $\pi^-$ + p($\Delta^{++}$) + $rho^0$($\pi^-$), Cherenkov mechanism for cross section behavior of, (T), 25:56498 (IFA-HE-76)
interactions $\pi^+$ + p → $\pi^+$ + $\pi^0$($\pi^+$) + p(n) at 13.1 GeV/c in hydrogen bubble chamber, diffractive $\pi$ + $\pi$ interactions in, (E), 25:56425 (COO-1428-294)
interactions $\pi^+$ + p at 10 to 17.5 GeV/c, polarization parameter in forward elastic, (E), 25:56437
interactions $\pi^-$ + p at 10 to 17.5 GeV/c, polarization parameter in forward elastic, (E), 25:56437
interactions $\pi^-$ + p at 20 to 65 GeV/c, energy dependence of total cross sections for, (E), 25:56433
interactions $\pi^+$ + p at 8 GeV/c in hydrogen bubble chamber, mass distributions and cross sections for resonance production and momentum and angular distributions for, (E), 25:56427 (IFA-HE-73)
interactions $\pi^+$ + p at 8 GeV/c in hydrogen bubble chamber, cross sections, kinematical behavior of secondaries, and K--anti K pairs and resonance production in four-prong, (E), 25:56428 (IFA-HE-75)
interactions with Alfven waves in magnetosphere, (T), 25:56011
mass difference (n - p), indefinite metric for electromagnetic, (T), 25:56547 (NYO-1932(2)-200)
modulation properties of solar low-energy acceleration-related, associated with propagating interplanetary shock waves, (E), 25:56020
observations of solar low-energy, during 1967 at widely separated locations, (E), 25:55956
precipitation in auroral region, simultaneous observations with auroral radar echoes, (E), 25:55963
production in four-prong $\pi^+$ + p interactions at 8 GeV/c in hydrogen bubble chamber, angular and momentum distributions for, (E), 25:56428 (IFA-HE-75)
production of low-energy, in cosmic particle reactions with nuclei above 100 GeV in emulsions, (E), 25:56429 (INP-754)
production of low-energy, in $\pi$ reactions with nuclei at 60 GeV in emulsions, (E), 25:56429 (INP-754)
radius in Bohr-like classical stochastic model of elementary particles, 25:56450
range in air, argon, nitrogen, and oxygen at 0.2 to 2.0 MeV as function of energy, (E), 25:56276
reaction with titanium, production of vanadium-48 by, 25:54677
reactions (p,2p) and (p,pn) with deuterium at 21.5 to 56.4 MeV, absolute cross sections for quasi-free scattering in, (E), 25:56640 (FRNC-CONF-8)
reactions (p,2p) with calcium-40, carbon-12, and silicon-28 at 600 MeV, distorted-wave impulse-approximation analysis of cross sections from, (E/T), 25:56711
reactions (p,2p) with calcium-40, carbon-12, silicon-28, vanadium-51, and zirconium-90 at 600 MeV, separation-energy spectra and momentum distributions of residual nuclei from, (E), 25:56706
reactions (p,2p) with carbon-12 at 1 GeV, Glauber multiple scattering theory for differential cross sections for quasi-free, (T), 25:56520 (IC-71/106)
reactions (p,2p) with deuterium at 28.6 MeV, differential cross section for, (E), 25:56644
reactions (p,3n$\gamma$) with lutetium-175 at 20 to 40 MeV, $\gamma$ spectra and excitation functions for, (E), 25:56796
reactions (p,4n) with manganese-55 at 65 MeV, production of iron-52 by, 25:54676
reactions (p,$\alpha$) with oxygen-18 at 500 to 750 keV, excitation function for, (E), 25:55384
reactions (p,d) with neodymium-142 and samarium-144 at 35 MeV, DWBA analysis of, (E), 25:56770
reactions (p,d) with neon-20, -21, and -22 at 40 MeV, differential cross sections for, (E), 25:56704
reactions (p,f) with radium-226 at 12.5 to 16.5 MeV, mass-yield curve for, (E), 25:56775
reactions (p,f) with radium-226 at 13 MeV, analysis using renormalized Fermi gas model and collective potential energy surface, (T), 25:56856
reactions (p,f) with thorium-232 at 20 to 85 MeV, fission yield and charge dispersion in, (E), 25:56805
reactions (p,f) with uranium at 30 to 160 MeV, yields and charge dispersion of antimony from, (E), 25:56757
reactions (p,$\gamma$) and (p,n) with carbon-14 at 2.3 to 2.6 MeV, excitation functions and gamma spectra from, (E), 25:56669
reactions (p,$\gamma$) on sodium-23, magnesium-24 photodisintegration rates from, 25:55703
reactions (p,$\gamma$) with deuterium at 0.8 to 3.2 MeV, angular distribution and cross section for, (E), 25:56645
reactions (p,n) with lithium-7 at 2 to 5.5 MeV, excitation function for, (E), 25:56752(R) (SUNI-14)
reactions (p,n$\gamma$) with zinc-66 at 6 to 6.8 MeV, $\gamma$ singles and coincidence spectra and angular distributions for, (E), 25:56732
reactions (p,xn) with uranium-238 at 750 MeV, neutron spectrum unfolding capability for, (E), 25:55038 (LA-DC-12314)
reactions with 12 < Z < 83 nuclei at 0.010 to 5 GeV, properties of low-energy nuclei from inelastic, (T), 25:56522(T) (ORNL-tr-2520)
reactions with aluminum, Mylar, nickel, and tantalum foils at 155 and 600 MeV, cross sections for electron capture in, (E), 25:55862
reactions with aluminum-27 at high energies, isobar model for analysis of meson ($\pi$) production in, 25:56530
reactions with cerium-140 at high energies, isobar model for analysis of meson ($\pi$) production in, 25:56530
reactions with chromium and vanadium, production of chromium-51 by, 25:54691
reactions with gases at 20 to 120 keV, cross sections for electron capture into n = 2 states of hydrogen in, (E), 25:55853
reactions with helium above 25 keV, excitation in, (T), 25:55842
reactions with helium and hydrogen molecules up to 5 MeV, cross sections for electron capture in, (T), 25:55837
reactions with hydrogen atoms at 10 to 2500 keV, excitation in, (T), 25:55841
reactions with hydrogen atoms at 30 and 50 eV, forced common turning-point treatment of excitation in, 25:55881
reactions with hydrogen atoms at 5 eV, cross sections for momentum transfer in, (E), 25:55840
reactions with hydrogen atoms, eikonal approximation for excitation of 2s state in, 25:55874
reactions with iron above 1.5 TeV, ionization spectrometer study of inelasticity coefficients for, (E), 25:56414 (INP-757)
reactions with lead-208 at high energies, isobar model for analysis of meson ($\pi$) production in, 25:56530
reactions with metal targets at 1.5 to 4.5 MeV, optical radiation from, (E), 25:55813 (JINR-P4-5957)
reactions with tin-116 at high energies, isobar model for analysis of meson ($\pi$) production in, 25:56530
reactions with zirconium-90 at high energies, isobar model for analysis of meson ($\pi$) production in, 25:56530
scattering by A = 50 to 66 nuclei at 6.9 MeV, distorted-wave analysis of differential and integrated cross sections for inelastic, (E), 25:56727
scattering by barium-138, lead-208, tin-120, and tin-124 with isobaric analog excitation, shell-model analysis of elastic, (E/T), 25:56769
scattering by boron-10 at 3.5 to 5 MeV, excitation functions for inelastic, (E), 25:56679
scattering by calcium-40, carbon-12, oxygen-16, and silicon-28, phase-shift analysis of polarization effects in elastic, (T), 25:56678
scattering by chlorine-35 at 5.47 to 5.61 MeV, excitation function for inelastic, (E), 25:56752(R) (SUNI-14)
scattering by even tin isotopes at 30.4 MeV, differential cross sections for elastic, (E), 25:56764
scattering by helium-4 below 50 MeV, analysis using nonlocal separable potential, (T), 25:56852
scattering by helium-4, analysis using separable nonlocal potential, (T), 25:56642 (LYCEN-7104, C5.1-15)
scattering by iron-54 and -56 at 9.6 MeV, optical-model analysis of elastic, (E/T), 25:56699
scattering by lithium-6 and -7 at 6.868 MeV, absolute cross section for elastic, (E), 25:56670
scattering by molybdenum-92, -94, -96, -98, and -100 at 15 MeV, coupled-channel analysis of elastic and inelastic, (E), 25:56774
scattering by neon-20 and -22 at 40 MeV, differential cross sections for elastic, (E), 25:56704
scattering by neon-20, -21, and -22 at 40 MeV, differential cross sections for inelastic, (E), 25:56704
scattering by nickel-60 at 11 MeV, differential cross sections for elastic, (T), 25:56789
scattering by nuclei at medium and high energies, cross sections for summed inelastic and quasi-elastic, (T), 25:56849
scattering by s-d shell nuclei, analysis of deformation in polarized inelastic, (T), 25:56828 (LYCEN-7104, S9.1-7)
scattering by sulfur-32 at 5 to 14 MeV, analysis of reaction mechanism in elastic and inelastic, (E), 25:56694

XUM

scattering by tin-120 at 9.6 MeV, S-matrix analysis of differential cross sections for elastic, (T), 25:56789
spallation of uranium at 5.5 GeV, yields of light elements in, (E), 25:56788
PROTONS (anti p)
interactions anti p + n + $\pi^+$ + 2$\pi^-$, mass and width of rho' in rising phase shift model for, (T), 25:56485 (ORO-3992-66)
interactions anti p + p + anti p + p + $\pi^0$ at 2.2 GeV/c, OPE models for, 25:56487
interactions anti p + p + anti p + p + $\pi^+$ + $\pi^-$ at 2.2 GeV/c, OPE models for, 25:56487
interactions anti p + p at rest, gauge-invariant chiral SU(3) x SU(3) symmetric Lagrangian model for two-meson production in s- and p-wave, (T), 25:56538 (ORO-3992-2)
interactions anti p + p at 10 and 14 GeV/c, polarization parameter in forward elastic, (E), 25:56438
interactions anti p + p at 20 to 65 GeV/c, energy dependence of total cross sections for, (E), 25:56433
PROTOTYPE FAST REACTOR
components for, design and performance requirements for, 25:57011
construction of, review of planning for, 25:56998
design parameters of, 25:57013
fuel elements for, performance requirements of, 25:57064
PROTOZOA
Trypanosoma equiperdum, immune reactions of rats to, studies on radioprotective effects of endotoxins using, 25:55267
PRUSSIAN BLUE
effects on distribution of mixed cesium and strontium radioisotopes in man following ingestion, 25:55113
PSORALEN
radiosensitizing effects on bacteriophage lambda, F' episomes, and Escherichia coli inactivation, uv, 25:55361
PUERTO RICO POWER REACTOR
fuel elements for, brazing methods for superheater shell of, 25:55425
PULSARS
JP 1933, distance from 21-cm line absorption profile, (E), 25:55724
JP 1933, scintillation parameters at 1420 MHz, (E), 25:55724
NP 0532, interpretation of precursor pulse in, (E/T), 25:55719
NP 0532, radiation mechanism for, (T), 25:55729
period--age distribution of, (E/T), 25:55687
search for, associated with Cyg X-1, (E), 25:55728
PULSE DISCRIMINATORS
design and performance of integral, for pulse-height analysis, 25:55073 (INR-1315)
PULSE GENERATORS (ELECTRONICS)
design of megavolt, for accelerator tubes, 25:56583 (IAE-1980)
PUMPS
design criteria for nuclear service, development program for, 25:57092(R) (ORNL-TM-3483)
design of glandless, for reactors, 25:54857
design problems for primary, in boiling water and pressurized water reactors, 25:57038
flow characteristics for boiling water and pressurized water power reactor cooling system, 25:57039
flow characteristics for boiling water and pressurized water power reactor cooling system, 25:57009
performance in sludge aeration operation, evaluation of, 25:54903
performance limits for boiling water reactor jet, optimum, 25:57037
standard for vertical shaft-sealed, motor-driven, single-stage centrifugal, 25:54831 (RDT-E-3-3-T)
PURINES
radiolysis of, rate constants for hydrogen atom reactions following electron, 25:55132
PYCNOMETERS
development of gas, for measuring swelling of boron carbide during irradiation, 25:54599 (ORNL-4717, p 117-24)
PYRIDINIUM COMPOUNDS
properties of pyridinium oxychlorouranate, 25:54541
PYRIMIDINE
effects of dimers of, in recovery of uv-irradiated Escherichia coli mutant, 25:55360
PYRIMIDINES
radiolysis of, rate constants for hydrogen atom reactions following electron, 25:55132
PYROCHLORES
separation of niobium as oxide from, 25:54741
PYROMETERS
design based on Nyquist noise theorem for in-core use, 25:55077(T) (LA-tr-71-71)

## Q

Q DEVICES
plasma confinement by electrostatic fields from electron beams in, alkali metal, (T), 25:56013
QUAD CITIES POWER REACTOR, UNIT 1
operation of, license for, 25:56944 (DOCKET-50254-52)
technical specifications for, 25:56944 (DOCKET-50254-52)
QUANTUM ELECTRODYNAMICS
electromagnetic operator in, test for isotensor component of, 25:56839
metric for neutron--proton electromagnetic mass difference and production of heavy photons in electromagnetic interactions, indefinite, 25:56547 (NYO-1932(2)-200)
QUANTUM FIELD THEORY
fields in, equivalence of Lorentz and Foldy--Wouthuysen transformations for free spinor, 25:56554
fields in, Lagrangian formalism for neutral massive spin-3, 25:56548 (ORO-3992-1)
formalism for quantized fields associated with annulus-type medium, canonical, 25:56563
formulation of action-at-distance, for particle interactions, 25:56550 (ORO-3992-14)
formulation of finite, review of, 25:56545 (IC-71/108)
formulation of, tempered distributions and departure from superposition principle in, 25:56544 (IC-71/71)
geometric structure of parity-conserving relativistic, 25:56557
Lagrangian formalism for neutral massive spin-3 fields in, 25:56548 (ORO-3992-1)
Lagrangians in, finite and unitary theory in highest perturbation orders for nonpolynomial, 25:56546 (JINR-P2-5998)
Lagrangians in, renormalization of nonpolynomial, 25:56549 (ORO-3992-9)
Lee model in, unified treatment of V--theta and V--2theta sectors of, 25:56553
Lorentz invariance and finite self-mass in local, 25:56564
particle interactions in action-at-distance, 25:56550 (ORO-3992-14)
quantization methods for tachyon fields, 25:56560
renormalization of nonpolynomial Lagrangians in, 25:56549 (ORO-3992-9)
scattering in, lectures on relativistic, 25:56571 (CERN-71-14, pp 229-87)
vertex functions in, Wilson expansions for small-distance behavior analysis for, 25:56543 (DESY-71/39)
Yang--Mills field in, Schwinger equations for, 25:56561
Yang--Mills theories in, higher groups for divergence of massive, 25:56542 (CNRS-CPT-71/P-378)
QUANTUM MECHANICS
angular momentum in, Bargmann space calculations for, 25:56395 (BNWL-1551(Vol.2)(Pt.1), pp 108-12)
Dirac equation for free electron, reduction to nonrelativistic form, 25:56391
energy states and statistics of atomic systems, 25:56397
formalism of relativistic, canonical proper-time, 25:56555
functionals in statistical and, subsidiary conditions for generating, 25:56556
integrals having both exponential and gaussian functions in, evaluation of, 25:56399
partition functions in, bound state and continuum contributions to two-body, 25:56396
Schroedinger equation in, method for reduction to one-dimensional integral equation, 25:56398
wave equations in, two-component spherical factorization of Klein--Gordon and Kramers, 25:56559
QUARTZ
analysis of standard, for bismuth, cadmium, mercury, and thallium by neutron activation and radiochemical separation, 25:54454
QUASARS
cosmic-particle absorption by high-energy, (T), 25:55908
energy sources for, supermassive objects as, (T), 25:55798
flux densities of four, daily and hourly variations of, (E), 25:55731
gravitational radiation in, conversion into electromagnetic waves, (T), 25:55805
gravitational redshifts in, (T), 25:55808
identification of southern, optical, (E), 25:55725
optical variability of 1215 + 30, (E), 25:55726
photon emission at 3 x $10^{10}$ eV from, (T), 25:55908

## R

RABBITS
plutonium-239 incorporation in hair of, effects of dose on rate of, 25:55116
prostaglandin radioimmunoassay in blood plasma of, using tritium, 25:55144
radiation effects on pulmonary blood circulation in, acute x, 25:55327
radioinduced cataracts in eyes of, effects of dose and LET on RBE for cobalt-60 $\gamma$, 2.5 and 14 MeV neutron, and 3 GeV proton, 25:55317 (CEA-CONF-1744)
RADAR
echoes from auroral region, simultaneous observaions with proton precipitation, (E), 25:55963
RADIATION
accidents involving, proposed USA registry for, 25:55250
dose calculations for infinitely thin source situated on boundary between two media, 25:55233
dose irregularities during neutron capture therapy,

local, 25:55212
dose rates from fission products in fallout from atmospheric nuclear explosions, calculation of, 25:55231
dose to human organs, terminology for expressing, 25:55251
dose to man in vicinity of nuclear fuel reprocessing plant, estimation of, 25:55237
dose to man near nuclear power plant sites, interpretation of emergency, 25:55242
dose to man, plutonium surface contamination levels for, 25:55195 (CONF-710401-, pp 352-64)
effectiveness for therapy of human tumors, effects of cell cycle synchronization on, 25:55306
effectiveness in inducing chromosome translocations in Vicia, 25:55191
effects on amino acid content of proteins in processed food, 25:55364
effects on aqueous solutions, ESR studies of free radicals produced by fast reaction flow systems from, 25:54662
effects on barley and maize, effects of developmental stage and dose on mutagenic, 25:55190
effects on calcium metabolism in rat bones, effects of sex on, 25:55331
effects on electrolyte metabolism in rats, combined effects of open skin lesions and, 25:55332
effects on germanium at low temperatures, review, 25:56303
effects on heating of plane bodies, tables for transient temperatures from, 25:56267
effects on hematopoiesis in active bone marrow, effects of dose fractionation on, 25:55326
effects on human bones following therapy of carcinomas, treatment of necrotic, 25:55270
effects on human chromosomes, bibliography on, 25:55178
effects on human tissues, effectiveness of additional treatment with iron and steroid preparations for minimizing therapeutic, 25:55303
effects on hydrocarbon--TBP mixtures, effects of nitric acid on, 25:54644
effects on II--VI compound semiconductors, review, 25:56291
effects on inorganic molecular ions, research progress on, 25:54633(R) (ORO-3660-4)
effects on monomer and polymer impregnants in cellulose and concrete, mechanical properties of products produced by, 25:55658
effects on polyoxymethylene, reduction of molecular weight and increase in thermal stability by, 25:54611(P)
effects on respiration rate in wheat seedlings, 25:55348
effects on semiconductors, review of important unanswered questions in, 25:56332
effects on silicon, structure of multiple-vacancy (oxygen) centers induced in, 25:56312
effects on solid organic compounds, effects of electron dislocation and molecular dimensions on, 25:54635
effects on space vehicle materials, 25:55576 (N-71-25034)
effects on storage life of fish, conference on, 25:55362 (LFEN-NI.-56a)
hazards to human population from nuclear power plant effluent, evaluation of, 25:55347
hazards to man from inhalation of reactor radioisotopes following accidental release, estimation of relative, 25:55202
use for cancer therapy, methods for altering sensitivity of host and tumor tissues during, 25:55265
use for tumor therapy in mice, comparison of effects of air and carbogen atmosphere on cure rate during, 25:55302

RADIATION CHEMISTRY
conference on progress and problems in contemporary, Tenth Czechoslovak, Marianske Lazne, Czechoslovakia, June 22-25, 1970, Vol. II, 25:54592 (CONF-700652-(Vol.2))
conference on progress and problems in contemporary, Tenth Czechoslovak, Marianske Lazne, Czechoslovakia, June 22-25, 1970, Vol. III, 25:54595 (CONF-700652-(Vol.3))
conference on progress and problems in contemporary, Tenth Czechoslovak, Marianske Lazne, Czechoslovakia, June 22-25, 1970, Vol. I, 25:54588 (CONF-700652-(Vol.1))
electron--ion recombination in, 25:54591 (CONF-700652-(Vol.1), pp 221-58)
ion pair mechanisms in, concentration dependence of, 25:54670
luminescence phenomena in, 25:54598 (CONF-700652-(Vol.2), pp 423-75)
mechanisms in, use of accelerated photoelelctrons to duplicate excitation, 25:54597
particle track structure in, models for, 25:54589 (CONF-700652-(Vol.1), pp 19-49)
radical pair formation in, 25:54665
reactions in solid organic materials, role of tunnel effect in postradiation, 25:54596
review on synthesis of organic compounds in liquid nonaqueous systems in, 25:54617
trapped electron production and reactions in, 25:54593 (CONF-700652-(Vol.2), pp 261-93)
trapped electron production and reactions in, 25:54594 (CONF-700652-(Vol.2), pp 331-64)
yield predictions for, current state of a priori, 25:54590 (CONF-700652-(Vol.1), pp 51-136)

RADIATION DETECTORS
background in Weber gravitational, experiments for estimation of upper limit for muon shower signal in, 25:56566
book: Radioactivity Measurements. Practical Manual on the Uses of Nuclear Radiation, 25:55020
calibration of stack-located, for monitoring reactor off-gases, neutron activation method for, 25:54986
calibration of, thermal neutron source for, 25:54892 (LA-4745)
design and construction of self-powered, for gamma radiation, 25:55011(P)
development of secondary-electron, for electron and photon beam energy measurements above 5 GeV, 25:56609(P)
readout electronics for ν + e interaction measurements, 25:55044 (JINR-E1-5818)
response of all-solid self-powered neutron flux, correlation of reactor power density profiles to, (E), 25:57017(R) (BAW-3647-22)

RADIATION DETECTORS, ACTIVATION
calibration of silver, for use with plasma focus experiment, 25:56214 (LGI-70/17/E)
fabrication of MgO--NiO and MgO--CoO, for in-core neutron flux monitoring, 25:55019(P)
handling and readout system for in-core neutron flux measurements, 25:55008(P)

RADIATION DETECTORS, BUBBLE CHAMBER
particle tracks in, automatic measurement of, 25:55047

RADIATION DETECTORS, CHERENKOV
development for beta detection in water, 25:55031

RADIATION DETECTORS, CRYSTAL
design of diamond, with radiator foil converter for neutron detection, 25:55009(P)

RADIATION DETECTORS, DIELECTRIC TRACK
particle tracks in glass, use of photoelectric colorimeter for counting, 25:55029
particle tracks in, elastically scattered recoil nuclei, 25:54999 (N-71-26447)
particle-track formation in, enhancement by exposure to oxygen and ultraviolet light, 25:55010(P)
performance for monitoring reactor power by nitrogen-17 decay, (E), 25:57124
performance of triacetate cellulose, for alpha dosimetry and spectroscopy, 25:55026

RADIATION DETECTORS, FISSION CHAMBER
readout in hard multiplying systems, asymptotic behavior of, (T), 25:55017

RADIATION DETECTORS, IONIZATION CHAMBER
amplifiers for, design of low-level, 25:55071 (CEA-N-1433)
description of, for personnel dosimetry, 25:55051(P)
design of boron trifluoride, for neutron detection, 25:55014(P)
design of universal portable, for dosimetry, 25:55052
development of boron coated, for power reactor in-core neutron monitoring, 25:57025
response to pulsed radiation using various filling gases, 25:55015

RADIATION DETECTORS, PROPORTIONAL
data acquisition from array of position-sensitive, correction for accidental coincidences in, 25:54997 (INSJ-128)
design for low-level tritium determination in biological and environmental samples, 25:55003 (UCRL-73128)
wall effects in tissue-equivalent, for microdosimetry, 25:55058
wall effects in, theory of, 25:55002 (NYO-2740-8, pp 7-146)

RADIATION DETECTORS, SCINTILLATION
design and performance of amphibious system containing, for in situ environmental radioactivity measurements, 25:55239
design and performance of combined solar battery--, for gamma and x radiation, 25:55005
design for neutron detection, 25:55012(P)
design of liquid, for low-level tritium determination in biological and environmental samples, 25:55003 (UCRL-73128)
design optimization of crystal, for low-level gamma activity measurements, 25:55024
development of improved, for use with video radioisotope scanning systems, 25:55278
development of miniaturized thallium-activated cesium iodide, for detecting radioactivity during thyroid surgery, 25:55018
development of NE-213, for fast neutron spectroscopy using off-line gamma-ray discrimination, 25:55033 (COO-2049-6)
development of NE-213, for neutron spectroscopy in aqueous media, 25:55034 (COO-2049-7)
performance of liquid, in radiation control laboratories, 25:55217
performance of organic, for x-ray detection, 25:55030
pulse-height response of activated alkali-metal iodide, to energetic heavy ions, (T), 25:55016
response function for sodium iodide, Monte Carlo

XUM

calculation of, 25:54994 (EGG-1183-2283)
sample positioning and rotation system for liquid, 25:55027(P)
temperature effects on thallium-activated sodium iodide, at 20 to 70°C, 25:55025
RADIATION DETECTORS, SEMICONDUCTOR
design of surface-barrier, for x rays and atomic particles, 25:55007(P)
development and uses of, 25:55000 (NP-19008)
RADIATION DETECTORS, SEMICONDUCTOR (GERMANIUM)
calibration of lithium-drifted, gamma energies and intensities of radium-226 source for, 25:55041 (ORNL-TM-3509)
performance of lithium-drifted, for measurement of fuel rod average burnup, 25:57201
preparation of lithium-drifted, 25:55013
time characteristics of lithium-drifted, computer programs for calculating, 25:55001 (NP-19011)
RADIATION DETECTORS, SEMICONDUCTOR (SILICON)
fabrication of surface-barrier ΔE, 25:54998 (JINR-P13-5970)
performance of lithium-drifted, for diagnosis of skin neoplasms using phosphorus-32, 25:55273
preparation of surface-barrier, 25:55013
RADIATION DETECTORS, SPARK CHAMBER
particle tracks in, automatic measurement of, 25:55047
particle tracks in, least squares fitting of, 25:55049
particle tracks in, stringing method for analysis of, 25:55048
RADIATION DOSE
calculation following fast reactor core failure accident, 25:57113 (HEDL-TME-71-33)
calculation of annual, from nuclear power plant-released krypton-85 in atmosphere to year 2000, 25:54781(T) (JPRS-53174)
estimation of personnel, for areas around radioactive objects, 25:54987
maximum permissible, evaluation of assumptions and methods used in calculating, 25:55254
RADIATION DOSIMETERS
development at Columbia Univ, 25:55002 (NYO-2740-8, pp 7-146)
development at Sloan-Kettering Institute during July 1, 1970 to June 30, 1971, 25:55208(R) (NYO-3510-18)
RADIATION DOSIMETERS, BIOLOGICAL
chromosome aberration frequency as, in accidentally exposed man, 25:55228
RADIATION DOSIMETERS, CHEMICAL
design of solid-electrolyte, for gamma rays and relativistic charged particles based on voltage change, 25:55054(P)
performance of fluorocarbons, based on radiolytic gas production, 25:55053
RADIATION DOSIMETERS, LUMINESCENT
response of Bragg--Gray-type anthracene--gelatin, for absorbed dose measurements, 25:55056
RADIATION DOSIMETERS, THERMOLUMINESCENT
data processing for multi-sphere polyethylene-moderated, for neutron spectroscopy, 25:55036 (HASL-244)
fabrication of small-grained aluminum oxide, 25:55055(P)
performance for fast neutrons in lucite phantoms, 25:55319 (UCD-472-118)
performance of encapsulated LiF, for dosimetry in bulk grain irradiator, 25:55234
RADIATION DOSIMETRY
research at Sloan-Kettering Institute during July 1, 1970 to June 30, 1971, 25:55208(R) (NYO-3510-18)
RADIATION PROTECTION
methods for operating personnel and population near pressurized-water reactor power plant in Japan, 25:54980
programs at Battelle plutonium facility, 25:54959 (CONF-710401-, pp 280-92)
standards of, Union of South Africa, 25:55245
RADIATION SOURCES
calibration of isotopic, development of equipment for, 25:55070(R) (BHO-67-2)
calibration of, at Cadarache, France, description of facility for, 25:54851
development of, technical progress review on, 25:57127
dose function of plane infinitely thin, situated on boundary between two media, 25:55233
holder for plesiotherapy, description of, 25:54902(P)
preparation of alpha--photon, 25:54887(R) (BNWL-1308-6)
production and uses of fission product, developments in, 25:54887(R) (BNWL-1308-6)
transfer between storage containers, design of cable-actuated device for remote, 25:54983(P)
RADIATION TARGET CANS
design of instrumented, for measuring thermal conductivity of uranium dioxide pellets, 25:55088
RADIATION TARGETS
design of absorbed deuterium--tritium, for neutron generators, 25:56626(P)
failure of natural uranium, contamination and radioprotection problems resulting from, 25:56582 (CEA-R-4188)
RADIATORS
mass of space power system, effects on system total mass, 25:54916
RADIO ASTRONOMY
survey of continuum radiation at 820 MHz between -7 and +85°, (E), 25:55787
RADIO TELESCOPES
development for molecular line radio astronomy, 25:55091
RADIO WAVES
absorption of auroral cosmic, relation to auroral vlf electromagnetic-wave emission, (E/T), 25:55999
emission from solar corona, slowly varying component of, (E), 25:55754
emission from Sun, (E), 25:55736
propagation across midlatitude polar cap, proton anomaly of PCA-associated very long, (E), 25:55996
transmission in ionospheric E region, detonation-wave effect on decameter-wavelength, (E/T), 25:55970
RADIOACTIVE CONTAMINATION
biological significance of, 25:55194 (70-CNA-641)
calculations for petroleum following production stimulation by contained nuclear explosions, 25:54826(T) (UCRL-Trans-10543, pp 99-116)
control on human clothing and skin, derivation of decision levels for, 25:55196 (LA-4558)
hazards from failure of natural uranium accelerator targets, systems for protection against, 25:56582 (CEA-R-4188)
hazards from underground nuclear explosion stimulation of gas and petroleum production, evaluation of, 25:54823(T) (UCRL-Trans-10543, pp 56-69)
monitoring in laboratories, use of liquid scintillation methods for, 25:55217
RADIOACTIVE MATERIALS
handling of, design of equipment for remote, 25:54853(P)
inventories at University of Colorado Medical Center, use of timesharing computer for maintaining and updating, 25:54984
processing buildings for, design of filter plenum heat exchangers for, 25:54950 (CONF-710401-, pp 162-80)
release to environment from nuclear power plants, estimation of effects on background radiation levels of long-term, 25:55200
shipping by rail and truck in Kentucky and Tennessee in 1968, shock and vibration data for container during, 25:54974 (SC-M-710241)
shipping through Mont Blanc Tunnel, safety evaluation of, 25:54973 (RT/PROT-(71)11)
storage of, design of fire-resistant container for, 25:54977(P)
transfer in and out of containers, design of leak-tight conveyer for, 25:54988(P)
transport of, civil responsibility and insurance in maritime, 25:55252 (NP-18752)
RADIOACTIVE MINERALS
processing of, efficiency of combined lump-and-batch method for industrial, (T), 25:54847
RADIOACTIVE WASTE
analysis of, nondestructive active and passive methods for, 25:55004(R) (WCAP-7562-4)
combustion of plutonium-bearing solid, 25:54715 (ORNL-4682, pp 95-113)
compaction for shipping and storage, equipment and methods for, 25:54975 (WASH-1167)
disposal at sea, international law regarding, 25:55252 (NP-18752)
disposal by hydraulic fracturing at ORNL, facility design and safety analysis for, 25:54971 (ORNL-4665)
disposal from pressurized-water reactor power plant in Japan, 25:54980
disposal in salt beds, research progress on, 25:54715 (ORNL-4682, pp 95-113)
disposal in salt mine repository, research progress on, 25:54758 (ORNL-4717, pp 109-15)
disposal of liquid metal fast breeder reactor fuel recycle complex, 25:54754
disposal of low- and medium-level, review of methods for, 25:54985
disposal of, review of environmental effects from, 25:54784
distribution of boiling power reactor, 25:56979
dose rates from boiling power reactor, 25:56979
fission product decay in glass cylinders containing, temperatures from, 25:54726
fixation in bitumen, mixer-evaporator and plant design for, 25:54981
incorporation in polyethylene, 25:54715 (ORNL-4682, pp 95-113)
incorporation of fuel reprocessing, in glass cylinders, 25:54726
management of power reactor, procedures and policies for, 25:57001
management of, engineering, economic, and safety evaluations of, 25:54715 (ORNL-4682, pp 95-113)
processing and storage of, review of corrosion problems in, 25:55390
processing of plutonium-contaminated liquid, methods and safety at Los Alamos plant for, 25:54708 (CONF-710401-, pp 369-85)
processing of, research progress on, 25:54715 (ORNL-4682, pp 95-113)
release from power reactors, effects on environment of, 25:56981
release limits for gaseous, derivation for power reactors of, 25:56980
release of liquid and gaseous, from power reactors,

25:56978
release of liquid, from West Valley fuel reprocessing plant, 25:54753
solidification in cement for disposal in seawater, 25:54979
storage of high-level, in solids, safety of, 25:54969 (JUL-766-CT)
storage of transuranic, site operation at NRTS for, 25:54965 (CONF-710401-, pp 365-8)
storage of, consideration of national and international radiation dose standards in planning for interim and long-term, 25:55253
volume reduction process for, at Rocky Flats, Colorado, 25:54709 (CONF-710401-, pp 386-91)
RADIOACTIVITY
book: Radioactivity Measurements. Practical Manual on the Uses of Nuclear Radiation, 25:55020
decay curves for, computer program for calculating half-lives and intensities of, 25:56695
deposition, diffusion, and transport of, comparison of US and USSR methods for calculating, 25:54782 (UCRL-51054)
estimation of induced, near activated objects, 25:54987
monitoring in aquatic environment of nuclear facility, role of stable element content measurements in pre-operational, 25:55240
monitoring in atmosphere and water, review of current methods for, 25:54784
monitoring in environment in United Kingdom, derivation and use of reference levels and working limits as standards for, 25:55241
monitoring in environment of nuclear power facility, consideration of ecological factors in developing program for, 25:55238
monitoring in gases surrounding contained nuclear explosion, method for, 25:54823(T) (UCRL-Trans-10543, pp 56-69)
simulation of, mathematical model for computer, (T), 25:54441
RADIOBIOLOGY
book: Physical and Radiobiological Investigations of Artificial Satellites of the Earth, 25:55342
book: Problems in Radiobiology, 25:55134
research at Columbia Univ., July 1, 1971, 25:55205(R) (NYO-2740-8)
RADIOCHEMICAL PROCESSING PLANTS
corrosion problems in fuel and waste processing, review on, 25:55390
criticality control in plutonium, administrative methods for, 25:54966 (CONF-710401-, pp 430-7)
design of plutonium, safety criteria for, 25:54967 (CONF-710401-, pp 438-53)
design of plutonium, using nitrogen processing atmospheres, 25:54943 (CONF-710401-, pp 69-82)
environmental monitoring and research on effects of Rocky Flats, 25:54964 (CONF-710401-, pp 316-19)
equipment development for TURF, 25:54716 (ORNL-4682, pp 133-43)
exhaust system for plutonium, design of filters for, 25:54947 (CONF-710401-, pp 118-32)
off-gas treatment from, in LMFBR fuel reprocessing, 25:54713 (ORNL-4682, pp 39-79)
operation of Rocky Flats, administrative procedures for, 25:54960 (CONF-710401-, pp 293-6)
radiation dose to man in vicinity of, estimation of, 25:55237
radioactive waste from liquid metal fast breeder reactor fuel recycle complex, 25:54754
safety aspects of proposed Rocky Flats, for plutonium recovery, 25:54961 (CONF-710401-, pp 297-9)
RADIOCHEMISTRY
research at Lyon Institute of Nuclear Physics in 1970, 25:56742(R) (LYCEN-7101)
RADIOFREQUENCY OSCILLATORS
quality factor of superconducting lumped-parameter, 25:55086
RADIOGRAPHY, BIOMEDICAL
bibliography on, 25:55274
RADIOGRAPHY, INDUSTRIAL
development and uses of neutron, 25:54930
equipment for neutron, design of, 25:54931(P)
facilities for neutron, at Sandia Laboratories, review of californium-252 and annular core pulse reactor, 25:54924 (SC-DR-710178)
method for detecting cracks in light alloy samples, optimization of, 25:54929
method for jet engine inspection using iridium-192 gamma source, 25:54927
RADIOISOTOPE SCANNING
effectiveness for diagnosis of human brain tumors in comparison with angiography, 25:55293
effectiveness for diagnosis of Paget's disease in comparison to biochemical methods and radiography, 25:55294
equipment for gamma emitters, description of, 25:55590(R) (EIR-192)
methods for combined skull and ventricular, for diagnosis of infantile hydrocephalus, 25:55290
methods for human thyroid, computer storage methods for evaluation of, 25:55282
methods using video systems, development of improved detector for, 25:55278
RADIOISOTOPES
accumulation by marine organisms, mechanisms of, 25:55154
accumulation by organisms in aquatic ecosystems, effects of stable element content on, 25:55158
book: Radioactivity Measurements. Practical Manual on the Uses of Nuclear Radiation, 25:55020
content and distribution of fallout, natural, and reactor produced, in Hudson River estuary, 25:55160
content of man, comparison of ICRP and MIRD methods for calculating maximum permissible, 25:55201
content of man, evaluation of assumptions and methods used in calculating maximum permissible, 25:55254
content of natural gas supplies, use of threshold limit values in establishing standards for, 25:55198
determination in mixtures, computer-assisted method for, 25:54441
determination of naturally unstable, α-, β-, and γ-emitting, review on effects of properties on radiometric, 25:54446
determination of, in mixtures, data unfolding techniques for, 25:54436 (ORNL-TM-3463)
development of, technical progress review on, 25:57127
distribution in rocks fractured by contained nuclear explosions, 25:54826(T) (UCRL-Trans-10543, pp 99-116)
effectiveness for renography in patients with cervical carcinomas in relation to prognosis, 25:55275
gamma angular distribution from polarized, system for measuring, 25:55089
inhalation of reactor inventory, estimation of relative radiation hazards to man from, 25:55202
neutron cross sections for, thermal, 25:54692(R) (NYO-3417-15)
preparation of colloids of, effects of hydroxide solubility products on, 25:54695
production and industrial uses of, selected abstracts of world literature on, 25:54894 (ORNL-IIC-37(Pt.2))
production and uses of, research progress on, 25:54887(R) (BNWL-1308-6)
production for medical uses, design of isotope generator for, 25:54909(P)
retention and excretion by peccaries following ingestion of debris from Schooner Event, 25:55124
separation by chromatography, automation of, 25:54727
separation of parent--daughter pairs, method for calculating cross contamination in column chromatographic, 25:54701
separation of short-lived, chemical problems in on-line, 25:54672
use as tracers in life sciences research since 1946, summary of, 25:55107
uses for studying blast-furnace ironmaking operations, 25:54906
uses in medicine, trends in, 25:56983 (NP-18992)
uses in pharmacy and clinical biochemistry, conference on, 25:55255
RADIOLOGY
research at Columbia Univ., July 1, 1971, 25:55205(R) (NYO-2740-8)
RADIOOPAQUE AGENTS
effectiveness of powdered tantalum, for radiography of upper respiratory mucosa, 25:55291
RADIOTHERAPY
dose distribution calculations for cobalt-60, development of computer program for, 25:55220
dose field in man during, standardization of isodose charts for expressing, 25:55211
dose field parameters for high energy bremsstrahlung, effects of electron component of beam on, 25:55209
dose planning for human, methods using digital computer for cobalt-60 γ, 25:55221
dose planning using IBM 1130 computer for calculation of treatment fields, 25:55218
source holder for, description of, 25:54902(P)
RADIUM
content in stratified uranium deposits, location of ore boundaries from gamma measurements of, 25:54808
dose distribution around sealed linear sources of, electronic calculations for, 25:54923
effectiveness for therapy of squamous epithelial cancer of mouth in comparison with ametohepazon, beta particles, gamma radiation, and 5-fluorouracil, 25:55345
effects on survival of hamster cells, RBE of, 25:55207 (NYO-2740-8, pp 220-59)
RADIUM ISOTOPES Ra-224
distribution in tissues of mice and rats following intraperitoneal injection, dose relation for radium-226 and, 25:55115
RADIUM ISOTOPES Ra-226
content in river waters in Czechoslovakia, (E), 25:54774
content of marine phytoplankton off coast of South Africa, 25:55155
content of uveal tissue in eyes of beagle dogs, use of autoradiography to measure, 25:55319 (UCD-472-118)
deuteron fission at 16 to 19 MeV, mass-yield curve for, (E), 25:56775
distribution in tissues of mice and rats, dose relation for radium-224 and, 25:55115
effects on bones of beagle dogs, estimation of hazards to

XUM

man from model for long-term low dose, 25:55319 (UCD-472-118)
handling and storage of sources of, equipment and methods for safe, 25:54936 (BRH/DMRE-71-3)
proton fission at 12.5 to 16.5 MeV, mass-yield curve for, (E), 25:56775
proton fission at 13 MeV, analysis using renormalized Fermi gas model and collective potential energy surface, (T), 25:56856
RADIUM ISOTOPES Ra-228
beta decay of, gamma ray intensities from, (E), 25:56747(T) (ORNL-tr-2531)
RADON
content in atmosphere at Plovdiv, Bulgaria during 1966 to 1969, 25:54792
content in uranium ores, effects on gamma spectrometric well logging measurements, 25:54759
content in USSR ground waters, effects of earthquakes on, 25:54775
content in waters of Bad Brambach, Germany, dual ionization chamber measurements of, 25:54766
decay products of, in surface layer of atmosphere, stationary vertical profiles for short-lived, 25:54787
diffusion in lunar rocks and soils, 25:54440
effects on ion balance in atmosphere, 25:54786
effects on lymphocytes in vitro following inhalation by patients with kidney diseases, 25:55346
monitoring in atmosphere, electrostatic sampler and detector system for, 25:55032
washout from atmosphere, method for measuring, 25:54802
RADON ISOTOPES Rn-220
content in atmosphere at Plovdiv, Bulgaria during 1966 to 1969, 25:54792
decay products of, in surface layer of atmosphere, stationary vertical profiles for short-lived, 25:54787
RADON ISOTOPES Rn-222
content in river waters in Czechoslovakia, (E), 25:54774
RAINWATER
fallout content in Hokkaido, Japan, following Sept. 1969 Chinese nuclear explosion, (E), 25:54789
RANCHO SECO POWER REACTOR
radioactive effluent treatment system for, operation of liquid, 25:56881
RARE EARTH ALLOYS AND SYSTEMS
book: Emissive Properties of Materials (Handbook), 25:56346
Al--La--rare earths, crystal field levels, superconducting transition temperature, and exchange parameters of, (T), 25:56359
rare earths--transition metals, preparation by heat treatment of amalgams of, 25:55401(T) (RFP-Trans-87)
RARE EARTH BROMIDES
formation of, estimation of free energies of, 25:54712 (ORNL-4682, pp 1-38)
RARE EARTH CHLORIDES
formation of, estimation of free energies of, 25:54712 (ORNL-4682, pp 1-38)
nuclear quadrupole resonance in, soft sphere model for, 25:57220 (COO-1533-15)
RARE EARTH HYDROXIDES
basicities of, 25:54718 (ORNL-4682, pp 168-81)
RARE EARTH ISOTOPES
energy levels of even--even deformed, structure and spin--spin correlations for collective $1^+$, (T), 25:56819 (JINR-P4-5889)
RARE EARTHS
chemical properties of aqueous solutions of, spectrophotometric studies on, 25:54578 (ORNL-4682, pp 215-17)
compounds, electron microscopic and thermal analysis of, 25:54671 (ORNL-4682, pp 114-32)
determination by spectroscopy of prompt $\gamma$ radiation following neutron capture, 25:54451
determination in fission product mixtures by ion exchange and $\beta$ counting, 25:54449
determination in lunar fines No. 10084 from Apollo 11 by ion exchange chromatography or high-voltage electrophoresis and neutron activation, 25:54475
determination in Mesozoic dolerite dikes, 25:54476
determination in meteorites and meteoritic phases by neutron activation and radiochemical separation, 25:54477
determination in powdered residues of thermal and surface water by mass and uv absorption spectrometry, 25:54409
determination in rocks by activation and high-pressure ion exchange, 25:54463
determination in rocks, chemical methods for, 25:54403
determination in yttrium by ion exchange and neutron activation, 25:54525
determination of, use of ion exchange in methods for, 25:54397
distribution between liquid bismuth and molten lithium halides, 25:54712 (ORNL-4682, pp 1-38)
Hall resistivity of, theory of anomalous, 25:56357
preparation using countercurrent electrophoresis, 25:54742
separation by displacement chromatography, 25:54723
separation by pressurized ion exchange, 25:54718 (ORNL-4682, pp 168-81)
separation from molten manganese nitrate hexahydrate or calcium chloride hexahydrate by solvent extraction using TBP, 25:54740
separation from MSBR fuel salt by metal transfer process, 25:54712 (ORNL-4682, pp 1-38)
separation from MSBR fuel solvent by extraction with bismuth--manganese alloys, 25:54534 (ORNL-4717, pp 43-56)
separation from pegmatitic ores, leaching studies for, 25:54752
separation of fission product, from irradiated LMFBR fuel by solvent extraction using dibutyl butylphosphonate, 25:54706 (BNWL-SA-3345)
separation of trace amounts of, from carbonate solutions by sorption on metal hydroxides, review on, 25:54734
solubility in liquid bismuth--lithium systems, 25:54712 (ORNL-4682, pp 1-38)
RATS
brain respiratory rate in $D_2O$, 25:55121
cesium-134 distribution in conceptus of pregnant, following injection, 25:55114
metabolism of lipids and proteins following ingestion of gamma irradiated beef, 25:55367
palladium-103 distribution in, following introduction into thigh muscle, effects of carrier on, 25:55112
radiation effects on bone marrow chromosomes of, x, 25:55192
radiation effects on calcium metabolism in, effects of sex on, 25:55331
radiation effects on electrolyte metabolism in, combined effects of open skin lesions and, 25:55332
radiation effects on enzyme activity and hematopoietic tissues in bone marrow of, effects of dose on x, 25:55330
radiation effects on hexokinase activity in brain, erythrocytes, and liver of, x, 25:55140
radiation effects on immune reactions to Trypanosoma, protective effects of endotoxins against x, 25:55267
radiation effects on olfactory bulb cells of, electron microscopy of x, 25:55336
radiation effects on response to tranquilizers, whole-body mixed $\gamma$ and neutron, 25:55325
radiation effects on taste threshold in, low dose x, 25:55322
radiation effects on thymidine incorporation into DNA of cultured thymus cells of, factors affecting x, 25:55127
radioinduced genetic damage in populations of, following repeated exposure over 13 generations, x, 25:55164
radioinduced osteosarcomas in, following injection of phosphorus-32, 25:55335
radium-224 distribution in tissues of, following intraperitoneal injection, dose relation for radium-226 and, 25:55115
toxicity of products of $\gamma$-irradiated DDT to, 25:55135
REACTIVITY
determination of pulsed, analysis of area-ratio method for, (T), 25:57185
REACTOR CONTAINMENT STRUCTURES
engineered safeguards equipment in, effects of post accident environments on performance of, (E), 25:57097 (WCAP-7744)
liner plate anchors for prestressed concrete, deformation of stud and rib type, (T), 25:56995
liners for prestressed concrete, matrix displacement method for buckling analysis of, 25:56994
performance of liquid metal cooled fast breeder reactor, effects of accidents on, 25:57069(R) (ANL-7800)
performance of, effects of internal explosions and pressure waves on, (E/T), 25:57070 (CEA-CONF-1796)
stress state of concrete, evaluation of safety margin of triaxial, 25:55659
REACTOR CONTAINMENT SYSTEMS
design requirements for core melt-through accident in liquid metal cooled fast breeder reactor, 25:57093 (ORNL-TM-3504)
spray solutions for, effects of organic materials on methyl iodide production in sodium hydroxide, 25:57092(R) (ORNL-TM-3483)
transients in boiling water power reactor pressure suppression, analytical modeling methods for coolant loss accident induced, 25:57057 (NEDO-10320(Suppl.1))
REACTOR CONTROL ELEMENTS
design requirements for 1000 MW(e) liquid metal cooled fast breeder reactor, 25:57069(R) (ANL-7800)
development of 1000 MW(e) liquid metal cooled fast breeder reactor, simulation studies for, 25:57069(R) (ANL-7800)
drives for rod, description of uniform motion hydraulic, 25:57200(P)
drives for, description and use of reluctance motors for, 25:54848
neutron absorption by cadmium, effects of rod interactions on, (E), 25:57205
neutron absorption by, effects of configuration on, (E), 25:57206
position indicator for rod, description of, 25:57204(P)
REACTOR COOLANTS
fission product control in gas, system for, 25:57033
REACTOR EXPERIMENTAL FACILITIES
design for radiation testing of fuels and materials, 25:55590(R) (EIR-192)
neutron spectra from horizontal channel of WWR-C-Prague, (E), 25:57125

rabbit system for IRT-M, design of pneumatic, 25:57130
survey of, 25:57122
REACTOR FUEL ELEMENTS
analysis of, nondestructive active and passive methods for, 25:55004(R) (WCAP-7562-4)
burnup calculations for, role in nuclear materials safeguards system, 25:54935 (BNWL-1599)
burnup of rod, performance of lithium-drifted germanium detector for measurement of average, 25:57201
cladding for, effects of coolant loss accident conditions on failure of Zircaloy, 25:57092(R) (ORNL-TM-3483)
cladding leaks in, remote detection using krypton-88, 25:54904
coatings for vitroceramic, chemical composition, deposition, and properties of aluminosilicate, 25:55613
coolant conditions in assemblies of, effects of interchannel thermal mixing on, (E/T), 25:57031 (WCAP-7755)
corrosion by liquid sodium of stainless steel clad mixed oxide, 25:57109 (ANL-7771)
cutting of irradiated, design of shears for, 25:54838(P)
decladding of stainless steel-clad spent, using hydrogen fluoride--oxygen mixtures, effects of temperature on, 25:54747
design characteristics of clusters of intermixed helical fin and plain rod, 25:57198(P)
end caps for, metallic joint for maintaining leak tightness of, 25:57195(P)
explosion in liqid sodium of uranium oxide ($UO_2$), mechanical energy conversion efficiency and particle size distribution from, (E/T), 25:57068(R) (AI-AEC-13006)
extrusion of aluminum alloy-clad ceramic dispersion, core and clad flow conditions during, 25:55420
failure detection system for heavy water moderated research reactor, performance of $\gamma$ radiation monitoring method for, 25:57118 (JAERI-Memo-4157, pp 44-50)
failure detection system for heavy water moderated research reactor, design parameters and performance of, 25:57117 (JAERI-Memo-4157, pp 23-43)
failure detection system for liquid metal cooled, development of delayed neutron monitoring, 25:57055 (JAERI-Memo-4157, pp 84-8)
failure detection system for water cooled research reactor, performance of delayed neutron monitoring method for, 25:57119 (JAERI-Memo-4157, pp 51-65)
failure detection system for, performance of precipitator and gas chromatography methods for, 25:57193 (JAERI-Memo-4157, pp 66-83)
failure detection systems for liquid sodium cooled, development of, 25:57056 (JAERI-Memo-4157, pp 89-100)
failure detection systems for, development and performance of, 25:57192 (JAERI-Memo-4157)
failure of liquid sodium cooled uranium oxide ($UO_2$) pellets, 25:57069(R) (ANL-7800)
failure of liquid sodium cooled, mockup testing facility for, 25:57092(R) (ORNL-TM-3483)
failure of sodium cooled, analysis of transient, (E/T), 25:57110 (CONF-710302-(Vol.1), pp 97-101)
failure propagation characteristics of liquid sodium cooled bundle arranged pin type, 25:57069(R) (ANL-7800)
failure propagation in rod, effects of coolant--molten fuel reactions on, 25:57083 (CONF-710302-(Vol.1), pp 241-58)
fission product release and detection of failed water cooled Zircaloy 2 clad uranium oxide ($UO_2$) rod, 25:57047 (JAERI-Memo-4157, pp 2-22)
heat conduction in, computer code for transient, 25:57094 (RISO-M-1391)
heat transfer to flowing liquids at supercritical pressures, effects of dimensions on, 25:54880
heat transfer to turbulently flowing coolants, effects of surface roughness on, 25:54874 (RD/B/N-1980)
holders and spacers for, testing in high-temperature sodium, 25:55379(R) (WARD-4210-T-1-2)
inspection of plutonium oxide ($PuO_2$)--uranium oxide ($UO_2$) rod type, 25:57111(R) (GEAP-10010-29)
performance of liquid metal cooled stainless steel clad uranium oxide ($UO_2$) pin type, effects of overpower transients on, 25:57046 (GEAP-13722)
performance of liquid metal cooled Type 347 stainless steel clad plutonium oxide ($PuO_2$)--uranium oxide ($UO_2$) pin type, effects of high temperature and burnup on, 25:57045 (GEAP-10385)
radiation effects testing of heavy water moderated gas cooled, 25:57050 (UJV-2551-RT)
radioinduced reactions between cladding and fuel in pin-type, in-pile, 25:55648 (RCN-144)
repair of instrumented plutonium oxide ($PuO_2$)--uranium oxide ($UO_2$) rod type, 25:57111(R) (GEAP-10010-29)
reprocessing of HTGR, development of head-end methods in, 25:54714 (ORNL-4682, pp 80-94)
reprocessing of LMFBR, head-end processes in, 25:54713 (ORNL-4682, pp 39-79)
reprocessing of, review of corrosion problems in, 25:55390
reprocessing of, safeguards capabilities of materials accounting systems in facilities for, 25:54968 (IAEA-R-878-F)
standards for Zircaloy clad uranium oxide ($UO_2$), for pressurized water reactors, 25:57049 (RDT-E-13-15-T)
REACTOR FUELS
analysis of reprocessing solutions of, for technetium, standard for colorimetric, 25:54429
burnup of gas cooled coated particle, computer program for calculation of, 25:57021 (JAERI-Memo-4449)
cycle analysis for, CITATION code for, 25:57183 (ORNL-TM-2496(Rev.2))
cycle for fluid and molten salt, computer program for calculation of optimum, 25:57048 (ORNL-TM-3359)
cycles for fast, TRACE code for analysis of equilibrium, 25:57020 (EUR-4709)
heat transfer characteristics in liquid sodium by debris pieces of, 25:57069(R) (ANL-7800)
irradiation testing of, diffusion of cesium through pyrocarbon coatings during, 25:55647 (ORNL-4717, pp 83-90)
performance of silicon carbide (SiC) coated particle type, high temperature, (E/T), 25:57053
processing of carbide, container materials for high temperature alkali metal salt, 25:55376 (CONF-690452-, Paper 9)
production of LMFBR, 25:54717 (ORNL-4682, pp 160-2)
properties of coated particles, for use in HTGR-type reactors, 25:57052
radiation effects on Dragon coated-particle, 25:55651
radiation properties and shielding requirements of LMFBR, 25:54713 (ORNL-4682, pp 39-79)
reprocessing of LMFBR, development of aqueous methods for, 25:54713 (ORNL-4682, pp 39-79)
reprocessing of LMFBR, integrated lanthanide--actinide solvent extraction process using dibutyl butylphosphonate in, 25:54706 (BNWL-SA-3345)
reprocessing of molten salt, by reductive extraction, 25:54712 (ORNL-4682, pp 1-38)
reprocessing of, disposal of wastes from, 25:54726
reprocessing of, kinetics of fluorination in, 25:54736
transfer during processing, design of hopper feeder for, 25:54841(P)
REACTOR LOADING MACHINES
design characteristics of liquid cooled shield penetrating, 25:57197(P)
design characteristics of overhead mechanical linkage, 25:57210(P)
shielding for, description of ring shaped support, 25:57209(P)
REACTOR SAFETY
coolant combustion in fast reactors, analysis of liquid sodium, (E/T), 25:57112 (HEDL-TME-71-31)
evaluation of, acceptable risk concept for, 25:56983 (NP-18992)
hydrodynamic aspects of accident conditions, use of computer codes for analysis of, (E/T), 25:57102
research and development program during May and June 1971, 25:57092(R) (ORNL-TM-3483)
research programs on, summaries of, 25:57096 (WCAP-7722)
research progress during June 1970 through May 1971, 25:57090 (ORNL-4717, pp 91-107)
REACTOR SAFETY EXPERIMENTS
experimental capabilities of TREAT, for liquid metal cooled fast breeder reactor safety programs, 25:57069(R) (ANL-7800)
fuel pin failures in TREAT sodium coolant loop, method for analysis of, (E/T), 25:57110 (CONF-710302-(Vol.1), pp 97-101)
REACTORS
chemistry of, research progress on, 25:54531(R) (ORNL-4717)
cooling system for, design of glandless pumps for, 25:54857
development of, conference on mathematics applications for, 25:57071 (CONF-710302-(Vol.1))
development of, conference on mathematics applications for, 25:57147 (CONF-710302-(Vol.2))
dynamics of cylindrical, COSTANZA (R,Z) code for analysis of transient, 25:57187 (EUR-4673)
materials for, selection criteria and machining aspects of, 25:57207
neutron flux distribution in non-uniform lattices in, modified collision probability method for calculation of, 25:57155 (CONF-710302-(Vol.2), pp 644-54)
neutron flux distribution in, determination of function moments of, (T), 25:57179
neutron flux distribution in, finite element solution of diffusion and transport equations for calculation of, 25:57159 (CONF-710302-(Vol.2), pp 723-38)
neutron flux distribution in, Monte Carlo calculation of adjoint, 25:57162 (CONF-710302-(Vol.2), pp 803-32)
neutron flux distribution in, non-iterative method for calculation of time dependent, 25:57157 (CONF-710302-(Vol.2), pp 679-700)
neutron flux distribution in, $P_3$ approximation for calculation of, 25:57149 (CONF-710302-(Vol.2), pp 561-4)
neutron flux distribution in, S/sub n/ programming techniques for calculation of, 25:57148 (CONF-710302-(Vol.2), pp 557-60)
neutron flux distribution in, solution of non-stationary and quasi-critical transport equations for, 25:57186
neutron flux distribution in, spherical harmonic equations for elimination of ray effects in, 25:57151

XUM

(CONF-710302-(Vol.2), pp 577-607)
neutron flux distribution in, synthetic transport theory method for calculation of, 25:57154 (CONF-710302-(Vol.2), pp 625-43)
neutron flux distribution in, time discretization of transport equation for calculation of, 25:57158 (CONF-710302-(Vol.2), pp 701-22)
neutron flux distribution in, variational treatment of DP-0 method for calculation of, 25:57152 (CONF-710302-(Vol.2), pp 608-16)
neutron flux distribution in, weighted diamond difference approximations for calculation of, 25:57150 (CONF-710302-(Vol.2), pp 565-76)
neutron leakage from, Monte Carlo method for calculation of, 25:57163 (CONF-710302-(Vol.2), pp 857-70)
physics calculations for, CITATION code for, 25:57169 (CONF-710302-(Vol.2), pp 939-52)
physics calculations for, computer equipment conversion of Argonne Reactor Computation system for, 25:57140 (CONF-710302-(Vol.1), pp 464-71)
physics calculations for, modularization of iteration procedures in, 25:57143 (CONF-710302-(Vol.1), pp 494-504)
physics calculations for, network organization of automated system for, 25:57146 (CONF-710302-(Vol.1), pp 516-30)
physics calculations for, summary of heterogeneous methods for, 25:57184
physics calculations for, survey of Danish Monte Carlo methods for, 25:57166 (CONF-710302-(Vol.2), pp 887-900)
physics calculations for, use of DATATRAN modular system for, 25:57141 (CONF-710302-(Vol.1), pp 472-7)
physics calculations for, user experience with Argonne Reactor Computation system for, 25:57142 (CONF-710302-(Vol.1), pp 478-93)
physics parameters of, methods for optimization of, (T), 25:57180
power distribution in non-uniform lattices in, nodal integral transport method for calculation of two-dimensional, 25:57156 (CONF-710302-(Vol.2), pp 655-78)
power distribution in, LEIDI code for calculation of, 25:57000
pressure vessels for, approximate method for calculation of time dependent stresses in prestressed concrete, 25:56988
pressure vessels for, axial rib effects on stresses in prestressed concrete, (T), 25:56990
pressure vessels for, design characteristics of steel lined prestressed concrete, 25:57203(P)
pressure vessels for, dynamic relaxation method for stress calculations for prestressed concrete, 25:56987
pressure vessels for, failure testing of prestressed concrete, 25:56992
pressure vessels for, overload and ultimate load behavior of end slabs of prestressed concrete, (E/T), 25:56986
pressure vessels for, stress-strain behavior of prestressed concrete, (E/T), 25:56993
pressure vessels for, structural mechanics of prestressed concrete, 25:56882
pressure vessels for, two-dimensional time-dependent deformation analysis of perforated end caps for prestressed concrete, (E/T), 25:56985
radiation conditions in, effects on californium-252 production of, 25:57067
radioactive effluents from, accumulation by marine organisms of, 25:55149 (BNWL-SA-4048)
shielding for, description of removable access well, 25:57199(P)
shielding for, RAGA code for γ-ray transport in multiregion slab, 25:57026 (RCN-146)
siting of, cloud gamma calculations for, 25:54797
siting of, conference on health physics aspects of, Vol. II, Idaho Falls, Idaho, Nov. 3 to 6, 1970, 25:55157
siting of, conference on health physics aspects of, Vol. III, Idaho Falls, Idaho, Nov. 3 to 6, 1970, 25:55193
siting of, conference on health physics aspects of, Vol. I, Idaho Falls, Idaho, Nov. 3 to 6, 1970, 25:57103
siting of, evaluation of steadiness of wind during stable conditions for, 25:54794
siting of, meteorological considerations in, 25:54793
transfer functions of, NOISE code for determination of, 25:57181 (BNWL-1609)

**REACTORS, AGR-TYPE**
moderator for, mathematical model of methane concentrations in graphite, 25:57044

**REACTORS, BOILING**
containment systems for power, analytical modeling methods for coolant loss accident induced transient in pressure suppression, 25:57057 (NEDO-10320(Suppl.1))
coolant channels in water-cooled, wick-boiling in porous magnetite-coated, (T), 25:54862 (AEEW-R-711)
coolant loss accident conditions in, analysis of pressure suppression containment system transients during, 25:57057 (NEDO-10320(Suppl.1))
excursions in, adiabatic aproximation model for analysis of control rod drop, (T), 25:57084 (CONF-710302-(Vol.1), pp 259-81)
fuel elements of water cooled, fission product release and detection of failed Zircaloy 2 clad uranium oxide ($UO_2$) rod, 25:57047 (JAERI-Memo-4157, pp 2-22)
hydrodynamics of, simulation of, (T), 25:57022 (MRR-73)
physics parameters of, heterogeneous method for calculation of, 25:57168 (CONF-710302-(Vol.2), pp 920-38)
pumps for power, flow characteristics for, 25:57009
pumps for power, flow characteristics for, 25:57039
pumps for, design problems for primary, 25:57038
pumps for, optimum performance limits for jet, 25:57037
radioactive effluents from power, distribution of and dose rates from, 25:56979
valve design for, 25:54842

**REACTORS, BREEDER**
economics of fast, in mixed electrical generating systems with light water reactors, (T), 25:57061 (MLM-1851)
economics of gas cooled fast, (T), 25:57065
fuel elements of liquid metal cooled fast, development of delayed neutron monitoring failure detection system for, 25:57055 (JAERI-Memo-4157, pp 84-8)
fuel elements of liquid sodium cooled fast, development of failure detection systems for, 25:57056 (JAERI-Memo-4157, pp 89-100)

**REACTORS, CANDU-TYPE**
coolant loss accidents in, PRESCON code for containment pressure transients from, 25:57087 (CONF-710302-(Vol.1), pp 436-51)

**REACTORS, FAST**
accidents in sodium cooled, limitation of hypothetical, 25:57072 (CONF-710302-(Vol.1), pp 1-24)
construction in United Kingdom, program for, 25:57012
cooling systems for space vehicle thermionic, calculations for heat pipes for, 25:57134
core vessel cover for, design characteristics of thermal insulated ductile pressure relieving, 25:57058(P)
core vessels for, effects of explosive loading on, (E/T), 25:57102
economics of gas cooled breeder, (T), 25:57065
economics of liquid metal cooled breeder, in mixed electrical generating systems with light water reactors, (T), 25:57061 (MLM-1851)
fuel cycles for, TRACE code for analysis of equilibrium, 25:57020 (EUR-4709)
fuel elements of liquid metal cooled breeder, development of delayed neutron monitoring failure detection system for, 25:57055 (JAERI-Memo-4157, pp 84-8)
fuel elements of liquid sodium cooled breeder, development of failure detection systems for, 25:57056 (JAERI-Memo-4157, pp 89-100)
physics calculations for, committee on computer code coordination for, 25:57018 (CONF-710302-(Vol.1), pp 452-63)
physics calculations for, neutron cross section 26 group set for, 25:57115 (HEDL-TME-71-65)
physics calculations for, space--energy factorization method for, 25:57170 (CONF-710302-(Vol.2), pp 953-67)
power transients in, effects of plutonium oxide ($PuO_2$) particle size on, 25:57107
shielding for, effects of iron contents on performance of concrete, (E), 25:57027 (RCN-147)

**REACTORS, FLUID-FUELED**
components for, review of corrosion problems in molten-salt, liquid-metal, and aqueous-slurry, 25:55395
core for, computer program for calculation of optimum design parameters of, 25:57048 (ORNL-TM-3359)
fuel cycle for, computer program for calculation of optimum, 25:57048 (ORNL-TM-3359)

**REACTORS, FRANCE**
development of, review of, 25:57002

**REACTORS, GAS-COOLED**
accidents in U.K., analysis of fission product release from pressure loss, 25:57106
components for, review of corrosion problems in, 25:55393
coolant for, system for control of fission products in, 25:57033
coolants for high temperature, properties of helium, 25:57040
cooling system for, description of flow regulating, 25:57041(P)
cooling systems for high temperature, fission product distribution in, 25:57092(R) (ORNL-TM-3483)
core structure of graphite moderated, description of graphite columns for, 25:57010(P)
economics of fast breeder, (T), 25:57065
fuel reprocessing for, development of head-end methods in, 25:54714 (ORNL-4682, pp 80-94)
fuel tubes for high temperature, calculation of stresses in graphite, (E/T), 25:57051
fuels for high temperature power, computer program for burnup calculations for coated particles, 25:57021 (JAERI-Memo-4449)
fuels for high temperature, properties of coated particle, 25:57052
fuels for, high temperature performance of silicon carbide (SiC) coated particle type, 25:57053
maintenance of power, procedures for remote, 25:57066
safety of, chemical aspects of, 25:57090 (ORNL-4717, pp 91-107)

**REACTORS, GRAPHITE-MODERATED**
core for, design characteristics of spaced graphite columns for, 25:57208(P)
core structure of gas cooled, description of graphite columns for, 25:57010(P)

XUM

neutron leakage from, pulsed-source measurements on effects of voids on, (E/T), 25:57190
neutron transport in, pulsed-source measurements on effects of voids on, (E/T), 25:57189
REACTORS, HEAVY WATER-MODERATED
coolant loss accidents in, calculation of containment pressure transient during, 25:57087 (CONF-710302-(Vol.1), pp 436-51)
coolant voiding accidents in fast, method for analysis of, 25:57082 (CONF-710302-(Vol.1), pp 215-40)
core melt-through accident in fast breeder, safety aspects and containment methods for, 25:57093 (ORNL-TM-3504)
fuel element failure in fast, effects on safety of propagation of, 25:57088 (GEAP-13639-1)
fuel element failure in fast, effects on safety of propagation of, 25:57089 (GEAP-13639-2)
pressure vessel for heavy water cooled, design of prestressed concrete, 25:56989
REACTORS, HETEROGENEOUS
core structure for, description of, 25:57015(P)
neutron spectra for, computer program calculation of resonance energy, 25:57182 (JAERI-Memo-4481)
REACTORS, HOMOGENEOUS
components for, review of corrosion problems in molten-salt, liquid-metal, and aqueous-slurry, 25:55395
REACTORS, LIQUID METAL-COOLED
accidents in fast breeder, analyses of dynamics of, 25:57069(R) (ANL-7800)
accidents in fast breeder, mathematical analysis of aerosol distribution following, 25:57105
accidents in sodium cooled, limitation of hypothetical, 25:57072 (CONF-710302-(Vol.1), pp 1-24)
components for, review of corrosion problems in, 25:55392
economics of fast, in mixed electrical generating systems with light water reactors, (T), 25:57061 (MLM-1851)
fuel elements of fast breeder, development of delayed neutron monitoring failure detection system for, 25:57055 (JAERI-Memo-4157, pp 84-8)
fuel elements of fast breeder, development of failure detection systems for, 25:57056 (JAERI-Memo-4157, pp 89-100)
heat transfer in coolant channels of, derivation of coefficients for forced-convection, 25:54864 (ANL-7754)
pressure vessels for, design of coolant seals for, 25:57043(P)
safety of, chemical aspects of, 25:57090 (ORNL-4717, pp 91-107)
REACTORS, MAGNOX
operation of power, review of capacity and availability factors for, 25:56893 (70-CNA-631)
REACTORS, MARITIME
economics for container ship propulsion, (T), 25:57138
REACTORS, MOLTEN-SALT
core for, computer program for calculation of optimum design parameters of, 25:57048 (ORNL-TM-3359)
fuel cycle for, computer program for calculation of optimum, 25:57048 (ORNL-TM-3359)
REACTORS, ORGANIC-COOLED
components for, review of corrosion problems in, 25:55394
REACTORS, ORGANIC-MODERATED
components for, review of corrosion problems in, 25:55394
REACTORS, PEBBLE-BED
fuel cycle for 2500 MW(t) high temperature, analysis of multizone core configuration for optimum economic thorium, 25:57060 (JUL-736-RG)
REACTORS, POWER
construction of fast, in United Kingdom, 25:57012
construction of, cost analysis for, 25:57059 (70-CNA-628)
containment systems for boiling water, analytical modeling methods for coolant loss accident induced transient in pressure suppression, 25:57057 (NEDO-10320(Suppl.1))
coolant for CIRENE, effects of channel configuration and heat flux on density of steam--water, (E), 25:57032
coolant loss accident in water cooled and moderated, analysis of fission product release during, 25:57104
cooling channels for CIRENE type, use of steady-state data for calculation of transient condition critical heat flux in, 25:57024
cooling system for thermal, surge and water hammer problems in condenser, 25:57036
cooling system for, flow characteristics and performance of equipment for, 25:57035
cost estimates for single unit pressurized water, computer program for calculation of conceptual, 25:57063 (ORNL-TM-3276)
costs for, effects of coolant type and fuel cycle on, 25:57059 (70-CNA-628)
design of advanced, use of graphic display computer systems for, 25:57008
design of advanced, use of graphic display computer systems for, 25:57007
development in Germany, planning for, 25:57003
development in Germany, review of, 25:56877 (CONF-700438)
development of, positive aspects of, 25:57004
development of, prospects for worldwide, 25:56999
dynamics for coupled core, calculation of domain asymptotic stability of nonlinear space-time, (T), 25:57188
dynamics of, noise analysis methods for, 25:57023
economics of dual purpose, in central heating stations, 25:57135
economics of fast, in mixed electrical generating systems with light water reactors, (T), 25:57061 (MLM-1851)
equipment for, earthquake stress resisting design requirements of Class 1, 25:57108
fission product production in, problems from iodine, 25:57100
fuel cycle for, development of optimum economic, 25:57062 (ORNL-4682, pp 240-1)
fuel tubes for high temperature gas cooled, calculation of stresses in graphite, (E/T), 25:57051
fuels for high temperature gas cooled, computer program for burnup calculations for coated particle, 25:57021 (JAERI-Memo-4449)
list of worldwide, 25:56984 (STI/PUB-194/4)
maintenance of gas cooled, procedures for remote, 25:57066
nuclear materials management at, safeguards aspects of, 25:54934 (BNWL-1598)
operation in Germany, review of, 25:56877 (CONF-700438)
operation of water cooled and Magnox, review of capacity and availability factors for, 25:56893 (70-CNA-631)
operation of, cost analysis for, 25:57059 (70-CNA-628)
power conversion system for, flow characteristics and performance of equipment for, 25:57035
pumps for boiling water and pressurized water, flow characteristics for, 25:57009
pumps for boiling water and pressurized water, flow characteristics for, 25:57039
radioactive effluents from boiling, distribution of and dose rates from, 25:56979
radioactive effluents from, effects on environment of, 25:56981
radioactive effluents from, radiation hazards from, 25:57099
radioactive effluents in Sweden from urban, calculations for, 25:56977
radioactive wastes from, procedures and policies for management of, 25:57001
safety aspects in Sweden for urban, 25:56977
siting in U.S. of, effects of public opinion on, 25:56976
siting of, analysis of characteristics and factors for, 25:56975
structures for, earthquake stress resisting design requirements of Class 1, 25:57108
REACTORS, PRESSURIZED-WATER
coolant loss accident conditions in, effects on core of, (E/T), 25:57095 (WCAP-7422)
coolant loss accidents in, numerical methods for analysis of pressure waves during, 25:57085 (CONF-710302-(Vol.1), pp 282-95)
core for, effects of coolant loss accident conditions on, (E/T), 25:57095 (WCAP-7422)
cost estimates for single unit power, computer program for calculation of conceptual, 25:57063 (ORNL-TM-3276)
economics of dual purpose, in central heating stations, 25:57135
engineered safeguards equipment for, effects of post accident containment environments on performance of, (E), 25:57097 (WCAP-7744)
fuel assemblies for, coolant mixing between subchannels in, (E/T), 25:57031 (WCAP-7755)
fuel elements for, standards for Zircaloy clad uranium oxide ($UO_2$), 25:57049 (RDT-E-13-15-T)
power density profiles in, correlation of neutron flux detector response to, (E), 25:57017(R) (BAW-3647-22)
pressurizers for, standards for electric heater and connector assembly for, 25:57030 (RDT-E-5-2-T)
pressurizers for, standards for electrically heated, 25:57029 (RDT-E-5-1-T)
pumps for power, flow characteristics for, 25:57039
pumps for power, flow characteristics for, 25:57009
pumps for, design problems for primary, 25:57038
radioactive wastes from Japanese, disposal of, 25:54980
safety of, summaries of reseach programs on, 25:57096 (WCAP-7722)
REACTORS, PROCESS HEAT
economics of dual purpose, in central heating stations, 25:57135
REACTORS, RESEARCH
construction in urban areas of U.S., licensing procedures for, 25:57131
design parameters of EWA-10, 25:57116 (INR-1303)
design parameters of L-88, for neutron radiography, 25:57128
experimental capabilities of EWA-10, 25:57116 (INR-1303)
experimental channel of WWR-C-Prague, neutron spectra from horizontal, (E), 25:57125
experimental facilities for HFR (Nederland), design parameters and operations of pressurized water in-pile loop, 25:57121 (RCN-145)
fuel elements of JRR-3, design parameters and performance of failure detection system for, 25:57117 (JAERI-Memo-4157, pp 23-43)


XUM

fuel elements of JRR-3, performance of γ radiation monitoring method for failure detection system for, 25:57118 (JAERI-Memo-4157, pp 44-50)
fuel elements of JRR-4, performance of delayed neutron monitoring method for failure detection system for, 25:57119 (JAERI-Memo-4157, pp 51-65)
in-pile loop for IRT Tbilisi, design of, 25:57129
irradiation channels for IRT-M, pneumatic rabbit system design for, 25:57130
irradiation services of, survey of, 25:57122
list of worldwide, 25:56984 (STI/PUB-194/4)
neutron spectrum for THOR, quadruple foil method for measurement of intermediate, 25:57126
operation in urban areas of U.S., licensing procedures for, 25:57131
photon field in RA core, spectrocalorimetric measurements of, 25:57123
power measurements in ASTRA, fission product track detector for, (E), 25:57124
radioactivity in cooling water of Slowpoke, 25:54587(R) (AECL-3909)
REACTORS, SWIMMING-POOL
neutron spectrum for, quadruple foil method for measurement of intermediate, 25:57126
REACTORS, THERMAL
cooling system for power, surge and water hammer problems in condenser, 25:57036
physics calculations for, comparison of ENDF/B-I and ENDF/B-II data for, 25:57019 (CONF-710302-(Vol.2), pp 1065-85)
shielding for, effects of iron contents on performance of concrete, (E), 25:57027 (RCN-147)
REACTORS, WATER-COOLED
components for, review of corrosion problems in, 25:55391
coolant boiling in, sensitivity of methods for detection of, (E), 25:56996
coolant interactions with molten aluminum cladding in, pressure generation from, (E/T), 25:57102
coolant loss accident in water moderated power, analysis of fission product release during, 25:57104
coolant loss accidents in, computer code for fuel rod heat conduction during, 25:57094 (RISO-M-1391)
coolant loss accidents in, program for analysis of core behavior during, 25:57101
cooling systems for, gaseous pressurizer performance for gas elution in primary, 25:57042
cooling systems of, effects of crud deposition on heat transfer in, (E/T), 25:57034
core components for, stability calculations for flow-induced vibrations of, 25:57086 (CONF-710302-(Vol.1), pp 356-9)
economics in mixed electrical generating systems with fast breeders, (T), 25:57061 (MLM-1851)
excursions in, adiabatic aproximation model for analysis of control rod drop, (T), 25:57084 (CONF-710302-(Vol.1), pp 259-81)
fluid flow in multirod coolant channels of, study of two-phase, (E), 25:54870(R) (GEAP-10347)
fuel elements of, fission product release and detection of failed Zircaloy 2 clad uranium oxide ($UO_2$) rod, 25:57047 (JAERI-Memo-4157, pp 2-22)
fuels for, high temperature performance of silicon carbide (SiC) coated particle type, 25:57053
heat transfer in multirod coolant channels of, study of boiling, (E), 25:54870(R) (GEAP-10347)
operation of power, review of capacity and availability factors for, 25:56893 (70-CNA-631)
pressure vessels for, stress analysis of prestressed concrete, (E/T), 25:56991
safety of, chemical aspects of, 25:57090 (ORNL-4717, pp 91-107)
shielding for, effects of configurations on performance of, 25:55043 (RD/B/N-2034)
standards for, development of engineering, 25:57092(R) (ORNL-TM-3483)
REACTORS, WATER-MODERATED
coolant loss accident in water cooled power, analysis of fission product release during, 25:57104
physics calculations for, comparison of ENDF/B-I and ENDF/B-II data for, 25:57019 (CONF-710302-(Vol.2), pp 1065-85)
physics calculations for, modular POWER-B code package for, 25:57172 (CONF-710302-(Vol.2), pp 983-90)
RECOILS
dose distributions in rabbit and rat phantoms from neutron beam, correlation of LET distributions and, 25:55229
REFRACTORY MATERIALS
book: Emissive Properties of Materials (Handbook), 25:56346
REFRIGERATION
design of helium-II, for 300 W at 1.8°K, 25:56118
systems for 1.0 to 1.85°K, large-scale, 25:56117
REGGE POLE THEORY
asymptotic behavior in, infinite one-particle-exchange type model from, 25:56579
cuts for strong interactions, review of, 25:56475 (RPP/C-24)
RELATIVE BIOLOGICAL EFFECTIVENESS
values for x-radioinduced inhibition of radish seed germination, effects of very high dose rate on, 25:55350
RELATIVITY THEORY
axiomatic foundations of special, 25:56562
group theory for general, nonlinear realizations in, 25:56549 (ORO-3992-9)
Lagrangian in quantized general, renormalization of nonpolynomial, 25:56549 (ORO-3992-9)
Lorentz covariance in, general, 25:56558
Lorentz transformations for invariant electric tension vector for motion of electric charges in electromagnetic field, 25:56567
scalar function in pseudoeuclidean space in, expansion in relativistic invariant functions of, 25:56577
tetrad theories as reference systems in general, 25:56568
REMOTE-HANDLING EQUIPMENT
description of hot cell, 25:57054 (ANL-EBR-30)
design for lifting and moving radioactive material, 25:54853(P)
design for poisonous or radioactive materials, 25:54978(P)
design of sealed master-slave, 25:54990(P)
development for radium-226 storage facility, 25:54936 (BRH/DMRE-71-3)
REPTILIA
Uta stansburiana, radiation effects on genetic variation in populations of, γ, 25:55320
REPUBLIC OF SOUTH AFRICA
radiation protection regulations of, 25:55245
radium-226 content of marine phytoplankton off coast of, 25:55155
RESISTORS
radiation effects on electric properties of black silicon-carbide varistors, neutron, 25:55103
radioinduced gas desorption from black silicon-carbide varistors, gamma, 25:55102
RESPIRATION
radiation effects on human external, following therapy of malignant chest tumors, γ, 25:55339
RESPIRATORS
performance for protection against radioactive and toxic contaminants, dioctyl phthalate man tests on, 25:55243 (CONF-710401-, pp 392-406)
RESPIRATORY SYSTEM
radiography of human, radioisotope scanning method for evaluating lung perfusion following, 25:55285
RHENIUM
casting by levitation melting using magnetic field, 25:55424
conductivity at 80 to 1900°K, electric and thermal, 25:55523
creep behavior of electron-beam melted, 25:55432 (N-71-23114)
creep properties of electron beam-melted and powder metallurgy, at 2200 to 4200°F, 25:55491
determination of trace amounts of, in molybdenum, review on, 25:54399
determination of, solvent extraction methods in, 25:54401
effects on properties and sintering of tungsten at 1000 to 2000°C, 25:55453
electron--phonon interaction in normal and superconducting states of high-purity, 25:56097
reactions with molten lithium perchlorate, Raman spectral studies on compounds produced by, 25:54538
superconducting-energy-gap behavior of single-crystal, tunneling study of, (E/T), 25:56067
RHENIUM ALLOYS AND SYSTEMS
C--Hf--Re--W, mechanical properties of, 25:55433 (N-71-23982)
Mo--Re--W, creep properties of, at 1800 to 4000°F, effects of grain size on, 25:55431 (N-71-23110)
Os--Re-base, sound velocity at room temperature in, 25:55078(R) (NYO-3906-5)
Pr-base--Re, phase diagram of, 25:55567
Re--Ta, hardening in monocrystals of, at 77 to 2000°K, solid-solution, 25:55457
Re--W, phase composition of, at 1500 to 1900°C, effects of aluminum oxide coating on, 25:55465
RHENIUM ISOTOPES Re-186
beta decay of, β-γ angular correlations and matrix elements for nonunique first-forbidden, (E), 25:56776
RHENIUM ISOTOPES Re-187
energy-level transitions in, nuclear structure effects on internal conversion of M1, 25:56756
RHODIUM
effects on properties and sintering of tungsten at 1000 to 2000°C, 25:55453
neutron resonance absorption in, self-shielding of, (E/T), 25:57196
RHODIUM ALLOYS AND SYSTEMS
Dy--Rh, hyperfine parameters of DyRh, Moessbauer-effect study of, 25:56382
Fe-base--Ni--Rh, use as filter in polarized iron-57 Moessbauer source, 25:56366
RHODIUM ISOTOPES Rh-103
energy levels from ruthenium-103 decay, spin--parity assignments for, (E), 25:56771
energy-level transitions from ruthenium-103 decay, internal conversion coefficients and multipolarities

for, (E), 25:56771
neutron capture at 14 MeV, γ spectra and cross section for, (E), 25:56729
RHODOPHYTA
Corallina sp., radioisotope content of Pacific Ocean, in environs of reactors, 25:55151 (CONF-710817-1)
Gelidium sp., radioisotope content of Pacific Ocean, in environs of reactors, 25:55151 (CONF-710817-1)
Phyllospadix sp., radioisotope content of Pacific Ocean, in environs of reactors, 25:55151 (CONF-710817-1)
RIBONUCLEASE
radioinduced inactivation of, conformational changes associated with uv, 25:55137
RIBOSOMES
radiation effects on synthesis of RNA precursor, in yeast, uv, 25:55138
RIVERS
radioisotope content of Czechoslovakian, measurement of natural, 25:54774
thorium content of Czechoslovakian, (E), 25:54774
uranium content of Czechoslovakian, (E), 25:54774
RNA NUCLEOTIDYLTRANSFERASE
radiation effects on activity of sugar beet, effects of dose on γ, 25:55351
ROBERT E. GINNA POWER REACTOR, UNIT 1
fuel elements of, inspection and replacement of defective, 25:56940 (DOCKET-50244-78)
power increase for, safety aspects of, 25:56941 (DOCKET-50244-79)
radioactive effluents from, excessive iodine-131 release on September 27 and 28, 1971, 25:56903 (DOCKET-50244-80)
ROCKS
age of worldwide, rubidium/strontium method for estimation of, 25:54757(R) (MIT-1381-18)
analysis by 14-MeV neutron activation and γ spectrometry, review of, 25:54465
analysis by activation, comparison of other methods with, 25:54458
analysis by alpha scattering, 25:54459
analysis by fast and thermal neutron and photon activation, 25:54463
analysis by instrumental activation, gamma--gamma coincidence spectrometry in, 25:54479
analysis by instrumental neutron activation and neutron activation with radiochemical separations, 25:54461
analysis by nondestructive 14-MeV neutron activation, computer program for analyzing γ spectra in, 25:54482
analysis for beryllium by alpha activation and prompt γ counting, 25:54467
analysis for gold by neutron activation of lead alloy obtained in cupel assay, 25:54521
analysis for noble metals by neutron activation and radiochemical separations, 25:54485
analysis of basic and ultrabasic, for thorium and uranium by neutron activation, 25:54495
analysis of standard, by neutron activation and γ spectrometry, 25:54464
analysis of standard, for bismuth, cadmium, mercury, and thallium by neutron activation and radiochemical separation, 25:54454
analysis of terrestrial and nonterrestrial, by atomic absorption spectroscopy, comparison of neutron activation analysis results with those from, 25:54511
analysis of terrestrial, for noble metals by neutron activation, 25:54484
analysis of ultramafic, for trace elements by neutron activation and γ spectrometry, 25:54496
argon-40 diffusion from, (E), 25:55672
book: Chemical Methods of Rock Analysis, 25:54403
radioisotope distribution in, fractured by contained nuclear explosion, 25:54826(T) (UCRL-Trans-10543, pp 99-116)
RODS
fluid flow through bundles of, convective heat transfer in axial turbulent, 25:54866 (EIR-198)
heat transfer in slender straight, calculation of, 25:54885
RUBIDIUM
determination in fission product mixtures by ion exchange and β counting, 25:54449
determination in sediments of Rhine River basin by x-ray fluorescence, 25:54408
determination in volcanic ash by neutron activation and γ spectrometry, 25:54513
diffusion in glass, effects of temperature on, 25:55611
separation from MSBR fuel solvent by extraction into bismuth by reduction with lithium at 650°C, 25:54534 (ORNL-4717, pp 43-56)
sorption of fission-product, by graphite at high temperatures, 25:55623
RUBIDIUM ALLOYS AND SYSTEMS
K--Na--Rb, phase studies of, thermal methods for, 25:55524(R) (COO-1707-11)
RUBIDIUM CHLORIDES
impurity location in crystals of, by axial channeling of helium ions and protons, 25:56337
RUBIDIUM FLUORIDES
$RbBF_4$--RbF, phase diagrams for, 25:54532 (ORNL-4717, pp 1-27)
RUBIDIUM FLUOROBORATES
$RbBF_4$--RbF, phase diagrams for, 25:54532 (ORNL-4717, pp 1-27)
RUBIDIUM IONS
reactions with tungsten, sputtering of secondary tungsten ions from, 25:55819
RUBIDIUM ISOTOPES
determination in rocks, methods and standards for, 25:54757(R) (MIT-1381-18)
RUBIDIUM ISOTOPES Rb-84
beta and electron-decay of, branching ratios and half-life for, (E), 25:56697
beta decay of, β-γ angular correlations and matrix elements for nonunique first-forbidden, (E), 25:56776
RUBIDIUM ISOTOPES Rb-87
energy level scheme from krypton-87 decay, (E), 25:56703
use as standard in nuclear metrology, 25:54901
RUBIDIUM PERCHLORATES
radiolysis of crystalline, effects of additives on yields from proton and γ, 25:54638
RUBIDIUM URANYL NITRATES
crystal growth and structure of $RbUO_2(NO_3)_3$, 25:54579
RUTHENIUM
casting by levitation melting using magnetic field, 25:55424
determination in geochemical samples by neutron activation, 25:54484
determination in geological sample by neutron activation and radiochemical separations, 25:54485
determination in presence of osmium, spectrophotometric, 25:54412
determination in silicate rocks and rock-forming minerals by neutron activation and radiochemical separations, 25:54486
determination of, use of ion exchange in methods for, 25:54397
effects on properties and sintering of tungsten at 1000 to 2000°C, 25:55453
properties of aerosols of, produced from solutions at high temperatures, chemical and physical, 25:54545
separation from iridium, palladium, or platinum on titanium tungstate papers by electrochromatography, 25:54744
separation from rhenium by solvent extraction, 25:54401
RUTHENIUM ALLOYS AND SYSTEMS
C--Ru--Th, phase studies of, 25:55640
Ce--Gd--Ru, critical magnetic field in superconducting, (E), 25:56074
Ce--Nd--Ru, critical magnetic field in superconducting, (E), 25:56074
Ce--Ru, critical magnetic field in superconducting intermetallic $CeRu_2$, (E/T), 25:56074
Ce--Ru--Y, critical magnetic field in superconducting, (E), 25:56074
Nb--Ru, diffusion in, effects of composition on mutual, 25:55452
Ru--Ta, hardening in monocrystals of, at 77 to 2000°K, solid-solution, 25:55457
Ru--Ta, thermionic properties of, relations with ruthenium content, 25:56350
Ru--V, phase transition of near-equiatomic, x-ray diffraction study of cubic--tetragonal, 25:55532
Ru--Zr, diffusion in, effects of composition on mutual, 25:55452
RUTHENIUM ISOTOPES Ru-103
beta decay of, conversion electron spectra and γ--γ angular correlations for, (E), 25:56771
RUTHENIUM ISOTOPES Ru-106
content in liquid radioactive waste effluents from Nuclear Fuel Services West Valley reprocessing plant, 25:54753
uptake by organisms of marine food chain, effects of physico-chemical form on, 25:55149 (BNWL-SA-4048)

## S

SACLAY PROTON SYNCHROTRON (SATURNE)
experimental facilities at, nuclear spectrometry, 25:56593 (LYCEN-7104, S7.1-2)
research on polarized proton reactions, 25:56688 (LYCEN-7104, S6.1-2)
SACLAY REACTORS (OSIRIS)
loop for, description of high-temperature in-pile, 25:54840
SAFETY
programs at Oarai Research Establishment in Japan during October through December 1970, 25:55247(R) (JAERI-Memo-4353)
SALICYLALDEHYDE
complexes with thorium, uranium, and/or yttrium, preparation and spectral properties of, 25:54539
SALIVA
analysis for iodine by neutron activation and radiochemical separation, 25:54509
SALT DEPOSITS
cavity excavation in underground, feasibility study of nuclear methods for storage, (E), 25:54824(T) (UCRL-Trans-10543, pp 70-80)
gas flow and diffusion in unconsolidated beds of, 25:54758 (ORNL-4717, pp 109-15)
radioactive waste disposal in German Asse, methods for low- and medium-level, 25:54985

XUM

radioactive waste storage in, safety of high-level, 25:54969 (JUL-766-CT)
SALTS
radiolysis of aqueous solutions of, 25:54758 (ORNL-4717, pp 109-15)
SAMARIUM
determination in fission product mixtures by ion exchange and β counting, 25:54449
determination in river water and seawater by neutron activation and radiochemical separation, 25:54504
determination in volcanic ash by neutron activation and γ spectrometry, 25:54513
determination of trace amounts of, in air by neutron activation and γ spectrometry, 25:54456
determination of trace amounts of, in nuclear grade uranium by x-ray excited optical fluorescence, 25:54428
mechanical properties at 78 to 600°K of polycrystalline, 25:55520
separation from aqueous solutions by solvent extraction using TTA, synergistic effects of 2,4-pentanedione on, 25:54731
separation from gadolinium and neodymium by liquid--liquid chromatography using bis(2-ethylhexyl) phosphate and sulfuric acid, 25:54745
separation from promethium by displacement chromatography using [(carboxymethylimino)bis(ethylenenitrilo)]tetraacetic acid, EDTA, and nitrilotriacetic acid, 25:54723
SAMARIUM ALLOYS AND SYSTEMS
Au--Sm, crystal structures and melting points of intermetallic, 25:55570
Fe--Sm, phase diagram and intermetallic compounds, 25:55569
SAMARIUM BORIDES
preparation and stoichiometry of $SmB_6$, 25:55601
SAMARIUM ISOTOPES Sm-139
beta decay of, half-life for, (E), 25:56761
energy levels from isomeric transition in, (E), 25:56761
energy-level transitions in, branching ratios, internal conversion coefficients, and multipolarities for, (E), 25:56761
isomeric transition in, half-life for, (E), 25:56761
SAMARIUM ISOTOPES Sm-143
energy levels from samarium-144 (p,d) reactions, neutron-hole structure of, (E), 25:56770
SAMARIUM ISOTOPES Sm-144
proton reactions (p,α) at 35 MeV, DWBA analysis of, (E), 25:56770
SAMARIUM ISOTOPES Sm-147
neutron reactions (n,α) at resonance energies, α widths and resonance spin assignments for, (E/T), 25:56754(T) (UCRL-Trans-10541)
SAMARIUM ISOTOPES Sm-149
neutron reactions (n,α) at resonance energies, α widths and resonance spin assignments for, (E/T), 25:56754(T) (UCRL-Trans-10541)
SAMARIUM ISOTOPES Sm-152
energy-level scheme from promethium-152 decay, (E), 25:56772
energy-level transitions from europium-152 decay, multipole mixing of, (E), 25:56777
SAMARIUM ISOTOPES Sm-153
energy levels of, model analysis for ΔN = 2 mixing in, (T), 25:56737 (JINR-E4-5877)
SAMARIUM ISOTOPES Sm-154
energy-level scheme from neutron inelastic scattering, (E), 25:56752(R) (SUNI-14)
neutron inelastic scattering at 1.5 MeV, γ spectra from, (E), 25:56752(R) (SUNI-14)
SAMARIUM ISOTOPES Sm-155
energy levels of, model analysis for ΔN = 2 mixing in, (T), 25:56737 (JINR-E4-5877)
SAMPLING
methods for environmental samples, evaluation of, 25:54779 (CONF-710401-, pp 347-51)
SAN ONOFRE POWER REACTOR, UNIT 1
core burnup limit for, revised Cycle 2, 25:56898 (DOCKET-50206-124)
emergency core cooling system for, improved performance and reliability of, 25:56936 (DOCKET-50206-125)
SANDS
moisture content of, radiometric gage for measuring, 25:55064(P)
SATURN (PLANET)
luminosity of, relation to solar activity, (T), 25:55766
SAXTON POWER REACTOR
cooling system for, inspection and leak detection procedures for, 25:56934 (DOCKET-50146-92)
fuel element assemblies for, revised technical specifications for plutonium oxide ($PuO_2$)--uranium oxide ($UO_2$), 25:56933 (DOCKET-50146-91)
SCANDIUM
abundance in solar atmosphere, (E/T), 25:55750
alpha reactions with, production of vanadium-48 by, 25:54677
determination in Australian tektites by neutron activation and gamma spectrometry, 25:54478
determination in rocks, chemical methods for, 25:54403
determination in standard aluminum--silicon system by neutron activation, 25:54455
determination in volcanic ash by neutron activation and γ spectrometry, 25:54513
determination of trace amounts of, in air by neutron activation and γ spectrometry, 25:54456
determination of trace amounts of, in ultramafic rocks by thermal neutron activation and γ spectrometry, 25:54496
effects on determination of calcium by nondestructive alpha activation, 25:54522
effects on solvolysis of tert-butyl halides, Broensted correlation for, 25:54548
lattice parameters of, effects of hydrogen on, 25:55549
phonon spectrum of, inelastic neutron scattering study of, (E/T), 25:56342
separation of trace amounts of, from carbonate solutions by sorption on metal hydroxides, review on, 25:54734
separation of uranium from, in methyl sulfoxide by cation exchange chromatography, 25:54728
SCANDIUM HYDROXIDES
preparation of ScOOH, high-pressure hydrothermal method for, 25:55602
SCANDIUM ISOTOPES Sc-48
energy-level scheme from calcium-48 (p,n) reactions, (E), 25:56752(R) (SUNI-14)
SCANDIUM OXIDES
properties at high temperatures, electric, mechanical, and thermal, 25:55620
SCATTERING
amplitudes in Regge pole model, analytic form of multiple, 25:56578
amplitudes of elastic, at extremely high energies, properties of, 25:56574
amplitudes of, relativistic expansions for, 25:56577
bounds for three-body, evaluation of upper and lower, using Hilbert-space results, 25:55876
description of elastic, using nonlocal separable potentials, 25:56852
elastic nuclear Coulomb, polarization forces in, (T), 25:56573
perturbation theory of inelastic, conservation of particle flux in, (T), 25:55877
phase shifts for one-dimensional, additivity of, 25:56576
potential, angular dependence of impact parameter for nonmonotonic, 25:56572
potential, approximate evaluation of relativistic correction in, 25:55846
quantum field theory of relativistic, lectures on, 25:56571 (CERN-71-14, pp 229-87)
theory for nonrelativistic three-body, Faddeev approach for, 25:56575
variational principle for multichannel, quasi-minimum, 25:55878
SCHEELITE
analysis of, from East Alps deposits by monstandard activation method, 25:54490
SCHIZOMYCOTA
Bacillus subtilis, radioinduced adenine auxotrophic mutations in, effects of aminopterin on uv, 25:55189
Bacillus subtilis, radiosensitivity of, mechanism of relation of dark-repair to uv, 25:55356
Escherichia coli B/8, radiosensitivity of, mechanism of relation of dark-repair to uv, 25:55356
Escherichia coli, radiation effects on donor ability of recA and recA+ strains of, γ, 25:55358
Escherichia coli, radiation effects on survival of mutant, temperature dependence of recovery from uv, 25:55360
Escherichia coli, radiation effects on survival of, effects of 2,4-dinitrophenol on recovery from x, 25:55355
Escherichia coli, radiation effects on thymineless death and liquid holding recovery in, synergistic uv and phosphorus-32, 25:55359
Escherichia coli, radioinduced adenine auxotrophic mutations in, effects of streptomycin on uv, 25:55189
Escherichia coli, radioinduced inactivation of, role of DNA cross-links in sensitizing effects of psoralen on uv, 25:55361
Mycobacterium phlei, mutation induction by 1-methyl-1-nitrosourea for pigment formation in, 25:55171
Mycobacterium phlei, radioinduced mutations for pigment formation in, uv, 25:55171
Salmonella sp., radiation effects on survival of, in smoked lake whitefish, effects of dose on γ, 25:55365
Vibrio sp., radioisotope accumulation by, 25:55154
SEALS AND GLANDS
design for sealing objects inside pressure tubes, 25:54845(P)
design of liquid metal cooled reactor pressure vessel coolant, 25:57043(P)
design of metallic, to maintain leak tightness of fuel element end caps, 25:57195(P)
SEAS
radioisotope uptake by organisms in, effects of physico-chemical form on, 25:55149 (BNWL-SA-4048)
SEAWATER
analysis for lanthanides by neutron activation and radiochemical separation, 25:54504
analysis for radioactive iodine as iodide and iodate by isotope exchange and scintillation counting, 25:54442
cerium content of, role of adsorption processes in,

XUM

25:54811
radioactive waste disposal in, solidification in cement for, 25:54979
separation of molybdenum from, by rapid adsorbing colloid flotation method, 25:54743
separation of uranium from, by adsorbing colloid flotation, 25:54738
uranium isotope distribution in, 25:54810
SEED
radioinduced chromosome aberrations in barley, method for metaphase analysis of x, 25:55175
radioinduced chromosome aberrations in wheat, effects of prolonged storage on repeated-exposure x, 25:55169
radioinduced inhibition of germination in radish, effects of very high dose rate on RBE for x, 25:55350
radioinduced mutations in barley and wheat, effects of ethylenimine on x, 25:55261
radioinduced mutations in Crepis capillaris, effects of water content on γ and x, 25:55167
radioinduced premutational oxygen-sensitive changes in chromosomes of Crepis capillaris, γ, 25:55168
strontium-90 content of hybrid wheat, in relation to phenotype, 25:55223
SEISMIC WAVES
ground motions from Rulison-produced, at Tosco mine and tower stations, 25:54813 (PNE-R-51)
polarization angles of S, from underground nuclear explosions, effects on earthquake occurrence, 25:54814
propagation in Sahara granite surrounding Monique nuclear explosion, (E), 25:54820(T) (UCRL-Trans-10543, pp 4-35)
spectra of San Fernando earthquake-generated, predictions for Glendale area, 25:54812 (NVO-1163-TM-30)
SELENIUM
alpha fission at 167 MeV, angular distributions and particle track lengths for, (E), 25:56806
analysis for chlorides, photometric, 25:54407
separation from tellurium by solvent extraction using Bismuthiol II, 25:54724
SELENIUM ISOTOPES Se-75
effectiveness of selenomethionine-incorporated, for scintiscanning of human pancreas, 25:55271(T) (LB/G-3059)
SEMICONDUCTORS
diffusion in, data tabulations on, 25:55509
electron transport theory using Monte Carlo methods, 25:56362
ion implantation in, review of analysis of lattice disorder in, 25:56304
positron lifetime measurements in single crystals of, 25:56360
radiation damage in II--VI compounds, review, 25:56291
radiation effects on, review of important unanswered questions in, 25:56332
SENA POWER REACTOR
fuel inventory for December 1970, 25:56918 (TID-25806)
fuel inventory for February 1971, 25:56920 (TID-25808)
fuel inventory for January 1971, 25:56919 (TID-25807)
fuel inventory for June 1971, 25:56923 (TID-25811)
fuel inventory for March 1971, 25:56921 (TID-25809)
fuel inventory for May 1971, 25:56922 (TID-25810)
fuel inventory for November 1970, 25:56917 (TID-25805)
maintenance during December 1970, 25:56918 (TID-25806)
maintenance during February 1971, 25:56920 (TID-25808)
maintenance during January 1971, 25:56919 (TID-25807)
maintenance during June 1971, 25:56923 (TID-25811)
maintenance during March 1971, 25:56921 (TID-25809)
maintenance during May 1971, 25:56922 (TID-25810)
maintenance during November 1970, 25:56917 (TID-25805)
operation during November 1970, 25:56917 (TID-25805)
operations during December 1970, 25:56918 (TID-25806)
operations during February 1971, 25:56920 (TID-25808)
operations during January 1971, 25:56919 (TID-25807)
operations during June 1971, 25:56923 (TID-25811)
operations during March 1971, 25:56921 (TID-25809)
operations during May 1971, 25:56922 (TID-25810)
SEPARATION PROCESSES
efficiency of combined lump-and-batch, for processing radioactive ores, (T), 25:54847
research progress on, 25:54718 (ORNL-4682, pp 168-81)
SEROTONIN
effects on sensitivity of guinea pigs and mice to transverse acceleration, 25:55264
radioprotective effects of, on mice, fast neutron and x, 25:55266
radioprotective effects on mice, effects of dose, sex, and strain on x, 25:55257
SERPUKHOV SYNCHROTRON
experimental facility for π + e interactions, readout electronics for multi-detector, 25:55044 (JINR-E1-5818)
SEWAGE
aeration of, evaluation of radiokrypton as indicator for oxygen mass transfer during, 25:54903
disposal of solid, description of BNL system for, 25:54843
SEWAGE SYSTEMS
description of pilot plant for nonpolluting operation, 25:54843
SEX
effects on radiosensitivity of rat bones, calcium metabolism studies on, 25:55331
SEYFERT GALAXIES
gravitational radiation in, conversion into electromagnetic waves, (T), 25:55805
SF MATERIALS ACCOUNTING
systems in uranium and plutonium scrap processing facilities, safeguards capabilities of, 25:54968 (IAEA-R-878-F)
SHEARON HARRIS POWER REACTOR, UNIT 1
construction of, permit application for, 25:56974 (DOCKET-50400-1)
operation of, license application for, 25:56974 (DOCKET-50400-1)
SHEARON HARRIS POWER REACTOR, UNIT 2
construction of, permit application for, 25:56974 (DOCKET-50400-1)
operation of, license application for, 25:56974 (DOCKET-50400-1)
SHEARON HARRIS POWER REACTOR, UNIT 3
construction of, permit application for, 25:56974 (DOCKET-50400-1)
operation of, license application for, 25:56974 (DOCKET-50400-1)
SHEARON HARRIS POWER REACTOR, UNIT 4
construction of, permit application for, 25:56974 (DOCKET-50400-1)
operation of, license application for, 25:56974 (DOCKET-50400-1)
SHEEP
iodine-125 and -131 transport across placenta in pregnant, 25:55319 (UCD-472-118)
SHELTERS
design of fallout, environmental factors in, 25:54933
SHIELDED CONTAINERS
design of fire-resistant, for radioactive materials, 25:54977(P)
design of pressure-relief plugged, for hazardous liquids, 25:54989(P)
development for safe handling and storage of radium-226 sources, 25:54936 (BRH/DMRE-71-3)
development for shipping irradiated LMFBR fuel, 25:54713 (ORNL-4682, pp 39-79)
safety evaluation of Types A and B, for shipping radioactive materials through Mont Blanc Tunnel, 25:54973 (RT/PROT-(71)11)
safety evaluation of, for shipping spent LMFBR fuel elements, 25:54972 (ORNL-TM-2723)
shock and vibration during rail and truck transport of radioactive materials, data tabulation on, 25:54974 (SC-M-710241)
testing of 10-ton cylindrical P-type, for shipping uranium hexafluoride, 25:54970 (KY-631)
SHIELDING
bremsstrahlung buildup factor, dependence on position between source and detector, 25:56280
calculations for lithium hydride and tungsten, for SNAP zirconium hydride reactor, 25:57133 (ORNL-TM-3366)
calculations for reactor multiregion slab, RAGA code for Monte Carlo, 25:57026 (RCN-146)
computer code for, Monte Carlo general purpose, 25:56262 (N-71-22378)
design characteristics of removable, for reactor access wells, 25:57199(P)
design characteristics of ring shaped, for reactor loading machine support, 25:57209(P)
design for radioactive areas in Battelle plutonium facility, 25:54959 (CONF-710401-, pp 280-92)
discrete ordinates method for anisotropically scattering multiplying particles in subcritical slab, convergence of, 25:56264 (ORNL-TM-3553)
gamma transport method for calculations of, three-dimensional stochastic, (T), 25:56273
neutron transport equation for slab geometry in, nonhomogeneous boundary-value problem for linear, (T), 25:56621
neutron transport in slabs of, orders-of-scattering method for fast-, 25:56258 (COO-2049-9)
neutron transport in, S/sub n/ discrete ordinate sets for deep-penetration, 25:57153 (CONF-710302-(Vol.2), pp 617-24)
radiation transport studies for, (E/T), 25:56255(R) (AD-721388)
SHIELDING MATERIALS
design of layered rubber--lead, for attenuation of streaming radiation, 25:55657(P)
evaluation of high boron and hydrogen content Cheatree, for neutrons, 25:54962 (CONF-710401-, pp 307-10)
SHIPPING
effects of rail and truck, on radioactive material shipping container, shock and vibration, (E), 25:54974 (SC-M-710241)
equipment and methods for spent LMFBR fuel elements, safety evaluation of, 25:54972 (ORNL-TM-2723)
regulations for overland, of sealed gamma sources for radiography, description of French, 25:54976
safety evaluation of radioactive material, through Mont Blanc Tunnel, 25:54973 (RT/PROT-(71)11)
SHIPPINGPORT PRESSURIZED-WATER REACTOR
maintenance during April through June 1971, 25:56894(R) (DLCS-5000271)
operation during April through June 1971, 25:56894(R)

XUM

(DLCS-5000271)
SHOCK WAVES
calculations for multi-dimensional magnetohydrodynamic, computer code for, 25:56192
effects on refractory nitride powders, 25:55618
magnetic-field microfluctuations on front of, model of, (E), 25:56009
models for collisionless, comparison of, 25:56189
particle velocity behind, use of magnetic field to measure, 25:57233 (LA-4545)
physical quantities behind, approximative method for calculation of, 25:57290(T) (UCRL-Trans-10539)
position indicator for, development of isotopic, 25:55065
propagation in collisionless magnetized plasma, kinetic model for unstable equilibrium, 25:56190
propagation in interplanetary space, association with directional and temporal properties of solar low-energy protons, (E), 25:56020
propagation in plasma, review of collisionless, (E/T), 25:56147
propagation of relativistic, astrophysical implications of, (T), 25:55668
SILANE
He--methane--$SiH_4$, radiation effects on, reactions of recoil tritium from neutron, 25:54678
SILICATE ROCKS
analysis for iridium, osmium, and ruthenium by neutron activation and radiochemical separations, 25:54486
analysis for trace bismuth, cadmium, mercury, and thallium by neutron activation and radiochemical separations, 25:54489
SILICIDES
diffusion in, data tabulations on, 25:55509
SILICON
abundance in B-type stars, (E), 25:55701
abundance in primary cosmic radiation, (E), 25:55911
alpha reactions at 160 MeV, cross sections and fission mechanism for lithium-9, carbon-16, and nitrogen-17 production in, (E/T), 25:56685 (FRNC-TH-48)
alpha reactions at 70 to 160 MeV, cross sections and fission mechanism for production of stable and neutron deficient nuclei in, (E/T), 25:56685 (FRNC-TH-48)
analysis for oxygen by helium-3 activation and γ spectrometry, 25:54502
analysis of pure, for calcium by nondestructive alpha activation, 25:54522
analysis of semiconductor, for boron and oxygen by alpha or proton activation, 25:54528
burning in stars, (E), 25:55703
determination in Australian tektites by 14-MeV neutron activation, 25:54478
determination in steel by fast neutron activation, 25:54519
effects of compounds of, on bubble formation during annealing of doped tungsten, 25:55511
ion implantation damage in, lateral-stress study of 220-keV, 25:56285 (SC-RR-710424)
radiation damage in carbon-doped, infrared absorption spectra of 130°K 2-MeV-electron, 25:56325
radiation damage in lithium-doped n-type, EPR study of lithium--defect interactions in 1-1.5-MeV electron, 25:56310
radiation damage in n- and p-type, EPR study of fast-neutron, 25:56324
radiation effects on cobalt-doped, iron-57 Moessbauer-effect study of fast-neutron, 25:56326
radioinduced defects in germanium-, oxygen-, and carbon-doped, infrared absorption spectral study of 90°K 2.8-MeV electron, 25:56297
radioinduced defects in lithium-compensated boron-doped, annealing of γ-, 25:56293
radioinduced defects in lithium-diffused n-type, 30-MeV-electron and fission-neutron, 25:56309
radioinduced defects in p-type, photoconductivity spectral study of 1.2-MeV-electron, 25:56308
radioinduced defects in, EPR study of structure of multiple-vacancy (oxygen), 25:56312
radioinduced divacancies in, absorption spectral study of growth and annealing of neutron-, at 76°K, 25:56311
radioinduced infrared absorption bands at 78°K, effects of uniaxial stress on fast-neutron, 25:56296
radioinduced luminescence spectra of, effects of annealing and lithium impurity on 3-MeV electron, 25:56294
radioinduced luminescence spectra of, effects of uniaxial stress and temperature on 2.5-MeV electron, 25:56295
separation from niobium by vacuum melting, 25:55403
surface wetting of molten, on boron nitride, mechanisms of, 25:55469
SILICON CARBIDES
properties of metal fiber reinforced composites of, review on, 25:55608(T) (LB/G-3074)
radiation effects on electric properties of varistors of black, neutron, 25:55103
radioinduced gas desorption from varistors of black, gamma, 25:55102
C--$HfB_2$--SiC, electric and thermal conductivity at 300 to 1300°K, 25:55627
C--SiC--$ZrB_2$, electric and thermal conductivity at 300 to 1300°K, 25:55627
SiC--$HfB_2$, electric and thermal conductivity at 300 to 1300°K, 25:55627
SiC--$ZrB_2$, electric and thermal conductivity at 300 to 1300°K, 25:55627
SILICON ISOTOPES Si-28
alpha elastic and inelastic scattering at 104 MeV, nuclear deformation study from differential cross sections for, (E), 25:56687 (KFK-1397)
alpha reactions (α,C-12) and (α,O-16) at 42 MeV, cross sections for, (E), 25:56659
alpha reactions (α,γ), at 1.4 to 2.75 MeV and at (0.3 to 3) x 10⁹ °K, rates for, (E/T), 25:55704
deuteron reactions (d,p) at 13.8 MeV, vector analyzing power for polarized, (E), 25:56724
electron inelastic scattering by, form-factor calculations using isotensor dipole sum rules, (T), 25:56868
helium-3 reactions (He-3,2p) and (He-3,d) at 40 MeV, DWBA analysis of angular distributions and spectra from, (E), 25:56713
nuclear deformation of, differential cross sections for alpha elastic and inelastic scattering by silicon-28 for determining, (E), 25:56687 (KFK-1397)
proton elastic scattering by, phase-shift analysis of polarization effects in, (T), 25:56678
proton reactions (p,2p) at 600 MeV, distorted-wave impulse-approximation analysis of cross sections from, (E/T), 25:56711
proton reactions (p,2p) at 600 MeV, separation-energy spectra and momentum distributions of residual nuclei from, (E), 25:56706
SILICON ISOTOPES Si-29
alpha reactions (α,n) at 2.8 to 4.1 MeV, excitation function for, (E), 25:56752(R) (SUNI-14)
SILICON JUNCTIONS
growth of n-type layers on p-type substrates, use of partially ionized vapor deposition method of epitaxial, 25:56347
radiation effects on junction capacitance of $n^+ - p - p^+$ power diode, fast-neutron, 25:55097 (N-71-25389)
radiation effects on p--n, gamma and neutron, (E/T), 25:55095(R) (COO-1624-41)
radiation effects on volt--ampere characteristics of diode, neutron, 25:55100
radioinduced currents in p--n diodes, minority carrier lifetime measurement using flash x-, 25:56336
SILICON NITRIDES
shock compression effects on powdered, x-ray-diffraction study of, 25:55618
SILICON OXIDES
carbon deposition on surfaces of, effects of chemical reactivity on pyrolytic, 25:55604
properties of metal fiber reinforced composites of, review on, 25:55608(T) (LB/G-3074)
SILICON SYSTEMS
Al--Si, analysis of standard, by neutron activation, 25:54455
C--Ca--Ce--Mg--Si, analysis for tellurium by gravimetry, 25:54416
C--Si, radioinduced dimensional changes in codeposited coatings of isotropic, fast neutron, 25:55652
Cu--Si, superconductivity in hcp phases of, (E), 25:56096
Fe-base--Si, magnetic properties at cryogenic temperatures, 25:56361
Ge--Si, fabrication of thermoelements of, hot pressing method for, 25:57267 (SC-DR-710438)
Hf--Si, properties of, thermochemical and thermophysical, 25:55644
Si--Zr, inflammability correlation of powdered, 25:55473
SILOXANES
radioprotective effects of poly-, uv, 25:55263
SILTS
analysis by fast and thermal neutron and photon activation, 25:54463
analysis of Alaskan, for gold by neutron activation, 25:54488
analysis of ocean, by nondestructive 14-MeV neutron activation, computer program for analyzing γ spectra in, 25:54482
analysis of Rhine basin, for metals by x-ray fluorescence, 25:54408
analysis of terrestrial, for noble metals by neutron activation, 25:54484
effects of lake bottom, on cesium-137 uptake by rainbow trout, 25:55159
SILVER
alpha fission at 167 MeV, angular distributions and particle track lengths for, (E), 25:56806
argon-ion reactions at 30 keV with surfaces of, charge states and kinetic energies of scattered and recoil ions from, (E), 25:55818
deposition on sodium fluoride, effects of electron irradiation on epitaxy of, 25:56322
effects on solvolysis of tert-butyl halides, Broensted correlation for, 25:54548
electron reactions at 0.5 to 15 keV, optical radiation from, (E), 25:55813 (JINR-P4-5957)
neutron resonance absorption in, self-shielding of, (E/T), 25:57196
proton reactions at 1.5 to 4.5 MeV, optical radiation from, (E), 25:55813 (JINR-P4-5957)

XUM

SILVER ALLOYS AND SYSTEMS
Ag--Al, diffusion in, 25:57238 (MLM-OP-71003)
Ag--Al, superconductivity in hcp phases of, (E), 25:56096
Ag--Cd, oxidation at 600 to 800°C, mechanisms of internal, 25:55381
Ag--Cd, search for superconductivity in fcc phases of, (E), 25:56096
Ag--Dy, hyperfine parameters in DyAg, Moessbauer-effect study of, 25:56382
Ag--In, search for superconductivity in fcc phases of, (E), 25:56096
Ag--Sb, superconductivity in hcp phases of, (E), 25:56096
Ag--Sn, superconductivity in hcp phases of, (E), 25:56096
Ag--Zn, diffusion in, 25:57238 (MLM-OP-71003)
SILVER ISOTOPES Ag-105
effectiveness for diagnosis of human inflammations, 25:55286
SILVER ISOTOPES Ag-108
ion elastic scattering in wide energy range, phase shift analysis of angular distributions for, (E), 25:56740 (JINR-P7-5884)
SILVER ISOTOPES Ag-110
content of metastable, in Pacific seaweeds in environs of reactors in comparison to other locations, 25:55151 (CONF-710817-1)
SILVER NITRATES
radiation effects on, on porous glass or silica gel surfaces, ESR studies of γ, 25:54607
radiation effects on, on porous glass or silica gel surfaces, ESR studies of γ, 25:54606
radiolysis of ices of, EPR studies on neutral silver trapping sites from γ, 25:54666
$AgNO_3$--KF, radiolysis of, EPR studies on neutral silver trapping sites from γ, 25:54666
SILVER OXALATES
radiolysis of crystalline, effects of cadmium on proton and γ, 25:54638
SKIN
radiation effects on human, following therapy of bone sarcomas, high energy bremsstrahlung, 25:55338
radioisotope contamination of human, derivation of decision levels for control of, 25:55196 (LA-4558)
SLURRIES
analysis of ore, by neutron activation, irradiator for on-stream, 25:54506
SNOW
density and thickness measurement of, development of airborne radiometric system for, 25:55065
strontium-90 content of Antarctic, 1955 and 1964 measurements of, 25:54788
SODIUM
abundance in primary cosmic radiation, (E), 25:55911
analysis for carbon and oxygen, development of meters for, 25:55379(R) (WARD-4210-T-1-2)
analysis of liquid, for oxygen by zirconium gettering-vacuum-fusion method, 25:54418
boiling in liquid metal cooled fast breeder reactor, detection and stability analysis of, 25:57069(R) (ANL-7800)
boiling in reactor cores, initiation and thermal hydraulics aspects of, (E/T), 25:57068(R) (AI-AEC-13006)
boiling of, effects of heat exchanger material and surface roughness on incipient, (E), 25:54868(T) (EURFNR-897)
combustion in fast test reactor, characteristics of, (E/T), 25:57112 (HEDL-TME-71-31)
combustion in reactor accidents, release and transport of aerosols and energy from, (E/T), 25:57068(R) (AI-AEC-13006)
content of diseased and normal human bones, neutron activation determination of, 25:55106
corrosive effects on niobium at 600°C, effects of oxygen on, 25:55386
corrosive effects on steels and stainless steels of liquid, 25:57109 (ANL-7771)
corrosive reactions with irradiated stainless steel, radioisotope deposition and transport from, 25:55370 (BNWL-SA-2335)
determination in Australian tektites by neutron activation and gamma spectrometry, 25:54478
determination in feldspar by neutron activation and γ spectrometry, 25:54494
determination in glass, by simultaneous measurement of scattered α particles and prompt protons, 25:56752(R) (SUNI-14)
determination in tourmaline, by deuteron activation analysis and γ counting, 25:56752(R) (SUNI-14)
determination in volcanic ash by neutron activation and γ spectrometry, 25:54513
determination of trace amounts of, in air by neutron activation and γ spectrometry, 25:54456
determination of trace amounts of, in ultramafic rocks by thermal neutron activation and γ spectrometry, 25:54496
diffusion in glass, effects of temperature on, 25:55611
diffusion in membranes and membrane model solutions, radiometric porous-frit method for measurement of self-, 25:54535 (ORNL-4717, pp 57-82)
distribution in metal transfer process for fission product removal from MSBR fuel solvent, 25:54534 (ORNL-4717, pp 43-56)
flow and pressure drop in multiple channels, effects of channel geometry on, 25:54863 (AI-AEC-13010)
heat transfer characteristics of debris pieces of reactor fuels in liquid, 25:57069(R) (ANL-7800)
impurities in liquid, calibration of devices for monitoring, 25:55069 (ANL-7804)
radiation effects on excretion of, in rat urine, combined effects of open skin lesions and, 25:55332
radiation effects on metabolism of, in man following therapy of diffuse toxic goiter, iodine-131, 25:55340
reactions of liquid, with acetylene, 25:54537
reactions with molten uranium oxide ($UO_2$) of liquid, 25:57069(R) (ANL-7800)
reactions with reactor materials, description of facility for studies of, 25:54839
separation, deactivation, and disposal of liquid, present with spent LMFBR fuels, 25:54713 (ORNL-4682, pp 39-79)
solvent properties of liquid, for argon and helium at 330 to 550°C, 25:54583
SODIUM ACETATES
radiolysis of crystals of, ESR studies on trapped $CH_2CO^-$ radicals produced by γ, 25:54652
SODIUM ACETYLIDES
equilibrium between $NaHC_2$ and $Na_2C$ in reactions of sodium with acetylene, 25:54537
SODIUM ALLOYS AND SYSTEMS
Ba--Na, phase diagram of, 25:55526
K--Na, electric conductivity of, to 300°C, 25:55527
K--Na, phase diagram of, 25:55527
K--Na--Rb, phase studies of, thermal methods for, 25:55524(R) (COO-1707-11)
SODIUM AZIDES
radiolysis of crystalline, effects of additives on yields from proton and γ, 25:54638
SODIUM CHLORIDES
diffusion of oxides on surface of, 25:54758 (ORNL-4717, pp 109-15)
effects on calcium-45 uptake and release by rat brain microsomes, 25:55120
effects on corrosion of superalloys by molten vanadium oxide, 25:55375 (CONF-690452-, Paper 8)
effects on separation of europium or lanthanum from acid solutions by solvent extraction using acidic esters of aminophosphonic acids, 25:54732
ion scattering by crystals of, channeling in, 25:54587(R) (AECL-3909)
plutonium diffusion in sodium chloride, 25:54758 (ORNL-4717, pp 109-15)
radioinduced reduction of cadmium ions in crystals of, magneto-optical study of x-,, 25:56320
SODIUM FLUORIDES
lattice sites of vanadium and manganese ions in crystals of, calculation and x-irradiation effects on, 25:56384
radiation effects on surfaces and deposit epitaxy of, electron, 25:56322
$BeF_2$--NaF, electric conductivity of molten, 25:54532 (ORNL-4717, pp 1-27)
$BeF_2$--NaF, glass transition temperatures of molten, 25:54532 (ORNL-4717, pp 1-27)
LiF--NaF--$ThF_4$,, phase equilibria in, high-temperature, 25:54532 (ORNL-4717, pp 1-27)
$NaBF_4$--NaF, potentiometric studies of euctectics of, 25:54532 (ORNL-4717, pp 1-27)
$NaBF_4$--NaF, solvent properties for hydrogen fluoride, 25:54532 (ORNL-4717, pp 1-27)
SODIUM FLUOROBORATES
$NaBF_4$--NaF, potentiometric studies of euctectics of, 25:54532 (ORNL-4717, pp 1-27)
$NaBF_4$--NaF, solvent properties for hydrogen fluoride, 25:54532 (ORNL-4717, pp 1-27)
SODIUM HYDROXIDES
positron annihilation in glassy ice of, effects of radioinduced trapped electrons on, (E), 25:55835
radiation effects on aqueous solutions of, ESR studies of ozonide ion formation from γ, 25:54608
SODIUM HYDROXYFLUOROBORATES
preparation by reaction of boron trifluoride gas and sodium hydrogen carbonate, 25:54532 (ORNL-4717, pp 1-27)
SODIUM IONS
reactions with oxygen ions ($O^-$) at 0.1 to 7 eV, merged-beam measurement of total cross sections for charge exchange in, 25:55859
reactions with tungsten, sputtering of secondary tungsten ions from, 25:55819
reactions with tungsten, sputtering of secondary tungsten ions from, 25:55819
SODIUM ISOTOPES Na-22
abundance in lunar materials, (E), 25:55772
SODIUM ISOTOPES Na-23
energy levels from neon-22 (p,γ) reactions, γ branching ratios for, (E), 25:56752(R) (SUNI-14)
neutron total cross sections for, transmission of fission spectra through thick samples for evaluation of minima in, (E), 25:56650 (COO-2049-5)
proton reactions (p,γ), magnesium-24 photodisintegration rates from, 25:55703


XUM

SODIUM NITRATES
radiation effects on dissociation of polycrystalline, 5-MeV proton and 20-MeV alpha, 25:56318
radiolysis of acetic acid solutions of, effects of diazo reagents on γ, 25:54657
radiolysis of crystalline, effect of adsorbed water on γ, 25:54649
radiolysis of, comparison of Ceric and Shinn methods for determining yield of nitrite ions from, 25:54633(R) (ORO-3660-4)
SODIUM OXIDES
effects on corrosion of superalloys by molten vanadium oxide, 25:55375 (CONF-690452-, Paper 8)
SODIUM SULFATES
effects on corrosion of superalloys by molten vanadium oxide, 25:55375 (CONF-690452-, Paper 8)
SODIUM TELLURATES
tellurium-125 Moessbauer spectral study of recoil effects in $Na_2H_4TeO_6$, 25:56381
SOILS
moisture measurements of, passive radiometric gage using cosmic ray neutrons for, 25:55061(P)
moisture--density of surface, tabulation of US state highway departments' uses of radiometric gages for measuring, 25:54907
photon reflection by, Monte Carlo calculation of effect of subterranean perturbations on, (T), 25:56274
plutonium content of desert, around Nevada Test Site, 25:54755 (CONF-710401-, pp 320-7)
radiation monitoring in environs of Ames Research Reactor during 1971, 25:55152 (IS-2658)
radioisotope content of clay and sandy, performance of airborne gamma spectrometer for measuring bismuth-214, potassium-40, and thallium-208, 25:54768
sorptive properties for calcium and strontium, effects of soil exchange sites on differential, 25:54778
sorptive properties of wet, for plutonium, theoretical studies of, 25:54756 (CONF-710401-, pp 411-29)
SOL-GEL PROCESS
development of, microcolumn studies on, 25:55590(R) (EIR-192)
microsphere production in, 25:54719 (ORNL-4682, pp 229-39)
research progress on, 25:55592 (ORNL-4682, pp 144-59)
sol droplet dehydration in, 25:54719 (ORNL-4682, pp 229-39)
SOLAR ACTIVE REGIONS
evolution of, Jan. 14--June 1, 1969, (E), 25:55753
magnetic-field strengths over, (E/T), 25:55755
relation to sector structure of interplanetary magnetic field, (E/T), 25:55765
SOLAR CELLS
performance in combination with scintillators for gamma and x-ray detection, 25:55005
radiation effects on silicon, high-energy proton, 25:55099
radiation effects on, spacecraft experiment for studying, 25:55098(R) (N-71-26389)
SOLAR CORONA
element abundances in, (E/T), 25:55750
magnetic loop systems in, rotation of, (E/T), 25:55743
model for, current sheet magnetic, (T), 25:55733 (N-71-23433)
radio emission from filaments and active streamers in, (E), 25:55754
radio-wave propagation in, (E/T), 25:55755
spectra of, identification of 417-A line in extreme-ultraviolet, (E), 25:55767
streamers in, morphological model for, (E), 25:55754
SOLAR FLARES
anisotropy during proton event of Nov. 18, 1968, (E), 25:55764
charged-particle emission mechanisms for, (T), 25:55769
development of, model using magnetic-energy conversion for, (T), 25:55773
effect of 2B, on electron-density enhancements in E and F regions in ionosphere, (E/T), 25:56035
effect of Dec. 27, 1968 chromospheric, on ionospheric parameters, (E/T), 25:55982
electron acceleration in, due to quasistatic electric fields, (T), 25:55760
emission from active regions during Jan. 14--June 1, 1969, (E), 25:55753
emissions during, relation of radio and x-ray, (E), 25:55759
gamma flux from, (T), 25:55762
history of, from study of aluminum-26 and sodium-22 in luner samples, (E), 25:55772
magnetohydrodynamic flow calculations for, 25:55940
neutron flux from, (T), 25:55761
particle propagation and density in interplanetary space from, effect of solar boundary conditions on, (T), 25:55738
physical processes in, (T), 25:55769
proton flux from July 7, 1966, Proton-3 measurement of, (E), 25:55991
radio emission from, (T), 25:55769
solar-particle anisotropy as function evolution of, (E/T), 25:55763
x-ray emission during Oct. 1969, Intercosmos-1 detection of polarization of, E), 25:55771
x-ray emission during, (E), 25:55737
x-ray emission during, flux, spectrum composition, and structure of regions of, (E), 25:55770
SOLAR GRANULES
intensity fluctuations of, rms, (E), 25:55744
SOLAR PARTICLES
anisotropy of low-energy, as function of solar-flare evolution, (E/T), 25:55763
anisotropy of, during proton event of Nov. 18, 1968, (E), 25:55764
emission of protons in relation to microwave bursts, (E), 25:55758
emission of protons in relations to microwave bursts, (E), 25:55757
energy dissipation of PCA-associated, in ionosphere, (T), 25:56005
observations of low-energy 0.3 MeV or greater, during 1967 at widely separated locations, (E), 25:55956
SOLAR PROMINENCES
formation of loop, thermal effects in, (T), 25:55752
SOLAR RADIO BURSTS
emission during solar flares, (E), 25:55737
emission of Type-III, association with interplanetary electrons and protons, (E/T), 25:55778
relation of Type-I, to polarity distribution in interplanetry magnetic field, (E/T), 25:55765
relation to proton emission, (E), 25:55757
relation to proton emission, (E), 25:55758
relation to x-ray bursts, (E), 25:55759
spectra of, (E/T), 25:55755
SOLAR SPICULES
position along limb of groups of, regularity in, (E), 25:55747
relation to disk structures, (E), 25:55746
SOLAR SYSTEM
cosmic-particle modulation by, Z = 20 to 30 primary, (E), 25:55909
cosmic-ray modulation by, step-like changes in long-term primary, (E), 25:55912
formation of, (T), 25:55781
interplanetary electron and proton association with Type-III solar radio bursts, (E/T), 25:55778
isotope abundance in targets aboard Soyuz space probes, helium-3 and tritium, (E), 25:55902
magnetic-field measurement in interplanetary space, north--south component of, (E), 25:55779
plasma observation by Vela 3 in interplanetary space, correlation with simultaneous Imp 3 interplanetary magnetic-field data, (E), 25:55780
SOLAR WIND
cosmic-ray modulation by, dimensions of region of, (E/T), 25:55901
effects on planetary luminosities, (T), 25:55766
interaction with geomagnetic field, dipole model of, (E), 25:56009
interactions with magnetosphere, simulation of, 25:55976
interactions with Moon, (E), 25:55810
kinetic energy in, conversion of magnetic-field energy into, (T), 25:55775
parameters of, relation with Pc-type steady Earth-current pulsations, (E/T), 25:56004
plasma instabilities with parallel magnetic fields, electromagnetic, (T), 25:56204
plasma penetration by Earth-associated electron beams, wave-generation mechanism of, (E/T), 25:56019
proton observations on Vela 3, correlation with simultaneous Imp-3 magnetic-field data, (E), 25:55780
shock waves in, reverse and forward slow, (E/T), 25:55735 (N-71-24166)
velocity of, estimate of magnetospheric electric-field dependence on, (T), 25:56039
SOLAR X-RAY BURSTS
emission during solar flares, (E), 25:55737
relation to microwave bursts, (E), 25:55759
spectra of, OSO-V experiment for, (E), 25:55734 (N-71-23434)
SOLID SOLUTIONS
interstitial solubility limit in, use of measured lattice parameter for determination of, 25:55568
SOLIDS
book:Tables for Calculating Nonstationary Temperatures of Plane Bodies During Heating by Irradiation, 25:56267
diffusion in, research progress on, 25:54587(R) (AECL-3909)
photoionization of nonpolar, properties of trapped electrons from, 25:54594 (CONF-700652-(Vol.2), pp 331-64)
temperature distribution in, finite element method for calculation of, 25:54882
thermal expansion to 2500°C, method and equipment for measurement of, 25:55493
SOLUTIONS
radiolysis of aqueous, ESR studies of free radicals produced by fast reaction flow systems in, 25:54662
radiolysis of glasses of alkaline, electron trapping in γ, 25:54627 (CONF-700652-(Vol.2), pp 295-330)
SOLVENT EXTRACTION PROCESSES
development of Lacex, for irradiated LMFBR fuel reprocessing using dibutyl butylphosphonate, 25:54706 (BNWL-SA-3345)
research progress on, 25:54718 (ORNL-4682, pp 168-81)

SOUND
velocity in osmium--rhenium alloys at room temperature, extensional, 25:55078(R) (NYO-3906-5)
SOUTHWEST EXPERIMENTAL FAST OXIDE REACTOR
experimental capabilities of, liquid metal cooled fast breeder reactor safety programs, 25:57069(R) (ANL-7800)
fuel elements for, inspection of plutonium oxide ($PuO_2$)--uranium oxide ($UO_2$) rod type, 25:57111(R) (GEAP-10010-29)
fuel elements for, repair of instrumented, 25:57111(R) (GEAP-10010-29)
maintenance during May to July 1971, 25:57111(R) (GEAP-10010-29)
operations during May to July 1971, 25:57111(R) (GEAP-10010-29)
physics measurements for plutonium oxide ($PuO_2$)--uranium oxide ($UO_2$) fueled, (E/T), 25:57111(R) (GEAP-10010-29)
pressure vessel for, installation of backup seal for head of, 25:57111(R) (GEAP-10010-29)
startup testing of plutonium oxide ($PuO_2$)--uranium oxide ($UO_2$) fueled, 25:57111(R) (GEAP-10010-29)
SOVIET UNION
nuclear explosions in, for petroleum production stimulation, 25:54822(T) (UCRL-Trans-10543, pp 42-55)
nuclear explosions in, review of program on possible peaceful uses of contained, 25:54821(T) (UCRL-Trans-10543, pp 36-41)
SPACE
cosmic-ray propagation through interstellar, to Earth, path-length determination for, (E/T), 25:55903
interplanetary, solar-flare particles propagation and density in, effect of solar boundary conditions on, (T), 25:55738
magnetic-field intensity in interplanetary, correlation with geomagnetic-field activity, (E), 25:56007
parameter variations of interplanetary, during solar cycle, 1959-1967, (E), 25:55992
SPACE FLIGHT
book: Physical and Radiobiological Investigations of Artificial Satellites of the Earth, 25:55342
planetary quarantine program for, 25:57283(R) (TID-25790)
SPACE VEHICLES
book: Physical and Radiobiological Investigations of Artificial Satellites of the Earth, 25:55342
materials for, effects of nuclear and space radiation on structural, 25:55576 (N-71-25034)
power supplies for, calculations for optimum economic heat pipe cooled fast thermionic reactor for, 25:57134
SPECTROMETERS
design of magnetic, first- and second-order matrix theory for, 25:56598 (SLAC-75(Rev.2))
performance and testing of electrostatic electron, 25:55083
pulse-height spectra unfolding for, computer program for, 25:55042 (RD/B/N-1963)
resolution of magnetic charged-particle, optimization of, 25:55037 (JUL-737-FF)
spectra from charged-particle electrostatic, method for evaluation of, 25:55082
SPECTROPHOTOMETRY
research progress on, 25:54578 (ORNL-4682, pp 215-17)
SPECTROSCOPY
Lie groups in atomic, survey of, 25:55882 (NYO-1447-64)
research progress on, 25:54587(R) (AECL-3909)
sources for electron, preparation of high-purity carrier-free cesium-131, 25:54889 (INR-P-1325)
SPERM
radiation effects on mouse, 25:55207 (NYO-2740-8, pp 220-59)
radiation effects on quality of bull, tonometer measurements on x, 25:55337
SPERMATOGONIA
radioinduced chromosome translocations in mouse, RBE for gamma, 25:55182
radioinduced recessive sex-linked lethal mutations in mouse, x, 25:55184
SPHERES
energy tensor of Einstein linear gravitational field theory for resting liquid, phenomenological, (T), 25:56565
heat transfer in small, calculation of, 25:54885
SPORES
radiation effects on survival of bacterial, parameters for heavy ion, 25:55313
STABLE ISOTOPES
content of aquatic environment, role of, in pre-operational environmental monitoring for nuclear facility, 25:55240
effects on radioisotope accumulation by organisms in aquatic ecosystems, 25:55158
production for research uses, review of, 25:54899
STACK DISPOSAL
plume rise from, method for calculating, (E/T), 25:54780 (CONF-710505-6)
STAINLESS STEEL
brazing for Bonus Reactor superheater shell, 25:55425
compatibility with uranium carbide, evaluation by carbon transfer measurements, 25:55589 (JAERI-Memo-4438)
corrosion by liquid sodium of Type 304 and Type 347, 25:57109 (ANL-7771)
corrosion of irradiated cladding of, by sodium, radioisotope deposition and transport from, 25:55370 (BNWL-SA-2335)
radiation effects on adhesion of epoxy cemented specimen couples of, gamma, 25:55666
radiation effects on creep in Type 316, at 750°C, relations of injected helium content with alpha, 25:55574 (JAERI-Memo-4408)
radioinduced reactions with uranium dioxide fuel pins, in-pile, 25:55648 (RCN-144)
radioinduced swelling of Types 304 and 316, relations of dose and temperature with fast neutron, 25:55572 (BLG-457)
radioinduced swelling of, fast neutron, 25:55581
reactions with sodium at 1000 to 1300°F, carbon and nitrogen mass transfer in, 25:55379(R) (WARD-4210-T-1-2)
sensitization by LACBWR cooling water, failure parameters from intergranular, 25:55378 (SWRI-1228-P-7-40)
testing of fuel tubes of, ultrasonic method for, 25:54926
welds in thin-wall tubes of Type 316, ultrasonic inspection of butt, 25:54928
STANDARDS
calculation of MPC and MPD, evaluation of assumptions and methods used in, 25:55254
Colorimetric Determination of Technetium in Aqueous Solutions ASTM-E417-70T, 25:54429
design and performance of air-cooled heat exchangers for nuclear steam-supplied systems, 25:54833 (RDT-E-4-18-T)
electric heat and connector assembly for pressurizer for pressurized water reactors, 25:57030 (RDT-E-5-2-T)
establishment for radioisotope content of natural gas supplies, use of threshold limit values in, 25:55198
fabrication and acceptance of shell and tube water-to-water heat exchangers, 25:54832 (RDT-E-4-17-T)
fuel assemblies for pressurized water reactors, 25:57049 (RDT-E-13-15-T)
listing of national and international nuclear, 25:57091 (ORNL-NSIC-94)
Measuring Fast Neutron Flux for Analysis for Barium-140 Produced by Uranium-238 Fission, ASTM E393-69T, 25:54444
pressurizer for pressurized water reactors, 25:57029 (RDT-E-5-1-T)
radiation protection, of Union of South Africa, 25:55245
radioactivity monitoring, derivation and use of reference levels and working limits as UK environmental, 25:55241
review of Moessbauer-spectroscopy, 25:56365
Selection of Neutron Activation Detector Materials, ASTM E419-70T, 25:54510
Specifications for Deuterium Oxide, ASTM D2032-68, 25:54529
strength and pressure integrity of vertical, shaft-sealed, motor-driven, single-stage centrifugal pump, 25:54831 (RDT-E-3-3-T)
Test for Consumption of Potassium Permanganate by Impurities in Deuterium Oxide, ASTM D2033-68, 25:54405
Test for Radioactive Tritium in Water, ASTM D2476-70, 25:54447
Testing Deuterium Oxide, ASTM D2184-68, 25:54430
STANFORD LINEAR ACCELERATOR
development and operation of, April 1--June 30, 1971, 25:56599(R) (SLAC-136)
development and operation, 1970, 25:56600(R) (TID-25781)
research at, 1970, high-energy physics, 25:56600(R) (TID-25781)
STAR CLUSTERS
tidal effects on small, (T), 25:55683
STARS
angular separation and position angle of close binary, (E), 25:55693
atmosphere analysis and abundance determinations for B-type, model, (E), 25:55701
atmospheres of O and B, model, (T), 25:55673
atmospheres of pole-on Be, Hα line profiles for model, (E/T), 25:55709
atmospheres of, computations for model, (T), 25:55713
atmospheres of, X and Y functions of radiative transfer, (T), 25:55676
book: Methods of Investigating Variable Stars, (T), 25:55674
book: Model Atmospheres for O and B Stars, (T), 25:55673
composition of horizontal-branch, (E/T), 25:55708
condensation of solid hydrogen in proto-, (T), 25:55785
convection in atmospheres of, asymptotic solutions in nonlinear thermal, (T), 25:55694
convection in atmospheres of, nonlinear thermal, (T), 25:55695
convection zones in, effects of metal abundance on structure of, (T), 25:55679
core structure of, Tolman's solutions of field equations for, (T), 25:55696
distribution in Cygnus, (E), 25:55790
element abundances in atmospheres of beta Cephei, (E/T), 25:55711
evolution of early-type close binary, (T), 25:55690
evolutionary models for 15- and 30-solar-mass, (T), 25:55691


XUM

evolutionary track for HD 49798, (E), 25:55682
existence of supermassive, evidence of, (T), 25:55798
formation of, importance of internal velocity field in, (T), 25:55706
gas motions in convective envelopes of, (T), 25:55707
helium burning in 15- and 30-solar-mass, (T), 25:55691
hydrogen-shell burning in open-cluster, (T), 25:55684
light variations in supergiant, in LMC, (E), 25:55705
luminosity of horizontal-branch, (E/T), 25:55708
luminosity of variable, (T), 25:55674
magnitudes of three new VV Cephei, absolute, (E), 25:55680
mass exchange in early-type close binary, (T), 25:55690
mass losses in hot, radiation-pressure effects on, (T), 25:55712
mass of horizontal-branch, (E/T), 25:55708
metal abundances in R Cyg and HD 35155, iron-group and heavy, (E), 25:55699
model for Cepheids, radiative-transfer, (T), 25:55710
model for IRC + 10216, (E), 25:55686
models for β Cephei, (T), 25:55688
nuclear reaction rates in, $^{28}Si(\alpha,\gamma)$ and $^{16}O(\alpha,\gamma)$, (E), 25:55704
observations of variable, (T), 25:55674
opacity in, (T), 25:55685
period of eclipsing binary TY Puppis, (E), 25:55675
period of variable, (T), 25:55674
photometry and spectral classification of OB, in region LF 5, (E), 25:55788
photometry of central, in bright condensation in NGC 2175, (E), 25:55681
physical characteristics of B-type, (E), 25:55701
pulsations of β Cephei, nuclear-energized, (T), 25:55688
radiative processes in, (T), 25:55685
rotation of, effects on Schoenberg--Chandrasekhar limit, (T), 25:55684
silicon burning in, (E), 25:55703
spectra of late-type, infrared, (E/T), 25:55698
spectra of three new VV Cephei, emission, (E), 25:55680
spectra of, interstellar absorption lines in, (E), 25:55717
spectral analysis of HD 49798, (E), 25:55682
spectral redshifts in superdense, 25:55808
velocities of 85 southern O and B, radial, (E), 25:55697

STEAM
corrosive effects on graphite, 25:57092(R) (ORNL-TM-3483)
$H_2O$--steam, density in tubular channels under adiabatic and heated conditions, (E), 25:57032
$H_2O$--steam, flow and heat transfer characteristics of, in multirod coolant channels, (E), 25:54870(R) (GEAP-10347)

STEAM POWER PLANTS
cost estimates for single unit, computer program for calculation of conceptual, 25:57063 (ORNL-TM-3276)
environmental effects of, estimate of potential, 25:57098

STEEL
analysis for silicon by fast neutron activation, 25:54519
corrosion by liquid sodium of tool, 25:57109 (ANL-7771)
crack arrest toughness of A533B, at -70 to 100°F, 25:55513
fracture of A533B, gross strain crack tolerance studies on, 25:55514
fracture of thick-section ASTM A533B, effects of mechanical constraint on, 25:55512
fracture toughness of A302B and A533, relations between stress intensity and microscopic strength, (T), 25:55503
fracture toughness of ASTM A533B, to 550°F, 25:55517
fracture toughness properties of heavy-section plates and arc weldments of A533B class 1, 25:55516
mechanical properties of pressure vessel, effects of microstructure changes on, 25:55466
neutron reflection from 6-in.-thick slab of, orders-of-scattering calculation of collimated polyenergetic fast-, 25:56257 (COO-2049-8)
neutron reflection from shielding slabs of, fast-, (E/T), 25:56258 (COO-2049-9)
properties of prestressing wires of, for use in concrete reactor pressure vessels, 25:55422
radiation effects on adhesion of epoxy cemented specimen couples of, gamma, 25:55666
radiation effects on Charpy-V performance and dynamic tear of plates and weld deposits of ASTM A533B, neutron, 25:55586
radiation effects on ductile-to-brittle transition temperature of thick-wall pressure vessel, neutron, 25:55588
radiation effects on fracture and tensile properties of A533B pressure vessel, fast neutron, 25:55587
radioinduced embrittlement of Types A302B and A533B, effects of impurity copper and phosphorus on neutron, 25:55577 (NRL-7310)
role of short fine wires of, for reinforcing concrete, 25:55662
welds in thin-walled tubes of, ultrasonic inspection of butt, 25:54928
Mn--Mo--Ni--steel, radiation effects on brittleness and strength of heavy-section plates and welds of, fast neutron, 25:55585

STELLAR WIND
radiation pressure effects in, (T), 25:55712

STEROIDS
effectiveness of nandrolon decanoate, combined with radiation for treatment of human tumors, 25:55303

STORAGE RINGS
beam collisions and crossings in Orsay, space charge effects in, 25:56592 (LAL-RT-43-70)
beam injection into, charge-exchange method for proton, 25:56590(T) (LA-tr-71-46)
development and operation of ACO, Sept. 1970, 25:56591 (LAL-RT-42-70)

STREPTOMYCIN
effects on mutation induction in uv irradiated Escherichia coli, 25:55189

STRESS
conference on analysis of, Fourth International, Cambridge, Eng., April 6 to 10, 1970, 25:54846
relaxation in in-pile materials, deformation model for analysis of uniaxial, 25:55579 (WAPD-TM-943)

STRONTIUM
alpha fission at 167 MeV, angular distributions and particle track lengths for, (E), 25:56806
determination in barium minerals by atomic absorption spectroscopy, 25:54413
determination in fission product mixtures by ion exchange and β counting, 25:54449
determination in rocks, chemical methods for, 25:54403
determination in sediments of Rhine River basin by x-ray fluorescence, 25:54408
determination of trace amounts of, in high-purity acids by emission spectrography, 25:54431
diffusion in glass, effects of temperature on, 25:55611
effects on radiolysis of crystalline potassium nitrate, 25:54638
effects on strontium-85 sorption by man, 25:55109 (COO-1231-67)
preparation using countercurrent electrophoresis, 25:54742
release from bonded beds of BISO-coated uranium dioxide particles during post irradiation annealing at 1250°C, 25:55647 (ORNL-4717, pp 83-90)
separation from magnesium on titanium tungstate papers by electrochromatography, 25:54744
separation from milk, double-bed ion exchange process for, 25:54722
separation from other alkaline earths by ionophoresis on filter paper and poly(vinyl alcohol), 25:54725
separation of uranium from, in methyl sulfoxide by cation exchange chromatography, 25:54728
sorption by soils, effects of soil exchange sites on differential, 25:54778
sorption on cation exchanger from strong acid in presence of iron, calculation of kinetics of, 25:54720 (UJV-2550-Ch)

STRONTIUM FLUORIDES
positron lifetimes in, empirical model for calculation of, 25:55834

STRONTIUM HAFNATES
thermal conductivity at high temperatures, 25:55637

STRONTIUM ISOTOPES
determination in rocks, methods and standards for, 25:54757(R) (MIT-1381-18)

STRONTIUM ISOTOPES Sr-85
decay of isomeric, beta--gamma branching ratio for, (E), 25:56722
effectiveness for diagnosis of human hypertrophic osteoarthropathy, 25:55298
effectiveness for scanning human sacroiliac joints in ankylosing spondylitis, 25:55287
energy levels from yttrium-85 decay, spin--parity assignments for, (E), 25:56722
metabolism in man following intravenous and oral administration, effects of calcium intake on, 25:55109 (COO-1231-67)
sorption by man, effects of lactose, lysine, stable strontium, and vitamin D on, 25:55109 (COO-1231-67)

STRONTIUM ISOTOPES Sr-87
alpha reactions (α,d) at 25 MeV, angular distributions for, (E), 25:56779
effectiveness of metastable, for diagnosis of human hypertrophic osteoarthropathy, 25:55298
helium-3 reactions (He-3,d) at 18 MeV, angular distributions for, (E), 25:56779

STRONTIUM ISOTOPES Sr-88
helium-3 reaction (He-3,t) at 23 MeV, analysis for reaction mechanism in, (E), 25:56779
shell-model analysis of isovector excitations in, (T), 25:56827 (LYCEN-7104, S8.1-10)

STRONTIUM ISOTOPES Sr-89
content in petroleum, following production stimulation by contained nuclear explosion, (E/T), 25:54826(T) (UCRL-Trans-10543, pp 99-116)
content ratio to strontium-90 in fallout, method for determining, 25:54803
distribution in man following ingestion, effects of calcium phosphate, methionine, Prussian blue, and sodium alginate on, 25:55113
effects on mice following chronic ingestion, tumorigenic, 25:55319 (UCD-472-118)

STRONTIUM ISOTOPES Sr-90
content in Antarctic snow cores, 1955 and 1964 measurements of, 25:54788
content in liquid radioactive waste effluents from Nuclear Fuel Services West Valley reprocessing plant, 25:54753
content of blood plasma in beagle dogs following prolonged ingestion, 25:55319 (UCD-472-118)
content of fish in Sweden, calculation of, 25:55156
content of hybrid wheat seeds in relation to phenotype, 25:55223
content ratio to strontium-89 in fallout, method for determining, 25:54803
determination of, use of ion exchange in methods for, 25:54397
distribution in man following ingestion, effects of calcium phosphate, methionine, Prussian blue, and sodium alginate on, 25:55113
effects on erythrocytes of beagle dogs, protective effects of hydrogen peroxide against, 25:55319 (UCD-472-118)
performance as beta source for neutralization of electrically charged flour, 25:54897
sorption by man, effects of calcium on, 25:55109 (COO-1231-67)
toxicity to animals, extrapolation to man of data for long-term, 25:55319 (UCD-472-118)
uptake by organisms of marine food chain, effects of physico-chemical form on, 25:55149 (BNWL-SA-4048)
uses as radiation source, development of market for, 25:54887(R) (BNWL-1308-6)
STRONTIUM PHOSPHATES
radioinduced paramagnetic centers in doped crystals of, EPR and annealing of gamma, 25:56339
STRONTIUM SULFATES
radioinduced paramagnetic centers in doped crystals of, EPR and annealing of gamma, 25:56339
STRONTIUM ZIRCONATES
thermal conductivity at high temperatures, 25:55637
STRUCTURAL BEAMS
creep strains in concrete, time-temperature extrapolation analysis of, 25:55663
STRUCTURES
fluid containment between walls of, design of device for, 25:54860(P)
STYRENE POLYMERS
preparation of blocks of, to correct for surface irregularities during tumor radiotherapy, 25:55244
radioinduced graft polymerization with lignin, γ, 25:54614
SUCCINATE DEHYDROGENASE
radiation effects on activity of in vitro rat liver, x, 25:55128
SUCROSE
effects on calcium-45 uptake and release by rat brain microsomes, 25:55120
SUGARS
radiation effects on content in processed garlic bulbs, γ, 25:55354
radiolysis of, rate constants for hydrogen atom reactions following electron, 25:55132
SULFATES
determination in water by precipitation with barium-133, radiometric, 25:54443
effects on corrosion of transition metals in alkali metal sulfate melts, 25:55373 (CONF-690452-, Paper 6)
effects on radiolysis of crystalline potassium nitrate, 25:54638
SULFUR FLUORIDES
effects on yields from radiolysis of butane, 25:54659
SULFUR IONS
implantation in gallium phosphide, gallium arsenide, and germanium at 20 and 40 keV, 25:56288
SULFUR ISOTOPES
determination of abundance of, in sulfur compounds, 25:56752(R) (SUNI-14)
SULFUR ISOTOPES S-32
deuteron reactions (d,p) at 13.8 MeV, vector analyzing power for polarized, (E), 25:56724
helium-3 reactions (He-3,pγ) at 8.00 to 9.00 MeV, proton spectrum and p--γ angular correlations in, (E), 25:56712
proton elastic and inelastic scattering at 5 to 14 MeV, analysis of reaction mechanism in, (E), 25:56694
SULFUR ISOTOPES S-33
deuteron reaction (d,p) at 12 MeV, angular distributions and Q-value for, (E), 25:56730
energy levels from phosphorus-31 (He-3,p) reactions, γ decay properties of isobaric analog, (E), 25:56715
energy levels from resonances in silicon-29 (α,n) reactions, spin assignments for, (E), 25:56752(R) (SUNI-14)
SULFUR ISOTOPES S-34
energy levels from sulfur-33 (d,p) reactions, spectroscopic factors for, (E), 25:56730
SULFUR ISOTOPES S-35
radioactivity of, liquid scintillators for absolute measurement of, 25:54697
SULFUR ISOTOPES S-37
energy levels from argon-40 (n,α) reactions, (E), 25:56718
SULFURIC ACID
proton transfer reactions in aqueous, effects of deuterium on, 25:54564
radiolysis of sulfuric acid solutions of, reactivity of tetravalent cerium from γ, 25:54647
SUN
activity of, effects on geophysical parameters of upper atmosphere, (E), 25:55981
boundary conditions at, effect on solar flare particles propagation and density in interplanetary space, (T), 25:55738
constant of, compilation of recent measurements, (T), 25:55742
cycle of 1959-1967, variations of interplanetary-space parameters during, (E), 25:55992
eclipse of Sept. 22, 1968, effect on ionosphere as observed at two stations, (E), 25:56000
helium abundance of, (E/T), 25:55751
neutrino production in, (E/T), 25:55741
radio emission at 2980 MHz, absolute calibration of flux density of, (E), 25:55756
radio emission from, (E), 25:55736
rotation of, streamlines from Doppler velocities in differential, (T), 25:55745
spectra between 12 and 24 μ, (E), 25:55739
spectra of, classification of highly ionized iron and nickel lines in euV, (E), 25:55774
spectra of, high-resolution extreme-ultraviolet, (E), 25:55740
spectral analysis of, (E/T), 25:55750
temperature of, effective, (T), 25:55742
x-ray emission from, (E), 25:55736
SUNSPOTS
fibrils near, topology of filaments and chromospheric, (E), 25:55749
SUPERCONDUCTIVITY
magnetic flux line heat transport and core fermion polarization, 25:56088
SUPERCONDUCTORS
cavity--vortex interaction in Type-II, (T), 25:56091
cooling of hollow, supercritical helium, (E/T), 25:56122
critical current of perfect Type-II, in mixed state, 25:56092
current of Type-II, maximum normalizing, (T), 25:56069
current-induced intermediate state in Type-I, structure of, (E/T), 25:56102
electron--phonon coupling parameter lambda for, model calculation of, 25:56106
fluxon motion and nucleation in, single, (E/T), 25:56098
hysteresis losses in hard, polygonal-section, 25:56101
magnetic flux line profiles derived from Tewordt's generalized Ginzburg--Landau functional, oscillatory, (T), 25:56070
nucleation field H/sub c4/ of, angular dependence of, (T), 25:56065
order parameter near T/sub c/ in, healing length of, (T), 25:56080
performance in lumped-parameter oscillator circuit, 25:55086
preparation by granule metallurgy, evaluation of, 25:55404
properties of micro-junctions near critical temperature, effect of external fluctuations on, 25:56090
relaxation processes in, kinetic equations for, 25:56093
sound excitation in Josephson junction, (T), 25:56089
theory of inhomogeneous, near T/sub c/, 25:56083
transitions at H/sub c1/ and H/sub c2/ in Type-II, first-order, (T), 25:56082
uses for energy storage and switching, 25:56110 (LA-DC-12990)
uses in electric power systems, 25:56114
uses in high-energy physics, 25:56116
uses of, in British industry, 25:56115
vortex flow in, with paramagnetic impurities, 25:56086
vortex interactions in Type-II, near T/sub c/, (T), 25:56081
SUPERFLUIDITY
Bose--Einstein condensation in one and two dimensions, possible existence of, 25:56049
energy gap of $^3P_2$ pairing in neutron-star matter, properties of anisotropic, (T), 25:55714
hydrodynamics of Bose fluid in terms of action-angle variables in quantum statistics, 25:56051
SUPERNOVA REMNANTS
W44, absorption of OH in direction of, (E), 25:55716
SURFACE WATERS
plutonium movement in, 25:55150 (CONF-710401-, pp 407-10)
SURFACES
chemistry of, research progress on, 25:54587(R) (AECL-3909)
effects of artificially roughened, on incipient boiling of sodium, (E), 25:54868(T) (EURFNR-897)
friction factor for rough, estimation from pressure distribution measurements in flow around roughness element, 25:54873 (RD/B/N-1967)
plutonium contamination levels for, based on radiation dose to humans, 25:55195 (CONF-710401-, pp 352-64)
SURRY POWER REACTOR, UNIT 1
buildings and structures for, safety analysis of earthquake stresses on, 25:56949 (DOCKET-50280-46)
construction of, request for continuing permit for,


XUM

25:56952 (DOCKET-50280-49)
coolant loss accident conditions in, safety analysis of, 25:56949 (DOCKET-50280-46)
cooling system for, inspection of Type 304 and Type 316 stainless steel weld joints in, 25:56948 (DOCKET-50280-45)
operations incidents in, response characteristics during, 25:56951 (DOCKET-50280-48)
piping systems of, performance of stainless steel welds in, 25:56950 (DOCKET-50280-47)
piping systems of, safety analysis of earthquake stresses on, 25:56949 (DOCKET-50280-46)
pumps for, qualification test of prototype vertical induction motor for containment recirculation spray, 25:56949 (DOCKET-50280-46)
SURRY POWER REACTOR, UNIT 2
buildings and structures for, safety analysis of earthquake stresses on, 25:56949 (DOCKET-50280-46)
construction of, request for continuing permit for, 25:56952 (DOCKET-50280-49)
coolant loss accident conditions in, safety analysis of, 25:56949 (DOCKET-50280-46)
operations incidents in, response characteristics during, 25:56951 (DOCKET-50280-48)
piping systems of, performance of stainless steel welds in, 25:56950 (DOCKET-50280-47)
piping systems of, safety analysis of earthquake stresses on, 25:56949 (DOCKET-50280-46)
pumps for, qualification test of prototype vertical induction motor for containment recirculation spray, 25:56949 (DOCKET-50280-46)
SWEDEN
strontium-90 content of fish in, calculation of, 25:55156
SWINE
promethium-147 metabolism in, in comparison to metabolism in man, 25:55108 (BNWL-SA-3747)
radiation effects on survival of, following bilateral and unilateral exposures, comparison of LD-50 for mixed fission neutron and γ, 25:55334
radioisotope retention and excretion by preccaries, following ingestion of debris from Schooner Event, 25:55124
SWITCHES
properties of superconducting, 25:56110 (LA-DC-12990)
SWITZERLAND
radiation monitoring in atmosphere of, 1969, 25:54791
SYMMETRY GROUPS
nuclear structure in, lectures on, 25:56838 (UR-875-350)
SL(2,C), representations as functions of eigenvalues of Casimir operators for, 25:56534 (KFKI-71-38)
SU(3) x SU(3) chiral breaking in phenomenological Lagrangians for meson interactions, 25:56533 (IFA-FT-85)
SU(3) x SU(3) chiral breaking terms in effective Lagrangian model for form factors of K → π + l + ν decay, 25:56537 (JINR-E2-5996)
SU(3) x SU(3) chiral Lagrangian model for two-meson production in anti p + p s- and p-wave interactions at rest, gauge-invariant, 25:56538 (ORO-3992-2)
SU(3) x SU(3) chiral, breaking parameter in hard-meson current algebraic tree-graph theory for, 25:56535 (ORO-3992-7)
SU(3) x SU(3), scalar meson masses in broken chiral, 25:56539 (ORO-3992-11)
SU(n), para-Fermi operators of order n for construction of generators of, 25:56536
Yang--Mills theories in higher, divergences of massive, 25:56542 (CNRS-CPT-71/P-378)
SYMMETRY GROUPS SU(3)
mass formulas in, classification of heavy octet hyperons from, 25:56540
mass formulas in, prediction of Ξ properties from, 25:56540
SYNCHROCYCLOTRONS
beam shape in center of, effects of acceleration voltage and magnetic field decay on, 25:56585 (JINR-P9-5945)
data acquisition system for Harwell, direct-access multi-user computer, 25:56612
experimental facility for 660-MeV, collector system for isotope separator, 25:56584 (JINR-P6-5888)
SYNCHROTRONS
beam injection system for JINR proton, performance of debuncher in, 25:56586 (JINR-P9-5956)
control system for proton, computer-based high-voltage, 25:56597 (SJC-A-71-3)
experimental facility at ITEP proton, for radiation therapy, 25:56581(T) (BNL-tr-442)
synchrotron radiation from Bonn 2.5-GeV electron, 25:56587 (JUL-748-PP)
SYSTEMS FOR NUCLEAR AUXILIARY POWER (SNAP)
design parameters for 600 kW(t) zirconium hydride moderated, reference, 25:57132 (AI-AEC-Memo-12715(Del.))
shielding for zirconium hydride reactor, Monte Carlo calculations for lithium hydride and tungsten, 25:57133 (ORNL-TM-3366)
SYSTEMS FOR NUCLEAR AUXILIARY POWER (SNAP-19)
heat sources for, design and fabrication of plutonium-238, 25:54893 (MLM-1736)
thermoelectric generator for, design and parametric safety studies of, 25:54895 (SC-RR-710353)

# T

T-111 (TANTALUM ALLOY)
corrosion by mercury at 1200°F, 25:55377 (N-71-26947)
TACHYONS
mass and width of complex-spin negative-mass-squared, in angular distributions of π + N charge-exchange interactions at 5.9 to 18.2 GeV/c, (T), 25:56500 (ORO-3992-18)
mass and width of negative-mass-squared, in π⁻ + p → π⁰ + n interactions at 5.9 to 18.2 GeV/c, (T), 25:56499 (ORO-3992-8)
production of complex-spin negative-mass-squared, in angular distributions of π + N charge-exchange interactions at 5.9 to 18.2 GeV/c, (T), 25:56500 (ORO-3992-18)
production of negative-mass-squared, in π⁻ + p → π⁰ + n interactions at 5.9 to 18.2 GeV/c, interpretation of angular distribution for, (T), 25:56499 (ORO-3992-8)
quantum field theory for, 25:56560
TANTALUM
analysis for nitrogen by fast neutron activation, 25:54501
argon-ion reactions at 30 keV with surfaces of, charge states and kinetic energies of scattered and recoil ions from, (E), 25:55818
casting by levitation melting using magnetic field, 25:55424
coating with zinc-plated aluminum silicide, corrosion protection by, 25:55398(P)
determination in rocks, chemical methods for, 25:54403
determination in volcanic ash by neutron activation and γ spectrometry, 25:54513
deuteron reactions at 80 MeV with foils of, cross sections for electron capture in, (E), 25:55862
effectiveness of powdered, as contrast medium for radiography of upper respiratory mucosa, 25:55291
effects on properties and sintering of tungsten at 1000 to 2000°C, 25:55453
emissivity at 4000 to 40000 A and 1200 to 2400°K, spectral, 25:55495
proton reactions at 155 and 600 MeV with foils of, cross sections for electron capture in, (E), 25:55862
radiation damage in discontinuous films of, electric conductivity and annealing of 30°K 150-keV proton, 25:56314
separation from pegmatitic ores, leaching studies for, 25:54752
sorptive properties for carbon monoxide, flash--mass spectrometric study of, 25:55441
thermal capacity at 1900 to 3000°K, pulse-heating method for measurement of, 25:55494
thermoelastic response of, Grueneisen coefficient for, 25:55436 (SC-RR-710314)
TANTALUM ALLOYS AND SYSTEMS
coating with zinc-plated aluminum silicide, corrosion protection by, 25:55398(P)
Fe--Ta, thermodynamic properties of intermetallic $TaFe_2$, 25:55508
Hf--Ta, hardening in monocrystals of, at 77 to 2000°K, solid-solution, 25:55457
Hf--Ta-base, oxidation behavior of polycrystals and single crystals of, at 750 to 1050°C, 25:55397
Mo--Ta, hardening in monocrystals of, at 77 to 2000°K, solid-solution, 25:55457
Mo--Ta--Ti, phase studies of, 25:55565
N--Ta, electric conductivity of films of, effects of glow discharge on, 25:55519
Nb--Ta, hardening in monocrystals of, at 77 to 2000°K, solid-solution, 25:55457
Re--Ta, hardening in monocrystals of, at 77 to 2000°K, solid-solution, 25:55457
Ru--Ta, hardening in monocrystals of, at 77 to 2000°K, solid-solution, 25:55457
Ru--Ta, thermionic properties of, relations with ruthenium content, 25:56350
Ta--Ti, elastic properties of, effects of composition and phase characteristics on, 25:55446
Ta--W, hardening in monocrystals of, at 77 to 2000°K, solid-solution, 25:55457
Ta--W, oxidation of single and polycrystals of, at 850 to 1100°C, 25:55385
TANTALUM BORIDES
stability in acids, 25:54543
TANTALUM CARBIDES
grain growth in liquid-phase sintering of, 25:55642
physical properties and stability to nitrogen, 25:55629
wetting by copper, effects of electronic structure on, 25:55643
TANTALUM IONS
effects on void production in vanadium at 7.5 MeV, 25:55573 (BNWL-SA-3962)
TANTALUM ISOTOPES Ta-181
energy-level transition in, calculation of γ circular polarization using parity-nonconserving potential, (T), 25:56768
energy-level transition in, nuclear current parameter for internal conversion of 6.21-keV, 25:56797
neutron elastic scattering at 7 MeV, S-matrix analysis of

XUM

differential cross sections for, (T), 25:56789
TANTALUM NITRIDES
physical properties of, 25:55629
TANTALUM OXIDES
ion implantation in anodic, 25:54587(R) (AECL-3909)
TARAPUR POWER REACTOR
radioactive effluents from, distribution of, 25:56978
TASTE
radiation effects on threshold of rat, low dose x, 25:55322
TD-NICKEL
mechanical properties of, at high temperatures, 25:55483
oxidation reactions of, kinetic studies on, 25:55387
strength of powder shapes of, effects of dispersion-, grain boundary-, and solid solution-hardening on, 25:55487
strengthening of, effects of substructure domain on dispersion, 25:55492
tensile strength at 1093°C, effects of thermomechanical processing on, 25:55486
TD-NICKEL CHROMIUM
production and properties of, for use in space shuttle, literature survey on, 25:55399 (N-71-27008)
strengthening of, effects of substructure domain on dispersion, 25:55492
TECHNETIUM
abundance in R Cyg and HD 35155, (E), 25:55699
determination in aqueous solutions from fuel reprocessing, standard for colorimetric, 25:54429
reactions with molten lithium perchlorate, Raman spectral studies on compounds produced by, 25:54538
TECHNETIUM ISOTOPES Tc-93
energy levels from molybdenum-92 (d,n) reactions, spectroscopic factors and spin--parity assignments for, (E), 25:56766
TECHNETIUM ISOTOPES Tc-95
energy levels from molybdenum-94 (d,n) reactions, spectroscopic factors and spin--parity assignments for, (E), 25:56766
TECHNETIUM ISOTOPES Tc-99
effectiveness of albumen-incorporated metastable, for scanning pulmonary arteries in patients with pulmonary hypertension, 25:55284
effectiveness of macroaggregated human serum albumin- and sulfur colloid-incorporated metastable, in combination with gamma camera for diagnosis of human lung embolism, 25:55296
effectiveness of sulfide-incorporated metastable, for diagnosis of human pericardial effusion, 25:55295
effects of metastable, on thyroid antibody production in children, immunofluorescent tests on, 25:55292
preparation of sulfur colloid macroaggregate-incorporated metastable, for human lung scanning, method for, 25:55297
production of metastable, by beta decay of molybdenum-99 and solvent extraction, 25:54675
use of metastable, for brain scanning in diagnosis of neurological disorders, role of prescanning cerebral angiography and pneumography in, 25:55281
use of metastable, for estimating late x radiation effects on circulation in brain, liver, lungs, and skin of rats, 25:55328
TEETH
radiography of human, clinical effectiveness of neutron, 25:55277
TEKTITES
analysis for tin by neutron activation using 40-min tin-123, 25:54480
analysis of Australian, by neutron activation, 25:54478
TELEMETERING SYSTEMS
design for wildlife research, 25:57266 (RLO-1929-16)
TELLURIC ACID
neutron reactions (n,γ) with tellurium-128 in, iodine-129 Moessbauer studies of recoil tellurium-129 reactions in, 25:54704
tellurium-125 Moessbauer spectral study of recoil effects in, 25:56381
tellurium-129m isomeric transition in, iodine-129 Moessbauer studies of chemical effects in, 25:54704
TELLURIUM
alpha fission at 167 MeV, angular distributions and particle track lengths for, (E), 25:56806
analysis for chlorides, photometric, 25:54407
analysis for trace amounts of copper by complexing with Bengal Rose and phenanthroline, spectrophotometric, 25:54414
determination by ultraviolet spectrophotometry, 25:54400
determination in fission product mixtures by ion exchange and polarography or β counting, 25:54449
determination in magnesium--silicon master alloys by gravimetry, 25:54416
determination in rocks, chemical methods for, 25:54403
neutron reactions (n,γ) with tellurium-128 in, iodine-129 Moessbauer studies of recoil tellurium-129 reactions in, 25:54704
radiation damage in, annealing recovery of 10°K 0.6- and 1-MeV-electron,, 25:56306
separation from selenium by solvent extraction using Bismuthiol II, 25:54724
sorption on nickel, 25:54587(R) (AECL-3909)
tellurium-129m isomeric transition in, iodine-129 Moessbauer studies of chemical effects in, 25:54704
TELLURIUM ISOTOPES Te-123
neutron reactions (n,α) at resonance energies, α widths and resonance spin assignments for, (E/T), 25:56754(T) (UCRL-Trans-10541)
TELLURIUM ISOTOPES Te-124
energy levels at 1156 and 2020 keV from iodine-124 decay, 0+, (E), 25:56781
energy-level transitions from iodine-124 decay, K-conversion coefficients and multipolarities for, (E), 25:56781
TELLURIUM ISOTOPES Te-125
Moessbauer spectra in telluric acid and sodium hydrogen tellurate, 25:56381
TELLURIUM ISOTOPES Te-126
energy levels at 1396 and 1685 keV from iodine-126 decay, 0+, (E), 25:56781
energy-level transitions from iodine-126 decay, K-conversion coefficients and multipolarities for, (E), 25:56781
TELLURIUM ISOTOPES Te-129
chemical state of recoil, in solid tellurium--oxygen compounds, iodine-129 Moessbauer studies of, 25:54704
isomeric transition in tellurium--oxygen compounds, iodine-129 Moessbauer studies of chemical effects of, 25:54704
TELLURIUM OXIDES
neutron reactions (n,γ) with tellurium-128 in, iodine-129 Moessbauer studies of recoil tellurium-129 reactions in, 25:54704
tellurium-129m isomeric transition in, iodine-129 Moessbauer studies of chemical effects in, 25:54704
TEMPERATURE
book:Tables for Calculating Nonstationary Temperatures of Plane Bodies During Heating by Irradiation, 25:56267
distribution in semi-infinite medium under transient thermal conditions, methods for calculating space--time, 25:54876 (RT/ING-(71)11)
measurement of, by x-ray diffraction analysis of defect annealing in irradiated diamonds, 25:55104
TERBIUM
determination in fission product mixtures by ion exchange and β counting, 25:54449
determination in river water and seawater by neutron activation and radiochemical separation, 25:54504
determination in volcanic ash by neutron activation and γ spectrometry, 25:54513
lattice parameters of, effects of hydrogen on, 25:55549
TERBIUM ALLOYS AND SYSTEMS
Au--Tb, crystal structures and melting points of intermetallic, 25:55570
TERBIUM ISOTOPES Tb-159
ion elastic scattering in wide energy range, phase shift analysis of angular distributions for, (E), 25:56740 (JINR-P7-5884)
TERPHENYL
boiling of high-boiling-point, critical heat transfer in, 25:54879
TESTES
radiation effects on function of bull, tonometer measurements on x, 25:55337
TEXAS
uranium deposits in, occurrence of, 25:54804
THALLIUM
determination by radiometric oxidimetric titration, 25:54448
determination in isoquinoline formate by polarography, 25:54421
determination in standard rocks and quartzes by neutron activation and radiochemical separation, 25:54454
determination of trace amounts of, in silicate rocks by neutron activation and radiochemical separations, 25:54489
effects of vapors of, on hydrogen isotope exchange at 300 to 500°C, 25:54552
effects on radiolysis of crystalline potassium nitrate, 25:54638
effects on solvolysis of tert-butyl halides, Broensted correlation for, 25:54548
neutron resonance absorption in, self-shielding of, (E/T), 25:57196
THALLIUM ALLOYS AND SYSTEMS
La--Tl, magnetic impurities effect on superconducting intermetallic $LaTl_3$, 25:56109
Pr-base--Tl, phase diagram of, 25:55567
Pr-base--Tl, phase diagram of, thermodynamic analysis of, 25:55566
THALLIUM BROMIDES
krypton-atom reactions with, crossed-beam measurements of cross sections for dissociative ionization in, 25:55879
xenon-atom reactions with, crossed-beam measurements of cross sections for dissociative ionization in, 25:55879
THALLIUM ISOTOPES Tl-208
content in sand and clay soils, performance of airborne gamma spectrometer system for measuring, 25:54768
THALLIUM SULFATES
radiolysis of, yields of hydrogen peroxide from γ, 25:54646


XUM

THERMAL INSULATION
performance in helium atmosphere of metallic, 25:56890
THERMAL PROPERTIES
conference on thermophysical properties, fifth, Boston, Mass., Sept. 30 to Oct. 2, 1970, 25:55624
THERMIONIC CONVERTERS
book: Emissive Properties of Materials (Handbook), 25:56346
design of radioisotope-fueled, for lunar base power supply, 25:54905(P)
design parameters of heat pipe cooled fast reactor powered, for space vehicle power supplies, 25:57134
insulators for, radiation effects on trilayer sheath, 25:55096 (N-71-24635)
THERMODYNAMIC PROPERTIES
tables of, for metals during oxidation and chlorination, 25:54586
THERMODYNAMICS
conference on thermophysical properties, fifth, Boston, Mass., Sept. 30 to Oct. 2, 1970, 25:55624
THERMOELECTRIC CONVERTERS
design and parametric safety studies of SNAP-19, for Nimbus B/Agena system, 25:54895 (SC-RR-710353)
THERMOLUMINESCENCE
method for estimating age of ancient pottery, principles and uses of, 25:54764
THERMOMETERS
development of ultrasonic, for LMFBR systems, 25:55078(R) (NYO-3906-5)
THERMONUCLEAR EXPLOSIONS
fuel burnup in, fractional, 25:54827
THERMONUCLEAR REACTORS
design of toroidal traps R-0 and RT-2 with steady and hf magnetic fields, 25:56221
energy balance calculations for, 25:56222
fuel balance calculations for, deuterium--helium-3, 25:56215 (N-71-25526)
magnetic configurations with helical magnetic axis in toroidal, resonance effects in, (T), 25:56209(T) (CTO-764)
magnetic fields for, energy storage and switching with superconductors for, 25:56110 (LA-DC-12990)
plasma confinement and turbulent heating in toroidal, (E), 25:56127
plasma temperature profiles in D--T fueled, 25:56216 (NP-19014)
THERMOSPHERE
hydrogen content from June 1966 to Jan. 1967 in, temporal variations from in situ, (E), 25:55973
parameters of, ground-based and satellite observations of solar-activity effects on geophysical, (E), 25:55981
THICKNESS GAGES
calibration of radiometric, frequency-response, 25:55060(P)
design of radiometric, for measuring uniformity of wires, 25:55062(P)
development of airborne radiometric, for snow, 25:55065
THORITES
effects on geochemistry of thorium and uranium deposits in Vosges Mountains, 25:54807
THORIUM
complexes with salicylaldehyde, preparation and spectral properties of, 25:54539
compounds, analysis for trace impurities by neutron activation, separation processes, and γ spectrometry, 25:54518
content in river waters in Czechoslovakia, (E), 25:54774
deposition on stainless steel from ammonium sulfate solutions, 25:54673
determination in Australian tektites by neutron activation and gamma spectrometry, 25:54478
determination in basic and ultrabasic rocks by neutron activation, 25:54495
determination in rocks, chemical methods for, 25:54403
determination in volcanic ash by neutron activation and γ spectrometry, 25:54513
distribution between bismuth--lead eutectic and MSBR fuel solvent, reductive extraction, 25:54534 (ORNL-4717, pp 43-56)
effects on solvolysis of tert-butyl halides, Broensted correlation for, 25:54548
electron band structure of, calculations for 5f states, 25:56388
fuel cycle for high temperature pebble bed reactor, analysis of multizone core configuration for optimum economic, 25:57060 (JUL-736-RG)
magnetic impurities effect on superconducting, 25:56109
preparation of sources of, for alpha spectrometry, 25:54673
separation from cerium and zirconium by reverse-phase partition chromatography on TTA-impregnated paper, 25:54746
separation from rare earth phosphors by precipitation as iodates, 25:54749(P)
separation of trace amounts of, from carbonate solutions by sorption on metal hydroxides, review on, 25:54734
separation of uranium from, in methyl sulfoxide by cation exchange chromatography, 25:54728
solubility in liquid bismuth--lithium systems, 25:54712 (ORNL-4682, pp 1-38)
THORIUM ALLOYS AND SYSTEMS
C--Ru--Th, phase studies of, 25:55640
Cu--Th, phase diagram and intermetallic compounds, 25:55571
THORIUM BROMIDES $ThBr_4$
complexes with N-substituted ureas, preparation and properties of, 25:54536
THORIUM CHLORIDES $ThCl_4$
complexes with N-substituted ureas, preparation and properties of, 25:54536
THORIUM DEPOSITS
geochemistry of Vosges Mountain, effects of thorite and zircon on, 25:54807
THORIUM FLUORIDES $ThF_4$
$BeF_2$--LiF--$ThF_4$, liquidus temperature of, 25:54534 (ORNL-4717, pp 43-56)
$BeF_2$--LiF--$ThF_4$, plutonium trifluoride solubility and absorption spectra in molten, effects of oxide on, 25:54532 (ORNL-4717, pp 1-27)
$BeF_2$--LiF--$ThF_4$--$UF_4$, separation of protactinium from molten, by oxide precipitation, 25:54712 (ORNL-4682, pp 1-38)
$BeF_2$--LiF--$ThF_4$--$UF_4$, separation of uranium from molten, by oxide precipitation, 25:54712 (ORNL-4682, pp 1-38)
$CeF_3$--$ThF_4$, phase studies in, 25:54532 (ORNL-4717, pp 1-27)
LiF--NaF--$ThF_4$, phase equilibria in, high-temperature, 25:54532 (ORNL-4717, pp 1-27)
THORIUM HIGH-TEMPERATURE REACTOR
pressure vessel for, design and stress analysis for, 25:56884
pressure vessel for, effects of helium on thermal insulation of, (E), 25:56890
pressure vessel for, elastic stresses near penetrations in, (E/T), 25:56887
pressure vessel for, stress load testing of models of, 25:56888
THORIUM ISOTOPES Th-222
photofission at 90 MeV, liquid-drop-model calculations of heavy-fragment masses in, (T), 25:56787
THORIUM ISOTOPES Th-228
energy level transitions from actinium-228 beta decay, (E), 25:56747(T) (ORNL-tr-2531)
THORIUM ISOTOPES Th-230
alpha fission at 25.7 and 29.5 MeV, analysis using renormalized Fermi gas model and collective potential energy surface, (T), 25:56856
content ratio to uranium-234 in fossil corals, accuracy of age estimates from, 25:54776
distribution in Pacific Ocean, 25:54810
THORIUM ISOTOPES Th-232
abundance in Galaxy, (T), 25:55781
alpha fission at 20 to 34 MeV, cross section and delayed neutron yields for, (E), 25:56803
alpha fission at 26.4 MeV, liquid-drop analysis of, (E/T), 25:56786
content in fossil corals, effects on accuracy of thorium-230/uranium-234 method for age estimation, 25:54776
heavy-ion reactions with, light-element yields from, (E), 25:56788
helium-3 fission at 20 to 34 MeV, cross section and delayed neutron yields for, (E), 25:56803
neutron fission at 14 MeV, liquid-drop-model calculations of heavy-fragment masses in, (T), 25:56787
neutron fission at 14.1 MeV, angular distributions for, (E), 25:56804
proton fission at 20 to 85 MeV, fission yield and charge dispersion in, (E), 25:56805
THORIUM OXALATES
thermal decomposition of hexahydrate of, thermogravimetric and differential thermal analysis studies of, 25:54544
THORIUM OXIDES $ThO_2$
analysis for uranium using Arsenazo III, spectrophotometric, 25:54420
defects in single crystals of, thermoluminescence study of electronic, 25:56315
desintering of sol-gel, 25:55594 (ORNL-4682, pp 218-28)
electric conductivity of yttrium oxide-doped solid electrolytes of, at 1200 to 1400°K, 25:56335
neptunium ion EPR spectrum in single crystals of, 25:56383
preparation of spheres of, by sol-gel process, 25:54716 (ORNL-4682, pp 133-43)
radiation effects on thermoluminescence of, 25:54587(R) (AECL-3909)
spectra of, color center identification in, 25:54587(R) (AECL-3909)
$ThO_2$--$UO_3$, preparation of spheres of, by sol-gel process, 25:54716 (ORNL-4682, pp 133-43)
Cu--$ThO_2$, production of plates, rods, sheets, and wires of high-conductivity high-strength, description of process for, 25:55417
Mo--Ni-base--$ThO_2$, tensile strength at 1093°C, effects of thermomechanical processing on, 25:55486
Ni--$ThO_2$, production of fine powders of, Microgel process for, 25:55419
$P_2O_5$--$ThO_2$--$ZrO_2$, phase studies on subsolidus equilibrium in, 25:55638
$ThO_2$--$UO_2$, preparation of spheres of, by sol-gel process, 25:54716 (ORNL-4682, pp 133-43)
THULIUM
determination in river water and seawater by neutron

XUM

activation and radiochemical separation, 25:54504
lattice parameters of, effects of hydrogen on, 25:55549
THULIUM ALLOYS AND SYSTEMS
Al--La--Tm, crystal field levels of La/sub 1-x/Tm/sub x/Al$_2$, (E), 25:56359
Au--Tm, crystal structures and melting points of intermetallic, 25:55570
THULIUM ISOTOPES Tm-167
use for bone scanning, 25:55279
THULIUM ISOTOPES Tm-170
beta decay of, β-γ angular correlations and matrix elements for nonunique first-forbidden, (E), 25:56776
THULIUM OXIDES
analysis for calcium by nondestructive alpha activation, 25:54522
THYMIDINE
effects of tritium-labeled, on cell renewal patterns of rat liver cells and spleen lymphocytes, 25:55110(R) (TID-25801)
radiation effects on incorporation of, into DNA of cultured rat thymus cells, factors affecting x, 25:55127
THYMINE
radioinduced free radicals in single crystals of, γ, 25:55130
THYROID GLAND
effects of functional state of, on strontium-85 sorption by man, 25:55109 (COO-1231-67)
radioinduced carcinoma in human, following iodine-131 therapy, 25:55343
radioisotope detection in, during surgery, miniaturized scintillation detector for, 25:55018
scanning of young human, using technetium-99m, immunofluorescent tests on antibody production following, 25:55292
scintiscanning of human, computer method for quantitative evaluation of, 25:55282
TIN
determination in geochemical and cosmochemical material by neutron activation using 40-min tin-123, 25:54480
determination in yttrium oxide by emission spectrometry, 25:54419
magnetic flux states of superconducting cylinders of, quantized, (E), 25:56064
phonon generation in superconducting, by ac Josephson effect, (E), 25:56073
separation of uranium from, in methyl sulfoxide by cation exchange chromatography, 25:54728
superconducting Josephson junctions of, generalized weak links in externally shunted, (E/T), 25:56094
superconducting transition temperature and effective interaction strength in, volume dependence, 25:56103
TIN ALLOYS AND SYSTEMS
Ag--Sn, superconductivity in hcp phases of, (E), 25:56096
Al--Cu--Fe--Sn--Ti-base--V, development and evaluation of high-strength, 25:55421
Al--Mo--Sn--Ti-base--Zr, welding of, properties of joints produced by friction, 25:55409
Al--Mo--Sn--U-base, tensile properties of dilute, at 23 to 600°C, 25:55429 (CEA-R-4177)
Al--Sn--Ti, mechanical properties of hot pressed powders of, for cryogenic uses, 25:55482
Au--Sn, superconductivity in hcp phases of, (E), 25:56096
Bi--Cd--Sn, electric transport of tin isotopes in 300°C melts of, 25:56349
In--Sn, phase diagrams of, relations with property--composition diagrams, 25:55546
La--Sn, magnetic impurities effect on superconducting intermetallic LaSn$_3$, 25:56109
La--Sn, magnetic properties of LaSn$_3$, NMR and susceptibility, 25:56353
Nb--Sn, fabrication of laminated superconducting Nb$_3$Sn, 25:56079(P)
Nb--Sn, niobium-93 in Nb$_3$Sn, 25:56373
Nb--Sn, phase transition in Nb$_3$Sn, neutron-scattering study of lattice-dynamical, 25:55545
Nb--Sn, phonon frequencies and susceptibility of Nb$_3$Sn, (T), 25:56344
Nb--Sn, superconducting critical current of intermetallic Nb$_3$Sn, effect of carbon on, 25:56084
Sn--Zn, diffusion in molten, kinetics of mutual, 25:55449
TIN ISOTOPES
electric transport in tin--bismuth--cadmium melts at 300°C, 25:56349
TIN ISOTOPES Sn-112
proton elastic scattering at 30.4 MeV, differential cross sections for, (E), 25:56764
TIN ISOTOPES Sn-114
proton elastic scattering at 30.4 MeV, differential cross sections for, (E), 25:56764
TIN ISOTOPES Sn-116
proton elastic scattering at 30.4 MeV, differential cross sections for, (E), 25:56764
proton reactions at high energies, isobar model for analysis of meson (π) production in, 25:56530
TIN ISOTOPES Sn-118
deuteron elastic and inelastic scattering at 13.6 MeV, strong-coupling analysis of, (T), 25:56780
proton elastic scattering at 30.4 MeV, differential cross sections for, (E), 25:56764
TIN ISOTOPES Sn-119
nuclear magnetic resonance in LaSn$_3$, 25:56353
TIN ISOTOPES Sn-120
neutron elastic scattering at 7 MeV, S-matrix analysis of differential cross sections for, (T), 25:56789
proton elastic scattering at 9.6 MeV, S-matrix analysis of differential cross sections for, (T), 25:56789
proton elastic scattering with isobaric analog excitation, shell-model analysis of, (E/T), 25:56769
TIN ISOTOPES Sn-122
proton elastic scattering at 30.4 MeV, differential cross sections for, (E), 25:56764
TIN ISOTOPES Sn-124
proton elastic scattering at 30.4 MeV, differential cross sections for, (E), 25:56764
proton elastic scattering with isobaric analog excitation, shell-model analysis of, (E/T), 25:56769
TISSUES
alpha-particle energy loss and straggling in tissue-equivalent gas, (E/T), 25:56279
analysis for trace metals by neutron activation, development of nonmetallic tools for sampling in, 25:54450 (TID-25773)
analysis of animal, for aluminum by separation and neutron activation, 25:54514
analysis of rat adipose, for chlorobiphenyl by neutron activation and radiochemical separation, 25:54500
effectiveness of γ-irradiated bovine fascia, for transplantation in dog brains for filling of defects in dura mater, 25:55148
radiation dosimetry of pelvic, for standardization of pendular cobalt-60 γ therapy, 25:55222
radiation effects on human, use of additional treatment with iron and steroid preparations for reducing therapeutic, 25:55303
radiation injuries to goat, pathology of γ, 25:55318(T) (LB/G-2995)
radioisotope distribution in, of uranium mining personnel, 25:55117
radiosensitivity of host and tumor, methods for altering, 25:55265
TITANIUM
abundance in solar atmosphere, (E/T), 25:55750
alpha reactions with, production of chromium-51 by, 25:54691
alpha reactions with, production of vanadium-48 by, 25:54677
analysis for nitrogen by fast neutron activation, 25:54501
casting by levitation melting using magnetic field, 25:55424
coating with zinc-plated aluminum silicide, corrosion protection by, 25:55398(P)
determination in stony meteorites by proton activation, 25:54466
deuteron reactions with, production of vanadium-48 by, 25:54677
diffusion of carbon in solid solutions of beta, 25:55479
diffusion of hydrogen in, at 450 to 600°F, effects of stress on, 25:55476
distribution coefficient of impurity of, in zirconium, measurement of, 25:55502
effects on properties and sintering of tungsten at 1000 to 2000°C, 25:55453
electric conductivity of, temperature dependence of, 25:55445
fabrication and tensile properties of composites, parts, and preforms of powder metallurgy, 25:55415
neutron reactions with, secondary gamma radiation in shielding from, 25:56277
proton reactions with, production of vanadium-48 by, 25:54677
separation from niobium by vacuum melting, 25:55403
separation of uranium from, in methyl sulfoxide by cation exchange chromatography, 25:54728
surface wetting of molten, on boron nitride, mechanisms of, 25:55469
thermoelectric properties of, at 0 to 1000°C, 25:56351
TITANIUM ALLOYS AND SYSTEMS
coating with zinc-plated aluminum silicide, corrosion protection by, 25:55398(P)
porosity of, effects of annealing and crystallization on micro-, 25:55462
preparation by granule metallurgy, evaluation of, 25:55404
Al--Co--Cr--Mo--Ni-base--Ti, fabrication of powdered, powder metallurgy and thermomechanical processes for, 25:55416
Al--Co--Cr--Mo--Ti--W, stress relaxation and surface hardening in, effects of high temperatures on, 25:55439
Al--Cr--Ni-base--Ti, corrosion by molten vanadium oxide, effects of chlorides, oxides, and sulfides of sodium on, 25:55375 (CONF-690452-, Paper 8)
Al--Cr--Ni-base--Ti, mechanical properties of dispersion-strengthened, at high temperatures, 25:55483
Al--Cu--Fe--Sn--Ti-base--V, development and evaluation of high-strength, 25:55421
Al--Fe--Ti, mechanical properties at 550 to 1100°C, 25:55501

XUM

Al--Fe--Ti, phase studies of, 25:55501
Al--Mo--Sn--Ti-base--Zr, welding of, properties of joints produced by friction, 25:55409
Al--Mo--Ti--V, corrosion cracking of, review on methods and problem of hot-salt stress, 25:55383
Al--Mo--Ti--V, diffusion of hydrogen in, at 450 to 600°F, effects of stress on, 25:55476
Al--Mo--Ti-base, embrittlement of two-phase, mechanisms of, 25:55450
Al--Sn--Ti, mechanical properties of hot pressed powders of, for cryogenic uses, 25:55482
Al--Ti, inflammability correlation of powdered, 25:55473
Al--Ti--V, corrosion cracking of, review on methods and problem of hot-salt stress, 25:55383
Al--Ti--V, fabrication and tensile properties of composites, parts, and preforms of powder metallurgy, 25:55415
Al--Ti--V, mechanical properties at 550 to 1100°C, 25:55501
Al--Ti--V, mechanical properties of hot pressed powders of, for cryogenic uses, 25:55482
Al--Ti--V, microstructure and properties of pressure-sintered powders of, 25:55413
Al--Ti--V, phase equilibria and properties along TiAl--$V_3Al_2$ section, 25:55537
Al--Ti--V, phase studies of, 25:55501
Al--Ti--V, properties of thin-film diffusion brazed joints in, corrosion, mechanical, and metallurgical, 25:55477
Al--Ti--V, sintering of powdered, electrically-activated pressure method for, 25:55413
Al--Ti-base--V, tensile properties of, effects of oxygen additions on, 25:55471
Al--Ti-base--V, welding of, properties of joints produced by friction, 25:55409
C--Co-base--Ti--W, mechanical properties of heat-treated, 25:55497
Cr--Ti-base, superconductivity and constitution of, 25:56108
Fe-base--Ti, stability of aluminum oxide dispersions in, at high temperatures, 25:55485
H--Ti--Zr, inflammability correlation of powdered, 25:55473
Hf--Nb--Ti--Zr, superconducting properties of, with, 25:56104
Mn--Ti, inflammability correlation of powdered, 25:55473
Mo--Ta--Ti, phase studies of, 25:55565
Mo--Ti, deformation mechanisms in, effects of temperature on, 25:55455
Mo--Ti-base, deformation of, effects of strain rate and temperature on, 25:55459
Nb--Ti, strengthening by step-aging, relations with microstructure, 25:55490
Nb--Ti--W--Zr, solidus volume of, simplex-lattice method for prediction of, 25:55529
Nb--Ti--Zr, phase studies of, 25:55564
Nb--Ti-base, superconductivity and constitution of, 25:56108
Nb--Ti-base, superconductivity of, relations with crystal structure, 25:55541
Nb-base--O--Ti, structure and tensile properties of, 25:55521
Nb-base--Ti, magnetization properties of superconducting, transporting sinusoidal alternating current in longitudinal magnetic field, (E/T), 25:56085
Ta--Ti, elastic properties of, effects of composition and phase characteristics on, 25:55446
Ti--V, tensile properties of, effects of oxygen additions on, 25:55471
Ti--V, thermodynamic interaction parameters in solid solutions of, Knudsen effusion--mass spectrometric study of, 25:55489
Ti--Zr, inflammability correlation of powdered, 25:55473
Ti-base--V, superconductivity and constitution of, 25:56108

TITANIUM BORIDES
stability in acids, 25:54543
wear resistance of deposited, on steels, 25:55619

TITANIUM CARBIDES
physical properties and stability to nitrogen, 25:55629
wetting by copper, effects of electronic structure on, 25:55643
Ni--TiC, grain growth in liquid-phase sintering of, 25:55642

TITANIUM CARBONITRIDES
preparation and properties of cemented, 25:55629

TITANIUM CHLORIDES
titanium nitride preparation from, chemical reactions for pyrolytic, 25:55605

TITANIUM ISOTOPES Ti-45
energy levels from phosphorus-31 (O-16,pnγ) reactions, lifetimes and transition probabilities for, (E), 25:56693
energy-level transitions from scandium-45 (p,nγ) reactions, internal conversion coefficients for, (E), 25:56693

TITANIUM ISOTOPES Ti-46
electron elastic scattering at 60 to 120 MeV, differential cross section for, (E), 25:56701
nuclear charge density from electron elastic scattering, (E), 25:56701

TITANIUM ISOTOPES Ti-48
deuteron elastic and inelastic scattering at 13.6 MeV, strong-coupling analysis of, (T), 25:56786
deuteron elastic scattering at 13.6 MeV, optical-model analysis of angular distributions from, (T), 25:56725
deuteron reactions (d,p) at 13.6 MeV, distorted-wave analysis of differential cross sections for, (T), 25:56725
electron elastic scattering at 60 to 120 MeV, differential cross section for, (E), 25:56701
nuclear charge density from electron elastic scattering, (E), 25:56701

TITANIUM ISOTOPES Ti-49
energy levels from titanium-48 (d,p) reactions, spectroscopic factors for, (T), 25:56725

TITANIUM ISOTOPES Ti-50
electron elastic scattering at 60 to 120 MeV, differential cross section for, (E), 25:56701
nuclear charge density from electron elastic scattering, (E), 25:56701

TITANIUM NITRIDES
physical properties of, 25:55629
production from titanium tetrachloride, chemical reactions for pyrolytic, 25:55605

TITANIUM OXIDES
abundance in atmospheres of late-type stars, (E/T), 25:55698

TOKAMAK DEVICES
design with superposed multipole magnetic fields, (T), 25:56211 (IPP-III-2)
plasma conductivity in T-3, mathematical model for, 25:56162 (CEA-CONF-1801)
plasma heating by increasing longitudinal magnetic field, (T), 25:56125
plasma heating by turbulence in, research on ohmic, (E), 25:56123(R) (ORO-4087-1)
plasma instabilities in, review of, 25:56198
plasma instabilities in, trapped-particle, (T), 25:56195 (JAERI-Memo-4483)

TOKAMAK MODEL ST
magnetic fields in, spatial determination of direction of, 25:56223
plasma conductivity in, mathematical model for, 25:56162 (CEA-CONF-1801)

TOURMALINES
analysis for aluminum, calcium, iron, lithium, magnesium, manganese, and sodium by deuteron activation analysis and γ counting, 25:56752(R) (SUNI-14)
analysis for boron in, by measurement of prompt proton spectra from (d,p) reactions, 25:56752(R) (SUNI-14)

TRACE ELEMENTS
uptake by organisms in marine food chains, effects of physico-chemical form on, 25:55149 (BNWL-SA-4048)

TRACER TECHNIQUES
summary of life sciences, since 1946, 25:55107
use of phosphorus-32, for measuring velocity of moving thread, 25:54900
uses of krypton-85, for studying atmospheric diffusion of plumes and puffs, 25:54908

TRANSACTINIDE ELEMENTS
production by nuclear reactions, chemical problems in, 25:54672

TRANSFERASES
reactions with pyridoxal-5-phosphate, fluorescence properties of products of, 25:57264(R) (ORO-3553-17)

TRANSITION METAL ALLOYS AND SYSTEMS
bond forces in d-intermetallic compounds, (T), 25:56386
Ga--transition metals--V, properties of ternary phases of, 25:55500
rare earths--transition metals, preparation by heat treatment of amalgams of, 25:55401(T) (RFP-Trans-87)

TRANSITION METAL CARBIDES
physical properties and stability to nitrogen, 25:55629
solubility and solid-phase reactions with copper and nickel at 1000 to 1200°C, 25:55464

TRANSITION METAL NITRIDES
physical properties of, 25:55629

TRANSITION METALS
binding energies of 5d atoms adsorbed on 5d, tight-binding calculations, 25:56385
corrosion by eutectic alkali metal sulfates, effects of polarization on, 25:55373 (CONF-690452-, Paper 6)

TRANSPORT THEORY
Boltzmann equation in spherical geometry and spherical symmetry, method for numerical solution of linear position-dependent, 25:56617 (JUL-765-RG)
discrete ordinates calculations in, quadrature variations in, 25:56278
discrete ordinates method for anisotropically scattering multiplying particles in subcritical slab, convergence of, 25:56264 (ORNL-TM-3553)
radiative transfer in, computational method for X and Y functions in, (T), 25:55676
radiative transfer, analytically solvable problems in, 25:56270

TRANSURANIUM ELEMENTS
bibliography on, First Quarter 1971 index to, 25:55369
purification of TRU product, 25:54671 (ORNL-4682, pp 114-32)
storage of waste, site operation at NRTS for, 25:54965 (CONF-710401-, pp 365-8)

TRANSURANIUM PROCESSING PLANT
operation of, 25:54671 (ORNL-4682, pp 114-32)
TRIBENZYLAMINE
solvent properties for antimony, arsenic, and gold, 25:54515
TRIFLUPROMAZINE
effects on whole-body mixed gamma and neutron irradiated rats, 25:55325
TRITIUM
abundance in targets aboard Soyuz space probes, (E), 25:55902
accumulation by marine phytoplankton, mechanisms of, 25:55154
content in liquid radioactive waste effluents from Nuclear Fuel Services West Valley reprocessing plant, 25:54753
content in moderator graphite from MSRE core, 25:54533 (ORNL-4717, pp 29-41)
decay to helium for studies of radiation effects in metals, 25:55575 (LA-DC-12996)
determination in biological and environmental samples, facility for low-level, 25:55003 (UCRL-73128)
determination in water by scintillation counting, standard for, 25:54447
distribution in neuronal and glial-enriched fractions of brain following in vitro and in vivo administration of leucine-incorporated, 25:55119
effects of thymidine-incorporated, on cell renewal patterns of rat liver cells and spleen lymphocytes, 25:55110(R) (TID-25801)
effects on benzene synthesis by water reaction with calcium carbide, 25:54735
exchange in molten fluoroborates, 25:54534 (ORNL-4717, pp 43-56)
exchange with deuterium between m-carborane and tert-butanol, ethanol, or liquid ammonia in metal alkoxide-catalyzed reactions, primary kinetic isotope effects in, 25:54555
helium-3 reactions (He-3,γ) at 0.5 to 20 MeV, angular distributions for, (E), 25:56646
helium-3 reactions (He-3,γ) at 9 to 26 MeV, differential cross section for, (E), 25:56664
incorporation in polypeptides, development of catalytic method for, 25:54693(P)
injection into metals, design of cathode for, 25:54858
radiation effects on exchange reactions of, with ethane, 25:54727
reactions of recoil atoms of, with cyclohexane, yields of alkanes from, 25:54685
reactions of recoil atoms of, with gaseous ethane, deuterated methane, and neon, kinetics of, 25:54684
reactions of recoil, with methane and silane system, 25:54678
use for radioimmunoassay of prostaglandins in blood plasma of rabbits, 25:55144
TRITIUM SYSTEMS
D--T, burnup in thermonuclear explosions, fractional, 25:54827
D--T, energy balance calculations for fusion reactor conditions, 25:56222
TRITONS
binding energy of, calculation using boundary-condition model, 25:56851
binding energy of, effect on singlet effective-range parameters in calculations using Mongan separable potential, (T), 25:56859
TROJAN POWER REACTOR, UNIT 1
construction of, effects on environment of, 25:56963 (DOCKET-50344-22)
operation of, effects on environment of, 25:56963 (DOCKET-50344-22)
TUBES
catalog of, tested at ORNL for use in water desalination equipment, 25:57247 (ORNL-TM-2713(Rev.1))
fluid flow through, convective heat transfer in axial turbulent, 25:54866 (EIR-198)
heat transfer in metal, containing boiling water, effects of pressure and surface roughness on, 25:54872 (JUL-740-RB)
heat transfer in slender straight, calculation of, 25:54885
TUNGSTEN
bubble formation in annealed, doped with aluminum, potassium, or silicon compounds, mechanisms and kinetics of, 25:55511
casting by levitation melting using magnetic field, 25:55424
crystallization of polycrystalline, effects of dislocation structure and deformation temperature on resistance to, 25:55558
deformation at 900 to 1700°K, effects of electrostatic fields on, 25:55451
determination in rocks, chemical methods for, 25:54403
effects on oxidation of niobium at 1500 to 2000°C and low pressures, 25:55380
electron reactions at 0.5 to 15 keV, optical radiation from, (E), 25:55813 (JINR-P4-5957)
erosion of sintered, in oil, design of equipment for measuring arc, 25:55454
impurity decomposition in, along grain boundaries, mechanisms of solid-solution, 25:55444
ion sputtering reactions with, secondary emission of W+ from alkali-metals, (E), 25:55819
mechanical properties of chemical vapor deposited rings of, design of apparatus for testing, 25:55440
microstructure of fracture surfaces in cast, effects of annealing and cold working on, 25:55542
neutron reactions at 10 to 30 GeV/c, total cross sections for, (E), 25:56421
oxidation at low pressures and high temperatures, steady-state nonequilibrium studies of, 25:55396
physical properties of plasma-sprayed spherical powders of, 25:55467
production of powdered, development of chloride process for, 25:55412
properties of powdered, produced from chloride process, 25:55412
properties of, effects of transition metal additions on, 25:55453
proton reactions at 1.5 to 4.5 MeV, optical radiation from, (E), 25:55813 (JINR-P4-5957)
separation from rhenium by solvent extraction, 25:54401
sintering at 1000 to 2000°C, effects of transition metal additions on, 25:55453
solubility in copper--nickel solid solutions in copper--nickel--tungsten alloys, limits of, 25:55447
sorptive properties for carbon monoxide, time-of-flight study of electron-stimulated, 25:55435 (RLO-2221-T-7-4)
sorptive properties for neodymium and ytterbium, heat of desorption of ions, 25:55533
welding of, evaluation and review of methods for, 25:55410
LiH--W, shielding properties of, calculation of, 25:57133 (ORNL-TM-3366)
TUNGSTEN ALLOYS AND SYSTEMS
welding of, evaluation and review of methods for, 25:55410
Al--Co--Cr--Mo--Ti--W, stress relaxation and surface hardening in, effects of high temperatures on, 25:55439
Al--Cr--Mo--Ni-base--W, fabrication of powdered, powder metallurgy and thermomechanical processes for, 25:55416
C--Co-base--Ti--W, mechanical properties of heat-treated, 25:55497
C--Co-base--W, mechanical properties of heat-treated, 25:55497
C--Hf--Re--W, mechanical properties of, 25:55433 (N-71-23982)
C--W, superconductivity of phases of, 25:56087
Co--Cr--Ni--W, physical properties of, effects of atomization media and consolidation methods on, 25:55480
Co--Fe--W, hardening of, kinetics of dispersion, 25:55423
Co-base--Cr--Mo--Nb--Ni--W, corrosion by molten vanadium oxide, effects of chlorides, oxides, and sulfides of sodium on, 25:55375 (CONF-690452-, Paper 8)
Cu--Ni--W, tungsten solubility in copper--nickel solid solutions of, limits of, 25:55447
Cu--W, preparation of composites of, by diffusion welding, 25:55405
Cu--W, thermal expansion of infiltrated pseudoalloys of, up to 1500°C, (E/T), 25:55468
Mo--Re--W, creep properties of, at 1800 to 4000°F, effects of grain size on, 25:55431 (N-71-23110)
Nb--Ti--W--Zr, solidus volume of, simplex-lattice method for prediction of, 25:55529
Ni--W-base, sintering of powdered dilute, effects of nickel content on, 25:55426
Re--W, phase composition of, at 1500 to 1900°C, effects of aluminum oxide coating on, 25:55465
Ta--W, hardening in monocrystals of, at 77 to 2000°K, solid-solution, 25:55457
Ta--W, oxidation of single and polycrystals of, at 850 to 1100°C, 25:55385
TUNGSTEN BORIDES
wear resistance of deposited, on steels, 25:55619
TUNGSTEN CARBIDES
production of cemented, from tungsten powders, 25:55412
properties of cemented, produced from tungsten powders, 25:55412
wetting by copper, effects of electronic structure on, 25:55643
Co--WC, composition and tensile properties of binder phase in, 25:55630
Co--WC, preparation of fine powdered mixtures of, using ultrasonic vibrations, 25:55598
Fe--Ni--WC, phase relations and tensile properties of sintered, 25:55631
Fe--WC, phase relations and tensile properties of sintered, 25:55631
TUNGSTEN ISOTOPES W-181
content in ground-level atmosphere in north Germany and north Norway during 1970 and 1971, (E), 25:54785
TUNGSTEN ISOTOPES W-182
Moessbauer effect in tungsten metal following Coulomb excitation by alpha particles, 25:56369
TUNGSTEN ISOTOPES W-183
Moessbauer effect in tungsten metal following Coulomb excitation by alpha particles, 25:56369


XUM

TUNGSTEN ISOTOPES W-184
Moessbauer effect in tungsten metal following Coulomb excitation by alpha particles, 25:56369
TUNGSTEN ISOTOPES W-186
Moessbauer effect in tungsten metal following Coulomb excitation by alpha particles, 25:56369
TUNNELS
planning and execution of Mt. Enasan, 25:57252(T) (ORNL-tr-2525)
TURBINES
design of carbon dioxide gas, for use with power reactor, 25:54856(P)
TZM (MOLYBDENUM ALLOY)
forgeability and tensile properties of powder metallurgy fabricated, 25:55418
radioinduced void production in, 5-MeV nickel ion, 25:55573 (BNWL-SA-3962)
Mo--TZM, deformation mechanisms in, effects of temperature on, 25:55455

## U

UDIMET 700
mechanical properties of sintered powder of, with particle boundary morphology, 25:55484
ULTRASONIC TESTING
method for inspection of butt welds in thin-walled tubes, 25:54928
method for pressure vessel nozzles, 25:54925
method for stainless steel and Zircaloy fuel cladding tubes, 25:54926
ULTRAVIOLET RADIATION
effects of solar extreme, on planetary luminosities, (T), 25:55766
effects on activity of ribonuclease, conformational changes associated with inhibitory, 25:55137
effects on bacteria in vacuo, mechanism of relation of dark repair to, 25:55356
effects on bacteriophage lambda, F' episomes, and Escherichia coli, role of DNA cross-links in sensitizing effects of psoralen on, 25:55361
effects on bacteriophage T4, recombination in mutant crosses following mutagenic, 25:55173
effects on branched alkane glasses, identification of free radicals from, 25:54648
effects on chemical, molecular biology, and physical processes in DNA, mechanism of, 25:55136
effects on Chlorella vulgaris, capacity for photoreactivation following mutagenic, 25:55172
effects on DNA and RNA synthesis in mouse kidney cells synchronized by medium change, 25:55129
effects on Escherichia coli, effects of 2,4-dinitrophenol on recovery from lethal, 25:55355
effects on HeLa cells following exposure of cytoplasm, nucleus, and whole cells, comparison of, 25:55312
effects on human skin, protective effects of polysiloxanes against, 25:55263
effects on incidence of adenine auxotrophic mutants in Bacillus subtilis, effects of aminopterin on, 25:55189
effects on incidence of adenine auxotrophic mutants in Escherichia coli, effects of streptomycin on, 25:55189
effects on incidence of dome mutants in Schizophyllum (mushroom), 25:55186
effects on Mycobacterium phlei, mutagenic, 25:55171
effects on N-acetylglycine in the presence of ammonia, 25:54650
effects on single- and double-strand breaks in DNA, mechanism of, 25:55308
effects on spontaneous recombination frequency of chromosomes of diploid yeast, 25:55180
effects on stability of silvered and aluminized FEP tefion second-surface mirrors, 25:55656 (N-71-27736)
effects on survival of Escherichia coli mutant, temperature dependence of recovery from, 25:55360
effects on survival of Escherichia coli, effects of dark-repair inhibitors and temperature on, 25:55357
effects on survival of yeast, effects of dehydration and vapor pressure on, 25:55183
effects on synthesis, of ribosomal precursor RNA in yeast, 25:55138
effects on thoria single crystals, electronic defects induced in, 25:56315
effects on thymineless death and liquid holding recovery in Escherichia coli, synergistic effects of phosphorus-32 on, 25:55359
effects on yeast, gene control of mutagenic, 25:55187
spectra of solar extreme-, (E), 25:55740
UNITED KINGDOM
irradiation facilities for commercial processing in, development of gamma, 25:55363
radioactivity monitoring in, derivation and use of reference levels and working limits as standards for, 25:55241
UNITED STATES
radiation accidents in, proposed registry for, 25:55250
UNIVERSE
gas density in, (E/T), 25:55806
gravitational instability in expanding, nonlinear theory of, (T), 25:55799
gravitational waves in closed, (T), 25:56570
opacity to high-energy cosmic photons, (T), 25:55908
structure of closed, detection of, (T), 25:55804
structure of, space--time, (T), 25:55802
URACIL, 5-BROMO-
radiosensitizing effects on Escherichia coli, effects of temperature on uv and x, 25:55357
URACIL, 5-FLUORO-
use for tumor cell cycle synchronization for improved efficiency of radiotherapy, 25:55306
URANIUM
analysis for hydrogen, design of instrument for, 25:54424
analysis of natural, for uranium-235 using hollow cathode discharge tube, spectrographic, 25:54435
analysis of nuclear grade, for rare earths at part per giga level by x-ray excited optical fluorescence, 25:54428
complexes with salicylaldehyde, preparation and spectral properties of, 25:54539
content in Japanese obsidian, (E), 25:54773
content in ores containing radon, gamma spectrometric measurements of, 25:54759
content in river waters in Czechoslovakia, (E), 25:54774
content in sand and clay soils, performance of airborne gamma spectrometer system for measuring, 25:54768
content in stratified uranium deposits, area-ratio method for determining, 25:54808
content in uranium deposits from Mizusawa area in Japan, (E), 25:54806
deposition on stainless steel from ammonium sulfate solutions, 25:54673
determination by controlled potential coulometry using rotated mercury cell, 25:54427
determination by dichrometric titration using triphenylmethane dyes as redox indicators, 25:54410
determination in basic and ultrabasic rocks by neutron activation, 25:54495
determination in isoquinoline formate by polarography, 25:54421
determination in rocks, chemical methods for, 25:54403
determination in thorium dioxide using Arsenazo III, spectrophotometric, 25:54420
determination in uranium minerals, γ spectrometric studies on uranium disintegration products following chemical treatment in, 25:54445
determination of, use of ion exchange in methods for, 25:54397
determination using benzoylacetanilide, spectrophotometric, 25:54423
determination using derivatography, extraction-photometric, and neutron activation methods, review on, 25:54734
diffusion in beta-zirconium films, 25:55498
oxidation of tetravalent to hexavalent, in hydrochloric acid, kinetic study of photosensitized, 25:54618
precipitation from molten halides using molten zinc cathode, 25:54580
preparation of sources of, for alpha spectrometry, 25:54673
preparation of trivalent, in hydrochloric, perchloric, and sulfuric acid solutions, 25:54540
processing of scrap, safeguards capabilities of materials accounting systems in facilities for, 25:54968 (IAEA-R-878-F)
production of enriched, Swedish studies on economics of, 25:54921
production of, corrosion of structural materials in, 25:55389
proton fission at 30 to 160 MeV, yields and charge dispersion of antimony from, (E), 25:56757
proton spallation at 5.5 GeV, yields of light elements in, (E), 25:56788
reactions in uranium nitrides in relation with nitrogen pressure and phase composition, vapor pressure studies on, 25:55617
reactions of tetravalent, with acetic acid or formic acid in aqueous benzene solutions, stability constants for complex ions produced by, 25:54581
separation from aqueous solutions as uranyl by solvent extraction using TTA, 25:54751
separation from bismuth on titanium tungstate papers by electrochromatography, 25:54744
separation from chromium, molybdenum, and tungsten by reverse-phase partition chromatography using TTA-impregnated paper, 25:54746
separation from fission products by fluorination process, 25:54736
separation from irradiated LMFBR fuel by solvent extraction using dibutyl butylphosphonate, 25:54706 (BNWL-SA-3345)
separation from MSBR fuel salt by oxide precipitation, 25:54712 (ORNL-4682, pp 1-38)
separation from other metals in methyl sulfoxide by cation exchange chromatography, 25:54728
separation from pegmatitic ores, leaching studies for, 25:54752
separation from phosphoric acid by solvent extraction, 25:54718 (ORNL-4682, pp 168-81)
separation from rhenium by solvent extraction, 25:54401
separation from seawater by adsorbing colloid flotation, 25:54738
separation of trace amounts of, from carbonate solutions

XUM

by sorption on metal hydroxides, review on, 25:54734
solidification of ingots of, mechanisms of, 25:55400 (NLCO-1077)
spectra of trivalent, in hydrochloric, perchloric, and sulfuric acid solutions, absorption, 25:54540
thermoelastic response of, Grueneisen coefficient for, 25:55436 (SC-RR-710314)

URANIUM ALLOYS AND SYSTEMS
analysis for hydrogen, design of instrument for, 25:54424
tensile properties of Sicral $F_1$, at 23 to 600°C, 25:55429 (CEA-R-4177)
Al--Mo--Sn--U-base, tensile properties of dilute, at 23 to 600°C, 25:55429 (CEA-R-4177)
C--N--O--Pu--U, preparation of carbides, carbonitrides, and hypostoichiometric oxides in, 25:55594 (ORNL-4682, pp 218-28)
C--Nb--U, phase diagram at 1000°C, carbide composition in, 25:55547
C--U--Zr, phase diagram at 950°C, carbide composition in, 25:55547
C--U--Zr, thermodynamic properties of, 25:55614
Mo--U, thermoelastic response of, Grueneisen coefficient for, 25:55436 (SC-RR-710314)

URANIUM BORIDES
physical properties of $UB_{12}$, 25:55622

URANIUM BROMIDES $UBr_4$
complexes with N-substituted ureas, preparation and properties of, 25:54536

URANIUM CARBIDES
compatibility with Type 304 stainless steel, evaluation by carbon transfer measurements, 25:55589 (JAERI-Memo-4438)
phase studies of, 25:55590(R) (EIR-192)
thermal capacity at 25 to 2790°C, 25:55626
PuC--UC, production of fuels of, development of process for, 25:55590(R) (EIR-192)

URANIUM CHLORIDES $UCl_4$
complexes with N-substituted ureas, preparation and properties of, 25:54536

URANIUM DEPOSITS
book: Essays on the Geology and Geochemistry of Ore Deposits, 25:54763
book: Prospecting for Uranium Deposits in Mountainous Taiga, 25:54805
distribution and formation of Mizusawa area, Japan, 25:54806
geochemistry of Vosges Mountain, effects of thorite and zircon on, 25:54807
occurrence in Texas, 25:54804
radium content of stratified, location of ore boundaries from gamma measurements of, 25:54808
uranium content of stratified, area-ratio method for determining, 25:54808

URANIUM FLUORIDES $UF_3$
disproportionation equilibria for dilute solutions of, in beryllium fluoride--lithium fluoride contained in graphite, 25:54532 (ORNL-4717, pp 1-27)

URANIUM FLUORIDES $UF_4$
$BeF_2$--LiF--$ThF_4$--$UF_4$, separation of protactinium from molten, by oxide precipitation, 25:54712 (ORNL-4682, pp 1-38)
$BeF_2$--LiF--$ThF_4$--$UF_4$, separation of uranium from molten, by oxide precipitation, 25:54712 (ORNL-4682, pp 1-38)

URANIUM FLUORIDES $UF_6$
equation of state of, at 99.1 to 320.3°C, use of constant-volume piezometric method for studying, 25:54582
shipping of, drop testing of 10-ton cylindrical containers for, 25:54970 (KY-631)

URANIUM ISOTOPES
content in USSR ground waters, effects of earthquakes on, 25:54775
separation of, review of new methods for, 25:54919

URANIUM ISOTOPES U-233
alpha decay of aligned, analysis of α angular distributions for, (E/T), 25:56749 (RCN-142)
neutron capture-to-fission ratios for, effects of EBR-II core position on, (E), 25:56982 (ANL-7791)
neutron fission of aligned, analysis of angular distributions for slow, (E/T), 25:56749 (RCN-142)
neutron fission of, liquid-drop-model calculations of heavy-fragment masses in thermal, (T), 25:56787
neutron fission of, prompt neutron yield from, (E), 25:56743 (NP-18966)
neutron fission of, yields from thermal, 25:54587(R) (AECL-3909)
storage and distribution of, 25:54716 (ORNL-4682, pp 133-43)

URANIUM ISOTOPES U-234
content ratio to thorium-230 in fossil corals, accuracy of age estimates from, 25:54776
distribution in seawater, 25:54810
energy levels from plutonium-238 alpha decay, (E), 25:56753 (UCRL-51087)

URANIUM ISOTOPES U-235
abundance in Galaxy, (T), 25:55781
alpha decay of aligned, analysis of α angular distributions for, (E/T), 25:56749 (RCN-142)
alpha reactions (α,2n) with, production of plutonium-237 by, 25:54674
content in highly enriched material, development of equipment for measuring, 25:55070(R) (BHO-67-2)
determination in human urine in presence of plutonium-239, radiochemical method for, 25:55197
determination in natural uranium using hollow cathode discharge tube, spectrographic, 25:54435
energy levels from plutonium-239 alpha decay, (E), 25:56753 (UCRL-51087)
neutron capture at 0.25 to 4 MeV with fission isomer excitation, excitation function for, (E), 25:56793
neutron capture-to-fission ratios for, effects of EBR-II core position on, (E), 25:56982 (ANL-7791)
neutron fission at 2 and 15 MeV, mass chain yield for, (T), 25:56816 (JAERI-Memo-4383)
neutron fission at 30 keV, time analysis of compound-nucleus decays in, (E), 25:56752(R) (SUNI-14)
neutron fission of aligned, analysis of angular distributions for slow, (E/T), 25:56749 (RCN-142)
neutron fission of, liquid-drop-model calculations of heavy-fragment masses in thermal, (T), 25:56787
neutron fission of, prompt neutron yield from, (E), 25:56743 (NP-18966)
neutron fission of, yields of light elements in thermal, (E), 25:56788
neutron reactions with, total γ spectrum above 1 MeV from, (E), 25:56745 (ORNL-4691)

URANIUM ISOTOPES U-236
energy levels from plutonium-240 alpha decay, (E), 25:56753 (UCRL-51087)

URANIUM ISOTOPES U-237
energy levels from plutonium-241 alpha decay, (E), 25:56753 (UCRL-51087)

URANIUM ISOTOPES U-238
abundance in Galaxy, (T), 25:55781
alpha fission at 20 to 34 MeV, cross section and delayed neutron yields for, (E), 25:56803
content in fossil corals, effects on accuracy of thorium-230/uranium-234 method for age estimation, 25:54776
content in highly enriched material, development of equipment for measuring, 25:55070(R) (BHO-67-2)
distribution in seawater, 25:54810
fission of isomeric, half-life for spontaneous, (E), 25:56801
fission of, delayed, (E), 25:56744(T) (NP-tr-1936)
helium-3 fission at 20 to 34 MeV, cross section and delayed neutron yields for, (E), 25:56803
ion elastic scattering in wide energy range, phase shift analysis of angular distributions for, (E), 25:56740 (JINR-P7-5884)
neutron capture below 600 eV, γ spectra and distribution of partial radiation widths in, (E), 25:56790
neutron capture-to-fission ratios for, effects of EBR-II core position on, (E), 25:56982 (ANL-7791)
neutron fission at 14 MeV, liquid-drop-model calculations of heavy-fragment masses in, (T), 25:56787
neutron fission at 14.1 MeV, angular distributions for, (E), 25:56804
neutron reactions with, total γ spectrum above 1 MeV from, (E), 25:56745 (ORNL-4691)
photofission at 35 MeV, liquid-drop-model calculations of heavy-fragment masses in, (T), 25:56787
photofission at 53 MeV, delay time for isomeric fission in, (E), 25:56801
proton reactions (p,xn) at 750 MeV, neutron spectrum unfolding capability for, (E), 25:55038 (LA-DC-12314)

URANIUM ISOTOPES U-239
energy levels from uranium-238 neutron capture, partial radiation widths for compound-nucleus, (E), 25:56790

URANIUM MINERALS
analysis for uranium, γ spectrometric studies on uranium disintegration products following chemical treatment in, 25:54445
distribution in igneous cumulates, use as indicator of mesostasis, 25:54809

URANIUM NITRIDES
photon reactions at 0 to 74 eV with UN, optical constants from, (E/T), 25:56345
reactions of uranium in, relations with nitrogen pressure and phase composition, vapor pressure studies on, 25:55617
thermal capacity at 25 to 2620°C, 25:55626

URANIUM ORE PROCESSING PLANTS
corrosion in, review of, 25:55389

URANIUM ORES
uranium content of, from Mizusawa area, Japan, (E), 25:54806

URANIUM OXIDES $UO_2$
mechanical properties of sintered, at room temperature, 25:55437(R) (TID-25784)
microstructure of sintered, 25:55437(R) (TID-25784)
physical properties of molten, measurement of high temperature, 25:57069(R) (ANL-7800)
preparation of sols of, by CUSP process, 25:55592 (ORNL-4682, pp 144-59)
preparation of spheres of, by sol-gel process, 25:54716 (ORNL-4682, pp 133-43)
preparation of uranium-233-enriched, process development and flowsheets for, 25:55593 (ORNL-4682, pp 163-7)
production of pellets of, relations of powder properties and process variables for, 25:55603
production of sols of, method for, 25:55590(R) (EIR-192)
radiation effects on bubble nucleation and re-solution

in, at high temperatures, fission and thermal neutron, 25:55649
radiation effects on fission gas release and swelling of clad pin-type fuels of, in-pile, 25:55648 (RCN-144)
radiation effects testing of BISO-coated particles of, release of cesium and strontium during annealing following, 25:55647 (ORNL-4717, pp 83-90)
radioinduced reactions with stainless steel, in-pile, 25:55648 (RCN-144)
reactions with fluorine and fluorine chlorides, kinetics of, 25:54736
reactions with liquid sodium of molten, 25:57069(R) (ANL-7800)
sorptive properties for nitric acid, 25:55594 (ORNL-4682, pp 218-28)
surface energy of, at 1500°C, 25:55616
thermal capacity at 25 to 3090°C, 25:55626
thermal conductivity during irradiation of, measurements of, 25:55647 (ORNL-4717, pp 83-90)
thermal conductivity of sintered pellets of, instrumented radiation target can for measuring, 25:55088
$Al_2O_3$--$Dy_2O_3$--$UO_2$, temperature distribution in irradiated fuels of, use of eutectic isotherm for monitoring, (E), 25:57194
Cu--$UO_2$, properties of, effects of stereometric microstructure on, 25:55628
Ni--$UO_2$, surface energy of, at 1500°C, 25:55616
$PuO_2$--$UO_2$, brittle-to-ductile transition temperature in blended fuels of, bend tests on, 25:55610
$PuO_2$--$UO_2$, dissolution rate of pellets of, 25:54713 (ORNL-4682, pp 39-79)
$PuO_2$--$UO_2$, physical properties of solid, measurement of high temperature, 25:57069(R) (ANL-7800)
$PuO_2$--$UO_2$, preparation by sol-gel process, 25:55592 (ORNL-4682, pp 144-59)
$PuO_2$--$UO_2$, preparation of enriched fuels of, method for safe and economical, 25:55597(P)
$PuO_2$--$UO_2$, preparation of powders of, 25:54717 (ORNL-4682, pp 160-2)
$PuO_2$--$UO_2$, radiation effects on fuel spheres of, at high burnups, 25:55590(R) (EIR-192)
$PuO_2$--$UO_2$, reactions of solid solutions of, with fluorine and fluorine chlorides, kinetics of, 25:54736
$ThO_2$--$UO_2$, preparation of spheres of, by sol-gel process, 25:54716 (ORNL-4682, pp 133-43)
URANIUM OXIDES $UO_3$
$ThO_2$--$UO_3$, preparation of spheres of, by sol-gel process, 25:54716 (ORNL-4682, pp 133-43)
URANIUM OXIDES $U_3O_8$
reactions with aluminum at 450°C, identification of phases in, 25:55609(T) (ORNL-tr-2456)
URANIUM SULFIDES
thermal capacity at 25 to 2725°C, 25:55626
thermodynamic properties of US, high-temperature, 25:54584
URANUS (PLANET)
luminosity of, relation to solar activity, (T), 25:55766
URANYL IONS
reduction in perchloric acid, disproportionation and ECE kinetics in, 25:54585
URANYL NITRATES
analysis for free acids, effects of solution age on, 25:54402
ion-exchange behavior of, effects of solution age on, 25:54402
UREA
complexes of N-substituted, with thorium and uranium tetrahalides, preparation and properties of, 25:54536
UREA, 1-METHYL-1-NITROSO-
effects on Mycobacterium phlei, mutagenic, 25:55171
URIDINE, 5-BROMO-2'-DEOXY-
effects on x radiosensitivity of synchronized cultures of Chinese hamster cells, 25:55258
URIDINE, 2'-DEOXY-5-IODO-
effects on renewal patterns of normal and tumor cells, 25:55110(R) (TID-25801)
URINE
americium-241 excretion in, of man following inhalation as oxide, effects of DTPA on, 25:55118
analysis for iodine by neutron activation and radiochemical separation, 25:54509
analysis for plutonium-239 and uranium-235 simultaneously, radiochemical method for, 25:55197
water recovery from human, design of spacecraft-carried radioisotope-heated distillation system for, 25:54911(P)

## V

VACUUM
measurement of ultrahigh, calibration of instruments for, 25:54992
VACUUM GAGES
development of hot-cathode ion, for use in magnetic fields, 25:56141
VALVES
design criteria for nuclear service, development program for, 25:57092(R) (ORNL-TM-3483)
design for Japanese boiling water reactors, 25:54842
VAN ALLEN RADIATION BELTS
electron intensity in outer, correlation patterns of magnetic activity and auroral activity with, (E/T), 25:55979
electron intensity of various energies and on different L shells in, exponential decrease of, (E), 25:55978
electron-flux profiles of pre-midnight asymmetry in outer, 40-keV, (E), 25:56045
formation of, from acceleration of near-Earth charged-particle bunches, (E/T), 25:56008
proton flux profiles near equator at L = 1.15 to 1.21 in 1967, 20 to 50, and greater than 100 MeV, (E), 25:55957
VAN DE GRAAFF ACCELERATORS
development and operation of RARAF, for radiological research, 25:55002 (NYO-2740-8, pp 7-146)
research and development at SUNI 5.5 MV, 25:56752(R) (SUNI-14)
VANADIUM
abundance in solar atmosphere, (E/T), 25:55750
coating with zinc-plated aluminum silicide, corrosion protection by, 25:55398(P)
de Haas--van Alphen frequencies for fields in (001) plane of single crystals of, (E/T), 25:56356
determination in magnetite by activation method, 25:54483
determination in rocks by activation and radiochemical separation, 25:54463
determination of trace amounts of, in high-purity acids by emission spectrography, 25:54431
deuteron reactions with, production of chromium-51 by, 25:54691
diffusion and internal friction of deuterium and hydrogen in, calculation from redistribution in periodic stress gradient, 25:55458
diffusion of carbon in solid solutions of, 25:55479
effects of additions of, on mechanical properties of ferritic iron and iron--vanadium alloys, 25:55478
preparation of high-purity, by molten salt electrorefining from carbothermic reduction of vanadium pentoxide, 25:55408
proton reactions with, production of chromium-51 by, 25:54691
radioinduced vacancies in, aggregate formation from laser-beam, 25:56313
radioinduced void production in, 7.5-MeV tantalum ion, 25:55573 (BNWL-SA-3962)
separation from rhenium by solvent extraction, 25:54401
separation of uranium from, in methyl sulfoxide by cation exchange chromatography, 25:54728
solvent properties for nitrogen at 300 to 1000°C, 25:55475
structure of thin films of, deposited on sapphire, epitaxy in, 25:55530
VANADIUM ALLOYS AND SYSTEMS
coating with zinc-plated aluminum silicide, corrosion protection by, 25:55398(P)
thermoelectric properties of, at 0 to 1000°C, 25:56351
Al--Cu--Fe--Sn--Ti-base--V, development and evaluation of high-strength, 25:55421
Al--Ge--V, phase formation in $V_3Al/sub\ x/Ge/sub\ 1-x/$ with A15 structure, 25:55539
Al--Mo--Ti--V, corrosion cracking of, review on methods and problem of hot-salt stress, 25:55383
Al--Mo--Ti--V, diffusion of hydrogen in, at 450 to 600°F, effects of stress on, 25:55476
Al--Ni--V, phase equilibria in intermetallic compounds of, 25:55562
Al--Ti--V, corrosion cracking of, review on methods and problem of hot-salt stress, 25:55383
Al--Ti--V, fabrication and tensile properties of composites, parts, and preforms of powder metallurgy, 25:55415
Al--Ti--V, mechanical properties at 550 to 1100°C, 25:55501
Al--Ti--V, mechanical properties of hot pressed powders of, for cryogenic uses, 25:55482
Al--Ti--V, microstructure and properties of pressure-sintered powders of, 25:55413
Al--Ti--V, phase equilibria and properties along TiAl--$V_3Al_8$ section, 25:55537
Al--Ti--V, phase studies of, 25:55501
Al--Ti--V, properties of thin-film diffusion brazed joints in, corrosion, mechanical, and metallurgical, 25:55477
Al--Ti--V, sintering of powdered, electrically-activated pressure method for, 25:55413
Al--Ti-base--V, tensile properties of, effects of oxygen additions on, 25:55471
Al--Ti-base--V, welding of, properties of joints produced by friction, 25:55409
Au--V, magnetic properties of, 25:56358
Co--Fe--V, magnetic properties at cryogenic temperatures, 25:56361
Fe-base--V, deformation and fracture at low temperatures, effects of vanadium content on, 25:55478
Ga--transition metals--V, properties of ternary phases of, 25:55500
Ga--V-base, properties of deformed superconducting, 25:56100
Hf--V, thermal capacity of superconducting intermetallic $HfV_2$, (E), 25:56072
Ru--V, phase transition of near-equiatomic, x-ray

XUM

diffraction study of cubic--tetragonal, 25:55532
Ti--V, tensile properties of, effects of oxygen additions on, 25:55471
Ti--V, thermodynamic interaction parameters in solid solutions of, Knudsen effusion--mass spectrometric study of, 25:55489
Ti-base--V, superconductivity and constitution of, 25:56108
V--Zr, thermal capacity of superconducting intermetallic $ZrV_2$, (E), 25:56072
VANADIUM BORIDES
stability in acids, 25:54543
VANADIUM CARBIDES
grain growth in liquid-phase sintering of, 25:55642
physical properties and stability to nitrogen, 25:55629
VANADIUM IONS
lattice sites in lithium fluoride and sodium fluoride crystals, calculation and x-irradiation effects, 25:56384
VANADIUM ISOTOPES V-48
production in cyclotron by α, deuteron, and proton reactions with chromium, scandium, or titanium, 25:54677
VANADIUM ISOTOPES V-51
neutron capture at 2.9 MeV, cross section for, (E), 25:56696
proton reactions (p,2p) at 600 MeV, separation-energy spectra and momentum distributions of residual nuclei from, (E), 25:56706
VANADIUM NITRIDES
physical properties of, 25:55629
VANADIUM OXIDES
abundance in atmospheres of late-type stars, (E/T), 25:55698
corrosive effects of melts of, on metals, relations with polarization, 25:55373 (CONF-690452-, Paper 6)
corrosive effects of molten, on nickel, mechanisms of, 25:55374 (CONF-690452-, Paper 7)
corrosive effects of molten, on superalloys, 25:55375 (CONF-690452-, Paper 8)
reduction of $V_2O_5$, to prepare high-purity vanadium, carbothermic, 25:55408
VANADIUM SILICIDES
magnetic susceptibility of $V_3Si$, (T), 25:56344
phonon frequencies of $V_3Si$, (T), 25:56344
VEGETABLES
potatoes, radiation processing of, equipment for gamma, 25:54837(P)
VESSELS
development of contactor, for reductive extraction reprocessing of molten salt fuels, 25:54712 (ORNL-4682, pp 1-38)
development of pulsed-clone contactor, 25:54719 (ORNL-4682, pp 229-39)
VITAMIN B GROUP
radioprotective effects on growth and survival of mice, x, 25:55268
VITAMIN D GROUP
effects on strontium-85 sorption by man, 25:55109 (COO-1231-67)
VOLCANIC ASH
analysis for trace elements by neutron activation and γ spectrometry, 25:54513


## W


WATER
abundance in atmospheres of late-type stars, (E/T), 25:55698
analysis for lanthanides by neutron activation and radiochemical separation, 25:54504
analysis for phosphorus-32 by Cherenkov radiation counting using liquid scintillation spectrometer, 25:54438
analysis for radioactive iodine as iodide and iodate by isotope exchange and scintillation counting, 25:54442
analysis for sulfates by precipitation with barium-133, 25:54443
analysis for tritium by scintillation counting, standard for, 25:54447
analysis of powdered residues of, by mass and uv absorption spectrometry, 25:54409
demineralization of reactor, by ion exchange, calculation and optimization of, 25:54737
diffusion in heated concrete, effects of pore pressure on, 25:55665
effects on plutonium sorption and reactions with soils, theoretical studies of, 25:54756 (CONF-710401-, pp 411-29)
effects on radiation chemical stability of crystalline sodium nitrate, 25:54649
electron reactions with, dependence of generalized oscillator strengths on momentum transfer in, (E), 25:55880
heat transfer by boiling, in metallic tubes, effects of pressure and surface roughness on, 25:54872 (JUL-740-RB)
heat transfer to high-pressure boiling, design and operation of loop for measuring, 25:54867 (EUR-4683)
mass transfer from sol droplets, 25:54719 (ORNL-4682, pp 229-39)
neutron diffusion constant and cooling coefficient for, calculation using modified classical monatomic gas model, (T), 25:56631
neutron reactions with, secondary gamma radiation in shielding from, 25:56277
neutron reflection from shielding slabs of, fast-, (E/T), 25:56258 (COO-2049-9)
neutron scattering in, computer program for analysis of thermal, 25:56638
radiation effects on distribution and permeability in frog muscle cells, x, 25:55323
radiation monitoring in environs of Ames Research Reactor during 1971, 25:55152 (IS-2658)
radioactivity monitoring in, review of current methods for, 25:54784
radiolysis of supercooled, yields from γ, 25:54663
radiolysis of, effects of temperature on absorption spectrum of hydrated electrons from electron, 25:54658
recovery from human urine, design of spacecraft-carried radioisotope-heated distillation system for, 25:54911(P)
separation of beryllium-7 from, by countercurrent electrophoresis, 25:54742
$D_2O$--$H_2O$, radiolysis of, isotopic separation factor for electron pulse, 25:54587(R) (AECL-3909)
$H_2O$--steam, density in tubular channels under adiabatic and heated conditions, (E), 25:57032
$H_2O$--steam, flow and heat transfer characteristics of, in multirod coolant channels, (E), 25:54870(R) (GEAP-10347)
WATER-$d_2$
analysis for hydrogen isotopes by specific gravity measurements, standard for, 25:54430
analysis for impurities by titration using potassium permanganate, standard for, 25:54405
effects on respiratory rate of rat brain slices, 25:55121
neutron diffusion constant and cooling coefficient for, calculation using modified classical monatomic gas model, (T), 25:56631
neutron scattering in, computer program for analysis of thermal, 25:56638
production by dual temperature process, stripping hydrogen sulfide from effluents for recycle in, 25:54918(P)
production by isotope exchange between ammonia and hydrogen, 25:54748
specifications for, as reactor moderator, standard for, 25:54529
thermal behavior of saturated, adiabatic calorimeter for studying, 25:55092
$D_2O$--$H_2O$, radiolysis of, isotopic separation factor for electron pulse, 25:54587(R) (AECL-3909)
WATER-t
analysis for tritium by scintillation counting, standard for, 25:54447
WATER-$t_2$
analysis for tritium by scintillation counting, standard for, 25:54447
monitoring in air, molecular sieve sampling method for, 25:54798
WATER VAPOR
effects on radioinduced reactions between carbon dioxide and graphite, 25:55654
WEISWEILER POWER REACTOR
development of, summary of program for, 25:57016
WELL LOGGING
equipment and method for gamma, for locating coal deposits, 25:54772
equipment and method for measuring neutron properties of material surrounding well bores, design of, 25:54769(P)
WELLS
control of runaway gas field, using contained underground nuclear explosions, 25:54825(T) (UCRL-Trans-10543, pp 81-98)
WEST VALLEY PROCESSING PLANT
design modifications of, seismic studies for, 25:54710 (DOCKET-50201-86)
operation for reprocessing of LMFBR fuel, feasibility of, 25:54713 (ORNL-4682, pp 39-79)
radioactive waste from, measurement of liquid, 25:54753
WHISTLERS
emission of magnetospheric triggered, effect of whistler-wave interaction with related resonating particles on, (E/T), 25:56038
relation of characteristics of, to spread F, (E), 25:55997
spectra of multicomponent and diffuse, associated with topside ionosphere ionization irregularities, (E), 25:55997
WHOLE-BODY COUNTERS
design and performance of Juelich, 25:55023
performance for determination of cesium-137 content of man, 25:55225
WINDOWS
materials for glove box, development of, 25:54939 (CONF-710401-, pp 17-25)
WIRES
thickness measurement of, radiometric gage for, 25:55062(P)


XUM

WYLFA REACTORS
pressure vessels for, prestressing and proof pressure testing of, (E/T), 25:56883
pressure vessels for, stresses in thermal insulation of, (E), 25:56889

# X

X RADIATION
detection of solar, OSO-V experiment for, (E), 25:55734 (N-71-23434)
detection of, design and performance of combined solar battery--scintillation detector for, 25:55005
detection of, performance of organic scintillators for, 25:55030
detection of, surface-barrier detector for, 25:55007(P)
dose distribution in man during radiography using single- and three-phase equipment, comparison of, 25:55227
dose to bone and muscle phantoms, use of tissue-equivalent organic scintillators in measurement of, 25:55213
dose to man in Japan from external occupational exposures, estimation of genetically significant equivalent, 25:55230
dose to medical personnel during cardiac catheterization procedure, 25:55226
dosimetry of 25- and 42-MV, in relation to tissue-maximum ratio, 25:55219
dosimetry using tissue-equivalent wall-less proportional detectors, 25:55002 (NYO-2740-8, pp 7-146)
effects on activity of NADP-dependent glyceraldehyde phosphate dehydrogenase in algae, effects of light on, 25:55353
effects on antigen retention system of mice, effects of injections of bone marrow, peritoneal exudate, spleen, or thymus cells on recovery from, 25:55147
effects on aqueous 2',4',5',7'-tetraiodofluorescein, 25:54664
effects on aqueous erythrosin, reaction mechanisms for lytic, 25:55139
effects on barley and wheat seeds, effects of ethylenimine on mutagenic, 25:55261
effects on cadmium ions in doped alkali-metal halide crystals, magneto-optical study of, 25:56320
effects on cardiovascular development in chick embryos, additive effects of hypothermia on, 25:55333
effects on cells of rat olfactory bulb, electron microscopy of, 25:55336
effects on cells, theory of dual action of, 25:55206 (NYO-2740-8, pp 147-219)
effects on chiasma frequency in grasshoppers, 25:55176
effects on chromosomes and mitoses in bone marrow of rats, single 800 R dose, 25:55192
effects on chromosomes in seeds of Crepis capillaris, effects of time of administration on additive or protective effects of ethylenimine on aberrant, 25:55260
effects on chromosomes of barley seeds, method for metaphase analysis of aberrant, 25:55175
effects on chromosomes of wheat seeds, effects of prolonged storage on aberrant, 25:55169
effects on circulation in brain, liver, lungs, and skin of rats following local exposure, use of radioisotopes for estimating late, 25:55328
effects on citrus fruits and peanuts, improved agricultural qualities in mutagenic, 25:55181
effects on compact traits of apples and pears, mutagenic, 25:55174
effects on cultured cells from hamster lung, daughter cell repair of lethal, 25:55311
effects on deuterated and normal glycine monocrystals at low temperature, ESR studies on, 25:54653
effects on developing ovaries of beagle dogs and monkeys following exposure in utero, effects of dose fractionation on sterilizing, 25:55319 (UCD-472-118)
effects on diploid yeast cells, lethal, 25:55165
effects on electrophoretic mobility of human lymphocytes, effects of phytohemagglutinin on, 25:55310
effects on enzyme activity and hematopoietic tissues in rat bone marrow, effects of dose on, 25:55330
effects on Escherichia coli, effects of 2,4-dinitrophenol on recovery from lethal, 25:55355
effects on function of bull testes, tonometer measurements on, 25:55337
effects on gastrointestinal tract of mice, effects of strain on protective effects of S-2-[3-aminopropylamino]ethylphosphorothioic acid against, 25:55259
effects on germination of radish seeds, effects of very high dose rate on RBE for inhibitory, 25:55350
effects on growth and survival of mice, protective effects of tetrahydrofolic acid against, 25:55268
effects on heredity of rats following repeated exposure over 13 generations, persistence of, 25:55164
effects on hexokinase activity in brain, erythrocytes, and liver of tumor-bearing rats, 25:55140
effects on immune reactions of rats to Trypanosoma, effects of endotoxins on, 25:55267
effects on impulse transmission in frog sciatic nerve, effects of LET on, 25:55215
effects on incidence of dominant lethal mutations in Drosophila, 25:55206 (NYO-2740-8, pp 147-219)
effects on incidence of recessive sex-linked lethal mutants in germ cells of mice, 25:55184
effects on L-penicillamine hydrochloride single crystals, ESR studies of, 25:54605
effects on lattice sites of vanadium and manganese ions in lithium and sodium fluorides, 25:56384
effects on lead azides, topography of evolution of products from, 25:54642
effects on leukosis and Rous sarcoma frequency in chickens, 25:55329
effects on life span of Habrobracon, mutagenic, 25:55185
effects on life span of mice, protective effects of AET, cysteamine, PAPP, and serotonin against, 25:55257
effects on mice, effects of radioprotective compounds on, 25:55266
effects on opacity of lens of mice, effects of dose fractionation on, 25:55206 (NYO-2740-8, pp 147-219)
effects on p--n silicon diodes of flash, currents induced in, 25:56336
effects on positron lifetimes in semiconductor single crystals, 25:56360
effects on potassium bromide crystals with and without copper dopant, thermoluminescent, 25:56323
effects on potassium hydrogen malonate monocrystals at 4.2°K, ESR spectral studies on production of radicals by, 25:54654
effects on pulmonary blood circulation in rabbits, acute, 25:55327
effects on seeds of Crepis capillaris, effects of water content on mutagenic, 25:55167
effects on single crystals of copper acetate monohydrate at 80 and 290°K, ESR studies on, 25:54610
effects on succinate dehydrogenase activity in rat liver in vitro, 25:55128
effects on survival of Escherichia coli, effects of dark-repair inhibitors and temperature on, 25:55357
effects on survival of hamster cells, 25:55207 (NYO-2740-8, pp 220-59)
effects on survival of synchronized L cells, effects of age on, 25:55309
effects on synchronized cultures of Chinese hamster cells, sensitizing effects of 5-bromodeoxyuridine on, 25:55258
effects on taste threshold in rats, low dose, 25:55322
effects on thymidine incorporation into DNA of cultured rat thymus cells, factors affecting, 25:55127
effects on water distribution and permeability in frog muscle cells, 25:55323
effects on yeast mutants, gene control of, 25:55187
emission from Coma Cluster, cosmological implications of, (E/T), 25:55806
emission from solar flares during Oct. 1969, detection of polarization of, (E), 25:55771
emission from solar flares, flux, spectrum composition, and structure of regions of, (E), 25:55770
emission from Sun, (E), 25:55736
emission of pulsed, from Cyg X-1, (E), 25:55727
reflection by soils at 70 to 200 keV, Monte Carlo calculation of effect of subterranean perturbations on, (T), 25:56274
scattering by three- and four-electron atoms and ions, form factors and scattering functions for coherent and incoherent, 25:56259 (EGG-1183-1479)
shielding for electrostatic accelerators, development of, 25:56603(P)
spectra of cosmic background, intensity and spatial, (E), 25:55734 (N-71-23434)
use for therapy of lymphogranulomatosis of bones, 25:55301
use for tumor therapy, preparation of Styrofoam compensators to correct for surface irregularities during, 25:55244
X-RAY FLUORESCENCE ANALYSIS
methods and standards for, of rocks, 25:54757(R) (MIT-1381-18)
XENON
gold-198 ranges in, from gold-197(n,γ) recoil, 25:56269
reactions with thallium bromides, crossed-beam measurements of cross sections for dissociative ionization in, 25:55879
uses of purified fission-product, evaluation of large-scale, 25:54887(R) (BNWL-1308-6)
XENON IONS
effects on silicon at 220 keV, lateral-stress study of damage produced in, 25:56285 (SC-RR-710424)
implantation in gallium arsenide at 151 keV, lattice disorder induced in, 25:56289
XENON ISOTOPES
abundance in meteorites, (E/T), 25:55670
nucleosynthesis in solar system, (E/T), 25:55670
XENON ISOTOPES Xe-126
energy-level transitions from iodine-126 decay, K-conversion coefficients and multipolarities for, (E), 25:56781
XENON ISOTOPES Xe-133
diffusion in cesium fluoride and iodide single crystals, effects of surface properties and structure on, 25:55633
release from failed water cooled Zircaloy 2 clad uranium oxide ($UO_2$) fuel rods, 25:57047 (JAERI-Memo-4157, pp

2-22)
use for estimating late x radiation effects on circulation in brain, liver, lungs, and skin of rats, 25:55328
use for lung scanning, health physics aspects of, 25:55248
use in hepatic blood flow measurement in dogs, 25:55123
XENON ISOTOPES Xe-135
release from failed water cooled Zircaloy 2 clad uranium oxide ($UO_2$) fuel rods, 25:57047 (JAERI-Memo-4157, pp 2-22)
XENON ISOTOPES Xe-138
release from failed water cooled Zircaloy 2 clad uranium oxide ($UO_2$) fuel rods, 25:57047 (JAERI-Memo-4157, pp 2-22)

# Y

YANKEE POWER REACTOR
operations during August 1971, 25:56897 (DOCKET-50029-158)
YTTERBIUM
desorption from tungsten, heat of, 25:55533
determination in river water and seawater by neutron activation and radiochemical separation, 25:54504
determination in volcanic ash by neutron activation and γ spectrometry, 25:54513
YTTERBIUM ALLOYS AND SYSTEMS
Au--Yb, crystal structures and melting points of intermetallic, 25:55570
YTTERBIUM ISOTOPES Yb-169
use of EDTA-incorporated, for brain and kidney scanning, 25:55272
YTTERBIUM ISOTOPES Yb-170
neutron capture at 8.1 to 73 eV, γ spectra from, (E), 25:56802
YTTERBIUM ISOTOPES Yb-171
energy levels from ytterbium-170 neutron capture, partial widths for, (E), 25:56802
YTTERBIUM ISOTOPES Yb-172
neutron capture at 140 to 202 eV, γ spectra from, (E), 25:56802
YTTERBIUM ISOTOPES Yb-173
energy levels from ytterbium-172 neutron capture, partial widths for, (E), 25:56802
YTTRIUM
analysis for rare earth impurities by ion exchange and neutron activation, 25:54525
complexes with salicylaldehyde, preparation and spectral properties of, 25:54539
determination in fission product mixtures by ion exchange and β counting, 25:54449
determination in rocks, chemical methods for, 25:54403
determination of, use of ion exchange in methods for, 25:54397
diffusion of interstitial carbon, nitrogen, and oxygen in, at 20 to 300°C, effects of dislocations on, 25:55461
lattice parameters of, effects of hydrogen on, 25:55549
properties of aerosols of, produced from solutions at high temperatures, chemical and physical, 25:54545
separation from cerium by extraction with bis(2-ethylhexyl) phosphate, 25:54750(P)
tensile properties of, relations with grain boundary twist, 25:55430 (IS-T-459)
YTTRIUM ALLOYS AND SYSTEMS
Al--Cu--Y, phase studies of, 25:55561
Ce--Ru--Y, critical magnetic field in superconducting, (E), 25:56074
YTTRIUM ISOTOPES Y-85
beta and electron-capture decay of ground-state and isomeric, branching ratios, gamma spectra, and log-ft values for, (E), 25:56722
YTTRIUM ISOTOPES Y-87
energy levels from zirconium-87 decay, spin--parity assignments for, (E), 25:56723
energy-level transitions from zirconium-87 decay, branching ratios for, (E), 25:56723
YTTRIUM ISOTOPES Y-88
energy levels from yttrium-89 (He-3,α) and zirconium-90 (d,α) reactions, spectroscopic factors for, (E), 25:56778
energy-level scheme, (E), 25:56779
YTTRIUM ISOTOPES Y-89
alpha elastic scattering at 20 MeV, angular distribution for, (E), 25:56778
energy levels from zirconium-89 decay, spin--parity assignments for, (E), 25:56723
energy-level transitions from zirconium-89 decay, branching ratios for, (E), 25:56723
helium-3 elastic scattering at 15 and 20 MeV, angular distributions for, (E), 25:56778
helium-3 reactions (He-3,α) at 15 MeV, DWBA analysis of, (E), 25:56778
helium-3 reactions (He-3,α) at 25 MeV, angular distributions for, (E), 25:56779
YTTRIUM OXIDES
analysis for calcium by nondestructive alpha activation, 25:54522
analysis for non-rare earth elements by emission spectrometry, 25:54419
preparation of dense ceramic, by sintering, 25:55606
properties of sintered, electric, mechanical, and physical, 25:55606
$CaO$--$Y_2O_3$--$ZrO_2$-base, thermal stability of solid solutions of, effects of yttrium oxide content on, 25:55636
$HfO_2$--$Y_2O_3$, thermal conductivity of solid solutions of, at high temperatures, 25:55637
$HfO_2$-base--$Y_2O_3$, properties as electrolyte, 25:56355
$MgO$--$Y_2O_3$--$ZrO_2$-base, thermal stability of solid solutions of, effects of yttrium oxide content on, 25:55636
$Y_2O_3$--Zr, strength of powder shapes of, effects of dispersion-, grain boundary-, and solid solution-hardening on, 25:55487

# Z

ZINC
argon-ion reactions at 30 keV with surfaces of, charge states and kinetic energies of scattered and recoil ions from, (E), 25:55818
determination in epitaxial films of gallium arsenide by neutron activation and radiochemical separation, 25:54512
determination in fission product mixtures by ion exchange and polarography or β counting, 25:54449
determination in sediments of Rhine River basin by x-ray fluorescence, 25:54408
determination in standard aluminum--silicon system by neutron activation, 25:54455
determination of trace amounts of, in air by neutron activation and γ spectrometry, 25:54456
determination of trace amounts of, in thorium and zirconium compounds by neutron activation, separation processes, and γ spectrometry, 25:54518
effects of vapors of, on hydrogen isotope exchange at 300 to 500°C, 25:54552
effects on solvolysis of tert-butyl halides, Broensted correlation for, 25:54548
potential for, method for modeling 1 = 2 component of, 25:56387
separation of uranium from, in methyl sulfoxide by cation exchange chromatography, 25:54728
ZINC ALLOYS AND SYSTEMS
preparation by granule metallurgy, evaluation of, 25:55404
Ag--Zn, diffusion in, 25:57238 (MLM-OP-71003)
Au--Zn, search for superconductivity in fcc phases of, (E), 25:56096
Ce--Zn-base, thermodynamics of molten, at 700 to 1000°K, emf studies of, 25:55442
Cu--Zn, search for superconductivity in fcc phases of, (E), 25:56096
Dy--Zn, hyperfine parameters of DyZn, Moessbauer-effect study of, 25:56382
Nb--Zn, phase and intermetallic compound formation in, 25:55534
Sn--Zn, diffusion in molten, kinetics of mutual, 25:55449
ZINC IONS
implantation in gallium arsenide at 140 keV, lattice disorder induced in, 25:56289
ZINC ISOTOPES Zn-60
binding energy, deformation, and single-particle spectra for, self-consistent calculation using Yukawa and Kuo-Brown matrix elements, (T), 25:56720
energy levels of, shell-model calculation with Reid and Yale potentials, 25:56857
ZINC ISOTOPES Zn-62
binding energy, deformation, and single-particle spectra for, self-consistent calculation using Yukawa and Kuo-Brown matrix elements, (T), 25:56720
ZINC ISOTOPES Zn-64
alpha elastic and inelastic scattering at 27.2 MeV, distorted-wave analysis of differential cross sections for, (T), 25:56726
binding energy, deformation, and single-particle spectra for, self-consistent calculation using Yukawa and Kuo-Brown matrix elements, (T), 25:56720
energy-level transitions from alpha inelastic scattering, distorted-wave calculation of probabilities for, (T), 25:56726
neutron reactions (n,α) at 281 and 2637 eV, α widths of levels in search for, (E), 25:56686 (JINR-P3-5875)
proton inelastic scattering at 6.9 MeV, distorted-wave analysis of differential and integrated cross sections for, (E), 25:56727
ZINC ISOTOPES Zn-65
uptake by organisms of marine food chain, effects of physico-chemical form on, 25:55149 (BNWL-SA-4048)
uptake by shell and soft tissues of oysters, effects of cobalt, iron, and species on, 25:55153
ZINC ISOTOPES Zn-66
alpha elastic and inelastic scattering at 27.2 MeV, distorted-wave analysis of differential cross sections for, (T), 25:56726
binding energy, deformation, and single-particle spectra for, self-consistent calculation using Yukawa and Kuo-Brown matrix elements, (T), 25:56720

XUM

energy-level transitions from alpha inelastic scattering, distorted-wave calculation of probabilities for, (T), 25:56726
proton inelastic scattering at 6.9 MeV, distorted-wave analysis of differential and integrated cross sections for, (E), 25:56727
proton reactions (p,nγ) at 6 to 6.8 MeV, γ singles and coincidence spectra and angular distributions for, (E), 25:56732
ZINC ISOTOPES Zn-67
neutron reactions (n,α) at 1548 eV, α widths of levels in search for, (E), 25:56686 (JINR-P3-5875)
ZINC ISOTOPES Zn-68
binding energy, deformation, and single-particle spectra for, self-consistent calculation using Yukawa and Kuo-Brown matrix elements, (T), 25:56720
neutron capture at 2.9 MeV, cross section for, (E), 25:56696
ZINC ISOTOPES Zn-70
alpha elastic and inelastic scattering at 27.2 MeV, distorted-wave analysis of differential cross sections for, (T), 25:56726
binding energy, deformation, and single-particle spectra for, self-consistent calculation using Yukawa and Kuo-Brown matrix elements, (T), 25:56720
energy-level transitions from alpha inelastic scattering, distorted-wave calculation of probabilities for, (T), 25:56726
ZINC SELENIDES
defects in wurtzite single crystals of, studies of growth and radioinduced, 25:56286
ZINC SULFIDES
defects in wurtzite single crystals of, studies of growth and radioinduced, 25:56286
ZION POWER REACTOR, UNIT 1
design parameters of, revised and additional data on, 25:56954 (DOCKET-50295-30)
operations aspects of, revised and additional data on, 25:56954 (DOCKET-50295-30)
ZION POWER REACTOR, UNIT 2
design parameters of, revised and additional data on, 25:56954 (DOCKET-50295-30)
operations aspects of, revised and additional data on, 25:56954 (DOCKET-50295-30)
ZIRCALOY
embrittlement of, effects of coolant loss accident conditions on, 25:57092(R) (ORNL-TM-3483)
testing of fuel tubes of, ultrasonic method for, 25:54926
ZIRCALOY-2
oxidation of, effects of coatings on high-temperature, 25:54587(R) (AECL-3909)
ZIRCONIUM
casting by levitation melting using magnetic field, 25:55424
coating with zinc-plated aluminum silicide, corrosion protection by, 25:55398(P)
compounds, analysis for trace impurities by neutron activation, separation processes, and γ spectrometry, 25:54518
deformation of alpha-phase, relations of aging with oxygen diffusion in, 25:55551
determination in fission product mixtures by ion exchange and β counting, 25:54449
determination in rocks, chemical methods for, 25:54403
determination in sediments of Rhine River basin by x-ray fluorescence, 25:54408
determination of trace amounts of, in high-purity acids by emission spectrography, 25:54431
diffusion of uranium in films of beta-, 25:55498
effects on oxidation of niobium at 1500 to 2000°C and low pressures, 25:55380
effects on solvolysis of tert-butyl halides, Broensted correlation for, 25:54548
electric conductivity of, temperature dependence of, 25:55445
iron impurity distribution in electric arc zone melted, measurement of coefficient of, 25:55502
oxidation of monocrystalline, effects of orientation on formation of monoclinic zirconium oxide in, 25:55540
preparation and uses of, newsletter on, 25:55406
properties and structure of, produced by sintering using systematic thermal fluctuations, 25:55414
properties of aerosols of, produced from solutions at high temperatures, chemical and physical, 25:54545
separation from cerium and thorium by reverse-phase partition chromatography on TTA-impregnated paper, 25:54746
separation from niobium by vacuum melting, 25:55403
separation of trace amounts of, from carbonate solutions by sorption on metal hydroxides, review on, 25:54734
separation of uranium from, in methyl sulfoxide by cation exchange chromatography, 25:54728
sorptive properties for nitrogen and oxygen at low pressures and high temperatures, 25:55463
titanium impurity distribution in electric arc zone melted, measurement of coefficient of, 25:55502
ZIRCONIUM ALLOYS AND SYSTEMS
coating with zinc-plated aluminum silicide, corrosion protection by, 25:55398(P)
corrosion studies on, 25:54587(R) (AECL-3909)
porosity of, effects of annealing and crystallization on micro-, 25:55462
preparation and uses of, newsletter on, 25:55406
thermoelectric properties of, at 0 to 1000°C, 25:56351
Al--Mg--Zr, cracking and mechanical properties of welded joints of, effects of long-term heating at 70°C on, 25:55470
Al--Mo--Sn--Ti-base--Zr, welding of, properties of joints produced by friction, 25:55409
Al--Zr, crystal structure of solidified, effects of cooling rate and supercooling on, 25:55550
Al-base--Zr, thermal expansion of quenched, 25:55499
C--Hf--Zr, thermodynamic properties of, 25:55614
C--Nb--Zr, thermodynamic properties of, relations with composition, 25:55615
C--U--Zr, phase diagram at 950°C, carbide composition in, 25:55547
C--U--Zr, thermodynamic properties of, 25:55614
Cr--Mo--Zr, phase diagram at 1150°C, 25:55538
Cu-base--Zr, microstructure of, potentiostatic studies on, 25:55555
H--Ti--Zr, inflammability correlation of powdered, 25:55473
Hf--Nb--Ti--Zr, superconducting properties of, with, 25:56104
Hf--Nb--Zr, superconducting properties of, 25:56105
Mg-base--Zr, oxidation above 400°C in presence of carbon dioxide, mechanisms of internal, 25:55382
Mg-base--Zr, structure of sintered, following high-temperature annealing, optical and electron microscopy studies of changes in, 25:55548
Nb--Ti--W--Zr, solidus volume of, simplex-lattice method for prediction of, 25:55529
Nb--Ti--Zr, phase studies of, 25:55564
Nb--Zr, microstructure of, isothermal omega transformation in, 25:55557
Nb--Zr-base, superconductivity of, relations with crystal structure, 25:55541
Nb-base--O--Zr, structure and tensile properties of, 25:55522
Nb-base--Zr, corrosion by mercury at 1200°F, 25:55377 (N-71-26947)
Nb-base--Zr, magnetization properties of superconducting, transporting sinusoidal alternating current in longitudinal magnetic field, (E/T), 25:56085
Nb-base--Zr, oxygen solubility limits in, lattice parameter measurements of, 25:55568
Nb-base--Zr, superconducting transition temperature of, effect of deformation on, (E/T), 25:56099
Pu--Zr, phase transformations in, during quenching, effects of composition and cooling rate on epsilon, 25:55528
Ru--Zr, diffusion in, effects of composition on mutual, 25:55452
Si--Zr, inflammability correlation of powdered, 25:55473
Ti--Zr, inflammability correlation of powdered, 25:55473
V--Zr, thermal capacity of superconducting intermetallic $ZrV_2$, (E), 25:56072
$Y_2O_3$--Zr, strength of powder shapes of, effects of dispersion-, grain boundary-, and solid solution-hardening on, 25:55487
ZIRCONIUM BORIDES
conductivity at 300 to 1300°K, electric and thermal, 25:55627
preparation and uses of, newsletter on, 25:55406
stability in acids, 25:54543
C--SiC--$ZrB_2$, electric and thermal conductivity at 300 to 1300°K, 25:55627
C--$ZrB_2$, electric and thermal conductivity at 300 to 1300°K, 25:55627
SiC--$ZrB_2$, electric and thermal conductivity at 300 to 1300°K, 25:55627
ZIRCONIUM CARBIDES
physical properties and stability to nitrogen, 25:55629
physical properties and structure of, review on effects of composition on, 25:55632
preparation and uses of, newsletter on, 25:55406
wetting by copper, effects of electronic structure on, 25:55643
NbC--ZrC, physical properties and structure of, review on effects of composition on, 25:55632
NbC--ZrC, wetting by copper at 1100°C, effects of electronic structure on, 25:55643
ZrC--ZrN, wetting by copper at 1100°C, effects of electronic structure on, 25:55643
ZIRCONIUM CHLORIDES
zirconium nitride preparation from, chemical reactions for pyrolytic, 25:55605
ZIRCONIUM HYDRIDES
neutron downscattering spectra of, effects of stoichiometry on structure in, 25:56343
neutron total cross section at subthermal energies, (E), 25:56623
ZIRCONIUM ISOTOPES Zr-87
beta decay of, branching ratios, gamma spectra, and log-ft and Q values for, (E), 25:56723
electron-capture decay of, branching ratios, gamma spectra, and log-ft and Q values for, (E), 25:56723
ZIRCONIUM ISOTOPES Zr-89
beta decay of ground-state and isomeric, branching ratios, gamma spectra, and log-ft values for, (E), 25:56723

electron-capture decay of ground-state and isomeric, branching ratios, gamma spectra, and log-ft values for, (E), 25:56723
ZIRCONIUM ISOTOPES Zr-90
deuteron reactions (d,α) at 15 MeV, DWBA analysis of, (E), 25:56778
energy levels from niobium-90 decay, spin--parity assignments for, (E), 25:56791
energy-level transitions from niobium-90 decay, K-conversion coefficients and multipolarities from, (E), 25:56791
helium-3 reactions (He-3,p) at 16.5 and 18 MeV, proton spectra and angular distributions for, (E), 25:56758
neutron elastic scattering at 7 MeV, S-matrix analysis of differential cross sections for, (T), 25:56789
proton reactions (p,2p) at 600 MeV, separation-energy spectra and momentum distributions of residual nuclei from, (E), 25:56706
proton reactions at high energies, isobar model for analysis of meson (π) production in, 25:56530
ZIRCONIUM ISOTOPES Zr-95
content in atmosphere during 1969, (E), 25:54803
distribution in mice following inhalation, effects of chemical form on, 25:55125
ZIRCONIUM NITRIDES
physical properties of, 25:55629
preparation and uses of, newsletter on, 25:55406
preparation of spheres of, for nitrogen diffusion studies, 25:55595
production from zirconium tetrachloride, chemical reactions for pyrolytic, 25:55605
shock compression effects on powdered, x-ray-diffraction study of, 25:55618
structure of spheres of, 25:55595
use in preparation of zirconium oxide microspheres using nitrogen plasma spraying, 25:55407
ZrC--ZrN, wetting by copper at 1100°C, effects of electronic structure on, 25:55643
ZIRCONIUM OXIDES
crystal structure of $ZrO_2$, polymorphic transformations in,, 25:55641
densification of hot pressing, 25:55600
particles of radioisotope-labeled, Coulter-type instrument for counting 10 μ-diameter, 25:55090
preparation and uses of, newsletter on, 25:55406
preparation of calcium oxide-stabilized electrolyte films of, by sintering for use in high-temperature fuel cells, 25:55596
preparation of hollow microspheres of, using nitrogen plasma spraying, 25:55407
production of monoclinic, by oxidation of single-crystal zirconium, 25:55540
properties of magnesium oxide-strengthened refractories of, mechanical and thermal, 25:55621
properties of sintered electrolyte films of, for use in high-temperature fuel cells, 25:55596
thermal conductivity at high temperatures, 25:55637
CaO--$Y_2O_3$--$ZrO_2$-base, thermal stability of solid solutions of, effects of yttrium oxide content on, 25:55636
CaO--$ZrO_2$, crystal structure of, polymorphic transformations in, 25:55641
CaO--$ZrO_2$, densification by hot pressing, 25:55600
$CaZrO_3$--$ZrO_2$, crystal structure of, polymorphic transformations in, 25:55641
MgO--$Y_2O_3$--$ZrO_2$-base, thermal stability of solid solutions of, effects of yttrium oxide content on, 25:55636
$P_2O_5$--$ThO_2$--$ZrO_2$, phase studies on subsolidus equilibrium in, 25:55638
ZIRCONIUM SILICIDES
preparation and uses of, newsletter on, 25:55406
ZIRCONS
analysis for hafnium by neutron activation and γ spectrometry of hafnium-179m, 25:54491
effects on geochemistry of thorium and uranium deposits in Vosges Mountains, 25:54807
properties of refractories of, mechanical and thermal, 25:55621

XUM

# REPORT NUMBER INDEX

Reports, conference papers and proceedings, numbered translations, and patents are included in this index. Each item is listed by report number; this is followed by the abstract number and a brief notation regarding public availability. The index entries show which reports are on file in the institutions listed on the back of the front cover (Dep.), which reports have been published in open-literature journals (journal citation), and which reports can be purchased (source and price). Whenever a report is identified by more than one number, the availability is given under the primary number, and a cross reference is given under the secondary report number.

The report number codes apply to USAEC reports unless designated otherwise. Non-USAEC reports are identified by parenthetical notes after the report codes; e.g., (non-AEC), (British), (Canadian), (French). The note (Misc.) identifies the codes used for both USAEC and non-USAEC reports. Patents are listed under the heading "PATENTS"; the country of origin is included in parentheses.

A comprehensive list of both USAEC and non-USAEC report codes is contained in the latest revision of TID-85, *Report Number Series Used by the Division of Technical Information in Cataloging Reports.* This information is also included in the Cumulative Report Number Index (issued annually).

## Availability of USAEC Reports

All USAEC Reports abstracted in *Nuclear Science Abstracts* are available through one or more of the following sources:

(1) University and public libraries in the United States. A list of these organizations appears on the inside front cover of each issue of *NSA*.

(2) NCR Microcard Editions in Microcard and micronegative form. Orders and inquiries should be sent to: Order Processing Department, 365 South Oak Street, West Salem, Wisconsin 54669.

(3) National Technical Information Service, U. S. Department of Commerce, Springfield, Virginia 22151.

(4) Superintendent of Documents, U. S. Government Printing Office, Washington, D. C. 20402.

(5) Microsurance, Inc., P. O. Box 3522, Oak Ridge, Tenn. 37830, in micronegative form. Purchase details available on request.

## Availability of Non-USAEC Reports

**U. S. Reports.** Reports of U. S. Government agencies are available to the public from the National Technical Information Service (NTIS). If specific availability is not shown, inquiries may be directed to NTIS.

**Non-U. S. Reports.** Reports of atomic energy organizations of other countries are available from NTIS for U. S. sale only. Specific availability in the country of origin is shown, when known, at the report number entry. Otherwise, inquiries should be made to the organizations listed below:

### AUSTRALIA

**Australian Atomic Energy Commission Research Establishment.** Available upon request from the Library, Australian Atomic Research Establishment, Private Mail Bag, Sutherland, New South Wales, Australia.

### BELGIUM

**Centre d'Étude de l'Energie Nucléaire.** Available upon request to individuals and organizations from the Centre d'Etude de l'Energie Nucléaire (C.E.N.), Studiecentrum voor Kernenergie (S.C.K.), Technical Information Dept., MOL-DONK (Belgium).

### CERN

**CERN European Organization for Nuclear Research.** Available without charge from CERN European Organization for Nuclear Research, Geneva 23, Switzerland. Copies are deposited in libraries throughout the world.

### FRANCE

**Commissariat à l'Energie Atomique.** Inquiries for reports numbered 1-2199 should be addressed to Service Central de Documentation du C.E.A., Centre d'Etudes Nucléaires de Saclay, Boîte postale n° 2, 91. GIF-sur-YVETTE, FRANCE. Reports numbered 2200 and above are available from La Documentation Française, 31 quai Voltaire, 75, PARIS (7e), FRANCE.

**Service Central de Protection contre les Rayonnements Ionisants.** Copies are available from Ministère de la Santé Publique, Service Central de Protection contre les Rayonnements Ionisants, B.P. n° 78 Le Vesinet (France) Telex 25667.

### GERMANY

**Deutsches Elektronen-Synchrotron DESY.** Copies are available from Deutsches Elektronen-Synchrotron DESY, Dokumentation, 2000 Hamburg 52, Notkestieg 1, Germany.

**Gesellschaft für Kernforschung mbH (KFK).** Copies are available from Gesellschaft für Kernforschung mbH, 75 Karlsruhe, Postfach 947, Germany. Copies are also deposited in many national nuclear centers in the world.

**Kernforschungsanlage.** Copies may be ordered from Zentralbibliothek der Kernforschungsanlage Jülich, Jülich, Bundesrepublik Deutschland.

**Hahn-Meitner-Institute für Kernforschung.** Available without charge from Hahn-Meitner-Institute für Kernforschung Ber-



XUM

lin, Bibliothek, Glienicker Strasse 100, 1 Berlin 39, Germany. Copies are deposited in many national nuclear centers in the world.

**Johann-Wolfgang-Goethe Universität, Frankfurt Am Main, Institut für Kernphysik, (IKF).** Copies are available from Gmelin Institut, 40–42 Varrentrappstrasse, Frankfurt (Main), West Germany.

**ISRAEL**

**Israel Atomic Energy Commission.** Available without charge from Israel Atomic Energy Commission, Soreq Nuclear Research Centre, Yavne, Israel.

**ITALY**

**Centro Informazioni Studi Esperienze (CISE).** For sale at CISE Press Office, Casella Postale 3986, Milano, Italy. Copies are deposited in the libraries of various nuclear centers in Italy and abroad.

**Comitato Nazionale per l'Energia Nucleare.** Copies are available from Comitato Nazionale per l'Energia Nucleare, Divisione Affari Internazionali e Studi Economici, Ufficio Pubblicazioni, Via Belisario, 15, Roma, Italy.

**JAPAN**

**Japan Atomic Energy Research Institute (JAERI).** Available from the Staff Supply Cooperative of Japan Atomic Energy Research Institute (JAERI), Tokai-mura, Naka-gun, Ibaraki-ken, Japan. Copies are deposited in depositories in Tokyo, Nagoya, and Osaka.

**Nagoya University.** Copies are available from Research Information Center, Institute of Plasma Physics, Nagoya University, Nagoya, Japan.

**University of Tokyo.** Available free of charge from Institute for Nuclear Study, University of Tokyo, Tanashi-Machi, Kitatama-gun, Tokyo, Japan.

**NETHERLANDS**

**Reactor Centrum Nederland.** For sale by Reactor Centrum Nederland, 112 Scheveningseweg, 's-Gravenhage, The Netherlands. Copies are deposited in university libraries in Holland and in many national nuclear centers in the world.

**NEW ZEALAND**

**Institute of Nuclear Sciences.** Copies are available from Librarian, N. Z. Institute of Nuclear Sciences, D.S.I.R., Private Bag, Lower Hutt, New Zealand. Copies are deposited in other countries.

**PAKISTAN**

**Atomic Energy Center.** Copies are available from Atomic Energy Center, P. O. Box 658, Lahore, (West Pakistan).

**POLAND**

Reports of the Polish nuclear institutes are published by the Nuclear Energy Information Center of the Government Commissioner for Use of Nuclear Energy. Copies are available free of charge from Nuclear Energy Information Center, Palace of Culture and Science, Warsaw, Poland.

**SPAIN**

**Junta de Energia Nuclear.** "JEN" reports are available without charge from Servicio de Documentation, Junta de Energia Nuclear, Ciudad Universitaria, Madrid (3), España.

**SWITZERLAND**

**Eidgenössisches Institut für Reaktorforschung.** "EIR" reports are available from Eidgenössisches Institut für Reaktorforschung, c/o Bibliothek, 5303 Würenlingen/Switzerland.

**TURKEY**

**Turkish Atomic Energy Commission.** Copies are available free of charge from T.A.E.C., Çekmece Nuclear Research Center, P. O. Box 1, Airport, Istanbul, Turkey.

## Conferences

Published conference proceedings as well as individual unpublished papers from conferences are included in this index. A CONF number is assigned to the conference if published proceedings are received and also if only a single paper is received. The base number used is year-month-sequence. Thus, the number CONF-650101 indicates that the conference was held in 1965, in January, and that this was the first January 1965 conference so received. This number would be assigned to complete published proceedings. If individual papers are received, the base number is extended to include a paper number, e.g., CONF-650101-1. As additional papers are received, they will be assigned consecutive numbers in the series, CONF-650101-1, CONF-650101-2, etc. This numbering system ensures that all papers received from a conference will be associated with that conference in this index.

If published proceedings are received after the receipt of individual papers, the complete proceedings will be abstracted and the abstract number will appear in this index with the base CONF number.

## Abbreviations Used in Availability Column

| | |
|---|---|
| AECL | Reports of the Atomic Energy of Canada Limited are for sale by the Scientific Document Distribution Office, Atomic Energy of Canada Limited, Chalk River, Ontario, Canada. |
| CFSTI | See NTIS |
| DENM | Reports of the Atomic Energy Commission Research Establishment, Risö, are available on exchange from the Library, Danish Atomic Energy Commission, Risö, Roskilde, Denmark. Also for sale at the price shown from Jul. Gjellerup, Booksellers, 87 Sölvgade, Kobenhavn K., Denmark.<br>Reports of Danatom are available on loan from Research Establishment, Risö, Roskilde, Denmark. Copies are available from Danatom, Aurehojvej 2, Hellerup, Denmark. |
| Dep. | AEC reports so designated are maintained in the organizations listed on the inside front cover of *NSA*. Prior to July 1, 1965, reports were deposited either in printed copy form or in microform. After that time, all reports have been in the form of micronegatives.<br>Reports from other countries so designated are available in the United States at the organizations listed on the inside front cover of *NSA*. |

XUM

DTIE — Available from the U. S. Atomic Energy Commission, Division of Technical Information Extension, P. O. Box 62, Oak Ridge, Tennessee 37830. (Conference papers are available on loan only.)

EM — Blueline prints of AEC engineering drawings are available from NTIS, U. S. Department of Commerce, Springfield, Virginia 22151. Current prices of the CAPE-packages may be obtained from this address. TID-4100, available from the Division of Technical Information Extension, P. O. Box 62, Oak Ridge, Tennessee 37830, contains information on all the CAPE-packages for sale.

EUR — For sale by Centrale de vente des publications des Communautés européennes 37, rue Glesener-Luxembourg.

GPO — For sale by the Superintendent of Documents, Government Printing Office, Washington, D. C. 20402.

IAEA — Available from the International Atomic Energy Agency, Vienna, Austria, and from its sales agencies in various countries throughout the world. A list of these agencies is found in each STI/DOC and STI/PUB publication.

INIS — Available on microfiche at $0.65 per document from INIS Section, International Atomic Energy Agency, P. O. Box 590 A-1011, Vienna, Austria

LMEC — Available *only to requesters within the United States* from the Liquid Metal Engineering Center, P. O. Box 1449, Canoga Park, CA 91304

NORW — Reports from Forsvarets Forskningsinstitutt are available from Norwegian Defense Research Establishment, Library, P. O. Box 25, Kjeller, Norway.
"KR" reports are available on an exchange basis from the Library, Institutt for Atomenergi, Box 40, Kjeller, Norway.
Reports of the Norwegian Reactor School are available from the Library, Institutt for Atomenergi, P. O. Box 40, Kjeller, Norway.

NRC — For sale by the National Research Council of Canada, Ottawa, Ontario, Canada.

NTIS — For sale by the National Technical Information Service (NTIS), U. S. Department of Commerce, Springfield, Virginia 22151 at the following prices for eye legible copy:

| | |
|---|---|
| 1–300 pages | $3.00 |
| 301–600 pages | $6.00 |
| 601–900 pages | $9.00 |

Documents over 900 pages have special prices which may be obtained from NTIS.
Microfiche copy of each separately bound document can be purchased for $0.95.
Reports issued by organizations outside the United States will be sold by NTIS *only to purchasers within the United States.*
Purchasers outside the United States may acquire such reports from the sources described elsewhere in these columns.

OECD — Available from O. E. C. D., Publications 2, rue, André-Pascal, 75 Paris 16$^{e}$, France, and from its sales agencies in various countries throughout the world. A list of these agencies is found in each OECD publication.

RSO — Available *only to requesters within the United States* from the Reactor Standards Office, Oak Ridge National Laboratory, P. O. Box X, Oak Ridge, TN 37830

SWED — "AE" reports are for sale from Aktiebolaget Atomenergi, Library Section, Box 43041, Stockholm 43, Sweden. Microcopy of these reports is available from the International Documentation Center, Turnba, Sweden.
Reports of the VDDIT-series may be obtained from Aktiebolaget Atomenergi, Information Office, Scientific and Technical Information, Box 43041, Stockholm 43, Sweden.
Other series are not generally available to the public. Organizations in the Atomic Energy field may obtain copies from Aktiebolaget Atomenergi.

UK — United Kingdom Atomic Energy Authority reports generally may be purchased from Her Majesty's Stationery Office, P. O. Box 569, London S.E.1. Copies of many UKAEA reports (particularly earlier ones) may be purchased in microcopy form from Micro Methods Ltd., East Ardsley, Wakefield, Yorkshire, England. Copies of UKAEA reports are deposited with the National Lending Library for Science and Technology and 10 public libraries in England; with the USAEC and (through USAEC) with NTIS; and in most national nuclear centers throughout the world. In the USA, UKAEA reports are available on a subscription basis, by subject category, from UNIPUB, Inc., P. O. Box 433, New York, NY 10016, USA; and from Pendragon House, Inc., 1093 Charter Avenue, Redwood City, CA 94063, USA.

UN — Mail orders should be directed to the Sales Section, Room 1059, United Nations Headquarters, New York, New York 10017.

ZAED — Available from Zentralstelle für Atomkernenergie Dokumentation, 6000 Frankfurt/Main 90, P. O. Box 901069, Westendstr. 21, West Germany

XUM

| Report No. | Abstract No. | Availability |
|---|---|---|
| AAEC/E- | (Australian) | |
| 219(Pt.1) | 25-57212 | Dep. NTIS (U. S. Sales Only), 29p. |
| AD- | (Misc.) | |
| 715563 | 25-56613 | NTIS, 53p. |
| 720974 | 25-54993 | NTIS, 14p. |
| 721388 | 25-56255 | NTIS, 60p. |
| 722012 | 25-56256 | NTIS, 57p. |
| 722031 | 25-54815 | NTIS, 19p. |
| AEC-tr- | | |
| 7240 | 25-55068 | Dep. NTIS |
| 7270 | 25-56224 | Dep. NTIS |
| AECL- | (Canadian) | |
| 3793 | 25-57213 | Dep. NTIS (U. S. Sales Only). AECL $1.00, 25p. |
| 3909 | 25-54587 | Dep. NTIS (U. S. Sales Only). AECL $2.00, 92p. |
| 3912 | 25-56733 | Dep. NTIS (U. S. Sales Only). AECL $2.00, 105p. |
| 3971 | 25-55893 | Dep. NTIS (U. S. Sales Only). AECL $2.00, 77p. |
| AEEW-R- | (British) | |
| 705 | 25-54861 | Dep. NTIS (U. S. Sales Only), 19p. |
| 711 | 25-54862 | Dep. NTIS (U. S. Sales Only), 10p. |
| AERE-Trans- | (British) | |
| 1137 | 25-56340 | Dep. NTIS (U. S. Sales Only). UK 13p |
| AI-AEC- | | |
| 13006 | 25-57068 | Dep. NTIS, 59p. |
| 13010 | 25-54863 | Dep. NTIS, 43p. |
| AI-AEC-Memo- | | |
| 12715(Del.) | 25-57132 | Dep. NTIS, 66p. |
| ANL- | | |
| 7714 | 25-56614 | Dep. NTIS, 455p. |
| 7754 | 25-54864 | Dep. NTIS, 31p. |
| 7771 | 25-57109 | Dep. NTIS, 43p. |
| 7791 | 25-56982 | Dep. NTIS, 32p. |
| 7800 | 25-57069 | Dep. NTIS, 462p. |
| 7804 | 25-55069 | Dep. NTIS, 36p. |
| ANL-EBR- | | |
| 27 | 25-57028 | Dep. NTIS, 53p. |
| 30 | 25-57054 | Dep. NTIS, 25p. |
| AWRE-O- | (British) | |
| 77/70 | 25-57214 | Dep. NTIS (U. S. Sales Only). UK 85p, 125p. |
| BAW- | (Misc.) | |
| 3647-22 | 25-57017 | Dep. NTIS, 26p. |
| BHO- | | |
| 67-2 | 25-55070 | Dep. NTIS, 10p. |
| BLG- | (Belgian) | |
| 457 | 25-55572 | Dep. NTIS (U. S. Sales Only), 32p. |
| BNL- | | |
| 16026 | 25-56580 | Dep. NTIS, 23p. |
| BNL-tr- | | |
| 442 | 25-56581 | Dep. NTIS |
| 446 | 25-56734 | Dep. NTIS |
| BNWL- | | |
| 1308-6 | 25-54887 | Dep. NTIS, 51p. |
| 1567 | 25-55427 | Dep. NTIS, 23p. |
| 1598 | 25-54934 | Dep. NTIS, 48p. |
| 1599 | 25-54935 | Dep. NTIS, 27p. |
| 1609 | 25-57181 | Dep. NTIS, 54p. |
| BNWL-B- | | |
| 108 | 25-55428 | Dep. NTIS, 68p. |
| BNWL-SA- | | |
| 2335 | 25-55370 | Dep. NTIS, 18p. |
| 3345 | 25-54706 | Dep. NTIS, 25p. |
| 3747 | 25-55108 | Dep. NTIS, 14p. |
| 3962 | 25-55573 | Dep. NTIS, 7p. |
| 4048 | 25-55149 | Dep. NTIS, 60p. |
| BRH/DMRE- | (Non-AEC) | |
| 71-3 | 25-54936 | GPO $0.30 |
| CALT- | | |
| 68-313 | 25-56452 | Dep. NTIS, 92p. |
| CEA-Bib- | (French) | |
| 198 | 25-57215 | Dep. NTIS (U. S. Sales Only), 27p. |
| 200 | 25-55246 | Dep. NTIS (U. S. Sales Only), 56p. |
| CEA-CONF- | (French) | |
| 1744 | 25-55317 | Dep. NTIS (U. S. Sales Only), 26p. |
| 1758 | 25-54865 | Dep. NTIS (U. S. Sales Only), 16p. |
| 1796 | 25-57070 | Dep. NTIS (U. S. Sales Only), 23p. |



| Report No. | Abstract No. | Availability |
|---|---|---|
| 1801 | 25-56162 | Dep. NTIS (U. S. Sales Only), 2p. |
| 1802 | 25-56225 | Dep. NTIS (U. S. Sales Only), 3p. |
| 1804 | 25-56226 | Dep. NTIS (U. S. Sales Only), 3p. |
| 1805 | 25-56227 | Dep. NTIS (U. S. Sales Only), 3p. |
| 1806 | 25-56228 | Dep. NTIS (U. S. Sales Only), 3p. |
| 1821 | 25-55645 | Dep. NTIS (U. S. Sales Only), 31p. |
| 1822 | 25-56282 | Dep. NTIS (U. S. Sales Only), 22p. |
| 1823 | 25-56283 | Dep. NTIS (U. S. Sales Only), 24p. |
| CEA-N- | (French) | |
| 1433 | 25-55071 | Dep. NTIS (U. S. Sales Only), 15p. |
| 1449 | 25-55203 | Dep. NTIS (U. S. Sales Only), 96p. |
| CEA-R- | (French) | |
| 4079 | 25-56132 | Dep. NTIS (U. S. Sales Only), 79p. |
| 4177 | 25-55429 | Dep. NTIS (U. S. Sales Only), 120p. |
| 4188 | 25-56582 | Dep. NTIS (U. S. Sales Only), 32p. |
| 4193 | 25-56412 | Dep. NTIS (U. S. Sales Only), 136p. |
| CERN- | (European Organization for Nuclear Research) | |
| 71-14 | 25-56807 | Dep. NTIS (U. S. Sales Only), 396p. |
| CNRS-CPT- | (French) | |
| 71/P-378 | 25-56542 | Dep. NTIS (U. S. Sales Only), 5p. |
| CONF-670992- | (Conference on Frozen and Irradiated Fish and Fishery Products, Madrid, Spain, Sept. 4-8, 1967) | |
| 1 | 25-55362 | See LFEN-NI.-56a |
| CONF-680535- | (14th National Conference of the Italian Association for Health Physics and Protection from Radiation, Formia, Italy, May 29-31, 1968) | |
| 21 | 25-54783 | Minerva Fisiconucl.; 13: 192-203(Jul-Sep 1969) |
| 25 | 25-54762 | Minerva Fisiconucl.; 13: 225-35(Jul-Sep 1969) |
| 26 | 25-54923 | Minerva Fisiconucl.; 13: 236-48(Jul-Sep 1969) |
| 27 | 25-55224 | Minerva Fisiconucl.; 13: 249-61(Jul-Sep 1969) |
| 28 | 25-55225 | Minerva Fisiconucl.; 13: 292-300(Oct-Dec 1969) |
| CONF-680933- | (Radioisotopes in Pharmacological and Clinical Biochemistry Meeting, Wiesbaden, Germany, Sept. 26-28, 1968) | |
| | 25-55255 | Stuttgart; F. K. Schattauer Verlag GmbH (1970). 757p |
| CONF-690128- | (Fuel Failure Detection Symposium, Tokyo, Japan, Jan. 31, 1969) | |
| | 25-57192 | See JAERI-Memo-4157 |
| CONF-690452- | (Meeting on Mechanisms of Corrosion by Molten Salts, Dusseldorf, Germany, Apr. 10, 1969) | |
| | 25-55371 | |
| CONF-690603- | (4th International Federation of Automatic Control Conference, Warsaw, Poland, June 16-20, 1969) | |
| (Absts.) | 25-55087 | Duesseldorf; International Federation of Automatic Control (1971). 348p |
| CONF-690609- | (15th Annual Meeting of the American Nuclear Society, Seattle, Wash., June 15-19, 1969) | |
| 29 | 25-55370 | See BNWL-SA-2335 |
| CONF-690663- | (Conference on the Application of the Mossbauer Effect, Tihany, Hungary, June 17-21, 1969) | |
| | 25-56374 | Budapest; Akademiai Kiado (1971). 808p |
| CONF-690706- | (Conference on Computational Physics, Culham, England, July 28-31, 1969) | |
| (Vols.1 and 2) | 25-56400 | London; Her Majesty's Stationery Office (1969). 255p. Pound 4 |
| CONF-690733- | (24th Annual Congress of ABM, Sao Paulo, Brazil, July 1969) | |
| 1 | 25-55609 | See ORNL-tr-2456 |
| CONF-690929- | (15th National Congress of the Italian Association for Health Physics and Protection Against Radiation, Cagliari, Italy, Sept. 29-Oct. 3, 1969) | |
| 7 | 25-54798 | Minerva Fisiconucl.; 14: 31-7(Jan-Mar 1970) |
| CONF-691065- | (6th International Symposium on Remote Sensing of Environment, Ann Arbor, Mich., Oct. 13-16, 1969) | |
| (Vol.1) | 25-54767 | Ann Arbor, Mich.; University of Michigan (1969). 697p |
| CONF-700114- | (6th Symposium on Mossbauer Effect | |

XUM

Report No. Abstract No. Availability

Methodology, Chicago, Ill., Jan. 25, 1970)
25-56364 Boston; New England Nuclear Corporation (1971). 244p

CONF-700402- (16th Annual Meeting on The Environmental Challenge of the 70'S, Boston, Mass., Apr. 12-12, 1970)
25-54932 Mt. Prospect, Ill,; Institute of Environmental Sciences (1970). 540p. $20.00

CONF-700424- (Symposium on The Past Decade in Particle Theory, Austin, Tex., Apr. 14-17, 1970)
2 25-56549 See ORO-3992-9

CONF-700427- (4th International Conference on Experimental Stress Analysis, Cambridge, England, Apr. 6-10, 1970)
25-54846 London; Institution of Mechanical Engineers (1971). 584p

CONF-700438- (Reactor Meeting, Berlin, Germany, Apr. 20-22, 1970)
25-56877

CONF-700445- (International Symposium on Computer Graphics, London, England, Apr. 14-16, 1970)
25-57007 New York; Plenum Publishing Corporation (1971). 1242p. $47.50

CONF-700505- (2nd Congress of the International Radiation Protection Association, Brighton, England, May 3-8, 1970)
25 25-54851 Radioprotection; 5: 323-8(1970)

CONF-700557- (Meeting on Mechanical Flow Processes in Gas Centrifuges, Porz-Wahn, Germany, May 14, 1970)
5 25-54888 Dep. NTIS (U. S. Sales Only), 23p.
7 25-54890 See K-Trans-61-3
8 25-54891 See K-Trans-61-5

CONF-700564- (10th Annual International Conference of the Canadian Nuclear Association, Toronto, Canada, May 24-27, 1970)
5 25-56893 See NUMERICAL 70-CNA-631
7 25-57059 See NUMERICAL 70-CNA-628
10 25-57211 See NUMERICAL 70-CNA-657
12 25-55194 See NUMERICAL 70-CNA-641

CONF-700605- (2nd International Conference on Nuclear Data for Reactors, Helsinki, Finland, June 15-19, 1970)
11 25-56835 See UCRL-Trans-10540
12 25-56754 See UCRL-Trans-10541
13 25-56836 See UCRL-Trans-10542

CONF-700627- (4th International Conference on Resonant Particles, Athens, Ohio, June 15-17, 1970)
2 25-56500 See ORO-3992-18

CONF-700628- (Cryogenic Engineering Conference, Boulder, Colo., June 17-19, 1970)
25-56113 New York; Plenum Publishing Corporation (1971). 518p. $30.00

CONF-700652- (10th Meeting on Radiation Chemistry, Marianske Lazne, Czechoslovakia, June 22-25, 1970)
(Vol.1) 25-54588
(Vol.2) 25-54592
(Vol.3) 25-54595

CONF-700658- (Siemens Process Calculator Utilization Conference, Julich, Germany, June 29-July 1, 1970)
25-55074 See JUL-Conf-5

CONF-700709- (International Powder Metallurgy Conference, New York, N.Y., July 12-16, 1970)
(Vol.4) 25-55411 New York; Plenum Publishing Corporation (1971). 603p. $29.50
(Vol.5) 25-55481 New York; Plenum Publishing Corporation (1971). 501p. $29.50

CONF-700824- (International Conference on Radiation Effects and Semiconductors, Albany, N.Y., Aug. 24-27, 1970)
3 25-56303 Radiat. Eff.; 9: No. 1-2, 27-36(May 1971)
4 25-56302 Radiat. Eff.; 9: No. 1-2, 37-40(May 1971)
5 25-56301 Radiat. Eff.; 9: No. 1-2, 41-5(May 1971)
6 25-56300 Radiat. Eff.; 9: No. 1-2, 47-9(May 1971)
7 25-56299 Radiat. Eff.; 9: No. 1-2, 51-5(May 1971)
8 25-56298 Radiat. Eff.; 9: No. 1-2, 57 (May 1971)
9 25-56297 Radiat. Eff.; 9: No. 1-2, 65-73(May 1971)
10 25-56296 Radiat. Eff.; 9: No. 1-2, 75-9(May 1971)
11 25-56294 Radiat. Eff.; 9: No. 1-2, 89-92(May 1971)
12 25-56293 Radiat. Eff.; 9: No. 1-2, 93-7(May 1971)
13 25-56292 Radiat. Eff.; 9: No. 1-2, 99-103(May 1971)
14 25-56291 Radiat. Eff.; 9: No. 1-2, 105-13(May 1971)
15 25-56290 Radiat. Eff.; 9: No. 1-2, 115-20(May 1971)
16 25-56289 Radiat. Eff.; 9: No. 1-2, 121-5(May 1971)
17 25-56288 Radiat. Eff.; 9: No. 1-2, 127-31(May 1971)
18 25-56287 Radiat. Eff.; 9: No. 1-2, 133-8(May 1971)
19 25-56286 Radiat. Eff.; 9: No. 1-2, 139-44(May 1971)
20 25-56332 Radiat. Eff.; 8: No. 3-4, 155-60(Apr 1971)
21 25-56331 Radiat. Eff.; 8: No. 3-4, 161-4(Apr 1971)
22 25-56330 Radiat. Eff.; 8: No. 3-4, 165-70 (Apr 1971)
23 25-56329 Radiat. Eff.; 8: No. 3-4, 171-5(Apr 1971)
24 25-56328 Radiat. Eff.; 8: No. 3-4, 177-82(Apr 1971)
25 25-56327 Radiat. Eff.; 8: No. 3-4, 183-8(Apr 1971)
26 25-56325 Radiat. Eff.; 8: No. 3-4, 189-93(Apr 1971)
27 25-56326 Radiat. Eff.; 8: No. 3-4, 195-201(Apr 1971)
28 25-56324 Radiat. Eff.; 8: No. 3-4, 203-11(Apr 1971)
29 25-56312 Radiat. Eff.; 8: No. 3-4, 213-19(Apr 1971)
30 25-56311 Radiat. Eff.; 8: No. 3-4, 221-7(Apr 1971)
31 25-56310 Radiat. Eff.; 8: No. 3-4, 229-37(Apr 1971)
32 25-56309 Radiat. Eff.; 8: No. 3-4, 239-44(Apr 1971)
33 25-56308 Radiat. Eff.; 8: No. 3-4, 245-8(Apr 1971)
34 25-56307 Radiat. Eff.; 8: No. 3-4, 249-53 (Apr 1971)
35 25-56306 Radiat. Eff.; 8: No. 3-4, 255-62(Apr 1971)
36 25-56305 Radiat. Eff.; 8: No. 3-4, 263-7(Apr 1971)
37 25-56304 Radiat. Eff.; 8: No. 3-4, 269-77(Apr 1971)
38 25-56295 Radiat. Eff.; 8: No. 1-2, 83-8(May 1971)

CONF-700846- (5th Symposium of the International Association for Hydraulic Research, Stockholm, Sweden, Aug. 23-26, 1970)
(Pt.1) 25-57035 Vaellingby, Sweden; Svenska Centralkommitten foer Internationella Ingenjoerskongresser (1970). 575p
(Pt.2) 25-57009 Vaellingby, Sweden; Svenska Centralkommitten foer Internationella Ingenjoerskongresser (1970). 315p

CONF-700901- (5th Symposium on Thermophysical Properties, American Society of Mechanical Engineers, Boston, Mass., Sept. 30-Oct. 2, 1970)
25-55624 New York; American Society of Mechanical Engineers (1970). 513p

CONF-700967- (Conference on the Physics and Chemistry of Aerosols, Fontenay-aux-Roses, France, Sept. 24-25, 1970)
25-54799 J. Aerosol. Sci.; 2: No. 2, 131-280(Jun 1971)

CONF-700968- (Conference on Activation Analysis in Geochemistry and Cosmochemistry, Kjeller, Norway, Sept. 7-12, 1970)
25-54457 Oslo; Universitetsforlaget (1971). 468p

CONF-701051- (3rd Russian-Italian Symposium on Chromatography, Tbilisi, U.S.S.R., Oct. 26-29, 1970)
25-54398 J. Chromatogr.; 58: No. 1, 1-135(10 Jun 1971)

CONF-701102- (Meeting of the American Nuclear Society, Washington, D.C., Nov. 15-19, 1970)
24 25-57093 See ORNL-TM-3504

| Report No. | Abstract No. | Availability |
|---|---|---|
| CONF-701106- | | (5th Annual Midyear Topical Symposium on Health Physics Aspects of Nuclear Facility Siting, Idaho Falls, Idaho, Nov. 3-6, 1970) |
| (Vol.1) | 25-57103 | Idaho Falls, Idaho; Burton R. Baldwin, Publications Chairman (1971). 259p |
| (Vol.2) | 25-55157 | Idaho Falls, Idaho; Burton R. Baldwin, Publications Chairman (1971). 288p |
| (Vol.3) | 25-55193 | Idaho Falls, Idaho; Burton R. Baldwin, Publications Chairman (1971). 256p |
| CONF-701121- | | (Meeting on Electron Synchrotron, Frascati, Italy, Nov. 5-7, 1970) |
| 8 | 25-56404 | Dep. NTIS (U. S. Sales Only), 53p. |
| CONF-701217- | | (Measurements and Instrumentation Symposium, Albuquerque, N. Mex., Dec. 9-10, 1970) |
| 1 | 25-54924 | See SC-DR-710178 |
| CONF-710108- | | (2nd Panel on the Peaceful Uses of Nuclear Explosions, Vienna, Austria, Jan. 18-22, 1971) |
| | 25-54818 | See UCRL-Trans-10543 |
| CONF-710216- | | (Conference on Some Microscopic Aspects of Nuclear Reactions, La Toussuire, France, Feb. 15-19, 1971) |
| | 25-56821 | See LYCEN-7104 |
| CONF-710302- | | (Meeting on New Development in Reactor Mathematics and Applications, Idaho Falls, Idaho, Mar. 29-31, 1971) |
| (Vol.1) | 25-57071 | Dep. NTIS, 569p. |
| (Vol.2) | 25-57147 | Dep. NTIS, 566p. |
| CONF-710304- | | (Symposium on Natural and Manmade Radiation in Space, Las Vegas, Nev., Mar. 1-5, 1971) |
| 13 | 25-57133 | See ORNL-TM-3366 |
| CONF-710314- | | (Symposium on Biophysical Aspects of Radiation Quality, Lucas Heights, Australia, Mar. 8-12, 1971) |
| 1 | 25-55317 | See CEA-CONF-1744 |
| CONF-710317- | | (16th Nuclear Congress, Rome, Italy, Mar. 25-26, 1971) |
| 2 | 25-54865 | See CEA-CONF-1758 |
| CONF-710331- | | (Isotopic Composition of Cosmic Ray Nuclei Conference, Lyngby, Denmark, Mar. 23-25, 1971) |
| 1 | 25-55894 | See LUIP-CR-71-4 |
| CONF-710401- | | (Rocky Flats Symposium on Safety in Plutonium Handling Facilities, Golden, Colo., Apr. 13-15, 1971) |
| | 25-54937 | Dep. NTIS, 463p. |
| CONF-710437- | | (International Symposium on High Energy Physics, Dresden, Germany, Apr. 19-26, 1971) |
| 1 | 25-56429 | See INP-754 |
| CONF-710438- | | (National Telemetering Conference, Washington, D.C., Apr. 12-15, 1971) |
| 1 | 25-57266 | See RLO-1929-16 |
| CONF-710505- | | (American Industrial Hygiene Conference, Toronto, Ontario, Canada, May 24-28, 1971) |
| 6 | 25-54780 | Dep. NTIS, 42p. |
| CONF-710527- | | (Physics Conference, Evian, France, May 25-29, 1971) |
| 2 | 25-56225 | See CEA-CONF-1802 |
| 4 | 25-56226 | See CEA-CONF-1804 |
| 5 | 25-56227 | See CEA-CONF-1805 |
| 6 | 25-56228 | See CEA-CONF-1806 |
| 7 | 25-56162 | See CEA-CONF-1801 |
| CONF-710606- | | (17th Annual Meeting of The American Nuclear Society, Boston, Mass., June 13-17, 1971) |
| 12 | 25-55038 | See LA-DC-12314 |
| 13 | 25-54436 | See ORNL-TM-3463 |
| CONF-710609- | | (International Conference on Elementary Particles, Amsterdam, Netherlands, June 30-July 6, 1971) |
| 8 | 25-56475 | See RPP/C-24 |
| 9 | 25-56547 | See NYO-1932(2)-200 |
| CONF-710612- | | (10th Biennial Conference on Carbon, Bethlehem, Pa., June 27-July 2, 1971) |
| 3 | 25-56283 | See CEA-CONF-1823 |
| 4 | 25-56282 | See CEA-CONF-1822 |
| 5 | 25-55645 | See CEA-CONF-1821 |
| CONF-710624- | | (International Working Session on Fusion Reactor Technology Conference, Oak Ridge, Tenn., June 28-July 2, 1971) |



| Report No. | Abstract No. | Availability |
|---|---|---|
| 2 | 25-55575 | See LA-DC-12996 |
| 3 | 25-56110 | See LA-DC-12990 |
| CONF-710625- | | (Thermonuclear Information Meeting, Oak Ridge, Tenn., June 1971) |
| 1 | 25-56580 | See BNL-16026 |
| CONF-710708- | | (Symposium on the Nuclear Three Body Problem and Related Topics, Budapest, Hungary, July 7-11, 1971) |
| 2 | 25-56817 | See JINR-E4-5836 |
| 3 | 25-56640 | See FRNC-CONF-8 |
| CONF-710709- | | (Annual Conference on Nuclear and Space Radiation Effects, Durham, N.H., July 20-23, 1971) |
| 3 | 25-55079 | See SC-DC-713696 |
| CONF-710710- | | (16th Annual Health Physics Society Meeting, New York, N.Y., July 12-16, 1971) |
| 10 | 25-55108 | See BNWL-SA-3747 |
| CONF-710809- | | (Tritium Symposium, Las Vegas, Nev., Aug. 30-Sept. 2, 1971) |
| 2 | 25-55003 | See UCRL-73128 |
| CONF-710810- | | (Meeting on Particles and Fields, Rochester, N.Y., Aug. 30-Sept. 2, 1971) |
| 3 | 25-56545 | See IC-71/108 |
| CONF-710813- | | (Meetings of the Genetics Society of America, Rochester, N.Y., Aug. 23-25, 1971) |
| (Absts.) | 25-55166 | Genetics; 68: No. 1, Suppl., s1-77(1971) |
| CONF-710816- | | (International Symposium on Electron and Photon Interactions, Ithaca, N.Y., Aug. 23-27, 1971) |
| 1 | 25-56452 | See CALT-68-313 |
| CONF-710817- | | (Plutonium Symposium, Los Alamos, N. Mex., Aug. 5, 1971) |
| 1 | 25-55151 | Dep. NTIS, 11p. |
| CONF-710819- | | (4th Topical Conference, Honolulu, Hawaii, Aug. 2-13, 1971) |
| 1 | 25-56482 | See COO-1195-224 |
| CONF-710902- | | (4th Annual Meeting of The International Metallographic Society, Denver, Colo., Sept. 21-23, 1971) |
| 2 | 25-57238 | See MLM-OP-71003 |
| 3 | 25-57239 | See MLM-OP-71004 |
| 6 | 25-57240 | See MLM-OP-71007 |
| CONF-710903- | | (1st International Conference on Structural Mechanics in Reactor Technology, Berlin, Germany, Sept. 20-24, 1971) |
| (Vol.3)(Pt. H) | 25-56882 | Luxemburg; Commission of the European Communities (1971). 492p |
| 3 | 25-57070 | See CEA-CONF-1796 |
| CONF-710911- | | (4th International Conference on High Energy Physics and Nuclear Structure, Dubna, U.S.S.R., Sept. 7-11, 1971) |
| 2 | 25-56589 | See LA-DC-12730 |
| 9 | 25-56520 | See IC-71/106 |
| CONF-710912- | | (Instrumentation Fair Conference, Washington, D.C., Sept. 9-10, 1971) |
| 1 | 25-55076 | See LA-DC-12576 |
| CONF-710914- | | (15th Solvay Conference, Brussels, Belgium, September 1971) |
| 1 | 25-55882 | See NYO-1447-64 |
| CONF-711001- | | (9th Rare Earth Research Conference, Blacksburg, Va., Oct. 10-14, 1971) |
| 2 | 25-54530 | See LA-DC-12469 |
| CONF-711005- | | (International Conference on Solid Surfaces, Boston, Mass., Oct. 11-15, 1971) |
| 1 | 25-55434 | See RLO-2221-T-7-3 |
| 2 | 25-55435 | See RLO-2221-T-7-4 |
| 3 | 25-57237 | See LBL-133 |
| CONF-711009- | | (Joint Meeting of the American Nuclear Society, Miami Beach, Fla., Oct. 17-21, 1971) |
| 3 | 25-55573 | See BNWL-SA-3962 |
| 6 | 25-54994 | See EGG-1183-2283 |
| 7 | 25-56260 | See EGG-1183-2284 |
| CONF-711012- | | (Symposium on Ion Sources and Formation of Ion Beams, Upton, N.Y., Oct. 19-21, 1971) |
| 6 | 25-55814 | See UCRL-73353 |
| 7 | 25-56217 | See UCRL-73387 |
| 8 | 25-56218 | See UCRL-73412 |
| 9 | 25-56208 | Dep. NTIS, 7p. |

XUM

| Report No. | Abstract No. | Availability |
|---|---|---|
| 10 | 25-56212 | See LBL-35 |
| 11 | 25-56213 | See LBL-327 |
| COO- | | |
| 1120-124 | 25-56812 | Dep. NTIS, 134p. |
| 1195-217 | 25-56423 | Dep. NTIS, 146p. |
| 1195-224 | 25-56482 | Dep. NTIS, 6p. |
| 1231-67 | 25-55109 | Dep. NTIS, 22p. |
| 1428-276 | 25-56440 | Dep. NTIS, 33p. |
| 1428-280 | 25-56424 | Dep. NTIS, 30p. |
| 1428-294 | 25-56425 | Dep. NTIS, 11p. |
| 1456-16 | 25-57216 | Dep. NTIS, 17p. |
| 1469-187 | 25-57217 | Dep. NTIS, 27p. |
| 1469-190 | 25-57218 | Dep. NTIS, 139p. |
| 1469-193 | 25-57219 | Dep. NTIS, 164p. |
| 1533-15 | 25-57220 | Dep. NTIS, 88p. |
| 1624-41 | 25-55095 | Dep. NTIS, 53p. |
| 1707-11 | 25-55524 | Dep. NTIS, 8p. |
| 1707-12 | 25-57221 | Dep. NTIS, 11p. |
| 1746-57 | 25-56813 | Dep. NTIS, 8p. |
| 2013-19 | 25-57222 | Dep. NTIS, 53p. |
| 2022-7 | 25-56814 | Dep. NTIS, 29p. |
| 2049-5 | 25-56650 | Dep. NTIS, 97p. |
| 2049-6 | 25-55033 | Dep. NTIS, 90p. |
| 2049-7 | 25-55034 | Dep. NTIS, 144p. |
| 2049-8 | 25-56257 | Dep. NTIS, 21p. |
| 2049-9 | 25-56258 | Dep. NTIS, 147p. |
| 2118-13 | 25-57223 | Dep. NTIS, 39p. |
| 2118-14 | 25-57224 | Dep. NTIS, 35p. |
| 2118-15 | 25-57219 | See COO-1469-193 |
| 2118-17 | 25-57225 | Dep. NTIS, 87p. |
| 2118-19 | 25-57226 | Dep. NTIS, 55p. |
| 2118-21 | 25-57227 | Dep. NTIS, 127p. |
| CPT- | (Non-AEC) | |
| 26 | 25-56548 | See ORO-3992-1 |
| 45 | 25-56535 | See ORO-3992-7 |
| 47 | 25-56499 | See ORO-3992-8 |
| 50 | 25-56549 | See ORO-3992-9 |
| 51 | 25-56484 | See ORO-3992-10 |
| 52 | 25-56539 | See ORO-3992-11 |
| 55 | 25-56550 | See ORO-3992-14 |
| 65 | 25-56500 | See ORO-3992-18 |
| 92 | 25-56453 | See ORO-3992-42 |
| 116 | 25-56485 | See ORO-3992-66 |
| CRD- | (Rumanian) | |
| 44-1970 | 25-55001 | See NP-19011 |
| CTO- | (Non-AEC) | |
| 764 | 25-56209 | Dep. NTIS (U. S. Sales Only) |
| DASA- | (Misc.) | |
| 2612 | 25-54815 | See AD-722031 |
| DESY- | (German) | |
| 71/33 | 25-56405 | Dep. NTIS (U. S. Sales Only), 18p. |
| 71/35 | 25-56406 | Dep. NTIS (U. S. Sales Only), 55p. |
| 71/39 | 25-56543 | Dep. NTIS (U. S. Sales Only), 85p. |
| DLCS- | | |
| 5000271 | 25-56894 | Dep. NTIS, 23p. |
| DOCKET-1155- | (LaCrosse Boiling Water Reactor) (AEC) | |
| 134 | 25-56925 | Dep. NTIS, 28p. |
| 135 | 25-56895 | Dep. NTIS, 46p. |
| DOCKET-50003- | (Indian Point Station; See Also DOCKET-50247, DOCKET-50286) (Non-AEC) | |
| 89 | 25-56926 | Dep. NTIS, 3p. |
| 90 | 25-56927 | Dep. NTIS, 29p. |
| 91 | 25-56928 | Dep. NTIS, 7p. |
| DOCKET-50010- | (Dresden Nuclear Power Station; See also DOCKET-50237 and DOCKET-50249) (Non-AEC) | |
| 95 | 25-56896 | Dep. NTIS, 2p. |
| DOCKET-50016- | (Enrico Fermi Atomic Power Plant) (Non-AEC) | |
| 127 | 25-56929 | Dep. NTIS, 10p. |
| 128 | 25-56930 | Dep. NTIS, 16p. |
| 129 | 25-56931 | Dep. NTIS, 2p. |
| DOCKET-50029- | (Yankee Atomic Electric Co.) (Non-AEC) | |
| 158 | 25-56897 | Dep. NTIS, 8p. |
| DOCKET-50133- | (Humboldt Bay Power Plant) (Non-AEC) | |
| 68 | 25-56932 | Dep. NTIS, 8p. |
| DOCKET-50146- | (Saxton Nuclear Experimental Corporation) (Non-AEC) | |
| 91 | 25-56933 | Dep. NTIS, 2p. |
| 92 | 25-56934 | Dep. NTIS, 4p. |
| DOCKET-50155- | (Big Rock Point Reactor) (Misc.) | |
| 92 | 25-56935 | Dep. NTIS, 17p. |
| DOCKET-50201- | (West Valley Reprocessing Plant--Formerly Spent Fuel Processing Plant) (Misc.) | |
| 86 | 25-54710 | Dep. NTIS, 9p. |

| Report No. | Abstract No. | Availability |
|---|---|---|
| DOCKET-50206- | (San Onofre Nuclear Generating Station) (Misc.) | |
| 124 | 25-56898 | Dep. NTIS, 12p. |
| 125 | 25-56936 | Dep. NTIS, 12p. |
| DOCKET-50219- | (Oyster Creek Nuclear Power Plant) (Non-AEC) | |
| 145 | 25-56937 | Dep. NTIS, 8p. |
| 146 | 25-56899 | Dep. NTIS, 36p. |
| 147 | 25-56900 | Dep. NTIS, 4p. |
| DOCKET-50220- | (Nine Mile Point Nuclear Station) (Non-AEC) | |
| 73 | 25-56901 | Dep. NTIS, 2p. |
| 74 | 25-56902 | Dep. NTIS, 2p. |
| DOCKET-50237- | (Dresden Nuclear Power Station, See also DOCKET-50249) (Non-AEC) | |
| 200 | 25-56938 | Dep. NTIS, 3p. |
| 201 | 25-56939 | Dep. NTIS, 14p. |
| DOCKET-50238- | (N.S. Savannah Safety Assessment) (Non-AEC) | |
| 83 | 25-57136 | Dep. NTIS, 126p. |
| 84 | 25-57137 | Dep. NTIS, 3p. |
| DOCKET-50244- | (Robert Emmett Ginna Nuclear Power Plant, Formerly Brookwood Nuclear Station) (Non-AEC) | |
| 78 | 25-56940 | Dep. NTIS, 35p. |
| 79 | 25-56941 | Dep. NTIS, 57p. |
| 80 | 25-56903 | Dep. NTIS, 3p. |
| DOCKET-50245- | (Millstone Point Nuclear Power Station) (Non-AEC) | |
| 89 | 25-56904 | Dep. NTIS, 4p. |
| 90 | 25-56905 | Dep. NTIS, 1p. |
| 91 | 25-56906 | Dep. NTIS, 2p. |
| 92 | 25-56907 | Dep. NTIS, 1p. |
| 93 | 25-56908 | Dep. NTIS, 1p. |
| DOCKET-50249- | (Dresden Nuclear Power Station; See also DOCKET-50237) (Non-AEC) | |
| 101 | 25-56909 | Dep. NTIS, 7p. |
| 102 | 25-56942 | Dep. NTIS, 14p. |
| 103 | 25-56943 | Dep. NTIS, 3p. |
| DOCKET-50254- | (Quad-Cities Station; See also DOCKET-50265) (Non-AEC) | |
| 52 | 25-56944 | Dep. NTIS, 269p. |
| DOCKET-50255- | (Palisades Plant) (Non-AEC) | |
| 53 | 25-56910 | Dep. NTIS, 5p. |
| 54 | 25-56911 | Dep. NTIS, 2p. |
| DOCKET-50261- | (H. B. Robinson) (Non-AEC) | |
| 73 | 25-56945 | Dep. NTIS, 80p. |
| DOCKET-50263- | (Monticello Nuclear Generating Plant) (Non-AEC) | |
| 82 | 25-56912 | Dep. NTIS, 2p. |
| 83 | 25-56946 | Dep. NTIS, 37p. |
| 84 | 25-56913 | Dep. NTIS, 2p. |
| 85 | 25-56914 | Dep. NTIS, 2p. |
| DOCKET-50265- | (Quad-Cities Station; See also DOCKET-50254) (Non-AEC) | |
| 44 | 25-56944 | See DOCKET-50254-52 |
| DOCKET-50266- | (Point Beach Nuclear Plant) (Non-AEC) | |
| 55 | 25-56947 | Dep. NTIS, 90p. |
| DOCKET-50269- | (Oconee Nuclear Station, See also DOCKET-50270, and DOCKET-50287) (Non-AEC) | |
| 37 | 25-56915 | Dep. NTIS, 51p. |
| DOCKET-50280- | (Surry Power Station, See also DOCKET-50281) (Non-AEC) | |
| 45 | 25-56948 | Dep. NTIS, 25p. |
| 46 | 25-56949 | Dep. NTIS, 277p. |
| 47 | 25-56950 | Dep. NTIS, 251p. |
| 48 | 25-56951 | Dep. NTIS, 84p. |
| 49 | 25-56952 | Dep. NTIS, 42p. |
| DOCKET-50281- | (Surry Power Station, See also DOCKET-50280) (Non-AEC) | |
| 44 | 25-56949 | See DOCKET-50280-46 |
| 45 | 25-56950 | See DOCKET-50280-47 |
| 46 | 25-56951 | See DOCKET-50280-48 |
| 47 | 25-56952 | See DOCKET-50280-49 |
| DOCKET-50282- | (Prairie Island Nuclear Generating Plant, See also DOCKET-50306) (Non-AEC) | |
| 40 | 25-56953 | Dep. NTIS, 547p. |
| DOCKET-50295- | (Zion Station Nuclear Power Plant. See also DOCKET-50304) (Non-AEC) | |
| 30 | 25-56954 | Dep. NTIS, 110p. |
| DOCKET-50298- | (Cooper Nuclear Station) (Non-AEC) | |
| 22 | 25-56955 | Dep. NTIS, 343p. |
| DOCKET-50301- | (Point Beach Nuclear Plant) (Non-AEC) | |
| 40 | 25-56947 | See DOCKET-50266-55 |

| Report No. | Abstract No. | Availability |
|---|---|---|
| DOCKET-50302- | | (Crystal River Nuclear Plant; see DOCKET-50303) (Non-AEC) |
| 25 | 25-56956 | Dep. NTIS, 103p. |
| DOCKET-50304- | | (Zion Station Nuclear Power Plant. See also DOCKET-50295) (Non-AEC) |
| 29 | 25-56954 | See DOCKET-50295-30 |
| DOCKET-50305- | | (Kewaunee Nuclear Power Plant) (Non-AEC) |
| 25 | 25-56957 | Dep. NTIS, 298p. |
| DOCKET-50306- | | (Prairie Island Nuclear Generating Plant, See also DOCKET-50282) (Non-AEC) |
| 39 | 25-56953 | See DOCKET-50282-40 |
| DOCKET-50309- | | (Maine Yankee Atomic Power Company) (Non-AEC) |
| 41 | 25-56958 | Dep. NTIS, 127p. |
| DOCKET-50313- | | (Russellville Nuclear Unit) (Non-AEC) |
| 31 | 25-56959 | Dep. NTIS, 133p. |
| DOCKET-50324- | | (Brunswick Steam Electric Plant, Units 1 and 2, See also DOCKET-50325) (Non-AEC) |
| 22 | 25-56960 | Dep. NTIS, 45p. |
| DOCKET-50325- | | (Brunswick Steam Electric Plant, Units 1 and 2, See also DOCKET-50324) (Non-AEC) |
| 22 | 25-56960 | See DOCKET-50324-22 |
| DOCKET-50333- | | (James A. Fitzpatrick Nuclear Power Plant) (Non-AEC) |
| 30 | 25-56961 | Dep. NTIS, 645p. |
| DOCKET-50334- | | (Beaver Valley Power Station) (Non-AEC) |
| 25 | 25-56962 | Dep. NTIS, 356p. |
| DOCKET-50344- | | (Trojan Nuclear Plant) (Non-AEC) |
| 22 | 25-56963 | Dep. NTIS, 43p. |
| DOCKET-50348- | | (Joseph M. Farley Nuclear Plant, Units 1 and 2, Formerly Seala Nuclear Plant, See also DOCKET-50364) (Non-AEC) |
| 24 | 25-56964 | Dep. NTIS, 12p. |
| 25 | 25-56965 | Dep. NTIS, 100p. |
| 26 | 25-56966 | Dep. NTIS, 6p. |
| DOCKET-50352- | | (Limerick Generating Station) (See also DOCKET-50353) (Non-AEC) |
| 19 | 25-56967 | Dep. NTIS, 210p. |
| 20 | 25-56968 | Dep. NTIS, 22p. |
| DOCKET-50353- | | (Limerick Generating Station) (See also DOCKET-50352) (Non-AEC) |
| 19 | 25-56967 | See DOCKET-50352-19 |
| 20 | 25-56968 | See DOCKET-50352-20 |
| DOCKET-50364- | | (Joseph M. Farley Nuclear Plant, Units 1 and 2, See also DOCKET-50348) (Non-AEC) |
| 18 | 25-56964 | See DOCKET-50348-24 |
| 19 | 25-56965 | See DOCKET-50348-25 |
| 20 | 25-56966 | See DOCKET-50348-26 |
| DOCKET-50366- | | (Edwin I. Hatch Nuclear Plant, Unit 2, Non-AEC) |
| 15 | 25-56969 | Dep. NTIS, 136p. |
| DOCKET-50367- | | (Bailly Generating Station Nuclear 1), (Non-AEC) |
| 21 | 25-56970 | Dep. NTIS, 351p. |
| 22 | 25-56971 | Dep. NTIS, 33p. |
| DOCKET-50376- | | (Aguirre Nuclear Plant) (Non-AEC) |
| 21 | 25-56972 | Dep. NTIS, 640p. |
| DOCKET-50398- | | (Mendocino Power Plant) (See Also DOCKET-50399) (Unit 1 and 2-NON-AEC) |
| 8 | 25-56973 | Dep. NTIS, 120p. |
| DOCKET-50399- | | (Mendocino Power Plant) (See Also DOCKET-50398) (Unit 1 and 2-NON-AEC) |
| 8 | 25-56973 | See DOCKET-50398-8 |
| DOCKET-50400- | | (Shearon Harris Nuclear Power Plant-See Also DOCKET-50401, 50402, 50403, NON-AEC) |
| 1 | 25-56974 | Dep. NTIS, 36p. |
| DOCKET-50401- | | (Shearon Harris Nuclear Power Plant-See Also DOCKET-50400, 50402, 50403, NON-AEC, Units 1, 2, 3, 4) |
| 1 | 25-56974 | See DOCKET-50400-1 |
| DOCKET-50402- | | (Shearon Harris Nuclear Power Plant-See Also DOCKET-50400, 50401, 50403, NON-AEC, Units 1, 2, 3, 4) |
| 1 | 25-56974 | See DOCKET-50400-1 |
| DOCKET-50403- | | (Shearon Harris Nuclear Power Plant-See Also Docket-50400, 50401, 50402, NON-AEC, Units 1, 2, 3, 4) |
| 1 | 25-56974 | See DOCKET-50400-1 |
| DP- | | |
| 929(Rev.1) (Suppl.3) | 25-57228 | Dep. NTIS, 23p. |
| 1275 | 25-55035 | Dep. NTIS, 40p. |
| DPC- | | |
| 851-31 | 25-56895 | See DOCKET-1155-135 |
| EGG- | | |
| 1183-1479 | 25-56259 | Dep. NTIS, 32p. |
| 1183-2283 | 25-54994 | Dep. NTIS, 15p. |
| 1183-2284 | 25-56260 | Dep. NTIS, 11p. |
| EIR- | | (Swiss) |
| 192 | 25-55590 | Dep. NTIS (U. S. Sales Only), 133p. |
| 198 | 25-54866 | Dep. NTIS (U. S. Sales Only), 154p. |
| EUR- | | (European Atomic Energy Community) |
| 4483 | 25-57229 | NTIS (U. S. Sales Only), 66p. |
| 4611 | 25-54995 | Dep. NTIS (U. S. Sales Only). EUR Lit. 620.-, 32p. |
| 4638 | 25-56879 | Dep. NTIS (U. S. Sales Only). EUR F.Fr. 18.35, 120p. |
| 4669 | 25-55246 | See CEA-Bib-200 |
| 4673 | 25-57187 | Dep. NTIS (U. S. Sales Only). EUR F.Fr. 13.08, 78p. |
| 4674 | 25-55646 | Dep. NTIS (U. S. Sales Only). EUR FF 4.45, 28p. |
| 4683 | 25-54867 | Dep. NTIS (U. S. Sales Only). EUR FF 7.75, 36p. |
| 4709 | 25-57020 | Dep. NTIS (U. S. Sales Only). EUR F.Fr. 5.60, 34p. |
| EUR-CEA-FC- | | (European Atomic Energy Community) |
| 598 | 25-56194 | Dep. NTIS (U. S. Sales Only), 14p. |
| 602 | 25-56229 | Dep. NTIS (U. S. Sales Only), 167p. |
| 603 | 25-56210 | Dep. NTIS (U. S. Sales Only), 29p. |
| EURFNR- | | (European Atomic Energy Community) |
| 897 | 25-54868 | Dep. NTIS |
| FEI- | | (Russian) |
| 202 | 25-56735 | Dep. NTIS (U. S. Sales Only), 11p. |
| 205 | 25-56683 | Dep. NTIS (U. S. Sales Only), 29p. |
| 216 | 25-56684 | Dep. NTIS (U. S. Sales Only), 49p. |
| 217 | 25-54869 | Dep. NTIS (U. S. Sales Only), 35p. |
| 233 | 25-56736 | Dep. NTIS (U. S. Sales Only), 25p. |
| FMRB- | | (German) |
| 37/71 | 25-56615 | Dep. NTIS (U. S. Sales Only), 25p. |
| FRNC-CONF- | | (French) |
| 8 | 25-56640 | Dep. NTIS (U. S. Sales Only), 2p. |
| FRNC-R- | | (French) |
| 1 | 25-56468 | Dep. NTIS (U. S. Sales Only), 12p. |
| FRNC-TH- | | (French) |
| 33 | 25-56497 | Dep. NTIS (U. S. Sales Only), 101p. |
| 48 | 25-56685 | Dep. NTIS (U. S. Sales Only), 101p. |
| 53 | 25-56426 | Dep. NTIS (U. S. Sales Only), 123p. |
| 54 | 25-55072 | Dep. NTIS (U. S. Sales Only), 97p. |
| 63 | 25-56474 | Dep. NTIS (U. S. Sales Only), 70p. |
| FTI- | | (Non-AEC) |
| 295 | 25-56224 | For translation see AEC-tr-7270 |
| GEAP- | | (Misc.) |
| 10010-29 | 25-57111 | Dep. NTIS, 74p. |
| 10347 | 25-54870 | Dep. NTIS, 76p. |
| 10385 | 25-57045 | Dep. NTIS, 60p. |
| 13639-1 | 25-57088 | Dep. NTIS, 133p. |
| 13639-2 | 25-57089 | Dep. NTIS, 382p. |
| 13722 | 25-57046 | Dep. NTIS, 56p. |
| GESP- | | (Non-AEC) |
| 199 | 25-55377 | See N-71-26947 |
| HASL- | | |
| 244 | 25-55036 | Dep. NTIS, 12p. |
| HEDL-TME- | | |
| 71-31 | 25-57112 | Dep. NTIS, 52p. |
| 71-33 | 25-57113 | Dep. NTIS, 37p. |
| 71-58 | 25-57114 | Dep. NTIS, 31p. |
| 71-65 | 25-57115 | Dep. NTIS, 19p. |
| 71-108 | 25-57230 | Dep. NTIS, 90p. |
| IAE- | | (Russian) |
| 1980 | 25-56583 | Dep. NTIS (U. S. Sales Only), 11p. |
| IAEA-R- | | (International Atomic Energy Agency) |
| 878-F | 25-54968 | |
| IC- | | (Italian) |
| 71/71 | 25-56544 | Dep. NTIS (U. S. Sales Only), 9p. |
| 71/106 | 25-56520 | Dep. NTIS (U. S. Sales Only), 18p. |
| 71/108 | 25-56545 | Dep. NTIS (U. S. Sales Only), 27p. |
| IFA-FT- | | (Rumanian) |

XUM

| Report No. | Abstract No. | Availability |
|---|---|---|
| 85 | 25-56533 | Dep. NTIS (U. S. Sales Only), 8p. |
| IFA-HE- | (Rumanian) | |
| 73 | 25-56427 | Dep. NTIS (U. S. Sales Only), 14p. |
| 75 | 25-56428 | Dep. NTIS (U. S. Sales Only), 17p. |
| 76 | 25-56498 | Dep. NTIS (U. S. Sales Only), 10p. |
| IFA-TR- | (Russian) | |
| 58 | 25-54871 | Dep. NTIS (U. S. Sales Only), 12p. |
| IKF- | (German) | |
| 28 | 25-54996 | Dep. NTIS (U. S. Sales Only), 93p. |
| INP- | (Polish) | |
| 741 | 25-56815 | Dep. NTIS (U. S. Sales Only), 41p. |
| 754 | 25-56429 | Dep. NTIS (U. S. Sales Only), 9p. |
| 756 | 25-56413 | Dep. NTIS (U. S. Sales Only), 20p. |
| 757 | 25-56414 | Dep. NTIS (U. S. Sales Only), 22p. |
| INR- | (Non-AEC) | |
| 1303 | 25-57116 | Dep. NTIS (U. S. Sales Only), 74p. |
| 1315 | 25-55073 | Dep. NTIS (U. S. Sales Only), 9p. |
| 1321 | 25-56230 | Dep. NTIS (U. S. Sales Only), 10p. |
| INR-P- | (Polish) | |
| 1322 | 25-56133 | Dep. NTIS (U. S. Sales Only), 7p. |
| 1325 | 25-54889 | Dep. NTIS (U. S. Sales Only), 10p. |
| 1327 | 25-55836 | Dep. NTIS (U. S. Sales Only), 10p. |
| INSJ- | (Japanese) | |
| 127 | 25-56651 | Dep. NTIS (U. S. Sales Only), 35p. |
| 128 | 25-54997 | Dep. NTIS (U. S. Sales Only), 21p. |
| INT- | (Misc.) | |
| 11 | 25-56341 | See NP-19010 |
| IPP- | (Non-AEC) | |
| 1/108 | 25-56149 | Dep. NTIS (U. S. Sales Only), 45p. |
| 4/82 | 25-56193 | Dep. NTIS (U. S. Sales Only), 94p. |
| IPP-III- | (German) | |
| 2 | 25-56211 | Dep. NTIS (U. S. Sales Only), 7p. |
| IS- | | |
| 2305 | 25-57231 | Dep. NTIS, 103p. |
| 2558 | 25-55152 | Dep. NTIS, 20p. |
| IS-T- | | |
| 459 | 25-55430 | Dep. NTIS, 129p. |
| 462 | 25-55525 | Dep. NTIS, 130p. |
| 494 | 25-57232 | Dep. NTIS, 120p. |
| JAERI-Memo- | (Japanese) | |
| 4157 | 25-57192 | |
| 4353 | 25-55247 | Dep. NTIS (U. S. Sales Only), 26p. |
| 4383 | 25-56816 | Dep. NTIS (U. S. Sales Only), 39p. |
| 4408 | 25-55574 | Dep. NTIS (U. S. Sales Only), 21p. |
| 4438 | 25-55589 | Dep. NTIS (U. S. Sales Only), 14p. |
| 4449 | 25-57021 | Dep. NTIS (U. S. Sales Only), 55p. |
| 4481 | 25-57182 | Dep. NTIS (U. S. Sales Only), 30p. |
| 4483 | 25-56195 | Dep. NTIS (U. S. Sales Only), 9p. |
| JINR- | (Russian) | |
| E1-5818 | 25-55044 | Dep. NTIS (U. S. Sales Only), 18p. |
| E2-5996 | 25-56537 | Dep. NTIS (U. S. Sales Only), 9p. |
| E2-6017 | 25-56483 | Dep. NTIS (U. S. Sales Only), 14p. |
| E4-5836 | 25-56817 | Dep. NTIS (U. S. Sales Only), 12p. |
| E4-5877 | 25-56737 | Dep. NTIS (U. S. Sales Only), 20p. |
| E4-5880 | 25-56818 | Dep. NTIS (U. S. Sales Only), 5p. |
| P1-5975 | 25-56521 | Dep. NTIS (U. S. Sales Only), 18p. |
| P1-6006 | 25-56739 | Dep. NTIS (U. S. Sales Only), 9p. |
| P2-5549 | 25-56522 | For translation see ORNL-tr-2520 |
| P2-5998 | 25-56546 | Dep. NTIS (U. S. Sales Only), 21p. |
| P3-5119 | 25-55039 | For translation see LB/G-3040 |
| P3-5875 | 25-56686 | Dep. NTIS (U. S. Sales Only), 11p. |
| P4-5889 | 25-56819 | Dep. NTIS (U. S. Sales Only), 17p. |
| P4-5954 | 25-56389 | Dep. NTIS (U. S. Sales Only), 42p. |
| P4-5957 | 25-55813 | Dep. NTIS (U. S. Sales Only), 22p. |
| P4-5986 | 25-56641 | Dep. NTIS (U. S. Sales Only), 13p. |
| P4-5997 | 25-56820 | Dep. NTIS (U. S. Sales Only), 14p. |
| P6-5888 | 25-56584 | Dep. NTIS (U. S. Sales Only), 19p. |
| P7-5584 | 25-56744 | For translation see NP-tr-1936 |
| P7-5884 | 25-56740 | Dep. NTIS (U. S. Sales Only), 18p. |
| P9-5945 | 25-56585 | Dep. NTIS (U. S. Sales Only), 12p. |
| P9-5956 | 25-56586 | Dep. NTIS (U. S. Sales Only), 9p. |
| P13-5970 | 25-54998 | Dep. NTIS (U. S. Sales Only), 17p. |
| P15-5959 | 25-56738 | Dep. NTIS (U. S. Sales Only), 7p. |
| JPRS- | (Non-AEC) | |
| 53174 | 25-54781 | NTIS |
| JUL- | (German) | |
| 635-RG | 25-55077 | For translation see LA-tr-71-71 |
| 731-FF | 25-56284 | Dep. NTIS (U. S. Sales Only), 66p. |
| 735-RW | 25-55591 | Dep. NTIS (U. S. Sales Only), 96p. |
| 736-RG | 25-57060 | Dep. NTIS (U. S. Sales Only), 84p. |
| 737-FF | 25-55037 | Dep. NTIS (U. S. Sales Only), 120p. |
| 739-PC | 25-55607 | Dep. NTIS (U. S. Sales Only), 60p. |
| 740-RB | 25-54872 | Dep. NTIS (U. S. Sales Only), 111p. |
| 748-PP | 25-56587 | Dep. NTIS (U. S. Sales Only), 89p. |
| 764-RG | 25-56616 | Dep. NTIS (U. S. Sales Only), 60p. |
| 765-RG | 25-56617 | Dep. NTIS (U. S. Sales Only), 52p. |
| 766-CT | 25-54969 | Dep. NTIS (U. S. Sales Only), 25p. |
| JUL-Conf- | (German) | |
| 5 | 25-55074 | |
| K- | | |
| 1817 | 25-55075 | Dep. NTIS, 7p. |
| K-Trans- | | |
| 61-3 | 25-54890 | Dep. NTIS |
| 61-5 | 25-54891 | Dep. NTIS |
| KFK- | (German) | |
| 1332 | 25-54868 | For translation see EURFNR-897 |
| 1397 | 25-56687 | Dep. NTIS (U. S. Sales Only), 78p. |
| KFKI- | (Hungarian) | |
| 71-35 | 25-56741 | Dep. NTIS (U. S. Sales Only), 8p. |
| 71-38 | 25-56534 | Dep. NTIS (U. S. Sales Only), 19p. |
| KHFTI- | (Russian) | |
| 70-72 | 25-56209 | For translation see CTO-764 |
| KY- | | |
| 631 | 25-54970 | Dep. NTIS, 17p. |
| LA- | | |
| 4490 | 25-55299 | Dep. NTIS, 211p. |
| 4535 | 25-56588 | Dep. NTIS, 76p. |
| 4545 | 25-57233 | Dep. NTIS, 14p. |
| 4558 | 25-55196 | Dep. NTIS, 115p. |
| 4721 | 25-57234 | Dep. NTIS, 9p. |
| 4728 | 25-57235 | Dep. NTIS, 12p. |
| 4745 | 25-54892 | Dep. NTIS, 6p. |
| 4774 | 25-56261 | Dep. NTIS, 4p. |
| LA-DC- | | |
| 12314 | 25-55038 | Dep. NTIS, 17p. |
| 12469 | 25-54530 | Dep. NTIS, 9p. |
| 12576 | 25-55076 | Dep. NTIS, 10p. |
| 12730 | 25-56589 | Dep. NTIS, 4p. |
| 12990 | 25-56110 | Dep. NTIS, 3p. |
| 12996 | 25-55575 | Dep. NTIS, 2p. |
| LA-tr- | | |
| 71-46 | 25-56590 | Dep. NTIS |
| 71-71 | 25-55077 | Dep. NTIS |
| 71-73 | 25-57236 | Dep. NTIS |
| LAL-RT- | (French) | |
| 42-70 | 25-56591 | Dep. NTIS (U. S. Sales Only), 13p. |
| 43-70 | 25-56592 | Dep. NTIS (U. S. Sales Only), 7p. |
| LB/G- | (British) | |
| 2995 | 25-55318 | Dep. NTIS (U. S. Sales Only) |
| 3040 | 25-55039 | Dep. NTIS (U. S. Sales Only) |
| 3059 | 25-55271 | Dep. NTIS (U. S. Sales Only) |
| 3074 | 25-55608 | Dep. NTIS (U. S. Sales Only) |
| LBL- | | |
| 35 | 25-56212 | Dep. NTIS, 5p. |
| 133 | 25-57237 | Dep. NTIS, 17p. |
| 327 | 25-56213 | Dep. NTIS, 2p. |
| LFEN-NI.- | (Portuguese) | |
| 56a | 25-55362 | Dep. NTIS (U. S. Sales Only), 75p. |
| LGI- | (Italian) | |
| 70/14/E | 25-56150 | Dep. NTIS (U. S. Sales Only), 27p. |
| 70/16/E | 25-56163 | Dep. NTIS (U. S. Sales Only), 51p. |
| 70/17/E | 25-56214 | Dep. NTIS (U. S. Sales Only), 24p. |
| 71/1/E | 25-56164 | Dep. NTIS (U. S. Sales Only), 15p. |
| LUIP-CR- | (Swedish) | |
| 71-2 | 25-55045 | Dep. NTIS (U. S. Sales Only), 85p. |
| 71-4 | 25-55894 | Dep. NTIS (U. S. Sales Only), 19p. |
| LYCEN- | (French) | |
| 7101 | 25-56742 | Dep. NTIS (U. S. Sales Only), 144p. |
| 7104 | 25-56821 | |
| MIT- | (Misc.) | |
| 1381-18 | 25-54757 | Dep. NTIS, 159p. |
| MLM- | | |
| 1736 | 25-54893 | Dep. NTIS, 57p. |
| 1851 | 25-57061 | Dep. NTIS, 198p. |
| MLM-OP- | | |
| 71003 | 25-57238 | Dep. NTIS, 9p. |
| 71004 | 25-57239 | Dep. NTIS, 13p. |
| 71007 | 25-57240 | Dep. NTIS, 20p. |
| MRR- | (West German) | |
| 73 | 25-57022 | Dep. NTIS (U. S. Sales Only), 87p. |
| MTP- | | |
| 6-2-332 | 25-54993 | See AD-720974 |

XUM

| Report No. | Abstract No. | Availability |
|---|---|---|
| N- | (Misc.) | |
| 71-16750 | 25-55046 | NTIS, 38p. |
| 71-22378 | 25-56262 | NTIS, 79p. |
| 71-23110 | 25-55431 | NTIS, 27p. |
| 71-23114 | 25-55432 | NTIS, 24p. |
| 71-23433 | 25-55733 | NTIS, 29p. |
| 71-23434 | 25-55734 | NTIS, 15p. |
| 71-23982 | 25-55433 | NTIS, 23p. |
| 71-24166 | 25-55735 | NTIS, 26p. |
| 71-24635 | 25-55096 | NTIS, 23p. |
| 71-24988 | 25-55895 | NTIS, 18p. |
| 71-25028 | 25-56196 | NTIS, 60p. |
| 71-25034 | 25-55576 | NTIS, 48p. |
| 71-25389 | 25-55097 | NTIS, 19p. |
| 71-25439 | 25-56231 | NTIS, 20p. |
| 71-25526 | 25-56215 | NTIS, 41p. |
| 71-26344 | 25-55669 | NTIS, 19p. |
| 71-26389 | 25-55098 | NTIS, 33p. |
| 71-26447 | 25-54999 | NTIS, 16p. |
| 71-26947 | 25-55377 | NTIS, 25p. |
| 71-27008 | 25-55399 | NTIS, 52p. |
| 71-27023 | 25-56146 | NTIS, 65p. |
| 71-27604 | 25-55952 | NTIS, 44p. |
| 71-27639 | 25-55896 | NTIS, 14p. |
| 71-27736 | 25-55656 | NTIS, 25p. |
| 71-27890 | 25-56165 | NTIS, 48p. |
| NASA-CR- | (Misc.) | |
| 1804 | 25-56146 | See N-71-27023 |
| 1811 | 25-55377 | See N-71-26947 |
| 118311 | 25-56196 | See N-71-25028 |
| 118657 | 25-54999 | See N-71-26447 |
| 118658 | 25-55669 | See N-71-26344 |
| 118660 | 25-55098 | See N-71-26389 |
| NASA-SP- | (Misc.) | |
| 8053 | 25-55576 | See N-71-25034 |
| NASA-TM-X- | (Misc.) | |
| 2263 | 25-56231 | See N-71-25439 |
| 2271 | 25-55096 | See N-71-24635 |
| 2280 | 25-56215 | See N-71-25526 |
| 64602 | 25-55399 | See N-71-27008 |
| 65440 | 25-55046 | See N-71-16750 |
| 65489 | 25-55735 | See N-71-24166 |
| 65496 | 25-55733 | See N-71-23433 |
| 65504 | 25-55734 | See N-71-23434 |
| 65506 | 25-55895 | See N-71-24988 |
| 65559 | 25-55656 | See N-71-27736 |
| 65562 | 25-55896 | See N-71-27639 |
| 65563 | 25-55952 | See N-71-27604 |
| NASA-TN-D- | (Misc.) | |
| 6170 | 25-56262 | See N-71-22378 |
| 6285 | 25-55431 | See N-71-23110 |
| 6291 | 25-55432 | See N-71-23114 |
| 6308 | 25-55433 | See N-71-23982 |
| 6330 | 25-55097 | See N-71-25389 |
| 6372 | 25-56165 | See N-71-27890 |
| NBS- | (Misc.) | |
| 10550 | 25-56255 | See AD-721388 |
| NBS-SPEC. PUBL- | (Non-AEC) | |
| 326 | 25-54878 | GPO $4.50 |
| NEDO- | (Non-AEC) | |
| 10320 (Suppl.1) | 25-57057 | |
| NLCO- | | |
| 1077 | 25-55400 | Dep. NTIS, 50p. |
| NOLTR- | (Misc.) | |
| 70-222 | 25-56256 | See AD-722012 |
| NP- | (AEC File No. for Non-AEC Reports) | |
| 18752 | 25-55252 | Dep. NTIS (U. S. Sales Only), 263p. |
| 18798 | 25-56265 | For translation see ORNL-tr-2518 |
| 18888 | 25-56415 | Dep. NTIS (U. S. Sales Only), 93p. |
| 18966 | 25-56743 | Dep. NTIS (U. S. Sales Only), 196p. |
| 18992 | 25-56983 | Dep. NTIS (U. S. Sales Only), 65p. |
| 18994 | 25-55040 | Dep. NTIS (U. S. Sales Only), 15p. |
| 18997 | 25-56441 | Dep. NTIS (U. S. Sales Only), 56p. |
| 18998 | 25-56594 | Dep. NTIS (U. S. Sales Only), 22p. |
| 19007 | 25-56595 | Dep. NTIS (U. S. Sales Only), 105p. |
| 19008 | 25-55000 | Dep. NTIS (U. S. Sales Only), 26p. |
| 19010 | 25-56341 | Dep. NTIS (U. S. Sales Only), 28p. |
| 19011 | 25-55001 | Dep. NTIS (U. S. Sales Only), 39p. |
| 19012 | 25-56166 | Dep. NTIS (U. S. Sales Only), 18p. |
| 19014 | 25-56216 | Dep. NTIS (U. S. Sales Only), 91p. |
| 19018 | 25-56643 | Dep. NTIS (U. S. Sales Only), 112p. |
| 19020 | 25-56232 | Dep. NTIS (U. S. Sales Only), 24p. |
| NP-tr- | (AEC File No. for Non-AEC Translations) | |
| 1936 | 25-56744 | |
| NRL- | (Misc.) | |
| 7310 | 25-55577 | |
| NYO- | | |



| Report No. | Abstract No. | Availability |
|---|---|---|
| 1163-TM-30 | 25-54812 | Dep. NTIS, 34p. |
| NYO- | | |
| 1447-64 | 25-55882 | Dep. NTIS, 16p. |
| 1480-179 | 25-57241 | Dep. NTIS, 75p. |
| 1932(2)-200 | 25-56547 | Dep. NTIS, 19p. |
| 2740-8 | 25-55205 | Dep. NTIS, 259p. |
| 3406-20 | 25-57242 | Dep. NTIS, 29p. |
| 3406-22 | 25-57243 | Dep. NTIS, 36p. |
| 3417-15 | 25-54692 | Dep. NTIS, 11p. |
| 3489-22 | 25-57244 | Dep. NTIS, 44p. |
| 3510-18 | 25-55208 | Dep. NTIS, 26p. |
| 3525-67 | 25-56832 | Dep. NTIS, 27p. |
| 3906-5 | 25-55078 | Dep. NTIS, 11p. |
| ORNL- | | |
| 4665 | 25-54971 | Dep. NTIS, 41p. |
| 4682 | 25-54711 | Dep. NTIS, 294p. |
| 4685 | 25-57245 | Dep. NTIS, 37p. |
| 4691 | 25-56745 | Dep. NTIS, 34p. |
| 4707 | 25-56746 | Dep. NTIS, 43p. |
| 4716 | 25-56263 | Dep. NTIS, 42p. |
| 4717 | 25-54531 | Dep. NTIS, 141p. |
| ORNL-IIC- | | |
| 37(Pt.2) | 25-54894 | Dep. NTIS, 45p. |
| ORNL-NSF-EP- | | |
| 8 | 25-57246 | Dep. NTIS, 10p. |
| ORNL-NSIC- | | |
| 94 | 25-57091 | Dep. NTIS, 129p. |
| ORNL-TM- | | |
| 2496(Rev.2) | 25-57183 | Dep. NTIS, 251p. |
| 2713(Rev.1) | 25-57247 | Dep. NTIS, 36p. |
| 2723 | 25-54972 | Dep. NTIS, 64p. |
| 2933 | 25-57248 | Dep. NTIS, 98p. |
| 3276 | 25-57063 | Dep. NTIS, 140p. |
| 3359 | 25-57048 | Dep. NTIS, 244p. |
| 3366 | 25-57133 | Dep. NTIS, 23p. |
| 3379 | 25-56655 | Dep. NTIS, 78p. |
| 3463 | 25-54436 | Dep. NTIS, 27p. |
| 3483 | 25-57092 | Dep. NTIS, 112p. |
| 3504 | 25-57093 | Dep. NTIS, 30p. |
| 3509 | 25-55041 | Dep. NTIS, 17p. |
| 3536 | 25-57249 | Dep. NTIS, 9p. |
| 3547 | 25-57250 | Dep. NTIS, 19p. |
| 3553 | 25-56264 | Dep. NTIS, 11p. |
| 3569 | 25-57120 | Dep. NTIS, 26p. |
| 3582 | 25-56134 | Dep. NTIS, 22p. |
| ORNL-tr- | | |
| 2456 | 25-55609 | Dep. NTIS |
| 2509 | 25-57251 | Dep. NTIS |
| 2518 | 25-56265 | Dep. NTIS |
| 2520 | 25-56522 | Dep. NTIS |
| 2525 | 25-57252 | Dep. NTIS |
| 2531 | 25-56747 | Dep. NTIS |
| ORO- | | |
| 2408-45 | 25-56748 | Dep. NTIS, 10p. |
| 2968-55 | 25-54621 | J. Polym. Sci., Part A-1; 9: No. 6, 1551-61(Jun 1971) |
| 2968-63 | 25-54667 | J. Phys. Chem.; 75: No. 19, 3023-4(16 Sep 1971) |
| 3195-41 | 25-57253 | Dep. NTIS, 19p. |
| 3195-42 | 25-57254 | Dep. NTIS, 26p. |
| 3195-43 | 25-57255 | Dep. NTIS, 21p. |
| 3195-44 | 25-57256 | Dep. NTIS, 29p. |
| 3195-45 | 25-57257 | Dep. NTIS, 16p. |
| 3195-46 | 25-57258 | Dep. NTIS, 21p. |
| 3195-47 | 25-57259 | Dep. NTIS, 51p. |
| 3195-48 | 25-57260 | Dep. NTIS, 39p. |
| 3195-49 | 25-57261 | Dep. NTIS, 32p. |
| 3195-50 | 25-57262 | Dep. NTIS, 27p. |
| 3195-51 | 25-57263 | Dep. NTIS, 28p. |
| 3553-17 | 25-57264 | Dep. NTIS, 19p. |
| 3660-4 | 25-54633 | Dep. NTIS, 10p. |
| 3765-31 | 25-56833 | Dep. NTIS, 13p. |
| 3765-32 | 25-56834 | Dep. NTIS, 42p. |
| 3871-6 | 25-56233 | Dep. NTIS, 15p. |
| 3883-3 | 25-57265 | Dep. NTIS, 7p. |
| 3992-1 | 25-56548 | Dep. NTIS, 22p. |
| 3992-2 | 25-56538 | Dep. NTIS, 38p. |
| 3992-7 | 25-56535 | Dep. NTIS, 10p. |
| 3992-8 | 25-56499 | Dep. NTIS, 14p. |
| 3992-9 | 25-56549 | Dep. NTIS, 25p. |
| 3992-10 | 25-56484 | Dep. NTIS, 23p. |
| 3992-11 | 25-56539 | Dep. NTIS, 10p. |
| 3992-14 | 25-56550 | Dep. NTIS, 41p. |
| 3992-18 | 25-56500 | Dep. NTIS, 14p. |
| 3992-42 | 25-56453 | Dep. NTIS, 14p. |
| 3992-66 | 25-56485 | Dep. NTIS, 7p. |
| 4087-1 | 25-56123 | Dep. NTIS, 23p. |
| PATENTS | (British) | |
| 1,224,599 | 25-54922 | |
| 1,226,690 | 25-54990 | |

XUM

| Report No. | Abstract No. | Availability |
|---|---|---|
| 1,226,928 | 25-54931 | |
| 1,227,540 | 25-54841 | |
| 1,229,375 | 25-54855 | |
| 1,229,773 | 25-54860 | |
| 1,230,005 | 25-54856 | |
| 1,230,258 | 25-54915 | |
| 1,230,301 | 25-54859 | |
| 1,230,550 | 25-54988 | |
| 1,233,548 | 25-54845 | |
| 1,235,745 | 25-54978 | |
| 1,236,808 | 25-55657 | |
| 1,240,379 | 25-55014 | |
| 1,240,767 | 25-55010 | |
| 1,241,407 | 25-56603 | |
| 1,241,614 | 25-55011 | |
| 1,242,419 | 25-55060 | |
| 1,243,056 | 25-56605 | |
| 1,243,262 | 25-56626 | |
| 1,243,471 | 25-54896 | |
| 1,243,486 | 25-54977 | |
| 1,243,625 | 25-54835 | |
| 1,245,917 | 25-55019 | |
| 1,246,235 | 25-56624 | |
| 1,246,306 | 25-55398 | |
| 1,246,372 | 25-55009 | |
| 1,246,578 | 25-56111 | |
| 1,247,138 | 25-55062 | |
| 1,247,319 | 25-56079 | |
| PATENTS | (Canadian) | |
| 865,022 | 25-54918 | |
| 872,722 | 25-55597 | |
| PATENTS | (French) | |
| 1,467,228 | 25-55068 | For translation see AEC-tr-7240 |
| 1,528,864 | 25-57195 | |
| 1,566,661 | 25-55027 | |
| 1,567,270 | 25-57204 | |
| 1,567,560 | 25-57041 | |
| 1,567,592 | 25-57015 | |
| 1,567,656 | 25-57199 | |
| 1,567,688 | 25-57209 | |
| 1,568,335 | 25-57200 | |
| 1,568,881 | 25-57010 | |
| 1,569,263 | 25-57197 | |
| 1,569,730 | 25-57208 | |
| 1,571,532 | 25-55913 | |
| 1,572,466 | 25-57058 | |
| 1,577,543 | 25-57203 | |
| 1,579,744 | 25-57198 | |
| 1,591,570 | 25-57236 | For translation see LA-tr-71-73 |
| 2,003,480 | 25-57043 | |
| 2,033,653 | 25-54902 | |
| 2,034,223 | 25-54838 | |
| 2,039,530 | 25-54693 | |
| 2,040,614 | 25-54619 | |
| PATENTS | (German) | |
| 1,464,988 | 25-57210 | |
| PATENTS | (Russian) | |
| 265,300 | 25-55051 | |
| 265,301 | 25-56609 | |
| 269,344 | 25-55012 | |
| 270,114 | 25-54837 | |
| PATENTS | (U. S.) | |
| 3,556,486 | 25-54853 | |
| 3,558,437 | 25-54911 | |
| 3,559,409 | 25-54854 | |
| 3,562,532 | 25-54983 | |
| 3,563,028 | 25-54910 | |
| 3,564,256 | 25-54909 | |
| 3,564,302 | 25-54905 | |
| 3,566,113 | 25-54849 | |
| 3,566,116 | 25-54769 | |
| 3,573,462 | 25-54989 | |
| 3,585,389 | 25-55054 | |
| 3,591,476 | 25-54625 | |
| 3,594,117 | 25-54749 | |
| 3,594,118 | 25-54750 | |
| 3,594,293 | 25-54611 | |
| 3,594,575 | 25-55059 | |
| 3,596,638 | 25-54836 | |
| 3,597,611 | 25-55063 | |
| 3,598,996 | 25-55008 | |
| 3,598,997 | 25-55007 | |
| 3,600,574 | 25-55064 | |
| 3,600,579 | 25-55055 | |
| 3,601,975 | 25-55085 | |
| 3,602,713 | 25-55061 | |
| PNE-R- | | |
| 51 | 25-54813 | Dep. NTIS, 6p. |
| 52 | 25-54817 | Dep. NTIS, 52p. |
| PR-CMa- | (Canadian) | |
| 16 | 25-54587 | See AECL-3909 |
| PR-P- | (Canadian) | |
| 89 | 25-56733 | See AECL-3912 |
| PURC- | | |
| 4159-42 | 25-56442 | Dep. NTIS, 77p. |
| RCN- | (Dutch) | |
| 142 | 25-56749 | Dep. NTIS (U. S. Sales Only), 171p. |
| 144 | 25-55648 | Dep. NTIS (U. S. Sales Only), 76p. |
| 145 | 25-57121 | Dep. NTIS (U. S. Sales Only), 20p. |
| 146 | 25-57026 | Dep. NTIS (U. S. Sales Only), 25p. |
| 147 | 25-57027 | Dep. NTIS (U. S. Sales Only), 59p. |
| RD/B/N- | (British) | |
| 1963 | 25-55042 | Dep. NTIS (U. S. Sales Only), 39p. |
| 1967 | 25-54873 | Dep. NTIS (U. S. Sales Only), 25p. |
| 1980 | 25-54874 | Dep. NTIS (U. S. Sales Only), 20p. |
| 1990 | 25-55578 | Dep. NTIS (U. S. Sales Only), 20p. |
| 2034 | 25-55043 | Dep. NTIS (U. S. Sales Only), 20p. |
| RDT-E- | | |
| 3-3-T | 25-54831 | RSO |
| 4-17-T | 25-54832 | RSO |
| 4-18-T | 25-54833 | RSO |
| 5-1-T | 25-57029 | RSO |
| 5-2-T | 25-57030 | RSO |
| 13-15-T | 25-57049 | RSO |
| RFP-Trans- | | |
| 82 | 25-54437 | Dep. NTIS |
| 87 | 25-55401 | Dep. NTIS |
| RHEL/R- | (British) | |
| 224 | 25-56501 | Dep. NTIS (U. S. Sales Only). UK Pound 1.00, 9ip. |
| RISO-M- | (Danish) | |
| 1391 | 25-57094 | Dep. NTIS (U. S. Sales Only), 57p. |
| RLO- | | |
| 1062-711 | 25-56689 | Dep. NTIS, 45p. |
| 1759-25 | 25-56750 | Dep. NTIS, 15p. |
| 1929-16 | 25-57266 | Dep. NTIS, 6p. |
| 2221-T-7-3 | 25-55434 | Dep. NTIS, 13p. |
| 2221-T-7-4 | 25-55435 | Dep. NTIS, 14p. |
| RMI-L- | | |
| 48 | 25-55402 | Dep. NTIS, 21p. |
| RPI- | (Misc.) | |
| 328-230 | 25-56618 | Dep. NTIS, 58p. |
| RPP/C- | (British) | |
| 24 | 25-56475 | Dep. NTIS (U. S. Sales Only), 59p. |
| RT/FI- | (Italian) | |
| (70)47 | 25-56690 | Dep. NTIS (U. S. Sales Only), 28p. |
| (70)49 | 25-56619 | Dep. NTIS (U. S. Sales Only), 27p. |
| (70)53 | 25-56620 | Dep. NTIS (U. S. Sales Only), 36p. |
| (70)55 | 25-56751 | Dep. NTIS (U. S. Sales Only), 19p. |
| RT/ING- | (Italian) | |
| (71)8 | 25-54875 | Dep. NTIS, 22p. |
| (71)11 | 25-54876 | Dep. NTIS (U. S. Sales Only), 27p. |
| RT/PROT- | (Italian) | |
| (70)3 | 25-54762 | Minerva Fisiconucl.; 13: 225-35(Jul-Sep 1969) |
| (71)11 | 25-54973 | Dep. NTIS (U. S. Sales Only), 34p. |
| SC-DC- | | |
| 713696 | 25-55079 | Dep. NTIS, 32p. |
| SC-DR- | | |
| 710178 | 25-54924 | Dep. NTIS, 46p. |
| 710438 | 25-57267 | Dep. NTIS, 30p. |
| 710463 | 25-57268 | Dep. NTIS, 19p. |
| 710472 | 25-57269 | Dep. NTIS, 25p. |
| SC-M- | | |
| 710241 | 25-54974 | Dep. NTIS, 318p. |
| 710527 | 25-57270 | Dep. NTIS, 30p. |
| SC-RR- | | |
| 710314 | 25-55436 | Dep. NTIS, 172p. |
| 710353 | 25-54895 | Dep. NTIS, 103p. |
| 710424 | 25-56285 | Dep. NTIS, 43p. |
| 710436 | 25-56596 | Dep. NTIS, 94p. |
| 710475 | 25-57271 | Dep. NTIS, 18p. |
| 710483 | 25-57272 | Dep. NTIS, 12p. |
| 710519 | 25-57273 | Dep. NTIS, 14p. |
| 710541 | 25-57274 | Dep. NTIS, 18p. |
| SC-T- | | |
| 713060 | 25-57275 | Dep. NTIS |
| 713061 | 25-57276 | Dep. NTIS |
| 713063 | 25-57277 | Dep. NTIS |
| 713064 | 25-56151 | Dep. NTIS |
| 713065 | 25-56152 | Dep. NTIS |
| 713066 | 25-57278 | Dep. NTIS |
| 713067 | 25-57279 | Dep. NTIS |

XUM

| Report No. | Abstract No. | Availability |
|---|---|---|
| SCL-DR-69-155 | 25-57280 | Dep. NTIS, 74p. |
| SGAE-RT-38/1971 | (Non-AEC) 25-54877 | Dep. NTIS (U. S. Sales Only), 109p. |
| SJC-A-71-3 | (Non-AEC) 25-56597 | Dep. NTIS (U. S. Sales Only), 18p. |
| SLAC-75(Rev.2) | 25-56598 | Dep. NTIS, 117p. |
| 136 | 25-56599 | Dep. NTIS, 60p. |
| SM-145/29 | (Misc.) 25-55317 | See CEA-CONF-1744 |
| SPP-17 | (Non-AEC) 25-55669 | See N-71-26344 |
| 20 | 25-54999 | See N-71-26447 |
| SRO-641-2 | (Misc.) 25-57281 | Dep. NTIS, 87p. |
| STI/PUB-194/4 | (International Atomic Energy Agency) 25-56984 | IAEA $2.00 |
| 259(Vol.1) | 25-56754 | For translation see UCRL-Trans-10541 |
| 259(Vol.2) | 25-56836 | For translation see UCRL-Trans-10542 |
| 259(Vol.2) | 25-56835 | For translation see UCRL-Trans-10540 |
| SUNI-14 | (South African) 25-56752 | Dep. NTIS (U. S. Sales Only), 67p. |
| SWRI-1228-P-7-40 | 25-55378 | Dep. NTIS, 29p. |
| TID-3916(Suppl. 1) | 25-57294 | See WASH-1182 |
| 25773 | 25-54450 | Dep. NTIS, 6p. |
| 25781 | 25-56600 | Dep. NTIS, 123p. |
| 25784 | 25-55437 | Dep. NTIS, 34p. |
| 25789 | 25-57282 | Dep. NTIS, 46p. |
| 25790 | 25-57283 | Dep. NTIS, 85p. |
| 25791 | 25-56916 | Dep. NTIS, 53p. |
| 25801 | 25-55110 | Dep. NTIS, 48p. |
| 25802 | 25-57284 | Dep. NTIS, 14p. |
| 25805 | 25-56917 | Dep. NTIS, 21p. |
| 25806 | 25-56918 | Dep. NTIS, 21p. |
| 25807 | 25-56919 | Dep. NTIS, 22p. |
| 25808 | 25-56920 | Dep. NTIS, 20p. |
| 25809 | 25-56921 | Dep. NTIS, 19p. |
| 25810 | 25-56922 | Dep. NTIS, 19p. |
| 25811 | 25-56923 | Dep. NTIS, 21p. |
| 25812 | 25-56924 | Dep. NTIS, 56p. |
| TRG-Report-1813 | (British) 25-57285 | Dep. NTIS (U. S. Sales Only). UK 50p, 77p. |
| 2086 | 25-55080 | Dep. NTIS (U. S. Sales Only). UK 9p, 6p. |
| UCD-472-118 | 25-55319 | Dep. NTIS, 143p. |
| UCLA-12-832 | 25-57286 | Dep. NTIS, 6p. |
| 34-P-88-32 | 25-54600 | Dep. NTIS, 28p. |



| Report No. | Abstract No. | Availability |
|---|---|---|
| UCRL-51054 | 25-54782 | Dep. NTIS, 52p. |
| 51065 | 25-56266 | Dep. NTIS, 30p. |
| 51075 | 25-57287 | Dep. NTIS, 55p. |
| 51087 | 25-56753 | Dep. NTIS, 26p. |
| 51088 | 25-57288 | Dep. NTIS, 101p. |
| 51098 | 25-57289 | Dep. NTIS, 16p. |
| 73128 | 25-55003 | Dep. NTIS, 10p. |
| 73353 | 25-55814 | Dep. NTIS, 7p. |
| 73387 | 25-56217 | Dep. NTIS, 9p. |
| 73412 | 25-56218 | Dep. NTIS, 9p. |
| UCRL-Trans-10539 | 25-57290 | Dep. NTIS |
| 10540 | 25-56835 | Dep. NTIS |
| 10541 | 25-56754 | Dep. NTIS |
| 10542 | 25-56836 | Dep. NTIS |
| 10543 | 25-54818 | Dep. NTIS |
| 10544 | 25-56837 | Dep. NTIS |
| UJV-2550-Ch | (Czechoslovakian) 25-54720 | Dep. NTIS (U. S. Sales Only), 58p. |
| 2551-RT | 25-57050 | Dep. NTIS (U. S. Sales Only), 45p. |
| UR-49-1515 | 25-57291 | Dep. NTIS, 50p. |
| 49-1516 | 25-57292 | Dep. NTIS, 133p. |
| 49-1517 | 25-57293 | Dep. NTIS, 116p. |
| 875-350 | 25-56838 | Dep. NTIS, 217p. |
| USIP-71-1 | (Swedish) 25-56416 | Dep. NTIS (U. S. Sales Only), 44p. |
| 71-3 | 25-56523 | Dep. NTIS (U. S. Sales Only), 63p. |
| 71-4 | 25-56417 | Dep. NTIS (U. S. Sales Only), 52p. |
| 71-6 | 25-56418 | Dep. NTIS (U. S. Sales Only), 69p. |
| WAPD-331 | (Misc.) 25-54834 | Dep. NTIS, 215p. |
| WAPD-TM-943 | (Misc.) 25-55579 | Dep. NTIS, 21p. |
| WARD-4210-T-1-2 | 25-55379 | Dep. NTIS, 67p. |
| WASH-1167 | 25-54975 | Dep. NTIS, 41p. |
| 1182 | 25-57294 | GPO $0.35 |
| WCAP-7422 | (Misc.) 25-57095 | |
| 7562-4 | 25-55004 | Dep. NTIS, 45p. |
| 7703 | 25-56940 | See DOCKET-50244-78 |
| 7722 | 25-57096 | |
| 7744 | 25-57097 | |
| 7755 | 25-57031 | |
| X-661-71-36 | (Misc.) 25-55046 | See N-71-16750 |
| Y-1790 | 25-57295 | Dep. NTIS, 134p. |
| Y-IA-92 | 25-57296 | Dep. NTIS, 13p. |
| ZJE-104 | (Czechslovakian) 25-56880 | Dep. NTIS (U. S. Sales Only), 28p. |

☆U. S. GOVERNMENT PRINTING OFFICE: 1971—745-063/12

XUM

UNITED STATES
ATOMIC ENERGY COMMISSION
P. O. BOX 62
OAK RIDGE, TENNESSEE 37830

OFFICIAL BUSINESS

POSTAGE AND FEES PAID
U. S. ATOMIC ENERGY COMMISSION

GOVI

ND FEES PAID
NT PRINTING OFFICE

U.S.MAIL

UNIVERSITY MICROFILMS
SERIAL PUBLICATIONS
300 NORTH ZEEB ROAD
ANN ARBOR MICHIGAN 48106

1

# nuclear-explosion seismology

AEC Critical Review Series

**Howard C. Rodean**
Seismic/Evasion Research
Lawrence Livermore Laboratory

September 1971
166 pages, 49 illustrations, 7 x 9¾ in.
Library of Congress Card Number: 73-170333

Mr. Rodean investigates the generation of seismic signals by underground nuclear explosions, including decoupling and low-coupling phenomena that minimize these signals. Careful throughout to define terms and avoid ambiguities, he describes the effects of rock-property variations on seismic-signal strength and summarizes principles of elastic-wave theory for compressional, shear, and Rayleigh waves. Theoretical compressional wave solutions are given for both ground motion and seismometer response to this motion. Available seismic-magnitude data are presented as a function of explosion yield and environment. Mr. Rodean concludes with a summary of what is and is not known about seismic-signal generation by underground nuclear explosions.

CONTENTS

Inelastic Response to Nuclear Explosions
Distribution of Energy from Underground Nuclear Explosions
Linear Elastic (Seismic) Waves from Explosions
Anelastic Attenuation of Seismic Signals
Seismometer Characteristics and Operating Environment
Distant Seismic Signals from Underground Nuclear Explosions
Techniques to Minimize Seismic Signals
References
Author and Subject Indexes

This book is available as TID-25572 for $3.00 from
National Technical Information Service, U. S. Department of Commerce,
Springfield, Virginia 22151

XUM

XUM